233093

– PUBLIC VERSION –
CONFIDENTIAL AND HIGHLY CONFIDENTIAL INFORMATION HAS BEEN REDACTED

BEFORE THE
SURFACE TRANSPORTATION BOARD

OCT 1 2012
RECEIVED

REASONABLENESS OF BNSF RAILWAY COMPANY COAL DUST MITIGATION TARIFF PROVISIONS	)))))	Finance Docket No. 35557

OPENING EVIDENCE AND ARGUMENT OF WESTERN COAL TRAFFIC LEAGUE, AMERICAN PUBLIC POWER ASSOCIATION, EDISON ELECTRIC INSTITUTE AND NATIONAL RURAL ELECTRIC COOPERATIVE ASSOCIATION

William L. Slover
John H. LeSeur
Andrew B. Kolesar III
Peter A. Pfohl
Slover & Loftus LLP
1224 Seventeenth St., N.W.
Washington, D.C. 20036
(202) 347-7170

Their Attorneys

Dated: October 1, 2012

TABLE OF CONTENTS

Page

SUMMARY 1

IDENTITY AND INTEREST 5

BACKGROUND 7

A. BNSF's Original Coal Dust Tariff 7

B. The Dust I Proceedings 9

C. BNSF's Revised Coal Dust Tariff 11

D. The Dust II Proceedings 12

ARGUMENT 15

I. The Revised Coal Dust Tariff is Unreasonable Because it is Based on Junk Science 15

A. The Board Rejected BNSF's Original Coal Dust Tariff Due to the Many Flaws in BNSF's Emission Monitoring and Emission Testing 16

B. BNSF's Dust II Tariff is Similarly Flawed 18

C. BNSF's Use of a "Safe Harbor" Does Not Excuse its Failed Science 20

D. Shippers Are Employing Cost-Effective Containment Practices 22

II. The Revised Coal Dust Tariff is Unreasonable Because it Requires Shippers to Bear All Compliance Costs 24

A. The Law Requires BNSF to Incur All Reasonable Spraying Costs 24

B. The Law Precludes BNSF from Requiring Shippers to Pay Twice for the Same Service 28

C. It is Fundamentally Unfair for Shippers to Pay More, While BNSF Pays Less 30

D. Requiring Shippers to Pay a Separate Charge for Coal Dust Mitigation is Contrary to Industry Practice 32

E. Fair Cost Sharing Requires BNSF to Reimburse Shippers for Their Reasonably Incurred Compliance Costs 33

III. The Revised Coal Dust Tariff is Unreasonable Because it Contains No Enforcement Provisions 33

IV. The Revised Coal Dust Tariff is Unreasonable Because BNSF's Train Profiling Monitoring Practices are Arbitrary 36

V. The Revised Coal Dust Tariff is Unreasonable Because BNSF Unlawfully Attempts to Insulate Itself from Liability 38

VI. Requested Relief 39

BEFORE THE
SURFACE TRANSPORTATION BOARD

REASONABLENESS OF BNSF RAILWAY COMPANY COAL DUST MITIGATION TARIFF PROVISIONS	)))))	Finance Docket No. 35557

OPENING EVIDENCE AND ARGUMENT OF WESTERN COAL TRAFFIC LEAGUE, AMERICAN PUBLIC POWER ASSOCIATION, EDISON ELECTRIC INSTITUTE AND NATIONAL RURAL ELECTRIC COOPERATIVE ASSOCIATION

In response to the Surface Transportation Board's ("STB" or "Board") decision served in this proceeding on July 31, 2012, the Western Coal Traffic League ("WCTL"), American Public Power Association ("APPA"), Edison Electric Institute ("EEI") and the National Rural Electric Cooperative Association ("NRECA") (collectively "Coal Shippers") present the following joint opening evidence and argument.

SUMMARY

In Dust I,[1] the Board found that BNSF's publication of the Original Coal Dust Tariff[2] was an unreasonable practice. The Board strongly admonished BNSF

[1] *Ark. Elec. Coop. Corp. – Petition for Declaratory Order*, STB Finance Docket No. 35305 ("Dust I").

[2] "Original Coal Dust Tariff" refers to Item 100, entitled "Coal Dust Mitigation Requirements," initially published on April 30, 2009 in Revision 011 to BNSF's Price List 6041-B and Item 101, entitled "Coal Dust Requirements Black Hills Sub-Division," initially published on May 27, 2009 in Revision 012 to BNSF's Price List 6041-B. The

Railway Company ("BNSF") to work collaboratively with its coal shippers to develop a reasonable alternative.[3] Unfortunately, BNSF failed to heed the Board's advice. As one BNSF manager put it, the "*substance*" of coal dust rules "is not a proper subject of negotiation between railroads and their shippers."[4] BNSF proceeded to ignore shippers and published its Revised Coal Dust Tariff[5] in July of 2011.

BNSF's failure to work with its shippers has led to this proceeding – Dust II. Coal Shippers' opening evidence and argument demonstrates that BNSF's unilateral actions have resulted in its repetition of the errors that led the Board to reject the Original Coal Dust Tariff. Specifically, Coal Shippers demonstrate in this opening submission:

- **The Revised Coal Dust Tariff, like the Original Coal Dust Tariff, is unreasonable because it is rooted in bad science.** Coal shippers presented detailed evidence in Dust I demonstrating that BNSF's Original Coal Dust Tariff was grounded in bad science, including a faulty and arbitrary attempt to measure coal dust emissions from moving coal cars. The Board agreed, stating that it "share[d]" shipper's concerns about

---

Original Coal Dust Tariff referred to an "IDV.2" value, which for ease of reference is referred to herein simply as an "IDV" value.

[3] Dust I, STB decision served March 3, 2011 at 14 ("Dust I Decision").

[4] Dust I, BNSF Railway Company's Reply to Western Coal Traffic League's Petition to Reopen and For Injunctive Relief Pending Board-Supervised Mediation, Verified Statement of Stevan B. Bobb ("Bobb V.S.") at 4 (Aug. 23, 2011) ("BNSF Dust I Reop. Reply") (emphasis in original).

[5] "Revised Coal Dust Tariff" refers to Item 100, entitled "Coal Dust Mitigation Requirements," as published on July 14, 2011 in Revision 016 to BNSF's Price List 6041-B, including subsequent revisions to date.

BNSF's coal dust science.[6] BNSF's Revised Coal Dust Tariff is similarly flawed, and must be rejected because it is predicated on faulty and arbitrary testing of coal dust emissions from moving coal cars.

- **The Revised Coal Dust Tariff, like the Original Coal Dust Tariff, is unreasonable because it places all compliance costs on coal shippers.** The Revised Coal Dust Tariff requires shippers to apply expensive surfactants to their coal cars, at a publicly estimated cost of between $50 to $150 million.[7] It is unreasonable for shippers to pay these huge sums because the law places the payment responsibility on BNSF and payment of the charges results in shipper's double paying for the same services. Payment of these additional sums is particularly outrageous because BNSF, and Union Pacific Railroad Company ("UP"), are already earning billions of profits annually on the coal traffic subject to the Revised Coal Dust Tariff.

- **The Revised Coal Dust Tariff, like the Original Coal Dust Tariff, is unreasonable because it contains no enforcement provisions.** In Dust I, shippers emphasized that the Original Coal Dust Tariff contained no enforcement provisions. The Board cited the lack of such provisions in rejecting the Original Coal Dust Tariff.[8] Nevertheless, the Revised Coal Dust Tariff contains no enforcement provisions, a particularly egregious oversight in light of statements reported in the trade press that BNSF may shut down coal trains or impose draconian financial penalties. Coal

---

[6] Dust I Decision at 13.

[7] *See* Dust I, Opening Statement of the National Coal Transportation Association ("NCTA") at 6 (March 16, 2010).

[8] Dust I Decision at 14.

transportation, as the Board has repeatedly observed, is vital to national energy security, and that security is too important for BNSF to be permitted to play cat and mouse games with its tariff enforcement.

- **The Revised Coal Dust Tariff, like the Original Coal Dust Tariff permits arbitrary train profile monitoring.** Several years ago, private sector negotiations led to an agreement between Powder River Basin ("PRB") coal shippers, PRB mine operators, and PRB railroads (BNSF and UP): mines would install loading chutes to load trains to meet a streamlined "profile" intended to reduce coal dust emissions from moving coal cars. All PRB mines now employ these chutes. Nevertheless, BNSF proposes to monitor compliance with its profiling requirements at locations that are far from PRB mines. This monitoring procedure produces arbitrary, skewed results, because once a train leaves the mine, train profiles can and do change for causes beyond shipper's control, including wind, train speed, and train vibration.

- **The Revised Coal Dust Tariff, like the Original Coal Dust Tariff, unlawfully limits BNSF's liability.** The Revised Coal Dust Tariff mandates that mine operators spray BNSF-approved surfactants on shippers' cars and then says, as did the Original Coal Dust Tariff, that shippers bear all liability – including liability for BNSF's own negligence – for any spray-related harm to "railroad employees, property, locomotives or owned cars." This attempt at liability shifting is blatantly unlawful. Liability to "railroad employees, property, locomotives or owned cars" is governed by state tort law, or other laws not administered by the STB. BNSF cannot rewrite this law through the publication of a common carrier tariff. It is also particularly arrogant for

BNSF to force shippers to spray their trains, and then try to exempt itself from ensuing liability.

In this opening submission, Coal Shippers present the expert verified statement of Dr. Mark J. Viz ("Viz V.S.") and the expert verified statement of Dr. Ralph W. Barbaro ("Barbaro V.S."). Dr. Viz is one of the nation's leading experts on fugitive dust emissions. Dr. Barbaro is a preeminent authority in matters related to coal production. Coal Shippers also rely on other verified evidence that WCTL tendered in Dust I, including evidence submitted by Paul H. Reistrup, one of the nation's foremost experts on rail operating practices, and Thomas D. Crowley, one of the nation's leading experts on railroad economics.[9]

IDENTITY AND INTEREST

WCTL is an association whose membership is composed of organizations that purchase and transport coal mined west of the Mississippi River. WCTL members transport over 140 million tons of coal annually, nearly all of which moves by rail. Since its formation in 1977, WCTL has actively participated in all major proceedings before the Board and its predecessor, the Interstate Commerce Commission ("ICC" or "Commission"), involving issues of concern to western coal shippers, including Dust I.

APPA is the national service organization representing the interests of over 2,000 municipal and other state- and locally-owned electric utilities in 49 states (all but

[9] The Board extended the protective order in Dust I to permit WCTL and BNSF to tender, in Dust II, confidential and highly confidential information they submitted in their Dust I pleadings. *See* Dust II, STB decision served Jan. 13, 2012 at 2.

Hawaii). Collectively, public power utilities deliver electricity to one of every seven electric consumers (approximately 46 million people), serving some of the nation's largest cities, but also many of its smallest towns. Over 40% of public power utilities generate power from coal.

EEI is the association of U.S. shareholder-owned electric utility companies. EEI's members serve 95 percent of the ultimate customers in the shareholder-owned segment of the industry, and they represent approximately 70 percent of the U.S. electric power industry. EEI's diverse membership includes utilities operating in all regions, including in regions with Regional Transmission Organizations and Independent System Operators, and companies supplying electricity at wholesale in all regions.

NRECA is the national service organization for more than 900 not-for-profit rural electric utilities that provide electric energy to approximately 42 million consumers in 47 states or 13 percent of the nation's population. Kilowatt-hour sales by rural electric cooperatives account for approximately 11 percent of all electric energy sold in the United States. NRECA members generate approximately 50 percent of the electric energy they sell and purchase the remaining 50 percent from non-NRECA members.

The vast majority of NRECA members are not-for profit, consumer-owned cooperatives. NRECA's members also include approximately 65 generation and transmission ("G&T") cooperatives, which generate and transmit power to 668 of the 841 distribution cooperatives. The G&Ts are owned by the distribution cooperatives they serve. Remaining distribution cooperatives receive power directly from other generation

sources within the electric utility sector. Both distribution and G&T cooperatives were formed to provide reliable electric service to their owner-members at the lowest reasonable cost.

Collectively, member companies of WCTL, APPA, EEI and NRECA comprise the vast majority of shippers that purchase, and pay for, the transportation of coal from PRB mines located in the states of Wyoming and Montana.

BACKGROUND

A. BNSF's Original Coal Dust Tariff

Dust I involved the legality of BNSF's Original Coal Dust Tariff. That Tariff called for BNSF's PRB coal shippers to "profile[]" their trains to meet a bread-loaf configuration specified by BNSF and to take steps to "ensure" that these trains would "not emit more than an Integrated Dust Value" ("IDV") of 300 "units" on the Joint Line[10] and 245 "units" on the Black Hills Subdivision. *Id.*

The Tariff further provided that coal shippers were to bear all liability for any "adverse[] impact[s]" to railroad employees or property caused by shipper efforts to comply with the IDV standards through use of train surfactants or other means. *Id.*

[10] The "Joint Line" refers to a line of railroad in the Wyoming PRB that is jointly owned by BNSF and UP. BNSF operates this line and establishes operating rules over the line. *See* Dust I Decision at 2 n.5.

Finally, BNSF published an operating rule that applied the Original Coal Dust Tariff requirements to UP trains moving over the Joint Line.[11]

Under BNSF's convoluted IDV-based tariff scheme, trains moved past "E-Samplers" which recorded emissions in the air.[12] The E-Sampler data was uploaded to a consulting firm in Charlottesville, Virginia, which then used a secret computer program to produce an IDV reading for each train.[13] BNSF asserted this IDV calculation measured "the volume of coal dust coming off the coal train over its entire length."[14]

BNSF also attempted to monitor compliance with its train profiling requirements by lasering trains at locations many miles away from PRB mines to see if the required profile remained intact.[15] The tariff did not contain any enforcement provisions, but BNSF officials were quoted in the trade press as saying that BNSF planned to shut-down trains, or impose penalties of $1.00 per ton (or both), if shippers failed to comply with the IDV and train profiling requirements.[16]

---

[11] Dust I, BNSF Railway Company's Opening Evidence and Argument at 26 (March 16, 2010) ("BNSF Dust I Op.").

[12] BNSF Dust I Op., Verified Statement of G. David Emmitt ("Emmitt V.S.") at 8 (Mar. 16, 2010).

[13] Dust I, Opening Evidence and Argument of Western Coal Traffic League and Concerned Captive Coal Shippers, V.S. of Dr. Mark J. Viz at 16 (Mar. 16, 2010) ("WCTL Dust I Op.").

[14] Original Coal Dust Tariff.

[15] Dust I, Rebuttal Evidence and Argument of Western Coal Traffic League and Concerned Captive Coal Shippers at 65 (June 4, 2010) ("WCTL Dust I Reb.").

[16] WCTL Dust I Op. at 49 n.24.

According to BNSF, the purpose of its convoluted IDV-based Original Coal Dust Tariff was to reduce coal dust emissions from the tops of moving coal cars by 85%.[17] BNSF believed this reduction would "substantially eliminate" coal dust in the ballast of the Joint Line and Black Hills Subdivision.[18] BNSF also opined that it was confident, based on IDV readings it had taken on "thousands" of PRB coal trains,[19] that shippers could meet the 85% reduction standard through train profiling, and spraying trains with surfactants – chemicals that are intended to bind coal.[20]

B. The Dust I Proceedings

Arkansas Electric Cooperative Corporation ("AECC") challenged the legality of BNSF's Original Coal Dust Tariff in a declaratory order action filed in October of 2009. In the ensuing proceedings at the STB, WCTL, and other coal shippers, submitted extensive evidence and argument demonstrating that BNSF's publication of the Original Coal Dust Tariff constituted an unreasonable practice.

These submissions proved that BNSF's IDV measurement system was not based on sound science; that there were no proven methods to comply with the IDV standards; that shippers were not legally required to pay for treatment of their trains with expensive surfactants; that the tariff unlawfully failed to state how the IDV standards would be enforced (and what penalties would apply if the standards were not met); that

---

[17] BNSF Dust I Op. at 15.

[18] *Id.* at 15.

[19] *Id.* at 6.

[20] *Id.* at 7, 13-14.

BNSF's proposed procedures to monitor compliance with the tariff train profiling monitoring requirements were arbitrary; that BNSF's attempts to insulate itself from all liability for application of surfactants were illegal; and that BNSF lacked the legal authority to compel UP shippers to comply with the tariff requirements.[21]

In its Dust I Decision served on March 3, 2011, the Board found that BNSF's publication of the Original Coal Dust Tariff constituted an unreasonable practice. The Board predicated this finding on three of the arguments raised by WCTL and other coal shippers: the IDV standards were not based on sound science;[22] there was no demonstrated compliance mechanism;[23] and the tariff did not set forth the penalties for non-compliance.[24] Because the Board found that the tariff was unreasonable on these three grounds, the Board determined it was unnecessary to address shippers' additional showings of tariff unreasonableness.[25] The Board proceeded to urge BNSF and its

---

[21] *See, e.g.*, WCTL Dust I Op. at 1-55; Reply Evidence and Argument of Western Coal Traffic League and Concerned Captive Coal Shippers at 1-32 (April 30, 2010) ("WCTL Dust I Reply"); WCTL Dust I Reb. at 1-76.

[22] *See* Dust I Decision at 13 ("The Board shares many of the Shipper Interests' concerns regarding the . . . proprietary IDV.2 measurement system.").

[23] *See id.* at 14 ("lacking some sort of safe harbor provision, no shipper can ever be confident that any particular movement it tenders will be in compliance.").

[24] *See id.* at 14 ("the tariff does not explain what consequences coal shippers would face if they are found to have tendered loaded coal cars to the railroad that subsequently released coal dust during transport").

[25] *See id.* at 15 ("there are multiple arguments that the Board does not address given our finding that the tariff is unreasonable").

customers to "collaborate" (*id.* at 14) to develop "cost-effective practices" to address "the coal dust problem."[26]

C. BNSF's Revised Coal Dust Tariff

BNSF ignored the Board's directive. Instead of working cooperatively with its shippers, BNSF unilaterally published its Revised Coal Dust Tariff in July of 2011. The Revised Tariff called for BNSF shippers originating coal from BNSF-served mines in Wyoming and Montana to reduce coal dust emissions from their loaded coal cars "by at least 85 percent" starting on "October 1, 2011." The Revised Coal Dust Tariff further provided that shippers would be "deemed to be in compliance" with the 85% reduction standard if they met train profiling requirements and properly applied a BNSF-approved surfactant or other form of BNSF-approved dust suppression.

BNSF listed three approved surfactants in the appendix to the Revised Coal Dust Tariff.[27] BNSF said that it had approved these surfactants based on the results of "recent tests carried out in the PRB."[28] The Revised Coal Dust Tariff also required, as did the Original Coal Dust Tariff, that shippers guarantee that application of BNSF approved surfactants "shall not adversely impact railroad employees, property, locomotives or owned cars."[29] The full text of the Revised Coal Dust Tariff is set forth in

---

[26] *See id.* at 5.

[27] *Id.* BNSF subsequently added two additional approved surfactants in Revision 18, and a third in Revision 20, to the Revised Coal Dust Tariff.

[28] *Id.*

[29] *Id.*

Counsel's Exhibit 1. Finally, BNSF issued a new Joint Line operating rule that required UP to comply with the terms of the Revised Coal Dust Tariff.[30]

In apparent response, UP published two new tariff rules. The first tariff rule "recommend[s]" that UP shippers purchasing PRB coal under contracts "issued on or prior to September 30, 2011" comply with the standards set forth in BNSF's Revised Coal Dust Tariff.[31] The second tariff rule "require[s]" that UP shippers purchasing PRB coal under contracts "issued after September 30, 2011" or under common carrier tariffs "effective October 1, 2011," comply with the standards set forth in BNSF's Revised Coal Dust Tariff.[32] The full text of these two UP tariff items, and their recent updates, is set forth in Counsel's Exhibit 2.

D. The Dust II Proceedings

On August 12, 2011, WCTL filed a petition asking the Board to reopen the Dust I case and to enjoin the application of the Revised Coal Dust Tariff pending the completion of a Board-supervised mediation.[33] WCTL took this action because BNSF had not adhered to the Board's admonition to work collaboratively with its shippers to develop reasonable coal dust practices, and, as a direct result, BNSF's Revised Coal Dust Tariff continued to be unreasonable because it was not based on sound science, it required shippers to bear all compliance costs, it failed to contain enforcement provisions,

---

[30] *See* BNSF Dust I Reop. Reply, Bobb V.S. at 8.

[31] UP Circular 6603-C, Item 215 (effective Sept. 30, 2011).

[32] UP Circular 6603-C, Item 216 (effective Sept. 30, 2011).

[33] *See* Dust I, Petition to Reopen and For Injunctive Relief Pending Board-Supervised Mediation (Aug. 11, 2011) ("WCTL Dust I Reop. Pet.").

it called for arbitrary monitoring of train profiling, and it attempted to insulate BNSF from liability. *Id.* at 7-8.

WCTL's petition was supported by all major coal shipper groups,[34] but opposed by BNSF and UP.[35] In its opposition filing BNSF made clear that in its view, collaboration was a one-way street. As one of BNSF's Vice Presidents put it, "the *substance* of operating rules is not a proper subject of negotiation between railroads and their shippers."[36] BNSF also argued that a stay of the Revised Coal Dust Tariff was unnecessary because BNSF would not enforce the Revised Tariff without giving affected shippers sixty days advance notice.[37]

The Board addressed WCTL's request for a stay in its decision served on August 31, 2011. The Board found that WCTL's request for a stay was effectively moot in light of BNSF's representations that it would not enforce the Revised Tariff. *See id.* at 3 ("shippers face[] no current possibility of a sanction for noncompliance"). The Board addressed WCTL's request to reopen, and for mediation, in its decision served on Nov 22, 2011.

---

[34] *See* Dust I, letter filed Aug. 23, 2011 (APPA, EEI and NRECA support WCTL's petition); letter filed Aug. 24, 2011 (NCTA supports WCTL's petition); letter filed Aug. 22, 2011 (CURE supports WCTL petition). AECC also filed a pleading supporting WCTL's petition on August 19, 2011.

[35] *See* BNSF's Dust I Reop. Reply at 1; Union Pacific Railroad Company's Reply to the Western Coal Traffic League's Petition to Reopen and for Injunctive Relief Pending Board-Supervised Mediation at 1 (Aug. 26, 2011).

[36] BNSF Dust I Reop. Reply, Bobb V.S. at 4.

[37] *Id.* at 7.

In this second decision, the Board concluded that the most effective way to address the issues raised in WCTL's petition was not to reopen Dust I, and mediate, but instead to institute a new proceeding.[38] As the Board explained, "[t]he new proceeding will allow parties to address issues raised by WCTL that are related to the reasonableness of the safe harbor provision, such as the absence of penalties for noncompliance, the lack of cost sharing, and shipper liability associated with the use of BNSF-approved topper agents."[39]

In the ensuing Dust II proceedings, the Board has entered a protective order;[40] modified the protective order it entered in Dust I to permit, *inter alia*, WCTL to utilize its confidential/highly confidential Dust I pleadings in Dust II;[41] resolved various discovery disputes;[42] and approved a procedural schedule permitting parties of record to submit three rounds of evidence and argument.[43]

---

[38] Dust II, STB decision served Nov. 22, 2011 at 4.

[39] *Id.* at 4 n.5. The Board later clarified that the issues that could be raised in this case were "not limited to" those it cited in this list. *See* Dust II, STB decision served March 19, 2012 at 1.

[40] *Id.*, Dust II, STB decisions served Jan. 13, 2012 and April 23, 2012,

[41] *Id.*

[42] *Id.*, Dust II, STB decisions served March 5, 2012, March 19, 2012, April 30, 2012 and June 25, 2012 (affirming Dust II Decision served Feb. 27, 2012).

[43] *Id.*, Dust II, STB decision served Dec. 16, 2011, as modified, Dust II, STB decisions served Feb. 27, 2012 and July 31, 2012.

ARGUMENT

The Revised Coal Dust Tariff appears to be BNSF's answer to the Board's Dust I Decision. However, the Board made it very clear in this decision that it "expect[ed] that railroads and their customers will collaborate" to "develop reasonable solutions to the problems presented in this case." Dust I Decision at 14. BNSF ignored the Board's directive. By pursuing unilateral action BNSF failed to adhere to the Board's Dust I Decision, and the resulting Revised Coal Dust Tariff continues to be unreasonable.

I.

THE REVISED COAL DUST TARIFF IS UNREASONABLE BECAUSE IT IS BASED ON JUNK SCIENCE

Coal Shippers demonstrated in Dust I that the coal dust mitigation standards in the Original Coal Dust Tariff were predicated on junk science, and that publication of a tariff based on junk science was an unreasonable practice. The Board agreed. BNSF has made the same mistake again. The coal dust mitigation standards in the Revised Coal Dust Tariff are based on junk science, and publication of a tariff based on this junk science is an unreasonable practice.[44]

---

[44] *See* Dust I, Reply Comments of the U.S. Department of Transportation at 1 ("DOT Dust I Reply") (to obtain regulatory approval, the "tariff rule at issue must be reasonable, which means that the Board must be satisfied that the methodology on which it is based is sound").

A. The Board Rejected BNSF's Original Tariff Due to the Many Flaws in BNSF's Emission Monitoring and Emission Testing

BNSF's Original Cost Dust Tariff's IDV methodology was developed in secret by BNSF with no meaningful input by rail shippers concerning the associated "science" behind the methodology. BNSF's closed-door policy left shippers with no alternative other than to challenge the Original Coal Dust Tariff in proceedings before this Board, and then use the Board's discovery processes to try to obtain the material necessary to understand and fairly evaluate BNSF's IDV "science."

Once BNSF's closed door was pried open in the Dust I proceedings, it was easy to see why BNSF did not want to let shippers see the innards of its IDV calculations. WCTL and other coal shippers demonstrated that BNSF's IDV-based approach to dust monitoring was fatally flawed in numerous respects: the E-Samplers BNSF relied on to collect dust from coal trains were not isolating coal dust; the E-Samplers produced wildly different readings in "side-by-side" testing; the E-Sampler filters were not being used, in contravention of the manufacturer's instructions; the IDV values purportedly being calculated using the E-Sampler results were the product of some unproduced computer program; and to the extent the program mechanics could be deciphered, they appeared to have significant statistical flaws.[45] In short, coal shippers demonstrated that BNSF's IDV-based system was based on garbage in/garbage out, rendering the IDV results unreliable, and a tariff based on them unreasonable.

---

[45] *See, e.g.*, WCTL Dust I Op. at 25-33; WCTL Dust I Reply at 17-19; WCTL Dust I Reb. at 30, 50.

In its Dust I Decision, the STB agreed with the coal shippers' demonstration:

> The Board is . . . concerned with technical aspects of BNSF's monitoring system and emission standards. The Shipper Interests claim that the monitoring system produces variable and unreliable results. For example, the Shipper Interests contend that the monitoring system does not account for the fact that dust dispersion is sporadic because of factors like wind speed, and they emphasize that when BNSF placed two E-Samplers next to each other for testing, one monitor had 31% higher readings than the other . . . .
>
> The Shipper Interests also claim that the monitors do not measure coal dust deposited on the tracks; instead, the monitors measure a variety of particles in the air many feet from the tracks. . . .
>
> The Shipper Interests assert that BNSF violated Board rules of practice when it did not provide the computer program it uses to convert the E-Sampler data into IDV.2 values, and that the "detailed logic and assumptions" that BNSF states it provided are insufficient for a full analysis. The Shipper Interests contend that the statistical analysis BNSF used to develop the IDV.2 standards is flawed and that BNSF was unable to find a third party to validate the methodology. . . .
>
> The Board shares many of the Shipper Interests' concerns regarding the methods of effective compliance and the proprietary IDV.2 measurement system. . . .
>
> . . . . [T]he railroad's trackside coal dust emission monitoring system raises additional questions. Shippers have raised legitimate concerns about their lack of access to equipment testing and other technical data before being asked to accept the equipment's measurements and the subsequent liability that would be triggered by those measurements.

Id. at 12-14 (footnotes omitted).[46]

B. BNSF's Dust II Tariff is Similarly Flawed

BNSF's Revised Coal Dust Tariff's "safe harbor" reflects the same closed-door/junk science approach. BNSF claims that "recent tests carried out in the PRB" demonstrate that three topper sprays, if properly applied and used in conjunction with train profiling, will reduce coal train emissions by 85%. *Id.* The "tests" BNSF is referring to are the so-called "Super Trial" tests BNSF conducted in 2010.[47]

The purpose of BNSF's Super Trial was to identify dust suppression sprays that, when applied to shippers' profiled trains, would meet BNSF's minimum IDV values.[48] 1,633 treated trains were tested, with IDV values calculated for 1,518 trains. BNSF claimed that the test results showed that different topically applied sprays produced different IDV values, but all produced dust reductions when compared to unsprayed trains.[49] The testing on these 1,518 trains must be thrown out for the same reasons the STB rejected the Original Coal Dust Tariff – BNSF's attempt to calculate train IDV does not produce reliable estimates of actual coal dust emissions.

---

[46] BNSF has now abandoned its IDV monitoring system for regulatory use. *See* BNSF Railway Company's Responses and Objections to Coal Shippers' First Set of Interrogatories and Document Requests at 11 (Jan. 9. 2012) ("BNSF Dust II Discovery Responses") ("BNSF states that it does not intend to use . . . E-Samplers to determine compliance with [the Revised Coal Dust Tariff]").

[47] *See* BNSF Dust I Reop. Reply at 9.

[48] *See* WCTL Dust I Reop. Pet., Verified Statement of Duane L. Richards ("Richards V.S."), Attachment 7 at 1.

[49] *Id.*, Attachment 8 at 2.

The remaining 115 trains – only 7% of the total trains tested – were composed of trains where one-half of the cars on a train were treated with a particular topper or full body spray and one-half of the cars on the same train were untreated. *Id.* at 1. BNSF placed passive collectors on a few treated and untreated cars in each train, collected particulate samples, and purported to process the results in a manner that identified the percent reduction in coal dust emissions between the sprayed and unsprayed particulate samples. *Id.*

WCTL asked Dr. Viz to review BNSF's passive collector study. He found that this study suffers from many of the same types of flaws that led the Board to reject BNSF's IDV study results, as well as additional new flaws:

- Dust sprays were designed for use in "static coal stockpiles at coal-burning power plants." Viz V.S. at 3. Sprays can "work when applied to a large pile of coal *that is stationary*, but there are still many aspects of their performance *in moving railcars* that have not yet been verified." *Id.* Indeed, in some instances, spraying can lead to increased dust emissions. *Id.*

- BNSF's 115 train size sample, as well as the much smaller sample sizes used to evaluate individual surfactants, were too small to "make any statistically significant inferences" concerning the effectiveness of broad-scale train spraying. *Id.* at 22-23.

- BNSF has failed to provide explanations or documents in discovery that explain key aspects of its passive collector measurements. *Id.* at 8-14, 16-20, 23.

- To the extent that Coal Shippers can decipher BNSF's passive collector measurements, it is clear that BNSF: {

}

- BNSF's passive collector testing was set up and supervised by the same consultants that produced the thoroughly discredited IDV measurement system, {

}

Based upon these, and other, "fundamental flaw[s]"[50] identified by Dr. Viz in BNSF's passive collector procedures, BNSF's passive collector study results, like its IDV results, do not provide a reasonable measure of actual coal dust emissions from any train, and certainly "cannot be used to scientifically establish the amount, if any, of fugitive particulate emissions from railcars with certainty, reliability or repeatability, nor can they be used to scientifically establish the quantitative effectiveness (in terms of percent reduction in dust emissions), if any, of the application of coal dust suppressants." *Id.* at 3.

C. BNSF's Use of a "Safe Harbor" Does Not Excuse its Failed Science

BNSF argues that even if its measurement of coal dust emissions produces wildly inaccurate measurements of coal dust, this result is of no practical consequence because "BNSF's coal dust rule gives shippers a safe harbor if they choose to use specific

[50] *Id.* at 7.

topper agents."[51] Of course, the existence of a "safe harbor" does not make the Revised Coal Dust Tariff reasonable.[52] Where, as here, the tariff is premised on studies of coal dust emissions that are fundamentally flawed, the tariff itself must be rejected. Shippers (or carriers) should not be required to expend millions to comply with a tariff that is not based on sound science.

The Department of Transportation ("DOT") reached the same conclusion in Dust I. DOT emphasized that any dust containment tariff must be based on a "sound" methodology for measuring coal dust emissions that has a "well-grounded scientific basis":

> [a]s a legal matter . . . the Board must be satisfied that BNSF's methodology and results are sound. In other words, that collection, measurement, and analysis of coal dust, as well as translation of these data into quantitative limits, all have a well-grounded scientific basis such that they accurately capture the extent of the emissions and effectively redress their impact. . . BNSF's emission limits would be unreasonable if they were based upon faulty collection, measurement, or analysis of coal dust emissions, or if they required steps that would not redress the problem.

DOT Dust I Reply at 6.

In the absence of any sound testing of coal dust emissions from moving coal cars, no valid conclusions can be drawn as to whether any percentage dust reduction

---

[51] BNSF Dust I Reop. Reply, Emmitt V.S. at 2. This position is inconsistent with the one taken by BNSF earlier in Dust I. *See* BNSF Dust I Op., Verified Statement of William VanHook ("VanHook V.S.") at 5 (coal dust mitigation should be "based on a solid factual and scientific basis").

[52] The Board itself has held that issues "relat[ing] to [BNSF's safe harbor] testing and performance of chemical agents for controlling coal dust" are "central to the subject matter of this proceeding." Dust II, STB decision served March 5, 2012 at 3.

target (be it 100%, 85%, 60% etc.) is achievable. Nor is it possible to determine the effectiveness of any proposed compliance mechanisms or perform any meaningful balancing of costs and benefits. *See* DOT Dust I Reply at 7 ("sound public policy militates in favor of resolving the problems posed by coal dust emissions in the most cost-effective way"); Dust I Decision at 5 ("a tariff should employ cost-effective practices").

BNSF does not care about flawed testing, etc., because it simply wants to force shippers to apply expensive surfactants. While BNSF may not care, shippers do, and the Board cannot approve an emissions-based tariff where, as here, the science underlying the emissions standards is fundamentally flawed.

D. Shippers Are Employing Cost-Effective Containment Practices

BNSF argues that Coal Shippers are not interested in seeking cost-effective solutions to coal dust mitigation.[53] However, that is not the case. All PRB coal shippers are profiling their trains, and most are replacing 2 inch coal with larger 3 inch coal. *See* Barbaro V.S. at 2-3.

BNSF's own studies of {

}:

- {

}[54]

[53] *See* BNSF Dust I Reop. Reply at 1-3, 10-14.

[54] *See* BNSF Dust I Op., VanHook V.S., Exhibit 5 at 65.

- {

}[55]

- {

}[56]

- {

}[57]

{

} valid testing may well show that a combination of profiling, use of larger coals, and appropriate maintenance, are a reasonable, cost-effective containment strategy. *See* Dust I Decision at 6 ("any tariff provision must be reasonably commensurate economically with the problem it addresses").

Coal Shippers note that BNSF's 85% reduction standard is one that BNSF conjured up based on the results of its thoroughly discredited IDV studies,[58] and one that BNSF has no incentive to modify since it is placing all compliance costs on coal shippers. BNSF would no doubt be taking a much closer look at its 85% reduction target, and the cost-effectiveness of spraying versus less expensive containment strategies, if it was footing the bill.

---

[55] *See id.* at 68

[56] *See id.* at 74, 76.

[57] *See* WCTL Dust I Op. at 23 (citing BNSF_COALDUST_0038717-38731, at 38726).

[58] *See* BNSF Dust I Op. at 14-15.

II.

THE REVISED COAL DUST TARIFF IS UNREASONABLE BECAUSE IT REQUIRES SHIPPERS TO BEAR ALL COMPLIANCE COSTS

BNSF's Revised Coal Dust Tariff, like the Original Coal Dust Tariff, requires that coal shippers bear all costs to comply with the tariff. The only BNSF-approved compliance option to date is profiling plus surfactant spraying, so compliance with the Revised Coal Dust Tariff terms requires that shippers pay to spray trains.

Spraying coal trains with surfactants is expensive. As noted above, the National Coal Transportation Association has estimated these costs in the $50 to $150 million range annually.[59] It is unreasonable for BNSF to unilaterally impose these costs on their coal shippers because: (1) the law places responsibility for spraying costs on BNSF; (2) the law precludes BNSF from requiring shippers to pay twice for the same service; and (3) it is fundamentally unfair for BNSF to reap all of the benefits (if any) from spraying, while incurring none of the costs; and (4) requiring shippers to pay to spray trains is contrary to current industry practice.

A. The Law Requires BNSF to Incur All Reasonable Spraying Costs

Governing law is clear here. The law requires whoever is supplying rail cars – be it the shipper or the railroad – supply a car that is properly loaded to permit safe

---

[59] {

}

transportation of freight.[60] The law also requires that the party (be it the shipper or the railroad) that seeks special car treatment or service – *i.e.*, service or treatment in addition to that needed for safe transportation of a shipper's freight in accordance with the shipper's instructions – bear the additional costs attributable to the special service.[61] Application of these basic principles here shows that BNSF is responsible for paying for any BNSF-mandated spraying of coal cars.

First, there is no question that coal can be carried safely in open-top coal cars without the application of surfactants. For over the past 100+ years coal has moved safely in open top cars without application of surfactants, and most coal transported today continues to move safely without application of surfactants. Application of surfactants is not a railcar safety issue, but instead a rail line maintenance-of-way issue.

---

[60] *See, e.g.*, 49 U.S.C. § 11706 (making common carriers by rail generally responsible for the safe transportation of the commodities they carry); *Waste Material Dealers Ass'n of Ark. v. Chicago, Rock Island & Pac. Ry.*, 226 I.C.C. 683, 688 (1938) ("It is the right and duty of the railroads to refuse to accept shipments that are not loaded in a safe manner."); *Consignees' Obligation to Unload Rail Cars in Compliance with Carriers' Published Tariffs*, 340 I.C.C. 405, 410 (1972) ("carriers may refuse for shipment articles tendered for transportation, unless in such condition and so prepared for shipment as to render the transportation thereof reasonably safe and practicable").

[61] *See, e.g.*, *Furnishing Suitable Cars For Loading Flour and Other Grain Products*, 128 I.C.C. 442, 444 (1927) ("It is well settled that a common carrier must furnish suitable equipment for safe transportation, and that special safeguards desired by the shipper should be furnished by him."); *Baltimore & Ohio R.R. v. United States*, 391 F. Supp. 249, 257 (E.D. Pa. 1975) ("it is inequitable to require shippers to pay additional charges for cars of different dimensions or capacity from those which would suit their needs"); *Radioactive Materials, Special Train Serv., Nationwide*, 359 I.C.C. 70, 91 (1978) ("[h]istorically special train service has been a privilege accorded the shipper, rather than any requirement imposed on a shipper").

The agency charged with regulating rail safety is the Federal Railroad Administration ("FRA") agrees. The FRA has promulgated many rules governing the safe operation of all railcars, including railcars used in coal service. The FRA has never deemed application of surfactants necessary for the safe transportation of coal, a position reaffirmed by the DOT in Dust I.

DOT explained in Dust I that coal cars could be safely transported with, or without, application of surfactants, so the issue before the Board was not one involving the safe loading of rail cars.[62] Instead, DOT said Dust I raised issues concerning proper ballast maintenance. *See id.* at 3 ("the [FRA] rules most germane to this proceeding are those governing ballast"). As described by DOT, FRA has adopted comprehensive standards governing ballast performance; directed railroads to comply with these standards; but left the specific steps for doing so with the railroads in the first instance rather than prescribing these steps:

> FRA has adopted comprehensive regulations that prescribe minimum track safety standards. 49 C.F.R. Part 213. Some provisions, like those on track structure, impose numerous detailed requirements for many physical aspects of railroad track . . . By contrast, the rules most germane to this proceeding are those governing ballast, and they are not prescriptive but performance-based:
>
> **Ballast; general.**
>
> Unless it is otherwise structurally supported, all track shall be supported by material which will—
> (a) Transmit and distribute the load of the track and railroad rolling equipment to the subgrade;

[62] *See* DOT Dust I Reply at 4.

> (b) Restrain the track laterally, longitudinally, and vertically under dynamic loads imposed by railroad rolling equipment and thermal stress exerted by the rails;
>
> (c) Provide adequate drainage for the track; and
>
> (d) Maintain proper track crosslevel, surface, and alignment.

49 C.F.R. § 213.103; *see also* 49 C.F.R. § 213.334.

> Ballast, then, must distribute loads while simultaneously maintaining specific track geometry metrics and providing adequate drainage. It can only perform these functions if it is at once strong, stable, and porous. FRA standards are performance-based because ballast must meet these needs in a variety of circumstances that defy uniformity. Accordingly, FRA does not prescribe the type of ballast or the amount of ballast that a track owner must use; compliance is determined by whether the ballast performs the functions that it is required to perform with respect to each specific segment of track.

Id. at 3-4 (footnotes omitted).

DOT went on to advise that BNSF could comply with FRA ballast requirements "in a variety of ways" including "via maintenance of way":

> Properly understood, FRA regulations require BNSF to ensure that the ballast of the PRB Joint Line track performs the functions specified. BNSF may do so in a variety of ways, as long as its choices do not themselves violate applicable regulations or otherwise threaten safety. None of the alternatives reflected in the record of this proceeding, whether undertaken by railroads (via maintenance of way) or coal shippers (by profile loading, spraying surfactant, etc.) do so.

Id. at 4.

Second, in this case, the party that is seeking to impose special treatment of safely loaded coal cars is BNSF, not its coal shippers. That treatment consists of

spraying coal cars, or application of any other BNSF-approved method. In either case, the Revised Coal Dust Tariff calls for the shipper, not BNSF, to pay for the special treatment. The costs associated with this special treatment must be borne by BNSF, the party seeking the special treatment.

B. The Law Precludes BNSF from Requiring Shippers to Pay Twice For the Same Service

The stated purpose of BNSF's Revised Coal Dust Tariff is to reduce the amount of coal dust that enters track ballast.[63] The law requires that BNSF – as a track owner – to properly maintain this ballast[64] and BNSF can collect payment from its shippers for providing this service. The same legal standards apply to UP.[65] However, the law does not permit BNSF or UP to force shippers to pay twice for the same maintenance service.[66] But that is exactly what they propose.

---

[63] *See* Revised Coal Dust Tariff (tariff rules intended "[t]o prevent contamination of the rail ballast"); Dust I Decision at 8 (coal dust raises "issues associated with maintenance").

[64] *See, e.g., R.R. Ventures, Inc. – Abandonment Exemption – Between Youngstown Ohio, & Darlington, Pa. In Mahong & Columbiana Cntys., Ohio, & Beaver Cnty., Pa.*, STB Docket No. AB-556 (Sub-2X) (STB served April 28, 2008) at 10 ("a common carrier [has] a duty to maintain its rail line in accordance with [governing] rules and regulations"); DOT Dust I Reply at 5 ("maintenance of way is a basic railroad responsibility").

[65] As discussed above, the Revised Coal Dust Tariff standards apply to UP trains, and BNSF and UP share ownership of the Joint Line.

[66] *See, e.g., Indiana Harbor Belt R.R. v. Gen. Am. Transp. Corp.*, 577 F.2d 394, 400 (7th Cir. 1978) (requiring shippers to pay twice for the same switching service is an unreasonable practice); *Rail Fuel Surcharges*, STB Ex Parte No. 661, at 10-11 (STB served Jan. 26, 2007) (requiring shippers to pay twice for the same fuel cost increase is an unreasonable practice).

BNSF stipulated in Dust I that it sets rates to cover all of its costs, including its maintenance costs:

> BNSF attempts generally to cover its variable costs, which would include maintenance costs relating to ballast cleaning, undercutting and shoulder cleaning, and to generate contribution that will assist in covering fixed costs.

WCTL Dust I Op., Verified Statement of Thomas D. Crowley ("Crowley V.S."), Exhibit TDC-2 at 1 (Letter from BNSF Counsel to WCTL Counsel (Feb. 26, 2010)).

Moreover, the rates BNSF and UP actually charge PRB shippers permit them to recover all of their PRB maintenance costs plus huge profits. BNSF's CEO has singled out BNSF's coal traffic as "the most profitable commodity we haul"[67] and, since 2003, rates BNSF and UP have charged on their PRB coal traffic have skyrocketed, generating billions in contribution and profits.[68]

PRB coal shippers are already paying rates that cover all of BNSF's, and UP's, PRB track maintenance costs. Requiring them to pay an additional $50 to $150 million annually to maintain PRB ballast – when they are already reimbursing the carriers for all ballast maintenance costs in their freight rates – is clearly an unreasonable practice.

---

[67] *Matt Rose Meets with Workforce at Town Hall*, Powder River Reflection, Sept./Oct. 2003 at 6.

[68] *See Competition in the R.R. Indus.*, STB Ex Parte No. 705, Comments of the Western Coal Traffic League, Richards V.S. at 18-19 (April 12, 2011); WCTL Dust I Reply, Crowley V.S. at 5-7.

C. It is Fundamentally Unfair for Shippers to Pay More While BNSF Pays Less

Under the Revised Coal Dust Tariff, shippers will pay more because they have to pay to spray their trains. On the other hand, BNSF concludes that it will incur substantially lower maintenance expense if shippers spray their trains.[69] Thus, under BNSF's proposal, shippers pay more and BNSF pays less. This result is a fundamentally unfair practice because shippers bear all the compliance costs, while BNSF obtains all the compliance benefits.[70]

BNSF argued in Dust I that it was fair for shippers to pay more, and BNSF pay less, because all shippers, other than coal shippers, are required to keep their freight in their cars.[71] BNSF's assertions are both misdirected and wrong. They are misdirected because most loading rules are directed at securing freight so it can be safely transported. Coal of course can be safely loaded and transported with or without spraying.[72]

---

[69] BNSF Dust I Reply, Van Hook V.S. at 25. {

}; *see also Major Issues in Rail Rate Cases*, STB Ex Parte No. 657 (Sub-No. 1) (STB served Oct. 30, 2006) at 43 ("[C]oal dust fouling a railroad's right-of-way is a source of maintenance expenses for railroads. Railroads and coal shippers are exploring ways to reduce the amount of coal dust lost in transit, such as altering the shape of car loads or spraying agents on the coal, thereby reducing the amounts necessary to be spent on maintenance.") (footnotes omitted).

[70] *See Kansas City Power and Light Co. v. Kansas City Southern Ry.*, 361 I.C.C. 848, 851 (1979) (finding carrier practice unreasonable where the practice was "fundamentally unfair" and resulted in a "windfall" for the carrier).

[71] *See* BNSF Dust I Op. at 5.

[72] *See* DOT Dust I Reply at 4.

They are wrong because most coal today moves without first being sprayed, as do other commodities that are transported in open top cars. As explained by Paul H. Reistrup, one of the nation's foremost authorities on railroad operations:

> During my many years of direct railroad operating experience and management, including overseeing all car operations for Illinois Central, I personally observed a variety of products that escape open top rail cars in addition to coal and coal dust, including wood chips, iron ore pellets, ballast, ballast dust, sand, gravel, crushed rock, crushed rock dust, other aggregates, and construction and demolition debris. Such occurrences were a regular part of operating the railroads I worked for and no special maintenance charges were assessed due to the escaped material.

WCTL Dust I Reb., Verified Statement of Paul H. Reistrup at 2.

Moreover, the amount of dust, if any, that may be emitted from the top of a loaded coal train turns on three principal factors: how the train is loaded, how it is operated, and the weather (including wind and rain).[73] Coal shippers have limited control over how their trains are loaded, and have no control whatsoever over how railroads operate those trains, or the weather. They should not have to bear all responsibility for actions that are, and always will be, beyond their control.

The equitable solution here is the same as the legal one. PRB coal shippers are already paying their full and fair share of BNSF's (and UP's) maintenance costs in their line haul rates. If BNSF (and UP) are going to require shippers to spray their trains, a reasonable and fair cost sharing approach is for BNSF and UP to reimburse shippers for

[73] *See* BNSF Dust I Op., VanHook V.S., Exhibit 5 at 29 ("[w]ind speed and train speed are two of the dominate factors controlling trains' dust emission"); Viz V.S. at 34-36.

the expenses they incur in complying with BNSF's spraying requirements, as those expenses – at least as BNSF and UP see it – should reduce substantially the maintenance costs that shippers are already paying.

Nothing in the Board's Dust I Decision compels a different answer. The Board held in Dust I that BNSF could adopt a "reasonable" loading rule directed at containing coal dust emissions in its ballast.[74] The important word is "reasonable" and what is reasonable and fair here is for BNSF (and UP) to reimburse their shippers for any reasonable costs they incur to comply with a reasonable loading rule directed at coal dust mitigation (should BNSF or UP ever promulgate such a rule).

D. Requiring Shippers to Pay a Separate Charge for Coal Dust Mitigation is Contrary to Industry Practice

In Dust I, BNSF pointed out that some Norfolk Southern Railway Company ("NS") trains, as well as some trains moved by railroads operating in foreign countries, were being sprayed with chemical surfactants.[75] However, BNSF pointed to no instances where NS, or a foreign carrier, was requiring shippers to enter into separate arrangements with coal suppliers to pay for the application of surfactants, and Coal Shippers are not aware of any such arrangements. Requiring shippers to enter into such arrangements is contrary to industry practice.

{

[74] Dust I Decision at 11.

[75] *See* BNSF Dust I Op., Emmitt V.S. at 13.

} *See* WCTL Dust I Op. at 36. As WCTL/CCCS correctly concluded in Dust I, {

} *Id.* at 36-37.

E. Fair Cost Sharing Requires BNSF to Reimburse Shippers for Their Reasonably Incurred Compliance Costs

BNSF could establish a fair cost sharing arrangement in a reasonable containment-based coal dust tariff by including a provision stating that it will reimburse shippers' reasonably incurred compliance costs or by including a provision containing a reasonable reimbursement at a specified per ton allowance. The choice is BNSF's in the first instance. UP could then follow suit. The absence of any such provisions, on the facts of this case, is an unreasonable practice.

III.

THE REVISED COAL DUST TARIFF IS UNREASONABLE BECAUSE IT CONTAINS NO ENFORCEMENT PROVISIONS

The Revised Coal Dust Tariff, like the Original Coal Dust Tariff, is unreasonable and unlawful because it does not inform shippers of the consequences of a shipper's failure to adhere to the tariff terms. BNSF's failure to include any enforcement provisions in the Original Coal Dust Tariff was one of the factors that led the Board to

find that the Original Coal Dust Tariff was unreasonable. *See* Dust I Decision at 14 ("the [Original Coal Dust] tariff does not explain what consequences coal shippers would face if they are found to have tendered loaded coal cars to the railroad that subsequently released dust during transport"). BNSF continues to ignore the Board's – and Coal Shippers' – concerns.

Most tariffs contain performance standards that explain the consequences of non-compliance. For example, tariffs will contain provisions establishing loading and unloading "free time," and then set forth the penalties that apply if a shipper fails to load or unload its trains during the "free time" allowed.[76] Similarly, tariffs will contain provisions governing payment of bills for services rendered, and then set forth penalties that apply if a shipper fails to pay its bills on time.[77] Tariffs are structured in this way so that carriers comply with governing law requiring that all pertinent transportation terms be clearly set forth in the tariff text.[78]

---

[76] *See, e.g.*, BNSF Price List 6041-B, Revision 20, Item 110 (establishing four hour free time for loading, and six hour free time for unloading, of PRB coal trains, and establishing a $600 per hour detention charge if trains are not loaded or unloaded during the specified free time).

[77] *See, e.g.*, BNSF Rules Book 6100-A, Revision 109, Item 3400G (establishing, *inter alia*, 15 day time period pay freight charges and setting forth finance charge of 0.033% per day for late payments).

[78] *See, e.g.*, *Birmingham Rail & Locomotive Co., Inc. v. Aberdeen & Rockfish R.R.*, 358 I.C.C. 606, 608 (1978) (tariff must contain "clear standards for application" and all governing rates, rules and policies "should be specifically defined as well as published"); *Radioactive Materials*, 359 I.C.C. at 73 (railroads must "plainly state their tariffs [] in order to inform all parties of their plain meaning and to avoid controversy") (internal quotation marks omitted).

The Revised Coal Dust Tariff contains many performance standards. Shippers are required to apply BNSF approved surfactants (or any other BNSF-approved dust mitigation method); shippers are required to "properly appl[y]" these approved surfactants; and shippers are required to "ensure" that trains meet BNSF's profiling requirements. *Id.* However, the Revised Coal Dust Tariff does not specify the consequences of a shipper's failure to comply with these standards.[79]

BNSF's failure to specify the consequences of non-compliance is particularly egregious in light of public reports that BNSF may shut down a shipper's trains, or impose draconian financial penalties, for claimed non-performance. *See UP Letter Mulls Implications of Coal Dust Rules*, Platt's Coal Trader, Oct. 19, 2009 ("A top BNSF official told utility customers this month that penalties for not meeting dust standards include a $1 per ton fine and possibly temporarily halting service.").

"Possibly temporarily halting train service" (*id.*) can be devastating to utilities that depend on coal as a utility boiler fuel and subverts national energy policy "[d]ue to the vital role transportation of coal by rail plays in the nation's energy supply and the economy in general." Dust I, STB decision served Dec. 11, 2009 at 1. Similarly, imposing a $1 per ton fine would produce huge fines approximating $17,000 per train for many trains.

[79] BNSF also has informed Coal Shippers that "no formal non-privileged consideration has been given to the implementation of specific enforcement measures" against BNSF or UP shippers for their failure to comply with the Revised Coal Dust Tariff standards. *See* BNSF Dust II Discovery Responses at 5, 7.

The law does not permit BNSF to play cat and mouse with tariff enforcement procedures. Nor is it sound public policy for shippers, and the Board, to be forced to guess what BNSF's enforcement policies may be based on trade publication reports, and industry conjecture. BNSF's failure – once again – to state its enforcement terms renders the Revised Coal Dust Tariff an unreasonable practice.

IV.

THE REVISED COAL DUST TARIFF IS UNREASONABLE BECAUSE BNSF'S TRAIN PROFILING PRACTICES ARE ARBITRARY

BNSF's Revised Coal Dust Tariff, like the Original Coal Dust Tariff, requires shippers to "ensure that loaded uncovered coal cars will be profiled in accordance with BNSF's published template entitled 'Redesigned Chute Diagram' located in Appendix A to this publication." *Id.* The "Redesigned Chute Diagram" reflects the results of private sector negotiations.

Several years ago, PRB coal shippers, mines, BNSF and UP agreed that PRB mines would modify their loading chutes to produce a bread-loaf profile shown in the Revised Chute Diagram. The bread-loaf shaped profile "is designed to reduce coal dust emission by reducing the effect of air currents on loaded coal."[80] All PRB mines have installed "redesigned chutes" and are using them.[81]

However, BNSF is not content with the parties' private sector bargaining. Instead, following the publication of the Original Coal Dust Tariff it began to "laser"

---

[80] Dust I Decision at 12.

[81] BNSF Dust I Op. at 13; Dust I Decision at 12.

trains[82] at locations many miles away from mine origins and, if BNSF's laser imaging indicated that trains did not meet the tariff profiling requirements, BNSF sent notices to coal shippers asserting that the shipper's trains were not in compliance with the tariff profiling requirements.[83] BNSF has now installed a permanent laser monitor near Milepost 91 on the Joint Line.[84]

BNSF's profile monitoring procedures are unreasonable. Once a train leaves a mine, any number of operating and weather factors can modify the train profile. *See* Viz V.S. at 30. Shippers should not be deemed to be in non-compliance with profiling standards due to events beyond their control.[85] Nor, unlike the application of surfactants, is there any "safe harbor" for train profiling.

BNSF could easily modify a reasonable containment-based coal dust tariff to address Coal Shippers' profile monitoring concerns by including language stating that a shipper will be deemed in compliance with BNSF's current Redesigned Chute Diagram

---

[82] BNSF refers to this laser-based equipment as its "Coal Car Loading Profiling System" or "CCLPS"). *See* BNSF Dust II Discovery Responses at 10.

[83] *See* WCTL Dust I Reb. at 65; BNSF Dust I Op., VanHook V.S. at 16.

[84] *See* Dust I, Opening Evidence and Argument of Union Pacific Railroad Company, Verified Statement of Douglas Glass at 10 (Mar. 16, 2010). The CCLPS at MP 91 is over 27 miles from the southern-most PRB mine (Antelope) and over 107 miles from the northern-most PRB mine (Buckskin). *See* BNSF Railway, Powder River Division, Timetable No. 8 (effective Nov. 29, 2006) *available at* www.huntsvillenewswire.com/RailroadInfo/BNSF%20Timetables/Powder%20River%20Division.pdf.

[85] *See* Dust I Decision at 13-14 ("After the loading has taken place, the shipment is under control of the railroad and subject to the vagaries of wind, weather, train speed, and track conditions. Once the movement is in transit, there is nothing the shipper can do to comply. Clearly, this suggests that the proper place to focus shipper efforts to minimize coal dust emissions must be at the load-out.").

if its mine operators have installed, and are using, loading chutes that conform to the Diagram specifications.

V.

THE REVISED TARIFF IS UNREASONABLE BECASE BNSF UNLAWFULLY ATTEMPTS TO INSULATE ITSELF FROM LIABILITY

The Revised Coal Dust Tariff provides that "[a]ny product including topper agents, devices, or appurtenance utilized by Shipper or Shipper's mine agents to control the release of coal dust shall not adversely impact railroad employees, property, locomotives or owned cars." *Id.* The Original Coal Dust Tariff contained similar text.

It is fundamentally unfair for BNSF to mandate train spraying, and train profiling, using BNSF-approved sprays and loading chutes, and then say that shippers are responsible for all liability arising from compliance with these mandates. BNSF wants it both ways: BNSF demands that shippers comply with its mandates, but then absolves itself from any corresponding responsibilities for liability to its employees, property, locomotives or owned cars, including liability arising from its own negligence or the negligence of its own employees.

Not only are BNSF's liability-shifting rules fundamentally unfair, they are also patently unlawful. Shipper, and BNSF, liability to BNSF's "employees, property, locomotives or owned cars" is governed by state tort law or other laws not administered by the STB. BNSF cannot use its tariff writing power to limit liability imposed by law. *See, e.g., Perishable Freight Investigation*, 56 I.C.C. 449, 483 (1920) ("tariff provisions

which purport to . . . fix limitations of the carriers' liability . . . [are] generally objectionable"); *Rules, Regulations, & Practices of Regulated Carriers With Respect to the Processing of Loss & Damage Claims*, 340 I.C.C. 515, 520 (1972) (common carriers may not "limit their liability for negligence"); *Provisions on Vegetables & Melons, Transcontinental*, 340 I.C.C. 807, 815 (1972) ("it would be an unreasonable practice . . . for a railroad to establish . . . claims rules that are clearly inconsistent with their liability under established law"); *Wooden Grain Doors, Burlington N., Inc.*, 350 I.C.C. 768, 774-75 (1975) (carriers may not promulgate tariff rules governing liability for torts "over which this Commission has no jurisdiction").

BNSF can simply and easily remedy this unreasonable practice by removing the liability limitations.

VI.

REQUESTED RELIEF

Coal Shippers request that the Board find that BNSF's publication of the Revised Coal Dust tariff constitutes an unreasonable practice. Coal Shippers further request that the Board once again urge BNSF to work collaboratively with its PRB coal shippers to devise a reasonable approach to coal dust mitigation issues. Finally, Coal Shippers request that the Board instruct BNSF that any new coal dust tariff provisions be based on sound emission testing; provide for the reasonable reimbursement of coal shippers' compliance costs; establish specific, reasonable enforcement terms; eliminate unfair coal profile monitoring; and remove all liability limitations.

Respectfully submitted,

By:

William L. Slover
John H. LeSeur
Andrew B. Kolesar III
Peter A. Pfohl
Slover & Loftus LLP
1224 Seventeenth St., N.W.
Washington, D.C. 20036
(202) 347-7170

Attorneys for Coal Shippers

Dated: October 1, 2012

CERTIFICATE OF SERVICE

I hereby certify that this 1st day of October, 2012, I have served a copy of the Opening Evidence and Argument of Western Coal Traffic League, American Public Power Association, Edison Electric Institute, and National Rural Electric Cooperative Association to be served via first-class mail, postage prepaid, upon counsel for BNSF Railway Company. I further certify that this 1st day of October, 2012, I have served public copies of the forgoing via first-class mail, postage prepaid, upon the parties of record to this case.

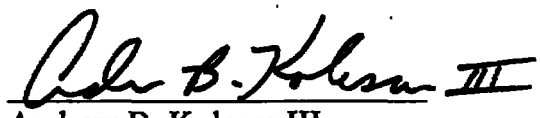

Andrew B. Kolesar III

Counsel's Exhibit No. 1

BNSF's Revised Coal Dust Tariff (excerpts)

BNSF 6041-B

Rev. 16, Issued July 14, 2011

Rev. 17, Issued July 20, 2011

Rev. 18, Issued September 15, 2011

Rev. 19, Issued September 19, 2011

Rev. 20, Issued September 26, 2011

BNSF 6041-B

Rev. 16, Issued July 14, 2011

BNSF PRICE LIST 6041-B
(Cancels BNSF Freight Tariff 6041-A)

PROVIDING

RULES AND REGULATIONS GOVERNING UNIT TRAIN AND VOLUME ALL-RAIL

COAL SERVICE, ALSO ACCESSORIAL SERVICES AND CHARGES THEREFOR

APPLYING AS PROVIDED IN PRICE LIST

ISSUED: July 14, 2011 EFFECTIVE: October 1, 2011
Issued by BNSF Price Management, P.O. Box 961069, Ft. Worth, TX 76161-0069

ITEM 100
COAL DUST MITIGATION REQUIREMENTS

1. To prevent contamination of the rail ballast caused by fugitive coal dust, BNSF is modifying the loading requirement applicable to all coal cars loaded at Powder River Basin ("PRB") mines by shippers whose coal transportation is subject to this Rules Book.

2. Effective October 1, 2011, shippers loading coal at any PRB mine must take measures to load coal in such a way that any loss in transit of coal dust from the shipper's loaded coal cars will be reduced by at least 85 percent as compared to loss in transit of coal dust from coal cars where no remedial measures have been taken. At least 30 days prior to loading cars for shipment by BNSF, a Shipper shall provide BNSF with written notice of compliance efforts.

3. A shipper will be deemed to be in compliance with the loading requirement set out in this Item if the shipper satisfies Sections 3.A and 3.B below or pursues the option in Section 4 below:

A. Shipper ensures that loaded uncovered coal cars will be profiled in accordance with BNSF's published template entitled "Redesigned Chute Diagram" located in Appendix A to this publication.

B. Shipper ensures that an acceptable topper agent (e.g., surfactant) will be properly applied to the entire surface of all loaded coal cars at an effective concentration level and in accordance with the manufacturer's specifications. An acceptable topper agent is one that has been shown to reduce coal dust loss in transit by 85%. In recent tests carried out in the PRB, three topper agents meet this criteria when properly applied. Appendix B to this publication lists these topper agents. Proper use of any one of the topper agents on the approved list in accordance with the manufacturer's specifications and at the application rates specified in Appendix B, will satisfy this safe harbor provision. BNSF will consider other topper agents to be acceptable for purposes of this safe harbor provision if the shipper can demonstrate that appropriate testing has shown that the topper agent achieves compliance with this Item. Guidelines for the testing of new topper agents will be provided upon request.

4. Shipper may seek inclusion of any other method of coal dust suppression (*e.g.*, compaction or other technology) in the safe harbor provision of Section 3.B above by submitting a compliance plan to BNSF that provides evidence demonstrating that an additional proposed compliance measure will result in compliance with this Item. Shipper must also satisfy the profiling requirement of Section 3.A above. Any product including topper agents, devices or appurtenance utilized by the Shipper or Shipper's mine agents to control the release of coal dust shall not adversely impact railroad employees, property, locomotives or owned cars.

APPENDIX A

REDESIGNED CHUTE DIAGRAM

Redesigned Chute Diagram

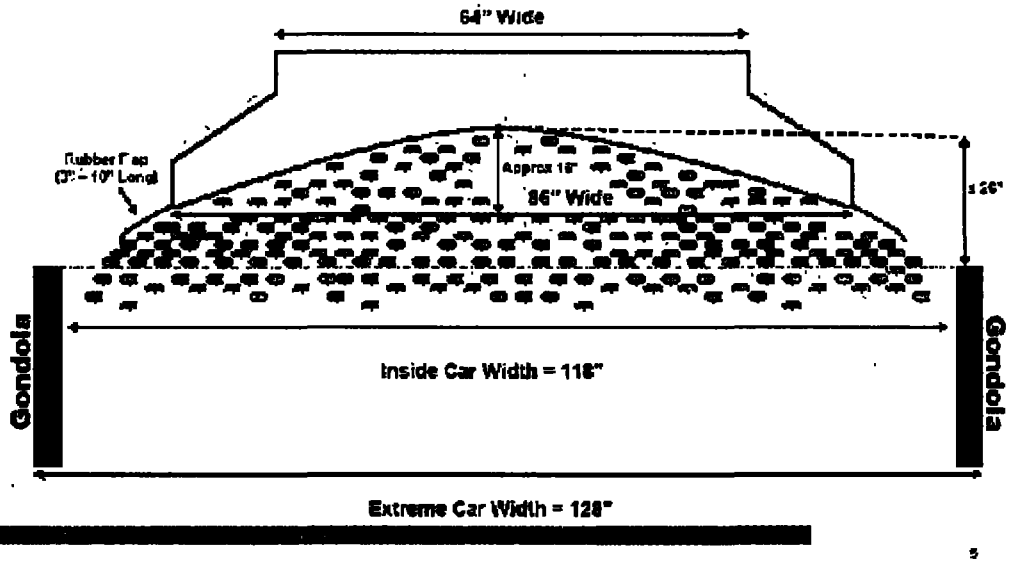

APPENDIX B

Acceptable Topper Agents and Application Rates

Topper Agents [1]	Concentration Rate per Car [2]	Total Solution Applied per Railcar [3]
Nalco Dustbind Plus	1.5 gal	15 gal
Midwest Soil-Sement	1.25 gal	18.75 gal
AKJ CTS-100	1.36 gal	15 gal

(1) For Topper Application only.
(2) The amount of topper agent mixed into a solution for each Railcar. These concentration rates were established during testing carried out in the PRB in 2010.
(3) The amount of topper agent applied to each Railcar.

BNSF 6041-B

Rev. 17, Issued July 20, 2011

BNSF PRICE LIST 6041-B
(Cancels BNSF Freight Tariff 6041-A)

PROVIDING

RULES AND REGULATIONS GOVERNING UNIT TRAIN AND VOLUME ALL-RAIL

COAL SERVICE, ALSO ACCESSORIAL SERVICES AND CHARGES THEREFOR

APPLYING AS PROVIDED IN PRICE LIST

ISSUED: July 20, 2011 EFFECTIVE: July 20, 2011
Issued by BNSF Price Management, P.O. Box 961069, Ft. Worth, TX 76161-0069

ITEM 100
COAL DUST MITIGATION REQUIREMENTS

1. To prevent contamination of the rail ballast caused by fugitive coal dust, BNSF is modifying the loading requirement applicable to all coal cars loaded at Powder River Basin ("PRB") mines by shippers whose coal transportation is subject to this Rules Book.

2. Effective October 1, 2011, shippers loading coal at any PRB mine must take measures to load coal in such a way that any loss in transit of coal dust from the shipper's loaded coal cars will be reduced by at least 85 percent as compared to loss in transit of coal dust from coal cars where no remedial measures have been taken. At least 30 days prior to loading cars for shipment by BNSF, a Shipper shall provide BNSF with written notice of compliance efforts.

3. A shipper will be deemed to be in compliance with the loading requirement set out in this Item if the shipper satisfies Sections 3.A and 3.B below or pursues the option in Section 4 below:

A. Shipper ensures that loaded uncovered coal cars will be profiled in accordance with BNSF's published template entitled "Redesigned Chute Diagram" located in Appendix A to this publication.

B. Shipper ensures that an acceptable topper agent (e.g., surfactant) will be properly applied to the entire surface of all loaded coal cars at an effective concentration level and in accordance with the manufacturer's specifications. An acceptable topper agent is one that has been shown to reduce coal dust loss in transit by 85%. In recent tests carried out in the PRB, three topper agents meet this criteria when properly applied. Appendix B to this publication lists these topper agents. Proper use of any one of the topper agents on the approved list in accordance with the manufacturer's specifications and at the application rates specified in Appendix B, will satisfy this safe harbor provision. BNSF will consider other topper agents to be acceptable for purposes of this safe harbor provision if the shipper can demonstrate that appropriate testing has shown that the topper agent achieves compliance with this Item. Guidelines for the testing of new topper agents will be provided upon request.

4. Shipper may seek inclusion of any other method of coal dust suppression (*e.g.*, compaction or other technology) in the safe harbor provision of Section 3.B above by submitting a compliance plan to BNSF that provides evidence demonstrating that an additional proposed compliance measure will result in compliance with this Item. Shipper must also satisfy the profiling requirement of Section 3.A above. Any product including topper agents, devices or appurtenance utilized by the Shipper or Shipper's mine agents to control the release of coal dust shall not adversely impact railroad employees, property, locomotives or owned cars.

APPENDIX A

REDESIGNED CHUTE DIAGRAM

Redesigned Chute Diagram

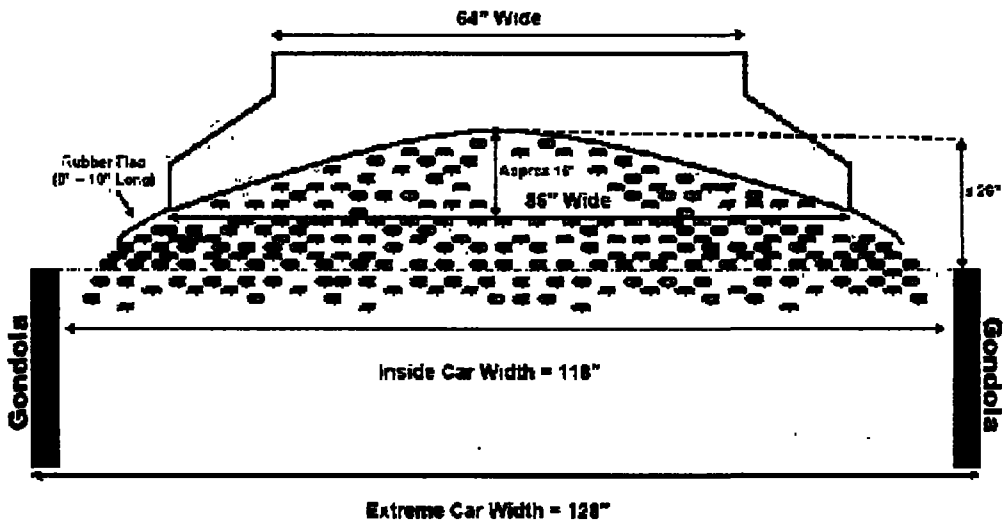

APPENDIX B

Acceptable Topper Agents and Application Rates

Topper Agents [1]	Concentration Rate per Car [2]	Total Solution Applied per Railcar [3]
Nalco Dustbind Plus	2.0 gal	20 gal
Midwest Soil-Sement	1.25 gal	18.75 gal
AKJ CTS-100	1.36 gal	15 gal

(1) For Topper Application only.
(2) The amount of topper agent mixed into a solution for each Railcar. These concentration rates were established during testing carried out in the PRB in 2010.
(3) The amount of topper agent applied to each Railcar.

BNSF 6041-B

Rev. 18, Issued September 15, 2011

BNSF PRICE LIST 6041-B
(Cancels BNSF Freight Tariff 6041-A)

PROVIDING

RULES AND REGULATIONS GOVERNING UNIT TRAIN AND VOLUME ALL-RAIL

COAL SERVICE, ALSO ACCESSORIAL SERVICES AND CHARGES THEREFOR

APPLYING AS PROVIDED IN PRICE LIST

ISSUED: September 15, 2011 EFFECTIVE: September 15, 2011
Issued by BNSF Price Management, P.O. Box 961069; Ft. Worth, TX 76161-0069

ITEM 100
COAL DUST MITIGATION REQUIREMENTS

1. To prevent contamination of the rail ballast caused by fugitive coal dust, BNSF is modifying the loading requirement applicable to all coal cars loaded at Powder River Basin ("PRB") mines by shippers whose coal transportation is subject to this Rules Book.

2. Effective October 1, 2011, shippers loading coal at any PRB mine must take measures to load coal in such a way that any loss in transit of coal dust from the shipper's loaded coal cars will be reduced by at least 85 percent as compared to loss in transit of coal dust from coal cars where no remedial measures have been taken. At least 30 days prior to loading cars for shipment by BNSF, a Shipper shall provide BNSF with written notice of compliance efforts.

3. A shipper will be deemed to be in compliance with the loading requirement set out in this Item if the shipper satisfies Sections 3.A and 3.B below or pursues the option in Section 4 below:

A. Shipper ensures that loaded uncovered coal cars will be profiled in accordance with BNSF's published template entitled "Redesigned Chute Diagram" located in Appendix A to this publication.

B. Shipper ensures that an acceptable topper agent (e.g., surfactant) will be properly applied to the entire surface of all loaded coal cars at an effective concentration level and in accordance with the manufacturer's specifications. An acceptable topper agent is one that has been shown to reduce coal dust loss in transit by 85%. Appendix B to this publication lists the topper agents that meet this criteria. Proper use of any one of the topper agents on the approved list in accordance with the manufacturer's specifications and at the application rates specified in Appendix B, will satisfy this safe harbor provision. BNSF will consider other topper agents to be acceptable for purposes of this safe harbor provision if the shipper can demonstrate that appropriate testing has shown that the topper agent achieves compliance with this Item. Guidelines for the testing of new topper agents will be provided upon request.

4. Shipper may seek inclusion of any other method of coal dust suppression (*e.g.*, compaction or other technology) in the safe harbor provision of Section 3.B above by submitting a compliance plan to BNSF that provides evidence demonstrating that an additional proposed compliance measure will result in compliance with this Item. Shipper must also satisfy the profiling requirement of Section 3.A above. Any product including topper agents, devices or appurtenance utilized by the Shipper or Shipper's mine agents to control the release of coal dust shall not adversely impact railroad employees, property, locomotives or owned cars.

APPENDIX A

REDESIGNED CHUTE DIAGRAM

Redesigned Chute Diagram

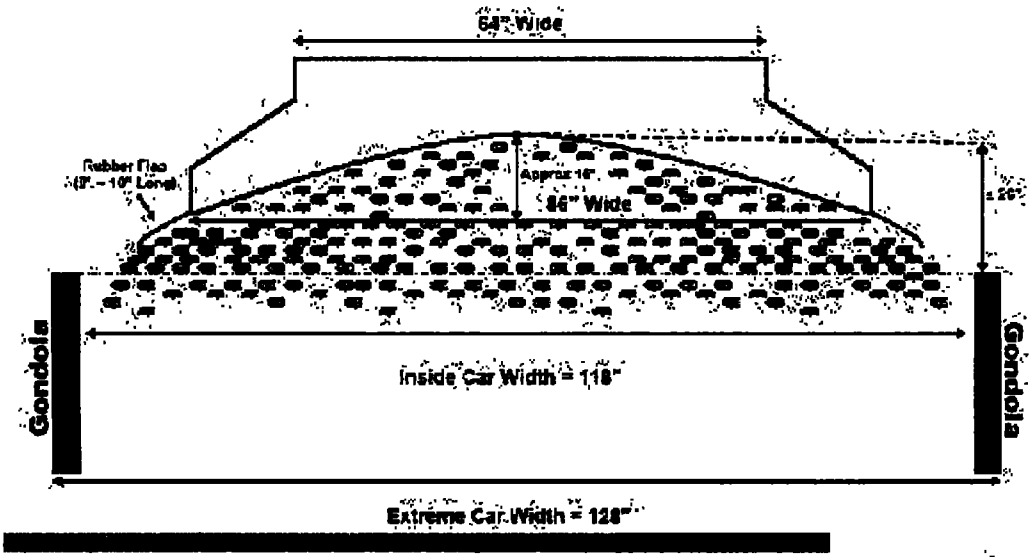

APPENDIX B

Acceptable Topper Agents and Application Rates

Topper Agents [1]	Concentration Rate per Car [2]	Total Solution Applied per Railcar [3]
Nalco Dustbind Plus	2.0 gal	20 gal
Midwest Soil-Sement	1.25 gal	18.75 gal
AKJCTX-100	1.36 gal[4]	15 gal
AKJ CTS-100C	1.36 gal[4]	15 gal
Rantec Capture 3000	2.5 lbs	20 gal

(1) For Topper Application only.
(2) The amount of topper agent mixed into a solution for each Railcar. These concentration rates were established during testing.
(3) The amount of topper agent applied to each Railcar.
(4) 1.36 gallons of concentrate (CTS-100C) mixed with 13.64 gallons of Water.

BNSF 6041-B

Rev. 19, Issued September 19, 2011

BNSF RAILWAY

BNSF PRICE LIST 6041-B
(Cancels BNSF Freight Tariff 6041-A)

PROVIDING

RULES AND REGULATIONS GOVERNING UNIT TRAIN AND VOLUME ALL-RAIL

COAL SERVICE, ALSO ACCESSORIAL SERVICES AND CHARGES THEREFOR

APPLYING AS PROVIDED IN PRICE LIST

ISSUED: September 19, 2011 EFFECTIVE: October 9, 2011
Issued by BNSF Price Management, P.O. Box 961069, Ft. Worth, TX 76161-0069

ITEM 100
COAL DUST MITIGATION REQUIREMENTS

1. To prevent contamination of the rail ballast caused by fugitive coal dust, BNSF is modifying the loading requirement applicable to all coal cars loaded at Montana and Wyoming mines by shippers whose coal transportation is subject to this Rules Book.

2. Effective October 1, 2011, shippers loading coal at any Montana and Wyoming mine must take measures to load coal in such a way that any loss in transit of coal dust from the shipper's loaded coal cars will be reduced by at least 85 percent as compared to loss in transit of coal dust from coal cars where no remedial measures have been taken.. At least 30 days prior to loading cars for shipment by BNSF, a Shipper shall provide BNSF with written notice of compliance efforts.

3. A shipper will be deemed to be in compliance with the loading requirement set out in this Item if the shipper satisfies Sections 3.A and 3.B below or pursues the option in Section 4 below:

A. Shipper ensures that loaded uncovered coal cars will be profiled in accordance with BNSF's published template entitled "Redesigned Chute Diagram" located in Appendix A to this publication.

B. Shipper ensures that an acceptable topper agent (e.g., surfactant) will be properly applied to the entire surface of all loaded coal cars at an effective concentration level and in accordance with the manufacturer's specifications. An acceptable topper agent is one that has been shown to reduce coal dust loss in transit by 85%. Appendix B to this publication lists the topper agents that meet this criteria. Proper use of any one of the topper agents on the approved list in accordance with the manufacturer's specifications and at the application rates specified in Appendix B, will satisfy this safe harbor provision. BNSF will consider other topper agents to be acceptable for purposes of this safe harbor provision if the shipper can demonstrate that appropriate testing has shown that the topper agent achieves compliance with this Item. Guidelines for the testing of new topper agents will be provided upon request.

4. Shipper may seek inclusion of any other method of coal dust suppression (*e.g.*, compaction or other technology) in the safe harbor provision of Section 3.B above by submitting a compliance plan to BNSF that provides evidence demonstrating that an additional proposed compliance measure will result in compliance with this Item. Shipper must also satisfy the profiling requirement of Section 3.A above. Any product including topper agents, devices or appurtenance utilized by the Shipper or Shipper's mine agents to control the release of coal dust shall not adversely impact railroad employees, property, locomotives or owned cars.

APPENDIX A

REDESIGNED CHUTE DIAGRAM

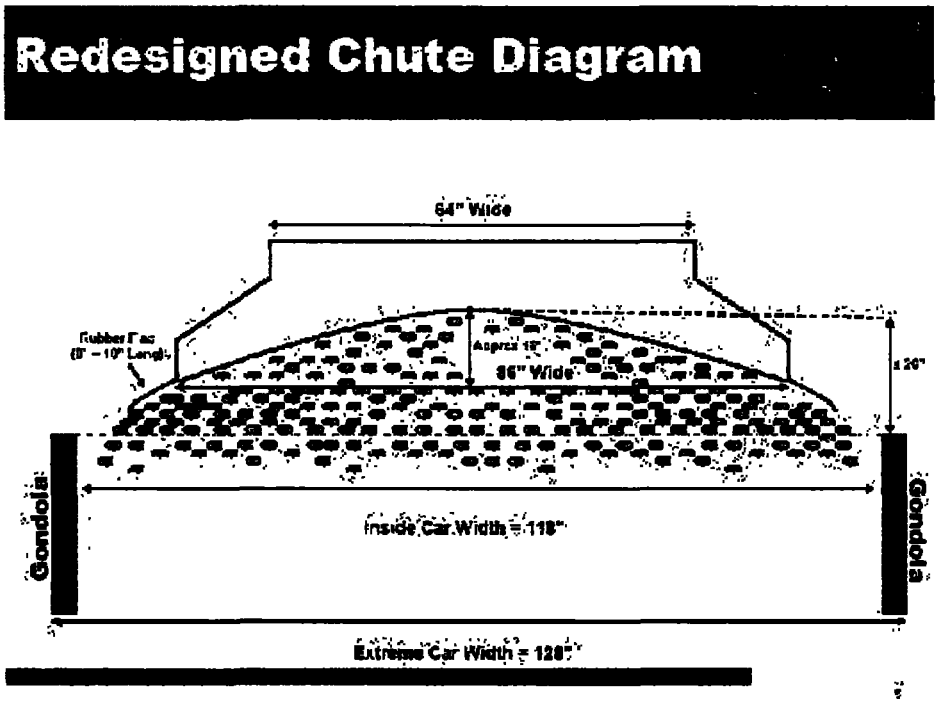

APPENDIX B

Acceptable Topper Agents and Application Rates

Topper Agents [1]	Concentration Rate per Car [2]	Total Solution Applied per Railcar [3]
Nalco Dustbind Plus	2.0 gal	20 gal
Midwest Soil-Sement	1.25 gal	18.75 gal
AKJ CTS-100	1.36 gal[4]	15 gal
AKJ CTS-100C	1.36 gal[4]	15 gal
Rantec Capture 3000	2.5 lbs	20 gal

(1) For Topper Application only.
(2) The amount of topper agent mixed into a solution for each Railcar. These concentration rates were established during testing. c
(3) The amount of topper agent applied to each Railcar.
(4) 1.36 gallons of concentrate (CTS-100C mixed with 13.64 gallons of water.

BNSF 6041-B

Rev. 20, Issued September 26, 2011

BNSF PRICE LIST 6041-B
(Cancels BNSF Freight Tariff 6041-A)

PROVIDING

RULES AND REGULATIONS GOVERNING UNIT TRAIN AND VOLUME ALL-RAIL

COAL SERVICE, ALSO ACCESSORIAL SERVICES AND CHARGES THEREFOR

APPLYING AS PROVIDED IN PRICE LIST

ISSUED: September 19, 2011 EFFECTIVE: October 9, 2011
Issued by BNSF Price Management, P.O. Box 961069, Ft. Worth, TX 76161-0069

ITEM 100
COAL DUST MITIGATION REQUIREMENTS

1. To prevent contamination of the rail ballast caused by fugitive coal dust, BNSF is modifying the loading requirement applicable to all coal cars loaded at Montana and Wyoming mines by shippers whose coal transportation is subject to this Rules Book.

2. Effective October 1, 2011, shippers loading coal at any Montana and Wyoming mine must take measures to load coal in such a way that any loss in transit of coal dust from the shipper's loaded coal cars will be reduced by at least 85 percent as compared to loss in transit of coal dust from coal cars where no remedial measures have been taken. At least 30 days prior to loading cars for shipment by BNSF, a Shipper shall provide BNSF with written notice of compliance efforts.

3. A shipper will be deemed to be in compliance with the loading requirement set out in this Item if the shipper satisfies Sections 3.A and 3.B below or pursues the option in Section 4 below:

A. Shipper ensures that loaded uncovered coal cars will be profiled in accordance with BNSF's published template entitled "Redesigned Chute Diagram" located in Appendix A to this publication.

B. Shipper ensures that an acceptable topper agent (e.g., surfactant) will be properly applied to the entire surface of all loaded coal cars at an effective concentration level and in accordance with the manufacturer's specifications. An acceptable topper agent is one that has been shown to reduce coal dust loss in transit by 85%. Appendix B to this publication lists the topper agents that meet this criteria. Proper use of any one of the topper agents on the approved list in accordance with the manufacturer's specifications and at the application rates specified in Appendix B, will satisfy this safe harbor provision. BNSF will consider other topper agents to be acceptable for purposes of this safe harbor provision if the shipper can demonstrate that appropriate testing has shown that the topper agent achieves compliance with this Item. Guidelines for the testing of new topper agents will be provided upon request.

4. Shipper may seek inclusion of any other method of coal dust suppression (*e.g.*, compaction or other technology) in the safe harbor provision of Section 3.B above by submitting a compliance plan to BNSF that provides evidence demonstrating that an additional proposed compliance measure will result in compliance with this Item. Shipper must also satisfy the profiling requirement of Section 3.A above. Any product including topper agents, devices or appurtenance utilized by the Shipper or Shipper's mine agents to control the release of coal dust shall not adversely impact railroad employees, property, locomotives or owned cars.

APPENDIX A

REDESIGNED CHUTE DIAGRAM

Redesigned Chute Diagram

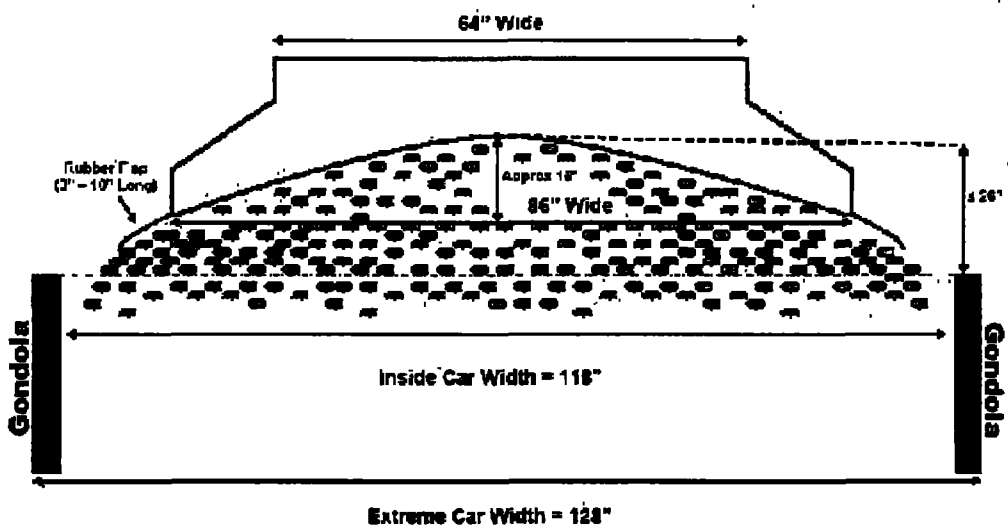

APPENDIX B

Acceptable Topper Agents and Application Rates

Topper Agents [1]	Concentration Rate per Car [2]	Total Solution Applied per Railcar [3]
Nalco Dustbind Plus	2.0 gal	20 gal
Midwest Soil-Sement	1.25 gal	18.75 gal
AKJ CTS-100	1.36 gal[4]	15 gal
AKJ CTS-100C	1.36 gal[4]	15 gal
Rantec Capture 3000	2.5 lbs	20 gal
MinTech Min Topper S+0150	1.1 gal	20 gal

(1) For Topper Application only.
(2) The amount of topper agent mixed into a solution for each Railcar. These concentration rates were established during testing. c
(3) The amount of topper agent applied to each Railcar.
(4) 1.36 gallons of concentrate (CTS-100C) mixed with 13.64 gallons of water.

Counsel's Exhibit No. 2

UP Coal Dust Tariff Rules

UP Circular 6603-C, Items 215 and 216

Issued September 8, 2011

UP Circular 6603-C, Items 215-A and 216-A

Issued September 26, 2012

UP Circular 6603-C, Items 215 and 216

Issued September 8, 2011

UP CIRCULAR 6603-C

Applying on Loading, Handling, Accessorial Charges,

Fuel Surcharges and

General Rules for Coal Trains Originating in Wyoming

Governed except as otherwise provided herein, by UFC 6000, OPSL 6000, UP 6004, and UP 6007-series.

Issued By:
E. A. HUNTER - MANAGER PRICING SERVICES
B. A. ROMMEL - MANAGER PRICING SERVICES

Union Pacific Railroad Company
1400 Douglas Street Omaha, NE 68179

Issued: March 3, 2006
Effective: March 15, 2006

RECOMMENDED LOADING MEASURES TO MITIGATE COAL DUST

This General Rule Item shall apply to contracts, transportation agreements or UPCQ's executed or issued on or prior to September 30, 2011.

1. For trains loaded at any Powder River Basin mine for subsequent movement on UP, Shipper is responsible for loading cars with coal in such a way that coal dust loss in transit from Shipper's loaded cars will be reduced by at least 85% as compared to loss of coal dust from loaded coal cars where no remedial measures were taken.

2. Loaded coal trains will be deemed to be in compliance with the standard in paragraph 1 if the trainloads meet the specifications in the General Order or Timetable for Powder River Division, Special Conditions involving Coal Mines issued by BNSF, the rail carrier designated by the ICC/STB as authorized to establish operating rules for the Joint Line ("Operating Rule"). Specifically either:

   a. Shipper or Shipper's Loading Operator should arrange (i) to load uncovered coal cars in accordance with the profile as published in the BNSF template drawing number 565000 http://www.bnsf.com/customers/what-can-i-ship/coal/coal-dust/pdf/q4.pdf and (ii) to properly apply an acceptable topper agent (e.g. surfactant) to the entire surface of coal in all cars in a trainload at an effective concentration level and in accordance with manufacturers' specifications. Topper agents and concentration rates currently considered as proven satisfactory by BNSF, if used in accordance with the manufacturers' specifications, are shown in table below:

Topper Agents (1)	Concentration Rate per Rail Car (2)	Total Solution Applied per Rail Car (3)
Nalco Dustbind Plus	2.0 gallons	20 gallons
Midwest Soil-Sement	1.25 gallons	18.75 gallons
AKJ CTS-100	1.36 gallons	15 gallons

   Notes to Table Above:
   (1) For Topper Application only.
   (2) The amount of topper agent mixed into a solution for each loaded Railcar. These concentration rates were established during testing carried out in PRB in 2010.
   (3) The amount of topper agent applied to each loaded Railcar.

   or

   b. Shipper or Shipper's Loading Operator may adopt an alternative coal dust mitigation plan involving other measures (e.g. compaction or other technology) and profiling in accordance with 2. a. (i) above; PROVIDED, HOWEVER, that Shipper or Shipper's Loading Operator must submit test results to BNSF that satisfy BNSF that the alternative proposed compliance measure(s) will result in compliance with paragraph 1. In addition, BNSF must be assured that any product involving topper agents. devices or appurtenances utilized to control the release of coal dust will not adversely impact railroad employees, property, locomotives or owned cars.

3. Shipper is encouraged to adopt measures to comply with Paragraph 2.a. as soon as practicable.

Continued on next page

a. If Shipper chooses to load its trains in accordance with paragraph 2. a., Shipper should notify UP in writing of the steps it has taken. or directed its Loading Operator to take, to comply with this Item for each mine or load out in the Powder River Basin where Shipper anticipates loading coal into trains that will subsequently be transported over UP. The notice should include the approximate date when those trainloads will be profiled and a topping agent will be applied. Shipper is requested to provide this notice to UP no later than October 7, 2011.

b. If Shipper proposes to comply by using either an alternative topping agent or an alternative measure, the notice to UP should provide a description of the alternative topping agent or measure and when Customer or Customer's loading agent proposes to obtain BNSF approval of the alternative topping agent or measure. Shipper may notify UP of its choice to use an alternative whenever Shipper decides that it will demonstrate to BNSF that the alternative should be accepted. Until BNSF notifies Shipper and UP in writing that BNSF considers the testing results adequate assurance that the alternative satisfies the standard in paragraph 1, however, Shipper or Shipper's Loading Operator should load its trains in accordance with paragraph 2.a.

REQUIRED LOADING MEASURES TO MITIGATE COAL DUST

This General Rule Item shall apply (a) to all tariffs effective October 1, 2011 and (b) to contracts, transportation agreements or UPCQ's executed or issued after September 30, 2011.

1. For trains loaded at any Powder River Basin mine for subsequent movement on UP, Shipper is responsible for loading cars with coal in such a way that coal dust loss in transit from Shipper's loaded cars will be reduced by at least 85% as compared to loss of coal dust from loaded coal cars where no remedial measures were taken.

2. Loaded coal trains will be deemed to be in compliance with the standard in paragraph 1 if the trainloads meet the specifications in the General Order or Timetable for Powder River Division, Special Conditions involving Coal Mines issued by BNSF, the rail carrier designated by the ICC/STB as authorized to establish operating rules for the Joint Line ("Operating Rule"). Specifically either:

   a. Shipper or Shipper's Loading Operator must arrange (i) to load uncovered coal cars in accordance with the profile as published in the BNSF template drawing number 565000 http://www.bnsf.com/customers/what-can-i-ship/coal/coal-dust/pdf/q4.pdf and (ii) to properly apply an acceptable topper agent (e.g. surfactant) to the entire surface of coal in all cars in a trainload at an effective concentration level and in accordance with manufacturers' specifications. Topper agents and concentration rates currently considered as proven satisfactory by BNSF, if used in accordance with the manufacturers' specifications, are shown in table below:

Topper Agents (1)	Concentration Rate per Rail Car (2)	Total Solution Applied per Rail Car (3)
Nalco Dustbind Plus	2.0 gallons	20 gallons
Midwest Soil-Sement	1.25 gallons	18.75 gallons
AKJ CTS-100	1.36 gallons	15 gallons

   Notes to Table Above:
   (1) For Topper Application only.
   (2) The amount of topper agent mixed into a solution for each loaded Railcar. These concentration rates were established during testing carried out in PRB in 2010.
   (3) The amount of topper agent applied to each loaded Railcar.

   or

   b. Shipper or Shipper's Loading Operator may adopt an alternative coal dust mitigation plan involving other measures (e.g. compaction or other technology) and profiling in accordance with 2. a. (i) above; PROVIDED, HOWEVER, that Shipper or Shipper's Loading Operator must submit test results to BNSF that satisfy BNSF that the alternative proposed compliance measure(s) will result in compliance with paragraph 1. In addition, BNSF must be assured that any product involving topper agents, devices or appurtenances utilized to control the release of coal dust will not adversely impact railroad employees, property, locomotives or owned cars.

3. In order for UP to comply with the BNSF Operating Rule regarding coal dust mitigation measures, Shippers must adopt measures to comply with this Item as soon as practicable.

Continued on next page

a. Shipper must notify UP in writing of the steps it has taken, or directed its Loading Operator to take, in accordance with paragraph 2.a. to comply with this Item for each mine or load out in the Powder River Basin where Shipper anticipates loading coal into trains that will subsequently be transported over UP. The notice must include the approximate date when those trainloads will be profiled and a topping agent will be applied. Shipper must provide this notice to UP no later than October 7, 2011.

b. If Shipper proposes to comply by using either an alternative topping agent or an alternative measure, the notice to UP should provide a description of the alternative topping agent or measure and when Customer or Customer's loading agent proposes to obtain BNSF approval of the alternative topping agent or measure. Shipper may notify UP of its choice to use an alternative whenever Shipper decides that it will demonstrate to BNSF that the alternative should be accepted. Until BNSF notifies Shipper and UP in writing that BNSF considers the testing results adequate assurance that the alternative satisfies the standard in paragraph 1, however, Shipper or Shipper's Loading Operator must load its trains in accordance with paragraph 2.a.

UP Circular 6603-C, Items 215-A and 216-A

Issued September 26, 2012

UP CIRCULAR 6603-C

Applying on Loading, Handling, Accessorial Charges,

Fuel Surcharges and

General Rules for Coal Trains Originating in Wyoming

Governed except as otherwise provided herein, by UFC 6000, OPSL 6000, UP 6004, and UP 6007-series.

Issued By:
E. A. HUNTER - MANAGER PRICING SERVICES
B. A. ROMMEL - MANAGER PRICING SERVICES

Union Pacific Railroad Company
1400 Douglas Street Omaha, NE 68179

Issued. March 3, 2006
Effective: March 15, 2006

RECOMMENDED LOADING MEASURES TO MITIGATE COAL DUST

This General Rule Item shall apply to contracts, transportation agreements or UPCQ's executed or issued on or prior to September 30, 2011.

1. For trains loaded at any Powder River Basin mine for subsequent movement on UP, Shipper is responsible for loading cars with coal in such a way that coal dust loss in transit from Shipper's loaded cars will be reduced by at least 85% as compared to loss of coal dust from loaded coal cars where no remedial measures were taken.

2. Loaded coal trains will be deemed to be in compliance with the standard in paragraph 1 if the trainloads meet the specifications in the General Order or Timetable for Powder River Division, Special Conditions involving Coal Mines issued by BNSF, the rail carrier designated by the ICC/STB as authorized to establish operating rules for the Joint Line ("Operating Rule"). Specifically either:

   a. Shipper or Shipper's Loading Operator should arrange (i) to load uncovered coal cars in accordance with the profile as published in the BNSF template drawing number 565000 http://www.bnsf.com/customers/what-can-i-ship/coal/coal-dust/pdf/q4.pdf and (ii) to properly apply an acceptable topper agent (e.g. surfactant) to the entire surface of coal in all cars in a trainload at an effective concentration level and in accordance with manufacturers' specifications. Topper agents and concentration rates currently considered as proven satisfactory by BNSF, if used in accordance with the manufacturers' specifications, are shown in table below: |c|

Topper Agents (1)	Concentration Rate per Rail Car (2)	Total Solution Applied per Rail Car (3)
Nalco Dustbind Plus	2.0 gallons	20 gallons
Midwest Soil-Sement	1.25 gallons	18.75 gallons
AKJ CTS-100	1.36 gallons (4)	15 gallons
AKJ CTS-100C	1.36 gallons (4)	15 gallons
Rantec Capture 3000	2.5 pounds	20 gallons
MinTech Min Topper S+0150	1.1 gallons	20 gallons

Notes to Table Above:
(1) For Topper Application only.
(2) The amount of topper agent mixed into a solution for each loaded Railcar. These concentration rates were established during testing carried out in the PRB.
(3) The amount of topper agent applied to each loaded Railcar.
(4) 1.36 gallons of concentrate (CTS-100C) mixed with 13.64 gallons of water.

or

   b. Shipper or Shipper's Loading Operator may adopt an alternative coal dust mitigation plan involving other measures (e.g. compaction or other technology) and profiling in accordance with 2. a. (i) above; PROVIDED, HOWEVER, that Shipper or Shipper's Loading Operator must submit test results to BNSF that satisfy BNSF that the alternative proposed compliance measure(s) will result in compliance with paragraph 1. In addition, BNSF must be assured that any product involving topper agents, devices or

Continued on next page

appurtenances utilized to control the release of coal dust will not adversely impact railroad employees, property, locomotives or owned cars.

3. Shipper is encouraged to adopt measures to comply with Paragraph 2.a. as soon as practicable.

   a. If Shipper chooses to load its trains in accordance with paragraph 2. a., Shipper should notify UP in writing of the steps it has taken, or directed its Loading Operator to take, to comply with this Item for each mine or load out in the Powder River Basin where Shipper anticipates loading coal into trains that will subsequently be transported over UP. The notice should include the approximate date when those trainloads will be profiled and a topping agent will be applied. Shipper is requested to provide this notice to UP no later than October 7, 2011.

   b. If Shipper proposes to comply by using either an alternative topping agent or an alternative measure, the notice to UP should provide a description of the alternative topping agent or measure and when Customer or Customer's loading agent proposes to obtain BNSF approval of the alternative topping agent or measure. Shipper may notify UP of its choice to use an alternative whenever Shipper decides that it will demonstrate to BNSF that the alternative should be accepted. Until BNSF notifies Shipper and UP in writing that BNSF considers the testing results adequate assurance that the alternative satisfies the standard in paragraph 1, however, Shipper or Shipper's Loading Operator should load its trains in accordance with paragraph 2.a.

REQUIRED LOADING MEASURES TO MITIGATE COAL DUST

This General Rule Item shall apply (a) to all tariffs effective October 1, 2011 and (b) to contracts, transportation agreements or UPCQ's executed or issued after September 30, 2011.

1. For trains loaded at any Powder River Basin mine for subsequent movement on UP, Shipper is responsible for loading cars with coal in such a way that coal dust loss in transit from Shipper's loaded cars will be reduced by at least 85% as compared to loss of coal dust from loaded coal cars where no remedial measures were taken.

2. Loaded coal trains will be deemed to be in compliance with the standard in paragraph 1 if the trainloads meet the specifications in the General Order or Timetable for Powder River Division, Special Conditions involving Coal Mines issued by BNSF, the rail carrier designated by the ICC/STB as authorized to establish operating rules for the Joint Line ("Operating Rule"). Specifically either:

   a. Shipper or Shipper's Loading Operator must arrange (i) to load uncovered coal cars in accordance with the profile as published in the BNSF template drawing number 565000 http://www.bnsf.com/customers/what-can-i-ship/coal/coal-dust/pdf/q4.pdf and (ii) to properly apply an acceptable topper agent (e.g. surfactant) to the entire surface of coal in all cars in a trainload at an effective concentration level and in accordance with manufacturers' specifications. Topper agents and concentration rates currently considered as proven satisfactory by BNSF, if used in accordance with the manufacturers' specifications, are shown in table below: [c]

Topper Agents (1)	Concentration Rate per Rail Car (2)	Total Solution Applied per Rail Car (3)
Nalco Dustbind Plus	2.0 gallons	20 gallons
Midwest Soil-Sement	1.25 gallons	18.75 gallons
AKJ CTS-100	1.36 gallons (4)	15 gallons
AKJ CTS-100C	1.36 gallons (4)	15 gallons
Rantec Capture 3000	2.5 pounds	20 gallons
MinTech Min Topper S+0150	1.1 gallons	20 gallons

Notes to Table Above:
(1) For Topper Application only.
(2) The amount of topper agent mixed into a solution for each loaded Railcar. These concentration rates were established during testing carried out in the PRB.
(3) The amount of topper agent applied to each loaded Railcar.
(4) 1.36 gallons of concentrate (CTS-100C) mixed with 13.64 gallons of water.

or

   b. Shipper or Shipper's Loading Operator may adopt an alternative coal dust mitigation plan involving other measures (e.g. compaction or other technology) and profiling in accordance with 2. a. (i) above; PROVIDED, HOWEVER, that Shipper or Shipper's Loading Operator must submit test results to BNSF that satisfy BNSF that the alternative proposed compliance measure(s) will result in compliance with paragraph 1. In addition, BNSF must be assured that any product involving topper agents, devices or

Continued on next page

appurtenances utilized to control the release of coal dust will not adversely impact railroad employees, property, locomotives or owned cars.

3. In order for UP to comply with the BNSF Operating Rule regarding coal dust mitigation measures, Shippers must adopt measures to comply with this Item as soon as practicable.

   a. Shipper must notify UP in writing of the steps it has taken, or directed its Loading Operator to take, in accordance with paragraph 2.a. to comply with this Item for each mine or load out in the Powder River Basin where Shipper anticipates loading coal into trains that will subsequently be transported over UP. The notice must include the approximate date when those trainloads will be profiled and a topping agent will be applied.

   b. If Shipper proposes to comply by using either an alternative topping agent or an alternative measure, the notice to UP should provide a description of the alternative topping agent or measure and when Customer or Customer's loading agent proposes to obtain BNSF approval of the alternative topping agent or measure. Shipper may notify UP of its choice to use an alternative whenever Shipper decides that it will demonstrate to BNSF that the alternative should be accepted. Until BNSF notifies Shipper and UP in writing that BNSF considers the testing results adequate assurance that the alternative satisfies the standard in paragraph 1, however, Shipper or Shipper's Loading Operator must load its trains in accordance with paragraph 2.a.

Viz

BEFORE THE
SURFACE TRANSPORTATION BOARD

FINANCE DOCKET NO. 35557

REASONABLENESS OF BNSF RAILWAY COMPANY COAL DUST MITIGATION TARIFF PROVISIONS

VERIFIED STATEMENT OF

MARK J. VIZ, Ph.D., P.E.

ON BEHALF OF

WESTERN COAL TRAFFIC LEAGUE, AMERICAN PUBLIC POWER ASSOCIATION, EDISON ELECTRIC INSTITUTE AND NATIONAL RURAL ELECTRIC COOPERATIVE ASSOCIATION

Public Version

Confidential and Highly Confidential Information has been Redacted

DATED: OCTOBER 1, 2012

1. Introduction.

a. My name is Mark J. Viz. I am a principal engineer with Exponent, Inc., an engineering, scientific, health and environmental consulting firm headquartered in Menlo Park, California. I am based in Exponent's Chicago, Illinois, office. For the past thirteen years I have performed engineering and/or engineering consultation work in a variety of aspects of mechanical performance, material handling, transportation and unintended releases of hazardous materials, and certain aspects of derailment cause and origin studies particular to rail transportation. From 2007 through 2009, I was the project manager and technical lead for a detailed study of coal loss, monitoring and measurement issues involving the movement of coal by rail on the "Joint Line" in the Powder River Basin. Part of that study involved the use of "Passive Dust Collectors," supplied to us by BNSF, for the performance of lengthy and detailed field testing of railcars loaded with coal and then profiled for full-scale wind testing. This study was funded by a consortium of member companies of the National Coal Transportation Association (NCTA). I have attached a copy of my current curriculum vitae (Exhibit MJV-1) to this statement.

b. Previously, I had been requested by the Western Coal Traffic League (WCTL) to analyze some of the means and methods that BNSF has used to attempt to monitor and measure coal dust emissions from loaded railcars in transit. These analyses are set forth in my Verified Statements submitted as part of WCTL's Opening, Reply, Rebuttal and Petition to Reopen filings in Surface Transportation Board ("STB" or "Board") Finance Docket No. 35305, Arkansas Electric Cooperative Corporation – Petition For Declaratory Order (so-called "Dust I").

c. Presently, I have been asked to comment on (1) BNSF's use of "Passive Dust Collectors" (also referred to as "passive collectors") as a means *to measure* the amount, if any, of fugitive coal dust emissions from moving coal railcars; (2) BNSF's use of laser scanning or other technology to monitor or "verify" that the

loaded top-of-car coal heap profile meets the precise requirements of BNSF's "bread loaf" railcar profiling requirements set forth in Appendix A to the Revised Coal Dust Tariff;[1] and (3) the factors that determine if, when and to what extent fugitive emissions will occur in the transportation of loaded railcars.

d. Passive Dust Collectors, as designed and implemented for use by BNSF's consultant, Simpson Weather Associates (SWA), and as used by BNSF (to the extent that BNSF and SWA's methods and procedures have been disclosed), cannot be used to scientifically establish the amount, if any, of fugitive particulate emissions from railcars with certainty, reliability or repeatability, nor can they be used to scientifically establish the quantitative effectiveness (in terms of percent reduction in dust emissions), if any, of the application of coal dust suppressants, in reducing fugitive particulate emissions with certainty, reliability or repeatability.

e. I also note at the outset that many if not all of the dust suppressants were designed for use in dust mitigation from static coal stockpiles at coal-burning power plants or similar facilities. In this regard these products are generally recognized to work when applied to a large pile of coal *that is stationary*, but there are still many aspects of their performance *in moving railcars* that have not yet been verified. I have observed from my own field work that crusting agents and other topper sprays essentially break apart when a railcar gets shaken or bumped going over the track. Frequently other events can also occur to either upset the efficacy of the topper agent or in certain cases to make the fugitive loss even worse by a process known as "saltation," i.e., the greater entrainment of particles in a moving air stream as a result of released particles impacting the surface and therefore releasing yet greater amounts of dust. The performance of suppressants during precipitation events and long exposure to wind and solar radiation are also not that well-understood.

[1] "Revised Coal Dust Tariff" refers to item 100, entitled "Coal Dust Mitigation Requirements," as first published on July 14, 2011, in Revision 016 to BNSF's Price List 6041-B and subsequent revisions thereto.

f. Dr. Emmitt in his August 23, 2012, Reply V.S. states at page 2 that "topper agents are used in Canada, Australia, China and by Norfolk Southern in Virginia to control coal dust losses. To suggest that application of topper agents may not be an appropriate method to control dust on loaded coal cars is without merit." Dr. Emmitt has missed my point. Suppressants can possibly reduce fugitive emissions under certain circumstances, but that is not the central issue with the requirements of the BNSF Tariff. The question is whether and to what extent those circumstances exist for railcars in motion and to what extent, if possible, that those reductions can be measured and verified using the techniques that BNSF and SWA have attempted to use.

2. Background.

a. BNSF's Original Coal Dust Tariff[2] required that coal trains moving over the PRB Joint Line "emit not more than an Integrated Dust Value (IDV.2) of 300 units" and that coal trains moving over the Black Hills Subdivision "not emit more than an (IDV.2) of 245 units." According to BNSF's filings in Dust I, BNSF had collected IDV.2 data "from thousands of trains passing Milepost 90.7 on the Joint Line and Milepost 558 on the Black Hills Subdivisions"[3] and had prepared a statistical analysis of these data showing that "there is a high degree of confidence that coal dust emissions would be reduced by at least 85%" at the mandated IDV.2 emission cap levels.[4] BNSF also claimed that if shippers applied appropriate suppressants and profiled their trains, they could meet the mandated IDV.2 standards.[5]

---

[2] "Original Coal Dust Tariff" refers to Item 100, entitled "Coal Dust Mitigation Requirements," initially published on April 29, 2009, in Revision 011 to BNSF's Price List 6041-B as amended through Revision 015 and Item 101, entitled "Coal Dust Requirements Black Hills Sub-Division," initially published on May 27, 2009, in Revision 012 to BNSF's Price List 6041-B, as subsequently amended.

[3] Dust I. BNSF Railway Company's Opening Evidence and Argument ("BNSF Dust I Opening") at 6.

[4] BNSF Dust I Opening, V.S. Sultana at 10.

[5] BNSF Dust I Opening. V.S. William Van Hook at 22: "We are confident that proper application of a quality surfactant onto a properly loaded coal car can reduce coal dust emissions from the rail car top by more than 85%."

b. In the Dust I case, I concluded that BNSF had not demonstrated that its IDV.2 calculations accurately measured fugitive coal emissions from moving coal railcars, or reductions in those emissions, if any, resulting from the application of suppressants. Reasons I cited for this conclusion included but were not limited to the following:

   i. BNSF attempted to collect coal dust emission data using MetOne E-Samplers on the Joint Line and on the Black Hills Subdivision, but BNSF failed to establish to a reasonable degree of engineering certainty that the E-Samplers accurately measure coal emissions, if any, from passing loaded coal railcars in a train.

   ii. BNSF failed to provide a reasoned explanation why its own studies of particulate measurements from E-Samplers located side-by-side in the field and in the laboratory produced substantially different IDV.2 results.

   iii. BNSF converted the E-Sampler output into IDV.2 values using a computer algorithm that it refused to produce, making it impossible to know how these values were being calculated and what they represented. BNSF's refusal to produce this computer algorithm was further exacerbated by the fact that the concept of "Integrated Dust Value" appears nowhere in the technical literature or regulations. In other words, the IDV concept is uniquely a creation of BNSF / SWA and has received no scrutiny or peer review from the appropriate technical community. This reality makes its meaning and applicability all the more suspect.

In its decision finding that BNSF's publication of the Original Coal Dust Tariff was an unreasonable practice, the Board stated that it "share[d]" many of these same concerns.[6]

c. BNSF published its Revised Coal Dust Tariff in July of 2011. This Tariff requires that PRB coal shippers "take measures to load coal in such a way that any loss in transit of coal dust from the shipper's loaded coal cars will be reduced by at least 85% as compared to loss in transit where no remedial measures have been taken." The Tariff further provides that "a shipper will be deemed to be in compliance" with the 85% reduction requirement if it profiles coal railcars in the same manner as was required under the Original Coal Dust Tariff and "properly" applies a BNSF-approved "topper agent" that has been shown to reduce coal dust loss in transit by 85%." The Revised Tariff, as originally published, also stated that "in recent tests carried out in the PRB, three topper agents meet this criteria when properly applied" and listed those agents in Appendix B to the Revised Tariff.

d. I was requested by WCTL in August of 2011 to review publicly available information concerning the "recent tests" referenced in the Revised Coal Dust Tariff. The "recent tests" BNSF was referencing was a study called the "Super Trial." In this series of tests, BNSF calculated IDV.2 values for 1,518 trains transported between March and September of 2010. Each of these trains had been treated with a specified coal dust suppression agent in either a body treatment or a topical treatment. A total of "seven different chemical agents" were used. In addition, "115 trains were tested using Passive Dust Collectors." BNSF explained its passive collector testing procedure as follows:[7]

> "On each of these 115 trains, half of the cars were treated with a coal dust suppression agent and the other half were untreated. Passive dust collectors were attached to the rear

[6] STB decision served March 3, 2011, at 13.

[7] Reference the publicly available document "Summary of BNSF/UP Super Trial 2010."

sill of seven treated and seven untreated cars on each train. The coal dust collected from the passive dust collectors during the train's movement was then analyzed to compare the amount of coal dust emitted from the treated and untreated cars."

The IDV.2 study data as arranged by BNSF in its "Summary" of the study results purported to show that shippers could comply with the IDV.2 standards set forth in the Original Coal Dust Tariff by applying topical suppressants, a result that BNSF said was "confirmed" by its passive dust collector results. BNSF also asserted that its passive dust collector results showed that "three topical treatment agents showed coal dust reductions of 85 percent or more – AKJ CTS-100, Midwest Soil-Sement and Nalco Dustbind Plus." These three suppressants were those BNSF identified in the Revised Coal Dust Tariff as approved suppressants.

e. The results of my initial review of BNSF's results were set forth in my Verified Statement accompanying WCTL's petition, filed with the Board on August 11, 2011. I concluded, based on public information then available to me, that BNSF's attempt to measure fugitive emissions from coal cars using its passive dust collector study method was riddled with fundamental flaws and, just like its prior IDV.2 studies, did not produce scientifically meaningful calculations of fugitive emissions from railcars with certainty, reliability or repeatability.

f. I have now had the opportunity to review additional materials produced in discovery in this case concerning BNSF's Super Trial study and additional post Super Trial studies that BNSF has conducted. I have also reviewed BNSF's filing responding to WCTL's August 11, 2011, petition. Based on this review, I reaffirm here the conclusions I reached in my August 11, 2011, Verified Statement: BNSF's attempt to quantitatively measure fugitive emissions, whether in an absolute or relative manner, from coal railcars using its passive collector methods was riddled with fundamental flaws and, just like its prior IDV.2 studies, did not

produce scientifically meaningful calculations of fugitive emissions from railcars with certainty, reliability or repeatability.

3. **A fundamental flaw with the passive dust collectors is that they collect particulate matter within a certain size range based on the particular design parameters of the collectors. No testing, calculations or other engineering data have been produced by SWA or BNSF to establish with certainty what the so-called "cut point" is for the collectors. In fact, it's quite possible that they simply do not know.**

   a. The passive dust collectors, as designed by SWA and used by BNSF, are essentially metal boxes that have an inlet opening with a certain cross-sectional area that is connected to a vertical channel that is then connected to a removable box at the bottom of the vertical channel (see Figure 1). To facilitate air flow through the collector, the vertical channel is equipped with a "volute," which is essentially a circular opening in the side of the channel that is then covered by a mesh screen. A combination of the fluid dynamics properties of the air flow in the channel and volute along with the "blocking" provided by the mesh screen allow entrained particles smaller than a certain size to exit the collector while larger particles drop into the collector box. The "cut point" that determines which particles pass-through and which are collected is to a large extent established by the detailed design and wind-tunnel testing of the collector. SWA has claimed that they have performed extensive wind-tunnel studies on their passive collector design; however, SWA neither presented any significant results from any such claimed testing nor have they published the results from any such claimed studies in the relevant technical literature. Given this lack of information and ability to verify the design and setting of the collector's cut point, neither SWA nor BNSF have offered reasonable scientific or engineering data to establish exactly what entrained particles the collectors actually collect.

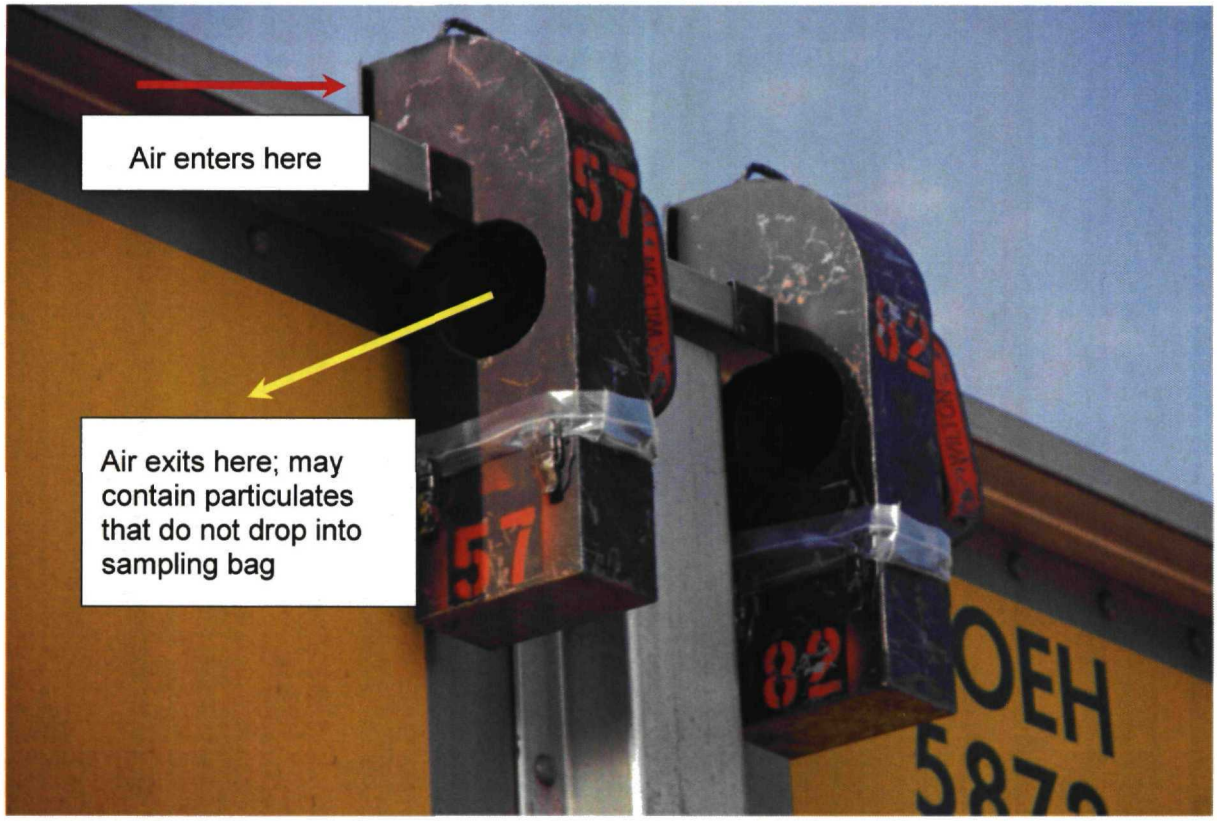

Figure 1.

b. In its response to WCTL's discovery requests, BNSF admits that its "passive collectors were not based upon a specified 'cut point' that distinguished between particles of different sizes"[8] but asserts that "analysis relating to a 'cut point' was not necessary because the passive collectors were designed to provide a relative measure of coal dust lost from rail cars in transit when they are attached to different rail cars to assess the effectiveness of different coal dust mitigation approaches."[9] However, BNSF's response begs the question as to whether the passive collectors retain the fugitive particles that allegedly cause the ballast fouling problems asserted by BNSF. It is self-evident that the passive collectors do not retain all of the particulate matter that enters them because the air that enters the collectors needs to exit the collectors (see arrows in Figure 1). But what range of particle size gets retained? If this reasoning were taken to its logical

[8] BNSF Railway Company's Responses and Objections to Coal Shippers' First Set of Interrogatories and Document Requests at 2, February 6, 2012 ("BNSF Feb. 6, 2012 Responses").

[9] Id.

conclusion that would mean that it would be possible to design the collectors with a high enough cut point such that most if not all entrained dust would then be able to pass through. Given this situation, it further would be logical to then conclude that no dust at all is emitted from moving railcars regardless if they are treated with a suppressant. It is well-established in the air sampling literature that sampling necessarily is associated with a particular range of particle size, whether it be PM10, PM2.5 or something else. Since BNSF / SWA have refused to address particle size issues at all in any of their work, this uncertainty remains with the passive collectors.

c. In addition to the ambiguity involved with the establishment of the cut point, the material that remains in the collector box can contain a whole variety of foreign, non-coal content such as insects, other organic matter, other airborne materials like pollen, etc. During the field testing that Exponent performed and that I directed (as mentioned in the **Introduction**), we experienced first-hand this phenomenon. We routinely found foreign matter such as insects and what appeared to be wood chips in the passive collector boxes that we used during our field testing. Exponent's understanding is that the passive collector samples taken during field testing performed by BNSF were also not checked for foreign content. This has been a concern regarding the use of the passive collector device as it will retain whatever is blown into it above a certain size. One solution to this clear problem is to perform a chemical or even simple visual / microscopic analysis of the materials found in each collector box. No evidence or data have been provided by BNSF or SWA to substantiate that the material they collected in each passive collector and then weighed to establish percentage dust reduction was actually all coal. BNSF claims that "large and obvious non-coal particles were removed before drying and weighing."[10] There are multiple problems with this approach to the disposal of suspected non-coal material found in the collectors:

[10] Id. at 3.

i. It introduces substantial bias into the already uncertain sampling approach because it relies upon a subjective norm to alter or reduce the collected sample (i.e., what one person in the field determines is "large and obvious" might not be the same as another person).

ii. It requires that the collected sample be manipulated in a manner that could significantly reduce (or potentially increase) the amount of material left in the sample bag. In some cases, the amount of material in the collector sample bag amounts to less than a gram ... roughly the mass equivalent of a small paper clip. In addition, this small amount of material would likely be present in the sample bag as a dust or fine granular material. Removing a large piece from the sample bag could easily change the total amount of remaining material in the bag to render its further use meaningless.

iii. Neither BNSF nor SWA appear to have created or disseminated a written protocol that establishes by what methods "large and obvious non-coal particles" should have been identified and removed.

d. Consider certain details from the technical literature that describe the use of passive collectors on tests of coal railcars in Europe: "All the dust collectors used in the four equipped wagons are of the same design, for the sake of comparison. Each wagon was equipped with a pair of dust collectors.... The lower part of each dust collector consists of a cylindrical container, where dust filters, previously weighted, were installed at the very beginning of the train run. At the end of the run, the weight of each filter was recorded, and qualitative analyses of the coal dust sample were conducted."[11] And from the same reference: "Due to the location of the flow sensors, specifically the proximity of the sensors to the wagon, it is expected that the measurements performed were influenced by the wagons and structures located upstream. Even so, since the flow erosion occurs

[11] Ferreira, A.D., Viegas, D.X. and Sousa, A.C.M., "Full-scale measurements for evaluation of coal dust release from train wagons with two different shelter covers," *J. Wind Eng. Ind. Aerodynamics*, v. 91, pp. 1271-1283, 2003.

through the top gap, the recorded information for the flow velocity and direction, near the top, is very important for the characterization of some parameters influencing the erosion process."

4. **Another fundamental flaw with the passive dust collectors is that no testing, calculations or other engineering data have been produced by SWA or BNSF to establish that the concentration of particulate matter in the entrained air flow "sampled" by the collector is the same as the concentration in the entire air flow over the top of the railcar so equipped. In addition, effects due to the collector geometry, dimensions and particle characteristics are not addressed by BNSF or SWA in any meaningful way.**

   a. Much like BNSF and SWA's failed efforts to show that the track-side E-Samplers are actually measuring something that is meaningful and able to be checked against a normative standard, this same general deficiency is present with the passive dust collectors. No evidence, wind tunnel test data, scale studies or calculations have been provided to establish that the entrained flow sampled by the passive collectors installed at certain locations on the top chord of the railcar is at all representative of the particulate concentrations found in the larger air flow currents over and around the entire railcar.

   b. A variety of citations in the relevant technical literature point to the importance of this very issue, sometimes referred to as "sampling efficiency." Consider the following excerpt: "There are many factors affecting the penetration efficiency, such as impaction, gravitational settling, and turbulent or laminar diffusion. After particles enter the sampling inlet, some particles are inevitably deposited on the internal walls by a combination of inertial impaction, gravitational deposition, diffusive deposition, and electrostatic deposition during transmission inside the sampling tube and the sampler. Such internal particle loss from the sampled air will lead to an effective reduction in the overall efficiency of sampling. The magnitude of this effect depends on the internal shape of the sampler, the

dimension of sampling tube, the sampling flow rate, and the physical properties of the particles."[12]

c. Consider another relevant excerpt from the technical literature: "Six sets of BSNE collectors [BSNE collectors operate on the same basic principle as a passive dust collector] were deployed at the windward and leeward positions in the field to measure saltation and suspension. One set of collectors consisted of five BSNE collectors mounted on a pole at heights of 0.1, 0.2, 0.5, 1, and 1.5 m. Two creep collectors were deployed at each field position to measure discharge to a height of 0.025 m. Sample collections were periodic due to the remoteness of the field sites and generally occurred immediately after a high-wind event. Sediment collected by BSNE and creep samplers was air-dried prior to weighing. For those events with sufficient sediment catch in the BSNE (more than 0.5 g), the sediment was separated into 10, 45, 100, and 150 μm diameter size fractions using a sonic sieve. Since the BSNE is inefficient in collecting all suspended sediment (Goossens and Offer, 2000), we ascertained the catch efficiency of the BSNE for suspended Ritzville silt loam sediment (particle size <125 μm) and PM10. Catch efficiency was determined in a wind tunnel by (1) placing a 50 mm extension on the front of a BSNE collector, (2) attaching a funnel to the top of the extension and (3) introducing a known amount of sediment or PM10 into the collector via the funnel. Catch efficiency was determined at wind speeds (measured using a pitot tube located adjacent to the opening of the BSNE collector) of 5, 10 and 18 m s^{-1} and computed as the ratio of mass of sediment or PM10 collected in the BSNE to the amount of sediment or PM10 introduced into the collector."[13]

d. In response to WCTL's discovery requests, BNSF states that it "is not aware of any 'testing, calculations, or other engineering data establishing that the

[12] Wang, X., Zhang, Y. and Tan, Z., "Comparison of different instruments for particle concentration measurements," *ASHRAE Trans., Part 2*, v. 111, pp. 467-475, 2005.

[13] Sharratt, B., Feng, G. and Wendling, L., "Loss of soil and PM10 from agricultural fields associated with high winds on the Columbia Plateau," *Earth Surf. Process. Landforms*, v. 32, pp. 621-630, 2007.

concentration of particulate matter in the entrained air flow sampled by the passive collectors was the same as the concentration in the entire air flow over the top of a rail car equipped with a passive collectors."[14] According to SWA's President, Dr. G. David Emmitt, "Dr. Viz's questions about 'sampling efficiency' and varying weather conditions might be worth considering if one were trying to predict the specific volume of coal dust that would be emitted from a train treated with a particular chemical binding agent but BNSF's objective was to determine whether a specific chemical could be expected to reduce coal dust losses by a certain percentage – 85%. Dr. Viz misunderstood, or ignored, BNSF's objective."[15]

e. To respond to Dr. Emmitt's assertion above, I neither "misunderstood" nor "ignored" BNSF's objective. Instead, I have relied upon the relevant technical literature and acceptable data reduction methods to support my conclusions, an approach that BNSF and SWA do not take. In response to Dr. Emmitt, reconsider the excerpt from Wang et al. just quoted above: "... After particles enter the sampling inlet, some particles are inevitably deposited on the internal walls by a combination of inertial impaction, gravitational deposition, diffusive deposition, and electrostatic deposition during transmission inside the sampling tube and the sampler. Such internal particle loss from the sampled air will lead to an effective reduction in the overall efficiency of sampling. [emphasis mine] The magnitude of this effect depends on the internal shape of the sampler, the dimension of sampling tube, the sampling flow rate, and the physical properties of the particles."[16] To calculate whether a "specific chemical could be expected to reduce coal dust losses by a certain percentage" as claimed by Dr. Emmitt, the total mass of material collected in each passive collector needs to be determined. If the collected mass were different from the total sampled mass for reasons such as those listed in Wang et al. (e.g., inertial impaction, gravitational deposition,

[14] BNSF Feb. 6, 2012 Responses at 3.

[15] STB Finance Docket No. 35305, BNSF Railway Company's Reply, V.S. Emmitt at 3-4, August 23, 2011 ("BNSF Aug. 23, 2011 Reply").

[16] Id. Wang et al.

diffusive deposition, electrostatic deposition, etc.), the calculated percentage difference between these two mass values would be different, but more importantly, incorrect. This point can be further illuminated by a simple example: Suppose the sampling efficiency of the passive collector is $X \pm 5\%$. If the mass of material collected in one sampling bag (from a collector on the treated portion of the train) is *1.00 g*, the actual mass could range from *0.95 g* to *1.05 g*. In a like manner, if the mass of material collected in one sampling bag (from a collector on the untreated portion of the train) is *2.00 g*, the actual mass could range from *1.90 g* to *2.10 g*. This would imply that the percentage reduction from the treated railcar compared to the untreated railcar could be anywhere from 44.7% to 54.8% – a significant range. So, to the contrary, Dr. Emmitt's conclusion that the sampling efficiency of the passive collectors, or how much internal particle loss occurs, is unnecessary "to determine whether a specific chemical could be expected to reduce coal dust losses by a certain percentage" is itself without merit, as the simple example presented above illustrates.

f. Regarding particle loss that occurs with the use of the passive collectors, Exponent found while performing the NCTA field studies that after the sampling bag was removed from the well of the passive collector, a significant amount of particulate material still remained attached or otherwise embedded in the structure of the collector. We used the technique of rapping the side of the collector body a few times before the sample bag was removed, but even then, additional rapping of the collector after the bag was removed produced a significant amount of particulates. For a total collected mass of just a few grams, the amount of material that could still be liberated from a collector after the sampling bag had been removed was occasionally significant and, based on our NCTA field studies, could easily double the total mass measurement or more.

5. **Field test results from BNSF / SWA and tests performed independently by Exponent show that the total amount of material retained in the collector can vary widely from fractions of a gram to hundreds of grams. It is difficult, if not**

impossible, to use a simple field measurement technique to establish a percentage reduction in particulate emissions when mass data from collector to collector can span 2 to 3 orders of magnitude in significant figures. Although in its response to Interrogatory No. 8 BNSF indicated that "more precise" measurements were taken in their lab, they have not provided any important details about how these measurements were taken. Given this lack of response, it is impossible to evaluate BNSF's claim that the lab measurements they performed were "more precise." Such details would provide critical information to be able to evaluate the validity of BNSF's sample collection and data reduction methods, but like the computer program BNSF and/or SWA use to compute IDV.2, this information has never been provided.

a. {

} Neither BNSF nor SWA have produced any detailed procedures as to what equipment was used to perform their field measurements of sample mass or whether their methods involved regular calibration traceable to a NIST standard. Without this basic information it is difficult, if not impossible, to establish any measure of repeatability or error in their measurements. Error estimates are extremely important when an attempt is made to establish a percentage reduction from one measurement to the next when the actual measured masses are each on the order of a gram or less.

b. In its Interrogatory No. 8, WCTL requested BNSF to describe the procedures it used to collect mass data from its passive collectors, including calibration traceable to a NIST standard and error measurements. In response, BNSF stated: "Field measurements were done with a weight-balance scale. However, field measurements were used only for purposes of preliminary and rough evaluation of

the results of dusting from a particular train movement. More precise measurements were performed by BNSF's Technical Research & Development (TR&D) Laboratory in a laboratory setting. The measurements done by BNSF's TR&D Laboratory were the basis for the test results that were used to evaluate the effectiveness of different topper agents."[17] Although in its response BNSF has indicated that "more precise" measurements were taken in their lab, they have not provided any important details about how these measurements were taken. Specifically, BNSF did not provide any information to WCTL's request for information regarding a description of the equipment used, whether the instruments were regularly calibrated to a NIST-traceable standard, the degree of precision associated with the measurements and an estimate of the measurement error. All of these parameters were explicitly requested in Interrogatory No. 8. Given the claimed importance that the passive collector measurements have in BNSF's fugitive dust mitigation program, it would seem reasonable and expected that this information would be available and supplied without hesitation. {

} In fact, an employee of BNSF did witness Exponent's static testing and sample handling / measurements during the Summer of 2008 at the AEP Cook Coal Terminal in Metropolis, Illinois.

6. **Passive dust collector handling, cleaning, installation and removal, sample removal and sample measurements all need to be performed in adherence to a well-defined, written protocol that all field personnel obey. No evidence has been produced by BNSF or SWA to substantiate that uniform procedures were in place and that they were being strictly followed.**

[17] BNSF Feb. 6, 2012 Responses at 3.

a. Field methods for measuring the mass of material samples from passive collectors should involve collection bag "blanking" and collector cleaning steps. Even then, sample mass measurements will still have variability. To my knowledge, neither BNSF nor SWA have ever produced any type of field procedure for sample handling and measurement nor has either performed any analysis to estimate variability associated with such measurements.

b. BNSF and/or SWA to our knowledge did not use certified-clean sample collection bags in the passive collectors used in field testing; the use of such collection bags constitutes good procedure. Such bags were used by Exponent in our field work. In our field work with passive collectors, each passive collector was equipped with a certified-clean, pre-weighed sample bag that once removed (performed inside a climate controlled structure) was measured two times for post-test mass gain and estimate of measurement repeatability.

c. No evidence has been produced to establish that either BNSF or SWA "conditioned" their material samples after they were removed from the collectors. "Conditioning" typically involves holding each sample for a fixed period of time in a controlled environment at a fixed temperature and relative humidity. In this manner sample mass variability attributed to moisture content can be normalized. In fact, no evidence has been provided to establish how BNSF / SWA accounted for moisture content in the passive collector samples. BNSF stated in its response to WCTL's discovery requests that "Once a train arrived to the rail yard for equipment removal, passive collectors were removed. The sampling bags were removed from the passive collectors, sealed and placed into a second sampling bag in case of spillage during shipping. All passive collector sampling bags were placed into a five-gallon bucket and shipped to BNSF's TR&D Laboratory for dry-weighted analysis."[18] However, neither BNSF nor SWA have provided any details as to what method was followed to establish "dry weights." In addition, it

[18] Id. at 3-4.

is not clear how a dry-weight analysis would be interpreted if the original moisture content of the coal was not determined from pre-departure sampling. Standardized methods do exist for the determination of the moisture content of a sample of coal, such as ASTM D3173, "Standard Test Method for Moisture in the Analysis Sample of Coal and Coke." However, neither BNSF nor SWA have provided any evidence that such consensus standards were referenced or followed.

d. It is my understanding that during BNSF-sponsored field testing from 2007 to 2009, field personnel were instructed to avoid applying passive dust collectors to railcars with "unusual loading profiles or unusual dimensions (height or capacity)." It is not clear if what constituted "unusual" was left to the discretion of the person involved in the field installation at the time. If an "unusual" profile or dimensions were observed, the field personnel were instructed to skip to the adjacent railcar or to apply the passive collectors to the most regular variety of railcar and coal profile seen in each particular consist.

e. {

} BNSF stated in response to WCTL's discovery

requests that "BNSF used RTEPS to determine the relative stressfulness of each rail trip test, including in particular whether any precipitation was experienced. RTEPS was not used to 'normalize' the passive collector data."[19]

f. It is not clear from any materials produced by BNSF if or how they or SWA quantitatively incorporate the "relative stressfulness" of each train trip into the method by which they analyze the sample mass measurements taken from the passive collectors. The use of "emission factors" that can be estimated from quantities such as the coal fines content, the mean local wind speed, train speed, the surface moisture content and more general weather data such as the number of dry days per month or per year in a specific region has been well-established in the technical literature for over 30 years.[20] In addition, the importance of including meteorological data in the general treatment of coal dust dispersion modeling and sampling has also been well-established.[21] Given the apparent complexity with which BNSF and SWA approached the analysis of E-Sampler data it is unclear why they did not attempt to normalize passive collector data by weather information.

Dr. Emmitt acknowledges that SWA / BNSF did not have a "well-defined, written protocol that all field personnel obey"[22] but claims that such a protocol was unnecessary. {

[19] Id. at 4.

[20] Stein, D. and Crow, G., "Problems in calculating fugitive-dust emissions for coal-handling facilities and storage piles," *Environmental Progress*, v. 3, n. 1, pp. 33-40, February 1984.

[21] Howroyd, G.C., "Technical guide for estimating fugitive dust impacts from coal handling operations," US Department of Energy report no. DOE/RG/10312-1, September 1984.

[22] BNSF Aug. 23, 2011 Reply, V.S. Emmitt at 4.

[23] Reference BNSF_COAL DUST II_00553765.

} It is difficult to imagine how Dr. Emmitt could conclude that a protocol was unnecessary given the extent of the field operations, the handling of numerous passive collector samples by multiple individuals and the apparent desire to measure and reduce the data from the passive collectors reliably and in a repeatable manner.

7. **During the Super Trial tests performed by BNSF in 2010, only 115 trains out of a population of 1,633 were equipped with passive dust collectors, and only 14 railcars in each of these 115 trains were equipped with passive collectors. Given the numerous sources of variability already described and the lack of any error analysis, it is highly unlikely that BNSF or SWA could make any statistically**

[24] Id.

[25] Id.

significant inferences about percentage dust reductions from the 115-train set behavior to the entire population of trains tested.

a. According to Dr. Emmitt, "It is possible to make a valid statistical inference based on a very small number of samples in tests such as those carried out with passive collectors in the super trial, where the relative impact of the topper agent is based on results from several treated cars and several untreated cars on the same train and thus experiencing the same weather and the same trip stresses."[26] However, the question is not so much if a statistical inference can be made but rather to what degree is that inference significant. As has been detailed throughout this statement, there have been and continue to be numerous uncertainties associated with the data collected and analyzed from the passive collectors. The central issue is not so much whether a passive collector will collect and retain particulate matter (some of which might be coal), but rather whether the information from the collected samples can be reliably used with certainty. That the information derived from the passive collectors can be used to roughly indicate that coal is being episodically emitted from a train is not the primary issue. The primary issue – and problem – with the passive collectors is that neither BNSF nor SWA have presented sufficient information, engineering analysis or third-party validation testing to show with quantifiable certainty that their use of the passive collectors can *measure* fugitive coal emissions in either an absolute or relative sense.

b. Only 115 trains were involved in the BNSF Super Trial tests performed in 2010, and each train was only equipped with 14 passive collectors each: seven installed on the untreated half of the train and seven installed on the treated half of the train. In addition, seven different suppressant chemicals were applied, some as full body applications, some as topper sprays and two as both. {

[26] BNSF Aug. 23, 2011, Reply, V.S. Emmitt at 4.

} In performing testing of this nature, particularly when there is a huge number of test variables each with its own uncertainty, it is preferable to attempt to measure and/or otherwise quantify the uncertainties and to use as large a sample size as possible in order to be able to increase the statistical confidence associated with the testing results. In addition, because the 115 trains were used to attempt to evaluate the performance of seven different suppressants, in reality results from very few trains were used to determine the effectiveness of each suppressant.[27]

c. As BNSF commented in the publicly available document "Summary of BNSF/UP Super Trial 2010," "field audits of treated trains showed that there was at times significant variation in the quality and consistency of the physical application of topical treatments at the mines." Given all of the different testing variables in addition to the uncertainty that is associated with each one of these variables, it seems inconceivable that a sample of 115 trains out of 1,633, as well as a smaller sample size to evaluate the performance of individual suppressants, could be sufficient to render any quantitative judgment about the effectiveness of suppressants. On a more technical level, the fundamental error that BNSF and SWA continuously have made in analyzing the results of these tests is that they never measure, determine or attach realistic uncertainties or variability to the quantities they are attempting to measure. For example, produced materials that have been made available for my review refer to passive collector total mass samples as straight numbers, X. But as we have shown in this statement and others, each collector mass sample needs to be stated as $X \pm Y\%$ or in some similar manner. This approach should be taken for the other relevant variables as well.

---

[27] {

}

Under this approach, the uncertainty portions of these quantities would need to be dealt with in a quantitative and statistically reliable manner because it is not just a matter of statistical inference but also one of certainty. In other words it is not just a question of what can be statistically inferred from the collected data, but to what degree of certainty can those inferences be made. No evidence has ever been produced in these proceedings to address the measurable uncertainties that are involved in the quantitative inputs to these studies.

d. {

}

{

b)

}

8. Even with the uncertainties and unreliability involved in the use of passive collectors, {

}

a. While I do not endorse the BNSF passive collector testing for the reasons discussed herein, it is possible that a valid study of fugitive coal emissions from railcars could show that a combination of profiling and increased coal size significantly reduces fugitive emissions and that the additional application of suppressants does not produce significant additional reductions in those emissions.

b. {

}

c. {

[28] Reference BNSF_COALDUST_0038717-0038731.

}

9. **BNSF's use of laser scanning or other technology to monitor or "verify" that the loaded top-of-car coal profile meets the precise requirements of BNSF's "bread loaf" railcar profiling requirements set forth in Appendix A to the Revised Coal Dust Tariff is inappropriate unless the laser profile measurement is made at or very near to the mine load-out location.**

   a. In my Opening V.S. (dated March 16, 2010) from the Dust I proceedings, I stated: "Furthermore, using laser scanning or other technology to monitor or 'verify' that the loaded top-of-car profile meets the precise requirements of BNSF's 'bread loaf' profile negates the reality that the profile will likely change shape and settle or become partially redistributed as each loaded railcar is exposed to train handling forces (e.g., buff, draft, slack action, possible emergency brake application) and vibrations that neither the mines nor the utilities can control." Top-of-car coal profiling appears to offer a significant benefit towards reducing fugitive coal dust emissions, but it is unfair and inappropriate to measure that profile once the railcar has experienced any significant handling or movement for the reasons noted above, i.e., train action and railcar vibration can cause the coal to settle or otherwise become redistributed in the railcar such that the original profile is no longer maintained.

[29] BNSF Dust I Op., Van Hook V.S., Exhibit 5 at 65.

[30] Id. at 68.

[31] Id. at 75.

10. By way of clarification, claims made by Dr. Emmitt in his V.S.[32] regarding the conclusions presented in the August 2009 Exponent final report to the NCTA are selectively referenced, incomplete and are quoted out of context. Dr. Emmitt's claims that the content of my August 11, 2011, V.S. is "contrary to the views he expressed in the prior Exponent report" are misquoted, incomplete and most importantly, incorrect.

a. In particular, in Dr. Emmitt's August 23, 2011, Reply, he cites a quotation from Exponent's August 2009 Report to the effect that it was possible that {

} From this premise, Dr. Emmitt claims that he is "surprised by the suggestion in [my] statement that the use of topper (or binding) agents on loaded coal cars may not be an effective way to address coal dust losses on moving coal cars."[34]

b. Dr. Emmitt has selectively quoted from my Report. In fact, my full statement emphasized that:

{

} [emphasis mine]

c. In addition, Dr. Emmitt asserts that Exponent's August 2009 Report {

}[36] In fact, Exponent's August 2009

[32] BNSF Aug. 23, 2011, Reply, V.S. Emmitt at 5.

[33] BNSF Aug. 23, 2011, Reply, V.S. Emmitt at 1-2 (citing NCTA Report at xiv).

[34] Id. at 1.

[35] Id. at xiv.

[36] BNSF Aug. 23, 2011, Reply, V.S. Emmitt at 5.

Report emphasized that {

}[37]

d. In addition, the Exponent August 2009 report also stated the following: {

}[38]

e. Finally, the Exponent August 2009 report also stated: {

[37] NCTA Report, August 2009, at xv.

[38] Id. at 124.

}[39]

f. Contrary to Dr. Emmitt's claims, {

} Moreover, this case involves studies and analyses *that BNSF says it relied upon* in developing its Revised Coal Dust standards, not the studies that Exponent performed in 2009. A primary issue is whether the passive collectors can be used as a *measurement of fugitive coal loss from a specific moving source*, and based on BNSF and SWA's work presented in these proceedings, they cannot. The BNSF passive collector studies at issue in this case are significantly flawed for the reasons discussed above.

11. The factors that determine if, when and to what extent fugitive emissions will occur in the transportation of loaded railcars were addressed in my Dust I Reply V.S. at 9-10. A review of the relevant technical literature clearly indicates that factors such as train speed (and therefore the resultant speed of the air over the top of loaded railcars when combined with local wind speed), train operation dynamics, weather and the properties of the coal itself are among the significant factors that determine if fugitive emissions will occur, when and to what extent. BNSF, in a variety of documents that they have either created or referenced, acknowledge the same factors.

a. One of the more relevant citations from the open literature includes: "The key factor that contributes to the emission rate of coal dust from wagons is the speed

[39] Id. at 157-158.

of the air passing over the coal surface. This is influenced by the train speed and the ambient wind speed. Other factors that are also found to contribute include: coal properties such as dustiness, moisture content and particle size; frequency of train movements; vibration of the [railcars]; profile of the coal load; transport distance; exposure to wind; and precipitation."[40,41,42]

b. Also consider the following citations all of which identify resultant wind speed over the top of loaded railcars as a significant causal factor: Ferreira and Vaz[43]; Leeder, Hutny and Price[44]; Noble, Sundberg and Bayard[45]; and Ferreira, Viegas and Sousa.[46]

{

[40] Interim Report issued by Connell Hatch for Queensland Rail titled, Environmental evaluation of fugitive coal dust emissions from coal trains, Goonyella, Blackwater and Moura Coal Rail Systems, Queensland Rail Limited, report no. H-327578, January 31, 2008.

[41] Draft Report issued by Connell Hatch for Queensland Rail titled, *Coal loss literature review, Coal loss management project, Queensland Rail Limited*, report no. H-327578-N00-CF00, January 11, 2008.

[42] Report issued by Simtars (a business unit of the Queensland government Department of Mines and Energy) titled. *Gladstone Airborne Coal Dust Monitoring: Complete Report for QR National*, report no. oe101776f3, January 18, 2008.

[43] A.D. Ferreira and P.A. Vaz, *Wind tunnel study of coal dust release from train wagons*, Journal of Wind Engineering and Industrial Aerodynamics, v. 92, 2004, pp. 565-577.

[44] R. Leeder, W. Hutny and J. Price, Train transportation coal losses – a wind tunnel study, Proceedings of the Iron and Steel Technology Conference, v. 1, 2007, pp. 129-138.

[45] G. Noble, S.E. Sundberg and M. Bayard, *Coal particulate emissions from rail cars*, Proceedings from the Air Pollution Control Association Specialty Conference on Fugitive Dust Issues in the Coal Use Cycle, rep. no. CONF-8304206, April 1983. pp. 82-92.

[46] A.D. Ferreira, D.X. Viegas and A.C.M. Sousa, *Full-scale measurements for evaluation of coal dust release from train wagons with two different shelter covers*, Journal of Wind Engineering and Industrial Aerodynamics, v. 91, 2003, pp. 1271-1283.

[47] BNSF March 15. 2010, V.S. Sultana at 5-6.

[48] Reference BNSF presentation { }
BNSF_COALDUST_0079702-0079717 at 24, 25 and 29.

d.

} factors such as train speed, train operation dynamics, weather and the properties of the coal itself are among the significant factors that determine if fugitive emissions will occur, when and to what extent.

VERIFICATION

I, Mark J. Viz, Ph.D., P.E., verify under penalty of perjury that I have read the foregoing Verified Statement and know the contents thereof; and that the same are true and correct. Further, I certify that I am qualified and authorized to file this statement.

Mark J. Viz

Executed on: October 1, 2012

Exhibit MJV-1

Exponent

Failure Analysis Associates

Exponent
525 W Monroe Street
Suite 1050
Chicago IL 60661

telephone 312-999-4200
facsimile 312 999 4299
www.exponent.com

Mark J. Viz, Ph.D., P.E.
Principal Engineer

Professional Profile

Dr. Mark J. Viz is a Principal Engineer in Exponent's Mechanical Engineering practice. He specializes in performance evaluation and mechanical analysis of railcar and aircraft structures. He also specializes in risk, reliability, and mechanical integrity assessments of a variety of process plant equipment such as pressure vessels and tanks, and certain types of transportation vessels including railcar tanks, intermodal vehicles, and over-the-road tank trailers. Dr. Viz also has experience in component life reliability assessments, "repair or replace" risk decisions, and statistical analysis of in-service component performance. Other areas of Dr. Viz's specific academic expertise include nonlinear finite element analysis, metal and composite material testing, fatigue and fracture mechanics, and statistical data reduction methods. He has investigated and/or consulted in matters involving railcar derailments, tank car ruptures, releases of hazardous materials in transportation, coal mining haulage accidents, rotor failures, bus rollovers, pressure vessel explosions, and other industrial accidents.

Given his expertise in engineering mechanics, Dr. Viz also performs engineering evaluations and analyses involving the mechanical performance of a variety of machines and products. Some of these devices include elements of cranes and lifting devices (e.g., wire rope failures, hydraulic and valve failures), elements of elevators, a variety of industrial machines (e.g., printing equipment, CNC machine tools, pumps, compressors), certain aspects of machine guarding and lock-out/tag-out procedures, and specialized evaluations of consumer products. Dr. Viz's involvement in these types of cases typically involves the synthesis and execution of a variety of engineering mechanics calculations and analyses.

Prior to joining Exponent, Dr. Viz was a Product Development Engineer at the GATX Rail Corporation. His responsibilities included new rail car design and development, budget and schedule management, and sales and marketing support. Dr. Viz was also heavily involved in the regulatory environment concerning the transportation of hazardous materials in rail tank cars. Dr. Viz also served as a Specialist Engineer in the Structural Damage Technology group at the Boeing Company. He was responsible for the durability and damage tolerance analysis and testing of a wide variety of aircraft structures from wing and fuselage sections to individual fasteners. He has also taught probability, statistics, and mechanics of materials at the college level.

Academic Credentials and Professional Honors

Ph.D., Cornell University, Theoretical and Applied Mechanics, 1996
B.S., Massachusetts Institute of Technology, Aeronautics and Astronautics, 1990

Licenses and Certifications

Licensed Professional Engineer, Illinois, #062.062247
Mining Safety and Health Administration (MSHA) Part 46 and Part 48 trained
Respirator and SCBA fit-tested and trained

Publications and Presentations

Viz MJ. Failure analysis in the design cycle. Presented as a guest lecture for CIV-ENG 395-0 Engineering Forensics course, Evanston, IL, April 16, 2008.

Viz MJ, Momsen RH. Reliability and risk management of railcar truck castings in high mileage, high gross rail load service: A case study. Presented at the Annual Meeting of the Society for Risk Analysis, Baltimore, MD, December 5, 2006.

Morrison III DR, Ogle RA, Viz MJ, Carpenter AR, Su YS. Investigating chemical process accidents: Examples of good practices. Process Safety Progress 2006; 25:71–77, March.

Ogle RA, Morrison III DR, Viz MJ. Emergency response to a non-collision HAZMAT release from a railcar. Process Safety Progress 2005; 24:81–85. June.

Morrison III DR, Ogle RA, Viz MJ, Carpenter AR, Su YS. Investigating chemical process accidents: Examples of good practices. Presented at the Process Plant Safety Symposium. 2005 Spring National Meeting, American Institute of Chemical Engineers. Atlanta, GA, April 11–13, 2005.

Zehnder AT, Viz MJ. Fracture mechanics of thin plates and shells under combined membrane, bending, and twisting loads. Applied Mechanics Reviews 2005; 58:37–48, January.

Ogle RA, Viz MJ, Morrison III DR, Carpenter AR. Bulk transportation of hazardous materials by rail: Lessons learned from non-collision accidents. Presented at the 2004 Annual Symposium, Mary Kay O'Connor Process Safety Center, Texas A&M University, College Station, TX, October 2004.

Ogle RA, Morrison III DR, Viz MJ. Emergency response to a non-collision HAZMAT release from a railcar. Presented at the 19th Annual CCPS International Conference, Emergency Planning: Preparedness, Prevention and Response, American Institute of Chemical Engineers, Orlando, FL, June 2004.

Ogle RA, Viz MJ, Carpenter AR. Lessons learned from HAZMAT accident investigations. Presented at the 17th Annual AAR/BOE Hazardous Materials Seminar, Association of American Railroads/Bureau of Explosives, Houston, TX, May 2004.

Zehnder AT, Potdar YK, Viz MJ. Fatigue fracture in plates in tension and out-of-plane shear. Fatigue and Fracture of Engineering Materials and Structures 2000; 23:403–415.

Viz MJ. Fatigue fracture of 2024-T3 aluminum plates under in-plane symmetric and out-of-plane anti-symmetric mixed-mode deformations. Ph.D. Dissertation, Cornell University, 1996.

Potyondy DO, Viz MJ, Zehnder AT. Rankin CC, Riks E. Computation of membrane and bending stress intensity factors for thin cracked plates. International Journal of Fracture 1995: 72:21–38.

Viz MJ, Zehnder AT, Bamford JD. Fatigue fracture of thin plates under tensile and transverse shear stresses. Fracture Mechanics, 26th Volume. ASTM STP 1256, Reuter WG, Underwood JH, and Newman JC (eds), American Society for Testing and Materials, pp. 631–651, 1995.

Viz MJ, Zehnder AT. Fatigue crack growth in 2024-T3 aluminum under tensile and transverse shear stresses. Proceedings, FAA/NASA International Symposium on Advanced Structural Integrity Methods for Airframe Durability and Damage Tolerance. NASA CP-3271, pp. 891–910, 1992

Viz MJ, Zehnder AT, Ingraffea AR. Fatigue fracture in thin plates subjected to tensile and shearing loads: Crack tip fields, j integral and preliminary experimental results. Proceedings, 7th International Congress on Experimental Mechanics, Society of Experimental Mechanics; 1992: 44–50.

Prior Experience

Director of Applied Mechanics, Packer Engineering, 2001–2003
Product Development Engineer, GATX Rail, 1999–2001
Specialist Engineer – Structural Damage Tolerance, Boeing, 1997–1999

Project Experience

Directed, managed, and performed numerous rail tank car failure cause and origin investigations, most involving the release of hazardous materials. Projects typically involve extensive field investigations, including confined space entry of tank cars, mechanical and metallurgical analysis, mechanical integrity assessments, non-destructive examination, and sample collection.

Managed and performed numerous rail tank car loading and unloading incident investigations, often involving worker injuries or fatalities.

Investigated the unintentional uncoupling of mining service cars in a Virginia underground coal mine. The uncoupling resulted in a runaway car situation that lead to the fatalities of two miners. Project work included incident modeling and reconstruction, performance calculations, and inspections.

Actively directing a lengthy study involving the investigation of railroad track ballast fouling and coal dust mitigation evaluations for coal transport out of the Powder River Basin in Wyoming. Project work includes measurement of fugitive dust emissions, static and dynamic

(over-the-road) monitoring of dust loss from railcars, cost analysis for proposed mitigation techniques, and analysis of health and safety issues.

Managed and performed projects for multiple clients involving the mechanical integrity assessment and fitness-for-service evaluations of railcar truck castings (bolsters and side frames). These projects have typically involved the development and implementation of non-destructive examination procedures for both on-car and off-car examination, cyclic fatigue testing, mechanical and metallurgical testing, engineering evaluation of test results with respect to mechanical performance, and development of engineering plans to manage fleet components over the projected remaining useful service life. Have presented findings to the Association of American Railroads (AAR) for multiple clients.

Performed risk, reliability, and mechanical integrity assessments for a variety of process plant equipment including piping and tanks. Select assignments have involved flash train tanks at a bauxite to alumina processing plant, piping and vessels at a district cooling ammonia refrigeration plant, liquid carbon dioxide storage tanks, baghouse equipment at cement kilns, and a variety of other equipment subject to OSHA PSM (process safety management) and EPA RMP (risk management plan) regulations.

Directed, managed, and performed numerous incidents involving the release of hazardous materials from transportation vessels, including rail tank cars, intermodal containers, and over-the-road tank trailers. Projects typically have involved extensive field investigations, including confined space entry of tank cars, mechanical and metallurgical analysis, mechanical integrity assessments, non-destructive examination, and sample collection.

Performed design evaluation and risk assessment of a manufacturer's new product offering that provides GPS location and condition monitoring of railcars while in-transit. System includes remote sensing, GPS and satellite uplink equipment, all packaged in a field-hardened package. Project work included FMEA (failure modes and effects analysis), reliability modeling, and predictions for warranty structuring and material compatibility analyses.

Performed mechanical performance and stress analysis calculations for a fleet of coal railcars that exhibited top chord and side sheet buckling failures. The project involved performing detailed field inspections of the damaged railcars, finite element analysis (FEA) of the cars, and a determination of the in-service loads that were needed to produce the exhibited damage.

Managed and performed a collision damage assessment and engineering repair oversight for a major accident involving a monorail train in the Pacific northwest. Project work included responsibility for oversight of repair plans, mechanical contractor selection and qualification review, quality assurance oversight, schedule analysis, and general technical consulting. Project involved extensive field work and multiple presentations to technical staff and insurance adjusters.

Performed numerous mechanical performance analyses/evaluations for a variety of machines and products including:

- Manufacturing machinery (printing and binding equipment, forming and cutting machines, product conveying equipment, certain types of CNC machine tools)
- Elements of machine guarding and lock-out/tag-out procedures (drum foamers, printing and binding equipment, packaging equipment)
- Elements of crane and lifting devices (e.g., scissor lifts), including wire rope failures, hydraulic cylinder failures, holding valve failures, and stability issues
- Elements of consumer product performance including structural performance and mechanical response.

Academic Appointments

- Adjunct Professor, Mathematics Department, Pierce College, WA

Professional Affiliations

- American Society of Mechanical Engineers—ASME (member)
- American Institute of Aeronautics and Astronautics—AIAA (member)
- Society for Risk Analysis—SRA (member)

Barbaro

BEFORE THE
SURFACE TRANSPORTATION BOARD

REASONABLENESS OF BNSF RAILWAY COMPANY COAL DUST MITIGATION TARIFF PROVISIONS	)))))	Finance Docket No. 35557

VERIFIED STATEMENT OF
DR. RALPH W. BARBARO

My name is Dr. Ralph W. Barbaro. I am the President of Energy Research Company ("ERC") and a former Principal of Energy Ventures Analysis ("EVA"). I am submitting this verified statement on behalf of the Western Coal Traffic League ("WCTL"), American Public Power Association ("APPA"), Edison Electric Institute ("EEI") and the National Rural Electric Cooperative Association ("NRECA") (collectively "Coal Shippers"). A copy of my curriculum vitae is attached hereto as Exhibit RWB-1.

I hold Bachelor of Science, Master of Science and Ph.D. degrees in Mining Engineering and Operations Research from Pennsylvania State University. I have been working in the coal and energy industries for the past 35 years, and am a Registered Professional Engineer. I have experience working on coal-related projects related to all of the major coal producing regions in the country, including the Powder River Basin ("PRB"). During my career as a consultant in the energy industry, I have performed numerous coal industry studies and analyses including supply studies, transportation analysis, coal mine valuation, due diligence reviews, strategic planning, performance and

reserve studies, market analysis, forecasting, coal procurement and bid evaluation, and coal suitability analysis. In addition, I have experience in other areas related to the energy industry, including natural gas supply and transportation issues, electricity generation cost analysis, dispatch analysis, power transmission issues, and environmental issues.

From 1980 to 1986, I was an instructor at Penn State in the Mining Engineering Department, teaching undergraduate and graduate courses and performing research on coal reserve estimation, production analysis techniques, and mine cost analysis. From 1976 to 1980, I worked for the North American Coal Company at the Helen Mine in Pennsylvania.

Coal Shippers have requested that I present testimony regarding the size of coal produced by Powder River Basin ("PRB") mines. Coal producers have the ability to regulate the size of the product that they load into railcars for delivery to shippers. This coal size is expressed in terms of the diameter of the largest pieces of coal in a given sample and is determined based upon the ability of the coal to pass through a given sieve size. Coal that is classified as 2" coal is coal that has been crushed to the point at which all pieces can pass through a 2" sieve. Coal that is classified as 3" coal, on the other hand, is coal that has been crushed only to the point at which all pieces can pass through a 3" sieve. Coal at the 3" size obviously requires less crushing by the producer than coal at the 2" size.

Traditionally, PRB coal was crushed to 2". However, to address railroad concerns about coal dust emissions from their trains, PRB coal suppliers have been

working with their customers to increase the standard PRB coal size from 2" to 3". This effort has been successful. Today, the current standard practice today is to crush PRB coal to 3".

Adjusting coal size is very straightforward for a PRB producer. Rather than having to replace existing equipment or to redesign their facilities in some manner, coal producers are able to adjust the size of the product that they deliver simply by adjusting a setting on their crusher equipment. This type of change is inexpensive and is not labor intensive.

VERIFICATION

I, Ralph W. Barbaro, Ph.D., verify under penalty of perjury that I have read the foregoing Verified Statement and know the contents thereof; and that the same are true and correct. Further, I certify that I am qualified and authorized to file this statement.

Ralph W. Barbaro

Executed on: September 27, 2012

Exhibit RWB-1

CURRICULUM VITAE
DR. RALPH WESLEY BARBARO, Ph.D., P.E.

CONTACT INFORMATION

Work address:	Energy Research Company LLC 13515 Hunting Hill Way North Potomac, MD 20878
Telephone numbers:	866-807-0191 (office) 866-807-0192 (fax) 301-807-6654 (cell)
Email:	ralph.barbaro@energyresearchco.com

EDUCATION

Years	Degree	School and Major
1981-1986	Dual Ph.D.	The Pennsylvania State University; Ph.D. degree in Mining Engineering and Operations Research. Thesis title: "Uncertainty and Risks of Reserve Estimation for Coal Quantity and Quality". (GPA: 3.92/4.0)
1980-1981	Dual M.S.	The Pennsylvania State University; Mining Engineering and Operations Research. Thesis title: "An Application of Mixed Integer Programming to the Optimal Siting and Production Scheduling for a Centralized Coal Preparation Plant". (GPA: 3.87/4.0)
1975-1980	B.S.	The Pennsylvania State University; Mining Engineering with Highest Distinction (GPA: 3.87/4.0)

PROFESSIONAL EXPERIENCE

Energy Research Company, LLC

President 2010-Current

Provide consulting services to energy companies, utilities, and other firms in numerous areas including:

- Coal markets studies and forecasting (national and regional)
  - Coal prices
  - Supply
  - Demand
- Coal mine analysis
  - Acquisition analysis/due-diligence
  - Financial/cost analysis (pro forma models)
  - Valuation analysis using DCF, comparables, and replacement costs
  - Mining conditions assessment
  - Management/operational review
  - Performance and benchmarking studies
  - Reserve analysis
- Coal transportation analysis
  - Rail
  - Barge

- Truck
- Conveyor
- Transloading
- Ocean vessels

- Coal contracting, procurement and administration
- Coal royalty/lease negotiations
- Coal contracts
  - Bidding and procurement
  - Bid evaluation
  - Due-diligence of potential suppliers
  - Escalation
  - Government Imposition evaluation and due-diligence
- Electricity markets
  - Wholesale electricity price forecasts
  - Retail electricity price forecast
  - Electricity demand forecast
  - Electricity capacity and generation forecasts
  - Power plant financial/cost analysis (pro forma models)
- Escalation forecasting
  - BLS energy related indicies
  - Labor costs
  - Coal production unit costs
  - Transportation units costs

Energy Ventures Analysis, Inc.

Principal	1989-2010
Associate	1986-1989

Provided consulting services to energy companies, utilities, and other firms in numerous areas including:

Energy and Electricity Supply/Demand/Price Forecasting

- Analyzed the electric utility, coal and natural gas industries for supply, demand and price forecasting of fossil fuels and electricity.
- Analyzed and forecasted the international coking and steam coal markets, prices, supply, exchange rates, shipping rates, etc.
- Developed and maintained computer models that analyze the generating capacity, output, delivered cost of fossil fuels, variable generation cost, and marginal generation cost for every power plant in the U.S.
- Forecasted load duration curves and price duration curves of wholesale electricity for all of the NERC regions and subregions.
- Tracked, analyzed and forecasted FOB mine, transportation and delivered coal prices
- Tracked, analyzed and forecasted wellhead, pipeline and delivered gas prices.
- Tracked changes in economics and technology of various generating technologies.
- Tracked and analyzed impact of environmental regulations on the energy industry.

Coal Supply Studies

Performed coal supply studies on coal supply and demand for all of the major U.S. producing regions including Northern Appalachia, Central Appalachia, Illinois Basin, Powder River Basin, and Western Bituminous

Coal Transportation Analysis

Performed transportation analysis including capital and operating costs, existing and future capacity, regulations, AAR indicies, market issues, etc. for various modes of transportation:

- Rail
- Barge
- Trucking
- Conveyors
- Transloading
- Ocean ships

Coal Mine Valuation, Due Diligence, Performance And Reserve Studies

Performed financial, discounted cash flow analysis, and/or operating performance evaluation of numerous coal companies, mines, and coal reserves.

Coal Contract Government Imposition and Force Majeure Analysis

Performed numerous reviews of government imposition and force majeure claims to verify their validity and the amount claimed.

Coal Market Analysis

Performed numerous coal market studies for all major U.S. coal supply regions including Northern Appalachia, Central Appalachia, Illinois Basin, and Western Bituminous, and for utility, metallurgical, industrial and export markets.

Economic and Cost Indices Forecasting

Performed forecasts of various economic parameters, such as GNP, inflation, RCAF, labor, material and supplies, fuel, power, medical, and other costs. Also, forecasted various BLS indices for several utilities.

Coal/Natural Gas Procurement And Contracting

Provided support to utilities in coal/natural gas procurement and contracting including preparing the contract terms and conditions for the bid solicitation, identifying likely suppliers, evaluating bids responses, evaluating the suppliers ability to meet the contract terms (mine audits), reviewing final contract terms, etc. for numerous utilities. Also assisted in several fuel supply audits.

Royalty Audits/Lease Negotiations

Performed audits of royalty payments including review of the sales price and volume calculations. Negotiated the terms and conditions of a coal lease. Reviewed many coal lease agreements as part of utility/mine audits of coal mines.

Litigation Support

Provided expert testimony and litigation support work for numerous arbitration and litigation proceedings.

The Pennsylvania State University

Instructor, Mineral Engineering Department 1981-1986
Graduate Assistant 1980-1981

Courses Taught

Taught or assisted several undergraduate and graduate courses including mine property valuation, mine cost analysis, mine operations analysis, mine system engineering, survey, ventilation.

Research

Performed various research on geostatistical reserve analysis applications to coal, variability of coal quality, statistical variation of coal washability characteristics, coal blending optimization models, mine production simulation models, queueing theory techniques to shovel-truck material haulage systems, etc.

North American Coal Corporation

Mining Engineering Department (1978-1979)

Worked a year in the engineering department at the Helen Mining Company in Homer City, PA, a one million tpy captive mine to the Homer City power plant. Prepared daily production and monthly royalty reports, and semi-annual ventilation and subsidence maps; assisted in preparation of mine plans and projections; performed both underground and surface surveying for property control, locating existing gas wells, and for siting a ventilation shaft; assisted supervision of 16 exploratory drill holes and the construction of a 15-foot-diameter raised-bored ventilation shaft; prepared permit to mine within 150 feet of a gas well; operated and maintained the mine sewerage treatment plant, etc.

Underground UMWA Laborer (1976-1977)

Worked a year in the UMWA as a miner helper, roof bolter helper, shuttle car operator, mechanics helper, supply man, belt man, brattice man and general laborer. Attended a special one-month training program, which covered mine machine operation, roof support, ventilation, health and safety, first aid, mine rescue, and general coal mining techniques.

PUBLICATIONS

Authored or co-authored papers that have been published in professional magazines and symposia including Coal Age, Mining Engineering, Application of Computers and Operations Research to the Mineral Industry, and Use of Computers in the Coal Industry. Has been quoted in national publications including Wall Street Journal, Forbes, Journal of Commerce, Power Market Week, etc.

CURRICULUM VITAE
DR. RALPH WESLEY BARBARO, Ph.D., P.E.

PROFESSIONAL ACTIVITIES

- Society of Mining Engineering of AIME, 1977-present
- Mining and Exploration Division - Operations Research Section for the SME-AIME
    - Scholarship Committee, 2001-03.
    - Executive Committee, 1988-89.
    - Program Chairman, 1987.
    - Program Planning, 1986.
    - Publications Chairman, 1985.
- Mining & Exploration Division's 1986 Peele Award Committee.
- President of Penn State's Student Chapter of SME-AIME, 1979-80.
- Washington D.C. AIME, 1986-present
- Operations Research Society, 1985-present

CERTIFICATIONS

- Registered Professional Engineer, PE-034293-E, 1985
- MSHA Instructor, 1982
- Mine Machine Operators School, 1976
- First Aid Training, 1976

AWARDS AND HONORS

- Centennial Fellow, College of Earth and Mineral Science, The Pennsylvania State University, 1996
- Best Student Paper - Graduate Division, Society of Mining Engineers, 1982
- Old Timers' Gold Watch Award (Outstanding Graduating Senior), The Pennsylvania State University, 1980
- First Place in the Health and Safety Contest, 1979
- Phi Kappa Phi Honor Society, 1979
- Alpha Lambda Delta Honor Society, 1976

ACADEMIC SCHOLARSHIPS AND FELLOWSHIPS

- Centennial Fellow, Earth & Mineral Science College, The Pennsylvania State University, 1996
- Mining and Mineral and Mineral Fuels Conservation Fellowship, 1980-81
- North American Coal Corporation Scholarship, 1979-80
- Donald MacIntire Scholarship, 1979-80
- Class of 1922 Scholarship, 1978
- Bayard D. Kunkle Scholarship, 1977-80
- Edwin L. Drake Memorial Scholarship, 1977-80
- Consolidation Coal Company Scholarship, 1975-77

COAL MINES EVALUATED/INSPECTED

Northern Appalachia

- AEP
  - Meigs 2 (OH)
  - Meigs 31 (OH)
  - Muskingum (OH)
  - Windsor (WV)
  - Martinka (WV)
- Alpha
  - Cumberland (PA)
  - Emerald (PA)
  - Nolo (PA)
  - Ondo (PA)
- Arch
  - Monongalia Strips (WV)
  - Sentenial (WV)
  - Spruce #1 (WV)
  - Spruce #2 (WV)
- Barnes and Tucker
  - 24B (PA)
  - Rushton
- Bethlehem
  - Fawn (PA)
- C&K Coal (PA)
- CONSOL
  - Bailey (PA)
  - Blacksville (PA)
  - Mine 84 (PA)
  - Quarto 4 (OH)
  - Pocahontas Div (VA)
- Helen Mining (PA)
- Murray Energy
  - Burrell (PA)
  - Canterbury/Diane (PA)
  - High Quality (PA)
  - Powhatan 6 (OH)
- Parkwood Resources (PA)
  - Cherry Tree (PA)
  - Genesis #17 (PA)
  - Parkwood (PA)
- Peabody
  - Federal #2
- R&P Coal
  - Emilie (PA)
  - Keystone (PA)
  - Florence (PA)
  - Robinson Run (PA)
- Rhino
  - Harrison (OH)
- Rosebud
  - Clementine (PA)
  - Josephine (PA)
  - Logansport (PA)
  - Stitt (PA)
  - Tracy Lynne (PA)

Central/Southern Appalachia

- Addington/Job 17 (KY)
- Alpha (WV, KY)
  - Cumberland Resources (KY/VA)
  - Delbarton (WV)
  - Elk Run (WV)
  - Logan County (WV)
  - Marfork (WV)
  - Marrowbone (WV)
  - Martin County (KY)
  - Omar (WV)
  - Peerless Eagle (WV)
  - Rawl (WV/KY)
  - Sidney (KY)
- Amvest
  - Powell Mountain (VA)
- Appolo Fuels (KY)
  - Appolo Prep (KY)
  - Hignite Strip/HWM (KY)
  - Jellico North (TN)
  - Low Splint – Wilco #2 (KY)
  - Poplar Lick Strip/HWM (KY)
  - Rich Mtn Strip/HWM (TN)
- Arch
  - Cumberland River (KY)
  - Dal-Tex (WV)
  - Samples (WV)
  - Ruffner (WV)
  - Lone Mountain (VA)
  - Lynch (KY)
- Black Diamond (KY)
  - Ivel Prep (KY)
  - Ivyton Strip (KY)
  - King Hamilton 2 (KY)
  - Martin Prep (KY)
  - Mitec 1 (KY)
  - Prater 2 (KY)
  - Prater 3 (KY)
  - Risner 3 Williams (KY)
  - RV-Margaret Fork (KY)
  - S&B Energy-Gunstock (KY)
  - Spurlock Prep (KY)
  - Turkey CreKY #2 (KY)
- Blue Gem (KY)
  - Bain Branch (KY)
  - Blue Gem #1 (KY)
  - D&R #1 (KY)
  - Harps Creek (KY)
  - Log Cabin (KY)
- Bluestone
  - Dynamic (WV)
  - Mine 65 (WV)
- Broken Ridge LLC (KY)
- Clearwater/Miller Bros (KY)
  - Combs Branch (KY)
  - Baker (KY)
  - Joes Branch (KY)
  - Panther (KY)
  - Trap Branch (KY)
  - Risner #2 (KY)
- CONSOL
  - Mill Fork (KY)
  - Millers Creek (WV)
- Costain
  - Prater Creek/Chaparral (KY)
- Cumberland Resources
  - Cloverlick (KY)
  - Panther #1 (KY)
  - North Fork #4 (KY)
  - Stillhouse (KY)
  - Nally & Hamilton (KY)
  - Bluff Spur (VA)
  - Dorchester #4 (VA)
- Dixie Fuels (KY)
- Eastern Associated
- Eastern Fuels (KY)
  - Coal Ridge (KY)
  - Goose Creek #1 (KY)
  - Goose Creek #2 (KY)
  - Goose Creek Prep (KY)
  - Gosling Branch (KY)
  - Martin Branch (KY)
  - Sly Branch (KY)
- Eagle Hawk/Laurel Creek (WV)
- Elkhorn Coal (KY)
- Energy Coal Partners
  - Alloy (SW)
  - Bent Mountain (KY)
  - Toney's Fork (SW)
- Fossil Fuels (KY)
- Golden Oak (KY)
- GTM Energy (AL)
- Hannah Energy
  - Cindas Creek (KY)
  - Moon Creek (KY)
  - Slater Branch-Pond Creek (KY)
  - Slater Branch-Cedar Grove (KY)
- Horizon (KY/WV)
- Ikerd Coal (KY)
  - Birdeye Hollow #1 (KY)
  - Flag Ridge (KY)
  - Little Round Mountain (KY)
  - Runyon Branch (KY)
  - Trace Branch (KY)
- Kentucky River Coal Company (KY)
- Logan Coal Partners/Madison Coal (WV)
- Miller Cove (VA)
- National Coal
  - Mann Steel Products (AL)
- Parkstone Energy
  - Chelyan Prep
  - Synergy (SW)
  - Essex (SW)
  - Miura #2 (SW)
  - Siata HWM (SW)
- Patriot
  - Jupiter (WV)
  - Panther (WV)
  - Remington (WV)
  - Rocklick (WV)
  - Wells (WV)
- Powell Mountain (VA)
- Progress Energy
  - Kelly Branch (KY)
- Quaker Coal (KY)
  - Beverly (KY)
  - Coal Prep (KY)
  - Road Creek (KY)
  - Sidewinder (KY)
- Sun Coal/Beechfork (KY)
- TECO
  - Premier Elkhorn (KY)
- Transco
  - Leeco (KY)

UNITED STATES ENVIRONMENTAL PROTECTION AGENCY
REGION 10
1200 Sixth Avenue, Suite 900
Seattle, WA 98101-3140

OFFICE OF
ECOSYSTEMS, TRIBAL AND
PUBLIC AFFAIRS

April 5, 2012

Mr. Steve Gagnon, Project Manager
U.S. Army Corps of Engineers
PO Box 2946
Portland, Oregon 97208-2946

Re: Comments on Public Notice for Permit Application under Section 10 of the Rivers and Harbors Act for a Coal Transloading Facility, Port of Morrow, Oregon.
U.S. Army Corps of Engineers No: NWP-2012-56
EPA Region 10 Project Number: 12-0013-COE.

Dear Mr. Gagnon:

The U.S. Environmental Protection Agency (EPA) has reviewed the above referenced March 6, 2012 Public Notice for Permit Application. We are submitting comments in accordance with our responsibilities under Section 102(2)(C) of the National Environmental Policy Act (NEPA) and Section 309 of the Clean Air Act.

We commend the Corps for a generally informative Public Notice and appreciate your clear disclosure of the project's purpose, to "Ship coal mined in Wyoming and Montana over-seas to Asia." We note that the Public Notice is soliciting comments to evaluate the impacts of the proposed activity and that comments will be used in the preparation of NEPA documents.

To assist your preparations for conducting an adequate NEPA analysis, we are sharing our perspective regarding potential environmental impacts. Our comments are structured in terms of the context and intensity components laid out in the Council on Environmental Quality's Regulations for Implementing the Procedural Provisions of the NEPA, 40 CFR Part 1508.27, as this structure is helpful in determining the significance of potential impacts.

Potential for significant impacts to public health: Transporting and transloading up to 8.8 million tons of coal with eleven trains, twelve loaded barge tows, and two Panamax ships per week has the potential to significantly impact human health and the environment. Two of our primary preliminary concerns relate to the potential for adverse effects from project-related coal dust and diesel pollution. Coal dust is a human health concern because it can cause pneumoconiosis, bronchitis and emphysema.[1] Coal dust is an environmental concern because it may settle on water, soil, or vegetation and impair biological processes such as photosynthesis. In addition, coal dust has been shown to cause tumors in experimental animals.[2] We are similarly concerned about diesel emissions because they can cause lung damage, aggravate existing respiratory disease such as asthma and are thought to be a human

[1] http://www.osha.gov/SLTC/healthguidelines/coaldust-less5percentsio2/recognition.html
[2] *Ibid.*

Printed on Recycled Paper

carcinogen. Diesel emissions have a high potential to impact people who are sensitive to the health effects of fine particles (e.g. children, the elderly, and those with existing heart or lung disease, asthma or other respiratory problems).[3]

We agree that all factors listed in the Public Notice[4] need to be considered as the process moves forward. Other factors, such as local air quality and haze may also require your consideration. We support and encourage your pursuit of a robust process to capture, understand and respond to concerns of the public, interest groups, and agencies.

Controversy: We are aware that there is a high level of interest and concern among communities, agencies, interest groups, and industries regarding proposals to ship coal mined in Wyoming and Montana to Asia. It is reasonable to expect that decision processes related to these proposals will be controversial.

Uncertainty and unique setting: The large quantity and high friability of Wyoming and Montana-mined coal contributes to the intensity and uncertainty of potential impacts from coal transport and transloading activities on the Columbia River - a federally designated National Scenic Area and one of our Nation's great waterbodies.

Effects on listed species, critical habitat and aquatic resources: According to the Public Notice, the project may affect an endangered or threatened species or its critical habitat. We would bring to your attention to the fact that impacts from project-related activities may affect critical habitat in the Port Westward area of the project corridor. A preliminary list of Endangered Species Act aquatic species with designated critical habitat likely to occur within the Port Westward area of the project corridor includes: lower Columbia River Chinook salmon ESU, upper Willamette River Chinook salmon ESU, Snake River fall run Chinook salmon ESU, Columbia River chum salmon ESU, middle Columbia River steelhead DPS, and, lower Columbia River steelhead DPS.

Effects on cultural resources: The project area may yield resources eligible for inclusion in the national Register of Historic Places, and project activities may affect cultural resources important to several tribes.

Contribution to cumulatively significant impacts: This project is one of at least six proposals to export coal from Oregon and Washington,[5] and one of at least three which will require permits from the Corps.[6] All of these projects – and others like them – would have several similar impacts. Consider, for example, the cumulative impacts to human health and the environment from increases in greenhouse gas emissions, rail traffic, mining activity on public lands, and the transport of ozone, particulate matter, and mercury from Asia to the United States. To address these and other cumulative impacts, we recommend

[3] http://www.epa.gov/otaq/toxics.htm#health

[4] "...conservation, economics, aesthetics, general environmental concerns, wetlands, historic properties, fish and wildlife values, flood hazards, floodplain values, land use, navigation, shoreline erosion and accretion, recreation, water supply and conservation, water quality, energy needs, safety, food and fiber production, mineral needs, consideration of property ownership, and, the needs and welfare of the people."

[5] http://ecotrope.opb.org/2012/04/desperate-to-export-a-coal-industry-close-up/

[6] Morrow Pacific Project (the subject of this Public Notice); Millennium Bulk Terminals – Longview in Longview, Washington; and, the Gateway Pacific Terminal in Bellingham, Washington

that the Corps conduct a thorough and broadly-scoped cumulative impacts analysis of exporting large quantities of Wyoming and Montana-mined coal through the west coast of the United States to Asia. This cumulative impacts analysis could be used in the environmental analyses of other proposed coal export projects of similar scope.

Finally, we encourage the Corps to integrate environmental review and consultation requirements into a single NEPA process. For example, integrating the NEPA process with those for permitting under Section 404 of the Clean Water Act and consultation under Section 106 of the National Historic Preservation Act would result in streamlined and consistent agency decision-making, enhanced public disclosure, and better predictability for the applicant.

We appreciate this opportunity to comment. If you have any questions or concerns I can be reached by email at kelly.kate@epa.gov, or by telephone at (206) 553-1271.

Sincerely,

Kate Kelly, Director
Office of Ecosystems, Tribal and Public Affairs

April 25, 2012

JOHN A. KITZHABER, MD
Governor

The Honorable John McHugh
Secretary of the Army
1400 Defense Pentagon
Washington, D.C. 20301-1400

The Honorable Ken Salazar
Secretary of the Interior
U.S. Department of the Interior
1849 C Street, NW, Room 5665
Washington, D.C. 20240

Major General Merdith W.B. (Bo) Temple
Headquarters
U.S. Army Corps of Engineers
441 G Street NW
Washington, D.C. 20314-1000

Mr. Robert Abbey, Director
Bureau of Land Management
U.S. Department of the Interior
1849 C Street, NW, Room 5665
Washington, D.C. 20240

Dear Sirs:

On behalf of the people of Oregon, I am writing to request that a federal agency prepare a programmatic and comprehensive environmental impact statement (EIS) under the National Environmental Policy Act to look at the unprecedented number of coal export proposals pending in the Pacific Northwest, as well as the potential effects in this country of the use of this coal in Asia. Currently, the United States annually exports between 80 and 100 million tons of coal from all ports in the United States. The current proposals for coal export facilities in Oregon and Washington could result in an *additional 157 million tons* of coal exports, more than doubling the U.S. coal export capacity.

Most of the environmental, community, economic, transportation, and energy security impacts associated with this tremendous increase in coal export would be shouldered by Oregon and Washington. In addition, the United States has the largest proven coal reserves in the world. Developing, transporting and using this resource for energy production in Asia will have significant implications for the trajectory of the world's transition to cleaner sources of energy and for our nation's energy security, as well as localized economic and environmental effects in our state. It is imperative that the federal government take seriously its responsibility to make informed decisions, and that there be a comprehensive look at the energy, environmental, and public health impacts of these proposals before the nation commits itself to this path.

Both the Army Corps of Engineers (Corps) and the Bureau of Land Management (BLM) have the responsibility to look at these impacts because both agencies are making decisions that will result in significant impacts that have not been analyzed. Previously, the Oregon Department of Environmental Quality (ODEQ) asked the BLM to prepare a supplemental EIS for the ongoing coal leasing and development activities on BLM lands in the Powder River Basin in Wyoming and Montana. Our prior request for a supplemental EIS was based on the fact the EIS that BLM

254 STATE CAPITOL, SALEM OR 97301-4047 (503) 378-3111 FAX (503) 378-6827
WWW.OREGON.GOV

prepared for its coal leasing program analyzed the environmental effects of transporting the coal to the mid-western and eastern United States, for domestic energy production. The BLM did not evaluate the effects of transporting substantial amounts of coal from the Powder River basin to the West Coast for export to overseas markets. BLM Director Abbey denied Oregon DEQ's request for a supplemental EIS on the grounds that the proposals for coal export through the west coast were too indefinite at that time. That lack of certainty has now changed, with several specific proposals now pending regulatory reviews, and others having secured initial property agreements. Now is the time for a programmatic EIS, before substantial and irreversible commitments of resources are made to this path.

The impacts from the transport of coal through Oregon and its communities would be significant. Areas of concern that merit a hard look, at a minimum, include:

Increased vessel traffic on the Columbia River, including navigational and maritime safety concerns
Protection of water quality, including increased risk of spills
Impacts to listed anadromous fish species
Coal dust emissions at the facilities and during product transport
Emissions of other air pollutants, including diesel particulate, ozone, mercury, and greenhouse gases and
Increased rail traffic, noise, and delay times for communities along the proposed rail lines, including emergency vehicles at rail crossings

I have already heard from many of our citizens and elected officials who are deeply concerned about the impacts of increased coal train traffic running through their communities. I share their concerns. This magnitude of coal moving through the region's rail system would represent a substantial increase in train traffic -- perhaps as many as 63 coal trains per day. The trains will travel through communities that have been identified as "choke points" along the line. This could significantly affect the transport of other export commodities and negatively impact plans to increase passenger rail. I am particularly concerned about a substantial increase in rail traffic through the Columbia Gorge National Scenic Area, where train noise, air emissions and coal dust could adversely affect the recreational and visual values protected by federal law.

The proposals could also cause significant vessel traffic impacts on the Columbia River. The Columbia River is a confined system, and the proposals could result in a 70% increase in ship traffic. The Columbia River has multiple ports, a breaking coastal bar at the entrance, and no federal vessel traffic system, all of which create significant potential for risk. Vessel traffic impacts from the proposals could be significant, and need to be analyzed.

Another major concern, and one not addressed by the prior BLM EIS for the Wright Area coal leases, is the impacts of increased or extended use of coal to generate electricity in Asia. Coal-fired energy production in Asia has been directly linked to increases in air pollution on the west coast of the United States. Studies that 84 percent of the mercury in the Columbia River basin is due to atmospheric deposition from global sources and 18 percent of mercury deposition recorded at one Oregon site can be traced to anthropogenic sources in Asia. Over the long term, these transported emissions could lead to economic as well as environmental and health impacts in our states, triggering additional costs in emissions controls for U.S. industries. The air quality impacts of the use of Powder River coal in Asia must be explored in the context of a comprehensive federal EIS.

Greenhouse gas emissions from the transport and combustion of coal are also a major concern. Two years ago, the Secretary of the Interior issued Order No. 3289, Amendment No. 1 (Feb. 22, 2010), which requires each bureau of the Department to consider and analyze potential climate change impacts when making major decisions regarding potential use of resources under the Department's purview. *See also* CEQ Draft NEPA Guidance on consideration of the Effects of Climate Change and Greenhouse Gas Emissions (Feb. 18, 2010). Oregon faces particular threats from climate change, including the reduction in the amount of precipitation falling as snow and the resulting effects on water supplies and fish and wildlife as well as power production from hydroelectric dams, more frequent and intense storm surges, more flooding, likely loss of land in coastal area, more frequent and severe forest fires and increased forest pests and diseases, and detrimental impacts to shellfish fisheries as a result of ocean acidification. As noted above, the United States has the largest proven coal reserves in the world. Developing that resource for energy production in Asia will extend the period of time that Asian nations are reliant on coal, resulting in greater worldwide emissions of greenhouse gases (and conventional air pollutants, as noted above). The impacts of United States coal exports on climate change are an issue of national concern that merits a hard look by a federal agency.

If the United States is going to embark on the large-scale export of coal to Asia it is imperative that we ask -- and answer -- the question of how such actions fit with the larger strategy of moving to a lower carbon future. In the absence of a clear federal policy on this point, we will simply be deciding by not deciding; locking ourselves into a coal-dependent future for Asia without the benefit of a full discussion, consideration and balancing of all the associated economic, environmental and health problems related to such a course of action. The decision must also be made only after we have full information about the short and long-term consequences. This critical step will fill significant information gaps that will benefit our nation, our states, and our communities. Since federal agencies will be making decisions whether to allow these projects to go forward, and because the impacts of the projects cross state boundaries, it is the responsibility of a federal agency to step up and do this analysis.

I strongly urge an immediate commitment to evaluating the impacts of these projects through a comprehensive, programmatic Environmental Impact Statement that examines both the cumulative effects of coal transport to the West Coast, and the effects of the use of that coal to produce energy in Asia here in the United States. The EIS must be prepared before regulatory or additional coal leasing decisions are made. Thank you. I look forward to your response.

Sincerely,

John A. Kitzhaber, M.D.
Governor

cc: Ray LaHood
Nancy Sutley
Joseph Szabo
Jack Lew
Steve Gagnon (re NWP-2012-56)

March 30, 2012

U.S. Army Corps of Engineers
Mr. Steve Gagnon; steven.k.gagnon@usace.army.mil
PO Box 2946
Portland, OR 97208-2946

RE: Comments on Permit Application NWP-2012-56

Dear Mr. Gagnon:

Thank you for the opportunity to provide comment on permit application NWP-2012-56, a proposed project to install a new transloading facility for coal at the Port of Morrow, Oregon, along the Columbia River. The Department of Natural Resources (DNR) is steward of state-owned aquatic lands on behalf of the people of Washington. DNR manages aquatic lands for current and future citizens of the state to sustain long-term ecosystem and economic vitality, and to ensure access to the aquatic lands and the benefits derived from them.

As discussed below, DNR strongly recommends that an environmental impact statement (EIS) be prepared to analyze the proposed project. As part of this analysis, the EIS should identify any potential impacts to Washington state-owned aquatic lands as a result of the proposed project and its connected actions, including construction and long-term operation of the transloading facility, existence of the completed facility, all new activities on the Columbia River, and rail transport of coal through the State of Washington. The EIS also should address the adequacy of the proposed compensatory mitigation measures, as well as the proposed best management practices (BMPs) to contain coal dust throughout the coal transportation process.

Per the public notice, the proposed project would involve construction of a new transloading facility for bringing coal in from Montana and Wyoming by rail and transferring it to barges on the Columbia River at the Port of Morrow, Oregon. This facility would include nine dolphins, walkways, a fixed dock, and a conveyor system for loading coal along with enclosed warehouses in the uplands for coal storage. Approximately 140 permanent piles ranging from 14 to 24 inches in diameter and 110 temporary 16-inch diameter piles would be installed to complete the project. Over 15,000 square feet of new overwater structure would be constructed.

Upon completion of the project, coal would then be shipped down the Columbia to Port Westward and loaded onto ocean-going vessels to be shipped to Asia. Approximately 3.85 million tons of coal would be shipped through the facility each year, which translates to approximately 5 trains to Port of Morrow, 5.5 loaded barge tows from Port of Morrow to Port

Westward, and 1 ship to Asia per week. Once at maximum capacity, the facility would handle 8.8 million tons of coal, which translates to 11 trains, 12 loaded barge tows, and 3 ships to Asia per week.

While the proposed project would be located on the Oregon side of the Columbia River, the facility operations involving coal transfer have the potential to nonetheless harm the long-term ecological and economic vitality of Washington state-owned aquatic lands. For instance, shoreline stabilization measures and overwater structures of the new facility could contribute to the destruction or outright elimination of habitat upon which numerous Columbia River species depend. In addition, any coal dust or debris, runoff, or other pollution that results from the facility, operations, barge tows, ocean-going vessels, and trains could degrade water quality and contribute to contamination of more than 200 river miles of Washington state-owned aquatic lands. This contamination would be toxic to aquatic life including submerged aquatic vegetation, shellfish, and other aquatic natural resources for which DNR is responsible. Further, any discharged pollution could contain bacteria and pathogens that would threaten public health and impair recreational opportunities for the citizens of Washington.

Given the aforementioned potential impacts to Washington state-owned aquatic lands, DNR strongly recommends that an EIS be prepared that analyzes any potential impacts of the project, as well as the adequacy of the BMPs and mitigation measures proposed by the applicant. Further, DNR suggests that these impacts be analyzed cumulatively within the context of other similar coal transport projects that have been proposed recently in Washington and Oregon.

Washington DNR appreciates the opportunity to comment on the permit application and looks forward to further contributing to this process in the months ahead. If you have any questions, please contact Mr. Chris Lyons, policy analyst, at chris.lyons@dnr.wa.gov or 360-902-1090.

Sincerely,

Kristin Swenddal
Aquatic Resources Division Manager

cc: Chris Lyons, Aquatics Policy Analyst

STATE OF WASHINGTON
DEPARTMENT OF ECOLOGY
PO Box 47600 • Olympia, WA 98504-7600 • 360-407-6000
711 for Washington Relay Service • Persons with a speech disability can call 877-833-6341

May 7, 2012

Mr. Steve Gagnon
U.S. Army Corps of Engineers
PO Box 2946
Portland, OR 97208-2946

RE: Public Notice of Permit Application for Coyote Island Terminals LLC; US COE Number NWP-2012-56

Dear Mr. Gagnon:

Thank you for the opportunity to comment on the above referenced permit application. The Washington State Department of Ecology (Ecology) believes that the project that Coyote Island Terminals seeks to permit could have the potential for significant adverse environmental impacts. Ecology is especially concerned about cumulative impacts because the present proposal is one of several proposed projects aimed at expanding coal export capacity within a defined geographic region (i.e., the states of Washington and Oregon). For that reason, and as more fully described in the enclosed comments, Ecology requests that the Corps prepare an Environmental Impact Statement (EIS) prior to making any decisions on the permit application.

Thank you for providing us the opportunity to comment and for your attention to the important issues raised by the present proposal. If you have any follow-up questions, please feel free to contact Brenden McFarland in our Shorelands & Environmental Assistance Program at 360) 407-6976 / brenden.mcfarland@ecy.wa.gov.

Sincerely,

Ted Sturdevant
Director

Enclosure

RESOLUTION No.

Adopt a policy opposing coal trains traveling through the City of Portland until an area-wide Environmental Impact Statement is completed. (Resolution)

WHEREAS, the City of Portland and State of Oregon have committed to greenhouse gas reduction goals; and

WHEREAS, in 2009 the City of Portland approved the Climate Action Plan, with a goal of achieving a 40 percent reduction in carbon emissions by 2030 and an 80 percent reduction by 2050; and

WHEREAS, burning coal releases harmful greenhouse gasses and contributes to global climate change and ultimately must be phased out and replaced with clean alternative renewable forms of energy production; and

WHEREAS, the City of Portland worked with Portland General Electric and many community partners to reach agreement to cease coal operations at the Boardman power plant, Oregon's only coal-burning power plant, by 2020 (Exhibit A); and

WHEREAS, toxic chemicals from coal-fired energy plants in Asia rise in the winds and are carried over the Pacific Ocean, resulting in increased air pollution on the west coast of the United States; and

WHEREAS, studies have shown that mercury— a potent neuro-toxin —is released from burning coal, and that nearly one-fifth of the mercury in the Willamette River originated in Asia; and

WHEREAS, many of the proposed coal export facilities will result in increased rail traffic through Portland, obstructing local roads; causing additional noise and air pollution; decreasing property values; and delaying emergency vehicles, commuters, passenger rail, business and domestic traffic in residential communities; and

WHEREAS, up to one ton of coal dust can escape from each rail car in transit which is a health concern because it can cause asthma attacks, pulmonary inflammation, bronchitis, emphysema, and cancer; and

WHEREAS, over 135 Oregon physicians, 180 health professionals and public health advocates, the Environmental Justice Task Force, the Chairs of 14 North Portland Neighborhood Associations, and the Yakama Nation have called on Governor Kitzhaber to review a comprehensive Health Impact Assessment before approving any coal export permits; and

WHEREAS, noise, diesel emissions, and toxic coal dust from the increased rail traffic will negatively impact the livability of Portland's neighborhoods and the health of our citizens; and

WHEREAS, increased rail traffic through the Columbia River Gorge National Scenic Area will impede Portlanders' access to this valuable recreational resource; and

WHEREAS, more than twenty cities and counties in the Northwest have passed resolutions or written letters expressing their concern about the potential adverse impacts of coal exports in their communities, and called for the Army Corps to study the cumulative and comprehensive impacts of coal exports; and

WHEREAS, local, state and federal officials including Mayor Sam Adams and Governor John Kitzhaber have expressed concerns about the real and potential harm to our collective communities, as well as called on the Army Corps of Engineers to require a comprehensive Environmental Impact Statement (EIS) for the proposed coal export facilities in Oregon and Washington (See Exhibits B-C); and

WHEREAS, the Linnton Neighborhood Association, the North Portland Coalition of Neighborhoods, and the Southeast Uplift Coalition of Neighborhoods, which are adjacent to rail lines, have called for an area-wide or programmatic Environmental Impact Statement to be performed; and

WHEREAS, the Cities of Hood River, Oregon; and Seattle, Washington have each stated opposition to transporting coal through their jurisdiction; and

WHEREAS, Environmental Assessments, as the Army Corps of Engineers currently requires, do not thoroughly review the impacts or allow for sufficient public input in the process; and

WHEREAS, coal trains traveling through our city will have significant consequences for Portlanders, and it is of paramount importance that community members are fully engaged in the decision-making process from the beginning; and

WHEREAS, an area-wide Environmental Impact Statement will ensure that the effects of increased coal export, its alternatives, and possible mitigations, are fully considered, and that the community has adequate opportunity to comment;

NOW THEREFORE BE IT RESOLVED that the City of Portland opposes coal export on trains through its jurisdiction until a complete National Environmental Policy Act process, including an area-wide Environmental Impact Statement, is completed; and

BE IT FURTHER RESOLVED that the City of Portland supports the development and review of a comprehensive Health Impact Assessment prior to approval of coal export permits by any state, regional or federal agency; and

BE IT FURTHER RESOLVED that the City of Portland requests that the Army Corps of Engineers require an area-wide Environmental Impact Statement that studies the

cumulative and comprehensive impacts of the five proposed coal export terminals in Oregon and Washington, before any coal export facility is approved; and

BE IT FURTHER RESOLVED that the City of Portland intends to address any impacts to public health, safety and property caused by the transport of coal through Portland by actively enforcing applicable local public health, safety, building, electrical and fire codes; and

BE IT FURTHER RESOLVED that the City of Portland intends to address any impacts to surface and groundwater caused by the transport of coal through Portland by actively enforcing any applicable environmental statutes delegated to the City of Portland; and

BE IT FURTHER RESOLVED that the City of Portland will request that the Railroad companies make public and properly notify citizens of any plans for new or expanded rail facilities or any anticipated increases in rail traffic volume; and

BE IT FURTHER RESOLVED that the City of Portland will request that the Railroads provide representatives to meet periodically with local citizen groups and local government officials to address local concerns; and

BE IT FURTHER RESOLVED that the City of Portland will request that the Railroads mitigate any public safety hazards created by the transport of coal through Portland; and

BE IT FURTHER RESOLVED that the City of Portland will request that the Railroads submit an emergency environmental cleanup plan in case of accidental derailment; and

BE IT FURTHER RESOLVED that the City of Portland supports economic growth that contributes to citizens' health, safety, and well-being, and that on balance, adheres to principles of sustainable development and an overall reduction of carbon emissions.

Adopted by the Council:

Commissioner Fritz
Prepared by: Milena Malone
Date Prepared: [Sept. 13th, 2012]

LaVonne Griffin-Valade
Auditor of the City of Portland
By

Deputy

EXHIBIT A

City of

PORTLAND, OREGON

Office of Mayor Sam Adams

Sam Adams, Mayor
1221 SW Fourth Avenue, Room 340
Portland, Oregon 97204-1994
(503) 823-4120
F: (503) 823-3588
E: mayorsam@ci.portland.or.us
www.mayorsamadams.com

October 5, 2009

Jim Piro
President and CEO
Portland General Electric
121 SW Salmon
Portland, Oregon 97201

Dear Jim,

I consider PGE to be one of Portland's most valued community partners and I am proud that Portland General Electric is an independent Portland-based company.

I would especially like to thank PGE for working closely with the City on the Clean Energy Works Portland pilot program, an integrated partnership to create green jobs, reduce carbon emissions and achieve energy bill savings. With our Clean Energy Works partners, we are showing how the public and private sectors, alongside community organizations and labor, can achieve real social, economic and environmental equity.

I appreciate the opportunity for public comment on your draft Integrated Resource Plan (IRP). It is on our firm foundation of partnership that I submit my proposed changes to your draft IRP and offer my help to make it happen.

Upfront, I want to laud the strategies that seek to advance a cleaner, more sustainable energy future for the Portland region. I'm pleased that the plan reflects a commitment to acquire clean energy resources in implementing Oregon's Renewable Energy Standard; pursues peak energy demand reduction; and conveys PGE's overall willingness to seek out new opportunities in sustainable energy resources.

My primary concern, however, is that the draft IRP relies on coal-based energy production and not enough on energy efficiency and clean technology. It is striking to me that the draft IRP shows the share of PGE's electricity from coal actually <u>increasing</u> over time, from 24 percent in 2010 to 25 percent in 2015.

I believe such a coal-dependent IRP is a poor long-term resource strategy as carbon regulation and firm targets for reducing greenhouse gas emissions are implemented. PGE's own assumptions about the future of Boardman are based on a regulatory environment that is certain to change and make coal still less affordable. I strongly urge you to evaluate phasing out Boardman and the procurement of coal-produced electricity by 2020 at the latest.

We want to help. This month, Portland City Council will be asked to approve a long-range climate protection policy, the Climate Action Plan. The Plan establishes a goal of reducing carbon emissions to 80 percent below 1990 levels—a target based on the latest science from the Intergovernmental Panel on Climate Change—and lays out a roadmap to transition our entire community from fossil-fuel dependence to a thriving, prosperous, low-carbon society.

Energy efficiency offers compelling advantages as a high-certainty, low-cost, zero-carbon resource that alleviates transmission issues and brings a host of related benefits. It can also keep business costs low, making our firms more competitive and growing the local economy. McKinsey's recent "Pathways to a Low-Carbon Economy" study, for example, found that about 75 percent of the total carbon-reduction potential in the building sector produces net economic benefits.[1]

I also note that the recent Sixth Power Plan from the Northwest Power and Conservation Council anticipates that energy efficiency can meet 85 percent of the increased need for electricity over the next 20 years for the entire region, considerably higher than PGE's own forecast of meeting half its demand growth with efficiency.[2] Recent experience suggests the Power Council's targets are realistic: The region has achieved 762 average megawatts of efficiency over the last four years, for example, already exceeding the five-year conservation target of 700 average megawatts adopted in the Fifth Power Plan in 2004.[3]

I see many opportunities to work together with PGE to dramatically ramp up energy efficiency, keeping costs low both for the utility and for Portland businesses and residents. The Clean Energy Works Portland program is just one example of how we can work together to scale up energy efficiency. Portland is currently seeking outside private and federal resources that can help lower the costs of acquiring efficiency still further, and the IRP should consider how these leveraged resources can help reduce PGE's overall resource-acquisition costs.

By shifting more of your focus to energy efficiency and clean technology, you also will help to better position the Portland region as the hub of the nation's clean technology industry, a key objective in our new Economic Development Strategy.[4]

---

[1] "Pathways to a Low-Carbon Economy," McKinsey & Co., 2009. URL: www.mckinsey.com/clientservice/ccsi/pathways_low_carbon_economy.asp

[2] "Draft Sixth Power Plan," Northwest Power and Conservation Council, September 2009. URL: http://www.nwcouncil.org/energy/powerplan/6/default.htm.

[3] "Draft Northwest Power Plan recommends mostly energy efficiency to meet future demand for electricity and reduce risk of future electricity shortages and high prices," Northwest Power and Conservation Council, September 3, 2009. URL: http://www.nwcouncil.org/library/releases/2009/0903.htm.

[4] http://pdxeconomicdevelopment.com/

Again thank you for being one of the City's most valued organizations. I support elements of the draft Integrated Resource Plan that seek to advance a cleaner, more sustainable energy future for the Portland region.

I welcome further discussion on these points. PGE's resource decisions have never been more important, and I look forward to participating in the formal IRP proceeding at the Public Utility Commission.

Sincerely,

Sam Adams

EXHIBIT B

OFFICE OF MAYOR SAM ADAMS
CITY OF PORTLAND

May 2, 2012

The Honorable John McHugh
Secretary of the Army
1400 Defense Pentagon
Washington, D.C. 20301-1400

The Honorable Ken Salazar
Secretary of the Interior
U.S. Department of the Interior
1849 C Street, NW, Room 5665
Washington, D.C. 20240

Major General Meredith W.B. (Bo) Temple
Headquarters
U.S. Army Corps of Engineers
1849 C Street NW, Room 5665
Washington, D.C. 20314-1000

Mr. Robert Abbey, Director
Bureau of Land Management
U.S. Department of the Interior
441 G Street NW
Washington, D.C. 20240

Brig. Gen. John McMahon
Commander and Division Engineer
U.S. Army Corps of Engineers
Northwestern Division
P.O. Box 2870
Portland, OR 97208-2870

Dear Sirs:

I am writing to urge you to undertake a programmatic and comprehensive review of the numerous coal-export facilities currently proposed in the Pacific Northwest. These facilities present potentially serious human and environmental health impacts in Portland and throughout Oregon.

To date, coal-export facilities have applied for permits and initiated the review process individually, yet it is their collective impact that poses the real concern. To adequately evaluate the risks to human and environmental health, I strongly urge you to view these various permit applications in context. While the impacts of any single facility alone are likely significant, the impacts collectively could be catastrophic.

1221 SW FOURTH AVENUE, SUITE 340 ♦ PORTLAND, OREGON 97204
(503) 823-4120 ♦ mayorsamadams.com

The Portland region was the first in the United States to adopt a Metro Export Initiative, and we are committed to the President's goal of doubling exports over the next five years. However, we believe that long term export growth will come from innovation and advanced manufacturing, and not from continued use of outdated technologies and the export of raw materials that pose significant risks.

Coal to and from several of these export facilities will be transported through Portland by rail or by barge and have the potential for major local impacts on human and environmental health. Of greatest concern are coal dust emissions from uncovered rail cars, which can significantly degrade local air quality. These impacts are compounded by a second wave of effects when the coal is eventually combusted, primarily in Asia, and prevailing winds carry the resulting air pollution to the Pacific Northwest. These impacts are not trivial: In the Columbia River basin more than 80 percent of the mercury pollution, a potent neurotoxin, is from overseas sources.

Prior to permitting any further facilities, I respectfully request that the Army Corps of Engineers evaluate the cumulative impacts of the various coal terminals in a single comprehensive Programmatic Environmental Impact Statement under the National Environmental Policy Act.

These facilities will be with us for decades, and I urge you to review these applications thoroughly and in context prior to reaching a decision.

Thank you for considering my request.

Sincerely,

Sam Adams, Mayor

cc: The Honorable Ron Wyden
The Honorable Jeff Merkley
The Honorable Suzanne Bonamici
The Honorable Earl Blumenauer
The Honorable Peter DeFazio
The Honorable Kurt Schrader
Governor John Kitzhaber
Steve Gagnon, U.S. Army Corps of Engineers (re: No. NWP-2012-56)

EXHIBIT C

JEFF MERKLEY
OREGON

COMMITTEES:
ENVIRONMENT AND PUBLIC WORKS
HEALTH, EDUCATION, LABOR, AND PENSIONS
BANKING, HOUSING, AND URBAN AFFAIRS
BUDGET

United States Senate

WASHINGTON, DC 20510

July 18, 2012

The Honorable John McHugh
Secretary of the Army
1400 Defense Pentagon
Washington, D.C. 20301-1400

The Honorable Ken Salazar
Secretary of the Interior
U.S. Department of the Interior
1849 C Street, NW, Room 5665
Washington, D.C. 20240

Dear Secretary McHugh and Secretary Salazar,

I have been talking with Oregonians in town hall meetings across the state, and have heard a great deal of input about the proposed coal export facilities in Oregon and Washington. These comments reflect a broad spectrum of opinions and some deep differences of opinion within and among communities that would be affected. Like many of the Oregonians I have heard from, I am supportive of efforts to increase exports of American products, especially through Oregon's ports. I recognize and appreciate that these projects would create much-needed jobs and economic development for local communities. Yet I also recognize and appreciate that many Oregonians have serious concerns relating to local and global impacts of these projects.

I am, therefore, writing to request that the Army Corps and the Bureau of Land Management conduct a comprehensive, expedited programmatic Environmental Impact Statement (EIS) for the proposed coal export facilities in Oregon and Washington.

The proposed export projects are a major undertaking but there has been significant uncertainty about the proposed facilities and communities are divided about the benefits and consequences of exporting coal. For that reason, I believe it is imperative that we do all we can to ensure there is full public disclosure of information about, and analysis of, the proposed facilities. A programmatic EIS would help put more information before the public and enable more comprehensive and informed public discourse. At the same time, the programmatic EIS should be conducted on the fastest timeline possible, preferably within one year, so as to not unnecessarily delay the decision-making process.

Some local communities see significant economic development opportunities and jobs in the potential coal export facilities. The potential benefits include the construction of coal transport infrastructure, jobs on trains and barges and at ports, and improvements to our region's rail and shipping infrastructure. In addition, it is likely that additional jobs for manufacturing and

313 HART SENATE OFFICE BUILDING
WASHINGTON, DC 20510
(202) 224-3753
FAX (202) 228-3997

121 S.W. SALMON STREET
SUITE 1400
PORTLAND, OR 97204
(503) 326-3386
FAX (503) 326-2900

operating barges would be created in Oregon. Permanent, family-wage jobs would be created through preliminary labor agreements between unions and the companies proposing the exports. At a time when we need to be doing everything possible to promote economic development and get Oregonians back to work, the proposals could have benefits for our state.

Some local communities have also expressed deep concerns about the impact of the proposed facilities. These include the impact of coal dust on public health or on local businesses, and the effects of increased rail congestion. Some residents have described their worry that small towns could essentially be divided in half by very lengthy coal trains for long periods of time.

Many people are concerned about larger-scale impacts. Conservation organizations have expressed concern that the proposed projects would offer developing Asian economies a significant new source of coal that they would otherwise not be able to access. They assert that this access, and the resulting effect on coal prices and demand, could change the fundamental economics of coal in Asia, increasing dependence on coal and slowing growth in the use of cleaner energy sources. Some are also concerned that further dependence on coal in Asia will lead the amount exported from the U.S. to increase significantly in the future. These developments could have a significant impact on climate change.

A programmatic EIS, or any type of EIS the Army Corps conducts, must be comprehensive in nature, and consider both local and global issues raised by the public. Relatively localized issues to be studied should include potential impacts on public health from coal dust and diesel pollution; effects on water quality; effects on listed species such as Chinook Salmon and steelhead in the Columbia and Willamette rivers; effects on other critical habitat and aquatic resources; effects on cultural resources and historic sites; and the effects of mining activity on public lands. In addition, the EIS should assess the impacts of increased vessel traffic on the Columbia River, including effects on navigational and maritime safety concerns; and the impacts of increased rail traffic, including noise and traffic delays for events such as emergency vehicles at rail crossings.

Global impacts of coal exports to be studied must include effects on climate change (including cumulative additions to global greenhouse gas emissions), global energy markets, energy security, and the clean energy economy. The changing climate is already altering our environment, and will have particularly significant negative impacts on our state, including sea level rise, ocean acidification, and an increase in the frequency and intensity of extreme weather events like storms, floods, and summer droughts.

These issues are complex and have major implications. They raise questions about whether global environmental and energy policy should be decided based on project-by-project applications or whether other policy forums should be engaged. A programmatic EIS would be one step toward ensuring more comprehensive analysis and informed decision-making. We should not make public policy decisions that could constitute significant moves toward a more coal-dependent future without gathering and publicly disclosing the best possible information and engaging in the appropriate analysis. I support an expedited programmatic EIS for that reason: it would enable a full and thorough examination of the issues to best inform public policy decisions for Oregon and for the nation.

Sincerely,

Jeffrey A. Merkley
United States Senator

Cc:
The Honorable Nancy Sutley
Chair, Council on Environmental Quality
Executive Office of the President
Washington, DC 20500

Major General Merdith W.B. (Bo) Temple
Headquarters
U.S. Army Corps of Engineers
441 G Street NW
Washington, D.C. 20314-1000

Mr. Robert Abbey, Director
Bureau of Land Management
U.S. Department of the Interior
1849 C Street, NW, Room 5665
Washington, D.C. 20240

Portland, Oregon

FINANCIAL IMPACT and PUBLIC INVOLVEMENT STATEMENT
For Council Action Items

(Deliver original to Financial Planning Division. Retain copy.)

1. Name of Initiator	2. Telephone No.	3. Bureau/Office/Dept.
Milena Malone	503-823-4124	Commissioner Fritz

4a. To be filed (date):	4b. Calendar (Check One)	5. Date Submitted to Commissioner's office and FPD Budget Analyst:
September 13th 2012	Regular ☒ Consent ☐ 4/5ths ☐	September 13, 2012

6a. Financial Impact Section:	6b. Public Involvement Section:
☒ Financial impact section completed	☒ Public involvement section completed

1) Legislation Title:

Adopt a policy opposing coal trains traveling through the City of Portland until an area-wide Environmental Impact Statement is completed. (Resolution)

2) Purpose of the Proposed Legislation:

The purpose of this legislation is to influence government partners, and railroad and coal companies to take specific actions to eliminate or mitigate community impacts of proposed coal export facilities.

3) Which area(s) of the city are affected by this Council item? (Check all that apply—areas are based on formal neighborhood coalition boundaries)?

☒ City-wide/Regional ☐ Northeast ☐ Northwest ☐ North
☐ Central Northeast ☐ Southeast ☐ Southwest ☐ East
☐ Central City
☐ Internal City Government Services

FINANCIAL IMPACT

4) Revenue: Will this legislation generate or reduce current or future revenue coming to the City? If so, by how much? If so, please identify the source.

No impact on current or future revenue coming to the City.

5) Expense: What are the costs to the City related to this legislation? What is the source of funding for the expense? *(Please include costs in the current fiscal year as well as costs in future years. If the action is related to a grant or contract please include the local contribution or match required. If there is a project estimate, please identify the* ***level of confidence****.)*

No costs to the City related to this legislation

6) **Staffing Requirements:**

- **Will any positions be created, eliminated or re-classified in the current year as a result of this legislation?** *(If new positions are created please include whether they will be part-time, full-time, limited term, or permanent positions. If the position is limited term please indicate the end of the term.)*

No positions will be created, eliminated or re-classified in the current year as a result of this legislation

- **Will positions be created or eliminated in *future years* as a result of this legislation?**

No positions be created or eliminated in future years as a result of this legislation

(Complete the following section only if an amendment to the budget is proposed.)

7) **Change in Appropriations** *(If the accompanying ordinance amends the budget please reflect the dollar amount to be appropriated by this legislation. Include the appropriate cost elements that are to be loaded by accounting. Indicate "new" in Fund Center column if new center needs to be created. Use additional space if needed.)*

Fund	Fund Center	Commitment Item	Functional Area	Funded Program	Grant	Sponsored Program	Amount

[Proceed to Public Involvement Section — REQUIRED as of July 1, 2011]

PUBLIC INVOLVEMENT

8) Was public involvement included in the development of this Council item (e.g. ordinance, resolution, or report)? Please check the appropriate box below:

☒ **YES**: Please proceed to Question #9.
☐ **NO**: Please, explain why below; and proceed to Question #10.

9) If "YES," please answer the following questions:

a) What impacts are anticipated in the community from this proposed Council item?

The purpose of this legislation is to influence government partners, and railroad and coal companies to take specific actions to eliminate or mitigate community impacts of proposed coal export facilities.

b) Which community and business groups, under-represented groups, organizations, external government entities, and other interested parties were involved in this effort, and when and how were they involved?

Many groups provided background information and suggestions, including but not limited to: several Neighborhood Associations, Friends of the Columbia River Gorge, Power Past Coal, the Sierra Club, and others. In addition, draft legislation was sent to a list of interested parties in advance and comments were solicited; several comments were incorporated into the final document.

c) How did public involvement shape the outcome of this Council item?

Community interest and advocacy led to the creation of this Resolution. Also, draft legislation was sent to a list of interested parties in advance and comments were solicited; several comments were incorporated into the final document.

d) Who designed and implemented the public involvement related to this Council item?

Commissioner Fritz and staff designed and implemented the public involvement.

e) Primary contact for more information on this public involvement process (name, title, phone, email):

Milena Malone, 503-823-4124, milena.malone@portlandoregon.gov

10) Is any future public involvement anticipated or necessary for this Council item? Please

describe why or why not.

Yes. If this legislation succeeds in influencing coal companies to produce an Environmental Impact Statement, the community will have further opportunity to comment on the proposed coal export facilities. Furthermore, this legislation seeks to influence local railroads to notify and meet with neighbors.

BUREAU DIRECTOR (Typed name and signature)

Resolution 2012-15

A Resolution stating the City of Hood River's concerns and opposition to transporting coal through the Columbia River Gorge

WHEREAS, The City of Hood River has committed itself to being a leader in protecting the environment, air quality, and water quality in the Columbia River Gorge, and

WHEREAS, burning coal leads to greenhouse gases, and the impacts of climate change on the Columbia River Gorge and other tourist attractions negatively impact Hood River's economy, and

WHEREAS, coal is commonly transported via open top rail cars, contaminating cities, towns, farmland, forestland, streams, and rivers within the Columbia River Gorge with coal dust and chunks of coal, and

WHEREAS, coal contains toxic heavy metals - including mercury, arsenic, lead, and uranium - and exposure to these toxic heavy metals in high concentrations is linked to a multitude of health problems, such as cancer and birth defects, and

WHEREAS, increased rail traffic will lead to an increase in diesel emissions in communities along rail lines, and

WHERAS, up to 54 additional trains per day will have detrimental effects on traffic congestion and air quality due to idling cars, and

WHEREAS, increased noise and vibration from large freight trains have been shown to have a negative impact on psychological health, and

WHEREAS, up to 54 additional trains per day may inhibit the travel of emergency vehicles in the Columbia River Gorge

WHEREAS, increased freight train traffic will have a negative effect on property values, and

WHEREAS, an increase in coal train traffic would raise the risk of a train derailment taking place, and communities within the Columbia River Gorge are not equipped to deal with the public safety and health risks caused by a coal train derailment, and

WHEREAS, public health risks associated with diesel emissions and other pollutants from coal trains disproportionately impact children, the elderly, and those with existing respiratory issues, and

WHEREAS, the route coal trains would follow through the Columbia River Gorge runs along the Columbia River through popular recreational areas, a major source of the economy in the Gorge, and

WHEREAS, the negative impacts of shipping coal by barge on the Columbia River will have similar effects on the Columbia River Gorge as those associated with shipping coal by rail.

Now therefore be it RESOLVED, that the City of Hood River opposes coal export projects that entail transporting coal through the Columbia River Gorge either by rail or by barge.

Be it further resolved, that the City of Hood River supports economic growth that does not jeopardize the City of Hood River's commitment to fight the serious impacts of climate change, and

Be it further resolved, that the City of Hood River urges the Governor and other decision makers to work on a comprehensive policy to prevent shipping/exporting coal through the Columbia River Gorge by rail or barge.

Be it further resolved, that the City of Hood River intends to address any impacts to public health and/or property caused by the transport of coal through The City of Hood River by actively enforcing local public health, safety, building, electrical, and fire codes, and

Be it further resolved that the City of Hood River intends to address any impacts to surface and/or groundwater caused by the transport of coal through The City of Hood River by actively enforcing applicable environmental statutes delegated to The City of Hood River, and

Be it further resolved that the City of Hood River strongly requests that the State of Oregon through its elected officials require the railroad and barge companies to mitigate any public safety hazards created by the transport of coal through the Columbia River Gorge such as access by emergency vehicles and

Be it further resolved that the City of Hood River requests that the railroad, and make public, any plans for new or expanded rail facilities or significant rail traffic volume increases within the Columbia River Gorge, and

Be it further resolved that the City of Hood River requests that the railroad and barge companies provide representatives to meet periodically with local citizen groups and local government officials from the Columbia River gorge to seek mutually acceptable ways to address local concerns, and

Be it further resolved that the City of Hood River requests that the railroad submit an emergency environmental clean-up plan in case of a derailment that affects local watersheds and recreational areas, and

Be it further resolved that the City of Hood River requests that the railroad and barge companies perform an Environmental Impact Study prior to approval of permits and later provide continued environmental monitoring of noise, air, groundwater, and surface water quality, including monitoring for the presence of coal dust, and that the results will be shared with local and state agencies, and

Be it further resolved that the City of Hood River requests that the railroad and barge companies carefully monitor the loading of coal at the coal mines as part of the contract(s) with the coal companies to assure best loading practices in order to reduce the amount of coal and coal dust coming out of the rail cars, and

Be it further resolved that the City of Hood River urges appropriate permitting authorities to require an environmental impact statement that identifies and measures the impacts on our community from a significant increase in coal train traffic, and

Be it further resolved that the City of Hood River urges appropriate permitting authorities to hold at least one environmental impact scoping hearing at a location in The City of Hood River, and

Be it further resolved that the City of Hood River transmits copies of this resolution to the Governor of Oregon, to all members of the Oregon State Division of Lands Board, and to each state Senator and Representative in both Oregon and Washington whose districts fall within Columbia River Gorge, the Washington Department of Ecology, and the Washington Department of Natural Resources, and

Be it further resolved that the City of Hood River transmits copies of this resolution to each Senator and Representative from Oregon and Washington in the Congress of the United States and

Be if further resolved that passage of this resolution shall not preclude the City of Hood River from taking additional actions to protect residents from the effects of coal trains in the future.

Approved by the Hood River City Council this 23rd day of April, 2012, to take effect immediately.

Arthur Babitz, Mayor

Jennifer Gray, City Recorder

RESOLUTION NO. 12-013

A RESOLUTION EXPRESSING CONCERN REGARDING POTENTIAL ADVERSE IMPACTS FROM INCREASING NUMBER OF TRAINS TRANSPORTING COAL THROUGH THE CITY OF THE DALLES, AND REQUESTING THE APPROPRIATE AUTHORITIES TO REQUIRE AN ENVIRONMENTAL IMPACT STATEMENT WHICH IDENTIFIES THE IMPACTS TO THE CITY OF THE DALLES

WHEREAS, there are currently a number of projects proposed which include the transportation of coal by train from the Powder River Basin in Wyoming to facilities located in the States of Oregon and Washington; and

WHEREAS, under these proposed projects, the potential exists for an increase in the number of trains transporting coal through the City of The Dalles; and

WHEREAS, the Union Pacific Railroad has track lines located in the City of The Dalles, including four at-grade crossings; and

WHEREAS, during two town hall presentations, the City Council heard public comment expressing concern for the potential for coal dust being generated by the trains, having a negative impact upon the residents of the City of The Dalles; and

WHEREAS, the City Council is concerned that the potential increase in train traffic used to transport coal could result in closure of at-grade crossings with greater frequency and for longer period of times, which could possibly contribute to traffic congestion and negatively impact emergency service response times; and

WHEREAS, the City Council is concerned about the impact on the community's health, environment, safety, and local business from coal dust and other particulates which may be blown from or fall from the train cars used to transport the coal; and

WHEREAS, the route which the coal trains would follow is adjacent to the historic downtown area of the City, and to the recently completed Lewis and Clark Festival Park, and the City Council is concerned about the potential negative impact of the increased number of coal trains upon customers of local businesses, and visitors to downtown area and the Festival Park;

NOW, THEREFORE, THE CITY COUNCIL OF THE CITY OF THE DALLES RESOLVES AS FOLLOWS:

Section 1. The City Council urges the appropriate authorities to require an environmental and economic impact statement which identifies and measures the impacts on the City of The Dalles and other communities located within the Columbia River Gorge from the increase in coal train traffic.

Section 2. The City Council urges the appropriate authorities to hold at least one of the environmental impact scoping hearings at a location within the City of The Dalles.

Section 3. This Resolution shall be effective as of September 24, 2012.

PASSED AND ADOPTED THIS 24TH DAY OF SEPTEMBER, 2012

Voting Yes, Councilors: Wood, Dick, McGlothlin, Spatz
Voting No, Councilors: Ahier
Abstaining, Councilors: None
Absent, Councilors: None

AND APPROVED BY THE MAYOR THIS 24TH DAY OF SEPTEMBER, 2012

BRIAN AHIER
MAYOR PRO TEM

James L. Wilcox, Mayor

ATTEST:

Julie Krueger, MMC, City Clerk

The New York Times

October 11, 2012

Tribes Add Potent Voice Against Plan for Northwest Coal Terminals

By KIRK JOHNSON

FERNDALE, Wash. — At age 94, Mary Helen Cagey, an elder of the Lummi Indian tribe, has seen a lot of yesterdays. Some are ripe for fond reminiscence, like the herring that used to run rich in the waters here in the nation's upper-left margin, near the border with Canada. Others are best left in the past, she said, like coal.

"I used to travel into Bellingham and buy my sack of coal," she said, standing in sensible shoes on a pebbled beach at a recent tribal news conference, talking about her girlhood of rural subsistence and occasional trips to the nearby market town. The idea that coal producers would make a comeback bid, with a huge export shipping terminal proposed at a site where she once fished, called Cherry Point, is simply wrong, she said. "It's something that should not come about," Ms. Cagey said.

Many environmental groups and green-minded politicians in the Pacific Northwest are already on record as opposing a wave of export terminals proposed from here to the south-central coast of Oregon, aiming to ship coal to Asia. But in recent weeks, Indian tribes have been linking arms as well, citing possible injury to fishing rights and religious and sacred sites if the coal should spill or the dust from its trains and barges should waft too thick.

And as history has demonstrated over and over, especially in this part of the nation, from protecting fish habitats to removing dams, a tribal-environmental alliance goes far beyond good public relations. The cultural claims and treaty rights that tribes can wield — older and materially different, Indian law experts say, than any argument that the Sierra Club or its allies might muster about federal air quality rules or environmental review — add a complicated plank of discussion that courts and regulators have found hard to ignore.

Lummi tribal leaders recently burned a mock million-dollar check in a ceremonial statement that money could never buy their cooperation. Last month, the Affiliated Tribes of Northwest Indians, a regional congress of more than 50 tribes in seven states, passed a resolution demanding a collective environmental impact statement for the proposed ports, rather than project-by-project statements, which federal regulators have suggested.

Leaders of the Columbia River Inter-Tribal Fish Commission, which focuses on fishing rights,

said in a statement in support of the resolution that moving millions of tons of coal through the region could affect a range of issues, like road traffic and economic life on the reservations, not to mention the environment.

“It brings another set of issues to the table,” said Gov. John Kitzhaber of Oregon, a Democrat who earlier this year asked for a broad federal environmental review that would examine implications of the coal plan from transit through the region by train or barge to the burning of the coal in China. The tribes, Mr. Kitzhaber said, have now added a voice that even a governor cannot match. “It definitely increases the pressure,” he said.

Coal producers across the nation have been wounded by a sharp drop in demand in the United States — down 16.3 percent in the period from April through June, compared with the same period in 2011, to the lowest quarterly level since 2005, according to the most recent federal figures. With prices falling and abundant supplies of natural gas flowing because of new fields and drilling technologies, especially hydraulic fracturing, or fracking, many electricity producers that can switch are doing so.

That has made coal exports, which have increased this year in every region of the country except the West, according to federal figures, even more crucial to the industry than they were when the six terminals on the Pacific Coast were first proposed. Jason Hayes, a spokesman for the American Coal Council, said that with coal-producing nations like Australia and Indonesia competing for Asian markets, a roadblock on the West Coast is an issue for the entire American economy.

The first public hearings for the terminal projects, conducted by the Army Corps of Engineers, are set to begin this month in Bellingham, near the Lummi reservation.

“The people that can produce efficiently and can ship quickly and reliably — those are the big things — they are going to be the ones that are chosen for being reliable business partners,” Mr. Hayes said. “If we can build the ports on the West Coast, then it just becomes that much more reliable.”

But by coincidence of history, geography, culture and law, the West Coast, especially Washington and Oregon, is also a center for Indian tribe muscle, legal scholars said.

Although many tribes around the nation received rights to hunt and fish in the treaty language of the 1800s that consigned them to reservations, few places had a focus on a single resource — fish, especially from the Columbia River and its tributaries — that tribes here did. They also, crucially, persisted in using the resources that the treaties had granted them; fishing did not become a hobby or a cultural artifact.

Then, in the 1970s, when the Indian rights and environmental movements were both surging, tribal timing was fortuitous in pushing court cases that reinforced their claims.

“They made really good use of those rights, and have become major players,” said Sarah Krakoff, a law professor at the University of Colorado who teaches Indian law and natural resources law. Tribal rights have been a cornerstone in the long battle over restoring salmon stocks in the Columbia River. This year, one of the biggest dam removal projects in the nation’s history reached a milestone when a section of the Elwha River near Olympic National Park in Washington was restored to wild flow, with fishing rights an important driver in the process.

Coal has also become an element in the presidential race, as energy executives have poured tens of millions of dollars into campaigns backing Mitt Romney, the Republican candidate, and accusing the Obama administration of harboring hostility to coal through tightened air pollution rules.

An executive order dating from the administration of Bill Clinton could give further ammunition to Northwest tribes in their coal fight, Professor Krakoff and other experts said. The order directs federal agencies to allow tribal access to sacred sites and to take into account religious practices in federal decision making.

Lummi leaders, in the protest this week where Ms. Cagey spoke, said the Cherry Point site in particular — though partly developed years ago by industry, with a major oil refinery nearby — is full of sacred sites and burial grounds. The tribe’s hereditary chairman, Bill James, said in an interview, however, that the tribe would not reveal the locations of the graves for fear of looting.

2012 Annual Convention
Pendleton, Oregon

RESOLUTION #12 - 53

"CALLING FOR FULL, TRANSPARENT ENVIRONMENTAL REVIEW OF THE PORT OF MORROW PROPOSAL, CONSULTATIONS, AND REGIONAL REVIEW OF ALL SIX NW COAL EXPORT PROPOSALS"

PREAMBLE

We, the members of the Affiliated Tribes of Northwest Indians of the United States, invoking the divine blessing of the Creator upon our efforts and purposes, in order to preserve for ourselves and our descendants rights secured under Indian Treaties, Executive Orders, and benefits to which we are entitled under the laws and constitution of the United States and several states, to enlighten the public toward a better understanding of the Indian people, to preserve Indian cultural values, and otherwise to promote the welfare of the Indian people, do hereby establish and submit the following resolution:

WHEREAS, the Affiliated Tribes of Northwest Indians (ATNI) are representatives of and advocates for national, regional, and specific tribal concerns; and

WHEREAS, ATNI is a regional organization comprised of American Indians/Alaska Natives and tribes in the states of Washington, Idaho, Oregon, Montana, Nevada, Northern California, and Alaska; and

WHEREAS, the health, safety, welfare, education, economic and employment opportunity, and preservation of cultural and natural resources are primary goals and objectives of the ATNI; and

WHEREAS, since time immemorial, our economy, culture, religion and way of life have centered around our fishing, hunting and gathering resources, and the lands and waters on which they depend, and we have been, and remain, careful and conscientious stewards over them to ensure their continued health and well-being; and

WHEREAS, the tribes of ATNI are sovereign and our people depend on the natural resources of this region; and

WHEREAS, the tribes of ATNI have an obligation to protect our First Foods and our most precious resource, water; and

WHEREAS, there are sweeping proposals for Powder River Basin coal to be shipped by rail and/or barge to West Coast ports: Cherry Point, Washington; Longview, Washington; Grays Harbor, Washington; Port of Morrow, Oregon; St. Helens, Oregon; and Coos Bay, Oregon; and

WHEREAS, the coal will then be shipped through our waters to Asia where it will then be burned in coal-fired power plants, emitting mercury and other toxins that return through the atmosphere to our homes; and

WHEREAS, the estimated coal export volumes from the proposed West Coast ports are unprecedented at over 150 million tons per year; and

WHEREAS, Northwest tribes have strong concerns about the impact of these proposals on tribal rights and resources, including but not limited to the following:

- Intrusions into traditional fishing, hunting and gathering sites;
- Destruction of our cultural and religious areas;
- Degradation of human health, related to fugitive coal dust and mercury poisoning;
- Interference with tribal business enterprises and opportunities, causing a loss of jobs, preventing jobs growth, and reducing tribal income, related to increased coal-train traffic;
- Declining water quality and loss of salmon and lamprey habitat from barging and shipping operations;
- Increases in emergency response times, interference with school functions, and fiscal impacts on other public services due to delays at train crossings;
- Filling of shorelines, wetlands, and streams, during expansion or reconstruction of rail lines along the Columbia River, the Salish Sea, and their tributaries;
- Climate change, sea level rise, and ocean acidification from coal-fired power plants; and
- Overall degradation of our natural resources and culture

; and

WHEREAS, Northwest tribes require transparency and ongoing consultation to ensure that the permitting and Environmental Impact Statements (EIS) for all of the proposed coal ports are consistent, in light of the fact that all of our waterways are connected to one another; and

WHEREAS, that ATNI hereby declares that a mere Environmental Assessment for the Port of Morrow facility, instead of an EIS, is completely unacceptable, based on a number of

deficiencies, including but not limited to the lack of Government-to-Government consultation required with all affected tribes in the region; now

THEREFORE BE IT RESOLVED, that ATNI hereby calls upon the White House Council on Environmental Quality to require immediate preparation of a comprehensive Environmental Impact Statement for the Port of Morrow proposed coal export facility; and

BE IT FURTHER RESOLVED, that ATNI hereby calls upon the White House Council on Environmental Quality to direct the U.S. Army Corps of Engineers (USACE) to develop a comprehensive EIS at the USACE Northwestern Division level, on the cumulative effects of all six currently proposed coal export proposals, and any future proposals, together, including analysis of the cumulative impacts of the proposals throughout the entire region and internationally, including their direct and indirect impacts on tribal cultural resources, treaty rights and interests (see attached letter); and

BE IT FURTHER RESOLVED, that ATNI hereby concludes that a separate EIS is also necessary for each of the coal export facilities individually; and

BE IT FINALLY RESOLVED, that ATNI hereby insists that the White House Council on Environmental Quality mandate all federal and state agencies to commence immediate Government-to-Government consultations with all tribes in the region, as our First Foods and resources, treaty rights and human health are directly impacted by the coal industry in the Northwest.

CERTIFICATION

The foregoing resolution was adopted at the 2012 Annual Convention of the Affiliated Tribes of Northwest Indians, held at Wildhorse Resort and Casino, Pendleton, Oregon on September 24 – 27, 2012 with a quorum present.

Fawn Sharp, President

Norma Jean Louie, Secretary

For Immediate Release: September 27, 2012

Distributed in conjunction with the Coast Salish Gathering and Association of Washington Tribes

Northwest Tribes say no short-cuts for coal export proposals

For more information contact:
Debra Lekanof, Swinomish Indian Tribal Community (360) 391-5296
Julie Carter, Columbia River Inter-Tribal Fish Commission (503) 238-0667

Mission, Oregon: Faced with the possibility of impacts to human health, natural resources and economies, leadership of Northwest tribes today called on the U.S. Army Corp of Engineers to conduct a full environmental analysis for all six proposals to transport and export coal through their shared lands and waters.

Today's action arose from the Northwest Tribal Coal Summit organized by the Association of Washington Tribes and the Coast Salish Gathering in conjunction with the Affiliated Tribes of Northwest Indians' fall convention hosted by the Confederated Tribes of the Umatilla Indian Reservation.

Driven by exploding Asian demand and declining domestic consumption of coal, export proposals have sprung up at Oregon and Washington ports. Six proposals call for transporting Powder River Basin coal from Montana through Indian and non-Indian lands in the Northwest via rail and barge.

Tribal communities are expressing grave concern about the health and safety impacts from environmental dangers of coal dust.

"Along the Columbia River it's cliff, highway, railroad, then river. Our communities are wedged between the railroad and the river. We've got nowhere to escape," said Paul Lumley, Executive Director of the Portland-based Columbia River Inter-Tribal Fish Commission. "If we cannot escape, neither will the coal."

The Tulalip Tribes expressed their concern both environmentally and economically. Tulalip is one of the largest economic engines in the region, along with Boeing. The Tulalips say that an increase in rail traffic along the I-5 corridor to as many as 18 trains a day will bring traffic in the area to a halt, blocking access to businesses, hospitals and fire stations.

"The risks not only to our tribe can be devastating, but also to the entire county," said Mel Sheldon, Chairman. "We've made substantial retail investments that depend heavily on quality of life, and we have collaborated with local citizens to restore and protect our watersheds. We are tracking this carefully, and plan to express our decision on this new threat in the near future."

Tribal leaders were addressed by Colonel Anthony Funkhouser, Commander of the Northwest Division of the U.S. Army Corps of Engineers, whose agency has federal permitting authority over coal export terminals through the Clean Water Act and Rivers and Harbors Act. The Corps of Engineers announced last week they would conduct an Environmental Assessment rather than a more rigorous Environmental Impact Statement on the Port of Morrow proposal for a new export coal terminal.

"We don't want the minimum protection any longer, we're used to getting the minimum", said Brooklyn Baptiste, Vice-Chairman of the Nez Perce Tribe. "We deserve the maximum attention and expect the lead and coordinating agencies to provide the full environmental studies on all ports, as they will be

making one of the largest decisions impacting human health, the environment and economies of not only our tribal communities, but of our neighboring citizens of the Northwest."

Kathryn "Kat" Brigham, member of the Confederated Tribes of Umatilla Board of Trustees, urged tribal leaders to reach out to neighboring communities, "they have something at risk too."

In addition to full environmental assessment the today's resolution passed by the fifty-seven member tribes of ATNI called for full transparency and government to government consultation throughout the entire decision making process the local, state, and federal levels.

"We believe the Northwest is interconnected through the families, resources and waterways, that these coal terminals and railway routes should be addressed in a holistic manner," expressed by Chairman Brian Cladoosby, Swinomish Tribe. "If a coal train or tanker were to spill on the route or in the river at Port Morrow in Oregon, the water ways will carry the pollution throughout the Northwest, and coal dust will be carried through the mountains in the air we all breath. "

Billy Frank Jr., Chairman of the Northwest Indian Fish Commission added, "The idea of a half-dozen new coal export terminals in western Washington and Oregon -- and the hundreds of trains and barges running from Montana and Wyoming every day to deliver that coal -- would threaten our environment and quality of life like nothing we have seen before. Coal may be a cheap source of energy for other countries, but these export facilities and increased train traffic would come at a great cost to our health, natural resources and communities."

# # # #

Confederated Tribes and Bands
of the Yakama Nation

Established by the
Treaty of June 9, 1855

May 3, 2012

Major General Merdith W.B. (Bo) Temple
Commanding General and Chief of Engineers, Acting
Headquarters
U.S. Army Corps of Engineers
441 G Street NW
Washington, DC 20314-1000

Brigadier General John McMahon
Commander and Division Engineer
Northwestern Division
U.S. Army Corps of Engineers
P.O. Box 2870
Portland, OR 97208-2870

Colonel John Eisenhauer
Commander, Portland District
U.S. Army Corps of Engineers
P.O. Box 2946
Portland, OR 97208-2946

Colonel Bruce Estok
Commander, Seattle District
U.S. Army Corps of Engineers
P.O. Box 3755
Seattle, WA 98124-3755

Re: Yakama Nation Comments NWP-2012-56 Coyote Island Terminal Coal Facility

Dear Sirs:

I am the Chairman of the Tribal Council for the Confederated Tribes and Bands of the Yakama Nation ("Yakama Nation" or "Nation"). The Nation is a federally recognized sovereign Indian tribe. The Yakama Nation reserved several rights under a treaty it signed with the Federal Government of the United States of America ("Treaty of 1855"), ratified by the United States Congress in 1859 (12 Stat. 951). Among various rights the Yakamas reserved to themselves and their progeny is the right to take fish in all usual and accustomed places, including the Columbia River. The Yakamas also secured the right to exclusive use and enjoyment of their Reservation. Implied within this right is the right to live free from environmental damages caused by nuisances, even those nuisances originating or transpiring outside the boundaries of the Yakamas' Reservation, such as the transportation of coal through the Nation's ancestral lands. The Coyote Island Terminal, and the regional plan of which it is unquestionably a part, implicates these rights and compels our Nation to submit this letter on behalf of our people, our ancestors who came before us, and those who've yet to come and have no voice to advocate for their rights.

This letter serves two purposes. First it is Yakama Nation's initial comments regarding the proposal for the Coyote Island Terminal, which is the first swell in the proposed regional tidal wave of coal transportation and exportation. Beyond the Coyote Island Terminal proposal we note that there are at least four additional coal export facilities planned for construction in Washington and Oregon. Therefore, through these comments we establish the basis for your agency to require a regional Programmatic Environmental Impact Statement ("PEIS") pursuant to the National Environmental Policy Act ("NEPA"). And we formally request a PEIS in this instance. A process to develop a PEIS would dispense with a piecemeal approach to review of

the regional plan the Coyote Island Terminal represents in favor of comprehensive and honest analyses. We find that a PEIS in this instance is a baseline for any valid analysis of the environmental and cultural impacts the proposed regional inundation of coal will have on the Yakama People, on all the residents of the northwestern states of our country, and the environment we all hold in trust for the benefit of generations to come.

With this prologue in mind, you'll find some of the apparent negative impacts associated with the Coyote Island Terminal application and the five other proposed coal export facilities in Washington and Oregon detailed in these comments. As we set forth below, the Coyote Island Terminal and its inextricable role in the regional plan to fashion the northwest into a coal transport and export hub will have lasting, detrimental impacts on the region's fisheries, its air quality, global climate change, and the Yakama Nation's cultural resources. And finally, both the letter and the spirit of the law require a PEIS to analyze these serious regional impacts, and mitigate those impacts.[1]

INTRODUCTION

Since we saw the first waves of outsiders settling here more than 150 years ago, their corporate enterprises and governments, their governmental policies, and the people that execute those policies have systematically ravaged the Yakama People's ancestral lands, waters, and air. They tell us these destructive plans are part of the march of progress. But their plans for progress have left a wake of destruction that has nearly eradicated our indigenous culture — a culture that teaches reverence for the environment and seeks to live in harmony with the world around it rather than exploit our resources as a parasite would see its host. These devastating waves have not only laid waste to our environment, they've swept away the resources upon which the Yakama People have relied for millennia. The next wave of so-called progress threatening my people is the coordinated plan to incrementally but totally transform our ancestral lands and the entire northwestern U.S. into a hub for the global exportation of coal.

As a specific historic example, we note the silence of Celilo Falls. This silence is a constant reminder of the destructive pattern the waves of progress sweeping through this region inflicted on the Columbia River Gorge ("CRG") and its native people. Fifty-five years ago, we watched as the closing of the floodgates at The Dalles Dam not only silenced Celilo Falls indefinitely, but also destroyed an area sacred to the Yakama People. Put simply, the eradication of Celilo Falls destroyed our Tribes' heartland. While the deliberate destruction of Celilo Falls and its surrounding villages provides an enduring symbol of the onslaught my people have suffered in the name of progress, Columbia River dams, like the Dalles Dam, had the immediate and

[1] By requesting a PEIS, the Yakama Nation in no way waives its right to oppose the Coyote Island Terminal and any of the other plans to increase coal through the Yakama Nation's ancestral lands. In fact, the Yakama Nation categorically opposes the Coyote Island Terminal and would prefer the government prevent further degradation of the Columbia River and the Gorge region through which it runs.

ongoing real-world effect of significantly eroding the Yakamas' right to take fish from the Columbia River and its tributaries. These consequences have rippled beyond the Columbia River, leaving the Nation deprived of its lifeblood; it's been forced to watch its culture slowly pass from existence as our youth now lack the opportunities to carry our customs and traditions forward. In sum, the Nation has been devastated by the waves of progress outsiders told us we must embrace.

Now we're told that what's best for us and our way of life is to embrace a staggering increase of coal transportation through the Yakamas' ancestral lands along the Columbia River. Like the dams of yesterday, the present plans to transform our region into a coal hub are championed as an essential element for progress. But the definition of "progress" cannot be limited to pecuniary progress without regard for the long-term damages those financial pursuits will cause. We must all do our part to ensure that real progress is made during our limited time on this earth, both economic and in many other more meaningful regards. For example, we have a duty to protect the environment not only because the law compels us to; we must protect our lands, our waters, and our air because our children and generations to follow will rely on them for sustenance, health, and security. We ask only that you do your duty and work with us to ensure that the waves we see on the horizon do not catch us unprepared and do not perpetuate the pattern of destruction the indigenous stewards of this region have endured for more than a century.

A. <u>The Scope And Bases For The Yakama Nation's PEIS Request</u>

A PEIS is a comprehensive review of a series of projects with impacts that are significantly interrelated; either programmatically, geographically, or environmentally. NEPA requires agencies to use this comprehensive method to review independent actions that have "cumulative" or "similar" impacts on an interrelated environment.[2] We urge your agency to carefully review federal environmental laws and what they have to say; not only regarding cumulative impacts, but also what the law mandates regarding the comprehensive analyses required for regional, multifaceted plans of development involving several projects — projects proponents may seek to have reviewed piecemeal for obvious, and I would argue short-sighted reasons. Particularly instructive is the language our nation's Supreme Court handed down three and a half decades ago in *Kleppe v. Sierra Club*.[3] While the Supreme Court ultimately decided in that case that the record before it at that point did not warrant a PEIS, it did agree that a PEIS would be necessary when several coal-related proposals will have significant impacts on a given region:

> " . . . when several proposals for coal-related actions that will have cumulative or synergistic environmental impact upon a region are pending concurrently before an agency, their environmental consequences must be considered together."[4]

---

[2] *See* 40 C.F.R § 1508.25.
[3] 427 U.S. 390 (1976)(internal citations and quotations omitted).
[4] *Id.* at 410.

The Supreme Court relied on two basic conclusions to find that no PEIS was required in the *Kleppe* case, neither of which are applicable here. First, the Supreme Court concluded that the various projects at issue in *Kleppe* were not part of a "proposal for regionwide action."[5] But here, the Port of Morrow Application ("Application") is part of a larger "regionwide" plan for to transport coal through, and export coal from Oregon and Washington's lands and waterways. Second, the Supreme Court upheld the agency's determination in *Kleppe* that the coal plans for the region at issue there were not sufficiently "programmatically, geographically, and environmentally related" to require a PEIS because it found the agency's determination was not arbitrary. In other words, the Supreme Court decided that the analysis of programmatic, geographic, and environmental interrelation "is a task assigned to the special competency of the appropriate agencies." And when the record in that case reflected a reasoned and competent approach by the agency, the Supreme Court would not to disturb the agency's expertly guided decision because that decision was not based on random or unreasoned whim. This second basis for the Supreme Court's decision in the *Kleppe* case — the deference the courts give to an agency's expertly guided and reasoned analysis — is especially critical here as your agency reviews this specific application and contemplates our request for a PEIS. As the *Kleppe* decision makes clear, your agency's judgment is given deference. But with that deference comes grave responsibility. As a lead federal agency, the U.S. Army Corps of Engineers ("Corps") is charged with utilizing its "special competency" to make an informed determination on whether the Application here is part of a regional plan that is sufficiently programmatically, geographically, and environmentally interrelated to warrant a PEIS. Even on the limited facts available to our staff, which have the various special competencies necessary for a complete environmental review, we find that there really is no reasonable debate on the matter of interrelatedness and the absolute necessity for a PEIS. The Port of Morrow is but the first of many planned coal-related projects that form a regional plan regarding coal transportation and exportation.

Presently, your agency is reviewing permits for several coal processing terminals in both Washington and Oregon. These multiple proposals represent an undeniably interrelated plan to turn our region into a hub for coal export. Permitting these proposals to move forward without a comprehensive environmental review through the completion of a PEIS may lead to the foundation of a global coal hub's infrastructure in our region; this could be a crack in the proverbial dam that will spread and cause a catastrophic flood of additional coal-related development projects, forever transforming this region for the worse. Each current project raises the specter of unique and seriously damaging environmental impacts in and around the areas proposed for development of coal terminals. But when you consider the various projects as a regional plan, the collective adverse environmental impacts come into focus, as explained in detail below. As an illustrative example, the completion of all proposals is estimated to add rail traffic through our region necessary to carry roughly 150 million tons of coal. The PEIS must consider the collective impacts of such a breathtaking increase in train traffic through our lands,

[5] *Id.* at 414-15.

among the myriad other significant impacts that will result from the interrelated plans for coal in our region.

The specific scope and prescribed contents of a PEIS should be determined through a full scoping process that includes public hearings around the region, in addition to government-to-government consultation between your agency and the elected officials of the Yakama Nation among other interested and affected indigenous peoples in and around the region. But as a baseline, the PEIS requested should analyze and mitigate impacts our region will sustain from the various projects' proposals to transport coal from the mountainous regions east of us, through Oregon, Washington, and on to Asia. The PEIS should also analyze and mitigate impacts resulting from the construction and operation of the export facilities within this region. And, beyond the region, the PEIS should consider the impacts that we all will suffer from burning the exported coal in Asia. It is critical that this PEIS is completed prior to any individual permit being issued at the local, state, or federal level.

Further, the Yakama Nation expects this PEIS will not be a substitute for project-specific EIS's that should follow the completion of a PEIS analyzing the regional plan's cumulative effects. In other words, the PEIS should supplement future EIS's if the regional plans move forward, and the PEIS should not serve as an excuse to forego future environmental analysis specific to one project or another. Moreover, until the cumulative impacts of all planned coal-related projects in the region have been identified and analyzed, and until the Federal Government consults with the Yakama Nation on a government-to-government level, no agency should make any decisions that would allow the commencement of any coal-related project. In other words, no agency should permit any application to advance this regional coal plan until the PEIS is complete, the specific EIS's are complete, and all interested parties have an opportunity to examine the regional coal plan holistically.

B. <u>Fisheries</u>

As indicated, the Treaty of 1855 reserved to the Nation the right to fish in perpetuity at all usual and accustomed places as they were known at the time of the Treaty signing. Though this right has been significantly diminished through the destruction of Celilo Falls and other "development" in the area, in the legal arena, this powerful right has been affirmed and re-invigorated through extensive litigation beginning with the *U.S. v. Winans* case in 1911 and culminating with *United States v Oregon*, which is still active. Today, the Yakama People continue to exercise their Treaty-reserved fishing rights on the Columbia River and its tributaries within the Nation's Ceded Lands and its usual and accustomed use areas. The site of the proposed action described in the Application is located completely within an area of active commercial gillnet fishing by members of the Yakama Nation.

Members of the Yakama Nation fish for subsistence and their livelihoods on the Columbia River using set gillnets that typically are anchored at one end to the river bank and to an anchored buoy up to 400 feet offshore in an orientation perpendicular to the flow of the river. Adult salmon and steelhead migrating upriver encounter the nets and become entangled in the gillnet webbing.

Fishers lift the nets 2-3 times per day from small, outboard-powered boats to harvest the fish from the webbing. Because the nets generally are most effective during hours of darkness, fishers typically visit the nets at least once — and often more frequently — during the night when fish are abundant. Several hundred tribal members utilize this method of fishing constantly during the fishing season. In aggregate, they may deploy over 1,000 such nets on the Columbia between Bonneville and McNary dams in the fishery administrative area known as Zone 6. Weekly fishing periods are established by tribal regulation depending on the availability of harvestable fish from mid-May to early October and February 1 to late March.

1. Impacts to Tribal Fishing Sites

The proposed coal export facilities throughout the CRG, including the coal loading dock identified as the Coyote Island Terminal, would have significant direct and indirect detrimental impacts to tribal fisheries in the project area. The construction and operation of the proposed terminal at the Port of Morrow will very likely destroy four tribal gillnet sites that Yakama members currently use to exercise their tribal fishing rights.[6] These particular threatened fishing sites are high quality and critically important to the tribal members who fish there. Construction of the proposed dock will at least interfere with — and very likely preclude — gillnet fishing at this location. From the Nation's experience with other docks and mooring dolphins, maneuvering barges into and out of the proposed dock will, again, at least interfere with, and perhaps preclude, fishing at sites adjacent to the proposed dock itself. It is important to note that these sites are not held or owned by individual tribal fishermen in the sense of title ownership. Rather, the Treaty-protected sites are held in trust by the Yakama Nation government for use by its enrolled members. The Nation authorizes tribal members to fish at certain sites on the Columbia through a site registration process administered by the Nation's Fisheries Program. Because the fishery is regulated in a site-oriented fashion, fishers authorized to fish at certain locations are not at liberty to simply move their fishing operation to another location on the river. The loss of fishing sites resulting from construction of the proposed dock would have the effect of disenfranchising the fishers authorized to fish at this location and would measurably diminish the number of fishing sites available to members of the Yakama Nation to exercise their Treaty-reserved right to fish at this usual and accustomed place. Put another way, construction of this project may directly violate the Treaty of 1855. Your agency must consider the potential treaty-violating effects of the Application.

2. Safety of Tribal Fisherman

Similarly, increased barge traffic through Zone 6 resulting from this project will impact the safety of tribal fishers exercising their Treaty-reserved fishing rights. Table 3.5 in the Biological Assessment (BA) for this project indicates that project-related barge traffic would nearly double the current volume of barge traffic on the Columbia River. Each additional barge, particularly those in transit during hours of darkness and/or foul weather, represents an increased safety risk

[6] This is qualified, because there is insufficient information to determine precisely how many fishing sites Ambre's project will destroy.

to fishers harvesting fish from their nets, operating small boats often times at night and in foul weather. Despite the fact that towboats are required to display lights indicating they are warped to one or more barges, the barges themselves are poorly lit and may obscure the lights of the towboat from the vantage point of a small boat. As tribal fishers may be hampered by foul weather gear, operating at night in otherwise dangerous conditions, and with barge lights obscured or confused by background lighting from Interstate 84 and fixed shore structures, increased barge traffic in the project area will considerably increase the safety risk to tribal fishers. The Application lacks any assessment of this increased hazard to tribal fishers and is thereby deficient. The Corps should not issue a permit without a PEIS addressing this matter comprehensively, and a project-specific EIS that considers safety hazards to tribal fishers.

Coal transportation by rail also poses a potential risk to human health and safety. Currently, there is a real risk of tribal fisherman being harmed or killed by trains traveling through the CRG. This risk would increase significantly with the addition of up to 60 coal trains moving through the Columbia Basin each day. Further, the coal residue that will be accumulating along the rail lines in the CRG poses yet another risk to human health that has not been evaluated in this application. Despite the Applicant's efforts to suppress the production of dust during transport by using surfactants and closed containers, coal will inevitably escape onto the railbed and eventually degrade to dust. Coal dust is a well-documented cause of disease in humans that sometimes results in death. Without adequate identification and analyses of these project-specific and general hazards posed by coal-related projects in the region, the Corps should not permit this Application to move forward.

3. *Impacts to Water Quality & Aquatic Species*

The BA prepared by Anderson Perry (April 2012) acknowledges that the project would have likely adverse effects on multiple endangered species, though it does not discuss how great those impacts would be or what would be done to mitigate for them. The potential significant increase of inadvertent coal spillage in the Columbia Basin could adversely affect Yakama Nation tribal resources including our tribal fisheries. Toxic effects are both acute and chronic to the Columbia Basins' aquatic food web and culturally important aquatic foods including salmon, sturgeon, and lamprey. Coal is associated with significant environmental problems including acidification of watersheds and metal contamination. Applicant's BA offers alleged assurances that Montana coal is considerably "cleaner" than other kinds but provides no list of contaminants present in the coal to be transported. Moreover, the chemical composition and biological effects of the surfactant sprayed on coal to reduce dust are not disclosed. The lack of this key information precludes a full analysis of potential biological impacts to water quality and associated aquatic biota in the likely event that coal enters the waters of the Columbia Basin. It is likely that this project will result in the contamination of the Columbia River as chunks of coal and coal dust inadvertently fall or spill into the waters of the Columbia Basin from trains traveling through the CRG. In fact, Burlington Northern Santa Fe has stated that up to 500 lbs. of coal per car is lost during rail transportation. Coal would also likely spill into the Columbia Basin during overwater barge loading, barge accidents, or train derailment. All of these types of accidents have been documented at least once and in some cases multiple times in the CRG within the past two

decades. The probability of future accidents and associated likely effects will significantly increase if this Application is approved, and they should be evaluated separately in a PEIS and for each project-specific review.

4. *Impacts to Habitat*

Along with the toxic properties of coal there are habitat threats associated with the construction of new coal facilities. Construction of the coal-loading facilities will impact habitat for species listed under the Endangered Species Act ("ESA") and will create possible habitat for native and nonnative predators. Destruction of habitat and negative impacts to ESA-listed species must be evaluated and fully considered. While the BA for this project describes in detail the range and nature of potential project impacts to Critical Habitat for ESA-listed species, it also acknowledges that it does not attempt to quantify the biological effects of such impacts on listed species. Absent specific quantitative assessments of project impacts, it is unclear how NMFS can issue a legally sufficient Biological Opinion that includes conservation measures and alternatives to mitigate project impacts. Without a viable BiOp, the Corps should not permit this Application.

In the single instance where quantitative data on biological effects are provided, the BA describes the potential for increased stranding of juvenile salmonids washed ashore in the wake of passing ocean-going vessels that would be associated with the proposed project. Unfortunately, neither the BA nor the cited original paper from which the data are drawn provide enough information to assess the cumulative effects of numerous such strandings over a broad geographic area. But the information given suggests that the effects could be significant and uniformly negative. The magnitude of this impact to listed salmonids and other aquatic resources critically important to the Yakama Nation should be analyzed before any BiOp or permit is issued for the project.

The Corps should consider whether and how this project is compatible with the ongoing regional effort to restore the Columbia Basin for fish and wildlife resources. Despite the BA's assertion of negligible or no project impacts to ESA-listed and other aquatic resources, the project represents an incremental, uniformly negative environmental stressor on an aquatic ecosystem that is already overstressed by existing human development. Allowing this project to move forward would fly in the face of the enormous regional investment in the recovery of our precious natural resources, especially the investment we've made in the salmon and steelhead that are iconic to the Pacific Northwest.

C. <u>Air Quality</u>

The Yakama Nation, federal agencies, and others have worked extensively over the past decade to identify, analyze, and address air quality concerns in the CRG. Through research and monitoring we have found the CRG to have some of the highest levels of air pollution and acid

rain in the Northwest.[7] Local coal-fired plants and China's massive coal burning industry have been identified as major sources of this harmful pollution in the CRG.[8]

Toxic pollutants like mercury from burning coal, and other fossil fuels from the diesel-powered locomotives and marine vessels within the CRG, continue to impact the Yakama People and their cultural, historic, and Treaty-reserved resources. Not only is this harmful pollution damaging our sacred and irreplaceable pictographs and petroglyphs, it continues to impact and threaten our People and the resources that we depend on as these contaminants move through the air, water, and soil.[9]

Though not occurring soon enough, the planned closures of the last two remaining coal-fired plants in Oregon and Washington — PGE Boardman and TransAlta — are enormous victories for the region and demonstrates the region's commitment to protecting human health and the environment. Given that we as a region rejected coal-fired plants, we must ask why then would we now allow and facilitate the export of up to 160 million tons of coal to be burned in China each year, only to have its harmful contaminants migrate back to pollute our region? The weekly increase of an additional 11 trains, 12 loaded barge tows from Port of Morrow to Port of Westward, and 3 Panamax ships moving through the Columbia River Basin to Asia from the proposed Coyote Islands Terminal alone, will greatly aggravate the detrimental air emissions and toxic pollutants in the CRG. The cumulative impacts from all 6 proposed coal export terminals would be catastrophic. Given the significant impacts that air pollutants from burning fossil fuels has on our People, cultural heritage and Treaty-reserved resources, it is imperative that the PEIS and project-specific EIS's quantify and analyze the effects of air emissions and associated acid deposition from the transport and burning of coal caused by the Coyote Island Terminal proposal and all others being considered in Oregon and Washington. Additionally, the Yakama Nation expects that transient coal dust from the transport and storage of coal at the transloading facilities will be quantified and its effects on human health and the environment will be fully analyzed.

D. Climate Change

Given all that we know about climate change – its causes and consequences – it is unconscionable to think that we as a country would accept building new infrastructure to export and facilitate the burning of up to 160 million tons of coal each year through ports in Washington and Oregon. This massive proposal is in direct conflict with the federal government's policies

[7] R. S. Sletten, "The Effects of Air Pollution on Rock Images in the Columbia River Gorge: A Sacred Breath Project of the Yakama Nation" (2011).

[8] See, Jaffee, D. A. & Reidmiller, D.R., "Now you see it, now you don't: Impact of temporary closures of a coal-fired power plant on air quality in the Columbia River Gorge National Scenic Area." Atmos. Chem. Phys. 9, 7997-8005 (2009); Jaffee, D.A. & Strode S., "Fate and Transport of Atmospheric Mercury from Asia." Journal of Environmental Chemistry 5(2), 121-126 (2008).

[9] R. S. Sletten, The Effects of Air Pollution on Rock Images in the Columbia River Gorge: A Sacred Breath Project of the Yakama Nation (2011); U.S. Environmental Protection Agency, Columbia River Basin: State of the River Report for Toxics (2009).

and commitment to reduce greenhouse gas emissions and to address and respond to climate change. Beyond policies, we as humans have a moral obligation to make every effort to stop the causes of climate change — such as burning coal — that has already had very real, profound impacts across the globe and especially upon indigenous people.

Climate change jeopardizes the Yakama Nation's traditional ways of life, especially the climate-change impacts upon water — both the quantity and quality — which, in turn, affects changes in flora and fauna in the region. Warming water temperatures associated with climate change have been shown to increase the levels of toxins in water bodies, thus increasing the amount of toxins that are taken up into fish and affecting human health. Research has shown specifically that the accumulation of methylized mercury in our fish and wildlife is linked to rising water temperatures in the Columbia Basin. This is only one example, among many, showing how climate change negatively impacts our people.

The transport and burning of 8.8 million tons of coal per year, as associated with the Coyote Island Terminal transloading facility alone, would have significant greenhouse gas emissions, thus contributing to and exacerbating climate change. The Yakama Nation expects that greenhouse gas emissions and climate change impacts associated with coal export through the Northwest will be quantified and analyzed, both independent of and in combination with all coal export facilities being proposed in Oregon and Washington. These analyses must consider all emissions from rail and barge shipments from Montana and Wyoming to Asia, operations at port terminals, as well as the burning of this coal in Asia.

E. Cultural Resources

Many known culturally sensitive sites are located along the rail routes and within close proximity to the proposed transloading facilities in both Washington and Oregon for the proposed coal transportation/exportation projects. The Yakama Nation is concerned that rail construction, increased barge traffic, and construction of the proposed transloading facilities will impact known archaeological sites, previously undocumented archaeological sites, and Traditional Cultural Properties.

The proposed Coyote Island Terminal is located within an area of extreme cultural sensitivity to the Yakama Nation. Prior to inundation by the dams, the Blalock Islands (including Coyote Island) were a river crossing and ancestral fishing area. Numerous burial sites, legendary sites, and village locations are known within close proximity to the proposed construction. The Coyote Island Terminal is within ¼ mile to the Coyote Island Burial Site, recorded as archaeological sites 45BN77. Though this site has been inundated by the backwaters of John Day Dam, potential impacts remain through construction, sedimentation changes during construction, construction-related dredging and filling, increased barge traffic over time, reservoir management changes required to accommodate increased shipping, and shipping accidents/spills. Further, many cultural sites similar to the Coyote Island Burial Site exist within close proximity and may be impacted by the proposed project.

The information provided regarding this Application is not sufficient to allow for examination of cumulative effects and impacts of this project on cultural resources over time. We request further information regarding the proposed life of the project, and information regarding the degree of dredge/fill operations for the construction area as well as dredge/fill of the shipping channel over time. Resources, though currently inundated, remain a high concern. Dredging/filling, will greatly impact cultural resources, fish habitat, ancestral fishing sites, Zone 6 Treaty Fishing Sites, and fishing sites throughout the upper and lower Columbia River in use today. We further request information regarding increased infrastructure requirements for overland transportation of coal to the Coyote Island Terminal; as such expansion will further impact these valued resources.

CONCLUSION

The Corps has a duty to ensure appropriate environmental analysis is completed on this Application before it moves forward in any respect. The Nation has considered both the environmental information and legal standards applicable here, and it is clear that a PEIS is warranted in this situation. We urge the Corps not just to take a "hard look" at this Application and its role in the broader plan for transforming our region into a coal hub. We request that you take your trust responsibility to the Yakama Nation seriously, and consider this Application in light of the decades upon decades of destructive waves that have decimated our culture, our people, and our land, water, and air, all advanced in the name of progress. As part of that trust responsibility, your agency has a duty under NEPA to demand a PEIS and a separate project-specific EIS that includes specific analyses of impacts this Application will have on the Yakama Nation. Additionally, your trust responsibility — in addition to federal regulations, policies, and various Presidential executive orders — requires the Corps to consult with the elected officials of the Yakama Nation on a government-to-government level. Thus, as a next step, please contact the Deputy Director of the Yakama Nation Department of Natural Resources to set up a meeting for the government-to-government consultation.

Sincerely,

Harry Smiskin
Yakama Tribal Council Chairman
Confederated Tribes and Bands of the Yakama Nation

Confederated Tribes and Bands
of the Yakama Nation

Established by the
Treaty of June 9, 1855

cc:

Governor Chris Gregoire, Washington State
Governor John Kitzhaber, Oregon State

Secretary Ken Salazar, U.S. Department of the Interior
Secretary Ray LaHood, U.S. Department of Transportation

Senator Patty Murray, U.S. Senate
Senator Ron Wyden, U.S. Senate
Senator Maria Cantwell, U.S. Senate
Senator Jeff Merkley, U.S. Senate

Congressman Norm Dicks, U.S. Congress
Congressman Peter DeFazio, U.S. Congress
Congressman Jim McDermott, U.S. Congress
Congressman Doc Hastings, U.S. Congress
Congressman Kurt Schrader, U.S. Congress
Congressman Adam Smith, U.S. Congress
Congressman Earl Blumenauer, U.S. Congress
Congressman Greg Walden, U.S. Congress
Congressman Rick Larsen, U.S. Congress
Congresswoman Cathy McMorris Rodgers, U.S. Congress
Congressman David Reichert, U.S. Congress
Congresswoman Jaime Herrera Beutler, U.S. Congress
Congresswoman Suzanne Bonamici, U.S. Congress

Lisa Jackson, U.S. Environmental Protection Agency
Dennis McClerran, U.S. Environmental Protection Agency
Steve Gagnon, U.S. Army Corps of Engineers
Samuel Rauch III, National Marine Fisheries Service
Will Stelle, National Marine Fisheries Service
Daniel Ashe, U.S. Fish & Wildlife Service
Robyn Thorson, U.S. Fish & Wildlife Service
Tom Tidwell, U.S. Forest Service
Kent Connaughton, U.S. Forest Service
Daniel Elliot III, Surface Transportation Board
Nancy Sutley, Council on Environmental Quality

Post Office Box 151, Fort Road, Toppenish, WA 98948 (509) 865-5121

Nez Perce

TRIBAL EXECUTIVE COMMITTEE
P.O. BOX 305 • LAPWAI, IDAHO 83540 • (208) 843-2253

By Electronic (Steven.K.Gagnon@usace.army.mil) Mail

May 3, 2012

Steve Gagnon
Regulatory Project Manager
U.S. Army Corps of Engineers
Portland District
PO Box 2946
Portland, OR 97208

Re: Nez Perce Tribe's comments on the March 6, 2012 Public Notice for Permit Application NWP-2012-56

Dear Mr. Gagnon:

The Nez Perce Tribe appreciates the opportunity to comment on the above-captioned Permit Application. The Tribe is concerned that this project may negatively affect Tribal treaty rights, ESA-listed fish and lamprey and their habitat, Tribal traditional use areas along the coal transportation corridor, tribal cultural resources, and Tribal member health arising from coal dust and diesel pollution. For the reasons below, the Tribe requests that the Corps prepare an Environmental Impact Statement under NEPA as part of its review of the project. The Tribe also requests government-to-government consultation with the Corps on this project consistent with Executive Order 13175, President Obama's November 2009 Memorandum on Consultation and Coordination with Tribal governments, and the Corps' implementing regulations.

Since time immemorial members of the Nez Perce Tribe have used and occupied the lands and waters of north-central Idaho, southwest Washington, northeast Oregon, and portions of western Montana for subsistence, ceremonial, commercial and religious purposes. In Article 3 of the 1855 Treaty with the United States, the Nez Perce Tribe reserved, and the United States secured, the right to take fish and at all usual and accustomed fishing places, and to hunt, gather and pasture on open and unclaimed lands. Treaty of June 9, 1855, with the Nez Perce Tribe, 12 Stat. 957 (1859). The waters within the Tribe's aboriginal territory continue to be used by the Nez Perce. Tribal members exercise their treaty-reserved rights, as well as observe ceremonial, cultural and religious practices within the Columbia River Basin, including usual and accustomed fishing places located within or adjacent to the project area on the Columbia River.

I. Project Description

According to the Public Notice, Coyote Island Terminals, LLC, and John Thomas, Ambre Energy North America are seeking a Corps Section 10 Rivers and Harbors Act permit to construct a new transloading facility for bringing coal in from Montana and Wyoming by rail and transferring it to barges on the Columbia River at the Port of Morrow. The purpose of the project is to "[s]hip coal mined from Wyoming and Montana overseas to Asia." The coal would be shipped down the Columbia to Port Westward and loaded onto ocean-going vessels to be shipped to Asia. Initially, approximately 3.85 million tons of coal would be shipped through the facility to Asia each year. At maximum capacity, the facility would be able to handle 8.8 million tons. That would translate to approximately 5 trains to Port of Morrow, 5.5 loaded barge tows from Port of Morrow to Port Westward, and one ship to Asia per week initially, increasing to 11 trains, 12 loaded barge tows, and three ships per week to Asia at full build out.

II. Comments

A. Impacts to Tribal treaty rights

The Tribe is concerned that this project will negatively affect tribal treaty rights. The Tribe reserves treaty-fishing rights at all usual and accustomed fishing places, including those places along the Columbia and Snake Rivers and their tributaries. As noted above, the permit application contemplates a significant increase in barge and rail traffic. The Tribe believes that the increase in barge traffic has the potential to directly interfere with tribal treaty fisheries. For example, drifting has become a major component of the commercial fishing in Zone 6 (between Bonneville and McNary Dams). Driftnetting downstream of the Port of Morrow would likely be affected by the increased barge traffic. In addition, the increased rail traffic may affect Tribal member access to usual and accustomed fishing places and other traditional use areas as well as interfere with Tribal member use of those places through increased noise disturbances, coal dust, and diesel pollution.

B. Impacts to ESA-listed fish and lamprey

According to the permit application, preliminary determinations indicate that the described activity may affect an endangered or threatened species or its critical habitat. There are several ESA-listed fish in the project corridor including Lower Columbia River Chinook Salmon ESU, Upper Willamette River Chinook Salmon ESU, Snake River Fall Chinook ESU, Columbia River chum salmon ESU, middle Columbia River steelhead DPS, and lower Columbia River steelhead DPS. These species are of critical importance to subsistence and culture of the Tribe.

In addition, lamprey, although currently are not a listed species, are also located in the project corridor.

C. Impacts to Tribal member health

Given the large amount of coal that is contemplated to be transported by barge and rail in connection with the project, the Tribe is very concerned of the project's potential impacts to Tribal member health. Coal dust and diesel emissions are known to cause respiratory disease, particularly affecting sensitive populations such as children and the elderly. In addition, the coal dust that settles on the water can have adverse environmental consequences to the river corridor.

Coal dust can affect natural biological processes and can potentially affect fish and other biota that reside in the rivers.

D. Indirect/Cumulative Impacts

Agencies conducting NEPA review must also consider the indirect effects of the proposed project. Indirect effects are those effects "caused by the [agency] action [that] are later in time or farther removed in distance, but are still reasonably foreseeable." 40 C.F.R. § 1508.8(b). Such effects "include growth inducing effects and other effects related to induced changes in the pattern of land use, population density or growth rate, and related effects on air and water and other natural systems, including ecosystems." *Id.*

Cumulative impacts are "the impact[s] on the environment which results from the incremental impact of the action when added to other past, present, and reasonably foreseeable future can actions regardless of what agency…or person undertakes such other actions. Cumulative impacts can result from individually minor but collectively significant actions taking place over a period of time. 40 C.F.R. § 1508.27(b)(7).

The Corps needs to analyze the indirect and cumulative effects associated with the increased barge and rail traffic the project will create. The Corps should analyze whether and how much dredging needs to occur on the river corridor to accommodate the increased traffic and how this dredging may affect the environment. In addition, the agency should assess the potential effect of accidents on the river caused by the increase in barge traffic. Finally, the Corps needs to analyze the cumulative effect of this project relative to the other coal export or similar projects that are proposed in the region.

E. Environmental Impact Statement

Given the potential impacts to tribal treaty rights, ESA-listed species, Tribal member health, and the indirect and cumulative effects that may result in Columbia River basin and the region, the Tribe requests that the Corps perform a full Environmental Impact Statement under NEPA. All of these issues cannot be properly assessed through an environmental assessment.

F. Conclusion

For the reasons above, the Tribe requests the Corps evaluate the project with an EIS so that a full exploration of the impacts of this controversial project can be thoroughly vetted. As part of this review, the Tribe looks forward to consulting with the Corps on a staff-to-staff and governmental basis before any formal action is taken on the proposal.

Please contact Mike Lopez, Nez Perce Tribal staff attorney, at (208) 843-7355 with any questions.

Sincerely,

Brooklyn Baptiste
Chairman

COLUMBIA RIVER INTER-TRIBAL FISH COMMISSION
729 NE Oregon, Suite 200, Portland, Oregon 97232 Telephone 503 238 0667
Fax 503 235 4228

May 7, 2012

Colonel John Eisenhauer
Commander, Portland District
U.S. Army Corps of Engineers
P.O. Box 2946
Portland, OR 972008-2946

RE: Public Notice for Permit Application, Coyote Island Terminals, LLC. U.S. Army Corps of Engineers No: NWP-2012-56

Dear Colonel Eisenhauer:

Since your arrival to the Portland district, I have truly appreciated the partnership and opportunities for collaboration between the U.S. Army Corps of Engineers (Corps) and the Columbia River Inter-Tribal Fish Commission (CRITFC) in the region's efforts to restore salmon and protect our member tribes' treaty fishing rights. The purpose of this letter is to provide CRITFC's comments regarding three project proposals to construct coal export terminals in the Columbia River Basin that threaten the forward progression of these efforts. Specifically, this letter includes our formal comments for one of the projects; the permit application for the Morrow Pacific Project.

CRITFC files these comments on behalf of its member tribes[1] and are in addition to the comments filed by the Yakama Nation and the Confederated Tribes of the Umatilla Indian Reservation, which are hereby incorporated by reference. The CRITFC tribes are very concerned about the Morrow Pacific Project because it will directly and negatively intrude on the tribes' exercise of their treaty fishing rights. The sparse information we currently have raises more questions than answers; it would be premature for the Corps to approve this permit application at this time. There are many other processes that need to occur before any approval is granted, and CRITFC recommends that the Corps suspend action on this permit application at this time.

Since time immemorial, the culture and livelihood of the Columbia River Basin tribes have been closely tied with the river. In the last century of modern development, this connection has been repeatedly broken. In 1977, the tribes resolved to restore fish to the

[1]The four member tribes are: the Confederated Tribes of the Umatilla Indian Reservation, the Confederated Tribes of the Warm Springs Reservation of Oregon, the Nez Perce Tribe, and the Confederated Tribes and Bands of the Yakama Nation. These tribes possess treaty rights to take fish that pass their usual and accustomed fishing places.

river and formed CRITFC to support and collaborate in their efforts to protect, promote, and enhance the anadromous fish resources consistent with their treaties. In the last decade, fish have been returning to the river in ever-increasing numbers and the tribes have been able to restore some of their traditional fisheries, but the balance is still fragile. Projects such as the Morrow Pacific Project will undoubtedly put more pressure on the fisheries and are a major step backward from the forward momentum of current efforts. If other projects proposed for the Columbia River, such as the "Longview Project" (proposed by Millennium Bulk Logistics) and the "St. Helens Project" (proposed by Kinder Morgan) are developed; the pressures on the Basin fish will be substantial. These projects will affect the tribes, and therefore, on behalf of our member tribes and in addition to the formal requests already made, CRITFC requests that the Corps to conduct formal government–to–government consultation on the effects of the Morrow Pacific Project as well as the effects of the other projects.

Environmental Justice and Public Interest

This project raises substantial environmental justice issues; the environmental and other costs will be significant, but the burden of the costs resulting from the projects will not be borne by those who will profit the most. The benefits of these proposals accrue to a only a few, that is, huge profits for large foreign and national coal companies coupled with the creation of few local jobs, whereas the larger burden and costs will be borne first by the tribal treaty fishers, their treaty fisheries, and all the small communities that line the Columbia River Gorge. The Treaty Tribes of the Columbia River Basin are tightly linked to the river, and throughout this century, they, and the salmon, have carried development on their backs. Over the past thirty years, the tribes have worked tirelessly to put fish back in the river with many successes. Approving the Morrow Pacific proposal – and any of the other coal export proposals – would be a significant step backwards for all those efforts.

The evaluation of a River & Harbors Act § 10 permit application must take into account the impacts to the public interest and will "reflect the national concern for both protection and utilization of important resources." Furthermore, the agency must weigh any benefits from the proposal against reasonably foreseeable detriments. Below we have listed several reasonably foreseeable impacts to our tribes and to the environment from the Morrow Pacific Project. It is clear from this initial list that the public interest would not in any way be served by approving this proposal; not in the short term and definitely not in the long term. In order to discuss these issues on a broad scale and in a transparent, open process, we request that the Corps hold public hearings on this application.

Environmental Review

As the Corps proceeds to the environmental review step in this process, on behalf of the tribes, we encourage the agency to prescribe a broad scope of review of the Morrow Pacific Project to include cumulative effects of both the construction of the dock at Port of Morrow as well as its connecting port at Port Westward. The current documents,

including the applicant's Biological Assessment, do not include very much information on the extent of work needed at the Port Westward site. Port Westward is within the Lower Columbia River Estuary and is near some particularly sensitive critical habitat for several salmonid stocks, including several listed as threatened or endangered under the Endangered Species Act (ESA). Restoration of habitat in the estuary is a key component to many of the anadromous fish processes in the Basin overseen by the National Marine Fisheries Service, or NOAA Fisheries.

CRITFC strongly recommends that the Corps initiate a programmatic environmental review to broadly analyze the other projects in the Basin, i.e., the Longview and the St. Helens projects. While each of these proposals will present unique circumstances, in the aggregate they create similar issues that will have profound detrimental effects to the tribes, the communities and the environment of the Columbia River.

Project proposals within the Northwest region, such as those proposed for Cherry Point, Grays Harbor Washington, and Coos Bay, Oregon, will also have synergistic effects on the Columbia River from increased train traffic to climate change effects.

Regulatory Review

Coal creates a myriad of ill effects on the environment in its removal, transport, and consumption. Of these, the transport and eventual consumption of this coal will create lasting and long-term effects on the Columbia River. Coal's characteristics and values vary according to where it is mined. Coal that is expected to be transported through the Columbia River will originate in the Powder River Basin, and is considered friable and volatile, e.g., easily broken down and easy to catch fire. While the proponent has argued that most of the coal dust "shakes out" within the first miles from its source, the reality is over the course of the long haul the coal will slowly break down into smaller pieces, creating more dust potential. Coupled with the gusty and intense Columbia River Gorge winds, coal dust is not some theoretical possibility, but a reality that tribal fishers have personally experienced with coal trains currently traversing the Gorge. Simply put, the current levels of coal dust are already unacceptable to tribal members living and working along the Columbia River and the railroad tracks that are immediately adjacent thereto. Increasing these impacts would be intolerable.

The Morrow Pacific Project attempts to address this issue by proposing fully enclosed storage and barging. However, the coal trains leading to the port are open. In addition, it is likely that coal dust will escape during the transfer process from the Port of Morrow site to the barge as well as the transfer between the barge and the panamax vessels at Port Westward. As noted in the letter from the U.S. EPA to the Corps (April 5, 2012), there is a potential for adverse effects in air quality from the airborne coal dust as well as the diesel used by the barges and ships.

Coal dust will also enter the river and effect water quality at both the Port of Morrow and Port Westward. While the biological impacts are not well-studied, coal's inherent

properties and the potential for fish ingestion is cause for concern. Since there are many questions and uncertainties, targeted analysis is needed before any permit is issued. We also encourage the State of Oregon to conduct a Clean Water Act section 401 water quality certification process for this project to examine the effects of the project on water quality.

The project will require extensive work in and over water, including building over 200 piles and adding 15,000 square feet of dock. Because of these additions to the Port, we recommend that the Corps require the applicant to apply for a Clean Water Act section 404 permit. While there are other docks at the site, this construction will bring new and expanded use to an area of navigable waters that will affect the flow of the river and will add new fill to the area.

This area is also within Traditional Cultural Property (TCP) designated land and is likely to have significant cultural resources. In addition, and as the application notes, there are ESA-listed aquatic species that migrate near and around the terminal. While the "Joint Permit Application Form" acknowledges these and other issues, it is clear that nothing has been addressed or reviewed in any detail, and none of CRITFC's member tribes have been consulted on any of these very important issues.

Treaty Fishing and Fishery Resources

In 1855, the CRITFC tribes signed treaties with the United States, peacefully ceding title to millions of acres of land in the Basin while reserving their rights to continue fishing at their usual and accustomed fishing places. The rights to access these sites have been fought for and preserved through the court system, and as a result, the tribes' treaty-protected right of access to usual and accustomed fishing grounds is firmly established as a matter of law.[2] After the construction of The Dalles Dam, and the subsequent flooding of Celilo Falls, the tribes and states agreed that the tribes would have exclusive access to commercial fishing in an area called "Zone 6", a section of the river extending from Bonneville to McNary dams. Tribal fishers conduct year-round subsistence, ceremonial and commercial fishing in that zone with fishing gear types regulated by the tribes but including hoopnets fished from platforms built by tribal members along the river and gillnets anchored to the shore or river bottom.

Shipping traffic has created many safety issues with gillnet fishers, and dock construction along the river has displaced fishing sites within Zone 6. The Port of Morrow is no different. Tribal members from the CRITFC tribes have fishers who lay their nets and make their livelihood within the Port of Morrow. There are numerous other sites within close vicinity up- and down-river from the Port as well. These are tribal people exercising

[2] The Supreme Court, and other federal courts, confirmed these rights in a number of cases. *See, e.g., Sohappy v. Smith,* 302 F.Supp. 899 (D.Or. 1969), *aff'd, United States v. Oregon,* 529 F.2d 570 (9th Cir. 1976); *Washington v. Washington State Commercial Passenger Fishing Vessel Ass'n,* 443 U.S. 658 (1979); *United States v. Winans,* 198 U.S. 371 (1905); *Confederated Tribes of the Umatilla Indian Reservation v. Alexander,* 440 F.Supp. 553 (D.Or. 1977).

their tribal treaty rights and projects such as the Morrow Pacific Project will directly and negatively interfere with the exercise of that right.

In addition to directly displacing fishing sites, the project brings concerns of increasing barge traffic by a magnitude of twenty-four barge trips each week. Barge traffic can interfere with fishing as well as be the leading cause of derelict nets, otherwise known as "ghost nets" in which nets are clipped and set adrift. These are very dangerous to aquatic creatures if left uncontrolled.

The Port of Morrow portion of the project is quite extensive and may harm the critical habitat that is designated near both parts of the project, i.e., Port Westward and the Port of Morrow. Before approving this permit application, the Corps needs to conduct significant environmental review, consult with the effected tribes, and initiate consultation with the resource agencies, NOAA Fisheries and U.S. Fish & Wildlife. Only after extensive review, analysis, and study, would it be appropriate to consider the permit application.

Climate Change and the Bigger Picture

Resource managers cannot make management decisions today without analyzing the potential for changes in the Earth's climate on the resources they are managing. There is no question that coal is a big problem on many levels and for many reasons with relation to climate change. Coal is the leading contributor to atmospheric carbon dioxide and will ultimately cause major effects to the Pacific Northwest. The environmental review needs to consider these potential effects and account for them.

Burning coal also emits significant amounts of mercury and fine particulates, which are known to travel across the Pacific via the "jet stream" from Asia and are deposited in Oregon, Washington, and California. Most of the industrial mercury in the Pacific Northwest comes from these global sources. In 2004, scientists from Oregon State University observed with instruments mounted atop Mount Bachelor's Summit Express ski lift an enormous Asian plume laced with mercury and ozone. The fine-particle concentration of this plume that had transited the Pacific Ocean was about 20 micrograms per cubic meter, compared with the federal air quality standard of an average 65 micrograms during a 24 -hour period. Oregon is already struggling to manage current levels of mercury pollution.

The coal proposed to be shipped through the Port of Morrow and the other proposed Northwest sites would add to this air pollution burden. The proposed development at the Port of Morrow and how it is evaluated by the reviewing agencies will ultimately be a reflection of the seriousness of United States government policy and commitments to reduce greenhouse gases and manage toxic pollutants. We believe that additional levels of air and water pollution associated with the project are not acceptable.

Conclusion

We appreciate your consideration of our comments and are available to answer any questions you have about our concerns. We also look forward to working with you on this project and expanding the analysis if possible. If you have any questions, please feel free to contact me or Julie Carter at 503-238-0667.

Sincerely,

Babtist Paul Lumley
Executive Director

Cc: Governor John Kitzhaber, State of Oregon
Governor Christine Gregoire, State of Washington
Lisa Jackson, Administrator, U.S. Environmental Protection Agency
Dennis McLerran, Administrator, Region 10, U.S. Environmental Protection Agency
Steve Gagnon, U.S. Army Corps of Engineers
J.R. Inglis, Tribal Liaison, Portland District, U.S. Army Corps of Engineers
Paul Cloutier, Tribal Liaison, Portland District, U.S. Army Corps of Engineers

Region 10 RTOC
Regional Tribal Operations Committee
"Tribes-RTOC-EPA: Working Together"
Port Graham Village Council, P.O. Box 5510 Port Graham, AK 99603
ph 907-284-2227 fax 907-284-2222 www.rtocregion10.org

May 15, 2012

Steve Gagnon
U.S. Army Corps of Engineers
P.O. Box 2946
Portland, OR 97208-2946

Kate Kelly, Director
Office of Ecosystems, Tribal and Public Affairs
U.S. Environmental Protection Agency
1200 Sixth Avenue, Suite 900
Seattle, WA 98101-3140

SENT VIA EMAIL

RE: Comments on Project No. NWP-2012-56 (Coal Terminal)

Dear Mr. Gagnon and Ms. Kelley:

This letter is sent on behalf of the Tribal Caucus members of EPA Region 10's Tribal Operations Committee ("RTOC"). This letter is not sent on behalf of EPA Region 10 or any employees of EPA, but solely tribal government representatives of the RTOC.

The intent of this letter is to express support for the April 5, 2012 letter submitted by EPA to the Corps urging that it thoroughly review the potential impacts of exporting large amounts of coal from Wyoming and Montana to Asia. As discussed by EPA, a project at Port of Morrow in Oregon has "the potential to significantly impact human health and the environment." The RTOC strongly agrees that the Corps should utilize the NEPA process to address overall impacts, including impacts to fisheries, cultural resources, the exercise of treaty-reserved rights, increases in greenhouse gas emissions, rail traffic, and mining activity on public lands. .

Given the magnitude of the coal export proposals associated with coal extraction in the Powder River Basin and the significant environmental and human health risks associated with these activities, the RTOC urges that the Corps join with other appropriate federal agencies and immediately begin the process of evaluating the cumulative impacts of coal extraction, shipping, export, and utilization in Asian power plants on human health and the environment through a comprehensive, programmatic Environmental Impact

Statement. This EIS must be completed prior to any decisions are made to permit shipping terminals or additional extraction.

In short, we believe that the Corps should consider the full scope of the impacts of coal to the environment.

The RTOC appreciates your consideration of these comments.

Sincerely,

/s/

Violet Yeaton
Region 10 RTOC
Tribal Caucus Co-chair

Cc: RTOC

Confederated Tribes *of the*
Umatilla Indian Reservation
Department of Natural Resources
Administration

46411 Timíne Way
Pendleton, OR 97801

www.ctuir.org ericquaempts@ctuir.org
Phone 541-276-3165 Fax: 541-276-3095

March 28, 2012

Steve Gagnon
Regulatory Project Manager
U.S. Army Corps of Engineers
Portland District
PO Box 2946
Portland, OR 97208

Submitted electronically to: Steven.K.Gagnon@usace.army.mil

Dear Mr. Gagnon:

The Confederated Tribes of the Umatilla Indian Reservation (CTUIR) Department of Natural Resources (DNR) appreciates the opportunity to comment on application NWP-2012-52. The CTUIR DNR has concerns that this project may impact Tribal treaty fisheries, nearby Tribal properties as well as traditional use areas, habitat and cultural resources along the rail transport corridors. Further, the CTUIR has concerns regarding the cumulative impacts of this project and others proposed in the area.

After careful consideration of the significant Tribal interests within our ceded, special use, and Tribally-owned lands, we recommend that the Corps of Engineers (Corps) undertake an Environmental Impact Statement (EIS). The EIS should include adequate information for the Corps and the CTUIR to make an informed judgment of the impacts to treaty rights, traditional use areas and other interests. We formally request consultation on a government-to-government basis concerning the impacts of this permit.

Due to the short timeframe for comments, DNR has prepared this letter documenting preliminary concerns. We look forward to working on this project with the Corps as the project develops and the National Environmental Policy Act (NEPA) documentation is prepared.

Fishing Site Impacts

The CTUIR holds treaty protected fishing rights at all usual and accustomed stations. These places include the Columbia River corridor and many of its tributaries. The proposed dock site is a usual and accustomed fishing station, but the overall project would also impact fishing stations downstream due to the increase in project related barge and train traffic.

The CTUIR worked with the Corps on the Willow Creek Barge Dock, NWP-2006-160. The revised Environmental Assessment, issued April 4, 2008, includes useful information regarding

the fishing issues presented by this application. The CTUIR intends to work with our Tribal fishermen to document their use of this area including timing and frequency.

The proposal also involves increasing the lockages on the Columbia River in Zone 6 between Bonneville and McNary dams. This increase would be between 550 and 1257 per year. However, it is unclear that there is an upper limit of barge lockages under the permit. Will there be a defined upper limit on the number of barge trips per year? Fishermen have reported that recently barges are entering areas where previously there was no barge traffic. This may be due to barge congestion or other factors. The Corps should quantify barge traffic on the Columbia and identify the potential impacts from increasing traffic at the dams. We note that 10 years ago there were roughly 1000 more lockages a year at the John Day dam. However, over the last 10 years fish runs have increased as have the number of fishermen and nets on the river. Documentation of barge/net interference over time would aid analysis of potential impacts.

Additionally, in 2008, the National Oceanic and Atmospheric Administration conducted a section 7 Endangered Species Act review of barge transport of baled municipal waste from Hawaii by way of barges up the Columbia River. This review was inadequate in many ways, not the least of which was the failure of NOAA to consult with the CTUIR. However, the review did analyze the impacts of the entire route of shipment of municipal waste from Hawaii to landfills in the northwest including ocean species impacts. Since the barges will be going to Asia, it is logical that NOAA be consulted regarding ocean impacts. Further, while the NOAA assessment determined there would be no impact to fisheries by the barges, that project included only 100 barges per year transporting garbage. This project has the potential for more than ten times that many barges. Analysis should also include potential barge accidents.

Cumulative Impacts

The shipment of hundreds of barges of coal down the Columbia River, coupled with other proposed projects such as the barging of municipal waste from Hawaii and the ZeaChem plant immediately adjacent to this project, necessitates analysis of the cumulative increase in barge traffic and the associated impacts. This impact will not just be on fishing sites or aquatic species, but traffic congestion on the river and the dam lockage infrastructure. The EIS would benefit from a discussion of the carrying capacity of the river for shipment of goods and materials.

Cultural Resources

In your February 27, 2012 email regarding this undertaking, you state, “The Corps believes this project will have No Effect to cultural resources based upon our review of available information. We reviewed Branch files and records, the latest published version(s) of the National Register, lists of properties determined eligible, and other appropriate sources of information in making our determination.” The CTUIR Cultural Resources Protection Program (CRPP) believes that finding is premature and incorrect.

Branch files should include site records for site 35MW13, which is both inundated by the John Day Reservoir and along the shoreline. This site has been recommended eligible for inclusion in the National Register of Historic Places. The proposed undertaking will certainly affect the site, and that effect will likely be adverse.

Branch files should also include a document by Teara Farrow and Thomas Morning Owl entitled *Addendum to the Identification of TCPs along Bonneville, The Dalles, and John Day Reservoirs*. This document was prepared for and submitted to the Corps Portland District in 2001. It identifies the Port of Morrow area as being located within Traditional Cultural Property 3. On what basis has your staff determined that the proposed undertaking will not affect this historic property?

Your email also describes the permit area as extending "from the Port of Morrow to Port Westward in light of increases in barge traffic due to the project." As you know neither the CTUIR nor the Advisory Council on Historic Preservation recognize Appendix C or the term "Permit Area" as being in compliance with National Historic Preservation Act (NHPA). To adequately address the permit application the CRPP will need a map of the area of potential effects (APE; including how far inland it extends) and a summary description of the potential effects the proposed undertaking will have on historic properties. This information will help us determine whether the proposed APE is appropriate. Please note that there are several parcels downstream on the Columbia River from the Port of Morrow which are held in trust for several tribes. Those parcels are overseen by Tribal Historic Preservation Offices (THPOs) rather than the State Historic Preservation Office (SHPO). Please make sure that you initiate consultation with the THPOs as well as the SHPOs for this undertaking.

In addition, as discussed below, the APE for this undertaking should include the rail transit, which passes adjacent to additional trust land and through additional traditional use areas. Information pertaining to changes in rail usage is necessary to assess the effects the proposed undertaking will have on those properties.

To conclude, the CRPP disagrees with your finding of effect for this undertaking and we require additional information regarding the APE. We look forward to further consultation to resolve these issues.

Air Quality

The CTUIR understands that much of the conveyance system for coal is going to be enclosed, limiting the release of coal dust. However, to what degree can/will the Corps mandate that the facility will not produce coal dust? Will there be air quality monitoring of all loading/offloading/transloading activities on the river? Will air releases of coal dust be reported? The CTUIR DNR requests a study documenting the impacts of coal dust release be conducted and the NEPA documentation identify release thresholds requiring environmental review. It is the hope of the CTUIR that there be as many protections as possible to prevent the release of

toxics into the river, including coal and coal dust. Additionally, information regarding air emissions of barge and rail traffic should be discussed.

Tribal Property

As noted above, the Area of Potential Effect/Permit Area impact analysis will be inclusive of the area between Port of Morrow and Port Westward, where the coal will be transloaded to the ocean-going barge. The CTUIR DNR recommends that the minimum area of the impact analysis should include both the transloading/barging activities as well as the associated rail transportation corridor traffic.

We are concerned about the associated rail transport impacts to Tribal properties, and traditional use areas. The CTUIR owns property near the applicant's proposed site. The property, referred to as Wanaket, has the Burlington Northern rail line along its southern boundary The property came into CTUIR ownership as one measure to specifically to mitigate for impacts to CTUIR treaty rights caused by the Corps and Bonneville Power Administration's hydropower impacts and operations. The CTUIR actively manages Wanaket for the preservation and enhancement of wildlife and related habitat purposes. Increased train travel will impact…?

Government-to Government Consultation

The CTUIR requests consultation on a government-to-government basis with the Corps on this permit. The Corps should provide adequate information to the CTUIR to make an informed analysis regarding its concerns and interests, as well including the CTUIR in the development of the NHPA and NEPA analysis of this permit.

Our designated staff member for coordination issues is our DNR Intergovernmental Affairs staff member, Audie Huber -- audiehuber@ctuir.org or (541) 429-7228.

Sincerely,

Eric Quaempts, Director
Department of Natural Resources

Cc: Chris Page, Corps Regulatory Archaeologist
Gail Celmer, Corps Division Archaeologist
Dennis Griffin, Oregon SHPO
John Pouley, Oregon SHPO

"AP-42 Continuous Drop Equation vs Stack Testing"

Southeastern Region IV Permitting Workshop
Tampa, Florida
May 9-11, 2007

Sterlin Woodard, P.E.
EPC-Hillsborough County

AP-42 Continuous Drop Equation vs Stack Testing

- *Why Is It Important?*
  - *Hillsborough County*
    - *7 Largest Port in United States*
    - *PM-RACT*
  - *Title V/PSD Applicability-PTE & Actuals*
    - *Rule 62-210(242)"Potential to Emit", F.A.C.-the maximum capacity of an emission unit or facility to emit a pollutant under its physical and operational design. Any physical or operational or operational limitation on the capacity of the emission unit or facility to emit a pollutant, including air pollution control equipment and restrictions on hours of operation or on the type or amount of material combusted, stored, or processed, shall be treated as part of its design if the limitation or the effect it would have on emissions is federally enforceable.*

AP-42 Continuous Drop Equation vs Stack Testing

- *Why Is It Important?*
  - *Title V/PSD Applicability-PTE & Actuals-*
    Rule 62-210.370, F.A.C. requires the use of the most accurate method:
    - *CEM*
    - *Mass Balance*
    - *EF based upon site-specific Stack Testing (eg. lb/ton)*
    - *Published EF directly applicable to the process*
    - *EF based upon a similar, but different process*

AP-42 Continuous Drop Equation vs Stack Testing

- *Started in 2000 with Permit 0570094-003-AC @ IMC Big Bend Facility in Hillsborough County*
  - *Scott McCann/Golder PM EF=0.00387 lb/ton using M=0.5%; U=1.3 mph from AP-42, Section 13.2.4 (AP-42 Continuous Drop Equation)*
  - *EPC Proposed PM EF-0.06 lb/ton from AP-42, Table 8.5.3-1 &*

    EAT Stack Test PM EF=0.05 lb/ton

AP-42 Continuous Drop Equation vs Stack Testing

- IMC agreed to PM Stack Test in June 2000
- Conducted by Dr. John Koogler on GTSP @ TP #3
- Results:
  - BH CE of 99%
  - PM EF of 0.01lb/ton for oiled GTSP
  - PM EF of 0.05 lb/ton for un-oiled GTSP
  - Permit 0570094-003-AC issued with 0.05 lb/ton un-oiled PM EF for each Transfer Point

AP-42 Continuous Drop Equation vs Stack Testing

- Continuous Drop Equation:
  AP-42, Section 13.2.4, Equation 1

$$PM = \frac{k(0.0032)(U/5)^{1.3}}{(M/2)^{1.4}} \text{(lb/ton)}$$

U= wind speed (1.3-15 mph)
M= moisture content (0.25-4.8%)
k=particle size multiplier (0.74 < 30 μm)
Silt Content Range:0.44-19%

- Predictive EF based upon dispersion modeling and Ambient PM monitoring. Only Measures up to PM_{30}

AP-42 Continuous Drop Equation vs Stack Testing

- Silt Content Missing From Continuous Drop Equation
  - No significant correlation with emissions
  - 200 Mesh Screen (ASTM-C-136) <= 75 µm
  - Typical Silt Content (AP-42 Table 13.2.4-1):
    - Limestone- 1.3%-1.9%
    - Coal-0.6%-4.8%
    - Fly Ash-78%-81%

AP-42 Continuous Drop Equation vs Stack Testing

- Stack Tests:
  - Based Upon EPA Method 1,2,4 and 5
  - Measures PM
  - Usually Well Designed Permanent Ventilation & Capture System
  - Permanent/Temporary Stack Sampling Platform

I. Phosphate Rock

A. AP-42, Section 13.2.4, Equation 1

$$PM = \frac{k(0.0032)(U/5)^{1.3}}{(M/2)^{1.4}} \text{(lb/ton)}$$

U= wind speed

M= moisture content

$$PM = \frac{0.74(0.0032)(8.4/5)^{1.3}}{(3/2)^{1.4}} = 0.0026 \text{ lb/ton}$$

B. CSX Ship Loading #7 BH, 11/15/97 Stack Test On 67 BPL Rock

$$PM = \frac{(6.07 \text{ lb/hr})}{(2500 \text{ tons/hr})} = 0.0024 \text{ lb/ton (controlled)}$$

PM = 0.24 lb/ton (uncontrolled) using 99% BH CE

Scale Factor = 92

*PM @ 1,000,000 tpy = 1.3 tpy vs 120 tpy

II. GTSP

A. AP-42, Section 13.2.4, Equation 1

$$PM = \frac{k(0.0032)(U/5)^{1.3}}{(M/2)^{1.4}} \text{(lb/ton)}$$

U= wind speed

M= moisture content

$$PM = \frac{0.74(0.0032)(8.4/5)^{1.3}}{(1.7/2)^{1.4}} = 0.006 \text{ lb/ton}$$

B. IMC Big Bend TP #3, 6/17-19/2000 Stack Test On GTSP

PM = 0.01 lb/ton (BH inlet controlled with DS)

PM = 0.05 lb/ton (uncontrolled) using 80% DS CE

Scale Factor = 8.3

*PM @ 1,000,000 tpy = 3 tpy vs 25 tpy

III. DAP

A. AP-42, Section 13.2.4, Equation 1

$$PM = \frac{k(0.0032)(U/5)^{1.3}}{(M/2)^{1.4}} \text{(lb/ton)}$$

U= wind speed

M= moisture content

$$PM = \frac{0.74(0.0032)(8.4/5)^{1.3}}{(1.7/2)^{1.4}} = 0.006 \text{ lb/ton}$$

B. CSX Ship Loading #7 BH, 5/22/03 Stack Test On DAP

$$PM = \frac{(0.23 \text{ lb/hr})}{(1815 \text{ tons/hr})} = 0.00013 \text{ lb/ton (controlled)}$$

PM = 0.065 lb/ton (uncontrolled) using 99% BH CE & 80% DS CE

Scale Factor = 10.8

*PM @ 1,000,000 tpy = 3 tpy vs 32.5 tpy

IV. AFI (Mono & Dicalcium Phosphate-Triple Super Phosphate)

A. AP-42, Section 13.2.4, Equation 1

$$PM = \frac{k(0.0032)(U/5)^{1.3}}{(M/2)^{1.4}} \text{(lb/ton)}$$

U= wind speed

M= moisture content

$$PM = \frac{0.74(0.0032)(8.4/5)^{1.3}}{(12/2)^{1.4}} = 0.00037 \text{ lb/ton}$$

B. Kinder Morgan-IMC Pt Sutton, 2/22/05 Stack Test On AFI

$$PM = \frac{(0.11 \text{ lb/hr})}{(684.9 \text{ tons/hr})} = 0.00016 \text{ lb/ton (controlled)}$$

PM = 0.016 lb/ton (uncontrolled) using 99% BH CE

Scale Factor = 43

*PM @ 1,000,000 tpy = 0.2 tpy vs 8 tpy

AP-42 Continuous Drop Equation vs Stack Testing

- *Not All Stack Tests Are Created Equal:*
  - *EPA Method 201A/5 using Temporary Ventilation & Capture System*
    - *Small 6 in Ducts*
    - *Usually S-Type Pitot Tube vs Required Standard Pitot Tube for Small Ducts (<12 inched in Diameter)*
    - *Vertical Traverses*
    - *Low Hood Capture Velocities*
    - *Low Duct Transport Velocities*
  - *EPA Method 201A/5 using Well Designed Permanent Ventilation & Capture System*
    - *Adequate Hood Capture Velocities-200-500 fpm (ACGIH Industrial Ventilation Manual & AP-40)*
    - *Adequate Duct Transport Velocities > 2000 fpm (ACGIH Industrial Ventilation Manual & AP-40)*

AP-42 Continuous Drop Equation vs Stack Testing

- Case Study-CEMEX
  - AP-42 Continuous Drop Equation=0.0011 lb/ton (U=5, M=2)
  - In response to an RAI, Conducted Stack Test @ Inglis
  - Based upon EPA Method 201 using Temporary Ventilation & Capture System (0.00087 lb/ton PM EF; M=7, S=0.7)
    - Small 6 in Ducts
    - S-Type Pitot Tube
    - Vertical Traverses
    - Inadequate Hood Design
    - Low Duct Transport Velocities < 1000 fpm
    - No VEs
  - Permit Issued-EPC Used Worst Case PM EF of 0.031 lb/ton (Uncontrolled AP-42 EF from Table 11.6-4 assuming 99% CE for BH & 90% CE for Water Spray)
  - *Scale Factor=28

AP-42 Continuous Drop Equation vs Stack Testing

- Case Study-Martin Marietta
  - Used AP-42, Table 11.19.2-2 for Crushed Stone 0.00014 lb/ton PM EF
  - AP-42 Continuous Drop Equation=0.0034 lb/ton (U=8.4, M=2.5)
  - Based upon EPA Method 201A/5 using Temporary Ventilation & Capture System @ MM North Carolina Facilities in mid 1990s
    - Small 6 in Ducts
    - S-Type Pitot Tube
    - Vertical Traverses
    - Inadequate Hood Design
    - Low Duct Transport Velocities < 1000 fpm
    - No VEs
    - John Richards,P.E.,Ph.D.-PM_{10}
  - Permit Denial/Issued-EPC Suggested Worst Case PM EF of 0.055 lb/ton (Granite with water spray @ 600 tph and M =0.29%)
  - *Scale Factor=393

AP-42 Continuous Drop Equation vs Stack Testing

- Conclusions:
  - AP-42 Continuous Drop Equation Grossly Underestimates PM emissions up to Several Orders of Magnitude
  - Previously Permitted Minor Sources May be Title V and/or PSD if throughputs are > 1,000,000 tpy
  - Developer of Continuous Drop Equation-High throughputs=Major Source

- Recommendations:
  - State-wide Consistency
    - Critically review the reasonableness of all EFs submitted in application
    - Compare EF vs Stack Test Data
    - Review Stack Test
    - Review the Ventilation & Capture System Design as part of PTE
  - State Sponsored Stack Testing

SCIENCE OF THE TOTAL ENVIRONMENT 407 (2009) 2461–2473

available at www.sciencedirect.com

ScienceDirect

www.elsevier.com/locate/scitotenv

Review

Native polycyclic aromatic hydrocarbons (PAH) in coals – A hardly recognized source of environmental contamination

C. Achten[a,b], T. Hofmann[a,*]

[a] University of Vienna, Department of Environmental Geosciences, Althanstr. 14, 1090 Vienna, Austria
[b] University of Münster, Department of Applied Geology, Corrensstr. 24, 48149 Münster, Germany

ARTICLE DATA

Article history:
Received 15 October 2008
Received in revised form
29 November 2008
Accepted 5 December 2008
Available online 4 February 2009

Keywords:
Native PAH
Bituminous coal
Hard coal
Sediment
Soil

ABSTRACT

Numerous environmental polycyclic aromatic hydrocarbon (PAH) sources have been reported in literature, however, unburnt hard coal/ bituminous coal is considered only rarely. It can carry native PAH concentrations up to hundreds, in some cases, thousands of mg/kg. The molecular structures of extractable compounds from hard coals consist mostly of 2–6 polyaromatic condensed rings, linked by ether or methylene bridges carrying methyl and phenol side chains. The extractable phase may be released to the aquatic environment, be available to organisms, and thus be an important PAH source. PAH concentrations and patterns in coals depend on the original organic matter type, as well as temperature and pressure conditions during coalification. The environmental impact of native unburnt coal-bound PAH in soils and sediments is not well studied, and an exact source apportionment is hardly possible. In this paper, we review the current state of the art.

© 2008 Elsevier B.V. All rights reserved.

Contents

1. Introduction . . . 2462
2. Reserves and production . . . 2462
3. Coal diagenesis and associated PAH formation . . . 2463
4. Coal classification . . . 2463
   4.1. Coal rank . . . 2464
   4.2. Types of fossil organic matter . . . 2464
   4.3. Coal maceral composition . . . 2464
5. Native PAH concentrations and distribution patterns: Occurrence and correlations with coal rank and type . . . 2465
6. Native hard coal-bound PAH in soils and sediments . . . 2467
   6.1. Unburnt coal particles in soils and sediments . . . 2467
   6.2. Identification, patterns and quantification of native PAH from unburnt coal particles in soils and sediments . . . 2469
7. Conclusions . . . 2470
References . . . 2470

* *Corresponding author.*
E-mail addresses: achten@uni-muenster.de (C. Achten), thilo.hofmann@univie.ac.at (T. Hofmann).

0048-9697/$ – see front matter © 2008 Elsevier B.V. All rights reserved.
doi:10.1016/j.scitotenv.2008.12.008

1. Introduction

Polycyclic aromatic hydrocarbons (PAH) comprise of many carcinogenic substances and are ubiquitous in the environment. The U.S. Environmental Protection Agency regulated 16 priority pollutant PAH (16 EPA-PAH) spanning from 2–6 condensed aromatic rings, which are commonly analyzed. The occurrence of PAH in soils and sediments is often correlated to pyrogenic non-point sources from incomplete combustion of (fossil) organic matter (Costa and Sauer, 2005; Lima et al., 2005; Müller et al., 1977; Suess, 1976). Point sources may originate from e. g. oil spills (Short et al., 2007), used motor oil (Stout et al., 2002b; Napier et al., 2008), or contaminated industrial sites such as manufactured gas plant sites (coal tar, coke) (Khalil and Ghosh, 2006; Saber et al., 2006; Stout and Wasielewski, 2004), sites of wood treatment with creosote (Murphy and Brown, 2005), aluminum production (Booth and Gribben, 2005) or steel works (Almaula, 2005). The occurrence of natural or industrially refined petrogenic PAH has been reported from crude oil/petroleum, naphtha, fuels, diesel, bunker C (marine) fuels and lubricating oil (Boehm et al., 1998, 2001; Short et al., 2007; Stout et al., 2002b; Wang and Fingas, 2006). Biogenic PAH such as retene (Simoneit et al., 1986), triaromatic triterpenoids/steroids (Tissot and Welte, 1978) or partially perylene (Meyers and Ishiwatari, 1993) have been identified.

Surprisingly, unburnt coal has rarely been considered as a PAH source in soils and sediments (Ahrens and Morrisey, 2005). In addition to sorbed PAH once being exposed to the environment, original hard coals from the seam can contain PAH up to hundreds and, in exceptional cases, thousands of mg/kg (Stout and Emsbo-Mattingly, 2008; Willsch and Radke, 1995). This neglect was expressed by Walker et al. (2005), who described coal as an unknown or unsuspected source of PAH. In coals of low rank, such as lignite, sub-bituminous coal or brown coal, significantly lower PAH concentrations were detected (e. g. 13 mg/kg EPA-PAH, Püttmann, 1988). Up to 30 mg/kg alkylnaphthalenes, but no EPA-PAH were observed by Bechtel et al. (2005). Their occurrence in brown coals is explained by degradation of pentacyclic angiosperm-derived triterpenoids (Püttmann and Villar, 1987; Tuo and Philp, 2005). In a sub-bituminous coal from the Wealden Basin at Zwischenahn, Germany, 243 mg/kg of total PAH and 14 mg/kg of EPA-PAH were detected (Radke et al., 1990). Kashimura et al. (2004) identified semi-quantitatively naphthalene, phenanthrene, anthracene, pyrene, chrysene, benzo[*a*]anthracene, perylene, benzo[*a*]pyrene, benzo[*e*]pyrene, benzo[*b*]chrysene, dibenzo[*a*, i]pyrene, dibenzo[*a*,*h*]pyrene, and coronene in Victorian brown coals from Australia. Other studies presented qualitative results only (Chaffee and Johns, 1982; Stout et al., 2002a).

Besides other environmental concerns regarding coal use and production, in theory their native PAH content could pose a risk to soils and sediments, however until today, no study clearly showed it. Whereas physical effects of coal dust on organisms have often been investigated (e. g. Ahrens and Morrisey, 2005 and references therein), less is known about chemical effects due to coal constituents such as PAH. The ecotoxicological impact of coal particles in soils and sediments has not yet been studied in detail (Ahrens and Morrisey, 2005, Chapman et al., 1996). It is well-known that non-native PAH and other hydrophobic contaminants present in the environment are effectively sorbed to simultaneously present coal particles (sink), which is explained by the strong sorption affinity, high sorption capacity, and slow desorption kinetics compared to other organic matter (Kleineidam et al., 2002; Wang et al., 2007; Yang et al., 2008a). However, little is known about desorption of native PAH from coal (Yang et al., 2008a,c and references therein).

Native PAHs in coal are of particular interest in environmental research since coal has been mined on a global scale for centuries at quantities reaching approx. 5 billion tons in 2005 (Thielemann et al., 2007). Unburnt coal particles can be released by open pit mining, spills during coal loading, and transport or accidents releasing coal into freshwater or marine systems (Fig. 1) (French, 1998; Johnson and Bustin, 2006; Pies et al., 2007). On industrial sites, coal is stored in stockpiles for the production of coke, gas or steam and is subject to erosion. Apart from coke and coal tar, manufactured gas plant sites are also known for present unburnt coal particles (Saber et al., 2006; Stout and Wasielewski, 2004). Recently, the addition of carbon particles like activated carbon and coke to reduce availability of organic contaminants has been discussed and investigated (Zimmerman et al., 2004; Werner et al., 2006; Brändli et al., 2008; Sun and Ghosh, 2008). Some of these materials may also contain PAH (e.g. coke) and add up to the total concentration present in sediments. In some areas, coal naturally eroded into aquatic systems from sedimentary rock outcroppings containing coal seams (Stout et al., 2002a). Finally, native and sorbed coal bound PAH may be relocated by colloidal/particulate transport of the coal particles themselves enhancing (or reducing) the mobility of hydrophobic organic contaminants (Hofmann 2002, Hofmann et al., 2003a, b; Hofmann and von der Kammer, 2008).

In this paper we focus on coal being a possible PAH source. The aim of this paper is to review the state of the art addressing the (1) characterization of PAH predominantly in hard coals/ bituminous coals, (2) the formation of PAH and influencing factors such as hard coal maturity and origin together with (3) the occurrence of hard coals and coal bound PAH in soils and sediments.

2. Reserves and production

Currently, the top eleven hard coal producing countries or countries with more than 10 billion tons of hard coal reserves are China, U.S.A., India, Australia, South Africa, Russia, Indonesia, Poland, Kazakhstan, Ukraine and Germany (World Coal Institute, 2007). Worldwide hard coal production has increased from less than 1 to 4.96 billon tons from 1900 to 2005 (Thielemann et al., 2007). The significance of coal as an energy source has recently been predicted to increase in the future (Massachusetts Institute of Technology, 2007). In 2004, China, the U.S.A. and India produced about 2, 1 and 0.4 billion tons of hard coal and held about 60, 100 and more than 80 billion tons of reserves, respectively. Australia, South Africa and Russia have reserves of about 40–50 billion tons of hard coal each and annual productions of less than 0.3 billion tons each. With a share of more than 70%, Australia is the largest

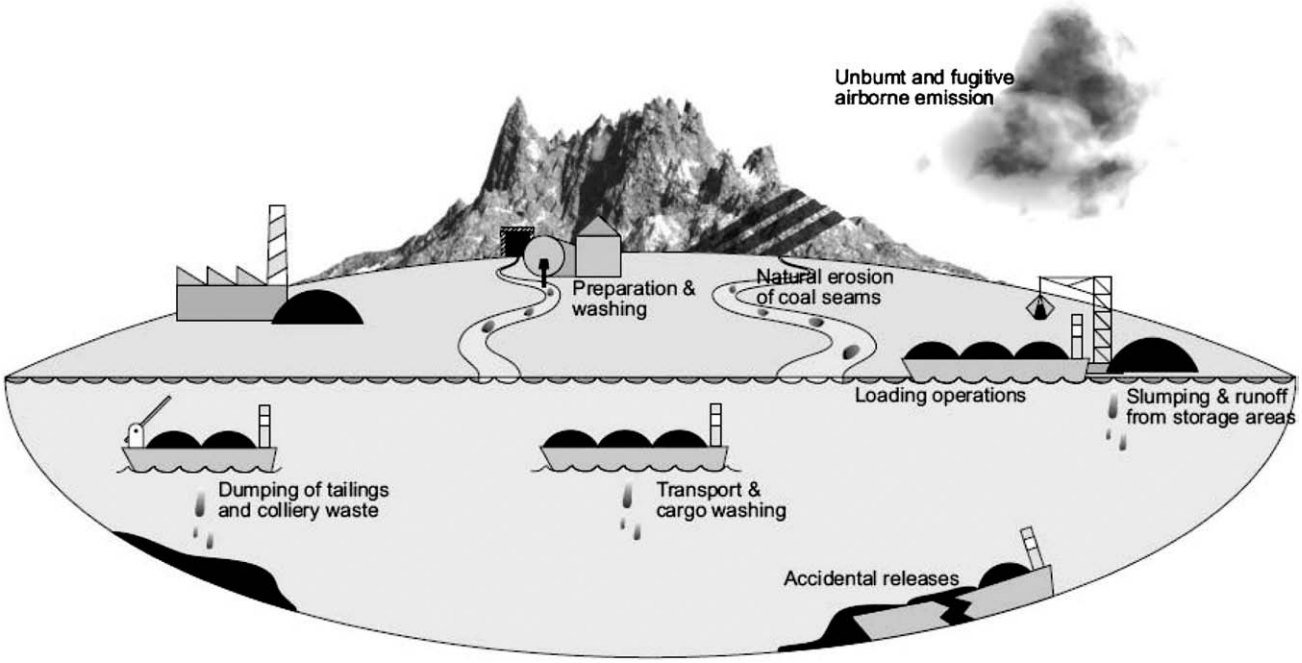

Fig. 1 – Coal emission sources to the aquatic environment (modified after Ahrens and Morrisey, 2005).

export country compared to 8%, 3% and no significant amounts of exports from the U.S.A., China and India, respectively (Max-Planck-Institut für Plasmaphysik, 2000; 2001a,b; 2002a,b). Due to the economic combination of large open pit mining near the East Coast and railway connections to several coal harbors, Australia is able to export 70% of the coal to Japan and other Asian countries and about 15% to Europe. Since the 1980s, the export of coal in Australia has doubled. In 1991, Russia was the largest hard coal exporting country worldwide, however since the break-up of the Soviet Union, the production and export numbers have reduced significantly.

3. Coal diagenesis and associated PAH formation

When remains of land plants, particularly peat, are buried, it is converted to coal by prolonged exposure to elevated temperatures and pressures in the subsurface. The concurrent physico-chemical changes are complex (Taylor et al., 1998). Generally, resistant plant biopolymers, e. g. lignin, are converted into highly aromatic, three-dimensional, network matrix in the order of increasing maturity: peat → lignite → sub-bituminous coal → bituminous coal → anthracite → graphite (Fig. 2). The proportion of conjugated aromatic rings per structural unit within the matrix determines the aromaticity and increases with increasing coalification, ultimately resulting in graphite. Dehydroxylation, demethylation and condensation reactions produce a relative increase in carbon combined with a decrease in oxygen and hydrogen as it is suggested in the van-Krevelen-diagram (Fig. 3, van Krevelen, 1993). Aromatic structures are commonly linked by ether or methylene bridges. Aliphatic side chains consist mainly of methyl, and less of ethyl, propyl or butyl functional groups. The average number of aromatic rings per structural unit in most coals is 3–5 (Stout et al., 2002b) with some individual units containing up to 10 rings. A typical hard coal is characterized by 2–6 PAH linked by methylene bridges with additionally bound aliphatic side chains and phenol functional groups. With increasing rank, aromatic units increase from 3–4 condensed rings at low rank to about 30 fused rings in anthracite. Concurrently, the lengths of side chains decrease.

In addition to the network structure, a multitude of small molecules, i.e. a 'mobile phase', is present within the network (Given, 1987) and is of particular environmental interest. These molecules can be released from the coal network more rapidly because they are less bound to the macromolecular matrix compared to the cross-linked molecules within the network. The type and rank of a coal influences the concentration and composition of the mobile phase, which is abundantly present in coals ranking within the oil generation window. The mobile phase is eliminated during hot steam treatment used for active carbon production from e. g. hard coal or charred coconut shells. During coal heating at manufactured gas plant sites, the linkages between some of the carbon units are cleaved, thereby releasing the conjugated aromatic rings into the mobile fraction (gas and coal tar).

4. Coal classification

Coal is being classified according to its various physico-chemical properties (van Krevelen, 1993). Due to the expected impact on the formation of PAH, we consider those classification systems, which are based on rank, types of fossil sedimentary organic matter and coal maceral composition.

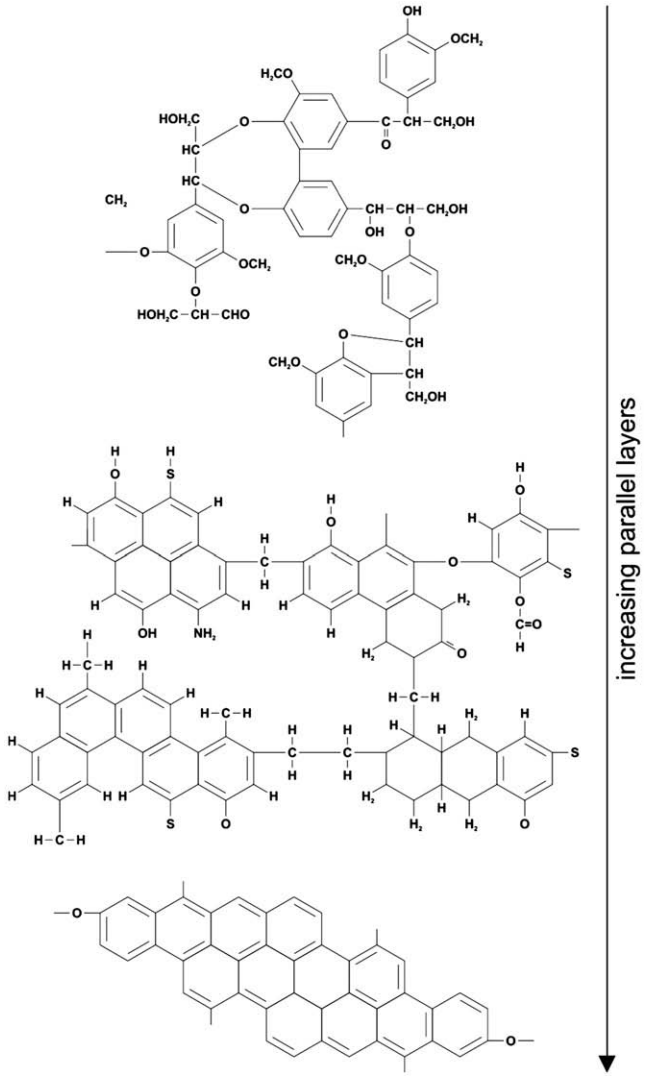

Fig. 2 – Small molecule sections of lignin (top), bituminous coal (middle) and anthracite (bottom) (modified after the College of Liberal Arts and Sciences, Western Oregon University, and after U.S., Lignin Institute, U.S.A.)

4.1. *Coal rank*

Volatile matter content, vitrinite reflectance (% R_o), carbon and water content, calorific value, hydrocarbon indices, temperature of maximum hydrocarbon formation during heating (T_{max}) and other factors (Tissot and Welte, 1978) are used to measure coal rank. Vitrinite reflectance is commonly used due to its stability over a wide range of coal rank, its abundance and independency on kerogen types or bitumen content (Stach et al., 1982). It is a measure of the percentage of light reflected from the vitrinite macerals at high magnification (×500) in oil immersion. Lignite is characterized by approx. 0.3% R_o, the transition zone from brown coal to hard coal is at approx. 0.65% R_o and from hard coal to anthracite approx. 2.2–2.5% R_o (Fig. 4). The oil generation window ranges from 0.5–1.3% R_o.

Various indices of parent and alkylated naphthalenes or phenanthrenes can also be applied. They are based on different stabilities of the alkyl functional groups at different positions on the molecules. The β-positions are more thermodynamically stable (e. g. 2- and 3-methylphenanthrenes) compared to the α-positions (e. g. 1- and 9-methylphenanthrenes) and their formation is preferred with increasing rank (Willsch and Radke, 1995). Trimethylnaphthalene ratios (TNR-1, TNR-2), methylphenanthrene ratio (MPR) (Radke and Welte, 1981), dimethylphenanthrene ratios (DPR-1, DPR-2), methylphenanthrene indices (MPI-1 and MPI-4) (Radke et al., 1982b; Radke et al., 1984; Willsch and Radke, 1995) and dimethylnaphthalene ratios (DNR-1 to -5) (Alexander et al., 1983, 1985) were described.

4.2. *Types of fossil organic matter*

Kerogen represents about 90% of the fossil organic carbon in sediments (van Krevelen, 1993). Three types can be recognized (Tissot and Welte, 1978); Type I is primarily derived from algal lipids (hydrogen-rich) and is mainly of aliphatic nature; Type II is primarily formed of marine plankton and bacteria (both exhibit a high gas and oil generating potential); Type III, the most common type of coal (humic coals, oxygen-rich) contains organic matter derived from terrestrial higher plants and exhibits a mostly aromatic nature. Its potential for oil generation is low. After successive alteration stages of diagenesis, catagenesis and metagenesis, finally, a chemically uniform product (graphite) is generated (Fig. 2).

4.3. *Coal maceral composition*

A classification system based on the fossilized plant remains (macerals) observed under the microscope is commonly used in coal research (Teichmüller, 1989). Three different maceral groups can be distinguished: (1) vitrinite, which may be considered the standard coalification product of woody tissue,

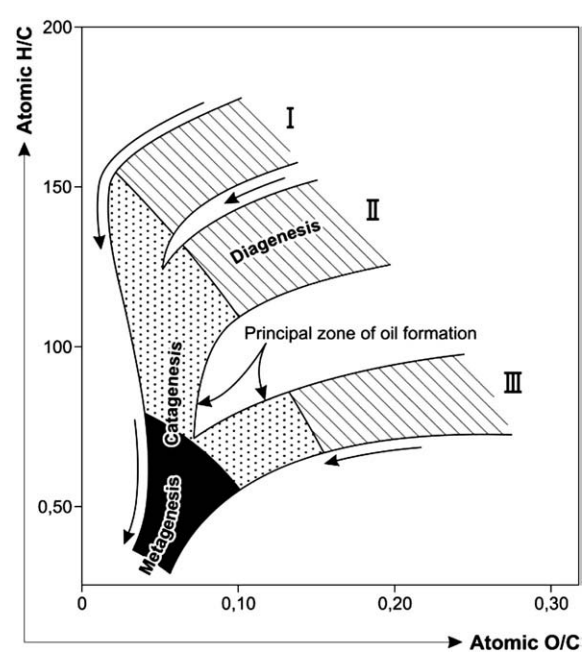

Fig. 3 – van Krevelen diagram (modified after van Krevelen, 1993).

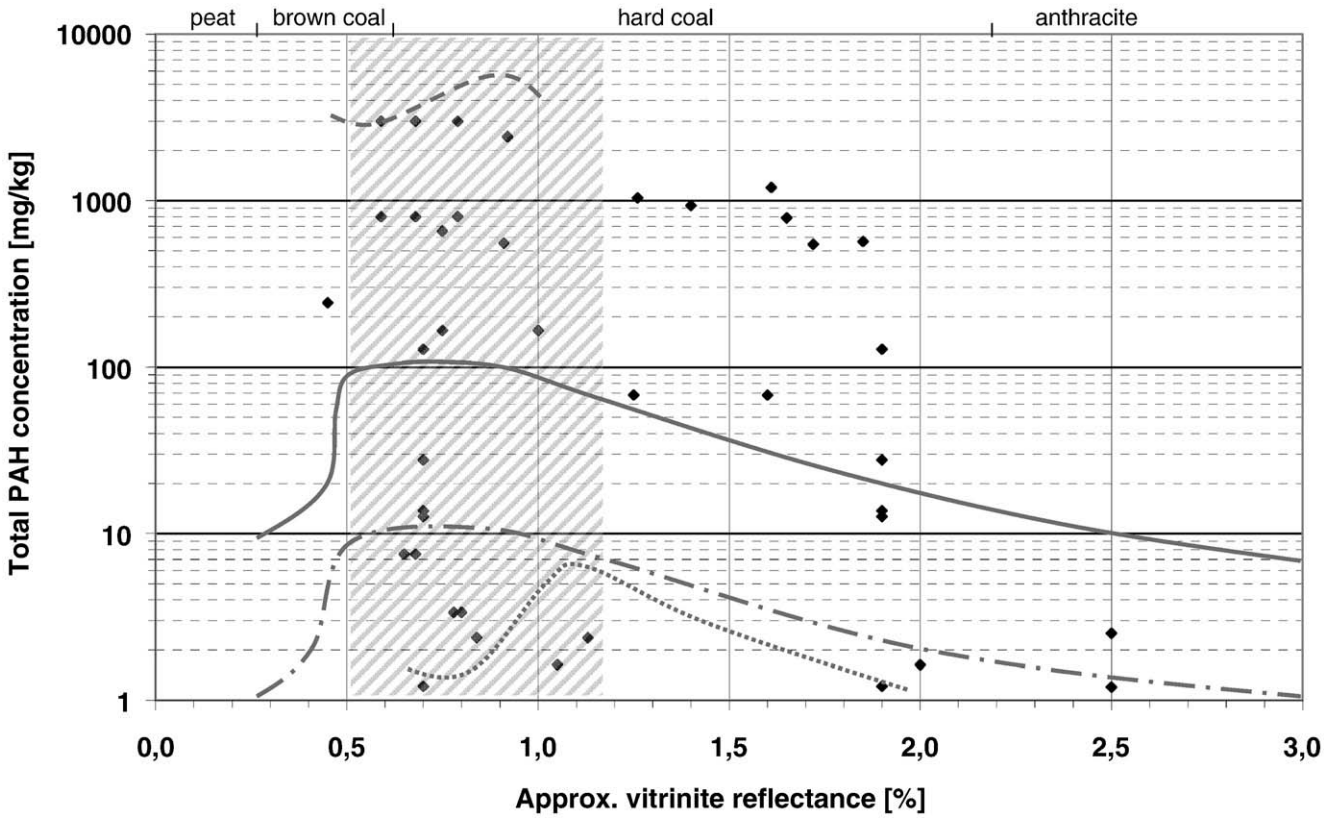

Fig. 4 – Total polycyclic aromatic hydrocarbon concentrations against coal rank of different coals. Dashed line: total aromatic hydrocarbons (Radke et al., 1990), solid line: total $PAH_{\Sigma 43}$ (Stout and Emsbo-Mattingly, 2008), dash-dotted line: EPA-PAH concentrations (Stout and Emsbo-Mattingly, 2008), dotted line: EPA-PAH concentrations (Zhao et al., 2000); (and data compiled from Chen et al., 2004; Pies et al., 2007; 2008a,b; Radke et al., 1990; Willsch and Radke, 1995; Van Kooten et al., 2002).

(2) liptinite, which has a higher hydrogen-content compared to vitrinite, and (3) inertinite, which shows a lower hydrogen-content compared to vitrinite. The maceral groups of vitrinite and liptinite form the reactive components in the carbonization and liquefaction processes of coal, whereas inertinite behaves as an inert additive (van Krevelen, 1993).

Macerals originating from woody and cortical tissues include the following (numbers in brackets refer to maceral groups):

- Vitrinite (with wooden structure: telinite, 1, without structure: collinite, 1),
- Fusinite (charred cell walls, characteristic maceral of fossil char coal, 3).

Macerals with a clear origin of plant material and other woody tissues include:

- Sporinite (fossil remains of spore exines, 2),
- Cutinite (constituent formed from cuticules, 2),
- Resinite (fossil remains of plant resins, 2),
- Alginate (remains of algae bodies, 2) and
- Sclerotinite (fossil remains of fungal sclerotia, 3).

The properties of different coals are strongly affected by the types and proportions of the various macerals present therein. The aromaticity of coal macerals in coals of different rank vary and at the same coal rank it decreases in the order inertinite > vitrinite > liptinite.

5. Native PAH concentrations and distribution patterns: Occurrence and correlations with coal rank and type

The presence of PAH in hard coals has been reported from several countries, e. g. Germany (76 samples) (Püttmann and Schaefer, 1990; Radke et al., 1982a, 1990; Radke and Welte, 1981; Willsch and Radke, 1995), Canada (34 samples) (Radke et al., 1982b; Willsch and Radke, 1995), U.S.A. (48 samples, including Alaska) (Hayatsu et al., 1978; Kruge, 2000; Kruge and Bensley, 1994; Stout et al., 2002a; Van Kooten et al., 2002; White and Lee, 1980; Zhao et al., 2000; Stout and Emsbo-Mattingly, 2008), Japan (3 samples) (Radke et al., 1990), France (1 sample) (Kruge, 2000), China (5 samples) (Chen et al., 2004; Tang et al., 1991) and Brazil (1 sample) (Püttmann, 1988). However, many studies present qualitative results only. A summary of the limited published quantitative PAH data available (Table 1) shows that concentrations vary widely, from 1 to about 2500 mg/kg. PAH in a sample set of several hard coals from international large coal basins are currently studied (Micic et al., 2007).

Detected compounds include 16 EPA-PAH, benzo[*e*]pyrene, perylene, coronene, and their alkylated derivatives (Püttmann, 1988; Van Kooten et al., 2002; Willsch and Radke, 1995), as well

Table 1 – Summary of total and 16 EPA polycyclic aromatic hydrocarbon concentrations in coals

	Total PAHs [mg/kg]	EPA-PAHs [mg/kg]	References
High volatile bituminous coal A, Elmsworth gasfield, 10-11-71-11W6, Canada	2429.1	152.1	Willsch and Radke (1995)
High volatile bituminous coal A, Elmsworth gasfield, 10-03-70-10W6, Canada	2412.3	136.6	
Medium volatile bituminous coal, Ruhr basin, Osterfeld, Germany	1037.2	153.3	
Medium volatile bituminous coal, Ruhr basin, Hugo, Germany	933.8	123.6	
Low volatile bituminous coal, Ruhr basin, Westerholt, Germany	1200.7	163.9	
Low volatile bituminous coal, Ruhr basin, Blumenthal, Germany	786.5	155.4	
Low volatile bituminous coal, Elmsworth gasfield, 06-19-68-13W6, Canada	546.4	98.6	
Low volatile bituminous coal, Ruhr basin, Haard, Germany	567.7	154.8	
High volatile bituminous coal, Wealden Basin, Nesselberg, Germany	656.2	43.1	Radke et al. (1990)
High volatile bituminous coal, Wealden Basin, Barsinghausen, Germany	554.4	56.7	
High volatile bituminous coal, Saar, Ensdorf, Germany	165.9	50.5	
Medium volatile bituminous coal, Germany	68.0	22.4	Pies et al. (2007)
Bituminous coal, Germany	127.6	28.7	
Lignite A, Northern Great Plains, Beulah, USA	8.5 [a]	1.2	Stout and Emsbo-Mattingly (2008)
Lignite A, Northern Great Plains, Pust, USA	6.5 [a]	1.0	
Sub-bituminous coal C, Northern Great Plains, Smith-Roland, USA	12.0 [a]	0.1	
Sub-bituminous coal C, Gulf Coast, Bottom, USA	14.0 [a]	1.6	
Sub-bituminous coal B, Northern Great Plaines, Dietz, USA	14.0 [a]	0.8	
Sub-bituminous coal B, Northern Great Plaines, Wyodak, USA	5.4 [a]	0.3	
Sub-bituminous coal A, Rocky Mountains, Deadman, USA	12.0 [a]	1.5	
High volatile bituminous coal C, Rocky Mountains, Blue, USA	77.0 [a]	5.3	
High volatile bituminous coal B, Eastern Coal, Ohio #4A, USA	60.0 [a]	8.2	
High volatile bituminous coal A, Rocky Mountains, Blind Canyon, USA	78.0 [a]	4.4	
High volatile bituminous coal A, Eastern Coal, Pittsburgh, USA	76.0 [a]	11.0	
Medium volatile bituminous coal, Rocky Mountains, Coal Basin M, USA	29.0 [a]	1.8	
Low volatile bituminous coal, Eastern Coal, Pocahontas #3, USA	20.0 [a]	3.8	
Semianthracite, Eastern Coal, PA Semi-Anth. C, USA	5.9 [a]	2.1	
Anthracite, Eastern Coal, Lykens Valley #2, USA	0.2 [a]	<0.1	
High volatile bituminous coal, Blind Canyon, USA	78.3	–	Stout et al. (2002b)
High volatile bituminous coal C-1, USA	7.5	0.5	
High volatile bituminous coal C-2, USA	3.4	0.4	
High volatile bituminous coal C-3, USA	2.4	0.3	
High volatile bituminous coal B-1, USA	1.6	0.3	
High volatile bituminous coal B-2, USA	12.7	2.4	
High volatile bituminous coal A-1, USA	13.7	5.4	Zhao et al. (2000)
High volatile bituminous coal A-2, USA	27.6	6.4	
Low volatile bituminous coal, USA	1.2	0.3	
Anthracite, China	2.5	1.8	Chen et al. (2004)
Bituminous coal, Brazil	13.0	–	Püttmann (1988)

[a] Sum of 43 PAHS.

as retene, methylated chrysenes, methylated picenes, tetrahydrochrysenes, hydropicenes and methylphenanthrenes in coals ranging from lignite to anthracite (Barrick et al., 1984).

Recently, 15 coal samples of different rank from the U.S.A. were analyzed for PAH concentrations and source characterization of coal (Stout and Emsbo-Mattingly, 2008). Low concentrations of 16 EPA-PAH from 0.035–11 mg/kg were observed with a mean of 3 mg/kg. Concentrations ranging from 0.18–78 mg/kg with a mean of 30 mg/kg were reported for 43 PAH compounds. Highest concentrations occurred in high volatile bituminous coals.

Considering the chemical processes during coalification, a systematic relationship between PAH concentrations and coal maturity is expected. In Fig. 4, total PAH concentrations from the literature are plotted against corresponding coal rank and no correlation can be deduced. However, if coals of similar origin are considered, the maximum total aromatic hydrocarbon yield (Radke et al., 1990) and maximum EPA-PAH concentrations (Zhao et al., 2000) were observed at 0.9% R_o and 1.1% R_o, respectively. Both measurements lie within the oil generation window. Stout et al. (2002b) and Stout and Emsbo-Mattingly (2008) observed maximum PAH concentrations in coals of about 0.5–0.9% R_o. Raises of PAH concentrations up to 1.1% R_o is explained by increasing condensation, carbon concentration and aromatization of coal with increasing maturity (Suggate and Dickinson, 2004). However, at high rank (>1.1% R_o) an increase of the polyaromatic compounds with more than 6 condensed rings may occur, at least partially, at the expense of 2–6 ring PAH due to rearrangement and fragmentation reactions. This process may be responsible for decreased total PAH (2–6 ring) concentrations in e. g. anthracite (Chen et al., 2004).

Not only PAH concentrations but also PAH patterns change with increasing rank. Sub-bituminous coals contain PAH, predominantly in the form of chrysene, picene and their alkylated derivatives. During coalification, PAH patterns change because primary products of higher thermodynamic stability are generated at the expense of less stable compounds. At the boundary between sub-bituminous/high

volatile bituminous coal (or brown/hard coal), distinct low molecular weight aromatic compounds are generated. Bi- and tricyclic PAH are formed mainly in the high volatile bituminous coal stage and provide a pattern of compounds showing a structural relationship to natural precursor molecules, e. g. phenanthrene derivatives, which are thought to be derived from plant resins and steroids (Püttmann and Schaefer, 1990). With increasing maturity, a shift occurs in the PAH pattern from high concentrations of naphthalene and its alkylated derivatives at low hard coal rank to a relative increase of 4–6-ring PAH at high rank (Ahrens and Morrisey, 2005). Simultaneously, the oxygen content is lowered, which results in lower concentrations of hydroxylated aromatic compounds, such as phenols, which are most prevalent in lignite. Due to rearrangement and fragmentation reactions at increasing rank, aromatic hydrocarbons are no longer directly derived from biological precursors. Similar distribution patterns compared to those of other coals of comparable rank occur and the individual PAH patterns of coals become less complex (Püttmann and Schaefer, 1990).

The changes in PAH patterns with increasing rank are shown in Fig. 5. At low hard coal rank (R_o<1%, Fig. 5a), C_0–C_4 alkylnaphthalenes (up to about 30%) are the dominant PAH group. C_0–C_3 alkylphenanthrenes rank second and typically comprise <10% of total PAH. Retene is present up to about 25%, whereas C_1+C_2 alkylfluorenes and methylfluoranthenes are only detected at low concentrations (up to about 2% each). Other PAH, if present, only occur at trace concentrations. With increasing rank (R_o=1.26–1.65%, Fig. 5b), the C_0–C_3 alkylnaphthalenes dominance is diminished, and C_4 alkylnaphthalenes and retene are no longer detected. In contrast, the phenanthrene dominance often increases with concentrations >10% of the total PAH present. C_1+C_2 alkylfluorene and methylfluoranthene concentrations increase, often reaching about 5% of the total aromatic hydrocarbons. Generally, higher molecular weight PAH concentrations are increased compared to those observed at lower hard coal rank, and C_0+C_1 alkylchrysenes and isomers are present up to about 4%. Significant increases in higher molecular weight PAH occur at high rank such as anthracite (R_o>2.5%, Fig. 5c). Here, naphthalenes are not present and the dominance of parent PAH and methylphenanthrenes is observed in the single reported sample. Higher molecular weight PAH such as benzo[*e*]pyrene and benzo[*b*]fluoranthene are detected at >10% each and coronene at >2%. The degree of alkylation of aromatic hydrocarbons decreases with increasing coal rank from low volatile bituminous coal to anthracite. In summary, a shift from alkylated bi- and tricyclic PAH at lower hard coal rank to higher molecular parent compounds in anthracite has been observed, which is in accordance with increasing carbon concentration and aromatization during the coalification process. Apparently, PAH patterns shift with increasing rank from a "bell-type" shape (C0-C4 naphthalenes and phenanthrenes) to a "slope-type" shape which is commonly known to be typical of a pyrogenic PAH origin.

Correlations between PAH distributions and the original organic matter type of coals are expected, since different coal macerals can produce different mixtures of aromatic compounds. For example, liptinites are known as sources for naphthalenes or vitrinite for biphenyls (Tang et al., 1991). Kruge (2000) observed correlations between dibenzothiophenes/-furans and dimethylphenanthrenes as an indicator for organic matter type I, II or III.

6. Native hard coal-bound PAH in soils and sediments

6.1. *Unburnt coal particles in soils and sediments*

The presence of unburnt coal particles has been reported from marine and freshwater sediments, as well as soils. In the marine environment, the *Exxon Valdez* oil spill in Alaska, U.S.A., triggered detailed discussion whether PAH in sediments of Prince William Sound originated from the spill or from naturally outcropping coal seams near the shore (Boehm et al., 2001; Short et al., 1999). In coastal sediments, coal particles in some cases reached sizes of some tens of centimeters in diameter, e. g. at Katalla beach. Earlier, Tripp et al. (1981) concluded that unburnt coal can be a significant source of sediment hydrocarbons in the coastal marine environment. Barrick et al. (1984) correlated hydrocarbons from 16 Western Washington coals to sediment samples from Puget Sound and Lake Washington.

Estuaries in the vicinity of mining activity can be impacted by coal emissions as reported from the Severn Estuary, Great Britain, where coal mining dates back to the mid-16th century (French, 1998). Intertidal mudflat sediments are estimated to hold around 10^5–10^6 tonnes of coal. Coal emissions into sediments were reported from harbors such as Hamilton Harbour (Curran et al., 2000) and Roberts Bank coal terminal, both in Canada (Johnson and Bustin, 2006). Coal particles present in sediments made up 10.5 to 11.9% dry weight of the soil mass in the vicinity of coal-loading terminals and was reported as non-hydrolysable solids. An increase of the coal concentration in the uppermost 2–3 cm within about 3 km^2 was observed from 1.8% to 3.6% during the time from 1977 to 1999 (Johnson and Bustin, 2006).

In freshwater sediments and floodplain soils, unburnt coal particles were identified at the Lippe (Klos and Schoch, 1993), Saar and Mosel rivers, Germany, due to former coal mining (Hofmann et al., 2007; Pies et al., 2007, 2008a; Yang et al., 2007). Hard coal particle concentrations of the heavily coal-impacted floodplain soil samples were in the range of 45–74 vol.% of the light fraction (the fraction with a density <2 g/cm^3, predominantly organic carbon). PAH concentrations of the light fractions in the samples ranged from 370–460 mg/kg (sum of EPA-PAH, 1- and 2- methylnaphthalenes) dry weight and thereby contributed 89.9% to the total (sum of EPA-PAH, 1- and 2- methylnaphthalenes) sediment PAH content (Yang et al., 2008b).

In soils, unburnt coal particles and elevated hydrocarbon concentrations were identified in dust and soil samples from the Ojców National Park, Poland (Schejbal-Chwastek and Marszalek, 1999). During the coal combustion process, fly ash notably still contains unburnt coal particles at low concentrations (Külaots et al., 2004; Lopez-Anton et al., 2007). These are not commonly investigated in soils and sediments. It cannot be excluded that native PAH from co-emitted unburnt coal particles contribute to health issues resulting from coal combustion linked emissions (Liu et al., 2008; Tremblay, 2007). For example, in China, since 2001 an increase

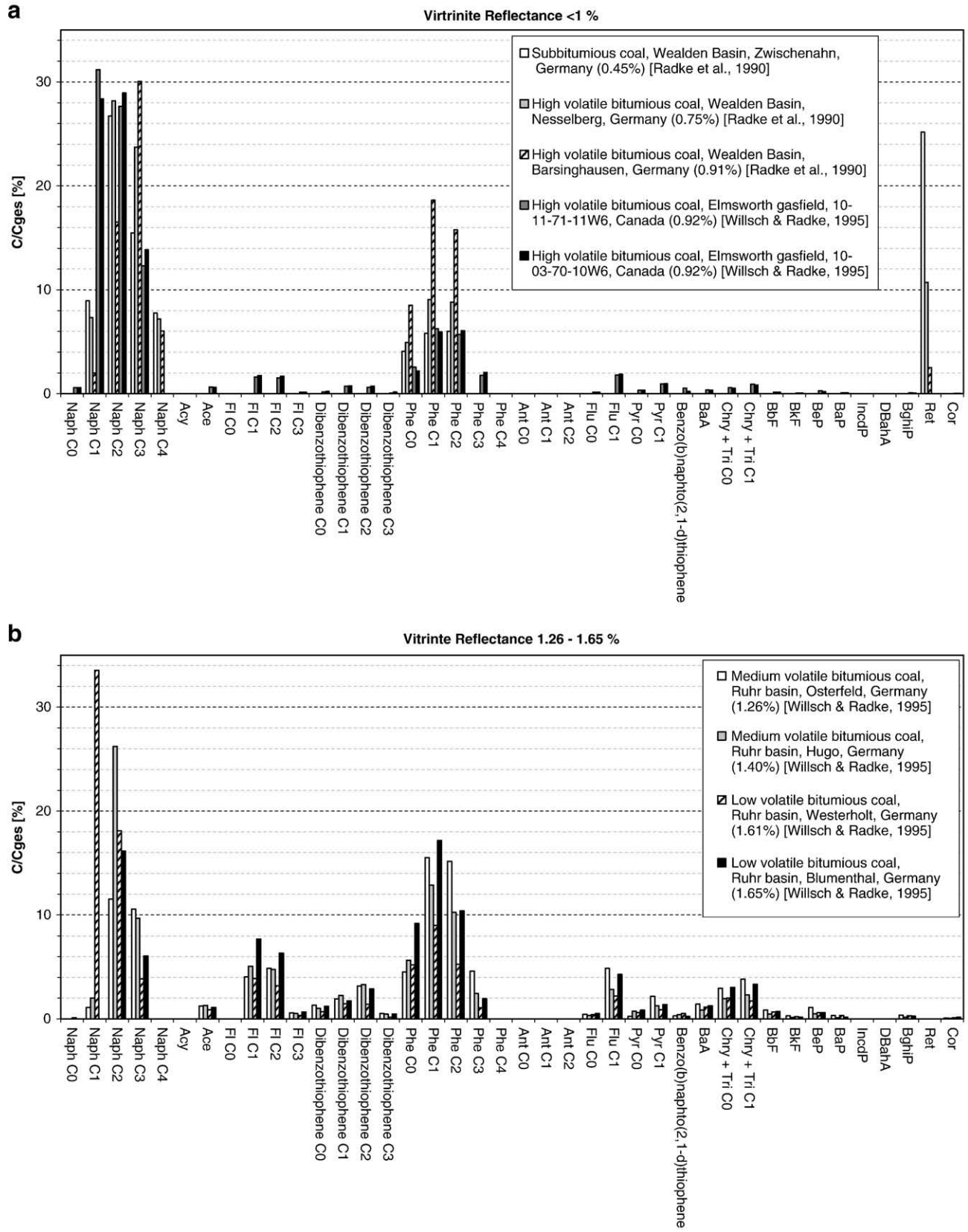

Fig. 5 – Total polycyclic aromatic hydrocarbon patterns at different coal ranks: a) <1% vitrinite reflectance (R_o), b) 1.26–1.65% R_o, and, c) >1.7% R_o; Naph: naphthalene, Acy: acenaphthylene, Ace: acenaphthene, Fl: fluorene, Phe: phenanthrene, Ant: anthracene, Flu: fluoranthene, Pyr: pyrene, BaA: benzo[*a*]anthracene, Chry + Tri: chrysene and triphenylene, BbF: benzo[*b*] fluoranthene, BkF: benzo[*k*]fluoranthene, Bep: benzo[*e*]pyrene, Bap: benzo[*a*]pyrene, Incdp: indeno[*1,2,3-cd*]pyrene, BghiP: benzo[*g,h,i*]perylene, Ret: retene, Cor: coronene, C0: parent compound, C1–C4: C_1–C_4 alkylated derivatives.

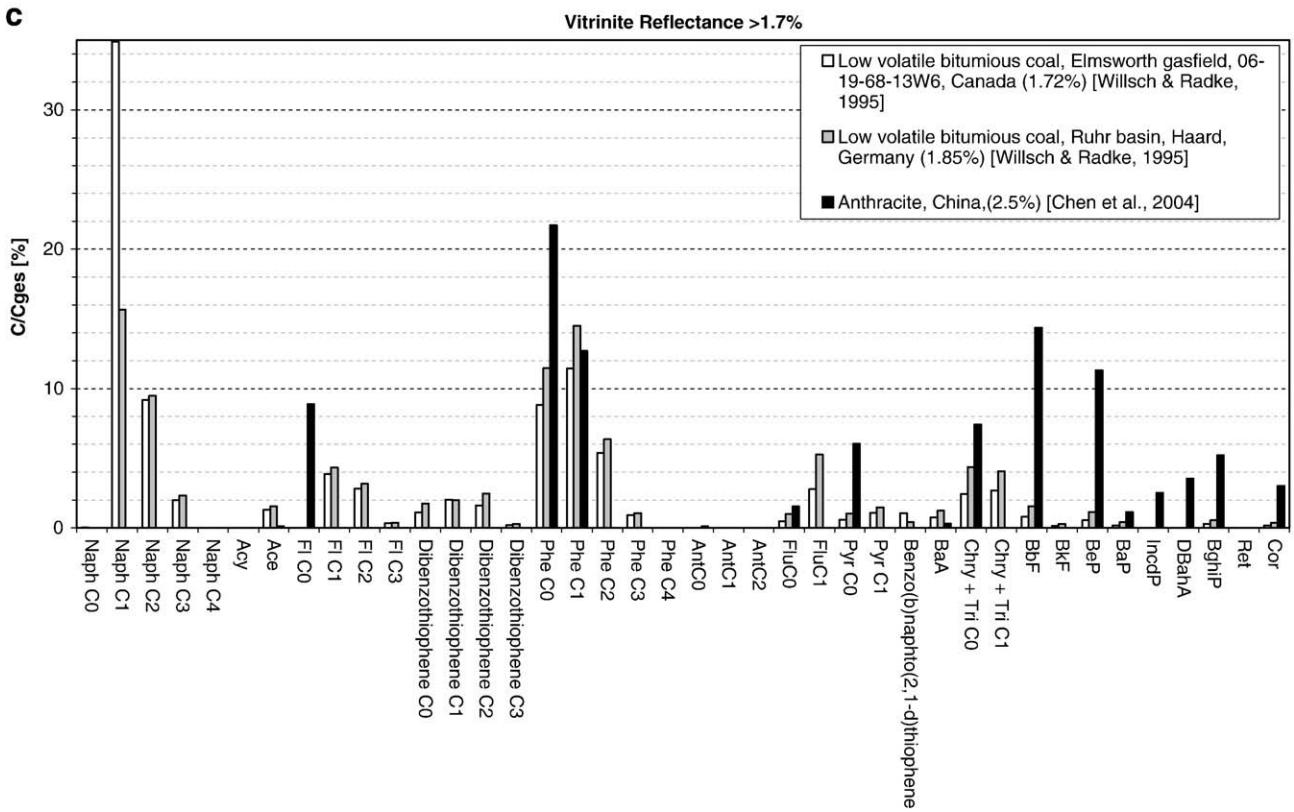

Fig. 5 (*continued*).

of 40% in birth defects was reported in regions of intensive coal mining and burning, i.e. in Shanxi Province. However, no statistical significance was detected between malformations during early embryogenesis and distance from coal plants (Gu et al., 2007).

Several investigations on emitted unburnt coal particles from opencast mining have been reported from India: Jharia coalfield (Ghose and Majee, 2000a,b), Raniganj coalfield (Singh and Sharma, 1992), Manuguru coal belt area of Andhra Pradesh (Sekhar and Rao, 1997) and Lakhanpur area of Ib Valley coalfield (Chaulya, 2004). In the Block II opencast project at the Jharia coalfield, different emission sources were quantified. Based on the project holding coal reserves of 37 Mt occupying 674 ha of land, an estimated total amount of 9368 kg/day of coal dust is emitted mainly due to mining activities and wind erosion of the exposed area (Ghose, 2007). The predominant emission sources were the crushing and feeding point for size reduction (40%), the unloading point of the conveyor belt (31%), wind erosion of the total area (17%), transportation on haul road (5.2%), loading into dumper (3%) and onto the conveyor belt (2%). Also, in the Manuguru coal belt area of Andhra Pradesh, an increase in coal emissions in recent years was observed (Sekhar and Rao, 1997).

6.2. *Identification, patterns and quantification of native PAH from unburnt coal particles in soils and sediments*

Unburnt coal particles in soils and sediments can be identified by coal petrography (Ligouis et al., 2005; Taylor et al., 1998; Yang et al., 2008b). However, since the method is complex and time-consuming it is seldom resorted to. In the coal mining area of Ruhr-Lippe, Klös and Schoch (1993) could correlate different historical periods of low coal-production due to an economic crisis to reduced PAH concentrations found in age-dated sediments. However, it was not investigated whether the PAH emissions originated from coal combustion or unburnt coal particles.

Frequently, hydrocarbon fingerprints and indices are used to distinguish between petrogenic and pyrogenic PAH in soils and sediments (Budzinski et al., 1997; Stout et al., 2002b; Wang, 2007; Pies et al., 2008b), but it is difficult to identify PAH derived from coal vs. PAH from oil. These uncertainties are assumed to be predominantly responsible for the lack of information on native coal-bound PAH in soils and sediments. This gap of knowledge can easily confound forensic attempts of source identification (Stout et al., 2002b), as evident in the case of the *Exxon Valdez* oil spill (Boehm et al., 1998, 2001; Short et al., 1999; Van Kooten et al., 2002). In the investigated sediments, Barrick et al. (1984) and Stout et al. (2002a,b) observed dominating alkylated naphthalenes with a "bell-shaped" pattern typical for petrogenic sources. Regarding the aliphatic fraction, n-alkanes exhibited a characteristic odd-even predominance within the C25-C31 range in a high volatile bituminous coal (Stout et al., 2002b). Low ratios of triaromatic steranes to methylchrysenes in coal (<0.2) compared to high ratios (11 and 13) were detected in oil (Short et al., 1999).

Barrick and Prahl (1987) described alkylphenanthrenes, alkylchrysenes and alkylpicenes concentrated in coal

fragments of sediments near river mouths in the central and southern Puget Sound region, U.S.A., originating from river systems draining coal-bearing strata. Surely, the most obvious characteristics of native PAH from coals are the predominance of naphthalene, phenanthrene and their alkylated derivatives, however, these are also typical of PAH from other petrogenic sources such as oil. Soil from a manufactured gas plant site contained a dominance of naphthalene, phenanthrene, chrysene and their alkylated derivatives in a coal sample separated from the soil, but not in other samples containing tar or residual petroleum (Stout and Wasielewski, 2004). EPA-PAH concentrations of the coal sample were around 10 mg/kg. Increased concentrations of fluoranthene, phenanthrene, pyrene and chrysene were reported from a coal pile runoff in Hamilton Harbour, Canada (Curran et al., 2000).

The PAH patterns of the coals investigated in the aftermath of the *Exxon Valdez* oil spill were also dominated by naphthalene, phenanthrene and alkylated derivatives (Short et al., 1999; Boehm et al., 2001). EPA-PAH concentrations are estimated at approx. 500 mg/kg in coals from the Kulthieth Formation (Van Kooten et al., 2002). In these coals, the presence of naphthalene, C1 and C2 naphthalenes tended to be greater than in seep oils, whereas the higher molecular weight PAH were more abundant in seep oils. Low molecular weight PAH can easily volatilize during sample preparation, e. g. if the extract is dried, which was not the case in this study. Naphthalenes volatilize more easily from oil or tar compared to coal since coal is a very strong sorbent. Therefore, the decrease in naphthalene concentrations in soils and sediments, after being subject to gentle evaporation, could be regarded as an indicator for oil-bound PAH but not coal-bound PAH. At the Mosel River, Germany, naphthalenes were also shown to be the key compounds for source apportionment of PAH. Native PAH in Saar coals (70–165 mg/kg EPA-PAH) are the major reason for elevated PAH concentrations in Saar and Mosel River floodplain soils downstream from mining activity (Hofmann et al., 2007; Pies et al., 2007, 2008a; Yang et al., 2007, 2008b,). Although major mining activity occurred between 200 to 50 years ago, naphthalenes and alkylated derivatives still dominate the PAH patterns in the floodplain soils (Pies et al., 2008a,b). Recently, Stout and Emsbo-Mattingly (2008) showed that PAH distributions and indices varied with coal rank and concluded that particulate coal in soils and sediments cannot be universally represented by a single set of diagnostic parameters based on the investigated samples.

7. Conclusions

Coal-bound native PAH in soils and sediments have been studied to a minor extent, despite 30 years of research on PAH in the environment. Their impact on the environment is not well understood. Unburnt hard / bituminous coal emissions from mining activity particularly impact those countries holding large coal basins. Coal particles were found in concentrations up to approx. 75 vol. % of the light fraction (<2 g/cm^3) of soils and sediments and they contain PAH concentrations ranges from trace level up to thousands of mg/kg.

Hard coal consists of a macromolecular network phase and a mobile phase, and PAH are part of both. However, the latter phase is of special environmental interest because it is more mobile and is expected to have higher bioavailability. Aromatization of coals increases with increasing rank from sub-bituminous coal to anthracite. In coals, oil (mobile phase, including 2–6 ring PAH) is generated at low to medium hard coal rank from 0.5–1.3% R_o. In this range also maximum PAH concentrations may occur but they also depend on origin (e. g. maceral composition). Naphthalene, phenanthrene, chrysene and alkylated derivatives are characteristic petrogenic PAH. To date, it is hardly possible to distinguish PAH derived from oil vs. PAH from coal. If other geosorbents such as black carbon are not present at higher levels, limited evaporation of naphthalenes compared to the greater losses in other samples may be a helpful indicator of the presence of coal. Other techniques, like organic petrography, are of major importance for source identification. The data is presently insufficient for us to ascertain if native PAH derived from unburnt hard coal particles pose a severe risk for humans or organisms of the benthos and soil. In addition, coal particles might also be relocated by wind erosion, transport/loading, or accidental releases (Ghoose and Majee, 2000a,b). Coal particles in the environment may sorb hydrophobic organic contaminants and enhance their relocation by colloidal/particulate transport (Hofmann et al., 2003a; Hofmann and Wendelborn, 2007; Hofmann and von der Kammer, 2008). For most of the large coal basins, these topics are not well studied. They should be included into an assessment of the environmental impacts of coal.

REFERENCES

Ahrens MJ, Morrisey DJ. Biological effects of unburnt coal in the marine environment. Oceanogr Mar Biol – Ann Rev 2005;43:69–122.

Alexander R, Kagi RI, Sheppard PN. Relative abundance of dimethylnaphthalene isomers in crude oils. Chromatorgraphy 1983;267:367–72.

Alexander R, Kagi RI, Roland SJ, Sheppard PN, Chirila TV. The effects of thermal maturity on distributions of dimethylnaphthalenes and trimethylnapthalenes in some ancient sediments and petroleums. Geochim Cosmochim Acta 1985;49:385–95.

Almaula S. Polycyclic aromatic hydrocarbons from steelmaking. Environ Forensics 2005;6:143–50.

Barrick RC, Prahl FG. Hydrocarbon geochemistry of the Puget Sound region – III. Polycyclic aromatic hydrocarbons in sediments. Estuar Coast Shelf Sci 1987;25:175–91.

Barrick RC, Furlong ET, Carpenter R. Hydrocarbon and azaarene markers of coal transport to aquatic sediments. Environ Sci Technol 1984;18:846–54.

Bechtel A, Sachsenhofer RF, Zdravkov A, Kostova I, Gratzer R. Influence of floral assemblage, facies and diagenesis on petrography and organic geochemistry of the Eocene Bourgas coal and the Miocene Maritza-East lignite (Bulgaria). Org Geochem 2005;36:1498–522.

Boehm PD, Page DS, Gifillan ES, Bence AE, Burns WA, Mankiewicz PJ. Study of the fates and effects of the *Exxon Valdez* oil spill on benthic sediments in two bays in Prince William Sound, Alaska. 1. Study design, chemistry, and source fingerprinting. Environ Sci Technol 1998;32:567–76.

Boehm PD, Page DS, Burns WA, Benze AE, Makiewicz PJ, Brown JS. Resolving the origin of the petrogenic hydrocarbon background

in Prince William Sound, Alaska. Environ Sci Technol 2001;35:471–9.
Booth R, Gribben K. A review of formation, environmental fate, and forensic methods for PAHs from aluminum smelting processes. Environ Forensics 2005;6:133–42.
Brändli RC, Hartnik T, Henriksen T, Cornelissen G. Sorption of native polyaromatic hydrocarbons (PAH) to black carbon and amended activated carbon in soil. Chemosphere 2008;73:1805–10.
Budzinski H, Baumard P, Papineau A, Wise S, Garrigues P. Focused microwave assisted extraction of polycyclic aromatic compounds from standard reference materials, sediments and biological tissues. Polycyc Aromat Compd 1997;9:1–4.
Chaffee AL, Johns RB. PAHs in Australian coals. I. Angularly fused pentacyclic tri- and tetraaromatic components of Victorian brown coal. Geochim Cosmochim Acta 1982;47:2141–55.
Chapman PM, Downie J, Maynard A, Taylors LA. Coal and deodorizer residues in marine sediments – contaminants or pollutants? Environ. Toxicol Chem 1996;15:638–42.
Chaulya SK. Assessment and management of air quality for an opencast coal mining area. J Environ Manag 2004;70/1:1–14.
Chen Y, Bi X, Mai B, Sheng G, Fu J. Emission characterization of particulate/gaseous phases and size association for PAHs from residential coal combustion. Fuel 2004;83:781–90.
Costa HJ, Sauer TCJ. Forensics approaches and consideration in identifying PAH background. Environ Forensics 2005;6:9–16.
Curran KJ, Irvine KN, Droppo IG, Murphy TP. Suspended solids, trace metal and PAH concentrations and loadings from coal pile runoff to Hamilton Harbour, Ontario. J Great Lakes Res 2000;26/1:18–30.
French PW. The impact of coal production on the sediment record of the Severn Estuary. Environ Pollut 1998;103:37–43.
Ghose MK. Generation and quantification of hazardous dusts from coal mining in the Indian context. Environ Monit Assess 2007;130:35–45.
Ghose MK, Majee SR. Assessment of the impact on the air environment due to opencast coal mining – an Indian case study. Atmos Environ 2000a;34:2791–6.
Ghose MK, Majee SR. Sources of air pollution due to coal mining and their impact in Jharia coalfield. Environ Int 2000b;26:81–5.
Given PH. The mobile phase in coals: its nature and modes of release. Final report – Part 2, U.S. Department for Energy; 1987.
Gu X, Lin L, Zheng X, Zhang T, Song X, Wang J, et al. High prevalence of NTDs in Shanxi Province: a combined epidemiological approach. Birth defects research Part A-clinical and molecular teratology, vol. 79; 2007. p. 702–7.
Hayatsu R, Winans RE, Scott RG, Moore LP, Studier MH. Trapped organic compounds and aromatic units in coals. Fuel 1978;57:541–8.
Hofmann T. An overview of factors influencing the colloid/particle favoured relocation of contaminants. IAHS-AISH Publication; 2002. p. 165–8.
Hofmann T, Baumann T, Bundschuh T, Kammer Fvd, Leis A, Schmitt D, et al. Aquatic colloids 1: definition and relevance – a review. Grundwasser 2003a;8:203–10.
Hofmann T, Baumann T, Bundschuh T, Kammer Fvd, Leis A, Schmitt D, et al. Aquatic colloids 2: sampling and characterization – a review. Grundwasser 2003b;8:213–23.
Hofmann T, Pies C, Yang Y. Elevated polycyclic aromatic hydrocarbons in a river flood plain soil due to mining activities. Water Sci Technol: Water Supply 2007;7:69–77.
Hofmann T, Wendelborn A. Colloid facilitated transport of polychlorinated dibenzo-p-dioxins and dibenzofurans (PCDD/Fs) to the groundwater at Ma Da area, Vietnam. Environ Sci Pollut Res 2007;14:223–4.
Hofmann T, von der Kammer F. Estimating the relevance of engineered carbonaceous nanoparticle facilitated transport of hydrophobic organic contaminants in porous media. Environ Pollut 2008, doi:10.1016/j.envpol.2008.10.022.
Johnson R, Bustin RM. Coal dust dispersal around a marine coal terminal (1977–1999), British Columbia: the fate of coal dust in the marine environment. Int J Coal Geol 2006;68:57–69.
Kashimura N, Hayashi J, Li C, Sathe C, Chiba T. Evidence of poly-condensed aromatic rings in a Victorian brown coal. Fuels 2004;83:97–107.
Khalil MF, Ghosh U. Role of weathered coal tar pitch in the partitioning of polycyclic aromatic hydrocarbons in manufactured gas plant site sediments. Environ Sci Technol 2006;40:5681–7.
Kleineidam S, Schüth C, Grathwohl P. Solubility-normalized combined pore-filling-partitioning sorption isotherms for organic pollutants. Environ Sci Technol 2002;36:4689–97.
Klös H, Schoch C. Historical trends of sediment loads – memory of an industrial region. Acta Hydrochim Hydrobiol 1993;21:32–7.
Kruge MA. Determination of thermal maturity and organic matter type by principal components analysis of the distributions of polycyclic aromatic compounds. Int J Coal Geol 2000;43:27–51.
Kruge MA, Bensley DF. Flash pyrolysis-gas chromatography/mass spectrometry of Lower Kittanning vitrinites: changes in the distributions of polyaromatic hydrocarbons as a function of coal rank. In: Mukhophadyay PK, Dow WG, editors. Vitrinite reflectance as a maturity parameter: applications and limitationsAmerican Chemical Society Symposium Series; 1994. p. 136–48.
Külaots I, Hurt RH, Suuberg EM. Size distribution of unburnt carbon in coal fly ash and its implications. Fuel 2004;83:223–30.
Ligouis B, Kleineidam S, Karapanagioti HK, Kiem R, Grathwohl P, Niemz C. Organic petrology: a new tool to study contaminants in soils and sediments. In: Lichtfouse E, Schwarzenbauer J, Robert D, editors. Environ. Chem. Germany: Springer Berlin Heidelberg; 2005. p. 89–98.
Lima ALC, Farrington JW, Reddy CM. Combustion-derived polycyclic aromatic hydrocarbons in the environment – a review. Environ Forensics 2005;6:109–31.
Liu G, Niu Z, Van Niekerk D, Xue T, Zheng L. Polycyclic aromatic hydrocarbons (PAHs) from coal combustion: emissions, analysis, and toxicology. Rev Environ Contam Toxicol 2008;192:1–28.
Lopez-Anton MA, Diaz-Somoano M, Martinez-Tarazona MR. Mercury retention by fly ashes from coal combustion: influence of the unburnt carbon content. Ind Eng Chem Res 2007;46:927–31.
Massachusetts Institute of Technology. The future of coal – an interdisciplinary MIT study; 2007. free access at http://web.mit.edu/coal/.
Max-Planck-Institut für Plasmaphysik. Kohle in den USA/ Coal in the U. S. Energie-Perspektiven online journal, 03; 2000. http://www.ipp.mpg.de/ippcms/ep/ausgaben/ep200003/0300_kohleusa_ep.html.
Max-Planck-Institut für Plasmaphysik. Kohle in China/ Coal in China. Energie-Perspektiven online journal, 01; 2001a. http://www.ipp.mpg.de/ippcms/ep/ausgaben/ep200101/0101_kohlechina_ep.html.
Max-Planck-Institut für Plasmaphysik. Kohle in Indien/ Coal in India. Energie-Perspektiven online journal, 03; 2001b. http://www.ipp.mpg.de/ippcms/ep/ausgaben/ep200103/0301_kohle_indien_ep.html.
Max-Planck-Institut für Plasmaphysik. Kohle in Australien/ Coal in Australia. Energie-Perspektiven online journal, 01; 2002a. http://www.ipp.mpg.de/ippcms/ep/ausgaben/ep200201/0102_kohle_australien_ep.html.
Max-Planck-Institut für Plasmaphysik. Kohle in Russland/ Coal in Russia. Energie-Perspektiven online journal, 04; 2002b. http://www.ipp.mpg.de/ippcms/ep/ausgaben/ep200204/0402_kohle_russland.html.

Meyers PA, Ishiwatari R. Lacustrine organic geochemistry—an overview of indicators of organic matter sources and diagenesis in lake sediments. Org Geochem 1993;20:867–900.
Micic V, Achten C, Schwarzbauer J, Hofmann T. Native PAHs in hard coal particles as a possible source of increased PAH concentrations in river sediments. Geochim. Cosmochim Acta 2007;15:A663.
Müller G, Grimmer G, Böhnke H. Sedimentary record of heavy metals and polycyclic aromatic hydrocarbons in Lake Constance. Naturwissenschaften 1977;64:427–31.
Murphy BL, Brown J. Environmental forensics aspects of PAHs from wood treatment with creosote compounds. Environ Forensics 2005;6:151–9.
Napier F, D'Arcy B, Jefferies C. A review of vehicle related metals and polycyclic aromatic hydrocarbons in the UK environment. Desalination 2008;226/1-3:143–50.
Pies C, Yang Y, Hofmann T. Polycyclic aromatic hydrocarbon (PAH) distribution in bank and alluvial soils of Mosel and Saar River. J Soils Sediments 2007;7:216–22.
Pies C, Hoffmann B, Petrowsky J, Yang Y, Ternes TA, Hofmann T. Characterization and source identification of polycyclic aromatic hydrocarbons (PAHs) in river bank soils. Chemosphere 2008a;72:1594–601.
Pies C, Ternes T, Hofmann T. Identifying sources of polycyclic aromatic hydrocarbons (PAHs) in soils: distinguishing point and non-point sources using an extended PAH spectrum and n-alkanes. J Soils Sediments 2008b;8:312–22.
Püttmann W. Analysis of polycyclic aromatic hydrocarbons in solid sample material using a desorption device coupled to a GC/MS system. Chromatography 1988;26:171–7.
Püttmann W, Villar H. Occurrence and geochemical significance of 1,2,5,6-tetramethylnaphthalene. Geochim Cosmochim Acta 1987;51:3023–929.
Püttmann W, Schaefer RG. Assessment of carbonization properties of coals by analysis of trapped hydrocarbons. Energy Fuels 1990;4:339–46.
Radke M, Welte DH. The Methylphenanthrene Index (MPI): a maturity parameter based on aromatic hydrocarbons. Adv Org Geochem 1981:504–12.
Radke M, Welte DH, Willsch H. Geochemical study on a well in the western Canada Basin: relation of the aromatic distribution pattern to maturity of organic matter. Geochim Cosmochim A 1982a;46:1–10.
Radke M, Willsch H, Leythaeuser D. Aromatic compounds of coal: relation of distribution pattern to rank. Geochim Cosmochim Acta 1982b;46:1831–48.
Radke M, Leythaeuser D, Teichmüller M. Relationships between rank and composition of aromatic hydrocarbons for coals of different origins. Org Geochem 1984;6:423–30.
Radke M, Willsch H, Teichmüller M. Generation and distribution of aromatic hydrocarbons in coals of low rank. Org Geochem 1990;15:539–63.
Saber D, Mauro D, Sirivedhin T. Environmental forensic investigation in sediments near a former manufactured gas plant site. Environ Forensics 2006;7:65–75.
Schejbal-Chwastek M, Marszalek M. Mineralogical and chemical impact of anthropogenic emissions on soils and rocks on the Ojcow National Park (Poland). Geol Carpath 1999;50:409–12.
Sekhar MC, Rao GA. Impact of opencast coal mining on the air environment. Eng Geol Environ 1997;1–3:2487–93.
Short JW, Kvenvolden KA, Carlson PR, Hostettler FD, Rosenbauer RJ, Wright BA. Natural hydrocarbon background in benthic sediments of Prince William Sound, Alaska: Oil vs coal. Environ Sci Technol 1999;33:34–42.
Short JW, Irvine GV, Mann DH, Maselko JM, Pella JJ, Lindeberg MR, et al. Slightly weathered Exxon Valdez oil persists in Gulf of Alaska beach sediments after 16 years. Environ Sci Technol 2007;41:1245–50.
Simoneit BRT, Grimalt JO, Wang TG, Cox RE, Hatcher RG, Nissenbaum A. Cyclic terpenoids of contemporary resinous plant detritus and of fossil woods, ambers and coals. Org Geochem 1986;10:877–89.
Singh G, Sharma RK. A study of spatial distribution of air pollutants in some coal mining areas of Raniganj coalfield, India. Environ Int 1992;18/2:191–200.
Stach E, Mackowsky MTh, Teichmüller M. Stach's Textbook of Coal Petrology. 3rd ed. Stuttgart, Germany: Borntraeger; 1982.
Stout SA, Wasielewski TN. Historical and chemical assessment of the sources of PAHs in soils at a former coal burning power plant, New Haven, Connecticut. Environ Forensics 2004;5:195–211.
Stout SA, Emsbo-Mattingly S. Concentration and character of PAHs and other hydrocarbons in coals of varying rank – Implications for environmental studies of soils and sediments containing particulate coal. Org Geochem 2008;39:801–19.
Stout SA, Emsbo-Mattingly S, Uhler AD, McCarthy K. Environmental forensics particulate coal in soils and sediments – recognition and potential influences on hydrocarbon fingerprinting and concentration. AEHS Magazine – Soil Sediment & Water (Environmental Forensics) June; 2002a. p. 12–5.
Stout SA, Uhler AD, McCarthy KJ, Mattingly SE. Chemical fingerprinting of hydrocarbons. In: Murphy BL, Morrison RD, editors. Introduction to environmental forensics. Amsterdam, Netherlands: Elsevier Academic Press; 2002b. p. 137–260.
Suess MJ. The environmental load and cycle of polycyclic aromatic hydrocarbons. Sci Tot Environ 1976;6:239–50.
Suggate RP, Dickinson WW. Carbon NMR of coals: the effects of coal type and rank. Int J Coal Geol 2004;57:1–22.
Sun X, Ghosh U. The effect of activated carbon on partitioning, desorption, and biouptake of native polychlorinated biphenyls in four freshwater sediments. Environ Toxicol Chem 2008;27:2287–95.
Tang D, Fermont WJ, Zhigui R, Püttmann W, Yang Q. Extraction yields and GC/MS characteristics of extracts from high rank coals and anthracites. Proceedings of the International Conference on Coal Science, 16–20 September 1991. U. K.: University of Newcastle-upon-Tyne; 1991.
Taylor GH, Teichmüller M, Davis A, Diessel CFK, Littke R, Robert P. Organic petrology. Berlin-Stuttgart: Gebrüder Borntraeger; 1998. Germany.
Teichmüller M. The Genesis of coal from the standpoint of coal petrology. Int J Coal Geol 1989;12:1–87.
Thielemann T, Schmidt S, Gerling C. Lignite and hard coal: energy suppliers for world needs until the year 2100 – an outlook. Int J Coal Geol 2007;72:1–14.
Tissot BP, Welte DH. Petroleum formation and occurrence. Berlin: Springer Verlag; 1978. Germany.
Tremblay GA. Historical statistics support a hypothesis linking tuberculosis and air pollution caused by coal. Int J Tuberc Lung Dis 2007;11/7:722–32.
Tripp BW, Farrington JW, Teal JM. Unburned coal as a source of hydrocarbons in surface sediments. Mar Pollut Bull 1981;12:122–6.
Tuo J, Philp RP. Saturated and aromatic diterpenoids and triterpenoids in Eocene coals and mudstones from China. Appl Geochem 2005;20:367–81.
Van Kooten GK, Short JW, Kolak JJ. Low-maturity Kulthieth Formation coal: a possible source of polycyclic aromatic hydrocarbons in benthic sediment of the Northern Gulf of Alaska. Environ Forensics 2002;3:227–41.
Van Krevelen DW. Coal, typology – physics – chemistry – constitution. 3rd ed. Amsterdam, The Netherlands: Elsevier Science Publishers B. V.; 1993.
Walker SE, Dickhut RM, Chisholm-Brause C, Sylva S, Reddy CM. Molecular and isotopic identification of PAH sources in a highly industrialized urban estuary. Org Geochem 2005;36:619–32.
Wang Z. Forensic identification and differentiation of pyrogenic PAHs from petrogenic PAHs. Proceedings The 21st

International Symposium for Polycyclic Aromatic Compounds, 05.–10.08.2007, Trondheim, Norway; 2007.
Wang Z, Fingas M. Oil and petroleum product fingerprinting analysis by gas chromatographic techniques. In: Nollet LML, editor. Chromatographic analysis of the environment. Boca Raton, U.S.: Taylor & Francis; 2006. p. 1028–98.
Wang G, Kleineidam S, Grathwohl P. Sorption/desorption reversibility of phenanthrene in soils and carbonaceous materials. Environ Sci Technol 2007;41:1186–93.
Werner D, Ghosh U, Luthy RG. Modeling polychlorinated biphenyl mass transfer after amendment of contaminated sediment with activated carbon. Environ Sci Technol 2006;40:4211–8.
White CM, Lee ML. Identification and geochemical significance of some aromatic components of coal. Geochim Cosmochim Acta 1980;44:1825–32.
Willsch H, Radke M. Distribution of polycyclic aromatic compounds in coals of high rank. Polycyc Aromat Comp 1995;7:231–51.
World Coal Institute. Top ten hard coal producing countries worldwide, 2004; 2007. http://www.worldcoal.org.
Yang Y, Hofmann T, Pies C, Grathwohl P. Occurrence of coal and coal-derived particle-bound polycyclic aromatic hydrocarbons (PAHs) in a river floodplain soil. Environ Pollut 2007;151:121–9.
Yang Y, Cajthaml T, Hofmann T. PAH desorption from river floodplain soils using supercritical fluid extraction. Environ Pollut 2008a;156:745–52.
Yang Y, Ligouis B, Pies C, Achten C, Hofmann T. Identification of carbonaceous geosorbents for PAHs by organic petrography in river floodplain soils. Chemosphere 2008b;71:2158–67.
Yang Y, Hofmann T, Pies C, Grathwohl P. Sorption of polycyclic aromatic hydrocarbons (PAHs) to carbonaceous materials in a river floodplain soil. Environ Pollut 2008c:1357–63.
Zhao ZB, Liu K, Xie W, Pan WP, Riley JT. Soluble polycyclic aromatic hydrocarbons in raw coals. J Hazard Mater 2000;73:77–85.
Zimmermann JR, Gosh U, Millward RN, Bridges TS, Luthy RG. Addition of carbon sorbents to reduce PCB and PAH bioavailability in marine sediments: physicochemical tests. Environ Sci Technol, 2004;38:5458–64.

World Journal of Microbiology & Biotechnology (2005) 21: 1237–1243
DOI 10.1007/s11274-005-1804-0
© Springer 2005

Effect of salinity on the tolerance to toxic metals and oxyanions in native moderately halophilic spore-forming bacilli

M.A. Amoozegar[1,*], J. Hamedi[1], M. Dadashipour[2] and S. Shariatpanahi[1]
[1]*Department of Biology, Faculty of Science, University of Tehran, Tehran, Iran*
[2]*Department of Biochemistry, Pasteur Institute of Iran, Tehran, 13164, Iran*
**Author for correspondence: Tel.: +98-21-6112622, Fax: +98-21-6492992, E-mail: alamoze@yahoo.com*

Received 4 October 2004; accepted 4 February 2005

Keywords: Chromate, halophilic bacteria, oxyanions, selenite, tellurite, tolerance, toxic metal

Summary

Ten moderately halophilic spore-forming bacilli were isolated from saline soils in Iran and their intrinsic high-level resistance to chromate, arsenate, tellurite, selenite, selenate and biselenite was identified by an agar dilution method. Minimum inhibitory concentration (MIC) for each oxyanion was determined. All isolates were resistant to higher concentrations of arsenate. The resistance level of the isolates to selenooxyanions was between 10 and 40 mM. Maximum and minimum tolerance against oxyanions was seen in selenite and biselenite, respectively. Although toxic metal resistance in the isolates was not different from non-halophilic bacteria that has been reported, unusual resistance to arsenate (250 mM), sodium chromate (75 mM) and potassium chromate (70 mM) was observed. The results obtained in this study revealed that all isolates were obviously susceptible to silver, nickel, zinc and cobalt, while seven isolates were resistant to lead. Susceptibility to copper and cadmium varied among the isolates. Silver had the maximum toxicity, whereas lead and copper showed minimum toxicity. The impact of salinity on the toxicity of oxyanions was also studied. Our results showed that in general an increase in salinity from 5% (w/v) to 15% (w/v) enhanced tolerance to toxic oxyanions.

Introduction

High concentrations of toxic metals have caused environmental pollution in agricultural soils, surface and underground water (Nriagu & Pacyna 1988; Kinkle *et al.* 1994). Microorganisms play a major role in bioremediation or biotransformation processes of these toxic elements, converting them to less toxic or non-toxic elements (Kinkle *et al.* 1994). *Acinetobacter*, *Rhodospirillum*, *Pseudomonas*, *Thiobacillus*, *Bacillus* and *Corynebacterium* have been reported as active biotransformers (Kessi *et al.* 1999; McLean & Beveridge 2001). Determining the potential of microorganisms and their tolerance against high concentrations of toxic metals will assist the selection of suitable species for bioremediation and biotransformation of toxic metals (Trevors *et al.* 1985; Burton *et al.* 1987). Halophilic and halotolerant microorganisms are suitable candidates for these processes as they have exceptional properties, that is high concentrations of anions and cations are necessary for the growth of halophilic microorganisms (Ventosa *et al.* 1998), hence they are not only naturally tolerant to some elements that are toxic to other microorganisms, but also they have a requirement for these elements. Furthermore, such information might be desirable, as some of these toxic metal-resistant halophilic bacteria could be used as bioassay indicator organisms in saline polluted environments (Nieto *et al.* 1989). Resistance to toxic metals is a widespread characteristic among bacteria isolated from several environments (Summers 1978, 1985; Trevors *et al.* 1985).

Recently, toxic heavy metal and oxyanion resistance was reported in halophilic microorganisms, e.g. *Halomonas* (Nieto *et al.* 1989; Ventosa *et al.* 1998; Souza *et al.* 2001) and *Pseudoalteromonas* (Rathgeber *et al.* 2002), but there is little work on the resistance of Gram-positive moderately halophilic bacilli to toxic heavy metals and oxyanions. In this study, we have isolated 10 moderately halophilic spore-forming bacilli from various saline soils in Iran, which were not contaminated with toxic oxyanions or heavy metals, and identified their intrinsic high-level resistance against these contaminants. Our aim was to determine resistance levels to toxic metals/oxyanions and the effect of various concentrations of NaCl on the minimum inhibitory concentration (MIC). This is the first report describing resistance to toxic oxyanions in moderately halophilic spore-forming bacilli.

Materials and methods

Bacterial isolation and identification

Ten Gram-positive spore-forming aerobic moderately halophiles were isolated from various concentrations of saline soils in Gheshm, Karaj, Tehran, Qom and Garmsar of Iran (Figure 1). About 1 g of soil samples was added to a 100 ml Erlenmeyer flask containing 20 ml nutrient broth plus maximum 10% (w/v) NaCl (Amoozegar *et al.* 2003). Inoculated flasks were incubated in an orbital shaker at 34 °C in 150 rev/min. Isolates colonies were taken by culturing the nutrient agar plus 10% (w/v) NaCl. The resistance of isolates to heavy metals was assayed on the nutrient agar plus 5, 10 and 15% (w/v) NaCl. If needed, the pH of the media adjusted at 7.2 ± 0.1 with 1 M KOH.

The morphological and physiological tests were conducted on the isolates. Purified isolates were identified by the Persian Type Culture Collection (PTCC), Tehran-Iran.

Chemicals

$Pb(NO_3)_2$, $AgNO_3$, $Cd(NO_3)_2$, $CoCl_2$, $NiCl_2$, $CuSO_4$, $ZnSO_4$, Na_2CrO_4, K_2CrO_4, Na_2SeO_3 and $NaHSeO_3$ were obtained from Merck. K_2TeO_3, Na_2SeO_4 and Na_2HAsO_4 were purchased from Sigma. Stock solutions of chemicals were dissolved in distilled water and sterilized with 0.22-μm bacteriological filters. Working solutions were stored in the refrigerator for up to 5 days.

Determining the toxic metal tolerance

The agar dilution method was used to determine the bacterial tolerance to toxic metals (Washington & Sutter 1980). Various concentrations of heavy metals (0.005, 0.01, 0.05, 0.1, 0.5, 1.0, 1.5, 2.0, 2.5, 3.0, 3.5, 4.0, 4.5, 5.0, 6.0, 7.0, 8.0, 9.0, 10.0, 12.0, 14.0, 16.0, 18.0 and 20.0 mM) and various concentrations of toxic oxyanions (0.05, 0.1, 0.3, 0.5, 1.0, 2.0, 3.0, 4.0, 5.0, 10.0, 15.0, 20.0, 25.0, 30.0, 35.0, 40.0, 45.0, 50.0, 55.0, 60.0, 65.0, 70.0, 75.0 and 80.0 mM) were examined. Sodium arsenate was an exception that was examined up to 300 mM, because the isolates were highly tolerant to it. Appropriate concentrations of heavy metals/toxic oxyanions were added to 100-ml Erlenmeyer containing 20 ml molten nutrient agar plus 10% (w/v) NaCl. Complete medium was poured in 8-mm glass Petri dishes. Then 10 μl of the bacterial suspension (1.5×10^8 c.f.u./ml) was inoculated and spread on the surface of each plate. The plates were incubated at 34 °C for 72 h. The MIC for each oxyanion was determined. The plates were prepared in triplicate.

Similar experiments were performed by nutrient agar containing 5 (w/v) and 15% (w/v) NaCl. Also, a control medium (without any metal/oxyanion) was used. The inoculated plates were incubated at 34 °C for 72 h. The minimum concentration of the metals/oxyanions that completely inhibited growth of the strain was reported as MIC. The MIC assay was performed in triplicate. It is well known that, unlike antibiotic resistance, which is evaluated with therapeutic doses, there are no standard acceptable metal concentrations used to specify metal or

Figure 1. Sampling sites for the isolation of moderately halophilic bacteria.

oxyanion resistance (Nieto *et al.* 1989; McLean & Beveridge 2001; Rathgeber *et al.* 2002). As mentioned above, this is the first report describing resistance to toxic oxyanions in moderately halophilic spore-forming bacilli, therefore, the interpretation of the bacterial resistance to oxyanions was based on the criteria used in previous studies carried out with other bacteria (Nieto *et al.* 1989; McLean & Beveridge 2001; Rathgeber *et al.* 2002). The strain was considered as resistant, when its growth was not inhibited by the resistance limit concentration of any metals/oxyanions. The resistance limit concentrations for arsenate, tellurite, selenate, selenite, biselenite, chromate, cadmium, cobalt, nickel, lead, zinc, silver and copper were 10, 0.5, 20, 20, 10, 5, 1, 1, 1, 1, 1, 1, 1, respectively.

Results

Isolation and identification

All isolates were Gram-positive rod-shaped spore-forming bacteria. The isolates were separated into groups A, B and C, according to the concentration of NaCl needed for growth. The optimum concentration of NaCl for the A, B and C groups was 15, 10 and 5%, respectively. The isolates could not grow in NaCl-deficient medium and thus were halophiles. The characteristics of the isolates are shown in Table 1. The morphological and physiological results obtained and other complementary tests that were done by the Persian Type Culture Collection (PTCC) revealed that all isolates were *Bacillus* sp.

Minimum inhibitory concentration of toxic metals

The MIC of the metals in the media containing 10% NaCl for each isolate is shown in Figure 2. 40% of the isolates were resistant to Cu^{2+} and Pb^{2+} and all strains were sensitive to Ag^{+}, Ni^{2+}, Zn^{2+}, Co and Cd^{2+}. The maximum tolerance to Pb^{2+} was seen with the strains named as C1 and C2, although most of the strains were sensitive to Ag^{+}, A3, C3 and C4 tolerated up to 0.05 mM Ag^{+}.

Minimum inhibitory concentration of toxic oxyanions

The MIC of the oxyanions in the media containing 10% NaCl for each isolate is shown in Figure 3. All of the strains tolerated selenite, selenate, tellurite and arsenate. Maximum tolerance was seen to arsenate (250 mM), although 90% of the strains were resistant to biselenite, sodium chromate and potassium chromate. C5 was sensitive to these oxyanions and tolerated only 4.5 mM of them. In addition, this strain showed minimum tolerance to biselenite and chromate (2.5 mM).

All strains were sensitive to Ni^{2+}, Ag^{+}, Zn^{2+} and Co^{2+}, but the strains named as A_1, B_2, C_1 and C_2 were not only resistant to $Pb(NO_3)_2$ and $CuSO_4$, but also showed the highest tolerance to toxic metals and oxyanions.

It must be emphasized that the isolates not only tolerated selenite, biselenite and tellurite, but also reduced these oxyanions. Reduction of tellurite and selenooxyanions by these bacteria resulted in black and dark-red colonies on agar plates, due to the accumulation of intracellular crystals of black elemental Te and

Table 1. Major characteristics of 10 Gram-positive rod-shaped spore-forming halophilic bacteria.

Characteristics	Strain									
	A1	A2	A3	B1	B2	C1	C2	C3	C4	C5
Pigment production	White	Cream	–	Cream	–	–	–	–	–	Cream
Spore location in the cell	Central	Central	Central	Sub-terminal	Central	Central	Central	Central	Central	Central
Motility	–	NA	+	–	–	+	–	–	–	–
Oxidase reaction	+	+	+	+	+	+	+	+	+	–
Growth on 0% NaCl	–	–	–	–	–	–	–	–	–	–
Growth on 1% NaCl	–	–	–	+	–	+	–	+	–	–
Growth on 25% NaCl	+	+	+	–	+	+	+	+	+	+
Optimum concentration of NaCl for growth	15%	15%	15%	10%	10%	5%	5%	5%	5%	5%
Acid production from										
Glucose	+	+	+	+	–	+	+	+	+	–
Galactose	–	+	–	–	–	+	–	+	–	–
Fructose	+	+	+	+	+	+	–	+	+	–
Sucrose	+	+	–	–	+	+	+	+	+	+
Maltose	+	+	+	+	+	+	+	+	+	+
Xylose	+	+	+	–	+	+	+	+	+	+
Mannitol	+	+	+	+	+	+	+	+	–	+
Hydrolysis of										
Gelatin	+	–	+	+	+	+	–	+	+	–
Casein	+	+	+	+	+	+	+	+	+	+
Starch	–	+	–	+	–	+	–	–	–	–
Tween 80	–	–	–	–	–	–	–	–	–	–
DNA	+	+	+	+	+	+	+	+	+	+
Nitrate reduction	–	–	–	–	–	–	–	–	–	–

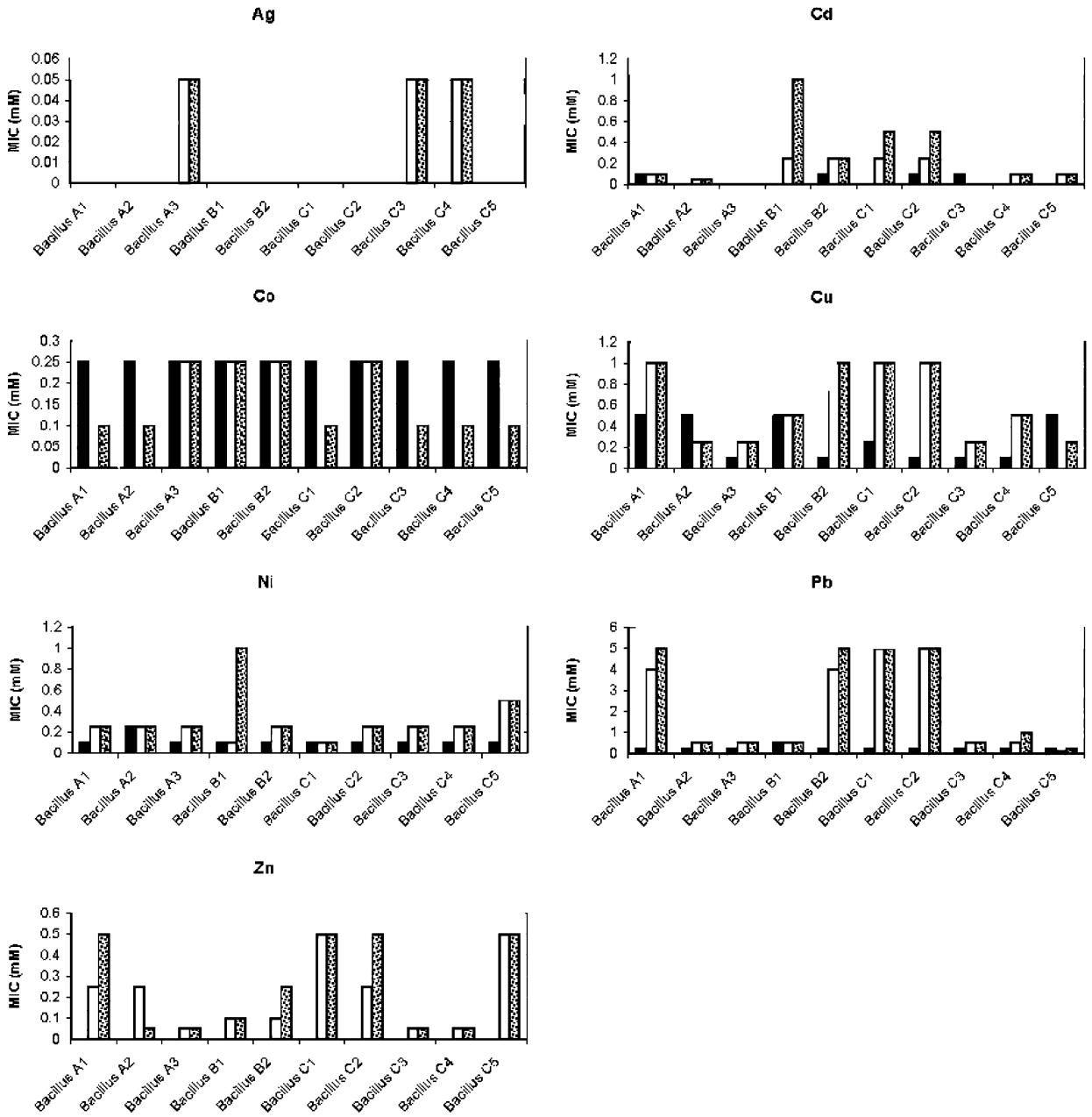

Figure 2. Toxic metal resistance of 10 halophilic spore-forming bacilli (expressed as MIC) in culture medium containing ■ 5%, □ 10% and ▚ 15% NaCl.

red, amorphous, elemental Se, respectively (Rathgeber *et al.* 2002).

Effect of NaCl concentrations on resistance of the strains to toxic metals and oxyanions

We examined the effect of the NaCl concentrations on the resistance of the strains to toxic metals and oxyanions and the results are shown in Figures 2 and 3, respectively. Although increasing the concentration of NaCl led to greater tolerance to chromate, selenate, selenite, biselenite and tellurite, the isolates had different tolerances to arsenate. The maximum effect of salt concentration was seen with the chromate anion. NaCl concentration increasing from 5 to 15% enhanced tolerance to sodium chromate and potassium chromate from 5 to 75 mM. The strains named A2 and B1 showed maximum tolerance to sodium chromate in the medium containing 15% NaCl.

With the exception of cobalt, for which the maximum tolerance was seen in 5% (w/v) NaCl-containing medium, generally, when the concentration of NaCl was increased from 5 to 15% (w/v), toxic metal tolerance was enhanced. The maximum effect of the NaCl concentration on the toxic metal resistance was seen in the Pb-containing medium.

As mentioned above, all isolates failed to grow in NaCl-deficient medium, while when some strains, such as B1 and C1, were cultured in the medium plus 30 and 20 mM sodium selenite, respectively, good growth was seen.

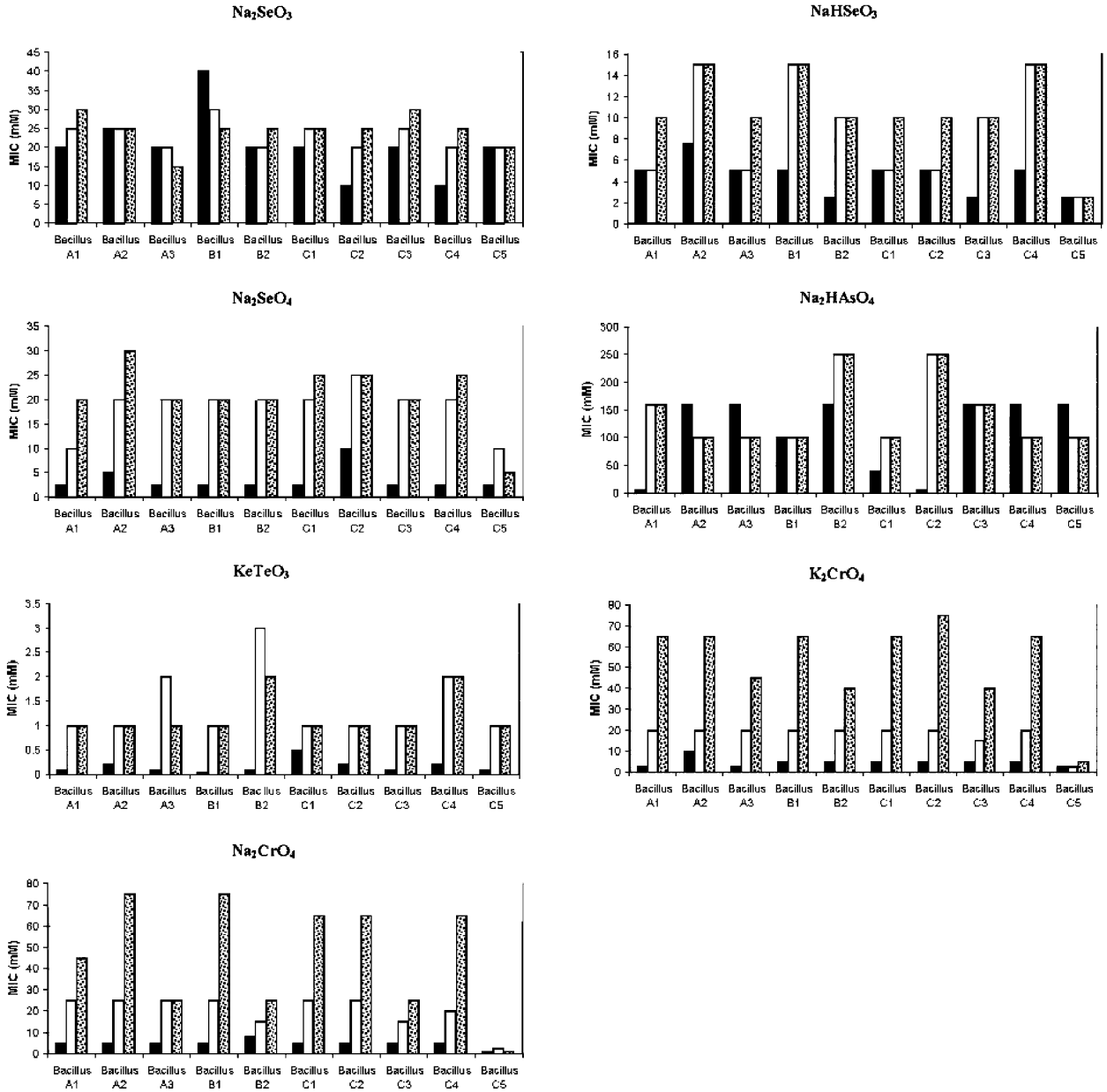

Figure 3. Toxic oxyanion resistance of 10 halophilic spore-forming bacilli (expressed as MIC) in culture medium containing ■ 5%, □ 10% and ▩ 15% NaCl.

Discussion

Moderately halophilic or halotolerant spore-forming Gram-positive rod-shaped bacilli are a diverse phylogenetic group of bacteria which have adapted to life at the lower range of salinities and with the possibilities of rapid adjustment to changes in the extreme salt concentration (Ventosa *et al.* 1998). Useful information has been published on the ecology and physiology of these bacteria (Oren 2002; Venosa 2004). These bacteria may be used for bioremediation of toxic metals from polluted environments; therefore, we studied the toxic metal and oxyanion tolerance in these bacteria.

The results obtained in this study showed that there were two patterns for tolerance in moderately halophilic bacilli. Although the spore-forming halophilic bacilli isolated had relatively low toxic metal tolerance (Figure 2), their resistance to toxic oxyanions was high (Figure 3). It seems that the presence of Na/K in chemical structure of the oxyanions studied was one of the reasons for the high tolerance to oxyanions. Sodium and potassium are necessary elements for the activity of enzymes and pumps in halophiles (Ventosa 1998); therefore, it seems that these elements enhanced the toxic metal tolerance.

We are the first to show high tolerance to the chromate anion in halophilic bacteria (75 mM). Tolerance to

chromate was reported in *Pseudomonas* CRB5 (10 mM) (Mclean & Beveradge 2001), *Salvibrio* (20 mM) (Ríos *et al.* 2001), *Arthrobacter* (100 mg/l) (Mgharaj *et al.* 2000) and *Corynebacterium hoagii* (22 mM) (Viti *et al.* 2003). Isolation of chromate-resistant, moderately halophilic bacilli provides additional bacterial models for studying the mechanisms of chromate resistance. In addition, these strains may have potential for bioremediation of chromate-contaminated saline soil, sediments and waste streams. The potential for biological treatment of chromate-contaminated waste is limited, as most microorganisms lose viability in the presence of high concentrations of chromate (Pattanapipitpaisal *et al.* 2001). Genes encoding chromate resistance in these strains may be useful for introduction into related halophilic bacteria used to degrade other pollutants in order to produce strains capable of bioremediation of mixed wastes. On the other hand, chromate-sensitive strains may be interest for future genetic works.

All isolates were resistant to arsenate and the highest resistance to this oxyanion was seen in the B2 and C2 strains (250 mM). Suresh *et al.* (2004) reported the maximum tolerance to 20 mM arsenate anion in a new bacterium, *Bacillus indicus*.

Our isolates had a relatively high tolerance to selenite, biselenite and tellurite oxyanions. This tolerance was comparable to that previously published (Kinkle *et al.* 1994; Souza *et al.* 2001; Rathgeber *et al.* 2002). The tolerance to these oxyanions was followed by reduction of toxic selenite or tellurite to their less toxic elemental forms. The reduction of soluble selenooxyanions and tellurite to elements could be an important mechanism for the removal of these elements from polluted hypersaline environments. Therefore, these strains may be good candidates for bioremediation of highly polluted effluents from industrial and mining operations. Conventional chemical methods for removing toxic oxyanions are expensive and require high energy or large quantities of chemical reagents, while microbial reduction of these toxic oxyanions is low in price and provides green technology. In addition, bacteria capable of reducing tellurite and selenite could be useful in the applied biometallurgy of tellurite and selenite, rare and expensive metals used extensively for their properties as semiconductors (Rathgeber *et al.* 2002).

Increasing industrial activities cause pollution of soil, water and atmosphere by chemicals such as toxic metals and oxyanions. Bioremediation is a good choice for removing the industrial pollution from the environment. There are two different strategies for bioremediation: (1) screening/development of potent and powerful microorganisms and (2) invention/optimization of bioremediation methods. In both approaches, high yield processes will be obtained by employing tolerant microorganisms. It seems that moderately halophilic spore-forming rod bacteria are useful candidates, because they are widely distributed in soil and resistant to such harsh environmental conditions. In this study, these bacteria were introduced for further studies as highly tolerant reducers of toxic metals and oxyanions such as chromate, arsenate and tellurite.

Acknowledgements

We are grateful to Persian Type Culture Collection of Microorganisms supervisor, Dr. F. Mohseni, and her colleagues for their technical assistance for identification of the isolates.

References

Amoozegar, M.A., Malekzadeh, F., Malik, K.A., Schumann, P. & Spröer, C. 2003 *Halobacillus karajensis* sp. nov., a novel moderate halophile. *International Journal of Systematic and Evolutionary Microbiology* **53**, 1059–1063.

Burton, G.A., Gidding, T.H., Debrine, P. & Fall, R. 1987 High incidence of selenite-resistant bacteria from a site polluted with selenium. *Applied and Environmental Microbiology* **53**, 185–188.

Kessi, J., Ramuz, M., Wehrli, E., Spycher, M. & Bachofen, R. 1999 Reduction of selenite and detoxification of elemental selenium by the phototrophic bacterium *Rhodospirillum rubrum*. *Applied and Environmental Microbiology* **65**, 4734–4740.

Kinkle, B.K., Sadowsky, M.J., Johnstone, K. & Koskinen, W.C. 1994 Tellurium and selenium resistance in Rhizobia ands its potential use for direct isolation of *Rhizobium meliloti* from soil. *Applied and Environmental Microbiology* **60**, 1674–1677.

McLean, J. & Beveridge, T.J. 2001 Chromate reduction by a Pseudomonad isolated from site contaminated with chromated copper arsenate. *Applied and Environmental Microbiology* **67**, 1076–1084.

Mgharaj, M., Avudainayagam, S. & Naidu, R. 2003 Toxicity of hexavalent chromium and its reduction by bacteria isolated from soil contaminated with tannery waste. *Current Microbiology* **47**, 51–54.

Nieto, J.J., Fernandez-Castillo, R., Marquez, M.C., Ventosa, A., Quesada, E. & Ruiz-Berraquero, F. 1989 Survey of metal tolerance in moderately halophilic eubacteria. *Applied and Environmental Microbiology* **55**, 2385–2390.

Nriagu, J.O. & Pacyna, J.M. 1988 Quantitative assessment of worldwide contamination of air, water and soils by trace metals. *Nature* **333**, 134–139.

Oren, A. 2002 *Halophilic Microorganisms and their Environments*, Dordrecht, The Netherlands: Kluwer Academic Publishers ISBN 1402008295.

Pattanapipitpaisal, P., Brown, N.L. & Macaskie, L.E. 2001 Chromate reduction and 16S rRNA identification of bacteria isolated from a Cr(VI)-contaminated site. *Applied Microbiology and Biotechnology* **57**, 257–261.

Rathgeber, C., Yurkova, N., Stackebrandt, E., Beatty, J.T. & Yurkov, V. 2002 Isolation of tellurite- and selenite-resistant bacteria from hydrotermal vents of the Juan de Fuca Ridge in the pacific ocean. *Applied and Environmental Microbiology* **68**, 4613–4622.

Ríos, M., García, M.T., Arahal, D.R. & Ventosa, A. 2001 *Salinivibrio kushnerii* sp. nov., a new moderately halophilic species tolerant to chromium. In *Proceedings of an International Conference on Halophilic Microorganisms held at Sevilla, Spain*. p. 9.

Souza, M.P., Amini, A., Dojka, M.A., Pickering, I.J., Dawson, S.C., Pace, N.R. & Terry, N. 2001 Identification and characterization of bacteria in a selenium contaminated hypersaline evaporation pond. *Applied and Environmental Microbiology* **67**, 3785–3794.

Summers, A. 1978 Microbial transformations of metals. *Annual Review of Microbiology* **32**, 637–672.

Summers, A. 1985 Bacteria resistance to toxic elements. *Trends in Biotechnology* **3**, 122–125.

Suresh, K., Prabagaran, S.R., Senqupta, S. & Shivaji, S. 2004 *Bacillus indicus* sp. Nov. an arsenic resistant bacterium isolated from an aquifer in West Bengal, India. *International Journal of Systematic and Evolutionary Microbiology* In press.

Trevors, J.T., Oddie, K.M. & Belliveau, B.H. 1985 Metal resistance in bacteria. *FEMS Microbiology Reviews* **32**, 39–54.

Ventosa, A., 2004 *Halophilic Microorganisms*, Berlin, Heidelberg, New York: Springer-Verlag ISBN 3540009264.

Ventosa, A., Nieto, J.J. & Oren, A. 1998 Biology of moderately halophilic aerobic bacteria. *Microbiology and Molecular Biology Reviews* **62**, 504–544.

Viti, C., Pace, A. & Giovannetti, L. 2003 Characterization of Cr (VI)-resistant bacteria isolated from chromium contaminated soil by tannery activity. *Current Microbiology* **46**, 1–5.

Washington, J.A. & Sutter, V.L. (1980). Dilution susceptibility test: agar and macro-broth dilution procedures, Manual of Clinical Microbiology. In E.H. Lennette, A. Balows, W.J. Hausler Jr., & J.P. Truant (Eds.), *Manual of Clinical Microbiology* (pp. 453–458). 3rd edition, American Society for Microbiology, Washington, D.C.ISBN: 1555812554.

(24) Logan, B. E.; Wilkinson, D. B. *Limnol. Oceanogr.* **1990**, *35*, 130-136.
(25) Friedlander, S. K. *J. Meterol.* **1960**, *17*, 373-374.
(26) Friedlander, S. K. *J. Meterol.* **1960**, *17*, 479-483.
(27) Alldredge, A. L.; Cole, J. J.; Caron, D. A. *Limnol. Oceanogr.* **1986**, *31*, 68-78.
(28) Faist, W. K. *Adv. Chem. Ser.* **1980**, *No. 189*, 259-282.
(29) Logan, B. E.; Wilkinson, D. B. *Biotechnol. Bioeng.* **1991**, *38*, 389-396.
(30) Logan, B. E.; Alldredge, A. L. *Mar. Biol.* **1989**, *101*, 443-450.
(31) Li, D.-h.; Ganczarczyk, J. J. *Environ. Sci. Technol.* **1989**, *23*, 1385-1389.
(32) Alldredge, A. L. University of California, Santa Barbara, unpublished.
(33) Adler, P. M. *J. Colloid Interface Sci.* **1981**, *81*, 531-535.
(34) Adler, P. M. In *The Fractal Approach to Heterogeneous Chemistry*; Avnir, D., Ed.; Wiley: New York, 1989; Chapter 4.2.

Received for review March 4, 1991. Revised manuscript received June 17, 1991. Accepted June 26, 1991. Funding for this research was provided through ONR Contracts N000014-88-K0387 and 423G004-01.

Interactions of Acidic Metal-Rich Coal Pile Runoff with a Subsoil

Michael A. Anderson,*,† Paul M. Bertsch,‡ Steven B. Feldman,§ and Lucian W. Zelazny§

Department of Soil and Environmental Sciences, University of California, Riverside, California 92521, Division of Biogeochemistry, University of Georgia, Savannah River Ecology Laboratory, Drawer E, Aiken, South Carolina 29801, and Department of Crop and Soil Environmental Sciences, Virginia Polytechnic Institute and State University, Blacksburg, Virginia 24061

■ Highly acidic and metal-rich runoff from coal storage facilities can have a dramatic impact on local surface water and groundwater quality. In order to identify important reactions governing metal transport within subsurface environments subject to infiltration of coal pile runoff (CPR), samples of uncontaminated subsoil adjacent to a coal stockpile runoff containment basin at the U.S. Department of Energy's Savannah River Site were collected and subjected to leaching with acidic, metalliferous CPR. Effluent was collected and multicomponent transport through the subsoil evaluated. Mass balance calculations, a sequential dissolution scheme in which column leaching was terminated and elements were partitioned to water, 1 M NH_4Cl, and ammonium oxalate in the dark-extractable phases, and mineralogical and surface chemical analyses were used to identify important chemical processes and mineralogical alterations occurring during leaching.

Introduction

Analogous to mining operations, the storage of coal can also generate highly acidic, metal-rich leachate resulting from the oxidation of sulfidic ores present in coal as impurities (*1*, *2*). Additional water quality concerns with regard to coal storage include that coal stockpiles are relatively abundant, not restricted to areas associated with mining operations, and often uncontrolled.

The interaction of these metalliferous acid leachates with more alkaline surface waters results in neutralization or dilution of acidity, precipitation of iron and aluminum hydroxides, oxyhydroxides, and/or basic sulfates (*3-6*), and sorption or coprecipitation of heavy metals to the freshly precipitated materials (*7-11*). Wangen and Jones (*12*) evaluated the capacity of different soils to neutralize coal mineral waste leachate and found that carbonate content governed acidity and also the metal concentrations of soil column effluent. A naturally acidic soil, with no free carbonates present, afforded little attenuation (*12*).

Inasmuch as a significant portion of the U.S. coal reserves and coal stockpiles resides within moderately to highly weathered geologic regions with limited carbonate alkalinity, an evaluation of the subsurface mobility of contaminants from coal pile runoff within a weathered, naturally acidic subsoil was undertaken.

Experimental Section

Study Site. Soil samples were collected from a site immediately adjacent to the D-area coal pile runoff (CPR) containment basin at the U.S. Department of Energy's Savannah River Site near Aiken, SC (Figure 1). The coal stockpile is 3.6 ha in areal extent, containing approximately 131 000 metric tons of low-S (1-2%) coal. The basin is 5.1 ha with a volume capacity near 3.8×10^{10} L. Monitoring well data (*13*) indicate significant degradation of groundwater downgradient of the coal pile and basin.

Soil Sampling and General Characterization. The basin was created by excavation and removal of the surficial 1-2 m of Fuquay soil (loamy, siliceous, thermic arenic Plinthic Paleudults). Subsoil was sampled 0.25-0.75 m below the basin surface, or approximately 2.25-2.75 m below the natural soil surface, by augering in uncontaminated soils adjacent to the basin. Bulk densities were determined on samples extruded from cores of known volume (*14*). The samples were weighed prior and subsequent to oven drying at 105 °C. Bulk densities were taken as the oven dry weight divided by core volume. Porosities were calculated from the bulk densities assuming a particle density of 2.65 g cm^{-3} (*15*). Particle-size distributions were determined via a modified pipet method (*16*).

Bulk soil samples were air-dried and passed through a 2-mm sieve. Soil pH was determined on 1:1 soil-water equilibrations (*17*). Noncrystalline and free oxide contents of triplicate 1-g (oven dry weight basis) subsamples were estimated via the 4-h ammonium oxalate in the dark (Ox) and dithionite-citrate-bicarbonate (DCB) procedures, respectively (*18*). Soil organic matter contents were determined with the Walkley-Black method (*19*). Cation-exchange capacities of the whole soils were determined by summation of native cations exchanged from triplicate 5-g (oven dry weight basis) subsamples with three 30-min extractions of 1 M NH_4Cl.

Column Leaching Experiments. Air-dried, <2-mm-diameter soils were packed into duplicate 25 cm × 2.54 cm columns to a uniform bulk density of 1.50 g cm^{-3}. Columns were then wet from the bottom with deionized water supplied at a constant flow equivalent to a Darcy velocity

† University of California.
‡ University of Georgia.
§ Virginia Polytechnic Institute and State University.

 0013-936X/91/0925-2038$02.50/0 © 1991 American Chemical Society

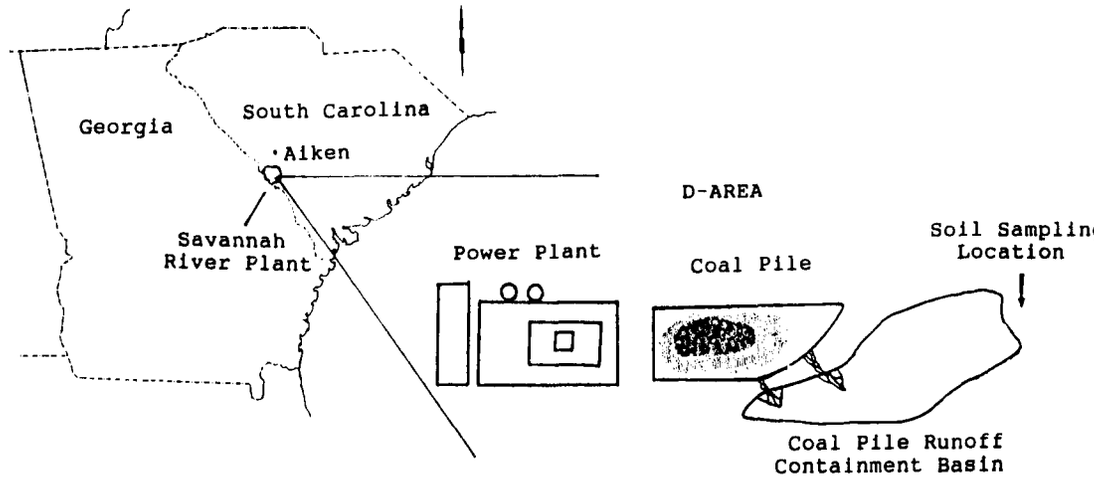

Figure 1. Study site.

(q) of 1.3 cm h^{-1} via a Dionex APM pump module (Dionex Corp., Sunnyvale, CA). Once steady saturated flow was attained, the columns were allowed to equilibrate overnight. Coal pile runoff collected from the basin was then supplied and the columns were leached under steady saturated flow (q = 1.3 cm h^{-1}). Effluent was collected via an LKB linear fraction collector. Column dispersivities were determined after leaching was completed via pulse injections equivalent to ~1 pore volume of 5 mM LiBr followed by additional runoff. Breakthrough data were then analyzed via the parameter estimation method of Parker and van Genucthen (*20*).

Results from the transport studies are presented using reduced values for time or, equivalently, as the number of pore volumes supplied to the columns (V/V_0), where V is the total volume supplied to the column and V_0 the total pore volume within the columns, and concentration (C/C_0), where C is the effluent concentration and C_0 the concentration of the influent.

Duplicated columns were also leached with 0–8, 12, and 60 pore volumes of CPR after which the leaching was stopped, and the soils were extruded and homogenized. The influence of increasing cumulative CPR influent flux on a number of chemical and mineralogical properties was then evaluated.

Element Partitioning. The partitioning of elements between operationally defined phases via sequential extraction techniques can be useful in assessing the bioavailability (*21*) and persistence (*22*) of metals within contaminated soils. For this investigation, elements were partitioned into three phases as a function of cumulative influent flux, water-soluble, 1 M NH_4Cl extractable, and ammonium oxalate extractable (Ox) fractions, corresponding roughly to water-soluble, exchangeable, and poorly crystalline phases (*18*), respectively. Water-soluble contents were determined from breakthrough curves. Dry weight samples (1.5-g equiv) were extracted twice with 7.5 mL of 1 M NH_4Cl and the supernatants combined, followed by a 10-mL deionized water wash, which was discarded. The previously extracted soils were then equilibrated with 30 mL of Ox reagent for 4 h in the dark (*18*).

Mineralogy. Silt (2–50 μm) and clay-sized (<2 μm) materials were separated from whole soils after Fe removal by DCB (*18*) via wet sieving and centrifugation (*23*). A tile mounting technique was used to prepare oriented clay mounts with Mg and K saturations (*24*). A clean, flat ceramic tile was placed in a suction apparatus and a clay suspension containing approximately 250 mg of sample was pipeted onto the tile. After free water had been drawn through the tile, 5 mL of 1 M KCl was added. This process was repeated a total of five times, followed by washing in a similar fashion with deionized water (five times). Analogously, Mg-saturated tiles were also prepared with 0.5 M $MgCl_2$, followed by one wash with 5 mL of 20% glycerol solution after the fifth water wash (Mg–gly).

The mounts were X-rayed with a Diano X-ray spectrometer (Diano Corp., Woburn, MA) from 2 to 32° 2θ at a step speed of 0.019° 2θ s^{-1} using a Cu source (wavelength 1.542 Å). The Mg–gly tile mounts were X-rayed at room temperature and after heating to 110 °C; the K-saturated tile mounts were X-rayed at room temperature and after heating to 110, 300, and 550 °C. Semioriented powder mounts of silt (2–50 μm) fractions (Na-saturated) were prepared by depositing oven-dried samples into a recessed holder and smoothing with a spatula. Clay (5 mg, <2 μm) subsamples from the K-saturated tile mounts were removed for analysis by differential scanning calorimetry (DSC). Samples were placed into gold pans and heated in an N_2 atmosphere to 625 °C at a rate of 20 °C min^{-1} with a Du Pont 1090 thermal analyzer (E. I. du Pont De Nemours and Co., Wilmington, DE).

Oxide mineralogy of the silt + clay (<50 μm) fractions were determined on nondeferrated samples by using X-ray diffraction (XRD). For these determinations, samples were scanned at a step speed of 0.00125° 2θ s^{-1}. A background diffractogram of a DCB-treated silt + clay sample (<50 μm) was subtracted from the oxide patterns.

Infrared Analysis. Fourier transform infrared analyses of silt + clay (<50 μm) fractions of soils leached with runoff were performed with a Digilab FTS-45 spectrophotometer (Bio-Rad, Digilab Division, Cambridge, MA) using diffuse reflectance (DRIFT). Sixty-four scans, sampled at 4-cm^{-1} resolution, were coadded to generate each spectrum.

Electrophoretic Mobility. Samples (~10 g) from soils leached with 0, 4, 8, 12, and 60 pore volumes of runoff from above were equilibrated with 30 mL of 1 M $NaClO_4$ and centrifuged; the supernatant was discarded. The process was repeated an additional four times, followed by two washes with 0.01 M $NaClO_4$. Samples were resuspended in 0.01 M $NaClO_4$ and wet sieved to remove >53-μm particles. The silt + clay (<50 μm) suspensions that passed the sieve were collected and 0.25-mL samples of these suspensions were then pipeted into 30-mL polycarbonate Oak Ridge tubes. Twenty-milliliter aliquots of 0.01 M $NaClO_4$ adjusted to pH 3, 4, 5, 7, and 9 with 0.1 M $HClO_4$ or NaOH were added; the resultant mixtures were equilibrated for 15 min and centrifuged and the supernatants

Table I. Composition of the Coal Pile Runoff Used in the Column Experiments

component	concn,[a] mg L^{-1}	component	concn,[a] mg L^{-1}
pH	2.13	K^+	1.668
		Li^+	0.232
Al^{3+}	101.0	Mg^{2+}	62.17
Be^{2+}	0.055	Mn^{2+}	7.302
Ca^{2+}	83.62	Na^+	11.52
Co^{2+}	0.461	Ni^{2+}	0.878
Cr^{3+}	0.010	H_4SiO_4	69.4
Cu^{2+}	0.262	SO_4^{2-}	2024
Fe^{2+}	4.70	Sr^{2+}	0.791
Fe^{3+}	119.5	Zn^{2+}	2.392

[a] Except pH.

discarded. Two additional treatments followed. The pH of an aliquot of the final wash was recorded before the sedimented material was resuspended (final suspension concentration was approximately 0.5 mg mL^{-1}).

The above treated suspensions were then analyzed for electrophoretic mobilities with a Zetasizer 3 (Malvern Instruments, Malvern, England). Cell chambers were filled with a solution equivalent in salt concentration and pH to that of the sample suspensions. Triplicate mobility determinations were made, with a 30-s count time and applied voltage and current of 80 mV and 3 mA, respectively.

Analytical. Hydrogen ion activities of the soil–water extracts and column effluent fractions were determined with a Radiometer GK2401C combined glass–calomel electrode and a Radiometer PHM 84 pH meter (Radiometer of America, Westlake, OH). Bromide concentrations were determined with a Fisher 13-620-520 Br^- ion specific electrode (Fisher Scientific, Fairlawn, NJ) and a Radiometer K401 reference electrode (Radiometer of America). Effluent fractions and extracts were analyzed for total dissolved major and trace element concentrations via inductively coupled plasma emission spectroscopy (ICPES). Sulfate analysis was performed using a Dionex System 2010i ion chromatograph (IC) (Dionex Corp.). Ferrous iron concentrations were determined via the *o*-phenanthroline method (*25*).

Speciation. Analytical speciation of elements was limited to S and Fe. Excellent agreement was obtained between total S via ICPES and S concentrations as SO_4^{2-} via IC (<1% deviation); as a result, all S was considered as SO_4^{2-} (Table I). Concentrations of Fe^{3+} were calculated from the difference between ICPES total Fe and *o*-phenanthroline-determined Fe^{2+}.

The CPR and column effluent samples were numerically speciated by use of MINTEQA2 (*26*) and saturation indexes (SI), defined as

$$\mathrm{SI} = \log (\mathrm{IAP}/K_{sp}) \quad (1)$$

where IAP is the ion activity product of a solution and K_{sp} is the solubility product for a given mineral phase, calculated. The reader is referred to ref 26 for a compilation of thermodynamic data used in these calculations.

Mass Balance. To properly account for components retained by the soil columns at any time, t, a mass balance about the column was calculated (Figure 2). The total volume of the column, V_T (L^3), was determined (127 cm^3). A total reactive mass of a component i, $M_{i,T}$ (M) was defined as

$$M_{i,T} = M_{i,aq} + M_{i,ex} + M_{i,ox} \quad (2)$$

where $M_{i,aq}$ is the total mass of component i in the aqueous phase, $M_{i,ex}$ is the total mass of component i on the exchange phase, and $M_{i,ox}$ is the total mass of component i that is extractable via the 4-h Ox procedure. Runoff of concentration $C_{i,in}$ ($M\ L^{-3}$) for each component (Table I) was supplied at constant volumetric flow Q, (for this investigation, 6.8 $cm^3\ h^{-1}$). Column effluent of concentration $C_{i,out}$ ($M\ L^{-3}$) was collected as a function of time. The change in total component mass within the column over time was, since V_T is constant, expressed by the equation

$$\Delta M_{i,T}/\Delta t = Q(C_{i,in} - C_{i,out}) \quad (3)$$

Solutions to eq 3 for the components evaluated were compared to that component mass which was recovered by the sequential extraction procedure.

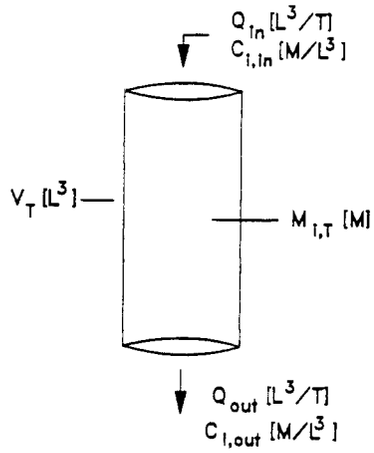

Figure 2. Mass balance about column.

Results and Discussion

Coal Pile Runoff. The CPR was highly acidic, with considerable dissolved SO_4^{2-}, Fe^{3+}, and Al concentrations (Table I). The runoff also had elevated concentrations of alkaline earth and transition metals (Table I). A redox potential of 0.77 V (pe = 13.05) was calculated for the CPR based upon Fe^{2+} and Fe^{3+} concentrations by use of MINTEQA2.

Results from MINTEQA2 speciations also indicated that the influent CPR was undersaturated with respect to a number of Al-bearing minerals, including jurbanite ($AlOHSO_4$) (SI = −0.51), gibbsite ($Al(OH)_3$) (SI = −5.95), and alunite ($KAl_3(SO_4)_2(OH)_6$) (SI = −5.65). The CPR was supersaturated with respect to Na–jarosite ($NaFe_3(SO_4)_2(OH)_6$), K–jarosite ($KFe_3(SO_4)_2(OH)_6$), H–jarosite ($HFe_3(SO_4)(OH)_6$, and goethite (α-FeOOH), however (SI = 2.56, 5.08, 4.72, and 1.42, respectively). The CPR was also supersaturated with respect to quartz (α-SiO_2) (SI = 0.87), though slightly undersaturated with respect to amorphous SiO_2 (SI = −0.43).

Jurbanite has been previously suggested as controlling Al solubility within acid mine drainage and acid sulfate soils (*27, 28*), though Nordstrom and Ball (*29*) and Filipek et al. (*30*) found that surface waters with pH <4.6 tended to transport Al conservatively and concluded that the semblance of dissolved Al to that predicted by jurbanite solubility is likely coincidental. Jarosite has been suggested as controlling Fe solubility within acid sulfate systems (*6*), though significant supersaturation of acid mine drainage with respect to jarosite, as observed here, has also been reported (*7, 30*).

Soil. The subsoil is characteristic of soils within the highly weathered southeastern Upper Coastal Plain region, having naturally low pH (4.96), a modest cation-exchange capacity (6.82 $cmol_c\ kg^{-1}$), a predominance of exchangeable Al (83.9%), and a coarse texture (sandy clay loam). The

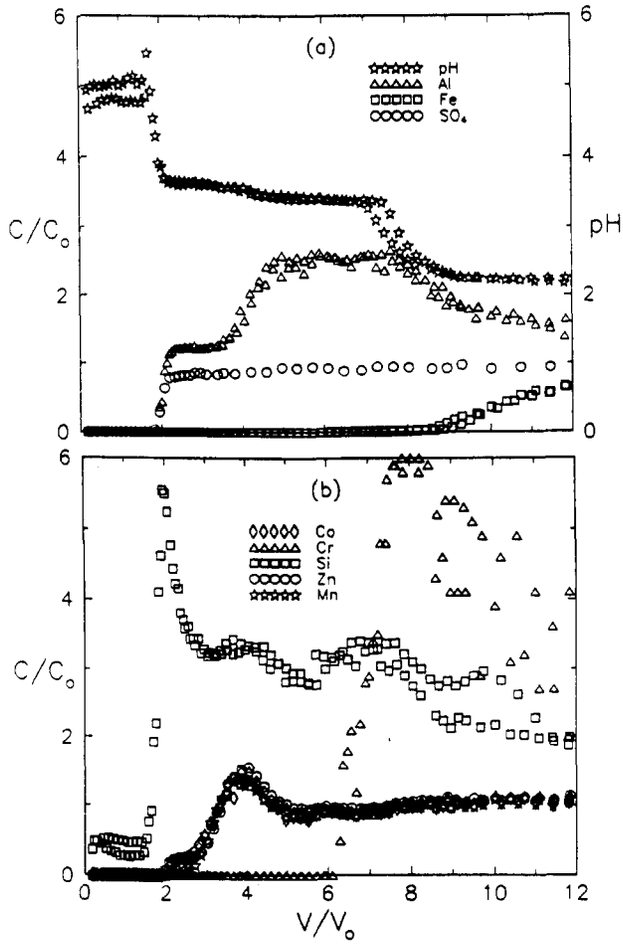

Figure 3. Column effluent concentration histories. (Data from duplicate columns provided.)

soil also had a low organic matter content (<0.15%). The bulk density for the first sampling depth (0–0.25 m beneath basin surface, or 2–2.25 m below natural soil surface) was 1.53 g cm^{-3}. A saturated hydraulic conductivity of approximately 1 cm h^{-1} was estimated from particle size and bulk density data (*31*). The subsoil possessed significant quantities of DCB- and Ox-extractable Fe (0.83 and 0.05% on a weight basis, respectively).

Quartz comprised the major mineral component within the subsoil (80%), accounting for all sand and silt-sized material. Kaolinite, a common 1:1 weathering product of 2:1 phyllosilicate minerals and a dominant mineral within the highly weathered Piedmont and Coastal Plain provinces, was the next most abundant mineral (13%). A number of 2:1 phyllosilicate minerals were also present (3% smectite, 1% mica, 2% randomly interstratified mica–vermiculite, and 1% hydroxy-interlayered vermiculite).

Element Mobility. Reproducibility of columns and column effluent concentration histories was very good. The duplicate columns yielded fitted dispersion coefficients of 2.00 and 2.02 cm^2 h^{-1}, as well as very similar column effluent concentration histories (Figure 3).

A range in relative mobilities of components within the CPR was observed (Figure 3). Transport of conservative, nonreactive solutes through homogeneous porous media should result in column effluent concentration histories in which $C/C_0 = 0.5$ at $V/V_0 = 1$; observed breakthrough behavior deviated significantly from this general trend. The classical, one-region, convection–dispersion equation (CDE) was found to accurately describe the breakthrough of Br^- (as LiBr), however ($R^2 = 0.98$).

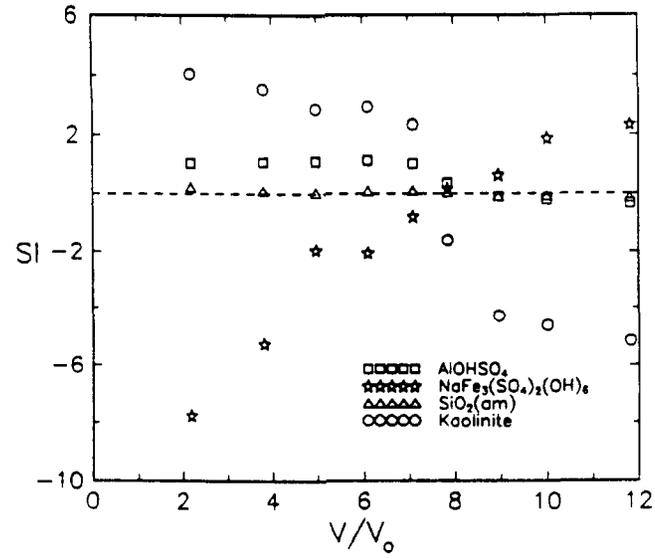

Figure 4. MINTEQA2-calculated saturation indexes for selected minerals from column effluent concentration data.

Hydrogen ion activity as a function of pore volume exhibited a two-step response. The pH remained essentially constant as the initial volumes of equilibrated deionized water were displaced with the CPR solution. After ~2 pore volumes, a slight rise in pH was observed, followed immediately by a rapid decrease to near pH 3.5 (Figure 3a). Apparent buffering reactions maintained effluent pH near 3.5 for an additional 5 pore volumes (despite supply of pH 2.1 influent solution) before descending toward the influent pH level (Figure 3a).

Appearance of both Al and SO_4^{2-} in the column effluent at a V/V_0 near 2 was also noted and coincided with the initial reduction in effluent pH (Figure 3a). Iron(III) was found within the column effluent when the effluent pH dropped below 3 (Figure 3a), where increased Fe solubility would be expected (*32*). Silicon slightly preceded sulfate and Al breakthrough (Figure 3b). Co, Mn, and Zn exhibited remarkably similar breakthrough behavior, appearing in the column effluent with sulfate, but reaching peak effluent concentrations closer to V/V_0 of 4 (Figure 3b). Chromium appeared in column effluent only after 6 pore volumes had passed the columns and pH descended below 3, and reached a peak effluent concentration at 8 pore volumes, the magnitude of which implies a net efflux from the soil.

Speciation of the column effluent yielded SIs for minerals that varied widely as a function of V/V_0 (Figure 4). The column effluent was slightly supersaturated with respect to jurbanite until approximately 8 pore volumes (Figure 4), which coincides with the decrease in effluent pH from 3.5 toward that of the influent (Figure 3a). Saturation indexes as a function of pore volume for H–, Na–, and K–jarosite all followed similar trends, with significant undersaturation at low V/V_0 and increasing SI with increasing V/V_0 (Figure 4). As with the CPR, under low-pH (high V/V_0) conditions, the column effluent was supersaturated with respect to the jarosites. The activity of Si in solution followed fairly closely that predicted from equilibrium with respect to an amorphous SiO_2 phase (Figure 4). While a number of solid phases have been proposed to control trace-metal solubilities in soils (*33*), no evidence for precipitation–dissolution reactions controlling metal mobility was found. The column effluent was also supersaturated with respect to kaolinite and other phyllosilicates at low V/V_0, whereas SI decreased below 0 at V/V_0 greater than 8 (Figure 4), which coincided with

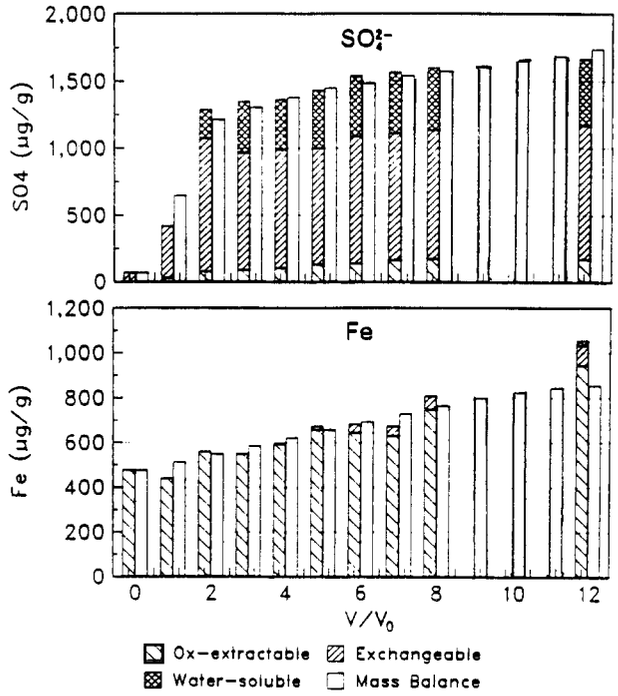

Figure 5. Mass balance and element partitioning results: SO_4^{2-} and Fe. (Element partitioning not determined on samples subjected to 9, 10, or 11 pore volumes of coal pile runoff.)

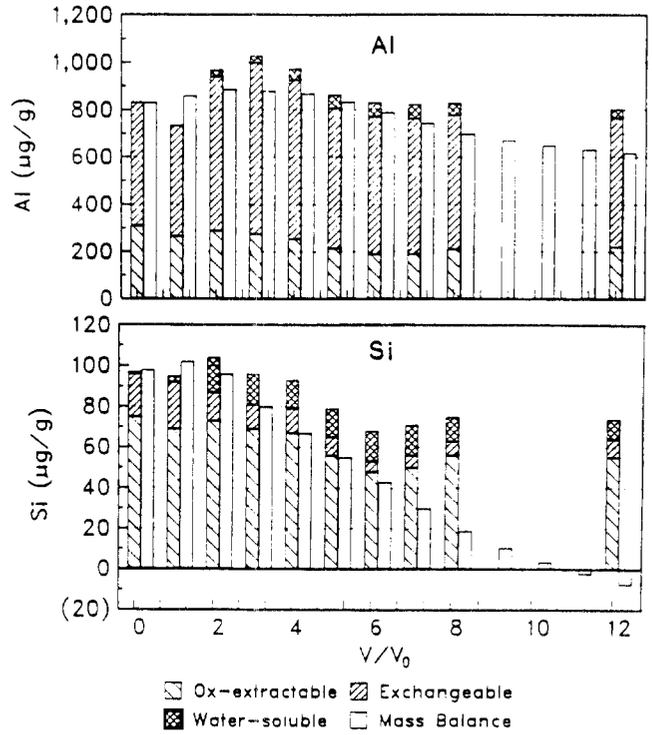

Figure 6. Mass balance and element partitioning results: Al and Si. (Element partitioning not determined on samples subjected to 9, 10, or 11 pore volumes of coal pile runoff.)

reduction in pH below 3.5 (Figure 3a). Thus, kaolinite and other minerals present in the soil matrix would be expected to dissolve and contribute structural elements to the solution (*30*, *34*).

Based upon observed effluent concentration histories and numerical speciation results, some reactions governing component mobility may be proposed. Given previous observations of sulfate sorption to soil and soil constituents (*35*, *36*) and precipitation of basic iron and aluminum sulfates (*6*, *28*), that sulfate is the predominant anion in the system, and the necessary condition of electroneutrality in solution, it appears that sulfate mobility governed initial appearance of certain cationic components in the column effluent. Sorption of sulfate via displacement of surface hydroxyls tends to increase pH (*35*) and accounts for the slight rise in pH noted (Figure 3a). Iron(III) flux through the soil exhibited a pronounced pH dependence, qualitatively following simple solubility–pH relations. Ion exchange apparently governed the mobility of Co, Mn, and Zn within the soil.

A feature common to all components except H^+, Fe^{3+}, and SO_4^{2-} is that of peak effluent concentrations exceeding influent or source concentrations (Table I). That is, the flux of CPR through soil generates so-called "concentration waves" via exchange, displacement of native soil cations, and precipitation–dissolution reactions. Such a phenomenon implies that even if runoff meets applicable water quality standards, groundwater downgradient may exceed concentration limits as the wave advances with the groundwater flow.

Element Partitioning. The distribution of elements between the water-soluble, 1 M NH_4Cl exchangeable, and Ox-extractable fractions varied for different components and as a function of CPR volume leached. Reproducibility of extractions was fair, with relative standard deviations (RSD) for triplicated extractions ranging from 2.9 to 12.2%, with an average RSD of 8.9%.

There was a modest amount of SO_4^{2-} initially present in the soil, which was recovered in the NH_4Cl extraction (Figure 5, SO_4^{2-}). Infiltration and movement of runoff through the soil column resulted in increasing total SO_4^{2-}, in good agreement with mass balance calculations (Figure 5, SO_4^{2-}). Extraction results indicated the SO_4^{2-} partitioned principally to the NH_4Cl-extractable fraction, with some residing within the aqueous and also the Ox-extractable phases (Figure 5, SO_4^{2-}). Total sorbed SO_4^{2-} (as sum of extractable SO_4^{2-}) measured near 1000 $\mu g\ g^{-1}$ of soil with nearly 80% recoverable in the NH_4Cl. Singh (*35*) reported a similar magnitude of SO_4^{2-} sorption (approximately 1000 $\mu g\ g^{-1}$) and noted increased sorption with decreasing pH; however, he found only 20% was desorbed with 0.01 M $Ca(NO_3)_2$. The difference in desorption efficiencies between the neutral salt extractants likely resulted from the significantly higher salt concentration used in this study. A monotonic increase in Ox-extractable sulfate with increasing V/V_0 was also noted in this investigation.

Iron was found to reside almost entirely within the Ox-extractable fraction prior to addition of CPR, with Ox-extractable Fe increasing steadily with increasing pore volumes (Figure 5, Fe). Partitioning of limited quantities of Fe first to the exchange phase, at pH 3.5, and subsequently to a water-soluble phase as the pH dropped near 2 (12 pore volumes) was also observed. The increase in Ox-extractable Fe between 0 and 8 pore volumes can be directly related to the retention of Fe within the soil column (i.e., the lack of Fe within the column effluent (Figure 3a)), in good agreement with mass retained via mass balance calculations (Figure 5, Fe). Mass balance calculations did, however, underestimate the extractable total reactive Fe for the sample subjected to 12 pore volumes (Figure 5, Fe). It appears that as the soil buffer capacity was exhausted and the pH dropped to near 2, additional native crystalline Fe phases were destabilized and thus became extractable in the Ox treatment.

Aluminum was distributed between the exchangeable and Ox-extractable pools prior to addition of leachate, as illustrated (Figure 6, Al). A maximum in exchangeable Al was noted after approximately 3 pore volumes of CPR were

supplied, preceding the wave of increased Al in fractions collected at subsequent pore volumes from the leaching experiments (Figure 3a), with some water-soluble Al also detectable after 2 pore volumes (corresponding to the reduction in effluent pH to 3.5) (Figure 6, Al). A gradual reduction in Ox-extractable Al with increasing pore volumes was also noted, implying dissolution of native poorly crystalline Al phases.

Silicon resided chiefly within the Ox and, to a lesser extent, exchangeable pools, though some Si was in solution prior to leaching (Figure 6, Si). Maximum water-soluble Si occurred at 2 pore volumes (Figure 6, Si). Leaching of the sample resulted in a gradual diminution in Ox-extractable Si to a minimum at 6 pore volumes, which was followed by increasing Ox-extractable Si. Mass balance calculations indicated a net export of Si out of the system, which completely exhausted the total initial reactive mass specified (Figure 6, Si). Deviation between observed and predicted total reactive Si indicates that an additional phase not initially accounted for is capable of transforming to these more labile phases represented by the NH_4Cl and Ox fractions. Desilication and formation of oxidic components is well-documented within soils subjected to naturally acidic conditions (e.g., spodic horizons formed under coniferous vegetation) as well as clays and sediments subjected to acid mine water (*30*, *34*).

No detectable Co or Zn was identified in the three pools prior to leaching with the CPR (Figure 7, Co and Zn). Exchangeable forms were noted after 1 pore volume, with additional exchangeable and also soluble metal contents occurring upon extraction after 2 pore volumes. Exchangeable Zn tended to decrease somewhat between 2 and 3 pore volumes (coincident with maximal exchangeable Al) before ascending again (Figure 7, Zn). Such behavior implies that Zn and Al are competing for available exchange sites within the soil. Cobalt exhibited somewhat different behavior in that exchangeable Co tended to increase generally with increasing leaching volumes (Figure 7, Co). In neither case was there evidence for sorption or precipitation of these metals. Manganese was found in minor quantities prior to leaching within an Ox-extractable phase (Figure 7, Mn). A maximum in exchange-phase Mn occurred at 2 pore volumes (Figure 7, Mn), with a minimum again coincident with peak effluent Mn concentration from the breakthrough experiments (Figure 3b) and maximum exchange-phase Al (Figure 6, Al). No evidence for accumulation in or mobilization from the Ox phase was apparent. Thus, under the conditions evaluated here, specific interactions with hydrous oxides and coprecipitation with solid phases were of secondary importance in regulating Co, Mn, and Zn mobility. Rather, simple partitioning between aqueous and exchange phases constituted the principal reactions governing transport within acid runoff percolating through the subsoil.

Chromium was found associated with the Ox-extractable phase for all treatments, including the native condition (Figure 7, Cr). Chromium partitioning was limited to this phase until the seventh pore volume, whereas Cr was found in both the exchange and water-soluble phases (Figure 7, Cr), which coincides with the onset of significant elution of Cr from the soil column (Figure 3b). This partitioning behavior contrasts with that for the previous transition metals and implies that a sorption or coprecipitation reaction controlled Cr mobility. The low concentrations of Cr in the runoff (10 $\mu g\ L^{-1}$) resulted in negligible loading to the soil.

Clay Mineralogy. The potential for alterations in phyllosilicate mineralogy upon leaching with the runoff

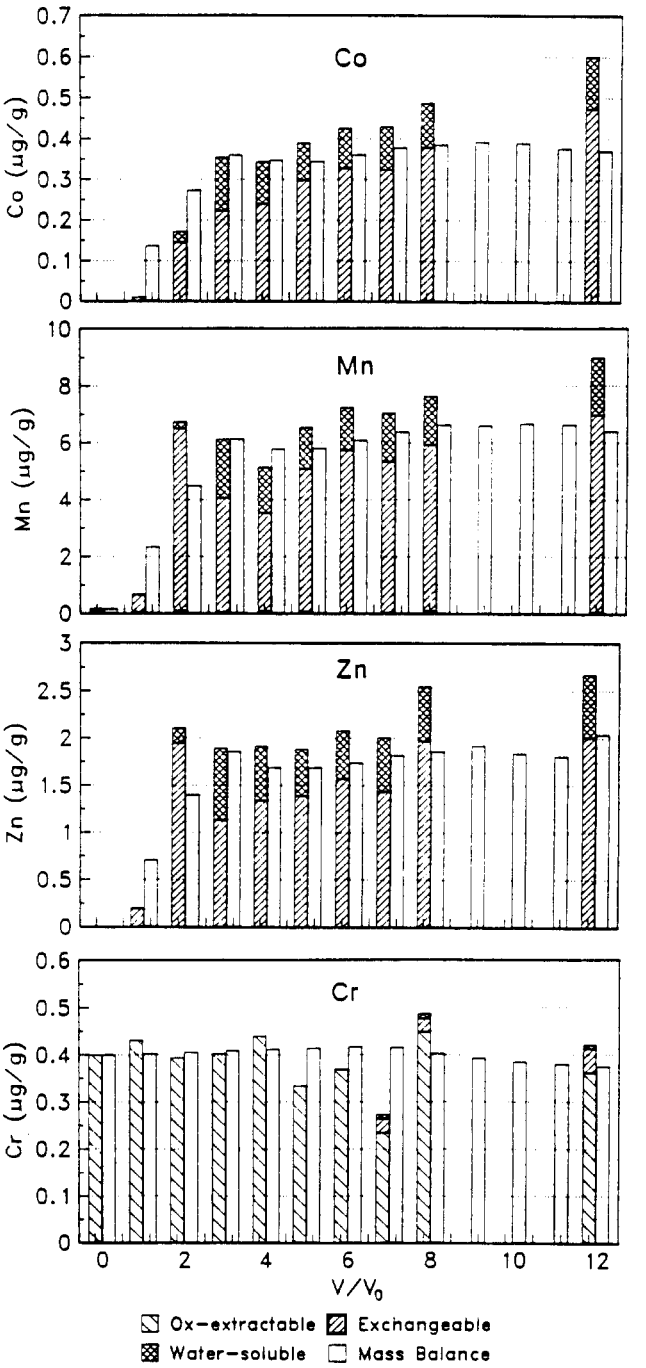

Figure 7. Mass balance and element partitioning results: Co, Mn, Zn, and Cr. (Element partitioning not determined on samples subjected to 9, 10, or 11 pore volumes of coal pile runoff.)

was evaluated through XRD and DSC analysis. Clay fractions from samples leached with 0, 4, 8, 12, and 60 pore volumes were X-rayed after Fe removal. Despite relatively high inputs of acidity, only subtle alterations were noted. For example, diffractograms of KCl, 25 °C treated clays showed no discernible differences in the dominant 7.2-(001) and 3.6-Å (002) reflections of kaolinite, suggesting that no substantial changes in the crystallinity of this mineral occurred after leaching (Figure 8). Some slight reduction in the broad low-angle reflection between 14 and 20 Å and a concomitant increase in the 10-Å reflection was noted, however (Figure 8), implying possible degradation of the weakly ordered interstratified mica–vermiculite mineral or dissolution of hydroxy–Al interlayers within hydroxy-interlayer vermiculite to yield a better defined 10-Å vermiculitic component upon prolonged leaching.

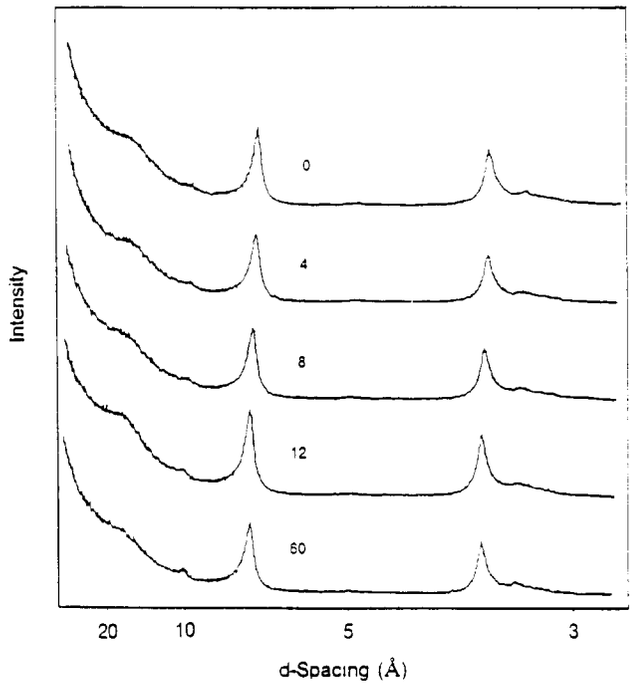

Figure 8. X-ray diffractograms of clay (<2 μm) fraction of subsoil after leaching with 0, 4, 8, 12, and 60 pore volumes of runoff (K-saturated, 25 °C).

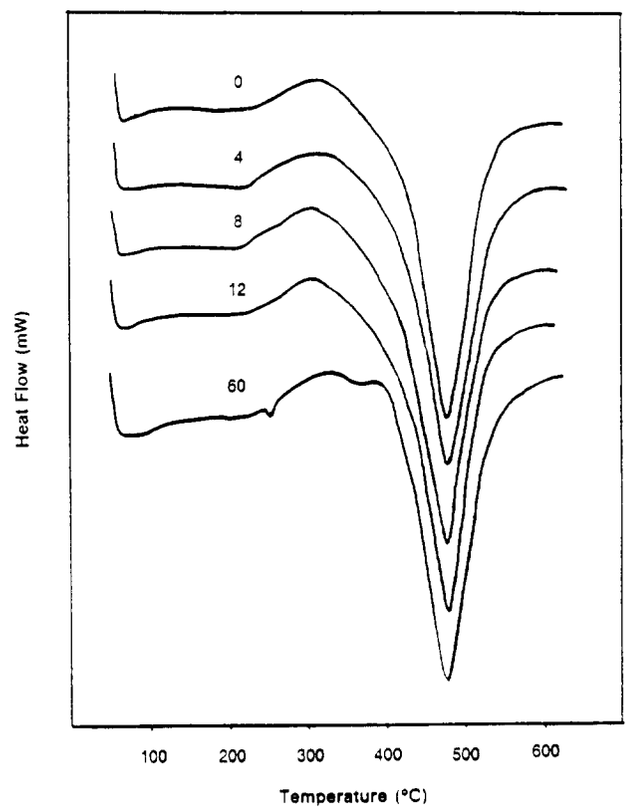

Figure 9. Thermograms of clay (<2 μm) fraction of subsoil after leaching with 0, 4, 8, 12, and 60 pore volumes of runoff.

Changes in DSC scans provided evidence for the dissolution of kaolinite and precipitation of gibbsite. There was a slight reduction in the area of the 480 °C kaolinite endotherm and the appearance of a subtle endotherm near 280 °C, characteristic for gibbsite, after leaching with 60 pore volumes of CPR (Figure 9). Gibbsite is a common weathering product resulting from desilication of phyllosilicates subjected to acidic conditions. The reduction in

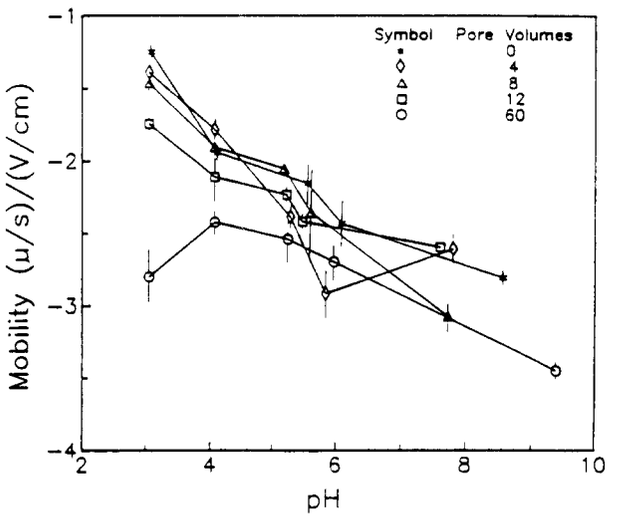

Figure 10. Electrophoretic mobility of silt + clay (<50 μm) fraction of subsoil after leaching with 0, 4, 8, 12, and 60 pore volumes of runoff.

the low-temperature skewness of the kaolinite endotherm with increasing pore volumes and emergence of a more symmetrical endotherm at 60 pore volumes suggests gradual dissolution of hydroxy-interlayer Al as inferred from XRD analyses.

The mineralogy of the oxidic phases was evaluated via differential XRD (i.e., subtraction of patterns of DCB-treated samples from that of untreated samples). Evidence for goethite (4.188-, 2.566-, 2.502-, 1.818-, and 1.515-Å reflections) and hematite (1.688- and 1.476-Å reflections) was found for the samples. No changes in the diffractograms with increasing pore volumes, and a general lack of characteristic peaks, including the strong jarosite reflection at 3.03 Å, suggest an absence of basic aluminum and iron sulfate phases forming during the leaching process, though analytical limitations on detection of small amounts of these phases preclude firm support for or against their existence.

Infrared Analysis. Infrared analysis of the samples yielded very similar spectra as well. Well-defined peaks at 3700, 3625, 1100, 1010, and 910 cm^{-1}, diagnostic for kaolinite (*37*), dominated the spectra. Broad absorbance bands centered near 3300 cm^{-1} and near 1640 cm^{-1} were also noted and correspond to water likely retained by swelling 2:1 minerals within the samples. Characteristic jarosite and sulfate absorbances at 1175, 1110, and 1020 cm^{-1} (*38*) were absent.

Electrophoretic Mobilities. Electrophoretic mobility of samples increased with increased leaching for any given suspension pH and increased with increasing suspension pH (Figure 10). The high mobilities even at low pH support the mineralogical data indicating appreciable constant-charge mineral content (*39*). The contribution of variable-charge minerals (e.g., kaolinite and oxyhydroxides) is also significant, as can be seen by the steep increase in mobility upon increasing suspension pH (Figure 10) (*40*). A somewhat flatter pH response with increasing pore volumes was observed (Figure 10). Additional charge was apparently generated via specific adsorption of sulfate to oxidic phases (*41*, *42*) and by dissolution of native constant charge-blocking oxidic phases.

Summary and Conclusions

Results of element partitioning via an operationally defined selective dissolution procedure were generally in good agreement with mass balance calculations and corroborate inferences made about element mobility from

breakthrough data. Iron was observed to accumulate within the soil column and was associated chiefly with the Ox-extractable phase. Aluminum was partitioned between the water, NH_4Cl-exchangeable, and Ox-extractable phases, with the water phase increasing and the Ox phase decreasing with increasing leaching. Silicon tended to follow Al to some extent, with Ox-extractable Si decreasing with increasing leaching. Cobalt and Zn were associated with the exchange phase early in the leaching process and then partitioned fairly consistently between the water and exchange phases, supporting the notion that ion exchange was the dominant mechanism governing mobility for these elements. Manganese followed the other divalent metal ions with the exception that a limited quantity was found associated with the Ox-extractable phase. Chromium departed significantly from the other first-row transition metals in that its mobility appeared to be governed by specific adsorption–desorption reactions.

Sustained leaching had little discernible effect on gross phyllosilicate mineralogy, though formation of gibbsite and limited degradation of hydroxy–Al interlayers within hydroxy-interlayered vermiculite was demonstrated after 60 pore volumes of CPR had been supplied to the column. Oxide mineralogy was fairly uniform, with goethite and hematite both present in the soils. Evidence for distinct basic aluminum or iron sulfate phases formed during leaching was generally lacking. Electrophoretic mobility increased (became more negative) with increased leaching, due in part to specific adsorption of sulfate and consequent generation of additional negative charge within the soil, and by dissolution of native charge-blocking oxidic phases.

These observations have a number of implications for soil and groundwater systems subject to infiltrating runoff from coal stockpiles and more generally from acid mine drainage. First of all, naturally acidic, noncarbonatic soils offer little resistance to subsurface migration of acidic, metal-rich runoff. As a result, coal stockpiles situated on such materials pose a serious threat to underlying groundwater systems. Facilities located on the Atlantic Coastal Plain, which possesses generally naturally acidic and often coarse-textured soils and relatively shallow aquifer systems, in particular are prone to degrade local water quality. The occurrence of both high industrial activity and urban populations over much of this physiographic province implies potentially severe local environmental problems.

The development of concentration waves attendant with infiltration and migration of runoff within subsurface materials further exacerbates potential water quality problems. That is, chromatographic and precipitation–dissolution reactions result in the development and movement of metals in waves of concentrations potentially greatly exceeding initial source concentrations. Discharge of effluent meeting appropriate water quality criteria may thus produce downgradient concentrations exceeding standards and source concentrations. This phenomenon poses difficult legal ramifications and also emphasizes the need for continued research evaluating multicomponent transport processes.

Acknowledgments

We thank Dr. Carl Strojan and Bruce Herbert for their thoughtful comments on an early draft of this manuscript.

Registry No. Al, 7429-90-5; Be, 7440-41-7; Ca, 7440-70-2; Co, 7440-48-4; Cr, 7440-47-3; Cu, 7440-50-8; Fe, 7439-89-6; K, 7440-09-7; Li, 7439-93-2; Mg, 7439-95-4; Mn, 7439-96-5; Na, 7440-23-5; Ni, 7440-02-0; Sr, 7440-24-6; Zn, 7440-66-6.

Literature Cited

(1) Davis, E. C.; Boegly, W. J. *J. Environ. Qual.* **1981**, *10*, 127–133.
(2) Swift, M. C. *Water Resour. Bull.* **1985**, *21*, 449–457.
(3) Theobald, P. K.; Lakin, H. W.; Hawkins, D. B. *Geochim. Cosmochim. Acta* **1963**, *27*, 121–132.
(4) Brady, K. S.; Bigham, J. M.; Jaynes, W. F.; Logan, T. J. *Clays Clay Miner.* **1986**, *34*, 266–274.
(5) Nordstrom, D. K.; Jenne, E. A.; Ball, J. W. In *Chemical Modeling of Aqueous Systems: Speciation, Sorption, Solubility, and Kinetics*; Jenne, E. A., Ed.; ACS Symposium Series 93; American Chemical Society: Washington, DC, 1979; pp 51–79.
(6) Nordstrom, D. K. In *Acid Sulfate Weathering*; Kittrick, J. A., Fanning, D. S., Hossner, L. R., Eds.; Soil Science Society of America Special Publication 10; Soil Science Society of America: Madison, WI, 1982; pp 37–56.
(7) Chapman, B. M.; Jones, D. R.; Jung, R. F. *Geochim. Cosmochim. Acta* **1983**, *47*, 1957–1973.
(8) Wangen, L. E.; Williams, J. M. *J.—Water Pollut. Control Fed.* **1982**, *54*, 1302–1310.
(9) Jones, K. C. *Environ. Pollut., Ser. B* **1986**, *12*, 249–263.
(10) Foster, P.; Hunt, D. T. E.; Morris, A. W. *Sci. Total Environ.* **1978**, *9*, 75–86.
(11) Robinson, G. D. *Chem. Geol.* **1981**, *33*, 65–79.
(12) Wangen, L. E.; Jones, M. M. *Environ. Geol. Water Sci.* **1984**, *6*, 161–170.
(13) *The Savannah River Plant's Groundwater Monitoring Program*; HP-88-098; Health Protection Department, Environmental Monitoring, Savannah River Plant, 1988.
(14) Blake, G. R.; Hartge, K. H. In *Methods of Soil Analysis, Part 1*; Klute, A., Ed.; Agronomy 9; American Society of Agronomy: Madison, WI, 1986; pp 363–382.
(15) Danielson, R. E.; Sutherland, P. L. In *Methods of Soil Analysis, Part 1*; Klute, A., Ed.; Agronomy 9; American Society of Agronomy: Madison, WI, 1986; pp 443–461.
(16) Miller, W. P.; Miller, D. M. *Commun. Soil Sci. Plant Anal.* **1987**, *18*, 1–15.
(17) McLean, E. O. In *Methods of Soil Analysis, Part 2*, Page, A. L., Miller, R. H., Keeney, D. R., Eds.; Agronomy 9; American Society of Agronomy: Madison, WI, 1982; pp 199–224.
(18) Jackson, M. L.; Lim, C. H.; Zelazny, L. W. In *Methods of Soil Analysis, Part 1*; Klute, A., Ed.; Agronomy 9; American Society of Agronomy: Madison, WI, 1986; pp 101–142.
(19) Allison, L. E. In *Methods of Soil Analysis, Part 2*; Black, C. A., Ed.; Agronomy 9; American Society of Agronomy: Madison, WI, 1965; pp 1367–1378.
(20) Parker, J. C.; van Genucthen, M. Th. Determining Transport Parameters from Laboratory and Field Tracer Experiments. *Va. Agric. Exp. Stn. Bull.* **1984**, *No. 84-3.*
(21) Jenne, E. A.; Luoma, S. N. In *Biological Implications of Metals in the Environment*; Proceedings, Hanford Life Science Symposium; Technical Information Center, Energy Research and Development Administration, Washington, DC, 1977; pp 110–143.
(22) Tessier, A.; Campbell, P. G. C.; Bisson, M. *Anal. Chem.* **1979**, *51*, 844–851.
(23) Whittig, L. D.; Allardice, W. R. In *Methods of Soil Analysis, Part 1*; Klute, A., Ed.; Agronomy 9; American Society of Agronomy: Madison, WI, 1986; pp 331–362.
(24) Rich, C. I.; Barnhisel, R. I. In *Minerals in Soil Environments*; Dixon, J. B., Weed, S. B., Eds.; Soil Science Society of America: Madison, WI, 1977; pp 797–808.
(25) *Standard Methods for the Examination of Water and Wastewater*, 17th ed.; American Public Health Association: Washington, DC, 1989; pp 3-102–3-106.
(26) Brown, D. S.; Allison, J. D. *MINTEQA2, an Equilibrium Metal Speciation Model*; EPA/600/3-87/012; U.S. EPA; Washington, DC, 1987.
(27) Van Breeman, N. *Soil Sci. Soc. Am. J.* **1973**, *37*, 694–697.
(28) Nordstrom, D. K. *Geochim. Cosmochim. Acta* **1982**, *46*, 681–692.
(29) Nordstrom, D. K.; Ball, J. W. *Science* **1986**, *232*, 54–56.

(30) Filipek, L. H.; Nordstrom, D. K.; Ficklin, W. H. *Environ. Sci. Technol.* **1987**, *21*, 388–396.
(31) Mishra, S.; Parker, J. C. *SOILPROP: A Program for Estimating Soil Hydraulic Properties and Their Uncertainty from Particle Size Data*; Center for Environmental and Hazardous Material Studies, Virginia Polytechnic Institute and State University, 1988; No. R8801.
(32) Baes, C. R., Jr.; Mesmer, R. E. *The Hydrolysis of Cations*; John Wiley and Sons: New York, 1976; pp 226–237.
(33) Lindsay, W. L. *Chemical Equilibria in Soils*; John Wiley and Sons: New York, 1979.
(34) Barnhisel, R. I.; Rotromel, A. L. *Soil Sci.* **1974**, *118*, 22–27.
(35) Singh, B. R. *Soil Sci.* **1984**, *138*, 346–353.
(36) Sigg, L.; Stumm, W. *Colloids Surf.* **1980**, *2*, 101–117.
(37) Farmer, V. C.; Palmieri, F. In *Soil Components. Inorganic Components*; Gieseking, J. E., Ed.; Springer-Verlag: New York, 1975; Vol. 2, pp 573–670.
(38) Omori, K.; Kerr, P. F. *Geol. Soc. Am. Bull.* **1963**, *74*, 709–734.
(39) Harsh, J. B.; Doner, H. E.; Fuerstenau, D. W. *Soil Sci. Soc. Am. J.* **1988**, *52*, 1589–1592.
(40) Williams, D. J. A.; Williams, K. P. *J. Colloid Interface Sci.* **1978**, *65*, 79–87.
(41) Rajan, S. S. S. *Soil Sci. Soc. Am. J.* **1978**, *42*, 39–44.
(42) Hansmann, D. D.; Anderson, M. A. *Environ. Sci. Technol.* **1985**, *19*, 544–551.

Received for review December 17, 1990. Revised manuscript received June 10, 1991. Accepted June 26, 1991. This research was partially supported by Contract DE-AC09-76SR00819 between the University of Georgia and the U.S. Department of Energy.

Parameterizing the Equilibrium Distribution of Chemicals between the Dissolved, Solid Particulate Matter, and Colloidal Matter Compartments in Aqueous Systems

James F. Pankow*,† and Stuart W. McKenzie‡

Department of Environmental Science and Engineering, Oregon Graduate Institute, 19600 N. W. Von Neumann Drive, Beaverton, Oregon 97006 and United States Geological Survey, Water Resources Division, 10615 S.E. Cherry Blossom Drive, Portland, Oregon 97216

■ The manner in which a chemical material partitions among the dissolved (D), particulate (P), and colloidal (C) phases affects both its chemical and physical behavior in the aquatic environment. The fractions of the chemical that are present in each of these three phases will be determined by the values of two simple parameters, K_pS_p/α_w and K_cS_c/α_w. The variables K_p and K_c are the particle/water and colloid/water partition constants (mL/g), respectively, S_p and S_c are the volume concentrations of particulate and colloidal material (mg/L), respectively, and α_w is the fractional volume of the system that is aqueous. This parameterization allows a rapid overview of how partitioning (1) changes as a function of chemical partitioning properties and water type, (2) affects *apparent* partition constants (i.e., K_p^{app} values) computed between the particulate phase and the remainder of the system, and (3) causes K_p^{app} values to become *independent* of chemical properties at high values of K_cS_c/α_w.

Introduction

The behavior and fate of an inorganic or organic species in an environmental system is closely tied to the manner in which that species is distributed between the various compartments present in that system. A priori, there is no limit on the number n_c of these compartments. For surface waters, it has currently become useful to take $n_c = 3$, with the three compartments corresponding to a dissolved, a suspended particulate solid, and a suspended colloidal matter phase (*1–6*). In groundwater and sediment/water systems, $n_c = 3$ is also often used, with the compartments considered including a dissolved, a stationary particulate solid, and a mobile colloidal matter phase.

In this paper, we will consider cases of the above type where $n_c = 3$. Thus, the term "dissolved (D) phase" will be used here when discussing the portion of some chemical that is dissolved and is surrounded only by the aqueous medium. "Particulate solid (P) phase" will be used when referring to the portion that is associated with particles that are sufficiently large that one can physically separate them from the remainder of the system. In the case of a sample of surface water, this separation might be carried out by filtration and/or centrifugation. "Colloidal (C) phase" will be used when referring to the portion that is associated with (1) very small particles that are difficult to remove by filtration or centrifugation *and/or* (2) dissolved humic molecules.

Unlike the D phase, under most circumstances neither the P phase nor the C phase will be a distinct thermodynamic phase. For example, the P phase will usually be composed of a variety of particle types, including various mineral phases as well as detrital organic matter. Nevertheless, since both D/P and D/C partitioning can be described by mean sorption constants (see below), then under conditions of constant pH, ionic strength, etc., both the particulate solid material and the colloidal material can be modeled as single phases.

The *distinction* between P-phase and C-phase material is always likely to be somewhat operational in nature. Indeed, the exact nature of this distinction will depend upon (1) the filtration process used to separate as many particles as possible from the D phase and (2) the degree of particulate loading on the filter and the manner in which that loading affects the particle-size-dependent efficiency of the filtration process.

The concentration of a species in the D phase is of interest because it affects the extent to which the species will be subject to transport by advection and molecular diffusion. In addition, the D-phase concentration is intimately related to the species' D-phase thermodynamic activity. This activity in turn reflects the positions of all chemical equilibria involving the species, including phase-partitioning equilibria. The amounts of the species that are associated with the P and C phases are of interest because those phases provide reservoirs for the release and storage of the species to and from the D phase, respectively. For

† Oregon Graduate Institute.
‡ United States Geological Survey.

 0013-936X/91/0925-2046$02.50/0 © 1991 American Chemical Society

Atmospheric Environment 54 (2012) 496–501

Contents lists available at SciVerse ScienceDirect

Atmospheric Environment

journal homepage: www.elsevier.com/locate/atmosenv

Short communication

Characterization of particulate matter (PM_{10}) related to surface coal mining operations in Appalachia

Viney P. Aneja [a,*], Aaron Isherwood [b], Peter Morgan [b]

[a] Department of Marine, Earth, and Atmospheric Sciences, North Carolina State University, Raleigh, NC 27695-8208, USA
[b] Sierra Club Environmental Law Program, San Francisco, CA 94105-3441, USA

ARTICLE INFO

Article history:
Received 20 June 2011
Received in revised form
13 February 2012
Accepted 15 February 2012

Keywords:
Surface coal mining
PM_{10}
Elemental analysis
Electron microscopy
Air toxic

ABSTRACT

This study investigates the environmental exposure of residents of a community in southwest Virginia to respirable concentrations of dust (PM-10 i.e. PM_{10}) generated by trucks hauling coal from surface coal mining operations. The study site is representative of communities in southwest Virginia and other parts of Appalachia that are located in narrow hollows where homes are placed directly along roads that experience heavy coal truck traffic.

Preliminary air sampling (Particulate Matter i.e. PM_{10}) was conducted for a period of approximately two weeks during early August 2008 in the unincorporated community of Roda, Virginia, at two locations (about a mile apart along Roda Road (Route 685) in Wise County, Virginia). For the purposes of this study (a combination of logistics, resource, and characterization of PM) we sited the PM samplers near the road to ascertain the micro exposure from the road. The results revealed high levels of PM_{10} (the mean adjusted 24-h concentration at the Campbell Site = 250.2 $\mu g\,m^{-3}$ ($\pm$135.0 $\mu g\,m^{-3}$); and at the Willis Site = 144.8 $\pm$ 60.0 $\mu g\,m^{-3}$). The U.S. 24-h national ambient air quality standard for PM_{10} is 150 $\mu g\,m^{-3}$. Elemental analysis for samples (blank-corrected) collected on Quartz filter paper (on one randomly selected day) at both the sites revealed the presence of antimony, arsenic, beryllium, cadmium, chromium, cobalt, lead, manganese, mercury, nickel, selenium. Electron micrographs reveal the morphology and habit (shapes and aggregates) of the particulate matter collected.

© 2012 Elsevier Ltd. All rights reserved.

1. Introduction

Surface coal mining has increased globally during the past 30 years. The use of coal is expected to increase by 60% over the next 20 years (http://www.worldcoal.org). This increase in coal usage raises a number of environmental challenges. Many of the environmental impacts of surface coal mining, particularly mountaintop removal mining in Appalachia, are well documented (Palmer et al., 2010; Gilbert, 2010). These impacts include loss of biodiverse native hardwood forests, burial of ecologically valuable headwater streams by valley fills, reduced soil infiltration capacity and increased runoff, and increased levels of acidity, electrical conductivity, total dissolved solids, and heavy metals in water bodies located downstream from mining operations. Less well known are the impacts to communities in Appalachia from air pollution caused by coal mining, and particularly by trucks that haul coal and other materials through residential areas (Aneja, 2009).

The central Appalachian region, including parts of Kentucky, Tennessee, Virginia, and West Virginia, is generally recognized to be one of most economically distressed regions in the United States (Appalachian Regional Commission, 2010). Within this region, the areas with the highest levels of poverty correspond to the areas with the greatest coal mining intensity (Hendryx, 2008). Central Appalachia also suffers from an excess of premature deaths (Halverson et al., 2004). Even adjusting for factors common to Appalachia such as poverty, smoking, and poor education, high age-adjusted mortality rates directly correlate with proximity to mining operations, with mortality rates increasing with increased coal production (Hendryx, 2008). The elevated adjusted mortality experienced in coal mining areas occurs in both males and females, suggesting that the cause is not occupational exposure but rather chronic exposure to air and water pollution caused by coal mining and related activities (Hendryx and Ahern, 2009). Human health impacts may come from water or exposure to airborne toxins and dust.

As described above, the impacts of surface coal mining on wetlands and water quality are well documented (Gilbert, 2010). Less well documented is the air pollution associated with surface

* Corresponding author. Tel.: +1 919 515 7808.
E-mail addresses: vpaneja@ncsu.edu, VINEY_ANEJA@NCSU.edu (V.P. Aneja).

1352-2310/$ – see front matter © 2012 Elsevier Ltd. All rights reserved.
doi:10.1016/j.atmosenv.2012.02.063

coal mining. Surface mines generate air pollution, primarily particulate matter, through blasting, wind erosion of exposed areas, and handling of coal at the mines, during transportation, and at processing plants. Because surface mining laws require a buffer between active mining operations and populated areas, the impacts of air pollution from blasting and wind erosion may not always be acutely experienced. Other forms of mining-related air pollution are harder for local residents to avoid.

After coal is removed from the ground, it is typically transported off-site via large trucks that travel on public roads. These coal trucks frequently travel through communities located in steeply sided valleys, or hollows, where homes are situated very close to the narrow roads. Some communities experience up to hundreds of truck trips a day. Coal trucks emit dust directly from their tires, bodies, and beds. They also track dirt and other materials from unpaved roads onto paved roads where the material dries and is re-entrained by the passage of subsequent vehicles.

The mountainous terrain of Appalachia both concentrates the air pollution associated with coal mining, and forces residents to place their homes in close proximity to roads and other sources of dust. Accordingly, typical methods of measuring regional air impacts – which involve placing monitors away from roads, among other precautions – may not accurately represent the actual exposure of residents of these communities. The objective of this study was to measure the exposure of residents of one community to respirable dust, and to correlate that exposure to dust sources including coal trucks.

2. Material and methods

During August 2008, two (2) PM_{10} air samplers were employed during a twelve day measurement period in the community of Roda in southwest Virginia where residents reported high truck traffic and significant dust problems (Fig. 1). PM_{10} samplers were located along a narrow, public road (Roda Road (Route 685) in Wise County, Virginia) that branches off of a state highway (Virginia State Route 78) and terminates approximately four miles later at the entrances to several coal mines. One sampler was located in the front yard of a residence located very close to the entrance to the coal mines ("Site Campbell") (36°57′35″N, 82°49′57″W, elevation 1942 feet MSL), and the second PM_{10} sampler was located in the front yard of a residence located approximately one mile further down the road, closer to the state highway ("Site Willis") (36°57′8″N, 82°49′14″W, elevation 1862 feet MSL). In both cases, the samplers were located

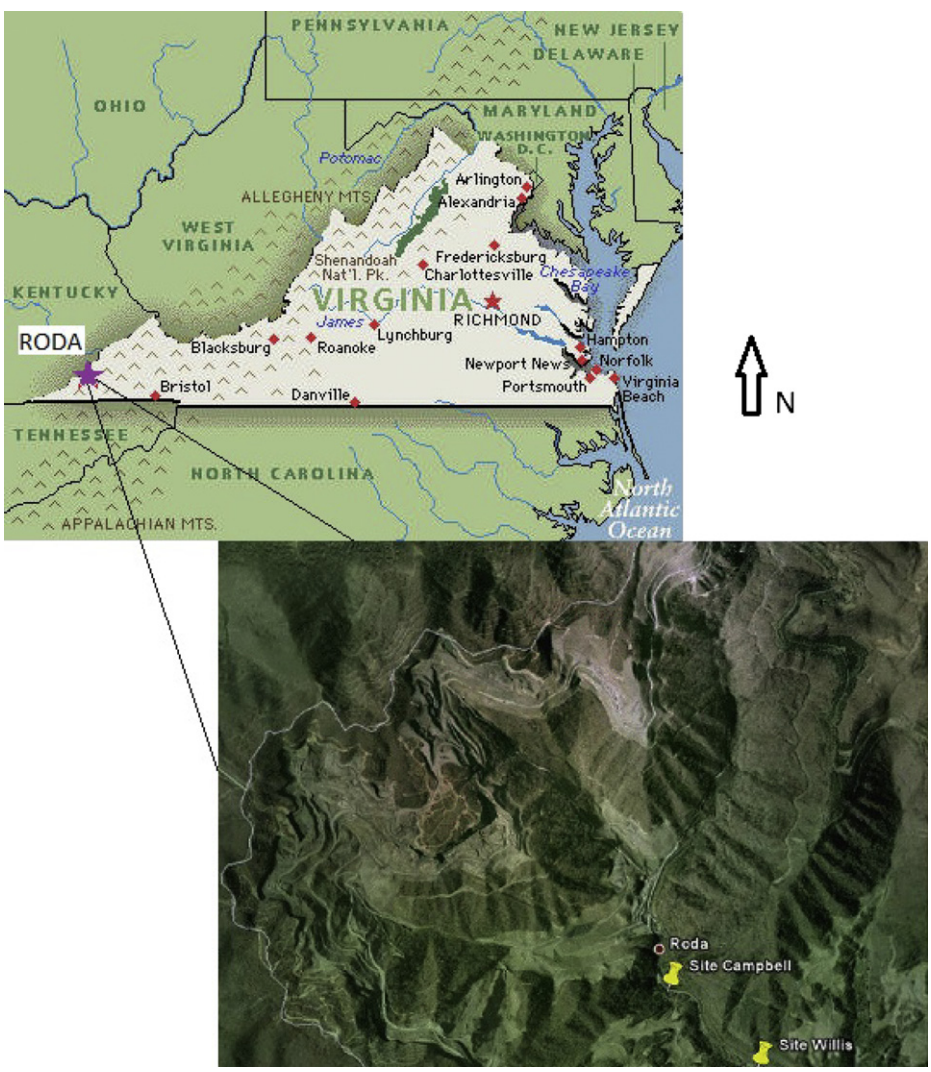

Fig. 1. Location of measurement sites in Roda, Virginia. Satellite image provides PM_{10} sampler locations (Site Campbell and Site Willis) along a narrow, public road (Roda Road (Route 685) in Roda, Wise County, Virginia) that branches off of a state highway (Virginia State Route 78) and terminates approximately four miles later at the entrances to several coal mines.

between the road and the front of the home, and within six (6) feet of the front of the home. The inlet height for both the samplers was ~5.5 feet. The topography around each monitoring site relative to the roadway was flat. These sampling locations were selected to represent micro to middle scale environments that are representative of the exposure of local residents. Because our goal was to record actual exposure levels experienced by local residents (special experiment) and not to evaluate regional air quality, we did not follow all of the United States Environmental Protection Agency (U.S. EPA) citing criteria for ambient air quality monitoring.

The PM_{10} samplers used were U.S. EPA reference method Andersen/GMW Model GUV-16H High Volume air samplers equipped with size selective inlets to collect ambient particulate matter with an effective aerodynamic size of less than ten microns. The samplers were calibrated in the laboratory immediately prior to the field deployment, and then calibrated and operated every day in accordance with the manufacturer's specifications and U.S. EPA methodology (US EPA, 1983, http://www.tisch-env.com/index8.asp). On-site calibrations included volumetric flow verification through the samplers via comparison of the calibrated orifice results to the volumetric flow controller tables. The samplers were operated continuously for twelve days, resulting in twelve 24-h samples from each location. Most of the particulate matter samples were collected onto 8-inch × 10-inch fiberglass filters, but on the same randomly determined day an 8-inch × 10-inch quartz fiber filter was used at each location. The quartz filters were equilibrated in an environmentally conditioned weighing room at ~70 °F and ~50% RH. The actual temperatures and humidities are in the research records at ERG. Binder-less Quartz filters were used directly from the manufacturer (Whatman) after equilibration and pre-weighing. Filters were handled with nitrile gloves and placed in glassene envelopes for shipping. Moreover, two blank quartz filter samples were also used (one for each site); and the blank corrections applied to the exposed quartz filters. The blank results are representative of a field sample because the blank samples were transported, prepared, digested and analyzed in the same way as the field sample. Analysis procedures for ambient quartz filters followed the Technical Assistance Document guidance for the National Air Toxics Trends Stations Program (http://www.epa.gov/ttnamti1/files/ambient/airtox/nattsTADRevision2_508Compliant.pdf).

Following the conclusion of sampling, the fiberglass filters were analyzed to determine mass, while the quartz filters were analyzed for mass and for the presence of a select group of metals. Filter tare weights were recorded prior to filter media shipment and use. Weight of the filter with the collected sample was measured following 24-h equilibration under environmentally controlled balance room conditions. The sample mass was determined by subtracting the original filter tare weight from the sample plus filter tare weight. Where the actual sampling exposure time for a filter was less than or greater than 24-h, we calculated the 24-h equivalent mass for the sample. A selection of the filters was subjected to scanning electron microscopy to confirm that the particles were consistent with the ten micron standard. The blank quartz filters were also analyzed for the presence of metals and used for blank correction for metal concentrations in the samples. A comprehensive US EPA based QA/QC protocol was in place for the entire experiment (Aneja, 2009).

A 4-inch × 1-inch portion of each of the two quartz filters was removed and the sample extracted in a 4% nitric acid solution via sonification for a total of 90 min, followed by the addition of 15 mL of water and sonification for an additional 90 min. The acid extractable fraction of each quartz filter portion was then analyzed by inductively coupled plasma mass spectrograph. This inorganic analysis followed the requirements in U.S. EPA compendium method IO-3.5. The US EPA IO-3.5 methods can be found at: http://www.epa.gov/ttnamti1/inorg.html.

3. Results

At the Campbell Site, our air sampling revealed adjusted 24-h concentrations of PM_{10} that ranged from 31.9 $\mu g\,m^{-3}$ to 469.7 $\mu g\,m^{-3}$ for the twelve sampling days. The mean adjusted 24-h concentration at the Campbell Site was 250.2 $\mu g\,m^{-3}$ ($\pm$135.0 $\mu g\,m^{-3}$). At the Willis Site, the adjusted 24-h concentrations of PM_{10} ranged from 19.2 $\mu g\,m^{-3}$ to 218.5 $\mu g\,m^{-3}$ for the twelve sampling days. The mean adjusted 24-h concentration at the Campbell Site was 138.5 $\mu g\,m^{-3}$ ($\pm$62.9 $\mu g\,m^{-3}$). The U.S. EPA National Ambient Air Quality Standard for 24-h concentrations of PM_{10} is 150 $\mu g\,m^{-3}$. Ten out of twelve samples taken at the Campbell site exceeded this limit, with one sample more than three times the national standard. Six out of twelve samples taken at the Willis site exceeded the national standard (Fig. 2). Moreover, a selection of the filters (collected at both sites on August 13, 2010) was subjected to scanning electron microscopy to confirm that the particles were consistent with the ten micron standard, and therefore that the samplers were measuring only respirable particles and that the results accurately represented the environmental exposure of the Roda community. The scanning electron microscopy further showed the morphology and habit (shapes and aggregates) of the particles, suggesting that particles that appeared at lower resolution to exceed ten microns in diameter had been subject to a growth mechanism owing to impaction and agglomeration on the filter media (Fig. 3).

Particulate matter is typically composed of a complex mixture of chemicals that is strongly dependent on source characteristics. Inorganic analysis of the two samples – one from each site – revealed the presence of antimony, arsenic, beryllium, cadmium, chromium, cobalt, lead, manganese, mercury, nickel, and selenium (Table 1). All of these metals present in the Roda samples are known to be present in coal (Finkelman, 1995).

4. Discussion and conclusions

Elevated levels of particulate matter have been associated with significant negative effects on human health. Significant and measurable reductions in life expectancy in the United States have been correlated to exposure to fine particulate matter (Pope et al., 2009). Exposure to PM_{10} is significantly correlated with all-cause, cardiovascular, and respiratory mortality (Zanobetti and Schwartz, 2009). In recognition of these health risks, the U.S. EPA has established health-based standards that provide maximum

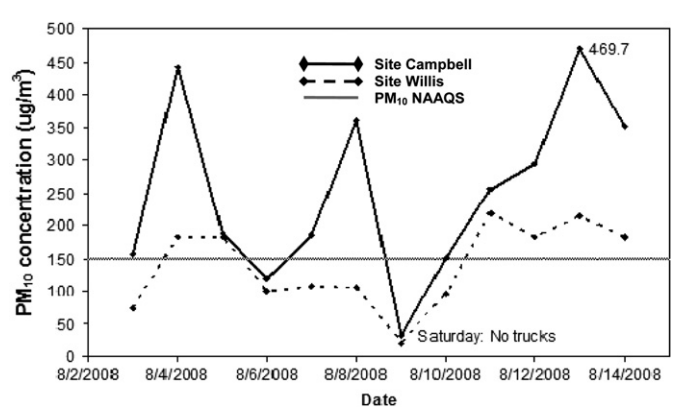

Fig. 2. Measurements of PM_{10} 24-h concentration at the two locations (Site Campbell and Site Willis) in Roda, Virginia, during August 2008.

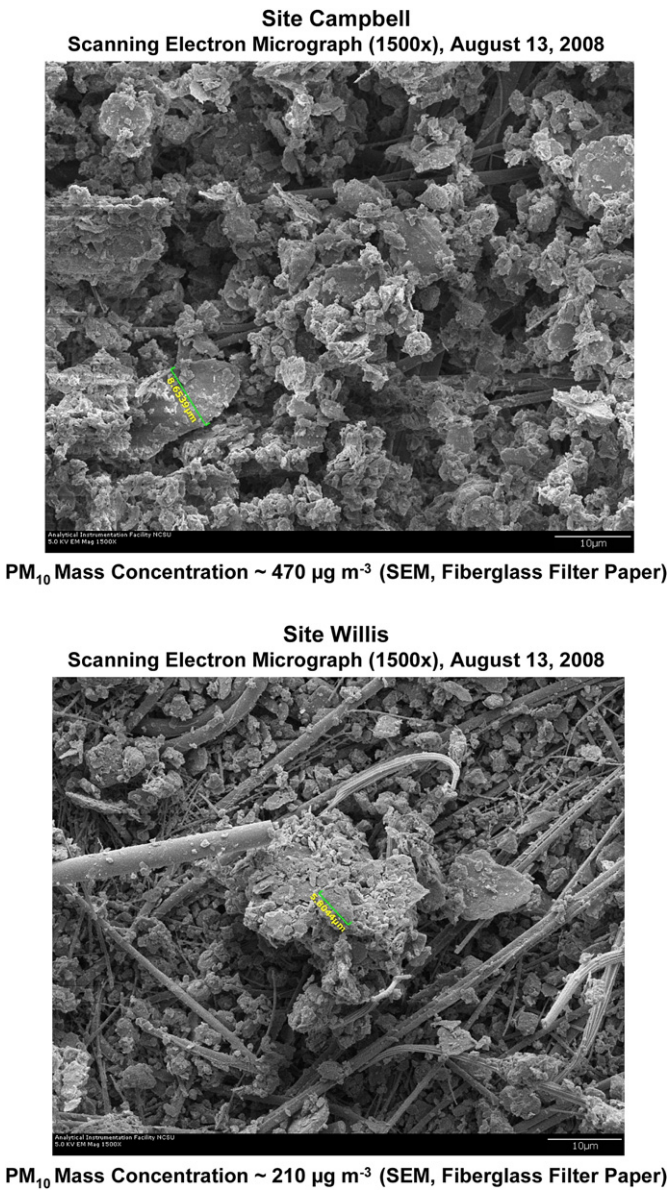

Fig. 3. Images from scanning electron microscopy.

ambient concentrations for particulate matter, including a standard of 150 $\mu g\,m^{-3}$ for 24-h concentrations for PM_{10}. U.S. EPA's recent draft policy assessment for particulate matter standards suggests a new 24-h PM_{10} standard in the range of 65–85 $\mu g\,m^{-3}$ for 24-h concentrations (U.S. EPA, 2010). Exposure to particulate matter that includes coal dust is particularly hazardous (Hendryx et al., 2008). The risks associated with coal dust exposure among mine workers are well studied. Recognizing the risk to the general public from exposure to particulate matter containing coal dust, the Wisconsin Department of Health and Family Services has proposed a risk-based ambient air concentration of 20 $\mu g\,m^{-3}$ for coal dust (WDHFS Letter, 2003).

The results of our recent air monitoring in Roda, Virginia, reveal that this community contends with exposure to particulate matter containing coal dust at levels far above what is considered safe. The extent of the community's exposure is not entirely understood at this time, as the study was limited to twelve consecutive days in August of one year, and particulate matter concentrations may vary seasonally. However, that multiple exceedances of the PM_{10} standards were documented within the limited sampling period strongly suggests that particulate matter exposure is a chronic problem for the Roda community, at least for portions of the year. In addition, there was insufficient data available from this study to assess the relative weight of the various factors (e.g. volume of truck traffic, weather conditions, additional sources of PM_{10}) that may have contributed to the variability of particulate matter concentrations recorded at each site. However, the near absence of detectable particulate matter on the one day when trucks were not running, combined with the consistent relative decrease in particulate matter levels between the site closest to the mine exit (Site Campbell) and the site approximately one mile further from the mine exit (Site Willis) (Fig. 2), strongly suggests that trucks carrying materials from the mines are a major contributor to the recorded particulate matter concentrations at this location.

Table 1
Inorganic analysis of particulate matter (PM_{10}) collected on quartz filters.

Analyte	PM_{10} mass concentration collected on the quartz filter paper ($ng\,m^{-3}$)	Time of exposure (h)	Normalized 24 h-Mass concentration ($ng\,m^{-3}$)[a]
Site Campbell – sample collected August 7, 2008			
Antimony	1.83	23.67	1.856
Arsenic	0.958	23.67	0.971
Beryllium	0.067	23.67	0.068
Cadmium	0.263	23.67	0.267
Chromium	2.74	23.67	2.778
Cobalt	0.915	23.67	0.928
Lead	3.9	23.67	3.954
Manganese	34.1	23.67	34.575
Mercury	0.14	23.67	0.142
Nickel	3.04	23.67	3.082
Selenium	0.613	23.67	0.623
PM_{10} mass	183,432	23.67	185,990
Site Willis – sample collected August 7, 2008			
Antimony	1.810	23.5	1.849
Arsenic	0.720	23.5	0.735
Beryllium	0.041	23.5	0.042
Cadmium	0.090	23.5	0.092
Chromium	3.600	23.5	3.166
Cobalt	0.697	23.5	0.991
Lead	3.320	23.5	3.391
Manganese	19.400	23.5	19.813
Mercury	0.972	23.5	0.993
Nickel	14.300	23.5	14.604
Selenium	0.568	23.5	0.592
PM_{10} mass	96,853	23.5	98,914

Volumetric flow rate of ambient air through the quartz filter paper: 40 $ft^3\,min^{-1}$.
[a] PM_{10} mass collected on the filter normalized to 24 h exposure.

Because this community is similarly situated to other communities in Appalachia where surface coal mining is common, it is very likely that these other communities contend with similar chronic exposure to particulate matter. However, additional study is required to confirm this hypothesis. Should further study demonstrate similar patterns of particulate matter exposure in other communities that experience high coal truck traffic, new regulations may be required to address the primary sources of this particulate matter.

Under the terms of the Clean Air Act, the U.S. EPA sets National Ambient Air Quality Standards (NAAQS) for a selection of air pollutants. Each state is then required to prepare and apply a State Implementation Plan (SIP) that describes how the state will attain and maintain those standards for each pollutant. The EPA has promulgated several NAAQS for particulate matter, including for PM_{10}. Many states, in turn, have adopted plans or control measures to limit emissions of particulate matter or fugitive dust. These SIPs for particulate matter or dust, however, are largely inadequate to address the problem of dust emitted by coal operations, including in particular the dust emitted by coal haul trucks.

Table 2
The particulate matter values from different regions of the world in or near an opencast coal mine.

Regions		$PM_{2.5}$ ($\mu g\,m^{-3}$)	PM_{10} ($\mu g\,m^{-3}$)	SPM or RPM ($\mu g\,m^{-3}$)
North East England (Pless-Mulloli et al., 2000)	Average	–	22.1	
Czech Republic (Hykysova and Brejcha, 2009)	Heating period	–	37	
	Non heating period	–	26	
	Transition period	–	33	
	Annual mean	–	33.5	
Turkey (Onder and Yigit, 2009)	Drilling	–	3080	
	Coal handling plant	–	1840	
	Stock yard	–	1670	
	Overburden loading	–	1350	
	Coal loading	–	1300	
Zonguldak City, Turkey (Tecer et al., 2008)	Winter	34.17	63.59	
	Spring	29.84	59.16	
	Summer	25.03	41.83	
	Autumn	23.03	39.66	
Jharia, India (Ghose and Majee, 2002)	Average (6 stations)	–	–	1473.66 (SPM); 197.79 (RPM)
Dhanbad, India (Dubey and Pal, 2012)	Average (31 stations)	–	194 ± 32 Range: (59–339)	
Present study	Campbell Site	–	250.2 ± 135.0 Range: (31.9–469.7)	
	Willis Site	–	144.8 ± 60.0 Range: (19.2–218.5)	

SPM is the suspended particulate matter and RPM is the respirable particulate matter.

In many states, the SIPs for particulate matter or fugitive dust require only that emitters employ "reasonable precautions" to prevent particulate matter from becoming airborne (Alaska SIP). A smaller subset of states provide examples of such reasonable precautions, but these examples fail to include those actions most likely to prevent the release of dust from trucks or from material tracked out onto roads (Virginia SIP). As a result, state and federal regulators are limited in their ability to enforce the standards, and emitters are not informed about actions they should take to reduce their dust emissions.

States, therefore, should consider revising their SIPs for particulate matter or fugitive dust to require that emitters take at least the following reasonable precautions: cover all loads transported by truck or railcar; promptly remove spilled or tracked materials from paved roads; wash all wheels, undercarriages, and other parts of every vehicle that hauls coal or other materials before or immediately after the vehicle leaves a dusty, dirty, or muddy surface; clean the empty bed and/or any other part of a vehicle that had recent contact with material capable of emitting dust; and install and use rumble strips, speed bumps, or other devices designed to reduce vehicle speed and to dislodge mud and other materials from tires and vehicle bodies before vehicles enter public roads.

We recently conducted monitoring in Roda, Virginia, a community that experiences heavy coal truck traffic and that is similarly situated to other communities in the steep hollows of Appalachia. Our monitoring revealed levels of respirable particulate matter (PM_{10}) up to three times the federal standard. The measured PM values are in the same range as the particulate matter values near an opencast coal mine in India, and significantly higher than particulate matter values near opencast coal mines in England and the Czech Republic (Table 2). The respirable particulate matter levels measured in Roda, therefore, are more closely aligned with those levels experienced in a newly industrialized nation than with the lower levels experienced in other developed nations. Without clear regulations and effective enforcement, communities like Roda will continue to contend with dangerous levels of particulate matter in dust generated by coal trucks.

Acknowledgments

We acknowledge support from the Southern Appalachia Mountain Stewards (SAMS) and the Sierra Club. We greatly appreciate the time and interest of the many volunteers, scientists, interest groups, and students (Mr. Saurabh Aneja, Ms. Megan Gore, Mr. William Blinn, and Mr. Ian Rumsey) who assisted us, and shared their knowledge and expertise to the development of the manuscript. We thank Ms. Lora S. Werner, Agency for Toxic Substances and Disease Registry (ATSDR), Region 3 Department of Health and Human Services, Philadelphia, PA; Dr. William Wilson, US Environmental Protection Agency, Research Triangle Park, NC; and Prof. Vivian E. Thomson, University of Virginia, Charlottesville, VA for the review of the manuscript.

References

Alaska SIP. 18 AK ADC 50.045(d). Available at: http://yosemite.epa.gov/r10/airpage.nsf/701092a6cfd3176c88256b6e000337d9/f9508a416b09305088256a080069469c!OpenDocument.
Aneja, V.P., 2009. Characterization of Particulate Matter (PM_{10}) in Roda, Virginia. http://www.nytimes.com/gwire/2009/04/24/24greenwire-dust-from-coal-trucks-poses-appalachian-health-10670.html, Report to the Virginia Air Resources Control Board, Richmond, VA. p. 19.
Appalachian Regional Commission. County Economic Status in Appalachia, FY 2010. http://www.arc.gov/assets/maps/related/County-Economic-Status_FY2010_Map.pdf.
Dubey, B., Pal, A.K., Singh, G., 2012. Trace metal composition of airborne particulate matter in the coal mining and non-mining areas of Dhanbad region. Atmospheric Pollution Research, Jharkhand, India. doi:10.5094/APR.2012.026.
Finkelman, R.B., 1995. Modes of occurrence of environmentally-sensitive trace elements in coal. In: Swaine, D.J., Goodarzi, F. (Eds.), Environmental Aspects of Trace Elements in Coal. Springer, New York, p. 25.
Gilbert, N., 2010. Mountain mining damages streams. Nature 466, 806.
Ghose, M.K., Majee, S.R., 2002. Assessment of the status of work zone air environment due to opencast coal mining. Environmental Monitoring and Assessment 71, 51–60.
Halverson, J.A., Ma, L., Harner, E.J., 2004. An Analysis of Disparities in Health Status and Access to Health Care in the Appalachian Region. Report Prepared for the Appalachian Regional Commission, Sept. 2004, p. xxi.
Hendryx, M., 2008. Mortality rates in Appalachian coal mining counties: 24 years behind the nation. Environmental Justice 1 (1), 5–11.
Hendryx, M., O'Donnell, K., Horn, K., 2008. Lung cancer mortality is elevated in coal mining areas of Appalachia. Lung Cancer 62 (1), 1–7.
Hendryx, M., Ahern, M., Jul–Aug 2009. Mortality in Appalachian coal mining regions: the value of statistical life lost. Public Health Reports 124, 541–550.
Hykysova, S., Brejcha, J., 2009. Monitoring of PM_{10} air pollution in small settlements close to opencast mines in the North-Bohemian Brown Coal Basin. WIT Transactions on Ecology and the Environment 123, 387–398.
Onder, M., Yigit, E., 2009. Assessment of respirable dust exposures in an opencast coal mine. Environmental Monitoring and Assessment 152, 393–401.
Palmer, M.A., et al., 2010. Mountaintop mining consequences. Science 327, 148–149.
Pless-Mulloli, T., King, A., Howel, D., Stone, I., Merefield, J., 2000. PM_{10} levels in communities close to and away from opencast coal mining sites in Northeast England. Atmospheric Environment 34, 3091–3101.

Pope 3rd, C.A., Ezzati, M., Dockery, D.W., 2009. Fine-particulate air pollution and life expectancy in the United States. New England Journal of Medicine 360, 376–386.

Tecer, L.H., Suren, P., Alagha, O., Karaca, F., Tuncel, G., 2008. Effect of meteorological parameters on fine and coarse particulate matter mass concentration in a coal-mining area in Zonguldak, Turkey. Journal of the Air & Waste Management Association 58, 543–552.

US EPA, 47 FR 54912, Dec. 6, 1982; 48 FR 17355, Apr. 22, 1983. Electronic Code of Federal Regulations. http://www.tisch-env.com/index8.asp.

U.S. EPA, 2010. Policy Assessment for the Review of the Particulate Matter National Ambient Air Quality Standards, Second External Review Draft. Available at: http://www.epa.gov/ttn/naaqs/standards/pm/data/20100630seconddraftpmpa.pdf (accessed 29.02.12).

Virginia SIP. 9 VAC 5-50-90. Available at: http://yosemite.epa.gov/r3/r3sips.nsf/9eeb842c677f8f5d85256cfd004c3498/623cab419b6ed41823d85256d24006297d2/$FILE/va_ch_50_part_II_article_1.pdf.

Wisconsin Department of Health and Family Services Letter to Wisconsin Department of Natural Resources Regarding Health Risks of Coal Dust Exposure, 2003. Available at: http://dnr.wi.gov/air/pdf/attach6_final_coaldust_dhfs_letter.pdf (accessed 06.08.10).

Zanobetti, A., Schwartz, J., 2009. The effect of fine and coarse particulate air pollution on mortality: a national analysis. Environmental Health Perspectives 117, 1–40.

WETLANDS AND URBANIZATION

Implications for the Future

Final Report of the Puget Sound Wetlands and Stormwater Management Research Program

1997

Edited by Amanda L. Azous and Richard R. Horner

Washington State Department of Ecology, Olympia, WA.
King County Water and Land Resources Division
and the
University of Washington, Seattle, WA.

Table of Contents

SECTION 1 OVERVIEW OF THE PUGET SOUND WETLANDS AND STORMWATER MANAGEMENT RESEARCH PROGRAM, *by Richard R. Horner* **1**

SECTION 2 DESCRIPTIVE ECOLOGY OF FRESHWATER WETLANDS IN THE CENTRAL PUGET SOUND BASIN **24**

CHAPTER 1 MORPHOLOGY AND HYDROLOGY, b*y Lorin E. Reinelt, Brian L. Taylor, and Richard R. Horner* **26**

CHAPTER 2 WATER QUALITY AND SOILS, *by Richard R. Horner, Sarah S. Cooke, Lorin E. Reinelt, Kenneth A. Ludwa and Nancy T. Chin* **40**

CHAPTER 3 CHARACTERIZATION OF PUGET SOUND BASIN PALUSTRINE WETLAND VEGETATION, *by Sarah S. Cooke and Amanda L. Azous* **59**

CHAPTER 4 EMERGING MACROINVERTEBRATE DISTRIBUTION, ABUNDANCE AND HABITAT USE, *by Klaus O. Richter and Robert W. Wisseman* **77**

CHAPTER 5 AMPHIBIAN DISTRIBUTION, ABUNDANCE AND HABITAT USE, *by Klaus O. Richter and Amanda L. Azous* **94**

CHAPTER 6 BIRD DISTRIBUTION, ABUNDANCE AND HABITAT USE, *by Klaus O. Richter and Amanda L. Azous* **109**

CHAPTER 7 SMALL MAMMAL DISTRIBUTION, ABUNDANCE AND HABITAT USE, *by Klaus O. Richter and Amanda L. Azous* **128**

SECTION 3 FUNCTIONAL ASPECTS OF FRESHWATER WETLANDS IN THE CENTRAL PUGET SOUND BASIN **139**

CHAPTER 8 EFFECTS OF WATERSHED DEVELOPMENT ON HYDROLOGY, *by Lorin E. Reinelt and Brian L. Taylor* **139**

CHAPTER 9 THE EFFECTS OF WATERSHED DEVELOPMENT ON WATER QUALITY AND SOILS, *by Richard R. Horner, Sarah S. Cooke, Lorin E. Reinelt, Kenneth A. Ludwa, Nancy T. Chin and Marian Valentine* **153**

CHAPTER 10 THE HYDROLOGIC REQUIREMENTS OF COMMON PACIFIC NORTHWEST WETLAND PLANT SPECIES, *by Sarah S. Cooke and Amanda L. Azous* **171**

CHAPTER 11 EMERGENT MACROINVERTEBRATE COMMUNITIES IN RELATION WATERSHED DEVELOPMENT, *by Klaus O. Richter, Kenneth A. Ludwa and Robert W. Wisseman* **190**

CHAPTER 12 BIRD COMMUNITIES IN RELATION TO WATERSHED DEVELOPMENT, *by Klaus O. Richter and Amanda L. Azous* **199**

SECTION 4 MANAGEMENT OF FRESHWATER WETLANDS IN THE CENTRAL PUGET SOUND BASIN **209**

CHAPTER 13 MANAGING WETLAND HYDROPERIOD: ISSUES AND CONCERNS, *by Amanda L. Azous, Lorin E. Reinelt and Jeff Burkey* **209**

CHAPTER 14 WETLANDS AND STORMWATER MANAGEMENT GUIDELINES, *by Richard R. Horner, Amanda A. Azous, Klaus O. Richter, Sarah S. Cooke, Lorin E. Reinelt and Kern Ewing* **222**

SECTION 1 OVERVIEW OF THE PUGET SOUND WETLANDS AND STORMWATER MANAGEMENT RESEARCH PROGRAM

by Richard R. Horner

INTRODUCTION

The Puget Sound Wetlands and Stormwater Management Research Program (PSWSMRP) was a regional research effort intended to define the impacts of urbanization on wetlands. The wetlands chosen for the study were representative of those found in the Puget Sound lowlands and most likely to be impacted by urban development. The program's goal was to employ the research results to improve the management of both urban wetland resources and stormwater.

This overview paper begins by defining the issues facing the program at its inception. It then summarizes the state of knowledge on these issues existing at the beginning and in the early stages of the program. The paper concludes by outlining the general experimental design of the study. Subsequent papers present the specific methods used in the various monitoring activities.

THE ISSUES

The PSWSMRP was inspired by proposals of stormwater managers and developers in the 1980s to store urban runoff in wetlands to prevent flooding and to protect stream channels from the erosive effects of high peak flow rates (see Athanas 1988 and McArthur 1989 for discussion of the use of wetlands for runoff quantity control). Stormwater managers were also interested in exploiting the known ability of wetlands to capture and to retain pollutants in stormwater, interrupting their transport to downstream water bodies (see Athanas 1988, Chan et al. 1981, Hickok 1980, Lakatos and McNemar 1988, Livingston 1988, and McArthur 1989 for discussion of the use of wetlands for runoff quality control).

In response to proposals to use wetlands for urban runoff storage, natural resources managers argued that flood storage and pollutant trapping are only two of the numerous ecological and social functions filled by wetlands. Among the other values of wetlands are groundwater recharge and discharge; shoreline stabilization; and food chain, habitat, and other ecological support for fish, waterfowl, and other species (Office of Technology Assessment 1984, Zedler and Kentula 1986). Resource managers further contended that using wetlands for stormwater management could damage their other functions (Livingston 1988; Newton 1989; Brown 1985; Canning 1988; ABAG 1986). They noted the general lack of information on the types and extent of impacts to wetlands used for stormwater treatment (Chan et al. 1981; Brown 1985; ABAG 1986; Canning 1988; Woodward-Clyde Consultants 1991).

Several researchers have suggested that findings about the impacts of municipal wastewater treatment in wetlands are relevant to stormwater treatment in wetlands (Chan et al. 1981; Silverman 1983). In some cases, wastewater treatment in wetlands has caused severe ecological disruptions (US EPA 1985), particularly when wastewater delivery is uncontrolled (Wentz 1987). A number of studies have raised concerns about possible long-term toxic metal accumulations, biomagnification of toxics in food chains,

nutrient toxicity, adverse ecological changes, public health problems, and other impacts resulting from wastewater treatment in wetlands (Benforado 1981; Guntspergen and Stearns 1981; Sloey, Spangler, and Fetter 1978; Dawson 1989).

Other researchers have reported negative impacts on wetland ecosystems from wastewater treatment. Wastewater additions can lead to reduced species diversity and stability, and a shift to simpler food chains (Heliotis 1982; Brennan 1985). Wastewater treatment in natural northern wetlands tended to promote the dominance of cattails (Typha sp.) (R. H. Kadlec 1987). In addition, animal species diversity usually declined. Discharge of wastewater to a bog and marsh wetland eliminated spruce and promoted cattails in both the bog and marsh portions (Stark and Brown 1988). Thirty years of effluent discharge to a peat bog caused parts of the bog to become monoculture cattail marsh (Bevis and Kadlec 1978). Application of chlorinated wastewater to a freshwater tidal marsh reduced the diversity of annual plant species (Whigham, Simpson, and Lee 1980). These findings on the effects of wastewater applications to wetlands have probable implications for the use of wetlands for stormwater treatment.

Despite the controversy over use of natural wetlands for stormwater treatment, it became apparent in early discussions on the subject that wetlands in urbanizing watersheds will inevitably be impacted by urbanization, even if there is no intention to use them for stormwater management. For example, the authors of a U.S. Environmental Protection Agency (US EPA) handbook on use of freshwater wetlands for stormwater management (US EPA 1985) stated that the handbook was not intended to be a statement of general policy favoring the use of wetlands for runoff management, but acknowledged that some 400 communities in the Southeast were already using wetlands for this purpose. Moreover, directing urban runoff away from wetlands in an effort to protect them can actually harm them. Such efforts could deprive wetlands of necessary water supplies, changing their hydrology (McArthur 1989) and threatening their continued existence as wetlands. In addition, where a wetland's soil substrate is subsiding, continuous sediment inputs are necessary to preserve the wetland in its current condition (Boto and Patrick 1978). Directing runoff to wetlands can help to furnish nutrients that support wetland productivity (McArthur 1989).

In its early years, the PSWSMRP focused on evaluating the feasibility of incorporating wetlands into urban runoff management schemes. Given this objective, the researchers initially viewed the issues more from an engineering than a natural science perspective. However, in later years, an appreciation of the fact that urban runoff reaches wetlands whether intended or not led the researchers to shift their inquiry to more fundamental questions about the impact of urbanization on wetlands. Thereafter, the Program's point of view ultimately merged natural science and engineering considerations. The information yielded by the Program will, therefore, be useful to wetland and other scientists, as well as to stormwater managers.

IMPACTS OF URBANIZATION ON WETLANDS

Urbanization impacts wetlands in numerous direct and indirect ways. For example, construction reportedly impacts wetlands by causing direct habitat loss, suspended solids additions, hydrologic changes, and altered water quality (Darnell 1976). Indirect impacts, including changes in hydrology, eutrophication, and sedimentation, can alter wetlands more than direct impacts, such as drainage and filling (Keddy 1983). Urbanization may affect wetlands on the landscape level, through loss of extensive areas, at the wetland complex level, through drainage or modification of some of the

units in a group of closely spaced wetlands, and at the level of the individual wetland, through modification or fragmentation (Weller 1988). Over the past several decades, it has become increasingly apparent that untreated runoff is the primary threat to the country's water quality. There has, consequently, been substantial research about the relationship between urbanization and runoff quality and quantity. However, the PSWSMRP focused primarily on the impacts of runoff on wetlands themselves, and not on the effects of urbanization on runoff flowing to wetlands.

Runoff can alter four major wetland components: hydrology, water quality, soils, and biological resources (US EPA 1993; Johnson and Dean 1987). Because impacts to wetland components are not distinct from one another but interact (US EPA 1993), it is difficult to distinguish between the effects of each impact or to predict the ultimate condition of a wetland component by simply aggregating the effects of individual impacts (Hemond and Benoit 1988). Moreover, processes within wetlands interact in complex ways. For example, wetland chemical, physical, and biological processes interact to influence the retention, transformation, and release of a large variety of substances in wetlands. Increased peak flows transport more sediment to wetlands that, in turn, may alter the wetlands' vegetation communities and impact animal species dependent on the vegetation.

SOURCES OF IMPACTS TO WETLANDS

Brief consideration of how urbanization affects runoff illustrates the potential for dramatic alteration of wetlands. Hydrologic change is the most visible impact of urbanization. Hydrology concerns the quantity, duration, rates, frequency and other properties of water flow. It has been called the linchpin of wetland conditions (Gosselink and Turner 1978) because of its central role in maintaining specific wetland types and processes (Mitsch and Gosselink 1993). Moreover, impacts on water quality and other wetland components are, to a considerable degree, a function of hydrologic changes (Leopold 1968). Of all land uses, urbanization has the greatest ability to alter hydrology. Urbanization typically increases runoff peak flows and total flow volumes and damages water quality and aesthetic values. For example, one study comparing a rural and an urban stream found that the urban stream had a more rapidly rising and falling hydrograph, and exhibited greater bed scouring and suspended solids concentrations (Pedersen 1981).

Pollutants reach wetlands mainly through runoff (PSWQA 1986; Stockdale 1991). Urbanized watersheds generate large amounts of pollutants, including eroded soil from construction sites, toxic metals and petroleum wastes from roadways and industrial and commercial areas, and nutrients and bacteria from residential areas. By volume, sediment is the most important nonpoint pollutant (Stockdale 1991). At the same time that urbanization produces larger quantities of pollutants, it reduces water infiltration capacity, yielding more surface runoff. Pollutants from urban land uses are, therefore, more vulnerable to transport by surface runoff than pollutants from other land uses. Increased surface runoff combined with disturbed soils can accelerate the scouring of sediments and the transport and deposition of sediments in wetlands (Loucks 1989; Canning 1988). Thus, there is an intimate connection between runoff pollution and hydrology.

INFLUENCE OF WETLAND AND WATERSHED CHARACTERISTICS ON IMPACTS TO WETLANDS

Watershed and wetland characteristics both influence how urbanization affects wetlands. For example, impacts of highways on wetlands are affected by such factors as highway location and design, watershed vulnerability to erosion, wetland flushing capacity, basin morphology, sensitivity of wetland biota, and wetland recovery capacity (Adamus and Stockwell 1983). Regional storm patterns also have a significant influence on impacts to wetlands (US EPA 1993). Hydrologic impacts are affected by such factors as watershed land uses; wetland to watershed areal ratios; and wetland soils, bathymetry, vegetation, and inlet and outlet conditions (Reinelt and Horner 1990; US EPA 1993). It is apparent that any assessment of the impacts of urbanization on a wetland should take into account the landscape in which the wetland is located. Whigham, Chitterling, and Palmer (1988), for example, suggested that a landscape approach might be useful for evaluating the effect of cumulative impacts on a wetland's water quality function. The rationale for such an approach is that most watersheds contain more than one wetland, and the influence of a particular wetland on water quality depends both on the types of the other wetlands present and their positions in the landscape.

IMPACTS OF URBANIZATION ON WETLANDS

Hydrologic Impacts

The direct impacts of hydrologic changes on wetlands are likely to be far more dramatic, especially over the short term, than other impacts. Hydrologic changes can have large and immediate effects on a wetland's physical condition, including the depth, duration, and frequency of inundation of the wetland. It is fair to say that changes in hydrology caused by urbanization can exert complete control over a wetland's existence and characteristics. A SWMM model run reported by Hopkinson and Day (1980) predicted that urbanization bordering a swamp forest would increase runoff volumes by 4.2 times. Greater surface runoff is also likely to increase velocities of inflow to wetlands, which can disturb wetland biota and scour wetland substrates (Stockdale 1991). Increased amounts of stormwater runoff in wetlands can alter water level response times, depths, and duration of water detention (US EPA 1993). Reduction of watershed infiltration capacity is likely to cause wetland water depths to rise more rapidly following storm events. Diminished infiltration in wetland watersheds can also reduce stream baseflows and ground water supplies to wetlands, lengthening dry periods and impacting species dependent on the water column (Azous 1991).

Water Quality Impacts

Direct Water Quality Impacts -- Prior to the PSWSMRP study, there was very little information specifically covering the impacts of urban runoff on water quality within wetlands (Stockdale 1991). On the other hand, there have been extensive inquiries into the effects of urbanization on runoff and receiving water quality generally. See, e.g., US EPA 1983, summarizing the results of the Nationwide Urban Runoff Program. Much of this information undoubtedly is suggestive of the probable effects of urban runoff on wetland water quality. There have also been numerous "before and after" studies evaluating the effectiveness of wetlands for treatment of municipal wastewater and urban runoff. See, e.g., ABAG 1986; Brown 1985; Chan et al. 1981; Dawson 1989;

Franklin and Frenkel 1987; Hickok et al. 1977; Hickok 1980; Lynard et al. 1980; Martin 1988; Morris et al. 1981; and Oberts and Osgood 1988. Many of these studies have focused on the effectiveness of wetlands for water treatment rather than on the potential for such schemes to harm wetland water quality.

Nevertheless, data on the quality of inflow to and pollutant retention by wetlands are likely to give some indication of the effects of urban runoff on wetland water quality. Studies on the effects of wastewater and runoff on other wetland components, such as vegetation, also may provide indirect evidence of impacts on wetland water quality. See, e.g., Bevis and Kadlec 1978; Brennan 1985; Chan 1979; Ehrenfeld and Schneider 1983; Isabelle et al. 1987; Morgan and Philipp 1986; Mudrock and Capobianco 1979; Stark and Brown 1988; Tilton and Kadlec 1979; and Whigham, Simpson, and Lee 1980. A number of researchers have warned of the risks of degradation of wetland water quality and other values from intentional routing of runoff through wetlands (see ABAG 1986; Brown 1985; Canning 1988; Chan et al. 1981; Galvin and Moore 1982; and Silverman 1983). Subsequent papers in this monograph describe the results of water quality impact studies performed by the program.

Hydrological Impacts on Water Quality -- Hydrology influences how water quality changes will impact wetlands. Hydrologic changes can make a wetland more vulnerable to pollution (Harrill 1985). Increased water depths or frequencies of flooding can distribute pollutants more widely through a wetland (Stockdale 1991). How wetlands retain sediment is directly related to flow characteristics, including degree and pattern of channelization, flow velocities, and storm surges (Brown 1985). Toxic materials can accumulate more readily in quiescent wetlands (Oberts 1977). In a study on use of wetlands for stormwater treatment, Morris et al. (1981) found that wetlands with a sheet flow pattern retained more phosphorus, nitrogen, suspended solids, and organic carbon than channelized systems, which were ineffective.

Changes in hydroperiod can also affect nutrient transformations and availability (Hammer 1992) and the deposition and flux of organic materials (Livingston 1989). Fries (1986) observed higher phosphorus concentrations in stagnant than in flowing water. In wetland soils, the advent of anaerobic conditions can transform phosphorus to dissolved forms (US EPA 1993). Lyon et al. (1987) reported that anaerobic conditions in flooded emergent wetlands increased nutrient availability to wetland plants, compared to infrequently flooded sites.

Impacts to Wetland Soils

Hydrologic Impacts to Wetland Soils -- Flow characteristics within wetlands directly influence the rate and degree of sedimentation of solids imported by runoff (Brown 1985). If unchecked, excessive sedimentation can alter wetland topography and soils, and ultimately result in the filling of wetlands. Alternatively, elevated flows can scour a wetland's substrate (Loucks 1989), changing soil composition, and leading to more channelized flow. Materials accumulated over several hundred years could, therefore, be lost in a matter of decades (Brinson 1988).

Water Quality Impacts to Wetland Soils -- The physical, chemical, and biological characteristics of wetland soils change as they are subjected to urban runoff (US EPA 1993). The physical effects of runoff on wetland soils, including changes in texture, particle sizes distributions, and degree of saturation are not well documented (US EPA

1993). However, a wetland's soil can be expected to acquire the physical characteristics of the sediments retained by the wetland.

Suspended matter has a strong tendency to absorb and adsorb other pollutants (Stockdale 1991). Sedimentation, therefore, is a major mechanism of pollutant removal in wetlands (Chan et al. 1981; Silverman 1983). Chemical property changes in wetland soils typically reflect sedimentation patterns (ABAG 1979; Schiffer 1989). Materials are often absorbed by wetland soils after entering a wetland, as well (Richardson 1989).

When nutrient inputs to wetlands rise, temporary or long-term storage of nutrients in ecosystem components, including soils, can increase (J.A. Kadlec 1987). Rates of nutrient transfer among ecosystem components and flow through the system may also accelerate. When chlorinated wastewater was sprayed onto a freshwater tidal marsh, surface litter accumulated nitrogen and phosphorus (Whigham, Simpson, and Lee 1980). However, although wetland soils can retain nutrients, a change of conditions, such as the advent of anaerobiosis and changed redox potential, can transform stored pollutants from solid to dissolved forms, facilitating export from the soil. (US EPA 1993). The capacity of wetland soils to retain phosphorus becomes saturated over time (Richardson 1985; Nichols 1983; R.W. Beck and Associates 1985). If the soil becomes saturated with phosphorus, release is likely.

Wetland soils can also trap toxic materials, such as metals (US EPA 1993). Horner (1988) found that there were high toxic metals accumulations in inlet zones of wetlands affected by urban runoff. Mudrock and Copobianco (1979) observed increased sediment metals concentrations in several locations in a wetland receiving wastewater. The quantity of metals that a wetland can absorb without damage depends on the rate of metals accretion and degree of burial (US EPA 1985). If stormwater runoff alters soil pH and redox potential, many stored toxic materials can become immediately available to biota (Cooke 1991).

Water quality impacts on wetland soils can eventually threaten a wetland's existence. Where sediment inputs exceed rates of sediment export and soil consolidation, a wetland will gradually become filled. Filling by sediment is a particular concern for wetlands in urbanizing areas (Stockdale 1991). Many wetlands have an ability to retain large amounts of sediment. For example, Hickok (1980) reported that a wetland captured 94% of suspended solids from stormwater. Oberts and Osgood (1988) observed that a stormwater treatment wetland lost 18% of permanent storage volume and 5% of total storage volume because of high rates of solids retention.

Impacts to Vegetation

Impacts on wetland hydrology and water quality can, in turn, affect wetland vegetation. Horner (1988) stated that emergent zones in Pacific Northwest wetlands receiving urban runoff are dominated by an opportunistic grass species, Phalaris arundinaceae, while non-impacted wetlands contain more diverse groupings of species. Ehrenfeld and Schneider (1983) observed marked changes in community structure, vegetation dynamics, and plant tissue element concentrations in New Jersey Pine Barrens swamps receiving direct storm sewer inputs, compared to swamps receiving less direct runoff. However, human impacts on wetland ecosystems can be quite subtle. For example, Keddy (1983), upon reconsidering data from two prior studies of ecological changes in wetlands, concluded that human influences, and not natural succession, as originally

believed, were the principal causes of change in the vegetation of two New England wetlands.

Hydrologic Impacts on Vegetation -- Hydrologic changes can have significant impacts on the livelihood of the whole range of wetland flora, from bacteria to the higher plants. Hickok et al. (1977) observed that microbial activity in wetland soils correlated directly to soil moisture. However, surface microbial activity decreased when soils were submerged and became anaerobic (Hickok 1980). To a greater or lesser degree, wetland plants are adapted to specific hydrologic regimes. For example, Bedinger (1978) observed that frequency and duration of flooding determined the distribution of bottomland tree species. Flood plain terraces with different flooding characteristics had distinct species compositions. Increased watershed imperviousness can cause faster runoff velocities during storms that can impact wetland biota (Stockdale 1991). However, as watersheds become more impervious, stream base flows and groundwater supplies can decline. As a result, dry periods in wetlands may become prolonged, impacting species dependent on the inundation (Azous 1991; US EPA 1985). Changes in average depths, duration, and frequency of inundation ultimately can alter the species composition of plant and animal communities (Stockdale 1991).

There have been numerous reports on the tolerance to flooding of wetland and non-wetland trees and plants. See, e.g., Green (1947); Brink (1954); Ahlgren and Hansen (1957); Rumberg and Sawyer (1965); Minore (1968); Gill (1970); Cochran (1972); Teskey and Hinckley (1977a, b, c, d); Bedinger (1978); Whitlow and Harris (1979); Davis and Brinson (1980); Walters et al. (1980); McKnight et al. (1981); Chapman et al. (1982); Jackson and Drew (1984); Kozlowski (1984); Thibodeau and Nickerson (1985); and Gunderson, Stenberg, and Herndon (1988). While flooding can harm some wetland plant species, it promotes others (US EPA 1993). There is little information available on the impacts of hydrologic changes on emergent wetland plants, although Kadlec (1962) identified several species that can tolerate extended dry periods. Rumberg and Sawyer (1965) reported that hay yields in native wet meadows increased with the length of flood irrigation if depths remained at 13 cm or less and declined if depths stayed at 19 cm for 50 days or longer.

Plant species often have specific germination requirements, and many are sensitive to flooding once established (Niering 1989). The life stage of plant species is an important determinant of their flood tolerances. While mature trees of certain species may survive flooding, the establishment of saplings could be retarded (Stockdale 1991). Where water levels are constantly high, wetland species may have a limited ability to migrate, and may be able to spread only through clonal processes because of seed bank dynamics (van der Valk 1991). The result may be reduced plant diversity in a wetland. However, anaerobic conditions can increase the availability of nutrients to wetland plants (Lyon, Drobney, and Olsen 1986).

Hydrologic impacts on individual plant species eventually translate into long-term alterations of plant communities (US EPA 1985). Changes in hydroperiod can cause shifts in species composition, primary productivity (US EPA 1985), and richness (Cooke 1991). Ehrenfeld and Schneider (1983) theorized that changes in hydrology were among the causes of a decline of indigenous plant species and an increase in exotic species in New Jersey Pine Barrens cedar swamps. In general, periodic inundation yields more plant diversity than either constantly wet or dry conditions (Conner et al. 1981; Gomez and Day 1982). However, early results of the PSWSMRP indicated that wetlands with wider water level fluctuations have lower species richness than systems

with lower water level fluctuations (Azous 1991, Cooke and Azous 1992). Monitoring in a Cannon Beach, Oregon wastewater treatment wetland revealed little change in herbaceous and shrub plant cover after two years of operation, except in channelized and deeply flooded portions, where herbaceous cover decreased (Franklin and Frenkel 1987). Slough sedge cover increased slightly in a shallowly flooded area. In 1986, flooding stress was observed in red alder trees in deeper parts of the wetland. Thibodeau and Nickerson (1985) examined a wetland, part of which was drained and part of which was impounded to a greater depth. Vegetation in the drained portion became more dense and diverse, but there was a marked decline in the number of species in the flooded portion after three years.

Please see Hydrologic Effects on Vegetation Communities, later in this volume, for the results of the PSWSMRP study on the effects of water level changes on wetland vegetation.

Water Quality Impacts on Vegetation -- High suspended solids inputs can reduce light penetration, dissolved oxygen, and overall wetland productivity (Stockdale 1991). However, inflow containing high concentrations of nutrients can promote plant growth. Tilton and Kadlec (1979) reported, for example, that in a wastewater treatment wetland, plants closer to the discharge point had greater biomass and higher concentrations of phosphorus in their tissues, and the cattails were taller. When nutrient inputs to wetlands increase, they may be stored either temporarily or over the long-term in ecosystem components, including vegetation (J.A. Kadlec 1987). Rates of nutrient movement, by transfer among ecosystems components and through the system, may accelerate.

Toxic materials in runoff can interfere with the biological processes of wetland plants, resulting in impaired growth, mortality, and changes in plant communities. The amount of metals absorbed by plants is, for some species, a function of supply. Ehrenfeld and Schneider (1983) reported that, in cedar swamps in the New Jersey Pine Barrens, plants took up more lead when direct storm sewer inputs were present than when runoff was less direct. The degree to which plants bioaccumulate metals is highly variable. Chan (1979) stated that pickleweed (Salicornia sp.) concentrated metals, especially zinc and cadmium, more than mixed marsh and upland grass vegetation. However, plants in a brackish marsh that had received stormwater runoff for more than 20 years did not appear to concentrate copper, cadmium, lead, and zinc any more than plants in control wetlands not receiving storm water (Chan et al. 1981).

While toxic metals accumulate in certain species, such as cattails, without causing harm, they interfere with the metabolism of other species (Stockdale 1991). Toxic metals can harm certain species by interfering with nitrogen fixation (Wickcliff et al. 1980). Metals can also impinge on photosynthesis in aquatic plants, such as water weed (Elide sp.) (Brown and Rattigan 1979). Portele (1981) reported that roadway runoff containing toxic metals had an inhibitory effect on algae. Marshall (1980) found in a bioassay study of the effects of stormwater on algae, that nutrients did not stimulate growth as much as predicted because of the presence of metals in the stormwater. Isabelle et al. (1987) found that the germination rates of wetland plants exposed to roadside snow melt in several concentrations varied inversely with snow melt concentration.

Changes in plant community composition may be the major impact of pollution in wetlands. Morgan and Phillip (1986) stated that the major effect of residential and agricultural runoff with high pH and nitrate concentrations was to cause indigenous

aquatic macrophytes of the New Jersey Pine Barrens to be replaced by non-native species. Ehrenfeld and Schneider (1983) also reported marked changes in plant community structure and vegetation dynamics in Pine Barrens cedar swamps where direct storm sewer inputs were present. Isabelle et al. (1987) found that, where wetland plants had been exposed to roadside snow melt in several concentrations, community biomass, species diversity, evenness, and richness after one month of growth varied inversely with snow melt concentration. Impacts were not as severe where runoff was less direct.

Impacts to Wetland Fauna

Hydrologic Impacts on Wetland Fauna -- Hydrologic changes can have as great an effect on wetland animal as on plant communities. Nordby and Zedler (1991) reported that, in two coastal marshes, animal species richness and abundance declined as hydrologic disturbance increased. Shifts in plant communities as a result of hydrologic changes can have impacts on the preferred food supply and cover of such animals as waterfowl.

Increased imperviousness in wetland watersheds can reduce stream base flows and groundwater supplies, prolonging dry periods in wetlands and impacting species dependent on the water column (Azous 1991). Many amphibians require standing water for breeding, development, and larval growth. Amphibians and reptile communities may experience changes in breeding patterns and species composition with changed water levels (Minton 1968 in Azous 1991). Because amphibians place their eggs in the water column, the eggs may be directly damaged by changes in water depth. Alterations in hydroperiods can be especially harmful to amphibian egg and larval development if water levels decline and eggs attached to emergent vegetation are exposed and desiccated (Lloyd-Evans 1989 in Azous 1991). Water temperature changes that accompany shifting hydrology may also impact egg development (Richter et al. 1991).

Hydrologic changes have implications for other wetland animals, as well. Alterations to water quality and wetland soils caused by hydrologic changes may negatively affect animal species. For example, increased peak flows that accelerate sedimentation in wetlands or cause scouring can damage fish habitat (Canning 1988). Mortality of the eggs and young of waterfowl during nesting periods may rise if water depths become excessive. (US EPA 1993). Johnsgrad (1956) reported that water level fluctuations resulting from an artificial impoundment in eastern Washington State caused a redistribution of bird populations. Flooding of potholes by the impoundment reduced waterfowl production and forced breeding waterfowl into the remaining smaller potholes. Hydrologic changes may impact mammal populations in wetlands by diminishing vegetative habitat and by increasing the potential for proliferation of disease organisms and parasites as base flows become shallower and warmer (Lloyd-Evans 1989). There is concern about maintaining habitat around wetlands that are receiving stormwater in order to permit free movement of animals during storm events (US EPA 1993).

Water Quality Impacts to Wetland Fauna -- Pollutants can have both direct and indirect effects on wetland fauna. Portele (1981) reported that road runoff containing toxic metals had an inhibitory effect on zooplankton, in addition to algae. Azous (1991) reported a significant negative correlation between water conductivity, a general indicator of dissolved substance concentrations, and amphibian species richness. Aquatic organisms, particularly amphibians, readily absorb chemical contaminants (Richter and Wisseman 1990). Thus, the status of such organisms is an effective

indicator of a wetland's health. The degree of bioaccumulation of metals in wetland animals varies by species. In a brackish marsh that had received storm runoff for 20 years, there was no observed bioaccumulation of metals in benthic invertebrates (Burstynsky 1986). However, a filter-feeding amphipod (Corophium sp.), known for its ability to store lead in an inert crystal form, accumulated significant amounts of lead. Water quality changes can indirectly harm fish and wildlife by reducing the coverage of plant species preferred for food and shelter (Mitsch and Gosselink 1993; Weller 1987 and Lloyd-Evans 1989 in Azous 1991).

Please see the discussions of amphibian, emergent aquatic insect, bird, and small mammal communities in relation to watershed development and habitat conditions, later in this volume, for the results of the PSWSMRP study on the effects of hydrologic and water quality changes on wetland animals.

Use of Wetlands for Stormwater Treatment

Impacts from intentional use of wetlands for stormwater management could be more harmful than those that would occur with incidental drainage from an urbanized watershed. For example, raising the outlet and controlling the outflow rate would, in general, change water depths and the pattern of rise and fall of water. Structural revisions to improve pollutant trapping ability would increase toxicant accumulations, in addition to the direct effects of construction. On the other hand, stormwater management actions could be linked with efforts to upgrade wetlands that are already highly damaged.

PUGET SOUND WETLANDS AND STORMWATER MANAGEMENT RESEARCH PROGRAM DESIGN

Representatives of the stormwater and resource management communities in the Puget Sound area of Washington State formed a committee in early 1986 to consider how to best resolve questions concerning wetlands and stormwater runoff. Committee members came from federal, state, and local agencies; academic institutions; and other local interests. The Resource Planning Section of the government of King County, Washington, coordinated the committee's work. The committee's initial effort was to enumerate the wetland resources that are implicated in urban stormwater management decisions and to identify the general types of effects that runoff could have on these resources. The committee members also oversaw the preparation of a literature review, designed to determine the extent to which previous work could address the issues before them, and a management needs survey.

Literature Review and Management Needs Survey

The principal activity of the Program's first year was a comprehensive literature review, which concluded with a report (Stockdale 1986a) and an annotated bibliography (Stockdale 1986b) covering the reported research and observations relevant to the issue of stormwater and wetlands. The review was updated in 1991 (Stockdale 1991). These reviews concentrated on what was known and what was not known about these issues at the time. Best known was the performance of wetlands in capturing pollutants, mostly derived from studies on their ability to provide advanced treatment to municipal wastewater effluents. Only a small body of information pertained to stormwater. The greatest shortcoming of the literature concerned the ecological impacts to wetlands

created by any kind of waste stream. The literature reviews also made clear the dearth of research on any aspect of Pacific Northwest wetlands, in contrast to some other areas of the country. Many detailed aspects of the subject of stormwater and wetlands were very poorly covered, including the relative roles of hydrologic and water quality modifications in stressing wetlands and the transport and fate of numerous toxicants in wetlands.

On the basis of their discussions and the literature review, the committee members participated in a formal survey designed to identify the most important needs for reaching the goal of protecting wetlands in urban and urbanizing areas, while improving the management of urban stormwater. The survey involved rating a long list of candidate management needs with respect to certain criteria. Computer processing of the ratings led to the following list of consensus high priority management needs:

- Definition of short and long-term impacts of urban stormwater on palustrine wetlands;
- Management criteria by wetland type;
- Allowable runoff storage schedules that avoid or minimize negative effects on wetlands and their various functions; and
- Features critical to urban runoff water quality improvement in wetlands.

Research Program Design

After completion of the literature review and management needs survey, the committee and staff assembled by King County turned to defining a research program to serve the identified needs. The program they developed included the following major components:

- Wetland survey;
- Water quality improvement study;
- Stormwater impact studies; and
- Laboratory and special field studies.

The purpose of the wetland survey was to provide a broad picture of freshwater wetlands representative of those in the Puget Sound lowlands. The survey covered 73 wetlands throughout lowland areas of King County. One important goal of the survey was to identify how urban wetlands differ from those that are lightly affected by human activity. The survey's design, results, and conclusions were reported by Horner et al. (1988) and Horner (1989). The survey results assisted in designing the remainder of the research program.

The water quality improvement study was an intensive, two-year (1988-1990) effort to answer remaining questions about the water quality functioning of wetlands. Reinelt and Horner (1995) discuss its methods and findings.

The results from the various portions of the Program were used to develop extensive guidelines for coordinated management of urban wetlands and stormwater. These guidelines have been continuously updated and refined throughout the program, as more information became available.

Wetlands Impacted by Urbanization in the Puget Sound Basin

The research program focused primarily on palustrine wetlands because urbanization in the Puget Sound region is impacting this wetland type more than other types. Palustrine wetlands are freshwater systems in headwater areas or isolated from other water bodies (Cowardin et al. 1979). They typically contain a combination of water and vegetation zones. Some palustrine wetlands consist of open water with only submerged or floating plants, or with no vegetation. Others include shallow or deep marsh zones containing herbaceous emergent plants, shrub-scrub vegetation, and/or a forested community.

Two “poor fens” being impacted by urban development were also monitored during the study. Poor fens, commonly confused with true bogs, are a special wetland type that is of considerable interest in northern regions. Under natural conditions, water supply to poor fens consists only of precipitation and groundwater. The lack of surface water inflow restricts nutrient availability, resulting in a relatively unusual plant community adapted to low nutrition and the attendant acidic conditions. Such a community is vulnerable to increased nutrient supply and buffering by surface water additions.

Stormwater Impact Studies

The stormwater impact studies formed the core of the program. This field research was supplemented by the laboratory and special field studies, which allowed investigation of certain specific questions under more control than offered by the broader field studies.

A special effort was made to ensure that research was conducted according to sound scientific design, so that the results and their application in management would be defensible. In order to approximate the classic "before/after, control/treatment" experimental design approach, the impact study included “control” and “treatment” wetlands. The stormwater impact study was conducted in 19 wetlands in King County, approximately half treatment and the remainder control sites. Figure 1 displays these 19 sites and four others, including three in Snohomish County to the north, where special studies were conducted.

The treatment wetlands, located in areas undergoing urban development during the course of the study, were monitored before, during, and after urbanization. The goals of studying these wetlands were to characterize preexisting conditions and to assess the consequences of any changes accompanying urbanization and modification of stormwater inflow. Not all of the treatment watersheds developed as much as anticipated at the outset of the study. The watersheds of the control wetlands ranged from no urbanization to relatively high levels. However, the watersheds of all of these wetlands were characterized by relative stability in land use during the study. The use of control sites made it possible to judge whether observed changes in treatment wetlands were the result of urbanization or of broader environmental conditions affecting all wetlands in the region. Control wetlands were paired with treatment sites on the basis of size, water and plant zone configuration, and vegetation community types. In recognition of the imperfect matches that occur in pairing natural systems, data analyses were performed for various groupings of sites and not just with respect to paired wetlands.

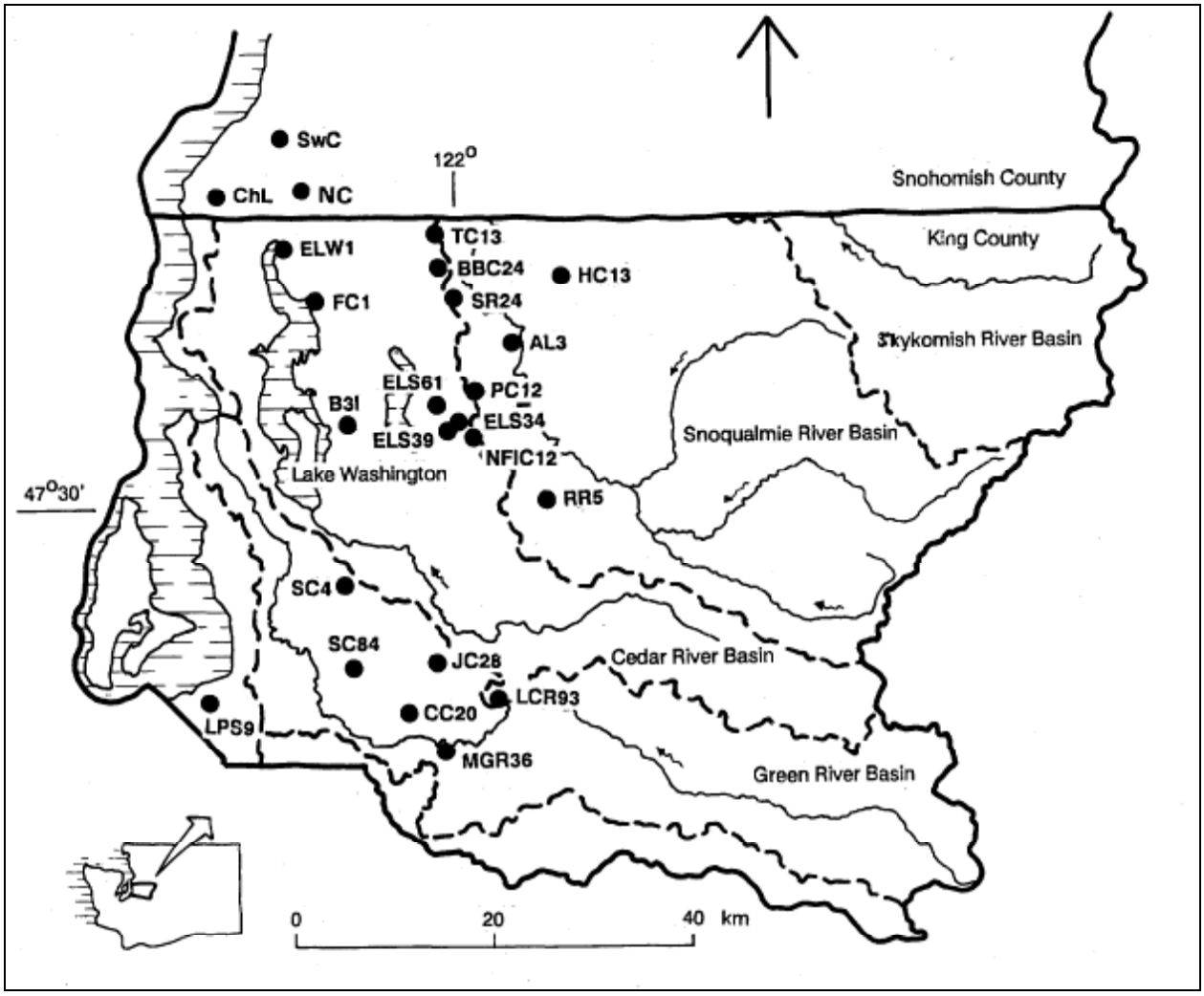

Figure 1. Puget Sound Wetlands and Stormwater Management Research Program study locations.

Because the program was interested in long-term as well as short-term effects, the impact monitoring was continued for eight years. Research in 1988 and 1989 generally provided the baseline data for the treatment wetlands. Data from 1990 reflected the early phase of urbanization in these wetlands. Monitoring resumed in 1993, generally shortly after a phase of building in the watersheds ended. Monitoring in 1995 was intended to document effects that took longer to appear.

Figure 2 illustrates the conceptual framework of the designs of the specific sampling programs pursued in the stormwater impact study and analyzing and interpreting the resulting data. The two blocks on the left of the diagram represent the driving forces determining a wetland's character (Watershed and Surrounding Landscape Conditions and Wetland Morphology). The term "surrounding landscape" signifies that not only a wetland's watershed (the area that is hydrologically contributory to the wetland) but also adjacent land outside of its watershed can influence the wetland. The surroundings include the wetland buffer, corridors for wildlife passage, and upland areas that provide for the needs of some wetland animals. Wetland morphology refers to form and

structure and embraces shape, dimensions, topography, inlet and outlet configurations, and water pooling and flow patterns.

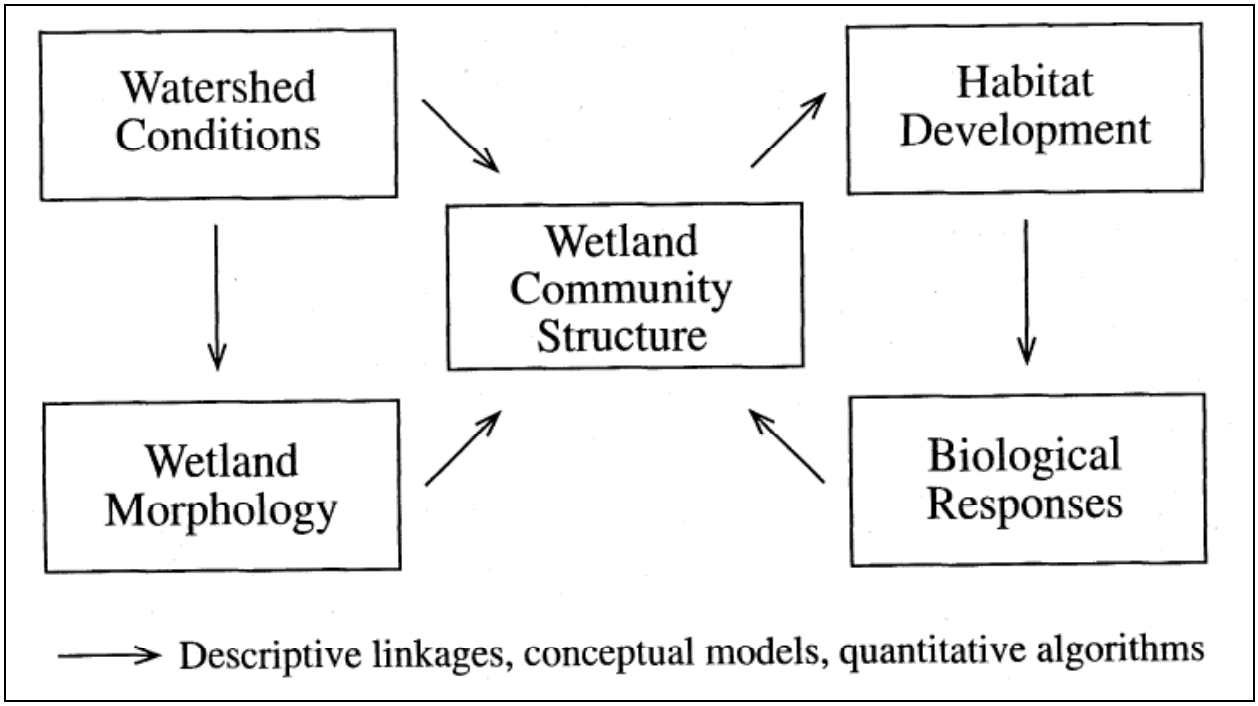

Figure 2. Puget Sound Wetlands and Stormwater Management Research Program experimental strategy.

The central block (Wetland Community Structure) represents the physical and chemical conditions that develop within a wetland and constitute a basis for its structure. Included are both quantity and quality aspects of its water supply and its soil system. Together these structural elements develop various habitats that can provide for living organisms, represented by the block at the upper right of the diagram. Biota will respond depending on habitat attributes, as illustrated by the block at the lower left. It is a fundamental goal of the Puget Sound Wetlands and Stormwater Management Research Program to describe these system components for the representative wetlands individually and collectively.

Connecting lines and arrows on Figure 2 depict the interactions among the components. It is a second fundamental goal of the program to understand and be able to express these interactions, toward the ends of advancing wetlands science and the management of urban wetlands and stormwater. Expression could come in the form of qualitative descriptions, relatively simple conceptual models, or more comprehensive mathematical algorithms. The extent to which definition of these interactions can be developed will determine the thoroughness with which management guidelines and new scientific knowledge can be generated by this research program.

The stormwater impact study examined the five major structural components of wetlands: (1) hydrology, (2) water quality, (3) soils, (4) plants, and (5) animals. Figure 3 presents a typical plan for monitoring of these components. A crest stage gage was used to register maximum water level since the preceding monitoring occasion, and a staff gage gave the instantaneous water level. These readings provided the basis for hydrologic analysis, as detailed in the paper on Morphology and Hydrology in Section 2.

Samples for water quality analysis were taken from the water column in an open water pool, and soil samples were collected at either three or four locations (see Water Quality and Soils in Section 2). Plant cover by species was determined along one or more transect lines, depending on wetland size and complexity of water and vegetation zones. Foliar tissue was sampled for analysis of metals content, and plant standing crop was cut for measurement of biomass gravimetrically. For more on the methods used in these monitoring activities refer to the Vegetation Community paper. Adult insect emergence was continuously monitored using triplicate emergence traps (see Emergent Aquatic Insect Community in Section 2). Amphibian breeding success was monitored along transects (labeled Herp. A, B in Figure 3). Adult amphibians as well as small mammals were live-trapped along other transects (labeled Mammal line A, B). The Section 2 papers titled Amphibian Community and Small Mammal Community elaborate on the methods. Birds were censused at one station as described by the Bird Community paper.

Definition of Watershed and Surrounding Landscape Characteristics

Essential to understanding the relationships between urban stormwater discharge and wetlands ecology was definition of the characteristics of wetland watersheds and surrounding landscapes. Each land use includes distinctive features, such as imperviousness and vegetative cover, that directly affect wetland conditions (Taylor 1993). Use of geographical information in the analysis of the effects of urbanization on wetlands allows the linking of effects with specific land use changes associated with urban development.

To this end, the program used a geographical information system (GIS) to inventory land uses in the watersheds of the study wetlands (Taylor 1993) (see Table 1). The GIS furnished quantitative and graphical representations of land use patterns. Study sites were located on U.S. Geographical Survey 7.5 minute series topographic maps

and the maps were used to locate wetland and watershed boundaries. Aerial photographs from 1989 were digitized into a computer data base and used to delineate wetland boundaries on the basis of wetland vegetation and open water. Land uses were classified according to a standard land use classification scheme. The GIS provided the areas of watersheds, wetlands, and land uses. These data were expressed in three ways: (1) wetland and watershed areas in hectares; (2) watershed land uses and vegetative cover as percentages of watershed areas; and (3) ratios of the areas of watersheds, land uses, and vegetative cover to wetland areas. The most important quantities yielded by the third method were the ratios of watershed and wetland areas (wetland areas were subtracted from their watershed areas in calculating these ratios). The method also was used to determine the ratios of impervious and forested areas to wetland areas. The 1989 GIS data were updated through manual examination of 1995 aerial photographs. In addition, in 1996, the same information was developed for 1000-meter wide bands of the surrounding landscapes using 1995 satellite images.

With regard to calculating watershed imperviousness, the program found that the relevant literature generally did not provide the level of detail necessary to establish the relationships between imperviousness and the land use definitions used in the GIS inventory. The program, therefore, relied on a variety of sources linking specific land uses to imperviousness levels. Estimates of imperviousness were made by using values from the literature for similar land uses (Alley and Veenhuis 1983; Prych and Ebbert 1986; Taylor 1993) and adjusting them according to best professional judgment.

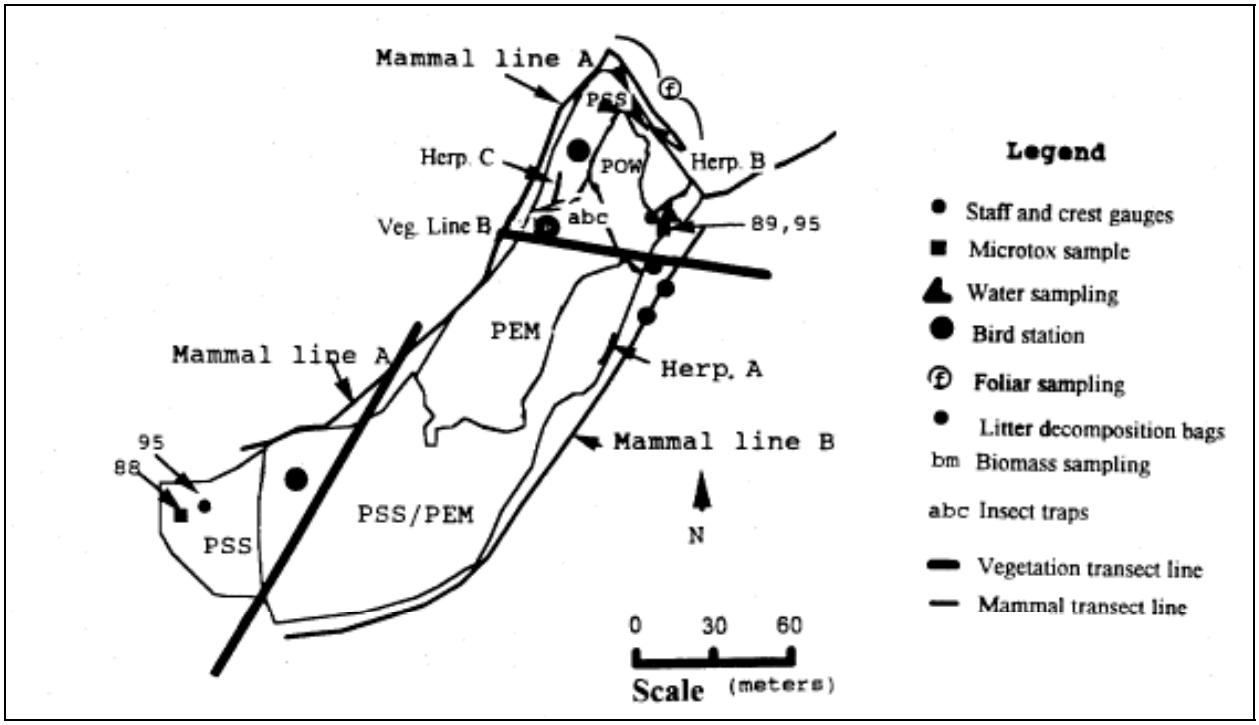

Figure 3. Typical monitoring plan (Patterson Creek 12 wetland).

Table 1. Landscape data for program wetlands.

Site	Watershed	Wetland	T/C	% Urban Cover			% Forest Cover			% Impervious Cover		
	Area	Area		1989	1995	Change	1989	1995	Change	1989	1995	Change
AL3	47.35	0.81	C	13.3	13.3	0.0	73.9	73.9	0.0	4.1	4.1	0.0
B3I	183.73	1.98	C	74.7	75.2	0.5	0.0	0.0	0.0	54.9	55.4	0.5
ELW1	54.63	3.84	C	56.6	56.6	0.0	0.0	0.0	0.0	19.9	19.9	0.0
FC1	357.34	7.28	C	81.2	81.2	0.0	14.7	14.7	0.0	30.8	30.8	0.0
HC13	359.36	1.62	C	1.5	1.5	0.0	76.6	75.1	-1.5	3.6	3.6	0.0
LCR93	198.22	6.09	C	12.8	11.0	-1.8	44.1	13.0	-31.1	5.8	6.1	0.3
LPS9	183.32	7.69	C	69.8	73.8	4.0	0.0	0.0	0.0	21.8	21.6	-0.2
MGR36	45.73	2.23	C	4.1	4.1	0.0	88.8	88.8	0.0	2.9	2.9	0.0
RR5	64.35	10.52	C	2.4	2.4	0.0	62.4	62.4	0.0	3.4	3.4	0.0
SC4	3.64	1.62	C	12.5	12.5	0.0	46.1	46.1	0.0	11.8	11.8	0.0
SC84	193.04	2.83	C	77.8	78.2	0.4	20.1	19.7	-0.4	18.5	17.0	-1.5
SR24	88.22	10.12	C	0.0	0.0	0.0	100.0	100.0	0.0	2.0	2.0	0.0
TC13	11.74	2.06	C	0.0	0.0	0.0	100.0	89.7	-10.3	2.0	2.3	0.3
BBC24	38.45	2.10	T	10.5	52.7	42.2	89.5	47.4	-42.1	3.4	10.6	7.2
ELS39	69.20	1.74	T	88.8	87.9	-0.9	18.5	10.8	-7.7	24.6	24.2	-0.4
ELS61	27.11	2.02	T	23.9	34.4	10.5	2.5	3.7	1.2	5.1	10.6	5.5
JC28	296.64	12.55	T	54.7	64.9	10.2	34.4	19.8	-14.6	20.0	20.6	0.6
NFIC12	3.24	0.61	T	0.0	100.0	100.0	100.0	0.0	-100.0	2.0	40.0	38.0
PC12	84.58	1.50	T	23.5	34.0	10.5	75.2	64.7	-10.5	5.1	6.8	1.7

a T=treatment wetlands; C=control wetlands.

b ELS39 developed was approximately 15% urban in 1988, before GIS analysis.

Effective Impervious Area (EIA) represents the impervious area that is actually connected to constructed drainage systems. This value was estimated as a proportion of Total Impervious Area (TIA) according to the formula EIA = 0.15 * TIA1.41 (Alley and Veenhuis 1983). This equation was developed in Denver and its accuracy (correlation coefficient = 0.98 and standard error = 0.075) probably varies in other areas. However, Alley and Veenhuis's estimates were compatible with those in Puget Sound lowland

hydrologic models (PEI 1990; SCS 1982). After determining EIA and TIA values for each land use. EIAs for entire watersheds were determined using the formula EIADB = $\Sigma 1 \rightarrow k$ (EIAk * LUk), where EIADB is the percentage of watershed area that is effectively imperviousness, k corresponds to the land uses inventoried in the basin, EIAk is the percentage of watershed area associated with land use k, and LUk is the percentage of the watershed classified as land use k. TIAs were calculated using the same formula.

ORGANIZATION OF THE MONOGRAPH

The papers that follow trace the major areas of progress in filling in the conceptual framework presented in Figure 2. The first series of papers provides a descriptive ecology of the palustrine wetlands of the central Puget Sound lowlands, organized according to the major structural components monitored during the program. The next series of papers assesses the effects of urban stormwater and other influences of urbanization observed during the study. The final series makes recommendations for managing urban stormwater and the wetlands subject to it.

REFERENCES

Adamus, P.R., and L.T. Stockwell. 1983. A Method for Wetland Functional Assessment: Volume 1 - Critical Review and Evaluation, FHWA-1P-82-23. U.S. Department of Transportation, Federal Highway Administration, Washington, DC.

Ahlgren, C.E., and H.L. Hansen. 1957. Some effects of temporary flooding on coniferous trees. Journal of Forestry 55: 647-650.

Alley, W.M., and J.E. Veenhuis. 1983. Effective impervious area in urban runoff modeling. J. Hydraulic Engineering 109(2): 313-319.

ABAG (Association of Bay Area Governments). 1979. Treatment of Stormwater Runoff by a Marsh/Flood Basin (Interim Report). Association of Bay Area Governments, Oakland, CA.

ABAG. 1986. Urban Stormwater Treatment at Coyote Hills Marsh. Association of Bay Area Governments, Oakland, CA.

Athanas, C. 1988. Wetlands creation for stormwater treatment. Pp. 61-66 in J. Zelanzny and J.S. Feierabend (eds.), Increasing Our Wetland Resources. National Wildlife Federation, Washington, DC.

Azous, A. 1991. An Analysis of Urbanization Effects on Wetland Biological Communities, M.S. thesis. University of Washington, Department of Civil Engineering, Environmental Engineering and Science Program, Seattle, WA.

Bedinger, M.W. 1978. Relation between forest species and flooding. In P.E. Greeson et al. (eds.), Wetland Functions and Values: The State of Our Understanding. American Water Resources Association, Minneapolis, MN.

Benforado, J. 1981. Ecological considerations in wetland treatment of wastewater. Pp. 307-323 in B. Richardson (ed.) Selected Proceedings of the Midwest Conference on

Wetland Values and Management, St. Paul, MN, June 17-19, 1981. Freshwater Society, Navarre, MN.

Bevis, F.B., and R.H. Kadlec. 1979. Effects of long-term discharge of wastewater on a northern Michigan wetland. In Abstracts of the Conference on Freshwater Wetlands and Sanitary Wastewater Disposal, Higgins Lake, MI, July 1979.

Boto, K.G., and W.H. Patrick, Jr. 1978. Role of wetlands in the removal of suspended sediments. Pp. 479-489 in P.E. Greeson et al. (eds.), Wetland Functions and Values: The State of Our Understanding. American Water Resources Association, Minneapolis, MN.

Brennan, K.M. 1985. Effects of wastewater on wetland animal communities. Pp. 199-223 in P.J. Godfrey et al. (eds.), Ecological Considerations in Wetlands Treatment of Wastewater. Van Nostrand Reinhold, New York, NY.

Brink, V.C. 1954. Survival of plants under flood in the lower Fraser River Valley, British Columbia. Ecology 35(1): 94-95.

Brinson, M.M. 1988. Strategies for assessing the cumulative effects of wetland alteration on water quality. Environmental Management 12(5): 655-662.

Brown, R.G. 1985. Effects of Wetlands on Quality of Runoff Entering Lakes in the Twin Cities Metropolitan Area, Minnesota, Water Resources Investigations Report 85-4170. U.S. Geological Survey, Washington, DC.

Brown, B.T., and B.M. Rattigan. 1979. Toxicity of soluble copper and other metal ions in Eleodea canadensis. Environ. Pollut. 21:303-314.

Bursztynsky, T.A. 1986. Personal communication to E.C. Stockdale, King County, Resources Planning Section (in Stockdale 1991).

Canning, D.J. 1988. Urban Runoff Water Quality: Effects and Management Options, Shorelands Technical Advisory Paper No. 4, 2nd ed. Washington Department of Ecology, Shorelands and Coastal Zone Management Program, Olympia, WA.

Chan, E. 1979. Treatment of Stormwater Runoff by a Marsh/Flood Basin. Association of Bay Area Governments, Oakland, CA.

Chan, E., T.A. Bursztynsky, N. Hantzsche, and Y.J. Litwin. 1981. The Use of Wetlands for Water Pollution Control, EPA-6-/S2-82-068, NTIS PB83-107466. U.S. Environmental Protection Agency, Municipal Environmental Research Laboratory, Cincinnati, Ohio.

Chapman, R.J., T.M. Hinckley, L.C. Lee, and R.O. Teskey. 1982. Impact of Water Level Changes on Woody Riparian and Wetland Communities: Volume X - Index and Addendum to Volumes I-VIII. U.S. Department of the Interior, Fish and Wildlife Service, Eastern Energy and Land Use Team, Kearneysville, WV.

Cochran, P.H. 1972. Tolerances of lodgepole pine and ponderosa pine seedlings to high water tables. N.W. Science 46(4): 322-331.

Conner, W.H., J.G. Gosselink, and R.T. Parrondo. 1981. Comparison of the vegetation of three Louisiana swamp sites with different flooding regimes. Am. J. Bot. 68: 320-331.

Cooke, S.S. 1991. The effects of urban stormwater on wetland vegetation and soils: a long-term ecosystem monitoring study. Pp. 43-51 in Puget Sound Research ‘91: Proceedings, January 4-5, 1991, Seattle, WA. Puget Sound Water Quality Authority, Olympia, WA.

Cowardin, L.M., V. Carter, F.C. Golet, and E.T. LaRoe. 1979. Classification of Wetlands and Deepwater Habitats of the United States, FWS/OBS-79/31. U.S. Fish and Wildlife Service, Biological Services Program, Washington, DC.

Darnell, R.M. 1976. Impacts of Construction Activities in Wetlands of the United States, EPA-600/3-76-045. U.S. Environmental Protection Agency, Environmental Research Laboratory, Corvallis, OR.

Dawson, B. 1989. High hopes for cattails. Civil Engineering, CEWRA9 59:5.

Davis, G.B., and M.M. Brinson. 1980. Responses of Submerged Vascular Plant Communities to Environmental Change, FWS/OBS-79/33. U.S. Department of the Interior, Fish and Wildlife Service, Office of Biological Services, Washington, DC.

Ehrenfeld, J.G., and J.P. Schneider. 1983. The Sensitivity of Cedar Swamps to the Effects of Nonpoint Source Pollution Associated with Suburbanization on the New Jersey Pine Barrens. Rutgers University, New Brunswick, NJ.

Franklin, K.T., and R.E. Frenkel. 1987. Monitoring a Wetland Wastewater Treatment System at Cannon Beach, Oregon. U.S. Environmental Protection Agency, Region 10, Seattle, WA.

Fries, B.M. 1986. Fate of Phosphorus from Residential Stormwater Runoff in a Southern Hardwood Wetland, M.S. thesis. University of Central Florida, Orlando, FL.

Galvin, D.V., and R.K. Moore. 1982. Toxicants in Urban Runoff, Toxicant Program Rept. No. 2. Municipality of Metropolitan Seattle, Seattle, WA.

Gill, C.J. 1970. The flooding tolerances of woody species: a review. Forestry Abstracts 31: 671-688.

Gomez, M.M., and F.P. Day. 1982. Litter nutrient content and production in the Great Dismal Swamp, Virginia. Am. J. Bot. 69: 1314-1321.

Gosselink, J.G., and R.E. Turner. 1978. The role of hydrology in freshwater wetland ecosystems. In R.E. Good et al. (eds.), Freshwater Wetlands: Ecological Processes and Management Potential. Academic Press, New York, NY.

Green, W.E. 1947. Effect of water impoundment on tree mortality and growth. Journal of Forestry 45(2): 118-120.

Gunderson, L.H., J.R. Stenberg, and A.K. Herndon. 1988. Tolerance of five hardwood species to flooding regimes. Pp. 119-132 in D.A.Wilcox (ed.), Interdisciplinary Approaches to Freshwater Wetlands Research. Michigan State University Press, East Lansing, MI.

Guntenspergen, G., and F. Stearns. 1981. Ecological limitations on wetland use for wastewater treatment. Pp. 272-284 in B. Richardson (ed.), Selected Proceedings of the Midwest Conference on Wetland Values and Management, St. Paul, MN, June 17-19, 1981. Freshwater Society, Navarre, MN.

Hammer, D.A. 1992. Creating Freshwater Wetlands. Lewis Publishers, Chelsea, MI.

Harrill, R.L. 1985. Urbanization, water quality and stormwater management: a Maryland perspective. Pp. 246-253 in Wetlands of the Chesapeake, Proceedings of the Conference Held April 9-11, 1985, Easton, Maryland.

Heliotis, F.D. 1982. Wetland Systems for Wastewater Treatment: Operating Mechanisms and Implications for Design, IES Report 117. Institute for Environmental Studies, University of Wisconsin, Madison, WI.

Hemond, H.F., and J. Benoit. 1988. Cumulative impacts on water quality functions of wetlands. Environmental Management 12(5): 639-653.

Hickok, E.A. 1980. Wetlands for the control of urban stormwater. Pp. 79-88 in W.L. Downing (ed.), Proceedings, National Conference on Urban Erosion and Sediment Control: Institutions and Technology, EPA 905/9-80-002. U.S. Environmental Protection Agency, Washington, DC.

Hickok, E.A., M.C. Hannaman, and N.C. Wenck. 1977. Urban Runoff Treatment Methods: Volume 1 - Non-Structural Wetlands Treatment, EPA-600/2-77-217. Minnehaha Creek Watershed District, Wayzata, MN.

Hopkinson, C.S., and J.W. Day, Jr. 1980. Modeling the relationship between development and stormwater and nutrient runoff. Environmental Management 4(4): 315-324.

Horner, R.R. 1989. Long-term effects of urban stormwater on wetlands. Pp. 451-465 in L.A. Roesner, B. Urbonas, and M.B. Sonnen (eds.), Design of Urban Runoff Controls. American Society of Civil Engineers, New York, NY.

Horner, R.R., F.B. Gutermuth, L.L. Conquest, and A.W. Johnson. 1988. Urban stormwater and Puget Trough wetlands. Pp. 723-746 in Proceedings, First Annual Meeting on Puget Sound Research, The Seattle Center, Seattle, WA, March 18-19, 1988. Puget Sound Water Quality Authority, Seattle, WA.

Isabelle, P.S., et al. 1987. Effects of roadside snowmelt on wetland vegetation: an experimental study. Journal of Environmental Management 25(1): 57-60.

Jackson, M.B., and M.C. Drew. 1984. Effects of flooding on growth and metabolism of herbaceous plants. Pp. 47-128 in T.T. Kozlowski (ed.), Flooding and Plant Growth. Academic Press, Inc.

Johnsgrad, P.A. 1956. Effects of water fluctuation and vegetation change on bird populations, particularly waterfowl. Ecology 37: 689-701.

Johnson, P.G., and L.F. Dean. 1987. Stormwater Management Guidebook for Michigan Communities. Clinton River Watershed Council, Utica, MI.

Kadlec, J.A. 1962. Effects of a drawdown on a waterfowl impoundment. Ecology 43: 267-281.

Kadlec, J.A. 1987. Nutrient dynamics in wetlands. Pp. 393-419 in K.R. Reddy and W.H. Smith (eds.), Aquatic Plants for Water Treatment and Resource Recovery. Magnolia Publishing, Orlando, FL.

Kadlec, R.H. 1987. Northern natural wetland water treatment systems. Pp. 83-98 in K.R. Reddy and W.H. Smith (eds.), Aquatic Plants for Water Treatment and Resource Recovery. Magnolia Publishing, Orlando, FL.

Keddy, P.A. 1983. Freshwater wetlands human-induced changes: indirect effects must also be considered. Environmental Management 7(4): 299-302.

Kozlowski, T.T. (ed.). 1984. Flooding and Plant Growth. Academic Press, Inc.

Lakatos, D.F., and L.J. McNemar. 1988. Wetlands and stormwater pollution management. Pp. 214-223 in J.A. Kusler and G. Brooks (eds.), Proceedings of a National Symposium: Wetland Hydrology. Association of State Wetland Managers, Berne, NY.

Leopold, L.B. 1968. Hydrology for Urban Land Planning: A Guidebook on the Hydrologic Effects of Urban Land Use, U.S. Geological Survey Circular 554. U.S. Department of the Interior, Geological Survey, Washington, DC.

Livingston, E.H. 1989. The use of wetlands for urban stormwater management. Pp. 467-489 in L.A. Roesner, B. Urbonas, and M.B. Sonnen (eds.), Design of Urban Runoff Quality Controls. American Society of Civil Engineers, New York, NY.

Lloyd-Evans, T.L. 1989. Use of Wetland for Stormwater Detention Effects on Wildlife Habitat. Manomet Bird Observatory (cited in Azous 1991).

Loucks, O.L. 1989. Restoration of the pulse control function of wetlands and its relationship to water quality objectives. Pp. 55-65 in J.A. Kusler and M.E. Kentula (eds.), Wetlands Creation and Restoration: The Status of the Science: Vol. II - Perspectives, EPA/600/3-89/038. U.S. Environmental Protection Agency, Environmental Research Laboratory, Corvallis, OR.

Lynard, W.G., E.J. Finnemore, J.A. Loop, and R.M. Finn. 1980. Urban Stormwater Management and Technology: Case Histories, EPA-600/8-80-035. U.S. Environmental Protection Agency, Washington, DC.

Lyon, J.G., R.D. Drobney, and C.E. Olson, Jr. 1986. Effects of Lake Michigan water levels on wetland soil chemistry and distribution of plants in the Straits of Mackinac. J. Great Lakes Res. 12(3): 175-183.

Marshall, W.A. 1980. The Effect of Stormdrain Runoff on Algal Growth in Nearshore Areas of Lake Sammamish, M.S. thesis. University of Washington, Department of Civil Engineering, Seattle, WA.

Martin, E.H. 1988. Effectiveness of an urban runoff detention pond wetlands system. Journal of Environmental Engineering - ASCE 114(4): 810-827.

McArthur, B.H. 1989. The use of isolated wetlands in Florida for stormwater treatment. Pp. 185-193 in D.N. Fisk (ed.), Wetlands: Concerns and Successes, Proceedings, American Water Resources Association Symposium, Tampa, FL, Sept. 17-22, 1989.

McKnight, J.S., D.D. Hook, O.G. Langdon, and R.L. Johnson. 1981. Flood tolerance and related characteristics of trees of the bottomland forest of the southern United States. Pp. 29-70 in J.R. Clark and J. Benforado (eds.), Wetlands of Bottomland Hardwood Forests. Elsevier Scientific Publishing Co., New York, NY.

Minore, D. 1968. Effects of Artificial Flooding on Seedling Survival and Growth of Six Northwestern Tree Species, Forest Service Reserve Note PNW-92. U.S. Department of Agriculture, Forest Service.

Minton, S.A., Jr. 1968. The fate of amphibians and reptiles in a suburban area. Journal of Herpetology 2(3-4): 113-116.

Mitsch, W.J., and J.G. Gosselink. 1993. Wetlands, 2nd ed. Van Nostrand Reinhold Co., New York, NY.

Morgan, M.D., and K.R. Philipp. 1986. The effect of agricultural and residential development on aquatic macrophytes in the New Jersey Pine Barrens. Biological Conservation 35: 143-158.

Morris, F.A., M.K. Morris, T.S. Michaud, and L.R. Williams. 1981. Meadowland Natural Treatment Processes in the Lake Tahoe Basin: A Field Investigation (Final Report), EPA-600/54-81-026, NTIS PB81-185639. U.S. Environmental Protection Agency, Washington, DC.

Mudrock, A., and J.A. Capobianco. 1979. Effects of treated effluent on a natural marsh. Journal Water Pollution Control Federation 51(9): 2243-2256.

Newton, R.B. 1989. The Effects of Stormwater Surface Runoff on Freshwater Wetlands: A Review of the Literature and Annotated Bibliography, Publication 90-2. University of Massachusetts, The Environmental Institute, Amherst, MA.

Nichols, D.S. 1983. Capacity of natural wetlands to remove nutrients from wastewater. Journal Water Pollution Control Federation 55(5): 495-505.

Niering, W.A. 1989. Effects of Stormwater Runoff on Wetland Vegetation. Unpublished report (cited in US EPA 1993).

Nordby, C.S., and J.B. Zedler. 1991. Responses of fish and macrobenthic assemblages to hydrologic disturbances in Tijuana Estuary and Los Peñasquitos Lagoon, California. Estuaries 14(1): 80-93.

Oberts, G.L. 1977. Water Quality Effects of Potential Urban Best Management Practices: A Literature Review, Technical Bulletin No. 97. Wisconsin Department of Natural Resources, Madison, WI.

Oberts, G.L., and R.A. Osgood. 1988. The water quality effectiveness of a detention/wetland treatment system and its effect on an urban lake, presented at the 8th Annual International Symposium on Lake and Watershed Management, November 15-19, 1988, St. Louis, MO. Metropolitan Council, St. Paul, MN.

PEI/Barrett Consulting Group. 1990. Snoqualmie Ridge Draft Master Drainage Plan. PEI/Barret Consulting Group, Bellevue, WA.

Pedersen, E.R. 1981. The Use of Benthic Invertebrate Data for Evaluating Impacts of Urban Stormwater Runoff, M.S. thesis. University of Washington, College of Engineering, Seattle, WA.

Portele, G.J. 1981. The Effects of Highway Runoff on Aquatic Biota in the Metropolitan Seattle Area, M.S. thesis. University of Washington, Department of Civil Engineering, Seattle, WA.

Prych, E. A., and J. C. Ebbert. 1986. Quantity and Quality of Storm Runoff from Three Urban Catchments in Bellevue, Washington, Water Resources Investigations Report 86-4000. U. S. Geological Survey, Tacoma, WA.

PSWQA (Puget Sound Water Quality Authority). 1986. Issue Paper: Nonpoint Source Pollution. PSWQA, Seattle, WA.

R.W. Beck and Associates. 1985. Marshland Wastewater Treatment Evaluation for the City of Black Diamond. R.W. Beck and Associates, Seattle, WA.

Reinelt, L.E., and R.R. Horner. 1990. Characterization of the Hydrology and Water Quality of Palustrine Wetlands Affected by Urban Stormwater. PSWSMRP, Seattle, WA.

Reinelt, L.E., and R.R. Horner. 1995. Pollutant removal from stormwater runoff by palustrine wetlands based on a comprehensive budget. Ecological Engineering 4: 77-97.

Richardson, C.J. 1985. Mechanisms controlling phosphorus retention in freshwater wetlands. Science 228: 1424-1427.

Richardson, C.J. 1989. Wetlands as transformers, filters and sinks for nutrients. In Freshwater Wetlands: Perspectives on Natural, Managed and Degraded Ecosystems - Ninth Symposium, Charleston, SC. University of Georgia, Savannah River Ecology Laboratory.

Richter, K.O., A. Azous, S.S. Cooke, R. Wisseman, and R. Horner. 1991. Effects of Stormwater Runoff on Wetland Zoology and Wetland Soils Characterization and Analysis. PSWSMRP, Seattle, WA.

Richter, K.O. , and R. Wisseman. 1990. Effects of Stormwater Runoff on Wetland Zoology. PSWSMRP, Seattle, WA.

Rumberg, C.B., and W.A. Sawyer. 1965. Response of wet meadow vegetation to length and depth of surface water from wild flood irrigation. Agron Journal 57: 245-247.

Schiffer, D.M. 1989. Effects of Highway Runoff on the Quality of Water and Bed Sediments of Two Wetlands in Central Florida, Rept. No. 88-4200. U.S. Department of the Interior, Geological Survey, Washington, DC.

Silverman, G.S. 1983. Seasonal Fresh Water Wetlands Development and Potential for Urban Runoff Treatment in the San Francisco Bay Area, Ph.D. thesis. University of California, Los Angeles, CA.

Sloey, W.E., F.L. Spangler, and C.W. Fetter, Jr. 1978. Management of freshwater wetlands for nutrient assimilation. Pp. 321-340 in R.E. Good et al. (eds.), Freshwater Wetlands: Ecological Processes and Management Potential. Academic Press, New York, NY.

SCS (U.S. Soil Conservation Service). 1982. (cited in Taylor)

Stark, J.R., and R.G. Brown. 1988. Hydrology and water quality of a wetland used to receive wastewater effluent, St. Joseph, Minnesota. In J.A. Kusler and G. Brooks (eds.), Proceedings of a National Symposium: Wetland Hydrology. Association of State Wetland Managers, Berne, NY.

Stockdale, E.C. 1986a. The Use of Wetlands for Stormwater Management and Nonpoint Pollution Control: A Review of the Literature. Washington Department of Ecology, Olympia, WA.

Stockdale, E.C. 1986b. Viability of Freshwater Wetlands for Urban Surface Water Management and Nonpoint Pollution Control: An Annotated Bibliography. Washington Department of Ecology, Olympia, WA.

Stockdale, E.C. 1991. Freshwater Wetlands, Urban Stormwater, and Nonpoint Pollution Control: A Literature Review and Annotated Bibliography. Washington Department of Ecology, Olympia, WA.

Surowiec, M.S. 1989. An Hydrogeologic and Chemical Characterization of an Urban and Nonurban Wetland, M.S. thesis. University of Washington, Department of Civil Engineering, Seattle, WA.

Taylor, B.L. 1993. The Influence of Wetland and Watershed Morphological Characteristics on Wetland Hydrology and Relationships to Wetland Vegetation Communities, M.S. thesis. University of Washington, Department of Civil Engineering, Environmental Engineering and Science Program, Seattle, WA.

Teskey, R.O., and T.M. Hinckley. 1977a. Impact of Water Level Changes on Woody Riparian and Wetland Communities: Volume I - Plant and Soil Responses to Flooding, FWS/OBS-77/58. U.S. Department of the Interior, Fish and Wildlife Service, Office of Biological Services, Washington, DC.

Teskey, R.O., and T.M. Hinckley. 1977b. Impact of Water Level Changes on Woody Riparian and Wetland Communities: Volume II - Southern Forest Region, FWS/OBS-77/59. U.S. Department of the Interior, Fish and Wildlife Service, Office of Biological Services, Washington, DC.

Teskey, R.O., and T.M. Hinckley. 1977c. Impact of Water Level Changes on Woody Riparian and Wetland Communities: Volume III - The Central Forest Region, FWS/OBS-77/60. U.S. Department of the Interior, Fish and Wildlife Service, Office of Biological Services, Washington, DC.

Teskey, R.O., and T.M. Hinckley. 1977d. Impact of Water Level Changes on Woody Riparian and Wetland Communities: Volume IV - Eastern Deciduous Forest Region, FWS/OBS-78/87. U.S. Department of the Interior, Fish and Wildlife Service, Office of Biological Services, Washington, DC.

Thibodeau, F.R., and N.H. Nickerson. 1985. Changes in a wetland plant association induced by impoundment and draining. Biological Conservation 33: 269-279.

Tilton, D.L., and R.H. Kadlec. 1979. The utilization of freshwater wetland for nutrient removal from secondarily treated wastewater effluent. Journal Environmental Quality 8: 328-334.

U.S. Congress, Office of Technology Assessment. 1984. Wetlands: Their Use and Regulation, OTA-0-206. U.S. Government Printing Office, Washington, DC.

U.S. Environmental Protection Agency. 1983. Results of the Nationwide Urban Runoff Program: Executive Summary. NTIS PB84-185545. U.S. Environmental Protection Agency, Water Planning Division, Washington, DC.

U.S. Environmental Protection Agency. 1985. Freshwater Wetlands for Wastewater Management: Environmental Assessment Handbook, EPA 904/9-85-135. U.S. Environmental Protection Agency, Region 4, Atlanta, GA.

U.S. Environmental Protection Agency. 1993. Natural Wetlands and Urban Stormwater: Potential Impacts and Management, 843-R-001. U.S. Environmental Protection Agency, Office of Water, Washington, DC.

van der Valk, A.G. 1991. Response of wetland vegetation to a change in water level. In C.M. Finlayson and T. Larson (eds.), Wetland Management and Restoration, Report 3992. Swedish Environmental Protection Agency, Stockholm, Sweden.

Walters, A.M., R.O. Teskey, and T.M. Hinckley. 1980. Impact of Water Level Changes on Woody Riparian and Wetland Communities: Volume VIII - Pacific Northwest and Rocky Mountain Regions, FWS/OBS-78/94. U.S. Department of the Interior, Fish and Wildlife Service, Office of Biological Services, Washington, DC.

Weller, M.W. 1987. The influence of hydrologic maxima and minima on wildlife habitat and production values of wetlands. In J.A. Kusler and G. Brooks (eds.), Wetland Hydrology. Association of State Wetland Managers, Chicago, IL.

Weller, M.W. 1988. Issues and approaches in assessing cumulative impacts on waterbird habitats in wetlands. Environmental Management 12(5): 695-701.

Wentz, W.A. 1987. Ecological/environmental perspectives on the use of wetlands in water treatment. Pp. 17-25 in K.R. Reddy and W.H. Smith (eds.), Aquatic Plants for Water Treatment and Resource Recovery. Magnolia Publishing, Orlando, FL.

Whigham, D.F., C. Chitterling, and B. Palmer. 1988. Impacts of freshwater wetlands on water quality: a landscape perspective. Environmental Management 12(5): 663-671.

Whigham, D.F., R.L. Simpson, and K. Lee. 1980. The Effect of Sewage Effluent on the Structure and Function of a Freshwater Tidal Marsh Ecosystem. Rutgers University, Water Resources Research Institute, New Brunswick, NJ.

Whitlow, T.H., and R.W. Harris. 1979. Flood Tolerance in Plants: A State of the Art Review, Technical Report E-79-2. U.S. Army Corps of Engineers, Waterways Experiment Station, Vicksburg, MS.

Wickcliff, C., H.J. Evans, K.K. Carter, and S.A. Russell. 1980. Cadmium effects on the nitrogen fixation system of red alder. J. Environ. Qual. 9: 180-184.

Woodward-Clyde Consultants. 1991. The Use of Wetlands for Controlling Stormwater Pollution (Draft). U.S. Environmental Protection Agency, Region 5, Water Division, Watershed Management Unit, Chicago, IL and U.S. Environmental Protection Agency, Office of Water Regulations and Standards, Office of Water Enforcement and Permits, and Office of Wetland Protection, Washington, DC.

Zedler, J.B., and M.E. Kentula. 1986. Wetlands Research Plan, EPA/600/3-86/009, NTIS PB86-158656. U.S. Environmental Protection Agency, Environmental Research Laboratory, Corvallis, OR.

Section 2 Descriptive Ecology of Freshwater Wetlands in the Central Puget Sound Basin

CHAPTER 1 MORPHOLOGY AND HYDROLOGY

by Lorin E. Reinelt, Brian L. Taylor and Richard R. Horner

INTRODUCTION

This chapter provides an overview of the morphologic and hydrologic characteristics of palustrine (isolated or depressional freshwater) wetlands and their watersheds in the central Puget Sound Basin. Natural and anthropogenic factors that affect wetland morphology and hydrology are discussed with particular attention to the effects of development (typically, the conversion of forested lands to urban areas) on changing watershed and wetland hydrology. It was concluded that wetland water level fluctuation (WLF) estimates, measured with staff and crest-stage gages, provide a good overall indicator of wetland hydrologic conditions. Analysis methods and materials used in the PSWSMRP are also presented.

Wetlands are ecosystems that develop at the interface of aquatic and terrestrial environments when hydrologic conditions are suitable. Wetlands are recognized as biologically productive ecosystems offering extensive, high-quality habitat for a diverse array of terrestrial and aquatic species, as well as multiple beneficial uses for humans, including flood control, groundwater recharge and water quality treatment. However, as urbanization of natural landscapes occurs, some or all of the functions and values of wetlands may be affected. Some wetlands may be impacted by direct activities such as filling, draining or outlet modification, while others may be affected by secondary impacts, including increased or decreased quantity and reduced quality of inflow water.

The morphology of a wetland and the wetland's position within the landscape greatly influences its' characteristics. Morphology is used here to describe the wetland's physical shape and form. As a result of a wetland's shape, it may contain significant pooled areas with little or no flow gradient (termed an open-water system), or alternatively, it may show evidence of channelization and contain a significant flow gradient (termed a flow-through system). In some instances, a wetland may also form in a local or closed depression (termed a depressional system).

The outlet condition of a wetland, as defined by the degree of flow constriction, has a direct effect on wetland hydrology and hydroperiod. Finally, a wetland's position in the landscape is also a key factor affecting wetland hydrologic conditions. Palustrine (isolated, freshwater) wetlands usually have relatively small contributing watersheds and often occur in areas with groundwater discharge conditions.

Hydrology is probably the single most important determinant for the establishment and maintenance of specific types of wetlands and wetland processes (Mitsch and Gosselink 1993). Water depth, flow patterns, and the duration and frequency of inundation influence the biochemistry of the soils and are major factors in the selection of wetland biota. Thus, changes in wetland hydrology may influence significantly the soils, plants

and animals of particular wetland systems. Precipitation, surface water inflow and outflow, groundwater exchange and evapotranspiration, along with the physical features noted above, are the major factors that influence the hydrology of palustrine wetlands.

PUGET SOUND WETLANDS AND STORMWATER MANAGEMENT RESEARCH PROGRAM

The Puget Sound Wetlands and Stormwater Management Research Program was established to determine the effects of urban stormwater on wetlands and the effect of wetlands on the quality of urban stormwater. There are two primary components of the research program: (1) a study of the long-term effects of urban stormwater on wetlands, and (2) a study of the water quality benefits to downstream receiving waters as urban stormwater flows through wetlands. In both studies, the hydrologic and morphologic conditions of the wetlands had a direct effect on observations involving water quality, soils, and the plant and animal communities.

This paper presents hydrologic information gained from a broad overview of the hydrology of 19 wetlands (representing a variety of watershed development conditions) studied from 1988-95, and specific information on the hydrology of two wetlands (one each in an urban and nonurban area) intensively studied from 1988-90 (B3I and PC12, respectively. (Study site locations are shown in Section 1, Figure 1).

WETLANDS IN URBANIZING AREAS

Wetlands have received increased attention in recent years as a result of continuing wetland losses and impacts resulting from new development. In urbanizing areas, the quantity and quality of stormwater can change significantly as a result of land-use conversion in a watershed. Increases in the quantity of stormwater may result from new impervious surfaces (e.g., roads, buildings), installation of storm sewer piping systems, and removal of trees and other vegetation. On the other hand, decreased inflow of water can result from modifications in surface and groundwater flows. For cases where wetlands are the primary receiving water for urban stormwater from new developments, it is hypothesized that the effects of watershed changes will be manifested through changes in the hydrology of wetlands.

Wetland hydrology is often described in terms of its hydroperiod, the pattern of fluctuating water levels resulting from the balance between water inflows and outflows, topography, subsurface soil, geology, and groundwater conditions (Mitsch and Gosselink, 1986). Wald and Schaefer (1986) referred to seasonal water level changes as the "heartbeat" of Pacific Northwest palustrine systems.

WETLAND HYDROLOGIC FUNCTIONS

Wetlands provide many important hydrologic, ecological, and water quality functions. Specific hydrologic functions include flood protection, groundwater recharge, and streamflow maintenance. Wetlands provide flood protection by holding excess runoff after storms, before slowly releasing it to surface waters. While wetlands may not prevent flooding, they can lower flood peaks by providing detention of storm flows.

Wetlands that are connected to groundwater or aquifers provide important recharge waters. Wetlands retain water, allowing time for surface waters to infiltrate into soils and replenish groundwater. During periods of low streamflow, the slow discharge of

groundwater maintains instream flows. The connection of wetlands with streamflows and groundwater make them essential in the proper functioning of the hydrologic cycle.

HYDROLOGY OF PALUSTRINE WETLANDS

The hydrology of palustrine wetlands is governed by the following components: precipitation, evapotranspiration, surface inflow, surface outflow, groundwater exchange, and change in wetland storage (Figure 1-1). In a hydrologic balance, these components are represented by the following equation (Reinelt et al., 1993):

$$P + I +/- G +/- S = ET + O \qquad (1)$$

where P = precipitation; I = surface inflow; G = groundwater exchange, S = change in wetland storage, ET = evapotranspiration; and O = surface outflow.

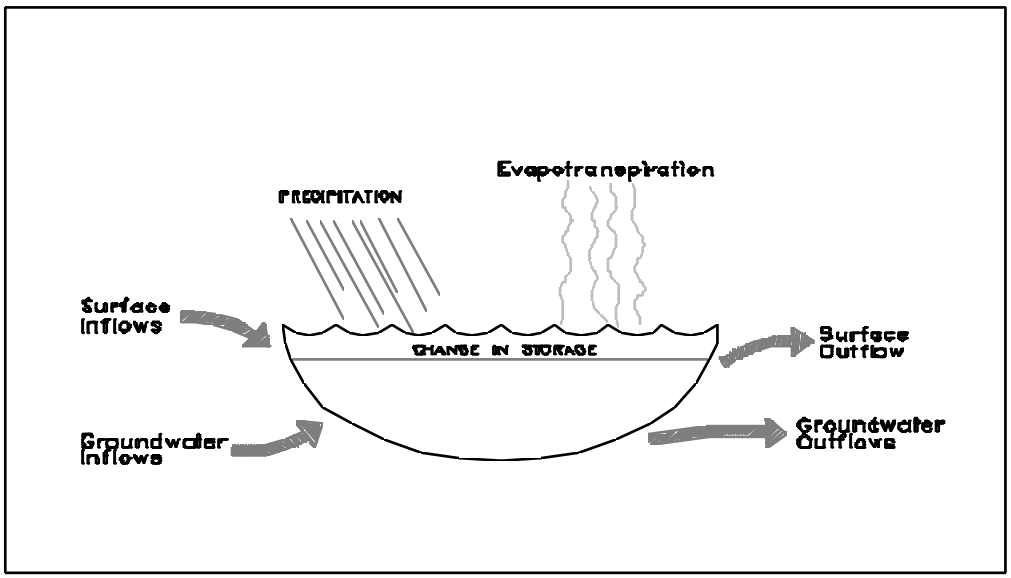

Figure 1-1. Wetland water budget components

Precipitation

Precipitation is determined by regional climate and topography. Approximately 75 percent of the total annual rainfall occurs from October to March during a well-defined wet season in the Puget Sound region. Generally, annual precipitation totals across central Puget Sound increase further east with increasing elevation. Rainfall tends to be more uniform geographically during the wet season, and more variable and intense during short dry-season cloud bursts.

Surface Inflows

Surface inflows result from runoff generation in the wetland's watershed. The quantity of surface inflows are determined by watershed land characteristics such as cover (e.g., impervious surface, forest), soils, and slope, as well as the wetland-to-watershed ratios. The rate of water delivery to the wetland is also affected by the predominant flow type in the watershed (e.g., overland or sheet flow, subsurface flow or interflow, concentrated

flow). Generally, as a watershed becomes more developed, with more constructed storm drainage systems, the more rapid the hydrologic response in the watershed.

Groundwater

The role and influence of groundwater on wetland hydrology are highly variable. The exchange of water between the wetland and groundwater is governed by the relative elevations of surface water in the wetland and surrounding groundwater, as well as soil permeability, local geology and topography. Numerous studies have discussed the importance of groundwater in maintaining wetland hydrology (Winter, 1988, Surowiec, 1989, Mitsch and Gosselink, 1986). Wetlands can be discharge or recharge zones for groundwater, or both depending on the time of year. The palustrine wetlands studied in this research are predominantly groundwater discharge zones (i.e., water discharges from groundwater to the wetland).

Groundwater flow to wetlands can be quantitatively estimated using Darcy's Law, an empirical law governing groundwater flow:

$$Q = K * (dH/dL) * A \qquad (2)$$

where K = hydraulic conductivity, dH/dL = the hydraulic or piezometric gradient and A = cross-sectional area or control surface across which groundwater flows.

In the detailed study of two wetlands, shallow and deep piezometers were installed at both wetlands to estimate the horizontal and vertical components, respectively, of groundwater flow to the wetlands.

Change in Wetland Storage

Wetland storage changes seasonally and in response to storm events. The water storage can be estimated as the mean water depth of the wetland multiplied by the areal extent of the wetland (Mitsch and Gosselink, 1986). Seasonal changes in wetland storage are attributable to the local patterns of precipitation and evapotranspiration.

Duever (1988) asserted that the prime factor controlling seasonal fluctuation is drainage basin topography and that wetland water levels generally coincide with regional groundwater levels. Surowiec (1989) noted that steep slopes adjacent to a wetland can also lead to increased groundwater inputs, particularly on a seasonal basis.

Event changes in wetland storage result from increased surface or ground water inputs associated with precipitation. Reinelt and Horner (1990), Azous (1991), and Taylor (1993) referred to this as water level fluctuation, and estimated it for an occasion i as the difference between a crest-stage measurement (peak water level since the previous sampling occasion) and the instantaneous staff-gage measurement.

Evapotranspiration

Evapotranspiration (ET) consists of water that evaporates from wetland water or soils combined with the water that passes through vascular plants that is transpired to the atmosphere. Solar radiation, temperature, wind speed and vapor pressure are the main factors influencing evaporation rates (Linsley et al., 1982).

The ratio of ET to evaporation varies widely depending on vegetation type and site conditions. Reported ET ratios vary between 0.67 and 1.9 (Dolan et al., 1984; Boyd,

1987; Koerselman and Beltman, 1988). Generally, emergent wetland vegetation transpires more than woody vegetation; however, factors such as plant density also effect transpiration rates. Evapotranspiration is greatest from May to August (exceeding 100 mm per month) and least from November to March.

Surface Outflow

Surface outflows are affected by all the hydrologic factors noted above. For wetlands with relatively large watersheds, outflows are often comparable in magnitude to inflows. The physical features that affect surface outflows include outlet conditions, wetland-to-watershed ratios, and wetland morphometry.

RESEARCH METHODS AND WETLAND DESCRIPTORS

Many of the methods and materials used for morphologic, hydrologic, and watershed data collection were previously reported in PSWSMRP papers (Reinelt and Horner, 1990; 1991; Taylor, 1993). This paper provides a summary of the methods, with additional information on data processing and analysis.

Wetland Morphology

Three different measures of wetland morphology that influence the hydrology and hydroperiod of wetlands were defined by Reinelt and Horner (1990): wetland shape/type (open water, flow through, depressional), outlet condition, and wetland-to-watershed ratio. Wetlands were classified as open-water systems if significant open water pools were present and surface water velocities were predominantly low (less than 5.0 cm/s). Wetlands were classified as flow-through systems if there was evidence of channelization and significant water velocities. All depressional wetlands are also open water wetlands.

Outlet conditions were defined by level of constriction (Reinelt and Horner, 1991; Taylor, 1993) as high (e.g., undersized culvert, closed depression, confined beaver dam), or low to moderate (e.g., overland flow to stream, oversized culvert, broad bulkhead or beaver dam). The wetland-to-watershed ratio was determined by the wetland and contributing watershed areas. Watershed areas were delineated based on USGS quadrangle map contours and wetland areas were obtained from the King County Wetlands Inventory (1992). The hydroperiod of wetlands with low wetland-to-watershed ratios (less than 0.05) tends to be dominated by surface inflows, whereas wetlands with higher ratios are more influenced by regional groundwater conditions.

Watershed Characteristics

Changes in land use ultimately affect wetlands receiving water from an urbanizing drainage basin. Different land uses have unique combinations of factors that directly affect watershed hydrology, such as imperviousness and vegetative cover. By collecting information about drainage basin land use, it is possible to link wetland hydroperiod characteristics to specific land uses, as well as general changes associated with urban development.

A geographic information system (GIS) was developed to manage land use data for the watersheds of the study wetlands, and to facilitate quantitative and graphical analysis of land-use patterns. Land-use classifications, based on a national standard (Anderson,

1976), were determined from 1989 aerial photographs and subsequently digitized into Arc/Info (Reinelt et al., 1991). For each study site, the GIS contained information about total watershed and wetland area, and the area and percent of watershed area for each land use type (e.g., urban, agriculture, forest).

Watershed Imperviousness

The literature consistently identifies hydrologic effects of urbanization with increased impervious areas within the watershed (Schueler, 1994). Impervious area increases within a watershed reduce evaporation and infiltration, and as a result of forest clearing for urban conversion also result in a loss of vegetative storage and decreased transpiration (Lazaro, 1979).

Imperviousness was estimated from aerial photos and empirical relationships between land uses and percent impervious cover (Table 1-1, Gluck and McCuen, 1975; Alley and Veenhuis, 1983; KCSWM, 1990). This estimation technique was found to produce results consistent with values used in Puget Sound lowland hydrologic models (PEI, 1990; SCS, 1982). Effective impervious areas (impervious surfaces connected to a storm drainage system) were also estimated according to a formula reported by Alley and Veenhuis (1983) based on drainage basins in the Denver area:

$$EIA = 0.15\ TIA1.41 \qquad (R\ 2 = 0.98,\ \text{standard error} = 7.5\%) \quad (3)$$

where EIA and TIA = percent effective and total impervious area, respectively.

Table 1-1. Impervious and effective impervious areas associated with land uses.

CODE	NATIONAL STANDARD	IA%	EIA%	Reference
111	Low Density SFR (<1 unit/acre)	<15	4	a
112	Med. Density SFR (1-3 unit/acre)	20	10	a
113	High Density SFR (3-7 units/acre)	40	25	a
114	Mobile Homes	70	60	b
115	Low Density MFR (>7 units/acre)	80	72	b
120	Commercial (general)	90	85	b
121	Retail sales and services	80	72	b
123	Offices and professional services	75	66	b
124	Hotels and Motels	75	66	c
131	Light Industrial	60	48	d
132	Heavy Industrial	80	72	c
144	Freeway Right-of-way	100	99	b
151	Energy Facilities	80	72	c
152	Water Supply Facilities	80	72	c
155	Utility Right-of-way	5	1.5	c
160	Community Facilities (general)	75	66	c
161	Educational Facilities	40	27	b
162	Religious Facilities	70	60	c
171	Golf Courses	20	10	b
172	Parks	5	1.5	b
190	Open Land (general)	2	1	c
192	Land being developed	50	37	c
193	Open space - designated	2	1	c
200	Agricultural Land	5	1.5	c
300	Grassland	2	0	c
400-430	Forest Lands	2	0	c
440	Clearcut areas	5	0	c

REFERENCES:

a. King County Surface Water Management (1990)
b. PEI (1990)
c. Estimate based on similar land uses
d. Alley and Veenhuis (1983)

WATERSHED SOILS

The Soil Conservation Service (SCS) Soil Survey for King County (Snyder et al., 1973) was used to evaluate the drainage characteristics of the soils in each of the 19 drainage basins. Two soil parameters were reviewed to determine which would be an appropriate index of the soil hydrologic characteristics relevant to the analysis: permeability and general drainage characteristics.

Soil permeability, is measured as a range of infiltration rates, the units of which are distance/time. Soil permeability for the majority of the soils found in the watersheds was in the range of 2.0 - 6.3 inches/hour. The drainage class is a more general description of the soil characteristics such as “Moderately well-drained” or “Somewhat excessively drained.” Many soils in the Pacific Northwest (e.g. Alderwood series) are underlain by glacial till, a hardpan layer that limits the ultimate depth of percolation and plays an important role in routing subsurface flow. Drainage class was therefore thought to be a

better estimator of the hydrologic role of the watershed soils than permeability because it represents the effects of the multiple soil horizons characterized as a particular soil type; an infiltration rate is based on the top soil layer.

For this study, a watershed soils index (WSI) was calculated as an area weighted mean of soil drainage classes found in the study basins. Each of six drainage classes described by the SCS was assigned a number that ranged from 1 to 6, with lower numbers representing poorly drained soils (Table 1-2). The range of the WSI corresponded with the SCS Hydrologic Soil groups, which are used in the Curve Number method of runoff estimation. The WSI was preferred for the analysis because it describes soil drainage to a finer level than the hydrologic soil group.

Table 1-2. Soil drainage classes and watershed soils index (WSI).

Drainage Class	WSI	SCS Hyd. Group (1)	Examples
Very poorly drained	1	(D)	(Muck)
Poorly drained	2	D	Norma, Bellingham
Somewhat poorly drained	3	(D)	(Oridia, Renton)
Moderately well drained	4	C	Alderwood, Kitsap
Well drained	5	B, C	Ragnar, Beausite
Somewhat excessively drained	6	A	Everett, Indianola

(1) Parenthesis indicates soils that were not found in any of the wetland watersheds.

WETLAND HYDROLOGY

Wetland Water Level Measurements and Fluctuation

Water level measurements in wetlands can be made using a variety of gages or instruments. Readings can be either instantaneous, continuous, or representative of a peak or base level since the last site visit. In the PSWSMRP, we utilized staff and crest stage gages to record instantaneous water levels and peak occasion water levels, respectively, during each site visit. At two wetlands (Bellevue 3I and Patterson Creek 12), continuous water levels were recorded over a two-year period (1988-90) using automatic data recorders. Gages were placed in open water areas or areas of channelized flow where water level measurements could be attained throughout most of the year.

The crest-stage and staff gage data were used to estimate wetland water level fluctuation. To estimate the water level fluctuation at a wetland site, two factors were considered: (1) the water level prior to the storm event, hereafter referred to as the base water level, and (2) the water level change resulting from the event. Four methods of calculating water level fluctuation were investigated in a preliminary analysis before choosing a preferred method to use in the analysis (Azous 1991, Taylor, 1993). The methods differed primarily in how the base water level prior to the stormwater influx was estimated. The fluctuation was then calculated as the difference between the maximum and base water levels. The selected method used the midpoint of the sampling interval to estimate the base water level:

$$WLFi = Ci - 0.5(Si + Si\text{-}1) \qquad (4)$$

where WLFi , Ci , and Si = the water level fluctuation, crest level, and base level, respectively for sampling occasion i, and Si-1 = the base level for occasion i-1.

The water level fluctuation data were used in three ways during the analysis. The data from each sampling occasion were used when evaluating the relationship between precipitation and water level fluctuation. Mean and maximum study period WLF values were used when assessing the effects of land use and wetland characteristics on the wetland hydroperiod.

Seasonal Fluctuation in Wetland Water Levels

Seasonal fluctuation in wetland water levels is probably the most important factor governing wetland development and functioning in the Pacific Northwest (Wald and Schaefer, 1986). A quantitative measure of seasonal WLF was developed based on an examination of the hydroperiod plots for the study wetlands.

May and October are months when the water level changes dramatically in those sites that undergo large seasonal fluctuations. Noting this, the dry season water level was estimated as the mean of staff gage measurements collected during the months June through September. Similarly, the wet season water level was estimated as the mean of staff gage measurements collected between November and May. Approximately equal sample sizes were used to calculate each of the seasonal mean water levels. The mean seasonal difference in water levels was calculated as the difference in these seasonal mean water levels. The data from the early study period (April 1988 - April 1991) were used to calculate seasonal WLFs.

A second measure of the seasonal WLF is the range of water levels observed. The water depth range was calculated as the difference between the study period maximum and minimum water levels. This measure, used with the mean seasonal water level difference described above, provided a picture of the wetland hydroperiod suitable for analysis, because both typical and extreme events were addressed.

Length of Summer Dry Period

The length of the summer dry period (as defined by the absence of surface water) was also analyzed; however, this dry period estimate was subject to the following limitations: (1) Estimating the length of the dry period was affected by the flow characteristics and topography within the wetland; that in turn determined which areas dry first. Because gages were placed in the wetland areas thought to be the last to dry out during the summer, a water level of 3 cm or less constituted “dry” in this analysis. (2) The exact length of the dry period was uncertain, because of the frequency of site visits. The approximate monthly sampling interval during the summer months did not allow for the determination of the date the water level reached “zero.” To compensate for this uncertainty, the transition from “wet” to “dry” (or vice versa) was assumed to occur at the midpoint of the sampling interval.

RESULTS AND THE CONCEPTUAL MODEL

Descriptive results of the morphologic and hydrologic analysis of the study wetlands are shown in Table 1-3. The various water level fluctuation patterns observed in the wetlands and a conceptual model relating wetland and watershed characteristics to wetland hydroperiod are also presented below.

Table 1-3. Wetland and watershed morphologic and hydrologic characteristics.

Wetland	Outlet Condition	Outlet Constriction	WLF Type	Dry in Summer?	System Type	% TIA 1989	% TIA 1995
AL3	None	high	FL	Y	OW/D	4	4
B3I	Culvert	high	SH	N	FT	55	55
BBC24	Beaver dam	low	SL	N	OW	3	11
ELS39	Culvert	high	FH	Y	OW	25	25
ELS61	Stream	low	FL	N	OW	5	11
ELW1	Lake	low	SH	N	FT	20	20
FC1	Beaver dam	moderate	S/FH	N	FT	31	31
HC13	Beaver dam	high	FL	N	OW	4	4
JC28	Stream	low	SL	Y	FT	20	21
LCR93	None	high	FH	Y	FT	6	6
LPS9	Drain inlet	high	FH	Y	FT	22	22
MGR36	Stream	low	SL	N	FT	3	3
NFIC12	None	high	FL	Y	OW/D	2	40
PC12	Beaver dam	high	FL	N	OW	5	7
RR5	Beaver dam	low	FL	N	OW	3	3
SR24	Road	low	FL	N	OW	2	2
SC4	Culvert	low	SL	Y	FT	12	12
SC84	Stream	low	FL	Y	OW	19	17
TC13	Drain inlet	moderate	FL	Y	OW	2	2

WATER LEVEL FLUCTUATION PATTERNS

Based on the water level fluctuation analysis, wetlands were classified into four distinguishable types of hydroperiods (Figure 1-2): (1) stable base water level with low event fluctuations (SL), (2) stable base water level with high event fluctuations (SH), (3) fluctuating base water level with low event fluctuations (FL), and (4) fluctuating base water level with high event fluctuations (FH). The four patterns were defined quantitatively using a threshold of 20 cm. Wetlands with a base water level range less than or greater than 20 cm were considered stable or fluctuating, respectively. Similarly, wetlands with event fluctuations less than or greater than 20 cm were considered low or high, respectively. Figure 1-2 shows the WLF pattern for the 19 study wetlands.

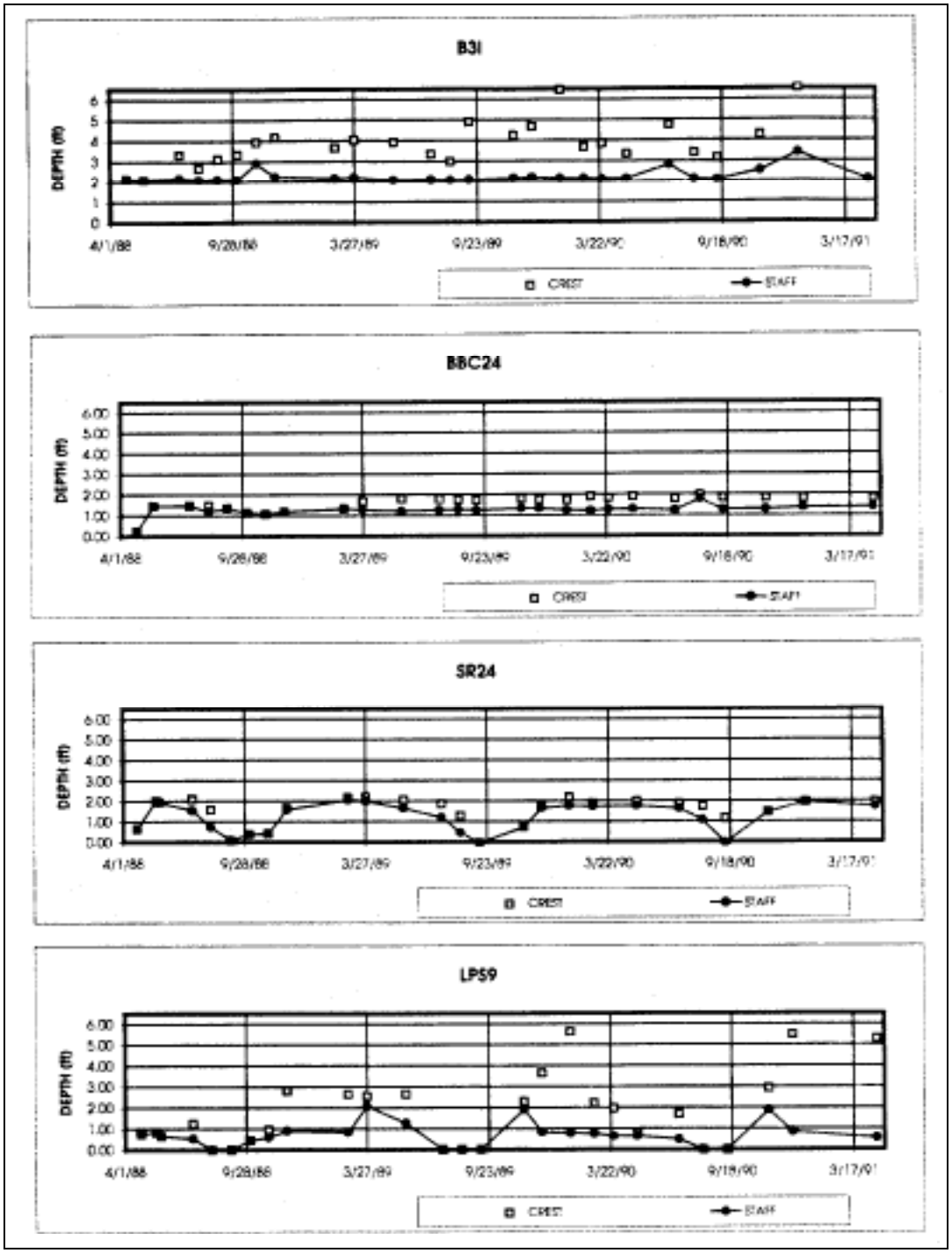

Figure 1-2. Four Water Level Fluctuation Patterns

CONCEPTUAL MODEL OF INFLUENCES ON WETLAND HYDROPERIOD

A conceptual model was developed by Taylor (1993) to characterize the relationships between watershed and wetland morphological characteristics and wetland hydroperiod (Figure 1-3). This model was used as a basis to examine, through application of a multivariate regression model, which wetland and watershed hydrologic processes, and factors governing these processes, had the greatest influence on wetland hydroperiod. Results from this analysis are presented in Section 3 of this report.

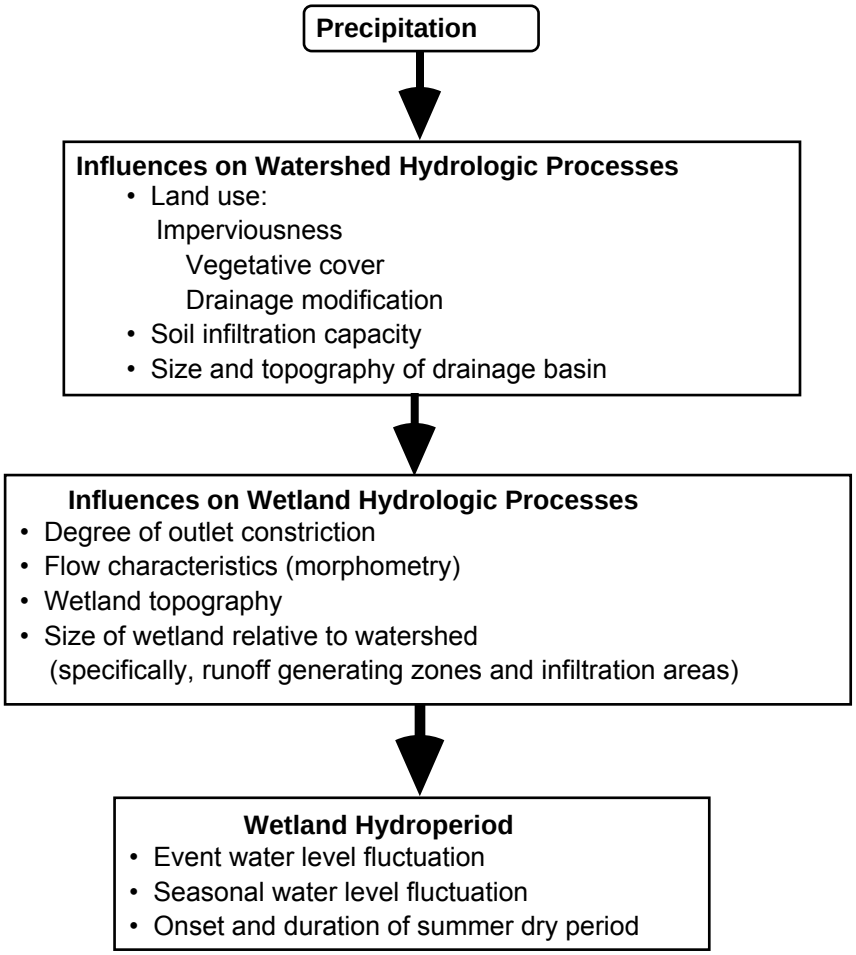

Figure 1-3. Conceptual model of influences on wetland hydroperiod.

CONCLUSIONS

There are many descriptive measures of the morphologic and hydrologic characteristics of freshwater wetlands in the central Puget Sound basin. This paper summarized those that were examined and utilized by the PSWSMRP. The physical shape or type of wetland (e.g., open water, flow-through), the wetland's position within the landscape (particularly as related to the wetland-to-watershed ratio), and the degree of outlet constriction were presented as key wetland characteristics affecting hydroperiods. The

imperviousness, land cover, and soils of the watershed were also found to be important characteristics affecting surface runoff and wetland hydrology.

The quantity of stormwater entering many wetlands in the central Puget Sound region has changed as a result of rapid development in urbanizing areas. These changes may affect the functions and values of wetlands by impacting the hydrology, which in turn may affect the plant and animal communities. If the relationships between watershed and wetland changes and their impacts on wetland hydroperiod can be characterized and documented, it may be possible to mitigate these effects through improved watershed controls or development regulations.

REFERENCES

Alley, W.M. and Veenhuis, J.E. 1983. Effective impervious area in urban runoff modeling. Journal of Hydraulic Engineering, 109(2): 313:319.

Anderson, 1976. USGS Paper 964.

Azous, A. 1991. An Analysis of Urbanization Effects on Wetland Biological Communities, M.S. thesis. University of Washington, Department of Civil Engineering, Environmental Engineering and Science Program, Seattle, WA.

Boyd, C.E. 1987. Evapotranspiration/Evaporation (E/Eo) Ratios for Aquatic Plants. J. Aquatic Plant Management, 25:1-3.

Dolan, T.J., Hermann, A.J., Bayley, S.E. and Soltek, J. 1984. Evapotranspiration of a Florida, U.S.A., Freshwater Wetland. Journal of Hydrology, 74:355-371.

Duever, M.J. 1988. Hydrologic processes for models of freshwater wetlands. In Wetland Modeling. Elsevier, New York, N.Y.

Gluck, W.R. and McCuen, R.H. 1975. Estimating land use characteristics for hydrologic models. Water Resources Research, 11(1): 177-179.

King County Surface Water Management. 1990. Surface Water Design Manual. King County Department of Public Works. Seattle, WA.

King County Wetlands Inventory. 1991. King County Resource Planning. King County, WA.

Koerselman, W. and Beltman, B. 1988. Evapotranspiration from Fens in Relation to Penman's Potential Free Water Evaporation (Eo) and Pan Evaporation. Aquatic Botany, 31:307-320.

Lazaro, T.R. 1979. Urban Hydrology: A Multidisciplinary Perspective. Ann Arbor Science Pub., Michigan.

Linsley, R.K. Jr., Kohler, M.A. and Paulhus, J.L.H. 1982. Hydrology for Engineers. McGraw-Hill.

Mitsch, W.J. and Gosselink, J.G. 1993. Wetlands 2nd Ed.. Van Nostrand Reinhold Co., New York.

PEI/Barrett Consulting Group. 1990. Snoqualmie Ridge Draft Master Drainage Plan.

Reinelt, L.E. and Horner, R.R. 1990. Characterization of the Hydrology and Water Quality of Palustrine Wetlands Affected by Urban Stormwater. King County Resource Planning, King County, WA.

Reinelt, L.E. and Horner, R.R. 1991. Urban stormwater impacts on the hydrology and water quality of palustrine wetlands in the Puget Sound region. In Puget Sound Research '91 Proceedings, 1: 33-42. Puget Sound Water Quality Authority.

Reinelt, L.E., Velikanje, J., and Bell, E.J. 1991. Development and application of a geographic information system for wetland/watershed analysis. Computers, Environment and Urban Systems, 15: 239-251.

Reinelt, L.E., Surowiec, M.S., and Horner, R.R. 1993. Urbanization effects on palustrine wetland hydrology as determined by a comprehensive water balance. King County Resource Planning. King County, WA.

Schueler, T.R. 1994. The importance of imperviousness. Watershed Protection Techniques, 1(3): 100-111.

Snyder, D.E., Gale, P.S., and Pringle, R.F. 1973. Soil Survey of King County Area, Washington. U.S. Dept. of Agriculture, Soil Conservation Service, Wash. D.C.

Surowiec, M.S. 1989. An Hydrogeologic and Chemical Characterization of an Urban and Nonurban Wetland. M.S.E. Thesis. Department of Civil Engineering, University of Washington.

Taylor, B.L. 1993. The Influence of Wetland and Watershed Morphological Characteristics on Wetland Hydrology and Relationships to Wetland Vegetation Communities. M.S.C.E. Thesis. Department of Civil Engineering, University of Washington.

Wald, A.R. and Schaefer, M.G. 1986. Hydrologic functions of wetlands of the Pacific Northwest. In Wetland Functions, Rehabilitation, and Creation in the Pacific Northwest: The State of Our Understanding. Washington State Dept. of Ecology.

Winter, T.C. 1988. A conceptual framework for assessing cumulative impacts on hydrology of nontidal wetlands. Environmental Management, 12(5): 605-620.

CHAPTER 2 WATER QUALITY AND SOILS

by Richard R. Horner, Sarah S. Cooke, Lorin E. Reinelt, Kenneth A. Ludwa and Nancy T. Chin

INTRODUCTION

This chapter emphasizes water and soil quality in wetlands without significant urbanization in their watersheds. Like other chapters in this section, its purpose is to characterize particular elements of Puget Sound Basin freshwater wetland ecology in a state relatively unaffected by human activity. The wetlands profiled in this group were those with < 4% impervious surface and ≥ 40% forested area in their watersheds. It is recognized that human influence is not entirely absent in these cases, but truly pristine examples do not exist in the lowlands of the Puget Sound Basin. While there are palustrine wetlands in the Pacific Northwest that are not directly affected by urbanization, it is difficult to locate wetlands that are completely unaffected by humans. Indeed, even where there is no human activity in a wetland's watershed, atmospheric pollutants from distant sources could still reach these "pristine" wetlands through rainfall. The wetlands considered here are regarded as representative of the closest to a natural state attainable in the ecoregion. Chapter 9 concentrates on water and soil quality in wetlands with watersheds that are moderately and highly urbanized, as well as those with watersheds that had new development during the years of the study.

It is important to reiterate that the research program concentrated on palustrine wetlands of the general type most prevalent in the lower elevations of the central Puget Sound Basin. The results and conclusions presented here are probably applicable to similar wetlands somewhat to the north and south of the study area, but may not be representative of higher, drier, or more specialized systems, like true bogs and “poor” (low nutrition) fens.

WATER QUALITY

Collection and Methods

Collection of samples for water quality analysis was performed in 1988-1990, 1993, and 1995. Sampling was concentrated during the wet and dry seasons, with fewer samples taken in the transition seasons between those periods. The reason for this scheduling was to concentrate effort when the most pollutants enter wetlands, during the runoff season, and when the decrease in surface water due to relatively low inflow and high evapotranspiration is expected to concentrate pollutants most.

In the last four of the five years' samples were collected in 19 wetlands on the following schedule: November 1-March 31--4 samples, April 1-May 31--1 sample, June 1-August 31--2 samples, and September 1-October 31--1 sample. Sampling occurred at about the same times each year in order to get a consistent view of seasonal water quality variation. The same general pattern was observed in 1988; but there were only 14 wetlands in the program at that time, sampling did not begin until May, and a total of seven instead of eight samples was taken. Some of the wetlands, in most years nine of the 19, had no surface water for varying lengths of time in the late spring, summer, and/or early fall and could not be sampled during those times.

Samples were taken from the largest open water pool in each wetland, if there was one. If not, they were collected near the outlet if surface water existed there or, otherwise downstream of the inlet. The standard grab method was generally used to collect the samples manually. A hand-pump-operated device (Horner and Raedeke 1989) was employed to take samples intended for dissolved oxygen analysis and in cases where shallow water prevented conventional grab sampling without entraining material from the bottom.

Temperature and pH were measured in the field, temperature either by mercury thermometer or electronic meter. The pH was determined with the electronic meter, in latter years a Beckman Model φ 11 instrument. Dissolved oxygen samples were stabilized in the field and transported on ice, along with samples for other analyses, to one of several laboratories used in the different years.

Water quality analyses varied somewhat from the beginning to the end of the program. Some analyses that did not produce much usable information in the early years were dropped. Analyses that were performed in all years and are the focus of this chapter are:

Temperature	Soluble reactive phosphorus (SRP)
pH	Total phosphorus (TP)
Dissolved oxygen (DO)	Fecal coliforms (FC)
Conductivity (Cond)	Total lead (Pb)
Total suspended solids (TSS)	Total copper (Cu)
Ammonia-nitrogen (NH3-N)	Total zinc (Zn)
Nitrate + nitrite-nitrogen (NO3+NO2-N)	

Among the analyses deleted after the early years were dissolved metals, which were usually below detection limits. It is probable that the use of exceptional methods would detect these constituents, but doing so was outside the objectives of this research. Enterococcus was dropped as a bacteriological measure because it did not yield the hoped for reduced variability often prevalent with fecal coliforms, and was never widely adopted as a standard analyte as had been anticipated 10 years ago. Oil and grease and total petroleum hydrocarbons were measured in a relatively small number of samples but were always present in the wetland water column in very small concentrations, with the exception of an isolated incident when an oil spill was suspected. In the final two years of sampling data became available on a number of metals in addition to the three of most interest since they were run routinely on the inductively coupled plasma-mass spectrometer (ICP-MS) used by the laboratory handling those samples.

Horner and Ludwa (1993) prepared a monitoring and quality assurance/quality control (QA/QC) plan that specifies in detail the sampling and analytical methods and QA/QC provisions for the last two years of the program, which were typical of all years. A report by Reinelt and Horner (1990) is the best source of detail on methods for the initial years. Water quality methods and results were also reported by King County Resource Planning Section (1988); Azous (1991); Reinelt and Horner (1991); Platin (1994); Ludwa (1994): Taylor, Ludwa, and Horner(1995); and Chin (1996).

Research Findings: A Portrait of Puget Sound Basin Wetland Water Quality

The main objective of this section is to develop a water quality profile of the least developed wetlands in the data set as presumably representative of the "best attainable" condition in the Puget Sound Basin lowlands. In developing this profile companion data are also presented for more urbanized cases, in part to allow some comparisons now and also for more extensive discussion of those cases in Chapter 9. Later in this chapter wetlands in the data set are classified according to morphological characteristics and again compared. These comparisons are performed with the use of basic summary statistics (primarily, means, standard deviations, and medians). For the most part, tests for statistical significance of differences and analyses of variance were not performed, because of lack of replication of conditions with any exactness, large natural variability, and relatively small sample sizes under any given set of conditions.

Table 2-1 gives a statistical summary of the water quality data gathered over the full project from wetlands whose watersheds did not experience significant urbanization change during that period (control wetlands) grouped by urbanization status. Chapter 9 takes up wetlands with watersheds that did change. Nonurban watersheds (N) were classed as those with both < 4% impervious land cover and ≥ 40% forest; highly urbanized watersheds (H) were considered to be those having both ≥ 20% impervious and ≤ 7% forest. Those not fitting either of the other categories were classified as moderately urbanized watersheds (M). Valentine (1994) developed this classification scheme for analysis of the probable origin of soil metals, and it is maintained here for water quality as well for consistency. Characteristics of the individual watersheds can be found in Section 1, Table 1. Indeterminate statistics (< or > a given value) are the result of some measurements being below detection or, in the case of FC, bacterial colonies too numerous to count in the dilutions analyzed in some very concentrated samples.

Examination of Table 2-1 reveals several general points about wetland water quality. First, excepting pH, concentrations were very variable, as indicated by the relatively high coefficients of variation (CV). The principal sources of water quality variability are examined later in the chapter. Fecal coliform was the most variable of the analytes overall, followed by TSS and NH3-N. Other than for pH, DO, and conductivity, medians were usually lower than arithmetic means, signifying the influence on means, but not on medians, exerted by a relatively few high values. This trend is consistent with a log-normal probability distribution of values, a distribution frequently observed in environmental data (Gilbert 1987).

Nonurban wetlands are the main focus of this chapter, and Chapter 9 further discusses the other categories. With a cursory comparison of the Table 2-1 medians, it can be seen that pH rose slightly and DO marginally declined with increasing urbanization. Conductivity and NH3-N increased substantially from nonurban to moderately urban wetlands but actually were a bit lower in highly urbanized cases. NO3+NO2-N and TP increased from N to M status but not further with H status. Cu showed little difference among categories, but many values were below detection. The remaining variables (TSS, SRP, FC, Pb, and Zn) all increased with each step up in urbanization level.

Table 2-1. Water quality statistics for wetlands not experiencing significant urbanization change (1988-1995).

Status	Statistic	pH		DO	Cond.		TSS		NH3-N	NO3+NO2-N		SRP	TP		FC		Cu		Pb		Zn
				(mg/L)	(µS/cm)		(mg/L)		(µg/L)		(µg/L)		(µg/L)		(CFU/100 mL)		(µg/L)		(µg/L)		(µg/L)
N	Mean	6.38		5.7	72.5	<	4.6	<	59.9	<	368.2	<	17.6	52.3	>	271.3	<	3.3	<	2.7	<	8.4
	Maximum	7.65		11.3	230.0		73.0		1373.0		3200.0		414.0	850.0		6240.0		15.0		21.0		49.0
	Std. Dev.	0.53		2.6	63.8	>	8.5	>	129.3	>	484.6	>	47.6	86.6	>	1000.4	>	2.7	>	2.8	>	8.3
	CV	8%		45%	88%	>	185%	>	216%	>	132%	>	271%	166%	>	369%	>	80%	>	105%	>	99%
	Median	6.36		5.9	46.0		2.0		21.0		111.5		6.0	29.0		9.0	<	5.0		1.0		5.0
	n	162		205	190		204		205		206		200	206		206		93		136		136.0
M	Mean	6.54	<	5.5	142.4	<	9.2	<	125.7	<	598.2	<	31.5	92.5	>	2664.8	<	3.7	<	3.4	<	9.8
	Maximum	7.88		14.8	275.0		180.0		2270.0		7210.0		280.0	780.0		359550.0		7.0		13.0		33.0
	Std. Dev.	0.82	>	3.6	72.8	>	21.6	>	266.8	>	847.2	>	37.9	91.8	>	27341.7	>	1.9	>	2.7	>	7.2
	CV	13%	>	66%	51%	>	235%	>	212%	>	142%	>	120%	99%	>	1026%	>	51%	>	79%	>	73%
	Median	6.72		5.1	160.0		2.8		43.0		304.0		16.0	70.0		46.0	<	5.0		3.0		8.0
	n	132		173	161		175		177		177		172	177		173		78		122		122.0
H	Mean	6.73	<	5.4	150.9	<	9.2	<	68.3	<	395.4		31.2	109.5	>	968.6	<	4.1	<	4.5	<	20.2
	Maximum	7.51		10.5	271.0		87.0		516.8		1100.0		79.0	1940.0		38000.0		12.0		22.0		73.0
	Std. Dev.	0.57	>	2.9	85.5	>	15.1	>	104.4	>	239.4		15.7	233.5	>	4752.8	>	2.5	>	4.0	>	16.7
	CV	9%	>	53%	57%	>	164%	>	153%	>	61%		50%	213%	>	491%	>	62%	>	89%	>	83%
	Median	6.88		6.3	132.2		4.0		32.0		376.0		28.2	69.0		61.0	<	5.0		5.0		20.0
	n	52		67	61		66		67		67		65	67		66		29		44		44.0

N = wetlands with nonurban watersheds; M = wetlands with moderately urbanized watersheds;
H = wetlands with highly urbanized watersheds; OW = open water wetland; FT = flow-through wetland

A water quality portrait of Puget Sound Basin lowland palustrine wetlands relatively unaffected by humans, then, shows slightly acidic (median pH = 6.4) systems with DO often well below saturation, and in fact sometimes quite low (< 4 mg/L). Dissolved substances are relatively low (most conductivity readings < 50 µS/cm) but somewhat variable. Suspended solids are routinely low but quite variable, reflecting the strong influence of storm runoff events on TSS. Median total dissolved nitrogen concentrations (the sum of ammonia, nitrate, and nitrite) are more than 20 times as high as dissolved phosphorus, suggesting general limitation of plant and algal growth by P. Some of the fairly abundant TP would become available over time to support photosynthesis, but probably not enough to modify the general picture. The low median fecal coliform indicates that most readings are very low (< 10 CFU/100 mL), but a small number is so high that the mean is 30 times the median. Both mean and median heavy metals concentrations are in the low parts per billion range, with standard deviations just about identical to the means.

Wetland Water Quality in Context

To proceed with a descriptive picture of regional wetland water quality, it is useful to provide some context for the quantitative information. This portion of the chapter discusses the statistical data with respect to informal criteria for separating the data into groups that can be associated with various factors that may influence the magnitudes. The account also gives a sense of how water quality compares in regional wetlands versus streams.

Reinelt and Horner (1990) first presented the informal criteria based on several considerations; they were slightly modified for this paper. Some are regulatory standards applied to other water body types (water quality standards have not yet been adopted for wetlands in Washington). Others have generally recognized biological relevance, but some are simply arbitrary breakpoints in the data distributions. In all cases professional judgment was applied in adopting a numerical informal criterion.

Table 2-2 gives the distribution of wetlands, using median values, among the three urbanization categories relative to the informal criteria. It also repeats the medians and means for each category from Table 2-1.

Some water quality variables did not appear to depend on urbanization. One site in each category had median pH < 6, apparently as a consequence of some presence of peat in soils and peat-forming vegetation. Each group also had DO distributed among the three criteria ranges. As discussed later, it seems that DO depends more heavily on wetland morphology than on urbanization.

Several variables exhibited rising medians with urbanization; but when viewed in terms of the criteria, low concentrations predominated, suggesting relatively light pollutant loading from stormwater runoff. Most NH3-N median values were in the lowest range in all categories. Wetlands produce ammonia in decomposing the abundant organic matter internally produced (Mitsch and Gosselink 1993); and, absent an elevated source, concentrations would not necessarily be expected to follow urbanization. Most NO3+NO2-N medians were also in the lowest range in the N and M wetlands but not in the most highly urbanized. For zinc, the most frequently detected metal, no median in any urbanization class approached the chronic criterion for the protection of aquatic life. In fact, the chronic criterion was violated in only one of these wetlands, a highly urbanized one, in individual samples during the entire program. Although not shown in the table, the same general situation prevailed for copper but not for lead, which has a very low chronic criterion in these generally soft waters (3.2 µg/L). As can be seen in Table 2-1, H wetlands had Pb medians above that concentration, and M wetlands fell close to it.

TSS, conductivity, TP, and fecal coliforms exhibited a general tendency toward more sites in the higher criteria ranges with increasing urbanization. Still, TSS medians were very low. A total phosphorus concentration > 20 µg/L is often recognized as one sign that a lake is eutrophic, and > 50 µg/L as an indication of a hypertrophic state (Welch 1980). No wetland had a median below 20 µg/L, and the majority of M and H wetlands fell above 50 µg/L. Wetlands are recognized as systems more prone to eutrophication than lakes for a number of reasons (e. g., rapid nutrient cycling, often having the entire water column in the photic zone). Even those subject to little or no urbanization appear to have a rather high trophic state, and more urbanized systems are even higher. However, since wetlands flush more rapidly than lakes, these elevated TP concentrations may be a lesser concern in wetlands than they would be in lakes. All but three wetlands would meet the 50 CFU/100 mL fecal coliform standard that applies to lakes and the highest class streams in Washington on the basis of their means. Two moderately and one highly urbanized site could not meet even the least stringent standard. Of course, a number of individual values were far higher.

For the least urbanized wetlands, the following general statements can be made to characterize the water quality of Puget Sound Basin lowland palustrine wetlands in a fairly natural state:

- These wetlands are highly likely (83% of cases observed) to have median conductivity < 100 µS/cm, NH3-N < 50 µg/L, TP in the range 20-50 µg/L, fecal coliforms < 50 CFU/100 mL, and total Zn < 10 µg/L.

- These wetlands are also likely (68% of cases observed) to have median TSS in the range 2-5 mg/L and NO3+NO2-N < 100 µg/L.
- The pH and DO in these wetlands are unpredictable from consideration of urbanization status alone, being dependent on other factors.

Table 2-3 statistically summarizes water quality data from 50 locations on western King County streams collected by the Municipality of Metropolitan Seattle during 1990-1993. These data represent grab samples taken on a regular schedule, by chance most often under baseflow conditions. In these ways they are comparable to the wetland data produced by the PSWSMRP. Unlike Tables 2-1 and 2-2, though, Table 2-3 mixes results from streams with very different influences. Nevertheless, it is useful to show how regional wetland and stream water quality compare.

While most wetlands tended strongly to be slightly acidic, and some were rather more so, streams tended just as strongly to be slightly alkaline. This difference is very likely the result of organic acid production by plants that are virtually absent in lotic systems. As expected, flowing streams were observed to be better oxygenated than wetlands, with median DO about twice as high. Streams at the median level were similar to moderately and highly urbanized wetlands in conductivity, but the nonurbanized wetlands had a central tendency below even the minimum measured stream value. TSS median concentrations were generally similar in the two types of water bodies. NH3-N was generally higher in wetlands, reflecting the relatively high production rate of this species accompanying organic matter decomposition. On the other hand, NO3+NO2-N was for the most part lower in the wetlands, perhaps because of slower nitrification in the more oxygen-depleted environment. Median stream TP fell between the levels in the nonurbanized and more highly urbanized wetlands. Stream median fecal coliforms were higher than in any wetland category, but there were no extremely high values such as were measured in the wetlands. This observation suggests that coliform organisms are able to reproduce more successfully in rich, quiescent wetland environments once they enter. All in all, the two sets of results exhibit rough comparability, with most deviations mirroring the physical and biological differences in the two systems.

Table 2-2. Comparison of medians of water quality variables for wetlands not experiencing significant urbanization change (1988-1995) with informal criteria.

Variable	Criterion	Nonurbanized			Moderately Urbanized			Highly Urbanized		
		Median	Mean	%[a]	Median	Mean	%[a]	Median	Mean	%[a]
pH	5-6	6.4	6.4	16.7	6.7	6.5	14.3	6.9	6.7	50.0
	6-7			67.7			57.1			0.0
	7-8			16.7			28.6			50.0
DO	< 4	5.9	5.7	33.3	5.1	< 5.5	57.1	6.3	< 5.4	50.0
(mg/L)	4-6			33.3			14.3			0.0
	> 6			33.3			28.6			50.0
Cond	< 100	46	72	83.3	160	142	28.6	132	151	50.0
(µS/cm)	100-200			16.7			42.8			0.0
	> 200			0.0			28.6			50.0
TSS	<2	2.0	< 4.6	33.3	2.8	< 9.2	14.3	4.0	< 9.2	50.0
(mg/L)	2-5			67.7			71.4			0.0
	> 5			0.0			14.3			50.0
NH_3-N	< 50	21	< 60	83.3	43	< 126	71.4	32	< 68	100.0
(µg/L)	50-100			16.7			14.3			0.0
	>100			0.0			14.3			0.0
NO3+NO2-N	< 100	112	< 368	67.7	304	< 598	57.1	376	< 395	0.0
(µg/L)	100-500			16.7			28.6			50.0
	> 500			16.7			14.3			50.0
TP	< 20	29	52	0.0	70	92	0.0	69	110	0.0
(µg/L)	20-50			83.3			42.8			0.0
	> 50			16.7			57.1			100.0
FC	< 50	9	> 271	83.3	46	> 266	71.4	61	> 969	50.0
(CFU/100 mL	50-100			16.7			0.0			0.0
	> 100			0.0			28.6[b]			50.0[b]
Zn	< 10	5.0	< 8.4	83.3	8.0	< 9.8	85.7	20.0	< 20.2	50.0
(µg/L)	> 10[c]			16.7			14.3			50.0

[a] % of sites with this urbanization status (see Table 1 for definitions) fitting the criterion.
[b] Medians are > 200.
[c] Highest median is 21 µg/L, in comparison to the 59 µg/L chronic criterion for the protection of aquatic life with a water hardness of 50 mg/L as $CaCO_3$.

Seasonal Variation

Wetlands are highly variable systems with annual, seasonal, and diurnal variability in water chemistry. They often have several sources of water supply, each possessing a distinctive chemical blend that varies from year to year. Many water quality parameters exhibited clear seasonal fluctuations in the wetlands studied. DO concentrations were generally higher from mid-November to mid-May than during the remainder of the year

(Reinelt and Horner 1990). This pattern is not surprising considering that most precipitation and runoff and the coolest temperatures in the Pacific Northwest occur during this period, and cooler, more turbulent water absorbs more oxygen.

Conductivity and pH did not exhibit such variation in most wetlands monitored. However, some had higher conductivity from May to November, when wetland water levels drop and dissolved substances become more concentrated (Reinelt and Horner 1990). Many wetlands had substantially higher TSS concentrations during the winter and early spring, the period of greatest runoff and erosion. However, colonial algae can cause high TSS readings in the late summer as well (Reinelt and Horner 1990).

Table 2-3. Distribution of water quality data for baseflow samples from 50 stream sites (Municipality of Metropolitan Seattle 1994).

	Maximum	75th Percentile	50th Percentile	25th Percentile	Minimum
Conductivity (µmho/cm)	30,900	203	130	104	53
Suspended solids (mg/L)	12.6	4.8	3.4	2.8	1.6
Ammonia (µg/L)	190	24	15	13	5
Nitrate+nitrite (µg/L)	3,000	1,100	630	320	73
Temperature (°C)	13.5	11.1	10.6	10	8.0
Dissolved oxygen (mg/L)	11.4	11.0	10.4	9.6	5.8
Turbidity (NTU)	16.5	2.7	1.8	1.4	0.7
Fecal coliform (org/100 mL)	900	220	100	49	7
Enterococcus (org/100 mL)	410	170	53	22	5
pH	8.2	7.6	7.5	7.3	6.9
Total phosphorus (µg/L)	150	66	48	32	13

While many wetlands monitored by the program had lower concentrations of NH3-N, SRP, and TP from November to May, they had higher nutrient concentrations in the other part of year possibly as a result of greater fertilizer applications and lower water levels that concentrate nutrients. NO3+NO2-N values fluctuated greatly in the program wetlands, and tended to vary directly with DO (Reinelt and Horner 1990). This association is another sign that nitrification moderated by the degree of aerobiosis has a strong influence on how much NO3+NO2-N will be found in a wetland water column.

Medians and geometric means of fecal coliform (FC) and enterococcus bacteria were highly variable. Peak counts occurred most frequently in late August and September, and least often from mid-November through February (Reinelt and Horner 1990). The monitoring program found that while most water quality parameters varied seasonally, NH3-N, SRP, TP, FC, and enterococcus were especially changeable (Reinelt and Horner 1990).

Variation with Wetland Morphology

Wetland morphology refers to its form and physical structure and embraces its shape; perimeter length; internal horizontal dimensions; topography (also termed bathymetry), which is the pattern of elevation gradients; water inlet and outlet configurations; and water pooling and flow patterns. These factors establish zonation at early successional stages by determining the extent of inundation from place to place and the hydrodynamic characteristics of flow. From these structural zones stem vegetation composition, distribution, and productivity, and, ultimately, the same features of the animal communities. Of course, these biota in turn influence morphological development over time through detrital and sediment accretion and animal activities like burrowing and dam building by beavers. The various morphological characteristics entirely determine the flood-flow storage and alteration function of wetlands. Along with the friction produced by vegetation, they set the residence time of water within the wetland, which is a key regulator of sediment trapping, nutrient processing, and other water quality functions.

Early work in the program determined that one aspect of morphology in particular, water pooling and flow patterns, had a substantial influence on wetland water quality (Reinelt and Horner 1990, 1991). The wetlands in the study were classified as either open-water (OW) or flow-through (FT) types. The OW systems contain significant pooled areas and possess little or no flow gradient, while the FT wetlands are often channelized and have a clear flow gradient.

Using the first three years of data (Reinelt and Horner 1990), it was found, unsurprisingly, that temperatures ranged higher in wetlands characterized by relatively large open pools, especially from May to September. On an annual basis, the photosynthetic pigments chlorophyll a and phaeophytin a attained higher concentrations in wetlands characterized by large open pools, which have greater light exposure and longer residence times, and ranged much higher than in flow-through wetlands during the growing season. Dissolved oxygen tended to be significantly lower than in flow-through wetlands during these periods.

Table 2-4 summarizes statistics for the wetlands whose watersheds stayed relatively stable during the program broken down by urbanization and morphological status. Comparing open water versus flow-through wetlands in the N and M categories, it can be seen that medians were higher, often substantially so, for flow-through than for open water wetlands in both urbanization categories for pH, DO, Cond, NO3+NO2-N, SRP, FC, and Pb. In addition, the flow-through means were higher in moderately urbanized wetlands for TSS, NH3-N, TP, Cu, and Zn. Over all levels of urbanization flow-through wetland medians were higher for all water quality variables reported in the table.

It is clear from these results that flow-through wetlands strongly tend to be less acidic and better oxygenated than open water sites, as would be expected. Humic acid-producing vegetation thrives in an environment with low inflow, and attendant nutrient

income. In these ponded systems oxygen renewal from the atmosphere is not as efficient as in flowing water, and they are warmer and hence have lower oxygen solubility. Also, more primary production and more oxygen-consuming organic decomposition occurs in the relatively long period of water residence. It is also clear that flow-through wetlands generally have higher pollutant concentrations, probably due to the greater loading of pollutants by the flow and reduced pollutant removal from the water column with the shorter hydraulic residence times.

Concentrations of NO3+NO2-N exhibited one of the greatest disparities between open water and flow-through wetlands. In addition to greater loading introduced by the flow, this phenomenon is probably partially due to higher oxygen levels in flow-through cases, which promote nitrification that converts ammonia to nitrite and then nitrate forms. In fact, ammonia differed between the two types of morphology much less than did NO3+NO2-N, suggesting that ammonia discharged to wetlands may be more effectively nitrified in flowing systems. Of course, these systems also support less decomposition by microorganisms and, thus, likely produce less ammonia internally than do open water wetlands.

Table 2-4. Water Quality Statistics for Wetlands Not Experiencing Significant Urbanization Change (1988-1995) Grouped by Urbanization and Morphological Status.

Status	Year	Stat.[a]	pH		DO	Cond.		TSS		NH_3-N		NO_3+NO_2-N		SRP		Tot P		FC		Tot Cu		Tot Pb		Tot Zn
					(mg/L)	(µS/cm)		(mg/L)		(µg/L)		(µg/L)		(µg/L)		(µg/L)		(CFU/100mL)		(µg/L)		(µg/L)		(µg/L)
N/OW	1995	Mean	33498.54		5.3	5	<	5.1	<	83	<	260	<	23		63	>	144	<	2.4	<	2.4	<	7.0
N/OW	1995	St. Dev.	935.94		2.6	3	>	7.8	>	154	>	487	>	59		103	>	702	>	3.7	>	3.1	>	8.4
N/OW	199500%	CV	3%		50%	50%	>	152%	>	186%	>	187%	>	258%		163%	>	488%	>	158%	>	131%	>	120%
N/OW	1995	Median	33092.00		5.3	5		2.4		35		49		6		31		5		0.9		1.0		2.5
N/OW	1995	n	136		135	135		109		104		107		121		136		115		23		21		65
N/FT		Mean	33443.64		6.6	7	<	6.6	<	65		672	<	11		31	<	327	<	1.6	<	5.3	<	4.4
N/FT		St. Dev.	919.99		2.3	2	>	11.7	>	133		417	>	19		27	>	855	>	2.6	>	0.0	>	5.8
N/FT		CV	3%		35%	35%	>	179%	>	206%		62%	>	165%		88%	>	262%	>	163%	>	0%	>	133%
N/FT		Median	33073.00		6.5	7		2.5		32		613		7		24		56		0.7		1.2		2.5
N/FT		n	70		70	70		54		46		70		62		70		65		8		6		29
M/OW	1995	Mean	33703.88	<	3.7	4	<	6.8	<	158	<	291	<	23		69	>	233	<	2.4	<	2.5	<	8.7
M/OW	1995	St. Dev.	851.14	>	2.7	3	>	14.7	>	371	>	401	>	41		69	>	769	>	2.0	>	2.2	>	6.7
M/OW	199500%	CV	3%	>	73%	74%	>	216%	>	235%	>	138%	>	178%		100%	>	331%	>	82%	>	88%	>	77%
M/OW	1995	Median	6.14		3.2	65		2.2		49		99		10		44		17		1.5		1.5		7.5
M/OW	1995	n	77		74	75		62		62		54		73		77		61		22		24		48
M/FT	1995	Mean	33505.61	<	7.0	7	<	12.4	<	127	<	912		39		111	>	4764	<	3.0	<	4.1	<	9.2
M/FT	1995	St. Dev.	918.20	>	3.6	4	>	26.4	>	200	>	989		35		103	>	37867	>	1.9	>	3.5	>	7.3
M/FT	199500%	CV	3%	>	51%	53%	>	214%	>	157%	>	108%		90%		93%	>	795%	>	62%	>	85%	>	79%
M/FT	1995	Median	33126.00		7.7	8		4.7		49		688		29		85		220		2.3		2.2		6.8
M/FT	1995	n	100		96	98		95		96		98		97		100		90		24		40		52
H/FT	1995	Mean	33436.94	<	5.4	5	<	10.5	<	81	<	401		31		110	>	1021	<	3.9	<	5.0	<	21.3
H/FT	1995	St. Dev.	914.79	>	2.8	3	>	15.8	>	111	>	236		16		233	>	4901.0	>	3.4	>	4.7	>	17.8
H/FT	199500%	CV	3%	>	52%	53%	>	150%	>	138%	>	59%		50%		213%	>	480%	>	88%	>	95%	>	84%
H/FT	1995	Median	33055.00		6.4	6		4.8		41		377		28		69		69		2.6		3.9		20.0
H/FT	1995	n	67		66	67		57		55		66		65		67		62		12		28		37
All		Median	6.16		4.6	39		2.3		39		70		7		35		8		1.1		1.4		5.2
OW		n	213		209	210		171		166		161		194		213		176		45		45		113
All		Median	7.00		6.9	183		4.2		42		510		21		60		110		2.3		3.0		6.9
FT		n	237		232	235		206		197		234		224	0	237		217		44		74		118

[a] See Table 1 for definitions of Status and Stat. abbreviations.

It must be noted that a preponderance of flow-through wetlands are in more urbanized areas, which certainly affects pollutant loading and may affect the strength of conclusions, although probably not the overall trends. It is possible that this skewed distribution is not just a coincidence but reflects the urban situation, in which higher peak

runoff flows, wetland filling, and stream channelization favor flow-through over open water wetland conditions.

SOILS

Collection and Methods

Soil samples were collected once from each wetland during the months July-September in 1988-1990, 1993, and 1995. Soil sampling areas were selected 3 meters to the side of vegetation transect lines at every point where the soil type appeared either to be transitional or completely different. Small soil cores or signs of vegetation change were the basis for judgment. Two to five samples, most commonly four, were collected from each wetland. The number had a relationship to the size and zonal complexity of the wetlands. This coverage was considered to be adequate because a synoptic study of 73 urban and rural wetlands early in the program found that there were no significant differences among wetland zones (e.g., open pool, inlet, scrub-shrub, and emergent) with respect to soil texture, organic content, pH, phosphorus, and nitrogen (Horner at al. 1988). Because oxidation-reduction potential and one metal were significantly different near inlets as compared to other locations, the inlet zone was emphasized in as one spot in choosing sampling areas, however.

Soil samples were collected with a corer consisting of a 10-cm (4-inch) diameter ABS plastic pipe section ground to a sharp tip. The corer was twisted into the soil with a wooden rod inserted horizontally through two holes near the top. Coring depth was 15 cm (6 inches). Samples were inserted immediately into plastic bags, air was extruded, and the bags were sealed with tape. They were then transported to one of several laboratories used in the different years.

A standard 60-cm (2-ft) deep soil pit was dug at each sampling point not inundated above the surface. The pit was observed and notes were recorded for depth to water table (if within 60 cm of the surface), horizon definition (thickness of each layer and boundary type between), color (using Munsell notations), structure (grade, size, form, consistency, and moisture), and presence of roots and pores.

Soil core samples were analyzed for:

General characteristics	Metals
Particle size distribution (PSD)	Arsenic (As)
% organics as loss on ignition (LOI)	Cadmium (Cd)
pH	Copper (Cu)
Oxidation-reduction potential (redox)	Lead (Pb)
Nutrients	Zinc (Zn)
Total phosphorus (TP)	
Total Kjeldahl nitrogen (TKN)	

A report by King County Resource Planning Section (1988) provides detail on the general analytical methods, as well as the sampling program design. A method for PSD, also termed soil texture, was developed during this program for soils with more than 5% organics, as most wetland soils have. Texture is the measurement of the proportions of the various sizes of mineral particles in a soil, classified from largest to smallest as sand, silt, and clay (gravel, when significant, is also recognized in the texture classification). The analysis of any soil with more than 5 % organic content must include a step that removes the organic material. Failure to remove the organic component may cause clumping of particles and render the results inaccurate. The new PSD method, which is provided in Appendix A of this chapter, is considered to be accurate for soils with up to 25% organics. At higher levels it is not accurate because of sample loss during organic removal preparation, especially in the clay component.

Publications by Cooke, Richter, and Horner (1989); Richter et al. (1991); Cooke (1991); and Cooke and Azous (1993) are additional sources of detail on methods and findings from the initial years. Soils methods and results were also reported by Azous (1991), Cooke (1991), and Platin (1994).

Research Findings: A Portrait of Puget Sound Basin Wetland Soils

General Soil Characteristics and Nutrients

As with water quality, this discussion is conducted mainly with reference to descriptive statistics. Tests for statistical significance of difference and analyses of variance generally were not performed, for the same reasons stated earlier in the chapter. Table 2-5 statistically summarizes the soils data, excluding PSD, for wetlands that did not experience significant urbanization change during the program. Metals are discussed in a later subsection. Nonurban wetlands are the main focus of this chapter, and Chapter 9 further discusses the other categories, as well as wetlands with watersheds that did change.

Like water quality, soil quality exhibited extensive variability. As with most water quality variables, coefficients of variation for the majority of the soil variables were generally in the approximate range 75-150%, although in both soil and water cases some were higher. CVs for pH were considerably lower than for other analytes for both soils and water, usually about 10 $\pm$ 3%. Again like water quality variables, the quantities in Table 2-5 usually exhibited medians lower than the means, except for redox and sometimes pH. Therefore, most of these data also are far from normally distributed, and are probably log-normal.

Most wetlands had at least some pockets of peat of mainly sedge and grass origins (Cooke 1991), and their soils accordingly tended to be acidic. Among the different groupings of data in Table 2-5, median pH values were $\leq$ 6.1, except for highly urbanized cases, which were both flow-through . Overall, highly urbanized sites had the highest median pH, followed by moderately urbanized and then nonurbanized locations. Flow-through wetlands overall and in the N and M categories had higher median pH than open water types.

These wetlands frequently had anaerobic soils, as indicated by median redox values often < 250 mv, the approximate point at which oxygen is fully depleted. The median for the most highly urbanized case was lower than for the N wetlands, which themselves had lower median redox than the M cases. Open water wetlands overall had higher

redox readings than flow-through ones. This result is somewhat surprising, in that open water wetlands are thought to host more oxygen-consuming decomposition and to have oxygen replenished from the atmosphere less efficiently than flow-through cases. It was found in the synoptic study of 73 wetlands at the beginning of the program that open water zones had the lowest redox readings (<100 mv) (Horner at al. 1988). Redox was below the level at which oxygen is generally depleted in the inlet, open water, and emergent zones but not in the scrub-shrub and forested zones. In another contrast with the more recent results, soils in the inlet zones of wetlands in nonurban wetlands had significantly ($P < 0.05$) lower redox than in urban wetlands.

The highest median TP occurred in moderately urbanized wetlands, and the highest TKN in nonurbanized ones. Open water systems were higher than flow-through cases in both nutrients overall, but that result was due to large differences between the two types of morphology in the M wetlands. This tendency was actually reversed in nonurbanized wetlands, which exhibited higher nutrients among the flow-through wetlands in that subset.

The N urbanization category had median organic content over 30%, although with extensive variation. The M and H sites overall had about half to two-thirds of that level. On the whole open water wetlands exceeded flow-through ones in organics, although again this tendency is due to the M wetland data. This finding is as expected, since ponded systems have more primary productivity and capability of settling solids.

Soil texture is important to the nutrition, structure, drainage, and erosion prevention characteristics of a soil. Nutrients are found in a soil attached to organic matter, clay particles, and metal oxides (especially iron oxides). Soils with a high portion of clay, organic material, or both adsorb water and nutrients much more readily than soils low in these components. Fine textured soils have a more compact structure, which may impede aeration of the soil. Clays adsorb water and if positioned lower down in the soil profile, can impede drainage, causing an impervious layer and creating a wetland. Sandy soils have very little cohesion and erode much more easily than silt- or clay-rich soils. One of the influences of urbanization on wetland ecosystems is deposition of sediments from development activities (clearing and grading).

Table 2-5. Soil quality statistics for wetlands not experiencing significant urbanization change (1988-1995) grouped by urbanization and morphological status.

Status [a]	Stat. [a]	pH	Redox. (mV)	TP (mg/kg)	TKN (mg/kg)	Org. (%)	Cu (mg/kg)	Pb (mg/kg)	Zn (mg/kg)	As (mg/kg)
N/OW	Mean	5.43	143	743	5261	45.5	58	65	27	6.5
	Maximum	6.67	649	6579	27369	97.3	2221	418	154	20
	St. Dev.	0.64	322	1087	5983	34.2	300	96	29	5.4
	CV	12%	225%	146%	114%	75%	515%	147%	106%	84%
	Median	5.40	153	251	2866	47.0	16	24	18	4.4
	n	47	46	55	58	58	54	54	54	54
N/FT	Mean	5.73	113	839	3899	36.1	21	33	31	15
	Maximum	7.12	629	8882	14223	97.3	40	322	103	225
	St. Dev.	0.48	296	1698	3297	28.8	13	60	30	42
	CV	8%	262%	202%	85%	80%	61%	184%	97%	284%
	Median	5.70	184	342	3799	34.1	17	18	17	6.6
	n	27	27	27	29	29	27	27	27	27
All N	Mean	5.54	132	775	4807	42.4	46	54	28	9.3
	Maximum	7.12	649	8882	27369	97.3	2221	418	154	225
	Std. Dev.	0.60	311	1310	5261	32.6	245	87	29	25
	CV	11%	236%	169%	109%	77%	536%	159%	103%	267%
	Median	5.60	184	283	2885	35.8	16	20	17	6.0
	n	74	73	82	87	87	81	81	81	81
M/OW	Mean	5.31	317	1114	6354	35.4	12	32	22	6.2
	Maximum	6.72	656	3827	22517	92.3	24	101	92	16
	St. Dev.	0.90	227	1019	5670	29.9	7	30	24	4.4
	CV	17%	72%	91%	89%	85%	60%	95%	107%	70%
	Median	5.11	362	945	5783	23.7	14	21	15	4.8
	n	26	26	25	25	25	28	28	28	28
M/FT	Mean	5.95	165	756	3999	25.7	18	77	60	8.1
	Maximum	6.96	611	2743	27967	92.3	63	530	334	25
	St. Dev.	0.51	279	819	5942	28.1	12	89	62	5.2
	CV	9%	169%	108%	149%	109%	68%	115%	104%	65%
	Median	6.09	226	481	2021	12.6	17	57	48	7.7
	n	45	43	41	43	47	43	43	43	43
All M	Mean	5.71	222	892	4865	29.1	16	59	45	7.3
	Maximum	6.96	656	3827	27967	92.3	63	530	334	25
	Std. Dev.	0.74	269	909	5912	28.9	11	75	53	5.0
	CV	13%	121%	102%	122%	99%	69%	126%	119%	68%
	Median	5.78	306	537	2764	15.1	15	34	33	6.2
	n	71	69	66	68	72	71	71	71	71
H/FT	Mean	5.88	87	654	2703	31.6	31	89	103	13
	Maximum	6.97	640	2995	11282	80.9	63	273	456	40
	St. Dev.	1.01	291	784	2892	26.3	17	68	112	9.4
	CV	17%	335%	120%	107%	83%	56%	76%	109%	74%
	Median	6.46	91	314	2033	22.8	30	64	65	10
	n	32	32	34	36	35	32	32	32	32
All OW	Mean	5.39	206	859	5590	42.4	43	54	25	6.4
	Maximum	6.72	656	6579	27369	97.3	2221	418	154	20
	St. Dev.	0.74	302	1074	5877	33.1	244	81	27	5.1
	CV	14%	147%	125%	105%	78%	572%	151%	107%	80%
	Median	5.35	305	414	3141	34.2	15	24	16	4.5
	n	73	72	80	83	83	82	82	82	82
All FT	Mean	5.87	127	744	3540	30.3	23	69	66	11
	Maximum	7.12	640	8882	27967	97.3	63	530	456	225
	St. Dev.	0.70	286	1102	4449	27.8	15	78	80	22
	CV	12%	226%	148%	126%	92%	67%	113%	123%	199%
	Median	5.92	162	378	2274	16.1	20	46	45	7.70
	n	104	102	102	108	111	102	102	102	102

[a] See Table 1 for definitions of abbreviations.

Table 2-6 presents a comparison of soil textures in 1989 and 1995 for the wetlands that did not experience significant watershed change. As was hypothesized for these cases,

little change occurred over these years regardless of urbanization or morphological status. The soils of the majority of these wetlands were dominated by silt-range particles, again irrespective of status. One N/OW and one M/FT site, located in different parts of the study area, had predominately sand. With two exceptions, the wetlands were found to have relatively little clay (≤ 20%). However, a wetland in north King County and one in south King County had about 30% and 50%, respectively. It bears noting that some of the samples contributing to these statistics had > 25% organic content, in the range where the analytical method is less accurate.

Table 2-6. Comparison changes in average particle size distributions from 1989 to 1995 in wetlands that experienced little urbanization change grouped by urbanization and morphological classifications.

Site[a]	Wetland Area (ha)	PSD 1989 (%sand/silt/clay)	PSD 1995 (%sand/silt/clay)
N/OW			
AL3	0.81	26/54/20	No data
HC13	1.62	47/47/6	45/37/18
RR5	10.52	74/15/11	68/21/11
SR24	10.12	1/89/10	6/75/19
N/FT			
LCR93	10.93	No data	30/50/20
MGR36	2.23	13/76/11	20/70/10
M/OW			
ELS39	2.02	35/49/16	15/69/16
SC84	2.83	4/81/15	11/73/16
TC13	2.06	30/41/29	38/32/30
M/FT			
ELW1	3.84	83/13/4	75/18/7
FC1	7.28	13/71/16	10/75/15
SC4	1.62	No data	No data
N/FT			
B3I	1.98	31/62/7	24/61/15
LPS9	7.69	30/16/54	32/20/48

[a]See Table 1 for definitions of abbreviations.

Analysis of the PSD measurements within individual wetlands indicates that PSD often varied substantially across wetlands and showed no trends with the amount of organic matter in the soil or the soil series. No association was seen between the total suspended solids in the surface water and changes in soil texture. However, soils located near the inlets of M and H wetlands were significantly ($P < 0.05$) more likely to have more sand than silt as compared to other locations.

METALS IN SOILS

Cadmium, lead, and zinc in wetland soils were observed to be highly variable from year to year, but copper and arsenic varied less. Overall, there was a declining trend in soil metal content over the years of the study. These results are somewhat surprising since the soil cores were 15 cm deep, representing soil horizons that would be expected to maintain fairly stable metals concentrations from year to year. Figure 2-1 shows that median concentrations of As, Cu, Pb, and Zn for all of the program wetlands generally declined each year. It is possible that metals enter and depart from wetland soils more easily than previously believed, permitting a rapid change in results in response to changes in inputs from the watershed. Declining metals pollution from vehicles and dissipating pollutants from industrial air pollution point sources, such as the closed ASARCO smelter in Tacoma, could explain the general decline of metals since the start of the program.

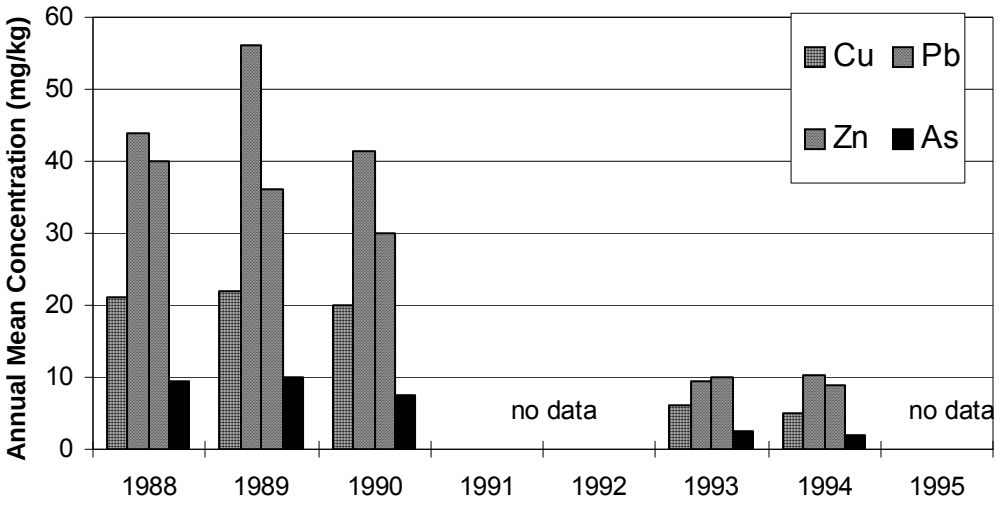

Figure 2-1. Annual mean metal concentration for all wetland samples in each year.

Cadmium was undetectable in the soils of most monitored wetlands, except in three that also had relatively high Pb. This result is consistent with the observation that metals often increase in tandem. Although the program detected substantial increases in Cd, Pb, and Zn at several wetlands between 1989 and 1990 (Richter et al. 1991), it is significant that there are no apparent common characteristics among these wetlands. They represent differing hydrology, ecology, and levels of watershed development.

It can be seen in reviewing the metals data in Table 2-5 that, like water quality and general soil characteristics, soil metals exhibited extensive variability. Again, too, medians were normally considerably less than means.

It is further apparent in Table 2-5 that median metals concentrations increased from nonurban to moderately urbanized and again from there to highly urbanized wetlands, except for a small drop in copper from N to M. Flow-through wetlands overall had higher median concentrations of all metals than did open water ones, although very marginally so for Cu. This tendency was again stronger for the moderately urbanized than the

nonurbanized wetlands. For the most part, then, soils exhibited the same trend as water quality, with quantities considered to be pollutants higher in FT than in the OW wetlands. It was thought that water column contaminants might be lower in open water wetlands because of losses to the soil. However, this supposition was not borne out by the soil results. Still, having the two most developed sites in the FT group may be skewing the results.

The Washington Department of Ecology (1991) set metals criteria for freshwater sediments in terms of lowest effect and severe effect thresholds. The criteria are:

	Lowest Effect Threshold (mg/kg dry soil)	Severe Effect Threshold (mg/kg dry soil)
Copper	16	110
Lead	31	250
Zinc	120	820

No mean or median value exceeded the severe effect criteria, and very few individual readings surpassed them at any time during the program. However, lowest effect thresholds were exceeded by some Cu and Pb means and even medians. Many individual readings in wetlands in all urbanization categories were beyond these lower limits.

Even though there is a trend toward increasing soil metals with urbanization, it is a fact that soil in either urban or nonurban wetlands can have elevated metals. These contaminants could be entering wetlands outside of urban areas in a variety of ways. Possibilities include via precipitation and atmospheric dryfall, dumping of metal trash, and leaching from old constructed embankments. Roads and narrow-gage railroad beds were built using mine tailings to serve logging operations in the last century in the vicinity of some of the wetlands. This phenomenon suggests the need for site-specific inquiries into metals pollution in Pacific Northwest palustrine wetlands, rather than reliance on broad patterns.

SUMMARY OF SOILS CHARACTERISTICS OF WETLANDS WITH NONURBANIZED WATERSHEDS

A soils portrait of Puget Sound Basin lowland palustrine wetlands relatively unaffected by humans shows a somewhat acidic condition; pH is very likely to be in the range 5-6. With redox as a basis, soils at many times and places will be anaerobic, but with great variability. Phosphorus is likely to be somewhere in the vicinity of 300 mg/kg, with nitrogen (TKN) approximately an order or magnitude higher. Based on these results, most soil samples from nonurban wetlands can be expected to have > 25% organics, and > 10% is extremely likely. Texture appears to be more a function of local conditions than a function of urbanization, or lack of it.

The metals As, Cu, Pb, and Zn, can range over two orders of magnitude, from a minimum in the low parts per million (mg/kg) region, in the soils of these nonurban wetlands. Most commonly, they appear to have approximately equal amounts of Cu, Pb, and Zn, around 20 mg/kg, and about one-quarter to one-third as much As. This level and the observed variation around it is sufficiently high to exceed lowest effect threshold freshwater sediment criteria for Cu often and for Pb occasionally, but very rarely for Zn.

REFERENCES

Azous, A. 1991. An Analysis of Urbanization Effects on Wetland Biological Communities, M.S. thesis. University of Washington, Department of Civil Engineering, Environmental Engineering and Science Program, Seattle, WA.

Chin, N. T. 1996. Watershed Urbanization Effects on Palustrine Wetlands: A Study of the Hydrologic, Vegetative, and Amphibian Community Response During Eight Years. M.S.C.E. thesis, University of Washington, Department of Civil Engineering, Environmental Engineering and Science Program, Seattle, WA.

Cooke, S.S. 1991. The effects of urban stormwater on wetland vegetation and soils: a long-term ecosystem monitoring study. Pp. 43-51 in Puget Sound Research '91: Proceedings, January 4-5, 1991, Seattle, WA. Puget Sound Water Quality Authority, Olympia, WA.

Cooke, S. S. and A. Azous. 1993. Characterization of Soils Found in Puget Lowland Wetlands. Engineering Professional Programs, University of Washington, Seattle, WA.

Cooke, S. S., K. O. Richter, and R. R. Horner. 1989. Puget Sound Wetlands and Stormwater Management Research Program: Second Year of Comprehensive Research. Engineering Professional Programs, University of Washington, Seattle, WA.

Gilbert, R. O. 1987. Statistical Methods for Environmental Pollution Monitoring. Van Nostrand Reinhold, New York, NY.

Horner, R. R. and K. A. Ludwa. 1993. Monitoring and Quality Assurance/Quality Control Plan for Wetland Water Quality and Hydrology Monitoring. Center for Urban Water Resources Management, University of Washington, Seattle, WA.

Horner, R. R. and K. J. Raedeke. 1989. Guide for Wetland Mitigation Project Monitoring. Washington State Department of Transportation, Olympia, WA.

King County Resource Planning Section. 1988. Puget Sound Wetlands and Stormwater Management Research Program: Initial Year of Comprehensive Research. Engineering Professional Programs, University of Washington, Seattle, WA.

Ludwa, K. A. 1994. Urbanization Effects on Palustrine Wetlands: Empirical Water Quality Models and Development of a Macroinvertebrate Community-Based Biological Index. M.S.C.E. thesis, University of Washington, Department of Civil Engineering, Environmental Engineering and Science Program, Seattle, WA.

Municipality of Metropolitan Seattle. 1994. Water Quality of Small Lakes and Streams, Western King County, 1990-1993. Municipality of Metropolitan Seattle, Seattle, WA.

Platin, T. J. 1994. Wetland Amphibians Ambystoma gracile and Rana aurora as Bioindicators of Stress Associated with Watershed Urbanization. M.S.C.E. thesis, University of Washington, Department of Civil Engineering, Environmental Engineering and Science Program, Seattle, WA.

Reinelt, L.E., and R.R. Horner. 1990. Characterization of the Hydrology and Water Quality of Palustrine Wetlands Affected by Urban Stormwater. Engineering Professional Programs, University of Washington, Seattle, WA.

Reinelt, L.E., and R.R. Horner. 1991. Urban stormwater impacts on the hydrology and water quality of palustrine wetlands in the Puget Sound region. Pp. 33-42 in Puget

Sound Research ‘91 Proceedings, Seattle, WA, January 4-5, 1991. Puget Sound Water Quality Authority, Olympia, WA.

Richter, K.O., A. Azous, S.S. Cooke, R. Wisseman, and R. Horner. 1991. Effects of Stormwater Runoff on Wetland Zoology and Wetland Soils Characterization and Analysis. PSWSMRP, Seattle, WA.

Taylor, B., K. A. Ludwa, and R. R. Horner. 1995. Urbanization effects on wetland hydrology and water quality. Pp. 146-154 in Puget Sound Research ‘95 Proceedings, Seattle, WA, January 12-14, 1995. Puget Sound Water Quality Authority, Olympia, WA.

Valentine, M. 1994. Assessing Trace Metal Enrichment in Puget Lowland Wetlands. Non-thesis paper for the M.S.E. degree, University of Washington, Department of Civil Engineering, Environmental Engineering and Science Program, Seattle, WA.

Washington Department of Ecology. 1991. Summary Criteria and Guidelines for Contaminated Freshwater Sediments. Washington Department of Ecology, Olympia, WA.

Welch, E. B. 1980. Ecological Effects of Waste Water. Cambridge University Press, Cambridge, England.

CHAPTER 3 CHARACTERIZATION OF PUGET SOUND BASIN PALUSTRINE WETLAND VEGETATION

by Sarah S. Cooke and Amanda L. Azous

INTRODUCTION

Nineteen wetlands in the Puget Sound Basin in King County, Washington were studied for five years between 1988 to 1995. An additional seven wetlands were studied infrequently over the same period. Our study attempted to understand the character and structure of wetland plant communities and, in particular, if and how wetland communities respond to changing land use and hydrology. The vegetation communities of each wetland were sampled and compared with land use and hydrologic conditions in the watershed.

Results from the early years of the study had shown that many plant species were found in only one or a few of the wetlands surveyed, suggesting that, regardless of size, wetland plant communities often have a few relatively uncommon species present (Cooke and Azous 1992). Early work had also shown a hydrologic measure, mean annual water level fluctuation, was negatively correlated with plant richness in wetlands. This chapter re-examines those earlier findings.

Plant richness and composition in wetlands was compared with wetland area, urbanization in the watershed and water level fluctuation. Community structure was examined through analysis of species richness, composition and percent cover. Ordination and classification analyses were used to identify distinct plant communities and examine relationships with the presence, abundance and distribution of invasive species.

Finally, the wetland indicator status of several common plant species, as assigned by Reed (1988, 1993), was examined. Comparisons were made between the Reed indicator status and a status assigned using quantitative data on species occurrence and hydrologic regime collected for our study.

METHODS

The wetlands surveyed were inland palustrine wetlands ranging in elevation from 50 m to 100 m above mean sea level and characterized by a mix of emergent, scrub-shrub, aquatic bed, and forested wetland vegetation classes. Wetlands were selected so that approximately half would be affected by urbanization sometime after the baseline year. Sites that remained unaffected by urbanization were expected to be the controls for those wetlands receiving urbanization treatment. The wetlands were matched, wherever possible, as treatment (new urban disturbance) and control (no new urban disturbance) pairs on the basis of morphological characteristics and vegetation zones (Cooke et al.'s 1989a, b, c).

Unfortunately, not all of the watersheds developed as predicted. Only six watersheds developed beyond 10% of the baseline developed area. This hindered the ability to statistically compare differences in plant community structure due to stormwater and urbanization effects between control and treatment pairs. Instead, differences in plant

communities related to stormwater and urbanization effects were identified by correlating conditions found at the wetlands with watershed conditions and analyzing all wetlands as a continuum. Together, over the study period, the wetlands represented a spectrum of watershed development conditions and hydrologic regimes that we were able to analyze and compare with respect to the plant communities observed.

Wetland sizes were estimated through analysis of USGS 7.5 minute series topographic maps and ranged from 0.4 to 12.4 hectares. Geographic Information Analysis (GIS) was also used to delineate land use and impervious areas within the watersheds (Taylor 1993). Land use classifications included agricultural lands, single and multiple family residential housing, commercial and industrial development, transportation corridors, and any other development within a watershed that reduced forest cover.

Plant communities in each wetland were characterized during a two to three week period during the active growing season between July and August, during the years 1988, 1989, 1990, 1993, and 1995. Plant community composition and percentage cover were sampled in permanent plots adjacent to linear transects established across the hydrologic gradients of each wetland. Species cover was recorded using a cover class system based on the Octave Scale (Barbour et al. 1987, Gauch 1982). Detailed protocols for the vegetation field work are documented in Cooke et al. (1989a). The data set also includes seven additional wetlands that were surveyed during the years 1993, 1994 and 1995 as part of several related studies.

Species were identified using Hitchcock et al. (1969) and were verified with specimens from the University of Washington Herbarium. Using the Cowardin classification system (Cowardin et al. 1979), sample plots were assigned a category based on the dominant structure of the vegetation community, such as aquatic bed (PAB), emergent (PEM), scrub-shrub (PSS), forested (PFO), upland, or some transition zone between them (e.g., PEM/PSS). The Cowardin classification system was selected because it is widely used in functional assessments, wetland protection, and mitigation criteria (Washington State Department of Ecology 1993). In some cases zones changed over time and were re-categorized as required. Upland zones were not included in the analyses of richness or disturbance, but were included in all other analyses.

The vegetation survey data were used to calculate the frequency with which plant species were observed among the wetlands surveyed. We also calculated total plant species richness for individual wetlands, and the total and average plant richness found in the different vegetation community zones of each wetland. Species were categorized according to wetland indicator status (Reed 1988, 1993) and included obligate (OBL), facultative wetland (FACW), facultative (FAC) and facultative upland (FACU) species. The indicator status in Reed is assigned based on qualitative expert experience of how frequently a plant species is found growing in wetland conditions (Table 3-1).

Table 3-1. Indicator status categories for wetland plant species.

Code	Designation	Wetlands Probability 1
OBL	Obligate wetland	> 99
FACW	Facultative wetland	67 to 99
FAC	Facultative	34 to 66
FACU	Facultative upland	1 to 33
UPL	Obligate upland	< 1
NI	No indicator status	

1Percent occurrence of plant found in a wetland

Community types were defined and described using ordination (DECORANA) and classification (TWINSPAN) comparisons (Hill 1979 a, b). Plant community data were tabulated in a two-way data matrix (species by cover). The classification method involved grouping similar vegetation units into categories (Cliffors and Williams 1973, Causton 1988). All of the species that composed more than 25 percent cover in the sample stations were included. Ordination was used to display the species data plots in graphical space where like-communities were plotted close together and dissimilar communities were plotted further apart (Hill 1979b, Gauch 1982). The frequency of species and the relative dominance of species were both described by the proportion of vegetation sampling plots in which the species were found.

Hydrologic measurements, including instantaneous water levels from staff gages and peak levels from crest gages, were recorded at least eight times annually while water was present in the wetlands (Reinelt and Horner 1990). Since we did not have a gage at each sample station, the hydrology at each vegetation sample station was calculated based on the elevation of the sample stations in relationship to the water levels measured at the wetland staff and crest gages. This method assumed that water levels were evenly distributed throughout the wetland varying only as elevation varied. In most cases this assumption was sufficiently accurate, however, the wetlands we studied were sometimes more hydrologically complex, so vegetation sample stations were field checked and eliminated if calculated water levels were inaccurate.

Each sample station was assigned an instantaneous water level and a maximum water level. Water level fluctuation (WLF) was computed as the difference between the peak level and the average of the current and previous instantaneous water levels for each four to six week monitoring period. Mean WLF was calculated by averaging all WLFs for a specific season, or the entire year. These data were averaged over the year and each of four seasons; the early growing (EG) (Mar 1-May 31), intermediate growing (IG) (June 1-August 30), senescence (Sept 1-Nov 15), and dormant (Nov 16-Feb 28) seasons.

The hydrologic data were used to compare the results of field measurements with Reed's categorization of wetland indicator plants. A status was assigned to each species based on the hydrologic regime observed at the vegetation sampling stations. If a station was inundated at any time during the year to within 30 cm of the surface of the sample station the station was considered wet and the plant categorized as growing in wet conditions. Water levels to within 30 cm of the soil surface at the station were used

in order to account for saturated soil conditions. All occurrences of individual species were evaluated and, based on the proportion in wet stations versus dry, categorized according to indicator status using Table 3-1.

RESULTS

Community Structure and Composition

Two hundred and forty-two plant species were identified in 26 wetlands over the study period (the list of species is provided in Appendix Table 3-1). Most were obligate (OBL) species (28%), followed by FAC (23%), FACU (22%), and FACW (16%) species. The remaining 11% had no assigned indicator status.

Forty-five species (19%) were found in only one (4%) of the wetlands surveyed. Over 38 percent of plant species were found in less than three wetlands (12%). The distribution of plants according to wetland indicator status was similar to the overall distribution. Forty percent of OBL, 35% of FAC, and 39 % of FACU species were also found in three or fewer wetlands. FACW species were generally more widely dispersed among wetlands, with all species observed in at least eight wetlands.

Most of the species observed were shrubs (35%), followed by herbs (25%) and ferns and horsetails (14%). Least commonly found were rushes (2%), sedges (3%), grasses (3%) and trees (13%). All of the exotic plant species identified in the study wetland plots were either herbs, shrubs, or rushes.

Rubus spectablilis, Rubus ursinus and Polystichum munitum were observed in all 26 wetlands, however, Spirea douglasii was considered to be the most dominant species as it occurred in 25 of 26 wetlands and covered greater than 64% of the sample station in more than 21% of the stations in which it was observed. Alnus rubra, Athyrium filix-femina, and Salix scoulerleriana were also found in 25 of 26 wetlands but rarely dominated the sample station. Phalaris arundinaceae, an invasive weed, was considered the second most dominant species, being found in 18 wetlands (69%) and dominating the sample station in 19% of the plots in which it was observed. Other invasive wetland species were Ranunculus repens found in 65% (17) of wetlands, and Juncus effusus, observed in 58% (15) of the wetlands. Lythrum salicaria, an exotic considered highly invasive, fortunately, was found in only one wetland. Table 3-2 shows some of the most common and least common plants we found categorized by occurrence and cover dominance.

Table 3-2. Species occurrence for different categories of plant type and cover dominance.

Cover Dominance Category	High Occurrence (>80% wetlands)	Low Occurrence (<10% wetlands)
Usually dominant. Greater than 64% coverage in more than 19 percent of observations.	Phalaris arundinaceae Spirea douglasii	Juncus supiniformis Menyanthes trifoliata
Dominance in plots varies	Alnus rubra Athyrium filix-femina Kalmia microphylla Lonicera involucrata Polystichum munitum Pteridium aquilinum Ranunculus repens Rhamnus purshiana Rubus laciniatus Rubus spectablilis Rubus ursinus Salix pedicellaris Salix scoulerleriana Salix sitchensis Vaccinium parvifolium	Azola mexicana Brasenia schribneri Eriophorum chamissonis Hippurus vulgaris Hydrocotyl ranunculoides Hydrophyllum tenuipes Nymphaea odorata Polygonum amphibium Potentilla gramineus Rhynchospora alba Sparganium eurycarpum Sagittaria latifolia Scirpus acutus Veronica americana
Always less than 1% coverage	no species	Mimulus guttatus Myosotis laxa Potamogeton diversifolius Ranunculus acris Rorippa curvisiliqua Rumex obtusifolius Trillium ovatum Vaccinium ovatum Vaccinium uliginosum Vicia sativa

Plant Community Zone Characterization

Twenty-four wetland vegetation community zones were encountered in the 26 study wetlands. These include the four Cowardin types PAB, PEM, PSS, PFO (Cowardin et al. 1979), an additional two zones called BOG and UPL (upland transition), and combinations of each. Table 3-3 lists the frequency of occurrence of each zone out of a total 465 vegetation stations sampled over the study. Shrub-scrub and forested wetlands were the most common vegetation zones sampled, 26 and 16 percent of the samples respectively. Emergent communities were 13 percent of the samples, and bogs (Sphagnum moss systems) 4.5 percent. Mixed communities were found in about one third of the stations sampled, though mosaic type communities, which include more than three mixed community types, were fairly rare.

Communities of the different vegetation zones were evaluated with respect to the dominant plants and their associated Reed indicator status. Most species found in PAB zones were obligate (74%) or FACW (17%). Six percent of species were FAC, and no FACU species were observed in PAB zones. As would be expected, PAB zones were

dominated by obligate herbs (67%), followed by obligate and FACW shrubs (15%), FACW herbs (3%), and rushes (3%).

Species most frequently observed in PEM communities were obligate herbs (31%) followed by FACW shrubs (8%) and FACU (8%) shrubs. Many more FAC (15%) and FACU (17%) species were present in emergent areas than were observed in aquatic bed areas.

Scrub-shrub zones were more evenly distributed between obligate (21%), FACW (22%), FAC (27%) and FACU (23%) species. PSS zones were comprised of 14% obligate herbs and 15% FACW shrubs. FAC and FACU shrubs were about 11% of the species observed in PSS communities.

Table 3-3. Plant community zone frequency of occurrence (descending order).

Plant Community Zone	Frequency	Plant Community Zone	Frequency
PSS	25.59%	PEM/PFO	1.29%
PFO	16.34%	PAB	1.29%
PEM	13.12%	PAB/PSS	1.08%
PEM/PSS	9.25%	PEM/UPL	0.86%
UPL	7.31%	PEM/BOG	0.22%
PSS/PFO	5.16%	PEM/PFO/UPL	0.22%
BOG	4.52%	PEM/PSS/PFO	0.22%
PFO/UPL	3.87%	PFO/PAB/PEM	0.22%
PAB/PEM	2.58%	PFO/PSS/UPL	0.22%
PSS/UPL	2.58%	PAB/PFO	0.22%
BOG/PSS	1.94%	PAB/PFO/UPL	0.22%
PAB/PEM/PSS	1.51%	UPL/PFO/PEM	0.22%

Shrubs made up about 36% of the species observed in PFO zones, and most of the shrubs observed were FAC (11%) or FACU (19 %) species. Upland tree species comprised about 17% of species observed in forested zones. FACW trees comprised less than 0.5% of the forested species observed. Thirteen percent of species observed in PFO zones were obligates, of which 9% were herbs.

A limited number of bog zones were also sampled. Obligate species made up 50% of the observations in bogs, and were mostly shrubs (21%) and herbs (18%). The remaining species found in bogs were primarily FACW shrubs (21%).

Wetland Plant Community Associations

Wetland vegetation sample plots were classified into eleven community types using TWINSPAN (Hill 1979a), on the basis of species composition and percent cover (Figure 3-1). The communities include the categories and species listed in Table 3-4.

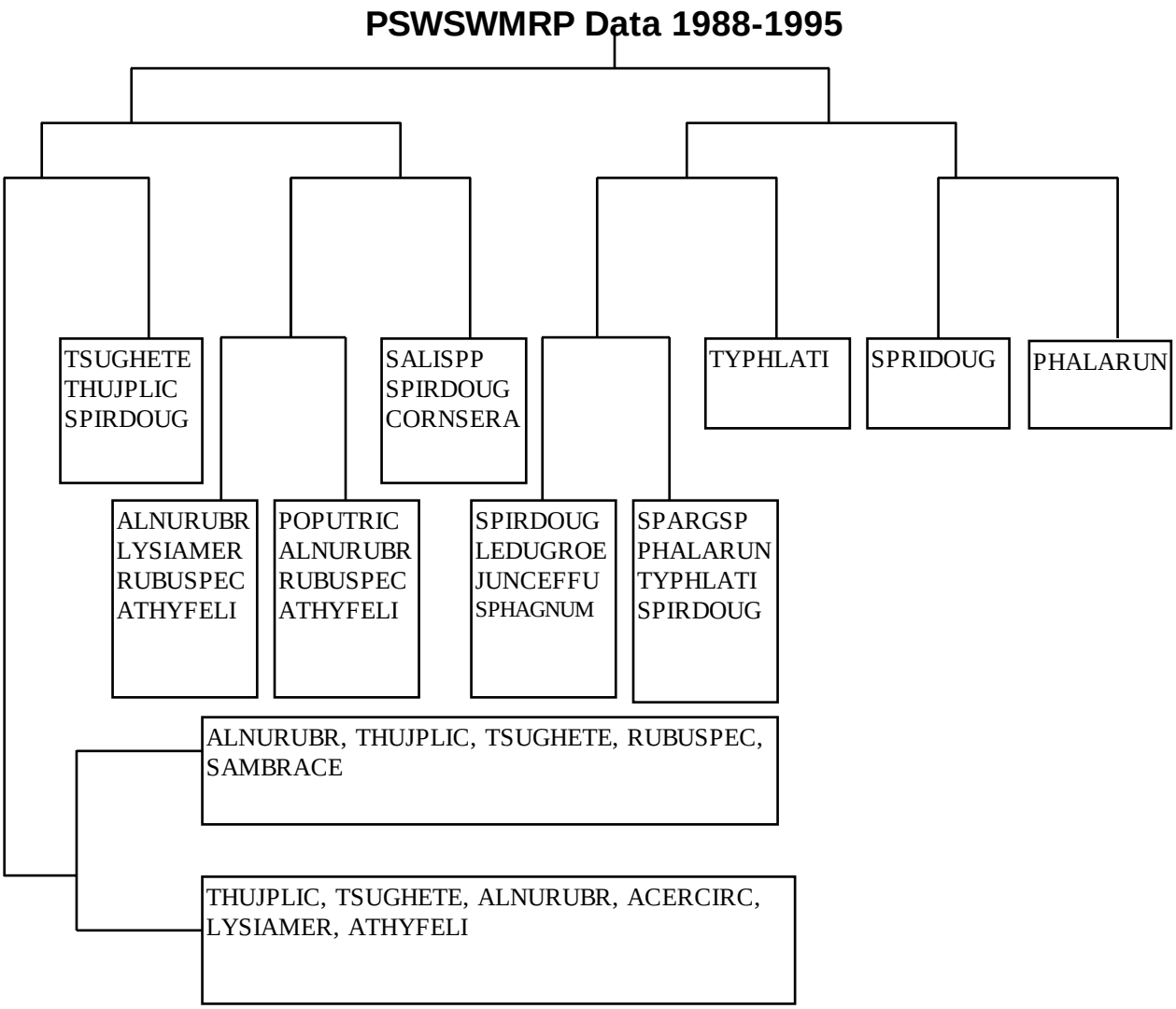

Figure 3-1 Classification of wetland community types present in the PSWSMRP study sites using TWINSPAN (Hill 1979a). (After Houck 1996).

All 24 of the community types listed in Table 3-3 are characterized by the dominant species associations shown in the of the TWINSPAN analysis (Figure 3-1), confirmed in the DECORANA analysis, and described in Table 3-4. These 11 basic community types were repeatedly observed in the study wetlands. Subdominant species changed and a single or a few uncommon species were sometimes present, but the dominant plant associations could be described by one of the eleven types. These communities may be used as a guide for understanding species composition and community structure in wetlands and are relevant to developing reference plant communities for palustrine wetlands in the Puget Basin.

Table 3-4. Wetland community type descriptions (Houck 1996).

Descriptive Name	Cowardin Community Type 1	Community Name 2	Dominant Species
Coniferous forest	PFO PFO/UPL PAB/PFO/UPL UPL	Tsuga-Thuja	Tsuga heterophylla Thuja plicata Spirea douglasii Gaultheria shallon Polystichum munitum
mixed coniferous-deciduous forest with shrub understory	PFO PSS/PFO PEM/PFO PEM/UPL PEM/PFO/UPL	Tsuga-Thuja-wet	Tsuga heterophylla Thuja plicata Acer macrophyllum Acer circinatum Lysichitum americanum
mixed coniferous-deciduous forest with little understory	PSS/UPL	Alnus-Thuja	Alnus rubra Thuja plicata Tsuga heterophylla Rubus spectabilis Sambucus racemosa
deciduous forest	PFO/PSS/UPL PFO/PSS	Populus	Populus balsamifera Alnus rubra Rubus spectabilis Athyrium filix-femina
deciduous forest	PEM/PSS/PFO PFO/PAB/PEM	Alnus	Alnus rubra Rubus spectabilis Cornus sericea Lysichitum americanum Athyrium filix-femina
mixed shrub scrub	PAB/PSS PAB/PFO	Salix-Spirea	Salix spp. Spirea douglasii Cornus sericea Cornus sericea Lonicera involucrata
bog	BOG, BOG/PSS	poor fen-shrub	Rhododendron groenlandicum (Ledum g.), Sphagnum Spirea douglasii
mixed emergent	PAB/PEM/PSS BOG/PEM	poor fen-marsh	Phalaris arundinacea Typha latifolia Rhododendron groenlandicum Sparganium spp Spirea douglasii
emergent	PAB, PAB/PEM	Typha	Typha latifolia Solanum dulcmara Lemna minor
emergent	PEM	Phalaris	Phalaris arundinaceae Solanum dulcmara Urtica dioica
scrub-shrub	PSS	Spirea	Spirea douglasii Salix sitchensis S. Alba

1- Community type used in Table 3-3 2- Community name used in Figure 3-2

The Abundance and Distribution of Invasive Plant Species

Patterns of invasive plant species distribution, dominance and abundance were compared among and within the wetland study sites (Houck 1996). The frequency of invasive species was found to be highly dependent on the conditions present, which varied for different species. For example, Phalaris arundinaceae, Rubus procerus and Solanum dulcamara were more abundant in urbanized watersheds, while Typha latifolia and Juncus effusus were generally more abundant in less urbanized watersheds (Houck 1996). Houck examined water level fluctuation, depth of flooding, and duration of inundation and found that only duration of flooding was associated with the abundance of some invasive species. Typha latifolia and Juncus effusus were generally more abundant in permanently flooded conditions, while Rubus procerus was found in sites where flooding seldom occurred.

Invasive species were most abundant in aquatic bed and emergent marsh communities. The species most frequently observed were Phalaris arundinaceae and Typha latifolia (Figure 3-2). Very few invasive species were found in coniferous forested communities in either the wetland or upland zones.

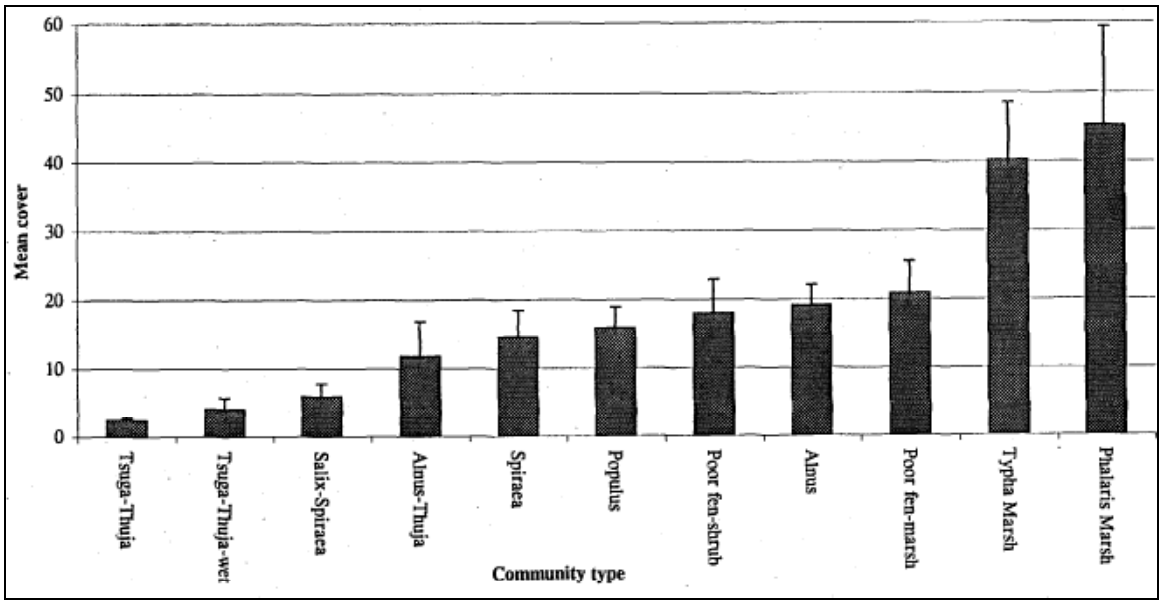

Figure 3-2. Abundance of invasive species within the community types found in the PSWSMRP study sites. Error bars are one standard error (Houck 1996).

Community Richness

At the completion of the study, total plant richness ranged from 35 to 109 species across the wetlands surveyed. Twelve of the wetlands had between 60 and 84 species. Seven had less than 60 species and seven had between 85 and 109 species.

Plant richness varied widely between and among the Cowardin vegetation types. Emergent type richness contained from two species to 33 and averaged 19 species per

station overall. Scrub-shrub types ranged from four to 27 species and averaged 11 species per station. Forested types had from five to 31 species and averaged 19. Aquatic bed types had the fewest species, from one to eight and averaging about four among the sample stations. The highest total plant richness was found in wetlands with the largest number of Cowardin community types (Fisher's r to z (Frz), R = 0.41, p = 0.0001).

Plant richness in wetlands and in the Cowardin et al. (1979) vegetation Aquatic bed was compared with wetland area, impervious area in the watershed and water level fluctuation. Total plant richness of a wetland was found to have no significant relationship to wetland area (Figure 3-3), nor did average wetland plant richness within community types, such as PEM and PSS, have any relationship to wetland area.

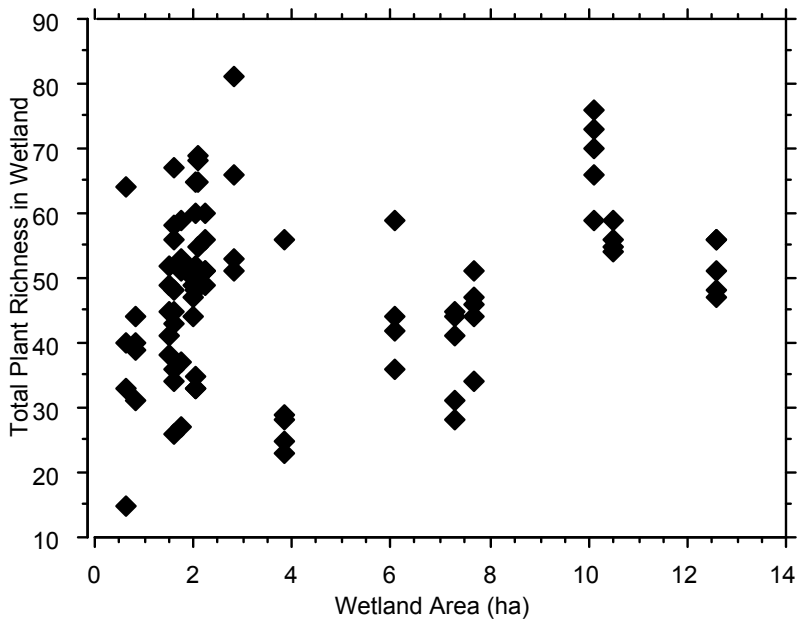

Figure 3-3. Plant richness and wetland area.

The percent of impervious area within the watershed was negatively correlated with average plant richness in the emergent zones and scrub-shrub community types (Figure 3-4). On average both types exhibited significantly lower species richness as the amount of impervious area in the watershed increased (Frz, PEM: R = 0.55, p = 0.002; PSS: R = 0.57, p = 0.001).

All years of data were examined for the relationship between mean annual WLF and plant richness with the following results. Total plant richness found in wetlands was unrelated to the degree of WLF. Average plant richness within the forested community type was also found to be unrelated to mean annual WLF. However, in both the emergent and scrub-shrub types, average plant richness was negatively correlated with mean annual WLF. Figure 3-5 shows plant richness in the these community types related to mean annual WLF for all years of data and all wetlands. The results showed a significant relationship in both types for all years combined (Frz, PEM: R = -0.38, p =

0.006; PSS: R=-0.5, p = .0001). When years were examined singly, both the emergent and scrub-shrub types showed significant negative correlations between plant richness and water WLF for three of the five years.

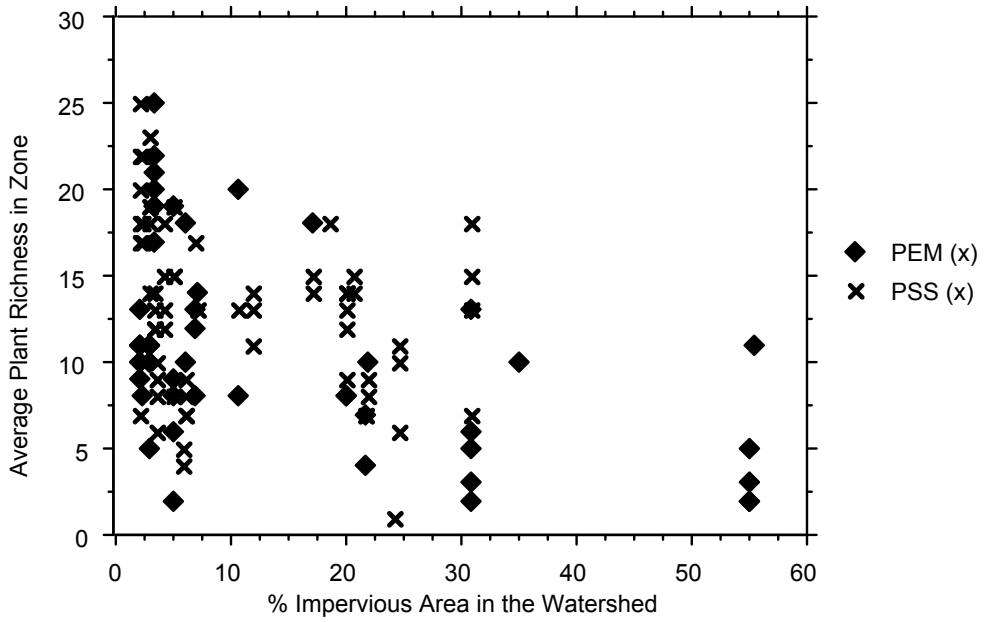

Figure 3-4. Richness in the emergent and scrub-shrub communities and impervious area in the watershed.

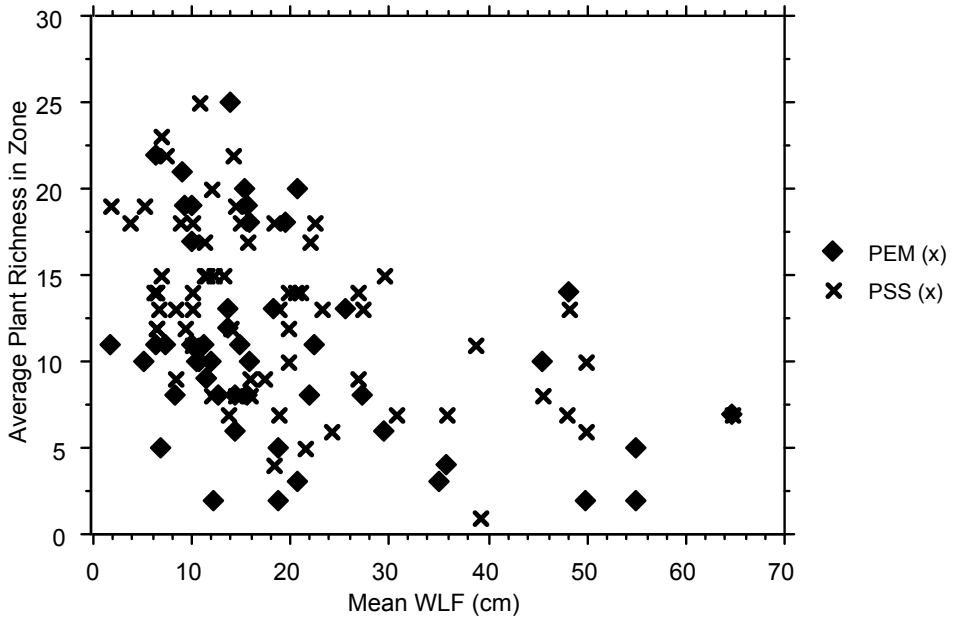

Figure 3-5. Plant richness in the emergent and scrub-shrub communities related to mean annual WLF.

Wetland Indicator Status

All 242 plant species found during our study were assigned an indicator status based on the hydrologic regimes observed at the study sample stations. Since upland zones represented only 18% of the stations sampled, it was expected that many transitional species would look wetter than indicated by Reed. However, for most species, the hydrology based assignments for indicator status matched Reed's assignments. Of the 93 that did not match, approximately 42% were eliminated because the number of observations was considered to be too low (less than 10) for an accurate assessment or because the water depths measured at the wetland gage did not accurately reflect the water depths at the vegetation sample stations. In addition, 27 species were eliminated as they were observed growing in conditions that were within 10% of the maximum and minimum range of observed frequency assigned by Reed (Table 3-1) and within the margin of error for measuring water levels. The remaining 27 species were selected as candidates for a change in the indicator status assigned by Reed and are shown in Table 3-5.

Interestingly, several species listed in the table are categorized as obligates by Reed but were found in wet zones in fewer than 88% of our observations. Most were observed in at least 25 sample stations. This study, however, was not able to measure hydrology at each plot but only calculate it based on events measured at the wetland gage station with respect to the elevation of the vegetation sample station. The remaining differences between the Reed categories and the hydrologically based categories may be due to the presence of hydrologic conditions not accounted for by our methods. Nevertheless, the number of observations and frequency of inundation recorded warrant a review of the species listed in Table 3-5.

Table 3-5. Comparison of indicator assignments for some plant species.

Plant Species	Form	Weed	Reed Wetland Indicator	Status Assigned Using PSWSMRP Study Data	Percent of Observations Plant Was Wet	Number of Observations
Epilobium ciliatum (watsonii)	herb	no	FAC	FACW	0.83	144
Acer circinatum	shrub	no	FACU	FAC	0.58	180
Dicentra formosa	herb	no	FACU	FAC	0.48	23
Dryopteris expansa (austriaca)	fern	no	FACU	FAC	0.62	143
Epilobium angustifolium	herb	no	FACU	FAC	0.6	15
Hypericum formosum	herb	no	FACU	FAC	0.65	17
Rubus procerus (discolor)	shrub	exotic	FACU	FAC	0.64	115
Sambucus racemosa	shrub	no	FACU	FAC	0.54	205
Stellaria media	herb	no	FACU	FAC	0.65	40
Tsuga heterophylla	tree	no	FACU	FAC	0.56	211
Rubus laciniatus	shrub	exotic	FACU	FACW	0.72	116
Carex hendersonii	sedge	no	none	FAC	0.33	21
Carex exsiccata (vesicaria)	sedge	no	OBL	FACW	0.85	13
Carex obnupta	sedge	no	OBL	FACW	0.67	72
Hypericum anagalloides	herb	no	OBL	FACW	0.8	25
Juncus acuminatus	rush	no	OBL	FACW	0.87	30
Ludwigia palustris	herb	no	OBL	FACW	0.75	24
Lycopus americanus	herb	no	OBL	FACW	0.74	50
Lycopus uniflorus	herb	no	OBL	FACW	0.7	44
Mimulus guttatus	herb	no	OBL	FACW	0.82	11
Myosotis laxa	herb	no	OBL	FACW	0.8	43
Salix pedicellaris	shrub	no	OBL	FACW	0.73	26
Scirpus atrocinctus	shrub	no	OBL	FACW	0.74	65
Scirpus microcarpus	shrub	no	OBL	FACW	0.74	42
Solanum dulcamara	herb	no	OBL	FACW	0.71	212
Veronica americana	herb	no	OBL	FACW	0.74	108
Veronica scutellata	herb	no	OBL	FACW	0.69	80

DISCUSSION

Wetland management regulations in the Puget Sound lowlands, for the most part, classify wetlands on the basis of area, the number and type of vegetation communities, and the presence of threatened or endangered species (King County 1990, Toshach 1991). Although one might rationalize that larger wetlands are more diverse ecosystems, we found that in the case of plants, wetland area is not directly related to the rarity or richness of the plant community.

Other factors, such as hydrologic regime and the kinds and frequency of disturbance, appeared to be more critical in determining the diversity and character of the wetland plant communities we studied. Generalized classifications of vegetation structure, such as forested, scrub-shrub and emergent, lend no insight into the presence or absence of unusual plant species, plant associations or the biodiversity value of a wetland to a

region. Our results suggest that selecting for wetland size and certain types of wetland plant communities will not insure protection of regional wetland values and functions.

Eleven distinct wetland plant communities were identified that are typical of the region. These communities were mostly found in mixed assemblages interspersed throughout individual wetlands. Most of the wetlands studied were characterized by several wetland plant community types with transition zones between them. In general, when several community types were present, plant richness was higher within individual communities, as many species were observed to transition between community types.

The presence of these zones is highly dependent on the hydrologic gradients at work in a wetland. Wetlands with the richest and most diverse plant communities were typically characterized by more complex hydrology and more variable morphology, providing many surfaces at different gradients for plant species to inhabit. Wetlands with simpler vegetation communities were more frequently topographically uniform, resulting in simpler hydrologic patterns. These differences may be traced, to some extent, to patterns of disturbance, including water level fluctuation.

It is important to focus our management efforts toward understanding the conditions required for wetland plant and animal diversity and to comprehensively mitigate the functions lost when wetlands are disturbed. In addition to preserving large wetlands with diverse hydrologic zones, we should consider addressing land use and development constraints to limit the extent of increases in water level fluctuations occurring in wetlands due to increased impervious area. Limiting other types of disturbance and monitoring invasive species presence also provide reasonable tools for maintaining species richness and regional biodiversity.

REFERENCES

Barbour, M.G., J.H. Burke, and W.P. Pitts. 1987. Terrestrial Plant Ecology. Benjamin Cummings Publ Co. CA.

Causton, D. R. 1988. An introduction to vegetation analysis. Unwin, Hyman, London.

Clifford, H.T. , and W. T. Williams. 1973. Classification dendograms and their interpretation. Aust J. Bot. 21:151:162.

Cooke, S.S., and Azous, A. 1992. Effects of Urban Stormwater Runoff and Urbanization on Palustrine Wetland vegetation. Report to U.S. Environmental Protection Agency, Region 10, by King County Resource Planning Section, Seattle, WA.

Cooke, S.S., R.R. Horner, C. Conolly, O. Edwards, M. Wilkinson, and M. Emers. 1989a. Effects of Urban Stormwater Runoff on Palustrine Wetland Vegetation Communities - Baseline Investigation (1988). Report to U.S. Environmental Protection Agency, Region 10, by King County Resource Planning Section, Seattle. WA.

Cooke, S., K. O. Richter and R. R. Horner. 1989b. Puget Sound Wetlands and Stormwater Management Research Program: Second Year of Comprehensive Research. Resource Planning Section of King County Parks, Planning and Resources Department, Seattle, WA.

Cooke, S., R. Horner and C. Conolly. 1989c. Effects of Urban Stormwater Runoff on Palustrine Wetland Communities- Baseline Investigation. King County, Natural Resources and Parks Division, King County, WA.

Cowardin, L. M., V. Carter, F. C. Goulet and E. T. LaRoe. 1979. Classification of wetlands and deepwater habitat of the United States. U. S. Fish and Wildlife Service, Washington D.C.

Gauch, H. G. 1982. Multivariate Analysis in Community Ecology. Cambridge University Press, Cambridge, England.

Hill, M.O. 1979a. TWINSPAN: A Fortran program for arranging multi-variate data in an ordered two-way table of classification of the individuals and attributes. Cornell University, Ithaca, NY.

Hill, M.O. 1979b. DECORANA: A Fortran program for detrending correspondence analysis and reciprocal averaging. Cornell University, Ithaca, NY.

Hitchcock, C. L., A. Cronquist, M. Ownbey, and J.W. Thompson. 1969. Vascular Plants of the Pacific Northwest, University of Washington Press, Seattle and London.

Houck, C. A. 1996. The distribution and abundance of invasive plant species in freshwater wetlands of the Puget Sound lowlands, King County, Washington. MS thesis. University of Washington. Seattle, WA.

King County. 1990. The King County Wetlands Inventory Notebook, Vol I-III. King County Environmental Section, Parks and Recreation Division, Bellevue, WA.

Kunze. Linda. 1994. Preliminary Classification of Native, Low Elevation, freshwater Wetland Vegetation in Western Washington. Washington Natural Heritage Program, Land and Water Conservation, Dept. of Natural Resources. Olympia, WA.

Reed, P. 1988. National List of Plant Species that Occur in Wetlands: Northwest Region 9. U.S. Fish and Wildlife Service, Biological Report 88(26.9).

Reed, P. 1993. Addendum to the National List of Plant Species that Occur in Wetlands: Northwest Region 9.

Reinelt, L. E. and R. R. Horner. 1990. Characterization of the Hydrology and Water Quality of Palustrine Wetlands Affected by Urban Stormwater. King County Resource Planning, King County, WA.

Taylor, B. 1993. The influence of wetland and watershed morphological characteristics on wetland hydrology and relationships to wetland vegetation communities. Masters thesis. University of Washington. Seattle, WA.

Washington State Department of Ecology. 1991. Washington State wetlands Rating System for Western Washington. Publication # 91-58, Olympia, WA.

Appendix Table 3-1. List of plant species and frequency found among 19 Puget lowland palustrine wetlands.

Plant Species	Number of Wetlands	Percent of All Wetlands	Plant Species	Number of Wetlands	Percent of All Wetlands
Adiantum pedatum	1	0.04	Rorippa calycina	5	0.19
Agrostis scabra	1	0.04	Rosa pisocarpa	5	0.19
Aira caryophyllea	1	0.04	Sium suave	5	0.19
Anthoxanthum odoratum	1	0.04	Utricularia minor	5	0.19
Arbutus menziesii	1	0.04	Agrostis gigantea (alba)	6	0.23
Asaurum caudatum	1	0.04	Crataegus monogyna	6	0.23
Berberis aquifolium	1	0.04	Fraxinus latifolia	6	0.23
Brasenia schribneri	1	0.04	Galium aparine	6	0.23
Carex athrostachya	1	0.04	Hypericum formosum	6	0.23
Carex stipata	1	0.04	Ludwigia palustris	6	0.23
Chenopodium alba	1	0.04	Rubus leucodermis	6	0.23
Cladina rangiferina	1	0.04	Smilacena racemosa	6	0.23
Convolvulus sepium	1	0.04	blue-green algae	6	0.23
Cornus canadensis	1	0.04	Anaphalis margaritacea	7	0.27
Echinochloa crusgalii	1	0.04	Festuca rubra	7	0.27
Festuca pratensis	1	0.04	Galium cymosum	7	0.27
Fragaria virginiana	1	0.04	Glyceria borealis	7	0.27
Goodyeara oblongifolia	1	0.04	Holodiscus discolor	7	0.27
Hippurus vulgaris	1	0.04	Juncus bufonius	7	0.27
Hydrocotyl ranunculoides	1	0.04	Lycopus americanus	7	0.27
Hydrophyllum tenuipes	1	0.04	Myosotis laxa	7	0.27
Juncus supiniformis	1	0.04	Potamogeton natans	7	0.27
Lamium purpurea	1	0.04	Rumex crispus	7	0.27
Lythrum salicaria	1	0.04	Carex lenticularis	8	0.31
Melilotus alba	1	0.04	Dactylis glomerata	8	0.31
Nymphaea odorata	1	0.04	Geranium robertianum	8	0.31
Poa palustris	1	0.04	Glyceria elata	8	0.31
Poa pratensis	1	0.04	Juncus acuminatus	8	0.31
Potamogeton diversifolius	1	0.04	Juncus ensifolius	8	0.31
Potamogeton gramineus	1	0.04	Rhododendron groenlandicum (Ledum g.)	8	0.31
Ranunculus acris	1	0.04	Nuphar polysepalum	8	0.31
Rhinanthus crista-galli	1	0.04	Oplopanax horridus	8	0.31
Ribes bracteosum	1	0.04	Potentilla palustris	8	0.31
Rorippa curvisiliqua	1	0.04	Ribes lacustre	8	0.31
Rosa nutkana	1	0.04	Stachys cooleyae	8	0.31
Rosa rugosa	1	0.04	Symphoricarpos albus	8	0.31
Rumex acetosella	1	0.04	Tiarella trifoliata	8	0.31
Sagittaria latifolia	1	0.04	Carex hendersonii	9	0.35
Scirpus acutus	1	0.04	Circium arvense	9	0.35
Solanum nigrum	1	0.04	Dicentra formosa	9	0.35
Stellaria longifolia	1	0.04	Rosa gymnocarpa	9	0.35
Tanacetum vulgare	1	0.04	Scirpus atrocinctus	9	0.35
Trifolium pratense	1	0.04	Sorbus scopulina	9	0.35
Vaccinium ovatum	1	0.04	Sphagnum spp.	9	0.35
Vicia sativa	1	0.04	Salix pedicellaris	10	0.38
Adenocaulon bicolor	2	0.08	Scirpus microcarpus	10	0.38
Alnus sinuata	2	0.08	Agrostis capillaris (tenuis)	11	0.42
Alopecurus pratensis	2	0.08	Callitriche heterophylla	11	0.42
Azola mexicana	2	0.08	Epilobium angustifolium	11	0.42
Bromus ciliatus	2	0.08	Lycopus uniflorus	11	0.42

Appendix Table 3-1 continued. List of plant species and frequency found among 19 Puget lowland palustrine wetlands.

Plant Species	Number of Wetlands	Percent of All Wetlands	Plant Species	Number of Wetlands	Percent of All Wetlands
Claytonia lanceolata	2	0.08	Rubus parviflorus	11	0.42
Cornus nuttallii	2	0.08	Scutellaria lateriflora	11	0.42
Elytrigia repens (Agropyron repens)	2	0.08	Sparganium emersum	11	0.42
Eriophorum chamissonis	2	0.08	Torreyochloa pauciflora (Puccinellia p.)	11	0.42
Glecoma hederacea	2	0.08	Veronica scutellata	11	0.42
Gnaphalium uliginosum	2	0.08	Equisetum hyemale	12	0.46
Gymnocarpium dryopteris	2	0.08	Equisetum telmateia	12	0.46
Hercaleum lanatum	2	0.08	Holcus lanatus	12	0.46
Hypochaeris radicata	2	0.08	Menziesia ferruginea	12	0.46
Impatiens noli-tangere	2	0.08	Polygonum hydropiper	12	0.46
Lolium mulitflorum	2	0.08	Typha latifolia	12	0.46
Lotus corniculatus	2	0.08	Bidens cernua	13	0.5
Menyanthes trifoliata	2	0.08	Carex arcta	13	0.5
Pinus monticola	2	0.08	Galium trifidum	13	0.5
Polygonum amphibium	2	0.08	Ilex aquifolia	13	0.5
Rhynchospora alba	2	0.08	Picea sitchensis	13	0.5
Rumex obtusifolius	2	0.08	Sorbus americana	13	0.5
Salix hookeriana	2	0.08	Berberis nervosa	14	0.54
Smilacena stellata	2	0.08	Carex utriculata =(rostrata)	14	0.54
Sparganium eurycarpum	2	0.08	Maianthemum dilatatum	14	0.54
Streptopus roseus	2	0.08	Salix alba	14	0.54
Taraxacum officinale	2	0.08	Tolmiea menziesii	14	0.54
Trfolium repens	2	0.08	Corylus cornuta	15	0.58
Vaccinium uliginosum	2	0.08	Juncus effusus	15	0.58
Vallisneria americana	2	0.08	Lemna minor	15	0.58
Actea rubra	3	0.12	Prunus emarginata	15	0.58
Alisma plantago-aquatica	3	0.12	Stellaria media	15	0.58
Carex exsiccata (vesicaria)	3	0.12	Trillium ovatum	15	0.58
Circium vulgare	3	0.12	Cornus sericea (stolonifera)	16	0.62
Cytisus scoparius	3	0.12	Geum macrophyllum	16	0.62
Dulichium arundinaceum	3	0.12	Oenanthe sarmentosa	16	0.62
Elodea canadensis	3	0.12	Acer macrophyllum	17	0.65
Lolium perenne	3	0.12	Carex obnupta	17	0.65
Mimulus guttatus	3	0.12	Ranunculus repens	17	0.65
Montia siberica	3	0.12	Rubus procerus (discolor)	17	0.65
Nasturtium officinale	3	0.12	Urtica dioica	17	0.65
Phleum pratense	3	0.12	Equisetum arvense	18	0.69
Ribes sanguineum	3	0.12	Glyceria grandis	18	0.69
Nastutium officinale	3	0.12	Luzula parviflora	18	0.69
Taxus brevifolia	3	0.12	Phalaris arundinaceae	18	0.69
Utricularia vulgaris	3	0.12	Populus balsamifera	18	0.69
Viola glabella	3	0.12	Blechnum spicant	19	0.73
Azolla filiculoides	4	0.15	Carex deweyana	19	0.73
Eleocharis ovata	4	0.15	Malus fusca (Pyrus f.)	19	0.73
Eleocharis palustris	4	0.15	Salix sitchensis	19	0.73
Hieracium pratense	4	0.15	Acer circinatum	20	0.77
Hypericum anagalloides	4	0.15	Lysichitum americanum	20	0.77
Iris pseudacorus	4	0.15	Polypodium glycyrrhiza	20	0.77

Appendix Table 3-1 continued. List of plant species and frequency found among 19 Puget lowland palustrine wetlands.

Plant Species	Number of Wetlands	Percent of All Wetlands	Plant Species	Number of Wetlands	Percent of All Wetlands
Kalmia microphylla	4	0.15	Pseudotsuga menziesii	20	0.77
Linnaea borealis	4	0.15	Salix lucida var. lasiandra	20	0.77
Mentha arvensis	4	0.15	Solanum dulcamara	20	0.77
Myosotis scorpioides	4	0.15	Thuja plicata	20	0.77
Petasites frigidus	4	0.15	Tsuga heterophylla	20	0.77
Physocarpus capitatus	4	0.15	Veronica americana	20	0.77
Plantago lanceolata	4	0.15	Oemleria cerasiformis	21	0.81
Plantoga major	4	0.15	Gaultheria shallon	22	0.85
Populus tremuloides	4	0.15	Sambucus racemosa	22	0.85
Solidago canadensis	4	0.15	Dryopteris expansa (austriaca)	23	0.88
Spirodela polyrhiza	4	0.15	Epilobium ciliatum (watsonii)	23	0.88
Streptopus amplexifolius	4	0.15	Lonicera involucrata	24	0.92
Vaccinium oxycoccos	4	0.15	Pteridium aquilinum	24	0.92
Agrostis oregonensis	5	0.19	Rhamnus purshiana	24	0.92
Amelanchier alnifolia	5	0.19	Rubus laciniatus	24	0.92
Betula papyrifera	5	0.19	Vaccinium parvifolium	24	0.92
Circaea alpina	5	0.19	Alnus rubra	25	0.96
Convolvulus arvensis	5	0.19	Athyrium filix-femina	25	0.96
Digitalis purpurea	5	0.19	Salix scoulerleriana	25	0.96
Drosera rotundifolia	5	0.19	Spirea douglasii	25	0.96
Hedera helix	5	0.19	Polystichum munitum	26	1
Lonicera ciliosa	5	0.19	Rubus spectablilis	26	1
Ribes divaricatum	5	0.19	Rubus ursinus	26	1

CHAPTER 4 EMERGING MACROINVERTEBRATE DISTRIBUTION, ABUNDANCE AND HABITAT USE

by Klaus O. Richter and Robert W. Wisseman

INTRODUCTION

Macroinvertebrates—particularly insects, are diverse and abundant zoological components of freshwater aquatic systems. Of all invertebrates, the trophic diversity and numerical abundance of insects, and especially the Diptera (true flies), make this group the most important taxa in streams, lakes and other water environments. Unique adaptations have evolved in their life-history patterns (breeding, oviposition, hatching and development), morphological and physiological characteristics (respiration) and behavioral traits (lotic/lentic habitat affinities, functional feeding groups) to enable them to occupy most wetland habitats and trophic levels.

Recent research focusing on aquatic invertebrates in wetlands, indicates the importance of insects in energy and nutrient transfer within aquatic ecosystems (Rosenberg and Danks 1987). They furnish food for other invertebrates (e.g., predatory insects and arachnids such as mites and spiders) and comprise significant portions of the nutritional requirements of amphibians, water birds and small mammals. They are especially important to rearing fish (e.g., Salmonidae, game fishes), contributing to commercial and sport fisheries.

Diptera as well as other aquatic insects are pivotal components of complex food webs, significantly increasing the number of links in the web with their richness and abundance. As filter feeders, shredders and scrapers they convert and assimilate microorganisms and vegetation into biomass of aquatic insects providing significant production available to secondary and tertiary consumers. Alternately, insects are sometimes thought detrimental to human health. Dipteran families including Simuliidae (black flies) and Culicidae (mosquitoes) are vectors of disease and can be pests to humans, livestock and other mammals. Consequently, they may be of medical and economic importance (Courtney et al. 1996).

The distribution and abundance of macroinvertebrates in running waters and lakes have long been recognized as important tools in describing and assessing the condition of these aquatic ecosystems (Rosenberg and Resh 1993). However, it has been relatively recently that they were identified as providing an indication of the condition of palustrine environments (Ludwa and Richter, this volume), particularly wetlands of watersheds undergoing urbanization (Ludwa 1994, Hicks 1996). This is primarily because basic information regarding their spatial and seasonal distribution and abundances in palustrine wetlands is uncommon. Moreover, specific hydrologic, water quality and other habitat characteristics that may account for invertebrate, and specifically insects, remain unavailable.

Consequently, in this paper we characterize the emergent macroinvertebrates in palustrine wetlands in the Pacific Northwest by describing the distribution and abundance of taxa collected in emergence traps at 19 wetlands of the Puget Sound region. Moreover, we determine characteristics of wetlands and watersheds that may account for their occurrences.

METHODS

We collected adult macroinvertebrates (e.g., most often insects of minimum of 5mm in size and easy to see with unaided eye), encompassing a wide diversity of taxa using emergence traps (Figure 4-1). We used emergence traps rather than dip nets (e.g., sweep nets) or benthic sampling because captures in emergent traps represent the final component of insect production, allows quantification of cumulative production over variable time periods and presorts species on their ability to climb or fly into the collecting chamber facilitating identification procedures. In addition, emergence traps exhibit less sampling variability compared to sediment sampling.

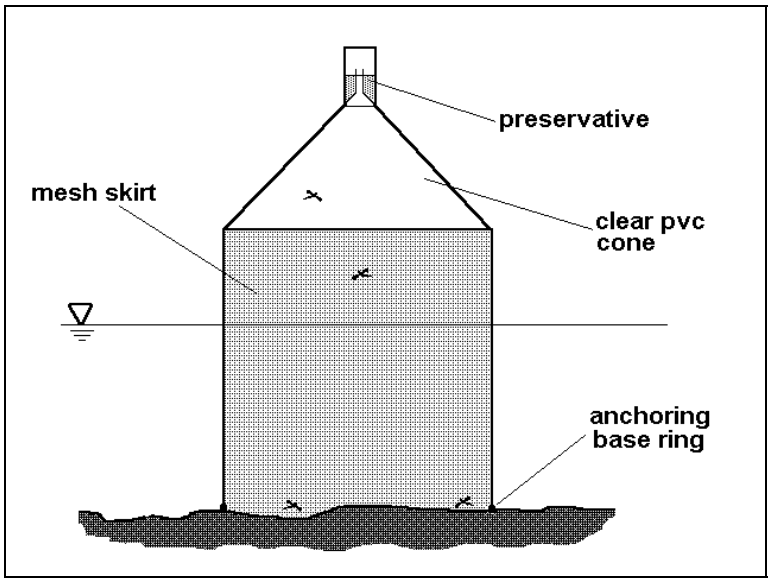

Figure 4-1. Side view cross-section of aquatic macroinvertebrate emergence trap.

The traps function by funneling emerging invertebrates upward into a glass jar at the top of the trap containing a liquid preservative. We placed three replicate traps, each covering a circular area of 0.25 M^2 within approximately one meter of each other in the deepest (maximum 1m deep) areas of wetlands that could be reached with chest waders during spring when invertebrates were first expected to emerge. Substrate and vegetation characteristics present at the trapping locations are described for individual wetlands in Table 4-1.

Traps were installed with base rings embedded in the substrate or flush to the ground. In September 1988 we installed traps in 14 wetlands with traps at five additional wetlands added in May 1989. We emptied traps semi-monthly. Traps were not emptied from mid-November 1988 to March 1989 and during other winter periods because of low or non-existent winter emergence. We attempted to empty traps within a three day period, although in some cases we took 19 days to collect samples. We captured and summarized macroinvertebrate data for all 19 wetlands in 1989 (including captures from September 15,1988 through September 31, 1989) and 1993 (including captures from April 10, 1993 through April 9, 1994). In 1995 we trapped in 18 wetlands (deleted TC13) from January 1, 1995 through October 30, 1995. Since winter emergence was low, our data essentially represents values for invertebrate years 1989, 1993 and 1995.

We identified emergent macroinvertebrates and placed them into broad groupings (adult arthropods, terrestrial arthropods, aquatic and semi-aquatic insects) for descriptive and statistical analysis. We use 1989 as our comprehensive description of macroinvertebrate distribution and abundance in Pacific Northwest wetlands in that we identified all invertebrates to the lowest taxa feasible—generally genus and species. In subsequent years we classified only to major taxa (e.g., Orders) except for Diptera, for which we identified captures to family and further limited our taxonomic efforts to the numerically dominant chironomid midges (suborder Nematocera, lower dipteran flies) with other Nematocera identified only to family. The suborder Brachycera (higher dipteran flies) were not identified because of the specialized expertise required for their taxonomy and because of the possibility they entered traps from adjacent areas during low water. We assigned the Dipterans to the aquatic group, since the vast majority of taxa within this order have larval stages developing in water or in saturated soils (Courtney et al. 1996). We identified wetland-associated terrestrial forms as species in which all life stages are found in terrestrial habitats.

The majority of the wetlands chosen for study are small palustrine systems ranging from several hectares to less than one hectare in size. We classified wetlands according to the level of development within their watersheds and flooding regime. Thus within watersheds of various levels of urbanization, wetlands were identified as to whether they were perennially or seasonally flooded during the monitoring year. Permanent wetlands exhibited standing water the entire year whereas seasonally flooded sites generally dried out between April and June and were re-flooded only after the onset of autumn rains in mid-October.

Table 4-1. Aquatic invertebrate emergence trap conditions (from Ludwa 1994).

	Flow		Substrate			Vegetation																						
Wetland	still water	discernible flow	gravel	sand	silt/mud	moss	periphyton	*Alnus rubra*	*Athyrium*	*Carex*	*Epilobium*	*Equisetum*	*Glyceria*	*Juncus*	*Lemna*	*Lysichtum*	*Nuphar*	*Oenanthe*	*Phalaris*	*Potentilla*	*Salix*	*Scirpus*	*Solanum*	*Sparganium emersum*	*Spirea*	*Typha*	*Veronica*	unidentified plants
AL3	×					×																						
B31		×	×	×	×			×		×		×							×			×						
BBC24	×																					×				×	×	
ELS39	×				×		×			×				×											×			
ELS61	×						×								×											×		
ELW1		×			×	×			×				×						×								×	
FC1		×			×		×						×		×				×									
HC13	×				×			×					×						×			×						
JC28	×				×			×								×												
LCR93		×															×	×							×	×		×
LPS9		×																×	×									
MGR36	×												×		×					×	×					×	×	
NFIC12	×				×	×	×							×														
PC12	×									×			×		×				×			×			×	×		
RR5	×									×				×								×						
SC4	×				×	×	×	×			×																×	
SC84	×					×	×											×					×				×	
SR24	×									×														×				
TC13	×				×	×	×											×				×				×	×	

We ran three Detrended Correspondence Analysis (DCA), iterations of the 1989 wetland data (Hill 1979, Hill & Gauch 1980) as follows; 1) all taxa; including terrestrial, aquatic and semiaquatic taxa identified to the lowest level reported, 2) all aquatic/semi-aquatic taxa, including the Brachycera, identified to the lowest level reported and 3) all chironomid midge taxa identified to the lowest level reported. Taxa abundances were log transformed prior to running the DCA program.

RESULTS AND DISCUSSION

Annual Overall Arthropod Richness and Abundance

Annual arthropod yield is presented in Table 4-2 (Table 4-2 and all subsequent tables may be found in Appendix 4-1). Terrestrial abundance was highest in 1989 (but see wetland NFIC12). Low numbers of arthropods were captured at wetlands both in 1993 and 1995. Total aquatic and semi-aquatic taxa richness and abundance varied widely between years and wetlands but were consistently dominated by Diptera in both categories. Aquatic and semi-aquatic abundance was highest in LCR93 with

21,501 invertebrates counted in 1995 and lowest in ELW1 with 256 animals tallied in 1995.

Terrestrial Arthropod Richness and Abundance

Arachnids and hexpods insects were the two terrestrial arthropod classes most frequently captured in emergence traps (Table 4-3). Arachnids are common predators (spiders) and parasites (mites) on aquatic insects and other invertebrates. Of the insects, we captured a total of nine terrestrial orders. Homoptera—particularly Aphididae (aphids), Coleoptera (beetles) and Hymenoptera (e.g., Parasitoid wasps) were represented in the greatest numbers. The captured taxa of these orders are often associated with emergent plant parts above water which were enclosed by the traps. That is probably why they were captured in our traps and not because they are obligate wetland species.

Total terrestrial arthropod richness ranged from a high of ten to a low of seven major invertebrate taxa in a single year (Table 4-3). Neuroptera were missing from eight wetlands (AL3, ELS39, ELW1, PC12, RR5, SC84, SR24 and TC13) and Hemiptera from five (AL3, BBC24, FC1, SR24 and TC13). Densities ranged from 56,439 M^2 in BBC24 for 1989 to a low of 9 M^2 at JC28 in 1993. The most abundant terrestrial taxa were Aphididae (e.g., aphids-Homoptera) mostly because of their reproductive characteristics, communal feeding and small size. Aphids frequently feed on exposed broad-leaved aquatic vegetation (personal observation) and therefore are abundant in open water wetlands that are characterized by water lilies such as found in BBC24. They are largely missing from forested and scrub-shrub wetlands without such plant species as for example JC28 and AL3.

Aquatic and Semi-Aquatic Insect Richness and Abundance

Five aquatic and semi-aquatic insect orders, Ephemeroptera (mayflies), Odonata (dragonflies/damselflies), Plecoptera (stoneflies), Trichoptera and Diptera, were collected within wetlands. Ephemeroptera were captured at 12 wetlands during the survey (Table 4-4). Their abundance was low (<25) except at LCR93 and JC28 at which maximum numbers were 232 and 206 individuals respectively. In the 1989 survey they represented only two taxa (Table 4-5). Ephemeroptera, in general, inhabit both lentic and lotic waters where adequate supplies of dissolved oxygen are found. The taxa we identified, *Callibaetis* and *Paraleptophlebia,* are also found mostly in perennial and seasonal wetlands respectively. Overall, Ephemeroptera richness and abundance were greater at perennial than in annually/seasonally flooded sites. Moreover, they were patchily represented in non-urbanized sites (AL3, SC4, HC13, LCR93, MGR36, SR24, TC13, PC12) and moderately urbanized (BBC24, ELW1, ELS61, ELS39, JC28, NFIC12, RR5, SC84, LPS9) sites but were not found at both highly urbanized sites (B3I and FC1).

Surprisingly, Odonata were captured at only three wetlands, and in low (<2 at ELS61 and LPS9, <25 at BBC24) numbers. A total of three species of damselflies were found at BBC24 and ELS61. Odonata require year-round standing water, and therefore are generally not found in temporary and seasonal wetlands.

Plecoptera, a lotic insect order, was encountered at eight wetlands. In 1989 this represented eight taxa including a new species, *Capni*. We found Plecoptera in large numbers (1576) at LCR93 in 1989, moderate numbers (101) at NFIC12 in 1995 and

low numbers of 42 and 32 animals/ M^2 in 1995 at RR5 and 1989 at JC28 respectively (Table 4-4). In all other wetlands and years they were collected in low numbers (<10). Plecoptera was usually found in wetlands with flow-through channels.

Trichoptera taxa richness is relatively high with 24 taxa identified during 1989 alone (Table 4-6). Regardless of wetland, the majority of larvae belonged to the family Limnephilidae. Oxyethira, a hydroptilid, was common at BBC24. Numbers of Trichoptera were low (<200) at many wetlands with the exception of 1995 at LPS9.

Insect emergence was clearly dominated by Diptera (Table 4-2). The abundance of individuals within these taxa often varied widely with the highest number of Diptera being as much as 13 times greater than the lowest numbers (e.g., ELS61 versus ELW1). Most often variations between high counts are between two to six times the low counts. More extreme are abundance data for chironomids in which numbers in high years are as much as 190, 84 and 36 times the numbers found in low year counts as in RR5, MGR36 and NFIC12, respectively, whereas the ranges at most other wetlands differed by five to 20. Nevertheless, the relative ranking of taxa abundance by wetlands was often relatively constant with the same wetlands retaining their lowest or highest relative ranking from among all wetlands. B3I and ELS61, for example, ranked in the top three in Cecidomyiidae and Tipulidae abundance in at least two of three years. Other common dipteran families captured included the Psychodidae, Tipulidae, and Empididae.

Actual dipteran numbers ranged from a high of high of 20,781 M^2 in ELS61 in 1989 to a low of 256 M^2 in ELW1 in 1995. In fact, ELW1 consistently had the lowest number and ELS61 the highest number of Diptera during the three-years of monitoring. Low dipteran numbers of under 1,000 M^2 in two out of three years were also identified at JC28 and high numbers of 10,000 M^2 or more at LCR93 and NFIC12. As expected significantly fewer aquatic and semi-aquatic forms and numbers were present in the higher dipteran suborder Brachycera, than the largely aquatic Nematocera (longhorned flies).

In the Nematocera, members of the family Chironomidae (midges) were clearly represented by the greatest number of taxa and often also by numbers. Chironomid midges have been found to be one of the most abundant and diverse groups in other regions of North America (Wrubleski 1987) and therefore these findings were expected. In 1989 we identified a high of 42 taxa in BBC24 and counted a high total abundance of 11,925 animals at ELS61 (Table 4-6). Chironomid taxa richness was consistently high in the perennial, non-urbanized wetlands, and consistently low in the non-urbanized wetlands that dried out in the summer. Table 4-7 provides the abundance rankings of all Chironomid taxa within our 1989 wetland characterization scheme.

Non-chironomid families of numerical importance include the Sciaridae, Cecidomyiidae (gall gnats that sometimes live in the tissues of live aquatic vegetation), Dixidae (dixid midges), and Tipulidae (crane flies). Rarely found non-Chironomids included the Anisopodidae, Bibionidae, Scatopsidae, Simuliidae (black flies) and Trichoceridae. Certain Psychodidae are often found in water and sewage-treatment facilities (Courtney at al. 1996). Psychodidae, Ptychopteridae and Syrphidae are collector-gatherers feeding on decaying fine organic matter associated with microorganisms. Collector-filterers include most Culicidae and Simuliidae. Tipulidae and Ephydridae are considered shredders.

Taxa richness of semi-aquatic and aquatic insects was generally higher (>40 taxa) in persistent than seasonal wetlands that dried out in summer (but see LCR93; Table 4-6). Both high and low richness was found in wetlands whose watersheds were largely non-urbanized depending on whether they remained flooded or dried out in summer. Interestingly, the three wetlands in non-urbanized watersheds that dried out in summer 1989 (AL3, NFIC12 and TC13) exhibited the lowest overall richness values as did the wetlands that dried out in highly urbanized watersheds (ELS39, LPS9, and SC84). Richness values for these wetlands ranged from 20-30 total taxa, with only 8-16 Chironomid taxa.

In 1989 we identified a high of 62 non-Brachycera taxa at BBC24 with 8570 animals M^2. The lowest richness of one third this highest value was observed at NFIC12, AL3 and ELS39. Densities were lowest at 655 animals M^2 in ELW1.

Shannon and Pielou diversity indices (Shannon and Weaver 1949, Pielou 1966) calculated for the full compliment of aquatic/semiaquatic invertebrates as well as the chironomid communities (Table 4-6) indicate that most wetlands within highly urbanized watersheds have lower richness than those in less urbanized watersheds. Most wetlands characterized by water permanence generally also exhibited higher richness than those that dried out.

In all three analyses using DCA, permanent wetlands were clearly distinguished from summer dry sites along axis 1 (Figures 4-2, 4-3 and 4-4). Axis 1 is most easily interpreted as representing a gradient progressing form wetlands experiencing lengthy summer drying, to wetlands having year-round standing water. Also, those summer dry site communities which experience highly fluctuating water levels are found at the extreme of axis 1, for example B3I, with one of the most urbanized watersheds. In general, insect communities of wetlands characterized by summer drought and flashy hydrology are harsh and unpredictable environments are less diverse; most likely because fluctuating environments generally exhibit simpler food chains or, fewer linkages per species, than stable ecosystems.

Axis 2 of the DCA plots are not satisfactorily related to an environmental gradient. Summer dry, moderately and highly urbanized sites were scattered more widely on this axis than were wet sites. The four wet, non-urbanized sites by being closely clustered and showing little separation on either axes, indicate very similar invertebrate communities. Though, the moderately and highly urbanized, wet sites could also be distinguished form the dry sites, they displayed more separation on both axis 1 and 2 than the non-urbanized wet sites. The BBC24 community was usually distant on axis 1 from the other wet sites. This wetland exhibited high taxa richness, and contained many Odonata, Trichoptera and Chironomidae taxa which were not typical of other wetlands.

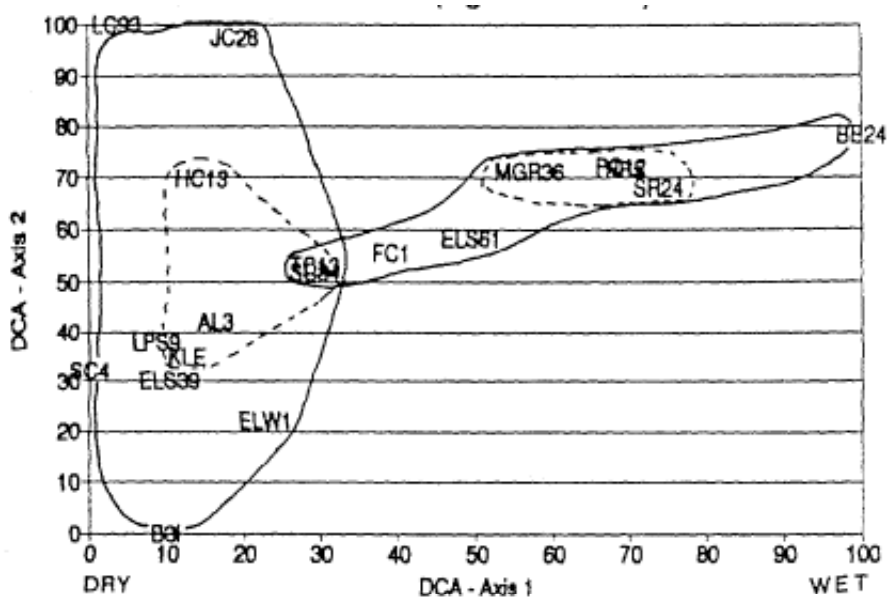

Figure 4-2. Terrestrial, aquatic and semi-aquatic taxa DCA analysis results.

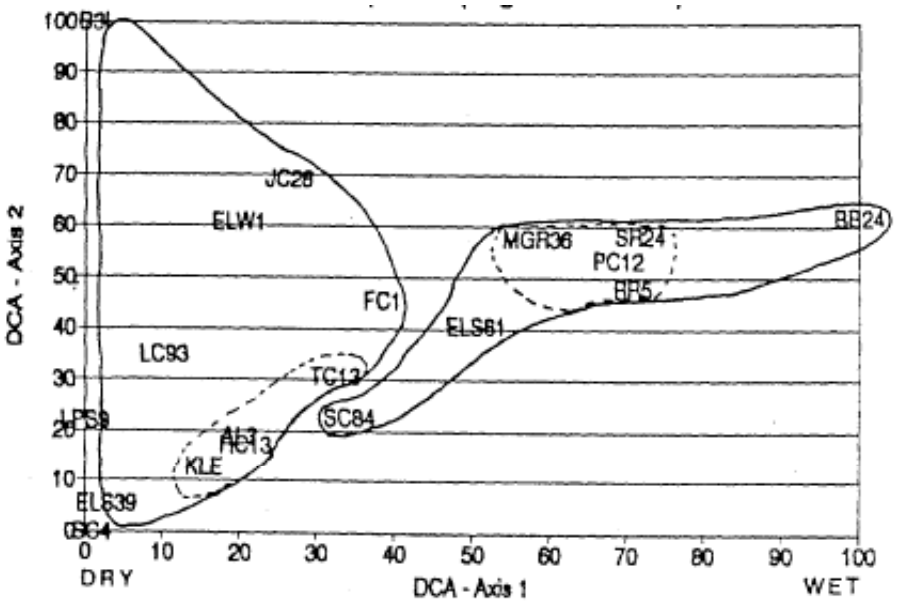

Figure 4-3. Aquatic and semi-aquatic taxa DCA analysis results.

On axis 2, communities of intermittent wetlands showed considerable separation from flooded wetlands indicating that seasonally flooded habitats were more variable in community structure than those with permanent standing water. As in the case for non-urbanized, wet sites, the four non-urbanized summer dry site insect communities clustered more closely together than the communities in moderately and highly urbanized site.

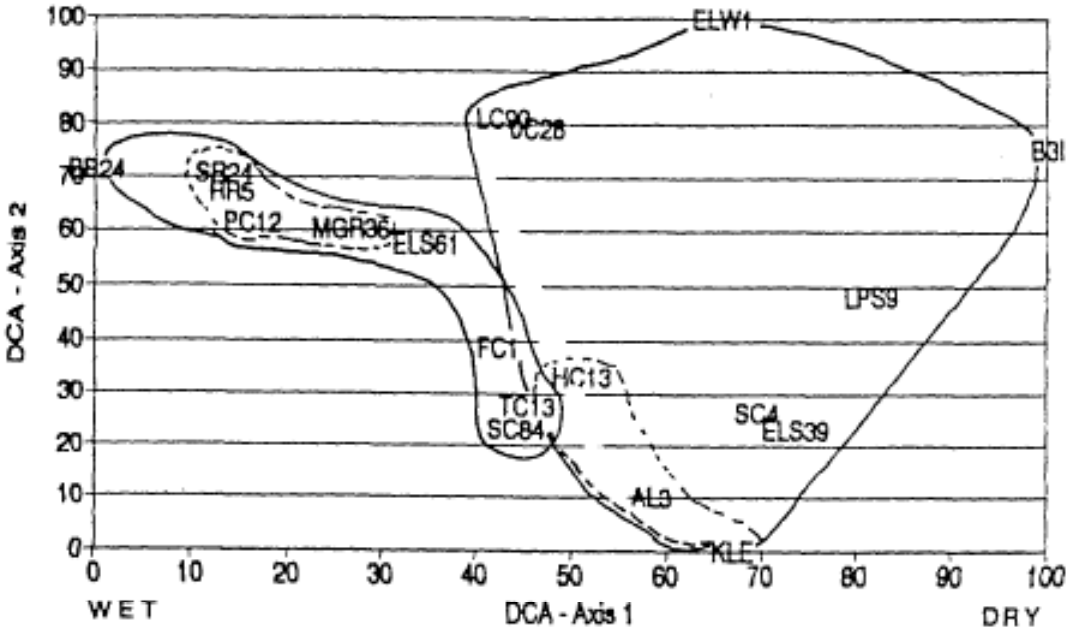

Figure 4-3. Midge taxa DCA analysis results.

CONCLUSION

Several studies have reported on invertebrates of lotic and lentic habitats. This paper is the most comprehensive to date on the distribution and abundance of emerging macroinvertebrates of palustrine wetlands in the Northwest. We feel confident that we have good descriptions of wetland emergent macroinvertebrates using the traps and conditions described from replicate captures among 19 wetlands during three years of survey between 1988 and 1995. Our descriptive statistical analysis of the high numbers of macroinvertebrates captured combined with estimates of variability among traps indicates that emergent trapping provides a good census of emerging aquatic insects in wetlands. Capture data further suggest that robust statistical comparisons of emergence data are possible by combining the three replicates at each site (Richter et. al. 1991). Nevertheless, increasing the number of replicates would be desirable and would provide additional power to our findings.

Our study is especially valuable in describing the chironomid midge communities. In North America, this group is represented by more species than all other orders of insects combined (McCafferty 1983). We identified 80 taxa in 1989 alone, including new species and extended the range extended extensions of several other taxa. Nearly half of the encountered taxa have not been previously reported in wetlands (Wrubeski 1987).

We identified 17 out of a total of 35 North American dipteran families associated with aquatic or semi-aquatic environments (McCafferty 1983) including several families not mentioned as found in marginal areas of shallow bodies of water including lakes, ponds, pools, marshes and bogs.

Non-dipteran aquatic and semi-aquatic insects identified within our survey were, for the most part, identified elsewhere in similar wetland ecosystems. The three taxa of

dragonflies (Odonata) and *Callibaetis* (Ephemeroptera) are commonly found in Canadian marshes (Rosenberg and Danks 1987), whereas *Paraleptophlebia* is common in ephemeral streams of the Pacific Northwest. Plecoptera taxa found are also the ones typically inhabiting small perennial or temporary streams.

LITERATURE CITED

Courtney, G. W., R. W. Merritt, H. J. Teskey and B. A. Foote. 1996. Aquatic Diptera Part 1. Larvae of Aquatic Diptera p 484-515 In: An Introduction to the Aquatic Insects of North America, Third Edition. R. W. Merritt and K. W. Cummins eds. Kendall/Hunt Publishing, Dubuque, IO, USA.

Hill, M. O. 1979. DECORANA—A FORTRAN program for detrended correspondence analysis and reciprocal averaging. Mimeographed Manuscript. Section of Ecology and Systematics, Cornell University, Ithaca, New York. USA.

Hill, M. O. and H. G. Gauch. 1980. Detrended Correspondence Analysis: An Improved Ordination Technique. Vegetatio 42:47-48.

Ludwa, K. A. 1994. Urbanization effects on palustrine wetlands: Empirical water quality models and development of macroinvertebrate community-based biological index. University of Washington, Seattle, WA, USA.

McCafferty, W. P. 1983. Aquatic Entomology. Jones and Bartlett Publishers. Boston, MA, USA.

Merritt, R. W. and K. W. Cummins, eds. 1996. An Introduction to the Aquatic Insects of North America, Third Edition. R. Kendall/Hunt Publishing, Dubuque, IO, USA.

Pielou, A. E. C. 1966. Species-diversity and pattern-diversity in the study of ecological successsion. J. Theoret. Biol. 10: 370-383.

Richter, K.O., A Azous, S. S. Cook, R.W. Wisseman and R.R. Horner. 1991. Effects of Stormwater runoff on wetland zoology and wetland soils characteristics and analysis. DOE Report Fourth Year Comprehensive Research. Puget Sound Wetlands and Stormwater Management Program. King County Resources Planning, Bellevue, WA. USA.

Rosenberg, D. M. and H. V. Danks (eds.). 1987. Aquatic Insects of Peatlands and Marshes in Canada. Mem. Ent, Soc. Canada. No. 140. The Entomology Society of Canada. Ottawa. Canada.

Rosenberg, D. M. and V. H. Resh (eds). 1993. Freshwater Biomonitoring and Benthic Macroinvertebrates. Chapman & Hall.

Shannon, C. E. and W. Weaver. 1949. The Mathematical Theory of Communication. Urbana, University of Illinois Press.

Turner, R. E. 1988. Secondary production in riparian wetlands. Trans. 53rd Wild. and Nat. Res. Conf., pp 491-501.

Wrubleski, D. A. 1987. Chironomidae (Diptera) of peatlands and marshes in Canada. Mem. Ent. Soc. Can. 140:141-161.

APPENDIX 4-1. TABLES OF ARTHROPOD YIELD.

Table 4-2. Annual arthropod yield (per M2) from 19 wetlands in King County, Washington. Measured with three emergence traps (0.25 M2 area) at each wetland site run continuously for "insect year" 1988* (9/15/88 - 9/30/89, 1993 (4/10/93 - 4/9/94) & 1995 (1/1/95 - 10/30/95).

Wetland	Year	TOTAL TERR. ARTHROPODS	TOTAL AQUATIC AND SEMI-AQUATIC TAXA	Ephemeroptera	Odonata	Plecoptera	Trichoptera	Diptera	Brachycera	Nematocera	Non-Chironomid Nematocera	Chironomidae
	1989	41	4408	0	0	0	9	4399	2428	1971	724	1247
AL3	1993	9	2134	0	0	0	0	2134	184	1950	584	1366
	1995	31	1323	1	0	0	36	1286	225	1061	354	708
	1989	589	3037	0	0	0	1	3035	888	2147	634	1513
B3I	1993	222	2360	0	0	0	0	2360	1107	1253	616	637
	1995	277	735	0	0	0	0	735	168	567	460	108
	1989	56439	8858	3	24	1	132	8698	267	8431	203	8228
BBC24	1993	172	7515	0	0	0	0	7515	136	7379	145	7234
	1995	289	3020	1	0	0	15	3004	94	2910	93	2816
	1989	1972	7337	0	0	0	9	7328	1016	6312	3552	2760
ELS39	1993	122	4229	0	0	0	0	4229	404	3825	1970	1855
	1995	509	3204	0	0	0	5	3199	304	2895	2299	596
	1989	25935	20828	19	1	0	27	20781	5488	15293	3368	11925
ELS61	1993	597	10844	0	0	0	0	10844	3779	7065	2902	4163
	1995	452	1612	0	0	7	5	1600	133	1467	484	983
	1989	336	1238	0	0	0	0	1238	583	656	485	171
ELW1	1993	73	339	0	0	0	0	339	55	284	269	15
	1995	90	256	0	0	0	0	256	140	116	105	11
	1989	1531	4736	0	0	0	1	4734	1575	3160	461	2699
FC1	1993	115	6767	0	0	0	0	6767	73	6694	301	6393
	1995	113	2899	0	0	0	5	2894	15	2879	35	2844
	1989	308	8753	0	0	5	40	8708	2169	6538	3525	3013
HC13	1993	113	2272	0	0	0	0	2272	44	2228	270	1958
	1995	69	1522	0	0	1	21	1500	33	1467	435	1032
	1989	97	1134	105	0	32	3	994	69	925	169	756
JC28	1993	8	2900	0	0	0	0	2900	7	2893	53	2840
	1995	28	702	206	0	7	24	465	28	437	134	303
	1989	5076	9691	232	0	1576	61	7821	2925	4896	2580	2316
LCR93	1993	45	6234	0	0	0	0	6234	128	6106	193	5913
	1995	217	21501	0	0	0	0	21501	880	20621	1605	19016
	1989	2836	5126	0	0	0	3	5124	1160	3964	3313	651
LPS9	1993	153	1076	0	0	0	1	1075	432	643	504	139
	1995	62	2964	8	2	0	231	2723	86	2637	382	2255
	1989	8067	7365	7	0	0	35	7324	2884	4440	1072	3368
MGR36	1993	243	6699	0	0	0	1	6698	39	6659	226	6433
	1995	294	1606	0	0	3	23	1580	234	1346	944	402
	1989	74	8870	0	0	0	7	8863	2984	5879	1127	4752
NFIC12	1993	282	13047	0	0	0	0	13047	368	12679	1340	11340
	1995	169	2256	5	0	101	9	2141	952	1189	877	313
	1989	575	5892	11	0	0	36	5845	484	5361	440	4921
PC12	1993	119	5683	0	0	0	0	5683	288	5395	437	4958
	1995	149	3159	0	0	0	13	3146	902	2244	313	1931
	1989	945	8621	3	0	0	28	8591	884	7707	500	7207
RR5	1993	60	2413	0	0	0	1	2412	35	2377	132	2245
	1995	127	2067	0	0	42	5	2020	307	1713	1676	38
	1989	308	2952	0	0	5	12	2935	887	2048	1232	816
SC4	1993	104	2186	0	0	0	0	2186	626	1560	678	882
	1995	84	1696	0	0	0	12	1684	189	1495	367	1128
	1989	115	3692	3	0	0	0	3689	1377	2312	449	1863
SC84	1993	25	1106	0	0	0	0	1106	20	1086	181	904
	1995	45	642	0	0	0	1	641	6	635	77	558
	1989	2590	5598	24	0	0	27	5547	467	5080	815	4265
SR24	1993	37	2506	0	0	0	0	2506	12	2494	82	2412
	1995	29	662	0	0	0	1	661	76	585	96	489
	1989	85	4658	0	0	0	1	4656	1043	3614	407	3207
TC13	1993	36	2116	0	0	0	0	2116	9	2107	104	2003
	1995											

Table 4-3. Annual terrestrial arthropod yield (per M^2) from 19 wetlands in King County, Washington. Measured with three emergence traps (0.025 M^2 area) at each wetland, run continuously for "insect year", 1989* (9/15/88-9/31/89), 1993 (4/10/93-4/9/94) and 1995 (1/1/95-10/30/95).

			INSECTA														
Wet-land	Year	**Arach-nida**	Collem-bola	Thysanop-tera	Psocop-tera	Hemip-tera	Homop-tera	Non Aphididae	Aphid-idae	Neurop-tera	Coleop-tera	Lepidop-tera	Hymenop-tera	Other Hymenop-tera	Parasit-oid	Formic-idae	TOTAL TERR. ARTHRO-PODS
AL3	1989	7	3	0	11	0	3	0	1	0	11	2	5	0	5	0	41
	1993	3	0	0	0	0	0	0	0	0	0	1	5	0	5	0	9
	1995	1	4	1	8	0	0	0	0	0	1	1	13	0	13	0	31
B3I	1989	35	124	13	41	9	124	0	113	9	11	7	216	0	212	4	589
	1993	4	1	4	20	1	110	5	105	3	12	7	60	7	51	3	222
	1995	3	37	1	20	0	165	1	163	0	0	0	51	0	51	0	277
BBC24	1989	33	179	17	144	0	55823	0	55797	7	56	7	173	1	171	1	56439
	1993	5	20	0	3	0	3	1	1	1	88	3	49	0	49	0	172
	1995	14	68	1	17	0	3	2	1	0	119	8	59	0	59	0	289
ELS39	1989	67	1043	33	4	1	281	0	133	0	40	8	495	4	505	5	1972
	1993	5	13	1	7	1	36	9	27	0	1	1	56	0	55	1	122
	1995	11	144	0	77	0	140	8	132	0	40	3	94	2	92	0	509
ELS61	1989	19	223	7	68	3	25155	0	25213	4	143	5	309	12	325	0	25935
	1993	12	72	4	0	3	210	13	197	0	37	24	235	1	234	0	597
	1995	13	337	4	4	0	31	23	8	0	11	9	44	1	43	0	452
ELW1	1989	19	131	0	47	12	44	0	17	0	1	1	81	1	79	1	336
	1993	13	4	0	24	0	3	1	1	0	8	0	21	0	21	0	73
	1995	8	36	3	15	1	1	1	0	0	11	1	15	1	13	0	90
FC1	1989	73	768	41	0	0	457	3	316	1	15	0	175	0	172	3	1531
	1993	20	7	5	9	0	48	25	23	0	8	0	17	0	17	0	115
	1995	9	11	5	70	0	1	1	0	0	3	1	12	0	12	0	113
HC13	1989	31	23	1	27	11	35	0	13	1	13	1	165	1	161	3	308
	1993	9	3	4	4	0	68	0	68	0	16	0	9	0	9	0	113
	1995	5	3	1	39	1	1	0	1	0	3	0	16	0	16	0	69
JC28	1989	11	32	1	20	4	7	0	5	0	1	0	21	0	21	0	97
	1993	1	1	0	0	0	0	0	0	3	0	0	3	0	3	0	8
	1995	3	7	1	11	1	1	1	0	0	3	1	0	0	0	0	28
LCR93	1989	88	21	57	129	15	4219	0	4055	3	101	1	441	0	439	3	74
	1993	11	0	5	1	0	8	3	5	0	9	0	11	0	11	0	282
	1995	16	19	0	0	0	100	0	100	2	9	1	69	1	68	0	169
LPS9	1989	57	197	15	4	5	2140	1	2084	5	55	1	388	8	380	0	5076
	1993	20	15	0	0	1	18	5	13	0	5	0	94	5	89	0	45
	1995	4	13	2	3	6	0	0	0	0	6	0	28	0	28	0	217
MGR36	1989	49	85	36	41	5	7645	0	7607	5	51	1	147	0	145	1	2868
	1993	43	5	4	5	1	4	1	3	0	7	0	174	0	174	0	153
	1995	23	132	11	0	0	9	4	5	0	15	8	97	0	94	3	62
NFIC12	1989	7	8	5	11	0	11	0	9	0	3	3	27	3	24	0	8067
	1993	4	11	4	16	5	7	1	5	1	3	0	231	4	227	0	243
	1995	12	5	1	68	1	16	11	5	0	17	1	47	0	47	0	294
PC12	1989	25	213	13	7	0	169	0	25	0	39	6	103	0	134	1	575
	1993	32	13	8	0	0	11	4	7	0	16	1	37	0	36	1	119
	1995	3	11	1	3	0	55	55	0	0	7	24	47	3	44	0	149
RR5	1989	21	137	15	39	3	219	3	75	0	261	23	228	1	213	13	945
	1993	1	3	3	1	0	4	1	3	0	19	3	27	0	27	0	60
	1995	21	41	0	1	0	0	0	0	0	17	3	43	0	43	0	127
SC4	1989	64	53	7	1	13	19	1	3	0	40	3	108	4	97	13	308
	1993	1	28	3	3	1	15	14	1	1	7	15	30	1	29	0	104
	1995	8	12	0	35	0	23	23	0	0	0	0	7	0	7	0	84
SC84	1989	12	11	5	3	0	24	0	1	0	1	0	59	7	43	9	115
	1993	4	0	0	10	2	2	2	0	0	0	0	7	0	7	0	25
	1995	5	15	0	4	0	10	10	0	0	5	0	5	0	5	0	45
SR24	1989	3	31	15	3	0	2375	16	2207	0	9	0	155	1	152	1	2590
	1993	5	0	1	3	0	9	5	3	0	12	0	7	0	7	0	37
	1995	3	8	1	7	0	0	0	0	0	5	0	5	0	5	0	29
TC13	1989	11	17	8	3	0	1	0	1	0	7	0	39	0	39	0	85
	1993	9	3	7	1	0	3	1	1	0	4	0	9	0	9	0	36
	1995																

Table 4-4. Annual aquatic/semi-aquatic insect yield (per M^2) from 19 wetlands in King County, Washington. Measured with three emergence traps (0.025 M^2 area) at each wetland site, run continuously for "insect year" 1989* (9/15/88 - 9/31/89), 1993 (4/10/93 - 4/9/94).

		TAXON																					
Wet-land	Year	Ephemer-optera	Odon-ata	Plecop-tera	Trichop-tera	Total Diptera/ Nemato-cera	Nema-tocera/ Chiron-omidae	Nema-tocera/ Non Chiron-omidae	Aniso-podi-dae	Bibion-idae	Cecid-omy-iidae	Cerat-opog-onidae	Chao-bori-dae	Culici-dae	Dixi-dae	Misc. Nema-tocera	Myce-tophil-idae	Psyc-hodi-dae	Scato-psi-dae	Sciar-idae	Simul-iidae	Tipuli-dae	Trichoc-eridae
	1989	0	0	0	9	724			0	0	159	53	5	3	100	0	52	120	0	137	0	95	0
AL3	1993	0	0	0	0	1950	584	1366	0	0	13	130	19	75	9	0	57	185	0	15	0	81	0
	1995	1	0	0	36	1061	354	708	0	0	5	25	72	13	19	0	4	21	0	9	0	185	0
	1989	0	0	0	1	624			1	0	407	71	0	1	1	1	8	32	4	13	0	84	0
B3I	1993	0	0	0	0	1253	616	637	1	0	246	1	0	0	5	0	76	16	0	21	0	249	0
	1995	0	0	0	0	567	460	108	0	0	301	3	0	0	0	0	9	5	0	19	0	122	0
	1989	3	24	1	132	203			0	0	11	121	11	1	33	15	0	1	0	9	0	0	0
BBC24	1993	0	0	0	0	7379	145	7234	0	0	3	25	35	39	28	0	0	8	0	5	0	3	0
	1995	1	0	0	15	2910	93	2816	0	0	5	15	33	8	7	0	4	9	0	11	0	1	0
	1989	0	0	0	9	3552			0	2	226	16	0	0	2	2	106	14	0	3152	0	32	0
ELS39	1993	0	0	0	0	3825	1970	1855	0	0	108	152	39	208	59	0	23	839	31	463	0	51	0
	1995	0	0	0	5	2895	2299	596	0	0	139	24	6	13	1	0	94	109	0	1906	0	7	0
	1989	19	1	0	27	3368			0	0	24	819	12	25	7	8	504	1449	1	336	0	183	0
ELS61	1993	0	0	0	0	7065	2902	4163	0	0	68	1886	0	37	20	0	218	315	0	153	0	205	0
	1995	0	0	7	5	1467	484	983	0	0	4	243	0	23	1	0	68	27	0	21	0	97	0
	1989	0	0	0	0	485			0	0	35	223	0	1	0	3	16	16	0	77	0	115	0
ELW1	1993	0	0	0	0	284	269	15	0	0	177	0	0	0	0	0	27	1	0	23	0	41	0
	1995	0	0	0	0	116	105	11	0	0	25	0	0	0	0	0	5	4	0	61	0	9	0
	1989	0	0	0	1	461			1	0	32	48	0	53	116	11	40	120	1	5	0	33	0
FC1	1993	0	0	0	0	6694	301	6393	0	0	1	29	0	33	181	0	0	52	0	3	0	1	0
	1995	0	0	0	5	2879	35	2844	0	0	3	3	0	0	18	0	0	3	0	8	0	1	0
	1989	0	0	5	40	3520			3	0	104	116	0	1	7	8	39	2421	0	509	4	308	0
HC13	1993	0	0	0	0	2228	270	1958	0	0	1	7	80	83	72	0	8	11	0	1	0	8	0
	1995	0	0	1	21	1467	435	1032	0	0	4	20	106	39	55	0	188	13	0	4	0	7	0
	1989	105	0	32	3	169			0	0	1	65	0	0	7	11	3	55	0	11	0	16	1
JC28	1993	0	0	0	0	2893	53	2840	0	0	8	0	0	0	29	0	8	5	0	1	0	1	0
	1995	206	0	7	24	437	134	303	0	0	11	19	0	1	15	0	16	15	0	40	0	19	0
	1989	232	0	1576	61	2579			31	0	241	764	0	0	191	229	177	367	0	129	152	297	0
LCR93	1993	4	0	0	9	6106	193	5913	0	0	11	21	0	1	48	0	31	0	0	3	25	53	0
	1995	0	0	0	0	20621	1605	19016	0	0	90	4	0	0	0	0	734	0	0	722	0	55	0
	1989	0	0	0	3	3313			4	0	1096	68	0	0	7	4	49	75	0	1528	0	483	0
LPS9	1993	0	0	0	1	643	504	139	0	0	130	9	0	0	1	0	82	1	0	266	0	15	0
	1995	8	2	0	231	2637	382	2255	0	0	7	289	0	25	22	0	4	13	0	21	0	0	0
	1989	7	0	0	35	1072			0	0	105	92	0	24	100	35	15	609	1	40	0	51	0
MGR36	1993	0	0	0	1	6659	226	6433	0	0	12	57	8	12	93	0	0	25	0	19	0	0	0
	1995	0	0	3	23	1346	944	402	0	0	57	44	0	0	0	0	41	1	0	497	0	303	0
	1989	0	0	0	7	1127			0	0	352	72	4	15	1	0	21	145	0	489	0	27	0
NFIC12	1993	0	0	0	0	12679	1340	11340	0	0	100	596	43	25	4	0	80	96	0	323	0	73	0
	1995	5	0	101	9	1189	877	313	0	0	138	67	0	0	20	0	67	61	0	448	4	72	0
	1989	14	0	0	36	437			1	0	15	84	0	23	1	24	8	179	1	64	0	37	0
PC12	1993	0	0	0	0	5395	437	4958	0	0	1	42	3	238	22	0	42	25	0	31	0	33	0
	1995	0	0	0	13	2244	313	1931	0	0	25	106	1	1	0	0	28	3	0	124	0	24	0
	1989	3	0	0	28	500			0	0	11	241	7	0	0	16	16	101	0	75	0	33	0
RR5	1993	0	0	0	1	2377	132	2245	0	0	3	114	3	3	0	0	3	0	0	4	0	3	0
	1995	0	0	42	5	1713	1676	38	0	0	91	3	0	161	0	0	55	15	0	1291	0	60	0
	1989	0	0	5	12	1232			0	0	299	3	0	16	0	3	7	117	0	728	0	60	0
SC4	1993	0	0	0	0	1560	678	882	0	0	122	37	0	120	15	0	57	131	0	120	0	75	0
	1995	0	0	0	12	1495	367	1128	0	0	4	5	133	71	112	0	1	28	0	9	0	4	0
	1989	3	0	0	0	449			0	0	65	33	7	1	12	4	9	84	0	79	0	155	0
SC84	1993	0	0	0	0	1086	181	904	0	0	9	0	80	18	61	0	2	10	0	2	0	0	0
	1995	0	0	0	1	635	77	558	0	0	11	6	11	6	3	0	22	10	0	7	0	0	0
	1989	24	0	0	27	815			0	0	107	189	7	19	48	132	163	84	0	27	0	40	0
SR24	1993	0	0	0	0	2494	82	2412	0	0	0	26	32	3	15	0	0	0	0	4	0	2	0
	1995	0	0	0	1	585	96	489	0	0	7	4	41	1	4	0	7	8	0	5	0	19	0
	1989	0	0	0	1	407			0	0	88	84	1	0	5	3	11	73	1	89	0	51	0
TC13	1993	0	0	0	0	2107	104	2003	0	0	7	39	17	8	24	0	0	5	0	4	0	0	0
	1995																						

Table 4-5. Annual aquatic/semi-aquatic insect yield (per M^2) from 19 wetlands in King County, Washington, as measured with 3 emergence traps (0.25 M^2 area) at each wetland site, run continuously between September 1988 and September 1989.

	AQUATIC AND SEMIAQUATIC INSECTS																		
	Non-Urbanized									Moderately Urbanized							Highly Urbanized		
	Perennial					Dry in Summer			Perrenial			Dry in Summer						Perennial	
TAXON	Mgr36	RR5	HC13	SR24	PC12	AL3	NFIC12	TC13	ELW1	BB24	ELS61	LCR93	LPS9	SC4	JC28	SC84	ELS39	B3I	FC1
Ephemeroptera	7	3	0	24	14	0	0	0	0	3	19	232	0	0	105	3	0	0	0
Callibaetis	0	3	0	24	13	0	0	0	0	3	19	0	0	0	0	3	0	0	0
Paraleptophlebia	7	0	0	0	1	0	0	0	0	0	0	232	0	0	105	0	0	0	0
Odonata	0	0	0	0	0	0	0	0	0	24	1	0	0	0	0	0	0	0	0
Ischnura cervula	0	0	0	0	0	0	0	0	0	20	1	0	0	0	0	0	0	0	0
Enallagma boreale	0	0	0	0	0	0	0	0	0	3	0	0	0	0	0	0	0	0	0
Coenagrion	0	0	0	0	0	0	0	0	0	1	0	0	0	0	0	0	0	0	0
Plecoptera	0	0	5	0	0	0	0	0	0	1	0	1576	0	5	32	0	0	0	0
Capnia nr. oregona	0	0	0	0	0	0	0	0	0	0	0	1	0	0	0	0	0	0	0
Paraleuctra? vershina	0	0	4	0	0	0	0	0	0	0	0	0	0	0	0	0	0	0	0
Malenka	0	0	0	0	0	0	0	0	0	0	0	83	0	0	0	0	0	0	0
Ostracerca dimicki	0	0	0	0	0	0	0	0	0	0	0	1	0	4	0	0	0	0	0
Podmosta delicatula	0	0	1	0	0	0	0	0	0	1	0	1325	0	1	1	0	0	0	0
Soyedina interrupta	0	0	0	0	0	0	0	0	0	0	0	137	0	0	31	0	0	0	0
Zapada cinctipes	0	0	0	0	0	0	0	0	0	0	0	1	0	0	0	0	0	0	0
Taenionema	0	0	0	0	0	0	0	0	0	0	0	27	0	0	0	0	0	0	0
Trichoptera	35	28	40	27	36	9	7	1	0	132	27	61	3	12	3	0	9	1	1
Unk. Trichoptera	0	0	0	0	6	0	0	0	0	0	0	0	0	0	0	0	0	0	0
Hydroptila	1	0	0	0	0	0	0	0	0	0	0	0	0	0	0	0	0	0	0
Oxyethira	0	1	0	0	0	0	0	0	0	112	0	0	0	0	0	0	0	0	0
Lepidostoma	0	0	0	0	0	0	0	0	0	0	0	0	0	0	3	0	0	0	1
Lepidostoma cinereum	0	0	0	0	0	0	0	0	0	0	0	3	0	0	0	0	0	0	0
Clistoronia	16	0	0	0	0	0	0	0	0	0	0	0	0	0	0	0	0	0	0
Clostoeca disjuncta	0	0	0	0	0	0	0	0	0	0	0	1	0	1	0	0	0	0	0
Glyphopsyche irrorata	0	0	0	0	0	0	0	0	0	1	0	0	0	0	0	0	0	0	0
Halesochila taylori	0	1	0	0	0	0	0	0	0	0	0	0	0	0	0	0	0	0	0
Lenarchus rho	0	4	0	1	1	0	3	0	0	0	3	0	0	0	0	0	0	0	0
Lenarchus vastus	0	12	36	0	5	9	3	0	0	0	0	4	0	0	0	0	4	0	0

Table 4-6. Diversity and richness of aquatic/semi-aquatic arthropod and Chironomidae communities found at 19 wetland sites in King County, Washington.

Diversity and Richness: All Aquatic/Semi-Aquatic Taxa Except Brachycera

	Non-Urbanized							Moderately Urbanized										Highly Urbanized	
	Perennial				Dry in Summer			Perennial			Dry in Summer							Perennial	
Wetland	MGR36	RR5	HC13	SR24	PC12	AL3	NFIC12	TC13	ELW1	BBC24	ELS61	LCR93	LPS9	SC4	JC28	SC84	ELS39	B3I	FC1
Taxa richness	40	52	40	47	52	21	20	27	27	62	47	62	22	29	39	29	21	31	34
Annual adult yield per m2	4433	7732	6585	5082	5407	1852	5884	3614	655	8570	15340	6761	3969	2065	1064	2307	6332	2139	3159
Shannon Diversity Index (log 2	4.27	2.76	3.04	4.13	3.83	3.1	2.27	2.73	3.12	3.72	2.6	4.2	2.48	2.58	3.53	3.19	1.79	3.08	2.98
Pielou Evenness Index	0.803	0.48	0.57	0.74	0.67	0.71	0.53	0.57	0.66	0.624	0.467	0.71	0.56	0.53	0.67	0.66	0.41	0.62	0.59

Diversity and Richness: All Chironomidae Taxa

Wetland	MGR36	RR5	HC13	SR24	PC12	AL3	NFIC12	TC13	ELW1	BBC24	ELS61	LCR93	LPS9	SC4	JC28	SC84	ELS39	B3I	FC1
Taxa richness	28	38	23	34	35	11	8	16	19	42	29	32	11	16	26	19	9	19	22
Annual adult yield per m2	3368	7207	3013	4265	4921	1247	4752	3207	171	8228	11925	2316	651	816	756	1863	2760	1513	2699
Shannon Diversity Index (log 2	3.83	2.4	2.54	3.56	3.44	1.67	1.44	2.18	2.88	3.49	1.7	3.07	1.79	1.4	2.66	2.45	0.87	2.42	2.31
Pielou Evenness Index	0.798	0.46	0.56	0.7	0.67	0.48	0.48	0.54	0.68	0.648	0.35	0.62	0.52	0.35	0.57	0.58	0.28	0.57	0.52

versity and Richness: Chironomidae Taxa without Unidentified Females

Wetland	MGR36	RR5	HC13	SR24	PC12	AL3	NFIC12	TC13	ELW1	BBC24	ELS61	LCR93	LPS9	SC4	JC28	SC84	ELS39	B3I	FC1
Taxa richness	24	34	19	30	31	8	6	13	15	38	26	28	10	13	22	16	7	16	18
Annual adult yield per m2	1726	1989	1062	1905	2993	215	1175	1172	56	4099	3000	861	226	212	379	864	608	777	689
Shannon Diversity Index (log 2	3.71	3.88	3.06	3.61	2.99	1.77	1.2	2.2	3.4	3.85	2.48	3.64	2.58	1.53	2.64	1.94	0.44	2.65	2.67
Pielou Evenness Index	0.809	0.76	0.72	0.74	0.6	0.59	0.46	0.59	0.87	0.734	0.528	0.76	0.78	0.41	0.59	0.49	0.16	0.66	0.64

Table 4-7. Annual adult Chironomidae yield (per M^2) from 19 wetlands in King County, Washington, as measured with 3 emergence traps (0.25 M^2 area) at each wetland site, run continuously between September 1988 and September 1989.

	CHIRONOMIDAE TAXA																		
	Non-Urbanized								Moderately Urbanized									Highly Urbanized	
	Perennial					Dry in Summer			Perennial			Dry in Summer						Perennial	
TAXON	MGR36	RR5	HC13	SR24	PC12	AL3	NFIC12	TC13	ELW1	BBC24	ELS61	LCR93	LPS9	SC4	JC28	SC84	ELS39	B3I	FC1
Diptera/Chironomidae																			
Boreochlus	145	0	8	0	0	0	0	0	0	0	0	0	0	3	0	0	0	0	0
Total Podonominae	145	0	8	0	0	0	0	0	0	0	0	0	0	3	0	0	0	0	0
Odontomesa	0	0	0	0	0	0	0	0	0	0	0	0	0	0	4	0	0	7	0
Prodiamesa	0	0	0	0	0	0	0	0	0	0	0	0	0	0	0	0	0	169	0
Total Prodiamesinae	0	0	0	0	0	0	0	0	0	0	0	0	0	0	4	0	0	176	0
Brillia	15	0	0	0	1	0	0	0	9	5	5	9	0	0	7	0	0	73	1
Chaetocladius	0	0	0	0	0	0	0	0	0	0	0	0	0	0	0	0	0	1	0
Corynoneura	161	40	35	523	83	0	0	1	0	40	11	37	0	0	17	0	0	0	24
Cricotopus	0	0	0	65	24	0	0	0	1	25	0	0	0	0	0	0	0	63	0
Cricotopus bifurcatus	0	0	0	0	0	0	0	0	3	0	0	0	0	0	0	0	0	0	0
Doithrix	0	0	0	0	0	0	0	0	0	0	0	0	0	1	0	0	0	0	4
Limnophyes	103	531	261	36	51	124	849	167	7	12	799	289	67	160	152	63	574	12	133
Mesosmittia	0	0	0	0	0	0	0	0	0	0	0	0	0	0	0	1	0	0	0
Metriocnemus	0	0	0	17	0	0	0	0	4	1	13	13	21	1	0	0	4	75	3
Nanocladius	0	43	0	0	0	0	0	0	0	8	0	39	0	0	1	0	0	0	0
Orthocladius	0	83	1	36	0	0	0	0	0	21	0	29	0	0	8	3	0	0	0
Parakiefferiella	0	0	0	0	0	0	0	0	1	0	0	3	0	3	0	0	0	0	0
Parametriocnemus	0	188	24	16	3	0	0	7	1	0	1439	29	7	1	11	0	0	1	0
Paraphaenocladius	17	0	0	0	0	0	1	0	0	0	0	0	0	0	0	0	0	1	0
Poryophaenocladius	0	0	0	0	0	0	0	0	0	5	0	0	0	0	0	0	0	0	0
Psectrocladius	1	285	0	11	32	0	0	15	0	21	15	0	0	0	0	0	0	0	0
Pseudosmittia	0	29	273	0	0	0	1	385	0	0	71	4	9	7	5	425	8	1	4
Rheocricotopus	0	0	3	0	1	0	0	0	0	0	1	29	43	0	1	1	0	0	0
Smittia	0	0	111	0	0	12	121	0	0	0	9	19	55	17	0	5	4	0	0
Thienemanniella	39	0	0	0	17	0	0	8	0	44	0	7	0	0	0	1	0	0	0
Orthocladiinae m.	3	73	5	5	17	0	0	3	1	0	4	53	19	5	4	0	2	253	0
Orthocladiinae fm.	657	4612	1632	877	512	716	3240	1685	77	119	8429	1083	423	583	325	721	2148	727	1395
Total Orthocladiinae	1004	5884	2345	1587	741	852	4213	2271	105	303	10796	1644	643	779	532	1221	2740	1208	1564
Chironomus decorus gr.	111	64	87	19	13	52	188	229	0	29	16	1	0	8	1	281	4	0	267
Chironomus riparius	0	0	0	0	0	1	0	0	0	0	0	0	0	0	0	0	0	0	0
Cladopelma viridula	0	20	0	7	1	0	0	0	0	68	0	0	0	0	0	0	0	1	0
Demicryptochironomus nr	0	0	0	5	0	0	0	0	0	0	0	0	0	0	0	0	0	0	0
Dicrotendipes	0	4	0	8	11	0	0	0	0	47	27	0	0	0	0	3	0	0	0
Endochironomus nigrican	0	5	0	56	24	0	0	0	0	19	71	3	0	0	0	1	0	0	0
Endochironomus subtend	0	0	0	0	4	0	0	0	0	0	0	0	0	0	0	0	0	0	0
Glyptotendipes	0	1	0	79	5	0	0	0	0	104	0	0	0	0	0	0	0	0	0
Kiefferulus dux	0	0	48	0	0	0	0	0	0	0	0	0	0	0	0	0	0	0	0
Microtendipes pedellus va	12	0	0	0	0	0	0	0	0	113	0	0	0	0	0	0	0	0	0
Microtendipes pedellus va	0	28	0	0	0	0	0	0	0	343	0	0	0	0	0	0	0	0	0
Parachironomus monochr	0	0	0	0	0	0	0	0	0	0	0	0	0	0	0	0	0	0	1
Parachironomus cf. forcep	0	4	0	0	0	0	0	0	0	0	0	0	0	0	0	0	0	0	0
Parachironomus sp. 1	0	44	0	4	0	0	0	0	0	0	0	0	0	0	0	0	0	0	0
Parachironomus sp. 2	0	47	0	15	0	0	0	0	0	7	1	5	0	0	0	0	0	0	0
Paratendipes	0	0	0	0	0	0	0	0	0	0	0	8	0	0	21	0	0	0	0
Paratendipes albimanus	3	0	0	0	0	0	0	0	0	8	0	0	0	0	0	0	0	0	0
Phaenopsectra flavipes	3	7	0	0	17	0	0	0	0	5	0	0	0	0	1	3	0	0	3
Phaenopsectra punctipes	0	0	1	0	0	0	0	0	0	4	3	0	0	0	0	0	0	0	0
Polypedilum illinoense	0	4	0	0	0	0	0	0	11	13	19	0	0	0	0	0	0	0	0
Polypedilum ophioides	0	0	0	0	0	0	0	0	0	13	0	0	0	0	0	0	0	0	0
Polypedilum cf. simulans	0	0	0	0	0	0	0	0	1	0	0	0	0	0	0	0	0	0	0
Polypedilum gr. 1	105	109	95	128	851	16	15	7	4	864	128	28	1	4	13	19	0	0	55
Polypedilum gr. 2	0	71	0	65	61	0	0	1	0	419	72	0	3	0	0	0	0	0	0
Stictochironomus	0	48	0	0	0	0	0	0	0	0	0	0	0	0	1	0	0	0	3
Xestochironomus	0	0	0	0	0	0	0	0	0	5	0	0	0	0	0	0	0	0	0
Unk. Chironomini genus	0	0	0	0	0	0	0	0	0	0	0	4	1	0	0	0	0	0	0
Chironomini m.	0	0	0	1	0	0	0	0	0	0	0	0	0	0	0	0	0	0	0
Chironomini fm.	253	400	232	540	680	184	336	347	23	1420	381	116	3	17	43	220	4	4	528
Total Chironomini	487	856	463	927	1668	253	539	584	39	3481	717	165	8	29	81	527	8	5	856

Table 4-7 Continued.

TAXON	MGR36	RR5	HC13	SR24	PC12	AL3	NFIC12	TC13	ELW1	BBC24	ELS61	LCR93	LPS9	SC4	JC28	SC84	ELS39	B3I	FC1
Chironomidae cont.																			
Ablabesmyia	57	33	0	335	35	0	0	0	0	275	68	1	0	0	0	0	0	0	11
Apsectrotanypus algens	129	3	0	0	0	0	0	0	0	80	0	15	0	0	117	0	0	0	0
Conchapelopia cf. currani	15	1	0	0	1	0	0	0	0	51	0	0	0	0	0	0	0	3	0
Conchapelopia dusena	0	0	1	0	0	0	0	0	0	0	0	0	0	0	0	0	0	112	8
Djalmabatista	0	3	0	0	0	0	0	0	0	0	0	0	0	0	0	0	0	0	0
Hayesumyia serata	0	0	0	0	0	0	0	0	1	0	0	0	0	0	0	0	0	0	0
Labrundinia	0	0	0	0	0	0	0	0	0	75	0	0	0	0	0	0	0	0	0
Larsia	0	51	1	36	5	0	0	0	0	0	0	0	0	0	0	0	0	0	3
Meropelopia nr. american	0	0	0	0	0	0	0	0	7	0	0	0	0	0	0	0	0	0	0
Natarsia miripes	0	0	0	0	0	0	0	0	0	0	0	111	0	0	3	0	0	0	0
Procladius bellus	0	59	0	8	5	0	0	0	0	0	0	0	0	0	0	0	0	0	1
Procladius nr. freemani	0	31	0	88	661	0	0	0	0	96	3	0	0	0	0	0	0	0	0
Procladius nr. sublettei	16	1	0	11	11	0	0	0	0	141	0	0	0	0	0	0	0	0	0
Procladius n. sp.?	0	0	0	1	0	0	0	0	0	0	0	0	0	0	0	0	0	0	0
Paramerina smithae	161	7	0	12	3	0	0	0	0	21	4	19	0	0	3	0	0	0	0
Psectrotanypus dyari	77	1	11	137	656	5	0	345	4	96	28	4	0	0	0	12	0	0	111
Tanypus cf. parastellatus	0	0	0	0	4	0	0	0	0	0	0	0	0	0	0	0	0	0	0
Zavrelimyia fastuosa	0	0	0	0	0	0	0	0	0	0	0	0	0	0	1	0	0	0	0
Zavrelimyia sinuosa	0	0	0	0	0	0	0	0	0	0	61	0	0	0	0	0	0	0	0
Zavrelimyia thryptica	133	0	5	0	35	4	0	0	0	5	104	9	0	1	4	1	0	0	13
Macropelopiini m.	3	0	0	0	0	0	0	0	0	0	0	0	0	0	0	0	0	1	0
Macropelopiini fm.	0	0	0	0	0	0	0	0	0	0	0	0	0	0	0	0	0	4	0
Pentaneurini m.	0	0	0	0	0	0	0	0	0	0	0	0	0	0	0	0	0	0	0
Pentaneurini fm.	283	64	13	75	33	4	0	0	1	19	7	113	0	3	3	0	0	7	9
Total Tanypodinae	875	253	32	703	1449	13	0	345	13	859	275	272	0	4	131	13	0	127	156
Micropsectra gr. 1	384	0	75	19	257	0	0	1	1	67	12	21	0	0	0	4	12	0	44
Micropsectra gr. 2	16	19	17	1	84	0	0	3	0	149	16	43	0	0	1	41	0	0	0
Rheotanytarsus	0	0	0	0	0	1	0	0	0	0	0	0	0	0	0	0	0	0	0
Tanytarsus	17	52	0	161	20	0	0	0	0	800	0	29	0	0	3	0	0	0	0
Tanytarsini fm.	407	141	76	827	701	0	0	3	12	2552	108	141	0	1	4	51	0	0	77
Total Tanytarsini	824	212	168	1008	1063	1	0	7	13	3588	136	235	0	1	8	96	12	0	121

CHAPTER 5 AMPHIBIAN DISTRIBUTION, ABUNDANCE AND HABITAT USE

by Klaus O. Richter and Amanda L. Azous

INTRODUCTION

Amphibians are a diverse vertebrate class in forests, wetlands and undisturbed areas. Although their role in ecosystem dynamics has not been intensively studied, their potential abundance suggest significant roles in energy transfers and nutrient cycling. Burton and Likens (1975) in the Hubbard Brook Experimental Forest of New Hampshire found salamander (primarily Plethodon cinereus) numbers to regularly exceed 2,000 per hectare, with concomitant biomass at 1.65 kg per hectare, equaling that of small mammals and twice that of birds. Amphibians also reduce eutrophication of wetlands by their net export of nitrogen. At some wetlands the nitrogen in tadpoles is more than double that of residual pond nitrogen. Furthermore, amphibians in some wetlands (e.g., Rana pipiens, R. catesbeiana, and Ambystoma spp.) collectively export six to 12 times more nitrogen from the ponds than imported through spawning by breeding adults (Seale 1980). Finally, tadpoles also reduce the biomass of nitrogen-fixing blue-green algae and primary production by feeding on all forms of algae (Seale 1980, Beebee 1996).

Some King County wetlands are used by breeding western toads (Bufo boreas) and red-legged frogs (Rana aurora) that produce thousands of eggs and larvae and hundreds of metamorphs and juveniles. At these sites algae-grazing frog and toad tadpoles may significantly influence water nutrient and energy dynamics and provide food for larger aquatic invertebrates and fish. Although salamanders spawn fewer eggs than frogs and toads, their invertebrate-eating larvae also play important roles in aquatic composition and predator-prey relationships. Hundreds of metamorphs are pivotal in transferring biomass from wetland to adjacent terrestrial systems and become prey for reptiles, birds and mammals.

Along with our recognition of the increasing ecological importance of amphibians, studies have shown significant decreases of some populations and extinctions of others (Corn 1994). These declines, however, have been difficult to document because of inadequate information on the geographic distributions and abundances of populations.

The occurrence of Northwest amphibians noted on range maps (Leonard et al. 1993) and spot maps (Nussbaum et al. 1983) indicates a potential of 14 species in King County, 12 of which are associated with aquatic environments and 10 particularly with marshes, swamps, bogs and other wetlands. Recently, we (Richter and Azous 1995) sighted 10 species (e.g., seven lentic-breeding, one lotic-breeding and two terrestrial-breeding) during a two-year survey of 19 wetlands in the Puget Sound Basin. Furthermore, we reported that their distribution was unrelated to wetland characteristics of size, vegetation classes, presence of vertebrate predators and water permanence. Correspondingly, from our watershed land cover analysis we found that larger water level fluctuations resulting from higher impervious areas in highly urbanized watersheds accounted for decreasing species richness.

This paper describes the geographic distribution and relative abundance of amphibians within these 19 palustrine wetlands after an additional two years of surveys in 1993, and

1995. Its companion paper, Chapter 12, reports on the effects of watershed development and habitat conditions on amphibian populations within these wetlands.

METHODS

Information about the locations and physical, hydrologic, chemical and vegetative conditions found in the study wetlands is presented in Section 1 and Chapters 1, 2, and 3 of Section 2.

We determined the distribution of amphibians primarily by autumn pitfall trapping when amphibians are more active than during the summer, and during which time animals migrate to winter hibernacula,. Egg mass sightings, aquatic funnel trapping and fortuitous observations by knowledgeable biologists at the sites for other monitoring purposes augment our distribution data. Relative abundances of trapable species (no Pacific treefrogs) were determined from the results of 14-day autumn pitfall trapping surveys standardized for equal trap nights and for favorable climatic conditions such as temperatures above 4°C (Beebee 1996). Site selection and trap installation procedures are described in Richter and Azous (1995). Trapped amphibians were identified to species and released.

Spring egg surveys were used to determine amphibian breeding in wetlands. Briefly, these included February through April searches of shoreline to 1-m deep palustrine aquatic bed (PAB) and shoreline palustrine scrub-shrub (PSS), palustrine emergent (PEM) and palustrine forested (PFO) habitat types. Detailed survey descriptions are provided in Richter and Roughgarden (1995). We also captured some species in aquatic funnel traps (Richter 1995) within some wetlands to augment diversity data.

We determined wetland boundaries, wetland size, habitat types and land cover conditions within the wetland's watershed and within select distances of each wetland. This data was obtained from King County's Wetlands Inventory, King County Surface Water Management Division's GIS system , and the 1992 Landsat Thematic Mapper for the Puget Sound Region (King County 1990, Puget Sound Regional Council 1994). From Landsat images we identified and characterized ten cover types: 1) impervious surfaces, 2) freeway/parking/gravel areas, 3) cleared land, 4) grasslands/golf courses, 5) multi-family housing, 6) single family residential, 7) single family forest, 8) agriculture/pasture lands, 9) forests, and 10) open water. These were collapsed into favorable amphibian breeding, feeding, migration and hibernation habitat (cover types 7-10) and unfavorable types (cover types 1-6).

We identified habitat structure categories (e.g., aquatic bed, herbs, shrubs and trees) according to Cowardin et al. (1979) from aerial photos recorded on maps (King County 1987), and refined those designations with field surveys that sampled vegetation along transects that crossed the hydrologic gradients represented in the wetlands. Life history characteristics discussed in the text were taken from Nussbaum et al. (1983) and our own observations (Richter and Roughgarden 1995, Richter 1996a, Richter 1996b).

RESULTS

Ten amphibian species, representing all but one (spotted frog) of the regional amphibian fauna, were identified at the 19 wetlands studied. Eight amphibian species was the highest richness found (at SR24) and included the introduced bullfrog. Seven species, the greatest number of native species at a wetland, and representing 70% of the total

potential native amphibian species, were identified at HC13, PC12 and SR24 east of Lake Sammamish. ELW1 had only one species captured, the bullfrog. Most wetlands exhibited five (50%) of the total potential native species. The most urbanized and isolated wetlands (B3I, FC1 and ELW1) had the lowest richness. Unexpected, however was the low richness at TC13 and RR5, relatively large wetlands in watersheds without extensive development. The proportional distribution of native amphibian richness within all wetlands is provided in Figure 5-1.

Sighted at 18 out of 19 wetland, the Pacific treefrog is likely the most broadly distributed amphibian (Table 5-1). Red-legged frogs, Northwestern salamanders, and long-toed salamanders were found in 16, 15 and 13 (84%, 79% and 68%respectively) of the wetlands surveyed. Of the two terrestrial-breeding buffer species Ensatina was found in 11 (58%) and Western red-backed salamanders in nine (47%) of wetlands.

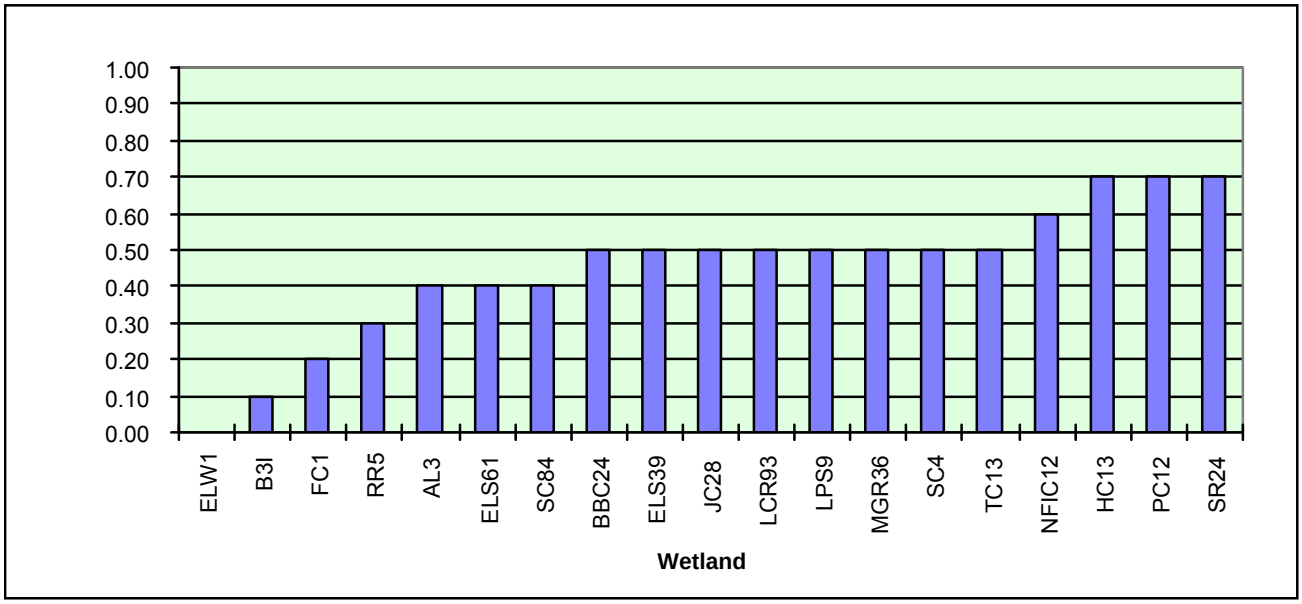

Figure 5-1. Proportional distribution of native amphibian richness within wetlands.

Table 5-1. Total amphibian fauna found in palustrine wetlands of the Puget Sound Basin.

Common Name	Scientific Name	Ames Lake 3	Bellevue 3l	Big Bear Creek 24	East Lake Sammamish 39	East Lake Sammamish 61	East Lake Washington 1	Forbes Creek 1	Harris Creek 13	Jenkin's Creek 28	Lower Cedar River 93	Lower Puget Sound 9	Middle Green River 24	North Fork Issaquah Creek 12	Patterson Creek 12	Raging River 5	Snoqualmie River 24	Soos Creek 4	Soos Creek 84	Tuck Creek 13	Percent of All Wetlands Species Was Present
Bullfrog	*Rana catesbeiana*			●		●	●	●	●					●			●			●	0.42
Ensatina	*Ensatina eschscholtzii*	●		●	●			●	●	●	●			●	●		●	●			0.58
Long-toed Salamander	*Ambystoma macrodactylum*	●	●		●	●		●	●		●	●	●		●		●		●	●	0.68
Northwestern Salamander	*Ambystoma gracile*			●	●	●			●	●	●	●	●	●	●	●	●	●	●	●	0.79
Pacific Giant Salamander	*Dicamptodon tenebrosus*														●		●				0.11
Pacific Treefrog	*Pseudacris regilla*	●	●	●	●	●		●	●	●	●	●	●	●	●	●	●	●	●	●	0.95
Red-legged Frog	*Rana aurora*	●		●	●	●			●	●	●	●	●	●	●	●	●	●	●	●	0.84
Roughskin Newt	*Taricha granulosa*			●		●				●											0.16
Western Red-backed Sa	*Plethodon vehiculum*	●		●					●	●	●	●	●					●	●		0.47
Western Toad	*Bufo boreas*								●						●	●	●				0.21

Spawn of the eggs of four species with large and readily identifiable eggs (Northwestern salamander, long-toed salamander, red-legged frog and Pacific treefrog) were identified at four wetlands, confirming breeding by these species at these sites. In contrast, eggs of the Western toad were not observed at any wetland, although metamorphs were sighted at BBC24 and RR5, corroborating that these wetlands are used by breeding toads. Though historically considered wide-spread (Nussbaum et al. 1983) roughskin newts were sighted in only three (16%) wetlands.

Lentic breeding species, as expected, were largely absent from wetlands with higher current velocities and channelized flows to which they are not well suited. High current velocity and water level fluctuations may thwart successful spawning, embryogenesis or larval survival of lentic breeding species. However, one lotic-breeding species, the Pacific giant salamander, was captured at PC12. Presumably, this animal was spawned in adjoining Patterson Creek, a cool, fast-running stream, similar to ones in which this species traditionally breeds.

We did not find spotted frogs, a native species. Historically never abundant in the Puget Sound Basin (McAllister and Leonard 1990, McAllister and Leonard 1991) spotted frogs were, nevertheless, expected at remote and undisturbed wetlands such as LCR93, MGR36, SR24 and RR5.

Bullfrogs were identified in several wetlands and in several drainages including Lake Sammamish (ELS61, NFIC12), Bear Creek (BBC24), Snoqualmie River (SR24), Tuck Creek (TC13), East Lake Washington (ELW1) and Harris Creek (HC13) drainages. Green frogs, another introduced species known to be in King County, were not seen within our wetlands. No native amphibians were captured in ELW1 although Pacific treefrogs were heard vocalizing. Although adult red-legged frogs were captured in

pitfalls at AL3, neither spawn nor juveniles were observed during spring egg searches and summer site visits.

There were significant differences between the abundance of species captured within wetlands between 1988 and 1995. 1988 and 1989 were ranked similarly with average capture rates of 2.8 and 4.1 individuals per 100 trap nights respectively but differed significantly from 1993 and 1995 in which average capture rates were 0.8 and 1.5, respectively (Friedman test, $\chi 2 = 19.6$, $p = .0002$). Over the study period, the number of amphibian captures per 100 trap nights declined in 12 of the 19 wetlands. Six wetlands showed the highest capture rates in 1989 and then declined. Only one wetland, SC84, showed a slight 0.3 increase in capture rate between 1988 and 1995 (Figure 5-2).

Overall, the most abundant amphibian captured in pitfall traps was the red-legged frog, with particularly high capture rates in 1988 and 1989. Long-toed salamanders, Northwestern salamanders and Western red-backed salamanders were also numerically important. Capture rates of individual species in wetlands for each study year ranged from a high of 9.7, representing 29 Northwestern salamander captured in one night at one wetland, BBC24, in 1989 to the most frequent capture rate of 0.33, representing one individual of one species captured in a wetland for one year's trapping period. Captures of the same species in different years was unpredictable. The number of captures per 100 trap nights, summarized for each species across all wetlands in Figure 5-3, varied but statistical significance could not be evaluated due to the low number of captures. With the exception of Northwestern salamander, long-toed salamander, Ensatina and red-legged frog, species capture rates were 2 individuals or fewer most years. Appendix Table 5-1 gives the capture rates of individual species for each study year in individual wetlands.

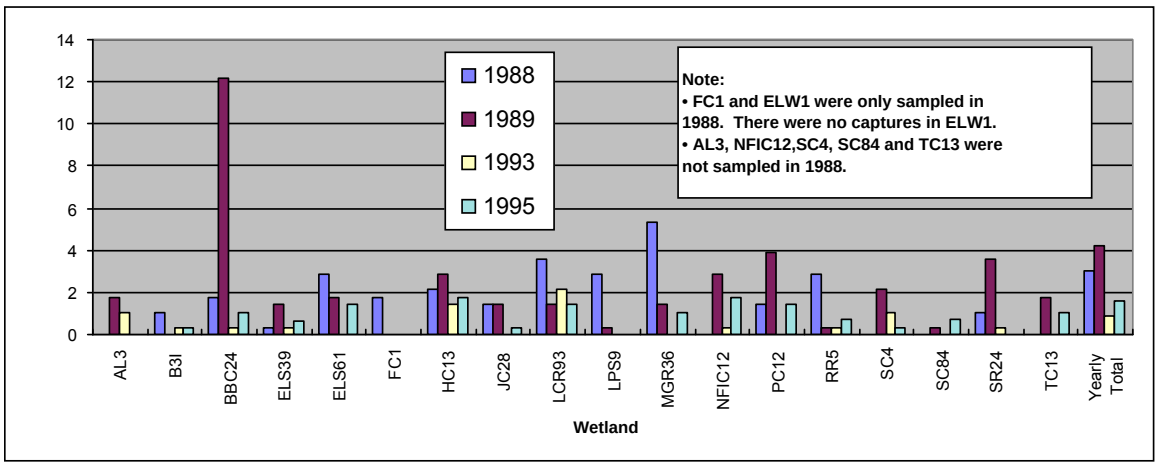

Figure 5-2. The number of total amphibian captures per 100 trap nights by wetland for each year of the study.

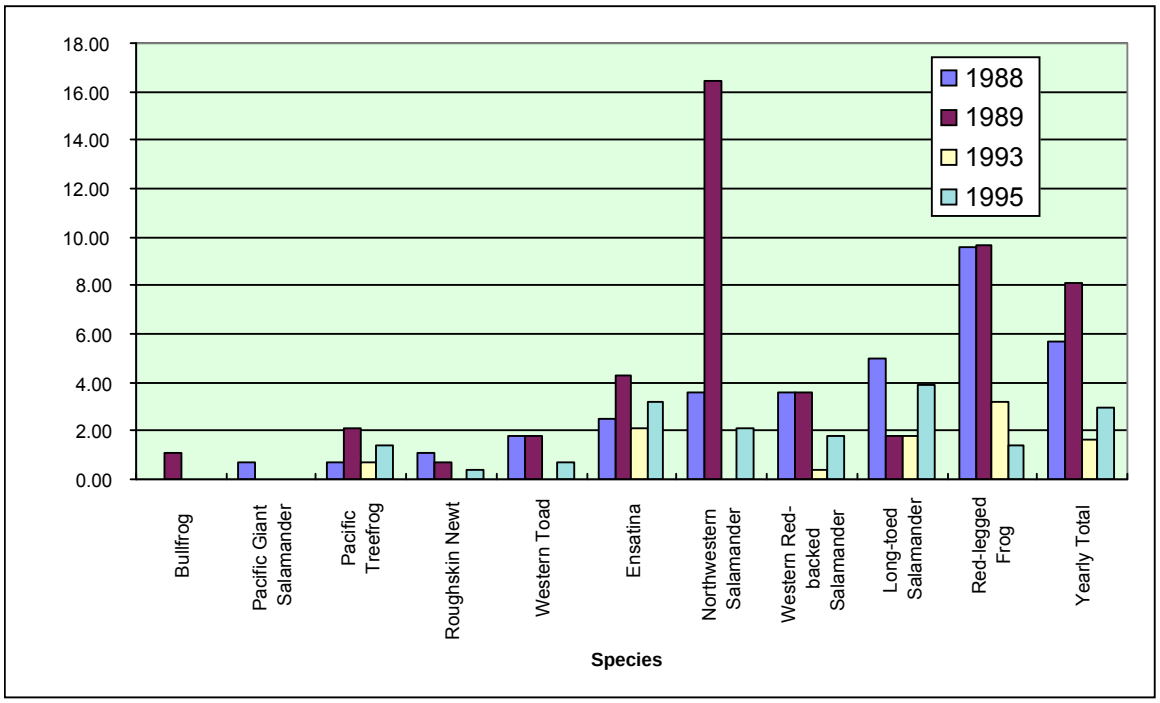

Figure 5-3. Number of captures per 100 trap nights for each species.

Land use in the watersheds of wetlands was related to amphibian richness. Wetlands with contributing watersheds in which more than 40 % of the land area was developed (usually housing with some commercial developments) were significantly more likely to have low amphibian richness of less than four species than wetlands within less urbanized watersheds, (Figure 5-4) ($\chi 2$, $P < 0.01$). Three wetlands with the highest native amphibian richness of more than 60% of all species observed, had very low watershed urbanization (less than 5%). Thirteen wetlands with medium amphibian richness of 40% to 60% of all species observed had urbanization ranging up to 90%. Three of the five wetlands with the highest urbanization had four or fewer species.

Since land use within the watershed wetland would directly affect hydrologic patterns in a wetland, we also evaluated whether minimum water levels, maximum water levels or the average range of fluctuation affected the richness of amphibian communities. Only average water level fluctuation (WLF) showed a statistically significant relationship with amphibian richness. When average WLF was 20 cm or more during the year, the number of amphibian species averaged three or fewer. Wetlands with lower WLFs (less than 20 cm) were significantly more likely to have a higher proportion of the potential amphibian richness, averaging five species (Mann Whitney, $p = 0.047$) (Figure 5-5).

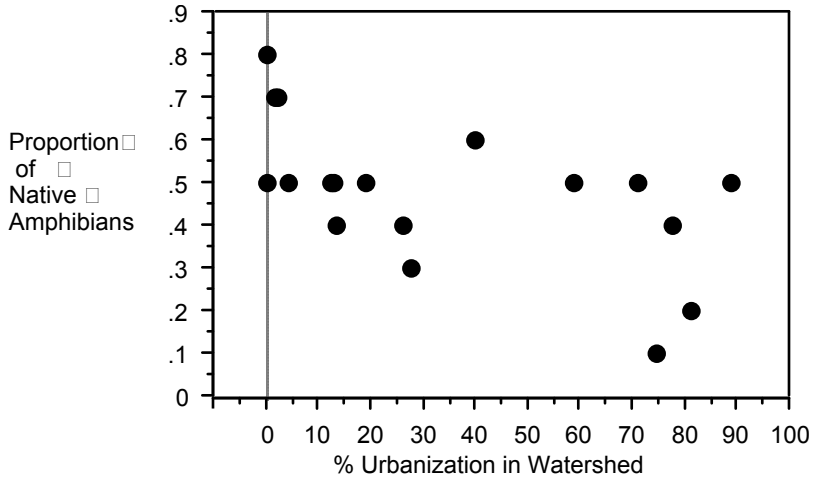

Figure 5-4. Relationship between the percent of native amphibian species present and percent of watershed urbanization.

Land use adjacent to a wetland was also found to be related to the richness of native amphibian populations. When land use within concentric areas of 10, 100, 500 and 1000 meters from the wetland were examined for statistically significant relations with amphibian richness we found that, within the distance encompassed by the 10 to 1000 M radii, amphibian richness was related to the percentage of favorable land available. Figure 5-6 shows the proportion of native species observed related to the percent of forest land within 10, 100, 500 and 1000 M of the wetland edge. In general, those wetlands which are adjacent to a high percentage of forest land were more likely to have richer populations of native amphibians. The significance of this relationship was weakest at 10 M ($R = 0.57$, $p = 0.01$) and strongest at 500 M ($R = 0.66$, $P = 0.004$). The graph shows that almost all wetlands had high proportions of forest land within 10 M and to a lesser extent at 100 M. But amphibian richness is highest in wetlands that retain at least 60% of adjacent area in forest land up to and exceeding 500 M. from the wetland and lowest in the wetlands that had a high proportion of forest land within 10 or 100 M but dropped significantly at 500 M and further from the wetland.

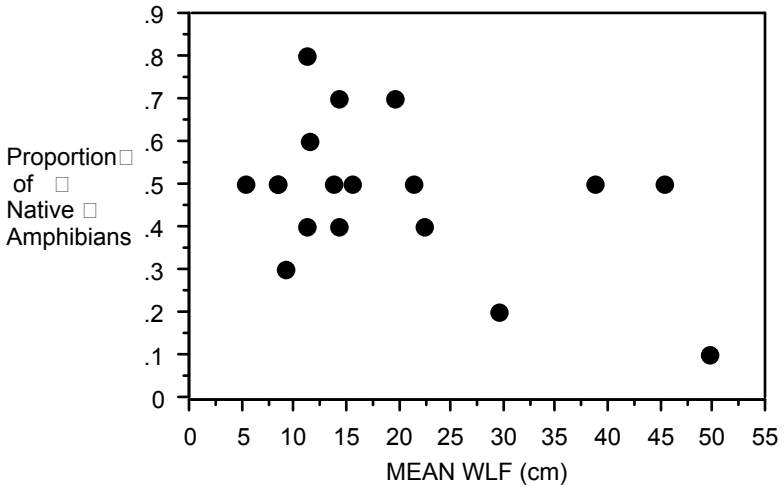

Figure 5-5. Relationship between the percent of possible amphibian species and average water level fluctuation.

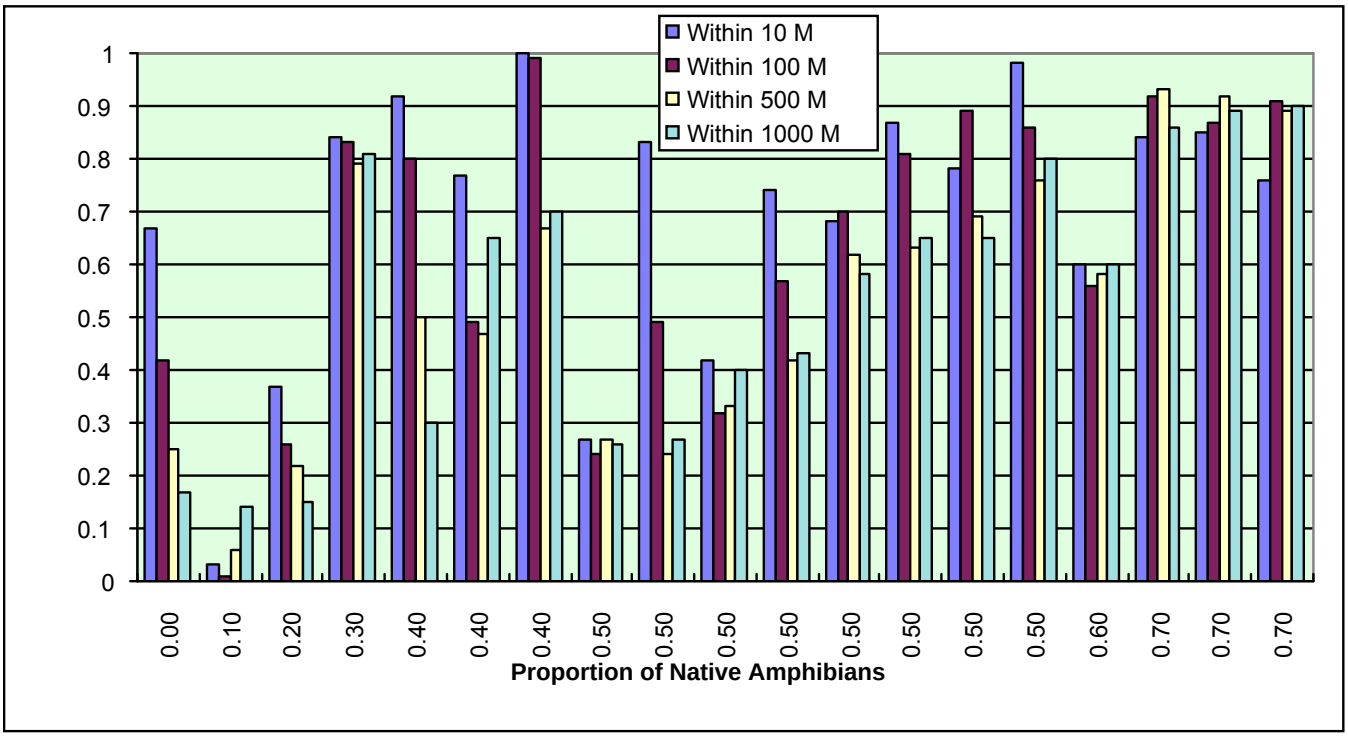

Figure 5-6. Plot of amphibian richness and the percent of favorable adjacent land.

DISCUSSION

Despite the low overall richness of amphibians within Puget Sound lowland palustrine wetlands when compared to the southeast (Gibbons and Semlitsch 1991) and central states (Clarke 1958, Clawson and Baskett 1982), the biomass of existing species may be high. The capture of 29 Northwestern salamander at one wetland on one night

clearly shows the numerical importance of this salamander, and underscores the ecological significance of amphibians in general, moreover, it demonstrates the abundance of this species at a site which, when censused on other nights, would falsely suggest fewer individuals. Other species are also likely to be significantly more abundant than the capture data suggest.

This research supports our earlier analysis of capture and observation data collected from 1988 to 1991 (Richter and Azous 1995) in that no new species were identified in 1993 or 1995. Consequently, our recent studies also show no relationships between the number of amphibian species and wetland size or the number of Cowardin et al. (1979) habitat classes. These data also confirmed the relationship we found in earlier years between spawning and select vegetation classes, showing that amphibians spawn within the thin stemmed (non-cattail) emergent zone and with salamanders particularly selecting thin-stemmed emergent vegetation and tiny branches and root hairs of submerged vegetation on which to spawn (Richter and Roughgarden 1995).

Our study shows large differences in amphibian richness, using diverse survey techniques, and varying abundance (captures per 100 trap nights) between the survey years suggesting that multiple year studies are a prerequisite to the accurate identification of a wetlands' amphibian fauna. Explanations accounting for the dramatic differences could be weather related, as almost all the wetlands we studied responded with similar declines in richness and abundance over the study period. Pechmann et al. (1991) and Hairston (1987), in analyzing data from long term studies, show that for many amphibians, populations normally fluctuate dramatically over short periods but remain stable over longer periods of five to ten years. The extent to which distinct local populations, such as those found in our wetlands, vary asynchronously within a given year and for what reasons remain to be investigated.

We also found differences in amphibians identified at wetlands depending on survey technique, suggesting that multiple methods should be employed to accurately assess a wetland's amphibian population. For example, Pacific treefrogs were not captured in pitfalls anywhere, and large numbers of Northwestern salamanders that were breeding at SR24 were never captured in pitfalls. Similarly, we captured roughskin newts in funnel traps at ELS61 in early spring but never saw or captured them in pitfall traps. Also significant is that wetlands in which adults were captured in pitfalls were not observed to have spawn. Pitfalls on either side of drift fences totally encircling wetlands would be a good method of capturing most species and measuring abundances but was not feasible in a study of thisd many wetlands.

Our estimates of the number of captures per 100 trap nights appear similar to amphibian capture data elsewhere in the Northwest (McComb et al. 1993a, McComb et al. 1993b, Aubry and Hall 1991). However, differences in habitats used, timing of censuses and field techniques, including the possibility of counting recaptures in our study, do not allow direct statistical comparisons of our results with those of others.

The reduced richness of amphibians in wetlands with highly urbanized watersheds is likely due, in part, to differences in hydrologic patterns related to land use. Average WLF increases as the frequency of peak flood events increases. Such conditions may result in a frequently wet buffer affecting habitat for terrestrial breeders which prefer well drained soils that are not extremely wet, and tend to avoid soaked or flooded sites (Aubry and Hall 1991, Gilbert and Allwine 1991). Low numbers in wet riparian as opposed to dryer upland habitats have, for example, been documented with Ensatina (E.

eschscholtzii) in red alder (McComb et al. 1993a, McComb et al. 1993b), second-growth conifer (Gomez and Anthony 1996) and unmanaged Douglas-fir (Aubry and Hall 1991, Gilbert and Allwine 1991) stands. Aquatic and semi-aquatic breeders may be similarly affected by the increased frequency of flooding in that flooded habitats with high water level fluctuation may have less large downed woody material, litter and other organic material that provide food, cover and oviposition sites. Clearly, hydrology may account for the richness of the amphibian communities in the wetlands we studied, but may, in addition, be related to the proportion of adjacent area comprised of favorable habitat.

REFERENCES

Aubry, K. B., and P. A. Hall. 1991. Terrestrial amphibian communities in the Southern Washington Cascade Range. Pages 327-338. In K. B. Aubry and M. H. Brookes, (eds.). Wildlife and Vegetation of Unmanaged Douglas-Fir Forests. U.S. Forest Service, Pacific Northwest Research station, Portland, OR, USA.

Beebee. 1996. Ecology and Conservation of Amphibians. Chapman & Hall, London, UK.

Brown, R. E. 1985. Management of Wildlife and Fish Habitats in the Forests of Western Oregon and Washington. U. S. Forest Service, Pacific Northwest Region, Portland, OR, USA.

Burton, T. M., and G. E. Likens. 1975. Salamander populations and biomass in the Hubbard Brook Experimental Forest, New Hampshire. Copeia 3:541-546.

Clarke, R. F. 1958. An ecological study of reptiles and amphibians in Osage County, Kansas. The Emporia State Research Studies 7:1-52.

Clawson, M. E. and T. S. Baskett. 1982. Herpetofauna of the Ashland wildlife area, Boone County, Missouri. Transactions, Missouri Academy of Science 16:5-16.

Corn, P. S. 1994. What we know and don't know about amphibian declines in the west. Pages 59-67. In T. C. W. Wallace Covington and Leonard F. DeBano, (eds.) Sustainable Ecological Systems: Implementing an Ecological Approach to Land Management. United States Department of Agriculture, Rocky Mountain Forest and Range Experiment Station, Fort Collins, CO, USA.

Cowardin, L. M., V. Carter, F. C. Goulet, and E. T. LaRoe. 1979. Classification of Wetlands and Deepwater Habitat of the United States. U. S. Fish and Wildlife Service, Washington D.C., USA.

Gibbons, J. M., and R. D. Semlitsch. 1991. Guide to the Reptiles and Amphibians of the Savannah River Site. The University of Georgia Press, Athens, Georgia, USA.

Gilbert, F. F., and R. Allwine. 1991. Terrestrial amphibian communities in the Oregon Cascade Range. Pages 319-324. In K. B. Aubry and M. H. Brookes, (eds.). Wildlife and Vegetation of Unmanaged Douglas-Fir Forests. U.S. Department of Agriculture, Forest Service, Pacific Northwest Research Station, Portland, OR, USA.

Gomez, D. M., and R. G. Anthony. 1996. Amphibian and reptile abundance in riparian and upslope areas of five forest types in Western Oregon. Northwest Science 70:109-119.

Hairston, N. G. 1987. Community Ecology and Salamander Guilds. Cambridge University Press, Cambridge, MA, USA.

King County. 1987. Wetland Characterizations. Resource Planning Section, King County, WA, USA.

King County, 1990. Wetlands Inventory. Three Volumes. King County Environmental Division. Bellevue, WA, USA.

Leonard, W. P., H. A. Brown, L. L. C. Jones, K. R. McAllister, and R. M. Storm. 1993. Amphibians of Washington and Oregon. Seattle Audubon Society, Seattle, WA, USA.

McAllister, K. R., and B. P. Leonard. 1990. Past Distribution and Current Status of the Spotted Frog (Rana pretiosa) in Western Washington. 1989 Progress Report. Washington State Department of Wildlife, Olympia, WA, USA.

McAllister, K. R., and B. P. Leonard. 1991. Past Distribution and Current Status of the Spotted Frog in Western Washington. 1990 Progress Report. Washington Department of Wildlife, Olympia, WA, USA.

McComb, W. C., C. L. Chambers, and M. Newton. 1993a. Small mammal and amphibian communities and habitat associations in red alder stands, central Oregon coast range. Northwest Science 67:181-188.

McComb, W. C., K. McGarigal, and R. G. Anthony. 1993b. Small mammal and amphibian abundance in streamside and upslope habitats of mature Douglas-fir stands, western Oregon. Northwest Science 67:7-14.

Nussbaum, R. A., D. B. Edmond, Jr, and R. M. Storm. 1983. Amphibians & Reptiles of the Pacific Northwest. University of Idaho Press, Moscow, Idaho, USA.

Pechmann, J. H. K., D. E. Scott, R. D. Semlitsch, J. P. Caldwell, L. J. Vitt, and J. W. Gibbons. 1991. Declining amphibian populations: The problem of separating human impacts from natural fluctuations. Science 253:892-895.

Puget Sound Regional Council. 1994. Satellite remote sensing project-land cover and change detection. Seattle, WA, USA.

Richter, K. O. 1995. A simple aquatic funnel trap and its application to wetland amphibian monitoring. Herpetological Review 26:90-91.

Richter, K. O. 1996a. Criteria for the restoration and creation of wetland habitats for lentic-breeding amphibians of the Puget Sound Basins: 1: site selection criteria (In review).

Richter, K. O. 1996b. Criteria for the restoration and creation of wetland habitats for lentic-breeding amphibians of the Puget Sound Basin 2: spawning habitat design criteria. (In review).

Richter, K. O. and A. L. Azous. 1995. Amphibian occurrence and wetland characteristics in the Puget Sound Basin. Wetlands 15:306-312.

Richter, K. O., and H. A. Roughgarden. 1995. Evaluating northwestern salamander and red-legged frog breeding environments and egg survivorship for habitat modeling and wetland evaluation. King County, Resource Planning Section, King County, Washington, USA.

Seale, D. B. 1980. Influence of amphibian larvae on primary production, nutrient flux, and competition in a pond ecosystem. Ecology 61:1531-1550.

APPENDIX TABLE 5-1. CAPTURE RATES OF AMPHIBIANS EACH YEAR IN INDIVIDUAL WETLANDS.

		Year			
Wetland	Data	Capture Rate 1988	Capture Rate 1989	Capture Rate 1993	Capture Rate 1995
AL3	AMGR				
	AMMA				
	ENES		0.667	0.333	
	BUBO				
	DITE				
	TAGR				
	RAAU		0.333		
	PSRE		0.333	0.333	
	PLVE		0.333	0.333	
	ENES		0.667	0.333	
B3I	AMGR				
	AMMA	1.000		0.333	0.333
	ENES				
	BUBO				
	DITE				
	TAGR				
	RAAU				
	PSRE				
	PLVE				
	ENES				
BBC24	AMGR	0.672	9.667		0.333
	AMMA	0.336	0.333		
	ENES		0.333	0.333	0.333
	BUBO				
	DITE				
	TAGR				0.333
	RAAU	0.672	1.000		
	PSRE				
	PLVE				
	ENES		0.333	0.333	0.333
ELS39	AMGR		0.333		
	AMMA				0.357
	ENES		0.667	0.333	0.357
	BUBO				
	DITE				
	TAGR				
	RAAU	0.333			
	PSRE		0.333		
	PLVE				
	ENES		0.667	0.333	0.357

Appendix Table 5-1 cont. Capture rates of amphibians each year in individual wetlands.

Wetland	Data	Capture Rate 1988	Capture Rate 1989	Capture Rate 1993	Capture Rate 1995
ELS61	AMGR	1.000	0.667		0.333
	AMMA	0.667	0.333		1.000
	ENES				
	BUBO				
	DITE				
	TAGR				
	RAAU	1.000	0.667		
	PSRE				
	PLVE				
	ENES				
ELW1	AMGR				
	AMMA				
	ENES				
	BUBO				
	DITE				
	TAGR				
	RAAU				
	PSRE				
	PLVE				
	ENES				
FC1	AMGR				
	AMMA	1.333			
	ENES	0.333			
	BUBO				
	DITE				
	TAGR				
	RAAU				
	PSRE				
	PLVE				
	ENES	0.333			
HC13	AMGR	0.333			
	AMMA			0.667	0.364
	ENES				0.364
	BUBO		0.333		
	DITE				
	TAGR				
	RAAU	1.357	1.667	0.667	0.727
	PSRE		0.333		
	PLVE	0.333	0.333		0.364
	ENES				0.364
JC28	AMGR	0.333			
	AMMA				
	ENES	0.333			
	BUBO				
	DITE				
	TAGR	0.333			
	RAAU		0.333		
	PSRE				
	PLVE	0.333	1.000		0.333
	ENES	0.333			

Appendix Table 5-1 cont. Capture rates of amphibians each year in individual wetlands.

Wetland	Data	Capture Rate 1988	Capture Rate 1989	Capture Rate 1993	Capture Rate 1995
LCR93	AMGR				
	AMMA		0.333		0.667
	ENES	0.333			0.333
	BUBO				
	DITE				
	TAGR				
	RAAU	2.333	0.667	2.000	0.357
	PSRE	0.333			
	PLVE	0.333	0.333		
	ENES	0.333			0.333
LPS9	AMGR	0.333			
	AMMA	1.000			
	ENES				
	BUBO				
	DITE				
	TAGR				
	RAAU	0.690	0.571		
	PSRE	0.333			
	PLVE	0.333			
	ENES				
MGR36	AMGR	0.333	0.667		0.333
	AMMA	0.333			
	ENES	1.000			
	BUBO				
	DITE				
	TAGR				
	RAAU	1.333			
	PSRE				
	PLVE	2.000	0.667		0.667
	ENES	1.000			
NFIC12	AMGR		1.345		
	AMMA				
	ENES		0.336	0.333	1.000
	BUBO				
	DITE				
	TAGR				
	RAAU		1.008		
	PSRE				0.333
	PLVE				0.333
	ENES		0.336	0.333	1.000
PC12	AMGR		0.667		
	AMMA				1.014
	ENES	0.333			
	BUBO		0.667		
	DITE	0.333			
	TAGR				
	RAAU	0.667	2.000		
	PSRE		0.333		0.338
	PLVE				
	ENES	0.333			

Appendix Table 5-1 cont. Capture rates of amphibians each year in individual wetlands.

Wetland	Data	Capture Rate 1988	Capture Rate 1989	Capture Rate 1993	Capture Rate 1995
RR5	AMGR	0.336	0.345		
	AMMA				
	ENES				
	BUBO	1.681			0.694
	DITE				
	TAGR				
	RAAU	0.672		0.333	
	PSRE				
	PLVE				
	ENES				
SC4	AMGR		1.000		0.333
	AMMA			0.333	
	ENES		0.667	0.333	
	BUBO				
	DITE				
	TAGR				
	RAAU				
	PSRE			0.333	
	PLVE		0.333		
	ENES		0.667	0.333	
SC84	AMGR				0.333
	AMMA				
	ENES				
	BUBO				
	DITE				
	TAGR				
	RAAU				0.392
	PSRE				
	PLVE		0.333		
	ENES				
SR24	AMGR				
	AMMA			0.333	
	ENES		1.000		
	BUBO		0.667		
	DITE	0.333			
	TAGR	0.667	0.667		
	RAAU		0.333		
	PSRE		0.667		
	PLVE				
	ENES		1.000		
TC13	AMGR		0.333		
	AMMA		0.333		
	ENES		0.333		0.667
	BUBO				
	DITE				
	TAGR				
	RAAU		0.667		
	PSRE				0.333
	PLVE				
	ENES		0.333		0.667

CHAPTER 6 BIRD DISTRIBUTION, ABUNDANCE AND HABITAT USE

by Klaus O. Richter and Amanda L. Azous

INTRODUCTION

Values and natural functions of wetlands gained growing recognition in the 1970s (Good et al. 1978, Greeson et al. 1979). Consequently, wetlands and are now considered sensitive habitats with diverse functions that are protected at federal, state and local levels. Of the many functions wetlands exhibit, their ability to provide resting, feeding and breeding habitat for a wide diversity of birds is among the most noticeable and appreciated. Abundant, often highly visible and unique avifauna are an important component of open space values, enriching quality of life. Despite these attributes, many hectares of marshes, swamps and other bird habitats are lost or impacted each year, in part due to our inadequate knowledge of how to protect the biologic function of wetlands.

Birds have been intensively studied in deciduous forests of east-central states (Blake and Karr 1984, Blake 1986), west coast coniferous forests (Artman 1990, Stofel 1993) and in other upland environments. Birds of coastal wetlands have also been widely studied (Craig and Beal 1992, Weller 1994). Fresh water wetland investigations, however, have been carried out by a relatively few biologists, who primarily documented the distribution and abundance of waterfowl and other marsh birds within pothole lakes and other wetlands in open landscapes of the Central Flyway (Weller and Spatcher 1965, Weller and Fredrickson 1974, Weller 1979). Although the importance of riparian corridors to avifauna, particularly passerines, woodpeckers and other non-game species has more recently been recognized (Brown and Dinsmore 1986, Knopf and Samson 1994), the avifauna of freshwater wetlands, specifically smaller palustrine wetlands distributed through forested landscapes, has not been well documented.

The purpose of this paper is to comprehensively describe palustrine wetland bird communities in the Lower Puget Sound Basin. The avifaunal literature is briefly reviewed to determine the uniqueness of palustrine wetland avifauna in a regional and landscape context. Then, we assess whether generalized landscape characteristics that account for bird distributions and abundances in upland ecosystems apply to predicting bird distributions within palustrine wetlands of the Northwest. We examined the diversity and proportional abundance of birds within the regional context of differing land use and the site-specific wetland attributes of size and vegetation structure, thereby building on the preliminary findings of Azous (1991) and Martin-Yanny (1992). The location, physical, chemical and vegetative description of the wetlands in this study are presented in Section 1 and Chapters 1, 2, and 3 of Section 2.

METHODS

The distribution and relative abundance of birds was determined based on surveys completed during the breeding period from late May to mid-June in 1988, 1989, 1991, 1992 and 1995. Birds were identified by non-territorial calls, territorial song, pecking and drumming, visual sightings and flyovers during 15-minute point counts (Johnston 1990, Verner 1985) at permanent census stations. Usually, four ornithologists surveyed each

wetland totaling one hour per station. Surveys commenced one half-hour after sunup to approximately 9:00 am and stations were surveyed in alternating order to minimize time biases.

We calculated the gamma diversity, the collective species identified across all wetlands (a landscape metric) and alpha diversity, the species identified at a single wetland (a site metric) (Whittaker 1975) by summing the number of species. We calculated all diversity measures only including species observed two or more times. Because alpha diversity measures are insensitive to bird species composition, we calculated diversity indices for birds with specific breeding habitats, versatility ratings, residency traits, and urbanization affinities. This paper reports on some of the more general overall diversity metrics analyzed to date.

We estimated relative abundances for each species at a wetland using average detection values calculated by dividing the total number of a species sighted at a wetland (derived by combining 15-minute station totals into a 1-hour station total and then combining station totals) by the total number of 15-minute observation periods at a wetland. Using this detection value we standardized the data among wetlands with unequal sampling effort (e.g., more stations and hence more time at large wetlands).

We relied on Paulson (1992) to identify total species potentially occurring in palustrine wetlands habitats (Appendix Table 6-1) of the Puget Sound Basin. Species were classified as common residents, rare residents, or migrants according to abundance ratings provided in Hunn (1982). Habitat versatility ratings for bird species were obtained from Brown (1985) and represent the sum total of the number of plant communities and stand conditions used for breeding plus the number of plant communities and stand conditions used for feeding by a species.

Bird preferences for National Wetlands Inventory (NWI) wetland habitat classes (Cowardin et al. 1979) identified at each wetland were converted to habitat preferences identified in Paulson (1992) as follows: open water/unconsolidated bottom = ponds and lakes; emergent wetland, persistent = fresh [water] marsh; forested wetland, needle-leaved evergreen = wet coniferous forest; forested wetland, broad-leaved deciduous = riparian woodland; emergent wetland, nonresistant = wet lowland meadow; scrub-shrub =shrub thickets, and unconsolidated shore. Alpha and gamma diversities within the study wetlands were compared against the potential species richness documented in the Lower Puget Sound Basin that were known to occur in these respective habitats. Habitat land cover and fragmentation was determined by quantifying land cover within 1000 m using remote sensing methods and a geographic information system.

Statistical analysis of correlations and hypothesis testing utilized parametric statistics when assumptions of normality were met and non-parametric statistics when assumptions were violated. We chose $P < 0.05$, and $P > 0.05$ and ≤ 0.10 with $r \geq 0.4$ as significant and weakly significant, respectively. Nevertheless, significance should be interpreted cautiously because of the high variability of the data and concomitantly unacceptably wide confidence intervals for predictive level of significance. This is due to the low number of replicates (e.g., wetlands undergoing significant impacts) and discontinuities in habitat characteristics (e.g., unequal representation of all wetland size classes, etc.).

RESULTS

Regional Species Richness (Beta Diversity)

A total of 94 species were identified and sighted on at least two or more occasions among all the wetlands (Table 6-1). This total wetland diversity of 94 species represents only 59% of the 158 species that could be expected to use habitats found at wetlands in the Lower Puget Sound Basin (Paulson 1992) (Appendix Table 6-1). This diversity, however, is significantly higher than the 56 species found by Stofel (1993), the 23 species identified by Artman (1990) in rural upland second-growth forest, and the 48 species by Gavareski (1976) in urban park environments. All the species identified in these studies were identified at our surveyed wetlands, with the exception of great horned owl, Northern harrier, Northern rough-winged swallow, luzuli bunting, and turkey vulture as well as a few high elevation species such as gray jay, blue grouse, golden-crowned sparrow.

The relative diversity across the study wetlands ranged from 38% to 72% of all birds collectively identified across all wetlands (Figure 6-1). No more than 42% (67 species) of potential regional bird diversity (per Paulson) was present in any one wetland. This represented 71% of our collective wetland sightings and was observed at SR24, a large, open-water, vegetatively rich, and undisturbed wetland. In contrast, the lowest diversity of 37 species (23% of potential regional and 39% of our collective wetlands) was identified at NFIC12 a small, highly disturbed wetland situated between a large subdivision and a roadway. The next lowest richness of 38 (40% of collective) and 39 (41% of collective) species were identified at AL3 and ELS39, respectively, both small, intermittently flooded wetlands.

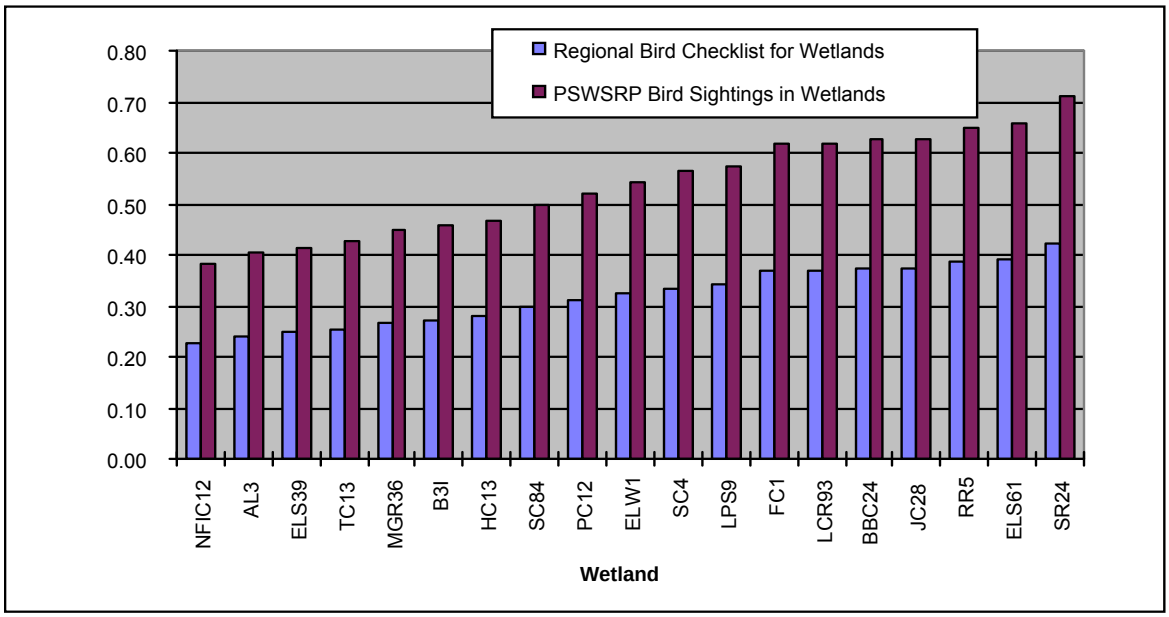

Figure 6-1. Percent of all species collectively found in wetlands.

Only three species, American robin, black-capped chickadee and song sparrow, and representing 3.2% of total diversity were shared between all 19 wetlands. Conversely, four species (4.3%), American coot, hooded merganser, savannah sparrow and spotted

sandpiper were found in only one wetland. Interestingly, 47 species (50% of total) were found in 53% or more of the wetlands.

Migrants accounted for 37% of species (35). Common and rare residents respectively numbered 17 and 42 species and comprised 18% and 45% of sightings thus significantly enhancing the diversity of wetland avifauna. Many residents were species of adjacent terrestrial habitats using wetlands to drink, augment diet, and support their young.

During the study period the observations of thirteen species declined including two rare residents, orange-crowned warbler and red crossbill. Nine other rare resident species showed no change and six weren't observed in sufficient numbers to determine. Forty-nine percent of species showed no change in population and ten species increased. We did not have enough observations of 25 species to determine changes in population status.

The observations of birds known to avoid suburban and urban development both declined and increased depending on species. Three avoiders declined including orange-crowned warbler, varied thrush and willow flycatcher while two increased, black-throated gray warbler and Swainson's thrush. Seven species known to be adaptable to urbanization increased while nine declined.

Species Richness by Wetland (Alpha Diversity)

Species richness varied widely within wetlands over the study period (Figure 6-2). Species richness for all years was higher because different species were observed in different years. We saw the highest richness in 1989 in virtually all wetlands and the lowest in the last year of our research, 1995.

Table 6-1. Species and life history traits of birds sighted at study wetlands.

Bird Species	Percent of Wetlands 1989	Percent of Wetlands 1991	Percent of Wetlands 1995	Percent of Wetlands All Years	Status	Population	Adapt-ability	Versatility Rating
American Coot	0.05	0.06	0.05	0.05	resident	insufficient data	Adapter	10
American Goldfinch	0.79	0.50	0.68	0.84	resident	declining	Adapter	23
American Robin	1.00	1.00	1.00	1.00	resident	increasing	Adapter	37
Anna's Hummingbird	0.11	0.00	0.05	0.16	rare resident	insufficient data	Adapter	25
Bald Eagle	0.00	0.06	0.11	0.11	migrant	insufficient data	Adapter	19
Barn Swallow	0.26	0.22	0.42	0.53	resident	increasing	Adapter	18
Black-capped Chickadee	1.00	0.94	1.00	1.00	migrant	declining	Adapter	28
Belted Kingfisher	0.26	0.22	0.21	0.58	resident	no change	Adapter	Undetermined
Bewick's Wren	0.68	0.89	0.74	0.95	resident	declining	Adapter	22
Brown-headed Cow Bird	0.58	0.33	0.63	0.95	migrant	insufficient data	Adapter	9
Band-tailed Pigeon	0.05	0.06	0.05	0.16	migrant	increasing	Adapter	17
Bushtit	0.84	0.61	0.21	0.95	migrant	no change	Adapter	10
Canada Goose	0.11	0.06	0.11	0.16	resident	declining	Adapter	22
California Quail	0.05	0.00	0.16	0.21	rare resident	no change	Adapter	8
Chestnut-backed Chickadee	0.79	0.78	0.47	1.00	resident	increasing	Adapter	27
Cedar Waxwing	0.84	0.78	0.53	0.89	resident	insufficient data	Adapter	28
Cliff Swallow	0.05	0.11	0.11	0.16	migrant	insufficient data	Adapter	12
Common Yellow-throat	0.58	0.67	0.47	0.68	rare resident	no change	Adapter	9
Dark-eyed Junco	0.68	0.50	0.37	0.84	migrant	insufficient data	Adapter	Undetermined
Downy Woodpecker	0.47	0.56	0.63	0.89	resident	insufficient data	Adapter	21
Fox Sparrow	0.05	0.00	0.11	0.16	resident	insufficient data	Adapter	34
Gadwall	0.11	0.06	0.05	0.11	resident	insufficient data	Adapter	10
Great Blue Heron	0.42	0.28	0.21	0.63	resident	no change	Adapter	27
Golden-crowned kinglet	0.95	0.94	0.37	1.00	resident	no change	Adapter	14
Glaucous-winged Gull	0.16	0.06	0.05	0.16	migrant	declining	Adapter	26
Hammond's Flycatcher	0.26	0.33	0.05	0.47	migrant	no change	Adapter	26
Hairy Woodpecker	0.79	0.50	0.32	0.79	rare resident	insufficient data	Adapter	10
House Finch	0.58	0.22	0.32	0.68	resident	no change	Adapter	28
Hutton's Vireo	0.42	0.06	0.11	0.47	resident	no change	Adapter	27
Killdeer	0.21	0.00	0.11	0.32	resident	no change	Adapter	28
Mallard	0.42	0.28	0.42	0.58	resident	no change	Adapter	10
Marsh Wren	0.68	0.22	0.16	0.68	resident	no change	Adapter	8
Northern Flicker	0.37	0.39	0.37	0.63	migrant	declining	Adapter	27
Northern Oriole	0.11	0.00	0.11	0.21	resident	no change	Adapter	33
Pied-billed Grebe	0.26	0.06	0.11	0.26	resident	no change	Adapter	Undetermined
Pacific-slope Flycatcher	0.95	1.00	0.84	1.00	migrant	insufficient data	Adapter	10
Purple Finch	0.63	0.44	0.47	0.79	migrant	increasing	Adapter	24
Red-breasted Nuthatch	0.53	0.56	0.63	0.84	migrant	insufficient data	Adapter	Undetermined
Red Crossbill	0.32	0.67	0.16	0.79	rare resident	declining	Adapter	29
Red-eyed Vireo	0.11	0.00	0.11	0.16	resident	no change	Adapter	26
Rufous-sided Towee	0.89	0.89	0.89	1.00	migrant	no change	Adapter	37
Rufous Hummingbird	0.21	0.17	0.16	0.32	resident	insufficient data	Adapter	28
Ruby Crowned Kinglet	0.53	0.44	0.63	0.89	resident	no change	Adapter	31
Red-winged Blackbird	0.53	0.33	0.53	0.68	rare resident	insufficient data	Adapter	22
Savannah Sparrow	0.00	0.06	0.00	0.05	resident	increasing	Adapter	11
Song Sparrow	1.00	1.00	1.00	1.00	resident	no change	Adapter	24
Sharp-shinned Hawk	0.21	0.00	0.00	0.21	rare resident	no change	Adapter	15
Steller's Jay	0.58	0.61	0.68	0.84	rare resident	insufficient data	Adapter	33
Tree Swallow	0.58	0.39	0.42	0.84	rare resident	no change	Adapter	22
Violet-green Swallow	0.47	0.39	0.79	0.79	rare resident	insufficient data	Adapter	28
Virginia Rail	0.26	0.11	0.16	0.32	migrant	no change	Adapter	33
White-crowned Sparrow	0.32	0.22	0.05	0.32	migrant	no change	Adapter	29
Western Wood-pewee	0.32	0.17	0.32	0.47	migrant	declining	Adapter	30
Winter Wren	0.95	0.94	0.68	1.00	resident	increasing	Adapter	27

Table 6-1 continued. Species and life history traits of birds sighted at study wetlands.

Bird Species	Percent of Wetlands 1989	Percent of Wetlands 1991	Percent of Wetlands 1995	Percent of Wetlands All Years	Status	Population	Adapt-ability	Versatility Rating
Wood Duck	0.32	0.22	0.37	0.63	rare resident	no change	Adapter	25
Yellow Warbler	0.74	0.72	0.21	0.95	migrant	declining	Adapter	19
Yellow-rumped Warbler	0.26	0.11	0.21	0.47	rare resident	no change	Adapter	31
Black Headed Grosbeak	0.84	0.61	0.79	1.00	rare resident	no change	Avoider	34
Brewer's Blackbird	0.21	0.39	0.11	0.47	migrant	no change	Avoider	28
Brown Creeper	0.26	0.28	0.16	0.47	resident	no change	Avoider	32
Black-throated Gray Warbler	0.53	0.39	0.47	0.79	migrant	increasing	Avoider	24
Blue-winged Teal	0.00	0.00	0.11	0.11	resident	no change	Avoider	29
Caspian Tern	0.00	0.00	0.11	0.11	migrant	insufficient data	Avoider	Undetermined
Chipping Sparrow	0.11	0.06	0.11	0.26	migrant	no change	Avoider	36
Cooper's Hawk	0.11	0.00	0.16	0.26	migrant	no change	Avoider	8
Common Raven	0.00	0.00	0.11	0.11	rare resident	insufficient data	Avoider	32
Evening Grosbeak	0.21	0.06	0.21	0.32	rare resident	no change	Avoider	33
Green Heron	0.11	0.06	0.05	0.16	migrant	no change	Avoider	6
Hermit Thrush	0.84	0.33	0.21	0.84	resident	no change	Avoider	22
Hooded Merganser	0.05	0.00	0.05	0.05	migrant	insufficient data	Avoider	25
MacGillivary's Warbler	0.11	0.00	0.21	0.26	migrant	insufficient data	Avoider	Undetermined
Northern Pigmy Owl	0.05	0.06	0.05	0.16	migrant	no change	Avoider	20
Orange-crowned Warbler	0.74	0.44	0.37	0.84	rare resident	declining	Avoider	31
Olive-sided Flycatcher	0.16	0.22	0.11	0.32	resident	no change	Avoider	36
Pine Siskin	0.26	0.00	0.26	0.47	resident	no change	Avoider	27
Pileated Woodpecker	0.21	0.00	0.11	0.26	resident	no change	Avoider	32
Red-breasted Sapsucker	0.21	0.00	0.21	0.37	resident	no change	Avoider	24
Red-eyed Vireo	0.05	0.06	0.11	0.16	resident	no change	Avoider	26
Ruffed Grouse	0.05	0.11	0.05	0.16	resident	insufficient data	Avoider	29
Sora	0.00	0.06	0.11	0.16	migrant	no change	Avoider	28
Solitary Vireo	0.21	0.39	0.21	0.58	migrant	insufficient data	Avoider	10
Spotted Sandpiper	0.05	0.00	0.00	0.05	rare resident	no change	Avoider	4
Swainson's Thrush	0.95	1.00	0.95	1.00	resident	increasing	Avoider	32
Townsend's Warbler	0.68	0.06	0.37	0.79	migrant	no change	Avoider	26
Varied Thrush	0.21	0.00	0.00	0.21	migrant	declining	Avoider	29
Vaux's Swift	0.58	0.44	0.16	0.68	migrant	no change	Avoider	34
Warbling Vireo	0.68	0.17	0.26	0.79	resident	insufficient data	Avoider	10
Western Tanager	0.47	0.33	0.42	0.63	migrant	no change	Avoider	34
Willow Flycatcher	0.84	0.83	0.79	0.95	migrant	declining	Avoider	20
Wilson's Warbler	0.89	0.78	0.63	1.00	migrant	no change	Avoider	33
American Crow	0.84	0.94	0.89	0.95	resident	declining	Exploiter	32
European Starling	0.42	0.28	0.16	0.53	resident	no change	Exploiter	27
House Sparrow	0.21	0.22	0.05	0.42	resident	insufficient data	Exploiter	12
Rock Dove	0.11	0.11	0.00	0.11	resident	increasing	Exploiter	Undetermined

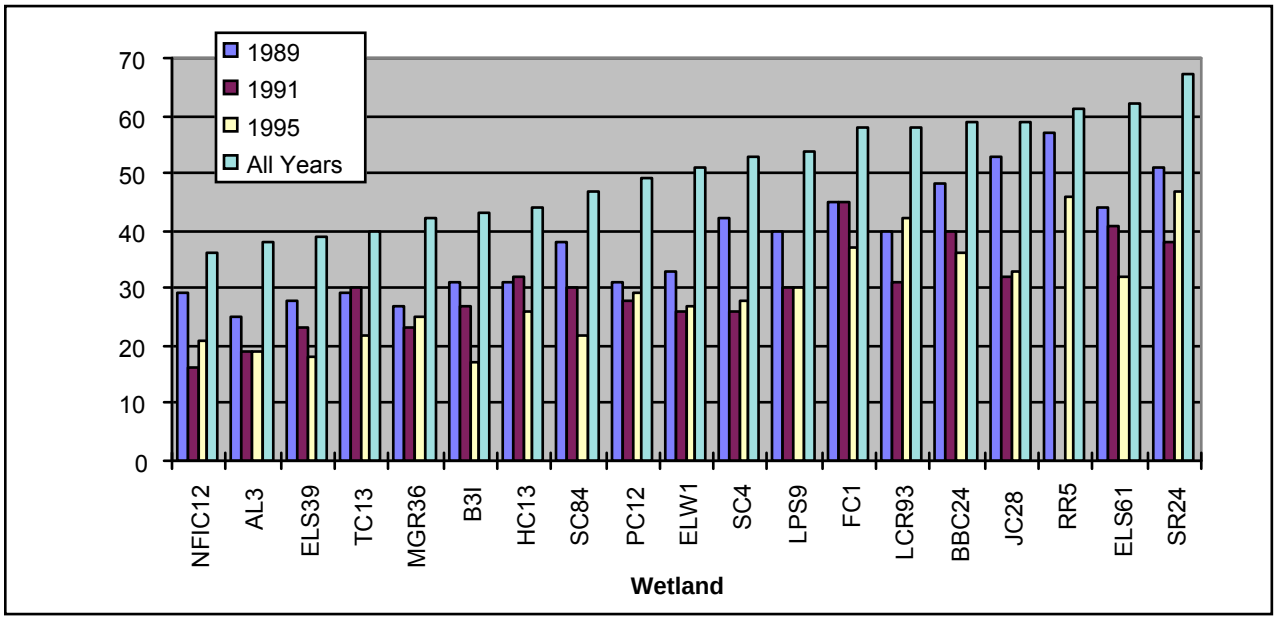

Figure 6-2. Total species diversity in wetlands for each study year.

We used total richness to measure species diversity and found it increased directly with wetland area (Fisher's r to z, R= 0.53, P= 0.018). Our study wetlands ranged from 0.6 to 12.6 ha with 13 wetlands less than four hectares. Among the six wetlands greater than four hectares, only one had less than 50 species present, whereas among the wetlands with less than four hectares, eight had richness of less than 50 (Figure 6-3).

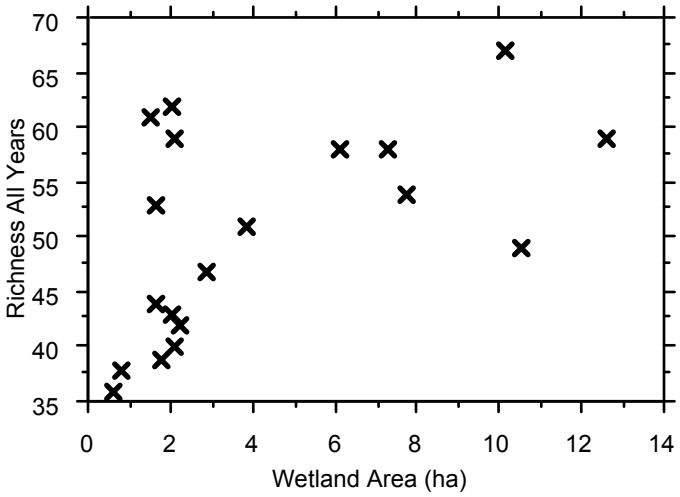

Figure 6-3. Relationship between bird species richness and wetland size.

Large wetland areas, while a major component of the most diverse bird communities we found, is not the only factor important as evidenced in that two of the smallest wetlands of less than two hectares had high richness of 61 and 62 species. Structural complexity was also found to be a contributing factor, as characterized by either the number of NWI vegetation (Fisher's r to z, R = 0.48, P = 0.04), or Paulson's habitat (Fisher's r to z, R = 0.6, P = 0.006) classes (Figure 6-4), though the statistical relationship was stronger with Paulson's habitat classifications. For example, three wetlands with only one NWI vegetation class had 55 bird species or more, representing the upper range of diversity, during the study period. The single NWI classifications used to describe the vegetation communities in those wetlands were equivalent to three of the bird habitat classifications probably better reflecting avian potential.

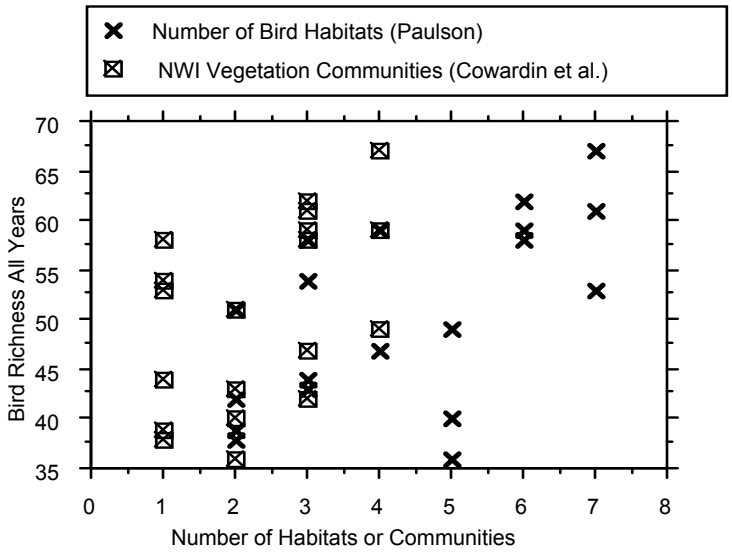

Figure 6-5. Relationship between bird species richness and vegetation community complexity.

Bird diversity in wetlands with adjacent lakes, for example FC1 and ELW1, and open water, such as SR28 and BBC24, was bolstered by waterfowl. Most frequent waterfowl encountered over the three years of complete surveys (e.g.,1989, 1991 and 1995) were mallard (99), Canada goose (10), pied-billed grebe (26), hooded merganser (9), and gadwall (7), with only occasional sightings of blue-winged teal (2), American widgeon (1), and lesser scaup (1).

Relative Abundance

Summary tables for species abundance determined by average detections are provided in Table 6-2, whereas detailed wetland-specific detections are provided in Appendix Tables 6-2. Found in each wetland and in decreasing order of abundance are song sparrow and American robin (both with at least one expected detection per visit), Swainsons thrush, red-wing blackbird and black-capped chickadees. Within selected other wetlands American crow, rufous-sided towhee and Pacific slope flycatchers, willow flycatcher winter wren and marsh wren were abundant.

DISCUSSION

Our bird diversities when compared with diversities observed in terrestrial habitats by others, indicate that wetlands are disproportionately used by birds and are probably the single most productive habitat for this vertebrate class in the Puget Sound Basin. Of all the species identified in Western Washington 82% are found in wetlands. Artman (1990) found only 23 species in 45-50 year old stands dominated by western hemlock but also containing Douglas-fir (*Pseudotsuga menziesii*), Pacific silver fir (*Abies amabilis*), and western red-cedar (*Thuja plicata*). Of the 48 species identified by Gavareski (1976) in 4-400 ha^2 diversely vegetated urban parks of Seattle only two (great horned owl and golden-crowned sparrow) were undetected at wetlands.

We also found significantly more species than identified by Milligan (1985) in a survey of wetlands of less than 4 ha^2 in urbanized areas of the Puget Sound Basin. From censuses in April, May and June of 1984, 60 species were found in combined wetland, and wetland and upland habitats, of 23 widely diverse sites characterized by varying density of development. Mulligan also found both total and average avifaunal diversity to be correlated to wetland habitat complexity measured by the number of NWI vegetation classes. Bird diversity was also found to correlate with the percentage of wetland buffered by shrubland or forest vegetation, although interestingly, there was only a minor predicted increase in diversity with increasing buffer width classes of 50, 100 and 200 feet from the wetland edge.

During the baseline surveys of wetlands for this study, Martin-Yanny (1992) listed 88 species. During subsequent surveys our study identified an additional six species, and presumably with continued surveys a few additional species may be expected at decreasing rates. Nevertheless it seems unlikely we would find the entire list of species identified by Paulson as potentially occurring in palustrine wetland habitats because of the limited geographic location of our wetlands within disturbed watersheds.

Paulson (1992) found that most resident species are maintaining their populations despite increasing urbanization. Our study results generally corroborate this finding though we did not have sufficient data to assess all species we observed. Declines were observed among some migrating species and some adapters.

Wetland area and habitat diversity were found to be critical factors in maintaining high biodiversity in wetland bird communities. When wetlands are assessed for function and value related to avian potential, methods based on bird preferences, such as the habitat classification by Paulson, would be more appropriate than the NWI classification system.

Table 6-2. Bird species abundance in order of increasing average detections.

Bird Species	1989	1991	1995	All Years	Detectability over all years, all wetland stations
Blue-winged Teal	0	0	2	2	0.0026
Savannah Sparrow	0	2	0	2	0.0026
Spotted Sandpiper	2	0	0	2	0.0026
Anna's Hummingbird	2	0	1	3	0.0039
Bald Eagle	0	1	2	3	0.0039
Northern Pigmy Owl	1	1	1	3	0.0039
California Quail	1	0	3	4	0.0052
Caspian Tern	0	0	4	4	0.0052
Northern Oriole	2	0	2	4	0.0052
Red-eyed Vireo	2	0	2	4	0.0052
Sharp-shinned Hawk	4	0	0	4	0.0052
Common Raven	0	0	5	5	0.0064
Rock Dove	2	3	0	5	0.0064
Ruffed Grouse	1	2	2	5	0.0064
Sora	0	2	3	5	0.0064
Chipping Sparrow	3	1	2	6	0.0077
Fox Sparrow	1	0	5	6	0.0077
Glaucous Winged Gull	3	1	2	6	0.0077
Gadwall	3	2	2	7	0.0090
Varied Thrush	7	0	0	7	0.0090
Band-tailed Pigeon	3	1	4	8	0.0103
MacGillivary's Warbler	2	0	6	8	0.0103
Red-breasted Sapsucker	4	0	4	8	0.0103
Red-eyed Vireo	2	1	5	8	0.0103
Cooper's Hawk	2	0	7	9	0.0116
Hooded Merganser	6	0	3	9	0.0116
Killdeer	6	0	3	9	0.0116
Canada Goose	2	2	6	10	0.0129
Green Heron	9	1	1	11	0.0142
House Sparrow	6	5	1	12	0.0155
Cliff Swallow	4	6	3	13	0.0168
Rufous Hummingbird	5	4	4	13	0.0168
Yellow-rumped Warbler	7	3	4	14	0.0180
American Coot	4	5	6	15	0.0193
Olive-sided Flycatcher	5	8	2	15	0.0193
Pileated Woodpecker	11	0	4	15	0.0193
Virginia Rail	7	3	5	15	0.0193
Evening Grosbeak	7	1	8	16	0.0206
Brewer's Blackbird	6	7	6	19	0.0245
Pine Siskin	7	0	12	19	0.0245
Belted Kingfisher	7	4	10	21	0.0271
Brown Creeper	9	7	5	21	0.0271
Hammond's Flycatcher	9	10	2	21	0.0271
Hutton's Vireo	19	1	2	22	0.0284
Solitary Vireo	5	13	4	22	0.0284
Wood Duck	9	4	9	22	0.0284
White-crowned Sparrow	14	9	1	24	0.0309

Table 6-2 continued. Bird species abundance in order of increasing average detections.

Bird Species	1989	1991	1995	All Years	Detectability over all years, all wetland stations
Pied-billed Grebe	8	2	16	26	0.0335
Western Wood-pewee	11	6	13	30	0.0387
Red Crossbill	9	23	4	36	0.0464
Vaux's Swift	17	13	8	38	0.0490
House Finch	23	8	8	39	0.0503
Great Blue Heron	17	7	17	41	0.0528
Northern Flicker	10	11	23	44	0.0567
Ruby Crowned Kinglet	19	9	20	48	0.0619
European Starling	32	11	9	52	0.0670
Townsend's Warbler	38	2	13	53	0.0683
Western Tanager	17	7	29	53	0.0683
Barn Swallow	12	11	31	54	0.0696
Downy Woodpecker	16	14	25	55	0.0709
Hairy Woodpecker	36	15	11	62	0.0799
Warbling Vireo	38	3	22	63	0.0812
Brown-headed Cow Bird	23	11	31	65	0.0838
Orange-crowned Warbler	38	23	11	72	0.0928
Black-throated Gray Warbler	25	13	44	82	0.1057
Dark-eyed Junco	40	17	25	82	0.1057
Purple Finch	24	22	38	84	0.1082
Red-breasted Nuthatch	15	29	40	84	0.1082
Violet-green Swallow	18	14	54	86	0.1108
Marsh Wren	55	19	23	97	0.1250
Bushtit	55	30	13	98	0.1263
Mallard	32	18	49	99	0.1276
Tree Swallow	43	27	31	101	0.1302
Hermit Thrush	84	11	8	103	0.1327
Golden-crowned kinglet	59	34	16	109	0.1405
Chestnut-backed Chickadee	41	37	38	116	0.1495
Steller's Jay	28	38	68	134	0.1727
Cedar Waxwing	57	41	42	140	0.1804
Yellow Warbler	67	50	26	143	0.1843
American Goldfinch	54	42	55	151	0.1946
Black Headed Grosbeak	56	37	64	157	0.2023
Bewick's Wren	48	42	68	158	0.2036
Common Yellow-throat	93	63	65	221	0.2848
Wilson's Warbler	115	71	77	263	0.3389
Winter Wren	109	85	114	308	0.3969
American Crow	73	106	134	313	0.4034
Rufous-sided Towee	99	94	140	333	0.4291
Willow Flycatcher	114	90	141	345	0.4446
Pacific-slope Flycatcher	127	147	145	419	0.5399
Black-capped Chickadee	152	138	170	460	0.5928
Red-winged Blackbird	280	147	165	592	0.7629
Swainson's Thrush	153	179	336	668	0.8608
American Robin	279	230	293	802	1.0335
Song Sparrow	454	389	395	1238	1.5954
Total Abundance	3426	2551	3337	9314	

References

Artman, V. L. 1990. Breeding bird population and vegetation characteristics in commercially thinned and unthinned Western Hemlock Forests of Washington. Pages 55. University of Washington, Seattle, WA, USA.

Azous, A. L. 1991. An analysis of urbanization effects on wetland biological communities. University of Washington, Seattle, WA, USA.

Blake, J. G. 1986. Species-area relationship of migrants in isolated woodlots in east-central Illinois. The Wilson Bulletin 98:291-296.

Blake, J. G., and J. R. Karr. 1984. Species composition of bird communities and the conservation benefit of large versus small forests. Biological Conservation 30:173-187.

Brown, M., and J. J. Dinsmore. 1986. Implications of marsh size and isolation for marsh bird management. J. Wildl. Manage. 50:392-397.

Brown, R. E. 1985. Management of Wildlife and Fish Habitats in the Forests of Western Oregon and Washington. U. S. Forest Service, Pacific Northwest Region, Portland, OR, USA.

Cowardin, L. M., V. Carter, F. C. Goulet, and E. T. LaRoe. 1979. Classification of wetlands and deepwater habitat of the United States. U. S. Fish and Wildlife Service, Washington D.C., USA.

Craig, R. J., and K. G. Beal. 1992. The influence of habitat variables on marsh bird communities of the Connecticut River Estuary. Wilson Bulletin 104:295-311.

Gavareski, C. A. 1976. Relation of park size and vegetation to urban bird populations in Seattle, Washington. Condor 78:375-382.

Good, R. E., D. F. Whigham, R. L. Simpson, and J. Jackson Crawford G , eds. 1978. Freshwater Wetlands: Ecological Processes and Management Potential. Academic Press, Inc., San Diego, CA, USA.

Greeson, P. E., J. R. Clark, and J. E. Clark, eds. 1979. Wetland Functions and Values: The State of Our Understanding. American Water Resources Association, Minneapolis, MN, USA.

Hunn, E. S. 1982. Birding in Seattle and King County. Seattle Audubon Society, Seattle, Washington, USA.

Knopf, F. L., and F. B. Samson. 1994. Scale perspectives on avian diversity in western riparian ecosystems. Conservation Biology 8:669-676.

Martin-Yanny, E. 1992. The impacts of urbanization on wetland bird communities. Pages 109. University of Washington, Seattle, WA, USA.

Milligan, D. A. 1985. The ecology of avian use of urban freshwater wetlands in King County, Washington. Pages 145. University of Washington, Seattle, WA.

Paulson, D. R. 1992. Northwest bird diversity: From extravagant past and changing present to precarious future. The Northwest Environmental Journal 8:71-118.

Stofel, J. L. 1993. Evaluating wildlife responses to alternative silvicultural practices. Pages 126. University of Washington, Seattle, Washington, USA.

Weller, M. W. 1979. Birds of some Iowa wetlands in relation to concepts of faunal preservation. Proc. Iowa Acad. Sci. 86:81-88.

Weller, M. W. 1994. Bird-habitat relationships in a Texas estuarine marsh during summer. Wetlands 14:293-300.

Weller, M. W., and L. H. Fredrickson. 1974. Avian ecology of a managed glacial marsh. The Living Bird 12:269-291.

Weller, M. W., and C. S. Spatcher. 1965. Role of habitat in the distribution and abundance of marsh birds. Pages 1-31. Iowa State University of Science and Technology, Ames, Iowa, USA.

Whittaker, R. H. 1975. Communities and Ecosystems. MacMillan, New York, New York, USA.

Appendix Table 6-1. List of bird species expected to be using palustrine wetlands in Western Washington.

		STATUS		BREEDING DISTRIBUTION							
SPECIES	Evolutionary Order	B	W	WA	PL	FM	WC	BF	RW	ST	WM
Common loon	1	x	x	o	SW						
Pied-billed grebe	2	x	x	x	R						
Horned grebe	3	x	x	o	SW						
Red-necked grebe	4	x	x	o	S						
Eared grebe	5	x	o	x	Sw						
Western grebe	6	o	x	x	SW						
Clark's grebe	7	o		o	S						
Double-crested cormorant	8	x	x	x	SW						
American bittern	9	x	o	x		SW					
Great blue heron	10	x	x	x		R					R
Great egret	11	o	o	o		S					
Black-crowned night-heron	12	o	o	x		SW					
Canada goose	13	x	x	x	R						R
Wood duck	14	x	o	x	R						
Green-winged teal	15	x	o	x	SW	SW					W
Mallard	16	x	x	x	R	R					W
Northern pintail	17	x	x	x	SW	SW					W
Blue-winged teal	18	x		x	S	S					
Cinnamon teal	19	o		x	S	S					
Northern shoveler	20	x	o	x	SW	SW					
Gadwall	21	x	x	x	SW	SW					W
American wigeon	22	x	o	x	SW	SW					W
Canvasback	23	x	x	x	SW	S					
Redhead	24	x	o	x	S	S					
Ring-necked duck	25	x	x	x	SW						
Barrow's goldeneye	26	x	x	x	S						
Bufflehead	27	x	x	o	SW						
Hooded merganser	28	x	x	x	SW						
Common merganser	29	x	x	x	W						
Ruddy duck	30	x	o	x	SW	S					
Bald eagle	31	x	x	x	R				R		
Northern harrier	32	x	x	x		SW					R
Sharp-shinned hawk	33	x	o	x			R	W	W	W	
Cooper's hawk	34	x	o	x			R	R	R		
Northern goshawk	35	x	x	x			R				
Red-tailed hawk	36	x	o	x			R	R	R		
American kestrel	37	x	x	x					R		
Peregrine falcon	38	o	o	x			r				
Spruce grouse	39	x	x	x			R*				
Blue grouse	40	x	x	x			R				
Ruffed grouse	41	x	x	x				R			
Sharp-tailed grouse	42	o	o	x					W		
Mountain quail	43	o	o	o						R	
Virginia rail	44	x	x	x		R					
Sora	45	x	o	x		SW					S
American coot	46	x	x	x	SW	S					
Sandhill crane	47	o	+	o		sM					sM
Killdeer	48	x	o	x	SW	SW					SW
Common snipe	49	x	o	x		SW					SW
Band-tailed pigeon	50	o	o	x			R	R			
Mourning dove	51	x	o	x				R	R		
Barn owl	52	o	o	x			r	R	R		
Western screech-owl	53	x	x	x			R	R	R		
Great horned owl	54	x	x	x			R	R	R		
Northern pygmy-owl	55	x	x	x			R				
Barred owl	56	x	x	x			R				
Long-eared owl	57	x	x	x					R		
Short-eared owl	58	x	x	x							R
Boreal owl	59	x	x	x			R*				
Northern saw-whet owl	60	x	x	x			R		W		

Appendix Table 6-1 cont'. List of bird species expected to be using palustrine wetlands in Western Washington.

		STATUS		BREEDING DISTRIBUTION							
SPECIES	Evolutionary Order	B	W	WA	PL	FM	WC	BF	RW	ST	WM
Common nighthawk	61	x		x			S		S		
Black swift	62	x		x			S				
Vaux's swift	63	x		x			S	S	S		
Black-chinned hummingbird	64	o		x				S	S		
Anna's hummingbird	65	o	o	o					R	R	
Calliope hummingbird	66	x		x				S	S		
Rufous hummingbird	67	x		x			S	S		S	
Belted kingfisher	68	x	x	x	SW						
Lewis' woodpecker	69	x	o	x					S		
Red-naped sapsucker	70	o		x				S	S		
Red-breasted sapsucker	71	x	o	x			R	R			
Downy woodpecker	72	x	x	x			r	R	R		
Hairy woodpecker	73	x	x	x			R	r			
Three-toed woodpecker	74	x	x	x			r*				
Black-backed woodpecker	75	x	x	x			R*				
Northern flicker	76	x	x	x			R	R	R		
Pileated woodpecker	77	x	x	x			R	R			
Olive-sided flycatcher	78	x		x			S	S			
Western wood-pewee	79	x		x			S	S	S		
Willow flycatcher	80	x		x					S	S	
Least flycatcher	81	x		o				S	S		
Hammond's flycatcher	82	x		x			S	S			
Pacific-slope flycatcher	83	x		x			S	S	S		
Ash-throated flycatcher	84	o		o					S		
Western kingbird	85	o		x					S		
Eastern kingbird	86	x		x					S		
Tree swallow	87	x		x	S				S		
Violet-green swallow	88	x		x	S		S				
Gray jay	89	x	x	x			R				
Steller's jay	90	x	x	x			R				
Black-billed magpie	91	x	x	x					R		
American crow	92	x	x	x			R	R			W
Common raven	93	x	x	x			R				
Black-capped chickadee	94	x	x	x				R	R	R	
Boreal chickadee	95	x	x	o			R				
Chestnut-backed chickadee	96	x	x	x			R				
Bushtit	97	o	o	x					R	R	
Red-breasted nuthatch	98	x	x	x			R	W	W		
White-breasted nuthatch	99	o	o	x				R			
Brown creeper	100	x	x	x			R	W	W		
Canyon wren	101	o	o	x					R		
Bewick's wren	102	o	o	x					R	R	
House wren	103	x		x				S	S	S	
Winter wren	104	x	x	x			R	R	W	M	
Marsh wren	105	x	o	x		R					w
Golden-crowned kinglet	106	x	x	x			R		W		
Townsend's solitaire	107	x	x	x			S*				
Veery	108	o		x				S	S		
Swainson's thrush	109	x		x			S	S			
Hermit thrush	110	x	o	x			S*				
American robin	111	x	x	x			R	R	S		W
Varied thrush	112	x	x	x			R	W	W		
Gray catbird	113	x		x				S	S	S	
American pipit	114	x	o	x		M					M
Bohemian waxwing	115	x	x	o			S		W		
Cedar waxwing	116	x	x	x			S	R	R		
Solitary vireo	117	x		x			S				
Hutton's vireo	118	o	o	o			R	R			
Warbling vireo	119	x		x			S	S		S	
Red-eyed vireo	120	x		x				S	S		
Orange-crowned warbler	121	x	+	x				S	S	Sw	

Appendix Table 6-1 cont'. List of bird species expected to be using palustrine wetlands in Western Washington.

		STATUS		BREEDING DISTRIBUTION							
SPECIES	Evolutionary Order	B	W	WA	PL	FM	WC	BF	RW	ST	WM
Nashville warbler	122	o		x					S	S	
Yellow warbler	123	x		x				S	S		
Yellow-rumped warbler	124	x	o	x			S*		Mw		
Black-throated gray warbler	125	o		x			S				
Townsend's warbler	126	x	o	x			S*				
Hermit warbler	127	o		o			S*				
American redstart	128	x		x				S	S		
Northern waterthrush	129	x		o					S		
MacGillivray's warbler	130	x		x				S	S	S	
Common yellowthroat	131	x		x		S					
Wilson's warbler	132	x		x			S	S		S	
Yellow-breasted chat	133	o		x					S	S	
Western tanager	134	x		x			S	S	S		
Black-headed grosbeak	135	x		x				S	S		
Lazuli bunting	136	x		x					S	S	
Rufous-sided towhee	137	x	o	x				R	R	R	
Savannah sparrow	138	x	o	x							S
Fox sparrow	139	x	x	x					S	SW	
Song sparrow	140	x	x	x		S			R	R	
Lincoln's sparrow	141	x	x	x		S*			M		
White-crowned sparrow	142	x	x	x			S		M	SR	
Dark-eyed junco	143	x	x	x			R	S	W	W	
Bobolink	144	o		o							S
Red-winged blackbird	145	x	o	x		SW					W
Yellow-headed blackbird	146	x	o	x		S					M
Brewer's blackbird	147	x	o	x					S		R
Brown-headed cowbird	148	x	o	x		S	S	S	S	S	
Northern oriole	149	o		x				S	S		
Pine grosbeak	150	x	x	x			R*				
Purple finch	151	x	x	x			R	R			
Cassin's finch	152	x	o	x			S*				
House finch	153	x	x	x					R	R	
Red crossbill	154	x	x	x			R				
White-winged crossbill	155	x	x	o			R*				
Pine siskin	156	x	x	x			R	W	W		
American goldfinch	157	o	o	x					R		
Evening Grosbeak	158	x	x	x			R	R			
Total:	158										
BREEDING SPECIES					66	38	84	65	69	30	19
NONBREEDING SPECIES					52	29	46	31	45	23	34
BREEDING HABITAT SPECIALISTS					34	13	31	4	5	2	5
NONBREEDING HABITAT SPECIALISTS					2	4	11	1	1	4	0

STATUS
B - breeding status

(also migratory status of nonbreeders)

S - summer
W - winter
M - migrant (spring and fall)
F - fall
W - wintering status
x - widespread
o - occurs in <33% of region
+ - occurs in <10% of region
c - coast only

DISTRIBUTION BY AREA
WA - Washington

x - widespread in area

o - occurs in <33% of area

Appendix Table 6-2. Detection rates for species within each wetland all years combined.

	Detection Rates																		
Species	AL3	B3I	BBC24	ELS39	ELS61	ELW1	FC1	HC13	JC28	LCR93	LPS9	MGR36	NFIC12	PC12	RR5	SC4	SC84	SR24	TC13
American Coot							1.25												
American Crow	0.67	1.50	0.33	0.92	0.83	1.00	1.67	0.67	3.08	0.58	3.58	1.92	0.75		1.67	1.92	3.75	0.33	0.92
American Goldfinch		1.08	0.33	0.25	0.33	0.08	0.50	0.25	2.75	0.42	4.42		0.17	0.08	0.42	0.42	0.25	0.83	
American Robin	0.67	2.42	5.75	0.75	3.33	2.92	2.42	1.75	6.00	5.17	5.92	2.58	1.17	2.25	3.00	8.42	5.25	5.50	1.58
Anna's Hummingbird			0.08		0.08													0.08	
Bald Eagle						0.08	0.17												
Barn Swallow		0.08	0.50		0.42	0.17	2.17		0.17		0.33				0.33	0.17		0.17	
Black-capped Chickadee	0.42	2.25	1.42	0.50	1.00	2.67	2.17	1.58	2.42	2.25	4.75	1.58	0.58	1.25	2.50	3.25	1.92	4.75	1.08
Belted Kingfisher			0.58		0.08	0.17	0.25	0.08	0.08	0.08		0.08			0.08	0.08		0.17	
Bewick's Wren	0.08	0.33		0.17	0.58	1.42	1.42	0.17	1.00	0.50	2.17	0.08	0.25	0.25	0.25	1.92	1.17	1.25	0.17
Brown-headed Cow Bird	0.17	0.42	0.33	0.17	0.42	0.08	0.25	0.08	0.50	0.42	0.50	0.08		0.33	0.50	0.08	0.17	0.83	0.08
Black Headed Grosbeak	0.17	0.42	1.50	0.17	1.42	0.67	0.83	0.33	0.58	1.25	1.33	0.17	0.08	0.50	0.58	0.67	0.17	2.00	0.25
Brewer's Blackbird		0.33		0.08	0.17		0.50			0.08	0.17	0.08				0.08		0.08	
Brown Creeper			0.33		0.08			0.08		0.08				0.17	0.42	0.17		0.25	0.17
Black-throated Gray Warbler	0.08		0.17		0.08			0.75	1.17	0.75	0.17	0.08	0.42	0.08	0.50	0.58	0.50	1.25	0.25
Band-tailed Pigeon								0.25								0.08		0.33	
Bushtit		0.50	0.08	0.17	0.33	0.17	0.50	0.17	0.33	0.42	2.33	0.33	0.25	0.25	0.25	1.00	0.08	0.75	0.25
Blue-winged Teal					0.08		0.08												
Canada Goose						0.42	0.33								0.08				
California Quail				0.08	0.08				0.08							0.08			
Caspian Tern						0.08	0.25												
Chestnut-backed Chickadee	0.17	0.17	0.67	0.17	0.33	0.17	0.25	0.17	1.00	0.58	0.42	0.25	0.42	0.25	1.00	0.92	0.42	2.08	0.25
Cedar Waxwing	0.08	1.00	1.00		0.50	0.42	1.25	0.50	0.92	0.67	0.17		0.17	1.25	1.08	0.67	0.33	1.50	0.17
Chipping Sparrow									0.17		0.08		0.08	0.08				0.08	
Cliff Swallow		0.08		0.08			0.92												
Cooper's Hawk	0.08				0.17				0.08	0.33								0.08	
Common Raven										0.17								0.25	
Common Yellow-throat		0.17	2.92		1.58	0.08	0.92	0.67	1.25	3.08	1.58	1.42		2.17	1.75			0.83	
Dark-eyed Junco	0.17		0.08	0.17	0.17			0.25	1.00	0.08	0.33	0.08	0.42	0.08	0.33	0.75	0.25	2.17	0.50
Downy Woodpecker	0.08	0.08	0.25		0.08	0.08	0.33	0.17	0.17	0.17	0.58	0.50		0.17	0.33	0.25	0.33	0.83	0.17
European Starling		0.92			0.17	0.33	1.42		0.50	0.17	0.50	0.08				0.17	0.08		
Evening Grosbeak	0.08								0.58	0.08	0.08				0.25			0.25	
Fox Sparrow		0.17	0.08							0.25									
Gadwall							0.50								0.08				
Great Blue Heron		0.17	0.17		0.25	0.50	1.17			0.08	0.17	0.08		0.17	0.17	0.08		0.42	
Golden-crowned kinglet	0.25	0.25	0.42	0.25	0.17	0.33	0.08	0.92	0.75	0.42	0.25	0.50	0.67	0.17	1.00	0.83	0.58	0.83	0.42
Green Heron		0.17					0.67					0.08							
Glaucous-winged Gull						0.08	0.33				0.08								
Hammond's Flycatcher	0.08				0.25			0.17			0.08	0.08		0.25	0.42		0.33	0.08	
Hairy Woodpecker		0.08	0.67		0.17	0.08		0.42	0.08	0.33		0.33	0.25	0.08	0.67	0.25	0.50	1.00	0.25
Hermit Thrush	0.25		0.50		0.42		0.08	0.67	0.25	0.92	0.08	0.50	0.42	0.67	0.58	0.42	0.92	1.58	0.33
House Finch	0.17	0.25	0.33	0.33	0.42	0.50	0.25		0.08		0.42				0.08	0.08	0.17	0.17	
Hooded Merganser															0.75				
House Sparrow		0.17		0.08	0.08	0.17	0.25		0.08					0.08	0.08				

Appendix Table 6-2 continued. Detection rates for species within each wetland all years combined.

	Detection Rates																		
Species	AL3	B3I	BBC24	ELS39	ELS61	ELW1	FC1	HC13	JC28	LCR93	LPS9	MGR36	NFIC12	PC12	RR5	SC4	SC84	SR24	TC13
Hutton's Vireo			0.17		0.17		0.08						0.08		0.42	0.50	0.17	0.08	0.17
Killdeer		0.08				0.17			0.25		0.08					0.08		0.08	
Mallard		0.17	1.25	0.08	0.83	0.17	3.75				0.17	0.58		0.17	0.75			0.33	
Marsh Wren			0.58	0.08		0.58	4.25		0.25	0.42	0.50	0.17		0.17	0.17	0.08	0.08	0.75	
MacGillivary's Warbler									0.17	0.25	0.08				0.08				0.08
Northern Flicker		0.33	0.83		0.33		0.08		0.08	0.17	0.08	0.33			0.42	0.33	0.42	0.25	
Northern Oriole			0.08				0.08					0.08			0.08				
Northern Pigmy Owl	0.08									0.08							0.08		
Orange-crowned Warbler		0.17	0.83	0.58	0.58	0.17	0.25	0.25	0.17	0.17	0.17			0.42	0.08	0.25	0.42	1.00	0.50
Olive-sided Flycatcher	0.08		0.08			0.08			0.33								0.50		0.17
Pied-billed Grebe					0.08	0.42	1.50								0.08			0.08	
Pine Siskin			0.08	0.08					0.58	0.08	0.08		0.08			0.08	0.33	0.17	
Pileated Woodpecker			0.42						0.08					0.08	0.58			0.08	
Pacific-slope Flycatcher	1.42	0.42	2.75	0.25	0.58	0.33	0.50	1.83	3.08	2.50	1.17	2.58	1.83	1.50	2.25	1.92	0.83	7.42	1.75
Purple Finch	0.08	0.17		0.17	0.25	0.08			1.25	0.50	0.58		0.33	0.25	1.25	0.83	0.33	0.83	0.08
Red-breasted Nuthatch	0.08		0.58	0.08	0.25	0.08		0.17	0.92	0.67	0.08		0.08	0.33	0.83	0.17	1.00	1.17	0.50
Red-breasted Sapsucker			0.08		0.08					0.08		0.08		0.08	0.17	0.08			
Red Crossbill			0.17		0.08	0.17		0.42	0.08	0.08	0.25	0.08	0.17	0.08	0.33	0.33	0.33	0.25	0.17
Red-eyed Vireo									0.08						0.08			0.17	
Red-eyed Vireo								0.17		0.25								0.25	
Rock Dove		0.17					0.25												
Rufous-sided Towee	0.25	0.83	0.33	1.00	1.17	1.58	0.17	0.33	2.08	0.42	4.58	0.17	2.00	1.33	0.75	5.42	2.58	1.75	1.00
Rufous Hummingbird			0.42	0.08	0.17		0.08							0.08				0.25	
Ruffed Grouse										0.08				0.08				0.25	
Ruby Crowned Kinglet	0.17	0.08	0.25	0.17	0.17			0.42	0.25	0.17	0.17	0.25	0.42	0.08	0.33	0.08	0.25	0.67	0.08
Red-winged Blackbird		0.08	13.33		9.67	1.00	9.50	0.25	0.08	2.75	6.33	5.42			0.42			0.33	0.17
Savannah Sparrow									0.17										
Sora			0.17				0.17			0.08									
Song Sparrow	1.17	4.08	10.33	1.58	3.17	4.33	5.92	3.92	6.00	6.50	14.42	3.92	1.83	3.50	4.58	9.50	6.83	10.08	1.50
Solitary Vireo	0.08		0.17		0.17		0.08		0.33		0.08			0.17		0.33	0.08	0.17	0.17
Spotted Sandpiper									0.17										
Sharp-shinned Hawk				0.08		0.08				0.08	0.08								
Steller's Jay	0.08	0.08	2.17		0.25	0.17		0.17	1.08	0.58	0.17		0.25	0.75	1.00	0.67	0.75	2.50	0.50
Swainson's Thrush	1.42	0.67	2.08	0.42	1.00	0.33	0.75	2.75	5.50	8.58	2.08	3.33	2.17	2.67	4.17	4.17	3.33	7.17	3.08
Townsend's Warbler	0.33		0.33	0.17	0.08	0.08		0.17	0.83	0.17		0.08	0.25		0.67	0.25	0.42	0.50	0.08
Tree Swallow	0.08	0.25	0.67	0.25	0.25	0.50	3.17		0.67		0.25	0.08	0.08	0.08	1.25	0.17	0.08	0.58	
Varied Thrush				0.08	0.08		0.33											0.08	
Vaux's Swift	0.25		0.25		0.17	0.25	0.17	0.75		0.08	0.08		0.08		0.33	0.08		0.42	0.25
Violet-green Swallow			1.33	0.08	0.50	0.42	1.17	0.08	0.83	0.17	0.67		0.17	0.25	0.17	0.33	0.25	0.75	
Virginia Rail			0.50		0.08		0.33			0.08		0.17		0.08					
Warbling Vireo		0.08	0.67	0.08	0.17	0.08	0.25	0.08	0.08	1.50	0.58	0.08			0.58	0.17	0.25	0.58	
White-crowned Sparrow	0.08			0.42	0.50		0.08		0.67							0.25			
Western Tanager	0.17		0.75					0.33	0.42	0.50	0.08			0.25	0.25	0.17	0.08	1.25	0.17
Western Wood-pewee	0.25		0.25		0.42	0.17		0.08						0.33	0.50		0.08		0.42

Appendix Table 6-2 continued. Detection rates for species within each wetland all years combined.

	Detection Rates																		
Species	AL3	B3I	BBC24	ELS39	ELS61	ELW1	FC1	HC13	JC28	LCR93	LPS9	MGR36	NFIC12	PC12	RR5	SC4	SC84	SR24	TC13
Willow Flycatcher	0.17	0.42	2.75	0.75	1.92	0.58	1.50	1.50	1.08	4.25	3.33	1.75	0.17	0.75	1.83		0.58	4.08	1.33
Wilson's Warbler	0.58	0.17	1.67	0.33	0.17	0.17	0.75	1.83	1.08	4.50	0.08	1.50	0.75	0.67	3.08	0.67	0.25	2.75	0.92
Winter Wren	1.67	0.25	3.92	0.25	0.25	0.58	0.50	1.42	2.83	1.33	0.42	1.08	0.33	1.08	2.42	0.92	0.42	4.00	2.00
Wood Duck			0.33		0.17	0.17	0.08			0.25		0.08	0.08	0.08	0.08		0.17	0.25	0.08
Yellow Warbler	0.25	0.67	0.92	0.25	0.42	0.83	1.08	0.25	0.67	3.17	0.50		0.25	0.17	0.25	0.58	0.17	1.33	0.17
Yellow-rumped Warbler		0.08	0.08					0.33	0.08		0.08		0.08	0.08		0.25		0.08	

CHAPTER 7 SMALL MAMMAL DISTRIBUTION, ABUNDANCE AND HABITAT USE

by Klaus O. Richter and Amanda L. Azous

INTRODUCTION

Small mammals are an integral component of most ecosystems. In the Northwest the regional distribution of small mammals has been described by Ingles (1965) and Maser et al. (1981). Within unmanaged (e.g., old growth) Douglas-fir forests, small mammals were described in Aubry et al. (1991) by numerous biologists. Mammals in second growth forests under differing cutting practices and intensity of landscaping and development were described by (Stofel 1993). Local small mammal species and distributions in urban parks varying in size of approximately four to 400 ha within urbanizing areas were described by (Gavareski 1976).

The distribution and abundance of small mammals, similar to that of macroinvertebrates, amphibians and birds may be indicators of the environmental health of wetlands. They also exhibit the ability to shape wetlands through their influence on soil, water and plants. Several species such as Trowbridge's shrew, marsh shrew, shrew-mole, western red-backed vole and creeping vole (See Table 7-1 for scientific names) are endemic to the Pacific Northwest (Corn and Bury 1991) and could be expected at pristine wetlands. Our objective in this chapter is to present the relative distribution and abundance of small mammals across the wetlands we studied. We also examine wetland conditions such as size, hydrology and vegetation complexity to gain insight into habitat characteristics important for maintaining diversity and unique species.

METHODS

We used pitfall and Sherman trap captures during autumn (mid-October to mid-November) as indicators of small mammal distributions. We installed traps along two 250-meter transects on opposite sides of each wetland. A combination of 10 pitfalls and 25 Sherman traps at 10 meter intervals was used without drift fences. To minimize the ejection of pitfalls due to hydrostatic pressure, transects were located above winter high-water levels. Pitfalls locations and trap installation procedures are described elsewhere (Richter 1995). Pitfalls were operated for a total of 14, mostly consecutive, days and Shermans for total of six days (alternating between wetlands for three consecutive days). We closed and removed traps vandalized or disturbed by dogs, cats, raccoons and other mammals and continued trapping after several days, when predators were no longer expected at traps. At wetlands in which trap nights were less than attempted (because of ongoing disturbance), captures were adjusted by calculating rates on available traps which was assumed to have been the total number set less one half the number of traps unavailable (Sherman's closed with no captures or treadle stuck; pitfall disturbed by dogs or wildlife), and extrapolated to the full monitoring period (Nelson and Clark 1973) and specifically noted within our discussion. We also relocated traps that became permanently flooded during our study to higher ground where possible. We used wood stakes to mark the beginning and end of transacts and blue flagging to distinguish the trap sites.

All small mammals were identified to species. Deer mice and forest deer mice were distinguished from each other by tail lengths in which adults with tails exceeding 96 mm were identified as deer mice as opposed to forest deer mice with tails less than or equal to 96 mm. Additionally, we aged all deer mice species as adults and subadults (coarse-brown versus soft-gray pelage and weight), sexed and marked by cutting the "pencil-hairs" from the tip of tails, allowing us to determine recaptures and hence rough indexes of abundances for this taxa. The high mortality of shrews in pitfall traps also enabled us to use their capture data in population estimations since recapture rate was low.

We compared the number of National Wetlands Inventory (NWI) (Cowardin et al. 1979) vegetation associations with the diversity of mammal communities. We looked at wetland size and land use, including degree of urbanization and amount forest land within 1000 meters of the wetland. Quantification of these habitat and landscape characteristics are described in the amphibian and bird chapters (five and six) of this report.

RESULTS

We captured a total of 21 small mammal species, 19 of which are native within the wetlands censused (Table 7-1), excluding Norway rat and black rat. The range of species diversity among wetlands varied widely from a low of just one species in ELW1, Norway rat, to a high of 13 species (70% of observed native species) in LCR93 (Figure 7-1).

Table 7-1. Small mammals captured and observed in palustrine wetlands of the Puget Sound Basin.

Common Name	*Scientific Name*	Ames Lake 3	Bellevue 3I	Big Bear Creek24	East Lake Sammamish 39	East Lake Sammamish 61	East Lake Washington 1	Forbes Creek 1	Harris Creek13	Jenkin's Creek 28	Lower Cedar River 93	Lower Puget Sound 9	Middle Green Rivers 36	North Fork Issaquah Creek 12	Patterson Creek 12	Raging River 5	Snoqualmie River 24	Soos Creek 4	Soos Creek 84	Tuck Creek 13
Black Rat	*Rattus rattus*		●									●		●						
Bushy-tailed Woodrat	*Neotoma cinerea*											●								
Creeping vole	*Microtus oregoni*	●	●	●	●	●		●	●		●		●	●	●	●		●		●
Deer Mouse	*Peromyscus maniculatus*	●	●	●	●	●		●	●	●	●	●	●	●	●	●	●	●	●	●
Douglas Squirrel	*Tamiasciurus douglasii*								●				●							
Ermine	*Mustela erminea*								●		●		●							
Forest Deer mouse	*Peromyscus oreas*	●	●	●	●	●			●	●	●	●	●	●	●	●	●	●	●	●
Long-tailed Vole	*Microtus longicaudus*			●							●	●		●						
Marsh Shrew	*Sorex bendirei*			●					●		●		●			●			●	●
Masked Shrew	*Sorex cinereus*										●									
Montane Shrew	*Sorex monticolus*				●	●			●		●	●	●		●	●			●	
Northern Flying Squirrel	*Glaucomys sabrinus*			●																
Norway Rat	*Rattus norvegicus*						●													
Pacific Jumping Mouse	*Zapus trinotatus*		●	●												●				
Shrew-mole	*Neurotricus gibbsii*			●					●		●		●		●	●	●			●
Southern Red-backed Vole	*Clethryonomys gapperi*		●		●						●								●	
Townsend's Chipmunk	*Eutamias townsendii*			●	●				●		●								●	●
Townsend's Vole	*Microtus townsendii*				●	●						●			●			●		
Trowbridge's Shrew	*Sorex trowbridgei*	●	●	●	●	●			●	●	●	●	●	●	●	●	●	●	●	●
Vagrant Shrew	*Sorex vagrans*	●	●	●	●	●		●	●		●	●	●	●	●	●		●	●	●
Water Shrew	*Sorex palustris*																			●

Sites severely altered by urbanization, and harboring minimal populations of native species, include ELW1 and FC1. Surprisingly, B3I, a small wetland almost totally surrounded by urbanization and containing black rats had seven native mammal species. Several wetlands were visited by free ranging dogs (BBC24), unidentified animals (most likely dogs, opossum, raccoon (LPS9), and bear and cougar (RR5), whose activities disrupted our trapping program.

Small mammal richness ranged widely between study years, shown for native species in Figure 7-2. For example, LCR93, which had the highest number of species over the whole study, had at least ten native species the first year, 1988, yet only five native species were collected or observed in 1993 and 1995. At another wetland, HC13, we identified eight, nine and seven species respectively in 1988, 1989 and 1995, yet in 1993, only three species were captured.

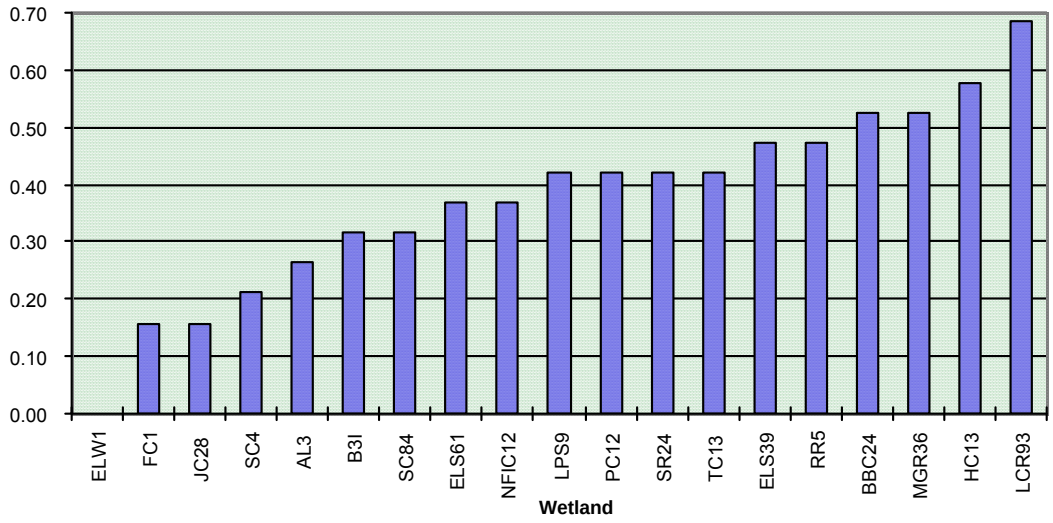

Figure 7-1. Proportional native species richness among 19 palustrine wetlands of the Puget Sound Region.

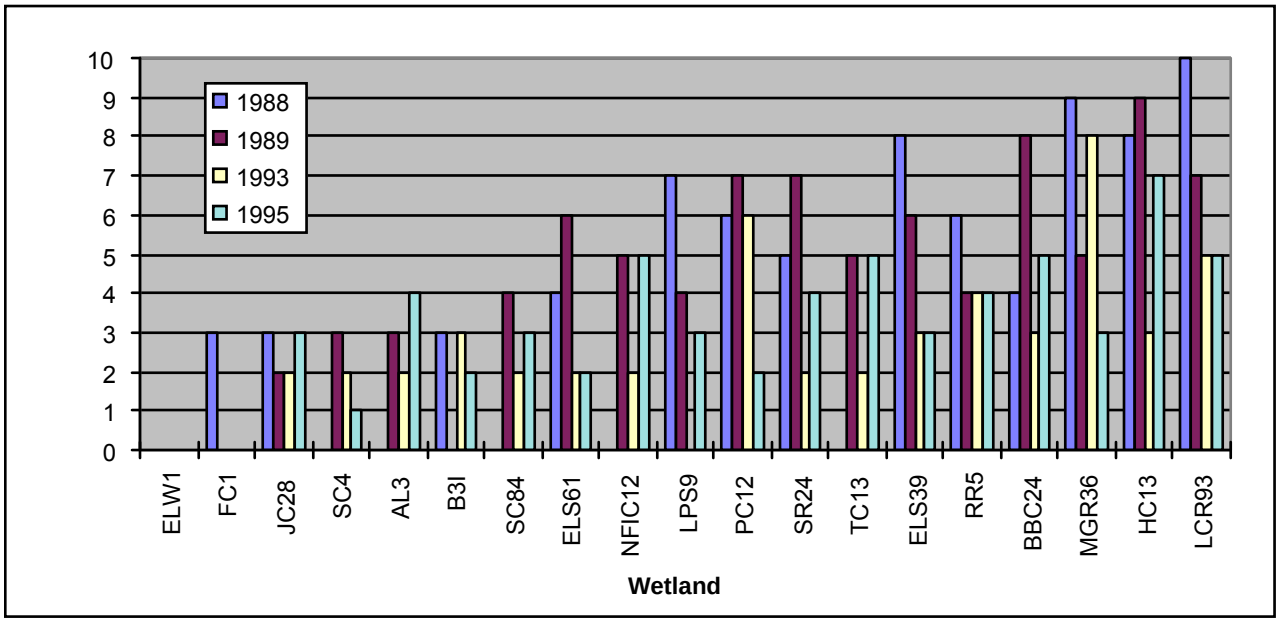

Figure 7-2. Native small mammal richness from 1988 to 1995 in study wetlands.

The abundance of deer mice and shrews varied widely between wetlands and between years. Table of capture rates of species by wetland and by year are available in Appendix Table 7-1. The deer mouse was by far the most abundant mammal captured in all years over all wetlands (Figure 7-3). The Montane shrew and forest deer mouse were the next most abundant and were captured in substantially fewer numbers than the deer mouse. The rarest capture was of the masked shrew, a fairly uncommon species in

this area. The most unusual capture was that of the northern flying squirrel, traditionally an arboreal species and consequently unlikely to be captured in traps on the ground.

Wetland size, by itself, was not found to be significant to mammal richness or abundance (measured as number of captures per 100 trap nights). This result was expected for abundance, however, we expected mammal richness to be strongly related to wetland size, since intuitively, one would expect larger wetlands to have more niches and habitat opportunities. But wetland size was not by itself a major factor and neither were the number of NWI habitat classes. However, the total area of adjacent development was found to be weakly correlated with mammal richness ($R = 0.4$, $p = 0.09$). Though adjacent development was a factor, more critical to highly diverse mammal communities was the percent of forest land immediately adjacent to the wetland within 500 to 1000 meters ($R \geq 0.55$, $p \geq 0.02$) (Figure 7-4). Forest land included all deciduous and coniferous forest and also included lands with single family dwellings within forested parcels. We found that wetlands were more likely to have diverse mammal communities if a substantial part of the adjacent land was not cleared and was retained in forest land.

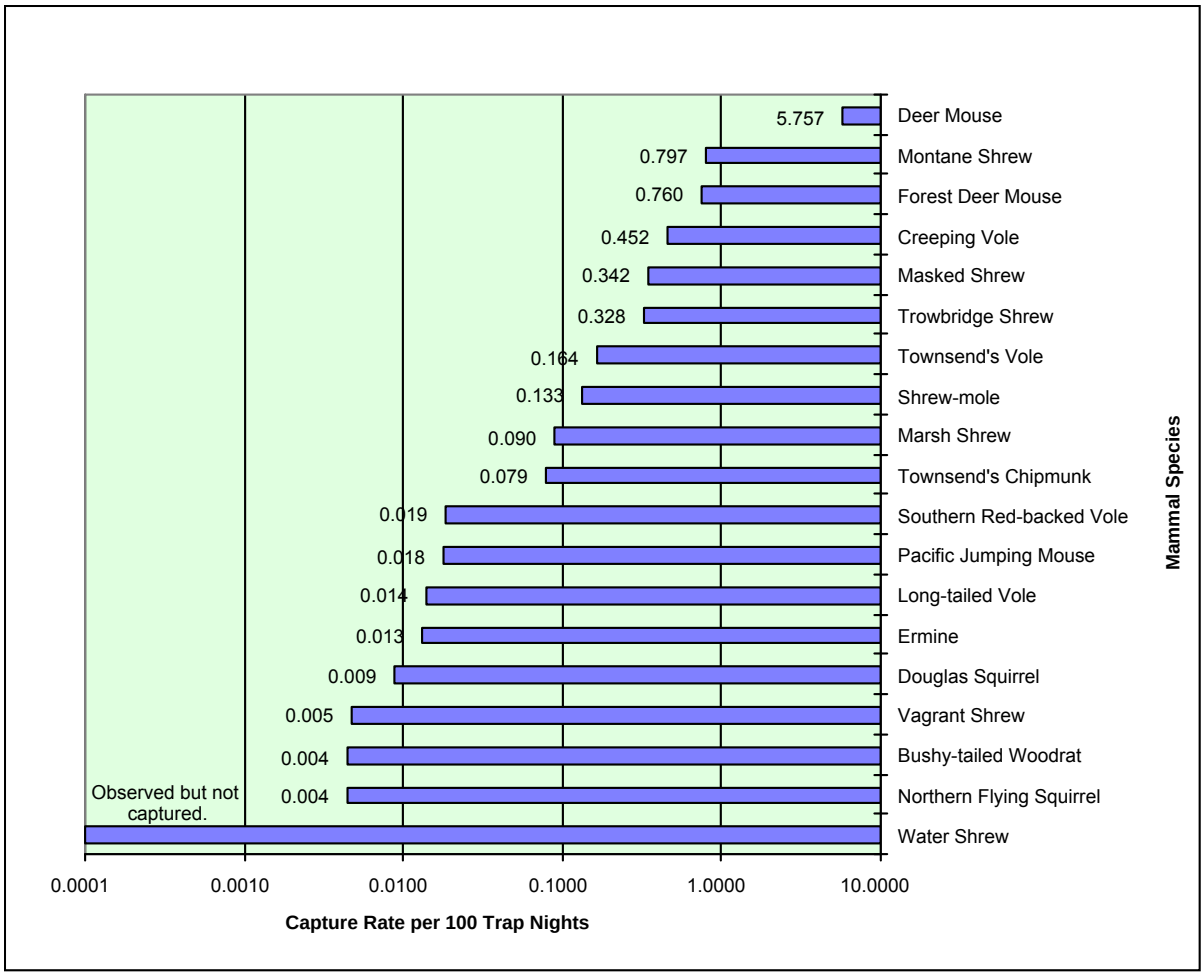

Figure 7-3. Capture rates of small mammals.

Large woody debris in the wetland buffer was also found to be a factor related to diversity. Small mammal richness was found to be associated with the combined factors of wetland size, adjacent land use and the relative quantity of large woody debris within the wetland buffer (Svendsen and Richter in prep.) (Figure 7-5).

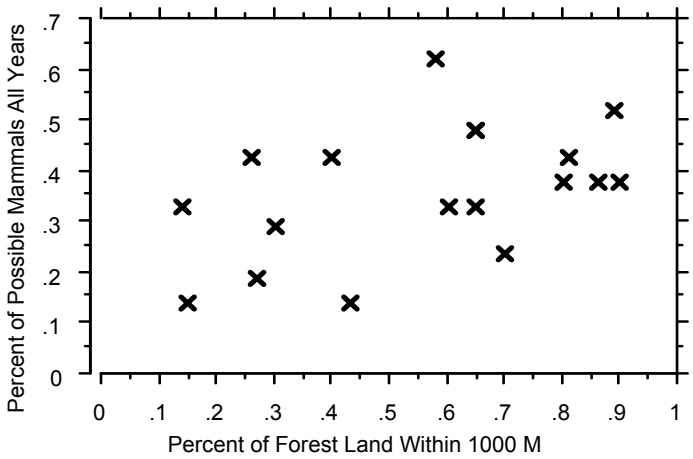

Figure 7-3. Relationship between small mammal diversity and forest land within 1000 meters of wetland.

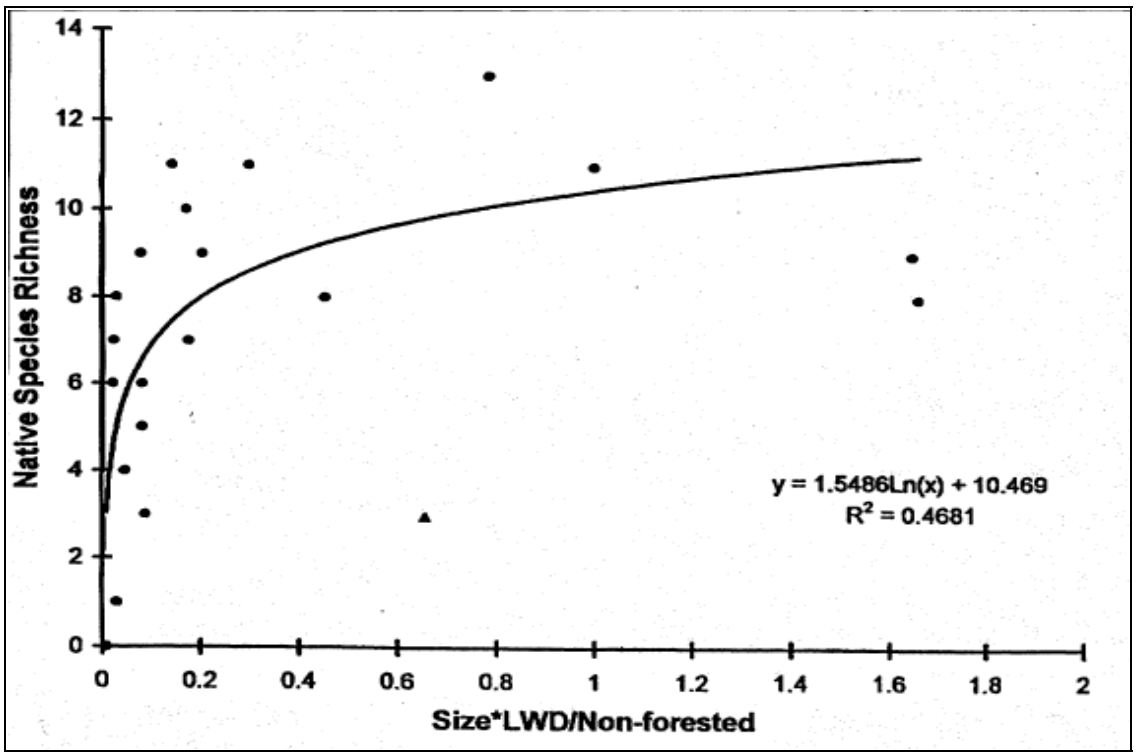

Figure 7-5. Relationship between small mammal species richness and habitat variables including wetland size, land use cover and large woody debris.

DISCUSSION

This study shows that the small mammal communities of wetlands are among the most diverse communities of mammals in the Puget Sound Basin. We captured 22 species (19 native), significantly more than in second-growth forests (Stofel 1993) and urban parks (Gavareski (1976). Because Northern flying squirrels, Douglas squirrels ermine, chipmunk and shrew moles are not well sampled by either pitfalls or Shermans, their true distribution and abundance remains unknown. We captured rats and mice (Muridae), which surprisingly Gavareski (1976) did not capture during her studies of urban parks. On the other hand, we did not capture or observe other non-native species of urban areas including Eastern-cottontail, (Sylvilagus floridanus), Fox squirrel (Sciurus niger) and Eastern gray squirrel (S. carolinensis).

Because of their numbers, deer mice most likely play important roles in trophic dynamics of palustrine wetlands. They appear to inhabit wetlands both in average years as well as in severe years, whereas other small mammals were not consistently captured.

Norway rats may be more damaging to native mammals than black rats in that wetlands with Norway rats appear to displace native species. This presumably happened in ELW1 and another wetland in a heavily urbanized landscape of Snohomish County studied by Svendsen and Richter (In press).

Perhaps one of the more significant findings is the importance of forest land and its consequent habitat component of large woody debris within the wetland buffer. Earlier statistical models that included the presence of vegetation structure (number of vegetation layers e.g., herb, shrub and tree cover), as well as the presence of development and its associated human and animal impacts (e.g., rats, cats and dogs) did not show the strong relationship that forest land and the presence large-woody debris exhibited. Consequently, this result suggests that a certain amount of development can occur and non-native mammals can be tolerated if enough forest land remains available for cover, food, shelter and microclimatic relief. Forest land can provide continuous production of large logs and tree stumps that provide habitat over time. These findings also point out the value of conserving and maintaining large woody debris in wetlands and wetland buffers to increase opportunities for small mammal habitat.

REFERENCES

Aubry, K. B., M. H. Brookes, (eds.). 1991. Wildlife and Vegetation of Unmanaged Douglas-fir Forests. U.S. Department of Agriculture, Forest Service, Pacific Northwest Research Station, Portland, OR, USA.

Corn, P. S., and R. B. Bury. 1991. Small mammal communities in the Oregon Coast Range. Pages 241-254. In K. B. Aubry and M. H. Brookes, (eds). Wildlife and Vegetation of Unmanaged Douglas-Fir Forests. U.S. Forest Service Pacific Northwest Research Station, Portland, OR, USA.

Cowardin, L. M., V. Carter, F. C. Goulet, and E. T. LaRoe. 1979. Classification of wetlands and deepwater habitat of the United States. U. S. Fish and Wildlife Service, Washington D.C., USA.

Gavareski, C. A. 1976. Relation of park size and vegetation to urban bird populations in Seattle, Washington. Condor 78:375-382.

Ingles, L. G. 1965. Mammals of the Pacific States. Stanford University Press, Stanford, CA, USA.

Maser, C., B. R. Mate, J. F. Franklin, and C. T. Dyrness. 1981. Natural History of Oregon Coast Mammals. Pages 496. U.S. Department of Agriculture, Forest Service, Pacific Northwest Forest and Range Experiment Station.

Nelson, L., Jr. And F.W. Clark. 1973. Correction for sprung traps in catch/effort calculations of trapping results. J. Mammal. 54:295-298.

Stofel, J. L. 1993. Evaluating wildlife responses to alternative silvicultural practices. Pages 126. University of Washington, Seattle, Washington, USA.

Svendsen, C. R., and K. R. Richter. In prep.. Small mammals in a restored urban wetland in response to biotic and landscape characteristics. Presented at Ecological Summit 96, Copenhagen, Denmark and to be published in Ecological Engineering).

Appendix Table 7-1. Pitfall capture rates of small mammals by wetland, species and year of capture.

Code	CLGA		EUTO			GLSA	MILO		
Species	Clethryonomys gapperi		Eutamias townsendii			Glaucomys grapperi	Microtus longicaudus		
Common Name	Southern Red-backed Vole		Townsend's Chipmunk			Northern Flying Squirrel	Long-tailed Vole		
Number of Captures per 100 Trap Nights									
SITE_ID	1988	1993	1988	1989	1995	1989	1988	1993	1995
AL3									
B3I	0.36								
BBC24						0.34		0.72	
ELS39	0.36		0.33	0.33	1.33				
ELS61									
ELW1									
FC1									
HC13				1.00					
JC28									
LCR93	0.33		2.33	0.67			0.36		
LPS9							0.33		
MGR36									
NFIC12									0.36
PC12									
RR5									
SC4									
SC84									
SR24		0.36		0.33					
TC13					0.33				

Code	MIOR				MITO				MUER	
Species	Microtus oregoni				Microtus townsendii				Mustela erminea	
Common Name	Creeping Vole				Townsend's Vole				Ermine	
Number of Captures per 100 Trap Nights										
SITE_ID	1988	1989	1993	1995	1988	1989	1993	1995	1988	1989
AL3				0.33						
B3I			0.36							
BBC24	1.37	1.01		2.15						
ELS39	5.95	1.00			7.24	2.07	0.36			
ELS61	1.36	0.33				0.33				
ELW1										
FC1	10.29									
HC13	4.02	0.67							0.33	
JC28										
LCR93	0.69			0.71						0.33
LPS9					1.05					
MGR36	6.90	0.69	0.36						0.33	
NFIC12		0.71		1.07						
PC12	1.71	1.33			1.69	1.33				
RR5	2.42									
SC4										
SC84		0.36				0.36				
SR24										
TC13		1.02								

Appendix Table 7-1. Pitfall capture rates of small mammals by wetland, species and year of capture.

Code	NECI	NEGI			PEMA			
Species	Neotoma cinerea	Neurotricus gibbsii			Peromyscus maniculatus			
Common Name	Bushy-tailed Woodrat	Shrew-mole			Deer Mouse			
Number of Captures per 100 Trap Nights								
SITE_ID	1989	1988	1989	1993	1988	1989	1993	1995
AL3						15.98	4.29	2.00
B3I					0.67		0.71	3.33
BBC24					3.70	14.48	0.72	13.01
ELS39					9.69	16.69	0.71	11.33
ELS61					8.00	12.38		2.02
ELW1								
FC1					8.67			
HC13			0.71		12.38	20.00	0.36	3.36
JC28					15.69	11.33	0.36	9.02
LCR93			0.36		32.40	7.33	2.86	8.67
LPS9	0.69				32.24	23.38		23.02
MGR36		0.36		0.36	7.79	14.74	4.64	9.05
NFIC12						9.64	0.36	2.33
PC12				1.07	3.69	11.05	5.00	9.02
RR5				3.21	8.42	10.11	1.79	4.05
SC4				0.36		14.76	0.36	23.00
SC84						73.50		16.33
SR24					1.67	19.02		2.00
TC13						0.67	1.43	3.38

Code	PEOR				RARA			SOBE		
Species	Peromyscus oreas				Rattus rattus			Sorax bendirei		
Common Name	Forest Deer Mouse				Black Rat			Marsh Shrew		
Number of Captures per 100 Trap Nights					1988	1989	1995	1988	1989	1993
SITE_ID	1988	1989	1993	1995						
AL3		1.67		3.33	1.33					
B3I				2.00					0.36	
BBC24	0.34	4.37		1.68						
ELS39				1.33						
ELS61	1.00	0.67		0.33						
ELW1										
FC1								0.71	0.36	
HC13	7.00	7.33		0.69						
JC28	6.33	1.00		0.67				0.71	1.07	
LCR93	5.36	2.67	0.36	0.67			1.67			
LPS9	1.33	0.33							0.36	1.43
MGR36	2.00	2.67	0.36	0.67						
NFIC12				0.67						
PC12		1.33	0.36	2.67				0.71		
RR5	1.68	1.34		0.34						
SC4		0.33								
SC84		6.02	0.36	1.67					0.36	
SR24	1.00	2.33		0.33					0.36	
TC13		0.33								

Appendix Table 7-1. Pitfall capture rates of small mammals by wetland, species and year of capture.

Code	SOCI	SOMO				SOTR			
Species	Sorex cinereus	Sorex monticolus				Sorex trowbridgei			
Common Name	Masked Shrew	Montane Shrew				Trowbridge Shrew			
	Number of Captures per 100 Trap Nights								
SITE_ID	1988	1988	1989	1993	1995	1988	1989	1993	1995
AL3								1.79	1.07
B3I								1.79	
BBC24						0.69	2.13	3.21	1.79
ELS39		1.38	1.38			0.36		0.36	
ELS61			2.79			1.05		0.71	
ELW1									
FC1									
HC13		0.36	1.79	0.36	1.79	0.71	0.36	0.71	1.07
JC28						0.67		1.07	0.36
LCR93	0.36	1.07		0.36		1.07	1.79	3.93	0.36
LPS9		0.69				2.45	2.76		0.36
MGR36		1.07		1.43		1.02	1.07	1.79	2.86
NFIC12			0.69				1.05	0.36	0.36
PC12		2.79	2.83	0.36		0.69	3.19	2.86	
RR5		0.34				3.21	1.05	2.14	
SC4							0.36		
SC84									0.71
SR24		0.36	0.71		0.36	0.71	3.21	2.14	1.43
TC13							0.36	0.71	1.79

Code	SOVA				TADO		ZATR	
Species	Sorax vagrans				Tamiasciurus douglasii		Zapus trinotatus	
Common Name	Vagrant Shrew				Douglas Squirrel		Pacific Jumping Mouse	
Number of Captures per 100 Trap Nights								
SITE_ID	1988	1989	1993	1995	1988	1995	1989	1995
AL3		2.12						
B3I	0.36							
BBC24		0.72					0.69	
ELS39	2.12	0.69						
ELS61		0.33	0.36					
ELW1								
FC1	0.33							
HC13	0.36	0.36		0.69		0.33		
JC28								
LCR93			0.36	0.33				
LPS9	1.40			0.71				
MGR36	0.69		1.43		0.33			
NFIC12		0.36						
PC12	1.07	1.76	2.14					
RR5		0.34	0.71					0.67
SC4								
SC84			0.36					
SR24	0.36	3.19						
TC13				1.07				

Section 3 Functional Aspects of Freshwater Wetlands in the Central Puget Sound Basin

CHAPTER 8 EFFECTS OF WATERSHED DEVELOPMENT ON HYDROLOGY

by Lorin E. Reinelt and Brian L. Taylor

INTRODUCTION

In urbanizing areas, the quantity (peak flow rate and volume) of stormwater can change significantly as a result of developments in a watershed. Increases in stormwater may result from new impervious surfaces, removal of forest cover, and installation of constructed drainage systems. Watershed development can also cause reduced recharge of groundwater and baseflow to streams, and less evapotranspiration.

Changes in hydrology, whether brought about intentionally or incidentally, have an influence on wetland systems. Wetlands will likely have a positive effect on downstream areas by dampening stormflows before discharging to streams and lakes. However, wetlands may also be adversely impacted by these same higher peak flows and volumes. For cases where wetlands are the primary receiving water for urban stormwater from new developments, it is hypothesized that the effects of watershed changes will be manifested through changes in the hydrology of wetlands.

Wetland hydrology is often described in terms of its hydroperiod, the pattern of fluctuating water levels resulting from the balance between inflows and outflows of water, landscape topography, and subsurface soil, geology, and groundwater conditions (Mitsch and Gosselink, 1993). Hydroperiod alterations are the most common effect of watershed development on wetland hydrology. This usually involves increases in the *magnitude*, *frequency* and *duration* of wetland water levels. In other words, increased stormwater flows tend to cause higher wetland water levels, on more occasions during the wet season, and for longer periods of time. These changes in wetland hydroperiod then result in impacts to plant and animal communities that were adapted to the pre-existing hydrologic conditions.

Puget Sound Wetlands and Stormwater Management Research Program

Palustrine wetland hydrology was studied as part of both components of the research program: (1) the study of the long-term effects of urban stormwater on wetlands, and (2) the study of the water-quality benefits to downstream receiving waters as urban stormwater flows through wetlands. This chapter presents results from the statistical analysis of 19 study wetlands from the long-term effects study, and from the water balance of two wetlands from the water-quality benefit study.

Research Objectives

The primary objective of this portion of the research program was to examine the effects of urban stormwater on wetland hydrology. However, there were also a variety of

specific hydrologic questions addressed throughout the research which developed into the following specific objectives:

1. Identify the wetland and watershed hydrologic processes, and the factors governing these processes.
2. Determine how urban catchments behave differently from forested catchments.
3. Determine the percent contribution of wetland hydrologic inputs and outputs.
4. Relate wetland hydrologic conditions to wetland/watershed characteristics.
5. Characterize wetland hydroperiods and develop a set of dependent variables for analysis.

DATA COLLECTION AND ANALYSIS METHODS

As noted in Chapter 1, a conceptual model was used to show the relationship between factors influencing wetland and watershed hydrologic processes and the wetland hydroperiod (Figure 1-4). In the conceptual model, some of the key factors thought to influence wetland water level fluctuation included: (1) forested area, (2) impervious area, (3) wetland morphology, (4) outlet constriction, (5) wetland-to-watershed area ratio, and (6) watershed soils. Statistical analyses were carried out to determine which factors were most important.

Statistical Analysis of Development Impacts on Wetland Hydrology

A variety of graphical and statistical techniques were used in identifying relationships between the watershed or wetland characteristics and wetland hydroperiod (Taylor, 1993). Microsoft EXCEL was used in processing the data and SYSTAT was used for statistical analyses.

Graphical Analysis

The objective of the graphical analysis was to identify trends and threshold levels that could then be statistically tested to determine which statistical methods (parametric or nonparametric) were appropriate. Graphical analysis provided insights into which factors correlated to specific aspects of the hydroperiod; however, it failed to show the effects of multiple factors or varying importance simultaneously.

Normality Testing

In order to determine which statistical tests were appropriate for a given hypothesis, the normality of the data was assessed. The Kolmogorov-Smirnoff test was used to compare the maximum difference between two cumulative distributions. The Lilliefors test was used when the mean and variance of the distribution were unknown, in order to automatically standardize the variables and test whether the standardized distributions were normally distributed (Wilkinson, 1990). The Lilliefors test was used to assess the distribution of water level fluctuation measurements. The significance level used in testing normality was alpha equal to 0.05.

Threshold Testing

Threshold testing was done when a scatterplot suggested one or more threshold levels in the response of wetland water level fluctuations to a specific watershed or wetland characteristic. The data were grouped categorically based on thresholds suggested in the scatterplots. These groups were compared in a test of the null hypothesis that all groups were from equivalent distributions.

Because the water level fluctuation measurements were not normally distributed for all of the study sites, nonparametric tests were used: the Mann-Whitney test for two groups and the Kruskal-Wallis test for more than two groups. These two tests are analogous to the independent groups t-test for normally distributed data, but are based on data ranks rather than the data values (Zar, 1984; Wilkinson, 1990). The Kruskal-Wallis test will reject the null hypothesis if *any* of the groups are significantly different; nonparametric multiple comparisons were done to identify *which* groups were significantly different (Zar, 1984). The significance level used in evaluating thresholds was alpha equal to 0.05.

Multivariate Regression Models

Multivariate, least squares, linear regression models were calibrated to the study data to show how various wetland and watershed factors combine to effect wetland hydroperiod (Taylor, 1993). Models were developed by: (1) using step regression to identify factors important to the aspect of wetland hydroperiod being investigated, (2) determining the best way to quantify or express this factor, (3) evaluating model fit, and (4) examining the sensitivity to the predictor variables. The data for each wetland were weighted by sample size when appropriate; mean water level fluctuation was weighted by the total number of observations used in its calculation while the length of the dry period and seasonal water level fluctuations were weighted by the number of years used in their calculation.

The fit of the regression models was evaluated through various methods: the coefficient of determination (r^2) and the F-ratio, which compares the explanation provided by each predictor to the residual associated with each observation. The final step in the generation of the multiregression models was to examine the sensitivity of each predictor variable. The standardized coefficient of each predictor variable provides a way to compare the significance of the variables (Wilkinson, 1990). Additionally, variables were removed from the final model one at a time to determine their effect on the model r^2 and the standard error of the estimate.

Data Collection and Analysis for the Wetland Water Balance

In the detailed study of two wetlands (Bellevue 3I and Patterson Creek 12), a complete water balance was performed (Reinelt et al., 1993). This consisted of independent measurements of the following components: precipitation, evapotranspiration, surface inflow, surface outflow, groundwater exchange, and change in wetland storage. Precipitation was measured using an event recorder connected to a tipping-bucket gauge that recorded each 0.25 mm of rainfall. Continuous water flow measurements were taken at the inlet and outlet of the two wetlands using a variety of different techniques (Reinelt et al., 1990).

Shallow (1.2 to 4 m) and deep (6 to 18 m) piezometers were installed at both wetlands to aid in the estimation of groundwater flow using Darcy's Law (see Chapter 1). The

hydraulic conductivity (K) of the underlying aquifer at both wetlands was determined using variable head pump and slug tests as described by Cedergren (1978) and Chapuis (1989). Piezometric head measurements were taken regularly to determine the hydraulic gradient (Surowiec, 1989). Control volumes were defined around each wetland to facilitate estimation of the horizontal and vertical components of groundwater flow.

Evapotranspiration was estimated from pan evaporation data from the Washington State University Extension Service Puyallup station representing the Puget Sound Lowlands region. Adjustments were made for differences between pan evaporation, open-water evaporation, and evapotranspiration by plants. Daily changes in wetland water depth (and corresponding storage volume) were estimated by correlating daily outflow data with regular gauge (water depth) readings. Storage volumes were determined for different water levels by multiplying the areal water coverage by water depth.

Identifying and describing seasonal differences in the hydrologic balance of the two wetlands was one objective of the study. Seasons were defined and analyzed by two classification methods. The first method included simply wet (October - March) and dry (April - September) seasons. The second method defined four seasons based on the climate of the Puget Sound region: wet (November-February), dry (June-September) and two transition (March-May; October) seasons. The division of data by season allowed for comparison of changes in the relative contributions of different inputs and outputs.

RESULTS AND DISCUSSION

Wetland Hydrology and Water Level Fluctuation

Three parameters were used to examine hydrologic conditions in the wetlands: water depth, water level fluctuation (WLF), and length of summer dry period. The minimum, maximum and range of water depths at the gauges are given in Table 8-1. Also given are the mean (according to equation 4 of Chapter 1) and maximum WLF, and days of summer drying in the wetland. Water depth and WLF varied widely for the 19 wetlands.

Table 8-1 Wetland watershed, outlet and hydrologic characteristics.

Wetland Name	Forest (%)	Imperv. Area (%)	Outlet Constr.	Range of Water Depth (m)	Mean WLF (m)	Max. WLF (m)	Mean Dry Period (days)	Calculated Mean WLF (m) Using Multiple Regression
AL3	73.9	3.4	1	0.00-0.62	0.07	0.31	101	0.21
MGR36	88.8	2.7	0	0.13-0.74	0.07	0.26	0	0.08
JC28	34.4	19.3	0	0.00-0.32	0.08	0.17	74	0.14
RR5	62.4	3.2	0	0.02-0.52	0.09	0.24	0	0.11
SC4	46.1	11.8	0	0.00-0.30	0.10	0.15	125	0.13
SR24	100.0	2.0	0	0.00-0.67	0.11	0.23	32	0.07
NFIC12	100.0	2.0	1	0.00-0.53	0.13	0.30	189	0.17
ELS61	0.0	3.9	0	0.05-0.84	0.14	0.33	0	0.19
PC12	75.2	3.9	1	0.20-1.19	0.14	0.84	0	0.20
BBC24	89.5	2.8	0	0.07-0.60	0.14	0.20	0	0.08
TC13	100.0	2.0	0	0.00-0.72	0.16	0.31	156	0.07
ELW1	0.0	19.9	0	0.00-0.66	0.22	0.44	19	0.19
HC13	76.6	3.6	1	0.09-1.56	0.24	0.41	0	0.20
SC84	20.1	15.9	0	0.00-1.08	0.26	0.53	62	0.16
FC1	14.7	30.8	0	0.11-1.01	0.28	0.62	0	0.38
LCR93	44.1	3.9	1	0.00-0.81	0.28	0.57	61	0.24
ELS39	0.0	28.0	1	0.00-1.61	0.46	1.29	151	0.51
B3I	0.0	54.9	1	0.63-2.37	0.57	1.54	0	0.51
LPS9	0.0	21.8	1	0.00-1.72	0.60	1.47	85	0.51

The largest range of water levels, as well as mean and maximum WLFs were found at B3I and LPS9, where the basins have among the highest percent of impervious area of any of the study sites and the wetland outlets are constricted (see B3I and LPS9 in Figure 8-1). Those wetlands with 90 percent or more forested cover and less than 3 percent impervious surfaces generally exhibited lower water ranges and low WLFs (see BBC24 and SR24 in Figure 8-1). As can be seen from Figure 8-1, these trends of low or high WLF are independent of whether the base level condition in the wetland is stable or fluctuating. Wetland JC28 was an exception to the normal relationship between high impervious area and high WLF; this was because the watershed soils are predominantly glacial outwash (highly permeable soils), thus reducing runoff volumes.

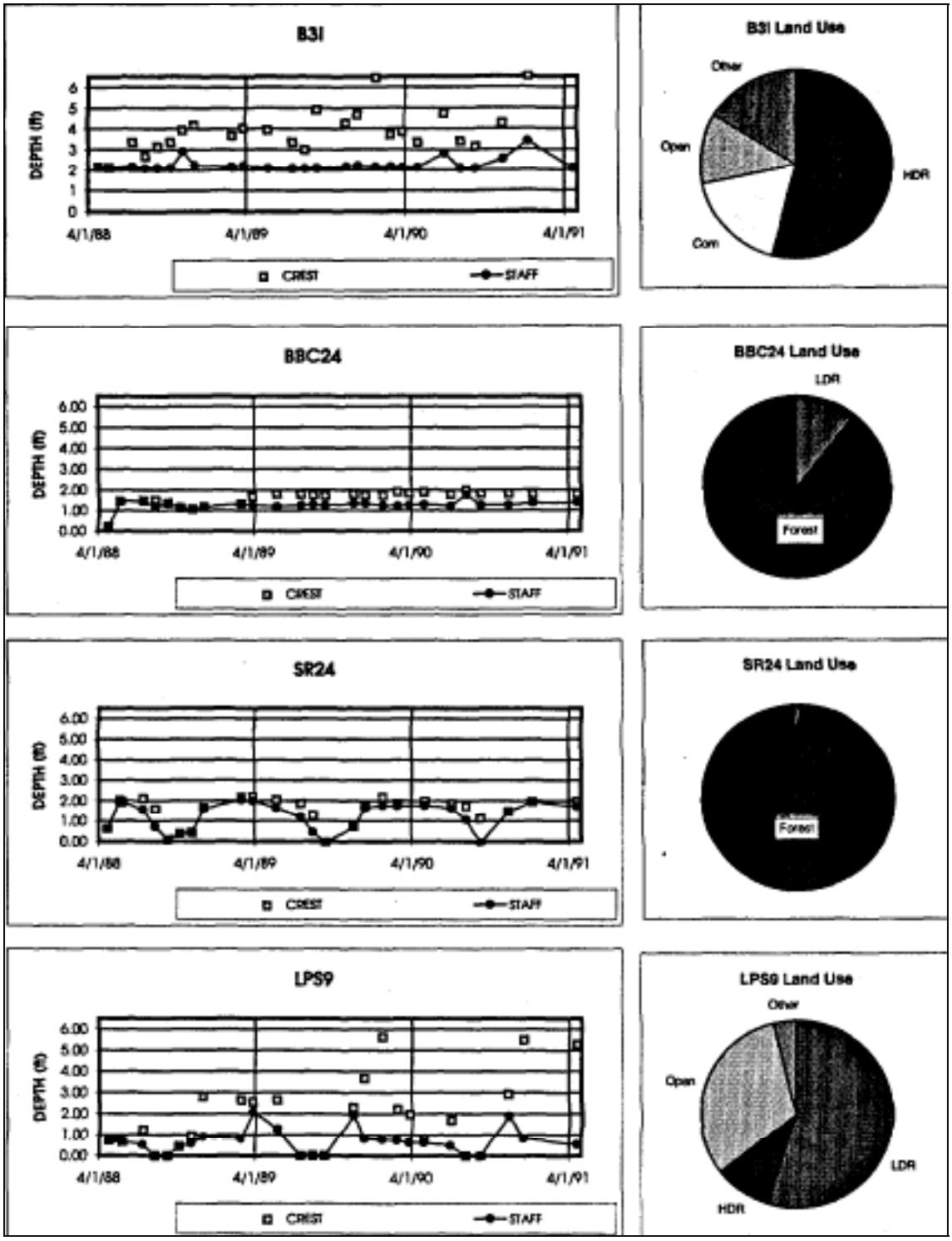

Figure 8-1. Wetland hydrographs (base and crest levels) and land use.

Threshold Level Analysis

Scatterplots of the event water level fluctuation data were plotted against the various wetland and watershed morphological parameters. Some of these plots showed

apparent thresholds that signify a range of the hydrologic parameter where the event fluctuation data are similarly distributed. Within these ranges, characteristics such as the mean and variance of the data were approximately equal. Table 8-2 shows significant threshold levels ($P < 0.05$ for all thresholds) and characterizes the water level fluctuation data within each range.

Table 8-2 Parameters significant to wetland water level fluctuation.

Parameter	Range (a)	Mean WLF (m)	Std. Dev. (m)	n
Forested area	forest = 0%	0.384	0.338	97
	forest ≥ 14.7%	0.151	0.138	224
Total impervious area	2.0 ≤ TIA ≤ 3.5%	0.105	0.072	105
	3.5 < TIA ≤ 20%	0.176	0.151	143
	21.8 < TIA ≤ 54.9%	0.478	0.348	73
Outlet constriction	low to moderate	0.148	0.119	198
	high	0.34	0.33	123
Wetland-to-watershed area ratio	0.005 ≤ W/Ws ≤ 0.04	0.304	0.301	169
	0.05 < W/Ws ≤ 0.44	0.129	0.091	152
Watershed soils index	3.9 ≤ WSI ≤ 4.1	0.247	0.279	209
	4.2 < WSI ≤ 5.8	0.174	0.143	112

(a) The upper and lower bounds are the maximum and minimum values of the parameter within the range.

A key index relating urbanization to WLF was basin imperviousness. Two thresholds were identified in the relationship between event WLF and impervious area (Figure 8-2). The first threshold (3.5% impervious area) may represent the level of urbanization where scattered clearing of forests is added to by larger developments, and storm drainage systems that route runoff to the wetland are developed. Development within the first range was usually below 15% low density residential (LDR), whereas the second range begins around 24% LDR. Wetlands HC13 and LCR93 (in the second range) were exceptions to this tendency, because of the large proportion of their watersheds that were clear-cut. The second threshold (20% impervious area) may represent the point that changes in storm runoff caused by urbanization (e.g., flow volumes, flashiness) become dominant over the other factors that influence wetland hydroperiod.

The amount of forested area in a watershed was expected to be inversely related to event WLF. Forests store rainwater in the canopy, return water to the atmosphere through evapotranspiration, and typically have a highly permeable litter zone on the soil surface, all of which act to reduce storm runoff volumes and reduce the delivery rate to receiving waters. Furthermore, in an area such as the Puget Sound lowlands which are primarily forested until urbanization begins, forested coverage is an index of urban development. The expected relationship was observed (Figure 8-2). Sites with highly constricted outlets were expected to exhibit higher event WLF than those with less constricted outlets due to backwater effects. Figure 8-2 shows that this trend was observed, particularly in the maximum levels of event WLF.

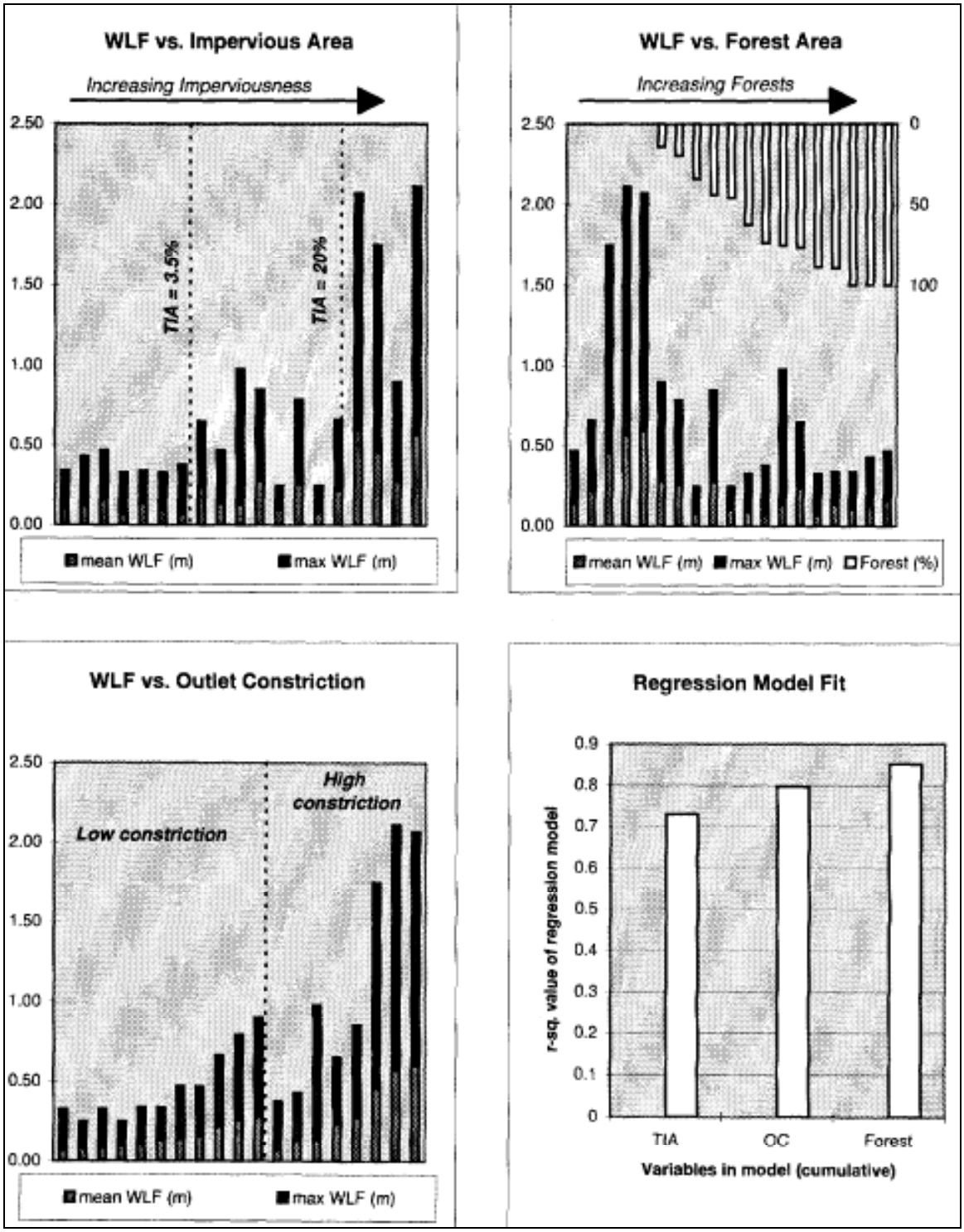

Figure 8-2. Relationships between water level fluctuations and imperviousness, forest area, and outlet constriction.

As shown in Table 8.2, there were two other variables that exhibited trends with wetland WLF: wetland-to-watershed area ratio and watershed soil index (WSI). The wetland-to-

watershed ratio can be thought of as a “loading” term. The lower the ratio, the less area available to store storm runoff, resulting in higher event WLF. The threshold observed (ratio = 0.045) corresponds with the recommended ratio for stormwater detention ponds, which is five percent (KCSWM, 1990). The WSI was developed to quantify the soil drainage characteristics; since higher values indicate soils with high infiltration capacity, these values were expected and found to be associated with low event WLF.

Multiple Regression Analyses

Multiple regression analyses were done on the mean event WLF data from 1988 through 1991. The mean WLF data were weighted by the sample size, with the size of the weighted data set consisting of 321 observations. The best model fit was found using three variables: impervious area, outlet constriction, and forested area (see Figure 8-2). The following equation produced the best fit when using percent impervious and forested areas as continuous variables, and outlet constriction as a binary variable (0 or 1):

$$\text{Mean WLF (m)} = 0.145 + 0.0052*(\text{Impervious}) + 0.141*(\text{OC}) - 0.0011*(\text{Forest})$$
$$\text{where } R^2 = 0.790 \text{ and SE} = 0.08 \text{ m.}$$

The model fit explained 79% of the variation in mean event WLF between sites. Residual analysis showed no deviations from the model assumptions. All the parameter coefficients were of the sign (positive or negative) expected. This model was tested in later years using data from 1993 through 1995 and not confirmed (Chinn 1996), however there were some significant differences in the assumptions guiding the selection of data between the two analyses which likely account for the different results.

Dry Period

The length of the summer dry period for the study sites ranged from zero for the sites with stable base flow to nearly 200 days (Table 8-1). A variety of approaches were used to evaluate which factors are important in determining the permanence of a site and the length of the dry period for those sites that dry in the summer. Spearman rank correlations were used to investigate the relation between the mean length of the summer dry periods and morphologic parameters at sites that dry during the summer. Significant negative correlation was found between the length of the dry period and the area of the wetland. The significance of the wetland area is attributable to two factors of the hydrologic balance, evapotranspiration and groundwater exchange. Because the correlation is negative, however, it is assumed that groundwater discharge to the wetlands is driving the relationship.

Hydrologic Characteristics of Two Intensively Studied Wetlands

A summary of the natural and hydrologic characteristics during the study period (1988-90) for the B3I and PC12 wetlands is given in Table 8-3. The hydrologic reactions to storms exhibited by the two wetlands are typical of the respective watershed land uses. The reaction of B3I inlet flows to storms is fast and dramatic. Flows increase almost immediately because of the large impervious land area and piped storm drain system. Similarly, when storms end, the flow recedes quickly to near baseflow conditions. The PC12 inlet flow, on the other hand, reacts relatively slowly to storms, with the receding

limb of the hydrograph extending much longer than at B3I. Significant inflows occurred at PC12 only from October to June; however, there was water in the wetland year round.

Table 8-3. Natural and hydrologic characteristics of two wetlands.

Variable (unit)	B3I Wetland	PC12 Wetland
Dominant land type	Urban	Forest
Watershed area (ha)	187	87
Wetland area (ha)	2	1.5
Wetland-to-watershed ratio	0.011	0.017
Total precipitation (mm)	1,813	1,934
Precip. volume (m^3) in drainage area	3.4×10^6	1.7×10^6
Mean daily inlet flow (m^3/s)	0.042	0.021
Maximum daily inlet flow (m^3/s)	0.75	0.22
Days with measurable flow during study	730	493
Total flow during study (m^3)	2.7×10^6	0.9×10^6
Wetland storage volume (m^3)[a]	400-5,000	600-7,000
Runoff/precipitation ratio	0.80	0.53

[a] Wetland storage volume varies depending on season and flow conditions.
(Note: Study period was two years for B3I and 20 months for PC12).

Nearly 80 % of the annual precipitation occurred between October and March. The maximum daily precipitation occurred on January 9, 1990 (approximately 80 mm at both sites). Pan evaporation data from the Puyallup station were used for ET estimates at the wetlands. The measured pan evaporation was greatest from May to August (exceeding 100 mm per month) and least from November to March. The maximum monthly and daily evaporation rates during the study were 160 mm (July 1989) and 16 mm (July 30, 1989), respectively.

Water storage volumes varied from 400 to 5,000 m^3 at B3I and from 600 to 7000 m^3 at PC12. Generally, changes in storage volume at B3I were short-term (on the order of hours) and directly related to storm events. Baseflow rates and water storage were comparable during the wet and dry seasons. At PC12, on the other hand, storage volumes changed during storm events and by season. Water volumes were greatest during large storms or groups of storms during the late wet season.

The results of the groundwater investigation indicate that both wetlands are discharge zones under most conditions meaning that groundwater discharges to the wetland and becomes surface water. Recharge wetlands, in contrast, replenish groundwater through infiltration of surface water. This was determined by the piezometric head measurements, and given the fact that groundwater flows from areas of high to low head. The head measurements in both wetlands generally increase with depth below the water table (as measured by the deep piezometer clusters) and distance from the wetland, indicating the groundwater flows both vertically and laterally to each wetland. Discharging wetlands have also been documented by other authors (Wilcox et al., 1986; Siegel and Glaser, 1987).

Wetland Hydrology by Season and Wetland

Table 8-4 summarizes the hydrologic inputs and outputs by season for the two wetlands. For both wetlands, surface water outflow accounted for greater than 99 % of the outputs during the study period. Thus, groundwater recharge and ET, the other potential sources of output, were insignificant on an annual basis. This is typical for wetlands that have a low wetland-to-watershed area ratio (1.1 and 1.7 % for B3I and PC12, respectively) and for wetlands that lie in a groundwater discharge area. For wetlands with low wetland-to-watershed ratios, inputs from the larger watershed (i.e., surface water flows) often dwarf the contributions from "in-wetland" components, such as groundwater and ET, because of the relatively small wetland area. Also, if groundwater exhibits mostly a discharge pattern as a result of topography and wetland location, then groundwater recharge is likely a minimal source of water output.

Table 8-4. Summary of hydrologic inputs and outputs by season (all values are in 1000 m^3; percent of total input or output in parentheses).

Wetland/ Season[a]	Precip-itation	Inputs Inflow	Ground-water[b]	Outputs Outflow	Evapo-ration	Error
B3I[c]						
Dry 88	2 (0.6)	289 (80.8)	66 (18.6)	319 (97.0)	10 (3.0)	28 (8.8)
Wet 88-89	12 (1.6)	639 (85.4)	99 (13.2)	762 (99.9)	1 (0.1)	-12 (-1.6)
Dry 89	6 (0.7)	668 (84.5)	116 (14.8)	627 (98.1)	12 (1.9)	150 (23.5)
Wet 89-90	14 (1.4)	863 (90.0)	82 (8.6)	989 (99.9)	0 (0.1)	-29 (-3.0)
Dry 90	2 (0.7)	239 (87.1)	33 (12.1)	231 (99.2)	2 (0.8)	40 (17.5)
Total	36 (1.2)	2,697 (86.1)	398 (12.7)	2,928 (99.2)	25 (0.8)	178 (6.0)
PC12[d]						
Wet 88-89	12 (2.1)	445 (79.5)	103 (18.4)	535 (99.9)	0 (0.1)	23 (4.4)
Dry 89	5 (3.9)	97 (72.4)	32 (23.8)	136 (93.6)	9 (6.4)	-9 (-6.4)
Wet 89-90	11 (2.5)	312 (74.1)	99 (23.4)	373 (99.9)	0 (0.1)	48 (13.0)
Dry 90	1 (2.5)	49 (82.3)	9 (15.2)	62 (97.7)	1 (2.3)	-4 (-6.4)
Total	29 (2.5)	904 (76.9)	243 (20.7)	1,105 (99.0)	11 (1.0)	58 (5.2)

[a] Dry season = April-September; wet season = October-March

[b] Positive groundwater values indicate groundwater discharge to wetlands.

[c] B3I study period: June 1988 - May 1990

[d] PC12 study period: October 1988 - May 1990

Surface water inflows accounted for 86 and 77% of the inputs for B3I and PC12, respectively, on an annual basis. Groundwater discharge to the wetlands accounted for most of the remaining input (13 and 21% for B3I and PC12, respectively). Direct precipitation inputs were quite small in the overall balance. During individual months or groups of months, however, groundwater and precipitation contributed substantially more to the wetland water inputs, particularly at PC12.

Differences also existed in the magnitudes of inputs and outputs for the wet and dry seasons. This was particularly true for precipitation, with 75 to 80% occurring during the wet season, and ET, with approximately 90% occurring during the dry season. At B3I, 60% of annual surface water flow occurred during the wet season, whereas at PC12 this component totaled approximately 80%. At PC12, ET accounted for greater than 50% of

the output from July to September 1989 when baseflows were minimal. During the same period, ET at B3I was less than 5% of the output, because of the stable and relatively high baseflow. The direct groundwater input to B3I was fairly steady throughout the year. However, at PC12, nearly 83% of the groundwater contribution to the wetland occurred during the wet season.

Urbanization and Other Factors Affecting Wetland Hydrology

The dynamics of wetland hydrology are governed by factors that may change seasonally or slowly over time. Seasonal changes result from variation in climate (e.g., precipitation, solar radiation), plant growth and groundwater recharge. Longer-term changes result from human activities, including watershed development, groundwater withdrawal, wetland outlet modification or drainage activities. Although this study was not designed to investigate change over time, some general conclusions can be drawn from comparisons between urbanized and nonurbanized catchments.

The runoff-to-precipitation ratios were 0.80 and 0.53 for B3I and PC12 wetland watersheds, respectively. Thus, more water is captured in the nonurbanized catchment, resulting in less runoff to the wetland. Potential pathways for the difference in water reflected in these numbers are ET, regional groundwater recharge and withdrawal in the watershed itself. The ET in the forested nonurbanized catchment of PC12 is undoubtedly greater than in the developed urbanized catchment of B3I. Regional or deep groundwater recharge within the PC12 watershed is also likely greater than in the case of B3I, because of milder topography and less impervious surface. Finally, groundwater withdrawal to meet local water needs is likely more significant in the PC12 watershed.

Water level fluctuation is perhaps the best single indicator of wetland hydrology, because it integrates nearly all hydrologic factors. The mean WLFs were 0.15 and 0.49 m for the PC12 and B3I wetlands, respectively. The higher mean occasion WLF at B3I reflects the effect of many factors, including its urbanized catchment, piped storm drain system and constricted outlet. The maximum study period WLFs were quite similar. This apparent discrepancy occurred because of the evaporation and lowered water level in PC12 during the summer. In summary, both wetlands experienced similar long-term fluctuations; however, the urban wetland was exposed to much more frequent and greater WLFs.

Hydrologic Components Error Analysis

By measuring all components of the water balance shown in Equation 1 (Chapter 1), it was possible to determine error estimates for the seasonal balances. The seasonal errors (Table 8-4) ranged from -6.4 to +23.5% of the total hydrologic outputs. For the entire study period, the errors were 6.0 and 5.2% for B3I and PC12, respectively. This reduction reflects the cancellation effect of positive and negative errors when summed over a longer time period. Generally, the larger percentage errors occurred during the dry seasons, reflecting the increased importance of groundwater inputs and ET in the overall balance at that time.

The type and magnitude of the errors associated with hydrologic or water balances may be characterized in several ways. These include errors associated with the: (1) equipment (e.g., inaccurate calibration), (2) measurements (e.g., representativeness of

measurement), (3) calculations (e.g., weak stage-discharge correlations, groundwater calculations), and (4) summation of balance components. It is important to note that these errors can improve or degrade the apparent accuracy of a water balance depending on the interaction between errors.

If precautions are taken to minimize the errors associated with the equipment, measurements and calculations, and if all components are included in a water balance, it is possible to reduce potential errors greatly. An assessment of the importance of the different components of a balance is a critical task in this process. Because of the above-noted errors, it is recommended that no components of a balance be estimated by difference. Using this technique simply masked the errors in the unknown or unmeasured component (usually ET, groundwater, or both).

CONCLUSIONS

The quantity of stormwater entering many palustrine wetlands in the Puget Sound region has changed as a result of rapid development in urbanizing areas. The purpose of this chapter has been to characterize the hydrology of wetlands affected by urban stormwater, in comparison to unaffected or forested systems. This information, then, may help to explain observed changes in wetland soils, plants and animals over time. Additionally, if observed effects of stormwater on wetlands can be documented, it may be possible to mitigate these effects through watershed controls and stormwater management efforts.

The hydrology of wetlands as measured by water level fluctuation was highly variable. Differences in water level fluctuation were attributed to level of watershed imperviousness, forested cover, and wetland outlet constriction. A multivariate model using these three parameters, calibrated to the study sites, was found to predict water level fluctuations relatively accurately. This model should be verified and tested further using similar data sets from all years of collection in future research efforts.

For the two study wetlands, surface water inflow and outflow were the dominant components in the water balance on an annual basis. It was concluded that this is typical for wetlands with low wetland-to-watershed ratios. The ET was insignificant in the overall water budget on an annual basis; however, it was the major source of water output from the PC12 wetland from July to September, when outflows were minimal. Both wetlands were identified as primarily groundwater discharge zones, with groundwater contributing significant inputs. Like ET, the influence of groundwater was greatest at PC12 during the summer months.

Differences were also identified in the hydrology of both wetlands because of the level of watershed urbanization. In the urbanized watershed, a greater proportion of the precipitation was realized as surface inflow to the wetland. Storm runoff was delivered more quickly and in greater short-term volumes to the urban wetland. The result of these conditions was greater and more rapid water level fluctuations in the urban wetland. This characteristic would probably be replicated in most wetlands where development occurs in the watershed.

REFERENCES

Cedergren, H.R. 1978. Seepage, Drainage and Flow Nets. John Wiley and Sons, Inc., New York, N.Y.

Chapuis, R.P. 1989. Shape factors for permeability tests in boreholes and piezometers. Ground Water, 27(5):647-654.

Chin, N. T. 1996. Watershed Urbanization Effects on Palustrine Wetlands: A Study of the Hydrologic, Vegetative, and Amphibian Community Response During Eight Years. M.S.C.E. thesis, University of Washington, Department of Civil Engineering, Environmental Engineering and Science Program, Seattle, WA.

King County Surface Water Management. 1990. King County Surface Water Design Manual. King County Department of Public Works, Seattle, WA.

Mitsch, W.J. and Gosselink, J.G. 1993. Wetlands, 2nd Ed.. Van Nostrand Reinhold Co., New York.

Reinelt, L.E. and Horner, R.R. 1990. Characterization of the Hydrology and Water Quality of Palustrine Wetlands Affected by Urban Stormwater. King County Resource Planning, King County, WA.

Reinelt, L.E., Horner, R.R., and Wittgren, H.B. 1990. Removal of sediment and nutrients in palustrine wetlands receiving runoff from urban and nonurban watersheds. In Reinelt, L. Nonpoint Source Water Pollution Management, Linköping Studies in Arts and Sciences 57, ISBN 91-7870-708-0.

Reinelt, L.E., Surowiec, M.S., and Horner, R.R. 1993. Urbanization effects on palustrine wetland hydrology as determined by a comprehensive water balance. (Manuscript).

Siegel, D.I. and Glaser, P.H. 1987. Groundwater flow in a bog-fen complex, Lost River Peatland, Northern Minnesota. J. of Ecology, 75:743-754.

Surowiec, M.S. 1989. An Hydrogeologic and Chemical Characterization of an Urban and Nonurban Wetland. M.S.E. Thesis. Department of Civil Engineering, University of Washington.

Taylor, B.L. 1993. The Influence of Wetland and Watershed Morphological Characteristics on Wetland Hydrology and Relationships to Wetland Vegetation Communities. M.S.C.E. Thesis. Department of Civil Engineering, University of Washington.

Wilcox, D.A., Shedlock, R.J. and Hendrickson, W.H. 1986. Hydrology, water chemistry and ecological relations in the raised mound of Cowles Bog. J. of Ecology, 74:1103-1117.

Wilkinson, L. 1990. SYSTAT: The System for Statistics. SYSTAT, Inc., Evanston, IL.

Zar, J.H. 1984. Biostatistical Analysis. Prentice Hall, Englewood Cliffs, N.J.

CHAPTER 9 THE EFFECTS OF WATERSHED DEVELOPMENT ON WATER QUALITY AND SOILS

by Richard R. Horner, Sarah Cooke, Lorin E. Reinelt, Kennneth A. Ludwa, Nancy Chin and Marion Valentine

INTRODUCTION

This chapter emphasizes water and soil quality in wetlands with significant urbanization in their watersheds. Like other chapters in this section, its purpose is to characterize particular elements of Puget Sound Basin freshwater wetlands having urbanized watersheds. The urbanized cases were divided into two major categories. The "treatment" group included the wetlands whose watersheds had a more than 10% rise in urbanization between 1989 and 1995. Conversely, the "control" category consisted of wetlands whose watersheds experienced a less than 10% increase in urban land cover between 1989 and 1995. The urban control wetlands were subdivided into two further classifications: (1) the most highly urbanized sites (H) had watersheds that were both ≥ 20% impervious and ≤ 7% forest by area; and (2) moderately urbanized wetlands (M) had watersheds that were 4-20% impervious and 7-40% forested by area. The nonurbanized category (N), with both < 4% impervious land cover and ≥ 40% forest, made up the balance. This latter category is emphasized in Chapter 2 but will be mentioned in this chapter at times for comparison. Table 1 of Section 1 gives characteristics of the individual watersheds.

This chapter first describes water quality conditions in urban control wetlands, and then discusses changes in these conditions in treatment wetlands. It then proceeds to cover soil characteristics in a similar way. Chapter 2 covers the methods with which the data were collected. Tables 1, 2, and 4 of Chapter 2 summarize water quality results for the urban control wetlands as well as the nonurbanized cases. Tables 5 and 6 in that chapter perform the same function for the soils data. These tables are not repeated in this chapter but are referenced here several times.

As has been stated elsewhere in this volume, the research program concentrated on palustrine wetlands of the general type most prevalent in the lower elevations of the central Puget Sound Basin. The results and conclusions presented here are probably applicable to similar wetlands to somewhat to the north and south of the study area but may not be representative of higher, drier, or more specialized systems, like true bogs and “poor” (low nutrition) fens.

THE EFFECTS OF WATERSHED DEVELOPMENT ON WATER QUALITY

This section first profiles the urban control wetlands, both moderately and highly urbanized, using the statistical summary data in Chapter 2, Tables 2-1, 2-2, and 2-4. Following the profiles is a more general summary of other applicable findings from the research.

Moderately Urbanized Wetlands

A water quality portrait of Puget Sound Basin lowland palustrine wetlands moderately affected by humans would show slightly acidic (median pH = 6.7) systems with DO often well below saturation, and in fact sometimes quite low (< 4 mg/L). Dissolved substances are fairly high relative to nonurbanized wetlands (median conductivity about three times as high) but somewhat variable. Suspended solids are only marginally higher than N wetlands but, like them, quite variable. Median total dissolved nitrogen concentrations (the sum of ammonia, nitrate, and nitrite) are more than 20 times as high as dissolved phosphorus, a ratio very similar to the nonurbanized wetlands but with higher magnitudes in both cases. Again, plant and algal growth is generally limited by P, rather than N. TP at the median level is more than twice as high in the M compared to the N wetlands (70 µg/L). The median fecal coliform concentration is close to the 50 CFU/100 mL criterion applied as a geometric mean to lakes and the highest class of streams by Washington state water quality criteria. This quantity is highly variable in all wetlands, most extremely so in those of the M class. More than half of the individual FC values for moderately urbanized flow-through wetlands exceeded the maximum 200 CFU/100 ml criterion applied to the lowest class streams (however, their geometric mean may not do so). As with N wetlands, both mean and median heavy metals concentrations in the moderately urbanized sites are in the low parts per billion range, with standard deviations just about identical to the means. The median lead concentration, however, is close to the chronic water quality criterion set for lakes and streams having hardness of 50 mg/L as $CaCO_3$.

In summary, the following general statements can be made to characterize the water quality of Puget Sound Basin lowland palustrine wetlands in a moderately urbanized state:

> These wetlands are highly likely (≥ 71% of cases observed) to have median conductivity > 100 µS/cm but median TSS in the range 2-5 mg/L, NH_3-N < 50 µg/L, and total Zn < 10 µg/L.
>
> Moderately urbanized wetlands are highly likely (71% of cases) to have median fecal coliforms < 50 CFU/100 mL, but also to have many individual measurements above 200.
>
> They are highly likely (100% of cases to have TP > 20 µg/L and likely (57% of cases) to have TP > 50 µg/L and NO_3+NO_2-N < 100 µg/L. The latter variable is highly likely (86% of case) to be < 500 µg/L.
>
> The pH and DO in these wetlands are unpredictable from consideration of urbanization status alone, being dependant on other factors.

Highly Urbanized Wetlands

Highly urbanized wetlands are harder to profile because of the small set of only two in the control group. Also, both of these wetlands are the flow-through type, not giving any picture of how morphology might affect the conclusions. What can be said is the following:

> There is some tendency for these wetlands to be the closest to neutral in pH among the three urbanization status categories. They tend to fall in the same region as the other classes in dissolved oxygen.

They most likely would have median conductivity > 100 µS/cm.

Like the other two classes, highly urbanized wetlands are very likely to have median NH_3-N < 50 µg/L.

Unlike the other two classes, they are very likely to have median NO_3+NO_2-N > 100 µg/L and TP > 50 µg/L.

These sites are likely, but somewhat less than the other categories, to have autotrophic growth limited by phosphorus.

They are likely to exceed the 50 CFU/100 mL level of fecal coliforms.

These wetlands have a higher tendency than the other categories to have Zn > 10 µg/L but in most instances still not to exceed the chronic criterion of 59 µg/L for relatively soft waters.

Other Findings

In a synoptic study of 43 urban and 27 nonurban wetlands during 1987, before routine sampling began, the program found that FC and enterococcus were significantly higher in urban wetlands (Horner et al. 1988). Although the mean counts for both types of bacteria were within water quality standards, bacteria substantially exceeded standards in wetlands in high density areas that showed evidence of human intrusion. The watersheds of most of the wetlands in which bacteria also exceeded standards were in watersheds characterized by low density residential development, while some of the watersheds of the remainder of the wetlands had high density residential development. None of the watersheds with bacteria in excess of standards were dominated by commercial development. Other than pH, FC count was the only water quality variable measured by the survey.

After four years of regular data accumulated, a major effort was undertaken to relate water quality conditions to watershed and wetland morphological circumstances. In this work it was found that certain water quality parameters varied in response to the changes in watershed wetland characteristics that can accompany urbanization (Ludwa 1994). The characteristics used as independent variables in this analysis included (1) percent forest cover, (2) percent total impervious area, (3) percent effective impervious area (the area actually linked to a storm drain system), (4) the ratio of wetland to watershed area, (5) the ratio of forest to wetland area, (6) wetland morphology (open water or flow-through), and (7) outlet contstriction. These measures may be expressed as either continuous (ranges) or categorical (binary or ternary) variables. Multivariate linear regressions were used to determine if there is an adequate relationship between these characteristics and water quality parameters. If there is such a relationship, the equations could be used to analyze probable changes in water quality following development.

Specific watershed land uses and wetland morphological values were significantly associated with most water quality values (Ludwa 1994). The dependent water quality variables exhibiting the best associations and most correctly predicted when verified with a portion of the data set held aside for verification were conductivity, pH, and TSS (Ludwa 1994). Pollutants that are often adsorbed to particulates, specifically TP, Zn, and FC, showed similar degradation across key levels of the independent variables. Conductivity, TSS, FC, and enterococcus degraded the most consistently between more highly developed watersheds and those that were moderately urbanized or rural (Taylor

et al. 1995). Conductivity, TSS, Zn, DO, and FC varied by the greatest amounts (Ludwa 1994).

Based on program data from 1988-93, percent forest cover was the best predictor of water quality for Pacific Northwest palustrine wetlands, followed by percent total impervious area, forest-to-wetland areal ratio, and morphology (Ludwa 1994). All variables except NO_3+NO_2-N were higher in wetlands with no forest in their watersheds compared to those in watersheds with at least 14.7% forest cover (Taylor et al. 1995). Conductivity, TP, and FC rose significantly when the percentage of impervious surface exceeded the values of 3.5% and 20% (Taylor et al. 1995). Forest-to-wetland areal ratio strongly influenced conductivity, TSS, NO_3+NO_2-N, TP, SRP, and FC, where the ratio was less than 7.2 (Taylor et al. 1995). Conductivity, TSS, NO_3+NO_2-N, TP, SRP, and FC, had significantly higher means in relatively channelized wetlands, although it should be noted that these results may have been influenced by extraneous factors (Taylor et al. 1995). Outlet constriction and wetland- to-watershed areal ratios had inconsistent roles in influencing water quality (Taylor et al. 1995). It should be noted that because the breakpoint values are expressed as fixed ranges, and it is unknown if thresholds exist or what they are, it is entirely possible that other water quality constituents also vary significantly with characteristics of urbanization on a continuous basis (Taylor et al. 1995).

The analysis indicated that, for similar watersheds in the region, there is a definite degree of deforestation and development above which average wetland water quality will become degraded. However, if amounts of forest remain above some minimum level, water quality will comply with criteria. It should be noted that because extremes in water quality often have greater impacts on biological resources than average conditions, attention should also be given to the relationships of conditions with minimum and maximum values. Minimums and maximums were found to vary widely across urbanization and morphological levels, so that entire ranges of water quality variables shift significantly to degraded conditions.

Ludwa (1994) found that the strongest regression relationships were for mean, maximum, and minimum conductivity, TSS, and DO. In view of the correlation coefficients, urbanization was consistently related to all water quality values except NH_3-N and SRP. The strong regressions of TSS and conductivity with urbanization suggested that an increase in watershed imperviousness will facilitate the movement to wetlands of runoff containing inorganic particulate and dissolved matter. Total suspended solids and conductivity are directly and indirectly harmful to wetland biological communities. Wetland morphological factors had similar effects, although they were less consistent for outlet constriction.

Predictions were generally better for mean and maximum values, since these values exhibited more variability than minimum values from site to site. The choice of factors to be included in the regression equations was manipulated to improve predictive value, although the process was somewhat subjective. Wetland-to-watershed areal ratio was the most frequently used factor. Although little can be done to affect this ratio other than by changing wetlands physically or by diverting inflows, the importance of this ratio does not suggest that development or deforestatation are unimportant. To the contrary, where a wetland covers a smaller portion of a watershed, the effect of deforestation may be magnified. Effective impervious area, which expresses how much land is actually drained by a storm drainage system, had more predictive power than total impervious area. However, there was no consistent relation between outlet constriction and water

quality. Categorical predictors seemed to have slightly better predictive value than continuous ones, and are also simpler to use.

The crucial values for water quality lie between 4 and 12% for total impervious area and 0 to 15% for forested area. Theory and observations in other regional ecosystems (e. g., Horner et al. in press) have demonstrated that there is likely to be a continuous and relatively rapid decline in various measures of ecosystem "quality" as forest begins to decrease in favor of impervious surfaces. As conversion progresses the decline is likely to slow in rate but to continue. Therefore, with a continuous pattern of variation normally prevailing, numerical values should not be regarded as thresholds but as points where degradation becomes evident and demonstrable, and where standards generally accepted as necessary to support biota probably will not be met, at least at times.

Ludwa recommended that total impervious area in Pacific Northwest watersheds with strong wetland protection goals be not more than 10% and that a forest cover of at least 15% be maintained. Whether more effective implementation of urban runoff best management practices would permit these thresholds to be shifted toward more urbanization is a matter only for conjecture. However, development and deforestation will ultimately have to be limited if high quality and well functioning wetland systems are to be preserved. Channelized sites usually had lower water quality, hence a shift to more channelized conditions intentionally or by inadvertant flooding resulting from increased urbanization should be avoided.

Treatment Wetlands

The treatment wetlands studied by the program were: Big Bear Creek 24 (BBC24), East Lake Sammamish 61 (ELS61), Jenkins Creek 28 (JC28), North Fork Issaquah Creek 12 (NFIC12), and Patterson Creek 12 (PC12). Their watersheds experienced increases of urbanization in the range of 10.2 to 10.5% in three of the five cases (JC28, ELS61, and PC12), 42.2% for BBC24, and 100% in the case of NFIC12. The most common change in land use was from forest to single family residential, a development pattern typical of the early stages of urbanization (Chin 1996). Table 9-1 shows land cover in 1995 and the changes since 1989.

This distribution of changes gave an opportunity to observe the relative effects with substantial compared to more limited watershed alterations. The timing of development in relation to the program's schedule also offered the chance to observe effects during the construction-phase, when soils are often bare for long intervals, versus the subsequent period when areas finished with construction are restabilized.

Table 9-1. Land cover in 1995 and the changes from 1989.

	Forest		Impervious Surface	
Wetland	1995(%)	Change(%)	1995(%)	Change(%)
JC28	19.8	-14.6	20.6	+0.6
ELS61	3.7	+1.2	10.6	+5.5
PC12	64.7	-10.5	6.8	+1.7
BBC24	47.4	-42.1	10.6	+7.2
NFIC12	0.0	-100.0	40.0	+38.0

In terms of the urbanization groupings used to classify the control wetlands, after the development that occurred through 1995 in the treatment watersheds, NFIC12 would be categorized as H and all of the others as M. Morphologically, JC28 is a flow-through type, and the remainder are all open water.

Observations for Individual Treatment Wetlands

Wetlands in urbanizing watersheds are especially vulnerable to erosion during the construction phase of development. Total suspended solids concentrations often increase greatly during such periods, but return to approximately pre-development levels as bare land is covered by structures and vegetation. During periods of construction, mean TSS values increase more dramatically than median values because of the influence of especially high concentrations. For instance, the ELS61 wetland recorded a median TSS concentration of 10.4 mg/L in 1989 and had a maximum concentration of 59 mg/L in August, as a result of construction site runoff. An increase in TSS at JC28 in 1989 was also linked to land disturbances. At both of these sites, TSS declined in the following year.

Elevated sediment in runoff from construction sites also corresponds to increases of concentrations of other pollutants, especially phosphorus and nitrogen), that are contained in soils (Novotny and Olem 1994). Subsequent to construction, application of fertilizers can further increase nutrient concentrations in runoff. In the JC28 wetland, land disturbances, including expansion of an adjacent golf course in 1989 marked the commencement of a regime of higher nutrient concentrations. Median NO_3+NO_2-N and SRP values increased by 63% and 96%, respectively, between 1988 and 1989, and continued to climb steadily from 1990 to 1995. The initial increases probably resulted from land disturbance, with the subsequent rises attributable to fertilizer runoff from the golf course. Mean NH_3-N also also rose sharply in 1989, with a maximum value of 619 μg/L, and median NH_3-N was higher in subsequent years. More than half of the NO_3+NO_2-N readings exceeded 500 μg/L.

At the ELS61 wetland, NH_3-N and NO_3+NO_2-N initially rose in 1989, but declined in 1993, although not to predevelopment levels. Concentrations of NH_3-N climbed again in 1993, while NO_3+NO_2-N greatly increased in 1995. Many NH_3-N and NO_3+NO_2-N concentrations exceeded 100 and 500 μg/L, respectively, during these years. Average SRP and TP concentrations were actually the highest in 1988, perhaps because of the operations at a small livestock farm next to the wetland. However, after declining from 1988 to 1990, SRP and TP concentrations were substantially higher in 1993 and 1995. One of the two highest chlorophyll a concentrations in the first two years of the program was recorded at ELS61 (Reinelt and Horner 1990).

NFIC12, the wetland that had the greatest amount of development in its watershed between 1989 and 1995, increasing from 0 to 100%, displayed different water quality patterns than ELS61 and JC28. Average values for TSS rose modestly from 1989 to 1995, with a maximum peak value of 16 mg/L in 1993. Average concentrations of NH_3-N and NO_3+NO_2-N did not appear to rise during this period, but NH_3-N and NO_3+NO_2-N did reach maximum concentrations 120 and 1400 μg/L, respectively, in 1993. Concentrations of SRP and TP, however, rose steadily, reaching median concentrations of 148 and 202 μg/L, respectively, in 1995. For all years, mean and median TP concentrations exceeded 50 μg/L.

Results were less conclusive for the other two treatment wetlands, PC12 and BBC24, demonstrating that there is not necessarily a link between development and water quality degradation, even for wetlands whose watersheds have undergone similar amounts of development. A possible explanation for the difference in results may be that the watersheds of PC12 and BBC24 remained approximately half forested, retarding transport of pollutants to the wetlands in runoff. The watersheds of JC28, ELS61, and NFIC12, on the other hand were only 0 to 19.8% forested by area. In addition, a large wet pond meeting current design standards was constructed to treat storm runoff from the development built adjacent to PC12. These observations are signs that concerted action to maintain forest cover and impose structural storm water management measures can avoid water quality degradation.

Increases in nutrient loadings can have serious consequences for normally nutrient-limited bogs and fens. In one of the bog-like wetlands covered by the program in a special study, East Lake Sammamish 34 (ELS34), also known as Queen's Bog, the *Sphagnum* mat was observed to be decomposing, probably because of stormwater inflow. Nitrogen input exponentially increases decomposition rates.

Profile of Treatment Wetlands

Table 9-2 shows statistics for the five treatment wetlands in the baseline period, when little or no urbanization had occurred (1988-1990), and then the later years (1993 and 1995), after most of the changes in land use were either well underway or complete. Very little change in pH was evident. DO exhibited some fluctuation in three wetlands, but only ELS61 registered a notable decline in the median level with time (≈ 2 mg/L).

Most direct comparisons for all of the other water quality variables and all wetlands indicated no change or reduction during the program, but there were some exceptions to that generality that bear examination. NH_3-N appeared to rise in ELS61 from predominantly < to > 50 μg/L values. NO_3+NO_2-N showed increases in all but NFIC12. Median concentrations still stayed mostly < 100 μg/L in PC12 and ELS61. The increase in BBC24 kept the median still below 500 μg/L. JC28 increased from an already relatively high median > 500 to > 1000 μg/L. In NFIC12 relatively high concentrations of SRP and TP increased further after development, reaching among the highest levels seen in the entire program. Increases in TP also occurred in JC28, but stayed in the 20-50 μg/L range, and in ELS61, where the median moved from the area of 50-100 to > 100 μg/L. Relatively small rises in fecal coliform statistics were registered in JC28 and ELS61, but medians remained below 50 CFU/100 mL. Although relatively high detection limits in the early years make comparisons more difficult for the metals, there was no sign that any of the three metals increased substantially anywhere or threatened a violation of the water quality criteria applied to other water bodies.

Wetlands in moderately and highly urbanized watersheds are generally profiled earlier in this chapter. Whether or not the treatment wetlands fit these profiles after going through development will now be examined. The four M wetlands all fit the profile for that category in the cases of conductivity, NH_3-N, zinc, and fecal coliforms. It should be noted that they almost always fit the same profile in the baseline years; thus, preexisting factors are most responsible for how these wetlands profile. ELS61 and JC28 failed to fit the profile for TP and NO_3+NO_2-N, respectively, being higher in both cases. In consequence, ELS61 did not appear to be generally phosphorus-limited in photosynthetic production, in contrast to the profile. A lack of fit occurred in only one other instance, TSS in BBC24, but the median was lower than the profile value. The only highly urbanized treatment wetland, NFIC12, exhibited fewer fits to the general H profile, but usually because it had lower values. This was the case for conductivity, NO_3+NO_2-N, and fecal coliforms. It did fit for NH_3-N, TP, and Zn, but actually fit in those cases before development too. This wetland also appears to tend toward nitrogen rather than phosphorus limitation, unlike the profile. Finally, it demonstrated no tendency toward more neutral pH, as the profile states. The humic acid-producing vegetation and peat prominent in this wetland apparently were not affected by the extensive urbanization, at least not yet.

Table 9-2. Water quality statistics for treatment wetlands in baseline and post-development years.

Site/ Years	Statistic	pH	DO (mg/L)	Cond. (µS/cm)	TSS (mg/L)	NH3-N (µg/L)	NO3+NO2-N (µg/L)	SRP (µg/L)	TP (µg/L)	FC (CFU/100ml)	Cu (µg/L)	Pb (µg/L)	Zn (µg/L)
JC28	Mean	6.59	6.9	99	< 5.68	< 72	710	17	44	< 237	< 5.0	< 5.5	< 28.9
88-90	St. Dev.	0.24	1.4	28	> 9.30	> 159	414	29	45	> 578	> 0.0	> 1.1	> 37.2
	CV	4%	21%	28%	164%	220%	58%	174%	101%	244%	0%	19%	129%
	Median	6.67	7.1	94	2.9	13	653	4	29	20	< 5.0	< 5.0	< 20.0
	n	19.00	19.0	16	19.0	19	19	19	19	19	8	8	8
93-95	Mean	6.74	6.9	98	< 4.9	< 34	1002	< 27	84	83	< 0.7	< 1.3	< 8.7
	St. Dev.	0.20	1.4	9	> 3.8	> 37	448	> 37	90	102	> 0.3	> 1.0	> 8.5
	CV	3%	20%	10%	78%	109%	45%	136%	107%	123%	45%	75%	98%
	Median	6.77	7.0	95	3.6	20	1080	8	43	36	0.6	< 1.0	< 5.0
	n	6.00	14.0	14	13.0	14	14	12	14	14	6	14	14
PC12	Mean	6.72	7.0	68	< 3.0	< 75	< 456	11	52	< 63	< 5.0	< 5.0	< 15.2
88-90	St. Dev.	0.32	3.4	11	> 2.6	> 76	> 551	10	45	> 146	> 0.0	> 0.0	> 5.4
	CV	5%	48%	15%	88%	101%	121%	89%	87%	233%	0%	0%	36%
	Median	6.62	7.5	71	2.4	35	108	7	40	8	< 5.0	< 5.0	16.0
	n	23.00	22.0	20	23.0	23	22	23	23	23	9	9	9
93-95	Mean	6.55	6.5	73	< 2.5	< 33	< 786	< 11	< 88	46	< 0.7	< 0.8	< 3.0
	St. Dev.	0.12	3.1	15	> 2.1	> 26	> 980	> 9	> 218	124	> 0.3	> 0.4	> 1.7
	CV	2%	48%	20%	87%	79%	125%	79%	248%	271%	40%	47%	57%
	Median	6.57	6.3	75	2.0	20	430	8	24	2	0.7	0.8	2.5
	n	8.00	16.0	16	16.0	15	13	15	15	16	8	16	16
ELS61	Mean	6.59	5.3	101	13.9	< 43	< 725	< 76	166	< 100	< 5.8	< 5.1	< 17.2
88-90	St. Dev.	0.27	3.1	19	16.8	> 94	> 1086	> 85	125	> 188	> 1.9	> 0.3	> 6.6
	CV	4%	58%	19%	121%	218%	150%	112%	76%	188%	32%	6%	38%
	Median	6.61	4.9	103	8.0	25	109	58	149	20	5.0	5.0	20.0
	n	23.00	23.0	20	23.0	23	17	22	23	23	10	10	10
93-95	Mean	6.31	< 3.8	91	< 9.5	< 136	< 527	35	101	321	< 0.9	< 0.8	< 2.3
	St. Dev.	0.19	> 2.8	19	> 20.9	> 190	> 592	41	95	992	> 0.3	> 0.3	> 1.2
	CV	3%	73%	21%	219%	140%	112%	116%	94%	309%	30%	34%	52%
	Median	6.28	3.4	90	3.0	74	344	21	62	39	< 0.9	< 0.8	< 2.5
	n	8.00	13.0	16	16.0	15	9	16	16	16	8	16	16

Table 9-2 continued. Water quality statistics for treatment wetlands in baseline and post-development years.

Site/ Years	Statistic	pH	DO (mg/L)	Cond. (µS/cm)	TSS (mg/L)	NH3-N (µg/L)	NO3+NO2-N (µg/L)	SRP (µg/L)	TP (µg/L)	FC (CFU/100ml)	Cu (µg/L)	Pb (µg/L)	Zn (µg/L)
BBC24	Mean	6.76	6.1	83	< 2.0	< 44	210	5	23	< 186	< 5.0	< 5.0	< 15.1
88-90	St. Dev.	0.25	1.9	19	> 2.0	> 35	183	3	13	> 542	> 0.0	> 0.0	> 5.6
	CV	4%	31%	23%	97%	80%	87%	64%	55%	292%	0%	0%	37%
	Median	6.77	5.4	84	1.1	31	189	4	21	14	< 5.0	< 5.0	17.0
	n	22.00	23.0	20	23.0	23	23	23	23	23	10	10	17
93-95	Mean	6.84	6.7	90	< 3.5	< 34	< 396	< 6	< 27	< 411	< 0.5	< 0.8	< 1.8
	St. Dev.	0.22	2.0	38	> 6.6	> 20	> 347	> 3	> 12	> 1492	> 0.0	> 0.4	> 1.3
	CV	3%	29%	43%	187%	57%	88%	51%	44%	362%	4%	50%	72%
	Median	6.82	7.5	82	1.7	30	323	5	28	18	0.5	0.8	2.5
	n	8.00	16.0	16	16.0	16	15	13	15	16	8	16	15
NFIC	Mean	5.08	3.4	50	< 2.3	< 41	< 54	75	119	< 2	< 5.0	< 5.0	< 19.0
88-90	St. Dev.	0.69	1.0	46	> 2.3	> 29	> 45	104	94	> 0	> 0	> 0	> 7
	CV	14%	29%	90%	98%	71%	83%	140%	79%	21%	0%	0%	37%
	Median	4.84	3.5	37	1.0	39	34	53	80	2	< 5.0	< 5.0	22.0
	n	12.00	12.0	10	12.0	12	10	12	12	12	5	5	5
93-95	Mean	4.72	< 3.6	43	< 4.0	< 40	< 477	126	253	8	2.9	< 2.2	19.6
	St. Dev.	0.18	> 2.3	13	> 5.1	> 41	> 799	95	303	16	1.1	> 1.7	9.6
	CV	4%	63%	31%	129%	102%	167%	76%	120%	207%	37%	78%	49%
	Median	4.74	3.2	39	2.0	20	20	115	177	2	2.9	1.9	18.9
	n	4.00	9.0	10	10.0	10	3	10	10	10	4	10	10

THE EFFECTS OF WATERSHED DEVELOPMENT ON SOILS

This section first profiles the soils of the urban control wetlands, both moderately and highly urbanized, using the statistical summary data in Chapter 2, Tables 2-5 and 2-6. Following the profiles is a more general summary of other applicable findings from the research.

Urbanized Wetland Soil Profiles

A soils portrait of Puget Sound Basin lowland palustrine wetlands moderately affected by urbanization shows a somewhat acidic condition, more so (by about 1 pH unit) in open water than flow-through wetlands. The range of median values can be expected to be approximately 5.1-6.1. These soils will be aerobic in many instances, but their redox potentials not infrequently are below the levels where oxygen is depleted. TP is likely to be in the range 500-1000 mg/kg, and TKN up to 10 times as high. Median levels of soil organic content are approximately 15%. No general statement is possible concerning particle size distribution. Metals appear to be less variable than in nonurban sites, but still have coefficients of variation ranging from about 60 to 100%. It is most likely for Cu concentration to be in the vicinity of 15 mg/kg, for Pb and Zn to be very roughly twice as high, and for As to be about half as concentrated. Copper and lead lowest effect threshold freshwater sediment criteria would be violated in some samples.

Only two sites represent the highly urban control sites, which is a very small sample from which to construct a profile. This group appears to have much less acidic soils than the other two, with median pH of 6.5. Soils in this urbanization category are the most likely to be anaerobic, with median redox less than 100 mv. Nutrients are no higher than in the moderately urbanized `wetlands, and may even be a bit lower. Median organic content in the small sample suggests a level of about 20%. Again, PSD is a function of local factors. The available values show metals to be distinctly higher than in the soils of the other urbanization categories, about double the values given in the preceding paragraph. These concentrations would routinely exceed lowest effect thresholds for Cu and Pb, but not for Zn. Severe effect thresholds would still not be approached often.

Other Findings

Before regular sampling began, the research program conducted a synoptic survey of 73 wetlands, about 60% urban and the balance nonurban. Samples were analyzed in the laboratory for 31 of the wetlands. In the data from this study, significant differences appeared in soil Pb concentrations between urban and nonurban wetlands in the inlet and emergent zones (Horner et al. 1988). There were also significant differences at α = 0.10 between the concentrations of both Cd and Zn in the emergent zones of urban and nonurban wetlands.

Metals accumulations may be linked to soil toxicity, as estimated by the Microtox method. The Microtox test assesses the potential toxicity of an environmental sample by measuring the reduction of the light output of bioluminescent bacteria when exposed to the sample for a period of time. The method yields the effective concentration (EC), which indicates the reduction of light output after a certain length of exposure. The

lower the EC value, the more toxic the sample is (Horner et al. 1988). In the synoptic study, urban open water zone soils had significantly lower ECs in both 5- and 15-minute tests and were, therefore, relatively more toxic. There was also a significant difference in emergent zone in the 15-minute test. However, there were no significant differences between the inlet and scrub-shrub zones of urban and nonurban wetlands.

Microtox analysis of wetland soils in 1993 failed to confirm the conclusion of Horner et al. (1988) that urban wetland soils were more toxic. It should be noted that only one 1993 sample from each wetland underwent Microtox analysis, and there was no attempt to compare the toxicity of various wetland zones, as in the synoptic study. Nevertheless, the 1993 results generally indicated that urban wetland soils were certainly no more toxic than those of rural wetlands. In fact, the three soils with the most toxic compounds came from less urbanized wetlands. The extraction and concentration of naturally occurring organic soil compounds in the laboratory, and not the presence of anthropogenic toxic substances, probably explained the results for these wetlands (Houck 1994). The results suggested that the soils of FC1, an urban wetland, and AL3, a rural wetland, possibly contained anthropogenic toxicants, because the results indicated toxicity in the absence of visible organic material. There were no evident accumulations of toxicants in the AL3 soil in 1993. The FC1 wetland, on the other hand, had the highest result for Cu (59 mg/kg), a Pb concentration (60 mg/kg) second only to the highly urban B3I, and a total petroleum hydrocarbon concentration (TPH) (840 mg/kg) more than three times greater than for any wetland except B3I, which exhibited an equally high value. That metals and TPH should be high at FC1 and B3I is not surprising in view of the intensity of commercial and transportation land uses in their watersheds.

Working with 1993 data, Valentine (1994) studied the efficacy of using regression relationships between widely distributed crustal metals (aluminum, Al, and lithium, Li) and toxic metals in relatively unimpacted wetlands to evaluate whether particular wetlands have enriched concentrations of toxic metals in their soils. The method was applied independently to the 1995 data. The regression analysis is based initially on relationships between crustal and heavy metals in relatively pristine wetlands that, it is assumed, have not received significant metal loadings of anthropogenic origin. These regressions must be developed for each region, since the natural background of metals varies with soils. If, in a given wetland, the concentration of a toxic metal is above a given confidence limit (95% in Valentine's study) of the linear regression, it is probable that there has been anthropogenic toxic metal pollution of the wetland's soil.

For the purpose of her 1994 study, Valentine divided the program wetlands into the same three groups outlined earlier in this chapter. She used the nomenclature Group 1 for nonurban (N) wetlands, Group 2 for moderately urbanized (M) ones, and Group 3 for highly urbanized (H) cases. In 1996, she employed only two groups, one less urban and the other more urban. Using the 1993 soil metals data, Valentine (1994) found that Li may be as good or better a reference metal than Al for As, Pb, and Zn. Nickel (Ni) bore a stronger relationship to Al, while Cu correlated equally well with both Al and Li.

Figures 9-1 and 9-2 illustrate the assessment tool using a nickel-aluminum pairing with 1993 and 1995 data, respectively. The regression line represents the best-fit line of the Group 1 (N) wetlands. The 95% confidence limits are the upper and lower bounds for one additional sample that is being assessed for Ni contamination. Sample contamination is gauged by considering the corresponding point’s location on the graph. If the point lies on or above the upper 95% confidence limit, then the sample is judged to

be enriched with the contaminating metal. Thus, in Figure 9-2, for example, seven samples above the line were judged to have Ni contamination of anthropogenic origin. The two relationships from the separate data sets exhibit a close correspondence.

Valentine (1994) found that the most urbanized wetlands had a higher rate of soil metals enrichment than moderately urbanized wetlands, considering both the Al and Li regressions. There were far fewer indications of metals enrichment in the moderately urbanized wetlands in 1993. The regressions of 1993 Pb with both Al and Li strongly agreed that most soil samples from each of the most urbanized wetlands were Pb enriched. The first set of regressions of As with both Al and Li generally agreed that soil samples from each of the most urbanized wetlands were As-enriched. Both Cu regressions using 1993 data indicated Cu enrichment in two of the most urbanized wetlands, which are also the wetlands listed as highly urbanized wetlands in Table 1 of Section 1. However the Li-Cu regression using 1995 data indicated enrichment in only two nonurban and one urban wetlands. The Al-Ni regression with 1993 data indicated Ni enrichment in three of the four most urban wetlands, although the Li-Ni relationship failed to show any enrichment in these sites. For 1995 data, no Ni enrichment appeared in the less urban wetlands, while there were five and six cases of enrichment according to the Al-Ni and Li-Ni regressions, respectively, in the more urbanized wetlands. The Li-Ni regression using 1995 data showed enrichment in all cases in which the Al-Ni regression also indicated enrichment. The first set of regressions for Zn showed a few cases of enrichment in the most urban group, although fewer in number and with less agreement between the regressions than for the other metals. The Li-Zn relationship in the 1995 data indicated Zn enrichment in ten of the more highly urbanized wetlands, in comparison to only one of the less urbanized wetlands.

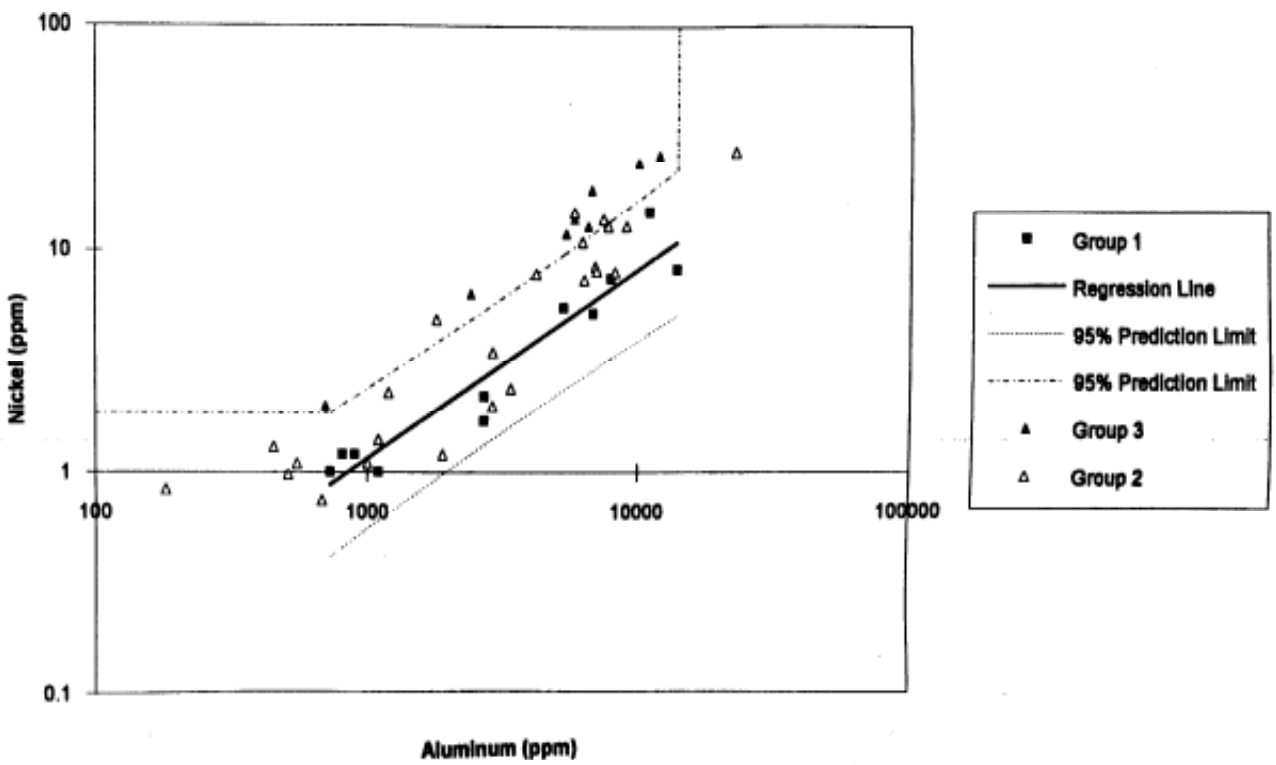

Figure 9-1. The Assessment Tool for NI Using AI as the Reference Element 1993 Data.

Although Valentine classified some of the wetlands in different groups than they would be in according to the GIS analysis, the results of her study agree well with observations based on the soil data statistics. Therefore, anthropogenic sources clearly impact the sediments of palustrine wetlands in the Puget Sound Basin. While wetlands can remove metals from the water column, the accumulation of metals could still harm wetland functions. Valentine noted that long-term effects of atmospheric emissions from past operations of the ASARCO smelter in Tacoma on wetland soils are unknown. It is possible that such distant sources could play a role in the enrichment of toxic metals wetlands. Rainfall removes such suspended metals from the atmosphere and provides the runoff which transports the metals to wetlands, where they accumulate in the sediments.

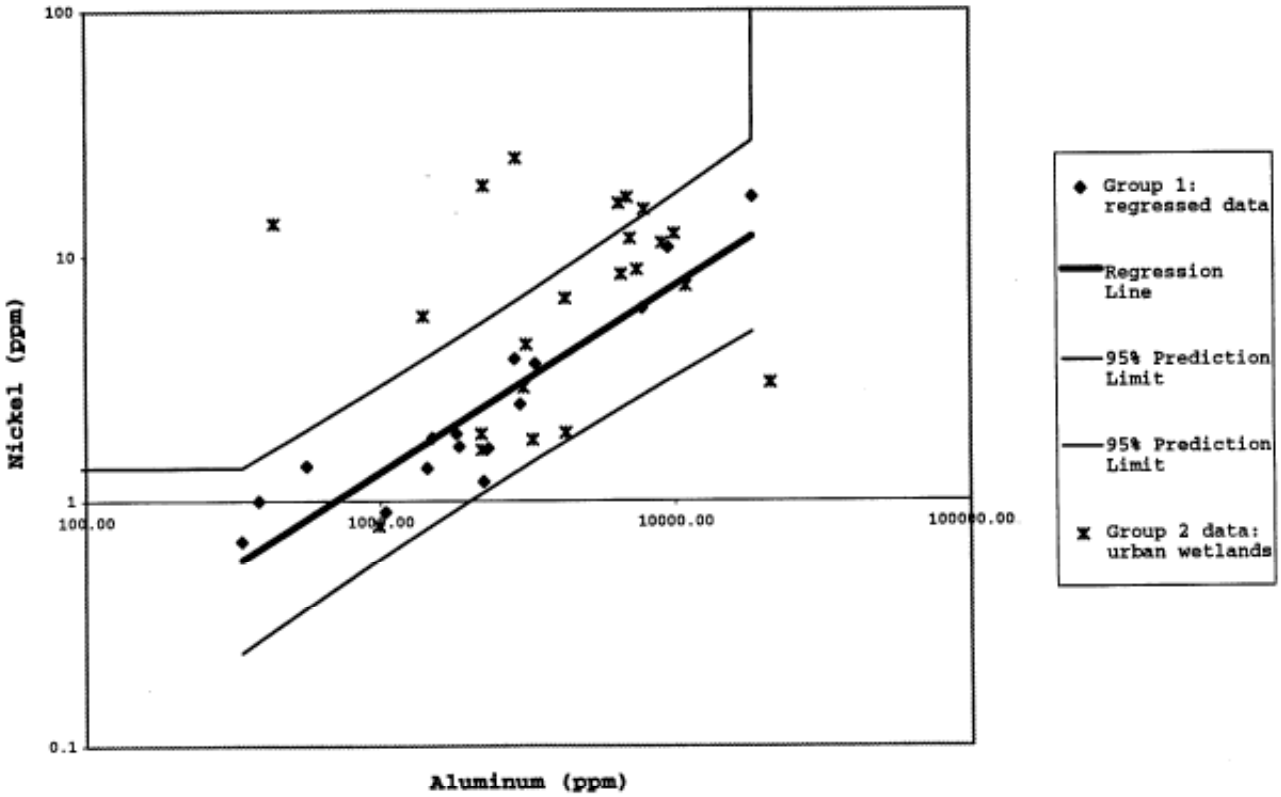

Figure 9-2. The Assessment Tool for NI Using AI as the Reference Element (1995 Data).

Treatment Wetlands

Table 9-3 shows soil statistics for the five treatment wetlands in the baseline period, when little or no urbanization had occurred (1988-1990), and then the later years (1993 and 1995), after most of the changes in land use were either well underway or complete.

It appears from program data that soil pH may have increased over the years at BBC24 and, especially, NFIC12, the wetlands whose watersheds underwent the greatest amounts of development. For NFIC12, rises in pH are entirely expected because (1) this wetland was a late successional peat bog that had the lowest soil pH readings of any of the wetlands, with no place to go except up; and (2) its watershed went from 0% to 100% urbanization between 1989 and 1995.

The treatment wetlands exhibited the particle size distributions in 1989 and 1995 shown in Table 9-4. BBC24 and ELS61 both registered transition from relatively sandy to silty soils, while clay stayed constant. NFIC12 exhibited a clay increase while sand was constant. The first result could be explained by sedimentation of finer particles over the pre-development substrate, but a 30% increase in clay is not easily explained.

Table 9-3. Soil statistics for treatment wetlands in baseline and post-development years.

Year	Stat.	pH	Redox. Potential (mV)	TP (mg/kg)	TN (mg/kg)	Volatile Solids (%)	Cu (mg/kg)	Pb (mg/kg)	Zn (mg/kg)	As (mg/kg)
JC28	Mean	5.89	12	964	6661	49.6	19.5	33.2	27.1	6.4
88-90	St. Dev.	0.11	240	637	4578	26.5	3.2	15.1	23.7	2.0
	CV	2%	2003%	66%	69%	53%	16%	46%	88%	31%
	Median	5.87	-20	578	6056	59.9	20.4	32.6	18.0	7.1
	n	7.00	7	7	8	9.0	7.0	7.0	7.0	7.0
93-95	Mean	5.63	545	153	1392	13.1	5.0	8.1	3.4	1.8
	St. Dev.	0.32	102	150	1241	1.2	2.6	2.3	2.4	1.6
	CV	6%	19%	98%	89%	9%	51%	28%	71%	89%
	Median	5.53	608	176	1980	12.8	4.3	8.5	2.7	1.2
	n	5.00	5	5	5	5.0	5.0	5.0	5.0	5.0
ELS61	Mean	5.70	162	755	4409	33.6	31.8	60.3	47.8	9.0
88-90	St. Dev.	0.34	187	716	3821	22.6	20.3	20.3	24.8	5.4
	CV	6%	115%	95%	87%	67%	64%	34%	52%	60%
	Median	5.84	70	1024	3443	29.5	31.0	32.4	56.6	9.2
	n	11.00	11	13	14	14.0	13.0	13.0	13.0	13.0
93-95	Mean	5.70	164	748	4382	33.8	31.6	60.2	47.6	9.0
	St. Dev.	0.71	298	973	5092	29.3	158.4	77.9	64.1	16.8
	CV	13%	182%	130%	116%	87%	502%	129%	135%	187%
	Median	5.67	547	69	537	8.1	12.7	9.5	14.3	2.8
	n	191.00	188	194	204	208.0	195.0	195.0	195.0	195.0
PC12	Mean	6.08	107	1285	8431	52.5	26.1	170.7	52.7	14.3
88-90	St. Dev.	0.29	291	1122	6813	23.2	8.7	197.8	31.5	7.2
	CV	5%	273%	87%	81%	44%	33%	116%	60%	50%
	Median	6.04	114	1089	6347	59.2	26.9	105.1	39.7	12.5
	n	7.00	7	6	7	6.0	6.0	6.0	6.0	6.0
93-95	Mean	6.15	351	111	911	6.9	3.7	9.1	7.5	1.7
	St. Dev.	0.14	99	115	866	1.5	0.9	6.0	3.2	0.5
	CV	2%	28%	104%	95%	21%	24%	65%	43%	32%
	Median	6.10	310	109	1060	7.0	3.6	10.3	6.6	1.8
	n	5.00	5	5	5	5.0	5.0	5.0	5.0	5.0
BBC24	Mean	5.90	-197	469	4171	22.7	19.1	44.9	39.0	11.0
88-90	St. Dev.	0.35	15	434	4802	17.6	12.4	25.2	16.5	5.5
	CV	6%	-8%	93%	115%	77%	65%	56%	42%	50%
	Median	5.73	-200	297	1692	15.3	17.9	51.6	48.0	10.7
	n	6.00	6	6	7	7.0	7.0	6.0	6.0	7.0
93-95	Mean	5.97	326	43	441	7.4	5.0	4.4	6.0	1.4
	St. Dev.	0.24	49	54	596	3.7	2.9	0.7	0.5	0.3
	CV	4%	15%	126%	135%	50%	58%	16%	9%	26%
	Median	5.97	326	43	441	7.4	5.0	4.4	6.0	1.4
	n	2.00	2	2	2	2.0	2.0	2.0	2.0	2.0

Table 9-3 continued. Soil statistics for treatment wetlands in baseline and post-development years.

Year	Stat.	pH	Redox. Potential (mV)	TP (mg/kg)	TN (mg/kg)	Volatile Solids (%)	Cu (mg/kg)	Pb (mg/kg)	Zn (mg/kg)	As (mg/kg)
NFIC12	Mean	3.97	144	2188	15984	76.0	19.5	48.6	10.4	9.2
88-90	St. Dev.	0.26	345	1138	7440	18.9	10.1	40.0	5.3	5.6
	CV	7%	240%	52%	47%	25%	52%	82%	51%	61%
	Median	3.94	140	2182	15698	81.0	16.3	44.4	10.9	9.9
	n	4.00	4	4	4	4.0	4.0	4.0	4.0	4.0
93-95	Mean	5.05	633	167	1950	12.5	2.5	10.3	3.0	2.2
	St. Dev.	1.05	2	67	113	0.7	0.3	0.8	2.2	0.3
	CV	21%	0%	40%	6%	6%	13%	8%	71%	13%
	Median	5.05	633	167	1950	12.5	2.5	10.3	3.0	2.2
	n	2.00	2	2	2	2.0	2.0	2.0	2.0	2.0

Table 9-4. Particle size distributions for treatment wetlands.

	%Sand/Silt/Clay	
Wetland	1989	1995
BBC24	61/29/10	45/47/8
ELS61	35/49/16	15/69/16
JC28	52/35/13	46/36/18
NFIC12	4/59/37	3/32/65
PC12	58/37/5	63/30/7

Otherwise, there was a strong trend for redox to rise but for nutrients, organic content, and metals all to fall from the pre-development to the post-development years. The reasons for these unexpected results can only be given speculation. What can be said is that, other than the pH increase at NFIC12, there is no obvious signal in the soils yet that negative changes may have accompanied recent urbanization.

REFERENCES

Azous, A. 1991. An Analysis of Urbanization Effects on Wetland Biological Communities, M.S. thesis. University of Washington, Department of Civil Engineering, Environmental Engineering and Science Program, Seattle, WA.

Chin, N. T. 1996. Watershed Urbanization Effects on Palustrine Wetlands: A Study of the Hydrologic, Vegetative, and Amphibian Community Response During Eight Years. M.S.C.E. thesis, University of Washington, Department of Civil Engineering, Environmental Engineering and Science Program, Seattle, WA.

Horner, R.R., F.B. Gutermuth, L.L. Conquest, and A.W. Johnson. 1988. Urban stormwater and Puget Trough wetlands. Pp. 723-746 *in* Proceedings, First Annual

Meeting on Puget Sound Research, The Seattle Center, Seattle, WA, March 18-19, 1988. Puget Sound Water Quality Authority, Seattle, WA.

Ludwa, K. A. 1994. Urbanization Effects on Palustrine Wetlands: Empirical Water Quality Models and Development of a Macroinvertebrate Community-Based Biological Index. M.S.C.E. thesis, University of Washington, Department of Civil Engineering, Environmental Engineering and Science Program, Seattle, WA.

Novotny, V. and H. Olem. 1994. Water Quality; Prevention, Identification, and Management of Diffuse Pollution. Van Nostrand Reinhold, New York, NY.

Taylor, B., K. Ludwa, and R. R. Horner. 1995. Urbanization effects on wetland hydrology and water quality. Pp. 146-154 *in* Puget Sound Research '95 Proceedings, Seattle, WA, January 12-14, 1995. Puget Sound Water Quality Authority, Olympia, WA.

Valentine, M. 1994. Assessing Trace Metal Enrichment in Puget Lowland Wetlands. Non-thesis paper for the M.S.E. degree, University of Washington, Department of Civil Engineering, Environmental Engineering and Science Program, Seattle, WA.

CHAPTER 10 THE HYDROLOGIC REQUIREMENTS OF COMMON PACIFIC NORTHWEST WETLAND PLANT SPECIES

by Sarah S. Cooke and Amanda L. Azous

INTRODUCTION

The vegetation and associated hydrologic regime of wetland study sites located in the Puget Sound Basin was evaluated between 1988 to 1995. Our study examined the role of hydrology in determining the vegetation composition of wetlands in the region. The observed hydrologic regime of common vegetation communities as defined by Cowardin et al. (1979) was evaluated and included forested, scrub-shrub, emergent, and aquatic bed type communities.

Additionally, the hydrologic requirements of individual species was examined in order to determine the optimal conditions and tolerances for some common wetland plants. Several hydrologic conditions present where plant species were growing, including water depth and water level fluctuation (WLF), were examined seasonally and annually. This paper presents an analysis of some of these vegetation and hydrology associations.

METHODS

The wetlands evaluated in this study are inland palustrine wetlands ranging in elevation from 50 m to 100 m above mean sea level and characterized by a mix of forested, scrub-shrub, emergent, and aquatic bed wetland vegetation classes. Twenty-six wetlands total were surveyed. In addition to the nineteen study wetlands surveyed at least three times between 1988 and 1995, the data set also includes seven other wetlands which were surveyed at least once during the years 1993, 1994 and 1995 as part of several related studies.

Sample plots were assigned a category based on the dominant structure of the vegetation community classified in the Cowardin system (Cowardin et al. 1979). The categories included aquatic bed (PAB), emergent (PEM), scrub-shrub (PSS), forested (PFO), upland, or some transition zone between them, for example, PEM/PSS. In some cases vegetation communities changed over time and were then re-categorized. Plant species presence was sampled in permanent plots established every 50 M installed along a gradient from the upland through the transition zones and, at intervals, crossing the different wetland vegetation communities.

The year was divided into four seasonal periods important to plant growth, early growing season, defined to be from March 1 through May 15, intermediate growing season which lasts from May 16 to August 31, senescence lasting from September 1 to November 15th and dormancy and decay, November 16 to February 28. The seasonal hydrologic regime was calculated for each vegetation sample station from 1988 to 1995. Species found in each sample station were associated with the seasonal hydrologic regime we observed at the station . This data was used to describe a hydrograph for many commonly found wetland plants showing typical conditions for mean and maximum water depths and water level fluctuation. This method presumes that plant species presence is associated with conditions favorable to their survival and that, with sufficient observations, ranges of hydrologic conditions successfully tolerated by species, could be determined.

Hydrologic measurements, including instantaneous water levels from staff gauges for measuring typical water level conditions and peak levels from crest gauges to measure depths from storm events occurring between gauge visits, were recorded at least eight times annually (measured every four to six weeks) while water was present in the wetlands (Reinelt and Horner 1990). Gauge measurements were averaged to obtain mean and maximum water depth for each season or for the year. Water level fluctuation (WLF) was computed as the difference between the peak level and the average of the current and previous instantaneous water levels for each four to six week monitoring period. Mean WLF was calculated by averaging all WLFs for a given season or year.

The elevation of each vegetation community was surveyed in order to tie the hydrologic conditions found at the gauge site with the vegetation communities observed at the sample stations. The elevation of all vegetation plots relative to the water depth measured at the wetland gauge was used to determine the likely water depths at the vegetation sample stations for a given sampling date (Figure 10-1).

The method assumed that the water depth measured at the staff gauge would accurately reflect the hydrologic conditions found throughout the wetland, after the data was corrected for elevation. This was not always true as hydrologic conditions in and around the plots sometimes varied from the conditions predicted through elevation change alone. Sometimes intervening topography or large woody debris would produce localized impoundments or dry hummocks unaccounted for in our methods which may affect the accuracy of our results. Whenever such plots were identified we made more accurate surveys or eliminated the plots from the analysis. In addition, our method did not determine whether soils were dry or saturated. We could only estimate saturation given the water depths found at the gauge.

$$D = G - E$$

where: D = water depth at the vegetation plot
G = gauge reading, depth above zero water level and
E = plot survey elevation above zero water level

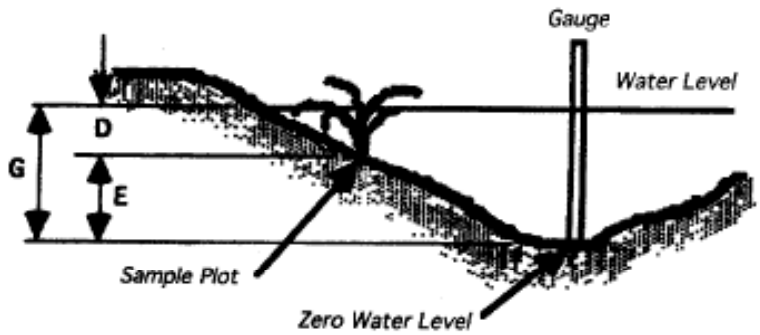

Figure 10-1 Relationship between water depth at vegetation sample plot and the depth at the water gauge (Taylor 1993).

Negative numbers in the hydrographs are interpreted as below the water surface, or inundated. Positive numbers represent the distance, in elevation, above the water surface. Negative numbers are interpreted as depth of inundation. Positive numbers indicate the plant or community being examined is dry during that period. Bar charts show the median and the central 80% of the range of observations for the condition being evaluated. The solid portion of the bar represents the central 50% of observations. We eliminated outliers from our analysis because we wanted to define the most likely range of wettest to driest conditions where particular wetland communities or species would be found.

RESULTS

Hydrologic Regimes By Community Type

The range of average conditions we calculated for instantaneous and maximum water depths found during the study period was in the PEM, PFO, PAB, and PSS communities are displayed in Figure 10-2. The solid bars in the figure show 50% of observations and, including the tails, represent 80% of observations. Forested communities were, as expected, the driest of the community types with a median of 62 cm above typical water levels, and ranged from about 12 cm inundation to about 210 cm above typical water levels. By contrast, the annual instantaneous median condition in the emergent zones was about 5 cm inundation and ranged from 96 cm of inundation to about 28 cm above typical water levels.

The biggest variation from wet to dry conditions through the year was observed in the PSS communities where the median condition for instantaneous water depths was 18 cm above water levels but decreased to 0 for maximum water depth conditions. This corresponds to field observations of different types of shrub communities. Willow

dominated communities (*Salix lucida* var. *lasiandra*, *S. sitchensis*) including red stem dogwood (*Cornus sericea*) represent the wetter shrub communities, while Scouler willow (Salix scouleriana), salmonberry (*Rubus spectabilis*), and black twinberry (*Lonicera involucrata*) represent the drier shrub communities. While the central 50% of observations depict the scrub-shrub communities as saturated to dry under normal conditions, during storm events, represented by the maximum depth, conditions in the PSS zones were much wetter, ranging between about 40 cm of inundation to 25 cm above water levels.

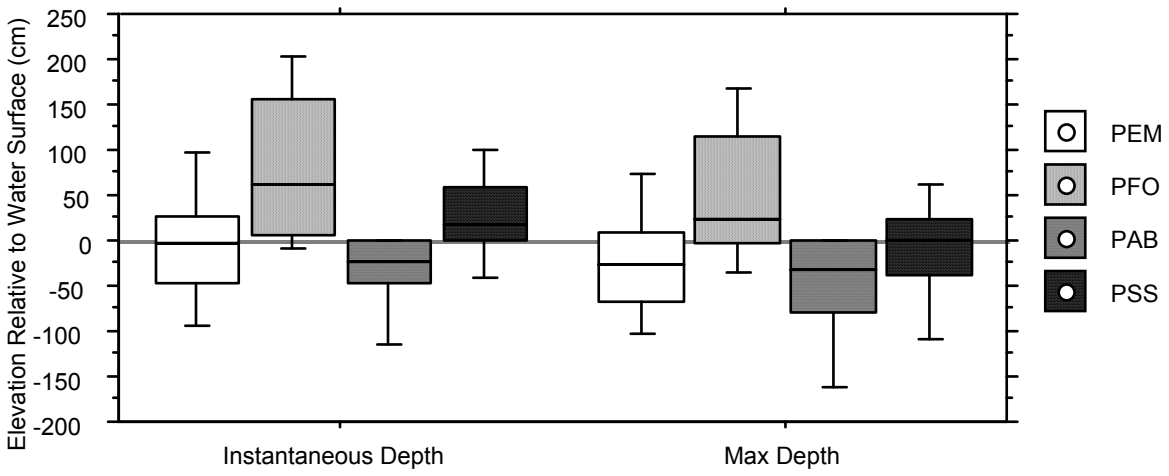

Figure 10-2. Annual mean instantaneous and maximum water depths (Max) associated with vegetation community types, 1988 through 1995.

In fact, annual water level fluctuation averaged 21 cm among all scrub-shrub zones as compared with about 12 cm in the aquatic bed communities and 14 cm in the emergent zones. Forested zones were usually at an elevation above surface inundation, so water level fluctuation was not a significant factor. Aquatic bed communities were observed to have very high water level fluctuations averaging 60 cm as compared with 11 cm and 18 cm, respectively, for emergent and scrub-shrub zones. Figure 10-3 shows the median and range of water level fluctuation calculated in each zone for all four seasons. Open water and scrub shrub zones showed the greatest variation in water level fluctuation between seasons while emergent zones were fairly stable. The median WLF for the aquatic bed zones was always less than 20 cm however the range of observations was quite a bit higher than seen in other community types, in all seasons, but particularly the early growing season of March through May.

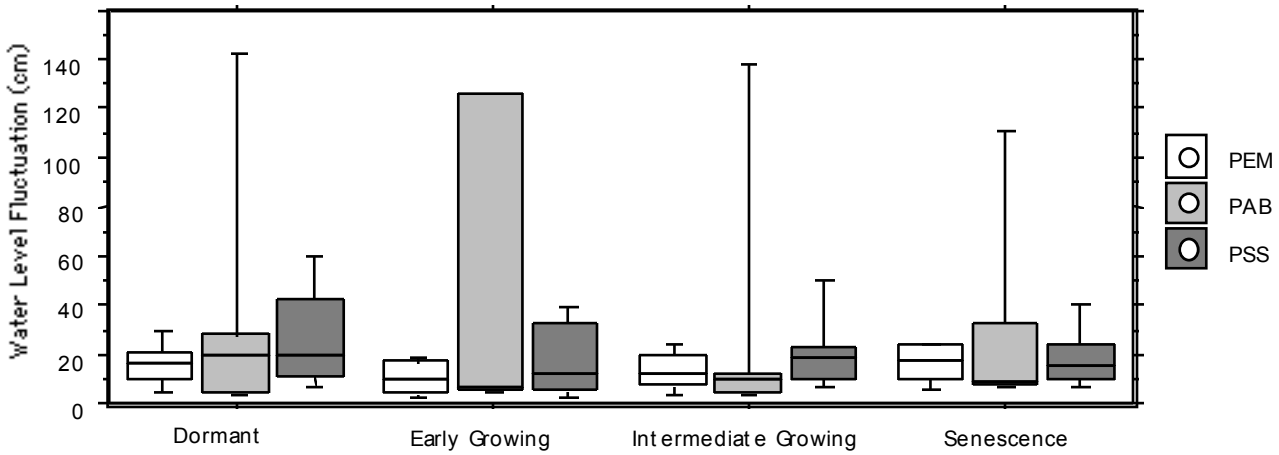

Figure 10-3. Water level fluctuation associated with vegetation community types in each season.

The range of instantaneous and maximum water levels for all seasons were plotted for each vegetation zone and are shown in Figures 10-4 through 10-7. The seasonal changes in each community are apparent in the box plots. The period of senescence, September through November is definitely drier in all zones, including the aquatic bed communities. Most aquatic bed zones had no surface water during this period except during storm events although many were observed to have saturated soils. Most emergent communities were inundated most of the year with the exception of during senescence. Forest wetland communities were relatively wetter during the early growing season than other seasons unlike the other community types which were mostly wettest during the dormant season.

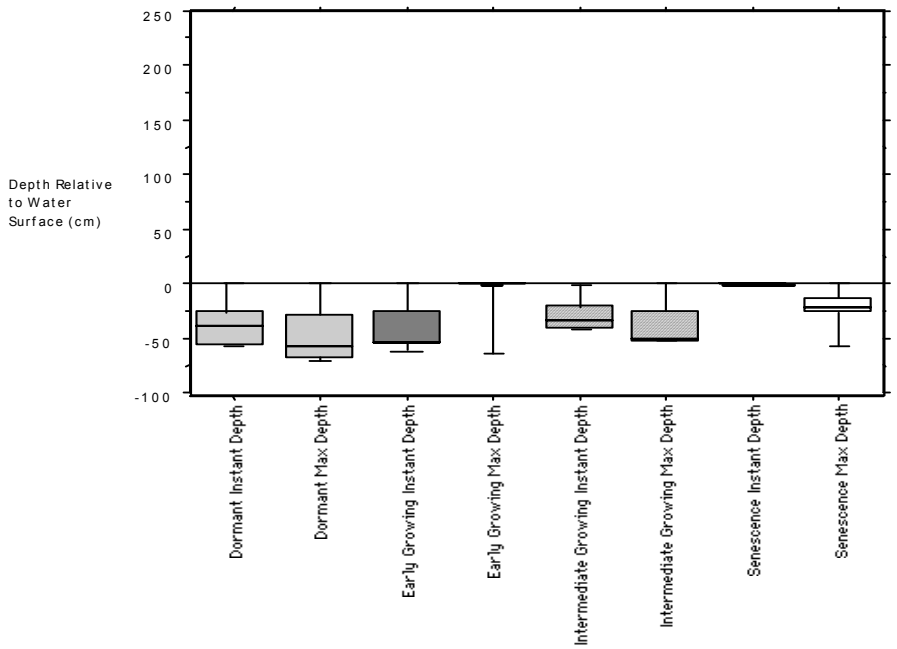

Figure 10-4. Seasonal hydrology associated with aquatic bed communities.

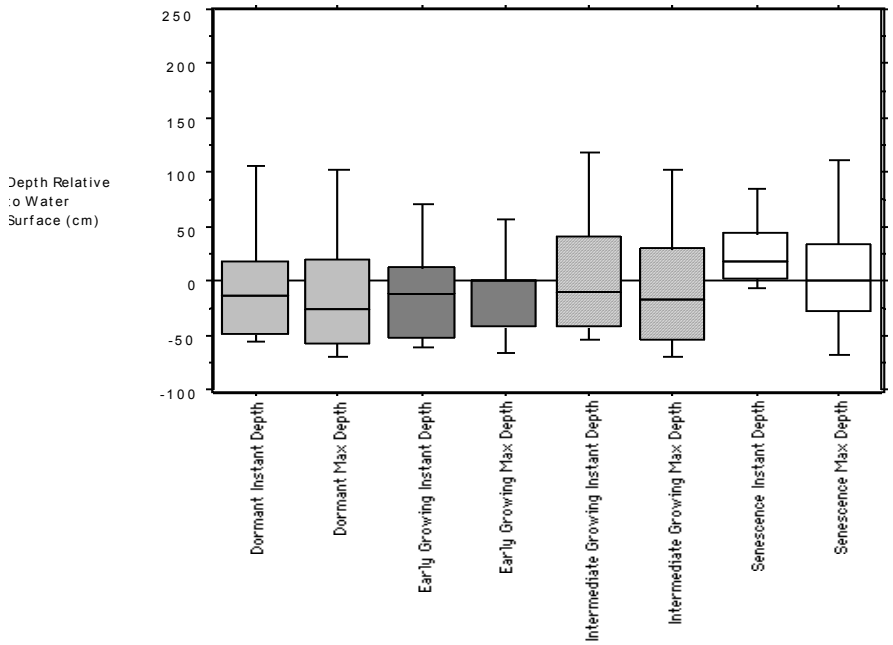

Figure 10-5. Seasonal hydrology associated with emergent communities.

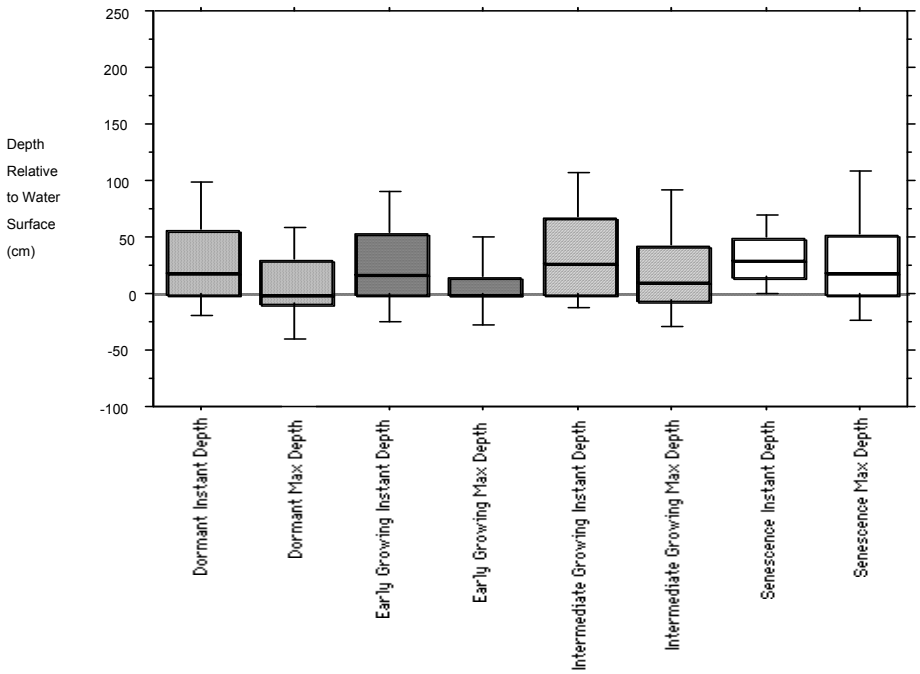

Figure 10-6. Seasonal hydrology associated with scrub-shrub wetland communities.

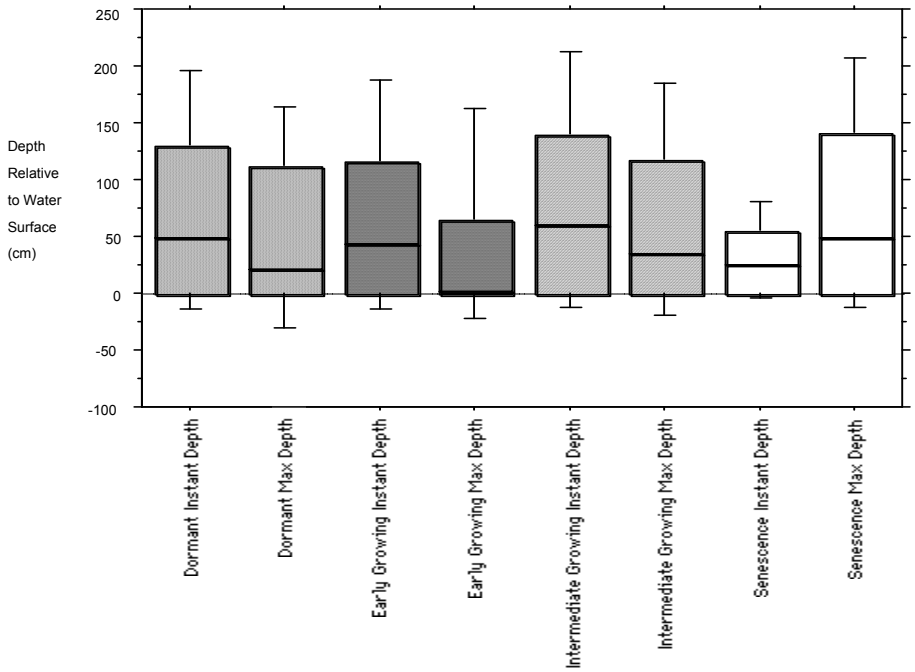

Figure 10-7. Seasonal hydrology associated with forested wetland communities.

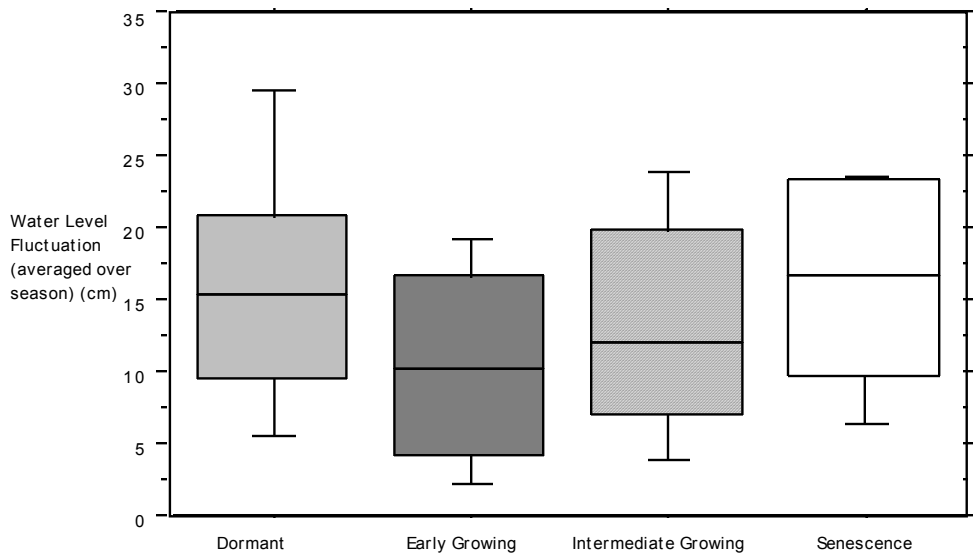

Figure 10-7. Seasonal WLF in the emergent zone.

Individual Plant Hydrologic Requirements

The hydrologic regime for some common wetland species was determined in the same manner as for the wetland zones. Black cottonwood (*Populus balsamifera* spp. *trichocarpa*) was mostly found in areas where there was little to no surface water during the active growing period but it was observed in stations which, on average, are inundated to 20 cm of water at some time during all seasons (Figure 10-8).

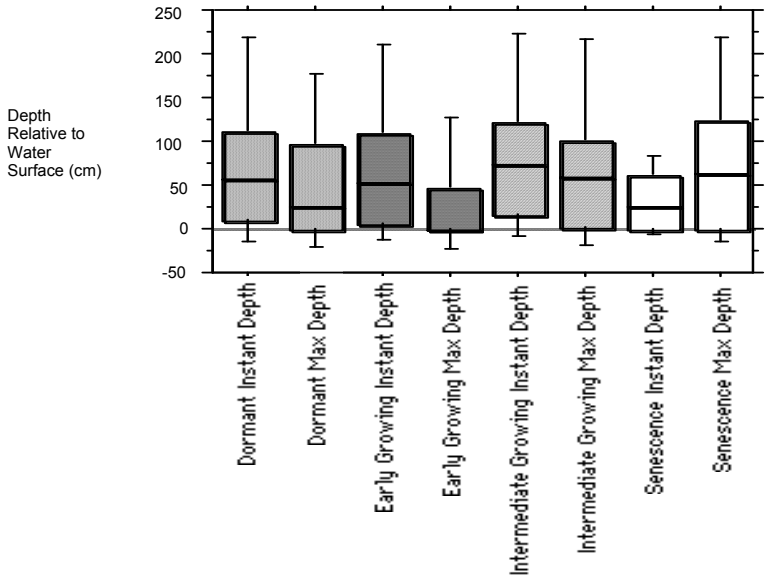

Figure 10-8. Hydrologic characteristics of instantaneous and maximum water depth (Max) of *Populus balsamifera*.

Hard hack spirea *(Spirea douglasii*) was found in a wide range of hydrologic conditions from typically dry through the year, to being frequently temporarily inundated, to complete inundation through both growing seasons (Figure 10-9). This adaptability is probably one reason why this species was among the most widely distributed in our study. In addition hard hack was found in wetlands with some of the highest water level fluctuations measured in our study, averaging as high as 57 cm in the dormant season and 35 cm in the early growing season.

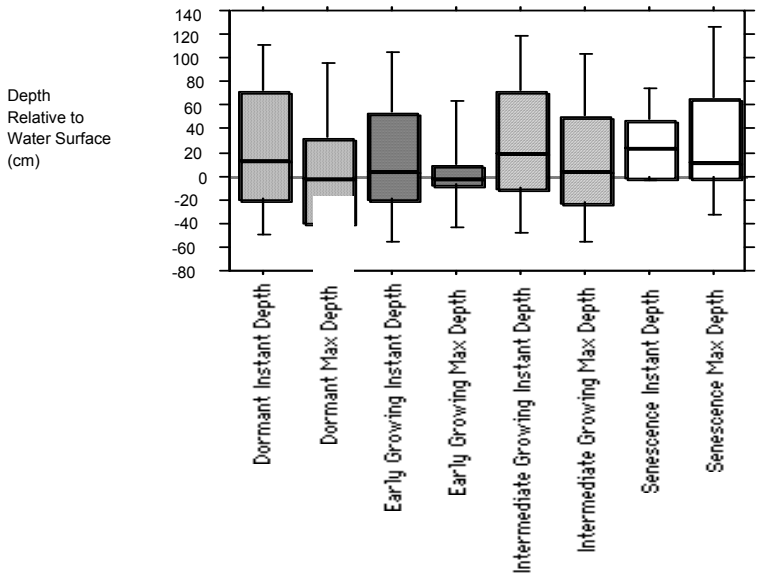

Figure 10-9 Hydrologic characteristics of instantaneous water depth, maximum water depth (Max) of *Spirea douglasii*.

Comparisons were made between plants that either fill the same niche, or are different species of the same genera but found in different habitats. Analysis of the hydrologic conditions where species were observed often showed seasonal hydrologic differences which may account for their distribution (Table 10-1). For example, two common wetland trees, red alder (*Alnus rubra)* and Oregon ash (*Fraxinus latifolia)* were both more prevalent on the drier sites we studied. Red alder differed, however, in that, it was found on many sites subjected to high average seasonal WLF (greater than 20 cm) during the early growing season, suggesting that it is frequently inundated for periods while Oregon ash was observed in areas with mostly stable water levels in the early growing season (Figure 10-10). Oregon ash was often observed in areas where the soil was organic rish and, though rarely inundated, soils were saturated for most of the growing season while red alder was mostly found growing in mineral soils that typically went dry in the summer.

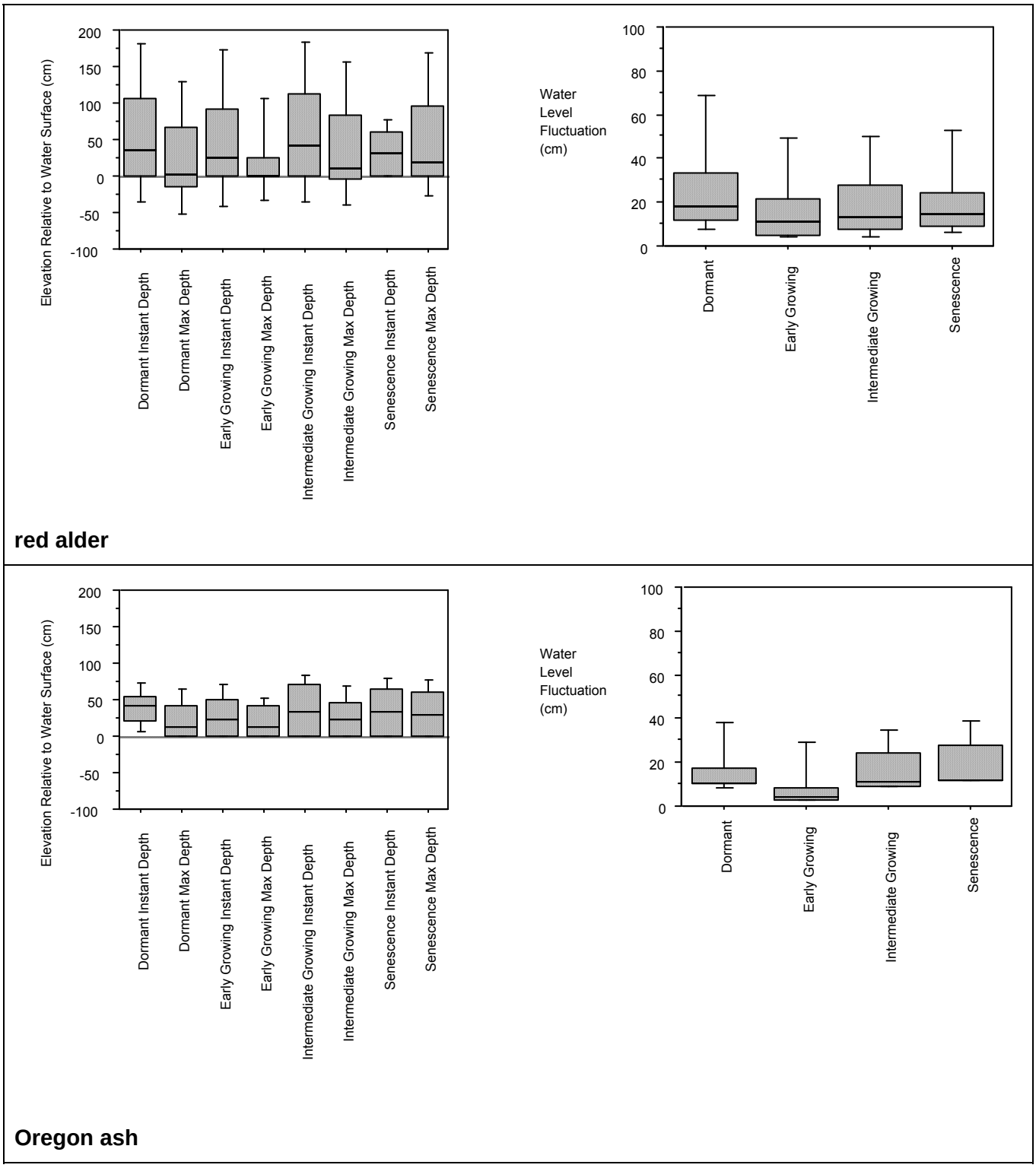

Figure 10-10. Seasonal hydrology and water level fluctuation of red alder and Oregon ash.

Scouler willow (*Salix scouleriana)* and Sitka willow *(Salix sitchensis*), two willows common in the Puget lowland, were both found in areas from inundated to dry in all seasons, but overall, the medians, means and most of the population data, indicate Sitka willow was growing closer to water than Scouler willow (Figure 10-11).

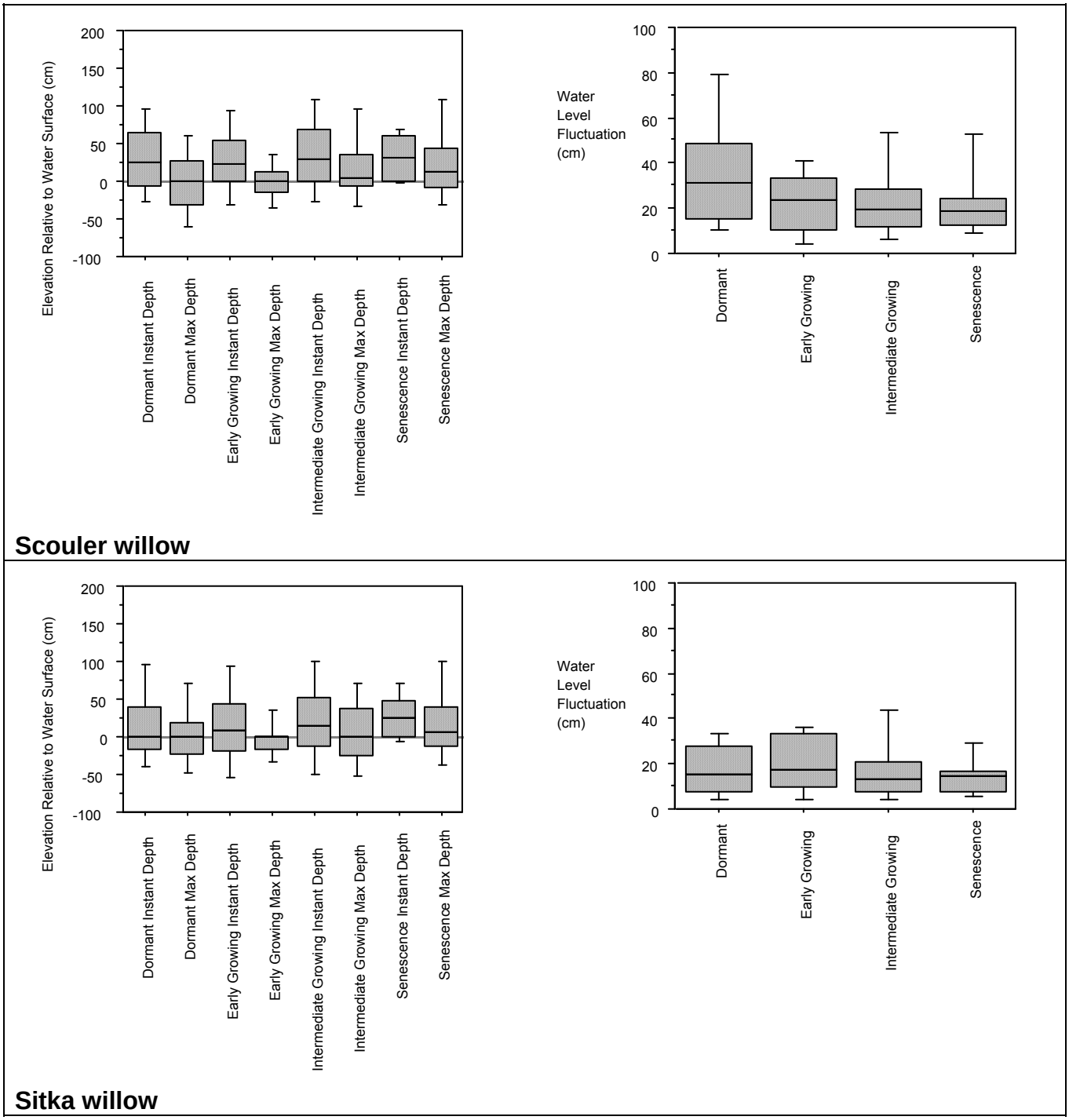

Figure 10-11. Seasonal hydrology and water level fluctuation of Scouler willow and Sitka willow.

Though both species were found growing in a similar range of conditions, tapertip rush (*Juncus acuminatus*) was found on more dry sites than soft rush (*Juncus effusus*) which was usually shallowly inundated during the early spring (Figure 10-12).

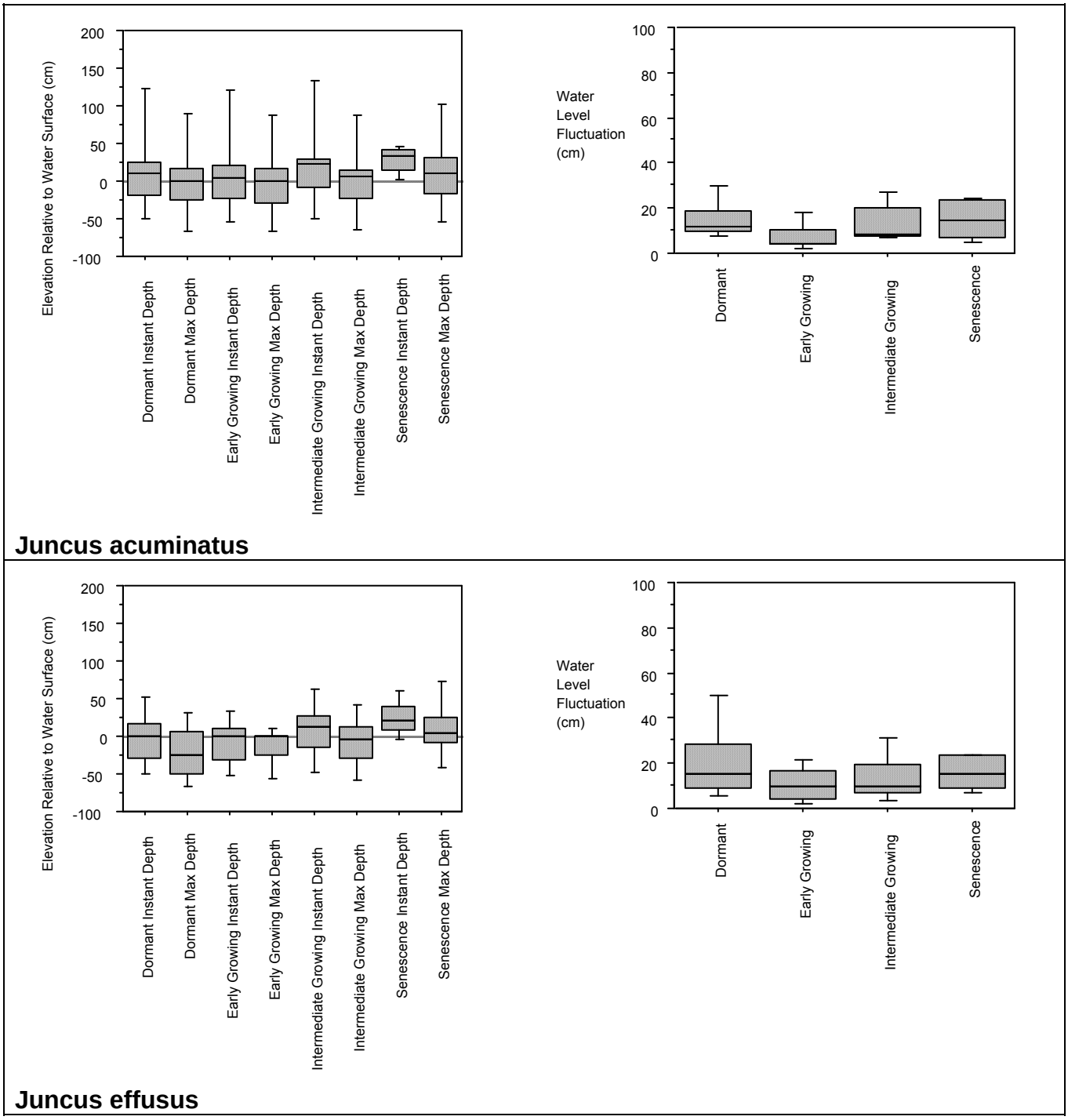

Figure 10-12. Seasonal hydrology and water level fluctuation of tapertip rush and soft rush.

Two sedges were evaluated, Slough sedge (*Carex obnupta)* which is very common in wetlands around the region, and inflated sedge (*Carex exsiccata*) (old name = *C. vesicaria*) which is found almost exclusively in relatively undisturbed wetlands (Figure 10-13). Slough sedge was found in drier areas above the water level during the early and intermediate growing seasons, while inflated sedge grew in saturated soils and areas of shallow inundation. Both species were found in areas inundated during the dormant season and both were found in conditions of high water level fluctuation.

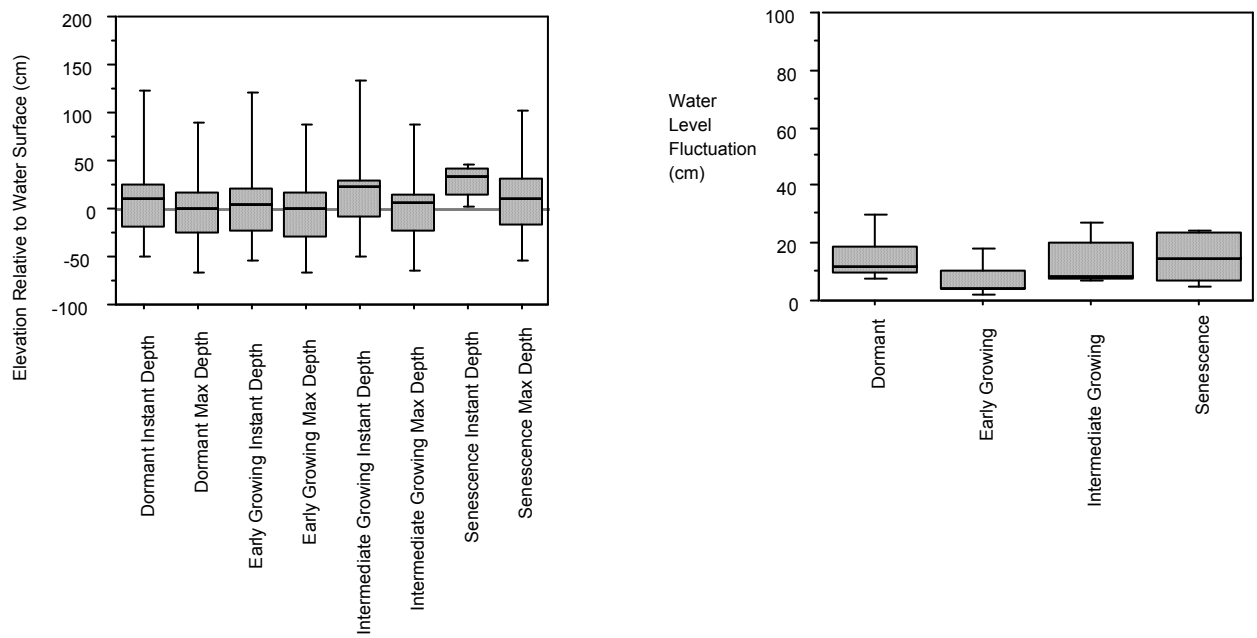

inflated sedge

Figure 10-13. Seasonal hydrology and water level fluctuation of inflated sedge and slough sedge (figure continued next page).

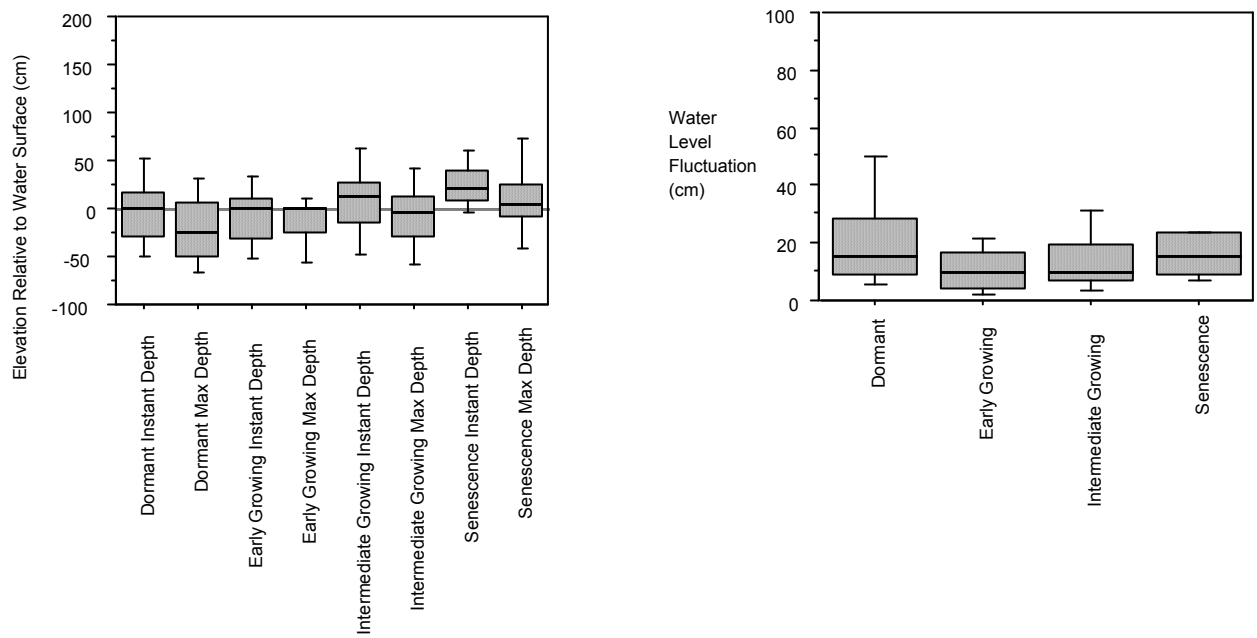

slough sedge

Figure 10-13 (continued). Seasonal hydrology and water level fluctuation of inflated sedge and slough sedge.

Small fruited bulrush, *Scirpus microcarpus*, found in disturbed wetlands, and wooly sedge, *Scirpus atrocinctus* (old name = *S. cyperinus*), found in relatively undisturbed wetlands, were observed growing in similar hydrologic conditions (Figure 10-14). Wooly sedge, however, was found in slightly wetter conditions during the early growing season. In addition, small-fruited bulrush was found in wetlands with high WLF throughout the growing season where wooly sedge was not.

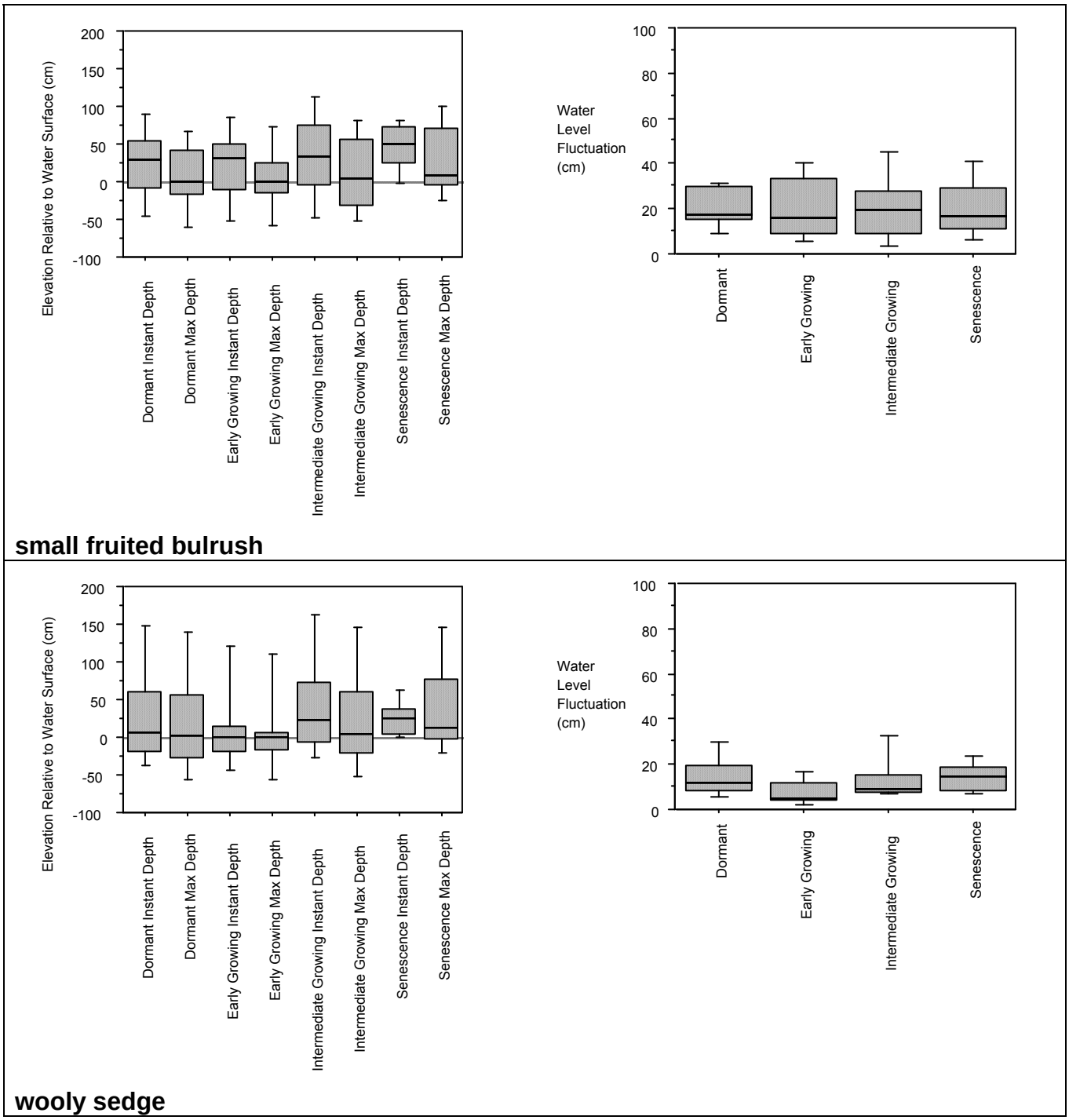

Figure 10-14. Seasonal hydrology and water level fluctuation of small fruited bulrush and wooly sedge.

Several invasive species including soft rush, reed canarygrass (*Phalaris arundinaceae)*, and cattail (*Typha latifolia)* were evaluated to see if there were hydrologic conditions common to aggressive species. Of the three, reed canarygrass grows in the driest areas, and cattail in the wettest (Figure 10-15). Reed canarygrass was found in many wetlands with very high seasonal WLF whereas cattail and soft rush were found in areas

where there is low WLF except during the dormant period. The only consistent hydrologic condition shared between these species was their distribution, most commonly within the emergent zones of wetlands.

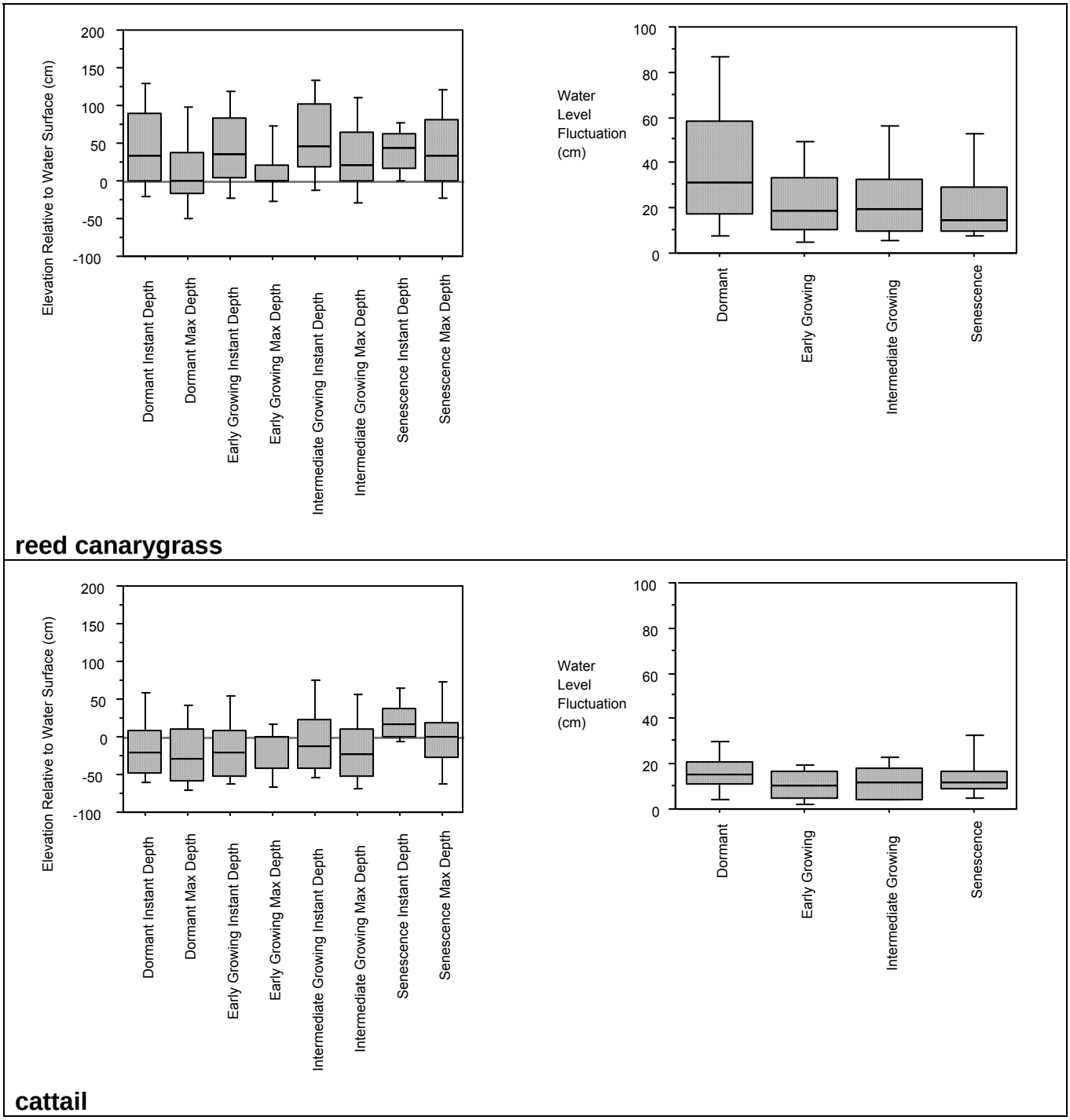

Figure 10-15. Seasonal hydrology and water level fluctuation of reed canarygrass and cattail.

Table 10-1 Comparison of different species and their hydrologic characteristics.

Measure Note: Negative numbers are depth under water. Positive numbers are distance from water surface.	Dormant Instant Depth	Dormant Max Depth	Dormant WLF	Early Growing Instant Depth	Early Growing Max Depth	Early Growing WLF	Inter-mediate Growing Instant Depth	Inter-mediate Growing Max Depth	Inter-mediate Growing WLF	Senes-cence Instant Depth	Senes-cence Max Depth	Senes-cence WLF
Species:	**Alnus rubra**											
Wettest Elevation From Water Surface (cm)	-97	-98	0	-98	-99	0	-97	-96	2	-10	-97	1
Driest Elevation From Water Surface (cm)	430	419	142	438	421	126	441	404	138	98	424	111
Median (cm)	35	2	18	25	0	11	41	11	13	30	20	15
Mean (cm)	58	32	30	48	21	21	60	41	21	33	51	21
Species:	**Fraxinus latifolia**											
Wettest Elevation From Water Surface (cm)	-55	-58	8	-62	0	2	-43	-56	9	-9	0	11
Driest Elevation From Water Surface (cm)	185	129	69	188	71	50	200	193	57	87	196	53
Median (cm)	42	13	10	23	12	4	34	23	11	33	29	12
Mean (cm)	40	22	18	31	20	9	43	31	18	36	37	20
Species	**Salix scouleriana**											
Wettest Elevation From Water Surface (cm)	-96	-98	4	-96	-100	0	-99	-99	0	-7	-94	5
Driest Elevation From Water Surface (cm)	286	261	139	237	194	116	233	185	95	82	235	84
Median (cm)	26	0	31	22	0	23	28	4	19	30	13	19
Mean (cm)	31	2	38	27	3	25	33	17	25	31	24	23
Species	**Salix sitchensis**											
Wettest Elevation From Water Surface (cm)	-97	-83	0	-98	-99	0	-97	-95	0	-9	-97	1
Driest Elevation From Water Surface (cm)	429	399	139	425	385	125	432	376	122	95	406	88
Median (cm)	0	0	15	8	0	17	15	0	13	25	6	15
Mean (cm)	18	8	22	17	3	23	24	10	19	28	20	16
Species:	**Juncus acuminatus**											
Wettest Elevation From Water Surface (cm)	-65	-82	5	-65	-79	2	-66	-79	6	-4	-82	5
Driest Elevation From Water Surface (cm)	169	156	135	166	158	125	182	153	122	88	182	88
Median (cm)	11	1	12	3	0	4	23	7	9	34	10	15
Mean (cm)	16	0	18	12	1	11	24	3	17	30	15	16
Species:	**Juncus effusus**											
Wettest Elevation From Water Surface (cm)	-68	-90	0	-64	-87	0	-60	-81	4	-9	-77	1
Driest Elevation From Water Surface (cm)	163	159	87	163	156	33	172	157	56	88	179	41
Median (cm)	0	-25	15	0	0	10	13	-3	10	21	5	15
Mean (cm)	1	-16	23	-5	-8	11	11	-4	14	26	10	15
Species:	**Carex exsiccata**											
Wettest Elevation From Water Surface (cm)	-23	-90	5	-31	-57	2	-16	-26	4	2	-21	17
Driest Elevation From Water Surface (cm)	106	102	77	75	65	27	117	103	32	87	111	27
Median (cm)	-11	-27	15	0	0	27	19	1	7	16	5	17
Mean (cm)	9	-16	31	0	-6	19	28	11	12	28	20	20

Table 10-1 (continued). Comparison of different species and their hydrologic characteristics.

Measure Note: Negative numbers are depth under water. Positive numbers are distance from water surface.	Dormant Instant Depth	Dormant Max Depth	Dormant WLF	Early Growing Instant Depth	Early Growing Max Depth	Early Growing WLF	Inter-mediate Growing Instant Depth	Inter-mediate Growing Max Depth	Inter-mediate Growing WLF	Senes-cence Instant Depth	Senes-cence Max Depth	Senes-cence WLF
Species:	**Carex obnupta**											
Wettest Elevation From Water Surface (cm)	-89	-95	4	-93	-94	0	-81	-92	2	0	-85	4
Driest Elevation From Water Surface (cm)	362	320	87	367	194	50	367	340	59	95	334	53
Median (cm)	26	0	17	20	0	11	31	10	19	25	20	19
Mean (cm)	43	19	26	40	11	16	51	31	22	35	39	22
Species	**Scirpus microcarpus**											
Wettest Elevation From Water Surface (cm)	-62	-93	8	-53	-70	5	-49	-68	4	-10	-70	4
Driest Elevation From Water Surface (cm)	175	162	69	173	162	50	188	162	57	90	173	53
Median (cm)	29	0	17	31	0	16	34	4	20	50	9	16
Mean (cm)	29	10	22	27	9	21	41	15	20	47	29	20
Species	Scirpus atrocinctus											
Wettest Elevation From Water Surface (cm)	-56	-90	5	-61	-78	2	-60	-81	6	-9	-77	5
Driest Elevation From Water Surface (cm)	187	173	77	181	176	34	202	182	37	88	199	41
Median (cm)	7	2	12	0	0	5	22	5	9	24	13	15
Mean (cm)	27	16	16	15	7	8	38	22	13	26	40	15
Species	**Phalaris arundinaceae**											
Wettest Elevation From Water Surface (cm)	-97	-93	0	-98	-99	0	-95	-88	0	-9	-97	1
Driest Elevation From Water Surface (cm)	430	419	142	438	421	126	441	395	138	99	424	111
Median (cm)	32	0	31	35	0	19	46	21	20	43	34	15
Mean (cm)	51	17	40	48	17	28	60	36	27	41	46	22
Species	**Typha latifolia**											
Wettest Elevation From Water Surface (cm)	-95	-98	0	-98	-98	0	-97	-96	4	-9	-97	1
Driest Elevation From Water Surface (cm)	308	283	50	259	185	40	157	146	57	86	175	41
Median (cm)	-20	-29	15	-21	0	10	-13	-23	12	17	0	12
Mean (cm)	-9	-17	17	-11	-13	11	-3	-14	13	22	3	15

DISCUSSION

Preliminary evaluations of the hydrologic characteristic of some common wetland species have shown that water level fluctuation and depth of inundation during the year, but especially the early growing season, can be key factors in the development of plant associations. The distribution of individual species or vegetation community are related to the hydrologic profile. If the hydrologic profile changes, such as through upstream controls, outlet controls or changing land use in the watershed, it is likely the plant community will shift towards the conditions produced by the new hydrograph. This can have both beneficial or negative consequences depending on the conditions created by management of the upstream watershed. For example, many common dominating species were found in a wider range of conditions of drought to inundation and water level fluctuation. In contrast, less common and less dominant species were almost always found in narrow ranges of hydrologic conditions.

Similarly, hydrologic profiles can help to determine the appropriate plantings for wetland design. The design and successful establishment of plant communities depends on whether individual species in those communities can flourish in the hydrologic regime. Planting designs should be developed based on the seasonal hydrologic conditions.

While our data is useful as a guideline, it is limited in its application. We did not measure plant responses or vigor with respect to hydrologic conditions. Ewing (1996), who measured and analyzed actual tree responses, observed that A. rubra was stressed by repeated cycles of inundation while Fraxinus shows no significant response to repeated inundation, provided the duration of the flooding was less than two to three days. Our methods did not measure such detailed impacts. We also did not accurately account for soil saturation and did not consider soil type which additionally effects species distribution.

REFERENCES

Cowardin, L. M., V. Carter, F. C. Goulet and E. T. LaRoe. 1979. Classification of wetlands and deepwater habitat of the United States. U. S. Fish and Wildlife Service, Washington D.C.

Ewing, K. 1996. Tolerance of four wetland plant species to flooding and sediment deposition. Journal of Experimental Botany. Vol. 36 (2): 131-146. Elsevier Science.

Hitchcock, C. L., A. Cronquist, M. Ownbey, and J.W. Thompson. 1969. Vascular Plants of the Pacific Northwest, University of Washington Press, Seattle and London.

Reinelt, L. E. and R. R. Horner. 1990. Characterization of the Hydrology and Water Quality of Palustrine Wetlands Affected by Urban Stormwater. King County Resource Planning, King County, WA.

Taylor, B. 1993. The influence of wetland and watershed morphological characteristics on wetland hydrology and relationships to wetland vegetation communities. Masters thesis. University of Washington. Seattle, Washington.

CHAPTER 11 EMERGENT MACROINVERTEBRATE COMMUNITIES IN RELATION WATERSHED DEVELOPMENT

by Klaus O. Richter, Kenneth A. Ludwa and Robert W. Wisseman

INTRODUCTION

Aquatic invertebrates play important roles in the food chain of fresh water wetlands. They are the pivotal link between the primary production and detrital trophic levels and higher level consumers including fish, amphibians and aquatic avifauna and mammals (Cummins and Merritt 1996). Moreover, aquatic macroinvertebrates have historically been used as biological indicators in riverine and lacustrine environments (Rosenberg and Resh 1996). Studies by scientists with the Puget Sound Wetlands and Stormwater Management Research Program (Ludwa 1994), (Azous 1991) and others (Murkin and Batt 1987), (Rosenberg and Danks 1987), (Wrubleski 1987), (Hicks 1995, Hicks 1996) have demonstrated the utility of macroinvertebrates as indicators of the health of palustrine environments, particularly for assessing the impacts of urbanization.

Macroinvertebrate communities are noted for their response to the four major wetland stresses identified by EPA's Environmental Monitoring and Assessment Program (EMAP): (1) altered hydroperiod, (2) excess sediment, (3) changes in nutrient cycling; and (4) contaminants (Liebowitz and Brown 1990). Unlike other wetland animal communities (amphibians, mammals, birds, fish) the larval forms of aquatic macroinvertebrates are completely confined to the water within a particular wetland, over entire growing seasons or years, until emergence. Therefore, the aquatic macroinvertebrate community is an excellent integrator of wetland impacts; it does not register impacts that may occur to other wetland animals that migrate outside the wetland for periods of time.

The goal of this study was to establish the impacts of watershed development and particularly, urban stormwater inputs on macroinvertebrate communities. Specific objectives included (1) developing a preliminary wetland macroinvertebrate community-based biotic index based on methods proven for streams, and (2) applying this index to examine the impacts of watershed urbanization on specific aspects of macroinvertebrate communities, over a range of watersheds with different levels of existing development, and within developing watersheds over time. The latter objective is based upon several hypotheses regarding the response of the aquatic macroinvertebrate community to anthropogenic changes to wetlands and their watersheds. These included (1) Changes in macroinvertebrate taxa richness and numbers of individual organisms will reflect changing land use, environmental pollution, direct habitat degradation, and general system health; (2) proportions of sensitive and tolerant taxa will change with increasing watershed urbanization and wetland habitat degradation; and (3) proportions of functional taxa groups will change with alterations to a wetland's nutrient cycle.

Although aquatic macroinvertebrates include non-insect taxa, the sampling device used in this study collected only adult aquatic insects. Therefore, the terms macroinvertebrates and insects shall be used interchangeably in this paper.

METHODS

We periodically monitored emergent aquatic macroinvertebrates in nineteen palustrine wetlands in the Puget Sound Basin from 1988 to 1995. These wetlands were located in watersheds in various stages of urban and suburban development and have been described in earlier chapters.

Trapping protocols are extensively described in Chapter 4 and are briefly summarized here. We made an attempt to place traps in conditions as similar as possible between wetlands (open still water, fine sediment). Location of traps was particularly important because the presence or absence of certain vegetation or substrate types can substantially influence the character of the aquatic macroinvertebrate community. We deployed the traps in each wetland over the periods listed in Table 1. Field staff collected the trap contents and replaced the preservative on an approximately monthly basis from April to September during each monitoring period, with a season-end collection also made in October and/or November. We made no collections from December through March because of low invertebrate activity during this period. The traps provided a cumulative measure of insect emergence between each occasion that the traps are emptied.

Table 11-1. Approximate aquatic invertebrate emergence trap sampling periods for growing seasons 1989, 1993, and 1995.

	1989	1993	1995
Start collection	September 1, 1988*	April 10, 1993	January 1, 1995
End collection	September 31, 1989	April 9, 1994	October 30, 1995

* Monitoring at Fourteen sites were started in September 1988; five more sites were added in April 1989.

We identified and enumerated the macroinvertebrates collected in 1989 to the lowest level possible, in most cases genus or species. We identified insects collected in 1993 and 1995 only to family for Dipteran taxa, and to order for all other taxa. We made identifications to a consistent level within each taxonomic group for all samples.

Using the 1989 data set, we developed a multimetric biological index based on principles of the Benthic Index of Biotic Integrity (Fore et al. 1995). We proceeded by first testing metrics to determine whether they differentiated between the two best and two worst sites; we then confirmed these metrics by testing them over the whole range of nineteen sites (Ludwa 1994) (Fore et al. 1995). We tested and adapted existing lotic macroinvertebrate community metrics to the wetland insect community, and tested and added new metrics unique to palustrine communities.

Because the level of taxonomic effort was considerably coarser for the 1993 and 1995 collections, we found it necessary to develop and test a new set of metrics suitable for that level of information. We performed this step with the 1989 collections by elevating the taxonomic data to the same levels as the 1993 and 1995 collections. Again, we followed the same procedures described by (Ludwa 1994). Most of the coarser-level metrics were based on, (Ludwa 1994) original metrics for the 1989 collections.

We tested the overall index scores against land use and wetland morphology thresholds reported by (Taylor et al. 1995) and Ludwa (Ludwa 1994) using the Mann-Whitney test (Zar 1984), the nonparametric equivalent of the independent groups t-test. We also

tested index scores against parameters for wetland hydrology and water quality, and separately against wetland morphology and watershed land use, using multiple regressions (Zar 1984). All statistical analyses were performed at a significance level of $p > 0.05$.

RESULTS

It is important to note that we designed and calculated the 1989 species/genus-level metrics using data spilt into distinct sampling periods: April-June, July-September, and October-November (Ludwa 1994). The data split into these periods, especially the two summer periods, responded more strongly to urbanization parameters than did the year-long data set. We designed and calculated the 1989 order/family-level metrics using the year-round data sets. Taxa richness values for the coarser-level data were too low for individual sampling periods to differentiate between sites. We assumed that the difference between the length of sampling periods between the three years (Table 1) did not significantly affect taxa richness values, but that it did affect total numbers of individuals collected. The metrics developed for the order/family-level data were taxa richness- and proportion-oriented; therefore we assumed that different sampling period lengths did not affect metric design or calculation.

The metrics recommended for further testing by (Ludwa 1994) for emergent collections with genus-species level taxonomy are listed in Table 2. Although taxa belonging to orders Ephemeroptera, Plecoptera, and Trichoptera are often the basis of stream biological metrics, we found a paucity of these taxa in the wetland insect collections (including order Odonata, these orders are referred to as EPOT). Therefore, although EPOT richness and abundance did yield two metrics, most of the metrics (numbers 7 through 22, including all new wetland- oriented metrics) related to order family Chironomidae of order Diptera (aquatic midges and true flies). Chironomids are a highly diverse family only sparsely detailed in ecological literature; although generally considered to be negative indicators for running waters, Chironomids are adapted to lentic environments, and therefore may be more appropriate indicators of their health.

Using an index composed of the metrics listed in Table 2, (Ludwa 1994) calculated index scores and compared them to direct and indirect measures of wetland stress. Ludwa (1994) emphasized that further verification of this index and its component metrics is necessary before it can be used as an independent measure of wetland ecological health. Conclusions drawn from (Ludwa 1994) analyses follow.

Table 11-2. Biotic index metrics recommended for use with wetlands, based on emergent macroinvertebrate collections with genus/species-level identification (Ludwa 1994).

Metrics Included in Final Wetland Biotic Index (Genus/Species-level Taxonomy)	
Adapted from stream metrics: 1. Taxa richness 2. Scraper and/or piercer taxa presence 3. Shredder taxa presence 4. Collector taxa richness 5. EPOT[1] taxa richness 6. Percent individuals as EPOT 7. Percent individuals as tanytarsini tribe 8. Tanytarsini tribe richness	Unique Wetland Metrics: 9. Percent individuals as Chironomini tribe 10. Chironomini tribe taxa richness 11. Percent individuals as Tanypodinae subfamily 12. Tanypodinae subfamily taxa richness 13. Presence *Thienemanniella* 14. Presence *Endochironomus nigricans* 15. Presence *Parachironomus* spp. 2 16. Presence *Polypedilum* gr.1 and 2 17. Presence A*blabesmyia* 18. Presence *Aspectrotanypus algens* 19. Presence *Paramerina smithae* 20. Presence *Psectrotanypus dyari* 21. Presence *Zavrelimyia thryptica* 22. Presence *Tanytarsus*

[1]EPOT = Ephemeroptera, Plecoptera, Odonata, and Trichoptera.

There appeared to be two primary periods of insect emergence, in the early summer and again in the late summer/early autumn; sampling periods in April-June and July-September were most appropriate for calculation of biotic index scores. Collections made in October-November did not appear to be as effective for purposes of bioassessment.

Biotic index scores responded significantly to land use and wetland morphology parameters. A multiple regression revealed that scores responded negatively to total watershed impervious area, wetland channelization, and incidence of dryness. The regression explained 67 percent of the variance in index scores. Threshold analyses also revealed that index scores were significantly higher with increasing watershed forest coverage and lower with increasing impervious area. Highly channelized sites had significantly lower scores, consistent with the observation of degraded water quality for most parameters in highly channelized sites.

A multiple regression indicated that water quality and hydrology parameters explained a significant amount of variation of the index scores (as high as 73 percent). Index scores responded negatively to hydrogen ion concentration (antilog pH), conductivity, suspended solids, water level fluctuation, and incidence of wetland dryness. Suspended solids, conductivity, and water level fluctuation were demonstrated by (Ludwa 1994), (Taylor et al. 1995), and (Chin 1996) to be the water quality and hydrology parameters in these sites most significantly degraded by increases in watershed impervious area and decreases in forest cover. This illustrates the interrelationship between a wetland's watershed, its physical and chemical parameters, and the health of its biological communities.

The order/family-level metrics developed with the 1989 data are listed in Table 3; Table 4 lists the resulting index scores calculated with these metrics for 1988, 1993, and 1995. Although the order/family-level metrics responded to indicators of urbanization, the overall index comprised of the metrics had much less power to discern between sites with different levels of urban impact. For example, the multiple regression of 1989 genus/species index scores versus total impervious area, wetland channelization, and incidence of dryness explained 67 percent of the index score variance. The same regression explained only 21 percent of the 1989 index score variance for the order/family data.

Table 11-3: Biotic index metrics recommended for use with wetlands, based on emergent macroinvertebrate collections with genus/species-level identification.

Metrics Included in Final Wetland Biotic Index (Order/Family-level Taxonomy)
• Family/Order Richness • Shredder Presence • Collector Richness • EPOT Order Richness • % Individuals as EPOT • % Individuals as Dixidae

After 1989, the next year in which land use data was available was 1995. The 1995 index scores were not significantly related to total impervious area or forested area, nor did the scores respond significantly in the multiple regression against total watershed impervious area, wetland channelization, and incidence of wetland dryness. Furthermore, the changes in index scores between 1989 and 1995 did not correspond to changes in land use. For example, NFIC12, which experienced an increase in impervious area from 2 percent to 40 percent, showed the highest percent increase in its index score, exactly opposite that which would be predicted (Figure 11-1).

Table 11-4. Order/Family macroinvertebrate index scores.

	Index Score		
	1989	1993	1995
AL3	16	10	20
B3I	12	8	6
BB24	26	10	16
ELS39	10	12	12
ELS61	18	10	18
ELW1	8	6	6
FC1	16	14	10
HC13	22	14	24
JC28	22	10	26
LCR93	28	16	6
LPS9	8	10	18
MGR36	20	12	16
NFIC12	10	10	24
PC12	18	10	10
RR5	10	6	18
SC4	16	10	12
SC84	14	14	12
SR24	18	10	14
TC13	10	12	10

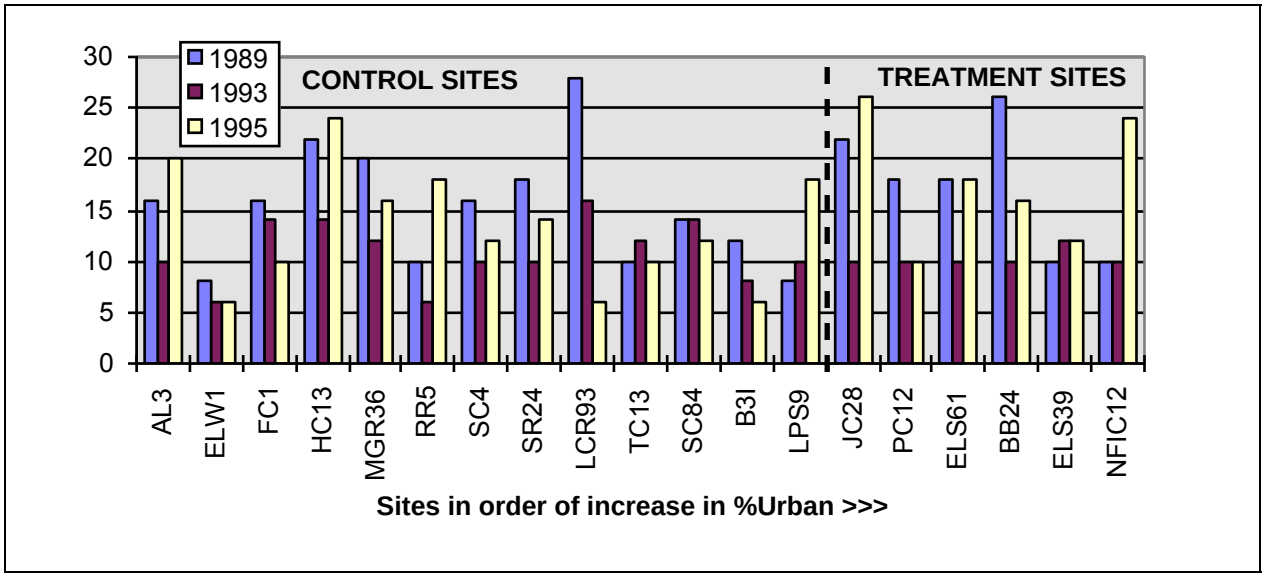

Figure 11-1. 1989, 1993, and 1995 Wetland macroinvertebrate index scores versus change in watershed urbanization.

In addition to relating index scores to changing watershed characteristics, we also examined changing taxa richness and abundance data to describe the impact of urbanization on emergent macroinvertebrates. Table 5 lists abundance and taxa

richness values for each site in each year. Multiple regressions and threshold tests revealed no significant patterns in order/family taxa richness related to impervious area, between sites or years. In other wetland animal communities, taxa richness of sensitive species is often more responsive to wetland degradation than is overall taxa richness (e.g., Power at. al., 1989). The index developed for the species/genus-level data incorporates this concept by including sixteen metrics based on the presence of taxa that are assumed to be more sensitive to disturbance. The order/family data does not allow enough resolution to indicate sensitive taxa. Numbers of individuals decreased from 1989 to 1995 in 14 out of 19 sites, but, as discussed above, we assume that this is primarily a function of a longer sampling period in 1989.

Table 11-5. Insect abundance and order/family richness: 1988, 1993, and 1995.

	Abundance			Taxa Richness		
	1989	1993	1995	1989	1993	1995
AL3	4408	3619	1946	12	11	13
B3I	3027	2219	988	14	10	8
BB24	8857	14742	5815	14	10	13
ELS39	7337	6267	3773	12	12	12
ELS61	20828	13457	2808	16	10	12
ELW1	1239	503	157	10	7	7
FC1	4736	13332	5751	14	9	9
HC13	8748	4436	2934	15	11	13
JC28	1133	5778	1251	13	8	13
LCR93	9689	12148	40464	15	12	7
LPS9	5127	1006	5490	12	10	12
MGR36	7365	13276	1918	14	10	10
NFIC12	8869	24866	2015	12	11	13
PC12	5893	10701	4350	15	11	11
RR5	8621	4748	2150	12	10	11
SC4	2952	2794	2962	12	10	12
SC84	3692	2159	1254	13	9	11
SR24	5598	4982	1140	14	8	12
TC13	4657	4204	4657	13	9	13

SUMMARY

We recommend further development of macroinvertebrate community-based biological indices for assessment of wetland biological health. Our results suggest that this kind of

index may be as useful as comparable indices established for running waters. Further testing of the metrics proposed by this study are necessary before the index may be used as an independent wetland assessment tool in the Puget Sound Ecoregion. Furthermore, refinement of insect tolerance and feeding group information may allow the index to be used as a diagnostic tool. Alternatively, in a set of proposed guidelines for assessing wetland health, Brooks and Hughes (1988) advocate a broad multi-taxa approach that not only includes invertebrates but plants and vertebrates as well.

We recommend genus and species-level taxonomic identification of macroinvertebrates for use of taxa richness values and calculation of biological indices. Coarser-level identifications do not appear to adequately discern insect functional groups, tolerance levels, and specific sensitive genera or species.

Results from the 1989 comparisons of insect data across wetlands with different levels of watershed development suggest that urbanization affects emergent macroinvertebrate communities by (1) decreasing overall taxa richness, (2) eliminating or reducing taxa belonging to scraper and shredder functional feeding groups (leaving a dominance of collector taxa), (3) reducing EPOT taxa richness and relative abundance, and (4) eliminating or reducing specific Dipteran taxa, particularly those belonging to the Chironomidae family.

REFERENCES

Azous, A. L. 1991. An analysis of urbanization effects on wetland biological communities. University of Washington, Seattle, WA, USA.

Brooks, R. P., and R. M. Hughes. 1988. Guidelines for assessing the biotic communities of freshwater wetlands. Pages 276-283. *In* J. A. Kusler, M. L. Quamen, and G. Brooks, eds. Proc. Nat. Wetlands Symposium: Mitigation of Impacts and Losses. Association of State Wetland Managers Inc., Berne, NY, USA.

Chin, N. T. 1996. Watershed urbanization effects on palustrine wetlands: A study of the hydrologic, vegetative, and amphibian community response during eight years. Pages 140. University of Washington, Seattle, WA, USA.

Cummins, K. W., and R. W. Merritt. 1996. Ecology and distribution of aquatic insects. Pages 74-86. *In* R. W. Merritt and K. W. Cummins, eds. An Introduction to the Aquatic Insects of North America. Kendall/Hunt Publishing Company, Dubuque, IO, USA.

Fore, L. S., J. R. Karr, and R. W. Wisseman. 1995. A benthic index of biotic integrity for streams in the pacific northwest. Journal of North American Benthological Society :2-31.

Hicks, A. L. 1995. Impervious surface area and benthic macroinvertebrate response as an index of impact from urbanization on freshwater wetlands. Pages 63. University of Massachusetts, Amherst, MA, USA.

Hicks, A. L. 1996. Aquatic invertebrates and wetlands: ecology, biomonitoring and assessment of impact from urbanization. Pages 130. *In* A. L. Hicks, (ed.) University of Massachusetts, Amherst, MA, Amherst, MA.

Liebowitz, N. C. and M. T. Brown. 1990. Indicator strategy for wetlands. *In* Environmental Monitoring and Assessment Program: Ecological Indicators, US Environmental Protection Agency. EPA/600/3-90/060. Office of Research and Development, Washington D.C. USA.

Ludwa, K. A. 1994. Urbanization effects on palustrine wetlands: Empirical water quality models and development of macroinvertebrate community-based biological index. University of Washington, Seattle, WA, USA.

Murkin, H. R., and B. D. J. Batt. 1987. The interactions of vertebrates and invertebrates in peatlands and marshes. Mem. Ent. Soc. Can. 140:15-30.

Power, T., K.L. Clark, A. Harfenist, and D.B. Peakall. 1989. A Review and Evaluation of the Amphibian Toxicological Literature. Canadian Wildlife Service, Headquarters, Ottawa, Canada.

Rosenberg, D. M., and H. V. Danks. 1987. Aquatic Insects of Peatlands and Marshes in Canada. Mem. of the Ent. Soc Canada No. 140:174.

Rosenberg, D. M., and V. H. Resh. 1996. Use of Aquatic Insects in Biomonitoring. Pages 87-97. *In* R. W. Merritt and K. W. Cummins, eds. An Introduction to the Aquatic Insects of North America. Kendall/Hunt Publishing Company, Dubuque, IO USA.

Taylor, B. L., K. A. Ludwa, and R. R. Horner. 1995. Urbanization effects on wetland hydrology and water quality. Pages 146-154. *In* R. Elizabeth, (ed.) Puget Sound Research '95 Proceedings. Puget Sound Water Quality Authority, Olympia, WA, USA.

Wrubleski, D. A. 1987. Chironomidae (Diptera) of peatlands and marshes in Canada. Mem. Ent. Soc. Can. 140:141-161.

Zar, J. H. 1984. Biostatistical Analysis, Englewood Cliffs, NJ, USA.

CHAPTER 12 BIRD COMMUNITIES IN RELATION TO WATERSHED DEVELOPMENT

by Klaus O. Richter and Amanda L. Azous

INTRODUCTION

Wetlands are recognized because of the disproportionate habitat value they provide for birds (Chapter 6 in this volume). Wetlands, however, are under increasing threat from watershed development in urbanizing areas. Landscape conversion from forests to residential housing and other developments remove or alter habitat immediately adjacent to wetlands and fragment habitat that remains. Moreover, wetlands themselves may be altered in their hydrology and water quality, directly influencing bird populations or indirectly affecting them by altering wetland vegetation. Collectively, these alterations may change breeding, nesting or feeding habitat and competitive interactions among and between species resulting in population shifts.

Striking bird population changes in terrestrial habitat within urbanizing landscapes have been documented. Blair (1996) in his review of researchers' findings of bird distributions along terrestrial gradients of urbanization, summarized that: (1) species composition changes in an area as it becomes urbanized; (2) almost always, the number of species decreases with increasing urbanization; and (3) all agree that bird density or abundance increases with urbanization. More specifically, urbanization is generally found to be correlated with increasing biomass and density and favoring dominance by a few urban ground gleaners where forest insectivores, canopy foliage gleaners or bark drillers used to forage (Beissinger and Osborne 1982).

Few studies, however, have investigated the impacts of watershed development on birds of wetlands. Birds of wetlands may directly be threatened by impacts to marshes, swamps and bogs and secondarily by habitat changes attributable to urbanization within the landscape. Foremost, wetland impacts include urban stormwater runoff that flood nest sites and disperses pollutants that may bio-acumulate in birds through aquatic food chains. Moreover, runoff may alter the areal extent of open water, existing hydrology, vegetation classes and other wetland characteristics influencing cover, nesting habitat and food distribution. Concomitantly, urbanization may influence wetland buffers and adjacent lands, which may also be reflected in changing bird distributions and abundances.

In this paper we describe the changing bird communities in wetlands across a gradient of increasing watershed development and within wetlands that have been altered during the duration of this study. We hypothesize that bird species diversity and abundance changes with increasing watershed development. Although total bird diversity may remain the same in wetlands, we predict that abundances of native species, especially urban-intolerant species, should decline and urban adapters and exploiters increase. Specifically, the proportion of species with low tolerances to habitat changes should be lower in wetlands affected by development than unaffected wetlands.

In part, these predicted changes are based on the fact that the distribution and abundance of birds are widely accepted as functions of vegetation structure and diversity which, in itself, is altered by development in watersheds. Therefore, we

hypothesize that bird species richness, diversity, and relative abundance reflect the structural diversity of vegetation at wetlands, with those wetlands with greatest vegetation changes exhibiting the greatest avifaunal changes.

METHODS

Bird survey methods are described in the companion paper on bird distributions in the wetlands of the Puget Sound Basin (Chapter 6). In this chapter we compare the pre-development and post-development alpha diversities of birds for life history characteristics covering adaptability and residency. We also evaluate bird density as measured by the average number of detections per visit to a wetland. Initially, to examine adaptability, we characterized species as invasive and non-invasive by identifying invasive birds as alien species spreading naturally (without the direct assistance of people) in natural or seminatural wetlands, to produce a significant change in terms of composition, structure or ecosystem process, which was a definition applied to invasive

vegetation by Cronk and Fuller (1995). Subsequently we identified species as 1) urban exploiters, 2) urban avoiders and 3) suburban adaptable using the criteria specified by Blair (1996) and based on species sensitivity to human-induced changes in wetlands and watersheds. We also characterize birds by whether they were common residents, rare residents or seasonal migrants according to Hunn (1982).

Wetland vegetation, hydrology and surrounding land use were measured as described in Sections 1 and 2 of this report. In addition, we characterize wetlands according to watershed condition and their level of disturbance, or treatment, during the course of our study. These experimental categories included wetlands in rural areas which did not change during our study (Rural Controls), wetlands which began the study in an urbanized area (Urban Controls) and wetlands which had 10% or more of their watershed develop, regardless of previous condition, during the study period (Treatments). We also examined the availability of suitable habitats for birds adjacent to wetlands, including forests, with and without single family housing, open water and shorelines. Undeveloped meadow and shrub-land were also evaluated as additions to suitable habitats whereas unsuitable habitat always included developed or cleared land and agricultural lands.

Statistical analysis of correlations and hypothesis testing utilized parametric statistics when assumptions of normality were met and non-parametric statistics when assumptions were violated. We chose $p \leq 0.05$ and $p \leq 0.10$ as significant and weakly significant, respectively, for reporting results. Nevertheless, significance should be interpreted cautiously because of the variability in sampling populations of species and the low number of wetlands undergoing impacts that could be observed in changing bird sightings during the period of our study.

RESULTS

Total alpha diversity decreased significantly among all wetlands between 1989 and 1995 (Friedman test (F), $\chi 2 = 18.3$, $p \leq 0.0001$). Total alpha diversity also decreased among all wetlands when analyzed by experimental category. Both wetlands in developed (urban controls) and undeveloped (rural controls) watersheds showed a significant decline in total diversity (F, $\chi 2 = 5.6$, $p = 0.06$ and F, $\chi 2 \geq 4.8$, $p = 0.09$, respectively), as

did wetlands in watersheds with increased development (treatments) during the study (F, $\chi 2$ = 9.0, p = 0.01).

Total diversity in a single wetland ranged from 16 to 57 species over the study period and averaged 38 among all wetlands in 1989, the year of highest recorded richness. During that same year, we observed an average of 37 bird species in both the urban control and rural control wetlands and an average of 38 in the treatment wetlands. By the last year of our surveys, 1995, total diversity within wetlands with undeveloped uplands averaged 31. In the treatment wetlands and in the urban control wetlands, an average of 28 species were detected.

Average alpha diversity, similar to total diversity decreased significantly for all wetlands (F, $\chi 2$ = 13, p = 0.0015). However, average alpha diversity only decreased significantly among the wetlands with watersheds affected by urbanization whether past (urban controls) (F, $\chi 2$ = 7.0, p = 0.03) or during the study period (treatments) (F, $\chi 2$ = 5.5, p = 0.06). Average diversity for all wetlands in undeveloped watersheds at the end of our study (controls) remained unchanged (F, $\chi 2$ = 3.1, p = 0.2) (Figure 12-1).

The average number of birds detected at all 19 wetlands slightly increased, from 1989 to 1995 (F, $\chi 2 \geq 4.8$, p = 0.09), but simultaneously, we found average detections unchanged among all experimental categories, the urban controls (F, $\chi 2 \geq 2.0$, p = 0.37), the treatment wetlands (F, $\chi 2 \geq .33$, p = 0.84) and among the rural control wetlands (F, $\chi 2 \geq 3.2$, p = 0.2) (Figure 12-2). A complete list of detection rates for all species is available in Appendix Table 12-1.

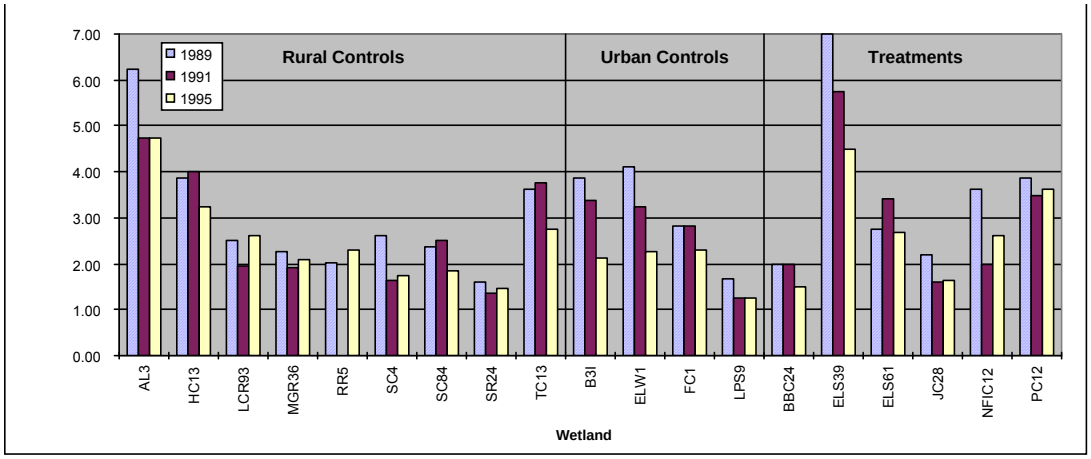

Figure 12-1. Average wetland alpha diversity over the study period by experimental category.

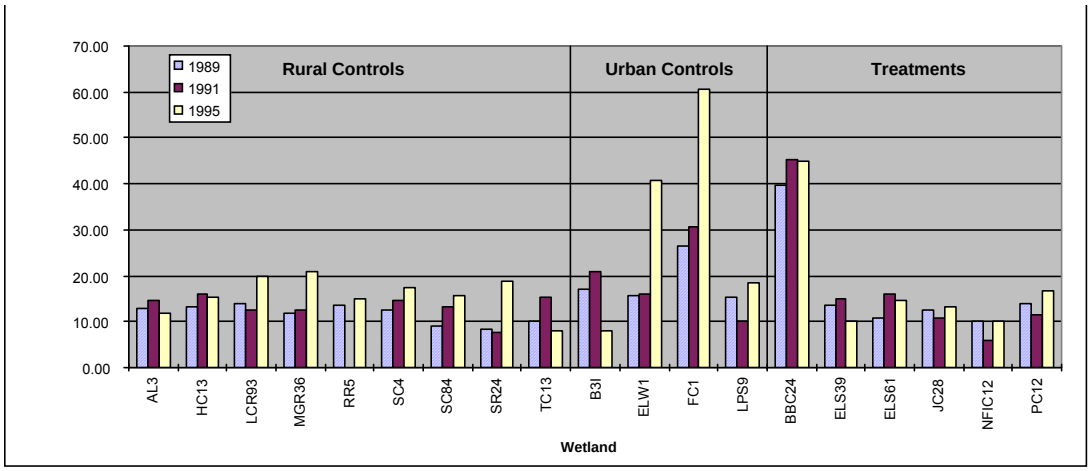

Figure 12-2. Average avian detection rate over the study period by wetland and experimental category.

We found that bird richness decreased and abundance remained the same in wetlands with developed or developing watersheds (urban control or treatment) but found richness unchanged in wetlands with rural, relatively pristine watersheds (rural controls).

Interestingly, although alpha bird diversity was statistically related to development in the watershed, we did not find diversity to be related to urbanization within 1000 meters of the wetlands. Although, increasing percentages of forest land within 1000 meters of the wetland did not add to diversity, the presence of forest land did affect the structure of bird communities from about 500 meters to 1000 meters (the maximum distance we studied). We found that species richness of birds known to avoid human development (avoiders) increased over the study period primarily in wetlands with high percentages of adjacent forest land within 500 meters (Mann-Whitney (MN), $p < 0.09$) whereas they decreased among the already urban wetlands and in those where land use changes decreased watershed habitat (Figure 12-3).

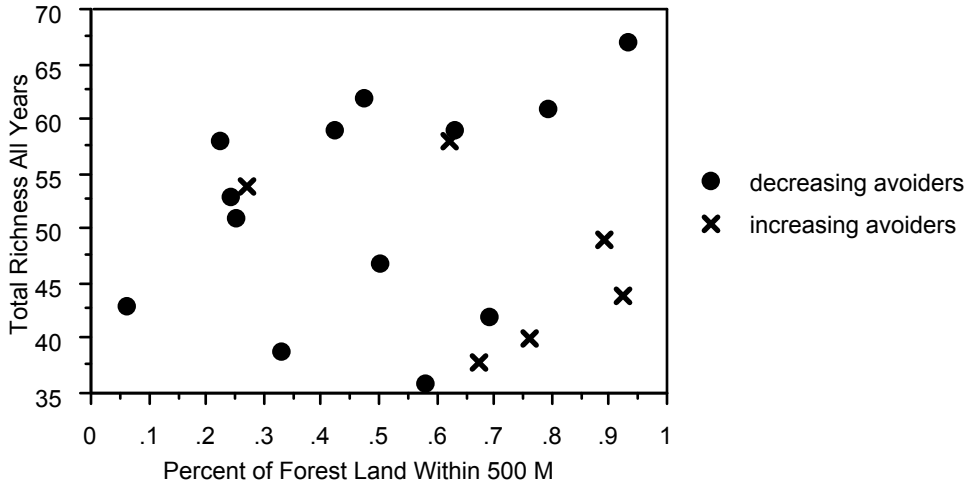

Figure 12-3. Species richness and whether the number of avoiders in the population increased or decreased related to the presence of forest land.

Detections of migrants declined during the study among all wetlands combined (F, $\chi 2$ = 31.6 $p \leq 0.0001$) as did rare residents (F, $\chi 2$ = 6.4, p = 0.04) while detections of residents remained the same. Migrants also declined within all experimental categories (F, $\chi 2 \geq 7.1$ $p \leq 0.02$) but detections of rare residents did not show any significant change within the experimental groups. Detections of resident species did not change among the rural control and treatment wetlands but declined in the urban control wetlands (F, $\chi 2$ = 5.1, p = 0.07).

Across all wetlands, the number of detections of species that avoid development and adaptive species declined during the study (F, $\chi 2 \geq 10.1$, $p \geq 0.007$) while densities of invasive or exploitive species stayed the same. Detections of avoiding species declined among the already urban and treatment wetlands but not the rural control wetlands (F, $\chi 2 \geq 9.1$, $p \leq 0.01$). The greatest declines of adaptive species occurred in treatment wetlands (F, $\chi 2 \geq 7.5$, $p \leq 0.02$). While exploitive species detections were not significantly different between years in wetlands overall, among the rural control wetlands in non-urbanized areas, densities of exploitive species increased significantly (F, $\chi 2$ = 5.6, p = 0.06) from 1989 to 1995. Density changes included increases in such invasive species as American crow, European starling and house sparrow.

Three wetlands, ELS39, ELS61 and NFIC12 exhibited dramatic vegetation changes during our study and also showed significant changes in bird species. At ELS39 species richness decreased from 28 to 23 and then to 18, from 1989, 1991 and 1995, respectively. Species disappearing included marsh wren, pine siskin and red-breasted nuthatch. Species increasing included, among others, urban habitat exploiters and adapters such as American crow, mallard, California quail, and rufous-sided towhee. At ELS61 species richness decreased from 44 to 32 species between 1989 and 1995 and at NFIC12 species decreased from 29 to 21. Within both wetlands sightings of American robin and black-capped chickadees increased.

DISCUSSION

Although our study intensively covers the wetlands of the lower Puget Sound region and represents a first comprehensive account of wetland bird diversity, we consider our work to date as a rough initial attempt to assess bird densities and population trends over the study period. Blair (1996) found that urbanization affects bird diversity in two distinct ways: moderate levels of development may both increase overall species diversity and decrease native bird diversity whereas increasingly severe development lowers total and native species diversity. Although moderate development increases diversity this increase seems attributable to the addition of widely distributed species at the expense of native species. Our findings agree with Blair in that, in general, we found average alpha diversity decreasing in wetlands in watersheds affected by urbanization but also in some wetlands not affected by urbanization. In addition, we found that abundance of birds (detection rate) increased among all the wetlands, yet remained unchanged in all experimental categories in undeveloped areas but decreased in those wetlands where development occurred or pre-existed. Moreover, detection of many native species that avoid urbanization decreased in all but rural wetlands in which development did not occur.

Decreasing diversity and increasing numbers in response to isolation were observed by Brown and Dinsmore (1986) who found that wetland size and isolation account for 75%

of the variation in species richness observed within prairie marshes. They also found that species richness was often greater in wetland complexes than in simple larger isolated marshes. Although, we found that the presence of forest within 0 to 500 meters was not correlated to avian richness or overall abundance, forests within the entire watershed did suggesting that wooded areas near but not adjacent to wetlands are important. We also found that wetlands with significant forest land remaining within 500 to 1000 meters, did account for increasing numbers of species that avoid urbanization, even though adaptable and exploitive species generally declined during the same period.

For the most part we found the wetland avifauna to be an extension of the upland avifauna. As expected, in wetlands of undisturbed landscapes (such as SR24 and RR5) species diversity is dominated by residents and migrants whereas wetlands in more urban areas (such as B3I and FC1) bird diversity is characterized by increasing numbers of non-native species including American crow, European starlings, house sparrows and some brown-headed cowbirds. We have seen European starlings displace cavity nesters including swallows and chickadees. Moreover, we have seen American Crows raid passerine nests. The shift of bird communities from predominantly native species in undisturbed areas to invasive species in highly developed areas is well documented in terrestrial environments (Blair 1996) and we saw similar shifts among some, but not all, wetlands within this study. Nevertheless, observations must be cautiously interpreted as recent literature suggests that determining bird diversity and abundance is extremely difficult (James et al. 1996, Thomas and Martin 1996), and furthermore, may be driven by immigration from few large regional source sites that produce surpluses (Brawn and Robinson 1996) rather than by more local conditions.

Based on these results, we predict that the distribution and abundance of species will change more dramatically as urbanization continues and becomes more severe. Specifically, we would expect decreasing diversity and abundances of migrants and residents and increasing nest predators including urban exploiters like the American crow and European starling as well as and nest parasites such as brown-headed cowbird. Other factors contributing to declines in birds that avoid urbanization are the density of predators like domestic cats and introduced rodents such as Norway rats and brown rats. We especially expect significant reductions in ground nesting species as increasing numbers of predators are introduced with human development.

Many wetlands in our study still exhibit a wide variety of vegetation structure and microhabitats that enable a rich diversity of birds to be found. However, with increasing urbanization and habitat fragmentation that separates wetlands from larger upland habitats and wetlands from each other, diversity of native species may be expected to decrease (as for example in urban areas, Milligan 1985). To avoid these effects, we recommend that forest land with complex structure be retained to the greatest extent possible in areas adjacent to wetlands. Dense stands of herbs and shrubs should also be retained to provide cover to birds and restrict the movement of avian predators. Access via roads, trails and footpaths that enable disturbance by humans and use by pets should be limited and edge habitat minimized as edge-related problems of thermo-regulation, predation and nest-parasitism increases along edges.

Our data supports the increasingly accepted view that total species richness is not an adequate measure of community condition under threat because the increasing diversity, attributable to urban exploiters and urban adaptable species, is in fact an indication of wetland functional deterioration. To maintain regional biodiversity, it is

critical to differentiate between native species with distinct habitat preferences and invasive species and adaptable species associated with urbanization, and to maintain habitat for native, specialized species rather than the increasingly common adptable birds. Finally, wetlands must be viewed as dynamic ecosystems which must be managed for diversity over the entire landscape and not just as individual isolated habitats.

REFERENCES

Batten, L. A. 1972. Breeding bird species diversity in relation to increasing diversity. Bird Study 19:157-166.

Beissinger, S. R., and D. R. Osborne. 1982. Effects of urbanization on avian community organization. Condor 84:75-83.

Blair, R. B. 1996. Land use and avian species diversity along an urban gradient. Ecological Applications 6:506-519.

Brawn, J. D., and S. K. Robinson. 1996. Source-sink population dynamics may complicate the interpretation of long-term census data. Ecology 77:3-12.

Brown, M., and J. J. Dinsmore. 1986. Implications of marsh size and isolation for marsh bird management. J. Wildl. Manage. 50:392-397.

Brown, R. E. 1985. Management of Wildlife and Fish Habitats in the Forests of Western Oregon and Washington. U. S. Forest Service, Pacific Northwest Region, Portland, OR, USA.

Cronk, C. B., and J. L. Fuller. 1995. Plant Invaders. Chapman and Hall, London, England. U.K.

Freemark, K. E., J. B. Dunning, S. J. Hejl, and J. R. Probst. 1995. A landscape ecology perspective for research, conservation, and management. Pages 381-421. *In* T. E. Martin and D. M. Finch, (eds). Ecology and Management of Neotropical Migratory Birds. Oxford University Press, New York, NY, USA.

Gavareski, C. A. 1976. Relation of park size and vegetation to urban bird populations in Seattle, WA. Condor 78:375-382.

Geis, A. D. 1974. Effects of urbanization and types of urban development on bird populations. Pages 97-105. *In* J. H. Noyes and. D. R. Propulske, (eds). Wildlife in an Urbanizing Environment. University of Massachusetts, Amherst, MA, USA.

Hunn, E. S. 1982. Birding in Seattle and King County. Seattle Audubon Society, Seattle, WA, USA.

Jackson, J. A. 1983. Adaptive response of Clapper Rails to unusually high water. Wilson Bulletin 95:308-309.

James, F. C., C. E. McCulloch, and D. E. Wiedenfeld. 1996. New approaches to the analysis of population trends in land birds. Ecology 77:13-27.

Lucid, V. J. 1974. Bird utilization of habitat in residential areas. Virginia Polytechnic Institute, Blacksburg, VA, USA.

Martin, A. C., H. S. Zim, and A. L. Nelson. 1951. American Wildlife and Plants: A Guide to Wildlife Food Habits. Dover, New York, N.Y., USA.

Milligan, D. A. 1985. The ecology of avian use of urban freshwater wetlands in King County, Washington. Pages 145. University of Washington, Seattle, WA. USA.

Thomas, L., and K. Martin. 1996. The importance of analysis method for breeding bird survey population trend estimates. Conservation Biology 10:479-490.

Villard, M. A., P. R. Martin, and C. G. Drummond. 1995. Dynamics in subdivided populations of Neotropical migratory birds in a fragmented temperate forest. Ecology 76:27-40.

Weller, M. W., and C. S. Spatcher. 1965. Role of habitat in the distribution and abundance of marsh birds. Iowa State University of Science and Technology, Ames, IA, USA.

Appendix Table 12-1. Abundance and detection rates of species over all wetlands.

	Abundance				Detection Rate			
Species	1989	1991	1995	All Years	1989	1991	1995	All Years
American Coot	4	22	9	35	0.014	0.087	0.034	0.045
American Crow	117	160	287	564	0.418	0.635	1.087	0.727
American Goldfinch	99	76	67	242	0.354	0.302	0.254	0.312
American Robin	294	239	322	855	1.050	0.948	1.220	1.102
Anna's Hummingbird	2		1	3	0.007	0.000	0.004	0.004
Bald Eagle		1	3	4	0.000	0.004	0.011	0.005
Barn Swallow	19	18	64	101	0.068	0.071	0.242	0.130
Black-capped Chickadee	213	194	245	652	0.761	0.770	0.928	0.840
Belted Kingfisher	7	4	10	21	0.025	0.016	0.038	0.027
Bewick's Wren	49	42	68	159	0.175	0.167	0.258	0.205
Brown-headed Cow Bird	23	16	39	78	0.082	0.063	0.148	0.101
Black Headed Grosbeak	57	38	64	159	0.204	0.151	0.242	0.205
Brewer's Blackbird	10	15	127	152	0.036	0.060	0.481	0.196
Brown Creeper	9	8	5	22	0.032	0.032	0.019	0.028
Black-throated Gray Warbler	25	13	44	82	0.089	0.052	0.167	0.106
Band-tailed Pigeon	4	2	4	10	0.014	0.008	0.015	0.013
Bushtit	126	88	141	355	0.450	0.349	0.534	0.457
Blue-winged Teal			2	2	0.000	0.000	0.008	0.003
Canada Goose	6	4	259	269	0.021	0.016	0.981	0.347
California Quail	1		3	4	0.004	0.000	0.011	0.005
Caspian Tern			13	13	0.000	0.000	0.049	0.017
Chestnut-backed Chickadee	63	77	74	214	0.225	0.306	0.280	0.276
Cedar Waxwing	111	74	110	295	0.396	0.294	0.417	0.380
Chipping Sparrow		1	2	3	0.000	0.004	0.008	0.004
Cliff Swallow	18	9	4	31	0.064	0.036	0.015	0.040
Cooper's Hawk	2		7	9	0.007	0.000	0.027	0.012
Common Raven			5	5	0.000	0.000	0.019	0.006
Common Yellow-throat	95	63	69	227	0.339	0.250	0.261	0.293
Dark-eyed Junco	40	17	32	89	0.143	0.067	0.121	0.115
Downy Woodpecker	16	14	28	58	0.057	0.056	0.106	0.075
European Starling	122	180	445	747	0.436	0.714	1.686	0.963
Evening Grosbeak	23	1	23	47	0.082	0.004	0.087	0.061
Fox Sparrow	1		5	6	0.004	0.000	0.019	0.008
Gadwall	5	4	4	13	0.018	0.016	0.015	0.017
Great Blue Heron	18	9	25	52	0.064	0.036	0.095	0.067
Golden-crowned kinglet	96	73	19	188	0.343	0.290	0.072	0.242
Green Heron	12	1	1	14	0.043	0.004	0.004	0.018
Glaucous Winged Gull	3	1	2	6	0.011	0.004	0.008	0.008
Hammond's Flycatcher	9	10	2	21	0.032	0.040	0.008	0.027
Hairy Woodpecker	40	17	13	70	0.143	0.067	0.049	0.090
Hermit Thrush	85	11	8	104	0.304	0.044	0.030	0.134
House Finch	23	8	16	47	0.082	0.032	0.061	0.061
Hooded Merganser	14		9	23	0.050	0.000	0.034	0.030
House Sparrow	9	5	2	16	0.032	0.020	0.008	0.021
Hutton's Vireo	21	1	3	25	0.075	0.004	0.011	0.032
Killdeer	6		4	10	0.021	0.000	0.015	0.013
Mallard	44	50	223	317	0.157	0.198	0.845	0.409
Marsh Wren	56	23	24	103	0.200	0.091	0.091	0.133
MacGillivary's Warbler	2		6	8	0.007	0.000	0.023	0.010
Northern Flicker	10	12	24	46	0.036	0.048	0.091	0.059
Northern Oriole	4		2	6	0.014	0.000	0.008	0.008

Appendix Table 12-1 continued. Abundance and detection rates of species over all wetlands.

	Abundance				Detection Rate			
Species	1989	1991	1995	All Years	1989	1991	1995	All Years
Northern Pigmy Owl		1	2	3	0.000	0.004	0.008	0.004
Orange-crowned Warbler	38	23	12	73	0.136	0.091	0.045	0.094
Olive-sided Flycatcher	5	8	2	15	0.018	0.032	0.008	0.019
Pied-billed Grebe	8	2	20	30	0.029	0.008	0.076	0.039
Pine Siskin	14		18	32	0.050	0.000	0.068	0.041
Pileated Woodpecker	13		4	17	0.046	0.000	0.015	0.022
Pacific-slope Flycatcher	127	147	145	419	0.454	0.583	0.549	0.540
Purple Finch	24	22	40	86	0.086	0.087	0.152	0.111
Red-breasted Nuthatch	15	29	42	86	0.054	0.115	0.159	0.111
Red-breasted Sapsucker	4		4	8	0.014	0.000	0.015	0.010
Red Crossbill	9	42	4	55	0.032	0.167	0.015	0.071
Red-eyed Vireo	2		9	11	0.007	0.000	0.034	0.014
Red-eyed Vireo	2	1	5	8	0.007	0.004	0.019	0.010
Rock Dove	5	4		9	0.018	0.016	0.000	0.012
Rufous-sided Towee	101	98	143	342	0.361	0.389	0.542	0.441
Rufous Hummingbird	6	5	4	15	0.021	0.020	0.015	0.019
Ruffed Grouse	1	2	2	5	0.004	0.008	0.008	0.006
Ruby Crowned Kinglet	21	10	20	51	0.075	0.040	0.076	0.066
Red-winged Blackbird	353	203	228	784	1.261	0.806	0.864	1.010
Savannah Sparrow		2		2	0.000	0.008	0.000	0.003
Sora		2	3	5	0.000	0.008	0.011	0.006
Song Sparrow	476	395	419	1290	1.700	1.567	1.587	1.662
Solitary Vireo	5	13	4	22	0.018	0.052	0.015	0.028
Spotted Sandpiper	3			3	0.011	0.000	0.000	0.004
Sharp-shinned Hawk	4			4	0.014	0.000	0.000	0.005
Steller's Jay	33	67	89	189	0.118	0.266	0.337	0.244
Swainson's Thrush	154	181	344	679	0.550	0.718	1.303	0.875
Townsend's Warbler	38	2	13	53	0.136	0.008	0.049	0.068
Tree Swallow	101	63	67	231	0.361	0.250	0.254	0.298
Varied Thrush	41			41	0.146	0.000	0.000	0.053
Vaux's Swift	18	13	8	39	0.064	0.052	0.030	0.050
Violet-green Swallow	56	68	151	275	0.200	0.270	0.572	0.354
Virginia Rail	9	3	6	18	0.032	0.012	0.023	0.023
Warbling Vireo	38	3	22	63	0.136	0.012	0.083	0.081
White-crowned Sparrow	14	9	1	24	0.050	0.036	0.004	0.031
Western Tanager	17	9	29	55	0.061	0.036	0.110	0.071
Western Wood-pewee	11	6	13	30	0.039	0.024	0.049	0.039
Willow Flycatcher	116	90	142	348	0.414	0.357	0.538	0.448
Wilson's Warbler	115	72	78	265	0.411	0.286	0.295	0.341
Winter Wren	109	85	115	309	0.389	0.337	0.436	0.398
Wood Duck	10	4	9	23	0.036	0.016	0.034	0.030
Yellow Warbler	67	50	26	143	0.239	0.198	0.098	0.184
Yellow-rumped Warbler	7	3	4	14	0.025	0.012	0.015	0.018
Totals	4203	3338	5215	12756	15.011	13.246	19.754	16.438

Section 4 Management of Freshwater Wetlands in the Central Puget Sound Basin

CHAPTER 13 MANAGING WETLAND HYDROPERIOD: ISSUES AND CONCERNS

by Amanda L. Azous, Lorin E. Reinelt and Jeff Burkey

INTRODUCTION

Land use changes and stormwater management practices usually alter hydrology within a watershed. A major finding of our study was that hydrologic changes were having more immediate and greater effects on the composition of vegetation and amphibian communities than other environmental conditions we monitored. Early study results showed wetland hydroperiod, which refers to the depth, duration, frequency and pattern of wetland inundation to be a key factor in determining biological responses.

Continuous recording gages were unavailable for the study, but we were able to monitor hydroperiod in the wetlands with instantaneous staff and crest stage gages. From these measurements a metric was developed called water level fluctuation (WLF) which showed statistically significant relationships with several measures of biological health (Azous 1991a). WLF is measured as the average difference between the maximum depth and average instantaneous or base depth in a time period (Taylor 1993, Taylor, Ludwa and Horner 1995).

Consistently we observed reduced numbers of plant and amphibian species when WLF was high in wetland areas (Azous 1991b, Cooke and Azous 1993, Richter and Azous 1995). As a result, substantial attention was given to understanding WLF and developing management guidelines for protecting wetland plants and animals.

A local jurisdiction, King County Surface Water Management (KCSWM) expressed an interest in developing wetland management guidelines that could be used in continuous flow event simulation computer models. In addition, only a few of the wetlands in the original 19 study wetlands showed extreme water level changes and we wanted to measure more plant and amphibian communities with high WLF conditions. We undertook a cooperative study to monitor the hydroperiods of six wetlands with continuous recording gages, and measure the plant and amphibian communities, in order to better understand the relationship between biological diversity, WLF, and the pattern of water depth, duration and frequency of inundation in wetlands.

This paper will discuss the methods and results of this study. The information has significant implications for evaluating the level of protection afforded wetlands from changing hydroperiod.

METHODS

Continuous recording gages were installed in six wetlands in late 1994 and early 1995. The gages were programmed to record water surface elevations at 15-minute increments. Two of the wetlands we monitored were in relatively undisturbed

watersheds and were already experimental controls in our ongoing study. The remaining four were recommended by KCSWM field staff as wetlands known to experience large changes in water depth throughout the year.

Water levels in all six wetlands were monitored over one year, however due to unexpected seasonable differences in rainfall and some losses of data due to malfunctioning equipment, there was only a partial water year for all the wetlands. The hydroperiod data was used to calculate WLF and to calibrate the computer model Hydrologic Simulation Program- FORTRAN (HSPF), a continuous event model with the ability to simulate hydrologic processes in a watershed. The model is used to predict rainfall runoff from different watershed conditions and is more accurate when field measurements are used to adjust runoff from simulated rainfall events with the outflows and stages resulting from actual events.

Of the six wetlands, two control wetlands were not calibrated nor modeled. The complexity of the wetlands' hydraulics were beyond the scope of this project. The remaining four wetlands all had well defined outlets, hydraulics and bethymetry which allowed reasonably accurate stage-storage-discharge relationships to be developed. Based on the margin of errors in the spatial distribution of precipitation represented by nearby gages and the length of the field record, the accuracy of the model's simulated wetland water levels to recorded water levels was limited to plus or minus 0.5 ft. (15 cm).

Emergent (PEM), scrub-shrub (PSS) and forested (PFO) wetland zones were surveyed and evaluated for plant species richness and the presence and dominance of exotic invasive species using the protocols for vegetation field work documented in Cooke et al. (Cooke et al. 1989). Disturbed commodities were those sample stations found to be dominated (>60%) by a weedy species. Amphibians were sampled during the fall and spring breeding seasons using methods described in Richter and Azous (1995).

The condition of plant and amphibian communities were compared with the observed and predicted water depths, the duration of storm events and the frequency of storm events for the whole season and the early growing season (March 1 through May 15). . We analyzed the emergent, scrub-shrub and forested zones to determine if there were significant differences in community composition related to hydroperiod regimes .

The six special study wetlands were also added to the larger database of 19 wetlands and all the data analyzed for differences corresponding to WLF conditions. All sample stations that were inundated at least once during the year were included in the analysis of water level fluctuation. The data was analyzed using StatView (Abacus Concepts Inc. 1993) statistical applications program. The plant richness data were not normal; therefore the non-parametric Kruskal-Wallace (KW) and Mann-Whitney (MW) tests were used to compare the distributions among categories, depending on the number of variables in the category being compared. Both tests indicate whether the underlying distributions for different groups are the same. Both use ranked data and are resistant to outliers.

Much of the data was categorized to provide more statistical rigor given the small data set and the 0.5 ft. (15 cm.) margin of error. Categories were based on frequency distributions of the data and a very limited sensitivity analysis of statistically significant breaks in the data.

We measured frequency of storm events in a hydroperiod by defining an event as an excursion which we define as a water level increase above the monthly average depth of

more than 0.5 ft. (15 cm.). Duration was defined as the time period of an excursion. In a stepwise regression, we looked at the statistical relationship between WLF, frequency and duration. Table 1 shows the categories used in the analysis.

Table 13-1. Category Definitions for Water Depth and Excursion Duration.

Frequency of Excursions	Water Depth*	Duration of Excursions
less than 6 per year	Greater than 2.0 ft. depth (>60 cm.)	less than 3 days
more than 6 per year	2 ft. to 0 ft. depth (-60 to 0 cm.)	3 to 6 days
	0 to 2.0 feet above water surface. (0 to +60 cm.)	more than 6 days

*Negative numbers are under water.

RESULTS

Plant richness in the sample stations ranged from three to 31 species in the POW zones, three to 22 in the PSS zones and 17 to 25 in the forested areas. Very few invasive weedy species were found and were dominant in only a few localized areas.

Frequency and Duration and Plant Richness

Plant richness was found to be significantly lower if water depths were usually deeper than 2 feet (60 cm.) (KW, $p < 0.0001$). To control for this, frequency and duration were evaluated separately for different water depths. The test for differences in duration and frequency showed that, in general, plant communities in areas subjected to more than six hydrologic excursions per year tended to have lower richness. In both the greater than 2.0 feet range and zero to 2.0 feet range the difference is statistically significant (MW, $p \leq 0.004$). It was not significant for the -2.0 to zero range (Figure 13-1).

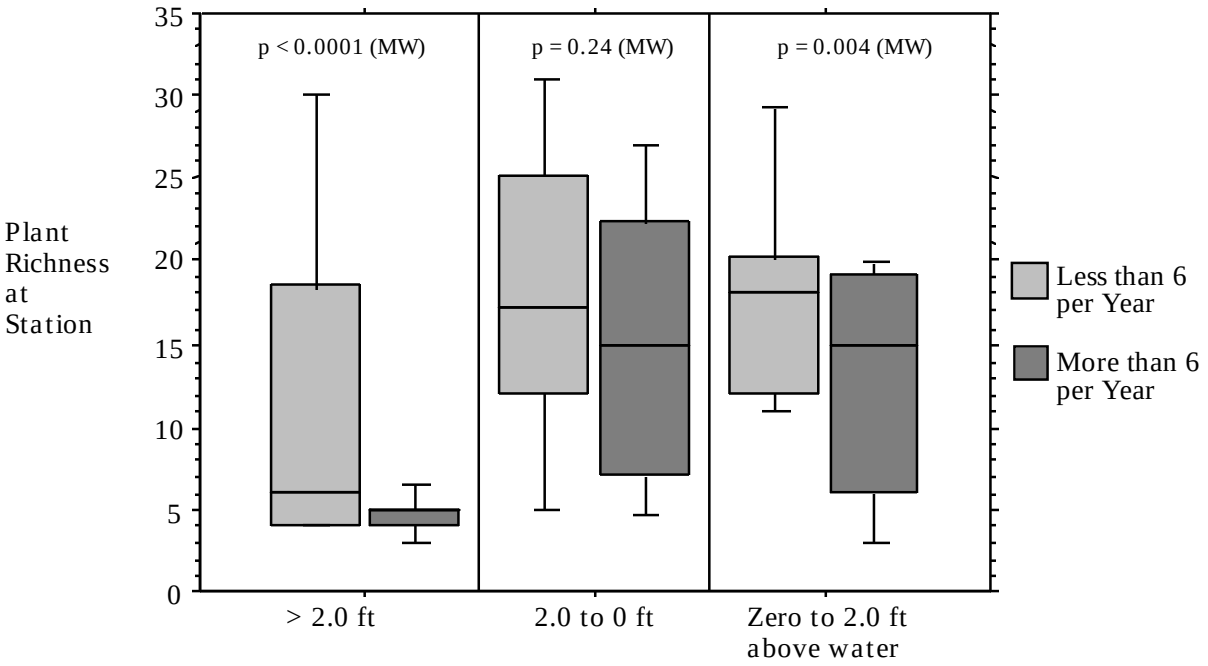

Figure 13-1. Plant richness, water depth and frequency of excursions.

The duration of excursions was compared to plant richness and water depth. Duration alone was a significant factor only in the deepest zones of -8.0 to -2.0 feet (KW, $p < 0.001$) (Figure 13-2). From -2.0 feet to 2.0 feet, increased duration did not significantly contribute to the variability of plant richness.

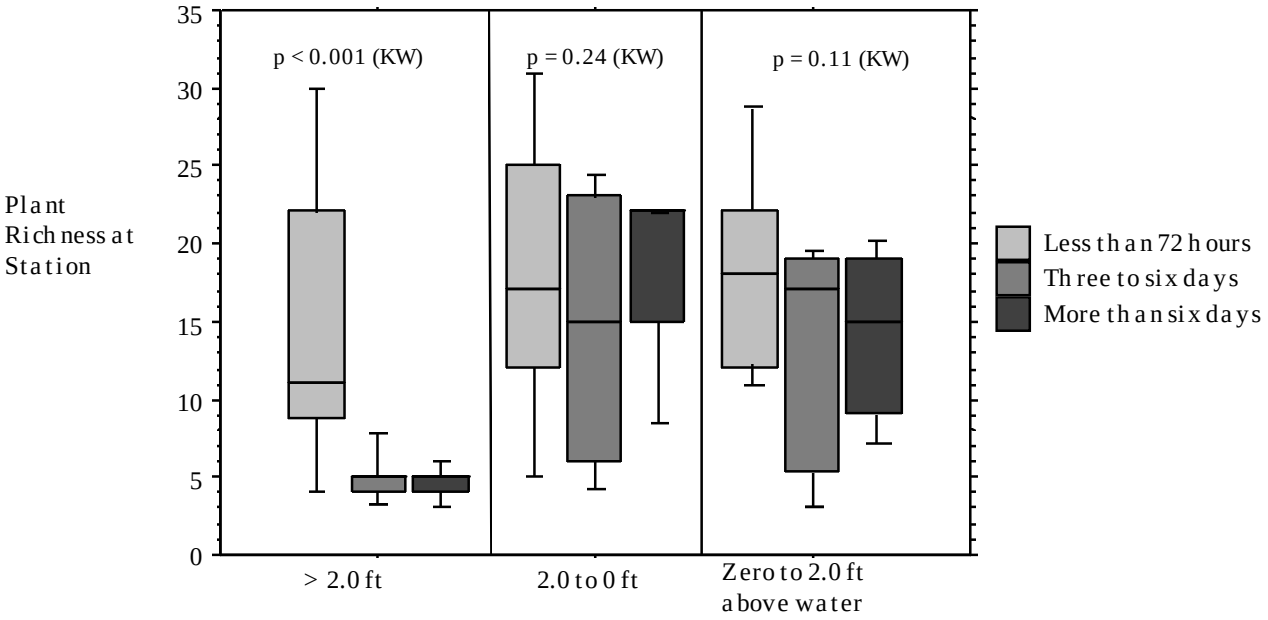

Figure 13-2. Plant richness, water depth and duration of excursions.

When the effects of excursion frequency and duration were combined, the relationship with plant richness was much stronger. Plant richness was found to decrease significantly with excursions longer than six days duration even with frequencies of less than six per year (KW, $p < 0.0001$). For excursion frequencies greater than six per year, richness dropped significantly when duration' exceeded three days per month (KW, $p < 0.0001$) (Figure 13-3)

These results were significant for both emergent and scrub-shrub zones and indicate that the average monthly duration of inundation can be significant to plant species richness, when the frequency of inundation is greater than six times per year on average or when the length of inundation exceeds three days per month. The frequency of excursions did not account for variability in species richness until excursion durations exceeded three days per month. There were an insufficient number of forested zones in the wetlands where frequency and duration were measured to adequately test for differences in the forested conditions and open water.

Water Level Fluctuation and Plant Richness

We looked at the relationship of water level fluctuation to plant richness in different zones of the wetlands. We examined all sample stations inundated at any time of the year and found richness was lower in wetlands with high WLF hydroperiods in the emergent and scrub-shrub zones but not the forested zones. There were not enough aquatic bed zones for adequate evaluation. Emergent zones subject to mean WLFs greater than 0.8 ft. (24 cm.) ranked significantly lower in the number of plant species present (MW, $U \geq 55$, $P \leq 0.003$) than emergent areas with mean WLF less than 0.8 ft. (24 cm.). This relationship was even more significant when richness was compared with water level fluctuation during the early growing season (Figure 13-4). Shrub-scrub zones also showed a significant difference in plant richness related to annual and early growing season water level fluctuation (MW, $U \geq 55$ $p < 0.0001$) (Figure 13-5). Forested zones showed no differences in richness accounted for by WLF.

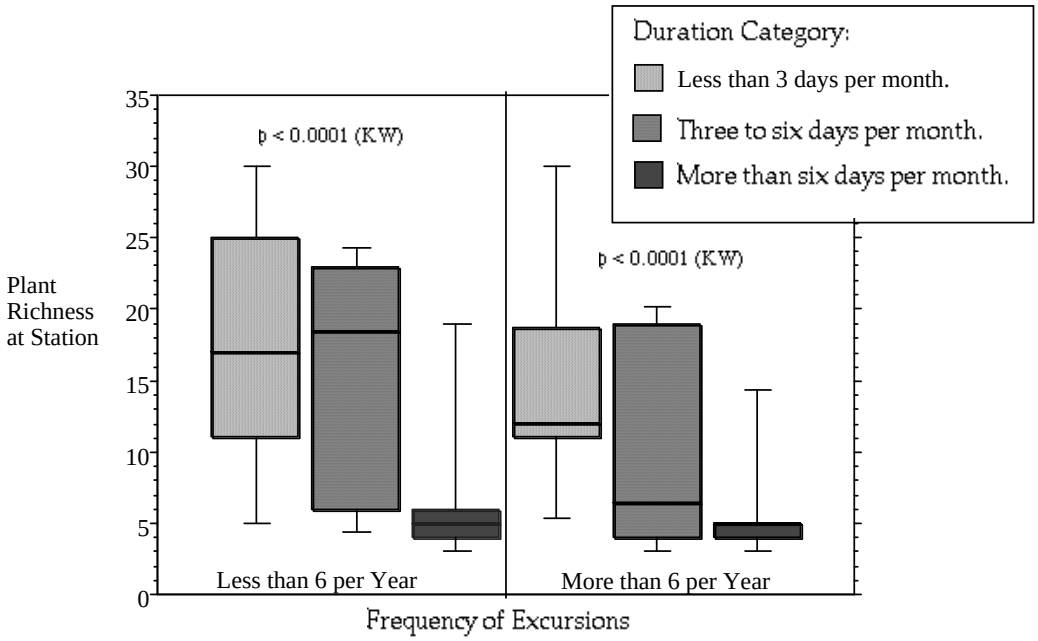

Figure 13-3. Plant richness, frequency and duration of excursions.

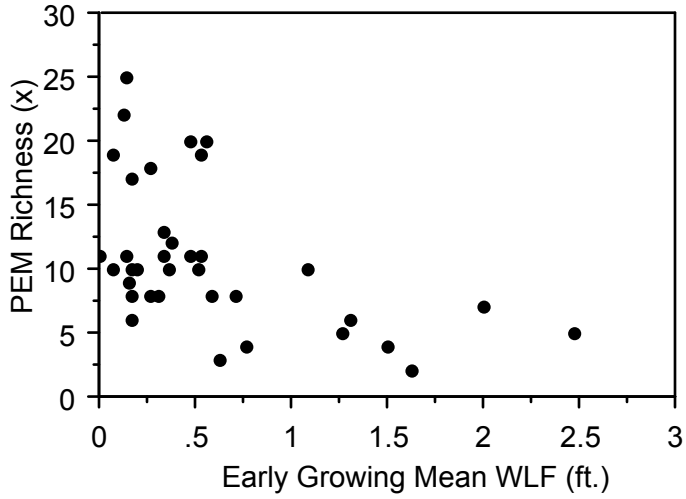

Figure 13-4. Plant rchness in the emergent zones in relation to mean WLF.

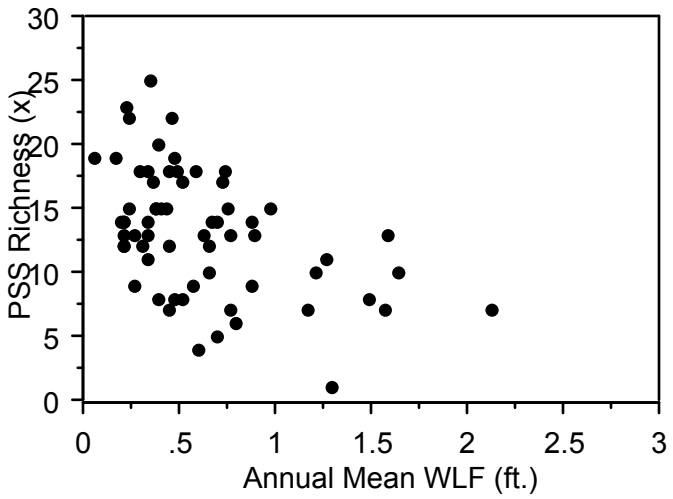

Figure 13-5. Plant richness in the scrub-shrub zones in relation to mean WLF.

Amphibian Results

Our study of amphibians left us with an incomplete picture. All of the wetlands in this study as well as the PSWSRP study had far fewer amphibian species in 1995 than collected in previously years. For example, seven species were collected in a rural wetland, BBC24, in 1989 and only three in 1995. Five species were collected in the urban surrounded wetland, LPS9, in 1989, compared with none in 1995. Eight were captured in SR24 in 1989 and again none were captured in 1995. Figure 13-6 shows amphibian richness for each wetland for both 1989 and 1995 trapping years. The lack of captures prevented analysis of frequency and duration effects for this study's wetlands.

Nevertheless, we were able to measure WLF relationships between amphibian communities over all years and all wetlands using the PSWSMRP wetlands database. The richness of amphibian communities was found to be lower in wetlands with WLF less than 0.8 ft. (24 cm). Wetlands with greater WLF were significantly more likely to have low amphibian richness with three or fewer different species present (*FE*, P = 0.046) as compared with four to eight.

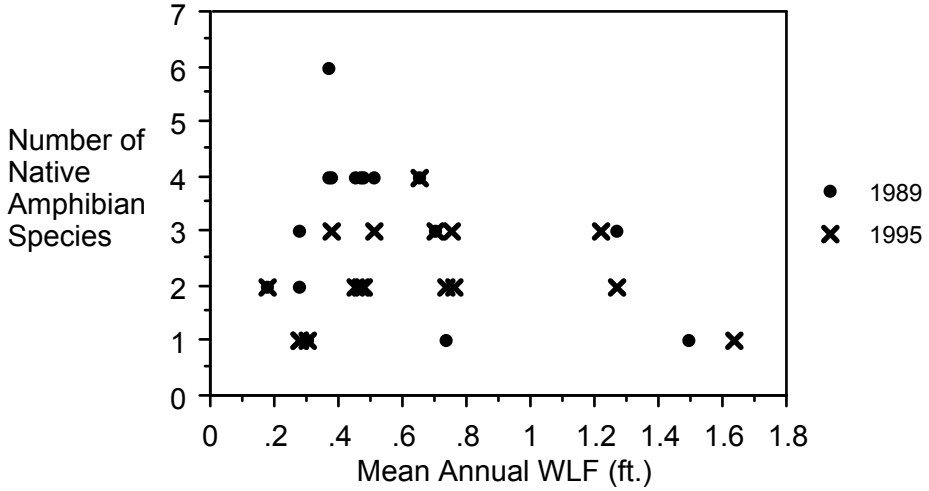

Figure 13-6. Amphibian richness as a function of mean WLF.

The reasons for the amphibian decline in 1995 are not understood. Amphibians sometimes breed in alternate years, hence in one year, populations could be much lower than the next. But we don't know if that phenomenon occurs across a population or just to particular individuals. The fact that low numbers were found in all wetlands suggests that it may be rainfall or climate related and 1995 was a drier spring than usual, but we are speculating.

WLF was found to be statistically related to excursion duration and frequency. Forty-one percent of the variation in WLF can be explained by the duration of events. Adding the effect of excursion frequency can explain as much as 53% of the variability in WLF ($p<0.0001$).

APPLICATION OF RESEARCH RESULTS

These results show that increasing the duration of storm events can be a significant factor in reducing wetland plant diversity. The frequency of storm peaks is also a factor and compounds the duration impact. Decreasing richness in the emergent and scrub-shrub zones and increasing frequency and duration are also associated with high mean water level fluctuation, annually, but particularly during the early spring growing season and amphibian breeding seasons.

Current stormwater protection measures primarily rely on stormwater detention for protecting wetlands. Detention acts to increase the duration of a storm event in order to reduce the peak depth. Water is captured, stored and released after the storm over a longer period of time. It was a management tool designed primarily for controlling floods and erosion in streams, however, it may operate counter to management goals as a tool for wetland protection.

The result of these findings has been to recommend for there to be limits on the durations of storm events as well as the frequency of excursions, when wetlands will be affected by changes in hydroperiod. The recommendations are that the frequency of water levels greater than 15 cm. (.5 ft.) above pre-development levels be limited to an annual average of six or less per year and that the durations of water levels greater than 15 cm. (.5 ft.) above or below pre-development levels be limited to less than three days per excursion.

The data set we analyzed was limited, as were time and funding and some questions remain about the potential for trading flood frequency and flood duration. For example, it might be possible to extend the durations of storm flows in wetlands if the frequency of those events is reduced. Similarly, it may also be possible to reduce durations in trade for allowing greater frequency. These areas of refinement remain largely unexplored.

Irrespective of any further results, it will be difficult for urbanizing jurisdictions to meet such standards in all areas. It is also not likely to happen if detention is the primary management tool. Achieving real resource protection of high value wetlands will require a more comprehensive approach.

Early in the research the PSWSRP learned that wetland management must be holistic, that wetlands are part of a system in a larger landscape and should be managed accordingly. This view has a number of implications for management:

- It is necessary to consider incidental effects on wetlands of activities in their watersheds, along with any engineering performed on the wetland itself for stormwater management purposes;
- Wetland response and management depend on a host of landscape factors, including retention of forest and other natural cover, maintenance of natural storage reservoirs and drainage corridors; the separation of human activities from wetlands; and public awareness.
- Wetland protection means finding root cause solutions e.g. source control practices that prevent or minimize quantities of runoff and release of pollutants, with downstream retention/detention for quantity control and treatment for pollutant capture regarded as secondary back-up measures where source controls alone can not ensure resource protection.
- Potential runoff infiltration opportunities should be explored and those that are found to be workable hydrogeologically and not threaten groundwater quality should be explored.

The experience of King County in its attempts to meet the PSWSRP recom-mendations is noteworthy and affords a view of some alternative approaches to detention.

The PSWSRP guidelines have been used in King County in both the basin and master drainage planning processes. Most of the applications have focused on minimizing water level fluctuation, as it was identified as the most direct effect on wetland functioning, vegetation communities, and habitat for breeding amphibians. Regulations governing factors that affect WLF have been targeted at new development on the urban side of the Urban Growth Boundary (UGB), where the most significant impacts are likely to occur. The general information on construction impacts generated by the Wetlands Research Program has also led to the application of seasonal clearing limits in the drainage areas of Class 1 wetlands.

Basin Planning

The basin planning process was developed by King County to address the significant and rapid land use changes occurring in the county that have an impact on water resources, including flooding, habitat, and water quality. The outcome of the basin planning process is a way of developing a comprehensive set of management recommendations that involve development regulations, capital improvement projects, education programs, improved maintenance practices, and monitoring.

The East Lake Sammamish Basin Plan (King County Surface Water Management Division (KCSWM) 1992) is an example where the results of the Wetlands Research Program were directly applied to management solutions. The East Lake Sammamish basin encompasses about 16 square miles east of Lake Sammamish. Since 1980, the basin has experienced rapid development, converting from low-density residential and forested land uses to higher density residential and some commercial uses. The diversity of the basin's more than 40 inventoried wetlands is as great as anywhere in King County, with nine wetlands ranked as unique and outstanding (Class 1 rating). As one of the prime resources in the basin, wetlands received significant attention for protection from the County and the citizenry.

Wetland Management Areas

Prior to adoption of the basin plan, wetland protection in King County was achieved primarily through the Sensitive Areas Ordinance (SAO). The wetland protection in the SAO provides for discrete buffer widths as a function of assigned rating (e. g., 100 feet for Class 1 wetlands). Although these buffers confer some protection to wetlands, they are inadequate to protect other functions influenced by the broader watershed and surrounding landscape. To address these issues, King County developed wetland management areas (WMA) focused on watershed-based controls to protect the nine Class 1 wetlands. The intent of these controls was to minimize the stormwater-related impacts on wetlands by minimizing impervious surfaces, retaining forests, clustering, and providing constructed infiltration systems, where feasible.

A major component of the wetland management strategy was the limitation of total impervious area in the catchment to eight percent, where allowed by zoning. From the Wetlands Research Program data, it was clear that there were significant increases in WLF between wetlands with watersheds less than 4 percent and those with watersheds greater than 12 percent impervious surface (Taylor 1993; Taylor, Ludwa, and Horner 1995). It was difficult to define this more precisely, because of the absence of impervious surfaces between 4 and 12 percent. Booth and Reinelt (1994) summarized several data sets showing loss of aquatic system function with impervious surface areas above about 10 percent, as measured by changes in channel morphology, fish and amphibian populations, habitat, and water chemistry. While the precise threshold will vary by watershed and the effectiveness of mitigation strategies, 8-10 percent impervious surface appears to be an appropriate threshold.

A requirement for 50 percent forest retention was also imposed in the catchments of some wetlands. This limitation is consistent with King County's reserve tract requirements associated with clustering and growth-reserve zoning. Taylor (1993) found a correlation between forest retention and reduced WLF, but no specific threshold was identified in this work. Clustering of development away from hydrologic source areas (landscape features transmitting water to wetlands during the wet season) was also recommended. An additional requirement in one wetland watershed was the use of constructed infiltration systems to reduce increases in stormwater volumes. This was feasible given the extensive glacial outwash soils in this watershed that were amenable to substantial infiltration. Finally, seasonal clearing limits for construction activities were imposed in eight of the nine watersheds. This limitation prevents clearing and grading during the wet season (October-April) when up to 88 percent of erosion occurs (KCSWM 1992).

King County has continued this approach of wetland management areas for protection of Class 1 wetlands in the Cedar River Basin Plan currently under development. Four Class 1 wetlands in the Cedar basin that are on the urban side of the UGB or that receive runoff from urban areas have been targeted.

Master Drainage Planning and Guidelines

King County uses the Master Drainage Planning (MDP) process for large or complex development sites to assess the potential impacts of development on aquatic resources (KCSWM 1993). The MDP process is required for Urban Plan Developments (UPD), for subdivisions with more than 100 single-family residences, and for projects which clear 500 acres or more within a subbasin. In addition, there are lower thresholds for

development in the drainage areas of Class 1 wetlands, regionally significant resource streams, or over sole source aquifers. For Class 1 wetlands, an MDP is required if a project seeks to convert more than 10 percent of the wetland's total watershed area to impervious surface.

The updated guidelines for MDP monitoring and studies (KCSWM 1993), supported in part by results of the Wetlands Research Program, require monitoring for purposes of: (1) assessing wetland functions in storing and releasing stormwater, (2) determining baseline WLF in relation to vegetation and amphibian communities, and (3) establishing baseline conditions from which to measure potential post-development changes. Specific concerns potentially resulting from development are: (1) loss of live storage and infiltration functions of wetlands, (2) stability of outlet control conditions, (3) the effects of increases in flow rates and volumes, (4) changes in spring WLF and resultant habitat changes, and (5) changes in groundwater and interflow.

For purposes of assessing wetland impacts, the MDP guidelines require determination of the following: bathymetry (morphometry) of the wetland; outlet control description and measurement; stage-discharge volume relationships; surface area of open water, including ordinary high water levels; and the dead and live storage maximum elevation and volume. Specific monitoring requirements are: (1) monthly instantaneous and crest water levels to determine WLF in the permanent pool area of the wetland; (2) inflow and outflow rates of the wetland; and (3) the duration of summer drying, if applicable.

For the North Fork Issaquah Creek Wetland 7 Management Area and Grand Ridge MDP, the East Sammamish Community Plan limited development in the drainage area tributary to North Fork Issaquah Creek Wetland 7 (NFIC-7), a Class 1 wetland, to no more than eight percent impervious surfaces and 65 percent forest retention. This condition applies to all development proposals submitted prior to adoption of the Issaquah Basin Plan (KCSWM 1994) and for all developments not going through the MDP process. In the basin plan, impervious surfaces are limited to a maximum of eight percent for all new subdivisions, short subdivision, and UPDs.

The proposed Grand Ridge development in the North and East Fork Issaquah Creek basins involved two development options: rural estates at a density of one unit per 5 acres and an urban proposal consisting of 580 acres of urban development and 1400 acres of permanent open space. In a study of potential development scenarios carried out using the Wetlands Research Program guidelines and a model developed by Taylor (1993), it was possible to examine the development impacts on the water level fluctuation of wetland NFIC-7. Based on the results of that analysis, mitigations were proposed that focused on maintaining greater forested area and utilizing infiltration to reduce stormwater volumes.

CONCLUSION

Fundamentally managing stormwater to protect wetland ecosystems must operate holistically within context of the hydrologic cycle. That requires that we consider infiltration and evapotranspiration in addition to storage, when we think about strategies. Controls focused on minimizing impervious surfaces and maximizing forest retention are likely to be the most widely usable effective strategies; however, additional mitigations that reduce stormwater volumes through infiltration are highly recommended when hydrogeological conditions permit.

REFERENCES

Azous, A. L. 1991a. An Analysis of Urbanization Effects on Wetland Biological Communities, M.S. Thesis. Department of Civil Engineering, University of Washington, Seattle, WA.

Azous, A. L. 1991b. Development of the Puget Sound Wetlands and Stormwater Management Guidelines *in* Development of Guidance for Managing Urban Wetlands and Stormwater. May 1991, Final Report, King County Resource Planning Section. Environmental Division.

Azous, A. 1995. Amphibian and Plant Community Responses to Changing Hydrology in Urban Wetlands. Proc. Third Puget Sound Research Meeting, Puget Sound Water Quality Authority, Olympia, WA.

Booth, D. B. and L. E. Reinelt. 1994. Consequences of Urbanization on Aquatic Systems--Measured Effects, Degradation Thresholds, and Corrective Strategies. Pp. 545-550, Proc. Watersheds '93 Conference, Alexandria, VA, March 21-24, 1993.

Cooke, S.S., R.R. Horner, C. Conolly, O. Edwards, M. Wilkinson, and M. Emers. 1989. Effects of Urban Stormwater Runoff on Palustrine Wetland Vegetation Communities - Baseline Investigation (1988). Report to U.S. Environmental Protection Agency, Region 10, by King County Resource Planning Section, Seattle.

Cooke, S. S. and A. Azous. 1993. Effects of Urban Stormwater Runoff on Palustrine Wetland Vegetation. Final Report to U. S. Environmental Protection Agency Region 10 and the Puget Sound Wetlands and Stormwater Research Program. March 1993.

Cooke, S. S. and A. Azous. 1995. Vegetation Species Responses to Changing Hydrology in Urban Wetlands. Proc. Third Puget Sound Research Meeting, Puget Sound Water Quality Authority, Olympia, WA.

Horner, R. R. 1995. Overview Of the Puget Sound Wetlands and Stormwater Management Research Program. Proc. Third Puget Sound Research Meeting, Puget Sound Water Quality Authority, Olympia, WA.

King County Surface Water Management Division. 1992. East Lake Sammamish Basin and Nonpoint Action Plan Volume 1. King County Public Works, Seattle, WA.

King County Surface Water Management Division. 1993. Master Drainage Planning for Large Site Developments - Proposed Process and Requirement Guidelines. King County Public Works, Seattle, WA.

King County Surface Water Management Division. 1994. Issaquah Creek Basin and Nonpoint Action Plan (Watershed Management Committee-proposed). King County Public Works, Seattle, WA.

Platin, T. J. and K. O. Richter. 1995. Effects of Changing Wetland Hydrology and Water Quality on Amphibian Breeding Success. Proc. Third Puget Sound Research Meeting, Puget Sound Water Quality Authority, Olympia, WA.

Puget Sound Wetlands and Stormwater Management Research Program. 1994. Wetlands and Stormwater Management (Preliminary Guidelines). King County Resource Planning Section, Bellevue, WA.

K. O. Richter and A. L. Azous. 1995. Amphibian Occurrence and Wetland Characteristics in the Puget Sound Basin. WETLANDS. Vol. 15. No. 3, pp 305-312.

Taylor, B. L. 1993. The Influence of Wetland and Watershed Morphological Characteristics on Wetland Hydrology and Relationships to Wetland Vegetation Communities. M. S. C. E. Thesis, Department of Civil Engineering, University of Washington, Seattle, WA.

Taylor B. L., K. Ludwa, and R. R. Horner. 1995. Urbanization Effects on Wetland Hydrology and Water Quality. Proc. Third Puget Sound Research Meeting, Puget Sound Water Quality Authority, Olympia, WA.

Washington Department of Ecology. 1992. Stormwater Management Manual for the Puget Sound Basin. Washington Department of Ecology, Olympia, WA.

CHAPTER 14 WETLANDS AND STORMWATER MANAGEMENT GUIDELINES

by Richard R. Horner, Amanda A. Azous, Klaus O. Richter, Sarah S. Cooke, Lorin E. Reinelt and Kern Ewing

If you are unfamiliar with these guidelines, read the description of the approach and organization that follows. If you are familiar, proceed directly to the appropriate guide sheet(s) for guidelines covering your issue(s) or objective(s):

Guide Sheet 1: Comprehensive Landscape Planning for Wetlands and Stormwater Management--page 202

Guide Sheet 2: Wetlands Protection Guidelines-- page 209

APPROACH AND ORGANIZATION OF THE MANAGEMENT GUIDELINES

Introduction

The Puget Sound Wetlands and Stormwater Management Research Program performed comprehensive research with the goal of deriving strategies that protect wetland resources in urban and urbanizing areas, while also benefiting the management of urban stormwater runoff that can affect those resources. The research primarily involved long-term comparisons of wetland ecosystem characteristics before and after their watersheds urbanized, and between a set of wetlands that became affected by urbanization (treatment sites) and a set whose watersheds did not change (control sites). This work was supplemented by shorter term and more intensive studies of pollutant transport and fate in wetlands, several laboratory experiments, and ongoing review of relevant work being performed elsewhere. These research efforts were aimed at defining the types of impacts that urbanization can cause and the degree to which they develop under different conditions, in order to identify means of avoiding or minimizing impacts that impair wetland structure and functioning. The program's scope embraced both situations where urban drainage incidentally affects wetlands in its path, as well as those in which direct stormwater management actions change wetlands' hydrology, water quality or both.

This document presents preliminary management guidelines for urban wetlands and their stormwater discharges based on the research results. The set of guidelines is the principal vehicle to implement the research findings in environmental planning and management practice.

Guidelines Scope and Underlying Principles

Note: For terms in **boldface** type see item 1 under Support Materials below.

1. These provisions currently have the status of guidelines rather than requirements. Application of these guidelines does not fulfill assessment and permitting requirements

that may be associated with a project. It is, in general, necessary to follow the stipulations of the State Environmental Policy Act and to contact such agencies as the local planning agency; the Washington Departments of Ecology, Fisheries, and Wildlife; the U. S. Environmental Protection Agency; and the U. S. Army Corps of Engineers.

2. Using the guidelines should be approached from a problem-solving viewpoint. The "problem" is regarded to be accomplishing one or more particular planning or management objectives involving a **wetland** potentially or presently affected by stormwater drainage from an urban or urbanizing area. The objectives can be broad, specific, or both. Broad objectives involve comprehensive planning and subsequent management of a drainage catchment or other **landscape unit** containing one or more wetlands. Specific objectives pertain to managing a wetland having particular attributes to be sustained. Of course, the prospect for success is greater with ability to manage the whole landscape influencing the wetland, rather than just the wetland itself.

3. The guidelines are framed from the standpoint that some change in the landscape has the potential to modify the physical and chemical **structure** of the wetland environment, which in turn could alter biological communities and the wetland's ecological **functions**. The general objective in this framework would be to avoid or minimize negative ecological change. This view is in contrast to one in which a wetland has at some time in the past experienced negative change, and consequent ecological degradation, and where the general objective would be to recover some or all of the lost structure and functioning through **enhancement** or **restoration** actions. Direct attention to this problem was outside the scope of the Puget Sound Wetlands and Stormwater Management Research Program. However, the guidelines do give information that applies to enhancement and restoration. For example, attempted restoration of a diverse amphibian community would not be successful if the water level fluctuation limits consistent with high amphibian species richness are not observed.

4. The guidelines can be applied with whatever information concerning the problem is available. Of course, the comprehensiveness and certainty of the outcome will vary with the amount and quality of information employed. The guidelines can be applied in an iterative fashion to improve management understanding as the information improves. Appendix A lists the information needed to perform basic analyses, followed by other information that can improve the understanding and analysis.

5. These guidelines emphasize avoiding structural, hydrologic, and water quality **modifications** of existing wetlands to the extent possible in the process of urbanization and the management of urban stormwater runoff.

6. In pursuit of this goal, the guidelines take a systematic approach to management problems that potentially involve both urban stormwater (quantity, quality, or both) and wetlands. The consideration of wetlands involves their areal extent, **values**, and functions. This approach emphasizes a comprehensive analysis of alternatives to solve the identified problem. The guidelines encourage conducting the analysis on a landscape scale and considering all of the possible stormwater management alternatives, which may or may not involve a wetland. They favor **source control best management practices** (BMPs) and **pre-treatment** of stormwater runoff prior to release to wetlands.

7. Furthermore, the guidelines take a holistic view of managing wetland resources in an urban setting. Thus, they recognize that urban wetlands have the potential to be affected structurally and functionally whether or not they are formally designated for stormwater management purposes. Even if an urban wetland is not structurally or hydrologically engineered for such purposes, it may experience altered hydrology (more or less water), reduced water quality, and a host of other impacts related to urban conditions. It is the objective of the guidelines to avoid or reduce the negative effects on wetland resources from both specific stormwater management actions and incidental urban impacts.

Support Material

1. The guidelines use certain terms that require definition to ensure that the intended meaning is conveyed to all users. Such terms are printed in **boldface** the first time that they appear in each guide sheet, and are defined in Appendix B.

2. The guideline provisions were drawn principally from the available results of the Puget Sound Wetlands and Stormwater Management Research Program, as set forth in Sections 2 and 3 of the program's summary publication, Wetlands and Urbanization, Implications for the Future (Horner et al. 1996). Where the results in this publication are the basis for a numerical provision, a separate reference is not given. Numerical provisions based on other sources are referenced. See Appendix C for references.

3. Appendix D presents a list of plant species native to wetlands in the Puget Sound Region. This appendix is intended for reference by guideline users who are not specialists in wetland botany. However, non-specialists should obtain expert advice when making decisions involving vegetation.

4. Appendix E compares the water chemistry characteristics of *Sphagnum* bog and fen wetlands (termed **priority peat wetlands** in these guidelines) with more common wetland communities. These bogs and fens appear to be the most sensitive among the Puget Sound lowland wetlands to alteration of water chemistry, and require special water quality management to avoid losses of their relatively rare communities.

GUIDE SHEET 1: COMPREHENSIVE LANDSCAPE PLANNING FOR WETLANDS AND STORMWATER MANAGEMENT

Wetlands in newly developing areas will receive urban effects even if not specifically "used" in stormwater management. Therefore, the task is proper overall management of the resources and protection of their general **functioning**, including their role in storm drainage systems. Stormwater management in newly developing areas is distinguished from management in already developed locations by the existence of many more feasible stormwater control options prior to development. The guidelines emphasize appropriate selection among the options to achieve optimum overall resource protection benefits, extending to downstream receiving waters and ground water aquifers, as well as to wetlands.

The comprehensive planning guidelines are based on two principles that are recognized to create the most effective environmental management: (1) the best management policies for the protection of wetlands and other natural resources are those that prevent or minimize the development of impacts at potential sources; and (2) the best management strategies are self-perpetuating, that is they do not require periodic infusions of capital and labor. To apply these principles in managing wetlands in a newly developing area, carry out the following steps.

Guide Sheet 1A: Comprehensive Planning Steps

1. Define the **landscape unit** subject to comprehensive planning. Refer to the definition of landscape unit in Appendix B for assistance in defining it.

2. Begin the development of a plan for the landscape unit with attention to the following general principles:

- Formulate the plan on the basis of clearly articulated community goals. Carefully identify conflicts and choices between retaining and protecting desired resources and community growth.

- Map and assess land suitability for urban uses. Include the following landscape features in the assessment: forested land, open unforested land, steep slopes, erosion-prone soils, foundation suitability, soil suitability for waste disposal, aquifers, aquifer recharge areas, wetlands, floodplains, surface waters, agricultural lands, and various categories of urban land use. When appropriate, the assessment can highlight outstanding local or regional resources that the community determines should be protected (e. g., a fish run, scenic area, recreational area, threatened species habitat, farmland). Mapping and assessment should recognize not only these resources but also additional areas needed for their sustenance.

3. Maximize natural water storage and infiltration opportunities within the landscape unit and outside of existing wetlands, especially:

- Promote the conservation of forest cover. Building on land that is already deforested affects basin hydrology to a lesser extent than converting forested land. Loss of forest cover reduces interception storage, detention in the organic forest floor layer, and water losses by evapotranspiration, resulting in large peak runoff increases and either their negative effects or the expense of countering them with structural solutions.

- Maintain natural storage reservoirs and drainage corridors, including depressions, areas of permeable soils, swales, and intermittent streams. Develop and implement policies and regulations to discourage the clearing, filling, and channelization of these features. Utilize them in drainage networks in preference to pipes, culverts, and engineered ditches.

- In evaluating infiltration opportunities refer to the stormwater management manual for the jurisdiction and pay particular attention to the selection criteria for avoiding groundwater contamination and poor soils and hydrogeological conditions that cause these facilities to fail. If necessary, locate developments with large amounts of impervious surfaces or a potential to produce relatively contaminated runoff away from groundwater recharge areas. Relatively dense developments on glacial outwash soils may require additional runoff treatment to protect groundwater quality.

4. Establish and maintain **buffers** surrounding wetlands and in riparian zones as required by local regulations or recommended by the Puget Sound Water Quality Authority's wetland guidelines. Also, maintain interconnections among wetlands and other natural habitats to allow for wildlife movements.

5. Take specific management measures to avoid general urban impacts on wetlands and other water bodies (e. g., littering, vegetation destruction, human and pet intrusion harmful to wildlife).

6. To support management of <u>runoff water quantity</u>, perform a hydrologic analysis of the contributing drainage catchment to define the type and extent of flooding and stream channel erosion problems associated with existing development, redevelopment, or new development that require control to protect the beneficial uses of receiving waters, including wetlands. This analysis should include assembly of existing flow data and hydrologic modeling as necessary to establish conditions limiting to attainment of beneficial uses. Modeling should be performed as directed by the stormwater management manual in effect in the jurisdiction.

7. In wetlands previously relatively unaffected by human activities, manage <u>stormwater quantity</u> to attempt to match the **pre-development hydroperiod** and **hydrodynamics**. In wetlands whose hydrology has been disturbed, consider ways of reducing hydrologic impacts. This provision involves not only management of high runoff volumes and rates of flow during the wet season, but also prevention of water supply depletion during the dry season. The latter guideline may require flow augmentation if urbanization reduces existing surface or groundwater inflows. Refer to Guide Sheet 2, Wetland Protection Guidelines, for detail on implementing these guidelines.

8. Assess alternatives for the control of <u>runoff water quantities</u> as follows:

a. Define the runoff quantity problem subject to management by analyzing the proposed land development action.

b. For existing development or **redevelopment**, assess possible alternative solutions that are applicable at the site of the problem occurrence, including:

- Protect health, safety, and property from flooding by removing habitation from the flood plain.

- Prevent stream channel erosion by stabilizing the eroding bed and/or bank area with **bioengineering** techniques, preferably, or by structurally reinforcing it, if this solution would be consistent with the protection of aquatic habitats and beneficial uses of the stream (refer to Chapter 173-201A of the Washington Administrative Code (WAC) for the definition of beneficial uses).

b. For new development or redevelopment, assess possible regulatory and incentive land use control alternatives, such as density controls, clearing limits, impervious surface limits, transfer of development rights, purchase of conservation areas, etc.

c. If the alternatives considered in Steps 8a or 8b cannot solve an existing or potential problem, perform an analysis of the contributing drainage catchment to assess possible alternative solutions that can be applied **on-site** or on a **regional** scale. The most appropriate solution or combination of alternatives should be selected with regard to the specific opportunities and constraints existing in the drainage catchment. For new development or redevelopment, on-site facilities that should be assessed include, in approximate order of preference:

- Infiltration basins or trenches;

- Retention/detention ponds;

- Below-ground vault or tank storage;

- Parking lot detention.

Regional facilities that should be assessed for solving problems associated with new development, redevelopment, or existing development include:

- Infiltration basins or trenches;

- Detention ponds;

- **Constructed wetlands**;

- Bypassing a portion of the flow to an acceptable receiving water body, with treatment as required to protect water quality and other special precautions as necessary to prevent downstream impacts.

d. Consider structurally or hydrologically engineering an existing wetland for water quantity control only if upland alternatives are inadequate to solve the existing or potential problem. To evaluate the possibility, refer to the Stormwater Wetland Assessment Criteria in Guide Sheet 1B.

9. Place strong emphasis on water resource protection during construction of new development. Establish effective erosion control programs to reduce the sediment loadings to receiving waters to the maximum extent possible. No preexisting wetland or other water body should ever be used for the sedimentation of solids in construction-phase runoff.

10. In wetlands previously relatively unaffected by human activities, manage stormwater quality to attempt to match pre-development water quality conditions. To support management of runoff water quality, perform an analysis of the contributing drainage catchment to define the type and extent of runoff water quality problems associated with existing development, redevelopment, or new development that require control to protect the beneficial uses of receiving waters, including wetlands. This analysis should incorporate the hydrologic assessment performed under step 6 and include identification of key water pollutants, which may include solids, oxygen-demanding substances, nutrients, metals, oils, trace organics, and bacteria, and evaluation of the potential effects of water pollutants throughout the drainage system.

11. Assess alternatives for the control of runoff water quality as follows:

a. Perform an analysis of the contributing drainage catchment to assess possible alternative solutions that can be applied on-site or on a regional scale. The most appropriate solution or combination of alternatives should be selected with regard to the specific opportunities and constraints existing in the drainage catchment. Consider both **source control BMPs** and **treatment BMPs** as alternative solutions before considering use of existing wetlands for quality improvement according to the following considerations:

- Implementation of source control BMPs prevent the generation or release of water pollutants at potential sources. These alternatives are generally both more effective and less expensive than treatment controls. They should be applied to the maximum extent possible to new development, redevelopment, and existing development.

- Treatment BMPs capture water pollutants after their release. This alternative often has limited application in existing developments because of space limitations, although it can be employed in new development and when redevelopment occurs in already developed areas. Following is a list of treatment BMPs that should be considered. Each has appropriate and inappropriate applications and advantages and disadvantages and must be carefully selected,

designed, constructed, and operated according to the specifications of the stormwater management manual in use in the jurisdiction.

— Infiltration basins or trenches;

— Constructed wetlands;

— Wet or extended-detention ponds;

— Biofiltration facilities (vegetated swales or filter strips);

— Filters with sand, compost, or other media;

— Water quality vaults;

— Oil/water separators.

b. Consider structurally or hydrologically engineering an existing wetland for water quality control only if upland alternatives are inadequate to solve the existing or potential problem. Use of Waters of the State and Waters of the United States, including wetlands, for the treatment or conveyance of wastewater, including stormwater, is prohibited under state and federal law. Discussions with federal and state regulators during the research program led to development of a statement concerning the use of existing wetlands for improving stormwater quality (**polishing**), as follows. Such use is subject to analysis on a case-by-case basis and may be allowed only if the following conditions are met:

- If **restoration** or **enhancement** of a previously **degraded** wetland is required, and if the upgrading of other wetland functions can be accomplished along with benefiting runoff quality control, <u>and</u>

- If appropriate source control and treatment BMPs are applied in the contributing catchment on the basis of the analysis in Step 10a and any legally adopted water quality standards for wetlands are observed.

If these circumstances apply, refer to the Stormwater Wetland Assessment Criteria in Guide Sheet 1B to evaluate further.

12. Stimulate public awareness of and interest in wetlands and other water resources in order to establish protective attitudes in the community. This program should include:

- Education regarding the use of fertilizers and pesticides, automobile maintenance, the care of animals to prevent water pollution, and the importance of retaining buffers;

- Descriptive signboards adjacent to wetlands informing residents of the wetland type, its functions, the protective measures being taken, etc.

- If beavers are present in a wetland, educate residents about their ecological role and value and take steps to avoid human interference with beavers.

Guide Sheet 1B: Stormwater Wetland Assessment Criteria

This guide sheet gives criteria that disqualify a natural wetland from being structurally or hydrologically engineered for control of stormwater quantity, quality, or both. These criteria should be applied only after performing the alternatives analysis outlined in Guide Sheet 1A.

1. A wetland <u>should not</u> be structurally or hydrologically engineered for runoff quantity or quality control and should be given maximum protection from overall urban impacts (see Guide Sheet 2, Wetland Protection Guidelines) under any of the following circumstances:

- In its present state it is primarily an **estuarine** or **forested wetland** or a **priority peat system**.

- It is a rare or irreplaceable wetland type, as identified by the Washington Natural Heritage Program, the Puget Sound Water Quality Preservation Program, or local government.

- It provides **rare, threatened, or endangered species** habitat that could be impaired by the proposed action. Determining whether or not the conserved species will be affected by the proposed project requires a careful analysis of its requirements in relation to the anticipated habitat changes.

In general, the wetlands in these groups are classified in Categories I and II in the Puget Sound Water Quality Authority's draft wetland guidelines.

2. A wetland <u>can be considered</u> for structural or hydrological modification for runoff quantity or quality control if most of the following circumstances exist:

- It is classified in Category IV in the Puget Sound Water Quality Authority's draft wetland guidelines. In general, Category IV wetlands have monotypic vegetation of similar age and class, lack special habitat features, and are isolated from other aquatic systems.

- The wetland has been previously **disturbed** by human activity, as evidenced by agriculture, fill, ditching, and/or introduced or **invasive weedy plant species**.

- The wetland has been deprived of a significant amount of its water supply by draining or previous urbanization (e. g., by loss of groundwater supply), <u>and</u> stormwater runoff is sufficient to augment the water supply. A particular

candidate is a wetland that has experienced an increased summer dry period, especially if the drought has been extended by more than two weeks.

- Construction for structural or hydrologic modification in order to provide runoff quantity or quality control will disturb relatively little of the wetland.

- The wetland can provide the required storage capacity for quantity or quality control through an outlet orifice modification to increase storage of water, rather than through raising the existing overflow. Orifice modification is likely to require less construction activity and consequent negative impacts.

- Under existing conditions the wetland's experiences a relatively high degree of water level fluctuation and a range of velocities (i. e., a wetland associated with substantially flowing water, rather than one in the headwaters or entirely isolated from flowing water).

- The wetland does not exhibit any of the following features:

  — Significant priority peat system or forested zones that will experience substantially altered hydroperiod as a result of the proposed action;

  — Regionally **unusual biological community types**;

  — Animal habitat features of relatively high value in the region (e. g., a protected, undisturbed area connected through undisturbed corridors to other valuable habitats, an important breeding site for protected species);

  — The presence of protected commercial or sport fish;

  — Configuration and topography that will require significant modification that may threaten fish stranding;

  — A relatively high degree of public interest as a result of, for example, offering valued local open space or educational, scientific, or recreational opportunities, unless the proposed action would enhance these opportunities;

- The wetland is threatened by potential impacts exclusive of stormwater management, and could receive greater protection if acquired for a stormwater management project rather than left in existing ownership.

- There is good evidence that the wetland actually can be restored or enhanced to perform other functions in addition to runoff quantity or quality control.

- There is good evidence that the wetland lends itself to the effective application of the Wetland Protection Guidelines in Guide Sheet 2.

- The wetland lies in the natural routing of the runoff. Local regulations often prohibit drainage diversion from one basin to another.

- The wetland allows runoff discharge at the natural location.

GUIDE SHEET 2: WETLAND PROTECTION GUIDELINES

This guide sheet provides information about likely changes to the ecological **structure** and **functioning** of **wetlands** that are incidentally subject to the effects of an urban or urbanizing watershed or are **modified** to supply runoff water quantity or quality control benefits. The guide sheet also recommends management actions that can avoid or minimize deleterious changes in these wetlands.

Guide Sheet 2A: General Wetland Protection Guidelines

1. Consult regulations issued under federal and state laws that govern the discharge of pollutants. Wetlands are classified as "Waters of the United States" and "Waters of the State" in Washington.

2. Maintain the wetland **buffer** required by local regulations or recommended by the Puget Sound Water Quality Authority's draft wetland guidelines.

3. Retain areas of native vegetation connecting the wetland and its buffer with nearby wetlands and other contiguous areas of native vegetation.

4. Avoid compaction of soil and introduction of exotic plant species during any work in a wetland.

5. Take specific site design and maintenance measures to avoid general urban impacts (e. g., littering and vegetation destruction). Examples are protecting existing buffer zones; discouraging access, especially by vehicles, by plantings outside the wetland; and encouragement of stewardship by a homeowners' association. Fences can be useful to restrict dogs and pedestrian access, but they also interfere with wildlife movements. Their use should be very carefully evaluated on the basis of the relative importance of intrusive impacts versus wildlife presence. Fences should generally not be installed when wildlife would be restricted and intrusion is relatively minor. They generally should be used when wildlife passage is not a major issue and the potential for intrusive impacts is high. When wildlife movements and intrusion are both issues, the circumstances will have to be weighed to make a decision about fencing.

6. If the wetland inlet will be modified for the stormwater management project, use a diffuse flow method, such as a spreader swale, to discharge water into the wetland in order to prevent flow channelization.

Guide Sheet 2B: Guidelines for Protection from Adverse Impacts of Modified Runoff Quantity Discharged to Wetlands

1. Protection of wetland plant and animal communities depends on controlling the wetland's **hydroperiod**, meaning the pattern of fluctuation of water depth and the frequency and duration of exceeding certain levels, including the length and onset of drying in the summer. A hydrologic assessment is useful to measure or estimate elements of the hydroperiod under existing **pre-development** and anticipated **post-development** conditions. This assessment should be performed with the aid of a qualified hydrologist. Post-development estimates of watershed hydrology and wetland hydroperiod must include the cumulative effect of all anticipated watershed and wetland modifications. Provisions in these guidelines pertain to the full anticipated build-out of the wetland's watershed.

This analysis hypothesizes a fluctuating water stage over time before development that could fluctuate more, both higher and lower after development; these greater fluctuations are termed **stage excursions**. The guidelines set limits on the frequency and duration of excursions, as well as on overall water level fluctuation, after development.

To determine existing hydroperiod use one of the following methods, listed in order of preference:

- Estimation by a continuous simulation computer model--The model should be calibrated with at least one year of data taken using a continuously recording level gage under existing conditions and should be run for the historical rainfall period. The resulting data can be used to express the magnitudes of depth fluctuation, as well as the frequencies and durations of surpassing given depths. [Note: Modeling that yields high quality information of the type needed for wetland hydroperiod analysis is a complex subject. Providing guidance on selecting and applying modeling options is beyond the scope of these guidelines but is being developed by King County Surface Water Management Division and other local jurisdictions. An alternative possibility to modeling depths, frequencies, and durations within the wetland is to model durations above given discharge levels entering the wetland over various time periods (e. g., seasonal, monthly, weekly). This option requires further development.]

- Measurement during a series of time intervals (no longer than one month in length) over a period of at least one year of the maximum water stage, using a crest stage gage, and instantaneous water stage, using a staff gage--The resulting data can be used to express water level fluctuation (WLF) during the interval as follows:

  Average base stage = (Instantaneous stage at beginning of interval + Instantaneous stage at end of interval)/2

  WLF = Crest stage - Average base stage

  Compute mean annual and mean monthly WLF as the arithmetic averages for each year and month for which data are available.

To forecast future hydroperiod use one of the following methods, listed in order of preference:

- Estimation by the continuous simulation computer model calibrated during pre-development analysis and run for the historical rainfall period--The resulting data can be used to express the magnitudes of depth fluctuation, as well as the frequencies and durations of surpassing given depths. [Note: Post-development modeling results should generally be compared with pre-development modeling results, rather than directly with field measurements, because different sets of assumptions underlie modeling and monitoring. Making pre- and post-development comparisons on the basis of common assumptions allows cancellation of errors inherent in the assumptions.]

- Estimation according to general relationships developed from the Puget Sound Wetlands and Stormwater Management Program Research Program, as follows (in part adapted from Chin 1996):

  — Mean annual WLF is very likely (100% of cases measured) to be < 20 cm (8 inches or 0.7 ft) if total impervious area (TIA) cover in the watershed is < 6% (roughly corresponding to no more than 15% of the watershed converted to urban land use).

  — Mean annual WLF is very likely (89% of cases measured) to be > 20 cm if TIA in the watershed is > 21% (roughly corresponding to more than 30% of the watershed converted to urban land use).

  — Mean annual WLF is somewhat likely (50% of cases measured) to be > 30 cm (1.0 ft) if TIA in the watershed is > 21% (roughly corresponding to more than 30% of the watershed converted to urban land use).

  — Mean annual WLF is likely (75% of cases measured) to be > 30 cm, and somewhat likely (50% of cases measured) to be 50 cm (20 inches or 1.6 ft) or higher, if TIA in the watershed is > 40% (roughly corresponding to more than 70% of the watershed converted to urban land use).

  — The frequency of stage excursions greater than 15 cm (6 inches or 0.5 ft) above or below pre-development levels is somewhat likely (54% of cases measured) to be more than six per year if the mean annual WLF increases to > 24 cm (9.5 inches or 0.8 ft).

  — The average duration of stage excursions greater than 15 cm above or below pre-development levels is likely (69% of cases measured) to be more than 72 hours if the mean annual WLF increases to > 20 cm.

2. The following hydroperiod limits characterize wetlands with relatively high vegetation species richness and apply to <u>all zones</u> within <u>all wetlands</u> over the <u>entire year</u>. If these limits are exceeded, then species richness is likely to decline. If the analysis described above forecasts exceedences, one or more of the management strategies listed in step 5 should be employed to attempt to stay within the limits.

- Mean annual WLF (and mean monthly WLF for every month of the year) does not exceed 20 cm. Vegetation species richness decrease is likely with: (1) a mean annual (and mean monthly) WLF increase of more than 5 cm (2 inches or 0.16 ft) if pre-development mean annual (and mean monthly) WLF is greater than 15 cm, or (2) a mean annual (and mean monthly) WLF increase to 20 cm or more if pre-development mean annual (and mean monthly) WLF is 15 cm or less.

- The frequency of stage excursions of 15 cm above or below pre-development stage does not exceed an annual average of six.

- The duration of stage excursions of 15 cm above or below pre-development stage does not exceed 72 hours per excursion.

- The total dry period (when pools dry down to the soil surface everywhere in the wetland) does not increase or decrease by more than two weeks in any year.

- Alterations to watershed and wetland hydrology that may cause perennial wetlands to become **vernal** are avoided.

3. The following hydroperiod limit characterizes **priority peat wetlands** (bogs and fens as more specifically defined by the Washington Department of Ecology) and applies to all zones over the entire year. If this limit is exceeded, then characteristic bog or fen wetland vegetation is likely to decline. If the analysis described above forecasts exceedence, one or more of the management strategies listed in step 5 should be employed to attempt to stay within the limit.

- The duration of stage excursions above the pre-development stage does not exceed 24 hours in any year.

- Note: To apply this guideline a continuous simulation computer model needs to be employed. The model should be calibrated with data taken under existing conditions at the wetland being analyzed and then used to forecast post-development duration of excursions.

4. The following hydroperiod limits characterize wetlands inhabited by breeding native amphibians and apply to breeding zones during the period 1 February through 31 May. If these limits are exceeded, then amphibian breeding success is likely to decline. If the analysis described above forecasts exceedences, one or more of the management strategies listed in step 5 should be employed to attempt to stay within the limits.

- The magnitude of stage excursions above or below the pre-development stage does not exceed 8 cm, and the total duration of these excursions does not exceed 24 hours in any 30 day period.

- Note: To apply this guideline a continuous simulation computer model needs to be employed. The model should be calibrated with data taken under

existing conditions at the wetland being analyzed and then used to forecast post-development magnitude and duration of excursions.

5. If it is expected that the hydroperiod limits stated above could be exceeded, consider strategies such as:

- Reduction of the level of development;
- Increasing runoff infiltration [Note: Infiltration is prone to failure in many Puget Sound Basin locations with glacial till soils and generally requires **pretreatment** to avoid clogging. In other situations infiltrating urban runoff may contaminate groundwater. Consult the stormwater management manual adopted by the jurisdiction and carefully analyze infiltration according to its prescriptions.];
- Increasing runoff storage capacity; and
- Selective runoff bypass.

6. After development, monitor hydroperiod with a continuously recording level gauge or staff and crest stage gauges. If the applicable limits are exceeded, consider additional applications of the strategies in step 5 that may still be available. It is also recommended that goals be established to maintain key vegetation species, amphibians, or both, and that these species be monitored to determine if the goals are being met.

Guide Sheet 2C: Guidelines for Protection from Adverse Impacts of Modified Runoff Quality Discharged to Wetlands

1. Require effective erosion control at any construction sites in the wetland's drainage catchment.

2. Institute a program of **source control BMPs** to minimize the generation of pollutants that will enter storm runoff that drains to the wetland.

3. Provide a water quality control facility consisting of one or more **treatment BMPs** to treat all urban runoff entering the wetland and designed according to the following criteria:

- The facility should be designed to remove at least 80 percent of the total suspended solids in the runoff.

- If the catchment could generate a relatively large amount of oil (e. g., certain industrial sites, bases handling large vehicles, areas where oil may be spilled or improperly disposed), the facility should include an appropriate oil control device.

- If the wetland is a **priority peat wetland** (bogs and fens as more specifically defined by the Washington Department of Ecology), the facility should include a BMP with the most advanced ability to control nutrients (e. g., an infiltration device, a wet pond or constructed wetland with residence time in the pooled storage of at least two weeks). [Note: Infiltration is prone to failure in many Puget Sound Basin locations with glacial till soils and generally requires **pretreatment** to avoid clogging. In other situations infiltrating urban runoff may contaminate groundwater. Consult the stormwater management manual adopted by the jurisdiction and carefully analyze infiltration according to its prescriptions.] Refer to Appendix E for a comparison of water chemistry conditions in priority peat versus more typical wetlands.

Refer to the stormwater management manual to select and design the facility. Generally, the facility should be located outside and upstream of the wetland and its buffer.

4. Design and perform a water quality monitoring program for priority peat wetlands and for other wetlands subject to relatively high water pollutant loadings. The research results (Horner 1989) identified such wetlands as having contributing catchments exhibiting either of the following characteristics:

- More than 20 percent of the catchment area is committed to commercial, industrial, and/or multiple family residential land uses; or

- The combination of all urban land uses (including single family residential) exceeds 30 percent of the catchment area.

A recommended monitoring program, consistent with monitoring during the research program, is:

- Perform pre-development **baseline sampling** by collecting water quality grab samples in an open water pool of the wetland for at least one year, allocated through the year as follows: November 1-March 31--4 samples, April 1-May 31--1 sample, June 1-August 31--2 samples, and September 1-October 31--1 sample (if the wetland is dry during any period, reallocate the sample(s) scheduled then to another time). Analyze samples for pH; dissolved oxygen (DO); conductivity (Cond); total suspended solids (TSS); total phosphorus (TP); nitrate + nitrite-nitrogen (N); fecal coliforms (FC); and total copper (Cu), lead (Pb), and zinc (Zn). Find the median and range of each water quality variable.

- Considering the baseline results, set water quality goals to be maintained in the post-development period. Example goals are: (1) pH--no more than "x" percent (e. g., 10%) increase (relative to baseline) in annual median and maximum or decrease in annual minimum; (2) DO--no more than "x" percent decrease in annual median and minimum concentrations; (3) other variables --no more than "x" percent increase in annual median and maximum concentrations; (4) no increase in violations of the Washington Administrative Code (WAC) water quality criteria.

- Repeat the sampling on the same schedule for at least one year after all development is complete. Compare the results to the set goals.

If the water quality goals are not met, consider additional applications of the source and treatment controls described in steps 2 and 3. Continue monitoring until the goals are met at least two years in succession.

Note: Wetland water quality was found to be highly variable during the research, a fact that should be reflected in goals. Using the maximum (or minimum), as well as a measure of central tendency like the median, and allowing some change from pre-development levels are ways of incorporating an allowance for variability. Table 14-1 presents data from the wetlands studied during the research program to give an approximate idea of magnitudes and degree of variability to be expected. Nonurbanized watersheds (N) are those that have both < 15% urbanization and < 6% impervious cover. Highly urbanized watersheds (H) are those that have both lost all forest cover and have > 20% impervious cover. Moderately urbanized watersheds (M) are those that fit neither the N nor H category.

Table 14-1. Water quality ranges found in study wetlands.

	N			M			H		
Metric	Median	Mean	Std.Dev./n[a]	Median	Mean	Std.Dev./n[a]	Median	Mean	Dev./n[a]
pH[b]	6.4	6.4	0.5/162	6.7	6.5	0.8/132	6.9	6.7	0.6/52
DO (mg/L)	5.9	5.7	2.6/205	5.1	5.53.6/173	6.3	5.4	2.9/67	
Cond. (µS/cm)	46	73	64/190	160	142	73/161	132	151	86/61
TSS (µg/L)	2.0	4.6	8.5/204	2.8	9.2	22/175	4.0	9.2	15/66
TP (µg/L)	29	52	87/206	70	93	92/177	69	110	234/67
N (µg/L)	112	368	485/206	304	598	847/177	376	395	239/67
FC (no./100mL)	9.0	271	1000/206	46	2665	27342/173	61	969	4753/66
Cu (µg/L)	<5.0	<3.3	>2.7/93	<5.0	<3.7	>1.9/78	<5.0	<4.1	<2.5/29
Pb (µg/L)	1.0	<2.7	>2.8/136	3.0	<3.4	>2.7/122	5.0	<4.5	>4.0/44
Zn (µg/L)	5.0	8.4	8.3/136	8.0	9.8	7.2/122	20	20	17/44

[a] Std. Dev.--standard deviation; n--number of observations.
[b] Values do not apply to priority peat wetlands. The program did not specifically study these wetlands but measured pH in three wetlands with "bog-like" characteristics. The minimum value measured in these wetlands was 4.5, and the lowest median was 4.8; but pH can be approximately 1 unit lower in wetlands of this type. Refer to Appendix E for a comparison of water chemistry conditions in priority peat versus more typical wetlands.

Guide Sheet 2D: Guidelines for the Protection of Specific Biological Communities

1. For wetlands inhabited by <u>breeding native amphibians</u>:

    - Refer to step 4 of Guide Sheet 2B for hydroperiod limit.
    - Avoid decreasing the sizes of the open water and aquatic bed zones.
    - Avoid increasing the channelization of flow. Do not form channels where none exist, and take care that inflows to the wetland do not become more concentrated and do not enter at higher velocities than accustomed. If necessary, concentrated flows can be uniformly distributed with a flow-spreading device such as a shallow weir, stilling basin, or perforated pipe. Velocity dissipation can be accomplished with a stilling basin or rip-rap pad.
    - Limit the post-development flow velocity to < 5 cm/s (0.16 ft/second) in any location that had a velocity in the range 0-5 cm/s in the pre-development condition.
    - Avoid increasing the gradient of wetland side slopes.

2. For wetlands inhabited by <u>forest bird species</u>:

    Retain areas of coniferous forest in and around the wetland as habitat for forest species.

Retain shrub or woody debris as nesting sites for ground-nesting birds and downed logs and stumps for winter wren habitat.

Retain snags as habitat for cavity-nesting species, such as woodpeckers.

Retain shrubs in and around the wetland for protective cover. If cover is insufficient to protect against domestic pet predation, consider planting native bushes such as rose species in the buffer.

3. For wetlands inhabited by **wetland obligate** bird species:

- Retain **forested zones**, sedge and rush meadows, and deep open water zones, both without vegetation and with submerged and floating plants.

- Retain shrubs in and around the wetland for protective cover. If cover is insufficient to protect against domestic pet predation, consider planting native bushes such as rose species in the buffer.

- Avoid introducing **invasive weedy plant species**, such as purple loosestrife and reed canarygrass.

- Retain the buffer zone. If it has lost width or forest cover, consider re-establishing forested buffer area at least 30 meters (100 ft) wide.

- If human entry is desired, establish paths that permit people to observe the wetland with minimum disturbance to the birds.

4. For wetlands inhabited by fish:

- Protect fish habitats by avoiding water velocities above tolerated levels (selected with the aid of a qualified fishery biologist to protect fish in each life stage when they are present), siltation of spawning beds, etc. Habitat requirements vary substantially among fish species. If the wetland is associated with a larger water body, contact the Department of Fisheries and Wildlife to determine the species of concern and the acceptable ranges of habitat variables.

- If stranding of protected commercial or sport fish could result from a structural or hydrologic modification for runoff quantity or quality control, develop a strategy to avoid stranding that minimizes disturbance in the wetland (e. g., by making provisions for fish return to the stream as the wetland drains, or avoiding use of the facility for quantity or quality control during fish presence).

APPENDIX A: INFORMATION NEEDED TO APPLY GUIDELINES

The following information listed for each guide sheet is most essential for applying the Wetlands and Stormwater Management Guidelines. As a start, obtain the relevant soil survey; the National Wetland Inventory, topographic and land use maps, and the results of any local wetland inventory.

Guide Sheet 1

1. Boundary and area of the contributing watershed of the wetland or other landscape unit

2. A complete definition of goals for the wetland and landscape unit subject to planning and management

3. Existing management and monitoring plans

4. Existing and projected land use in the landscape unit in the categories commercial, industrial, multi-family residential, single-family residential, agricultural, various categories of undeveloped, and areas subject to active logging or construction (expressed as percentages of the total watershed area)

5. Drainage network throughout the landscape unit

6. Soil conditions, including soil types, infiltration rates, and positions of seasonal water table (seasonally) and restrictive layers

7. Groundwater recharge and discharge points

8. Wetland category (I - IV in draft Puget Sound Water Quality Authority wetland protection guidelines); designation as rare or irreplaceable. Refer to the Washington Natural Heritage Program data base. If the needed information is not available, a biological assessment will be necessary.

9. Watershed hydrologic assessment

10. Watershed water quality assessment

11. Wetland type and zones present, with special note of estuarine, priority peat system, forested, sensitive scrub-shrub zone, sensitive emergent zone and other sensitive or critical areas designated by state or local government (with dominant plant species)

12 . Rare, threatened, or endangered species inhabiting the wetland

13. History of wetland changes

14. Relationship of wetland to other water bodies in the landscape unit and the drainage network

15. Flow pattern through the wetland

16. Fish and wildlife inhabiting the wetland

17. Relationship of wetland to other wildlife habitats in the landscape unit and the corridors between them

Guide Sheet 2

1. Existing and potential stormwater pollution sources

2. Existing and projected landscape unit land use (see number 4 under Guide Sheet 1)

3. Existing and projected wetland hydroperiod characteristics

4. Wetland bathymetry

5. Inlet and outlet locations and hydraulics

6. Landscape unit soils, geologic and hydrogeologic conditions

7. Wetland type and zones present (see number 11 under Guide Sheet 1)

8. Presence of breeding populations of native amphibian species

9. Presence of forest and wetland obligate bird species

10. Presence of fish species

APPENDIX B: DEFINITIONS

Baseline sampling: Sampling performed to define an existing state before any modification occurs that could change the state.

Bioengineering: Restoration or reinforcement of slopes and stream banks with living plant materials.

Buffer: The area that surrounds a wetland and that reduces adverse impacts to it from adjacent development.

Constructed wetland: A wetland intentionally created from a non-wetland site for the sole purpose of wastewater or stormwater treatment. These wetlands are not normally considered Waters of the United States or Waters of the State.

Degraded (disturbed) wetland (community): A wetland (community) in which the vegetation, soils, and/or hydrology have been adversely altered, resulting in lost or reduced functions and values; generally, implies topographic isolation; hydrologic alterations such as hydroperiod alteration (increased or decreased quantity of water), diking, channelization, and/or outlet modification; soils alterations such as presence of fill, soil removal, and/or compaction; accumulation of toxicants in the biotic or abiotic components of the wetland; and/or low plant species richness with dominance by invasive weedy species.

Enhancement: Actions performed to improve the condition of an existing degraded wetland, so that functions it provides are of a higher quality.

Estuarine wetland: Generally, an eelgrass bed; salt marsh; or rocky, sandflat, or mudflat intertidal area where fresh and salt water mix. (Specifically, a tidal wetland with salinity greater than 0.5 parts per thousand, usually semi-enclosed by land but with partly obstructed or sporadic access to the open ocean).

Forested communities (wetlands): In general terms, communities (wetlands) characterized by woody vegetation that is greater than or equal to 6 meters in height; in these guidelines the term applies to such communities (wetlands) that represent a significant amount of tree cover consisting of species that offer wildlife habitat and other values and advance the performance of wetland functions overall.

Functions: The ecological (physical, chemical, and biological) processes or attributes of a wetland without regard for their importance to society (see also Values). Wetland functions include food chain support, provision of ecosystem diversity and fish and wildlife habitat, flood flow alteration, groundwater recharge and discharge, water quality improvement, and soil stabilization.

Hydrodynamics: The science involving the energy and forces acting on water and its resulting motion.

Hydroperiod: The seasonal occurrence of flooding and/or soil saturation; encompasses the depth, frequency, duration, and seasonal pattern of inundation.

Invasive weedy plant species: Opportunistic species of inferior biological value that tend to out-compete more desirable forms and become dominant; applied to non-native species in these guidelines.

Landscape unit: An area of land that has a specified boundary and is the locus of interrelated physical, chemical, and biological processes.

Modification, Modified (wetland): A wetland whose physical, hydrological, or water quality characteristics have been purposefully altered for a management purpose, such as by dredging, filling, forebay construction, and inlet or outlet control.

On-site: An action (here, for stormwater management purposes) taken within the property boundaries of the site to which the action applies.

Polishing: Advanced treatment of a waste stream that has already received one or more stages of treatment by other means.

Pre-development, post-development: Respectively, the situation before and after a specific stormwater management project (e. g., raising the outlet, building an outlet control structure) will be placed in the wetland or a land use change occurs in the landscape unit that will potentially affect the wetland.

Pre-treatment: An action taken to remove pollutants from runoff before it is discharged into another system for additional treatment.

Priority peat systems: Unique, irreplaceable fens that can exhibit water pH in a wide range from highly acidic to alkaline, including fens typified by *Sphagnum* species, *Rhododendron groenlandicum* (Labrador tea), *Drosera rotundifolia* (sundew), and *Vaccinium oxycoccos* (bog cranberry); marl fens; estuarine peat deposits; and other moss peat systems with relatively diverse, undisturbed flora and fauna. Bog is the common name for peat systems having the *Sphagnum* association described, but this term applies strictly only to systems that receive water income from precipitation exclusively.

Rare, threatened, or endangered species: Plant or animal species that are regional relatively uncommon, are nearing endangered status, or whose existence is in immediate jeopardy and is usually restricted to highly specific habitats. Threatened and endangered species are officially listed by federal and state authorities, whereas rare species are unofficial species of concern that fit the above definitions.

Redevelopment: Conversion of an existing development to another land use, or addition of a material improvement to an existing development.

Regional: An action (here, for stormwater management purposes) that involves more than one discrete property.

Restoration: Actions performed to reestablish wetland functional characteristics and processes that have been lost by alterations, activities, or catastrophic events in an area that no longer meets the definition of a wetland.

Source control best management practices (BMPs): Actions that are taken to prevent the development of a problem (e. g., increase in runoff quantity, release of pollutants) at the point of origin.

Stage excursion: A post-development departure, either higher or lower, from the water depth existing under a given set of conditions in the pre-development state.

Structure: The components of an ecosystem, both the abiotic (physical and chemical) and biotic (living).

Treatment best management practices (BMPs): Actions that remove pollutants from runoff through one or more physical, chemical, biological mechanisms.

Unusual biological community types: Assemblages of interacting organisms that are relatively uncommon regionally.

Values: Wetland processes or attributes that are valuable or beneficial to society (also see Functions). Wetland values include support of commercial and sport fish and wildlife species, protection of life and property from flooding, recreation, education, and aesthetic enhancement of human communities.

Vernal wetland: A wetland that has water above the soil surface for a period of time during and/or after the wettest season but always dries to or below the soil surface in warmer, drier weather.

Wetland obligate: A biological organism that absolutely requires a wetland habitat for at least some stage of its life cycle.

Wetlands: Lands transitional between terrestrial and aquatic systems that have a water table usually at or near the surface or a shallow covering of water, hydric soils, and a prevalence of hydrophytic vegetation.

APPENDIX C: REFERENCES

Chin, N. T. 1996. Watershed Urbanization Effects on Palustrine Wetlands: A Study of the Hydrologic, Vegetative, and Amphibian Community Response over Eight Years. M. S. C. E. Thesis, University of Washington, Seattle, WA.

Horner, R. R. 1989. Long-term effects of urban runoff on wetlands. Pp. *in* L. A. Roesner, B. Urbonas, and M. B. Sonnen (eds.), Design of Urban Runoff Controls, American Society of Civil Engineers, New York, NY.

Horner, R. R., J. J. Skupien, E. H. Livingston, and H. E. Shaver. 1994. Fundamentals of Urban Runoff Management: Technical and Institutional Issues. Terrene Institute, Washington, D. C.

Horner, R. R., S. S. Cooke, K. O. Richter, A. L. Azous, L. E. Reinelt, B. L. Taylor, K. A. Ludwa, and M. Valentine. 1996. Wetlands and Urbanization, Implications for the Future. Puget Sound Wetlands and Stormwater Management Research Program, Engineering Professional Programs, University of Washington, Seattle, WA.

APPENDIX D: NATIVE AND RECOMMENDED NONINVASIVE PLANT SPECIES FOR WETLANDS IN THE PUGET SOUND BASIN

Caution: Extracting plants from an existing wetland donor site can cause a significant negative effect on that site. It is recommended that plants be obtained from native plant nursery stocks whenever possible. Collections from existing wetlands should be limited in scale and undertaken with care to avoid disturbing the wetland outside of the actual point of collection. Plant selection is a complex task, involving matching plant requirements with environmental conditions. It should be performed by a qualified wetlands botanist. Refer to Restoring Wetlands in Washington by the Washington Department of Ecology for more information.

Plants preferred in Puget Sound Basin freshwater wetlands

Open water zone:
Potamogeton species (pondweeds)
Nymphaea odorata (pond lily)
Brasenia schreberi (watershield)
Nuphar luteum (yellow pond lily)
Polygonum hydropiper (smartweed)
Alisma plantago-aquatica (broadleaf water plantain)
Ludwigia palustris (water purslane)
Menyanthes trifoliata (bogbean)
Utricularia minor, *U. vulgaris* (bladderwort)

Emergent zone:
Carex obnupta, *C. utriculata, C. arcta, C. stipata, C. vesicaria C. aquatilis, C. comosa, C. lenticularis* (sedge)
Scirpus atricinctus (woolly bulrush)
Scirpus microcarpus (small-fruited bulrush)
Eleocharis palustris, E. ovata (spike rush)
Epilobium watsonii (Watson's willow herb)
Typha latifolia (common cattail) (Note: This native plant can be aggressive but has been found to offer certain wildlife habitat and water quality improvement benefits; use with care.)
Veronica americana, V. scutellata (American brookline, marsh speedwell)
Mentha arvensis (field mint)
Lycopus americanus, L. uniflora (bugleweed or horehound)
Angelica species (angelica)
Oenanthe sarmentosa (water parsley)
Heracleum lanatum (cow parsnip)
Glyceria grandis, G. elata (manna grass)
Juncus acuminatus (tapertip rush)

Juncus ensifolius (daggerleaf rush)
Juncus bufonius (toad rush)
Mimulus guttatus (common monkey flower)

Scrub-shrub zone:
Salix lucida, S. rigida, S. sitchensis, S. scouleriana, S. pedicellaris (willow)
Lysichiton americanus (skunk cabbage)
Athyrium filix-femina (lady fern)
Cornus sericea (redstem dogwood)
Rubus spectabilis (salmonberry)
Physocarpus capitatus (ninebark)
Ribes species (gooseberry)
Rhamnus purshiana (cascara)
Sambucus racemosa (red elderberry) (occurs in wetland-upland transition)
Loniceria involucrata (black twinberry)
Oemleria cerasiformis (Indian plum)
Stachys cooleyae (Stachy's horsemint)
Prunus emarginata (bitter cherry)

Forested zone:
Populus balsamifera, ssp. *trichocarpa* (black cottonwood)
Fraxinus latifolia (Oregon ash)
Thuja plicata (western red cedar)
Picea sitchensis (Sitka spruce)
Alnus rubra (red alder)
Tsuga heterophylla (hemlock)
Acer circinatum (vine maple)
Maianthemum dilatatum (wild lily-of-the-valley)
Ivzula parviflora (small-flower wood rush)
Torreyochloa pauciflora (weak alkaligrass)
Ribes species (currants)

Bog:
Sphagnum species (sphagnum mosses)
Rhododendron groenlandicum (Labrador tea)
Vaccinium oxycoccos (bog cranberry)
Kalmia microphylla, ssp. *occidentalis* (bog laurel)

Exotic plants that should not be introduced to existing, created, or constructed Puget Sound Basin freshwater wetlands

Hedera helix (English ivy)
Phalaris arundinacea (reed canarygrass)
Lythrum salicaria (purple loosestrife)
Iris pseudacorus (yellow iris)
Ilex aquifolia (holly)
Impatiens glandulifera (policeman’s helmet)
Lotus corniculatus (birdsfoot trefoil)

Lysimachia thyrsiflora (tufted loosestrife)
Myriophyllum species (water milfoil, parrot's feather)
Polygonum cuspidatum (Japanese knotweed)
Polygonum sachalinense (giant knotweed)
Rubus discolor (Himalayan blackberry)
Tanacetum vulgare (common tansy)

Native plants that should not be introduced to existing, created, or constructed Puget Sound Basin freshwater wetlands

Potentilla palustris (Pacific silverweed)
Solarum dulcimara (bittersweet nightshade)
Juncus effusus (soft rush)
Conium maculatum (poison hemlock)
Ranunculus repens (creeping buttercup)

APPENDIX E: COMPARISON OF WATER CHEMISTRY CHARACTERISTICS IN *SPHAGNUM* BOG AND FEN VERSUS MORE TYPICAL WETLANDS

Water Quality Variable	Typical Wetlands	*Sphagnum* Bogs and Fens
pH	6 - 7	3.5 - 4.5
Dissolved oxygen (mg/L)	4 - 8	Shallow surface layer oxygenated, anoxic below
Cations	Divalent Ca, Mg common	Divalent Ca, Mg uncommon; Univalent Na, K predominant
Anions	HCO_3^-, CO_3^{2-} predominant	Cl^-, SO_4^{2-} predominant; almost no HCO_3^-, CO_3^{2-} (organic acidsform buffering system)
Hardness	Moderate	Very low
Total phosphorus (µg/L)	50 - 500	5 - 50
Total Kjeldahl nitrogen (µg/L)	500 - 1000	~ 50

REFERENCES

Clymo, R. S. 1963. Ion exchange in *Sphagnum* and its relation to bog ecology. Annals of Botany 27 (106):310-324.

Cooke, S. S., Puget Sound Wetlands and Stormwater Management Research Program, unpublished Queen's Bog data.

Meyer, J., L. Vogel, and T. Duebendorfer, East Lake Sammamish wetland no. 21 unpublished data, submitted to L. Kulzer, King County Surface Water Management Division.

Moore, P. D. and D. J. Bellamy. 1974. Chapter 3, The Geochemical template. Peatlands. Elek Science, London, U. K.

Thurman, E. M. 1985. Organic Geochemistry of Natural Waters. Martinus Nijhoff/Dr W. Junk Publishers, Dordrecht, The Netherlands.

Vitt, D. H., D. G. Horton, N. G. Slack, and N. Malmer. 1990. *Sphagnum*-dominated peatlands of the hyperoceanic British Columbia coast: Patterns in surface water chemistry and vegetation. Canadian Journal of Forest Research 20:696-711.

Water Air Soil Pollut (2007) 185:195–207
DOI 10.1007/s11270-007-9442-9

Arsenic Addition to Soils from Airborne Coal Dust Originating at a Major Coal Shipping Terminal

William J. Bounds · Karen H. Johannesson

Received: 15 February 2007 / Accepted: 17 May 2007 / Published online: 21 June 2007
© Springer Science + Business Media B.V. 2007

Abstract Soil samples were collected from Norfolk, Virginia in order to examine the extent of particulate coal, and associated arsenic (As) deposition to local soils. The particulate coal originates from the adjacent coal shipping terminal at the Lambert's Point Docks, which is the largest marine coal shipping terminal in the Northern Hemisphere. Particulate coal was separated from soil samples using heavy liquid (i.e., sodium polytungstate) extraction. Sand-sized coal separates isolated from the soil samples were subsequently digested using concentrated nitric and sulfuric acid, and analyzed for As by high-resolution inductively coupled plasma mass spectrometry (HR-ICP-MS). Selected total soil digests were also analyzed for As by HR-ICP-MS. Results indicate particulate coal ranges from less than 1% up to ~20%, by weight, of the soil samples analyzed. Arsenic concentrations in sand-sized particulate coal extracted from these sediments range from undetectable levels (i.e., <3 ng/kg) up to 17.4 mg/kg, whereas total As concentrations in the soils range from 3 to 30.5 mg/kg. The data indicate that particulate coal originating at the Lambert's Point Docks is an additional source of As to local soils, especially sites proximal to the shipping terminal. Although the particulate coal itself likely poses only minor health hazards (if any), the environmental consequences of As transported with the particulate coal is not known.

Keywords Coal dust · Arsenic · Soils · Airborne transport · Coal shipping terminal · Virginia

W. J. Bounds
Department of Ocean, Earth and Atmospheric Sciences,
Old Dominion University,
Norfolk, VA 23529-0275, USA

K. H. Johannesson (✉)
Department of Earth and Environmental Sciences,
Tulane University,
New Orleans, LA 70118-5698, USA
e-mail: kjohanne@tulane.edu

1 Introduction

Environmental concerns over the use of coal as a fossil fuel have commonly focused on the impact that mining, coal combustion, and the resultant fly ash has on environmental quality (e.g., Querol et al. 1991, 1992, 1999; Kizilshtein and Kholodkov 1999; Feng et al. 2000; Finkelman et al. 2002, 2006; Fuge 2005; Yudovich and Ketris 2005; Greb et al. 2006; Kolker et al. 2006). It is generally accepted, for example, that combustion of high-sulfur coal has contributed to the occurrence of acid rain and the consequent acidification of watersheds with low acid buffering capacity (Gupta 1999). Moreover, because fly ash generated from coal combustion can be enriched in many trace elements, including a number of potentially toxic trace elements such as arsenic (As), selenium (Se), cadmium (Cd), chromium (Cr), and mercury (Hg), studies have

examined the impact of trace element loading to the environment from fly ash fall-out (Eskenazy 1995; Querol et al. 1999; Fuge 2005; Mastalerz and Drobniak 2007). However, the environmental impact of and/or the potential human health issues arising from transport and shipping of coal, and subsequent inhalation of resulting "environmental" coal dust, have typically not been examined, although occupational inhalation has been extensively studied (e.g., coal workers' pneumoconiosis; Attfield et al. 1997, 1998; Finkelman et al. 2002; Centeno et al. 2005). Recent investigation of coal workers' pneumoconiosis (also known as black lung disease) suggests that finely disseminated pyrite grains within coat dust may be responsible for the inflammation of lung tissue that leads to development of lung fibrosis (Finkelman et al. 2006). Possible human health issues may also arise from inhalation of airborne "environmental" particulate coal owing to the fact that: (1) it can occur in size fractions (e.g., $PM_{2.5}$; <2.5 μm) that are potentially hazardous (Zheng et al. 1999); and (2) because it may be enriched in pyrite and/or toxic trace elements such as As, Hg, Se, Cd, and Cr (Eskenazy 1995; Smith et al. 1998; Querol et al. 1999; Finkelman et al. 2006).

The facility at the Lambert's Point Docks in Norfolk, Virginia (Fig. 1) is home to North America's largest coal shipping terminal in terms of total tonnage shipped. Specifically, more than 28 million tons of coal is shipped from Lambert's Point Docks annually (Dinsmore 1999). The method used to load coal from railroad cars to waiting ships involves overturning each coal-filled railroad car and dumping the coal onto a conveyor belt leading to the transport ship, where it is dumped again into the ship's hold. Owing to the nature of the process, the coal loading method generates "environmental" coal dust that is subsequently transported into nearby regions of Norfolk and Portsmouth, Virginia (Fig. 1). The Virginia Department of Environmental Quality (VDEQ (Virginia Department Environmental Quality) 2002) estimates that the coal pier at Lambert's Point released approximately 35 tons of particulate coal into the air during 2000, although it is permitted to release up to 50 tons/year. It is important to note that this permitted release

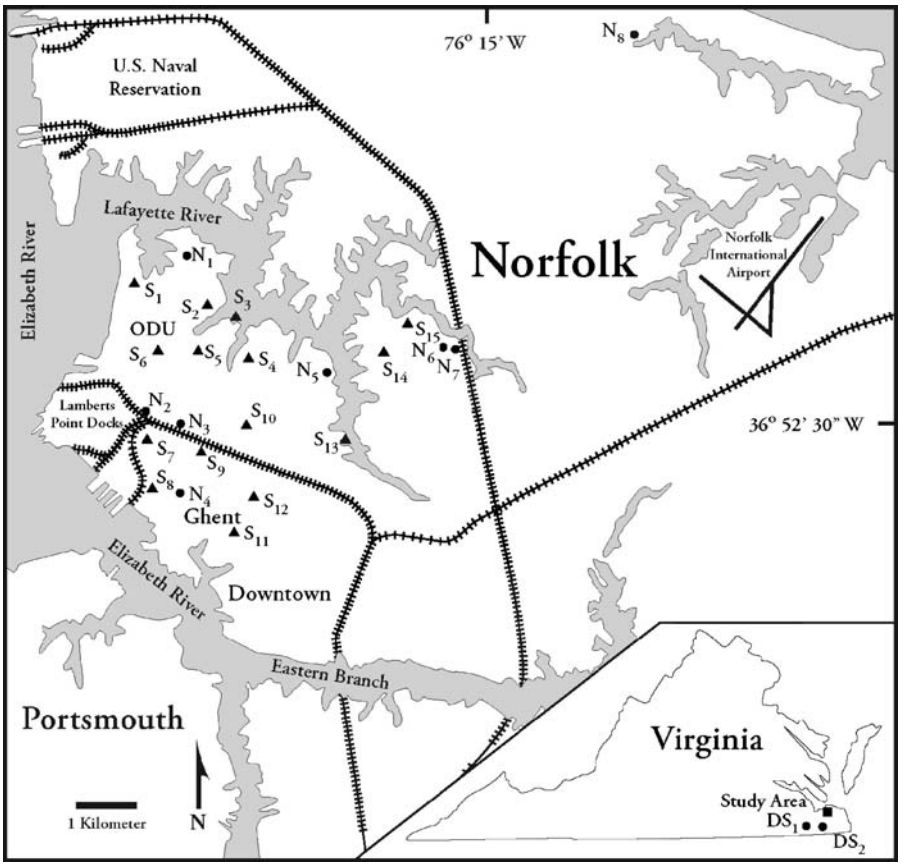

Fig. 1 Map showing the location of the study region in southeastern Virginia, USA (*insert*) and the locations of soil cores (N_1 through N_8, DS_1 and DS_2), and surface soil samples (S_1 through S_{15}), within the city of Norfolk, Virginia. Soil cores are shown as *filled circles*, whereas the surface sample locations are depicted as *filled triangles*. In addition, major railway lines (++++) within the city of Norfolk are also shown along with a number of landmarks and neighborhoods. Old Dominion University is shown as ODU

level for airborne coal dust was exceeded in 1999 (VDEQ 2002). Black, gritty veneers of what appears to be particulate coal coating objects (e.g., automobiles, window sills, plants, etc.) are common in both Norfolk and Portsmouth, Virginia, and anecdotal accounts suggest that such veneers are more prevalent in the West Ghent neighborhood of Norfolk, proximal to the Lambert's Point Docks. These thin coatings of probable coal dust suggest that airborne transport of coal dust from the Lambert's Point Docks is prevalent in the region. It should be mentioned that coal has also been transported into the study area via railways for reasons other than immediate export via the Lambert's Point Docks, including its use in household heating, storage for future shipment, and for burning in local coal-fired power plants.

2 Study Site

The study area is located in the southeast corner of the State of Virginia, on the east coast of the USA (Fig. 1). It is bounded by the Elizabeth River (i.e., tidal) along the west and south, the Lafayette River (also tidal) to the north, and thus includes a significant portion of the city of Norfolk, Virginia. The Lambert's Point Docks are located within Norfolk's city limits, along the Elizabeth River (Fig. 1). The region surrounding the docks is highly urbanized and characterized by low elevation and relatively flat terrain (Mixon et al. 1989).

The study region is underlain by the Tabb Formation, which was deposited during several high and low stands of sea-level during the Pleistocene (Mixon et al. 1989). The youngest member of the Tabb Formation is the Poquoson Member, which is a medium to coarse sand that grades upwards to clayey sands. The Poquoson Member is characterized by ridge and swale topography and achieves a maximum thickness of 4.6 m (Mixon et al. 1989). The Poquoson Member, however, is not exposed within the city of Norfolk (Mixon et al. 1989). Beneath the Poquoson Member is the Lynnhaven Member, which was deposited during a high stand of sea-level in the Pleistocene. The Lynnhaven Member is the chief member of the Tabb Formation that outcrops in the study region. The Lynnhaven Member consists of fine to coarse sands that grade upwards to sandy silts. It is cross-bedded at the base and has several channel cuts filled with clayey silt and organic material. The Lynnhaven Member is an extensive surficial deposit that averages roughly 6 m in thickness and has a toe altitude of 5.4 m above mean sea-level (Mixon et al. 1989). Underlying the Lynnhaven Member is the Segfield Member, the oldest member of the Tabb Formation. The Segfield Member is composed of clayey sand that grades upwards to clayey silt. The Segfield Member also contains numerous channel fills at its base and is cross-bedded with clayey sands and clayey silts throughout. The Segfield Member ranges up to 15.2 m thick, and is assigned an approximate age of 71,000 years based on uranium-series dating of coral *(Astrangia* sp.) that occurs within the deposit (Mixon et al. 1989).

Soils in the study region are classified as urban soils (e.g., Brady and Weil 1996); hence, detailed descriptions of the soil have not been published. However, the soils in the study area closely resemble soil units common to southeastern Virginia including the Sassafras fine sandy loam, the Woodstown fine sandy loam, and the Keyport very fine sandy loam (Henry et al. 1959). All of these specific soils are found outside of the immediate study area, within the broader Hampton Roads region of southeastern Virginia. The Sassafras fine sandy loam is a friable, red/brown soil that grades to yellow/red, and is typically well drained. The Woodstown fine sandy loam is a moderately well drained friable soil that ranges from brown through yellow/brown to yellow in color. The Keyport very fine sandy loam is a moderately well drained soil that is characterized by high water holding capacity. The Keyport ranges from gray/brown to yellow/brown in color, and is mottled at depth (Henry et al. 1959).

The study area is characterized by warm humid summers, with a mean high temperature of 25.3°C, and mild winters with an average low temperature of 6.5°C (Henry et al. 1959). The area's annual precipitation is ~1,100 mm/year with the majority falling during the winter months (Henry et al. 1959). Prevailing winds for the area are from the west (Halpern et al. 2001).

3 Materials and Methods

3.1 Sample Collection and Textural Classification

Eight 32 cm deep soil cores were collected from the city of Norfolk, with seven of these cores from the

immediate study area (labeled N_i, where i identifies the core number on Fig. 1). Two additional soil cores were also obtained from the Great Dismal Swamp outside of the immediate study (i.e., identified as DS_i on insert map of Virginia of Fig. 1). In addition, 15 surface soil samples, collected at a depth of 4 cm, were obtained from the study region (marked S_i on Fig. 1). Sample locations were chosen primarily based on accessibility (i.e., public property or permission from title holder) and location relative to the Lambert's Point Docks. The soil cores from the Great Dismal Swamp (i.e., DS_1 and DS_2; Fig. 1) were collected as controls in order to determine the amount of particulate coal present in soils from regions we initially considered to be unaffected by deposition of particulate coal originating from the Lambert's Point Docks.

All soil core samples where collected to an approximate depth of 32 cm using a stainless steel hand auger. The auger was rinsed with ultra-pure Milli-Q water (18 MΩ-cm) before commencing each coring. The soil samples were then extracted from the top of the auger and sampled at depth increments of 4.5 cm (i.e., 4 cm after accounting for soil expansion). Each soil sample was removed from the auger by scraping it off with a pre-cleaned (i.e., nitric acid rinsed) plastic spatula. Soil samples where then placed into pre-labeled, Ziplock®-style polyethylene bags, returned to the laboratory, and subsequently dried in an oven before analysis.

The textural classification of each soil sample was determined (i.e., Bounds 2001) by adding 40 g aliquots of dried soil to a 10 mL solution of sodium hexametaphosphate in 100 ml of Milli-Q water. The soil solution slurry was subsequently stirred to disperse the soil. After dispersal, the slurry was transferred to a 1,000 mL graduated cylinder, and filled to 700 mL with Milli-Q water (Bounds 2001). The slurry was shaken and allowed to settle for 40 s at which point a hydrometer reading was obtained. The hydrometer reading was used to determine the weight of the soil remaining in the water after the sand has settled out. Temperature was measured to correct the hydrometer reading. The same procedure was then repeated for the clay fraction, however; in this case, the hydrometer was read after 1.5 h, which allows for both the sand and silt fraction to settle (e.g., see Gee and Bauder 1986, for method details, and Table 2 of Bounds 2001, for details concerning the distribution of sand-, silt-, and clay-sized particles in each soil sample). Briefly, the sand-sized fraction of the sediment cores ranges from 50 to 80 wt.%. The silt-sized fraction accounts for between 10 to 40 wt.%, whereas the clay-sized fraction accounts for 9–20 wt.% of each sample (Bounds 2001).

3.2 Coal Particle Separation

In order to extract the coal particles from the soil samples, 10 g of each soil was first placed into separate 150 mL beakers along with a solution consisting of 15 mL of sodium hypochlorite ("Baker Analyzed," reagent grade) in 100 mL of Milli-Q water (18 MΩ-cm). It should be noted that all separations and sample handling were conducted in a class 100 laminar flow bench to minimize potential contamination from particles. The soil slurries were subsequently allowed to sit for a period of 1–5 days. The sodium hypochlorite procedure was chosen because Lewis and McConchie (1994) argue that it destroys the soil organic matter but does not affect coal particles. Indeed, no visible effects of the sodium hypochlorite on coal particles were observed in preliminary tests using crushed coal particles. Each soil sample was then wet sieved using sieves of 250 μm, followed by 63 μm, to separate the fine and coarse sand-size fractions from one another, and to separate the silt/clay fraction. Sample aliquots that passed through each sieve were collected in 600 mL beakers. Upon completing the sieving, the size fractions (i.e., >250 μm, >63 μm, and silt/clay fractions) were dried and weighed (Bounds 2001).

For the sand fraction of each soil sample, 25 mL of sodium polytungstate (ρ=2.0 g/cm^3; Fisher Scientific, ACS certified) was added in order to separate the coal from the rest of the soil. Sodium polytungstate was used because its density is greater than that of coal, but less than the density of the silicates and metal oxides in the soil. Consequently, the coal generally floats in the solution, whereas the silicates and metal oxides sink. Because coal particles containing finely disseminated pyrite could potentially sink in the heavy liquid solution, we cannot entirely rule out some loss of coal during the separation (see Section 4.2 below). After a period of 1 h, the sodium polytungstate and suspended coal particles were decanted and filtered through a number 41 Whatman filter to separate the coal from the heavy liquid. The

recovered coal particles were then washed with Milli-Q water, dried, and weighed (Bounds 2001).

Because only the >63 μm fraction of coal (i.e., sand-sized) was analyzed for As (see below), the <63 μm coal fraction (i.e., the silt/clay fraction) was subsequently subjected to digestion with hydrogen peroxide ("Baker Analyzed," reagent grade). The hydrogen peroxide attacks the coal but does not affect the silt or clay minerals (e.g., Lewis and McConchie 1994). Before the coal was digested with hydrogen peroxide, the weight of the silt/clay fraction was measured. The remaining silt/clay fraction was then dried and weighed, and the weight of the coal digested determined by difference (Bounds 2001). It should be noted that because the hydrogen peroxide may also dissolve sulfides, sulfates, and carbonates, the calculated difference gives a maximum value for the weight of the coal fraction.

3.3 Arsenic Analysis

As mentioned above, only the sand-sized coal fraction from each soil sample was analyzed for arsenic (As) in the recovered coal. Aliquots of the sand-sized coal fraction were crushed, reweighed, and then placed in 180 mL borosilicate glass digestion beakers along with 10 mL of concentrated Trace Metal Grade HNO_3 (Fisher Scientific) and 1 mL of concentrated Trace Metal Grade H_2SO_4 (Fisher Scientific). The sample slurry was then allowed to sit covered overnight in a class 100 laminar flow hood. The coal samples were subsequently heated at 110°C on a hotplate for 4 h. The samples were then removed from the hotplate and allowed to cool for 15 min, after which 5 mL of 30% v/v ultra-pure H_2O_2 (Suprapur® grade) was added, and the samples returned to the hotplate for another 90 min. The samples were then removed from the hotplate and 10 mL of Milli-Q water was added. At this point, the samples were allowed to cool, and were subsequently filtered through number 41 Whatman filter, to remove any remaining silicate, into 100 mL volumetric flasks, rinsed with Milli-Q water, and the volume made up to 100 mL with Milli-Q water. The samples were then transferred to pre-cleaned (i.e., acid-washed; Johannesson et al. 2004) high density polyethylene sample bottles and stored until analysis. Similar procedures were followed for the total soil As analysis, however, instead of a combined HNO_3 and H_2SO_4 digestion, only 15 mL of Trace Metal Grade HNO_3 (Fisher Scientific) was used to digest the soil (Bounds 2001). The procedural blanks, consisting initially of 10 mL of Milli-Q water, were subjected to the same reagents to assess their potential as sources of As contamination during the digestion procedure.

Arsenic concentrations in the soil coal digests and bulk soil digests were measured by high-resolution inductively coupled plasma mass spectrometry (HR-ICP-MS; VG Axiom) at the Harry Reid Center for Environmental Studies, University of Nevada, Las Vegas (Dr. J. Cizdziel, analyst). The HR-ICP-MS was calibrated and the sample concentrations verified using a series of As calibration standards of known concentrations (1, 5, 15, 100 μg/kg). The calibration standards were prepared from NIST traceable High Purity Standards (Charleston, SC). In addition, a check standard (16.8 μg/kg) was prepared from a Perkin Elmer As standard and analyzed regularly during the analyses to certify accuracy. Platinum was added to each sample prior to analysis as an internal standard to monitor for matrix effects, differences in sample viscosity, solute build-up on the sampler and skimmer cones, and instrument drift during the analyses (Guo 1996). Analytical precision was on the order of 5.9% relative standard deviation (RSD) for arsenic concentrations at 1 μg/kg, and 3.1% RSD at 100 μg/kg arsenic. The analytical precision of the check standards analyses was 2.2% RSD. Detection limits for As were ~ 3 ng/kg using our approach, and As concentrations in procedural blanks were generally at or below detection (Bounds 2001).

4 Results and Discussion

4.1 Soil Textual Classification

Soils were matched to the *Soil Survey of Norfolk County* (i.e., Henry et al. 1959) based on color and textural classification. Texturally, all collected soil cores are sandy loams, and can be classified as belonging to the Woodstown, Sassafras, and Keyport soil types of Henry et al. (1959). Based on soil colors, seven samples including the Manchester Avenue (N_1), 37th Street (N_2), 35th Street (N_3), 39th Street (N_5), Silbert Road (N_6), Beckner Street (N_7), and the Dismal Swamp East (DS_2) belong to the Keyport soil type. The Princess Anne Road (N_4) and the Dismal Swamp West (DS_1) samples, however, fit the descrip-

tion of the Woodstown soil type, whereas the Capeview Avenue (N_8) sample shares characteristics with the Sassafras soil (see Henry et al. 1959; Bounds 2001).

4.2 Soil Separation Testing

In order to establish the recovery efficiency of the extraction procedure used here to separate particulate coal from silicates, metal oxides, and organic matter in local soil samples (Section 3.2), the separation method was first applied to a simulated test soil sample containing a known amount of coal particles (see Bounds 2001 for details). Briefly, 9 g of sand and 1 g of crushed coal (collected from the Lambert's Point Docks) were mixed to create the test soil. Five separate aliquots from this test soil were then processed using the heavy liquid procedure described above in Section 3.2. Recoveries of coal particles from each of these test soil aliquots were 95, 81, 87, 84, and 87%, with a mean recovery (± standard deviation) of 86±5.2% (Bounds 2001). The mean recovery indicates that the soil coal extraction method is relatively accurate, although it generally leads to an underestimate of the actual amount of particulate coal present in the soils. The underestimates may reflect some loss during the sodium polytungstate separation owing to sinking of coal particles containing heavy minerals like pyrite. Therefore, our estimates of the amount of particulate coal present in soils from Norfolk, Virginia likely err on the low side. The actual amount of particulate coal may exceed the estimates by as much as 17%, on average (Bounds 2001).

Precision for the separation technique was quantified by using a second soil core collected from the Manchester Avenue site in Norfolk (location N_1), and subjecting six different replicates of this soil sample to the heavy liquid separation procedure. The replicate analyses produced a relative standard error of ± 8.46%, indicating that the separation procedure produces relatively consistent results (i.e., better than ± 10%; Bounds 2001).

4.3 Particulate Coal Distribution

The distribution of coal (in wt.%) in the soil cores and surface samples are presented in Tables 1 and 2, respectively. The surface soil samples (i.e., S_1 through S_{15}, Table 2), which were collected at depths of 4 cm, are comparable to the shallowest samples from each soil core (Table 1). The amount of particulate coal that occurs in the surface soil samples (i.e., 4 cm depth) of the study area varies from a high of ~ 20% by weight, to a low of 1 wt %, exhibiting a mean value (± standard deviation) of 7.1±3.9 wt. %. The surface sample (4 cm) from the 37th Street core (i.e., N_2) exhibits the highest amount of particulate coal (i.e., 19.9 wt. %). The 37th Street core is located less than 1 km east of the Lambert's Point Docks (Fig. 1). The surface sample (4 cm depth) of the Silbert Road core (N_6), which is located approximately 5.5 km to the east of the Lambert's Point Docks (Fig. 1), has 3.4 wt. % particulate coal, whereas the surface sample from the

Table 1 Amount of particulate coal (in weight %) recovered from soil cores collected within Norfolk (N) and the Great Dismal Swamp (DS) in southeastern Virginia

Depth (cm)	N_1	N_2	N_3	N_4	N_5	N_6	N_7	N_8	DS_1	DS_2
4	4.56	19.9	7.88	7.82	10	3.45	7.42	1.08	1.23	1.59
8	2.2	20	7.29	7.22	9.84	3.95	6.72	0.83	1.33	1.47
12	3.79	18.1	7	7	9.59	3.57	5.38	0.48	1	2.02
16	3.75	16.2	6.87	6.87	8.33	3.55	5.57	0.68	1.31	1.74
20	3.98	14	6.62	6.62	6.42	3.34	4.21	0.05	1.12	1.26
24	3.03	10.4	5.91	5.91	6.15	2.78	3.1	0.01	1.29	1.63
28	1.77	7.46	5.2	5.2	5.32	2.79	1.82	0.04	1.12	1.42
32	2.12	8.82	4.64	4.64	3.88	3.88	1.56	0.05	1.07	1.59

N_1 Manchester Avenue, *N_2* 37th Street, *N_3* 35th Street, *N_4* Princess Anne Road, *N_5* 39th Street, *N_6* Silbert Road, *N_7* Beckner Street, *N_8* Capeview Avenue, *DS_1* collected along the Washington Ditch in the Great Dismal Swamp[a], and *DS_2* collected at Arbuckle Landing, near the outflow of the Feeder Ditch[a]

[a] See Johannesson et al. (2004).

Table 2 Amount of particulate coal (in weight %) recovered from surface samples (collected at ~4 cm depth) from Norfolk, Virginia

	Weight % coal
S_1	4.73
S_2	5.36
S_3	4.89
S_4	6.07
S_5	6.23
S_6	7.03
S_7	14.6
S_8	7.49
S_9	9.56
S_{10}	8.93
S_{11}	3.87
S_{12}	4.82
S_{13}	4.35
S_{14}	3.77
S_{15}	3.24

Capeview Avenue core (N_8), roughly 12 km northeast of the docks, exhibits 1.1 wt % particulate coal (Table 1). The decrease in the amount of particulate coal within the surface soils with increasing distance from Lambert's Point Docks, and the fact that the prevailing wind direction for the region is from the west (Halpern et al. 2001), suggests that the docks are the chief source of particulate coal to these soils. Similar areal distribution patterns of particulate coal occur at depths in these soils (Bounds 2001). Soil samples collected proximal to the railroad tracks in the study region (e.g., N_7, S_{10}, S_7, and S_9) also exhibit relatively high particulate coal levels (Tables 1 and 2). These elevated soil coal levels indicate that coal cars transporting coal into the city along existing rail lines are also a source of particulate coal to local soils. Others have also recognized the importance of railway lines as sources of potential contaminants (Smith et al. 2006).

The amount of particulate coal in each soil core collected from the city of Norfolk (i.e., N_1 through N_8) decreases with increasing depth (Fig. 2). The decrease in particulate coal with depth is most evident for soil core N_2, located less than a km from the Lambert's Point Docks (Figs. 1 and 2). For the Capeview Avenue core (N_8), the amount of particulate coal decreases from ~1.1 wt. % at a depth of 4 cm to below detection at 20 cm, where it remains with increasing depth (to 32 cm, Fig. 2, Table 1). The two soil cores from the Great Dismal Swamp (DS_1 and DS_2) exhibit low, but constant amounts of particulate coal with depth (Fig. 2; Table 1). Both Great Dismal Swamp soil cores have amounts of particulate coal at the surface (i.e., 4 cm depth) that are comparable to the Capeview Avenue (N_8) core (1.23 and 1.59 wt. % vs. 1.08 wt. %, respectively), but have higher amounts of particulate coal at depth (Table 1, Fig. 2). The Great Dismal Swamp cores exhibit similar amounts of particulate coal at depth to the Manchester Avenue (N_1), Silbert Road (N_6), and Beckner Street (N_7) cores from within the city of Norfolk (Table 1; Fig. 2). Hence, the Great Dismal Swamp soil cores indicate that much of the Hampton Roads region of southeastern Virginia has experienced atmospheric deposition of particulate coal originating from the Lambert's Point Docks, or possibly other coal shipping docks in the region (e.g., Newport News, Virginia).

Assuming a uniform distribution of particulate coal in the surface soils equal to the mean amount of coal estimated from our soil core and surface samples (i.e., 4 cm depth, 7.1±3.9 wt. %, n=22), and an approximate bulk density for the soil of 1.9 g/cm^3 (ρ_{solids}= 2.65 g/cm^3 with porosity ~30%), the amount of particulate coal contained within the top 4 cm of the soils can be roughly estimated for the immediate study area (Norfolk south of the Lafayette River, north of the Eastern Branch of the Elizabeth River, and west of the railway line to the U.S. Naval Reservation; Fig. 1, ~33 km^2). These values lead to an estimate of 1.8×10^8 ($\pm10^5$) kg of particulate coal in the top 4 cm of soil within the immediate study area. It is important to stress that this estimate is severely compromised by the limited sample coverage in the study region and the assumption of a uniform distribution of coal, which the data demonstrate varies as a function of distance from the Lambert's Point Docks. Thus, the actual inventory of particulate coal in these soils could conceivable differ by orders of magnitude. It is noteworthy, however, that this rough, first approximation of the particulate coal inventory in Norfolk surface soils seems high compared to the permitted amount of particulate coal that the State of Virginia allows the Lambert's Point Docks to release annually (i.e., 50 tons: VDEQ (Virginia Department Environmental Quality) 2002). The estimate suggests that the our approach overstates the amount of particulate coal in Norfolk soils (laboratory experiments indicate, however, that the method under-

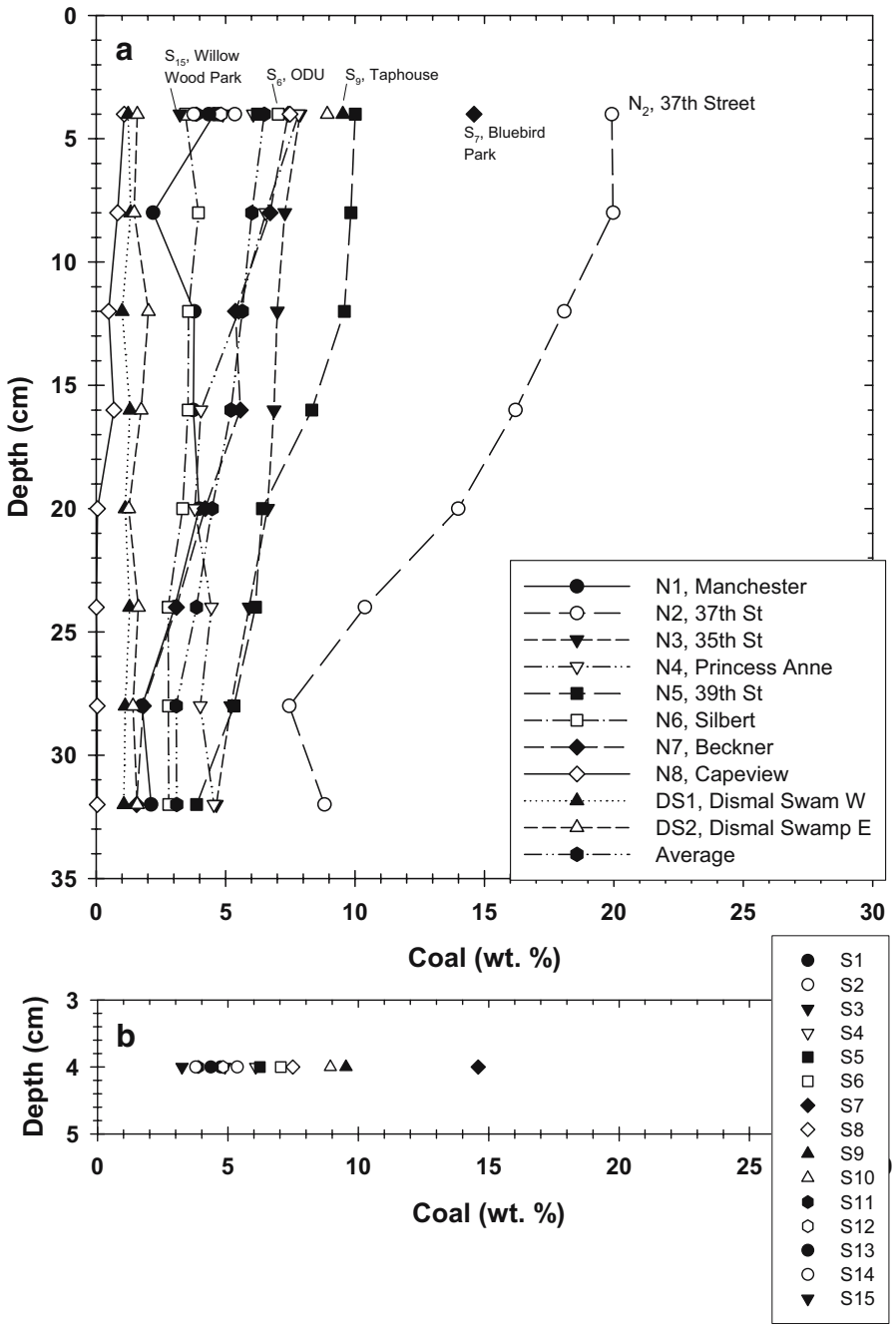

Fig. 2 Concentrations, in weight percent, of particulate coal from **a** soil profiles resulting for the soil cores (N_1 through N_8, DS_1 and DS_2), and **b** the surface soil samples (S_1 through S_{15}). The surface samples are included in panel **a** but are reproduced in panel **b** for clarity

estimates the amount of coal present, Section 4.2), that other sources of particulate coal dust, such as the coal shipping terminal in nearby Newport News, Virginia, local railway lines, etc., contribute coal dust to Norfolk soils, and/or that the Lambert's Point Dock commonly exceeds its permitted release levels of particulate coal to the atmosphere. Clearly, more study of the fluxes of particulate coal in the Hampton Roads region of Virginia is warranted to better constrain the sources and mass balance of particulate coal.

4.4 Soil Arsenic Concentrations

Coal shipped to and from the Lambert's Point Docks originates from mines in Alabama, Indiana, Illinois, Kentucky, Tennessee, Ohio, Pennsylvania, Virginia,

and West Virginia (Norfolk Southern 2007). Coal from these states, which are located within the Appalachian and Eastern Interior coal basins, have As concentrations that range, on average, from 20 to 70 mg/kg (Kolker et al. 2006; Mastalerz and Drobniak 2007; and references therein). The mean As concentration of coal from Virginia is 20.2 mg/kg (Henderson et al. 1985; Hower et al. 1997). These mean values are between an order of magnitude to as much as ~45 times greater than upper continental crust As concentrations (1.5–2.0 mg/kg; Taylor and McLennan 1985; Wedepohl 1995). Hence, because of the relatively high As concentrations that characterize some coal from the Appalachian and Eastern Interior coal basins, we chose to evaluate whether the particulate coal dispersed to Norfolk soils has enriched As in these soils.

Arsenic values for the sand-sized coal particles extracted from cores N_1 through N_7 range from a high of 17.4 mg/kg at 8 cm depth within the 37th Street core (N_2), to below detection (i.e., <3 ng/kg) at 16 cm and 32 cm depths within the Silbert Road core (N_6; Fig. 3; Table 3). Because no sand-sized coal particles were recovered from the Capeview Avenue core (N_8), or the Great Dismal Swamp cores (DS_1, DS_2), we did not determine the coal-dust associated As in these cores using the methods employed in this study. Nonetheless, the mean As concentration for sand-sized coal particles collected from all depths in cores N_1 through N_7 is 7.3 mg/kg.

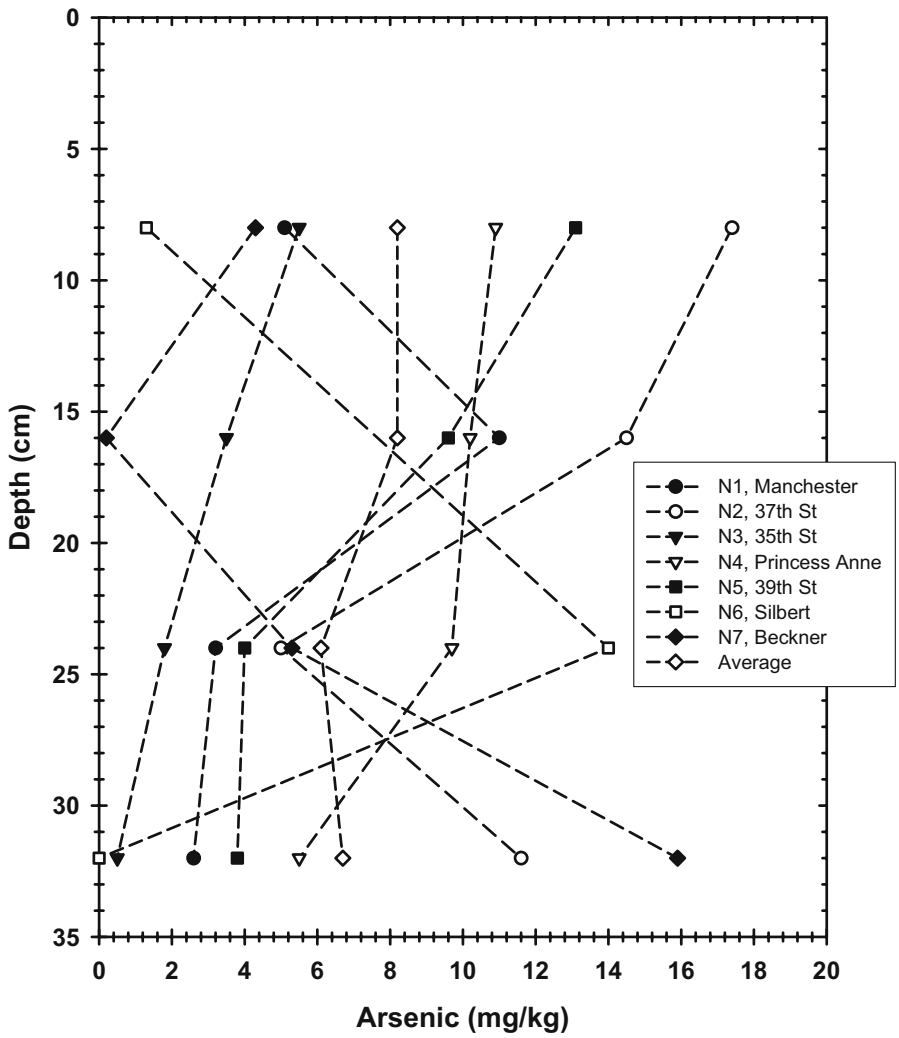

Fig. 3 Concentrations of arsenic in mg/kg in sand-size coal particles separated from soil core samples collected at 8, 16, 24, and 32 cm depth

Table 3 Arsenic concentrations (in mg/kg) of sand-sized particulate coal recovered from soil cores collected from Norfolk, Virginia[a]

Depth (cm)	N_1	N_2	N_3	N_4	N_5	N_6	N_7	Mean	Max	Min
8	5.1	17.4	5.5	10.9	13.1	1.3	4.3	8.2	17.4	1.3
16	11	14.5	3.5	10.2	9.6	BD	0.2	8.2	14.5	BD
24	3.2	5	1.8	9.7	4	14	5.3	6.1	14	1.8
32	2.6	11.6	0.5	5.5	3.8	BD	15.9	6.7	15.9	0.5

[a] No sand-sized particulate coal was recovered from N8, DS1, or DS2, hence, we did not analyze this absent coal size fraction for As.
BD below detection

Arsenic concentrations of sand-sized coal particles from Norfolk soil cores are all lower than the mean As values reported for coal from the Appalachian and Eastern Interior coal basins (Kolker et al. 2006), as well as the average As concentration reported for Virginia coals (i.e., 20.2 mg/kg; Henderson et al. 1985). We expect that the As concentration of the sand-sized coal particles recovered from Norfolk soils to generally be lower than bulk coal samples from the Appalachian and Eastern Interior coal basin owing to: (1) selective mining that extracts low As coals; (2) coal cleaning that can reduce As in coal by as much as 50%; (3) physical separation of As-bearing pyrite during transport and shipping; and (4) possible loss of some As-rich coal particles during our laboratory separations where denser pyrite containing particles may sink (R.B. Finkelman, 2007, personal communication). Nevertheless, As concentrations of sand-sized coal particles recovered from Norfolk soils are similar to those measured in coals samples (n=3) obtained from the Lambert's Point Docks (i.e., 12.6 mg/kg; Bounds 2001). Arsenic concentrations measured in sand-sized particulate coal from the Norfolk soil core samples are, therefore, enriched by 4–5 times, on average, over that of the upper continental crust.

A recent survey of As levels in surficial deposits (i.e., soils and sediments) of North America indicates that background As concentrations range from crustal values (1–2 mg/kg) up to ~7 mg/kg in soil/sediments of southeastern Virginia, with the highest levels centered in Norfolk (Grosz et al. 2004). These preliminary data suggest that background As concentrations in soils/sediments from the Norfolk region are, to a first approximation, similar to average soil As concentrations in the USA (e.g., 5–7 mg/kg; Shacklette and Boerngen 1984; Yang and Donahoe 2007). However, the observation that directly to the west of the city of Norfolk, the background surficial As concentrations drop to crustal or lower values from a high of ~7 mg/kg within the city center (Grosz et al. 2004), supports the hypothesis that coal shipping through the Lambert's Point Docks is at least partially responsible for elevating soil zone As concentrations within the city.

Arsenic concentrations for the total (i.e., bulk) soil digests (silicate minerals, metal oxides, amorphous phases, organic matter, and particulate coal), performed on aliquots from 8 cm depth for each soil core, ranged from a high of 30.5 mg/kg to a low of 3.0 mg/kg, with a mean As value of 13.3 mg/kg (Table 4). The total soil digests indicate that Norfolk soils (from a depth of 8 cm) are enriched in As by a factor of 2 to 20 times over upper continental crustal abundances (Taylor and McLennan 1985; Wedepohl 1995), and by as much as five times over background soil concentrations (Shacklette and Boerngen 1984; Grosz et al. 2004; Yang and Donahoe 2007). Therefore, it can be inferred from these data that a substantial amount of the total As in Norfolk soils (at 8 cm depths) reflects the presence of sand-sized, particulate coal in these soils (Fig. 4). More specifi-

Table 4 Arsenic concentrations (in mg/kg) of total soil digests of soil samples collected from 8 cm depth in each soil core from the study region

	As (mg/kg)
N_1	8.1
N_2	16.6
N_3	7.8
N_4	20.7
N_5	30.5
N_6	3
N_7	12.1
N_8	25.9
DS_1	3.2
DS_2	5.1
Mean	13.3
Max	30.5
Min	3

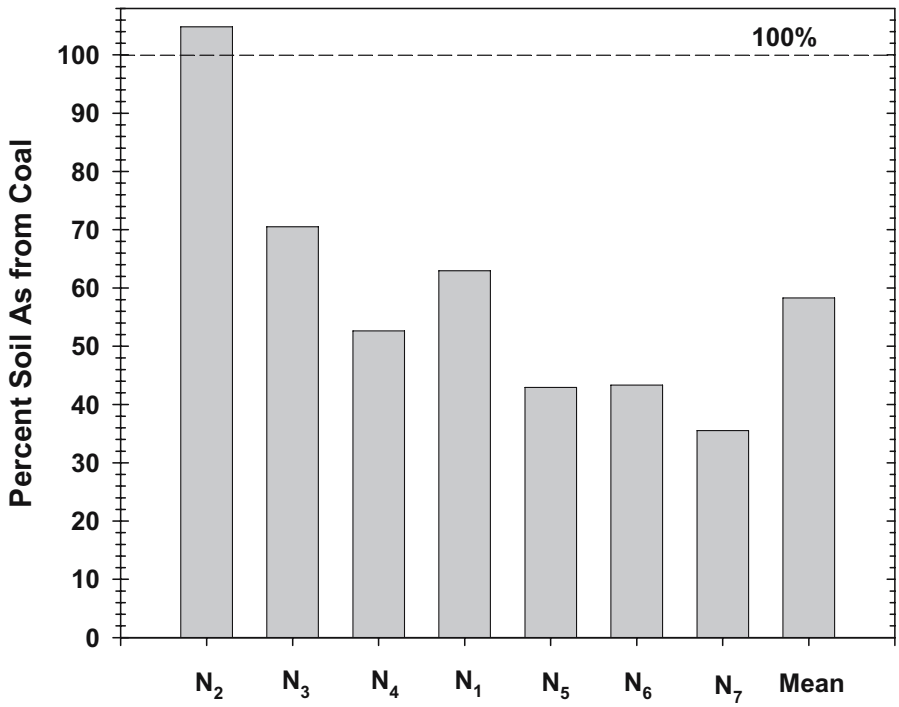

Fig. 4 Percent of soil arsenic that can be attributed to particulate coal within the sand-size fractions of the 8 cm depth samples of soil cores N_1 through N_7, plotted as a function of relative distance from Lambert's Point Docks. In addition, the mean value is also shown. Note there is a general decrease in the percentage of As in these samples that can be ascribed to particulate coal as distance increases away from the Lambert's Point Docks

cally, the amount of As in these soils from 8 cm depth that owes its origin to sand-sized coal particles ranges from ~36% for the Beckner Street (N_7) sample up to ~100% for the 37th Street core (N_2), with an overall mean of ~58% (Table 4; Fig. 4). Another important feature of the percentage of As in these soil core samples that is attributable to particulate coal is that this percentage generally decreases with distance from the Lambert's Point Docks (Fig. 4). Note that essentially all of the As within the 8 cm sample from the 37th Street core (N_2), which is located within 1 km of the Lambert's Point Docks, can be attributed to particulate coal, whereas only ~36% of the As from the 8 cm sample of the Beckner Street core (N_7), approximately 5.5 km from the Docks, can be ascribed to particulate coal. Thus, particulate coal originating from Lambert's Point Dock is an important source of As to the local soils, especially for soils located in close proximity to the Docks.

Because we have only analyzed As in sand-sized coal particles extracted from the soil samples, and owing to the fact that our soil-coal separation techniques tends to underestimate the amount of coal dust in the soils (Section 4.1), the actual percentage of As in these soils due to particulate coal originating from Lambert's Point Docks may be higher than indicated in Fig. 4. Nevertheless, these data suggest that coal shipping through the Lambert's Point Docks is adding particulate coal and As to the soils of Norfolk, Virginia. The significance of this additional As to human and/or environmental health in southeastern Virginia is currently unknown. However, application of phosphorous-rich fertilizers to these soils, many of which are overlain by lawns, could potentially lead to the mobilization of the added As in Norfolk soils (e.g., Peryea and Kammereck 1997). Furthermore, a recent study demonstrated that children playing in playgrounds with chromated copper arsenate treated wooden playground structures or with sand that has come in contact with such structures, acquire more soluble As on their hands compared to children not exposed to such structures or the associated sand (Kwon et al. 2004). Moreover, children that live near open-pit coal mines more frequently complain of respiratory distress to family physicians than children living more distal to such operations (Howel et al. 2001; Moffatt and Pless-Mulloli 2003). Hence it seems reasonable to investigate more fully the possible health effects of particulate coal and associated As, if any, on the local populace of Hampton Roads. Finally, on a related topic, Reidel et al. (2000) presents data that strongly suggests that meteoric water interacting with standing coal piles in the region can significantly increase the As loading to

local surface water bodies. Further investigation of Norfolk's groundwater, as well as the estuarine waters surrounding the city, may shed additional light on the potential impact of particulate coal derived As on these waters and the local environment.

5 Conclusions

Substantial amounts of particulate coal originating from the Lambert's Point Docks are documented in soil samples from Norfolk, Virginia, with regions closest to the shipping terminal containing the most particulate coal by weight. Along with the particulate coal, arsenic associated with the coal is also enriched in these soils by 2 to 20 times over upper crustal abundances, and by ~five times over estimated background soil As concentrations. The data presented here indicate that the Lambert's Point Docks is a significant source of particulate coal to the local environment, and further, that this coal contributes As to the local soils.

Acknowledgements The authors wish to thank Drs. J. Sanders and J. Rule for reading an earlier version of this manuscript and providing important and helpful input for this project. We are also especially grateful to Drs. K. Stetzenbach and J. Cizdziel of the Harry Reid Center (HRC) for Environmental Studies at the University of Nevada, Las Vegas for arranging and performing the arsenic analyses. We wish to thank N. McGinnis and J. Daniels, also at the HRC, for helping with the soil sample collection, and S. Haque and M. Vessely (The University of Texas at Arlington) for editorial assistance. The Department of Ocean, Earth, and Atmospheric Sciences at Old Dominion University, the Commonwealth of Virginia, and the American Association of Petroleum Geologists provided funding for the project. We thank J. Quintans of The University of Texas at Arlington Office of University Publications for drafting the map. Finally, we express our gratitude to R.B. Finkelman and two anonymous reviewers whose comments greatly improved this manuscript.

References

Attfield, M., Kuempel, E., & Wagner, G. (1997). Exposure-response for coal workers' pneumoconiosis in underground coal miners: A discussion of issues and findings. *The Annals of Occupational Hygiene, 41*(Suppl. 1), 341–345.

Attfield, M. D., Petsonk, E. L., & Wagner, G. R. (1998). Coal workers' lung diseases. In J. M. Stellman (Ed.), *Encyclopaedia of occupational health and safety* (4th ed., pp. 10.46–10.50). Geneva: International Labor Office.

Brady, N. C., & Weil, R. R. (1996). *The nature and properties of soils*. Upper Saddle River, NJ: Prentice-Hall.

Bounds, W. J. (2001). *The distribution of airborne coal dust in soil profiles of Norfolk, VA and its implications for arsenic loading to these soils*. MS thesis. Virginia: Old Dominion University.

Centeno, J. A., Mullick, F. G., Ishak, K. G., Franks, T. J., Burke, A. P., Koss, M. N., et al. (2005). Environmental pathology. In O. Selinus, B. J. Alloway, J. A. Centeno, R. B. Finkelman, R. Fuge, U. Lindh, et al. (Eds.), *Essentials of medical geology: Impacts of the natural environment on public health* (pp. 563–594). Amsterdam: Elsevier.

Dinsmore, C. (1999). *Loads of coal Norfolk southern terminal marks its 1 billionth ton*. Norfolk, VA: The Virginian-Pilot, September 4, D1.

Eskenazy, G. M. (1995). Geochemistry of arsenic and antimony in Bulgarian coals. *Chemical Geology, 119*, 239–254.

Feng, X., Hong, Y., Hong, B., & Ni, J. (2000). Mobility of some potentially toxic trace elements in the coal of Guizhou, China. *Environmental Geology, 39*, 372–377.

Finkelman, R. B., Belkin, H. E., & Centeno, J. A. (2006). Health impacts of coal: Should we be concerned? *Geotimes, 51*, 24–28.

Finkelman, R. B., Orem, W., Castranova, V., Tatu, C. A., Belkin, H. E., Zheng, B., et al. (2002). Health impacts of coal and coal use: Possible solutions. *International Journal of Coal Geology, 50*, 425–443.

Fuge, R. (2005). Anthropogenic sources. In O. Selinus, B. J. Alloway, J. A. Centeno, R. B. Finkelman, R. Fuge, U. Lindh, et al. (Eds.), *Essentials of medical geology: Impacts of the natural environment on public health* (pp. 43–60). Amsterdam: Elsevier.

Gee, G. W., & Bauder, J. W. (1986). Particle size analysis. Methods of soil analysis, Part 1. *Physical Mineralogical, 9*, 383–411.

Greb, S. F., Eble, C. F., Peters, D. C., & Papp, A. R. (2006). *Coal and the environment* (p. 64). Alexandria, Virginia: AGI Environmental Awareness Series, American Geological Institute.

Grosz, A. E., Grossman, J. N., Garrett, R., Friske, P., Smith, D. B., Darnley, A. G., et al. (2004). A preliminary geochemical map of arsenic in surficial materials of Canada and the United States. *Applied Geochemistry, 19*, 257–260.

Guo, C. (1996). *Determination of fifty-six elements in three distinct types of geological materials by inductively coupled plasma-mass spectrometry.* MS thesis, Nevada: University of Nevada, Las Vegas.

Gupta, D. C. (1999). Environmental aspects of selected trace elements associated with coal and natural waters of Pench Valley Coalfield of India and their impact on human health. *International Journal of Coal Geology, 40*, 133–149.

Halpern, D., Woiceshy, P. M., Zlotnicki, V., Brown, O. B., Feldman, G. C., Freilich, M. H., et al. (2001). *An atlas of monthly mean distribution of SSMI surface wind speed, A VHRR sea surface temperature, TNI sea surface temperature, AMI surface wind velocity, Sea WiFS Chlorophyll-a, and TOPEX/POSEIDON sea surface topography during 1999*. Pasadena, California: Jet Propulsion Laboratory.

Henderson, J. A. Jr., Wilkes, G. P., Bragg, L. J., & Oman, C. L. (1985). *Analyses of Virginia coal samples collected 1978–1980*. Charlottesville, Virginia: Virginia Division of Mineral Resources, Publication 63.

Henry, E. F., Chudoba, J., Porter, H. C., & Ligon, W. S. (1959). *Soil survey*. Norfolk County Virginia: United States Department of Agriculture.

Howel, D., Pless-Mulloni, T., & Darnell, R. (2001). Consultations of children living near open-cast coal mines. *Environmental Heath Perspectives, 109*, 567–571.

Hower, J. C., Robertson, J. D., Wong, A. S., Eble, C. F., & Ruppert, L. F. (1997). Arsenic and lead concentrations in the pond creek and fire clay coal beds, eastern Kentucky coal field. *Applied Geochemistry, 12*, 281–289.

Johannesson, K. H., Tang, J., Daniels, J. M., Bounds, W. J., & Burdige, D. J. (2004). Rare earth element concentrations and speciation in organic-rich blackwaters of the Great Dismal Swamp, Virginia, USA. *Chemical Geology, 209*, 271–294.

Kizilshtein, L. Y., & Kholodkov, Y. I. (1999). Ecologically hazardous elements in coal of the Donets Basin. *International Journal of Coal Geology, 40*, 189–197.

Kolker, A., Palmer, C. A., Bragg, L. J., & Bunnell, J. E. (2006). Arsenic in coal. *U.S. Geological Survey Fact Sheet*, 2005–3152.

Kwon, E., Zhang, H., Wang, Z., Jhangri, G. S., Lu, X., Fok, N., et al. (2004). Arsenic on the hands of children after playing in playgrounds. *Environmental Health Perspectives, 112*, 1375–1380.

Lewis, D. W., & McConchie, D. (1994). *Analytical sedimentology*. New York: Chapman & Hall.

Mastalerz, M., & Drobniak, A. (2007). Arsenic, cadmium, lead, and zinc in the Danville and Springfield coal members (Pennsylvanian) from Indiana. *International Journal of Coal Geology, 71*, 37–53.

Mixon, R. B., Berquist, C. R., Newell, W. L., Johnson, G. H., Powars, D. S., Schindler, J. S., et al. (1989). *Geologic map and generalized cross sections of the Coastal Plain and adjacent parts of the Piedmont Virginia*. Washington, DC: US Geological Survey.

Moffatt, S., & Pless-Mulloli, T. (2003). It wasn't the plague we expected. Parents' perceptions of the health and environmental impact of opencast coal mining. *Social Science & Medicine, 57*, 437–451.

Norfolk Southern Corporation (2007). Website accessed 1 May 2007 http://www.nscorp.com/nscportal/nscorp/Customers/Coal/Mine%20Operations/index.html).

Peryea, F. J., & Kammereck, R. (1997). Phosphate-enhanced movement of arsenic out of lead arsenate-contaminated topsoil and through uncontaminated subsoil. *Water, Air, & Soil Pollution, 93*, 243–254.

Querol, X., Alastuey, A., Lopez-Soler, A., Plana, F., Mantilla, E., Juan, R., et al. (1999). Characterisation of atmospheric particulates around a coal-fired power station. *International Journal of Coal Geology, 40*, 175–188.

Querol, X., Fernandez, J. L., Lopez, A., & Duran, M. E. (1992). Trace elements in high-S subbituminous coals from the Teruel Mining District, northeast Spain. *Applied Geochemistry, 7*, 547–561.

Querol, X., Fernandez, J. L., Lopez, A., Hagemann, H. W., Dehmer, J., Juan, R., et al. (1991). Distribution of sulfur in coals of the Teruel Mining District, Spain. *International Journal of Coal Geology, 18*, 327–346.

Riedel, G. F., Williams, S. A., Reidel, G. S., Gilmour, C. C., & Sanders, J. G. (2000). Temporal and spacial patters of trace elements in the Patuxent River: A whole watershed approach. *Estuaries, 23*, 521–535.

Shacklette, H. T., & Boerngen, J. G. (1984). Element concentrations in soils and other surficial materials of the conterminous United States. U.S. Geological Survey Professional Paper 1270.

Smith, E., Naidu, R., & Alston, A. M. (1998). Arsenic in the soil environment: A review. *Advances in Agronomy, 64*, 149–195.

Smith, E., Smith, J., & Naidu, R. (2006). Distribution and nature of arsenic along former railway corridors of South Australia. *Science of the Total Environment, 363*, 175–182.

Taylor, S. R., & McLennan, S. M. (1985). *The continental crust: Its composition and evolution*. Boston: Blackwell Scientific Publications.

VDEQ (Virginia Department Environmental Quality) (2002). http://www.deq.state.va.us/.

Wedepohl, K. H. (1995). The composition of continental crust. *Geochimica et Cosmochimica Acta, 59*, 1217–1232.

Yang, L., & Donahoe, R. J. (2007). The form, distribution and mobility of arsenic in soils contaminated by arsenic trioxide, at sites in southeast USA. *Applied Geochemistry, 22*, 320–341.

Yudovich, Ya. E., & Ketris, M. P. (2005). Arsenic in coal: A review. *International Journal of Coal Geology, 61*, 141–196.

Zheng, B., Ding, Z., Haung, R., Zhu, J., Yu, X., Wang, A., et al. (1999). Issues of health and disease related to coal use in southwestern China. *International Journal of Coal Geology, 40*, 119–132.

Hydrobiologia (2006) 559:161–168
DOI 10.1007/s10750-005-1095-3
© Springer 2006

Primary Research Paper

Physiological and behavioral effects of zinc and temperature on coho salmon (*Oncorhynchus kisutch*)

Lizabeth Bowen[1,2,*], Inge Werner[3] & Michael L. Johnson[2]
[1]*Department of Pathology, Microbiology and Immunology, School of Veterinary Medicine, University of California, Davis, CA 95616, USA*
[2]*John Muir Institute of the Environment, University of California, Davis, CA 95616, USA*
[3]*Department of Anatomy, Physiology and Cell Biology, School of Veterinary Medicine, University of California, Davis, CA 95616, USA*
*(*Author for correspondence: Tel.: +530-754-8096; Fax: +530-752-3349; E-mail: lbowen@ucdavis.edu)*

Received 3 December 2004; in revised form 5 August 2005; accepted 27 August 2005

Key words: zinc, temperature, hsp-70, salmon, behavior, growth

Abstract

Pacific salmon species including the U.S. federally endangered coho salmon (*Oncorhynchus kisutch*) and the U.S. federally threatened steelhead trout (*Oncorhynchus mykiss*) have declined at an alarming rate in the last 40 years. Two of the main causes for the decline in coastal coho populations include increases in temperature and contaminant loads in coastal watersheds. Zinc, in particular, is one of the most common contaminants in aquatic systems. Using an experimental mesocosm design, we examined physiological, biochemical, and behavioral responses of coho salmon to excess dietary zinc and increased temperatures, with the ultimate goal of relating results to wild populations of coho salmon and steelhead in the Navarro River, California. Fish were obtained from a hatchery and divided into four treatments: low water temperature-no dietary zinc, high temperature-no zinc, low temperature-zinc, and high temperature-zinc. Each treatment had four replicate tanks. Zinc concentrations in liver increased during exposure to a high zinc diet. Iron concentrations in liver increased during simultaneous exposure to high zinc diet and increased temperature, and growth was reduced in this experimental treatment. Expression of hsp-70 was not significantly different between treatments, but showed decreasing trends with high dietary zinc and high temperature. Feeding rate increased with exposure to a high zinc diet. Comparison with steelhead trout samples from the Navarro River, California, showed levels of zinc, iron, and hsp-70 greater than those found in the experimental Coho salmon. All comparisons between the hatchery coho salmon and wild steelhead should be viewed with caution due to the differences between species, the laboratory and natural environment, and the genetic differences between wild and hatchery fish.

Introduction

Pacific salmon species including the U.S. federally endangered coho salmon (*Oncorhynchus kisutch*) have declined at an alarming rate in the last 40 years (Brown & Moyle, 1991). During this time, 40% of California streams have lost their historic coho runs; 25% of the streams have intermittent runs of very few fish and only a few streams still retain self-sustaining runs of this once abundant salmon species (Brown & Moyle, 1991). Coho populations along the coast of California are currently perhaps at 6% of the levels seen in the 1890s (Brown et al., 1994). The main causes for the decline in coastal coho populations include alteration of stream systems and water quality from

factors such as logging and urbanization, periodic floods and drought, hatchery operations, disease, over harvest, and climate change (Brown et al., 1994). Many of these can lead to reduced stream flows and higher water temperatures, and the delivery of contaminants to the stream system.

Zinc is one of the most common contaminants in aquatic systems and is associated with urban runoff, soil erosion, industrial discharges, pharmaceuticals, and pesticides (Krenkel et al., 1975, Irwin, 1997). In some locations up to 50% of the zinc delivered to stream systems comes from highway runoff (Krenkel et al., 1975). Zinc is easily bioaccumulated in stream invertebrates – an important food source for juvenile salmonids while rearing in freshwater systems. Recent studies demonstrate that fish fed diets contaminated with zinc exhibited reduced survival, growth, and increased incidence of disease (Farag et al., 1994, Balasubramanian et al., 1995).

Water temperatures in most Northern California coastal watersheds are higher than historic levels, mostly due to the degradation of riparian vegetation and therefore reduced shading (Brown & Moyle, 1991). Coldwater, anadromous fishes in particular, may be subjected to sublethal heat stress due to large temperature fluctuations in shallow or unshaded streams (Wedemeyer, 1973). Studies of the acute effects of extreme temperatures (upper thermal tolerance limit) of salmonids have been numerous, but the consequences of sublethal temperature stress (thermal additions) have received less attention (Wedemeyer, 1973). One of the most common features of the sublethal response to temperature stress and exposure to xenobiotic compounds such as heavy metals is the increased cellular production of heat-shock or stress proteins (hsps) (Iwama et al., 1998, 1999). Hsps play a vital role in maintenance of protein integrity, preventing premature folding and aggregation of proteins (Iwama et al., 1998, 1999). Under normal conditions, cells produce relatively small amounts of hsps. However, the level of hsp production increases and regular protein synthesis is repressed during environmental conditions that result in thermal or proteotoxic stress to an organism (Sanders, 1993). Genes encoding hsps are grouped into four gene families, hsp-83, hsp-70, hsp-60 and the small hsps. The hsp70 family is the most highly conserved of the hsps and is found widely across species (Feige et al., 1996). Increased levels of hsp-70 protect cells from the deleterious effects of elevated temperatures or other stressors (Sanders, 1993).

While the effects of temperature and contaminants on fish have been studied as individual stressors (Hodson & Sprague, 1975), there is relatively little information about the combined effects of such stressors on growth and fitness of Pacific salmon. The combined effects of multiple stressors on organisms can be complex. For example, while zinc has been found to be more acutely toxic to fish at higher temperatures than at lower temperatures, water temperature can also reduce the toxicity of zinc (Hodson & Sprague, 1975, Donker et al., 1998) by increasing its metabolic elimination or detoxification rate, and by changing the physiological state of the animal (e.g. by induction of protective enzymes such as heat shock proteins) (Donker et al., 1998). Sublethal stress caused by exposure to elevated water temperature and high concentrations of zinc may also modify behavior (Hogstrand & Wood, 1996, Shumway, 1999). Metals have been shown to reduce aggression at sublethal concentrations (Henry & Atchison, 1986, Atchison et al., 1987). Toxicants can also affect swimming performance and compromise the ability to escape predators, impair predator detection abilities, and increase conspicuousness due to erratic behavior or hyperactivity (Mesa, 1994, Weis et al., 1999).

The objective of this study was to examine the physiological, biochemical, and behavioral responses of coho salmon to excess dietary zinc and increased temperatures, and to determine if the combination of stressors acts synergistically.

Materials and methods

Experimental conditions

Juvenile coho salmon (approximately two to three months old) were obtained from the Cascade Fish Hatchery in Cascade Locks, Oregon, and transported in chilled (10 °C) water to the University of California, Davis, CA. Fish were acclimated at 10 °C for 7 days and then randomly separated into 16 tanks (40 l each), 6 fish per tank at 10 °C. Temperature in eight tanks was increased by 1 °C per

day to a final temperature of 15 °C. Fish were acclimated to final experimental temperatures for 14 days. During the course of the experiments, ambient air temperatures reached 43 °C, contributing to intermittent breakdown of the water-cooling system. As a result, temperatures in the 10° tanks averaged between 8.6° and 11.5° during the experiment. Temperatures in the 15° tanks averaged between 13.8° and 16.2° prior to the experiment and between 14.6° and 15.9° during the experiment.

During acclimatization, all fish were fed 2.5% of their body weight twice per day with Biodiet Oregon 1-mm pellet size. Prior to introducing the experimental diet, all fish were weighed to the nearest 0.5 g and measured to the nearest millimeter. Fish were not individually marked, and all growth measurements were based on averages for each replicate tank.

On day 1 of the experimental phase, the diet in eight tanks (4 at 10 °C, 4 at 15 °C) was changed to a zinc-enhanced diet. The zinc-enhanced diet was prepared by mixing distilled water and $ZnCl_2$ with 1-mm pellet size Biodiet Oregon. The mixture was then freeze-dried, ground, and passed through a 1 mm mesh sieve. The final zinc concentration was 1900 ppm as analyzed by the California Veterinary Diagnostic Laboratory (CVDLS) at the University of California at Davis. During the exposures, fish were fed 2.5% of their body weight twice per day of either Biodiet Oregon or zinc-enhanced Biodiet Oregon. Fish were exposed for 21 days to one of four combinations of diet and temperature, high zinc/high temperature (15 °C), control/high temperature, high zinc/low temperature (10 °C), and control/low temperature. End points included length, weight, tissue metal accumulation, heat shock protein expression, aggression, and feeding frequency.

Chemical analysis of liver samples

Portions of fish livers were composited by tank and sent to the CVDLS at the University of California at Davis for analysis. Livers were analyzed according to methods described by Martin et al. Briefly, livers were analyzed using an ICP analytical procedure for nine metals. Samples were prepared by nitric acid/hydrochloric acid digestion. Based on a one gram sample size, this screen quantitates for Fe >0.2 ppm, Mn >0.04 ppm, Cu >0.1 ppm, Zn >0.1 ppm, Cd >0.3 ppm, and Mo >0.4 ppm, while semi-quantitative results were obtained for Pb >1 ppm, and Hg >1 ppm. On day 21, fish were removed from the tanks individually, weighed, measured, and sacrificed. Fish were placed in liquid nitrogen for immediate freezing. Condition factor was determined by the equation: C.F. = body weight (g)/length^3 (cm). All fish were stored in a −80° freezer until dissection for heavy metal and hsps analysis. Fish were dissected and gill, muscle, and 1/2; liver were removed for analysis of hsp induction.

Hsp-70 analysis

Hsp-70 proteins were analyzed using Western blotting techniques following methods described by Werner et al. (2001). Muscle and gill tissues were separated into two fractions, a supernatant or soluble fraction and a pellet (5% sodium dodecyl sulfate – SDS) fraction containing membranes and subcellular organelles. For liver tissue only the soluble fraction was analyzed. Briefly, samples were homogenized in a hypotonic solution containing 66 mM Tris–HCl (pH 7.5), 0.1% Nonidet, 10 mM EDTA, 10 mM DTT and protease inhibitors, i.e. 10 mM benzamidine, 5 μM pepstatin, 0.001% aprotinin, and 0.1 mM phenylmethylsulfonyl fluoride (PMSF). Homogenates were centrifuged, supernatants were collected then pellets resuspended in homogenization buffer containing 5% SDS, vortexed for 10 s, centrifuged and sample buffer added. Total protein concentration in each fraction was determined using the Biorad DC Protein Assay based on Lowry et al., (1951).

Subsamples of equal total protein content (50 μg) were separated by SDS-PAGE on 10% polyacrylamide gels with 5% stacking gels (Blattler et al., 1972) using the buffer system described by Laemmli (1970). Hsp-70 antigen was applied to one lane per gel to serve as an internal standard for blotting efficiency. Proteins were separated then electroblotted onto Immobilon-P membrane at constant voltage (40 V) over night. Membranes were blocked with 5% skim milk in 20 mM tris buffer and 0.4 M NaCl (pH 7.5) with 0.05% Tween-20 for 30 min. A monoclonal antibody for hsp70 (1:500; Affinity Bioreagents, MA3-001) was used as probe. Blots were incubated for 1 h 30 min with primary antibody, then washed three times for 30 min in tris-buffered saline solution containing 0.05% Tween-20. Alkaline phosphatase-conjugated

goat-anti-rat IgG (1:30000; Sigma) was used to detect hsp-70 probes. Bound antibody was visualized by a chemiluminescent substrate (CDP-Star; Tropix, Bedford, MA), and protein bands were quantified by densitometry (Biorad GS710).

Behavioral endpoints

Each fish was observed for a total of 5 h over the course of the 21-day experiment (each tank was observed for 30 min every other day). Fish were monitored for aggression measured as strikes/minute against conspecifics, and for feeding activity measured as strikes/minutes at food pellets.

Statistical analysis

To reduce handling stress, fish were not individually marked. Instead, all differences in behavior, growth and condition factor were based on averages of individuals in each tank. Data were analyzed using a 2-way Analysis of Variance with temperature and zinc as the main treatment effects. In tests of the effects of diet and temperature on post-trial condition factor and aggression (strikes/min), pretrial condition factor and post-trial condition factor, respectively, were used as covariates. Because multiple tests were performed, we used a Bonferroni correction to adjust the Type I error rate to the 0.05 level across all statistical tests performed. The Bonferroni correction is simply the 0.05 error rate divided by the number of tests performed. It is generally acknowledged that the Bonferroni correction is conservative in that it makes statistical significance more difficult to demonstrate (Perneger, 1998). Removing the effect of the covariates significantly reduced the possibility that differences in post-trial condition factor could be due to pre-trial condition or that changes in aggression could result from differences in body size of the fish. For correlated response variables like behavioral measures or fish size, condition factor, MANOVAs were performed.

Results

Pre-experiment conditions

After random assignment of fish to treatments, fish did not differ in condition factor. However, there was a statistically significant difference in body mass and length between temperature treatments (Table 1) with the fish at 15 °C being heavier ($F = 8.54$, $p = 0.012$) and longer ($F = 15.6$, $p = 0.002$). The fish in the 15 °C/high zinc treatment were slightly heavier (~13%) than fish in the two 10 °C treatments. Fish in the 15 °C/control diet treatment were almost 1 g heavier and 8 mm longer (~12%) than fish in both 10 °C treatments. In the analyses of post-treatment results, pre-treatment length was used as a covariate. However, the covariate was not significant in the majority of the analyses and is not reported unless it is significant.

Growth and condition factor

Growth, measured as increased length, differed slightly between treatments. Fish not exposed to zinc grew approximately 15% longer during the course of the experiment (17% at 10 °C, 14% at 15 °C), while fish on high-zinc diets experienced a lower growth rate of 6% (8% at 10 °C, 5% at 15 °C). The two-way ANOVA indicated that the difference due to zinc was significant ($F = 23.8$, $p < 0.001$) The effect of temperature on these results was not significant ($F = 1.46$, $p = 0.250$), and there was no interaction between temperature and zinc ($F = 0.031$, $p = 0.863$). There was a significant difference in growth of body mass due to temperature with fish at the lower temperatures growing heavier than at higher temperatures ($F = 8.9$, $p = 0.011$). The change in condition factor between pre-treatment and post-treatment was positive (increase in condition factor) in all treatments. The increase in condition factor was significantly less in the high zinc treatments ($F = 18.93$, $p = 0.000$) than in fish fed control diets OK. Pretrial condition factor used as a covariate was not significant, indicating that the change in condition factor was not a function of the condition of the fish prior to the initiation of the experiment. There was also an effect of temperature on change in condition factor ($F = 6.02$, $p = 0.03$) with lower temperatures exhibiting a greater increase in condition factor. Change in length, change in weight, and post-test condition factor were combined into a single response variable in a two-way MANOVA. There were significant differences between temperatures (Wilkes

Table 1. Effects of temperature and zinc treatments on physiological and behavioral parameters in coho salmon (Oncorhynchus kisutch)

Parameter	Treatment			
	10 °C – no zinc	10 °C – zinc	15 °C – no zinc	15 °C – zinc
Pretreatment length (mm)	60.1	60.9	64.5	65.0
Post-treatment length (mm)	70.3	65.7	73.5	68.1
Growth (mm)	10.2	4.7	9.0	3.1
Pretreatment mass (g)	4.6	4.6	5.5	5.2
Post-treatment mass (g)	14.2	14.2	14.3	14.1
Growth (g)	9.6	9.5	8.8	9.0
Pretreatment condition factor	0.021	0.020	0.021	0.019
Post-treatment condition factor	0.041	0.050	0.036	0.045
Zinc in liver (ppm)	20.0	21.5	19.5	23.0
Fe in liver (ppm)	51.0	66.3	85.8	120.0
Aggression (Strikes/minute)	3.6	1.3	2.5	1.3
Feeding (Strikes/minute)	9.5	15.2	11.2	18.0
Hsp-70 (muscle)	8.41 (1.26) 17.16 (3.48)	9.00 (1.76) 14.74 (2.86)	6.9 (2.02) 12.55 (3.35)	7.9 (1.12) 14.58 (4.44)
Hsp-70 (liver)	17.38 (2.76)	15.44 (3.21)	16.67 (3.93)	12.66 (3.55)
Hsp-70 (gill)	8.1 (3.41)	6.96 (2.95)	5.82 (2.23)	4.25 (3.42)

$\lambda = 0.264$, $F = 9.26$, $p = 0.003$), zinc treatment (Wilkes $\lambda = 0.286$, $F = 8.32$, $p = 0.005$), but no interaction (Wilkes $\lambda = 0.951$, $F = 0.17$, $p = 0.91$).

Zn and Fe

No pretreatment measurements of zinc or iron in liver were available due to the limited number of fish. Therefore fish fed control diets, i.e. not exposed to zinc were used as the control for concentration measurements of zinc and iron in the liver. Zinc in liver increased significantly ($F = 5.00$, $p = 0.045$) with exposure to a high-zinc diet. Fe in the liver increased with exposure to both zinc and high temperature. The increase due to zinc in the diet was significant ($F = 5.63$, $p = 0.035$), and the increase due to temperature was highly significant ($F = 17.98$, $p = 0.001$). No temperature–zinc interaction was present in either analysis. Also, no factor such as length, body mass, or condition factor was significant as a covariate, indicating that there was no size dependence in zinc or iron processing.

Differences in hsp-70 levels were not statistically significant, but several trends could be observed. Overall, expression of hsp-70 in both muscle and liver supernatant extractions was higher in the 10 °C treatments than in the 15 °C treatments. Expression of hsp-70 in liver was lower than controls in the zinc-exposed fish.

Behavior

Exposure to high-zinc diet decreased aggression as measured by the number of strikes per minute at other fish in the tank ($F = 11.65$, $p = 0.005$). Condition factor used as a covariate was not significant indicating that larger fish were not more aggressive. Feeding rate increased with exposure to zinc ($F = 15.41$, $p = 0.002$).

Discussion

One of the primary results of this 21-day study was the lack of a significant interaction between temperature and zinc. Statistical analyses demonstrated that there was no interaction for any of the experimental endpoints measured indicating that there are neither synergistic nor antagonistic effects between exposure to a diet containing 1900 ppm zinc and a moderately elevated temperature (15 °C).

Increased dietary zinc reduced incidents of intraspecific aggressive behaviors, but caused a significant increase in feeding rate, (Table 2). Environmental stressors have been shown to impair predator avoidance (Weis et al., 1999) and would potentially affect competitive behaviors in general. Less time spent defending resources would allow for additional time spent feeding. However, even with increased feeding rates, growth of fish from this treatment was lower than that of control fish. This indicates that there was a significant diversion of energy due to uptake of zinc, and that fish may have tried to compensate for this energetic demand by increasing their food intake. It is known that there is a large energetic cost associated with the induction of stress-responsive and detoxifying enzymes (Barton & Schreck, 1987). Zinc can induce metal-specific detoxifying enzymes such as metallothionein as well as components of the cellular response to oxidative stress.

Exposure to elevated temperature (15 °C) also reduced growth rate, a common result in studies of this type. Increasing temperature results generally in an increase in metabolic rate and, consequently, in energy demand. If food is supplied at a greater rate, growth rate can in fact increase. However, we kept the feeding rate constant at 2.5% body mass and therefore likely placed the fish in an energetic deficit resulting in a reduced growth rate at higher temperature.

It is generally believed that juvenile salmonids cannot tolerate temperatures greater than 23–26 °C, and the preferred temperature of juvenile coho salmon is about 10–12 °C (Konecki et al., 1995). We chose treatment temperatures of 10 °C (control) and 15 °C (experimental thermal stress) in order to investigate response to continuous thermal stress. We were surprised to see a decreased rather than increased expression of heat shock proteins in livers of fish in increased temperature and zinc treatment groups (1900 ppm zinc/15 °C). The same trend was seen in gill tissues of these fish. Although a decreased expression of hsps in apparently stressed organisms has been observed in other studies (Werner & Hinton, 1999, Kohler, 1999, Kohler, 2001, Viant et al., 2004, Werner, 2004) we still lack the mechanistic understanding for this phenomenon. Viant et al. (2004) suggest that steelhead trout are able to adapt to a constant 5 °C elevation in temperature, from 15 to 20 °C, within ca. 3 weeks. Induction of hsps may also depend more upon the relative increase in environmental temperature than upon the absolute temperature experienced by these fish (Fader et al.,

Table 2. Results of two-way ANOVA analyses on the physiological and behavioral parameters. All values are p values. Bonferroni correction factors for the number of tests resulted in $p = 0.0036$ as the alpha value that allowed an experiment-wide type I error rate of $p = 0.05$. All significant results at the $p = 0.0036$ level are in bold

Variable	Model Terms				
	Model	Covariate	Diet	Temp	Diet × Temp (Interaction Term)
Pre-trial condition factor	0.124	N/A	N/A	N/A	N/A
Growth (length/mm)	**0.003**	N/A	**0.000**	0.250	0.863
Growth (weight/g)	0.066	N/A	0.782	0.011	0.532
Zinc in liver	0.168	N/A	0.045	0.663	0.389
Iron in liver	**0.003**	N/A	0.035	**0.001**	0.381
Hsp-70 Muscle supernatant	0.036	N/A	0.102	0.008	0.680
Hsp-70 Muscle pellet	**0.000**	N/A	0.753	0.234	0.016
Hsp-70 Gill supernatant	0.182	N/A	0.947	0.110	0.227
Hsp-70 Gill pellet	0.772	N/A	0.351	0.729	0.493
Hsp-70 Liver supernatant upper band	0.580	N/A	0.425	0.453	0.327
Hsp-70 Liver supernatant lower band	0.009	N/A	0.004	0.072	0.259
Aggression (strikes/min)	0.023	N/A	0.005	0.305	0.349
Feeding (strikes/min)	0.011	N/A	**0.002**	0.192	0.736

1994). It has also been hypothesized that a lack of energy, potentially stemming from increased metabolic demands related to stressors, leads to a reduction in cellular protein expression (Sanders et al., 1991, Werner & Hinton, 1999). It has also been suggested that the basis of the decrease in stress protein levels may lie in the pharmacological kinetics of the hsp70 level in response to increasing intensity of stressors; the induction of hsp70 follows an optimum curve with an optimum stress response (Kohler et al., 2001). Vijayan et al. (1998) demonstrated a surpassing of the stress response optimum and declining hsp70 levels following exposure to increasing concentrations of chemical stressors. While increasing temperature alone has been shown to induce an optimum hsp70 response, in theory, high temperature is potentially capable of reducing contaminant-induced hsp70 levels when they occur together (Kohler et al., 2001).

Increasing concentrations of iron in the liver, as measured in fish exposed to dietary zinc and elevated temperature, are considered to be an indicator of liver damage (Skibba & Gwartney, 1997, Mori & Hirayama, 2000) in mammals. Mammalian hepatotoxicity in response to hyperthermia may be the result of oxidative stress from superoxide generation, and ferritin released from the liver appears to play a central role in hyperthermic toxicity (Martin et al., 1998). Whether this same phenomenon is occurring in fish and by what mechanism is unknown, but livers did accumulate iron in response to increasing temperature and increasing zinc indicating that hepatotoxicity was occurring.

As populations of coho salmon in many Pacific North coast watersheds are federally listed, field experimentation and investigation of this species is nearly impossible. Coho salmon used in this experiment were obtained from hatchery stock considered genetically different from wild coho salmon. Since differences in tolerance to environmental factors appear to have a genetic basis, results may not be directly transferable to field situations (Weis et al., 1999). Additionally, methods used to incorporate metals into fish diets can influence the degree of toxicity caused by metals (Farag et al., 1994). When metals were added surficially to commercial diets, the toxicity to trout was less than when zinc occurred naturally in the diet. Thus, although the concentrations of metals in diets may be similar, toxicological effects of those diets can differ (Farag et al., 1994).

Species with similar life history strategies and habitat requirements such as steelhead may be studied in the field to gain insights into the complex interactions and subsequent population consequences of environmental stressors. In the Navarro River, for example, we have examined steelhead in an attempt to gain insight into the decline of the coho salmon populations in that watershed. Preliminary investigations have shown levels of zinc in steelhead livers averaging 32.8 ppm, approximately 1.5 times the levels found in livers of our experimental coho. Levels of iron in livers taken from Navarro steelhead averaged 114 ppm, while values from our experimental coho averaged 66 ppm (10° + Zn), 51 ppm (10°), 120 ppm (15° + Zn), and 86 ppm (15°). Hsp levels in a small sample of Navarro steelhead averaged 9.6, while levels in our experimental coho averaged approximately 8.05 (muscle supernatant) and 7.05 (muscle pellet). These values demonstrate strong responses to environmental stressors present in the Navarro River. Clearly, however, further research is necessary in order to begin to separate the multiple factors involved in declines of fish species and populations.

References

Atchison, G. J., M. G. Henry & M. B. Sandheinrich, 1987. Effects of metals on fish behavior a review. Environmental Biology of Fishes 18: 11–26.

Balasubramanian, S., R. Pappathi & S. P. Raj, 1995. Bioconcentration of zinc, lead and chromium in serially-connected sewage-fed fish ponds. Bioresource Technology 51: 193–197.

Barton, B. A. & C. B. Schreck, 1987. Metabolic cost of acute physical stress in juvenile steelhead. Transactions of the American Fisheries Society 116: 257–263.

Brown L. R., & P. B. Moyle, 1991. Status of Coho Salmon in California. In Report submitted to the National Marine Fisheries Service.

Brown, L. R., P. B. Moyle & R.M. Yoshiyama, 1994. Historical decline and current status of coho salmon in California. North American Journal of Fisheries Management. 14: 237–261.

Donker, M. H., H. M. Abdel-Lateif, M. A. Khalil, B. M. Bayoumi & N. Straalen, 1998. Temperature, physiological time, and zinc toxicity in the isopod Porcellio scaber. Environmental Toxicology and Chemistry 17: 1558–1563.

Fader, S. C., Z. Yu & J. R. Spotila, 1994. Seasonal variation in heat shock proteins (hsp70) in stream fish under natural conditions. Journal of Thermal Biology 19: 335–341.

Farag, A. M., C.J. Boese, D. F. Woodward & H. L. Bergman, 1994. Physiological changes and tissue metal accumulation in rainbow trout exposed to foodborne and waterborne metals. Environmental Toxicology and Chemistry 13: 2021–2029.

Feige, Morimoto Yahara Polla 1996. Stress-Inducible Cellular Responses. Birkhauser Verlag, Basel, Switzerland.

Henry, M. G. & G. J. Atchison, 1986. Behavioral changes in social groups of bluegills [Leponis macrochirus] exposed to copper. Transactions of the American Fisheries Society 115: 590–595.

Hodson, P. V. & J. B. Sprague, 1975. Temperature-induced changes in acute toxicity of zinc to Atlantic salmon (Salmo salar). Journal of the Fisheries Research Board of Canada 32: 1–10.

Hogstrand, C. & C. M. Wood, 1996. The physiology and toxicology of zinc in fish. In Taylor, E. W. & M. Murphy (eds), SEB Seminar Series - Aquatic Toxicology, 57th edn. Cambridge University Press, Cambridge, U.K: 61–84.

Irwin, R. J., 1997. Environmental Contaminants Encyclopedia. National Park Service.

Iwama, G. K., M. Vijayan, C.F. Mazur, P. Ackerman. 1998. Heat shock proteins and physiological stress in fish. American Zoologist 38: 71A.

Iwama, G. K., M. M. Vijayan, R. B. Forsyth & P. A. Ackerman, 1999. Heat shock proteins and physiological stress in fish. American Zoologist 39: 901–909.

Kohler, H. R., H. Eckwert, R. Triebskorn & G. Bengtsson, 1999. Interaction between tolerance and 70kDa stress protein (hsp70) induction in collemolan populations exposed to long-term metal pollution. Applied Soil Ecology 11: 43–52.

Kohler, H. R., C. Bartussek, H. Eckwert, K. Farian, S. Granzer, T. Knigge & N. Kunz, 2001. The hepatic stress protein (hsp70) response to interacting abiotic parameters in fish exposed to various levels of pollution. Journal of Aquatic Ecosystem Stress and Recovery 8: 261–279.

Konecki, J. T., C. A. Woody & T. P. Quinn, 1995. Temperature preference in two populations of juvenile coho salmon, Oncorhynchus kisutch. Environmental Biology of Fishes 44: 417–421.

Krenkesh Peter, A., 1975. Heavy Metals in the Aquatic Environment Proceedings of the International Conference Held in Nashville, Tennessee, December 1973. Pergamon Press, New York.

Martin, M., C. Hernandez, G. Bodega, I. Suarez, M. Del Carmen Boyano & B. Fernandez, 1998. Heat-shock proteins expression in fish central nervous system and its possible relation with water acidosis resistance. Neuroscience Research 31: 97–106.

Mesa, M. G., 1994. Effects of multiple acute stressors on the predator avoidance ability and physiology of juvenile Chinook salmon. Transactions of the American Fisheries Society 123: 786–793.

Mori, N. & K. Hirayama, 2000. Long-term consumption of a methionine-supplemented diet increases iron and lipid peroxide levels in rat liver. Journal of Nutrition 130: 2349 2355.

Perneger, T. V, 1998. What is wrong with Bonferroni adjustments. British Medical Journal 136: 1236–1238.

Sanders, B. M, 1993. Stress proteins in aquatic organisms: An environmental perspective. Critical Reviews in Toxicology 23: 49–75.

Sanders, B. M., L. S. Martin, W. G. Nelson, D. K. Phelps & W. Welch, 1991. Relationships between accumulation of a 60 kDa stress protein and scope-for growth in *Mytilus edulis* exposed to a range of copper concentrations. Marine Environmental Research 31: 81–97.

Skibba, J. L. & E. A. Gwartney, 1997. Liver hyperthermia and oxidative stress: role of iron and aldehyde production. International Journal of Hyperthermia 13: 215–226.

Shumway, C. A., 1999. A neglected science: Applying behavior to aquatic conservation. Environmental Biology of Fishes 55: 183–201.

Vijayan, M. M., C. Pereira, G. Kruzynski & G. K. Iwama, 1998. Sublethal concentrations of contaminant induce the expression of hepatic heat shock protein 70 in two salmonids. Aquatic Toxicology 40: 101–108.

Wedemeyer, G., 1973. Some Physiological aspects of sublethal heat stress in the juvenile steelhead trout (*Salmo gairdneri*) and coho salmon (*Oncorhynchus kisutch*). Journal Fisheries Research Board of Canada 30: 831–834.

Weis, J. S., G. M. Smith & T. Zhou, 1999. Altered predator/prey behavior in polluted environments: Implications for fish conservation. Environmental Biology of Fishes 55: 43 51.

Werner, I. & D. E. Hinton, 1999. Field validation of hsp70 stress proteins as biomarkers in Asian clam (*Potamocorbula amurensis*): is downregulation an indicator of stress? Biomarkers 4: 473–484.

Werner, I., C. S. Koger, J.T. Hamm & D.E. Hinton, 2001. Ontogeny of the heat shock protein, hsp70 and hsp60, response and developmental effects of heat-shock in the teleost, medaka (*Oryzias latipes*). Environmental Sciences 8: 13–30.

Copyright of Hydrobiologia is the property of Springer Science & Business Media B.V. and its content may not be copied or emailed to multiple sites or posted to a listserv without the copyright holder's express written permission. However, users may print, download, or email articles for individual use.

Copyright of Hydrobiologia is the property of Springer Science & Business Media B.V. and its content may not be copied or emailed to multiple sites or posted to a listserv without the copyright holder's express written permission. However, users may print, download, or email articles for individual use.

Journal of Toxicology and Environmental Health, Part A, 70: 1897–1911, 2007
Copyright © Taylor & Francis Group, LLC
ISSN: 1528-7394 print / 1087-2620 online
DOI: 10.1080/15287390701551159

Heavy Metals in Pacific Cod *(Gadus macrocephalus)* from the Aleutians: Location, Age, Size, and Risk

Joanna Burger
Division of Life Sciences, Environmental and Occupational Health Sciences Institute (EOHSI), and Consortium for Risk Evaluation with Stakeholder Participation (CRESP), Rutgers University, Piscataway, New Jersey

Michael Gochfeld and Tara Shukla
Environmental and Occupational Health Sciences Institute (EOHSI) and Consortium for Risk Evaluation with Stakeholder Participation (CRESP), Rutgers University, Piscataway, New Jersey, and Environmental and Occupational Medicine, University of Medicine and Dentistry of New Jersey-Robert Wood Johnson Medical School, Piscataway, New Jersey

Christian Jeitner, Sean Burke, Mark Donio, and Sheila Shukla
Division of Life Sciences, Environmental and Occupational Health Sciences Institute (EOHSI), and Consortium for Risk Evaluation with Stakeholder Participation (CRESP), Rutgers University, Piscataway, New Jersey

Ronald Snigaroff, Daniel Snigaroff, and Timothy Stamm
Villages of Atka and Nikolski, Aleutians, Alaska

Conrad Volz
Department of Environmental and Occupational Health, Graduate School of Public Health, University of Pittsburgh, Pittsburgh, Pennsylvania, USA

Received 22 March 2007; accepted 16 May 2007.

We thank the people who contributed to the development and execution of the Amchitka Science Plan, which provided the initial framework for this project, including Charles Powers, David Kosson, Barry Friedlander, John Eichelberger, David Barnes, and Lawrence Duffy., as well as Monica Sanchez, Runore Wycoff, and Peter Sanders (Department of Energy, National Nuclear Security Administration, Nevada), Jenny Chapman (Desert Research Institute), Anne Morkill and G. Siekaniec (U.S. Fish and Wildlife Service), Robert Patrick (Aleutian/Pribilof Island Association), Ron King, David Rogers, and Doug Dasher (Alaska Department of Environmental Conservation), and the people of the villages of Unalaska, Nikolski, Atka, and Adak in the Aleutians. Over the years our thinking about the risks from consumption of fish has also been influenced by A. Stern, C. Chess, M. A. Gallo, B. D. Goldstein, K. Kirk-Pflugh, and K. Cooper. Several people aided in some aspects of the research, including S. Jewett, V. Vyas, and H. Mayer. We thank the entire crew of the *Ocean Explorer*, Captain Ray Haddon, mate Glenn Jahnke, cook Don Dela Cruz, and Bill Dixon, Joao Do Mar, and Walter Pestka, for making our field work possible and pleasant, and for bringing us safely back to port. We also thank the Captain of the *Gladiator* trawler and his crew for aiding our collecting, and M. E. Wilkins of NOAA for allowing us to participate on their cruise. The research was conducted under an approved Rutgers University Protocol, and supported by NIEHS Center grant (P30ES005022), Consortium for Risk Evaluation with Stakeholder Participation (Department of Energy, numbers DE-FC01-95EW55084, DE-FG 26-00NT 40938, DE-FC01-06EW07053), Wildlife Trust, the Tiko Fund, and EOHSI. The views expressed in this article are solely those of the authors and do not represent the funding agencies.

Address correspondence to Joanna Burger, Division of Life Sciences, Rutgers University, 604 Allison Road, Piscataway, NJ 08854-8082, USA. E-mail: burger@biology.rutgers.edu

Considerable attention has been devoted to the risks from mercury (Hg) and polychlorinated biphenyls (PCB) to high-level predators (including humans) who consume freshwater fish. Although the U.S. Food and Drug Administration (FDA) issued advisories because of Hg for four marine fish species, there are few data on lead (Pb), cadmium (Cd), or other metals in Bering Sea fish generally, or on the risk these levels pose to the fish themselves or to consumers of marine fish. Levels of arsenic (As), Cd, chromium (Cr), Pb, Hg, and selenium (Se) levels were examined in muscle and liver of 142 Pacific Cod (*Gadus macrocephalus*) collected in 2004 at Nikolski, Adak, Amchitka, and Kiska Islands in the Aleutian Chain (Alaska) in the Bering Sea/North Pacific Ocean, a major source of commercial fishing. One key objective was whether there were location, age, gender, and size effects on tissue concentration that might pose a risk to the fish or their predators (including humans). All fish were measured and weighed, and a subset was aged by examining otolith layers. As was higher in liver than in muscle (geometric mean 2420 versus 1590 ng/g or ppb wet weight), as were Cd (GM 224 versus 1.92) and Se (GM 1380 versus 165). Conversely, Cr was higher in muscle (76.8 versus 45 ppb), as were Pb (23.7 vs 12 ppb) and surprisingly Hg (128 versus 82 ppb). Adak, until recently a large military base, had the highest levels of As, Hg, and Se, while Amchitka had the highest Pb levels, but Nikolski, which generally had the lowest levels, had relatively high Pb in liver. In general, interisland differences were significant for most metals in muscle, but only for Cr in liver. Weight and length were positively related to age, but age tended to explain more of the variance in metal levels. The multiple regression relationships differed by tissue in an unanticipated manner. Location contributed significantly to the models for muscle Cd, Pb, Hg, and Se, but not for liver levels. Conversely the length by weight interaction entered all of the liver models but none of the muscle models. Se and Hg were positively but weakly correlated in both liver (tau=+0.16) and muscle tissue (tau=0.12). Hg was positively correlated with length, weight, and age in muscle, but not in liver. As showed a significant negative correlation with size variable in both tissues, and Cr was negatively correlated in muscle. Cd was positively correlated with Hg, Se, and As. Between liver and muscle there were significant positive correlations for Hg (tau=.24), As (tau=.407), and Cr (tau=0.17), but not for Pb, Cd, or Se. In this study, the only metals that might pose a risk to cod-eating predators is Hg, as well as some of the higher values of Pb at Amchitka and Nikolski . The U.S. Environmental Protection Agency (EPA) reference dose (RfD) (not available for lead) was used to evaluate the risk to people consuming an 8-ounce (228g) meal of cod once per day and once per week, and to calculate risk using the levels found in this study. If a subsistence fisher from one of the Aleut villages ate one meal of cod per week for As, or one meal per day for Hg, they would exceed the U.S. EPA reference dose for As and Hg (set at a level to be without adverse effect for any person with this average daily exposure).

The importance of pollutants to exposed aquatic organisms, and to the species that depend upon them for food, can be studied in part by measuring the levels of contaminants in organisms. Subsequently these levels are compared to those known to produce adverse effects in the organisms themselves, and to higher trophic level organisms consuming them. Fish are often used as bioindicators because of their role in aquatic food chains and their importance as a human food. In many parts of the world fish provide the major source of protein (Toth & Brown, 1997; Fleming et al., 1995; Burger, 2000, 2002; Bayen et al., 2005; Jorgensen et al., 2006), particularly for native populations and subsistence peoples (Harris & Harper, 1998; Burger, 1999; Burger et al., 1999). Fish are an excellent, low-fat source of protein and provide many benefits, such as contributing to low blood cholesterol (Anderson & Wiener, 1995). The omega-3 (*n*-3) fatty acids in fish reduce cholesterol levels and the incidence of heart disease, stroke, and pre-term delivery (Anderson & Wiener, 1995; Daviglus et al., 2002; Patterson, 2002).

Levels of contaminants in fish are of considerable interest because of potential effects on the fish themselves or the organisms that consume them, including top-level receptors (Hylland et al., 2006). The primary contaminants of concern in fish are methylmercury (MeHg) and polychlorinated biphenyls (PCBs), which are sufficiently high in some fish to produce adverse human health effects in people consuming large quantities (Stern, 1993; IOM, 1991; Gochfeld, 2003; Hightower & Moore, 2003; Consumer Reports, 2003; Hites et al., 2004). Maternal exposures to metals may threaten the developing fetus because chemicals are transferred across the placenta (Gulson et al., 1997). There is also lactational transfer affecting nursing infants (Berlin et al., 2002). Much of the increasing concern about the safety of fish revolves around self-caught fish (both sport and subsistence fishing) from freshwater lakes and rivers, which are under consumption advisories in most states (U.S. EPA, 2004). Yet the levels of metals other than mercury are rarely measured.

In this study the levels of arsenic, cadmium, chromium, lead, mercury, and selenium were examined in Pacific cod (*Gadus macrocephalus*) from the Aleutians. Of particular interest were locational differences that might affect the potential risk to top level predators of cod, including humans. Arsenic and selenium are technically metalloids. In addition, differences in metal levels were examined as a function of age and size of the fish. Some of the mercury data were published separately (Burger & Gochfeld., 2007), but this article focuses on other metals, in the comparison between these metals, and in the risk posed to humans and wildlife from the levels of Pacific cod from the Aleutians.

Contaminants are of special concern to people living in the Arctic and sub-Arctic region because fish are an important dietary item (NRC, 1996; Egeland & Middaugh, 1997; Berti et al., 1998; Egeland et al., 1998; Chan & Receveur, 2000; Duchesne et al., 2004; Duhaime et al., 2004; Hansen et al., 2004). This is especially true for people living on the Aleutian and Pribilof Islands in the northern Pacific/Bering Sea region (APIA, 2002; Hamrick & Smith, 2003). From 30 to 90% of the food consumed by people in the Aleutians is subsistence food (Patrick, 2002), and cod is one of their preferred foods (APIA, 2002; Patrick, 2002; Hamrick & Smith, 2003). Some fish analyzed in this report were caught by Aleut fishermen; the fish

represent those that would be consumed by subsistence peoples (Gerstenberger & Dellinger, 2002). Pacific cod are one of the 25 commercially important species of fish in the region (NRC, 1996), and are common even in East Coast markets (Burger et al., 2004).

Cod are also of interest as components of ecosystems because they are broadly distributed in the North Pacific at depths of 80–260 m, particularly on the shelf and upper slope (Bakkala, 1984; Allen & Smith, 1988). They migrate seasonally between the continental slope/shelf and along the continental slope, and are generally bottom-dwellers (Simenstad et al., 1977).

Pacific Cod are an important commercial fish of the Bering Sea/North Pacific region. They were one of the species making up the bulk of the commercial fishery by the early 1980s, and Merrell (1977) correctly predicted that catches would continue to increase. The catch of Pacific cod in the eastern Bering Sea increased from the early 1960s to over 180 metric tons by the late 1980s (NRC, 1996), and it remains an important commercial fish today. Further, it is an important subsistence fish for the Aleuts living in the Aleutian Islands (Patrick, 2002; APIA, 2002; Hamrick & Smith, 2003).

Fishing poles were used, rather than the more customary method of trawling because of the importance of obtaining fish the way the Aleuts who are at risk obtain them. Trawling results in fish of all sizes, not just those that are of a legal limit or that subsistence fishermen take home. Catching fish with a pole best approximated the fishing method of the Aleuts and a comparison of fish obtained by the scientist team and Aleut team validated this approach (Burger et al., 2006).

Pacific cod are also important in the marine ecosystem. Cod are eaten by larger fish, such as halibut, by fur seals and whales, and of course, by humans. Cod are thus relatively high on the food chain, and are expected to have intermediate or higher levels of contaminants, compared to other fish (see later discussion). Cod are also scavenged by seabirds from the intertidal, from behind factory ships, and from canneries, and eagles catch intermediate-sized cod. Thus, levels of heavy metals in cod are indicative of both their prey base, and may serve as a bioindicator of exposure for their predators that are higher on the food chain, including people.

Pacific cod range in age up to 25 yr (Merrell, 1977: Munk, 2001), although in this study the oldest cod was only 11 yr. Cod are associated with Pacific halibut (*Hippoglossus stenolepis*) and other flounders (Simenstad et al., 1977). They feed on benthic epifauna, shrimps and crabs, and juvenile fish, such as pollock (*Theragra chalcogramma*; Hood & Calder, 1981), although in some places they eat mainly fish and crabs (Tokranov & Vinnikov, 1991). Tokranov and Vinnikov (1991) found that nearly 70% of the diet of cod was pollock, and the relative percentage increased with size of the cod. Cod are relatively high on an index of trophic level for the Bering Sea (Mito et al., 1999). Juvenile cod live in the kelp and eelgrass communities near shore (Dean et al. 2000), while older cod move offshore. Small juvenile cod may remain within vegetation beds for protection from predators (Heck & Orth, 1980), and they eat primarily copepods, invertebrate larvae, and small bivalves (Dean et al., 2000). Most cod occur at depths from 50 to 300 m, on or close to the continental shelf (Bakkala, 1984; Allen & Smith, 1988). Tagging studies, however, indicate that there is little movement of cod among areas (Canada, 2006).

METHODS

Study Areas

Pacific cod were collected at Nikolski (n = 16), Adak (n = 6), Amchitka (n = 77) and Kiska (n = 42) Islands in the Aleutian Chain of Alaska (Figure 1). Although Amchitka and Kiska had military occupation during the Second World War, they are not currently occupied, and are part of the Alaska Maritime National Wildlife Refuge, established in 1913 by executive order of President Taft (ATSDR, 2004). Amchitka was also the site of three underground nuclear tests from 1965 to 1971 (Powers et al., 2005). From around 1940 through the 1990s, Adak was home to a large U.S. Naval base, since closed, and is now occupied by a community of about 200. Nikolski, the longest continually occupied community in the Western Hemisphere, is home to a permanent Aleut community of about 40 people.

Protocol

Under appropriate permits from the State of Alaska's Department of Fish and Game (number CF-04-043), cod (n = 141)

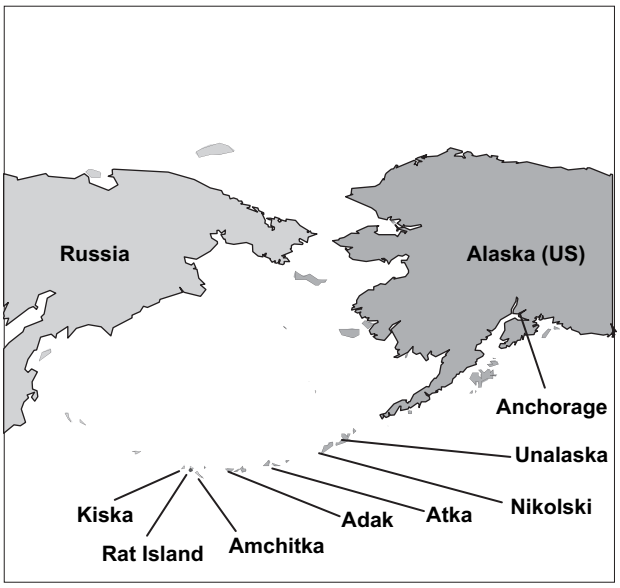

FIG. 1. Map of the Aleutians, showing the location of islands where Pacific cod were collected, including Nikolski, Amchitka, and Kiska.

were collected by rod and reel in June and July 2004 from the dock at Adak, and from small skiffs deployed from the *Ocean Explorer*, and from trawling aboard the National Oceanic and Atmospheric Administration (NOAA) survey vessel *Gladiator*. Fish were collected by researchers and an Aleut team from the multiuniversity Consortium for Risk Evaluation with Stakeholder Participation (CRESP) as part of an independent assessment, examining radionuclide levels related to former nuclear testing at Amchitka (Powers et al., 2005). Cod were also collected by TS on Nikolski in the summer of 2005 as part of subsistence fishing. Fish were measured (standard length = snout to base of caudal fin), weighed, and dissected, and samples of liver and muscle were frozen for later analysis. Liver samples were collected as indicators of potential risk to the fish themselves, and muscle was taken as an indicator of risk to consumers, including humans. Otoliths were removed from a selected sample (n = 49), and aged by Delsa Anderl of the National Oceanic and Atmospheric Administration (NOAA).

Fish were shipped frozen to the Environmental and Occupational Health Sciences Institute (EOHSI) of Rutgers University for metal analysis (for information on radionuclide analysis see Powers et al., 2005). At EOHSI, a 2-g (wet weight) sample of fish tissue was digested in ultrex ultrapure nitric acid in a microwave (MD 2000 CEM), using a digestion protocol of 3 stages of 10 min each under 50, 100, or 150 pounds per square inch (3.5, 7, and 10.6 kg/cm^2) at 70× power. Digested samples were subsequently diluted to 25 ml with deionized water. All lab equipment and containers were washed in 10% HNO solution and deionized water rinse, prior to each use (Burger et al., 2001a).

Mercury was analyzed by the cold vapor technique using the Portable Zeeman Lumex (RA-915) mercury analyzer, with an instrument detection level of 0.2 ng/g, and a matrix level of quantification of 0.002 μg/g. All other metals were analyzed by graphite furnace atomic absorption, with Zeeman correction. Concentrations are expressed in parts per billion (ppb= ng/g on a wet weight basis). Values are for total mercury, not methylmercury, but it is reasonable to assume that about 90% of the total mercury is methylmercury (Bloom, 1991). All specimens were run in batches that included blanks, a standard calibration curve, two spiked specimens, and one duplicate. The accepted recoveries for spikes ranged from 85 to 115%; no batches were outside of these limits. Ten percent of samples were digested twice and analyzed as blind replicates (with agreement within 15%). A DORM-2 certified dogfish tissue was used as the calibration verification standard. Recoveries between 90 and 110% were accepted to validate the calibration.

Kruskal–Wallis nonparametric one-way analysis of variance (ANOVA, generating a χ^2 statistic) was used to examine differences among tissues and study sites. ANOVA with Duncan's multiple range test was used on log-transformed data to identify the significant differences (SAS, 1995). Table 1 provides geometric as well as arithmetic means, and numbers are rounded to no more than three significant figures. Kendall correlations were used to examine relationships between metals, size, and weight. Multiple regression procedures were used to determine the variables that contributed to variations in concentrations of metals (PROC GLM, SAS, 1995). Variables that vary colinearly are entered only if they add independently to explaining the variance (r^2). The level for significance was designated as $p < .05$, although levels of $p < .1$ are given because of the small sample sizes and limited power.

Finally, metal levels obtained for the cod were used to evaluate potential risk. The U.S. Environmental Protection Agency (EPA) reference dose (RfD) was used to evaluate risk to people consuming one 8-ounce (228g) meal of cod per day, per week and per month, given the levels found in cod from the Aleutians.

RESULTS

There were significant interisland differences in the weights, sizes, and ages of the Pacific cod (Table 1). The youngest and smallest cod were collected at Kiska. There were significant interisland differences for all metals except chromium in the muscle of cod, yet conversely, chromium was the only element that had significant inter-island differences in liver. In muscle, Adak cod had the highest levels of cadmium, mercury, and selenium, while Amchitka had the highest levels of lead. Nikolski cod had significantly lower levels of cadmium and selenium than fish from the other islands. Amchitka had the highest chromium levels in liver (Table 1).

Multiple regression models (SAS PROC GLM) were run for the 49 fish that had been aged (Table 2) and then separately for the entire sample of 142 fish (without the age variable (Table 3). For muscle, the models explained between 32 and 74% of the variances in levels of all metals except chromium, with age entering the models first, although length contributed to the r^2 for cadmium and mercury. The models were less predictive with r^2 from .25 to .35 for chromium, arsenic, and selenium; again, age entered the models first. Gender and weight did not contribute to the models.

In the larger data set, there were significant models for muscle arsenic, cadmium, mercury, and selenium, with island as the most predictive variable for these elements. Length and weight also entered the mercury model, but their interaction did not. Conversely, for the liver models, the length by weight interaction entered all models and island by length interaction entered significantly for arsenic, cadmium, and mercury. Gender only entered the muscle cadmium model.

As expected, there was a positive correlation between length and weight, and between these size variables and age (Table 4). Older fish were heavier and longer. However, metals were not uniformly associated with size. As in many studies, mercury in muscle (but not liver) showed a positive correlation with age and size. However, cadmium levels were generally negatively correlated with age and size (Table 4). Cadmium levels were significantly correlated with lead in muscle, mercury in liver, and selenium in both tissues. Selenium and mercury were also positively correlated in both tissues (Table 3).

TABLE 1
Metal Levels (ppb, wet weight)(ng/g) in Muscle and Liver of Pacific Cod Collected from Four Islands of the Aleutian Chain in Alaska

	Entire sample	Nikolski (Umnak I)	Adak	Amchitka	Kiska	Kruskal-Wallis X^2 (p)
	n=141	n=16	n=6	n=77	n=42	
standard length (cm)	56.3 ± 1.5	64 ± 3	54 ± 1	61 ± 2	47 ± 1	33 (0.0001)
range	18–107	43–90	50–61	18–107	38–91	
weight (g)	4060 ± 434	4183 ± 776	2920 ± 336	5310 ± 710	1890 ± 450	23 (0.0001)
range	200–23600	850–11300	2100–4500	200–23600	670–15900	
number aged	49	16	0	28	5	
age (years)	6.3 ± 0.28	6 ± 0.5	…	6.6 ± 0.35	4 ± 0	9 (0.009)
range	4–11	4–11		4–10	4	
MUSCLE						
arsenic[a]	2180 ± 231	2680 ± 382	2750 ± 596	1710 ± 355	538 ± 60	8.5 (0.04)
range	60–9770	481–5560	1510–4670	358–6600	60–9770	
GM	1592	2230	2460	1250	1330	
Duncan MRT		(A)	(A)	(A)	(A)	
cadmium	8.53 ± 0.95	0.57 ± 0.46	13.0 ± 4	11.8 ± 1	4.93 ± 1	41.0 (0.0001)
range	0.01–49	0.01–7	3–31	0.1–46	0.01–49	
GM	1.92	0.02	9.3	5.0	1.52	
Duncan MRT		(C)	(A)	(A,B)	(B,C)	
chromium	115 ± 11.7	84.7 ± 14	40.6 ± 10	112 ± 15	145 ± 27	6.1 (0.10)
range	2–890	32–254	12–71	17–793	2–890	
GM	76.8	73.1	33.5	77.5	86.4	
Duncan MRT		(A)	(A)	(A)	(A)	
lead	60.6 ± 5.8	60.5 ± 14	22.0 ± 11	76.0 ± 9	38.0 ± 6	11.6 (0.009)
range	0.1–395	9–254	0.1–74	0.1–395	0.1–193	
GM	23.7	45.0	3.9	34.7	12.0	
Duncan MRT		(A,B)	(B)	(A)	(A,B)	
mercury	173 ± 11.5	148 ± 24	316 ± 70	201 ± 17	111 ± 12	18.8 (0.0003)
range	8–859	20–323	75–603	8–859	10–426	
GM	12.8	114	268	155	86.1	
Duncan MRT		(B)	(A)	(B)	(B)	
selenium	183 ± 6.6	119 ± 16	282 ± 67	182 ± 7	195 ± 11	16.1 (0.001)
range	9–602	9–219	160–602	50–401	58–326	
GM	165	95	252	171	181	
Duncan MRT		(C)	(A)	(B)		
LIVER						
arsenic[a]	3420 ± 369	3110 ± 607	4330 ± 681	3630 ± 744	3240 ± 698	NS
range	203–12910	628–9308	3000–6750	890–12910	203–12100	
GM	2420	2400	4140	2620	1950	
Duncan MRT		(A)	(A)	(A)	(A)	
cadmium	387 ± 41	335 ± 87	519 ± 274	390 ± 52	382 ± 89	NS
range	1–3740	8–1138	99–1880	1–2270	11–3740	
GM	224	167	323	222	244	
Duncan MRT		(A)	(A)	(A)	(A)	
chromium	73.7 ± 7.9	51.5 ± 5	13.9 ± 4	92 ± 14	57.8 ± 6	11.5 (0.009)
range	1–758	24–102	2–32	3–758	1–174	
GM	45	48	9.7	54.5	38.3	
Duncan MRT		(A,B)	(B)	(A)	(A,B)	

(*Continued*)

TABLE 1
(*Continued*)

	Entire sample	Nikolski (Umnak I)	Adak	Amchitka	Kiska	Kruskal-Wallis X^2 (p)
lead	39.4 ± 4.3	45.9 ± 13	20.2 ± 8	46.3 ± 7	27.2 ± 5	NS
range	0.1–243	0.1–145	0.1–51	0.1–243	0.1–141	
GM	12.1	15	4.1	12.5	12.4	
Duncan MRT		(A)	(A)	(A)	(A)	
mercury	114 ± 11.5	94 ± 13	135 ± 35	113 ± 13	122 ± 29	NS
range	14–1250	17–188	27–279	17–644	14–1250	
GM	82	77	109	81.7	80.1	
Duncan MRT		(A)	(A)	(A)	(A)	
selenium	1570 ± 64	1450 ± 110	1703 ± 264	1620 ± 97	1514 ± 110	NS
range	68–4000	835–2289	991–2550	281–4000	68–3730	
GM	1380	1390	1590	1400	1300	
Duncan MRT		(A)	(A)	(A)	(A)	

[a]Arsenic was analyzed in only 60 fish.

Note. Given are arithmetic means plus/minus standard error. Geometric means (GM) are listed in second row. Right-hand column gives Kruskal–Wallis nonparametric analysis of variance among islands yielding chi square statistic and *p* values. Duncan Multiple Range Test performed on log-transformed values, with unlike letters indicating significant difference of means.

TABLE 2
Multiple Regression Models (SAS PROC GLM) Explaining Variances in Levels of Metals and Metalloids in Pacific Cod Collected From the Aleutians, With Df for Model=6 and Error=38 Except for Arsenic (6, 29)

MUSCLE:	arsenic[a]	cadmium	chromium	lead	mercury	selenium
Model						
r^2	0.57	0.74	0.04	0.32	0.52	0.49
F	6.21	17.60	0.30	3.07	6.94	6.22
P	0.0003	<0.0001	NS	0.015	<0.0001	<0.0001
Factors entering at 0.10 level						
F (P)						
island	13.1(<0.0001)	43(<0.0001)	NS	7.3(0.002)	NS	14.9(<0.0001)
sex	NS	NS	NS	NS	NS	NS
age	8.0(0.008)	8.7(0.005)	NS	3.0(0.09)	34(<0.0001)	5.73(0.025)
length	NS	3(0.027)	NS	NS	3.0(0.09)	NS
weight	NS	NS	NS	NS	NS	NS
LIVER:						
Model						
r^2	0.32	0.15	0.25	0.15	0.16	0.35
F	2.31	1.12	2.08	1.17	1.25	3.41
P	0.06	NS	0.08	NS	NS	0.009
Factors entering at 0.10 level						
F (P)						
island	NS	NS	2.98(0.06)	NS	NS	NS
sex	NS	3.59(0.07)	NS	NS	NS	NS
age	10.9(0.002)	NS	NS	NS	2.86(0.10)	5.11(0.03)
length	NS	NS	NS	4.47(0.04)	NS	9.57(0.004)
weight	NS	NS	NS	NS	NS	NS

[a]= arsenic was analyzed in only 39 of the 49 known-age fish.

Note. NS=not significant. Models only include the 49 cod that were aged.

TABLE 3
Multiple Regression Models (SAS PROC GLM) Explaining Variances in Levels of Metals and Metalloids in Pacific Cod Collected from the Aleutians for the Entire Data Set of 141 Cod, With Model DF=16 and Error DF=108, Except for Arsenic (16, 37)

MUSCLE:	arsenic[a]	cadmium	chromium	lead	mercury	selenium
Model						
r^2	0.43	0.28	0.09	0.16	0.45	0.22
F	1.74	2.63	0.74	1.3	5.75	2.02
P	0.083	0.002	NS	NS	<0.0001	0.02
Factors entering at 0.10 level						
F (P)						
island	NS	9.36(<0.0001)	NS	2.96(0.04)	8.9(<0.0001)	6.2(0.0007)
sex	NS	4.1(0.046)[b]	NS	NS	NS	NS
length	9.7(.004)	NS	3.62(0.06)	NS	51(<0.0001)	NS
weight	NS	3.7(0.06)	NS	5.75(0.02)	6.2(0.014)	NS
island × sex	NS	NS	NS	NS	NS	NS
island × length	NS	NS	NS	NS	NS	2.43(0.07)
island × weight	NS	NS	NS	NS	NS	NS
length × weight	NS	NS	NS	NS	NS	NS
LIVER:						
Model						
r^2	0.46	0.35	0.15	0.21	0.40	0.18
F	1.98	3.64	1.20	1.79	4.56	1.48
P	0.04	<0.0001	NS	0.04	<0.0001	NS
Factors entering at 0.10 level						
F (P)						
island	NS	NS	NS	NS	NS	NS
sex	NS	NS	2.81 (0.10)[b]	NS	NS	NS
length	8.1(0.007)	NS	NS	NS	10.8(.002)	13.1(0.0004)
weight	NS	NS	NS	NS	NS	NS
island × sex	NS	0.10	NS	NS	NS	NS
island × length	4.92(0.027)	11.1(<0.0001)	NS	NS	15.1(<0.0001)	NS
island × weight	NS	3.4(0.02)	NS	NS	2.14(.10)	NS
length × weight	0.033	4.8(0.03)	5.32(0.025)	16.5(<0.0001)	5.19(0.025)	4.20(0.043)

Note. NS=not significant.
[a]=arsenic was analyzed in only 60 fish and was not speciated.
[b]=males had higher levels than females.

DISCUSSION

Locational, Size, and Age Differences

One of the primary objectives of the research was to determine whether there were locational, size, gender, or age differences in metal levels in cod. All of the islands where fish were collected were occupied by Aleuts for centuries, and Adak and Nikolski still have Aleut communities. Adak, Amchitka, and Kiska saw military occupation, Adak until 1997. Amchitka was used for underground nuclear testing (1965–1971), but most surface contamination was cleaned up. Kiska has not had permanent occupation since the 1940s. The expected result was that any geographic differences in levels of contaminants in this study, as well as radionuclides in the larger Amchitka study (Powers et al., 2005), might relate to human activities on the islands themselves, as well as regional contamination from hazardous waste dumping or even at-sea waste disposal from the former Soviet Union (Fisher et al., 1999). In this study there was a significant locational difference in muscle for all metals except chromium; conversely, for liver there was a significant difference only for chromium. The highest levels of cadmium, mercury, and selenium in muscle were found in cod from Adak, and the highest levels of lead in muscle were found on Amchitka. Of the islands studied, Adak is the one with the greatest population size, with the largest and longest military occupation, with the most diverse population, and with a port

TABLE 4

Correlation of Standard Length, Weight, Age, and Contaminant Levels in Pacific Cod from the Aleutians (All Islands Combined, n=141), With Correlations for Muscle Above the Diagonal and Liver Below (Given are Kendall Tau Correlations)

	cadmium	chromium	lead	mercury	selenium	arsenic[a]	length	weight	age[b]
cadmium	**********	(NS)	(NS)	0.14(0.01)	0.11(0.04)	−0.19(0.04)	(NS)	0.11(0.05)	(NS)
chromium	NS	**********	0.12(0.04)	(NS)	(NS)	(NS)	−0.16(0.005)	−0.18(0.001)	(NS)
lead	NS	(NS)	**********	(NS)	(NS)	(NS)	(NS)	0.09 (0.09)	(NS)
mercury	0.28(<0.0001)	(NS)	(NS)	**********	0.12(0.03)	(NS)	0.38(<0.0001)	0.38 (0.0001)	0.45(0.0001)
selenium	0.29(<0.0001)	(NS)	(NS)	0.16(0.005)	**********	(NS)	(NS)	(NS)	(NS)
arsenic[a]	0.27(0.003)	(NS)	(NS)	0.28(0.001)	0.32(0.0003)	**********	−0.32(0.0004)	−0.30(0.0008)	−0.56(<0.0001)
length	−0.18(0.002)	(NS)	(NS)	(NS)	−0.23(<0.0001)	−0.31(0.0006)	**********	0.84(<0.0001)	0.72(<0.0001)
weight	−0.18(0.002)	(NS)	−0.10(0.09)	(NS)	−0.28(<0.0001)	−0.3(0.0007)	0.84(<0.0001)	**********	0.65(<0.0001)
age[b]	−0.23(0.03)	(NS)	(NS)	(NS)	−0.19(0.08)	−0.50(<0.0001)	0.72(<0.0001)	0.66(<0.0001)	**********

[a]Only 60 fish were analyzed for arsenic.
[b]Only 49 fish were aged by microscopic examination of otoliths.

active for the longest period. Nikolski does not have a port (no harbor is deep enough), Kiska was used only during the Second World War, and Amchitka was also used only during the Second World War and during the nuclear activities. The higher activity level likely contributed to greater environmental disposition of contaminants on land, and in the surrounding marine environment.

Julshamn et al. (1982) used differences in mercury levels to identify populations of cod, and tagging studies indicate that there is very little movement of cod among areas (Canada, 2006). Mainly cod move inshore and offshore in the same general area. The locational differences in metal levels were not due only to size because location entered the models independently of size (island × length, or island × weight).

For some contaminants, particularly mercury, levels increase with the size of the fish (Lange et al., 1994; Bidone et al., 1997; Burger et al., 2001a, 2001b; Pinho et al., 2002; Green & Knutzen, 2003). However, this is not always the case (Stafford & Haines, 2001), and at low contaminant levels, the size relationships may not hold (Park & Curtis, 1997), resulting in "correlational-chaos" (Gochfeld & Burger, 1987). Storelli et al. (2002) reported that size and mercury levels were highly correlated for swordfish (*Xiphias gladius*) and bluefin tuna (*Thunnus thynnus*) from the Mediterranean Sea. However, while yellowfin tuna (*Thunnus albacares*) showed a positive relationship between mercury and size, albacore tuna (*Thunnus alalunga*) did not (Fiji, 2006). Luten et al. (1987) found a positive correlation between size and mercury content in Atlantic cod. Interpreting correlation coefficients requires caution. The correlations may be highly significant, but the correlation coefficient may not be high; the significance derives largely from the sample sizes. In the present study, mercury levels were highly correlated with age (tau=0.45) and weight (tau=0.38) in muscle tissue, but the correlations in liver were not high (refer to Table 4). Conversely arsenic was highly negatively correlated with age (tau=−0.50) and both weight and length (tau=−0.3) in both tissues. Chromium also showed negative correlation with length and weight (tau=−0.16 and −0.18) in muscle but not liver.

Age is unknown for most fish, and size is used as a surrogate (Boening, 2000). Thus, it is usually difficult to correlate contaminant levels, size, and age. However, Braune (1987) found that in known-aged herring (*Clupea harengus harengus*), age was more strongly correlated with mercury levels than were weight or length, and the same was found to be true for the Pacific cod in this study. Although Staveland et al. (1993) found that mercury content rose markedly with increasing age for 16 cod; size relationships were not given. There are no studies where size, age, and contaminant levels were examined in the same study for cod. Contaminants that show a generally positive correlation with size and age are presumed to bioaccumulate throughout life, with length or weight representing a surrogate for age. The negative correlation, in a rapidly growing fish such as cod, probably

represents dilution by growth, as tissue mass accumulates more rapidly than the pollutant. Since there were only age data on about 40% of the cod sample in this study, the relationships with length and weight independent of age was also examined. The surprising finding was that the interaction of length × weight was more strongly related to metal levels in liver for all six metals than either length or weight alone, and that neither was predictive of muscle levels (Table 4).

In this study otolith examination was used to establish age. The relationship between mercury, size and age has been studied (Burger & Gochfeld, 2007), but has largely been ignored for other metals. In this study, there were no positive correlations in muscle with age except for mercury (tau=0.45), while in liver there were negative correlations for arsenic (tau= −0.50), cadmium (tau= −0.23), and selenium (tau= −0.19). Thus with increasing length, weight, and age, levels of cadmium and chromium declined, while mercury rose in muscle. Thus, consumers or ecological receptors cannot decrease their exposure to several metals by simply eating smaller fish.

Geographical Comparisons of Metals in Fish Muscle

One way to place contaminant levels in context is to compare levels among geographical areas. The following comparisons are for muscle only. According to the National Contaminant Biomonitoring Program (NCBP) of fish collected at 109 stations nationwide, concentrations of most heavy metals declined from 1976 through 1984 (Schmitt & Brumbaugh, 1990). The NCBP measured contaminant loads in whole fish, including stomach contents, scales, and bones. This provides a useful method for comparing levels among species, but does not provide useful information on potential adverse effects either to fish or consumers. Contaminant levels were measured only in muscle and liver, rather than in the entire fish because of interest in the possible adverse effects of the metals on the cod themselves, and on the organisms that consumed them. Unfortunately, no studies determined concentrations of metals in both whole body and muscle, which is necessary to compare such studies. Later in this section are summarized the major findings with whole body burdens for comparison, and data on muscle levels for direct comparison. It should be noted, however, that most of the data are for freshwater fish, and considerably more attention needs to be devoted to metals (other than mercury) in saltwater fish (Burger & Gochfeld, 2005, 2006; Burger et al., 2005).

Whole-body burdens of arsenic in fish from the United States overall average 140 ppb, with the maximum being 1500 ppb (wet weight; Schmitt & Brumbaugh,1990). Saiki et al. (1992) reported mean whole-body arsenic values as high as 1050 ppb (dry weight, = approximately 340 ppb wet weight) in bluegills, and 322 ppb dry weight (= ~110 ppb wet weight) in largemouth bass (*Micropterus salmoides*) from the contaminated San Joaquin valley in California, which were higher than the reported values for the United States generally. For saltwater fish purchased from markets in New Jersey, Burger and Gochfeld (2005) reported mean arsenic levels in muscle that ranged from 230 ppb (wet weight) for red snapper (*Lutjanidae* family) to 3300 ppb for flounder (*Pleuronectes americanus*); the average value for cod was 2200 ppb. Since the Atlantic cod fishery was essentially closed at the time, these fish in New Jersey markets were presumed to be Pacific cod and the result is similar to the mean of 2750 ppb for the cod from the Aleutians presented in this article. In seafood, most arsenic is in the form of organic compounds such as arsenobetaine, which is generally recognized to exert low toxicity (ATSDR, 2000).

Overall whole-body burdens of cadmium in fish from the United States average 30 ppb, with the maximum average being 220 ppb (wet weight; Schmitt & Brumbaugh, 1990). Harrison and Klaverkamp (1990) examined levels in several fish near a smelter in Manitoba. Cadmium levels averaged as high as 100 ppb (all wet weight) in pike and <10 ppb in sucker. These levels were similar to those found in other lakes in Ontario (Bradley & Morris, 1986). In freshwater fish muscle from Bangladesh, levels of cadmium ranged from 40 to 130 ppb (wet weight; Sharif et al., 1993). Levels in arctic fish are often relatively low, with means for cadmium of 1 to 294 ppb (Allen-Gill & Martynov, 1995). Arctic cod (*Boreogadus saida*) averaged 190 ppb in the Alaskan and Canadian Arctic (Dehn et al., 2005). For saltwater fish purchased in New Jersey supermarkets, Burger and Gochfeld (2005) reported mean cadmium levels in muscle that ranged from 0.50 (cod) to 30 ppb for yellowfin tuna. Nikolski cod averaged 0.57 ppb, close to the New Jersey supermarket value, while the other island averages ranged from 5 to 13 ppb, lower than most of the levels in the literature cited.

Whole-body burdens for chromium were not examined in the Schmitt and Brumbaugh (1990) study. However, Johnson (1987) reported average chromium levels of 190 to 270 ppb (wet weight) for whole fish from Ontario lakes. Levels in the muscle of *Tilapia* sp. from Baja California ranged from 140 to 13,300 ppb for chromium (Galindo et al., 1989). Saiki et al. (1992) reported average whole-body chromium levels as high as 280 ppb (dry weight, wet weight approximately 90 ppb) in largemouth bass from the contaminated San Joaquin Valley in California. Fish muscle from the Savannah River averaged from 150 to 340 ppb (wet weight) of chromium, which are similar to levels from elsewhere. For saltwater fish purchased in New Jersey supermarkets, Burger and Gochfeld (2005) reported mean chromium levels in muscle that ranged from 70 ppb in whiting (*Merluccius* spp.) to 340 ppb for cod. Thus the average levels of up to 145 ppb chromium in the cod from this study are lower than those found in other studies.

Whole-body burdens of lead in fish from the United States overall average 110 ppb, with the maximum being 4880 ppb (wet weight; Schmitt & Brumbaugh, 1990), and levels in

muscle can average 300 ppb (wet weight), a level that is hazardous to humans (Schmitt et al., 1984). Levels in Arctic fish are often relatively low, with means for lead of 10 to 810 ppb (wet weight; Allen-Gill & Martynov, 1995). Lead levels in fish muscle near Chernobyl were mostly less than 150 ppb (dry wgt), ranging up to 1760 ppb (about 400 ppb wet weight) (Jagoe et al., 1998). For saltwater fish purchased in New Jersey supermarkets, Burger and Gochfeld (2005) reported mean lead levels that ranged from 40 ppb in yellowfin tuna to 140 ppb in porgy (*Stenotomus chrysops*); cod averaged 120 ppb. Thus, the levels in cod from the Aleutians, which averaged up to 76 ppm, are within, or lower than, those reported from elsewhere.

For mercury, there are comparative values for cod from the literature. Mercury levels in muscle of Atlantic cod (*Gadus morhua)* range from 10 ppb in the Barents Sea and Faeroe Islands, to 330 ppb in the Wadden Sea (Zauke et al., 1999; Vos et al., 1986). For fish purchased in New Jersey supermarkets, Burger and Gochfeld (2005) reported mean mercury levels in muscle that ranged from 50 ppb in flounder to 650 ppb for yellowfin tuna; cod averaged of levels 110 ppb (wet weight). In a similar study of fish from markets in Chicago, Burger and Gochfeld (2006) reported mean mercury levels in fish muscle that ranged from 30 ppb in salmon (*Salmo* spp.) to 1070 ppb in swordfish (*Xiphias gladius*). The Pacific cod from the Aleutians averaged up to 316 ppb, higher than the cod reported from supermarkets.

Whole-body selenium concentrations range from 700 to 820 ppb (Schmitt & Brumbaugh, 1990), up to 1200 ppb in bass from the San Joaquin Valley. Freshwater fish from the Savannah River averaged 210–640 ppb (Burger et al., 2001a). In the New Jersey study of 9 fish species, mean selenium ranged from 50 to 1020 ppb, with 700 ppb in cod (Burger & Gochfeld, 2005). Arctic cod (*Boreogadus Saida*) from Alaskan Arctic averaged 2990 ppb selenium (Dehn et al., 2005). Selenium in muscle of 25 species of marine fish purchased commercially in Italy ranged from 73 to 734 ppb, with Atlantic Cod averaging 188 ppb (Plessi et al., 2001), compared to 183 ppb in this study. Overall, the levels of these metals and metalloids in the cod from the Aleutians were within the levels reported for saltwater fish from elsewhere, although arsenic was at the high end of published values.

Effects in Wildlife

Arsenic poisoning is relatively rare in wildlife (Eisler, 1994). Most arsenic in fish is organic arsenic, which is less toxic than inorganic arsenic species (Eisler, 1994; ATSDR, 2000). Most lab studies dealing with chronic exposure do not examine the levels in the tissues consumed that result in lethality or other adverse effects. This suggests a critical need for studies that relate levels in prey organisms, level in tissues, and dose, to adverse effects.

Cadmium is a teratogen, carcinogen, and a possible mutagen. Adverse effects of cadmium in fish and wildlife are pronounced or probable when cadmium exceeds 3 ppb in freshwater, 4.5 ppb in saltwater, and 1000 ppb in the diet (Eisler, 1985). In this study, concentrations in liver averaged 387 ppb. Concentrations in vertebrate liver that exceed 10 ppm (wet weight) need to be viewed as producing sublethal effects, and 200 ppm (wet weight) in the liver is life threatening (Eisler, 1985). In general, marine organisms are less sensitive than freshwater organisms, and mammals and birds are comparatively resistant to Cd (Eisler, 1985). Thus, the effects on mammalian consumers from cadmium in fish are expected to be low. Seabirds accumulate metals, notably cadmium and mercury, to relatively high concentrations (Thompson et al., 1993; Burger & Gochfeld, 1999). For seabirds that have evolved in marine environments with exposure to cadmium, toxic thresholds may be considerably greater (Furness, 1996), although seabirds would obviously be eating smaller cod than examined in this study. Fish themselves are affected by chronic cadmium exposure to the eggs or fry (Prager, 1995), including growth deficits, hatching rates, and spinal deformities (Williams & Holdway, 2000; Hansen et al., 2002). There is a great of variation among species (Wren et al., 1995). Salmonids, for example, are more sensitive than other fish species, and juvenile stages of fish are more sensitive than embryos (Wren et al., 1995). Adverse effects from cadmium occur in fish with dietary levels of 1000 ppb (Eisler, 1985). Whole body burdens of cadmium in fish from the United States overall averaged 30 ppb (wet weight), with the maximum being 220 ppb (Schmitt & Brumbaugh, 1990), but current levels range as high as 540 ppb in free-ranging fish (Burger et al., 2002). The geometric means concentration of cadmium in liver (224 ppb), is below the 1000 ppb cadmium effects level, but is high enough to warrant future monitoring and research.

Levels of 10,000 ppb chromium in the diets of birds are considered to cause adverse effects in some species (Eisler, 1986). Levels in the Aleutian cod were well below these levels, suggesting that predators or scavengers are not at risk from chromium if they eat cod in the Aleutian marine environment. The main human health concern for chromium is the carcinogenicity of hexavalent chromium [Cr(VI)], which may be the case with wildlife, but chromium both is an essential trace element and may manifest noncancer toxicity (Burger and Gochfeld, 1995).

Lead is a neurotoxin that produces behavioral deficits in vertebrates (Weber & Dingel, 1997), and decreases in survival, growth rates, learning, and metabolism (Eisler, 1988; Burger & Gochfeld, 2000). Levels of 50,000 ppb in the diet may produce adverse reproductive effects in some predators, and dietary levels as low as 100 to 500 ppb are associated with learning deficits in some vertebrates (Eisler, 1988). In this study, the levels of lead in liver (39 ppb) and muscle (61 ppb) of cod were below the adverse effects level, suggesting that predators would not be adversely affected by lead.

In some fish, mercury concentrations of 5000 ppb (wet weight) in muscle were associated with emaciation, decreased coordination, loss of appetite and mortality (Eisler, 1987), while concentrations of 15,000 ppb are required for adverse effects in other species (Wiener & Spry, 1996). However, sensitive birds that consume fish exhibit adverse effects at dietary mercury concentrations of 50 to 500 ppb. For sensitive mammals, harmful effects occur at dietary levels of 1100 ppb Eisler, 1987; WHO, 1990, 1991). In this study, mercury levels were 173 ppb in muscle, and 114 ppb in liver. Thus, it appears that some sensitive birds or mammals might be adversely affected if they consume the fish with the highest mercury levels. However, it is unlikely that any ecological receptors (such as birds or most mammals) would always obtain the largest fish to eat. People, however, may always eat the larger fish because they prefer the largest fish to take home or are required to release undersized fish.

Selenium is an essential micronutrient, but it may be toxic at high levels (Coyle et al., 1993). A concentration of about 1000 ppb (wet weight) in prey is the threshold for selenium toxicity in some fish, while muscle concentrations of 2600 ppb are associated with adverse effects in the fish themselves (Lemly, 1993). Further, selenium concentrations of 1000 ppb in food are toxic to other wildlife that consume them (Lemly, 1993). Selenium concentrations in the cod from the Aleutians were 183 ppb in muscle and 1570 ppb in liver, and were well below any of these effects levels.

Thus overall, the only metal that might pose a risk to predators consuming the cod is mercury, with the possibility of some of the higher values of lead at Amchitka and Nikolski posing a risk. The possible risk from mercury to marine birds and mammals, however, is lower than for terrestrial birds and mammals because they are less sensitive (Furness, 1996).

Human Health Risk

There are no uniform sources of guidance or standards for most metal residues in fish (Burger & Gochfeld, 2005). The U.S. EPA Integrated Risk Information System (IRIS) database does not specify values for fish, but inferences are drawn by comparing the chronic oral references doses (not available for lead or chromium). This is the dose expressed in milligrams per kilogram of body weight per day, which can be consumed on a daily basis over a 45-yr life span without adverse effect, and the RfD is considered protective even of sensitive subpopulations (Barnes & Dourson, 1988). "In general, the RfD is an estimate (with uncertainty spanning perhaps an order of magnitude) of a daily exposure to the human population (including sensitive subgroups) that is likely to be without an appreciable risk of deleterious effects during a lifetime." (EPA IRIS database). The dose in μg/kg = body weight/day divided by the RfD yields the Hazard Quotient (HQ) shown in the right hand column of Table 5. If HQ > 1 it indicates potential excess risk. The RfD and risk assessment in general are subject to criticism (Graham, 1995). The Rfd has been considered overprotective (due to conservative assumptions) and underprotective (averaging intermittent peak exposures).

Methylmercury is one of the main contaminants of concern in fish. The U.S. Food and Drug Administration (FDA) action level for methylmercury in fish is 1 μg/g (ppm w/w) (U.S. FDA 2001), but this is a regulatory action level, rather than a risk level. The United Kingdom and the European Union established criteria for certain metals in fish (e.g., the level for mercury is 0.5 ppm in edible fish), while China has set standards for methylmercury in canned fish (ppm wet weight) of 0.5 ppm (except 1 ppm is allowed in shark, sailfish, tuna, pike, and other high-mercury fish). In 1982 the European Commission set an Environmental Quality Standard for mercury of 0.3 ppm (wet weight).

Mercury in the muscle of cod in this study averaged about 0.17 ppm, with 13% of the cod having levels above 0.3 ppm; thus, they generally do not pose a risk to human consumers. However, although the general U.S. population would likely not eat one meal per week of cod, it is possible for subsistence Aleuts to eat five or more fish meals a week, particularly in the smaller villages on islands where planes and boats are irregular. When salmon are running, some Aleuts eat mainly salmon, but when they are not, they sometimes eat other species of fish on a daily basis. From 30 to 90% of the food consumed by people in the Aleutians is subsistence food (Patrick, 2002), and cod is one of their preferred foods (APIA, 2002; Patrick, 2002; Hamrick & Smith, 2003).

The U.S. EPA RfD was used to evaluate the risk to people consuming one 8-ounce (228 g) meal of cod per day, per week or per month, given the levels found in cod from the Aleutians (Table 5). If a person ate two meals of cod per week or even one meal per day, they would not exceed the U.S. EPA reference dose for cadmium, chromium, or selenium, but would exceed the RfD for arsenic and mercury (no RfD has been set for lead). Even one cod meal per week exceeds the U.S. EPA reference dose for mercury and arsenic. Metals were not "speciated" (i.e., did not measure separately the organic and inorganic forms of mercury or arsenic). For both elements, the organic compounds predominate in fish. However, organic arsenic compounds are much less toxic than the inorganic arsenicals on which the RfD is based, while the converse is true for mercury. Methylmercury is the predominant mercury species in fish, and also the most toxic form. The reference dose approach suggests (Table 5) that a person could eat 1 cod meal every 10 days (or 36 meals per year) for the whole year without exceeding the reference dose for mercury. However, since subsistence diets must cope with seasonal availability, the effect of eating 36 cod meals on 36 consecutive days, would need to be considered. Ginsberg and Toal (2000) suggested that there may be risk during pregnancy for exposure to a single-meal of high mercury if it occurred at a critical period. While the cod in this study generally did not have high mercury levels, some reached 0.3 ppm.

TABLE 5

Risk Evaluation for Human Consumption of Pacific Cod from the Aleutians, Based on the Average Metal Level (Converted to μg/g or ppm on Wet Weight Basis), With Assumptions that Include a "Typical" 70-kg Adult, Consuming One 228-g (8 ounce) Meal per Day (Top Panel), One Meal per Week (Middle Panel), and One Meal per Month (Bottom Panel)

	Highest Island Average		One meal per day	Intake/70 kg body wgt	EPA chronic oral Rfd	
Element	Island	Mean (μg/g)	μg/228 g	μg/kg/day	μg/kg/day	Hazard quotient
Arsenic	Adak	2.75	627.00	8.96	0.3	29.86
Cadmium	Adak	0.013	2.96	0.04	10	0.004
Chromium	Kiska	0.145	33.06	0.47	1500	0.000
Lead	Amchitka	0.076	17.33	0.25	10	0.02
Mercury	Adak	0.316	72.05	1.03	0.1	10.29
Selenium	Adak	0.282	64.30	0.92	5	0.18

	Highest Island Average		Average daily intake from one 8 ounce meal/week	Intake/70 kg body wgt	EPA chronic oral Rfd	
Element	Island	Mean (μg/g)	μg/228 g	μg/kg/day	μg/kg/day	Hazard quotient
Arsenic	Adak	2.75	89.57	1.28	0.3	4.27
Cadmium	Adak	0.013	0.42	0.01	10	0.001
Chromium	Kiska	0.145	4.72	0.07	1500	0.000
Lead	Amchitka	0.076	2.48	0.04	10	0.00
Mercury	Adak	0.316	10.29	0.15	0.1	1.47
Selenium	Adak	0.282	9.19	0.13	5	0.03

	Highest Island Average		Average daily intake from one 8 ounce meal/month	Intake/70 kg body wgt	EPA chronic oral Rfd	
Element	Island	Mean (μg/g)	μg/228 g	μg/kg/day	μg/kg/day	Hazard quotient
Arsenic	Adak	2.75	20.90	0.30	0.3	1.00
Cadmium	Adak	0.013	0.10	0.00	10	0.00
Chromium	Kiska	0.145	1.10	0.02	3	0.01
Lead	Amchitka	0.076	0.58	0.01	10	0.00
Mercury	Adak	0.316	2.40	0.03	0.1	0.34
Selenium	Adak	0.282	2.14	0.03	5	0.01

[a]The RfD is for inorganic arsenic. Most of the arsenic in seafood is organic arsenic with low toxicity.

[b]Chromium in the form of Cr-III is an essential trace element and an allowable daily intake of 1500. The RfD of 0.3 mg/kg/day is set for Cr-VI. For the sake of this risk assessment, the chromium in fish is assumed to be hexavalent.

[c]Lead does not have an oral RfD. We have arbitrarily assigned it the same value as cadmium.

REFERENCES

Agency for Toxic Substances and Disease Registry. 2000. *Toxicological profile for arsenic.* Atlanta, GA: ATSDR.

Agency for Toxic Substances and Disease Registry. 2004. *Public health assessment: Naval Air Facility, Adak.* http://www.atsdr.cdc.vog/HAC/PHA/adak/ada_p1.html (accessed 9/15/04).

Allen, M. J., and Smith, G. B. 1988. *Atlas and zoogeography of common fishes in the Bering Sea and north Pacific.* Seattle, WA: NOAA Tech. Rep. NMFS-NWFSC 66.

Allen-Gill, S. M., and Martynov, V. G. 1995. Heavy metal burdens in nine species of freshwater and anadromous fish from the Pechora River, northern Russia, *Sci. Total Environ.* 160:653–659.

Anderson, P.D. and Wiener, J.B. 1995. Eating fish. In *Risk versus risk: Tradeoffs in protecting health and the environment*, eds. J. D. Graham ad J. B. Wiener, pp. 104–123. Cambridge, MA: Harvard University Press.

APIA (Aleutian Pribilof Islands Association). 2002. *Atka traditional food sampling survey.* Anchorage, AL: APIA.

Bakkala, R.G. 1984. Pacific cod of the eastern Bering Sea. *Int. North Pacific Fish. Comm. Bull.* 42:157–179.

Barnes, D. G., and Dourson, M. 1988. Reference dose (RfD): Description and use in health risk assessments. *Regul. Toxicol. Pharmacol.* 8:471–486.

Bayen, S., Giusti, P., Lee, H. K., Barlow, P. J., and Obard, J. P. 2005. Bioaccumulation of DDT pesticide in cultured Asian seabass following dietary exposure. *J. Toxicol. Environ. Health A* 68:51–65.

Berlin, C. M., Jr., Kacew, S., Lawrence, R., LaKind, J. S., and Campbell, R. 2002. Criteria for chemical selection for programs on human milk surveillance and research for environmental chemicals. *J. Toxicol. Environ. Health A* 65:1839–1851.

Berti, P. R., Receveur, O., Chan, H. M., and Kuhnlein, H. V. 1998. Dietary exposure to chemical contaminants from traditional food among adult Dene/Metis in the Western Northwest Territories, Canada. *Environ. Res.* 76:131–142.

Bidone, E. D., Castilhos, Z. C., Santos, T. J. S., Souza, T. M. C. and Lacerda, L. D. 1997. Fish contamination and human exposure to mercury in Tartarugalzinho River, Northern Amazon, Brazil. A screening approach. *Water Air Soil Pollut. 97*:9–15.

Bloom, N. S. 1991. On the chemical form of mercury in edible fish and marine invertebrate tissue. *Can. J. Fish. Aquat. Sci.* 49:1010–1017.

Boening, D. W. 2000. Ecological effects, transport, and fate of mercury: A general review. *Chemosphere* 40:1335–1351.

Bradley, R. W., and Morris, J. R. 1986. Heavy metals in fish from a series of metal-containing lakes near Sudbury, Ontario. *Water, Air Soil Pollut.* 27:341–354.

Braune, B. M. 1987. Mercury accumulation in relation to size and age of Atlantic herring (*Clupea harengus harengus*) from the southwestern Bay of Fundy, Canada. *Arch. Environ. Contam. Toxicol.* 16:311–320.

Burger, J. 1999. American Indians, hunting and fishing rates, risk and the Idaho National Engineering and Environmental Laboratory. *Environ. Res.* 80:317–329.

Burger, J. 2000. Consumption advisories and compliance: The fishing public and the deamplification of risk. *J. Environ. Plan. Manage.* 43:471–488.

Burger, J. 2002. Consumption patterns and why people fish. *Environ. Res.* 90:125–135.

Burger, J., and Gochfeld, M. 1995. Growth and behavioral effects of early postnatal chromium and manganese exposure in herring gull (*Larus argentatus*) chicks. *Pharmacol. Biochem. Behav.* 50:607–612.

Burger, J., and Gochfeld, M. 1999. Interspecific and locational differences in heavy metal levels in four species of birds near Sydney, Australia. *Environ. Monit. Assess.* 58:105–119.

Burger, J.,and Gochfeld, M. 2000. Effects of lead on birds (Laridae): A review of laboratory and field studies. *J. Toxicol. Environ. Health* 3:59–78.

Burger, J., and Gochfeld, M. 2004. Mercury in canned tuna: white versus light and temporal variation. *Environ. Res.* 96:239–249.

Burger, J., and Gochfeld, M. 2005. Heavy metals in commercial fish in New Jersey. *Environ. Res.* 99:403–412.

Burger, J., and Gochfeld, M. 2006. Mercury in fish available in supermarkets in Illinois: Are there regional differences. *Sci. Total Environ.* (in galley).

Burger, J., and Gochfeld, M. 2007. Risk to consumers from mercury in Pacific cod (*Gadus macrocephalus*) from the Aleutians: Age and size effects. *Environ. Res.* 105:276–284.

Burger, J., Pflugh, K. K., Lurig, L., von Hagen, L. A. and von Hagen, S. A. 1999. Fishing in urban New Jersey: Ethnicity affects information sources, perception, and compliance. *Risk. Anal.* 19:217–229.

Burger, J., Gaines, K. F., Boring, C. S., Stephens, W. L., Jr., Snodgrass, J., and Gochfeld, M. 2001a. Mercury and selenium in fish from the Savannah River: Species, trophic level, and locational differences. *Environ. Res.* 87:108–118.

Burger, J., Gaines, K. F., and Gochfeld, M. 2001b. Ethnic differences in risk from mercury among Savannah River fishermen. *Risk. Anal.* 21:533–544.

Burger, J., Gaines, K. F., Boring, C. S., Stephens, W. L., Snodgrass, J., Dixon, C., McMahon, M., Shukla, S., Shukla, T. and Gochfeld, M. 2002. Metal levels in fish from the Savannah River: Potential hazards to fish and other receptors. *Environ. Res.* 89:85–97.

Burger, J., Stern, A. H., Dixon, C., Jeitner, C., Shukla, S., Burke, S. and Gochfeld, M. 2004. Fish availability in supermarkets and fish markets in New Jersey. *Sci. Total Environ.* 333:89–97.

Burger, J., Stern, A. H. and Gochfeld, M. 2005. Mercury in commercial fish: Optimizing individual choices to reduce risk. *Environ. Health Perspect.* 113:266–270.

Burger, J., Gochfeld, M., Burke, S., Jeitner, C.W., Jewett, S., Snigaroff, D., Snigaroff, R., Stamm, T., Harper, S., Hoberg, M., Chenelot, H., Patrick, R., Volz, C.D., and Weston, J. 2006. Do scientists and fishermen collect the same size fish? Possible implications for exposure assessment. *Environ. Res.* 101:34–41.

Canada. 2006. Groundfish—Pacific cod. http://www-comm.pac.dfo-mpo.gc.ca/publications/speciesbook/groundfish/cod_e.htm. (accessed February 2006).

Chan, H. M., and Receveur, O. 2000. Mercury in the traditional diet of indigenous peoples of Canada. *Environ. Pollut.* 110:1–2.

Consumer Reports. 2003. American's fish: fair or foul? http://www.consumerreports.org/special/consumerInteret/Reports/0102fis0.html (accessed 1 April 2004). New York: Consumers Union.

Coyle, J. J., Ingersoll, D. R., Fairchild, C. G., and May, T. W. 1993. Effects of dietary selenium on the reproductive success of bluegills (Lepomis macrochirus). *Environ. Toxicol. Chem.* 12:551–565.

Daviglus, M., Sheeshka, J., and Murkin, E. 2002. Health benefits from eating fish. *Comments Toxicol.* 8:45–374.

Dean, T. A., Haldorson, L., Laur, D. R., Jewett, S. C., and Blanchard, A. 2000. The distribution of nearshore fishes in kelp and eelgrass communities in Prince William Sound, Alaska: Associations with vegetation and physical habitat characteristics. *Environ. Biol. Fish.* 57:271–287,

Dehn, L. A., Sheffield, G. G., Follmann, E. H., Duffy, L. K., Thomas, D. L., Bratton, G. R., Taylor, R. J., and O'Hara, T. M. 2005. Trace elements in tissues of phocid seals harvested in the Alaskan and Canadian Arctic: influence of age and feeding ecology. *Can. J. Zool.* 83:726–746.

Duchesne, J. F., Levesque, B., Gauvin, D., Braune, B., Gingras, S., and Dewailly, E. 2004. Estimating the mercury exposure dose in a population of migratory bird hunters in the St. Lawrence River region, Quebec, Canada. *Environ. Res.* 95:207–214.

Duhaime, G., Chabot, M., Frechette, P., Robichaud, V., and Proulx, S. 2004. The impact of dietary changes among the Inuit of Nunavik (Canada): A socioeconomic assessment of possible public health recommendations dealing with food contamination. *Risk. Anal.* 24:1007–1018.

Egeland, G. M., Feyk, L. A., and Middaugh, J. P. 998. The use of traditional foods in a healthy diet in Alaska. Juneau: Alaska Division of Public Health.

Egelend G. M., and Middaugh, J. P. 1997. Balancing fish consumption benefits with mercury exposure. *Science* 278:904–1906.

Eisler, R. 1985. Cadmium hazards to fish, wildlife, and invertebrates: A synoptic review. Washington, DC: U.S. Fish and Wildlife Service Rep. 85(1.2).

Eisler, R. 1986. Chromium hazards to fish, wildlife, and invertebrates: A synoptic review. Washington, DC: U.S. Fish and Wildlife Service Rep. 85(1.6).

Eisler, R. 1987. Mercury hazards to fish, wildlife, and invertebrates: A synoptic review. Washington DC: U.S. Fish and Wildlife Service Rep. 85(1.10),.

Eisler, R. 1988. Lead hazards to fish, wildlife, and invertebrates: A synoptic review. Washington, DC: U.S. Fish and Wildlife Service.

Eisler, R. 1994. A review of arsenic hazards to plants and animals with emphasis on fishery and wildlife resources. In Arsenic in the environment, Part II, ed. J. O Nriagu, pp. 185–259. New York: John Wiley.

Fiji. 2006. Mercury levels in Fijian seafood. http://www.wpro.who.int/NR/rdonlyres/437775AO-671F-41AE-A068 (accessed February 10, 2006).

Fisher, N.S., Fowler, S. W., Boisson, F., Carroll, J., Rissanen, K., Salbu, B., Sazykina, T. G., and Sjoeblom, K. L. 1999. Radionuclide bioconcentration factors and sediment partition coefficients in Arctic Seas subject to contamination from dumped nuclear wastes. *Environ. Sci. Technol.* 33:1979–1982.

Fleming, L. E., Watkins, S., Kaderman, R., Levin, B., Ayyar, D. R., Bizzio, M., Stephens, D., and Bean, J. A. 1995. Mercury exposure in humans through food consumption from the Everglades of Florida. *Water Air Soil Pollut.* 80:41B48.

Furness, R. W. 1996. Cadmium in birds. In *Environmental contaminants in wildlife: Interpreting tissue concentrations*, eds. W. N. Beyer, G. H. Heinz, and A. W. Redmon-Norwood, pp. 389–404. Boca Raton, FL: Lewis.

Galindo, G., Munoz, E. F., and Reynosa, V. M. 1989. Trace metals in fish from the Mexicali Valley, Mexico. *Ciencias Marinas* 15:105–115.

Gerstenberger, S. L., and Dellinger, J. A. 2002. PCBs, mercury, and organochlorine concentrations in lake trout, walleye, and whitefish from selected tribal fisheries in the Upper Great Lakes region. *Environ. Toxicol.* 17:513–519.

Ginsberg, G. L., and Toal, B. F. 2000. Development of a single-meal fish consumption advisory for methylmercury. *Risk Anal.* 20:41–47.

Gochfeld, M. 2003. Cases of mercury exposure, bioavailability, and absorption. *Ecotoxicol. Environ. Safety* 56:174–179.

Gochfeld, M., and Burger, J. 1987. Factors affecting tissue distribution of heavy metals: Effects of age on correlation patterns in common terns *Sterna hirundo*. *Biol. Trace Element Res.* 12:389–399.

Graham, J. D. 1995. Historical perspective on risk assessment in the federal government. *Toxicology* 102:29–52.

Green, N. W., and Knutzen, J. 2003. Organohalogens and metals in marine fish and mussels and some relationships to biological variables at reference localities in Norway. *Mar. Pollut. Bull.* 46: 362–377.

Gulson, B. L., Jameson, C. S., Mahaffey, K. R., Mizon, K. J., Korsch, M. J., and Vimpani, G. 1997. Pregnancy increases mobilization of lead from maternal skeleton. *J. Lab. Clin. Med.* 130:51–62.

Hamrick, K., and Smith, J. 2003. Subsistence food use in Unalaska and Nikolski. Anchorage, AL: Aleutian Pribilof Island Association.

Hansen, J. A., Welsh, P. G., Lipton, J., and Suedkamp, M. J. 2002. The effects of long-term cadmium exposure on the growth and survival of juvenile bull trout (*Salvelinus confluentus*). *Aquat. Toxicol.* 58:165–174.

Hansen, J. C., Deutch, B., and Pedersen, H. S. 2004. Selenium status in Greenland Inuit. *Sci. Total Environ.* 331:207–214.

Harris, S. G., and Harper, B. L. 1998. Native American exposure scenarios and a tribal risk model. *Risk Anal.* 17:789–785.

Harrison, S. E., and Klaverkamp, J. F. 1990. Metal contamination in liver and muscle of northern pike (*Esox lucious*) and white sucker (*Catostomus commersoni*) and in sediments from lakes near the smelter at Flin Flon, Manitoba. *Environ. Toxicol. Chem.* 9:941–956.

Heck, K. L., and Orth, R. J. 1980. Seagrass habitats: The roles of habitat complexity, competition and predation in structuring associated fish and motile macroinvertebrate assemblages. In *Estuarine perspectives*, ed. V. S. Kenedy, pp. 449–464. New York: Academic Press.

Hightower, J. M., and Moore, D. 2003. Mercury levels in high-end consumers of fish. *Environ. Health Perspect.* 111:604–608.

Hites, R. A., Foran, J. A., Carpenter, D. O., Hamilton, M. C., Knuth, B. A., and Schwager, S. J. 2004. Global assessment of organic contaminants in farmed salmon. *Science* 303:226–229.

Hood, D. W., and Calder, J. A., eds. 1981). The eastern Bering Sea shelf: Oceanography and resources. Washington, DC: U.S. Departments of Commerce and Interior, U.S. Bureau of Land Management, NOAA.

Hylland, K., Beyer, J., Bertssen, M., Klungsoyr, J., Land, T., and Balk, L. 2006. May organic pollutants affect fish populations in the North Sea? *J. Toxicol. Environ. Health A* 69:125–138.

Institute of Medicine. 1991. *Seafood safety*. Washington, DC: National Academy Press.

Jagoe, C. H., Dallas, C. E., Chesser, R. K., Smith, M. H., Lingenfelser, S. K., Lingenfelser, J. T., Holloman, K., and Lomakin, M. D. 1998. Contamination near Chernobyl: Radiocesium, lead and mercury in fish and sediment radiocesium from waters within the 10 km zone. *Ecotoxicology* 7:1–9.

Jensen, J., Adare, K., and Shearer, R. 1997. Canadian Arctic contaminants assessment report. Indian and Northern Affairs, QS-8525-000-EE-A1, Ottawa, Canada.

Johnson, M. G. 1987. Trace element loadings to sediments of fourteen Ontario lakes and correlations with concentrations in fish. *Can. J. Fish. Aquat. Sci.* 44:3–13.

Jorgensen, E. H., Vijayan, M. M., Killie, J. A., Aluru, N., Aas-Hansen, O., and Maule, A. 2006. Toxicokinetics and effects of PCBs in Arctic fish: A review of studies of Arctic charr. *J. Toxicol. Environ. Health A* 69:37–52.

Julshamn, K., Ringdal, O., and Braekkan, O. R. 1982. Mercury concentration in liver and muscle of cod (*Gadus morhua*) as evidence of migration between waters of different levels of mercury. *Bull. Environ. Contam. Toxicol.* 29:544–549.

Lange, T. R., Royals, H. E., and Connor, L. L. 1994. Mercury accumulation in largemouth bass (*Micropterus salmoides*) in a Florida Lake. *Arch. Environ. Contam. Toxicol.* 27:466–471.

Lemly, D. A. 1993. Guidelines for evaluating selenium data from aquatic monitoring and assessment studies. *Environ. Monit. Assess.* 28:83–100.

Luten, J. B., Bouquet, W., Riekwel-Booy, G., Rauchbaar, A. B., and Scholte, M. W. M. 1987. Mercury in flounder, *Platichtys flesus*, cod, *Gadus morhua*, and perch, *Perca fluviatilis*, in relation to their length and environment. *Bull. Environ. Contam. Toxicol.* 38:318–323.

Merrell, T. R., Jr. 1977. Fishery resources of the Western Aleutians. In *The environment of Amchitka Island, Alaska*, eds. M. L. Merritt and R. G. Fuller, pp. 315–330 . Washington, DC: TIC, Energy Research and Development Administration.

Mito, K., Nishimura, A., and Yanagimoto, T. 1999. Ecology of groundfishes in the eastern Bering Sea, with emphasis on food habits. In *Dynamics of the Bering Sea*, eds. T. R. Laughlin and O. Kiyotaka, pp. 537–580. Fairbanks: Universty of Alaska, SeaGrant.

Munk, K. M. 2001. Maximum ages of groundfishes in waters off Alaska and British Columbia and considerations of age determination. *Alaska Fish. Res. Bull.* 9:13–21.

National Research Council. 1996. *The Bering Sea ecosystem.* Washington DC: National Academy Press.

Park, J. G., and Curtis, L. R. 1997. Mercury distribution in sediments and bioaccumulation by fish in two Oregon reservoirs: Point-source and nonpoint source impacted systems. *Arch. Environ. Contam. Toxicol.* 33:423–429.

Patrick, R. 2002. How local Alaska native communities view the Amchitka issue. *Proc. Amchitka long-term stewardship workshop.* Fairbanks: CRESP/University of Alaska.

Patterson, J. 2002. Introduction—Comparative dietary risk: Balance the risks and benefits of fish consumption. *Comments Toxicol.* 8:337–344.

Pinho, A. P., Guimaraes, J. R. D., Marins, A. S., Costa, P. A. S., Olavo, G., and Valentin, J. 2002. Total mercury in muscle tissue of five shark species from brazilian offshore waters: Effects of feeding habit, sex and length. *Environ. Res.* 89:250–258.

Plessi, M., Bertelli, D., and Monzani A. 2001. Mercury and selenium content in selected seafood. *J. Food Compos. Anal.* 14:461–467.

Powers, C. W., Burger, J., Kosson, D., Gochfeld, M., and Barnes, D., eds. 2005. Biological and geophysical aspects of potential radionuclide exposure in the Amchitka marine environment. Piscataway, NJ: CRESP.

Prager, J. C. 1995. *Environmental contaminant reference databook*, vol. 1. New York: Van Nostrand Reinhold.

Saiki, M. K., Jennings, M. R., and Ma, T. W. 1992. Selenium and other elements in freshwater fishes from the irrigated San Joaquin valley, California. *Sci. Total Environ.* 126:109–137.

Schmitt, C. J., and Brumbaugh, W. G. 1990. National contaminant biomonitoring program: Concentrations of arsenic, cadmium, copper, lead, mercury, selenium and zinc in U.S. Freshwater fish, 1976–1984. *Arch. Environ. Contam. Toxicol.* 19:731–747.

Schmitt, C. J., Dwyer, F. J. and Finger, S. E. 1984. Bioavailability of Pb and Zn from mine tailings as indicated by erythrocyte α-aminolevulinic acid dehydratase (ALA-D) activity in suckers (Pisces: Catostomidae). *Can. J. Fish. Aquat. Sci.* 41:1030–1040.

Sharif, A. K. M., Alamgir, M., Mustafa, A. I., Hossain, M. A., and Amin, M. N. 1993. Trace element concentrations in ten species of freshwater fish of Bangladesh. *Sci. Total Environ.* 138:117–126.

Simenstad, C. A., Isakson, J. S., and Nakatani, R. E. 1977. Marine fish communities. In *The environment of Amchitka Island, Alaska,* eds. M. L. Merritt and R. G. Fuller, pp. 451–492. Washington, DC: TIC, Energy Research and Development Administration.

Stafford, C. P., and Haines, T. A. 2001. Mercury contamination and growth rate in two piscivore populations. *Environ. Toxicol. Chem.* 20: 2099–2101.

Statistical Analysis System (SAS). 1995. *SAS users' guide*. Cary, NC: Statistical Institute, Inc.

Staveland, G., Marthinsen, I., Norheim, G., and Julshamn, K. 1993. Levels of environmental pollutants in flounder (*Platichthys flesus* L.) and cod (*Gadus morhua* L.) caught in the waterway of Glomma, Norway. II. Mercury and arsenic. *Environ. Contam. Toxicol.* 24:187–193.

Stern, A. H. 1993. Re-evaluation of the reference dose for methylmercury and assessment of current exposure levels. *Risk Anal.* 13:355–364.

Storelli, M. M., Stuffler, R. G., and Marcotrigiano, G. O. 2002. Total and methylmercury residues in tuna-fish from the Mediterranean Sea. *Food Addit. Contam.* 19:715–720.

Thompson, D. R., Becker, P. H., and Furness, R. W. 1991. Long-term changes in mecury concentrations in herring gulls *Larus argentatus* and common terns *Sterna hirundo* from the German North Sea Coast. *J. Applied Ecol.* 30:316–320.

Toth, J. F., Jr., and Brown, R. B. 1997. Racial and gender meanings of why people participate in recreational fishing. *Leisure Sci.* 19:129–146.

Tokranov, A. M., and Vinnikov, A. M. 1991. Diet of the Pacific cod *Gadus morhua marcocephalus* and its position in the food chain in Kamchatkan coastal waters. *J. Ichthyol.* 31:84–98.

U.S. Environmental Protection Agency. 2004. National listing of fish advisories. Cincinnati, OH: U.S. EPA. http//map1.epa.gov (accessed 30 October 2004).

U.S. Food and Drug Administration. 2001. FDA consumer advisory. Washington, DC: U.S. Food and Drug Administration. http//www.fda.gov/bbs/topics/ANSWERS/2000/advisory.html. (accessed 1 December 2001).

Weber, D. N., and Dingel, W. M. 1997. Alterations in neurobehavioral responses in fishes exposed to lead and lead-chelating agents. *Am. Zool.* 37:354–362.

Wiener, J. G., and Spry, D. J. 1996. Toxicological significance of mercury in freshwater fish. In *Environmental contaminants in wildlife: Interpreting tissue concentrations*, eds, W, N. Beyer, G. H. Heinz, and A. W. Redmon-Norwood, pp. 297–339. Boca Raton, FL: Lewis.

Williams, N. D., and Holdway, D. A. 2000. The effects of pulse-exposed cadmium and zinc on embryo hatchability, larval development, and survival of Australian crimson spotted rainbow fish (*Melanotaenia fluviatalis*). *Environ. Toxicol.* 15:165–173.

World Health Organization. 1990. IPCS Methylmercury. Environmental Health Criteria 101. Geneva: WHO.

World Health Organization. 1991. IPCS Inorganic mercury. Environmental Health Criteria 118. Geneva: WHO.

Wren, C. D., Harris, S., and Harttrup, N. 1995. Ecotoxicology of mercury and cadmium. In Handbook of ecotoxicology, eds. D. J. Hoffman, B. A. Rattner, G. A, Burton, Jr., and J. Cairns, Jr., pp. 392–423. Boca Raton, FL: Lewis.

Zauke, G. P., Savinov, V. M., Ritterhoff, J., and Savinova, T. 1999. Heavy metals in fish from the Barents Sea (summer 1994). *Sci. Total Environ.* 227:161–173.

Copyright of Journal of Toxicology & Environmental Health: Part A is the property of Taylor & Francis Ltd and its content may not be copied or emailed to multiple sites or posted to a listserv without the copyright holder's express written permission. However, users may print, download, or email articles for individual use.

Copyright of Journal of Toxicology & Environmental Health: Part A is the property of Taylor & Francis Ltd and its content may not be copied or emailed to multiple sites or posted to a listserv without the copyright holder's express written permission. However, users may print, download, or email articles for individual use.

Science of the Total Environment 416 (2012) 208–214

Contents lists available at SciVerse ScienceDirect

Science of the Total Environment

journal homepage: www.elsevier.com/locate/scitotenv

Genotoxic effects in blood cells of *Mus musculus* and *Iguana iguana* living near coal mining areas in Colombia

Maria Cabarcas-Montalvo, Jesus Olivero-Verbel *, Homer Corrales-Aldana

Environmental and Computational Chemistry Group, Faculty of Pharmaceutical Sciences, University of Cartagena, Cartagena, Colombia

ARTICLE INFO

Article history:
Received 3 September 2011
Received in revised form 29 November 2011
Accepted 30 November 2011
Available online 4 January 2012

Keywords:
Coal mining
Comet assay
DNA damage
Micronucleus test
Genotoxicity
Environmental monitoring

ABSTRACT

Coal is a mixture of chemicals with the capacity of promoting biochemical changes that may lead to DNA damage. In this study, the comet assay in peripheral blood cells, and the micronucleus test in blood smears were used to evaluate potential genotoxic effects derived from exposure to coal mining activities on wild populations of *Mus musculus* and *Iguana iguana*. Four locations from Colombia were evaluated: La Loma and La Jagua de Ibirico, two municipalities located near coal mining fields at the Department of Cesar; and Valledupar and Arjona, cities used as reference sites, both localized at least 100 and 200 km far from the mines, respectively. Compared to Valledupar and Arjona, animals collected in close proximity to coal mining areas showed highest percentages of DNA damage for both species, evidencing that living around coal mining fields may result in an increase of DNA lesions in blood cells of rodents and reptiles. The results for micronucleus test were conflicting. Mice from Arjona had greater number of cells with micronucleus than those from the other studied locations, probably as a result of infection found by blood parasites. In summary, it was demonstrated that animals living around coal mining areas have a greater chance of having DNA damage, as measured by the comet assay, than those from sites far from the coal dust source.

© 2011 Elsevier B.V. All rights reserved.

1. Introduction

Coal is a key mineral used as an energy source for many countries (Bian et al., 2010). It is a complex mixture of chemicals that is not always homogeneous and depends on the source and rank of the coal (Donbak et al., 2005). It is made of carbon, hydrogen, oxygen, nitrogen, inorganic minerals, quartz, trace metals, and other contaminants (Castranova and Vallyathan, 2000). Many of the coal components are mutagenic and carcinogenic (da Silva et al., 2000a); for instance, quartz could be a prominent risk factor for lung cancer in coal miners (Borm and Tran, 2002), and the International Agency for Research on Cancer (IARC) classified it into IARC's Group 1 (carcinogenic to humans), due to sufficient evidence for carcinogenicity in experimental animals and in humans (IARC, 2010). Heavy metals such as arsenic, cadmium, as well as, polycyclic aromatic hydrocarbons (PAHs), present in coal, are also well recognized carcinogens (da Silva et al., 2000a, 2000b).

Coal dust extracts have also been reported to be cytotoxic and mutagenic in mammalian systems (Ulker et al., 2008). Oxidative DNA damage was observed to be significantly higher in lymphocytes of retired coal miners than in controls (Shins et al., 1995). Besides, there was an increase in the frequencies of sister chromatid exchanges, chromosomal aberrations, and micronucleus in underground coal miners, indicating the genetic damage due to coal dust exposure (Donbak et al., 2005).

Studies of genetic toxicology have given rise to a number of testing procedures, designed to assess the effects of substance exposure on genetic mechanisms and the consequent risk to organisms, including humans (Krishna and Hayashi, 2000). One of the tools aimed to evaluate genotoxic effects in the biota is the neutral comet assay, an electrophoresis-based method that is able to detect the actual single-strand (SS) and double-strand (DS) breaks in individual cells (Collins et al., 2008; Tice et al., 2000). This test has shown to be a simple, fast, and effective assay to detect DNA damage (Mitchelmore and Chipman, 1998). It has been already used to assess environmental genotoxicity in coal mining areas (León et al., 2007) and for the detection of early biological effects of DNA damaging agents (Sasaki et al., 1998) such as radiation, chemotherapeutic agents, and reactive oxygen radicals, in both environmental and occupational settings (Fairbairn et al., 1995; Moller et al., 2000). Another toxicity test widely used to measure genotoxicity is the micronucleus assay (MN) in peripheral blood. This assay, when performed appropriately, detects both clastogenicity (chromosome breakage) and aneugenicity (chromosome lagging due to dysfunction of mitotic apparatus) (Krishna and Hayashi, 2000).

Colombia is the country with the largest coal reserves in Latin America. It has potential resources of 16,992 million tons (UPME, 2007), being the sixth largest exporter of coal in the world. Most

* Corresponding author at: Environmental and Computational Chemistry Group, Faculty of Pharmaceutical Sciences, University of Cartagena, Zaragocilla Campus, Cartagena, Colombia. Tel.: +57 5 6698179, +57 5 6698180; fax: +57 5 6698323.
E-mail addresses: joliverov@unicartagena.edu.co, jesusolivero@yahoo.com (J. Olivero-Verbel).

0048-9697/$ – see front matter © 2011 Elsevier B.V. All rights reserved.
doi:10.1016/j.scitotenv.2011.11.080

coal reserves and mines (95%) are located in the Departments of La Guajira and Cesar (UPME, 2005). There are several coal mines operated by different companies in the Department of Cesar, and the most important are located in the towns of La Loma and La Jagua de Ibirico. In 2004, La Loma produced 38%, and La Jagua de Ibirico about 10% of the total Colombian Atlantic Coast exports (UPME, 2006b). For 2005, the coal mine in La Loma (Cesar) had the second largest coal production in Colombia, which was estimated at 16.5 million tons (UPME, 2006a).

The goal of this research was to evaluate the potential genotoxic damage in peripheral blood cells of *Mus musculus* (mice) and *Iguana iguana* (iguana) living near coal mining polluted areas at the Department of Cesar, Colombia, using the neutral comet assay and the micronucleus test in blood smears.

2. Materials and methods

2.1. Study area

This study was performed between August 2010 and April 2011 in different areas of the Departments of Cesar and Bolivar, at the north of Colombia. Two towns located next to the most important coal mines in the Department of Cesar were evaluated: La Jagua de Ibirico (10°31′19″ N, 73°18′56″ W) and La Loma (10°23′58″ N, 75°30′9″ W). The municipality of La Jagua de Ibirico is located in the central region of the department, at the foothills of the Colombian Andean Eastern Mountain Range. Its land area is 728.9 km^2 with an average altitude of 150 m.a.s.l. and an estimated population of 21,386 inhabitants (DANE, 2005). The village of La Loma, located 28.74 km far from La Jagua de Ibirico, has the second largest coal mine in the country.

Mice were also collected from two different reference sites: The urban area of Valledupar (10°28′06″ N, 73°15′04″ W), the capital of the Department of Cesar, approximately 100 km far from the coal mining area (Fig. 1), and Arjona (10°15′17″ N, 75°20′32″ W), a small town at the Department of Bolivar, at least 200 km far from the mines. The city of Valledupar covers an area of 4493 km^2, with 169 m.a.s.l., and an expected population of 413,301 habitants in 2011 (DANE, 2009). Its average annual temperature is 28.4 °C, with highs and lows of 22 °C and 34 °C, respectively (Ortega-Montero, 2007). The topography of the municipality of Arjona is slightly undulating, with elevations not exceeding 200 m.a.s.l, and a calculated population of 67,325 inhabitants (DANE, 2009). The specimens of *I. iguana* were captured only in 2011, in rural areas of La Loma and near to the natural reserve Los Besotes, at the north of Valledupar (10°34′26″N, 73°16′19″W).

2.2. Sampling methods

The specimen collection procedure was conducted with permission of CORPOCESAR, the environmental protection agency for the Department of Cesar (Resolution No. 739, dated June 22, 2010). Characteristics of collected specimens are shown in Table 1. *M. musculus* specimens were collected by a capture-removal method using Sherman live-capture traps (8×9×23 cm; Sherman Traps, Inc., Tallahassee, FL). These were placed inside houses between 04:00 and 06:00 pm and picked up the following day between 06:00 and 07:30 am. Iguanas were captured during early morning hours with the help of local farmers.

The rodents were processed in the field according to established biosafety guidelines (Mills et al., 1995). Mice were treated intraperitoneally

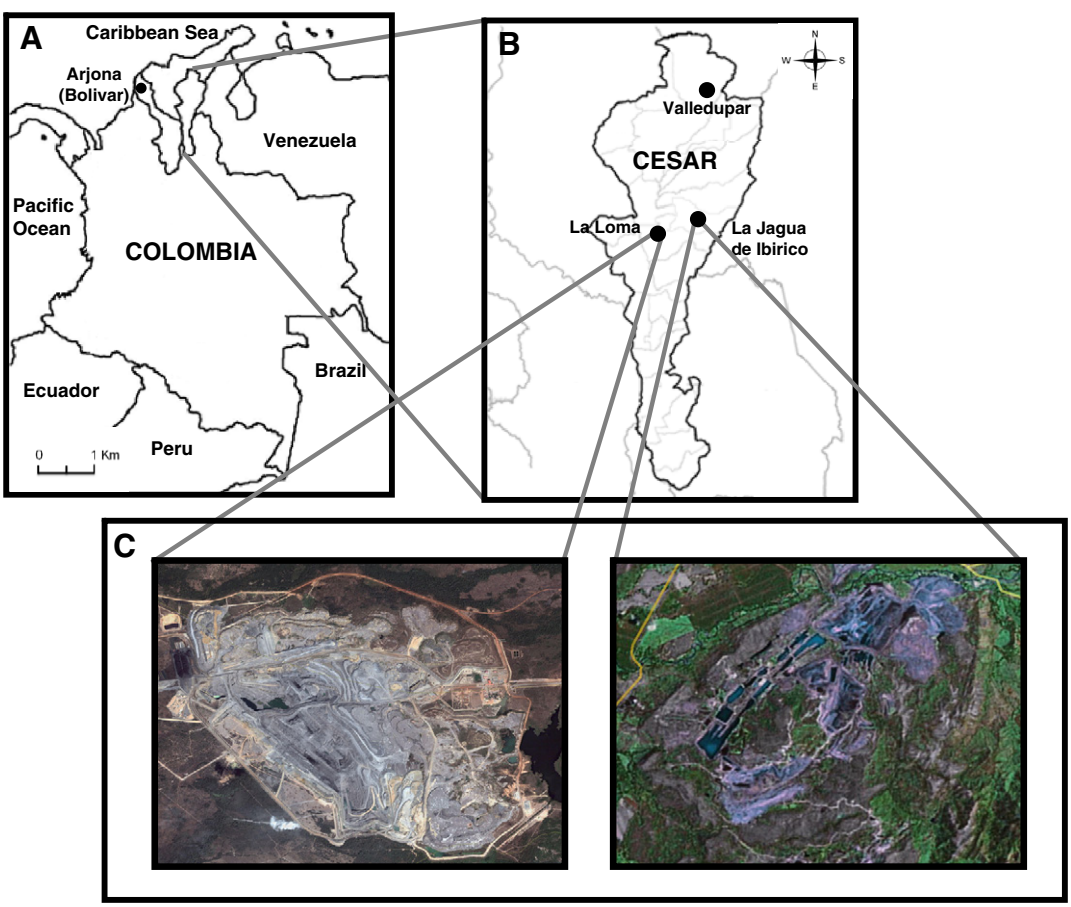

Fig. 1. Map of Colombia showing the geographic localization of sampling areas. A. Arjona (Department of Bolívar). B. La Loma. La Jagua and Valledupar (Department of Cesar). C. Satellite images of the coal mines.

Table 1
Characteristics of collected specimens from sampling sites.

Study area		*Mus musculus*						*Iguana iguana*		
		2010			2011			2011		
		Male	Female	Total	Male	Female	Total	Male	Female	Total
Arjona	Juvenile	1	1	2	1	3	4	*N.A.	N.A.	N.A.
	Adult	9	2	11	4	4	8	N.A.	N.A.	N.A.
	Total	10	3	13	5	7	12	N.A.	N.A.	N.A.
Valledupar	Juvenile	2	1	3	0	4	4	2	7	9
	Adult	4	9	13	8	5	13	1	0	1
	Total	6	10	16	8	9	17	3	7	10
La Jagua	Juvenile	3	0	3	3	2	5	N.A.	N.A.	N.A.
	Adult	3	2	5	2	2	4	N.A.	N.A.	N.A.
	Total	6	2	8	5	4	9	N.A.	N.A.	N.A.
La Loma	Juvenile	3	0	3	2	3	5	3	2	5
	Adult	3	5	8	5	8	13	4	2	6
	Total	6	5	11	7	11	18	7	4	11
Total	28	20	48	25	31	56	10	11	21	

* N.A. not available.

with sodium thiopental and iguanas with ketamine until a level of deep anesthesia was attained. Blood samples were obtained from the caudal vena cava and collected in tubes containing 3.8% sodium citrate, stored at 4 °C and protected from light until processed. All samples were analyzed within 24 hours.

2.3. Comet assay

The neutral comet assay was performed following the method proposed by Trevigen (Trevigen; Gaithersburg, MD) with some modifications (Yang et al., 2011). Blood samples were combined with 0.5% low melting agarose in a 1:12.5 and 1:75 (v/v) ratio for mice and iguanas, respectively. Then, 10 μL of the cell suspension were dispensed into two-well Comet Slide™ (Trevigen; Gaithersburg, MD). After gel solidification, slides were submerged in pre-cooled lysis solution (2.5 M NaCl, 10 mM Tris base, 1% sodium dodecyl sulfate, 10% dimethyl sulfoxide, and 1% Triton X-100) at 4 °C for 1 h. Once lysed and rinsed, slides were equilibrated in prechilled neutral electrophoresis buffer (1.0 M Tris base, 3.0 M sodium acetate) for 30 min at 4 °C, and then electrophoresed at 300 mA for 60 min in darkness. Slides were then immersed in DNA precipitation solution (1.5 M ammonium acetate in absolute ethanol) for 30 min at room temperature, followed by immersion in 70% ethanol for 30 min at room temperature. Once dried, slides were stained for 30 min with SYBR Green and observed under fluorescence microscope equipped with a green filter of 540 nm.

At least, images of 1000 randomly selected cells from the two wells were analyzed using a Nikon fluorescence microscope. Based on tail intensity and length, DNA damage was quantified by visual classification of nucleoids into five comet classes, from undamaged (class 0), to maximum DNA damage (class 4) (Fig. 2), resulting in a single DNA damage score for each specimen (Collins, 2004). Besides,

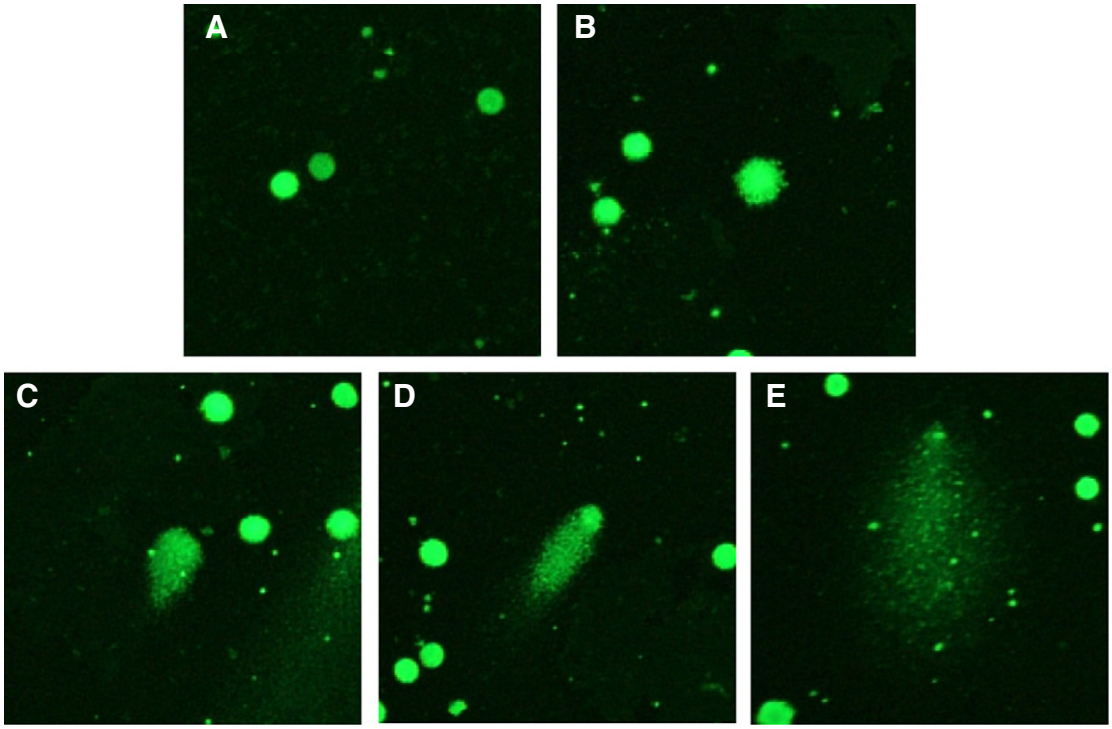

Fig. 2. Classification of blood cells in the comet assay. A. Class 0. no visible DNA migration from the nucleoid. B. Class 1. minimal DNA migration with an intact nucleoid. C. Class 2. moderate DNA migration with reduction in the size of the nucleoid. D. Class 3. extensive DNA migration with only a remaining pinpoint nucleoid. E. Class 4. complete migration of DNA into a comet tail with no visible nucleoid.

the total score expressed as a genetic damage indicator (GDI) was calculated multiplying the percentage of nucleoids in each class by the corresponding factor (Azqueta et al., 2009), according to the formula:

$$\begin{aligned}\text{GDI} = {} & [(\%\ \text{nucleoids class } 0) \times 0] + [(\%\ \text{nucleoids class } 1) \times 1] \\ & + [(\%\ \text{nucleoids class } 2) \times 2] + [(\%\ \text{nucleoids class } 3) \times 3] \\ & + [(\%\ \text{nucleoids class } 4) \times 4].\end{aligned}$$

In order to improve the reading of the expression of the DNA damage extent (Çavaş and Könen, 2007; Palus et al., 1999), the subtotal frequency of nucleoids (F_{2+3+4}) with medium, high, and complete damaged DNA was calculated as the sum of cells in classes 2, 3, and 4.

2.4. Micronucleus in peripheral blood smears

Blood smears were made on clean glass slides and air-dried. At least five blood smears were prepared per animal. The slides were stained using Wright-Giemsa stains (Schlegel and MacGregor, 1982), and the mean frequency of erythrocytes with MN in peripheral blood smears was scored by random analysis of five slides, examining 10 fields per slide, with approximately 2500 cells per slide.

2.5. Data analysis

Kruskal–Wallis test was used to compare means between sampling sites, followed by the Dunn's Multiple Comparisons test. A *P*-value<0.05 was set as statistically significant.

3. Results

DNA damage was assessed in peripheral blood cells of mice and iguanas collected near coal mining areas and from reference sites, at the north of Colombia.

3.1. Comet assay

The results of the comet assay performed in blood samples from mice collected during 2010 and 2011 are shown in Table 2. In 2010, mice from La Loma had the highest GDI and the highest F_{2+3+4} for both male and female groups. Compared to Arjona, the extent of DNA migration in peripheral blood leukocytes from male animals, measured as GDI and F_{2+3+4}, was statistically greater in La Jagua de Ibirico. This difference was maintained when data for both sexes were combined (Table 2). When independent data for each sex in animals from La Jagua de Ibirico were compared to those from Valledupar, no statistical differences were observed. However, significant differences were detected between these two sampling sites when data were pooled.

In 2011, GDI data for each sex group from Arjona were significantly different than those collected from both mining areas. This was not observed when Valledupar was compared to these places. Regarding La Jagua, statistical differences were found only when GDI pooled data were compared with Valledupar. During this year, similar results were obtained for F_{2+3+4}, although Arjona presented significant differences also with Valledupar (Table 2).

The results obtained for comet assay in blood cells of *I. iguana* are shown in Table 3. GDI values obtained for male and female specimens captured in La Loma were statistically different when compared to those from Valledupar. Values for F_{2+3+4} presented differences with Valledupar only for females (Table 3). When males and females were pooled, results for both GDI and F_{2+3+4} were statistically different when comparing both sampling sites.

Table 2
GDI and subtotal frequency of nucleoids from *M. musculus* blood scored for DNA damage based on tail intensity and length.

Year	Capture area	Sex	N	GDI ± SD	F_{2+3+4} ± SD
2010	Arjona	Male	10	1.06 ± 0.46	0.09 ± 0.11
		Female	3	1.11 ± 0.67	0.06 ± 0.07
		Total	13	1.07 ± 0.48	0.09 ± 0.10
	Valledupar	Male	6	1.62 ± 1.04	0.38 ± 0.32
		Female	10	2.56 ± 2.06	0.38 ± 0.40
		Total	16	2.20 ± 1.77	0.35 ± 0.36
	La Jagua de Ibirico	Male	6	22.78 ± 11.09*	5.27 ± 2.94*
		Female	2	29.40 ± 9.92	11.27 ± 2.52
		Total	8	24.43 ± 10.55*,**	6.77 ± 3.85*,**
	La Loma	Male	6	45.15 ± 22.05*,**	10.55 ± 6.63*,**
		Female	5	50.89 ± 53.49*,**	18.60 ± 26.30*,**
		Total	11	47.76 ± 37.37*,**	13.03 ± 17.45*,**
2011	Arjona	Male	5	0.37 ± 0.38	0.03 ± 0.05
		Female	7	0.26 ± 0.21	0.04 ± 0.06
		Total	12	0.31 ± 0.28	0.04 ± 0.05
	Valledupar	Male	8	3.39 ± 3.07	0.85 ± 0.79
		Female	9	2.27 ± 1.71	0.76 ± 0.65*
		Total	17	2.80 ± 2.43	0.81 ± 0.69*
	La Jagua de Ibirico	Male	5	16.23 ± 5.62*	1.64 ± 0.56*
		Female	4	17.96 ± 7.94*	1.86 ± 1.72*
		Total	9	17.00 ± 6.34*,**	1.74 ± 1.13*
	La Loma	Male	7	6.38 ± 4.37*	1.43 ± 1.81*
		Female	11	5.35 ± 6.06*	1.15 ± 1.62*
		Total	18	5.75 ± 5.35*	1.26 ± 1.65*

* Significantly different (P<0.05) when compared to Arjona. ** Significantly different (P<0.05) when compared to Valledupar.

3.2. Micronucleus test in blood smears

Some images of micronuclei observed in blood samples from examined mice and iguanas are shown in Fig. 3. However, the results of MN in blood smears showed that mice captured in areas affected by coal mining (La Jagua de Ibirico and La Loma) had percentages of MN similar to those obtained from Valledupar, for both sampling years and sexes (Table 4). It was also noted the presence of protozoan parasites in smears of some animals from Arjona.

The results of MN in peripheral blood smears of *I. iguana* specimens are also presented in Table 4. It is observed that blood cells from iguanas collected from a site near a coal mine (La Loma) have a tendency to present greater values for MN (Table 4) that those from individuals not impacted by this activity (Valledupar). However, this difference was not statistically significant.

4. Discussion

The results obtained for *M. musculus* and *I. iguana* showed a clear relationship between their habitats and the frequency of DNA-damaged blood cells. Mice (Table 2) and iguanas (Table 3) living near coal mining operations, such as in La Loma and La Jagua de Ibirico, exhibited a significantly greater extent of DNA damage, measured as GDI and F_{2+3+4}, compared to specimens from reference sites (Fig. 4). It is interesting to mention that regarding these biomarkers, the obtained pattern for males and females is similar to that seem when data are pooled. In other words, the extent of the damage is independent from the sex of the animal. To the best of our knowledge, this is the first report on DNA damage assessed by the comet assay in

Table 3
GDI and subtotal frequency of nucleoids from *I. iguana* blood scored for DNA damage based on tail intensity and length.

Capture area	Sex	N	GDI ± SD	F_{2+3+4} ± SD
Valledupar	Male	3	0.46 ± 0.14	0.03 ± 0.03
	Female	7	0.55 ± 0.28	0.02 ± 0.04
	Total	10	0.53 ± 0.24	0.02 ± 0.04
La Loma	Male	7	15.39 ± 8.80**	0.80 ± 0.68
	Female	4	27.34 ± 12.58**	0.68 ± 0.33**
	Total	11	19.73 ± 11.42**	0.76 ± 0.56**

** Significantly different (P<0.05) when compared to Valledupar.

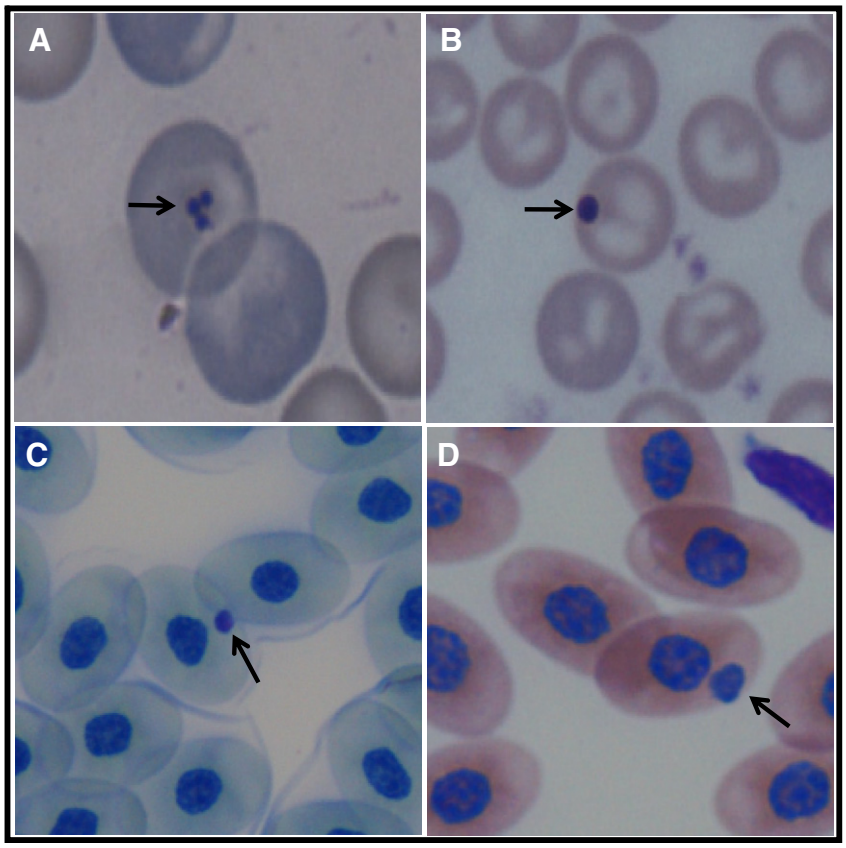

Fig. 3. Images of micronuclei observed in *Mus musculus* (A. B) and *Iguana iguana* (C. D) red blood cells. The micronuclei are shown by an arrow.

Table 4
Percentage of micronuclei found in *M. musculus* and *I. iguana* blood cells.

Species	Year	Capture area	Sex	N	%MN ± SD
Mus musculus	2010	Arjona	Male	10	0.19 ± 0.07
			Female	3	0.38 ± 0.49
			Total	13	0.23 ± 0.23
		Valledupar	Male	6	0.07 ± 0.03*
			Female	10	0.06 ± 0.02
			Total	16	0.07 ± 0.03*
		La Jagua de Ibirico	Male	6	0.07 ± 0.03*
			Female	2	0.09 ± 0.01
			Total	8	0.08 ± 0.03
		La Loma	Male	6	0.06 ± 0.02*
			Female	5	0.06 ± 0.02
			Total	11	0.06 ± 0.02*
	2011	Arjona	Male	5	0.13 ± 0.07
			Female	7	0.19 ± 0.49
			Total	12	0.16 ± 0.12
		Valledupar	Male	8	0.05 ± 0.03*
			Female	9	0.03 ± 0.04*
			Total	17	0.04 ± 0.04*
		La Jagua de Ibirico	Male	5	0.03 ± 0.02*
			Female	4	0.03 ± 0.03
			Total	9	0.03 ± 0.02*
		La Loma	Male	7	0.06 ± 0.05*
			Female	11	0.03 ± 0.03*
			Total	18	0.05 ± 0.04*
Iguana iguana	2011	Valledupar	Male	3	0.01 ± 0.02
			Female	7	0.02 ± 0.05
			Total	10	0.02 ± 0.04
		La Loma	Male	7	0.10 ± 0.11
			Female	4	0.03 ± 0.03
			Total	11	0.07 ± 0.09

* Significantly different ($P<0.05$) when compared to Arjona.

wild iguanas. Therefore, the information collected in this study, is a useful baseline for future research.

The presence of DNA damage in cells from the biota of coal mining areas is not surprising. Coal open-cast mining extraction is an activity considered an important source of pollutants (Bian et al., 2010). Coal itself has been described as the most significant pollutant of all fossil fuels, containing a heterogeneous mixture of contaminants (Leffa et al., 2010). Moreover, airborne coal particles as well as coal tailings are rich in potentially toxic hydrocarbons and genotoxic metals, among other contaminants (Celik et al., 2007), that ultimately may lead to profound changes in cells, tissues, populations, and ecosystems (Leffa et al., 2010).

Some of the DNA damaging agents can be breathed and therefore increase the risks of health hazards (NIOSH, 1995). Coal ash residues as well as dust from polluted areas by coal mining operations have been shown to contain significant amounts of heavy metals (Bai et al., 2004; Mugica et al., 2003; O'Shea, 2001; Tiwary, 2001), some of which have been considered to possess carcinogenic properties, including nickel, chromium, mercury, and cadmium. DNA lesions attributable to metal exposure are known to be driven by mechanisms involving the generation of highly reactive oxygen species (Hartwig, 2000), and interference with DNA repair processes (Kasprzak, 1991). However, the molecular interactions that lead to tumor formation after exposure to metal mixtures remain poorly understood.

Contrasting GDI and F_{2+3+4} data from mice collected in 2011 with those obtained in 2010, it is possible to observe differences in the registered percentages for each one of the comet classes, being 2010 the year with greater DNA damage (Table 2).

It is interesting that in 2011, the sampling sites close to mine showed statistical significance only with Arjona. These results seem to be due to the wide distance between Arjona and sampling sites of the Department of Cesar. The values generated for GDI and F_{2+3+4} show that, after the rainy season occurred in 2011, the sampling

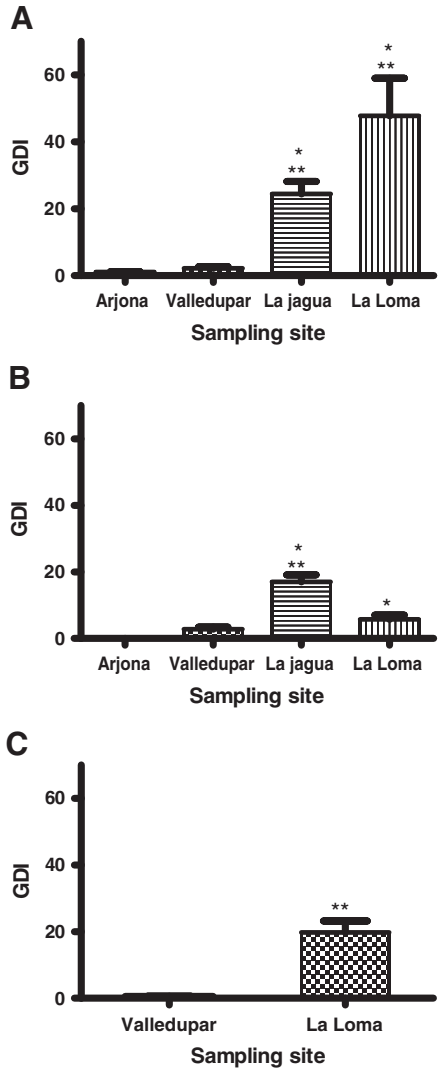

Fig. 4. Bar chart showing the GDI scores of *Mus musculus* blood cells for 2010 (A). and 2011 (B); and *Iguana iguana* (C). *. Significantly different ($P<0.05$) when compared to Arjona. **. Significantly different ($P<0.05$) when compared to Valledupar.

sites from the Department of Cesar behave similarly to each other when compared to Arjona. This observation allows us to suggest that samples from Arjona are a reliable control baseline group in this study.

Some authors have reported higher levels of DNA damage in summer than in winter (Verschaeve et al., 2007; Moller et al., 2002), which may indicate a direct relationship between DNA damage and increased intensity sunlight (Verschaeve et al., 2007), as well as greater exposure to PAHs (Moller et al., 2002), as a result of the phototoxicity of PAHs, which have been listed as photomutagenic (Yan et al., 2004). The last two months of 2010 and the first months of 2011, periods used for specimen collections, were particularly abundant in heavy rains that triggered deadly floods and landslides; the heaviest rainfall since records began in 1969 (World Meteorological Organization, 2010). Water droplets can capture coal dust, and this is an efficient method to decrease respirable coal dust. In fact, water spray has become a strategy for longwall mining machines during underground mining operations (Kilau, 1993). Given the strong rainy season that took place in late 2010 and early 2011 in Colombia, the concentrations of genotoxic compounds could have decreased as a result of heavy precipitations.

Regarding MN data for mice and iguanas (Table 4), it may be stated that blood smear was not as sensitive as the comet assay to detect genotoxic effects, as no difference was detected among the coal polluted sampling sites and Valledupar (Fig. 5). The greater MN average found in blood cells of mice collected in Arjona (control site) could had been the result of protozoa parasite infections, as it has been previously reported (Dertinger et al., 2000). These negative results observed by MN assay in blood smear for both species, agree with data from other authors, which did not detect a significant increase of MN in mice exposed to coal dust (Ong et al., 1985; da Silva et al., 2000a). Undefined factors may also influence the sensitivity of this method (Speit and Schmid, 2006). Besides, the frequency of micronuclei in reticulocytes may be low due to the efficiency by which the spleen sequesters and destroys these aberrant cells (Dertinger et al., 2003). Some authors suggested that the *in vivo* comet assay can compensate the limitations of the micronucleus assay in blood smear (Sasaki et al., 1998).

5. Conclusion

Biota residing near coal mining activities in La Loma and La Jagua de Ibirico, Cesar, Colombia, presents greater risk of DNA damage in blood cells than those living far from these sites. Moreover, *M. musculus* and *I. iguana* showed to be sensitive and suitable organisms to investigate environmental genotoxicity derived from coal mining activities.

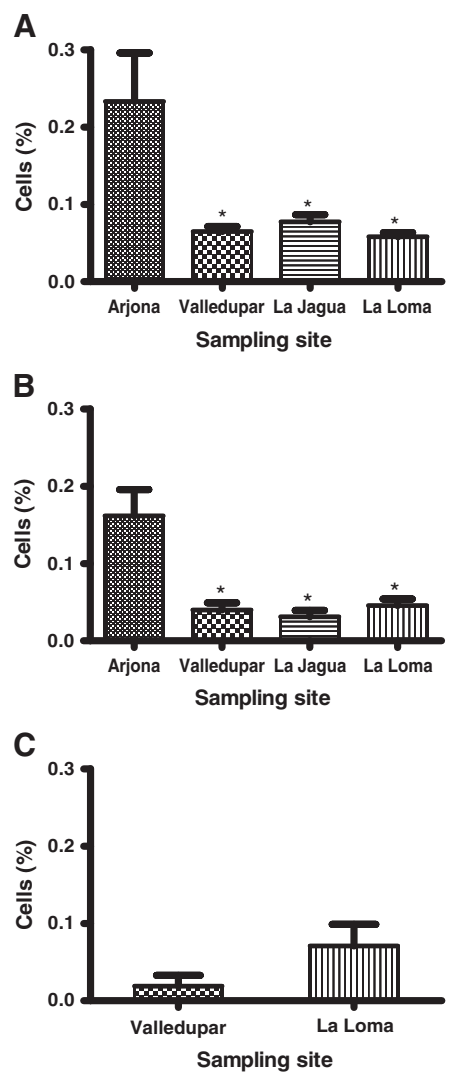

Fig. 5. Percentage of blood cells with micronucleus found in *Mus musculus* in 2010 (A) and 2011 (B); and *Iguana iguana* (C). *. Significantly different ($P<0.05$) when compared to Arjona. **. Significantly different ($P<0.05$) when compared to Valledupar.

Acknowledgements

The authors wish to thank Department of Cesar, and the University of Cartagena-Colciencias (Colombia) for their financial support (Contract 1235/09 and Grant 110749326186, respectively), as well as Leonor Cervantes, Tony Muñoz, Mayra Rivera and Liliana Carranza for their expertise and the Biomedical Research Group at the University of Sucre for providing the Sherman traps. Homer Corrales-Aldana is sponsored by the "Virginia Gutierrez de Pineda" Young Investigators Program of Colciencias-Universidad de Cartagena (2010–2011).

References

Azqueta A, Shaposhnikov S, Collins AR. DNA oxidation: investigating its key role in environmental mutagenesis with the comet assay. Mutat Res-Gen Tox En 2009;674:101–8.
Bai JF, Shi YH, Cui LP, Tang XY. The impact of heavy metals from coal mine-spoil heaps on soil. J Anhui Univ Sci Technol (Nat Sci) 2004;24:10–5.
Bian Z, Inyang HI, Daniels JL, Otto F, Struthers S. Environmental issues from coal mining and their solutions. Min Sci Technol 2010;20:215–23.
Borm PJA, Tran L. From quartz hazard to quartz risk: the coal mines revisited. Ann Occup Hyg 2002;46:25–32.
Castranova V, Vallyathan V. Silicosis and coal workers' pneumoconiosis. Environ Health Perspect 2000;108:675–84.
Çavaş T, Könen S. Detection of cytogenetic and DNA damage in peripheral erythrocytes of goldfish (Carassius auratus) exposed to a glyphosate formulation using the micronucleus test and the comet assay. Mutagenesis 2007;22(4):263–8.
Celik M, Donbak L, Unal F, Yüzbasıoglu D, Aksoy H, Yılmaz S. Cytogenetic damage in workers from a coal-fired power plant. Mutat Res 2007;627:158–63.
Collins AR. Comet assay for DNA damage and repair: principles, applications and limitations. Mol Biotechnol 2004;26:249–61.
Collins AR, Oscoz AA, Brunborg G, Gaivão I, Giovannelli L, Kruszewski M, et al. The comet assay: topical issues. Mutagenesis 2008;23:143–51.
Da Silva J, de Freitas TRO, Heuser V, Marinho JR, Bittencourt F, Cerski CTS, et al. Effects of chronic exposure to coal in wild rodents (Ctenomys torquatus) evaluated by multiple methods and tissues. Mutat Res 2000a;470:39–51.
Da Silva J, de Freitas TRO, Heuser V, Marinho JR, Erdtmann B. Genotoxicity biomonitoring in coal regions using wild rodent Ctenomys torquatus by comet assay and micronucleus test. Environ Mol Mutagen 2000b;35:270–8.
DANE. Departamento Administrativo Nacional de Estadística. Censo general 2005. Nivel nacional. ISBN 978-958-624-072-7. Bogotá – Colombia. [cited 2011 Jun 9]. Available from:http://www.dane.gov.co/censo/files/libroCenso2005nacional.pdf 2005. [Internet].
DANE. Departamento Administrativo Nacional de Estadística. Proyecciones nacionales y departamentales de población 2005–2020. Estudios postcensales No. 7. ISBN 978-958-624-078-9. Bogotá – Colombia. [cited 2011 Jun 9]. Available from:http://www.colombiajoven.gov.co/Es/documentacion/Documents/Sistema%20Nacional%20de%20Informaci%C3%B3n%20de%20Juventud/7Proyecciones_poblacion.pdf2009. [Internet].
Dertinger SD, Torous DK, Hall NE, Tometsko CR, Gasiewicz TA. Malaria-infected erythrocytes serve as biological standards to ensure reliable and consistent scoring of micronucleated erythrocytes by flow cytometry. Mutat Res 2000;464:195–200.
Dertinger SD, Chen Y, Miller RK, Brewer KJ, Smudzin T, Torous DK, et al. Micronucleated CD71-positive reticulocytes: a blood-based endpoint of cytogenetic damage in humans. Mutat Res 2003;542:77–87.
Donbak L, Rencuzogulları E, Yavuz A, Topaktas M. The genotoxic risk of underground coal miners from Turkey. Mutat Res 2005;588:82–7.
Fairbairn DW, Olive PL, O'Neil KL. The comet assay: a comprehensive review. Mutat Res 1995;339:37–59.
Hartwig A. Recent advances in metal carcinogenicity. Pure Appl Chem 2000;72:1007–14.
IARC. A review of human carcinogens. Monographs on the evaluation of the carcinogenic risk of chemicals to humansGenova: IARC Pres; 2010.
Kasprzak KS. The role of oxidative damage in metal carcinogenicity. Chem Res Toxicol 1991;4:604–15.
Kilau HW. The wettability of coal and its relevance to the control of dust during coal mining. J Adhes Sci Technol 1993;7:649–67.
Krishna G, Hayashi M. In vivo rodent micronucleus assay: protocol, conduct and data interpretation. Mutat Res 2000;455:155–66.
Leffa DD, Damiani AP, da Silva J, Zocche JJ, dos Santos CE, Boufleur LA, et al. Evaluation of the genotoxic potential of the mineral coal tailings through the *Helix aspersa* (Müller, 1774). Environ Contam Toxicol 2010;59:614–21.
León G, Pérez LE, Linares JC, Hartmann A, Quintana M. Genotoxic effects in wild rodents (Rattus rattus and Mus musculus) in an open coal mining area. Mutat Res 2007;630:42–9.
Mills JN, Childs J, Ksiazek G, Peters C. Methods for trapping and sampling small mammals for virologic testing. Atlanta, Georgia: US Department of Health and Human Services, Centers for Disease Control and Prevention; 1995. p. 14–32.
Mitchelmore CL, Chipman JK. DNA strand breakage in aquatic organisms and the potential value of the comet assay in environmental monitoring. Mutat Res 1998;399:135–47.
Moller P, Knudsen LE, Loft S, Wallin H. The comet assay as a rapid test in biomonitoring occupational exposure to DNA-damaging agents and effect of confounding factors. Cancer Epidemiol Biomarkers Prev 2000;9:1005–15.
Moller P, Wallin H, Holst E, Knudsen LE. Sunlight-induced DNA damage in human mononuclear cells. FASEB J 2002;16:45–53.
Mugica V, Amador MA, Torres M, Figueroa JJ. Mercurio y metales tóxicos en cenizas provenientes de procesos de combustión e incineración. Rev Int Contam Ambient 2003;19:93-100.
NIOSH. Criteria for a recommended standard—occupational exposure to respirable coal mine dust. DHHS (NIOSH) Publ; 1995. p. 95-106.
O'Shea TJ. Impacts of mine related contaminants on bats. In: Vories KC, Throgmorton D, editors. Proceedings of bat conservation and mining: a technical interactive forum held. St. Louis: U.S. Dept. of Interior, Office of Surface Mining; 2001. p. 205–16.
Ong T, Whong WZ, Xu J, Burchell B, Green FHY, Lewis T. Genotoxicity studies of rodents exposed to coal dustand diesel emission particulates. Environ Res 1985;37:399–409.
Ortega-Montero C. Valledupar. In: Hermelin M, editor. Entorno natural de 17 ciudades de Colombia. Medellín: Ediciones Universidad Eafit; 2007. p. 333–42.
Palus J, Dziubaltowska E, Rydzynski K. DNA damage detected by the comet assay in the white blood cells of workers in a wooden furniture plant. Mutat Res 1999;444:61–74.
Sasaki YF, Saga A, Akasaka M, Ishibashi S, Yoshida K, Su YQ, et al. Detection of in vivo genotoxicity of haloalkanes and haloalkenes carcinogenic to rodents by the alkaline single cell gel electrophoresis comet assay in multiple mouse organs. Mutat Res 1998;419:13–20.
Schlegel R, MacGregor JT. The persistence of micronuclei in peripheral blood erythrocytes: detection of chronic chromosome breakage in mice. Mutat Res 1982;104:367–9.
Shins RPF, Schilderman PAEL, Borm PJA. Oxidative damage in peripheral blood lymphocytes of coal workers. Int Arch Occup Environ Health 1995;67:153–7.
Speit G, Schmid O. Local genotoxic effects of formaldehyde in humans measured by the micronucleus test with exfoliated epithelial cells. Mutat Res 2006;613:1–9.
Tice RR, Agurell E, Anderson D, Burlinson B, Hartmann A, Kobayashi H, et al. Single cell gel/comet assay: guidelines for in vitro and in vivo genetic toxicology testing. Environ Mol Mutagen 2000;35:206–21.
Tiwary RK. Environmental impact of coal mining on water regime and its management. Water Air Soil Pollut 2001;132:185–99.
Ulker OC, Ustundag A, Duydu Y, Yucesoy B, Karakaya A. Cytogenetic monitoring of coal workers and patients with coal workers' pneumoconiosis in Turkey. Environ Mol Mutagen 2008;49:232–7.
UPME. Unidad de Planeación Minero Energética. Información Sectorial y Potencialidades del Carbón. [cited 2011 Jun 9]. Available from:http://www.upme.gov.co/ 2005. [Internet].
UPME. Unidad de Planeación Minero Energética. Boletín Estadístico de Energía y Minas 1999–2005. [cited 2011 Jun 9]. Available from:http://www.upme.gov.co/2006a. [Internet].
UPME. Unidad de Planeación Minero Energética. El Carbón colombiano, fuente de energía para el mundo. [cited 2011 Jun 9]. Available from:http://www.upme.gov.co/ 2006b. [Internet].
UPME. Unidad de Planeación Minero Energética. Mercado nacional e internacional del carbón colombiano. [cited 2011 Jun 9]. Available from:http://www.upme.gov.co/ 2007. [Internet].
Verschaeve L, Koppen G, Gorp UV, Schoeters G, Jacobs G, Zwijzen C. Seasonal variations in spontaneous levels of DNA damage; implication in the risk assessment of environmental chemicals. J Appl Toxicol 2007;27:612–20.
World Meteorological Organization. WMO statement on the status of the global climate in 2010. Geneva, Switzerland: Chair, Publications Board; 2010.
Yan J, Wang L, Fu PP, Yu H. Photomutagenicity of 16 polycyclic aromatic hydrocarbons from the US EPA priority pollutant list. Mutat Res 2004;557:99-108.
Yang ES, Nowsheen S, Wang T, Thotala DK, Xia F. Glycogen synthase kinase 3beta inhibition enhances repair of DNA double-strand breaks in irradiated hippocampal neurons. Neuro Oncol 2011;13(5):459–70.

Available online at www.sciencedirect.com
ScienceDirect
Chemosphere 69 (2007) 1100–1110
CHEMOSPHERE
www.elsevier.com/locate/chemosphere

Study of trace metal leaching from coals into seawater

Jean Yves Cabon [a,*], Laure Burel [a], Cathy Jaffrennou [a], Philippe Giamarchi [a], François Bautin [b]

[a] *UMR CNRS 6521 UBO, 6, Avenue Le Gorgeu, 29200 Brest, France*
[b] *Total Gaz Electricité Holdings, 2 Place de La Coupole La Défense 6, 92078 Paris la Défense-Cedex, France*

Received 29 March 2007; received in revised form 4 April 2007; accepted 4 April 2007
Available online 22 May 2007

Abstract

The behaviour of three South African coals in water and, particularly in seawater, was examined. A sequential speciation procedure used to evaluate trace metal partitioning in coal has shown that trace metals will not be easily released from these coals into environmental ecosystems. Only a few trace elements are slightly leached from these coals into water or seawater at pH around 8. On the other hand, Mn is highly leached from these coals into water or seawater. It has been clearly shown that Mn concentrations are highly correlated to sulfate and calcium concentrations indicating that Mn is mainly solubilized into water simultaneously to gypsum; the leaching efficiency being severely reduced for coal having a high calcite content. The leaching percentage of Mn into seawater is enhanced by the presence of seawater salts that increases gypsum solubility. The leaching process of Mn from coal into water or seawater is governed by gypsum solubilization and is relatively rapid during the first thirty minutes, then very slow. In this study, it has been also shown that, depending on their physico-chemical properties, trace metals may be removed from seawater solutions in the presence of coal having a high calcite content. In this work, it has been also shown that some elements, particularly Fe, are greatly solubilized into seawater in the presence of a strong chelating agent like EDTA. Like for Mn, the leaching rate of metals from coal in the presence of EDTA is relatively rapid during the first 30 min then much slower, suggesting a solubilization process simultaneously to gypsum or/and calcite solubilization.
© 2007 Elsevier Ltd. All rights reserved.

Keywords: Coal; Trace metals; Gypsum; Calcite; Leaching; Seawater

1. Introduction

In recent years, there has been an increasing interest to evaluate the environmental impact of trace element pollution by coal. Because trace metals enter the environment mainly through the atmosphere during coal combustion, most studies are mainly dealing with the elemental analysis of trace metals in coals. To reduce their emission into the atmosphere during coal combustion, different chemical pretreatments may be used, like acid leaching in order to minimize metal contents (Seferinoglu et al., 2003; Sakanishi et al., 2004). However, there are many cases in which phreatic aquifer or rivers may be impacted by waste from coal processing activities (Binotto et al., 2000; Teixeira et al., 2000). Nowadays, traffic shipping of coal is very important. Therefore, shipwreck liability and potential impact of important quantity of coal into seawater and sediments have to be considered. Consequently, understanding the leaching process of toxic metals from coal to seawater appears to be very important. Except Ohki et al. paper (2004), there are no detailed papers dealing with this subject. In their paper, Ohki et al. examined the leaching of various metals from coals into water, with or without the presence of different leaching agents. They showed that the percent metal leaching from coal by HNO_3 and EDTA agents could be important for some elements, like Ca, Cu, Fe, Mg, Mn, Pb and Zn. However, except Ca and Mg, leachable trace metal concentrations in water were below detection limits of the ICP-AES technique. The aim of

* Corresponding author. Tel.: +33 298016254; fax: +33 298017001.
E-mail address: Jean-Yves.Cabon@univ-brest.fr (J.Y. Cabon).

0045-6535/$ - see front matter © 2007 Elsevier Ltd. All rights reserved.
doi:10.1016/j.chemosphere.2007.04.018

our study was to evaluate the behaviour of coal in seawater and the risks of trace metal pollution through the leaching process; for this purpose three South African Reference Materials (SARM 18, SARM 19 and SARM 20) having different matrix and metal compositions were chosen. Our study was focused upon the determination of trace metals in leachates by electrothermal atomic absorption spectrometry that has generally lower detection limits than ICP-AES for many elements. In order to get a better understanding of the leaching process and, because coal may be mixed to marine sediments, we apply to the three types of coals the speciation protocol previously used for marine sediments (Marin et al., 1997; Larner et al., 2006). The coal to water or seawater ratio used in the leaching process was also varied. The kinetics of the leaching process from the three different coals was examined by following the concentration of Mn. Because humic acids present in coal may interact with trace metals (Ibarra and Orduna, 1986; Cezikova et al., 2001; Madronova et al., 2001; Martyniuk and Wieckowska, 2003; Burns et al., 2004), we also examined the ability of coal to remove trace metals from seawater solution.The leaching of metals from coal into seawater in the presence of a chelating agent was also examined.

2. Materials and methods

2.1. Coals and chemicals

Three South African certified reference coals (SARM) prepared by the Council for Mineral Technology (MINTEK), South Africa, were used. SARM 18 is a high volatile, low-rank bituminous coal with a rank in the vitrinite category V_7. SARM 19 is a subbituminous to bituminous coal and is generally very low rank (average V_4). SARM 20 is a subbituminous to bituminous coal and is of generally low rank (average V_6). The particle size of SARM coals were under 106 μm. Table 1 presents the certified elemental analysis of these coals. Hydrochloric, hydrofluoric and nitric acids were suprapur Merck products. Acetic acid was a pro analysi Merck product. Hydrogen peroxide about 30%, hydroxylammonium chloride and ammonium acetate were normapur Prolabo products. Ethylenediaminetetraacetic acid disodium salt was an Aldrich product. Standard sulfate solution was 1 g l^{-1} Merck solution. Standard solutions of Al, Cr, Cu, Fe, Mn, Ni, Pb and Cd used for ETAAS calibrations were 1 g l^{-1} in 0.5 M HNO_3 Merck solutions. 10 g $Pd(NO_3)_2$ in ~15% HNO_3 solution from Merck was used as a chemical matrix modifier. All solutions and dilutions were prepared in Milli Q water (18.2 M cm^{-1}). Coastal surface seawater was manually collected near Brest (Mer d'Iroise) with FLPE Nalgene bottles during winter then filtered with 0.45 μM Sartorius filters.

Table 1
Composition of SARM coals

	SARM 18	SARM 19	SARM 20
Loss on ignition (%)	90.11	71.28	64.66
Al (%)	1.36	4.24	5.96
Ca (%)	0.13	0.99	1.34
Cr (μg g^{-1})	16	50	67
Cu (μg g^{-1})	5.9	13	18
Fe (%)	0.2	1.22	0.82
Mg (%)	0.066	0.12	0.26
Mn (μg g^{-1})	22	157	80
Na (%)	0.013	0.22	0.2
Ni (μg g^{-1})	10.8	16	25
Pb (μg g^{-1})	5	20	26
S (%)	0.56	1.49	0.51
Si (%)	2.9	7.01	8.26
Ti (%)	0.068	0.204	0.38
Zn (μg g^{-1})	5.5	12	17

2.2. XRD analysis

X-ray powder diffraction analysis of coal was performed with the use of a D8 advance apparatus from Bruker. Minerals present in coal have been identified with the use of Eva software.

2.3. Sequential extraction procedure

Step 1 20 ml acetic acid (0.11 mol l^{-1}) are added to 0.2 g of coal in a 30 ml PTFE flask. The flask is shaken for 24 h at room temperature on a end-over-end mechanical shaker at a speed of 60 rpm. The supernatant is separated from the solid residue by centrifugation at 3600 rpm for 30 min, removed with a pneumatic syringue and filtered. The volume is then adjusted to 50 ml with water.

Step 2 20 ml hydroxylammonium chloride (0.1 mol l^{-1}, adjusted to pH = 2 with nitric acid) are added to the residue from step 1. The extraction procedure is then repeated as described in step 1.

Step 3 5 ml hydrogen peroxide (8.8 mol l^{-1}) are added to the residue of step 2. Flasks are introduced into a Stuart block heater and digestion is performed at 85 °C for 1 h; the solution is then reduced to a small volume (1–2 ml) at about 110 °C; the treatment is repeated three times. 20 ml ammonium acetate (1 mol l^{-1}, adjusted to pH = 2 with nitric acid) are then added to the residue. The extraction procedure is then conducted as in step 1.

2.3.1. Residual metals

The metal amount remaining in the residue after step 3 has been calculated by substracting the sum of the metal amounts released during the first three steps to the certified values of SARM coals (Table 1).

2.4. Leaching procedure

A determined mass of coal was weighed in 30 ml Teflon flasks; 20 ml of a water or a seawater solution were then added and shaken at room temperature for a definite period, at ambient temperature on a end-over-end mechanical shaker at a speed of 60 rpm.

A filtration was performed to separate the coal from the solution (0.45 μm Sartorius membrane filters).

2.5. Determination of metals

The determination of metal concentrations in the different solutions was conducted by electrothermal atomic absorption spectrometry. A Perkin–Elmer SIMAA 6100 working in the single element monochromator mode was used for all atomic absorption measurements. End-capped pyrolytic coated graphite tubes equipped with integrated platforms were used. The inert gas was argon. Samples were delivered to the furnace using a Perkin–Elmer AS-800 autosampler and stored in acid washed polypropylene cups prior to injection. The light sources were Perkin–Elmer hollow cathode lamps. Calibration curves were constructed and, when necessary, filtrates were diluted before measurements. Dilutions were carried out with calibrated Gilson Pipetman pneumatic syringes. Experimental protocols for the direct determination of Cr, Cu, Mn and Pb in seawater by ETAAS have been previously described (Cabon and Le Bihan, 1994, 1995, 1996). Similar experimental conditions were used for Al, Fe and Ni: 10 μg Pd was added as a chemical modifier for all measurements in water and seawater solutions. Atomisation temperatures close to the temperatures recommended by the manufacturer were used (2000–2400 °C). No pretreatment step was used for the determination of metals in water solutions. In the case of seawater, a pretreatment step at about 1300 °C (30 s) was used all for the determination of metals, in order to remove interfering sodium species before atomisation. Such a pretreatment step could not be used for the determination of Cd due to losses of analyte at this temperature. Therefore, for the determination of Cd in seawater, HF was used as a chemical modifier (Cabon, 2002). Indeed, the use of HF permits the atomization of Cd at a low temperature (around 1300 °C) below the vaporization of seawater salts. The detection limits of metals were respectively: 0.06 $\mu g\,l^{-1}$ for Cr, 0.2 $\mu g\,l^{-1}$ for Cu, 0.05 $\mu g\,l^{-1}$ for Cd, 0.5 $\mu g\,l^{-1}$ for Ni, 0.2 $\mu g\,l^{-1}$ for Fe, 1 $\mu g\,l^{-1}$ for Al, 0.05 $\mu g\,l^{-1}$ for Zn and 0.5 $\mu g\,l^{-1}$ for Pb.

2.6. Determination of sulfate

Sulfate concentrations were determined by ion chromatography. The sulfate concentration was measured with a Dionex DX-100 ion chromatograph equipped with an AS9-SC column and an ASRS-I anion self generating suppressor; the eluent being a 1.7 mM $NaHCO_3$/1.8 mM Na_2CO_3 solution.

3. Results and discussion

3.1. Sequential extraction of coal

It is now widely accepted that total metal concentration is not sufficient to evaluate trace element impact in environmental ecosystems. Indeed, the availability and toxicity of metals depend upon the chemical form in which a metal can exist. For marine sediments, different methods have been proposed to identify and quantify various physicochemical forms. The proposed methods, many of which being variants of Chester and Hughes (1967) and Tessier et al. (1979) procedures, enable to access to chemical speciation by using a sequential extraction protocol. In order to permit the comparison of the different works, the European Communities Bureau of reference has proposed a sequential extraction protocol (Ure et al., 1992), based on the scheme of Salomons and Forstner (1984), for European interlaboratory comparisons. This speciation protocol has then been evaluated and recommended by Marin et al. (1997) and Larner et al. (2006). Because this protocol may help to understand leaching process of trace metals from coal to seawater, it appeared interesting to us to apply this protocol to SARM 18, SARM 19 and SARM 20 coal samples in order to evaluate the risks of pollution by immerging coal into seawater. The results obtained with the use of this sequential procedure for speciation of different metallic elements are presented in Table 2.

Step 1 Metals extracted at step 1 are mainly those which are exchangeable and soluble in acetic acid solution at pH about 3, i.e. weakly adsorbed metals on coal surface, metals that can be released by ion-exchange processes and metals co-precipitated with sulfate or carbonate. The results obtained for the three coal samples for Al, Cr, Cu, Fe, Mn, Ni, Pb and Zn, expressed as a percentage of the total metal contents are presented in Table 2. As shown, the metal fraction released in acetic solution at pH = 3 is very low for Al (below 2%) that is mainly present in SARM coals as a very low soluble kaolinite form ($Al_2SiO_2(OH)_4$) (Fig. 1). Similarly, the metal fraction released in acetic acid solution at pH = 3 is very low for Fe (below 3%) that is mainly present in SARM coals also as a very low soluble pyrite form (FeS_2) (Fig. 1). Cr is also poorly released in acetic solution at pH = 3 (below 0.5%). For Cu and Pb, the metal fraction released in acetic acid solution at pH = 3 from the three SARM coals is higher and depends on the type of coal; the % metal released from coal shows a similar variation: SARM 18 $\gg$ SARM 19 > SARM 20. It may be noted that the more important metal fraction is released from SARM 18 coal that has the lower carbonate (calcite) and sulfate (gypsum) contents (Fig. 1). This may suggest the presence of labile organic complexes in this coal. For Ni and Zn and particularly Mn, more important fractions are released from the three SARM coals in acetic acid solution at pH = 3, probably through the solubilization of their carbonate or/and sulfate mineral forms associated to calcite or/and gypsum and, eventually also through the solubilization of labile organic complexes.

Table 2
Partitioning of metals in SARM 18, SARM 19 and SARM 20 (%)

	Step 1	Step 2	Step 3	Residual
Al				
SARM 18	1.8 ± 0.1	3.7 ± 0.2	11.1 ± 0.2	83.4
SARM 19	1.6 ± 0.2	5.0 ± 0.2	8.7 ± 0.1	84.7
SARM 20	0.9 ± 0.1	1.6 ± 0.1	5.9 ± 0.1	91.6
Fe				
SARM 18	3.3 ± 0.3	9.0 ± 0.3	18.1 ± 0.5	69.6
SARM 19	0.9 ± 0.3	15.6 ± 0.8	15.8 ± 1.1	67.8
SARM 20	1.7 ± 0.5	12.6 ± 1.0	12.8 ± 0.7	72.9
Cr				
SARM 18	0.3 ± 0.1	1.4 ± 0.1	47.5 ± 1.3	50.7
SARM 19	0.2 ± 0.1	0.7 ± 0.1	25.3 ± 1.7	73.8
SARM 20	0.5 ± 0.1	1.0 ± 0.1	22.4 ± 0.6	76.2
Cu				
SARM 18	23.2 ± 0.9	2.5 ± 0.7	29.2 ± 1.6	45.1
SARM 19	2.7 ± 0.1	1.3 ± 0.4	35.2 ± 1.9	60.6
SARM 20	1.0 ± 0.1	1.4 ± 0.3	36.9 ± 0.4	60.8
Mn				
SARM 18	55.5 ± 2.4	11.4 ± 0.1	10.9 ± 0.3	22.3
SARM 19	26.8 ± 2.9	11.9 ± 0.9	11.9 ± 0.5	49.4
SARM 20	35.0 ± 3.4	18.0 ± 1.5	6.3 ± 0.1	40.7
Ni				
SARM 18	3.0 ± 0.3	1.5 ± 0.1	33.6 ± 1.3	42.4
SARM 19	11.4 ± 0.6	10.2 ± 1.0	22 ± 0.2	47.9
SARM 20	4.7 ± 0.2	6.9 ± 0.4	6.5 ± 0.5	62.1
Pb				
SARM 18	9.9 ± 0.3	33.5 ± 1.3	22.0 ± 0.7	34.6
SARM 19	1.8 ± 0.1	26.2 ± 1.7	28.2 ± 0.7	43.9
SARM 20	1.1 ± 0.1	10.6 ± 0.8	30.4 ± 0.7	58
Zn				
SARM 18	20.4 ± 1.1	4.5 ± 0.2	13.8 ± 1.2	61.3
SARM 19	15.8 ± 1.4	10.0 ± 0.1	6.6 ± 0.8	67.6
SARM 20	12.4 ± 0.8	4.0 ± 0.3	6.3 ± 0.4	77.4

Mean of four replicates.

Step 2 Metals extracted at step 2 are defined as oxide species unstable under reducing conditions. Under these experimental conditions, Al, Cu, Cr and Ni are slightly extracted from SARM coals (<10%). Fe, Mn, Zn and particularly Pb are more leached from coals with the use of this treatment (~10–20%).

Step 3 The use of strong oxidising conditions leads to the degradation of organic matter and to the release of trace metals bound to it. Trace metals bound to sulfide may be also solubilized during this treatment. For all trace metals, an important release from coals is observed under these experimental conditions. The most important metal fractions are observed for Fe, Cr, Cu, Ni and Pb for the three SARM coals; this may result from the degradation of their organic complexes or/and to an oxidative release of mineral sulfides.

Step 4 The residual fraction should contain minerals which may hold trace metals within their crystalline matrix. As expected for Al (kaolinite) and Fe (pyrite), this insoluble oxide or sulfide fraction represents the most important part of coal content. For all other metals, this refractory fraction is variable and represents between 20% and 75% of their total content in the different coals.

These results show that trace metals are diversely distributed between different phases in coal. Therefore, the release of trace metals will highly depend on physico-chemical treatments and only a very small fraction is susceptible to be easily released in natural waters. The release of trace metals will depend also on coal composition and on physico-chemical properties of each metal.

3.2. Coal leaching into water

SARM 18, SARM 19 and SARM 20 coals were subjected to a leaching procedure by shaking different masses of coal (0.1 g to 2 g of coal with 20 ml of water during 24 h); in the French standard lixiviation procedure AFNOR (1992), a liquid/solid mass ratio of 10, i.e. 2 g solid for 20 ml solution is recommended. As shown in Fig. 2, SARM 19 and SARM 20 solutions are slightly basic and lead to pH around 8. SARM 18 solutions are slightly less basic and pH value increases from 6 to 8 with the increase of the coal mass from 0.1 g to 2 g. pH values are mainly governed by the solubilization of the carbonate mineral content of coal, mainly calcite, that appears to be more important in SARM 19 and 20 coals than in SARM 18 coal (Fig. 1). Chloride concentrations in water shaken with the three coal samples are below 1 mg l^{-1}, confirming the low chloride content in SARM 18, SARM 19 and SARM 20. For the three types of coal, the concentration of sulfate measured in water is much higher and varies linearly with the mass of coal. As checked for a 200 mg mass of SARM 18, 19 and 20 coals leached with water, sulfate and calcium concentrations are highly correlated indicating that the main origin of leached sulfate is gypsum. This observation was also confirmed by X-ray powder analysis showing the disparition of gypsum peaks observed for SARM 19 and 20 (Fig. 1) after a leaching treatment of these coals with water. The non-correlation of soluble sulfate with S content can be attributed to the presence of other non soluble S species, like mainly FeS_2 or eventually organic sulphide compounds.

As observed in Fig. 2, leached manganese concentrations from coal into water may be very high, particularly for SARM 19. For this coal, Mn concentration varies linearly with the mass of coal; the percentage of leached Mn being around 15%. For SARM 18, the variations of coal with the mass of coal is also relatively close to the linearity with a percentage of leached manganese varying from about 30% for 0.1 g coal mass to about 15% for a 2 g coal mass. For these two coal samples, the sulfate and Mn concentrations leached into water are highly correlated ($R^2 \sim 0.99$) indicating that this released fraction of Mn is a sulfate form probably co-precipitated with gypsum in

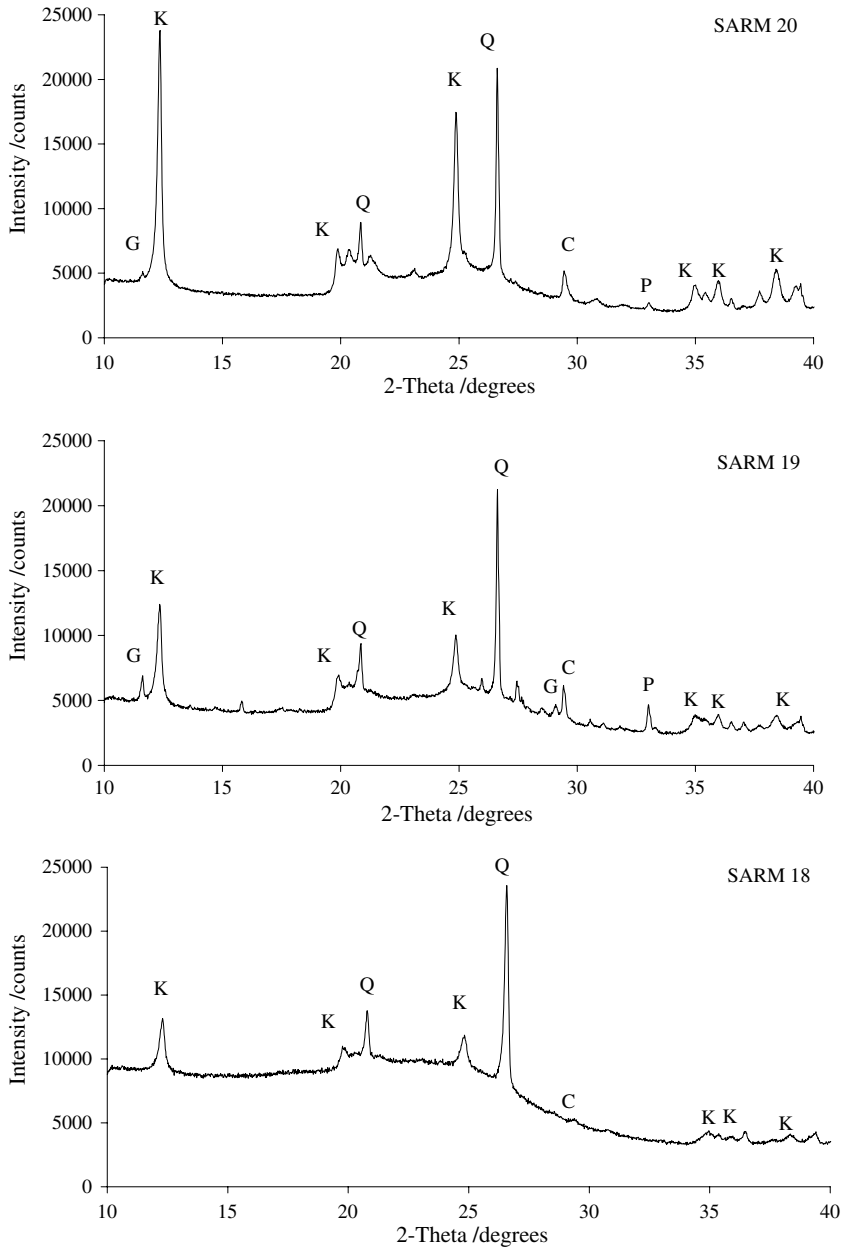

Fig. 1. X-ray powder diffractograms of SARM 18, 19 and 20 coals. Only the scan interval from 10° to 45° 2-theta is shown. Major peaks are identified as follows: Q = quartz; K = kaolinite; G = gypsum; C = calcite; P = pyrite.

coal. In the case of SARM 20, manganese amount leached into water is much lower; the variations of manganese concentrations with the mass of coal are not linear. The percentage of leached manganese varies from 3% for 0.1 g coal mass to only 1% for 2 g mass of SARM 20. The much lower leaching percentage is probably due to the simultaneous solubilization of the important calcite content of this coal that hinders the solubilization of Mn (Fig. 1). Indeed, Mn carbonate form is much less soluble (65 mg l^{-1}, Handbook of Chemistry and Physics, Lyde, 1991–1992) than its sulfate form (520 g l^{-1}, Handbook of Chemistry and Physics, Lyde, 1991–1992) in water solution at pH $\sim$ 8. As expected, due to its main kaolinite form (Fig. 1), the percentage of Al leached into water is very low (0.001–0.2%). However, despite this low percentage, the concentration level of Al leached from coal into water may be relatively important (5–200 μg l^{-1}). Al concentrations decrease with increasing masses of coal, due to the increase of pH values. The pH effect is much more important on the release of Al, for pH values below $\sim$7, in the case of SARM 18 that has a lower calcite content. Similarly, for Cu, in this hydrogeno-carbonate medium, significant values are obtained for SARM 18 only for pH values below 7; as in the case of Al, leached Cu concentrations decrease when the mass of coal is increased due to the increase of pH values. For Ni, only SARM 19 leads to significant leached

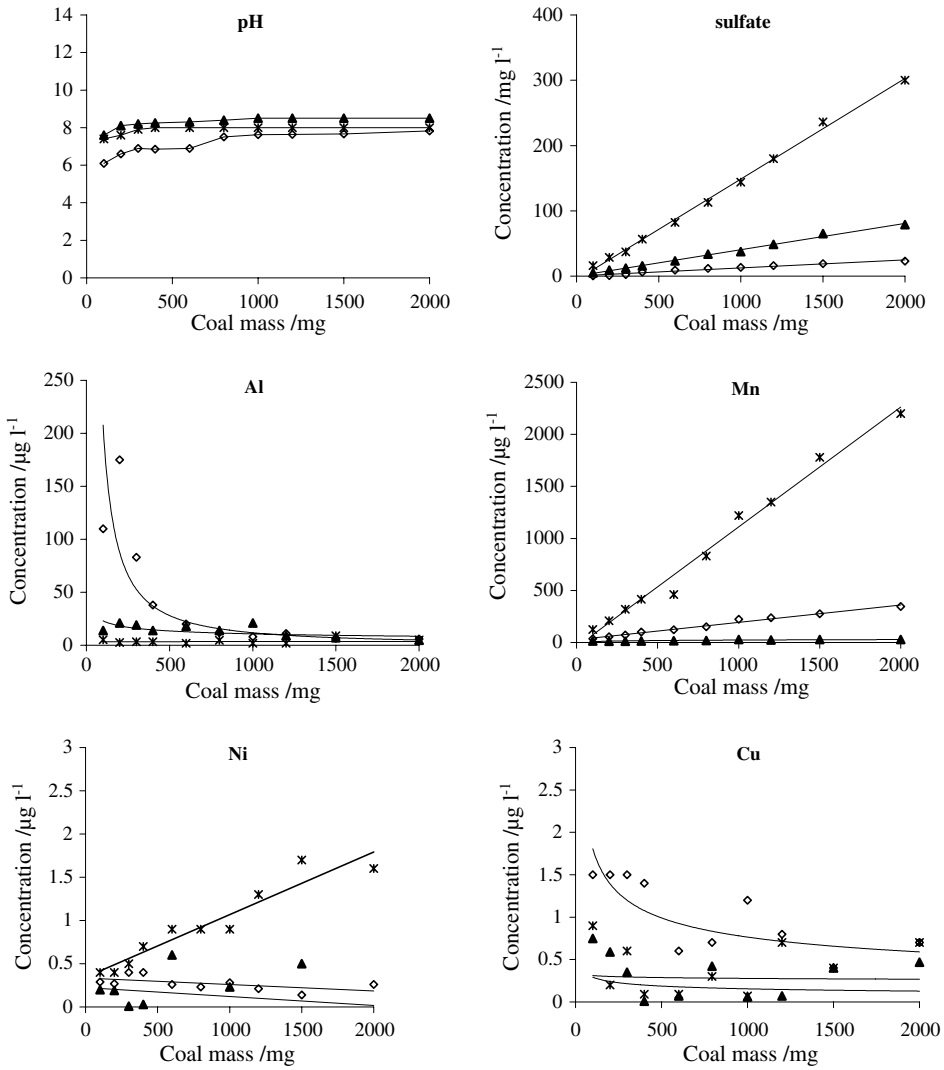

Fig. 2. Variations of pH and sulfate, Al, Mn, Ni and Cu concentrations in water (20 ml) shaken for 24 h with different SARM 18 (◊), SARM 19 (∗) and SARM 20 (▲) coal masses.

concentrations in water; Ni concentration varying linearly with coal masses and, probably like Mn, through solubilization of its sulfate form co-precipitated with gypsum in coal. For Cr, Fe, Pb and Zn, leached concentrations are very low in hydrogeno-carbonate solutions around pH ∼ 6–8 values and, close to or below the detection limits. No significant trend was observed for these metals when the mass of coal was increased.

3.3. Coal leaching into seawater

As was done for water, the three types of coal were subjected to the same leaching procedure by shaking various masses of coal with 20 ml of seawater during 24 h. Due to the calcite content of coal and the pH buffering effect of seawater (HCO_3^- 140 mg l^{-1}), pH values of seawater solutions shaken with the different coals were close to the pH of seawater, i.e. about 8.1. Therefore, trace metals can be distributed in this medium as free ion, chloride, hydroxy, hydrogeno-carbonate, sulfate or possibly organic forms according to their different physico-chemical properties (Zirino and Yamamoto, 1972; Stumm and Brauner, 1975; Dyrssen et al., 1975; Ahrland, 1975; Florence and Batley, 1976; Millero, 2003; Bruland and Lohan, 2003). As shown in Fig. 3, Mn concentrations leached from SARM coals into seawater may be very high, particularly for SARM 19. Manganese concentrations in seawater are about twice as high for SARM 18, 3 times as high for SARM 19 and 20 times as high for SARM 20 as in water. For these coals, seawater salts favour the leaching of Mn, probably by increasing the solubility of gypsum from 2.9 g l^{-1} to 3.8 g l^{-1} due to the ionic strength effect (Kopittke et al., 2004). Like in water, leachable Mn concentrations vary linearly with the masses of coal in the case of SARM 18 and 19. Like in water, variations of leached Mn concentrations with increasing masses of coal are not linear in the case of SARM 20, also due to its important calcite content. As shown in Fig. 3, seawater salts also favour the solubilization of Ni

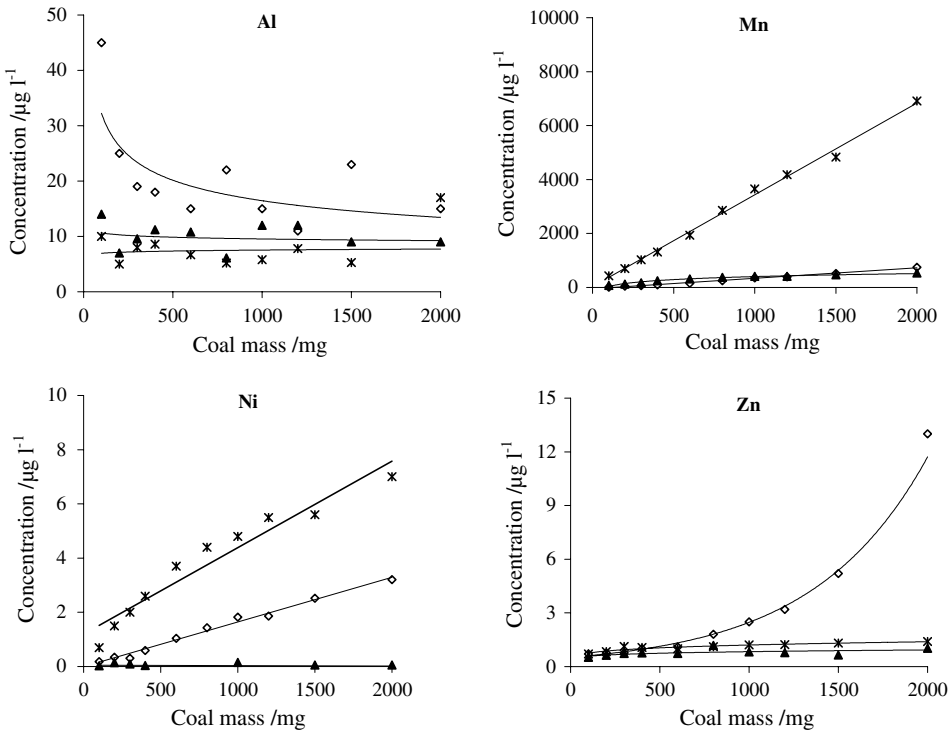

Fig. 3. Variations of Al, Mn, Ni and Zn concentrations in seawater (20 ml) shaken for 24 h with different SARM 18 (◊), SARM 19 (∗) and SARM 20 (▲) coal masses.

from coal, probably also through the higher solubilization of sulfate species; like Mn, leachable Ni concentrations increase linearly with the masses of coal in the case of SARM 18 and SARM 19. Similarly, seawater components favours also significantly the leaching of Zn, particularly for SARM 18. On the other hand and like in water, Cu, Cr, Fe and Pb are not significantly leached from coals into seawater; metal concentrations in seawater being close or below their ETAAS detection limits. For Cu, Fe and Pb, their leaching from coal into seawater is probably mainly governed by the hydrogeno-carbonate system that does not favour their solubilization into seawater. Humic substances present in coal or in seawater do not favour their transfer from coal into seawater.

3.4. Leaching rate of Mn from coal into seawater

Leaching rate of elements from solid and heterogeneous materials are generally relatively slow and contact time is an important parameter. Moreover, when immerged into seawater, coal will be subject to a continuous renewal of seawater; therefore, it appeared important to us to examine the rate of transfer of metals from coal into seawater. Because Mn appears to be an interesting element to follow the presence of a pollution from coal, we examined the rate of leaching of this element from SARM 18, SARM 19 and SARM 20 into seawater. As shown in Fig. 4a, the variations of the concentrations of Mn leached into seawater with time is relatively similar for the three different types of coal and, probably governed by gypsum solubilization; the major part of Mn being leached into seawater during the first 60 min. As shown in Fig. 4b, a similar trend was obtained when SARM 19 was shaken with water; Mn concentrations being lower in water than in seawater due to its ionic strength effect. As also shown in this figure, sulfate and Mn are simultaneously leached from SARM 19 into water. Their strong correlation during the leaching process confirms that the rate of leaching of Mn from coal is probably mainly governed by gypsum solubilization.

When immerged into seawater, coal will be probably continuously leached by renewed seawater. To evaluate this phenomenon, percolation studies through a column filled with coal may be an interesting approach. However, due to the clogging effect of 0.45 µm filters by fine particles of coal, it does not appear possible to maintain a constant continuous flow of the eluent solution through the filter. Therefore, we used a different protocol by submitting coal to successive extractions. For this purpose, a 0.1 mg SARM 19 coal sample was placed onto a 0.45 µm filter in a filtration unit, and leached by successive 20 ml clean seawater samples. Because the leaching of Mn was relatively slow, the contact time in the filtration unit was varied. As shown in Fig. 4c, about 20% of Mn was released from coal after 4 min by leaching coal with ten successive 20 ml seawater volumes; a similar leaching efficiency was obtained only after 30 min by leaching coal with a single 20 ml seawater volume. So, the rate of transfer of manganese from coal into seawater will depend both on contact time, on seawater volume and on renewal of seawater in contact with coal. It has been also noted that a small agita-

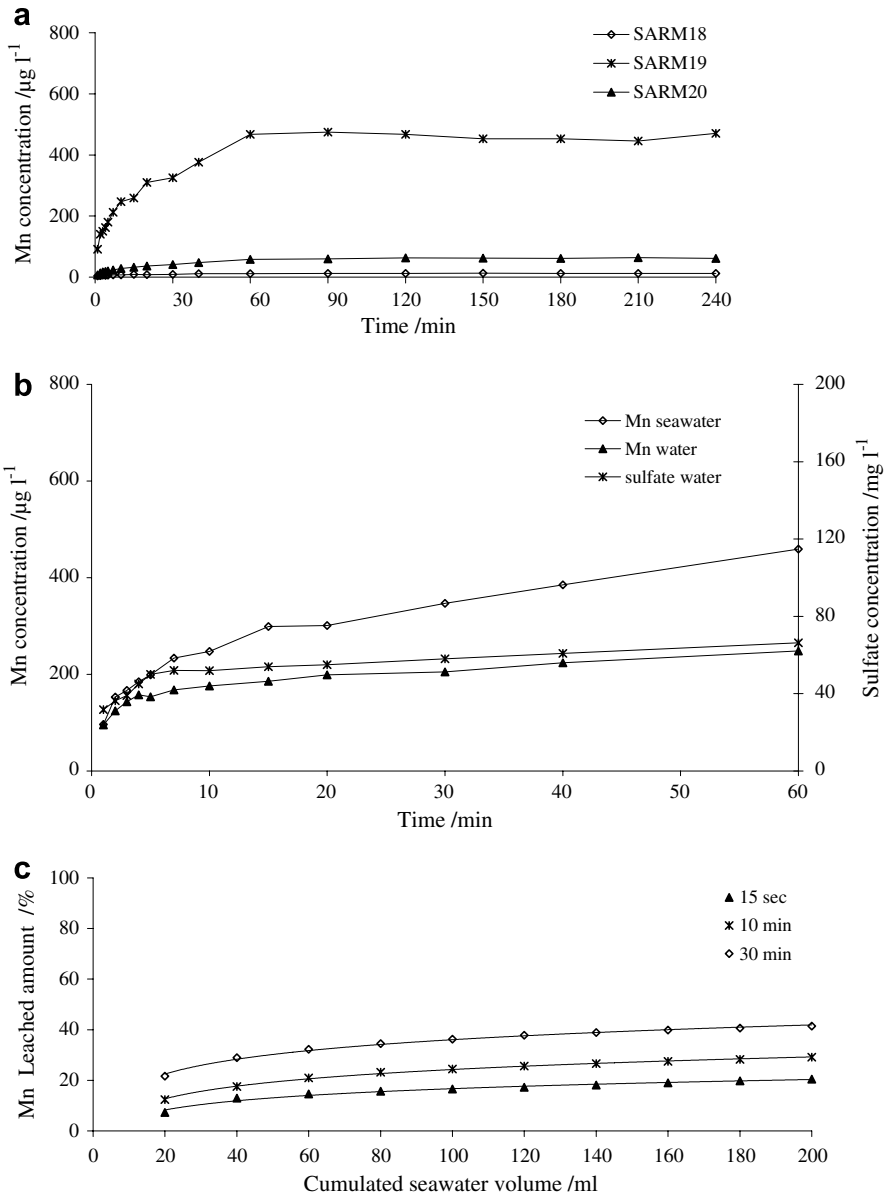

Fig. 4. (a) Variations with time of Mn concentration in seawater (20 ml) shaken with 0.2 g of SARM 18 (◊), SARM 19 (∗) or SARM 20 (▲) coal; (b) variations with time of Mn concentration in seawater (20 ml) (◊) shaken with 0.2 g SARM 19 coal and of Mn (▲) and sulfate (∗) concentrations in seawater (20 ml) shaken with 0.2 g SARM 19 coal; (c) Variation of the percent of leached Mn with cumulated seawater extracts (20 ml) of a 0.1 mg SARM 19 coal sample for various contact times: 15 s (▲), 10 min (∗) and 30 min (◊).

tion could also increase the leaching rate by a factor of about two.

3.5. Adsorption of metals from seawater upon coals

From our upper results, it appears that, despite their relatively high contents in coal, some trace elements like Cd, Cu, Pb or Zn (except SARM 18), are not significantly leached from the considered coals into seawater. This result may be explained both by the complexing properties of different ligands present in seawater towards trace metals, i.e. hydroxy-carbonate system, chloride, sulfate or organic ligands, or/and by the physico-chemical properties of coal. In order to examine this problem, we followed the behaviour of Cd, Cu, Pb and Zn dissolved in seawater when shaken with these coals.

As shown in Fig. 5, both these metals and the three types of coal present different behaviours. In the presence of SARM 18 that has the largest organic and the lowest calcite contents, no significant decrease of Cu, Pb, Zn and Cd concentrations in seawater is observed indicating that these metals are not fixed onto humic substances present in coal. On the other hand, a strong decrease of the concentrations of Cu and Pb was observed when seawater solutions were shaken with SARM 20. An important decrease was also noted for Zn concentration but only a small

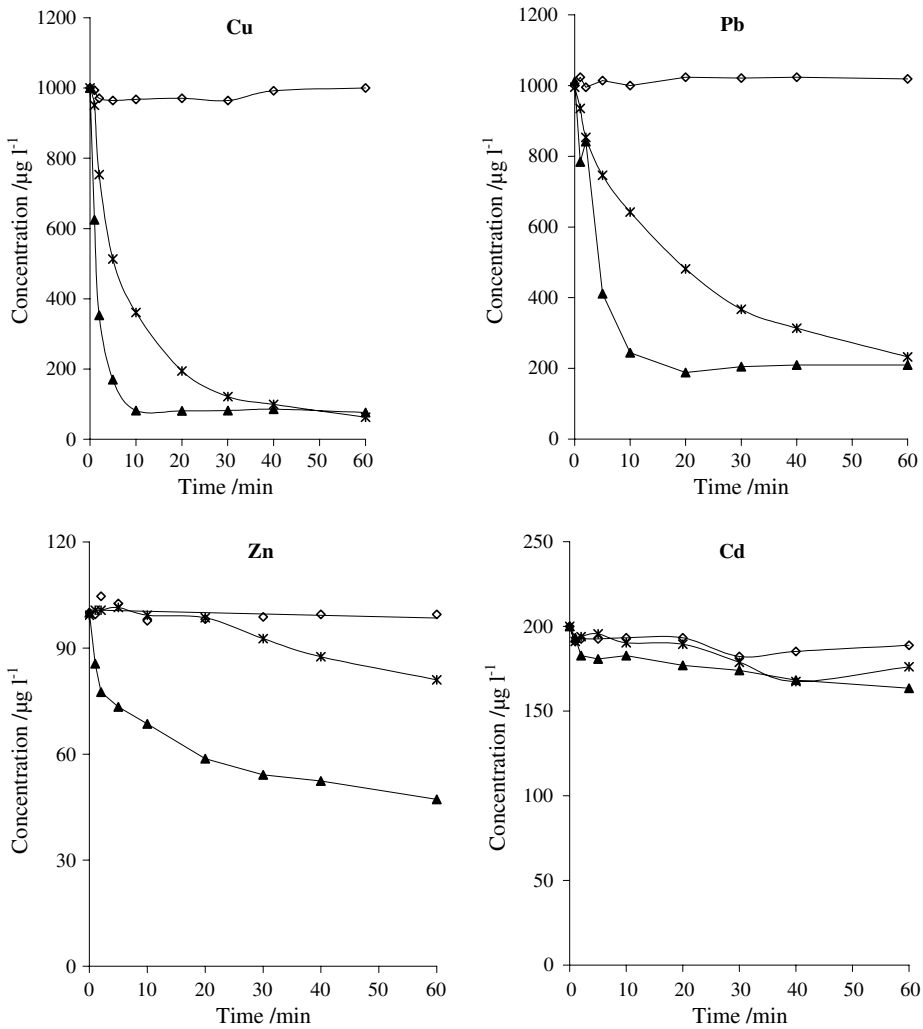

Fig. 5. Variation with time of Cu, Pb, Zn and Cd concentrations in seawater (20 ml) shaken with 0.2 g of SARM 18 (◊), SARM 19 (∗) or SARM 20 (▲) coal.

decrease for Cd concentration. An intermediate behaviour was observed when trace metal solutions were shaken with SARM 19. From this study, it appears that Cu and Pb distribution between SARM coals and seawater appears to be mainly governed by the hydroxy-carbonate system; their solubility in seawater is reduced when a higher calcite mass is dissolved from coal into seawater (SARM 20 > SARM19 > SARM18). On the other hand, inorganic Zn, and particularly Cd, that are less subject to hydroxy-carbonate complexation but are mainly distributed between chloride and sulfate species in seawater (Zirino and Yamamoto, 1972; Dyrssen et al., 1975; Florence and Batley, 1976) are much less removed from seawater solutions. So from Fig. 5, it appears that the removal of metals from seawater solution will depend on the nature of the coal material and physico-chemical properties of each metal; their removal can be very rapid, particularly for Cu and Pb, in the presence of coals having a high calcite content. The leaching of metals from these SARM coals into seawater appears to be mainly governed by inorganic speciation and humic substances present in coal or in seawater do not influence their exchange between coal and seawater.

3.6. Leaching of metals from coal into seawater in the presence of a complexing agent

As seen above, humic substances present in coal and seawater do not favour the leaching of trace metals from coal into seawater. However, according to location, depth or period of seawater sampling, the presence of a biological activity may increase the concentration and nature of organic ligands in seawater that are likely to complex metals and susceptible to facilitate their transfer to the marine ecosystem. Therefore, it appeared interesting to us to examine this possibility with the use of EDTA as a model of stronger chelating agent. For this purpose, 0.2 g of each SARM coal sample was shaken for 24 h with 20 ml EDTA seawater solutions. The EDTA concentrations (<0.05 mM) used being low enough to keep the seawater

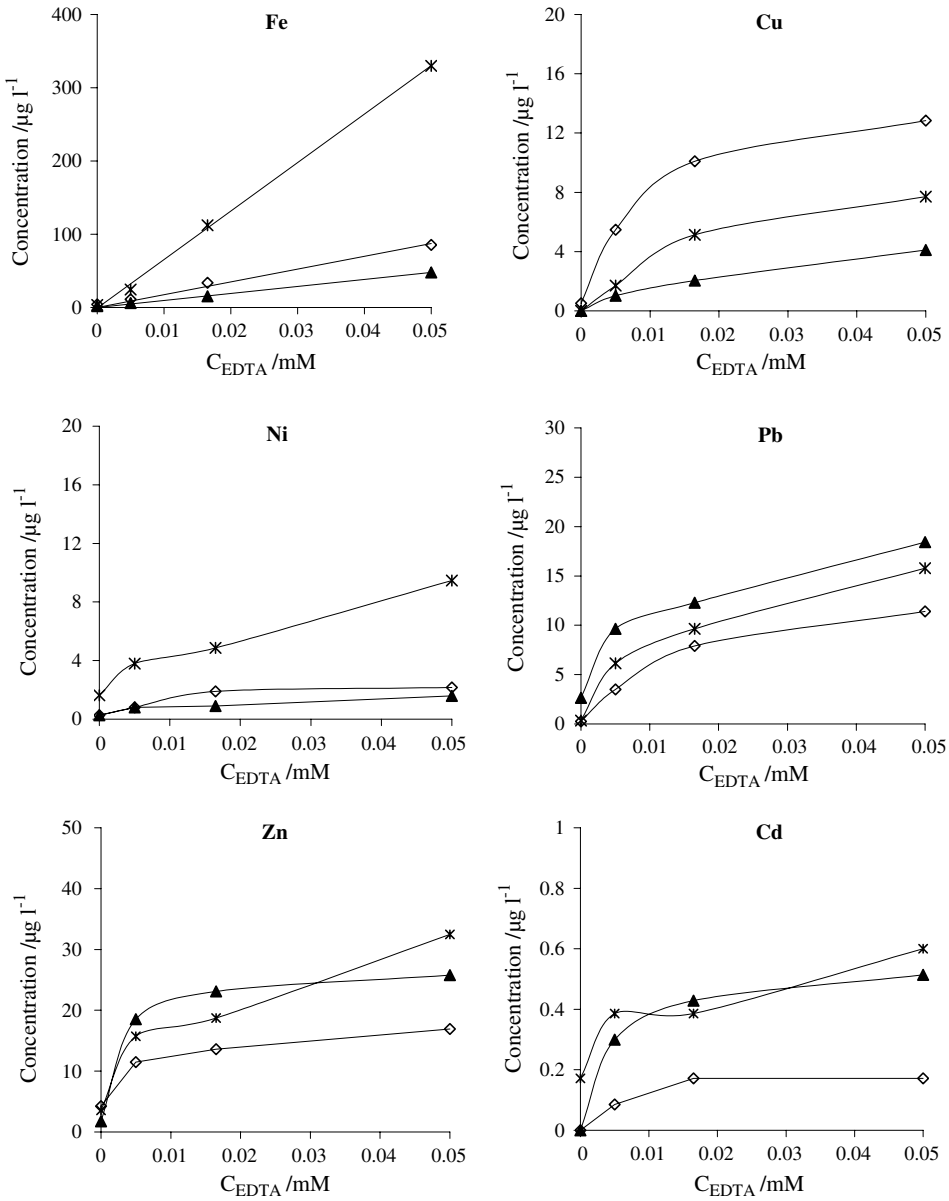

Fig. 6. Variations of Fe, Cu, Ni, Pb, Zn and Cd concentrations in EDTA seawater solutions (20 ml) shaken with 0.2 g SARM 18 (◊), SARM 19 (∗) or SARM 20 (▲) coal with EDTA concentrations.

pH unchanged. As shown in Fig. 6, leaching of all trace metals from coal into seawater was highly enhanced through their chelate formation with EDTA. In the considered EDTA concentration range, high concentrations of Fe were leached into seawater from the different coals, increasing linearly with increasing concentration of EDTA. By complexing Fe, probably liberated during the dissolution of carbonate or sulfate minerals (calcite, gypsum), EDTA favours its transfer into seawater. These results are in accordance with oceanographic observations showing that the solubility of Fe(III) in seawater carbonate system is greatly increased by the presence of natural organic ligands (Millero, 2003). In the case of Cd, Cu, Ni, Pb and Zn, high concentrations were also obtained by shaking EDTA seawater solutions with the three different types of coal; the variation of metal concentrations being not linear in these cases (Fig. 6). For these metals, the correlation ($R^2 = 0.78$) between their % leaching from coal with acetic acid at pH = 3 and with 5 mM EDTA indicates a similar solubilization process. This has been also confirmed by following the variations of the concentrations of leached metals with time in a EDTA seawater solution shaken with SARM 19 coal. Indeed, it appears that metals, like Fe and Cu, have a relatively similar behaviour: their leaching from coal by EDTA seawater solutions is rapid during the first thirty minutes and much slower thereafter. These curves are relatively similar to the leaching curve of Mn from SARM coals suggesting that these metals may be released simultaneously to the dissolution of minerals, like calcite or gypsum and, significantly

solubilized in seawater, only in the presence of a strong complexing organic agent.

4. Conclusion

This study has shown that the chemical impact of a coal pollution in seawater through leaching process will depend on various parameters: composition and physico-chemical properties of coal, coal mass to seawater ratio, time contact and agitation of seawater. Most hazardous trace metals will not be released from coal into seawater and, on the contrary are likely to be removed from seawater solution in the presence of coal having a high calcite content. However, Mn has a remarkable behaviour because a high labile fraction may be solubilized into seawater that may lead to an important pollution level, higher than the toxicity limit; its leaching from coal being mainly governed by the solubilization of soluble sulfate minerals like gypsum but reduced for coals having a high calcite content. In this study, we have also shown that the presence of strong chelating agents produced during biological activity periods may favour the solubilization of significant concentrations of trace metals from coals into seawater. From this work, it appears also clearly that leaching process depends on speciation of metals in coal and its distribution between the different mineral phases. Therefore, the determination of total metal content in coal is not sufficient to predict trace metal pollution through leaching process into seawater and the knowledge of major mineral composition of coal is essential, particularly its gypsum and calcite content.

Acknowledgements

The authors wish to thank Yves Fouquet from Ifremer, Centre de Brest, France, for XRD analysis of coals.

References

Association Française de Normalisation (AFNOR), 1992. Standard Methods for Leaching of Solid Wastes X31-210, France, p. 13.

Ahrland, S., 1975. Metal complexes present in seawater. In: Goldberg, E.D. (Ed.), The Nature of Sea Water. Dahlem Konferenzen, Berlin.

Binotto, R.B., Teixeira, E.C., Sanchez, J.C.D., Migliavacca, D., Nanni, A.S., 2000. Environmental assessment: contamination of phreatic aquifer in areas impacted by waste from coal processing activities. Fuel 79, 1547–1560.

Bruland, K.W., Lohan, M.C., 2003. Controls of trace metals in seawater. In: Elderfield, H., Holland, H.D., Turekian, K.K. (Eds.), The Oceans and Marine Geochemistry, Treatise On Geochemistry, Vol. 6. Elsevier–Pergamon, Oxford, pp. 23–44.

Burns, C.A., Boily, J.F., Crawford, R.J., Harding, I.H., 2004. Cd(II) binding by particulate low-rank coals in aqueous media: sorption characteristics and NICA-Donnan models. J. Colloid Interface Sci. 278, 291–298.

Cabon, J.Y., 2002. Determination of Cd and Pb in seawater by graphite furnace atomic absorption spectrometry with the use of hydrofluoric acid as a chemical modifier. Spectrochim. Acta 57B, 513–524.

Cabon, J.Y., Le Bihan, A., 1994. Direct determination of zinc in seawater using electrothermal atomization atomic absorption spectrometry with Zeeman-effect background correction. Chemical and spectral interference effects. J. Anal. Atom. Spectrom. 9, 477–481.

Cabon, J.Y., Le Bihan, A., 1995. The determination of Cr, Cu and Mn in seawater with transversely heated graphite furnace atomic absorption spectrometry. Spectrochim. Acta, Part B 50, 1703–1716.

Cabon, J.Y., Le Bihan, A., 1996. Determination of lead in seawater by electrothermal atomic absorption spectrometry with transversely heated furnace by using oxalic acid or Pd/Mg as modifiers. Spectrochim. Acta, Part B 51, 1245–1251.

Cezikova, J., Kozler, J., Madronova, L., Novak, J., Janos, P., 2001. Humic acids from coals of the North-Bohemian coal field II. React. Func. Polym. 47, 111–118.

Chester, R., Hughes, M.J., 1967. Chem. Geol. 2, 249–262.

Dyrssen, D., Wedborg, M., Goldberg, E.D., 1975. Equilibrium calculations of the speciation of elements in seawater. In: The Sea, vol. 5. Wiley J. and sons, New York.

Florence, T.M., Batley, G.E., 1976. Trace metal species in sea water. Talanta, 23–179.

Ibarra, J.V., Orduna, P., 1986. Variation of the metal complexing ability of humic acids with coal rank. Fuel 65, 1012–1016.

Kopittke, P.M., Menzies, N.W., Fulton, I.M., 2004. Gypsum solubility in seawater, and its application to bauxite residue amelioration. Aust. J. Soil Res. 42 (8), 953–960.

Larner, B.L., Seen, A.J., Townshend, A.T., 2006. Comparative study of optimised BCR sequential extraction scheme and acid leaching of elements in the certified reference material NIST 2711. Anal. Chim. Acta 556, 444–449.

Lyde, D.R., 1991–1992. Handbook of Chemistry and Physics, 72nd ed. CRC Press, Boca Raton, Ann Arbor, Boston.

Madronova, L., Kozler, J., Cezikova, J., Novak, J., Janos, P., 2001. Humic acids from coal of the North-Bohemia coal field III. Metal-binding properties of humic acids-measurements in a column arrangement. React. Func. Polym. 47, 119–123.

Marin, B., Valladon, M., Polve, M., Monaco, A., 1997. Reproducibility testing of a sequential extraction scheme for the determination of trace metal speciation in a marine reference sediment by inductively coupled plasma-mass spectrometry. Anal. Chim. Acta 342, 91–112.

Martyniuk, H., Wieckowska, J., 2003. Adsorption of metal ions on humic acids extracted from brown coals. Fuel Process. Technol. 84, 23–36.

Millero, F.J., 2003. Physicochemical Controls on Seawater. In: Elderfield, H., Holland, H.D., Turekian, K.K. (Eds.), The Oceans and Marine Geochemistry, Treatise On Geochemistry, Vol. 6. Elsevier-Pergamon, Oxford, pp. 1–21.

Ohki, A., Nakajima, T., Yamashita, H., Iwashita, A., Takanashi, H., 2004. Leaching of various metals from coal into aqueous solutions containing an acid or a chelating agent. Fuel Process. Technol. 85, 1089–1102.

Sakanishi, K., Akashi, E., Nakazato, T., Tao, H., Kawashima, H., Saito, I., Takarada, T., 2004. Characterisation of eluted metal components from coal during pretreatment and solvent extraction. Fuel 83, 739–743.

Salomons, W., Forstner, U., 1984. Metals in the Hydrocycle. Springer-Verlag, New York.

Seferinoglu, M., Paul, M., Sandström, A., Köker, A., Toprak, S., Paul, J., 2003. Acid-leaching of coal and coal ashes. Fuel 82, 1721–1734.

Stumm, W., Brauner, P.A., 1975. Chemical speciation. In: Riley, J.P., Skirrow, G. (Eds.), Chemical Oceanography, Vol. 1. Academic Press, New York.

Teixeira, E.C., Sanchez, J.C.D., Migliavacca, D., Binotto, R.B., Fachel, J.M.G., 2000. Environmental assessment: study of metals in fluvial sediments in sites impacted by coal processing and steel industry activities. Fuel 79, 1539–1546.

Tessier, A., Campbell, P.G.C., Bisson, M., 1979. Anal. Chem., 51–844.

Ure, A.M., Quevauviller, P., Muntau, H., Griepink, B., 1992. EUR. Report N14763, CEC, Brussels.

Zirino, A., Yamamoto, S., 1972. A pH-dependent model for the chemical speciation of copper, zinc, cadmium and lead in sea water. Limnol. Oceanogr. 17, 661.

ELSEVIER

Aquatic Toxicology 38 (1997) 1–15

AQUATIC TOXICOLOGY

Increased CYP1A1 and ribosomal protein L5 gene expression in a teleost: The response of juvenile chinook salmon to coal dust exposure

P.M. Campbell[1,*], R.H. Devlin

Department of Fisheries and Oceans, 4160 Marine Drive, West Vancouver, V7V 1N6, BC, Canada

Accepted 11 November 1996

Abstract

Molecular studies on the sublethal physiological effects of coal dust exposure in vertebrates are sparse. Coal dust contamination of the marine environment occurs, for example, around coal loading and storage terminals. To determine the potential impact of coal dust exposure on juvenile chinook salmon, fish were exposed for an 8 day period to 60 mg L^{-1}, 200 mg L^{-1} or 500 mg L^{-1} of coal dust in sea water and the levels of CYP1A1 mRNA quantitated using RT-cPCR. Two control groups were utilized; one 'negative' control group was maintained in sea water only, whilst the second 'positive' control group was i.p. injected with β-naphthoflavone (BNF: 50 mg kg^{-1}). There was a significant increase in CYP1A1 expression in fish exposed to coal dust (ANOVA; $P < 0.001$), and in fish injected with BNF (t-test; $P < 0.001$), relative to controls. In addition, RT-PCR analysis indicated increased expression of a second gene in the fish exposed to coal dust. Sequence analysis identified the second coal-dust-inducible gene as ribosomal protein L5. Both of these genes, CYP1A1 and L5, encode proteins vital in cellular metabolism. The enzyme encoded by CYP1A1 (P4501A1) plays an important role in the metabolic activation of PAHs to carcinogenic and mutagenic metabolites. L5 plays a crucial role in ribosome biogenesis. At present, the significance of the increased hepatic expression of L5 in coal dust exposed fish is unclear and warrants further investigation.

Keywords: CYP1A1; Ribosomal protein L5; Coal dust; Chinook salmon; RT-cPCR; Liver; Gene expression

*Corresponding author. Procter and Gamble, European Technical Center, Temselaan 100 B-1853 Strombeek-Bever, Brussels, Belgium. Tel: (02) 456 24 97; fax: (02) 460 25 80. e-mail: campbell.pm@pg.com.

[1] *Present address:* Procter and Gamble, Professional and Regulatory Services, European Technical Center, Temselaan 100 B-1853 Strombeek-Bever, Brussels, Belgium.

0166-445X/97/$17.00 © 1997 Elsevier Science B.V. All rights reserved.
PII S0166-445X(96)00848-X

1. Introduction

Molecular physiological studies on the sublethal effects of coal dust exposure in vertebrates are sparse. There are, however, a few indications in the literature, based almost exclusively on lung pathophysiological studies, that coal dust exposure causes changes in cellular metabolism that can ultimately be manifest as tissue damage and reduced health (Kuhn et al., 1990; Heederik et al., 1994; Lee et al., 1994). However, despite the fact that coal dust contains planar PAHs capable of inducing CYP1A1 (a gene encoding the xenobiotic-metabolizing enzyme P4501A1), previous studies on the response of mammals to coal dust exposure indicated no effect on P4501A1-associated enzyme activities in either liver or lung microsomes (Rabovsky et al., 1984).

The potential impact of coal dust exposure on species living in environs immediately surrounding sources of coal dust contamination have received little attention. Coal dust can enter the marine environment around coal ports through storm water discharge, coal pile drainage run-off, and when coal dust from storage piles, transfer conveyer belts and rail cars becomes airborne and is deposited in the surrounding environment (i.e. fugitive coal dust)(Xuan and Robins, 1994). The practice of using additives, such as surfactants, in the water being used for surface wetting of coal piles can increase the solubility of hydrophobic compounds and thus their mobility in the aquatic environment (Enzminger and Ahlert, 1987).

Coal dust contamination of estuarine habitat can occur around coal loading and storage terminals and hence may impinge on vital habitat for juvenile chinook salmon (*Oncorhynchus tshawytscha*)(Levings and Riddell, 1992; Macdonald et al., 1988). Previous studies have shown that low tide use of habitats immediately surrounding coal ports on the British Columbia coast by juvenile Pacific salmon is extensive (Levings, 1985). Chinook salmon may be exposed to coal-dust-derived PAHs through contaminated water and via their food since chironomid larvae, a significant food source for juvenile salmon, have been shown to bioaccumulate PAHs in estuaries contaminated with coal byproducts (Dickmann et al., 1992). The construction and expansion of coal terminals has already exerted some pressure on the survival of some stocks of Pacific salmon since this activity has reduced the amount of suitable estuarine habitat available for juvenile salmonids (Levings, 1985; Levings and Riddell, 1992). The exposure of Pacific salmon to pollution is of some concern since it is one of the contributing factors implicated in the depletion of some chinook salmon stocks on the West Coast of Canada over the past decade (Rogers et al., 1988 and Rogers et al., 1989; Birtwell and Kruzynski, 1989; Servizi et al., 1993; Kruzynski et al., 1994).

The P450 system in vertebrates is responsible for the metabolism of a wide range of endogenous and xenobiotic compounds and consequently plays vital roles in the toxicology, metabolism, activation and excretion of drugs, pollutants and potentially carcinogenic compounds. Unlike mammals, in which two forms of CYP1A (P4501A) are found (CYP1A1 and CYP1A2) only one form, CYP1A1, is known in teleosts (Heilmann et al., 1988; Stegeman and Hahn, 1994), although this gene is duplicated in salmonids (Berndston and Chen, 1994). The induction of CYP1A1 has

been used as a sensitive marker for the exposure, and the responsiveness, of animals to organic pollutants including PAHs. In this study, hepatic CYP1A1 mRNA levels were quantitated using a recently developed, sensitive RT-cPCR assay (Campbell and Devlin, 1996) to determine the response of chinook salmon to coal dust exposure. In addition, it was noted that coal dust exposure caused increased hepatic expression of a second gene which was subsequently identified as ribosomal protein L5.

2. Materials and methods

2.1. Materials

Lab chemicals were purchased from commercial suppliers (Sigma Chemicals, St. Louis, MO). Enzymes were purchased from Gibco BRL (Burlington, Ont.) and Perkin Elmer Cetus (Norwalk, CT). Deoxynucleotides were purchased from Pharmacia Canada (Baie d'Urfe, Qué.). Sequenase PCR product sequencing kits were purchased from Amersham Life Sciences Inc., (IL, USA).

2.2. Experimental animals

Juvenile chinook salmon (mean weight (g) 23.49 ± 4.19, $n = 50$) were maintained outdoors in large (1500 L), circular, fibreglass tanks each supplied with an independent, constant flow of sea water (8.7 ± 0.5°C) until required for experiments. At the start of the experiment the fish were transferred to 200 L indoor fibreglass aquaria, also supplied with a constant flow of sea water. The fish were allowed to acclimate in the indoor aquaria with sea water flow-through for 6 days. Fish were fed once daily with extruded dry pellets (Moore-Clark, La Connor, WA). Fish were not fed 24 h before, or during, the exposure period.

2.3. Treatment and sampling method

For the 8 day exposure period a static system was utilized: the tanks were filled with sea water only or sea water containing either 60 mg L^{-1}, 200 mg L^{-1} or 500 mg L^{-1} coal dust. These concentrations were chosen since present regulations in British Columbia (Environment Canada) limit levels of suspended solids in coal terminal effluent to 60 mg L^{-1} however, consideration is presently being given to a request that allowable levels of suspended solids in coal terminal effluent be raised to 200 mg l^{-1}. The use of submersible pumps ensured that the water in each tank was constantly recirculated, and in-tank cooling coils equilibrated the temperature to 12°C. The tanks were covered to exclude light during the exposure period. The sea water, or sea water containing the appropriate concentration of coal dust, was replaced in each tank every 2 days. In addition, two control groups of fish were utilized: A 'negative' control group which were held in sea water only, and a 'positive' control group which were held in sea water only but were also anaesthe-

tized with MS-222 (100 mg L^{-1}, buffered with 100 mg L^{-1} sodium bicarbonate) and intraperitoneally injected at the start of the 8-day experiment with 50 mg kg^{-1} body weight β-naphthflavone (BNF) dissolved by sonication in corn oil (5 mg ml^{-1}). At the end of the exposure period eight fish were sampled from each treatment group. Fish were rapidly removed from the tanks and anaesthetized in water containing MS-222, weights and lengths were recorded, and the fish were then killed instantly with a sharp blow to the head. Livers were rapidly removed, cut into 8–10 pieces using fine scissors, and immediately placed in tubes containing 10 ml 95% ethanol. The alcohol-fixed livers were stored at room temperature prior to analysis. This method of sampling tissue (as an alternative to freezing of tissue) prior to mRNA analysis by RT-cPCR has been validated previously (see Campbell et al., 1996).

2.4. RNA isolation and RT-cPCR

Total RNA was isolated using the single step method of Chomczynski and Sacchi (1987), and the RT-cPCR analysis carried out using the method of Campbell and Devlin (1996).

2.5. Sequence analysis

The RT-PCR products obtained from coal dust exposed fish were electrophoretically separated in a 1% TAE agarose gel (Ultrapure, Gibco BRL), the 270 bp and 300 bp bands excised, and purified using the freeze/thaw method of Qian and Wilkinson (1991). The purified fragments were then amplified by PCR in 100 μl reaction volumes containing purified cDNA, PCR premix [50 mM KCl, 10 mM Tris (pH 8.3), 1.5 mM $MgCl_2$, 100 μg ml^{-1} gelatin; Gibco BRL), dNTPs (0.2 mM each)], 3′ primer 1A1-2 (50 pmol) and 5′ primer 1A1-3 (50 pmol) and Taq DNA polymerase (0.05 u μl^{-1}). After an initial denaturation of 95°C for 3 min, reactions were run for 30 cycles with a 60°C annealing cycle (1 min), 72°C extension cycle (2 min), and a 95°C denaturing cycle (1 min) in a Perkin Elmer Cetus DNA thermal cycler followed by a final incubation at 72°C for 10 min. Both purified fragments, the 270 bp CYP1A1 fragment, and the 300 bp second gene product (subsequently identified as rp L5) were then sequenced using a Sequenase PCR product sequencing kit (Amersham Life Science Inc., IL, USA).

2.6. Particle size and PAH analysis

Coal-dust contaminated sea water samples were collected from the coal-pile run-off collecting lagoon of a major coal terminal. Particle size analysis was accomplished by the Elzone 280PC method, i.e. electronic size analysis using a particle size counter following preparation of the sample in 1% sodium chloride, with a drop of Triton X-100 added as a dispersant, and subsequent sonication for 15 min and filtration through a 0.45 μm filter. The presence of coal dust derived PAHs in sea water were analyzed by GC/MS. The contaminated sea water from the collecting lagoon was analyzed for PAH content. The sea water contaminated with coal dust

which contained 100 mg L^{-1}total suspended solids (90% of coal particles <8 μm diameter) was allowed to settle for 24 h. The supernatant, which contained 36 mg L^{-1} of non-settleable solids, was solvent extracted for 16 h with 15% acetone in dichloromethane using a separatory funnel technique. The extracts were then concentrated on a rotary evaporator at 35°C, and the final sample held in 2.0 ml of toluene for analysis at 4°C. Samples were analyzed on a Hewlett-Packard Model 5988A gas chromatograph/mass spectrophotometer (GC/MS) operated in selected ion mode. The GC/MS was equipped with a 30 mm×0.25 mm fused silica DB-5 capillary column and a split/splitless injection port. The method used was based on the EPA Method 8270 SW-846 (BCRI, 1995). Coal dust was obtained from the same coal terminal for the exposure experiments—a subsample of this coal was added to sea water (100 mg L^{-1}) and analyzed for the presence of PAHs to ensure that the coal dust suspensions used in the exposure experiments, and the relative amounts of PAHs leached from these suspensions, were representative of the coal-contaminated sea water present in coal-terminal collecting lagoons.

2.7. Statistical analysis

The levels of CYP1A1 mRNA in the livers of the juvenile chinook were analysed by one-way analysis of variance (ANOVA; Sigmastat, Jandel Scientific, San Rafael, CA). Pairwise comparisons were conducted using Student-Newman-Keuls multiple comparison test or *t*-test. Where appropriate, log transformations were selected to improve the homogeniety of variance. The level of significance was derived from these analyses, although data are presented as arithmetic means ± SEM.

3. Results

3.1. Detection of CYP1A1 expression: RT-PCR

CYP1A1 mRNA isolated from the livers of juvenile chinook was converted to cDNA using primer 1A1-3, and the CYP1A1 mRNA levels were detected using RT-PCR. The 1A1-1/1A1-3 primer pair amplifies a 270 bp fragment from CYP1A1 mRNA—this band is strongly evident in the samples obtained from the BNF-treated fish (see Fig. 1, Lanes 3 and 4), but barely detectable in the samples from the negative control fish (Fig. 1, Lanes 1 and 2). This 270 bp band is also evident in the samples from the coal dust exposed fish, with the intensity of the band increasing between the samples taken from fish exposed to 200 mg L^{-1} (Fig. 1, Lanes 5 and 6) and 500 mg L^{-1} (Fig. 1, Lanes 7 and 8) of coal dust. In addition, a second gene product was amplified from the samples obtained from coal-dust-exposed fish, this is evidenced by the second band at 300 bp obtained following RT-PCR (Fig. 1, Lanes 5–8). The 300 bp band was faint in the 60 mg L^{-1} group but increasingly evident in the 200 mg L^{-1} and 500 mg L^{-1} group. This 300 bp fragment is not seen in either of the control groups (Fig. 1, Lanes 1–4).

Fig. 1. Photograph of an agarose gel showing an example of RT-PCR results using RNA isolated from the livers of two fish from each of the following treatment groups: Controls held in sea water only (Lanes 1 and 2); Positive controls injected with 50 mg kg^{-1} BNF (Lanes 3 and 4); Fish exposed to 200 mg L^{-1} coal dust (Lanes 5 and 6) and fish exposed to 500 mg L^{-1} coal dust (Lanes 7 and 8). The band at 270 bp indicates amplification from CYP1A1 mRNA whereas the band at 300 bp indicates amplification from ribosomal protein L5.

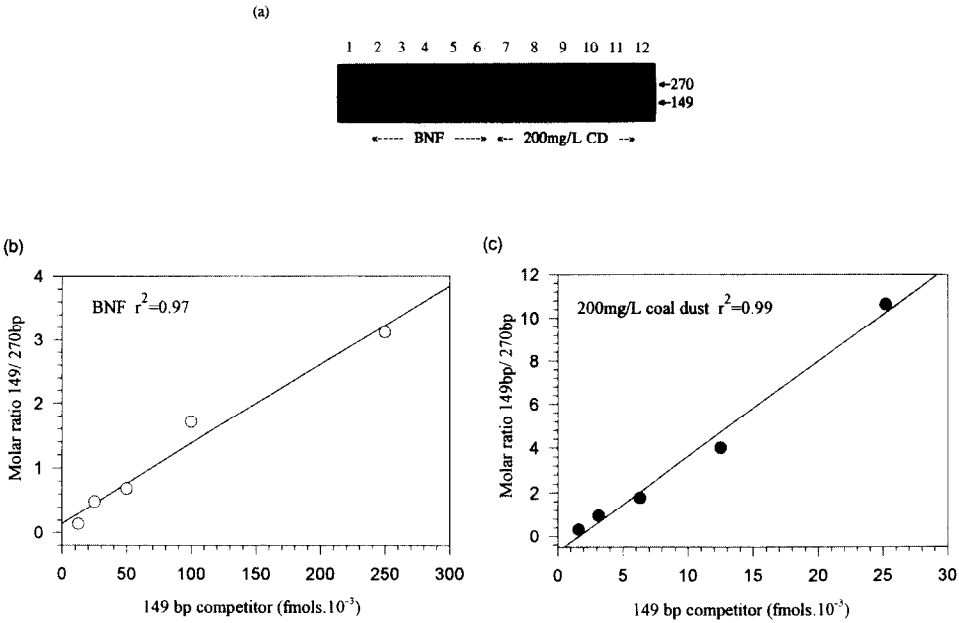

Fig. 2. Quantitation of CYP1A1 expression in liver samples from juvenile chinook salmon using RT-cPCR. An agarose gel (a) shows examples of RT-cPCR results obtained from a positive control fish injected with BNF (Lanes 2–6) and a fish exposed to 200 mg L^{-1} coal dust (Lanes 7–11). Following densitometric scanning of these RT-cPCR results the appropriate regressions were obtained for the BNF-treated fish (b) and the coal-dust exposed fish (c) and the CYP1A1 mRNA levels quantitated. Amplification from CYP1A1 cDNA results in the production of a 270 bp band, whereas amplification from the competitor results in the production of a 149 bp band.

3.2. Quantitation of CYP1A1 expression using RT-cPCR

The CYP1A1 mRNA levels in the liver samples were quantitated using the method of Campbell and Devlin (1996). Fig. 2 shows the results of two such RT-cPCR analyses; Lanes 2–6 of the gel shown in Fig. 2(a) show the results obtained using RNA from the liver of a BNF-treated fish, whereas Lanes 7–11 show the results obtained using RNA isolated from the liver of a fish exposed to 200 mg L^{-1} coal dust. For each analysis, five equal aliquots of RNA were prepared and the CYP1A1 mRNA within these samples was converted to cDNA. Two-fold dilutions of the 149 bp competitor DNA were added to each tube. The two fragments, the 270 bp fragment from the CYP1A1 cDNA and the control 149 bp fragment, then competed for amplification within the PCR. Fig. 2 shows that as the amount of competitor increases, the amount of CYP1A1 cDNA being amplified decreases; hence the ratio of the two bands changes between Lanes 2–6 and between Lanes 7–11. After densitometric scanning, the molar ratio of the competitive DNA to CYP1A1 cDNA products was regressed against the amount of competitor added. The results for the BNF-treated fish are shown in Fig. 2(b), and the results for the 200 mg L^{-1} coal dust exposed fish in Fig. 2(c). In these examples, the amount of CYP1A1 cDNA in the sample from the BNF-treated fish was 69.0 attomols μg^{-1} RNA (Fig. 2(b)) compared with 3.94 attomols μg^{-1} RNA Fig. 2(c)) for the sample from the coal dust (200 mg l^{-1}) exposed fish.

The 300 bp band seen in the results from RT-PCR analysis of RNA from coal dust exposed fish was found to be barely detectable or undetectable in the results of RT-cPCR analysis of the same samples (compare Fig. 1, Lanes 5–6 and Fig. 2, Lanes 7–11) suggesting it does not amplify effectively within the highly competitive conditions within the RT-cPCR.

The RT-cPCR assay was used to quantify CYP1A1 mRNA levels in the livers of juvenile chinook following the 8 day exposure period (Fig. 3). The mean levels of CYP1A1 mRNA in the livers of the control fish maintained in sea water only were

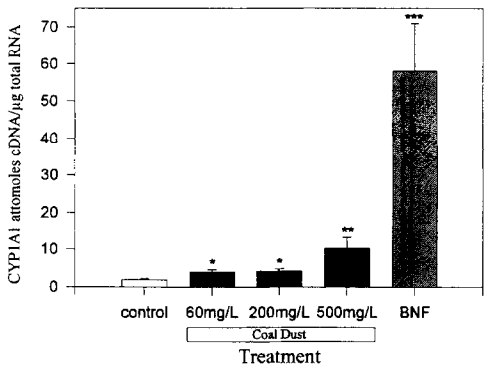

Fig. 3. Hepatic CYP1A1 mRNA levels in juvenile chinook salmon quantitated by RT-cPCR, asterisks indicate mean CYP1A1 levels which are significantly ($^{*}P<0.05$, $^{**}P<0.01$, $^{***}P<0.001$) different from control values.

```
(a)

PR1 TTC ACC ATC CCI CAC AGC AC→ --- --- --- --- --- --- --- --- ---
RAT TTA TCT ATC CCC CAT AGT ACC AAA CGA TTC CCT GGC TAT GAC TCT GAA
XEN TTA TCT ATT CCA CAC AGT ACC AAG CGT TTC CCT GGC TAT GAC TCT GAA
CHK --- --- --- --- --- --- --C AAA CGT TTC CCT GGG TAT GAT GCT GAG
    **. .*. **. **. **. **. *** **. **. *** *** **. *** **. .** **.

RAT AGC AAG GAA TTC AAT GCA GAG GTG CAC CGG AAG CAC ATC ATG GGT CAG
XEN AGC AAA GAA TTC AAT CCT GAG GTC CAC CGC AAG CAC ATC TTT GCC CAG
CHK AGC AAA GAA TTC AAT GCG GAG GTC CAC CGC AAG CAC ATC ATG GGC CAG
    *** **. *** *** *** .*. *** **. *** **. *** *** *** .*. *.. ***

RAT AAT GTG GCA GAC TAC ATG CGC TAC CTG ATG GAG GAG GAT GAG GAT GCG
XEN AAC GTT GCA GAG TAC ATG CGT CTT CTG ATG GAA GAA GAT GAA GAT GCG
CHK AAC GTT GCA GAG TAC ATG CGT TAC CTG ATG GAG GAA GAT GAA GAT GCA
    **. **. *** **. *** *** **. ... *** *** **. **. *** **. *** **.

RAT TAT AAG AAA CAG TTC TCT CAG TAC ATC AAG AAC AAC GTG ACT CCA GAC
XEN TAT AAA AAG CAG TTC TCT CAA TAC ATA AAG AAT GGT GTG ACT GCA GAC
CHK TAC AAA AAG CAG TTC TCC CGC TTC ATC AAG AAT GGC GTG GTT CCT GAC
    **. **. **. *** *** **. *.. *.* **. *** **. ... *** ..* .*. ***

RAT --- ATG GAG GAG ATG TAT AAG AAA GCT CAT GCT GCT ATC CGA GAG AAT
XEN CAG GTG GAA GAC CTG TAC AAA AAG GCT CAT GCA GGT ATT CGG GAG AAT
CHK AAG GTG GAA GAA ATG TAC AAA AAG GCT CAC GCT GGC ATT CGG GAG AAT
    ... .** **. **. .** **. **. **. *** **. **. *.. **. **. *** ***

RAT CCA GTC TAC GAG AAG AAG CCC AAG AGA GAA GTG AAG AAG AAG AGG TGG
XEN CCA GTG CAC GAA AAG AAA CCC AAG AAG GAA GTC AAA AAG AAG AGG TGG
CHK CCA CTG CAC GAA AAG AAA CCC AAG AAG GAA GTC AAG AAG AA- --- ---
PR2 --- --- --- --- --- --- --- --- --- --- --- --- --- ←G AGG TCT
    *** .*. .** **. *** **. *** *** *.. *** **. **. *** *** *** *..

RAT AAT CGT CCC AAA
XEN AAC CGT GCC AAA
CHK --- --- --- ---
PR2 TCC TCT TCC TGG
    ... ..*  ** ...

(b)
        180                     200                     220
RAT   KRFPGYDSESKEFNAEVHRKHIMGQNVADYMRYLMEEDEDAYKKQFSQYIKNNVTPD
XEN   KRFPGYDSESKEFNPEVHRKHIFAQNVAEYMRLLMEEDEDAYKKQFSQYIKNGVTAD
CHK   KRFPGYDAESKEFNAEVHRKHIFAQNVAEYMRYLMEEDEDAYKKQFSRFIKNGVVPD
      *******.******.*******..****.***.**************.****.*..*


          240                     260
RAT   -MEEMYKKAHAAIRENPVYEKKPKREVKK
XEN   QVEDLYKKAHAGIRENPVHEKKPKKEVKK
CHK   KVEEMYKKAHAGIRENPLHEKKPKKEVKK
        .*..******.*****..*****.****
```

Fig. 4. A comparison of the (a) nucleotide sequences of a portion (between nucleotides 594 and 888) of rat L5 cDNA (Chan et al., 1987), Xenopus L5a cDNA (Wormington, 1989), and the 300 bp fragment isolated from coal dust exposed fish. The corresponding amino acid sequence alignment is also shown (b). The oligonucleotide primers 1A1-1 (PR1) and 1A1-3 (PR2) are also shown. Asterisks (*) show that a position in the alignment has been perfectly conserved, a period (.) shows that a position is well conserved (2/3 of sites). Dashes indicate spaces inserted for alignment purposes.

1.83 attomols μg^{-1} RNA. The mean CYP1A1 mRNA levels in the coal dust exposed fish were significantly elevated above control values (ANOVA; $P < 0.001$) with RT-cPCR analysis revealing mean CYP1A1 mRNA levels of 3.9 attomols μg^{-1} RNA (Student-Newman-Keuls; $P < 0.05$), 4.23 attomols μg^{-1} RNA (Student-Newman-Keuls; $P < 0.05$) and 10.28 attomols μg^{-1} RNA (Student-Newman-Keuls; $P < 0.01$) for the 60 mg L^{-1}, 200 mg L^{-1} and 500 mg L^{-1} coal dust

```
1A1-1 --------------------->
TROUT TTCACCATCC CACACTGCAC AGTCAAGGAT ACATCGCTCA ATGGCTACTT
CHK                         AGTCAAGGAT ACATCTCCTC ATGGCTGCTT
                            ********** ***** *    ****** ***

TROUT CATTCCCAAG GACACCTGTG TCTTCATCAA CCAGTGGCAG GTCAACCATG
CHK   CATTCCCAAG GACACCTGTT TCTTCATCAA CCAGTGGCAG GTCAACCATG
      ********** *********  ********** ********** **********

TROUT ACCCGGAGCT GTGGAAGGAG CCTTCTTCAT TCAACCCTGA CCGTTTCCTG
CHK   ACCCGGAGCT GTGGAAGGAG CCTTCTTTAT TCAACCCTGA CCGTTTCCTG
      ********** ********** ******* ** ********** **********

TROUT AGTGCTGATG GCACAGAACT CAACAAATTG GAGGGGGAGA AGGTGCTCGT
CHK   AGTGCTGATG GTACAGAACT CAACAAGCTG GAGGGGGAGA AAGTGCTCGT
      ********** * ******** ******  ** ********** * ********

TROUT ATTTGGCATG GGCAAGCGCC GCTGCATAGG TGAGGCCATC GGACGCAATG
CHK   ATTCGGGATG GGCAAGCGCC GCAGCATCGG TGAGGCCATC GGACGCAAC
      *** ** *** ********** ** **** ** ********** ********
                                                          ←1A1-3
                                                          (cont.)
TROUT AGGTCTACCT CTTCTTGG
CHK
      ←------------------1A1-3
```

Fig. 5. Comparison of the nucleotide sequence of a portion (between nucleotides 1164 and 1432) of trout CYP1A1 cDNA (Heilmann et al., 1988) and the 270 bp fragment isolated from coal dust exposed fish. Asterisks (*) show that a position in the alignment has been perfectly conserved.

exposures, respectively. The mean levels of CYP1A1 mRNA in the BNF-treated fish were 58.1 attomols μg^{-1} RNA and hence were very significantly elevated above control values (t-test; $P < 0.001$).

3.3. Sequence analysis

The additional 300 bp fragment obtained by RT-PCR analysis of RNA from coal-dust-exposed fish was sequenced. A Genbank search revealed that the nucleotide sequence of the 300 bp fragment had very high homology with the nucleotide sequences of ribosomal protein L5 from other vertebrates including rat rp L5 (Accession # M17419), *Xenopus laevis* (both L5a, Accession # M29032 and L5b, Accession # M29033), chicken rp L5 (Accession # X57016) and human rp L5 (Accession # U14966). A comparison of the nucleotide sequences, specifically the region containing the putative RNA binding domain, of rat L5, *Xenopus* ribosomal protein L5a and the 300 bp fragment isolated from coal dust exposed fish is shown in Fig. 4(a). This figure illustrates an 87% similarity between the 300 bp fragment (excluding primer sequences) and *Xenopus* L5a, and an 80% similarity with rat L5. Comparison of the deduced amino acid sequence for the 300 bp fragment with the protein sequences of rat L5 (85% similar) and *Xenopus* L5a (91% similar) is shown in Fig. 4(b) and provides further evidence that the 300 bp fragment is indeed amplification of a region of chinook salmon L5 mRNA, and indicates that this region of the protein has been very well conserved throughout evolution. The 270 bp fragment amplified from coal dust exposed fish was also sequenced and confirmed to be amplification from chinook salmon CYP1A1 cDNA with 94% similarity with rainbow trout CYP1A1 (Heilmann et al., 1988) (see Fig. 5).

Table 1
Polynuclear aromatic hydrocarbons (PAHs) present in coal dust contaminated sea water. The coal dust sample analyzed was obtained from the coal pile run-off collecting lagoon of a major coal terminal and contained 100 mg L^{-1} total suspended solids, 36 mg L^{-1} non-settleable solids (NSS) and 5577 ng L^{-1} total PAHs. Coal dust obtained from the same terminal was used in the exposure experiments and, for comparative purposes, 100 mg L^{-1} of this sample was placed in sea water and was found to yield 51 mg L^{-1} of non-settleable solids and 4906 ng L^{-1} total PAHs

Compound	Limit of quantitation (ng L^{-1})	Blank (ng L^{-1})	Coal dust leachate (ng L^{-1})
Low molecular weight PHAs			
Naphthalene	1.0	nd	408
Acenaphthylene	1.0	nd	nd
Acenaphthene	1.0	nd	nd
Fluorene	1.0	nd	280
Phenanthrene	1.0	nd	2037
Anthracene	1.01	nd	143
Total LMW PAHs			2868
High molecular weight PAHs			
Fluoranthrene	1.0	nd	353
Pyrene	1.0	nd	373
Benzo(a)anthracene	1.0	nd	285
Chrysene/Triphenylene	1.0	nd	466
Benzo(b/k)fluoranthrene	1.0	nd	417
Benzo(a)pyrene	1.0	nd	233
Indeno(1,2,3-cd)pyrene	1.0	nd	134
Benzo(g,h,i)perylene	1.0	nd	292
Dibenzo(a,h)anthracene	1.0	nd	156
Total HMW PAHS			2709
Total PAHS			*5577*

nd: not detected.

3.4. PAH analysis

The analysis of total PAHs leached from coal dust into sea water, in a sample collected from a coal terminal collecting lagoon which had been allowed to settle for 24 h (100 mg L^{-1} total suspended solids; 36 mg L^{-1} non-settleable solids), revealed the presence of 5577 ng L^{-1} total PAHs with 2868 ng L^{-1} total low molecular weight PAHs and 2709 ng L^{-1} total high molecular weight PAHs. The PAH analysis is presented in detail in Table 1 and indicates that procarcinogens including benzo(a)pyrene, dibenzo(a,h)anthracene, indeno(1,2,3-*cd*)pyrene and benzo(g,h,i)-perylene are present in coal dust contaminated sea water that is eventually released in coal terminal effluent. To ensure that the method used to prepare the coal dust suspensions for the exposures resulted in suspensions that were representative of the coal-dust contaminated sea water found in coal terminal collecting lagoons, the coal used in the exposure experiments was added to sea water at 100 mg L^{-1} and

analyzed for total PAHs. It was found that 100 mg L^{-1} of the coal dust used in the exposure experiments yielded 51 mg L^{-1} non-settleable solids and 4706 mg L^{-1} total PAHs when added to sea water and allowed a 24 h settling period. Hence the coal dust samples suspended in sea water and used to expose the fish were similar to the coal suspensions found in the coal terminal collecting lagoon, i.e. for the same level of coal dust, a similar level of non-settleable solids and total PAHs was found in both types of sample.

4. Discussion

The results of this study directly demonstrate that juvenile chinook salmon exposed to coal dust exhibit increased hepatic expression of both L5 and CYP1A1, genes which encode proteins which play crucial roles in cellular metabolism. This is the first study, to our knowledge, to partially characterize L5 from a teleost and to show that L5 expression can be altered by contaminant exposure.

In this study, mean hepatic CYP1A1 mRNA levels increased up to 6-fold following the 8-day exposure of juvenile salmon to the highest concentration of coal dust (500 mg L^{-1}). Previous studies have indicated similar fold increases (3-fold to 8-fold) in CYP1A1-associated enzyme activity in fish exposed to refinery effluent containing PAHs (Imber et al., 1995), and in fish sampled from a coal tar contaminated estuary (Vignier et al., 1994). Hence the level of CYP1A1 induction observed in this study corresponds well with the levels of induction noted previously in fish exposed to environmentally relevant doses of PAHs derived from coal byproducts. Chemical analysis of the PAHs which leach from coal dust into sea water revealed the presence of procarcinogens e.g. benzo(*a*)pyrene and dibenzo(a,h)anthracene which can be converted by P4501A1 into active carcinogens (Varanasi et al., 1986, 1987; Stegeman and Hahn, 1994). The induction of hepatic CYP1A1 in juvenile chinook living in coal-contaminated estuaries could therefore result in the production of mutagenic metabolites and hence have profound physiological consequences (Varanasi et al., 1989; Stein et al., 1990). These results are, however, in contrast to the information available on mammals in which coal dust exposure has not been shown to induce CYP1A1 in either liver or lung despite prolonged exposure (Rabovsky et al., 1984). This discrepancy could arise from the fact that teleosts may be more sensitive than mammals to some CYP1A1 inducers, e.g. 2,3,7,8-tetrachlorodibenzofuran, (Hahn and Stegeman, 1994) and this may also be true for some of the CYP1A1-inducing components in coal dust. It is also possible that CYP1A1-inducing components were extracted from the coal dust by the sea water and hence were more bioavailable in the present study.

The results of this study also indicated that coal dust exposure caused an increase in hepatic L5 gene expression, although the physiological consequences of this are presently unclear. It is well established in other vertebrate species, including mammals and *Xenopus laevis*, that L5 plays a vital role in ribosome biogenesis (Mager, 1988; Steitz et al., 1988; Wormington, 1989).

The region of L5 amplified by RT-PCR from coal dust exposed fish contained the

sequence encoding the putative RNA binding domain of this protein (Wormington, 1989). It is interesting to note that L5 does not share any sequence similarities to the highly conserved RNA recognition motif (RRM), which has been identified in a large number of RNA-binding proteins (Bandziulis et al., 1989; Kenan et al., 1991), indicating that alternative structures contribute to its specific interaction with 5S rRNA.

Ribosomal constituents, 3–4 rRNAs and 60–80 ribosomal proteins, are assembled in a precise and efficient manner, and the rate of ribosome formation is accurately tuned to the cellular need for protein biosyntheic capacity (Mager, 1988). Not only must the appearance of various ribosomal components be coordinated on the transcriptional level, but those that are not synthesized in the nucleolus (5S and ribosomal proteins) must become specifically concentrated there. There is much evidence that L5 specifically binds 5S rRNA and acts as a nuclear shuttling protein (Guddat et al., 1990). It is interesting to note that a direct inhibitory effect of coal dust on protein synthesis was noted by Lee et al. (1994) however, despite continued exposure, this inhibitory effect gradually disappeared. In this study, an upregulation of L5 expression following exposure to coal dust may indicate a compensatory response to these inhibitory effects on protein synthesis, since increased L5 expression may indicate enhanced or restored cellular protein biosynthesizing capacity.

The expression of ribosomal proteins, including L5, has also been shown in mammals to be senescence-regulated (Seshadri et al., 1993) and this down-regulation in senescent cells, coupled with the fact that increased expression of ribosomal proteins is observed in hepatocellular carcinomas (Frigerio et al., 1995), is thought to reflect an altered state of differentiation (Seshadri et al., 1993). These observations suggest that overexpression of a subset of ribosomal proteins is associated with cell growth and proliferation.

The mechanisms underlying the increased expression of L5 in coal dust exposed fish remains to be established. In fact, relatively little is known of the mechanisms that control vertebrate L5 gene expression. In contrast, the mechanisms by which CYP1A1 expression is controlled have been studied extensively. CYP1A1 gene expression can be induced by PAHs through both the well defined Ah receptor-dependent pathway (Whitlock, 1990; Okey, 1990) and the more recently elucidated and much less well defined AhR-independent pathway (Raha et al., 1995). The AhR-dependent pathway involves the binding of certain organic compounds (e.g. dioxin) to the Ah receptor complex (Whitlock, 1990; Neuhold et al., 1989; Okey, 1990; Wen et al., 1990; Reyes et al., 1992). The AhR-independent mechanisms are thought to involve the activation of a 33-kDal protein, recently identified as glycine *N*-methyltransferase (GNMT) (Raha et al., 1995). A nuclear protein of approximately the same size has also been shown to bind to the promotor regions of L5 and is thought to play a role in transcriptional regulation of this gene (Kenmochi and Tanaka, 1993). Whether a PAH-binding protein, such as the AhR or GNMT, could simultaneously influence the expression of both CYP1A1 and L5 remains to be established.

It is clear that coal dust has effects on the expression of several genes in juvenile chinook salmon. It is also possible that these sublethal effects may become manifest

at higher levels of biological organization. Coal byproducts and specific components found in coal dust leachate have been shown to reduce the growth rate of trout (Herbert and Richards, 1963), cause oocyte atresia and reduced ovarian growth in crayfish (Sarojini et al., 1995) and to promote DNA adduct formation and hepatocellular carcinoma in fish (Hendricks et al., 1985; Varanasi et al., 1986; Stein et al., 1990). It is known that CYP1A1 plays a role in the activation of procarcinogens and the formation of DNA adducts (Varanasi et al., 1986, 1989; Okey, 1990). However, to a large extent the mechanisms underlying the physiological disruptions observed in animals living in polluted environments is unknown. It is likely that these physiological effects are mediated through a number of mechanisms including the altered expression of several genes, only one of which is CYP1A1 (Gaido and Maness, 1994). Since L5 plays such a crucial role in ribosome biogenesis and cellular metabolism it is certainly plausible that the altered expression of this gene by contaminant exposure may ultimately have physiological consequences. The results of this study also indicate that alterations in the expression of L5 may potentially be used as a biomarker of specific PAH exposure in teleosts.

Acknowledgements

This work was supported by Canadian Department of Fisheries and Oceans Toxic Chemicals Green Plan and The Leverhulme Trust (UK). The authors are grateful to D. Hervio for assistance with the DNA sequencing. The authors acknowledge the assistance of Drs. D. Poon and D. Goyette (Environment Canada) and the funding contributed by PERD (Panel on Energy Research and Development), and are grateful to BCRI, especially M. McLeay, J. Pickard, G.J. Pasek and J.W. McKinley, for the PAH analysis information and technical assistance.

References

Bandziulis, R.J., Swanson, M.S. and Dreyfuss, G., 1989. RNA-binding proteins as developmental regulators. Genes Develop., 3: 431–437.

Berndston, A.K. and Chen, T.T., 1994. Two unique CYP1A genes are expressed in response to 3-methylcholanthrene treatment in rainbow trout. Arch. Biochem. Biophys., 310: 187–195.

Birtwell, I.K. and Kruzynski, G.M., 1989. In situ and laboratory studies on the behaviour and survival of Pacific salmon (genus *Oncorhynchus*). Hydrobiologica, 188/189: 543–560.

BCRI Environmental Sciences and Engineering, 1995. Impact of coal dust on the marine environment. BCRI report No. 2-11-0753, prepared for Environmental Protection, Environment Canada - Pacific and Yukon Division, 224 West Esplanade, North Vancouver, BC.

Campbell, P.M. and R.H. Devlin, R.H., 1996. Expression of CYP1A1 in livers and gonads of Pacific salmon: Quantitation of mRNA levels by RT-cPCR. Aquat. Toxicol., 34: 47–69.

Campbell, P.M., Kruzynski, G.M., Birtwell, I.H. and Devlin, R.H., 1996. The quantitation of dose-dependent increases in CYP1A1 mRNA levels in juvenile chinook salmon exposed to treated BKME using two field sampling techniques. Environ. Toxicol. Chem., 15: 1119–1123.

Chan, Y-L., Lin, A., McNally, J. and Wool, I.G., 1987. The primary structure of rat ribosomal protein L5. J. Biol. Chem., 262: 12879–12886.

Chomczynski, P. and Sacchi, N., 1987. Single step method of RNA isolation by acid guanidinium-thiocyanate-phenol-chloroform extraction. Anal. Biochem., 162: 156–159.

Dickmann, M., Brindle, I. and Benson, M., 1992. Evidence of teratogens in sediments of the Niagara River watershed as reflected by chironomid (Diptera: Chironomidae) deformities. J. Great Lakes Res., 18: 467–480.

Enzminger, J.D. and Ahlert, R.C., 1987. Environmental fate of polynuclear aromatic hydrocarbons in coal tar. Environ. Tech. Lett., 8: 269–278.

Frigerio, J-M., Dagorn, J.-C. and Iovanna, J.L., 1995. Cloning, sequencing and expression of the L5, L21, L27a, L28, S5, S9, S10 and S29 human ribosomal protein mRNAs. Biochim. Biophys. Acta, 1262: 64–68.

Gaido, K.W. and Maness, S.C., 1994. Regulation of gene expression and acceleration of differentiation in human keratinocytes by 2,3,7,8-tetrachlorodibenzo-p-dioxin. Toxicol. Appl. Pharmacol., 127: 199–208.

Guddat, U., Bakken, A.H. and Pieler, T., 1990. Protein-mediated nuclear export of RNA: 5S rRNA containing small RNPs in *Xenopus* oocytes. Cell, 60: 619–628.

Hahn, M.E. and Stegeman, J.J., 1994. Regulation of cytochrome P4501A1 in teleosts: Sustained induction of CYP1A1 mRNA, protein, and catalytic activity by 2,3,7,8-tetrachlorodibenzofuran in the marine fish *Stenotomus chrysops*. Toxicol. Appl. Pharmacol., 127: 187–198.

Heederik, D., De Cock, J. and Endlich, E., 1994. Dust exposure indices and lung function changes in longshoremen and dock workers. Am. J. Ind. Med., 26: 497–509.

Heilmann, L.J., Sheen, Y.Y., Bigelow, S.W. and Nebert, D.W., 1988. Trout P450IA1: cDNA and deduced protein sequence, expression in liver, and evolutionary significance. DNA, 7: 379–387.

Hendricks, J.D., Meyers, T.R., Shelton, D.W., Casteel, J.L. and Bailey, G.S., 1985. Hepatocarcinogenicity of benzo(a)pyrene to rainbow trout by dietary exposure and intraperitoneal injection. J. Natl. Cancer Inst., 74: 839–852.

Herbert, D.W.M. and Richards, J.M., 1963. The growth and survival of fish in some suspensions of solids of industrial origin. Int. J. Wat. Pollut., 7: 297–302.

Imber, B.E., Spence, B., Chan, Z. and Van Aggelen, G., 1995. Temporal variation in hepatic mixed-function oxidase (MFO) induction in rainbow trout exposed to industrial effluent. Mar. Poll. Bull., 30: 558–562.

Kenmochi, N. and Tanaka, T., 1993. A common nuclear factor that binds to the transcriptional control regions of ribosomal protein L5 and 5S rRNA genes. Biochem. Biophys. Res. Comm., 194: 1131–1134.

Kenan, D.J., Query, C.C. and Keene, J.D., 1991. RNA recognition: towards identifying determinants of specificity. TIBS, 16: 214–220.

Kruzynski, G.M., Birtwell, I.K. and Chew, G.L., 1994. Behavioural approaches to demonstrate the ecological significance of exposure of juvenile Pacific salmon (genus *Oncorhynchus*) to the antosapstain fungicide TCMTB. J. Aquat. Ecosys. Health, 3: 113–127.

Kuhn, D.C., Stanley, C.F., Nadia, E.-A. and Demers, L.M., 1990. Effect of in vivo coal dust exposure on arachidonic acid metabolism in the rat alveolar macrophage. J. Toxicol. Environ. Health, 29: 157–168.

Lee, Y.-C., Hogg, R. and Rannels, D.E., 1994. Extracellular matrix synthesis by coal dust-exposed type II epithelial cells. Am. J. Physiol., 267: 365–374.

Levings, C.D., 1985. Juvenile salmonid use of habitats altered by a coal port in the Fraser River Estuary, British Columbia. Mar. Poll. Bull., 16: 248–254.

Levings, C.D. and Riddell, B.E., 1992. Salmonids and their habitat in Howe Sound Basin: Status of knowledge. In: C.D. Levings, R.B. Turner and B. Ricketts (Editors). Proceedings of the Howe Sound Environmental Workshop. Can. Tech. Rep. Fish. Aquat. Sci., 1879: 65–83.

Macdonald, J.S., Levings, C.D., McAllister, C.D., Fagerlund, U.H.M. and McBride, J.R., 1988. A field experiment to test the importance of estuaries for chinook salmon (*Oncorhynchus tshawytscha*) survival: short term results. Can. J. Fish. Aquat. Sci., 45: 1366–1377.

Mager, W.H., 1988. Review: Control of ribosomal protein gene expression. Biochim. Biophys. Acta, 949; 1–15.

Neuhold, L.A., Shirayoshi, Y., Ozato, K., Jones, J.E. and Nebert, D.W., 1989. Regulation of mouse CYP1A1 gene expression by dioxin requirement of two cis-acting elements during induction. Mol. Cell. Biol., 9: 2378–2386.

Okey, A.B., 1990. Enzyme induction in the cytochrome P-450 system. Pharma. Ther., 45: 241–298.

Qian, L. and Wilkinson, M., 1991. DNA fragment purification: removal from agarose 10 minutes after electrophoresis. Biotechniques, 10: 736–737.

Rabovsky, J., Petersen, M.R., Lewis, T.R., Marion, K.J. and Groseclose, R.D., 1984. Chronic inhalation of diesel exhaust and coal dust: Effect of age and exposure on selected enzyme activities associated with microsomal cytochrome P-450 in rat lung and liver. J. Toxicol. Environ. Health, 14: 655–666.

Raha, A., Joyce, T., Gusky, S. and Bresnick, E., 1995. Glycine N-methyltransferase is a mediator of cytochrome P4501A1 gene expression. Arch. Biochem. Biophys., 322: 395–404.

Reyes, H., Reisz-Porszasz, S. and Hankinson, O., 1992 Identification of the Ah receptor nuclear translocator protein (Arnt) as a component of the DNA binding form of the Ah receptor. Science, 256: 1193–1195.

Rogers, I.H., Servizi, J.A. and Levings, C.D., 1988. Bioconcentration of chlorophenols by juvenile chinook salmon (*Oncorhynchus tshawytscha*) overwintering in the upper Fraser River: laboratory and field tests. Wat. Poll. Res. J. Can., 23: 100–113.

Rogers, I.H., Levings, C.D., Lockhart, W.L. and Norstrom, R.J., 1989. Observations on overwintering juvenile chinook salmon (*Oncorhynchus tshawytscha*) exposed to bleached kraft mill effluent in the upper Fraser River, British Columbia. Chemosphere, 19: 1853–1868.

Sarojini, R., Nagabhushanam, R. and Fingerman, M., 1995. Naphthalene-induced atresia in the ovary of the crayfish, *Procambarus clarkii*. Ecotoxicol. Environ. Saf., 13: 76–83.

Stegeman, J.J. and M.E. Hahn (1994) Biochemistry and molecular biology of monooxygenases. In: D.C. Malins and G.K. Ostrander (Editors). Aquatic Toxicology; Molecular, Biochemical and Cellular Perspectives, CRC Press, Boca Raton, FL, pp. 87–207.

Servizi, J.A., Gordon, R.W., Martens, D.W., Lockhart, W.L., Metner, D.A., Rogers, I.H., McBride, J.R. and Norstrom, R.J., 1993. Effects of biotreated effluent on fingerling chinook salmon (*Oncorhynchus tshawytscha*). Can. J. Fish. Aquat. Sci., 50: 846–857.

Seshadri, T., Uzman, J.A., Oshima, J. and Campisi, J., 1993. Identification of a transcript that is down-regulated in senescent human fibroblasts. J. Biol. Chem., 268: 18474–18480.

Stein, J.E.,e Reichert, W.L., Nishimoto, M. and Varanasi, U., 1990. Overview of studies on liver carcinogenesis in English sole from Puget Sound; Evidence for a xenobiotic chemical etiology II: Biochemical studies. Sci. Total Environ., 94: 51–69.

Steitz, J.A., Berg, C., Hendrick, J.P., La Branche-Chabot, H., Metspalu, A., Rinke, J. and Yario, T., 1988. A 5S rRNA/L5 complex is a precursor to ribosome assembly in mammalian cells. J. Cell Biol., 106: 545–556.

Varanasi, U., Nishimoto, M., Reichart, W.L. and Le Eberhart, B.-T., 1986. Comparative metabolism of benzo(a)pyrene and covalent binding to hepatic DNA in English Sole, starry flounder and rat. Cancer Res., 46: 3817–3824.

Varanasi, U., Stein, J.E., Nishimoto, M., Reichert, W.L. and Collier, T.K., 1987. Chemical carcinogenesis in feral fish: uptake, activation, and detoxification of organic xenobiotics. Environ. Health Perspect., 71: 155–165.

Varanasi, U., Reichert, W.L. and Stein, J., 1989. 32P-postlabelling analysis of DNA adducts in liver of wild english sole (*Parophrys vetulus*) and winter flounder (*Pseudopleuronectes americanus*). Cancer Res., 49: 1171–1180.

Vignier, V., Vandermeulen, J.H., Singh, J. and Mossman, D., 1994. Interannual mixed function oxidase (MFO) activity in winter flounder (*Pleuronectes americanus*) from a coal tar contaminated estuary. Can. J. Fish. Aquat. Sci., 51: 1368–1375.

Wen, L.-P., Koieman, N. and Whitlock, J.P., 1990. Dioxin-inducible Ah receptor-dependent transcription in-vitro. Proc. Natl. Acad. Sci. USA, 87: 8545–8549.

Whitlock, J.P., 1990. Genetic and molecular aspects of 2,3,7,8-tetrachlorodibenzo-p-dioxin. Ann. Rev. Pharmacol. Toxicol., 30: 251–277.

Wormington, W.M., 1989. Developmental expression and 5S rRNA-binding activity of *Xenopus laevis* ribosomal protein L5. Mol. Cell. Biol., 9: 5281–5288.

Xuan, J. and Robins, A., 1994. The effects of turbulence and complex terrain on dust emissions and depositions from coal stockpiles. Atmos. Environ., 28: 1951–1960.

October 26, 2006

Puget Sound Partnership
c/o Puget Sound Action Team,
P.O. Box 40900
Olympia, WA 98504-0900

Dear Puget Sound Partners

SUBJECT: PARTNERSHIP RECOMMENDATIONS TO:

IMPROVE WATER QUALITY AND HABITAT BY MANAGING STORMWATER RUNOFF

PROTECT ECOSYSTEM BIODIVERSITY AND RECOVER IMPERILED SPECIES

PROVIDE WATER FOR PEOPLE, FISH AND WILDLIFE, AND THE ENVIRONMENT

We, the undersigned members of Washington State's scientific community, have been studying impacts of urbanization on habitat and aquatic life for decades. There is a large body of literature regarding the relationship of urban runoff and the health of waterbodies. We have had the privilege of contributing papers describing the status and trends in Northwest rivers, wetlands, and coastal environments, the impacts of urban runoff (and other effects of human activities on Puget Sound waters), the effectiveness of mitigation measures, and original and effective methods for monitoring waterbody health. All undersigned have credentials to comment on effective approaches for urban runoff management.

These comments are in response to preliminary recommendations by the Puget Sound Partnership, dated October 2006, for action to preserve and recover Puget Sound.

IMPORTANCE OF STORMWATER RUNOFF MANAGEMENT IN THE PUGET SOUND BASIN

Urban runoff scours streams, destroys aquatic life characteristic of a healthy ecosystem, and carries enormous loads of contaminants to Puget Sound. Stormwater is most likely a primary source of destructive flows and contaminants leading to the precipitous decline in the health of the Puget Sound ecosystem.

Because of urbanization, peak stormwater flows can increase stream discharge by factors of up to 10-fold over predevelopment peaks. Annual flow volumes can double.

Contaminants in and volumes of urban runoff discharged to streams change the types and numbers of aquatic species, changes that are key signals of declining ecological health.

The decline in stream health begins with the clearing of the forest and modification of river channels in a watershed. Stream flow usually increases dramatically after clearing and often streams are devastated even before any development takes place. Every square foot of effective impervious surface then added to a watershed counts further toward the stream's decline. ("Effective" impervious area is that connected by a conveyance system to surface water.) With the first increments of effective impervious area in a watershed, the numbers of the most sensitive species decline dramatically. Contrary to popular dogma, there is no threshold of development below which there will be no biological degradation.

Although all groups of aquatic organisms are affected by the actions of humans, anadromous fish in our region are the most widely understood and appreciated species that suffer enormously in streams draining urbanized watersheds. Salmon and sea-run cutthroat trout spawned and nurtured in Puget Sound's streams are important for several reasons: regional icons, contributors to regional economies, and key players in the food webs that range from mountain forests to the health of Puget Sound orcas. In short, a healthy Puget Sound depends on a healthy regional biota, especially anadromous fish populations.

END-OF-PIPE TREATMENT AND DETENTION DISCREDITED

"End-of-Pipe" management of stormwater refers to the practice of treating and detaining runoff from urban land uses before discharging it to surface water. Underlying the employment of end-of-pipe management is the assumption that forested watersheds can be converted to any type of land use (including 100% impervious) and that the impacts of these changes on receiving waters can be negated through the use of engineered stormwater-management hardware.

The prescriptions and methods for design of such hardware are found in drainage design manuals in use by every jurisdiction in the basin. An example of such a manual is the DOE's "Stormwater Management Manual for Western Washington". Newly written NPDES permits require that jurisdictions use this manual (or its equivalent) in mitigating for urban runoff. However, the DOE manual itself disavows claims to protect aquatic life. From Volume 1, Section 1.7.5: …*land development as practiced today is incompatible with the achievement of sustainable ecosystems*. And also from Volume 1, Section 1.7.5: *The engineered stormwater … systems advocated by this and other stormwater manuals … cannot replicate … hydrologic functions of the natural watershed that existed before development, nor can they remove sufficient pollutants to replicate the water quality of predevelopment conditions*.

End-of-pipe stormwater management has been and continues to be a failure at adequately protecting streams, wetlands, and Puget Sound. The literature in the past 30 years documents the negative effects of stormwater discharges on receiving waters.

In the past 5 years several papers have been published describing the marginal differences in stream damage between those watersheds where treatment and detention is installed and those where discharges are unmitigated. Hydrological studies are available that show that no amount of end-of-pipe mitigation can protect streams from urban runoff. In short, conversion of forests to traditional urban land uses cannot be mitigated by end-of-pipe prescriptions.

Since 1996, the correlation between urbanization (and concomitant decline in forest cover, loss of stream buffers, new impervious area) and stream health has been documented in detail. It is now possible to predict, with considerable confidence, the ill-effect of continuing urbanization on the last vestiges of healthy streams in the basin if such development follows the same formula employed in the past.

THE PARTNERSHIP LEANS ON FAILED PRACTICES FOR PROTECTION

The following is the stormwater recommendation from the latest draft of Puget Sound Partners recommendations (dated October 2006):

> *1. Issue NPDES Phase I and Phase II permits that brings 80% of the Puget Sound's population (and some 80 cities) into active stormwater management. Also:*
>
> > *a. Implement a coordinated water quality monitoring program.*
> > *b. Expand programs to maximize stormwater infiltration.*
> > *c. Promote a basin approach to stormwater by sponsoring pilot projects.*
> > *d. Increase funding for Low Impact Development (LID) demonstration projects and develop incentives to encourage the use of LID.*

The Partnership recommendation to issue NPDES permits is unnecessary in that this will be done regardless of Partnership stance.

Furthermore it is widely known that NPDES offers little hope of protecting streams and Puget Sound. NPDES permits issued by Washington State require only that permittees adhere to the state's "Stormwater Management Manual for Western Washington", a set of prescriptions for end-of-pipe engineering hardware. The manual recognizes that end-of-pipe engineering will not protect streams and source control is necessary (Volume 1). But, in the subsequent volumes containing its prescriptions, the manual is silent about the advisability of conversion of forests to intense forms of land use. The manual allows development projects that convert up to 100% of a forested site to impervious area. The manual's prescriptions are concerned only with sizing of hardware. The scientific literature demonstrates that it is not possible to fully mitigate for any such conversions regardless of hardware size.

The Partnership should not expect that NPDES or continued end-of-pipe management of runoff will lead to the protection or recovery of Puget Sound.

Encouraging infiltration (in the absence of LID standards) is meaningless ("*b*." above). For traditional high-impact development, jurisdictions disallow infiltration on till soils. Encouragement to "maximize" infiltration will not make soils more porous. And the Partnership should not be "encouraging" anything. The Partnership should be describing practices and standards that are vital to Sound recovery and recommending that they be implemented and enforced.

More low impact development pilot and demonstration projects, at best, will delay essential action ("*c"* and "*d*." above). We have sufficient experience with traditional end-of-pipe stormwater management to know that it is not an alternative and we must turn from it as quickly as possible. Sufficient projects have been constructed to show that LID projects can be successful at retaining runoff on project site. To recommend more such projects (in the absence of action to introduce changes into development code to require them) reflects unjustifiable timidity in the face of great danger to the Sound. Moreover, the Partnership recommendation for incentives ("d" above) to abide by LID standards, in the absence of regulations to force such changes, is destined to fall far short of the goal to protect and restore Puget Sound.

We regrettably conclude that, if the above is the extent of the Partnership recommendations regarding stormwater, little hope should be held for restoration of Puget Sound. Indeed it is far more likely, with the arrival of millions more newcomers and concomitant high-impact development, that the health of Puget Sound will continue in its precipitous decline.

PRACTICES THAT MUST BE IMPLEMENTED IF PUGET SOUND IS TO BE SAVED

Science supports the following actions and practices related to land use as necessary to halt the decline of Puget Sound ecosystem, provide for recovery of anadromous fish, halt the increase in and reduce the load of pollutants carried by stormwater to Puget Sound, and begin the steep climb toward restoration. This list is not all-inclusive. It is left to others to urge the many other action items needed to restore Puget Sound and other regional water bodies to healthy condition.

1. **Preserve Existing Least-Disturbed Watersheds and Subwatersheds**. The scientific literature is clear that the healthiest and most biologically productive streams are found in undisturbed watersheds. Very small levels of disturbance in the healthiest watersheds immediately start their inevitable biological or ecological decline, beginning with the loss of their most sensitive species, to decline in predators and to the increase in the most tolerant species.

Such watersheds and associated streams should be set aside and protected from disturbance. If we are serious about preserving Puget Sound, we must identify those watersheds that we can characterize as in good or excellent condition and preserve them. The means employed for preservation must ensure that it is certain and permanent.

2. **No Net Loss of Forest Cover in the Puget Sound Basin**. Forest loss must be limited in the process of conversion to urban purposes, and such loss must be balanced by increasing/restoring forest cover in disturbed areas within the basin.

   Forest loss owing to new development should be limited through development code. An example of such code can be found in DOE's "Stormwater Management Manual for Western Washington", Volume V, BMP T5.30. The Partnership should recommend that this code be used to guide all new development.

   To mitigate for the fraction of forest cleared in each new development (i.e. the fraction not preserved by code), the Partnership should recommend a program of clearing trading rights. Such a program would ensure that for each portion of a site cleared for development an equivalent forest area is restored elsewhere in the basin. (Forest restoration in disturbed areas can be affected by a variety of programs. Restoration of buffers along urban streams is an example.)

3. **Halt Runoff From New Impervious Area in the Puget Sound Basin**. Methods for eliminating runoff from impervious surfaces include (but are not limited to) using pervious paving materials, associating impervious area with bioretention facilities, reducing such areas to functional minimums, and so on.

   The Partnership should recommend code changes requiring that most new paving and roofing be constructed using materials and practices to prevent them from generating runoff to surface water.

   These methods are some of the tools in the practice of "low impact development".

4. **Preserve Existing and Restore Destroyed Buffer Areas Adjacent to Streams**. Destroyed buffers are often found in private ownership. The Partnership should recommend that these be purchased, or otherwise protected, and that soil and riparian vegetation be restored. The protection of Puget Sound as a public good requires creative approaches to these activities. The Partnership should recommend that jurisdictions adopt a system of prioritization of stream buffers to be restored and a time table for restoration. Obviously, restoration of existing problem-buffers may take decades; even so, the Partnership should set reasonable targets for buffer restoration for year 2020 and other milestone dates.

5. **Reduce the Amount of Runoff From Existing Impervious Area**. Much existing impervious area is unnecessary and should be removed. (For example, two-way streets could be converted to one-way and a lane eliminated.) Existing impervious area could be disconnected from surface water by repaving using pervious materials or bordering with bioretention facilities or both.

   The Partnership should recommend a program of prescriptions and incentives to reduce existing total and effective impervious area.

The Puget Sound Partnership has a daunting task and carries the burden of responsibility for the fate of the basin's ecosystem. We the undersigned applaud the effort, and offer our services in making the best possible recommendations to the Governor.

Sincerely,

Douglas Beyerlein, Professional Hydrologist and Professional Engineer
Susan Bolton, PhD, Professional Engineer
Derek B. Booth, PhD, Professional Engineer and Professional Geologist
Thomas W. Holz, Professional Engineer
Thom Hooper, Fisheries Biologist
Richard R. Horner, PhD, Environmental Engineering Research
James R. Karr, PhD, Ecologist
DeeAnn Kirkpatrick, Fisheries Biologist
John Lombard, Planner and Environmental Policy Analyst
Christopher W. May, PhD
Gary Minton, PhD, Professional Engineer
David R. Montgomery, PhD, Professor of Geomorphology
David Somers, Fisheries Biologist
Cleve Steward, Fisheries Biologist

ENVIRONMENTAL IMPACTS OF ACID LEACHATE DERIVED FROM COAL-STORAGE PILES UPON GROUNDWATER

ANGIE M. COOK and STEVEN J. FRITZ*
Purdue University, West Lafayette, IN, U.S.A.
(author for correspondence, e-mail: sfrito@eas.purdue.edu, Phone (765) 494–3276, Fax (765) 496–1210)*

(Received 21 June 2000; accepted 18 May 2001)

Abstract. Leachate emanating from a coal-storage area at an electric utility plant in Northwest Indiana (U.S.A.) is impacting groundwater quality. This assessment is based on results of a long-term groundwater monitoring program conducted at Purdue University's Wade Utility Plant where a monthly average of 32,000 metric tons of both high- and low-sulfur coal are stored. Groundwater from both a perched and major aquifer (the Wabash Valley Aquifer) as well as surface water from a large retention pond were sampled monthly for 34 consecutive months. Such a long-term, continuous sampling scheme proved beneficial in identifying seasonal trends and anomalies within the chemistry of ground- and surface waters. Data show elevated concentrations of sulfate and hardness in the perched zones and the Wabash Valley Aquifer (WVA). Lead in the WVA has also been reported at a concentration greater than the state maximum contaminant level, while several metals (Be, Cd, Cu, Pb, Ni, Se, and Zn) contained within retention-pond sediments have the highest concentrations in aquatic sediments ever reported within the State of Indiana.

Due to the buffering capacity of carbonate minerals in underlying unconsolidated deposits, the acidic pH of coal-pile leachate is raised to values typical for groundwater in carbonate terrain common in Northwest Indiana. Further ameliorating the input of acid percolation is the dilution capabilities of both the WVA and the recharge pond. Hence, sites without such advantages would exhibit a greater degree of groundwater contamination than what is observed at Purdue's coal-storage facility.

Keywords: acidity, coal, coal storage, groundwater, leachate, power plant

1. Introduction

The United States relies on the combustion of approximately 800 million metric tons of coal per year to generate 53% of its electricity. Coal-fired power plants typically store a 30–90 day supply of coal for their operations, and at year-end 1997 there were approximately 100 million metric tons of coal in storage in the United States at electric utility plants alone (Energy Information Administration, 1998). There are currently no federal design requirements in the United States for a coal-storage facility; hence, coal is typically stored in direct contact with the ground and without a liner or leachate collection system. Since acidic, metal-rich leachate is produced when sulfur-bearing coal is exposed to the atmosphere, this type of storage poses a threat to both ground- and surface water.

Water, Air, and Soil Pollution **135:** 371–388, 2002.
© 2002 *Kluwer Academic Publishers. Printed in the Netherlands.*

Coal leachate characteristics have been studied extensively in the laboratory via coal-leaching experiments (Anderson and Youngstrom, 1976; Cox *et al.*, 1977; Wachter and Blackwood, 1978). This study presents a long-term field investigation to evaluate the impact of acidic coal-pile leachate upon underlying aquifers. Results of 34 months of continuous sampling of ground- and surface water at the coal-fired power plant located at Purdue University (West Lafayette, Indiana, U.S.A) are reported. The plant burns both low-sulfur (1 to 2%) and high-sulfur (3.5 to 4.5%) coal, and approximately 32,000 metric tons of coal are piled in a 14-hectare area (Figure 1).

Published investigations concerning impact of coal-pile leachate on water quality (Brookman *et al.*, 1977; Carlson, 1990) discuss results of only few samplings distributed over a period of time no longer than 6 months. We show that continuous monthly sampling of observation wells permits a better interpretation of hydrogeochemical impacts of coal-pile leachate because seasonal trends and periodic anomalies can be better identified. This was particularly true of this field area because a contaminant-free recharge pond pushes leachate at varying rates toward the aquifer. An assessment of the buffering ability of carbonate terrain is also examined in this study, which is an aspect of coal-pile leachate that has never been assessed in a field study.

2. Site Characteristics

2.1. Coal storage information

Two spreader-stoker boilers and a fluidized-bed boiler operate at Wade Utility Plant, and an average of 114,000 metric tons of coal are combusted per year at the plant. There are three types of coal storage at the plant: active, short-term, and long-term. The active piles are replenished by daily coal deliveries and do not have sufficient residence time for leachate production to occur. Short-term storage consists mainly of low-sulfur coal, while long-term storage is a mixture of both types of coal. Approximately 75% of the total amount of coal storage on site is contained within the long-term storage pile, which has an estimated turnover rate of 5 to 6 yr.

2.2. Hydrogeologic setting

According to Weinreb (1987), the general geology of the immediate region consists of a heterogeneous layering of glacially derived outwash and till deposits capping Devonian and Mississippian age shales. The study area is located on the Maumee outwash terrace which consists mainly of sand and gravel deposits.

There are three main hydrated zones within the study area: the Wabash Valley Aquifer (WVA), a perched aquifer system, and three recharge ponds. The extensive WVA is contained within the water-bearing sand and gravel outwash deposits and

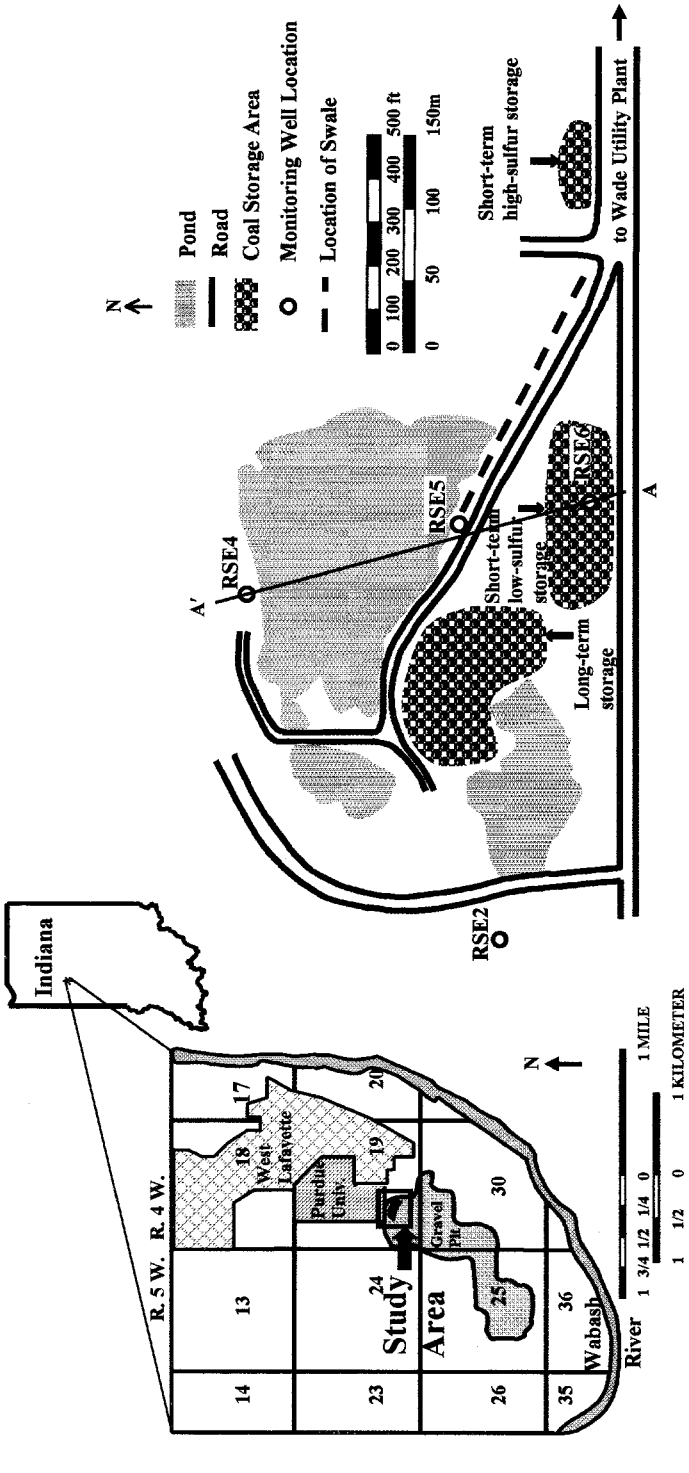

Figure 1. The study area is situated on the south side of the Purdue University West Lafayette campus in Northwest Indiana, U.S.A. Cross-section A-A' is shown in Figure 2.

is the source of drinking water for Purdue University and surrounding communities. Interspersed lenses of till within the sand and gravel configure the shallow, discontinuous perched aquifer system which is less productive than the WVA. The main recharge pond is located on the northern perimeter of the study area (Figure 1) and receives a combined average of 5.3 million liters per day of waste air-conditioning and cooling water from campus buildings and stormwater runoff from campus streets (Bjelke, 1960). The water level within the pond has remained constant for many years, indicating that the pond is in a near hydraulic steady state *vis-á-vis* inflow versus outflow. Thus, the pond serves as a major source of recharge to underlying aquifers.

The WVA is unconfined in the vicinity of the study area and has a hydraulic conductivity ranging from 38 to 91 m day^{-1} (Weinreb, 1987). Recharge to the aquifer in the area underlying the coal piles is supplied largely by the recharge pond; however, lateral underflow from the northwest as well as vertical infiltration of precipitation are additional sources of recharge. The hydraulic gradient of the aquifer is estimated as 0.0019 and flow within the WVA is toward the southeast (Weinreb, 1987). Groundwater ultimately discharges into the Wabash River (Figure 1), although during periods of high river stage, the river may also serve as a source of recharge (Weinreb, 1987). Discharge also occurs via pumpage from the three main groundwater users in the area: Purdue University, West Lafayette Water Company, and Eli Lilly Company. Total discharge by these three entities is estimated at 55 million liters per day (Weinreb, 1987).

Four monitoring wells are present at the study area, each consisting of PVC casing and screened at the top of the respective aquifer that each well taps. Wells RSE2 and RSE4 tap a perched aquifer while RSE5 and RSE6 tap the WVA. A cross-section trending SE/NW through the study area (Figure 1) was constructed using well-log data from the current study and subsurface interpretations of Weinreb (1987) (Figure 2).

3. Methodology

Continuous monthly sampling of the monitoring wells and recharge pond began in September, 1996 and ended in June, 1999. Between December, 1996 and April, 1997 sampling was conducted biweekly in order to better pinpoint lag-times of chloride spikes originating in the recharge pond and subsequently traveling through the aquifers. This period coincided with peak road-salting operations following winter storms.

Depth-to-water, temperature, dissolved oxygen (DOX), pH, and alkalinity were measured at each sampling site. Sulfate and nitrate were performed using a *Dionex*® model 4000i ion chromatograph, while Mg^{+2}, Na^{+}, and K^{+} were measured using a *Varian*® model SpectrAA-20 atomic absorption spectrophotometer. Chloride, alkalinity, and hardness were determined by standard titrimetric techniques

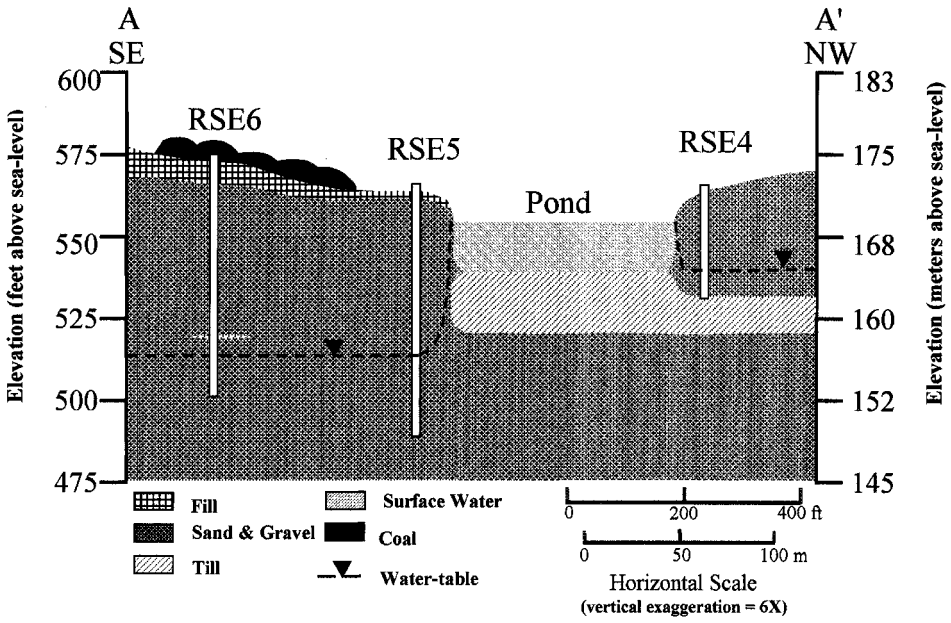

Figure 2. Cross-section trending SE/NW through the study area. Subsurface deposits consist mainly of sand and gravel with interspersed lenses of till. The pond is in near-hydraulic steady state leaking approximately 5.3 million liters per day to the subsurface. Hence, wells RSE4 and RSE5 are significantly influenced by pond water.

(Franson, 1980). Trace metals (As, Cd, Cr, Cu, Pb, Hg, Se) were analyzed on three occasions during the course of the study by an outside laboratory.

Recharge pond samples were collected by mixing approximately 500 ml of water from both the main pond and the small pond directly west of the main pond. This stirred mixture was then split into two portions: one for measurement of field parameters and the other for filtration of sample. The elevation of the main pond was gauged by measuring the water level relative to the top of a culvert of known elevation.

A column experiment was performed to better gauge the groundwater chemistry in terms of the type and magnitude of acid leachate emanating from the coal piles. These leachate experiments allowed us to recognize signatures of contamination and also to determine how effectively site characteristics (such as dilution and carbonate mineral dissolution) reduce the contamination potential of coal-pile leachate. The experimental setup consisted of two PVC columns, each 2 m long with a 10 cm inner diameter. One column was packed with low-sulfur coal (0.60% S), while the other was packed with high-sulfur coal (2.92% S). Both samples are Indiana coals mined from the eastern limb of the Illinois Basin. Each of these columns was subjected to the addition of 1.3 cm of deionized water every 5 days for

TABLE I

Chemical characteristics of leachates generated in coal-leaching experiments. Coal-packed columns were subjected to the addition of 1.3 cm of deionized water every five days for a 30 day period. Leachates were collected and analyzed every 5 days, and the reported data are results of analyses on day 30

	pH	Hardness	Fe_T	SO_4^{-2}	Alkalinity	Acidity
Low-sulfur coal (0.60% S)	5.94	120.2	0.32	597.9	17.34	0.00
High-sulfur coal (2.92% S)	2.22	0.66	15,700	33,766	0.00	36,380

All ion concentrations in terms of mg L^{-1}.
Alkalinity and acidity in terms of $CaCO_3$ L^{-1}.

a 30 day period. The resulting leachate was collected every fifth day and chemically analyzed.

4. Results and Discussion

4.1. Sulfate as an indicator of contamination

Coal-leaching experiments conducted with samples of coal stored at the study area indicate that coal-pile leachate is responsible for elevated concentrations of sulfate. Leachate produced from the addition of 1.3 cm of deionized water every five days to low-sulfur coal (0.6% S) had a sulfate concentration of 12.5 meq L^{-1} (597.9 mg L^{-1}) after 30 days, while high-sulfur coal (2.92% S) produced leachate with a sulfate concentration of 703 meq L^{-1} (33,766 mg L^{-1}) when subjected to the same conditions (Table I). Due to the large amount of dilution associated with the recharge pond and the WVA, concentrations of sulfate in groundwater underlying the coal piles are typically on the order of what is observed for low-sulfur coal leachates.

Data obtained from groundwater sampling at Wade Utility Plant are summarized in Table II, which displays the average of 34 months of data for each measured parameter. A comparison is made between the averages for each individual well and the overall county average, which is based on quarterly measurements of 30 wells in an 1100 km^2 area in Tippecanoe County. Upon cursory examination of these data it is apparent that concentrations of sulfate are above average in every well on the site and are significantly elevated in RSE5 and RSE6, which are wells located most adjacent to the coal piles.

TABLE II

A comparison of parameter averages within each well to the respective county average. Uncertainty associated with the averages are $\pm 1\sigma$ relative to the reported average. Average concentrations of SO_4^{-2}, Ca^{+2}, and Mg^{+2} are elevated above the county average because coal-pile leachate dissolves calcite and dolomite contained within unconsolidated deposits beneath the coal-piles

	RSE2 Average	RSE4 Average	RSE5 Average	RSE6 Average	County[a] Average
Water Elevation (m)	163.48 ± 0.67	164.30 ± 0.49	156.70 ± 0.70	156.60 ± 0.70	–
Temperature (°C)	16.5 ± 1.9	14.1 ± 6.5	17.1 ± 4.8	19.1 ± 1.9	13.0 ± 1.5
pH	6.89 ± 0.10	7.47 ± 0.18	7.19 ± 0.23	6.96 ± 0.13	7.25 ± 0.11
–log pCO_2 (atm)	1.26 ± 0.12	2.06 ± 0.23	1.76 ± 0.33	1.43 ± 0.14	1.82 ± 0.10
DOX	3.0 ± 1.0	4.4 ± 1.9	6.9 ± 1.7	4.0 ± 1.0	–
Na^+	1.21 ± 0.31	1.19 ± 0.82	0.85 ± 0.37	0.76 ± 0.08	0.62 ± 0.54
K^+	0.34 ± 0.08	0.08 ± 0.01	0.11 ± 0.03	0.16 ± 0.02	0.07 ± 0.03
Ca^{+2}	9.84 ± 1.9	3.57 ± 0.43	8.61 ± 4.4	12.49 ± 2.0	3.93 ± 1.1
Mg^{+2}	2.95 ± 0.48	2.24 ± 0.30	3.28 ± 1.5	4.71 ± 0.68	2.57 ± 0.66
Cl^-	0.86 ± 0.43	1.35 ± 0.90	0.76 ± 0.49	0.62 ± 0.23	0.56 ± 0.67
$SO_4{}^{-2}$	5.74 ± 2.0	1.08 ± 0.27	7.29 ± 6.2	11.61 ± 2.6	1.04 ± 0.75
Alkalinity	7.68 ± 0.63	4.55 ± 0.54	4.78 ± 1.1	5.86 ± 0.31	5.25 ± 0.92
$NO_3{}^-$	0.05 ± 0.07	0.04 ± 0.03	0.02 ± 0.036	0.09 ± 0.11	–

[a] County average based on 30 wells sampled by Harvey (1990) and reported by Fritz *et al*. (1994). Average for RSE2 based upon 33 samplings, while averages for the other 3 wells are based upon 39 samplings. All concentrations in milliequivalents L^{-1} with the exception of DOX which is reported in mg L^{-1}.

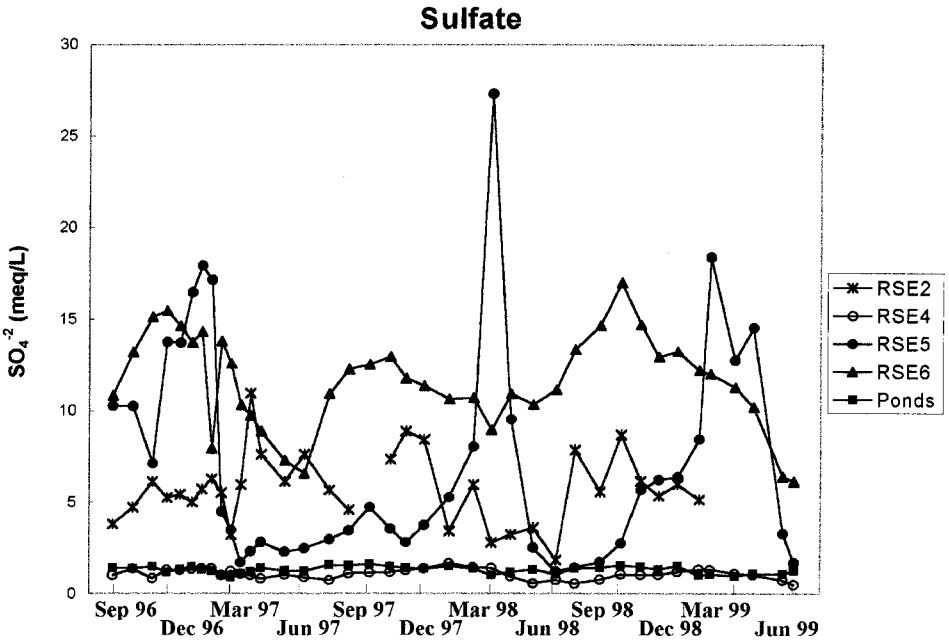

Figure 3. Concentration of sulfate vs. time. Seasonal fluctuation is observed in RSE6 which can be correlated with the amount of coal storage present, e.g. sulfate concentrations are greater during winter months when more coal is stockpiled. Spikes of sulfate observed in RSE5 can be explained in the context of precipitation (Figure 5).

4.2. Trends in Sulfate Data

The data continuum provided by continuous monthly sampling allows one to better analyze trends in sulfate data and to pinpoint outlying concentrations of sulfate (Figure 3). This was essential for recognizing factors that influence the magnitude of high-sulfate leachate that invades groundwater beneath the coal piles. Such factors include: the amount of storage present, the influence of precipitation, and the effect of dilution from the pond. Monthly sampling provides sufficient resolution to discern that RSE6 has the most consistent and highest average sulfate concentration relative to the other wells at the study area (Figure 3). This is not surprising as RSE6 is positioned in the center of the short-term coal storage piles. It is also apparent that sulfate concentrations are greatest in RSE6 in early autumn when coal stocks are increased for winter demand and lowest in late spring when stocks have diminished. Correspondingly, the average temperature of water in RSE6 (19.1 $\pm$ 1.9 °C) is higher than in any other well and is considerably elevated above the county average of 13 °C (Figure 4). This temperature anomaly is due to the heat produced by the oxidation of organic carbon and pyrite in the coal. Other wells influenced by coal-pile leachate, as evidenced by elevated sulfate concentrations

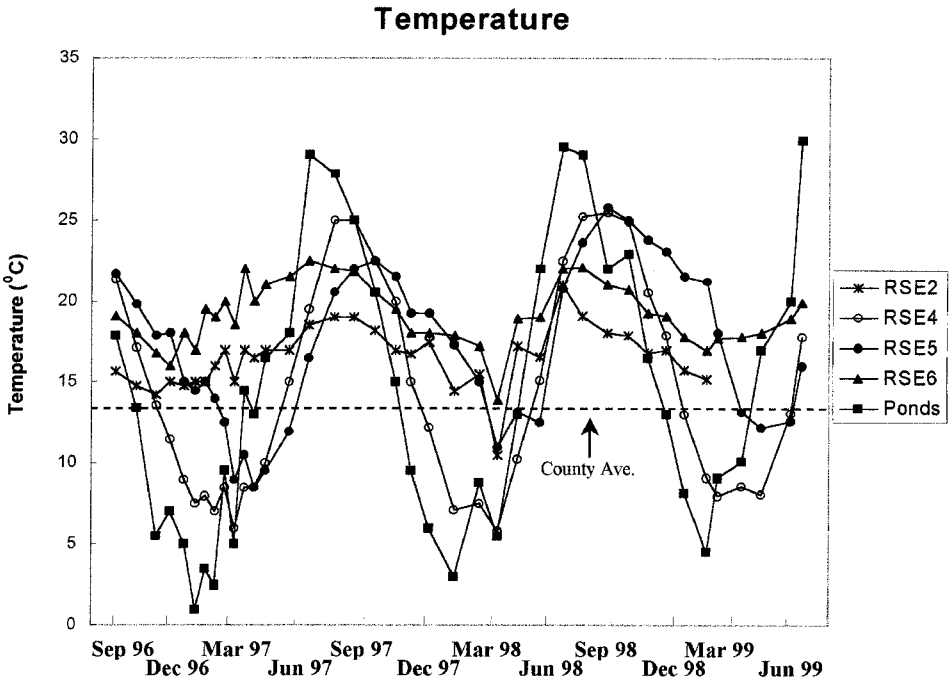

Figure 4. Temperature vs. time. The data portray an obvious seasonal trend with maxima corresponding to summer months and minima to winter months. The key aspect of this figure is that wells most impacted by coal-pile leachate (RSE5, RSE6, and RSE2) have the highest average temperature due to the heat of oxidation associated with leachate production. The horizontal dashed line shows the average groundwater temperature based on quarterly measurements of 30 wells (> 10 m depth to water) in a 1100 km^2 area in Tippecanoe County.

(RSE2 and RSE5), also have average temperatures elevated above the county mean (Table II).

Perhaps the most striking aspects of the sulfate data are the large spikes of sulfate that appear in RSE5. A particularly large spike of sulfate (27.28 mN) was noted in RSE5 in March, 1998. Since the amount of coal storage is relatively low in March (and would not likely influence a well to the extent of 27.28 mN sulfate even if stocks were high at the time) it was necessary to explore an alternate explanation for this spike. Figure 5 illustrates how this spike relates to precipitation preceding the sampling event. Although rainfall does not control the amount of sulfate produced, it can influence the concentration. During periods of little-to-no precipitation (like the period between the January 1998 sampling and several days before the March 1998 sampling) acid leachate that has been neutralized by reaction with carbonate minerals in the vadose zone can produce a sulfate-rich caliche. Such a phenomenon has been documented by Everett (1985) who noted that acidic pore waters migrate upward along capillary pathways during prolonged dry periods, which results in the precipitation of salts as the waters evaporate. When

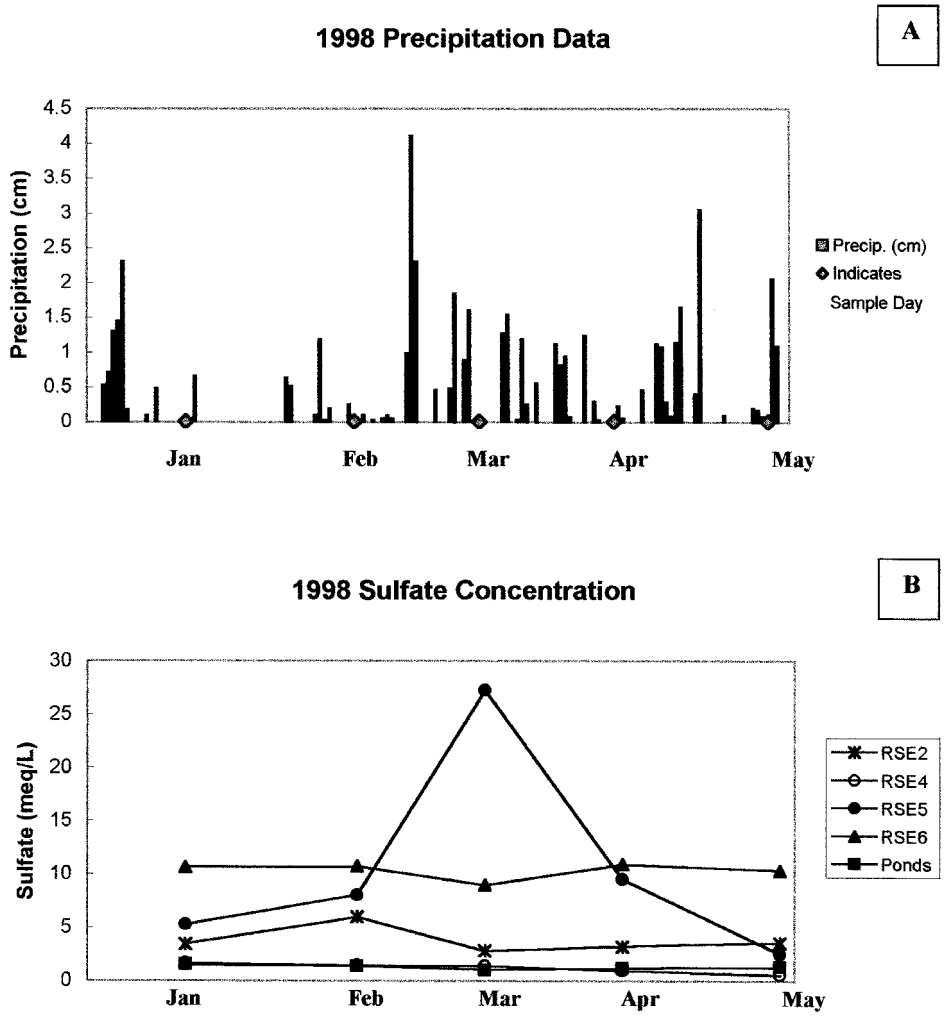

Figure 5. An amplified representation of the March 1998 sulfate spike observed in RSE5 (B), and the amount of precipitation measured prior to the observation of the spike (A). These figures illustrate that a prolonged dry period was likely responsible for a build-up of sulfate in the unsaturated zone that was flushed into the saturated zone following significant rainfall.

a significant flushing event finally occurs, the caliche is dissolved and the result is a highly concentrated sulfate solution.

Although no physical evidence was obtained to substantiate the presence of a caliche, chemical data suggest this as the most likely explanation for spikes of sulfate in RSE5. However, this interpretation alone does not explain why similar spikes don't appear in the remainder of the wells at the study area. This is best explained in terms of the position of RSE5 relative to the high-sulfur coal piles, which produce leachates with sulfate concentrations orders of magnitude

greater than low-sulfur coal (Table I). After a storm event, channels of overland flow containing leachate derived from these piles often terminate in a topographic depression near RSE5, while the other wells are located up-slope from these piles.

The baseline established by monthly sampling also provides insight into the extent to which each well is influenced by pond dilution, which considerably minimizes the impact of leachate on groundwater near the study area. Since the pond water exhibits low concentrations of sulfate (an average of 1.29 ± 0.19 mN), those wells most influenced by pond water infiltrating to the subsurface will likely exhibit low or reduced concentrations of sulfate. For example, Figure 3 shows that RSE4 typically has concentrations very similar to the pond, which indicates that the water in this well is strongly influenced by pond water. Conversely, the concentration of sulfate in water from RSE6 is often ten times the concentration in the pond. Water from RSE6 is nearly immune to pond influence not only because of its large distance from the pond relative to the other wells, but also because of its close proximity to the coal. For this reason, RSE6 serves as the best indicator of the contaminant potential of coal-pile leachate in the WVA. Pond dilution can also be attributed to the fact that RSE5 has sulfate concentrations similar to RSE2 (which is not as influenced by pond water) even though RSE5 is located much closer to the coal piles.

4.3. Indicators of Acid Neutralization

Dissolution of calcite and dolomite contained within the underlying till at the study area is responsible for neutralizing leachate acidity. This conclusion is supported by neutral pH, elevated hardness concentrations, and increased pCO_2 for all of the analyzed well waters. Upon cursory examination of the data, neutral pH is the first indication that neutralization has occurred since the average pH of leachates generated in the column experiments was 6.36 for low-sulfur coal and 2.21 for high-sulfur coal. In contrast, the lowest average pH for a well at the study area was 6.89 (Table II) while none of the 147 groundwater pH measurements was below 6.6. In addition, field evidence shows that at locales where the buffering influence of carbonate minerals is not present, groundwater pH will be depressed when influenced by coal leachate. Such data are presented in a study of a reject coal-pile conducted by Carlson (1990) at the U.S. Department of Energy's Savannah River Site in South Carolina, which is an area dominated by low pH, clayey soils. Results of that study showed that pore water within the rooting zone was highly acidic with pH values as low as 2.2.

Hardness concentrations elevated above the county average (Table II) as well as increased pCO_2 are two other indications that calcite and dolomite dissolution contributes to leachate neutralization. Elevated calcium and magnesium concentrations are relatively simplistic indicators because calcium and magnesium ions are released to solution upon the dissolution of calcite or dolomite; however, increased pCO_2 requires a more detailed explanation.

There are two possible mechanisms to explain high partial pressures of CO_2 in the gravel pits relative to the $10^{-1.82}$ atmosphere county average (Table II). The first is dissolution of calcite and/or dolomite in the *saturated zone*, which liberates CO_2:

$$CaCO_3 + H_2SO_4 \rightarrow Ca^{+2} + SO_4^{-2} + CO_2 + H_2O$$

The second possible mechanism involves neutralization in the *vadose* zone. In this case, the dissolution reaction proceeds in the same manner as shown in the above reaction with the exception that CO_2 is permitted to leave solution leaving a calcium sulfate rich solution. When this solution enters the saturated zone, which is presumed to be saturated with respect to calcite in a carbonate terrain like northwest Indiana, calcite precipitates due to the common ion effect. This reaction also liberates CO_2:

$$CaSO_4 + Ca^{+2} + 2HCO_3^- \rightarrow Ca^{+2} + SO_4^{-2} + CaCO_3 + H_2O + CO_2$$

The elevated pCO_2 observed in groundwater at the study area is likely due to the liberation of CO_2 as described by one of the above reactions; however, chemical data from the vadose zone would be necessary to differentiate between mechanisms.

4.4. Trace metals

High concentrations of trace metals, such as arsenic and selenium, are typically associated with coal-pile leachate. However, since groundwater underlying the coal piles at this study area retains near-neutral pH, concentrations of trace metals in groundwater are typically minimal. Results of the 1996 trace metal analyses in groundwater showed that all metals, with the exception of lead, were either below detection limits or were well below their respective maximum contaminant level (MCL) established by the State of Indiana. Lead was measured at a concentration of 62 ppb in RSE6, which greatly exceeds the state MCL of 15 ppb. The 1998 analyses showed similarly low concentrations for all analyzed metals; however, on this occasion arsenic was elevated to a level very near the MCL in RSE2. In 1999, all metals (including lead and arsenic) were either below detection limits or present at small concentrations. It is likely that the reduction in total metals concentration in 1999 was aided by the construction of a limestone swale which extends from the termination of the concrete slab southwest of the high-sulfur coal piles to the edge of the pond near RSE5 (Figure 1).

Although groundwater concentrations of trace metals are typically low at the study area, it appears as though recharge-pond sediments serve as a sink for metals. Metals concentrations found in pond sediment samples (collected by the consulting firm Ontario Environmental), as well as the mean and maximum concentrations found in Indiana lakes and streams are shown in Table III. According to the Indiana

TABLE III

Comparison of metals concentrations in aquatic sediments contained within the Purdue recharge pond with background values for the State of Indiana. Bold values indicate concentrations higher than maximum background sediment concentrations for Indiana lakes and streams

	Purdue recharge pond sediment[a,b]		Indiana lakes and streams background sediment concentrations[a,c]	
	Mar-90	Duplicate	Mean	Maximum
Al	5668	5334	2600	9400
Sb	< 30	< 30	0.16	0.49
As	22	25	2.8	29
Ba	108	92		
Be	**1.08**	**1.25**	**0.7**	**0.7**
Cd	**5.33**	**5.33**	**0.78**	**1**
Cr	15.8	21.7	13	50
Co	15.0	14.2	10	20
Cu	**91.7**	**70**	**10**	**20**
Pb	**167**	**233**	**17**	**150**
Hg	< 0.13	< 0.125	0.05	0.44
Ni	**33**	**35**	**9.9**	**21**
Se	**2.33**	**< 0.50**	**0.29**	**0.55**
Ag	< 0.50	< 0.50	< 0.5	< 0.5
Tl	< 25	> 25	< 3.8	< 3.8
V	22	23		
Zn	**233**	**233**	**38**	**130**
Mn	283	250	400	1700

[a] All concentration in ppm.
[b] Samples collected and analyzed by Ontario Environmental (1991) in a study commissioned by Purdue University.
[c] Background concentrations presented in 'Background Levels of Potential Toxicants in Indiana Stream and Lake Sediments' by Greg R. Bright, Indiana Department of Environmental Management, 1996.

Department of Environmental Management (IDEM), the best criterion for determining whether an aquatic soil has been subjected to anthropogenic pollutants is to compare individual metal concentrations with the maximum observed concentration within Indiana aquatic soils. Those parameters exceeding their respective state maximum concentration (Be, Cd, Cu, Pb, Ni, Se, and Zn) have been highlighted in bold. It was noted that results for zinc, cobalt, copper, and barium were considered suspect due to laboratory contamination (Ontario Environmental, 1991).

4.5. Rate and Extent of Contaminant Flow

The rate at which coal-pile leachate is pushed through the aquifers in the vicinity of the study area is largely controlled by the recharge pond, which is in near hydraulic steady state, leaking approximately 5.3 million liters per day to the subsurface (Weinreb, 1987). The close proximity of the sampled wells to the pond provides an opportunity to compare variations of well-water temperature and chloride concentration with that of the pond to discern lag times at which pond water reaches the individual wells. Coupling lag times with the distance between the pond and an individual well yields an approximation of the potential rate of travel of coal-pile leachate through an aquifer.

Temperature data serve as a good indicator of flow within the aquifers. Well RSE4 is in very close hydraulic communication with the pond as its temperature fluctuation is very similar to that of the pond (Figure 4). For example, from the period between January 17, 1997, and March 14, 1997, the temperature fluctuation patterns in the pond and RSE4 are identical. Since sampling occurred biweekly within this time period, lag time would be estimated at two weeks or less. However, data also show a lag time of up to a month in instances such as the 27.8 °C temperature peak in the pond on June, 1997 that was not recognized in RSE4 until one month later. Although RSE5 is roughly the same distance to the pond as RSE4, the influence of pond water is not as pronounced. Since RSE5 is screened deeper than RSE4 and taps the voluminous WVA, it is not as susceptible to temperature changes brought about by dilution from pond water. However, it is evident from Figure 4 that RSE5 does fluctuate in a similar pattern as the pond but with a larger lag time (1–2 months) than seen with RSE4. Wells RSE2 and RSE6 are less affected by pond water as evidenced by their smaller temperature fluctuations relative to RSE4 and RSE5. On occasion, however, a significant increase or decrease in temperature in these two wells can be correlated with fluctuations in pond temperature, which typically suggest a lag time of approximately two months from the pond to both RSE2 and RSE6.

Spikes of chloride can also be used as tracers to determine travel times between the RSE wells and the pond. In order to more accurately pinpoint travel times, the wells and pond were sampled biweekly between December, 1996 and April, 1997. This period corresponds to times when road-salt is most likely to enter the pond through campus storm drains. Figure 6 shows an amplified graph of the chloride data collected during biweekly sampling. On February 14, 1997, the largest spike of chloride ever observed in the pond (3.89 mN) was recorded, which is considerably higher than the county average for chloride in surface water which is 0.96 mN (Leap *et al.*, 1990). This spike appears in RSE4 with greater magnitude one month later. Since it is unlikely that the concentration in RSE4 would surpass that of the pond, one might suggest that the peak concentration in the pond probably occurred slightly later than the February 14th sampling. If this were the case, the lag time of water between RSE4 and the pond would be slightly less than one month, which

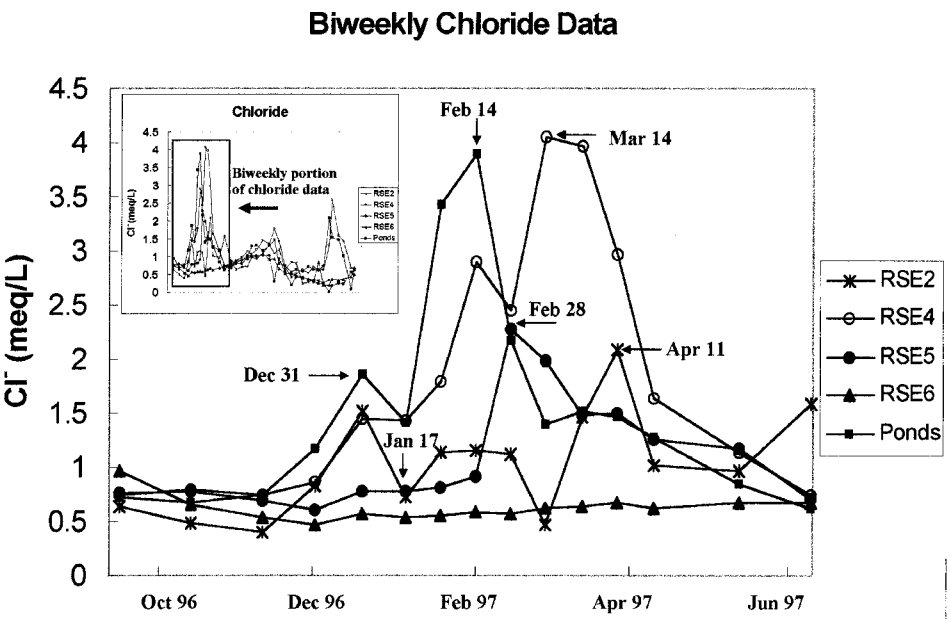

Figure 6. Chloride data for samples collected at 2-week intervals between December, 1996 and April, 1997. Chloride spikes appear in the pond in response to application of road-salt to streets after snowfall events. The resolution provided by biweekly data allows for more accurate interpretation of lag times between the pond and the wells.

correlates well with lag time estimates derived from temperature data. The same chloride spike was detected in RSE5 in only two weeks time and in RSE2 in about two months time but was never detected in RSE6.

An understanding of lag-times and flow-path connectivity between the pond and the RSE wells provides a basis for the discussion of contaminant transport at the study area. A simple method for estimating flow rate is to use the hypotenuse of a right triangle in which one apex is the pond's mean surface elevation and another apex is a well's mean water elevation. Dividing the hypotenuse distance of this triangle by the lag time observed between the pond and well yields a rough approximation of groundwater velocity within the aquifers. This, of course, ignores porosity and tortuosity; nevertheless, this technique provides a guideline for a reasonable flow rate. Utilizing this method with the assumption of a lag time of two months between the pond and both RSE2 and RSE6 (the slowest lag time observed between the pond and RSE6), a contaminant originating in the pond could be transported through the perched aquifer at a rate of 3.3 m/day and through the main aquifer at a rate of 1.5 m/day. It should be noted, however, that groundwater contamination in the area originates from the coal piles and not the pond. Hence the travel times derived from the pond to the wells are intended for interpretation as a general extrapolation for the aquifers in the study area.

It is interesting to compare the 1.5 m/day velocity estimated from lag times with the velocity calculated from 'typical' values of hydraulic conductivity (K), effective porosity (n_e), and hydraulic gradient (dh/dl) for the WVA. According to Leap *et al*. (1990), hydraulic conductivity for the WVA is estimated as 110 ft/day, the gradient is approximately 0.0019, and average effective porosity is 30%. The average linear velocity, V_x, was determined to be 0.70 m/day using the following equation:

$$V_x = K\,(dh\ dl^{-1})\,(1/n_e)$$

A comparison of the two velocities reveals little variation between the two indicating that the lag-time method provides a good estimation of velocity.

The extent of the coal leachate contamination can be determined by examining sulfate data from the Purdue well field and from the Wabash River. The Purdue Water Works Annual Reports for fiscal years 1997 and 1998 (Morrison *et al*., 1997 and Morrison *et al*., 1998) both report that a 'typical' sulfate concentration in the production wells is 80 mg L^{-1} which is approximately 1.67 mN. This value falls within the range of one standard deviation unit from the average sulfate concentration in groundwater in Tippecanoe County (1.04 $\pm$ 0.75 mN), suggesting that these wells are not impacted by coal-pile leachate. This is not surprising as the Purdue well field is located approximately 1.5 km up-gradient from the coal piles.

In order to gauge the impact of coal-pile leachate down-gradient from the power plant, sulfate data from the Wabash River was obtained from the U.S. Environmental Protection Agency's (USEPA) STORET database. Data from locations both upstream and downstream of the Utility Plant were compared. The upstream sampling location is located approximately 1.5 km upstream of the point on the Wabash River where groundwater from the study area would likely discharge while the downstream location is approximately 13 km from this point. The average concentration of sulfate (calculated from monthly data spanning a five-year period) at the upstream site is 1.32 mN while the average concentration at the downstream site is 1.39 mN. These values are very close to the county average for sulfate in surface waters which is 1.35 $\pm$ 0.49 mN (Leap *et al*., 1990).

Although there is little difference in the *average* upstream and downstream concentrations, it is interesting to note that during winter months, when coal storage is greatest, the difference between the two is typically the greatest. For example, in November, 1983 the upstream sulfate concentration was 1.65 mN while the downstream concentration was 1.94 mN. Given the velocity estimate of 1.5 m/day for the WVA, roughly 21 months would be required for leachate to travel approximately 975 m to the Wabash River. Hence, if coal-pile leachate is responsible for elevated sulfate in the river during winter months, the observed sulfate would likely be associated with leachate produced two winters prior. Since sulfate is also elevated upstream of the power plant in winter months, it is possible that a different source of sulfate is responsible for elevated concentrations.

5. Summary and Conclusions

Data obtained from groundwater monitoring at Wade Utility Plant reflect a site in which the impacts of coal-pile leachate are largely ameliorated by carbonate mineral dissolution and by dilution. This is supported by near-neutral groundwater pH, minimal concentrations of metals, and limited geographic extent of sulfate contamination. However, a significant accumulation of trace metals in recharge pond sediments indicates that the site is not completely immune to the negative impacts of coal-pile leachate. Without the ameliorating effects of carbonate minerals to neutralize acid leachate and immobilize trace elements, above-ground storage of coal piles in non-carbonate terrain may be compromising the water quality of underlying aquifers.

Long-term monthly sampling of the RSE wells and the recharge pond was essential in providing a necessary baseline for interpretation of data trends. This continuum revealed that RSE6 is most impacted by acid leachate and that fluctuations in sulfate concentration in this well can be correlated with the amount of coal in storage. In addition, large spikes of sulfate in RSE5 were clearly viewed as anomalous in the context of the established baseline. Pinpointing these anomalies was a key factor in recognizing that extended dry periods followed by precipitation events yield sulfate-rich spikes to underlying groundwater from dissolution of gypsum caliche in the vadose zone. Monthly sampling (as opposed to quarterly sampling) was also essential for interpreting lag times of water movement between the pond and wells since none of the observed lag times was greater than 2 months.

Acknowledgements

The authors would like to thank the Purdue University Physical Plant for providing partial funding for this study. Thanks are also offered to Greg Chmiel, John Foster, and Sandra Mansilla who assisted in the field and laboratory during the early stages of this project.

References

Anderson, M. A., Bertsch, P. M., Feldman, S. B. and Zelazny, L. W.: 1991, 'Interactions of acidic metal-rich coal pile runoff with a subsoil', *Env. Sci. Technol.* **25**, 2038–2046.

Anderson, W. C. and Youngstrom, M. P.: 1976, 'Coal pile leachate-quantity and quality characteristics', Journal of Sanitary Engineering, Division of the American Society of Civil Engineering, 102(EE6), p. 1239–1253.

Bjelke, W.: 1960, 'Recharge capacity of the Purdue Gravel Pit', M.S. Thesis, Dept. of Civil Engineering, Purdue University, 150 pp.

Bright, G. R.: 1986, 'Background levels of potential toxicants in Indiana stream and lake Sediments', Indiana Department of Environmental Management.

Brookman, G. T., Binder, J. J. and Wade III, J. A.: 1977, 'Measurement and modeling of storm water runoff from coal storage piles and the impact on receiving waters', in Proc. 3rd Symp. on Coal Preparation NCA/BCR Coal Fon. and Expo IV, Washington, D.C., 18–20 Oct. 1977, p. 214–242.

Carlson, C. A.: 1990, 'Subsurface leachate migration from a reject coal pile in South Carolina', *Water, Air, and Soil Pollut.* **53**, p. 345–366.

Cox, D. B., Chu, T. Y. J. and Ruane, R. J.: 1977, 'Quality and treatment of coal-pile runoff', in Proc. 3rd Symp. On Coal Preparation NCA/BCR Coal Conf. and Expo IV, Washington, D.C., 18–20 Oct. 1977, p 252–277.

Energy Information Administration: 1998, Electric Power Annual, 1997'. DOE/EIA-0348(97), July 14, 1998.

Everett, L. G.: 1985, Groundwater Monitoring Handbook for Coal and Oil Shale Development, Elsevier, New York, 305 pp.

Franson, M. A. H. (ed.): 1980, Standard Methods for the Examination of Water and Wastewater, 15th edition, 1134 pp.

Fritz, S. J., Bryan, J. D., Harvey, F. E. and Leap, D. I.: 1994, 'A geochemical and isotopic approach to delineate landfill leachates in a RCRA study', *Ground Water* **32**(4), 743–750.

Harvey, F. E.: 1990, 'A hydrogeochemical investigation of the aquifer system near West Lafayette, Indiana', M.S. Thesis, Dept. of Earth and Atmospheric Sciences, Purdue University. 319 pp.

Leap, D. I., Fritz, S. J. Bryan, J. D. Clabaugh, B. D. Henderson, M. E. Lee, K. K. Roberts, R. L. and Smith, W. R.: 1990, 'Final report of the results of a RCRA facilities investigation of solid waste management units on the Horticulture Research Farm and the Thomas Farm, Purdue University, Tippecanoe County, Indiana', *Water Resources Research Center, Tech. Report* **61**, 107 pp.

Morrison, D. V., Gemmecke, D. L., Hudson, S. A., Baxter, D. M. and Nethercutt, T.A.: 1997, 'Water works annual report', Purdue University, West Lafayette Campus.

Morrison, D. V., Gemmecke, D. L., Hudson, S. A., Baxter, D. M. and Nethercutt, T. A.: 1998, 'Water works annual report', Purdue University, West Lafayette Campus.

Ontario Environmental: 1991, 'Evaluation of environmental and regulatory issues associated with Purdue University's south campus gravel pit pond: Report of Findings', 38 pp.

STORET, U.S. EPA on-line database, <http://www.epa.gov/OWOW/STORET/index.html>.

Wachter, R. A. and Blackwood, T. R.: 1978, 'Source assessment: water pollutants from coal storage areas', EPA-600-2-78-004M. Industrial Environ. Res. Lab., Off. of Res. and Dev., U.S. Environmental Protection Agency, Cincinnati, Ohio.

Wangen, L. E. and Jones, M. M.: 1984, 'The attenuation of chemical elements in acidic leachates from coal mineral wastes by soils', *Environmental Geology and Water Science* **6**, p. 161–170.

Weinreb, G.: 1987, 'A hydrogeological investigation of thermal contamination within the Wabash Valley Outwash Aquifer, West Lafayette, Indiana', M.S. Thesis, Department of Earth and Atmospheric Sciences, Purdue University, 170 pp.

Zelmanowitz, S., Boyle, W. C., Armstrong, D. E. and Park, J. K.: 1995, 'Ability of subsoils to buffer extremely acidic simulated coal-pile leachates', Journal of Environmental Engineering, vol. 121, no. 11, p. 816–823.

ADVERTISING
SONY. give Cheer, give the Best, give Sony. SEATTLE PREMIUM OUTLETS Sony Outlet I-5, Exit 202, Near Marysville Click Here for a Special Offer
EXPLORE seattletimes.com / entertainment

ADVERTISING
Go Huskies! Go Mobile! Follow UW Men's Basketball anytime, anywhere with real-time news, stats, scores, commentary and much more. Get Husky Basketball 2010-11 app now!

My Health. On My Time. MyChart. The Everett Clinic For the whole you

Originally published May 11, 2008 at 12:00 AM | Page modified May 14, 2008 at 12:53 PM

E-mail article Print view

The painful cost of booming growth

The loggers arrived in July, toppling 35 acres of Douglas firs and cedars. The bulldozers and excavators followed, scraping away the topsoil...

By Warren Cornwall
Seattle Times environment reporter

The loggers arrived in July, toppling 35 acres of Douglas firs and cedars.
The bulldozers and excavators followed, scraping away the topsoil and leveling the land to golf-course smoothness. By this summer, the first of 166 homeowners will move here, to a place called McCormick Woods, west of Port Orchard in Kitsap County and a mile upstream from Puget Sound.

It's an unremarkable transformation that happens every day. And it's one of the biggest threats to Puget Sound.

The way we grow is undermining our promises to protect and restore Puget Sound, and could hobble a new rescue plan on which we may be asked to commit as much as $18 billion on top of the $9 billion we already expect to spend by 2020.

It happens one creek at a time as bulldozers and pavement disrupt the natural flow of water through the ecosystem, destroying habitat and sending billions of gallons of polluted runoff into the Sound.

At McCormick Woods the next victim is Anderson Creek, once one of the most unspoiled streams flowing to Sinclair Inlet. Today, there are plans to build hundreds of homes around it.

"Bye-bye, Anderson Creek," said Ed O'Brien, a stormwater engineer for the state Department of Ecology.

Even as we continue to push to protect Puget Sound, the entire effort is up against the fact that we also need to make room for as many as 4 million more people who could move here this century.

And as we do, we are gradually eating away at the Sound's finely tuned water-cleaning system by leveling as much as 10,000 acres of forest every year.

There's no overt conspiracy to hurt the Sound. Instead, the damage is happening in the pursuit of cheaper land and economic development, a longing for big backyards and a resistance to urban density,

PREV 1 of 4 NEXT

enlarge STEVE RINGMAN / THE SEATTLE TIMES
A McCormick Woods development takes shape near Port Orchard, a mile upstream from Puget Sound. Trees were felled and topsoil scraped away, disrupting the natural flow of water through the ecosystem — a common process as homes are built, but one that's also harmful to the Sound.

Related

- New ideas | Project meets challenge of runoff
- Graphic | How development harms Puget Sound (PDF)
- Audio Slideshow | Eiichi "Jerry" Yamashita, oyster farmer
- Scientists warn the current approach to stormwater threatens Puget Sound (PDF)
- Master Builders Association of King and Snohomish Counties critique (PDF)
- Consultants and engineers critique the scientist's letter (PDF)
- The Washington Chapter of the American Public Works Association letter concurring with scientists (PDF)
- Internal Ecology memo discusses political strategy for stormwater regulation (PDF)
- Resources
- Are we striking the right balance between protecting

More Local News

NEW - 5:02 PM
4 accused of taking dead veterans' benefits
Tales of a nightmare commute
NEW - 5:10 PM
Heading east? Prepare for bitter cold
La Niña can be 'tough nut to crack'
More snow and cold temperatures ahead

ADVERTISING
Create the restful surroundings babies need to wake up happy.
lightcatcher baby
Other curtains just hang there
Available exclusively at
buybuy BABY Buy Now

Video

West Seattleites talk about Monday's commute
Following Monday's snowfall, West Seattle residents talk about their commutes home as they head back out to work on Tuesday morning, November 23, 2010.

Columbia City snowball fight
Kite Hill sledding at Gas Works Park
Radio traffic with SPD dispatch after the shooting of John T. Williams
Seattle Police Department dashcam video | Part Two

More videos

Marketplace

Explore your options. Get inspired. Make connections. nwjobs.
Resumes and Job Hunt
With more than 22,000 members, Linked:Seattle is a force in networking
Post a comment

and a need to keep home prices within reach of average people.

There are success stories. Cities no longer routinely pump partially treated sewage into the water. Some of the most polluted places, such as bays next to cities, are getting cleaned up. Some toxic chemicals are on the decline in animals. Factories today are much more restricted than 40 years ago in the pollution they pump into the Sound.

Yet we still struggle to protect Puget Sound and at the same time make room for everyone to live the way they want.

• Efforts to regulate stormwater are politically toxic, and state officials have balked at tougher, more costly controls.

the Sound and making room for growth?
Seattle Times Special Report | Failing our Sound

Who's in charge of stormwater?

Washington Department of Ecology: Sets overall standards for stormwater controls under the federal Clean Water Act.

Local governments: Create and implement most land-use regulations, with guidance from the state Growth Management Act.

Puget Sound Partnership: New state agency currently creating a 2020 cleanup plan for the Sound. Not responsible for creating or enforcing regulations. Replaced the Puget Sound Action Team.

Governor's Puget Sound Commission: A 2006 gathering of political, business, tribal and environmental leaders that met to discuss Puget Sound issues. Confusingly, it was also called the Puget Sound Partnership, though it was a different group than the new agency.

• The developments we allow lag behind the latest stormwater designs, because many county and city goverments are still using 16-year-old rules.

• Even the newest engineering standards, some of the strictest in the country and ones that could add thousands of dollars to the cost of a home, aren't enough to stop the damage.

• Perversely, developers who try promising new approaches to addressing stormwater face red tape that creates costly delays or hurts effectiveness.

"The implications for the Sound are dire," said Gene Duvernoy, president of the Cascade Land Conservancy, a Seattle-based nonprofit that works to preserve undeveloped land.

"Puget Sound is a funnel. Anything that we do at the top end of the funnel comes out at the bottom end."

The damage runoff does

Four decades ago, stormwater runoff wasn't considered an environmental problem. After all, it wasn't chemical pollution pouring from factory pipes or sewage plants. So builders dug ditches and laid pipes to send runoff to the handiest stream.

The result was quiet environmental decay.

Surging water flooded and scoured streams. Rain rushed off roads and rooftops, washing pollution into rivers.

Today, stormwater flowing into Puget Sound is a slow-motion oil spill, amounting to millions of gallons a year.

Leaking septic tanks ruin shellfish beds. Pesticides wash off lawns into streams. Copper poisons salmon, scrambling their ability to smell predators. Toxic flame retardants used in everything from televisions to mattresses enter the Puget Sound food chain, winding up in harbor seals and orcas. Dirt smothers fish eggs.

Coho salmon have been filmed going belly-up in Seattle streams after encountering a gush of stormwater. Creeks now go dry in the summer because we've messed with the groundwater that used to replenish them.

The state first tried to tackle the problem 16 years ago. In 1992, the state Department of Ecology issued an engineering manual describing how to build the pipes and ponds that cope with the rainwater flowing from developments around Puget Sound.

The approach called for channeling water into big holding ponds, where water would dribble out, reducing creek erosion from uncontrolled gushes. Dirt and pollutants would settle to a pond's bottom instead of washing out to creeks and eventually the Sound.

But within a few years, it became clear the designs weren't working well enough. The man-made holding ponds were too small to handle a good Puget Sound winter soaker.

So Ecology tried again with new engineering manuals that called for bigger and more costly ponds to catch even more stormwater.

But the state didn't make them mandatory. So most local jurisdictions haven't made changes.

At McCormick Woods near Port Orchard, Kitsap County commissioners promised in 2003 to require builders to follow the most up-to-date stormwater standards. At the same time, they approved what will

Post a Resume
Search for a Job
Go
Advanced Search
Salary Advice
Career Center
Employers: Post a Job
Education Center

Nine to Thrive
A NWjobs blog about finding work life balance
How to fess up to your workplace foul-ups
Post a comment

Hire Ground
A NWjobs blog about landing your dream job in Seattle
Turning that seasonal job into a permanent gig
Post a comment

Every day, we're working to help set opportunity in motion in Seattle.
Bank of America
EXPLORE MORE

Most read | Most commented | Most e-mailed

1. More snow, wind on the way Monday evening
2. More snow and cold temperatures ahead
3. 747 slides off runway at Sea-Tac airport | The Weather Beat
4. Salt treatment no match for temperature drop
5. UPDATE: Man killed with hatchet near Seattle U. | The Blotter
6. Huskies crush Virginia in Maui opener, 106-63
7. Map | Snow photos and videos from around the region | The Weather Beat
8. Videos show Williams' numerous encounters with police
9. La Niña can be 'tough nut to crack'
10. Man arrested in fatal hatchet attack had been jailed before

Most viewed images

amount to a small city with a business park, shopping, and more than 4,000 homes and apartments, ranging from big houses along a golf course to modest ones aimed at first-time buyers.

Yet they didn't change any county stormwater rules. Kitsap County still follows the 1992 manual.

That's not unusual. Snohomish, Skagit, Pierce, Thurston, Mason and Island counties all follow the 1992 manual, and so do countless cities.

Kitsap County hasn't wanted to commit the time and effort to overhaul its engineering standards, which it adopted in 1997, said Jeff Rowe-Hornbaker, assistant director of the Community Development Department. He also questioned the worth of the state's newer standards.

"Until it's mandated, most organizations don't really act," he said.

New rules, same problems

Now most local governments don't have a choice. The Ecology Department plans to force many, including Kitsap County, to adopt its newest stormwater engineering manual by August 2009.

But scientists — and even the Ecology Department's own experts — say the new standards won't protect Puget Sound either.

The simple fact is this: It's nearly impossible to get pipes and ponds to imitate a forest.

The new stormwater designs screen out some pollution, but not all of it. And pavement still prevents rain from soaking into the ground.

Even a little development can do a lot of damage. Stormwater scientists have found that when the amount of roads, rooftops and parking lots surrounding a stream — called "impervious surfaces" — goes above even 5 percent, it means environmental decline.

That's trouble for Anderson Creek at McCormick Woods, currently home to steelhead, coho and chum-salmon runs. When construction is finished, the creek is expected to be 40 percent surrounded by impervious surface. At that level, scientists expect a big drop in wildlife, including fish, songbirds and amphibians.

Two years ago, a group of 14 scientists and engineers finally had enough. They wrote a letter to a 2006 Puget Sound commission appointed by Gov. Christine Gregoire, saying "little hope should be held for restoration of Puget Sound" if sweeping changes weren't made to address stormwater.

The scientists called for severely restricting new construction near healthy streams, stopping deforestation, engineering developments to let rain soak into the ground, and replacing antiquated stormwater systems.

But the proposal was dismissed as "wholly unrealistic and naive" by the Master Builders of King and Snohomish Counties, one of the state's most powerful building lobbies.

The association's executive, Sam Anderson, said new stormwater systems hadn't been used long enough to declare them a failure.

Ignored, developers say, is the cost more regulation adds to the price of new homes, putting them further out of reach of average people. Builders complain that the newest stormwater requirements will add thousands to the costs of building each house. They point to a new study from a University of Washington economist saying land-use regulations have already added $200,000 to the price of an average Seattle home.

Peter Orser, president of Quadrant Homes of Bellevue, the arm of Weyerhaeuser that starts five new homes around Puget Sound every workday, argues that new-home builders shouldn't bear all the burdens of restoring Puget Sound.

After all, there are plenty of older neighborhoods that dump stormwater into the Sound with virtually no control.

"We don't go in there to rape the land," he said. "Everything we do is done in the lowest-impact development we can."

Do permits have teeth?

This is the climate that Jay Manning, the state Ecology director, landed in last year when he announced reforms meant to change the way we deal with stormwater.

Manning praised the new approach as "one of the most important steps that this agency has taken in many years" to deal with the problem. But the new rules — contained in a permit most cities and counties need under the Federal Clean Water Act — were compromised from the start because of opposition from business and local governments.

Under the permit rules, which the Ecology Department wrote, dozens of Puget Sound cities and counties would finally have to start following Ecology's latest engineering manual.

To upgrade antiquated stormwater systems in most places around the Sound, developers who tear down an old building to put up a new one would need to control more runoff. And some counties and cities, for the first time, would have to start monitoring stormwater systems to see if they work.

But Mike Grady, a top policy adviser for the Seattle office of the National Marine Fisheries Service, the federal agency in charge of protecting Puget Sound chinook and orcas, says the permit doesn't go far enough. It sets no limits on the amount of toxic chemicals allowed in stormwater, he said. The permit also doesn't require any of the latest, environmentally friendly development methods.

"To me it comes down to, when are you going to draw a line in the sand and say, 'These standards are not protective to fish, so let's not pretend that they are,' " Grady said.

The Environmental Protection Agency, the U.S. Fish and Wildlife Service and the fisheries service have told the state Ecology Department that the permit should go further.

But department leaders have been unwilling to try, in part because of politics, according to internal memos.

In 2003, Bill Moore, the department's lead stormwater-policy adviser, acknowledged in a memo to top Ecology department managers that fully protecting water quality would require much stricter rules. But that would mean a bruising backlash from business and local government that could hurt the chances for progress, he said.

Moore recommended that the department instead aspire to a permit that was "adequate-to-good."

For example, the Ecology Department decided counties and cities can let developers in most places off the hook in following the new standards, if they build on less than an acre. That was despite opposition from some of the agency's own experts, who warned research showed many small developments could add up to significant damage.

Environmental groups are now suing the Ecology Department to get tougher rules. But on the other side, a host of cities and counties are suing to block the new permit, which they argue is unduly burdensome and costly.

In a recent interview, Moore defended his agency's position. Stormwater permits alone, he said, can't conquer a much more fundamental issue affecting Puget Sound: where and how we build.

Think low-impact

So where and how should we be building around Puget Sound, a place where millions of new residents will all want their own places to call home?

Environmentalists and some developers say low-impact development is one answer. The state is starting to promote it, and some local governments say they want to change their rules to allow it.

It turns out it's easier said than done.

The idea sounds simple: Design developments to act more like forests by allowing rainwater to soak into the ground through permeable pavement with tiny holes. Build special gardens to soak up the rain that sluices from gutters. Some even suggest building houses on short columns that leave the forest floor untouched.

But the concept runs up against decades of habits and rules: the assembly-line methods of major developers, concerns that low-impact methods are unproven and bureaucrats wedded to old methods.

Today, only a few adventurous developers dare to try new approaches. But many complain of costly delays, roadblocks and outright opposition from government officials resistant to trying something new.

At McCormick Woods, Kitsap County promised to encourage developers to use these low-impact techniques. But there's little sign of it at a new Quadrant Homes project under construction there.

The company says that a layer of tough, claylike earth — a common problem in Western Washington — makes novel approaches to stormwater management unworkable because the water won't quickly soak into the ground.

Quadrant made a similar argument in Snoqualmie, persuading the City Council to reject a plan requiring low-impact development for much of its massive Snoqualmie Ridge development. The company is trying it in a few places there.

Still, Orser, Quadrant's president, says he's afraid the low-impact approach will make homes hard to sell to people unaccustomed to the look. He also worries the novel strategies will fail if homeowners don't

maintain things like rain gardens.

But some of the area's top low-impact experts say the builders are copping out, and low-impact methods can still work with customized approaches to each project, instead of cookie-cutter formulas.

"It's way easier for those guys to come in and do what they've always done until there's some regulation that comes in and tells them to do something else," said Curtis Hinman of Washington State University, who has written a widely used manual on low-impact development.

Partners in restoration

In 2007, with huge fanfare, the Legislature approved a new state agency, The Puget Sound Partnership. It's supposed to lead a restoration of the Sound by 2020. As it formulates an overarching strategy, its leaders have vowed that stormwater and development issues will be prominent parts of the effort.

"We have to grow differently," said David Dicks, the partnership's executive director. "There's just no two ways about it."

In a recent draft report, a group of experts convened by the partnership called for a dramatic overhaul of the state's myriad environmental laws, instead creating a single set of rules governing the land around Puget Sound. It also recommended a single group or superagency to oversee the new regulations.

"We do not reach this conclusion lightly," said the report, which is meant to be part of a broader study underpinning the final cleanup plan. "However, in this case we believe it is warranted. The region has tried the uncoordinated, diffuse approach and it has not achieved success."

But the Puget Sound Partnership has little power to create rules or enforce standards. Instead, the agency has been assigned the task of writing a recovery plan, doling out money to governments and nonprofit groups, drumming up public support and nudging local and state agencies in the right direction.

Brad Ack, who headed the state's previous Puget Sound agency, the Puget Sound Action Team, points to recent compromises as a possible preview of things to come.

The governor's 2006 Puget Sound commission recommended incremental improvements in the handling of stormwater, triggering criticism from scientists who said it wasn't nearly enough. When the commission responded by suggesting a task force to look at the problem, the builders' lobby fought back. The task force was quietly scrapped.

Stormwater was "the gorilla in the room that we came right up to and touched ... but nobody was willing to confront," said Ack, who now works for a group that promotes sustainable seafood harvesting.

"People just said, 'We don't have time to deal with that. It's too controversial. It's too complex.' "

Warren Cornwall: 206-464-2311 or wcornwall@seattletimes.com

Copyright © 2008 The Seattle Times Company

E-mail article Print view Share: Digg Newsvine More Local News headlines...

ADVERTISING

Ads by Google

Seattle Homes for Sale
Find homes, condos, townhomes and real estate listings in Seattle
www.welcome2seattle.com

Homes For Rent Seattle Wa
Find more sources/options for Homes For Rent Seattle Wa
www.webcrawler.com

Frank Unlimited, LLC
Award Winning Advertising Agency. Creative. Strategic. Results driven
www.frankunlimited.com

Site map

Search

Our network sites seattletimes.com | Advanced

The Seattle Times Company
About the company
Employment opportunities
Seattle Times store
Advertise with us
Newspapers in Education

Services
Your account / Log in
E-mail newsletters
Contact us
Feedback and questions
Submit listings
Send us news tips
Historical archive

News
Home
Local
Nation/World
Business/Tech
Entertainment
Living
Travel
Sports
Opinion
Extras
Today's news index

Marketplace
Jobs
Autos
Homes
Rentals
Classifieds
Shopping
Personals
Post an ad

Getting Your Newspaper
Home delivery
Temporary stops
Subscriber services

Other editions
News by e-mail
Mobile
RSS feeds
e-Edition
Low-graphic
Twitter
Social media

Malware attacks are a growing problem on all Web sites. Read more about what to do if you see something suspicious.

Privacy statement | Terms of service
Copyright © 2010 The Seattle Times Company

Royal Swedish Academy of Sciences

Ecotoxicological Determination of Pigmented Salmon Syndrome: A Pathological Condition of Atlantic Salmon Associated with River Pollution

Author(s): Bronwen Croce, Ronald M. Stagg, Nicholas C. Everall, David B. Groman, Christopher G. Mitchell, Roger Owen

Source: *Ambio*, Vol. 26, No. 8 (Dec., 1997), pp. 505-510
Published by: Springer on behalf of Royal Swedish Academy of Sciences
Stable URL: http://www.jstor.org/stable/4314657
Accessed: 31/01/2011 22:45

Your use of the JSTOR archive indicates your acceptance of JSTOR's Terms and Conditions of Use, available at http://www.jstor.org/page/info/about/policies/terms.jsp. JSTOR's Terms and Conditions of Use provides, in part, that unless you have obtained prior permission, you may not download an entire issue of a journal or multiple copies of articles, and you may use content in the JSTOR archive only for your personal, non-commercial use.

Please contact the publisher regarding any further use of this work. Publisher contact information may be obtained at http://www.jstor.org/action/showPublisher?publisherCode=springer.

Each copy of any part of a JSTOR transmission must contain the same copyright notice that appears on the screen or printed page of such transmission.

JSTOR is a not-for-profit service that helps scholars, researchers, and students discover, use, and build upon a wide range of content in a trusted digital archive. We use information technology and tools to increase productivity and facilitate new forms of scholarship. For more information about JSTOR, please contact support@jstor.org.

Springer and *Royal Swedish Academy of Sciences* are collaborating with JSTOR to digitize, preserve and extend access to *Ambio*.

http://www.jstor.org

Article

Bronwen Croce, Ronald M. Stagg, Nicholas C. Everall, David B. Groman, Christopher G. Mitchell and Roger Owen

Ecotoxicological Determination of Pigmented Salmon Syndrome

A Pathological Condition of Atlantic Salmon Associated with River Pollution

The 'Pigmented Salmon Syndrome' is a noninfectious haemolytic anaemia with associated clinical jaundice of Atlantic salmon (*Salmo salar*), caused by exposure to a combination of chemical pollutants. The disease has been restricted to the migrating adult Atlantic salmon population of the River Don, Aberdeenshire, Scotland, UK, where it reached epidemic proportions in the early 1980s. Effluents from paper mills, from the oil-servicing industry and from an airport were implicated as causative factors in the syndrome. Subsequent experiments showed that symptoms of the syndrome could be reproduced by the sequential or combined exposure to petroleum hydrocarbons (such as diesel) and resin acids. The Pigmented Salmon Syndrome has not recurred in wild River Don salmon since 1989, and our research suggests that this is due to directed improvements in the water quality of the River Don. The disease is a good example of how multiple contaminants can collectively cause biological effects which are not apparent from exposure to single substances. This article describes how the causes of the disease were determined.

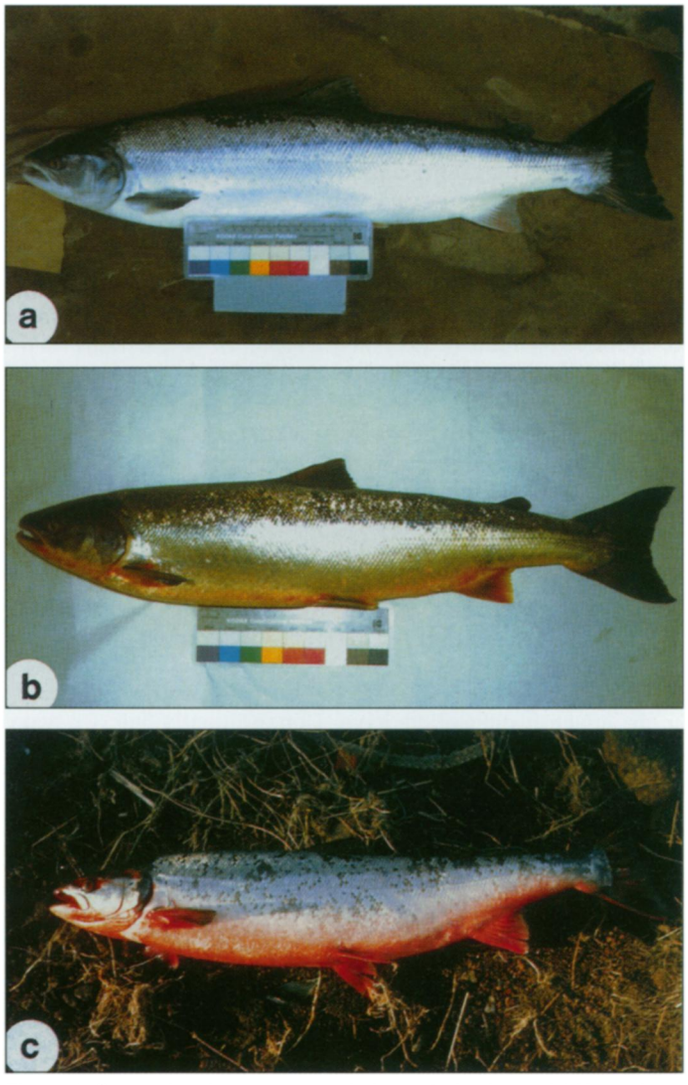

Figure 1. Gross visual appearance of pigmented salmon. (a) Normal Atlantic salmon. (b) Yellow/golden pigmented salmon. (c) Red pigmented salmon. Photos: D. Groman.

INTRODUCTION

Atlantic salmon (*Salmo salar*) are anadromous fish, feeding in the sea and returning to their natal rivers to spawn in the headwaters. In Scotland, spawning usually takes place between October and February (1). The mature adult Atlantic salmon does not feed when in freshwater, and so during its spawning migration undergoes an extensive mobilization of its body lipid and protein to provide energy to sustain basic metabolism and for the additional requirements of gonadal development and increased muscle activity for swimming upstream (2, 3). In the absence of feeding, waste products accumulate in the gall-bladder (4).

In the mid-1970s Atlantic salmon in the lower reaches of the River Don (Aberdeenshire, Scotland, UK) began to appear with abnormal pigmentation ranging from yellow to orange and red, especially around the eyes, fin bases and ventral surface (Fig.1). In the winter of 1981–1982, the 'Pigmented Salmon Syndrome' (PSS), as it had by then been named, reached epidemic levels (5). The condition accounted for the death of hundreds of mature adult salmon, prior to spawning; the impact on recruitment could not be assessed. National and international enquiries suggested that this phenomenon was restricted to River Don stock. The syndrome—or at least the visual manifestations of it—also appeared to be restricted specifically to the adult Atlantic salmon returning to spawn. Although the incidence of ulcerative dermal necrosis has been reported in all Scottish East Coast rivers, pathological investigations of PSS affected salmon revealed that this condition had not been caused by a bacterial, viral or parasitic agent, suggesting that the syndrome might be due to a toxic chemical in the river. The specific nature of the condition implied that either the toxic agent was unique to the river or that River Don salmon were particularly susceptible to it.

There are many research programs involved in determining correlations between chemical contamination and overt fish pathology (6), but the cases where a clear cause-effect relationship between fish disease and pollution exposure has been demonstrated are confined to liver pathology with a cancerous aetiology (7, 8). Ten years of research into the problem of PSS has provided a detailed description of the clinical pathology and epidemiology of this disease. In addition, the aetiology of PSS has been directly linked to a combination of two industrial effluents, and symptoms of PSS have been reproduced in experiments where salmon were exposed to key chemicals from these effluents. This article presents the findings of this research as a complete account for the first time.

WATER QUALITY AND ASSOCIATED HYDROLOGY OF THE RIVER DON

The River Don is the sixth largest river in Scotland with a length of 120 km; its source is in the Grampian Mountains and it enters the North Sea at its estuary in the city of Aberdeen.

The lower 14 km stretch of the River Don has received high domestic and industrial pollution loads for over 150 years (Fig. 2). In the mid-1960s the main discharges to the river were from two meat-processing factories, a paper mill, a board mill, and

© Royal Swedish Academy of Sciences 1997
http://www.ambio.kva.se

local authority sewers. The lower Don was grossly polluted until the 1970s when a major sewage-treatment works was completed, which dealt with the domestic sewage and some industrial discharges. The paper and board mill continued to discharge largely untreated effluent into the river until the late 1980s when effluent-treatment plants were commissioned. A further paper mill, situated 32 km upstream of the river mouth, began full treatment of its effluent in 1991. In the early 1970s, the discovery of oil and gas in the North Sea led to the development of several new industrial estates of ancillary servicing companies and the expansion of an airport in the lower Don catchment, all of which contributed to the contamination of surface waters with fuel oils, cleaning agents and other organic contaminants.

Above the uppermost paper mill the River Don is of Class 1 status, which is defined as "high quality, potable water, able to support game or other high-class fisheries, with a diverse invertebrate fauna, a sparse microbial population and a high amenity value" (9). Before effluent treatment was instigated, the water of the lower Don was attributed Class 2 or 3 status due to the high biological oxygen demands (exceeding 3 mg L^{-1}). Despite this pollution, the River Don has always allowed the passage of migratory fish (10), unlike rivers such as the Thames in England where the polluted and deoxygenated state of the lower reaches caused the extinction of the salmon run by the early 19th century (11).

PSS was most prevalent in the autumn and winter prior to the higher river flows associated with increased rainfall and snowmelt. Low river flows are likely to have increased the concentration of contaminants in the river and, in addition, restricted the upstream progression of salmon from the sea. The latter situation was compounded by the presence of several large weirs in the lower reaches of the River Don, originally built for water abstraction purposes. Flows in the River Don can range from 5 to 50 $m^3 s^{-1}$, dependent on season; there was a run of dry years between 1971 and 1976 in which there were exceptionally low mean annual flows (the mean for these years was 15 $m^3 s^{-1}$, data provided by the North East River Purification Board). Between 1984 and 1987, a survey of rod-caught salmon in the lower reaches of the River Don found a higher percentage of fish showing symptoms of PSS in months where flows were below 30 $m^3 s^{-1}$ (5).

PIGMENTED SALMON PATHOLOGY

An investigation of the blood chemistry and pathophysiology of affected fish led to the formal diagnosis of the PSS as a noninfectious haemolytic anaemia.

The pigments responsible for the overt symptoms of PSS were deposited in the muscle tissue, organs, brain and cartilage and were identified as the haem pigments bilirubin (yellow), haemosiderin (golden) and haemoglobin (red). The severity of the disease showed a positive correlation with the plasma concentrations of bilirubin and haemoglobin. The condition may have been exacerbated for adult Atlantic salmon, which do not feed on returning from the sea to the river for spawning. The release of bile from the liver into the gut (via the gall bladder) ceases in the absence of feeding (anorexia). However, bile production continues because it is an important means by which waste products are removed from the body, including blood pigment breakdown products and certain foreign compounds such as toxic chemicals. The bile produced during anorexia accumulates in the gall bladder (4).

Pigmented salmon haematology was characterized by reduced red-blood cell counts, whole blood haemoglobin concentrations and haematocrit values in conjunction with marked increases in the concentration of haemoglobin and bilirubin in the plasma (12). Differential blood-cell counts indicated significant differences in the ratios of mature, immature, reticulocytic and pyknotic erythrocytes in diseased fish. Figures 3a and 3b show

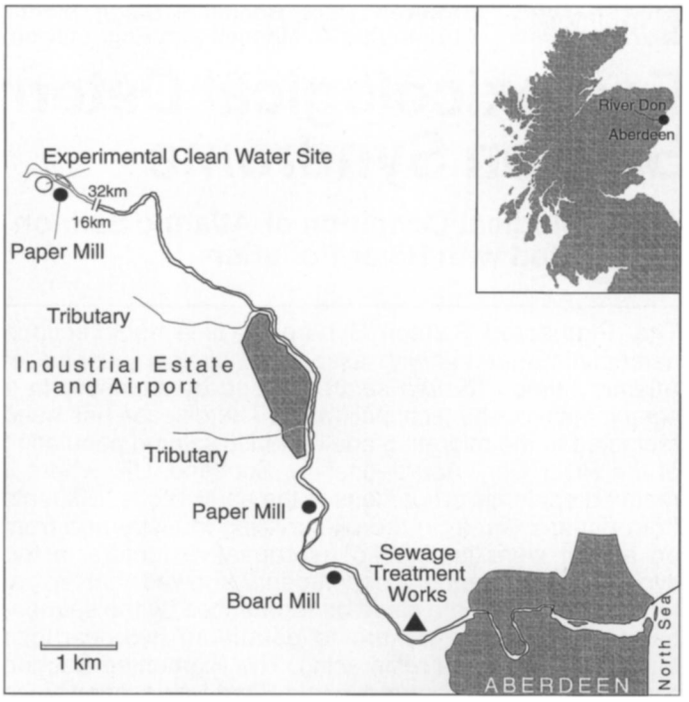

Figure 2. Map of the industrial region of the River Don, Aberdeenshire. Inset, location of the River Don in Scotland.

haematological profiles for yellow and red pigmented salmon and Table 1 provides median values for the parameters constituting these profiles.

Histological examinations of pigmented salmon revealed significant pathology in the gills and kidneys. Gill damage was consistent with that normally associated with polluted water, where swelling of the epithelium combined with shrinkage of the blood spaces leads to severe respiratory distress, in this case distress also resulted from the anaemia (13). The kidney and spleen had accumulations of macrophages, which contained the breakdown products (haemosiderin) of effete red blood cells (Fig. 4). In addition, the examination of the ultrastructure of hepatocytes showed the endoplasmic reticulum within these cells to be expanded and that these cells contained a large number of degenerating mitochondria. Histopathologically, the disease was described as an intravascular haematotoxic erythrocytic necrosis accompanied by respiratory epithelial, hepatic and renotubular degeneration (5).

AETIOLOGY OF PSS

Captive Fish Studies

To identify the source of the toxic agents in the river attempts were made to reproduce the disease in healthy fish under experimental conditions. Early work could not demonstrate PSS in rainbow trout or immature salmon, this restricted the experiments to the use of adult, wild Atlantic salmon. Each effluent was treated as a point source and exposures involved holding groups of three to five salmon in tanks sited at different locations along the Don, each receiving a continuous supply of water from the river or a diluted industrial discharge at that point (Fig. 2). By compiling haematological profiles a direct comparison was made between the experimentally exposed fish and the abnormally pigmented fish occurring in the River Don (5, 14).

The exposure experiments took place between 1985 and 1988, over which time major improvements in water quality were occurring. Initial experiments took place whilst the paper and board mill in the lower Don were still discharging untreated effluent to the river; the lowest source of haemolytic agents (defined by salmon haematological parameters, Table 1) was established to

© Royal Swedish Academy of Sciences 1997
http://www.ambio.kva.se

be below the board mill, but above the sewage treatment works. Experiments continued, working upstream to determine the highest source of haemolytic agents. The paper- and board mill effluents contained components that were toxic to the salmon, but the effluents upstream of these sources also contained haemolytic agents and, for the first time, the industrial estates were implicated in the cause of PSS (5). The paper mill 32 km from the river mouth was determined to be the highest source of haemolytic agents (14).

Exposure to Combinations of Effluents

The experiments provided proof that the waters and effluents from the River Don were causing some symptoms of PSS, but holding fish at any single point effluent source did not produce the gross visual appearance associated with the syndrome. Captive fish had been exposed to controlled doses of isolated effluents for approximately three weeks, but there were no means of assessing the duration and degree of effluent exposure endured by the wild salmon in the river. It was hypothesized that the differences in symptoms between the experimental fish and wild pigmented salmon were because wild fish would pass through the whole industrial area and might be exposed to a plethora of chemicals emanating from several different sources. A further series of experiments was designed to test whether more than one type of effluent might be involved in causing PSS.

Groups of five adult Atlantic salmon were sequentially exposed to a 400-fold dilution of water from an industrial tributary of the river Don for two weeks, followed by a further two weeks exposure to a 200-fold dilution of a paper-mill effluent. These fish developed a yellow pigmentation and had identical haematological profiles to pigmented salmon occurring in the river (Fig. 3c). This tributary had been selected because the experimental fish could be sited within the security of the airport premises; this choice of location did not eliminate other similar industrial drains and burns in the area as causative factors of the pollution. Captive fish studies concluded that the disease was caused by exposure to a combination of effluents from paper mills and the industrial area housing North Sea oil servicing industries and the airport (15).

The Atlantic salmon used in these experiments had been obtained from the estuaries of two neighboring rivers (the Dee and North Esk) neither of which had recorded PSS in their stocks. It was now evident that the haemolytic anaemia was not due to a genetic susceptibility in the River Don Atlantic salmon population. In the knowledge that exposure to a combination of paper-mill effluent and contaminated surface water drainage caused salmon to develop PSS, further research was undertaken to determine the chemicals that had caused PSS. The paper and board mills were all by now biologically treating their effluent, but a reoccurrence of PSS could not be ruled out without some clarification of the active chemical compounds in the two identified sources.

Table 1. Median values of haematological parameters associated with PSS.

Parameter	North Esk	Salmon type Don (yellow)	Don (red)
Haematocrit (%)	44.0	34.4	11.4
Red blood cell count (x 10^6 mm^{-3})	1.2	1.0	0.4
Immature red blood cell count (%)	0.3	7.0	0.6
Whole blood haemoglobin (g dl^{-1})	13.0	7.6	4.9
Mean corpuscular volume (fl)	327.0	332.5	355.0
Plasma bilirubin (µmol L^{-1})	4.0	49.9	96.2
Plasma lactate dehydrogenase (IU ml^{-1})	1.0	1.6	1.7
Plasma glutamic oxaloacetic transaminase (IU ml^{-1})	0.6	1.0	0.7
Plasma alkaline phosphatase (IU ml^{-1})	0.6	0.4	0.4

Values are the medians of samples from 21 River North Esk salmon (healthy control group) and 12 River Don yellow or red pigmented salmon.

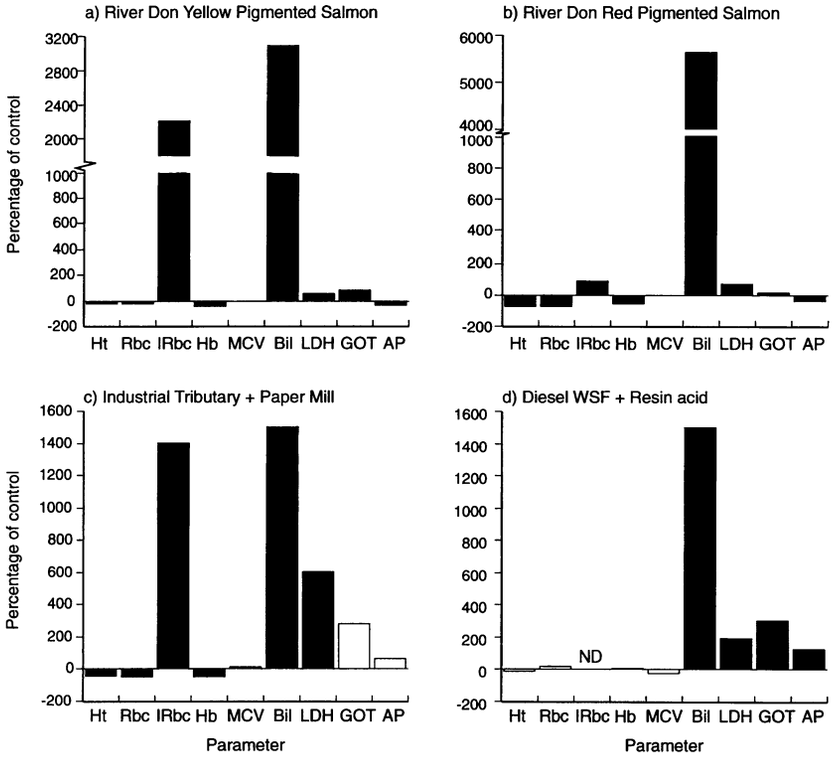

Figure 3. Clinical profiles of yellow (a) and red (b) pigmented Atlantic salmon from the River Don. The profiles are compared to those from: (c) adult Atlantic salmon sequentially exposed to water from a tributary of the River Don and paper mill effluent; and (d) S2 Atlantic salmon parr exposed to a water soluble fraction of diesel fuel oil and a 50 mg L^{-1} mixture of the resin acids dehydroabietic, abietic and isopimaric acids in a continuous flow of water. Values are expressed as a percentage of the relevant control salmon in each case; solid bars represent significance ($p < 0.05$) in a Kruskal-Wallis one-way analysis of ranks. ND, not determined. Ht, haematocrit; Rbc, red-blood cell count; IRbc, immature red blood cell count; Hb, whole blood haemoglobin concentration; MCV, mean corpuscular volume; Bil, plasma bilirubin concentration; LDH, plasma lactate dehydrogenase; GOT, plasma glutamic oxaloacetic transaminase; AP, plasma alkaline phosphatase.

Contaminated Surface Water

Gas chromatographic and fluorometric fingerprinting of petroleum hydrocarbons in water extracts from streams and surface waters in the industrial area of the Don catchment had repeat-

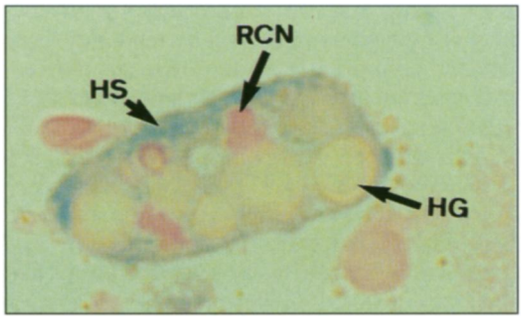

Figure 4. Kidney macrophage from a red pigmented salmon stained with Bunting's Prussian Blue, showing red blood cell breakdown products. RCN, red blood cell nucleus; HG, haemoglobin; HS, haemosiderin. Photographed through a Zeiss automatic exposure microscope, magnification, x 2000. Photo: C. Mitchell.

© Royal Swedish Academy of Sciences 1997
http://www.ambio.kva.se

edly shown diesel fuel oil to be the predominant contaminant (5, 16, Fig. 5). Analysis of muscle tissue from pigmented salmon for hydrocarbons was inconclusive, although some diseased fish had elevated levels of aliphatic hydrocarbons, and River Don salmon were often reported as being tainted with petroleum (5). In addition, pigmented salmon had elevated levels of hepatic cytochrome P450 compared to control fish (Fig. 6) (17): suggesting that salmon affected by PSS had been exposed to petroleum-type compounds. The cytochrome P450 1A subfamily of enzymes are induced upon exposure to planar polyaromatic hydrocarbons and have been extensively used as a monitoring tool to assess the exposure of fish to some types of environmental pollutants (18). Petroleum derived oils are also known to act as haemolytic agents (19).

Trace-metal analysis of tissues from pigmented salmon had shown no significant elevations in heavy metal content, and X-ray microanalysis of the macrophages in their kidney tissues showed no traces of heavy metals (5). In addition, metallothionein levels were not significantly elevated in pigmented salmon (17), thus heavy metal pollutants were not suspected of causing PSS.

Other suspect chemicals from the industrial area contaminating the lower Don were surfactants and de-icing compounds. A vast array of anionic, cationic and non-ionic surfactants were recorded to be in use by Donside Industries in the mid-1980s, and surfactants are known to have haemolytic properties (5). In the past, urea was the major runway de-icing chemical used at Aberdeen Airport, but it has not been used since January 1993; bacteria convert urea to ammonia, which is toxic to fish and macroinvertebrate species (20). It was noted that the elevated concentrations of ammonia in the River Don did not coincide with the occurrence of pigmented salmon, which were generally seen in early autumn (5). Smaller proportions of glycol-based de-icing compounds were used for aircraft de-icing, the major problem associated with glycol contamination is that their degradation by microorganisms causes a depletion in the oxygen available to other organisms in the receiving water. If glycol compounds contributed to causing PSS it is more likely that the toxicity would have been due to the short-chain alcohol and aldehyde metabolites of biodegradation.

Paper-mill Effluent

The environmental impact of effluents from mills producing wood pulp has been well documented (21). Within these effluents some of the most toxic components to fish have been ascertained to be chlorinated phenols produced in bleaching processes and resin acids (diterpene constituents of the bark of certain softwood trees). Chemical analysis of the River Don paper-mill effluent that had reproduced PSS in the combined effluent exposure experiments, found a predominance of resin acids with lesser amounts of chlorinated hydrocarbons (derived from cleaning solvents) and benzothiazoles (from biocides) (15). The majority of the wood pulp used by the River Don mills is now elemental chlorine free, thus, chemicals derived from bleaching processes are not likely to be significant to PSS. In pulp production, resin acids are liberated from the bark, and are present in pulp and paper-mill effluents (22). Exposure to resin acids has been reported to cause jaundice both in sockeye salmon, *Oncorhynchus nerka* (23) and in rainbow trout, *Oncorhynchus mykiss* (24); however, the concentrations of bilirubin in the plasma of pigmented salmon were an order of magnitude greater than those reported in these studies.

Jaundice (an accumulation of the pigment bilirubin in the tissues) is common to several different pathological disorders, impairment of the liver conjugation enzymes results in some types of jaundice (25). Uridine diphosphate glucuronyl transferase (UDPGT) catalyzes the attachment of glucuronic acid to an acceptor compound (known as conjugation). This process favors

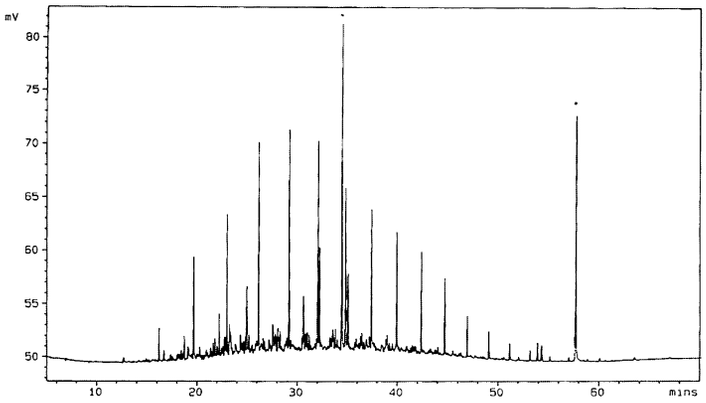

Figure 5. GC-FID chromatogram of a dichloromethane extract of water from a River Don tributary taken during a sampling program in 1992. This trace is typical of diesel fuel oil.
***, Dichlorobenzylether internal standards.**

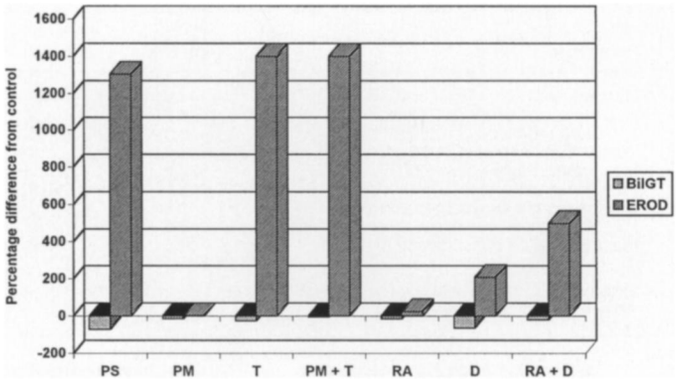

Figure 6. Xenobiotic metabolizing enzymes in pigmented and experimental salmon. PS, pigmented salmon; PM, adult Atlantic salmon exposed to a 200-fold dilution of a paper mill effluent; T, adult Atlantic salmon exposed to a 400-fold dilution of water from an industrial tributary of the River Don; PM + T, adult Atlantic salmon sequentially exposed to T followed by PM; RA, S2 salmon parr exposed to a 50 mg L^{-1} resin acid mixture; D, S2 salmon parr exposed to a 2 mg L^{-1} water soluble fraction of diesel fuel oil; RA + D, S2 salmon parr simultaneously exposed to RA and D. The enzymes measured were cytochrome P450 1A (as ethoxyresorufin-*O*-deethylase, EROD, activity) and Bilirubin UDP-glucuronosyl transferase.
Mean values are expressed as a percentage of the mean value of the relevant control salmon in each case.

the excretion of the conjugated compound from the body rather than its accumulation in the fatty tissues due to the increases both in its molecular mass and in its water solubility. UDPGT exists in several different isozymic forms (26), substrates include steroids, bilirubin and many xenobiotics. Bilirubin is mainly excreted from the liver into the bile as a bilirubin glucuronide; measurements of bilirubin UDPGT in liver samples from a small number of pigmented salmon showed lower values than those measured in healthy River Don salmon (Fig. 6) (17). Resin acids are also excreted as glucuronides (27), and liver UDPGT activity has been used as an indicator of the exposure of rainbow trout to resin acids (24).

Toxicity Testing with Suspected Chemicals

Although resin acids do not induce cytochrome P450 1A (28), it was demonstrated that they could interact with cytochrome P450 1A in a 20 d exposure (via intraperitoneal injection) of groups of 12 starved salmon parr to a mixture of three pure resin acids (dehydroabietic, abietic and isopimaric acids) in combination with a model cytochrome P450 1A inducer (8-naphthoflavone, BNF). These resin acids are some of the most predominant and persistent in pulp-mill effluents (29). Cytochrome P450

© Royal Swedish Academy of Sciences 1997
http://www.ambio.kva.se

1A in microsomes prepared from the livers of the experimental fish (measured as ethoxyresorufin-*O*-deethylase, EROD, activity) was not induced by resin acids at any of the concentrations tested (1.2, 12 and 120 mg kg^{-1}) but in the presence of BNF (200 mg kg^{-1}) the resin acids enhanced EROD activity at the lowest concentration used and depressed EROD activity at the mid concentration. Exposure to BNF in combination with resin acids also caused significant elevations in the plasma bilirubin concentrations compared to fish receiving either chemical alone: bilirubin-UDPGT activity showed significant decreases in fish treated with the mid-concentration of resin acids (both in the absence and the presence of BNF) when compared to control fish. BNF alone also decreased the bilirubin-UDPGT activity (30).

The fuel oil contamination of lower Don surface water was the most likely source of P450 inducing chemicals in PSS, thus further controlled exposure experiments used diesel fuel oil water-soluble-fractions (WSF) in combination with resin acids to attempt to reproduce PSS symptoms in experimental fish. A 9-day waterborne exposure of groups of 9 starved salmon parr to the same mixture of resin acids (at 10, 50 and 100 μg L^{-1}) in combination with a WSF of diesel fuel oil (2 mg L^{-1}) in a continuous flow system demonstrated that this chemical combination, in part, mimicked the cocktail of chemicals that gave rise to PSS (16). In the treatments where fish had received a combination of diesel WSF and resin acids many had yellow pigmentation on the ventral surface and around the gill arches, those given the highest resin acid dose in the absence of diesel were also yellow. Salmon in the treatments receiving 50 and 100 μg L^{-1} resin acid mixture in combination with the diesel WSF had significantly elevated plasma bilirubin concentrations. Exposure to diesel WSF and resin acids either alone or in combination did not elicit an anaemic response, but combined exposure did cause an increase in the concentrations of the enzymes alkaline phosphatase, glutamic oxaloacetic acid transaminase and lactate dehydrogenase in the plasma (Fig. 3d), indicating the occurrence of liver damage. Diesel WSF alone caused a significant reduction in bilirubin UDPGT and was capable of inducing EROD activity, although the latter was not as pronounced as that seen in pigmented salmon or in salmon exposed to water from the industrial tributary (Fig. 6). Because bilirubin UDPGT is essential to remove bilirubin from the body, the repression caused by the diesel WSF exposure may explain the increased plasma bilirubin concentrations in those fish having to deal with the additional burden of a resin acid exposure.

The incomplete matches in haematological profiles between pigmented salmon and those exposed to combinations of resin acids with a diesel WSF (particularly in the anaemic response) may be due to physiological differences between starved salmon parr and anorexic mature salmon or a reflection on exposure times—a chronic exposure to low doses of toxicants over several months may have reproduced these effects. Alternatively, another type of chemical, for example, surfactants, could have been additionally involved in causing PSS. Nevertheless, the results demonstrated that some key symptoms of PSS could be reproduced by exposing experimental salmon to a combination of chemicals known to have contaminated the River Don at the time of the PSS epidemic.

Riverine Concentrations of Chemicals

A total resin acid concentration of 38 μg L^{-1} was measured in River Don water, 100 m below the uppermost paper mill in 1988 (at that time the mill had not installed its effluent treatment plant). A concentration of 30 μg L^{-1} resin acid was also recorded in the test waters of the combined effluent exposure experiment that produced experimental yellow salmon (15). The resin acid dehydroabietic acid has been reported to produce physiological disturbances in rainbow trout down to a 'minimum effective concentration' of 20 μg L^{-1} (31); the relative toxicity of other resin acids is greater (32). Changes to, and improvements in, mill processes have resulted in lower concentrations of resin acids in present-day mill raw effluents and the biological treatment of these wastewaters is over 90% efficient at removing resin acids (16). Approximately 10 mg of resin acids per liter of mill effluent currently enter the River Don (16), where they are further diluted—a 100-fold dilution factor would be expected at an average river flow of about 30 m^3 s^{-1}.

Composite samples of water from the industrial tributary taken in 1992 recorded diesel concentrations in the 0.5–5.0 mg L^{-1} range (16). Since that time there has been a concerted effort to improve the water quality of this part of the River Don catchment. For example, local sewerage authorities have sealed leaks in the surface-water sewer and repaired an oil interceptor treating the surface water from one of the industrial estates while local industries have instigated measures to reduce the impact of their activities on the watercourse.

In 1995, a fluorimeter which could continuously record aromatic hydrocarbon fluorescence (excitation 310 nm, emission 360 nm) *in situ* was deployed in the River Don at a site below the industrial estates (Fig. 7). Readings generally corresponded to 2 μg L^{-1} diesel equivalents, however, several events occurred over a 12-day monitoring period in which there were dramatic increases in the recorded fluorescence. A small episode saw concentrations increase to an average of 40 μg L^{-1} over a 24 hr period and included two peaks of 4 mg L^{-1}. Another event was detected over a 5 hr period on a separate day, over which time concentrations in the region of 3 mg L^{-1} were sustained (16). Although data were only collected over a relatively short period they provided some interesting information on the nature of oil pollution in the River Don. It would appear that organisms within the water may experience both short-duration exposures to high concentrations of oil or longer exposures to lower levels, this being dependent on position in the water column as well as position in the river.

CONCLUSIONS

PSS demonstrates a strong cause-effect relationship between water pollution and a fish disease. Controlled exposure experiments with Atlantic salmon were able to show that effluents from two distinct sources acted synergistically to cause the disease. Further experiments demonstrated that exposure to a combination of specific chemicals from these effluents, resin acids and diesel-fuel oil, at concentrations that had been recorded in the River Don, reproduced PSS symptoms in experimental salmon parr. A decline in the occurrence of PSS and its eventual disappearance from River Don stock coincided with improvements in river water quality, brought about in particular by the introduction of biological effluent treatment plants at the River Don

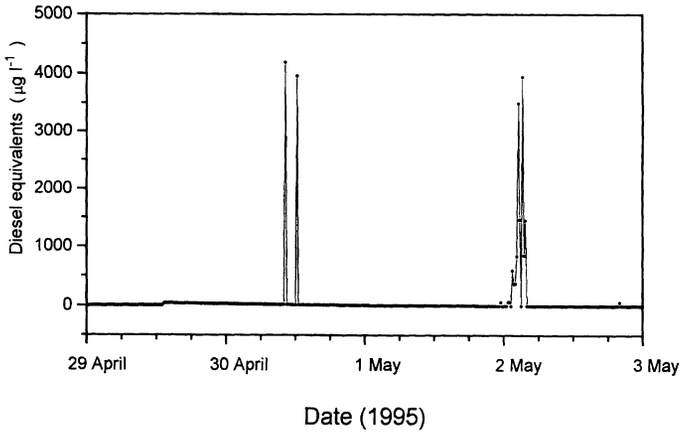

Figure 7. *In situ* fluorimetry of the lower River Don in 1995. The instrument was calibrated against a water soluble fraction of diesel fuel oil.

© Royal Swedish Academy of Sciences 1997
http://www.ambio.kva.se

paper and board mills; biological treatment was subsequently shown to be highly efficient at removing resin acids from mill wastewaters.

The pigmented salmon scenario highlights the complex interactions of pollutants in the environment and the importance of incorporating ecotoxicological parameters into industrial-discharge consents, drawn up by regulatory bodies. By using an ecologically relevant test species, methods for detecting sub-lethal effects of toxicants can be developed that may provide early indications of pollutant exposure. These studies also demonstrate that toxicity assessment of individual chemicals is not sufficient to allow predictions of their effects upon discharge to natural systems, where they may act synergistically with other chemicals.

References and Notes

1. Shearer, W.M. 1992. *The Atlantic Salmon. Natural History, Exploitation and Future Management*. Blackwell, Oxford, UK, 244 pp.
2. Walton, M.J. and Cowey, C.B. 1982. Aspects of intermediary metabolism in salmonid fish. *Comp. Biochem. Physiol 73B*, 59–79.
3. Jonsson, N., Jonsson, B. and Hansen, L.P. 1991. Energetic costs of spawning in male and female Atlantic Salmon (*Salmo salar* L.). *J. Fish Biol. 39*, 739–744.
4. Talbot, C. and Higgins, P.J. 1982. Observations on the gall bladder of juvenile Atlantic salmon. *J. Fish Biol. 21*, 663–669.
5. Groman, D.B., Mitchell, C.G. and Miller, K. 1987. *Pigmented Salmon Project. Interim Project Completion Report (1984-1987)*. North East River Purification Board, Aberdeen, UK, 215 pp.
6. Vethaak, A. D. 1992. Gross pathology and histopathology in fish: summary. *Mar. Ecol. Prog. Ser. 91*, 171–172.
7. Malins, D.C., Krahn, M.M., Brown, D.W., Rhodes, L.D., Myers, M.S., McCain, B.B. and Chan, S.-L. 1985. Toxic chemicals in marine sediment and biota from Mukilteo, Washington: relationships with hepatic neoplasms and other hepatic lesions in English sole (*Parophrys vetulus*). *J. Natl Cancer Inst. 74*, 487–494.
8. Peters, N., Köhler and Kranz, H. 1987. Liver pathology in fishes from the Lower Elbe as a consequence of pollution. *Dis. Aquat. Org. 2*, 87–97.
9. Scottish Development Department. 1972. *Report of a Rivers Pollution Survey of Scotland, Towards Cleaner Water*. Her Majesty's Stationery Office Press, Edinburgh, UK.
10. Owen, R. 1991. The recovery from organic pollution and the search for the cause of pigmented salmon syndrome in the river Don, Aberdeenshire. In: *Interactions between Fish and the Environment. Proceedings of the Institute of Fisheries Management, 22nd Annual Study Course*. University of Aberdeen, Aberdeen, pp. 65–80.
11. Banks, J.W. 1990. Fisheries management in the Thames Basin, England, with special reference to the restoration of a salmon population. In: *Proceedings of the European Inland Fisheries Advisory Commission on Management of Freshwater Fisheries*. Van Densen, W.L.T., Steinmetz, B. and Hughes, R.H. (eds). Pudoc, Wageningen, Netherlands, pp. 511–519.
12. Groman, D.B. and Miller, K. 1987. Haemolytic anaemia of Atlantic salmon: haematology and chemical pathology. *Aquaculture 67*, 210–211.
13. Bruno, D.W. and Poppe, T.T. 1996. *A Colour Atlas of Salmonid Diseases*. Academic Press, London, pp.123–124.
14. Everall, N.C., Mitchell, C.G., Groman, D.B. and Johnston, J.A.A. 1991. Tracing of haematotoxic agents in water with the aid of captive fish: a study with captive adult Atlantic salmon, *Salmo salar*, in the river Don, Aberdeenshire, Scotland. *Dis. Aquat. Org. 10*, 75–85.
15. Everall, N.C., Mitchell, C.G., and Robson, J.N. 1992. Effluent causes of the "pigmented salmon syndrome" in wild adult Atlantic salmon, *Salmo salar*, from the river Don in Aberdeenshire. *Dis. Aquat. Org. 12*, 199–205.
16. Croce, B. and Stagg, R.M. 1997. Exposure of Atlantic salmon parr (Salmo salar) to a combination of resin acids and a water soluble fraction of diesel fuel oil. A model to investigate the chemical causes of Pigmented Salmon Syndrome. Environ. Toxicol. Chem. 16, 1921–1929.
17. George, S.G., Groman, D., Brown, S. and Holmes, K. 1992. Studies of a fatal pollutant-induced hyperbilirubinaemia in spawning Atlantic salmon. *Mar. Environ. Res. 34*, 81–86.
18. Goksrøyr, A. and Förlin, L. 1992. The cytochrome P450 system in fish: aquatic toxicology and environmental monitoring. *Aquat. Toxicol. 22*, 287–312.
19. Couillard, C.M. and Leighton, F.A. 1993. In vitro red blood cell assay for oxidant toxicity of petroleum oil. *Environ. Toxicol. Chem. 12*, 839–845.
20. Turnball, D.A. and Bevan, J.R. 1995. The impact of airport de-icing on a river: the case of the Ouseburn, Newcastle upon Tyne. *Environ. Pollut. 88*, 321–332.
21. Owens, J.W. 1991. The hazard assessment of pulp and paper effluents in the aquatic environment: a review. *Environ. Toxicol. Chem. 10*, 1511–1540.
22. Lee, H.-B., Peart, T.E. and Carron, J.M. 1990. Gas chromatographic and mass spectrometric determination of some resin and fatty acids in pulpmill effluents as their pentafluorobenzyl ester derivatives. *J. Chromatog. 498*, 367–379.
23. Kruzynski, G.M. 1979. *Some Effects of Dehydroabietic Acid (DHAA) on Hydromineral and Other Physiological Parameters in Juvenile Sockeye Salmon* Onchorhynchus nerka. PhD thesis, University of British Columbia, Canada.
24. Matsoff, L. and Oikari, A. 1987. Acute hyperbilirubinaemia in rainbow trout (*Salmo gairdneri*) caused by resin acids. *Comp. Biochem. Physiol. 88C*, 263–268.
25. Chowdhury, N.R., Chowdhury, J.R., Gross, F. and Arias, I.M. 1982. Bile pigment metabolism. *Liver Annual 4*, 372–393.
26. Leaver, M.J., Clarke, D.J. and George, S.G. 1992. Molecular studies of the phase II xenobiotic conjugative enzymes of marine Pleuronectid flatfish. *Aquat. Toxicol. 22*, 265–278.
27. Oikari, A., Ånäs, E., Kruzynski, G. and Holmbom, B. 1984. Free and conjugated resin acids in the bile of rainbow trout, *Salmo gairdneri*. *Bull. Environ. Contam. Toxicol. 33*, 233–240.
28. Oikari, A. and Lindström-Seppä, P. 1990. Responses of biotransformation enzymes in fish liver: experiments with pulpmill effluents and their components. *Chemosphere 20*, 1079–1085.
29. Oikari, A., Holmbom, B., Ånäs, E. and Bister, H. 1980. Distribution in a receipient lake and bioaccumulation in fish of resin acids from kraft pulp mill waste waters. *Pap. ja Puu 62*, 193–202.
30. Croce, B., Stagg, R.M. and Smith, M. 1995. Effects of exposure to a combination of 8-naphthoflavone and resin acids on biotransformation enzymes in Atlantic salmon parr (*Salmo salar*). *Aquat. Toxicol. 32* 161–176.
31. Oikari, A., Lönn, B.-E., Castren, M., Nakari, T., Snikars-Nikinmaa, B., Bister, H. and Virtanen, E. 1983. Toxicological effects of dehydroabietic acid (DHAA) on the trout, *Salmo gairdneri* Richardson, in fresh water. *Water Res. 17*, 81–89.
32. Wang, Z., Chen, T., Gao, Y., Breuil, C. and Hiratsuka, Y. 1995. Biological degradation of resin acids in wood chips by wood-inhabiting fungi. *App. Environ. Microbiol. 61*, 222–225.
33. Copies of the reports cited in references 5 and 16 can be obtained from SEPA (formally the North East River Purification Board), Greyhope House, Greyhope Road, Aberdeen, AB11 9RD, UK.

34. This research was funded by the North East River Purification Board, The Scottish Office Agriculture and Fisheries Department, The Scottish Office Environment Department, Grampian Regional Council Water Services Department, Federal Tait Paper and Aberdeen Airport Ltd.
35. First submitted 2 April 1996. Accepted for publication after revision 26 November, 1996.

Bronwen Croce is a biochemist with a PhD in pollutant biodegradation by microalgae. She has worked on the chemical and ecotoxicological aspects of the Pigmented Salmon Project since 1992. Her main interests are in the areas of biochemical toxicology and detoxification processes.

Ron Stagg is an ecotoxicologist with a PhD on the effects of heavy metals on osmoregulation in fish. He leads an ecotoxicology section at the Marine Laboratory in Aberdeen with research interests in the use of biomarkers to assess the effects of pollution in the marine environment. He works on programs involved in monitoring the impact of the offshore oil industry in the North Sea and has research interests in P450 1A, tumor genes and metallothioneins in fish.

Their address: Scottish Office Agriculture, Environment and Fisheries Department, Marine Laboratory, P.O. Box 101, Victoria Road, Aberdeen, AB11 9DB, UK.

Nick Everall is a fisheries biologist with a PhD in aquatic ecotoxicology. He worked on the Pigmented Salmon Project between 1987 and 1990. He is currently a senior assessor for biological issues with Severn Trent Water Ltd. His research interests include the use of decomposing straw for control of algal blooms and water quality assessments and biorehabilitation using biological techniques. His address: Severn Trent Water Ltd, Quality and Environmental Services, PO Box 51, Raynesway, Derby, Derbyshire, DE21 7JA, UK.

David Groman, is a fish pathologist with an MSc in pathobiology and a PhD in aquaculture and fish health management. He worked on the Pigmented Salmon Project between 1984 and 1987. He is now an adjunct professor of Fish Health at the Atlantic Veterinary College. He works primarily in the field of diagnostic fish pathology, servicing the Canadian aquaculture industry. His research interests include fish pathology, clinical chemistry and haematology as well as applied aquaculture topics. His address: Department of Pathology and Microbiology, Atlantic Veterinary College, University of Prince Edward Island, Charlottetown, C1A 4P3, Canada.

Chris Mitchell is a fish biologist with an MSc in applied fish biology. He worked on the Pigmented Salmon Project between 1986 and 1989. Today, he represents the Scottish Office Agriculture Environment and Fisheries Department in Shetland as a Fish Health Inspector, where he services the local salmon farming industry. In addition to aquaculture technology, his interests include management issues in a scientific context, for which he has almost completed an MBA at the University of Aberdeen. His address: Scottish Office Agriculture, Environment and Fisheries Department, Marine Laboratory, PO Box 101, Victoria Road, Aberdeen, AB11 9DB, UK.

Roger Owen is a biologist with a PhD in technological economics from Stirling University. He is Head of Biology for the Scottish Environmental Protection Agency in Aberdeen. He has been involved in research into the biological effects of waterborne pollutants since 1976 and is responsible for biological water quality monitoring in the North of Scotland. His address: Scottish Environmental Protection Agency, Greyhope House, Greyhope Road, Aberdeen, AB11 9RD, UK.

© Royal Swedish Academy of Sciences 1997
http://www.ambio.kva.se

Pergamon

Spill Science & Technology Bulletin, Vol. 7, Nos. 5–6, pp. 257–278, 2002
Crown Copyright © 2002 Published by Elsevier Science Ltd. All rights reserved
Printed in Great Britain
1353-2561/02 $ - see front matter

PII: S1353-2561(02)00043-9

RESEARCH

Experimental Tainting of Marine Fish by Three Chemically Dispersed Petroleum Products, with Comparisons to the *Braer* Oil Spill

H.K. DAVIS†, C.F. MOFFAT‡* & N.J. SHEPHERD‡
†*Central Science Laboratory, Sand Hutton, York, YO41 1LZ, UK*
‡*FRS Marine Laboratory, Victoria Road, Aberdeen, AB11 9DB, UK*

Fish tainting thresholds, and rates of development and loss of taint, have been measured using two salmonid and two shellfish species exposed to three petroleum products in a study concurrent with the examination of fish affected by the spillage of oil from the wreck of MV *Braer*. The range of (24 h) fish tainting thresholds varied from 0.098 to 0.331 mg/l for trout exposed to the three oils, and was no greater than the difference between the values obtained for the diesel oil used in this study and another sample examined previously by the same group. Thresholds were little different for salmon and trout exposed to the same (Forties) crude oil but, although the lowest tainting threshold was observed with mussels (0.032 mg/l), crabs appeared to show some resistance to tainting. The rate of induction of oil into fin-fish and mussels produced a readily detectable taint within 6 h of exposure to oil-contaminated water, but rates of uptake, and losses after transfer to clean water, contrasted with the measured fish tainting thresholds for the three different products. Diesel-derived taint persisted for over 10 weeks, much longer than both the medium fuel oil and the Forties crude oil-derived taints, and depuration time increased with oil loading and duration of exposure. Data from analyses of hydrocarbons in depurating salmon are presented, and criteria used to declare fish to be tainted or untainted are discussed.
Crown Copyright © 2002 Published by Elsevier Science Ltd. All rights reserved.

Keywords: **Fish, oil taint, threshold, uptake, depuration, hydrocarbons, *Braer* oil spill**

Introduction

When fresh, the skeletal muscle of most species of marine fish is highly palatable. In benthic species, such as cod, this fillet meat is composed mainly of white muscle with a small proportion of dark muscle that is rich in haem pigments and lipid. Fillets of pelagic species, such as herring, contain more of the dark muscle. Cooked flesh of fish is typically sweet, with a range of flavours characteristic of the species. There are, however, occasions when the flesh acquires strong, atypical flavours that arise from exposure to odorous substances dissolved in the fishes' ambient water. Water-soluble substances are readily absorbed into fish, and when they reach a concentration at which they can be detected sensorily the fish are said to be tainted. Taints can appear as a result of natural causes, such as the earthy taste often associated with freshwater fish, but can also arise from industrial activity, notably from spillage of crude oil or oil products into marine and fresh waters. Persson (1984) has reviewed the published work on uptake and release of a wide range of fish taints caused by environmental contamination by industrial activity. In a more recent essay on tainting of foods, Howgate (1999) presented a

*Corresponding author. Tel.: +44-1224-876544; fax: +44-1224-295511.
E-mail addresses: h.davis@totalise.co.uk (H.K. Davis), moffatc@marlab.ac.uk (C.F. Moffat).

Taint: Taint is a sensory experience, defined by the International Standards Organisation (ISO) as 'an odour or flavour foreign to the product', that can only be measured by a sensory procedure using human assessors, and ignores any subjective judgement of pleasant or unpleasant. Usually, however, work on taints is conducted where the effects are generally perceived to be deleterious. Note that although sometimes used synonymously, this definition serves to distinguish between 'taint' and 'off-flavours' that may appear in, for example, microbiologically spoiled foods. The distinction is that taints are derived from materials present in the surroundings of the product; off-odours and off-flavours are produced by processes within the product.

Do untainted fish usually taste the same? No, edible fish have naturally occurring flavours that vary, depending upon factors such as where they live, the season, intrinsic condition, and time elapsed since slaughter. When fresh, and through the early stages of decay, they have a range of flavours that are regarded as characteristic for the species.

How do fish become tainted? Substances that impart a taste or smell may appear in the edible portions of fish as a result of some component in their food or taken up directly, through their gills and skin, from the water in which they live.

Are all taints in fish the result of industrial pollution? No, naturally occurring phenomena occasionally cause fish to have odours and flavours significantly beyond the normal range.

Does tainting of fish really matter? Yes, for the many people, including fishermen, fish traders, and restaurateurs whose livelihood may be taken away, or severely damaged, by the closure of fishing grounds or markets by regulatory authorities, or from the loss of business following reports of tainted fish having been sold.

Do the 'naturally occurring' seepages of oil into the oceans create a 'background level'? Oil components from natural and industrial sources are ubiquitous in the marine environment but, mostly, the levels are too low to cause an effect that can be recognised as taint. There is at least one report of fish caught in industrially polluted waters, and where oil taint is said to be commonly detectable in fish accepted for sale for human consumption. In addition, there have been a number of reports relating to tainting by chronic discharges of petroleum or petroleum related chemicals into rivers, estuaries or inshore waters.

detailed summary of taints affecting aquatic products, together with an exposition of the methods employed for their assessment. GESAMP (1993) contains a summary, with references to earlier reviews, of published work on the contamination of fish and shellfish by oil, and consequent chemical and tainting effects.

Fish do not always avoid chemical pollutants (Sprague & Drewery, 1969), and migratory behaviour of salmon has been reported to be unaffected by experimental exposures to oil (GESAMP, 1993). Much of the potential for taint that is presented by a large discharge of oil into a commercial fishing area appears not, however, to be realised, in part presumably because, generally, fish will try to move away from large spills of oil. Also, the chances of large numbers of tainted fish being found on quayside markets will rapidly diminish as affected stocks disperse. That is not to say that there is little commercial significance as public confidence may collapse following any reported discovery of tainted fish. For some fisheries, the problem can be much more apparent and more demanding of action by regulatory bodies and insurers. Farmed fish held in freshwater ponds, marine fish held in cages in estuarine or inshore waters, and many shellfish species that do not rapidly move large distances are all more vulnerable to acute spills. Growth of the aquaculture industry in coastal waters (e.g. production of Atlantic salmon (*Salmo salar*) in Scotland has increased from 10,337 tonnes in 1985 to 128,959 tonnes in 2000) has been a particular spur to the investigation of oil taints. This is because cages containing large numbers of fish are often very close to shipping channels that are vulnerable to tanker accidents.

Taints are sensory phenomena and, although chemical analyses have a role, their investigation depends primarily on sensory analytical techniques. There are various systems that may be used, and which can be operated in a highly objective manner. This study aimed to determine the degree of exposure to oils that would cause a consequent change to the taste of fish and shellfish, and to examine patterns of change of intensity during exposure and subsequent depuration in clean water. The former required a discriminative test, where panellists make direct comparisons of exposed and unexposed reference samples. Human senses can detect small differences in such tests but, because individuals vary considerably, large num-

Don't fish die when exposed to oil? Oil spills result in the death of many marine organisms, including fish, but many survive short-term, high exposures. Farmed salmon have been seen leaping through oil floating on the surface in their attempts to escape major oil spills when trapped in pens.

Wouldn't fish swim away from an oil spill? Fish will often try to avoid pollutants when they can, but may be trapped (accidentally, or in fish farm cages) or, compelled by reproductive instincts, to swim through oil towards their mating grounds. Others, including many valuable shellfish species, have a sedentary habit and cannot quickly move away. After a sudden, large release, those fish that can swim away might be exposed to a significant quantity of oil before escaping.

Would taint be better measured using chemical analytical techniques? Taint is a sensory experience and can only be detected and measured by sensory procedures, i.e. by smelling or tasting the fish or shellfish suspected of being tainted. Chemical tests can be useful for monitoring but, ultimately, a sensory test is needed because chemical data can only predict that a food might be tainted. Non-sensory tests can only help if it is known what substance caused the taint, and if the relationship between concentration and sensory response for the substance is also known. Human olfactory responses to volatile compounds vary considerably, with some being barely detectable, whilst others have a powerful impact, the perceived character of which may change with concentration.

bers of assessors are needed to obtain an overall measure of the sensitivity of a population.

Estimations of quantity are less precise than direct comparisons of samples. Only a small number of intensity score intervals can be differentiated because of the exponential relationship between amount of a stimulus and the perceived intensity. Despite this limitation, assessment of intensity can be used to examine patterns of change such as those that occur in the flavour of fish flesh after exposure of the live fish to oil-contaminated water, and again after transfer to clean water. Continuous monitoring by a discriminative test procedure would add considerably to the practical difficulties, as well as the cost, of sensory assessment.

For application to the monitoring of real spill events, the difficulties are compounded by the absence of true control samples which, for work of this nature, can only be obtained in experimental situations. A controlled testing procedure that was developed by ECETOC (1987) for measuring fish tainting thresholds of individual compounds was used in this study to measure the tainting thresholds of the three test oils. The same exposure system, except for being on a bigger scale, was also used to produce stocks of fish that had been subjected to a range of exposure and depuration regimes. Here, the sensory discrimination testing method was inappropriate because, for most of the samples, the challenge to assessors was to record the intensity of oil taint, using their experience and training to apply a common scale. If the end point of the depuration trials could have been predicted the more sensitive discrimination procedure could have been used. But the greater amount of material required, and the need for the batches of fish to be assessed out of sequence to avoid a predictive influence on the assessors, militated against that option.

Chemical tests appeal as offering a totally objective measure that should avoid the need for relatively large numbers of experienced people in taste panels. They are costly, however, having only limited throughput, and little is known about the compounds in oil that are responsible for the oily tastes. There is certainly no single cause; the taste results from a large number of components though it may be that a relatively small number predominate. The contributing components probably differ considerably in their water solubilities, flavour strength, and amounts that are present in oil

What factors affect the intensity of taint in fish exposed to a pollutant? Odour/taste sensitivity of humans to the pollutant, its concentration in the water in which the fish live, and the period of time that the fish has been exposed to the pollutant and, subsequently, to clean water.

How does insoluble oil induce taint in fish? Components of extremely low solubility in water will have little tainting effect. Also, components of high solubility but only weak odours will also have little effect. Crude oil, and associated distillates, consists of a variable mixture of hundreds of components of widely differing water solubility, many of which can dissolve in the water and thence pass into the fish. Where those components also have low tainting thresholds (have strong odours/flavours), they will cause the fish to be tainted.

What are the benefits of sensory assessment following an oil spill? The assessment of taint in fish and shellfish samples has the advantage that:

- it is rapid, enabling relatively large numbers of individual fish and shellfish to be tested; and
- it permits targeting of the appropriate samples for chemical analyses.

from different sources. Following an oil spill, the polycyclic aromatic hydrocarbon (PAH) concentration of water, biota, and sediment is routinely determined. This, in part, results from the carcinogenic potential of some of the larger PAHs. In addition, however, the naphthalenes (which dominate the PAHs in crude and diesel oils) are strongly odiferous and are more soluble than the three-ring PAHs. Indeed, there is often an increase in the proportion of naphthalenes observed in fish flesh relative to the original oil. Comparisons have, therefore, been made between the PAH concentration and taint in an attempt to assess if a direct association can be made between the totally objective chemical tests and the sensory data. A tentative association was observed in field samples obtained following an incident in the Moray Firth, Scotland. Comparison of the PAH data with sensory analysis showed that PAH concentrations of <10 ng/g wet weight of *Nephrops norvegicus* resulted in no taint. *Nephrops* which contained between 35 and 60 ng/g wet weight PAHs were rated as having a 'suspect taint' while a sample of *Nephrops* containing 363 ng/g PAHs was reported as being tainted. In this case the *Nephrops* contained approximately equal amounts of naphthalenes and phenanthrenes (Moffat *et al.*, 1998). More recent studies with rainbow trout (*Oncorhynchus mykiss*) have shown a correlation between increasing concentration of naphthalenes and development of a taint. The presence of a taint was noted when the total naphthalene concentration (naphthalenes represented upwards of 95% of the PAHs in the flesh) was 130 ng/g wet weight and increased with increasing naphthalene concentration (Tenaud & Moffat, unpublished data). Whilst not intended as fully addressing this major analytical problem, the opportunity was taken to include in the present study some analyses of oil components. Analytical methods in routine use for the analysis of petrogenic hydrocarbons were applied to a batch of salmon recovering in clean water after an experimental exposure to crude oil.

This investigation is presented as three sub-topics:

- *thresholds*: the determination, for various combinations of oil products and fish species, of statistically derived exposure concentrations that can be expected to cause taint detectable by 50% of a group of people;
- *uptake*: the patterns of induction of the oily taste during periods of exposure of fish to oil; and
- *depuration*: the patterns of loss of oily taste from fish as they recover in clean water after an exposure to oil.

(*Note*: The term threshold implies a minimum concentration required to produce a detectable response, but can never be derived with certainty. Here, the term refers to the median effect concentration, TC_{50}, analogous to the lethal concentration LC_{50} as used in toxicity studies (GESAMP, 1989). For all bar the lowest of oil exposure levels examined, concentrations are nominal values because not all the oil would be completely solubilised.)

Materials

Test oils

Three test oils were used. Two (1 and 2 below) were supplied by the UK Department of Transport's Ma-

Fish tainting threshold: The minimum concentration for a substance to be detected by smell is called the odour threshold. For similar measurements of taste thresholds, the medium in which the test compound is dissolved (usually water) must be defined because of the potential for interference by the matrix. For practical reasons, however, fish tainting threshold is defined not as the minimum concentration in the fish meat, but as the minimum concentration in the water to which the fish are exposed (for 24 h) for a taint to be detected.

Why does the tainting threshold need to be defined and determined differently from other thresholds? The material being tested may be a mixture of many compounds, and the amount of each that transfers from water into a live fish may be very different from the composition of the original mixture. Even for a single substance, it is difficult to obtain a representative mixture of a solute in fish meat by mechanical homogenisation.

What period of exposure is needed to taint fish? This will depend upon the tainting threshold of the pollutant and its concentration in the exposure water. Because of the rapid transfer of molecules across the membranes of fish gills, and thence into the bloodstream, induction of a taint into fish is a matter of minutes rather than days. Under experimental conditions, a taint can be detected after only 30 min exposure to a crude oil.

If taint can appear rapidly in fish, will it not also disappear quickly when the cause is removed? If the cause of the taint is a highly water-soluble substance, then the taint may disappear in a few days. But when the cause of the taint is oil or a more lipophilic substance (i.e. $\log K_{ow} >\sim 3.3$) it will transfer to lipid tissues. When moved from contaminated water to clean water, transfer of such substances back into the aqueous phase is slow, and thus depuration of the substance from the fish, and loss of taste in the flesh, can take many weeks or months.

rine Pollution Control Unit (MPCU), and the third was obtained from a local environmental services company. Characteristics of the test oils were:

1. Forties crude oil blend used in other MPCU projects, labelled 1267 3WE MPCU Dune Disposal Project. Density $(d) = 0.817$ g/ml, sulphur content $(S) = 0.04\%$;
2. medium fuel oil labelled 31/E 1268. $d = 0.976$ g/ml, $S = 1.10\%$;
3. diesel oil. $d = 0.856$ g/ml, $S = 0.19\%$.

Dispersant

Three commercial oil spill dispersant formulations were considered for mixing with the test oils during exposure treatments. These included a hydrocarbon-based mixture with a specific gravity of 0.85, a mixture that had 2-butoxyethanol as the active component and a specific gravity of 0.99, and Noble Superdispersant NS25, an aqueous mixture of glycol, glycol ether co-solvents, non-ionic and ionic surfactants, with a specific gravity of 0.99–1.01. Following an assessment of the potential for the dispersant formulations to cause taint it was concluded that Noble Superdispersant NS25 had the least potential to cause a taint in fish.

Holding facilities

Fresh water and sea water were supplied at controlled rates, via separate intermediate tanks of ~10,000 l, to holding tanks of 600 or 1000 l capacity which were used for maintaining most stocks of fish and shellfish (6500 l for salmon). Sea water was pumped ~1 km, from a sand-filtered intake located about 50 m from the northwestern shore of Nigg bay, into the laboratory facilities at Torry, Aberdeen. Fresh water was taken from the local mains supplies. Water in the holding tanks was continually aerated and recirculated through sponge filters, with new water added at ~2–3% per hour. Holding tanks were filled and operated for at least 1 week of normal operation to condition and stabilise the test water and system before fish were introduced.

Test fish

The test organisms were selected in an attempt to cover a variety of form and habit within a small number of readily available species of commercially exploited fish. Most of the testing utilised rainbow trout (*Oncorhynchus mykiss*), chosen by ECETOC (1987) as the preferred fish species for general use because of its worldwide availability, moderate fat content, and adaptability to fresh or sea water. They were purchased from local freshwater fish farms and gradually acclimated to ~90–95% sea water. Salmon (*Salmo salar*) were purchased as smolts and similarly adapted to 100% sea water. Farmed mussels (*Mytilus edulis*) and wild crabs (*Cancer pagurus*) were purchased from commercial wholesalers and transferred directly to tanks containing sea water. The trout and salmon were fed on appropriate commercial pelleted feeds, and the crabs were fed sparingly with strips of fresh, raw marine fish. Feeding was discontinued at least 4 days before fish were to be exposed to oil. The sponge filters were removed from tanks containing mussels as they were given no food other than might have been present in the seawater supplies.

When slaughtered, eviscerated fish weights were:

- *Threshold experiments*
  - *trout*: 127–332 g,
  - *salmon*: 180–341 g,
  - *mussels* (averages per batch of cooked/shucked meats): 1.6–3.5 g,
  - *crabs*: not determined;
- *Uptake experiments*
  - *trout*: 139–252 g,
  - *salmon*: 282–408 g,
  - *mussels*: same stock as threshold, i.e. ~2.3 g per cooked and shucked meat;
- *Depuration experiments* (batch average weights)
  - *trout*: 120–506 g,
  - *salmon*: 217–360 g,
  - *mussels and crabs*: not determined.

Fat contents, as occasionally determined on bulked samples by a modified Bligh and Dyer (1959) method, were:

- *trout*: 1.3–4.3%;
- *salmon*: 2.6–6.8%;
- *mussels*: 4.7%.

Experimental Methods

All the exposure systems, and assessments of tainting thresholds, were conducted according to the recommended procedures established conjointly by ECETOC (1987) and GESAMP (1989). Most evaluations of fish in the studies of uptake and depuration were dealing with much stronger odours and flavours that required an assessment of the intensity of taint by experienced, trained panellists using the same scoring procedure as used in an earlier study (Davis *et al.*, 1992).

Exposure of test fish to oils and dispersants

Test fish were transferred from stock tanks to exposure tanks that had been set up at least 15 h earlier with oil and/or a spill dispersant injected at the required rates into the inflowing water supply. Accord-

Fish tainting threshold

Exposure: Batches of fish or shellfish were exposed to a range of different concentrations of the test material for 24 h, slaughtered, wrapped in aluminium foil, blast-frozen, and then stored at −30 °C until required. At the same time, similar batches were exposed only to the test water.

Sensory assessment, three-alternative forced choice test (3-AFC): The thawed fish were cooked, and edible portions from fish within each batch were mixed and dispensed to cups which were set out in groups of three. For each test concentration, two cups contained untainted reference material, and one cup contained material from the exposed fish. Assessors were required to identify the sample that had an oily taint. The tainting threshold is the concentration of test material in exposure water at a panel detection level, in the fish, of 66.7%, the mid-point between detection by all the panellists (100%) and the level that is to be expected by chance even when no difference exists (33.3%).

Uptake

Exposure: Larger batches of fish or shellfish, in similar but larger facilities, were exposed to water containing known amounts of test oil, and samples of fish removed at intervals and slaughtered, wrapped, and blast frozen.

Sensory assessment, numerical scalar assessment of intensity of taint: The thawed fish were cooked by microwave cooking (fin-fish) and presented to the panel members in lidded casseroles (Whittle *et al.*, 1997b). Each assessor was asked, independently, to allocate a score for the intensity of oil taint, on a 0 (absence of taint) to 5 (extremely strong) numerical scale. The average scores, when plotted against time, indicate the times required for a taint to be detected and the rates at which the intensity then increased.

Depuration

Exposure: Large batches of fish or shellfish were exposed for fixed intervals to water containing known amounts of test oil. The fish were then transferred to clean, flowing water, and samples of fish removed at intervals, slaughtered, wrapped, and then blast-frozen.

Sensory assessment, numerical scalar assessment of intensity of taint: The thawed fish were cooked by microwave cooking (fin-fish) and presented to the panel members in lidded casseroles. Each assessor was asked, independently, to allocate a score for the intensity of oil taint, on a 0 (absence of taint) to 5 (extremely strong) numerical scale. The average scores, when plotted against time, indicate the rates at which the intensity of taint decreased as the oil components responsible for the taint were depurated from the fish tissues.

Chemical determinations of oil components: Portions of raw edible flesh from each of the samples of salmon taken from the batch that had been exposed to Forties crude oil, and then transferred to clean, flowing water, were saponified with methanolic sodium hydroxide and extracted with *iso*-hexane. The *iso*-hexane solution was dried with anhydrous sodium sulphate and evaporated down to a small volume for injection onto a high performance liquid chromatography (HPLC) column to separate the aliphatic and aromatic hydrocarbons. The aliphatic fraction was analysed using gas chromatography with flame ionisation detection (GC-FID), and the aromatic fraction by GC with mass selective detection (GC-MSD) using selected ion monitoring (Topping *et al.*, 1997; Whittle *et al.*, 1997b).

Can the exposure system realistically mimic an oil spill? That is not the purpose of the procedure employed for exposure of fish to controlled amounts of chemicals. Every spill is different, both in the amounts and properties of the oil involved and the weather and geographical/hydrographic influences on the consequences of the spill. What is needed is a reproducible test with the exposure parameters defined as precisely as is possible. Studies of fish tainting that, for example, have used oil floated onto the surface of the water will be more difficult to accurately reproduce, and the data will be of limited relevance to other studies.

ing to nomograms given by Sprague (1973), flow rates in all the exposure tanks were sufficient to give 99% replacement of water in approximately 5 h.

For measurements of fish tainting thresholds, all test fish were removed from the exposure tanks and slaughtered within 10 min of the allotted 24 h exposure period. Smaller variations from the nominal exposure times were allowed for shorter duration uptake experiments. Apart from the initial, zero time interval, samples, fish that had been exposed in preparation for depuration studies were not transferred immediately from the exposure tank. Instead, inflow of oil and dispersant was halted and the rate of water exchange temporarily accelerated by releasing approximately one-third of the water whilst maintaining the inflow of clean water.

Thresholds. To confirm the suitability of NS25, and for measurement of tainting thresholds of the three oils, preparation and assessment of fish employed procedures based on the methods established conjointly by ECETOC (1987) and GESAMP (1989). Syringe pumps pushing gas-tight syringes were used to inject test substances into heated, aerated water flowing at ~1.5 l/min into a series of 100 l covered aquaria. Inflow was to the bottom of each exposure tank, with overflow spigots at the opposite end taking water from the surface to waste. Fish (three to five), having a total weight of ~1 kg, were introduced to each tank, and removed 24 h later.

The test water conditions for trout were:

- temperature: 10.5–14.8 °C;
- salinity: 27.2–31.1‰;
- dissolved oxygen: 70.8–88.5% saturation;
- pH: 6.6–7.2.

Conditions for the other species, where appreciably different, were:

- *salmon*: 13.0–13.7 °C, 35.0‰ salinity (100% sea water), pH = 7.37;
- *crabs*: 35.0‰ salinity (100% sea water);
- *mussels*: 35.0‰ salinity (100% sea water).

Where tainting thresholds were measured with dispersant, NS25 and oil were pre-mixed according to the manufacturer's recommendation of one part dispersant in 20 parts oil (w/w). Fish intended as control samples were subjected to the same procedures as the test fish except for injection of oil and dispersant.

Uptake. In order to examine the rates at which oil taints developed in fish, the exposure system was scaled up so that sufficient fish could be exposed to permit samples to be removed at intervals up to 24 h. The larger tank (600 l) had a siphon system that was adjusted so that outflow included both a surface skim as well as water from the bottom of the tank. Water conditions were:

- *trout*: 16.4–16.5 °C and 27.2‰ salinity;
- *salmon*: 12.0 °C and 35.7‰ salinity (100% sea water);
- *mussels*: 9.4 °C and 36.3‰ salinity (100% sea water).

Depuration. The same 600 l exposure system was used to provide batches of tainted fish for depuration studies. Water conditions were:

- *trout*: 10.5–17.6 °C, 21.8–31.1‰ salinity;
- *salmon*: 11.5–14.5 °C, 33.6–35.7‰ salinity (100% sea water);
- *crabs*: 9.7–15.0 °C, 27.2–35.0‰ salinity (100% sea water);
- *mussels*: 7.4–9.4 °C, 33.6–36.3‰ salinity (100% sea water).

Immediately after removal from the exposure or depuration tanks, fin-fish were slaughtered, gutted, washed, wrapped in aluminium foil, blast-frozen, and held at ~−30 °C until needed for sensory assessment. Salmon that were to be analysed for petrogenic hydrocarbons were wrapped in aluminium foil that was pre-washed with *iso*-hexane to minimise possible interference from this source. The shellfish were cooked before being frozen. Crabs were drowned in fresh water before the temperature was raised to boiling point and maintained for 20 min, removed from the water and cooled, vacuum-packed whole, and frozen. Mussels were cooked for 3 min in a shallow pan of water to release the meats from the shell, and the shucked meats were vacuum-packed before freezing.

Isn't sensory testing very subjective? Although responses to sensory stimuli differ between people according to individual sensitivities, and cultural influences, the use of multiple assessors and training (where appropriate to the method selected), and a disciplined approach to the construction of the test systems, can make testing for taint objective. The disciplines that are needed for sensory work are essentially the same as for chemical and physical techniques of investigation, and any results obtained without them would be equally suspect.

What are 'objective' sensory tests? They can be considered as two groups: 'expert' and 'non-expert' tests. The 'expert' test used here requires a panel of assessors to be trained to recognise a particular odour/flavour (oil taint in this case) and to allocate a score on a 0 (absent) to 5 (extremely strong) scale. After training, performance is enhanced by accumulated experience. Panellists make their assessments individually, and their scores are averaged or subjected to other statistical treatments. Because of the limitations of the human senses when estimating amounts, the results are subject to relatively large error bounds. A popular non-expert test is called the triangle test, but a more powerful variant is called the three-alternative forced choice test (3-AFC).

The *triangle test* requires each assessor to examine samples that are presented in groups of three. Each group of three samples contains one or two test samples and one or two control samples, and the assessor has to select the one that they believe is different.

In the *3-AFC*, the single sample in each group of three is always the test sample, and assessors are asked to identify the test sample. Both of these tests gain from the greater power of human senses to discriminate when making direct comparisons between samples, and the lack of need for training of the assessors.

Sampling intervals for studies of uptake and depuration necessarily entailed some guesswork, aided by limited data, as most samples could not be assessed in time for the work to gain the benefit of feedback into the design of subsequent experiments. When needed for analysis, batches of samples were removed from frozen storage in a random manner and left to thaw overnight in a refrigerator (~+4 °C). The storage conditions used ensured that cold-storage flavours were not introduced to the product.

Sensory assessment

Sensory assessments of taint were made by two panels of volunteers from the staff of CSL Food Science Laboratory, Torry, Aberdeen (formerly known as the Ministry of Agriculture, Fisheries and Food, Torry Research Station). Threshold measurements required a panel of 18 people from a total of 42 that were used at some time. The group included a wide range of people from across all work areas, with some having little or no previous experience of sensory testing. Assessments of intensity of taint were made by a smaller, 'expert' group of 5–11 (usually 9 or 10) trained assessors from a panel of 14. All members of this panel had considerable experience of assessment of fin-fish and oil taints, but were less familiar with the two shellfish species.

In view of the smaller amounts of test material required, the widely differing experience of the assessors, and previous observations of the methods (Davis *et al.*, 1992), the 3-AFC procedure was considered to be more appropriate than triangle tests for the measurements of tainting thresholds. The 3-AFC method is similar to, but a more powerful means of discrimination than, the triangle test which is recommended in the ECETOC/GESAMP procedures for measurement of tainting thresholds. After cooking transverse steaks of fin-fish in a microwave oven, the flesh of all samples within a treatment group was mixed and dispensed to expanded polystyrene cups closed with plastic lids. The cups were presented in groups of three to each assessor, with the groups presented in order of increasing oil concentration of the exposed samples. Within each group, one cup contained test material taken from all the exposed stock within one oil treatment. The other two cups contained similarly treated control material. For each group, each assessor was required to identify the sample that had an oily taint.

The 3-AFC procedure was used in one experiment on the uptake of taint, but otherwise sensory evaluation of uptake and depuration of taint employed the expert panel to assess intensity of taint. The 14 members of this panel had been trained to recognise petroleum tastes in fish, and to apply a 0 (absent) to 5 (extremely strong) intensity scale. Although an untainted reference sample was usually provided, the essence of the task for each assessor was to judge the test samples against their accumulated knowledge of the range of flavours of the relevant species.

All assessments of intensity of taint in uptake and depuration experiments were conducted on discrete batches of fish, by the same procedure that was used on samples of fish and shellfish taken from waters near acute oil spill incidents. Batches were removed from

frozen storage in a random manner and prepared for assessment by cooking whole fillets, in separate lidded glass casseroles, in a microwave oven, to a centre temperature of 65 °C. Mussels were similarly assessed after thawing and then heating the shucked meats for $1\frac{1}{2}$ min in a microwave oven. After thawing, the whole crabs, white (claw and leg) and brown (hepatopancreas) meats were removed and assessed separately without re-heating. Most of the work was conducted alongside assessments of samples (over 4000 in total) submitted as part of the monitoring work following large oil spills from the tankers *Braer* (at Garths Ness, Shetland) and *Sea Empress* (on the Welsh coast at Milford Haven). These incidents added hugely to the demands on the assessors. On balance, however, both this experimental study and the spill monitoring work probably benefited from the additional experience that each contributed to the progress of the other.

Chemical analysis of petrogenic hydrocarbons

Samples of the petroleum products, fish food, and flesh from the same oil-exposed and control samples of salmon were analysed to determine concentrations of *n*-alkanes and PAHs. Tainted salmon were taken, at intervals, from a batch that had been exposed to Forties crude oil and then allowed to depurate in clean water. Hydrocarbons were isolated by refluxing the samples with a methanolic solution of sodium hydroxide, after addition of known amounts of aliphatic and aromatic standard solutions. The aqueous saponified mixtures were extracted with a non-miscible solvent, *iso*-hexane, and the solvent solution washed with methanol and water before passing through a column of anhydrous sodium sulphate, and reduced in volume. Alkane and PAH fractions were separated by injecting the resultant concentrated solution onto an unmodified (normal phase) silica HPLC column, being eluted at 2 ml/min with *iso*-hexane. The alkanes and PAHs were collected in two separate fractions, volume-reduced, and transferred to small vials which were crimp-capped and stored in a refrigerator until analysed. The hydrocarbons were analysed using GC with determination of alkanes by flame ionisation (GC-FID), and the PAH compounds determined by mass spectrometry (GC-MS) using selected ion monitoring.

GC-FID analyses of aliphatic hydrocarbons employed a fused silica capillary column (25 m × 0.25 mm id) coated with a 0.33 μm film of a cross-linked methyl silicone gum, Ultra-1 (Hewlett Packard, Bracknell, Berkshire, UK), with nitrogen at 16 psi used as the carrier gas. The initial oven temperature was 60 °C and, after 3 min, the temperature was elevated at 4 °C/min up to 280 °C. In the presence of an unresolved complex mixture (UCM), *n*-alkane peaks were quantified using the UCM as the baseline. GC-MSD analyses of PAHs used a 25 m × 0.20 mm id fused silica column coated with a 0.33 μm film of Ultra-1, with helium carrier gas at 7 psi. After an initial isothermal period of 3 min, the temperature was elevated at 20 °C/min up to 100 °C, and then at 4 °C/min up to a final temperature of 270 °C, and held constant for another 32 min. The mass selective detector was set up for selective ion monitoring according to the procedure detailed by Topping *et al.* (1997).

Data treatments

Thresholds were estimated by fitting a logistic curve to the 3-AFC data, running from 0.333, the probability of correctly selecting the test sample by chance in the absence of an effect, to 1.0, correct selection by all the assessors. The fish tainting threshold concentration is defined as the concentration in ambient water which induces a taint with a probability of detection of 0.5. For data obtained from 3-AFC tests, calculated threshold values needed to be determined as the (nominal) concentrations for which the probability of correct selection was 0.667, i.e. midway between the theoretical asymptotes. The data were processed using a computer programme developed by the University of Birmingham School of Psychology during previous work on this topic (Davis *et al.*, 1992). The programme was written to calculate the best fit using the criterion of maximum likelihood and to derive confidence bounds around the threshold estimates. Microcal Origin (version 3.0) technical graphics package was used to prepare the figures and for curve fitting of uptake and depuration data.

Is sensory testing more expensive than chemical tests? Apart from the costs of employing a panel of assessors, the equipment requirements for sensory testing are simple and cheap compared with, for example, gas chromatography. The relative costs for staff are more difficult to compare; the sensory expertise needed to design and organise the testing is scarce and, as members of assessment panels are often employed mainly for other tasks, the true costs of panellists, sometimes a hidden cost, can vary considerably. But, again, it must be remembered that any inappropriate test will be the most expensive. The role of chemical analysis in taint assessment has to be supportive, for example, monitoring components that are known or strongly suspected to cause taint, in order to reduce the burden on sensory assessors.

Results

Impact of dispersant NS25

From 18 assessments of trout exposed for 24 h to dispersant NS25 at loadings of 0.96 and 9.6 mg/l, there were, respectively, five and seven correct selections of the oil-tainted sample using the 3-AFC procedure. This is below the minimum (10) needed to indicate a detection significant at the 95% confidence level. With such a high fish tainting threshold, the dispersant would not be expected to have any significant influence on the taste of fish in any of the oil and dispersant, or control sample exposure regimes, and was excluded from the treatment applied to the control fish. At very high oil concentrations, oil taint would swamp any contribution there might be from the dispersant which, being readily water soluble, would also be rapidly lost from the tissues of fish used for depuration studies.

Tainting thresholds of three oils applied to trout

Estimated thresholds for the six tainting regimes applied to trout, i.e. three oils with and without NS25 dispersant, are presented in Table 1. As the differences between results obtained with and without dispersant were not significant, they were combined to give better estimates for each type of oil. The combined data were also used to produce the overall patterns of panel responses, presented in Fig. 1 as the fitted curves with individual data points illustrated for two exposure regimes: Forties crude oil alone and pre-mixed with NS25 dispersant. The results indicate that the samples of diesel or medium fuel oil had similar fish tainting thresholds but Forties crude oil was an appreciably more powerful tainting substance.

Table 1 Fish (trout; *Oncorhynchus mykiss*) tainting threshold values for three oils tested with and without dispersant

Exposure mixture		Fish tainting threshold value (mg/l)	Confidence boundaries ($p = 0.05$)	
Oil	Dispersant		Upper	Lower
Diesel	⌛	0.224	0.272	0.185
	🗐	0.265	0.298	0.237
	Combined data	0.248	0.276	0.224
Medium fuel	⌛	0.294	0.355	0.241
	🗐	0.383	0.549	0.267
	Combined data	0.331	0.406	0.269
Forties crude	⌛	0.076	0.109	0.053
	🗐	0.137	0.192	0.098
	Combined data	0.098	0.127	0.076

⌛ = absent; 🗐 = present.

Tainting thresholds for Forties crude oil applied to different fish species

Forties crude oil was used to compare sensory responses to different types of fish and shellfish after similar exposures to oil. There was no significant difference between the tainting thresholds for trout and salmon, but sensory responses to the two shellfish species were very different (Table 2). Confidence boundaries for the taint threshold in mussels overlap with those for salmon and trout because of one, seemingly aberrant, data point (61% detection after exposure to oil at 0.77 mg/l despite progressive increases with increasing exposure concentration, to

Summary

	Test animal	Forties crude oil	Medium fuel oil	Diesel fuel
Tainting thresholds (mg/l)	Trout	0.10	0.33	0.25
	Salmon	0.11		
	Crab (white meat)	>7.7		
	Crab (brown meat)	>7.7		
	Mussels	0.03		
Uptake: increase of taint with exposure time (in hours to average score = 3 (strong taint))	Trout	~5.5 @ 34.1 mg/l	<0.5 @ 5.9 mg/l	
	Salmon	~7.5 @ 23.3 mg/l		
	Mussels	~3.0 @ 25.7 mg/l		
Depuration: loss of taint after transfer to clean water (in days to detection of oil taint by 20% of panel members: equivalent to an average score of 0.5 (no certain detection))	Trout	~35 (after 10.7 mg/l for <5 h)	~47 (after 111.7 mg/l for 96 h)	~114 (after 21.8 mg/l for 240 h)
	Salmon	~45 (after 30.0 mg/l for 124 h)		
	Crab	~18 days (after 19.8 mg/l for 96 h)		
	Mussels	>65 days (after 25.7 mg/l for 240 h)		
PAHs: Reduction to 95% of induced level/reduction to normal background	Salmon	~23 days/~55 days (after 30.0 mg/l for 124 h)		

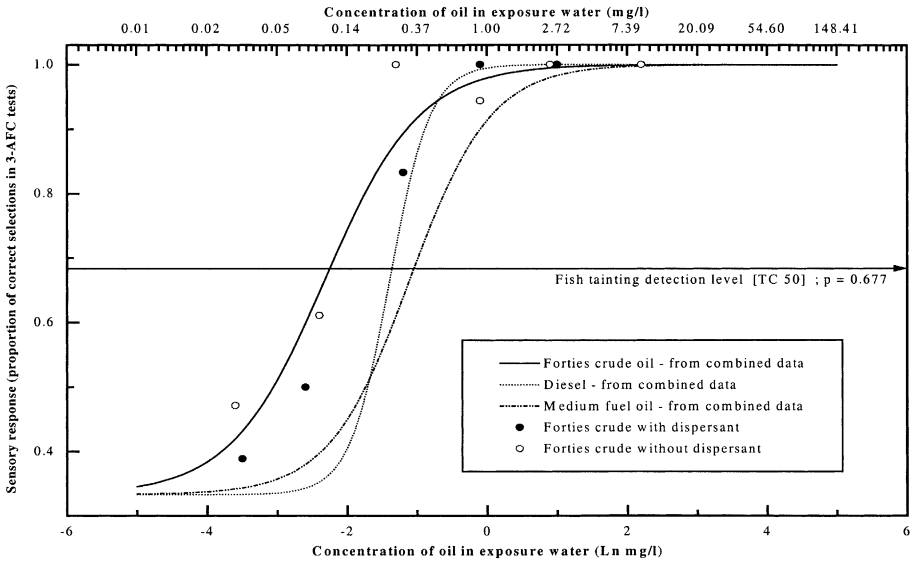

Fig. 1 Proportions of correct responses in the 3-AFC procedure: (a) logistic curves fitted to combined (±dispersant) data for trout exposed to Forties crude diesel and medium fuel oils; (b) individual data points for taint in trout exposed to Forties crude oil.

100% detection at 0.10 mg/ml). Otherwise, taint appeared to be detectable in mussels after exposure to oil concentrations of more than one order of magnitude less than was needed to taint the fin-fish.

A response similar to that obtained with mussels was expected for the brown meat of edible crabs. Shortage of suitable test animals meant that only three exposure regimes could be examined, which is insufficient to make a reliable estimation of thresholds. Further, panel responses to both the white and brown meats from crabs exposed to the highest oil concentration were lower than for the intermediate concentration. When the results were combined, in order to treat as a single test, the proportion of correct responses from these two exposure regimes was still too low to indicate detection with a probability $\geqslant 0.5$. Thus, being above the highest concentration that was applied, the tainting thresholds for both types of crab-meat were at least two orders of magnitude higher than those for the skeletal muscle of salmonid fish.

Table 2 Tainting threshold values for Forties crude oil applied to trout (*Oncorhynchus mykiss*), salmon (*Salmo salar*), edible crabs (*Cancer pagurus*), and mussels (*Mytilus edulis*)

	Tainting threshold (mg/l)	Confidence boundaries ($p = 0.05$)	
		Upper	Lower
Trout	0.098	0.127	0.076
Salmon	0.109	0.169	0.070
Crab—white meat	>7.7		
Crab—brown meat	>7.7		
Mussels	0.0323	0.210	0.005

Note: the threshold values and width of the confidence boundaries for salmon and, particularly, the mussels were raised due to the influence in each instance of one low detection by the panel.

Effect of duration of exposure on detection of oil taints

The 24 h exposure regime for measurement of threshold assumes that the capacity of the test substance to cause taint will be at or close to maximum within that time. The series of tests to examine rates of increase was conducted with high oil concentrations to ensure that assessors were presented with samples that would have variable levels of taint detectable by the scoring procedure. There would also be some parallel with farmed fish and other stocks unable to flee from a sudden, but sub-lethal, release of a large amount of oil.

When the 3-AFC procedure was used to examine taint in trout exposed to high concentrations of Forties crude oil (26.5 mg/l) with NS25, for periods of up to 4 h, a plateau was reached within that period ('×' in Fig. 2), though not 100% detection. Figure 2 also shows how scores for intensity of taint in salmon exposed to a similar oil concentration (Forties crude oil at 23.3 mg/l, with NS25, for up to 24 h) changed more slowly. Although still increasing, intensity scores had almost reached an asymptote within 24 h. The error bars show ±1 standard error of the mean (SE), reflecting the combined variations within the group of fish and the different sensitivities and interpretations of the assessors. When all intensity scores above zero were treated simply as detections, regardless of magnitude, the pattern of detection rates ('•' in Fig. 2) changed in an almost identical manner to the 3-AFC scores. After an initial period of rapidly increasing detection levels, the panel consistently showed 100%

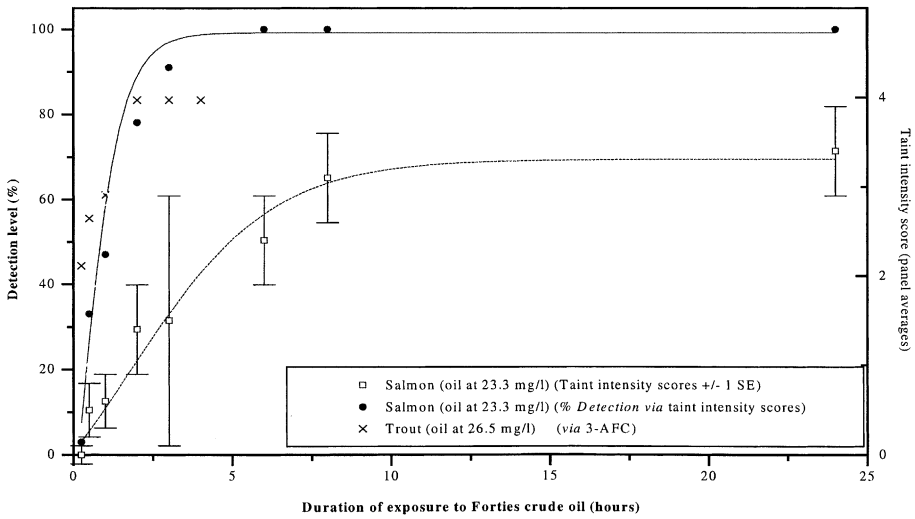

Fig. 2 Detection of taint in salmon and trout exposed to Forties crude oil.

detection in assessments of samples taken at three intervals between 6 and 24 h of exposure.

Two groups of trout exposed to two different oils, at concentrations calculated to give similar tainting capacity (concentration × tainting threshold), produced an unexpected contrast with the threshold measurements. The concentrations were: Forties crude, 31.1 mg/l; medium fuel oil, 111.7 mg/l. These values represent similar multiples of their fish tainting thresholds (respectively, 317 and 337 times). Both regimes resulted in high taint scores but, although exposure to Forties crude oil led to results for the trout that were similar to those for salmon (Table 3), exposure to medium fuel oil produced detection levels of 100% after a considerably shorter duration. The Forties data were also consistent with those from the similar exercise using the 3-AFC procedure, where trout exposed to similar concentrations of the oil for 2, 3, and 4 h resulted in taint detection levels of 83% ('×' in Fig. 2).

High scores after short exposure times could be expected with mussels exposed to Forties crude oil at

Table 3 Panel mean scores for intensity of oil taint induced into trout (*Oncorhynchus mykiss*), salmon (*Salmo salar*), and mussels (*Mytilus edulis*) during exposure to oil

Exposure time (h)	Intensity of taint		Detection rate (%)	Intensity of taint		Detection rate (%)
	Mean score	SE		Mean score	SE	
	Trout Forties crude oil: 31.1 mg/l (+1.6 mg/l NS25) (≡ 317 × threshold for the oil)			Trout Medium fuel oil: 111.7 mg/l (+5.9 mg/l NS25) (≡ 337 × threshold for the oil)		
0.5	1.6	1.3	72	3.1	0.9	100
1.0	1.3	1.2	69	3.2	1.0	100
2.0	1.2	1.0	73	3.7	1.0	100
4.0	2.6	1.2	97	4.2	0.7	100
8.0	3.6	1.2	100	4.0	1.0	100
15.0				4.1	1.0	100
16.0	3.7	1.1	100			
24.0	3.3	1.1	99	4.7	0.5	100
	Salmon Forties crude oil: 23.3 mg/l (+1.2 mg/l NS25) (≡ 214 × threshold for the oil) (≡ 238 × trout threshold)			Mussels Forties crude oil: 25.7 mg/l (+1.4 mg/l NS25) (≡ 796 × threshold for the oil) (≡ 262 × trout threshold)		
0.25	0.0	0.1	3			
0.5	0.4	0.3	33	2.4	0.2	81
1.0	0.6	0.3	47	2.6	0.2	84
2.0	1.4	0.5	78			
3.0	1.5	0.4	91	2.6	0.2	84
6.0	2.4	0.5	100	3.3	0.2	95
8.0	3.1	0.5	100	3.2	0.2	92
24.0	3.4	0.5	100	3.1	0.2	87

approximately 800 times threshold concentration. But the scores should also have quickly approached the maximum of the scale and 100% detection. The relatively low values shown in Table 3 probably reflect the unfamiliarity of the panel to the normal range of mussel flavours.

Loss of taint after transfer of oil-contaminated fish to clean water

Depuration experiments required assessment of intensity of oil taint after subjecting each test species to oil at a selection of different concentrations and periods of exposure, followed by periods of depuration in clean water. Table 4 records all the exposure regimes together with assessment score averages and standard errors. Initial tainting impacts, as shown by the average taint scores at the end of the exposure period (zero depuration time), increased with exposure concentration and duration. Comparing the three oils when applied to trout, persistence of oil taint during depuration in clean water contrasted with the tainting threshold values. Most scores for Forties crude-derived taint had fallen to 0.5 or below within 11 days except for fish exposed for the shortest time, when depuration to this level took almost twice as long. A relatively long period of uncertainty followed before most assessors felt confident that all samples showed no signs of oil taint. Longer periods of depuration were needed following exposure to similar or lower concentrations of the sample of diesel oil, but exposure to a very high concentration of the medium fuel oil for 96 h required a depuration time that was intermediate between the diesel and Forties crude oils.

Patterns of loss of taint were examined by fitting the data to exponential decay algorithms (Table 5). For any one type of oil, depuration time was dependent on the total load (L: exposure concentration $\times$ duration). Data for loss of diesel-derived taint from trout fitted well to a single exponential function, and a log–log plot of decay constant (t) against L showed a near-linear relationship:

$$\log t = 0.23 \log L + 1.1 \quad (r = 0.978).$$

Omitting the least reliable data point, that from the weakest tainting regime (diesel at 0.9 mg/l for 24 h), for which there were few depuration data points, gave:

$$\log t = 0.16 \log L + 1.2 \quad (r = 0.998).$$

Data from the medium fuel and Forties crude oils fitted better to more complex algorithms containing two exponential decay functions, but insufficient data were generated to determine comparable relationships

Table 4 Panel scores for intensity of taint in oil-exposed fish allowed periods of depuration in clean water

Time in clean water (days)	No. of fish/ shellfish	Taint intensity scores	
		Average	SE
Trout + diesel: 21.8 mg/l for 240 h			
0	2	4.5	0.2
4	3	4.8	0.1
7	3	4.6	0.2
11	3	3.9	0.1
16	3	3.6	0.5
21	3	3.3	0.3
25	3	3.2	0.2
30	3	1.4	0.6
35	3	2.7	0.7
40	3	2.1	0.1
45	3	1.5	0.2
50	3	1.5	0.2
56	3	1.3	0.1
60	3	0.7	0.3
65	3	0.9	0.2
70	3	1.3	0.2
75	3	0.7	0.3
80	3	0.1	0.1
88	3	0.4	0.2
100	3	1.1	0.1
110	3	0.3	0.2
120	2	0.0	0.0
Trout + diesel: 8.7 mg/l for 96 h			
0	8	3.6	0.1
10	8	2.7	0.1
31	8	1.3	0.1
52	8	0.7	0.1
67	8	0.4	0.1
81	8	0.1	0.1
94	8	0.0	0.0
105	5	0.0	0.0
Trout + diesel: 8.4 mg/l for 24 h			
0	8	1.9	0.1
27	8	0.6	0.2
45	8	0.3	0.1
59	8	0.2	0.0
73	8	0.0	0.0
87	8	0.1	0.0
101	8	0.0	0.0
Trout + diesel: 0.9 mg/l for 24 h			
0	8	1.6	0.1
18	8	0.4	0.1
31	9	0.0	0.0
54	9	0.0	0.0
Trout + MFO: 111.7 mg/l for 96 h			
0	6	4.8	0.0
6	6	3.8	0.1
13	6	3.2	0.1
20	6	2.3	0.2
42	6	0.2	0.1
52	6	0.4	0.1
66	6	0.1	0.1
80	6	0.0	0.0
102	6	0.0	0.0
Trout + FCO: 22.6 mg/l for 24 h			
0	6	3.0	0.1
3	6	0.9	0.1
6	6	0.2	0.1
10	6	0.7	0.1
24	6	0.2	0.1
38	6	0.1	0.1
59	6	0.0	0.0
87	6	0.0	0.0

(*continued on next page*)

Table 4 (*continued*)

Time in clean water (days)	No. of fish/ shellfish	Taint intensity scores	
		Average	SE
Trout + FCO: 3.0 mg/l for 24 h			
0	6	2.9	0.1
3	6	1.3	0.2
7	6	0.6	0.1
11	6	0.5	0.1
16	6	0.0	0.0
19	6	0.1	0.0
24	6	0.1	0.0
31	6	0.0	0.0
38	6	0.0	0.0
45	6	0.0	0.0
91	6	0.0	0.0
Trout + FCO: 10.7 mg/l for <5 h			
0	6	3.7	0.1
4	6	3.4	0.1
9	6	1.7	0.1
16	6	0.9	0.2
23	6	0.1	0.0
37	6	0.5	0.1
51	6	0.1	0.1
58	6	0.2	0.1
100	6	0.0	0.0
Salmon + FCO: 30.0 mg/l for 240 h			
0	6	4.2	0.2
2	6	3.8	0.1
4	6	2.9	0.1
8	6	2.4	0.1
12	6	2.3	0.1
17	6	1.8	0.2
27	6	0.7	0.2
35	6	0.5	0.1
45	6	0.5	0.1
52	6	0.1	0.0
59	6	0.0	0.0
Mussels + FCO: 25.7 mg/l for 240 h			
0	56	4.4	0.2
4	54	2.6	0.2
8	55	2.4	0.1
15	53	2.0	0.2
25	54	1.5	0.2
35	53	1.2	0.1
45	43	0.8	0.3
65	53	0.8	0.0
Crabs + FCO: 19.8 mg/l for 96 h			
White (claw and leg) meat			
0	5	0.2	0.1
43	5	0.1	0.0
Brown (hepatopancreas) meat			
0	5	2.1	0.1
43	5	0.1	0.1

MFO = medium fuel oil; FCO = Forties crude oil.

between oil loading and subsequent rates of loss of taint.

The depuration data can be used simply as positive or negative indicators of detection in the same manner as the earlier treatment of uptake data. All the results obtained in this manner for trout exposed to diesel are presented in Fig. 3, and all three oils are compared in Fig. 4. The principal feature to note is how the initial panel response to diesel-derived taint increased with concentration and duration of exposure, to the point where 100% detection extended through $3\frac{1}{2}$ weeks of depuration. For the three greatest exposures to diesel, once the detection levels (D%) started to fall below maximum, the rates at which they fell were very similar (0.90–0.97 D%/day). Again, comparisons of the three oils (Fig. 4) contrasted with the threshold results. A shorter period of maximum detection was obtained with trout exposed to a much greater concentration of medium fuel oil (of similar tainting threshold as the diesel), and there was little prolongation of maximum D% with increased loadings of Forties crude oil, the strongest tainter of the oils tested.

Average scores and standard errors for Forties crude-derived oil taints in salmon, mussels, and crabs are shown in Table 4, and detection rates in Fig. 5. Forties crude oil-derived taint was lost from salmon at a faster rate than taint derived from a similar exposure of trout to diesel. Initial intensity scores for salmon exposed to Forties crude oil for 10 days were correspondingly higher than for the 1 day exposure applied to trout, and there was some extension of a near-maximum detection rate. Otherwise, there was little difference in the patterns of loss of taint from these salmonids. The long exposure applied to the crabs showed that the brown meat was vulnerable to tainting by oils but, again, there was little effect on the white meat. The taint effectively disappeared within 6 weeks, the only sampling interval employed for crabs. Oil taint appeared to persist longer in mussels than in the other species but, although the experiment was concluded before an asymptote could be confidently established, there remains the suspicion that a significant contribution arose from the assessors' lack of experience with this substrate.

Depuration of hydrocarbons from oil-contaminated salmon

n-Alkanes. Concentrations of *n*-alkanes (nC_{12} to nC_{33}) in the samples of Forties crude oil, diesel oil, and medium fuel oil were 49, 126, and 17 mg/g respectively. Concentrations of individual *n*-alkanes in the Forties crude oil declined progressively from nC_{12} (~5 mg/g) to nC_{33} (~0.5 mg/g). The distribution in diesel oil showed a peak at nC_{14} with a progressive decline either side; the pattern for the medium fuel oil was more irregular between nC_{12} and nC_{21}. The salmon feed pellets contained *n*-alkanes at total concentrations that were much lower than for the hydrocarbon oils. In addition, the distribution in the salmon food was irregular, and only nC_{15}, nC_{17}, nC_{24}, nC_{26}, and nC_{28} were present at concentrations above 1 μg/g.

Table 5 Constants calculated for the exponential loss of taint from fish subjected to different exposure regimes

Fish/Shellfish species	Oil	Exposure concentration (mg/l)	Exposure time (hours)	Decay constants		Amplitude	
				t_1 *	t_2 **	A_1 *	A_2 **
Trout	Diesel	21.8	240	41.01		5.16	
Trout	Diesel	8.7	96	29.50		3.67	
Trout	Diesel	8.4	24	23.91		1.90	
Trout	Diesel	0.9	24	11.56		1.61	
Trout	MFO	111.7	96	21.54		5.01	
Trout	FCO	22.6	24	1.36	17.62	2.27	0.71
Trout	FCO	3.0	24	3.92	13.07	2.54	0.35
Trout	FCO	10.7	<5	12.17	94.12	3.76	0.17
Salmon	FCO	30.0	240	18.01	16.36	2.69	1.33
Mussels	FCO	25.7	240	0.31	25.22	1.26	2.58
Salmon	FCO	30.0	240				
	PAH			0.46	8.56	748	2878
	Naphthalenes			4.25	13.75	2.88	981
	Phenanthrenes			4.33	53.20	57	6

Derived by fitting of exponential decay functions, given below, to data for loss of taint and petrogenic hydrocarbons from the muscle of fish and shellfish after exposures to petroleum products:

$y = y_0 + A_1 e^{-(x-x_0)/t_1} \ldots * \ldots$ a single exponential decay function

$y = y_0 + A_1 e^{-(x-x_0)/t_1} + A_2 e^{-(x-x_0)/t_2} \ldots ** \ldots$ a double exponential decay function

where: y = panel mean score for intensity of taint; y_0 = asymptote; x = depuration time (days); x_0 = start of depuration (=0 days); A = amplitude = y(max) − y(asymptote); t_1, t_2 = relative rate of decay constants.

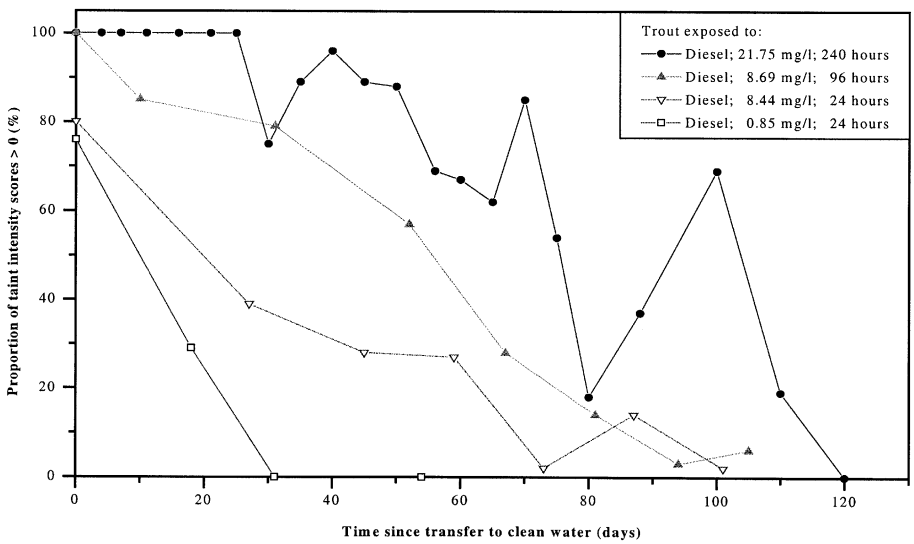

Fig. 3 Loss of oil taint from trout transferred to clean water following exposure to different amounts of diesel fuel.

n-Alkanes present in the flesh of salmon that were used as controls showed an irregular distribution with nC_{15} and nC_{17} the main homologues, each at >0.1 μg/g in a total *n*-alkane concentration of ~0.8 μg/g, while the $nC_{24,26,28}$ homologues were not significant components.

Concentrations of pristane and, particularly, phytane were much lower in the feed than in the hydrocarbon oils, and the high ratio of pristane/phytane in the fish flesh was the same as in the feed. The amounts of pristane and phytane in the flesh appeared to be unaffected by exposure to the Forties crude oil.

Apart from nC_{15} and nC_{17}, concentrations of individual *n*-alkane homologues up to nC_{23} were slightly higher in the salmon exposed to Forties crude oil than in the control fish. But total concentrations of *n*-alkanes averaged only 555 (SE = 150) ng/g (wet weight) immediately following exposure to the oil compared with 768 (SE = 232) ng/g in the control samples. Distributions of individual homologues in the oil-exposed fish largely

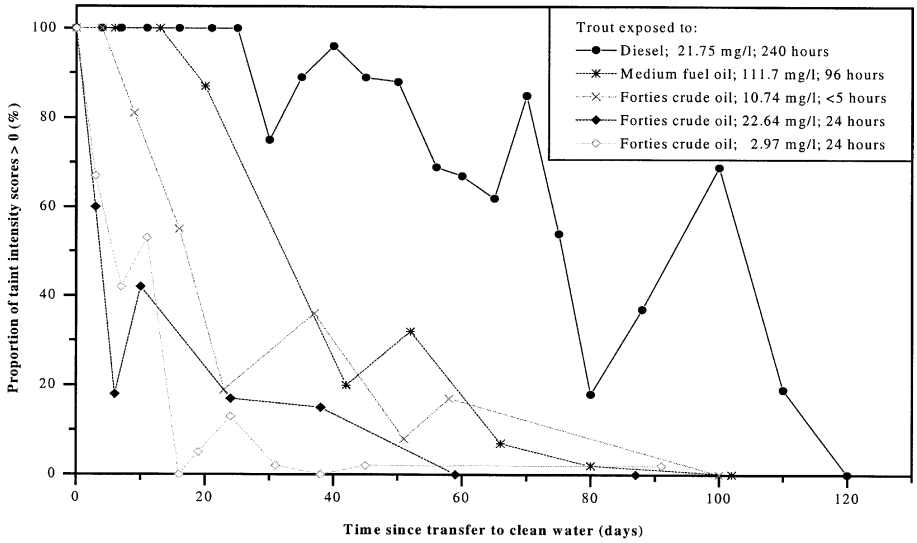

Fig. 4 Loss of oil taint from trout transferred to clean water following exposure to different fuel oils.

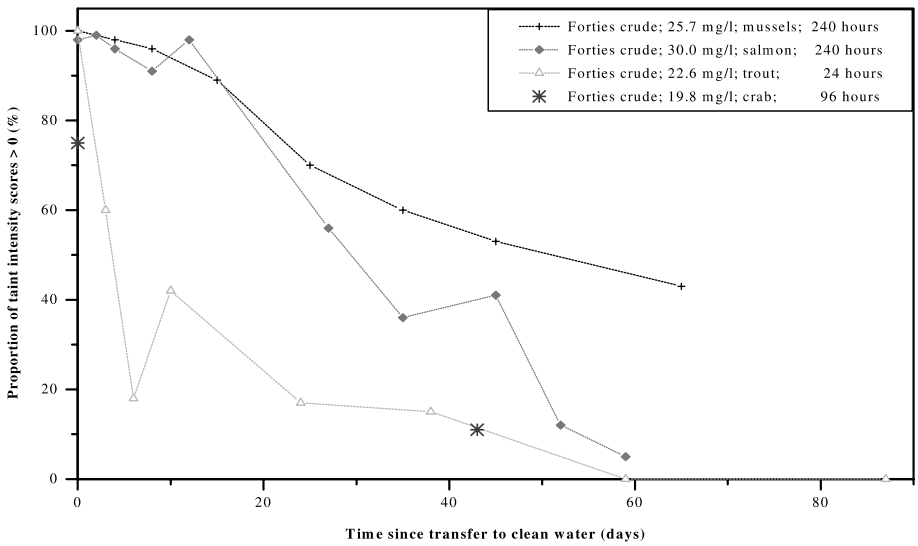

Fig. 5 Loss of oil taint from mussels, crabs, salmon, and trout following different exposures to Forties crude oil.

reverted to the pattern seen in control fish within 2 days of transfer to clean water. Average concentrations during the subsequent 59 days varied between 2216 (SE = 1660) ng/g (due to a short period of abnormally high concentrations of nC_{29}, nC_{31}, and nC_{33} alkanes) and 358 (SE = 61) ng/g. Hence, the fish had established an equilibrium state before the deliberate exposure to oil, and the Forties crude oil contributed little extra that could be accumulated.

Polycyclic aromatic hydrocarbons (PAHs). Total concentrations (sum of 2- to 6-ring parent and branched PAHs) of PAHs in the salmon feed and the three oils were: feed, 0.2 μg/g; diesel, 5603 μg/g; medium fuel oil 6132 μg/g; Forties crude oil, 19,260 μg/g. The muscle of salmon control samples contained 0.02 μg/g PAH (average of all the control samples) with average values for total naphthalenes equivalent to 82% of the total PAH content (compared with 43% in the salmon food and 70% in Forties crude oil); phenanthrenes, 13% (29% and 18%); dibenzothiophenes (DBTs) 1% (22% and 7%); fluoranthene and pyrenes, 2% (5% and 4%); and traces of benzophenanthrenes and benzofluoranthenes which were detected in the feed at 1.7% and 0.4%, respectively, and in the Forties crude oil at 1% and 0.5%, respectively.

The same 2- and 3-ring compounds most abundant in the feed, oils, and fish muscle before the salmon were exposed to Forties crude oil were similarly dominant in the PAH composition of salmon muscle

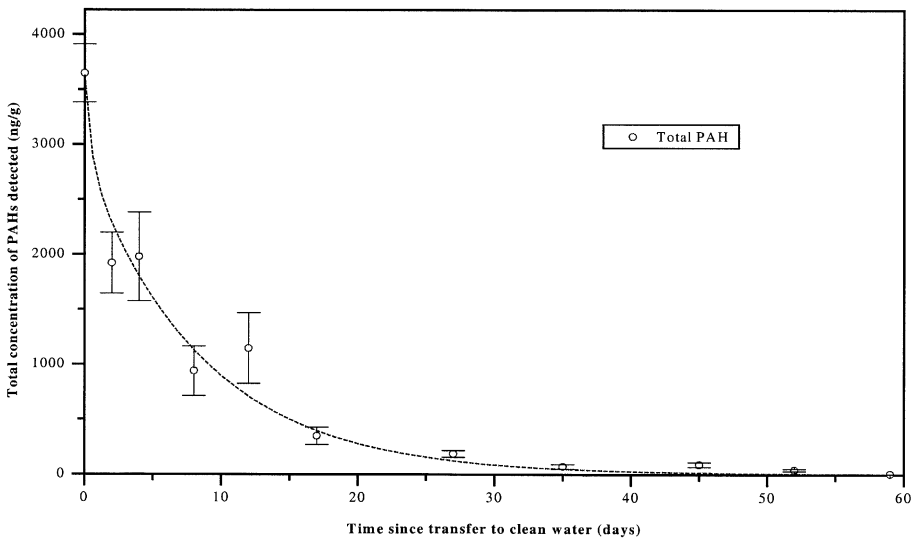

Fig. 6 Loss of total (2- to 6-ring parent and branched) polycyclic aromatic hydrocarbons (PAH ± 1 SE) from skeletal muscle of salmon transferred to clean water following exposure to Forties crude oil at 30.0 mg/l.

after exposure to the oil. A problem with the HPLC separation column that affected retention of DBTs, and was discovered after most of the analyses had been completed, led to very erratic results for this group. The highest concentrations of DBTs found in individual fish were 393 and 164 ng/g, after depuration for 12 and 17 days, respectively. In both instances, DBT comprised >75% of this group, with 15% and 13% of the C_1, and 7% and 12% of the C_2 homologues, respectively. Thus, despite the analytical problem, it is clear that DBTs transferred to the fish muscle. If, as suspected, these sulphur-containing compounds do contribute to oily taint, they remained long enough to have contributed to the pattern of slow decline.

Throughout the study, the general pattern of distribution showed a predominance of 2-methyl and 1-methyl-naphthalenes, and the C_2 homologues, with smaller contributions from naphthalene and the C_3 homologue. Figure 6 shows the exponential pattern of change in total PAH, which consisted almost entirely (90–99%) of naphthalenes during the first 35 days of depuration. Thereafter, the proportion of PAHs that comprised naphthalenes decreased to 81% after 45 days and 75% after 52 days. At the end of the depuration period (59 days) the naphthalenes again comprised greater than 90% of the PAHs but the total PAH concentration was only 15.9 ng/g wet weight of flesh (Fig. 6). The fluoranthene/pyrene group showed an almost identical pattern at total concentrations that were approximately $\frac{1}{60}$th of the naphthalenes. As noted earlier for the taint intensity data for depuration of Forties crude oil-derived taint, a 2-exponent curve gave the best fits to the phenanthrenes, naphthalenes, and total PAH depuration data.

Discussion

Uptake of tainting components into the edible flesh

Movement of contaminants into the flesh of fish requires that they are solubilised in water so that they may readily pass via the gills into the bloodstream, thence to circulate throughout the tissues. Neff *et al.* (1976) found that concentrations of oil components in muscle of fish exposed to water-solubilised fractions (WSF) of fuel oil increased rapidly, reaching a maximum within approximately 1 h. Continued exposure led to accumulation of these lipophilic substances in lipid-rich tissues such as the liver. Vapour pressures of oil-soluble components will be higher in an aqueous system than in lipids. Consequently, despite variable amounts of lipid in fish muscle, the effect on taste after short exposures to oil is likely to be governed by lower concentrations of tainting components present in the aqueous phase. Thus, fish tainting threshold will, normally, be a function of the odour threshold for the substance dissolved in water, and the variable degree of masking caused by the different intrinsic flavours, and muscle lipid contents, of the test species.

The absence of an apparent dispersant effect appears to contradict other published work, such as that of Martinsen *et al.* (1992), but the difference is almost certainly due to the different exposure systems employed. The degree of exposure of fish to oil is dependent upon the solubilisation of oil components which, in turn, depends upon the amount of energy in the system that is available for mixing the oil and water. Dispersants cannot change the ultimate solubility of oil components; their action is to increase the rate of dispersion and the speed with which maximum

solubility is approached. Where oil is floated onto the surface of slowly moving water, the amount of mixing, and subsequent tainting of fish in that water, will be highly variable, and such a system will be difficult to replicate exactly. The mixing will largely depend upon the limited turbulence at the surface, increasing with the rate of flow and aeration, and the presence of a dispersant could reasonably be expected to exert a measurable influence. The results in our study indicate that, even without added dispersant, oil was mixed with the inflowing water with sufficient energy to have achieved near-maximum solubilisation of the components that cause the oil taint.

The negligible extent of retention of aliphatic hydrocarbons beyond the existing background levels in the flesh of salmon is consistent with the observations of Hardy *et al.* (1974), who found high concentrations of *n*-alkanes in liver, but not in muscle, of cod that had been fed on a diet containing Kuwait crude oil.

Tainting thresholds for oil products in fish and shellfish

Detection levels increased rapidly with duration of exposure. Exposure loadings were relatively high, but the results are similar to the oil uptake results of Neff *et al.* (1976) and support the 24 h exposure period used in the ECETOC/GESAMP tainting threshold test.

The three oils showed distinctly different sensory properties. The samples of diesel and medium fuel oil had similar fish tainting thresholds that were significantly higher than the Forties crude oil, but the steeper curve for diesel (Fig. 1) indicates a narrower distribution of sensitivities to that taste than to the other two oils. In an earlier study, however, the same research group (Davis *et al.*, 1992) obtained a fish tainting threshold of 0.082 mg/l for a different sample of diesel fuel, i.e. almost the same as determined here for the Forties crude oil. The chemical composition of crude oils from different sources can differ considerably (GESAMP, 1993), and so it is to be expected that thresholds for an oil product such as diesel should have at least as great a range as those observed for the different types of product. The entire span of tainting thresholds for the fin-fish, from the lowest confidence boundary of the most powerful tainter to the highest boundary for the weakest tainter, was, however, contained within one order of magnitude.

The edible portion of mussels included the entire contents of the shell. Thus, with mussels and the brown meat of crabs, assessors may have been responding to relatively high concentrations of oil components accumulated within fatty tissues of digestive organs, which are not usually regarded as part of the edible portion of fin-fish. To a considerable extent, however, the crabs proved resistant to the induction of taint. Howgate *et al.* (1977) found that oily taints were readily induced into other crustaceans, scampi (*Nephrops norvegicus*) and shrimps, placed on an oil-contaminated sediment. But Kneiper and Culley (1975) found that with two Louisiana crude oils, concentrations of 49–160 mg/l were needed to induce oily taint in two species of shrimp, and 620–1250 mg/l for white meat of crab (*Callinectes sapidus*). These are relatively high concentrations even after allowing for differences which will arise from a different methodology, principally that the oil was floated onto the surface of the water. If low vapour pressures over lipid rich tissue was sufficient to inhibit detection of taint in the crab brown meat, then similar exposures could be expected to have had a similar effect on mussels. Ingestion of oil particles by filter-feeding molluscs has been strongly implicated as a major source of PAH (Topping *et al.*, 1997), and could account for the lower threshold for oil taint obtained with mussels.

The ECETOC/GESAMP procedure recommends rainbow trout, or similar alternatives, as a general test organism because of worldwide availability, adaptability to fresh or sea water, and fat contents that are normally intermediate in the range. Such a choice is appropriate for the purpose of generating comparable data on a variety of test substances. But, as the results for crabs and mussels show, threshold values for oil taint in some species are influenced by more than a masking effect of intrinsic flavours of white muscle on the taste of the analyte. Where the interest is more concerned with a specific fishery, trials should use the relevant species, with appropriate regard to any seasonal effects and post-harvest treatments.

Experimental systems for exposure of aquatic organisms to fuel oils

The ECETOC (1987) method for the evaluation of fish tainting was intended to standardise the generation of data on the potential of industrial chemicals to cause fish to become tainted. The method was not designed specifically to accommodate fuel oils. The general suitability of the method was demonstrated in a small collaborative trial (ECETOC, 1987; Poels *et al.*, 1988) applied to four chemicals selected to provide a range of octanol/water partition coefficients, toxicities, and solubilities in water. But the least soluble of the substances tested had a saturation solubility of approximately 100 mg/l, which is greater than for many of the components of crude oil. There is some guidance on dealing with substances of low solubility (<10 mg/l), which is practical only for testing in static tanks, and mixtures are not included.

Of the little that has been published on the potential of crude oils or products to cause taint in fish, most

refer to aqueous extracts of oil as the test material. For example, Ernst *et al.* (1989) exposed fish to WSF for 24 h to compare the tainting impacts of four crude oils. In triangle tests on the fish, all the oils were found to cause taint but at concentrations of total hydrocarbons in the exposure water of approximately one order of magnitude higher than results obtained here with a whole-oil exposure system.

Very low solubilities present difficulties to design, implementation, and interpretation of laboratory studies of environmental impacts of fuel oils. Laboratory experiments address small, specific issues of the consequences of a spill, and their relevance depends upon the clarity of the (inevitably limited) relationship with real spills. There are unavoidable problems of scale as complex changes take place, e.g. as large spills of oil spread through a body of water, and no one system can satisfy all requirements. The crux of the problem is that solubilities of individual components of a fuel oil vary considerably, and the composition of aqueous extracts depends upon the extraction ratio. With correction of an experimental observation for the dilution factor, very different results will be produced from essentially the same experiment conducted with different extraction ratios. Nevertheless, many toxicological as well as tainting studies have used aqueous extracts of oils as the source, and attempts have been made to standardise both the water/oil ratios and duration of the extraction procedure. Even so, the same difficulty limits application of results to spills, where the relative volumes of water are so much greater. Although no single system can overcome all the limitations, whole-oil experimental systems should correspond more reliably to real oil spills, and the threshold results presented here confirm the value of whole oil injection into continuous-flow exposure tanks as the preferred test protocol.

Depuration

Oil components rapidly accumulate in fish tissues but depurate at a considerably slower rate. Naphthalenes are one group of oil components which have distinct, powerful odours and which, almost certainly, will make a significant, but not necessarily dominant, contribution to oil taints in fish. Neff *et al.* (1976) found that naphthalenes which had accumulated in fish exposed to a WSF of a No. 2 fuel oil at ~2 mg/l for 2 h returned to background levels within 10 days. This is consistent with taint depuration times reported for fish experimentally exposed to oils, for periods of 1–3 days, via WSF (Ernst *et al.*, 1987; Lockhart & Danell, 1992; Heras *et al.*, 1993).

After exposure to whole oil in the system used here, depuration times varied with the type of oil and with the total exposure level. With higher loadings and longer exposure periods, greater amounts of oil components will have accumulated, and taken correspondingly longer to clear. After a 10 day exposure of salmon to Forties crude oil, depuration took several weeks, with naphthalenes and taint both persisting for 50–60 days. This might be a largely fortuitous association, but there is a notable parallel with the observations of Whittle *et al.* (1997a,b) on samples of salmon affected by a different oil, Gullfaks crude, after the grounding of the tanker *Braer*. They found that the proportion of C1 substituted naphthalenes closely matched the proportion of assessors able to detect oily taint. Although proportions of C2, C3, and C4 substituted naphthalenes differed between the two studies, both showed a similar relationship between C1 naphthalenes and rates of detection of taint (Fig. 7).

The appreciably longer depuration time that was needed for taint derived from exposure to diesel indicates that, even if such an association presented a fair reflection of the significance of naphthalenes, some oils present additional problems. Scrutiny of the hydrocarbon composition of the three oils, and the rates of depuration of taint from fish exposed to them, sheds little additional light on the probable main causes of oil taint. Most studies of the causes of oil taint, as here, have concentrated on a limited range of hydrocarbons. As Malins and Hodgins (1981) noted in a wider context, most work has been restricted to analytical procedures designed primarily as measures of petroleum contamination. Many more compounds escape detection.

Loss of Forties-derived taint from mussels was a slower process than from fin-fish, complicated by a greater degree of assessor uncertainty, but faster than has been observed for some mussels affected by oil spills. Some stocks affected by oil from the tanker *Braer* were found to be tainted 18 months after the incident (Topping *et al.*, 1997). There is conflicting evidence as to whether PAHs in filter-feeding bivalves are derived principally from the dissolved phase or from ingestion as particulate-adsorbed oil (Naes *et al.*, 1995). Kaag *et al.* (1997) reported that uptake of contaminants by mussels appeared to be independent of concentrations in the sediment. That, seemingly perverse, observation was based on a relatively static experimental system. It is, however, consistent with the observation of a tidal-linked pulse of hydrocarbon contamination in an area where oysters were still affected 7 years after the *Amoco Cadiz* oil spill in 1978 (Berthou *et al.*, 1987). They suggested that oil buried in sediments is released by turbulent weather. Similarly, Webster *et al.* (1997), observing a seasonal variation in the PAH concentration of mussels, attributed increasing concentrations in winter to

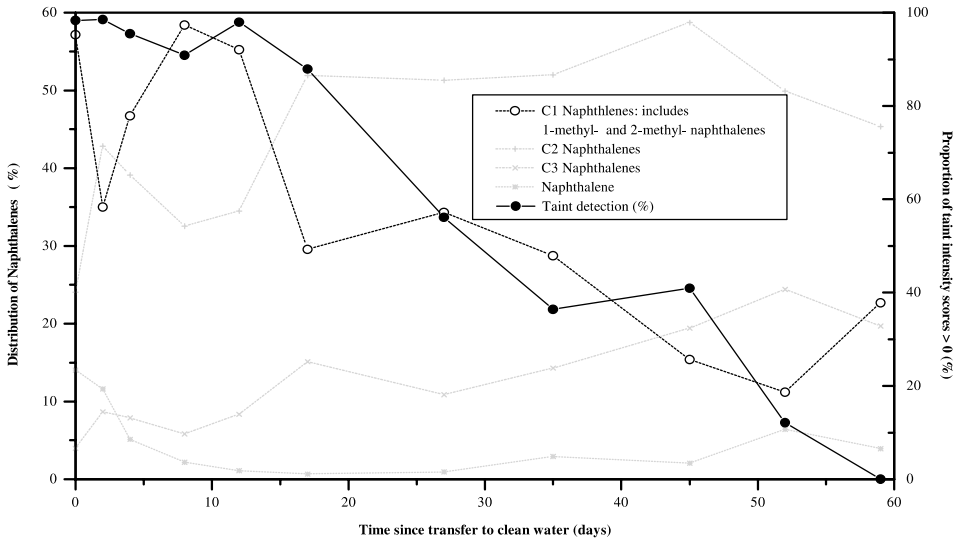

Fig. 7 Changes in proportions of naphthalenes and detections of taint in the flesh of salmon transferred to clean water following exposure to Forties crude oil at 30.0 mg/l.

increased lipid content of the mussels and to storms causing exposure to resuspended sediments. Declining concentrations in spring were associated with mobilisation of lipids during gametogenesis.

The degree of resistance to induction of taint shown by crabs, and the rapid loss after taint was induced, has some support from other published work. Greater concentrations of oil components have been found in body meats of crustaceans than in white meats (Uthe & Musial, 1986; Melzian & Lake, 1986/7; Hale, 1988; Williams *et al.*, 1989; Hellou *et al.*, 1994). With prolonged exposure, continued uptake to the lipid-rich tissues of the hepatopancreas is to be expected. But when Kneiper and Culley (1975) examined different portions from an oil-tainted crab, they observed differences in the intensity of taint in muscle from anterior and posterior segments and appendages. Such differences might arise from the open vascular circulation of crabs with, compared to other animals, a relatively restricted blood flow to muscles of locomotion. Another powerful influence is the induction of xenobiotic-metabolising enzymes which catalyse the transformation of lipophilic contaminants into more soluble compounds that are more readily excreted. Induction of enzymes requires exposure above some minimum effective dose (Binder *et al.*, 1984), though this is unlikely to account for the inversion of depuration rates observed with different loadings of Forties crude oil (Table 4). There are, also, considerable differences within and between different species, in the capacity to metabolise contaminants (Mothershead *et al.*, 1991), but little attention has been paid to the activity of these systems in crustacean species.

Although the scale of oil spills into fresh waters is relatively small, many do occur and have similar consequences to spills at sea, including the appearance of taints in wild and farmed fish. Uptake of petroleum compounds into the fish may be different, being affected by solubility of the compound (lower in sea water than fresh water) and drinking rates of the fish (higher in marine fish). The toxicity of petroleum compounds is known to be influenced by salinity (Thomas & Rice, 1986), but there are no specific comparisons of induction and loss of taint. In experiments using radioisotope-labelled hydrocarbons in fish food, Thomas and Rice (1986) showed much greater amounts of toluene and naphthalene transferring to the muscle of fish in fresh water than in sea water. This limited evidence suggests that a spill in fresh water presents the greater initial risk of tainting. Conversely, as higher concentrations of labelled metabolites appeared in the freshwater fish, depuration might proceed at a faster rate.

Criteria for classifying fish of uncertain origin as not tainted

To determine if fish are tainted, criteria need to be established for the interpretation of analytical data. This is as true of chemical as it is of sensory analyses. Evidence from chemical analyses may be a useful adjunct but, as can be seen from the analyses of depurating salmon, suspected contributors to taint were present in the control samples. The primary judgement rests on sensory assessments which have varying degrees of positive bias (Howgate, 1999). In this work, assessors were allowed to use half-mark intervals for intensity of taint. Hence, the lowest score, other than zero, was 0.5. With a positive bias present in the sys-

tem simply by virtue of presenting assessors with the question, some threshold average score needs to be exceeded for fish to be declared tainted. This is a matter of judgement as there are no absolute criteria. Where some process is being examined, as in the monitoring of farmed fish after an oil spill, then the general pattern of change enables some reasonable attempt at prediction and choice of safety margin. Assessment of isolated batches inevitably requires that greater regard is paid to the differences within a panel and the distribution of scores from individual assessors.

Judgements based on average scores were avoided during monitoring of the *Braer* and *Sea Empress* oil spills, in favour of the detection levels that any score above zero indicated (Topping *et al.*, 1997). This does not avoid inherent bias or the need to establish criteria for their interpretation, but makes use of the variability within a panel. The same 50% level used in measurements of tainting thresholds was too high for use as the only criterion because the products offered for sale would have a taint that was detectable by half the population. Some arbitrarily selected lower level was needed. A three-tier system was chosen whereby a batch of fish having 50% detection was regarded as definitely tainted; between 20% and 50% detection, fish were suspected as tainted; and batches showing less than 20% detection were deemed to be clear. The 20% level accommodated the area of uncertainty due to inherent bias and equates to an intensity score of ~0.5.

Applying the 20% detection criterion to all the data in this study of experimentally exposed depurated fish, the longest depuration time was approximately 114 days for trout exposed to diesel at 21.8 mg/l for 10 days. That exposure level is greater than the concentrations as measured in water at fish farms close to the spill of Gullfaks crude oil shortly after the grounding of the tanker *Braer*. Unfortunately there are no other data on the tainting properties of that oil, or details from the site, to explain the much longer persistence of taint, more than 20 weeks in some instances (Ritchie & O'Sullivan, 1994). As most of the fish (farmed salmon) were free of taint much sooner than that, it is probable that there remained some source of continuing contamination.

Summary and Conclusions

Some oily taint was detected in fin-fish within 30 min of transfer to sea water containing crude oil at between 20 and 31 mg/l; a strong taint was evident within 3–4 h. For the products tested, the range of thresholds of detection of oil taint in fin-fish was similar to the difference between two samples of diesel; all fell within one order of magnitude, from 0.08 to 0.38 mg/l, though the range of test materials was necessarily limited. In a high energy mixing system, the presence of a dispersant had no effect on the fish tainting threshold value. Tainting thresholds for Forties crude oil applied to two salmonid species were close, but very different from the thresholds obtained when the same oil was applied to two types of shellfish. Limited data suggest that the tainting threshold for oil in mussels was almost one order of magnitude lower than for the fin-fish, but crabs displayed some degree of resistance to becoming tainted by oil. Tainting thresholds for Forties crude oil in crab meats, both the white and brown, were higher than 7 mg/l.

When oil-contaminated fish were transferred to clean water, intensities of oil taint fell exponentially for all intensities, but persisted for considerably longer than they took to induce. Using simple proportions of positive detections of taint, detection levels at, or close to, 100% persisted longer as concentration and duration of the initial exposure treatment increased.

Detection levels then declined at a rate that, for diesel, was reasonably consistent. Medium fuel- and Forties crude oil-induced taints were lost at faster rates than the diesel. Forties crude, the most powerful tainter of the three samples, had the least persistent taint but remained longer in mussels than in fin-fish. When oil taint was induced in crabs by a prolonged exposure to Forties crude oil similar to that applied to the other species, the brown meat was the most tainted; and that taint was lost at least as quickly as from the fin-fish.

Measurement of petroleum hydrocarbons in tainted salmon confirmed that naphthalenes made the greatest contribution to the PAH fraction. This pattern was maintained during depuration in clean water. Having strong, characteristic odours, naphthalenes will undoubtedly contribute to oil taints, but their impact relative to other components remains unknown. Among the individual naphthalenes, an earlier observation on the relationship between levels of detection of taint and the amounts of methyl naphthalenes relative to the total was seen to be repeated.

Acknowledgements—This work was funded by the Marine Pollution Control Unit of the Department of the Environment, Transport and the Regions' Maritime and Coastguard Agency. The authors wish to express their gratitude to all those members of staff of the CSL Food Science Laboratory, Torry (now closed), in Aberdeen whose voluntary efforts as members of the sensory panels was crucial to the conduct of this work. For those most involved, Mr. R.S. Anderson, Mr. N. Brown, Mrs. E. Campbell, Mrs. A.E. Craig, Mrs. P. Cruickshank, Mr. E.J. Dalgarno, Dr. E.T. Griffiths, Mr. J. McDermott, Mr. B. McGregor, Miss S. Miller, Mrs. J.A. Morrison, Dr. P. Reece, and Mrs. V.J. Russell, the requirements of this experimental study added to the considerable burden made by the *Braer* and *Sea Empress* monitoring, and other work. Thanks are also due to Mr. P.F. Howgate and Dr. K.J. Whittle (formerly FSL, Torry) and Dr. A.W. MacRae (School of Psychology, University of Birmingham) for helpful contributions in planning and during the course of the project.

References

Berthou, F., Balouet, G., Bodennec, G., Marchand, M., 1987. The occurrence of hydrocarbons and histopathological abnormalities in oysters for seven years following the wreck of the *Amoco Cadiz* in Brittany (France). Marine Environmental Research 23, 103–133.

Binder, R.L., Melancon, M.J., Lech, J.J., 1984. Factors influencing the persistence and metabolism of chemicals in fish. Drug Metabolism Reviews 15, 697–724.

Bligh, E.G., Dyer, W.J., 1959. A rapid method of total lipid extraction and purification. Canadian Journal of Biochemistry and Physiology 37 (8), 911–917.

Davis, H.K., Geelhoed, E.N., MacRae, A.W., Howgate, P., 1992. Sensory analysis of trout tainted by diesel fuel in ambient water. Water Science and Technology 25 (2), 11–18.

ECETOC, 1987. Evaluation of fish tainting. Technical Report No. 25, European Chemical Industry Ecology and Toxicology Centre, Brussels, Belgium.

Ernst, R.J., Ratnayake, W.M.N., Farquharson, T.E., Ackman, R.J., Tidmarsh, W.G., 1987. Tainting of fin-fish by petroleum hydrocarbons. Environmental Studies Research Funds Report No. 080, Ottawa, Canada.

Ernst, R.J., Ratnayake, W.M.N., Farquharson, T.E., Ackman, R.J., Tidmarsh, W.G., Carter, J.A., 1989. Tainting of Atlantic cod (*Gadus morhua*) by petroleum hydrocarbons. In: Engelhardt, A.H., Ray, J.P., Gillam, A.H. (Eds.), Drilling Wastes. Elsevier Applied Science, Sussex, England, pp. 827–839.

GESAMP, 1989. The evaluation of the hazards of harmful substances carried by ships: revision of GESAMP Reports and Studies No. 17. Reports and Studies No. 35, IMO/FAO/UNESCO/WMO/IAEA/UN/UNEP Joint Group of Experts on the Scientific Aspects of Marine Pollution, International Maritime Organisation, London.

GESAMP, 1993. Impact of oil and related chemicals and wastes on the marine environment. Reports and Studies No. 50, IMO/FAO/UNESCO/WMO/IAEA/UN/UNEP Joint Group of Experts on the Scientific Aspects of Marine Pollution, International Maritime Organisation, London.

Hale, R.C., 1988. Disposition of polycyclic aromatic compounds in blue crabs, *Callinectes sapidus*, from the southern Chesapeake bay. Estuaries 11 (4), 255–263.

Hardy, R., Mackie, P.R., Whittle, K.J., McIntyre, A.D., 1974. Discrimination in the assimilation of *n*-alkanes in fish. Nature 252, 577–578.

Hellou, J., Upshall, C., Taylor, D., O'Keefe, P., O'Malley, V., Abrajno, T., 1994. Unsaturated hydrocarbons in muscle and hepatopancreas of two crab species, *Chionoecetes opilio* and *Hyas coarctatus*. Marine Pollution Bulletin 28, 482–488.

Heras, H., Zhou, S., Ackman, R.G., 1993. Uptake and depuration of petroleum hydrocarbons by Atlantic salmon: effect of different lipid levels. In: Proceedings of the 16th Arctic and Marine Oil Spill Program Technical Seminar, Calgary, Alta., June 7–9, 1993, pp. 343–351.

Howgate, P., 1999. Tainting of food by chemical contaminants. In: Moffat, C.F., Whittle, K.J. (Eds.), Environmental Contaminants in Food. Sheffield Academic Press, Sheffield, UK, pp. 430–470.

Howgate, P., Mackie, P.R., Whittle, K.J., Farmer, J., McIntyre, A.D., Eleftheriou, A., 1977. Petroleum tainting in fish. Rapports et Procès-verbaux des Réunions—Conseil permanent international pour l'Exploration de la Mer 171, 143–146.

Kaag, N.H.B.M., Foekema, E.M., Schloten, M.C.Th., van Strallen, N.M., 1997. Comparisons of contaminant accumulation in three species of marine invertebrates with different feeding habits. Environmental Toxicology and Chemistry 16 (5), 837–842.

Kneiper, L.H., Culley, D.D., 1975. The effects of crude oil on the palatability of marine crustaceans. The Progressive Fish Culturalist 37 (1), 9–14.

Lockhart, W.L., Danell, R.W., 1992. Field and experimental tainting of arctic freshwater fish by crude and refined petroleum products. In: Proceedings of the 15th Arctic and Marine Oil Spill Program Technical Seminar, Edmonton, Canada, June 10–12, 1992, pp. 763–771.

Malins, D.C., Hodgins, H.O., 1981. Petroleum and marine fishes: a review of uptake, disposition, and effects. Environmental Science and Technology 15 (11), 1272–1280.

Martinsen, C., Lauby, B., Nevissi, A., Brannon, E., 1992. The influence of crude oil and dispersant on the sensory characteristics of steelhead (*Oncorhynchus mykiss*) in marine waters. Journal of Aquatic Food Product Technology 1 (1), 37–51.

Melzian, B.D., Lake, J., 1986/7. Accumulation and retention of No. 2 fuel oil compounds in the blue crab, *Callinectes sapidus* Rathbun. Oil and Chemical Pollution 3, 367–399.

Moffat, C.F., McIntosh, A.D., Webster, L., Shepherd, N.J., Dalgarno, E.J., Brown, N.A., Moore, D.C., 1998. Determination and environmental assessment of hydrocarbons in fish, shellfish and sediments following an oil spill at the Captain Field. Fisheries Research Services Report No. 9/98.

Mothershead, R.F., Hale, R.C., Greaves, J., 1991. Xenobiotic compounds in blue crabs from a highly contaminated urban subestuary. Environmental Toxicology and Chemistry 10, 1341–1349.

Naes, K., Bakke, T., Konieczny, R., 1995. Mobilization of PAH from polluted seabed and uptake in the blue mussel (*Mytilus edulis* L.). Marine and Freshwater Research 46, 275–285.

Neff, J.M., Dixit, D., Anderson, J.W., 1976. Accumulation and release of petroleum-derived aromatic hydrocarbons by four species of marine animals. Marine Biology 38, 279–289.

Persson, P.-E., 1984. Uptake and release of environmentally occurring odorous compounds by fish. Water Research 18 (10), 1263–1271.

Poels, C.L.M., Fischer, R., Fukawa, K., Howgate, P., Maddock, B.G., Persoone, G., Stephenson, R.R., Bontinck, W.J., 1988. Establishment of a test guideline for the evaluation of fish tainting. Chemosphere 17 (4), 751–765.

Ritchie, W., O'Sullivan, M., 1994. The environmental impact of the wreck of the *Braer*. A report by the Ecological Steering Group on the Oil Spill in Shetland, The Scottish Office, Edinburgh.

Sprague, J.B., 1973. The ABC's of pollutant bioassay using fish. In: Special Technical Publication No. 528. American Society for Testing and Materials, Philadelphia, pp. 6–30.

Sprague, J.B., Drewery, D.E., 1969. Avoidance reactions of salmonid fish to representative pollutants. Advances in Water Pollution Research 4, 169–179.

Thomas, R.E., Rice, S.D., 1986. The effects of salinity on uptake and metabolism of toluene and naphthalene by Dolly Varden, *Salvelinus malma*. Marine Environmental Research 18, 203–214.

Topping, G., Davies, J.M., Mackie, P.R., Moffat, C.F., 1997. The impact of the *Braer* spill on commercial fish and shellfish. In: Davies, J.M., Topping, G. (Eds.), The Impact of an Oil Spill in Turbulent Waters: The *Braer*. The Stationery Office Ltd., Edinburgh, pp. 121–143.

Uthe, J.F., Musial, C.J., 1986. Polycyclic aromatic hydrocarbon contamination of American lobster, *Homarus americanus*, in the proximity of a coal-coking plant. Bulletin of Environmental Contamination and Toxicology 37, 730–738.

Webster, L., Angus, L., Topping, G., Dalgarno, E.J., Moffat, C.F., 1997. Long-term monitoring of polycyclic aromatic hydrocarbons in mussels (*Mytilus edulis*) following the *Braer* oil spill. Analyst 122, 1491–1495.

Whittle, K.J., Anderson, D.A., Davis, H.K., Lavèty, J., Mackie, P.R., McGill, A.S., Moffat, C.F., Shepherd, N.J., McVicar, A.H., 1997a. Tainting of caged salmon (*Salmo salar*) as a consequence of the *Braer* oil spill. In: Luten, J.B., Børresen, T., Oehlenschläger, J. (Eds.), Seafoods from Producer to Consumer, an Integrated Approach. Proceedings of the International Seafood Conference, Noordwijkerhout, Netherlands, November 13–16, 1995. Elsevier Science, New York, pp. 665–679.

Whittle, K.J., Anderson, D.A., Mackie, P.R., Moffat, C.F., Shepherd, N.J., McVicar, A.H., 1997b. The impact of the *Braer* oil on caged salmon. In: Davies, J.M., Topping, G. (Eds.), The Impact of an Oil Spill in Turbulent Waters: The *Braer*. The Stationery Office Limited, Edinburgh, pp. 144–160.

Williams, U.P., Kicenuik, J.W., Fancey, L.L., Botta, J.R., 1989. Tainting and depuration of taint by lobsters (*Homarus americanus*) exposed to water contaminated with a No. 2 fuel oil: relationship with aromatic hydrocarbon content in tissue. Journal of Food Science 54 (2), 240–257.

Environ. Sci. Technol. **2009,** *43,* 5864–5870

Unlike PAHs from Exxon Valdez Crude Oil, PAHs from Gulf of Alaska Coals are not Readily Bioavailable

HALAMBAGE UPUL DEEPTHIKE,[†] ROBIN TECON,[‡] GERRY VAN KOOTEN,[§] JAN ROELOF VAN DER MEER,[‡] HAUKE HARMS,[||] MONA WELLS,*[,||] AND JEFFREY SHORT[⊥]

Department of Chemistry, Tennessee Technological University, Cookeville, Tennessee 38505, Department of Fundamental Microbiology, University of Lausanne, Lausanne, CH 1015, Switzerland, Department of Geology, Geography, and Environmental Studies, Calvin College, Grand Rapids, Michigan 49546, Department of Environmental Microbiology, Helmholtz Centre for Environmental Research, Permoserstraβe 15, Leipzig, 04318, Germany, and Oceania, 175 S. Franklin St, Juneau, Alaska 99801

Received March 9, 2009. Revised manuscript received June 3, 2009. Accepted June 8, 2009.

In the wake of the 1989 Exxon Valdez oil spill, spatially and temporally spill-correlated biological effects consistent with polycyclic aromatic hydrocarbon (PAH) exposure were observed. Some works have proposed that confounding sources from local source rocks, prominently coals, are the provenance of the PAHs. Representative coal deposits along the southeast Alaskan coast (Kulthieth Formation) were sampled and fully characterized chemically and geologically. The coals have variable but high total organic carbon content, technically classifying as coals and coaly shale, and highly varying PAH contents. Even for coals with high PAH content (~4000 ppm total PAHs), a PAH-sensitive bacterial biosensor demonstrates nondetectable bioavailability as quantified, based on naphthalene as a test calibrant. These results are consistent with studies indicating that materials such as coals strongly diminish the bioavailability of hydrophobic organic compounds and support previous work suggesting that hydrocarbons associated with the regional background in northern Gulf of Alaska marine sediments are not appreciably bioavailable.

Introduction

The T/V *Exxon Valdez* discharged at least 41 000 m^3 of Alaska North Slope crude oil onto the waters of Prince William Sound, Alaska, polluting 2000+ km of shorelines along the coast up to 750 km to the southwest. Long-term biological damage attributed to lingering oil is inferred from spill-related spatial and temporal patterns in biochemical responses, characteristic of polycyclic aromatic hydrocarbon (PAH) exposure of monitored species, including cytochrome P450 1A (CYP1A) induction and detection of fluorescent aromatic compounds (FAC) in bile (*1*−*3*). However, geological background sources of PAHs in marine sediments of the northern Gulf of Alaska have been imputed as confounding PAH sources. These deposits, including organic-rich hydrocarbon source rocks, coals, and natural oil seeps (*4*−*7*), have been proposed as alternative sources for the observed biochemical responses (*8*, *9*). The basis for such conclusions is debatable (*10*, *11*), and claims are difficult to evaluate given source chemical complexity and the lack of a controlled setting for monitoring exposure (*12*). This study addresses the difficulty by focusing on an end-member of interest (coals) and by employing a controlled setting for exposure.

The proposed provenance of confounding sources is organic-rich hydrocarbon source rock exposed along the Alaskan coast southeast of Prince William Sound from Katalla to Yakutat. These include organic-rich shale from the Poul Creek Formation, coals from the Kulthieth Formation, and oil seeps from both (*13*). Regional glaciation produces PAH bearing particulates that are carried to the coast by rivers and streams, where larger particles are deposited with marine sediment. Smaller particulates remain suspended and are transported by the Alaska Coastal Current westward to Prince William Sound, settling to the seafloor in the more quiescent waters (*6*, *7*). Sterane and triterpane biomarkers indicate that the geologic deposit-derived PAHs predominately originate from the Kulthieth Formation (*13*, *14*). Whereas putative organic-rich hydrocarbon source rock in the Kulthieth Formation may lie inaccessible beneath glaciers, numerous coal outcrops are accessible. These oil-prone coals are the likely source of oil seeps in the Yakataga region (*14*). While these seeps are too small to plausibly contaminate a large area of marine sediments, association of finely divided coal particles with siliciclastic material could account for all or most of the marine sediment PAH burden attributed to regional hydrocarbon source rock (*13*).

Here we use engineered bacterial biosensors (bioreporters) to investigate the bioavailability of PAHs in Kulthieth Formation coals, an end-member contribution to Gulf of Alaska marine sediments. Pollutant bioavailability as a risk assessment parameter has been of interest for regulatory purposes as early as 1989 (*15*). Lack of a standard definition or standardized methods for quantification causes difficulty in implementing bioavailability for risk-based applications (*16*), with additional complication in reconciling the related term, bioaccessibility. The term bioavailability references only the amount of a substance available to an organism at some time, and bioaccessibility relates to the amount of a substance that is *and could potentially become* available, i.e., for toxic response (*16*). In a quantifiable or mathematical sense, bioavailability is an instantaneous quantity and bioaccessibility is bioavailability integrated over time. Thus terms such as "bioavailable fraction" allude to bioaccessibility (i.e., the total fraction or load available *or* potentially available). Most measurement methods, whether chemical or ecotoxicological, are performed over short periods of time compared to the time scale for slow desorption in environmental settings, hence represent an incomplete measurement of bioaccessibility. Nonetheless such methods are used and accepted, as we have previously discussed, ad hoc, and the ad hoc quantity correlates with theoretical ($t = \infty$) bioaccessibility due to its asymptotic approach to same (see ref *17* and references therein). Viewed thus, bioavailability is an objective rate descriptor and bioaccessibility is an operational end-point descriptor. Here we use the term bioavailability loosely as others do, a sort of common misnomer that refers to ad hoc bioaccessibility. Bioaccumulation represents a third

* Corresponding author e-mail: mona.wells@ufz.de.
[†] Tennessee Technological University.
[‡] University of Lausanne.
[§] Calvin College.
[||] Helmholtz Centre for Environmental Research.
[⊥] Oceania.

10.1021/es900734k CCC: $40.75
© 2009 American Chemical Society
Published on Web 06/22/2009

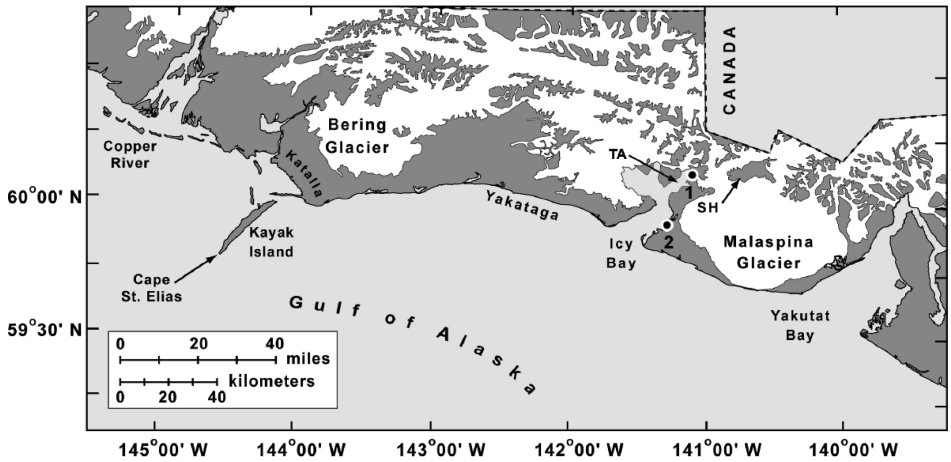

FIGURE 1. Map of Icy Bay, Southeast Alaska: 1 sampling site of coal seams (referred to as Tyndall Arm, TA, lying to the west of the Samovar Hills, SH), and 2 sampling site of floating particulate coal where the Caetani River flows into outer Icy Bay.

distinct quantity, sometimes confused with bioavailability and/or bioaccessibility, but not relevant to this study.

Measuring bioavailability with bioreporters combines the advantages of chemical and ecotoxicological approaches. Chemical techniques are static vis a vis living organisms' dynamic interactions with chemically complex matrices (*17*); ecotoxicological methods are dynamic but only measure bioavailability indirectly via toxic effects (*18*). The bioreporter used here employs sensor and regulator proteins of a metabolic pathway (i.e., not an intracellular pathway for toxicity response) and exhibits increasing response with increasing analyte concentration, characteristic of chemical approaches, while reflecting the biological system dynamics, characteristic of ecotoxicological approaches (*19*−*22*). Further, we previously documented that for experiments with biocided sediments and model materials, i.e., removing biological dynamics, bioreporter measured bioavailability correlates strongly with bioavailability approximated chemically (Tenax extraction) (*23*). Results from this study demonstrate strong and dose dependent bioreporter response from Exxon Valdez crude oil (EVCO) exposure and no discernible response for Kulthieth Formation coals.

Experimental Section

Field Area and Sample Suite. Icy Bay (60° 01′ N, 141° 20′ W) is a coastal fjord 100 km northwest of Yakutat, Alaska, and 275 km east of Prince William Sound, Alaska. Four fjords radiate from inner Icy Bay, one of which is Taan Fjord (called Tyndall Arm as the upper Taan Fjord terminates at the retreating toe of the Tyndall glacier). Eocene Kulthieth Formation oil-prone bituminous coals occur along ∼130 km of the coastal margin between Cape Yakataga and the Samovar Hills, including Icy Bay (*14*). Coal samples were taken along a vertical section from dipping beds exposed on the east side of upper Tyndall Arm and from riverine coal floats (Figure 1). Exposed coal seams range from 6 cm to 1.5 m thick. Coal samples with a large PAH content range were chosen for this study; additional information is in the Supporting Information (SI). An EVCO sample was also used. The sample was collected by Dr. David Shaw (University of Alaska Fairbanks) directly from the cargo hold of the T/V *Exxon Valdez* after its stranding on Bligh Reef. Portions were subsequently stored in airtight containers in the dark at −20 °C.

Materials. Dialysis tubing was from Spectrum (Spectra/Por, MWCO: 6000−8000). Chemicals and media were obtained from Fisher, Fisher Biotech, and Sigma Aldrich.

Bioreporter Studies. *Bacterial Strain and Culture Conditions.* The bioreporter, *Burkholderia sartisoli* sp. strain RP037 (*24*), carries a plasmid (pJAMA37) with a second copy of the PhnR regulatable promoter, P_{phnS} transcriptionally fused to the reporter gene, *egfp*. When PAHs bind to a repressor protein, it activates transcription of the reporter gene to produce a reporter mRNA, which undergoes translation to produce EGFP, a stable variant of green fluorescent protein GFP (vide infra). Naphthalene was used for calibration, since the organism is most sensitive to naphthalene, although it also reacts to phenanthrene and some other PAHs. To culture, a −80 °C stored portion was thawed and grown overnight (∼16 h) in Luria Broth (LB) at 26 °C, shaking at 150 rpm, to an optical density at 600 nm of 1 ($OD_{600} = 1$). The overnight culture was diluted 1:50 in LB and regrown under like conditions to $OD_{600} = 1.0$. All LB media contained 50 mg/L kanamycin for maintaining the reporter construct. Cells were centrifuged at 1800 rcf for 5 min, and the cell pellet was resuspended in minimal medium (MM, details in SI) to $OD_{600} = 0.20$. Fresh cultures prepared in this manner were used for bioassays.

Preparation of Amended Kaolinite and Coal Samples for Biological Analysis. Naphthalene-amended kaolinite samples were prepared by spiking 1 g of kaolinite with 20 μL methanolic solutions of naphthalene at various concentrations and thoroughly mixing. Kaolinite samples amended with various concentrations of EVCO were prepared likewise by adding a weight-range of small portions of the crude oil. Coal samples were prepared by grinding and sieving (100 μm metal sieve). For coal, varying PAH concentrations were obtained by using samples having different natural PAH contents.

Activation and Response Measurement. Samples (1 g) were each placed in a 30 cm long piece of dialysis tube. Loaded tubes were suspended in sterilized 125 mL Erlenmeyer flasks and 30 mL of bioreporter culture was added to each flask, submerging the sample containing portion of the tube in culture. Flasks were incubated at 26 °C and shaken at 150 rpm. Periodically (times reported below by experiment), 3.0 mL was removed from each flask and used to measure both the OD_{600} and the fluorescence emission spectrum (Varian Cary Eclipse, 480 nm excitation). EGFP fluorescence emission peak area was taken as bioreporter response. Additional information on cultures and cell viability is in the SI.

Chemical and Geological Studies. *Pyrolysis and TOC Analysis of Coals.* Samples for total organic carbon (TOC) analysis and pyrolysis analysis were ground and sieved to <250 μm. For TOC, samples were weighed (∼0.1 g) and acid washed (HCl, minimum 2 h to remove carbonates), then filtered through a glass microfiber filter. The filter was heated in crucible in a LECO 600 carbon analyzer to 1100 °C to oxidize organic matter; TOC was determined according to CO_2 evolved. Rock-Eval (Rock-Eval II with TOC, Vinci

TABLE 1. Results from TOC and Rock-Eval Analysis on Icy Bay Samples[a]

sample ID	TOC (%)	S1 mg/g	S2 mg/g	S3 mg/g	T_{max} (°C)	calc R_o (%)	HI	OI	S2/S3	S1/TOC	PI	notes
PKC-A	36	7.3	121	2.1	456	1.05	339	6	58	21	0.06	n;lts2p
PKC-B	82	10.1	300	3.6	447	0.89	365	4	84	12	0.03	n;lts2p
PKC-C	76	22.2	252	2.9	449	0.92	332	4	87	29	0.08	n;lts2p
PKC-D	50	8.9	146	2.5	453	0.99	294	5	59	18	0.06	n;lts2p
PKC-E	76	15.2	263	2.4	446	0.87	345	3	110	20	0.05	n;lts2p
PKC-F	80	11.5	300	2.6	450	0.94	375	3	115	14	0.04	n;lts2p
PKC-G	76	10.1	277	2.2	446	0.87	366	3	127	13	0.04	n;lts2p
PKC-H	25	3.2	87	7.1	444	0.83	353	29	12	13	0.04	n;lts2p

[a] Measured quantities are thermally released bitumen (S1, pyrosylate or S2, i.e., from thermal cracking of kerogen, carbon dioxide or S3, and temperature at maximum pyrosylate yield, T_{max}; calculated quantities are R_o, hydrogen index (HI or 100 × S2/TOC), oxygen index (OI or 100 × S3/TOC), S2/S3, S1/TOC, and production index (PI or S1/(S1 + S2)). S1 reflects free hydrocarbons in sample while S2 is generated hydrocarbons. T_{max} is a maturity parameter, HI and OI reflect the type of kerogen, S1/TOC is normalized oil content, and PI reflects maturity. Under notes, *n* indicates normal program and lts2p indicates low temperature S2 shoulder.

TABLE 2. Results from PAH Analysis of Crude Oil and Coal Samples Used in This Study

sample ID:	Exxon Valdez crude oil EVCO	Tyndall Glacier coal seam PKC-A	Tyndall Glacier coal seam PKC-B	Tyndall Glacier Coal seam PKC-C	Tyndall Glacier coal seam PKC-D	Tyndall Glacier coal seam PKC-E	Tyndall Glacier coal float PKC-F	Tyndall Glacier coal seam PKC-G	Caetani River coal float PKC-H
concentrations (mg/g):									
Nap	0.72	0.010	0.004	0.13	0.020	0.063	0.004	0.001	0.033
2-methyl nap	1.33	0.046	0.020	0.39	0.070	0.17	0.010	0.006	0.096
1-methyl nap	1.02	0.053	0.040	0.37	0.076	0.16	0.035	0.022	0.078
nap-2	3.15	0.23	0.16	0.61	0.24	0.43	0.095	0.095	0.18
nap-3	2.35	0.33	0.37	0.47	0.22	0.34	0.16	0.21	0.17
nap-4	0.60	0.16	0.20	0.16	0.067	0.11	0.10	0.17	0.066
Phe	0.25	0.080	0.061	0.090	0.051	0.074	0.047	0.042	0.035
phe-1	0.75	0.22	0.20	0.23	0.12	0.18	0.15	0.19	0.081
phe-2	0.89	0.21	0.24	0.22	0.11	0.15	0.15	0.24	0.072
phe-3	0.56	0.12	0.15	0.11	0.058	0.078	0.092	0.15	0.034
phe-4	0.17	0.010	0.006	0.008	0.005	0.005	0.005	0.015	0.003
ΣPAH[a]	14.7	2.18	2.14	3.56	1.49	2.33	1.33	1.85	1.04

[a] See the Supporting Information.

Technologies) pyrolysis was performed to assess coal thermal maturity and quality as oil bearing source rock (*25, 26*). Samples (~0.1 g) were incrementally heated under a helium atmosphere; the heating regime was 300 °C for 3 min (producing peak S1, i.e., volatilization of free/unbound hydrocarbons) followed by heating at 25 °C/minute to 600 °C (producing peak S2 representing heavy hydrocarbons, > C_{40}, and cracking of kerogen, i.e., the bound/generated fraction). S1 and S2 are detected by flame ionization detection, but during thermal cracking carbon dioxide (peak S3) is also liberated (at 300−390 °C) and trapped; after S2 measurement the instrument heats the trap, driving off carbon dioxide that a thermal conductivity detector measures. The temperature at which peak S2 reaches a maximum (T_{max}) is measured as an indicator of coal maturity as source rock (T_{max} also varies by organic matter type). Table 1 contains data on the TOC and Rock-Eval analyses. Additional analyses (specific macerals, mineral content, and vitrinite reflectance) are in the SI.

Crude Oil and Coal PAH Analysis. Samples were analyzed for aliphatic and aromatic hydrocarbons following previously described procedures ((*27*), and see the SI). Coal samples were pulverized and a sieved (<63 μm-mesh) fraction was added to anhydrous sodium sulfate (dehydration), then spiked with 500 μL of a hexane solution containing 11 perdeuterated surrogate hydrocarbon standards prior to extraction with dichloromethane (using a Dionex accelerated solvent extractor). Extract volumes were reduced over steam and exchanged with hexane to a final volume of ~1 mL, then separated into aliphatic and aromatic hydrocarbon fractions using 5%-deactivated silica gel/activated-alumina (20:10 g, +5 g activated Cu for sulfur removal) column chromatography. Aliphatics were eluted with 50 mL of pentane, followed by elution of aromatics with 250 mL of 1:1 pentane: dichloromethane. Both fractions were reduced over steam to a final volume of ~0.5 mL, and the aromatic fraction was further purified by gel-permeation high performance liquid chromatography (HPLC).

Purified aromatic fractions were analyzed using selective-ion-monitoring (SIM) mode gas chromatography−mass spectrometry (GC-MS, HP Ultra 2 column, 25 m × 0.25 mm × 0.33 μm). PAHs analyzed included both parent homologue and alkyl-substituted naphthalenes (nap-*X*), fluorenes, dibenzothiophenes, phenanthrenes/anthracenes (phe-*X*), and chrysenes/benzanthracene; for nap-*X* and phe-*X*, *X* = the number of alkyl-substituted carbon atoms ranging from 0 to 4. Table 2 contains abridged data for coal and EVCO PAH content.

Naphthalene Sorption Tests. Naphthalene crystals were suspended in sterile deionized water for several days; immediately prior to use the solution was filtered through a glass fiber filter. Triplicate 100 mg portions of samples (coals, kaolinite, or activated charcoal) were ground and sieved, and naphthalene solution (15 mL) was added to each; triplicate control samples with 15 mL aliquots of aqueous naphthalene solution (without solid) were also prepared. Samples were kept tightly sealed on a mechanical shaker at 26 °C and 150 rpm for 5 h, then each solution was filtered through an alumina syringe filter (Anatop 10; 0.2 μm, 10 mm, Whatman). To 10 mL portions of filtrate, 5 mL of HPLC grade

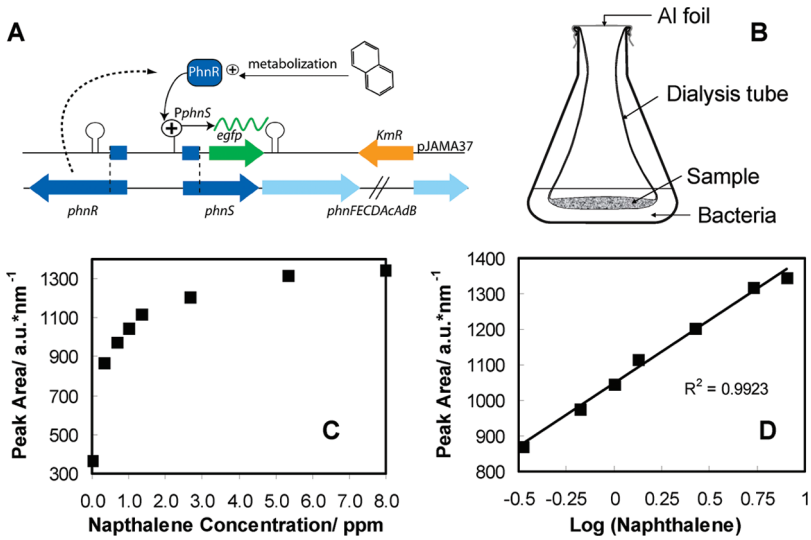

FIGURE 2. Genetic circuitry leading to RP037 expression of EGFP in response to naphthalene (A), and scheme of the experimental setup for solid samples (B); quantitative response of RP037 to naphthalene concentration, without solid phase, is shown in linear (C) and logarithmic representation (D).

heptane was added, then samples were kept tightly sealed on a mechanical shaker at 26 °C and 150 rpm for 15 h. Following this extraction, the heptane layers were analyzed by GC-MS (Varian CP-3800 gas chromatograph/Saturn 2200 mass spectrometer/CTC Analytics Combi-PAL autosampler). Naphthalene sorbed in such tests was expressed as a percent of the naphthalene control solution, and used to estimate the concentration of naphthalene in the solid (C_s) and aqueous (C_{aq}) phases (equilibrium calculations indicate that the vapor phase is negligible). Sorption is expressed as a single-point apparent distribution coefficient K'_d, where $K'_d = C_s/C_{aq}$. The experimental conditions were chosen after rough testing of the saturation behavior to ensure that the final sorption tests were performed in the linear part of the isotherm.

Results and Discussion

Figure 2 provides background information about RP037; Figure 2A illustrates how the RP037 sensing element expresses EGFP in response to PAH activation (previously reported (*24*)). Figure 2B shows the dialysis tube setup, and Figure 2C and D show RP037 logarithmic response as a function of naphthalene concentration in solution (no solid). Logarithmic response has been observed for similar bacterial systems, depending upon concentration range and other factors (refs *19*−*22*, *28*, *29*, and references therein). The sensitivity of response is influenced by, for example, stage of growth phase upon activation; however, Figure 2D is representative and readily reproducible with high precision (typically R^2 > 0.99 as shown).

We have previously demonstrated that kaolinite is a good model solid for use in bioreporter studies, representing, as we prepare it, a solid from which naphthalene is 100% bioavailable (*23*). Thus, kaolinite amended with naphthalene or EVCO represents a benchmark by which 100% bioavailability is assessed and is not intended to represent sediments per se. Though we have used sediments to validate this approach in a previous study, the point here is not to study sediments (i.e., as previous studies with reference to bioavailability and environmental materials in the Gulf of Alaska or Prince William Sound), but rather specifically to contrast bioavailability of PAHs from EVCO to those from Kulthieth Formation coals, to wit, potential sources. Kaolinite provides a proxy to the solid support of a geomaterial (PAH-bearing sediments or coals) without introduction of collateral bioavailability modifying parameters such as the complex assemblages of organic matter/coal in natural sediments. EVCO-amended kaolinite can be viewed as the crude oil end-member analog to be contrasted with the coal end-member.

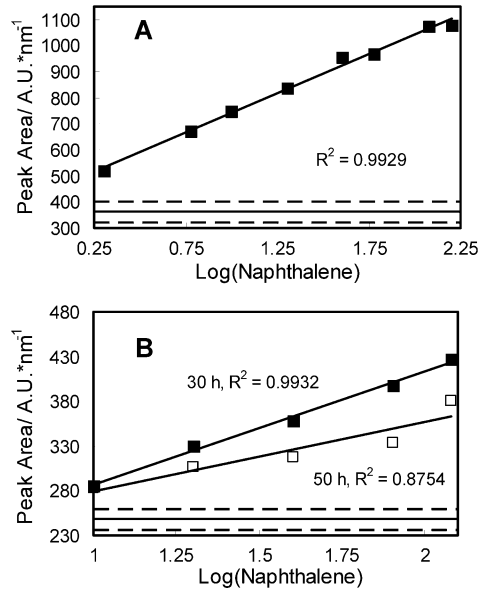

FIGURE 3. RP037 response to naphthalene-amended kaolinite. Panels A and B show different experiments, and Panel B the effect of long activation times. Naphthalene concentrations are in ppm; control response (0 ppm naphthalene) is represented by the solid horizontal line, ± uncertainty represented by dashed horizontal lines.

Solids can interfere with bioreporter response measurement (e.g., via sample autofluorescence), and bacteria allowed to freely mix with a solid sample are difficult to recover for response measurement. For these reasons, we use the dialysis tube assay. Amending kaolinite with naphthalene or crude oil results in a solid-phase material that may be handled in the same way as coal samples. Results of calibration experiments with naphthalene-amended kaolinite confirm the practicability of our approach. Figure 3A shows response taken after 16 h activation. We consistently observe an optimum response between ~12 and 18 h in terms of both sensitivity and precision. Curves from a separate calibration experiment in Figure 3B show that even after

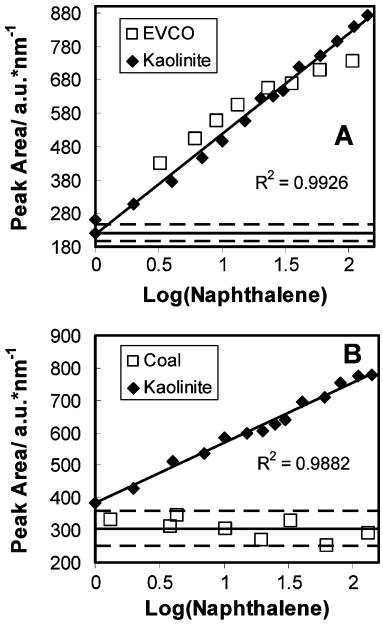

FIGURE 4. RP037 response to different quantities of EVCO (A), and Kulthieth Formation coals of different PAH contents (B). Control experiments (simultaneous) using naphthalene-amended kaolinite are included for reference. Naphthalene concentrations are in ppm; control response (0 ppm naphthalene) is represented by the solid horizontal line, ± uncertainty represented by dashed horizontal lines.

30 h activation precision is still acceptable, but after 50 h there is a decline in sensitivity and precision, possibly due to poststationary lysis.

Figure 4 shows representative results from RP037 studies on EVCO-amended kaolinite (Figure 4A) and coal samples from Icy Bay, Alaska (Figure 4B), along with naphthalene-amended kaolinite for reference. For EVCO composition is fixed, so dose dependency is demonstrated by amending kaolinite samples with increasing amounts of EVCO. At lower concentrations, the magnitude of the EVCO response is slightly higher than for the naphthalene-amended kaolinite reference samples. At higher concentrations, the EVCO response becomes nonlinear. These observations are consistent with a priori expectations: EVCO response should be higher than for the calibrant because it is a complex material with bioreporter-inducing PAHs other than naphthalene, and at higher PAH concentrations, i.e., as the ratio of EVCO increases relative to a fixed amount of kaolinite, the thickness of the oil rime around kaolinite grains increases, and physical resistance to mass transport begins to increase nonlinearly (surface area:volume effect). In the case of coal samples, PAH composition varies substantially (Tables 1−2 and SI Tables S1−S2), and so a range of naphthalene/PAH concentrations was achieved by use of multiple samples, none of which was artificially amended. Figure 4B shows that there was essentially baseline bioreporter response to coal samples. Results from chemical and Rock-Eval analyses in Tables 1 and 2 indicate a substantial organic content of EVCO and coal samples. For coals, the TOC results correlate with S1 + S2 from the Rock-Eval analysis at $R^2 = 0.98$. Based on TOC results, five Icy Bay samples with TOC >50% classify as coal (TOC from 76 to 82%), two samples classify as coaly shale (TOCs of 25 and 46%), and one is in between (50%). Normalizing the S2 and S3 peaks to TOC content yields hydrogen index (HI) and oxygen index (OI), which indicate if generated hydrocarbons are likely to be oil or gas. The uniformly high HI and low OI values indicate the coals are oil prone, converting 25−30% by weight into oil upon heating; the remainder/coaly shales are also oil prone and convert 9−15% by weight to oil (Table 1, S2).

TABLE 3. Estimated K_d's for Coals and Model Calibrants

sample ID/sample description	K'_d
PKC-A	2700
PKC-B	1700
PKC-C	1200
PKC-D	1000
PKC-E	600
PKC-F	1300
PKC-G	2000
PKC-H	1700
kaolinite	0.01
activated charcoal	47 000

High HI values and low S1/TOC ratios suggest that most of the organic matter in the Icy Bay samples is not labile, and over most of the naphthalene concentration range in Figure 4 biosensor response for kaolinite amended with different amounts of crude oil is nearly superimposable with the results for naphthalene-amended kaolinite, whereas coal samples show baseline response. Qualitatively it is clear that PAHs from EVCO are highly available and PAHs from coal, even these oil prone coals, are entirely unavailable. Quantitatively, Exxon Valdez crude oil has essentially 100% bioavailability of PAH as compared to 0% bioavailability of PAH in Icy Bay coals. Viability measurements demonstrated no evidence of compromised cells (i.e., no toxicological effect) during the course of studies on EVCO and coal (see SI).

After the Exxon Valdez oil spill, a comprehensive effort was undertaken to study exposure to and effect of hydrocarbons in the affected area, of which PAHs are a toxic fraction (more especially the higher molecular weight PAHs, which are both more slowly degraded and weathered). Subsequently, some investigators have proposed that the source of toxicologically active PAHs is a geological/indigenous "regional background", based on inconclusive biochemical evidence from resident biota. The results here and recent reports on the effects of black carbon on bioavailability contradict this suggestion. Coal particles in marine sediments of the northern Gulf of Alaska could even act as a PAH sink and reduce PAH bioavailability (*30*−*36*). While Figure 4B demonstrates that there is no bioreporter response for these coals, a slight negative slope (not statistically differentiable from zero slope, $p < 0.05$) with increasing concentration could indicate that more oil-prone coals have less available PAHs. From the results for coal in Figure 4B, we estimated the relative sorptive capacities of the coal samples and results for naphthalene are tabulated in Table 3 as apparent distribution coefficients, K'_d.

The results in Table 3 show that the coals sorb naphthalene much more effectively than kaolinite, yet less effectively than activated charcoal. The K'_d of kaolinite, at 0.01, is effectively 0, i.e., a prerequisite to the observation in this and our previous work of 100% bioavailability for this material. The value obtained for activated charcoal (47 000, Table 3) is consistent with a literature-averaged estimate of K'_d for naphthalene on black carbon (37 000) (*23*). The average K'_d of Icy Bay samples (1500) is roughly 2-fold higher than K'_d calculated (i.e., $K'_{oc} \times f_{oc,avg} \sim 800$, where K'_{oc} is the effective organic carbon−water distribution coefficient (*37*), and $f_{oc,avg}$ is the average TOC from Table 1), which may reflect the coals' oil prone nature and diagenetic maturity. Values for K'_d show a weak correlation with indigenous vitrinite reflectance ($R^2 = 0.72$), which is one indicator of diagenetic maturity (see SI).

Biological results indicate that PAHs in Icy Bay coals are unavailable (Figure 4B), and geological results support this

finding (Table 1 and SI Table S1), as do results from chemical sorption tests (Table 3, and consistent with environmental literature on coals and black carbon). A self-consistent conclusion emerges that although the coal particles found in continental shelf sediments of the Gulf of Alaska contain suites of PAHs resembling crude oils (e.g., ref *7*), they have the capacity to remove PAHs from seawater and are more likely a sink than a source. Though there is a growing consensus in the environmental literature that PAHs from coal are not bioavailable, there is hardly a consensus within the greater scientific community. In the emerging field of medical geology reports document release of PAHs from coal, in some cases linking release of organics from coal with putative adverse health effects. Such studies underscore the importance of linking biological effect to coal characterization (chemical) and understanding of geological context (*38*−*43*).

Due to the high chemical resistance to mass transport (release) of PAHs from the coal samples used here, the corresponding dominant desorption kinetics will be very slow, obviously much slower than the time scale of measurement employed here. We and other authors have addressed this point from many perspectives, full consideration of which is beyond the scope of the present manuscript. In brief, it is difficult to extend bioreporter studies past the time periods used here. However, most measurements of bioavailability are similarly restricted to measurement periods of a few hours or even weeks, i.e., periods equally inadequate to slow desorption (many months to years; with reference to the Valdez spill, some studies address this point of very slow desorption (*13*), others overlook it). One highly cited work on chemical extraction demonstrated that the bioremediable (i.e., perforce ad hoc bioaccessible) fraction of desorbing PAHs over two years is captured in the amount desorbed to Tenax over the same time frame as used in the present experiments (*44*). This result stems from the quasi-infinite sink nature of the Tenax extractant's driving release in conjunction with the aforementioned asymptotic approach of ad hoc bioaccessibility to the theoretical limit. Bacteria that metabolize PAHs, bioreporters inclusive, also function as a quasi-infinite sink, as we have before documented (*17*), which is in accord with our previous demonstration of a 1:1 correspondence between bioreporter measured bioavailability and Tenax measured bioavailability (*23*).

PAH-sensitive bioreporter bacteria demonstrate a very strong and dose dependent bioavailable response from EVCO exposure and no response for Kulthieth Formation coals for the same range of PAH loading. These results corroborate earlier work suggesting that hydrocarbons associated with the regional background in northern Gulf of Alaska marine sediments are not appreciably bioavailable. Taken in the context of literature reports on black carbon, the present results are consistent with other spill-related spatial and temporal patterns in long-term indications of toxic stress resulting from exposure to the release of EVCO into the environment. One reviewer of this manuscript mandated mention of another possibility for the role of these coals in the environment: because of their capacity to sorb PAHs, rates of other processes of natural attenuation (photooxidation, biodegradation) could be diminished, diminishing the immediate PAH burden, but enhancing the persistence of toxic PAHs. While we mention this possibility, it is tangential to our main study objectives and findings. Our primary finding, based on quantitative results from the present end-member study of bioavailability, is that bioavailable PAHs do not originate from organic-rich source rock associated with the Poul Creek and Kulthieth Formations east of Prince William Sound. EVCO represents the primary known source of bioavailable PAHs in the region.

Acknowledgments

H.U.D. acknowledges the TTU Center for the Management, Protection and Utilization of Water Resources for a graduate fellowship and associated funding and support, and we thank Dick Drozd of Humble Geochemical for consultation regarding TOC, Rock-Eval, and petrographic work.

Supporting Information Available

Additional information on methods, chemical and geological characterization of samples, and studies on cell viability. This material is available free of charge via the Internet at http://pubs.acs.org.

Literature Cited

(1) Bodkin, J. L.; Ballachey, B. E.; Dean, T. A.; Fukuyama, A. K.; Jewett, S. C.; McDonald, L.; Monson, D. H.; O'Clair, C. E.; Van Blaricom, G. R. Sea otter population status and the process of recovery from the 1989 'Exxon Valdez' oil spill. *Mar. Ecol.: Prog. Ser.* **2002**, *241*, 237–253.

(2) Hom, T.; Varanasi, U.; Stein, J. E.; Sloan, C. A.; Tilbury, K. L.; Chan, S.-L. In *Proceedings of the Exxon Valdez Oil Spill Symposium*; Rice, S. D., Spies, R. B., Wolfe, D. A., Wright, B. A., Eds.; American Fisheries Society Symposium: Anchorage, AK, 1996; Vol. 18, pp 856−866.

(3) Trust, K. A.; Esler, D.; Woodin, B. R.; Stegeman, J. J. Cytochrome P450 1A induction in sea ducks inhabiting nearshore areas of Prince William Sound, Alaska. *Mar. Pollut. Bull.* **2000**, *40*, 397–403.

(4) Bence, A. E.; Kvenvolden, K. A.; Kennicutt, M. C. II Organic geochemistry applied to environmental assessments of Prince William Sound, Alaska, after the Exxon Valdez oil spill—A review. *Org. Geochem.* **1996**, *24*, 7–42.

(5) Boehm, P. D.; Page, D. S.; Burns, W. A.; Bence, A. E.; Mankiewicz, P. J.; Brown, J. S. Resolving the origin of the petrogenic hydrocarbon background in Prince William Sound, Alaska. *Environ. Sci. Technol.* **2001**, *35*, 471–479.

(6) Page, D. S.; Boehm, P. D.; Douglas, G. S.; Bence, A. E.; Mankiewicz, P. J. The natural petroleum hydrocarbon background in subtidal sediments of Prince William Sound, Alaska, USA. *Environ. Toxicol. Chem.* **1996**, *15*, 1266–1281.

(7) Short, J. W.; Kvenvolden, K. A.; Carlson, P. R.; Hostettler, F. D.; Rosenbauer, R. J.; Wright, B. A. Natural hydrocarbon background in benthic sediments of Prince William Sound, Alaska: Oil vs. Coal. *Environ. Sci. Technol.* **1999**, *33*, 33–42.

(8) Huggett, R. J.; Stegeman, J. J.; Page, D. S.; Parker, K. R.; Brown, J. S. Biomarkers in fish from Prince William Sound and the Gulf of Alaska: 1999−2000. *Environ. Sci. Technol.* **2003**, *37*, 4043–4051.

(9) Page, D. S.; Huggett, R. J.; Stegeman, J. J.; Parker, K. R.; Woodin, B.; Brown, J. S.; Bence, A. E. Polycyclic aromatic hydrocarbon sources related to biomarker levels in fish from Prince William Sound and the Gulf of Alaska. *Environ. Sci. Technol.* **2004**, *38*, 4928–4936.

(10) Short, J. W.; Springman, K. R.; Lindeberg, M. R.; Holland, L. G.; Larsen, M. L.; Sloan, C. A.; Khan, C.; Hodson, P. V.; Rice, S. D. Semi-permeable membrane devices link site-specific contaminants to effects: Part II—A comparison of lingering Exxon Valdez oil with other potential sources of cytochrome P450 1A inducers in Prince William Sound, Alaska. *Mar. Environ. Res.* **2008**, *66*, 487–498.

(11) Springman, K. R.; Short, J. W.; Lindeberg, M. R.; Maselko, J. M.; Khan, C.; Hodson, P. V.; Rice, S. D. Semi-permeable membrane devices link site-specific contaminants to effects: Part I - Induction of CYP 1A in rainbow trout from contaminants in Prince William Sound, Alaska. *Mar. Environ. Res.* **2008**, *66*, 477–486.

(12) Springman, K. R.; Short, J. W.; Lindeberg, M.; Rice, S. D. Evaluation of bioavailable hydrocarbon sources and their induction potential in Prince William Sound, Alaska. *Mar. Environ. Res.* **2008**, *66*, 218–220.

(13) Short, J. W.; Kolak, J. J.; Payne, J. R.; Van Kooten, G. K. An evaluation of petrogenic hydrocarbons in northern Gulf of Alaska continental shelf sediments - The role of coastal oil seep inputs. *Org. Geochem.* **2007**, *38*, 643–670.

(14) Van Kooten, G. K.; Short, J. W.; Kolak, J. J. Low-maturity Kulthieth Formation coal: A possible source of polycyclic aromatic hydrocarbons in benthic sediment of the northern Gulf of Alaska. *J. Environ. Forensics* **2002**, *3*, 227–242.

(15) Maddaloni, M. A. Bioavailability of soil-borne chemicals: a regulatory perspective. *Hum. Ecol. Risk Assess.* **2004**, *10*, 657–663.

(16) Semple, K. T.; Doick, K. J.; Jones, K. C.; Burauel, P.; Craven, A.; Harms, H. Defining bioavailability and bioaccessibility of contaminated soil and sediment is complicated. *Environ. Sci. Technol.* **2004**, *38*, 228A–231A.
(17) Wells, M.; Wick, L. Y.; Harms, H. A Model Polymer Release System study of PAH bioaccessibility: the relationship between "rapid" release and bioaccessibility. *Environ. Sci. Technol.* **2005**, *39*, 1055–1063.
(18) Kimball, K. D.; Levin, S. A. Limitations of laboratory bioassays: The need for ecosystem-level testing. *BioScience* **1985**, *35*, 165–171.
(19) Belkin, S. Microbial whole-cell sensing systems of environmental pollutants. *Curr. Opin. Microbiol.* **2003**, *6*, 206–212.
(20) Daunert, S.; Barrett, G.; Feliciano, J. S.; Shetty, R. S.; Shrestha, S.; Spencer, W. S. Genetically engineered whole-cell sensing systems: coupling biological recognition with reporter genes. *Chem. Rev.* **2000**, *100*, 2705–2738.
(21) Hansen, L. H.; Sorensen, S. J. The use of whole-cell biosensors to detect and quantify compounds or conditions affecting biological systems. *Microb. Ecol.* **2001**, *42*, 483–494.
(22) van der Meer, J. R.; Tropel, D.; Jaspers, M. Illuminating the detection chain of bacterial bioreporters. *Environ. Microbiol.* **2004**, *6*, 1005–1020.
(23) Kohlmeier, S.; Mancuso, M.; Deepthike, U.; Tecon, R.; van der Meer, J. R.; Harms, H.; Wells, M. Comparison of naphthalene bioavailability determined by whole-cell biosensing and availability determined by extraction with Tenax. *Environ. Pollut.* **2008**, *156*, 803–808.
(24) Tecon, R.; Wells, M.; van der Meer, J. R. A new gfp-based bacterial biosensor for analyzing phenanthrene fluxes. *Environ. Microbiol.* **2006**, *8*, 697–708.
(25) Peters, K. E. Guidelines for evaluating petroleum source rock using programmed pyrolysis. *AAPG Bull.* **1986**, *70*, 318–329.
(26) Peters, K. E.; Cassa, M. R. Applied source rock geochemistry. In *The Petroleum System—From Source to Trap: AAPG Memoir*; Magoon, L. B., Dow, W. G., Eds.; AAPG: Tulsa, OK, 1994; Vol. 60, pp 93−120.
(27) Barrona, M. G.; Carls, M. G.; Short, J. W.; Rice, S. D.; Heintz, R. A.; Rau, M.; Di Giulioc, R. Assessment of the phototoxicity of weathered Alaska North Slope crude oil to juvenile pink salmon. *Chemosphere* **2004**, *60*, 105–110.
(28) Bechor, O.; Smulski, D. R.; Van Dyk, T. K.; LaRossa, R. A.; Belkin, S. Recombinant microorganisms as environmental biosensors: pollutants detection by Escherichia coli bearing fabA':lux fusions. *J. Biotechnol.* **2002**, *94*, 125–132.
(29) Wells, M.; Gösch, M.; Rigler, R.; Harms, H.; Lasser, T.; van der Meer, J. R. Ultra-sensitive reporter protein detection in genetically-engineered bacteria. *Anal. Chem.* **2005**, *77*, 2683–2689.
(30) Accardi-Dey, A.; Gschwend, P. M. Assessing the combined roles of natural organic matter and black carbon as sorbents in sediments. *Environ. Sci. Technol.* **2002**, *36*, 21–29.
(31) Accardi-Dey, A.; Gschwend, P. M. Reinterpreting literature sorption data considering both absorption into organic carbon and adsorption onto black carbon. *Environ. Sci. Technol.* **2003**, *37*, 99–106.
(32) Ghosh, U.; Zimmerman, J. R.; Luthy, R. G. PCB and PAH speciation among particle types in contaminated harbor sediments and effects on PAH bioavailability. *Environ. Sci. Technol.* **2003**, *37*, 2209–2217.
(33) Hong, L.; Ghosh, U.; Mahajan, T.; Zare, R. N.; Luthy, R. G. PAH sorption mechanism and partitioning behavior in lampblack-impacted soils from former oil-gas plant sites. *Environ. Sci. Technol.* **2003**, *37*, 3625–3634.
(34) Karapanagioti, H. K.; Childs, J.; Sabatini, D. A. Impacts of heterogeneous organic matter on phenanthrene sorption: different soil and sediment samples. *Environ. Sci. Technol.* **2001**, *35*, 4684–4690.
(35) Lohmann, R. The emergence of black carbon as a super-sorbent in environmental chemistry: The end of octanol. *Environ. Forensics* **2003**, *4*, 161–165.
(36) Cornelissen, G.; Gustafsson, O.; Bucheli, T.; Jonker, M. O.; Koelmans, A.; van Noort, P. C. Extensive sorption of organic compounds to black carbon, coal, and kerogen in sediments and soils: mechanisms and consequences for distribution, bioaccumulation, and biodegradation. *Environ. Sci. Technol.* **2005**, *39*, 6881–6895.
(37) EPA, U. S. *Region 9 Preliminary Remediation Goals*; U.S. EPA Region 9: San Franciso, 1996.
(38) Bunnell, J. E.; Finkelman, R. B.; Centeno, J. A.; Selinus, O. Medical Geology: a globally emerging discipline. *Geol. Acta* **2007**, *5*, 273–281.
(39) Feder, G. L.; Radovanovic, Z.; Finkelman, R. B. Relationship between weathered coal deposits and the etiology of Balkan Endemic Nephropathy. *Kidney Int.* **1991**, *40*, S9−S11.
(40) Finkelman, R. B.; Orem, W.; Castranova, V.; Tatu, C. A.; Belkin, H. E.; Zheng, B. S.; Lerch, H. E.; Maharaj, S. V.; Bates, A. L. Health impacts of coal and coal use: possible solutions. *Int. J. Coal Geol.* **2002**, *50*, 425–443.
(41) McElmurry, S. P.; Voice, T. C. Screening methodology for coal-derived organic contaminants in water. *Int. J. Environ. Anal. Chem.* **2004**, *84*, 277–287.
(42) Orem, W.; Tatu, C.; Pavlovic, N.; Bunnell, J.; Lerch, H.; Paunescu, V.; Ordodi, V.; Flores, D.; Corum, M.; Bates, A. Health effects of toxic organic substances from coal: Toward "panendemic" nephropathy. *Ambio* **2007**, *36*, 98–102.
(43) Orem, W. H.; Feder, G. L.; Finkelman, R. B. A possible link between Balkan endemic nephropathy and the leaching of toxic organic compounds from Pliocene lignite by groundwater: preliminary investigation. *Int. J. Coal Geol.* **1999**, *40*, 237–252.
(44) Cornelissen, G.; Rigterink, H.; Ferdinandy, M. M. A.; Van Noort, P. C. M. Rapidly desorbing fractions of PAHs in contaminated sediments as a predictor of the extent of bioremediation. *Environ. Sci. Technol.* **1998**, *32*, 966–970.

ES900734K

Supporting Information

Supplemental Experimental Details, Data, and Commentary

Field area and sample suite

Seven Kulthieth Formation coal samples were chosen for use in this study as well as a riverine coal float sample. The latter, collected at the mouth of the Caetani River, was from fine grained particulate coal mixed with silty sediments discharged into Icy Bay where fresh river water mixes with marine. This sample was finely ground by the Malaspina Glacier from coals and coaly shales beneath the ice and represents a natural mix from various coaly sources not exposed at the surface. Van Kooten et al. (*S1*) documented a probable genetic link between Kulthieth coal and regional oil seeps along the Sullivan Anticline east of Cape Yakataga, that is supported by: 1) coincident distribution of coals and seeps, 2) petrographic identification of lipid organic material in the Kulthieth coal, 3) similarity of resistant sterane biomarkers between Kulthieth coal and weathered oil, and 4) absence of other identified source rocks. Petrographic examination of coals from the Taan Fjord outcrops have identified abundant lipid-rich vitrinite (mainly desmocollinite). The lipid component within the desmocollinite grains is dispersed as tiny grains that are integrated within the detrital vitrinite macerals. The lipid material is possibly derived from algae and bacteria growing in clear water swamps, subsequently mixed with detrital, degraded vitrinite, and is evidently responsible for the oil generative potential of the Kulthieth coals. In addition to TOC and Rock-Eval

analyses, petrographic maceral analysis (specific maceral content and vitrinite reflectance) were conducted as detailed below.

Biological Studies

Minimal Medium (MM). The MM was prepared by dissolving 1.00 g NH_4Cl, 7.02 g $Na_2HPO_4 \times 12H_2O$, and 2.77 g KH_2PO_4 in a liter of water (pH adjusted to 6.8), sterilizing the solution by autoclaving at 120°C for 20 minutes, adding to the cool solution 1) 20 mL of sterile Hutner's vitamin free mineral base (10 g/L nitriloacetic acid, dissolved and neutralized with KOH, 14.45 g/L $MgSO_4 \times 7H_2O$, 3.33 g/L $CaCl_2 \times 2H_2O$, 9.74 g/L $(NH_4)_6Mo_7O_{24} \times 4H_2O$, 99 mg/L $FeSO_4 \times 7H_2O$, and 50 mL Metals 44 solution, final solution autocleaved at 120°C for 20 minutes), and 2) 2.0 mL sterile filtered vitamin solution (5 mg/L biotin, 0.5 g/L nicotinic acid, 0.25 g/L thiamin hydrochloride, final solution sterile filtered, 0.2 μm). Metals 44 solution is 3.87 g/L $Na_4EDTA \times 4H_2O$, 10.95 g/L $ZnSO_4 \times 7H_2O$, 9.14 g/L $FeSO_4 \times 7H_2O$, 1.54 g/L $MnSO_4 \times H_2O$, 0.392 g/L $CuSO_4 \times 5H_2O$, 0.248 g/L $Co(NO_3)_2 \times 6H_2O$, 0.177 g/L $Na_2B_4O_7 \times 10H_2O$, and five drops of 6 N H_2SO_4, final solution sterile filtered (0.2 μm). After preparation, but prior to use with the bioreporter, a portion of MM was taken and kanamycin, sodium acetate, and NaCl were dissolved in it. This was then sterile filtered back into a larger portion of MM to obtain final concentrations of 50 mg/ L kanamycin, 0.82 g/L sodium acetate and 2.9 g/L NaCl).

Culture ODs. The OD_{600} of each sample culture were routinely measured. To within normal variation for separate suspensions of a culture, these were invariant for activation times up to 24 h. For instance, OD_{600} relative standard deviations for Figure 3A and 4A were 0.9 and 0.5%, respectively. For the coal results in Figure 4B, the relative standard

deviation was somewhat higher at 2.5%, however there was no trend with respect to concentration (zero slope, $p < 0.05$). Trends in OD_{600} were observed at longer activation times (e.g. Figure 3B). However, normalization of individual sample data to sample optical density (factor was OD_{sample}/OD_{avg}), produced calibration slopes that were not statistically differentiable from those of raw response data.

Cell Viability. To assure that there was not a toxicological effect during the course of studies on crude oil and coal, a propidium iodide (PI) viability assay was performed. PI has useful characteristics for viability assays in that its emission is not influenced by EGFP expression (hence its use also in LIVE/DEAD assays wherein the LIVE portion of the assay is much akin to EGFP spectrally). For these, selected coal samples and concentrations of crude oil amended kaolinite samples were prepared as described in the Experimental Section, and used to induce strain RP037, also as previously described. Flasks with only 30 mL of the culture were additionally prepared for positive and negative controls. At various induction times, triplicate 500 μL portions of the bacteria cultures were placed into 1.5-mL microcentrifuge tubes and 1 mL of deionized water was added to each tube, mixed well, and centrifuged at 10,000 rcf for 5 mins. Afterwards, 1.4 mL of the supernatant was removed from each tube without disturbing the bacterial cell pellet and PI (1 mg/ mL aqueous solution, Invitrogen) staining was performed. For PI staining, a 1.4 mL aliquot of an aqueous solution of 0.025 mg/mL PI was added to each tube and bacterial cells were resuspended in it by vortexing for 3 minutes. Tubes were then incubated at 26°C for 25 minutes. After that tubes were centrifuged at 10,000 rcf for 5 minutes and the supernatant was removed without disturbing the resulting pellet. Then the pellet was resuspended in 1.5 mL of deionized water and fluorescence emission spectra were obtained (535 nm excitation) with response taken as PI fluorescence

emission peak area. Positive (dead cells) and negative (live cells) controls (no naphthalene) were processed in the same manner, except for positive controls after the bacterial cultures were loaded into microcentrifuge tubes 1.0 mL of ethanol was added to each tube to kill cells. Tubes were incubated for 1 hour at 26°C and then centrifuged at 10,000 rcf for 5 minutes. Supernatant ethanol was completely removed with care not to disturb the cell pellet and 100 μL of deionized water was added to each tube followed by PI staining and measurement.

PI staining is a test of membrane integrity as PI is an intercalating agent that binds to nucleic acids in a manner that both drastically increases its fluorescence and shifts the wavelength of fluorescence. As it is essentially membrane impermeant it is excluded from functioning cells with viable membranes, and hence can be used as a measure of compromised and dead cells in a population. Representive oil and coal samples were chosen to span naphthalene concentrations from low to high, and samples were assayed with PI staining across a two day window. Figure S1 shows representative results. The negative control consists of RP037 only, and the positive control is a sample of the same cells after exposure to ethanol to induce cell death. None of the coal or oil sample signals lie between the two, and in fact, all lie below that of the negative control. Though the error bars appear small in the figure, analysis of variance indicates that individual EVCO samples are not statistically different from each other at 95% confidence, and not different from the negative control. Previous work with this assay for bacteria and other cell assays has not indicated negative interference of PAHs with the assay (*S2*-*S3*), and there are no avenues for spectral contamination (particularly since the below baseline response would not involve such). However, the coal samples do show response that is statistically speaking lower than that of EVCO or the negative control. While the coals

may sorb hydrophobic compounds such as PAHs, they also contain a rich complement of more soluble/less sorptive organic materials, some of which may serve to enrich the complexity of the background support media, hence actually improving overall cell health (i.e. as this strains does much better with compositionally complex rich media such as LB compared to the minimal medium used).

It should be strongly emphasized that many engineered biosensors are useful as such precisely because their particular regulatory machinery and/or engineering offer a means by which they are resistant to toxic insult that could be harmful to other organisms in the natural environment. Indigenous organisms do not share the engineered strain's genetic advantage and must fend off bioavailable compounds in crude oil on their own recognizance. Thus while the levels of toxic compounds present in the Icy Bay coals and EVCO samples do not evoke a positive PI response (diminished viability) for the bioreporter, this is anticipated due to the choice of engineered strain.

Chemical and Geological Studies

Petrographic analysis of coals. For petrographic analyses, samples were crushed to < 20 mesh, mounted in epoxy, and polished. Polished samples were subjected to incident and transmitted light maceral analysis (discrete particles of sedimentary organic matter) and reflectance analysis (Leitz Amistemp Microscope). For maceral analysis, individual maceral constituents were identified via visual inspection of samples under white and blue light and determining volume percent by a microscopic point count method. Vitrinite macerals are particles of sedimentary organic matter derived from wood, and their reflectance of incident light under oil immersion is used to assess the thermal maturity of a sample. Vitrinite reflectance ($\%R_0$) increases with increased depth of burial (i.e., increased thermal exposure), and is an indication of thermal maturity or

coal rank. Reflectance measurements for sample phytoclasts were measured and plotted as frequency histograms and polymodal histograms were edited to exclude recycled and contaminant vitrinites (i.e. providing a measure of indigenous vitrinite reflectance). Table S1 summarizes results of petrographic analysis.

Crude oil and coal chemical analyses. Sample extraction and extract cleanup were performed as described in the Experimental Section, and separated aliphatic and aromatic fractions were analyzed. The extraction method reported here (accepted variant of EPA method) has been vetted independently in our laboratory and found to have the approximate extraction efficiency of three serial 6 hour Soxhlet extractions in dichloromethane. Aliphatics from extracts were analyzed on a gas chromatograph (GC) equipped with a flame ionization detector (FID). The aliphatic hydrocarbons analyzed included the *n*-alkanes from *n*-nonane (nC_9) through *n*-tetratriacontane (nC_{34}), pristane (2,6,10,14-tetramethylhexadecane; abbreviated as Pr) and phytane (2,6,10,14-tetramethylheptadecane; Ph). These aliphatic hydrocarbons were separated on an HP Ultra 2 column (25 m x 0.25 mm x 0.33 μm). Aliphatic hydrocarbon concentrations were determined using an internal-standard method employing a five-point calibration curve for each target analyte, with the perdeuterated surrogate standards treated as the internal standards. The unresolved complex mixture was determined as the difference between the total FID response and the cumulative response of the resolved peaks. This difference was converted to a concentration using the response calibration curve for hexadecane (*S4*). In addition to data shown in the results, the full suite of PAHs analyzed also included both parent homolog and alkyl-substituted fluorenes, dibenzothiophenes, fluoranthenes/pyrenes, and chrysenes/benzanthracenes (abbreviated as flu-X, DBT-X, fp-

X, and chr-X, where X = number of alkyl-substituted carbon atoms ranging from 0 to 3 or 4), along with biphenyl (bip), acenaphthene (ace), acenaphthylene (acn), anthracene (ant), fluoranthene (fla), pyrene (pyr), methyl-fluoranthene/pyrene (fp-1), benzo-[*a*]-anthracene (baa), benzo-[*b*]-fluoranthene (bbf), benzo-[*k*]-fluoranthene (bkf), benzo-[*e*]-pyrene (bep), benzo-[*a*]-pyrene (bap), perylene (per), indeno-[1,2,3-*c,d*]-pyrene (icp), dibenzo-[*a,h*]-anthracene (dba), and benzo-[*g,h,i*]-perylene (bgp). The concentrations of N-1 and the unsubstituted PAHs were determined in a manner similar to that used for the aliphatic hydrocarbons. Calibration curves for the other alkyl-substituted PAHs were calculated using the most similar PAHs: 2,6-dimethylnaphthalene was used for nap-2; 2,3,5-trimethylnaphthalene was used for nap-3 and nap-4; and 1-methylphenanthrene was used for the phe-1-phe-4 homologues. Table S2 provides additional results from chemical analysis.

Samples were extracted and analyzed in batches of 12 along with two reference samples, a method blank and a spiked method blank for quality control. Method detection limits (MDLs) varied inversely with sample aliquot size and are summarized in Short et al. (*S4*). These MDLs are approximately 2-20 ng g^{-1} dry wt. sediment for the coal samples, and 100 – 15,000 ng g^{-1} dry wt. for the crude oil sample. Sample precision is generally better than ± 20% based on the combined results of the reference samples, and accuracy is generally better than ± 15% based on comparison with National Institute of Standards and Technology standards used for the spiked blanks.

Supporting Information References

(S1) Van Kooten, G. K.; Short, J. W.; Kolak, J. J. Low-maturity Kulthieth Formation coal: A possible source of polycyclic aromatic hydrocarbons in benthic sediment of the northern Gulf of Alaska. *J. Environ. Forensics* **2002**, *3*, 227-242.

(S2) Gagne, F.; Trottier, S.; Blaise, C. ; Sproul, J.; Ernst, B. Genotoxicity of sediment extracts obtained in the vicinity of a creosote-treated wharf to rainbow-trout hepatocytes. *Toxicol. Lett.* **1995**, *78*, 175-182.

(S3) Shi, L.; Muller, S.; Harms, H.; Wick, L. Y. Effect of electrokinetic transport on the vulnerability of PAH-degrading bacteria in a model aquifer. *Environ. Geochem. Health* **2008**, *30*, 177-178.

(S4) Short, J. W.; Jackson, T. J.; Larsen, M. L.; Wade, T. L. 1996. Analytical methods used for the analysis of hydrocarbons in crude oil, tissues, sediments, and seawater collected for the natural resources damage assessment of the *Exxon Valdez* oil spill. *Edited by* S.D.Rice, R.B.Spies, D.A.Wolfe, and B.A.Wright. American Fisheries Society Symposium 18, Bethesda, Maryland pp. 140-148.

.

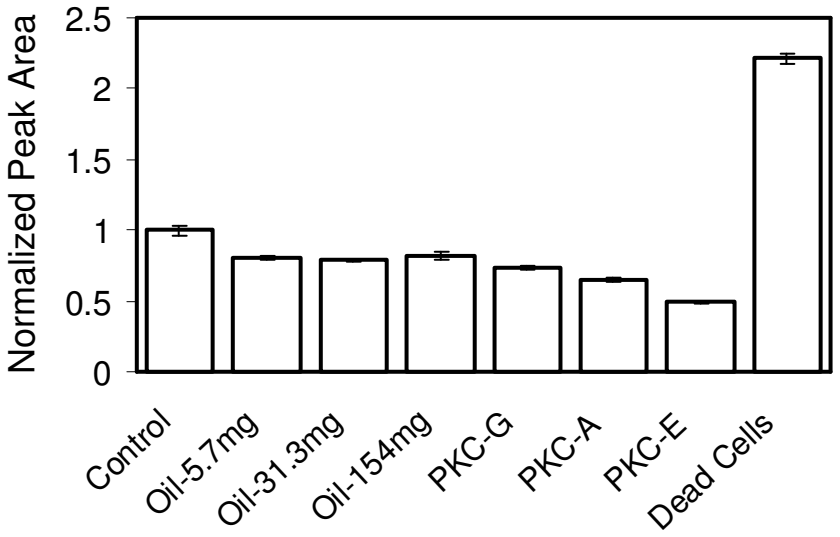

Figure S1. Results of cell viability assay using PI staining with positive staining representative of dead cells. "Control" denotes negative control – i.e. no naphthalene, and "Dead Cells" are positive control with no naphthalene wherein cells were killed prior to staining. Other labels correspond to sample IDs in Table 1, except coal numerical sample IDs have been truncated to last three digits for legibility.

Table S1. Complete results for petrographic analysis for samples in Table 1.

Sample ID	Telocollinite	Gelocollinite	Desmocollinite	Vitrodetrinite	Saprovitrinite	Fusinite/Semifusinite/Sclerotinite	Macrinite/Inertodetrinite	Micrinite	Sporinite/Cutinite/Suberinite	Resinite	Liptodetrinite	Alginite	Amorphous OM/Bituminite	Exsudatinite/Solid Bitumen	Mineral Matter (clays + pyrite)	Total Vitrinite (volume %)	Total Inertinite (volume %)	Total Liptinite (volume %)	Total Mineral Matter (volume %)	# of Readings	Total Sample (% Ro)	# of Indigeonus Readings	Indigenous Vitrinite (% Ro)	Comments
PKC-A	1	29	54	6	6	0	0	0	1	0	0	0	0	0	3	96	0	1	3	51	0.92	45	0.89	Abundant suppressed
PKC-B	3	7	34	7	0	0	1	0	5	0	0	0	0	0	43	51	1	5	43	50	0.92	41	0.90	Mixture of clay minerals and framboidal pyrite
PKC-C	2	18	54	15	4	0	1	0	1	1	0	1	0	0	3	93	1	3	3	50	0.99	42	0.96	
PKC-D	1	8	25	21	3	0	0	0	4	0	0	0	0	0	38	58	0	4	38	51	0.96	43	0.93	Abundant framboidal
PKC-E	2	15	44	10	4	0	3	0	3	1	0	0	0	1	17	75	3	5	17	51	0.99	43	0.97	Abundant framboidal
PKC-F	1	5	83	6	2	0	0	0	2	0	0	0	0	0	1	97	0	2	1	50	0.92	45	0.92	
PKC-G	1	11	40	12	8	1	0	0	0	1	0	0	0	0	26	72	1	1	26	50	0.93	47	0.90	Mostly framboidal pyrite; some clay
PKC-H	1	4	44	4	24	0	3	0	2	15	0	0	0	0	3	77	3	17	3	50	0.88	41	0.93	Abundant suppressed

Table S2. Complete results from chemical analysis of crude oil and coal samples used in this study.

	Exxon Valdez	Tyndall Glacier	Tyndall Glacier	Tyndall Glacier	Tyndall Glacier	Tyndall Glacier	Tyndall Glacier	Tyndall Glacier	Caetani River
	Crude oil	coal seam	coal seam	coal seam	coal seam	coal seam	coal float	coal seam	coal float
Lab ID:	EVCO	PKC-A	PKC-B	PKC-C	PKC-D	PKC-E	PKC-F	PKC-G	PKC-H
PAH concentrations (ng/g):									
Nap	7.24E+05	1.04E+04	4.35E+03	1.33E+05	1.98E+04	6.28E+04	3.86E+03	1.33E+03	3.28E+04
2-methylnap	1.33E+06	4.60E+04	2.00E+04	3.91E+05	6.97E+04	1.67E+05	1.02E+04	6.26E+03	9.63E+04
1-methylnap	1.02E+06	5.32E+04	3.96E+04	3.67E+05	7.61E+04	1.64E+05	3.47E+04	2.15E+04	7.81E+04
2,6-dimethylnap	7.55E+05	5.47E+04	3.00E+04	1.68E+05	6.27E+04	1.15E+05	1.59E+04	1.33E+04	5.70E+04
nap-2	3.15E+06	2.30E+05	1.59E+05	6.09E+05	2.38E+05	4.29E+05	9.46E+04	9.47E+04	1.78E+05
2,3,5-trimethylnap	3.69E+05	7.08E+04	9.08E+04	7.90E+04	4.41E+04	6.27E+04	3.02E+04	4.42E+04	3.51E+04
nap-3	2.35E+06	3.35E+05	3.67E+05	4.75E+05	2.19E+05	3.41E+05	1.60E+05	2.14E+05	1.70E+05
nap-4	5.98E+05	1.58E+05	2.02E+05	1.63E+05	6.66E+04	1.10E+05	1.05E+05	1.65E+05	6.60E+04
Bip	1.83E+05	1.86E+04	1.27E+04	5.48E+04	2.25E+04	4.46E+04	7.31E+03	5.31E+03	1.32E+04
can	1.39E+04	0.00E+00	0.00E+00	0.00E+00	0.00E+00	0.00E+00	0.00E+00	0.00E+00	0.00E+00
Ace	1.74E+04	1.68E+03	1.17E+03	8.81E+02	7.51E+02	1.16E+03	1.21E+03	1.58E+03	7.21E+02
Flu	9.11E+04	1.76E+04	8.61E+03	1.65E+04	2.43E+04	2.42E+04	1.12E+04	9.60E+03	9.79E+03
flu-1	2.25E+05	6.39E+04	3.83E+04	4.56E+04	5.49E+04	5.14E+04	2.82E+04	4.70E+04	2.03E+04
flu-2	1.91E+05	8.39E+04	7.10E+04	8.34E+04	6.07E+04	5.42E+04	5.03E+04	9.09E+04	2.94E+04
flu-3	1.51E+05	3.25E+04	2.40E+04	4.05E+04	1.98E+04	1.34E+04	2.31E+04	3.64E+04	6.24E+03
flu-4	NR	1.19E+04	1.20E+04	1.10E+04	4.59E+03	4.63E+03	7.99E+03	1.36E+04	1.85E+03
Dbt	1.95E+05	1.76E+04	1.60E+04	3.75E+04	2.43E+04	3.74E+04	4.35E+03	5.93E+03	3.97E+03
dbt-1	4.17E+05	5.65E+04	5.92E+04	6.82E+04	4.28E+04	6.61E+04	1.99E+04	3.96E+04	9.33E+03
dbt-2	5.70E+05	6.09E+04	7.00E+04	5.21E+04	3.78E+04	5.73E+04	2.16E+04	5.52E+04	6.66E+03
dbt-3	4.81E+05	2.84E+04	3.50E+04	2.73E+04	1.54E+04	2.04E+04	9.51E+03	2.74E+04	2.94E+03
dbt-4	NR	1.10E+04	1.27E+04	4.29E+03	5.42E+03	3.97E+03	3.37E+03	1.03E+04	5.18E+02
Phe	2.55E+05	7.96E+04	6.10E+04	9.03E+04	5.14E+04	7.44E+04	4.65E+04	4.20E+04	3.52E+04
1-methylphe	1.97E+05	4.88E+04	4.49E+04	5.33E+04	2.69E+04	3.81E+04	3.31E+04	3.86E+04	1.84E+04
phe-1	7.55E+05	2.23E+05	2.00E+05	2.34E+05	1.23E+05	1.77E+05	1.48E+05	1.94E+05	8.09E+04
phe-2	8.92E+05	2.13E+05	2.42E+05	2.18E+05	1.06E+05	1.48E+05	1.54E+05	2.43E+05	7.19E+04
phe-3	5.58E+05	1.22E+05	1.54E+05	1.11E+05	5.80E+04	7.82E+04	9.16E+04	1.48E+05	3.36E+04
phe-4	1.66E+05	9.70E+03	6.37E+03	8.47E+03	4.78E+03	4.85E+03	5.14E+03	1.47E+04	3.46E+03
Ant	ND	8.74E+02	6.27E+02	6.99E+02	4.92E+02	7.44E+02	3.94E+02	5.18E+02	6.73E+02
Fla	9.09E+03	2.25E+03	1.63E+03	2.30E+03	1.14E+03	1.69E+03	2.30E+03	2.36E+03	1.14E+03
Pyr	1.47E+04	6.24E+03	5.66E+03	6.12E+03	2.82E+03	4.13E+03	6.87E+03	6.99E+03	2.26E+03
fp-1	7.16E+04	3.63E+04	3.03E+04	3.43E+04	1.98E+04	2.65E+04	3.17E+04	3.89E+04	1.29E+04
fp-2	NR	5.75E+04	5.05E+04	6.53E+04	3.20E+04	3.73E+04	4.89E+04	6.95E+04	1.87E+04
fp-3	NR	3.13E+04	4.12E+04	4.04E+04	1.80E+04	2.10E+04	3.36E+04	4.63E+04	1.16E+04
fp-4	NR	5.53E+03	7.30E+03	8.77E+03	3.57E+03	4.64E+03	7.42E+03	1.06E+04	1.34E+03
Baa	ND	3.96E+03	3.25E+03	4.03E+03	1.74E+03	2.65E+03	2.20E+03	2.96E+03	1.25E+03
Chr	4.92E+04	1.71E+04	1.64E+04	1.94E+04	8.03E+03	1.11E+04	2.25E+04	2.27E+04	5.88E+03
chr-1	8.02E+04	4.43E+04	4.56E+04	4.08E+04	1.64E+04	2.81E+04	3.46E+04	4.96E+04	1.13E+04
chr-2	1.06E+05	5.77E+04	7.85E+04	5.71E+04	2.27E+04	3.02E+04	4.96E+04	6.44E+04	1.52E+04
chr-3	3.62E+04	2.18E+04	2.98E+04	1.89E+04	8.56E+03	1.17E+04	2.13E+04	2.90E+04	4.63E+03
chr-4	ND	1.54E+03	1.35E+03	6.02E+02	6.46E+02	7.99E+02	1.79E+03	1.80E+03	1.60E+02
Bbf	6.44E+03	3.10E+03	3.17E+03	5.50E+03	2.15E+03	2.51E+03	8.20E+03	5.97E+03	1.72E+03
Bkf	ND	8.02E+02	7.71E+02	9.07E+02	0.00E+00	4.27E+02	0.00E+00	0.00E+00	3.17E+02
Bep	1.19E+04	5.33E+03	5.74E+03	6.08E+03	2.37E+03	2.76E+03	1.33E+04	9.16E+03	1.66E+03
Bap	ND	2.12E+03	1.80E+03	1.78E+03	6.69E+02	1.21E+03	2.19E+03	2.11E+03	7.93E+02
Per	ND	1.56E+02	2.89E+02	1.09E+02	5.97E+01	8.45E+01	2.26E+02	2.44E+02	9.73E+02
Icp	ND	2.84E+02	9.59E+01	2.27E+02	1.47E+02	2.02E+02	4.18E+02	2.62E+02	1.29E+02

Dba	ND	8.62E+02	6.61E+02	1.18E+03	4.64E+02	6.94E+02	1.22E+03	1.02E+03	2.69E+02
Bgp	2.93E+03	1.67E+03	1.49E+03	1.69E+03	7.46E+02	8.72E+02	4.61E+03	2.46E+03	7.03E+02
Alkane concentrations (ng/g):									
C9	NR	2.08E+04	6.40E+03	5.84E+04	5.21E+04	7.83E+04	2.01E+03	3.60E+03	8.95E+03
C10	4.82E+06	8.41E+04	4.89E+04	1.33E+05	8.17E+04	1.36E+05	1.62E+03	1.27E+04	5.92E+04
C11	3.99E+06	6.32E+04	3.09E+04	1.15E+05	2.60E+04	3.53E+04	4.50E+03	1.13E+04	2.75E+04
C12	4.18E+06	6.69E+04	3.40E+04	9.02E+04	2.18E+04	3.14E+04	2.56E+03	1.71E+04	2.56E+04
C13	4.42E+06	7.76E+04	4.13E+04	8.56E+04	2.74E+04	3.49E+04	6.16E+03	2.26E+04	2.94E+04
C14	3.56E+06	5.66E+04	5.03E+04	4.50E+04	2.49E+04	2.77E+04	7.33E+03	3.40E+04	2.27E+04
C15	3.30E+06	5.22E+04	2.26E+04	3.41E+04	3.38E+04	2.34E+04	7.99E+03	1.40E+04	2.20E+04
C16	2.90E+06	4.92E+04	6.85E+04	3.75E+04	2.32E+04	2.29E+04	1.32E+04	4.82E+04	1.89E+04
C17	2.60E+06	3.70E+04	4.38E+04	2.91E+04	1.69E+04	1.88E+04	1.11E+04	2.55E+04	1.63E+04
Pr	2.31E+06	3.85E+04	9.63E+04	3.58E+04	2.54E+04	2.47E+04	2.10E+04	1.46E+05	3.41E+04
C18	2.89E+06	4.55E+04	2.75E+04	3.96E+04	1.71E+04	2.06E+04	1.76E+04	1.29E+04	1.65E+04
Ph	1.80E+06	1.36E+04	1.45E+04	1.39E+04	1.02E+04	6.41E+03	7.50E+03	1.42E+04	4.06E+03
C19	1.97E+06	3.55E+04	1.93E+04	3.45E+04	1.24E+04	1.79E+04	1.57E+04	9.37E+03	1.46E+04
C20	2.37E+06	3.64E+04	2.27E+04	3.58E+04	1.51E+04	1.81E+04	1.74E+04	1.23E+04	1.39E+04
C21	1.93E+06	2.88E+04	1.96E+04	2.97E+04	1.04E+04	1.44E+04	1.62E+04	1.13E+04	1.24E+04
C22	1.47E+06	2.84E+04	1.99E+04	3.11E+04	1.13E+04	1.50E+04	2.00E+04	1.40E+04	1.47E+04
C23	1.36E+06	2.43E+04	1.79E+04	2.88E+04	9.86E+03	1.30E+04	2.12E+04	1.48E+04	1.45E+04
C24	1.31E+06	2.08E+04	1.63E+04	2.76E+04	8.11E+03	1.05E+04	2.25E+04	1.55E+04	1.20E+04
C25	1.21E+06	1.96E+04	1.67E+04	2.65E+04	7.62E+03	1.01E+04	2.52E+04	1.70E+04	1.37E+04
C26	9.21E+05	1.66E+04	1.40E+04	2.28E+04	6.29E+03	8.25E+03	2.62E+04	1.61E+04	9.53E+03
C27	8.74E+05	1.21E+04	9.15E+03	1.67E+04	4.16E+03	5.46E+03	2.38E+04	1.23E+04	1.22E+04
C28	8.77E+05	1.14E+04	1.07E+04	1.86E+04	3.98E+03	5.19E+03	2.58E+04	1.42E+04	7.91E+03
C29	7.17E+05	8.41E+03	7.66E+03	1.54E+04	2.98E+03	3.88E+03	2.22E+04	1.16E+04	1.13E+04
C30	5.76E+05	2.85E+03	4.42E+03	9.87E+03	1.92E+03	2.35E+03	2.13E+04	8.65E+03	6.02E+03
C31	NR	5.12E+03	4.23E+03	9.98E+03	1.74E+03	2.07E+03	1.37E+04	7.24E+03	7.00E+03
C32	3.61E+05	4.38E+03	6.15E+03	5.91E+03	1.67E+03	1.33E+03	1.01E+04	6.56E+03	3.07E+03
C33	NR	2.02E+03	2.11E+03	3.96E+03	0.00E+00	6.96E+02	6.33E+03	3.60E+03	2.32E+03
C34	3.87E+05	1.33E+03	0.00E+00	6.73E+03	0.00E+00	0.00E+00	6.10E+03	3.87E+03	0.00E+00
C35	NR	2.05E+03	0.00E+00	4.02E+03	0.00E+00	0.00E+00	4.07E+03	1.51E+03	0.00E+00
C36	NR	0.00E+00	0.00E+00	0.00E+00	0.00E+00	0.00E+00	2.08E+03	0.00E+00	0.00E+00

Department of Ecology
Water Quality Program

AUG 1 3 2003
POSTED

SO3-001528D
INDUSTRIAL STORMWATER GENERAL PERMIT
DISCHARGE MONITORING REPORT

MONITORING PERIOD for (year/quarter): 2003 (year) Jan/Feb/Mar (Apr/May/Jun) Jul/Aug/Sep Oct/Nov/Dec

Facility/Site Information

BURLINGTON NORTHERN SANTE FE BALMER
Location: 3600 GILMAN AVE W
County: KING
Primary SIC Code: 4011

Mailing Information

BNR AND SANTE FE RAILWAY CO
2454 OCCIDENTAL AVE S SUITE 1A
SEATTLE WA 98134

You must send a Discharge Monitoring Report (DMR) to Ecology **every quarter**. If there was **no discharge** *or* you have **suspended sampling** because of consistent attainment of benchmark values, mark the appropriate boxes and send the DMR to Ecology. Please read the instructions before completing the DMR.

Discharge Point #1

X There was no qualifying storm event this quarter so no values are entered below (see explanation)

Quarterly Monitoring		AVERAGE	MAXIMUM	UNITS	Sample Type	Events Sampled
Turbidity	Consistent Attainment			NTU		
pH	Consistent Attainment			Standard Units		
Zinc (total)	Consistent Attainment			µg/L		
Oil & Grease	Consistent Attainment			mg/L	**Grab**	

I CERTIFY UNDER PENALTY OF LAW THAT I HAVE PERSONALLY EXAMINED AND AM FAMILIAR WITH THE INFORMATION SUBMITTED HEREIN AND BASED ON MY INQUIRY OF THOSE INDIVIDUALS IMMEDIATELY RESPONSIBLE FOR OBTAINING THE INFORMATION. I BELIEVE THE SUBMITTED INFORMATION IS TRUE, ACCURATE, AND COMPLETE. I AM AWARE THAT THERE ARE SIGNIFICANT PENALTIES FOR SUBMITTING FALSE INFORMATION INCLUDING THE POSSIBILITY OF FINE AND IMPRISONMENT. SEE 18 USC § 1001 AND 33 USC § 1319. *(PENALTIES UNDER THESE STATUES MAY INCLUDE FINES UP TO $10,000.00 AND OR MAXIMUM IMPRISONMENT OF BETWEEN SIX MONTHS AND FIVE YEARS.)*

Jennifer Anderson
NAME/TITLE PRINCIPAL EXECUTIVE OFFICER (TYPED OR PRINTED)

8/11/03
DATE: MO DAY YEAR

SIGNATURE OF PRINCIPAL EXECUTIVE OFFICER OR AUTHORIZED AGENT

206-625-6034
TELEPHONE NUMBER

COMMENTS / EXPLANATIONS

No discharge from site during observed qualifying rain events. Site is covered largely in gravel, which allows for rapid infiltration of stormwater.

Entered 2/20/05 CO

SO3-001528D

INDUSTRIAL STORMWATER GENERAL PERMIT
DISCHARGE MONITORING REPORT

MONITORING PERIOD for (year/quarter): 2003 (year) **Jan/Feb/Mar** **Apr/May/Jun** **Jul/Aug/Sep** **Oct/Nov/Dec**

Facility/Site Information

BURLINGTON NORTHERN SANTE FE - BALMER
Location: 3600 GILMAN AVE W
County: KING

Primary SIC Code: 4011

Mailing Information

BURLINGTON NORTHERN SANTE FE RAILROAD
2454 OCCIDENTAL AVE SOUTH, SUITE 2D
SEATTLE, WA 98134

Department of Ecology
Water Quality Program
NOV 17 2003

You must send a Discharge Monitoring Report (DMR) to Ecology **every quarter**. If there was **no discharge** *or* you have **suspended sampling** because of consistent attainment of benchmark values, mark the appropriate boxes and send the DMR to Ecology. Please read the instructions before completing the DMR.

Discharge Point #1

(X) There was no qualifying storm event this quarter so no values are entered below (see explanation)

Quarterly Monitoring		AVERAGE	MAXIMUM	UNITS	Sample Type	Events Sampled
Turbidity	Consistent Attainment			NTU		
pH	Consistent Attainment			Standard Units		
Zinc (total)	Consistent Attainment			µg/L		
Oil & Grease	Consistent Attainment			mg/L	**Grab**	

I CERTIFY UNDER PENALTY OF LAW THAT I HAVE PERSONALLY EXAMINED AND AM FAMILIAR WITH THE INFORMATION SUBMITTED HEREIN AND BASED ON MY INQUIRY OF THOSE INDIVIDUALS IMMEDIATELY RESPONSIBLE FOR OBTAINING THE INFORMATION, I BELIEVE THE SUBMITTED INFORMATION IS TRUE, ACCURATE, AND COMPLETE. I AM AWARE THAT THERE ARE SIGNIFICANT PENALTIES FOR SUBMITTING FALSE INFORMATION INCLUDING THE POSSIBILITY OF FINE AND IMPRISONMENT. SEE 18 USC § 1001 AND 33 USC § 1319. *(PENALTIES UNDER THESE STATUES MAY INCLUDE FINES UP TO $10,000.00 AND OR MAXIMUM IMPRISONMENT OF BETWEEN SIX MONTHS AND FIVE YEARS.)*

Jennifer Anderson
NAME/TITLE PRINCIPAL EXECUTIVE OFFICER (TYPED OR PRINTED)

11/14/03
DATE: MO DAY YEAR

For Jennifer Anderson
Agent of BNSF
SIGNATURE OF PRINCIPAL EXECUTIVE OFFICER OR AUTHORIZED AGENT

206-625-6034
TELEPHONE NUMBER

COMMENTS / EXPLANATIONS

No discharge from site during observed qualifying rain events. Site is covered largely in gravel, which allows for rapid infiltration of stormwater.

SO3-001528D

INDUSTRIAL STORMWATER GENERAL PERMIT
DISCHARGE MONITORING REPORT

MONITORING PERIOD for (year/quarter): 2003 (year) Jan/Feb/Mar Apr/May/Jun Jul/Aug/Sep X Oct/Nov/Dec

Facility/Site Information

Burlington Northern Santa Fe - BALMER
Location: 3600 Gilman Ave. W, Seattle Washington
County: KING

Primary SIC Code: 4011

Mailing Information

Burlington Northern Santa Fe Railroad
2454 Occidental Ave. South, Suite 2D
Seattle, WA 98134

Department of Ecology
Water Quality Program
FEB 13 2004
Entered 25 Feb 05

You must send a Discharge Monitoring Report (DMR) to Ecology **every quarter**. If there was **no discharge** *or* you have **suspended sampling** because of consistent attainment of benchmark values, mark the appropriate boxes and send the DMR to Ecology. Please read the instructions before completing the DMR.

Discharge Point #1

There was no qualifying storm event this quarter so no values are entered below (see explanation)

Quarterly Monitoring		AVERAGE	MAXIMUM	UNITS	Sample Type	Events Sampled
Turbidity	Consistent Attainment	526	526	NTU	Grab	10/15/03
pH	Consistent Attainment	6	6	Standard Units	Grab	10/15/03
Zinc (total)	Consistent Attainment	125	125	µg/L	Grab	10/15/03
Oil & Grease	Consistent Attainment	ND	ND	mg/L	Grab	10/15/03

I CERTIFY UNDER PENALTY OF LAW THAT I HAVE PERSONALLY EXAMINED AND AM FAMILIAR WITH THE INFORMATION SUBMITTED HEREIN AND BASED ON MY INQUIRY OF THOSE INDIVIDUALS IMMEDIATELY RESPONSIBLE FOR OBTAINING THE INFORMATION, I BELIEVE THE SUBMITTED INFORMATION IS TRUE, ACCURATE, AND COMPLETE. I AM AWARE THAT THERE ARE SIGNIFICANT PENALTIES FOR SUBMITTING FALSE INFORMATION INCLUDING THE POSSIBILITY OF FINE AND IMPRISONMENT. SEE 18 USC § 1001 AND 33 USC § 1319. *(PENALTIES UNDER THESE STATUES MAY INCLUDE FINES UP TO $10,000.00 AND OR MAXIMUM IMPRISONMENT OF BETWEEN SIX MONTHS AND FIVE YEARS.)*

Jennifer Anderson
NAME/TITLE PRINCIPAL EXECUTIVE OFFICER (TYPED OR PRINTED)

February 11, 2004
DATE: MO DAY YEAR

Jennifer Anderson
SIGNATURE OF PRINCIPAL EXECUTIVE OFFICER OR AUTHORIZED AGENT

206-625-6034
TELEPHONE NUMBER

COMMENTS / EXPLANATIONS

Entered 5-7-04

SO3-001528D

INDUSTRIAL STORMWATER GENERAL PERMIT
DISCHARGE MONITORING REPORT

MONITORING PERIOD for (year/quarter): 2004 (year) X Jan/Feb/Mar Apr/May/Jun Jul/Aug/Sep Oct/Nov/Dec

Facility/Site Information

Burlington Northern Santa Fe - BALMER
Location: 3600 Gilman Ave. W, Seattle Washington
County: KING
Primary SIC Code: 4011

Mailing Information

Burlington Northern Santa Fe Railroad
2454 Occidental Ave. South, Suite 2D
Seattle, WA 98134

Department of Ecology
Water Quality Program
MAY 1 9 2004

You must send a Discharge Monitoring Report (DMR) to Ecology **every quarter**. If there was **no discharge** *or* you have **suspended sampling** because of consistent attainment of benchmark values, mark the appropriate boxes and send the DMR to Ecology. Please read the instructions before completing the DMR.

Discharge Point #2

There was no qualifying storm event this quarter so no values are entered below (see explanation)

Quarterly Monitoring		AVERAGE	MAXIMUM	UNITS	Sample Type	Events Sampled
Turbidity	Consistent Attainment	94.3	94.3	NTU	Grab	03/25/04
pH	Consistent Attainment	6	6	Standard Units	Grab	03/25/04
Zinc (total)	Consistent Attainment	132	132	µg/L	Grab	03/25/04
Oil & Grease	Consistent Attainment	ND	ND	mg/L	Grab	03/25/04

I CERTIFY UNDER PENALTY OF LAW THAT I HAVE PERSONALLY EXAMINED AND AM FAMILIAR WITH THE INFORMATION SUBMITTED HEREIN AND BASED ON MY INQUIRY OF THOSE INDIVIDUALS IMMEDIATELY RESPONSIBLE FOR OBTAINING THE INFORMATION, I BELIEVE THE SUBMITTED INFORMATION IS TRUE, ACCURATE, AND COMPLETE. I AM AWARE THAT THERE ARE SIGNIFICANT PENALTIES FOR SUBMITTING FALSE INFORMATION INCLUDING THE POSSIBILITY OF FINE AND IMPRISONMENT. SEE 18 USC § 1001 AND 33 USC § 1319. *(PENALTIES UNDER THESE STATUES MAY INCLUDE FINES UP TO $10,000.00 AND OR MAXIMUM IMPRISONMENT OF BETWEEN SIX MONTHS AND FIVE YEARS)*

Jennifer Anderson
NAME/TITLE PRINCIPAL EXECUTIVE OFFICER (TYPED OR PRINTED)

May 15, 2004
DATE: MO DAY YEAR

SIGNATURE OF PRINCIPAL EXECUTIVE OFFICER OR AUTHORIZED AGENT

206-625-6034
TELEPHONE NUMBER

COMMENTS / EXPLANATIONS

Entered 8/2/05 C

AUG 10 2004
Department of Ecology Water Quality Program

SO3-001528D
INDUSTRIAL STORMWATER GENERAL PERMIT
DISCHARGE MONITORING REPORT

MONITORING PERIOD for (year/quarter): 2004 (year) Jan/Feb/Mar X Apr/May/Jun Jul/Aug/Sep Oct/Nov/Dec

Facility/Site Information

Burlington Northern Santa Fe - BALMER
Location: 3600 Gilman Ave. W, Seattle Washington
County: KING
Primary SIC Code: 4011

Mailing Information

Burlington Northern Santa Fe Railroad
2454 Occidental Ave. South, Suite 2D
Seattle, WA 98134

You must send a Discharge Monitoring Report (DMR) to Ecology **every quarter**. If there was **no discharge** *or* you have **suspended sampling** because of consistent attainment of benchmark values, mark the appropriate boxes and send the DMR to Ecology. Please read the instructions before completing the DMR.

Discharge Point #1

X There was no qualifying storm event this quarter so no values are entered below (see explanation)

Quarterly Monitoring		AVERAGE	MAXIMUM	UNITS	Sample Type	Events Sampled
Turbidity	Consistent Attainment			NTU		
pH	Consistent Attainment			Standard Units		
Zinc (total)	Consistent Attainment			µg/L		
Oil & Grease	Consistent Attainment			mg/L		

I CERTIFY UNDER PENALTY OF LAW THAT I HAVE PERSONALLY EXAMINED AND AM FAMILIAR WITH THE INFORMATION SUBMITTED HEREIN AND BASED ON MY INQUIRY OF THOSE INDIVIDUALS IMMEDIATELY RESPONSIBLE FOR OBTAINING THE INFORMATION, I BELIEVE THE SUBMITTED INFORMATION IS TRUE, ACCURATE, AND COMPLETE. I AM AWARE THAT THERE ARE SIGNIFICANT PENALTIES FOR SUBMITTING FALSE INFORMATION INCLUDING THE POSSIBILITY OF FINE AND IMPRISONMENT. SEE 18 USC § 1001 AND 33 USC § 1319. *(PENALTIES UNDER THESE STATUES MAY INCLUDE FINES UP TO $10,000.00 AND OR MAXIMUM IMPRISONMENT OF BETWEEN SIX MONTHS AND FIVE YEARS.)*

Jennifer Anderson
NAME/TITLE PRINCIPAL EXECUTIVE OFFICER (TYPED OR PRINTED)

August 9 2004
DATE: MO DAY YEAR

SIGNATURE OF PRINCIPAL EXECUTIVE OFFICER OR AUTHORIZED AGENT

206-625-6034
TELEPHONE NUMBER

COMMENTS / EXPLANATIONS
No discharge was present at the site during observed qualifying rain events. Site is covered largely in gravel, which allows for rapid infiltration of stormwater.

Entered 8 Nov 05

SO3-001528D
INDUSTRIAL STORMWATER GENERAL PERMIT
DISCHARGE MONITORING REPORT

MONITORING PERIOD for (year/quarter): 2004 (year) **Jan/Feb/Mar** **Apr/May/Jun** X **Jul/Aug/Sep** **Oct/Nov/Dec**

Facility/Site Information

Burlington Northern Santa Fe - BALMER
Location: 3600 Gilman Ave. W, Seattle Washington
County: KING
Primary SIC Code: 4011

Mailing Information

Burlington Northern Santa Fe Railroad
2454 Occidental Ave. South, Suite 2D
Seattle, WA 98134

You must send a Discharge Monitoring Report (DMR) to Ecology **every quarter**. If there was **no discharge** *or* you have **suspended sampling** because of consistent attainment of benchmark values, mark the appropriate boxes and send the DMR to Ecology. Please read the instructions before completing the DMR.

Discharge Point #1

There was no qualifying storm event this quarter so no values are entered below (see explanation)

Quarterly Monitoring		AVERAGE	MAXIMUM	UNITS	Sample Type	Events Sampled
Turbidity	Consistent Attainment	**1990**	**1990**	NTU	**grab**	**9/1/2004**
pH	Consistent Attainment	**7**	**7**	Standard Units	**grab**	**9/1/2004**
Zinc (total)	Consistent Attainment	**1,180**	**1,180**	µg/L	**grab**	**9/1/2004**
Oil & Grease	Consistent Attainment	**4.9**	**4.9**	mg/L	**grab**	**9/1/2004**

I CERTIFY UNDER PENALTY OF LAW THAT I HAVE PERSONALLY EXAMINED AND AM FAMILIAR WITH THE INFORMATION SUBMITTED HEREIN AND BASED ON MY INQUIRY OF THOSE INDIVIDUALS IMMEDIATELY RESPONSIBLE FOR OBTAINING THE INFORMATION, I BELIEVE THE SUBMITTED INFORMATION IS TRUE, ACCURATE, AND COMPLETE. I AM AWARE THAT THERE ARE SIGNIFICANT PENALTIES FOR SUBMITTING FALSE INFORMATION INCLUDING THE POSSIBILITY OF FINE AND IMPRISONMENT. SEE 18 USC § 1001 AND 33 USC § 1319. *(PENALTIES UNDER THESE STATUES MAY INCLUDE FINES UP TO $10,000.00 AND OR MAXIMUM IMPRISONMENT OF BETWEEN SIX MONTHS AND FIVE YEARS.)*

Jennifer Anderson
NAME/TITLE PRINCIPAL EXECUTIVE OFFICER (TYPED OR PRINTED)

11-15-04
DATE: MO DAY YEAR

SIGNATURE OF PRINCIPAL EXECUTIVE OFFICER OR AUTHORIZED AGENT

206-625-6034
TELEPHONE NUMBER

COMMENTS / EXPLANATIONS

3-9-05ca

SO3-001528D
INDUSTRIAL STORMWATER GENERAL PERMIT
DISCHARGE MONITORING REPORT

MONITORING PERIOD for (year/quarter): 2004 (year) Jan/Feb/Mar Apr/May/Jun Jul/Aug/Sep X Oct/Nov/Dec

Facility/Site Information

Burlington Northern Santa Fe - BALMER
Location: 3600 Gilman Ave. W, Seattle Washington
County: KING
Primary SIC Code: 4011

Mailing Information

Burlington Northern Santa Fe Railroad
2454 Occidental Ave. South, Suite 2D
Seattle, WA 98134

You must send a Discharge Monitoring Report (DMR) to Ecology **every quarter**. If there was **no discharge** *or* you have **suspended sampling** because of consistent attainment of benchmark values, mark the appropriate boxes and send the DMR to Ecology. Please read the instructions before completing the DMR.

Discharge Point #1

There was no qualifying storm event this quarter so no values are entered below (see explanation)

Quarterly Monitoring		AVERAGE	MAXIMUM	UNITS	Sample Type	Events Sampled
Turbidity	Consistent Attainment	**290**	**290**	NTU	**grab**	**12/13/2004**
pH	Consistent Attainment	**7**	**7**	Standard Units	**grab**	**12/13/2004**
Zinc (total)	Consistent Attainment	**240**	**240**	µg/L	**grab**	**12/13/2004**
Oil & Grease	Consistent Attainment	**ND**	**ND**	mg/L	**grab**	**12/13/2004**

I CERTIFY UNDER PENALTY OF LAW THAT I HAVE PERSONALLY EXAMINED AND AM FAMILIAR WITH THE INFORMATION SUBMITTED HEREIN AND BASED ON MY INQUIRY OF THOSE INDIVIDUALS IMMEDIATELY RESPONSIBLE FOR OBTAINING THE INFORMATION, I BELIEVE THE SUBMITTED INFORMATION IS TRUE, ACCURATE, AND COMPLETE. I AM AWARE THAT THERE ARE SIGNIFICANT PENALTIES FOR SUBMITTING FALSE INFORMATION INCLUDING THE POSSIBILITY OF FINE AND IMPRISONMENT. SEE 18 USC § 1001 AND 33 USC § 1319. *(PENALTIES UNDER THESE STATUES MAY INCLUDE FINES UP TO $10,000.00 AND OR MAXIMUM IMPRISONMENT OF BETWEEN SIX MONTHS AND FIVE YEARS.)*

Jennifer Anderson
NAME/TITLE PRINCIPAL EXECUTIVE OFFICER (TYPED OR PRINTED)

2-14-05
DATE: MO DAY YEAR

SIGNATURE OF PRINCIPAL EXECUTIVE OFFICER OR AUTHORIZED AGENT

206-625-6034
TELEPHONE NUMBER

COMMENTS / EXPLANATIONS

SO3-001528D

INDUSTRIAL STORMWATER GENERAL PERMIT
DISCHARGE MONITORING REPORT

Department of Ecology
Water Quality Program
MAY 16 2005

MONITORING PERIOD for (year/quarter): 2005 (year) X Jan/Feb/Mar Apr/May/Jun Jul/Aug/Sep Oct/Nov/Dec

Facility/Site Information

Burlington Northern Santa Fe - BALMER
Location: 3600 Gilman Ave. W, Seattle Washington
County: KING

Primary SIC Code: 4011

Mailing Information

Burlington Northern Santa Fe Railroad
2454 Occidental Ave. South, Suite 2D
Seattle, WA 98134

You must send a Discharge Monitoring Report (DMR) to Ecology **every quarter**. If there was **no discharge** *or* you have **suspended sampling** because of consistent attainment of benchmark values, mark the appropriate boxes and send the DMR to Ecology. Please read the instructions before completing the DMR.

Discharge Point #1

X There was no qualifying storm event this quarter so no values are entered below (see explanation)

Quarterly Monitoring		AVERAGE	MAXIMUM	UNITS	Sample Type	Events Sampled
Turbidity	Consistent Attainment			NTU		
pH	Consistent Attainment			Standard Units		
Zinc (total)	Consistent Attainment			µg/L		
Oil & Grease	Consistent Attainment			mg/L		
Lead (total)	Consistent Attainment			µg/L		
Oil & Grease	Consistent Attainment			mg/L		
Hardness	**N/A – Discharge to Marine Water.**					

I CERTIFY UNDER PENALTY OF LAW THAT I HAVE PERSONALLY EXAMINED AND AM FAMILIAR WITH THE INFORMATION SUBMITTED HEREIN AND BASED ON MY INQUIRY OF THOSE INDIVIDUALS IMMEDIATELY RESPONSIBLE FOR OBTAINING THE INFORMATION, I BELIEVE THE SUBMITTED INFORMATION IS TRUE, ACCURATE, AND COMPLETE. I AM AWARE THAT THERE ARE SIGNIFICANT PENALTIES FOR SUBMITTING FALSE INFORMATION INCLUDING THE POSSIBILITY OF FINE AND IMPRISONMENT. SEE 18 USC § 1001 AND 33 USC § 1319. *(PENALTIES UNDER THESE STATUES MAY INCLUDE FINES UP TO $10,000.00 AND OR MAXIMUM IMPRISONMENT OF BETWEEN SIX MONTHS AND FIVE YEARS.)*

Jennifer Anderson
NAME/TITLE PRINCIPAL EXECUTIVE OFFICER (TYPED OR PRINTED)

5/13/05
DATE: MO DAY YEAR

SIGNATURE OF PRINCIPAL EXECUTIVE OFFICER OR AUTHORIZED AGENT

206-625-6034
TELEPHONE NUMBER

COMMENTS / EXPLANATIONS
No discharge was observed during qualifying rain events.
Due to site improvements, the sampling point will be relocated.

SO3-001528D

INDUSTRIAL STORMWATER GENERAL PERMIT
DISCHARGE MONITORING REPORT

Department of Ecology
Water Quality Program
AUG 16 2005

MONITORING PERIOD for (year/quarter): 2005 (year) Jan/Feb/Mar **X** Apr/May/Jun Jul/Aug/Sep Oct/Nov/Dec

Facility/Site Information

BNSF - BALMER
Location: 3600 Gilman Ave. W, Seattle Washington
County: KING
Primary SIC Code: 4011

Mailing Information

BNSF Railway
2454 Occidental Ave. South, Suite 2D
Seattle, WA 98134

Entered 23 Aug 05

You must send a Discharge Monitoring Report (DMR) to Ecology **every quarter**. If there was **no discharge** *or* you have **suspended sampling** because of consistent attainment of benchmark values, mark the appropriate boxes and send the DMR to Ecology. Please read the instructions before completing the DMR.

Discharge Point #1

X There was no qualifying storm event this quarter so no values are entered below (see explanation)

Quarterly Monitoring		AVERAGE	MAXIMUM	UNITS	Sample Type	Events Sampled
Turbidity	Consistent Attainment			NTU		
pH	Consistent Attainment			Standard Units		
Zinc (total)	Consistent Attainment			µg/L		
Copper (total)	Consistent Attainment			µg/L		
Lead (total)	Consistent Attainment			µg/L		
Oil & Grease	Consistent Attainment			mg/L		
Hardness	**N/A – Discharge to Marine Water.**					

I CERTIFY UNDER PENALTY OF LAW THAT I HAVE PERSONALLY EXAMINED AND AM FAMILIAR WITH THE INFORMATION SUBMITTED HEREIN AND BASED ON MY INQUIRY OF THOSE INDIVIDUALS IMMEDIATELY RESPONSIBLE FOR OBTAINING THE INFORMATION, I BELIEVE THE SUBMITTED INFORMATION IS TRUE, ACCURATE, AND COMPLETE. I AM AWARE THAT THERE ARE SIGNIFICANT PENALTIES FOR SUBMITTING FALSE INFORMATION INCLUDING THE POSSIBILITY OF FINE AND IMPRISONMENT. SEE 18 USC § 1001 AND 33 USC § 1319. *(PENALTIES UNDER THESE STATUES MAY INCLUDE FINES UP TO $10,000.00 AND OR MAXIMUM IMPRISONMENT OF BETWEEN SIX MONTHS AND FIVE YEARS.)*

Jennifer Anderson
NAME/TITLE PRINCIPAL EXECUTIVE OFFICER (TYPED OR PRINTED)

8/11/05
DATE: MO DAY YEAR

Jennifer Anderson for BNSF
SIGNATURE OF PRINCIPAL EXECUTIVE OFFICER OR AUTHORIZED AGENT

206-625-6034
TELEPHONE NUMBER

COMMENTS / EXPLANATIONS
No discharge was observed during qualifying rain events.

Department of Ecology
Water Quality Program
OCT 11 2005

SO3-001528D

INDUSTRIAL STORMWATER GENERAL PERMIT
DISCHARGE MONITORING REPORT

MONITORING PERIOD for (year/quarter): 2005 (year) Jan/Feb/Mar Apr/May/Jun X Jul/Aug/Sep Oct/Nov/Dec

Facility/Site Information

BNSF - BALMER
Location: 3600 Gilman Ave. W, Seattle Washington
County: KING
Primary SIC Code: 4011

Mailing Information

BNSF Railway
2454 Occidental Ave. South, Suite 2D
Seattle, WA 98134

Entered 12 Oct 05

You must send a Discharge Monitoring Report (DMR) to Ecology **every quarter**. If there was **no discharge** *or* you have **suspended sampling** because of consistent attainment of benchmark values, mark the appropriate boxes and send the DMR to Ecology. Please read the instructions before completing the DMR.

Discharge Point #1

X There was no qualifying storm event this quarter so no values are entered below (see explanation)

Quarterly Monitoring		AVERAGE	MAXIMUM	UNITS	Sample Type	Events Sampled
Turbidity	Consistent Attainment			NTU		
pH	Consistent Attainment			Standard Units		
Zinc (total)	Consistent Attainment			µg/L		
Copper (total)	Consistent Attainment			µg/L		
Lead (total)	Consistent Attainment			µg/L		
Oil & Grease	Consistent Attainment			mg/L		
Hardness	**N/A – Discharge to Marine Water.**					

I CERTIFY UNDER PENALTY OF LAW THAT I HAVE PERSONALLY EXAMINED AND AM FAMILIAR WITH THE INFORMATION SUBMITTED HEREIN AND BASED ON MY INQUIRY OF THOSE INDIVIDUALS IMMEDIATELY RESPONSIBLE FOR OBTAINING THE INFORMATION, I BELIEVE THE SUBMITTED INFORMATION IS TRUE, ACCURATE, AND COMPLETE. I AM AWARE THAT THERE ARE SIGNIFICANT PENALTIES FOR SUBMITTING FALSE INFORMATION INCLUDING THE POSSIBILITY OF FINE AND IMPRISONMENT. SEE 18 USC § 1001 AND 33 USC § 1319. *(PENALTIES UNDER THESE STATUES MAY INCLUDE FINES UP TO $10,000.00 AND OR MAXIMUM IMPRISONMENT OF BETWEEN SIX MONTHS AND FIVE YEARS.)*

Jennifer Anderson
NAME/TITLE/PRINCIPAL EXECUTIVE OFFICER (TYPED OR PRINTED)

10/10/05
DATE: MO DAY YEAR

SIGNATURE OF PRINCIPAL EXECUTIVE OFFICER OR AUTHORIZED AGENT

206-625-6034
TELEPHONE NUMBER

COMMENTS / EXPLANATIONS
No discharge was observed at the site during the quarter.

SO3-001528D

INDUSTRIAL STORMWATER GENERAL PERMIT
DISCHARGE MONITORING REPORT

MONITORING PERIOD for (year/quarter): 2005 (year) Jan/Feb/Mar Apr/May/Jun Jul/Aug/Sep X Oct/Nov/Dec

Facility/Site Information

BNSF - BALMER
Location: 3600 Gilman Ave. W, Seattle Washington
County: KING
Primary SIC Code: 4011

Mailing Information

BNSF Railway
2454 Occidental Ave. South, Suite 2D
Seattle, WA 98134

Water Quality Program
FEB 14 2006

You must send a Discharge Monitoring Report (DMR) to Ecology **every quarter**. If there was **no discharge** *or* you have **suspended sampling** because of consistent attainment of benchmark values, mark the appropriate boxes and send the DMR to Ecology. Please read the instructions before completing the DMR.

Discharge Point #1

X There was no qualifying storm event this quarter so no values are entered below (see explanation)

Quarterly Monitoring		AVERAGE	MAXIMUM	UNITS	Sample Type	Events Sampled
Turbidity	Consistent Attainment			NTU		
pH	Consistent Attainment			Standard Units		
Zinc (total)	Consistent Attainment			µg/L		
Copper (total)	Consistent Attainment			µg/L		
Lead (total)	Consistent Attainment			µg/L		
Oil & Grease	Consistent Attainment			mg/L		
Hardness	**N/A – Discharge to Marine Water.**					

I CERTIFY UNDER PENALTY OF LAW THAT I HAVE PERSONALLY EXAMINED AND AM FAMILIAR WITH THE INFORMATION SUBMITTED HEREIN AND BASED ON MY INQUIRY OF THOSE INDIVIDUALS IMMEDIATELY RESPONSIBLE FOR OBTAINING THE INFORMATION, I BELIEVE THE SUBMITTED INFORMATION IS TRUE, ACCURATE, AND COMPLETE. I AM AWARE THAT THERE ARE SIGNIFICANT PENALTIES FOR SUBMITTING FALSE INFORMATION INCLUDING THE POSSIBILITY OF FINE AND IMPRISONMENT. SEE 18 USC § 1001 AND 33 USC § 1319. *(PENALTIES UNDER THESE STATUES MAY INCLUDE FINES UP TO $10,000.00 AND OR MAXIMUM IMPRISONMENT OF BETWEEN SIX MONTHS AND FIVE YEARS.)*

Jennifer Anderson
NAME/TITLE PRINCIPAL EXECUTIVE OFFICER (TYPED OR PRINTED)

2/15/2006
DATE: MO DAY YEAR

SIGNATURE OF PRINCIPAL EXECUTIVE OFFICER OR AUTHORIZED AGENT

206-625-6034
TELEPHONE NUMBER

COMMENTS / EXPLANATIONS
No discharge was observed at the site during the qualified rain events.

POSTED
DATE: 5/12/06
INITIALS: JAN

MAY 1 0 2006

SO3-001528D

INDUSTRIAL STORMWATER GENERAL PERMIT
DISCHARGE MONITORING REPORT

MONITORING PERIOD for (year/quarter): 2006 (year) **X** Jan/Feb/Mar Apr/May/Jun Jul/Aug/Sep Oct/Nov/Dec

Facility/Site Information

Burlington Northern Santa Fe - BALMER
Location: 3600 Gilman Ave. W, Seattle Washington
County: KING
Primary SIC Code: 4011

Mailing Information

Burlington Northern Santa Fe Railroad
2454 Occidental Ave. South, Suite 2D
Seattle, WA 98134

You must send a Discharge Monitoring Report (DMR) to E as **no discharge** *or* you have **suspended sampling** because of consistent attainment of be priate boxes and send the DMR to Ecology. Please read the instructions before compl

A & B
LEVEL ONE RESPONSES

Discharge Point #1

There was no qualifying storm event this quarter so no values are entered below (see explanation)

Quarterly Monitoring		AVERAGE	MAXIMUM	UNITS	Sample Type	Events Sampled
Turbidity	Consistent Attainment	**490**	**490**	NTU	**grab**	**01/16/2006**
pH	Consistent Attainment	**7.1**	**7.1**	Standard Units	**grab**	**01/16/2006**
Zinc (total)	Consistent Attainment	**590**	**590**	µg/L	**grab**	**01/16/2006**
Oil & Grease	Consistent Attainment	**ND**	**ND**	mg/L	**grab**	**01/16/2006**
Lead (total)	Consistent Attainment	**110**	**110**	µg/L	**grab**	**01/16/2006**
Copper (total)	Consistent Attainment	**130**	**130**	µg/L	**grab**	**01/16/2006**
Hardness	**N/A – Discharge to Marine Water.**					

I CERTIFY UNDER PENALTY OF LAW THAT I HAVE PERSONALLY EXAMINED AND AM FAMILIAR WITH THE INFORMATION SUBMITTED HEREIN AND BASED ON MY INQUIRY OF THOSE INDIVIDUALS IMMEDIATELY RESPONSIBLE FOR OBTAINING THE INFORMATION, I BELIEVE THE SUBMITTED INFORMATION IS TRUE, ACCURATE, AND COMPLETE. I AM AWARE THAT THERE ARE SIGNIFICANT PENALTIES FOR SUBMITTING FALSE INFORMATION INCLUDING THE POSSIBILITY OF FINE AND IMPRISONMENT. SEE 18 USC § 1001 AND 33 USC § 1319. *(PENALTIES UNDER THESE STATUES MAY INCLUDE FINES UP TO $10,000.00 AND OR MAXIMUM IMPRISONMENT OF BETWEEN SIX MONTHS AND FIVE YEARS.)*

Jennifer Anderson
NAME/TITLE PRINCIPAL EXECUTIVE OFFICER (TYPED OR PRINTED)

DATE: MO 5 DAY 12 YEAR 06

SIGNATURE OF PRINCIPAL EXECUTIVE OFFICER OR AUTHORIZED AGENT

206-625-6034
TELEPHONE NUMBER

COMMENTS / EXPLANATIONS

INCOMPLETE
APP FORM

JK

DEPARTMENT OF ECOLOGY

JUN 2 1 2007
WATER QUALITY PROGRAM

SO3-001528D

INDUSTRIAL STORMWATER GENERAL PERMIT DISCHARGE MONITORING REPORT

MONITORING PERIOD for (year/quarter): 2006 (year) X Jan/Feb/Mar Apr/May/Jun Jul/Aug/Sep Oct/Nov/Dec

Facility/Site Information

Burlington Northern Santa Fe - BALMER
Location: 3600 Gilman Ave. W, Seattle Washington
County: KING

Primary SIC Code: 4011

Mailing Information

Burlington Northern Santa Fe Railroad
2454 Occidental Ave. South, Suite 2D
Seattle, WA 98134

You must send a Discharge Monitoring Report (DMR) to Ecology **every quarter**. If there was **no discharge** *or* you have **suspended sampling** because of consistent attainment of benchmark values, mark the appropriate boxes and send the DMR to Ecology. Please read the instructions before completing the DMR.

Discharge Point #1 #2 MB

There was no qualifying storm event this quarter so no values are entered below (see explanation)

Quarterly Monitoring		AVERAGE	MAXIMUM	UNITS	Sample Type	Events Sampled
Turbidity	Consistent Attainment	490	490	NTU	grab	01/16/2006
pH	Consistent Attainment	7.1	7.1	Standard Units	grab	01/16/2006
Zinc (total)	Consistent Attainment	590	590	µg/L	grab	01/16/2006
Oil & Grease	Consistent Attainment	ND	ND	mg/L	grab	01/16/2006
Lead (total)	Consistent Attainment	110	110	µg/L	grab	01/16/2006
Copper (total)	Consistent Attainment	130	130	µg/L	grab	01/16/2006
Hardness	**N/A – Discharge to Marine Water.**					

I CERTIFY UNDER PENALTY OF LAW THAT I HAVE PERSONALLY EXAMINED AND AM FAMILIAR WITH THE INFORMATION SUBMITTED HEREIN AND BASED ON MY INQUIRY OF THOSE INDIVIDUALS IMMEDIATELY RESPONSIBLE FOR OBTAINING THE INFORMATION, I BELIEVE THE SUBMITTED INFORMATION IS TRUE, ACCURATE, AND COMPLETE. I AM AWARE THAT THERE ARE SIGNIFICANT PENALTIES FOR SUBMITTING FALSE INFORMATION INCLUDING THE POSSIBILITY OF FINE AND IMPRISONMENT. SEE 18 USC § 1001 AND 33 USC § 1319. *(PENALTIES UNDER THESE STATUES MAY INCLUDE FINES UP TO $10,000.00 AND OR MAXIMUM IMPRISONMENT OF BETWEEN SIX MONTHS AND FIVE YEARS.)*

Jennifer Anderson
NAME/TITLE PRINCIPAL EXECUTIVE OFFICER (TYPED OR PRINTED)

DATE: MO. 5 DAY 12 YEAR 06

SIGNATURE OF PRINCIPAL EXECUTIVE OFFICER OR AUTHORIZED AGENT

206-625-6034
TELEPHONE NUMBER

COMMENTS / EXPLANATIONS

POSTED
DATE:
INITIALS:

SO3-001528D

INDUSTRIAL STORMWATER GENERAL PERMIT
DISCHARGE MONITORING REPORT

MONITORING PERIOD for (year/quarter): 2006 (year) ☐ Jan/Feb/Mar X Apr/May/Jun ☐ Jul/Aug/Sep ☐ Oct/Nov/Dec

Facility/Site Information

Burlington Northern Santa Fe - BALMER
Location: 3600 Gilman Ave. W, Seattle Washington
County: KING
Primary SIC Code: 4011

Mailing Information

Burlington Northern Santa Fe Railroad
2454 Occidental Ave. South, Suite 2D
Seattle, WA 98134

You must send a Discharge Monitoring Report (DMR) to Ecology every quarter. If there was no discharge *or* you have suspended sampling because of consistent attainment of benchmark values, mark the appropriate boxes and send the DMR to Ecology. Please read the instructions before completing the DMR.

Discharge Point #1

X There was no qualifying storm event this quarter so no values are entered below (see explanation)

Quarterly Monitoring		AVERAGE	MAXIMUM	UNITS	Sample Type	Events Sampled
Turbidity	☐ Consistent Attainment			NTU	NA	NA
pH	☐ Consistent Attainment			Standard Units	NA	NA
Zinc (total)	☐ Consistent Attainment			µg/L	NA	NA
Oil & Grease	☐ Consistent Attainment			mg/L	NA	NA
Lead (total)	☐ Consistent Attainment			µg/L	NA	NA
Copper (total)	☐ Consistent Attainment			µg/L	NA	NA
Hardness	N/A – Discharge to Marine Water.					

I CERTIFY UNDER PENALTY OF LAW THAT I HAVE PERSONALLY EXAMINED AND AM FAMILIAR WITH THE INFORMATION SUBMITTED HEREIN AND BASED ON MY INQUIRY OF THOSE INDIVIDUALS IMMEDIATELY RESPONSIBLE FOR OBTAINING THE INFORMATION, I BELIEVE THE SUBMITTED INFORMATION IS TRUE, ACCURATE, AND COMPLETE. I AM AWARE THAT THERE ARE SIGNIFICANT PENALTIES FOR SUBMITTING FALSE INFORMATION INCLUDING THE POSSIBILITY OF FINE AND IMPRISONMENT. SEE 18 USC § 1001 AND 33 USC § 1319. (PENALTIES UNDER THESE STATUTES MAY INCLUDE FINES UP TO $10,000 AND OR MAXIMUM IMPRISONMENT OF BETWEEN SIX MONTHS AND FIVE YEARS)

Jennifer Anderson
NAME/TITLE PRINCIPAL EXECUTIVE OFFICER (TYPED OR PRINTED)

6-11-06
DATE: MO DAY YEAR

SIGNATURE OF PRINCIPAL EXECUTIVE OFFICER OR AUTHORIZED AGENT

206-625-6034
TELEPHONE NUMBER

COMMENTS / EXPLANATIONS
Sampling personnel made several attempts to retrieve a sample at this site during a qualifying rain event. As per letter from Washington State Department of Ecology, BNSF understands it can grab a sample during a non-qualifying event. Procedures have been modified and will be reflected in future sampling activities. Attempts to retrieve a non-qualifying event sample in the second half of the quarter were unsuccessful.

DEPARTMENT OF ECOLOGY
JUN 21 2007
WATER QUALITY PROGRAM

503-001528D
INDUSTRIAL STORMWATER GENERAL PERMIT
DISCHARGE MONITORING REPORT

MONITORING PERIOD for (year/quarter): 2006 year ☐ Jan/Feb/Mar X Apr/May/Jun ☐ Jul/Aug/Sep ☐ Oct/Nov/Dec

Facility/Site Information
Burlington Northern Santa Fe - BALMER
Location: 1600 Gilman Ave. W, Seattle Washington
County: KING
Primary SIC Code: 4011

Mailing Information
Burlington Northern Santa Fe Railroad
2454 Occidental Ave. South, Suite 2D
Seattle, WA 98134

You must send a Discharge Monitoring Report (DMR) to Ecology every quarter. If there was no discharge *or* you have suspended sampling because of consistent attainment of benchmark values, mark the appropriate boxes and send the DMR to Ecology. Please read the instructions before completing the DMR.

Discharge Point #2 MB

X There was no qualifying storm event this quarter so no values are entered below (see explanation)

Quarterly Monitoring		AVERAGE	MAXIMUM	UNITS	Sample Type	Events Sampled
Turbidity	☐ Consistent Attainment			NTU	NA	NA
pH	☐ Consistent Attainment			Standard Units	NA	NA
Zinc (total)	☐ Consistent Attainment			µg/L	NA	NA
Oil & Grease	☐ Consistent Attainment			mg/L	NA	NA
Lead (total)	☐ Consistent Attainment			µg/L	NA	NA
Copper (total)	☐ Consistent Attainment			µg/L	NA	NA
Hardness	N/A – Discharge to Marine Water.					

I CERTIFY UNDER PENALTY OF LAW THAT I HAVE PERSONALLY EXAMINED AND AM FAMILIAR WITH THE INFORMATION SUBMITTED HEREIN AND BASED ON MY INQUIRY OF THOSE INDIVIDUALS IMMEDIATELY RESPONSIBLE FOR OBTAINING THE INFORMATION, I BELIEVE THE SUBMITTED INFORMATION IS TRUE, ACCURATE, AND COMPLETE. I AM AWARE THAT THERE ARE SIGNIFICANT PENALTIES FOR SUBMITTING FALSE INFORMATION INCLUDING THE POSSIBILITY OF FINE AND IMPRISONMENT. SEE 18 USC § 1001 AND 33 USC § 1319. (PENALTIES UNDER THESE STATUTES MAY INCLUDE FINES UP TO $10,000 AND OR MAXIMUM IMPRISONMENT OF BETWEEN SIX MONTHS AND FIVE YEARS)

Jennifer Anderson
NAME OF PRINCIPAL EXECUTIVE OFFICER (TYPED OR PRINTED)

6-11-06
DATE: MO DAY YEAR

206-625-6034
TELEPHONE NUMBER

SIGNATURE OF PRINCIPAL EXECUTIVE OFFICER OR AUTHORIZED AGENT

COMMENTS / EXPLANATIONS
Sampling personnel made several attempts to retrieve a sample at this site during a qualifying rain event. As per letter from Washington State Department of Ecology, BNSF understands it can grab a sample during a non-qualifying event. Procedures have been modified and will be reflected in future sampling activities. Attempts to retrieve a non-qualifying event sample in the second half of the quarter were unsuccessful.

E ivecl

DEPARTMENT OF ECOLOGY
NOV 1 5 2006
WATER QUALITY PROGRAM

SO3-001528D

INDUSTRIAL STORMWATER GENERAL PERMIT
DISCHARGE MONITORING REPORT

MONITORING PERIOD for (year/quarter): **2006** (year) ☐ Jan/Feb/Mar ☐ Apr/May/Jun **X** Jul/Aug/Sep ☐ Oct/Nov/Dec

Facility/Site Information

Burlington Northern Santa Fe - BALMER
Location: 3600 Gilman Ave. W, Seattle Washington
County: KING
Primary SIC Code: 4011

Mailing Information

Burlington Northern Santa Fe Railroad
2454 Occidental Ave. South, Suite 2D
Seattle, WA 98134

You must send a Discharge Monitoring Report (DMR) to Ecology **every quarter**. If there was **no discharge** *or* you have **suspended sampling** because of consistent attainment of benchmark values, mark the appropriate boxes and send the DMR to Ecology. Please read the instructions before completing the DMR.

Discharge Point #1

X There was no qualifying storm event this quarter so no values are entered below (see explanation)

Quarterly Monitoring		AVERAGE	MAXIMUM	UNITS	Sample Type	Events Sampled
Turbidity	☐ Consistent Attainment			NTU		
pH	☐ Consistent Attainment			Standard Units		
Zinc (total)	☐ Consistent Attainment			µg/L		
Oil & Grease	☐ Consistent Attainment			mg/L		
Lead (total)	☐ Consistent Attainment			µg/L		
Copper (total)	☐ Consistent Attainment			µg/L		
Hardness	**N/A – Discharge to Marine Water.**					

I CERTIFY UNDER PENALTY OF LAW THAT I HAVE PERSONALLY EXAMINED AND AM FAMILIAR WITH THE INFORMATION SUBMITTED HEREIN AND BASED ON MY INQUIRY OF THOSE INDIVIDUALS IMMEDIATELY RESPONSIBLE FOR OBTAINING THE INFORMATION, I BELIEVE THE SUBMITTED INFORMATION IS TRUE, ACCURATE, AND COMPLETE. I AM AWARE THAT THERE ARE SIGNIFICANT PENALTIES FOR SUBMITTING FALSE INFORMATION INCLUDING THE POSSIBILITY OF FINE AND IMPRISONMENT. SEE 18 USC § 1001 AND 33 USC § 1319. *(PENALTIES UNDER THESE STATUES MAY INCLUDE FINES UP TO $10,000.00 AND OR MAXIMUM IMPRISONMENT OF BETWEEN SIX MONTHS AND FIVE YEARS.)*

Jennifer Anderson
NAME/TITLE PRINCIPAL EXECUTIVE OFFICER (TYPED OR PRINTED)

11-13-06
DATE: MO DAY YEAR

SIGNATURE OF PRINCIPAL EXECUTIVE OFFICER OR AUTHORIZED AGENT

206-625-6034
TELEPHONE NUMBER

COMMENTS / EXPLANATIONS
No qualifying rain events were observed during this quarter. Attempts to retrieve a non-qualifying event sample in the second half of the quarter were unsuccessful.

DEPARTMENT OF ECOLOGY
JUN 21 2007
WATER QUALITY PROGRAM

SO3-001528D
INDUSTRIAL STORMWATER GENERAL PERMIT
DISCHARGE MONITORING REPORT

MONITORING PERIOD for (year/quarter): 2006 (year) ☐ Jan/Feb/Mar ☐ Apr/May/Jun X Jul/Aug/Sep ☐ Oct/Nov/Dec

Facility/Site Information

Burlington Northern Santa Fe - BALMER
Location: 3600 Gilman Ave. W, Seattle Washington
County: KING
Primary SIC Code: 4011

Mailing Information

Burlington Northern Santa Fe Railroad
2454 Occidental Ave. South, Suite 2D
Seattle, WA 98134

You must send a Discharge Monitoring Report (DMR) to Ecology **every quarter**. If there was **no discharge** *or* you have **suspended sampling** because of consistent attainment of benchmark values, mark the appropriate boxes and send the DMR to Ecology. Please read the instructions before completing the DMR.

Discharge Point #1 #2 MB

X There was no qualifying storm event this quarter so no values are entered below (see explanation)

Quarterly Monitoring		AVERAGE	MAXIMUM	UNITS	Sample Type	Events Sampled
Turbidity	☐ Consistent Attainment			NTU		
pH	☐ Consistent Attainment			Standard Units		
Zinc (total)	☐ Consistent Attainment			µg/L		
Oil & Grease	☐ Consistent Attainment			mg/L		
Lead (total)	☐ Consistent Attainment			µg/L		
Copper (total)	☐ Consistent Attainment			µg/L		
Hardness	N/A – Discharge to Marine Water.					

I CERTIFY UNDER PENALTY OF LAW THAT I HAVE PERSONALLY EXAMINED AND AM FAMILIAR WITH THE INFORMATION SUBMITTED HEREIN AND BASED ON MY INQUIRY OF THOSE INDIVIDUALS IMMEDIATELY RESPONSIBLE FOR OBTAINING THE INFORMATION, I BELIEVE THE SUBMITTED INFORMATION IS TRUE, ACCURATE, AND COMPLETE. I AM AWARE THAT THERE ARE SIGNIFICANT PENALTIES FOR SUBMITTING FALSE INFORMATION INCLUDING THE POSSIBILITY OF FINE AND IMPRISONMENT. SEE 18 USC § 1001 AND 33 USC § 1319. *(PENALTIES UNDER THESE STATUES MAY INCLUDE FINES UP TO $10,000.00 AND OR MAXIMUM IMPRISONMENT OF BETWEEN SIX MONTHS AND FIVE YEARS.)*

Jennifer Anderson
NAME/TITLE PRINCIPAL EXECUTIVE OFFICER (TYPED OR PRINTED)

11-13-06
DATE: MO DAY YEAR

SIGNATURE OF PRINCIPAL EXECUTIVE OFFICER OR AUTHORIZED AGENT

206-625-6034
TELEPHONE NUMBER

COMMENTS / EXPLANATIONS
No qualifying rain events were observed during this quarter. Attempts to retrieve a non-qualifying event sample in the second half of the quarter were unsuccessful.

ENTERED

DEPARTMENT OF ECOLOGY
FEB 09 2007
WATER QUALITY PROGRAM

SO3-001528D

INDUSTRIAL STORMWATER GENERAL PERMIT
DISCHARGE MONITORING REPORT

MONITORING PERIOD for (year/quarter): **2006** (year) **Jan/Feb/Mar** **Apr/May/Jun** **Jul/Aug/Sep** **X Oct/Nov/Dec**

Facility/Site Information

Burlington Northern Santa Fe - BALMER
Location: 3600 Gilman Ave. W, Seattle Washington
County: KING

Primary SIC Code: 4011

Mailing Information

Burlington Northern Santa Fe Railroad
2454 Occidental Ave. South, Suite 2D
Seattle, WA 98134

You must send a Discharge Monitoring Report (DMR) to Ecology **every quarter**. If there was **no discharge** *or* you have **suspended sampling** because of consistent attainment of benchmark values, mark the appropriate boxes and send the DMR to Ecology. Please read the instructions before completing the DMR.

Discharge Point #1

X There was no qualifying storm event this quarter so no values are entered below (see explanation)

Quarterly Monitoring		AVERAGE	MAXIMUM	UNITS	Sample Type	Events Sampled
Turbidity	Consistent Attainment			NTU		
pH	Consistent Attainment			Standard Units		
Zinc (total)	Consistent Attainment			µg/L		
Oil & Grease	Consistent Attainment			mg/L		
Lead (total)	Consistent Attainment			µg/L		
Copper (total)	Consistent Attainment			µg/L		
Hardness	**N/A – Discharge to Marine Water.**					

I CERTIFY UNDER PENALTY OF LAW THAT I HAVE PERSONALLY EXAMINED AND AM FAMILIAR WITH THE INFORMATION SUBMITTED HEREIN AND BASED ON MY INQUIRY OF THOSE INDIVIDUALS IMMEDIATELY RESPONSIBLE FOR OBTAINING THE INFORMATION, I BELIEVE THE SUBMITTED INFORMATION IS TRUE, ACCURATE, AND COMPLETE. I AM AWARE THAT THERE ARE SIGNIFICANT PENALTIES FOR SUBMITTING FALSE INFORMATION INCLUDING THE POSSIBILITY OF FINE AND IMPRISONMENT. SEE 18 USC § 1001 AND 33 USC § 1319. *(PENALTIES UNDER THESE STATUES MAY INCLUDE FINES UP TO $10,000.00 AND OR MAXIMUM IMPRISONMENT OF BETWEEN SIX MONTHS AND FIVE YEARS.)*

Jennifer Anderson
NAME/TITLE PRINCIPAL EXECUTIVE OFFICER (TYPED OR PRINTED)

2-2-07
DATE: MO DAY YEAR

SIGNATURE OF PRINCIPAL EXECUTIVE OFFICER OR AUTHORIZED AGENT

206-625-6034
TELEPHONE NUMBER

COMMENTS / EXPLANATIONS

Due to continuous rain during the first half of the fourth quarter, a qualifying rain event that produced enough runoff to sample was not witnessed. In the second half of the fourth quarter, attempts to retrieve a sample during a non-qualifying event were also unsuccessful due to insufficient runoff during site visits.

DEPARTMENT OF ECOLOGY

JUN 21 2007

WATER QUALITY PROGRAM

SO3-001528D

INDUSTRIAL STORMWATER GENERAL PERMIT
DISCHARGE MONITORING REPORT

MONITORING PERIOD for (year/quarter): 2006 (year) Jan/Feb/Mar Apr/May/Jun Jul/Aug/Sep X Oct/Nov/Dec

Facility/Site Information

Burlington Northern Santa Fe - BALMER
Location: 3600 Gilman Ave. W, Seattle Washington
County: KING

Primary SIC Code: 4011

Mailing Information

Burlington Northern Santa Fe Railroad
2454 Occidental Ave. South, Suite 2D
Seattle, WA 98134

You must send a Discharge Monitoring Report (DMR) to Ecology **every quarter**. If there was **no discharge** *or* you have **suspended sampling** because of consistent attainment of benchmark values, mark the appropriate boxes and send the DMR to Ecology. Please read the instructions before completing the DMR.

Discharge Point ~~#1~~ #2 MB

X There was no qualifying storm event this quarter so no values are entered below (see explanation)

Quarterly Monitoring		AVERAGE	MAXIMUM	UNITS	Sample Type	Events Sampled
Turbidity	Consistent Attainment			NTU		
pH	Consistent Attainment			Standard Units		
Zinc (total)	Consistent Attainment			µg/L		
Oil & Grease	Consistent Attainment			mg/L		
Lead (total)	Consistent Attainment			µg/L		
Copper (total)	Consistent Attainment			µg/L		
Hardness	N/A – Discharge to Marine Water.					

I CERTIFY UNDER PENALTY OF LAW THAT I HAVE PERSONALLY EXAMINED AND AM FAMILIAR WITH THE INFORMATION SUBMITTED HEREIN AND BASED ON MY INQUIRY OF THOSE INDIVIDUALS IMMEDIATELY RESPONSIBLE FOR OBTAINING THE INFORMATION, I BELIEVE THE SUBMITTED INFORMATION IS TRUE, ACCURATE, AND COMPLETE. I AM AWARE THAT THERE ARE SIGNIFICANT PENALTIES FOR SUBMITTING FALSE INFORMATION INCLUDING THE POSSIBILITY OF FINE AND IMPRISONMENT. SEE 18 USC § 1001 AND 33 USC § 1319. *(PENALTIES UNDER THESE STATUES MAY INCLUDE FINES UP TO $10,000.00 AND OR MAXIMUM IMPRISONMENT OF BETWEEN SIX MONTHS AND FIVE YEARS.)*

Jennifer Anderson
NAME/TITLE PRINCIPAL EXECUTIVE OFFICER (TYPED OR PRINTED)

2-2-07
DATE: MO DAY YEAR

SIGNATURE OF PRINCIPAL EXECUTIVE OFFICER OR AUTHORIZED AGENT

206-625-6034
TELEPHONE NUMBER

COMMENTS / EXPLANATIONS

Due to continuous rain during the first half of the fourth quarter, a qualifying rain event that produced enough runoff to sample was not witnessed. In the second half of the fourth quarter, attempts to retrieve a sample during a non-qualifying event were also unsuccessful due to insufficient runoff during site visits.

POSTED
DATE: 05/9/07
INITIALS: JK

SO3-001528D

INDUSTRIAL STORMWATER GENERAL PERMIT
DISCHARGE MONITORING REPORT

MONITORING PERIOD for (year/quarter): **2007** (year) **X** Jan/Feb/Mar Apr/May/Jun Jul/Aug/Sep Oct/Nov/Dec

Facility/Site Information

BNSF Railway - BALMER
Location: 3600 Gilman Ave. W, Seattle Washington
County: KING
Primary SIC Code: 4011

Mailing Information

BNSF Railway
2454 Occidental Ave. South, Suite 1A
Seattle, WA 98134

You must send a Discharge Monitoring Report (DMR) to Ecology **every quarter**. If there was **no discharge** *or* you have **suspended sampling** because of consistent attainment of benchmark values, mark the appropriate boxes and send the DMR to Ecology. Please read the instructions before completing the DMR.

Discharge Point #1

X There was no qualifying storm event this quarter so no values are entered below (see explanation)

Quarterly Monitoring		AVERAGE	MAXIMUM	UNITS	Sample Type	Events Sampled
Turbidity	Consistent Attainment			NTU		
pH	Consistent Attainment			Standard Units		
Zinc (total)	Consistent Attainment			µg/L		
Oil & Grease	Consistent Attainment			mg/L		
Lead (total)	Consistent Attainment			µg/L		
Copper (total)	Consistent Attainment			µg/L		
Hardness	**N/A – Discharge to Marine Water.**					

I CERTIFY UNDER PENALTY OF LAW THAT I HAVE PERSONALLY EXAMINED AND AM FAMILIAR WITH THE INFORMATION SUBMITTED HEREIN AND BASED ON MY INQUIRY OF THOSE INDIVIDUALS IMMEDIATELY RESPONSIBLE FOR OBTAINING THE INFORMATION, I BELIEVE THE SUBMITTED INFORMATION IS TRUE, ACCURATE, AND COMPLETE. I AM AWARE THAT THERE ARE SIGNIFICANT PENALTIES FOR SUBMITTING FALSE INFORMATION INCLUDING THE POSSIBILITY OF FINE AND IMPRISONMENT. SEE 18 USC § 1001 AND 33 USC § 1319. *(PENALTIES UNDER THESE STATUES MAY INCLUDE FINES UP TO $10,000.00 AND OR MAXIMUM IMPRISONMENT OF BETWEEN SIX MONTHS AND FIVE YEARS.)*

Jennifer Anderson
NAME/TITLE PRINCIPAL EXECUTIVE OFFICER (TYPED OR PRINTED)

5-8-07
DATE: MO DAY YEAR

SIGNATURE OF PRINCIPAL EXECUTIVE OFFICER OR AUTHORIZED AGENT

206-625-6034
TELEPHONE NUMBER

COMMENTS / EXPLANATIONS

Attempts to collect stormwater samples on 3/9/07 and 3/15/07 were not successful. No flow was observed upon arrival at the facility.

DEPARTMENT OF ECOLOGY

JUN 21 2007
WATER QUALITY PROGRAM

SO3-001528D
INDUSTRIAL STORMWATER GENERAL PERMIT DISCHARGE MONITORING REPORT

MONITORING PERIOD for (year/quarter): 2007 (year) X Jan/Feb/Mar Apr/May/Jun Jul/Aug/Sep Oct/Nov/Dec

Facility/Site Information

BNSF Railway - BALMER
Location: 3600 Gilman Ave. W, Seattle Washington
County: KING
Primary SIC Code: 4011

Mailing Information

BNSF Railway
2454 Occidental Ave. South, Suite 1A
Seattle, WA 98134

You must send a Discharge Monitoring Report (DMR) to Ecology **every quarter**. If there was **no discharge** *or* you have **suspended sampling** because of consistent attainment of benchmark values, mark the appropriate boxes and send the DMR to Ecology. Please read the instructions before completing the DMR.

Discharge Point ~~#1~~ #2 MB

X There was no qualifying storm event this quarter so no values are entered below (see explanation)

Quarterly Monitoring		AVERAGE	MAXIMUM	UNITS	Sample Type	Events Sampled
Turbidity	Consistent Attainment			NTU		
pH	Consistent Attainment			Standard Units		
Zinc (total)	Consistent Attainment			µg/L		
Oil & Grease	Consistent Attainment			mg/L		
Lead (total)	Consistent Attainment			µg/L		
Copper (total)	Consistent Attainment			µg/L		
Hardness	**N/A – Discharge to Marine Water.**					

I CERTIFY UNDER PENALTY OF LAW THAT I HAVE PERSONALLY EXAMINED AND AM FAMILIAR WITH THE INFORMATION SUBMITTED HEREIN AND BASED ON MY INQUIRY OF THOSE INDIVIDUALS IMMEDIATELY RESPONSIBLE FOR OBTAINING THE INFORMATION, I BELIEVE THE SUBMITTED INFORMATION IS TRUE, ACCURATE, AND COMPLETE. I AM AWARE THAT THERE ARE SIGNIFICANT PENALTIES FOR SUBMITTING FALSE INFORMATION INCLUDING THE POSSIBILITY OF FINE AND IMPRISONMENT. SEE 18 USC § 1001 AND 33 USC § 1319. *(PENALTIES UNDER THESE STATUES MAY INCLUDE FINES UP TO $10,000.00 AND OR MAXIMUM IMPRISONMENT OF BETWEEN SIX MONTHS AND FIVE YEARS.)*

Jennifer Anderson
NAME/TITLE PRINCIPAL EXECUTIVE OFFICER (TYPED OR PRINTED)

5-8-07
DATE: MO DAY YEAR

SIGNATURE OF PRINCIPAL EXECUTIVE OFFICER OR AUTHORIZED AGENT

206-625-6034
TELEPHONE NUMBER

COMMENTS / EXPLANATIONS

Attempts to collect stormwater samples on 3/9/07 and 3/15/07 were not successful. No flow was observed upon arrival at the facility.

WRONG OP

DEPARTMENT OF ECOLOGY
JUL 27 2007
WATER QUALITY PROGRAM

SO3-001528D

INDUSTRIAL STORMWATER GENERAL PERMIT
DISCHARGE MONITORING REPORT

MONITORING PERIOD for (year/quarter): 2007 (year) ☐ Jan/Feb/Mar X Apr/May/Jun ☐ Jul/Aug/Sep ☐ Oct/Nov/Dec

Facility/Site Information

BNSF Railway - BALMER
Location: 3600 Gilman Ave. W, Seattle Washington
County: KING
Primary SIC Code: 4011

Mailing Information

BNSF Railway
2454 Occidental Ave. South, Suite 1A
Seattle, WA 98134

You must send a Discharge Monitoring Report (DMR) to Ecology **every quarter**. If there was **no discharge** *or* you have **suspended sampling** because of consistent attainment of benchmark values, mark the appropriate boxes and send the DMR to Ecology. Please read the instructions before completing the DMR.

Discharge Point #2

X There was no qualifying storm event this quarter so no values are entered below (see explanation)

Quarterly Monitoring		AVERAGE	MAXIMUM	UNITS	Sample Type	Events Sampled
Turbidity	☐ Consistent Attainment			NTU		
pH	☐ Consistent Attainment			Standard Units		
Zinc (total)	☐ Consistent Attainment			µg/L		
Oil & Grease	☐ Consistent Attainment			mg/L		
Lead (total)	☐ Consistent Attainment			µg/L		
Copper (total)	☐ Consistent Attainment			µg/L		
Hardness	**N/A – Discharge to Marine Water.**					

I CERTIFY UNDER PENALTY OF LAW THAT I HAVE PERSONALLY EXAMINED AND AM FAMILIAR WITH THE INFORMATION SUBMITTED HEREIN AND BASED ON MY INQUIRY OF THOSE INDIVIDUALS IMMEDIATELY RESPONSIBLE FOR OBTAINING THE INFORMATION, I BELIEVE THE SUBMITTED INFORMATION IS TRUE, ACCURATE, AND COMPLETE. I AM AWARE THAT THERE ARE SIGNIFICANT PENALTIES FOR SUBMITTING FALSE INFORMATION INCLUDING THE POSSIBILITY OF FINE AND IMPRISONMENT. SEE 18 USC § 1001 AND 33 USC § 1319. *(PENALTIES UNDER THESE STATUES MAY INCLUDE FINES UP TO $10,000.00 AND OR MAXIMUM IMPRISONMENT OF BETWEEN SIX MONTHS AND FIVE YEARS.)*

Jennifer Anderson
NAME/TITLE PRINCIPAL EXECUTIVE OFFICER (TYPED OR PRINTED)

7-12-07
DATE: MO DAY YEAR

Jennifer Anderson for BNSF
SIGNATURE OF PRINCIPAL EXECUTIVE OFFICER OR AUTHORIZED AGENT

206-625-6034
TELEPHONE NUMBER

COMMENTS / EXPLANATIONS

An attempt to collect a stormwater sample on 6/14/07 was not successful. No flow was observed upon arrival at the facility.

WRONG DP

DEPARTMENT OF ECOLOGY
NOV 07 2007
WATER QUALITY PROGRAM

SO3-001528D

INDUSTRIAL STORMWATER GENERAL PERMIT
DISCHARGE MONITORING REPORT

MONITORING PERIOD for (year/quarter): 2007 (year) ☐ Jan/Feb/Mar ☐ Apr/May/Jun X Jul/Aug/Sep ☐ Oct/Nov/Dec

Facility/Site Information

BNSF Railway - BALMER
Location: 3600 Gilman Ave. W, Seattle Washington
County: KING
Primary SIC Code: 4011

Mailing Information

BNSF Railway
2454 Occidental Ave. South, Suite 1A
Seattle, WA 98134

You must send a Discharge Monitoring Report (DMR) to Ecology **every quarter**. If there was **no discharge** *or* you have **suspended sampling** because of consistent attainment of benchmark values, mark the appropriate boxes and send the DMR to Ecology. Please read the instructions before completing the DMR.

Discharge Point #2

☐ There was no qualifying storm event this quarter so no values are entered below (see explanation)

Quarterly Monitoring		AVERAGE	MAXIMUM	UNITS	Sample Type	Events Sampled
Turbidity	☐ Consistent Attainment	**130**	**130**	NTU	**Grab**	**9/16/07**
pH	☐ Consistent Attainment	**7.4**	**7.4**	Standard Units	**Grab**	**9/16/07**
Zinc (total)	☐ Consistent Attainment	**1,310**	**1,310**	µg/L	**Grab**	**9/16/07**
Oil & Grease	☐ Consistent Attainment	**8**	**8**	mg/L	**Grab**	**9/16/07**
Lead (total)	☐ Consistent Attainment	**312**	**312**	µg/L	**NA**	**9/16/07**
Copper (total)	☐ Consistent Attainment	**194**	**194**	µg/L	**NA**	**9/16/07**
Hardness	**N/A – Discharge to Marine Water.**					

I CERTIFY UNDER PENALTY OF LAW THAT I HAVE PERSONALLY EXAMINED AND AM FAMILIAR WITH THE INFORMATION SUBMITTED HEREIN AND BASED ON MY INQUIRY OF THOSE INDIVIDUALS IMMEDIATELY RESPONSIBLE FOR OBTAINING THE INFORMATION, I BELIEVE THE SUBMITTED INFORMATION IS TRUE, ACCURATE, AND COMPLETE. I AM AWARE THAT THERE ARE SIGNIFICANT PENALTIES FOR SUBMITTING FALSE INFORMATION INCLUDING THE POSSIBILITY OF FINE AND IMPRISONMENT. SEE 18 USC § 1001 AND 33 USC § 1319. *(PENALTIES UNDER THESE STATUES MAY INCLUDE FINES UP TO $10,000.00 AND OR MAXIMUM IMPRISONMENT OF BETWEEN SIX MONTHS AND FIVE YEARS.)*

Jennifer Anderson
NAME/TITLE PRINCIPAL EXECUTIVE OFFICER (TYPED OR PRINTED).

11 - 05 - 07
DATE: MO DAY YEAR

SIGNATURE OF PRINCIPAL EXECUTIVE OFFICER OR AUTHORIZED AGENT

206-625-6034
TELEPHONE NUMBER

COMMENTS / EXPLANATIONS

DEPARTMENT OF ECOLOGY

JAN 31 2008

WATER QUALITY PROGRAM

POSTED DATE: INITIALS:

SO3-001528D

INDUSTRIAL STORMWATER GENERAL PERMIT
DISCHARGE MONITORING REPORT

MONITORING PERIOD for (year/quarter): 2007 (year) ☐ Jan/Feb/Mar ☐ Apr/May/Jun ☐ Jul/Aug/Sep X Oct/Nov/Dec

Facility/Site Information

BNSF Railway - BALMER
Location: 3600 Gilman Ave. W, Seattle Washington
County: KING
Primary SIC Code: 4011

Mailing Information

BNSF Railway
2454 Occidental Ave. South, Suite 1A
Seattle, WA 98134

POSTED DATE: 1/22/08 INITIALS: [illegible]

You must send a Discharge Monitoring Report (DMR) to Ecology **every quarter**. If there was **no discharge** *or* you have **suspended sampling** because of consistent attainment of benchmark values, mark the appropriate boxes and send the DMR to Ecology. Please read the instructions before completing the DMR.

Discharge Point #2

☐ There was no qualifying storm event this quarter so no values are entered below (see explanation)

Quarterly Monitoring		AVERAGE	MAXIMUM	UNITS	Sample Type	Events Sampled
Turbidity	☐ Consistent Attainment	**1,100**	**1,100**	NTU	**Grab**	**12/27/07**
pH	☐ Consistent Attainment	**7.3**	**7.3**	Standard Units	**Grab**	**12/27/07**
Zinc (total)	☐ Consistent Attainment	**1,950**	**1,950**	µg/L	**Grab**	**12/27/07**
Oil & Grease	☐ Consistent Attainment	**ND (<7)**	**ND (<7)**	mg/L	**Grab**	**12/27/07**
Lead (total)	☐ Consistent Attainment	**1,980**	**1,980**	µg/L	**NA**	**12/27/07**
Copper (total)	☐ Consistent Attainment	**522**	**522**	µg/L	**NA**	**12/27/07**
Hardness	**N/A – Discharge to Marine Water.**					

I CERTIFY UNDER PENALTY OF LAW THAT I HAVE PERSONALLY EXAMINED AND AM FAMILIAR WITH THE INFORMATION SUBMITTED HEREIN AND BASED ON MY INQUIRY OF THOSE INDIVIDUALS IMMEDIATELY RESPONSIBLE FOR OBTAINING THE INFORMATION, I BELIEVE THE SUBMITTED INFORMATION IS TRUE, ACCURATE, AND COMPLETE. I AM AWARE THAT THERE ARE SIGNIFICANT PENALTIES FOR SUBMITTING FALSE INFORMATION INCLUDING THE POSSIBILITY OF FINE AND IMPRISONMENT. SEE 18 USC § 1001 AND 33 USC § 1319. *(PENALTIES UNDER THESE STATUES MAY INCLUDE FINES UP TO $10,000.00 AND OR MAXIMUM IMPRISONMENT OF BETWEEN SIX MONTHS AND FIVE YEARS.)*

Jennifer Anderson
NAME/TITLE PRINCIPAL EXECUTIVE OFFICER (TYPED OR PRINTED)

1-23-08
DATE: MO DAY YEAR

SIGNATURE OF PRINCIPAL EXECUTIVE OFFICER OR AUTHORIZED AGENT

206-625-6034
TELEPHONE NUMBER

COMMENTS / EXPLANATIONS

POST
DATE:
INITIALS:

DEPARTMENT OF ECOLC

MAY 15 2008
WATER QUALITY PROGR

SO3-001528D

INDUSTRIAL STORMWATER GENERAL PERMIT
DISCHARGE MONITORING REPORT

MONITORING PERIOD for (year/quarter): **2008** (year) **X** Jan/Feb/Mar Apr/May/Jun Jul/Aug/Sep Oct/Nov/Dec

Facility/Site Information

BNSF Railway - BALMER
Location: 3600 Gilman Ave. W, Seattle Washington
County: KING
Primary SIC Code: 4011

Mailing Information

BNSF Railway
2454 Occidental Ave. South, Suite 1A
Seattle, WA 98134

You must send a Discharge Monitoring Report (DMR) to Ecology **every quarter**. If there was **no discharge** *or* you have **suspended sampling** because of consistent attainment of benchmark values, mark the appropriate boxes and send the DMR to Ecology. Please read the instructions before completing the DMR.

Discharge Point #2

There was no qualifying storm event this quarter so no values are entered below (see explanation)

Quarterly Monitoring		AVERAGE	MAXIMUM	UNITS	Sample Type	Events Sampled
Turbidity	Consistent Attainment	**84**	**84**	NTU	**Grab**	**3/13/08**
pH	Consistent Attainment	**7.6**	**7.6**	Standard Units	**Grab**	**3/13/08**
Zinc (total)	Consistent Attainment	**1,030**	**1,030**	µg/L	**Grab**	**3/13/08**
Oil & Grease	Consistent Attainment	**ND (<6)**	**ND (<6)**	mg/L	**Grab**	**3/13/08**
Lead (total)	Consistent Attainment	**484**	**484**	µg/L	**NA**	**3/13/08**
Copper (total)	Consistent Attainment	**279**	**279**	µg/L	**NA**	**3/13/08**
Hardness	**N/A – Discharge to Marine Water.**					

I CERTIFY UNDER PENALTY OF LAW THAT I HAVE PERSONALLY EXAMINED AND AM FAMILIAR WITH THE INFORMATION SUBMITTED HEREIN AND BASED ON MY INQUIRY OF THOSE INDIVIDUALS IMMEDIATELY RESPONSIBLE FOR OBTAINING THE INFORMATION, I BELIEVE THE SUBMITTED INFORMATION IS TRUE, ACCURATE, AND COMPLETE. I AM AWARE THAT THERE ARE SIGNIFICANT PENALTIES FOR SUBMITTING FALSE INFORMATION INCLUDING THE POSSIBILITY OF FINE AND IMPRISONMENT. SEE 18 USC § 1001 AND 33 USC § 1319. *(PENALTIES UNDER THESE STATUES MAY INCLUDE FINES UP TO $10,000.00 AND OR MAXIMUM IMPRISONMENT OF BETWEEN SIX MONTHS AND FIVE YEARS.)*

Jennifer Anderson
NAME/TITLE PRINCIPAL EXECUTIVE OFFICER (TYPED OR PRINTED)

5-1-08
DATE: MO DAY YEAR

SIGNATURE OF PRINCIPAL EXECUTIVE OFFICER OR AUTHORIZED AGENT

206-625-6034
TELEPHONE NUMBER

COMMENTS / EXPLANATIONS

SO3-001528D

INDUSTRIAL STORMWATER GENERAL PERMIT
DISCHARGE MONITORING REPORT

MONITORING PERIOD for (year/quarter): **2008** (year) ☐ Jan/Feb/Mar **X** Apr/May/Jun ☐ Jul/Aug/Sep ☐ Oct/Nov/Dec

Facility/Site Information

BNSF Railway - BALMER
Location: 3600 Gilman Ave. W, Seattle Washington
County: KING
Primary SIC Code: 4011

Mailing Information

BNSF Railway
2454 Occidental Ave. South, Suite 1A
Seattle, WA 98134

You must send a Discharge Monitoring Report (DMR) to Ecology **every quarter**. If there was **no discharge** *or* you have **suspended sampling** because of consistent attainment of benchmark values, mark the appropriate boxes and send the DMR to Ecology. Please read the instructions before completing the DMR.

Discharge Point #2

X There was no qualifying storm event this quarter so no values are entered below (see explanation)

Quarterly Monitoring		AVERAGE	MAXIMUM	UNITS	Sample Type	Events Sampled
Turbidity	☐ Consistent Attainment			NTU	**Grab**	
pH	☐ Consistent Attainment			Standard Units	**Grab**	
Zinc (total)	☐ Consistent Attainment			µg/L	**Grab**	
Oil & Grease	☐ Consistent Attainment			mg/L	**Grab**	
Lead (total)	☐ Consistent Attainment			µg/L	**NA**	
Copper (total)	☐ Consistent Attainment			µg/L	**NA**	
Hardness	**N/A – Discharge to Marine Water.**					

I CERTIFY UNDER PENALTY OF LAW THAT I HAVE PERSONALLY EXAMINED AND AM FAMILIAR WITH THE INFORMATION SUBMITTED HEREIN AND BASED ON MY INQUIRY OF THOSE INDIVIDUALS IMMEDIATELY RESPONSIBLE FOR OBTAINING THE INFORMATION, I BELIEVE THE SUBMITTED INFORMATION IS TRUE, ACCURATE, AND COMPLETE. I AM AWARE THAT THERE ARE SIGNIFICANT PENALTIES FOR SUBMITTING FALSE INFORMATION INCLUDING THE POSSIBILITY OF FINE AND IMPRISONMENT. SEE 18 USC § 1001 AND 33 USC § 1319. *(PENALTIES UNDER THESE STATUES MAY INCLUDE FINES UP TO $10,000.00 AND OR MAXIMUM IMPRISONMENT OF BETWEEN SIX MONTHS AND FIVE YEARS.)*

Jennifer Anderson
NAME/TITLE PRINCIPAL EXECUTIVE OFFICER (TYPED OR PRINTED)

7-29-08
DATE: MO DAY YEAR

SIGNATURE OF PRINCIPAL EXECUTIVE OFFICER OR AUTHORIZED AGENT

206-625-6034
TELEPHONE NUMBER

COMMENTS / EXPLANATIONS

An attempt to collect a stormwater sample on 6/27/08 was not successful. No rainfall occurred on this day.

DEPARTMENT OF ECOLOGY

NOV 12 2008

WATER QUALITY PROGRAM

SO3-001528D

INDUSTRIAL STORMWATER GENERAL PERMIT
DISCHARGE MONITORING REPORT

MONITORING PERIOD for (year/quarter): 2008 (year) ☐ Jan/Feb/Mar ☐ Apr/May/Jun X Jul/Aug/Sep ☐ Oct/Nov/Dec

Facility/Site Information

BNSF Railway - BALMER
Location: 3600 Gilman Ave. W, Seattle Washington
County: KING

Primary SIC Code: 4011

Mailing Information

BNSF Railway
2454 Occidental Ave. South, Suite 1A
Seattle, WA 98134

POSTED
DATE _____
INITIALS _____

You must send a Discharge Monitoring Report (DMR) to Ecology **every quarter**. If there was **no discharge** *or* you have **suspended sampling** because of consistent attainment of benchmark values, mark the appropriate boxes and send the DMR to Ecology. Please read the instructions before completing the DMR.

Discharge Point #2

X There was no qualifying storm event this quarter so no values are entered below (see explanation)

Quarterly Monitoring		AVERAGE	MAXIMUM	UNITS	Sample Type	Events Sampled
Turbidity	☐ Consistent Attainment			NTU	**Grab**	
pH	☐ Consistent Attainment			Standard Units	**Grab**	
Zinc (total)	☐ Consistent Attainment			µg/L	**Grab**	
Oil & Grease	☐ Consistent Attainment			mg/L	**Grab**	
Lead (total)	☐ Consistent Attainment			µg/L	**NA**	
Copper (total)	☐ Consistent Attainment			µg/L	**NA**	
Hardness	**N/A – Discharge to Marine Water.**					

I CERTIFY UNDER PENALTY OF LAW THAT I HAVE PERSONALLY EXAMINED AND AM FAMILIAR WITH THE INFORMATION SUBMITTED HEREIN AND BASED ON MY INQUIRY OF THOSE INDIVIDUALS IMMEDIATELY RESPONSIBLE FOR OBTAINING THE INFORMATION, I BELIEVE THE SUBMITTED INFORMATION IS TRUE, ACCURATE, AND COMPLETE. I AM AWARE THAT THERE ARE SIGNIFICANT PENALTIES FOR SUBMITTING FALSE INFORMATION INCLUDING THE POSSIBILITY OF FINE AND IMPRISONMENT. SEE 18 USC § 1001 AND 33 USC § 1319. *(PENALTIES UNDER THESE STATUES MAY INCLUDE FINES UP TO $10,000.00 AND OR MAXIMUM IMPRISONMENT OF BETWEEN SIX MONTHS AND FIVE YEARS.)*

Jennifer Anderson
NAME/TITLE PRINCIPAL EXECUTIVE OFFICER (TYPED OR PRINTED)

11-6-08
DATE: MO DAY YEAR

SIGNATURE OF PRINCIPAL EXECUTIVE OFFICER OR AUTHORIZED AGENT

206-625-6034
TELEPHONE NUMBER

COMMENTS / EXPLANATIONS

No rainfall occurred during site inspections at the Interbay facility on 8/20/08 and 9/19/08.

SO3-001528D

INDUSTRIAL STORMWATER GENERAL PERMIT
DISCHARGE MONITORING REPORT

MONITORING PERIOD for (year/quarter): **2008** (year) ☐ Jan/Feb/Mar ☐ Apr/May/Jun ☐ Jul/Aug/Sep **X** Oct/Nov/Dec

Facility/Site Information

BNSF Railway - BALMER
Location: 3600 Gilman Ave. W, Seattle Washington
County: KING
Primary SIC Code: 4011

Mailing Information

BNSF Railway
2454 Occidental Ave. South, Suite 1A
Seattle, WA 98134

You must send a Discharge Monitoring Report (DMR) to Ecology **every quarter**. If there was **no discharge** *or* you have **suspended sampling** because of consistent attainment of benchmark values, mark the appropriate boxes and send the DMR to Ecology. Please read the instructions before completing the DMR.

Discharge Point #2

X There was no qualifying storm event this quarter so no values are entered below (see explanation)

Quarterly Monitoring		AVERAGE	MAXIMUM	UNITS	Sample Type	Events Sampled
Turbidity	☐ Consistent Attainment			NTU	**Grab**	
pH	☐ Consistent Attainment			Standard Units	**Grab**	
Zinc (total)	☐ Consistent Attainment			µg/L	**Grab**	
Oil & Grease	☐ Consistent Attainment			mg/L	**Grab**	
Lead (total)	☐ Consistent Attainment			µg/L	**NA**	
Copper (total)	☐ Consistent Attainment			µg/L	**NA**	
Hardness	**N/A – Discharge to Marine Water.**					

I CERTIFY UNDER PENALTY OF LAW THAT I HAVE PERSONALLY EXAMINED AND AM FAMILIAR WITH THE INFORMATION SUBMITTED HEREIN AND BASED ON MY INQUIRY OF THOSE INDIVIDUALS IMMEDIATELY RESPONSIBLE FOR OBTAINING THE INFORMATION, I BELIEVE THE SUBMITTED INFORMATION IS TRUE, ACCURATE, AND COMPLETE. I AM AWARE THAT THERE ARE SIGNIFICANT PENALTIES FOR SUBMITTING FALSE INFORMATION INCLUDING THE POSSIBILITY OF FINE AND IMPRISONMENT. SEE 18 USC § 1001 AND 33 USC § 1319. *(PENALTIES UNDER THESE STATUES MAY INCLUDE FINES UP TO $10,000.00 AND OR MAXIMUM IMPRISONMENT OF BETWEEN SIX MONTHS AND FIVE YEARS.)*

Jennifer Anderson
NAME/TITLE PRINCIPAL EXECUTIVE OFFICER (TYPED OR PRINTED)

1-14-09
DATE: MO DAY YEAR

SIGNATURE OF PRINCIPAL EXECUTIVE OFFICER OR AUTHORIZED AGENT

206-625-6034
TELEPHONE NUMBER

COMMENTS / EXPLANATIONS

An attempt to collect a stormwater sample on 12/12/08 was not successful. No flow was observed upon arrival as the stormwater conveyance line was determined to be plugged as a result of recent construction activities to install a sampling port. The line was cleaned by jet-rodding. The sampling port is being evaluated.

SO3-001528D

INDUSTRIAL STORMWATER GENERAL PERMIT
DISCHARGE MONITORING REPORT

MONITORING PERIOD for (year/quarter): **2009** (year) **X** Jan/Feb/Mar Apr/May/Jun Jul/Aug/Sep Oct/Nov/Dec

Facility/Site Information

BNSF Railway - BALMER
Location: 3600 Gilman Ave. W, Seattle Washington
County: KING
Primary SIC Code: 4011

Mailing Information

BNSF Railway
2454 Occidental Ave. South, Suite 1A
Seattle, WA 98134

You must send a Discharge Monitoring Report (DMR) to Ecology **every quarter**. If there was **no discharge** *or* you have **suspended sampling** because of consistent attainment of benchmark values, mark the appropriate boxes and send the DMR to Ecology. Please read the instructions before completing the DMR.

Discharge Point #2

X There was no qualifying storm event this quarter so no values are entered below (see explanation)

Quarterly Monitoring		AVERAGE	MAXIMUM	UNITS	Sample Type	Events Sampled
Turbidity	Consistent Attainment			NTU	**Grab**	
pH	Consistent Attainment			Standard Units	**Grab**	
Zinc (total)	Consistent Attainment			µg/L	**Grab**	
Oil & Grease	Consistent Attainment			mg/L	**Grab**	
Lead (total)	Consistent Attainment			µg/L	**NA**	
Copper (total)	Consistent Attainment			µg/L	**NA**	
Hardness	**N/A – Discharge to Marine Water.**					

I CERTIFY UNDER PENALTY OF LAW THAT I HAVE PERSONALLY EXAMINED AND AM FAMILIAR WITH THE INFORMATION SUBMITTED HEREIN AND BASED ON MY INQUIRY OF THOSE INDIVIDUALS IMMEDIATELY RESPONSIBLE FOR OBTAINING THE INFORMATION, I BELIEVE THE SUBMITTED INFORMATION IS TRUE, ACCURATE, AND COMPLETE. I AM AWARE THAT THERE ARE SIGNIFICANT PENALTIES FOR SUBMITTING FALSE INFORMATION INCLUDING THE POSSIBILITY OF FINE AND IMPRISONMENT. SEE 18 USC § 1001 AND 33 USC § 1319. *(PENALTIES UNDER THESE STATUES MAY INCLUDE FINES UP TO $10,000.00 AND OR MAXIMUM IMPRISONMENT OF BETWEEN SIX MONTHS AND FIVE YEARS.)*

Jennifer Anderson
NAME/TITLE PRINCIPAL EXECUTIVE OFFICER (TYPED OR PRINTED)

4-20-09
DATE: MO DAY YEAR

SIGNATURE OF PRINCIPAL EXECUTIVE OFFICER OR AUTHORIZED AGENT

206-625-6034
TELEPHONE NUMBER

COMMENTS / EXPLANATIONS

An attempt to collect a stormwater sample on 2/25/09 was not successful. Construction of a new sampling port is underway. The previous sampling port became clogged and was not repairable.

SO3-001528D

INDUSTRIAL STORMWATER GENERAL PERMIT
DISCHARGE MONITORING REPORT

MONITORING PERIOD for (year/quarter): 2009 (year) Jan/Feb/Mar X Apr/May/Jun Jul/Aug/Sep Oct/Nov/Dec

Facility/Site Information

BNSF Railway - BALMER
Location: 3600 Gilman Ave. W, Seattle Washington
County: KING
Primary SIC Code: 4011

Mailing Information

BNSF Railway
2454 Occidental Ave. South, Suite 1A
Seattle, WA 98134

You must send a Discharge Monitoring Report (DMR) to Ecology **every quarter**. If there was **no discharge** *or* you have **suspended sampling** because of consistent attainment of benchmark values, mark the appropriate boxes and send the DMR to Ecology. Please read the instructions before completing the DMR.

Discharge Point #2

X There was no qualifying storm event this quarter so no values are entered below (see explanation)

Quarterly Monitoring		AVERAGE	MAXIMUM	UNITS	Sample Type	Events Sampled
Turbidity	Consistent Attainment			NTU	**Grab**	
pH	Consistent Attainment			Standard Units	**Grab**	
Zinc (total)	Consistent Attainment			µg/L	**Grab**	
Oil & Grease	Consistent Attainment			mg/L	**Grab**	
Lead (total)	Consistent Attainment			µg/L	**NA**	
Copper (total)	Consistent Attainment			µg/L	**NA**	
Hardness	**N/A – Discharge to Marine Water.**					

I CERTIFY UNDER PENALTY OF LAW THAT I HAVE PERSONALLY EXAMINED AND AM FAMILIAR WITH THE INFORMATION SUBMITTED HEREIN AND BASED ON MY INQUIRY OF THOSE INDIVIDUALS IMMEDIATELY RESPONSIBLE FOR OBTAINING THE INFORMATION, I BELIEVE THE SUBMITTED INFORMATION IS TRUE, ACCURATE, AND COMPLETE. I AM AWARE THAT THERE ARE SIGNIFICANT PENALTIES FOR SUBMITTING FALSE INFORMATION INCLUDING THE POSSIBILITY OF FINE AND IMPRISONMENT. SEE 18 USC § 1001 AND 33 USC § 1319. *(PENALTIES UNDER THESE STATUES MAY INCLUDE FINES UP TO $10,000.00 AND OR MAXIMUM IMPRISONMENT OF BETWEEN SIX MONTHS AND FIVE YEARS.)*

Jennifer Anderson
NAME/TITLE PRINCIPAL EXECUTIVE OFFICER (TYPED OR PRINTED)

8-4-09
DATE: MO DAY YEAR

SIGNATURE OF PRINCIPAL EXECUTIVE OFFICER OR AUTHORIZED AGENT

206-625-6034
TELEPHONE NUMBER

COMMENTS / EXPLANATIONS

Rainfall resulting in a qualified event occurred on May 5, 2009; however, no flow was observed upon arrival at the facility. The majority of precipitation fell before 8 am on May 5, 2009.

SO3-001528D

INDUSTRIAL STORMWATER GENERAL PERMIT
DISCHARGE MONITORING REPORT

MONITORING PERIOD for (year/quarter): 2009 (year) **Jan/Feb/Mar** **Apr/May/Jun** X **Jul/Aug/Sep** **Oct/Nov/Dec**

Facility/Site Information

BNSF Railway - BALMER
Location: 3600 Gilman Ave. W, Seattle Washington
County: KING
Primary SIC Code: 4011

Mailing Information

BNSF Railway
2454 Occidental Ave. South, Suite 1A
Seattle, WA 98134

You must send a Discharge Monitoring Report (DMR) to Ecology **every quarter**. If there was **no discharge** *or* you have **suspended sampling** because of consistent attainment of benchmark values, mark the appropriate boxes and send the DMR to Ecology. Please read the instructions before completing the DMR.

Discharge Point #2

There was no qualifying storm event this quarter so no values are entered below (see explanation)

Quarterly Monitoring		AVERAGE	MAXIMUM	UNITS	Sample Type	Events Sampled
Turbidity	Consistent Attainment	**69.5**	**69.5**	NTU	**Grab**	**8/11/09**
pH	Consistent Attainment	**9.6**	**9.6**	Standard Units	**Grab**	**8/11/09**
Zinc (total)	Consistent Attainment	**166**	**166**	µg/L	**Grab**	**8/11/09**
Oil & Grease	Consistent Attainment	**38.9**	**38.9**	mg/L	**Grab**	**8/11/09**
Lead (total)	Consistent Attainment	**44.6**	**44.6**	µg/L	**NA**	**8/11/09**
Copper (total)	Consistent Attainment	**81.0**	**81.0**	µg/L	**NA**	**8/11/09**
Hardness	**N/A – Discharge to Marine Water.**					

I CERTIFY UNDER PENALTY OF LAW THAT I HAVE PERSONALLY EXAMINED AND AM FAMILIAR WITH THE INFORMATION SUBMITTED HEREIN AND BASED ON MY INQUIRY OF THOSE INDIVIDUALS IMMEDIATELY RESPONSIBLE FOR OBTAINING THE INFORMATION, I BELIEVE THE SUBMITTED INFORMATION IS TRUE, ACCURATE, AND COMPLETE. I AM AWARE THAT THERE ARE SIGNIFICANT PENALTIES FOR SUBMITTING FALSE INFORMATION INCLUDING THE POSSIBILITY OF FINE AND IMPRISONMENT. SEE 18 USC § 1001 AND 33 USC § 1319. *(PENALTIES UNDER THESE STATUES MAY INCLUDE FINES UP TO $10,000.00 AND OR MAXIMUM IMPRISONMENT OF BETWEEN SIX MONTHS AND FIVE YEARS.)*

Jennifer Anderson
NAME/TITLE PRINCIPAL EXECUTIVE OFFICER (TYPED OR PRINTED)

11 - 6 - 09
DATE: MO DAY YEAR

SIGNATURE OF PRINCIPAL EXECUTIVE OFFICER OR AUTHORIZED AGENT

206-625-6034
TELEPHONE NUMBER

COMMENTS / EXPLANATIONS

Rainfall resulting in a qualified event occurred on August 11, 2009. Since the date of this sampling event, it has been determined that stormwater represented by this data discharges to the municipal combined sewer system. A permit Notice of Termination form has been submitted to Ecology.

SO3-001528D

INDUSTRIAL STORMWATER GENERAL PERMIT
DISCHARGE MONITORING REPORT

MONITORING PERIOD for (year/quarter): **2009** (year) **Jan/Feb/Mar** **Apr/May/Jun** **Jul/Aug/Sep** **X** **Oct/Nov/Dec**

Facility/Site Information

BNSF Railway - BALMER
Location: 3600 Gilman Ave. W, Seattle Washington
County: KING
Primary SIC Code: 4011

Mailing Information

BNSF Railway
2454 Occidental Ave. South, Suite 1A
Seattle, WA 98134

You must send a Discharge Monitoring Report (DMR) to Ecology **every quarter**. If there was **no discharge** *or* you have **suspended sampling** because of consistent attainment of benchmark values, mark the appropriate boxes and send the DMR to Ecology. Please read the instructions before completing the DMR.

Discharge Point #2

There was no qualifying storm event this quarter so no values are entered below (see explanation)

Quarterly Monitoring		AVERAGE	MAXIMUM	UNITS	Sample Type	Events Sampled
Turbidity	Consistent Attainment			NTU		
pH	Consistent Attainment			Standard Units		
Zinc (total)	Consistent Attainment			µg/L		
Oil & Grease	Consistent Attainment			mg/L		
Lead (total)	Consistent Attainment			µg/L		
Copper (total)	Consistent Attainment			µg/L		
Hardness	**N/A – Discharge to Marine Water.**					

I CERTIFY UNDER PENALTY OF LAW THAT I HAVE PERSONALLY EXAMINED AND AM FAMILIAR WITH THE INFORMATION SUBMITTED HEREIN AND BASED ON MY INQUIRY OF THOSE INDIVIDUALS IMMEDIATELY RESPONSIBLE FOR OBTAINING THE INFORMATION, I BELIEVE THE SUBMITTED INFORMATION IS TRUE, ACCURATE, AND COMPLETE. I AM AWARE THAT THERE ARE SIGNIFICANT PENALTIES FOR SUBMITTING FALSE INFORMATION INCLUDING THE POSSIBILITY OF FINE AND IMPRISONMENT. SEE 18 USC § 1001 AND 33 USC § 1319. *(PENALTIES UNDER THESE STATUES MAY INCLUDE FINES UP TO $10,000.00 AND OR MAXIMUM IMPRISONMENT OF BETWEEN SIX MONTHS AND FIVE YEARS.)*

Jennifer Wiener
NAME/TITLE PRINCIPAL EXECUTIVE OFFICER (TYPED OR PRINTED)

1-22-10
DATE: MO DAY YEAR

SIGNATURE OF PRINCIPAL EXECUTIVE OFFICER OR AUTHORIZED AGENT

206-625-6034
TELEPHONE NUMBER

COMMENTS / EXPLANATIONS

This is the final DMR for the BNSF Balmer Yard. A notice of termination for the Balmer ISWGP was granted by Ecology on December 8, 2009.

Marine Environmental Research 69 (2010) 172–177

Contents lists available at ScienceDirect

Marine Environmental Research

journal homepage: www.elsevier.com/locate/marenvrev

Oxidative damage in trout erythrocyte in response to "in vitro" copper exposure

Donatella Fedeli, Manuel Carloni, Giancarlo Falcioni *

Department of Molecular Cellular and Animal Biology, University of Camerino, Via Gentile III da Varano, 62032 Camerino MC, Italy

ARTICLE INFO

Article history:
Received 3 April 2009
Received in revised form 2 October 2009
Accepted 4 October 2009

Keywords:
Copper
Trout erythrocyte
Hemoglobin
Hemolysis
DNA damage

ABSTRACT

The oxidative action of copper on different trout *Oncorhynchus mykiss* erythrocyte components was studied. The results indicate that:

- cupric ions differently influence the oxidative status of two trout hemoglobin components I and IV (HbI and HbIV) having different structural and functional properties;
- reactive oxygen species (ROS) production associated with hemoglobins autoxidation is not influenced by the presence of copper sulfate;
- the susceptibility to hemolysis increases in the presence of copper only when the erythrocyte suspension is incubated in air; the effect of copper is almost absent for carbon monoxide-saturated erythrocyte suspensions;
- DNA damage due to copper was not observed in our experimental conditions.

The data obtained are important for the analysis of the environmental risks produced by copper on fish.

© 2009 Elsevier Ltd. All rights reserved.

1. Introduction

Copper is an essential trace metal for living organisms and its role as cofactor for crucial enzymes (cytochrome c oxidase, superoxide dismutase, ceruloplasmin, monooxygenases) has been well established. Most of these enzymes catalyze oxidation/reduction reactions that have molecular oxygen as co-substrate. However, if copper is present at relatively high concentrations in the environment, toxicity to aquatic organisms can occur (Winger et al., 2000; Marcano et al., 1996; Roche and Boge, 1996). In aquaculture systems, copper is regularly used in the form of copper sulfate as a therapeutic agent and it is widely used to control alga blooms and aquatic macrophyte infestations (Boyd and Massaut, 1999).

There is no doubt that exposure to excess copper can damage cells and organs because copper ion and its complexes can induce formation of reactive oxygen species that can damage biomolecules such as lipids, proteins and DNA. Copper toxicity at the cellular level depends on the permeability of cell membranes to copper ions and on its participation in redox reactions because it easily cycles between the cuprous and cupric state.

$$Cu^{2+} + O_2^{\cdot -} \rightarrow Cu^{+} + O_2 \quad (1)$$

$$Cu^{+} + H_2O_2 \rightarrow Cu^{2+} + OH^{\cdot} + OH^{-} \quad (2)$$

This paper focuses on the "in vitro" effects of copper ions on oxidative damage in trout *Oncorhynchus mykiss* erythrocytes. The effect of copper ions on the oxidation of trout hemoglobin components either as purified proteins or in the whole hemolysate was examined. It is worth recalling that contrary to mammals and birds, a multiplicity of hemoglobin components is generally present in erythrocytes of fish. In the case of nucleated erythrocytes from trout *O. mykiss*, four different hemoglobin components are present; they are characterized by functional differences which have been correlated with different physiological roles (Brunori, 1975). Trout hemoglobin components according to their anionic mobility have been called HbI, HbII, HbIII and HbIV. These hemoglobins are prone to oxidation and this property permits to follow "in vitro" the autoxidation process over a relatively short time. The production of reactive oxygen species during the hemoglobin oxidation was also evaluated. The measurements regarding purified hemoglobins were performed on HbI and HbIV. These two trout hemoglobin components represent, respectively, about 20% and 60% of the whole pigment present inside trout erythrocytes and have very different oxygen binding properties (Brunori, 1975). The mechanism of copper-induced met-hemoglobin formation has been described in detail for human hemoglobin solutions (Bonaventura et al., 1999) but this is not well understood for fish hemoglobins that have different structures. Furthermore, the influence of copper on the extent of hemolysis and on the susceptibility of DNA to oxidative damage was assessed.

* Corresponding author. Tel.: +39 0737 403211; fax: +39 0737 403290.
E-mail address: giancarlo.falcioni@unicam.it (G. Falcioni).

0141-1136/$ - see front matter © 2009 Elsevier Ltd. All rights reserved.
doi:10.1016/j.marenvres.2009.10.001

2. Materials and methods

All the reagents used were of analytical grade.

2.1. Samples

Red blood cells were obtained from *O. mykiss* trout, coming from the fish farm "Eredi Rossi Silvio" Sefro MC, Italy. The fish were kept in tanks containing water from Scarsito River, a tributary of the Potenza River, and fed with commercial fish food obtained from Hendrix S.p.A (Mozzecane, VR, Italy). Blood was extracted by puncturing the lateral tail vein. After washing with isotonic medium at pH 7.8 (0.1 M phosphate buffer 0.1 M NaCl, 0.2% citrate, 1 mM EDTA) the cells were suspended in the desired isotonic buffer.

2.2. Separation of hemoglobin components and carbon monoxide hemoglobin (HbCO) formation

Separation of the various hemoglobins, as described previously (Binotti et al., 1971) was carried out by column chromatography on DEAE-Spehadex A-50; their homogenity was tested by electrophoresis.

Experiments involving carbon monoxide (CO) hemoglobin were carried out after exposure of the oxygenated derivative to a weak vacuum by using a rotary vane pump and then to pure CO gas. The vacuum, performed for a few seconds, permits the removal of part of the oxygen thus making the formation of CO hemoglobin easier (Hb affinity for CO is greater than that for O_2 by about 250-fold).

2.3. Ferric hemoglobin (Met-Hb) formation and hemoglobin precipitation

The rate of met-Hb formation in the hemolyzates and in two electrophoretically distinct hemoglobin components called hemoglobin trout I and IV (HbI and HbIV) was followed in a Cary 219 spectrophotometer in the visible region; reference value (i.e. complete oxidation) was estimated by addition of ferricyanide. Absorbance at 700 nm was followed as an index of turbidity to monitor the onset of hemoglobin precipitation.

2.4. Reactive oxygen species production during Hb oxidation

ROS production associated with Hb autoxidation was evaluated by monotoring the oxidation of non-fluorescent dichlorofluorescein (DCFH) to fluorescent DCF.

A solution of 1 mg ml^{-1} of HbI or HbIV was incubated for 1 h in phosphate buffer 50 mM pH 7.5 at different temperatures and in the presence of 0.036 μm DCFH and of 10 or 100 μM $CuSO_4$. DCFH oxidation was measured fluorimetrically on these solutions at excitation and emission wavelengths of 498 nm and 520 nm, respectively.

2.5. Hemolysis

In order to evaluate the hemolysis rate, the erythrocytes were suspended in isotonic medium at pH 6.3 at 35 °C. The degree of hemolysis was determined spectrophotometrically at 540 nm as previously described (Falcioni et al., 1987) either in the presence or absence of the desired amount of copper sulfate. In particular, hemolysis was determined as $100 \times A/10 \times A^{*} \times 100\%$ where A is the optical density of Hb present in the supernatant after centrifugation of red cell suspension and $A^{*} \times 100\%$ is the optical density of the red cell suspension after complete lysis with 10 volumes of distilled water at zero time incubation.

2.6. Single-cell gel electrophoresis (comet assay)

The "comet" assay was performed on trout erythrocytes (1×10^6 cells ml^{-1}) incubated in a pH 6, 3 isotonic buffer at 35 °C for 1 h in the presence and absence (control) of 50 μM copper sulfate. After incubation, the erythrocytes were suspended in 0.7% low melting agarose in phosphate buffer saline (PBS) and pipetted on microscope slides pre-coated with a layer of 1% normal melting agarose. The agarose with the cell suspension was allowed to set on the pre-coated slides at 4 °C for 10 min. Subsequently, another top layer of 0.7% low melting agarose was added and allowed to set at 4 °C for 10 min. The slides were then immersed in lysis solution (1% sodium *n*-lauroyl-sarcosinate, 2.5 M NaCl, 100 mM Na_2EDTA, 10 mM Tris HCl pH 10, 1% Triton X-100 and 10% dimethyl sulfoxide for 1 h at 4 °C in the dark, in order to lyse the embedded cells and to permit DNA unfolding. After incubation in lysis solution, slides were exposed to alkaline buffer (1 mM Na_2EDTA, 300 mM NaOH buffer, pH >13) for 20 min; in this condition RNA is completely degraded. The slides were subjected to 20 min electrophoresis at 25 V in the same alkaline buffer and finally washed with 0.4 M Tris HCl buffer (pH 7.5) to neutralize excess alkali and to remove detergents before staining with ethidium bromide (2 μg ml^{-1}).

Cells were examined with an Axioskop 2 plus microscope (Carl Zeiss, Germany) equipped with an excitation filter of 515–560 nm and a magnification of ×20. Imaging was performed using a specialized analysis system ("Metasystem" Altlussheim, Germany) to determine tail moment (TM), tail length (TL) and tail intensity (TI), parameters correlated with the degree of DNA damage in each single cell. Experiments were performed three times and data (at least 150 scores per sample) are the mean values plus/minus the standard error of the mean (SEM). Statistical analysis was performed using the student *t*-test and differences were regarded as statistically significant when p values were <0.05.

3. Results

3.1. Met-Hb rate formation in hemolysates

Fig. 1 is one representative set of tracings from a total of at least three experiments and shows the time course of hemoglobin autoxidation during incubation at 35 °C in 50 mM phosphate buf-

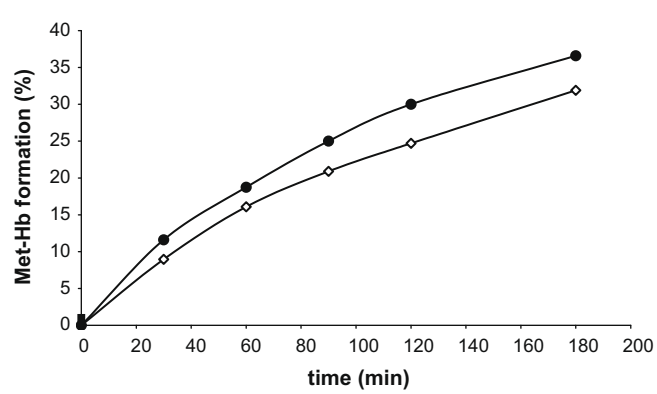

Fig. 1. Time course of Hb autoxidation in trout hemolysate containing Hb (1 mg ml^{-1}) during incubation at 35 °C in phosphate buffer 50 mM pH 7.5 in the presence and in the absence of 10 μM $CuSO_4$. Data are from one representative set of tracings from a total of three experiments. (◇) control and (●) +10 μM $CuSO_4$.

fer, pH 7.5, of trout hemolysate in the absence and presence of 10 μM $CuSO_4$. As can be observed, the presence of 10 μM $CuSO_4$ increases the met-Hb formation rate; after 2 h of incubation, the level of met-Hb was ~30% and ~25% in the presence and absence of copper sulfate, respectively. The statistical analysis of the three experiments give a p value <0.05.

3.2. Met-Hb rate formation in purified hemoglobin components HbI and HbIV

Fig. 2 shows the time course of HbI autoxidation when the protein was incubated at 35 °C and pH 7.5. The presence of high amounts of $CuSO_4$ (up to 100 μM) does not influence the HbI oxidation rate with respect to the control (HbI alone without $CuSO_4$) during our incubation time.

It was not possible to perform similar experiments with HbIV because this hemoglobin component is less stable and tends to precipitate under these experimental conditions. The presence of copper sulfate accelerates the protein denaturation rate. A similar behaviour was also observed at lower incubation temperatures (30 °C).

3.3. Reactive oxygen species production during Hbs incubation

ROS production associated with Hb autoxidation was followed by means of fluorescence deriving from DCFH oxidation. Figs. 3 and 4 show the time course of DCF fluorescence generated during 1 h incubation of HbI or HbIV followed at different temperatures. After 1 h of HbI incubation at 20 °C and 25 °C there is no ROS formation and this is in agreement with the absence of HbI oxidation. When the HbI solution is incubated for 1 h at 35 °C ROS formation due to the partial oxidation of the protein was observed (Fig. 3). Similar experiments were performed with HbIV (the highest temperature was 30 °C) (Fig. 4). A slight ROS production was present also at 25 °C which increased at 30 °C. For both hemoglobins the level of ROS production was not influenced by the presence of copper sulfate. It is possible to avoid the formation of met-Hb by adding carbon-monoxide (CO) before incubation. Experiments performed with HbCO did not show ROS formation at any temperature (data not shown). This behaviour is due to the stability versus the oxidation of the carbomonoxy-derivative; in other words, HbCO does not lead to the ferric form during incubation.

3.4. Hemolysis rate

By varying pH and temperature, it is possible for trout erythrocytes suspended in isotonic medium to follow "in vitro" the hemolytic event over a relatively short time (Falcioni et al., 1987); the hemolytic process is characterized by the presence of a long lag phase. The influence of a fixed amount (50 μM) of copper sulfate on the rate of hemolysis in trout erythrocytes during incubation in isotonic buffer at 35 °C and pH 6.3 was investigated and reported in Fig. 5. The figure is one representative set of tracings from a total of at least three experiments. The susceptibility to hemolysis increases in the presence of copper only when the erythrocyte suspension was incubated in air; a dose-dependent effect of copper was absent for CO-saturated erythrocyte suspensions exposed to air under identical conditions. The half time ($t/2$) of hemolysis (expressed as the time necessary for 50% hemolysis to occur) and determined from Fig. 5 is 160 min, 186 min, 148 min and 183 min for red blood cells (RBC) suspension in air, RBC suspension with CO, RBC suspension in air with 50 μM $CuSO_4$ and RBC suspension with CO and 50 μM $CuSO_4$, respectively. The statistical analysis of the three experiments give a p value <0.05.

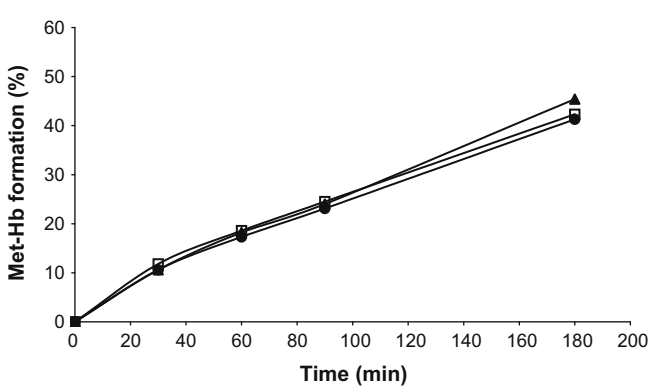

Fig. 2. Time course of 1 mg ml^{-1} HbI autoxidation during incubation at 35 °C in phosphate buffer 50 mM pH 7.5 in the presence and in the absence of 10 and 100 μM $CuSO_4$. Data are from one representative set of tracings from a total of three experiments. (●) control; (□) +10 μM $CuSO_4$ and (▲) +100 μM $CuSO_4$.

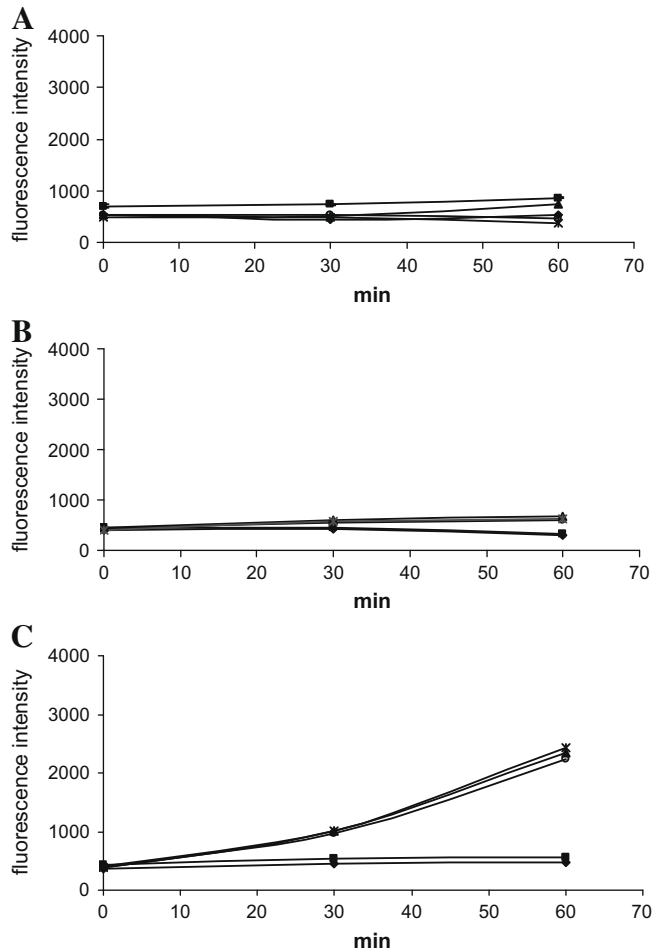

Fig. 3. Time course of DCFH (0.036 μM) fluorescence generated during 1 h incubation of HbI (1 mg ml^{-1}) in phosphate buffer 50 mM pH 7.5 at 20 °C (Panel A), at 25 °C (Panel B) and at 35 °C (Panel C) in the presence and absence of 10 and 100 μM $CuSO_4$. Data are from one representative set of tracings from a total of three experiments. (♦) Phosphate buffer + DCFH; (■) phosphate buffer + 100 μM $CuSO_4$ + DCFH; (▲) phosphate buffer + HbI + DCFH; (O) phosphate buffer + HbI + 10 μM $CuSO_4$ + DCFH and (∗) phosphate buffer + HbI + 100 μM $CuSO_4$ + DCFH.

3.5. Comet assay

The "comet assay" or single-cell gel electrophoresis was performed on trout erythrocyte suspension to explore if the copper salt under study influenced the DNA status in these nucleated cells.

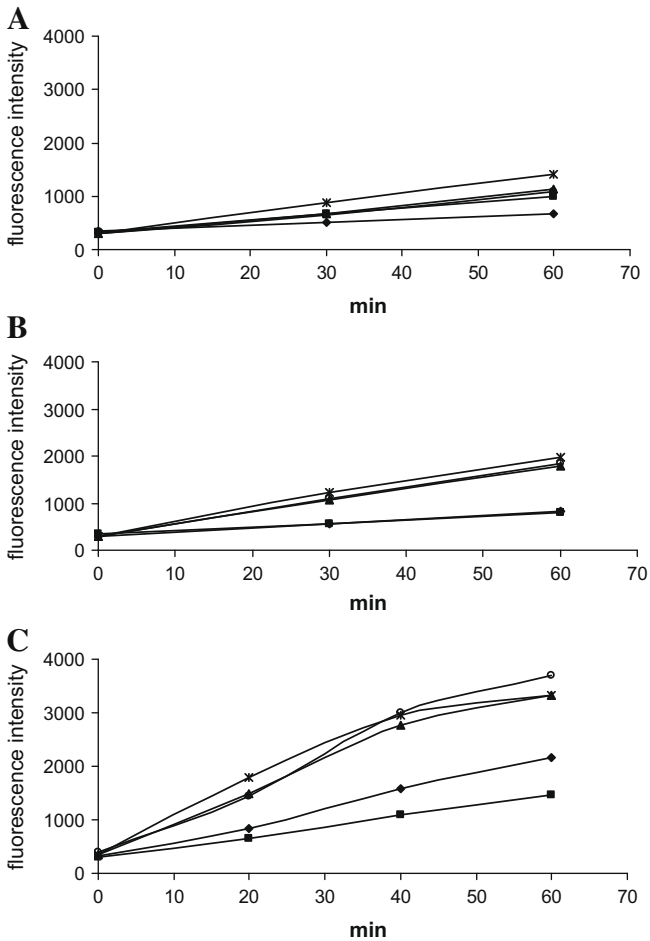

Fig. 4. Time course of DCFH (0.036 μM) fluorescence generated during 1 h incubation of HbIV (1 mg ml^{-1}) in phosphate buffer 50 mM pH 7.5 at 20 °C (Panel A), at 25 °C (Panel B) and at 30 °C (Panel C) in the presence and absence of 10 and 100 μM $CuSO_4$. Data are from one representative set of tracings from a total of three experiments. (♦) Phosphate buffer + DCFH; (■) phosphate buffer + 100 μM $CuSO_4$ + DCFH; (▲) phosphate buffer + HbIV + DCFH; (O) phosphate buffer + HbIV + 10 μM $CuSO_4$ + DCFH and (∗) phosphate buffer + HbIV + 100 μM $CuSO_4$ + DCFH.

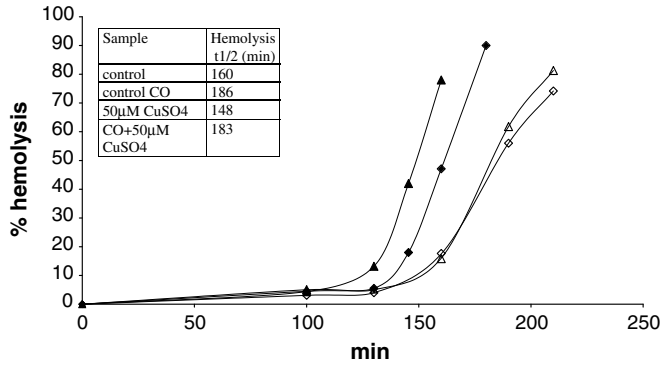

Sample	Hemolysis t1/2 (min)
control	160
control CO	186
50μM CuSO4	148
CO+50μM CuSO4	183

Fig. 5. Time course of hemolysis of trout erythrocyte suspensions (Hb = 30 mg ml^{-1}) incubated in isotonic buffer pH 6.3 and at 35 °C in presence and absence of carbon monoxide and 50 μM $CuSO_4$. Data are from one representative set of tracings from a total of three experiments. (♦) control; (▲) + 50 μM $CuSO_4$; (◇) control CO and (Δ) CO + 50 μM $CuSO_4$.

This test has become increasingly popular for the measurement of DNA damage in individual cells and consists of embedding cells in agarose, followed by lysis, electrophoresis and staining to visualize DNA damage using fluorescence microscopy. Cells with increased DNA damage display an increased migration of genetic material in the direction of the electrophoresis. The extent of DNA damage is quantified by measuring the displacement of the genetic material between the cell nucleus ("comet head") and the resulting "tail". The parameters used as an index of DNA damage are tail length, tail intensity and tail moment and they are calculated by computerized image analysis. The "comet assay" was performed on trout erythrocyte suspensions incubated at pH 6.3 and 35 °C for 60 min in the presence of 50 μM copper sulfate. Fig. 6 clearly shows that all the considered comet parameters (tail length, tail intensity and tail moment) increased after 1 h. The increase for tail length and tail moment was independent of the presence of copper

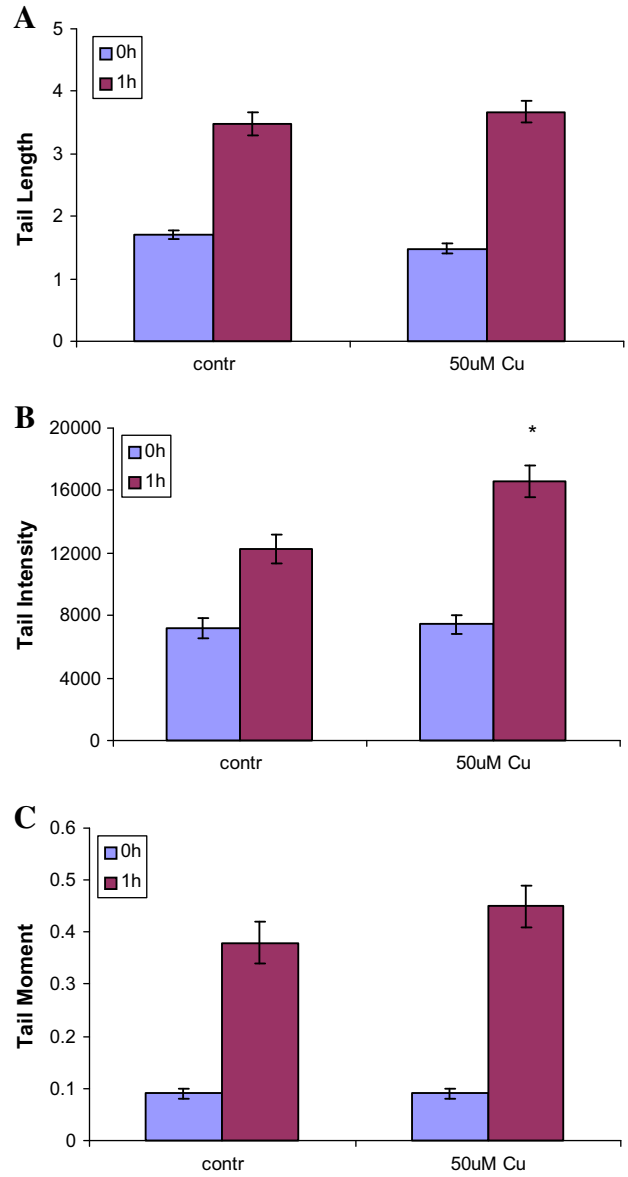

Fig. 6. Tail length (A), tail intensity (B) and tail moment (C) comet parameter (mean ± s.e.m) measured on trout erythrocyte suspension incubated in isotonic buffer at pH 6.3 and at 35 °C for 1 h in the presence and in the absence of carbon monoxide and 50 μM $CuSO_4$. $^{*}p < 0.05$ compared to control 1 h.

sulfate in the incubation medium; a slight increase was instead measured for tail intensity.

4. Discussion

It is well known that copper can induce damage to cells through radical-formation (Valko et al., 2005; Gaetke and Chow, 2003). Furthermore it is important to remember that copper, together with iron and selenium, control the activity of those enzymes involved in the defence mechanisms against reactive oxygen species (superoxide dismutase, catalase and glutathione peroxidase). The results reported here clearly show that the presence of copper can influence the redox state of HbIV and disrupts the plasma membrane. However, under our experimental conditions DNA damage due to the presence of copper was not observed, except for a slight increase in tail intensity.

There is evidence that copper catalyzes human oxyhemoglobin oxidation also at very low concentrations (Rifkind, 1974; Winterbourn and Carrel, 1997) while other metal ions have no significant effect even at high concentrations. The copper induced met-Hb formation mechanism has been described in detail for human hemoglobin (Bonaventura et al., 1999). It is probable that ferric hemoglobin formation, in general, involves an electron transfer from Fe^{++} to Cu^{++} as suggested for human hemoglobin (Bonaventura et al., 1999). Our results on the effect of copper on autoxidation of trout hemoglobins clearly show that the effect of the metal is different in the two hemoglobin fractions HbI and HbIV that have different aminoacid sequences, and as a consequence, different tridimensional structures and functional properties (Barra et al., 1983; Petruzzelli et al., 1989).

The involvement of the sulphydryl group in β-93 position in hemoglobin autoxidation has been reported in the literature (Rifkind, 1972). The effect of copper on Hb oxidation during the hemolysate incubation reported in Fig. 1 could imply that the hemoglobin component oxidized is HbIV and not HbI. This is due to the fact that HbI in the presence of copper at the highest concentration and in the same experimental conditions was not oxidized.

It is worth pointing out that the autoxidation of oxygenated Hbs can be followed by the transformation of the oxidized molecule (high-spin Fe^{3+}) into a species absorbing as a low-spin Fe^{3+} compound, that is a hemichrome which tends to precipitate. The overall process may be described according to the following scheme:

HbO_2 – met Hb – hemicrome – precipitate

The presence of different antioxidant enzymes (superoxide dismutase, catalase and glutathione peroxidase) in the hemolysate could reduce the oxidation rate of HbIV and thus avoiding the formation of HbIV precipitate.

The conversion of oxyhemoglobin into met-Hb is associated with superoxide production (Misra and Fridovich, 1972; Brunori et al., 1975) and thereby of products such as H_2O_2 or hydroxyl radical, which can derive from $O_2^{\cdot-}$ itself.

We have observed that the presence of copper sulfate does not influence the level of ROS during 1 h of HbI or HbIV incubation (Figs. 3 and 4). This result could be due to the direct interaction between heme–iron and copper or to the participation of copper in redox reactions involving ROS.

The presence of Cu^{++} in the trout erythrocyte suspension influences the hemolytic process (Fig. 5) when the cells are exposed to air. The effect of Cu^{++} is absent when the experiment was performed with CO-saturated erythrocytes; the presence of CO leads to insignificant hemoglobin auto-oxidation over the same time range. These data appear to indicate that the effect of Cu^{++} on lysis is also correlated with hemoglobin oxidation. The hemolytic event is a complex process due to more than one type of biochemical damage. The difference in the rate of hemolysis between red blood cells saturated with either CO or O_2 was due to the consequences following hemoglobin oxidation (Falcioni et al., 1987). Recently, Labieniec et al. (2009) found that incubation with copper of marine fish erythrocytes from *Dicentrarchus labrax* increased hemolysis of cells; a significant decrease in the hemoglobin content and red blood cells after exposure of fish *Channa punctatus* to sublethal concentration of copper sulfate has been reported by Singh et al. (2008). On the membrane surface as well as at the cytosol level, copper ions are involved in various redox reactions that lead to an increased radical production followed by oxidative damage and lipid bilayer destruction. Cupric but not cuprous ions are responsible for met-Hb formation that can contribute to the hemolytic event. The reduction of cupric to cuprous ion can occur at the membrane surface level (Bogdanova et al., 1999) by the involvement of sulphydryl groups. Both cupric and cuprous ions can interact with transport systems outside and inside the membrane leading to its perturbation (Bogdanova et al., 2002).

5. Conclusions

In conclusion, the environmental risks from the use of copper compounds should be evaluated in order to control biological damage to fish. The results here presented indicated that an eventual "in vivo" alteration following copper exposure could induce plasma membrane perturbation with a mechanism involving methemoglobin formation.

References

Barra, D., Petruzzelli, R., Bossa, F., Brunori, M., 1983. Primary structure of hemoglobin from trout (*Salmo irideus*) amino acid sequence of the beta chain of trout HbI. Biochimica Biophysica Acta 742, 72–77.

Binotti, I., Giovenco, S., Giardina, B., Antonini, E., Brunori, M., Wyman, J., 1971. Studies of the functional properties of fish hemoglobins. II. The oxygen equilibrium of the isolated hemoglobin components from trout blood. Archives of Biochemistry Biophysics 142, 274–280.

Bogdanova, A.Y., Virkki, L.V., Gusev, G.P., Nikinmaa, M., 1999. Copper effects on ion transport across lamprey erythrocyte membrane: Cl (−)/OH (−) exchange induced by cuprous ions. Toxicology Applied Pharmacology 159, 204–213.

Bogdanova, A.Y., Gassmann, M., Nikinmaa, M., 2002. Copper ion redox state is critical for its effects on ion transport pathways and methaemoglobin formation in trout erythrocytes. Chemico–Biological Interaction 139, 43–59.

Bonaventura, C., Godette, G., Tesh, S., Holm, D.E., Bonaventura, J., Crumbliss, A.S., Pearce, J., Peterson, J., 1999. Internal electron transfer between hemes and Cu (II) bound at cysteine beta93 promotes methemoglobin reduction by carbon monoxide. Journal Biological Chemistry 274, 5499–5507.

Boyd, C.E., Massaut, L., 1999. Risk associated with the use of chemicals in pond aquaculture. Aquacultural Engineering 20, 113–132.

Brunori, M., 1975. Molecular adaptation to physiological requirements: the hemoglobin system in trout. Current Topics in Cellular Regulation 9, 1–39.

Brunori, M., Falcioni, G., Fioretti, E., Giardina, B., Rotilio, G., 1975. Formation of superoxide in the autoxidation of isolated a and b chains of human hemoglobin and its involvement in the hemicromes precipitation. European Journal Biochemistry 53, 99–104.

Falcioni, G., Cincolà, G., Brunori, M., 1987. Glutathione peroxidase and oxidative hemolysis in trout red blood cells. Febs Letters 221, 355–358.

Gaetke, L.M., Chow, C.K., 2003. Copper toxicity, oxidative stress and antioxidant nutrients. Toxicology 189, 147–163.

Labieniec, M., Milowska, K., Balcerczyk, A., Rucinska, A., Sadowska, M., Jokiel, M., Brichon, G., Gabryelak, T., 2009. Interaction of free copper (II) ions alone or in complex with iron (III) ions with erythrocytes of marine fish *Dicentrarchus labrax*. Cell Biology International 33, 941–948.

Marcano, L., Nusetti, O., Rodriguez-Grau, J., Vilas, J., 1996. Uptake and regulation of copper and zinc in relation to metal-binding protein in the Polychaete Eurythoe complanata. Comparative Biochemistry Physiology 114C (3), 179–184.

Misra, H.P., Fridovich, I., 1972. Generation of superoxide radical during the autoxidation of haemoglobin. Journal Biological Chemistry 247, 6960–6962.

Petruzzelli, R., Barra, D., Sensi, L., Bossa, F., Brunori, M., 1989. Amino acid sequence of alpha-chain of hemoglobin IV from trout (*Salmo irideus*). Biochimica Biophysica Acta 995, 255–258.

Rifkind, J.M., 1972. The autoxidation of horse hemoglobin: the effect of glutathione. Biochimica Biophysica Acta 273, 30–39.

Rifkind, J.M., 1974. Copper and autoxidation of hemoglobin. Biochemistry 13, 2475–2481.
Roche, H., Boge, G., 1996. Fish blood parameters as potential tool for identification of stress caused by environmental factors and chemical intoxication. Marine Environmental Research 41 (1), 27–43.
Singh, D., Nath, K., Trivedi, S.P., Sharma, Y.K., 2008. Impact of copper on haematological profile of freshwater fish, *Channa punctatus*. Journal Environmental Biology 29 (2), 253–257.
Valko, M., Morris, H., Cronin, M.T., 2005. Metal, toxicity and oxidative stress. Current Medicinal Chemistry 12, 1161–1208.
Winger, P.W., Lasier, P.J., White, D.H., Seginak, J.T., 2000. Effect of contaminants in dredge material from the lower Savannah River. Archives Environmental Contaminants and Toxicology 28 (1), 128–136.
Winterbourn, C.C., Carrel, R.W., 1997. Oxidation of human hemoglobin by copper. Biochemical Journal 165, 141–148.

ELSEVIER

Aquatic Toxicology 78 (2006) 59–65

AQUATIC TOXICOLOGY

www.elsevier.com/locate/aquatox

Effects of Cu on plasma cortisol and cortisol secretion by adrenocortical cells of rainbow trout (*Oncorhynchus mykiss*)

Alexandra Gagnon [a], Catherine Jumarie [a], Alice Hontela [b,*]

[a] *Département des Sciences Biologiques, TOXEN Research Centre, Université du Québec à Montréal, C.P. 8888, Suc. Centre-ville, Montréal, Que., Canada H3C 3P8*

[b] *Department of Biological Sciences, University of Lethbridge, 4401 University Dr., Lethbridge, Alta., Canada T1K 3M4*

Received 2 November 2005; received in revised form 13 February 2006; accepted 15 February 2006

Abstract

Fish are exposed to multiple stressors, often acting concurrently, in their environment. To evaluate the potential of Cu to act as a chemical stressor, rainbow trout (*Oncorhynchus mykiss*) were exposed to Cu (30 or 80 μg/l) for 30 days in the laboratory and they were subjected to a physical stressor (1 min air exposure) before sampling. Physiological stress indicators in the whole fish as well as cortisol secretion by adrenocortical cells in vitro were measured. Fish exposed to Cu had a lower condition factor, hepatosomatic index, plasma glucose, hepatic glycogen and gill Na^+/K^+-ATPase activity compared to controls. Exposure to Cu did not have an effect on basal plasma cortisol (fish sampled without air exposure stress) however, the air exposure-induced increase in plasma cortisol was lower in fish exposed to Cu. Cortisol secretion stimulated by ACTH in vitro was greater in adrenocortical cells isolated from fish exposed to Cu in vivo but in vitro exposure to Cu consistently impaired cortisol secretion. Our results indicate that Cu at high concentrations disrupts cortisol secretion through a direct toxic effect on adrenocortical cells while low concentrations resulting from a 30-day exposure to environmentally relevant Cu concentrations enhances cortisol secretion in response to ACTH in vitro.
© 2006 Elsevier B.V. All rights reserved.

Keywords: Cu; Fish; Cortisol; In vitro; Acclimation; Glucose; Glycogen; Na^+/K^+-ATPase

1. Introduction

Copper (Cu), an essential element for cellular metabolism, is a cofactor of redox reactions involving intracellular enzymes and proteins such as cytochrome oxidase, lysyl oxidase and superoxide dismutase. The redox nature of Cu is essential to cellular respiration, free-radical defence and cellular Fe metabolism. However, at high concentrations Cu becomes toxic to fish. Loss of appetite, reduced growth, ion loss, decreased aerobic scope, histological alterations in kidney and gill, and mortality are some of the manifestations of Cu toxicity (Marr et al., 1996; McGeer et al., 2000a; Handy, 2003; Mazon et al., 2004). Although Cu concentrations rarely exceed 3 μg/l in pristine waters, in polluted waters they may surpass 63 μg/l and reach the toxicity threshold for some fish species (Taylor et al., 2003).

There is evidence to suggest that Cu concentrations in the body are regulated—a characteristic compatible with the essentiality of this metal and its toxicity at high concentrations. Grosell et al. (1997, 1998) reported that Cu-acclimated fish had reduced Cu concentrations in plasma compared with unacclimated fish, with no apparent change in gill Cu uptake. The difference in Cu concentrations was attributed to increased hepatic clearance of the newly accumulated Cu. Other investigators demonstrated that acclimation to Cu enhances tolerance to acute challenges with Cu and other metals, partly through metallothionein induction (Carvalho et al., 2004; van Heerden et al., 2004). Hansen et al. (2002) reported that while naïve trout suffered over 80% mortality when subjected to an acute 96 h challenge with 91 μg/l Cu, trout acclimated to 36 μg/l Cu for 56 days suffered only 20% mortality when challenged. Although it is known that liver, gill and the gut are the organs that mediate acclimation to Cu (Kamunde et al., 2002; Niyogi and Wood, 2003), how the acclimation processes influence sensitivity to Cu in other tissues has not been investigated.

The hypothalamo-pituitary-interrenal (HPI) axis of fish is activated during acute exposures to stressors (Hontela, 2005), including 24–96 h exposures to relatively high (up to 100 μg/l) concentrations of Cu (De Boeck et al., 2001; Teles et al., 2005).

* Corresponding author.
E-mail address: alice.hontela@uleth.ca (A. Hontela).

0166-445X/$ – see front matter © 2006 Elsevier B.V. All rights reserved.
doi:10.1016/j.aquatox.2006.02.004

The effects of chronic Cu exposure on the HPI axis and related parameters are less well understood. Plasma cortisol levels increased in rainbow trout exposed to 26.9 μg/l Cu for 3 days, however they returned to normal by day 21 (Dethloff et al., 1999a). There were no effects on plasma parameters, including plasma cortisol, at 14 μg/l Cu (Dethloff et al., 1999b). Given the controversy regarding the protective effect of cortisol during exposure to metals (Bury et al., 1998; De Boeck et al., 2003; Mazon et al., 2004), it is important to characterize the physiological stress response to chronic Cu exposure in fish and determine whether pre-exposure to Cu protects cells against Cu toxicity. Cortisol secretion by adrenocortical cells of rainbow trout and yellow perch is impaired by in vitro exposure to Cd or Hg (Leblond and Hontela, 1999; Lacroix and Hontela, 2004) and by chronic field exposures to metals including Cu in lakes situated in a mining region (Lévesque et al., 2003). However, the effects of chronic waterborne or acute in vitro exposures to Cu on cortisol secretion by the adrenocortical cells have not yet been investigated.

Thus the objective of the present study is to evaluate the impact of chronic exposure to Cu on the stress-related physiological responses (plasma cortisol, glucose, thyroid hormones, hepatic glycogen and gill Na^+/K^+ ATPase activity) in rainbow trout to determine whether at environmentally relevant concentrations Cu is recognized by the fish as a chemical stressor. To test the hypothesis the pre-exposure to Cu in vivo protects the adrenocortical cells against the toxic effects of an in vitro Cu challenge, the adrenal bioassay will be used in vitro with cells from fish chronically exposed to Cu in vivo.

2. Materials and methods

2.1. Fish and maintenance conditions

Juvenile rainbow trout (average body weight 88.5 ± 7.3), *Oncorhynchus mykiss,* were obtained from a commercial fish supplier (Pisciculture Laurentienne, Québec) in April–July. Fish were held in flow-through holding tanks (600 l) at 15 °C and a 12L:12D photoperiod. The tanks were supplied with Montreal city tap water which had been dechlorinated (by activated charcoal, UV irradiation plus thiosulfate titration to remove chloramines), degassed and reoxygenated to saturation. The entire plumbing system was constructed of PVC to circumvent metal toxicity. The water conductivity was 294 μS/cm, pH 7.2, alkalinity 125 mg/l $CaCO_3$, Ca 33 mg/l, Na 12 mg/l, K 1.51 mg/l, Cl 22 mg/l and background Cu at 4 μg/l. Fish were fed Purina trout Chow daily at 7 h at the manufacturer's recommended rate (10 g/kg of fish).

2.2. Experimental treatments

Following acclimation, fish were exposed to $CuSO_4$ (Fisher) through water at 0, 30 and 80 μg/l Cu for 30 days. The water Cu concentrations were maintained at a constant level with Mariotte bottles, test solutions were added to the tank at a flow rate of 2 ml/min. The nominal concentrations of $CuSO_4$ were fractions (15–40%) of 200 μg/l, the 96 h LC50 reported for rainbow trout maintained in Montreal water (Spear and Anderson, 1975). The concentration of 30 μg/l Cu represents environmental concentrations in some lakes in Sudbury (Ontario, Canada), an important mining area with smelting and refining complexes (Iles and Rasmussen, 2005). Water samples for Cu analyses were taken in the middle of the tank at days 5, 10, 20 and 30; Cu was measured by inductively coupled plasma atomic emission spectrophotometry (ICP-AES). Mean measured water Cu concentrations were within the expected range: 2.09 ± 1.02 μg/l in the control tank; 28.5 ± 2.43 μg/l in the 30 μg/l Cu treatment tank, and 87.7 ± 3.37 μg/l in the 80 μg/l Cu treatment tank.

2.3. Sampling

One week before sampling, fish in each experimental tank were separated into two equal groups by a mesh compartment. The system of two compartments permitted sampling fish in one compartment without disturbing fish in the other compartment of the same tank (same Cu exposure, same treatment) and stagger the sampling over two days. Fish were sampled between 9 h00 and 10 h30 in all treatments to minimize variations in the hormonal responses caused by diel endocrine cycles.

For basal cortisol levels (sampling without the air exposure stress), all fish in one compartment were removed quickly with the net to standardize the handling procedure, and they were immediately anaesthetized with MS 222. For sampling with the air exposure stress, all fish in one compartment were removed with the net, held in the air for 1 min and returned to the tank to be sampled 45 min later. Fish were weighed, fork length was recorded, and plasma was collected for glucose and hormone analyses. Fish were then perfused through the caudal vein with 0.7% saline, in preparation for the in vitro experiments with the adrenocortical cells. Livers were dissected, weighed and frozen for glycogen and Cu analyses. Kidneys were dissected and frozen for Cu analyses and gills for Na^+/K^+-ATPase analyses. The head kidneys were dissected for the in vitro experiments (see Section 2.6).

2.4. Analyses of Cu

Concentration of Cu were measured by inductively coupled plasma atomic emission spectrophotometry (ICP-AES) in water, and in kidney, interrenal tissue and liver, using tissue homogenates corresponding to 100 mg dry weight, as described previously by Laflamme et al. (2000). A mass of 1 μg/g dry weight corresponds to approximately 0.29 μg/g wet weight.

2.5. Biochemical analyses

2.5.1. Hormone analyses

Plasma cortisol, T3 and T4 were assayed with commercial radioimmunoassay kits (No. 07-221102 for cortisol and No. 838 for T3, ICN Biochemicals Canada, Ltd., Montreal, Que.). The characteristics of the assays were described in Hontela et al. (1995).

2.5.2. Glucose and glycogen

Plasma glucose was determined with a colometric enzymatic method using glucose oxidase (GOD-PAP) (Boehnringer Mannheim, Diagnostica). Liver glycogen was assayed with a method described in Lévesque et al. (2002). Frozen liver (≈0.1 g) was digested in 10% KOH and hydrolysed with amyloglucosidase (Sigma). Glucose was then assayed with GOD-PAP method.

2.5.3. Na^+/K^+ -ATPase

ATPase activity was measured with the methods described in Lévesque et al. (2003). Briefly, the gill Na^+/K^+-ATPase activity was calculated as the difference in inorganic phosphate production between the reactions in two different media (buffer A without ouabain and Buffer B with ouabain). The assay period was 30 min at 30 °C.

2.6. In vitro exposure to Cu

Adrenocortical cell suspensions were prepared as described by Leblond and Hontela (1999). Head kidneys were dissected, digested with collagenase/dispase in Minimum Essential Medium (MEM), and the individualized cells (75×10^6 cells/ml) were plated in a 96-well microplate. Cells were preincubated for 2 h in MEM, centrifuged, then exposed to Ringer solution with or without $CuSO_4$ at the selected Cu concentration for 1 h at 15 °C. Following exposure to Cu, cells were washed and stimulated with 1 U/ml ACTH in MEM, and incubated for 60 min. Cortisol in the supernatants was determined by radioimmunoassay.

To determine in vitro the EC_{50} of Cu (the effective concentration that reduces cortisol secretion by 50%), adrenocortical cells from control fish (not exposed to Cu in vivo) were exposed to various concentrations of Cu in vitro and cortisol secretion in response to stimulation with ACTH was measured. The EC_{60} (200 μM $CuSO_4$, a simple solution to prepare) was the concentration of Cu used in subsequent in vitro exposures of the adrenocortical cells isolated from fish exposed to waterborne Cu for 30 days. Cell viability was assessed by flow cytometry using the exclusion dye propidium iodide. To perform the viability test, 5 μl sample from each well of the microplate was resuspended in a test tube containing 370 μl of MEM with propidium iodide (1 μg/ml). Cells were analyzed using a FACscan (Becton Dickinson), equipped with an argon laser emitting at 488 nm and 10,000 events were analyzed for each sample. Data analyses were performed with a Consort 32 system and LYSIS-II program. Cells viability was used to determine the LC_{50} of Cu (lethal concentration that kills 50% of cells).

2.7. Statistical analysis

Differences among groups were tested using one-way analysis of variance (ANOVA), followed by a Dunnett's test to compare treated groups with control or Tukey–Kramer test to compare more than two groups. Data were transformed when necessary to obtain normality. A statistical significance level of $P \leq 0.05$ was used.

3. Results

3.1. Copper concentrations

Fish exposed to 30 or 80 μg/l Cu for 30 days had higher liver and kidney Cu concentrations than controls; the differences in interrenal Cu between the groups were not significant (Table 1). Concentrations of Cu were consistently (17–90-fold) higher in the liver, compared with kidney and the interrenal tissue. There was no mortality in control fish and fish exposed to 30 μg/l Cu for 30 days, however five fishes from a total of 35 died after 5 days of exposure to 80 μg/l Cu.

3.2. Morphological characteristics of rainbow trout

Fish exposed to 30 and 80 μg/l Cu for 30 days and sampled without air exposure stress had a lower condition factor (ratio weight to length) and a lower hepatosomatic index (ratio liver weight to body weight) than controls (Table 1). A similar trend was detected in fish sampled with air exposure stress but the differences were not significant (data not shown).

3.3. Plasma cortisol, T3 and T4

Plasma cortisol levels measured in fish sampled without air exposure stress (basal cortisol) were below 5 ng/ml in controls, indicating that fish were not stressed by removal from the tank. Exposure to 30 and 80 μg/l Cu for 30 days had no effect on basal plasma cortisol (Fig. 1). Air exposure challenge increased plasma cortisol levels in all treatment groups but the magnitude of the increase was lessened in a Cu concentration-dependent pattern. Plasma T3 and T4 of fish exposed to Cu and sampled with or without air exposure stress were not different from their controls (data not shown). The average plasma T3 and T4 level

Table 1
Concentrations of Cu (mean ± S.E., *N*) and gross morphology of rainbow trout exposed to 0, 30 and 80 μg/l Cu for 30 days[a] in the laboratory

Treatment	Liver Cu (μg/g)	Interrenal Cu (μg/g)	Kidney Cu (μg/g)	Condition factor	Hepatosomatic index
Control	84.60 ± 12.48 (7)	2.44 ± 0.14 (7)	6.45 ± 0.22 (7)	1.09 ± 0.01 (32)	1.33 ± 0.03 (32)
30 μg/l Cu	147.39 ± 16.74 (7)	2.41 ± 0.15 (7)	8.64 ± 0.77* (7)	1.03 ± 0.01* (30)	1.08 ± 0.04* (30)
80 μg/l Cu	283.38 ± 56.12* (7)	3.00 ± 0.49 (7)	8.46 ± 0.74* (7)	1.02 ± 0.14* (30)	1.17 ± 0.32 (30)

[a] Fish were sampled without the air exposure stress.
* Indicates means significantly different from the control (Dunnett's test, $P < 0.05$).

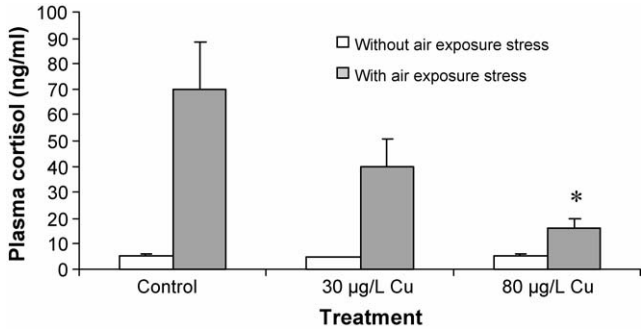

Fig. 1. Plasma cortisol levels (mean ± S.E.) in fish exposed to 0, 30 and 80 µg/l Cu for 30 days and sampled without air exposure stress (white bars, $N = 30$) and with air exposure stress (gray bars, $N = 17–20$). Means indicated by * are significantly different from the control (Dunnett's test, $P < 0.05$).

for all groups was 7.12 ± 0.2 ng/ml and 15.99 ± 0.45 ng/ml, respectively.

3.4. Plasma glucose, liver glycogen and gill Na^+/K^+ ATPase

Plasma glucose was significantly lower, compared with controls, in fish exposed to 80 µg/l Cu and sampled without air exposure stress (Fig. 2). There were no differences in plasma glucose in fish exposed to various concentrations of Cu and sampled with air exposure stress. Liver glycogen (Fig. 3A) and the activity of gill Na^+/K^+ ATPase (Fig. 3B) were also lower, compared with controls, in fish exposed to 30 and 80 µg/l Cu.

3.5. Adrenotoxicity of Cu and cortisol secretion in vitro

Fig. 4 shows a dose-response curve and the toxicological characteristics of Cu in the in vitro bioassay using adrenocortical cells. The EC_{50} of Cu (effective concentration that reduces cortisol secretion by 50%) is 180 µM and the LC_{50} (lethal concentration that kills 50% of cells) is 1200 µM. The concentration of 200 µM of Cu was selected for subsequent in vitro exposure experiments with adrenocortical cells isolated from control fish and fish exposed to Cu in vivo, sampled without or with air exposure stress.

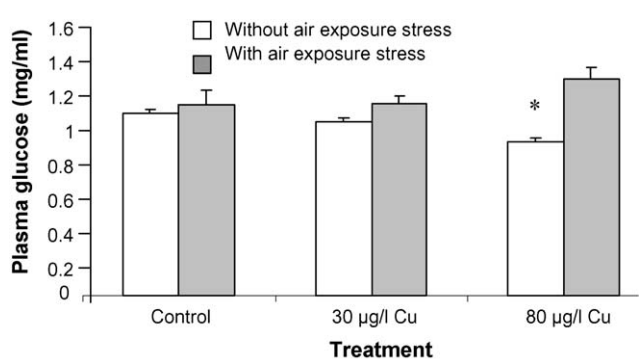

Fig. 2. Plasma glucose (mean ± S.E.) in fish exposed to 0, 30 and 80 µg/l Cu for 30 days and sampled without air exposure stress (white bars, $N = 30$) and with air exposure stress (gray bars, $N = 17–20$). Means indicated by * are significantly different from the control (Dunnett's test, $P < 0.05$).

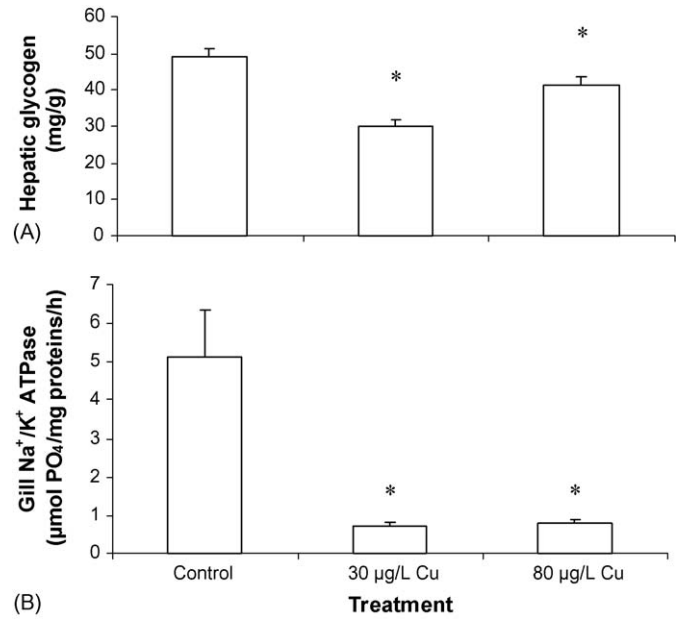

Fig. 3. Hepatic glycogen (A) and gill Na^+/K^+-ATPase activity (B) (mean ± S.E.) in fish exposed to 0, 30 and 80 µg/l Cu for 30 days and sampled without air exposure stress. Means indicated by * are significantly different from the control (Dunnett's test, $P < 0.05$). For each treatment, $N = 30$.

In a medium without Cu, cells isolated from fish exposed to 80 µg/l Cu in vivo and sampled without air exposure stress secreted more cortisol in response to a standardized stimulation by ACTH (1 IU/ml for 60 min) than cells from control fish (not exposed to Cu in vivo) or cells from fish exposed to Cu at 30 µg/l (Fig. 5A). This pattern was also detected in cells isolated from fish sampled with air exposure stress (Fig. 5B), although the overall level of secretion was lower in these fish. Consistently, exposure of adrenocortical cells to Cu (200 µM of Cu) in vitro, reduced the ACTH-stimulated secretion of cortisol by cells isolated from fish (controls and those exposed to Cu in vivo), sampled without or with air exposure stress (Fig. 5A and B).

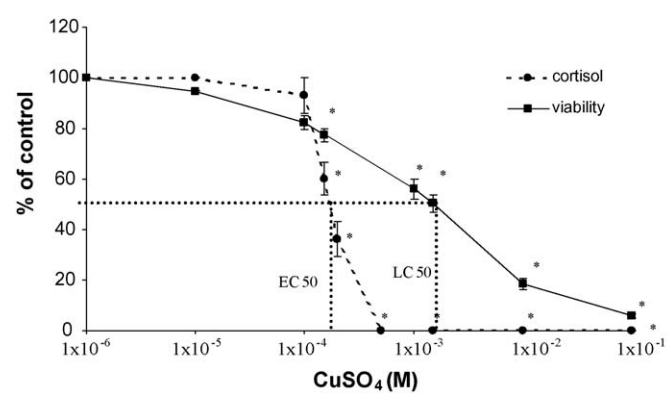

Fig. 4. Viability and cortisol secretion by adrenocortical cells (means ± S.E.) stimulated with 1.0 U/ml ACTH following an in vitro exposure to $CuSO_4$ for 60 min. Means indicated by * are significantly different from controls (100%) (Dunnett's test, $P < 0.05$). The concentration of Cu that reduced cortisol secretion by 50% (EC_{50}) was 180 µM, concentration that reduced cell viability by 50% (LC_{50}) was 1200 µM. Adrenocortical cells obtained from the interrenal tissue of one fish correspond to $n = 1$ ($n = 6$ for viability, $n = 10$ for cortisol secretion).

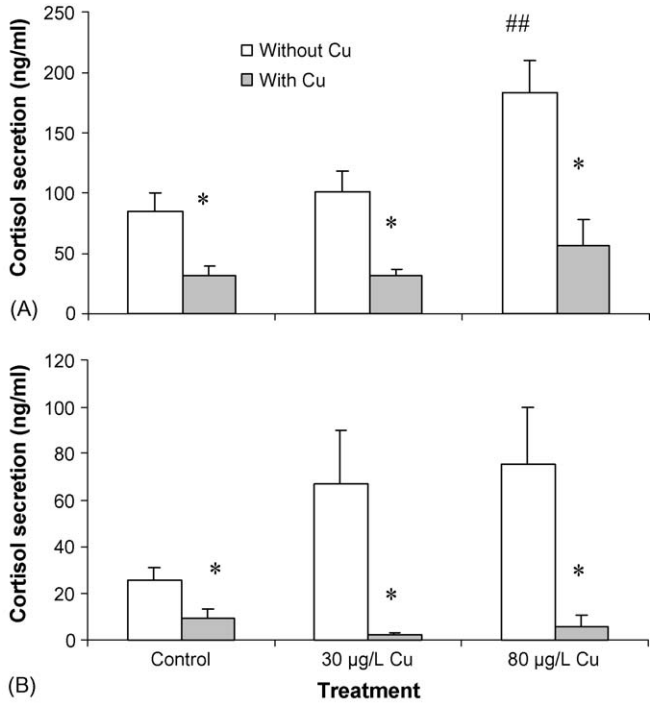

Fig. 5. Cortisol secretion (mean ± S.E.) by adrenocortical cells stimulated with 1.0 U/ml ACTH. Adrenocortical cells isolated from fish exposed to 0, 30 and 80 μg/l Cu for 30 days and sampled without air exposure stress (A) and with air exposure stress (B) were exposed in vitro for 60 min to 200 μM $CuSO_4$ (EC_{60}) (gray bars) or to saline (white bars). Mean followed by ## is significantly different from control treatment (Dunnett's test, $P < 0.05$). Means with Cu followed by * are significantly different from means without Cu in same treatment (Dunnett's test, $P < 0.05$). For fish without air exposure stress $N = 15$, for fish with air exposure stress $N = 11$.

4. Discussion

The present study was designed to evaluate the impact of Cu on the physiological status and the hypothalamo-pituitary-interrenal (HPI) axis of rainbow trout, and test the hypothesis that pre-exposure to Cu in vivo protects cells against adverse effects of subsequent exposures to this metal. The water Cu concentrations used in this study were environmentally relevant and did result in accumulation of Cu in fish tissues. Moreover, Cu concentrations in livers of trout exposed to the higher concentration (80 μg/l) were similar to levels reported by Laflamme et al. (2000) in perch from field studies in the mining area of Abitibi, Qc. Similar to other laboratory and field studies, liver was the principal organ of Cu accumulation, followed by other tissues (McGeer et al., 2000b; Audet and Couture, 2003; Lévesque et al., 2003; Giguere et al., 2004).

Morphological characteristics were used in the present study, along with physiological responses, as indicators of effects of metal exposure. Numerous field studies reported that the condition factor is lower in fish exposed to mixtures of metals, through alterations of enzymatic capacity (Lévesque et al., 2003; Couture and Kumar, 2003) and in some situations, alterations of the food basis in contaminated lakes (Sherwood et al., 2000; Iles and Rasmussen, 2005). Exposure to Cu alone decreased the condition factor and hepatosomatic index in this study, however whether these effects were caused by reduced food consumption or a less efficient capacity to transform food into biomass was not determined. Trout exposed to Cu for 30 days and sampled without air exposure stress also had lower plasma glucose levels, as has been reported for other fish species (Dhanapakiam and Ramasamy, 2001), and lower liver glycogen reserves. Fish exposed to Cu were however able to maintain their plasma glucose as did the control fish, when challenged by air exposure stress. Exposure to Cu thus seems to mobilize glycogen reserves and modify glucose metabolism, possibly through a higher turnover and use of glucose by tissues challenged by Cu. Further studies are required to characterize the effects of Cu on metabolic capacities of fish under controlled exposures.

Exposure to Cu had no effect on plasma thyroid hormone levels of rainbow trout, in contrast to studies with other fish species (Lévesque et al., 2003; Teles et al., 2005); possibly because the concentrations used in the present study (30 and 80 μg/l) were too low to influence thyroid function in rainbow trout. In contrast, these exposures clearly decreased the activity of gill Na^+/K^+-ATPase. There is some disagreement about the effects of Cu on this enzyme and it has been proposed that differences in the degree of acclimation to Cu influence its activity (Laurén and McDonald, 1987). Acute laboratory exposure to Cu decreased gill Na^+/K^+-ATPase activity in common carp and rainbow trout (Laurén and McDonald, 1987; De Boeck et al., 2001). Chronic exposures however led to either a return to normal activity of the gill Na^+/K^+-ATPase (Laurén and McDonald, 1987) or an increase (McGeer et al., 2000a). Field studies with yellow perch sampled in lakes contaminated by mixtures of metals, including Cu, reported both lower activities (Lévesque et al., 2003) and higher activities (Audet and Couture, 2003), compared to reference fish. Our results with rainbow trout exposed in the laboratory indicate that a 30 day exposure to 30 or 80 μg/l of Cu inhibits the activity of gill Na^+/K^+-ATPase, possibly because the fish were not fully acclimated to the metal.

The main objective of this study was to determine whether Cu at environmentally relevant concentrations is recognized by the fish as a chemical stressor and if in vivo pre-exposure to Cu protects cells from potentially deleterious effects of subsequent exposures. Plasma cortisol is an excellent indicator of functional alterations in the HPI axis (Hontela, 2005) and air exposure stress did increase plasma cortisol as expected. Exposure to Cu did not have an effect on basal plasma cortisol, however challenging the fish with air exposure stress revealed a Cu concentration-dependant impairment of the capacity to raise plasma cortisol. This finding is highly relevant for fish in their natural habitat where they may be subjected to multiple stimuli, including those that activate the physiological stress response. Socially subordinate fish have higher plasma cortisol levels than dominant fish and their ionoregulation is altered (Sloman et al., 2004). Exposure to metals and other toxicants that impair cortisol secretion could then influence social interactions and cortisol-dependant processes. Scott et al. (2003) reported that plasma cortisol levels in rainbow trout increased when fish were exposed to an alarm substance, a chemical released from skin epithelium, and this increase was inhibited by Cd. Other studies provided evidence that the capacity to raise plasma cortisol is impaired in

fish exposed to organic pollutants (Aluru et al., 2004) and metals (Brodeur et al., 1997; Norris, 2000; Lévesque et al., 2002). Our data indicate that exposure to Cu alone disrupts the HPI axis since fish exposed to Cu exhibited an impaired cortisol stress response. Since this effect of Cu could be mediated through a decreased synthesis of pituitary ACTH, the hormone that stimulates cortisol secretion, or through a direct toxic effect of Cu on the interrenal steroidogenic cells, the in vitro approach was used to further investigate the mechanisms of endocrine toxicity of Cu.

First, the toxicological characteristics of Cu were determined in vitro as adrenotoxicity, defined as loss of capacity to secrete cortisol in vitro ($EC_{50} = 180\ \mu M$), and cytotoxicity defined as the capacity to kill cells ($LC_{50} = 1200\ \mu M$). Comparing with other toxicants investigated previously (Leblond and Hontela, 1999), toxicity of Cu (as $CuSO_4$) was lower than that of $HgCl_2$ but higher than $ZnCl_2$ and $CdCl_2$. The ratio LC50/EC50 of Cu was 6.6, indicating that the endocrine disrupting effects occur at substantially lower concentrations than those causing cell death. To investigate the effect of in vivo pre-exposure to Cu on the subsequent response to the metal in vitro, adrenocortical cells isolated from fish exposed to waterborne Cu for 30 days were exposed for 60 min to Cu ($EC_{60} = 200\ \mu M$ of $CuSO_4$) in vitro and their capacity to secrete cortisol in response to a standard stimulation by synthetic ACTH was then assessed. Cells isolated from fish exposed to waterborne Cu secreted more cortisol in response to ACTH in vitro than cells from control fish. This pattern was observed for fish sampled with air exposure stress (Fig. 5A) or without (Fig. 5B), although cells isolated from fish stressed by air exposure secreted overall less cortisol (maximum 80 ng/ml) compared to about 200 ng/ml in fish sampled without air exposure stress, as has been reported by others (Rotlland et al., 2003). Thus even though the capacity to elevate plasma cortisol in response to air exposure stress was impaired by the 30-day exposure to Cu, as was observed with whole fish in vivo, the adrenocortical cells were not impaired by this exposure, their capacity to respond to a stimulation by ACTH was in fact enhanced. A mechanism of Cu toxicity compatible with the in vitro and in vivo results in the present study is a disruptive effect of Cu on pituitary ACTH secretion. A Cu-induced decrease in ACTH secretion would result in lower plasma cortisol levels in response to air exposure stress in fish exposed to Cu, with a normal or even enhanced steroidogenic capacity of the interrenal tissue. It is not known at present whether the effect of Cu on the steroidogenic capacity of the interrenal tissue is mediated through effects on the ACTH receptors and their sensitivity or numbers, or through alterations in plasma ACTH dynamics.

The influence of the in vivo pre-exposure to Cu on the sensitivity of the interrenal tissue to a subsequent in vitro exposure to the same metal was investigated next. Although several studies investigated the acclimation process, using for example survival parameters (Hansen et al., 2002), this study is first to address the issue of acclimation to a metal in fish endocrine cells. When cells were exposed in vitro to Cu, cortisol secretion was reduced in fish from all the in vivo treatments, in controls and in fish pre-exposed to Cu for 30 days. Thus exposure to Cu in vivo did not protect the cells from the effects of Cu in vitro. The reduction in cortisol secretion when Cu was added to the incubation media was expected to be 60% since the EC60 (200 μM $CuSO_4$), identified by the in vitro dose-response study, was used. Such a decrease was observed in control fish (not exposed to waterborne Cu in vivo) sampled either without or with air exposure stress. An even greater decrease in cortisol secretion in response to the in vitro exposure to Cu was observed in cells from fish exposed to Cu in vivo. Cells from fish challenged by the air exposure stress (Fig. 5B) were particularly vulnerable to Cu in vitro, as indicated by more than 95% reduction in their secretory capacity. Even though the Cu concentration chosen for the in vitro exposure (200 μM $CuSO_4$) is high compared to plasma Cu levels measured in fish exposed to waterborne Cu in other laboratory studies (Grosell et al., 1997, 2001), our results indicate that Cu does have the potential for adrenotoxicity when it is directly available to the adrenocortical cells. Moreover, our study provides evidence that additional stressors (e.g. air exposure) render these cells even more vulnerable to Cu toxicity and that exposure to environmentally relevant waterborne Cu concentrations do not protect the adrenocortical cells against Cu toxicity in vitro.

In conclusion, the present study provided evidence that exposure to waterborne Cu for 30 days impairs the capacity to elevate plasma cortisol in rainbow trout but does not disrupt, in fact enhances, the secretory response of the interrenal tissue to stimulation by ACTH in vitro. These results are compatible with the hypothesis that prolonged exposure to waterborne Cu at concentrations that did not lead to a detectable accumulation in the interrenal tissue, may impair pituitary ACTH secretion. Our study also provided evidence that Cu does have an adrenotoxic potential since exposure to Cu in vitro impaired the secretory capacity of the adrenocortical cells. Pre-exposure to waterborne Cu did not protect the adrenocortical cells from Cu toxicity and air exposure stress together with in vitro exposure to Cu increased the vulnerability of the cells. Our study provides evidence that fish subjected to a metal-induced stress may not be able to respond to additional stressors imposed upon them. Fish exhibiting an impaired cortisol stress response may be at a disadvantage in coping with environmental stressors.

Acknowledgments

We thank V. Leblond, and M. Camiré for laboratory help. We also thank S. Prémont for metal analyses (INRS-ETE University of Quebec). This study was funded by MITE-RN (Impacts) and FCAR bursary to AG.

References

Aluru, N., Jorgensen, E.H., Maule, A., Vijayan, M.M., 2004. PCB disruption of the hypothalamo-pituitary-interrenal axis involves brain glucocorticoid receptor downregulation in anadromous Arctic charr. Am. J. Physiol. 287, R787–R793.

Audet, D., Couture, P., 2003. Seasonal variation in tissue metabolic capacities of yellow perch (*Perca flavescens*) from clean and metal-contaminated environments. Can. J. Fish. Sci. 60, 269–278.

Brodeur, J.C., Sherwood, G., Rasmussen, J.B., Hontela, A., 1997. Impaired cortisol secretion in yellow perch (*Perca flavescens*) from lakes contam-

inated by heavy metals: in vivo and in vitro assessment. Can. J. Fish. Aquat. Sci. 54, 2752–2758.

Bury, N.R., Jie, L., Flik, G., Lock, R.A., Wendelaar Bonga, S.E., 1998. Cortisol protects against copper induced necrosis and promotes apoptosis in fish chloride cells in vitro. Aquat. Toxicol. 40, 193–202.

Carvalho, C.D., de Araujo, H.S.S., Fernandes, M.N., 2004. Hepatic metallothionein in a teleost (*Prochilodus scrofa*) exposed to copper at pH 4.5 and pH 8.0. Comp. Biochem Physiol. B 137, 225–234.

Couture, P., Kumar, P.R., 2003. Impairment of metabolic capacities in copper and cadmium contaminated wild yellow perch (*Perca flavescens*). Aquat. Toxicol. 64, 107–120.

De Boeck, G., Vlaeminck, A., Balm, P.H.M., Lock, R.A.C., de Wachter, B., Blust, R., 2001. Morphological and metabolic changes in common carp, *Cyprinus carpio*, during short-term copper exposure: interactions between Cu^{2+} and plasma cortisol elevation. Environ. Toxicol. Chem. 20, 374–381.

De Boeck, G., de Wachter, B., Vlaeminck, A., Blust, R., 2003. Effect of cortisol treatment and/or sublethal copper exposure on copper uptake and heat shock protein levels in common carp, *Cyprinus carpio*. Environ. Toxicol. Chem. 22, 1122–1126.

Dethloff, G.M., Schlenk, D., Khan, S., Bailey, H.C., 1999a. The effects of copper on blood and biochemical parameters of rainbow trout (*Oncorhynchus mykiss*). Arch. Environ. Contam. Toxicol. 36, 415–423.

Dethloff, G.M., Schlenk, D., Hamm, J.T., Bailey, H.C., 1999b. Alterations in physiological parameters of rainbow trout (*Oncorhynchus mykiss*) with exposure to copper and copper/zinc mixtures. Ecotoxicol. Environ. Saf. 42, 253–264.

Dhanapakiam, P., Ramasamy, V.K., 2001. Toxic effects of copper and zinc mixtures on some haematological and biochemical parameters in common carp, *Cyprinus carpio* (Linn). J. Environ. Biol. 22, 105–111.

Giguere, A., Campbell, P.G.C., Hare, L., McDonald, D.G., Rasmussen, J.B., 2004. Influence of lake chemistry and fish age on cadmium, copper, and zinc concentrations in various organs of indigenous yellow perch (*Perca flavescens*). Can. J. Fish. Aquat. Sci. 61, 1702–1716.

Grosell, M.H., Hogstrand, C., Wood, C.M., 1997. Cu uptake and turnover in both Cu-acclimated and non-acclimated rainbow trout (*Oncorhynchus mykiss*). Aquat. Toxicol. 38, 257–276.

Grosell, M.H., Hogstrand, C., Wood, C.M., 1998. Renal Cu and Na excretion and hepatic Cu metabolism in both acclimated and non acclimated rainbow trout (*Oncorhynchus mykiss*). Aquat. Toxicol. 40, 275–291.

Grosell, M., McGeer, J.C., Wood, C.M., 2001. Plasma copper clearance and biliary copper excretion are stimulated in copper-acclimated trout. Am. J. Physiol. Regulat. Integr. Comp. Physiol. 280, R796–R806.

Handy, R.D., 2003. Chronic effects of copper exposure versus endocrine toxicity: two sides of the same toxicological process? Comp. Biochem. Physiol. A 135, 25–38.

Hansen, J.A., Lipton, J., Welsh, P.G., Morris, J., Cacela, D., Suedkamp, M.J., 2002. Relationship between exposure duration, tissue residues, growth, and mortality in rainbow trout (*Oncorhynchus mykiss*) juveniles subchronically exposed to copper. Aquat. Toxicol. 58, 175–188.

Hontela, A., 2005. Adrenal toxicology: environmental pollutants and the HPI axis. In: Mommsen, T.P., Moon, T.W. (Eds.), Biochemistry and Molecular Biology of Fishes, vol. 6. Elsevier B.V., pp. 331–363.

Hontela, A., Dumont, P., Duclos, D., Fortin, R., 1995. Endocrine and metabolic dysfunction in yellow perch, *Perca flavescens*, exposed to organic contaminants and heavy metals in the St. Lawrence River. Environ. Toxicol. Chem. 14, 725–731.

Iles, A., Rasmussen, J.B., 2005. Indirect effects of metal contamination on bioenergetics of yellow perch (*Perca fjlavescens*) in Sudbury area lakes resulting from food web simplification. Fresh Water Biol. 50, 976–992.

Kamunde, C., Clayton, C., Wood, C.M., 2002. Waterborne vs. dietary copper uptake in rainbow trout and the effects of previous waterborne copper exposure. Am. J. Physiol. 283, R69–R78.

Lacroix, A., Hontela, A., 2004. A comparative assessment of the adrenotoxic effects of cadmium in two teleost species, rainbow trout, *Oncorhynchus mykiss*, and yellow perch, *Perca flavescens*. Aquat. Toxicol. 67, 13–21.

Laflamme, J.S., Couillard, Y., Campbell, P.G.C., Hontela, A., 2000. Interrenal metallothionein and cortisol secretion in relation to Cd, Cu and Zn exposure in yellow perch, *Perca flavescens*, from Abitibi lakes. Can. J. Fish. Aquat. Sci. 57, 1692–1700.

Laurén, D.J., McDonald, D.G., 1987. Acclimation to copper by rainbow trout, *Salmo gairdneri*: biochemistry. Can. J. Fish. Aquat. Sci. 44, 105–111.

Leblond, V.S., Hontela, A., 1999. Effects of in vitro exposures to cadmium, mercury, zinc, and 1-(2-chlorophenyl)-1-(4-chlorophenyl)-2,2-dichloroethane on steroidogenesis by dispersed interrenal cells of rainbow trout (*Oncorhynchus mykiss*). Toxicol. Appl. Pharmacol. 157, 16–22.

Lévesque, H., Moon, T.W., Campbell, P.G.C., Hontela, A., 2002. Seasonal variation in carbohydrate and lipid metabolism of cortisol-impaired metal-exposed yellow perch (*Perca flavescens*). Aquat. Toxicol. 60, 257–267.

Lévesque, H.M., Dorval, J., Van Der Kraak, G.J., Campbell, P.G.C., Hontela, A., 2003. Hormonal, morphological and physiological responses of yellow perch (*Perca flavescens*) to chronic environmental metal exposures. J. Toxicol. Environ. 66, 87–106.

Marr, J.C.A., Lipton, J., Cacela, D., Hansen, J.A., Bergman, H.L., Meyer, J.S., Hogstrand, C., 1996. Relationship between copper exposure duration, tissue copper concentration, and rainbow trout growth. Aquat. Toxicol. 36, 17–30.

Mazon, A.F., Nolan, D.T., Lock, R.A.C., Fernandes, M.N., Wendelaar Bonga, S.E., 2004. A short-term in vitro gill culture system to study the effects of toxic (copper) and non-toxic (cortisol) stressors on the rainbow trout, *Oncorhynchus mykiss* (W.). Toxicol. In Vitro 18, 691–701.

McGeer, C.J., Szbedinszky, C., McDonald, D.G., Wood, C.M., 2000a. Effects of chronic sublethal exposure to waterborne Cu, Cd or Zn in rainbow trout. 1. Iono-regulatory disturbance and metabolic costs. Aquat. Toxicol. 50, 231–243.

McGeer, C.J., Szbedinszky, C., McDonald, D.G., Wood, C.M., 2000b. Effects of chronic sublethal exposure to waterborne Cu, Cd or Zn in rainbow trout. 2. Tissue specific metal accumulation. Aquat. Toxicol. 50, 245–256.

Niyogi, S., Wood, C.M., 2003. Effects of chronic waterborne and dietary metal exposure on gill metal-binding: implications for the biotic ligand model. Human Ecol. Risk Assess. 9, 813–846.

Norris, O.D., 2000. Endocrine disruptors of the stress axis in natural populations: How can we tell? Am. Zoolog. 40, 393–401.

Rotlland, J., Ruane, N.M., Caballero, M.J., Montero, D., Tort, L., 2003. Response to confinement in sea bass (*Dicentrachus labrax*) is characterized by an increased biosynthetic capacity of interrenal tissue with no effect on ACTH sensitivity. Comp. Biochem. Physiol. A 136, 613–620.

Scott, G.R., Sloman, K.A., Rouleau, C., Wood, C.M., 2003. Cadmium disrupts behavioural and physiological responses to alarm substance in juvenile rainbow trout (*Oncorhynchus mykiss*). J. Exp. Biol. 206, 1779–1790.

Sherwood, G.D., Rasmussen, J.B., Rowan, D.J., Brodeur, J., Hontela, A., 2000. Bioenergetic costs of heavy metal exposures in yellow perch (*Perca flavescens*): in situ estimates with a radiotracer (^{137}Cs) technique. Can. J. Fish Aquat. Sci. 59, 1–5.

Sloman, K.A., Scott, G.R., McDonald, D.G., Wood, C.M., 2004. Diminished social status affects ionoregulation at the gills and kidney in rainbow trout (*Oncorhynchus mykiss*). Can. J. Fish. Aquat. Sci. 61, 618–626.

Spear, P.A., Anderson, P.D., 1975. Fish size as a quantitative function of tolerance to heavy metals. Water Pollut. Res. Can. 10, 170–179.

Taylor, L.N., Wood, C.M., McDonald, D.G., 2003. An evaluation of sodium loss and gill metal binding properties in rainbow trout and yellow perch to explain species differences in copper tolerance. Env. Toxicol. Chem. 22, 2159–2166.

Teles, M., Pacheco, M., Santos, M.A., 2005. Physiological and genetic responses of European eel (*Anguilla anguilla* L.) to short-term chromium or copper exposure—influence of preexposure to a PAH-like compound. Environ. Toxicol. 20, 92–99.

Van Heerden, D., Vosloo, A., Nikinmaa, M., 2004. Effects of short-term copper exposure on gill structure, metallothionein and hypoxia-inducible factor-1 alpha (HIF-1 alpha) levels in rainbow trout (*Oncorhynchus mykiss*). Aquat. Toxicol. 69, 271–280.

Environ. Sci. Technol. **2010,** *44,* 1431–1437

Copper Binding Dynamics and Olfactory Impairment in Fathead Minnows (*Pimephales promelas*)

WARREN W. GREEN,[†,‡,§] REEHAN S. MIRZA,[†,‡] CHRIS M. WOOD,[†] AND GREG G. PYLE*[,‡,||]

Department of Biology, McMaster University, Hamilton, Ontario, L8S 4K1 Canada, and Department of Biology, Nipissing University, North Bay, Ontario, P1B 8L7 Canada

Received August 7, 2009. Revised manuscript received January 12, 2010. Accepted January 13, 2010.

When fish are exposed to sublethal, environmentally relevant Cu concentrations, olfactory acuity is impaired. The goals of the present study were to investigate the binding dynamics of waterborne Cu in the olfactory epithelium (OE), to examine the influence of calcium (Ca^{2+}) on Cu binding, and to link Cu-OE binding to changes in olfactory acuity. Using short-term in vivo waterborne exposures to ^{64}Cu, we found that Cu accumulates rapidly in the OE, reaching a plateau by 3 h. The binding affinity (log K_{Cu-OE}) and binding capacity (B_{max}) of ^{64}Cu in the OE were 6.7 and 10.0 nmol Cu g^{-1}, respectively. As waterborne Ca^{2+} was increased from 50 to 1000 μM L^{-1}, the B_{max} of Cu decreased by ~50% while the log K_{Cu-OE} remained constant, indicative of noncompetitive inhibition. Using electro-olfactograms (EOG), short-term exposures to 160 and 240 nmol Cu L^{-1} were found to reduce olfactory responses to 10^{-5} M L-arginine by 72 and 79%, respectively. Short-term exposure to 160 nmol Cu L^{-1} also caused a 15-fold reduction in behavioral responses to a food stimulus. Interestingly, increasing waterborne Ca^{2+} did not reduce the effects of Cu on EOG or behavioral responses. These results demonstrate that short-term, environmentally realistic concentrations of Cu not only bind to the OE of fathead minnows but also impair their olfactory sensitivity and behavioral responses to olfactory stimuli. Waterborne Ca^{2+} reduces Cu–OE binding but does not protect against olfactory impairment.

Introduction

The biotic ligand model (BLM) (*1–3*) uses laboratory-derived gill-metal binding constants log *K* (binding affinity, an index of the strength of binding between the metal and the biotic ligand) and B_{max} (binding capacity, the maximum number of binding sites on the biotic ligand) as well as site-specific water chemistry in order to predict acute metal toxicity in fishes (i.e., 96 h LC50) (*4, 5*). The Cu gill–metal binding constants have been determined, as well as how a variety of different water quality variables (e.g., Ca^{2+}, Na^{+}, Mg^{2+}, H^{+}, DOC) influence gill–Cu accumulation (*6–9*) ultimately leading to the production of a Cu BLM for both fathead minnows (*Pimephales promelas*) and rainbow trout (*Oncorhynchus mykiss*, RBT) (*2, 3*).

Fish gills are appropriate as biotic ligands for predicting acute toxicity because they are physiologically sensitive to metals (*10*) and BLM predictions typically correspond to laboratory-derived acute toxicity data (*3*). However, predictions of Cu toxicity may be inappropriate using a gill-based BLM when fish are exposed to chronic sublethal waterborne and/or dietary metal concentrations because gill-metal binding characteristics (log K_{Cu} and B_{max}) may shift due to acclimation (*11*). Furthermore, when Cu concentrations are too low to cause mortality, they still may cause disruption of physiological processes in other tissues (*11*).

One such target tissue is the olfactory epithelium (OE). Olfaction is particularly important in aquatic environments for communication, especially at night or when the water is turbid (*12*). Olfactory chemical cues play a crucial role in locating food (*13*), assessing mating potential (*14*), recognizing kin (*15, 16*), and avoiding predators (*12, 17, 18*). The OE of fishes is in constant contact with the aquatic environment and does not possess a protective membrane, which can make it susceptible to toxicants (*19*). Waterborne concentrations of Cu can vary greatly and have been found in the range of 2–25 μg Cu L^{-1} in lakes along a metal contamination gradient (*20*). Exposure to dissolved Cu can cause degeneration of the OE via apoptosis, thereby reducing the number of ciliated and microvillar olfactory sensory neurons (OSN) (*21–23*). Furthermore, exposures to environmentally relevant concentrations of Cu (1–20 μg Cu L^{-1}; 15.6–312.5 nmol L^{-1}) impair peripheral olfactory responses (EOG–electro-olfactogram) and central olfactory responses (EEG–electroencephalogram) to a variety of olfactory stimuli (i.e., amino acids, bile salts, alarm cues) in juvenile coho salmon (*Oncorhynchus kisutch*) (*24–26*). Copper-impaired EOG responses to conspecific skin extracts (i.e., alarm substance) are correlated to decreases in behavioral responses to the same stimuli (*26*). Thresholds for sublethal olfactory Cu toxicity in juvenile coho salmon were determined to be ~3 μg Cu L^{-1} (~47 nmol L^{-1}) based on a 25% reduction in EOG response to standardized chemical stimuli (*24*).

Our aim was to quantify the binding of waterborne Cu to the OE of fathead minnows using an environmentally relevant range of Cu concentrations and to examine how increasing waterborne Ca^{2+} influences this binding. In order to link Cu/Ca^{2+} binding dynamics in the OE with a biological effect we examined the influence of waterborne Cu and Ca^{2+} concentrations on EOG and behavioral responses to a suite of odorants. By understanding Cu–OE binding constants, the influence of water chemistry on ligand binding, and ethological or ecological end points such as the inability to detect chemical cues that facilitate predator avoidance, we may be able to develop a model to predict metal toxicity in the OE. Such a model may be useful in devising environmental regulations to protect against sublethal metal toxicity in fishes.

Experimental Procedures

Acclimation of Experimental Animals. Adult fathead minnows (3–5 g) were acclimated for 2+ weeks to either synthetic softwater (SSW- a mixture of dechlorinated Hamilton, ON municipal water and reverse osmosis water) (mean ± SEM; Ca^{2+} = 122.7 ± 4.4 μM, Na^{+} = 106.6 ± 6.6 μM, Mg^{2+} = 35.7 ± 1.3 μM, dissolved organic carbon ~ 1 mg L^{-1}, temperature = 12 ± 1 °C) for ligand binding experiments or dechlorinated North Bay, ON municipal water (Ca^{2+} = 167.5 ± 2.0 μM, Na^{+}

* Corresponding author phone: 1-807-766-7149; fax: 1-807-346-7796; e-mail: gpyle@lakeheadu.ca.
† McMaster University.
‡ Nipissing University.
§ Present address: Department of Biological Sciences, University of Windsor, 401 Sunset Avenue, Windsor, Ontario N9B 3P4 Canada.
|| Present Address:Department of Biology, Lakehead University, 955 Oliver Road, Thunder Bay, Ontario P7B 5E1 Canada.

10.1021/es9023892 © 2010 American Chemical Society
Published on Web 01/26/2010

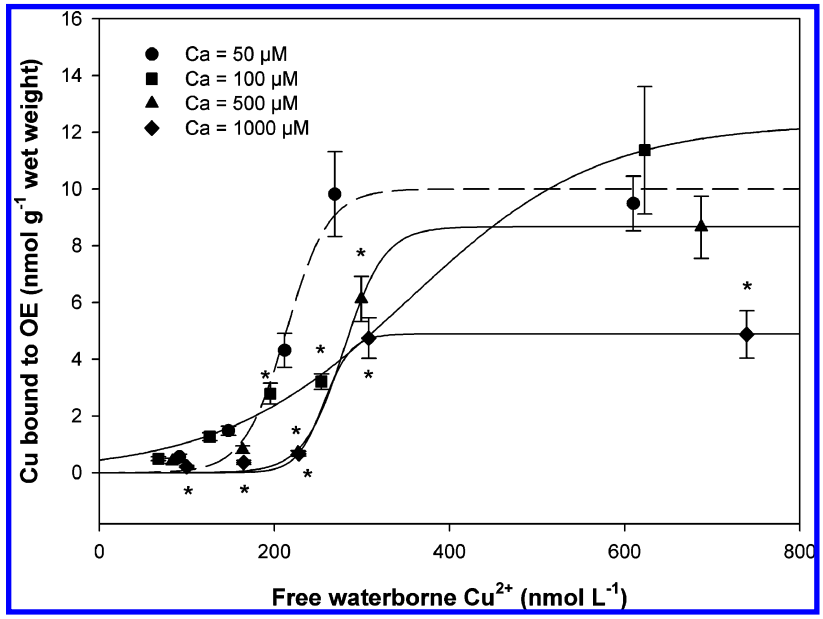

FIGURE 1. New copper binding to the olfactory rosettes of fathead minnows across a range of waterborne Cu concentrations in different waterborne Ca^{2+} concentrations after a short-term 3 h copper exposure. Means ± SEM (n = 6−7). Asterisks represent significant difference of Cu binding from Cu binding in baseline softwater (hatched line) within the respective Cu concentration.

= 560.9 ± 12.5 μM, Mg^{2+} = 63.3 ± 2.3 μM, temperature = 19 ± 1 °C) for electro-olfactogram and behavioral experiments. Fish were kept on a 16 h:8 h light:dark cycle. The pH of the experimental water was measured (PHM 82 standard pH meter with a GK2401C electrode, Radiometer Copenhagen) before all experiments, and was always in the range 6.72−6.93.

Effect of Ca on Cu−OE binding. Five 2 L Cu-exposure treatments were prepared in aerated SSW (mean ± SEM; Ca^{2+} = 41.7 ± 2.2 μM, Na^{+} = 51.6 ± 0.9 μM, Mg^{2+} = 11.1 ± 0.06 μM, dissolved organic carbon ~ 0.3 mg L^{-1}, temperature = 14 °C). Treatments were spiked with ^{64}Cu to yield concentrations of (nominal) 79, 160, 236, 315, and 787 nmol L^{-1} (5, 10, 15, 20, 50 μg L^{-1}) (measured: 100.5 ± 8.2 nmol L^{-1}, 176.7 ± 10.8 nmol L^{-1}, 252.9 ± 9.2 nmol L^{-1}, 331.7 ± 15.2 nmol L^{-1}, 780.9 ± 36.2 nmol Cu L^{-1}). Radioactive ^{64}Cu [as $Cu(NO_3)_2$] was created by irradiation in the McMaster University Nuclear Reactor (specific activity = 2 μCi μg^{-1}; half-life = 12.9 h). Exposure solutions were also prepared at three additional dissolved Ca^{2+} concentrations (nominal 100, 500, and 1000 μM Ca; measured 104.1 ± 0.9 μM, 474.7 ± 2.1 μM, 971.5 ± 5.8 μM Ca) in order to test the effect of Ca^{2+} on Cu−OE binding. Calcium concentrations were manipulated by adding measured quantities of $Ca(NO_3)_2$ (Fisher Scientific, Oakville, ON) to SSW to yield the desired concentrations.

Seven fathead minnows were randomly assigned to each exposure treatment. We found that Cu reaches a plateau in OE after 3 h (Supporting Information (SI) Figure S1) so at this time, fish were euthanized in an overdose of buffered MS222 (500 mg L^{-1}; ethyl 3-aminobenzoate methanesulfonate salt, Sigma, Oakville, ON, Canada) and rinsed in SSW to remove any loosely bound ^{64}Cu. Both olfactory rosettes were removed, rinsed in SSW, blotted dry, weighed and counted for ^{64}Cu activity on a Canberra-Packard Minaxi Auto-Gamma 5000 series gamma counter with on-board decay correction for ^{64}Cu (Canberra-Packard Instruments, Meriden, CT). Duplicate 10 mL water samples were collected from each treatment at the beginning and end of the exposure period, passed through a 0.45 μm filter, and acidified to 1% with trace metal grade HNO_3 (Fisher Scientific, Oakville, ON). Dissolved Cu concentrations were determined using graphite furnace atomic absorption spectroscopy (GFAAS) (Varian GTA 110, Varian Scientific, Mulgrave, Australia). A certified reference material (SLRS-5) from the National Research Council of Canada was used to ensure accuracy. Ca^{2+}, Na^{+}, and Mg^{2+} concentrations in water samples were measured using flame atomic absorption spectroscopy (FAAS) (Varian SpectrAA-220 FS, Varian Scientific, Australia) against reference standards from Fisher Scientific, U.S.

Effect of Cu on EOG Response. The olfactory stimulus, 10^{-4} M L-arginine, was used to examine the effect of Cu on EOG response. The stimulus solution was prepared fresh daily from a stock solution (prepared fresh weekly) and SSW. Two experimental blank solutions were also prepared with SSW or SSW + Cu, where the Cu concentration corresponded to the exposure treatment (see below). All solutions were stored at 4 °C and brought to room temperature when needed.

Fathead minnows were anaesthetized in buffered MS222 (185 mg L^{-1}), immobilized by an epaxial intramuscular injection of Flaxedil (gallamine triethiodide, 3 mg kg^{-1} body mass, Sigma, Oakville, ON, Canada) (*27*), and wrapped in wet tissue to prevent desiccation, leaving the head and tail regions exposed. Fish were secured and electrically grounded in an acrylic glass perfusion chamber where the gills were perfused via a tube inserted into the mouth with a constant supply of aerated holding tank water containing 50 mg L^{-1} MS222 (*27*). The right olfactory rosette was exposed by removing the nasal septum, and the exposed olfactory chamber was irrigated with SSW prior to EOG testing. After this 1 h stabilization period, an EOG signal was continuously monitored throughout the course of the experiment. See SI for details of the EOG recording setup.

Experimental stimuli were delivered directly to the olfactory chamber in three phases: (i) a 30 min premetal exposure, (ii) a 60 min metal exposure, and (iii) a 30 min postmetal exposure. During the premetal exposure phase, experimental stimuli were delivered sequentially in 3 s pulses once every 10 min via a gravity-fed delivery system. Immediately following a 3 s stimulus pulse, the irrigation stream was switched back to SSW, thus maintaining a continuous flow to the olfactory chamber. A minimum of 2 min of continuous SSW irrigation was maintained between successive stimulus deliveries to minimize olfactory attenuation.

During the 60 min metal exposure phase, the irrigation stream was switched from SSW to SSW + Cu, where the nominal dissolved Cu concentration was one of 80, 160, or 240 nmol L^{-1} (5, 10, 15 μg L^{-1}) (measured: 74.5 ± 2.2, 134.6 ± 4.4, 163.1 ± 5.5 nmol L^{-1}). Successive olfactory stimulus delivery of 10^{-4} M L-arginine continued in 10 min intervals

as described above, and EOG signals continued to be recorded. During the 30 min postmetal exposure period, Cu was removed from the irrigation stream leaving only SSW perfusing the olfactory chambers. Again, experimental stimuli were delivered in 10 min intervals and EOG responses were recorded. Gill perfusion water, irrigation water, and all experimental stimuli were at room temperature (18−22 °C).

Effect of Ca on Cu-Impaired EOG Responses. To test whether dissolved Ca^{2+} could protect against Cu-impaired EOG responses, fathead minnows ($n = 4$) were randomly assigned to one of three pre-exposure treatments, where Cu concentrations were held constant at 160 nmol L^{-1} (10 μg L^{-1}) but Ca^{2+} concentrations increased (100, 500, or 1000 μM Ca^{2+}), and one control treatment (no Cu + 100 μM Ca^{2+}). Fish were pre-exposed to these solutions for 3 h prior to EOG testing. Olfactory stimuli were delivered successively in 10 min intervals as described above, and included 10^{-4} M L-arginine as well as two additional stimuli, 10^{-4} M L-alanine and the bile acid 10^{-5} M TCA. Irrigation water was SSW and did not include Cu. Each stimulus was delivered three times to each fish.

Behavioral Experiments. Fathead minnows ($n = 15$) were randomly assigned to one of four pre-exposure treatments corresponding to those of the previous section (i.e., constant 160 nmol L^{-1} Cu in 100, 500, and 1000 μM Ca^{2+}, and a control of no Cu in 100 μM Ca^{2+}). Pre-exposures were for 3 h.

Behavioral trials were conducted in 36 × 80 cm Y-mazes. Each Y-maze consisted of a large plastic container with an acclimation chamber located at one end and a corrugated plastic barrier separating each arm to prevent any mixing of chemicals. A removable barrier was placed between the acclimation zone and both arms (SI Figure S2). Arm preference trials found there was no significant difference in the amount of time spent in either arm ($t = 0.861$, df = 11, $p = 0.408$). A food stimulus to induce attraction was prepared from 500 mg of frozen brine shrimp in 250 mL of SSW, and filtered to remove large particles. For each trial one arm of the maze (SI Figure S2) was randomly assigned as experimental (food stimulus) and the other as control (SSW). Stimuli were injected into the distal end of each maze arm at the same time that a single fish from one of the four pre-exposures was introduced to the acclimation area at the proximal end. During a 20 min acclimation period, fish were prevented from accessing either arm of the maze. At the end of the acclimation period, the barrier was lifted and the fish's location was recorded every 10 s. Each trial ran for 10 min and was conducted in SSW (18−20 °C).

Calculations and Statistical Analysis. The amount of newly bound Cu (nmol g^{-1}) to the OE was calculated using

$$a(bc^{-1})^{-1}$$

where a = radioactivity counts in the OE (cpm g^{-1} wet tissue weight); b = radioactivity counts in the water (cpm L^{-1}); c = dissolved metal concentration in the water (nmol L^{-1}).

Nonlinear regressions (Sigmaplot 8.0 for Windows) were employed for the analysis of metal binding to the OE using a sigmoid 3-parameter curve fit:

$$y = \frac{a}{1 + \exp^{-}\left(\frac{x - x_0}{b}\right)}$$

B_{max} (binding capacity) and log K (binding affinity) were determined from these regressions. B_{max} was the value on the y-axis where the maximum amount of metal binding occurred (represented by "a" in the above equation). Log K was determined as the negative logarithm of the free Cu^{2+} ion concentration in the water ("x_0" in the above equation, in molar units) that provides metal binding equivalent to half the B_{max}. Free Cu^{2+} ion concentrations were estimated using measured water chemistry values and the aquatic chemistry program MINEQL+.

TABLE 1. Log K and B_{max} Values for Cu Binding to the Olfactory Epithelium (OE) and Gill Epithelium of Fathead Minnows in Artificial Softwater with Low Concentrations of Competitive Ions and Other Complexing Agents (e.g., DOC)[a]

metal	tissue	$[Ca^{2+}]$ (μM)	B_{max} (nmol g^{-1})	Log K
Cu	OE	50	10.0	6.7
		100	12.3	6.5
		500	8.7	6.6
		1000	4.9	6.6
Cu	Gill		10.0*	7.4*

[a] Values for the OE are after a 3 h exposure to waterborne Cu and are shown as a function of increasing waterborne $[Ca^{2+}]$. Asterisks indicate values from ref *7* and *8*.

The magnitude of an EOG response to an odor stimulus was measured as the difference between baseline and peak depolarization for each odor delivery. Relative responses to a particular odorant (e.g., 10^{-5} M L-arginine) were calculated by dividing each response value for a given fish by the corresponding premetal exposure (control) response average for that odorant.

All data are presented as means ± SEM (n) where n = number of fish. The effects of increasing waterborne [Cu] and $[Ca^{2+}]$ on metal−OE accumulation were examined by two-way ANOVA. Subsequent ANOVA's with a Tukey−Kramer HSD post hoc tests were used to determine if increasing waterborne $[Ca^{2+}]$ reduced Cu−OE accumulation at each of the Cu concentrations tested. To determine the effect of Cu exposure on EOG response to 10^{-5} M L-arginine throughout the entire testing period, repeated measures two-way ANOVA were utilized. The responses from the Cu/Ca exposure EOG data were analyzed by conducting three one-way ANOVA among Cu/Ca concentrations (one for each chemical stimulus) followed by post hoc Tukey analysis. In the behavioral trials, the difference in time spent between the two arms was calculated (experimental−control) for each Cu/Ca concentration. The differences among Cu/Ca concentrations were analyzed with one-way ANOVA followed by post hoc Tukey HSD tests. All statistical analyses employed a significance level of 0.05, and were performed using JMP statistical software (v.5.0; SAS, Cary, NC).

Results

Metal−ligand Binding Experiments. The concentration-dependence of ^{64}Cu binding was measured using a 3 h assay to establish the affinity (log K) and binding capacity (B_{max}) of Cu to the OE in baseline SSW. The curve representing Cu binding to the OE was S-shaped over the [Cu] range of 0−800 nmol L^{-1} (0 − 50 μg L^{-1}). Cu−OE binding increased significantly above [Cu] of ∼177 nmol L^{-1} (11 μg L^{-1}) and reached a plateau at ∼330 nmol L^{-1} (21 μg L^{-1}) ($F_{4,30} = 26.70$; $p < 0.0001$) with Cu−OE binding increasing by ∼1600% over the [Cu] range tested. Log K_{Cu-OE} was calculated to be 6.7, representing a free Cu^{2+} concentration of 214 nmol L^{-1} (13.5 μg L^{-1}), and B_{max} was 10.0 nmol g^{-1} (Figure 1, Table 1).

Increasing waterborne $[Ca^{2+}]$ from 50 μM (baseline SSW) to 100, 500, or 1000 μM (2, 4, 20, 40 mg L^{-1}) reduced Cu−OE binding between 200 and 600% relative to Cu−OE binding in baseline SSW at each of the waterborne [Cu] tested (whole model $F_{19,119} = 22.28$; $p < 0.0001$) (Figure 1). However, at Cu concentrations ≤160 nmol L^{-1} (≤10 μg L^{-1}), Cu−OE binding was significantly reduced only at waterborne Ca^{2+} concentrations of 1000 μM L^{-1} (40 mg L^{-1}). Notably, as waterborne $[Ca^{2+}]$ increased, the B_{max} of Cu decreased by up to 50% while the log K_{Cu-OE} remained the same (Table 1), indicative of noncompetitive inhibition.

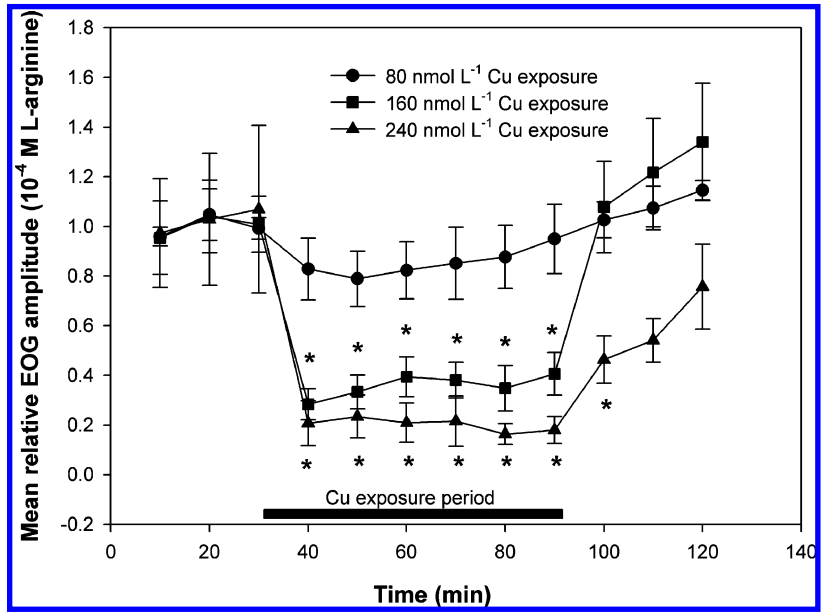

FIGURE 2. Mean ± SEM (n = 5) of the relative EOG response of fathead minnows to 10^{-4} M L-arginine for the precopper, copper exposure, and postcopper exposure periods at concentrations of 80, 160, and 240 nmol Cu L^{-1}. Relative responses were determined by dividing each response value for a given fish by the respective premetal exposure response average. Plotted means were determined by averaging the response to 10^{-4} M L-arginine of all five fish for a given time period. Repeated measures two-way ANOVA was conducted for each Cu concentration and asterisks indicate significant differences from the respective premetal exposure responses ($p \leq 0.05$). The solid bar indicates the copper exposure period.

Electro-Olfactogram Experiments. Exposure to 160 and 240 nmol Cu L^{-1} (10 and 15 μg L^{-1}) for 10 min reduced the EOG responses to 10^{-4} M L-arginine by approximately 72 and 79%, respectively, relative to controls ($F_{11,121} = 3.47$, $p < 0.0001$) (Figure 2). This inhibition continued throughout the Cu exposure period. Interestingly, even after a 1 h exposure to 80 nmol Cu L^{-1} (5 μg L^{-1}), EOG responses to 10^{-4} M L-arginine were not affected (Figure 2). During the post-Cu exposure period, the EOG response to 10^{-4} M L-arginine returned to pre-Cu exposure levels within 10 min after a 160 nmol Cu L^{-1} (10 μg L^{-1}) exposure and 20 min after a 240 nmol Cu L^{-1} (15 μg L^{-1}) exposure, indicating relatively rapid recovery. Further electrophysiological experiments using additional odorants revealed that increasing Ca^{2+} concentrations from 100 to 1000 μM had no protective effect against a 160 nmol Cu L^{-1} (10 μg L^{-1}) exposure (Figure 3a).

Behavioral Experiments. Fathead minnows not exposed to Cu spent 15-fold more time in the experimental arm with the food stimulus compared to fathead minnows exposed to any of the Cu/Ca combinations ($F_{3,56} = 6.03$, $p = 0.001$). The behavioral responses paralleled the EOG results in that increasing Ca^{2+} concentrations from 100 to 1000 μM did not have a protective effect against a 3 h, 160 nmol Cu L^{-1} (10 μg L^{-1}) exposure (Figure 3b) regardless of the fact that increasing waterborne Ca reduced B_{max} by up to 50%.

Discussion

It is well established that waterborne Cu concentrations above 80 nmol L^{-1} (~5 μg L^{-1}) can be toxic to the olfactory system of fishes causing reduced olfactory sensitivity and impaired behavioral responses (*26, 28, 29*). A recent study by the authors (*30*) demonstrated that waterborne Cu also alters EOG and behavioral responses in wild yellow perch chronically exposed to metals. The results shown here are in general agreement with previous studies and build upon our previous research in order to characterize Cu−OE binding and provide insight into the potential mechanism of Cu toxicity in the OE. These results are the first to demonstrate that increasing water Ca^{2+} noncompetitively inhibits Cu−OE binding. In addition, our results show that although increases in waterborne Ca^{2+} reduce Cu-OE binding they do not protect against Cu induced impairment of olfactory sensitivity or behavioral responses.

Copper binding in the OE is thought to occur on cellular surface proteins, membrane structures, and internal organelles. At high concentrations Cu accumulation is known to cause cell death via apoptosis (*21, 22, 31*). Moreover, Cu may disrupt odor responses by blocking ligand-gated and (or) voltage-gated ion channels (*32*). Our results demonstrate that both EOG and behavioral responses of FHM were significantly reduced at an exposure of 160 nmol Cu L^{-1} (~10 μg Cu L^{-1}). Previous studies in salmon have also found that Cu (as low as ~31−47 nmol L^{-1} (2−3 μg Cu L^{-1})) reduces EOG responses and impairs behavioral responses (at ~80 nmol L^{-1} (≥5 μg Cu L^{-1})) of fishes to a variety of odorants (*24−26, 28*). In addition, our previous research has shown that wild yellow perch chronically exposed to sublethal metal concentrations, including Cu (~140 − 390 nmol L^{-1}), actually exhibited increased EOG responses, presumably in compensation for prolonged exposure, but behavioral responses to a variety of odorants were still inhibited (*30*). In the current study, increasing waterborne Ca^{2+} concentrations up to 1000 μM L^{-1} did not restore EOG responses during a 160 nmol L^{-1} (10 μg L^{-1}) Cu exposure. Similar results in salmon have shown that increasing water hardness up to ~6000 μM L^{-1} (240 mg Ca L^{-1}) does not restore EOG responses to a variety of odorants during exposures of 10−20 μg Cu L^{-1} (~160−320 nmol L^{-1}) (*24, 33*). Similarly, our current study shows that increasing waterborne Ca^{2+} up to 1000 μM L^{-1} does not restore behavioral responses to a food stimulus during a low, sublethal Cu exposure (160 nmol L^{-1} (10 μg L^{-1}). Overall, our findings demonstrate that the effects of Cu on the olfactory system occur at approximately 160 nmol L^{-1}. Interestingly, the binding curve data show that at 160 nmol Cu L^{-1}, calcium does not reduce OE Cu binding and therefore does not provide a protective benefit. In fact, calcium only provides a protective benefit against Cu-binding at much higher Cu concentrations. This suggests that Cu and Ca could be binding at two different sets of binding sites in the OE. However, another possible explanation for the effect of Ca on Cu

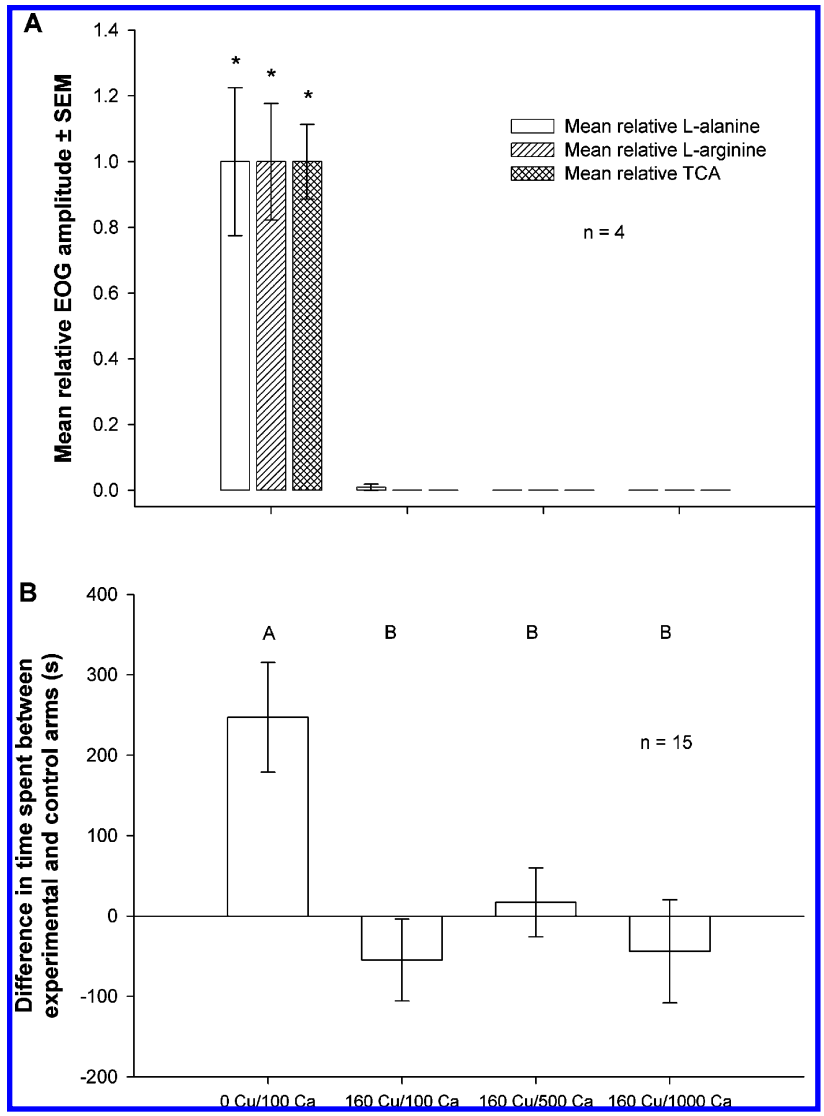

FIGURE 3. Mean ± SEM of (A) relative EOG response of adult fathead minnows to 10^{-4} M L-alanine, 10^{-4} M L-arginine and 10^{-5} M taurocholic acid (TCA) and (B) difference in time spent between experimental (brine shrimp stimulus) and control (blank water) arms of a Y-maze after 3 h exposure to waterborne copper/calcium solutions of 0 nmol Cu L^{-1} /100 μM Ca L^{-1}, 160 nmol Cu L^{-1} /100 μM Ca L^{-1}, 160 nmol Cu L^{-1} /500 μM Ca L^{-1}, and 160 nmol Cu L^{-1} /1000 μM Ca L^{-1}. $n = 15$/treatment. * indicates a significant difference at $p < 0.001$. Separate comparisons were conducted between Cu/Ca combinations for each stimulus. Different letters above bars indicate a significant difference ($p \leq 0.05$).

binding at the OE is the change in plasma membrane surface potential following increases of ionic strength in the exposure medium (*34*).

Recently, it has been shown that the current gill-based BLM does not adequately predict and protect against Cu induced toxicity in the olfactory epithelium (*33*). Specifically, gill BLM LC50 and OE IC50 predictions for Cu exposure were compared across a range of calcium, bicarbonate, and dissolved organic matter concentrations with calculated gill BLM LC50 values in each instance being higher than OE IC50 values (*33*). Increases in calcium over the range of ~0−1500 μM had little effect on predicted OE IC50 values, which were always <10 μg Cu L^{-1} (~160 nmol L^{-1}), whereas calculated gill LC50 values were 3 times higher (*33*). The results of the current experiments also demonstrate that Cu toxicity in the OE occurs at ~160 nmol L^{-1} despite the fact that the binding capacity for Cu in the OE was decreased by up to 50% with increasing calcium. In addition, BLM predicted gill LC50 values using our reported water chemistry data for SSW in the EOG and behavioral experiments are ~416 nmol Cu L^{-1} and increase up to ~800 nmol Cu L^{-1} as Ca concentrations increase from ~50 to 1000 μM. Therefore, a distinct set of binding constants and end points for the olfactory system are required in order to produce a model that adequately predicts metal binding at the OE and protects against toxicity.

The log *K* values for the OE are ~1 log unit lower than that estimated for the gill of fathead minnows, but the B_{max} values are very similar (Table 1). This indicates that although OE Cu affinity is approximately 10-fold lower than gill Cu affinity, the OE has a relatively large binding capacity for Cu, probably due to the fact that its normal function is to bind odor molecules from the water column. Interestingly, as waterborne [Ca^{2+}] increased from ~50 to 1000 μM, the Cu B_{max} decreased but log *K* remained the same (i.e., unchanged binding affinity), indicative of noncompetitive inhibition. The binding and consequent toxic effects of Cu in fish gills are mainly reduced with increasing waterborne [Ca^{2+}] (*6, 7, 35*) and partly by increasing waterborne [Na^{+}] (*3, 35, 36*). This may be because Ca^{2+} controls the permeability of the membrane, thereby reducing Na^{+} and Cl^{-} loss through paracellular pathways (*36*). In the BLM approach, this effect at the gills is implicitly assumed to occur by competitive inhibition (*1−5*), but the original experiments (*3, 6−9, 35, 37*)

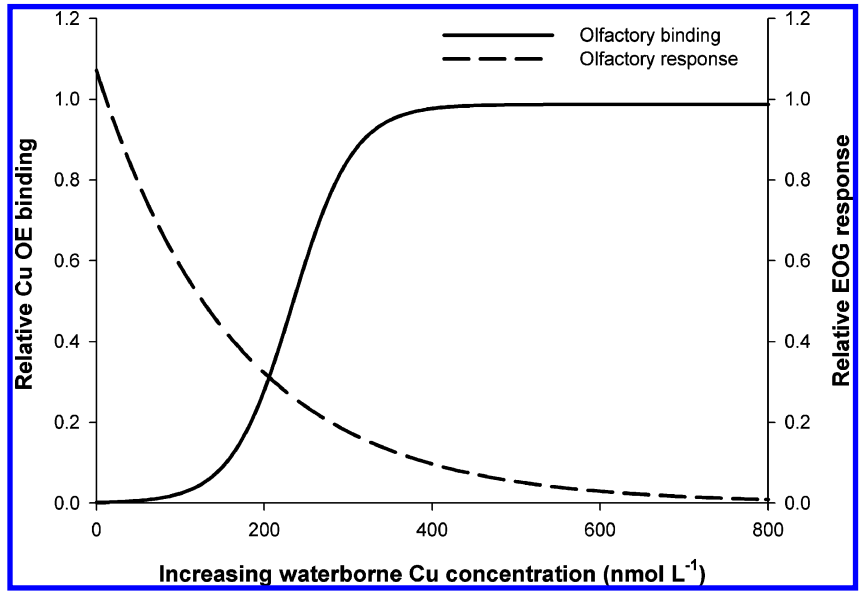

FIGURE 4. Diagram of the relationship between increasing copper binding to the olfactory epithelium and decreasing electro-olfactogram responses in fathead minnows exposed to increasing waterborne copper concentrations. Diagram based on data presented in Figures 1 and 2 in baseline synthetic softwater. All data on *y*-axes are relative to their respective no-copper control responses.

were not done in such a manner as to distinguish competitive from noncompetitive inhibition. Predictions of the gill BLM do not protect the OE from Cu toxicity, despite the fact that the log *K* values for the OE are 10-fold lower than that of the gill epithelium because changes in water chemistry do not reduce toxicity at the OE and ligand binding at the OE does not follow competitive binding principles of the BLM. In addition, toxicity at the OE occurs at lower waterborne Cu concentrations than at the gill epithelium (*33*). Combined, these findings indicate that the OE is more sensitive than the gill to Cu toxicity. The inhibition of peripheral olfactory function by sublethal Cu exposure has implications for the survival and reproductive success of fishes in metal-contaminated aquatic habitats (*12, 18, 28*).

When examining the binding dynamics of Cu in the OE and the inhibition of EOG responses across the same range of environmentally relevant Cu concentrations, it is clear that as little as a 15% increase in Cu accumulation in the OE can lead to more than a 50% decrease in EOG response (Figure 4). Furthermore, as our results show, a 50% or greater loss of olfactory response leads to a loss of behavioral responses to ecologically important odorants (*12, 18*). By understanding the relationship between metal binding dynamics in the OE and inhibition of peripheral olfactory function, it may be possible to develop a model to predict sublethal metal toxicity to the olfactory system of freshwater fishes. Such a model may be used to relate metal accumulation in the olfactory rosettes and site-specific water chemistry to predict end points such as a 50% inhibition of olfactory response leading to impaired behavioral responses. This may ultimately lead to improved ecological risk assessment.

Acknowledgments

We thank the NSERC-MITHE (Metals in the Human Environment) Strategic Network for funding G.G.P. and C.M.W., and Dr. Jasim Chowdhury, Dr. Tania Ng, and Sunita Nadella, for all of their help. W.W.G. was funded through an NSERC postgraduate scholarship. C.M.W. and G.G.P. are supported by the Canada Research Chair Program.

Supporting Information Available

Additional information regarding the experimental methods and results of the metal ligand binding and electro-olfactogram experiments. Figure S1 illustrates the time course of Cu binding to the OE of fathead minnows over a 24-h period. Figure S2 is a diagram of the Y-maze utilized for behavioral experiments. This material is available free of charge via the Internet at http://pubs.acs.org.

Literature Cited

(1) McGeer, J. C.; Playle, R. C.; Wood, C. M.; Galvez, F. A physiologically based biotic ligand model for predicting the acute toxicity of waterborne silver to rainbow trout in freshwaters. *Environ. Sci. Technol.* **2000**, *34*, 4199–4207.
(2) Di Toro, D. M.; Allen, H. E.; Bergman, H. L.; Meyer, J. S.; Paquin, P. R.; Santore, R. C. Biotic ligand model of the acute toxicity of metals. 1. Technical basis. *Environ. Toxicol. Chem.* **2001**, *20*, 2383–2396.
(3) Santore, R. C.; Di Toro, D. M.; Paquin, P. R.; Allen, H. E.; Meyer, J. S. Biotic ligand model of the acute toxicity of metal. 2. Application to acute copper toxicity in freshwater fish and *Daphnia*. *Environ. Toxicol. Chem.* **2001**, *20*, 2397–2402.
(4) Paquin, P. R.; Gorsuch, J. W.; Apte, S.; Batley, G. E.; Bowles, K. C.; Campbell, P. G. C.; Delos, C. G.; Di Toro, D. M.; Dwyer, R. L.; Galvez, F.; Gensemer, R. W.; Goss, G. G.; Hogstrand, C.; Janssen, C. R.; McGeer, J. C.; Naddy, R. B.; Playle, R. C.; Santore, R. C.; Schneider, U.; Stubblefield, W. A.; Wood, C. M.; Wu, K. B. The biotic ligand model: a historical overview. *Comp. Biochem. Physiol. Part C.* **2002**, *133*, 3–35.
(5) Niyogi, S.; Wood, C. M. Biotic ligand model, a flexible tool for developing site-specific water quality guidelines for metals. *Environ. Sci. Technol.* **2004**, *38*, 6177–6192.
(6) Playle, R. C.; Gensemer, R. W.; Dixon, D. G. Copper accumulation on gills of fathead minnows: influence of water hardness, complexation and pH of the gill micro-environment. *Environ. Toxicol. Chem.* **1992**, *11*, 381–391.
(7) Playle, R. C.; Dixon, D. G.; Burnison, K. Copper and cadmium binding to fish gills: modification by dissolved organic carbon and synthetic ligands. *Can. J. Fish. Aquat. Sci* **1993**, *50*, 2667–2677.
(8) Playle, R. C.; Dixon, D. G.; Burnison, K. Copper and cadmium binding to fish gills: estimates of metal-gill stability constants and modelling of metal accumulation. *Can. J. Fish. Aquat. Sci* **1993**, *50*, 2678–2687.
(9) MacRae, R. K.; Smith, D. E.; Swoboda-Colberg, N.; Meyer, J. S.; Bergman, H. L. Copper binding affinity of rainbow trout (*Oncorhynchus mykiss*) and brook trout (*Salvelinus fontinalis*) gills: implications for assessing bioavailable metal. *Environ. Toxicol. Chem.* **1999**, *18*, 1180–1189.
(10) Wood, C. M. Toxic responses of the gill. In *Target Organ Toxicity in Marine and Freshwater Teleosts, Vol. 1, Organs*; Schlenk, D., Benson, W.H., Eds.; Taylor & Francis: London, 2001.
(11) Niyogi, S.; Wood, C. M. Effects of chronic waterborne and dietary metal exposures on gill metal-binding: implications for the biotic ligand model. *Hum. Ecol. Risk Assess.* **2003**, *9*, 813–846.

(12) Wisenden, B. D. Scents of danger: the evolution of olfactory ornamentation in chemically-mediated predator-prey interactions. In *Animal Signals: Signalling and Signal Design in Animal Communication*; Espmark, Y., Amundsen T., Rosenqvist G., Eds.; Tapir Academic Press: Trondheim, 2000.
(13) Hara, T. J. Role of olfaction in fish behaviour. In *Behaviour of Teleost Fishes*; Pitcher, T.J., Ed.; Croom Helm: London, 1986.
(14) Yambe, H.; Shindo, M.; Yamazaki, F. A releaser pheromone that attracts males in the urine of mature female masu salmon. *J. Fish. Biol.* **1999**, *55*, 158–171.
(15) Brown, G. E.; Brown, J. A. Kin discrimination in salmonids. *Rev. Fish. Biol. Fish.* **1996**, *6*, 201–219.
(16) Olsen, K. H.; Grahn, M.; Lohm, J.; Langefors, A. MHC and kin discrimination in juvenile Arctic charr *Salvelinus alpinus*. *Anim. Behav.* **1998**, *56*, 319–327.
(17) Smith, R. J. F. Alarm signals in fishes. *Rev. Fish. Biol. Fish.* **1992**, *2*, 33–63.
(18) Chivers, D. P.; Smith, R. J. F. Chemical alarm signalling in aquatic predator-prey systems: A review and prospectus. *Écoscience.* **1998**, *5*, 338–352.
(19) Klaprat, D. A.; Evans, R. E.; Hara, T. J. Environmental contaminants and chemoreception in fishes. In *Fish Chemoreception*; Hara, T. J., Ed.; Chapman and Hall: London, 1992.
(20) Pyle, G. G.; Rajotte, J. W.; Couture, P. Effects of industrial metals on wild fish populations along a metal contamination gradient. *Ecotox. Environ. Safety.* **2005**, *61*, 287–312.
(21) Julliard, A. K.; Saucier, D.; Astic, L. Time-course of apoptosis in the olfactory epithelium of rainbow trout exposed to a low copper level. *Tissue Cell.* **1996**, *28*, 367–377.
(22) Hansen, J. A.; Rose, J. D.; Jenkins, R. A.; Gerow, K. G.; Bergman, H. L. Chinook salmon (*Oncorhynchus tshawytscha*) and rainbow trout (*Oncorhynchus mykiss*) exposed to copper: Neurophysiological and histological effects on the olfactory system. *Environ. Toxicol. Chem.* **1999**, *18*, 1979–1991.
(23) Bettini, S.; Ciani, F.; Franceschini, V. Recovery of the olfactory receptor neurons in the African *Tilapia mariae* following exposure to low copper level. *Aquat. Toxicol.* **2006**, *76*, 321–328.
(24) Baldwin, D. H.; Sandahl, J. F.; Labenia, J. S.; Scholz, N. L. Sublethal effects of copper on coho salmon: impacts on non-overlapping receptor pathways in the peripheral olfactory nervous system. *Environ. Toxicol. Chem.* **2003**, *22*, 2266–2274.
(25) Sandahl, J. F.; Baldwin, D. H.; Jenkins, J. J.; Scholz, N. L. Odor-evoked field potentials as indicators of sublethal neurotoxicity in juvenile coho salmon (*Oncorhynchus kitsutch*) exposed to copper, chlorpyrifos, or esfenvalerate. *Can. J. Fish. Aquat. Sci* 2004*61*, 404–413.
(26) Sandahl, J. F.; Baldwin, D. H.; Jenkins, J. J.; Scholz, N. L. A sensory system at the interface between urban stormwater runoff and salmon survival. *Environ. Sci. Technol.* **2007**, *41*, 2998–3004.
(27) Sveinsson, T.; Hara, T. J. Olfactory sensitivity and specificity of Arctic char, *Salvelinus alpinus*, to a putative male pheromone, prostaglandin F2α. *Physiol. Behav.* **2000**, *69*, 301–307.
(28) Scott, G. R.; Sloman, K. A. The effects of environmental pollutants on complex fish behaviour: integrating behavioural and physiological indicators of toxicity. *Aquat. Toxicol.* **2004**, *68*, 369–392.
(29) Pyle, G. G.; Mirza, R. S. Copper-impaired chemosensory function and behavior in aquatic animals. *Human Ecol. Risk Assess.* **2007**, *13*, 492–505.
(30) Mirza, R. S.; Green, W. W.; Connor, S.; Weeks, A. C. W.; Wood, C. M.; Pyle, G. G. Do you smell what I smell? Olfactory impairment in wild yellow perch from metal-contaminated waters. *Ecotox. Environ. Saf.* **2009**, *72*, 677–683.
(31) Brown, S. B.; Evans, R. E.; Thompson, B. E.; Hara, T. J. Chemoreception and aquatic pollutants. In *Chemoreception in Fishes*; Hara, T.J. , Ed.; Elsevier: Amsterdam, 1982.
(32) Sandahl, J. F.; Miyasaka, G.; Koide, N.; Ueda, H. Olfactory inhibition and recovery in chum salmon (*Oncorhynchus keta*) following copper exposure. *Can. J. Fish. Aquat. Sci* **2006**, *63*, 1840–1847.
(33) McIntyre, J. K.; Baldwin, D. H.; Meador, J. P.; Scholz, N. L. Chemosensory deprivation in juvenile coho salmon exposed to dissolved copper under varying water chemistry conditions. *Environ. Sci. Technol.* **2008**, *42*, 1352–1358.
(34) Kinraide, T. B. Plasma membrane surface potential (Ψ_{PM}) as a determinant of ion bioavaialability: a critical analysis of new and published toxicological studies and a simplified method for the computation of plant ΨPM. *Environ. Toxicol. Chem.* **2006**, *25* (12), 3188–3198.
(35) Grosell, M.; Wood, C. M. Copper uptake across rainbow trout gills: mechanisms of apical entry. *J. Exp. Biol.* **2002**, *205*, 1179–1188.
(36) Hunn, J. B. Role of calcium in gill function in freshwater fishes. *Comp. Biochem. Physiol.* **1985**, *82A*, 543–547.
(37) Erickson, R. J.; Benoit, D. A.; Mattson, V. R.; Nelson, H. P., Jr.; Leonard, E. N. The effects of water chemistry on the toxicity of copper to fathead minnows. *Environ. Toxicol. Chem.* **1996**, *15*, 181–193.

ES9023892

Hydrobiologia (2005) 544:241–247
DOI 10.1007/s10750-005-0862-5
© Springer 2005

Primary Research Paper

Effects of pulsed and pressed disturbances on the benthic invertebrate community following a coal spill in a small stream in northeastern USA

Matthew P. Harper[1] & Barbara L. Peckarsky[1, 2]
[1]*Departments of Entomology, Ecology and Evolutionary Biology, Cornell University, Ithaca, NY USA 14853*
[2]*Rocky Mountain Biological Laboratory, Crested Butte, CO USA 81224*
*(*Author for correspondence: E-mail: mph26@cornell.edu)*

Received 19 May 2004; in revised form 14 December 2004; accepted 18 January 2005

Key words: Cayuga Inlet, channelization, coal spill, human disturbance, long-term recovery, stream invertebrates

Abstract

In September 1999, a coal-carrying train derailed and spilled 180,000–270,000 kg of coal into the Cayuga Inlet near Ithaca, New York. This study determined the immediate effects of the coal spill and the clean up procedures on the aquatic invertebrate community, and whether the stream recovered from this event after 2 years. Benthic invertebrate samples were taken both upstream and downstream of the coal spill immediately following clean-up efforts and two years later. Just after the coal spill, the total abundance and species richness of aquatic invertebrates were significantly lower downstream of the spill, suggesting that the disturbance caused increased mortality and/or emigration compared to a reference site upstream. Taxa affected most were grazers and turbidity-susceptible invertebrates. Two years later the invertebrate communities were similar upstream and downstream of the spill, except for an increase in the percent of the dominant genus, *Hydropsyche* (Trichoptera: Hydropsychidae). We speculate that long-term effects of channelization of the stream that occurred during the clean-up prevented the invertebrate assemblage from returning to the conditions observed in a reference site upstream of the coal spill. We propose that large scale environmental clean-ups should be designed to avoid altering ecosystems permanently, and that streams should be allowed to recover naturally without destructive human intervention.

Introduction

Pulsed disturbances from catastrophic spills of hazardous materials can result in short-term effects on aquatic environments. For example, coal spills in streams have been shown to cause simplification of food chains (Cherry & Guthrie, 1977), reduction in fish populations (Cherry et al., 1976), and reduction in both aquatic invertebrate densities and species richness (Guthrie et al., 1978; Cherry et al., 1979a, b; Scullion & Edwards, 1980; Forbes & Magnuson, 1981; Larrick et al., 1981; Duchrow, 1982; VanHassel & Wood, 1984). These effects have been attributed to two different mechanisms. First, physical disturbance, such as increased turbidity and smothering of substrates caused by the coal can have detrimental effects on invertebrates with higher oxygen requirements, exposed gills, or preferences for low-sediment environments (Duchrow, 1982; Cherry et al., 1979a). Second, the chemical effects of the coal indirectly lower invertebrate abundance, because reduced water quality kills bacteria and fungi negatively affecting the decomposing detritus or biofilm on which the

invertebrates graze (Guthrie, et al., 1978, Cherry et al., 1979b, Forbes & Magnuson, 1981, Larrick et al., 1981, VanHassel et al., 1984).

The objectives of this study were to quantify the short-term effects of a coal spill and its subsequent clean-up on the aquatic invertebrate community, and to determine the extent to which it had recovered two years later. Previous research indicated that short-term negative effects would occur on abundance and species richness of invertebrates, especially grazers and taxa sensitive to increases in turbidity. We hypothesized that the invertebrate community would recover completely two years following the coal spill (Duchrow, 1982, Specht et al., 1984). However, we suspected that recovery might be incomplete if channelization permanently altered the channel (Yount & Niemi, 1990).

Materials and methods

At 16:48 on 1 September 1999 five coal-carrying cars of a Norfolk-Southern railroad train derailed, three of which spilled their contents into the Cayuga Inlet, a third order stream running parallel to the tracks in Tompkins County, NY. Clean-up crews estimated between 180,000 and 270,000 kg of coal entered the stream. Norfolk-Southern and New York State Department of Environmental Conservation officials began an extensive clean-up effort the same day that the spill occurred, which included constructing an impoundment of boulders and cobble across the stream to provide a road for large vehicles to access the railroad tracks. They also stabilized the bank adjacent to the tracks with rip rap, attempted to contain the coal by placing large plastic curtains along the river bank, and mechanically removed large amounts of coal from the stream and its banks.

Whereby the coal spill was a "pulsed" disturbance, the clean-up activities could be considered a "pressed" disturbance, because they more permanently altered the channel downstream of the spill (Yount & Niemi, 1990). After the 2–3 week clean-up was completed, the dam was removed, and a large flood occurred on the 16–17 September that raised the water level and removed the majority of the residual coal out of the river or downstream of the area of immediate impact.

To measure the effect of the coal spill and subsequent clean up activities on the stream communities, invertebrate samples were taken from the Cayuga Inlet in Tompkins County, NY near Blacksler Hill Road on 21 September 1999 at one site upstream (reference) and one site downstream (impact) of the coal spill and the temporary impoundment. On 15 October 2001, $\sim$ two years later, invertebrate samples were taken at the same locations to quantify the extent of recovery of the invertebrates from the effects of the coal spill and clean-up activities.

Six traveling kick samples were taken from riffles immediately upstream (reference site) and downstream (impact site) of the coal spill and the temporary impoundment and consisted of a sampler moving across a transect of the stream collecting invertebrates in a D-frame net (mesh size 0.8 mm) for a period of one minute. All invertebrates were preserved in 70% ethanol and identified in the laboratory to the lowest taxonomic level possible, which was genus in most cases. Chironomidae (Diptera) and Tubificidae (Oligochaeta) were identified to family.

Total invertebrate abundance was measured by counting all individuals obtained during the 1-min traveling kick samples. Taxonomic richness was also measured from all invertebrates collected in each sample. Two other metrics were obtained using random subsamples of 100 invertebrates from each sample: proportion of EPT, and percent of the dominant taxon. Proportion of EPT was calculated as the fraction of individuals in the sample that belonged to Ephemeroptera, Plecoptera, and Trichoptera, which are three orders that are generally most sensitive to reduced water quality (Eaton & Lenat, 1981). The percentage of the dominant taxon provides a measure of evenness of distribution of individuals among taxa. Abundance and richness of grazers were also compared between upstream and downstream sites (Ephemeroptera: *Baetis, Caenis, Eurylophella, Stenonema*, Trichoptera: *Helicopsyche*, Coleoptera: *Psephenus*, and Gastropoda: *Physella*), which we suspected would be selectively affected by the coal spill. Finally, abundance and richness of invertebrates belonging to orders that Duchrow (1982) found to be highly sensitive to increases in turbidity (Trichoptera, Megaloptera, Ephemeroptera, and Isopoda) were compared.

Non-parametric (distribution free) Wilcoxon Rank Sum tests were used to compare the upstream and downstream sites in both 1999 and 2001 with respect to total invertebrate abundance, taxon richness, proportion EPT, and percent dominant taxon. Wilcoxon Rank Sum tests were also used to compare the effects of the coal spill on grazers and invertebrates susceptible to turbidity during these two different collection periods (SAS Institute, 2001).

Results

Immediately following the coal spill (1999) there were significantly lower total invertebrate abundance and taxon richness at the site downstream than upstream of the impoundment and the coal spill (Fig. 1a and b). Abundance of total invertebrate grazers was also significantly reduced at the site downstream of the coal spill in 1999 (Fig. 2a), while the taxon richness of grazers did not differ between upstream and downstream sites ($Z_1 = 1.77$, df = 1, $p = 0.077$; Table 1). Abundance of invertebrates in the orders especially vulnerable to turbidity (Trichoptera, Megaloptera, Ephemeroptera, and Isopoda) was also significantly reduced at the site downstream of the coal spill 1999 (Fig. 3a), while the taxon richness of those orders did not differ between sites upstream and downstream of the coal spill ($Z_1 = 1.44$, df = 1, $p = 0.150$; Table 1). Finally, the proportion of EPT ($Z_1 = 1.73$, df = 1, $p = 0.084$; Table 1) and percent dominant taxon (Fig. 4a) did not differ between the upstream and downstream sites indicating that these aspects of the invertebrate community were not affected by the coal spill in the short term.

Results of samples taken two years later (2001) suggested that the invertebrate community had completely recovered from the coal spill and clean-up, because total invertebrate abundance, taxon richness (Fig. 1c and d), and grazer abundance (Fig. 2b) no longer differed between the upstream and downstream sites. Furthermore, taxon richness ($Z_1 = 0.00$, df = 1, $p = 1.000$) and proportion EPT ($Z_1 = 0.16$, df = 1, $p = 0.871$) remained similar between upstream and downstream sites as in 1999 (Table 1). Abundance of turbidity-susceptible invertebrates had also recovered two years after the coal spill (Fig. 3b), and taxon richness of turbidity-susceptible invertebrates no longer differed between upstream and downstream sites ($Z_1 = 0.08$, df = 1, $p = 0.932$; Table 1).

Hydropsyche spp. (Trichoptera, Hydropsychidae) was the dominant taxon in the benthic community at all sites in both 1999 and 2001 (Fig. 4a). However, the only difference between the upstream and downstream invertebrate communities two years after the coal spill was that the percent of this dominant taxon was significantly higher at the site downstream of the coal spill in 2001 (Fig. 4b).

Discussion

Previous research conducted on streams directly affected by coal particles has shown that the benthic invertebrate communities initially suffer an impact characterized by a decline in total abundance and species richness.(Guthrie et al., 1978; Cherry et al., 1979a, b; Scullion & Edwards, 1980; Forbes & Magnuson, 1981; Larrick et al., 1981; Duchrow, 1982; VanHassel & Wood, 1984). These same trends were observed in the benthic communities of the Cayuga Inlet following a coal spill in September 1999. However, two years following the stress, the aquatic invertebrate communities had not completely recovered with respect to evenness of distribution of individuals among taxa. These findings suggest that the pressed disturbance of channel modification during the clean-up may have had long-term effects on the stream invertebrate communities.

The significant decline in total invertebrates and taxa richness following the coal spill with no significant effects on EPT demonstrated that the negative effects of the coal spill were not limited to the most sensitive invertebrates of the community. These effects could be attributed to two different mechanisms. First, a change in water chemistry could have caused invertebrate mortality, due to increased levels of $Fe(OH)_x$ and a decline in pH that occur when coal is added to water (Vinikour, 1979; Cherry et al., 1979b; Scullion & Edwards, 1980). Second, Cherry et al. (1979a) reported that in some cases the physical effects of increased turbidity and smothering by the coal particles are more deleterious than the toxicity created by the

coal/water mixture. Turbidity may have played an extremely important role in the Cayuga Inlet since a temporary impoundment was constructed, then removed, and coal was then removed from the stream bank by bulldozers before the first samples were collected. This suggests that the turbidity caused by coal particles and sediment stirred up during the clean-up phase contributed in part to the generalized taxonomic effects that were observed. The same patterns that Cherry

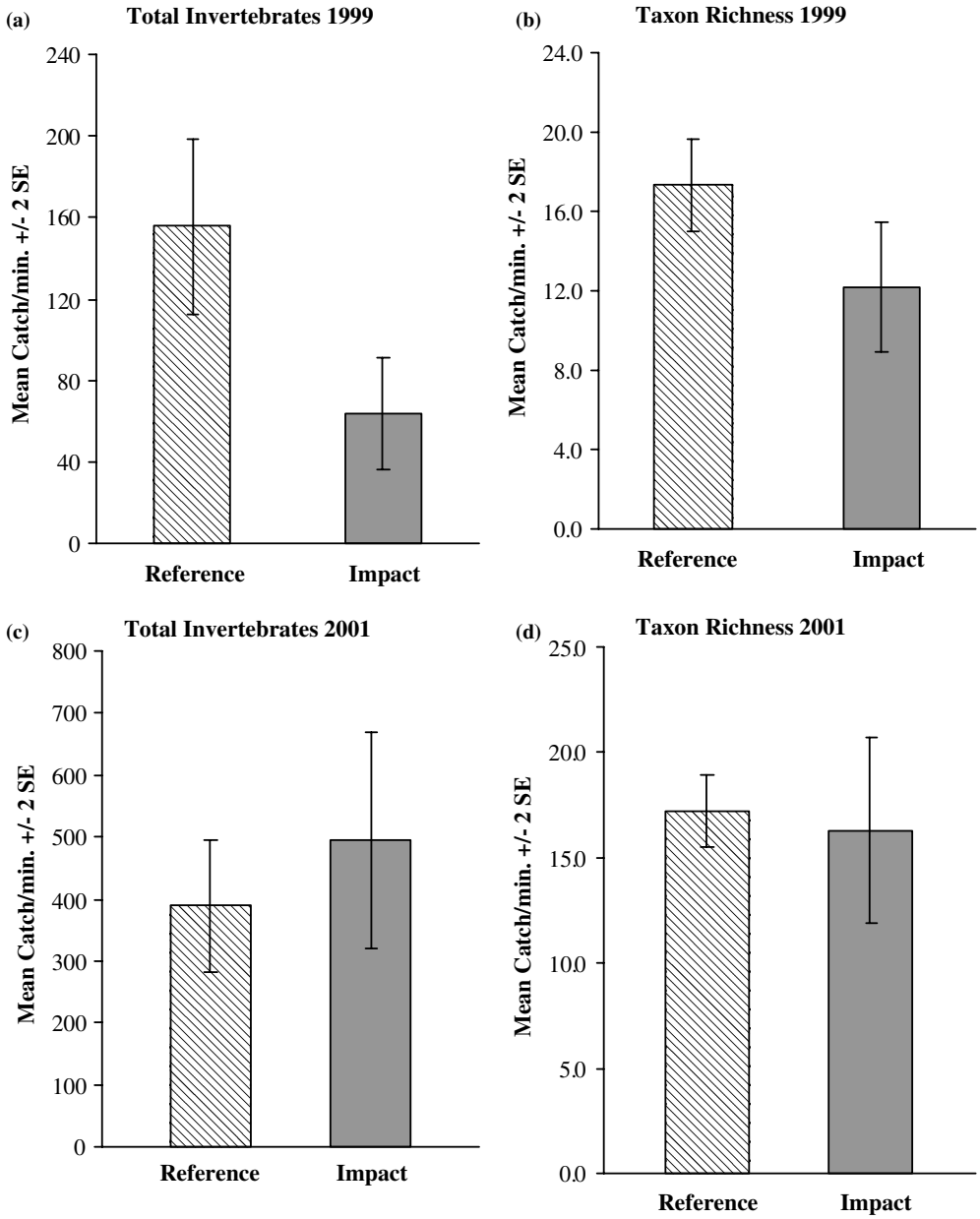

Figure 1. Mean abundance of total invertebrates and taxon richness ($\pm$2SE) at reference site (upstream) and impact site (downstream) of the coal spill in 1999 and 2001. (a) Total abundance ($Z_1 = 2.32$, df = 1, $p = 0.020$) and (b) taxon richness ($Z_1 = 2.49$, df = 1, $p = 0.013$) were significantly reduced at the impact site of the coal spill in 1999. (c) In 2001, total invertebrate abundance ($Z_1 = -0.72$, df = 1, $p = 0.471$) and (d) taxon richness ($Z_1 = 0.72$, df = 1, $p = 0.466$) did not differ between reference and impact sites.

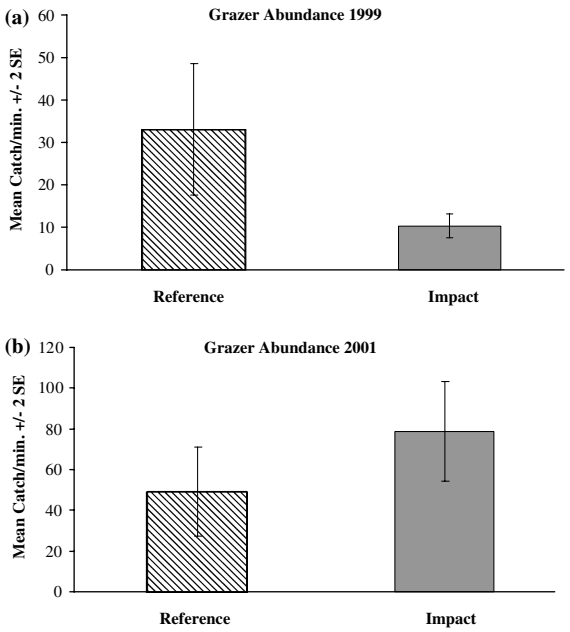

Figure 2. (a) In 1999, mean ($\pm$2SE) abundance of invertebrate grazers was significantly reduced at the impact site ($Z_1 = 2.81$, df = 1, $p = 0.005$); (b) In 2001, grazer abundance did not differ between impact and reference sites ($Z_1 = -1.68$, df = 1, $p = 0.092$).

et al. reported in 1979 are supported by the observation that insect orders more susceptible to turbidity suffered disproportionately greater declines than those with low tolerance to reduced oxygen (e.g., mayflies and stoneflies, Duchrow, 1982).

The EPT index did not vary between reference and impact sites on either sampling date, suggesting that the coal disturbance did not target Ephemeroptera, Plecoptera, and Trichoptera, which are insect orders that are generally less tolerant to disturbance (Eaton & Lenat, 1991). However, the immediate impact of the coal spill was most pronounced in grazer species, which may have been due to an indirect effect of chemical inhibition of their algal or bacterial food sources (VanHassel et al., 1984). Therefore, both smothering effects and the change in water chemistry caused by the addition of coal to the channel may have contributed to the immediate invertebrate kill or emigration observed in the stream following the coal spill.

Two years later we expected the effects of the coal spill to have dissipated, but the stream remained channelized as a result of the clean-up. At that time all of the invertebrate bioassessment indices measured indicated that the stream had fully recovered, except for the significantly higher percent dominance of the Trichoptera, *Hydropsyche*. This observation suggests that a factor other than the coal spill had a long-term impact on the distribution of individuals within taxa, which is one of the components of the diversity of the invertebrate assemblage of this stream (Yount & Niemi, 1990). During the clean-up of the coal spill, the stream channel of the Cayuga Inlet was modified and rip-rap was added to stabilize the banks. The resultant substrate in the

Table 1. Mean values (and 2 SE) of the invertebrate metrics that showed no significant differences between reference and impact sites in 1999 or 2001

Invertebrate metrics	Location	Mean	2 SE
Grazer taxon richness 1999	Reference	4.7	0.8
	Impact	3.7	1.0
Turbidity susceptible invertebrate taxon richness 1999	Reference	7.3	1.1
	Impact	6.2	1.7
EPT 1999	Reference	8.3	0.8
	Impact	6.7	1.8
EPT 2001	Reference	9.0	1.5
	Impact	9.0	2.5
Grazer taxon richness 2001	Reference	5.7	0.7
	Impact	5.8	1.6
Turbidity susceptible invertebrate taxon richness 2001	Reference	10.7	0.8
	Impact	10.8	2.9

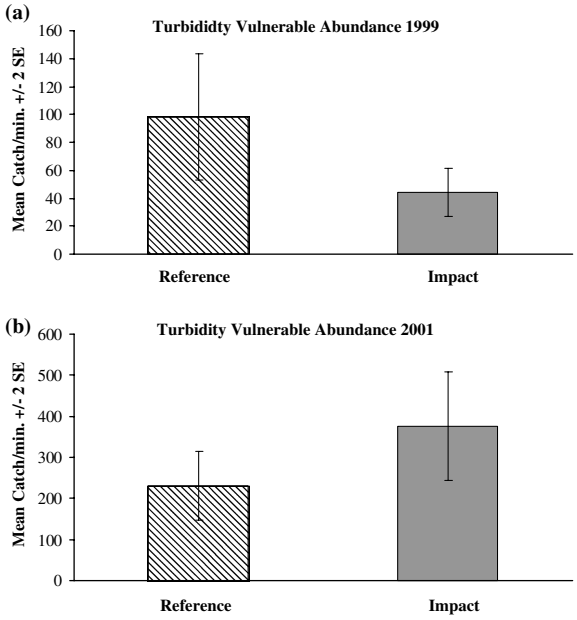

Figure 3. (a) In 1999, the abundance of invertebrates belonging to orders vulnerable to turbidity (Trichoptera, Megaloptera, Ephemeroptera, and Isopoda) was significantly reduced at the impact site ($Z_1 = 2.00$, df = 1, $p = 0.045$); (b) In 2001, abundance of turbidity-sensitive invertebrates did not differ between impact and reference sites ($Z_1 = -1.52$, df = 1, $p = 0.128$).

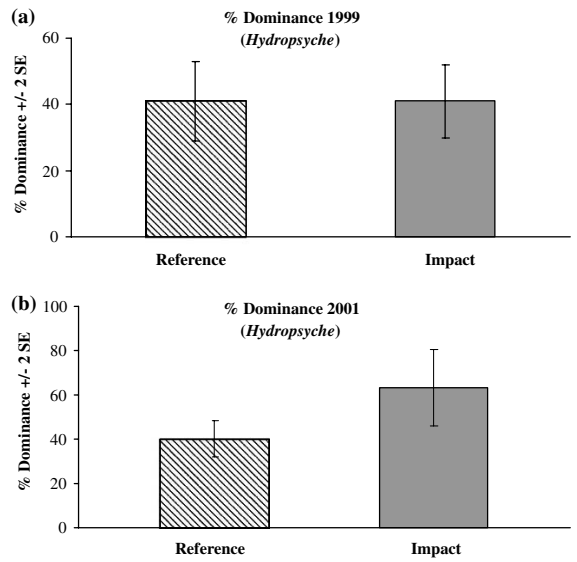

Figure 4. (a) In 1999, mean (± 2SE) percent dominant taxon did not differ between the reference and impact sites ($Z_1 = -0.08$, df = 1, $p = 0.936$); (b) In 2001, mean percent dominance was significantly higher in the impact than in the reference site ($Z_1 = -2.82$, df = 1, $p = 0.005$).

modified stream channel was highly uniform and comprised predominantly of medium-sized cobbles, which could have provided optimal suspension-feeding habitat for *Hydropsyche* to attach their retreats and silken catch nets (Georgian & Thorp, 1992).

The recovery process after any disturbance involves an adjustment of the community to a new steady state determined by a change in carrying capacity. Longest recovery times are generally associated with stressors leading to long-term alterations in physical stream habitat. If a river channel never returns to its pre-disturbance state, then the macroinvertebrate composition may be changed forever (Yount & Niemi, 1990). Although Whitaker et al. (1979) found that macroinvertebrate communities quickly stabilized after channel modification, returning to their steady state one year after the initial disturbance, most studies have shown that channelization is one of the most detrimental long-term stressors to stream communities (Zimmer & Bachman, 1978, Haynes & Makarewicz, 1982, Yount & Niemi, 1990). Further sampling of these sites on the Cayuga Inlet will determine whether *Hydropsyche* will eventually return to the reference condition.

Overall, grazers and turbidity-susceptible invertebrates were more negatively affected by the disturbance. Although the stream had generally recovered from the effects of the coal spill two years later, the proportion of the dominant taxon, the net-spinning caddisfly, *Hydropsyche*, increased in the area of the stream receiving the initial impact. Because coal has not been reported to alter stream invertebrate community structure beyond one year, we suspect that some other factor, such as the channelization of the stream during clean up, has altered the stream community structure over the long term (pressed disturbance). Thus, while negative effects of coal were short-term, environmental managers should place more emphasis on minimizing potential long-term consequences of invasive clean up measures. With less human intervention after such disturbances, streams may have a better chance of eventually returning to their natural condition (Poff et al., 1997), rather than changing the stream and its inhabitants indefinitely.

Acknowledgments

We thank the following people who helped collect samples: Keith Sendziak, Nate Hardy, Andrea Encalada, Jonas Dahl, and Steve Horn. Brad Taylor, Kate Macneale and Andrea Encalada helped with the statistics. We thank the Cornell Presidential Research Scholars for funding MPH, and HATCH grant No. 139402 to BLP.

References

Cherry, D. S. & R. K. Guthrie, 1977. Toxic metals in surface waters from coal ash. Water Resource Bulletin 13: 1227–1236.

Cherry, D. S., R. K. Guthrie, F. F. Sherberger & S. R. Larrick, 1979a. The influence of coal ash and thermal discharges upon the distribution and bioaccumulation of aquatic invertebrates. Hydrobiologia 62: 257–267.

Cherry, D. S., S. R. Larrick, R. K. Guthrie, E. M. Davis & A. F. Sherberger, 1979b. Recovery of invertebrate and vertebrate population in a coal ash stressed drainage system. Journal of Fisheries Research Board Canada 36: 1089–1096.

Duchrow, R. M., 1982. Effects of barite tailings on benthos and turbidity of two Ozark streams. Transactions of the Missouri Academy of Science 16: 55–66.

Eaton, L. E. & D. R. Lenat, 1991. Comparison of a rapid bioassessment method with North Carolina's qualitative macroinvertebrate collection method. Journal of the North American Benthological Society 10: 335–338.

Forbes, A. M. & J. J. Magnuson, 1981. Decomposition and microbial colonization of leaves in a stream modified by coal ash effluent. In Krumholz L. A. (ed.), The Warmest Streams Symposium. Southern Division, American Fisheries Society: 241–249.

Georgian, T. J. & J. H. Thorp, 1992. Effects of microhabitat selection on feeding rates of net-spinning caddisfly larvae. Ecology 73: 229–240.

Guthrie, R. K., D. S. Cherry & F. L. Singleton, 1978. Responses of heterotrophic bacterial populations to pH changes in coal ash effluent. Water Resource Bulletin 14: 803–808.

Haynes, J. M. & J. C. Makarewicz, 1982. Comparison of benthic communities in dredged and undredged areas of the St. Lawrence River, Cape Vincent, NY. Ohio Journal of Science 82: 165–169.

Larrick, S. R., J. R. Clark, D. S. Cherry & J. Cairns, Jr., 1981. Structural and functional changes of aquatic heterotrophic bacteria to thermal, heavy and fly ash effluents. Water Research 15: 875–880.

Poff, N. L., J. D. Allan, M. B. Bain, J. R. Karr, K. L. Prestegaard, B. D. Richter, R. E. Sparks & J. C. Stromberg, 1997. The natural flow regime. BioScience 47: 769–784.

SAS Institute, 2001. JMP IN Statistical Discovery Software; Version 4. SAS Institute Inc., Cary, North Carolina, USA.

Scullion, J. & R. W. Edwards, 1980. The effects of coal industry pollutants on the macroinvertebrate fauna of a small river in the South Wales coalfield. Freshwater Biology 10: 141–162.

Specht, W. L., D. S. Cherry, R. A. Lechleitner & J. Cairns, Jr., 1984. Structural, functional, and recovery responses of stream invertebrates to fly ash effluent. Canadian Journal of Fisheries and Aquatic Sciences 41: 884–896.

VanHassel, J. H. & K. V. Wood, 1984. Factors affecting aquatic macroinvertebrates below a fly ash pond discharge. Journal of Freshwater Ecology 2: 571–586.

Vinikour, W. S., 1979. Coal slurry observed as habitat for semiaquatic beetle *Lanternarius brunneus* (Coleoptera: Heteroceridae) with notes on water quality conditions. Entomology News 90: 203–204.

Whitaker, G. A., R. H. McCuen & J. Brush, 1979. Channel modification and macroinvertebrate community diversity in small streams. Water Resources Bulletin 15: 874–879.

Yount, J. D. & G. J. Niemi (eds), 1990. Recovery of lotic communities and ecosystems following disturbance: theory and applications. Environmental Management 14: 515–762.

Zimmer, D. W. & R. W. Bachman, 1978. Channelization and invertebrates in some Iowa streams. Water Resources Bulletin 14: 868–883.

Copyright of Hydrobiologia is the property of Springer Science & Business Media B.V. and its content may not be copied or emailed to multiple sites or posted to a listserv without the copyright holder's express written permission. However, users may print, download, or email articles for individual use.

NOAA Technical Memorandum NMFS-NWFSC-83

An Overview of Sensory Effects on Juvenile Salmonids Exposed to Dissolved Copper:

Applying a Benchmark Concentration Approach to Evaluate Sublethal Neurobehavioral Toxicity

October 2007

U.S. DEPARTMENT OF COMMERCE
National Oceanic and Atmospheric Administration
National Marine Fisheries Service

NOAA Technical Memorandum
NMFS-NWFSC Series

The Northwest Fisheries Science Center of the National Marine Fisheries Service, NOAA, uses the NOAA Technical Memorandum NMFS-NWFSC series to issue scientific and technical publications. Manuscripts have been peer reviewed and edited. Documents published in this series may be cited in the scientific and technical literature.

The NMFS-NWFSC Technical Memorandum series of the Northwest Fisheries Science Center continues the NMFS-F/NWC series established in 1970 by the Northwest & Alaska Fisheries Science Center, which has since been split into the Northwest Fisheries Science Center and the Alaska Fisheries Science Center. The NMFS-AFSC Technical Memorandum series is now being used by the Alaska Fisheries Science Center.

Reference throughout this document to trade names does not imply endorsement by the National Marine Fisheries Service, NOAA.

This document should be referenced as follows:

Hecht, S.A., D.H. Baldwin, C.A. Mebane, T. Hawkes, S.J. Gross, and N.L. Scholz. 2007. An overview of sensory effects on juvenile salmonids exposed to dissolved copper: Applying a benchmark concentration approach to evaluate sublethal neurobehavioral toxicity. U.S. Dept. Commer., NOAA Tech. Memo. NMFS-NWFSC-83, 39 p.

NOAA Technical Memorandum NMFS-NWFSC-83

An Overview of Sensory Effects on Juvenile Salmonids Exposed to Dissolved Copper:

Applying a Benchmark Concentration Approach to Evaluate Sublethal Neurobehavioral Toxicity

Scott A. Hecht,[1] David H. Baldwin, Christopher A. Mebane,[2]
Tony Hawkes,[1] Sean J. Gross,[3] and Nathaniel L. Scholz

Northwest Fisheries Science Center
Ecotoxicology and Environmental Fish Health Program
2725 Montlake Boulevard East
Seattle, Washington 98112

[1] National Marine Fisheries Service
Office of Protected Resources, Endangered Species Division
510 Desmond Drive Southeast
Lacey, Washington 98506

[2] U.S. Geological Survey
NMFS Liaison
10095 West Emerald Street
Boise, Idaho 83704

[3] National Marine Fisheries Service
Washington State Habitat Office
7600 Sand Point Way Northeast
Seattle, Washington 98115

October 2007

U.S. DEPARTMENT OF COMMERCE
National Oceanic and Atmospheric Administration
National Marine Fisheries Service

Most NOAA Technical Memorandums NMFS-NWFSC are available online at the Northwest Fisheries Science Center web site (http://www.nwfsc.noaa.gov)

Copies are also available from:
National Technical Information Service
5285 Port Royal Road
Springfield, VA 22161
phone orders (1-800-553-6847)
e-mail orders (orders@ntis.fedworld.gov)

Table of Contents

List of Figures v
List of Tables vii
Executive Summary ix
Acknowledgments xi
Introduction 1
Previous Studies on the Effects of Copper 3
Application of the Benchmark Concentration Analysis 9
Results of the Benchmark Concentration Analysis 11
Discussion of Site Specific Considerations for Sensory System Effects 14
  Impairment from Short-term Increases of dCu 14
  Calculating an Acute Criterion Maximum Concentration 14
  Salmonids Are Typically Exposed to Multiple Stressors 15
  Bioavailability of dCu 15
  Olfactory Toxicity in Saltwater 16
  Avoiding Short-term Increases in dCu 17
  Coho Salmon–derived BMCs Should Apply to Other Salmonids 17
Conclusions 18
Glossary 19
References 21
Appendix A: Other Salmonid Sensory Effects of dCu 27
  Migratory Disruption 27
  Laboratory Avoidance Studies 28
  Other Adverse Effects 31
Appendix B: Supplementary Bibliography 33
  Copper Sources 33
  Benchmark Concentration/Dose 33
  Copper and Neurobiology 33
  Reviews 35
  Studies with Other Metals 36
  Selected Behavioral Studies 37
  Recovery of Olfactory Epithelium after Damage 38
  Additional Endpoints 38

List of Figures

Figure 1. Recording methods and features of the salmon peripheral olfactory system. 6

Figure 2. Copper-induced reductions in juvenile salmonid olfactory response and behavior are significantly correlated..... 8

Figure 3. Using a benchmark concentration approach to estimate a threshold for dCu toxicity in the salmonid olfactory system. 12

Figure A-1. Reduction in downstream migration of yearling coho salmon following 6-days exposure to copper at various concentrations..... 29

List of Tables

Table 1. Selected examples of adverse effects with copper to salmonids or their prey. 4

Table 2. Benchmark responses and benchmark concentrations for juvenile salmon exposed to dCu for 3 hours. 13

Executive Summary

Dissolved copper (dCu) is a ubiquitous surface water pollutant that causes a range of adverse effects in fish as well as in aquatic invertebrates and algae. This technical memorandum is a summary and targeted synthesis regarding sensory effects to juvenile salmonids from low-level exposures to dCu. As such, the material presented here serves to summarize scientific research on dCu and its impacts on salmonid sensory systems. In addition, this document provides a benchmark analysis of empirical data generated in recent National Marine Fisheries Service investigations that have focused on salmon olfactory function. The review section, Appendix A, discusses peer reviewed and gray literature on the effects of dCu on salmonid sensory systems, associated sensory-mediated behaviors, and physiology. It is intended to facilitate understanding of the effects of dCu on sensory system–mediated behaviors that are important to survival, reproduction, and distribution of salmonids. The review does not address the effects of dCu on salmonid habitats, although copper is also highly toxic at low µg/L concentrations to aquatic primary producers and invertebrates (i.e., the aquatic food web). Undoubtedly, new information will become available that enhances our current understanding of copper's effect on threatened and endangered salmonids and their supporting habitats.

A large body of scientific literature has shown that fish behaviors can be disrupted at concentrations of dCu that are at or slightly above ambient concentrations (i.e., background). In this document, background is operationally defined as surface waters with less than 3 µg/L dCu, as experimental water had background dCu concentrations as high as 3 µg/L dCu. Sensory system effects are generally among the more sensitive fish responses and underlie important behaviors involved in growth, reproduction, and (ultimately) survival (i.e., predator avoidance). Recent experiments on the sensory systems and corresponding behavior of juvenile salmonids contribute to more than four decades of research and show that dCu is a neurotoxicant that directly damages the sensory capabilities of salmonids at low concentrations. These effects can manifest over a period of minutes to hours and can persist for weeks.

To estimate toxicological effect thresholds for dCu in surface waters, benchmark concentrations (BMCs) were calculated using a U.S. Environmental Protection Agency methodology. This paper presents examples of BMCs for juvenile salmonid olfactory function based on recent data. BMCs ranged 0.18–2.1 µg/L, corresponding to reductions in predator avoidance behavior of approximately 8–57%. The BMC examples represent the dCu concentration (above background) expected to affect the ability of juvenile salmonids to avoid predators in freshwater. These concentration thresholds for juvenile salmonid sensory and behavioral responses fall within the range of other sublethal endpoints affected by dCu such as behavior, growth, and primary production, which is 0.75–2.5 µg/L.

The paper also discusses the influence of water chemistry on the bioavailability and toxicity of copper to fish sensory systems. Studies exploring behavioral avoidance as well as representative studies of other effects to salmonids are also summarized. Salmon may be able to

avoid dCu in environmental situations where distinct gradients occur. However, avoidance of dCu originating from nonpoint sources appears unlikely. Given the large body of literature on copper and responses of aquatic ecosystems, we focused on a subset of fish sensory system studies relevant to anadromous salmonids.

Point and nonpoint source discharges from anthropogenic activities frequently exceed these thresholds by one, two, and sometimes three orders of magnitude, and can occur for hours to days. The U.S. Geological Survey ambient monitoring results for dCu representing 811 sites across the United States detected concentrations ranging 1–51 µg/L, with a median of 1.2 µg/L. Additionally, typical dCu concentrations originating from road runoff from a California study were 3.4–64.5 µg/L, with a mean of 15.8 µg/L. Taken together, the information reviewed and presented herein indicates that impairment of sensory functions important to survival of juvenile salmonids is likely to be widespread in many freshwater aquatic habitats. Impairment of these essential behaviors may manifest within minutes and continue for hours to days depending on concentration and exposure duration. Therefore, dCu has the potential to limit the productivity and intrinsic growth potential of wild salmon populations by reducing the survival and lifetime reproductive success of individual salmonids.

Acknowledgments

The authors thank Jim Meador, Lyndal Johnson, and Karen Peck for insightful and critical reviews of prior versions of this document. We also thank Jenifer McIntyre, Neil Rickard, and Scott Anderson for fruitful discussions and comments.

Introduction

Copper, a naturally occurring element, is an essential micronutrient for plants and animals. However, copper is also recognized as a priority pollutant under the U.S. Clean Water Act. Historical and current anthropogenic activities have mobilized significant quantities of copper. Vehicle emissions and brake pad dust (Drapper et al. 2000), pesticides (USEPA 2005), industrial processes, municipal discharges, mining, and rooftops (Good 1993, Thomas and Greene 1993) are a few of the sources of copper in the environment. These various human activities may lead to the unintended and, in some circumstances, intended introduction of copper into aquatic ecosytems (Sansalone and Buchberger 1997, Wheeler et al. 2005). Once in the aquatic environment, copper is detected in multiple forms. It can be dissolved, or bound to organic and inorganic materials either in suspension or in sediment. This so called speciation of copper is dependent on site specific abiotic and biotic factors. As an element, copper will persist and cycle through ecosystems. Copper in its dissolved state is worthy of particular scrutiny as it is highly toxic to a broad range of aquatic species including algae, macrophytes, aquatic invertebrates, and fishes. The latter include anadromous salmon and steelhead within the *Oncorhynchus* and *Salmo* genera that are, in part, managed by the National Marine Fisheries Service.

Currently, anadromous salmonid populations inhabit waters of Alaska, Oregon, Washington, California, Idaho (*Oncorhynchus* spp.), and Maine (Atlantic salmon [*Salmo salar*]). Dissolved copper (referred to as dCu herein) is consistently detected in salmonid habitats including areas important for rearing, migrating, and spawning (Alpers et al. 2000, Soller et al. 2005). Dissolved copper is known to affect a variety of biological endpoints in fish (e.g., survival, growth, behavior, osmoregulation, sensory function, and others, as reviewed in Eisler 1998). More than three decades of experimental results have shown that the sensory systems of salmonids are particularly vulnerable to the neurotoxic effects of dCu. Recent experimental evidence showed that juvenile sensory system–mediated behaviors are also affected by short-term exposures to dCu.

Given the ecological significance of these behaviors to salmonids, it is important to characterize the potential effects from dCu. The growing body of scientific literature indicates that dCu is a potent neurotoxicant that directly damages the sensory capabilities of salmonids at low concentrations (see the Previous Studies on the Effects of Copper section). These concentrations may stem from anthropogenic inputs of dCu to salmonid habitats. Salmonid sensory systems mediate ecologically important behaviors involved in predator avoidance, migration, and reproduction. Impairment of these behaviors can limit an individual salmonid's potential to complete its life cycle and thus may have adverse consequences at the scale of wild populations.

The purpose of this paper is to: (1) summarize information on the effects of dCu to the sensory systems of juvenile salmonids in freshwater (also see Appendix A), (2) conduct a

benchmark concentration analysis to generate examples of dCu effect thresholds, and (3) to discuss site-specific considerations for sensory system effects. As such, it focuses on a single contaminant (dCu), two relevant sensory system endpoints (olfaction and alarm response behavior), and a single salmonid life stage (juvenile, <10 months old).

Previous Studies on the Effects of Copper

Examples of copper's effects on a suite of selected biological endpoints from laboratory and field exposures are presented in Table 1. Additionally, Appendix A contains a targeted review and summary of some of the previous studies showing copper's effect on salmonid behavior, including avoidance and migratory disruptions. Appendix B is a supplementary bibliography that provides further information sources on salmonid sensory systems. The following analysis of sensory effects on juvenile salmonids primarily emphasizes recent and ongoing research conducted at the National Marine Fisheries Service's Northwest Fisheries Science Center. However, the phenomenon that copper and some other trace metals can interfere with chemoreception, alter behaviors, and influence the movements of fish was first described at least 40 years ago, and a large body of knowledge on the adverse effects of dCu has subsequently developed (Table 1).

The salmonid olfactory sensory system relies on olfactory receptor neurons (ciliated ORNs) to detect and respond to cues in the aquatic environment. The receptors are in direct contact with the aqueous environment. Olfactory receptors detect chemical cues that are important in finding food, avoiding predators, navigating migratory routes, recognizing kin, reproducing, and avoiding pollution. The architecture of the salmon olfactory system consists of a pair of olfactory rosettes, each positioned within an olfactory chamber near the midline of the fish's rostrum (Figure 1A). Each rosette contains ORNs that respond to dissolved odorants as water passes through the olfactory chamber (Figure 1B) and over the surface of the rosette in which the receptor neurons are embedded (Figure 1C). These chemical cues convey important information about the surrounding aquatic environment.

Direct exposure to dCu can impair and destroy olfactory sensory neurons, although the precise mechanism by which dCu interferes with the normal function of ORNs remains unknown (Hansen et al. 1999b, Baldwin et al. 2003, Sandahl et al. 2006, Sandahl et al. 2007). Impairment of olfaction (i.e., smell) can be measured by an electrophysiological technique called the electro-olfactogram (EOG) (Figure 1) (Scott and Scott-Johnson 2002, Baldwin and Scholz 2005, Sandahl et al. 2006). The EOG measures olfactory response of a population of receptor neurons in fish. Reductions in the EOG amplitude of copper-exposed fish compared to unexposed fish reflect functional losses in sensory capacity. Dissolved copper's toxic effect to olfactory sensory neurons is observable as a reduction in or elimination of the EOG amplitude to a recognizable odor (Figure 1D).

Several recent studies highlight some important aspects of copper olfactory toxicity (Baldwin et al. 2003, Sandahl et al. 2004, 2007). Baldwin et al. (2003) found that the neurotoxic effects of copper in coho salmon (*Oncorhynchus kisutch)* manifest over a timescale of minutes. At 10 minutes, EOG amplitude reductions were observed in juvenile coho exposed to 2, 5, 10, and 20 µg/L dCu above experimental background (3 µg/L). After 30 minutes at 2 µg/L dCu above experimental background, the EOG amplitude from juvenile coho to odors was reduced by approximately 25% compared to controls; in 20 µg/L dCu after 30 minutes by approximately

80%. Sandahl et al. (2004) found similar effects following 7 days of exposure (both in EOG reductions and copper concentrations). This result indicated that the juvenile olfactory system does not appear to be able to adapt or otherwise compensate for continuous copper exposure for durations up to 7 days.

Table 1. Selected examples of adverse effects with copper to salmonids or their prey.[a]

Species (lifestage)	Effect	Effect concentra-tion (µg/L)[b]	Effect statistic	Hardness (mg/L)[c]	Exposure duration	Source
	Sensory and behavioral effects					
Coho salmon (juvenile)	Reduced olfaction and compromised alarm response	0.18–2.1	EC_{10} to EC_{50}	120	3 hours	Sandahl et al. 2007
Chinook salmon (*O. tshawytscha)* (juvenile)	Avoidance in laboratory exposures	0.75	LOEC	25	20 minutes	Hansen et al. 1999a
Rainbow trout (*O, mykiss)* (juvenile)	Avoidance in laboratory exposures	1.6	LOEC	25	20 minutes	Hansen et al. 1999a
Chinook salmon (juvenile)	Loss of avoidance ability	2	LOEC	25	21 days	Hansen et al. 1999a
Atlantic salmon (juvenile)	Avoidance in laboratory exposures	2.4	LOEC	20	20 minutes	Sprague et al. 1965
Atlantic salmon (adult)	Spawning migrations in the wild interrupted	20	LOEC	20	Indefinite	Sprague et al. 1965
Chinook salmon (adult)	Spawning migrations in the wild apparently interrupted	10–25	LOEC	40	Indefinite	Mebane 2000
Coho salmon	Delays and reduced downstream migration of dCu-exposed juveniles	5	LOEC	95	6 days	Lorz and McPherson 1976, 1977
Rainbow trout	Loss of homing ability	22	LOEC	63	40 weeks	Saucier et al. 1991
	Ecosystem effects					
NA[d]	Ecosystem function: Reduced photosynthesis	2.5	LOEC	49	≈ 1 year	Leland and Carter 1985
NA[d]	Ecosystem structure: loss of invertebrate taxa richness in a mountain stream	5	LOEC	49	≈ 1 year	Leland et al. 1989
	Other sublethal effects					
Chinook salmon	Reduced growth (as weight)	1.9	EC_{10}	25	120 days	Chapman 1982
Rainbow trout	Reduced growth (as weight)	2.8	EC_{10}	25	120 days	Marr et al. 1996

Table 1 continued. Selected examples of adverse effects with copper to salmonids or their prey.[a]

Species (lifestage)	Effect	Effect concentra-tion (µg/L)[b]	Effect statistic	Hardness (mg/L)[c]	Exposure duration	Source
	Other sublethal effects (cont.)					
Coho salmon	Reduced growth (as weight)	21–22	NOEC	24–32	60 days	Mudge et al. 1993
Steelhead (*O. mykiss*)	Reduced growth (as weight)	45 to >51	NOEC	24–32	60 days	Mudge et al. 1993
	Direct lethality[e]					
Chinook salmon (fry)	Death	19	LC_{50}	24	96 hours	Chapman 1978
Coho salmon (fry)	Death	28–38	LC_{50}	20–25	96 hours	Lorz and McPherson 1976
Steelhead/rain-bow trout (fry)	Death	9–17	LC_{50}	24–25	96 hours	Chapman 1978, Marr et al. 1999
Coho salmon (adult)	Death	46	LC_{50}	20	96 hours	Chapman and Stevens 1978
Steelhead (adult)	Death	57	LC_{50}	42	96 hours	Chapman and Stevens 1978
Coho salmon (juvenile)	Death	21–22	NOEC	24–32	60 days	Mudge et al. 1993
Steelhead (juvenile)	Death	24–28	NOEC	24–32	60 days	Mudge et al. 1993
Steelhead (egg-to-fry)	Death	11.9	EC_{10}	25	120 days	Chapman 1982

[a] Abbreviations: LOEC = Lowest observed adverse effect concentration (and most LOEC values given are not thresholds, but were simply the lowest concentration tested); NOEC = No observed adverse effect concentration; LC_{50} = the concentration that kills 50% of the test population; ECp = effective concentration adversely affecting (p) percent of the test population or percent of measured response, e.g., 10% for an EC10, etc.; and Indefinite = field exposures without defined starting and ending times. NA = not applicable.
[b] Effects and exposure durations stem from laboratory and field experiments, therefore in some experiments multiple routes of exposure may be present (i.e., aqueous and dietary) and water chemistry conditions will likely differ (see reference for details).
[c] Hardness is reported, as it can influence the toxicity of copper.
[d] This study examined ecosystems consisting of a number of species or unidentified species.
[e] Acute sensitivity of salmonids to copper probably varies by life stage, and the swim-up fry stage is probably more sensitive than older juvenile life stages such as parr and smolts or adults.

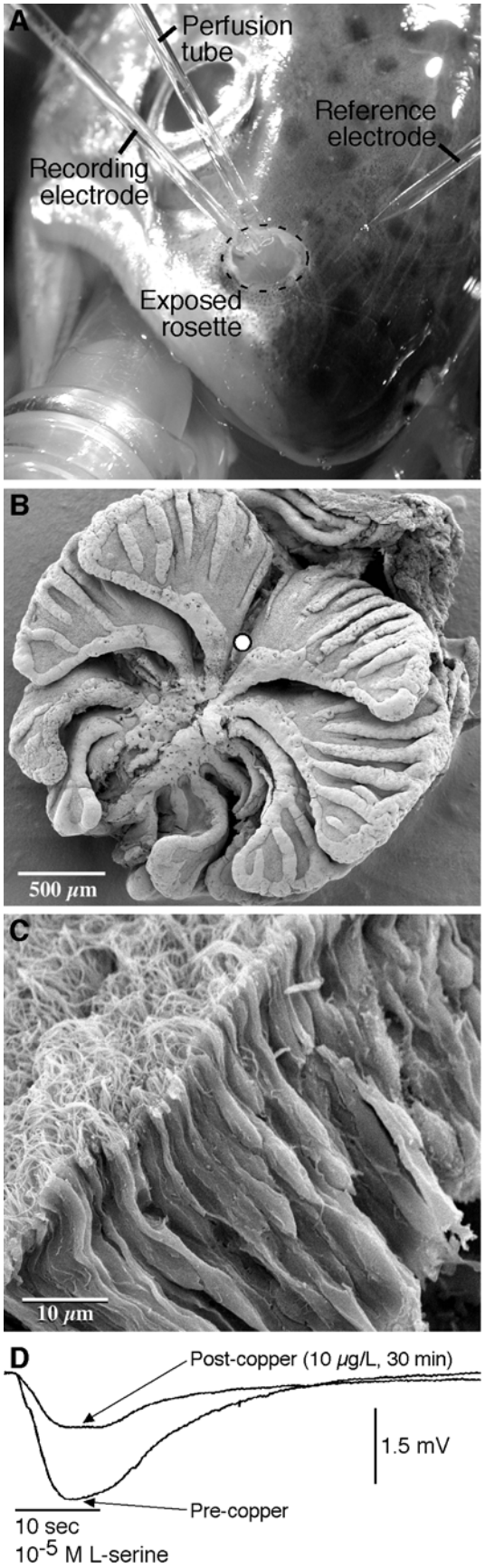

Figure 1. Recording methods and features of the salmon peripheral olfactory system. A) Photograph showing the rostrum of a coho salmon during the recording of electro-olfactograms (EOGs). The mouthpiece provides chilled, anaesthetized water to the gills, while the perfusion tube delivers odor-containing solutions to the olfactory chamber. The recording electrode in the olfactory chamber and reference electrode in the skin monitor the response of the olfactory system to an odor. B) Scanning electron micrograph showing a rosette, located within an olfactory chamber of a juvenile coho salmon. Each rosette consists of lamellae (lobes) covered by an epithelium containing regions of sensory neurons. The open circle denotes the location and approximate size of the tip of the recording microelectrode. C) Scanning electron micrograph showing a cross section from a region of sensory epithelium of a lamella. In the upper left is the apical surface containing the cilia and microvilli of the olfactory receptor neurons (ORNs). The dendrites and somata of the ORNs appear in the center within the epithelium, while the axons of the ORNs emerge from the basal surface at the lower right to produce the olfactory nerve. D) Typical odor-evoked EOGs obtained from a salmon before and after exposure to copper. A 10-second switch to a solution containing 10^{-5} M L-serine is shown with a horizontal bar. The EOG evoked by the odor pulse consists of a negative deflection in the voltage. A 30-minute exposure to copper reduced the amplitude of the EOG evoked in the same fish by 57%. (Photos courtesy of Carla Stehr. Figure adapted from Baldwin and Scholz 2005).

Recently, using EOG measurements in combination with a predator avoidance assay, Sandahl et al. (2007) presented the first evidence that impaired olfaction (smell) resulted in a direct suppression of predator avoidance behavior (alarm response) by juvenile coho salmon at environmentally relevant dCu exposures (≥2.0 µg/L; 3 hr exposure). Unexposed juveniles (control treatment) reduced their swimming speed on average by 74% (alarm response) in response to an alarm odor (conspecific skin extract). A reduction in swimming speed is a typical predator avoidance response for salmonids and many other fish. In unexposed fish, the alarm odor elicited a mean EOG response of 1.2 mV. Juvenile coho salmon exposed to 2-20 µg/L copper exhibited measurable reductions in both EOG (50–92%) and alarm response (47 to >100%) (derived from data in Figure 2 of Sandahl et al. 2007). Juvenile coho exhibited statistically significant decline in antipredator behavior at 5, 10, and 20 µg/L dCu (Figure 2).

Importantly, concentrations of dCu below 2 µg/L were not tested in Sandahl et al. (2007). This is notable because all concentrations tested (between 2 and 20 µg/L) significantly affected olfaction with reductions in EOG ranging ≈50–92%. Because individual juvenile coho were significantly affected at the lowest concentration tested (2 µg/L), uncertainty remains with respect to the precise threshold for olfactory impairment. The results of this last study provide evidence that juvenile salmon exposed to sublethal dCu concentrations at 2 µg/L (resulting in approximately 50% reductions in EOG), and likely even lower, might not recognize and respond to a predation threat, and therefore have an increased risk of being eaten by other fishes or birds (a form of ecological death, Kruzynski and Birtwell 1994).

Typically dCu concentrations in road runoff are well within the range affecting antipredator behavior, for example, 3.4–64.5 µg/L, with a mean of 15.8 µg/L (Soller et al. 2005). A 3 hour exposure is also likely to be environmentally relevant, as stormwater runoff durations from roads typically range from a few minutes to several hours (Sansalone and Buchberger 1997). Fish may regain their capacity to detect odors fairly quickly in some cases; physiological recovery of olfactory neuron function is dose-dependent and occurs within a few hours at low copper concentrations (i.e., <25 µg/L dCu, Baldwin et al. 2003). However, long-term damage to the sensory epithelia has also been documented. Where cell death occurs (i.e., ≥25 µg/l copper, Hansen et al. 1999a, 1999b) recovery is on the order of weeks (Moran et al. 1992) and in some cases months (Evans and Hara 1985).

Interestingly, another fish sensory system, the lateral line, is also a target for the neurotoxic effects of dCu. It is composed of mechanosensory neurons (hair cells) that respond to surface water vibrations, flow, and other types of mechanical cues in the aquatic environment. The lateral line system thereby mediates shoaling, pursuit of prey, predator avoidance, and rheotaxis (orientation to flow). In a recent study, dCu (i.e., ≥20 µg/L; 3 hour exposure) killed 20% of hair cells in zebrafish (*Danio rerio*) (Linbo et al. 2006). As mentioned earlier, juvenile salmon ORNs may also be killed at higher concentrations of dCu, highlighting the similar sensitivity of olfactory and lateral line receptors to this toxic metal. Consequently, dCu may damage or destroy either or both of these important sensory systems. Currently, we are not aware of any research on the effects of dCu to the lateral line of salmonids, although the comparable sensitivity of the olfactory system across species suggests that the salmon lateral line is likely to be vulnerable as well.

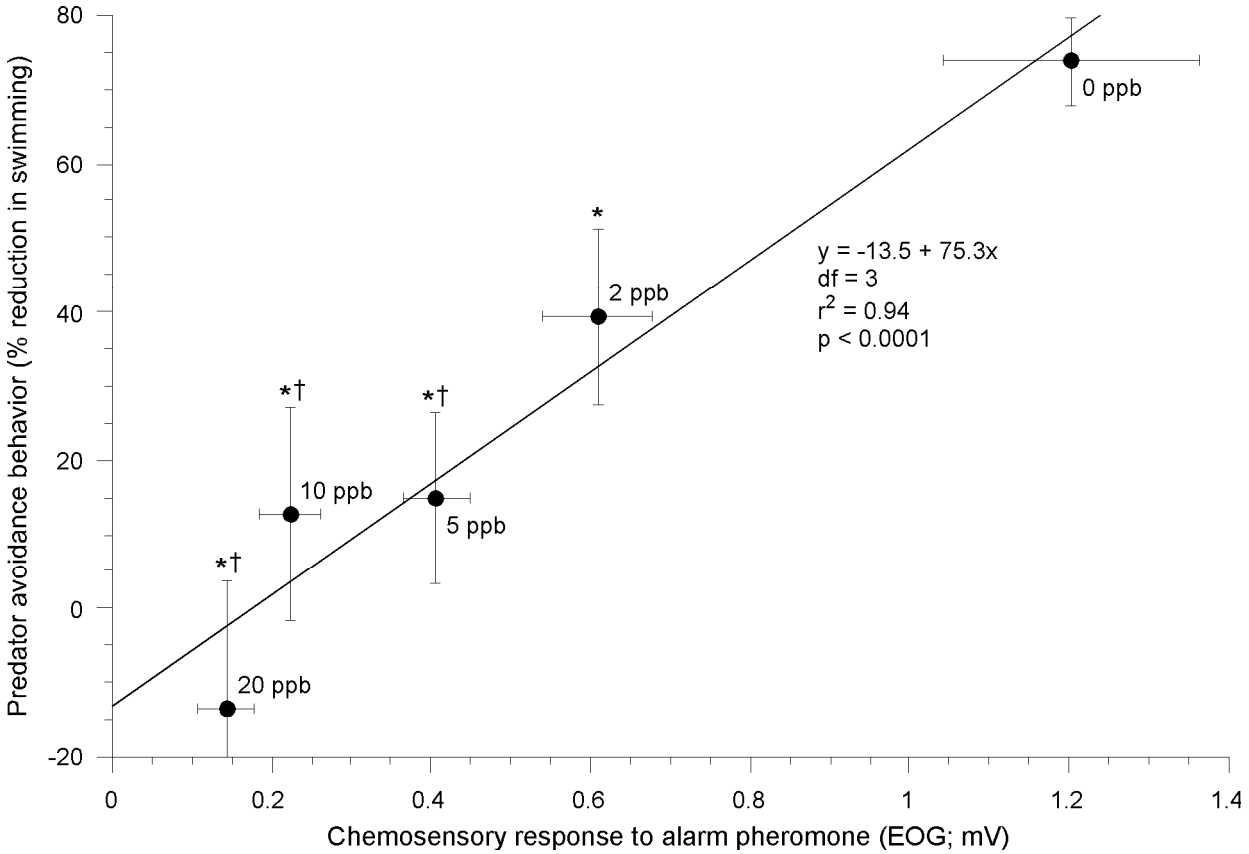

Figure 2. Copper-induced reductions in juvenile salmonid olfactory response and behavior are significantly correlated. Fish exposed to dCu (3 hours) showed reduced olfactory sensitivity and corresponding reduction in predator avoidance behavior. Values represent treatment means (with copper exposure concentration labeled to the right); error bars represent one standard error; n = 8–12 individual coho salmon; asterisk (*) represents a statistically significant difference in olfactory response (EOG data) compared to controls (one-way ANOVA with Dunnett post hoc test, $p < 0.05$); †represents statistically significant difference in behavioral response to skin extract (% reduction in swimming) compared to controls (one-way ANOVA with Dunnett post hoc test, $p < 0.05$). The line represents a statistically significant linear regression based on treatment means (n = 5; $p < 0.0001$; $r^2 = 0.94$). 1 ppb = 1 µg/l. (Adapted from Figure 2C in Sandahl et al. 2007.)

In this paper, a benchmark dose (concentration) analysis (USEPA 1995) is applied to recent data from dose-response experiments on juvenile salmonids exposed to dCu (Sandahl et al. 2007) to determine the exposure concentrations that may adversely affect salmonid sensory systems. In previous studies, benchmark concentrations (BMCs) were determined for olfactory responses, however, concomitant behavioral responses were not measured (Baldwin et al. 2003, Sandahl et al. 2004). The BMC analysis conducted herein determined concentrations of dCu that could be expected to affect juvenile salmonid olfaction and, by extension, alarm response behavior involved in predator avoidance.

Application of the Benchmark Concentration Analysis

The BMC, also referred to as a benchmark dose, is a method that has been used since 1995 by agencies such as the U.S. Environmental Protection Agency (EPA) to determine no observable adverse effect level (NOAEL) values. The method statistically fits dose-response data to determine NOAEL values (EPA 1995). This is in contrast to other methods (e.g., using an analysis of variance) that rely on finding a no observable effect concentration (NOEC) and lowest observable effect concentration (LOEC) to establish the NOAEL. Multiple difficulties arising from the traditional approach of selecting a NOAEL from dose-response data were previously identified by the EPA. Specific shortcomings associated with traditional methods included: 1) arbitrary selection of a NOAEL based on scientific judgments; 2) experiments involving fewer animals produced higher NOAELs; 3) dose-response slopes were largely ignored; and 4) the NOAEL was limited to the doses tested experimentally (EPA 1995). These as well as other concerns with selection of a NOAEL led to the development of an alternative approach, the BMC analysis. The BMC approach uses the complete dose-response data set to identify a NOAEL, thereby selecting an exposure concentration that may not have been tested experimentally.

The BMC is statistically defined as the lower confidence limit for a dose that produces a predetermined adverse effect relative to controls. This effect is referred to as the benchmark response (BMR) (EPA 1995). Unlike the traditional method of selecting the NOAEL (e.g., establishing a NOEC), the BMC takes into account the full range of dose-response data by fitting it with an appropriate regression equation. These can be linear, logarithmic, sigmoidal, etc. The BMR is generally set near the lower limit of responses (e.g., an effect concentration of 10%) that can be measured directly in exposed or affected animals.

In the present context, a BMC approach was used to estimate thresholds for dCu's sublethal effects on the chemosensory physiology and predator avoidance behaviors of juvenile coho salmon (Sandahl et al. 2007). An example of this approach is shown in Figure 3. This methodology has been used previously to determine toxicity thresholds in Pacific salmon (Sandahl and Jenkins 2002, Baldwin et al. 2003, Sandahl et al. 2004). The dose-response relationship for copper's effect on the EOG was described by fitting the data with a sigmoid logistic model:

$$y = m/[1+(x/k)^n]$$

where m is maximum EOG amplitude (fixed at the control mean of 1.2 mV), y is EOG amplitude, x is copper concentration, k is copper concentration at half-maximum EOG amplitude (EC_{50}), and n is slope.

For this nonlinear regression, the average olfactory response of the control fish to a natural odor was used to constrain the maximum odor evoked EOG (m in the above equation). Consequently, the control fish were not used in the regression other than to set m. The regression incorporated the individual response of each exposed fish (n = 44 total) rather than the average values for each exposure group. As shown in Figure 3, the sigmoid logistic model was a very good fit for both the sensory and behavioral data ($r^2 = 0.94$, $p < 0.0001$). Benchmark concentrations were then determined based on the concentration at which the estimated curve intersected benchmark responses.

Results of the Benchmark Concentration Analysis

Examples of benchmark concentrations and responses are presented in Figure 3 and Table 2. The EPA methodology recommends using the concentration that represents a 10% reduction in response compared to controls when limited biological effects data are available (EPA 1995). This is the BMC_{10} and is synonymous with the concentration producing an effect of 10% (EC_{10}), in this case a 10% reduction in the recorded amplitude of the salmon's chemosensory response (EOG). Since the predicted fish EOG response at the BMC_{10} falls well within the olfactory response of unexposed juveniles, that is, 95% CI (control fish, Figure 3), it is more than likely that this individual response (1.08 mV) at the BMC_{10} (0.18 µg/L) would not be detectable or biologically significant as an adverse response.

Other BMCs were derived using statistical criteria to determine benchmark responses. For example, Table 2 shows two BMCs that were determined using the statistical departure of the lower-bound confidence interval (CI) of the control mean (unexposed fish), 1.2 mV (either the 90 or 95% CI). The selection of different CIs results in different BMCs. The CI-derived BMCs represent a reasonable estimate of when an individual salmonid is likely to have a biologically significant reduction in olfaction and a concomitant reduction in predator avoidance behavior. The relative departures from controls in Table 2 are equivalent to effective concentrations for olfactory inhibition, that is, at the lower-bound 90% CI a BMC of 0.59 µg/L equates to a $BMC_{24.2}$. Put another way, the BMC analysis predicts a substantial 24.2 % reduction in olfaction (i.e., EOG amplitude) at 0.59 µg/L dCu. At the lower-bound 95% CI a 29.2% reduction in olfaction is predicted to occur at 0.79 µg/L.

The BMC_{50} is equivalent to the EC_{50} for olfactory responses (2.1 µg/L) and is very similar to the lowest observable effect concentration (LOEC) of 2 µg/L. Since the EC_{50} approximately equals the LOEC, it is almost certain that effects to juvenile salmonid olfaction will occur at lower concentrations than those measured. Therefore it is appropriate and useful to apply a BMC analysis to these data to predict effects occurring between 0 and 2 µg/L dCu. The predicted effect thresholds for sensory responses in juvenile coho salmon ranged 0.18–2.1 µg/L, which corresponded to reductions in predator avoidance behavior (i.e., reduced alarm response) of 8–57%. Comparatively, the other two studies that conducted a BMC approach with salmon olfaction data sets (e.g., EOG measures) estimated dCu BMCs of 3.6–10.7 µg/L (BMC_{20}–BMC_{50}) (Sandahl et al. 2004) and 2.3–3.0 µg/L (BMC_{25}) (Baldwin et al. 2003).

Together these three studies highlight that different experimental conditions including age of fish, exposure duration, and experimental background of dCu may influence BMCs. Importantly, of the three experiments that derived BMCs for olfactory impairment, the data set used in this technical memorandum from Sandahl et al. (2007) empirically linked impaired olfaction to an ecologically relevant behavior, that is, reduced alarm behavior (Figure 2).

Therefore, we believe that the dCu BMC analysis herein is derived from the most ecologically relevant of the three studies.

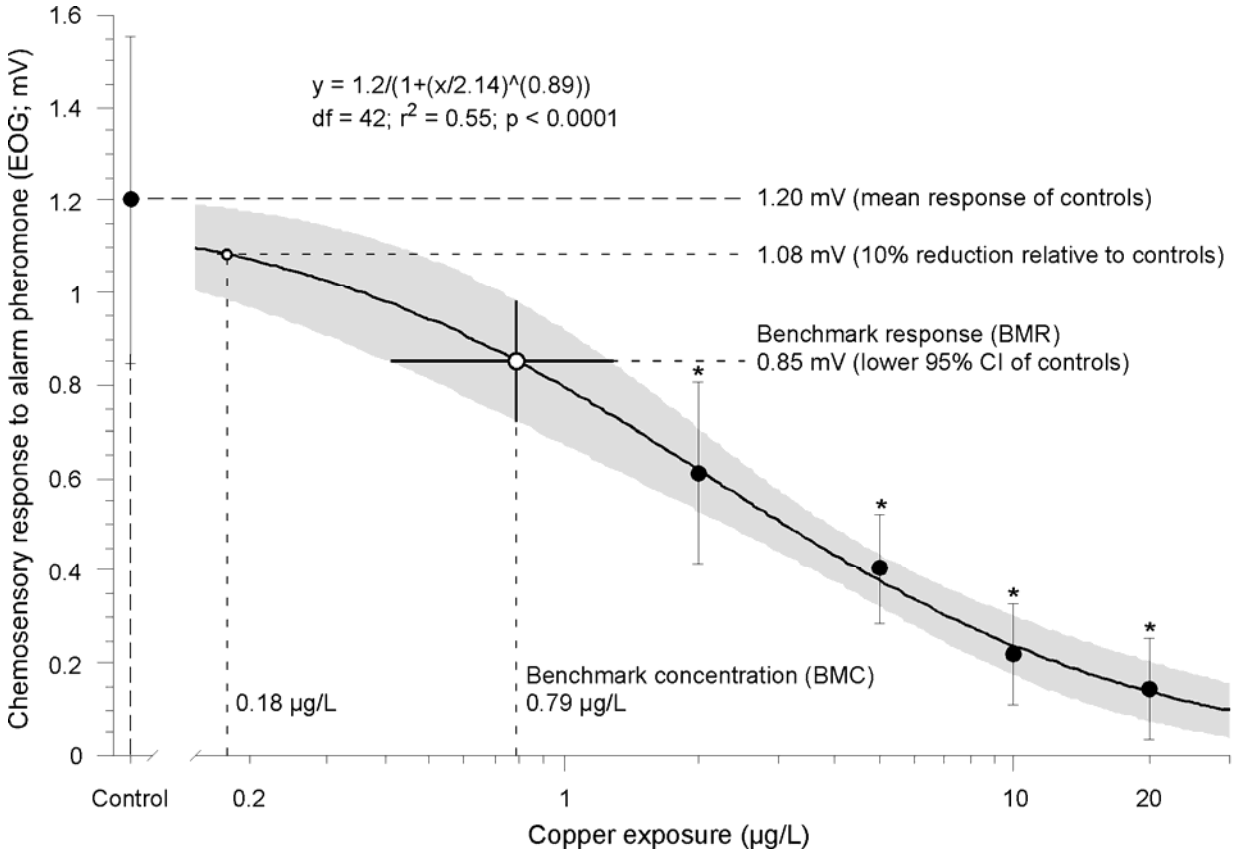

Figure 3. Using a benchmark concentration approach to estimate a threshold for dCu toxicity in the salmonid olfactory system. Filled circles represent treatment means; error bars represent the 95% confidence interval for each mean (n = 8–12 individual coho salmon). An asterisk (*) indicates a statistically significant difference in the size of the olfactory response (EOG data) compared to controls (one-way ANOVA with Dunnett post hoc test, $p < 0.05$). The line represents a statistically significant nonlinear regression based on individual fish (n = 44, $p < 0.0001$, $r^2 = 0.55$). The gray shading shows the 95% confidence band for the nonlinear regression. The regression used a standard sigmoid function with the maximum constrained to the control mean (1.2 mV, indicated by the upper horizontal dashed line). Therefore, the control fish were not included in the nonlinear regression. The lower bound of the 95% confidence interval of the control mean (0.85 mV) is indicated by the lower horizontal dashed line and is an example of a BMR. The large open circle shows where the regression line crosses the BMR and denotes the corresponding BMC, which in this case is a dCu concentration of 0.79 µg/L. Horizontal and vertical lines through the open circle highlight the 95% confidence intervals for the BMC based on the results of the nonlinear regression. The small open circle shows where the regression line crosses the BMR (1.08 mV) and denotes the corresponding BMC_{10} (0.18 µg/L) at which a 10% reduction in olfactory capacity is expected. (Data from Sandahl et al. 2007.)

Table 2. Benchmark responses and benchmark concentrations for juvenile salmon exposed to dCu for 3 hours. Benchmark response values represent a reduction in olfactory response to an alarm pheromone as measured via EOG recordings. Behavioral impairment indicates a predicted decrease in predator recognition and avoidance as indicated by a reduced alarm response. CI = confidence interval; NA = not applicable.

Benchmark responses[a]		**Benchmark concentrations**[b]		**Behavioral impairment (predicted)**[c]
Departure from mean of controls				Departure from mean of controls
Statistical[d] (CI of control mean)	Relative[e] (% reduction in olfactory response)	Value[f] (µg/l)	95% CI[g] (µg/l)	Relative[h] (% reduction in alarm response)
NA	10.0	0.18	0.06–0.52	8.3
Lower 90%	24.2	0.59	0.30–1.16	25.6
Lower 95%	29.2	0.79	0.44–1.42	31.8
NA	50.0	2.10	1.60–2.90	57.2

[a] The predetermined level of altered response or risk at which the benchmark dose (concentration) is calculated (EPA/630/R-94/007, 02/1995).
[b] The dose (concentration) producing a predetermined, altered response for an effect (EPA/630/R-94/007; 02/1995).
[c] Based on the linear regression shown in Figure 2; note behavioral responses were determined by inputting the Benchmark response value (EOG, mV) into the regression equation.
[d] Location of the value with respect to a confidence interval of the mean of the controls.
[e] Amount of reduction in the olfactory response represented by the value relative to the mean of the controls.
[f] Corresponding concentration; see Figure 3 and text for calculation method.
[g] Confidence interval for the value based on the nonlinear regression.
[h] Amount of reduction in alarm response represented by the value relative to the mean of the controls.

Discussion of Site Specific Considerations for Sensory System Effects

Below we identify several issues to consider when using the BMCs to evaluate dCu concentrations under natural conditions.

Impairment from Short-term Increases of dCu

These BMCs reflect expected impairment of chemosensory systems from short-term increases of dCu above ambient concentrations (defined here as < 3 µg/L) (Baldwin et al. 2003, Sandahl et al. 2004, 2007) and are not expected to be alleviated by homeostatic mechanisms. Specifically, the BMCs are predicated on increases of dCu in salmon habitats that result from specific human activities. Effects to juvenile salmonid olfaction are expected following a few minutes of exposure. Salmonids are capable of regulating the amount of internal copper via uptake and elimination processes. These so called homeostatic mechanisms (such as metallothionein induction) can reduce copper's toxic effects and may result in acclimation. Consequently, fish may tolerate certain dCu exposures without showing overt toxicological responses; however, at higher levels these mechanisms could ultimately fail.

Initial evidence indicates that homeostatic mechanisms are not likely to reduce copper toxicity to the olfactory sensory system for pulsed or short-term exposures lasting less than a week (Hansen et al. 1999a) or for chronically exposed fish (McPherson et al. 2004). Moreover, lateral line neurons exposed continuously to dCu for 72 hours showed no signs of acclimation within this exposure interval (Linbo et al. 2006). For other measures of copper toxicity from long-term exposures, evidence suggests that olfactory acclimation may not occur (Table 1, Appendix A). Fish exposed to higher dCu concentrations for longer periods may lose much of their olfactory function. For example, field evidence suggests that wild fish living in heavy metal contaminated lakes where total copper concentrations ranged 9.7–15 µg/L showed reduced olfactory-mediated predator avoidance behavior; that is, homeostatic mechanisms appeared insufficient to alleviate metal toxicity, including copper (McPherson et al. 2004).

Calculating an Acute Criterion Maximum Concentration

The EPA sets acute water quality criteria by calculating an acute criterion maximum concentration (CMC) (Stephan et al. 1985). The CMC is an estimate of the highest concentration of a substance in surface water to which an aquatic community can be exposed briefly without resulting in an unacceptable effect (EPA 2002).We calculated an acute CMC using the Biotic Ligand Model (BLM) (EPA 2007). Interestingly, the estimated acute CMC based on the BLM using measured and estimated water quality parameters from Sandahl et. al. (2007) was 0.63 µg/L with a range from 0.34 to 3.2 µg/L, while the EPA hardness-based acute CMC (EPA 2002) was 6.7 µg/L. Because the BLM-based acute criterion is sensitive to pH and

DOC, the range of measured test pH values (6.5–7.1) and the range of estimated DOC values (0.3–1.5 mg/L) produced this range of BLM-based acute criterion values. It is also interesting that the acute CMC range (0.34–3.2 µg/L) overlapped with the olfactory-based BMC range (0.18–2.1 µg/L).

Salmonids Are Typically Exposed to Multiple Stressors

These BMCs are specifically focused on the impact of dissolved copper alone on olfaction and predator avoidance behavior. Salmonids are rarely exposed to dCu only under natural conditions. In fact, exposure to complex environmental mixtures of other toxic compounds (e.g., metals, pesticides, PAHs, etc.) in conjunction with other stressors (e.g., elevated temperatures, low dissolved oxygen, etc.,) is the norm for many salmonid-bearing habitats. Equally important are exposure routes other than the water column, such as consumption of contaminated prey items (dietary) or direct contact with contaminated sediments. Threshold examples (BMCs) presented here are based solely on juvenile salmonids exposed to dCu. Presently, these thresholds do not take into account multiple routes of exposure or the potential impacts of complex mixtures of contaminants on olfaction. That said, several studies have shown a greater than expected toxicity (i.e., nonadditive) to other fish endpoints from mixtures of metals (Sprague et al. 1965, Norwood et al. 2003). For example, mixtures containing zinc and copper were found to have greater than additive toxicity to a wide variety of aquatic organisms including freshwater fish (Eisler 1998). Other metal mixtures also yielded greater than additive toxic effects at low dissolved concentrations (Playle 2004). The toxic effects of metals to salmonids may also be exacerbated by other types of contaminants such as pesticides (Forget et al. 1999). While interactions among multiple stressors, including contaminant mixtures, are beyond the scope of this document, they warrant careful consideration in site-specific assessments.

Bioavailability of dCu

These BMCs were derived from experiments using a single freshwater source (dechlorinated, soft municipal water). Hardness, alkalinity, and dissolved organic carbon (DOC) are known to alter the bioavailability of dissolved copper in surface waters to ligands in the fish gill. These water chemistry parameters can therefore influence the potential for dCu exposure in the field to cause an acute fish kill. Acute copper lethality mediated via the gill route of exposure is typically estimated using the Biotic Ligand Model (BLM; reviewed by Niyogi and Wood 2004). However, recent unpublished research by McIntyre et al. (in press) suggest that these parameters may have less of an influence on salmonid olfactory function across environmentally realistic ranges of hardness, alkalinity, and DOC.

To date, the U.S. Geological Survey (USGS) has monitored hardness, alkalinity, and DOC for more than 10 years in many West Coast river basins including the Willamette River basin, Puget Sound basin, Yakima River basin, and the Sacramento-San Joaquin River basin (USGS no date). Several at-risk species of anadromous salmonids inhabit these basins. The monitoring data indicate that surface waters within these basins typically have very low hardness and alkalinity and seasonally affected DOC concentrations. Hardness, alkalinity, and DOC levels found in most freshwater habitats occupied by Pacific salmonids would be unlikely to

confer substantial protection against dCu olfactory toxicity (Winberg et al. 1992, Bjerselius et al. 1993, Baldwin et al. 2003, McIntyre et al. in press).

Recent experimental results suggest that significant amelioration of olfactory toxicity due to hardness is unlikely in typical Pacific salmonid freshwater habitats. The experiment showed that hardness at 20, 120, and 240 mg/L Ca (experimentally introduced as $CaCl_2$) did not significantly protect juvenile coho salmon from olfactory toxicity following 30 minute laboratory exposures to 10 µg dCu/L above an experimental background of 3 µg/L (Baldwin et al. 2003). In another experiment, a 20 µg dCu/L exposure (30 minutes) in water with low hardness and alkalinity and no DOC produced an 82% inhibition in juvenile coho olfactory function (McIntyre et al. in press). A hardness of ≥82 mg/L Ca was needed to reduce the level of olfactory inhibition to ≤50% at 20 µg/L dCu (McIntyre et al. in press). However, 82 mg/L was never exceeded in any of the surface water samples from USGS-sampled NAWQA basins (McIntyre et al. in press).

Typical alkalinity values from Pacific Northwest and California freshwater surface waters are also unlikely to protect salmonids from olfactory toxicity (USGS no date). Some reduction in dCu olfactory toxicity was observed in a recent study (McIntyre et al. in press). However, only 0.4% of stream samples contained alkalinity levels sufficient to reduce olfactory toxicity of dCu by half (McIntyre et al. in press). Bjerselius et al. (1993) and Winberg et al. (1992) also found that hardness and alkalinity provided limited amelioration of olfactory responses in juvenile Atlantic salmon exposed to dCu.

Increases in DOC showed greater protection to dCu compared to increases in alkalinity and hardness. Twenty-nine percent of USGS surface water samples from West Coast basins had a DOC concentration sufficient to limit olfactory impairment to 50% or less at 20 µg dCu /L (McIntyre et al. in press). Only a small fraction (6%) of all samples contained DOC levels (greater or equal to 6 mg/L) sufficient to completely protect the olfactory responses of juvenile coho salmon from the toxic effect of 20 µg dCu /L (McIntyre et al. in press). This information underscores the importance of evaluating site-specific DOC data to address the potential influence of this water quality parameter on olfactory toxicity.

Because the typical range of hardness, alkalinity, and DOC concentrations are unlikely to confer substantial protection against dCu toxicity, we expect that the BMC thresholds presented in this document will be applicable for most of the freshwater environments that provide migrating, spawning, and rearing habitats for salmonids.

Olfactory Toxicity in Saltwater

Dissolved copper's effect on salmonid olfaction in saltwater environments remains a recognized data gap and it is presently uncertain whether the BMC thresholds derived in this document apply to salt water environments. Estuarine and nearshore salt water environments, despite their higher salinity (in part due to increased cation concentrations) and hardness may or may not confer protection against dCu-induced olfactory toxicity. One source of this uncertainty is whether or not free copper (Cu^{2+}) is the sole species of copper responsible for olfactory toxicity. In freshwater, evidence suggests that Cu^{2+} is not the only toxic species that adversely affects olfaction in fish (McIntyre et al. in press) as well as more conventional endpoints such as

mortality (Niyogi and Wood 2004). Other copper species (e.g., CuOH; Cu^{1+}) will also bind to the gill, thereby causing toxicity (Niyogi and Wood 2004). While the physiological basis for salmonid olfaction is well characterized, the transition to saltwater may involve important changes in olfactory receptor neuron function that ultimately influence the expression of the as yet unidentified ligands for dCu.

Avoiding Short-term Increases in dCu

Salmonids may or may not avoid short-term increases in dCu. Salmonids will actively avoid water containing dCu if they can detect it. As a consequence, fish may not use otherwise high quality rearing and spawning habitats. In addition, the presence of dCu may affect migratory routes of juveniles and adults. Smith and Bailey (1990) and Mebane (2000) derived regulatory "zones of passage" around wastewater discharges that were based on salmonid avoidance responses. However, in areas with diffuse, nonpoint source pollution, or multiple point source discharges, it may be difficult to apply "zones of passage", and in some cases available zones of passage may not exist. Despite a fish's preference to avoid dCu, circumstances may force migrating juveniles and adults to be exposed. For dCu contaminated, high quality rearing habitats, juveniles could either remain and be exposed or move to lower quality habitats. Juveniles could therefore suffer either reduced predator avoidance or reduced growth. For contaminated spawning habitats, adult salmon may either remain and be exposed as well as their offspring or move to lower quality habitats. Both of these scenarios result in potential reductions in reproductive success.

Coho Salmon–derived BMCs Should Apply to Other Salmonids

These BMCs were derived using data from juvenile coho salmon, but should apply to other fish species. The examples of BMC thresholds were derived from data based on juvenile coho salmon (4–5 month old, mean of 0.9 grams wet weight). However, we expect these BMC examples to be generally applicable to other species of salmon, trout, and steelhead in freshwater habitats. For example, 3 hour exposures of 4-month-old steelhead to a similar range of dCu produced comparable olfactory toxicity to that reported for 4-month-old coho salmon (Baldwin et al. in prep.). Studies on 10-month-old juvenile coho had similar reductions in olfaction compared to 4-month-old fish (Baldwin et al. 2003, Sandahl et al. 2004). Juvenile chum salmon (*O. keta)* (2–3 month old) also showed a dose dependent reduction in EOG amplitude following exposure to dCu (3–58 µg/L) (Sandahl et al. 2006). Taken together these findings suggest that the BMC threshold derived herein should be applicable to juvenile life stages of coho, Chinook, sockeye (*O. nerka)*, and pink salmon (*O. gorbuscha*) as well as steelhead, bull trout (*Salvelinus confluentus*), and other members of the family Salmonidae. As noted earlier, the toxicity of dCu to other life stages (particularly marine phases of life) remains to be determined.

Conclusions

Dissolved copper (dCu) is a ubiquitous, bioavailable pollutant that can directly interfere with fish sensory systems and by extension important behaviors that underlie predator avoidance, juvenile growth, and migratory success (see Appendix A). Recent research shows that dCu not only impairs sensory neurons in a salmonid's nose, but also impairs juvenile salmonids' ability to detect and respond to predation cues. A juvenile salmonid with disrupted predator avoidance behaviors stands a greater risk of mortality and by extension a reduction in the likelihood of surviving to reproduce. The degree to which effects on individual behavior and survival impact a given population will depend in part on the number of the individuals affected and the status of the population (numbers, distribution, growth rate, etc.).

In this report, BMCs were calculated using an EPA methodology to provide examples of effect thresholds of dCu's impacts on salmonid sensory biology and behavior. The BMC examples represent increases in the dCu concentration above background or ambient levels (where background is less than or equal to 3 µg/L) expected to affect juvenile salmonid ability to avoid predators in fresh water. Benchmark concentrations ranged 0.18–2.1 µg/L, corresponding to reductions in predator avoidance behavior (alarm reaction) that ranged approximately 8–57%. Taking into account the olfactory responses of unexposed fish, a more biologically relevant range of BMCs is 0.59–2.1 µg/L (Table 2). This second range of BMC thresholds is similar to or slightly less than documented effects to other copper-affected sublethal endpoints such as behavior and growth that range 0.75–2.5 µg/L (see Table 1).

The primary objective of this report was to present examples of threshold concentrations for effects of dCu on a critical aspect of salmonid biology: olfaction. A secondary objective of this paper was to summarize a selection of recent and historical information related to the effects of dCu on salmonid sensory systems. This document is based on the current state of the science. Importantly, this overview is not a comprehensive summary of the myriad effects of copper to anadromous salmonids. As such, new information will undoubtedly become available that enhances our understanding of copper's effect on salmonid populations and their supporting habitats. The information reviewed and presented herein indicates that significant impairment of sensory functions important to survival of threatened and endangered juvenile salmonids is likely to be widespread in many freshwater aquatic habitats. Impairment of these essential behaviors may occur following 10 minutes of exposure and continue for hours to weeks depending on concentration and duration.

Glossary

Acute exposure. Short-term continuous exposure usually lasting 96 hours or less.

BLM. Biotic Ligand Model

Chronic exposure. Longer-term continuous or pulsed exposures generally lasting greater than 96 hours.

Confidence interval (CI). A random interval constructed from data in such a way that the probability that the interval contains the true value can be specified before the data are collected.

dCu. dissolved copper.

DOC. dissolved organic carbon.

EC_p. Effective concentration adversely affecting (p) percent of the test population or percent of measured response, for example, 10% for an EC_{10} and so forth.

EOG. electro-olfactogram.

LC_{50}. The aqueous concentration of a substance that kills 50% of the test population.

Lower-bound 90% confidence interval. The lower half of the 90% confidence interval of the mean.

Lower-bound 95% confidence interval. The lower half of the 95% confidence interval of the mean.

LOEC. lowest observable effect concentration.

Mean. The average of the response values in a treatment population. Numerically the mean represents the sum of the individual response values divided by the number of individuals in a treatment.

mV. millivolts.

NOAEL. no observable adverse effect level.

NOEC. no observable effect concentration.

ORN. olfactory receptor neuron.

ppb. part(s) per billion, equivalent to µg/L.

Relative departure from control response. A user selected level of response compared to control response; for example, a 10% reduction from the control response (unexposed individuals).

Statistical departure from control response. Uses statistical methods to select a response based on the distribution of responses seen in unexposed individuals. For example, the 95% lower bound confidence interval of the mean response from controls (unexposed individuals).

References

Alpers, C. N., R. C. Antweiler, H. E. Taylor, P. D. Dileanis, and J. L. Domagalski. 2000. Metals transport in the Sacramento River, California, 1996–1997, Volume 2: Interpretation of metal loads. U.S. Geological Survey water resources investigation report 2000–4002.

Baldwin, D. H., J. F. Sandahl, J. S. Labenia, and N. L. Scholz. 2003. Sublethal effects of copper on coho salmon: Impacts on nonoverlapping receptor pathways in the peripheral olfactory nervous system. Environ. Toxicol. Chem. 22:2266–2274.

Baldwin, D. H., and N. L. Scholz. 2005. The electro-olfactogram: An in vivo measure of peripheral olfactory function and sublethal neurotoxicity in fish. *In* G. K. Ostrander (ed.), Techniques in aquatic toxicology, Volume 2, p. 257–276. CRC Press, Inc., Boca Raton, FL.

Baldwin, D.H., C. Tatara, and N.L. Scholz. In prep. Olfactory sensitivity and copper toxicity in steelhead salmon raised in natural and hatchery environments. (Available from D. Baldwin, NWFSC, 2725 Montlake Blvd. E., Seattle, WA 98112.)

Bjerselius, R., S. Winberg, Y. Winberg, and K. Zeipel. 1993. Ca2+ protects olfactory receptor function against acute Cu(II) toxicity in Atlantic salmon. Aquat. Toxicol. 25:125–138.

Chapman, G. A. 1978. Toxicities of cadmium, copper, and zinc to four juvenile stages of Chinook salmon and steelhead. Trans. Am. Fish. Soc. 107:841–847.

Chapman, G. A. 1982. Chinook salmon early life stage tests with cadmium, copper, and zinc. Letter of December 6, 1982 to Charles Stephan, EPA Environmental Research Laboratory, Duluth. Environmental Protection Agency, Corvallis, Oregon. Online at http://www.epa.gov/ow/docket.html [accessed 27 September 2007].

Chapman, G. A. Unpubl. data. Acclimation, life stage differences in lethality and behavioral effects of chronic copper exposures with steelhead. Letter of July 5, 1994 to Chris Mebane, NOAA liaison to EPA Region 10, Seattle, WA. (Available from EPA Coastal Ecosystems Team, Newport, OR.)

Chapman, G. A., and D. G. Stevens. 1978. Acutely lethal levels of cadmium, copper, and zinc to adult male coho salmon and steelhead. Trans. Am. Fish. Soc. 107:837–840.

Damkaer, D. M., and D. B. Dey. 1989. Evidence of fluoride effects on salmon passage at John Day Dam, Columbia River, 1982–1986. N. Am. J. Fish. Manag. 9:154–168.

Drapper, D., R. Tomlinson, and P. Williams. 2000. Pollutant concentrations in road runoff: Southeast Queensland case study. J. Environ. Eng.-ASCE 126:313–320.

Eisler, R. 1998. Copper hazards to fish, wildlife, and invertebrates: A synoptic review. U.S. Geological Survey, Biological Resources Division, Biological science report USGS/BRD/BSR-1997-0002.

EPA (U.S. Environmental Protection Agency). 1995. The use of the benchmark dose approach in health risk assessment. EPA/630/R-694/007. Office of Research and Development, Washington, DC.

EPA (U.S. Environmental Protection Agency). 2002. National recommended water quality criteria. EPA-822-R-02-047. Environmental Protection Agency, Washington, DC.

EPA (U.S. Environmental Protection Agency). 2005. Ecological risk assessment for re-registration copper-containing pesticides (Case#0636 copper sulfate, Case#0649 Group II copper compounds, Case#4029 copper salts, and Case#4025 copper and oxides (Cuprous oxide)). Screening level risk assessment. Environmental Protection Agency, Office of Pesticide Programs, Washington, DC.

EPA (U.S. Environmental Protection Agency). 2007. Aquatic life ambient freshwater quality criteria - copper, 2007 revision. EPA-822-R-07-001. Environmental Protection Agency, Office of Water, Office of Science and Technology, Washington, DC.

Evans, R. E., and T. J. Hara. 1985. The characteristics of the electro-olfactogram (EOG): Its loss and recovery following olfactory nerve section in rainbow trout (*Salmo gairdneri*). Brain Res. 330:65–75.

Farag, A. M., C. J. Boese, D. F. Woodward, and H. L. Bergman. 1994. Physiological changes and tissue metal accumulations of rainbow trout exposed to foodborne and waterborne metals. Environ. Toxicol. Chem. 13:2021–2030.

Farag, A. M., D. Skaar, D. A. Nimick, E. MacConnell, and C. Hogstrand. 2003. Characterizing aquatic health using salmonid mortality, physiology, and biomass estimates in streams with elevated concentrations of arsenic, cadmium, copper, lead, and zinc in the Boulder River watershed, Montana. Trans. Am. Fish. Soc. 132:450–467.

Folmar, L. C. 1976. Overt avoidance reaction of rainbow trout fry to nine herbicides. Bull. Environ. Contam. Toxicol. 15:509–514.

Forget, J., J. Pavillon, B. Beliaeff, and G. Bocquene. 1999. Joint action of pollutant combinations (Pesticides and metals) on survival (LC50 values) and acetylcholinesterase activity of *Tigriopus Brevicornis* (Coperpoda, Harpacticoida). Environ. Toxicol. Chem. 18:912–918.

Giattina, J. D., R. R. Garton, and D. G. Stevens. 1982. The avoidance of copper and nickel by rainbow trout as monitored by a computer-based aquisition system. Trans. Am. Fish. Soc. 111:491–504.

Good, J. C. 1993. Roof runoff as a diffuse source of metals and aquatic toxicity in storm water. Water Sci. Technol. 28:317–321.

Hansen, J. A., J. C. A. Marr, J. Lipton, D. Cacela, and H. L. Bergman. 1999a. Differences in neurobehavioral responses of Chinook salmon (*Oncorhynchus tshawytscha*) and rainbow trout (*Oncorhynchus mykiss*) exposed to copper and cobalt: Behavioral avoidance. Environ. Toxicol. Chem. 18:1972–1978.

Hansen, J. A., J. D. Rose, R. A. Jenkins, K. G. Gerow, and H. L. Bergman. 1999b. Chinook salmon (*Oncorhynchus tshawytscha*) and rainbow trout (*Oncorhynchus mykiss*) exposed to copper: Neurophysiological and histological effects on the olfactory system. Environ. Toxicol. Chem. 18:1979–1991.

Hartwell, S. I., D. S. Cherry, and J. J. Cairns. 1987. Field validation of avoidance of elevated metals by fathead minnows (*Pimephales promelas*) following in situ acclimation. Environ. Toxicol. Chem. 6:189–200.

Korver, R. M., and J. B. Sprague. 1989. Zinc avoidance by fathead minnows: Computerized tracking and greater ecological significance. Can. J. Fish. Aquat. Sci. 46:494–502.

Kruzynski, G. M., and I. K. Birtwell. 1994. A predation bioassay to quantify the ecological significance of sublethal responses of juvenile Chinook salmon (*Oncoryhynchus tshawytscha*) to the antisapstain fungicide TCMTB. Can. J. Fish. Aquat. Sci. 51:1780–1790.

Leland, H. V., and J. L. Carter. 1985. Effects of copper on production of periphyton, nitrogen-fixation and processing of leaf litter in a Sierra-Nevada, California, stream. Freshw. Biol. 15:155–173.

Leland, H. V., S. V. Fend, T. L. Dudley, and J. L. Carter. 1989. Effects of copper on species composition of benthic insects in a Sierra-Nevada, California, stream. Freshw. Biol. 21:163–179.

Linbo, A. O., C. M. Stehr, J. P. Incardona, and N. L. Scholz. 2006. Dissolved copper triggers cell death in the peripheral mechanosensory system of larval fish. Environ. Toxicol. Chem. 25:597–603.

Lorz, H. W., and B. P. McPherson. 1976. Effects of copper or zinc in freshwater on the adaptation to sea water and ATPase activity, and the effects of copper on migratory disposition of the coho salmon (*Oncorhynchus kisutch*). J. Fish. Res. Board Can. 33:2023–2030.

Lorz, H. W., and B. P. McPherson. 1977. Effects of copper and zinc on smoltification of coho salmon. EPA 600/3-77-032. Oregon Department of Fish and Wildlife and U.S. EPA Environmental Research Laboratory, Corvallis, OR.

Lorz, H. W., R. H. Williams, and C. A. Futish. 1978. Effects of several metals on smolting of coho salmon. EPA 600/3-78-090. Oregon Department of Fish and Wildlife and U.S. EPA Environmental Research Laboratory, Corvallis, OR.

Marr, J. C. A., J. Lipton, D. Cacela, M. G. Barron, D. J. Beltman, C. Cors, K. LeJune, A. S. Maest, T. L. Podrabsky, H. L. Bergman, J. A. Hansen, J. S. Meyer, and R. K. MacRae. 1995. Fisheries toxicity injury studies, Blackbird Mine site, Idaho. Contract 50-DGNC-1-00007, task order 50084. Prepared by RCG/Hagler Bailly and the University of Wyoming for NOAA, Boulder, CO, and Laramie, WY.

Marr, J. C. A., J. Lipton, D. Cacela, J. A. Hansen, H. L. Bergman, J. S. Meyer, and C. Hogstrand. 1996. Relationship between copper exposure duration, tissue copper concentration, and rainbow trout growth. Aquat. Toxicol. 36:17–30.

Marr, J. C. A., J. Lipton, D. Cacela, J. A. Hansen, J. S. Meyer, and H. L. Bergman. 1999. Bioavailability and acute toxicity of copper to rainbow trout (*Oncorhynchus mykiss*) in the presence of organic acids simulating natural dissolved organic carbon. Can. J. Fish. Aquat. Sci. 56:1471–1483.

McIntyre, J. K., D. H. Baldwin, J. P. Meador, and N. L. Scholz. In press. Chemosensory deprivation in juvenile coho salmon exposed to dissolved copper under varying water chemistry conditions. Environ. Sci. Technol.

McKim, J. M. 1985. Early life stage toxicity tests. *In* G. M. Rand and S. R. Petrocelli (eds.), Fundamentals of aquatic toxicology: Methods and applications, p. 58–95. Hemisphere Publishing, New York.

McKim, J. M., and D. A. Benoit. 1971. Effects of long-term exposure to copper on survival, growth, and reproduction of brook trout (*Salvelinus fontinalis*). J. Fish. Res. Board Can. 28:655–662.

McPherson, T. D., R. S. Mirza, and G. G. Pyle. 2004. Responses of wild fishes to alarm chemicals in pristine and metal-contaminated lakes. Can. J. Zool. 82:604–700.

Mebane, C. A. 1994. Blackbird Mine preliminary natural resource survey. NOAA, Hazardous Material Assessment and Response Division, Seattle, WA.

Mebane, C. A. 2000. Evaluation of proposed new point source discharges to a special resource water and mixing zone determinations: Thompson Creek Mine, upper Salmon River subbasin, Idaho. Idaho Department of Environmental Quality, Boise, ID.

Meyer, J. S. 2005. Toxicity of dietborne metals to aquatic organisms. Society of Environmental Toxicology and Chemistry, Pensacola, FL.

Moran, D. T., J. C. Rowley, G. R. Aiken, and B. W. Jafek. 1992. Ultrastructural neurobiology of the olfactory mucosa of the brown trout, *Salmo trutta*. Microscopy Res. Tech. 23:28–48

Mudge, J. E., T.E. Northstrom, G.S. Jeane, W. Davis, and J. L. Hickam. 1993. Effect of varying environmental conditions on the toxicity of copper to salmon. *In* J. W. Gorsuch, F. J. Dwyer, C. G. Ingersoll, and T. W. La Point, (eds.), Environmental toxicology and risk assessment, ASTM STP 1216, p. 19–33. American Society for Testing and Materials, Philadelphia, PA.

Niyogi, S., and C. M. Wood. 2004. Biotic ligand model, a flexible tool for developing site-specific water quality guidelines for metal. Environ. Sci. Technol. 38:6177–6192.

Norwood, W. P., U. Borgmann, D. G. Dixon, and A. Wallace. 2003. Effects of metal mixtures on aquatic biota: A review of observations and methods. Hum. Ecol. Risk Assess. 9:795–811.

Playle, R. C. 2004. Using multiple metal-gill binding models and the toxic unit concept to help reconcile multiple-metal toxicity results. Aquat. Toxicol. 67:359–370.

Sandahl, J. F., D. H. Baldwin, J. J. Jenkins, and N. L. Scholz. 2004. Odor-evoked field potentials as indicators of sublethal neurotoxicity in juvenile coho salmon (*Oncorhynchus kisutch*) exposed to copper, chlorpyrifos, or esfenvalerate. Can. J. Fish. Aquat. Sci. 61:404–413.

Sandahl, J. F., D. H. Baldwin, J. J. Jenkins, and N. L. Scholz. 2007. A sensory system at the interface between urban storm water runoff and salmon survival. Environ. Sci. Technol. 41:2998–3004.

Sandahl, J. F., and J. J. Jenkins. 2002. Pacific steelhead (*Oncorhynchus mykiss*) exposed to chlorpyrifos: Benchmark concentration estimates for acetylcholinesterase inhibition. Environ. Toxicol. Chem. 21:2452–2458.

Sandahl, J. F., G. Miyasaka, N. Koide, and H. Ueda. 2006. Olfactory inhibition and recovery in chum salmon (*Oncorhynchus keta*) following copper exposure. Can. J. Fish. Aquat. Sci. 63:1840–1847.

Sansalone, J. J., and S. G. Buchberger. 1997. Partitioning and first flush of metals in urban roadway storm water. J. Environ. Monit. 123:134–143.

Saucier, D., L. Astic, and P. Rioux. 1991. The effects of early chronic exposure to sublethal copper on the olfactory discrimination of rainbow trout, *Oncorhynchus mykiss*. Environ. Biol. Fishes 30:345–351.

Saunders, R. L., and J. B. Sprague. 1967. Effects of copper-zinc mining pollution on a spawning migration of Atlantic salmon. Water Res. 1:419–432.

Scherer, E., and R. E. McNoil. 1998. Preference-avoidance responses of lake whitefish (*Coregonus clupeaformis*) to competing gradients of light and copper, lead, and zinc. Water Res. 32:494–502.

Schreck, C. B., and H. W. Lorz. 1978. Stress response of coho salmon (*Oncorhynchus kisutch*) elicited by cadmium and copper and potential use of cortisol as an indicator of stress. J. Fish. Res. Board Can. 35:1124–1129.

Scott, J. W., and P. E. Scott-Johnson. 2002. The electroolfactogram: A review of its history and uses. Microscopy Res. Tech. 58:152–160.

Seim, W. K., L. R. Curtis, S. W. Glenn, and G. A. Chapman. 1984. Growth and survival of developing steelhead trout (*Salmo gairdneri*) continuously or intermittently exposed to copper. Can. J. Fish. Aquat. Sci. 41:433–438.

Smith, E. H., and H. C. Bailey. 1990. Preference/avoidance testing of waste discharges on anadromous fish. Environ. Toxicol. Chem. 9:77–86.

Soller, J., J. Stephenson, K. Olivieri, J. Downing, and A. W. Olivieri. 2005. Evaluation of seasonal scale first flush pollutant loading and implications for urban runoff management. J. Environ. Manag. 76:309–318.

Sorensen, E. M. B. 1991. Chapter VII: Copper. *In* E. M. B. Sorensen (ed.), Metal poisoning in fish, p. 235–284. CRC Press, Boca Raton, FL.

Sprague, J., P. Elson, and R. Saunders. 1965. Sublethal copper-zinc pollution in a salmon river—A field and laboratory study. Int. J. Air Water Pollut. 9:531–543.

Stephan, C. E., D. I. Mount, J. A. Hansen, J. H. Gentile, G. A. Chapman, and W. A. Brungs. 1985. Guidelines for deriving numerical national water quality criteria for the protection of aquatic organisms and their uses. National Technical Information Service, Springfield, VA.

Stevens, D. G. 1977. Survival and immune response of coho salmon exposed to copper. EPA 600/3-77-031. U.S. EPA Environmental Research Laboratory, Corvallis, OR.

Sutterlin, A., and R. Gray. 1973. Chemical basis for homing of Atlantic salmon (*Salmo salar*) to a hatchery. J. Fish. Res. Board Can. 30:985–989.

Thomas, P. R., and G. R. Greene. 1993. Rainwater quality from different roof catchments. Water Sci. Technol. 28:291–299.

USGS (U.S. Geological Survey). No date. National Water Information System databases. Online at http://waterdata.usgs.gov/nwis [accessed 27 September 2007].

Waiwood, K. G., and F. W. H. Beamish. 1978a. The effect of copper, hardness, and pH on the growth of rainbow trout, *Salmo gairdneri*. J. Fish Biol. 13:591–598.

Waiwood, K. G., and F. W. H. Beamish. 1978b. Effects of copper, pH, and hardness on the critical swimming performance of rainbow trout (*Salmo gairdneri*). Water Res. 12:611–619.

Wheeler, A. P., P. L. Angermeier, and A. E. Rosenberger. 2005. Impacts of new highways and subsequent landscape urbanization on stream habitat and biota. Rev. Fish. Sci. 13:141–164.

Winberg, S., R. Bjerselius, E. Baatrup, and K. B. Doving. 1992. The effect of Cu(II) on the electro-olfactogram (EOG) of the Atlantic salmon (*Salmo salar L.*) in artificial freshwater of varying inorganic carbon concentrations. Ecotoxicol. Environ. Saf. 24:167–178.

Appendix A:
Other Salmonid Sensory Effects of dCu

In this appendix, results are highlighted from several studies that we thought were particularly relevant, including comparing the concentrations that have caused sensory effects to concentrations causing lethality or growth reductions in field and laboratory experiments. As such, the following review is not an exhaustive summary of copper's adverse effects to anadromous salmonids. We emphasize studies that were conducted in waters with low alkalinity and hardness (<50 mg/L as calcium carbonate), and if reported, low concentrations of dissolved organic material. These conditions were emphasized since we believe these are the most relevant water quality conditions for an area of particular concern to us—freshwater habitats used by juvenile salmonids in the Pacific Northwest and California.

Migratory Disruption

Laboratory and field experiments with salmonids have shown avoidance of low concentrations of copper, disruption of downstream migration by juvenile salmonids, loss of homing ability, and loss of avoidance response to even acutely lethal concentrations of copper following long-term habituation to low level copper exposure. Saucier et al. (1991) examined the impact of a long-term sublethal copper exposure (22 µg/L, 37–41 weeks in duration) on the olfactory discrimination performance in rainbow trout (*Oncorhynchus mykiss*). When controls were given a choice between their own rearing water or other waters, they significantly preferred their own rearing water, whereas both copper-exposed groups showed no preference. They concluded that their results demonstrate that a long-term sublethal exposure to copper, as it commonly occurs under "natural" conditions, may result in olfactory dysfunction with potential impacts on fish survival and reproduction.

Field studies have reported that copper impairs both upstream spawning migration of salmonids and downstream outmigration of juveniles. Avoidance of copper in the wild has been demonstrated to delay upstream passage of Atlantic salmon (*Salmo salar*) moving past copper-contaminated reaches of the river to their upstream spawning grounds, cause unnatural downstream movement by adults away from the spawning grounds, and increase straying from their contaminated home stream into uncontaminated tributaries. Avoidance thresholds in the wild of 0.35 to 0.43 toxic units were about seven times higher than laboratory avoidance thresholds (0.05 toxic units), perhaps because the laboratory tests used juvenile fish rather than more motivated spawning adults. For this study 1.0 toxic unit was defined as an incipient lethal level (ILL, essentially a time independent LC_{50}), of 48 µg/L in soft water (Sprague et al. 1965, Saunders and Sprague 1967). Studies of home water selection with returning adult salmon showed that addition of 44 µg/L copper to their home water reduced the selection of their home stream by 90% (Sutterlin and Gray 1973). Releases of about 20 µg/L from a mine drainage into a salmon spawning river resulted in 10–22% repulsion of ascending salmon during four consecutive years compared to 1–2% prior to mining (Sutterlin and Gray 1973). The upstream

spawning migration of Chinook salmon (*O. tshawytscha*) in Panther Creek, Idaho, may have been interrupted during the 1980s and early 1990s when the fish encountered dCu concentrations of 10–25 µg/L. In Panther Creek, the majority of spawning habitat and historical locations of Chinook salmon spawning were high in the watershed, upstream of copper discharges. However, Chinook salmon were only observed spawning below the first major diluting tributary, a point above which copper concentrations averaged about 10–25 µg/L during the times of the spawning observations (Mebane 1994, 2000).

Sublethal copper exposure has been shown to interfere with the downstream migration to the ocean of yearling coho salmon (*O. kisutch*). Lorz and McPherson (1976, 1977) and Lorz et al. (1978) evaluated the effects of copper exposure on salmon smolts' downstream migration success in a series of 14 field experiments. Lorz and McPherson (1976, 1977) exposed yearling coho salmon for six to 165 days to nominal copper concentrations varying from 0–30 µg/L. They then marked and released the fish during the normal coho salmon migration period and monitored downstream migration success. The fish were released simultaneously, allowing for evaluation of both copper exposure concentrations and exposure duration on migration success. All dCu exposures resulted in reduction of migration compared with unexposed control fish. Migration success decreased with both increasing copper concentrations and increased exposure time for each respective concentration. Exposure to 30 µg/L dCu for as little as 72 hours caused a considerable reduction in migration (≈60%) compared to control fish. The reductions in migration following short-term exposures to dCu are illustrated in Figure A-1. Following exposure to 30 µg/L dCu, 80% of coho did not reach the migratory point in 49 days. These concentrations (5-20 µg/L) were one-tenth to one-third the 96-hour LC_{50} for the same stock of juvenile coho salmon in the same water. Lorz et al. (1978) further tested downstream migration with yearling coho salmon previously exposed to copper, cadmium, copper-cadmium mixtures, zinc, and copper-zinc mixtures. Copper concentrations in all tests were held at 10 µg/L. In all cases, the copper exposed fish again had poorer migratory success than did controls. The other metals did not show the dose-dependent result found for copper. These studies suggest that exposure to copper concentrations at levels found in streams subject to nonpoint copper pollution may impair downstream migration, a result of direct and indirect effects to salmon smolts, including reproductive success.

Laboratory Avoidance Studies

Studies have shown that salmonids can detect and avoid copper at low concentrations when tested in troughs or streams that allow them to choose between concentration gradients. To our knowledge, the lowest copper concentration reported to cause avoidance in laboratory conditions was 0.1 µg/L (Folmar 1976). However, these results may have low applicability to ambient conditions because copper exposure concentrations were not analytically verified. Avoidance thresholds of 2 µg/L copper have been reported for Atlantic salmon (*Salmo salar*), concentrations that are less than one-tenth of acute LC_{50} values (Saunders and Sprague 1967). Giattina et al. (1982) reported that rainbow trout appeared to detect copper concentrations down to 1.4–2.7 µg/L, because declines in residence time started to occur at these lower concentrations. However, the responses were only statistically significant at 4.4 to 6.4 µg/L depending on whether fish were exposed to a gradually increasing or abruptly increasing concentration gradient respectively. At exposure to extremely high dCu levels, for example,

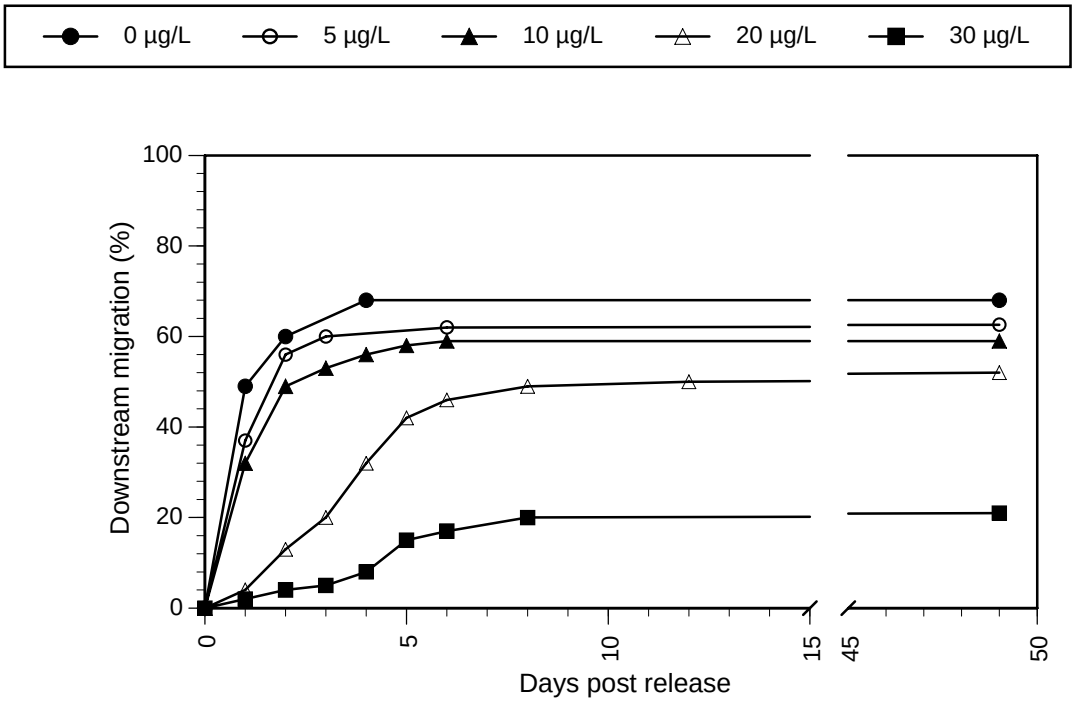

Figure A-1. Reduction in downstream migration of yearling coho salmon following 6 days of exposure to copper at various concentrations. (Redrawn from Lorz and McPherson 1977, their Figure 19.)

330–390 µg/L, trout showed diminished avoidance and sometimes attraction to acutely lethal concentrations (Giattina et al. 1982, Hansen et al. 1999a, Chapman unpubl. data).

Chapman (unpubl. data) reported that long-term sublethal copper exposures had impaired the avoidance performance of salmonids. Steelhead (*O. mykiss*), acclimated to low copper levels by surviving about 3 months early life stage toxicity testing, subsequently failed to avoid much higher, acutely lethal concentrations. Following about 3 month continuous exposure to 9 µg/L copper (from fertilization to about 1 month after swim up) the copper-acclimated fish and control fish with no previous copper exposure were exposed to a range of copper concentrations from 10 to 80 µg/L in avoidance-preference testing. The tests used the same counter flow avoidance-preference test chambers described by Giattina et al. (1982). The acclimated steelhead failed to avoid even the highest copper concentrations while most of the unexposed fish avoided all concentrations.

Hansen et al. (1999a) and Marr et al. (1995) conducted a variety of behavioral and other toxicity studies with Chinook salmon and rainbow trout exposed to copper. In these studies they used well water that was diluted with deionized water and spiked with copper to obtain a hardness, alkalinity, and pH that simulated those in Panther Creek, a mine-affected stream in Idaho. The avoidance response of the Chinook salmon was statistically significant for 0.8 and 2.8–22.5 µg/L copper but was not significant for a 1.6 µg/L copper treatment. Since the avoidance responses (percent time spent in test water) were similar between the 0.8, 1.6, and 3 µg/L treatments, but the 1.6 µg/L treatment had fewer replicates than the other treatments (10 vs. 20), the lack of statistical significance for the 1.6 µg/L treatment was probably an artifact of the

different sample sizes rather than a true lack of response. Rainbow trout consistently avoided copper at concentrations of 1.6 µg/L and above. To simulate avoidance responses that might result on exposing fish to background levels of copper, Hansen et al. (1999a) acclimated both Chinook salmon and rainbow trout to 2 µg/L copper for 25 days, and repeated the avoidance experiments. They observed that the avoidance response of Chinook salmon was greatly dampened such that no copper treatments resulted in statistically significant responses. In contrast, the avoidance response of rainbow trout was unaffected by the acclimation. This dramatic difference between Chinook salmon and rainbow trout avoidance was so unexpected that Hansen et al. (1999a) ran a second set of experiments that yielded the same results. Background dCu concentrations (<4 µg/L) are commonly observed in natural waterways, yet Chinook salmon failed to avoid any higher dCu concentrations following an acclimation to a nominal 2 µg dCu/L. Importantly, if Chinook salmon will not avoid any dCu concentrations following acclimation to low dCu concentrations, the behavioral defense against chronic and acute exposures to dCu is lost, and high mortality or chronic physiological effects are probable if subsequent higher levels of dCu exposure occur. Unlike Chinook salmon, dCu-acclimated rainbow trout preferred clean water and avoided higher dCu concentrations. Other differences between Chinook salmon and rainbow trout avoidance responses to copper were that addition of 4 and 8 mg/L dissolved organic carbon (DOC) did not appreciably affect the avoidance response of Chinook salmon to copper, nor did altering pH across a range of 6.5 to 8.5. In contrast, the addition of DOC (4 and 8 mg/L) did reduce the avoidance response of rainbow trout to copper. Although variable, avoidance responses of rainbow trout were slightly stronger at pH 7.5 and 8.5 than at 6.5 (Marr et al. 1995).

A further repeated finding from these laboratory avoidance tests was that although rainbow trout, steelhead, and Chinook salmon avoided low concentrations of dCu, they were apparently intoxicated and sometimes attracted to very high concentrations (Giattina et al. 1982, Hansen et al. 1999a, Chapman unpubl. data). The direct relevance of laboratory avoidance studies to the behaviors of fish in the wild is debatable since in natural waters fish likely select and move among habitats based on myriad reasons such as access to prey, shelter from predators, shade, velocity, temperature, and interactions with other fish. In contrast, laboratory preference/avoidance tests are commonly conducted under simple, highly artificial conditions to eliminate or minimize confounding variables other than the water characteristic of interest. Laboratory tests may overestimate the actual protection this behavior provides fish in heterogeneous, natural environments (Hartwell et al. 1987, Korver and Sprague 1989, Scherer and McNoil 1998).

However, at least one study suggested that experimental avoidance responses observed with salmonids are relevant to fish behaviors in the wild. From 1980 to 1982, sublethal levels of a contaminant (fluoride) from an aluminum mill at the John Day Dam on the Columbia River were associated with a significant delay in salmon passage and decreased survival (Damkaer and Dey 1989). Salmon took an average of 36 hours to pass up the fish ladder at the Bonneville and McNary dams compared to 157 hours delay at the John Day Dam. Greater than 50% mortality occurred between the Bonneville and McNary dams (above and below the John Day dam), compared to about 2% mortality associated with the other dams. Damkaer and Dey (1989) introduced similar levels of the contaminant in streamside test flumes alongside a salmon spawning stream (Big Beef Creek, Washington). Significant numbers of adult Chinook salmon failed to move out of their holding area and continue upstream; those that did move upstream

chose the noncontaminated side of the flume. By adjusting the dose, Damkaer and Dey (1989) predicted a threshold detection limit for avoidance by salmon. The mill subsequently reduced its release of the contaminant to below these experimental threshold levels, which did not show a response in the streamside tests. Afterwards, fish passage delays and salmon mortality between the dams decreased to 28 hours and <5%, respectively (Damkaer and Dey 1989). This study suggested that the delay due to avoidance of a chemical affected the spawning success of migrating adult salmonids. These results are also consistent with the field studies of salmon migration in copper-contaminated streams and from laboratory avoidance/preference testing. Experimental avoidance/preference testing thus appears to be relevant to fish behavior in nature.

Other Adverse Effects

The focus of this literature synthesis is sensory effects of copper on juvenile salmonids. However, other adverse effects of copper to salmonids reported in the literature include weakened immune function and disease resistance, increased susceptibility to stress, liver damage, reduced growth, impaired swimming performance, weakened eggshells, and direct mortality (McKim and Benoit 1971, Stevens 1977, Schreck and Lorz 1978, Waiwood and Beamish 1978a, 1978b, Chapman 1982, Farag et al. 1994, Marr et al. 1996, Farag et al. 2003). While a comprehensive review of other adverse effects of copper on fish is beyond the scope of this synthesis, we discuss several studies of interest below.

Stevens (1977) reported that preexposure to sublethal levels of dCu interfered with the immune response and reduced the disease resistance in yearling coho salmon. Juvenile coho salmon were vaccinated with the bacterial pathogen *Vibrio anguillarum* prior to copper exposure to investigate the effects of copper upon the immune response and survival. Following copper exposure (9.6–40 µg/L), surviving juveniles were challenged under natural conditions to *V. anguillarum*, the causative agent of vibriosis in fish. Vibriosis is a disease commonly found in wild and captive fish from marine environments and has caused deaths of coho and Chinook salmon. Coho salmon were exposed to constant concentrations of dCu for about one month at levels that covered the range from no effect to causing 100% mortality, 9.6–40 µg/L. The antibody titer level against *V. anguillarum* was significantly reduced in fish exposed to 13.9 µg/L of dCu when compared to that developed in control fish. The survivors of the dCu bioassays were then exposed in saltwater holding ponds for an additional 24 days to the *V. anguillarum* pathogen. The unvaccinated, non-dCu exposed control fish had 100% mortality and the vaccinated, non-dCu exposed fish had the lowest mortality. The vaccinated, dCu-exposed fish had increasing mortality corresponding to the lower antibody titer levels which in turn corresponded to the increasing dCu exposure levels. Therefore, dCu exposure can significantly reduce a fish's immune function and disease resistance at concentrations as low as 13.9 µg/L following 30 days of exposure (Stevens 1977).

Schreck and Lorz (1978) studied the effects of copper exposure to stress resistance in yearling coho salmon. Fish that were exposed for 7 days to 15 µg/L dCu and unexposed control fish were subjected to severe handling and confinement stress. Copper-exposed fish survived this additional stress for a median of 12–15 hours while control fish experienced no mortality at 36 hours. Schreck and Lorz (1978) concluded that exposure to copper placed a sublethal stress on the fish which made them more vulnerable to handling and saltwater adaptation. Further,

they hypothesized that dCu exposure may make salmonids more vulnerable to secondary stresses such as disease and pursuit by predators.

Exposure of brook trout (*Salvelinus fontinalis*) eggs to 17.4 µg dCu/L for 90 days resulted in weakened chorions (eggshells) and embryo deformities. After hatching, poor yolk utilization and reduced growth were demonstrated. These overall weakened conditions may reduce survival chances in the wild (McKim and Benoit 1971, McKim 1985). Copper accumulation in the liver of rainbow trout caused degeneration of liver hepatocytes, which resulted in reduced ability to metabolize food, reduced growth, or eventual death (Leland and Carter 1985, Farag et al. 1994, Meyer 2005). Waiwood and Beamish (1978a), Chapman (1982), Seim et al. (1984), McKim and Benoit (1971), and Marr (1996) have also observed reduced growth of salmonids in response to chronic copper exposures as low as 1.9 µg/L. Waiwood and Beamish (1978b) reported that rainbow trout exposed to copper levels had reduced swimming performance (10, 15, 20, 30 µg/L dCu) and reduced oxygen consumption (25, 40 µg/L dCu) apparently due to gill damage and decreased efficiency of gas exchange.

In sum, there is a large body of literature showing that behavior of salmonids and other fishes can be disrupted at concentrations of dCu that are only slightly elevated above background concentrations. Further, dCu stress has been shown to increase the cost of maintenance to fish and to limit oxygen consumption and food metabolism. Reduced growth may result in increased susceptibility to predation, and impaired swimming ability may result in reduced escape reaction and prey hunting, with a possible consequence of reduced survival at the population level. We summarize selected examples of effect concentrations reported with copper for several different types of effects in Table 1 of this technical memorandum. In general, typical copper exposures probably do not kill juvenile salmonids directly until concentrations greater than about 10 times that of sensory thresholds, and then only if the concentrations are sustained for at least several hours. In selecting these examples, we sought to list representative effects and concentrations rather than extreme values that could be gleaned from the literature. However, the selected examples do not constitute an exhaustive review of the effects of copper to fish; more general reviews of effects of copper to fish and other aquatic organisms are available elsewhere (Leland and Carter 1985, Sorensen 1991, Eisler 1998, USEPA 2007).

Appendix B: Supplementary Bibliography

Copper Sources

Good, J. C. 1993. Roof runoff as a diffuse source of metals and aquatic toxicity in storm water. Water Sci. Technol. 28:317–322.

Thomas, P. R., and G. R. Greene. 1993. Rainwater quality from different roof catchments. Water Sci. Technol. 28:291–297.

Benchmark Concentration/Dose

Crump, K. S. 1995. Calculation of benchmark doses from continuous data. Risk Anal. 15:79–89.

Sandahl, J. F., and J. J. Jenkins. 2002. Pacific steelhead (*Oncorhynchus mykiss*) exposed to chlorpyrifos: Benchmark concentration estimates for acetylcholinesterase inhibition. Environ. Toxicol. Chem. 21:2452–2458.

Slikker, W., K. S. Crump, M. E. Andersen, and D. Bellinger. 1996. Biologically based, quantitative risk assessment of neurotoxicants. Fundam. Appl. Toxicol. 29:18–30.

U.S. Environmental Protection Agency. 1995. The use of the benchmark dose approach in health risk assessment. EPA 630/R-94/007. EPA Office of Research and Development, Washington, DC.

Copper and Neurobiology

Baldwin, D. H., J. F. Sandahl, J. S Labenia, and N. L. Scholz. 2003. Sublethal effects of copper on coho salmon: Impacts on nonoverlapping receptor pathways in the peripheral olfactory nervous system. Environ. Toxicol. Chem. 22:2266–2274.

Baldwin, D. H., and N. L. Scholz. 2005. The electro-olfactogram: An *in vivo* measure of peripheral olfactory function and sublethal neurotoxicity in fish. *In* G. K. Ostrander (ed.), Techniques in aquatic toxicology, Volume 2, p. 257–276. CRC Press, Boca Raton, FL.

Bettini, S., F. Ciani, and V. Franceschini. 2006. Recovery of the olfactory receptor neurons in the African *Tilapia mariae* following exposure to low copper level. Aquat. Toxicol. 76:321–328

Beyers, D. W., and M. S. Farmer. 2001. Effects of copper on olfaction of Colorado pikeminnow. Environ. Toxicol. Chem. 20:907–912.

Bjerselius, R, S. Winberg, Y. Winberg, and K. Zeipel. 1993. Ca^{2+} protects olfactory receptor function against acute copper (II) toxicity in Atlantic salmon. Aquat. Toxicol. 25:125–138.

Carreau, N. D., and G. G. Pyle. 2005. Effect of copper exposure during embryonic development on chemosensory function of juvenile fathead minnows (*Pimephales promelas*). Ecotoxicol. Environ. Saf. 61:1–6.

Chai, M., and X. Chen. 1999. Inhibition of Cd^{2+}, Hg^{2+} and Pb^{2+} on EOG responses of *Tilapia* sp. Journal of Fishery Sciences of China/Zhongguo Shuichan Kexue Beijing 6:89–92.

Chai, M., and Z. Huang. 1996. Effect of Ca^{2+} on the EOG of *Tilapia* sp. and exploration of detoxifying feasibility. Journal of Xiamen University Natural Science/Xiamen Daxue Xuebao Xiamen 35:941–946.

Chai, M., and L. Pan. 1996. Effects of heavy metal (Cu^{2+}, Zn^{2+}) on the EOG response of fish (*Tilapia* sp.). Journal of Xiamen University Natural Science/Xiamen Daxue Xuebao Xiamen 35:94–99.

Goldstein, J. N., D. F. Woodward, and A. M. Farag. 1999. Movements of adult Chinook salmon during spawning migration in a metals-contaminated system, Coeur d'Alene River, Idaho. Trans. Am. Fish. Soc. 128:121–129.

Hansen, J. A., J. C. A. Marr, J. Lipton, D. Cacela, and H. L. Bergman. 1999. Differences in neurobehavioral responses of Chinook salmon (*Oncorhynchus tshawytscha*) and rainbow trout (*Oncorhynchus mykiss*) exposed to copper and cobalt: Behavioral avoidance. Environ. Toxicol. Chem. 18:1972–1978.

Hansen, J. A., J. D. Rose, R. A. Jenkins, K. G. Gerow, and H. L. Bergman. 1999. Chinook salmon (*Oncorhynchus tshawytscha*) and rainbow trout (*Oncorhynchus mykiss*) exposed to copper: Neurophysiological and histological effects on the olfactory system. Environ. Toxicol. Chem. 18:1979–1991.

Hara, T. J., Y. M. C. Law, and S. Macdonald. 1976. Effects of mercury and copper on the olfactory response in rainbow trout. J. Fish. Res. Board Can. 33:1568–1573.

Hernández, P. P., V. Moreno, F. A. Olivari, and M. L. Allende. 2006. Sublethal concentrations of waterborne copper are toxic to lateral line neuromasts in zebrafish (*Danio rerio*). Hear. Res. 213:1–10.

Julliard, A. K., D. Saucier, and L. Astic. 1993. Effects of chronic low-level copper exposure on ultrastructure of the olfactory system in rainbow trout (*Oncorhynchus mykiss*). Histol. Histopathol. 8:655–672.

Julliard, A. K., D. Saucier, and L. Astic. 1995. Metal X-ray microanalysis in the olfactory system of rainbow trout exposed to low level of copper. Biol. Cell 83:77–86.

Julliard, A. K., D. Saucier, and L. Astic. 1996. Time-course of apoptosis in the olfactory epithelium of rainbow trout exposed to a low copper level. Tissue Cell 28:367–377.

Kasumyan, A. O. 2001. Effects of chemical pollutants on foraging behavior and sensitivity of fish to food stimuli. J. Ichthyol. 41:76–87.

Kasumyan, A. O., and A. M. H. Morsi. 1998. Effect of heavy metals on the feeding activity and taste behavior responses of carp *Cyprinus carpio*: 1. Copper, cadmium, zinc, and lead. J. Ichthyol. 38:393–409.

Klima, K. E., and F. M. Applehans. 1990. Copper exposure and the degeneration of olfactory receptors in rainbow trout (*Oncorhynchus mykiss*). Chem. Speciat. Bioavailab. 2:149–154.

Linbo, A. O., C. M. Stehr, J. P. Incardona, and N. L. Scholz. 2006. Dissolved copper triggers cell death in the peripheral mechanosensory system of larval fish. Environ. Toxicol. Chem. 25:597–603.

Little, E. E., R. D. Archeski, B. A. Flerov, and V. I. Kozlovskaya. 1990. Behavioral indicators of sublethal toxicity in rainbow trout. Arch. Environ. Contam. Toxicol. 19:380–385.

Little, E. E., and S. E. Finger. 1990. Swimming behavior as an indicator of sublethal toxicity in fish. Environ. Toxicol. Chem. 9:13–19.

McPherson, T. D., R. S. Mirza, and G. G. Pyle. 2004. Responses of wild fishes to alarm chemicals in pristine and metal-contaminated lakes. Can. J. Zool. 82:694–700.

Moran, D. T., J. C. Rowley, and G. Aiken. 1986. Trout olfactory receptors degenerate in response to waterborne ions: A potential bioassay for environmental neurotoxicology? Chem. Senses 11:642.

Moran, D. T., J. C. Rowley, G. R. Aiken, and B. W. Jafek. 1992. Ultrastructural neurobiology of the olfactory mucosa of the brown trout, *Salmo trutta*. Microscopy Res. Tech. 23:28–48.

Rehnberg, B., and C. B. Schreck. 1986. Acute metal toxicology of olfaction in coho salmon: Behavior, receptors, and odor-metal complexation. Bull. Environ. Contam. Toxicol. 36:579–586.

Sandahl, J. F., D. H. Baldwin, J. J. Jenkins, and N. L. Scholz. 2007. A sensory system at the interface between urban stormwater runoff and salmon survival. Environ. Sci. Technol. 41:2998–3004.

Sandahl, J. F., D. H. Baldwin, J. J. Jenkins, and N. L. Scholz. 2004. Odor-evoked field potentials as indicators of sublethal neurotoxicity in juvenile coho salmon (*Oncorynchus kisutch*) exposed to copper, chlorpyrifos, or esfenvalerate. Can. J. Fish. Aquat. Sci. 61:404–413.

Saucier, D., and L. Astic. 1995. Morphofunctional alterations in the olfactory system of rainbow trout (*Oncorhynchus mykiss*) and possible acclimation in response to long-lasting exposure to low copper levels. Comp. Biochem. Physiol. A Physiol. 112:273–284.

Saucier, D., L. Astic, and P. Rioux. 1991. The effects of early chronic exposure to sublethal copper on the olfactory discrimination of rainbow trout, *Oncorhynchus mykiss*. Environ. Biol. Fishes 30:345–351.

Saunders, R. L., and J. B. Sprague. 1967. Effects of copper-zinc mining pollution on a spawning migration of Atlantic salmon. Water Res. 1:419–432

Starcevic, S. L., and B. S. Zielinski. 1997. Neuroprotective effects of glutathione on rainbow trout olfactory receptor neurons during exposure to copper sulfate. Comp. Biochem. Physiol. C 117C:211–219.

Tjalve, H., and J. Henriksson. 1999. Uptake of metals in the brain via olfactory pathways. Neurotoxicology 20:181–195.

Weis, J. S., and P. Weis. 1996. The effects of using wood treated with chromated copper arsenate in shallow-water environments: A review. Estuaries 19:306–310.

Winberg, S., R. Bjerselius, E. Baatrup, and K. B. Døving. 1992. The effect of copper (II) on the electro-olfactogram (EOG) of the Atlantic salmon (*Salmo salar L.*) in artificial freshwater of varying inorganic carbon concentrations. Ecotoxicol. Environ. Saf. 24:167–178.

Reviews

Brown, G. E. 2003. Learning about danger: Chemical alarm cues and local risk assessment in pre fishes. Fish Fish. 4:227–234.

Døving, K. B. 1991. Assessment of animal behaviour as a method to indicate environmental toxicity. Comp. Biochem. Physiol. C 100:247–252.

Eisler, R. 1998. Copper hazards to fish, wildlife, and invertebrates: A synoptic review. Report No. USGS/BRD/BSR--1998-0002. U.S. Geological Survey, Biological Resources Division.

Halpern, B. P. 1982. Environmental factors affecting chemoreceptors: An overview. Environ. Health Perspect. 44:101–105.

Hara, T. J. 1972. Electrical responses of the olfactory bulb of Pacific salmon *Oncorhynchus nerka* and *Oncorhynchus kisutch*. J. Fish. Res. Board Can. 29:1351–1355.

Hara, T. J. 1992. Mechanisms of olfaction. *In* T. J. Hara (ed.), Fish chemoreception, p. 150–170. Chapman & Hall, London.

Kats, L. B., and L. M. Dill. 1998. The scent of death: Chemosensory assessment of predation risk by prey animals. Ecoscience 5:361–394.

Klaprat, D. A., R. E. Evans, and T. J. Hara. 1992. Environmental contaminants and chemoreception in fishes. *In* T. J. Hara (ed.), Fish chemoreception, p 321–342. Chapman & Hall, London.

Scott, J. W., and P. E. Scott-Johnson. 2002. The electroolfactogram: A review of its history and uses. Microscopy Res. Tech. 58:152–160.

Scott, G. R., and K. A. Sloman. 2004. The effects of environmental pollutants on complex fish behaviour: Integrating behavioural and physiological indicators of toxicity. Aquat. Toxicol. 68:369–392.

Shumway, C. A. 1999. A neglected science: Applying behavior to aquatic conservation. Environ. Biol. Fishes 55:183–201.

Smith, R. J. F. 1992. Alarm signals in fishes. Rev. Fish Biol. Fish. 2:33–63.

Sorensen, E. M. B. 1991. Chapter VII: Copper. *In* E. M. B. Sorensen (ed.), Metal poisoning in fish, p. 235–284. CRC Press, Boca Raton, FL.

Sutterlin, A. M. 1974. Pollutants and the chemical senses of aquatic animals—perspective and review. Chem. Senses Flavor 1:167–178.

Studies with Other Metals

Baatrup, E. 1991. Structural and functional effects of heavy metals on the nervous system, including sense organs, of fish. Comp. Biochem. Physiol. C 100:253–257.

Baatrup, E., and K. B. Døving. 1990. Histochemical demonstration of mercury in the olfactory system of salmon (*Salmo salar* L.) following treatments with dietary methylmercuric chloride and dissolved mercuric chloride. Ecotoxicol. Environ. Saf. 20:277–289.

Baatrup, E., K. B. Døving, and S. Winberg. 1990. Differential effects of mercurial compounds on the electroolfactogram (EOG) of salmon (*Salmo salar L.*). Ecotoxicol. Environ. Saf. 20:269–276.

Baker, C. F., and J. C. Montgomery. 2001. Sensory deficits induced by cadmium in banded kokopu, *Galaxias fasciatus*, juveniles. Environ. Biol. Fishes 62:455–464.

Beauvais, S. L., S. B. Jones, J. T. Parris, S. K. Brewer, and E. E. Little. 2001. Cholinergic and behavioral neurotoxicity of carbaryl and cadmium to larval rainbow trout (*Oncorhynchus mykiss*). Ecotoxicol. Environ. Saf. 49:84–90.

Chakrabarti, P., M. Ghosal, and D. K. Mandal. 1994. Microanatomical and histopathological sequels of cadmium intoxication on the olfactory epithelium of the fish *Mystus vittatus* (Bloch). Environ. Ecol. 12:540–544.

Hernadi, L. 1993. Fine structural characterization of the olfactory epithelium and its response to divalent cations Cd^{2+} in the fish *Alburnus alburnus* (Teleostei, Cyprinidae): A scanning and transmission electron microscopic study. Neurobiology 1:11–31.

Scott, G. R., K. A. Sloman, C. Rouleau, and C. M. Wood. 2003. Cadmium disrupts behavioural and physiological responses to alarm substance in juvenile rainbow trout (*Oncorhynchus mykiss*). J. Exp. Biol. 206:1779–1790.

Selected Behavioral Studies

Berejikian, B. A., R. J. Smith, E. P. Tezak, S. L. Schroder, and C. M. Knudsen. 1999. Paired chemical alarm signals and complex hatchery rearing habitats affect predator behavior and survival of Chinook salmon (*Oncorhynchus tshawytscha*) juveniles. Can. J. Fish. Aquat. Sci. 56:830–838.

Brown, G. E., J. C. Adrian Jr., T. Patton, and D. P. Chivers. 2001. Fathead minnows learn to recognize predator odor when exposed to concentrations of artificial alarm pheromone below their behavioral-response threshold. Can. J. Zool. 79:2239–2245.

Brown, G. E., and R. J. Smith. 1997. Conspecific skin extracts elicit antipredator responses in juvenile rainbow trout (*Oncorhynchus mykiss*). Can. J. Zool. 75:1916–1922.

Døving, K. B., H. Westerberg, and P. B. Johnsen. 1985. Role of olfaction in the behavioral and neuronal responses of Atlantic salmon, *Salmo salar*, to hydrographic stratification. Can. J. Fish. Aquat. Sci. 42:1658–1667.

Hatfield, C. T., and J. M. Anderson. 1972. Effects of two pesticides on the vulnerability of Atlantic salmon (*Salmo salar*) parr to brook trout (*Salvenius fontinalis*) predation. J. Fish. Res. Board Can. 29:27–29.

Hatfield, C. T., and P. H. Johansen. 1972. Effects of four insecticides on the ability of Atlantic salmon parr (*Salmo salar*) to learn and retain a simple conditioned response. J. Fish. Res. Board Can. 29:315–321.

Hiroven, H., E. Ranta, J. Piironen, A. Laurila, and N. Peuhkuri. 2000. Behavioural responses of naive Artic charr young to chemical cues from salmonid and nonsalmonid fish. Oikos 88:191–199.

Kruzynski, G. M., and I. K. Birtwell. 1994. A predation bioassay to quantify the ecological significance of sublethal responses of juvenile Chinook salmon (*Oncoryhynchus tshawytscha*) to the antisapstain fungicide TCMTB. Can. J. Fish. Aquat. Sci. 51:1780–1790.

McLennan, D. A., and M. J. Ryan. 1997. Responses to conspecific and heterospecific olfactory cues in the swordtail *Xiphophorus cortezi*. Anim. Behav. 54:1077–1088.

Mirza, R. S., and D. P. Chivers. 2001. Chemical alarm signals enhance survival of brook charr (*Salvelinus fontinalis*) during encounters with predatory chain pickerel (*Esox niger*). Ethology 107:989–1005.

Poulin, R., D. Marcogliese, and J. McLaughlin. 1999. Skin-penetrating parasites and the release of alarm substances in juvenile rainbow trout. J. Fish Biol. 55:47–53.

Wisby, W. J., and A. D. Hasler. 1954. Effect of occlusion on migrating silver salmon (*Oncorhynchus kisutch*). J. Fish. Res. Board Can. 11:472–478.

Recovery of Olfactory Epithelium after Damage

Evans, R. E., and T. J. Hara. 1985. The characteristics of the electro-olfactogram (EOG): its loss and recovery following olfactory nerve section in rainbow trout (*Salmo gairdneri*). Brain Res. 330:65–75.

Zielinski, B. S., and T. J. Hara. 1992. Ciliated and microvillar receptor cells degenerate and then differentiate in the olfactory epithelium of rainbow trout following olfactory nerve section. Microscopy Res. Tech. 23:22–27.

Additional Endpoints

Ali, A., S. M. Al-Ogaily, N. A. Al-Asgah, and J. Gropp. 2003. Effect of sublethal concentrations of copper on the growth performance of *Oreochromis niloticus*. J. Appl. Ichthyol. 19:183–188.

Beaumont, M. W., P. J. Butler, and E. W. Taylor. 2003. Exposure of brown trout *Salmo trutta* to a sublethal concentration of copper in soft acidic water: Effects upon gas exchange and ammonia accumulation. J. Exp. Biol. 206:153–162.

Bielmyer, G. K., D. Gatlin, J. J. Isely, J. Tomasso, and S. J. Klaine. 2005. Responses of hybrid striped bass to waterborne and dietary copper in freshwater and saltwater. Comp. Biochem. Physiol. C Toxicol. Pharmacol. 140:131–137.

Brix, K. V., D. K. DeForest, and W. J. Adams. 2001. Assessing acute and chronic copper risks to freshwater aquatic life using species sensitivity distributions for different taxonomic groups. Environ. Toxicol. Chem. 20:1846–1856.

Buckley, J. T., M. Roch, J. A. McCarter, C. A. Rendell, and A. T. Matheson. 1982. Chronic exposure of coho salmon to sublethal concentrations of copper. 1. Effect on growth, on accumulation and distribution of copper, and on copper tolerance. Comp. Biochem. Physiol. C Pharmacol. Toxicol. Endocrinol. 72:15–19.

Campbell, H. A., R. D. Handy, and D. W. Sims. 2002. Increased metabolic cost of swimming and consequent alterations to circadian activity in rainbow trout (*Oncorhynchus mykiss*) exposed to dietary copper. Can. J. Fish. Aquat. Sci. 59:768–777.

Campbell, H. A., R. D. Handy, and D. W. Sims. 2005. Shifts in a fish's resource holding power during a contact paired interaction: The influence of a copper-contaminated diet in rainbow trout. Physiol. Biochem. Zool. 78:706–714.

Darwish, A. M., D. L. Straus, and B. R. Griffin. 2005. Histologic evaluation of the safety of copper sulfate to channel catfish. N. Am. J. Aquacult. 67:122–128.

De Boeck, G., A. Vlaeminck, and R. Blust. 1997. Effects of sublethal copper exposure on copper accumulation, food consumption, growth, energy stores, and nucleic acid content in common carp. Arch. Environ. Contam. Toxicol. 33:415–422.

Diamond, J., M. Bowersox, H. Latimer, C. Barbour, J. Bearr, and J. Butcher. 2005. Effects of pulsed contaminant exposures on early life stages of the fathead minnow. Arch. Environ. Contam. Toxicol. 49:511–519.

Furuta, T., N. Iwata, K. Kikuchi, and K. Namba. 2005. Effects of copper on survival and growth of larval false clown anemonefish *Amphiprion ocellaris*. Fish. Sci. 71:884–888.

Galvez, F., and C. M. Wood. 2002. The mechanisms and costs of physiological and toxicological acclimation to waterborne silver in juvenile rainbow trout (*Oncorhynchus mykiss*). J. Comp. Physiol. B Biochem. Syst. Environ. Physiol. 172:587–597.

Hansen, J. A., J. Lipton, P. G. Welsh, D. Cacela, and B. MacConnell. 2004. Reduced growth of rainbow trout (*Oncorhynchus mykiss*) fed a live invertebrate diet pre-exposed to metal-contaminated sediments. Environ. Toxicol. Chem. 23:1902–1911.

Hansen, J. A., J. Lipton, P. G. Welsh, J. Morris, D. Cacela, and M. J. Suedkamp. 2002. Relationship between exposure duration, tissue residues, growth, and mortality in rainbow trout (*Oncorhynchus mykiss*) juveniles subchronically exposed to copper. Aquat. Toxicol. 58:175–188.

Hansen, J. A., P. G. Welsh, J. Lipton, and D. Cacela. 2002. Effects of copper exposure on growth and survival of juvenile bull trout. Trans. Am. Fish. Soc. 131:690–697.

Lorz, H. W., and B. P. McPherson. 1976. Effects of copper or zinc in freshwater on adaptation to seawater and Atpase activity, and effects of copper on migratory disposition of coho salmon (*Oncorhynchus kisutch*). J. Fish. Res. Board Can. 33:2023–2030.

Marr, J. C. A., J. Lipton, D. Cacela, J. A. Hansen, H. L. Bergman, J. S. Meyer, and C. Hogstrand. 1996. Relationship between copper exposure duration, tissue copper concentration, and rainbow trout growth. Aquat. Toxicol. 36:17–30.

Rajotte, J. W., and P. Couture. 2002. Effects of environmental metal contamination on the condition, swimming performance, and tissue metabolic capacities of wild yellow perch (*Perca flavescens*). Can. J. Fish. Aquat. Sci. 59:1296–1304.

Roch, M., and J. A. McCarter. 1984. Metallothionein induction, growth, and survival of Chinook salmon exposed to zinc, copper, and cadmium. Bull. Environ. Contam. Toxicol. 32:478–485.

Sloman, K. A., D. W. Baker, C. G. Ho, D. G. McDonald, and C. M. Wood. 2003. The effects of trace metal exposure on agonistic encounters in juvenile rainbow trout, *Oncorhynchus mykiss*. Aquat. Toxicol. 63:187–196.

Sloman, K. A., D. W. Baker, C. M. Wood, and G. McDonald. 2002. Social interactions affect physiological consequences of sublethal copper exposure in rainbow trout, *Oncorhynchus mykiss*. Environ. Toxicol. Chem. 21:1255–1263.

Sloman, K. A., T. P. Morgan, D. G. McDonald, and C. M. Wood. 2003. Socially induced changes in sodium regulation affect the uptake of waterborne copper and silver in the rainbow trout, *Oncorhynchus mykiss*. Comp. Biochem. Physiol. C Toxicol. Pharmacol. 135:393–403.

Recent NOAA Technical Memorandums

published by the
Northwest Fisheries Science Center

NOAA Technical Memorandum NMFS-NWFSC-

82 **Helser, T.E., I.J. Stewart, C.E. Whitmire, and B.H. Horness. 2007.** Model-based estimates of abundance for 11 species from the NMFS slope surveys. U.S. Dept. Commer., NOAA Tech. Memo. NMFS-NWFSC-82, 145 p. NTIS number pending.

81 **Hard, J.J., J.M. Myers, M.J. Ford, R.G. Cope, G.R. Pess, R.S. Waples, G.A. Winans, B.A. Berejikian, F.W. Waknitz, P.B. Adams. P.A. Bisson, D.E. Campton, and R.R. Reisenbichler. 2007.** Status review of Puget Sound steelhead *(Oncorhynchus mykiss)*. U.S. Dept. Commer., NOAA Tech. Memo. NMFS-NWFSC-81, 117 p. NTIS number PB2008-100451.

80 **Berntson, E.A., P.S. Levin, and P.C. Moran (editors). 2007.** Conservation of North Pacific rockfishes: Ecological genetics and stock structure. Proceedings of the workshop, March 2-3, 2004, Seattle, Washington. U.S. Dept. Commer., NOAA Tech. Memo. NMFS-NWFSC-80, 80 p. NTIS number PB2007-111137.

79 **Lawson, P.W., E.P. Bjorkstedt, M.W. Chilcote, C.W. Huntington, J.S. Mills, K.M.S. Moore, T.E. Nickelson, G.H. Reeves, H.A. Stout, T.C. Wainwright, and L.A. Weitkamp. 2007.** Identification of historical populations of coho salmon *(Oncorhynchus kisutch)* in the Oregon coast evolutionarily significant unit. U.S. Dept. Commer., NOAA Tech. Memo. NMFS-NWFSC-79, 129 p. NTIS number PB2007-111607.

78 **Ruckelshaus, M.H., K.P. Currens, W.H. Graeber, R.R. Fuerstenberg, K. Rawson, N.J. Sands, and J.B. Scott. 2006.** Independent populations of Chinook salmon in Puget Sound. U.S. Dept. Commer., NOAA Tech. Memo. NMFS-NWFSC-78, 125 p. NTIS number PB2007-104920.

77 **Sloan, C.A., D.W. Brown, G.M. Ylitalo, J. Buzitis, D.P. Herman, D.G. Burrows, G. Yanagida, R.W. Pearce, J.L. Bolton, R.H. Boyer, and M.M. Krahn. 2006.** Quality assurance plan for analyses of environmental samples for polycyclic aromatic compounds, persistent organic pollutants, fatty acids, stable isotope ratios, lipid classes, and metabolites of polycyclic aromatic compounds. U.S. Dept. Commer., NOAA Tech. Memo. NMFS-NWFSC-77, 30 p. NTIS number PB2007-104919.

76 **Gustafson R.G., J. Drake, M.J. Ford, J.M. Myers, E.E. Holmes, and R.S. Waples. 2006.** Status review of Cherry Point Pacific herring *(Clupea pallasii)* and updated status review of the Georgia Basin Pacific herring distinct population segment under the Endangered Species Act. U.S. Dept. Commer., NOAA Tech. Memo. NMFS-NWFSC-76, 182 p. NTIS number PB2007-104918.

75 **Keller, A.A., B.H. Horness, V.J. Tuttle, J.R. Wallace, V.H. Simon, E.L. Fruh, K.L. Bosley, and D.J. Kamikawa. 2006.** The 2002 U.S. West Coast upper continental slope trawl survey of groundfish resources off Washington, Oregon, and California: Estimates of distribution, abundance, and length composition. U.S. Dept. Commer., NOAA Tech. Memo. NMFS-NWFSC-75, 189 p. NTIS PB2006-111432.

Most NOAA Technical Memorandums NMFS-NWFSC are available online at the Northwest Fisheries Science Center web site (http://www.nwfsc.noaa.gov)

The Effects of Coal Dust on Ventilation and Oxygen Consumption in the Dungeness Crab, *Cancer magister*

Betty A. Hillaby

Field Services Branch
Habitat Management Division
Water Quality Unit
Department of Fisheries and Oceans
Vancouver, B.C. V6E 2P1

DEPT. OF FISHERIES & OCEANS
NOV 13 1981
REGIONAL LIBRARY, PACIFIC

August 1981

Canadian Technical Report of Fisheries and Aquatic Sciences No. 1033

Government of Canada Fisheries and Oceans
Gouvernement du Canada Pêches et Océans

Canadian Technical Report of Fisheries and Aquatic Sciences

These reports contain scientific and technical information that represents an important contribution to existing knowledge but which for some reason may not be appropriate for primary scientific (i.e. *Journal*) publication. Technical Reports are directed primarily towards a worldwide audience and have an international distribution. No restriction is placed on subject matter and the series reflects the broad interests and policies of the Department of Fisheries and Oceans, namely, fisheries management, technology and development, ocean sciences, and aquatic environments relevant to Canada.

Technical Reports may be cited as full publications. The correct citation appears above the abstract of each report. Each report will be abstracted in *Aquatic Sciences and Fisheries Abstracts* and will be indexed annually in the Department's index to scientific and technical publications.

Numbers 1-456 in this series were issued as Technical Reports of the Fisheries Research Board of Canada. Numbers 457-714 were issued as Department of the Environment, Fisheries and Marine Service, Research and Development Directorate Technical Reports. Numbers 715-924 were issued as Department of Fisheries and the Environment, Fisheries and Marine Service Technical Reports. The current series name was changed with report number 925.

Details on the availability of Technical Reports in hard copy may be obtained from the issuing establishment indicated on the front cover.

Rapport technique canadien des sciences halieutiques et aquatiques

Ces rapports contiennent des renseignements scientifiques et techniques qui constituent une contribution importante aux connaissances actuelles mais qui, pour une raison ou pour une autre, ne semblent pas appropriés pour la publication dans un journal scientifique. Il n'y a aucune restriction quant au sujet, de fait, la série reflète la vaste gamme des intérêts et des politiques du Ministère des Pêches et des Océans, notamment gestion des pêches, techniques et développement, sciences océaniques et environnements aquatiques, au Canada.

Les Rapports techniques peuvent être considérés comme des publications complètes. Le titre exact paraîtra au haut du résumé de chaque rapport, qui sera publié dans la revue *Aquatic Sciences and Fisheries Abstracts* et qui figurera dans l'index annuel des publications scientifiques et techniques du Ministère.

Les numéros 1-456 de cette série ont été publiés à titre de Rapports techniques de l'Office des recherches sur les pêcheries du Canada. Les numéros 457-714, à titre de Rapports techniques de la Direction générale de la recherche et du développement, Service des pêches et de la mer, ministère de l'Environnement. Les numéros 715-924 ont été publiés à titre de Rapports techniques du Service des pêches et de la mer, Ministère des Pêches et de l'Environnement. Le nom de la série a été modifié à partir du numéro 925.

La page couverture porte le nom de l'établissement auteur où l'on peut se procurer les rapports sous couverture cartonnée.

Canadian Technical Report of

Fisheries and Aquatic Sciences

August 1981

DEPT. OF FISHERIES & OCEANS
NOV 13 1981
REGIONAL LIBRARY, PACIFIC

THE EFFECTS OF COAL DUST ON VENTILATION AND OXYGEN CONSUMPTION IN THE DUNGENESS CRAB, *Cancer magister*

by

Betty A. Hillaby

Field Services Branch

Habitat Management Division

Water Quality Unit

Department of Fisheries and Oceans

Vancouver, British Columbia V6E 2P1

© Minister of Supply and Services Canada 1981

Cat. No. Fs 97-6/1033 ISSN 0706-6457

Correct citation for this publication:

Hillaby, Betty A. 1981. The effects of coal dust on ventilation and oxygen consumption in the Dungeness crab, *Cancer magister*. Can. Tech. Rep. Fish. Aquat. Sci. 1033: vi + 18 p.

CONTENTS

List of Tables iv

List of Figures v

Abstract/Résumé vi

Introduction 1

Materials and Methods 3

Respiration Chambers and Substrates 3

Experimental Animals 5

Experimental Protocol 7

Calculations 7

Oxygen Consumption 7

Scaphognathite Activity 8

Histology 9

Statistical Anaylsis 9

Results 9

Oxygen Consumption 9

Control Chambers 9

Chambers with Crabs 10

Scaphognathite Activity 10

Burrowing Activity 12

Histology 12

Discussion 12

Acknowledgments 16

References 17

LIST OF TABLES

Table		Page
1	Particle sizes of sand and coal	5
2	Characteristics of seawater flowing into the respiration chambers	9
3	Oxygen consumption of crabs in experimental substrates at 7, 14, and 21 days	10
4	Scaphognathite activity of crabs in sand and coal substrates	13
5	Oxygen consumption rates of *Cancer* species	14

LIST OF FIGURES

Figure		Page
1	Lower Fraser River estuary showing the general location of the study area	2
2	Lateral view of experimental plexiglass respiration chamber	4
3	Schematic representation of ventral view of a crab, with one leg removed in illustration to show location of cannula	6
4	Two minute record of scaphognathite activity showing reversed and forward pumping and pausing of scaphognathite of Crab C10 after 7 days on a coal substrate	11

ABSTRACT

Hillaby, Betty A. 1981. The effects of coal dust on ventilation and oxygen consumption in the Dungeness crab, *Cancer Magister*. Can. Tech. Rep. Fish. Aquat. Sci. 1033: vi + 18 p.

Dungeness Crabs, *Cancer magister*, were placed in respirometers containing substrates of various concentrations of coal dust mixed with aquarium sand to determine if oxygen consumption or gill ventilation would be affected by the coal. Additional crabs were placed on sand substrates as controls. Oxygen consumption of the crabs was calculated from various measurements, and movements of water through the branchial chambers of the crabs (gill ventilation) were monitored indirectly. Although trace amounts of coal were deposited on the gill lamellae of the crabs in coal, oxygen consumption of these crabs after seven, fourteen, and twenty-one days on the coal substrates was not significantly different than oxygen consumption of crabs on sand after the same periods of time. Crabs in coal ventilated their gills in the reversed direction for similar periods of time as the crabs in sand. Crabs in sand and crabs in coal demonstrated respiratory pausing behaviour. From these experiments it is apparent that coal dust in the substrate (up to 75% coal-to-sand by volume) has no measureable effect on the oxygen consumption or gill ventilation of crabs over an exposure period of twenty-one days.

Key Words: Crabs, oxygen consumption, scaphognathite activity, coal dust.

RÉSUMÉ

On a mis des crabes de Dungeness (Cancer magister) dans différents respiromètres au fond desquels on a placé un mélange de sable d'aquarium et de charbon en poussière dans des proportions variées, afin de déterminer si l'absorption d'oxygène ou le mouvement de l'eau à travers les branchies sont affectés par la présence de charbon. Au cours de la même expérience, on a mis d'autres crabes sur un fond de sable afin de disposer d'un point de comparaison. On a mesuré l'absorption d'oxygène de plusieurs moyens différents en même temps que l'on mesurait de façon indirecte le mouvement de l'eau passant dans les chambres branchiales des crabes (à travers les branchies). Bien que l'on ait relevé des dépôts de charbon à l'état de traces sur les lamelles des branchies des crabes placés sur le charbon, on n'a pas constaté de différence notable dans l'absorption d'oxygène entre les crabes mis en présence de charbon et les autres, après des périodes de 7, 14 et 21 jours. Après avoir soumis les deux groupes à une expérience de même durée, on a constaté que le mouvement de l'eau à travers les branchies se faisait de la même façon que chez les crabes placés sur un fond de sable, soit en direction inverse de l'écoulement normal. On peut conclure qu'au terme d'une expérience de 21 jours, la présence de charbon en poussière dans le substrat (le charbon occupant jusqu'à 75% du volume total) n'affecte pas de façon mesurable l'absorption d'oxygène ou le mouvement de l'eau à travers les branchies.

Mots-clés: crabe, absorption d'oxygène, battements du scaphognathite, charbon en poussiére.

INTRODUCTION

Roberts Bank, which forms part of British Columbia's Fraser River estuary, supports a substantial commercial fishery for the edible crab, *Cancer magister*. Results from mark and recapture studies carried out in 1981 by Fisheries and Oceans, Canada, estimate that the adult crab population inhabiting the area between the coal port causeway and the Tsawwassen ferry terminal causeway (Figure 1) is between 1.8 to 14.2 crabs per square metre (Bruce Hillaby, unpublished data).

Since April 1970, coal has been shipped from Westshore Terminals, Roberts Bank coal port, located at the southern tip of the Roberts Bank causeway (Figure 1). Coal arrives at the facility by rail, is unloaded, and stockpiled uncovered until loaded by conveyor belt onto ships.

The unloading, stockpiling, and loading practices at the coal port result in coal dust becoming airborne and eventually settling on the water surrounding the facility. The accumulation of coal in bottom sediments around the coal port was documented between March 1970 and October 1971 (Butler 1972). A subsequent study in July 1975 (Pearce and McBride 1977) confirmed the continued increase in sediment coal content around the coal terminal.

Pearce and McBride (1977) assessed the acute toxicity of coal dust to *C. magister* under laboratory conditions. Coal dust was not acutely toxic to the crabs after twenty-two days of exposure to seawater containing a mixture of commercial aquarium sand and coal dust, up to a maximum of 50% coal-to-sand by weight. However, there was a progressive increase in the concentration of coal particles in interlamellar spaces in the gills of the crabs with exposure to higher concentrations of coal, up to 50% by weight.

The gills of crabs are used for gas exchange between their blood and the external environment. Movements of the scaphognathites bring water into the branchial chamber, and determine the direction of water flow over the gills (Hughes *et al.* 1969; McDonald *et al.* 1977). During periods of normal flow, the scaphognathites move water in an anterior direction: water enters the branchial chambers through openings at the bases of the chelipeds and walking legs, is moved anteriorly over the gills, and exits through paired openings between the antennae and mouth parts. A less than ambient pressure, relative to the external water pressure, is maintained inside the branchial chambers during this forward pumping by the scaphognathites. Periodically the scaphognathites also move water in the reverse direction through the branchial chambers creating a higher than ambient pressure within the branchial chambers (McDonald *et al.* 1977). Both scaphognathites may beat at once, moving water in either the forward or reversed direction, only one may beat (unilateral pumping) or both may cease beating (pausing) (McDonald *et al.* 1977; McDonald *et al.* 1980).

Reversed pumping may serve to clean the gills of suspended material (Hughes *et al.* 1969), or to flush out the epibranchial space (Arudpragasam and Naylor 1966). Pausing behaviour may aid in concealing a crab from a predator,

FIGURE I—LOWER FRASER RIVER ESTUARY SHOWING THE GENERAL LOCATION OF THE STUDY AREA

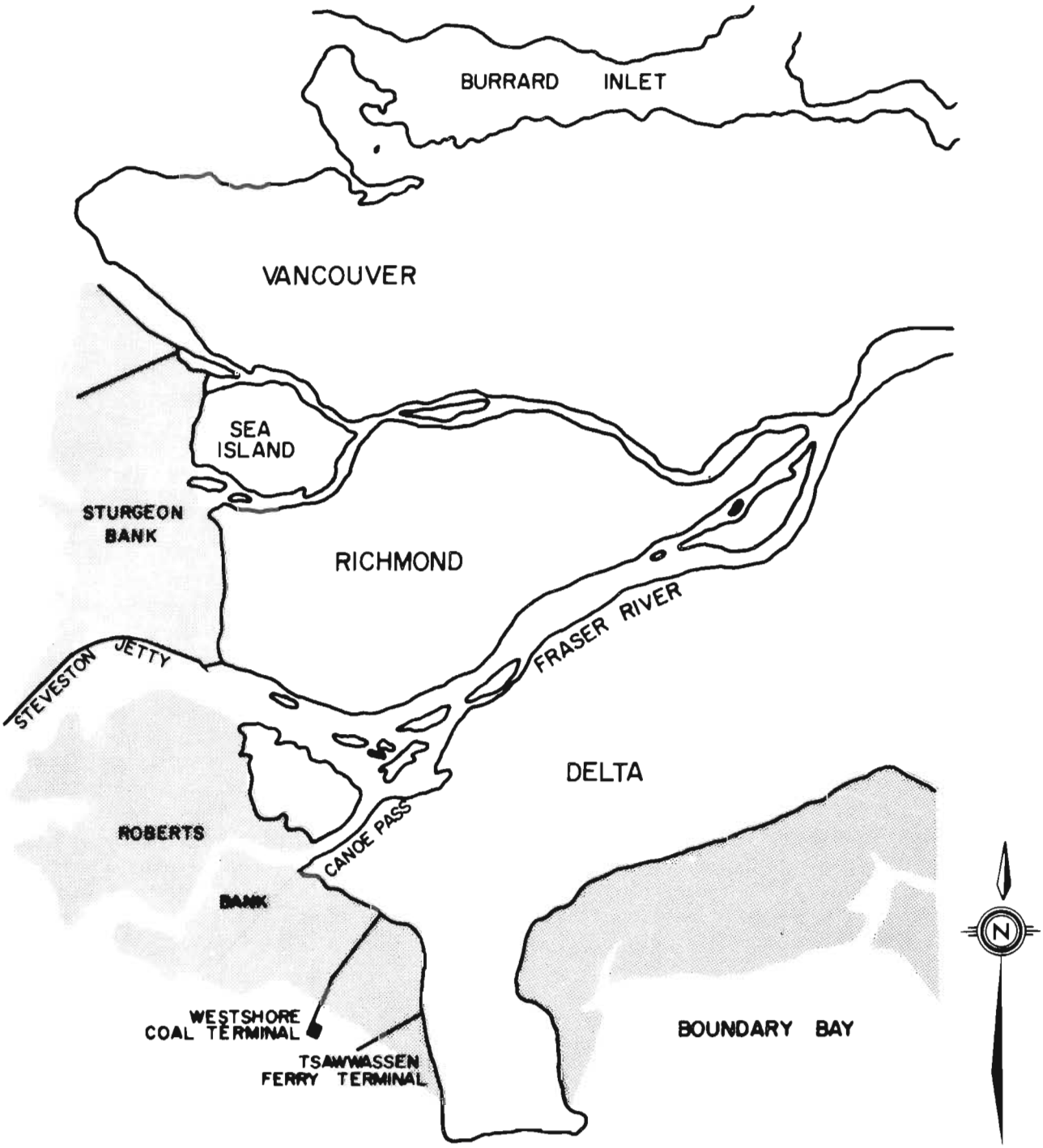

SCALE APPROX.: 1cm. = 2·28 km.

and may be initiated by abrupt external stimulation of sensory receptors (Wilkens *et al.* 1974). In *Cancer productus*, McMahon and Wilkens (1977) demonstrated that pausing behaviour was highest in resting crabs in well-aerated water, and was reduced by conditions which increased oxygen demand or reduced oxygen supply. Changes in scaphognathite activity, whether occurring spontaneously or in response to external stimuli, are considered part of the normal respiratory cycle of crabs (McDonald *et al.* 1977).

If reversals serve as a cleaning function, then particles, such as coal dust, deposited on the gill surface should increase the incidence of reversals in crabs. However, an increase in reversed pumping could result in less efficient oxygen extraction from the water by disrupting the blood-water counter-current flow (Hughes *et al.* 1969). In addition, deposition of coal particles on the gill surface could reduce the area available for respiratory exchange. Increased reversal behaviour and a reduction in respiratory surface could result in less oxygen being extracted from the water by crabs, and therefore either unilateral pumping or pausing would not be expected to occur.

This study was initiated as a result of a proposal to expand the coal shipping facilities at Westshore Terminals on Roberts Bank. Although coal dust settles on the water surface surrounding the terminals, no study has been undertaken to determine the amount of coal suspended in the water column. Coal dust accumulation in the sediments, however, has been well-documented. Therefore, these experiments were designed to determine the effects of various concentrations of coal dust in sediments on both scaphognathite activity and oxygen consumption of the crab, *C. magister*. The objective was to test the hypothesis that coal dust might lead to respiratory impairment in this crab.

MATERIALS AND METHODS

RESPIRATION CHAMBERS AND SUBSTRATES

Respiration chambers (Figure 2) were constructed of "smoked" plexiglass to reduce effects of external stimuli on the crabs. Substrates were placed in the respiration chambers to a depth of 6.4 cm, and seawater was supplied to the chambers in a constant, flow-through arrangement.

Coal dust, collected from beneath a conveyor belt at Westshore Terminals, was screened to obtain a fine fraction. A mixture of coal dust and heat-sterilized commercial aquarium sand was added to the chambers to form a substrate (Table 3). The substrates were placed in the chambers and seawater was allowed to flow through the chambers. The crabs were placed in the chambers fifteen to thirty-one days later. During the course of the experiment a small amount of coal washed out of the chambers.

Most of the sand particles were distributed between 500 and 2000 µm, while most of the coal dust particles were fairly evenly distributed between 3.9 and 500 µm (Table 1).

FIGURE 2-LATERAL VIEW OF EXPERIMENTAL PLEXIGLASS RESPIRATION CHAMBER (A, crab; C, pressure cannula; I, input of fresh seawater; L, sealed removeable lid; S, substrate; X, outflow of seawater)

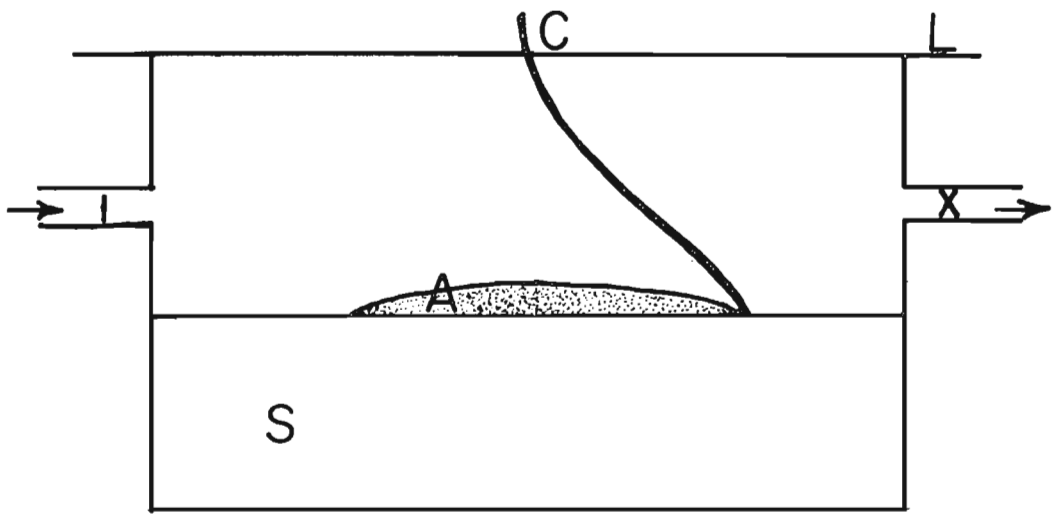

SCALE: 1 cm = 2.54 cm

TABLE 1. Particle sizes of sand and coal.

	Size (μm)	Per Cent of Total Weight
Sand:	4000 - 2000	1.5
	2000 - 1000	27.3
	1000 - 500	64.2
	500 - 250	6.3
	250 - 125	0.3
	125 - 62.5	0.3
	62.5 - 3.9	0.3
Coal:	1000 - 500	0.6
	500 - 250	21.0
	250 - 125	28.7
	125 - 62.5	21.6
	62.5 - 3.9	28.1

EXPERIMENTAL ANIMALS

Dungeness crabs *(Cancer magister)* of both sexes weighing 359±103.8 g, carapace width 134±13.8 mm, ($\bar{x}$±SD, n=16), were used. The crabs, obtained from a commercial crab fisherman, were collected in June of 1977 from live traps at Sturgeon Bank, British Columbia, and transported on the day of capture, to an outdoor seawater tank at the West Vancouver Laboratory, West Vancouver British Columbia. The crabs were maintained in the outdoor tank for up to fifty-one days prior to the experiment, and were fed freshly killed fingerling salmonids.

Experiments were carried out between July and September 1977, in an indoor laboratory with artificial light on a natural photoperiod, and with a constant supply of seawater, at temperatures from 10.5 to 15 °C, salinities from 26.88 to 29.88 °/oo, and oxygen tension from 94 to 132 torr. The seawater was taken from an intake pipe located 18 m below zero tide, and was not aerated as oxygen uptake in *C. magister* has been shown to be relatively independent of external oxygen availability to oxygen tensions as low as 50 torr (Johansen *et al.* 1970).

Prior to placement in respiration chambers, the crabs were scrubbed to remove algal growth, and drilled with a dental drill through the ventral edge of the carapace. A cannula of Intramedic (Clay Adams, Inc.) PE 60 tubing was inserted through the hole to the branchial cavity (Figure 3). The cannula was held in place by the size of the hole.

Crabs were initially placed on a sand substrate (D, 0:100 coal-to-sand, by volume), to serve as their own control, one per respiration chamber, for seven days then measurements were taken for the calculation of oxygen consumption and scaphognathite activity. The crabs were then moved to a chamber containing a sand and coal substrate. Four crabs remained on substrate (D) for the duration of the experiment, and four crabs were placed on each of substrates (A, 25:75 coal-to-sand), (B, 50:50 coal-to-sand), and (C, 75:25 coal-to-sand). One chamber per substrate contained no crab in order to check for possible oxygen uptake by the system.

FIGURE 3—SCHEMATIC REPRESENTATION OF VENTRAL VIEW OF A CRAB, WITH ONE LEG REMOVED IN ILLUSTRATION TO SHOW LOCATION OF CANNULA

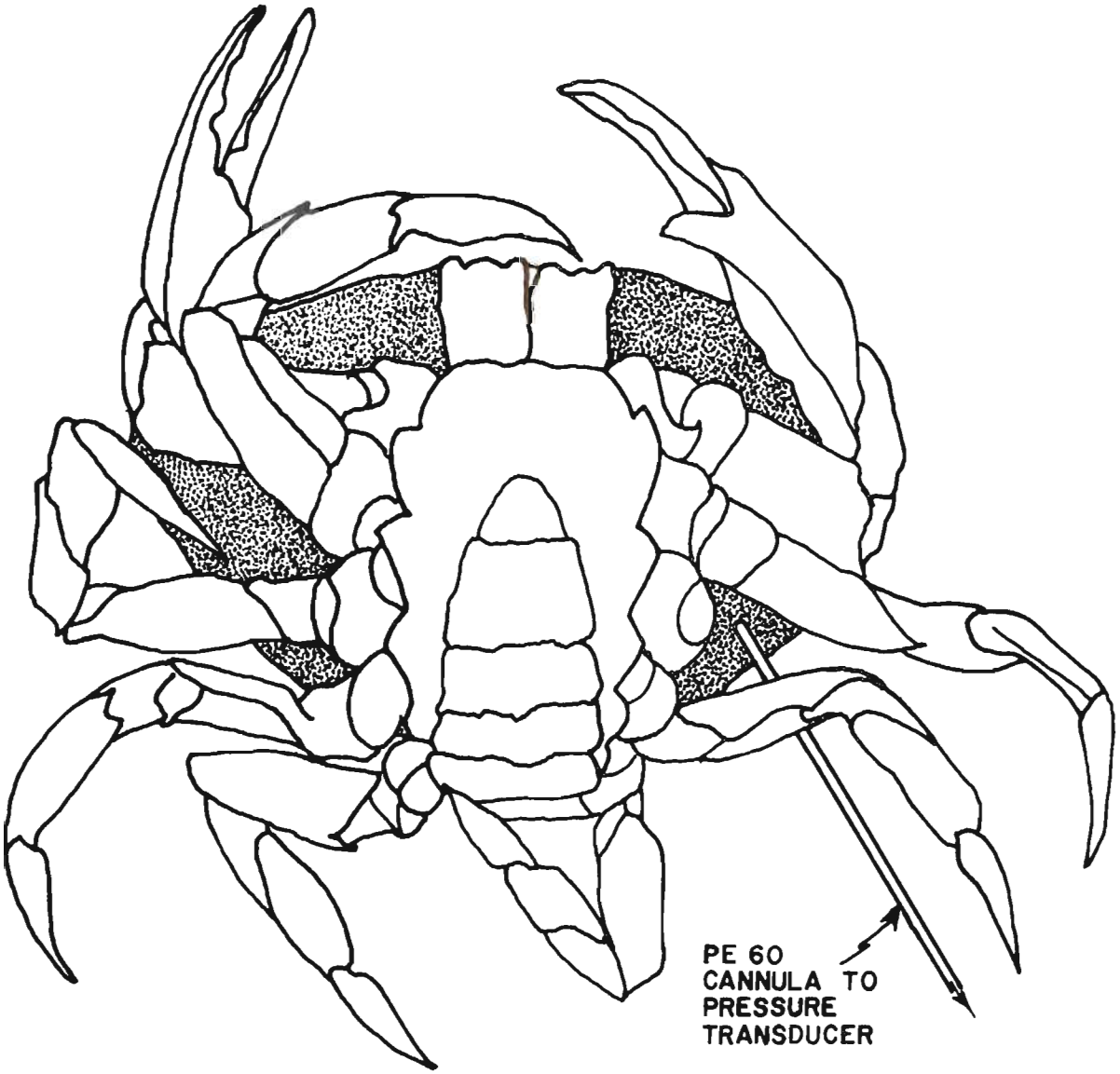

SCALE: 1 mm = 1.21 mm

EXPERIMENTAL PROTOCOL

The following protocol was followed before measurements were made: cannulae previously inserted in the drilled holes were visually examined to determine if still intact, and reinserted if necessary. The lids of the respiration chambers were then sealed, and water flow through the chambers was regulated between 40 to 60 $mL \cdot min^{-1}$ during measurments. The crabs were allowed a recovery period of 2.5 hours before measurements were made. Following the measurements for oxygen consumption and scaphognathite activity, the crabs were fed fingerling coho, and any uneaten food was then removed from the chamber. During the days between measurements, the lids of the respiration chambers were fastened loosely and water flow through the chambers was increased.

CALCULATIONS

Oxygen consumption of the respiration chamber ($\dot{V}_{O_{2(r)}}$), in mL $O_2 \cdot h^{-1}$:

(1) $$\dot{V}_{O_{2(r)}} = (P_{I_{O_2}} - P_{E_{O_2}}) \times \alpha\omega O_2 \times F$$

where $P_{I_{O_2}}$ and $P_{E_{O_2}}$ are the partial pressures of oxygen in water, in torr, flowing into and out of the respiration chamber, respectively, $\alpha\omega O_2$ is the oxygen solubility coefficient in water at the test temperature, in mL $O_2 \cdot$mL $H_2O^{-1} \cdot torr^{-1}$, and F is the flow of water through the chamber, in mL $H_2O \cdot h^{-1}$. $\alpha\omega O_2$ was calculated from daily salinity and temperature measurements (Truesdale *et al.* 1957).

Oxygen consumption per unit weight of a crab ($\dot{V}_{O_{2(c)}}$), in mL $O_2 \cdot kg^{-1} \cdot h^{-1}$:

(2) $$\dot{V}_{O_{2(c)}} = \frac{((P_{I_{O_2}} - P_{E_{O_2}}) \times \alpha\omega O_2 \times F) - V_{O_{2(r)}}}{W}$$

where W is the weight of the crab, in kg.

OXYGEN CONSUMPTION

Measurements of water flow and partial pressure of oxygen in the water, used in the calculation of oxygen consumption, were made for the control chambers without crabs, and for chambers containing crabs on a sand substrate, and at seven, fourteen, and twenty-one days following placement of the crabs in the experimental substrates, over a twenty-five day period from 19 August to 12 September 1977.

Oxygen consumption of the crabs was corrected for the oxygen consumption of the control chambers. In those cases where the control chamber oxygen consumption was greater than crab oxygen consumption, the crab oxygen consumption was considered to be zero.

As time constraints prevented measurements being made on all crabs on the same day (four replicates of four crabs on each of the four substrates), measurements were made on only four crabs per day, one crab per substrate. The order of measurement was preplanned from a random number table.

Oxygen consumption was not calculated when the crabs had been on the sand substrate for seven days prior to being moved to the coal substrates, and for the first crabs on each substrate after seven days on the respective substrates due to difficulties encountered with the oxygen electrode. Data were discarded for one crab which was observed at the end of the experiment to be carrying eggs, and for two crabs when measurements were made two days following feeding, as preliminary data analysis demonstrated that oxygen consumption was significantly higher in these crabs than in crabs on the same substrates when measurements were made four or more days following feeding. All of the crabs offered food did not eat each time so there was a range of four to twenty days between feeding and measurements in those crabs used in the calculation of oxygen consumption.

P_{O_2} measurements were made with a Radiometer P_{O_2} electrode connected to a Radiometer PHM 72 acid-base analyser. The electrode was contained in a thermostated cell and maintained at the same temperature as the crabs. The electrode was set to zero daily with commercial oxygen-free solution (Radiometer Copenhagen), maintained at the same temperature as the electrode. The electrode was calibrated with water vapour equilibrated with atmospheric air, checked after one or two measurements, and readjusted as necessary.

SCAPHOGNATHITE ACTIVITY

Scaphognathite activity, for one branchial chamber only, was measured indirectly by monitoring pressure changes in the branchial chamber via a pressure transducer system (Statham P23BB and Beckman RM Dynograph Recorder) connected to a water-filled cannula of Intramedic PE 60 tubing inserted into the branchial chamber. The system was set to zero prior to each recording, but was not calibrated.

As only one scaphognathite per crab was monitored, it was not possible to differentiate between pausing (cessation of pumping by both scaphognathites) and unilateral pumping (cessation of pumping by one scaphognathite) (McDonald *et al.* 1980) so the term "pausing" as used herein could refer to either case.

The total recording time for each crab was divided into periods of ten minutes each and the number of reversals or pauses for each period was noted. The ten minute periods were further divided into sixty second periods and the forward pumping rates were calculated as beats per minute (BPM) of the scaphognathite.

Duration of forward pumping was the time spent in forward pumping of the scaphognathite between either reversed pumping or pausing. Duration of reversed pumping (or pausing) was the time spent in the respective activity. As the total recording times of scaphognathite activity varied for each animal, values for scaphognathite activity were averaged over the total recording time of each animal.

HISTOLOGY

At the end of the experiment gill sections were removed from two crabs from each treatment, and retained for histological examination.

STATISTICAL ANALYSIS

Unless otherwise reported, values are given as the mean plus or minus one standard deviation ($\bar{x}\pm SD$). The level of significance used for all statistical tests was $P \leq 0.05$.

In order to take repeated measurements on the same animal (used in the calculation of oxygen consumption) into consideration, analysis of variance was performed only on data from crabs which were measured at each of seven, fourteen, and twenty-one days on the experimental substrates.

As a result of poor recordings, or no recordings, of scaphognathite activity from many of the crabs, the data obtained from crabs in all coal substrates were combined for comparison with crabs on the sand substrate.

RESULTS

OXYGEN CONSUMPTION

The oxygen content of the seawater flowing into the respiration chambers ranged between 59.3 to 83.5 (average 68.2) per cent of air saturation. Mean incoming water P_{O_2}, oxygen content, temperature, and salinity are shown in Table 2.

TABLE 2. Characteristics of seawater flowing into the respiration chambers ($\bar{x}\pm SD(n)$).

$P_{I_{O_2}}$ (torr)	O_2 Content ($mL \cdot L^{-1}$)	Temperature (^oC)	Salinity ($^o/oo$)
107.7±0.54(188)	4.21±0.02(188)	11.5±0.24(11)	28.57±0.26(11)

Analysis of the oxygen consumption data indicated the following:

Control Chambers

Analysis of variance using a 4 x 3 factorial, with repeated measures (Winer 1962) on data from the control chambers containing no crabs revealed that the variable "time" had a significant effect on the oxygen consumption of the chambers, but that the variables "substrate" and "time and substrate interaction" had no significant effects. Subsequent analysis using the Newman-Keuls Procedure (Winer 1962) demonstrated that oxygen consumption of the chambers was greatest after twenty-one days, and ranged between 0.14 to 0.72 mL $O_2 \cdot h^{-1}$ over the total time.

Chambers With Crabs

Oxygen consumption of the crabs ranged between 0 to 22.17 mL $O_2 \cdot kg^{-1} \cdot h^{-1}$ (Table 3). Analysis of variance using a 4 x 3 factorial, with repeated measures (Winer 1962) on data from the chambers containing crabs with various substrates indicated no significant differences in oxygen consumption with respect to the variables "time", "substrate", or "time and substrate interaction". As there were no significant differences, oxygen consumption data of the crabs were combined to give an average rate of 10.46±4.53 (n=24) mL $O_2 \cdot kg^{-1} \cdot h^{-1}$.

TABLE 3. Oxygen consumption of crabs in experimental substrates at 7, 14, and 21 days (each value is calculated from four measurements made throughout the day on a single crab, and is reported as $\bar{x}$±SD).

Substrate (% Coal:Sand)	Crab Number	$V_{O_{2(c)}}$ (mL $O_2 \cdot kg^{-1} \cdot h^{-1}$) at: 7 Days	14 Days	21 Days
25: 75 (A)	A 1	--[a]	9.40±4.08	14.43±1.39
"	A 2	12.19±1.43	6.70±3.76	9.68±2.64
"	A 3	10.01±2.75	11.56±1.69	10.87±2.07
50: 50 (B)	B 4	--[a]	5.01±0.59	9.19±2.56
"	B 5	11.73±4.56	22.17±1.42	14.74±1.35
"	B 6	--[a]	13.57±2.46	2.37±3.20
"	B 7	14.51±1.96	12.54±2.12	10.79±2.12
75: 25 (C)	C 8	--[a]	9.53±2.64	0.81±1.62
"	C 9	1.48±2.34	7.25±2.61	0[b]
"	C10	10.56±0.92	15.52±0.94	11.75±0.49
0:100 (D)	D11	--[a]	11.53±3.95	7.64±3.29
"	D12	9.74±4.52	9.75±0.33	4.91±2.93
"	A 2	7.13±4.79	--[c]	--[c]
"	D13	10.62±4.69	13.64±1.66	8.22±1.31

[a] "--" P_{O_2} measurements not recorded because of difficulties with the oxygen electrode

[b] "0" oxygen uptake by the system was greater than oxygen consumption of the crab

[c] "--" crab was moved to a coal substrate

SCAPHOGNATHITE ACTIVITY

A typical recording, illustrating both forward and reversed pumping, and pausing, is shown in Figure 4.

In comparison to crabs in coal, crabs in sand spent significantly more time in forward pumping by the scaphognathite. The scaphognathite forward pumping rate was significantly faster for crabs in sand (107±29.1

FIGURE 4—TWO MINUTE RECORD OF SCAPHOGNATHITE ACTIVITY SHOWING REVERSED (R) AND FORWARD (F) PUMPING AND PAUSING (P) IN CRAB C10 AFTER 7 DAYS ON COAL SUBSTRATE C (Top trace is chart speed at 1mm per second)

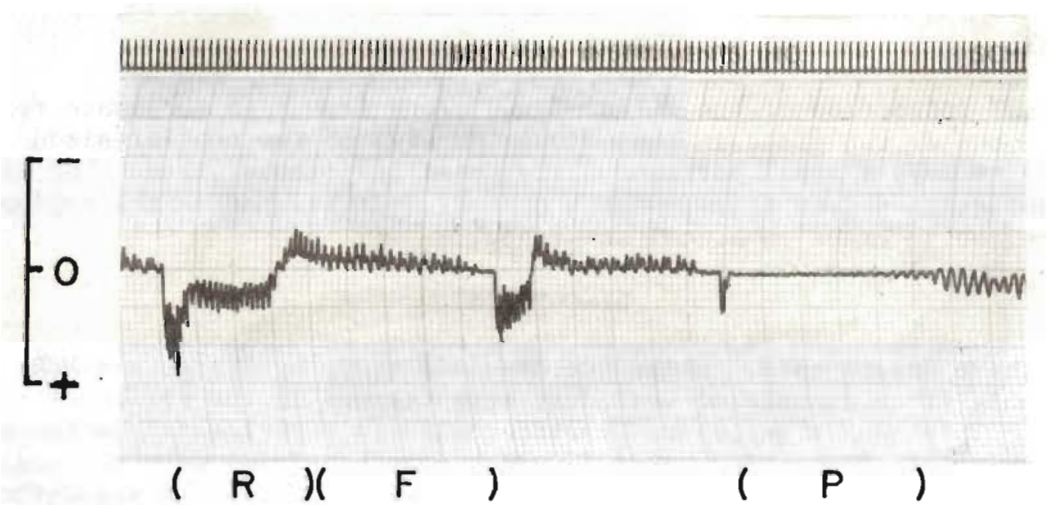

29.1 (n=40) beats per minute (BPM)) than for crabs in coal (79±28.7 (n=87) BPM, Table 4, Student's t-test).

There were no differences in the time spent in reversed pumping, nor in the number of reversals per ten minute period, between crabs in sand and crabs in coal (Table 4, Student's t-test).

Only one crab in sand demonstrated pausing behaviour with the pauses ranging from sixteen seconds to fourteen minutes in length. Four of the crabs in coal demonstrated pausing behaviour, with the pauses ranging from three seconds to greater than twenty-four minutes in length.

BURROWING ACTIVITY

The burrowing reaction of the crabs differed with the four substrates. Crabs in sand (substrate D) never completely burrowed, but remained either completely exposed, or with only a fraction of the rear portion of their carapace buried. The proportion of carapace buried increased with increasing amounts of coal in the substrate, so that in substrate (C) the crabs burrowed completely under the surface, with only eyes and antennae remaining visible.

HISTOLOGY

Visual inspection of the gills of two crabs from each substrate revealed damage to one or two gills in the cannulated area of the smaller-sized crabs, amounting to only a small portion of the total respiratory area. The histological examination showed trace amounts of coal dust trapped in the region of the gill lamellae in crabs on a coal substrate.

DISCUSSION

In these experiments, unlike the previous study by Pearce and McBride (1977), only trace amounts of coal dust were trapped in the region of the gill lamellae. This can be explained by differences in experimental design between the two studies: Pearce and McBride used a static system, with the coal and sand mixed with the water so that some coal always remained in suspension, in order to test the toxicity of coal dust to crabs; in my experiments the crabs were placed on the appropriate substrates in flow-through chambers for calculation of oxygen consumption of the crabs and to test the effects of coal in the substrate on the oxygen consumption and ventilation of the crabs.

In comparison with literature values for oxygen consumption of *Cancer* species (Table 5), the average resting rate from this study is equivalent to the average standard rate of *C. pagurus* (Aldrich 1975), and lies within the lower range for routine respiration of *C. pagurus* (Ansell 1973) and *C. magister* (Prentice and Schneider 1979). However, oxygen consumption rates from this study are lower than those reported for *C. magister* by Johansen *et al.* (1970) and by McDonald *et al.* (1980).

TABLE 4. Scaphognathite activity of crabs in sand and coal substrates ($\bar{x}$±SD, (n)).

Crab Number	Substrate (% Coal: Sand)	Time in Substrate (d)[a]	Duration of Periods of Forward Pumping (s)[b]	Duration of Periods of Reversed Pumping (s)	Duration of Periods of Pausing (s)	Scaphognathite Forward Pumping Rate (BPM)[c]	Number of Reversals Per Ten Minutes	Number of Pauses Per Ten Minutes
A 2	0:100(D)	14	561±357.1(4)	15± 1.7(6)	0	112±119.0(11)	1 ±1.2 (3)	0 ±0 (3)
D 3	"	8	746±509.1(9)	57± 90.9(9)	426±346.8(6)	69± 19.3(10)	0.5 ±0.51(17)	0.7±0.69(17)
D 9	"	13	454±225.1(5)	13± 3.7(6)	0	133± 6.3(10)	1 ±0.96(4)	0 ±0 (4)
D10	"	6	347±270.0(8)	18± 9.0(9)	0	--[d]	2 ±0.82(4)	0 ±0 (4)
D12	"	14	97 (1)	10± 5.5(3)	0	102± 22.3(9)	0 (1)	0 (1)
	Overall Mean:		522±396.0(27)	27± 49.5(33)	426±346.8(6)	107± 29.1(40)	0.86±0.90(29)	
A 1	25:75(A)	9	98± 76.0(21)	18± 4.7(20)	13± 6.3(6)[e]	82± 9.7(10)	3 ±2.8 (8)	1 ±0.83(8)
B 4	50:50(B)	9	414±366.5(4)	24± 15.9(5)	0	66± 5.0(10)	1 ±0 (3)	0 ±0 (3)
B 5	"	14	395±183.7(17)	15± 2.2(18)	0	130± 6.2(10)	2 ±0.52(11)	0 ±0 (11)
C 8	75:25(C)	9	413±355.6(11)	0±	36± 18.0(11)	88± 6.6(10)	0 ±0 (8)	2 ±0.76(8)
C 9	"	9	713±656.5(10)	0±	24± 10.7(11)[f]	44± 24.2(17)	0 ±0 (12)	1 ±1.0 (12)
C10	"	7	57± 40.5(14)	56±100.3(10)	11± 9.5(6)	73± 25.7(10)	5 ±2.8 (2)	2 ±2.8 (2)
C10	"	14	292±188.8(9)	26± 11.7(11)	0	83± 8.7(10)	2 ±1.3 (5)	0 ±0 (5)
C10	"	21	580±522.6(11)	29± 19.3(12)	0	95± 9.0(10)	1 ±0.77(11)	0 ±0 (11)
	Overall Mean:		329±378.3(97)	26± 38.3(78)	24± 15.9(34)	79± 28.7(87)	1.2 ±1.60(60)	

[a] "d" days

[b] "s" seconds

[c] "BPM" beats per minute

[d] "--" unable to determine rate

[e] crab paused for +1960 seconds at the end of recording

[f] crab paused for + 750 seconds at the end of recording

TABLE 5. Oxygen consumption rates of *Cancer* species.

Species	Activity	$\dot{V}_{O_2}$ (mL $O_2 \cdot kg^{-1} \cdot h^{-1}$)	Source
Cancer magister	resting - average	10.46	This study
	- range	0 to 22.17	
C. magister	routine respiration	7 to 50	approximated from graph by Prentice and Schneider (1979)
C. magister	resting (but including spontaneous activity)	25.2 to 50.4	Johansen *et al.* (1970)
C. magister	forward pumping	25.27	converted for comparison from McDonald *et al.* (1980)
	reverse pumping	16.26	
	before pausing	21.10	
	after pausing	38.84	
C. pagurus	minimum standard rate	4.0	converted for comparison from Aldrich (1975)
	average standard rate	10.0	
	average starved excited rate	17.0	
	average fed standard rate	22.5	
	average fed excited rate	25.5	
	maximum fed excited rate	53.0	
C. pagurus	routine respiration	9.6 to 78.8	converted for comparison from Ansell (1973)

Prentice and Schneider (1979) transferred their crabs to the respirometers immediately prior to measuring oxygen consumption, therefore the higher range reported could be as a result of insufficient acclimation time.

McDonald *et al.* (1977) reported ventilation levels (branchial water flow) in *C. magister* as high as those reported by Johansen *et al.* (1970) only after some type of disturbance to the crabs. The lower values for oxygen consumption obtained in my experiment from undisturbed crabs maintained in the respiration chambers for the total length of the experiment suggest that oxygen consumption values reported by Johansen *et al.* (1970) also may not be from resting crabs. Crabs maintained in respirometers tend to be more inactive than crabs kept in aquaria, and would be expected to spend more time in unilateral pumping or pausing behaviour, resulting in low oxygen consumption rates (D.G. McDonald, personal communication).

Although no significant differences were found in the oxygen consumption between crabs on the four substrates over the period of the experiment, differences may have been obscured by the great variability between crabs under the same treatment conditions. In order to overcome this individual variability, a much larger number of experimental animals should have been used.

Variability in oxygen consumption between crabs on the same substrate may also be attributed to other factors such as:

1. Many of the animals used in this study ecdysed while in the outdoor holding tank prior to commencement of the experiments. Lewis and Haefner, Jr. (1976) reported that respiratory rates of *Callinectes sapidus* varied with the stage of molt.

2. The use of wet weights in calculating oxygen consumption may introduce variability as the amount of water retained in the branchial chambers may vary with each crab (Lewis and Haefner, Jr. 1976).

3. Oxygen consumption could differ with the degree of burrowing by the crabs in the substrate; crabs on the surface may be in a state of apparent greater alertness. Ansell (1973) reported higher rates of oxygen consumption in *Cancer pagurus* when the body was held above the substrate.

The second objective of this experiment was to determine any effects of coal dust on scaphognathite activity. Coal was deposited on the gill lamellae only in crabs in a coal substrate. However, no significant differences were found in either the number of reversals or the length of reversals between crabs in sand and crabs in coal. A greater number of crabs were observed to pause in coal than in sand. Coal dust in the substrate, under these experimental conditions, neither had an affect on the respiratory reversal activity of the crabs, nor prevented pausing behaviour.

The faster scaphognathite forward pumping rate for crabs in sand (107 $\pm$ 29.9 (n=40) BPM) compared to crabs in coal (79 $\pm$ 28.7 (n=87) PBM) in these experiments could be the result of the crabs remaining on the surface of the sand, and therefore exhibiting a greater degree of alertness than the crabs in coal which were burrowed under the surface. McDonald *et al.*(1977) reported scaphognathite forward pumping rates of 104 BPM in crabs which burrowed following a disturbance, and of 50 BPM for crabs prior to the onset of unilateral pumping.

Because of the individual variability of the crabs, as well as the variability between crabs under the same treatment conditions, a much larger number of animals should have been used in these experiments. However, the presence of both pausing and reversal behaviour even in crabs in the highest coal concentration (substrate C) suggests that resting oxygen demands can be adequately met with coal dust on the gill lamellae and in the substrate at the experimental levels.

Further studies, using a much larger number of animals, should be carried out to determine if oxygen demands of active crabs can be adequately met in the presence of suspended coal dust in seawater.

ACKNOWLEDGMENTS

I wish to thank G. Primrose for collecting the crabs, B. Pearce for his aid in collecting the coal dust and for discussions relating to his experiments, J. McBride for the histology work, I. Birtwell for his aid in designing the experiment and his comments and review of the final report, M. Nassichuk for his comments and review of the final report, and a special thanks to W. Burggren for drilling the hole in the crabs for cannulae, and D. Randall and J. Davis for their discussion throughout the experiment, and for reviewing and commenting on the data and final report.

REFERENCES

Aldrich, John C. 1975. On the oxygen consumption of the crabs *Cancer pagurus* (L.) and *Maia squinado* (Herbst). Comp. Biochem. Physiol. 50A: 223-228.

Ansell, A.D. 1973. Changes in oxygen consumption, heart rate and ventilation accompanying starvation in the decapod crustacean *Cancer pagurus*. Neth. J. Sea Res. 7: 455-475.

Arudpragasam, K.D., and E. Naylor. 1966. Patterns of gill ventilation in some Decapod Crustacea. J. Zool. Soc. 150: 401-411.

Butler, T.H. 1972. Interim report on occurrence of coal in bottom sediments from Roberts Bank. MS Rep. Fish. Res. Bd. Canada. 7 p. plus figures and tables.

Hughes, G.M., B. Knights, and C.A. Scammell. 1969. The distribution of PO_2 and hydrostatic pressure changes within the branchial chambers in relation to gill ventilation of the shore crab *Carcinus maenas* L. J. Exp. Biol. 51: 203-220.

Johansen, K., C. Lenfant, and J.A. Mecklenburg. 1970. Respiration in the crab, *Cancer magister*. Zeitsch. vergl. Physiol. 70: 1-19 (now J. Comp. Physiol.A).

Lewis, Elizabeth G., and Paul A. Haefner, Jr. 1976. Oxygen consumption of the blue crab *Callinectes sapidus* Rathbun, from proecdysis to postecdysis. Comp. Biochem. Physiol. 54A: 55-60.

McDonald, D.G., B.R. McMahon, and C.M. Wood. 1977. Patterns of heart and scaphognathite activity in the crab *Cancer magister*. J. Exp. Zool. 202(1): 33-44.

McDonald, D.G., C.M. Wood, and B.R. McMahon. 1980. Ventilation and oxygen consumption in the Dungeness Crab, *Cancer magister*. J. Exp. Zool. 213: 123-136.

McMahon, B.R., and J.L. Wilkens. 1977. Periodic respiratory and circulatory performance in the red rock crab *Cancer productus*. J. Exp. Zool. 202(3): 363-374.

Pearce, B.C., and J. McBride. 1977. A preliminary study on the occurrence of coal dust in Roberts Bank sediments and the effect of coal dust on selected fauna. FMS Tech. Rep. Ser. No. PAC/T-77-17. 43 p.

Prentice, E.J., and D.E. Schneider. 1979. Respiration and thermal tolerance of the Dungeness Crab, *Cancer magister* Dana. Comp. Biochem. Physiol. 63A: 591-597.

Truesdale, G.A., and A.L.H. Gameson. 1957. The solubility of oxygen in saline water. Extr. J. Cons., Cons. Int. Explor. Mer. 22: 163-166.

Wilkens, J.L., L.A. Wilkens, and B.R. McMahon. 1974. Central control of cardiac and scaphognathite pacemakers in the crab, *Cancer magister*. J. Comp. Physiol. 90: 89-104.

Winer, B.J. 1962. Statistical Principles in Experimental Design. McGraw-Hill Book Company. New York. pp. 140-378.

PRB COAL DEGRADATION – CAUSES AND CURES

By

Roderick J. Hossfeld
Jenike & Johanson, Inc.
1 technology Park Drive
Westford, MA 01886-3189
978.392.0300 (voice) 978.392.9980 (fax)
rjhossfeld@jenike.com

Rod Hatt
Coal Combustion Inc.
114 South Main Street
Versailles, KY
859.873.0188 (voice)
rod_hatt@coalcombustion.com

Introduction

The coals produced in the Powder River Basin (PRB) are environmentally and economically attractive to power companies. This type of coal has made enormous inroads to power plants due to these factors regardless of any difficulties plant personnel might experience. The difficulties in handling and storing PRB coal are due to fines generation and spontaneous combustion issues. Many [1-9] have worked on addressing these concerns and how we can improve our utilization of these fuels. Refer to APPENDIX A for basic bulk solids handling considerations for PRB coal.

PRB coal is extremely friable and will break down into smaller particles virtually independent of how the coal is transported or handled. PRB represents the extremes of handling problems: *dust* is an issue when the coal is fine and dry; *plugging* in bunkers and chutes is an issue when the same fine coal is wet. Once PRB coal is exposed by mining, the degradation process begins – the majority of the damage can occur in a very short time, even as short as a few days. The extent of the degradation that occurs depends in large part on the distance to the plant from the mine, i.e., how long the coal is exposed to the atmosphere during transportation. Additional factors such as crushed run of mine (CROM) size, and specific handling procedures also impact the degradation process. Additional decomposition occurs during handling and storage in a pile and bunker, bin or silo. We believe the root cause of the degradation is loss of moisture that impacts the coal both mechanically and chemically, through the generation of additional surface reaction area. The combination of the two is what makes PRB coal so difficult to handle.

This paper focuses on the mechanisms, both inherent and external, that cause this rapid degradation of the coal particles. Some of the questions are posed that could lead to preventing, or at least retarding the degradation of the particles, thus avoiding the results of the associated problems with handling and storage, such as dust, perceived loss of inventory, bunker hang-ups and especially spontaneous combustion.

What is PRB coal?

The Powder River Basin extends from Wyoming into Southeast Montana, with the bulk of the PRB coal being supplied from the Southern Powder River Basin (Wyoming). PRB is classified by the American Society for Testing and Materials (ASTM) as a sub-bituminous A or B [10] coal. Scientists report that these coals have been burning naturally for over 2 million years. Early Native Americans held these coal fired lands to be spiritual. Prehistoric inhabitants of the Powder River Basin used porcellanite as weapons and tools. Porcellanite is formed from the intensively coal baked shale or siltstone near or in the coal as it burned. We know this material today as *slag*. The fires are in part caused by the spontaneous combustion of coal. These same properties show up at the plant as hot coal, fires and explosions. While low in sulfur (0.4 to 1.4 LB/MMBTU), PRB coal is also low in heating value (8,000 to 8,800 BTU/LB, on an *as received* basis for Southern PRB, with one or two mines in the north going as high as 9,400 BTU/LB). Additionally, its friability results in fines and, when dry, the dust (Fig. 1) increases the explosion hazard potential. On the other hand, this same fine coal can be high in moisture content (Fig. 2), which increases its handling difficulty in equipment. Most of the plants currently burning or converting to burn PRB coal have difficulty with these characteristics.

Fig. 1 PRB coal – *dry*

Fig. 2 PRB coal – *wet*

The relatively low ranking of PRB coal means that the coal is relatively young. Specific ASTM ranking is just a laboratory method for drawing a line in the sand to differentiate different types of coals. It is basically describing the geological process of transforming plant material to anthracite. The first phase of coalification (fossilization) is to preserve the plant material from oxidation. This peat moss like material is still basically plant material. The first coal-like material formed is lignite, or brown coal. The coalification process basically squeezes out oxygen and water. As the plant material becomes less like wood and more like oil, the pore structure constricts, limiting the water retention capacity of a coal chemically; as the oxygen content decreases the coal becomes more hydrophobic or water repelling (water and oil don't mix). This water retention capacity is measured using the equilibrium moisture test. Sub-bituminous coals like the PRB coals are the next step up in the coal ranking system. Then comes the low ranked Bituminous C type coal. This is the ranking of many Illinois Basin coals. The higher ranked Bituminous B and C coals are generally found in the Appalachian coalfields. Most of the coal tests that ASTM has standardized were written around higher ranked bituminous and anthracite coals. The tight pore structures of these coals limit the amount of inherent moisture they can hold. Typically these high ranked coals have equilibrium moistures of between 1 and 10. The first step of determining coal quality in the lab is to air-dry the

sample to near equilibrium with the laboratory humidity levels. This is done to minimize any impact on lab results of additional drying or absorption of water from the air. In high rank coals, the moisture lost in the air-drying step is near equivalent to the surface moisture.

The residual moisture is that moisture that is still locked up in the coal after air-drying. The higher ranked coals that ASTM standards were based on possess this well-defined split between the air-dried or surface moisture and the residual or near equilibrium moisture. This is not the case for low rank coals like PRB coal. The sponge-like or wood like nature of PRB coals make the split between surface moisture and inherent moisture a rather fuzzy line.

Most of the quality differences between PRB coal and the higher ranked coal are due to the PRB coal's looser pore structure and additional moisture retention capacity. PRB coal also has more oxygen chemically bonded to the coal, which makes the coal hydrophilic (water-liking). This helps explain why the PRB coal is likely to reabsorb water after it has dried and degraded.

Self-heating characteristics

Spontaneous combustion of coal is a well-known phenomenon, especially with PRB coal. This high-moisture, highly volatile sub-bituminous coal will not only smolder and catch fire while in storage piles at power plants and coal terminals, but has been known to be delivered to a power plant with the rail car or barge partially on fire.

An "explosive" case study [11] was presented at the PRBCUG (Powder River Basin Coal Users Group) Annual Meeting in Houston, March 2003 that is a case in point. The dust in a tripper room ignited, causing a major explosion (Figure 3) at Wisconsin Public Service J.P. Pulliam Generating Station in Green Bay Wisconsin in June 1991. At the time, the plant was burning a 50/50 blend of PRB coal and bituminous coal, and a fire existed in one of the coal bunkers. Dust within the atmosphere of the tripper room was ignited by a minor explosion, or *puff*, within the bunker, which triggered a massive explosion in the tripper room, blowing out the outer building walls and roof. While fires prior to this were not uncommon with bituminous coal in the bunker, this was the first serious dust explosion.

Figure 3. Tripper room after explosion at WPS J. P. Pulliam Generating Station

The coal properties that affect spontaneous combustion risk include [12]:

- Moisture content of the PRB coal - or how much drying and rewetting occurs during handling.
- Friability - or how much size degradation occurs.
- Particle size - or exposed surface reaction area.
- Rank - PRB coal contains a high percentage of reactive components that tend to decompose as a coal's rank increases to Bituminous and Anthracite.
- Pyrite concentrations greater than two percent - PRB coal is low in pyrite, so the risk due to this effect is low.

These properties primarily influence the rate of heat generation during the self-heating of coal. Since most of the combustible matter in coal is carbon, when coal is stored in an atmospheric environment, the carbon slowly oxidizes to form carbon dioxide and carbon monoxide. PRB coal is also one of the highest hydrogen content coals. The oxidation reaction with hydrogen forms water. The production of both water and carbon gases in the coal will not help the situation. These reactions produce heat; since coal is a relatively good insulator, much of this heat is trapped, increasing both the temperature and the rate of oxidation. Depending on how the coal is stored, heat production may substantially exceed heat loss to the environment, and the coal can self-ignite.

Self-heating occurs when the rate of heat generation exceeds the rate of heat dissipation. Two mechanisms contribute to the rate of heat generation, coal oxidation and the adsorption of moisture. The reactivity of coal is a measure of its potential to oxidize when exposed to air. The mechanism of coal oxidation is not completely understood. The coal's minimum Self Heating Temperature (SHT) is sometimes used as a relative indication of its reactivity. There are various methods used to determine a coal's minimum SHT, but they all require running a test in real time and monitoring the temperature of the coal as any reaction occurs. These tests are typically a relative measure of a coal's propensity to self-ignite. In general, a coal's reactivity increases with decreasing rank.

The moisture content of a coal is also an important parameter in the rate of heat generation of the coal. Drying coal is an endothermic process, in which heat is absorbed, and the temperature of the coal is lowered. The adsorption of moisture on a dry coal surface is an exothermic process, with a heat producing reaction. If it is partially dried during its mining, storage, or processing, coal has the potential to readsorb moisture, thus producing heat. Therefore, the higher the moisture content of the coal, the greater the potential for this to occur. The most dangerous scenario for spontaneous combustion is when wet and dry coals are combined; the interface between wet and dry coal becomes a heat exchanger [13]. If coal is either completely wet or completely dry, the risk is substantially reduced. In general, the moisture content of coal increases with decreasing rank. For example, PRB coal has a higher inherent moisture content than bituminous B type coal.

Friability and previous oxidation of the coal are also important factors in the self-heating process. The friability of the coal is a measure of the coal's ability to break apart into smaller pieces. This exposes fresh coal surfaces to air and moisture, where oxidation and moisture adsorption can occur. Previous oxidation makes coal more friable. Although the oxidized matter is less reactive, the porous nature of the oxidized coal makes the coal more susceptible to air and water leakage when exposed to higher pressure differentials, such as in a pile or bunker.

The oxidation of sulfur in pyrite is also a heat producing reaction. The heat generated can cause the temperature of the surrounding coal to increase, thus increasing the rate of oxidation. Also, as it oxidizes, the sulfur expands, causing coal degradation to occur. Fortunately, PRB coal contains less than the minimum two percent concentration of pyrite considered necessary for a reaction.

Causes of degradation

From the time it leaves the mine, PRB coal starts to degrade. The most dramatic result of this can be found by observing the top surface of an open railcar delivering PRB coal to the plant from the mine. The large particles have distinct cracks and will shatter into smaller pieces when dropped from a height of only 6 feet. Particles contained deeper in the bed of coal within the railcar do not appear to be similarly affected.

The root cause of this degradation of PRB is the drying and resultant cracking and particle size degradation and oxidation. There are many variables that are potential contributors to attrition of PRB coal once it is exposed to air: ambient temperature (heat), moisture (addition and loss), compaction, impact (drop height), interparticle motion (due to general handling), and time. It is felt that all of these variables impact the total degradation process, however the loss of moisture appears to dominate the process.

The moisture that contributes to the problem of spontaneous combustion comes from humidity and from other PRB coal. New PRB coal added over old PRB coal seems to create more heat at that interface. The fine particles typically have a higher total moisture content compared to the coarse particles, due to their larger surface area per unit volume. Generally, each time a particle diameter is reduced by half due to breakage, the surface area doubles. This is true for smooth surface spheres or cubes. Coals, especially those low in rank, have a significant amount of surface area that resides *within* the pore structure. This would indicate there is a potential for significantly more surface area being available when fines are generated. Also, this available surface area increases as the particle becomes drier, and the pores that were filled with moisture become available for oxygen adsorption.

Test program

The test program investigated the influence of one variable on the degradation process – *time*. In a relatively dry environment, as time proceeded, the coal dried out. As it dried out, the coal cracked and broke down into smaller particles. The role that particle size plays in this process can be investigated by exposing both large and small particles to a controlled environment (temperature and moisture), and monitoring the weight loss (moisture and/or volatiles loss) over time.

Two different types of tests were run.

Test Program 1. Large PRB coal particles were exposed to ambient conditions (inside a building) for 6 days.

Test Program 2. Both fines (-1/4 in. particles) and coarse (3 inch particles) were placed in an environmental chamber at controlled conditions (72°F and approximately 45% Relative Humidity, with some excursions) for 16 days.

Results of Test Program 1

The first test simply allowed large PRB coal particles to sit at ambient conditions (inside a building) for 6 days while photos were taken. Figures 4a–4f show a series of photos of one particle over time.

Figure 4a. PRB coal at start of test.

Figure 4b. PRB coal after 5 hours.

Figure 4c. PRB coal after 2 days.

Figure 4d. PRB coal after 4 days.

Figure 4e. PRB coal after 6 days.

Figure 4f. PRB coal after 6 days.

As is evident from the photos, degradation of the coal starts immediately upon exposure to the environment. In fact, cracks started to appear within one hour after the start of the test!

Results of Test Program 2

Three samples of fines (-1/4 in. particles) and three samples of coarse (3 inch) particles were placed on individual trays and placed in an environmental chamber. The temperature was kept constant at 72°F and the Relative humidity at approximately 45% RH (with some excursions). The test was run over a period of 16 days. The weight of the samples was monitored and recorded over that time period. The temperature of the coal was monitored also, using multiple thermocouples, but no change in temperature of the samples was noted. It was not anticipated that any heat would be generated because drying of coal (loss of moisture) is an endothermic reaction. It is likely that even if any small amount of heat were generated due to the slight gain in moisture (exothermic reaction) on one of the large particles, the heat would quickly dissipate because the coal surface area was relatively small compared to the environmental room. The effect of moisture addition on heat generation would be a good candidate for further study. The test results are shown in Figure 5.

Figure 5. Cummulative % Moisture/Volatiles Loss/Gain for PRB Coal exposed to atmosphere

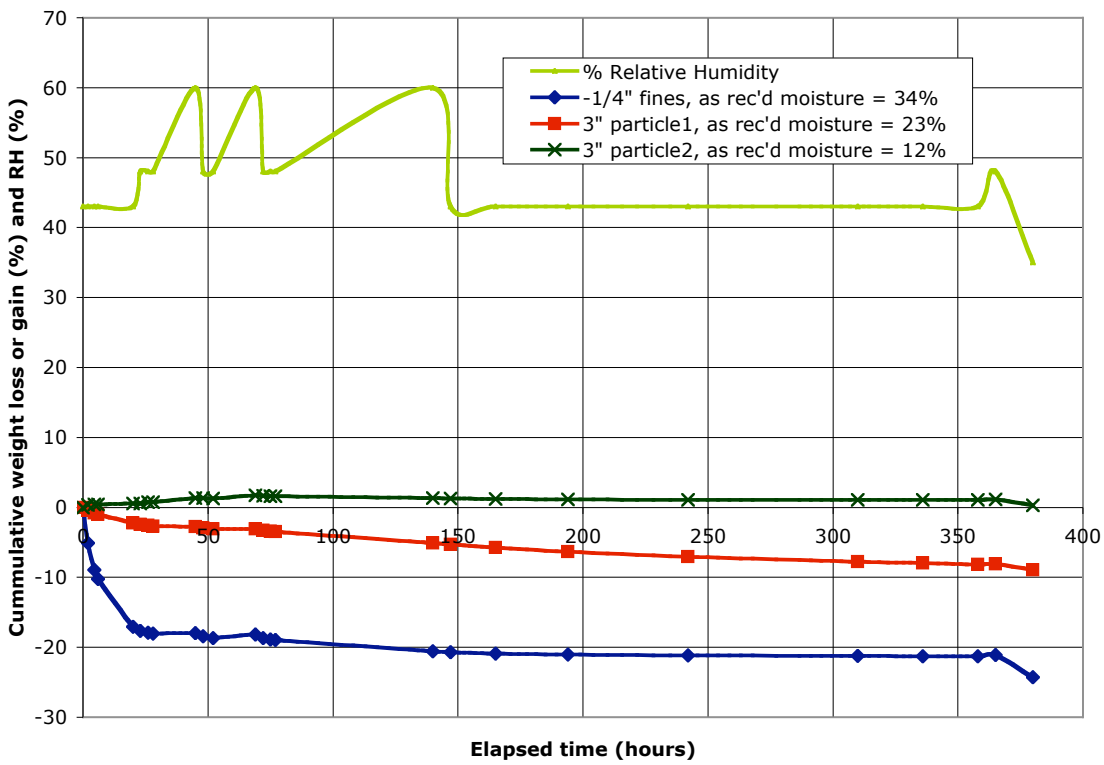

The moisture values were determined by drying small samples at 107°C in a forced convection oven and recording the weight change, until no additional weight loss was recorded. The loss in weight of each sample, divided by its original weight before drying, is denoted as the *moisture*. The fines, with an *as received* (starting) moisture of 34%, lost the largest percentage of weight (18%) during the first 24 hours compared to the coarse particles. One coarse particle (particle2) with a starting moisture of 23%, lost only 3% of its weight during the first 24 hours and 9% over 16 days; another

coarse particle (particle1) with a starting moisture of only 12%, actually *gained* weight (0.75% in 24 hours, with a net gain of 0.3% over 16 days). The *equilibrated* moisture content of the samples at the end of the test was determined to be approximately 10% for the fines and 13% for the coarse particles. As shown in Figure 5, the *rate* of moisture loss (or gain) decreased well before the test ended. For example, both the fines and coarse particle2 approached their *equilibrated* moisture content after 7 days. However, particle1 still had not reached its *equilibrated* moisture by the end of the test (16 days).

Test conclusions

One of the six samples, particle2, showed an indication of the potential for coal to adsorb more moisture. If more moisture, i.e., humidity, were available, it is likely that particle2 had the potential for adsorbing more moisture, setting up the conditions for self-heating. As discussed previously, the adsorption of moisture on a dry coal surface is an exothermic process, with a heat producing reaction. A Wyoming University/Wyoming State Geological Survey [5] study found that larger, partially dried particles produce heat as they adsorb moisture. However, as was the case with our tests, the Wyoming study dealt mostly with dry coal, so data on this effect is limited.

Preventing and/or retarding degradation

Some of the same procedures that are followed to minimize the potential for spontaneous combustion can be followed to prevent particle attrition:

Coal Handling (in general)

- Incorporate any process that can minimize additional drying of the coal
- Use larger, slower moving belts
- Minimize drop heights to control drying, especially in open air in windy conditions
- Minimize drop heights to control attrition due to impact.

Coal pile

- Seal the pile to minimize air ingress and air movement in the pile. This also helps prevent moisture loss and size degradation.
- Protect the pile from the wind. A steeper slope creates greater wind resistance, forcing air into the pile; protecting the pile from the wind (e.g., wind screens) minimizes air movement through the pile.

Coal bunker

- Design for a mass flow pattern [3, 4, 11] (see APPENDIX A).
- Provide an inerting agent or atmosphere (not recommended on a normal basis)

Considerations for further study

The following are areas of study that the authors feel may assist in our further understanding of PRB coal degradation:

- The effect of moisture addition on heat generation. Particles that are partially dried could be subjected to varying levels of increased relative humidity, while monitoring the internal temperature of the large coal particle or bed of coal fines.
- Particle porosity vs. particle size; particle porosity vs. moisture content.
- Moisture gain and loss due to changes in relative humidity.
- How various substances/additives retard the loss and adsorption of moisture.

References

1. Primer on Spontaneous Heating and Pyrophoricity (DOE-HDBK-1081-94), U.S. Department of Energy, Washington, D.C. 20585
2. Chakraborti, S.K., "Bulk Solids Handling – American Electric Power's Coal Pile Management Program", 15(3), pp 421-428, July-September, 1995.
3. NFPA 850 "Recommended Practices for Fire Protection for Electric Generating Plants and High Voltage Direct Converter Stations", 2000 ed. (section 5-4.2, Bins, Bunkers, and Silos).
4. NFPA 85 "Boiler and Combustion Systems Hazards Code", 2001 ed. (note: supercedes NFPA 8503 "Standard for Pulverized Fuel Systems", 1997 ed.)
5. Lyman, Robert M. and Volkmer, John E., "Pyrophoricity (spontaneous combustion) of Powder River Basin coals – considerations for coal bed methane development." Coal Report CR01-1, Wyoming State Geological Survey, Laramie, Wyoming, March 2001.
6. Craig, D. A., R. J. Hossfeld: Measuring Powder-Flow Properties, Chemical Engineering, September 2002, pp. 41-46.
7. Craig, D. A., R. J. Hossfeld: Keeping Coal Flowing, World Coal, January 2003, pp. 17-22
8. Chakraborti, S.K., R. J. Hossfeld, R. A. Mesing, K. Steppling: How to Achieve Reliable Coal Flow and Maintain Plant Availability, Presented at Power-Gen International, Orange County Convention Center, Orlando, FL, December 11, 2002.
9. Hatt, Rod: Sticky When Wet, World Coal, August 1997
10. "Standard Classification of Coal by Rank, American Society for Testing and Materials (ASTM), D 388-98a, (1998).
11. Dantoin, B., R. J. Hossfeld, K. L. McAtee: Improving Fuel Handling with PRB Coal by Converting a Bunker from Funnel Flow to Mass Flow, Presented at the Electric Power 2003 Conference & Exhibition PRB Coal Users Group Annual Meeting, Houston, TX, March 5, 2003.
12. Kim, A. G. Laboratory Studies on Spontaneous Combustion of Coal, US Bureau of Mines IC 8756, p 13 1997
13. Smith A. C. and others Large-scale studies of spontaneous combustion of coal, US Bureau of Mines ROI 9346, p30 1991

APPENDIX A
BASIC BULK SOLIDS HANDLING CONSIDERATIONS FOR PRB COAL

MASS FLOW: ESSENTIAL FOR SAFE COAL STORAGE

Common flow problems

Two of the most common flow problems experienced in an improperly designed silo are no-flow and erratic flow.

No-flow [Fig. A1] from a silo can be due to either arching (bridging) or ratholing.

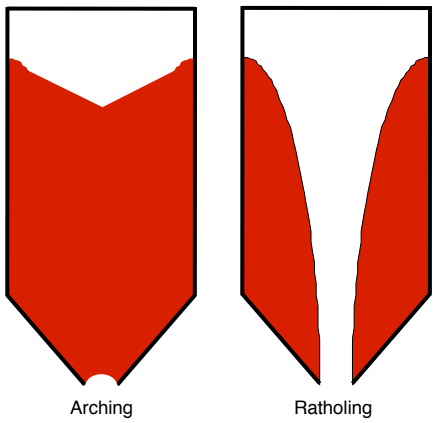

Figure A1. No Flow

Arching occurs when an obstruction in the shape of an arch or bridge forms above the outlet of a hopper and prevents any further discharge. This cohesive arch occurs when particles pack together to form such an obstruction.

Ratholing can occur in a silo when flow takes place in a channel located above the outlet. If the coal being handled has sufficient cohesive strength, the stagnant material outside of this channel will not flow into it. Once the flow channel has emptied, all flow from the silo stops.

Erratic flow is often the result of an obstruction alternating between an arch and a rathole. A rathole may fail due to an external force, such as ambient plant vibrations, vibrations created by a passing train, or vibrations from a flow aid device such as an air cannon, vibrator, etc. While some coal discharges as the rathole collapses, falling material often gets compacted over the outlet and forms an arch. This arch may break due to a similar external force, and material flow resumes until the flow channel is emptied and a rathole forms again.

Results of flow problems

Delayed startup time caused by problems related to fuel handling can add significantly to the cost of a plant. While flow stoppages alone can be very costly problems, any stagnant region in a silo can be dangerous, especially when handling coals that are prone to spontaneous combustion. If flow takes place through a channel within the silo, the material outside of this channel may remain stagnant for a very long time (depending on how often the silo is completely emptied or refilled), increasing the likelihood of fires.

Collapsing ratholes and arches can cause silos to shake or vibrate [A1]. They can also impose significant dynamic loads that can result in structural failures of hoppers, feeders or silo supports. In addition, non-symmetric flow channels alter the loading on the cylinder walls and can lead to silo deformation or buckling [A2, A3].

Flow patterns

There are two basic types of flow [A4]: *funnel flow* and *mass flow*. In *funnel flow*, some material moves while the rest remains stationary during discharge from the silo (see Fig. A2).

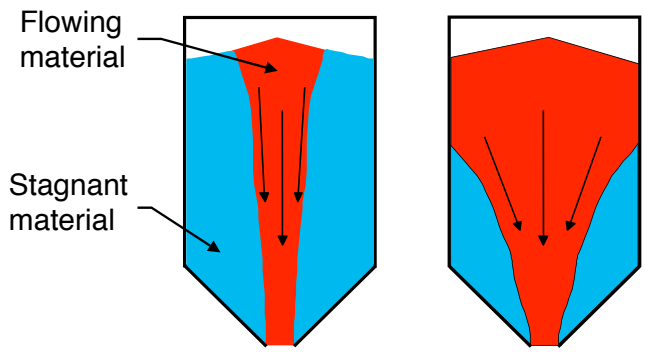

Fig. A2: Funnel Flow Pattern

Funnel flow occurs when the sloping hopper walls of a silo are not steep enough and sufficiently low in friction for material to flow along them. Under these conditions, particles slide on themselves rather than the hopper walls, and an internal flow channel develops.

Mass flow is defined as the flow pattern where upon withdrawal of any material, all of the material in a silo moves (see Fig. A3).

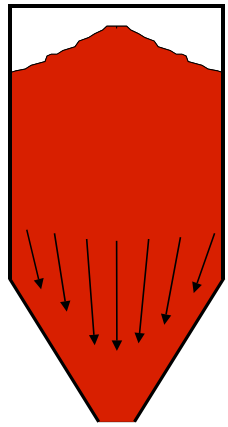

Fig. A3: Mass Flow Pattern

Mass flow occurs when particles slide along sloping hopper walls during discharge. Mass flow eliminates ratholing, stagnant material and the associated problem of spontaneous combustion, and maximizes the usable (live) capacity of the silo. In order to achieve mass flow, two conditions must be met: the sloping hopper walls must be steep enough and low enough in friction for the particles to slide along them; and the hopper outlet must be large enough to prevent arching.

TYPICAL SOLUTIONS

The key to reliability is to design the handling system equipment based on the measured flow properties of the coal being handled. As discussed above, given the variability of coals, it is essential to test samples from multiple sources over the expected range of moisture contents.

However, if the plant is already built, there are three methods available to address the types of problems mentioned here - change the material, change the operating procedures or change the equipment. The methods described here also apply to new plant design.

Change the material

The material can be changed by any of the following methods. The moisture of the coal can be lowered by covering the storage pile, by mechanical drying, or by blending wet and dry materials. Increasing the particle size by screening lowers the cohesive strength (arching/ratholing tendency); however, this is not always a practical consideration, especially for plants that use finer coal for greater boiler efficiency. The composition of the coal can be changed by finding another source of coal or by blending coal from different sources.

Change the operating procedures

Often changing the operational procedures is extremely effective in reducing handling problems, and in many cases is the most economical solution. If the coal gains cohesive strength after being stored at rest for extended periods, limiting the time of storage at rest can reduce its arching or ratholing tendency. If the combination of the silo design and the coal flow properties result in stagnant material, reducing the amount of material being stored (limit silo capacity and thus reduce head pressure) can reduce the amount of material remaining stagnant. Frequently drawing the material down to low levels, or emptying the silo on a regular basis, can help with clean-off and reduce the amount of stagnant material.

Flow aids can be very effective in breaking arches when used only after an arch has formed (due to material impact upon filling or after storage at rest) and turned off once flow has resumed; however, if material flow has not resumed and the flow aids are used repeatedly, the coal will become more compacted, and restarting flow with these devices will be futile.

If the coal silo has multiple outlets, all outlets must be used simultaneously. Use of only one outlet will likely result in severe eccentric silo wall loading and compacted, stagnant material over the non-flowing outlet(s).

Change the equipment

Consideration should be given to changing the equipment only after measuring or confirming the flow properties of the coal to be handled, thus eliminating guesswork. This is particularly wise given the significant capital investment that was laid out for this equipment in the first place. Thus, unnecessary changes should be avoided, if at all possible; however, changes to the equipment may be the most effective and long-term economic solution. Based on the measured flow properties of the coal being handled, the required modifications can range from simply lining the existing hopper with a less frictional liner to changing the hopper geometry more significantly by such measures as enlarging the outlet, steepening the angle of the lower hopper section, and/or adding an insert. Changes to the feeder, standpipe and/or the feeder interface may also be required.

The chutes at belt conveyor transfer points may need modifications as well, ranging from simple liners to a complete change in geometry to minimize impact points, while ensuring a consistent velocity to prevent adhesion to the chute surface.

HOW TO DESIGN EQUIPMENT FOR RELIABLE COAL HANDLING

To be confident that the coal storage and handling equipment will operate with few or no problems due to solids flow, the handling system should be designed utilizing a proven scientific and practical method.

Achieving mass flow

In order to achieve mass flow, two conditions must be met: the sloping hopper walls must be steep enough and low enough in friction for the coal particles to slide along them; and the hopper outlet must be large enough to prevent the coal from arching.

Hopper angle and smoothness. How steep and how smooth must a hopper surface be? This answer depends on the friction that develops between the particles and the hopper surface. This friction can be measured in a laboratory using an ASTM test method [A5]. A small sample of coal is placed in a test cell and slid along wall surfaces of interest (*e.g.* stainless steel with #2B, #1 or mill finish, and polyethylene liners). As various forces are applied normal (perpendicular) to the cell cover, the shear force is measured. These measurements are used to calculate the wall friction angle, which also can be expressed as a coefficient of friction. From the wall friction angles, limiting hopper angles for mass flow can be determined using a method developed by Dr. Andrew Jenike [A4]. These angles are used as design criteria for achieving mass flow in new silo installations, and are invaluable when considering retrofit options using liners, coatings and polished surfaces with existing designs [A6].

In general, a number of factors can affect wall friction for a given coal, such as:

- *Wall material*. Generally, smoother wall surfaces result in lower wall friction (there are exceptions), thus allowing shallower hopper angles to be sufficient for mass flow to take place.
- *Bulk solid condition*. Moisture content, variations in material composition and particle size can affect wall friction.
- *Time at rest*. Some coals adhere to a wall surface if left at rest in a hopper. Wall friction tests can be performed to measure the increase in wall friction (if any) due to storage at rest. If adhesion takes place, steeper hopper angles are required to overcome it.
- *Corrosion*. Wall materials that corrode with time generally become more frictional.
- *Abrasive wear*. Often, abrasive wear results in smoother wall surfaces; therefore, designs based on an unpolished surface are usually conservative. However, abrasive wear can occasionally result in a more frictional surface, which can disrupt mass flow. When handling abrasive materials, wear tests can be performed to determine the effect on wall friction, as well as calculate the amount of wear expected. A patented wear tester developed by Jenike & Johanson, Inc. can be used to estimate the amount of abrasive wear in a particular silo due to solids flow [A7]. These tests allow for a prediction of the useful life of a liner or surface based on its thickness, which can be an important economic consideration.

Hopper outlet size. The second requirement for mass flow is that the outlet must be large enough to prevent arching. Two types of arches are possible. Interlocking arches can be overcome by ensuring that the outlet diameter is at least six to eight times the largest particle size in a circular opening, or the width is at least three to four times the largest particle size in a slotted opening. (Slotted outlets must be at least three times as long as they are wide for such conditions to apply.)

The second type of arch, namely a cohesive arch, can be analyzed by determining the cohesive strength of the material. First the flow function of the coal (*i.e.,* its cohesive strength as a function of consolidating pressure) is measured through laboratory testing. Tests are conducted using an ASTM described direct shear tester [A5]. In this test, consolidating forces are applied to material in a test cell, similar to the wall friction test, and the force required to shear the material is measured. The measured property directly relates to a coal's ability to form a cohesive arch or a rathole. Once the flow function is determined, minimum outlet sizes to prevent arching or ratholing (in funnel flow) can be calculated through a series of design charts also published by Jenike [A4].

A number of factors affect the minimum outlet sizes required, including:

- *Particle size*. Generally as particle size decreases, cohesive strength increases, requiring larger outlets to prevent arching.
- *Moisture*. Increased moisture content generally results in an increase in cohesive strength, with the maximum typically occurring between 70% and 90% of saturation moisture. At moistures higher than these, many bulk solids (including coal) tend to become slurry-like and their cohesive strength decreases.
- *Time at rest*. Similar to wall friction, some coals exhibit an increase in their cohesive strength if left at rest for some period of time. Cohesive strength can be measured using a direct shear tester simulating storage time at rest.

Waste coals (such as bituminous gob and anthracite culm) are inherently difficult to handle because they are high in everything that contributes to flow problems: high fines, high ash (much of which is clay in waste coals), high moisture and storage time at rest. PRB and lignite, while low in ash, are high in just about everything else that contributes to handling difficulties. A robust design requires testing samples from multiple sources over a range of moisture contents.

Feeder design

In addition to ensuring that reliable flow takes place in the silo, it is also necessary for the entire cross-sectional area of the outlet to be active. A restricted outlet, such as due to a partially open slide gate, will result in funnel flow with a small active flow channel regardless of the hopper design. It is therefore imperative that a feeder be capable of continuously withdrawing material from the entire outlet of the hopper [A8]. This feature allows mass flow to take place in the silo above, if it is so designed. It also reduces the potential for ratholing in funnel flow by keeping the active flow channel as large as possible.

A hopper with an elongated, or slotted, outlet is often the preferred geometry due to its effectiveness in preventing arching compared to a circular outlet. When using a slotted outlet, it is essential that the feeder capacity increase in the direction of flow. As an example, when using a belt feeder, this increase in capacity is achieved by using a tapered interface as shown in Fig. A4.

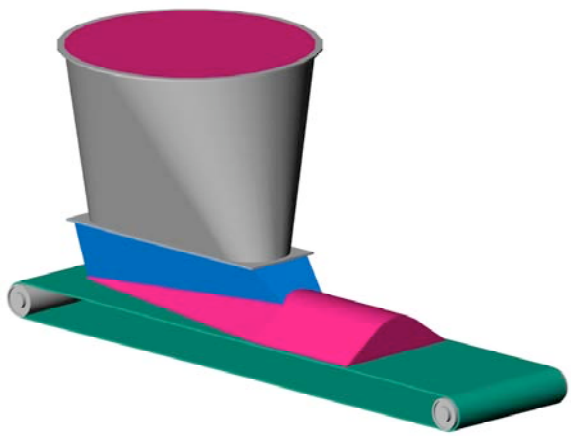

Figure A4. Mass Flow Belt Feeder Interface

Standpipe design

There are two purposes for a standpipe: to minimize the amount of gas leakage into the silo from a pressurized boiler and/or mill, and to minimize the upward (positive) gas pressure gradient that can in turn actually increase the arching potential of the coal, depending on the permeability of the coal. The finer the coal, the more adverse this latter effect will be - this applies to atmospheric boilers as well, if the seal air is supplied by positive pressure fans. Proper analysis must be used to determine the minimum height requirement for the standpipe.

When dealing with the high cohesive strength associated with waste coals and other fine, high moisture coals, the use of slotted outlets is becoming more common. This type of outlet requires a rectangular shaped standpipe (Fig. A5) between the hopper and feeder. The long slot makes the feeder interface design even more critical, compared to a typical round standpipe, to ensure a fully active flow channel within the standpipe and to avoid belt slippage, as well as minimize belt wear, by reducing the material head pressure on the belt. To provide additional stress relief, alternate design concepts may be needed.

Figure A5. Rectangular standpipe

References (APPENDIX A)

A1. Purutyan, H., Bengston, K.E. and Carson, J.W.: Identifying and Controlling Silo Vibration Mechanisms: Part I, Powder and Bulk Engineering, 1994, pp. 58-65.

A2. Carson, J.W. and T. Holmes: Why Silos Fail, Powder and Bulk Engineering, November 2001, pp. 31-43.

A3. Carson, J.W. and Jenkyn, R.T.: Load Development and Structural Considerations in Silo Design, Presented at Reliable Flow of Particulate Solids II, Oslo, Norway, 1993.

A4. Jenike, A.W.: *Storage and Flow of Solids*, University of Utah Engineering Experiment Station, Bulletin No. 123, 1964.

A5. "Standard Test Method for Shear Testing of Bulk Solids Using the Jenike Shear Cell," American Society for Testing and Materials (ASTM), D 6128-00, 2000.

A6. Purutyan, H., Pittenger, B.H. and Carson, J.W.: Solve Solids Handling Problems by Retrofitting, Chemical Engineering Progress, Vol. 94, No. 4, 1998, pp. 27-39.

A7. Johanson, J.R. and Royal, T.A.: Measuring and Use of Wear Properties for Predicting Life of Bulk Materials Handling Equipment, Bulk Solids Handling, Vol. 2, No. 3, 1982, pp. 517-523.

A8. Carson, J.W. and Petro, G.J.: Feeder Selection Guidelines, Chemical Processing, Powder Solids Annual, 1997, pp. 40-43.

Arch. Environ. Contam. Toxicol. 28, 93–107 (1995)

ARCHIVES OF
Environmental
Contamination
and Toxicology
© 1995 Springer-Verlag New York Inc.

Polycyclic Aromatic Hydrocarbon and Petroleum Hydrocarbon Contamination in Sediment from the Newark Bay Estuary, New Jersey

S. L. Huntley[1], N. L. Bonnevie, R. J. Wenning

ChemRisk®—A Division of McLaren/Hart, Stroudwater Crossing, 1685 Congress Street, Portland, Maine 04102, USA

Received: 2 May 1994/Revised: 7 June 1994

Abstract. The presence of numerous industrial and municipal sources such as former creosote wood preserving facilities, petroleum storage and refinery facilities, paint and chemical manufacturers, combined sewer overflows, and sewage treatment facilities along the shores of Newark Bay, New Jersey and its major tributaries suggests the potential for widespread contamination by polycyclic aromatic hydrocarbons (PAHs) and petroleum hydrocarbons. In this study, the concentrations and distributions of 19 PAHs and total extractable petroleum hydrocarbon (TEPH) were determined in 213 sediment samples obtained from 58 sediment cores collected between November 1991 and March 1993 from the Arthur Kill, Elizabeth River, Hackensack River, Kill Van Kull, Newark Bay, Upper New York Bay, and Rahway River. Chronological profiles of PAH and TEPH deposition from pre-1930 to the present were determined in each sediment core using ^{137}Cs and ^{210}Pb radioisotope measurements. The concentrations of total PAHs (tPAH) and individual PAHs were compared to National Oceanic and Atmospheric Administration (NOAA) benchmark sediment effects-range median (ER-M) values. The objectives of this study were to: (a) determine the spatial and temporal distributions of PAHs in sediments; (b) identify their possible sources; and (c) assess the potential for sediment toxicity within the estuary. The results indicate elevated concentrations of PAHs and TEPH in surface and buried sediments throughout the estuary, particularly in the Elizabeth River, the Arthur Kill, and in the Passaic River above the Dundee Dam and below the Jackson Street Bridge. Sediments collected from ship berths at Port Newark and Port Elizabeth in Newark Bay were also found to contain elevated levels of PAHs and TEPH. The concentrations of PAHs and TEPH in sediment generally increase with depth throughout the estuary. Comparisons to NOAA ER-M values indicate that the concentrations of many PAHs in surface and buried sediments at several locations in the estuary pose a significant hazard to aquatic organisms. Radiodating of sediment cores reveals that the highest concentrations of PAHs, and the greatest potential hazards to aquatic biota, occur in sediments deposited during the 1950s. Although the major inputs of PAHs are probably combustion sources and urban runoff entering the estuary through combined sewer overflows and storm drains, the unusually high concentrations of PAHs and TEPH found in some sediments may be best explained by point source inputs or catastrophic oil spills.

The accumulation of high concentrations of polycyclic aromatic hydrocarbons (PAHs) in the sediments of industrialized and densely populated bays and estuaries has been well established (NOAA 1988, 1991). During the past century, these levels have increased due to the escalating use of petroleum products, post-World War II economic expansion, and greater reliance on marine transportation of oil (O'Connor and Hugget 1988). As a result of their hydrophobicity and strong affinity for organic matter, PAHs accumulate in sediments at levels several orders of magnitude higher than those found in source effluents (Herbes and Schwall 1978). Since these compounds are biologically available, PAH-contaminated sediment can adversely affect biota or result in high concentrations in the tissues of indigenous organisms (Pruell *et al.* 1984). It is well known that even moderate concentrations of certain PAHs and petroleum hydrocarbons in sediment can have a detrimental effect on aquatic organisms (Hollister *et al.* 1980; Catallo and Gambrell 1987).

In the Newark Bay Estuary, numerous studies have been conducted to determine the extent of chemical contamination in sediment and biota, but most have focused on other persistent compounds such as dioxins, PCBs, and metals (Wilber and Hunter 1973, 1979; Suszkowski 1978; Williams *et al.* 1978; Meyerson *et al.* 1981; NOAA 1982, 1984a, 1984b; O'Keefe *et al.* 1984; NJDEP 1985; Bopp 1988; Goeller 1989; HMDC 1989; Moser 1990; Bopp *et al.* 1991; Bonnevie *et al.* 1992, 1993; Gillis *et al.* 1993; Wenning *et al.* 1992). It has been shown in whole sediment bioassays that PAHs may act synergistically to elicit toxic responses similar to those demonstrated for dioxins (Brunström *et al.* 1992); therefore, it is important to consider these compounds when evaluating the overall toxicity of sediments.

In general, high PAH concentrations in sediment have been linked to a wide variety of combustion sources and creosote

Correspondence to: S. L. Huntley

wood preserving facilities (USEPA 1982; Mueller *et al.* 1989) as well as tanker spills, oil seeps, and other petroleum-related industries (NOAA 1991). Since the early 1800s, a myriad of activities have resulted in the pollution of Newark Bay and its tributaries from municipal and industrial wastewaters, stormwater runoff, accidental spills, direct dumping of wastes, and atmospheric deposition (Olsen *et al.* 1984; HydroQual 1991). The presence of hundreds of industrial and municipal facilities including paint and chemical manufacturing facilities, metal scrapyards and refineries, wood treatment plants, and petroleum terminals provides strong impetus for examining PAH and petroleum hydrocarbon sediment concentrations in the estuary.

In this study, the concentrations of 19 PAHs and TEPH (measured as diesel) were determined in sediments collected from the Newark Bay Estuary, specifically the Arthur Kill, Elizabeth River, Hackensack River, Kill Van Kull, Newark Bay, Passaic River, Upper New York Bay, and Rahway River. The age of the sediment at different depths was established from ^{137}Cs measurements and confirmed by the distribution of the ^{210}Pb radioisotope using the dating techniques of Faure (1986). The geochemical data were used to assess historic and current ecological conditions, identify potential sources, and provide information for evaluating future dredging and disposal options in the estuary.

Materials and Methods

Sediment Sampling

Two hundred and thirteen sediment samples from 58 sediment cores were collected throughout the estuary during November/December 1991 (stations 1–59), December 1992 (stations 60–72), and March 1993 (stations 73–89). The study area and core sampling stations are shown in Figure 1. With the exception of sediments collected from the Port Newark and Port Elizabeth navigation channels in Newark Bay, sampling stations were located outside of designated ship navigation channels in stable depositional reaches to minimize the impacts associated with dredging activities and ship traffic, and to obtain undisturbed sedimentation profiles. The selection of sampling locations was biased toward areas of apparent high sediment accumulation and current or historical industrial activity. At most locations, cores ranging in length from 1.5 to 4.5 m were collected. However, due to anticipated high rates of sediment accumulation in the lower Passaic River (IT 1986), 6.0 m cores were collected below the Jackson Street Bridge (stations 13–22) during November/December 1991 sampling.

At all stations, except 1, 2, 5, and 49, a Model 1400 Vibracore unit equipped with a 1.5, 3.0, 4.5, or 6.0 m stainless steel core barrel and Lexan liner was used to obtain sediment cores from water depths averaging less than 3.0 m to as much as 8.0 m. A portable Vibracore unit with a 3.0 m, unlined, aluminum core tube was used at stations 1, 2, 5, and 49. All field sampling and sample processing equipment used in the November/December 1991 sampling (core barrels and Lexan liners) was rinsed with acetone and hexane (50:50), analyte-free trichloroethylene, and analyte-free deionized water prior to the collection of sediment cores. In the 1992 and 1993 sampling events, decontamination of sampling equipment consisted of a hexane rinse, followed by isopropanol and deionized water. Field equipment rinsate samples were utilized to verify the levels, if any, of residual contamination. Sediment samples were collected from the intact Lexan liner at up to eight depths for chemical (5.0 cm subsection) and radioisotope (2.5 cm subsection) analyses. The outermost layer of sediment was discarded to minimize contamination from vertical mixing of sediments during core collection. In accordance with USEPA Contract Laboratory Program (CLP) requirements, samples were transferred to precleaned amber glass containers, sealed, and maintained at 4°C prior to chemical analysis.

Fig. 1. Sediment sampling locations in the Newark Bay Estuary, New Jersey

Chemical Analysis

Sediments were assayed for base/neutral and acid extractable (BNA) organic chemicals by S-Cubed Laboratory (San Diego, CA) using gas chromatography/mass spectroscopy (GC/MS) according to USEPA Method 8310 (USEPA 1991), and for total extractable petroleum hydrocarbons (TEPH) using a modification of SW-848 USEPA Method 8015. For TEPH analyses, sediments were extracted with methylene chloride by sonication and analyzed on a GC equipped with a flame ionization detector. Diesel was used as the calibration standard.

^{210}Lead and ^{137}Cesium Analyses

Sediments were assayed for ^{210}Pb and ^{137}Cs activity by Teledyne Isotopes (Westwood, NJ). ^{210}Lead activity was determined by radiochemical separation and assay of the ^{210}Bi daughter product. Sediments were leached with 6M hydrochloric acid together with stable lead and bismuth carriers. Sample filtrate was evaporated, oxidized with nitric acid, and dissolved in 1.8M hydrochloric acid. Using an anion exchange column, lead was eluted with 0.05M hydrochloric acid followed by 9M hydrochloric acid and deionized water. Bismuth was then eluted with 2M sulfuric acid. The bismuth was precipitated as the oxychloride and collected on a 2.5 cm glass fiber filter. Bismuth yield was determined gravimetrically. Beta activity of the bismuth precipitate was measured using a low level, gas-flow proportional counter. ^{137}Cesium activity was determined by gamma spectral analysis of sediment for at least five hours using lithium-drifted germanium and high purity (>55 cc) germanium detectors. The activity of ^{137}Cs was measured by integrating its gamma emission at 661.6 KeV.

Sediment Accumulation Rates

^{210}Lead analyses were conducted prior to ^{137}Cs analyses to more accurately predict the depth interval of the ^{137}Cs 1954 horizon in each sediment core. The ^{210}Pb-derived sediment accumulation rates were estimated using Eqs. (1) and (2) as described by Faure (1986). For ^{210}Pb activities, the time (t) that correlates to a specific depth (h) is described by

$$t_h = \frac{1}{\lambda} \log(^{210}Pb_A^0 / {}^{210}Pb_A) \qquad (1)$$

where $^{210}Pb_A^0$ is the unsupported activity (pCi/g) in surface sediments, $^{210}Pb_A$ is the unsupported activity (pCi/g) at a specific sediment depth, λ is the ^{210}Pb decay constant (3.11×10^{-2} yr^{-1}), and t_h is the estimated age (years) of the sediment at a given depth. The ^{210}Pb-derived sediment accumulation rate (R_{Pb}; cm/yr) is based on the slope (m) of the regression line of log ($^{210}Pb_A - {}^{210}Pb_{As}$) versus depth as described in

$$R_{Pb} = \frac{-\lambda}{m} \qquad (2)$$

Based on the calculated sediment accumulation rates, approximate dates of deposition were determined for each sample. These approxi-

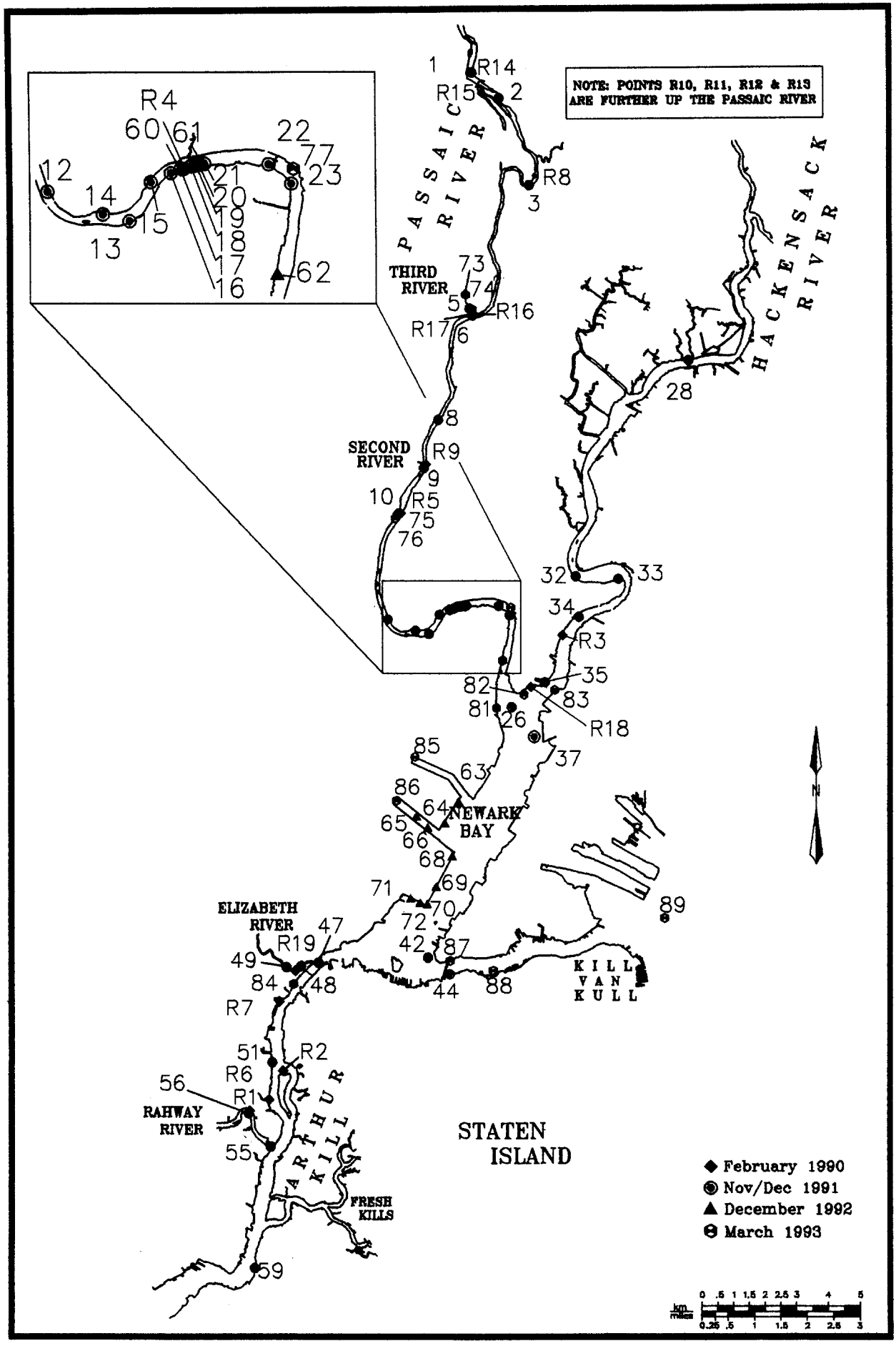
NOTE: POINTS R10, R11, R12 & R13 ARE FURTHER UP THE PASSAIC RIVER
PASSAIC RIVER
HACKENSACK RIVER
THIRD RIVER
SECOND RIVER
NEWARK BAY
ELIZABETH RIVER
RAHWAY RIVER
ARTHUR KILL
KILL VAN KULL
FRESH KILLS
STATEN ISLAND
February 1990
Nov/Dec 1991
December 1992
March 1993
km
miles

mate dates were used to determine depth intervals for ^{137}Cs analyses in each sediment core. The precise depth interval of the 1954 horizon was confirmed by determining the depth of diminished ^{137}Cs activity along the length of the sediment core. Point estimates of the ^{137}Cs sediment accumulation rates (R_{Cs}; cm/yr) in each sediment core were determined using

$$R_{Cs} = \frac{d}{\Delta t} \quad (3)$$

where d is the depth (cm) of the 1954 horizon and Δt is the period of time from 1954 to the date when the sediment core was collected. The depth of the 1954 horizon (d) was assumed to be the midpoint of the depth interval bounded by the deepest depth at which ^{137}Cs activity was detected and the shallowest depth at which ^{137}Cs activity was not detected in sediment.

Data Analysis

Summary statistics (arithmetic mean, standard deviation, median, and upper 90% confidence limit on the mean) were calculated for individual PAHs, total PAHs (tPAH), and TEPH for the Arthur Kill, Hackensack River, Kill Van Kull, Newark Bay, and Passaic River. Statistical summaries for the Newark Bay consisted of measurements from six areas, including Port Elizabeth Channel, Port Elizabeth Pierhead, Port Elizabeth South Channel, Port Newark Channel, the Northern Reach adjacent to Kearny Point, and the Southern Reach adjacent to Shooter's Island. Similarly, summary statistics for the Arthur Kill include Elizabeth River and Rahway River data. Total PAHs were calculated as the sum of the 19 individual PAHs. The upper 90% confidence limit on the mean was determined for individual PAHs, tPAH, and TEPH and compared to specific concentrations found at each depth and location. Chemical concentrations exceeding the 90% upper confidence limit were considered significantly elevated above the mean concentration for the purposes of evaluating inputs from point and non-point sources. Historical trends were evaluated by grouping PAH and TEPH results into 10-year intervals, calculating the mean PAH and TEPH concentrations for each decade, and plotting concentration against time. All statistical analyses were performed using one-half the analytical detection limit for non-detected values, as described by Haas and Scheff (1990).

Assessment of Aquatic Hazards

As part of ongoing studies associated with the National Oceanic and Atmospheric Administration's (NOAA) National Status and Trends Program, NOAA has derived effects-range low (ER-L) and effects-range median (ER-M) benchmark sediment toxicity values for predicting the potential for adverse effects of persistent chemicals (Long and Morgan 1991). For 18 PAHs, NOAA determined the distribution of sediment concentrations that were associated with any degree of toxicity to freshwater, marine, and estuarine organisms. The 50th percentile of the distribution was identified as the effects range-median (ER-M) value and the 10th percentile of the distribution was identified as the effects range-low (ER-L) value. Although these values are not intended for use as regulatory guidelines, they provide useful benchmarks for assessing the potential toxicity of contaminated sediments. The NOAA ER-M and ER-L values used in this analysis are presented in Table 1.

Using NOAA ER-M values, hazard ratios were calculated for individual PAHs and tPAH for both mean surface sediment concentrations and for mean sediment concentrations across the entire core depth. A hazard ratio of greater than 1 indicates that chemical concentrations may pose a potential hazard to aquatic organisms. Surface sediments were evaluated separately to assess current potential hazards to aquatic organisms. Hazard ratios were calculated for buried sediments to assess the possible impacts associated with dredging and other disturbances of these sediments. Generally, when dredging has occurred in the Newark Bay Estuary, the upper Passaic River channel has been dredged to approximately 3 m, the middle Passaic River channel to approximately 5 m, and the lower Passaic River channel to a depth of 6–9 m. The lower Hackensack River channel, below the turning basin, has typically been dredged to a depth of 9 m (ACOE 1988). Therefore, all sediment sample depths evaluated in the present investigation were included in the evaluation of buried sediments and the effects of dredging.

Table 1. Benchmark sediment quality values (mg/kg) proposed by NOAA for polycyclic aromatic hydrocarbons (PAHs)

	United States NOAA	
Chemical[a]	ER-L values	ER-M values
Acenaphthene	0.15	0.65
Anthracene	0.085	0.96
Benzo(a)anthracene	0.23	1.6
Benzo(a)pyrene	0.40	2.5
Chrysene	0.40	2.8
Dibenzo(a,h)anthracene	0.06	0.26
Fluoranthene	0.60	3.6
Fluorene	0.035	0.64
2-Methylnaphthalene	0.065	0.67
Naphthalene	0.34	2.1
Phenanthrene	0.225	1.38
Pyrene	0.35	2.2
Total PAHs	4	35

[a]NOAA has not derived toxicity values for six of the PAHs evaluated in this study

Results

The range of PAH and TEPH concentrations varied considerably, both vertically and spatially, throughout the estuary as shown in Table 2 (Arthur Kill and Hackensack River), Table 3 (Kill Van Kull and Newark Bay), and Table 4 (Passaic River). The very high standard deviations for many of the chemicals and waterways is indicative of the large degree of variation in the data. For example, the concentration of phenanthrene in the Arthur Kill varied by over 2 orders of magnitude, ranging from 0.36 to 89 mg/kg (Table 5). Similarly, the concentrations of tPAH in the Arthur Kill ranged from 0.31 to 420 mg/kg with a mean concentration of 37 mg/kg (s.d., 81.7 mg/kg). In contrast to the relatively high tPAH concentrations found in Arthur Kill sediments, the concentration of tPAH in Hackensack River sediments ranged from 2.2 to 71 mg/kg. Kill Van Kull sediments were to found to be contaminated with relatively lower concentrations of tPAH ranging from 1.9 to 36 mg/kg. The levels of tPAH in Newark Bay (0.22–400 mg/kg) were comparable to Arthur Kill concentrations. The Passaic River was found to be the most highly contaminated of the five waterways examined. Total PAH concentrations in sediment ranged from 0.22 to 8,000 mg/kg (Table 5) with a mean concentration of 145 mg/kg (s.d., 739 mg/kg; Table 4).

The frequency of detection for many of the compounds was highly variable due, in part, to a high degree of variability in detection and quantitation limits. The relatively high detection limits reported for the various PAHs were attributed to matrix

Table 2. Polycyclic aromatic hydrocarbons (PAHs) and petroleum hydrocarbons (mg/kg, d.w.) in Arthur Kill and Hackensack River sediments

	Arthur Kill (n = 24)			Hackensack River (n = 12)		
Chemical	Median	Mean ± s.d.	90% UCL	Median	Mean ± s.d.	90% UCL
Acenaphthene	0.75	2.4 ± 6.88	4.3	0.41	0.74 ± 0.78	1.0
Acenaphthylene	0.65	0.73 ± 0.626	0.90	0.40	0.54 ± 0.32	0.66
Anthracene	0.83	2.3 ± 6.12	3.9	0.96	1.3 ± 1.22	1.8
Benzo(a)anthracene	0.83	1.6 ± 2.46	2.3	1.3	1.8 ± 1.55	2.4
Benzo(a)pyrene	0.80	1.4 ± 2.19	2.0	1.3	1.8 ± 1.51	2.4
Benzo(b)fluoranthene	0.76	1.3 ± 1.77	1.8	0.82	1.6 ± 1.53	2.2
Benzo(g,h,i)perylene	0.62	0.72 ± 0.528	0.86	0.96	1.1 ± 0.613	1.3
Benzo(k)fluoranthene	0.77	1.3 ± 1.84	1.8	0.90	1.3 ± 0.827	1.6
Carbazole	0.70	0.78 ± 0.530	0.93	0.65	0.60 ± 0.258	0.70
Chrysene	0.91	1.9 ± 2.79	2.6	1.7	2.1 ± 1.89	2.9
Dibenzo(a,h)anthracene	0.70	0.68 ± 0.274	0.8	0.58	0.56 ± 0.287	0.68
Dibenzofuran	0.65	0.88 ± 1.12	1.2	0.58	0.57 ± 0.280	0.68
Fluoranthene	1.6	5.2 ± 13.2	8.7	3.1	3.7 ± 3.26	5.0
Fluorene	0.75	1.4 ± 3.34	2.3	0.52	0.72 ± 0.56	0.93
Indeno(1,2,3-cd)pyrene	0.56	0.74 ± 0.625	0.91	0.91	1.0 ± 0.648	1.3
2-Methylnaphthalene	0.70	1.6 ± 4.36	2.8	0.59	0.63 ± 0.42	0.80
Naphthalene	0.75	3.0 ± 10.9	5.9	0.60	0.77 ± 0.77	1.1
Phenanthrene	0.80	5.8 ± 18.0	11	1.5	2.7 ± 3.33	4.0
Pyrene	1.6	3.6 ± 5.59	5.1	2.6	3.0 ± 2.58	4.1
tPAH[a]	17	37 ± 81.7	59	23	27 ± 19.3	34
TEPH[b]	205	703 ± 1184	1020	106	119 ± 86.89	153

[a]PAH = polycyclic aromatic hydrocarbon
[b]TEPH = total extractable petroleum hydrocarbon

Table 3. Polycyclic aromatic hydrocarbons (PAHs) and petroleum hydrocarbons (mg/kg, d.w.) in Kill Van Kull and Newark Bay sediments

	Kill Van Kull (n = 12)			Newark Bay (n = 45)		
Chemical	Median	Mean ± s.d.	90% UCL	Median	Mean ± s.d.	90% UCL
Acenaphthene	0.40	0.41 ± 0.204	0.49	0.60	2.3 ± 5.45	3.4
Acenaphthylene	0.40	0.45 ± 0.233	0.55	0.55	1.5 ± 4.14	2.3
Anthracene	0.40	1.3 ± 2.58	2.3	0.55	2.4 ± 5.57	3.5
Benzo(a)anthracene	0.57	0.94± 0.832	1.3	0.62	2.2 ± 4.74	3.1
Benzo(a)pyrene	0.52	1.0 ± 0.849	1.3	0.56	1.7 ± 4.22	2.5
Benzo(b)fluoranthene	0.44	1.0 ± 0.864	1.3	0.61	1.8 ± 4.26	2.7
Benzo(g,h,i)perylene	0.36	0.52 ± 0.426	0.69	0.46	1.5 ± 4.16	2.3
Benzo(k)fluoranthene	0.41	0.92 ± 0.989	1.3	0.55	1.7 ± 4.20	2.5
Carbazole	0.40	0.58 ± 0.505	0.77	0.55	1.7 ± 4.23	2.5
Chrysene	0.52	1.0 ± 0.862	1.3	0.65	2.2 ± 4.90	3.2
Dibenzo(a,h)anthracene	0.40	0.44 ± 0.233	0.54	0.55	1.5 ± 4.14	2.3
Dibenzofuran	0.40	0.44 ± 0.233	0.54	0.60	2.0 ± 4.60	2.8
Fluoranthene	0.74	1.6 ± 1.75	2.3	1.0	5.3 ± 15.0	8.2
Fluorene	0.39	0.44 ± 0.228	0.53	0.60	2.1 ± 5.60	3.1
Indeno(1,2,3-cd)pyrene	0.41	0.53 ± 0.381	0.68	0.49	1.8 ± 4.31	2.7
2-Methylnaphthalene	0.36	0.44 ± 0.235	0.53	0.60	1.5 ± 4.15	2.3
Naphthalene	0.40	0.44 ± 0.233	0.54	0.55	1.8 ± 4.44	2.7
Phenanthrene	0.45	0.85 ± 0.796	1.2	0.55	4.7 ± 15.8	7.7
Pyrene	0.97	1.5 ± 1.33	2.0	0.91	3.9 ± 9.76	5.8
tPAH[a]	7.9	15 ± 11.9	19	14	44 ± 98.5	63
TEPH[b]	77.5	370 ± 797.0	684	149	339 ± 534.8	441

[a]PAH = polycyclic aromatic hydrocarbon
[b]TEPH = total extractable petroleum hydrocarbon

effects associated with significant organic chemical and petroleum contamination. The individual PAHs that were consistently measured at the highest concentrations in the Newark Bay Estuary were acenaphthene, benzo(a)anthracene, benzo(a) pyrene, benzo(b)fluoranthene, benzo(k)fluoranthene, chrysene, fluoranthene, phenanthrene, and pyrene.

Nearly half of the 58 sediment cores collected from the Newark Bay Estuary contained PAH concentrations that were statistically ($p < 0.05$) elevated above the mean concentration for their respective waterways for at least one individual PAH or for tPAH (Table 5). Geographically, these 27 sampling locations were grouped into seven different areas: the Passaic

Table 4. Polycyclic aromatic hydrocarbons (PAHs) and petroleum hydrocarbons (mg/kg, d.w.) in the Passaic River

Chemical	Passaic River Median	Mean ± s.d.	90% UCL
Acenaphthene	0.68	13 ± 93.0	24
Acenaphthylene	0.65	2.9 ± 8.86	3.9
Anthracene	0.75	8.3 ± 47.0	14
Benzo(a)anthracene	1.4	7.4 ± 30.5	11
Benzo(a)pyrene	1.5	5.5 ± 20.1	7.9
Benzo(b)fluoranthene	1.4	4.2 ± 11.2	5.5
Benzo(g,h,i)perylene	0.90	2.8 ± 6.12	3.5
Benzo(k)fluoranthene	1.2	3.9 ± 11.2	5.3
Carbazole	0.70	2.3 ± 6.41	3.1
Chrysene	1.9	7.9 ± 32.2	12
Dibenzo(a,h)anthracene	0.65	2.2 ± 5.21	2.8
Dibenzofuran	0.65	2.6 ± 8.04	3.6
Fluoranthene	3.2	10 ± 40.2	15
Fluorene	0.65	7.7 ± 49.3	14
Indeno(1,2,3-cd)pyrene	0.88	3.0 ± 6.96	3.9
2-Methylnaphthalene	0.70	11 ± 80.0	21
Naphthalene	0.70	16 ± 123	31
Phenanthrene	1.8	19 ± 113	33
Pyrene	3.4	14 ± 61.9	22
tPAH[a]	1960	145 ± 739	232
TEPH[b]	294	1520 ± 5,970	2,230

[a]PAH = polycyclic aromatic hydrocarbon
[b]TEPH = total extractable petroleum hydrocarbon

River, above the Dundee Dam and below Second River; the Hackensack River, adjacent to the Koppers Coke hazardous waste site and the former federal ship terminal at the confluence of Newark Bay; the Kill Van Kull near Bergen Point; the upper portion of the Arthur Kill and in the Elizabeth River adjacent to the Chemical Control Superfund site; and at the end of the Port Newark navigation channel. TEPH concentrations were statistically elevated above mean concentrations for their respective waterways at 20 sampling locations throughout the estuary, which generally correspond to areas with elevated PAH concentrations. Significantly elevated TEPH levels were also found in sediments at Kearny Point, as well as in southern reaches of the Arthur Kill adjacent to Tremley Point and the Fresh Kills Landfill (Table 5, Figure 1). The concentrations of tPAH and TEPH were generally higher in buried sediments than in surface sediments at most locations (Table 5).

Sediment accumulation rates derived from ^{210}Pb and ^{137}Cs measurements for 52 of the 58 sediment cores are presented in Table 6. The six sediment cores collected in the Port Newark and Port Elizabeth navigation channels were not assayed for ^{210}Pb and ^{137}Cs because sediments in these areas represent only accumulation after the completion of the last dredging project in 1989. Sediment accumulation rates throughout the estuary ranged from 0.41 to 8.9 cm/year. Sediment cores from the lower Passaic River were found to have the highest depositional rates (3.8–8.9 cm/year), confirming those reported in a previous study (IT 1986). The lower Passaic River, between the Pulaski Skyway Bridge and just above the Clay Street Bridge, has not been dredged by U.S. Army Corps of Engineers since 1949 (IT 1986); the high sedimentation rates estimated in the present study indicate that as much as 240 cm or more of sediment has accumulated in the Brown Street storm sewer outfall area (adjacent to station 17) since that time. The varied distributions of ^{210}Pb activity in several cores that could not be dated suggest that sediments at these locations are well mixed, precluding a retrospective evaluation of chemical deposition and sediment accumulation.

Using sediment accumulation rates calculated from ^{137}Cs measurements (Table 6), profiles of mean concentrations of PAHs and TEPH in sediment were determined according to the decade of deposition from pre-1930 to the present in the Passaic River and the Newark Bay Estuary. The results are presented in Figure 2. In both the Passaic River and the estuary, the mean concentrations of tPAH associated with sediments deposited prior to 1940 ranged from 75 to 95 mg/kg. Mean tPAH concentrations declined during the 1940s (45–55 mg/kg), reached their maximum in the 1950s, and then declined during the 1960s and 1970s to pre-1940 levels. Mean concentrations of tPAHs have further declined since the 1980s to levels ranging from 27 to 40 mg/kg. The mean concentration of TEPH in sediments deposited prior to 1960 ranged from 1,000 to 1,300 mg/kg in the Newark Bay Estuary and the Passaic River and peaked during the 1960s (2,300–3,100 mg/kg). Mean TEPH concentrations have declined since the 1970s in both the Passaic River and elsewhere in the estuary to levels ranging from 240 to 280 mg/kg, respectively.

The hazard ratios for individual PAHs present in Newark Bay Estuary sediments are presented in Figure 3. In surface sediments, all 12 PAHs evaluated, except benzo(a)pyrene and chrysene, pose a potential hazard to aquatic organisms, as indicated by the hazard ratios exceeding a value of 1. In general, buried Newark Bay Estuary sediments posed nearly three times more of a toxic hazard than surface sediments. In the Passaic River, buried sediments pose, on average, approximately six times more of a toxic hazard than surface sediments (Figure 3). The high hazard associated with buried sediments in the estuary is attributed primarily to acenaphthene, anthracene, dibenzo (a,h)anthracene, fluorene, 2-methylnaphthalene, naphthalene, and phenanthrene. These same compounds also appear to be responsible for most of the potential toxicity due to PAHs in buried Passaic River sediments. Further assessment of the relative toxicity of sediments in the lower reach of the Passaic River indicates that hazard ratios for tPAH in surface and buried sediments are higher in the lower reach of the river than elsewhere in the Passaic River and the Newark Bay Estuary.

Discussion

The results of this investigation indicate that sediments throughout the Newark Bay Estuary contain elevated levels of PAHs and TEPH. These findings are consistent with a previous study of surface sediments in the Arthur Kill, Hackensack River, Newark Bay, and the Passaic River (USEPA 1981). In that study, tPAH concentrations exceeded 100 mg/kg in the lower reaches of the Passaic River and above the Dundee Dam (USEPA 1981). The concentrations of PAHs and TEPH exceeding the 90% UCL in some areas of the Arthur Kill and the Passaic River strongly suggest that current and historical levels are the result of point source discharges, rather than nonpoint sources.

Numerous point sources of PAH compounds have been identified in the environment. High levels of PAHs have been

Table 5. Polycyclic aromatic and total extractable petroleum hydrocarbons in Newark Bay Estuary sediments (mg/kg, dry weight)[a]

Field ID	Depth (cm)	ACE	ACY	ANT	BAA	BAP	BBF	BGP	BKF	CAR	CHR	DBA	DBF	FLA	FLU	IND	MET	NAP	PHE	PYR	tPAH[b]	TEPH
Arthur Kill																						
47/001	0	34*	3.4*	31*	12*	11*	8.7*	2.8*	9.3*	2.5*	14*	1.2*	6.0*	66*	17*	3.3*	22*	54*	89*	27*	410*	2,150*
47/005	20	0.26	(0.76)	(0.76)	(0.76)	(0.76)	(0.76)	(0.76)	(0.76)	(0.76)	(0.76)	(0.76)	(0.76)	(0.76)	(0.76)	(0.76)	0.46	0.37	0.45	0.17	7.0	(30)
47/010	46	(0.77)	(0.77)	(0.77)	(0.77)	(0.77)	(0.77)	(0.77)	(0.77)	(0.77)	(0.77)	(0.77)	(0.77)	(0.77)	(0.77)	(0.77)	(0.8)	(0.77)	(0.77)	(0.77)	7.3	(30)
48/001	0	7.5*	(1.6)	3.3	1.4	1.1	0.66	0.46	0.75	(1.6)	1.5	(1.6)	0.59	3.2	0.75	0.51	(1.6)	(1.6)	6.3	4.5	37	(56)
48/005	20	1.6	0.48	1.2	2.5*	2.1*	2.3*	0.86	1.7	0.34	2.6*	(1.5)	0.62	5.0	1.4	1.2*	1.8	2.2	5.1	6.5*	40	310
48/010	46	2.3	0.36	1.3	(1.6)	1.4	1.5	0.68	1.8*	(1.6)	1.9	(1.6)	0.48	3.8	1.4	0.81	2.1	1.9	5.0	4.3	33	850
49/001	0	(0.84)	(0.84)	(0.84)	0.3	0.47	0.42	0.33	0.6	(0.84)	0.39	(0.84)	(0.84)	0.74	(0.84)	0.3	(0.84)	(0.84)	0.36	0.99	8.7	70
49/010	46	(0.76)	(0.76)	(0.76)	(0.76)	(0.76)	(0.76)	(0.76)	(0.76)	(0.76)	(0.76)	(0.76)	(0.76)	(0.76)	(0.76)	(0.76)	(0.76)	(0.76)	(0.76)	(0.76)	7.2	(30)
49/020	97	(1.3)	(1.3)	(1.3)	(1.3)	0.31	(1.3)	(1.3)	(1.3)	(1.3)	(1.3)	(1.3)	(1.3)	(1.3)	(1.3)	(1.3)	(1.3)	(1.3)	(1.3)	(1.3)	12	(48)
51/001	0	(0.87)	(0.87)	(0.87)	0.32	0.31	0.29	(0.87)	0.2	(0.87)	0.4	(0.87)	(0.87)	0.59	(0.87)	(0.87)	(0.87)	(0.87)	0.55	0.69	8.1	50
51/010	46	0.67	(1.3)	1.7	2.9*	2.4*	1.3	1.3*	2.6*	(1.3)	3.6*	0.69	(1.3)	6.0	0.74	1.2*	(1.3)	(1.3)	5.2	5.4*	39	430
51/020	97	(1.4)	(1.4)	(1.4)	(1.4)	0.77	(1.4)	(1.4)	(1.4)	(1.4)	(1.4)	(1.4)	(1.4)	(1.4)	(1.4)	(1.4)	(1.4)	(1.4)	(1.4)	(1.4)	13	(50)
55/001	0	(1.2)	(1.2)	(1.2)	(1.2)	(0.69)	0.65	0.5	0.7	(1.2)	0.74	(1.2)	(1.2)	1.6	(1.2)	0.43	(1.2)	(1.2)	(1.2)	1.6	13	490
55/010	46	(1.7)	(1.7)	0.81	1.4	(1.7)	1.1	0.62	1.3	(1.7)	1.7	(1.7)	(1.7)	2.9	0.78	0.64	(1.7)	(1.7)	2.3	3.4	24	5,130*
55/020	97	(0.86)	(1.4)	1.6	1.8	(1.5)	1.4	0.66	1.2	(1.4)	2.2	(1.4)	(1.4)	4.8	(1.4)	0.74	(1.4)	(1.4)	0.51	4.6	26	2,320*
56/001	0	(2.2)	(2.2)	(2.2)	(2.2)	0.92	0.95	(2.2)	1.0	(2.2)	1.2	(2.2)	(2.2)	1.9	(2.2)	0.53	(2.2)	(2.2)	0.78	1.6	21	80
56/010	46	(1.8)	(1.8)	(1.8)	(1.8)	0.5	0.82	(1.8)	1.1	(1.8)	0.57	(1.8)	(1.8)	0.78	(1.8)	(1.8)	(1.8)	(1.8)	(1.8)	0.73	16	440
56/020	97	(1.7)	(1.7)	(1.7)	(1.7)	0.79	0.64	(1.7)	1.1	(1.7)	0.9	(1.7)	(1.7)	1.6	(1.7)	0.42	(1.7)	(1.7)	(1.7)	1.4	17	450
59/001	0	(2.4)	(2.4)	(2.4)	(2.4)	(2.4)	0.84	0.61	0.79	(2.4)	0.81	(2.4)	(2.4)	1.3	(2.4)	0.58	(2.4)	(2.4)	(2.4)	1.6	21	100
59/010	46	(1.6)	(1.6)	0.61	(1.6)	(1.6)	0.55	0.38	0.38	(1.6)	0.92	(1.6)	(1.6)	1.4	(1.6)	(1.6)	(1.6)	(1.6)	(1.6)	1.8	16	1,480*
59/020	97	(1.6)	(1.6)	1.4	(1.6)	(1.6)	1.2	0.53	0.94	(1.6)	2.8*	(1.6)	(1.6)	3.7	(1.6)	0.53	(1.6)	(1.6)	(1.6)	4.5	24	1,950*
84/001	0	(0.45)	(0.45)	0.26	0.98	0.83	0.87	(0.45)	0.55	(0.45)	1.0	(0.45)	(0.45)	1.9	(0.45)	(0.45)	(0.45)	(0.45)	0.83	2.2	12	95
84/012	56	(0.40)	(0.40)	0.2	0.61	0.58	0.62	0.29	0.58	(0.40)	0.71	(0.40)	(0.40)	1.2	(0.40)	0.27	(0.40)	(0.40)	0.58	1.1	8.3	34
84/024	117	1.3	0.37	2.9	5.2*	3.6*	4.2*	1.2*	3.1*	2.1*	4.0*	0.6	1.2*	13*	1.6	1.4*	0.57	1.3	14*	11*	73*	309
Hackensack River																						
28/001	0	(2.0)	(2.0)	(2.0)	(2.0)	0.5	(2.0)	(2.0)	(2.0)	(2.0)	0.49	(2.0)	(2.0)	0.67	(2.0)	(2.0)	(2.0)	(2.0)	(2.0)	0.57	17	60
28/010	46	(0.81)	(0.81)	(0.81)	(0.81)	(0.81)	(0.81)	(0.81)	(0.81)	(0.81)	(0.81)	(0.81)	(0.81)	(0.81)	(0.81)	(0.81)	(0.81)	(0.81)	(0.81)	(0.81)	7.7	(30)
28/020	97	(0.79)	(0.79)	(0.79)	(0.79)	(0.79)	(0.79)	(0.79)	(0.79)	(0.79)	(0.79)	(0.79)	(0.79)	(0.79)	(0.79)	(0.79)	(0.79)	(0.79)	(0.79)	(0.79)	7.5	(30)
32/001	0	(1.5)	0.58	2.0*	3.4*	4.1*	4.8*	2.2*	2.6*	(1.2)	4.2*	0.75*	0.45	8.0*	0.67	2.3*	0.28	3.0*	2.2	5.1*	48*	190
32/010	46	3.1*	1.1*	4.7*	5.0*	4.7*	3.4*	1.4*	2.7*	(1.5)	6.6*	0.75*	(1.5)	8.3*	2.2*	1.8*	1.6*	1.0	12*	8.4*	70*	250*
32/020	97	0.72	0.32	1.7	1.7	1.5	0.69	(1.4)	1.4	(1.4)	2.2	0.35	(1.4)	3.0	1.2*	(1.4)	0.78	0.32	4.2*	3.2	26	90
35/001	0	(1.7)	(1.7)	0.66	(1.4)	1.7	1.6	1.3*	1.6*	(1.7)	1.8	(1.7)	(1.7)	3.2	(1.7)	1.1	(1.7)	(1.7)	0.72	2.3	23	(60)
35/010	46	0.38	0.35	0.95	1.7	1.9	(1.6)	1.8*	(1.6)	(1.6)	2.3	(1.6)	(1.6)	3.8	0.34	1.1	(1.6)	(1.6)	1.3	3.4	25	150
35/020	97	0.39	(1.6)	0.96	1.3	1.1	(1.6)	0.91	(1.6)	(1.6)	1.6	(1.6)	(1.6)	3.7	0.47	0.82	(1.6)	(1.6)	1.9	2.9	22	270*
83/001	0	(0.43)	(0.43)	0.28	0.6	0.61	0.54	0.37	0.52	(0.43)	0.68	(0.43)	(0.43)	1.3	(0.43)	0.34	(0.43)	(0.43)	0.9	1.0	8.9	122
83/012	56	0.41	(0.41)	1.9*	4.2*	3.6*	3.9*	1.7*	2.1*	0.4	3.8*	(0.41)	0.20	9.7*	0.56	1.9*	(0.41)	(0.41)	5.6*	6.8*	48*	159
83/024	117	0.27	(0.48)	0.57	1.2	1.1	0.84	0.62	0.71	(0.48)	1.2	0.24	(0.48)	1.8	0.28	0.56	(0.48)	(0.48)	1.7	2.0	14	79.1
Kill Van Kull																						
42/001	0	(0.95)	(0.95)	0.21	(0.95)	0.33	0.25	0.21	0.23	(0.95)	0.33	(0.95)	(0.95)	0.48	(0.95)	0.2	(0.95)	(0.95)	(0.95)	0.53	7.5	(43)
42/010	46	(0.83)	(0.83)	(0.83)	(0.83)	(0.83)	(0.83)	(0.83)	(0.83)	(0.83)	(0.83)	(0.83)	(0.83)	(0.83)	(0.83)	(0.83)	(0.83)	(0.83)	(0.83)	(0.83)	7.9	(31)
42/020	97	(0.77)	(0.77)	(0.77)	(0.77)	(0.77)	(0.77)	(0.77)	(0.77)	(0.77)	(0.77)	(0.77)	(0.77)	(0.77)	(0.77)	(0.77)	(0.77)	(0.77)	(0.77)	(0.77)	7.3	(29)
44/001	0	(1.5)	(1.5)	1.4	1.0	1.4*	1.2	0.85*	1.5*	(1.5)	(1.5)*	(1.5)	(1.5)	2.3*	(1.5)	0.79*	(1.5)	(1.5)	1.2*	1.7	21	135
44/005	20	0.41	(1.6)	1.1	2.5*	2.9*	2.2*	1.6*	3.5*	(1.6)	2.9*	(1.6)	(1.6)	5.7*	0.39	1.5*	(1.6)	(1.6)	2.7*	4.0*	36*	160
44/010	46	(1.7)	(1.7)	1.0	1.1	1.6*	1.9*	0.95*	0.96	(1.7)	1.4*	(1.7)	(1.7)	2.4*	(1.7)	0.87*	(1.7)	(1.7)	1.3*	1.7	22	110
87/001	0	(0.85)	0.52	9.4*	2.6*	2.1*	2.7*	0.6	2.0*	2.0*	2.1*	(0.85)	(0.85)	4.1*	0.76*	0.71	0.34	(0.85)	1.9*	4.0*	38*	895*
87/012	56	(0.67)	0.35	0.92	1.3*	1.2	1.2	(0.67)	0.82	(0.67)	1.2	(0.67)	(0.67)	1.8	(0.67)	0.4	(0.67)	(0.67)	0.96	2.1*	15	2,780*
87/024	117	(0.43)	(0.43)	(0.43)	0.26	0.46	0.34	0.18	0.35	(0.43)	0.3	(0.43)	(0.43)	0.3	(0.43)	(0.43)	(0.43)	(0.43)	(0.43)	0.64	5.2	44.9
88/001	0	(0.47)	(0.47)	(0.47)	0.2	0.25	0.26	(0.47)	0.2	(0.47)	0.21	(0.47)	(0.47)	0.36	(0.47)	(0.47)	(0.47)	(0.47)	(0.47)	0.41	4.7	24
88/012	56	(0.48)	(0.48)	0.23	0.66	0.58	0.47	(0.48)	0.4	(0.48)	0.62	(0.48)	(0.48)	1.0	(0.48)	(0.48)	(0.48)	(0.48)	0.24	1.3	7.9	206
88/024	117	(0.42)	(0.42)	(0.42)	0.33	0.41	0.32	(0.42)	0.25	(0.42)	0.3	(0.42)	(0.42)	0.34	(0.42)	0.42	(0.42)	(0.42)	(0.42)	0.43	5.1	37.9
Newark Bay																						
26/001	0	(1.3)	(1.3)	(1.3)	0.38	0.53	0.47	0.39	0.36	(1.3)	0.49	(1.3)	(1.3)	0.61	(1.3)	0.29	(1.3)	(1.3)	(1.3)	0.69	11	(48)
26/010	46	(1.0)	(1.0)	(1.0)	(1.0)	(1.0)	(1.0)	(1.0)	(1.0)	(1.0)	(1.0)	(1.0)	(1.0)	(1.0)	(1.0)	(1.0)	(1.0)	(1.0)	(1.0)	(1.0)	9.5	(41)
26/020	97	(1.1)	(1.1)	(1.1)	(1.1)	(1.1)	(1.1)	(1.1)	(1.1)	(1.1)	(1.1)	(1.1)	(1.1)	(1.1)	(1.1)	(1.1)	(1.1)	(1.1)	(1.1)	(1.1)	10	(38.0)
37/001	0	(1.0)	(1.0)	(1.0)	(1.0)	(1.0)	(1.0)	(1.0)	(1.0)	(1.0)	(1.0)	(1.0)	(1.0)	(1.0)	(1.0)	(1.0)	(1.0)	(1.0)	(1.0)	(1.0)	9.5	(40)

Table 5. *Continued*

Field ID	Depth (cm)	ACE	ACY	ANT	BAA	BAP	BBF	BGP	BKF	CAR	CHR	DBA	DBF	FLA	FLU	IND	MET	NAP	PHE	PYR	tPAH[b]	TEPH
37/010	46	(1.2)	(1.2)	(1.2)	(1.2)	(1.2)	(1.2)	(1.2)	(1.2)	(1.2)	(1.2)	(1.2)	(1.2)	(1.2)	(1.2)	(1.2)	(1.2)	(1.2)	(1.2)	(1.2)	11	(50)
37/020	97	(4.3)	(4.3)	(4.3)	(4.3)	(4.3)	(4.3)	(4.3)	(4.3)	(4.3)	(4.3)	(4.3)	(4.3)	(4.3)	(4.3)	(4.3)	(4.3)	(4.3)	(4.3)	(4.3)	41	(180)
63/001	0	(2.0)	(2.0)	(2.0)	(2.0)	0.48	0.48	(2.0)	(2.0)	(2.0)	0.51	(2.0)	(2.0)	0.96	(2.0)	(2.0)	(2.0)	(2.0)	(2.0)	0.89	17	121
63/013	61	(1.6)	(1.6)	0.37	(1.6)	0.73	0.77	0.45	0.61	(1.6)	0.75	(1.6)	(1.6)	1.5	(1.6)	0.53	(1.6)	(1.6)	0.4	1.3	15	142
63/025	48	(1.3)	(1.3)	0.63	(1.3)	0.79	0.81	0.43	0.57	(1.3)	1.0	(1.3)	(1.3)	2.6	(1.3)	0.46	(1.3)	(1.3)	0.55	2.3	16	283
64/001	0	(1.8)	(1.8)	0.4	(1.8)	0.7	0.84	0.46	0.47	(1.8)	0.78	(1.8)	(1.8)	1.6	(1.8)	0.46	(1.8)	(1.8)	0.64	1.4	16	197
64/013	61	(1.6)	(1.6)	(1.6)	(1.6)	0.94	0.92	0.54	0.66	(1.6)	1.4	(1.6)	(1.6)	2.2	(1.6)	0.53	(1.6)	(1.6)	1.2	2.8	19	149
64/025	122	(35)	(35)	(35)	(35)	(35)	(35)	(35)	(35)	(35)	(35)	(35)	(35)	(35)	(35)	(35)	(35)	(35)	(35)	(35)	330	176
65/001	0	(46)	(46)	(46)	(46)	(46)	(46)	(46)	(46)	(46)	(46)	(46)	(46)	(46)	(46)	(46)	(46)	(46)	(46)	(46)	440	116
65/013	61	(0.86)	(0.86)	(0.86)	(0.86)	(0.86)	(0.86)	(0.86)	(0.86)	(0.86)	(0.86)	(0.86)	(0.86)	(0.86)	(0.86)	(0.86)	(0.86)	(0.86)	(0.86)	(0.86)	8.2	(16.2)
65/025	122	(0.87)	(0.87)	(0.87)	(0.87)	(0.87)	(0.87)	(0.87)	(0.87)	(0.87)	(0.87)	(0.87)	(0.87)	(0.87)	(0.87)	(0.87)	(0.87)	(0.87)	(0.87)	(0.87)	8.3	(16.4)
66/001	0	(0.87)	(0.87)	(0.87)	(0.87)	(0.87)	(0.87)	(0.87)	(0.87)	(0.87)	(0.87)	(0.87)	(0.87)	(0.87)	(0.87)	(0.87)	(0.87)	(0.87)	(0.87)	(0.87)	8.3	(16.5)
66/013	61	(0.87)	(0.87)	(0.87)	(0.87)	(0.87)	(0.87)	(0.87)	(0.87)	(0.87)	(0.87)	(0.87)	(0.87)	(0.87)	(0.87)	(0.87)	(0.87)	(0.87)	(0.87)	(0.87)	8.3	(16.4)
66/025	122	(0.87)	(0.87)	(0.87)	(0.87)	(0.87)	(0.87)	(0.87)	(0.87)	(0.87)	(0.87)	(0.87)	(0.87)	(0.87)	(0.87)	(0.87)	(0.87)	(0.87)	(0.87)	(0.87)	8.3	(16.4)
68/001	0	(1.6)	(1.6)	(1.6)	(1.6)	0.43	0.4	(1.6)	(1.6)	(1.6)	0.49	(1.6)	(1.6)	0.78	(1.6)	(1.6)	(1.6)	(1.6)	0.45	0.69	14	173
68/013	61	(1.5)	(1.5)	(1.5)	(1.5)	0.39	0.49	0.5	0.31	(1.5)	(1.5)	0.5	(1.5)	(1.5)	0.74	(1.5)	(1.5)	(1.5)	(1.5)	(1.5)	0.69	13
68/025	122	(1.1)	(1.1)	(1.1)	(1.1)	0.28	0.27	(1.1)	(1.1)	(1.1)	0.29	(1.1)	(1.1)	0.5	(1.1)	(1.1)	(1.1)	(1.1)	(1.1)	0.46	9.5	197
69/001	0	(1.5)	(1.5)	(1.5)	(1.5)	(1.5)	(1.5)	(1.5)	(1.5)	(1.5)	(1.5)	(1.5)	(1.5)	0.36	(1.5)	(1.5)	(1.5)	(1.5)	(1.5)	0.31	13	92.9
69/013	61	(1.5)	(1.5)	0.35	(1.5)	0.78	0.7	0.46	0.47	(1.5)	0.74	(1.5)	(1.5)	1.3	(1.5)	0.43	(1.5)	(1.5)	0.57	1.2	14	109
69/025	122	0.26	(1.1)	0.27	(1.1)	0.32	0.3	(1.1)	(1.1)	(1.1)	0.37	(1.1)	(1.1)	0.99	(1.1)	(1.1)	(1.1)	(1.1)	0.38	0.78	9.7	166
70/001	0	(1.7)	(1.7)	0.94	(1.7)	0.66	0.59	0.43	0.37	(1.7)	0.65	(1.7)	(1.7)	1.1	(1.7)	0.4	(1.7)	(1.7)	0.5	1.1	14	108
70/013	61	(1.6)	(1.6)	(1.6)	(1.6)	0.74	0.61	0.48	0.46	(1.6)	0.65	(1.6)	(1.6)	1.0	(1.6)	0.45	(1.6)	(1.6)	(1.6)	0.91	14	221
70/025	122	(1.3)	(1.3)	0.84	(1.3)	0.68	0.61	0.42	0.51	(1.3)	0.77	(1.3)	(1.3)	1.7	(1.3)	0.42	(1.3)	(1.3)	1.1	1.5	14	417
71/001	0	(0.93)	(0.93)	(0.93)	(0.93)	(0.93)	(0.93)	(0.93)	(0.93)	(0.93)	(0.93)	(0.93)	(0.93)	(0.93)	(0.93)	(0.93)	(0.93)	(0.93)	(0.93)	(0.93)	8.8	(17.6)
71/013	61	(0.88)	(0.88)	(0.88)	(0.88)	(0.88)	(0.88)	(0.88)	(0.88)	(0.88)	(0.88)	(0.88)	(0.88)	(0.88)	(0.88)	(0.88)	(0.88)	(0.88)	(0.88)	(0.88)	8.4	(16.7)
71/025	122	(0.87)	(0.87)	(0.87)	(0.87)	(0.87)	(0.87)	(0.87)	(0.87)	(0.87)	(0.87)	(0.87)	(0.87)	(0.87)	(0.87)	(0.87)	(0.87)	(0.87)	(0.87)	(0.87)	8.3	(16.4)
72/001	0	(2.0)	(2.0)	(2.0)	0.57	0.43	0.59	(2.0)	1.0	(2.0)	(2.0)	(2.0)	(2.0)	3.0	(2.0)	4.3*	(2.0)	(2.0)	1.7	2.1	25	194
72/013	61	(1.9)	(1.9)	(1.9)	0.45	0.44	0.49	(1.9)	0.56	(1.9)	(1.9)	(1.9)	(1.9)	1.2	(1.9)	6.8*	(1.9)	(1.9)	0.47	0.95	22	188
72/025	122	(0.97)	(0.97)	(0.97)	(0.97)	(0.97)	(0.97)	(0.97)	(0.97)	(0.97)	(0.97)	(0.97)	(0.97)	0.36	(0.97)	7*	(0.97)	(0.97)	(0.97)	0.32	15	124
81/001	0	(0.47)	(0.47)	0.38	0.61	0.61	0.7	(0.47)	0.19	(0.47)	0.56	(0.47)	(0.47)	1.3	(0.47)	0.25	(0.47)	(0.47)	0.52	1.2	8.4	201
81/012	56	(0.69)	(0.69)	0.74	1.4	1.2	1.2	(0.69)	1.1	(0.69)	0.94	(0.69)	(0.69)	2.3	(0.69)	(0.69)	(0.69)	(0.69)	1.1	2.5	16	919*
81/024	117	(0.49)	(0.49)	0.44	0.97	0.7	0.95	(0.49)	0.58	(0.49)	0.69	(0.49)	(0.49)	2.0	0.59	(0.49)	0.63	(0.49)	1.8	2.2	14	1,480*
82/001	0	(0.60)	0.29	0.33	0.83	1.1	0.73	0.43	0.69	(0.60)	0.99	(0.60)	(0.60)	1.7	(0.60)	0.58	(0.6)	(0.60)	(0.60)	1.4	11	716*
82/012	56	(0.51)	(0.51)	(0.51)	(0.51)	(0.51)	(0.51)	(0.51)	(0.51)	(0.51)	(0.51)	(0.51)	(0.51)	(0.51)	(0.51)	(0.51)	(0.5)	(0.51)	(0.51)	0.22	4.8	156
82/024	117	(0.57)	(0.57)	(0.57)	(0.57)	0.52	(0.57)	(0.57)	(0.57)	(0.57)	(0.57)	(0.57)	(0.57)	(0.57)	(0.57)	(0.57)	(0.6)	(0.57)	(0.57)	(0.57)	5.7	(21.7)
85/001	0	2.7	(1.3)	3.1	4.0*	2.1	2.7*	1.1	2.1	(1.3)	4.4*	(1.3)	(1.3)	15*	0.6	1.0	(1.3)	(1.3)	1.6	10*	54	889*
85/012	56	17*	0.94	15*	9.8*	4.9*	6.9*	1.9	3.7*	3.8*	12*	1.1	9.0*	43*	9.1*	1.9	(1.2)	3.7*	38*	25*	210*	1,820*
85/024	117	20*	0.99	23*	15*	6.1*	6.1*	1.9	5.6*	6.8*	16*	(0.99)	13*	90*	19*	2.0	2.8*	12*	98*	57*	400*	1,780*
86/001	0	(0.98)	(0.98)	0.52	0.62	0.56	0.72	(0.98)	0.43	(0.98)	0.84	(0.98)	(0.98)	1.9	(0.98)	(0.98)	(0.98)	(0.98)	0.77	1.5	13	2,260*
86/012	56	0.6	(0.90)	0.86	1.1	0.78	1.1	(0.90)	0.66	(0.90)	1.1	(0.90)	(0.90)	3.0	0.39	(0.90)	(0.90)	(0.90)	1.2	2.6	17	684
86/024	117	1.3	(0.82)	1.8	1.9	0.42	1.5	(0.82)	0.84	0.48	1.8	(0.82)	0.87	7.1	1.6	(0.82)	(0.82)	(0.82)	6.3	4.3	33	766
Passaic River																						
01/001	0	0.33	0.54	0.94	1.9	1.9	1.2	1.0	1.3	(0.96)	2.2	(0.96)	(0.96)	3.2	0.49	0.88	(0.96)	(0.96)	3.2	4.3	26	130
01/010	46	1.2	1.7	2.1	5.1	5.2	3.6	2.1	4.6	(1.0)	5.8	1.3	(1.0)	7.2	1.2	2.4	0.36	0.28	6.2	9.2	61	160
01/020	97	36*	4.3*	32*	22*	16*	11*	(1.2)	10*	(1.2)	17*	0.58	2.1	37*	26	1.9	6.1	19	91*	52*	390*	11,330*
02/001	0	(9.4)	(9.4)	1.9	3.5	3.5	2.4	2.4	3.8	(9.4)	3.6	(9.4)	(9.4)	6.7	(9.4)	(9.4)	(9.4)	(9.4)	6.2	5.6	82	(39)
02/005	20	(9.7)	(9.7)	(9.7)	(9.7)	(9.7)	(9.7)	(9.7)	(9.7)	(9.7)	(9.7)	(9.7)	(9.7)	2.1	(9.7)	(9.7)	(9.7)	(9.7)	(9.7)	2.3	87	100
02/010	46	(5.0)	1.2	1.5	4.6	4.7	3.6	3.9*	2.6	(5.0)	5.3	1.4	(5.0)	6.7	(5.0)	3.1	(5.0)	(5.0)	4.0	8.5	66	590
05/001	0	(1.4)	(1.4)	0.44	1.5	1.8	1.1	0.9	0.49	(1.4)	2.0	0.44	(1.4)	3.7	(1.4)	1.0	(1.4)	(1.4)	2.2	3.6	24	(59)
05/005	20	(1.2)	(1.2)	0.4	1.2	1.3	0.73	0.68	0.53	(1.2)	1.6	(1.2)	(1.2)	3.1	(1.2)	0.84	(1.2)	(1.2)	2.0	3.1	20	110
05/010	46	(1.1)	0.95	0.58	2.5	2.9	1.0	0.93	0.78	(1.1)	2.9	0.36	(1.1)	2.5	(1.1)	1.0	(1.1)	(1.1)	1.1	4.0	25	60
06/001	0	0.43	(0.87)	0.65	1.3	1.2	1.2	0.98	1.1	0.26	1.5	0.24	0.23	2.6	0.44	0.8	(0.87)	0.32	2.3	2.5	19	(32)
06/010	46	(0.92)	(0.92)	0.35	1.1	1.1	1.0	0.71	0.93	(0.92)	1.3	(0.92)	(0.92)	2.2	(0.92)	0.61	(0.92)	(0.92)	1.5	2.3	17	390
06/020	97	(0.78)	(0.78)	(0.78)	(0.78)	(0.78)	(0.78)	(0.78)	(0.78)	(0.78)	(0.78)	(0.78)	(0.78)	0.24	(0.78)	(0.78)	(0.78)	(0.78)	(0.78)	0.25	7.1	(29)
08/001	0	(17)	(17)	(17)	(17)	(17)	(17)	(17)	(17)	(17)	(17)	(17)	(17)	(17)	(17)	(17)	(17)	(17)	(17)	(17)	160	895
08/012	56	(15)	(15)	(15)	(15)	(15)	(15)	(15)	(15)	(15)	(15)	(15)	(15)	8.1	(15)	(15)	(15)	(15)	11	9.4	150	770
08/024	117	(0.42)	(0.42)	0.39	0.97	0.92	0.56	0.55	0.51	(0.42)	0.87	(0.42)	(0.42)	1.1	(0.42)	0.46	(0.42)	(0.42)	0.26	1.7	90	250
09/001	0	0.51	0.69	1.8	4.9	3.8	4.7	1.8	2.2	0.48	5.3	0.58	0.6	7.4	1.3	1.8	0.25	0.52	7.1	9.4	55	540

Table 5. *Continued*

Field ID	Depth (cm)	ACE	ACY	ANT	BAA	BAP	BBF	BGP	BKF	CAR	CHR	DBA	DBF	FLA	FLU	IND	MET	NAP	PHE	PYR	tPAH[b]	TEPH
09/005	20	(0.80)	(0.80)	(0.80)	0.5	0.45	0.47	0.37	0.37	(0.80)	0.58	(0.80)	(0.80)	0.98	(0.80)	0.3	(0.80)	(0.80)	0.42	1.0	9.0	(31)
09/010	46	0.19	(0.81)	0.21	0.65	0.57	0.53	0.45	0.52	(0.81)	0.76	(0.81)	(0.81)	1.2	(0.81)	0.35	(0.81)	(0.81)	0.7	1.3	10	440
12/001	0	(1.3)	0.33	0.8	2.3	2.8	4.2	1.8	6.3*	0.31	2.9	0.62	(1.3)	5.2	(1.3)	1.5	(1.3)	(1.3)	1.8	5.6	40	120
12/010	46	1.6	(0.99)	1.2	1.8	1.5	1.0	0.67	1.3	(0.99)	2.0	0.29	(0.99)	3.6	(0.99)	0.75	(0.99)	(0.99)	2.8	3.9	25	1,170
12/017	81	(0.71)	(0.71)	(0.71)	(0.71)	(0.71)	(0.71)	(0.71)	(0.71)	(0.71)	(0.71)	(0.71)	(0.71)	(0.71)	(0.71)	(0.71)	(0.71)	(0.71)	(0.71)	(0.71)	6.7	(27)
13/001	0	1.3	1.0	2.6	5.8	4.0	2.8	1.5	5.6*	(0.84)	5.9	0.69	0.25	11	0.3	1.6	(0.84)	(0.84)	4.1	11	61	200
13/010	46	110*	8.9*	62*	48*	38*	29*	13*	30*	(8.6)	52*	1.9	5.1*	91*	39*	13*	(8.6)	5.7	180*	100*	840*	3,760*
13/020	97	(1.3)	(1.3)	(1.3)	(1.3)	0.27	(1.3)	(1.3)	0.31	(1.3)	0.29	(1.3)	(1.3)	0.56	(1.3)	(1.3)	(1.3)	(1.3)	0.28	0.41	11	(50)
13/047	234	(1.0)	(1.0)	(1.0)	(1.0)	0.22	(1.0)	(1.0)	(1.0)	(1.0)	(1.0)	(1.0)	(1.0)	(1.0)	(1.0)	(1.0)	(1.0)	(1.0)	(1.0)	(1.0)	9.2	(39)
13/074	371	0.2	(0.84)	(0.84)	1.6	1.6	1.5	0.88	1.2	(0.84)	1.6	(0.84)	(0.84)	3.3	0.18	(0.84)	(0.84)	(0.84)	1.5	2.3	19	(31)
13/098	493	(0.77)	(0.77)	(0.77)	(0.77)	(0.77)	(0.77)	(0.77)	(0.77)	(0.77)	(0.77)	(0.77)	(0.77)	(0.77)	(0.77)	(0.77)	(0.77)	(0.77)	(0.77)	(0.77)	7.3	(30)
14/001	0	0.32	0.25	(1.1)	1.3	1.4	1.3	(1.1)	2.1	(1.1)	1.7	(1.1)	(1.1)	2.9	(1.1)	0.69	(1.1)	(1.1)	0.9	3.1	20	50
14/010	46	1.4	0.29	0.8	2.3	2.6	1.6	1.1	1.9	(1.2)	2.8	(1.2)	(1.2)	4.7	0.27	0.98	(1.2)	(1.2)	1.1	5.7	31	(44)
14/020	97	(1.2)	(1.2)	(1.2)	(1.2)	(1.2)	(1.2)	(1.2)	(1.2)	(1.2)	(1.2)	(1.2)	(1.2)	(1.2)	(1.2)	(1.2)	(1.2)	(1.2)	(1.2)	(1.2)	11	(46)
14/047	234	(0.98)	(0.98)	(0.98)	(0.98)	(0.98)	(0.98)	(0.98)	(0.98)	(0.98)	(0.98)	(0.98)	(0.98)	(0.98)	(0.98)	(0.98)	(0.98)	(0.98)	(0.98)	(0.98)	9.3	(35)
14/074	371	(1.1)	(1.1)	(1.1)	(1.1)	0.25	(1.1)	(1.1)	(1.1)	(1.1)	(1.1)	(1.1)	(1.1)	(1.1)	(1.1)	(1.1)	(1.1)	(1.1)	(1.1)	(1.1)	10	(43)
14/116	584	(1.2)	(1.2)	(1.2)	(1.2)	(1.2)	(1.2)	(1.2)	(1.2)	(1.2)	(1.2)	(1.2)	(1.2)	(1.2)	(1.2)	(1.2)	(1.2)	(1.2)	(1.2)	(1.2)	11	(45)
15/001	0	0.27	0.32	0.86	2.0	2.3	2.0	0.43	2.0	(1.3)	2.6	(1.3)	(1.3)	4.6	(1.3)	0.6	(1.3)	(1.3)	2.0	5.3	12	140
15/010	46	(1.2)	(1.2)	(1.2)	(1.2)	(1.2)	(1.2)	(1.2)	(1.2)	(1.2)	(1.2)	(1.2)	(1.2)	(1.2)	(1.2)	(1.2)	(1.2)	(1.2)	(1.2)	(1.2)	11	(47)
15/020	97	(1.3)	(1.3)	(1.3)	(1.3)	(1.3)	(1.3)	(1.3)	(1.3)	(1.3)	(1.3)	(1.3)	(1.3)	(1.3)	(1.3)	(1.3)	(1.3)	(1.3)	(1.3)	(1.3)	12	(47)
15/047	234	(1.3)	(1.3)	(1.3)	(1.3)	(1.3)	(1.3)	(1.3)	(1.3)	(1.3)	(1.3)	(1.3)	(1.3)	(1.3)	(1.3)	(1.3)	(1.3)	(1.3)	(1.3)	(1.3)	12	(51)
15/074	371	(0.78)	(0.78)	(0.78)	(0.78)	(0.78)	(0.78)	(0.78)	(0.78)	(0.78)	(0.78)	(0.78)	(0.78)	(0.78)	(0.78)	(0.78)	(0.78)	(0.78)	(0.78)	(0.78)	7.4	(30)
15/098	493	(0.85)	(0.85)	(0.85)	(0.85)	(0.85)	(0.85)	(0.85)	(0.85)	(0.85)	(0.85)	(0.85)	(0.85)	(0.85)	(0.85)	(0.85)	(0.85)	(0.85)	(0.85)	(0.85)	8.1	(31)
15/114	574	(0.82)	(0.82)	(0.82)	(0.82)	(0.82)	(0.82)	(0.82)	(0.82)	(0.82)	(0.82)	(0.82)	(0.82)	(0.82)	(0.82)	(0.82)	(0.82)	(0.82)	(0.82)	(0.82)	7.8	(31)
16/001	0	(1.6)	(1.6)	0.55	1.9	1.8	2.0	1.2	1.6	(1.6)	2.4	(1.6)	(1.6)	3.2	(1.6)	1.0	(1.6)	(1.6)	1.5	3.9	27	(62)
16/010	46	(2.8)	(2.8)	0.81	(2.8)	2.3	2.3	1.4	1.5	(2.8)	3.0	(2.8)	(2.8)	4.0	(2.8)	1.2	(2.8)	(2.8)	2.1	5.1	36	440
16/020	97	(3.2)	(3.2)	1.1	1.7	(1.8)	(1.8)	(1.3)	(1.4)	(3.2)	2.2	(3.2)	(3.2)	4.0	(3.2)	(1.1)	(3.2)	(3.2)	2.2	4.9	33	1,210
16/047	234	(2.8)	(2.8)	1.1	(2.8)	1.7	1.8	1.1	1.5	(2.8)	2.4	(2.8)	(2.8)	4.1	(2.8)	0.92	(2.8)	(2.8)	2.9	5.3	35	1,380
16/074	371	5.9	1.4	6.6	7.5	5.4	4.4	1.7	2.8	(2.3)	7.6	0.56	(2.3)	9.6	3.4	1.6	(3.3)	1.7	16	17	99	2,380
16/095	478	(0.72)	(0.72)	(0.72)	(0.72)	(0.72)	(0.72)	(0.72)	(0.72)	(0.72)	(0.72)	(0.72)	(0.72)	(0.72)	(0.72)	(0.72)	(0.72)	(0.72)	(0.72)	(0.72)	6.8	(27)
16/113	569	(0.74)	(0.74)	(0.74)	(0.74)	(0.74)	(0.74)	(0.74)	(0.74)	(0.74)	(0.74)	(0.74)	(0.74)	(0.74)	(0.74)	(0.74)	(0.74)	(0.74)	(0.74)	(0.74)	7.0	(27)
17/001	0	(1.6)	(1.6)	(1.6)	(1.6)	1.0	1.1	0.81	0.83	(1.6)	1.3	(1.6)	(1.6)	1.7	(1.6)	0.62	(1.6)	(1.6)	0.68	1.9	18	174
17/010	46	(1.4)	(1.4)	0.57	(1.4)	1.3	1.3	0.63	1.0	(1.4)	1.6	(1.4)	(1.4)	2.4	(1.4)	0.55	(1.4)	(1.4)	1.7	3.3	21	2,200
17/020	97	(0.36)	(1.5)	0.79	(1.5)	1.4	1.7	0.79	1.1	(1.5)	1.9	(1.5)	(1.5)	3.4	0.33	(1.5)	(1.5)	(1.5)	1.8	4.8	24	1,900
17/047	234	(1.5)	(1.5)	0.52	(1.5)	1.2	1.1	0.9	1.0	(1.5)	1.6	(1.5)	(1.5)	2.6	0.35	0.92	(1.5)	(1.5)	2.0	3.6	22	1,030
17/074	371	0.99	0.74	1.3	3.2	2.6	2.8	0.96	1.8	(2.6)	3.9	(2.6)	(2.6)	6.1	1.1	0.91	0.67	2.1	5.0	8.8	47	3,200
17/095	478	1.2	0.79	7.7	13*	9.3*	8.4*	4.4*	5.2	(1.7)	12*	2.4	(1.7)	18*	0.98	4.7*	(1.7)	(1.7)	12	21	124	1,700
17/101	508	(0.75)	(0.75)	(0.75)	(0.75)	(0.75)	(0.75)	(0.75)	(0.75)	(0.75)	(0.75)	(0.75)	(0.75)	(0.75)	(0.75)	(0.75)	(0.75)	(0.75)	(0.75)	(0.75)	7.1	NA[c]
18/001	0	(3.8)	(3.8)	(3.8)	1.8	(3.4)	1.7	1.6	1.3	(3.8)	2.4	(3.8)	(3.8)	4.0	(3.8)	1.2	(3.8)	(3.8)	1.5	4	38	800
18/010	46	(3.4)	(3.4)	(3.4)	1.5	(3.4)	1.6	1.2	1.1	(3.4)	1.9	(3.4)	(3.4)	3.2	(3.4)	1.1	(3.4)	(3.4)	2.0	3.7	34	1,540
18/020	97	(0.57)	(2.8)	1.0	2.6	(2.8)	2.6	2.0	2.2	(2.8)	3.6	(2.8)	(2.8)	5.2	(2.8)	1.9	(2.8)	(2.8)	3.0	7.5	43	3,040
18/032	157	(1.8)	(1.0)	1.8	5.0	4.6	4.1	3.7*	4.0	(2.5)	6.4	1.1	(2.5)	7.9	0.81	3.0	(2.5)	(2.5)	5.0	10	64	2,030
18/047	234	2.2	0.73	2.4	4.2	(3.2)	2.6	2.4	2.6	(2.6)	5.0	0.52	(2.6)	6.5	1.6	2.3	2.3	2.8	6.9	9.1	58	2,410
18/062	310	17	2.1	14*	14*	9.7*	7.0*	2.6	4.8	(2.7)	15*	1.1	1.0	16*	10	2.6	20	22	35*	34*	230	1,690
18/074	371	3.1	0.87	5.0	7.6	5.7	5.7*	3.7*	2.7	(1.6)	8.0	1.2	0.42	11	2.4	3.7	1.5	2.5	11	13	90	3,840
18/084	422	(0.74)	(0.74)	(0.74)	(0.74)	(0.74)	(0.74)	(0.74)	(0.74)	(0.74)	(0.74)	(0.74)	(0.74)	0.18	(0.74)	(0.74)	(0.74)	(0.74)	(0.74)	0.21	6.7	(29)
18/090	452	(0.76)	(0.76)	(0.76)	(0.76)	(0.76)	(0.76)	(0.76)	(0.76)	(0.76)	(0.76)	(0.76)	(0.76)	(0.76)	(0.76)	(0.76)	(0.76)	(0.76)	(0.76)	(0.76)	7.2	(27)
19/001	0	(3.5)	(3.5)	3.5	1.7	(3.5)	1.9	1.9	1.3	(3.5)	2.4	(3.5)	(3.5)	3.8	(3.5)	1.4	(3.5)	(3.5)	1.6	3.9	37	440
19/010	46	0.61	0.63	1.1	3.4	(3.3)	2.6	2.7	3.0	(3.0)	4.7	(3.0)	(3.0)	6.2	(3.0)	2.1	(3.0)	(3.0)	2.2	8.8	49	1,140
19/020	97	0.68	0.59	1.3	3.6	(3.2)	3.5	1.7	2.7	(2.8)	4.6	(2.8)	(2.8)	6.3	(2.8)	2.0	(2.8)	(2.8)	3.3	9.9	50	1,600
19/047	234	1.8	1.4	4.4	8.3	5.5	4.7	2.7	3.4	(2.4)	8.8	0.98	0.71	13	2.3	2.5	0.93	1.6	8.7	16	89	1,230
19/074	371	43	33*	40*	29*	18*	10*	(39)	11*	(39)	34*	(39)	(39)	41*	42*	(39)	180*	290*	110*	60*	1040*	15,690
19/095	478	(0.76)	(0.76)	(0.76)	(0.76)	(0.76)	(0.76)	(0.76)	(0.76)	(0.76)	(0.76)	(0.76)	(0.76)	(0.76)	(0.76)	(0.76)	(0.76)	(0.76)	(0.76)	(0.76)	7.2	210
19/107	538	(0.77)	(0.77)	(0.77)	(0.77)	(0.77)	(0.77)	(0.77)	(0.77)	(0.77)	(0.77)	(0.77)	(0.77)	(0.77)	(0.77)	(0.77)	(0.77)	(0.77)	(0.77)	(0.77)	7.3	(29)
20/001	0	1.9	0.52	3.3	5.2	3.7	3.4	2.5	2.5	(1.5)	5.0	0.77	0.4	9.7	1.4	2.2	1.1	2.6	9.2	9.1	65	30
20/010	46	1,000*	80*	500*	320*	210*	110*	46*	110*	(110)	340*	29*	74*	420*	530*	55*	850*	1,300*	1,200*	650*	7,900*	61,380
20/020	97	57	11*	68*	47*	29*	16*	9.8*	16*	(25)	49*	(25)	7.7	73*	34	9.8*	(25)	22	180*	97*	760*	3,090
20/047	234	(0.77)	(0.77)	(0.77)	(0.77)	(0.77)	(0.77)	(0.77)	(0.77)	(0.77)	(0.77)	(0.77)	(0.77)	(0.77)	(0.77)	(0.77)	(0.77)	(0.77)	(0.77)	(0.77)	7.3	(29)

Table 5. *Continued*

Field ID	Depth (cm)	ACE	ACY	ANT	BAA	BAP	BBF	BGP	BKF	CAR	CHR	DBA	DBF	FLA	FLU	IND	MET	NAP	PHE	PYR	tPAH[b]	TEPH
20/074	371	(0.61)	(0.86)	1.5	4.6	4.5	4.2	3.1	2.9	(2.7)	5.6	0.84	(2.7)	7.8	0.68	2.6	(2.7)	(2.7)	4.7	9.8	59	1,760
20/095	478	1.1	1.0	1.7	4.3	3.7	4.6	3.2	2.6	(2.5)	5.5	0.88	(2.5)	7.6	0.65	2.7	0.75	1.8	2.5	9.8	57	1,140
20/116	584	0.32	(0.78)	0.32	0.37	0.28	0.24	(0.78)	0.2	(0.78)	0.41	(0.78)	(0.78)	0.88	0.16	(0.78)	0.20	0.36	(1.0)	0.97	8.1	(29)
21/001	0	(3.4)	(3.4)	0.74	2.4	2.7	2.8	2.2	2.2	(3.4)	3.4	(3.4)	(3.4)	4.7	(3.4)	2.3	(3.4)	(3.4)	1.9	5.5	44	300
21/010	46	0.7	0.67	1.4	4.1	3.6	3	2.9	2.9	(2.1)	5.0	0.82	(2.1)	7.4	0.69	2.4	(2.1)	(2.1)	3.1	9.3	52	1,230
21/020	97	0.68	0.81	1.4	4.8	4.3	3.9	2.8	3.9	(2.7)	6.1	0.8	(2.7)	(9.0)	0.75	2.6	(2.7)	(2.7)	5.1	12	64	2,110
21/047	234	1.4	1.2	2.0	5.5	4.4	4.3	2.5	3.3	(2.7)	6.4	(2.7)	(2.7)	8.1	1.1	2.8	(2.7)	0.96	5.9	14	69	1,430
21/074	371	24*	3.8	22*	23*	15*	11*	2.6	9.9*	0.94	22*	0.9	4.5*	24*	17*	2.5	31*	27*	52*	49*	340*	1,810
21/095	478	0.29	(0.83)	0.18	(0.83)	(0.83)	(0.83)	(0.83)	(0.83)	(0.83)	0.18	(0.83)	(0.83)	0.22	(0.83)	(0.83)	(0.83)	(0.83)	0.61	0.36	7.2	(30)
21/109	549	(0.80)	(0.80)	(0.80)	(0.80)	(0.80)	(0.80)	(0.80)	(0.80)	(0.80)	(0.80)	(0.80)	(0.80)	(0.80)	(0.80)	(0.80)	(0.80)	(0.80)	(0.80)	(0.80)	7.6	(30)
22/001	0	(1.5)	(1.5)	0.35	1.0	1.3	1.5	(1.5)	1.0	(1.5)	1.4	(1.5)	(1.5)	2.2	(1.5)	0.62	(1.5)	(1.5)	0.82	1.8	19	170
22/010	46	0.44	(1.4)	1.6	1.3	1.3	1.3	0.64	2.0	(1.4)	2.1	(1.4)	(1.4)	4.1	(1.4)	0.64	(1.4)	(1.4)	0.94	3.3	25	830
22/020	97	0.73	(1.5)	(1.5)	1.4	1.4	(1.5)	(1.5)	(1.5)	(1.5)	2.0	(1.5)	(1.5)	3.8	0.58	(1.5)	(1.5)	(1.5)	2.2	3.6	24	910
22/047	234	5.1	3.6	11	46*	11*	10*	3.5*	4.3	(1.6)	36*	(1.6)	1.2	17*	5.2	3.7	6.2	3.3	24	100*	290*	1,160
22/074	371	0.53	0.18	0.83	1.1	0.99	0.67	0.5	0.68	(0.82)	1.3	0.18	(0.82)	2.0	0.58	0.44	0.40	0.51	2.6	2.4	17	(31)
22/098	478	(0.81)	(0.81)	(0.81)	(0.81)	(0.81)	(0.81)	(0.81)	(0.81)	(0.81)	(0.81)	(0.81)	(0.81)	(0.81)	(0.81)	(0.81)	(0.81)	(0.81)	(0.81)	(0.81)	7.7	(30)
22/109	549	(0.81)	(0.81)	(0.81)	(0.81)	(0.81)	(0.81)	(0.81)	(0.81)	(0.81)	(0.81)	(0.81)	(0.81)	(0.81)	(0.81)	(0.81)	(0.81)	(0.81)	(0.81)	(0.81)	7.7	(29)
23/001	0	(1.5)	(1.5)	0.31	1.0	1.2	1.1	0.65	1.4	(1.5)	1.3	1.5	(1.5)	2.2	(1.5)	0.63	(1.5)	(1.5)	0.86	2.3	2.0	70
23/010	46	(1.6)	(1.6)	(1.6)	0.93	1.2	1.1	0.48	1.2	(1.6)	1.3	(1.6)	(1.6)	1.9	(1.6)	0.52	(1.6)	(1.6)	0.82	2.3	19	105
23/020	97	(1.6)	(1.6)	0.48	1.2	1.5	1.6	(1.6)	1.5	(1.6)	1.8	(1.6)	(1.6)	2.7	0.32	0.33	(1.6)	(1.6)	1.6	3.3	23	670
60/001	0	(2.2)	(2.2)	0.73	(2.2)	2.1	2.0	1.3	2.1	(2.2)	2.2	(2.2)	(2.2)	4.4	(2.2)	1.5	(2.2)	(2.2)	1.6	4.4	32	456
60/013	61	(4.7)	(4.7)	(4.7)	(4.7)	(4.7)	(4.7)	(4.7)	(4.7)	(4.7)	(4.7)	(4.7)	(4.7)	(4.7)	(4.7)	(4.7)	(4.7)	(4.7)	(4.7)	(4.7)	66	1,540
60/025	122	(2.3)	(2.3)	(2.3)	12*	8.4*	9.5*	(2.3)	8.1*	(2.3)	13*	(2.3)	(2.3)	24*	(2.3)	(2.3)	(2.3)	(2.3)	6.7	19	110	8,910*
61/001	0	(1.6)	(1.6)	0.33	1.1	1.2	1.2	1.1	0.86	(1.6)	1.5	0.52	(1.6)	2.3	(1.6)	0.94	(1.6)	(1.6)	0.79	2.2	20	198
61/012	56	(48)	(48)	(48)	(48)	(48)	(48)	(48)	(48)	(48)	(48)	(48)	(48)	(48)	(48)	(48)	(48)	(48)	(48)	(48)	460*	1,070
61/024	117	(57)	(57)	(57)	(57)	(57)	(57)	(57)	(57)	(57)	(57)	(57)	(57)	(57)	(57)	(57)	(57)	(57)	(57)	(57)	540*	2,140
62/001	0	(1.8)	(1.8)	0.5	0.88	1.1	0.65	0.91	1.0	(1.8)	1.1	(1.8)	(1.8)	1.8	(1.8)	0.77	(1.8)	(1.8)	0.58	1.6	18	166
62/012	56	0.8	0.43	(1.6)	1.7	1.7	1.8	1.4	1.2	(1.6)	1.8	0.56	0.5	4.2	0.95	1.2	0.38	(1.6)	3.5	3.4	28	527
62/024	117	(47)	(47)	(47)	(47)	(47)	(47)	(47)	(47)	(4.7)	(47)	(47)	(47)	(47)	(47)	(47)	(47)	(47)	(47)	(47)	430*	570
77/001	0	(0.82)	(0.82)	0.63	1.6	1.6	1.4	1.1	1.1	(0.82)	1.7	(0.82)	(0.82)	3.3	0.34	1.0	(0.82)	0.55	2.1	2.6	21	515
77/012	56	1.0	(0.78)	2.0	1.4	1.4	1.4	1.0	1.0	0.4	1.6	(0.78)	0.62	3.7	1.8	0.93	6.3	(0.78)	5.1	3.2	34	1,850
77/024	117	(6.9)	(6.9)	(6.9)	(6.9)	(6.9)	(6.9)	(6.9)	(6.9)	(6.9)	(6.9)	(6.9)	(6.9)	5.2	(6.9)	(6.9)	(6.9)	(6.9)	2.9	5.6	69	1,570
73/001	0	(0.42)	(0.42)	(0.42)	0.34	0.36	0.37	0.2	0.38	(0.42)	0.39	(0.42)	(0.42)	0.84	(0.42)	0.19	(0.42)	(0.42)	0.44	0.66	6.1	(15.8)
74/001	0	(0.79)	(0.79)	0.45	2.0	1.9	2.6	0.99	1.8	(0.79)	2.3	(0.79)	(0.79)	4.4	(0.79)	0.99	(0.79)	(0.79)	2.2	4.0	27	117
74A012	56	(1.1)	(1.1)	(1.1)	(1.1)	0.9	(1.1)	(1.1)	(1.1)	(1.1)	(1.1)	(1.1)	(1.1)	(1.1)	(1.1)	(1.1)	(1.1)	(1.1)	(1.1)	(1.1)	11	(43.3)
74A024	117	(0.48)	(0.48)	(0.48)	(0.48)	0.41	(0.48)	(0.48)	(0.48)	(0.48)	(0.48)	(0.48)	(0.48)	(0.48)	(0.48)	(0.48)	(0.48)	(0.48)	(0.48)	(0.48)	4.7	(18.3)
75/001	0	(1.0)	(1.0)	(1.0)	1.2	1.0	1.2	0.9	0.71	(1.0)	1.4	(1.0)	(1.0)	2.2	(1.0)	0.83	(1.0)	(1.0)	0.88	1.9	17	428
75/012	56	(0.69)	(0.69)	0.49	1.1	0.93	0.94	0.73	0.65	(0.69)	1.1	0.3	(0.69)	2.0	(0.69)	0.68	(0.69)	(0.69)	0.86	1.8	14	1,490
75/024	117	(19)	(19)	(19)	(19)	(19)	(19)	(19)	(19)	(19)	(19)	(19)	(19)	(19)	(19)	(19)	(19)	(19)	(19)	(19)	181	1,190
76/001	0	(0.42)	(0.42)	(0.42)	0.31	0.3	0.31	0.21	0.2	(0.42)	0.4	(0.42)	(0.42)	0.66	(0.42)	0.2	(0.42)	(0.42)	0.26	0.63	5.4	102
76/012	56	(0.38)	(0.38)	0.28	0.76	0.77	0.78	0.39	0.43	(0.38)	0.83	(0.38)	(0.38)	1.9	(0.38)	0.34	(0.38)	(0.38)	0.55	1.5	10	288
76/024	117	(14)	(14)	(14)	11*	10*	(14)	(14)	(14)	(14)	12	(14)	(14)	19*	(14)	(14)	(14)	(14)	17	26*	186	737
Upper New York Bay																						
89/001	0	(0.51)	(0.51)	(0.51)	0.47	0.71	0.45	(0.51)	0.61	(0.51)	0.49	(0.51)	(0.51)	0.51	(0.51)	(0.51)	(0.51)	(0.51)	(0.51)	0.92	4.0	130
89/012	56	(0.44)	(0.44)	(0.44)	(0.44)	(0.44)	(0.44)	(0.44)	(0.44)	(0.44)	(0.44)	(0.44)	(0.44)	(0.44)	(0.44)	(0.44)	(0.44)	(0.44)	(0.44)	(0.44)	ND	(16.6)
89/024	117	(0.41)	(0.41)	(0.41)	(0.41)	(0.41)	(0.41)	(0.41)	(0.41)	(0.41)	(0.41)	(0.41)	(0.41)	(0.41)	(0.41)	(0.41)	(0.41)	(0.41)	(0.41)	(0.41)	ND	(15.7)

[a] Data presented in parentheses are detection limits

[b] Calculated as the sum of 19 PAHs; when a compound was not detected, one-half the analytical detection limit was used to estimate concentrations

[c] Not analyzed

* Statistically elevated ($p < 0.05$) above the arithmetic mean concentration for the respective waterway

ACE = acenapthene, ACY = acenaphthylene, ANT = anthracene, BAA = benzo(a)anthracene, BAP = benzo(a)pyrene, BBR = benzo(b)fluoranthene, BGP = benzo(g,h,i)perylene, BKF = benzo(k)fluoranthene, CAR = carbazole, CHR = chrysene, DBA = dibenzo(a,h)anthracene, DBF = dibenzofuran, FLA = fluoranthene, FLU = fluorene, IND = indeno(1,2,3-cd)pyrene, MET = 2-methylnaphthalene, NAP = naphthalene, PHE = phenanthrene, PYR = pyrene, tPAH = total PAH, TEPH = total extractable petroleum hydrocarbons

Table 6. Sediment accumulation rates derived from ^{137}Cs and ^{210}Pb assay results

Station	Rate (cm/yr)	Station	Rate (cm/yr)	Station	Rate (cm/yr)	Station	Rate (cm/yr)
1	0.61	17	8.9	37	[a]	74	1.2
2	1.3	18	3.8	42	[a]	75	3.6
3	6.6	19	5.3	44	>4.8	76	[a]
5	>1.2	20	[a]	47	[a]	77	>3.0
6	4.6	21	6.1	48	2.0	81	>3.0
8	[a]	22	6.1	49	0.66	82	[a]
9	>4.8	23	>7.4	51	[a]	83	2.0
10	3.0	26	0.61	55	0.58	84	2.8
12	0.66	28	0.99	56	6.4	85	5.1
14	0.99	32	[a]	59	3.3	86	10.7
13	0.66	33	[a]	60	3.8	87	[a]
15	0.41	34	[a]	61	>3.3	88	[a]
16	8.6	35	>6.9	62	>3.3	89	[a]

[a]Derivation of rates was not possible due to inability to identify the ^{137}Cs 1954 horizon, unacceptable scatter of ^{210}Pb activities, and/or ^{210}Pb activities near the supported level

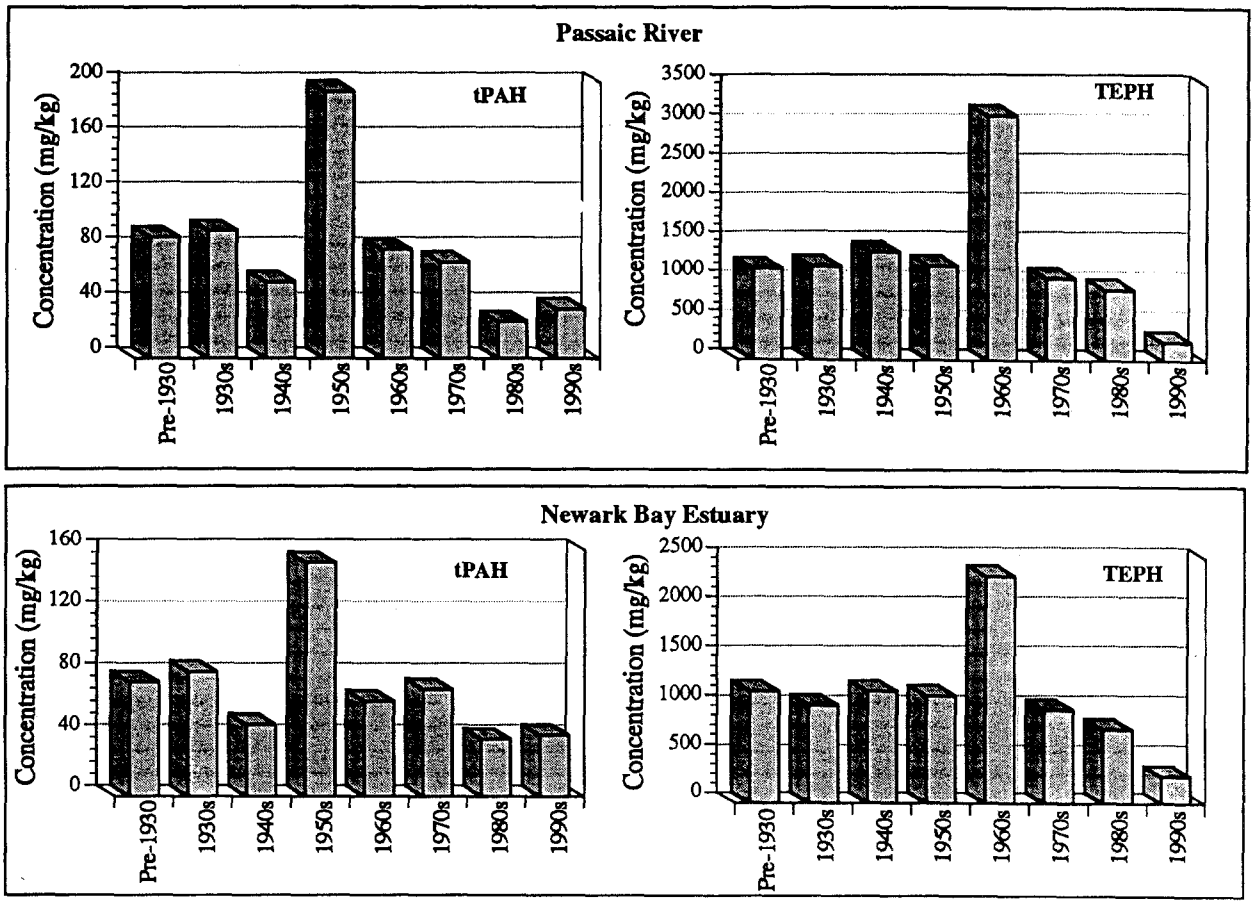

Fig. 2. Temporal distributions (mean concentrations, mg/kg) of TEPH and tPAH in the Passaic River and Newark Bay Estuary

detected near wood preserving facilities (Zitco 1978; Neff 1980). Creosote used as a wood preservative contains approximately 80–85% PAHs (Ehrlich *et al.* 1982; USEPA 1988). Mueller *et al.* (1989) reported that coal tar creosote consists of a variety of PAHs, predominately naphthalene, 2-methylnaphthalene, phenanthrene, and anthracene as well as 1-methylnaphthalene, fluorene, fluoranthene, chrysene, pyrene, and benzo(a)pyrene. Because of its predominance in coal tar creosote, naphthalene has been used as a chemical marker for distinguishing inputs from wood preserving industry effluent (USEPA 1982). Catallo and Gambrell (1987) characterized PAH contamination of surface sediments associated with the Bayou Bonfouca Superfund site in Louisiana and found that the most extremely contaminated area had levels ranging from 610 mg/kg for benzo(a)pyrene to as high as 2,931 mg/kg for phenanthrene. The authors estimated that this sample contained

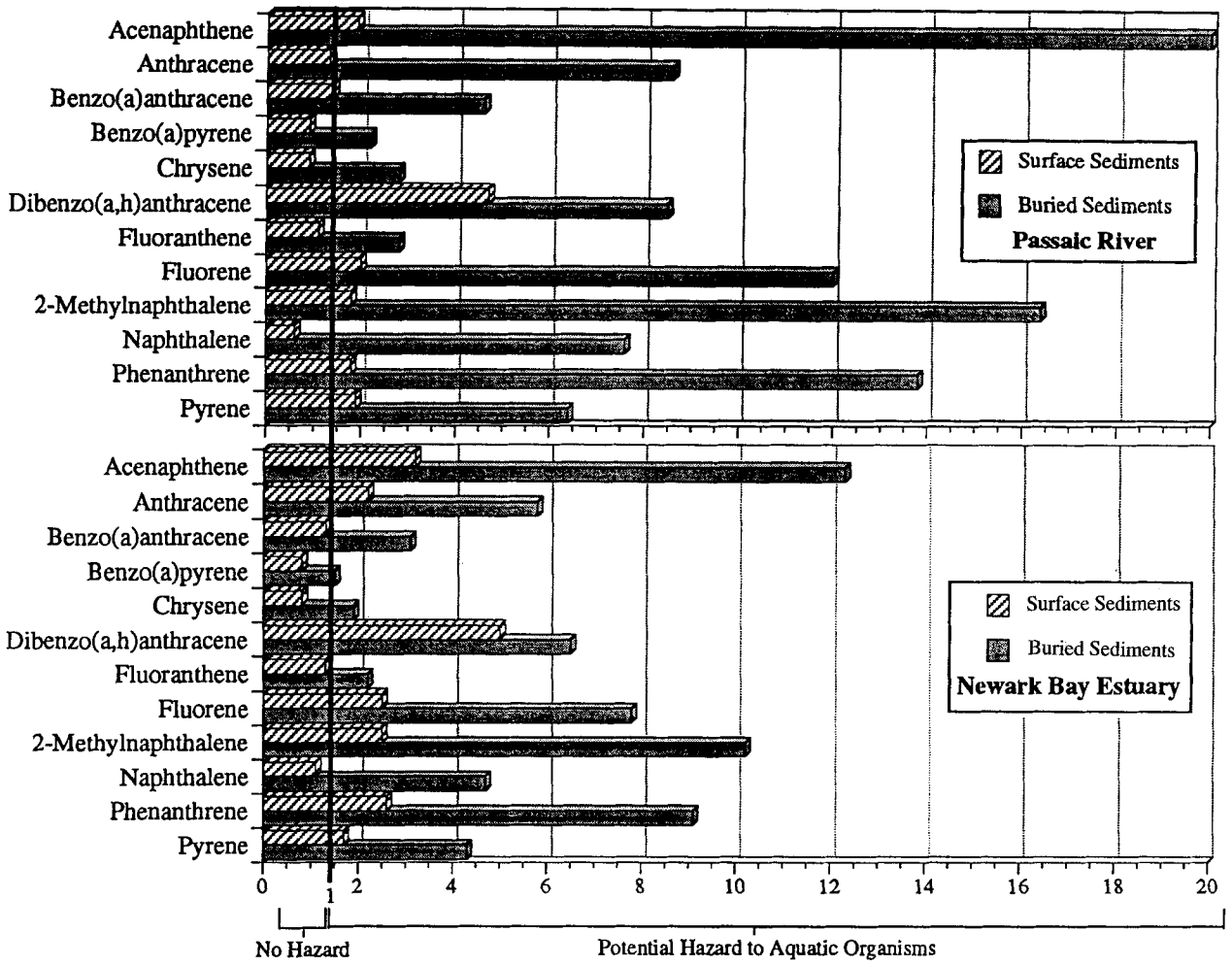

Fig. 3. Comparison of PAH hazard ratios in Passaic River and Newark Bay Estuary buried and surface sediments

approximately 25% creosote based on a comparison of phenanthrene concentrations in the sample and site creosote.

The highest levels of PAHs and TEPH were found in the lower Passaic River in the depositional reach between the Jackson Street bridge and New Jersey Turnpike. The highest concentrations were found near Frank Creek at station 20; at 46 cm, all PAHs except carbazole, were significantly elevated above mean Passaic River concentrations. Very high hazard ratios ranging up to 320 and 330 for 2-methylnaphthalene and acenaphthene were estimated for this location. Unfortunately, radionuclide activities at this station were not sufficient to allow an accurate estimate of sediment accumulation rates. Sediment accumulation at the nearest upstream and downstream sampling locations (station 19, 5.3 cm/yr; station 21, 6.1 cm/yr) suggest that the rate of accumulation at station 20 is approximately 5.8 cm/yr. Based on this estimate, the 46 cm sediments at station 20 were likely deposited in the early 1980s. Frank Creek has been known as a source of oil pollution in the Passaic River since the early 1970s (PVSC 1970); the 6.1% TEPH measured in these sediments (Table 5) strongly suggests that petroleum contamination may be the source of PAHs in this reach of the river.

Clearly, many sources may have contributed to the excessive PAH concentrations in the lower Passaic River and elsewhere in the Newark Bay Estuary. The elevated PAH concentrations measured in the lower reach are likely influenced by numerous stormwater and sewer outfalls and industrial sites located upstream (Brydon 1974). This is consistent with other heavily used estuaries such as the Southern California Bight, for example, where several sources of PAHs, including treated sewage (Eganhouse *et al.* 1981; SCCWRP 1988), stormwater run-off (Eganhouse and Kaplan 1982; SCCWRP 1988), and oil spills (Hyland *et al.* 1989), provide considerable inputs to the aquatic environment. The Roanoke Street combined sewer outfall (CSO) located adjacent to station 23 and the Brown Street CSO located adjacent to station 17 have been identified as two of Newark's most contaminated discharge sewers (PVSC 1970). This area of the river is also of particular interest because of historical chemical and paint manufacturing dating back to the 1930s. However, given the high levels of TEPH found in PAH-contaminated sediments, petroleum-related sources provide the most plausible explanation for the significantly elevated levels found in the lower Passaic River sediments. Many petroleum terminals are located along the Passaic River and have operated since the first half of the century (RPI 1989). Furthermore, numerous oil spills have been documented throughout the Newark Bay Estuary (NOAA 1982; Gunster *et al.* 1993a, 1993b.). The percentage of PAHs in crude oil, Bunker C oil, and No. 2 diesel oil are about 1%, 4%, and 9% by weight, respectively (NRC 1985), while refinery sludges contain approximately 1 to 3% PAHs (API 1984).

The highest PAH concentrations in Arthur Kill sediments were measured in a core collected at the mouth of the Elizabeth River. Nineteen PAH compounds were significantly elevated ($p<0.05$) above mean concentrations in surficial sediments at station 47, downstream of the Chemical Control Superfund Site. Fourteen PAHs were detected in surficial sediments at station 48, located in the Elizabeth River upstream from the Chemical Control site, at concentrations about 1 order of magnitude lower than at the confluence. The Chemical Control Superfund Site is a former waste treatment and storage facility that received hazardous wastes from chemical manufacturers, metal finishers and processors, waste haulers, paper companies, home care product manufacturers, oil refineries, and paint and varnish manufacturers (USEPA 1987; NJDEP 1989). The facility operated from 1970 to 1979. During cleanup operations in 1980, an explosion and fire at the site sent drums of hazardous waste into the Elizabeth River. In addition, there had been reports that Chemical Control had dumped wastes directly into the river, and that the sewage system discharged directly into the Arthur Kill (USEPA 1987). Several other industries are also located proximate to that portion of the river, including petroleum refineries and metal processing facilities. For example, a chemical manufacturer and an oil refining company were located directly across the Elizabeth River from the Chemical Control facility during this period (ACOE 1965; USEPA 1987). Although sediments at station 47 could not be dated, sediments from the surface and 20 and 46 cm at station 48 correlate approximately to 1990, 1980, and 1967, respectively.

Hackensack River sediments appear to be moderately contaminated with PAHs and TEPH compared to either the Arthur Kill or the Passaic River. Sediment samples collected from the northern-most sampling station on the Hackensack River (station 28) were relatively uncontaminated compared to Arthur Kill samples and samples collected in southern reaches of the Hackensack River. Sediments collected at station 32, located just downstream of the Standard Chlorine and Koppers Coke hazardous waste sites, had the highest PAH concentrations. Nine PAHs in surface sediments and 11 PAHs and TEPH at 46 cm had concentrations that were significantly elevated ($p < 0.05$) above mean concentrations. The relatively high concentrations of naphthalene found in surface sediments at this location warrant further investigation of discharges from the nearby abandoned Koppers Coke site. The site was a naphthalene refining facility during the 1950s (NJDEP 1989). Radiodating results could not be interpreted for sediments collected at this station.

Among the more interesting findings of this investigation were the high levels of PAHs and TEPH in the 97 cm deep sediments collected above the Dundee Dam on the Passaic River. These sediments, which date back to the mid-1800s, had detectable PAH concentrations ranging from 0.58 to 91 mg/kg and a TEPH concentration of 11,330 mg/kg. Ten PAHs were significantly elevated above mean Passaic River concentrations. Although hazard ratios indicate only a slight potential hazard associated with surface sediments above the Dundee Dam, the hazards associated with the mean concentration in buried sediments is appreciable, particularly with respect to phenanthrene, fluoranthene, acenaphthene, and anthracene. Early industrial activities on the Passaic River are known to have had a significant impact on the aquatic ecosystem. The dam was constructed in 1859 (Brydon 1974), and by the late 1880s, numerous silk-dying facilities were discharging millions of gallons of colored dyestuffs into the river at Paterson, several miles upstream of the Dundee Dam (Brydon 1974; Galishoff 1988).

Although grain size and total organic carbon are known to influence the concentrations of organic chemicals in sediments (McCain *et al.* 1992), the data presented in this study strongly suggest the presence of multiple point sources. In general, the very highest levels of PAH and petroleum hydrocarbon contamination appear in sediments dated to the years ranging from about the 1950s to 1960s, corresponding to periods of heavy industrialization in the region. PAH concentrations in the lower Passaic River were elevated relative to other areas of the estuary even when these data were normalized to total organic carbon.

Conclusions

Polycyclic aromatic hydrocarbon and petroleum hydrocarbon contamination is widespread in the Newark Bay Estuary. Severely high concentrations in sediments occur in several areas, including the upper Arthur Kill near its confluence with the Elizabeth River, in the Passaic River above the Dundee Dam, and in the lower Passaic River, the lower Hackensack River, and the Port Newark navigation channel in Newark Bay. These chemical hot spots are proximate to suspected point sources and to combined sewer outfalls. PAH contamination is also evident in the Third River and at the confluence of the Rahway River and the Arthur Kill. The historical distribution of PAHs in sediments throughout the estuary is consistent with post World War I and World War II economic expansion and is consistent with the standard waste disposal practices at that time. The results indicate that PAH concentrations in the majority of surface and buried sediments in the Newark Bay Estuary are potentially toxic to aquatic biota. The concentrations of most PAHs in surface sediments pose less of a potential hazard. Although PAHs in lower Passaic River surface sediments pose a low hazard to aquatic biota, severely elevated concentrations in buried sediments raise concerns regarding their potential hazard to aquatic organisms if these sediments are disturbed by dredging or other activities. These data provide a strong impetus for conducting aquatic bioassays on these sediments to determine the relative toxic contribution of each class of chemicals.

References

Army Corps of Engineers (1965) Port facilities at Port of New York, Arthur Kill, NY and NJ. Map Nos. 47 and 50, NY

———(1988) The Port of New York, NY and NJ and Ports of Long Island, NY. Port Series No. 5. U.S. Army Water Resources Support Center, Fort Belvoir, VA

American Petroleum Institute (1984) The land treatability of Appendix BIII constituents present in petroleum industry wastes. Document No. B-974-220

Bonnevie NL, Gunster DG, Wenning RJ (1992) Lead contamination in surficial sediments from Newark Bay, New Jersey. Environ Int 18(5):497–508

Bonnevie NL, Wenning RJ, Huntley SL, Bedbury H (1993) Distribution of inorganic compounds in sediments from three waterways in northern New Jersey. Bull Environ Toxicol Chem 51:672–680

Bopp RF (1988) Dioxins in Newark Bay. In: Annual report. Lamont-Doherty Geological Observatory of Columbia University, pp 8–11

Bopp RF, Gross ML, Tong H, Simpson HJ, Monson SJ, Deck BL, Moser FC (1991) A major incident of dioxin contamination: Sediments in New Jersey estuaries. Environ Sci Technol 25(5):951–956

Brunström B, Broman D, Dencker L, Näf C, Vejlens E, Zebuhr Y (1992) Extracts from settling particulate mater collected in the Stockholm Archipelago waters: Embryolethality, immunotoxicity and EROD-inducing potency of fractions containing aliphatics/monoaromatics, diaromatics or polyaromatics. Environ Toxicol Chem 11:1441–1449

Brydon NF (1974) The Passaic River: Past, present, future. Rutgers University Press, New Brunswick, NJ, 376 pp

Catallo WJ, Gambrell RP (1987) The effects of high levels of polycyclic aromatic hydrocarbons on sediment physicochemical properties and benthic organisms in a polluted stream. Chemosphere 16(5):1053–106

Eganhouse RP, Simoneit BRT, Kaplan IR (1981) Extractable organic matter in urban stormwater runoff. 2. Molecular characterization. Environ Sci Technol 15(3):315–326

Eganhouse RP, Kaplan IR (1982) Extractable organic matter in municipal wastewaters. 1. Petroleum hydrocarbons: temporal variations and mass emission rates to the ocean. Environ Sci Technol 16(3):180–186

Ehrlich GG, Goerlitz DF, Godsy EM, Hult MF (1982) Degradation of phenolic contaminants in groundwater by anaerobic bacteria: St. Louis Park, Minnesota. Groundwater 20(4):703–710

Faure, G (1986) Principles of isotope geology. John Wiley & Sons, NY

Galishoff S (1988) Newark, the nation's unhealthiest city. Rutgers, The State University, NJ, 260 pp

Gillis CA, Bonnevie NL, Wenning RJ (1993) Mercury contamination in the Newark Bay Estuary. Ecotoxicol Environ Saf 25: 214–226

Goeller AF (1989) Heavy metals and radionuclides in sediments of the Hackensack River, New Jersey. MS Dissertation, Rutgers University, New Brunswick, NJ, October

Gunster DG, Bonnevie NL, Gillis CA, Wenning RJ (1993a) Assessment of chemical loadings to Newark Bay, New Jersey from petroleum and hazardous chemical accidents occurring from 1986 to 1991. Ecotoxicol Environ Safety 25:202–213

Gunster DG, Gillis CA, Bonnevie NL, Abel TB, Wenning RJ (1993b) Petroleum and hazardous chemical spills in Newark Bay, New Jersey, USA from 1982 to 1991. Environ Pollut 82:245–253

Herbes SE, Schwall LR (1978) Microbial transformation of polycyclic aromatic hydrocarbons in pristine and petroleum-contaminated sediments. Appl Environ Microbiol 35(2):306–316

Hackensack Meadowlands Development Commission (1989) Inventory of fisheries resources of the Hackensack River within the jurisdictional boundary of the Hackensack Meadowlands Development Commission from Kearny, Hudson County, to Ridgefield, Bergen County, New Jersey, May

Hollister TA, Ward GS, Parish PR (1980) Acute toxicity of a #6 fuel oil to marine organisms. Bull Environ Contam Toxicol 24:656–661

HydroQual (1991) Assessment of pollutant loadings to New York–New Jersey Harbor. Prepared for U.S. Environmental Protection Agency, January

Hyland J, Kennedy J, Campbell J, Williams S, Boehm P, Uhler A, Steinhaver W (1989) Environmental effects of the Pacific Baroness oil and copper spill. In: Proceedings 1989 oil spill conference (prevention, behavior, control, cleanup), San Antonio, TX, February 13–16 American Petroleum Institute, Washington, DC, pp 413–419

International Technology Corporation (1986) Passaic River sediment study, final report. Prepared by International Technology Corp, Pittsburgh, PA for the New Jersey Department of Environmental Protection, Trenton, NJ, March

Long ER, Morgan LG (1991) The potential for biological effects of sediment-sorbed contaminants tested in the National Status and Trends Program. NOAA Tech Memo NOS OMA 52. National Oceanic and Atmospheric Administration, Coastal and Estuarine Assessment Branch, Seattle, WA

McCain BB, Chan S-L, Krahn MK, Brown DW, Myers MS, Landahl JT, Pierce S, Clark RC Jr., Varansi U (1992) Chemical contamination and associated fish diseases in San Diego Bay. Environ Sci Technol 26(4):725–733

Meyerson AL, Luther GW, Krajewske J, Hires RI (1981) Heavy metal distribution in Newark Bay sediments. Marine Pollut Bull 12:244–250

Moser FC (1990) Toxic levels in water, sediment and biota, and their effects in the Hudson–Raritan Estuary, Long Island Sound and New York Bight. In: Cleaning up our coastal waters: An unfinished agenda. A regional conference, March 12–14, Manhattan College, Riverdale, NY. Dynamic Corp., NY

Mueller JG, Chapman PJ, Pritchard PH (1989) Creosote-contaminated sites. Environ Sci Technol 23(10):1197–1201

Neff JM (1980) Polycyclic aromatic hydrocarbons in the aquatic environment. Applied Science Publishers, London, 262 pp

National Oceanic and Atmospheric Administration (1982) Contaminant inputs to the Hudson-Raritan Estuary. NOAA Tech Bull OMPA-21. Boulder, CO

———(1984a) A geochemical assessment of sedimentation and contaminant distributions in the Hudson-Raritan Estuary. NOAA Tech Memo NOS OMS-2. Rockville, MD

———(1984b) Chemical pollution of the Hudson-Raritan estuary. NOAA Tech Memo NOS OMA-7. Rockville, MD

———(1988) A summary of selected data on chemical contaminants in sediments collected during 1984, 1985, 1986, and 1987. NOS OMA-44. Rockville, MD

———(1991) Contaminant trends in the Southern California bight: Inventory and assessment. NOAA Tech Memo NOS ORCA 62. Seattle, WA

New Jersey Department of Environmental Protection (1985) A study of dioxin (2,3,7,8-tetrachlorodibenzo-p-dioxin) contamination in select finfish, crustaceans, and sediments of New Jersey waterways. Office of Science and Research, Trenton, NJ, 101 pp

———(1989) 1989 Status report on the hazardous waste management program in New Jersey. Site Specific Information, October. Trenton, NJ

National Research Council (1985) Oil in the sea. Inputs, fates, and effects. National Academy Press, Washington, DC

O'Connor JM, Huggett RJ (1988) Aquatic pollution problems, North Atlantic coast, including Chesapeake Bay. Aquat Toxicol 11:163–190

O'Keefe P, Hilker D, Meyer C, Aldous K, Shane L, Donnelly R, Smith R, Sloan R, Skinner L, Horn E (1984) Tetrachlorodibenzo-p-dioxins and tetrachlorodibenzofurans in Atlantic coast striped bass and in selected Hudson River fish, waterfowl, and sediments. Chemosphere 13:849–860

Olsen CR, Larsen IL, Brewster RL, Cutshall NH, Bopp RF, Simpson H (1984) A geochemical assessment of sedimentation and contaminant distributions in the Hudson-Raritan Estuary. NOS OMS 2. June. National Oceanic and Atmospheric Administration, Rockville, MD

Pruell RJ, Hoffman EJ, Quinn JG (1984) Total hydrocarbons, polycyclic aromatic hydrocarbons, and synthetic organic compounds in the hard shell clam, *Mercenaria mercenaria*, purchased at commercial seafood stores. Mar Environ Res 11:163–181

Passaic Valley Sewerage Commissioners (1970) Annual Report to Commissioners. Newark, NJ, pp 12–13

Research Planning, Inc. (1989) Oil and hazardous substances pollution incidences-planning and response considerations: The Port of

New York/New Jersey, Vol. 3. Prepared for National Oceanic and Atmospheric Administration, Ocean Assessments Division, Rockville, MD. pp 1–18

Southern California Coastal Water Research Project (1988) Annual Report, 1987. Long Beach, CA, pp 101

Suszkowski DJ (1978) Sedimentology of Newark Bay, New Jersey: An urban estuarine bay. PhD Dissertation, University of Delaware, Newark, DE

U.S. Environmental Protection Agency (1981) Unpublished data.

———(1982) An exposure and risk assessment for benzo(a)pyrene and other polycyclic aromatic hydrocarbons: Vol II. Naphthalene. Office of Water Regulations, Washington, DC

———(1987) Record of decision. Chemical Control Corporation. Region II. September 3. NY

———(1988) Characterization and laboratory soil treatability studies for creosote and pentachlorophenol sludges and contaminated soil. USEPA-600/2-88/055. Research Triangle Park, NC

———(1991) Contract Laboratory Program statement of work for organic analysis, Multi-Media, Multi-Concentration. ILMO1.6, March. Research Triangle Park, NC

Wenning RJ, Harris MA, Ungs MJ, Paustenbach DJ, Bedbury H (1992) Chemometric comparisons of polychlorinated dibenzo-*p*-dioxin and dibenzofuran residues in surficial sediments from Newark Bay, New Jersey and other industrialized waterways. Arch Environ Contam Toxicol 22:397–413

Wilber WG, Hunter JV (1973) The impact of urbanization on the distribution of heavy metals in bottom sediments of the Saddle River. Water Res Bull 15:790–800

———(1979) Distribution of metals in street sweepings, stormwater solids, and urban aquatic sediments. J Water Pollut Control Fed 51:2811–2822

Williams SC, Simpson HJ, Olsen CR, Bopp RF (1978) Sources of heavy metals in sediments of the Hudson River estuary. Mar Chem 6:195–213

Zitko V (1978) Aromatic hydrocarbons in aquatic fauna. Bull Environ Contam Toxicol 14:621–631

REMOVAL AND RECOVERY OF METALS FROM A COAL PILE RUNOFF

VICTOR M. IBEANUSI*, DONNA PHINNEY and MICHELLE THOMPSON
Environmental Science Program, Spelman College, Atlanta, Georgia, U.S.A.
(author for correspondence, e-mail: vibeanus@spelman.edu.)*

Abstract. The removal and recovery of heavy metals from a coal pile runoff water using a mixture of multiple metal-tolerant bacterial strains of ATCC 55673, and ATCC 55674 and a *Pseudomonas sp.* was investigated. The analysis of elemental composition of metal precipitates recovered from the bacterial biomass by transmission electron microscopy and energy dispersive X-ray analysis revealed the presence of metals originally present in the wastewater. In addition, analysis of metals in culture supernatant and bacterial biomass by inductively coupled plasma emission spectroscopy (ICP-ES) indicated a removal range of 82–100% and a recovery of 15–58% of metals from the wastewater and bacterial biomass, respectively.

Keywords: coal pile run off, metal precipitates, metal removal, metal recovery, and bacterial biomass

1. Introduction

The extent to which microbial systems can be used in metal recovery varies with the species and may be complicated by the nature of both the absorbent and the metal species in aqueous solution. Therefore, bioremediation strategies that involve the use of microbial biomass in metal treatment depend to a larger degree on their ability to accumulate a variety of metal ions before the cells become affected by metal toxicity.

Wastewater effluents from coal pile run off are of major concern because of the acidity and presence of several dissolved metals in the waste stream. Similar to acid mine drainage (AMD), the chemical and biological reactions of pyrite in coal pile run off generate acidic minerals, which can oxidize to form sulfuric acid, ferrous sulfate and associated toxic metals. Two major reactions have been noted to be responsible for the oxidation process (Lovell, 1983, Allen *et al.*, 1996a; Allen *et al.*, 1996b; Vinyard 1996 and Sreekrishnan 1994).

$$FeS_2 + 7\ Fe(SO_4)_3 + H_2O \rightarrow 15Fe_2SO_4 + 8\ H_2SO_4 \quad (1)$$

$$2\ FeS_2 + 2\ H_20 \rightarrow 2\ FeSO_2 + 2\ H_2SO_4 \quad (2)$$

Since reactions 1 and 2 are pH sensitive, the rate law could be represented as:

$$-d\ [Fe^{2+}]/dt = K\ [Fe^{2+}]\ [O_2\ (aq)]/[H^+]^2 \quad (3)$$

Environmental Monitoring and Assessment **84:** 35–44, 2003.
© 2003 *Kluwer Academic Publishers. Printed in the Netherlands.*

The re-oxidation of ferrous ions in reaction 2 can be accelerated by sulfur-oxidizing acidophilic bacteria such as Thiobacillus ferrooxidans, and other acidophilic microbes (Baillet *et al.*, 1998, Foos 1996, Strasser *et al.*, 1995, and Lovell 1983). Furthermore, Lovell (1983) had noted that in the presence of air and water, it is possible to generate various insoluble iron sulfides, such as $FeSO_4 \cdot H_2O$ (ferrous sulfate), $FeSO_4 \cdot 7\ H_2O$ (Melanterite), and $Fe(SO_4)_3 \cdot 9\ H_2O$ (Coquimbite). Unlike a typical AMD, in which the major metal ions are Fe^{2+} and Fe^{3+}, the coal pile runoff used in this study presented unique and complex chemical dynamics due to the prevalence of several dissolved toxic metals (Al, As, Be, Cd, Cr, Cu, Fe, Ni, Pb, Se and Zn) in the wastewater.

Conventional methods of treating such metal-contaminated wastewater require the use of lime or other chemical processes that raise the pH to near neutral and above (Brower *et al.* 1997, Ehrlich 1996 and Lyew 1997). Due to large chemical sludge resulting from such chemical treatment processes, there is the need to develop biological systems that generate non-toxic biodegradable by-products, and as well favor the recovery of metals for potential reuse. The objectives of this present study were to evaluate the use of specific bacterial biomass in the removal and recovery of metals in coal pile runoff waters.

2. Materials and Methods

2.1. Coal pile run-off

The coal pile run off water was collected from a coal-fired plant at the Savannah River Site near Aiken, SC. During rain events, coal pile runoff is diverted bya series of interconnected ditches into a catchment basin. Associated with the coal pile run off in the catchment basin were several dissolved metals, such as: Al, As, Cd, Be, Cu, Cr, Fe, Pb, Ni, Se, and Zn. In all cases of our sampling, the concentrations of Al and Fe were predominantly high, ranging from 2.50–2.937 mg L^{-1} or 838–979% above drinking water standards. Other notable metals in the wastewater with concentrations above drinking water include: As (> 0.0945 mg L^{-1} or 89%), Cd (0.0109 mg L^{-1} or 9%), Pb (> 0.9 mg L^{-1} or 80%), Se (0.0149 mg L^{-1} or 49%), and Zn (6.65 mg L^{-1} or 33%).

2.2. Water sampling and metal analysis

Water samples and associated microbial biomass were initially digested with a CEM Microwave Digestion System (MDS 2000, CEM Corporation) and subse-

quently analyzed by Inductively Coupled Plasma Emission Spectroscopy (ICP, Perkin Elmer Plasma 400). Metal concentrations were calculated as:

$$\textit{Metal conc } (mg\ l^{-1}) = \frac{\textit{Conc. metal in digested sample } (mg\ l^{-1}) \times \textit{final vol. digested soln } (ml)}{\textit{Sample volume } (ml)} \quad (4)$$

$$\textit{Metal conc } (mgkg^{-1})\ \textit{drywt.} = \frac{\textit{Conc. metal in digested sample } (mg\ l^{-1}) \times \textit{final vol. } (L)}{\textit{dry weight of sample } (Kg)} \quad (5)$$

2.3. Metal treatment and removal experiments

In each test, triplicate cultures containing 150 ml of coal pile runoff wastewater from the catchment basin were inoculated with a mixture of mid log 10^6 cell ml^{-1} of each bacterial strain and compared with two sets of control flasks with no microbial addition. One set of the control flasks contained wastewater only, while the second set had wastewater plus nutrients. This experimental set up allowed us to evaluate the role of the bacterial strains and the effects of nutrients on the metal removal and recovery process. Growth nutrients (in grams per liter) were ammonium sulfate, 0.5; ammonium nitrate, 0.5; potassium phosphate, 0.5; pyruvic acid, 1.2; and oxalic acid, 1.2. Pyruvic and oxalic acids were added to specifically inhibit the growth of indigenous bacteria, such as *Thiobacillus feroxidans*, and other acidophiles, which are usually associated with coal pile run off waters (Lyew 1997, and Vinyard 1996). Culture flasks were grown at 35 °C in a shaker agitated at 160 rpm for 21 days. Metal removal was calculated as described below:

$$\textit{Metal Removal } (0\%) = \frac{\textit{Amt. of } M(mg),\ \textit{in UTW} - \textit{Amt. of } M(mg) \textit{ in TW} \times 1000}{\textit{Amt. of metal } (mg),\ \textit{in UTW}} \quad (6)$$

M = metals; UTW = untreated water in control; TW = Treated water.

2.4. Metal recovery

Bacterial biomass was harvested by centrifugation of culture flasks at 10,000 rpm for 10 min. The bacterial biomass from each flask was air dried and weighed. Metal removal and recovery in mg kg^{-1} dry weight of biomass were calculated as follows:

$$\textit{Metal Removal } (\%) = \frac{\textit{Amt. of } M(mg),\ \textit{in TW} - \textit{biomass} \times 1000}{\textit{Amt. of } M(mg),\ \textit{in UTW}} \quad (7)$$

2.5. Metal recovery index

The metal recovery index in Table III was calculated as:

$$\frac{\textit{Percent (\%) metal removed from wastewater}}{\textit{Percent (\%) metal recovered from bacterial biomass}} \tag{8}$$

2.6. Electron microscopy and X-ray analyses

In order to correlate harvested bacterial biomass with metal removal and recovery, samples were assayed by electron microscopy and X-ray microanalyses. Harvested cells were air dried overnight and fixed in 2.5% glutaraldehyde and dehydrated in graded ethanol-oxide series. Samples were carefully mounted on carbon stubs and examined by transmission electron microscopy (ETEC OMINSCAN, Kevex Corporation). Energy dispersive X-ray analysis was performed with a Tracor Northern 5500 X-ray. Unstained samples were employed for TEM, relying upon complexed metal on bacterial biomass for electron scatter.

3. Results and Discussions

3.1. Electron microscopy and X-ray analysis

In Figure 1, results of the transmission electron microscopy indicated various stages of intracellular complexation of metal precipitates within the cytoplasm and cell membranes of the bacterial cells. Ultimately, the metal ions were sequestered outside the cells as metal precipitates (Figure 1e). The x-ray microanalysis of precipitates revealed the presence of most of the metals (As, Al, Cu, Cr, Fe, Pb and Zn) originally present in the wastewater (Figure 2). The presence of Ca, P, and S in Figure 2 suggested that most of the metals could possibly precipitate as metal carbonates, phosphates and sulfides.

3.2. Metal removal

In Table I, concentrations of all metals present in the wastewater were reduced significantly in culture flasks containing the microbes, compared to control flasks with wastewater plus nutrients or wastewater only. In the latter, metal removal and recovery remained virtually unchanged. The percent removal of metals in treatment flasks inoculated with the specific bacterial strains ranged from 82–100.

3.3. Metal recovery

Table II showed that the metals removed from the wastewater by the microbes could possibly be recovered from the bacterial biomass. Recovery of the metals

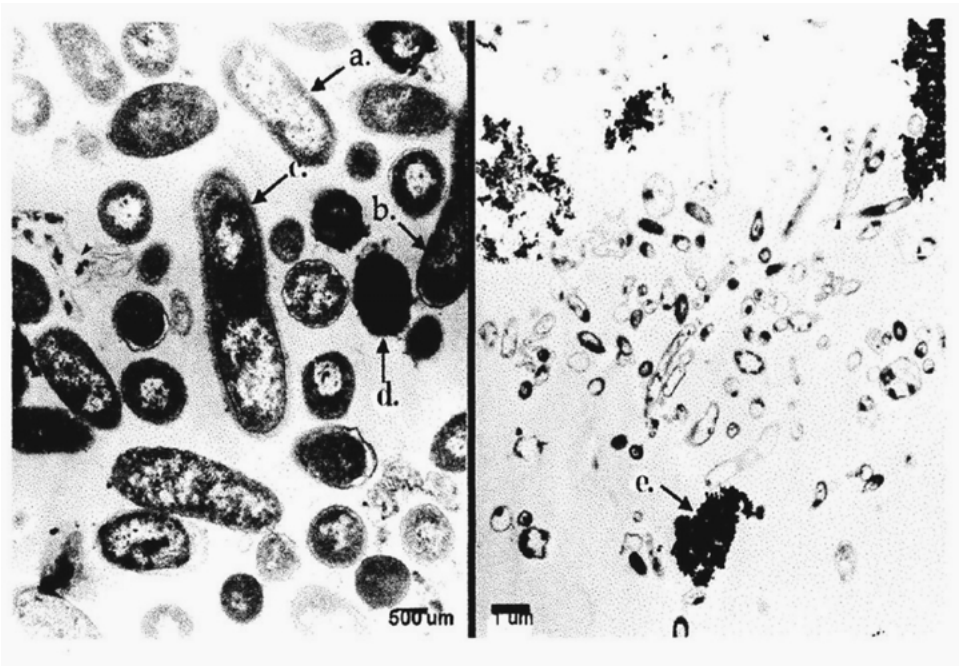

Figure 1. Metal Binding and Recovery Process in Bacterial Cells. [Material for TEM were prepared from unstained samples, relying on sorbed metals for metal electron scatter. (a-d) Metal binding and crystallization on cell membrane and cytosol of bacterial cells; (e) Extracellular metal precipitates].

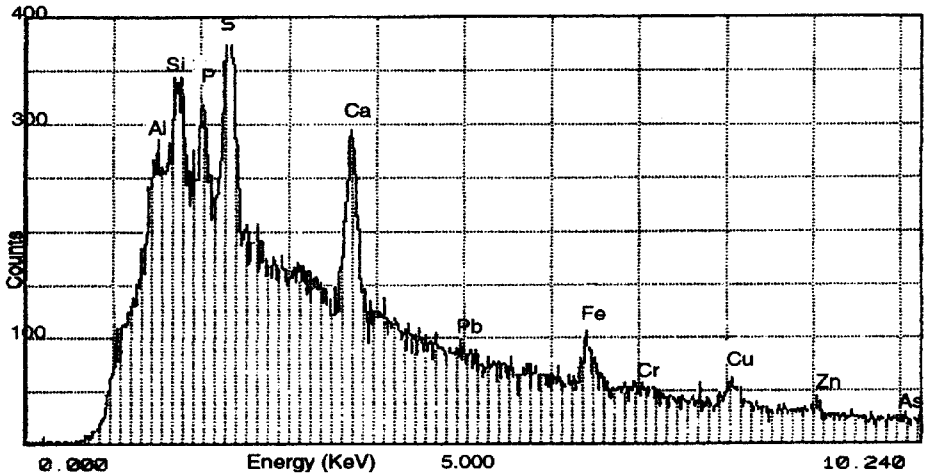

Figure 2. EDX Spectra of Metal Precipitates. [Peaks from the x-ray microanalysis represent metals bound on the bacterial biomass].

TABLE I

Treatment and removal of metals (mg L^{-1}) from coal pile run off

	As	Se	Cr	Zn	Cd	Ni	Pb	Cu	Fe	Al
Table IA										
Day 0	1.5	0.47	0.1	1.7	0.1	1.5	1.13	0.4	250.9	97.13
Day 7	1.4	0.43	0.1	1.6	0.1	1.43	1.33	0.53	246.03	92.4
Day 14	1.47	0.47	0.1	1.6	0.13	1.47	1.13	0.43	245.97	96.83
Day 21	1.53	0.5	0.13	1.57	0.1	1.47	1.23	0.47	251.3	96.17
% Removal	0	0	0	7.84	0	2.22	3.03	0	0.11	1.67
Table IB										
Day 0	1.4	0.5	0.1	1.7	0.1	1.5	1.2	0.5	252.1	98.4
Day 7	1.4	0.5	0.1	1.7	0.1	1.4	1.1	0.5	254.2	95.4
Day 14	1.5	0.5	0.1	1.6	0.1	1.5	1.0	0.4	250.4	93.7
Day 21	1.4	0.5	0.1	1.7	0.1	1.5	1.1	0.5	251.3	96.4
% Removal	0	0	0	0	0	0	8.33	0	0.32	2.03
Table IC										
Day 0	1.27	0.5	0.2	1.63	0.2	1.3	1.17	0.4	233.33	87.5
Day 7	0.2	0.13	0.03	0.23	0.0	0.63	0.57	0.13	75.57	24.0
Day 14	0.1	0.15	0.03	0.1	0.0	0.4	0.4	0.03	6.53	5.17
Day 21	0.07	0.0	0.0	0.03	0.0	0.2	0.2	0.03	1.0	0.5
% Removal	94.07	100	100	98.04	100	85.19	82.86	91.67	99.57	99.38

Table 1A (Control 1) = untreated wastewater. Table IB (Control 2) = wastewater + nutrients. Table IC (Treatment) = wastewater + nutrients + bacteria.

ranged from 15–58% indicating differences in the binding affinities of each metal to the bacterial biomass. This observation was supported by the results presented in Table III, which showed differences in the recovery index for each metal. These differences could also be attributed to the varied degrees of metal resistance of the bacterial strains.

The results of these experiments had clearly demonstrated the effectiveness of the microbial system in metal removal and recovery process. There are several published reports on individual metal binding by specific bacterial strains (Ehrlich 1997, Dressler *et al.*, 1991, Levy *et al.*, 1997, Hu *et al.*, 1996, Latinwo *et al.*, 1998, Faison *et al.*,1990, and Albrechtsen *et al.*, 1994, and Watson 1990). The uniqueness of this present study, was the effectiveness of using an integrated mixed microbial system to enhance the removal of multiple metals in a conglomerate solution. The removal of these metals from coal pile run off and their subsequent recovery in the bacterial biomass provides a potential mechanism for metal recycling and reuse. For example, in an activated sludge wastewater treatment system, where the system

TABLE II
Recovery of metals from coal pile run off

Treatment Flasks	As	Se	Cr	Zn	Cd	Ni	Fe	Pb	Al	Be	Cu
Table IIA											
Untreated Water	0.16	0.04	0.02	0.19	0.01	0.14	24.13	0.09	10.48	0.002	0.04
biomass	0	0	0	0	0	0	0	0	0	0	0
% Recovery	0	0	0	0	0	0	0	0	0	0	0
Table IIB	0.14	0.03	0.01	0.17	0.01	0.119	18.33	0.06	8.989	0.002	0.035
Wastewater + nutrients											
biomass	0.00	0.00	0.00	0.00	0.00	0.000	0.14	0.00	0.006	0.000	0.000
% Recovery	1.41	0	0	1.16	0	0	0.75	0	0.07	0	0
Table IIC											
Treatment: wastewater + nutrients + bacteria	0.01	0.01	0.00	0.01	0.00	0.033	0.098	0.01	0.079	0.000	0.014
biomass	0.05	0.02	0.01	0.07	0.00	0.017	7.745	0.03	3.369	0.001	0.005
% Recovery	37.6	45.6	58.0	39.8	54.3	14.62	42.25	47.8	37.47	50.00	15.43

Table IIA (Control 1) = untreated wastewater. Table IIB (Control 2) = wastewater + nutrients. Table IIC (Treatment flasks) = wastewater + nutrients + bacteria

is primarily used for the biodegradation of BODs (biochemical oxygen demanding compounds), the incorporation of this microbial system, could potentially enhance the simultaneous removal of BODs and dissolved metals. In this context, the pro-

TABLE III
Metal recovery index from coal pile run off

Metals	Al	As	Cd	Cr	Cu	Fe	Ni	Pb	Se	Zn
% Removal	99.4	94.1	100	100	91.67	99.57	85.2	82.9	100	98.04
% Recovered	37.5	37.6	54.3	58	15.43	42.25	14.6	47.8	45.6	39.77
Recovery Index[a]	2.65	2.50	1.84	1.72	5.94	2.36	5.83	1.73	2.19	2.47

Sequence of metal recovery from coal pile run off

cess could potentially save the cost of further tertiary treatment of the effluent from an activated sludge treatment tank.

The above observation was particularly significant considering that the Resource Conservation and Recovery Act (RCRA) of 1984 encourages waste management options, which include mechanisms for waste recycling (United States EPA Report, 1991). As a result, several metal recovery technologies have been designed to support this regulation. These technologies include high-temperature metals recovery (HTMR), electrolyte recovery or 'electrowinning', leaching, chemical precipitation, membrane separation, evaporation, and ion exchange. There are major drawbacks in using these traditional technologies, such as the lack of flexibility, and requirements for initial wastewater processing before they can be used. For example, the use of HTMR requires preprocessing that includes the addition of additives, and drying of feed sludges; chemical precipitation requires an initial removal of grease and oil, and is influenced by the concentration of dissolved solids; membrane separation requires a combination of ultrafiltration and microfiltration, because individual units are not effective in removing significant amounts of the metals from wastewater; and electrolyte recovery can only be used for noble metals, and is ineffective in the recovery of metals in low concentrations.

The microbial/bioremediation system used in this study did not require preprocessing of the wastewater. The system was effective in changing the pH and redox from < 2 to > 7, and 350 mV to –70 mV, respectively without any pretreatment of the wastewater (Ibeanusi and Wilde, 1998). Significant removal of each metal in the coal pile run off was achieved, even for those that existed in low concentrations, such as beryllium and selenium. In this context, this bioremediation system could potentially be used for metal polishing applications, in which initial treatments failed to remove metals at low concentrations, and the removal of metals in high concentrations. Notice that in Tables I and II, Al and Fe were effectively removed from the wastewater almost in the same percentage as Cr and Se, which existed in relatively low concentrations. From highest to lowest, the percent metal removal were: (Se, Cr, Cd) → Fe → Al → Zn → As → Cu → Ni → Pb.

In metal recovery, the order was: Cr → Cd → Be → Pb → Se → Fe → Zn → As → Al → Cu → Ni. Apart from Al, Pb, and Se, the percent metal removed from the wastewater followed similar trend with the percentage recovered. However, when the sequence of metal recovery were compared with the metal recovery index, stronger correlations were observed (Table III).

The order of the metal recovery index was: Cr → Pb → Cd → Se → Fe → Zn → As → Al → Cu. In practice, these trends are important in wastewater treatment, because it provides the end users of this bioremediation technology the means to target the system to specific metal contaminated sites where the metals may be highly prevalent.

Acknowledgments

The author acknowledges the excellent contributions of Fares Elkatri and Alicia Bonhart for their technical assistance. This research was supported through a Department of Energy, Environmental Restoration Division Grant No. DE-FG09-95SR18534-A003.

References

Albrechtsen, H. and Christensen, T.: 1994, 'Evidence for microbial iron reduction in a landfill leacheate-polluted aquifer', *Appl. Environ. Microbiol.* **60**, 3920–3925.

Allens, S., Allen, J. and Lucas, S.: 1996a, 'Concentration of contaminants in surface water samples collected in West Central Indiana impacted by acidic mine drainage', *Environ. Geology.* **27**, 34–37.

Allen, J., Lucas, S. and Allen, S.: 1996b, 'Formation of hydroxy radical in illminated surface waters contaminated with acidic mine drainage', *Environ. Toxicol. Chem.* **15**. 107–113.

Baillet, F., Margnin, J., Cheruy, A. and Ozil, P.: 1998, 'Chromium precipitation by acidophilic bacterium *Thiobacillus ferroxidans*', *Biotechn. Lett.* **20**, 95–99.

Brower, J., Ryan, R. and Paziraandeh, M.: 1997, 'Comparison of ion exchange resins and biosorbents for the removal of heavy metals from plating factory wastewater', *Environ. Sci Technol.* **31**, 2910–2914.

Dressler, C., Kues, U., Nies, D. and Friedrich, B.: 1991, 'Determinants encoding resistance to several heavy metals in newly isolated copper-resistant bacteria', *Appl. Environ. Microbiol.* **57**, 3079–3085.

Ehrlich, H. L.: 1997, 'Microbes and metals', *Appl. Microbiol. Biotechnol.* **48**, 687–692.

Foos, A.: 1996, 'Geochemical modeling of coal mine drainage, Summit County, Ohio', *Environ. Geol.* **31**, 205–210.

Faison, B., Cancel, C., Lewis, S. and Alders, H.: 1990, 'Binding of dissolved strontium by *Micrococcus luteus*', *J. Appl. Environ.* **56**, 3649–3656.

Hu, M., Norman, J. and Faison, B.: 1996, 'Biosorption of uranium by *Pseudomonas aeroginosa* strain CSU: Characterization and comparison studies', *Biotechnol. Bioeng.* **51**, 237–247.

Ibeanusi, V. and Wilde, E.: 1998, 'Bioremediation of coal pile run off waters using an integrated microbial ecosystem', *Biotechnol. Lett.* **11**, 1077–1079.

Latinwo, L., Donald, C., Ikediobi, C. and Simon, S.: 1998, 'Effects of intracellular glutathione on sensitivity of *Escherichia coli* to mercury and arsenite', *Biolog. Biophys. Res. Commun.* **242**, 67–70.

Levy, D., Cutis, W. and Rock, P.: 1997, 'The aqueous geochemistry of the abandoned spenceville copper pit, Nevada County, California', *J. Environ. Quality.* **26**, 233–243.

Lovell, H.: 1983, 'Coal mine drainage in the United States – an overview', *Wat. Sci Tech.* **15**, 1–25.

Lyew, D. and Sheppard, J.: 1997, 'Effects of physical parameters of a gravel bed on the activity of sulphate-reducing bacteria in the presence of acid mine drainage', *J. Chem. Technol. Biotechnol.* **70**, 223–230.

Masscheleyn, P., Delaune, R. and Patrick W.: 1991, 'Effects of redox potential and pH on arsenic speciation and solubility in a contaminated soil', *Environ. Sci. Technol.* **25**, 1414–1419.

Streekrishnan, T. and Tyagi, R.: 1994, 'Heavy metal leaching sewage sludges: A techno-economic evaluation of the process options', *Environ. Technol.* **15**, 531–543.

Strasser, H., Brunner, H. and Schinner, F.: 1995, 'Leaching of iron and toxic heavy metals from anaerobically-digested sewage sludge', *J. Indust. Microbiol.* **14**, 281–287.

United States Environmental Protection Agency: 1991. 'Recovery of Metals from Sludge', *EPA/600/82-91/041*. Washington D.C.

Vinyard, G.: 1996, 'A chemical and biological assessment of water quality impacts from acid mine drainage in first order mountain stream and comparison of two bioassay techniques'. *Environ. Technol.* **17**, 273–281.

Watson, J., Scott, C. and Faison, B.: 1990, 'Evaluation of a Cell-Biopolymer Sorbent for Uptake of Strontium from Dilute Solutions', in *Emerging Technologies in Hazardous waste Management*, pp. 172–184.

Trace Element Chemistry of Coal Bed Natural Gas Produced Water in the Powder River Basin, Wyoming

RICHARD E. JACKSON AND K. J. REDDY*
Department of Renewable Resources, University of Wyoming, P.O. Box 3354, Laramie, Wyoming 82071-3354

Coal bed natural gas (CBNG) produced water is usually disposed into nearby constructed disposal ponds. Geochemistry of produced water, particularly trace elements interacting with a semiarid environment, is not clearly understood. The objective of this study was to collect produced water samples at outfalls and corresponding disposal ponds and monitor pH, iron (Fe), aluminum (Al), chromium (Cr), manganese (Mn), lead (Pb), copper (Cu), zinc (Zn), arsenic (As), boron (B), selenium (Se), molybdenum (Mo), cadmium (Cd), and barium (Ba). Outfalls and corresponding disposal ponds were sampled from five different watersheds including Cheyenne River (CHR), Belle Fourche River (BFR), Little Powder River (LPR), Powder River (PR), and Tongue River (TR) within the Powder River Basin (PRB), Wyoming from 2003 to 2005. Paired *t* tests were conducted between CBNG outfalls and corresponding disposal ponds for each watershed. Results suggest that produced water from CBNG outfalls is chemically different from the produced water from corresponding disposal ponds. Most trace metal concentrations in the produced water increased from outfall to disposal pond except for Ba. In disposal ponds, Ba, As, and B concentrations increased from 2003 to 2005. Geochemical modeling predicted precipitation and dissolution reactions as controlling processes for Al, Cu, and Ba concentrations in CBNG produced water. Adsorption and desorption reactions appear to control As, Mo, and B concentrations in CBNG water in disposal ponds. Overall, results of this study will be important to determine beneficial uses (e.g., irrigation, livestock/wildlife water, and aquatic life) for CBNG produced water in the PRB, Wyoming.

Introduction

Several western states within the United States (e.g., Wyoming, Colorado, Montana, North Dakota, New Mexico, and Utah) are exploring natural gas extraction from coal resources to meet the nation's energy demands. Coal bed natural gas (CBNG) is formed in confined coal bed aquifers through complex biogeophysical processes and remains trapped by aquifer pressure. Natural gas extraction is facilitated by pumping water from the aquifer. This water is commonly referred to as CBNG produced water. A single CBNG extraction well in the Powder River Basin (PRB) can discharge 8−80 L of produced water per minute, but this water production varies between aquifers and well density (*1*). The Wyoming State Geological Survey predicts 2−3 billion m^3 of produced water will eventually be discharged from CBNG extraction in Wyoming (*1*). Commonly, 2−10 CBNG extraction wells are combined together at a single outfall to discharge produced water and release it into constructed disposal ponds, stream channels, or re-inject into shallow groundwater aquifers. However, the majority of CBNG-produced water is discharged into unlined disposal ponds.

CBNG produced water can have high concentrations of soluble salts, and when confined in disposal ponds, can have increased concentrations of trace elements (*2*−*7*). These trace elements can be essential or toxic to plants and animals depending on their ionic species and concentrations. Geochemical processes such as mineral dissolution, precipitation, and ion adsorption/desorption control trace metal bioavailability and subsequent toxicity (*8*, *9*).

The Wyoming Department of Environmental Quality (WYDEQ) considers CBNG produced waters as surface water of the state with Class 4C designation, allowing for agricultural, industrial, wildlife, and recreational uses (*10*). This water classification has raised concerns from landowners due to potential harmful effects CBNG produced water could have on surrounding soils, vegetation, wildlife, and livestock. Beneficial uses proposed for CBNG produced water include irrigation, livestock and wildlife drinking water, aquatic life, and human drinking water (*10*). However, any potential beneficial use of produced water depends on its water quality.

A few studies have examined the quality of CBNG produced water and associated disposal ponds in the PRB (*3*, *4*). For example, McBeth et al., (*3*) monitored CBNG produced water quality at outfalls and associated disposal ponds on the western edge of the PRB. These studies established seven sites in the Little Powder River Basin, four sites in the Belle Fourche River Basin, and three sites in the Cheyenne River Basin and monitored water quality during the summers of 1999 and 2000. McBeth et al., (*3*) found that concentrations of dissolved Ba, Mn, and Cr decreased while concentrations of dissolved Al, Fe, As, and Se increased in disposal ponds. Our study is similar to McBeth et al. (*3*); however, in our study several sites from two different watersheds were added. Furthermore, CBNG outfalls and disposal ponds were monitored for 3 years, and geochemical changes over time were reported. Studies conducted by Rice et al. (*4*) examined the chemistry of CBNG discharge water from the well head at forty seven locations throughout the central PRB and found that trace elements were at or below the detection limits. Overall, both Rice et al. (*4*) and McBeth et al. (*3*) studies found that dissolved concentrations of most trace elements from CBNG well heads, outfalls and disposal pond waters were very low (below the EPA primary drinking water's maximum contaminant levels) (*11*). In these studies, no statistical analyses were conducted to determine changes in the concentration or distribution of trace elements from outfall to corresponding disposal pond.

In conjunction with CBNG energy development, there is a need to protect the environment. Potential water quality problems from CBNG-produced water disposal could affect energy extraction, impacting the nation's current energy crisis. To effectively manage CBNG produced water, there is a need to understand geochemical changes that occur in CBNG disposal ponds. Management decisions could be made from this information to identify beneficial uses for CBNG produced water such as irrigation and livestock/wildlife use, and prevent ecological problems such as trace metal

* Corresponding author e-mail: katta@uwyo.edu.

10.1021/es062504o CCC: $37.00 © 2007 American Chemical Society
Published on Web 07/20/2007

contamination of water and soils, and subsequent toxicity to plants and animals. The objective of this study was to collect and monitor Al, As, Ba, B, Fe, Cd, Cu, Cr, Mn, Mo, Se, Pb, and Zn from CBNG produced water samples at outfalls and associated disposal ponds from 2003 to 2005. From the monitoring data, we conducted paired *t* tests to identify statistical differences between outfalls and associated disposal ponds by individual watershed. Geochemical modeling was used to identify mineral precipitation/dissolution processes affecting water quality in these CBNG produced waters; likewise, CBNG produced water quality parameters were compared to common water use criteria to determine possible beneficial uses. Major anion (alkalinity, SO_4^{2-}, Cl^-, F^-, NO_3^-, and PO_4^{3-}) and cation (Ca, Mg, Na, and K) concentrations were also monitored (in Table S3), and their results were reported by Jackson and Reddy (*6*).

Materials and Methods

Study Area Description. Most CBNG development in Wyoming occurs in the eastern portion of the PRB. This basin is part of the Great Plains Missouri Plateau. The PRB is semiarid with average annual precipitation ranging from 30 to 60 cm. The basin is bounded by the Black Hills on the east, the Hartville Uplift to the south, the Big Horn Mountains on the west, and the Yellowstone River to the north (*12*). The PRB generally consists of high plains with elevations from 1640−1800 m above sea level with rolling hills capped with clinker (*12*).

Major coal formations in the PRB include the Tertiary Wasatch Formation and the Tertiary Tongue River Member of the Fort Union Formation (*5*). Soils in the PRB are dominated by Ustic Haplargids (clay loam), Ustic Calciargids (fine loamy), and Ustic Torriorthents (loamy) (*5*). The major river systems in the PRB include the Cheyenne River, Belle Fourche River, Little Powder River, Powder River, and Tongue River. The Cheyenne River drains the southeast portion of the PRB; the Belle Fourche River drains the eastern portion of the basin; the Little Powder River and Powder River drain the northern portion of the basin; and the Tongue River drains the northwestern portion of the basin. These are perennial rivers and tributaries of the Missouri River.

Surface streams that contribute to CHR, BFR, LPR, PR, and TR have intermittent or ephemeral flows based on snowmelt or storm events. Major land uses in the PRB include ranching, livestock production, coal and uranium extraction, and natural gas extraction (*5*). Discharge of CBNG produced water increases overall flow of receiving tributaries, which drain through local soils and plant communities. Subsequently, these processes influence the quality of the receiving water.

Site Selection. Site selection was based on geographic location and extensive CBNG development in the Tongue River, Powder River, and Little Powder River watersheds. Twenty-six sites were selected within the five Wyoming watersheds to obtain CBNG produced water discharge points and associated disposal pond samples. Figure 1 identifies sampling locations that include seven sites each within the LPR and PR watersheds, three sites from the CHR watershed, four sites from the BFR watershed, and five sites from the TR watershed.

Sample Collection and Analysis. *Sampling.* CBNG water samples from each outfall and corresponding disposal pond were collected during the summers of 2003, 2004, and 2005. Before sample collection, field measurements including pH, conductivity, temperature, oxidation and reduction potential (ORP), and dissolved oxygen were taken from each CBNG outfall and associated disposal pond with an Orion model 1230 Multi-Probe. Exact locations for pond measurements were taken from within the disposal pond directly away from the outfall, at the point where disposal pond pH stabilized (typically 2−3 meters into the disposal pond). The disposal pond water samples and field measurements were collected far from any sediment disturbances caused by movement in the disposal pond.

Chemical Analysis. Duplicate water samples from outfalls and disposal ponds were taken from each site. Samples were transported in ice coolers (2 °C) to the University of Wyoming Water Quality Laboratory. Each sample was filtered through a 0.45 μm filter and subdivided: half were acidified to a pH of 2.0 with HNO_3, and half were left unacidified. Acidified samples were analyzed for Ca, Na, Mg, K, Fe, Al, Cr, Mn, Pb, Cu, Zn, As, Se, Mo, Cd, Ba, and B by inductively coupled plasma-mass spectrometry (ICP−MS), and unacidified samples were analyzed for SO_4^{2-}, Cl^-, F^-, NO_3^-, and PO_4^{3-} using ion chromatography (IC). Total alkalinity of unacidified samples was determined by the acid titration method.

Geochemical Modeling. The geochemical model MINTEQA2 was used to verify analytical data accuracy and predict ion activities and saturation indices (*13*). This model used chemical data, pH, ORP, alkalinity, and redox couples to calculate ion speciation, ion activities, ion complexes, and saturation indices.

Quality Control. The quality control/quality assurances protocols such as duplicate sampling and analysis, trip blanks, and known concentrations of reference standards were included. Standard laboratory procedures were used for all analytical analyses including pH, electrical conductivity, and alkalinity measurements. All analyses were performed following the EPA Code of Federal Regulations (CFR) 40, Part 1, Chapter 36 procedures (*14*).

Statistical Analysis. Due to a "natural pairing" of the outfall and an associated disposal pond, paired *t* tests were used to identify these differences between water types (outfalls vs associated disposal ponds) which were separated by individual watershed (alpha = 0.05) (*15*). Residual normality was obtained for all measured parameters except Se, Cd, and Mn, which were removed from statistical analysis.

Results and Discussion

Samples from outfalls and corresponding disposal ponds varied in pH and ORP throughout the watersheds (Figure 2). The pH of outfall samples ranged from 7.1 to 7.5 among all watersheds, while samples from disposal ponds ranged from 8.1 to 9.4. Though some individual CBNG water sample pH ranges overlapped, outfalls typically had lower pH than their corresponding disposal ponds. Outfall water pH was stable and controlled by the geologic formation and the concentration of dissolved CO_2 confined in the aquifer, whereas the disposal pond water pH was varied because of the degassing of CO_2 from the produced water and its interaction with local soils (*2*). The ORP followed a trend similar to that of pH, in that the ORP samples from outfalls typically were lower (−109 to 161 mV) than the ORP of samples from disposal ponds (−17 to 121 mV). These results were expected due to a reduced environment where CBNG is produced, and the relative oxidized environment in the disposal ponds.

Mean trace metal concentrations and standard errors for water samples from CBNG outfalls and disposal ponds, separated by watershed, are presented in Table 1. Iron (1.28−8.27 μM/L), Al (6.71−67.35 μM/L), Ba (0.95−4.47 μM/L), and B (5.89−15.20 μM/L) were the major constituents of trace metal concentrations, while Cd and Pb concentrations were the lowest at <0.01 μM/L for both elements. Most trace elements increased in concentration from the CBNG outfall to the disposal pond. Barium was an exception because it significantly decreased from the outfall to the disposal pond in all watersheds (Figure 3). Though most trace elements increased in disposal ponds, only Al, Cu, Ba, As, Mo, and B were statistically different from outfalls to disposal ponds (alpha 0.05) and will be discussed in the subsequent sections.

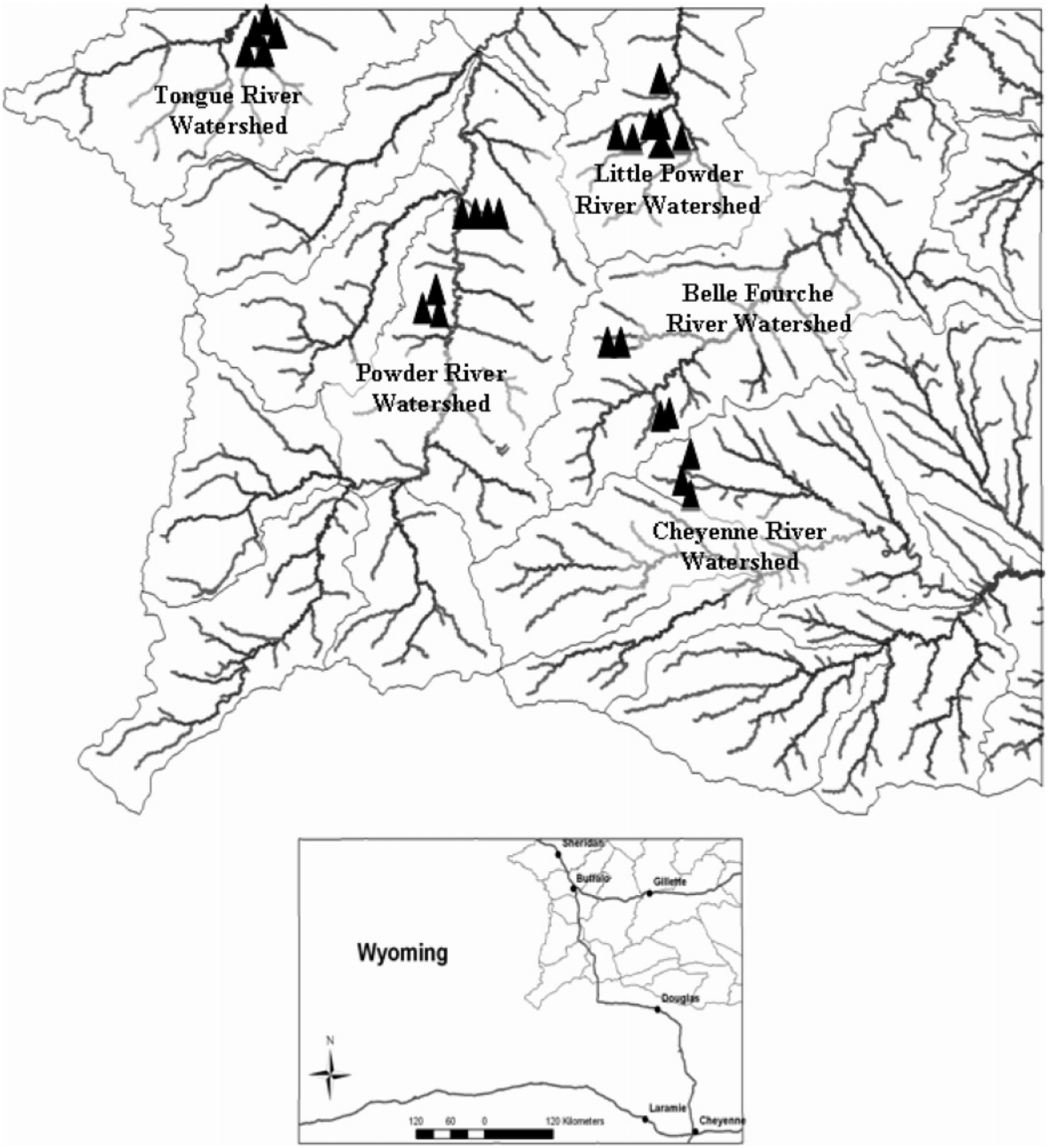

FIGURE 1. Sample site locations in the Powder River Basin, Wyoming.

Yearly mean concentrations of Al, Cu, Ba, As, Mo, and B are presented in Table S1. Of those trace elements (Al, Cu, Ba, As, Mo, and B), Al and Cu concentrations decreased between years in disposal ponds, while Ba, As, and B concentrations increased between years; however, Mo concentrations remained the same in most watersheds.

Aluminum. Aluminum concentrations varied between outfalls and disposal ponds across watersheds (Figure 3). The BFR, LPR, and PR Al concentrations were significantly different between outfalls and disposal ponds (*t* test *p*-values 0.05, 0.02, and 0.02). In the BFR, Al concentrations tended to be higher in outfalls than in disposal ponds (18.83−10.72 μM/L), but in the LPR and PR, disposal ponds had higher Al concentrations (LPR 11.27−21.24 μM/L and PR 6.71−9.29 μM/L).

Disposal pond Al concentrations tended to decrease from 2003 to 2005 in most watersheds. In BFR, LPR, PR, and TR disposal ponds, overall Al concentrations decreased. For example, in LPR disposal ponds, Al concentrations decreased from 2003 to 2004 from 49.16 to 10.70 μM/L, and decreased to 0.97 μM/L in 2005. It is interesting to observe that disposal pond Al concentrations in CHR did not follow the other four watersheds' decreasing Al trend, but increased in concentration from 10.53 μM/L in 2003 to 35.08 μM/L in 2005.

Dominant Al species data in outfalls and disposal ponds across all watersheds are presented in Tables 2 and 3. For all produced water sampled, $Al(OH)_4^-$ was the dominant dissolved ionic species. McBeth et al. (*3*) found similar results in CBNG produced waters in CHR, BFR, and LPR watersheds, and Stumm and Morgan (*9*) also predicted $Al(OH)_4^-$ as a dominant species in natural waters.

The CHR and TR Al concentrations were not significantly different between outfalls and disposal ponds (*t* test *p*-values 0.22 and 0.42), but Al mean concentrations in TR outfalls were much higher (67.35 μM/L) than all other watersheds. The unusually high Al concentrations can be attributed to a common remediation technique used by CBNG producers in the TR that acidifies the produced water with sulfuric acid.

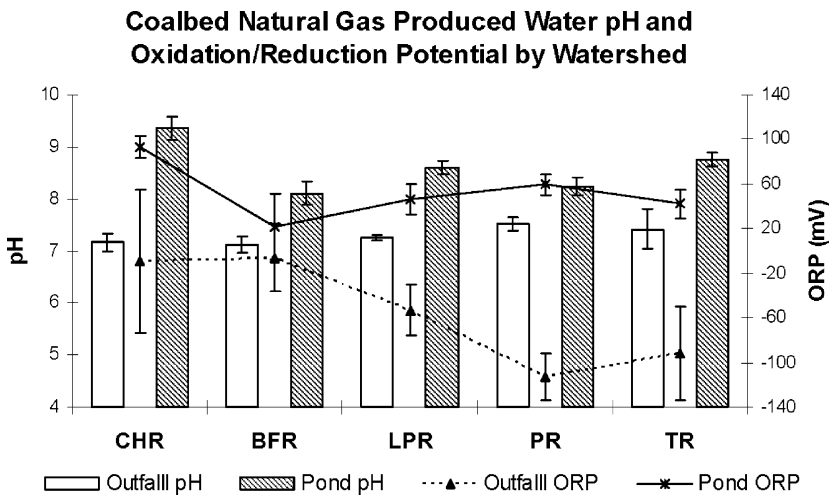

FIGURE 2. The pH and oxidation/reduction potential (ORP) measured in millivolts (mV) of coal bed natural gas (CBNG) produced waters in Cheyenne (CHR), Belle Fourche (BFR), Little Powder (LPR), Powder (PR), and Tongue River (TR) watersheds. Error bars denote one standard error of the mean.

This process is used to lower the sodium adsorption ratio (SAR), but it also affects many other trace elements, such as Al, causing them to become soluble and mobile (*8*, *9*). MINTEQA2 results from TR suggest that $AlSO_4^+$ is the dominant species in sulfuric acid treated produced waters, but $Al(OH)_4^-$ is dominant in outfalls and disposal pond waters before and after the acid treatment. The geochemical model suggests that when sulfuric acid treated produced water enters disposal ponds, $AlSO_4^+$ is the dominant Al species. As the disposal ponds equilibrate, $Al(OH)_4^-$ becomes the dominant ionic species.

Copper. Mean copper concentrations are given in Figure 3. The results indicate a significant increase from outfalls to disposal ponds across all watersheds except in TR watershed (*t* test *p*-value 0.08). Outfall concentrations across all watersheds ranged from 0.11 to 0.17 μM/L, and the disposal ponds ranged between 0.18 and 0.31 μM/L. Overall copper concentrations in disposal ponds tended to decrease between 2003 and 2005 in all watersheds. For instance, in CHR, Cu concentrations slightly increased from 2003 to 2004 from 0.39 to 0.43 μM/L, and then decreased to 0.11 μM/L in 2005.

MINTEQA2 predicted $CuCO_3^0$ as the dominant Cu species in CBNG outfalls (Table 2). The geochemical prediction for the dominant Cu species in CBNG disposal ponds varied between $Cu(CO_3)_2^{-2}$ and $CuCO_3^0$ equally. Based on a thermodynamic approach, Strumm and Morgan also predicted $CuCO_3^0$ and $Cu(CO_3)_2^{-2}$ as a predominant dissolved Cu species in natural waters with a near neutral to alkaline pH (*9*).

MINTEQA2 analyses further suggested that dissolved Cu concentrations across all watershed outfalls were close to the solubility of chalcocite (Cu_2O) and cuprite (Cu_2S), while dissolved Cu concentrations in disposal ponds were close to the solubility of tenorite (CuO). This finding is expected due to the highly reduced environment of the CBNG outfalls (ORP of most outfalls is between −240 and −4 mV) and the somewhat oxidized environment of the ponds (ORP of most ponds is between 6 and 158 mV).

Barium. Unlike the previous elements, Ba concentrations significantly decreased from outfall to disposal pond across all watersheds (*t* test *p*-values: CHR 0.03, BFR 0.02, LPR <0.01, PR <0.01, and TR <0.01) (Figure 3). McBeth et al. (*3*) reported similar results in CBNG produced waters in CHR, BFR, and LPR watersheds. Mean discharge well concentrations ranged from 1.97 to 4.47 μM/L, and disposal ponds ranged from 0.95 to 2.43 μM/L. In disposal ponds, Ba concentrations tend to increase in BFR, LPR, PR, and TR between years; however, Ba decreased in CHR disposal ponds. MINTEQA2 results suggested that the dominant Ba dissolved species in outfalls and disposal ponds was Ba^{+2} (Table 2 and 3), and dissolved Ba concentrations were near the solubility of Barite ($BaSO_4$). Increased pH in disposal ponds (8.1−9.4) may result in Barite mineral precipitation and an overall decrease in Ba concentrations within disposal ponds (*3*).

Arsenic. Mean As concentrations in water samples from outfalls and from disposal ponds across watersheds are presented in Figure 4. Results suggest that As concentration increases from the outfalls to the disposal ponds. Arsenic was statistically higher in samples from the disposal ponds in all watersheds (*t* test *p*-values: CHR 0.01, LPR >0.01, PR 0.01, and TR 0.04) except BFR (*t* test *p*-value 0.07). Outfall sample concentrations ranged from 0.01 to 0.02 μM/L, whereas disposal pond sample concentrations ranged from 0.02 to 0.13 μM/L.

Recently, As has been identified as a major contaminant of groundwater resources and a public health concern. Further investigation of As concentrations in water samples from disposal ponds revealed an incremental increase from year to year across all watersheds. For example, As increased in CHR disposal ponds from 2003 to 2005 from 0.03 to 0.12 uM/L. Many studies have identified that As solubility is directly related to adsorption and desorption processes of metal oxides and hydroxides (*9*, *16*). In semi-arid alkaline environments, mineral oxides and hydroxides tend to have a negative surface charge. In nature, As is an anion, thus it is expected to be soluble and mobile in these watersheds and increase in concentration over time in disposal ponds.

Molybdenum. Mean Mo concentrations are presented in Figure 4. Though all concentrations were low, across all watersheds, Mo increased from outfalls to disposal ponds. Outfall sample concentrations were ≤0.01 μM/L and disposal pond sample concentrations ranged from 0.02 to 0.03 μM/L. Statistically, only water samples from BFR and TR outfalls and disposal ponds were significantly different (*t* test *p*-values 0.04), while there was little difference in Mo concentrations between years. Like As, Mo solubility is directly related to adsorption and desorption processes of metal oxides and hydroxides and its concentration increases in disposal ponds (*9*). There is a positive correlation between CBNG discharge pond concentrations of Mo and Fe. Reddy et al., (*17*) found similar correlations between dissolved Mo and Fe in soil solutions.

Boron. Outfall and disposal pond sample B concentrations are presented in Figure 4. Boron concentrations increase in

TABLE 1. Mean Element Concentrations (μM/L) with One Standard Error of the Mean for Coal Bed Natural Gas (CBNG)-Produced Waters in Cheyenne (CHR), Belle Fourche (BFR), Little Powder (LPR), Powder (PR), and Tongue River (TR) Watersheds

	CHR		BFR		LPR		PR		TR	
	outfalls	disposal ponds	outfalls	disposal ponds	outfalls	disposal Ponds	outfalls	disposal ponds	outfalls	disposal ponds
iron (Fe)	2.05± 0.23	5.88 ± 2.09	2.04 ± 0.46	8.27 ± 2.66	2.22 ± 0.20	3.88 ± 1.91	1.45 ± 0.24	3.64 ± 1.61	1.28 ± 0.61	2.60 ± 0.83
aluminum (Al)	8.07 ± 6.09	19.84 ± 8.99	18.83 ± 13.39	10.72 ± 5.13	11.27 ± 4.89	21.24 ± 9.87	6.71 ± 2.99	9.29 ± 3.52	67.35 ± 43.52	13.37 ± 6.01
chromium (Cr)	0.10 ± 0.03	0.13 ± 0.03	0.09 ± 0.01	0.10 ± 0.02	0.17 ± 0.02	0.17 ± 0.03	0.23 ± 0.05	0.22 ± 0.03	0.16 ± 0.03	0.18 ± 0.03
manganese (Mn)	0.09 ± 0.03	0.19 ± 0.09	0.47 ± 0.32	1.19 ± 0.79	0.23 ± 0.07	0.21 ± 0.15	0.15 ± 0.04	0.06 ± 0.02	0.14 ± 0.05	0.13 ± 0.04
lead (Pb)	<0.01 ± 0.01	<0.01 ± 0.01	<0.01 ± 0.01	<0.01 ± 0.01	<0.01 ± 0.01	<0.01 ± 0.01	<0.01 ± 0.01	<0.01 ± 0.01	<0.01 ± 0.01	<0.01 ± 0.01
copper (Cu)	0.11 ± 0.03	0.31 ± 0.06	0.12 ± 0.03	0.18 ± 0.05	0.17 ± 0.02	0.30 ± 0.07	0.12 ± 0.04	0.31 ± 0.03	0.17 ± 0.03	0.27 ± 0.03
zinc (Zn)	0.13 ± 0.05	0.17 ± 0.05	0.16 ± 0.05	0.13 ± 0.04	0.12 ± 0.03	0.14 ± 0.03	0.11 ± 0.03	0.16 ± 0.05	0.16 ± 0.06	0.28 ± 0.08
arsenic (As)	0.02 ± 0.01	0.07 ± 0.02	0.01 ± 0.01	0.05 ± 0.02	0.01 ± 0.01	0.13 ± 0.09	0.01 ± 0.01	0.05 ± 0.01	0.01 ± 0.01	0.02 ± 0.01
selenium (Se)	0.01 ± 0.01	0.01 ± 0.01	0.01 ± 0.01	0.01 ± 0.01	0.02 ± 0.01	0.02 ± 0.01	0.02 ± 0.01	0.03 ± 0.01	0.01 ± 0.01	0.01 ± 0.01
molybdenum (Mo)	<0.01 ± 0.01	0.02 ± 0.01	0.01 ± 0.01	0.02 ± 0.01	<0.01 ± 0.01	0.03 ± 0.02	0.01 ± 0.003	0.02 ± 0.01	<0.01 ± 0.01	0.02 ± 0.01
cadmium (Cd)	<0.01 ± 0.01	<0.01 ± 0.01	<0.01 ± 0.01	<0.01 ± 0.01	<0.01 ± 0.01	<0.01 ± 0.01	<0.01 ± 0.01	<0.01 ± 0.01	<0.01 ± 0.01	<0.01 ± 0.01
barium (Ba)	2.46 ± 0.16	1.23 ± 0.25	2.55 ± 0.17	1.71 ± 0.31	4.47 ± 0.36	2.43 ± 0.26	3.74 ± 0.72	2.07 ± 0.45	1.97 ± 0.19	0.95 ± 0.17
boron (B)	5.89 ± 0.27	8.36 ± 0.83	6.45 ± 0.42	7.72 ± 0.63	9.19 ± 0.44	11.66 ± 1.78	13.08 ± 1.99	15.20 ± 1.14	10.08 ± 0.63	11.44 ± 0.62

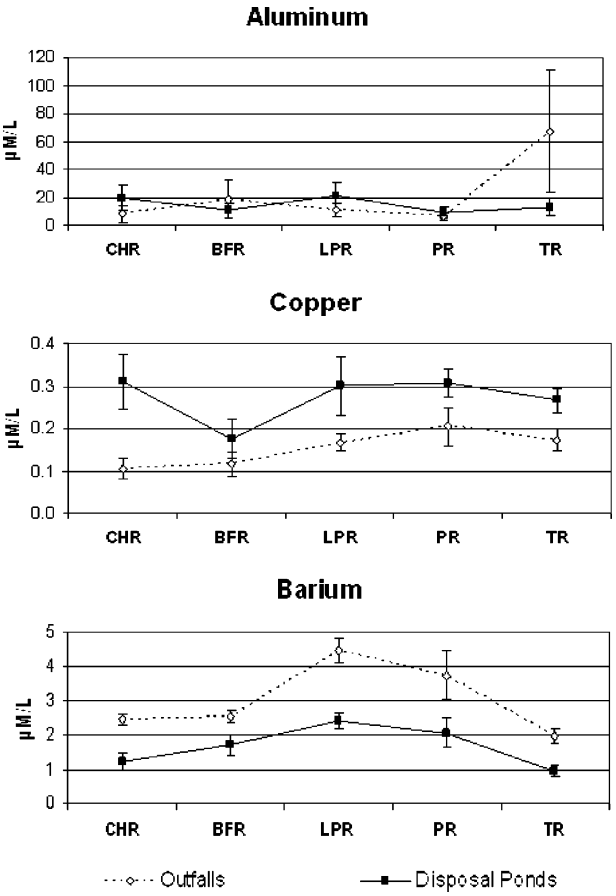

FIGURE 3. Mean aluminum, copper, and barium concentrations in coal bed natural gas (CBNG) produced waters in Cheyenne (CHR), Belle Fourche (BFR), Little Powder (LPR), Powder (PR), Tongue River (TR) watersheds. Error bars denote one standard error of the mean.

TABLE 2. Average Aluminum, Copper, Barium, and Iron Ion Percentages for Samples Collected between 2003 and 2005 in Coal Bed Natural Gas (CBNG) Outfalls Across Cheyenne (CHR), Belle Fourche (BFR), Little Powder (LPR), Powder (PR), and Tongue River (TR) Watersheds[a]

	CHR	BFR	LPR	PR	TR
	% dissolved aluminum				
$Al(OH)_4^-$	74.3	72.8	85.7	91.9	88.0
$Al_2(OH)_2CO_3^{+2}$	11.9	11.8	3.9	0.3	NA
$Al(OH)_3^0$	8.6	8.2	7.7	6.5	1.8
$AlSO_4^+$	NA	NA	NA	NA	7.5
	% dissolved copper				
$CuCO_3^0$	85.9	85.9	90.1	87.6	74.5
Cu^{+2}	8.5	8.6	3.2	1.5	6.5
$CuHCO_3^+$	2.0	2.6	1.6	1.4	1.6
$Cu(CO3)_2^{-2}$	1.9	1.5	4.3	8.2	13.8
	% dissolved barium				
Ba^{+2}	96.5	95.8	93.0	88.4	89.6
$BaHCO_3^+$	3.3	3.6	6.6	10.8	5.3
	% of dissolved iron				
$Fe(OH)_2^+$	97.6	99.2	99.0	97.8	85.5
$Fe(OH)_3^0$	1.7	0.6	0.7	1.3	2.3
$Fe(OH)_4^-$	1.2	0.1	0.2	0.9	2.6

[a] NA identifies no appreciable percentage of that species.

samples from outfalls to ponds across all watersheds, but were only statically significant in TR (t test p-value 0.04). Outfall sample concentrations ranged from 5.89 to 13.08 μM/L, and disposal pond sample concentrations ranged from 7.72 to 15.20 μM/L. Boron concentrations in disposal ponds increased overall between years across all watersheds. For example, disposal pond B concentrations in CHR increased

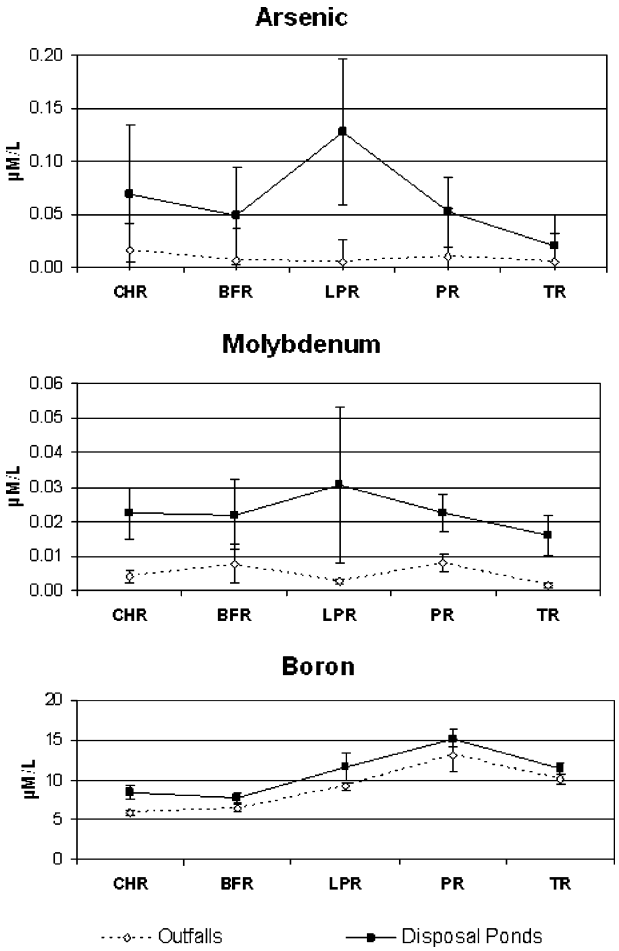

FIGURE 4. Mean arsenic, molybdenum, and boron concentrations in coal bed natural gas (CBNG) produced waters in Cheyenne (CHR), Belle Fourche (BFR), Little Powder (LPR), Powder (PR), Tongue River (TR) watersheds. Error bars denote one standard error of the mean.

TABLE 3. Average Aluminum, Copper, Barium, and Iron Ion Percentages for Samples Collected between 2003 and 2005 in Coal Bed Natural Gas (CBNG) Disposal Ponds Across Cheyenne (CHR), Belle Fourche (BFR), Little Powder (LPR), Powder (PR), and Tongue River (TR) Watersheds

	CHR	BFR	LPR	PR	TR
% dissolved aluminum					
$Al(OH)_4^-$	99.7	97.3	99.4	97.4	99.3
% dissolved copper					
$Cu(CO_3)_2^{-2}$	47.9	18.8	52.3	51.1	58.0
$CuCO_3^0$	43.4	76.4	46.5	2.2	40.6
$Cu(OH)_2^0$	5.7	0.7	0.4	45.5	0.4
% dissolved barium					
Ba^{+2}	88.5	90.7	84.8	80.0	80.4
$BaCO_3^0$	8.6	2.3	8.9	10.4	9.8
$BaHCO_3^+$	2.7	3.7	6.1	8.8	5.7
% dissolved iron					
$Fe(OH)_4^-$	82.1	24.5	55.1	46.1	63.1
$Fe(OH)_2^+$	15.3	71.3	39.9	50.8	31.8

from 6.03 to 10.68 μM/L from 2003 to 2004, then slightly decreased in 2005 to 8.39 μM/L. Solubility of B is related to sorption and desorption processes (*18*). Like As and Mo, B is an anionic species and, in semiarid alkaline environments, mineral oxides and hydroxides tend to have a negative surface charge, causing B solubility and mobility to increase in these watersheds.

Water Quality Standards. Existing uses for water from CBNG disposal ponds include irrigation and drinking water for livestock, wildlife, and aquatic life. Table 1 identifies trace metal concentrations in CBNG-produced waters by watershed. Table S2 identifies water quality standards for human consumption, agricultural, livestock and wildlife drinking water, and aquatic life chronic values. Comparisons with these standards suggest that many of the CBNG produced water samples contain low concentrations of trace elements. The most restrictive use, based solely on trace metal concentrations, is aquatic life. Most CBNG produced water samples exceeded the aquatic life criteria for Al and Cu. Based on secondary water quality standards, many CBNG outfall water samples are not suitable for human drinking water due to high Fe and Al concentrations. These results suggest that many of the CBNG produced waters across the PRB can be used for agriculture and livestock/wildlife drinking water.

Our studies suggest that, though trace metal concentrations were low in both CBNG outfalls and disposal ponds, a statistically significant increasing trend was observed for most trace elements between the outfalls and disposal ponds. Reactions governing the trace metal changes are precipitation/dissolution of geologic material for Al, Cu, and Ba and adsorption/desorption for As, Mo, and B. Mean concentrations of Al and Cu decreased over time in disposal ponds, whereas Ba, As, and B concentrations increased over time. Molybdenum concentrations remained the same in most watersheds. Most CBNG-produced waters examined were unsuitable for human drinking water and aquatic life, but were suitable for agricultural uses and livestock and wildlife drinking water. If the trace elements continue to increase and accumulate in CBNG disposal ponds, there may be a point in time when the concentrations of these trace elements could exceed standards for agricultural uses and livestock and wildlife drinking water. Overall, this study's results will be useful for water quality managers, industry, and landowners in properly managing and developing best uses for produced water in the PRB, Wyoming.

Acknowledgments

We thank the U.S. Geological Survey and Wyoming Water Development Commission for funding this project. We appreciate input from Professors R. Olson, D. Legg, and L. Munn from the Department of Renewable Resources and from Professor D. Johnson from the Department of Civil and Architectural Engineering, University of Wyoming. We also thank local landowners who participated in this project and without whom this project could not have succeeded. Finally, we would like to thank all the graduate and undergraduate students who graciously helped collect field samples and provided data entry.

Supporting Information Available

Table S1 contains yearly element concentration means for coal bed natural gas (CBNG) disposal pond waters in Cheyenne, Belle Fourche, Little Powder, Powder, and Tongue River watersheds. Maximum trace metal concentrations in water for human consumption, agricultural use, livestock and wildlife, and aquatic life values from various published water standards are presented in Table S2. Cation (Na, Ca, Mg, K) and anion (alkalinity, SO_4^{2-}, Cl^-, NO_3^-) concentrations from CBNG outfall and disposal pond waters are presented in Table S3. This material is available free of charge via the Internet at http://pubs.acs.org.

Literature Cited

(1) DeBruin, R. H.; Lyman, R. M.; Jones, R. W.; Cook, L. W. *Coal Bed Methane Development in Wyoming*; Information Pamphlet number 7; Wyoming State Geological Survey: Laramie, WY, 2000.

(2) McBeth, I. H.; Reddy, K. J.; Skinner, Q. D. Chemistry of coalbed methane product water in three Wyoming watersheds. *J. Am Water Res.* **2003a**, *39*, 575−586.

(3) McBeth, I. H.; Reddy, K. J.; Skinner, Q. D. Chemistry of trace elements in coalbed methane product water. *Water Res.* **2003b**, *37*, 884−890.
(4) Rice, C. A.; Ellis, M. S; and Bullock, J. H., Jr. *Water Co-produced with Coalbed Methane in the Powder River Basin, Wyoming: Preliminary Compositional Data*; U.S. Geological Survey Open-File Report 00−0372; USGS: Reston, VA, 2000; http://pubs.usgs.gov/of/2000/ofr-00−372/.
(5) U.S. Department of Interior, Bureau of Land Management. *Final Environmental Impact Statement and Proposed Plan Amendment for the Powder River Basin Oil and Gas Project*; Buffalo Field Office: Buffalo, WY, 2003; Vol. 1−3.
(6) Jackson, R. E.; Reddy, K. J. Geochemistry of coalbed natural gas (CBNG) produced water in Powder River Basin, Wyoming: salinity and sodicity. *Water, Air, Soil Pollut.* **2007**, DOI: http://www.springerlink.com/content/100344/?sortorder=asc&Content+Status=Accepted.
(7) van Voast, W. A. Geochemcial signature of formation waters associated with coalbed methane. *AAPG Bull.* **2003**, *87*, 667−676.
(8) Drever, J. I. *The Geochemistry of Natural Waters, Surface and Groundwater Environments*; Prentice Hall: Upper Saddle River, NJ, 1997.
(9) Strumm, W.; Morgan, J. J. *Aquatic Chemistry, Chemical Equilibria and Rates in Natural Waters*, 3rd ed.; John Wiley and Sons: Toronto, Canada, 1996.
(10) Wyoming Department of Environmental Quality. *SAP: Water Quality Rules and Regulations*; Chapter 1; Department of Environmental Quality and Water Quality Division: Cheyenne, WY, 2001; http://deq.state.wy.us/wqd/WQDrules/Chapter_01.pdf.
(11) U.S. Environmental Protection Agency. *Drinking Water Contaminants*; EPA Office of Water: Washington, DC, 2001; www.epa.gov/safewater/mcl.html.
(12) Lowry, M. E.; Wilson, J. F. *Hydrology of Area 50, Northern Great Plains and Rocky Mountain Coal Provinces, Wyoming and Montana*; Open-File Report 83−545; U.S. Geological Survey: Reston, VA, 1986.
(13) Brown, D. S.; Allison, J. D. *MINTEQA2: An Equilibrium Metal Speciation Model*; Environmental Research Laboratory, Office of Research and Development, U.S. Environmental Protection Agency: Athens, GA, 1992.
(14) American Public Health Association. *Standard Methods for the Examination of Water and Wastewater*; American Public Health Association: Washington DC, 1992.
(15) SAS (SAS Institute). *SAS Proprietary Software Release 9.0*; SAS Institute: Raleigh, NC, 2000.
(16) Mok, W. M.; Wai, C. M. Mobilization of Arsenic in Contaminated River Waters. In *Arsenic in the Environment: Part I Cycling and Characterization*; Nriagu, O. J., Ed.; Wiley: New York, 1994.
(17) Reddy, K. J.; Munn, L. C.; and Wang, L. Chemistry and Mineralogy of Molybdenum in Soils. In *Soils and Plant Molybdenum and Its Significance in Crops and Livestock*; Cambridge University Press: Cambridge, 1997.
(18) Elrashidi, M. A.; O'Connor, G. A. Boron sorption and desorption in soils. *Soil Sci. Soc. Am.* **1982**, *46*, 27−31.

Received for review October 18, 2006. Revised manuscript received June 3, 2007. Accepted June 20, 2007.

ES062504O

Available online at www.sciencedirect.com
SCIENCE DIRECT®
International Journal of Coal Geology 68 (2006) 57–69
International Journal of COAL GEOLOGY
www.elsevier.com/locate/ijcoalgeo

Coal dust dispersal around a marine coal terminal (1977–1999), British Columbia: The fate of coal dust in the marine environment

Ryan Johnson, R.M. Bustin *

Department of Earth and Ocean Sciences, The University of British Columbia, Vancouver, B.C., Canada V6T 1Z4

Received 1 April 2005; received in revised form 24 October 2005; accepted 24 October 2005
Available online 30 March 2006

Abstract

A 1999 assessment of sediments, adjacent to the Roberts Bank coal terminal in Delta, British Columbia, Canada, shows that the concentration of coal particles (reported as non-hydrolysable solids or NHS) has increased substantially since a prior study in 1977. NHS concentrations have doubled from a mean concentration of 1.80% in 1977 to 3.60% in 1999. Overall the dispersal distance of coal has not increased over the 22-year period but rather the abundance of coal in the surface sediment within the dispersal area has increased. Since 1977 the main deposition of coal has occurred in the vicinity of the coal-loading terminals, where concentrations of 10.5% and 11.9% NHS (non-hydrolysable solids = coal) occur.

The settling properties of fresh and oxidized coal particles (<53 μm up to >2.36 mm) were examined in order to better understand the dispersal of coal in marine waters. No change in settling velocity of coal particles occurred with increasing oxidation. However, the proportion of buoyant coal particles decreases with oxidation in all size fractions, reflecting the decrease of coal hydrophobicity with oxidation.

The distribution of coal around the terminals agrees with measured particle settling velocity and current velocity, with coal concentration decreasing rapidly away from the terminal. Coarser sediment fractions contain the highest coal (NHS) concentrations and carbon/nitrogen ration when compared to finer fractions. Coal particles with >2.36 mm diameter (settling velocities ≤10.54 cm/s) settle out close to the terminal (depending on currents), whilst small (<53 μm) and weakly oxidized coal particles travel further and take longer to settle out (settling velocities ≥0.16 cm/s). This results in a wider dispersal of coal particles, and a corresponding decrease in the coal concentration.

Coal distribution would likely affect those benthic flora and fauna, most susceptible to coal dust coverage and possible anoxic conditions that might arise during coal oxidation within very close proximity (0–100 m) to the coal-loading terminal.
© 2006 Elsevier B.V. All rights reserved.

Keywords: Coal contamination; Coal environment; Coal settling velocity

1. Introduction

The Roberts Bank coal terminal has been in business for over thirty years and is presently operated by Westshore Terminals Ltd (Fig. 1). Located on Roberts Bank in the municipality of Delta, British Columbia, Canada, it is the first stage in a proposed development of a major bulk-loading port and industrial park, as the major terminals in Burrard Inlet (Vancouver, B.C.) exceed their exporting and development capacities.

However, Roberts Bank is not naturally a deep-sea port and is located in one of the most ecologically

* Corresponding author.
E-mail address: bustin@unixg.ubc.ca (R.M. Bustin).

0166-5162/$ - see front matter © 2006 Elsevier B.V. All rights reserved.
doi:10.1016/j.coal.2005.10.003

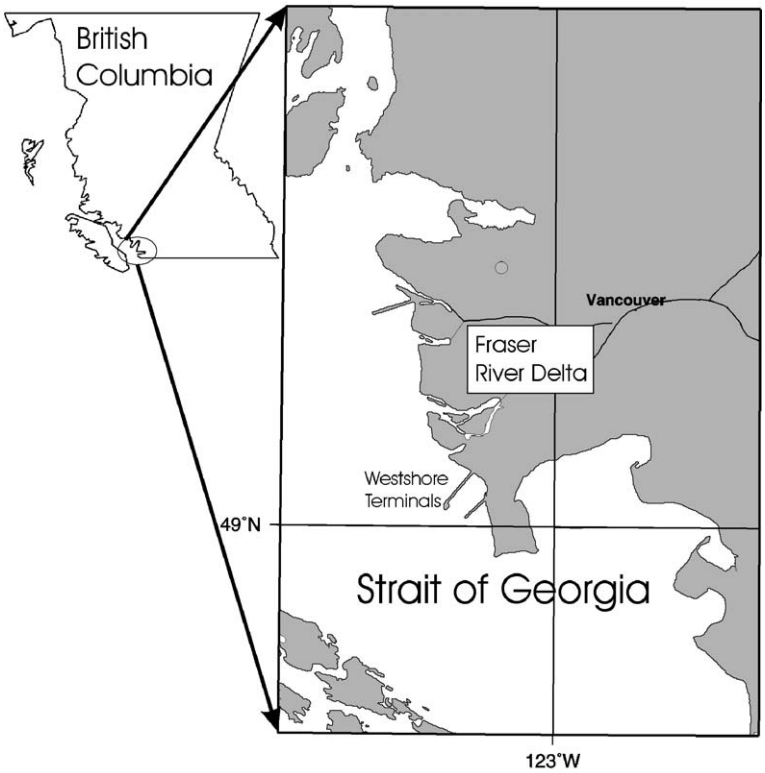

Fig. 1. Location of Westshore Terminals and Fraser River Estuary, British Columbia, Canada.

important estuaries on the west coast of North America. The construction of the coal terminal has had numerous effects on the local ecology, and the release of coal dust has had a detrimental impact on the region.

This paper investigates the coal content of the sediments in the vicinity of the coal loading facility, and reveals significant changes in sediment coal content and distribution in the 23 years since the previous study. An assessment of the settling properties and velocities of the coal particles in the water column were conducted to predict coal particle dispersal around the terminal, and these results are compared with the observed distribution of coal in the sediments adjacent to the coal loading facility. Some of the effects of this coal accumulation on the local ecology are also discussed.

2. History and previous studies

In April 1970, shipments of coal mined in the interior of British Columbia and Alberta began from the Roberts Bank coal terminal located south of the Main Arm of the Fraser River, just south of Vancouver (Fig. 1). The present facility consists of a 96-hectare man-made island situated at the end of a 4.8-km long causeway, serviced by a 20-m deep dredged waterlot and a large ship turning basin located between the terminal and the Tsawwassen Ferry terminal (Fig. 2).

Westshore Terminals handle approximately 30% of the shipping volumes of the British Columbia Lower Mainland. Approximately 90% of this volume is coal that is transported to the facility in unit trains, where the coal is unloaded and stored in large unprotected stockpiles. The coal is subsequently loaded aboard ships ranging in size form 45 000 deadweight tonnes (DWT) to 250 000 DWT for export from two major coal-loading terminals, referred to as pods #1 and 2 (Fig. 2). Coal shipments have increased from 10.6 million metric tonnes in 1980 to a maximum of 23.5 million in 1997. Estimates forecast a continued increase of 4% per annum until 2010 (Fraser River Estuary Management Program (FREMP), 1990a,b). Annual shipments are projected to reach 30 million metric tonnes of coal only with modification of Pod #3, as this terminal is presently being used as a bulk cargo terminal (Deltaport).

In 1975, Westshore Terminals Ltd. applied for a permit under the British Columbia Pollution Control Act, 1967 (Emissions), to discharge “unknown and immeasurable” quantities of coal dust to the air (Pearce and McBride, 1977) as they had previously operated

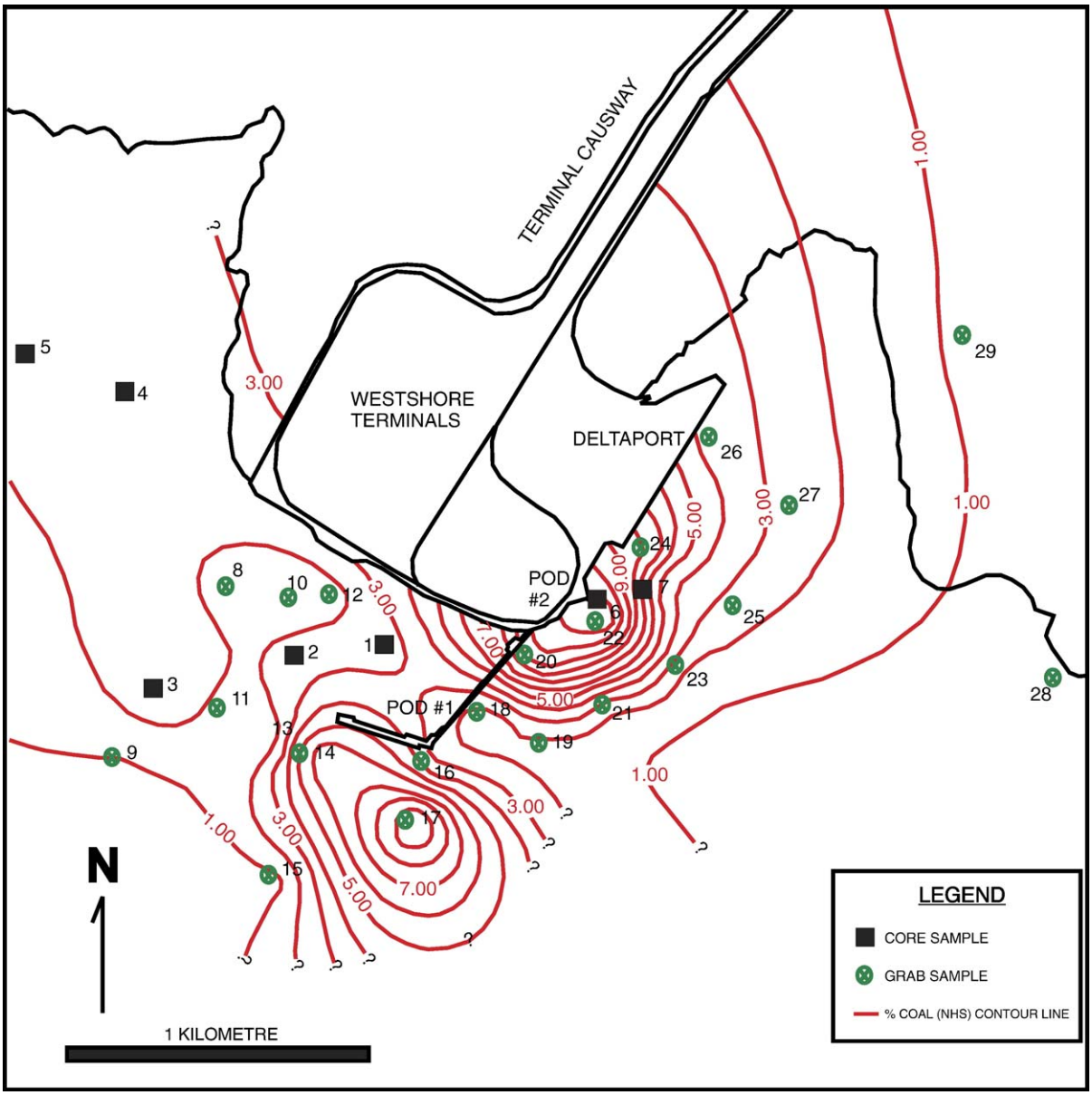

Fig. 2. Sample location and coal dust distribution in surface sediment as measured in weight percent NHS.

without a Pollution Control Branch permit. Local residents as far away as Pt. Roberts, have often complained of the coal dust escaping the terminal (Department of Fisheries and Environment Canada, 1978) from the incoming loaded rail cars, conveyor belts, and returning empty trains during the loading processes. Emissions from open stockpiles also contribute to the coal dust (especially during high wind periods), though it occurs to a lesser degree due to the use of resin binders such as polyvinyl acetate (Pearce and McBride, 1977).

Coal accumulation in bottom sediments, documented by Butler (1972) and Butler and Longbottom (1970) stimulated the Habitat Protection staff of the Fisheries and Marine Service to undertake a limited program in 1975 to study the further accumulation of coal in marine sediments around the terminal, and the possible effect of this coal accumulation on the local ecology. Pearce and McBride conducted the last of these studies in 1977 (Darrel Dejerdin, Vancouver Port Authority, Environmental Services, pers. Comm., 1999) and concluded that the coal content of the

sediments adjacent to the Roberts Bank (reported as non-hydrolysable solids) increased only slightly in the five years since Butler's investigation.

3. Study area

Historically, man's encroachment upon, and development of the ecologically important Fraser Estuary/Delta has generally been both ad hoc and unrestricted. This uncoordinated approach to resource use, without regard to, or knowledge of effects on the environment has led to very significant changes in the environment. Since the 1800's, roughly 70% of the estuary's original wetlands have been lost to dyking, dredging, draining, and filling (FREMP, 1997). However, the total area of freshwater and brackish marshes on the outer estuary may have increased in the last century due to the accretion of mudflats on Sturgeon and Roberts Banks (FREMP, 1996).

3.1. Physical environment

Annual deposits on Roberts Bank of approximately 17 million tonnes of sediment are supplied by the Fraser River (FREMP, 1996), the largest river on the west coast of North America (Fig. 1). This sedimentation plays a vital role in the creation of much of the aquatic habitat on Roberts Bank, and is in a dynamic state due to interacting and variable river flows and tides. Constant dredging is necessary to maintain depths of navigable shipping lanes in the vicinity of Westshore Terminals, and recent applications (Westshore Terminals Administrative Department, 1998) have been submitted to dredge approximately 4000 m^3 in the immediate vicinity of Pod #2, (Fig. 2; Dariah Hasselman, FREMP, Project Review Coordinator, pers. comm.).

Roberts Bank comprises approximately 8000 of the total 14,000 hectares of tidal flat associated with the Fraser River Delta. The dominant platform of Roberts Bank is over 6-km wide and slopes gently from the dyked delta lowlands out to a distinct break in slope, approximately 9 m below the lowest normal tide level (Fig. 2). In the vicinity of the Westshore Terminals causeway, the intertidal area exposed between high and low water is approximately 3000-m wide. Tidal channels, current, and wave ripples interrupt the otherwise featureless bank (Luternauer and Murray, 1973; Luternauer, 1974.

3.2. Estuarine ecology

The Fraser River estuary is notable for its biological productivity. This is especially evident between the Roberts Bank Coal Loading Port and the Tsawwassen Ferry Terminal, home to tidal flats, wetlands and eelgrass beds. These habitats form the basis for populations of varied estuarine life forms (in addition to the large numbers of migratory salmon and waterfowl) including the benthos, plankton and fish (Federal Environmental Assessment Review Office, 1979; Fraser River Estuary Management Program, 1989, 1991a, 1991b, 1993, 1994).

The benthos, composed of organisms dwelling on the sea bottom and in sediments are the most greatly affected due to the disturbance of the bottom caused by deposition of coal particles. Anoxic conditions, evident from the presence of hydrogen sulphide, in the sediments receiving very high levels of organic input (including coal), caused by the consumption of oxygen during the degradation (oxidation) of organic matter, would likely have the most detrimental impact on the benthic florae and faunae.

The ecological contribution of bottom microinvertebrates is very significant, as larvae from clams, mussels, barnacles, and crabs drift out to sea and constitute a substantial proportion of the seasonal food for juvenile salmonids and herring. Damage to the benthos therefore has serious implications for both the mature invertebrate populations as well as those creatures that predate upon the benthic larvae.

The Fraser River and its estuary support one of the largest commercial, recreational, and aboriginal salmon fisheries in British Columbia, which includes salmon, surf smelt, eulachon, cutthroat trout, steelhead trout, white sturgeon, mountain whitefish, and Dolly Varden. The annual commercial fishery of Fraser River salmon between 1989 and 1992 was valued of over $115 million (Canadian dollars), with a post-processing wholesale value of over $230 million (Environment Canada and Fisheries and Oceans Canada, 1995). Additionally, sport fishing throughout British Columbia earns about $180 million/year in direct revenues, with Fraser River Chinook and Coho comprising a large percentage of this catch (Environment Canada and Fisheries and Oceans Canada, 1995). Furthermore, seven native bands (Musqueam, Tsawwassen, Semiahmoo, Coquitlam, Katzie, Matsqui, and Langley) participate in the aboriginal food fishery in the Fraser River Estuary.

On Roberts Bank, the Dungeness crab is the only species that is exploited commercially and recreationally, representing approximately 10% of the total catch in British Columbia (Environment Canada and Fisheries and Oceans Canada, 1995). The reported darker coal-coloration of some crabs taken from Roberts Bank is a concern of local fishermen who find the darker crabs more difficult to market.

4. Material and methods

4.1. Sediment and sample collection

A benthic sample of the sediments was collected from each of 29 subtidal sampling stations (Fig. 2). The station locations were established using a differential GPS device and cross-referenced with the Canadian Hydrographic Chart #3492 (Fig. 2) and were chosen at roughly 200 m intervals radiating from the two main coal-loading terminals (pods #1 and 2). Stations 28 and 29 were situated closer to the Tsawwassen ferry terminal to act as 'controls'.

A gravity impact corer was used to collect the first seven samples at high tide on October 22, 1999 and a Shipek© model sediment sampler was used to collect the last 22 samples on November 26, 1999.

Upon retrieval, the uppermost 2–3 cm (approximately 200 g) of the samples were removed and placed in sealed plastic bags while the remainder of the samples were placed in larger bags, or retained in the core tubes. The samples were transported immediately to the laboratory and placed in a freezer to prevent decomposition.

Two coal samples (samples 30 and 31) from the Balmer seam (R_0 ~1.4%) of the Early Cretaceous Mist Mountain Formation (Kootney Group) were used in both the sediment coal content and coal settling property analyses, as these metallurgical coal samples are representative of the majority of coal exported from the Westshore Terminals facility.

4.2. Analytical techniques

4.2.1. Sediment coal content analysis

Determination of the coal content in the 29 sediment samples (each measured in duplicate) was performed using a modified hydrochloric acid hydrolysis method, mimicking the analytical procedure of Pearce and McBride (1977). During this process hydrolysable protein and acid-soluble carbonates are removed by hydrochloric acid hydrolysis with the remaining non-hydrolysable organic matter being removed by hydrogen peroxide oxidation.

Coal is essentially unaffected by the peroxide oxidation and hydrolysis, and its concentration is determined by subsequent gravimetric analysis and ashing. Coal content is reported here as percent total non-hydrolysable solids (NHS), while the organic content is reported as the percent total hydrolysable solids (HS).

The percent NHS is not a measure of the actual coal content of the marine sediments, mainly due to the presence of hydrolysis-resistant organic material such as wood, charcoal, and bark. Post-hydrolysis combustion of such materials would provide an overestimate of the actual coal content by resulting in an elevated NHS value. Despite this source of error, investigations have shown that NHS values do provide an indication of the coal content in marine sediments (Pearce and McBride, 1977).

Two coal samples from the Balmer seam were also analyzed to allow an estimate of coal lost during the digestion process as well as determining the ash content.

4.2.2. Sediment particle size analysis

Sediment particle size analyses were performed on the seven core samples using the wet sieve method described by Morgans (1956) to minimize the loss of particles and reduction in their grain size. The sediments were sieved into five different size fractions and then dried at 50 °C for 3 h prior to being weighed. Cumulative weight percents were plotted against grain size values to obtain an estimate of the grain size distribution in the vicinity of Westshore Terminals, as well as the degree of sediment sorting. Individual sieve fractions were examined with a microscope to determine an estimate of the fractions in which most of the coal grains occur.

4.2.3. Sediment organic/inorganic carbon and nitrogen analysis

Upon completion of the sediment particle analysis, samples were ground to less than 53 μm using a mortar mill. The organic carbon content for the various sediment size fractions was determined from the difference between total carbon content and inorganic carbon (IOC) content, with IOC content being determined by coulometric analysis.

Sediment total organic carbon (TOC) and nitrogen content for the sediment size fractions were determined using an instantaneous oxidation of the sample by 'flash combustion' and subsequent chromatographic analysis.

4.2.4. Coal settling properties analysis

A series of settling velocity experiments were performed to determine the settling characteristics of coal under various conditions in an attempt to explain the distribution of coal in the sediments surrounding Westshore Terminals. The effects of moisture and various degrees of oxidation on the hydrophobicity of the coal particles were investigated to determine the conditions under which various size fractions would float or sink, as well as to determine their settling velocities.

Coal samples from the Mist Mountain Formation were crushed using a mortar and pestle, dry sieved to the desired size fractions, and placed in sealed plastic containers. Five, 1-g samples of the smallest coal size fraction (<53 μm) were gently placed on the surface of 200 ml of seawater in open jars, and left exposed to the atmosphere for a month without agitation.

The remaining samples of the larger size fractions were divided into four subsamples. One group remained in the sealed plastic containers; the second group was placed on open aluminum foil trays at approximately 25 °C; the third group was placed in open beakers an oven at 50 °C; and the fourth group was placed in open beakers in the oven at 100 °C.

Settling velocities were determined in a 1000-ml test tube filled with 25 °C seawater by dropping individual coal particles from 8 cm above the water surface (to partially overcome surface tension), and the settling time was recorded for individual particles to settle 30 cm in the test tube. Ten trials were run for each size fraction, and an average of the trials was calculated. The number of buoyant coal particles was also recorded, as well as whether agitation was necessary to initiate particle settling. Agitation of the samples involved gently pushing the samples below the water surface with a glass rod; their displacement being factored into the settling times.

The settling velocities of the thirteen different coal size fractions of the first group of 'fresh' (least oxidized) coal samples were measured immediately, while the other three groups were allowed to oxidize for a week at temperatures of 25, 50, and 100 °C. The '100 °C' group of coal particles was returned to the oven for further oxidation and their settling properties were measured on a weekly basis for the following two weeks. Oxidation was confirmed by measuring the loss of caking ability of the coal. Because of the fine particle size, petrographic observations of the samples by light microscopy was not possible.

The densities of the coal samples (larger than 2.36 mm) were measured for the fresh, saturated, and oxidized (25, 50, and 100 °C) groups by weighing the samples in air and in toluene. Specific gravities were determined from the particles' displacement in toluene.

5. Results

5.1. Sediment coal content

The coal and organic content of the sediments, expressed as the percentage of non-hydrolyzable solids and hydrolysable solids respectively, are shown in Table 1.

Based on the sediment NHS content, the subtidal coal distribution in the area around the coal terminal is shown in Fig. 2. The area of greatest accumulation (>11%) is located directly southeast of the Pod #2 coal-loading terminal. This region of high concentration is limited to within a hundred metre radius of the loading facility, and the coal concentration diminishes rapidly to less than 1% within 700 to a 1000 m. A second region of elevated coal dust concentration (>10%) is found approximately 200 m directly south of the Pod #1 coal-loading terminal. Samples were not taken closer to Pod #1 (between stations 14 and 16) because a large coal transport ship was moored at the terminal on both sample collection dates. This region around Pod #1 is

Table 1
Sample location with average total organic carbon content and average coal content (NHS)

Sample station	Average OM content (%)	Average coal content (%)	Sample station	Average OM content (%)	Average coal content (%)
1	17.98	2.74	16	18.62	3.02
2	12.71	2.66	17	31.47	10.47
3	14.46	2.97	18	18.92	1.20
4	14.47	2.52	19	15.45	1.61
5	15.61	2.31	20	14.02	9.90
6	15.17	10.85	21	19.60	2.14
7	22.92	4.22	22	16.12	11.90
8	23.95	1.74	23	16.48	1.95
9	18.28	0.91	24	23.10	7.80
10	17.01	1.62	25	18.26	2.48
11	15.79	1.52	26	24.26	3.29
12	20.74	1.82	27	31.70	2.58
13	14.86	1.04	28 (control)	14.02	0.77
14	14.02	6.72	29 (control)	13.71	0.65
15	13.06	0.92	30 (coal)	0.12	94.89
			31 (coal)	0.77	93.41

also characterized by a high NHS concentration gradient, dropping to levels less than 1% within 500 to 1000 m. An area of moderate accumulation (1–3%) completely surrounds the coal terminal and extends outward for at least 1000 m to the north (limit of sampling), west, and east, and 800 m towards the south. Contouring of Fig. 2 south of stations 15 and 16 is based on limited data. Subtidal control samples collected at stations 28 and 29 (near the Tsawwassen ferry terminal and causeway) contained low (<0.8%) NHS concentrations.

The coal content in the sediments decreased significantly with distance from the terminal (Fig. 3).

Concentrations of hydrolysable matter, assumed to represent organic matter (OM) content, consistently exceeded the non-hydrolysable (coal) content in the sediments in each of the twenty-nine stations sampled. OM was found to compose at least 12% (by weight) of the surface sediment content on Roberts Bank, with a maximum of 31 OM at station 17 (Table 1).

The two Mist Mountain coal samples have an average of 0.44% HS. However, this apparent hydrolysable solid content most likely represents the irremovable coal residue in the test tubes upon completion of the digestion process. The coal samples were analyzed to contain an average of 94.15% NHS, with the decreased mass likely representing the ash content of the coal.

5.2. Sediment particle size

Results from the physical analysis of the sediment samples from the core samples are presented in Figs. 4–6. Subtidal grain sizes range between silt and clay to medium grained sand (<53 to >355 μm). The sediments to the north and northwest of the terminal are primarily silt and fine sand (<53 to 250 μm), while the area to the south and east is dominated by fine to medium sand (125 to 500 μm). The nearshore area adjacent to the coal terminal in the lee of the Pod #1 terminal (Core #1) is dominated by fine sediments in the silt and clay range (<63 μm).

Quartz grains dominate the sand, though a high abundance of lithic grains, shell fragments and mica also occur. Large coal fragments (up to 2 cm in diameter) occur in several of the core and grab samples, and are especially abundant in sample locations 6, 17, 20, and 22. The sediments have a moderate to poor degree of sorting and the larger grains are predominantly subangular with a moderate degree of sphericity. Both the degree of angularity and the composition of these sediments are indicative of poor to moderate chemical and physical maturity.

5.3. Sediment organic/inorganic carbon and nitrogen content

Results from the analysis of the total organic carbon (TOC) indicate that the TOC is highest in the coarser sediment size fractions (>250 μm), with a maximum of 16.8% in Core #6 (Fig. 4). TOC values in the smaller size fractions are generally less than 2%, and the lowest values occur in the 150-μm size fraction.

The inorganic carbon (IOC) values are generally less than 0.7%, with a maximum value of 1.2% occurring in the coarsest fraction (355 to 500 μm) in cores 1 and 7.

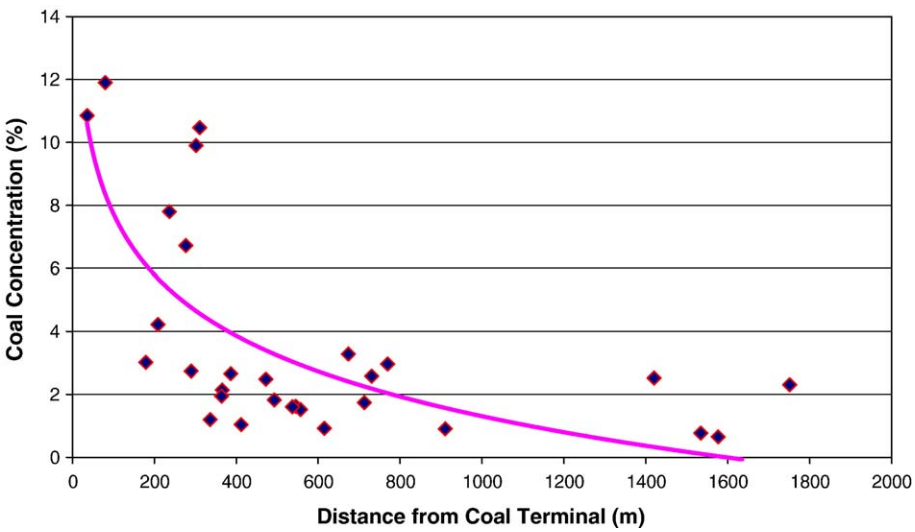

Fig. 3. Coal concentration (wt.%) with distance from the coal terminal.

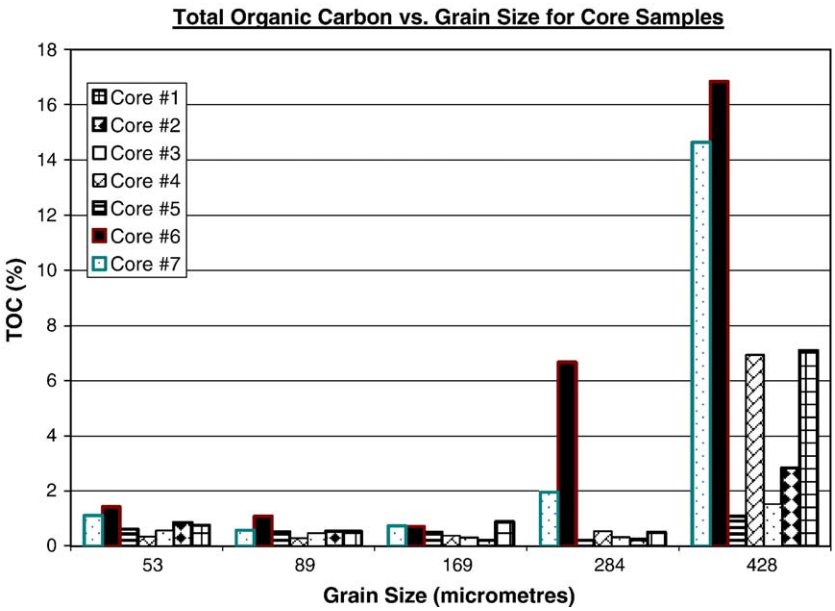

Fig. 4. Total organic carbon content vs. particle size distribution of samples for cores collected across study area (core locations are shown in Fig. 2).

Minimum values of IOC content are found to coincide with a grain size of approximately 200 μm, albeit a poor correlation.

Trends in the sediment nitrogen concentrations are found to generally conform to those of the TOC concentrations, although the nitrogen concentrations are considerably less (Fig. 5). Maximum nitrogen concentrations reached 0.34% in the largest size fraction (355 to 500 μm), while the nitrogen content in the majority of the other size fractions rarely exceed 0.10%. Minimum concentrations of approximately 0.03% nitrogen occur near the 200 μm size fraction.

A ratio between the carbon and nitrogen was plotted against the various core sample grain size fractions to determine whether or not the carbon being measured was from a terrestrial or marine source. Terrestrial carbon sources are known to generally have a higher C/N ratio than their marine counterparts (Mayer, 1994).

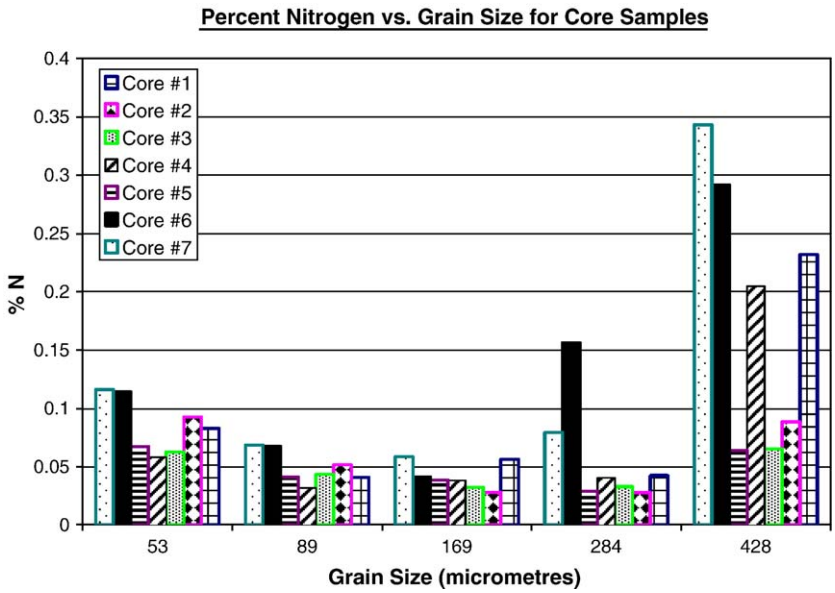

Fig. 5. Particle size distribution of samples vs. the total nitrogen content for cores collected across study area (core locations are shown in Fig. 2).

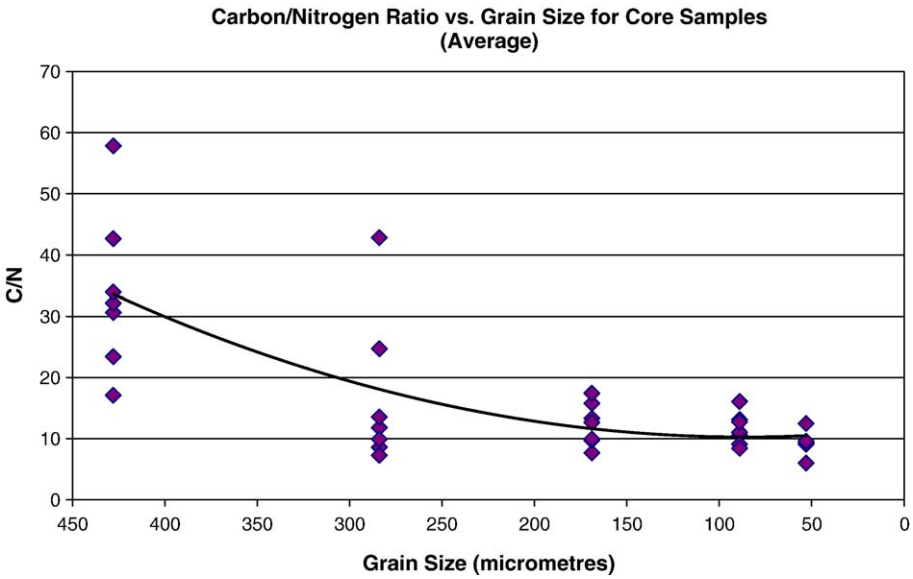

Fig. 6. Carbon to nitrogen ratio vs. grain size.

The highest C/N values occurred in the larger size fractions, and the C/N ratios generally decrease with decreasing particle size (Fig. 6). Cores 6 and 7 have the greatest C/N ratios, with a maximum value of approximately 68 for the 355 to 500 μm size fraction of Core 6. These elevated C/N values generally coincide with the maximum TOC and nitrogen values in the larger size fractions (Figs. 4 and 5), while the lowest C/N values have an approximate correlation with the minimum TOC and nitrogen values of cores 3 and 5 in the smaller size fractions. Cores 1, 2, and 4 lacked correlation between the TOC, nitrogen, and C/N values, although the same general trend can be observed.

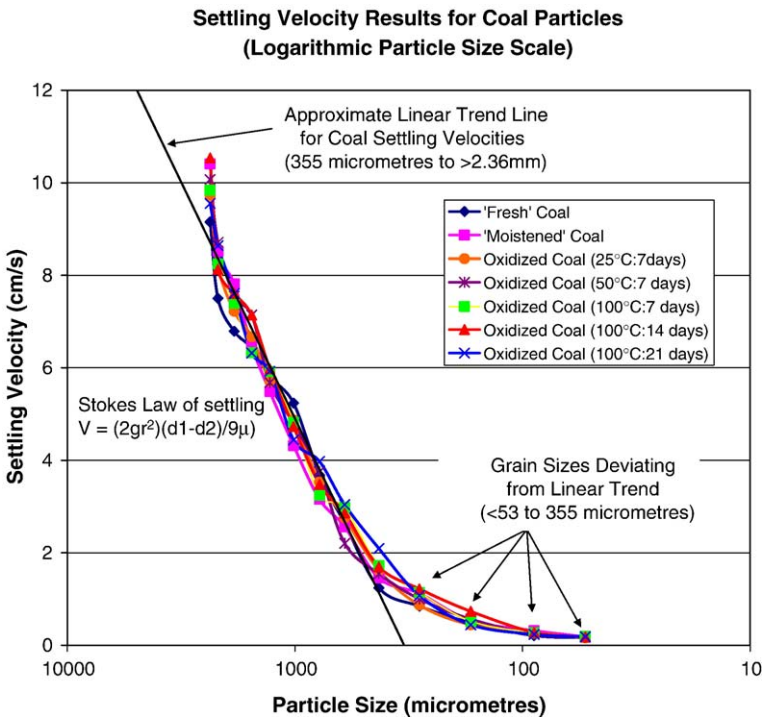

Fig. 7. Variation in coal particle settling velocity with particle size and degree of oxidation. For most particle sizes settling rates follow Stoke's Law.

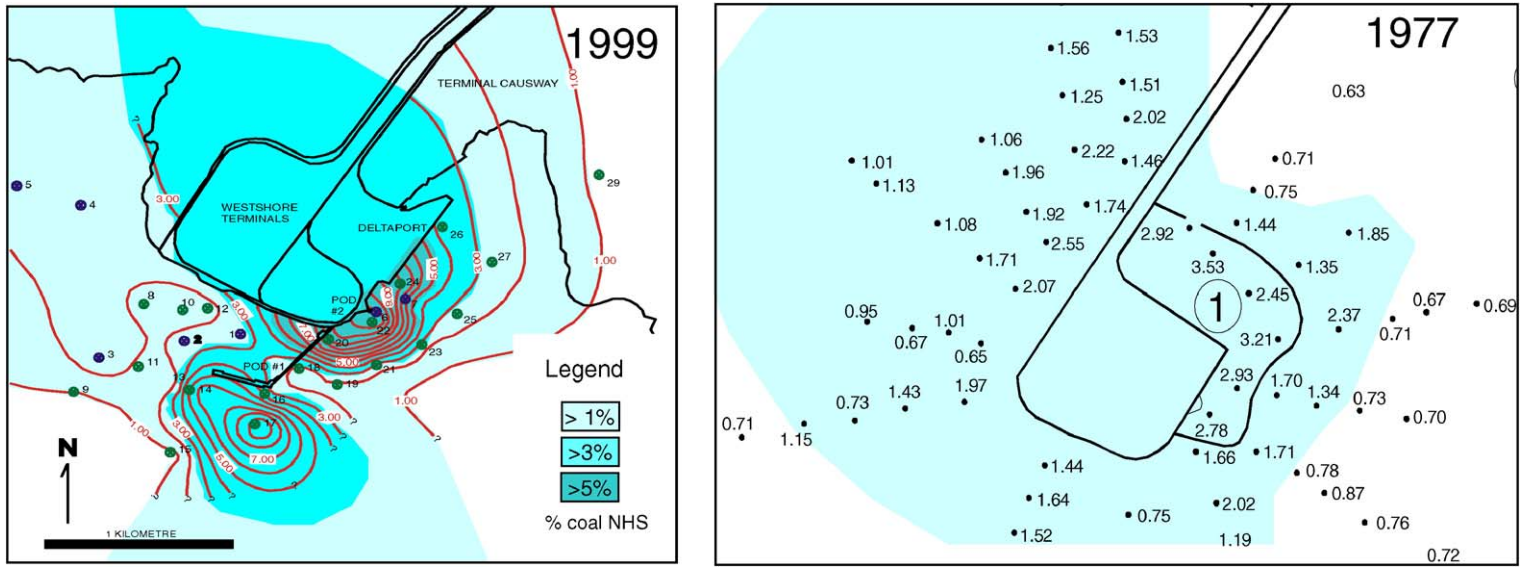

Fig. 8. Comparison of coal distribution (NHS) in 1977 and 1999 in the vicinity of the Terminal. Scale on each map is approximately the same. The aerial extent of the coal has changed little between 1977 and 1999 however the abundance of coal is markedly higher in surface sediments in 1999. The scale for both maps is the same.

5.4. Coal settling properties

The settling velocity results are presented in Figs. 7 and 8. The vast majority (>99%) of the five smallest samples (<53 μm) placed in open jars of quiescent seawater remained on the surface after a month; agglomerating into balls up to 1 cm in diameter. This agglomeration is likely the result of a weak electrostatic attraction between the fine coal particles as they also aggregate in a dry container, disintegrating only when shaken vigorously. The rest of the coal dust remained on the surface as a thin film, attesting to the hydrophobicity of the coal. The resistance to settling of the coal particles could also be due to surface tension, although one would expect this effect to be overcome when the particles were temporarily immersed in the water during vigorous shaking of the jars. Larger particles that did not settle, aggregated at the surface, even when initially separated by up to 5 cm. This attraction might be due to electrostatic forces and mutual repulsion from the water (hydrophobicity). The particles remained bound even after agitation and would settle at a greater velocity due to their combined radii.

The settling velocities of the different coal size fractions did not change significantly with oxidation, as illustrated by the similar trends in settling velocities in Fig. 7. Nonetheless, the settling velocities for the larger grain sizes (1.7 to >2.36 mm) increased slightly when the samples were moistened and exposed to various degrees of oxidation. The settling velocity for coal grains larger than 2.36 mm increased from a minimum of 9.15 cm/s ('fresh' coal) to 10.54 cm/s (100 °C: 14 days). However, exposure of the coal to 25, 50, and 100 °C oxidation conditions over the course of the experiment did not result in a consistent increase in settling velocity for the remaining grain size fractions.

As predicted by Stokes Law, the settling velocities decreased exponentially with decreasing particle size (diameter) for the majority of the grain sizes. The approximate linear trend line illustrated in Fig. 7 when the particle sizes are plotted on a logarithmic scale demonstrates this relationship. The smaller grain sizes (<53 to 355 μm) deviated from this trend, with a reduced rate of settling velocity increase with increasing particle size.

Although the settling velocities of the coal did not change significantly with oxidation, there was a consistent decrease in the size fraction where agitation was necessary. The least oxidized coal samples (based on time of exposure and confirmed by loss of caking ability) were found to have a greater proportion of particles that would float than those oxidized more thoroughly. Agitation was generally necessary for grain sizes smaller than 500 μm.

The specific gravities of the coal particles did not change dramatically under the various exposure conditions averaging 1.39±0.05 for all of the subgroups. However, the specific gravity did vary by as much as 0.10 within each group, attesting to the heterogeneity of the small coal samples.

6. Discussion and conclusion

An assessment of the benthic sediments adjacent to the Westshore Terminals coal terminal on Roberts Bank has shown that the concentrations of coal in the sediments (reported as NHS) has increased substantially since it was last investigated in 1977, having doubled from a concentration of 1.8% in 1975 to a mean concentration of 3.60% in 1999. NHS concentrations range from 0.65% in the 'background' samples 1.5 km away up to 11.90% in the immediate vicinity of the coal loading terminals. Since 1977 the main deposition of coal appears to have occurred in the vicinity of Pods #1 and 2 coal loading terminals, although limited samples were taken on the north side of the coal terminal causeway (Fig. 8). Coal concentrations in the sediments generally decrease rapidly with increasing distance from the terminal. Overall, the dispersal distance of coal has not increased over the 22-year period but rather the abundance of coal in the surface sediment within the dispersal area has increased.

The settling velocities of coal particles ranging from <53 to >2.36 mm did not change significantly with increased saturation and oxidation, although the saturated samples and those that were oxidized did settle faster in the largest size fraction (>2.36 mm). However, the proportion of buoyant coal particles decreased with increasing exposure to oxygen and temperature of heating throughout the range of coal size fractions examined, supposedly reflecting the decrease of coal hydrophobicity with increased oxidation.

Settling velocities for the coal particles in sea water analyzed in this experiment range from 0.16 to 10.54 cm/s for the <53 μm and >2.36 mm size fractions, respectively. These size fractions represent the majority of coal that could escape in the local winds (via deflation and saltation) during the loading processes and from the stockpiles themselves. Local winds average between 10–15 km/h throughout the year and attain speeds in excess of 60 km/h, especially during the winter months (Environment Canada, 1963–1990).

The regions around the coal terminal with the highest coal concentrations average depths between 5–20 m (Fig. 2). According to this experiment, the largest size

fraction (>2.36 mm) would take between 47 s and 3 min to settle 5 and 20 m, respectively. Assuming that the smallest fraction (<53 μm) would settle, it would take coal particles of this size fraction between 52 min and 21 h to settle the same depths. However, both of these calculations assume that the water column lacks any vertical or horizontal currents. Such conditions are rare at Roberts Bank, and would only occur at slack tide on an extremely calm day. The action of any currents in the water column would have drastic repercussions on the settling velocities of the coal particles, especially for the smaller size fractions. ` On Roberts Bank, normal maximum tidal currents alone can reach 0.051–0.76 m/s near Pod #1 (Canadian Hydrographic Service). In such currents the coal particles larger than 2.36 mm could travel laterally up to approximately 60 m to settle 5 m through the water column, and travel 230 m to settle 20 m. In the same currents, the smallest size fraction could travel between 4 and 96 km laterally to settle to the same depths (although it is highly unlikely that maximum tidal currents could be sustained for the 21 h necessary for 96 km of dispersal). Upwelling currents and turbulence would also contribute to the residence time of the coal particles in the water column. Furthermore, these calculations assume that the particles would settle in the first place, though the waves and currents would undoubtedly agitate the coal particles to a degree and initiate settling.

The hydrophobicity of the coal particles would result in particles staying afloat longer than assumed in the above calculations. During the sampling a thin layer of small coal particles floating on calm water approximately 200 m east of Pod #2 was observed. This film of fine coal particles was observed when there was no coal loading activities in progress, and no ship was docked.

The distribution of coal around Westshore Terminals is in agreement with the data from the analysis of the coal settling properties. The sediments that contain the highest coal concentrations are in the coarser size fractions in close proximity to the coal loading facility. The experiments studying the settling velocities of the coal particles indicate that the larger coal particles (with settling velocities of up to 10.54 cm/s) settle out within the first few hundred metres of the terminal (depending on the currents). The degree of coal oxidation would dictate which coal size fraction would readily settle, with the increasingly oxidized particles tending to settle due to their decreased hydrophobicity. The smaller particles (as well as those oxidized to a lesser degree) would float longer and take longer to settle (with minimum velocities of 0.16 cm/s) through the water column, resulting in an increased dispersal of the coal, and coincident decrease in the sediment coal content. These low concentrations would be difficult to detect using the hydrolysis method of this study.

Benthic flora and fauna, which are most susceptible to coal dust coverage and possible anoxic conditions that might arise due to the oxidation of the coal, would likely only be affected on sediments within very close proximity (0–300 m) to the coal loading terminals at pods #1 and 2. Creatures dwelling further away would unlikely experience coal concentrations sufficient to blanket the bottom (thereby decreasing insulation) and give rise to anoxic conditions in the upper sediments. Furthermore, in all of the sediments sampled in this study, the hydrolysable organic matter content of the sediments ranged between one-and-a-half to 20 times the coal content (NHS) of the sediments. If anoxic conditions were to arise, they would likely be the result of the natural organic detritus rather than the coal content. Inspection of the sediments around Westshore Terminals failed to reveal any evidence of anoxic conditions in the upper sediments. If anoxic conditions did prevail, the sediments (at a variable depth below the sediment–water interface, depending on the degree of oxidation) would be expected to have a dark (black) coloration and pungent aroma. Such characteristics would reflect a reducing environment in which bacterial degradation of the organic matter (as well as the activities of detritivores) was inhibited by a lack of oxygen.

The benthic creatures dwelling in the sediments adjacent to the coal terminal would more likely be adversely affected by the alteration of their habitat through changes in the physical nature of the substrate such as size, weight, particle shape, porosity, permeability, and stability of the sediments (Pearce and McBride, 1977) due to the dredging operations in the area.

Though this report does not directly address the amount of suspended solid levels (i.e. coal) in the waters around Westshore Terminals, Shelton (1971) documented the effects of dumping annually 6.2 million metric tonnes of fine coal, fly ash and other colliery wastes off the north coast of England. Investigations demonstrated that the growth of periphytic (attached) algae was inhibited by the reduction of light penetration from increased levels of suspended solid load, adversely affecting the fauna associated with the attached algae. While the volume of coal dust settling on Roberts Bank is undoubtedly much less than that documented by Shelton (1971), the study does indicate the effects of suspended coal levels may have on marine flora and fauna.

Acknowledgements

The authors acknowledge the financial support of the Natural Sciences and Engineering Council, Canada.

References

Butler, T.H., 1972. Interim report on the occurrence of coal in bottom sediments from Roberts Bank. Manuscript Report of the Fisheries Research Board of Canada. 7 pp.

Butler, T.H., Longbottom, M.R., 1970. The determination of organic matter in marine muds: the effect of the presence of coal in the routine determination of protein. Journal of Marine Biological Ecology 5, 158–169.

Department of Fisheries and Environment Canada, 1978. Roberts Bank Port Expansion: A Compendium of Written Submissions to the Environmental Assessment Panel. 463 pp.

Environment Canada, 1963–1990. Environment Canada Wind Data Analysis for Tsawwassen Ferry Terminal. Queens Printer, Government of Canada, Vancouver, 13 pp.

Environment Canada and Fisheries and Oceans Canada, 1995. The Fraser Fishery: A Valuable Resource-Fact Sheet. Fraser River Action Plan. Vancouver, British Columbia.

Federal Environmental Assessment Review Office, 1979. Report of the Environmental Assessment Panel: Roberts Bank Port Expansion. 75 pp.

Fraser River Estuary Management Program, 1989. Proceedings from the Third Annual Fraser River Estuary Workshop On Monitoring And Research. Walton, D.G. (Chairman). February, 1989. 57 pp.

Fraser River Estuary Management Program, 1990a. Port/Industrial Land Supply and Demand Study. Port/Industrial Land Development Activity Work Group. 100 pp.

Fraser River Estuary Management Program, 1990b. Potential surface water contamination from miscellaneous sources in the Fraser River Estuary. In: Hagen, M.E. (Ed.), Waste Management Activity Program Working Group Report. December, 23 pp.

Fraser River Estuary Management Program, 1991a. A Recommended Port and Industrial Development Strategy. Port and Industrial Development Activity Work Group. February, 45 pp.

Fraser River Estuary Management Program, 1991b. Navigation, dredging and environment in the Fraser river estuary. Navigation and Dredging Workshop Report. 89 pp.

Fraser River Estuary Management Program, 1993. Compilation and Interpretation of Data on Contaminant Concentrations in Fraser River Estuary Sediments. Anderson, B.E., Technical Report WQWM 93-03. 46 pp.

Fraser River Estuary Management Program, 1994. An Estuary Management Plan for the Fraser River: A Living Working River. 113 pp.

Fraser River Estuary Management Program, 1996. Environmental Quality Report. October, 164 pp.

Fraser River Estuary Management Program, 1997. An Estuary Management Plan for the Fraser River: A Living Working River (1997 Update). 28 pp.

Luternauer, J.L., 1974. Geology. In: Hoos, L.M., Packman, G.A. (Eds.), The Fraser River Estuary: Status of Environmental knowledge to 1974. Special Estuary Series, vol. 1. Environment Canada, pp. 10–29. 517 pp.

Luternauer, J.L., Murray, J.W., 1973. Sedimentation on the western delta front of the Fraser River, British Columbia. Canadian Journal of Earth Sciences 10, 1642–1663.

Mayer, L.M., 1994. Surface area control of organic carbon accumulation in continental shelf sediments. Geochimica et Cosmochimica Acta 58 (4), 1271–1284.

Morgans, J.F.C., 1956. Notes on the analysis of shallow water soft substrata. Journal of Animal Ecology. Vol.25: pp376–387 *in* Pearce, B.C., and McBride, J., 1977. A Preliminary Study on the Occurrence of Coal Dust in Roberts Bank Sediments and the Effect of Coal Dust on Selected Fauna. Fisheries and Marine Service Technical Report No. PAC/T-77-17. 25 pp.

Pearce, B.C., McBride, J., 1977. A preliminary study on the occurrence of coal dust in Roberts Bank Sediments and the effect of coal dust on selected fauna. Fisheries and Marine Service Technical Report No. PAC/T-77-17. 25 pp.

Shelton, R.G.J., 1971. Some effects of dumped, solid wastes on marine life and fisheries. North Sea Science, NATO North Sea Science Conference. Aviemore, Scotland, November 15–20th. Ed. Edward D. Goldbury *in* Pearce, B.C., and McBride, J., 1977. A Preliminary Study on the Occurrence of Coal Dust in Roberts Bank Sediments and the Effect of Coal Dust on Selected Fauna. Fisheries and Marine Service Technical Report No. PAC/T-77-17. 25 pp.

Westshore Terminals Administration Department, 1998. Application for Dredging Permit submitted to FREMP on October 11, 1998. 10 pp.

Available online at www.sciencedirect.com
ScienceDirect
Mutation Research 630 (2007) 42–49
Genetic Toxicology and Environmental Mutagenesis
www.elsevier.com/locate/gentox
Community address: www.elsevier.com/locate/mutres

Genotoxic effects in wild rodents (*Rattus rattus* and *Mus musculus*) in an open coal mining area

Grethel León [a], Lyda Espitia Pérez [a], Juan Carlos Linares [b], Andreas Hartmann [c], Milton Quintana [a,*]

[a] *Laboratorio de Investigación Biomédica y Biología Molecular, Universidad del Sinú, Campus Elías Bechara Zainúm, Calle 38 Cra.1W Barrio Juan XXIII, Montería, Córdoba, Colombia*
[b] *Departamento de Biología, Universidad de Córdoba, Colombia*
[c] *Novartis Pharma AG, Basel, Switzerland*

Received 28 December 2006; received in revised form 16 February 2007; accepted 26 February 2007
Available online 1 March 2007

Abstract

Coal is a mixture of a variety of compounds containing mutagenic and carcinogenic polycyclic aromatic hydrocarbons. Exposure to coal is considered as an important non-cellular and cellular source of reactive oxygen species that can induce DNA damage. In addition, spontaneous combustion can occur in coal mining areas, further releasing compounds with detrimental effects on the environment. In this study the comet assay was used to investigate potential genotoxic effects of coal mining activities in peripheral blood cells of the wild rodents *Rattus rattus* and *Mus musculus*. The study was conducted in a coal mining area of the Municipio de Puerto Libertador, South West of the Departamento de Cordoba, Colombia. Animals from two areas in the coal mining zone and a control area located in the Municipio de Lorica were investigated. The results showed evidence that exposure to coal results in elevated primary DNA lesions in blood cells of rodents. Three different parameters for DNA damage were assessed, namely, DNA damage index, migration length and percentage damaged cells. All parameters showed statistically significantly higher values in mice and rats from the coal mining area in comparison to the animals from the control area. The parameter "DNA Damage Index" was found to be most sensitive and to best indicate a genotoxic hazard. Both species investigated were shown to be sensitive indicators of environmental genotoxicity caused by coal mining activities. In summary, our study constitutes the first investigation of potential genotoxic effects of open coal mining carried out in Puerto Libertador. The investigations provide a guide for measures to evaluate genotoxic hazards, thereby contributing to the development of appropriate measures and regulations for more careful operations during coal mining.
© 2007 Elsevier B.V. All rights reserved.

Keywords: Genotoxicity; Coal dust; Rodents; Comet assay

1. Introduction

The mining of coal is an activity with a high potential for pollution of the environment. Coal has been described as the most significant pollutant of all fossil energy sources containing important polluting compounds as sulfur dioxide and its derivatives [1]. The activities of stripping of coal liberate large quantities of pollutants into the atmosphere. In addition, ashes and products of liquefaction and combustion of coal contain polycyclic aromatic hydrocarbons (PAH), which constitute a significant risk to the environment. Several of these PAH

* Corresponding author. Tel.: +57 4 7841961; fax: +57 4 7841961.
E-mail address: quintanaso@yahoo.com (M. Quintana).

1383-5718/$ – see front matter © 2007 Elsevier B.V. All rights reserved.
doi:10.1016/j.mrgentox.2007.02.007

exhibit well-known mutagenic and carcinogenic activity, and therefore, more rigorous control measures have been established by international organizations with regards to the presence of coal in the environment [2].

Colombia possesses the biggest natural reserves of coal in Latin America and it is the fifth biggest exporter of thermal coal in the world. The mining region of the Atlantic Coast, conformed by the departments Guajira, Cesar and Córdoba, produces 90% of the thermal coal of the country that in turn corresponds to 98% of the national coal resources [3]. The carboniferous area of the Departamento de Córdoba is located the South West, in the Municipio de Puerto Libertador, Alto San Jorge. The coal mined in the area is classified as sub-bituminous, of low quality and caloric power, with a content of total sulfur of 1.31%. Coal it is openly mined, with middle-sized mining systems, meaning that although more advance technology exists stripping of the material is conducted with a minimum degree of environmental surveillance. The operations carried out in Puerto Libertador consist of two activities: stripping (extraction of coal) and crushing (mincing of coal for transporting) which have been acknowledged to release fugitive particles into the environment [4]. For example, stripping of coal releases significant quantities of potentially toxic substances into the atmosphere where they constitute complex mixtures [5]. The exposure to a combination of compounds is considered to present a higher health risk due to potential synergistic effects of the resulting mixture [6]. Once in the environment pollutants resulting from coal mining have the potential to penetrate into water sources of the biota or into the atmosphere in significant amounts, thus presenting potential hazards for the environment and human health [7]. The pollution resulting from coal mining and the potentially genotoxic effects on organisms have been investigated using bacteria [8], earthworms [9], fish [10], plants [11], rodents [12,13] and human cells [8,14].

The comet assay is recognized as one of the most sensitive methodologies available for DNA damage detection [15], and is distinguished by being simple, fast, and effective, especially for small samples sizes and is applicable to cells from virtually any organ of eukaryotic organisms [16]. The comet assay has several advantages over other in vivo genotoxicity test methods as cytogenetic evaluations, such as the micronucleus test or the chromosome aberration assay applicable to proliferating cells only. However, there are relatively few limitations of the comet assay, very short lived primary DNA lesions, such as single-strand breaks, which may undergo rapid DNA repair could be missed when using inadequate sampling times. However, an appropriate study design should ensure that these lesions are captured at higher dose levels, at which DNA repair may be significantly slowed down or even overwhelmed [17].

The aim of the present study was to evaluate genotoxic effects of coal mining activities on two species of rodents (rat, *Rattus rattus* and mouse, *Mus musculus*) using the comet assay. The studies demonstrate that this test system is a useful tool to assess environmental genotoxicity in polluted areas and demonstrate the importance of such investigations to assess environmental hazards resulting from open coal mining.

2. Materials and methods

2.1. Sampling procedures

The study on the rodent populations was started in August 2005 and it continued until March of the 2006. Each of the field work phases consisted of a period of 15 days, during which the animals were captured and slide preparation for the comet assay was carried out. The capture of the animals was authorized by the CVS (the official Cordoba's environmental protection agency). The procedure for obtaining the different species of rodents was the capture-removal method, which means that the captured animals were not returned to their place of origin. For the capture of the animals three areas were selected, two located inside the area of coal mining in the Municipio de Puerto Libertador (Departamento de Córdoba, Colombia) and a third area located in the Municipio de Lorica (Departamento de Córdoba, Colombia) approximately to 151 km of the mining area. The later served as a control area to investigate animals that were not exposed to residuals of the mining of coal (Fig. 1). The two areas inside the coal mining area consisted of a stripping zone and crushing zone. Animals were trapped using 60 medium-size Sherman traps located in each of the three designated areas. Each group of traps was posted in the designated area between 05:00 and 06:00 pm and picked up the following day between 06:00 and 07:00 am.

No previous records on the diversity and density of wild rodents in the region were available. Therefore, the species for this study were only chosen after the captures. Three criteria were established: the distribution range (that the two species were present in both areas), populational density (sufficient individuals to ensure a meaningful sample size of each species) and sympatry. Based on these criteria and on the results of the captures, two species of wild rodents were chosen: rat (*R. rattus*) and mouse (*M. musculus*) which are species that are commonly used in genotoxicity testing, and well-known as species with peridomestic habits. The captured animals were anesthetized to facilitate the blood sampling and recording of morphometric data. Peripheral blood of the animals was obtained from tail pricks with the help of capillaries.

In parallel to the collection of the animal blood samples additional samples of human blood by finger pricks were collected and processed under the same conditions. These samples

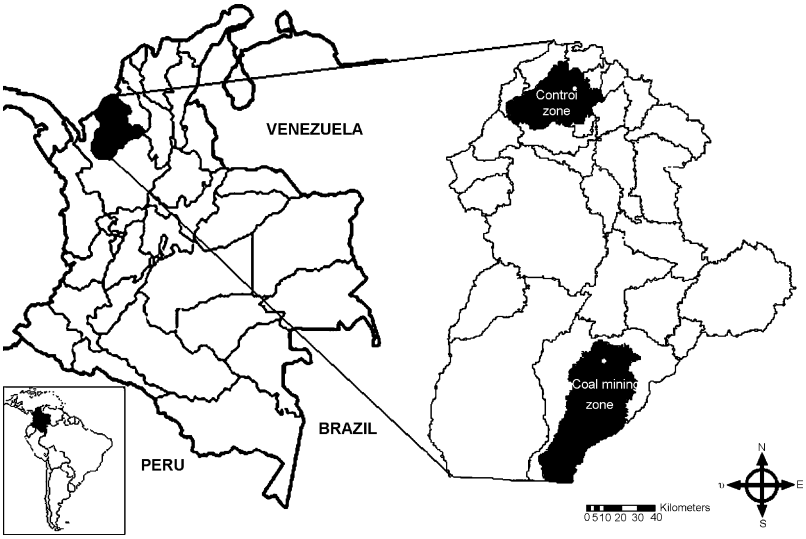

Fig. 1. Geographic localization of sampling areas: Puerto Libertador (coal mining area) and Lorica (control area).

were used as internal standards to allow for the detection of potential confounding factors that may have been caused by sample handling or transportation to the laboratory.

2.2. Comet assay

Prior to the initiation of the field study, the comet assay procedure was established in the laboratory using whole blood samples from healthy volunteers. For this purpose, samples were treated for 2 h with methyl methanesulfonate (MMS, Sigma) at 1×10^{-5} M in Hank's balanced salt solution (HBSS, Sigma). For negative control samples whole blood in HBSS was used. The samples were incubated for 2 h at 37 °C. This concentration was used to demonstrate different levels of damage and the sensitivity of the electrophoresis and test conditions used.

The comet assay was carried out according to of the original methodology (alkaline version) described by Singh et al. [18] with modifications. Additional modifications for field work were integrated [12]. For the preparation of the samples, 5 μl of whole blood were mixed with heparin and 120 μl of low melting point agarose (LMA)(Invitrogen) at 37 °C. This mixture was placed in a slide previously covered with 1.5% of normal melting point agarose (NMA) (Cambrex Bioscience Rockland) processed at 60 °C. The mixture of LMA and blood on the slide was covered with a cover slip. After solidifying of the gel on the slides, the cover slip was removed and the slides were immersed in lysis solution (2.5 M NaCl, 100 mM EDTA and 10 mM Tris, pH 10.0–10.5, 1% with freshly added 1% Triton X-100 and 10% DMSO) at 4 °C. The slides remained for two weeks in this solution until transport to the laboratory where they were further processed. Direct light exposure of the samples was avoided during the whole process. The slides were removed of lysis solution and placed for 30 min close to the anode of an electrophoresis box containing alkaline buffer at 4 °C (300 mM NaOH and 1 mM EDTA, pH > 13). The electrophoresis was carried out for 30 min at 25 V and 300 mA. Afterwards the alkalinity was neutralized with 0.4 M Tris (pH 7.5) with washes of 5 min for each slide. Finally, the DNA was stained with ethidium bromide solution (2 μl/ml) and assessed using a fluorescence microscope equipped with a green filter of 540 nm.

For each sample images of 100 randomly selected cells (50 cells from each of two replicate slides) were analyzed from each animal. DNA migration length (nuclear region plus tail) were measured in microns (μm) using the Motic® Images 2000 software version 1.2. In addition, the cells were classified according to tail size into five classes ranging from undamaged (0) to maximally damaged (4) (Fig. 2), obtaining a measure of the individual damage for each animal and consequently for each analyzed group. The calculation of the damage index was car-

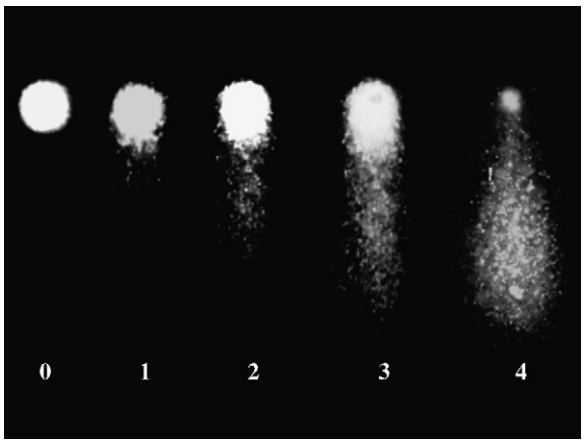

Fig. 2. Visual DNA damage classification of the nuclei in the range of 0–4.

Table 1
Average values of DNA damage index, DNA migration length and percentage damaged cells of controls and cultures treated with methyl methanesulfonate (MMS)

DNA damage parameter	Average value of four experiments [range]	
	Control (HBSS)	MMS (10^{-5})
Migration length (μm)*	21.5 [18.1–25.0]	42.7 [33.5–48.6]
Damage index*	70.3 [47–94]	134 [94–181]
Percentage damaged cells*	41.8 [34–50]	49.0 [42–61]

* Average of four independent experiments per data point, mean of 100 cells per experiment.

ried out according to the visual classification system [15]. The values for the damage index can range from 0 (100 cells class 0) up to 400 (100 cells class 4). Similarly, the frequencies of damaged cells were calculated for each one of the areas under investigation. This parameter was based on the number of cells with tail versus number of cells without tail. Statistical analysis of the data was conducted by means of the variance analysis using the statistical software SPSS (version 12.0) with a level of established significance ($\alpha = 0.05$). The statistical test used in these hypothesis tests (significance in the values of each area) was the *F*-test (Fisher).

3. Results

Prior to conducting the field study, the comet assay procedure was established in our laboratory. In order to demonstrate that a genotoxic effect can be detected by the procedure and results are reproducible, human blood samples were treated with saline solution or 10^{-5} M methyl methanesulfonate (MMS). The results of four independent experiments (average values of the four experiments and range) are shown in Table 1. The results demonstrate that a genotoxic effect was reproducibly identified in each of the independent experiments. While the parameters "DNA migration length" and "DNA Damage Index" found to sensitively demonstrate the induction of genotoxicity by MMS, the parameter "Percentage Damaged Cells" was less sensitive.

In the field study, a total of 22 rodents were investigated in the open mining areas of which 10 were trapped in the crushing zone and 12 inside the stripping zone. In total, 7 males and 5 females mice (*M. musculus*) and 5 males and 5 females rats (*R. rattus*) were investigated. In the control area five rats (two males, three females) and four mice (two males, two females) were investigated. During the field studies, additional finger-prick samples of human blood were taken in parallel to the animal samples and were used as internal controls. These controls were included into every electrophoresis run to assure acceptable levels of DNA damage. The values for DNA damage of animal samples were considered acceptable

Table 2
Average values of DNA damage parameters of mice and rats from coal mining and control areas

Species	Area	*n*[a]	Gender	DNA damage index[b,c]	DNA migration length (μm)[b,c]	Percentage damaged cells (%)[b,c]
M. musculus	Crushing	3	Female	197.6 ± 61.4	28.3 ± 3.2	71.0 ± 21.0
		3	Male	212 ± 42.5	29.5 ± 10.1	90.6 ± 14.4
	Stripping	2	Female	195 ± 77.7	20.4 ± 1.4	48.0 ± 7.0
		4	Male	186 ± 19.2	28.9 ± 4.2	77.2 ± 18.7
	Control	2	Female	38.0 ± 29.6	11.8 ± 1.7	16.5 ± 10.6
		2	Male	12.5 ± 3.5	14.0 ± 4.2	12.0 ± 2.8
R. rattus	Crushing	3	Female	188 ± 77.1	34.1 ± 10.6	76.0 ± 18.5
		3	Male	221 ± 56.4	31.1 ± 9.0	71.0 ± 16.0
	Stripping	2	Female	191 ± 31.8	17.0 ± 4.1	84.0 ± 5.6
		2	Male	208 ± 45.9	53.0 ± 9.7	27.2 ± 5.6
	Control	3	Female	90.6 ± 37.0	16.2 ± 5.0	40.6 ± 1.2
		2	Male	69.5 ± 19.0	16.3 ± 3.0	37.5 ± 3.5

[a] Number of animals per group.
[b] Average values of 100 cells per animal.
[c] Average value ± standard deviation.

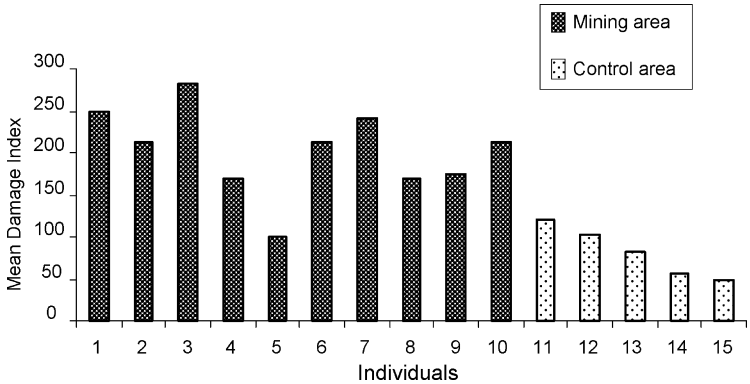

Fig. 3. Individual DNA damage index values for rats from coal mining areas and control area.

when the following values were achieved with the finger-prick samples—DNA damage index: 100 ± 59.1; DNA migration length: 17.7 ± 14.0 μm; percentage damaged cells: 49.0 ± 38.1.

Table 2 summarizes the mean values of all animals investigated from the crushing, stripping and control areas. The average values and standard deviations are presented for damage index, migration length, and the percentage of damage cells. Mice as well as rats from both coal mining areas presented clearly higher values for DNA damage compared to animals from the control area. The values obtained for the crushing and stripping areas were comparable for each parameter; however, the difference between the two mining areas was not statistically significant. When comparing the different DNA damage parameters, it is obvious that the parameter "DNA Damage Index" showed the clearest separation between animals from the mining areas and the control area. As this parameter was found the most sensitive for the indication of a genotoxic effect in rodents, values for the "DNA Damage Index" of the individual animals are presented in Figs. 3 and 4. This comparison clearly demonstrates higher levels of DNA damage in individuals of both species from the coal mining areas compared to the control area. The differences between the "DNA Damage Index" for mining and control zone were statistically significant.

It is interesting that all mice from the coal mining areas exhibited clearly higher DNA damage values when compared to the controls. As for rats, there was one individual animal from the coal mining area showing a DNA damage value which was comparable to control area values. Such a clear separation between the mining and control areas was not observed for the parameters "DNA Migration Length" or "Percentage Damaged Cells" (individual data not shown). In spite of this, difference between males and females were not significant. Fig. 5 compares the average group parameters for both species from the mining and control areas. The statistical analysis shows that all parameters for DNA damage measured in the animals from the coal mining areas were significantly elevated above the respective controls.

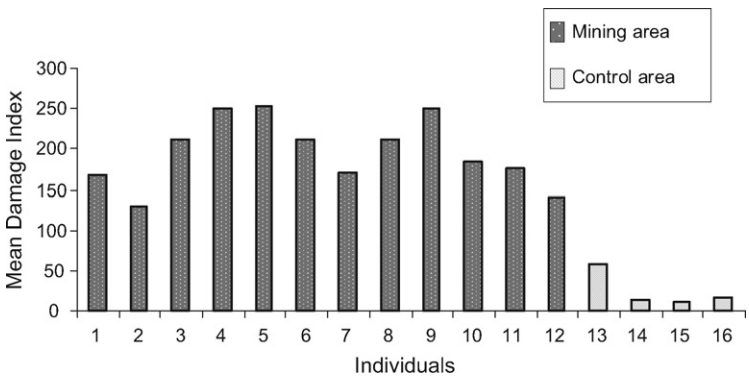

Fig. 4. Individual DNA damage index values for mice from coal mining areas and control area.

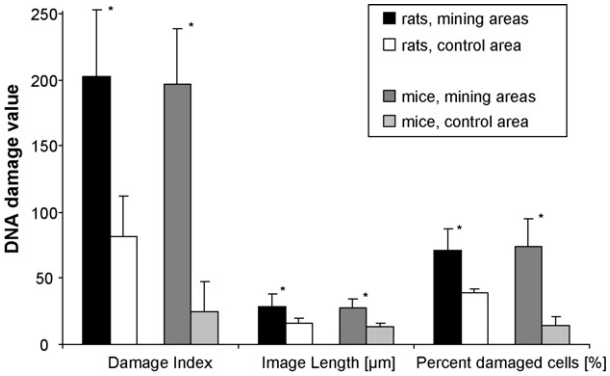

Fig. 5. Comparison of average group values and standard deviations of mice and rats from coal mining and control areas. Asterisk (*) indicates statistically significant difference of average group mean vs. control.

4. Discussion

Coal is a heterogeneous mixture of more than 50 elements, including oxides and other elements as silica, PAH, heavy metals and ash. During the processes of coal extraction, large amounts of these substances can be liberated to the atmosphere, where they constitute complex mixtures. Complex mixtures have been considered to present a significant risks for health taking into account potential synergistic effects cause by combination of individual compounds [6]. Only a few studies in mammals have been conducted to assess the environmental mutagen hazards of coal and complex mixtures that it forms with other substances [12,13,19,20]. In the present study, wild rodents were investigated for the potential genotoxicity of exposure to coal. We applied the comet assay to compare the extent of primary DNA damage in peripheral blood cells of rodents from areas subject to open coal mining activities and a control area.

The data clearly demonstrate that mice and rats originating from the coal mining area exhibited a significantly higher extent of DNA damage as assessed by length of DNA migration, damage index and percentage of damaged cells compared to animals from a non-polluted control area. The parameter "DNA Damage Index" was found to best demonstrate a difference between the control and mining area groups. A more pronounced difference in average DNA damage index was observed in mice compared to rats: while the DNA damage index in mice from the mining area was approximately 8-fold higher than that of mice from the control area, the difference between the rat populations was only 2.5-fold. This difference between the species may in part be explained by the comparatively low baseline value in mice from the control area. Although underlying mechanisms for the difference were not investigated and samples from animals under controlled conditions (e.g., laboratory studies) were not available, a potential cause for the interspecies difference may be differences in DNA repair mechanisms.

In contrast, the extent of the DNA damage index found in mice and rats from the coal mining area were comparable. This observation may point towards a difference in baseline DNA damage values in the species investigated. However, it has to be emphasized that the total number of both, rats and mice investigated from the control area is rather limited and the use of a larger number of individuals may result in more similar baseline values in both species. Besides the DNA damage index, the parameters "Percentage Damaged Cells" and "Migration Length" also showed a statistically significant difference in the average values between the groups from the mining and control areas. The parameter "Percentage Damaged Cells" is considered a simple method for the collection of comet assay data and can easily be compared between laboratories [21].

The rodent species investigated in the mining area are subject to exposure due to different mining activities, specifically, stripping and crushing of coal. The first activity includes the extraction of rocks and transportation to the crushing machines. During the crushing procedure, coal is processed into small particles in order to enable transportation. These activities are liberating great quantities of fugitive particles into the environment which contain ashes including PAHs and toxic gases [4]. During the crushing process of the coal large quantities of coal dust particles can be spread into the surrounding environment and they are deposited on the surfaces of the plants or in river beds. Results similar to ours were obtained in a biomonitoring study conducted in a carboniferous areas using wild rodent species *Ctenomys torquatus* [12]. The study investigated micronucleus and comet formation in areas of coal mining and showed elevated DNA and chromosomal lesions in peripheral blood cells of rodents. Other species have been used as well to study genotoxic and toxic effects of coal mining. Using the comet assay, increased DNA damage was observed in liver and blood cells of fish exposed to wastewaters from coal mining areas [22]. Other environmental studies include the evaluation of genotoxicity of rodents exposed to coal dust and diesel emissions [19], the evaluation of carcinogenic effects from emissions of mines and plants of coal [20], and the effects of coal ashes on the lungs of guinea pigs [13]. In addition, in vitro investigations have demonstrated hazardous effects of coal and its derivatives [23,24]. Significant inter-individual differences were observed in all populations of rats and mice of our study. While the variability in rat populations

from both areas was comparable, the inter-individual difference in mice was much higher in the polluted compared to the control area. This observation may indicate differences in the individual exposure of mice to genotoxic agents or may point towards different amounts of toxicants in the coal mining area.

The mined coal of Puerto Libertador, Córdoba, is classified as sub-bituminous and is characterized by a low content of carbon. This type is expected to undergo reactions of spontaneous combustion to a significantly higher degree as compared to other classes of coal. Indeed, upon processing of coal into finer particles by a crushing process, the exposure to ambient oxygen and the sun can result in a combustion process within the stored material. A further source of environmental pollution is the processing of coal which releases significant amounts of fine particles into the surrounding environment. The results obtained indicate the presence of a genotoxic hazard towards the rodent populations in the coal mining area, however, in this type of study is a complicated task mainly because of the relatively low levels of genotoxicants and the existence of multiple potential genotoxic pollutants often encountered as complex mixtures [16]. The interactions between these genotoxicants and the organism's DNA can lead to a variety of damage [25]. The detected DNA damage in the comet assay in rodents residing in close proximity to coal mines is thought to be attributed to coal or its by-products; however, other environmental factors (water, other genotoxicants) cannot be totally ruled out since these factors were not controlled for in the present study design.

The comparatively high average DNA damage values in samples of rodents from the coal mining area may point towards the type of DNA lesions induced in the animals. The comet assay is particularly sensitive towards direct and indirect DNA strand breakage and alkaline–labile sites in the DNA. These types of DNA damage are usually induced by most of the genotoxic agents [26], which induce breaks in the phosphodiester skeleton or between bases and sugars of the DNA resulting in abasic sites. It is known that coal mining activities liberate significant quantities of fugitive particles and toxic gases as sulfur dioxide into the environment [4]. Therefore, the large extent of DNA damage observed in the present study may be related to oxidative damage caused by reactive substances contained in the coal, such as iron and sulfur [24]. In addition, since large amounts of mutagenic compounds, such as PAHs derived from coal combustion products are liberated into the atmosphere [2], DNA adduct formation by PAH is likely an important contributing to the high extent of DNA damage observed.

In conclusion, the results obtained in our study demonstrate that coal mining activities in Puerto Libertador–Córdoba-Colombia present a genotoxic hazard to wild rodents. The two species investigated were shown to be sensitive and suitable to investigate environmental genotoxicity caused by coal mining activities.

Acknowledgements

We thank very cordially Dr. Juliana Da Silva to guide us along of this study, Carbones del Caribe Company S.A. for the financial support to this work, Juan Carvajal, Harold González, Raúl Pedroza, Alvaro Miranda and Ronald Ayazo for their great help during the field work.

References

[1] S.F. Zakrewski, Principles of Environmental Toxicology, American Chemical Society, Washington, DC, 1991, p. 270.

[2] M.C.R. Peralba, Caracterização química dos hidrocarbonetos de betumes de carvões sul-brasileiros, in: Dissertação de Doutorado, Instituto de Física e Química de São Carlos, USP, 1990, 126 pp.

[3] UPME, Unidad de Planeación Minero Energética, Plan de expansión de referencia generación–transmisión (Versión preliminar), vol. 2019 (2005) p. 148, www.upme.gov.co.

[4] Carbones del Caribe S.A., Plan de Manejo Ambiental, Flanco Occidental del Sinclinal del Río San Pedro Módulo D (Wenceslao), Departamento de Planeación, 1996.

[5] C. Stephens, M. Ahern, Worker and Community Health impacts related to mining operations internationally: a rapid review of the literature, Mining, Minerals and Sustainable Development Project (MMSD), Institute for Environment and Development (IIED), World Business Council, for Sustainable Development (WBCSD), 2001, p. 59.

[6] L.A. Gold, B.N. Ames, Too many rodent carcinogens? Science 249 (1990) 970–997.

[7] Managing coal combustion residues in mines, Committee on Mine Placement of Coal Combustion Wastes, National Research Council, ISBN: 0-309-65889-6, (2006) p. 300.

[8] J.C. Kleinjans, Y.M. Janssen, B. van Agen, G.J. Hageman, J.G. Schreurs, Genotoxicity of Coal Fly Ash, Assessed In Vitro in *Salmonella typhimurium* and human lymphocytes, and in vivo in an occupationally exposed population, Mutat. Res. 224 (1989) 127–134.

[9] L. Verschaeve, J. Gilles, Single cell gel electrophoresis assay in the earthworm for the detection of genotoxic compounds in soils, Bull. Environ. Contam. Toxicol. 54 (1995) 112–119.

[10] R. Pandrangi, M. Petras, S. Ralph, M. Vrzoc, Alkaline single cell gel (comet) assay and genotoxicity monitoring using bulheads and carp, Environ. Mol. Mutagen. 26 (1995) 345–356.

[11] G. Naidoo, D. Chirkoot, The effects of coal dust on photosynthetic performance of mangrove *Avicennia marina* in Richards Bay, South Africa, Environ. Pollut. 127 (2004) 359–366.

[12] J. Da Silva, T.R.O. De Freitas, V. Heuser, J. Marinho, B. Erdtmann, Genotoxicity biomonitoring in coal regions using wild rodent *Ctenomys torquatus* by Comet Assay and Micronucleus Test, Environ. Mol. Mutagen. 35 (2000) 270–278.

[13] L.C. Chen, H.F. Lam, E.J. Kim, J. Guty, M.O. Amdur, Pulmonary effects of ultrafine coal fly ash inhaled by guinea pigs, Toxicol. Environ. Health 29–32 (1990) 169–184.
[14] W.Z. Whong, R. Long, R.G. Ames, T. Ong, Role of Nitrosation in the mutagenic activity of coal dusts: a postulation for gastric carcinogenesis in coal miners, Environ. Res. 32 (1983) 298–304.
[15] A.R. Collins, V.L. Dobson, M. Dusinská, G. Kennedy, R. Štetina, The comet assay: what can it really tell us? Mutat. Res. 375 (1997) 183–193.
[16] C.L. Mitchelmore, J.K. Chipman, DNA strand breakage in aquatic organisms and the potential value of the comet assay in environmental monitoring, Mutat. Res. 399 (1998) 135–147.
[17] A. Hartmann, M. Schumacher, U. Plappert-Helbig, P. Lowe, W. Suter, L. Mueller, Use of the alkaline *in vivo* Comet assay for mechanistic genotoxicity investigations, Mutagenesis 19 (2004) 51–59.
[18] N.P. Singh, M.T. MCcoy, R.R. Tice, E.L. Schneider, A simple technique for quantitation of low levels of DNA damage in individuals cells, Exp. Cell Res. 175 (1988) 184–191.
[19] T. Ong, W.Z. Whong, J. Xu, B. Burchell, F.H.Y. Green, T. Lewis, Genotoxicity studies of rodents exposed to coal dust and diesel emission particulates, Environ. Res. 37 (1985) 399–409.
[20] S.A. Persson, M. Ahlberg, L. Berghem, E. Konberg, G.F. Nordberg, F. Bergman, Long-term carcinogenicity study in Syrian golden hamster of particulate emissions from coal- and oil-fired power plants, Environ. Health Perspect. 77 (1988) 109–120.
[21] E. Rojas, M.C. Lopez, M. Valverde, Single cell gel electrophoresis assay: methodology and applications, J. Chromatogr. B 722 (1999) 225–254.
[22] J.C. Benassi, R. Laus, R. Geremias, P.L. Lima, C.T. Menezes, M.C. Laranjeira, D. Wilhelm-Filho, V.T. Favere, R.C. Pedrosa, Evaluation of remediation of coal mining wastewater by chitosan microspheres using biomarkers, Arch. Environ. Contam. Toxicol. 51 (2006) 633–640.
[23] M. Granella, E. Clonfero, Sensitivity of different bacterial assays in detecting mutagens in urine of humans exposed to polycyclic aromatic hydrocarbons, Mutat. Res. 268 (1992) 131–137.
[24] R. Schins, P. Borm, Mechanisms and mediators in coal dust induced toxicity: a review, Ann. Occup. Hyg. 32 (1999) 7–33.
[25] A. Schnurstein, T. Braunbeck, Tail moment versus tail length–application of an in vitro version of the comet assay in biomonitoring for genotoxicity in native surface waters using primary hepatocytes and gill cells from zebrafish (*Danio reio*), Ecotoxicol. Environ. Saf. 49 (2001) 187–196.
[26] R.R. Tice, E. Agurell, D. Anderson, B. Burlinson, A. Hartmann, H. Kobayashi, Y. Miyamae, E. Rojas, J.C. Ryu, Y.F. Sasaki, Single cell gel/comet assay: guidelines for in vitro and in vivo genetic toxicology testing, Environ. Mol. Mutagen. 35 (2000) 206–221.

OVERVIEW OF MINERAL MATTER IN U.S. COALS

R. D. Harvey and R. R. Ruch

Illinois State Geological Survey
Champaign, IL 61820

INTRODUCTION

Minerals in coal have been a subject of much interest during the past 20 years. Early studies approached the subject somewhat indirectly by means of chemical analysis of high temperature ash and back calculation to obtain estimates of the mineral matter (1). Others supplemented chemical studies by hand picking the coarser minerals or making density separations for chemical tests and optical microscopic study (2,3). With the advent of radio frequency ashing at low temperature (<150°C) it became possible to directly investigate all the mineral constituents (4). This led to progress in quantitative analyses of the mineral composition by x-ray diffraction methods (5-8). This paper summarizes some geological aspects related to minerals, their classification and occurrences in coal, and presents a compilation of available data on the mineralogical composition in coals from some of the major coal basins in the United States.

CLASSIFICATION OF MINERAL MATTER IN COAL

Coal is a sedimentary rock composed of three categories of substances: organic carbonaceous matter, termed macerals, inorganic (mainly crystalline) minerals, and fluids. The latter occur in pores within and between the other two solid constituents. The fluids in coal prior to mining are mainly moisture and methane. Applied to coal, the term mineral matter is an inclusive term that refers to the mineralogical phases as well as to all other inorganic elements in the coal; that is, the elements that are bonded in various ways to the organic (C,H,O,N,S) components. The term mineral refers only to the discrete mineral phases.

Because coal is a type of sedimentary rock, 100 or so different minerals can occur in coals; however, only about 15 are abundant enough to have high importance. These are listed in table 1 along with the stoichiometric chemical formula of each. It must be noted that minor impurities commonly substitute for the major cations as well as some anions which account for a considerable fraction of the minor and trace elements reported in coals (9-10).

Minerals in coal occur as discrete grains or flakes in one of five physical modes: (1) disseminated, as tiny inclusions within macerals; 2) layers or partings (also lenses) wherein fine-grained minerals predominate; 3) nodules, including lenticular or spherical concretions; 4) fissures (cleat and fracture fillings and also small void fillings); 5) rock fragments, megascopic masses of rock replacements of coal as a result of faulting, slumping, or related structures.

The minerals listed in table 1 are classified by their physical modes of occurrences. Description of mineral impurities in coal deposits, based on this classification is useful in a number of ways. Thick layers and abundant nodules or rock fragments hamper mining operations, but are easily removed by standard coal preparation (cleaning) facilities. On the other hand, disseminated minerals and the thinner (microscopic) layers are not much removed by existing preparation facilities. The latter two modes are dominated by mixtures of illite, quartz, and pyrite (table 1).

Useful also is a genetic classification of minerals in coal, wherein they are classified according to Mackowsky (11) as detrital, syngenetic, or epigenetic (table 1). Detrital minerals are those that were deposited in a coal forming peat swamp from slowly moving water or wind currents. Flakes of illite clay and microscopic grains of quartz, feldspars, zircon, apatite, rutile and perhaps others were deposited as discrete grains which became interbedded with peat and ultimately with the resultant coal. Most wind deposited minerals are recognized as such by the presence of certain high temperature phases. These are therefore, dust particles derived from distant volcanoes. Layered deposits of these dusts are termed tonsteins.

Syngenetic minerals are those that formed within the peat during the early stages of its coalification - before the peat was deeply buried by other sediments, probably by not more than about 50 feet. Under these conditions disseminated pyrite is thought to have formed in sulfate bearing peat by bacterial reduction of the sulfur. Much of this type of pyrite has a spherical form and is described as framboidal pyrite. Nodules of peat mineralized with various carbonates and nodules comprised of microcrystalline quartz and/or hematite formed early in the development of coal. Ultra-small crystallites of some minerals disseminated within macerals may also be syngenetic in origin, notably micrometer sized crystals of kaolinite and possibly illite observed by Strehlow, et al. (12) and by Wert and Hsieh (13). These crystallites, as well as some of the tiny disseminated grains of quartz are thought by some to have crystallized from inorganic matter inherited from the original plant material (2,3,14).

Epigenetic minerals are mainly those found in fissures and void fillings. Much of the calcite in coals as well as part of the pyrite and kaolinite in coals are recognized as epigenetic. This class of minerals formed long after the peat was consolidated and coalified enough to allow joints to develop where in these minerals precipitated. For most coals, this precipitation probably occurred during the late lignite or early subbituminous stages of coalification.

DISTRIBUTION OF MINERALS IN COALS

Typically, different layers of a seam vary considerably in their mineral matter as well as specific mineral components (fig. 1). The thin layer labeled BB is a carbonaceous shale and it contains the highest amount of mineral matter, which is mainly comprised of clay (illite, kaolinite, and smectite minerals) and quartz. At one site in the mine studied this layer was enrichedin pyrite (see lower part of the figure). The pyrite distribution at the four sites is fairly consistent in the upper layers at each site, but this epigenetic type of mineral is enriched in the lowest layer at three of the four sites (fig. 1). At this mine, and elsewhere, the conditions under which peat accumulated are thought to have been fairly consistant over regional geographical areas, much as they are today in existing peat swamps. Therefore, comparisons of mineral matter between coals are usually made by comparing analyses of channel samples that represent all layers in the seam (10).

ANALYTICAL TECHNIQUES

There are numerous instrumental techniques that can be applied to the characterization of mineal matter in coal. Probably the most widely used technique is x-ray diffraction analysis because of its availability and extensive development by mineralogists (5,6,7). Infrared spectroscopy has been successfully applied toward the analyses of common minerals found in coal (15). Differential Thermal Analysis (DTA) under nitrogen atmosphere can be used for the identification of certain minerals (16) by monitoring decomposition temperatures. Scanning electron microscopy with an energy dispersive x-ray analysis accessory unit has been used to identify various minerals as hosts for specific elements in coal (17,18). The

ion microprobe has also been applied to the study of minerals in coal (19). Mössbauer Spectroscopy has recently become very important in the study of iron sulfide minerals in coal (20). Preconcentrating the mineral matter in coal by radio frequency low-temperature ashing has been well established and is extensively practiced (4,9,14,22). It effectively removes the carbonaceous matter while causing only minor changes in the remaining minerals. The advantages are higher sensitivity for most instrumental techniques used.

Extensive elemental analyses has primarily been carried out on coal samples or ashes of coals for purposes of distribution studies and has been reviewed (21). Chemical analyses of separated coal minerals are also available confirming element-mineral associations derived from float-sink studies (14,22).

MINERAL COMPOSITION IN SOME SAMPLES FROM VARIOUS COAL BASINS

Results of mineralogical analyses of low temperature ashes by x-ray diffraction were compiled from the files of the Illinois State Geological Survey (table 2). Samples representative of the two most mined coals in the Illinois Basin provide a good statistical bases for evaluating this basin; however, this is not the case for results listed for other basins. To date, there is insufficient mineralogical data on these coal basins to draw many conclusions. Nonetheless, these data were generated in one laboratory, using the same procedures, and they provide a basis for some preliminary comparisons. The results show the following increasing compositional trends of the mean values, expressed by the state abbreviations given in table 1.

Mineral matter: AZ<TN<MT,ND,WY = So.WV<No.WV<IL<AL<IA

Pyrite (FeS_2): AZ = MT,ND,WY = So.WV<TN<AL = IL<No.WV<IA

The samples from the Black Mesa Basin in Arizona indicate the seams mined there are lowest in mineral matter and pyrite contents; those in Iowa appear to be the highest in both of these constitutents. However, the range of mineral contents is generally high and dictates that the quality of each deposit be considered on its own quality parameters for possible feed stock to coal processing plants.

REFERENCES

1. S. W. Parr, University of Illinois Engineering Experiment Station Bull. 180, 1928, 62 pp.

2. C. G. Ball, Illinois State Geological Survey Report Invest. 33, 1935, 106 pp.

3. G. C. Sprunk and H. J. O'Donnell, U.S. Bureau of Mines Technical Paper 648, 1942, 67 pp.

4. H. J. Gluskoter, Fuel, 44, 285-291 (1965).

5. C. Prasada Rao and H. J. Gluskoter, Illinois State Geological Survey Circular 476, 1973, 56 pp.

6. J. J. Renton, U.S. Dept. Energy, Morgantown Energy Research Center MERC/CR-77/10, 1977, 20 p.

7. S. J. Russell and S. M. Rimmer, "Analysis of Mineral Matter in Coal, Coal Gasification Ash, and Coal Liquefaction Residues by Scanning Electron Microscopy and X-ray Diffraction," in Analytical Methods for Coal and Coal Products, C. Kan Jr., ed., Academic Press, NY, 1979, pp. 133-162.

8. A. S. Pavlovic, J. M. Cook, and J. J. Renton, Proc. International Conference on Coal Science, Düsseldorf 7-9.9, 1981, pp. 828-834.

9. J. V. O'Gorman and P. L. Walker, Jr., Fuel, 50, 1971, 135-151.

10. H. J. Gluskoter, R. R. Ruch, W. G. Miller, R. A. Cahill, G. B. Dreher, and J. K. Kuhn, Illinois State Geological Survey, Circular 477, 1977, 154 pp.

11. M.-Th. Mackowsky, in E. Stach, et al. "Coal Petrology," 3rd revised ed., Gebruder Borntraeger, Berlin, 1982, pp. 153-171.

12. R. A. Strehlow, L. A. Harris, and C. S. Yust, Fuel, 57, 1979, 185-186.

13. C. A. Wert and K. C. Hzieh, Proc. International Conference on Coal Science, Düsseldorf 7-9.9, 1981, p. 780-785.

14. C. B. Cecil, R. W. Stanton, and F. T. Dulong, U.S. Geological Survey Open-File Report 81-953-A, 1981, 92 pp.

15. P. A. Estep, J. J. Kovach, and Clarence Karr, Jr. Anal. Chem., 40 (2) 358-363 (1968).

16. James V. O'Gorman and P. L. Walker, Fuel 52, 71-79 (1973).

17. R. R. Ruch, H. J. Gluskoter, and N. F. Shimp, Illinois State Geological Survey Environ. Geology Note No. 72, 1974.

18. H. J. Gluskoter and P. C. Lindahl, Science, 181 264-166 (1973).

19. P. H. Ribbe, Abstr. Geol. Soc. Am. Abstracts with Programs, 7 (7) 1244 (1975).

20. Gerald V. Smith, Juei-Ho Lin, Mykola Saporoschenko, and Richard Shiley, Fuel 57 (1), 41-45 (1978).

21. Harold J. Gluskoter, Neil F. Shimp, and Rodney R. Ruch, "Coal Analyses, Trace Elements, and Mineral Matter," in Chemistry of Coal Utilization, Second Supplementary Volume, Martin A. Elliott, ed., John Wiley and Sons, 1981, pp. 369-424.

22. R. D. Harvey, R. A. Cahill, C.-L. Chou, and J. D. Steele, US EPA Grant R 806654, Final Report, 1983, 162 pp.

Table 1. Minerals frequently occurring in coals, their stoichometric compositions, their modes of occurrences, and relative abundance (11).

Mineral	Composition	Chief occurrences		Abundance in min. matter
		Physical*	Genetic**	
Clay minerals				
illite (sericite, K-mica)	$KAL_2(AlSi_3O_{10})(OH)_2$	D,L	d,s(?)	common
smectite (mixed layered)	$Al_2Si_4O_{10}(OH)_2 \cdot H_2O$ (with Na, Mg and Others)	D,L	d,s(?)	common
kaolinite group	$Al_4Si_4O_{10}(OH)_8$	L,F	e,d,s(?)	common
Sulfides				
pyrite	FeS_2 (isometric)	D,N,F	s,e	variable
marcasite	FeS_2 (orthorhombic)	D(?)	s(?)	rare
sphalerite	ZnS	F	e	rare
others: greigite, galena, chalcopyrite and pyrrhotite are reported as very rare				
Carbonates				
calcite	$CaCO_3$	N,F	e,s	variable
dolomite, incl. ankerite (Fe)	$Ca(Mg,Fe)(CO_3)_2$	N	s,e	variable
siderite	$FeCO_3$	N	s,e	variable
Oxides				
hematite	Fe_2O_3	N	s	rare
quartz	SiO_2	D,L,N	d	common
others: magnetite and rutile are reported as very rare				
Others				
limonite-goethite	FeOOH	N	e	rare
apatite, incl.	$Ca_5(PO_4)_3(F,Cl,OH)$	D	d,s(?)	rare
sulfates, mainly gypsum, barite, and several iron-rich ones				
feldspars	$K(Na)AlSi_3O_8$	D,L	d	rare
zircon	$ZrSiO_4$	D,L	d	rare
others: many others reported as very rare (11)				

* D = disseminated; L = layers (partings); N = nodules; F = fissures (cleat). Each mineral listed may often occur in rock fragments within coal beds.

** d = detrital; e = epigenetic, second state of coalification (mainly along joints (cleat) in coal beds); s = syngenetic, first stage of coalification (disseminated, intimately intergrown with macerals). The first listed occurrence is the more common one in U.S. coals; others are reported in some coal fields.

Table 2. Mineral composition of channel samples in various US coals*

Minerals	Great Plains Basins MT,ND,WY %	(range)	Western Interior Basin IA %	(range)	Illinois Basin IL,IN,W-KY %	(range)	Central Appalachian Basin Southern WV %	(range)	Central Appalachian Basin Northern WV+PA %	(range)
No. Samples	23		3		107		3		6	
LTA**	13	(7-27)	28	(23-34)	16	(9-28)	13	(13-14)	14	(10-15)
Pyrite	<1	(0-2)	8	(7-9)	2	(<1-12)	<1	(<1-1)	4	(2-5)
Quartz	2	(<1-6)	4	(1-7)	2	(<1-5)	1	(<1-3)	2	(1-2)
Calcite	<1	(0-3)	4	(1-7)	1	(<1-5)	<1	(0-<1)	1	(<1-3)
Clays†	11	(4-25)	13	(9-16)	9	(3-19)	11	(10-12)	8	(6-9)
Others (traces)	sulfates &/or nitrates feldspar aragonite chlorite		none det.		sulfates marcasite sphalerite feldspar hematite		siderite ankerite		siderite feldspar	

	Black Mesa Basin AZ %	(range)	Southern Appalachian Basin AL %	(range)	Southern Appalachian Basin TN %	(range)
No. Samples	3		5		4	
LTA	9	(5-12)	18	(13-28)	12	(10-16)
Pyrite	<1	(<1)	2	(0-6)	1	(<1-1)
Quartz	2	(2-3)	2	(<1-4)	1	(<1-2)
Calcite	<1	(0-1)	<1	(0-1)	none det.	
Clay†	6	(2-9)	18	(12-21)	11	(9-14)
Others (traces)	none det.		siderite apatite sericite		none det.	

* Mean weight percent and range on a whole coal basis.
** Total mineral matter by low temperature ashing methods.
† By difference.

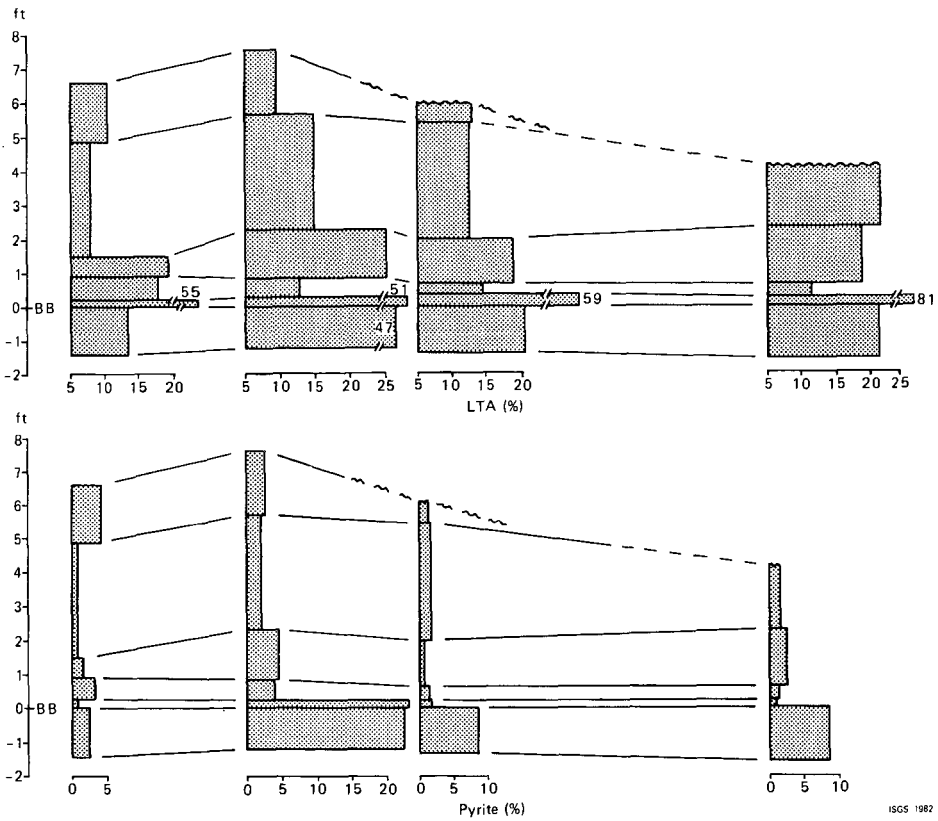

Figure 1. Vertical variation of mineral matter within a seam at four sites in a large mine: the total mineral matter content is shown in the upper diagram and the pyrite (FeS_2) fraction below. Geological analysis of the layers indicated that the upper most layer at three sites was not present at the fourth, shown on the right.

Influence of Environments of Deposition on the Inorganic Composition of Coals

S. M. Rimmer[1] and A. Davis[2]

[1]Department of Geology, University of Kentucky, Lexington, KY 40506
[2]Department of Geosciences, The Pennsylvania State University, University Park, PA 16802

Introduction

The mineral composition of coal is the result of physical, chemical and biological processes acting on the system from the time of peat accumulation, through burial and subsequent increase in rank, to the present. With respect to origin, inorganic constituents may be classified as: inherent (being derived from inorganic components within the peat-forming plants) or adventitious (being derived from outside the peat swamp and forming either during or after peat accumulation); and detrital (those transported into the peat swamp) or authigenic (those formed within the environment). Mackowsky (1) further differentiates between syngenetic minerals, formed during the accumulation of peat, and epigenetic minerals, which formed later.

In recent years considerable controversy has surrounded the origin of minerals in coal: the question is whether most of these materials are derived from inorganic substances originally contained within peat-forming plants (inherent), or from sources outside the peat swamp (detrital).

Studies of modern peat-forming environments have emphasized the importance of detrital influx (2,3), syngenetic formation of pyrite (4) and biogenic silica (2,5), and in-situ mixing with underlying sediments (2,6) to account for mineral constituents in coal. Within the peat environment certain unstable detrital clays may undergo alteration or dissolution (3,7); other clays, such as kaolinite, may form authigenically; and biogenic silica dissolves, possibly contributing to later authigenic mineralization (3,5). In coals, authigenic kaolinite formation along cleats is common (8,9). Clays may also form by alteration of volcanically-derived material (10). Opposing the concept of a major detrital input, Cecil and his co-workers (11,12) consider the major source of ash components to be the inorganic fraction of peat-forming plants, and total mineral content to be a function of the degree of peat degradation.

While this controversy still lingers, its appears that several origins are possible for minerals in peat and coal, including detrital influx, biogenic input, and precipitation either during or after peat accumulation, including some contribution from inorganic substances derived from plants. Various studies have attempted to relate inorganic composition to conditions existing at the time of peat accumulation. Pyrite has frequently been associated with marine and brackish peats (4,13), and the pyrite content of coal has been related to roof lithology (14,15). Clay assemblages of coals and underclays also have been related to depositional environment (9,16).

The purpose of this paper is to decribe variability in the inorganic content of a single coal and attempt to explain the distribution of minerals in a framework of depositional environments. In western Pennsylvania, the Lower Kittanning seam provides an opportunity to study coal that was influenced by freshwater, brackish and marine conditions, as indicated by a previous study of the overlying shale (17). Several geologic controls are thought to have influenced deposition during this time: differential subsidence resulted in a thickening of sediments (and coal) towards the center of the basin; a basement high to the north of the field area may have supplied clastic material, adding

to a predominantly eastern sediment source; and active folds and variations in paleotopography may have also influenced sedimentation patterns (18).

Sampling and Methods

Forty-three channel samples of the Pennsylvanian-aged Lower Kittanning coal (Kittanning Formation, Allegheny Group) were collected in western Pennsylvania. Samples are representative of all three suggested depositional environments (Figure 1) and also of the increase in rank from high volatile bituminous in the west to low volatile bituminous in the southeast. Analyses included major and minor elements, total sulfur and sulfur forms, and low-temperature ashing. LTA's were obtained according to standard procedures (19). X-ray diffraction analysis of LTA's provided qualitative, quantitative (for quartz and pyrite), and semi-quantitative (for clays in the < 2 µm fraction) data using procedures modified from Russell and Rimmer (20). Kaolinite was quantitified using infra-red spectroscopy. Mineral composition was also calculated by normative techniques modified from Pollack (21) and Given et al., (22).

Results and Discussion

The major mineral components of this coal include quartz, pyrite (and marcasite), and clays (predominantly kaolinite and illite/mica, with lesser amounts of expandable clays). Total mineral content (percent LTA) varies considerably across the basin, with very high ash contents occurring in the center of the basin and along sections of the Allegheny Front. To further understand these variations, individual mineral distributions were examined.

Pyrite distribution shows a definite basinal trend, with high pyrite contents occurring across the center of the basin (Figure 2). Whereas much of this area underlies marine and brackish roof rocks, the relationship is not perfect. Highest pyrite content appears to be most closely related to the eastern brackish zone. Factors influencing the distribution of sulfur in peat and coals include availability of iron and sulfate, and pH. Sulfate is thought to be introduced by marine and brackish waters (4). Recent work on pyrite distribution in the Florida Everglades (23) indicates highest pyrite content is associated with brackish environments rather than marine, and this has been related to the availability of iron. In freshwater, iron is transported in organic colloids which flocculate quickly upon entering brackish water, resulting in a higher availability of iron in brackish environments (24). pH is also a factor, as much of the pyrite appears to form as a by-product of sulfate-reducing bacteria (4). Compared to the more acidic freshwater environments, higher levels of microbial activity would occur in the neutral to basic pH conditions existing in marine or brackish waters. Pyrite content is therefore highest in areas that were influenced at least by brackish conditions.

The central part of the basin was experiencing more rapid subsidence than the margins, thus any marine influence would be greater in this area. Apparent discrepencies in the relationship between pyrite content and roof lithology may be explained on the basis of iron availability. (Data to be discussed later suggest a detrital influence towards the eastern margin of the basin, providing clay-rich sediments which may have contributed to the supply of iron). Other workers have also commented on this lack of correlation and suggest epigenetic pyrite formation along cleats and joints may be responsible (25). A third alternative is that the zone of maximum brackish and marine influence shifted during the history of the peat swamp.

Quartz content is highest in the north-central part of the basin, with isolated quartz-rich pods along the Allegheny Front. The origin of quartz in coal has been debated at length. Detrital quartz has been distinguished by many

authors (1,3) while other workers (11,12) believe much of this quartz is derived from silica originally contained within the plants. Petrographic observations of quartz in this coal revealed an association with attrital bands, suggesting a detrital origin. The distribution may be related to the basement high that existed to the north during this time (18). Transportation within the swamp of quartz-rich sediments derived from this high was possibly restricted by the baffling effect of vegetation, a phenomenon noted in modern swamps (2). In addition, lesser amounts of quartz may have been carried in from the east. Sediment derived from this latter source appears to have been predominantly clay. Comparable quartz distributions were noted in the underclay (26), thus the influence of in-situ mixing also exists.

Kaolinite is the major clay constituent of the coal and occurs in highest concentrations along the basin margins, with illite increasing towards the central part of the basin. Once again a similar distribution wasnoted in the underclays (26). Differential flocculation within the basin, together with chemical regrading of clays, could be used to explain this distribution. Holbrook (26) argues against this mechanism for the underclays on the basis of flocculation studies in modern environments, and suggests differential leaching related to variations in paleotopography may have been important. Another control could be the effect of peat chemistry on the clay assemblage. Kaolinite appears to be highest in freshwater environments where, under lower pH conditions, it would be the most stable clay mineral. Thus, in these areas not only could kaolinite be detrital, but also the product of clay alteration and authigenesis. The presence of high-temperature polytypes suggest a detrital origin for illite/mica in the Lower Kittanning coal and underclay, as discussed by Davis et al. (3) and Holbrook (26). Detrital illite/mica would be better preserved in more basinward areas.

One additional control on the clay mineral assemblage could be rank. With the increase in rank exhibited by this coal, certain diagenetic changes might be expected. No consistent trends in mineralogy were observed, however a general lack of smectite and highly-expandable clays (which can be seen in lower rank coals) was noted. This could be related to rank, or be a function of provenance.

Summary

The distribution of minerals within the Lower Kittaning coal can be related to depositional environments. Total mineral content varies considerably across the basin, and variations can be explained by examining the distributions of individual minerals.

Pyrite content is controlled by availability of sulfate and iron, and pH. Highest concentrations are seen towards the center of the basin where subsidence was more rapid and marine and brackish influences (affecting sulfate availability and pH) were felt during and after peat accumulation. Iron availability may have been associated with the transport of organic colloids or clay into the basin.

Quartz appears to be limited to the northern part of the field area and isolated areas along the Allegheny Front. It is suggested that quartz-rich sediments were derived from a positive area to the north. Much of the sediment brought in from the east appears to have been clay-rich.

The chemistry of the peat may have had a strong influence on clay mineral assemblage. Kaolinite may have been both detrital and authigenic, whereas illite/mica appears to be detrital. Rank has had little effect on the overall clay assemblage.

References

(1) Mackowsky, M-Th. (1968). In "Coal and Coal-Bearing Strata" (D. Murchison and T.S. Westoll, eds.), pp. 325-345, American Elsevier, New York.

(2) Otte, L.J. (1984). Geol. Soc. Am., Abstr. Programs 16, 3, 185.

(3) Davis, A., Russell, S.J., Rimmer, S.M., and Yeakel, J.D. (1984) Int. J. Coal Geol., 3, 293-314.

(4) Casagrande, D.J., Siefert, K., Berschinski, C., and Sutton, N. (1977) Geochim. Cosmochim. Acta, 41, 161-167.

(5) Andrejko, M.J., Raymond, R. Jr., and Cohen, A.D. (1983). In "Mineral Matter in Peat: Its Occurrence, Form, and Distribution" (R. Raymond, Jr., and M.J. Andrejko, eds.), pp. 25-37, Proc. Workshop, Los Alamos Natl. Lab., Los Alamos, New Mexico.

(6) Andrejko, M.J., Cohen, A.D., and Raymond, R. Jr. (1983). In "Mineral Matter in Peat: Its Occurrence, Form, and Distribution" (R. Raymond, Jr., and M.J. Andrejko, eds.), pp. 3-24, Proc. Workshop, Los Alamos Natl. Lab., Los Alamos, New Mexico.

(7) Staub, J.R., and Cohen, A. (1978). J. Sed. Pet., 48, 203-210.

(8) Ball, C.G. (1934). Econ. Geol., 29, 757-776.

(9) Gluskoter, H.G. (1967). J. Sed. Pet., 37, 205-214.

(10) Bohor, B.F., Pollastro, R.M., and Phillips, R.E. (1978) 27th. Ann. Clay Min. Conf., Prog. and Abstr., 47.

(11) Renton, J.J., and Cecil, C.B. (1980). In "Carboniferous Coal Short Course and Guidebook, Vol. 3" (A.C. Donaldson, M.K. Presley, and J.J. Renton, eds.), AAPG Seminar, pp. 103-128, Morgantown, W.Va.

(12) Renton, J.J., Cecil, C.B., Stanton, R., and Dulong, F. (1980). In "Carboniferous Coal Short Course and Guidebook, Vol. 3" (A.C. Donaldson, M.K. Presley, and J.J. Renton, eds.), AAPG Seminar, pp. 57-101, Morgantown, W.Va.

(13) Spackman, W., Cohen, A.D., Given, P.H., and Casagrande, D.J. (1976) A Field Guide to Aid in the Comparative Study of the Okefenokee Swamp and the Everglades-Mangrove Swamp-Marsh Complex of Southern Florida: The Pennsylvania State University Coal Research Section Short Course, University Park, PA.

(14) Williams, E.G., and Keith, M.C. (1963). Econ. Geol., 58, 720-729.

(15) Kravits, C.M., and Crelling, J.C. (1981). Int. J. Coal Geol., 1, 195-212.

(16) Parham, W.E. (1966). Proc. Int. Clay Conf., 1, 135-145, Jerusalem, Isreal.

(17) Williams, E.G. (1960). J. Paleontol., 34, 908-922.

(18) Williams, E.G. and Bragonier, W.A. (1974). Geol. Soc. Am. Spec. Paper 148, 135-152.

(19) Gluskoter, H.G. (1965) Fuel, 44, 285-291.

(20) Russell, S.J., and Rimmer, S.M. (1979). In "Analytical Methods for Coal and Coal Products, Vol. III" (C. Karr, Jr., ed.), pp. 133-162, Academic Press, New York.

(21) Pollack, S. (1979). Fuel, 58, 76-78.

(22) Given, P.H., Weldon, D., and Suhr, N. (1980). Investigation of the Distribution of Minerals in Coal by Normative Analysis: Tech. Rept. 2, Pennsylvania State University to U.S. Dept. Energy, Rept. No. FE-2494-TR-2.

(23) Cohen, A.D., Spackman, W., and Dolsen, P. (1983). In "Mineral Matter in Peat: Its Occurrence, Form and Distribution" (R. Raymond, Jr., and M.J. Andrejko, eds.), pp.87-112, Proc. Workshop, Los Alamos Natl. Labs., Los Alamos, New Mexico.

(24) Sholkovitz, E.R., Boyle, E.A., and Price, N.B. (1978). Earth and Planet. Sci. Newsletter, 40, 130-136.

(25) Davies, T.D., and Raymond, R. Jr. (1983). In "Mineral Matter in Peat: Its Occurrence, Form and Distribution" (R. Raymond, Jr., and M.J. Andrejko, eds.), pp. 123-139, Proc. Workshop, Los Alamos Natl. Labs., Los Alamos, New Mexico.

(26) Holbrook, P.W. (1973) Geologic and Mineralogic Factors Controlling the Properties and Occurrences of Ladle Brick Clays: Unpubl. PhD. Thesis, The Pennsylvania State University, University Park, PA.

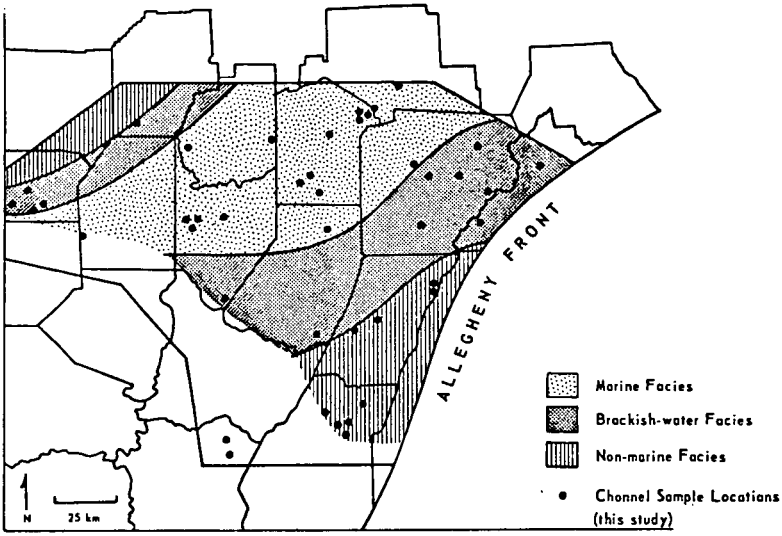

FIGURE 1. DISTRIBUTION OF SAMPLES IN WESTERN PENNSYLVANIA IN RELATION TO SUGGESTED ENVIRONMENTS OF DEPOSITION FOR THE OVERLYING SHALE

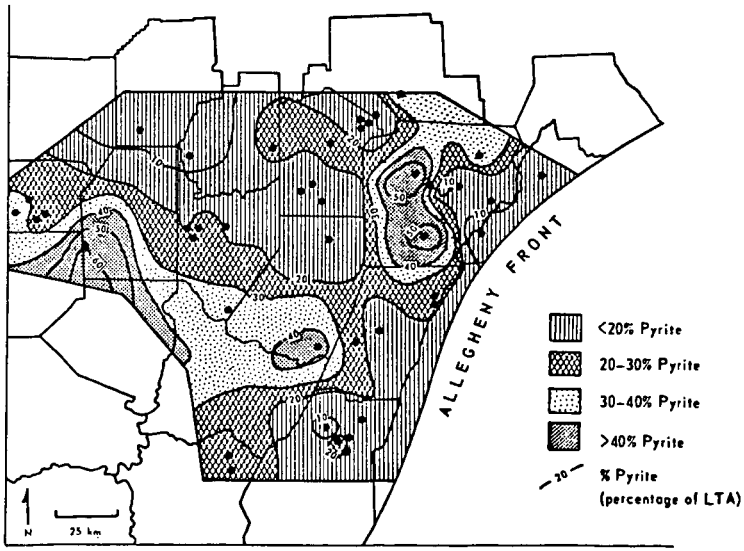

FIGURE 2. LATERAL VARIABILITY IN PYRITE CONTENT (LTA BASIS), AS DETERMINED BY X-RAY DIFFRACTION ANALYSIS

The Origin of Quartz In Coal

Leslie F. Ruppert, C. Blaine Cecil, and Ronald W. Stanton
U.S. Geological Survey, National Center, MS 956, Reston, Va. 22092

Introduction

Mineral matter in coal can originate as (1) inorganic elements from plants that were incorporated during peat formation, (2) wind- or water-borne detritus that settled in the peat-forming environment, and (3) epigenetic minerals that formed during or after burial of the peat (Stach and others, 1982). The latter two processes generally are considered to be the principal contributors to the amount and variety of minerals in coal of commercial quality. Certain physical properties, such as the shape of quartz grains, have led some workers to postulate that quartz in coal is primarily of detrital origin (Finkelman, 1981a, 1982b; Davis and others,1981); however, evidence for such a hypothesis may be highly subjective and inconclusive. In contrast, Cecil and others (1982) suggested that mineral matter in the Upper Freeport coal bed is dominantly authigenic, on the basis of statistical relationships among major-, minor-, and trace-element, maceral, and mineral data. Mineral matter in coal, exclusive of pyrite and calcite, was probably derived from plants that contributed to peat formation (Stevenson, 1913; Cecil and others, 1982).

Cathodoluminescence (CL) petrography was used in the present investigation to obtain quantitative data on the amounts of authigenic and detrital quartz in the Upper Freeport coal bed. CL is the emission of visible light during electron bombardment. It is used widely as a tool in sandstone petrology to distinquish between detrital and authigenic quartz grains. CL in quartz results from molecular or other lattice imperfections; molecular imperfections which include the addition of "activator" ions (Al^{+3} or Ti^{+3} that substitute for Si^{+4}), and other lattice imperfections are related to temperature (Zinkernagel, 1978). Zinkernagel observed three distinct types of luminescence in quartz grains that included (1) "violet" luminescing quartz (spectral peaks at 450 and 610-630 nm), (2) "brown" or orange luminescing quartz (spectral peaks at 610-630 nm), and (3) non-luminescing quartz. He examined quartz from 46 localities and ranging in age from Precambrian to Tertiary, and in all cases the CL color was dependent on the temperature of crystallization. "Violet" or blue luminescing quartz was characteristic of fast-cooled volcanic, plutonic, and high-grade metamorphic rocks that were formed at temperatures greater than 573°C. "Brown" or orange luminescing quartz was characteristic of high-grade slow-cooled metamorphic rocks formed at temperatures ranging from 573° C to 300° C. Quartz that was formed at temperatures below 300°C and that was not heat tempered did not luminesce in the visible range. The origin of quartz can be inferred from CL data because detrital quartz, which has a high- temperature origin (>300°C), luminesces in the visible range whereas authigenic quartz, formed at low temperatures (<300° C) does not luminesce.

Methodology

Both a scanning electron microscope (SEM) and an electron microprobe (EMP) were used in this study to analyze the CL properties of quartz grains in samples of the Upper Freeport coal bed because quartz grains in coal are small (silt sized) and below the resolution capabilities of a standard luminoscope. Quartz grains were identified by the detection of silicon alone with energy dispersive X-ray units attached to both the SEM and the EMP.

The SEM was used to observe and photograph the quartz grains. The EMP which was equipped with both a photomultiplier tube (spectral response 185-930 nm) and a monocrometer, was used to measure wave length and intensity of CL. The EMP, instrument conditions were calibrated using a reference sample of the upper part of the Raleigh Sandstone Member of the New River Formation (Pennsylvanian age), which contained both orange and blue luminescent detrital quartz grains and non-luminescent authigenic overgrowths of low-temperature origin (fig. 1).

Quartz grains from the Upper Freeport coal bed were analyzed in (1) ash samples that were prepared by low-temperature plasma ashing (LTA) of facies channel samples, (2) pulverized coal samples of size-gravity separates, and (3) oriented blocks of mineral-rich bands, vitrain, fusain, clay-rich parting material, and roof-shale that were each cut from a coal core. All samples were mounted in epoxy and polished prior to analysis.

Results

All the Upper Freeport coal bed samples examined contained both luminescent and non-luminescent quartz grains (table 1, fig. 2). More than 200 grains were visually examined, and 76 measured spectra were obtained.

In the LTA samples, 95 percent of the quartz particles examined were non-luminescent and 5 percent were luminescent. Most grains luminesced in the orange range.

Twenty-nine measured spectra of quartz grains were obtained from the lightest (1.275 float) and the heaviest (1.800 sink) size-gravity separates. Only nine grains were analyzed in the lightest gravity separates because of the paucity of mineral matter. All nine grains were non-luminescent and were associated with vitrain. In the heaviest gravity separates, 60 percent of the quartz was non-luminescent; this quartz is petrographically associated with both vitrain, mineral-rich bands, and shale partings. The remaining 40 percent of the quartz grains in the heavy gravity separates were luminescent and are associated with mineral-rich bands and shale parting material.

Data from CL analyses of the blocks of coal from the core revealed that luminescing quartz was relatively rare and is associated only with mineral-rich bands. Of the 29 quartz grains analyzed, only 17 percent luminesced. The non-luminescent grains are petrographically associated with both vitrain and mineral-rich bands.

Roof-shale samples from the core were also examined. Ninety-three percent of the quartz analyzed was luminescent and only 7 percent was non-luminescent. The quartz grains analyzed were similar in size to the quartz grains in coal.

Conclusions

Seventy-six percent of the quartz grains examined in the Upper Freeport coal samples are non-luminescent; therefore the quartz is interpreted to be domininantly authigenic. The authigenic quartz is petrographically associated with both vitrain and mineral-rich bands. The remaining 23 percent of the quartz analyzed luminesced in the visible range and is therefore interpreted to be detrital in origin. Detrital quartz was petrographically associated with mineral-rich bands and clay-parting material.

In contrast, quartz grains in the samples of shale directly overlying the Upper Freeport coal bed are interpreted to be predominantly detrital in origin. The quartz grains are in the same size range as quartz grains in the coal samples.

Data from CL petrography support the interpretation of Cecil and others (1982) that quartz in Upper Freeport coal bed is primarily authigenic and derived from plant ash. Although it is impossible to ascertain the ash content of Pennsylvanian plants that grew in the Upper Freeport paleo-peat forming environment, it seems reasonable that the plants did contain silica, as do most modern plants. Biogenic silica can be preserved as phytoliths (Smithson, 1956; Baker, 1960; and Jones, 1964; Andrejko and others, 1983) and quartz grains in coal are similiar in size to plant phytoliths (Wilding and Drees, 1974).

Most quartz grains in the commercial-quality Upper Freeport coal bed samples are authigenic in origin, but this interpretation does not rule out a detrital source for areas of the bed containing higher amounts of ash (approximately 20 percent) or for other high ash bituminous coal beds. The percentage of detrital quartz would be expected to increase approaching stream channels and the margins of the paleoswamp environment, but vegetal matter is probably the dominant source for quartz in interior portions of the paleoswamp.

Table 1. CATHODOLUMINESCENT AND PETROGRAPHIC CHARACTERISTICS OF QUARTZ GRAINS IN COAL AND SHALE

[Determined by using an electron microprobe (EMP). TNA, Total number of grains analyzed; Nonlum, nonluminescent grains: Lum, Luminescent grains; *, data was not obtained because coal was crushed; N/A, not applicable.]

	LOW-TEMPERATURE ASH (Facies channel samples)		SIZE-GRAVITY SEPARATES			
			Float 1.275 (TNA = 9)		Sink 1.800 (TNA = 20)	
	Nonlum	Lum	Nonlum	Lum	Nonlum	Lum
Number of grains	39	2	9	0	12	8
Grain size range (in µm)	*	*	6-22	N/A	5-14	9-32
Mean grain size (in µm)	*	*	9.9	N/A	8.4	18.9
Percent of total	95	5	100	N/A	60	40
Association	*	*	Vitrain	N/A	Vitrain Mineral-rich band Shale parting	Mineral-rich band Shale parting

	COAL BLOCKS (TNA = 9)		ROOF-SHALE (TNA = 15) BLOCKS	
	Nonlum	Lum	Nonlum	Lum
Number of grains	24	5	1	14
Grain size range (in µm)	8-20	7-22	N/A	6-32
Mean grain size (in µm)	12	14.8	7	13.5
Percent of total	83	17	7	93
Association	Vitrain	Mineral-rich	Shale	Shale

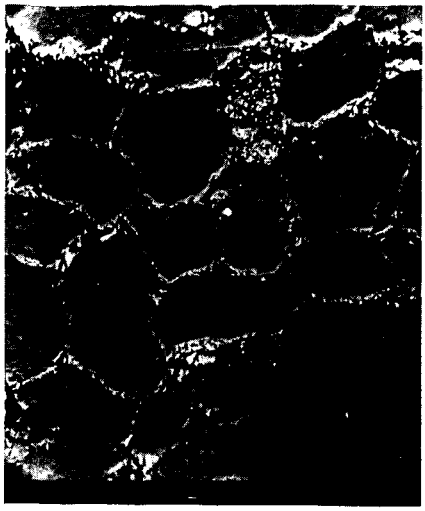

a

b

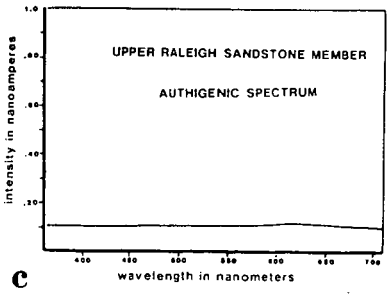

c

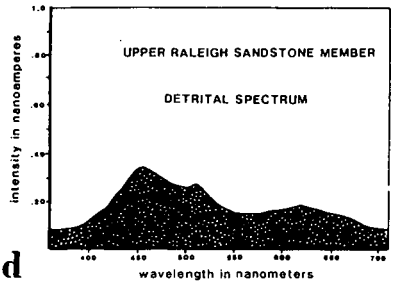

d

Figure 1 - Reference sample for EMP. (a) SEM backscatter electron photomicrograph, (b) CL SEM photomicrograph. Note luminescing detrital quartz grains, (c) EMP CL spectrum of non-luminescing authigenic overgrowth, (d) EMP CL spectrum of blue luminescing detrital quartz grain.

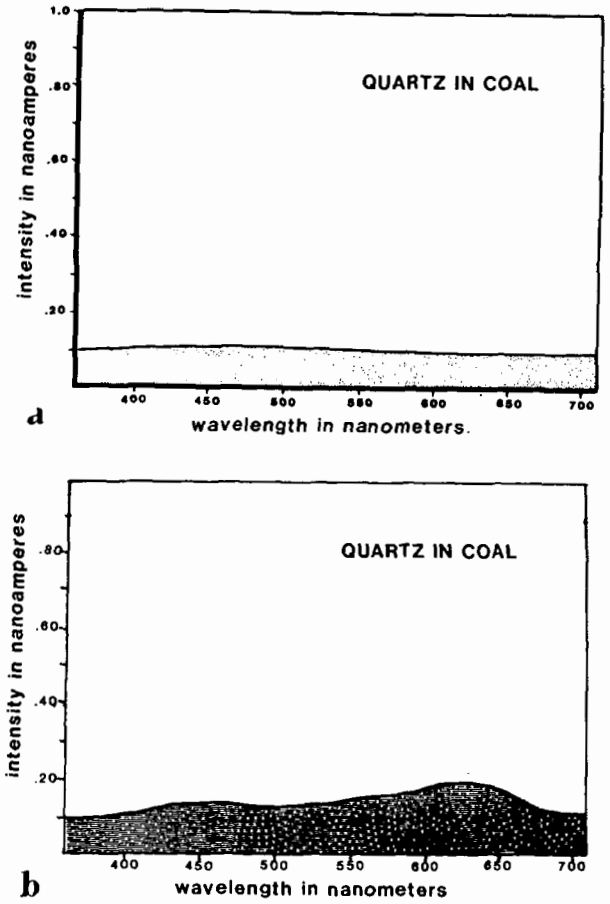

Figure 2 - EMP CL spectra of quartz in the Upper Freeport coal bed. (A) Non-luminescing authigenic spectrum, (B) Luminescing detrital spectrum.

References

Andrejko, M.J., Raymond, R., and Cohen, A.D., 1983, Biogenic silica in peats: Possible Sources for Chertification in Lignite: in Raymond, R., and Andrejko, M.J., eds,. Mineral Matter in Peat: Its Occurrence, Form, and Distribution: Los Alamos National Lab., Los Alamos, N.Mex., 1983.

Baker, G., 1960, Opal phytoliths in some Victorian soils and "red rain" residues: Australian Journal of Botany, v. 7, p. 64-87.

Cecil, C.B., Stanton, R.W., Dulong, F.T., and Renton, J.J., 1982, Geologic factors that control mineral matter in coal; in Filby, R.H., Carpenter, B.S., and Ragina, R.C., eds., Atomic and Nuclear Methods in Fossil Research: Plenum Press, New York, p. 323-325.

Davis, A., Rimmer, S.M., Russell, S.J., and Yeakel, J.D., 1981, Some observations on the origin of common minerals in coals and their relationship to the organic petrology [abs]: Geological Society of America, Abstracts with Programs, v. 13, no. 7, p. 436.

Finkelman, R., 1981a, The origin, occurrence, and distribution of the inorganic constituents in low-ranked coals, in Proceedings of the Basic Coal Science Workshop, Houston, Texas, Dec. 8-9, 1981, p. 69-90.

----1981b, Recognition of authigenic and detrital minerals in coal [abs]; Geological Society of America, Abstracts with Programs, v. 13, no. 7, p. 451.

Jones, R.L., 1964, Note on the occurrence of opal phytoliths in some Cenozoic sedimentary rocks; Journal of Paleonotology, v. 38, p. 773-775.

Smithson, F., 1956, Silica particles in some British soils: Journal of Soil Science, v. 7, no. 1, p. 122-129.

Stach, E., Mackowsky, M-Th., Teichmuller, M., Taylor, G.H., Chandra, D., and Teichmuller, R., 1982, Stach's textbook of coal petrology: Gebruder Borntraeger, Berlin, p. 156.

Stevenson, J.J., 1913, Formation of coal beds: Proceedings of the American Philosophical Society, v. 52, p. 100-108.

Wilding, L.P., and Drees, L.F., 1974, Contributions of forest opal and associated crystalline phases of fine silt and clay fractions of soils; Clay Mineralogy, v. 22, p. 295-306.

Zinkernagel, U., 1978, Cathodoluminescence of quartz and its application to sandstone petrology: Contributions to Sedimentology, no. 8, 69 p.

SEMI QUANTITATIVE DETERMINATION OF COAL MINERALS BY X-RAY DIFFRACTOMETRY

John J. Renton

Department of Geology
West Virginia University
Morgantown, West Virginia 26506

INTRODUCTION

The purpose of this paper is to present and support the argument that abundance estimates of the minerals in coal based upon x-ray diffraction data can only be considered semi-quantitative with expected errors of determination of 10 percent or more of the reported values. The compositional and physical characteristics of the low temperature ash components of coal relative to the preparation and mounting of ash for XRD analysis must also be considered.

MINERALS IN COAL

The minerals commonly found in coal are listed in Table 1. In the average coal, clay minerals may constitute up to 60 weight percent of the mineral matter (1,2). Quartz is usually the second most abundant mineral, with up 20 weight percent being common. The carbonate minerals (calcite, siderite and to a lesser extent, dolomite and ankerite) and the iron disulphide minerals (pyrite and marcasite) make up, on the average, about 10 weight percent each group. Sulphate minerals of calcium and iron and the feldspar minerals are commonly present but rarely in concentrations of more than a few weight percent. Except for unusual cases such as the sulphide rich coals of the northern Illinois Basin, the occurrence of the other minerals in concentrations exceeding a few percent is rare. It must, however, be kept in mind that the mineralogy of the inorganic portion of coal shows systematic variation both geographically and locally reflecting the geochemistry of the original peat forming environment (3). As a result, "average" values of concentration may have little practical meaning.

Most coals considered for conversion processes such as liquifaction, and thereby those of prime interest to chemists, are generally high in ash (>10 weight percent) and sulfur (>1 weight percent). In such coals, illite would invariably be the dominant clay material, constituting, in some coals, up to half or more of the mineral content. Most of the sulfur contained in these coals will be in the form of pyrite although marcasite may be locally dominant (4).

QUANTIFICATION BY X-RAY DIFFRACTION

The most commonly employed quantitative XRD procedure used to evaluate the concentration of mineral components in a multicomponent mixture of minerals compares the Bragg intensity data of unknowns to those generated from a suite of known standard samples. Mineral specimens are acquired to represent each of the minerals expected in the unknowns. The specimens are ground to a uniformly small size (less than 44 microns) and mixed together in concentrations which represent the range of concentrations expected for each mineral. An internal standard such as calcium fluoride, aluminum oxide or powdered aluminum is usually added in order to monitor and correct for variations in sample absorption and instrumental variables. Working curves are then prepared by plotting the ratio of intensity (preferably integrated intensity) of the Bragg reflection chosen to quantify the mineral to that chosen for the standard versus the weight percent of the mineral in the standard samples.

This procedure will provide analyses of high precison provided certain basic assumptions are met: (1) the high composition and crystallinity (degree of ordering) of the individual minerals in the unknowns are both reasonably constant from sample to sample and (2) the composition and crystallinity of the standard minerals chosen for the preparation of the standard samples reasonably duplicate the composition and crystallinity of the respective minerals in the unknowns. The purpose of the following discussion is to demonstrate that, in the case of coal minerals, neither of the above assumptions is valid and as a result, any such quantitative procedure will reflect the inherent degree of departure from these basic assumptions and will therefore be semi-quantitative. Other procedures using data normalized to the total integrated intensity and quantification procedures utilizing weighting factors based upon standard chemical formulae for the minerals can be used but with no improvement in quantitative errors (5,6).

Illite and pyrite were specifically cited in the above discussion to make a point relative to the precision and accuracy with which coal minerals can be quantified by XRD. First, illite is NOT a mineral. Illite is "...a general term for the clay mineral constituents of argillaceous sediments belonging to the mica group (7). To a clay mineralogist, the term illite is synonomous with variability in both composition and crystallinity (8). The situation is even further complicated by the fact that much of the material in coal referred to a "illite" is actually an illite dominated mixed layered clay wherein the illite lattices are randomly interstratified with 14A clay lattices; usually chlorite. This mixing of clay mineral lattices further adds to the inherent variability in both composition and crystallinity of the illite material. The constitution of "illite" can therefore be expected to vary significantly from sample to sample. It should be quite apparent from the above discussion that no "standard" illite exists that could be used to represent illite in standard samples.

The iron disulphides may represent 10 weight percent or more of high ash-sulphur coal ashes. Usually, pyrite is the major disulphide. Pyrite occurs in coal in a number of morphological forms and sizes (9). Not only does the pyrite in coal vary in morphology and size but also in stoichiometry and crystallinity. Studies have been conducted in the author's laboratory on cut and polished surfaces of coal blocks wherein the blocks have been exposed to the atmosphere and the pyrites observed over a period of time. Some pyrite grains, the

euhedral forms, remain bright and show little tendency to react. The massive forms of pyrite, on the other hand, show a wide variation in apparent reactivity with crystals of ion sulfates being observed to form on some pyrite surfaces within a matter of hours and in some cases, within minutes.

Another study involved in quantification of pyrite in different coal lithotypes. Coals are described megascopically based upon the degree of bright and dull banding. Zones are delineated within the coal and designated as a "lithotype" based on the relative percentage of bright and dull bands within the zone (10). Dominantly bright bands are called "VITRAIN", dull bands, DURAIN and those intermediate between the two; "CLARAIN". Although the designation as to lithotype is solely made depending upon megascopic description, the lithotypes differ in basic organic composition as illustrated by the data for the Waynesburg Coal shown in Table 2.

TABLE 2. COMPOSITION OF LITHOTYPES OF THE WAYNESBURG COAL

LITHOTYPE	%VITRINITE	%EXINITE	%INERTINITE	%MINERAL MATTER
Vitrain	93.1	1.8	2.4	2.7
Clarain	84.2	4.4	5.6	5.8
Durain	43.4	17.8	24.9	13.9

The low temperature ash of each lithotype was then submitted to XRD analysis. The integrated intensities of each of the selected analytical Bragg reflections selected for the individual minerals were summed for all minerals present in each sample to give a "total integrated intensity". This value was then divided into the integrated intensity of the pyrite analytical Bragg reflection to give the "percent of total integrated intensity". The data are summarized in Figure 1. It is apparent that there is a systematic relationship between the composition/crystallinity of the pyrite and the basic organic makeup of the coal. Most important is the observation that equal concentrations of pyrite give different intensity responses. Volume for volume, the pyrite contained within the bright coal (Vitrain) showing significantly higher Bragg intensities than the pyrite contained in the duller coals.

To compound the problem, marcasite for reasons unknown to the author, does not show the intensity reponse, volume for volume as pyrite. It has been the author's experience that the marcasite coals that have been shown by optical examination to be insignificant concentration show almost no indication of being present on a diffractogram generated from the low temperature ash.

It must be apparent from the above discussion that the great number of variables other than concentration affect the intensities of mineral pattern as observed on a diffractogram. Inasmuch as they cannot be monitored and compensated for mathmetically, these variations must be reflected in the error of determination. This would be true regardless of the quantification procedure employed. The conclusion, therefore, is that the inherent variability in composition and/or crystallinity that exists within the major mineral components of the low temperature ashes of coal will be reflected in the statistical error of determination and that error will be of sufficient magnitude to preclude the use of the term "quantitative" to describe the procedure. Therefore, any procedure using x-ray diffraction to determine the minerals in coal must be considered semi-quantitative at best.

SAMPLE PREPARATION & MOUNTING

Any procedure for the preparation and mounting of coal low temperature ashes for XRD analysis MUST take two properties of the material into account: (1) minerals exist which react with water to produce acidic solutions (the iron disulphides) which in turn dissolve acid soluble components such as calcite and (2) the clay minerals by virtue of exceptionally well developed (001) cleavage surfaces have a dominant platey crystal form. The significance of the first attribute is that the ashes cannot be placed in water thereby precluding certain sample preparation techniques such as dispersion in water followed by vacuum mounting on filters or ceramic blocks. The second characteristic, possession of a platey crystal form, precludes the attainment of the theoretically required randomly oriented sample. Those who work with the clay minerals, realizing a random sample cannot be prepared and that the clay particles will deposit in preferred orientation, purposely prepare and mount the samples such that the preferred orientation of the individual platelets is maximized and thereby minimize any variations in diffraction intensity due to variations in particle alignment within the sample. The orientation of the clay platelets parallel to the sample surface positions the "C" crystallographic axis perpendicular to the sample surface. Because the diagnostic interplanar spacing for the clay minerals is along the "C" crystallographic direction, such an orientation is ideal for clay mineral identification. The simplest method to mount a low temperature ash for XRD analysis is to press the ash onto the surface of a pellet prepared from the coal from which the ash was derived.

FUTURE PROSPECTS

A few years ago, and ad hoc group of workers interested in coal minerals, The Mineral Matter in Coal Group, prepared and distributed a round-robin low temperature ash to ten laboratories. Each laboratory was to prepare, mount and quantify the mineral components in the ash by their respective XRD techniques. The data were then compared. Even though a wide variety of techniques was used for each phase of the analysis, with the exception of the clay mineral estimates made by one laboratory (significantly lower than the others) and the pyrite estimate made by another (too high), the data compared reasonably well. The averages of all the submitted estimates are summarized in Table 3.

TABLE 3. RESULTS OF ROUND ROBIN L.T.A. ANALYSIS

MINERAL	AVE. CONC. WT%	S.DEV.	C.V.
Illite+Mix L	30	7.07	0.24
Kaolinite	18	4.85	0.27
Quartz	21	6.31	0.30
Calcite	10	3.59	0.36
Pyrite	18	4.93	0.27

Another objective of the exercise was to discuss the results and procedures used and come to some agreement on a "standard" procedure for sample preparation, mounting and quantification that would be acceptable to all the workers. The agreement that was reached was that no agreement would be forthcoming on any of the phases of the analysis. With no one procedure demonstratably better than the other, each laboratory was expected to maintain their own procedure. As long as a procedure is scientifically and analytically sound and reflects a thorough understanding of the characteristics of minerals contained in coal and the requirements and limitations of x-ray diffraction, one procedure will probably be as good as another but none will be better than semi-quantitative. With all its shortcomings, x-ray diffraction is still the best and most practical method for the estimation of the abundance of the individual minerals in coal.

REFERENCES CITED

1. Renton, J. J., 1982, in Coal Structure, R. Meyers ed., Academic Press, p. 283-326.

2. Renton, J. J., 1978, Energy Sources, Vol. 43, No. 2, p. 91-112.

3. Renton, J. J., C. B. Cecil, 1979, in "Carboniferous Coal Guidebook", A. C. Donaldson, M. W. Presley and J. J. Renton, eds., West Virginia Geological and Economic Survey, Morgantown, W. Va., p. 103-128.

4. King, H. M., 1978, Masters Thesis, Dept. of Geology, W. Virginia.

5. Renton, J. J., 1977, U. S. Dept. of Energy, MERC/CR-77/10, 20pp.

6. Renton, J. J., 1979, U. S. Dept. of Energy, METC/CR-79/5, 22pp.

7. Grim, R. E., et al, 1937, Amer. Min., Vol. 22, pp. 813-829.

8. Brown, G., 1961, Mineralogical Soc. of London, Clay Mineral Group, London, 544pp.

9. Grady, W. C., 1977, AIME Transactions, Vol. 262, p. 268-274.

10. Stopes, M. C., 1919, Proc. Roy Soc. B., 90, 470-487, London.

TABLE 1

COMMON COAL MINERALS

Major	Silicates	Clay Minerals	Kaolinite	$Al_2Si_2O_5(OH)_4$
			Illite	a
			Mixed Layer	b
			Chlorite	$(MgfFeAl)_6(SiAl)_4O_{10}(OH)_8$
			Quartz	SiO_2
Minor		Carbonates	Calcite	$CaCO_3$
			Dolomite	$(Ca,Mg)(CO_3)_2$
			Ankerite	$Ca(Fe,Mg)CO_3$
			Siderite	$FeCO_3$
		Disulfides	Pyrite	FeS_2 (cubic)
			Marcasite	FeS_2 (orthorhombic)
		Sulfates	Coquimbite	$Fe_2(SO_4)_3 \cdot 9H_2O$
			Szmolnokite	$FeSO_4 \cdot H_2O$
			Gypsum	$CaSO_4 \cdot 2H_2O$
			Bassanite	$CaSO_4 \cdot \frac{1}{2}H_2O$
			Anhydrite	$CaSO_4$
			Jarosite	$KFe_3(SO_4)_2(OH)_6$
		Feldspars	Plagioclase	$(NaCa)Al(AlSi)Si_2O_8$
			Orthoclase	$KAlSi_3O_8$

[a]Illite has a composition similar to muscovite-$KAl_2(Si_3Al)O_{10}(OH)_2$, except for less K+ and more SiO_2 and H_2O

[b]Mixed layered clays are usually randomly interstratified mixtures of illitic lattices with montmorillonitic and/or chloritic lattices.

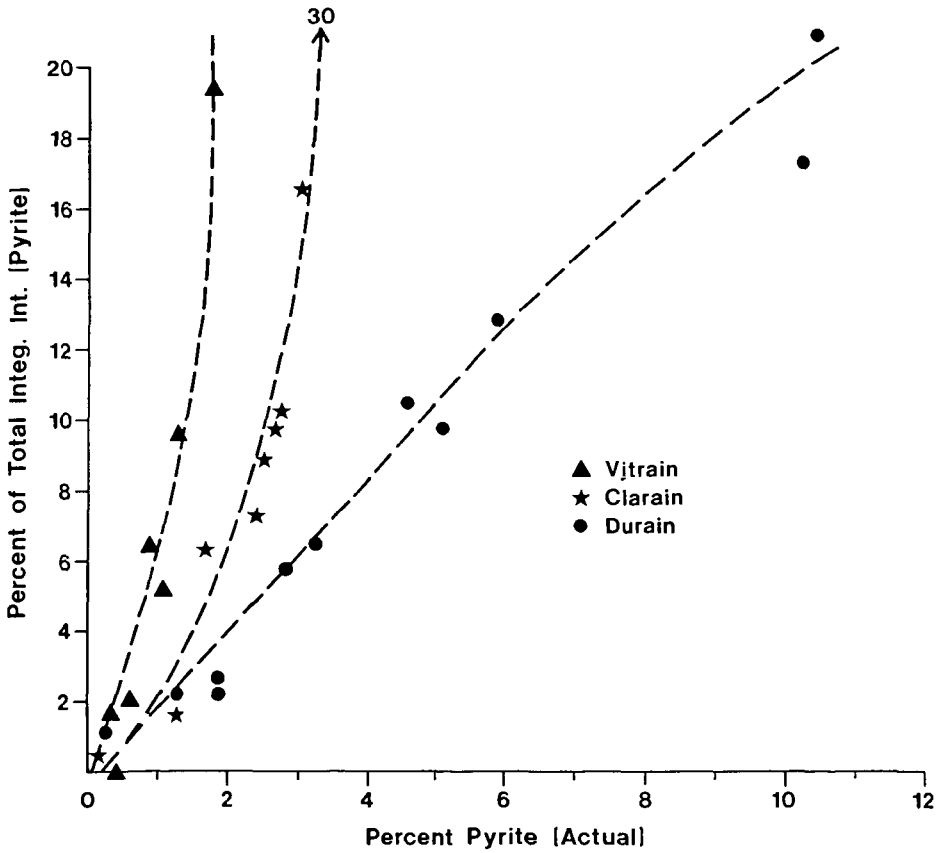

Figure 1. Relationship between actual pyrite composition and relative percent total integrated intensity of pyrite in low temperature ashes of Waynesburg coal lithotypes.

FACTORS INFLUENCING TRACE ELEMENT VARIATIONS IN U.S. COALS

Peter C. Lindahl

Analytical Chemistry Laboratory
Chemical Technology Division
Argonne National Laboratory
9700 South Cass Avenue
Argonne, IL 60439

Robert B. Finkelman

Reservoir and Facies Division
Exxon Production Research Company
P.O. Box 2189
Houston, TX 77001

INTRODUCTION

Although trace element data exist for thousands of coal samples, more will be required to better elucidate trace element trends within coal basins and to help decipher the geological and geochemical controls on trace element distribution and mode of occurrence. However, increased numbers of analyses will not necessarily provide all the answers. We run the risk of ending up information rich but knowledge poor.

The purpose of this paper is to give our analysis of coal trace element data in the literature. Several valuable compilations of trace element data exist for U.S. coal (1-4). We have borrowed freely from these compilations to illustrate their value in elucidating just one aspect of coal geochemistry: the factors influencing trace element variations.

Trace elements are generally defined as those elements with concentrations below 0.1 wt. % (1000 ppm). Despite concentrations in the parts-per-million range, certain trace elements can have a significant impact on coal utilization. For example, the chalcophile elements As, Cd, Hg, Pb, and Se, which are released during coal combustion or leached from coal waste products, can present significant environmental hazards; halogens such as Cl and F can cause severe boiler corrosion, and volatilized Ni or V can cause corrosion and pitting of metal surfaces. Moreover, although not strictly a trace element, sodium, even in small concentrations, can contribute to boiler fouling or to agglomeration of fluidized-bed reactors. On the positive side, some trace elements (e.g., Ge, Zn, U, Au) may eventually prove to be economic by-products, and others may be useful in helping to understand depositional environments (e.g., B) and to correlate coal seams (5,6).

In early studies of trace elements in coal (7-11), coal ash was analyzed using emission spectroscopy. Recent studies (3,4,12,13) have employed quantitative multielement instrumental methods. Because a particular analytical technique is better suited for certain elements than for others, a combination of methods is usually necessary to determine all elements of interest. Methods for determining trace elements in coal must be accurate and precise. In addition, if possible, they should determine a large number of elements of interest simultaneously, require relatively little sample preparation, be capable of automation, produce an output compatible with computerized data processing, and be rapid.

Trace element concentrations in coal show variations from a microscopic to a worldwide scale. From a resource evaluation perspective, the most significant variations occur within and between coal basins. The rest of the paper will discuss factors that cause these variations.

DISCUSSION

Ash Related Variations

The amount of ash in a coal is a major factor influencing trace element content. In general, trace element concentrations increase as ash content increases. This relationship reflects the fact that most inorganic elements in coal are associated with minerals (5). Figures 1 and 2 illustrate this relationship for K in eastern Kentucky coals and for Ti in coals from the Uinta Region.

The above relationship also holds when comparing trace element concentrations among coal basins. Table I compares trace element data for coals from the Black Mesa Field, the Powder River Region, and the San Juan Region. As shown in Table I, the concentrations of the following elements increase as the ash contents of the coals increase: Si, Al, Na, K, Cu, Th, V, Li, Pb, and Se. The reason for the variation of these elements with ash content is that most are, or were, associated with the silicate (detrital) minerals brought into the depositional basins during the formation of the coals. Chemical alteration of minerals within the coal basin can remobilize some elements, which then precipitate as authigenic nonsilicate minerals, e.g., Cu and Pb, as sulfides or selenides (14). The good correlation between element concentration and ash content indicates that most elements have remained within the coal basin despite remobilization (15).

Table I. Concentrations of Selected Elements in Coal Samples from Black Mesa, Powder River, and San Juan Regions[1]

	Black Mesa	Powder River	San Juan
Ash, %	8.0	9.9	21.1
Si, %	1.1	1.5	5.4
Al, %	0.69	0.78	2.7
Ca, %	0.78	1.1	0.67
Mg, %	0.1	0.2	0.1
Na, %	0.09	0.1	0.2
K, %	0.04	0.05	0.16
Fe, %	0.31	0.54	0.54
Ti, %	0.05	0.04	0.11
Cu, ppm	5.5	11.2	13.3
Th, ppm	2.2	4.3	5.9
Zn, ppm	5.6	20	15.1
Cr, ppm	3	7	5
Ni, ppm	2	5	3
V, ppm	7	15	20
Mn, ppm	9.7	51	29
Li, ppm	3.9	5.9	19.7
Pb, ppm	2.7	5.6	13.1
Se, ppm	1.6	1.7	2
Ba, ppm	300	300	300
Sr, ppm	150	200	100
Nb, ppm	1.5	1.5	3
Zr, ppm	15	15	50

[1]Data from Reference 4; results are calculated on a moisture-free coal basis (mf coal).

Elements not increasing in concentration with ash content are generally those with (a) organic affinities (Ca, Mg, Sr, Ba); (b) sulfide affinities (Fe, Zn); (c) carbonate affinities (Ca, Mn, Mg); or (d) sulfate affinities (Ba, Sr, Ca). Sulfides, carbonates, and sulfates are generally epigentic phases. Presence of these phases affects element concentration more than ash content. The concentrations of Zr and Nb would be expected to increase with ash content. The reason that this

behavior is not apparent in Table I may be the poor resolution of the technique (semiquantitative spectrographic analysis) used to obtain the data.

Rank-Related Variations

Several elements exhibit a distinct variation in concentration with coal rank. Table II illustrates the general decrease in concentration of alkaline-earth elements (Mg, Ca, Sr, Ba), Na, and B with increasing coal rank. It is generally accepted that these elements are associated with organic functional groups (e.g., carboxylic acids) in low-rank coals. With increasing coal rank, these groups are destroyed, thus displacing organically associated inorganic trace elements.

Table II. Rank-Related Variations[1]

	Anthracite	Bituminous	Subbituminous	Lignite
Ca, %	0.07	0.33	0.78	1.2
Mg, %	0.06	0.08	0.18	0.31
Na, %	0.05	0.04	0.10	0.21
B, ppm	10	50	70	100
Ba, ppm	100	100	300	300
Sr, ppm	100	100	100	300

[1]Data from Reference 1; mf coal.

Organic association has been proposed for other trace elements, such as Be, Sb, Ge, U, and some halogens (3,16). Finkelman (15) suggests that organic association of these elements is significant mainly for low-rank, low-ash coals.

Concentrations of organically bound elements in coal can decrease with increasing amount of detritus (Figure 3). Also, note that the concentrations of boron decrease with increasing ash contents (Table I).

Variations Due to Geochemical Factors

Geochemical factors, such as Eh and pH during and subsequent to coal formation, can have dramatic effects on trace element contents. The effect of these geochemical factors can be seen in Table III, in which selected data for Appalachian and Interior Province coals are compared. Coals from both areas are similar in rank and ash content, but the Interior Province coals have significantly higher contents of all six trace elements. The higher content of Ca is perhaps due to carbonate mineralization (high pH), whereas that of Fe, Cd, Pb, and Zn is attributable to sulfide mineralization (low Eh). The higher content of B is perhaps attributable to greater marine influence (high salinity).

Table III. Concentrations of Selected Elements in Coal Samples from Appalachian and Interior Coal Basins

	Appalachian[1]	Interior[2]
Ash, %	13.3	15.7
Ca, %	0.12	1.2
Fe, %	1.9	3.3
Cd, ppm	0.7	7.1
Pb, ppm	15.3	55
Zn, ppm	20	373
B, ppm	30	100

[1]Data from Reference 2; mf coal.
[2]Data from Reference 4; mf coal.

The occurrence of cleat-filling sphalerite and galena in the Interior Province coals is a classic example of how epigentic mineralization can affect trace element content (17). Dramatic intra- and interseam variations are common. Cobb (18) reports that zinc content from benches of the Herrin (No. 6) coal varied from 20 to 14,900 ppm.

Variations Due to Geologic Factors

Ash chemistry is another important factor affecting trace element variations. Its influence is, however, generally more subtle than the other factors. In Table IV the trace element contents are compared for Appalachian Province coals and Wasatch Plateau coals. Both are bituminous coals with similar ash contents and rank. However, with a few exceptions, the trace element contents of the Wasatch coals are lower than those of Appalachian coals. The lower content of chalcophile elements in Wasatch coals may be due to a lower pyrite content. The lower concentration of lithophile elements (e.g., Li, Zr, Nb, Th, Sc, Y) but higher Si content may reflect a higher quartz content in the detrital component of Wasatch coals; this, in turn, may be a reflection of differences in the mineralogy of the source rocks.

Table IV. Concentrations of Selected Elements in Coal Samples from Appalachian Province and Wasatch Coal Field

	Appalachian[1]	Wasatch[2]
Ash, %	13.3	11.3
Ca, %	0.2	0.41
Fe, %	1.9	0.26
Cd, ppm	0.7	0.06
Li, ppm	27.6	16
Pb, ppm	15.3	5.8
U, ppm	1.4	1.2
Zn, ppm	20	11
B, ppm	30	100
Nb, ppm	5	0.3
Ni, ppm	15	5
Zr, ppm	50	30
As, ppm	27	0.8
Cu, ppm	24	9.3
F, ppm	80	67
Th, ppm	4.9	1.8
Ba, ppm	100	70
Co, ppm	7	1.5
Cr, ppm	20	10
Mo, ppm	3	0.7
Sc, ppm	5	3
V, ppm	20	15
Y, ppm	10	7

[1]Data from Reference 6; mf coal.
[2]Data from Reference 19; mf coal.

Other Factors Affecting Trace Element Content

Other factors that could modify the ash chemistry or the availability of trace elements include the salinity of waters in contact with the coal or peat, the type of chemical weathering process (arid vs. humid), and hydrologic conditions (Br and Cl may be especially sensitive to this factor). In general, these factors are still poorly understood.

CONCLUDING COMMENTS

In this paper, we made several broad generalizations regarding factors that influence trace element variations. We urge that in interpretative work these generalizations be applied carefully.

A critical evaluation of existing trace element data would probably result in identification of anomalous values and elimination of suspect data. Several questions might be answered by such an evaluation; for example, do the two K values in the high-ash region of Figure 1 deviate significantly from the trend of the other data because of analytical errors or recording errors? Are they legitimate geochemical anomalies? We encourage analytical chemists and geologists to interact closely because this is one of the best ways to improve the quality of analytical methodology and data, and geological interpretation.

The nature of trace element variations, for whatever cause, highlights the need to more judiciously select representative samples for reliable quantitative analyses.

Statistical techniques, such as principal component analysis, should help in resolving the influence of the factors affecting trace element variations in coal.

It is hoped that this paper will encourage more detailed study of factors influencing trace element variations in coals.

ACKNOWLEDGMENT

Portions of this work were performed under the auspices of the U.S. Department of Energy.

REFERENCES

1. Swanson, V. E., Medlin, J. H., Hatch, J. R., Coleman, S. L., Wood, G. H., Jr., Woodruff, S. D., Hildebrand, R. T. Geol. Surv. Open-File Rep. (U.S.) 1976, No. 76-468.
2. Zubovic, P., Oman, C., Coleman, S. L., Bragg, L., Kerr, P. T., Kozey, K. M., Simon, F. O., Rowe, J. J., Medlin, J. H., Walker, F. E. Geol. Surv. Open-File Rep. (U.S.) 1979, No. 79-665.
3. Gluskoter, H. J., Ruch, R. R., Miller, W. G., Cahill, R. A., Dreher, G. B., Kuhn, J. K. Circ.-Ill. State Geol. Surv. 1977, No. 499.
4. Hatch, J. R., Swanson, V. E. Resour. Serv. (Colo. Geol. Surv.) 1977, 1 (Geol. Rocky Mt. Coal-Symp., 1976), 143-164.
5. Finkelman, R. B. Ph.D. Dissertation, University of Maryland, College Park, MD, 1980.
6. Swaine, D. J. In "The Significance of Trace Elements in Solving Petrogenetic Problems and Controversies," Theophrastus Publications S.A.; Athens, Greece, 1983; p. 521-532.
7. Abernethy, R. F., Peterson, M. J., Gibson, F. H. Bur. Mines Rept. Inv. (U.S.) 1969, No. 7281.
8. Zubovic, P., Stadnichenko, T., Sheffey, N. B. Geol. Surv. Bull. (U.S.) 1961, No. 1117-A.
9. Zubovic, P., Stadnichenko, T., Sheffey, N. B. Geol. Surv. Bull. (U.S.) 1964, No. 1117-B.
10. Zubovic, P., Stadnichenko, T., Sheffey, N. B. Geol. Surv. Bull. (U.S.) 1966, No. 1117-C.
11. Zubovic, P., Sheffey, N. B., Stadnichenko, T. Geol. Surv. Bull. (U.S.) 1967, No. 1117-D.
12. Swanson, V. E., Huffman, J. C. Geol. Surv. Circ. (U.S.) 1976, No. 735.
13. Ruch, R. R., Gluskoter, H. J., Shimp, N. F. Environ. Geol. Notes (Ill. State Geol. Surv.) 1974, No. 72.
14. Cecil, C. B., Stanton, R. W., Allshouse, S.C., Finkelman, R. B. "Abstracts of Papers," Chemical Congress - 177th National Meeting of the American Chemical Society and 39th National Meeting of the Chemical Society of Japan, Honolulu, HI, April 1979; American Chemical Society: Washington, DC, 1979; FUEL 48.
15. Finkelman, R. B. "Proceedings," Basic Coal Science Workshop, Houston, TX, Dec. 1981; Energy Resources Co., Inc.: Cambridge, MA, 1982; 69-90.
16. Miller, R. N., Given, P. H. State College, PA, 1978, DOE Report FE-2494-TR-1.
17. Hatch, J. R., Gluskoter, H. J., Lindahl, P. C. Econ. Geol. 1976, 71, 613-624.
18. Cobb, J. C., Masters, J. M., Treworgy, C. G., Helfinstine, R. J. Ill. Mineral Note 1979, No. 71.
19. Hatch, J. R., Affolter, Davis, F. D. Spec. Stud.-Utah Geol. Miner. Surv. 1979, No. 49, 69-102.

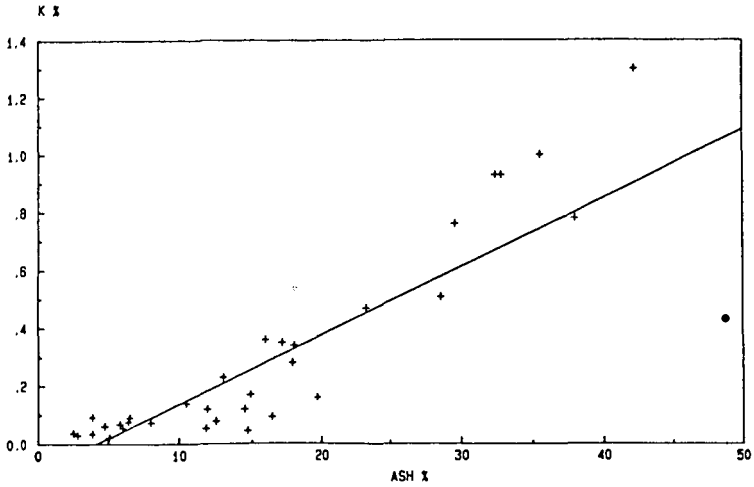

Figure 1. Relationship between K concentration in the coal and ash content for 34 coals from eastern Kentucky. R = 0.86. Data from Reference 1.

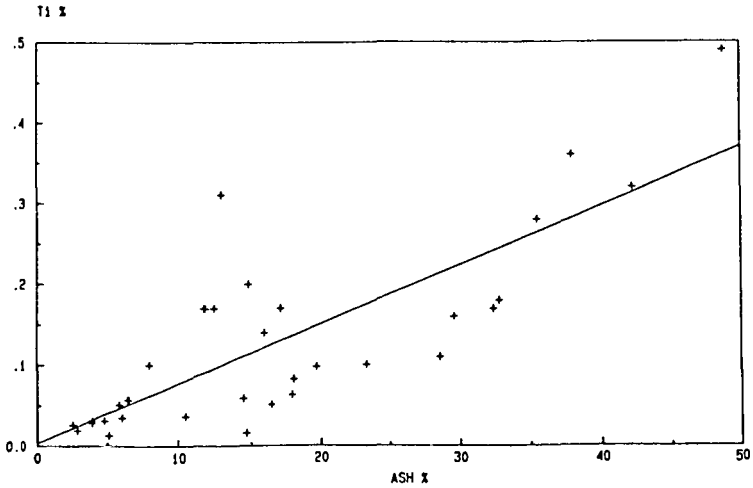

Figure 2. Relationship between Ti concentration in the coal and ash content for 26 coals from the Uinta Region. R = 0.86. Data from Reference 1.

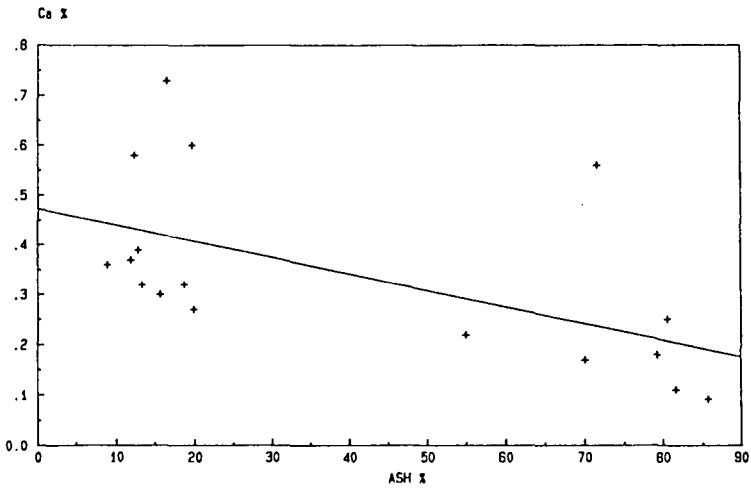

Figure 3. Relationship between Ca concentration in the coal and ash content for 17 coals and shales from the Emery Coal Field. R = -0.57. Data from Reference 18.

ELEMENTAL DISTRIBUTION AND ASSOCIATION WITH INORGANIC AND ORGANIC COMPONENTS IN TWO NORTH DAKOTA LIGNITES

S.A. Benson, S.K. Falcone, and F.R. Karner

University of North Dakota
Energy Research Center
Box 8213, University Station
Grand Forks, North Dakota 58202

Introduction

The associations of major, minor, and trace elements in lignite-bearing strata of the Fort Union Region present a challenge in understanding their geochemical relationships and history. In an earlier work (1), the spatial patterns of elemental distribution within a lignite-bearing sequence were examined and were related to factors of accumulation of vast amounts of plant materials and to the depositional and post-depositional influx of inorganic matter. Lignite-bearing sediments, including the lignite, lignite overburden, and underclay, were sampled from two beds, the Kinneman Creek and the Beulah-Zap, which are part of the Sentinel Butte Formation of North Dakota. These samples were examined to determine the spatial patterns of elemental distribution within the lignite seam, modes of elemental occurrence, and organic/inorganic affinities of the inorganic constituents.

The inorganic constituents within lignites from the Fort Union Region have been classified as being very heterogeneous (2), which leads some investigators to believe that the study of geochemical relationships is futile. The modes of occurrences of the elements are generally similar from one mine to another within the Fort Union Region lignites (3). The inorganic matter in the lignites is distributed as adsorbed ions on the organic acid groups, coordinated species, detrital minerals, and authigenic minerals. The distribution of elements is determined by natural processes, and, therefore, is expected to be systematic even though complex.

The methods to qualitatively identify the interrelationships of major, minor, and trace elements include examining the spatial patterns of distribution of elements within a stratigraphic sequence (1), consideration of results of chemical fractionation procedures (4), and evaluation of organic/inorganic affinities (5,6). The spatial pattern of elemental distribution was correlated with the chemical fractionation behavior, organic/inorganic affinities, and ionic potentials of elements to infer the association or combination of associations an element may have within these coals.

Methods and Procedures

The samples were collected from freshly exposed faces within open pit mines. The lignite, lignite overburden, and underclay were collected from two pits at the Beulah Mine where lignite is mined from the Beulah-Zap seam. Samples were also collected from the Kinneman Creek seam in the Center mine. The sample collection procedures have been summarized by Karner (7) and Benson (8). Bulk channel samples were also collected and homogenized to provide large quantities for additional experiments.

The lignite samples collected at various intervals within the stratigraphic sequence were subjected to the following analyses: proximate, ultimate, heating value, ash analysis, and trace element analysis by neutron activation analysis (NAA) (9) and x-ray fluorescence (10). Minerals in the coal and the associated sediments were determined by x-ray diffraction and by scanning electron microscopy and electron microprobe analysis. A split from the bulk sample was examined by chemical

fractionation to selectively extract inorganic constituents based on how they are bound in the coal. Briefly, the chemical fractionation procedure involves extracting the coal with 1M ammonium acetate to remove soluble and ion-exchangeable inorganic components. The coal is subsequently extracted with 1M hydrochloric acid to remove elements present as carbonates, oxides, or coordinated species. The extracts and residues from the chemical fractionation procedure are analyzed by a combination of NAA, XRF, inductively coupled argon plasma (ICAP), and atomic absorption spectroscopy (AA).

Results and Discussion

The major, minor, and trace element determinations along with locations within the seams and lithology of the stratigraphic sequence are summarized in Tables I and II for the Beulah coals. The data from Center Mine stratigraphic sequence was summarized in a previous report by Karner and others (1).

In previous work (1), the spatial distribution of elemental constituents has been described as fitting into several patterns: 1) concentration at one or both margins, 2) even distribution, and 3) regular patterns. The various ways inorganic constituents accumulated in the lignite during and after deposition affect where certain elements will concentrate within the seam. The detrital constituents carried in by wind and water will most likely be enriched near the margins of the coal seam. Included in this group of inorganic constituents are clay minerals, quartz, and volcanic ash. Solutions containing ions flowing through the lignite can exchange with the coal matrix and precipitate as stable authigenic phases. Inorganic constituents are also present in the original plant material that was deposited. Even patterns of elemental distribution are characteristic of organically bound elements. Irregular distribution patterns are characteristic of concentrated occurrences of authigenic minerals.

Table I includes data from two seams within the south Beulah mine. Table II summarizes the data from a high-sodium pit (Orange Pit) of the Beulah mine. The Center mine data used in this work was reported by Karner and others (1).

In this study, the spatial patterns of enrichment and depletion of major, minor, and trace elements have been expanded to include four categories: 1) even distribution, 2) enrichment at margins (top, bottom, or both), 3) enrichment at the center of the seam, and 4) irregular. The patterns of enrichment and depletion are listed in Table III for Beulah and Center mine lignite seams.

The bulk coals were subjected to chemical fractionation analysis (3) which can be used to categorize how a particular element is associated in the coal. The elemental associations within the coal were divided into three categories: 1) ion-exchangeable, 2) acid-soluble, and 3) residual. The elements are associated in the coal in one or more of the groups described above. The categories for the elements are listed in Table III.

The organic and inorganic affinities of elemental constituents have been determined by a number of investigators (5,6). The relationship between the concentration of an element in moisture-free coal and the ash content can be used as a guide to the affinity of that element for, or incorporation in, the mineral matter or the carbonaceous material. If the concentration of an element increases with increasing ash content that element may be characterized as being associated with the inorganic species that form ash, or in other words may be said to have an inorganic affinity. If the concentration shows no correlation with ash content, that element may be said to have an organic affinity. Linear least squares correlation coefficients were calculated for the concentrations of the elements versus the ash content. For example, organic and inorganic affinities for elements from the Center mine indicate the following affinities. Seven elements - Na, Ca, Mn, Br, Sr, Y, and Ba - had correlation coefficients below 0.200 and thus show organic affinity in this suite of samples. An additional seven elements - Mg, K, Cu, As, Rb, Ce, and Eu - had correlation coefficients ranging from 0.201 to 0.600

and may be associated with both the carbonaceous and mineral portions of the coal. The remaining 24 elements show inorganic affinity.

The ionic potentials of all the elements, Z/r, where Z is the ionic charge and r is the ionic radius, are summarized in Table III. The ionic potentials of elements have a large effect on the association of the element in mineral-forming processes (13). Elements having low ionic potential ($Z/r < 3$), such as sodium, magnesium, and calcium, associate as hydrated cations. Insoluble hydrolysates have ionic potential of $3 < Z/r < 12$, which include, for example, the elements aluminum, silica, and titanium.

The elements displaying an even distribution within the coal seams have the following characteristics: 1) ion-exchangeable, 2) organic affinity or both organic and inorganic, and 3) ionic potential less than 3. The elements that are included in this group are Na, Mg, Ca, Mn, Sr, and Ba. Slight variations in distribution patterns and chemical fractionation behavior may be indicated; these generalizations were made on the basis of average trends. The elements showing enrichment of the margins in the lignite seams display the following characteristics: 1) chemical fractionation suggests association with the acid soluble and residue portions or, in some cases, distribution in all three groups, 2) inorganic affinity, and 3) ionic potential $3 < Z/r < 12$. The elements that have these characteristics include Al, Si, Cl, K, Sc, Ti, V, Cr, Co, Br, Zr, Ra, Cs, La, Ce, Sm, Eu, Yb, Th, and U. These elements are primarily associated with detrital constituents. The elements that have a random or irregular distribution within the coal seams, for the most part, have the following characteristics: 1) chemical fractionation behavior which suggests that the elements are insoluble and remain in the residue, 2) inorganic affinity, and 3) formation by authigenic mineralization. The elements included in this group are Fe, Ni, Zn, As, Se, Cd, and Sb. The irregular distribution of these elements is the result of syngenetic and epigenetic mineralization in the formation of sulfides. All of these elements have chalcophilic characteristics.

The possible associations of the elements included in this study are given in Table IV which summarizes distribution patterns, chemical fractionation behavior, organic and inorganic affinities, and ionic potential.

Acknowledgment

The authors would like to thank Robin G. Roaldson for his assistance in sample preparation and data handling.

Literature Cited

1. Karner, F.R.; Benson, S.A.; Schobert, H.H.; and Roaldson, R.G. ACS Div. Fuel Chem. Preprints, 28 (4), 123-137 (1983).
2. Sondreal, E.A.; Kube, W.R.; and Elder, J.L. BuMines R.I. 7158, 94 pp. (1968).
3. Hurley, J.P.; and Benson, S.A. ACS Div. Fuel Chem. Preprints, to be presented at the Philadelphia ACS Meeting, August 1984.
4. Benson, S.A.; and Holm, P.L. ACS Div. of Fuel Chem. Preprints, 28 (2), 234 (1983).
5. Gluskoter, H.J.; Ruch, R.R.; Miller, W.G.; Cahill, R.A.; Dreker, G.B.; and Kuhn, J.K. Trace Elements in Coal: Occurrence and Distribution, Illinois State Geological Survey Circular 499, p. 109 (1977).
6. Nicholls, G.D. The Geochemistry of Coal-Bearing Strata in Murchison, D., and T.S. Westoll, editors. Coal and Coal-Bearing Strata: American Edition, New York, American Elsevier, p. 269-307 (1968).
7. Karner, F.R.; White, S.F.; Brekke, D.W.; and Schobert, H.H. Geologic Sampling of Lignite Mines in Mercer and Oliver Counties, North Dakota. DOE/FC/FE-1, 1983 (in preparation).
8. Benson, S.A.; Kleesattel, D.; and Schobert, H.H. ACS Div. of Fuel Chemistry Preprints, 29 (1), pp. 108-113, 1984.

9. Weaver, J.N. in Analytical Methods for Coal and Coal Products, Vol. 1, p. 377-401, Karr, C., Jr. (Ed.), Academic Press, Inc., New York (1978).
10. Benson, S.A. Proceedings, North Dakota Academy of Science, 34 (10), 1980.
11. Mason, B. Principles of Geochemistry. John Wiley and Sons Inc., New York, 2nd Ed., 1964, pp. 155-157.
12. Kleesattel, D.R. "Distribution, Abundance, and Maceral Content of the Lithotypes of the Beulah-Zap Bed of North Dakota." For Presentation at the Rocky Mountain Coal Symposium. Bismarck, North Dakota, October 2-4, 1984.

Table I. Elemental Analysis of a Stratigraphic Sequence Containing Two Lignite Seams at the Beulah Mine, North Dakota, part per million unless otherwise indicated, dry coal basis

ID	Lithology	Height, m*	% Ash[1]	Na	Mg	Al	Si**	P**	S**	Cl	K	Ca	Sc	Ti
3-1-A	Underclay	-0.3	--	1964	10364	84699	321178	436	2803	750	10062	3398	11.7	3574
3-2-A	Lignite	0.0	17.0	7767	722	8394	19572	679	17182	100	530	6888	11.9	829
3-3-A	Lignite	0.1	8.47	14348	678	1935	5068	332	10142	8	500	6101	2.1	207
3-4-A	Lignite	0.5	7.30	3479	642	2584	3139	286	8302	100	500	7249	4.9	100
3-5-A	Lignite	0.9	22.20	753	1598	27082	34145	387	13513	100	1908	2191	10.6	438
3-6-A	Clay	1.0	--	1821	13741	113270	298737	0	8009	750	13269	3720	15.0	4211
3-7-A	Clay	1.6	--	2159	12454	111945	307620	0	3204	750	13585	2559	16.1	4560
2-1-A	Lignite	1.7	10.80	3991	671	9428	10956	282	8823	16	500	7062	10.8	125
2-2-A	Lignite	2.1	7.20	7497	707	5192	3971	471	7698	100	500	5281	0.9	119
2-3-A	Lignite	2.6	7.60	9482	717	4542	5045	364	8522	100	713	6206	0.8	140
2-5-A	Lignite	2.9	7.10	6598	731	3431	3086	0	8046	100	500	6031	1.7	226
2-6-A	Lignite	3.3	7.40	6988	571	3886	4981	355	9720	100	500	3973	0.5	59
2-7-A	Lignite	3.4	5.60	6692	564	2664	11048	122	3453	24	500	4615	0.3	100
2-8-A	Lignite	3.6	15.28	6583	3386	7312	10072	800	20071	100	500	8261	0.8	502
2-10-A	Lignite	4.2	6.40	5907	472	4308	5475	223	6561	100	500	12635	2.4	77
2-11-A	Lignite	4.8	12.0	5631	1242	7557	12398	366	10476	100	500	8927	6.1	121
2-13-A	Top of Lignite	5.1	9.10	5561	914	5937	5360	436	10823	100	500	6423	11.5	196
2-14-A	Clay	5.2	--	3518	16012	118373	290790	436	4405	750	16692	4520	15.5	3647
2-15-A	Clay	6.3	--	4385	14031	88995	293127	0	1201	750	15654	4983	13.9	3630
2-16-A	Silt	7.3	--	3440	14605	88403	288453	0	2803	750	9177	2880	12.0	3082
2-17-A	Chert	7.5	--	464	3800	13052	56100	0	9211	1250	1000	1709	12.1	1000
2-18-A	Sandstone	7.8	--	4084	9826	49621	250117	0	2803	750	7608	27085	8.3	2426
2-19-A	Clay	8.9	--	1771	14771	81163	287518	436	4405	750	4162	6110	14.5	4017

Table I. Elemental Analysis of a Stratigraphic Sequence Containing Two Lignite Seams at the Beulah Mine, North Dakota, part per million unless otherwise indicated, dry coal basis (Continued)

ID	Lithology	V	Cr	Mn	Fe	Co	Ni	Cu	Zn	As	Se	Br	Ru	Cd	Sb
3-1-A	Underclay	99	66	177	24853	5.9	>25	150	66	2.51	0.20	1.10	86.00	2.50	0.65
3-2-A	Lignite	66	37	44	15358	5.5	>20	58	19	21.8	1.42	1.70	12.00	1.00	4.61
3-3-A	Lignite	4	5	42	6580	4.0	9	10	25	22.5	0.69	4.98	5.00	1.00	0.05
3-4-A	Lignite	6	6.5	40	2561	1.7	>25	11	25	2.17	0.55	1.69	5.00	1.00	0.04
3-5-A	Lignite	148	39	57	26129	13.0	90	25	9	374	4.28	3.28	16.00	1.00	5.74
3-6-A	Clay	205	91	96	15258	18.0	95	150	30	24.1	0.20	0.77	108.00	1.00	1.78
3-7-A	Clay	181	94	98	11929	2.7	>25	150	94	6.66	4.12	0.76	126.00	2.50	1.35
2-1-A	Lignite	25	16	36	3100	1.9	>25	52	33	11.5	0.43	1.73	3.26	1.20	1.33
2-2-A	Lignite	3	2.8	41	1502	1.2	>25	25	8	3.55	0.10	1.18	5.00	1.00	0.12
2-3-A	Lignite	2	2.9	46	1467	1.1	>25	25	25	5.18	0.52	1.25	5.00	1.00	1.28
2-5-A	Lignite	5	3.1	46	1489	0.7	>25	48	0	2.22	1.00	1.29	5.00	1.00	0.04
2-6-A	Lignite	3	2.5	31	6193	1.0	>25	25	30	31.5	0.39	0.45	1.42	0.65	0.01
2-7-A	Lignite	1	1.3	36	1035	1.1	>25	25	25	0.66	0.32	0.53	5.00	1.00	0.03
2-8-A	Lignite	1	4.4	58	2928	0.6	>25	25	25	4.37	0.59	0.46	5.00	1.00	0.21
2-10-A	Lignite	6	8.6	27	8711	5.2	>25	25	20	21.2	1.27	0.55	5.18	1.00	0.34
2-11-A	Lignite	5	6.5	79	2821	1.5	7	25	19	3.45	0.56	1.24	5.00	1.00	0.29
2-13-A	Top of Lignite	34	9.3	70	2405	3.0	10	10	25	7.03	0.20	1.16	5.00	1.00	0.60
2-14-A	Clay	177	81	212	22282	17.0	121	150	30	14.8	0.20	0.50	115.00	2.50	1.52
2-15-A	Clay	144	64	735	27448	12.0	15	150	30	2.63	0.20	0.50	90.00	2.50	1.04
2-16-A	Silt	136	56	1000	28123	11.0	>20	150	30	2.75	0.20	0.89	77.80	2.50	0.63
2-17-A	Chert	73	18.9	8046	273475	2.7	>25	300	200	0.50	0.20	0.89	10.00	2.50	0.19
2-18-A	Sandstone	73	55	611	15853	8.6	>20	150	52	6.09	0.54	0.25	50.64	2.50	0.49
2-19-A	Clay	134	68	738	35592	12.0	>20	150	30	2.48	3.22	1.12	87.00	2.50	0.73

Table I. Elemental Analysis of a Stratigraphic Sequence Containing Two Lignite Seams at the Beulah Mine, North Dakota, part per million unless otherwise indicated, dry coal basis (Continued)

ID	Lithology	Cs	Ba	La	Ce	Sm	Eu	Yb	U
3-1-A	Underclay	4.96	786	32.18	48.66	2.51	1.36	1.59	1.91
3-2-A	Lignite	5.50	746	8.07	19.81	1.31	0.71	2.22	2.09
3-3-A	Lignite	0.02	756	1.29	8.46	1.42	0.36	1.37	0.50
3-4-A	Lignite	0.05	1114	2.95	9.21	1.04	0.46	1.62	0.23
3-5-A	Lignite	4.56	683	45.36	71.90	8.29	1.95	1.38	3.32
3-6-A	Clay	8.10	676	45.36	41.00	2.45	1.13	1.20	3.32
3-7-A	Clay	10.00	644	36.00	45.32	2.58	0.98	1.60	2.34
2-1-A	Lignite	1.49	1005	2.49	8.32	1.05	0.49	1.41	1.86
2-2-A	Lignite	0.05	988	9.75	14.35	0.52	0.21	0.40	0.41
2-3-A	Lignite	0.05	1158	3.75	6.98	0.35	0.12	0.38	0.36
2-5-A	Lignite	0.05	1284	11.36	16.00	0.43	0.11	0.41	0.56
2-6-A	Lignite	0.16	844	0.84	1.00	0.17	0.07	0.11	0.23
2-7-A	Lignite	0.12	1041	0.58	1.66	0.17	0.06	0.07	0.10
2-8-A	Lignite	0.05	21	2.07	4.08	0.42	0.26	0.63	0.50
2-10-A	Lignite	1.15	3045	7.47	39.27	0.63	0.55	0.42	0.24
2-11-A	Lignite	0.34	1749	4.06	9.69	0.81	0.37	1.11	0.90
2-13-A	Top of Lignite	0.02	226	3.52	6.77	0.82	0.43	1.39	2.08
2-14-A	Clay	8.50	811	36.20	52.50	2.73	1.11	1.72	2.88
2-15-A	Clay	5.31	813	35.00	45.61	3.28	1.30	1.83	1.82
2-16-A	Silt	4.35	613	28.00	39.00	2.54	1.06	1.17	2.30
2-17-A	Chert	0.40	274	11.60	10.00	1.27	0.40	1.09	0.20
2-18-A	Sandstone	3.00	725	26.70	37.00	2.65	1.18	1.26	1.54
2-19-A	Clay	5.28	851	25.60	46.70	2.63	1.43	1.81	1.75

*Height from base of first seam.
**Determined by x-ray fluorescence.
†Ash on a moisture-free basis

Table II. Elemental Analysis of a Stratigraphic Sequence Containing One Lignite Seam from the Orange Pit of the Beulah Mine, North Dakota, ppm (dry basis)

ID	Lithology	Height, m*	Ash, %	Na	Mg	Al	Si**	S**	Cl	K	Ca	Sc	Ti	V
B-1	Lignite	-0.5	7.1	7041	1041	2824	10800	65890	44.3	500	7317	2.16	132	3.02
B-2	Lignite	0.00	6.8	5178	1004	3107	12950	46240	43.9	500	9072	0.64	132	2.84
B-3	Lignite	0.50	6.7	5833	1150	3472	7940	50030	52.8	500	8891	0.57	138	2.73
B-4	Lignite	1.00	6.8	6018	1043	2675	16760	51530	41.8	500	7803	0.57	144	2.22
B-5	Lignite	1.50	13.0	5826	3526	6710	12580	65160	132.7	500	8016	0.38	326	5.84
B-6	Lignite	2.00	6.9	5313	1238	2793	39940	59750	49.2	500	7828	0.36	150	2.20
B-7	Lignite	2.50	8.5	6169	1292	4348	93000	64240	63.2	500	11998	0.43	162	2.50
B-8	Lignite	3.00	15.7	6278	1449	5869	44510	64020	70.9	500	10872	0.48	167	2.12
B-9	Lignite	3.50	10.4	5096	1483	7929	104700	56470	54.1	500	11876	1.05	226	4.85
BR-1	Overburden	3.60	--	2246	15718	91958	275900	3130	750	9724	7094	15	2390	136.00
BR-3	Overburden	4.14	--	2773	13226	89901	259700	1100	750	14994	6673	18	4256	165.00
BR-5	Overburden	4.80	--	3098	15480	97158	281400	497	100	8653	7342	16	3880	158.00
BR-6	Overburden	5.10	--	2619	15475	84893	288900	1480	100	10800	6197	5.1	3674	134.00
BR-9	Overburden	6.10	--	2389	16774	88663	294000	1350	750	14971	9553	15.8	4557	142.00
BR-11	Overburden	6.70	--	2082	9982	51610	187700	3220	750	14971	9465	18.7	2760	119.00
BR-13	Overburden	7.30	--	2842	12634	66743	277400	12710	750	6441	12042	8.97	3796	80.1
BR-13A	Overburden	7.35	--	3028	14339	78427	284900	840	150	8994	123401	12.9	4131	117.0
BR-18	Overburden	8.90	--	3028	12471	75153	286200	1070	750	8994	13916	14.0	4360	117.0
BR-19	Overburden	9.20	--	2863	12793	78030	290700	<100	750	10006	14862	14.0	3451	117.0

Table II. Elemental Analysis of a Stratigraphic Sequence Containing One Lignite Seam from the Orange Pit of the Beulah Mine, North Dakota, ppm (dry basis) (Continued)

ID	Lithology	Cr	Mn	Fe	Co	Ni	Cu**	Zn	As	Se	Br	Sr**	Y**	Zr**
B-1	Lignite	2.24	22	5147	1.68	5.75	53	12.62	10.67	0.05	1.62	360	6	8
B-2	Lignite	1.62	28	3261	0.75	10.23	33	5.48	3.90	0.40	1.40	445	6	11
B-3	Lignite	1.41	29	3462	0.70	10.71	53	6.08	3.52	0.39	1.49	480	4	13
B-4	Lignite	1.37	28	3289	0.39	13.17	58	4.78	3.34	0.50	1.04	410	2	9
B-5	Lignite	2.08	136	22202	0.37	5.00	23	25.00	27.18	0.91	0.84	320	2	<5
B-6	Lignite	1.89	37	3308	0.80	15.34	64	25.00	5.24	0.54	0.99	360	2	8
B-7	Lignite	2.30	33	1706	0.59	11.36	59	3.46	3.55	0.49	0.55	520	2	15
B-8	Lignite	2.60	48	30530	0.69	15.66	30	25.00	39.17	0.79	0.81	330	2	10
B-9	Lignite	3.51	47	2897	0.70	9.36	62	8.57	7.85	0.36	0.92	520	6	17
BR-1	Overburden	86.2	611	36878	14.02	28.88	86	30.00	12.66	1.56	0.92	262	26	112
BR-3	Overburden	93.2	2092	50756	13.57	72.84	73	30.00	2.50	0.57	1.05	223	28	94
BR-5	Overburden	92.4	467	30865	10.97	22.93	87	30.00	5.25	1.40	0.27	239	26	109
BR-6	Overburden	32.4	979	14308	3.99	95.69	81	25.00	6.23	0.42	0.55	234	31	126
BR-9	Overburden	88.0	885	39106	13.78	63.45	84	30.00	3.52	1.25	0.92	230	25	108
BR-11	Overburden	72.3	3542	147377	11.26	39.66	46	30.00	2.50	0.20	1.07	104	18	66
BR-13	Overburden	63.0	308	36902	10.14	50.09	64	30.00	27.16	1.01	1.41	255	22	169
BR-13A	Overburden	78.7	424	26437	9.95	20.00	71	30.00	5.01	0.84	1.46	274	28	165
BR-18	Overburden	90.8	670	31472	11.33	45.09	80	30.00	5.01	0.53	1.46	285	25	131
BR-19	Overburden	90.8	435	28566	11.44	36.64	73	30.00	3.34	1.08	1.08	265	27	164

Table II. Elemental Analysis of a Stratigraphic Sequence Containing One Lignite Seam from the Orange Pit of the Beulah Mine, North Dakota, ppm (dry basis) (Continued)

ID	Lithology	Ru	Ag	Cd	Sb	Cs	Ba	La	Ce	Sm	Eu	Yb	Th	U
B-1	Lignite	2.00	0.15	5.00	0.01	0.01	714	7.84	8.30	0.53	0.11	0.36	0.57	0.40
B-2	Lignite	1.37	0.53	5.00	0.04	0.04	917	3.30	5.61	0.49	0.09	0.28	0.75	0.24
B-3	Lignite	2.00	0.48	5.00	0.10	0.03	943	3.62	6.39	0.43	0.06	0.24	0.81	0.23
8-4	Lignite	2.00	0.79	0.34	0.10	0.03	844	3.24	4.92	0.24	0.05	0.09	0.83	0.75
B-5	Lignite	2.00	0.05	1.10	0.07	0.01	930	12.78	13.14	0.34	0.03	0.01	0.78	0.40
B-6	Lignite	2.00	0.53	0.19	0.01	0.03	704	0.98	2.42	0.26	0.01	0.06	0.49	0.31
B-7	Lignite	2.00	0.75	5.00	0.06	0.03	1138	1.52	3.18	0.31	0.05	0.09	1.01	0.56
B-8	Lignite	2.00	0.37	1.87	0.04	0.05	1242	2.20	9.98	0.28	0.07	0.08	1.12	1.26
8-9	Lignite	2.00	0.15	5.00	0.22	0.08	720	2.38	4.97	0.55	0.12	0.38	1.75	0.99
BR-1	Overburden	114.48	0.08	2.50	0.44	6.57	1075	12.19	63.46	1.17	1.30	1.07	10.37	1.51
BR-3	Overburden	131.48	0.08	2.50	0.50	7.56	732	14.58	67.26	1.23	1.29	1.77	10.14	1.03
BR-5	Overburden	164.19	0.08	2.50	0.49	7.53	685	13.82	61.24	1.25	1.12	1.33	9.50	0.80
BR-6	Overburden	35.87	0.49	5.00	0.51	0.79	285	12.70	18.50	1.26	0.31	0.73	3.26	0.76
8R-9	Overburden	127.44	0.08	2.50	0.38	6.38	567	12.31	61.70	1.12	1.33	1.59	9.39	1.09
BR-11	Overburden	77.75	0.00	2.50	0.69	4.50	401	16.88	82.93	1.59	1.37	1.46	7.02	2.99
BR-13	Overburden	72.16	0.08	2.50	0.40	3.39	444	12.36	69.63	1.15	1.26	1.15	7.84	1.12
BR-13A	Overburden	108.76	20.08	2.50	0.38	4.53	619	14.57	63.00	1.28	1.35	1.50	9.35	0.80
BR-18	Overburden	101.83	0.08	2.50	0.38	5.10	567	14.00	63.00	1.35	1.43	1.52	9.45	1.27
BR-19	Overburden	94.82	0.08	2.50	0.30	4.69	511	13.55	64.46	1.22	1.46	1.71	10.18	1.13

*Height from base of first seam.
**Determined by x-ray fluorescence.
† Ash on a moisture-free basis

Table III. Qualitative Geochemical Relationships Between Geochemical Properties and Elemental Distribution Within Seams

	Distribution Within Lignite Seams at the Beulah Mine					Distribution Within Lignite Seam at the Center Mine			
		Beulah							
	Beulah Orange Pit	Upper Seam	Lower Seam	Chemical Fractionation Behavior	Affinity	Center	Chemical Fractionation Behavior*	Affinity	Ionic Potential Z/r
Na	E	E	CE	IE	Organic	E	IE	Organic	1.0
Mg	E	E	E	IE	NC	E	IE>>AS	NC	3.0
Al	T-MA	MA	B-MA	AS, RS	Inorganic	MA	AS, RS	Inorganic	5.9
Si	T-MA	IR	E	RS	Inorganic	MA	RS	Inorganic	9.5
P	ND	IR	B-MA	ND	Inorganic	IR	ND	Inorganic	14.3
S	IR	IR	MA	RS, IE	Organic	MA	RS, IE	Organic	17.1
Cl	E	E	E	ND	NC	B-MA	ND	Inorganic	
K	E	E	E	RS, AS	Inorganic	B-MA	IE, AS, RS	Inorganic	0.13
Ca	E	CE	E	IE, AS	NC	E	IE, AS	NC	2.0
Sc	MA	MA	MA	RS, AS	NC	MA	AS, RS	Inorganic	3.7
Ti	T-MA	IR	B-MA	RS	Inorganic	B-MA	RS	Inorganic	5.9
V	E	MA	B-MA	AS	NC	B-MA	AS, RS	Inorganic	4.0
Cr	MA	MA	B-MA	RS	Inorganic	B-MA	RS	Inorganic	4.8
Mn	E	T-MA	T-MA	AS, IE	NC	E	AS, IE	NC	2.5/6.7
Fe	IR	IR	B-MA	RS, AS	Inorganic	MA	AS	Inorganic	2.7/4.7
Co	B-MA	ND	ND	AS, RS	Inorganic	MA	AS, RS	Inorganic	2.8
Ni	IR	E	MA	RS	Inorganic	MA	RS	Inorganic	3.0
Cu	IR	E	B-MA	ND	Inorganic	B-MA	RS	Inorganic	1.0/2.8
Zn	IR	ND	ND	RS	Inorganic	MA	ND	Inorganic	.88/2.7
Ge	ND	ND	ND	ND	ND	B-MA	ND	ND	2.7/7.5
As	IR	IR	IR	RS	Inorganic	MA	RS	NC	10.8
Se	CE	IR	B-MA	RS	Inorganic	B-MA	RS, IE	Inorganic	14.3
Br	B-MA	MA	CE	ND	NC	ND	ND	Organic	
Rb	ND	ND	ND	ND	ND	IR	RS, AS	ND	0.68
Sr	E	ND	ND	IE	Organic	E	IE	Organic	1.8
Y	MA	ND	ND	ND	ND	IR	ND	ND	3.4
Zr	T-MA	ND	ND	RS	ND	MA	ND	Inorganic	5.1
Ru	E	E	B-MA	ND	Inorganic	B-MA	ND	Inorganic	6.0
Ag	IR	ND	ND	ND	ND	MA	ND	Inorganic	2.2
Cd	ND	E	E	RS	NC	IR	ND	Inorganic	.87/2.1
Sb	IR	B-MA	B-MA	RS	Inorganic	B-MA	AS, RS	Inorganic	4.0
Cs	T-MA	B-MA	B-MA	RS	Inorganic	B-MA	RS	Inorganic	0.6
Ba	E	T-MA	T-MA	IE, AS	NC	MA	IE, AS	NC	1.5
La	B-MA	IR	MA	AS, RS	Inorganic	B-MA	AS, RS	Inorganic	2.6
Ce	B-MA	IR	B-MA	AS, RS	Inorganic	MA	AS, RS	NC	2.9
Sm	MA	MA	E	AS, RS	Inorganic	MA	AS	Inorganic	3.1
Eu	MA	MA	MA	AS, RS	Inorganic	MA	AS	NC	3.2
Yb	MA	MA	MA	AS, RS	NC	MA		Inorganic	
Th	T-MA	MA	B-MA	RS	Inorganic	MA	RS	Inorganic	3.9
U	T-MA	MA	B-MA	AS, RS	Inorganic	MA	AS, RS	Inorganic	4.2

Patterns of Distribution

E - Even Distribution
MA - Enrichment at both margin
T-MA - Enrichment at top margin
B-MA - Enrichment at bottom margin
CE - Enrichment at the center of the seam
IR - Irregular

*Chemical Fractionation Behavior

IE - Ion-exchangeable
AS - Acid soluble
RS - Remains in the residue
NC - No Correlation
ND - Not Determined

Table IV. Association of Elements in North Dakota Lignites

Element		Possible Association
Na	-	Organically bound
Mg	-	Organically bound, carbonates
Al	-	Clay minerals, possibly hydroxide or coordinated
Si	-	Clay minerals, quartz
P	-	Organically bound, phosphates*, associated with rare earth elements
S	-	Sulfides, sulfates, organically bound
Cl	-	Inorganic association
K	-	Associated with illite and other k-bearing minerals, organically bound
Ca	-	Organically bound, carbonates
Sc	-	Inorganic association, clay minerals
Ti	-	Rutile, associated with quartz
V	-	Possibly has both an organic and inorganic association
Cr	-	Totally an inorganic association
Mn	-	Organically bound, carbonate minerals
Fe	-	Oxides, hydroxides, sulfides
Co	-	Inorganic association, possibly sulfides
Ni	-	Inorganic association, possibly sulfides
Zn	-	Inorganic association, possible sulfides
As	-	Inorganic association, possible sulfides
Se	-	Inorganic association, possibly sulfides
Br	-	May have an organic association
Rb	-	Organically bound
Sr	-	Organically bound
Y	-	Inorganic association, possibly carbonates
Zr	-	Zircon
Ru	-	Inorganic
Ag	-	Inorganic, possibly sulfides
Cd	-	Inorganic, possibly sulfides
Ba	-	Organic, sulfates
La	-	Detrital inorganic, phosphates*
Ce	-	Detrital inorganic, phosphates*
Sm	-	Detrital inorganic
Eu	-	Detrital inorganic
Yb	-	Detrital inorganic
Th	-	Detrital inorganic
U	-	Detrital inorganic

*Monazite has been found in Beulah lignite samples (12).

VOLCANIC ASH LAYERS IN COAL: ORIGIN, DISTRIBUTION, COMPOSITION AND SIGNIFICANCE

Don Triplehorn and Bruce Bohor

Geology/Geophysics Program, University of Alaska, Fairbanks, Alaska 99701, and U.S. Geological Survey, Federal Center, Denver, Colorado 80225

INTRODUCTION

The main purpose of this paper is to call attention to volcanic eruptions as a source of mineral matter in coal. Volcanic material is apt to have mineral and chemical compositions as well as patterns of distribution different from the more usual types of mineral matter in coal. Recognition of volcanic material requires some understanding of the process of origin, an awareness of the considerable variety of materials involved, and an appreciation of the tendency of volcanic materials to undergo substantial alteration so that their genesis is obscured.

Some comments on terminology are necessary. "Volcanic ash partings" here refers to sedimentary units bounded by organic-rich material (coal, lignite, or organic shale) and which were deposited as air-fall volcanic ash with essentially no subsequent transport or mixing with terrigenous detrial silicates (clay, mud and sand). No specific grain size or composition is implied. The term "tephra" is now commonly used for modern, unaltered, uncompacted material, while the term "tuff" is used for the compacted (rock) equivalent.

A volcanic origin is obvious where there is glass, volcanic phenocrysts, characteristic mineralogy, or absence of terrigenous detritus and lack of sedimentary structures formed by moving water. With increasing age, however, there is progressive alteration and loss of recognizable volcanic features; the product is generally some kind of clay unit. As a general term they might be called altered tuffs. In marine shales they are known as bentonites; these are usually montmorillonitic (smectitic), light-colored, and sticky when wet. In coals, particularly Carboniferous coals, they are usually kaolinitic, light-colored and firm. We prefer the general term "altered volcanic ash" because there is considerable range in physical appearance, original and secondary mineralogy, as well as in the type of enclosing sediment.

ORIGIN

Volcanic ash partings in coals should not be surprising. The recent eruption of Mt. St. Helens spread volcanic ash across several western states and traces of the dust traveled around the world. Consider, however, where a recognizable layer of this ash is likely to be preserved. On land, almost all of it will be eroded by wind and water, mixed with terrigenous sand and clay, and ultimately dispersed into lakes or the ocean. An important exception is to be found in marshes or swamps, the general setting in which plant material accumulates to eventually become coal. Once deposited in a coal swamp, an ash fall has a good chance of

remaining undisturbed because the shallow water, low stream gradients, lack of relief, and sediment baffling effects of vegetation minimize processes that could cause reworking. Portions of such swamps may be so distant from major streams that they receive little or no mud from overbank floods. Thus it is likely that some ash falls would be buried in organic debris (coal) and remain free of non-volcanic material from fluvial sources.

It follows then that there is a genetic relationship between volcanic ash partings and the coals that contain them: environments of coal deposition provide one of the best places for preservation of air-fall volcanic materials.

Not all kinds of volcanic ash have the same chance of such preservation, however. Many volcanoes, such as those in Hawaii, are characterized by relatively quiet eruptions of mostly fluid lava. Though spectacular on a human scale, these involve only minor injection of fine-grained material into the upper atmosphere where it can be carried long distances by prevailing winds. Only volcanoes characterized by particularly violent eruptive styles are likely to be important in producing the thin, widespread units of ash most commonly preserved in the geologic record. The explosiveness of eruptions is related to several factors, including gas content and geometry of the vent. Of most importance here, however, is silica content: silica increases the viscosity of magma and the tendency toward explosive eruptions rather than quiet flows. Thus volcanic ash partings in coals are primarily the product of such silica-rich eruptions; this has important consequences in terms of the composition of the ash, as will be discussed later.

FIELD APPEARANCE OF VOLCANIC ASH PARTINGS IN COALS

Most volcanic ash partings are thin, ranging from 1 mm to a few cm. A few, however, attain thicknesses of more than 1 m. Some are uniform in thickness and have either sharp or gradational boundaries with the enclosing coal. Many, however, pinch and swell rapidly and may consist of a series of lenses rather than continuous beds, a feature they share with Carboniferous tonsteins (Williamson, 1970). Light shades of gray, brown, or yellow are most common, reflecting a lower organic content than the adjacent coal. Black and dark brown partings also occur, and sometimes these become obvious only after weathering; the oxidation of organic matter then results in a light-colored surface layer of siliceous material. Figure 1 shows the most common field appearance; in this case for a Cretaceous example from southern Alaska.

To a large extent the grain size and degree of induration of these partings depends upon the amount of post-depositional alteration; this in turn is largely a function of age and depth of burial. For example, lignites almost 4-5 m.y. old in southern Alaska contain partings that are loose and sandy; in fact they are clearly recognizable volcanic ash consisting mostly of glass shards. In contrast, 300 m.y. old partings in Kentucky bituminous coal are hard and very fine grained. The latter probably was similar to the Alaskan example at first, but has completely altered to a compact variety of kaolin known as flint clay.

COMPOSITION

Composition of the partings is a function of both the original materials and conditions, and the kind and extent of post-depositional modification. Therefore it is necessary to consider the primary composition (original) separately from the secondary composition (altered).

Primary Composition

The solid products of explosive volcanism include individual glass fragments, individual crystals (phenocrysts), and aggregates of these known as rock fragments. Glass is perhaps the most common component but there is a great variety among modern volcanics. A given volcano may eject different material over its eruptive lifespan. Even a single eruption, lasting perhaps only a few days, may involve changes in ash composition.

Volcanic ashes are characterized by a limited suite of mineral components. By far the most abundant are quartz, sanidine and plagioclase feldspars, certain pyroxenes and amphiboles, magnetite, apatite, biotite, and zircon. The presence of these minerals and the absence of others constitute evidence of a volcanic origin. Certain crystal forms, such as the beta form of quartz and hexagonal prisms of biotite, are particularly useful indicators of origin. Similarly, the presence of sanidine, the high-temperature form of potassium feldspar, suggests a volcanic origin. On the other hand, the presence of non-volcanic minerals such as muscovite and garnet indicates a non-volcanic origin or at least some admixture of non-volcanic (probably fluvial) material.

The specific minerals present reflect the original compositions of the magma. As noted earlier, explosive behavior, the kind most likely to produce ash partings in coals, is characteristic of silica-rich magmas. Thus the minerals cited above, and those to be expected in volcanic ash partings, are those associated with silica-rich magmas. The glass phase will, of course, also reflect this silica-rich tendency.

Original grain size of an ash parting reflects the texture of the material produced by a given volcano plus the progressive loss of coarser and denser components as an ash cloud moves downwind. In other words, texture is in part a function of distance from the source volcano. By far the most common ash partings in coal are thin, uniform and widespread. These probably were derived from distant volcanoes and consisted originally of silt-and clay-sized particles carried by high-altitude winds. Conversely, where ash partings are coarse-grained, thick, and abundant, the volcanic source is assumed to have been relatively close.

Secondary Composition

The primary composition discussed above is important here in that it determines in part the final products of alteration. It should be noted, however, that the factors controlling the degree and direction of alteration have not been thoroughly studied. In our opinion, chemical alteration in the environment of deposition and the length of time involved are probably more important than original composition in determining the final product.

The main secondary products are clay minerals, either smectite or kaolinite. These clay minerals are derived mainly and most readily from glass, but feldspars, amphiboles, pyroxenes, and biotite also alter in part to clay minerals. The alteration to kaolinite involves essentially complete removal of soluble components such as Na, Ca, Mg, K and Fe as well as considerable silica. Pure kaolinite consists of equal parts of silica and alumina and virtually nothing else--this is thus the product of very intensive leaching. Smectite on the other hand requires some Mg and more silica; it is thus the product of less intensive leaching than that which produces kaolinite.

It is uncertain whether the path of alteration can lead directly to kaolinite or must pass through a smectite intermediate stage. Certainly the thickness of the original ash can play a role: thin partings may be altered completely to kaolinite while adjacent thicker partings contain substantial smectite (Triplehorn and Bohor, 1981; Reinink-Smith, 1982). Given more time and further leaching, these smectitic partings presumably would eventually be altered to kaolinite. On the other hand, individual minerals such as feldspars and biotite can be observed altering directly to kaolinite without any smectite involvement.

A variety of other secondary minerals may occur in altered volcanic ash partings. Some of these may be related to modification of the primary constituents but others are more likely introduced by ground water taking advantage of the higher permeabilities of volcanic ash layers relative to the adjacent organic material (now coal). Carbonate minerals in quantities too large to have been derived entirely from the primary volcanic material are not uncommon. Siderite is most abundant although dolomite sometimes is present. Such cementation may obscure the volcanic origin of the original layer because well cemented partings are similar in appearance to the purely sedimentary carbonate layers that are very commonly associated with coals.

Recently occurrences of unusual aluminum phosphate minerals have been found with ash partings in coals (Triplehorn and Bohor, 1983). Since that report we have found a number of occurrences in Alaska and one in the Appalachian area. These minerals were grouped by Palache _et al._ (1951) as the plumbogummite series, with the general formula $X\,Al_3(PO_4)_2(OH)_5H_2O$. End members of interest here include goyazite (where X = Sr), gorceixite (Ba), crandallite (Ca), and florencite (Ce, U, and other rare earths). Some layers in Alaska are sufficiently radioactive to give a distinct reading on hand-held radiation detectors in the field.

DISTRIBUTION

Because many geologists are not aware that volcanic ash partings occur in coals it is difficult to interpret the absence of published reports regarding their occurrences. The abundance of such partings is probably much greater than presently recognized. The following generalities regarding their distribution are mainly limited to North America and are based primarily on our own observations, discussions with others, and interpretation of published reports. Specific references to recognized volcanic ash partings in coals are relatively few and restricted mostly to the past few years.

In simple terms ash partings are relatively abundant in Cretaceous and Tertiary coals of the West and rare in Carboniferous coals of the East. We are less certain of the Gulf Coast Tertiary lignites but they appear to have at least a moderate abundance of such partings. To a degree this apparent distribution is related to the fact that the volcanic origin of the younger ash beds is more apparent, while older partings commonly appear as kaolinitic clay beds with little evidence of their volcanic heritage (see Bohor and Triplehorn, 1981). Even so, there is no question that the absolute frequency is higher in the West.

Locally the abundance can be highly variable. Where many coals are present ash partings may be distributed sparsely but uniformly or concentrated in just a few coals. Figure 2 shows an example in Southwestern Washington, in this case including both kaolinitic and smectitic partings (Reinink-Smith, 1982). In the West, where most of our work has been, volcanic ash partings are known from numerous coals in Utah, New Mexico, Colorado, Wyoming, Montana and Washington (Bohor, et al. 1978; Triplehorn and Bohor, 1981). Again, the frequency is highly variable. Individual coals in Montana and Colorado contain up to twenty or more ash partings, while the unusually thick coals of the Powder River Basin contain almost none. In Alaska, volcanic ash partings are present in all of the Cretaceous and Tertiary coals we have examined, but appear to be particularly abundant in the Cook Inlet area.

In the Appalachian coal basin and the Eastern Interior Basin, where we have had less experience, ash partings appear to be rare (Bohor and Triplehorn, 1982). The lack of ash partings in Carboniferous coals of eastern North America contrasts with their abundance in European coals of the same age. These have been studied for over a century although their volcanic origin was not generally accepted until the last few decades. Bouroz, et al. (1983) provides a good recent summary of some of this work in English.

SIGNIFICANCE

The geologic importance of volcanic ash partings in coals has been summarized previously by Triplehorn (1976). Of greatest importance is their use in correlation, the process of determining the time relationships among rocks exposed at different localities. The simplest use is as marker beds, where individual ash falls can be recognized and distinguished from others on the basis of some textural or compositional aspect. Beds containing the same ash layer (whether in coal or any other rock type) are the same age, although the absolute age (in years) is not indicated. Happily, the absolute age can sometimes be determined by radiometric age dating of certain minerals in the ashes. Potassium-argon dating is used for such minerals as feldspar and hornblende, while fission-track dating may be used for zircon and apatite.

It may be of interest here to note that Williamson (1970) mentioned the high radioactivity of certain ash partings (he called them tonsteins) that made them useful in bore-hole studies because they appeared as sharp maxima on gamma-ray logs of coal beds. Such maxima are conspicuous because coals are generally known for their absence of radioactivity.

He ascribed the high radioactivity of these partings to an unusual abundance of zircons. We have no specific knowledge of these occurrences, but suggest that the high radioactivity might instead be related to uranium-bearing phosphate minerals.

Thus far geologists have paid little attention to the significance of ash partings as indicators of processes and conditions in the coal-forming environment. For example, thin widespread partings without penetrating plant material suggest that these originated as ashes that fell into shallow standing water. Thick ashes should have affected the kind and amount of vegetation, and indirectly the nature of the coal immediately overlying thick ash beds. As yet there is little data in these aspects because geologists have not recognized the potential value of such studies.

For those interested in mineral matter in coal an awareness that some partings may be of volcanic origin may be useful in explaining the distribution of some of these layers and the occurrences of some unusual components, such as strontium, phosphate, or uranium. Volcanic ash partings are likely to be more widespread and uniform in texture, composition and thickness than the more common partings of fluvial origin. They are also more likely to show marked differences from layer to layer, and more likely to contain exotic mineral or chemical components.

REFERENCES

Bohor, B.F., R.M. Pollastro, and R.E. Phillips, 1978, Mineralogical evidence for the volcanic origin of kaolinite partings (tonstein) in Upper Cretaceous and Tertiary coals of the Rocky Mountain region (abstr.): The Clay Mineral Soc., 15th Ann. Mtng., 27th Ann. Clay Minerals Conf. Bloomington, Indiana, Program and Abstracts, p. 47.

Bohor, B.F., and D.M. Triplehorn, 1982, Volcanic origin of the Flint Clay parting in the Hazard #4 (Fire Clay) coal bed of eastern Kentucky, field trip guidebook, Geological Society of America Ann. Mtng., Oct., 1981, issued by Kentucky Geological Survey, 1982, p. 49-53.

Bouroz, A., D.A. Spears, and F. Arbey, 1983, Review of the formation and evolution of petrographic markers in coal basins: Societe Giologique du Nord, Memoires Tome XVI, 115 pp.

*Triplehorn, D.M., 1976, Volcanic ash partings in coals: characteristics and stratigraphic significance, The Neogene Society, Spring, 1976, Pacific Section, Society of Economic Paleontologists and Mineralogists, p. 9-12.

Triplehorn, D.M. and B.F. Bohor, 1981, Altered volcanic ash partings in the C-coal, Ferron Sandstone member of the Mancos Shale, Emery County, Utah, U.S. Geol. Surv. Open-File Report 81-775, 49 pp.

Triplehorn, D.M., and B.F. Bohor, 1983, Goyazite in kaolinitic altered tuff beds of Cretaceous age near Denver, Colorado: Clays and Clay Minerals, 31/4, p. 299-304.

Triplehorn, D.M., D.L. Turner, and C.W. Naeser, 1977, K-Ar and fission-track dating of ash partings in Tertiary coals from the Kenai Peninsula, Alaska: a radiometric age for the Homerian-Clamgulchian stage boundary: Geological Society of Am. Bull, 88, pp. 1156-1160.

Turner, D.L., D.M. Triplehorn, C.W. Naeser, and V.A. Wolfe, 1980, Radiometric dating of ash partings in Alaskan coal beds and upper Tertiary paleobotanical stages: Geology, 8, p. 92-96.

Williamson, I.A., 1970, Tonsteins--their nature, origin, and uses: The Mining Magazine, 112, p. 119-125, 200-209.

*Reinick-Smith, L., 1982, The Mineralogy, Geochemistry and Origin of Bentonite Partings in the Eocene Skookumchuck Formation, Centralia Mine, S. W. Washington. Unpublished M. S. Thesis, W. Washington Univ., 179 pp.

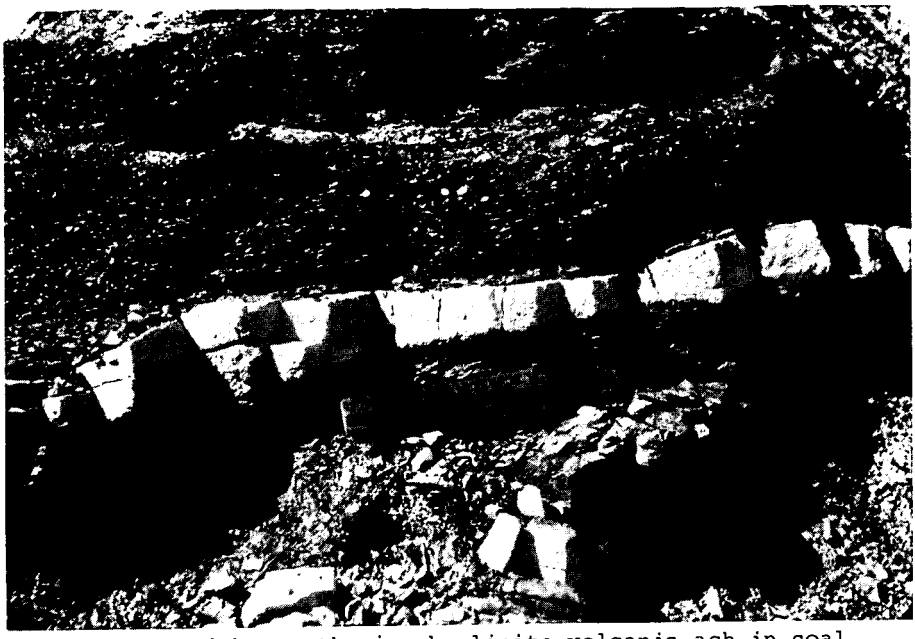

Figure 1. Light weathering kaolinite volcanic ash in coal, southern Alaska.

Figure 2. Multiple smectitic and kaolinitic ash partings in the Big Seam, southeastern Washington.

REACTIONS AND TRANSFORMATIONS OF COAL MINERAL MATTER AT ELEVATED TEMPERATURES

G. P. Huffman and F. E. Huggins

U. S. Steel Corporation Technical Center
Monroeville, PA

Introduction

Coal contains a variety of inorganic constituents that exhibit deleterious behavior in most processes that attempt to convert the energy in coal to a useful form. As coal is heated, the inorganic phases undergo transformations and reactions that yield a complex mixture of solid, molten, and volatile species. These species give rise to slagging and fouling deposits, corrosion, pollution, and other problems. Although such problems are usually associated with the combustion of coal to produce electrical power, they are also common in coal gasification and liquefaction, cokemaking, and iron production.

The current paper will briefly review research on this topic.

Nature of the Inorganic Constituents of Coal

It is common practice to make a distinction between the inorganic constituents of so-called "Eastern" and "Western" coals. By definition, Western coals are those for which the CaO+MgO content exceeds the Fe_2O_3 content of the ash, while the reverse is true for Eastern coals.[1] The inorganic constituents in Eastern coals, which are principally bituminous in rank, are predominantly in the form of discrete mineral particles. Clay minerals (kaolinite, illite) are usually dominant, followed by quartz and pyrite. The range and typical values of the mineral distribution and ash chemistry of Eastern coals are shown in Table I. These data were determined from computer-controlled scanning electron microscopy (CCSEM), Mössbauer spectroscopy, and other measurements on over a hundred coals.

Western coals are usually lignites or subbituminous coals. The range and typical values of the inorganic phase distribution and ash chemistry of approximately 20 Western coals examined in this laboratory are shown in Table II. In a recent paper, we discussed the differences between the inorganic constituents of low-rank coals and those of bituminous coals.[2] These differences occur in the calcium-, iron-, and alkali-containing phases. In bituminous coals, the calcium content is typically low (CaO <5% of ash) and all calcium is contained in the mineral, calcite. The calcium content of lignites is high (CaO ~10 to 30% of ash) and the calcium is molecularly dispersed throughout the coal macerals as salts of carboxylic acids. The latter point has been directly confirmed by EXAFS (extended X-ray absorption fine structure) spectroscopy.[2,3] Similar differences occur for the alkali elements. Minerals such as illite, which accounts for most of the potassium in bituminous coal, are usually low in lignite and subbituminous coal (see Tables I and II). In lignites, sodium and potassium are believed to occur as salts of humic or carboxylic acids. Montmorillonite and halite (NaCl) are the dominant Na-containing minerals, and they occur in both bituminous and lower rank coal. The iron-bearing minerals in unoxidized bituminous coals include pyrite, ferrous-bearing clays (illite, chlorite), and carbonates (siderite, ankerite).[4] In lignites, only pyrite and its weathering products (iron sulfates and oxyhydroxides) are normally observed.[2]

The diversity of transformations and reactions that such complex assemblages of inorganic matter can undergo when coal is combusted or otherwise converted to a more useful form of energy is too complex to be discussed in any detail in a short article. Our intention, therefore, is simply to outline some of the major phenomena and to provide the reader with useful references. Most of the article will deal with reactions and transformations related to coal combustion, with a short section devoted to other conversion processes.

Slagging Behavior; Ash Melting

During pulverized-coal combustion, atmospheric conditions within the coal flame are considered to be reducing in the sense that the stable ionic form of iron is ferrous. After ash particles have left the flame region, they encounter a more oxidizing environment, yielding deposits and fly ash in which the iron may be predominantly ferric or a mixture of ferrous and ferric, dependent on the air-to-fuel ratio. Consequently, it is important to understand the high temperature reactions of ash constituents in both types of environment. This point is recognized in the ASTM ash-fusion test[5] which specifies measurement of the fusion temperatures of ash cones in both a reducing (60% CO, 40% CO_2) and an oxidizing (air) atmosphere. Numerous empirical formulae have been developed to predict ash-fusion temperatures (AFTs) and the viscosities of molten coal-ash slags at higher temperatures from ash composition. Detailed discussions of these formulae and their physical basis have been given by Winegartner and his associates,[1,6,7] by Watt and Fereday,[8,9] and in a recent review article by Reid.[10] The dominant parameter in these relationships is usually the base-to-acid ratio, where "base" and "acid" are simply the sums of the weight percentages of the basic and acidic oxides:

$$\text{Base} = Fe_2O_3 + CaO + K_2O + Na_2O + MgO \quad (1)$$

$$\text{Acid} = SiO_2 + Al_2O_3 + TiO_2 \quad (2)$$

Recently, we examined the behavior of ash fusion temperatures in the context of ternary phase diagrams.[11] Significant similarities were observed between the dependence of AFTs on chemical composition and the liquidus curves in appropriate regions of the $FeO-SiO_2-Al_2O_3$, $CaO-SiO_2-Al_2O_3$, and $K_2O-SiO_2-Al_2O_3$ phase diagrams. The development of the $Base-SiO_2-Al_2O_3$ phase diagrams for the prediction of ash behavior appears to be a fruitful area for future research. An example of such a phase diagram is shown in Figure 1 where ash-softening temperatures (ST, reducing) are plotted in what is effectively the "mullite" region of a $Base-SiO_2-Al_2O_3$ phase diagram. The curves of equal ST exhibit great similarity to the liquidus curves in true ternary diagrams.[12]

The arrow in Figure 1 illustrates the use of the phase diagram to predict STs. In this instance, a bituminous coal with a low ST was blended with two other coals to yield a product with a much higher ST. The blend was chosen with the aim of moving the composition of ash in a direction approximately normal to the equal ST curves. The predicted and observed STs of the original coal and the blend are shown in the inset of Figure 1. The predicted values are probably not as accurate as could be obtained with existing empirical formulae,[6] but they are nevertheless quite reasonable.

Ternary and more complex phase diagrams can also contribute to interpretation of the reactions that lead to ash melting. In a reducing environment

(60%CO-40%CO_2), the important reactions for Eastern coals occur primarily within the $FeO-SiO_2-Al_2O_3$ phase diagram.[13,14] Using a variety of techniques [Mossbauer spectroscopy, computer-controlled scanning electron microscopy (CCSEM), X-ray diffraction (XRD)] to investigate quenched ash samples heat treated under conditions similar to the ASTM ash-fusion test, it was established that most Eastern coal ashes exhibit behavior similar to that shown in the schematic diagram of Figure 2. Here, phases that are molten at elevated temperatures appear as glass phases in the quenched specimens. The potassium-containing clay mineral, illite, appears to be the first phase converted to a partially molten form; presumably this is because of the numerous low-temperature eutectic points in the $K_2O-SiO_2-Al_2O_3$ phase diagram.[12] At approximately 900°C, wustite, derived from pyrite and other iron-rich minerals, begins to react with quartz and aluminosilicates derived from clay minerals to produce a mixture of wustite, fayalite (Fe_2SiO_4), and ferrous-containing melt phase. At somewhat higher temperatures (~1050°C), fayalite has been largely incorporated into the melt phase, and ferrous iron may react with aluminosilicates to form hercynite ($FeAl_2O_4$). This reaction retards melting somewhat and its importance is related to the Al_2O_3 content of the ash. Essentially all of the iron is contained in the melt phase for samples quenched from above 1200°C, as shown in Figure 3. Above 1200°C, reducing, most Eastern ashes (%Base <30%) are a mixture of molten aluminosilicates, mullite, quartz, and minor constituents such as iron sulfide, which is also molten, but is immiscible with the viscous silicate melt.

Similar, but less extensive experiments have also been performed on ash samples quenched from high temperatures in air.[13] Below approximately 1200°C, essentially all of the glass observed in the samples is derived from the potassium-bearing clay mineral illite. Melting accelerates above approximately 1300°C and approaches completion for most Eastern ashes at temperatures of the order of 1500°C. In an oxidizing environment, calcium appears to be a more effective flux than ferric iron.

In both reducing and oxidizing atmospheres, significant partial melting of ash occurs at temperatures well below the initial deformation temperature (IDT). It is not uncommon to observe up to 50 percent of the ash in the form of glass at quenching temperatures as low as 200 to 400°C below the IDT. Such partial melting is important in deposit formation. Not surprisingly, the amount of glass observed at a given temperature in an oxidizing atmosphere is significantly less than that in a reducing atmosphere.[13,14]

Fouling; Volatile Species

Fouling generally refers to the formation of deposits on convective heat-transfer surfaces at relatively low temperatures (600 to 1000°C). Excellent discussions of this problem have recently been given by Wibberly and Wall[15] and in the general review article by Reid.[10] Alkali elements (Na, K) are the principal culprits in the formation of such deposits. Within the flame, these elements become volatilized. The ease of volatilization is related to the form in which the alkalies are present in the coal. Organically bound alkalies would be expected to be easily volatilized at typical flame temperatures (1400-1500°C), as would NaCl, the most common form of sodium in bituminous coal. Potassium contained in illite would not be expected to volatilize as readily; illite should rapidly convert to a molten slag at these temperatures. For this reason, the water-soluble alkali content of coal[1] is considered to be a more reliable indicator of fouling than the total alkali content, at least for Eastern coals. Wibberly and Wall[15] list Na, NaOH, and NaCl as likely gaseous species, dependent on chlorine content of

the coal, flame temperature, and oxygen potential. Nonchloride species are probably rapidly converted to oxides (Na_2O, K_2O) on leaving the flame front. The volatile alkalies may condense on the surfaces of fly-ash particles carried by the flue gas or on cooler boiler surfaces. Wibberly and Wall[15] performed drop-tube experiments in which silica particles were exposed to synthetic combustion gases containing sodium at temperatures of 1200 to 1600°C. Sodium silicate layers ranging in thickness from 0.03 to 0.3 μm were observed on the particle surfaces, and sintered deposits formed rapidly on stainless steel probes inserted into the lower part of the furnace. Such alkali-silicate layers are molten at the temperatures of interest. The thickness of the sodium silicate layers was decreased by a factor of three when the sodium was introduced in the form of NaCl, rather than in chlorine-free forms.

An excellent review of the role of alkali sulfates is given by Reid.[10] Below 1100°C, alkali oxides and chlorides react rapidly with SO_2 and O_2 or SO_3 to form condensed sulfates on fly-ash particles and metal surfaces. Because of their low melting points, alkali sulfates are very corrosive, and form strongly bonded deposits. The melting points of the most easily formed sulfates, Na_2SO_4 and K_2SO_4, are 882°C and 1075°C, respectively, and the minimum melting point of Na_2SO_4-K_2SO_4 mixtures is 833°C. K_2SO_4-$CaSO_4$ and Na_2SO_4-$CaSO_4$ are also commonly observed mixtures, which exhibit melting points in the range from 870 to 970°C. If the SO_3 content of the atmosphere is sufficiently high, the pyrosulfates, $K_2S_2O_7$ and $Na_2S_2O_7$, may be formed from K_2SO_4 and Na_2SO_4. These phases melt at very low temperatures: 400°C for $Na_2S_2O_7$ and 300°C for $K_2S_2O_7$. Crossley[16] has suggested that rapid metal wastage is caused by the reaction of the pyrosulfates with Fe_2O_3 to form low-melting point (<600°C) alkali-iron trisulfates:

$$3M_2S_2O_7 + Fe_2O_3 \rightarrow 2M_3Fe(SO_4)_3 \qquad (3)$$

where M = Na or K. This point of view is supported by the work of Coats et al.[17] which established that liquid melts containing up to 90 percent pyrosulfate can be formed from Na_2SO_4-K_2SO_4 mixtures in SO_3 pressures of 100 to 300 ppm at temperatures down to 335°C. Such SO_3 levels can be readily reached via catalytic oxidation of SO_2 in the presence of Fe_2O_3.[10]

CCSEM analyses of fouling deposits from a boiler furnace in which a North Dakota lignite had been fired are given in Table III. Although the deposits consisted principally of calcium-enriched aluminosilicates, they also contained small but significant amounts of alkali sulfates, intermixed with calcium sulfate. Recently, we conducted potassium K-edge X-ray absorption spectroscopy (XAS) measurements on one of these samples at the Stanford Synchrotron Radiation Laboratory. The X-ray absorption near-edge structure, or XANES, shown in Figure 4, is nearly identical to that of a $K_2S_2O_7$ standard sample. It appears that XAS will be a very useful method of investigating the structure of individual elements in complex deposits.

Reactions and Transformations of Interest for Other Coal Conversion Processes

In this section, examples of the high-temperature behavior of inorganic phases in other conversion processes will be given.

Liquefaction - Montano et al.[18] have investigated the transformation of pyrite to pyrrhotite in coal liquefaction environments. They conducted in situ Mossbauer

spectroscopy measurements on coals maintained at 1.24 MPa nitrogen pressure and observed changes in the isomer shift at approximately 300°C that signalled the beginning of the transformation of pyrite to pyrrhotite. The transformation accelerated between 300 and 400°C, and from 20 to 80 percent of the pyrite in four different coals was transformed after one hour at 440°C. From close examination of both the in situ spectra and the spectra of cooled residues, they concluded that the pyrrhotite underwent covalent bonding to the coal molecules, causing a catalytic effect on coal liquefaction.

Carbonization - When coal is heated to temperatures ∿900 to 1200°C in the absence of air, most of the volatile matter is driven off, leaving a char, or, in the case of metallurgical bituminous coal, a coke. The atmosphere in a coke oven consists principally of hydrogen and methane. Consequently, pyrite is reduced to a mixture of iron sulfide (troilite and pyrrhotite) and iron metal.[19] The amount of iron metal formed depends on both the temperature and the composition of the coke-oven gas. The reduction of iron sulfide to iron metal is desirable since blast furnace operation is more efficient with low sulfur coke. Calcite reacts with the liberated sulfur to form calcium sulfate, thus retaining sulfur in the coke. In Figure 5, the calcium XANES spectrum of a coke produced from a Pittsburgh seam coal in which all calcium was initially present as calcite is shown. The spectrum establishes that approximately 70 percent of the calcite was converted to calcium sulfate during coking.

Gasification

Iron exhibits a great diversity of reactions at elevated temperatures when the reaction environment encompasses both reducing and oxidizing conditions at different stages of the process. For example, it is not unusual to observe five or six different iron-bearing compounds in three different oxidation states in char and ash samples obtained from coal-gasification systems. In Figure 6, the Mossbauer spectrum of a char residue from a bench-scale gasification system at the Institute of Gas Technology is shown. The input atmosphere to the gasifier was approximately 5.2% O_2, 21.2% H_2O, and the remainder N_2, and the average temperature was 1800°F. As indicated in Figure 6, six iron-bearing phases exhibiting three different oxidation states are observed: iron metal, iron sulfide (principally FeS), fayalite (Fe_2SiO_4), magnetite (Fe_3O_4), hematite (Fe_2O_3), glass, wustite, and possibly other minor phases. A more detailed discussion of this work has been given by Mason et al.[20]

Conclusions

Even from this brief overview, it is clear that much remains to be done in the area of understanding mineral-matter behavior in coal combustion and other conversion technologies and even more in combating the sticky problems arising from this component in coal. In particular, we feel there is a great need for much more detailed investigations of full-scale technological processes, especially now that a number of relatively new and sophisticated techniques are available that can be used to characterize mineral-matter related phenomena in ways that were not possible a few years ago. Such techniques include Mossbauer and EXAFS spectroscopies, which we have highlighted in this article, that have the ability to focus on specific critical elements (Fe, K, S, etc.), and reveal very detailed information about the behavior of that element. However, the observed phenomena in full-scale processes will also need to be interpreted in terms of both kinetic (e.g., drop-tube experiments[15]) and thermodynamic (e.g., phase diagram analysis[11]) approaches, as

well as to take into account the form of the mineral matter and its distribution in the original coal. These areas, we feel, should be important areas for research on mineral-matter related problems in the immediate future.

Acknowledgements

We are grateful to Ken Ho of the Babcock and Wilcox Company and Dave Mason of the Institute of Gas Technology for providing several of the samples discussed in this paper. We would also like to acknowledge the Stanford Synchrotron Radiation Laboratory for providing beam-time for the XAS experiments and our collaborators in those experiments, F. W. Lytle and R. B. Greegor of The Boeing Company.

References

1. Coal Fouling and Slagging Parameters, E. C. Winegartner, Ed., ASME Special Publication, 1974.

2. G. P. Huffman and F. E. Huggins, "Analysis of the Inorganic Constituents in Low-Rank Coals," to be published in Chemistry of Low-Rank Coal," H. H. Schobert, Ed., ACS Advances in Chemistry Series.

3. F. E. Huggins, G. P. Huffman, F. W. Lytle, and R. B. Greegor, Proceedings of the International Conference on Coal Science, International Energy Agency, NY, 1983, 679-682.

4. G. P. Huffman and F. E. Huggins, Fuel, 1978, 57, 592-604.

5. 1976 Annual Book of ASTM Standards, Pt. 26, American Society for Testing and Materials, Philadelphia, PA, 263-268.

6. E. C. Winegartner and B. T. Rhodes, Trans. ASME, J. Eng. for Power, (Series A) 1975, 97, 395-406.

7. E. C. Winegartner and A. A. Ubbens, Trans. AIME 1976, 260, 67-70.

8. J. D. Watt and F. Fereday, J. Inst. Fuel 1969, 42, 99-103.

9. J. D. Watt, J. Inst. Fuel 1969, 42, 131-134.

10. W. T. Reid, "Coal Ash--Its Effect on Combustion Systems," Chap. 21, 1389-1446 in Chemistry of Coal Utilization, M. A. Elliott, Ed., J. Wiley, NY, 1981.

11. F. E. Huggins, D. A. Kosmack, and G. P. Huffman, Fuel 1981, 60, 577-584.

12. E. M. Levin, H. F. McMurdie, and H. P. Hall, Phase Diagrams for Ceramists, Amer. Ceramic Soc., Inc., Columbus, Ohio, 1964.

13. G. P. Huffman, F. E. Huggins, and G. R. Dunmyre, Fuel 1981, 60, 585-597.

14. G. P. Huffman and F. E. Huggins, Fouling and Slagging Resulting from Impurities in Combustion Gases, R. W. Bryers, Ed., pp. 259-280, Engineering Foundation, New York, NY, 1983.

15. L. J. Wibberly and T. F. Wall, Fouling and Slagging Resulting from Impurities in Combustion Gases, R. W. Bryers, Ed., pp. 493-513, Engineering Foundation, New York, NY, 1983.

16. H. E. Crossley, J. Inst. of Fuel 1967, 40, 342-347.

17. A. W. Coats, D. J. A. Dear, and D. Penfold, J. Inst. of Fuel 1968, 41, 129-132.

18. A. S. Bommannavar and P. A. Montano, Fuel, 1982, 61 523-528.

19. G. P. Huffman and F. E. Huggins, Chapter 12, 265-301 in Mossbauer Spectroscopy and Its Chemical Applications, J. G. Stevens and G K. Shenoy, Eds., ACS Adv. in Chem. Series 194, 1981.

20. Coal Gasification Research Studies, Proj. 61063, Quart. Report for Aug. 1983 through Nov. 1983, DOEMC/19301-5.

Table 1

Inorganic Constituents of Eastern Coals

Mineral Distribution			Typical Ash Chemistry	
Mineral	Range	Typical	Species	Weight %
Quartz	5-44	18	SiO_2	54
Kaolinite	9-60	32	Al_2O_3	29
Illite	2-29	14	Fe_2O_3	8
Chlorite	0-15	2	CaO	2
Mixed Silicates	5-31	17	MgO	1
Pyrite	1-27	8	K_2O	2
Calcite	0-14	3	Na_2O	1
Siderite/Ankerite	0-11	2	TiO_2	1
Other Minerals	0-12	4	P_2O_5	0.2
			SO_3	2

Table II

Inorganic Constituents of Western Coals

Mineral Distribution			Typical Ash Chemistry	
Mineral	Range	Typical	Species	Weight %
Quartz	7-22	15	SiO_2	30
Kaolinite	13-45	30	Al_2O_3	15
Illite	0-12	2	Fe_2O_3	10
Mixed Silicates	0-22	8	CaO	20
Pyrite	1-26	7	MgO	8
Fe Sulfates	0-5	1	K_2O	0.7
Fe-rich*	0-14	2	NaO	0.6
Ca-rich**	7-49	25	TiO_2	0.7
Other minerals***	1-10	7	P_2O_5	0.4
			SO_3	15

*Principally iron oxyhydroxide.
**Principally calcium bonded to carvoxyl groups in the macerals.
***Barite, apatite, montmorillonite, and others.

Table III

CCSEM Analyses of Fouling Deposits

CCSEM Category	Sec. Superheater, 990-1050°C	Preheater 750°C
Ca-rich aluminosilicate*	55	63
Ca- and Fe-rich aluminosilicate**	7	6
Alkali sulfate***	2	2
Calcium sulfate + alkali sulfate	4	6
SiO_2	3	2
Ca-rich	10	6
Hematite	2	1
Ca-Fe ferrite	2	1
Ca-Mg sulfate	3	2
Al-Si rich	5	2
Unidentified, mixed phases	7	5

*Approximate average composition (mole %) determined from CCSEM energy dispersive X-ray fluorescence spectra was 37% Ca, 8% Mg, 4% Fe, 41% Si, 10% Al.

**Average composition - 31% Ca, 7% Mg, 21% Fe, 32% Si, 9% Al.

***Average composition - $Na_{33}Ca_{16}K_3S_{48}$.

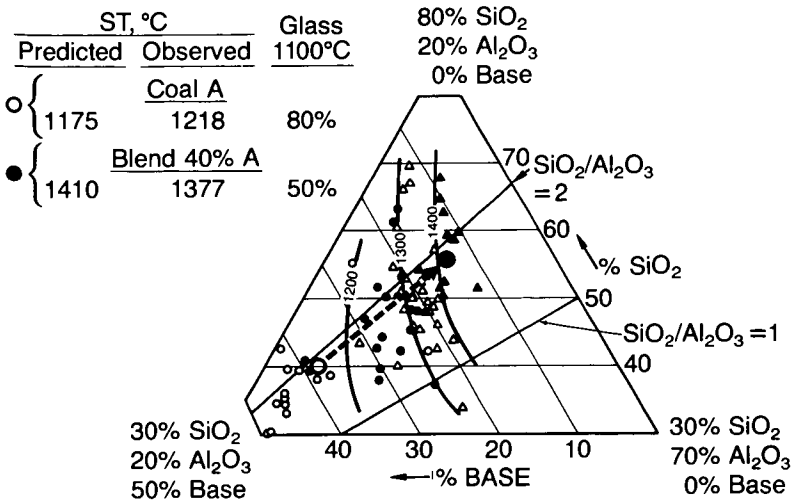

Figure 1 Pseudoternary phase diagram (Base - Al_2O_3 - SiO_2) showing spherical temperature (ST) contours. See text for discussion of points connected by arrow.

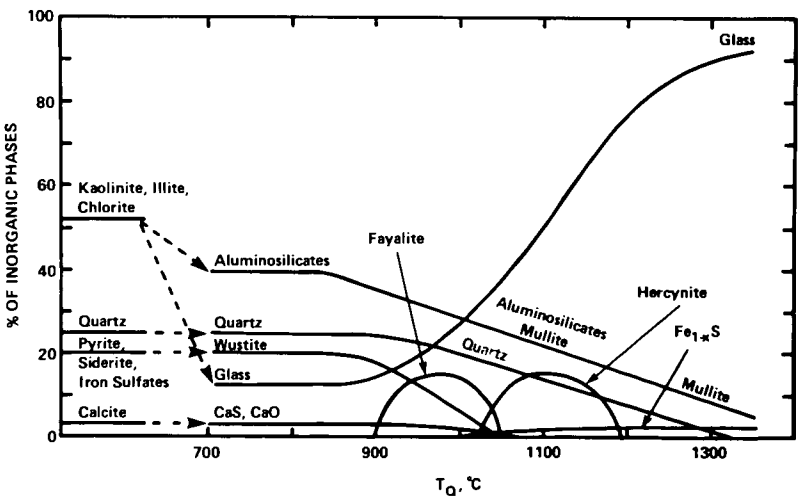

Figure 2 Schematic diagram illustrating high-temperature reactions for minerals in an Eastern-type coal under reducing conditions.

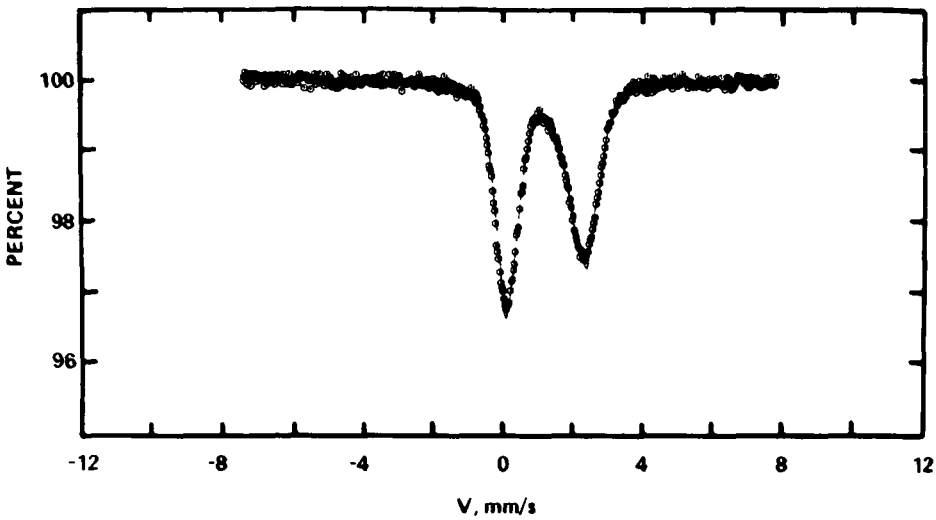

Figure 3 Mössbauer spectrum of Somerset C ash quenched from 1260°C under reducing conditions. Asborption derives entirely from Fe^{2+} in glass.

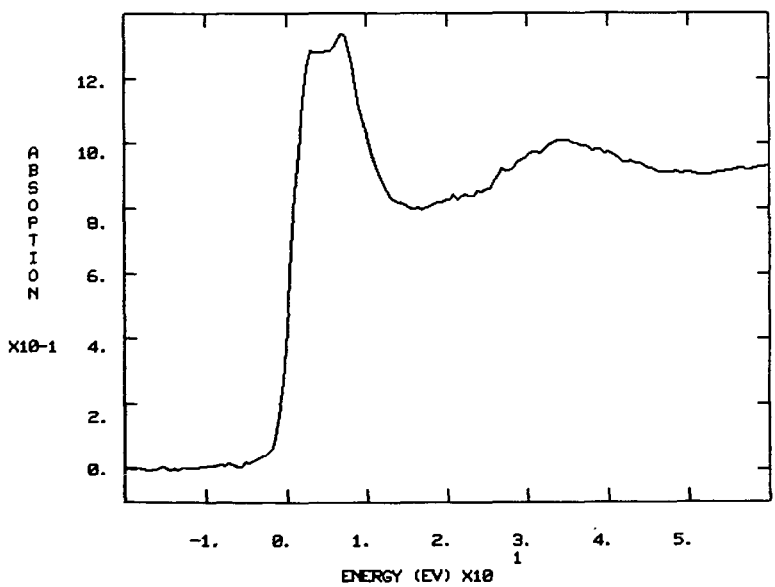

Figure 4 XANES for potassium (K edge) in the fouling deposit resulting from lignite combustion.

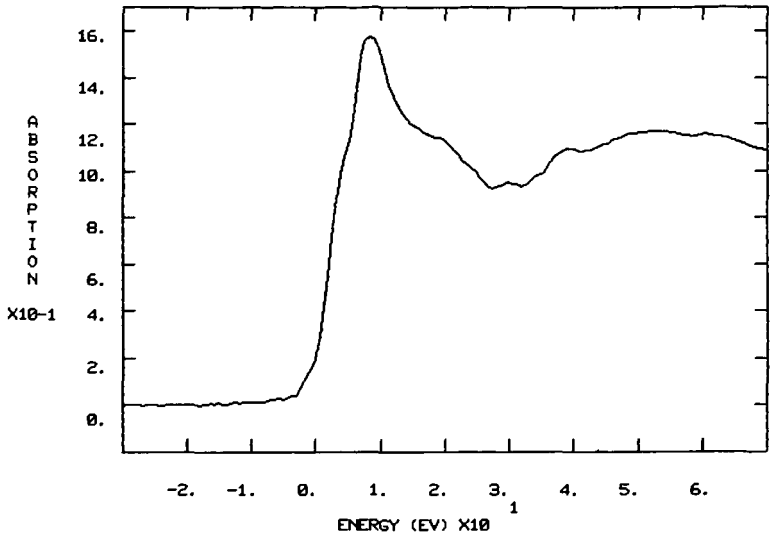

Figure 5 XANES for calcium (K edge) in coke made from high-sulfur coal from Pittsburgh seam.

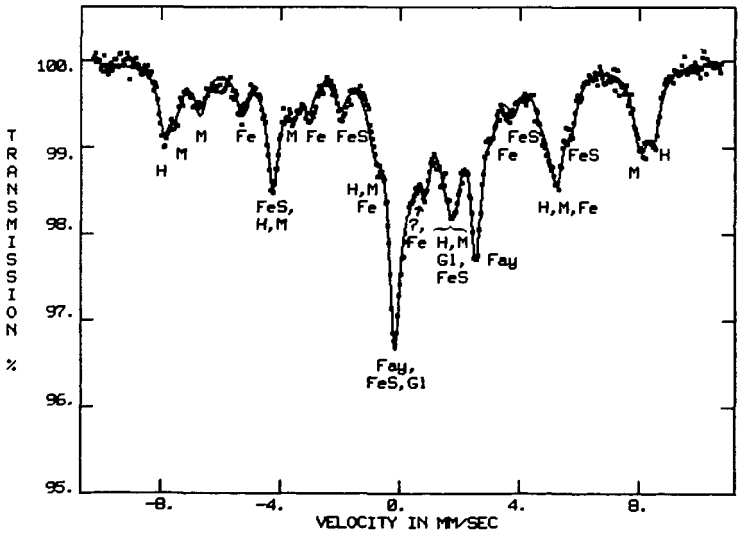

Figure 6 ^{57}Fe Mössbauer spectra of gasification char residue showing peaks from hematite (H), magnetite (M), iron metal (Fe), iron sulfides (FeS), fayalite (Fay), glass ± wustite (Gl), and an unknown phase (?).

Microstructural Changes in Coal During Low-temperature Ashing*

R. W. Carling, R. M. Allen

Sandia National Laboratories
Livermore, CA 94550

and

J. B. VanderSande

Massachusetts Institute of Technology
Cambridge, MA 02139

Introduction

In the present work, the microstructural changes occurring in two U. S. coals during low temperature ashing (LTA) have been examined using a scanning transmission electron microscope (STEM) and automated image analysis in an electron microprobe. The latter, a computer based technique, can be used to provide a quantitative analysis, by species, of the mineral particles >0.2 μm in diameter in petrographic samples of powdered coal. A full description of the operation of automated image anaylsis routines for coal science application may be found elsewhere(1-5). The STEM, by comparison, with its high spatial resolution for imaging and compositional analysis, can be used to examine ultra-fine mineral particles (diameters <0.2 μm) in coal(6-9), and also to directly determine the principal inorganic elements chemically bound in the organic coal matrix(9). These two techniques therefore can be used together in a complementary manner to provide a detailed characterization of the mineral matter in coal samples(9). For the present task, their ability to work directly on either raw coal or ash samples was also a great advantage.

In support of the electron optical analysis of LTA transformations, complex thermochemical calculations have also been made. These calculations serve two purposes. The first is to provide a more fundamental thermodynamic understanding of mineral matter behavior under LTA conditions. Secondly, the calculations assist the electron microscopist in identifying species by predicting the possible products of observed reactants. This serves as guide when it becomes necessary to distinguish various species by electron diffraction, rather than energy-dispersive X-ray spectrometry (as when dealing with the many oxides, sulfides, and sulfates of iron). The limitation on this computational technique is that chemical equilibrium is assumed but may not be reached over the duration of a typical LTA experiment.

*This work supported by U.S. Department of Energy, DOE, under contract DE-AC04-76DP00789.

Experimental

The coals used in the present experiments were PSOC 98, a high-volatile-C bituminous coal from Wyoming (Bed #80 seam), and PSOC 279, a high-volatile-B bituminous coal from Indiana (Indiana #3 seam) obtained from the Penn State Coal Bank. The low temperature asher used in the present work was an LTA-504 from LFE Corporation. During ashing, small specimens were removed from a sample of each coal after 1, 3, 6, 12, 24, 48, and 72 hours of ashing. These partially-ashed samples were used for subsequent STEM analyses.

Thermochemical Modeling

The complex equilibrium code used in this work was an extension of the code originally developed by Erickson(10-12) and later modified by Bessman(13). The code, SOLGASMIX-PV, has been interfaced with a data base that is a compilation of thermodynamic data from JANAF(14) and the U.S. Geological Survey(15).

The elements included in the equilibrium calculations were: H, C, O, Mg, Al, Si, S, Ca, and Fe. The numbers of moles of each element (based on the analyses of each coal) were entered as oxides. An excess of oxygen was included to simulate the oxygen-rich environment of the LTA. The equilibrium temperature was set at 150°C with a pressure of one atmosphere. The list of species investigated for equilibrium stability is too long to present here, but included all of the combinations of the above elements given in the JANAF data base as well as many carbonates, sulfates, alumino-silicates, and sodium-aluminum silicates tabulated by the U.S. Geological Survey.

Results

PSOC 98

Low temperature ashing produced radical structural changes in PSOC 98 which resulted in individual ash particles having a gauzy appearance in the STEM. Stereomicroscopic examination revealed that the "gauze" was a fine three-dimensional network with denser particles suspended within the ash matrix. STEM microanalysis showed these dense particles to be the same sort of mineral inclusions observed in the raw coal. Electron diffraction patterns taken of the ash showed crisp rings characteristic of crystalline material. Analysis of the ash matrix in the STEM revealed Ca and S, as in the raw coal matrix. With this additional compositional information, the diffraction patterns were indexed and the presence of the mineral bassanite, $CaSO_4.1/2H_2O$, was established. The grain size of the bassanite networks forming the matrices of the ash particles was on the order of 30 nm, as determined from standard dark field images formed from portions of the bassanite ring pattern.

Subsequent X-ray diffraction analysis of the material ashed for 72 hours showed bassanite to be one of the three principal minerals found after LTA (together with quartz and kaolinite).

PSOC 279

The raw particles of PSOC 279 were similar in appearance to those of PSOC 98. The most commonly observed type of ash particle, however, consisted of an agglomeration of mineral particles, principally quartz, clays, and pyrite. These were the predominant mineral species found in the raw coal by the electron microprobe analysis. These were also the three major species found by X-ray diffraction in the material ashed for 72 hours.

"Gauzy" ash particles, very similar in appearance to those in the PSOC 98 ash, were less common than the agglomerate type but were also found in the STEM samples. The characteristic inorganic signature of the organic matrix of raw PSOC 279 particles was a combination of an Al and a Si signal. Again, the same combination was carried over into the matrices of the gauzy type or ash for this coal.

STEM examination of the low temperature ash of PSOC 279 showed that much of the pyrite in the starting coal survived the full 72 hours of ashing. This was confirmed by the X-ray diffraction analysis of the ash, as mentioned earlier. STEM analysis was also done on particles of small (<80 nm diameter) crystals. These particles were Fe and S rich, but with much lower S:Fe ratios than pyrite. A significant portion of these particles had a cubic morphology. No minerals of this type were observed during STEM examination of the raw Indiana coal.

Modeling Results

Figure 1 illustrates the stable condensed phases predicted by the equilibrium calculations for low temperature ashing conditions. The results shown are for PSOC 98 but apply as well for PSOC 279 except for the relative amounts of each specie.

Discussion

Bassanite formation is commonly observed during low temperature ashing, particularly for western coals. It is believed to form by three means: dehydration of gypsum ($CaSO_4.2H_2O$) found in the raw coal(16,17), reaction of organic S and the mineral calcite ($CaCO_3$)(18),and direct reaction of organic Ca and S(19,20). These reactions have proven to be hard to distinguish, because of the difficulty of analyzing the starting mineral content of raw coal samples by conventional techniques, and the inability of these same techniques to find and examine partially-ashed

particles to observe the reaction in progress. The use of the electron-optical analysis techniques described in this paper, however, overcame both of these problems, as will now be described.

The STEM results for PSOC 98 indicate that the organic matrix of the raw coal contained Ca and S in a non-crystalline form. This is consistent with the Penn State sulfur-forms analysis which indicates that most of the S in the coal is in an organic form. It also explains the relatively small percentages of Ca-bearing minerals found by the electron microprobe, since other information indicates that PSOC 98 contains a relatively large amount of calcium.

Apparently, the organic matrix of the coal itself was the origin of the Ca and S needed for bassanite formation. The fact that calcium sulphate would form under these conditions was confirmed by the results of the thermochemical calculations (see Fig. 1) which indicated that sufficient sulfur was present in the coal to react with the calcium and prevent the formation of other species, such as calcium carbonate (calcite).

The details of this LTA reaction process were brought to light by the STEM examination of the partially-ashed samples. In general, these samples were simply made up of mixtures of raw coal and fully-ashed particles in varying proportions, based on the amount of ashing time they had seen. However, it was still possible to find individual particles which themselves were only partially ashed.

In such a particle it appears that the fine bassanite network forms continuously as the organic material is burned away and the Ca and S are freed from the matrix. Mineral inclusions originally present in the raw coal particle often remain entrapped within this network as it forms. The bassanite network created thus determines the structure of the low temperature ash of PSOC 98.

It is interesting to speculate on the possible origin of the "gauze" developed by this reaction. It is well known that for coals from the western U.S., organic Ca is readily ion-exchangeable(21). This indicates that the Ca has ready access to the pore structure of the coal. If, during LTA, the Ca in the raw coal reacts in place with the organic S and the oxygen plasma, it could be that the bassanite gauze produced has a network structure related to the pore structure of the raw coal. The 30 nm size of the bassanite crystallites is also comparable to the diameters of a significant portion of the pores likely to be found in coal(22). It may therefore be possible to obtain heretofore unobtainable topographical information of the pore structure of pulverized coal particles by careful LTA experiments. This information would be of great use for modeling the combustion of such particles in commercial boilers. Further work is under way to investigate this possibility.

Although most of the ash produced from PSOC 279 consisted of particles

which appeared to be agglomerates of the mineral inclusions found in the raw coal, some "gauzy" particles were also generated during ashing. In analogy to the results from PSOC 98 just described, this suggests that the gauze was produced from inorganic elements chemically bound in the organic matrix of the starting coal. Unlike the Wyoming coal, however, the coal from Indiana had a matrix that contained primarily Al and Si. This combination of elements has been found by STEM analysis in the matrix of another midwestern coal as well(9). The STEM analysis of the gauzy ash particles for PSOC 279 also showed principally Al and Si. It appears that for this coal, the Al and Si from the organic matrix could react during ashing to produce new crystalline mineral matter. This transformation during LTA has not been previously reported.

The thermochemical modeling of the system indicated that Al and Si should preferentially react together with the oxygen of the LTA plasma to form one or more alumino-silicate compounds, as opposed to the separate formation of alumina and silica. This could not be directly confirmed by electron diffraction in the STEM, for several reasons. First, the mineral inclusion content of the gauzy particles was much higher for this coal than for PSOC 98. In addition, the microprobe results show that nearly 30 percent of these inclusions were alumino-silicates of various types. Selected area diffraction patterns of portions of gauzy particles therefore tended to be quite complex, and not readily amenable to interpretation. An attempt was made to use microdiffraction on the small regions of the network matrix which appeared to be relatively inclusion-free. However, the material was quickly destroyed by the high beam currents involved. The most that can be said from the present work is that STEM microanalysis supports the prediction of the thermochemical model by confirming the combined presence of Al and Si in the matrix of the gauzy ash particles from PSOC 279.

The thermochemical modeling also predicts another LTA transformation for PSOC 279. The modeling results indicate that pyrite is not a stable phase under the low temperature ashing conditions, and is expected to transform to an $Fe_2(SO_4)_3$-type compound. Sulfur is expected to leave the system as SO_3 vapor.

A variety of LTA transformations involving Fe- and S-bearing compounds have been reported previously. Pyrite has been reported as either remaining unchanged(16,25), reacting to form coquimbite and other Fe^{3+} sulfates(17,24,25), or oxidizing to hematite(19). It is generally accepted that rozenite and other Fe^{2+} sulfates oxidize to Fe^{3+} sulfates during LTA(17,23-25). Indeed, in the most recent of these papers it was shown by Mossbauer spectroscopy that, for the LTA conditions used, all of the Fe^{3+} sulfate produced during LTA originated from the Fe^{2+} sulfate in the starting coal, while the pyrite remained unaffected(23).

The STEM results of the present work indicate that a significant amount of pyrite did appear to react during LTA. The pyrite that survived the LTA retains its dense appearance under STEM examination, along with its cubic morphology and high sulfur to iron ratio. By comparison, the

decomposition product has a highly porous structure, a much lower S:Fe ratio, and, in many (but not all) instances, has apparently lost its overall cubic shape. It was difficult to obtain electron diffraction patterns from these latter particles because of their unstable nature under the electron beam. In the few instances where a diffraction pattern was successfully recorded, the best fit for indexing the pattern appeared to be the Fe^{3+} sulfates, coquimbite and para-butlerite. The large proportion of these low S:Fe ratio particles (relative to surviving pyrite particles) observed in the ashed PSOC 279 rules out the possibility of their formation being completely the result of the oxidation of the starting iron sulfates in this coal. Only a very small fraction of the starting mineral matter in the coal was present in the form of Fe^{2+} sulfate.

For the LTA conditions used in the present work, pyrite in the starting coal did partially decompose. This appeared to occur on a particle-by-particle basis; no intermediate reaction products were observed. The rather sporadic nature of the decomposition of pyrite during LTA has been shown previously in tests where pyrites from different sources were subjected to LTA(19). The reason for this behavior is still not known.

One additional prediction of the thermochemical modeling requires comment. SiO_2 is not thermodynamically stable under LTA conditions, but instead should be reacting with other compounds to form alumino-silicates. However, silica particles were still easily identifiable as a specie surviving LTA. There are at least two possible explanations for this. The first is that silica was generally found in relatively large particles, and so was not able to mix intimately with other compounds. Secondly, the kinetics of many ractions may be too slow for them to take place in the time frame of a LTA experiment. As was pointed out earlier, the thermodynamic models assume that equilibrium is reached.

References

1. Walker, P. L., Jr., Spackman, W., Given, P. H., White, E. W., Davis, A., and Jenkins, R. G., "Characterization of Mineral Matter in Coals and Coal Liquefaction Residues", 1st Annual Report to EPRI, Project RP-366-1 (Palo Alto, CA, 1975).

2. Walker, P. L., Jr., Spackman, W., Given, P. H., White, E. W., Davis, A., and Jenkins, R. G., "Characterization of Mineral Matter in Coals and Coal Liquefaction Residues", EPRI AF-417, Project RP-366-1 (Palo Alto, CA, 1977).

3. Lee, R. J., Huggins, F. E., and Huffman, G. P., in Scanning Electron Microscopy/1978/I (Ed. O. Johari), Scanning Electron Microscopy, Inc. (AMF O'Hare, IL, 1978) p. 561.

4. Huggins, F. E., Kosmack, D. A., Huffman, G. P., and Lee, R. J., in Scanning Electron Microscopy/1980/I (Ed. O. Johari), Scanning Electron Microscopy, Inc. (AMF O'Hare, IL, 1980) P. 531.

5. Huggins, F. E., Huffman, G. P., and Lee, R. J., in Coal and Coal Products: Analytical Characterization Techniques (Ed. E. L. Fuller, Jr.), ACS Symposium Series, No. 205, ACS (New York, 1977) p. 239.

6. Harris, L. A., Braski, D. N., and Yust, C. S., in Microstructural Science, Vol. 5 (Ed. J. D. Braun, H. W. Arrowsmith, and J. L. McCall), Elsevier North-Holland, Inc. (New York, 1977) p. 351.

7. Hsieh, K. C. and Wert, C. A., Mat. Sci. Eng., 50, 117 (1981).

8. Heinemann, H. in Proceedings of the International Conference on Coal Science, Dusseldorf, 7-9 Sept. 1981, Verlag Gluckauf (Essen, 1981) p. 567.

9. Allen, R. M. and VanderSande, J. B., Fuel, 63, 24 (1984).

10. Erickson, G., Acta Chem. Scand., 25, 2651 (1971).

11. Erickson, G. and Rosen, E., Chemica Script, 4, 193 (1973).

12. Erickson, G., Chemica Scripta, 8, 100 (1975).

13. Bessman, T. M., "SOLGASMIX-PV, a Computer Program to Calculate Equilibrium Relationships in Complex Chemical Systems", ORNL/TM-5775, Oak Ridge National Laboratory (1977).

14. JANAF Thermochemical Tables, 2nd edition, Ed. D. R. Stull and H. Prophet, U. S. Dept. of Commerce, National Bureau of Standards Publication NSRDS-NBS 37 (1971).

15. Robie, R. A., Hemingway, B. S., Schafer, C. M., and Haas, J. L., Jr., "Heat Capacity Equations for Minerals at High Temperatures", U.S. Geological Survey Rep. 78-934, U.S. Dept. of the Interior (1978).

16. Gluskoter, H., Fuel, 44, 285 (1965).

17. Mitchell, R. S. and Gluskoter, H. J., Fuel, 55, 90 (1976).

18. Painter, P. C., Coleman, M. M., Jenkins, R. G., Whang, P. W., and Walker, P. L., Jr., Fuel, 57, 337 (1978).

19. Miller, R. N., Yarzab, R. F., and Given, P. H., Fuel, 58, 4 (1979).

20. Morgan, M. E., Jenkins, R. G., and Walker, P. R., Jr., Fuel, 60, 189 (1981).

21. Durie, R. A., Fuel, 40, 407 (1961).

22. Gan, H., Nandi, S. P., and Walker, P. L., Jr., Fuel, 51, 272 (1972).

23. Guilianelli, J. L. and Williamson, D. L., Fuel, 61, 1267 (1982).

24. Montano, P. A., Fuel, 56, 397 (1977).

25. Huggins, F. E. and Huffman, G. P., in Analytical Methods for Coal and Coal Products, Vol. III, (Ed. C. Karr, Jr.), Academic Press (New York, 1979) p. 371.

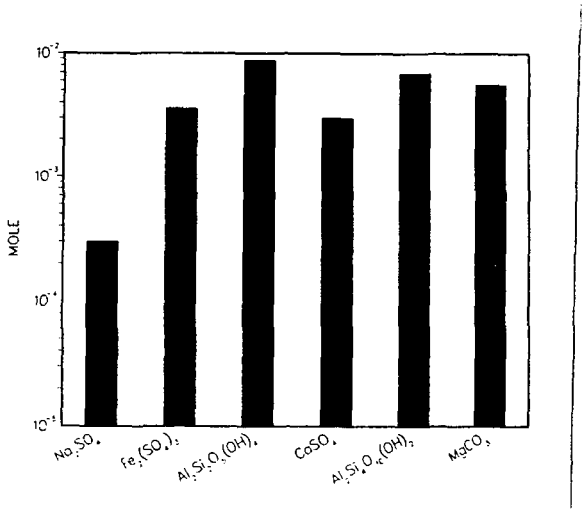

Figure 1 - Thermodynamically stable condensed phase species as predicted by the equilibrium thermochemical modeling. The plot shows the number of moles of each stable specie that would be produced after equilibrium was reached under LTA conditions. The starting material was 100 g of PSOC 98.

MINERAL TRANSFORMATIONS DURING ASHING AND SLAGGING OF SELECTED LOW-RANK COALS

S.K. Falcone, H.H. Schobert, D.K. Rindt, and S. Braun

University of North Dakota Energy Research Center
Box 8213, University Station
Grand Forks, North Dakota 58202

Introduction

Inorganic species are incorporated in low-rank coals in many ways: as ion-exchangeable cations, as coordination complexes, and as a diverse array of discrete minerals. In some cases an element will be present in more than one form; potassium, for example, occurs both as an exchangeable cation and in association with clay minerals. The variation in association of inorganics among the multiple modes of occurrence results in a very complex series of reactions and mineral transformations when low-rank coals are ashed or slagged. The behavior or the inorganic components can be at least as important to effective operation as the behavior of the carbonaceous portion in low-rank coal utilization processes. The determination of the extent of the changes in bulk composition and in mineral phases during controlled laboratory ashing is very important in developing an understanding of ash or slag behavior during coal processing and how such changes are related to process conditions.

In the past, mineralogical determinations using ash formed at the standard temperature of 750°C identified minerals which were not originally present in the raw coal but which were artifacts of the ashing procedure. This was due to the alteration of minerals by oxidation, dehydration and other processes at high temperatures. Recent studies by Miller et al (1), Frazer and Belcher (2), and O'Gorman and Walker (3) have concentrated on relating raw coal mineralogy to ash mineralogy generated at low temperatures. Low-temperature ashing (LTA) theoretically would enable one to obtain the true mineralogical composition of a coal since little mineral alteration occurs up to 125°C. Mitchell and Gluskoter (4) expanded this concept to study low to high temperature mineral transformations in ash of subbituminous and bituminous coals. With few exceptions the application of LTA in ash mineralogy studies has been primarily associated with subbituminous and bituminous coals (5). In fact, Miller et al (1) and Frazer and Belcher (2) state that LTA may be unsuitable for obtaining the original mineralogy in lignites without appropriate pretreatment. This is due to the high organic oxygen content with associated inorganic exchangeable cations characteristic of lignites. The presence of organically-bonded inorganics drastically increases the ashing time thereby increasing the chances of mineral alteration by oxidation. In addition, the release of organically-bound cations and organic sulfur in contact with mineral matter can alter the original coal mineralogy with an extended period of low-temperature ashing.

The purpose of this study is to identify mineral transformations in low to high temperature ashes (125°, 750°, and 1000°C) and slags (1300°C) characteristic of lignites. The processes responsible for certain mineral transformation are also examined.

Twelve low-rank coals were selected from the northern Great Plains and Gulf Coast. Nine North Dakota lignites, two Gulf Coast (Texas and Alabama) lignites, and one subbituminous coal from Montana were studied (Table I).

Experimental

The mineral matter composition of each coal sample was determined directly by X-ray diffraction (XRD) of low temperature ash (LTA). A LFE Model 504 four-chamber oxygen

Table I. Location and Inorganic Analyses (XRF) of Coals Studied. All Coals are Lignites Except for Absaloka Subbituminous

Coal Name	Locality	Major and Minor Elements (Percent)									
		Si	Al	Fe	Mg*	Ca	Na*	S	K	Ti	Ba*
+Absaloka	Big Horn Co., Montana	< 3.5	1.61	2.58	0.08	0.37	0.33	3.92	0.12	0.06	0.03
Beulah Low Sodium	Mercer Co., North Dakota	0.90	0.54	1.02	1.18	1.57	0.14	2.01	0.09	0.05	0.02
Beulah High Sodium	Mercer Co., North Dakota	0.35	0.29	0.52	0.67	1.81	0.46	0.75	ND	0.06	0.04
Center	Oliver Co., North Dakota	0.66	0.44	0.89	0.94	1.70	0.40	0.65	0.08	0.32	0.04
Choctaw	Choctaw, Alabama	1.06	0.49	1.87	0.56	0.84	0.09	2.50	0.10	0.04	ND
Falkirk	McLean Co., North Dakota	0.86	0.50	0.48	0.91	2.60	0.01	0.55	0.15	0.04	0.02
Gascoyne Blue	Bowman Co., North Dakota	1.09	0.73	0.25	0.38	2.28	0.27	0.93	0.14	0.05	0.13
Gascoyne Red	Bowman Co., North Dakota	2.86	0.87	0.39	0.59	1.74	0.13	1.12	0.13	0.12	0.06
Indian Head	Mercer Co., North Dakota	0.71	0.49	0.68	0.97	1.56	0.62	0.44	0.12	0.04	0.05
Pike	Pike County, Alabama	1.11	0.66	0.36	0.11	1.77	NA	2.28	0.10	0.65	NA
San Miguel	Atascosa Co., Texas	3.58	1.06	0.47	ND	1.20	0.60	1.88	0.35	0.08	NA
Velva	McHenry Co., North Dakota	0.56	0.33	0.26	0.11	0.98	0.09	NA	0.05	0.02	0.03

*Concentrations measured by neutron activation analyses (NAA).
+Absaloka coal analysis completely by NAA.
NA (Not Available) ND (Not Detected)

plasma low temperature asher was used. The ashing procedures used were modified after Miller and Givens' (6) technique for low temperature ashing of subbituminous and bituminous coals. One set of samples was ion-exchanged in 1N ammonium acetate at 70°C for 24 hours and freeze-dried prior to low temperature ashing. This procedure was repeated three times to ensure removal of ion-exchangeable cations. Another, but untreated, sample set was also ashed. Preliminary comparison of sample sets showed the exchanged samples to have reduced ashing time and identical mineralogy except for the presence of bassanite in non-exchanged samples. This difference will be discussed later.

Modifications in operating procedures are as follows: an RF Power of approximately 150W and an oxygen flow of 100cc/min at 2 psi were maintained along with a chamber pressure of 1mm Hg. Samples were stirred once every 2 hours during the first eight hours and every eight hours during the remaining ashing time.

Samples were also ashed at 750°C in accordance with ASTM procedure D3174-73 and will be referred to as ASTM samples (7). Samples were then ashed at 1000°C following the same procedure for 750°C coal ashing and will be referred to as HTA (high temperature ash) samples. Finally raw coal samples were heated to 1300°C forming slag. All slag samples were air quenched.

Mineralogical composition of ash samples was analyzed by XRD. X-ray fluorescence (XRF) analysis was also used for bulk ash analysis. Raw coal analysis was performed by XRF and neutron activation (NAA). XRF elemental analyses of raw coal samples are listed in Table I.

Results and Discussion

Mineralogical phases formed at different temperatures for each coal sample are summarized in Table II. The major mineral phases detected by XRD in LTA samples are quartz, pyrite, bassanite, kaolinite and plagioclase. The processes responsible for mineral transformations include oxidation, vaporization, sulfur fixation, dehydration, solid-state interactions, and recrystallization. The temperatures at which specific transformations occur are based on previous experimental work by Mitchell and Gluskoter (4) and published chemical data in the Handbook of Chemistry and Physics (8). In addition to mineral-mineral interactions it is believed that reactions between minerals and exchangeable cations occur (9).

Pyrite (FeS_2) is present in all LTA samples. While Miller et al (1) stated that pyrite may be oxidized with increased low temperature ashing time in lignites no evidence of oxidized forms of iron was seen by XRD. This may be attributed to the pretreatment of samples with ammonium acetate, thereby reducing ashing times as much as 50%. In ASTM samples pyrite is oxidized to hematite (Fe_2O_3) and magnetite (Fe_3O_4). According to Miller and Gluskoter (4), pyrite oxidizes at 500°C. With the oxidation of pyrite to iron oxide rather than iron sulfate, pyritic sulfur is released. The formation of sodium and calcium sulfates, detected in ASTM ash, may be associated with the release of pyritic sulfur. The source of such sulfates may be the interaction of pyritic sulfur released during pyrite oxidation with carbonates as well as with organically-bound calcium and sodium.

Bassanite ($CaSO_4.5H_2O$) is present in some of the sample LTAs. Bassanite most likely forms from the dehydration of gypsum ($CaSO_4.2H_2O$) at 65°C. Gypsum was detected by scanning electron microscopy (SEM) in raw coal samples. Another source of calcium or sodium sulfate may be the fixation of organic sulfur by organically-bound calcium or sodium cations (9, 10). In this case, bassanite is simply an artifact of the low temperature ashing procedure. This phenomenon is typical of coals having abundant alkali cations associated with carboxyl groups. Continued increases in ashing temperature results in complete dehydration of bassanite to anhydrite ($CaSO_4$) at 400°C. Anhydrite is a major mineral phase in ASTM and HTA samples and is present in most slags.

Kaolinite ($Al_2Si_2O_5(OH)_4$) is present in only LTA samples. Kaolinite dehydration occurs approximately from 400° to 525°C (4). With removal of water by dehydration, the kaolinite structure collapses, retaining some degree of order forming

Table II. Mineralogical Composition of Ash and Slag Samples Determined by XRD*

Sample	LTA (∿125°C)	ASTM (750°C)	HTA (1000°C)	Slag(1300°C)
Absaloka	Quartz Pyrite Kaolinite Plagioclase Bassanite	Quartz Anhydrite Hematite	Anhydrite Magnetite Hematite Quartz Melilite Plagioclase Nepheline	Plagioclase Hematite Magnetite Quartz
Beulah-Low Sodium	Quartz Pyrite Kaolinite Bassanite	Quartz Hematite Magnetite Anhydrite	Anhydrite Pyroxene Magnetite Hauyne Hematite Quartz	Anhydrite Pyroxene Magnetite
Beulah-High Sodium	Quartz Bassanite Kaolinite Pyrite	Anhydrite Hematite Magnetite Quartz Melilite Hauyne	Anhydrite Melilite Magnetite Hematite Hauyne Quartz Corundum	Melilite Hauyne Nepheline Magnetite Quartz Corundum
Center	Quartz Bassanite Pyrite Kaolinite	Anhydrite Hematite Quartz	Anhydrite Hauyne Pyroxene Melilite Hematite Quartz	
Choctaw	Quartz Pyrite Kaolinite Bassanite Plagioclase	Anhydrite Quartz Hematite Magnetite Plagioclase Pyroxene	Anhydrite Hematite Quartz Magnetite Plagioclase	
Falkirk	Quartz Kaolinite Pyrite	Anhydrite Quartz Hematite Magnetite Melilite (trace)	Anhydrite Quartz Melilite Hematite Magnetite Hauyne	Melilite (Akermanite) Anhydrite Pyroxene Hematite
Gascoyne Blue-High Sodium	Quartz Kaolinite Pyrite Calcite Sodium Sulfate (trace)	Anhydrite Quartz Hematite Magnetite Nosean Melilite	Anhydrite Melilite Hauyne Quartz	Anhydrite Pyroxene Spinel Melilite Magnetite

Table II. Mineralogical Composition of Ash and Slag Samples Determined by XRD*--Continued

Sample	LTA (∿125°C)	ASTM (750°C)	HTA (1000°C)	Slag(1300°C)
Gascoyne Red-Low Sodium	Quartz Kaolinite Pyrite	Quartz Anhydrite Hematite Magnetite	Quartz Anhydrite Pyroxene Hematite Hauyne	(Amorphous)
Indian Head-High Sodium	Quartz Pyrite Kaolinite Bassanite	Anhydrite Quartz Hematite Nosean Melilite Hauyne Sodium Sulfate (?)	Melilite Hematite Anhydrite Hauyne Magnetite Pyroxene	
Pike	Quartz Pyrite Kaolinite	Anhydrite Quartz Pyrite	Anhydrite Hematite Melilite Anorthite Quartz	
San Miguel	Zeolite (Heulandite) Quartz Kaolinite Pyrite Bassanite Plagioclase	Zeolite Anhydrite Hematite Quartz Plagioclase (Anorthite) Melilite	Plagioclase (Anorthite) Hematite Quartz Magnetite Anhydrite	(Amorphous)

*Minerals listed in decreasing order of peak intensities and occurrence.

metakaolin. No metakaolin was detected by XRD in ASTM samples perhaps due to its poorly defined crystalline structure. However, it is believed that the basic kaolinite components are present in an amorphous form in ASTM ash. With increasing temperature the collapsed kaolinite structure forms corundum ($\gamma \cdot Al_2O_3$). While mullite ($3Al_2O_8 \cdot 2SiO_2$) and cristobalite (SiO_2) have been reported to form from well-ordered kaolinites in bituminous coals at 1000°C (4) neither were observed in HTA samples. According to Grim (11), the absence of mullite suggests that the original kaolinitic structure was poorly defined. It has also been suggested by Grim (11) that the presence of impurities in the form of alkali ions, such as in lignites, retards the development of mullites and cristobalite. The mechanism for this is not fully understood.

The collapsed kaolinitic structure acts as a source or framework for several different alumino-silicate complexes formed in HTA and slag samples. Common minerals found are as follows: anorthite ($CaAl_2Si_2O_8$), pyroxenes ($(Ca,Na)(Mg,Fe,Al)(Si,Al)_2O_6$), melitites ($(Na,Ca)_2(Mg,Fe,Al)(Si,Al)_2O_7$, hauyne ($(Na,Ca)_{4-8}(AlSiO_4)(SO_4)_{1-2}$, nosean ($Na_8Al_6Si_6O_{24}SO_4$) and nepheline ($(Na,K)AlSiO_4$). At 1000°C alumino-silicates minerals form from solid-state reactions of kaolinitic material with cations derived from carbonates, oxides, or sulfates. Interstitial substitution of alkali cations occurs within the dehydrated kaolinite structure with with increasing temperature due to thermal expansion. In some coals, particularly those high in sodium, these alumino-silicates are also seen in ASTM samples.

At 1300°C inorganics are in a liquid phase. Upon quenching some sample slags remain amorphous due to rapid cooling thereby inhibiting nucleation of elements preventing the formation of crystalline structures. Other samples recrystallized upon cooling forming previously existing and new alumino-silicate structures. Differences between sample slagging behavior can be traced to silica content of the raw coal. Samples high in silica, such as Gascoyne Red and San Miguel coals, formed amorphous slags upon cooling. Samples having relatively low silica contents such as Absaloka, Beulah High and Low Sodium, Falkirk and Gascoyne Blue coals, formed crystalline slags when cooled. Anhydrite and magnetite are still present at 1300°C.

Minor amounts of calcite ($CaCO_3$) were detected in raw coal samples by SEM. XRD failed to detect calcite in LTA samples possibly due to extraction by ammonium acetate or because the amounts of calcite were below detection limits ($\sim$5%). For the most part, calcium is supplied to the system by gypsum and organically-bound calcium. As previously discussed, calcium whether in the form of bassanite, calcite, or cations in LTA samples forms anhydrite in ASTM samples. In HTA samples calcium reacts primarily with dehydrated kaolinite forming alumino-silicates discussed under kaolinite reactions.

Quartz (SiO_2) is stable throughout the ash samples at varying temperatures up to 1000°C. In slag analysis, quartz is not always present in crystalline form but forms an amorphoua substance along with other compounds.

With increasing temperature quartz peak intensities in HTA samples decrease or disappear while various alumino-silicate peaks increase in intensity and number. According to Rindt et al (12) localized reducing areas are present within coal particles during combustion. In these areas, reactions between volatilized sodium and quartz occur forming sodium silicates (13). The sodium is fixed and not readily released on further heating.

Figure 1 displays a typical X-ray diffractogram sequence from LTA sample through slagging of the Beulah High Sodium lignite. Predominant peaks are identified according to the mineral phases present. Mineral transformations at higher temperatures are characterized by the presence of numerous alumino-silicate solid-solution series. Often several members of a particular solid-solution series have almost identical diffractogram patterns making identification by XRD difficult. When comparing several of these diffractograms there is little difference between LTA samples while ASTM, HTA, and slag samples are quite different. When comparing mineralogical differences to raw coal elemental compositions of various coals samples containing higher amounts of sodium tend to form alumino-silicates at lower temperatures (750°C) than samples high in calcium. High sodium coals such as Beulah

High Sodium and Gascoyne Blue develop complex silicates in ASTM samples and are known to be high fouling coals. Typical of such alumino-silicates in ASTM, HTA and slag samples are melilites, hauyne, nepheline, nosean and pyroxenes. Commonly these are minerals found in combustion fouling deposits of most lignites.

Concluding Remarks

The results of this study reflect the preliminary stage of investigation into the mineral phase transformations seen in low-rank coals. The original mineralogies of coals sampled do not vary a great deal. Quartz, kaolinite, pyrite, and bassanite are found in abundance in each LTA sample. Greater differences between samples are apparent at higher temperatures where complex alumino-silicates predominate. Perhaps this is a reflection of differences not so much in original mineral matter but in the total inorganic composition of the coal, specifically the presence of exchangeable alkali cations. The interactions of such organically-bound cations with crystalline inorganic phases in lignites account for differences in ashing and slagging behavior between coal samples (9).

The processes responsible for most reactions identified are oxidation, dehydration, sulfur fixation, solid-state interactions, vaporization, and recrystallization. Isolating specific reactions occurring in a multi-component system is difficult at best. Understanding the thermodynamics of mineral transformations is a necessity and will be pursued in future study. In addition, future studies isolating mineral pairs to observe phase transformations at various temperatures will support or refute results presented here.

Literature Cited

1. Miller, R.N.; Yarzab, R.F.: and Given, Peter. Fuel 1979, 58, 4.
2. Frazer, F.W.; and Belcher, C.B. Fuel 1973, 52,41.
3. O'Gorman, J.V.: and Walker, P.L. Fuel 1973, 52,71.
4. Mitchell, R.S.; and Gluskoter, H.J. Fuel 1976, 55,90.
5. Gluskoter, J.J. Fuel 1965, 44, 285.
6. Miller, R.N.; and Given, Peter. 'A Geochemical Study of the Inorganic Constituents in Some Low-Rank Coals' Technical Report, Pennsylvania State University to the U.S. Department of Energy, Rep. FE-2494-TR-1, 1978.
7. Annual Book of American Society of Testing Materials Standards 1979, Part 26: Gaseous Fuels; Coal and Coke; Atmospheric Analysis.
8. Handbook of Chemistry and Physics 54th edition, Chemical Rubber Company, 1973.
9. Morgan, M.E.; Jenkins, R.G.; and Walker, P.L. Jr. Fuel 1981, 60, 189.
10. Painter, P.C.; Coleman, M.M.: Jenkins, R.G.; and Walker, P.L. Jr. Fuel 1978, 57, 125.
11. Grim, R.E. Clay Mineralogy, McGraw-Hill, New York, 1968, Chapter 9.
12. Rindt, D.K.: Selle, S.J.; and Beckering, W. 1979 American Society of Mechanical Engineers, Corrosion and Deposits Division, Reprint 79-WA/CS-5.
13. Boow, J. Fuel 1972, 51, 170.

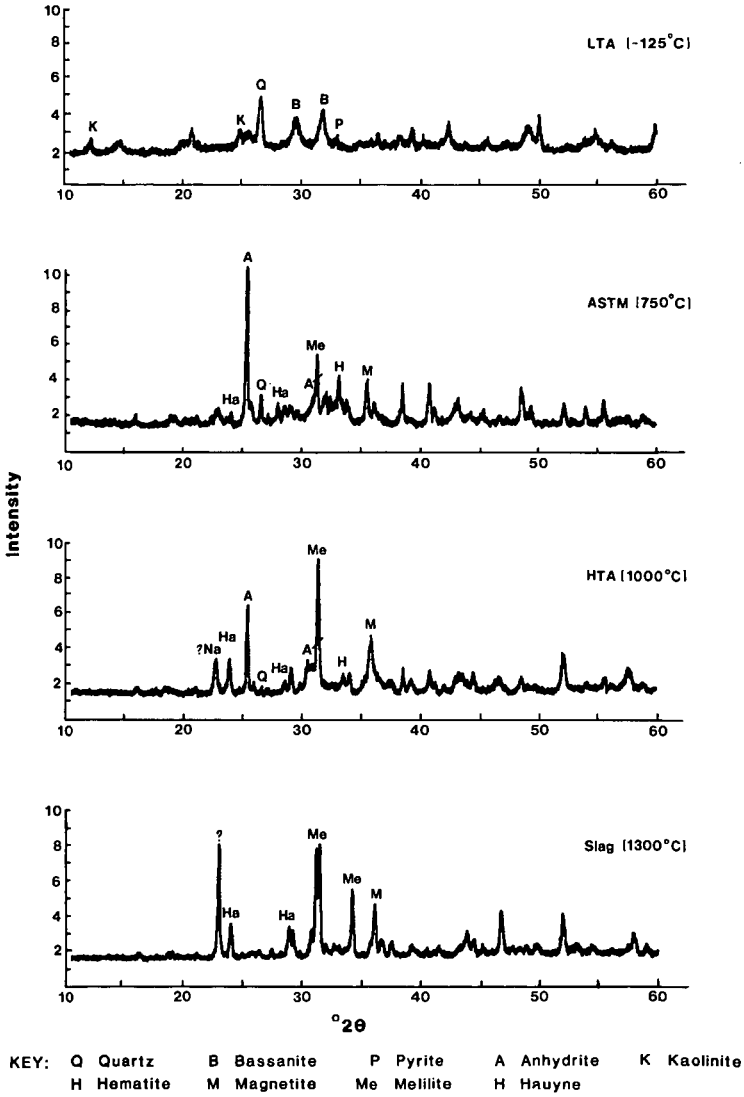

Figure 1. X-ray diffractograms of LTA, ASTM, HTA, and slag samples of Beulah high sodium coal.

HIGH TEMPERATURE INTERACTIONS AMONG MINERALS OCCURRING IN COAL

BY
DONALD L. BIGGS AND CURTIS G. LINDSAY

AMES LABORATORY*, IOWA STATE MINING AND MINERAL RESOURCES RESEARCH INSTITUTE, AND THE DEPARTMENT OF EARTH SCIENCES, IOWA STATE UNIVERSITY
AMES, IOWA 50011

INTRODUCTION

Mineral impurities in coal are known to be primary contributors to the slagging and fouling of utility boilers, fly ash and bottom ash production as well as atmospheric pollution. They also produce undesirable effects in some parts of hydrogenation processes such as liquifaction and gasification (1,2,3). Despite a long history of investigation prompted by these observations, many questions remain unanswered.

Simple empirical relationships between fusion temperature of the furnace deposits and the mineralogy of coals have been proposed (4,5,6). More recently attempts have concentrated on a physico-chemical view of the problem comparing ash fusion temperatures with phase relations in three-component chemical systems (7,8). This method of attack has yielded some significant results, but at least some researchers (8) have questioned the assumption that these processes occur under conditions of equilibrium.

The aim of the research described here is to observe interactions between minerals known to occur in coals in the most direct fashion possible and in the simplest conditions consistent with causing the reactions to occur. It is considered that observation of simple mixtures of minerals observed to enter into reaction may make possible a better accounting of the processes by which slag and fouling deposits form in furnaces.

EXPERIMENTAL METHODS

ISOLATION AND IDENTIFICATION OF COAL MINERALS. Two coal samples collected from different coal basins in the United States (see Table I), were subjected to low-temperature ashing as described by Gluskoter (9). This process avoids destruction of the minerals while oxidizing the organic portion of the coal. This ashing procedure occurs at a much lower temperature than that of the American Society for Testing and Materials (ASTM) method it is given the name of "low-temperature ash" and generally abbreviated, LTA. In formation of a mineral concentrate by low-temperature ashing (LTA) a few changes are anticipated; some clays are reversibly dehydrated, hydrated sulfates are reduced to the hemihydrate form, for instance gypsum is converted to bassanite. Because these changes are known in advance, due allowance can be made for them.

*Operated for the U. S. Dept. of Energy by Iowa State Univ. under contract No. W-7405 Eng-82.

TABLE I

Coal Samples, Localities of Origin, and Analyses
(all samples run-of-mine)

Seam: Illinois #6
Locality: St. Clair County, Illinois

Analysis:

	9 mesh x 0 Raw	9 x 32 mesh Float	9 x 32 mesh Sink
Moisture (%):	5.31	5.44	2.55
Ash, ASTM (%):	32.86	7.10	68.05
Pyritic Sulfur (%):	2.46	0.76	5.08
Total Sulfur (%):	4.57	4.57	5.94
Heating Value (BTU/lb.):	9,039	13,248	3,574

Seam: Upper Freeport
Locality: Grant County, West Virginia

Analysis:

	9 mesh x 0 Raw	9 x 32 mesh Float	9 x 32 mesh Sink
Moisture (%):	0.30	0.68	0.93
Ash, ASTM (%):	35.90	7.26	72.10
Pyritic Sulfur (%):	1.58	0.27	2.62
Total Sulfur (%):	2.18	1.06	3.00
Heating Value (BTU/lb.):	9,695	13,365	3,086

Mineral constituents of the LTA concentrates were identified by x-ray diffraction techniques. Illite, kaolinite, quartz and pyrite are ubiquitous in the mineral suites; calcite occurs in most concentrates. Many other minerals have been identified in coals, but were not observed in these specimens.

HEATING-STAGE MICROSCOPIC OBSERVATIONS. Following the characterization of the mineral suites by x-ray diffraction techniques, each LTA concentrate was heated in a heating stage mounted on a microscope fitted for observation in vertically incident light. Concentrates examined in this way and the product phases are found in Table II.

TABLE II

LTA Samples and Heating Products

LTA Sample	T_{max} (°C)	Phases Identified
Upper Freeport raw	560	quartz, illite, pyrrhotite
	1410	quartz, mullite[a]
Upper Freeport 1.40 float	1031	quartz[b]
	1250	quartz[b]
Upper Freeport 1.40 sink	635	quartz, illite, pyrrhotite
	1150	quartz, pyrrhotite, illite[c]
Illinois #6 raw	880[d]	quartz, illite, pyrrhotite, oldhamite(?)
Illinois #6 1.40 float	625	quartz, illite, pyrrhotite, troilite (?)
	1370	quartz, pyrrhotite
Illinois #6 1.40 sink	920	quartz, illite, pyrrhotite, oldhamite
	1334	quartz, pyrrhotite, oldhamite

NOTES:

[a]XRD peaks occurred at the correct diffraction angles for mulite, but were to weak to permit accurate intensity comparisons.

[b]The overall pattern was similar to the one for the illite-kaolinite pair heated to 1410°C, except that stronger peaks for quartz were found in the LTA XRD pattern.

[c]Peaks were detected at some of the diffraction angles for illite, but the intensities were not comparable with standard patterns; it is possible thast these were relict peaks of illite as it began to alter.

[d]Another sample of Illinois #6 raw LTA was heated to 1421°C; it formed a hard, dark-coloured glass at about 1400°C, and this material could not be removed from the heating-stage crucible.

The heating stage is limited to inert atmosphere or vacuum operation. Therefore, reactions sensitive to atmospheric conditions, such as partial pressure of oxygen cannot be studied. Furthermore, the extremely small particle size of the sample resulted in inability to observe changes occurring below the mount surface, and to resolve the specific minerals entering into a reaction at any point in the run.

These difficulties were met by obtaining samples of the minerals identified in the LTA concentrate before heating, grinding them to approximately the same size consist as the concentrate, and mounting them in separate domains in the heating stage crucible. The geometry of these mounts is shown in Fig. 1.

EXPERIMENTS WITH KNOWN MINERALS

EXPERIMENTS WITH INDIVIDUAL MINERALS. Single mineral mounts in the heating-stage crucible yielded the expected products, that is, pyrite yielded pyrrhotite and troilite, calcite gave lime and carbon dioxide, and clays reacted under high temperature condtions to yield a silicate glass.

EXPERIMENTS WITH PAIRS AND TRIPLETS OF KNOWN MINERALS. In these experiments, known minerals were ground and placed in the heating- stage crucible in separate domains as pairs or triplets of minerals. The pairs and triplets were heated and the behavior at their boundaries observed. Table III lists the minerals used in pair mounts and the reaction products obtained by heating.

TABLE III

Mineral Pairs and Heating Products

Mineral Pair	t_{max} (°C)	Products Identified[a]
calcite-illite	1310	lime (CaO)
calcite-kaolinite	1322	lime (CaO)
calcite-montmorillonite	1285	(indeterminate)[b]
calcite-pyrite	1253	lime, pyrrhotite ($Fe_{1-x}S$), oldhamite (CaS)
calcite-quartz	1467	quartz (SiO_2), lime (CaO)
illite-kaolinite	1410	mullite ($Al_6Si_2O_{13}$)
illite-montmorillonite	662	(indeterminate)[b]
illite-montmorillonite	1212	(indeterminate)[b]
illite-pyrite	1519	pyrrhotite, troilite (FeS)
illite-quartz	1450	quartz
kaolinite-montmorillonite	1403	mullite (poorly-crystalline)[c]
kaolinite-pyrite	1445	mullite
kaolinite-quartz	1220	quartz
montmorillonite-pyrite	1053	(indeterminate)
montmorillonite-quartz	1492	quartz
pyrite-quartz	1571	quartz

Notes:
[a]Only those products are listed which could be positively identified by XRD; no attempt is made here to deduce the composition of amorphous products.
[b]XRD patterns for these heating products did not match any standard pattern closely; attempts to match with computer routines produced results of low reliability.
[c]"Poorly crystalline" means that diffraction maxima were found corresponding to the indicated phase, but peaks were not sharp and did not have the correct relative intensities in all cases.

Because the most reactive phases found in the experiments with pairs of minerals were clays, calcite, and pyrite, these were prepared in triplet mounts. In trials using either montmorillonite or illite with calcite and pyrite, a liquid formed at the mutual boundary of the latter pair at 600 - 650°C. Pyrite and calcite had, of course, previously reacted and this liquid therefore occurred between the product phases pyrrhotite and lime. Subsequent x-ray analysis showed the presence of pyrrhotite, lime, and oldhamite. In both instances, the temperature of this reaction was lower than that obtained in the pair mount of calcite and pyrite, 1140°C. When kaolinite was in the mount with calcite and pyrite, the same reaction occurred at 750 - 760°C. Though the fluxing action of the clays is not presently understood, the differences in reaction temperature with and without clay is considered significant.

The most obvious reaction of the clays themselves during these experiments was a darkening beginning with pyrite decompositon. This was more marked in the case of illite and montmorillonite. It is considered that in all cases, the clay mineral present formed a silicate glass, much like those found in furnace slags, but having, perhaps, less oxygen.

SUPPORTING EXPERIMENTS. To examine the effect of oxidizing and reducing atmosphere on these materials, graphite crucibles 10mm in diameter and 5mm deep were packed in the same manner described above and heated in a furnace fitted to permit introduction of controlled gases during heating. After heating, the samples were examined by scanning electron microscopy and energy dispersive x-ray spectroscopy (SEM/EDS). Samples treated in this way are listed in Table IV.

TABLE IV

Subjects of Supporting Experiments

Assemblage	Atmosphere	T (°C)	Duration (min)
calcite-kaolinite	inert	1400	60
calcite-quartz	inert	1400	60
pyrite-quartz	oxidizing	1200	30
pyrite-quartz	reducing	1200	30
pyrite-calcite	reducing	1200	30
pyrite-kaolinite	oxidizing	1200	30
pyrite-kaolinite	reducing	1200	30
pyrite-montmorillonite	inert	800	15
pyrite-montmorillonite	reducing	800	15
py.-calc.-kao.	reducing	1200	30
py.-calc.-mont.	inert	800	15
py.-calc.-mont.	reducing	800	15

NOTE:
The indicated temperature was the steady-state temperature for the trial. The indicated duration was the period of time for which that steady-state temperature was maintained.

In all these cases where pyrite was used with a clay, iron was found to have migrated from the region that was originally iron sulfide into the clay. Elemental mapping showed the presence of iron to have completely pervaded the region formerly occupied by clay. In the calcite-pyrite pair mount, the iron was lost. EDS mapping showed the presence of abundant calcium and sulfur, but iron was present in small amount. In all mounts containing calcite and pyrite, the calcium and sulfur peaks were present in the region originally occupied by calcite, and sometimes found in the region that had been pyrite-filled.

SUMMARY AND CONCLUSIONS

It is apparent that the phenomena described here are not complete processes terminating in equilibrium assemblages. The times of reaction are too short for many of the products of silicates such as clays and quartz to come to thermodynamic equilibrium at the new temperature. That this is indeed the case in operation of power-plant boilers is obvious from the consideration of the amount of glass found in furnace slags and fly-ash.

Illite and montmorillonite are similar in structure and differ slightly from kaolinite in this regard. The first two are composed of two silicon-oxygen layers per octahedral layer containing iron, magnesium and aluminum and in kaolinite the ratio of tetrahedral and octahedral layers is 1. In these crystals, thermal modification is easier because the bonds formed between the Al, Fe, and Mg atoms and oxygen are weaker than the Si-O bonds. Clays, therefore are expected to be more reactive than the silica crystals. There is evidence that some glass is formed in the clay mineral domains during thermal treatment and that iron diffuses into the mass. Further inquiries are in progress to answer these questions.

Calcite appears largely inert until temperatures approaching 600°C in the presence of some of the clay minerals and inert until about 900°C in their absence. The cause of this fluxing is not well understood at this time, but investigations are planned to elucidate this behavior. At whatever temperature, the reaction observed is for the calcite to decompose to lime (CaO) and carbon dioxide. The extent to which carbon dioxide fluxes further reaction is not known, but must be considered as an important step in complete explanation.

Like calcite, pyrite is quite reactive and its thermal behavior is influenced by the presence of clay minerals. The initial reaction temperature of pyrite alone or in the presence of calcite alone is to produce pyrrhotite, ($Fe_{1-x}S$) and at the highest temperature, troilite (FeS). The loss of sulfur is obvious and continues over an appreciable temperature range. T

The most important reaction products are those of the iron enrichment of the clay minerals, probably a precursor of the iron oxide and glass mixtures commonly observed in slags and fly-ashes, and the formation of the sulfide of calcium, oldhamite. That oldhamite is observed in all experiments where calcite and pyrite interact, and that anhydrite is observed only where they have reacted in the presence of an oxygen-rich atmosphere supports the conclusion that oldhamite, formed in the reducing part of a flame, is a necessary precursor to the formation of the sulfate, anhydrite.

Acknowledgements

This material is based, in part, on work supported by the U.S. Bureau of Mines, Department of the Interior, under Grant No. G1106002. Any opinions, findings, and conclusions or recommendations expressed in this publication are those of the authors and do not necessarily reflect the views of the U.S. Bureau of Mines, Department of the Interior.

Work on other parts of this publication was performed in Ames Laboratory and was supported by the Assistant Secretary of Fossil Energy, Division of Coal Utilization through the Pittsburgh Energy Technology Center, Coal Preparation Branch.

REFERENCES

(1)Mukkherjee, D.K., and Chowdhury, B. : Fuel, 55, pp.4-8 (1976).

(2)Wakely, L.D., Davis,A., Jenkins,R.G., Mitchell,G.D., and Walker, P.L.Jr. :Fuel, 58,pp.379-385 (1979).

(3)Gray, D. : Fuel, 57, pp.213-216 (1978).

(4)Moody, A.H., and Langhan, D.D. : Combustion, 6, pp.13-20 (1935)

(5)Gauger, A.W. : Procedures of the American Society of Testing Materials 37, Part I, pp.376-401 (1937).

(6)Palmenburg, O.W. : Industrial and Engineering Chemistry, 31, pp. 1058-1059. (1939).

(7)Electric Power Research Institute (EPRI) Report CS-1418, Research Project 736; prepared by Battelle, Columbus Laboratories (1980).

(8)Huggins, F.E., Kosmack, D.A., and Huffman, G.P. : Fuel, 60, pp. 577-584 (1981).

(9)Gluskoter, H.J. : Fuel, 44, pp. 285-291 (1965)

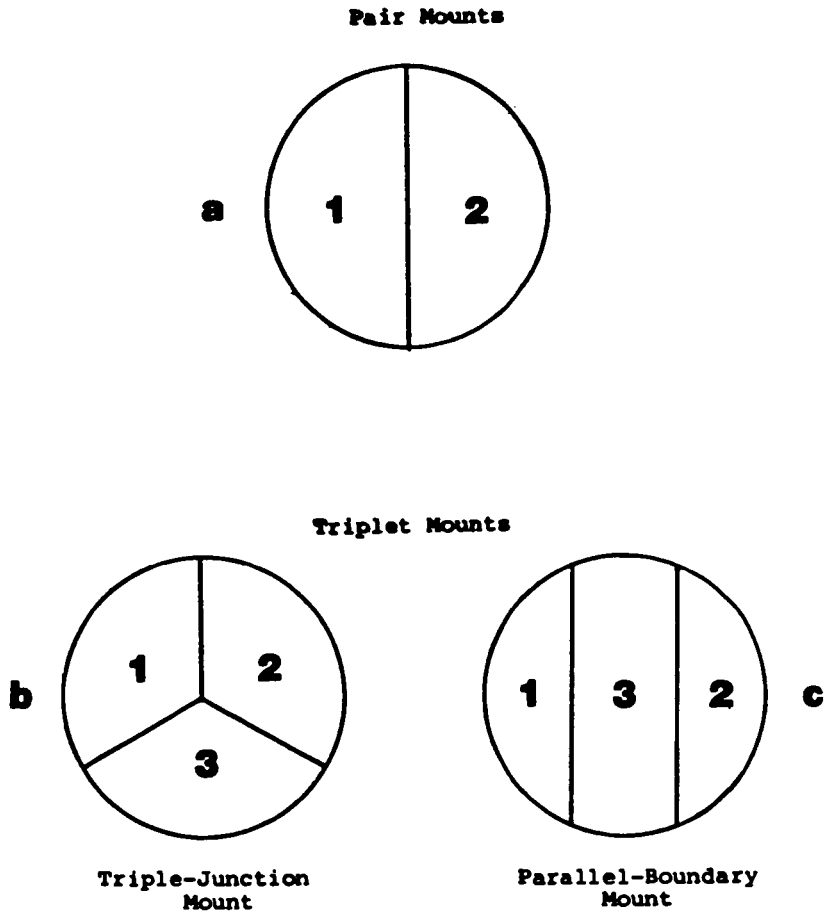

Figure 1. Geometric arrangements of mineral pairs and triplets used in heating-stage microscopic experiments and in supporting experiments. Approximate diameters of actual mounts: for heating-stage experiments--5 mm; for supporting experiments--11 mm. In all triplet mounts, mineral "3" was a clay mineral.

FLAME VITRIFICATION AND SINTERING CHARACTERISTICS OF SILICATE ASH

ERICH RAASK

Technical Planning and Research Division of Central Electricity Generating Board, Kelvin Avenue, Leatherhead, Surrey, UK

The silicate species constitute the bulk of the mineral matter in most coals, and the formation of boiler deposits depends largely on the physical and pyrochemical changes of the ash residue constituents. In this work the mode of occurence of coal silicate minerals, and the flame induced vitrification and sodium initiated sintering mechanisms have been studied. The pulversized coal flame temperature is sufficiently high to vitrify the quartz particles. On cooling some devitrification occurs and the rate of sintering depends largely on the ratio of glassy phase to crystalline species in the ash. The flame volatile sodium captured by the vitrified silicate particles can initiate the coalescence of deposited ash by viscous flow and the rate of sintering is markedly increased by the alkali-metal dissolved in the glassy phase.

The flame imprinted characteristics of pulverized coal ash relevant to boiler slagging, corrosion and erosion have been discussed previously (1,2). The silicate minerals constitute between 60 and 90 per cent of ash in most coals and boiler deposits are largely made up from the silicious impurity constituents. This work sets out first to examine the mode of occurrence of the silicate mineral species in coal followed by a characterization assessment of the flame vitrified and sodium enriched silicate ash particles. The ash sintering studies are limited to investigations of the role of sodium in initiating and sustaining the bond forming reactions leading to the formation of boiler deposits.

SILICA (QUARTZ) AND SILICATE MINERAL SPECIES IN COAL

The quartz and alumino-silicate species found in most coals constitute the bulk of combustion ash residue. The alumino-silicates include muscovite and illite which contain potassium, and kaolinite species (3,4,5,6). The silica (SiO_2) and alumina (Al_2O_3) as determined by chemical analysis are present in alumino-silicates on an average weight ratio of 1.5 to 1 as reported by Dixon et al. (6). The excess of silica represents the amount of quartz in coal mineral matter:

$$(SiO_2)_q = (SiO_2)_t - 1.5(Al_2O_3) \qquad 1)$$

Where $(SiO_2)_q$, $(SiO_2)_t$ and (Al_2O_3) denote respectively the quartz, total silica and alumina contents of ash.

An approximate amount of potassium alumino-silicates in coal mineral matter can be obtained from the potassium oxide (K_2O) content of ash. The amount of non-silicate potassium species is small in most coals and the silicate minerals contain on average 11 per cent K_2O by weight (6). Thus the potassium alumino-silicate content of coal mineral matter (K_{AL-SIL}) by weight per cent is:

$$K_{AL-SIL} = \frac{K_2O}{0.11} = 9.1\ K_2O \qquad 2)$$

where K_2O denotes the potassium oxide content of ash.

The total amount of silicate minerals equals approximately the sum of SiO_2, Al_2O_3 and K_2O in ash, and an estimate of kaolinite species is thus given by:

$$\text{Kaolinite} = (SiO_2 + Al_2O_3 + K_2O) - (\text{Quartz} + \text{Potassium Silicates}) \quad 3)$$

Table 1 gives the SiO_2, Al_2O_3 and K_2O contents of some US and British bituminous coal ashes (4,7) which were used to calculate the approximate amounts of quartz, potassium alumino-silicate and kaolinite species in the mineral matter.

Table 1: Silicate Species in Mineral Matter of British and US Bituminous Coals

Type of Coal		Ash Constituents, Weight Per Cent of Ash			Mineral Species, Weight Per Cent of the the Total		
		SiO_2	Al_2O_3	K_2O	Quartz	Pot. Alum. Silicates	Kaolinite
Low Silica	British	31.1	18.1	1.2	3.9	10.9	26.2
	US	29.2	14.2	1.5	7.9	13.6	23.6
Medium Silica	British	46.5	22.8	2.8	12.3	25.5	34.3
	US	46.6	27.8	1.1	4.9	10.0	60.6
High Silica	British	55.5	30.0	2.7	10.5	24.5	53.2
	US	56.5	32.2	2.6	8.0	23.6	59.7

Table 1 shows that the kaolinite species constitutes up to 60 per cent of the coal mineral matter. The amount of potassium alumino-silicates, chiefly muscovite and illite is between 10 and 25 per cent, and the quartz content is usually below 12 per cent. The alumino-silicate minerals contain frequently iron, calcium, magnesium and sodium as part replacement for potassium and partly incorporated in the kaolinite structure. Also, the silicate minerals occur as hydrated species with the inherent water content of between 2 to 5 per cent, thus the silicious mineral contents are likely to be about 5 per cent higher than those given in Table 1.

The silica and alumina contents of the first two samples are exceptionally low for bituminous coal ashes. The usual concentration range of silica is 35 to 55 per cent and that of alumina is 20 to 30 per cent thus the alumino-silicate species together with quartz constitute between 6o to 90 per cent of the bituminus coal mineral matter.

The silicate species occur in coal chiefly as separate strata and large particle inclusions, and this mode of occurrence is termed the "adventitious" mineral matter. Fig. la shows a typical sample of the adventitious silicate mineral particles, density separated from pulverized coal. The density separation technique does not remove the small silicate particles, chiefly alumino-silicate species dispersed in the coal substance (Fig. lb). The average ash content of bituminous coals utilized in electricity generating power stations is usually between 12 and 20 per cent (4,8) and about one quarter, 3 to 5 per cent fraction is present as the inherent ash.

The mineral elements can be held in the coal substance as organo-metal salts, and also as a result of molecular adsorption and co-valent bonding. The mineral species dissolved in coal pore water, chiefly chlorides can also be considered as a part of the inherent mineral matter. The lignites and sub-bituminous coals can have a high fraction of the mineral elements, chiefly sodium, calcium and also aluminium and iron chemically combined in the fuel substance (9,10). The chemical reactivity and porosity of the fuel matrix decreases with the increase of coal age from lignite to bituminous rank. The loss of carboxyl, hydroxyl and quinone bonding sites in the fuel matrix results in a low "chemical" mineral matter content of bituminous coals.

CHLORIDE IN COAL PORE AND SEAM WATER

Chloride minerals are rarely found in coal in the form of solid species because of high solubility of sodium, calcium and trace metal chlorides in coal strata waters. The "inherent" water content of coal is related to its porosity and thus the moisture content of lignite deposits can exceed 40 per cent decreasing to below 5 per cent in fully matured bituminous coals (11). Chlorides, chiefly associated with sodium and calcium constitute the bulk of water-soluble matter in British bituminous coals (12) and Skipsay (13) has found that the distribution of chlorine coals was closely related to the salinity of mine waters. Hypersaline brines with concentrations of dissolved solids up to 200 kg m^{-3} occur in several of the British coalfields.

The mode of formation of hypersaline brines has been discussed by Dunham (14) concluding that the connate waters were of marine origin formed by the osmotic filtration through clay and shale deposits. The salinity of the brine ground waters increases with depth and when they are in contact with fuel bearing strata, correspondingly more chloride is taken up by the fuel. However, according to Skipsey (13) the high rank bituminous coals because of their low porosity are unable to take up large amounts of the chloride and associated cations, and the chlorine content rarely exceeds 0.2 per cent. The chlorine content of low rank bituminous coals can reach one per cent and correspondingly the sodium fraction associated with chlorine will amount up to 0.4 per cent of coal. That is, the ash from a high chlorine coal can contain up to 3 per cent of flame volatile sodium. The chlorine content of lignites and sub-bituminous coals is usually low, below 0.1 per cent, and sodium is held chiefly in the fuel substance in the form of organo-metal components (9,10).

All coals contain some sodium combined in the alumino-silicate species which will remain largely involatile in the flame. The ratio of the silicate sodium to non-silicate sodium varies over a wide range. The alkali-metal is present chiefly in the silicates in low chlorine bituminous coals, but in the high chlorine bituminous coals and in many lignites and sub-bituminous coals it is present mainly in a flame volatile form.

FLAME VITRIFICATION OF SILICA MINERALS

A characteristic feature of flame heated ash is that the particles are spherical in shape as shown in Fig. 2. The transformation of the angular silicate mineral particles in pulverized coal to spherical particle ash is a result of the surface tension force acting on the vitrified species. The stress (f) on a non-spherical surface section of the particle is:

$$f = 2\gamma/\rho \qquad 4)$$

where γ is the surface tension of glassy silicate and ρ is the radius of curvature. It is evident from equation (4) that the stress is inversely proportional to the radius of curvature and thus the small sharp-edged particles are first to take a spherical form.

Frenkel (15) has shown that time (t) required to transform an angular particle to sphere is given to first approximation by:

$$r = r_0 e^{-t/z} \qquad 5)$$

where

$$z = 4\pi\eta r_0/\gamma \qquad 6)$$

and r is the distance of a point on the original surface from the center of a sphere of equivalent volume having radius r_0, η is the viscosity and γ is the surface tension.

Equation 5 can be used to calculate the approximate time required for a particle to assume a spherical shape when the surface tension, viscosity, size and initial shape of particle are known. Alternatively, an estimate of the viscosity for the change to take place, can be made when the residence time of particles at a given temperature is known. Table 1 gives the calculated values of viscosity when the time for the change is one second. It was assumed that the thickness of moving surface layer was about ten per cent of the radius, and the surface tension of fused ash was taken to be 0.32 N m^{-1} as measured previously (16).

Table 2: Calculated Viscosities for Spheridization of Different Size Silicate Particles

Particle Radius, μm	0.01	0.1	1	10	100
Viscosity, N s m^{-2}	2.5×10^7	2.5×10^6	2.5×10^5	2.5×10^4	2.3×10^3

Table 2 shows that the small irregularly shaped particles transform to spheres in a coal flame when the viscosity of the material is several orders higher than that required for bulk flow under gravity, which is about 25 N s m^{-2}. A laboratory technique was used to determine the minimum temperature at which coal mineral species are transformed to spherical shapes (17). Particles of 10 to 200 μm in diameter were introduced into a gas stream and then passed through a vertical furnace. The temperature of the furnace was varied from 1175 to 2025 K and was measured by a radiation pyrometer and by thermocouples placed in the furnace. The residence time of particles in the furnace was between 0.2 and 0.5 sec. depending on the particle size.

Fig. 3a shows a surface-fused silicate particle heated to a temperature some 25 K lower than that required for its spheridization. Fig. 3b shows a spheridized particle heated in the laboratory furnace. Fig. 4 shows the temperature range at which the shape change of different coal mineral particles occurred. The chlorite mineral contain some quartz and the two species spheridized at markedly different temperatures as shown by curves D_1 and D_2.

The temperature of mineral particles in the pulverized coal flame exceeds 1800 K (Fig. 5), and it is therefore to be expected that all particles with the exception of large size quartz will vitrify and change to spherical shapes. Fig. 6a shows a surface-fused but non-spherical quartz particle found in a sample of fly ash captured in the electrical precipitator. Occasionally ellipsoidal particles of alumino-silicates (Fig. 6b) can be found in the ash indicating that the high temperature residence time was slightly too short for complete spheridization. However, the majority of the ash particles appear to be spherical as shown in Fig. 2.

The spherical silicate ash particles, when viewed at close-up range appear to host a large number of sub-micron particles at the surface (Fig. 6c). The microids could be silicate crystalloids precipitated from the vitrified phase or sulphate fume particles formed from the non-silicate coal minerals (18). The latter are soluble in a dilute acid (HCl) solution and Fig. 6d shows the acid etched particles. Clearly, most of the microid particles were dissolved and the leach solution contained sodium and potassium sulphates.

Another diagnostic test for silicate ash is to treat the particles with hydrofluoric (HF) acid solution (18,19,20). The acid will dissolve the glassy phase revealing skeletons of crystalline species which may be in the form of mullite needles (Fig. 6e) or quartz crystalloids (Fig. 6f). The ratio of the glassy phase to crystalline species varies from particle to particle depending on the original composition of the silicate minerals, the capture of volatile sodium and the rate of cooling of the flue gas borne ash.

The flame imprinted characteristics of silicate mineral species from the point of view of subsequent sintering are summarized in Table 3.

Table 3: Flame Vitrification and Recrystallization of Silicates

Constituent Species	Particle Vitrification		Recrystallization Tendency	Glass Content
	Temperature Range, K	Extent		
Quartz	1700 to 1900	Medium	Low	Medium
Kaolinite	1600 to 1700	High	High	Medium
Potassium Alumino-silicates	1400 to 1600	High	Low	High

The relative amount of coal mineral quartz surviving in the pulverized fuel flame depends on the particle size and temperature. In the intense combustion of cyclone fired boilers the flame temperature exceeds 2000 K and the quartz particles of all sizes will vitrify. Some quartz particles in the crystalline form will survive the flame treatment in pulverized coal fired boilers and the ash may contain 25 per cent of the original coal quartz in the crysalline form (21).

The kaolinite mineral species in coal contain some sodium, calcium and iron in the crystalline structure (6) and the presence of fluxing metals enhances vitrification of the flame heated particles. The high temperature crystalline form of kaolinite species is mullite and the characteristic needle shapes of mullite (Fig. 6e) are frequently found in large, above 5 μm diameter particles. The mullite needle crystals in ash are always embedded in a glassy phase of the large particles and it appears that the small, below 5 μm diameter particles of the flame heated kaolinite species are not extensively recrystallized on cooling. The crystalline species of illite and muscovite are not found in the flame heated ash and thus it is likely that the potassium alumino-silicates remain on cooling largely in the form of glassy particles.

The inherent silicate ash (Fig. 1b) will coalesce on combustion first to a sintered matrix inside the burning coal particle and also to small slag globules at the surface of coke residue. Fig. 7a shows the slag globules on a coke particle separated from pulverized coal ash and Fig. 7b shows a lace skeleton of sintered ash in another coke particle revealed after combustion at 900 K.

During combustion of the mineral rich coal particles in the pulverized fuel flame ash envelopes may be created which can take the form of cenospheres as shown in Fig. 7c and d. The gas bubble evolution leading to cenosphere formation has been discussed previously (16,22) and the fly ash usually contains between 0.1 and 2 per cent by weight of the lightweight ash. The mineral rich coal particles may leave the combustion ash residue also in the form of plerosphere (spheres-inside-sphere) as shown in Fig. 7e.

The above examples show that the inherent silica ash particles undergo extensive coalescence by sintering and slagging during combustion of the host coal particles. However, the adventitious ash retain the particle identity in the flame and the processes of sintering and slagging take place after deposition on boiler tubes.

TRANSFER OF FLAME VOLATILE SODIUM TO SILICATES.

The coal sodium originally present as chloride or organo-metal compounds is rapidly volatilized in the pulverized coal flame (23). Subsequently the volatile species are partly dissolved in the surface layer of flame heated silicate particles and partly sulphated in the flue gas (8). The formation of sodium sulphate can proceed via two routes:

Route 1 - In the Flue Gas

$$\underset{2NaX}{2X} + \underbrace{\left[2Na + H_2O + SO_2 + \frac{1}{2}O_2\right] \rightarrow 2HCl + Na_2SO_4}_{\text{Vapour phase reactions}} \rightarrow \underset{\text{Particles}}{\overset{\text{Fume}}{Na_2SO_4}}$$

Route 2 - At the Surface of Ash Particles

$$\underset{2NaX}{2X} + \underbrace{\left[2Na + H_2O\right] \rightarrow 2HCL + Na_2O}_{\text{Vapour phase reactions}} \rightarrow \underbrace{Na_2O + SO_2 + \frac{1}{2} \rightarrow Na_2SO_4}_{\text{Reactions at ash surface}}$$

Route 1 for genesis of sodium sulphate fume can be described as the non-captive formation and route 2 as the captive formation.

Some potassium sulphate can also be formed via the two routes. Potassium is present in coal chiefly in the form of potassium alumino-silicates (Table 1) and a large part of the alkali-metal will remain involatile in the flame heated silicate particles. Some 5 to 20 per cent of the potassium is released for sulphation (24) which takes place partly at the surface of the parent particles (25) and partly via the volatilization routes as described above. However, sodium sulphate content of fly ash and chimney content of fly ash and chimney solids is always higher than that of potassium sulphate.

The distribution of the flame volatile sodium between the ash silicate and sulphate phases is markedly influenced by the temperature and residence time of the ash particles in the flame. The high temperature of large boiler flame reduces the viscosity of vitrified silicate particles and as a result a large fraction of the volatile sodium is dissolved in the silicate phase. On average 60 per cent of the sodium is dissolved in the silicate ash particles (6) the remainder being present as suphate fume particles in the flue gas (20).

THE MECHANISM AND MEASUREMENTS OF SODIUM ENHANCED SINTERING

The formation of sintered ash deposits on boiler tubes requires first a close, molecular distance contact between the particles followed by a growth of particle-to-particle bridges chiefly by viscous flow. Sodium sulphate phase together with some potassium sulphate may play a significant role in the initial stage of sintering by bringing the silicate particles together as a result of surface tension. Sodium sulphate melts at 1157 K but mixed alkali-metal sulphates can form a molten phase at lower temperatures (26).

Once the close contact between the silicate particles has been established a viscous flow of the particle surface layer can commence and the sinter bonds are established according to Equation 7 as discussed by Frenkel (15):

$$\frac{x^2}{r^2} = \frac{3\gamma t}{2\eta r} \qquad 7)$$

where x is the radius of neck growth between the spherical particles of radius r, γ is the surface tension, η is the viscosity of fused ash, and t is the time. The $(x/r)^2$ ratio can be taken as a criterion of the degree of sintering, i.e. the strength of boiler deposit (s) developed in time t, that is:

$$s = k\left(\frac{x}{r}\right)^2 \qquad 8)$$

and the rate of deposit strength development is:

$$\frac{ds}{dt} = \frac{3k\gamma}{2\eta r} \qquad 9)$$

where k is a constant.

Equation 9 shows that the rate of ash sintering, i.e. the development of cohesive strength of a deposit matrix is proportional to the surface tension and inversely proportional to the viscosity. The surface tension and particle size are not markedly changed by dissolution of sodium, iron or calcium oxides in the glassy phase of silicate ash. However, the viscosity is markedly changed by the oxides. In particular, an enrichment of sodium in the surface layer of the silicate ash particles can lead to a high rate of sintering.

Some of the flame volatile sodium is dissolved in the vitrified silicate ash particles before deposition and an additional amount of sodium is transferred from the sulphate to silicate phases during sintering. The reaction between sodium sulphate and silicates at ash sintering temperatures has been monitored by thermo-gravimetric measurements. Some of the results are given in Table 4.

Table 4: Weight Loss of Sulphates and Sulphate/Silicate Mixtures

Sample	Na_2SO_4	Na_2SO_4/Kaolin	Na_2SO_4/Ash	$CaSO_4$	$CaSO_4$/Kaolin	$CaSO_4$/Ash
Loss Initiation Temperature, K	1425	1085	1175	>1525	1275	1275

Anhydrous sulphate samples and the suphate/silicate mixtures (50 per cent by weight sulphate) were heated in air at the rate of 6 K per minute.

The results in Table 4 show that the reaction between sodium sulphate and kaolin commenced at 1085 K with the release of SO_2 and SO_3

$$Al_2O_3 + xNa_2SO_4 \rightarrow xNa_2O.Al_2O_3.2SiO_2 + x(SO_2, SO_3) \qquad 10)$$

A typical bituminous coal ash required a higher temperature of 1175 K for the sulphate decomposition reaction.

The transfer of sodium from the sulphate of silicate phase will reduce the viscosity of the glassy material resulting in an enhanced rate of sintering. At higher temperatures, above 1275 K, calcium sulphate starts to dissociate in the preence of kaolin and thus calcium oxide will be available for the sintering reactions. The specific roles of coal calcium and also the iron mineral species in ash sintering and slag formation have been discussed previously (2).

The sintering rates of bituminous, sub-bituminous and lignite coal ashes of different sodium contents can be determined by the electrical conductance measurements. In this method the conductance across an ash compact is measured and it is an indication of the degree of sintering (27). The sodium ions in the low viscosity glass and molten sulphate are the conductive species and the conductance continuity is provided by the sinter bridges between the particles.

Fig. 8 (curve B) shows that sub-bituminous coal ash of high (6.3 per cent) sodium oxide content commenced sintering at 1100 K as determined by the conductance measurements. The results (27) suggest that the amount of sodium in some ashes are sufficiently high both to initiate and sustain a rapid rate of sintering below 1200 K. In contrast, with low sodium coals the rate of ash sintering and the formation of boiler deposits are related to the calcium and iron contents of coal mineral matter. Several empirical formulae have been proposed for predicting the deposit forming propensity of the lignitic and bituminous coal type ashes based on the sodiu content (28). These formulae indicate that a rapid build-up of boiler deposit is to be expected when sodium (Na_2O) content of bituminous coal exceeds 2.5 per cent, and that of lignite and sub-bituminous coal ashes is above 4 per cent.

The lignite type ashes have comparatively low fouling propensity when the sodium content is below 4 per cent because of the limited amount of clay minerals available for sintering reaction. That is, in some lignite and sub-bituminous coals there is an excess of sodium and calcium available for the high temperature reactions, and the rate of deposit formation depends on the silicate content of ash (2,9,30). The bituminous coal type ash has an excess of silicates, i.e. the ash is pyrochemically acidic snd the rate of sintering depends on the availability of sodium, calcium and iron species in the flame heated deposit material.

The formation of sintered ash deposits is governed chiefly by viscous flow, and the rate of sintering (S_r) can be expressed in terms of the ratio of glassy material to crystalline species of silicate ash ($R_{g/c}$) and the viscosity of the glassy phase (η):

$$S_r = \kappa_1 (R_{g/c}) \frac{1}{\eta} \qquad 11)$$

where κ is a constant. The characteristics of flame heated silicate particles, (Fig. 4 and Table 3 in Sect. 4) suggest that the vitrified potassium alumino-silicate particles and the below 5 μm diameter kaolinite particles are first to sinter after deposits. The particles will have a high glass content and the small size enhances sintering as evident from equation (10). It is therefore to be expected that the presence of floor material (6) should enhance sintering and

large particle quartz particles would retard the deposit formation. This applies in the absence of large concentrations of the flame volatile sodium, and non-silicate calcium and iron compounds. The flux material oxides will both increase the ash glass content and reduce the viscosity for sintering, Equation 11, and the composition of original silicate species is less important.

CONCLUSIONS

Silicate Minerals in Coal

The silicate minerals, kaolinite and potassium alumino-silicate species together with quartz constitute the bulk of mineral matter in most coals. The approximate amounts of different silicate species of the bituminous coal mineral matter can be estimated from ash analysis.

Flame Volatile and Silicate Sodium in Coal

Sodium is rapidly volatilized in the flame when it occurs in a non-silicate compound form, chiefly associated with chlorine in bituminous coals and combined with organic compounds in the lignite and sub-bituminous fuels. The fraction of sodium combined with coal silicates remains largely involatile in the pulverized fuel flame.

Flame Vitrification and Spheridization of Silicate Particles

The alumino-silicate particles vitrify and take a spherical shape in the flame and are partially recrystallized on cooling. Micro-needles of mullite up to 10 μm long and crystalloids of quartz are the principal devitrification products enveloped in a glassy material matrix. Large quartz particles originally present in coal are only surface vitrified and do not spheridize in the flame. The coalescence by sintering and fusion of the small alumino-silicate particles dispersed in the fuel substance occurs when the host coal particles burn in the flame. The products are sintered ash skeletons, censopheres and plerospheres up to 250 μm in diameter.

Sodium Transfer to Silicate and Sulphate Phases

The flame volatile sodium is partly dissolved in the surface layer of vitrified silicate ash particles and partly sulphated. The sulphate particles, 0.1 to 2 μm in diameter can form on the surface of ash particles or in th flue gas via vapour phase reactions followed by sublimation on cooling. Some potassium sulphate is also formed from a fraction of the alkali-metal released on vitrification of potassium alumino-silicates in the flame.

Initial Stage in Ash Sintering

The sulphate phase can initiate ash sintering by bringing the silicate particles to close contact as a result of the surface tension force. Subsequent sintering proceeds by viscous flow and the rate of sinter bond growth is proportional to the surface tension of silicate glassy phase and inversely proportional to the particle size and the viscosity. The latter changes exponentially with temperature and thus the viscosity of silicate ash particles governs the rate of sintering at different temperatures.

Decomposition of Sulphate on Silicate Ash Sintering

Sodium sulphates in the initial material deposited on boiler tubes will be decomposed by the pyrochemically acidic silicates in ash when the deposit temperature exceeds 1085 K. The transfer of sodium from the sulphate to silicate

phase reduces the viscosity of the glassy material of silicate ash thus increasing the rate of sintering.

Sintering of High Sodium Coal Ashes

Some lignite and sub-bituminous coal ash contain sufficiently high quantities of the flame volatile sodium to initiate and subsequently to sustain a high rate of ash sintering leading to a rapid build-up of boiler deposit. With most bituminous coal ashes the volatile sodium plays a role in initiating sintering but the subsequent deposit and slag formation depends largely on the presence of calcium and iron flux oxides. In general terms, the rate of ash sintering is governed by the ratio of glassy material to crystalline species and the viscosity of the glassy phase.

ACKNOWLEDGEMENT

The work was carried out at the Central Electricity Research Laboratories and the paper is published by permission of the Central Electricity Generating Board.

LITERATURE CITED

1. Raask, E., "Flame Imprinted Characteristics of Ash Relevant to Boiler Slagging, Corrosion and Erosion", Jour. Eng. Power (1982), 104, 858.

2. Raask E., "Mineral Impurities in Coal Combustion - The Behaviour, Problems and Remedial Measures", Hemisphere Publishing Corp., New York (1984).

3. Gumz, W., Kirsch, H. and MacKowsky, M-T., "Slagging Studies: Investigations of Minerals in Fuel and Their Role in Boiler Operation", Springer-Verlag, Berlin (1958).

4. O'Gorman, J.V. and Walker, P.L. "Mineral Matter and Trace Elements in US Coals", Dept. Interior Office of Coal Res. and Dev. Report No. 61, Washington, USA (1972).

5. Rao, C.P. and Gluskoter, J.H., "Occurrence and Distribution of Minerals in Illinois Coals", III. State Geol. Survey, Circular No. 476, Urbana, USA (1973).

6. Dixon, K., Skipsey, E. and Watts, J.T., "The Distribution and Composition of Inorganic Matter in British Coals: Part 2 - Alumino-Silicate Minerals in the Coal Seams of the East Midlands Coalfields", Jour Inst. Fuel (1970), 43, 124.

7. BCURA, "The Chemical Composition and the Viscometric Properties of the Slags Formed from Ashes of British Coals", British Coal Utilization Research Association, Leatherhead, UK (1963).

8. Raask, E., "Sulphate Capture in Ash and Boiler Deposits in Relation to SO_2 Emission", Prog. Energy Combust. Sci., (1982), 8, 261.

9. Sondreal, E.A., Kube, W.R. and Elder, J.L., "Analysis of the Northern Great Province Lignites and Their Ash: A Study of Variability", US Bureau of Mines, Report No. 7158, Washington, USA (1968).

10. Kiss, L.T., "The Mode of Occurrence and Distribution of Inorganic Elements in Australian Brown Coal", Coal Science Conference, E7 p. 774, Dusseldorf, W. Germany (1981).

11. Francis, W., "Coal, its Formation and Deposition", Arnold, London (1961).

12. Daybell, G.N., "The Relationship between Sodium and Chlorine in Some British Coals", Jour. Inst. Fuel (1967), 40, 3.

13. Skipsey, E., "Relationship between Chlorine in coal and the Salinity of Strata Waters", Fuel (1975) 54, 121.

14. Dunham, K.C., "Mineralization by Deep Formation Waters: A Review", Trans. Inst. Min. Metal, (1970), 79, B127.

15. Frenkel, J.S., "Viscous flow at Crystalline Bodies under the Action of Surface Tension", Jour. Phys. (Moscow) (1945), 9, 385.

16. Raask, E., Slag-Coal Interface Phenomena, ASME Jour Eng. Power (1966), Jan. p. 40.

17. Raask, E., "Fusion of Silicate Particles in Coal Flames", Fuel (1969), 48, 366.

18. Raask, E. and Goetz, L., "Characterization of Captured Ash, Chimney Stack Solids and Trace Elements", Jour. Inst. Energy, (1981), 54, 163.

19. Raask, E. and Bhaskar, M.C., "Pozzolanic Activity of Pulverized Fuel Ash", Concrete Res., (1975), 5, 363.

20. Raask, E., "Surface Properties of Pulverized Coal Ash and Chimney Solids", (1981), 1, 233.

21. Raask, E., "Quartz, Sulphates and Trace Elements in PF Ash", Jour. Inst. Energy, (1980), 53, 70.

22. Raask, E., "Cenospheres in Pulverized Fuel Ash", Jour. Inst. Fuel (1968), 43, 339.

23. Halstead, W.D. and Raask, E., "The Behaviour of Sulphur and Chlorine Compounds in Pulverized Coal Fired Boilers", Jour. Inst. Fuel (1969), 42, 344.

24. Raask, E., "The Behaviour of Potassium Silicates in Pulverized Coal Firing", VGB Mitteillungen (Essen Germany) (1968) 48, 348.

25. Stinespring, C.D. and Stewart, G.W., "Surface Enrichment of Alumino-Silicate Minerals and Coal Combustion Ash Particles", Atm. Envir. (1981), 15, 307.

26. Adams, A.M. and Raask, E., "Complete Sulphates in Coal Fired Boiler Plant", Conf. Mechanism of Corrosion by Fuel Impurities, p. 196, Marchwood U.K., Butterworths Publ., London (1963).

27. Raask, E., "Sintering Characteristics of Coal Ashes by Simutaneous Dilatometry and Electrical Conductance Measurements", Jour. Therm. Anal. (1979), 16, 91.

28. Winegartner, E.C., "Coal Fouling and Slagging Parameters", ASME Research Committee Publication on Corrosion and Deposits from Combustion Gases, New York (1974).

29. Tufte, P.H., Gronhovd, G.H., Sondreal, E.H. and Selle, S.J., "Ash Fouling Potentials of Western Sub-Bituminous Coal as Determined in a Pilot Plant Test Furnace", Am. Power Conf., Chicago, USA (1976).

30. Sondreal, E.A., Gronhovd, G.H., Tufte, P.H. and Beckering, W., "Ash Fouling Studies of Low Rank Western US Coals", Conf. Ash Deposition and Corrosion due to Impurities in Combustion Gases, p. 85, Edited by R.W. Bryers, Hemisphere Publishing Corp. Washington (1978).

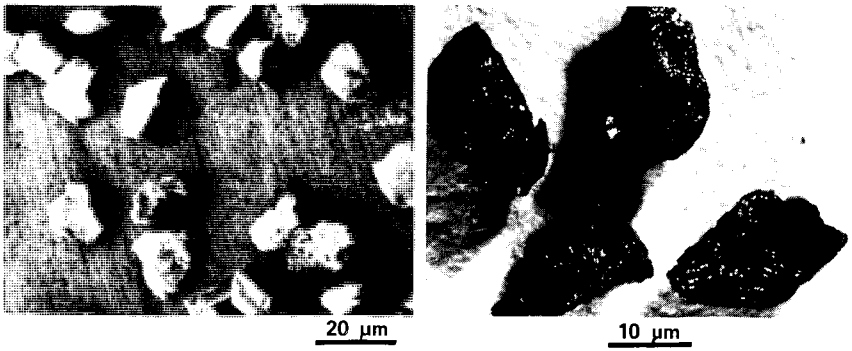

(a) ADVENTITIOUS (b) INHERENT-WHITE PARTICLES

FIG. 1 MINERAL MATTER IN COAL

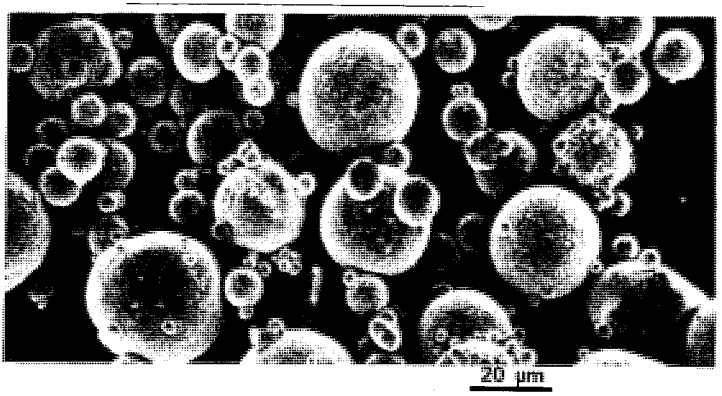

FIG. 2 PULVERIZED COAL ASH

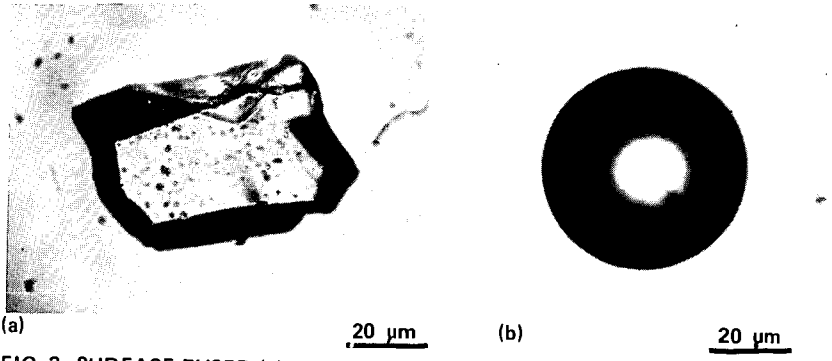

FIG. 3 SURFACE FUSED (a) AND SPHERIDIZED (b) SILICATE PARTICLES

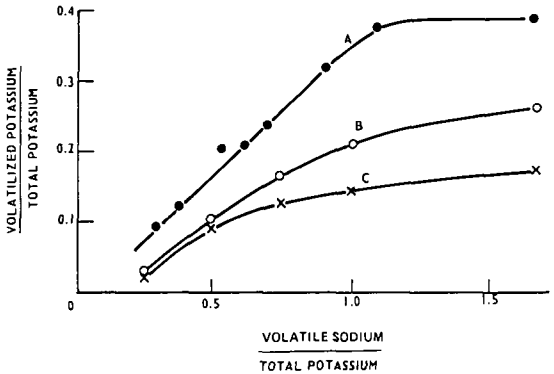

FIG.4 THE EFFECT OF SODIUM CHLORIDE ON RELEASE POTASSIUM FROM SILICATES

A – COAL SILICATES
B – MUSCOVITE
C – ORTHOCLASE

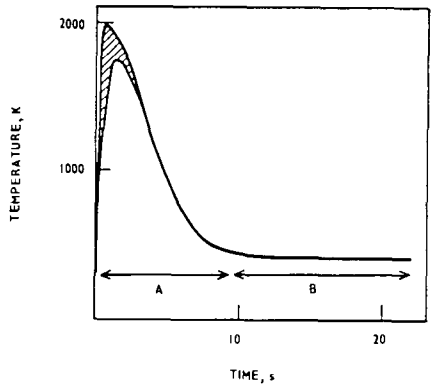

FIG.5 TEMPERATURE/TIME PLOT FOR ASH PARTICLES IN A 500 MW PULVERIZED COAL FIRED BOILER – 0.1 μm (TOP CURVE) TO 100 μm (LOWER CURVE) SIZES

SECTION A COMBUSTION AND HEAT EXCHANGE CHAMBERS
SECTION B ELECTRICAL PRECIPITATORS AND CHIMNEY

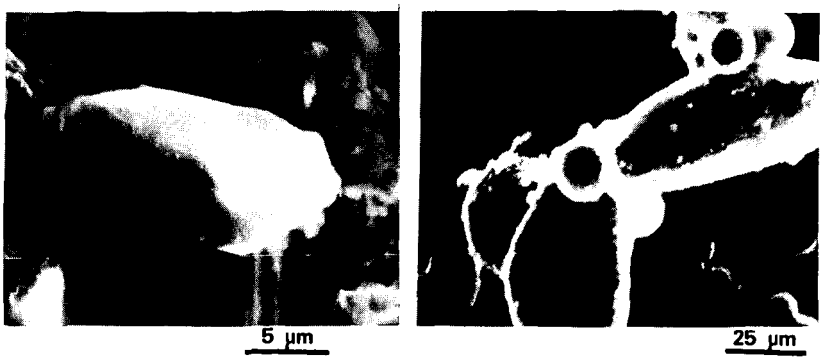

(a) UNFUSED QUARTZ PARTICLE

(b) ELONGATED SILICATE PARTICLES

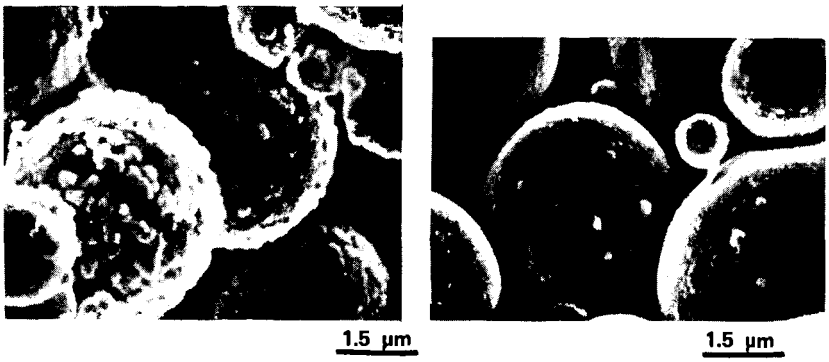

(c) MICROIDS ON ASH

(d) ACID CLEANED ASH

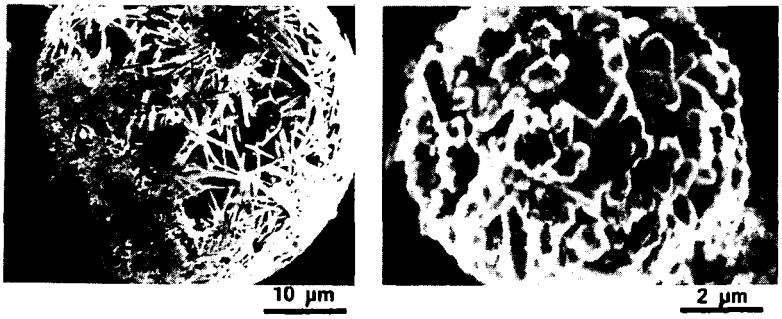

(e) MULLITE NEEDLES IN ASH

(f) QUARTZ CRYSTALLOIDS

FIG. 6 DIAGNOSTIC FEATURES OF FLAME HEATED ASH

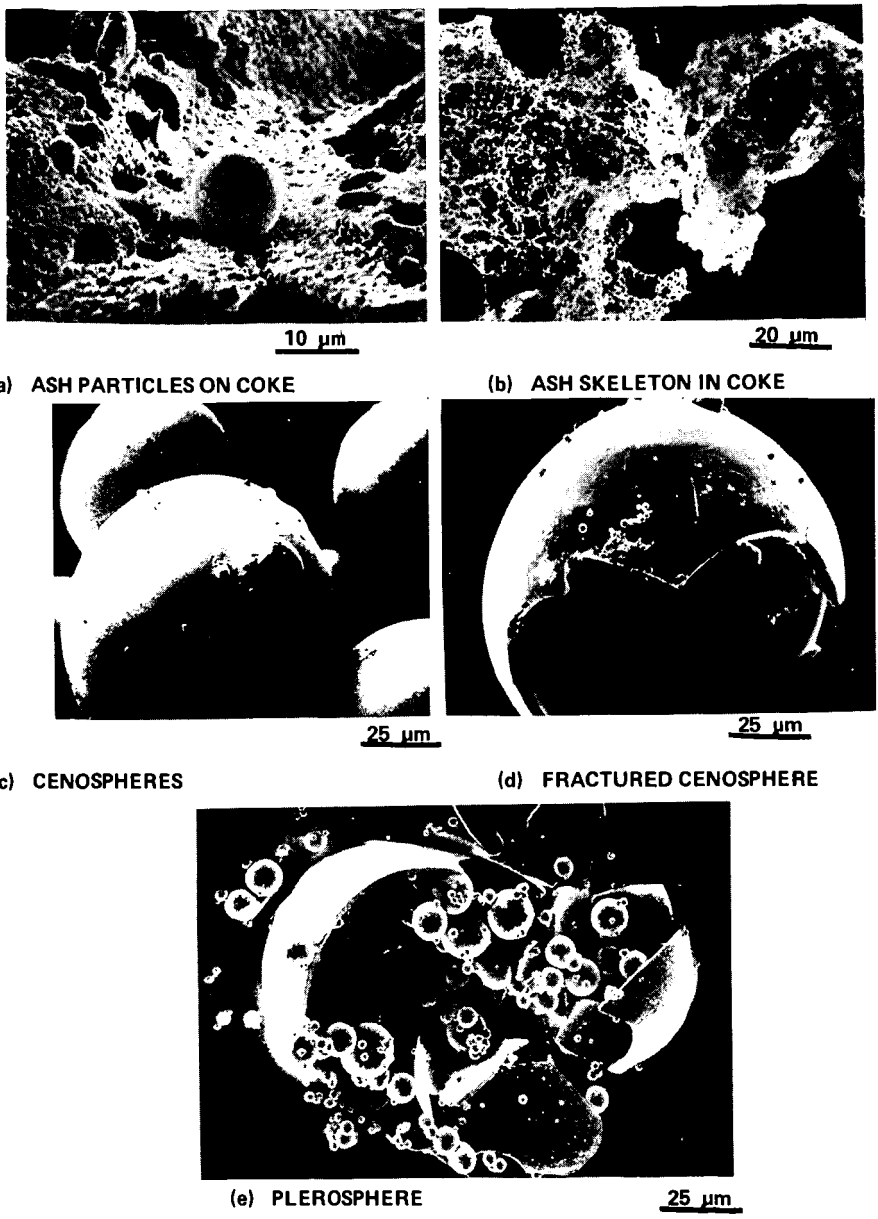

(a) ASH PARTICLES ON COKE

(b) ASH SKELETON IN COKE

(c) CENOSPHERES

(d) FRACTURED CENOSPHERE

(e) PLEROSPHERE

FIG. 7 COALESCENCE PRODUCTS OF INHERENT ASH IN FLAME

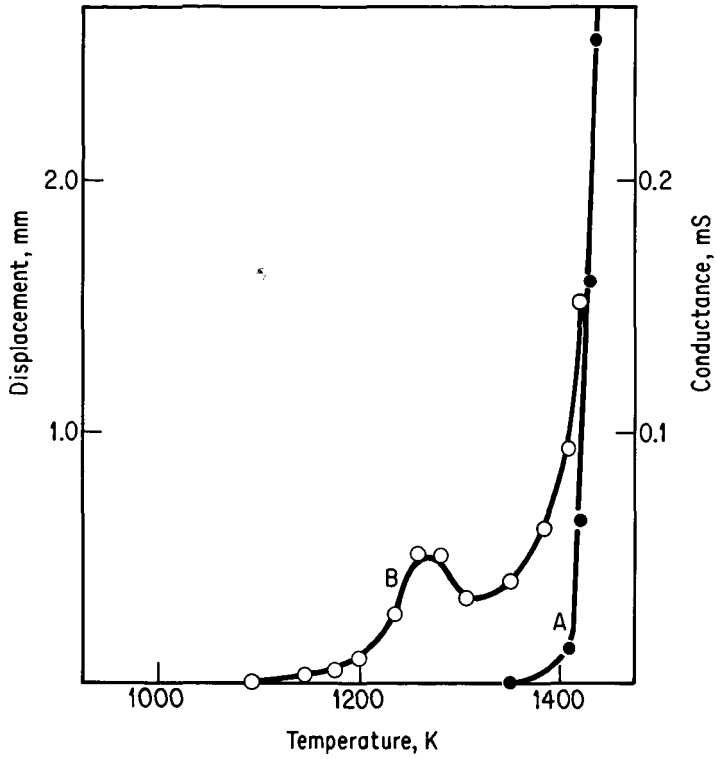

FIG. 8 SIMULTANEOUS SHRINKAGE AND CONDUCTANCE MEASUREMENTS LEIGH CREEK (AUSTRALIA) COAL ASH

A – SHRINKAGE
B – CONDUCTANCE

VISCOSITY OF SYNTHETIC COAL ASH SLAGS

Karl S. Vorres and Sherman Greenberg†

Chemistry Division, Building 211
†Materials Science and Technology Division, Building 212
Argonne National Laboratory
9700 South Cass Avenue
Argonne, Illinois 60439

INTRODUCTION

Coal used for energy conversion contains a considerable amount of mineral matter. During the conversion process the mineral matter is heated, and in the higher temperature reactors is converted to a molten material which flows from the reactor at a rate dependent on the viscosity of the slag. In studies of coal slags obtained from electric utility boilers (1,2,3) this behavior has been studied and correlations have been determined between the viscosity of the slag and the chemical composition. These studies have been carried out in a range of gaseous environments typical of the combustion furnace with a range of oxygen concentrations from almost zero to 15%.

The purposes of this study included a determination of the viscosity behavior of synthetic slags over a range of compositions and temperatures characteristic of slagging gasifier operation. The compositions were chosen to be broadly representative of a range of coals from both the eastern and western U.S. The temperatures were chosen to be in the range of satisfactory gasifier operation, and within the limits of the experimental equipment. The gaseous environments were selected to have the low oxygen partial pressure (about 10-8 to 10-9 atm) typical of the slagging gasifier.

The viscosity data were to be used as input for an associated refractory/slag corrosion program. Accordingly, the data obtained for the first few slags were compared with correlations developed by Watt and Fereday (1,2) based on chemical composition and by Hoy, Roberts and Williams (3), using a modified version of the silica ratio. In order to simplify the systems for study, the synthetic slags were limited to the five components: SiO_2, Al_2O_3, FeO, CaO and MgO. Since they contained no Na_2O or K_2O, the slag compositions were outside the range of the earlier correlations. If this difference was neglected, then the composition of all but four of the synthetic slags used in this program fell outside the range of the compositions for which the correlations were developed (10% Al_2O_3 or 0% MgO or low silica ratio or high SiO_2/Al_2O_3 ratio) and the correlations did not, in general, represent the data obtained for the synthetic slags.

EXPERIMENTAL

Slag: The viscosities of 21 synthetic slags, covering the range of compositions expected in slags derived from American coals were determined in this

study. The synthetic slags were prepared from reagent grade chemicals. The synthetic slags were mixed with water and pressed into pellets using a pressure of 15000 psig. The pellets had a slightly smaller diameter than that of the containment crucible. The composition of the slags is given in Table 1.

Viscometer: The apparatus and technique have been described in detail (4). Essentially a Brookfield Rheolog(TM) was used to replace the sample head in the rotating cylinder slag corrosion apparatus used in slag/refractory corrosion studies at ANL (5). Appropriate seals and ceramic structural components permit maintenance of the desired low oxygen activity within the measuring chamber. The viscosity measuring "bob" was a cylinder 12.7 mm diameter and 11.1 mm high. For measurement at lower oxygen partial pressures the "bob" and connecting shaft were fabricated of molybdenum; in an air environment the molybdenum was replaced by platinum. The slag was contained in Al2O3 crucibles. The "bob" and measuring system were calibrated at room temperature using a series of NBS oils ranging from 10 to 600 poise.

Procedure: Viscosity measurements were usually made in a decreasing temperature mode at 50 C. intervals after the slag sample had been slowly heated to the desired temperature, typically about 1400-1550 C. The slag was kept at each temperature long enough to demonstrate constant viscosity (about 30-60 minutes). In one case, slag 12, measurements were also made in an increasing temperature mode to determine if there were hysteresis effects. None were observed in this slag and other work confirmed this (4). Measurements made in other laboratories with other slags have shown hysteresis (6). The desired oxygen partial pressure was maintained by flowing H_2-CO_2-N_2 (or A) mixtures of the required composition through the interior of the measuring chamber throughout the experiment. The variation of oxygen partial pressure with gas composition and temperature was calculated using a NASA-developed code (4).

RESULTS AND DISCUSSION

The data obtained were plotted as viscosity versus temperature for the different materials and displayed the expected exponential increase in viscosity as the temperature decreased. In most of the runs a characteristic sudden increase in viscosity was noted, as in some related studies (1,3). Some typical results are shown and compared with the Watt-Fereday and modified silica ratio projections, assuming a liquid phase, in Figures 1 and 2, (slags 1 & 12).

To understand the Newtonian characteristics of the slags, plots of logarithm of viscosity versus temperature were made. These indicated straight lines or two line segments. For runs with a sudden increase in viscosity at lower temperatures, two segments were observed. Shear rates were not varied and the various types of non-Newtonian behavior were not explored. The observed straight lines are consistent with Newtonian behavior.

Arrhenius plots were then made. These plots typically involve the logarithm of a rate constant and the reciprocal of the absolute temperature. Viscosity is not a rate parameter, but is defined as the shear stress divided by the shear rate. The reciprocal of the viscosity is the shear rate per unit shear stress and was used in the plots. A typical example is shown in Figure 3. Slag 1 shows a typical high temperature low activation energy regime with a transition to a high activation energy, low temperature regime. This behavior was noted in most of the

runs. The other behavior was, as in the case of slag 12, a single straight line covering the range of the data. The slopes and activation energies for runs without the transition tended to be intermediate in the range of the values for runs with the transition.

In order to compare the viscosity behavior of the different compositions for the higher temperature regime and the slags with no transitions, separate plots superimposing the sample series with a constant weight % SiO_2 were made and are shown in Figures 4,5 and 6. Note the vertical change in scale in Figure 6. The solid portion of the lines represents the actual range of data. The dashed part of the lines was added to facilitate visual comparison. Examination of the plots shows two general tendencies. The reciprocal viscosities or fluidities tend to increase for series with lesser amounts of SiO_2 in them. Although the envelopes of data are broad, this observation can be made. Additionally, for a given series with a fixed weight % SiO_2, the fluidities are greater for the lower amounts of Al_2O_3.

A similar study of the lower temperature regime will be made later.

Activation energies and the temperature range of data are given in Table 2. Initial statistical analyses have not shown a strong correlation of activation energies with any of the slag constituents.

A wide range of activation energies with very high values was obtained for the lower temperature regime. The transition from the higher to the lower temperature regime generally occurred in the 1300-1400 C range. In order to interpret the data the ternary equilibrium phase diagrams for the systems SiO_2-Al_2O_3-MO were examined where MO is either CaO, FeO, or MgO. The mole fractions of each of the constituents were calculated as also shown in Table 2, and the ternary diagram corresponding to the major base in the group CaO, FeO or MgO was selected. Usually a ternary eutectic was found in the temperature region which would be expected for a system most closely corresponding to the sample composition. This eutectic temperature was close to the observed transition temperatures in the viscosity data. Many of the highest temperatures used were significantly below those associated with the appearance of a solid phase from the melt. This solid phase could have been present through the entire series of measurements on the slag.

CONCLUSIONS

A series of 21 synthetic coal ash slags were studied. It was observed that: (1) Plots of the logarithm of viscosity versus temperature showed one or two straight line segments, indicating Newtonian behavior in the temperature range studied. (2) Plots of the logarithm of the reciprocal of viscosity versus reciprocal of absolute temperature also showed one or two straight line segments, indicating one or two mechanisms were operative over the temperature range. (3) For three series, varying in SiO_2 content, those with the greatest SiO_2 content had the highest viscosities. (4) Within a series of given SiO_2 content, those members with the highest Al_2O_3 content had the highest viscosity. (5) For slags exhibiting a transition in behavior, the transition temperature could usually be associated with a ternary eutectic temperature in the phase equilibrium diagram for the most closely related ternary system. (6) Many of the slags probably had a

solid phase precipitating from the liquid phase during the cooling period before the transition temperature.

ACKNOWLEDGMENTS

The authors gratefully acknowledge the support of the U. S. Department of Energy. KSV acknowledges support from the Chemical Sciences Division of the Office of Basic Energy Sciences, while SG acknowledges support from the Surface Gasification Materials Program.

REFERENCES

1. J. D. Watt and F. Fereday, "The Flow Properties of the Slags Formed from the Ashes of British Coals. Part I. Viscosity of Homogeneous Liquid Slags in Relation to Slag Composition", J. Inst. Fuel 42, 101 (1969).

2. J. D. Watt, "The Flow Properties of Slags Formed from the Ashes of British Coals. Part 2. The Crystallizing Behavior of the Slags", J. Inst. Fuel 42, 131 (1969).

3. H. R. Hoy, A. G. Roberts, and D. M. Williams, "Behavior of Mineral Matter in Slagging Gasification Processes", IGE Journal 5, 444 (1965).

4. J. Chen, S. Greenberg, and R. Poeppel, "The Viscosity of Coal Slags as a Function of Composition, Temperature and Oxygen Partial Pressure", ANL/FE-83-30 (in press).

5. S. Greenberg, R. Poeppel et al, "The Corrosion of Ceramic Refractories in Synthetic Coal Slags Using the Rotating Cylinder Technique: An Interim Report", ANL/FE-83-31 (in press).

6. R. C. Streeter, E. K. Diehl and H. H. Schobert, "Measurement and Prediction of Low-Rank Coal Viscosity", Preprints Am. Chem. Soc. Div. Fuel Chem. 28(4) 174 (1983).

TABLE 1 SLAG COMPOSITIONS

COMPOSITION	NO. 1	2	3	4	5	6	7
SiO_2	50	50	50	50	50	50	50
CaO	5	5	5	5	5	5	5
Al_2O_3	10	10	20	20	20	30	30
FeO	15	25	25	15	5	15	5
MgO	20	10	0	10	20	0	10
	8	9	10	11	12	13	14
SiO_2	40	40	40	40	40	40	40
CaO	15	15	15	15	15	15	15
Al_2O_3	10	10	20	20	20	30	30
FeO	15	25	25	15	5	15	5
MgO	20	10	0	10	20	0	10
	15	16	17	18	19	20	21
SiO_2	30	30	30	30	30	30	30
CaO	25	25	25	25	25	25	25
Al_2O_3	10	10	20	20	20	30	30
FeO	15	25	25	15	5	15	5
MgO	20	10	0	10	20	0	10

Table 2. Activation Energies, Range of Temperatures and Mole Fractions

Slag #	Ea	Temperature Range	Mole Fractions SiO2	Al2O3	CaO	FeO	MgO
1	43.9	1440-1332	.483	.057	.052	.121	.288
2	44.2	1460-1314	.515	.061	.055	.215	.154
3	42.0	1456-1350	.568	.134	.061	.237	.000
4	40.1	1513-1337	.529	.125	.057	.133	.158
5	60.2	1462-1312	.495	.117	.053	.041	.295
6	366	1550-1500	.584	.209	.063	.147	.000
7	65.2	1515-1415	.543	.192	.058	.045	.162
8	77.6	1353-1192	.384	.056	.154	.120	.286
9	13.1	1455-1297	.409	.060	.164	.214	.152
10	55.5	1454-1335	.451	.133	.181	.235	.000
11	37.6	1439-1310	.420	.124	.169	.132	.156
12	103	1436-1262	.393	.116	.158	.041	.293
13	36.9	1535-1447	.464	.205	.186	.145	.000
14	50.8	1484-1401	.431	.190	.173	.045	.161
15	104	1434-1339	.286	.056	.255	.119	.284
16	77.6	1390-1265	.272	.060	.272	.212	.151
17	29.5	1451-1299	.335	.132	.299	.234	.000
18	106	1448-1377	.313	.123	.279	.131	.155
19	20.0	1459-1352	.293	.115	.261	.041	.291
20	55.1	1402-1294	.345	.203	.308	.144	.000
21	116	1532-1415	.321	.189	.286	.045	.159

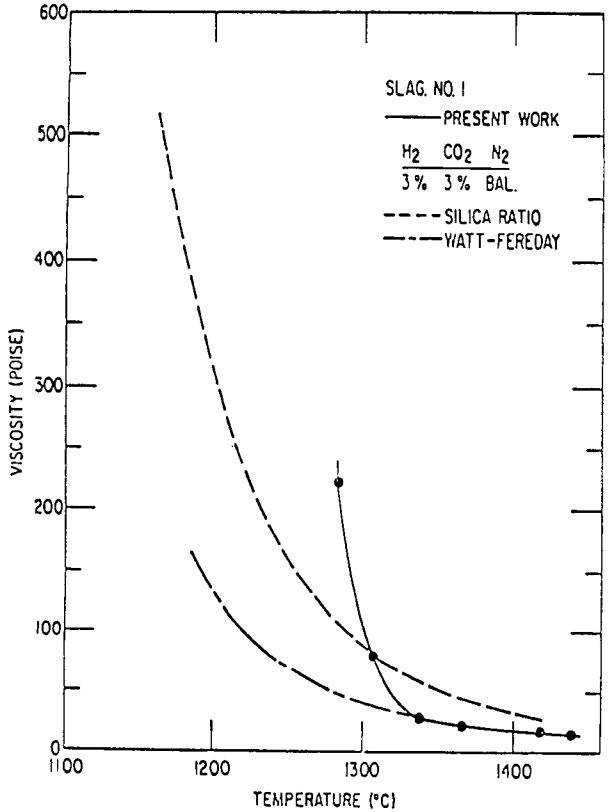

Figure 1. Viscosity of Slag 1

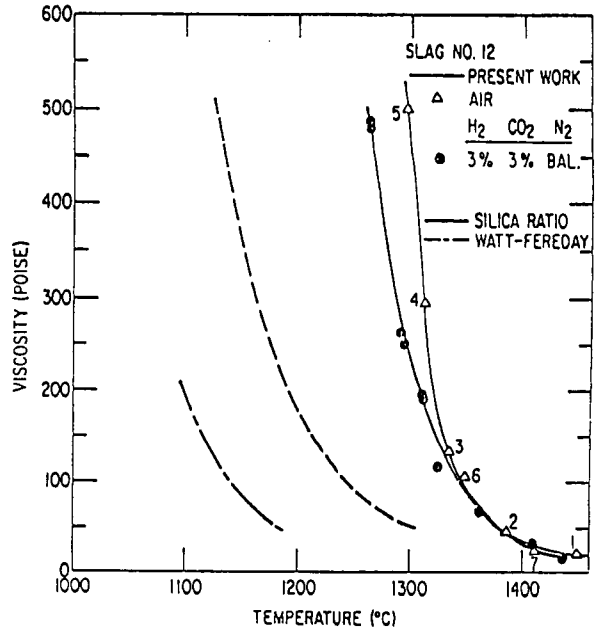

Figure 2. Viscosity of Slag 12

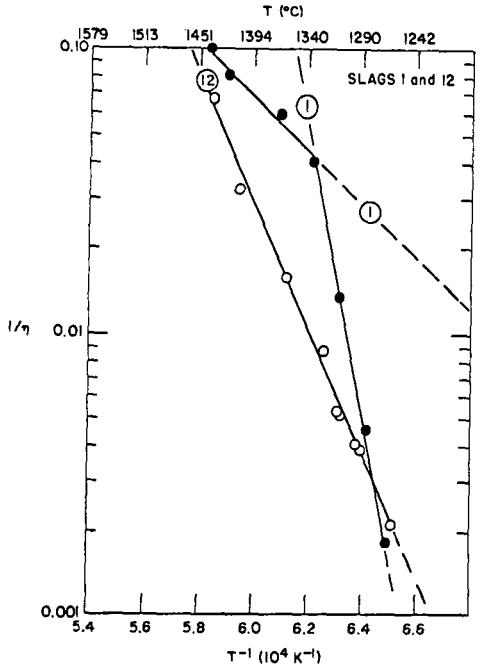

Figure 3. Typical Arrhenius Plots

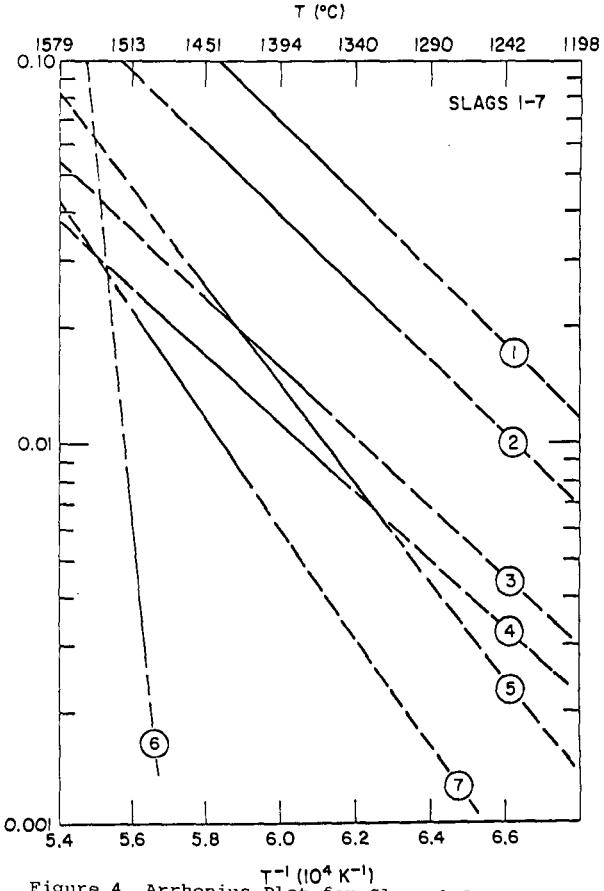

Figure 4. Arrhenius Plot for Slags 1-7

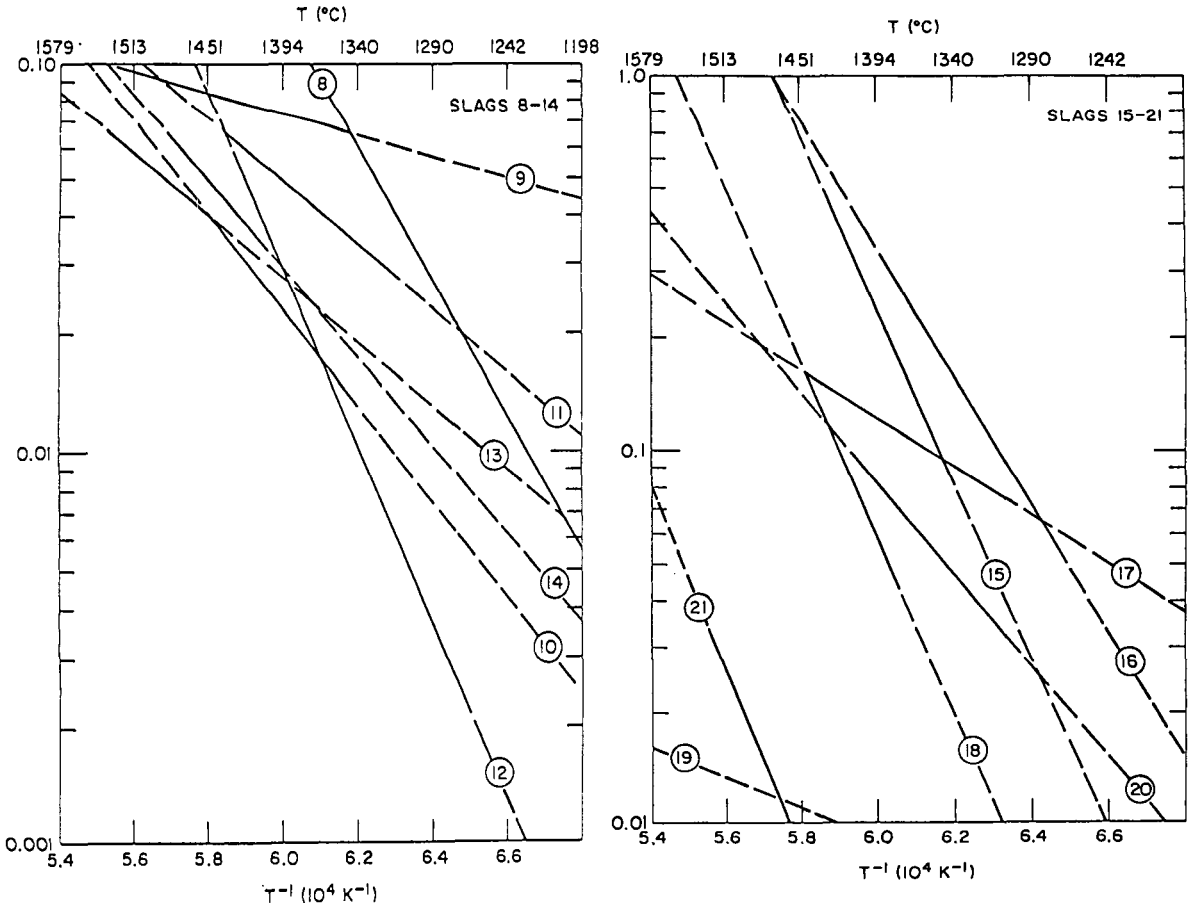

Figures 5 and 6. Arrhenius Plots of Logarithm of Reciprocal Viscosity and Reciprocal Absolute Temperatures for Slags 8-14 and 15-21

SULFUR SOLUBILITY IN SLAGS FOR CYCLONE COAL COMBUSTORS

by

David H. DeYoung

Smelting Process Development Division
Alcoa Laboratories
New Kensington, PA 15068

I. INTRODUCTION

This study was conducted to select potential slag compositions for use in a slagging, staged, cyclone coal combustor, and to obtain the necessary data to evaluate the desulfurizing ability of the combustor. The first stage of such a combustor would be operated quite reducing to facilitate sulfur removal by a slag formed from the coal ash and inorganic additives (e.g., lime). A tangential motion imparted to the gas would throw ash, coal, and additives to the combustor wall where they would combine to form a molten slag. This slag, containing some dissolved sulfur, would continually drain out of a taphole at the exit end of the horizontally-placed cylindrical combustor. Advantages of this type of combustor are removal of some sulfur, low particulate emissions, and low NO_x emissions.

This paper will be divided into three parts. First, the selection of slag compositions will be outlined. Second, sulfide capacity measurements of these slags will be discussed. Third, the desulfurizing potential of a slagging, cyclone combustor will be evaluated using these measurements.

II. SLAG COMPOSITION SELECTION

The strategy was first to select possible additives, then locate phase diagrams for systems of major ash components plus additives, and finally, select low-melting eutectic compositions as candidate slags. Additives were chosen for their known ability to form low-melting silicates (e.g., the alkalis) or for their known ability for desulfurization (e.g., the alkaline earth elements). An eastern coal was used for tests of a pilot combustor. Its ash composition, used to calculate additive compositions, is given in Table I. Major components, SiO_2, Al_2O_3, and Fe_2O_3, account for approximately 80% of the ash.

Ternary phase diagrams for the SiO_2-Al_2O_3-additive and SiO_2-FeO-additive systems were investigated for possible slag compositions. Unless otherwise noted, all phase diagrams were taken from Levin, et al (1-3) or Roth, et al (4). The selected compositions which were tested are given in Table II, as are estimated liquidus temperatures. Obviously, the liquidus temperature of the slag consisting of coal ash and the additive will be different from those given by the phase diagrams because of the minor components of the ash. However, the phase diagrams provide reasonable initial selections. Additive compositions and quantities are given in Table III.

III. SULFIDE CAPACITY MEASUREMENTS

Sulfide capacities of the selected slag compositions were measured to rate the slags and to provide data for evaluation of the operation of a combustor with these slags.

Chemistry of Sulfur in Slags: There has been considerable research on the chemistry of sulfur in slags reported in the literature. Most was aimed toward understanding and improving the desulfurization of iron and steel. These studies (5-7) have shown that at high oxygen potentials sulfur dissolves in slags as a sulfate, and at low oxygen potentials, the condition relevant to the two-stage combustor, sulfur dissolves as a sulfide. This can be represented by the reaction,

$$1/2\ S_2(g) + \left(O^{2-}\right) = 1/2\ O_2(g) + \left(S^{2-}\right). \qquad 1)$$

A quantity called the sulfide capacity (6) can be defined as:

$$C_S \equiv (\text{wt \% S}) \left(\frac{P_{O_2}}{P_{S_2}}\right)^{1/2} \qquad 2)$$

where wt % S refers to sulfur dissolved in the slag, and P_{O_2} and P_{S_2} are the partial pressures of oxygen and sulfur in the atmosphere with which the slag is equilibrated. The sulfide capacity for many slags has been found (5,6) to be independent of sulfur and oxygen potentials for wide ranges, and therefore is a useful quantity for rating slags. One exception relevant to this study is that, for slags containing FeO, C_S is expected to change with oxygen potential as the ratio of ferrous to ferric ions in the slag changes.

A review of the literature (5-22) showed that virtually all work on sulfur in slags was on systems relevant to the desulfurization of iron and steel and at temperatures ranging from 1400-1600°C. No data were found for low-melting slags (liquidus temperatures, approximately 1000-1100°C), and particularly for the iron-alkali-aluminosilicates from which many of the proposed compositions are composed. Therefore, experimental measurements were necessary to obtain the data needed for selection of slags.

Experimental Method: An equilibration technique was chosen to measure the sulfide capacities of the candidate slags. Slag samples were equilibrated with a $CO-CO_2-SO_2$ gas mixture having fixed oxygen and sulfur potentials, quenched to room temperature, and analyzed for sulfur. Sulfide capacities were then calculated from the sulfur concentrations using Equation 2. This technique was chosen because it is a direct method, and because the oxygen and sulfur potentials could be accurately controlled, and, if necessary, these could be set to match the activities for oxygen and sulfur which were anticipated in the actual coal combustor. The apparatus used for sulfide capacity measurements is shown schematically in Figure 1.

Slags were prepared by mixing preweighed amounts of additives and coal ash. The coal ash was obtained from Bituminous Coal Research, Inc. It was prepared by ashing Loveridge Seam, West Virginia coal in air at 750°C, followed by a reduction in a 60%CO-40%CO_2 gas at 1000°C, then cooled under nitrogen.

The gas compositions for each experiment were chosen to obtain as low an oxygen potential as possible, without reducing FeO to Fe metal. They were also chosen to obtain as low a sulfur potential as possible to match anticipated conditions in the actual combustor, yet large enough so that they could be prepared by mixing gases. The equilibration time for slag samples was determined by periodic analyses of the gas exiting the reactor. Quenched slag samples were analyzed for sulfur using a Leco titrator, and were analyzed for Si, Al, Fe, Na, K, Ca, Mg, Ti, and P by atomic absorption.

Results: Table IV gives the results for all sulfide capacity measurements. Figures 2 and 3 show ternary phase diagrams for selected systems on which the results are shown. Compositions shown were obtained by taking the three major components from the slag analyses and normalizing to 100%. The sulfide capacities are shown as a function of basicity in Figure 4, which summarizes all results of this study. Molar basicities (Σmole fraction bases/Σmole fraction acids) were calculated from the slag analyses.

It was found that after equilibration with the sulfurizing gas, certain slags in the $FeO-Al_2O_3-SiO_2$ system consisted of two immiscible liquids at 1100°C. One phase was a glass. The other phase had a metallic appearance and will be referred to as the "matte phase". The sulfide capacities for these slags should be considered as "apparent" because the sulfide capacity is defined for a single liquid phase. The matte phase in all of these double-phased slags contained 27-31% S, while the glass phase contained from 0.2 to 13% S. X-ray diffraction analyses showed the glass phase to be amorphous and the matte phase to contain FeS and FeS_2.

Discussion: Slag compositions 2-A-1, 2-A-7, 2-B-2, 2-C-1, 2-D-2, and 2-E-1 were closest to the coal ash composition given in Table I, containing 25-38% additive. As seen from Table IV, log C_S ranged from approximately -3.8 to -5.5 at 1100°C. Using the basicity of the ash calculated from Table I and the data shown in Figure 4, the sulfide capacity for pure ash is estimated to be approximately log C_S = -5.2. This is quite low as compared to results obtained for slags containing significant quantities of additives. As will be demonstrated later in the report, sulfur captured by coal ash slag with this sulfide capacity would be insignificant even at very favorable conditions - very low oxygen potential and low temperature.

There is a general correlation between sulfide capacity and basicity for a given system, as shown in Figure 4. There is a sharp drop in sulfide capacity between basicities of 1.0 to 0.5, which corresponds to the metasilicate to disilicate compositions in a binary silicate. For a given basicity, systems 2-A (FeO) and 2-C (FeO, CaO) have significantly higher sulfide capacities than systems 2-D (Na_2O) and 2-E (CaO), so that for a given basicity, FeO is superior to CaO and Na_2O as an additive. This is not what would be expected considering the standard free energies of formation of the sulfides and oxides of Fe, Ca, and Na.

Considering standard free energies for the formation of metal sulfides from metal oxides, FeO and CaO should be approximately equivalent desulfurizers and Na_2O should be superior. However, slags are far from ideal solutions because of the strong interactions among species -- particularly with SiO_2. This is why experimental measurements of sulfide capacities were needed. Free energy of mixing data (24) for Na_2O, CaO, and FeO binary silicates show that the chemical interaction with silica decreases in the order Na_2O, CaO, FeO, and for a given basicity, the activity of the basic oxide in the silicates increase in the order Na_2O, CaO, and FeO. On this basis, FeO should be a better desulfurizer than CaO or Na_2O. This is consistent with the present results. Not surprisingly, the metal oxide-silica interaction is a major factor in the desulfurization ability of the slag.

Several modifications of slags based on the $FeO-Al_2O_3-SiO_2$ system were tested to determine if a less expensive additive could be substituted for some of the iron or if additives could be used to reduce liquidus temperatures. Figure 4 shows that replacing a portion of the iron oxide in slags of the $FeO-Al_2O_3-SiO_2$ system with CaO (5 wt %) or MgO (12 wt %) had no effect on the sulfide capacities. Results for composition 2-C-1 also support this conclusion, because for this composition approximately 14% of the FeO of an equivalent composition in the $FeO-Al_2O_3-SiO_2$ system was replaced by CaO, with only a slight decrease in sulfide capacity. Replacement of portions of the SiO_2 in $FeO-Al_2O_3-SiO_2$ slags by B_2O_3 or P_2O_5 has no effect on sulfide capacities; therefore, these additives are potentially useful for reducing slag liquidus temperatures.

Figure 5 compares some results of this study to those found in the literature for similar slags at higher temperatures. These literature data were adjusted to a basicity of 1.65 using data given in Figure 4. The data from this study are quite consistent with the literature data. The linearity of the sulfide capacity with inverse temperature is consistent with the theoretical relationship,

$$\frac{d \ln C_S}{d(1/T)} = -\Delta H^\circ/R + H^M_{FeO}/R - H^M_{FeS}/R \qquad 3)$$

where ΔH° is the standard enthalpy change for the reaction,

$$1/2\ S_2(g) + FeO = 1/2\ O_2(g) + FeS \qquad 4)$$

and H^M_{FeO} and H^M_{FeS}

are the partial molar enthalpies of mixing of FeO and FeS in the slag. This relationship can be derived from Equation 2, the equilibrium constant for Equation 4 and the Gibbs-Helmholtz equation.

Most of the slags tested were found to have been partially or completely melted at 1100°C. However, at 1000°C, all slags from the $FeO-Al_2O_3-SiO_2$ system were not molten. It is thought that for these compositions the entire additive reacted with sulfur species in the atmosphere while none reacted with the SiO_2 or with other components in the ash. Hence, sulfide capacities measured from this experiment are not true sulfide capacities of the slags. Another point which supports this is that the "measured" sulfide capacities at 1000°C are greater than those at 1100°C, while Figure 5 shows the opposite trend for results for molten slags. Also, other literature data show that sulfide capacities generally increase with temperature.

This points out an inherent disadvantage in using a coal ash slag for desulfurization. When silica reacts with the desulfurizing agent, e.g., lime, the effectiveness of the desulfurizing compound is greatly reduced. Hence, it is desirable to design a desulfurizing combustor in which the ash does not react with the desulfurizing material.

IV. EVALUATION OF A PILOT COMBUSTOR

Calculations: The measured sulfide capacities were used to estimate sulfur emissions from a staged, slagging, cyclone combustor operating close to equilibrium. To calculate sulfur emissions, an equation for gas-slag chemical equilibrium for sulfur (Equation 2) and a mass balance for sulfur are solved simultaneously. First, the equilibrium gas compositions were calculated for the combustion of coal with air for a range of sulfur concentrations in the coal. This was done using Alcoa's Chemical Equilibrium Computer Program (23). Next, the concentrations of sulfur in the slags for equilibrium with the combustion gases were calculated. Finally, the quantity of additives needed to obtain these compositions were calculated from sulfur mass balances.

Results: Figure 6 shows an example of the results for these calculations, for combustion with 55% of stoichiometric air (stage 1) at 1100°C. A reasonable goal for the sulfur capture, considering projections of future EPA regulations, is 70%. The slag mass can vary between 85 and 350 g/kg coal (the upper limit was

established from a heat balance for Alcoa's pilot combustor), so the necessary log C_S for a 70% sulfur removal is between -2.75 and -3.3. A sulfide capacity of log C_S = -3.3 at 1100°C was obtained for certain slags based on the $FeO-Al_2O_3-SiO_2$ system, e.g., compositions 2-A-3 or 2-A-10.

As the combustion stoichiometry is decreased, the curves in Figures 6 are rotated counterclockwise about the origin, i.e., the sulfur removal is increased. An increase in temperature will have the opposite effect. The curves are rotated clockwise about the origin. However, for a particular slag composition the sulfide capacity increases with temperature, as shown in Figure 5. The net result of the two opposing effects (using the temperature behavior shown in Figure 5) is that the sulfur removal decreases with increasing temperature. In the range of coal-sulfur contents investigated, 2-6%, the fraction of sulfur removed by slag does not change with sulfur content in the coal. The total sulfur emitted increases with increasing sulfur concentration in the coal, but the sulfur removal by the slag also increases.

A final point to note regarding sulfur removal is that as the concentration of hydrogen in the combustion gases is decreased, the sulfur removal by the slag will increase. This is due to the high stability of the hydrogen-sulfur species, such as $H_2S(g)$, as compared to the carbon-sulfur species, such as COS. Thus, drying and charring of coal would significantly increase the theoretical removal of sulfur by the slag.

These calculations assume gas-slag equilibrium with respect to sulfur. This is probably only approached at the gas-slag surface near the exit of the first stage. At the entrance end of the combustor, the conditions would probably be more oxidizing than conditions calculated from the overall combustion stoichiometry, Ø, and thus sulfur solubility in the slag would be less than that calculated. At some depth below the slag surface near this entrance end of the first stage, the conditions would be more reducing than those calculated from the overall combustion stoichiometry. This would result in increased sulfur solubility. The actual combustion process and sulfur removal processes are quite complex, and the extent of sulfur removal will depend on the combustion kinetics. For example, consider two extreme situations. In one, where most coal is combusted after it hits the slagged wall, sulfur removal should be relatively good. In the other extreme, where all the coal is combusted before it reaches the slagged wall, sulfur removal would be relatively poor because it would be dependent on mass transport through the gas phase, and the gas has a relatively short residence time.

In summary, the kinetics of the combustion process is important with regard to sulfur removal. The kinetics must be considered either by modelling or experimentation before a final judgment on desulfurization in a slagging, cyclone combustor can be made. The results of this study show that it is theoretically possible.

V. CONCLUSIONS

Sulfide capacity measurements of relatively low melting (approximately 1100°C in most cases) slags based on the $FeO-Al_2O_3-SiO_2$, $FeO-Na_2O-SiO_2$, $FeO-CaO-SiO_2$, $Na_2O-Al_2O_3-SiO_2$, and $CaO-Al_2O_3-SiO_2$ systems but composed of coal ash + additives, have shown that the $FeO-Al_2O_3-SiO_2$-based slags had the highest sulfide capacities. For a given basicity, the sulfide capacities could be ranked in the following order: $FeO-Al_2O_3-SiO_2 > FeO-CaO-SiO_2 > FeO-Na_2O-SiO_2 > CaO-Al_2O_3-SiO_2 > Na_2O-Al_2O_3-SiO_2$. The chemical interaction of the basic oxides with silica appears to be a dominant factor controlling the sulfide capacity. There was good correlation between sulfide capacity and slag basicity, and sulfide capacities increased with temperature.

Calculations of the equilibrium sulfur removal for a commercial combustor using the measured sulfide capacities, showed that it was theoretically possible to remove 70% or more of the sulfur in coal. The sulfur removal increases with decreasing temperature, decreasing combustion stoichiometry in the first stage of the burner, increasing slag flow, and decreasing content of hydrogen in the fuel. This work showed that a slagging, cyclone combustor can remove sulfur into the slag, but kinetic modelling and/or experimentation is needed to prove whether or not the concept will work.

VI. ACKNOWLEDGEMENT

This work was sponsored by the U.S. Department of Energy under Contract No. DE-AC07-78CS40037, "Pulverized Coal Firing of Aluminum Melting Furnaces."

VII. REFERENCES

1. E. M. Levin, C. R. Robbins, and H. F. McMurdie: Phase Diagrams for Ceramists, American Ceramic Society, Columbus, OH (1964).
2. E. M. Levin, C. R. Robbins, and H. F. McMurdie: Phase Diagrams for Ceramists, 1969 Supplement, American Ceramic Society, Columbus, OH (1969).
3. E. M. Levin and H. F. McMurdie: Phase Diagram for Ceramists, 1975 Supplement, American Ceramic Society, Columbus, OH (1975).
4. R. S. Roth, T. Negas, and L. P. Cook: Phase Diagrams for Ceramists, Volume IV, American Ceramic Society, Columbus, OH (1981).
5. G. R. St. Pierre and J. Chipman: Trans. AIME, v. 206, pp. 1474-1483 (1956).
6. C.J.B. Finchman and F. D. Richardson: Proc. R. Soc. Series A223, 40 (1954) and J. Iron Steel Ins. 178, 4 (1954).
7. F. D. Richardson: Physical Chemistry of Melts in Metallurgy, v. 2, pp. 291-304, Academic Press, London (1974).
8. P. T. Carter and T. G. McFarlane: J. Iron Steel Inst., 185, 54 (1957).
9. K. P. Abraham, M. W. Davies, and F. D. Richardson: J. Iron Steel Inst., v. 196, pp. 309-312 (1960).
10. K. P. Abraham and F. D. Richardson: J. Iron Steel Inst., v. 196, pp. 313-317 (1960).
11. E. W. Dewing and F. D. Richardson: J. Iron Steel Inst., v. 194, pp. 446-450 (1960).
12. R. A. Sharma and F. D. Richardson: J. Iron Steel Inst., v. 198, pp. 386-390 (1961).
13. R. A. Sharma and F. D. Richardson: J. Iron Steel Inst., v. 200, pp. 373-379 (1962).
14. G.J.W. Kor and F. D. Richardson: J. Iron Steel Inst. v. 206, pp. 700-704 (1968).
15. G.J.W. Kor and F. D. Richardson: Trans. AIME, v. 245, pp. 319-327 (1969).
16. R. J. Hawkins, S. G. Meherali, and M. W. Davis: J. Iron Steel Inst., v. 209, pp. 646-657 (1971).
17. A. Bronson and G. R. St. Pierre, Met. Trans. B, v. 10B, pp. 375-380 (1979).
18. A. Bronson and G.R. St. Pierre: Met. Trans. B, v. 12B, pp. 729-731 (1981).
19. H. B. Bell: Can. Met. Quart., v. 20 (2), pp. 169-179 (1981).
20. J. D. Shim and S. Ban-ya: Tetsu-to-Hagane, v. 68, pp. 251-60 (1982).
21. S. D. Brown, R. J. Roxburgh, I. Ghita, and H. B. Bell: Ironmaking and Steelmaking, v. 9, pp. 163-67 (1982).
22. I. Ghita and H. B. Bell: Ironmaking and Steelmaking, v. 9, pp. 239-43 (1982).
23. W. E. Wahnsiedler: "Chemical Equilibrium Package Users Manual," Alcoa Laboratories Report No. 7-78-25.
24. D. R. Gaskell: Metallurgical Treatises, J. K. Tien and J. F. Elliott, ed., p. 60, TMS-AIME, Warrendale, PA (1981).

TABLE I. ASH FROM LOVERIDGE SEAM (WEST VIRGINIA) COAL

Component	Ash Analysis: Wt Pct.	Ash Analysis: Normalized (excluding sulfur and taking iron as FeO)
Al_2O_3	18.4	24.1
SiO_2	44.5	47.8
Fe_2O_3	15.9	17.4 (FeO)
CaO	4.56	4.9
MgO	1.08	1.2
Na_2O	1.10	1.5
K_2O	1.11	1.3
TiO_2	1.20	1.1
SO_3	9.02	--
P_2O_5	0.33	0.5

TABLE II. NORMALIZED COMPOSITIONS OF CANDIDATE SLAGS - MAJOR COMPONENTS ONLY

Slag No.	Composition, Wt. Pct. SiO_2	Al_2O_3	FeO	Na_2O	CaO	Liquidus Temperature (°C) (Major Components Only)
2-A-1	46.0	19.9	34.1			1205
2-A-2	40.0	12.0	48.0			1083
2-A-3	18.1	5.9	76.0			1148
2-A-7	43.3	19.8	36.9			1220
2-A-8	35.3	14.1	50.6			1200
2-A-9	27.0	8.3	64.4			1150
2-A-10	23.6	5.9	70.4			1155
2-B-1	39.3		48.0	12.7		1000
2-B-2	56.4		21.8	21.8		?
2-B-3	33.2		26.2	40.6		1050
DSE-1	42.5		28.9	28.6		900
DSE-2	37.0		26.0	37.0		
2-C-1	37.7		46.4		15.7	1093
2-D-1	43.8	18.2		37.9		915
2-D-2	62.7	23.2		14.0		1063
2-D-3	61.6	12.2		26.2		732
2-E-1	42.1	20.1			37.8	1265
2-I-1	55.3	21.5	10.0	13.1		990

TABLE III. ADDITIVE COMPOSITIONS FOR CANDIDATE SLAGS

Slag No.	Additive Mass g/g Ash	Additive Composition, Wt. Pct.					
		SiO_2	Al_2O_3	Fe_2O_3	Na_2CO_3	CaO	Other
2-A-1	0.34	22.9		77.1			
2-A-2	1.20	27.0		73.0			
2-A-3	3.52	7.4		92.6			
2-A-4	3.74	7.0		87.2			5.8 % CaF_2
2-A-5	3.52	1.6		92.6			5.8 % B_2O_3
2-A-6	3.52	1.6		92.6			5.8 % P_2O_5
2-A-7	0.36	13.9		86.1			
2-A-8	0.89	13.9		86.1			
2-A-9	2.19	13.9		86.1			
2-A-10	3.47	13.9		86.1			
2-A-10b	4.07	11.8		73.5			14.7 % MgO
2-A-11	3.49	7.5		86.7		2.5	3.4 % CaF_2
2-A-12	4.99	13.9		86.1			
2-B-1	0.69			65.7	34.2		
2-B-2	0.30			3.9	96.1		
2-B-3	1.20			18.9	81.1		
DSE-1	0.69			24.2	75.8		
DSE-2	0.97			18.5	81.5		
2-C-1	0.61			75.5		24.5	
2-D-1	0.93	10.9			89.1		
2-D-2	0.40	43.8			56.2		
2-D-3	1.60	46.3			53.7		
2-E-1	0.43	6.3				93.7	
2-I-1	0.99	49.1	13.5		37.4		

TABLE IV. SULFIDE CAPACITY MEASUREMENTS

Exp't. No.	T (°C)	Run Time (h)	Slag Composition	Wt % S	Log C_S	Comments
2*	1100	24	DSE-1	4.22	-4.31	
			"	5.34	-4.21	
			2-B-1	6.05	-4.16	
			2-B-2	0.26	-5.52	
			2-D-1	0.96	-4.96	
			2-D-2	0.87	-5.00	Did not melt
			2-D-3	0.69	-5.10	
4**	1100	115	DSE-1	4.31	-4.06	
			2-A-1	4.80	-4.01	
			2-A-2			Sample crept out
			2-A-3	22.5	-3.34	2 phases
			2-A-4	23.5	-3.32	2 phases
			2-C-1	7.91	-3.79	
5**	1100	144.6	2-A-5	20.2	-3.38	2 phases
			2-A-6	13.4	-3.56	2 phases
			2-A-7	5.06	-3.99	
			2-A-8	9.81	-3.70	
			2-A-9	16.6	-3.47	2 phases
			2-A-10	19.1	-3.41	2 phases
			2-A-11			Sample crept out
			2-B-3	2.65	-4.27	
7***	1000	168.75	2-A-3	25.4		Did not melt
			2-A-4	25.1		" " "
			2-A-5	25.5		" " "
			2-A-6	24.1		" " "
			2-A-10	23.6		" " "
			2-A-11	24.2		" " "
			2-A-12	25.8		" " "
			2-A-3a	26.3		" " "
			2-I-1	0.44	-5.04	
11****	1300	70.0	2-A-3	2.67	-2.86	
			2-A-10	1.97	-3.00	
			2-A-10b	3.10	-2.80	

* Gas Composition - 70%CO-29.5% CO_2-0.5%SO_2

$X_{O_2} = 7.2 \times 10^{-14}$, $X_{S_2} = 5.4 \times 10^{-4}$

** Gas Composition - 70.2%CO-29.6%CO_2-0.25%SO_2

$X_{O_2} = 6.8 \times 10^{-14}$, $X_{S_2} = 1.6 \times 10^{-4}$

*** Gas Composition - 74.5%CO-25.3%CO_2-0.18%SO_2

$X_{O_2} = 6.8 \times 10^{-14}$, $X_{S_2} = 1.6 \times 10^{-4}$

**** Gas Composition - 66.3%CO-33.6%CO_2-0.14%SO_2

$X_{O_2} = 4.9 \times 10^{-11}$, $X_{S_2} = 1.9 \times 10^{-4}$

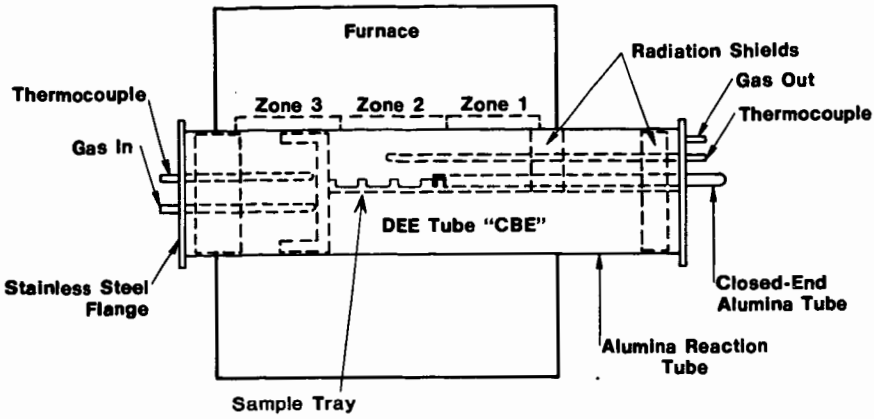

FIGURE 1. REACTOR USED FOR SULFIDE CAPACITY MEASUREMENTS.

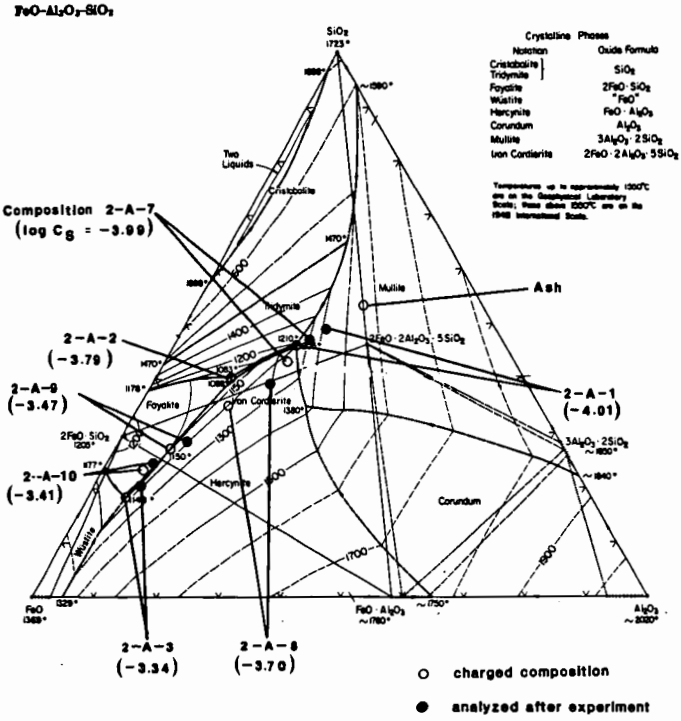

FIGURE 2. THE $FeO-Al_2O_3-SiO_2$ SYSTEM (2-A) WITH MEASURED SULFIDE CAPACITIES INDICATED. PHASE DIAGRAMS TAKEN FROM REFERENCE (1). OXIDE PHASES IN EQUILIBRIUM WITH METALLIC IRON.

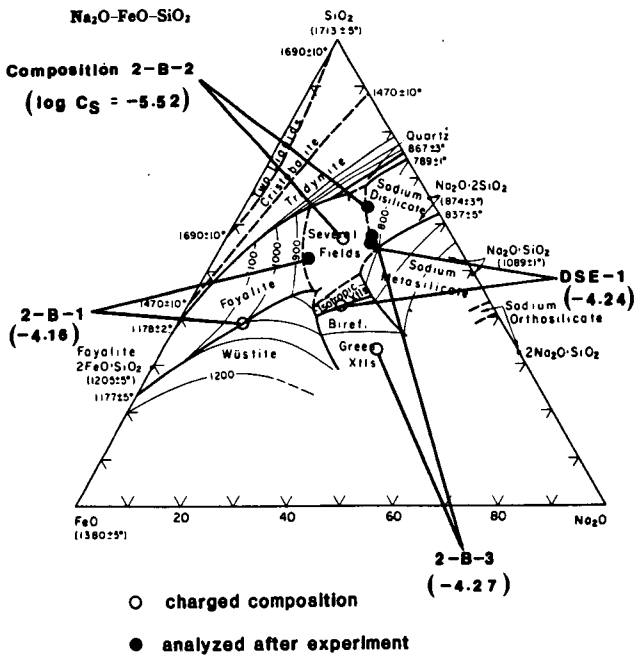

FIGURE 3. THE $FeO-Na_2O-SiO_2$ SYSTEM (2-B) WITH MEASURED SULFIDE CAPACITIES INDICATED. PHASE DIAGRAM TAKEN FROM REFERENCE (2). OXIDE PHASES IN EQUILIBRIUM WITH METALLIC IRON.

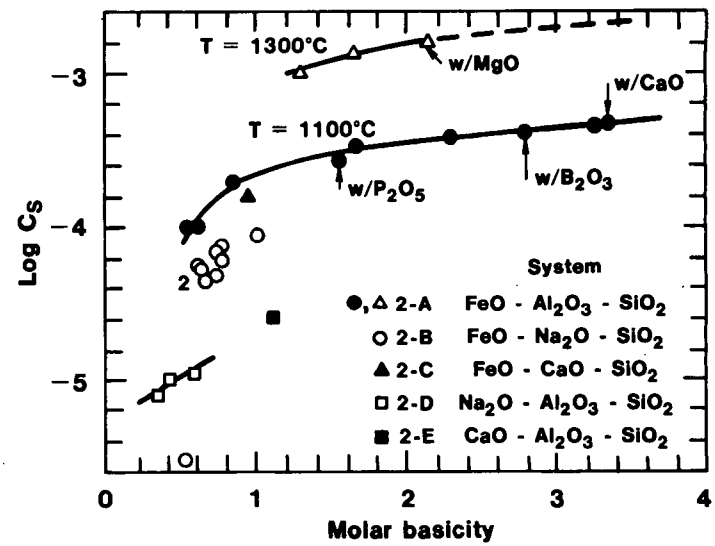

FIGURE 4. MEASURED SULFIDE CAPACITIES OF CANDIDATE SLAGS. BASICITY CALCULATED FROM CHEMICAL ANALYSES. POINTS DENOTED BY w/P_2O_5 AND w/B_2O_3, REPRESENT SLAGS IN WHICH 5% SiO_2 WAS REPLACED BY 5% OF THESE OXIDES. POINT DENOTED BY w/CaO IS FOR SLAG TO WHICH 5% CaF_2 WAS ADDED, BUT ALL FLUORINE WAS LOST DURING EXPERIMENT. POINT DENOTED BY w/MgO FOR SLAG TO WHICH 12% MgO WAS ADDED.

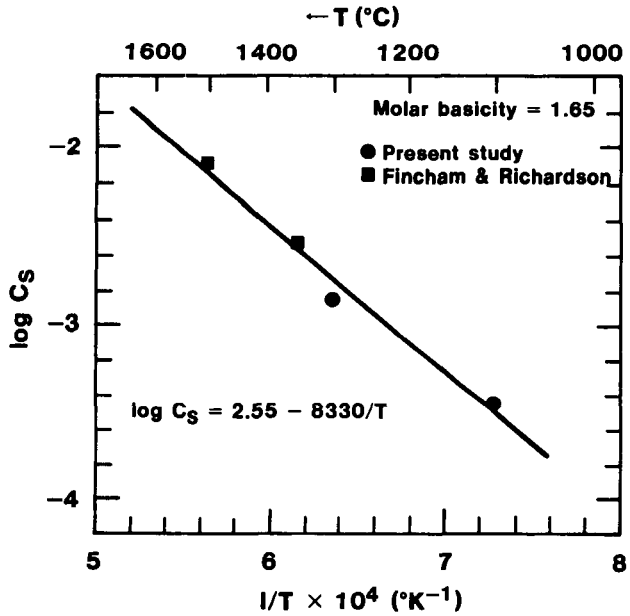

FIGURE 5. COMPARISON OF RESULTS FROM THIS STUDY TO THOSE OF FINCHAM AND RICHARDSON (6) FOR AN IRON SILICATE WITH MOLAR BASICITY OF 1.65. DATA FROM FINCHAM AND RICHARDSON WERE FOR PURE IRON SILICATES WHILE THESE FROM THE PRESENT STUDY CONTAINED SOME COAL ASH. DATA FROM FINCHAM AND RICHARDSON WERE CORRECTED FOR BASICITY USING DATA FROM THE PRESENT STUDY.

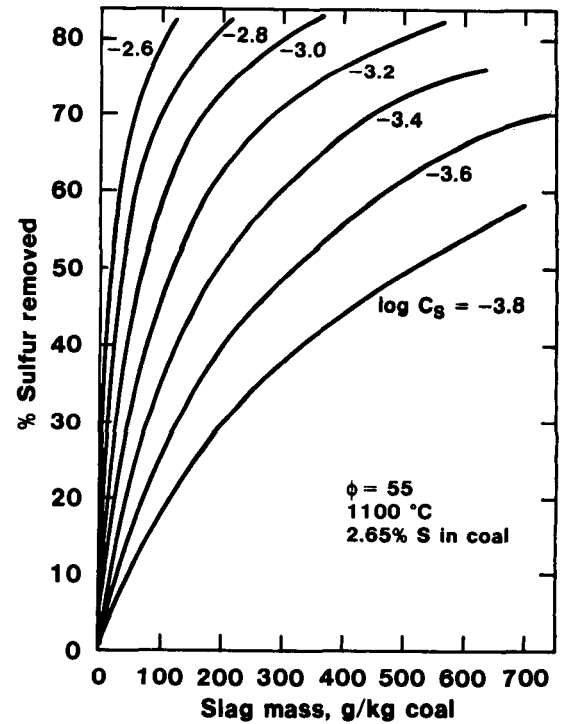

FIGURE 6. EQUILIBRIUM SULFUR REMOVAL BY SLAG FOR A COMBUSTOR OPERATING WITH LOVERIDGE SEAM (WEST VIRGINIA) COAL.

The Thermodynamic Properties of Molten Slags

Milton Blander* and Arthur D. Pelton†

INTRODUCTION

Silica based slag systems are highly ordered liquids which have been a difficult class of materials on which to perform thermodynamic analyses.[1–5] To our knowledge, no satisfactory, self-consistent prior method of analysis has been developed for systems as ordered and complex as silicates which incorporates all known data in a meaningful way. In this paper, we discuss the results of a method of analysis which permits one to simultaneously analyze a large amount of different types of data on binary systems. The calculations lead to a small set of parameters which permit one to calculate the thermodynamic properties of slag solutions as a function of temperature and composition. The thermodynamic self-consistency and the form of the equations used provide some confidence in the use of the results for interpolations and extrapolations outside the range of data. In addition, for systems in which silica is the only acid constituent, we propose a theoretically justified combining rule to calculate the properties of ternary systems based solely on data for the three subsidiary binaries. The results are in good agreement with available data.

The ionic nature of molten silicates suggests that many of the theories and correlations developed for molten salts[6] can be applied to the development of correlations between the relative magnitudes of the deviations from ideal solution behavior in terms of ionic radii, charges, polarizabilities, dispersion interactions and ligand field effects.

CALCULATIONAL METHOD[7]

The molar free energy of mixing, ΔG_m of a silicate is represented by the expression

$$\Delta G_m = \sum_i RTX_i ln X_i + \sum_i RTX_i ln\gamma_i = \Delta G_m^{ideal} + \Delta G^E \qquad (1)$$

where X_i is the mole fraction of component i, γ_i, the activity coefficient, represents deviations from ideal solution behavior of component i, ΔG_m^{ideal} is the molar free energy of mixing of a hypothetical ideal solution and ΔG^E is the molar excess free energy of mixing which represents the deviations from ideality of the molar free energy of solution. The conventional representation of $\ln\gamma_i$ and ΔG^E is a power series in mole fractions. The complexity of ordered solutions would require a very long power series in order to obtain a reasonable representation of their properties. This arises from the tendency of such solutions to have a "V" shaped dependence of the enthalpy of mixing and an "m" shaped dependence of the entropy of mixing on concentration.[1] The fitting of data using a long polynomial will generally be poor and ambiguous in such systems. In order to obtain reasonable fits, one must use equations which inherently have the concentration and temperature dependence of ordered solutions built in.

We have deduced a set of equations with such properties based on empirical modifications of the quasi-chemical theory. An energy parameter in the theory, W, is represented by a power series

*Argonne National Laboratory, Argonne, IL 60439

†Ecole Polytechnique, Université de Montréal, Montréal, Québec, Canada, H3C3A7

$$W = \sum_{j=0} C_j y^j \qquad (2)$$

where y is an equivalent fraction of one of the components (silica is always chosen if present). For binary systems, the parameters C_j are deduced from a complex optimization procedure which performs a global and simultaneous analysis of all thermodynamic data on a system. This includes liquidus phase diagrams, activity data, data on miscibility gaps, enthalpies of fusion, free energies of formation of compounds, etc. The small set of resultant parameters (seven at most including temperature coefficients of some) are then used to recalculate the input data to double check the accuracy of the curve fitting procedure and the efficacy of the use of the equations for representing the data. The results were generally very good.

For multicomponent systems, we developed an asymmetric combining rule such that *e.g.* for a system 1–2–3 where 1 is silica, W_{12} and W_{13} which represent energies related to interactions of silica with the other two components, are a function only of y_1, and W_{23} is related to the ratio $y_3/(y_2 + y_3)$. A partial theoretical justification for such a method can be based on theories for ternary systems.[8]

RESULTS OF THERMODYNAMIC ANALYSES

We have performed analyses of ten of the fifteen binary systems and six of the twenty ternary systems containing the components MgO, FeO, CaO, Na_2O, Al_2O_3, and SiO_2.[7,9]

Table I
Systems Which Have Been Analyzed

Binary Systems		Ternary Systems
CaO-SiO_2	CaO-$AlO_{1.5}$	CaO-$AlO_{1.5}$-SiO_2
FeO-SiO_2	$NaO_{0.5}$-$AlO_{1.5}$	$NaO_{0.5}$-CaO-SiO_2
MgO-SiO_2	MgO-FeO	$NaO_{0.5}$-$AlO_{1.5}$-SiO_2
$NaO_{0.5}$-SiO_2	MgO-CaO	CaO-FeO-SiO_2
$AlO_{0.5}$-SiO_2	CaO-FeO	CaO-MgO-SiO_2
		MgO-FeO-SiO_2

We illustrate our calculations for one ternary system below. The analysis of the three binary subsystems and the ternary system CaO-FeO-SiO_2 was performed using as input the liquidus phase diagram,[10] activities of CaO,[11] and SiO_2,[12], the free energies of formation of $CaSiO_3$ and Ca_2SiO_4,[13] and the miscibility gap[14] in the CaO-SiO_2 system, measured activities of FeO in the CaO-FeO system,[15] and the activities of FeO,[16,17,18] the phase diagram[19] and the free energy of formation of Fe_2SiO_4[13] in the FeO-SiO_2 system. To illustrate some of the results, we exhibit (1) the calculated phase diagram of the FeO-SiO_2 system in Fig. 1 along with measured values of the invariant points and (2) a comparison of activities of "FeO" measured in the iron saturated molten FeO-SiO_2 system with calculated values in Fig. 2.

Using our "asymmetric" combining rules, the data for the binary systems were combined and led to the results for ternary systems given in Fig. 3; this figure illustrates the correspondence between calculated and measured values[20] of the activities of FeO in the CaO-FeO-SiO_2 system. The differences are well within the uncertainties in the measurements. We find that this method essentially permits us to make predictions in ternary systems based solely on data for the three

subsidiary binary systems for cases in which silica is the only acid component. When alumina and silica are both present, a more complex representation is necessary.

The good correspondence of calculations with the complex concentration dependence of activities in the CaO-FeO-SiO_2 system illustrates the fact that our equations properly take into account the kinds of ternary interaction terms known to exist in such systems.[8,21] This feature lends confidence in the use of our equations for predictions in multicomponent systems (containing only silica as an acid component) based solely upon the subsidiary binaries. If, as it appears, this is generally true, our method provides an important predictive capability.

CORRELATIONS OF PROPERTIES

Theories and concepts which have been developed for molten salt solutions can be used to correlate the thermodynamic properties of silicates.[6] Coulomb interactions lead to a dependence of thermodynamic functions on the inverse of the cation-anion interatomic distance. Thus, by analogy with molten salts, one would expect a linear dependence of the magnitudes of free energies of mixing on this parameter which is in a direction such that negative deviations from ideality increase in the order Li^+, Na^+, K^+, Rb^+, Cs^+, and Mg^{++}, Ca^{++}, Sr^{++}, and Ba^{++}. In addition, monovalent alkali oxides should exhibit more negative deviations from ideality than divalent alkaline earth oxides. The polarizability of oxide anions leads to an additional contribution with a similar dependence on cations. The magnitude of cation-cation dispersion interactions are related to the polarizabilities, ionization potentials and interaction distances. Thus, the disolution of oxides of cations with large dispersion interactions leads to a loss of this negative energy and hence to a positive contribution to deviations from ideality. In addition ligand field effects for divalent transition metals tend to contribute to negative deviations from ideal solution behavior in molten salts with monovalent cations. The effective charge of Si is greater than two and one would thus expect a positive contribution to deviations from ideal solution behavior from this source. The effect for Mn^{2+} which has a half filled shell for example, should be much less positive than for Fe^{2+}.

The data for testing these influences on solution behavior are too sparse to reach quantitative conclusions. However, the general trends are in the right direction. Measured deviations from ideality of silicates with divalent oxides become more negative (or less positive) in the order Fe^{+2}, Mn^{2+}, Pb^{2+}, Mg^{2+}, Ca^{2+}.[1,7,9,22] In this view, ligand field effects lead to Fe^{2+} preceding Mn^{2+} and Mn^{2+} preceding even Mg^{2+} which has a smaller radius; dispersion interactions lead to Pb^{2+} preceding even Mg^{2+} even though its radius is larger than Ca^{2+} and Sr^{2+}; finally, coulomb and polarization interactions lead to Mg^{2+} preceding Ca^{2+}. With careful measurements of a larger number of binary silicate systems, it should be possible to develop useful correlations and a means of making reasonable predictions of the magnitudes of thermodynamic properties of silicates.

CONCLUSIONS

There are several significant conclusions which can be reached.

1. We have performed analyses of thermodynamic data on binary silicate systems which lead to a unique and accurate mathematical representation of their known properties.
2. Our use of equations which have the properties of ordered liquids built in appears to have the innate capability for representing a mass of different types of data on binary systems measured in various ranges of temperature and composition. This result lends confidence in the use of our analyses for interpolations and extrapolations outside the range of measurements.

3. We can theoretically justify an "asymmetric" combining rule which, for cases in which silica is the only acid component, leads to *a priori* predictions for ternary systems based on data for the three subsidiary binaries. It appears likely that such predictions would be valid for multicomponent systems.
4. A preliminary examination of themodynamic data on silicates indicates that correlations developed for molten salts may be useful in understanding and ultimately in predicting magnitudes of the thermodynamic solution properties of silicates.

FIGURE CAPTIONS

1. Calculated phase diagram of the FeO-SiO_2 system. Numbers in parentheses are measured values from Muan and Osborne[10] and Robie, et al.[13]
2. Activities of "FeO" measured in iron saturated molten FeO-SiO_2 at 1325°C (Δ)[17], 1785°C (O)[16], 1880°C (◇)[16], and 1960°C (□)[16]. The two solid lines represent calculated points at 1325°C and 1880°C. The filled circles along one solid line represent individual calculated points and the three filled circles labeled 1960, 1880, and 1785 represent calculated points at three temperatures and fixed composition which illustrate the calculated temperature dependence.
3. Activities of FeO in iron saturated CaO-FeO-SiO_2 at 1550°C. Dashed lines are from Timucin and Morris[20] and the solid lines represent our calculations.

REFERENCES

1. P. L. Lin and A. D. Pelton, Metall. Trans. 10B, 667–676 (R1979).
2. C. R. Masson, I. B. Smith, and S. G. Whiteway, Can. J. Chem. 48, 1456–1464 (1977); Proc. 11th International Congress on Glass, J. Gotz, Ed., Vol. 1, pp. 3–41, Prague (1977).
3. D. R. Gaskell, Metall. Trans. 8B, 131–145 (1977).
4. C. J. B. Fincham and F. D. Richarson, Proc. Roy. Soc. 223, 40 (1954).
5. G. W. Toop and C. S. Samis, Trans. TMS-AIME 224, 878–887 (1962).
6. M. Blander, "Thermodynamic Properties of Molten Salt Solutions," Molten Salt Chemistry, M. Blander, Ed., Interscience, N.Y., pp. 127–237 (1964).
7. M. Blander and A. D. Pelton, Computer Assisted Analyses of the Thermodynamic Properties of Slags in Coal Combustion Systems, ANL/FE-83-19, Argonne National Laboratory, Argonne, IL (1983) Available from NTIS, U.S. Dept. of Commerce, Washington, D.C.
8. M.-L. Saboungi and M. Blander, J. Chem. Phys., 63, 212–220 (1975); J. Amer. Ceram. Soc. 58, 1–7 (1975).
9. A. D. Pelton and M. Blander, in preparation.
10. A. Muan and E. F. Osborne, Phase Equilbria Among Oxides in Steelmaking, Addison-Wesley Publishing Co., Reading, Mass. (1965).
11. R. A. Sharma and F. D. Richardson, J. Iron Steel Inst. 200, 373 (1962); 198, 308 (1961).
12. R. H. Rein and J. Chipman, Trans. AIME 233, 415–425 (1965).
13. R. A. Robie, B. S. Hemingway, and J. R. Fisher, Thermodynamic Properties of Minerals and Related Substances at 298.15 K and 1 Bar Pressure and at Higher Temperatures, Geologic Survey Bulletin 1452, U.S. Govt. Printing Office, Washington, D.C. (1978).
14. Ya. I. Ol'shanskii, Dokl. Akad. Nauk. SSR 76, 94 (1951); J. D. Tewhey and P. C. Hess, Phys. Chem. Glasses, 20, 41-53 (1979)
15. J. F. Elliott, Trans. AIME, 203, 485 (1955).
16. P. A. Distin, S. G. Whiteway, and C. R. Masson, Can. Met. Quart., 10, 73(1971).
17. R. Schuhmann and P. Ensio, J. Metals, 3, 401 (1951).
18. C. Bodsworth, J. Iron and Steel Inst., London, 193, 13 (1959).
19. E. M. Levin, C. R. Robbins, and H. F. McMurdie, Phase Diagrams for Ceramists, Am. Ceram. Soc., Columbus, Ohio (1964); Supplement, (1969); E. M. Levin and H. F. McMurdie, Supplement (1975).
20. M. Timucin and A. E. Morris, Met. Trans., 1, 19 (1970).
21. M. Blander, "Some Fundamental Concepts in the Chemistry of Molten Salts" in Molten Salts, G. Mamantov, ed., Marcel Dekker, New York (1969).
22. H. Gaye and P. Riboud, Donnèes Experimentales sur les Activitès des Constituants de Laitiers, IRSID PCM-RE 337, St. Germain-en-Laye, France (1976).

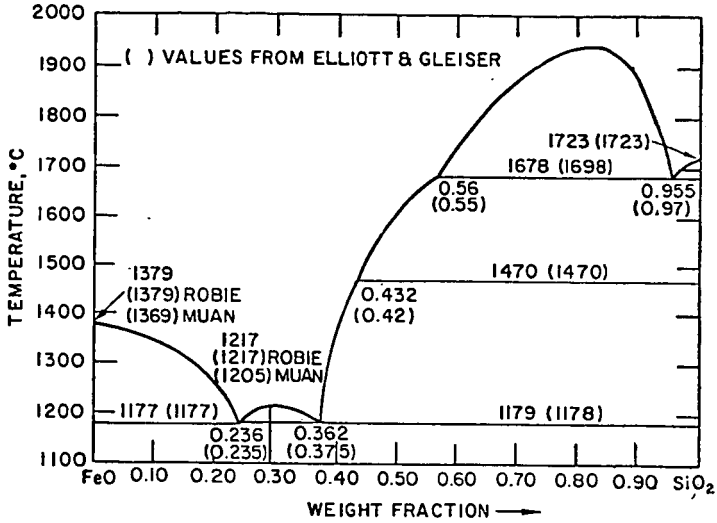
( ) VALUES FROM ELLIOTT & GLEISER
TEMPERATURE, °C
2000
1900
1800
1700
1600
1500
1400
1300
1200
1100
1723 (1723)
1678 (1698)
0.56
(0.55)
0.955
(0.97)
1379
(1379) ROBIE
(1369) MUAN
1470 (1470)
0.432
(0.42)
1217
(1217) ROBIE
(1205) MUAN
1177 (1177)
1179 (1178)
0.236
(0.235)
0.362
(0.375)
FeO 0.10 0.20 0.30 0.40 0.50 0.60 0.70 0.80 0.90 SiO2
WEIGHT FRACTION

Fig. 1

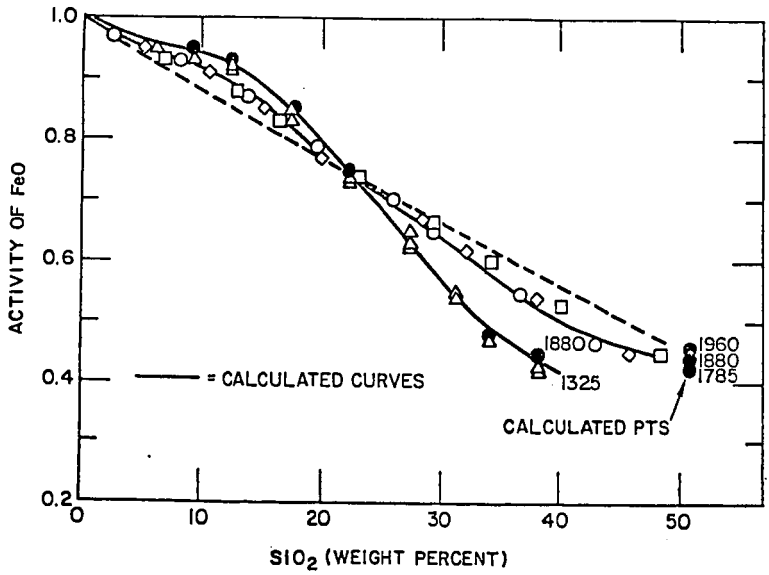
ACTIVITY OF FeO
1.0
0.8
0.6
0.4
0.2
= CALCULATED CURVES
1880
1325
1960
1880
1785
CALCULATED PTS
0 10 20 30 40 50
SiO2 (WEIGHT PERCENT)

Fig. 2

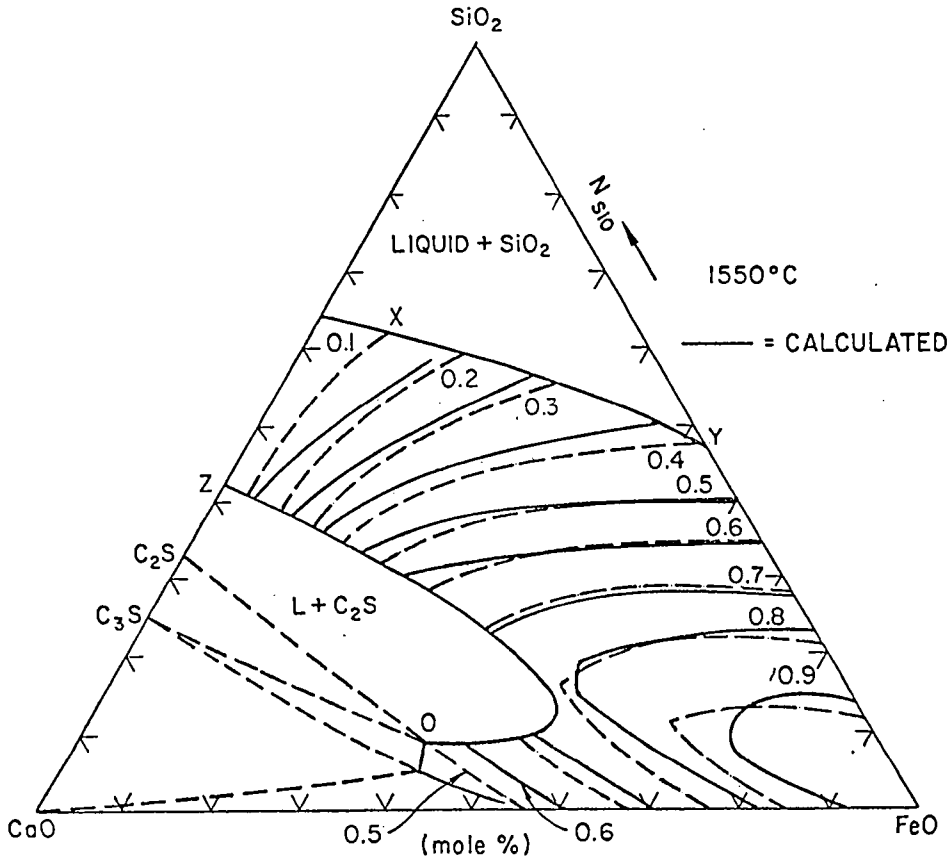
SiO2
LIQUID + SiO2
N SiO
1550°C
= CALCULATED
X
Y
Z
O
0.1
0.2
0.3
0.4
0.5
0.6
0.7
0.8
0.9
C2S
C3S
L + C2S
CaO
FeO
0.5
0.6
(mole %)

Fig. 3

ESTIMATION OF PHYSICO-CHEMICAL PROPERTIES OF COAL SLAGS AND ASHES

K C MILLS
National Physical Laboratory, Teddington, Middx, TW11 OLW, UK.

1. INTRODUCTION.

Slags formed during the gasification of coal usually contain SiO_2, Al_2O_3, iron oxides, CaO, Na_2O and K_2O with minor amounts of various other oxides. A knowledge of the physico-chemical properties of these slags can improve the control of the process eg. the amount of flux required to bring the slag viscosity to a level suitable for tapping can be calculated from viscosity-composition relations. Physical property data for the coal slags can also improve process design by the development of reliable mathematical models of the process eg. thermal properties of the slags are needed for heat balance calculations. There is an appreciable variation in the compositions of slags formed from various coals and even from different batches of the same stock on occasions and these compositional variations can give rise to considerable differences in the physical properties. As the chemical analysis is frequently available on a routine basis it would be particularly desirable to have reliable models for the prediction of physico-chemical properties from their chemical composition. Furthermore such models would have the further advantage that they would eliminate the need for arduous interpolations on pseudo-ternary plots for slags which are really multicomponent and interactive systems.

The properties of slags are dependent not only upon chemical composition, but upon other factors also. The most pronounced deviations from addivity rules based on composition arise in the estimation of those properties which involve ionic transport such as electrical conductivity. However surface tension values estimated from additivity rules are frequently in error as bulk thermodynamic properties do not apply at surfaces. Furthermore, virtually all the physical properties of slags are, to some extent, dependent upon the structure of the slag (viz. the length of silicate chains,degree of crystallinity etc.) thus estimation procedures have to accommodate these structural factors, where possible.

There is only a limited amount of physical property data available for coal slags and consequently it has been necessary to examine a much broader range of silicates including magmatic liquids and those slags encountered in steelmaking, glassmaking and non-ferrous processes. Thus the models cited here should have a much wider range of application than coal gasification.

A critical evaluation of the extant physical property data has shown that virtually every physical property is markedly dependent upon the distribution of iron in the slag between FeO, Fe_2O_3 and free iron. Frequently these distributions are not reported and they can not be easily predicted as they are very dependent upon (i) the partial pressure of oxygen, p_{O_2} (1) (ii) temperature (1) T and (iii) the nature of the other oxides present, eg CaO, Na_2O and K_2O (1)(2)(3) increase the amount of Fe_2O_3 and SiO_2 increases the amount of FeO present. Even when the iron distributions are cited they are vulnerable to error owing to difficulties in chemical analysis and the possibility of some redistribution of the $Fe/Fe^{2+}/Fe^{3+}$ ratios during the quench. Nevertheless it is strongly recommended that all future physical property determinations on coal slags should be accompanied by chemical analysis for Fe(free), FeO and Fe_2O_3 on the quenched specimen as the surface tension, absorption coefficient, melting range etc. fluctuate dramatically with the iron distribution.

2. MODELS FOR ESTIMATING PHYSICO-CHEMICAL PROPERTIES.

2.1 Melting Range

Empirical rules have been formulated[4-6] for the estimation of melting range on the basis of the basicity of the slag or ash. However the various constants used in the calculations are applicable to very narrow compositional ranges and thus a large number of constants are required to represent the slags formed from different coals.

A more universal approach has been adopted recently by Gaye[7,8] who expressed, the dependency of liquidus temperature, T_{liq}, upon chemical composition as polynomial for each of the phases (or compounds) formed by the slag. The *maximum* calculated value of T_{liq} value for the various phases is the T_{liq} value. Good agreement was obtained between the calculated and experimental values for T_{liq} for the $SiO_2 + Al_2O_3 + MgO + FeO$ and the $SiO_2 + Al_2O_3 + MgO + CaO$ systems. However development of this model to cover the multicomponent coal slags could prove difficult.

A second model due to Gaye[9] would appear to offer more promise; it is based on the Kapoor-Frohberg model for the estimation of activities and assumes that both acidic and basic oxides are made up of symmetrical cells and that these interact to form assymmetrical cells. The activities of the various oxides calculated for quaternary slags with this model are in excellent agreement with those determined experimentally. Values of T_{liq} for a given composition can be derived by determining the temperature at which the solid phase formed has an activity of one. The model has been developed for systems based on seven components, SiO_2, Al_2O_3, CaO, MgO, FeO, Fe_2O_3 and MnO. The model will have to be enlarged to include Na_2O etc. before it can be used for the reliable estimation of T_{liq} of coal slags but it would seem to have considerable promise and has the decided advantage that it also produces activity data for the various component oxides.

2.2 Viscosity (η)

Several models have been reported for the estimation of viscosities (η) of silicate melts to cover the compositional ranges of glasses[10,11] steelmaking slags[12-14], *magmas*[15-18] and coal slags and ashes[19-24]. The temperature (T) dependence of the viscosity is expressed in the form of the Arrhenius relationship (equation 1)) or the Frenkel relationship (equation 2) which is sometimes known as the Weymann equation) where A and B are constants, E is the activation energy and R is the Gas Constant.

$$\eta = A \exp. (E/RT) \qquad 1)$$

$$\eta = AT \exp.(E/RT) \qquad 2)$$

Estimated viscosities have been calculated using these various models and the closest agreement with experimental values was obtained with the models due to Riboud *et al*[13] and Urbain *et al*[17,18]. These estimation procedures use the Frenkel relationship and thus their superiority may be largely due to the use of equation 2). The model due to Schobert which involves petrographic classification of the coal slag has not been checked and this procedure may provide reliable estimates of viscosity for coal slags but could not be applied to slags covering a wide range of composition. Thus effort in the present study was focussed predominantly on the Riboud and Urbain models.

Model due to Riboud et al[13]

The slag constituents are classified in five different categories in this model. The mole fractions (x) for those categories being given by

(i) $x("SiO_2") = x(SiO_2) + x(PO_{2.5} + x(TiO_2) + x(ZrO_2)$

(ii) $x("CaO") = x(CaO) + x(MgO) + x(FeO) + x(FeO_{1.5})$

(iii) $x(Al_2O_3)$

(iv) $x(CaF_2)$ and

(v) $x("Na_2O") = x(Na_2O) + x(K_2O)$.

The parameters A and B of equation 2) are calculated from the mole fraction of the five categories by using equations 3) and 4).

$$A = \exp(-19.81+1.73x("CaO")+5.82x(CaF_2)+7.02x(Na_2O)-33.76x(Al_2O_3)) \quad 3)$$

$$B = +31140-23896x("CaO")-46356x(CaF_2)-39159x("Na_2O")+68833x(Al_2O_3) \quad 4)$$

Subsequently, from the values of A and B it is possible to calculate the viscosity for the temperatures in question by use of equation 2).

Model due to Urbain et al[18]

In this model the parameters A and B are calculated by dividing the slag constituents into three categories (i) "glass formers", $x_G = x(SiO_2) + x(P_2O_5)$ (ii) "modifiers", $x_M = (CaO) + x(MgO) + x(Na_2O) + x(K_2O) + 3x(CaF_2) + x(FeO) + x(MnO) + 2x(TiO_2) + 2x(ZrO_2)$ (iii) "amphoterics", $x_A = x(Al_2O_3) + x(Fe_2O_3) + x(B_2O_3)$.

However we consider that Fe_2O_3 behaves more like a modifier than an amphoteric and in our revised programme $1.5\ x(FeO_{1.5})$ has been added to x_M and $x(Fe_2O_3)$ deducted from x_A. "Normalized" values x_G^* and x_M^* and x_A^* are obtained by dividing the mole fractions, x_G, x_M and x_A by the term $(1 + 2x(CaF_2) + 0.5\ x(FeO)_{1.5}) + x(TiO_2) + x(ZrO_2))$. Urbain proposed that the parameter B was influenced both by the ratio, $\beta = [x_M^*/(x_M^* + x_A^*)]$ and by x_G^*. The parameter B can be expressed in the form of equation (5) where B_1, B_2 and B_3 can be obtained by equation (6).

$$B = B_o + B_1\ x_G^* + B_2(x_G^*)^2 + B_3(x_G^*)^3 \quad 5)$$

$$B_i = a_i + b_i\beta + c_i\beta^2 \quad 6)$$

B_o, B_1, B_2 and B_3 can be calculated from the equations listed in Table 1 and these parameters are then introduced into equation 5) to calculate B. The parameter A can be calculated from B by equation 7) and the viscosity of the slag (in PaS) can then be determined using equation 8).

$$-\ln A = 0.2693\ B + 11.6725 \quad 7)$$

$$\eta = 0.1[AT \exp(10^3\ B/T)] \quad 8)$$

TABLE 1

$B_o = 13.8 + 39.9355\beta - 44.049\beta^2$

$B_1 = 30.481 - 117.1505\beta + 129.9978\beta^2$

$B_2 = -40.9429 + 234.0486\beta - 300.04\beta^2$

$B_3 = 60.7619 - 153.9276\beta + 211.1616\beta^2$

Modifications to the Urbain model

Urbain[18] has recently modified the model to calculate separate B values for different individual modifiers, CaO, MgO and MnO. The global B value for a slag containing all three oxides can be derived using equation 9)

$$B(\text{global}) = \frac{x(CaO)B(CaO) + x(MgO)B(MgO) + x(MnO)B(MnO)}{x(CaO) + x(MgO) + x(MnO)} \qquad 9)$$

Assessment of the viscosity models

These two models have been used to calculate the viscosities of slags with widely-varying compositions and it has been found that both give values which agree well with experiment.

The model of Urbain gives a slightly better fit than the Riboud model. The discrepancies between the experimental values and the predicted values are of the order of $\pm$ 30% which are of similar magnitude to the experimental uncertainties for viscosity measurements.

2.3 Density (ρ)

Recently Keene[25] has reported that the density at 1673K of molten slags can be obtained within $\pm$ 5% using the equation 10)

$$\rho\ /gcm^{-3} = 2.46 + 8.018\ (\%\ FeO + \%\ Fe_2O_3 + \%\ MnO + \%\ NiO) \qquad 10)$$

An additive method for the estimation of densities (ρ) in slags has been widely used for some time[26,27]. In this method, the molar volume, V, can be obtained from equations 11) and 12) below, where M, x and $\bar{V}$ are the molecular weight, mole fraction and the partial molar volume, respectively, and 1, 2 and 3 denote the various oxide constituents of the slag.

$$V = M_1x_1 + M_2x_2 + M_3x_3 \qquad 11)$$

$$V = x_1\bar{V}_1 + x_2\bar{V}_2 + x_3\bar{V}_3 \qquad 12)$$

The partial molar volume is usually assumed to be equal to the molar volume of the pure component (V^o). Bottinga and Weill[28] produced a series of values of $\bar{V}$ for various oxides assuming a constant value for $\bar{V}(SiO_2)$ and it was claimed that good estimations of the density could be obtained for compositions containing between 40 and 80% SiO_2. Two more recent studies[29,30] also concluded that $\bar{V}$ (SiO_2) was independent of composition and have revised the $\bar{V}$ values for the various oxides. However it has been pointed out[31,32] that the density of the slag is also related to its structure. Silicate slags contain a mixture of chains, rings and basic silicate units, which are dependent upon the silica concentration and upon the nature of the cations present. Thus the densities of silicate slags estimated using a constant value for $\bar{V}(SiO_2)$ will be subject to error as the arrangement of these silicate chains varies with silica concentration.

Furthermore Grau and Masson[31] pointed out that for the series M_2O, M_2SiO_2 the partial molar volume of SiO_2 is not constant. They calculated a $\Delta\bar{V}$ term for the differences between any two members of the series and in this way calculated values were derived for the systems FeO + SiO_2, PbO + SiO_2, FeO + MnO + SiO_2 and FeO + CaO + SiO_2 for compositions in the range x_{SiO_2} = 0.5 to 1.0. However this method is not suitable for calculating densities of multicomponent systems.

Very recently, Bottinga et al[33] have presented a model in which the partial molar volumes of alumina-silicate liquids were considered to be composition-dependent.

New model for calculating the densities of slags

Slags containing SiO_2, Al_2O_3 and P_2O_5 consist of chains, rings and complexes which are dependent upon the amount and nature of the cations present. Thus it is necessary to make the partial molar volumes dependent upon composition for oxides of this type. If in a binary system, equation 12) were applicable and if $\bar{V}_i = V_i^o$ ie. $\bar{V}$ is independent of composition, then the curve of V as a function of composition will be that shown by the solid line in Figure 1a and the two $x_i\bar{V}_i$ contributions by the dotted lines. If we now consider a binary silicate system the molar volume (V) would have the form shown as a solid line in Figure 1b. It is reasonable to assume that $\bar{V}(M_xO)$ is independent of composition and would have the form of $x_1\bar{V}_1$ in Figure 1b. The parameter $x_2\bar{V}_2$ can be derived for SiO_2 by use of equation 13) below.

$$x_2\bar{V}_2 = V - x_1\bar{V}_1 \qquad 13)$$

Thus $x_2\bar{V}_2$ will have the form of the curve shown in Figure 1b.

It is possible to derive $x\bar{V}$ for SiO_2 in ternary and quaternary slags by using equation 14). Values for $x\bar{V}$ (SiO_2) have been derived using experimental density data for the systems, $FeO + SiO_2$, $CaO + SiO_2$, $MnO + SiO_2$, Na_2O+SiO_2, $K_2O + SiO_2$ and $CaO + FeO + SiO_2$ and are plotted against $x(SiO_2)$ in Figure 2. It can be seen from this figure that there is excellent agreement between the $x\bar{V}(SiO_2)$ calculated from different sources, with the exception of that for the $MnO + SiO_2$ system; however the reliability of the experimental data for this system, have been questioned previously. From this curve for $x\bar{V}(SiO_2)$ we can derive the relationship, $V(SiO_2) = 19.55 + 7.966.x(SiO_2)$. The recommended values for $\bar{V}$ for the various oxides at 1500°C are given in Table 2.

$$xV(SiO_2) = V - x_1\bar{V}_1 - x_2\bar{V}_2 - x_3\bar{V}_3 \qquad 14)$$

Values for $x\bar{V}$ (Al_2O_3) were determined in a similar manner by using experimental density data for the systems, $CaO + Al_2O_3$, $CaF_2 + Al_2O_3$, $CaF_2 + Al_2O_3$, $SiO_2 + Al_2O_3$, $MgO + CaO + Al_2O_3$ and $MnO + SiO_2 + Al_2O_3$. The xV (Al_2O_3) results are plotted in Figure 3 and the relationship $\bar{V}(Al_2O_3) = 28.31 + 32\,x(Al_2O_3) - 31.45\,x^2(Al_2O_3)$ was derived from this curve.

There are few experimental data for the density of phosphate slags, $x\bar{V}(P_2O_5)$ values were derived from data for the systems $CaO - FeO - P_2O_5$ and $Na_2O - P_2O_5$. A constant value of $\bar{V} = 65.7\ cm^3\ mol^{-1}$ was obtained from the selected linear relationship.

TABLE 2

Recommended values for the partial molar volumes, $\bar{V}$, of various slag constituents at 1500°C

SiO_2	$19.55 + 7.966\,x(SiO_2)$	FeO	15.8	K_2O	51.8
Al_2O_3	$28.31 + 32\,x(Al_2O_3) - 31.45\,x^2(Al_2O_3)$	Fe_2O_3	38.4	CaF_2	31.3
CaO	20.7	MnO	15.6	P_2O_5	65.7
MgO	16.1	Na_2O	33	TiO_2	24

Units of $\bar{V} = cm^3\ mol^{-1} = 10^{-6}\ m^3\ mol^{-1}$

In order to provide a temperature coefficient, the temperature dependencies of

the molar volumes (dV/dT) of many slag systems were examined and a mean value of 0.01% K^{-1} was adopted.

Assessment of density models.

An analysis of the uncertainties associated with the estimated of densities with this model has not been completed yet. However on the basis of those values obtained so far the standard deviation of the factor '[(ρest-ρexpt/ρexpt] is between 1 and 2% and less than that recorded vary the method due to Bottinga et al[33]. The experimental uncertainties associated with density measurements for slags are i.e. ± 2%.

2.4 Surface tension (γ)

Methods for estimating the surface tension of slags based on the addition of the partial molar contributions ($\bar{\gamma}$) of the individual constituents have been reported by Appen[34] by Boni and Derge[35] and by Popel[36]. All these methods make use of equation 13a where 1,2,3 etc denote the various slag constituents.

$$\gamma = x_1\bar{\gamma}_1 + x_2\bar{\gamma}_2 + x_3\bar{\gamma}_3 + \ldots\ldots \qquad 13a)$$

Values of $\bar{\gamma}_i$ are often taken to be the surface tension of the pure components, γ_i^o, and have also been obtained by reiterative procedures. Figure 4a shows a typical plot of γ as a function of x for a binary slag and the individual $x_i\bar{\gamma}_i$ contributions have been included These methods work well for certain slag mixtures but break down when surface-active constituents, such as P_2O_5, are present. Surface active components migrate preferentially to the surface and cause a sharp decrease in the surface tension and only very small concentrations are required to cause an appreciable decrease in γ if the constituent is concentrated in the surface layer. Thus some unreported or undetected impurity could have a marked effect on the surface tension of the slag and consequently produce an apparent error in the value estimated by the model. In this aspect surface tension differs from all the other physical properties which are essentially bulk properties.

Model for calculating the surface tension of slags

Figure 4a shows the surface tension of two slag constituents which are not surface active. For a binary mixture with one surface active component the surface tension-composition relationship will have the form of that shown in Figure 4b where 2 denotes the surface-active constituent. If we assume that $x\bar{\gamma}$ for component 1 is unaffected then the term $\gamma_2 x_2$, the partial molar contribution of the surface active material, can be calculated by equation 14a below. The term $(x_2\bar{\gamma}_2)$ can similarly be calculated for ternary and quaternary systems providing there is only one surface active component. The compositional dependence of the $(x_2\bar{\gamma}_2)$ term is shown in

$$x_2\bar{\gamma}_2 = \gamma - x_1\bar{\gamma}_1 \qquad 14a)$$

Figure 4b and it should be noted that as $x_2 \rightarrow 1$ then $x_2\bar{\gamma}_2 \rightarrow \gamma_2^o$. Values of $(x\bar{\gamma})$ for various surface active materials derived from experimental surface tension data are shown in Figures 5a. It is possible to deal with the compositional dependence of these $(x\bar{\gamma})$ values by considering two curves viz. one operating up to the point N and the other representing values of x where x > N. The partial surface tension for non-surface active constituents is shown in Table 3 and the equations for calculating $\bar{\gamma}$ for surface active components and values of N are given in Table 4. There is a considerable discrepancy in the $x_2\bar{\gamma}_2 - (x_2)$ relationships for B_2O_3 obtained from experimental data on two different systems,

consequently a mean value has been adopted until further data become available.

TABLE 3
Partial molar surface tension, $\bar{\gamma}$, at 1500 °C
for different slag constituents

Oxide	SiO_2	CaO	Al_2O_3	MgO	FeO	MnO	TiO_2
$\bar{\gamma}$/mNm^{-1}	260	625	655	635	645	645	360

TABLE 4
Values of $x_i\bar{\gamma}_i$ at 500°C for surface-active constituents

Slag Constituent	$x_i\bar{\gamma}_i$ for x < N	N	$x_i\bar{\gamma}_i$ for x > N
Fe_2O_3	$-3.7 - 2972\,x + 14312\,x^2$	0.125	$-216.2 + 516.2\,x$
Na_2O	$0.8 - 1388\,x - 6723\,x^2$	0.115	$-115.9 + 412.9\,x$
K_2O	$0.8 - 1388\,x - 6723\,x^2$	0.115	$-94.5 + 254.5\,x$
P_2O_5	$-5.2 - 3454\,x + 22178\,x^2$	0.12	$-142.5 + 167.5\,x$
B_2O_3	$-5.2 - 3454\,x + 22178\,x^2$	0.10	$-155.3 + 265.3\,x$
Cr_2O_3	$- 1248\,x + 8735\,x^2$	0.05	$-84.2 + 884.2\,x$
CaF_2	$-2 - 934\,x + 4769\,x^2$	0.13	$-92.5 + 382.5\,x$
S	$-0.8 - 3540\,x + 55220\,x^2$	0.04	$-70.8 + 420.8\,x$

The reported values of $(d\gamma/dT)$ for various slag systems were examined and a mean value of -0.15 mN m^{-1} K^{-1} was applied as a temperature coefficient.

Assessment of the model

The standard deviation of the factor $[(\gamma_{est} - \gamma_{expt})/\gamma_{expt}]$ was ca. $\pm$ 10%. Undoubtedly much of the uncertainty arises from experimental errors, where the effect of unreported surface active impurities and the nature of the gaseous atmosphere could have a marked effect on the value of surface tension.

Another major source of error is the amount of Fe_2O_3 present in the slag, this investigation has shown clearly that Fe_2O_3 is very surface active. Few investigators cite the (Fe^{3+}/Fe^{2+}) ratio which in turn is dependent upon, (i) p_{O_2} (ii) T and (iii) the nature and amount of other oxides present and furthermore the ratio, when quoted, is vulnerable to error. Thus the problem arises if a decrease in γ is recorded when Na_2O is added to the slag, is this decrease due to a increase in Fe_2O_3 content or due to the surface activity? In this investigation attempts were made to compensate γ for an increase in Fe_2O_3 content but the effects of basic oxides on the Fe distribution are not well documented and some error may ensue.

A major unresolved problem concerns the situation where the slag contains more than one surface active component. It is possible that there is some competition for sites on the surface and hence the decrease in γ would not be as sharp as that calculated from the summation of $(x_A\bar{\gamma}_A + x_B\bar{\gamma}_B)$ where A and B denote surface active constituents. In this case the model may overestimate the decrease in γ. There are no extant data to confirm this possibility, we have, however, considered $(Na_2O + K_2O)$ as one contribution in the model.

2.5 Thermal Properties

The computation of the thermal losses in the converter by conductive and radiative processes requires knowledge of the following thermal properties, heat capacity, enthalpy, thermal conductivity, absorption coefficient and emissivity.

2.5.1 Heat capacity C_p and enthalpy $(H_T - H_{298})$ of slags

When a silicate liquid is cooled the structure of the solid formed is dependent upon the cooling rate and the thermal history of the sample. Consider a liquid at a temperature corresponding to the point C in Figure 6, a rapid quench will produce a glass and the enthalpy evolved will follow the path CLGA. By contrast, a very slow cooling rate will result in the formation of a crystalline slag, the enthalpy evolution following the path CL DB. It will be noted from Figure 6 that $(H_T - H_{298})_{cryst} = (H_T - H_{298})_{glass} + \Delta H^{vit}$, where ΔH_{vit} is enthalpy of the endothermic transformation of (crystal $\longrightarrow$ glass). The C_p values for the various phases can be summarized as:

$$C_p(\text{crystal}) \simeq C_p(\text{glass}) < C_p\ (\text{supercooled liquid}) \simeq C_p\ (\text{liquid})$$

It can be seen from Figure 6 that at the glass temperature (T_{gl}) there is a sudden increase in C_p (ΔC_p^{gl}) as the glass transforms into a supercooled liquid. Drop calorimetry studies on the glass phase at temperatures between T_{gl} and T_{liq} will produce progressively more crystallization as T_{liq} is approached and consequently the $(H_T - H_{298})$ - T relationship will be similar to that depicted by the dots in Figure 6 and not the path, AGLC; the magnitude of the apparent enthalpy of fusion (ΔH^{fus}) will be dependent upon the fraction of the sample crystallized during annealing at temperatures between T_{gl} and T_{liq}. The C_p values for the liquid and supercooled liquids have been reported to be constant and independent of temperature[37]. It follows from the triangle GEL in Figure 6 that $\Delta C_p^{gl}(T_{liq} - T_{gl}) = \Delta H^{fus}$. Thus it is possible to estimate the enthalpy of a slag with a glassy structure from estimates of C_p(glass) C_p(liq) and T_{gl}. However the estimation of T_{gl} is difficult as it can vary between ~ 700 and 1100 K and the various estimation rules suggested are known to be prone to appreciable errors[38]. Inspection of literature data[38,39] indicates that the glass transformation occurs when C_p attains a value of ca. 1.1 J $K^{-1}g^{-1}$; this rule has been used in the development of the following model for the estimation of $(H_T - H_{298})$ and C_p of slags with a glassy structure.

The C_p for glass, liquid and supercooled liquid phases can be estimated from the slag composition using partial molar heat capacities ($\bar{C}_p$) as shown in equation 15).

$$C_p = x_1\bar{C}_{p_1} + x_2\bar{C}_{p_2} + x_3\bar{C}_{p_3} + x_4\bar{C}_{p_4} \ldots \qquad 15)$$

For most materials the temperature dependence of C_p is usually expressed the form given by equation 16) where a, b and c are constants

$$C_p = a + bT - c\,T^{-2} \qquad 16)$$

The enthalpy at T relative to 298 K (25 °C) is obtained from equation 17) for the glass phase

$$(H_T - H_{298}) = \int_{298}^{T} Cp = a(T-298) + \frac{b}{2}(T^2 - 298^2) + \frac{C}{T} - \frac{C}{298} \qquad 17)$$

Values of a, b and c for the various slag components are given in Table 5 and it should be noted that the P_2O_5 and S in the slag were calculated as CaP_2O_6 and $CaSO_4$, respectively. The amount of CaO used in the calculation of $x\bar{C}_p$ (CaO) should be adjusted by the relationship x(CaO) = x(CaO ,total) - x(P_2O_5) - x(S) to account for the CaO in CaP_2O_6 and $CaSO_4$. The model also takes into account the presence of free iron in the slag.

TABLE 5

Slag Component	M	$\bar{C}_p$(glass)/calK^{-1}mol^{-1}=a+bT -c/T^2 a	b.10^3	c.10^5	$\bar{C}_p$(liq) cal K^{-1}mol^{-1}
SiO_2	60.09	13.38	3.68	3.45	20.79
CaO	56.08	11.67	1.08	1.56	19.3
Al_2O_3	101.96	27.49	2.82	8.4	35
MgO	40.31	10.18	1.78	1.48	21.6
K_2O	94.2	15.7	5.4	0	17.7
Na_2O	61.98	15.7	5.4	0	22
TiO_2	79.9	17.97	0.28	4.35	26.7
MnO	70.94	11.11	1.94	0.88	19.1
FeO	71.85	11.66	2.0	0.67	18.3
Fe_2O_3	159.7	23.49	18.6	3.55	45.7
Fe	55.85	3.04	7.58	-0.6	10.5
P_2O_5	141.91	43.63	11.1	10.86	58
CaF_2	78.08	14.3	7.28	-0.47	23
SO_3	80.06	16.78	23.6	0	42

1 cal = 4.184 J; T in K

The values of $\bar{C}_p$ for the liquid and supercooled liquid given in Table 5 are those reported by Carmichael et al[40] except $\bar{C}_p$ values for Al_2O_3 and Fe_2O_3, where other values have been preferred.

Thus ($H_T - H_{298}$) values for a liquid slag at temperature T can be estimated by determining T_{gl} (ie temperature at which C_p = 1.1 J K^{-1} g^{-1}) and calculating ($H_{T_{gl}} - H_{298}$) from equation (17) and ($H_T - H_{T_{gl}}$) from C_p(liq).(T-T_{gl}).

Values of C_p(glass) obtained with this model lie within 2% of the experimental values and the C_p(liq) values also appear to agree with experimental data; values of ΔC_p at T_{gl} calculated using the model lie within the range of experimental values[38,39] of 0.15 to 0.30 J K^{-1} g^{-1}. One major uncertainly would appear to lie in the calculation of T_{gl}, however it can be shown that an error in T_{gl} of 100 K would only produce an error of ca. 1% in the value of ($H_{1900} - H_{298}$) for the slag. The most serious source of error would thus appear to arise through crystallization of the sample during quenching, as few data are available for ΔH^{vit}, the magnitude of errors arising from this source have not been evaluated.

2.5.2 Heat transfer in slags

Heat is transferred through slags by a variety of mechanisms which include convection, radiation and various thermal conduction processes, viz. thermal ("phonon") conductivity, (k_c), electronic conductivity (k_{el}) and radiation conductivity (k_R). Methods for estimating the various physical properties involved in these processes are considered below.

2.5.3 Thermal conductivity (k)

Heat is transferred by phonons which are quanta of energy associated with each mode of vibration in the sample. Scattering of the phonons causes a decrease in the thermal conductivity and thus the conductivity is sensitive to the structure of the slag and consequently those factors affecting structure such as the basicity. Despite this structure dependence, estimation rules based on the additivity principle (equation 18)) have been proposed[41,42]. Other models have been developed which relate k to the volume concentration of the oxides in the

glass[43] and a third approach[44] relates the thermal resistance (1/k) to $x_i m_i$ where m_i is the effectiveness of modifier of component i in scattering phonons.

$$k \doteq (\%i)k_i + (\%j)k_j + \ldots\ldots \qquad 18)$$

However in coal slags there is frequently an appreciable degree of crystallization and the thermal conductivity value varies with the thermal history of the sample[45], and consequently rules developed for glasses may not apply well for coal slags. Recent work carried out on a large number of silicate slags[46] indicated that the thermal diffusivity, a, ($a=k/C_p.\rho$) of various slags was independent of both composition and temperature in the range (500-1300 K) with a(glass) = $4.5(\pm 0.5)\times10^{-7}$ m^2s^{-1} ; a(cryst) = 6×10^{-7} m^2s^{-1} and a(liq) $\cong$ a(glass). These data are consistent with values reported for coal slags[45] and steelmaking slags[47]. However, the values reported by Nauman et al[48] indicate that at high FeO contents (> 20%) both k and a increase with increasing FeO content ($k = 0.8 + 1.7\times10^{-2}$(% FeO) $Wm^{-1}K^{-1}$).

2.5.4 Absorption coefficient (α)

Radiation conductivity (k_R) can be the predominant mode of heat transfer through semi-transport media like glasses and the magnitude of k_R is determined largely by the optical properties such as the absorption coefficient (α) and the refractive index (n). The value of k_R increases as the slag thickness (d) is increased until a critical point is attained, above this point k_R remains constant and independent of thickness. Above this critical point the slag is said to be "optically thick, this condition applies when $\alpha d > 3.5$ and values of k_R can be calculated using equation 19), where σ is the Stefan-Boltzmann constant.

$$k_R = \frac{16\, n^2 T^3 \sigma}{3\,\alpha} \qquad 19)$$

No formulae exist for the calculation of k_R for optically thin conditions. The absorption coefficient (α) is markedly dependent upon the amounts of Fe^{2+} and Mn^{2+} present in the slag[49]; levels for FeO < 5% the following relationship can be applied, $\alpha(cm^{-1}) = 11(\%FeO)$. Temperature appears to have little effect on the absorption coefficient of glasses but the absorption coefficients of magmas have been reported to increase with increasing temperature[50,51]. Crystallization of the slag will result in a large increase in the absorption (or extinction) coefficient which could reduce k_R to virtually zero.

The importance of radiation conduction in heat transfer through coal slags can readily be demonstrated, for a slag with an appreciable FeO content (7%) Fine et al[47] recorded $\alpha \cong 50$ cm^{-1} at 298 K using this value and equation 19), a value of $k_R = 0.9$ $Wm^{-1}K^{-1}$ can be calculated for 1873 K. As $k_c \cong 1.5$ $Wm^{-1}K^{-1}$ it can be seen that about 40% of the heat is transferred by radiation conduction.

2.5.5 Emissivity (ε)

The emissivity (ε) of a semi-transparent medium, is a bulk property cf. ε(metal) which is solely dependent upon the surface. In the basis of the spectral and total normal emissivity data reported for coal and metallurgical slags the value $\varepsilon = 0.8 \pm 0.1$ can be adopted for coal slags in the range (1100 - 1900 K).

CONCLUSIONS

1) Estimation procedures based on the chemical composition of the slag have now been developed for the prediction of viscosity, surface tension, density and heat capacity.
2) The accuracy of these estimation routines for some physical properties (eg viscosity, surface tension) can be improved when more reliable experimental data become available.
3) The distribution of iron in the slag betwen free Fe, FeO and Fe_2O_3 has a pronounced effect of virtually all the physical properties and it is recommended that experimental data for the properties of the slag should always be accompanied by values for the distribution of iron.
4) The development of models for the prediction of some physical properties (thermal conductivities, absorption coefficient) is restricted by the limited amount of experimental data available.

REFERENCES

1) DARKEN, L.S. and GURRY, R.W. J. Am. Chem. Soc. 1946, 68, 798.

2) LARSON, H. and CHIPMAN, J. J. Metals, 1953, Sept., 1089.

3) BANYA, S. and SHIM, J.D. Canad. Metall. Q., 1982, 21, 319.

4) SONDREAL, E.A. and ELLMAN, R.C. Fusibility of ash from lignite and its correlation with ash composition. US Energy Res. and Develop. Admin. GFERC/RI-75-1, Pittsburgh, 1975.

5) WINEGARTNER, E.C. and RHODES, B.T. J. Eng. Power, 1975, 97, 395.

6) BRYERS, R.W. and TAYLOR, T.E. J. Eng. Power, 1976, 98, 528.

7) STEILER, J.M. Commission of the European Communities Research Contract, 7210 CA/3/3/03. Thermodynamic data for steelmaking. 1981, Eur N7820, BP 1003, Luxembourg 1982.

8) GAYE, H. Ironmaking and Steelmaking, 1984, in press.

9) GAYE, H. Paper presented at Metallurgical Conference, Centenary of Teaching of Metallurgy, held at Strathclyde University, 25/26 June 1984.

10) OCHOTIN, M.W. Steklo Keram., 1954, 11, 7.

11) LYON, K.C. J. Res. Natl. Bur. Stand., 1974, 78, 497.

12) MCCAULEY, W.D. and APELIAN, D. Canad. Metall. Quart., 1981 20, 247.

13) RIBOUD, P.V., ROUX, Y, LUCAS, L.D. and GAYE, H. Fachber. Huttenpraxis Metallveiterverarb., 1981, 19, 859.

14) MAIRY, B. Private communication, Centre Recherches Metallurgique, Liege, Belgium.

15) BOTTINGA, Y. and WEILL, D.F. Am. J. Sci., 1972, 272,

16) SHAW, H. Am. J. Sci., 1972, 272, 870.

17) URBAIN, G., CAMBIER, F., DELETTER, M. and ANSEAU, M.R. Trans. J. Brit. Ceram. Soc., 1981, 80, 139.

18) URBAIN, G. Private communication, CNRS, Laboratoire de Ultra-Refractaires, Odeillo, France. Jan. 1983.

19) WATT, J.D. and FEREDAY, D. J. Instr. Fuel, 1969, 338, 99.

20) BOKAMP, . Inst. of Gas Technol. Preparation of a coal conversion systems Technical Data Book. Energy Res. and Dev. Admin. Report FE-1730-21 (1976).

21) CAPPS, W. and KAUFFMAN, D. Natl. Bur. Stand. Quart. Prog. Rept. to Office of Coal Res., Dept. Interior, 30/9/74.

22) SCHOBERT, H.H. Div. Fuel Chem. Prep., 1977, 22, 143.

23) SCHOBERT, H.H. and WITTHOEFFT, C. Fuel Proc. Technol., 1981, 5, 157.

24) HENSLEE, S.P. and KELSEY, P.V. Jr. US Dept. of Energy Report, EGG-FM-6049, Sept. 1982.

25) KEENE, B.J. National Physical Laboratory Report, DMA(D)75, Feb. 1984.

26) MOREY,G.H. Properties of Glasses. Rienhold,New York,1954,217.

27) HUGGINS,M.L;SUN,K.H. J.Am.Ceram.Soc. 1948,26,4.

28) BOTTINGA, H. and WEILL, D.E. Am. J. Sci., 1972, 272 438.

29) NELSON, S.A. and CARMICHAEL, I.S.E. Contrib. Mineral Petrol, 1979, 71, 117.

30) MO, Y., CARMICHAEL, I.S.E., RIVERS, M. and STEBBINS, J. Mineralog. Mag., 1982, 45, 237.

31) GRAU, A.E. and MASSON, C.R. Canad. Metall. Quart., 1976, 15, 367.

32) LEE, Y.E., GASKELL, D.R. Metall. Trans., 1974, 5, 853.

33) BOTTINGA, Y., WEILL, D.E. and RICHET, P. Geochim Cosmochim. Acta, 1982, 46, 909.

34) APPEN, A.A., SHISHKOV, K.A. and KAYALOVA, S.S. Zhur. Fiz. Khim, 1952, 26, 1131.

35) BONI, R.E. and DERGE, G. J. Metals, 1956, 8, 53.

36) POPEL, S.E. Metallurgy of slags and their use in building. 1962, 67.

37) RICHET, P. and BOTTINGA, Y. Geochim. Cosmochim Acta, 1984, 44, 1533.

38) BACON, C.R. Am. J. Sci., 1977, 277, 109.

39) MOYNIHAN, C.T., EASTEAL, A.J., TRAN, D.C., WILDER, J.A. and DONOVAN, E.P. J. Am. Ceram. Soc., 1976, 59, 137.

40) CARMICHAEL, I.S.E., NICHOLLS, J., SPERA, F.J., WOOD, B.J. and NELSON, S.A. Phil. Trans. Roy. Soc. (London), 1977, A286, 373.

41) MOREY, G.W. Properties of Glass. Reinhold, New York, 1954, 217.

42) ABAKOVA, I.G. and SERGEEV, O.A. Thermophysical properties of glasses. Proc. of Metrological Inst. of USSR, No.129 (189), Moscow-Leningrad, 1971, 13.

43) MISNAR, A. Thermal conductivity of solid, gases and composite materials. Leningrad, 1968.

44) VAVILOU, Y.V., KOMAROV, V.E. and TABUNOVA, W.A. Phys. Chem. Glasses, 1982, 8, 472.

45) GIBBY, R.L. and BATES, J.L. 10th Thermal Conductivity Conf. held Newton, Mass. Sept. 1970, IV-7,8.

46) TAYLOR, R. and MILLS, K.C. Unpublished work, 1984.

47) FINE, H.A., ENGH, T. and ELLIOTT, J.F. Metall. Trans. B. 1976, 7B, 277.

48) NAUMAN, J., FOO, G. and ELLIOTT, J.F. Extractive Metallurgy of Copper. Chapter 12, 237.

49) STEELE, F.N. and DOUGLAS, R.W. Phys. Chem. Glasses, 1965, 6, 246.

50) FUKAO, Y., MITZUTANI, H. and UYEDA, S. Phys. Earth Planet Interiors, 1968, 1, 57.

51) ARONSON, J.R., BELLOTI, L.H., ECKROAD, S.W., EMSLIE, A.G., MCCONNELL, R.K. and THUNA, P.C., von. J. Geophys. Res., 1970, 75, 3443.

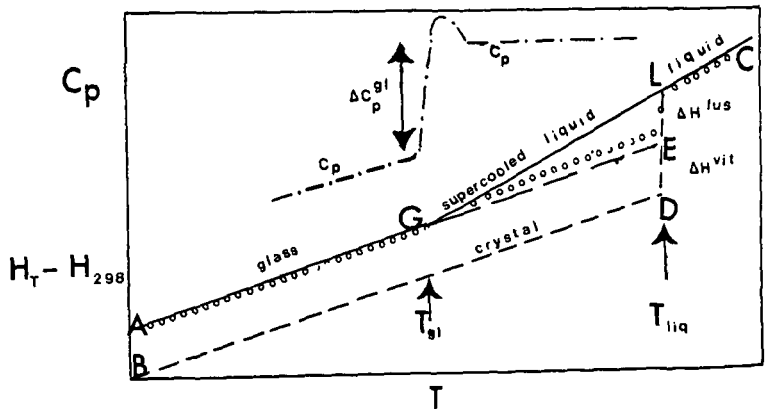

Figure 6 Cp and $(H_T - H_{298})$ for glassy and crystalline phases of a slag; O, indicates typical drop calorimetry results.

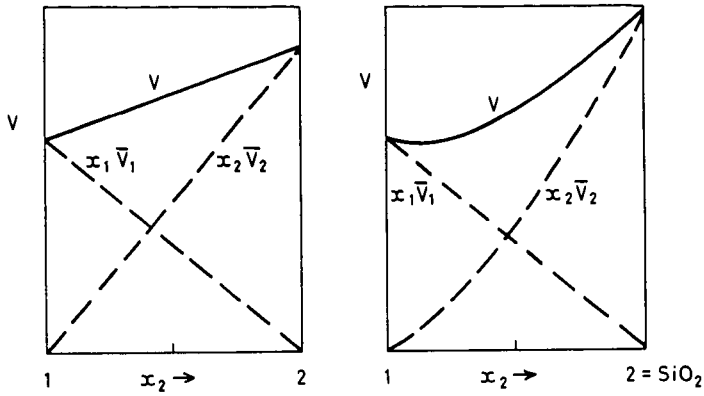

Figures 1a The molar volume of binary slag system as a function of composition and 1b. showing the individual $x_i\bar{V}_i$ contributions.

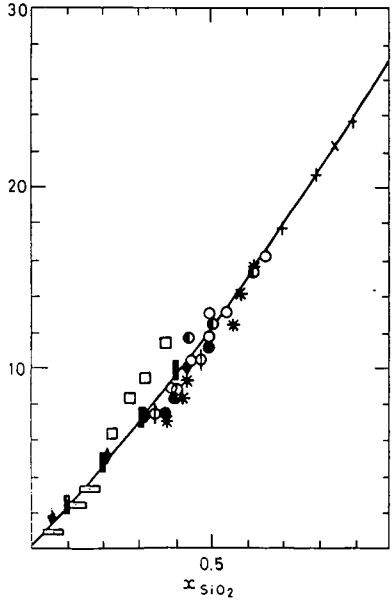

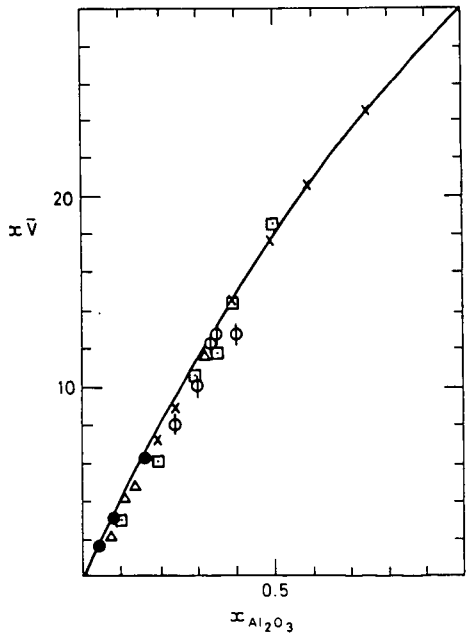

Figure 2. $x\bar{V}(SiO_2)$ as a function of $x(SiO_2)$

Figure 3. $x\bar{V}(Al_2O_3)$ as a function of $x(Al_2O_3)$

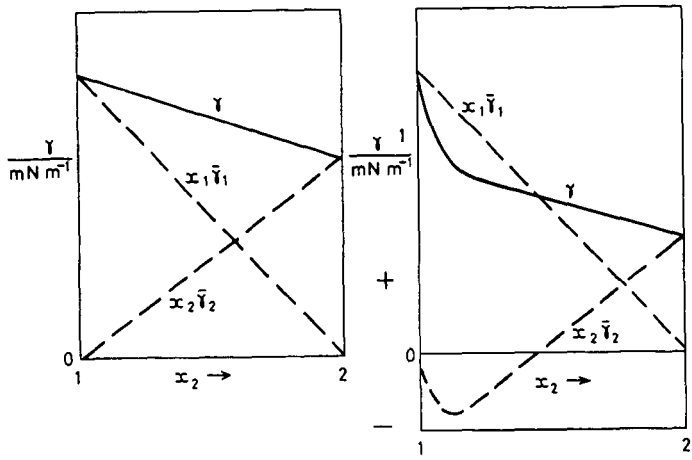

Figure 4a. The compositional dependence of , $x_1\bar{\gamma}_1$ and $x_2\bar{\gamma}_2$ for a binary slag system with non-surface active constituents

Figure 4b. with one surface active constituent (2).

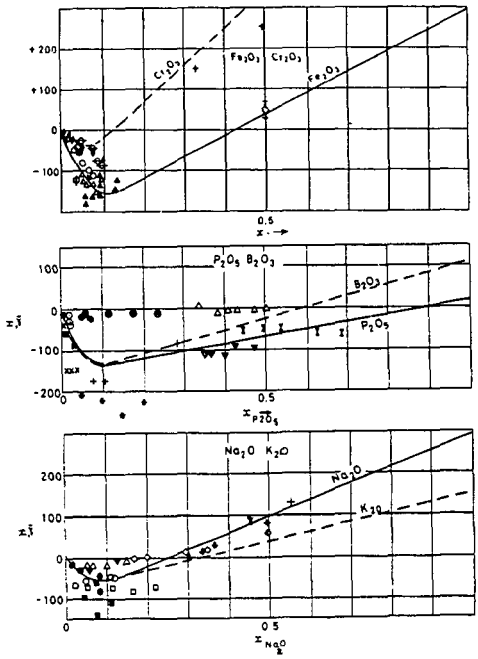

Figure 5 The compositional dependence of $x_i\bar{\gamma}_i$ for various surface-active constituents.

Viscosity of Fluxes for the Continuous Casting of Steel

W. L. McCauley and D. Apelian

Materials Engineering, Drexel University, Philadelphia, PA, 19104

Mold fluxes are routinely used in both continuous casting and bottom pouring of steel. These fluxes are generally calcium-silicate based compositions with alkali oxides [(Li, Na, K)$_2$O] and fluorides [CaF_2, NaF] added as fluidizers. The compositions are sometimes based on the blast furnace slag [Al_2O_3-SiO_2] system, but the fly ash [CaO-SiO_2] system is more common.

A variety of properties of the flux must be controlled, including fusion characteristics (fusion temperature range and sintering characteristics, flow properties of the powder, viscosity of the molten flux, and non-metallic absorption ability. The viscosity influences the consumption rate of flux, heat transfer in the mold, and non-metallic dissolution rate, and has been the subject of a great deal of published and unpublished work over the last ten years. The purpose of this paper is to discuss the expression of viscosity as a function of composition and temperature in separate relations.

In a previously published work (1), fluxes based on the CaO-SiO_2 system were examined to determine the effects of basicity ratio and alkali oxide and fluoride additions on the viscosity of oxide melts in the mold flux composition range. Those results showed that for that range of compositions, the viscosity at a given temperature could be expressed as a function of the silica content squared. In this work, an expression for viscosity as a function of temperature is derived from the Claussius-Clapeyron equation.

Previous Work - Viscosity vs. Composition

The viscosity of twenty controlled composition fluxes was measured as a function of temperature. The compositions, given in Table 1, were selected to fit a second order statistical design in the variables V-ratio, %Na_2O and %CaF_2. The V-ratio [wt%CaO/wt%SiO_2] was varied from 0.6 to 1.3, Na_2O from 4 to 19wt%, and CaF_2 from 2 to 12wt%. Al_2O_3 was kept constant at 10wt%. The viscosity was measured using a rotating type viscometer with a molybdenum spindle in an argon atmosphere. Details of the experimental technique were reported earlier (1).

A summary of the experimental results is given in Table 2. Viscosity decreased with increasing V-ratio, CaF_2 content and Na_2O content as shown in Figures 1, 2 and 3, respectively. A plot of viscosity vs. silica content, Figure 4, shows that silica has a predominating effect on viscosity. A simple quadratic relation of viscosity with wt% silica or mole fraction of silicon cations produced a better fit of the data than a model containing the design variables. The best fit of data was obtained with a quadratic relation of the ratio of network forming cations [Si, Al and Zr] to total anion concentration [O and F]. Specifically,

$$\eta_{1500°C} = 6.338 - 43.44K + 75.03K^2$$

where

$$K = \frac{X_{Si} + X_{Al} + X_{Zr}}{X_O \quad X_F}$$

The log of viscosity versus reciprocal absolute temperature showed a distinct non-linearity as evidenced by the typical results shown in Figure 5. This is not a complete surprise, but a simple Arrhenius type equation is not adequate to describe the viscosity/temperature relationship.

Viscosity vs. Temperature

Viscosity can be considered as a measure of the ease of movement of molecules in a liquid undergoing shear. Several factors may influence this ease of movement including molecule size and intermolecular attraction, but a major factor is the amount of space available between the molecules, hence, the variety of models incorporating a free volume term.

The Claussius-Clapeyron equation relates pressure with temperature, enthalpy, and volume, and has been used to develop semi-theoretical expressions of vapor pressure (2). Many properties, including viscosity, can be related to an energy barrier, free volume and temperature. The attempt here is to express viscosity in the form of the Claussius-Clapeyron equation.

The Claussius-Clapeyron equation can be written

$$\frac{dP}{dT} = \frac{H}{T\,\Delta V} = \frac{\Delta H}{T(V-V_o)} \qquad 1)$$

where P, T, and ΔH have their usual meaning. For this discussion, ΔV is a measure of free volume or the difference between the volume at temperature and the volume at some standard state, e.g., at absolute zero.

Equation 1 can be rewritten as

$$\frac{d(\ell nP)}{d(1/T)} = -\frac{\Delta H}{R\,\Delta z} \qquad 2)$$

where $\Delta z = PV/RT - PV_o/RT$

Expanding ΔH to the Taylor series form and integrating with respect to 1/T yields

$$\ell nP = \frac{1}{R}\left(a - \frac{\Delta Ho}{T} + b\ell nT + dT + \frac{e}{2}T^2 + \ldots\right) \qquad 3)$$

If the higher order terms are ignored, the expression reduces to

$$\ell nP = A - \frac{B}{T} + C\ell nT \qquad 4)$$

Such a derivation was originally developed and used by Kirchoff [1858] and Rankine [1849] (2) to express the temperature dependence of vapor pressure. It was also successfully used by Brostow (3) to express the temperature dependence of the isothermal compressibility of a wide variety of organic liquids, some metallic liquids and water. By a similar analogy, we have used it to express the viscosity of liquid mold fluxes.

Regression Analysis

The flux viscosity data was fitted to the Kirchoff-Rankine equation as,

$$\eta = \exp(C_1 + \frac{C_2}{T} + C_3 \ln T) \quad 5)$$

and to the Andrade-Arrhenius equation

$$\eta = A \exp(E/RT) \quad 6)$$

using the Marquardt method of non-linear least squares regression in the Statistical Analysis Systems [SAS] program package (4). The results of the regression are given in Table 3. The standard deviation and an average difference between calculated and measured values are given in Table 4.

In some cases, viz., Fluxes 5, 6 and 13 in Table 3, the signs of the coefficients are reversed, and a concave downward curve is generated. This is most likely caused by the regression being trapped at a local minimum in the data and assuming convergence at that point. It is required for these cases that the size of the regression step should be increased to avoid the local minima, which SAS does not allow. Also, there may not be enough data points to expand the regression step as is probably true for Fluxes 6 and 13.

For the majority of fluxes evaluated, the standard deviation, s, and the average percent variation, $\overline{\Delta\%}$, is lower for the Kirchoff-Rankine fitted equation vs. the Andrade-Arrhenius model, indicating a better fit of the experimental data. The average percent variation between calculated and experimental values is lower for the Kirchoff-Rankine equation, and the difference is most pronounced for those fluxes where the non-linearity of the experimental $\ln \eta$ vs. $1/T$ data is greatest.

Discussion

When the non-linearity of the log viscosity vs. reciprocal temperature data was first observed, tests were made to insure that the curvature was real and not an artifact of the experimental apparatus. Hysteresis curves and constant temperature for extended time tests showed that the non-linearity was not caused by volatilization of alkali or fluoride constituents or from thermal deviations in the furnace setup. The observed curvature of the data was not an artifact and represented the true physical behavior of the materials. The application of the Kirchoff-Rankine equation produced a more accurate description of the temperature dependence of viscosity.

Additional work on liquid metals, simple chloride salts and some small molecule organic liquids (5) indicates that the advantage of the Kirchoff-Rankine equation over the Andrade-Arrhenius equation improves as the size of the melt species increases. The improvement in the description of viscosity vs. temperature for metals and simple salts [e.g., NaCl and $BiCl_2$] is not great, but for materials with larger melt species, there is a distinct improvement.

References

(1) W. L. McCauley and D. Apelian, *Canadian Metallurgical Quarterly*, 20(2) 1984, pp. 247-262.

(2) G. W. Thomson, *Chemical Review*, 38, February 1946.

(3) W. Brostow and P. Maynadier, *High Temperature Science*, 11 1979, pp. 7-21.

(4) SAS User's Guide, SAS Institute, Inc., Cary, North Carolina, 1979.

(5) W. L. McCauley and D. Apelian, "Temperature Dependence of the Viscosity of Liquids," to be presented at the International Symposium on Slags and Fluxes, TMS-AIME Fall Meeting, Lake Tahoe, NV, November 1984; to be published.

Table 1. Experimental Fluxes - Frit Composition, wt%

Flux	SiO_2	Al_2O_3	CaO	Na_2O	CaF_2	MgO	ZrO_2	Total	V-ratio
1	34.8	10.2	32.7	10.7	7.6	0.9	0.6	97.5	0.94
2	34.4	9.8	32.1	10.9	8.4	0.7	0.6	96.9	0.93
3	34.5	10.0	32.7	11.0	7.6	0.7	0.7	97.2	0.95
4	34.6	10.1	32.5	10.8	7.8	0.6	0.6	97.0	0.94
5	34.6	10.3	32.3	10.9	8.0	0.7	0.5	97.3	0.93
6	34.7	10.1	33.0	10.8	7.2	0.6	0.6	97.0	0.95
7	26.7	9.8	31.8	14.4	11.7	0.6	1.9	96.9	1.19
8	30.7	8.9	32.6	12.9	2.3	0.7	8.8	96.9	1.06
9	31.2	10.4	40.3	5.7	7.6	0.8	0.7	96.7	1.29
10	35.2	10.3	40.8	5.7	3.3	0.9	0.8	97.0	1.16
11	33.5	10.4	24.9	15.1	11.5	0.5	0.4	96.3	0.77
12	38.8	10.4	26.2	15.1	3.5	0.7	0.9	95.6	0.67
13	41.9	10.6	29.5	6.8	7.8	0.7	0.9	98.2	0.77
14	48.0	10.6	28.6	6.5	3.3	0.8	1.4	99.2	0.60
15	46.8	10.4	22.2	10.7	5.5	0.6	2.7	98.9	0.47
16	30.6	10.0	36.2	10.3	7.0	1.0	2.1	97.2	1.18
17	30.0	10.2	27.8	18.6	8.2	0.8	1.6	97.2	0.93
18	39.6	10.4	35.7	4.0	4.7	1.0	1.3	96.7	0.90
19	32.4	10.4	30.4	10.8	11.7	0.7	1.1	97.5	0.94
20	39.1	10.4	32.6	11.3	1.7	0.9	1.2	97.2	0.83

Table 2. Summary of Flux Viscosities

Flux	Viscosity at 1300°C, Ns m^{-2}	Viscosity at 1400°C, Ns m^{-2}	Viscosity at 1500°C, Ns m^{-2}
1	0.395	0.230	0.135
2	0.310	0.175	0.112
3	0.340	0.205	0.128
4	0.485	0.235	0.125
5	0.290	0.190	0.088
6	0.510	0.230	0.122
7	0.110	0.065	0.035
8	NA*	NA*	NA*
9	0.280	0.160	0.080
10	6.00	0.360	0.180
11	0.270	0.150	0.114
12	0.930	0.460	0.270
13	1.15	0.530	0.280
14	2.80	1.30	0.710
15	2.40	1.30	0.725
16	7.00	0.170	0.090
17	0.160	0.115	0.059
18	1.40	0.670	0.380
19	0.250	0.130	0.094
20	1.40	0.720	0.410

*Not available

Table 3. Regression Analysis Results

	Andrade-Arrhenius Equation				Kirchoff-Rankine Equation					
Flux	A (Pa s)	E (cal/mole)	s†	$\overline{\Delta\%}$††	C_1	C_2	C_3	s	$\overline{\Delta\%}$	n†††
1	8.831E-6	33783	7.03E-3	2.40	-184.35	51341	20.502	6.36E-3	1.94	12
2	2.704E-6	36304	1.99E-2	7.98	-282.59	68183	32.337	1.27E-2	3.47	6
3	2.332E-6	30095	8.92E-3	2.08	-184.30	47516	20.792	5.68E-3	1.42	6
4	8.016E-7	41748	1.82E-2	2.73	-278.11	71633	31.502	1.67E-2	3.20	6
5	2.528E-5	29493	2.15E-2	4.14	132.94	-10764	-17.290	2.10E-2	3.91	14
6	8.079E-7	41814	2.33E-2	5.41	123.80	-5309	-16.447	2.29E-2	5.68	7
7	1.963E-7	41439	1.31E-2	7.01	-1511.91	297516	179.394	5.72E-3	3.91	5
9	1.496E-5	30736	1.22E-2	3.15	-1626.10	321853	192.942	1.11E-2	3.62	6
10	7.5E-3	36000*	-	-	-8603.16	1735752	1019.0	2.83E-2	3.97	18
11	7.820E-6	32510	1.43E-2	3.15	-276.14	63473	31.935	5.81E-3	1.52	7
12	4.828E-7	45110	6.00E-2	2.95	-239.51	62253	27.155	3.35E-2	1.10	12
13	2.661E-6	40700	5.19E-2	4.69	169.80	-13879	-21.843	5.00E-2	3.89	8
14	5.488E-8	48579	2.26E-1	13.00	-987.72	212141	116.012	9.85E-2	5.30	11
15	5.761E-6	40568	1.32E-1	5.57	-233.90	60668	26.660	6.26E-2	3.07	10
16	2.0E-2	30000*	-	-	-42701.6	8456727	5071.8	8.69E-2	15.8	17
17	5.469E-6	32981	8.65E-3	5.05	-483.18	105664	56.221	1.60E-3	0.84	5
18	4.126E-6	39880	2.66E-2	3.01	-200.79	56382	22.457	1.66E-2	1.84	6
19	7.393E-6	32313	1.48E-2	7.39	-377.12	85334	43.656	8.69E-3	4.89	7
20	1.493E-7	50240	1.62E-1	16.46	-517.30	116706	60.246	5.32E-2	4.46	8

† $s = \sqrt{\epsilon(\eta^2_{exp} - \eta^2_{calc})/(n-1)}$

†† $\overline{\Delta\%} = \frac{1}{n}\left(\frac{\eta_{exp} - \eta_{calc}}{\eta_{exp}}\right) \times 100$

††† n = number of observations

* estimated

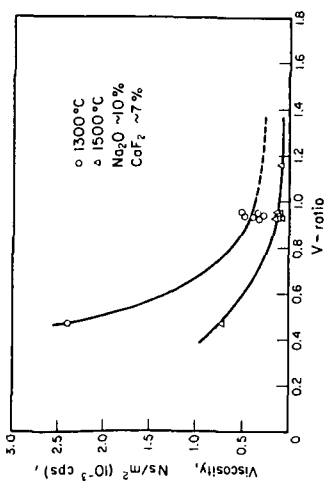

Figure 1. Viscosity vs. V-ratio

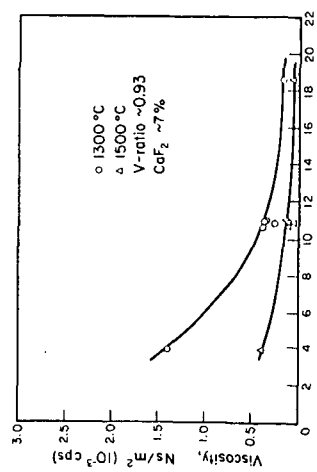

Figure 2. Viscosity vs. Na_2O Content

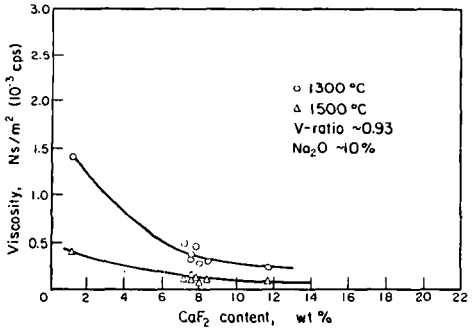

Figure 3. Viscosity vs. CaF_2 Content

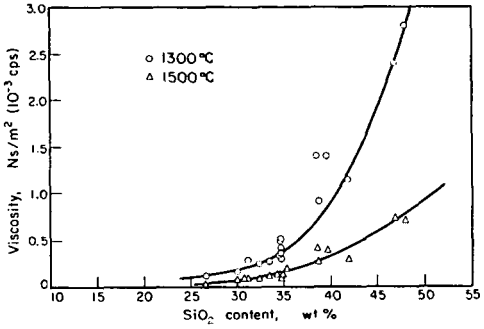

Figure 4. Viscosity vs. SiO_2 Content

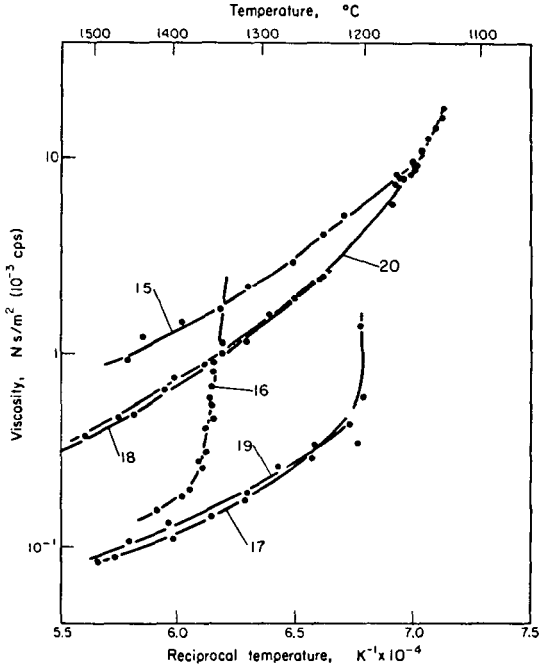

Figure 5. Typical viscosity results vs. reciprocal temperature

RHEOLOGICAL PROPERTIES OF MOLTEN KILAUEA IKI BASALT CONTAINING SUSPENDED CRYSTALS

H. C. Weed, F. J. Ryerson, and A. J. Piwinskii

University of California, Lawrence Livermore National Laboratory
Livermore, CA 94550

INTRODUCTION

In order to understand the flow behavior of molten silicates containing suspended crystals, we need to know the rheological behavior of the system as a function of volume fraction of the suspended crystalline phases at appropriate temperatures, oxygen fugacities and bulk compositions. This approach can be applied to magma transport during volcanic eruptions, large scale convective and mixing processes in magmatic systems, and fouling of internal boiler surfaces by coal ash slags in plants burning pulverized coal.

EXPERIMENTAL METHODS

We are currently determining the dynamic viscosity and crystallization sequence for a basalt from Kilauea Iki, Hawaii at 100 kPa total pressure. The oxygen fugacity is controlled by mixing CO and CO_2. The mixing proportions are chosen to yield oxygen fugacities corresponding to the high temperature extrapolation of quartz-fayalite-magnetite buffer (i.e. QFM, see Huebner (1)). Viscosities are being measured in an iron-saturated, Pt-30% Rh, rotating-cup viscometer of the Couette type from 1250° to 1150°C. The temperature interval for the crystallization sequence ranges from 1270° to 1130°C; the oxygen fugacity is maintained by flowing CO/CO_2 mixtures and is monitored by a ZrO_2 sensor cell. Low temperature limits on the investigated crystallization sequence are dictated by the sluggish kinetics encountered in this system.

RESULTS

The major element bulk composition of the starting material used in our experiments is given in Table 1:

TABLE 1. Analyses of Starting Material

Oxide	Kilauea Iki	Shaw *et. al*(2)
SiO_2	46.29	50.14
Al_2O_3	10.44	13.37
MgO	17.90	8.20
FeO*	11.34	10.13
Fe_2O_3	-	1.21
CaO	8.49	10.80
Na_2O	1.84	2.32
P_2O_5	0.22	0.27
K_2O	0.40	0.53
TiO_2	1.89	2.63
MnO	0.19	0.17
TOTAL	99.90	99.77

*All iron as FeO

The crystallization experiments were carried out employing a specimen of Kilauea Iki whole rock powder. The experimental results obtained at the QFM buffer are listed in Table 2. Olivine and chrome spinel are the only crystalline phases which occur between 1240°and 1179°C; clinopyroxene and plagioclase feldspar crystallize at approximately 1170°C.

Approximately 30 weight per cent crystallization occurs between 1250° and 1180°C. The liquid line of descent is characterized by a slight SiO_2, Al_2O_3 and alkali enrichment and an FeO and MgO depletion.

The volume percentage of melt as a function of temperature is shown in Figure 1. The break in slope at approximately 1170°C, corresponds to the appearance of clinopyroxene and plagioclase feldspar (see Table 2).

TABLE 2. Results of Selected Kilauea Iki Liquidus Experiments

Exp't No.	Time (Hrs)	Temp (°C)	Experiment Products	Vol % Melt[a]	Wt % Melt[b]
14	93.0	1240	olivine, chrome spinel, glass	71.8	78.1
9	189.5	1230	olivine, chrome spinel, glass	80.2[c]	76.1
8	24.0	1219	olivine, chrome spinel, glass	77.3	74.8
10	290.0	1209	olivine, chrome spinel, glass	76.2	74.2
12	289.0	1189	olivine, chrome spinel, glass	63.8	72.5
13	364.0	1179	olivine, chrome spinel, glass	71.8	71.5
16	380.0	1170	olivine, chrome spinel, clino-pyroxene, plagio-clase, glass	69.6	68.5
19	400.0	1160	olivine, chrome spinel, clino-pyroxene, plagio-clase, glass	54.7	53.5
20	400.0	1149	olivine, chrome spinel, clino-pyroxene, plagio-clase, glass	40.7	49.8

a) Volume percent of melt was determined by a 1000 point mode on metallograph.
b) Weight percent of melt was determined by constrained least squares analysis of phase compositions.
c) Volume percent glass was determined by 850 point mode on metallograph.

This volume percentage of melt, V_m, is given by Equations 1 and 2:

$$V_m\ (Ol+Chsp) = 0.157\ T(°C) - 114.0, \text{ where } T(°C) \geq 1170, \qquad 1)$$

$$V_m\ (Ol+Chsp+Cpx+Plag) = 1.36\ T\ (°C) - 1522.7, \text{ where } T\ (°C) \leq 1170. \qquad 2)$$

Extrapolation of Equation 1 to $V_m = 100$ corresponds to T = 1360°C for the liquidus. Extrapolation of Equation 2 to $V_m = 0$ yields T = 1119°C for the disappearance of liquid, the solidus temperature.

The measured apparent viscosities of the Kilauea Iki molten basalt between 1250° and 1150°C varied from 30 to 2000 Pa·s. Sigmoidal torque versus rotation speed curves were obtained at all investigated temperatures. The curves are linear at low rotation speeds, less than 0.4 revolutions/second, with a positive slope. This corresponds to Newtonian behavior. However, at higher rotation speeds, the curves are concave toward the rotation speed axis, indicating pseudoplastic behavior. This pseudoplastic behavior becomes more

pronounced at low temperature as the volume per cent of suspended crystals increases. We have analyzed the results in terms of an extended the power law indicated by Equation 3:

$$\log \tau_{yx} = A_1 + A_2\left(\log \left(\frac{du}{dx}\right)\right) + A_3\left(\log \left(\frac{du}{dx}\right)\right)^2 \qquad 3)$$

where τ_{yx} is the stress, and $(\frac{du}{dx})$ the strain rate. The apparent viscosity, μ, is given by Equation 4:

$$\mu = \tau_{yx} \Big/ \left(\frac{du}{dx}\right) \qquad 4)$$

Figure 2 is a plot of Equation 3 portraying experimental results obtained at the 1236°C isotherm. Figure 3 is a log-log plot of apparent viscosity as a function of shear rate at the same temperature. The apparent viscosity decreases with increasing shear rate, which is common for pseudoplastic liquids. The log of the viscosity at unit shear rate, log μ_0, is calculated from Equation 3 as $\log \mu_0 = A_1$.

Log μ_0 is plotted as a function of reciprocal temperature in an Arrhenius diagram given in Figure 4. The log viscosity curves illustrated there show a sharp break in slope with decreasing temperature. Data above and below this break have been fitted by limiting straight lines from which apparent activation energies can be calculated. The apparent activation energy in the temperature interval 1250° - 1170°C is 65 + 30 kcal mol^{-1}. For temperatures below 1170°C where appreciable crystallization occurs (see Table 2 and Figure 1) and the system exhibits strongly pseudoplastic behavior, the apparent activation energy is 341 + 42 kcal mol^{-1}. Also shown in Figure 4 are the results of Shaw (3) obtained on a Hawaiian basalt similar to our Kilauea Iki specimen (see Table 1). The general trend of the two sets of data is similar, but the break in the slope of Shaw's data occurs at a lower temperature than it does in ours, presumably because of the change from Newtonian to pseudoplastic behavior in his system. In both studies, the break in the slope of the viscosity curves occurs at 20 to 30 volume percent of suspended crystals. The non-Newtonian behavior of these molten silicate suspensions appears to arise from the increasing volume of suspended crystals in the melt. This suggests that in modeling fluid flow in silicate liquids, power law behavior should be considered when the suspended crystal volume exceeds 20 percent.

REFERENCES

(1) Huebner, J. S. (1971) in Research Techniques for High Pressure and High Temperature, Ulmer, E. C. ed., Springer-Verlag (1971), p. 146.
(2) Shaw, H. R., Wright, T., Peck, D. L. and Okamura, R. (1968) Amer. Jour. Sci., Vol. 266, p. 225-264.
(3) Shaw, H. R. (1969) Jour. Petrology, Vol. 10, p. 510-535.

This work was performed under the auspices of the U. S. Department of Energy by the Lawrence Livermore National Laboratory, under Contract No. W-7405-ENG-48.

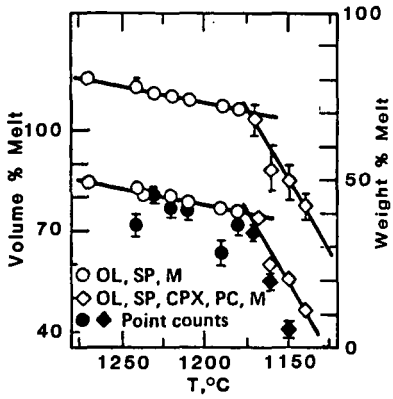

Fig. 1. Volume percent and weight percent melt as a function of temperature for Kilauea Iki basalt. The upper curve gives weight percent melt, indicated by the right ordinate. Open symbols on the lower curve give volume percent melt remaining (left ordinate), calculated from weight percent data and densities of phases. Solid symbols are from modal analyses.

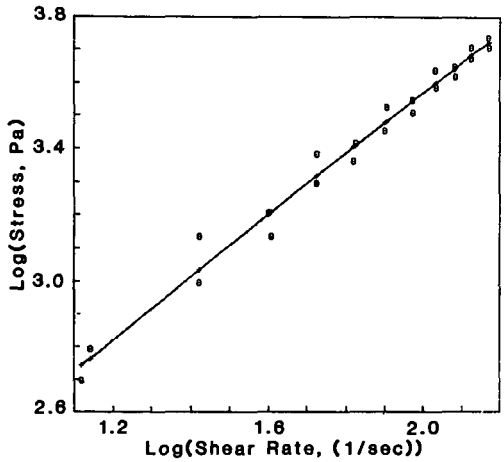

Fig. 2. Log (Stress) as a function of log (Shear Rate) for Kilauea Iki basalt melt at 1236°C.

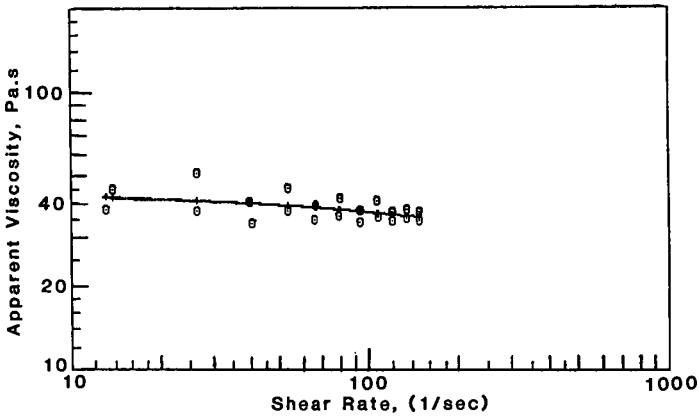

Fig. 3. Apparent viscosity of Kilauea Iki basalt melt as a function of shear rate at 1236°C.

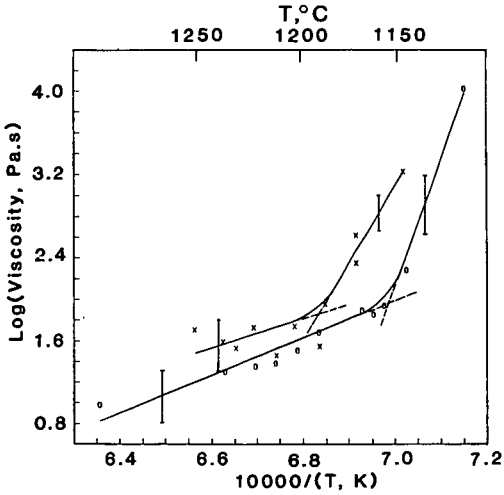

Fig. 4. Log (Apparent Viscosity) as a function of a reciprocal temperature. Present study, X; Shaw (1969), θ.

CRYSTALLISATION OF COAL ASH MELTS

David P. Kalmanovitch and J. Williamson[+]

Energy Research Laboratories, CANMET, 555 Booth St., Ottawa, K1A 0G1, Canada
[+]Department of Metallurgy and Materials Science, Imperial College of Science and Technology, Prince Consort Rd., South Kensington, London, SW7, England.

The formation of ash deposits within p.f. coal-fired boilers may cause severe reduction in heat transfer and thermal efficiency. These deposits vary in nature from friable, slightly sintered fouling to dense, semi-vitreous slags. Utility boiler designers and operators use a variety of methods (9) to ascertain various design criteria or the likelihood of the ash to form deposits (its slagging or fouling propensity). The major technique used is the standard ash fusion test (2) in which a cone or pyramid of coal ash is heated at a given rate, both in air and a mildly reducing atmosphere, while the temperatures at which various degrees of deformation occur are recorded. This method is known to give inaccurate indications of slagging propensity due mainly to the subjective nature of the test and the fact that the technique does not duplicate the thermal history experienced by coal matter in a p.f. boiler.

Various laboratory studies, (5,6) have shown that significant fusion of coal mineral matter, the precursor to ash, occurs within a very short time-frame at temperatures analagous to those in the combustion zone of a boiler (about 1550–1650°C). This is confirmed by microscopical studies of p.f. fly ash. Despite total flight times of about 2s (6) and a temperature gradient ranging from 1650°C to about 300°C the characteristic nature of fly ash, that of hollow cenospheres is due to the presence of significant liquid phase at some stage of the particles' histories. This is further confirmed by mineralogical studies of the particles which sometimes reveals the presence of a refractory phase which had crystallised from a liquid and was not the product of thermal decomposition of an individual coal mineral (4,6). Raask has shown that the growth of deposits is by initial adhesion of fly ash particles to the surface of deposits already present. This adhesion is due to the liquid phase present and the rate of assimilation of the captured particle will be by sintering by viscous flow. From the theory of sintering (6) the rate of increase in strength (s) i.e. growth, of the deposit is given by:

$$\frac{ds}{dt} = \frac{3\gamma k}{2\eta r}$$

Where γ is the surface tension coefficient of the viscous phase, k a constant, r the initial radius of the particles and η the viscosity of the liquid. It can be seen that the nature of a deposit can be described by the degree of sintering which has taken place. For a given coal ash the parameters r and γ are effectively constant with respect to the variability of the viscosity. Therefore the factors which affect the rheological behaviour will determine to a great extent the rate of growth by viscous flow. For homogeneous melts the determining factors are temperature and chemical composition. Lauf has observed that the amount of fly ash particles collected at the outlet of various boilers was inversely proportional to the calculated viscosity (taking account of the different ash contents between the parent coals). (4) The viscosity was calculated by two methods based on the chemical composition; those of Watt and Fereday and Reid. (7,8) The observations confirm the viscosity relation above, albeit qualitatively and the assumption of complete melting of the coal mineral matter. A factor which has not received attention in the literature is the crystallisation of ash particles and/or the deposits already present. With devitrification of a phase from homogeneous melt the composition of the liquid phase will change depending on the precipitating phase and the degree of crystallisation. This in turn will directly affect the viscosity and hence the rate of growth of the deposits.

subjected to a series of crystallisation treatments within the reducing atmosphere. The quenched samples were analysed for phases present by X-ray diffraction and for the ratio of ferrous to ferric iron by a wet chemical technique.

The major observation of the crystallisation study of the ash melts was that the phase or phases which were precipitated contained only the predominant components, the minor components remaining in the liquid phase. Another observation was the reluctance of the melt to crystallise to the expected number of phases; only anorthite ($CaO.Al_2O_3.2SiO_2$) was determined to crystallise for the two western type ashes and mullite ($3Al_2O_3.2SiO_2$) as the primary phase with a secondary phase of iron spinel; a member of the solid solution series magnetite ($FeO.Fe_2O_3$) - hercynite ($FeO.Al_2O_3$), only for the eastern type ash.

The crystallisation of the ternary compositions is discussed with respect to that predicted for each from the phase diagram for the system. The normalized ternary compositions of the two western type ashes were plotted on the phase diagram and the observed crystallisation compared with that predicted from the diagram and the behaviour of the model compositions. The system was found not to be able to correctly predict the primary crystalline phase for one of the two ashes but could account for the crystallisation of anorthite only for the other ash.

As quaternary systems are quite complex both the representation and crystallisation of compositions are discussed in the presentation. Planes of constant MgO content was used as the method of representation of the $CaO-MgO-Al_2O_3-SiO_2$, with planes at 5, 10 and 15 wt% prepared from literature sources and results of this study (3). The observed crystallisation of the glasses studied is discussed in terms of the equilibrium system, a striking observation being the apparent low solubility of magnesia in the compositions studied; a magnesia bearing phase precipitating for nearly all the glasses as primary or secondary phase. The corresponding normalised composition of the western type ashes were plotted on the 5% plane and the observed behaviour compared with the predicted crystallisation behaviour. As with the ternary system the four-component system only correctly predicted the primary crystalline phase for one of the ashes. Also the system would predict that a secondary phase containing magnesia would be expected to crystallise; behaviour which was not observed.

The true representation of the system $CaO-Al_2O_3-SiO_2$-iron oxide is as a quinary system which is too complex for normal analysis. The results of the ferrous to ferric ratio of the quenched samples showed significant amount of ferric iron present. Fortunately analysis of the crystalline phases shows that predominantly the ferrous iron is taken up by the iron bearing phase (there was some evidence of solid solution of ferric iron in the iron spinel phase) and therefore the system could be approximated by the quaternary system $CaO-FeO-Al_2O_3-SiO_2$. Planes of constant FeO content (5-30 wt% at 5% increments) have been prepared from literature sources and the results of the crystallisation studies of the glasses are discussed in terms of the system. Unlike the quaternary system above the iron oxide remains in solution compared with magnesia. This would be predicted from the planes of the system and was observed in the crystallisation studies; no primary phase containing iron oxide was determined even for the glasses containing 20 wt% equivalent FeO. The corresponding normalised composition of the three ashes (iron oxide expressed as equivalent FeO) was plotted on the relevant plane of the system and the observed behaviour compared with that predicted from the phase diagram and the behaviour of the model compositions. The system correctly predicted the primary crystalline phase for all the ashes and could account for the crystallisation of anorthite only for the two western type ashes. While initially the system could not predict the crystallisation of iron spinel as the secondary phase for the eastern type ash analysis of the

Thus it will be of great value to be able to predict to some extent the crystallisation behaviour of coal ash melts. For simplicity it is initially necessary to consider that the crystallisation will be from a homogeneous melt. The data obtained can be extended to the phenomena of boiler deposits by using an accurate model of viscosity of ash melts based on chemical composition. The main aim of the study presented here was to obtain relevant crystallisation data of coal ashes and to model the behaviour so as to be able to predict the devitrification of a given ash. Coal ash is usually described as a mixture of up to 11 oxide components and though various investigators (1) have attempted to simplify the system by using certain equivalences the authors have chosen to use the major three or four components to model the observed behaviour.

For eastern type coal ashes the major components are silica, alumina, iron oxide and lime, whereas for western type ashes the major components are silica, alumina, lime and iron oxide or magnesia. In both cases these may comprise 90 wt% or more of the total composition of the ash. Sanyal and Williamson have shown that the initial crystallisation of two western type ashes of low iron oxide content (5% or less) could be described by the normalised composition on the ternary equilibrium diagram of the system $CaO-Al_2O_3-SiO_2$. The study presented here has extended the investigation to the devitrification of eastern type ash as well as two western type ashes and the crystallisation of model compositions corresponding to the normalised compositions of coal ashes. The systems studied were; $CaO-Al_2O_3-SiO_2$, $CaO-MgO-Al_2O_3-SiO_2$ and $CaO-Al_2O_3-SiO_2$-iron oxide, to ascertain which system or systems govern the behaviour most adequately.

The crystallisation of three coal ashes (two western and one eastern type) was determined under laboratory conditions by fusing a sample in an electric muffle furnace to achieve complete melting of the coal minerals. Devitrification was induced by reducing the temperature to a given level and leaving the sample for a given time. The sample was then quenched, effectively freezing the phases present at the elevated temperatures. The sample was analysed by petrographic microscopy and X-ray diffraction. The treatment was repeated over a range of temperatures and times for each sample.

For the study of the crystallisation of the model compositions five ternary CaO, Al_2O_3 and SiO_2 compositions were chosen which were expected to exhibit different behaviour (from the corresponding phase diagram) while being in the compositional region relevant to coal ashes. Homogenous glasses were produced by fusing the correct mixture of the oxide components. The crystallisation of the glasses was determined in an analagous manner to that used for the ash melts. The same five compositions were used as the basis for the study of the crystallisation of the system $CaO-MgO-Al_2O_3-SiO_2$. Two series of compositions were prepared based on the ternary compositions with 5 and 10 wt% MgO respectively. Glasses were produced and the liquidus and crystallisation behaviour determined by a quenching technique.

As iron oxide exists in two oxidation states (ferrous and ferric) in p.f. ash deposits it was necessary to study the crystallisation of glasses in the system $CaO-Al_2O_3-SiO_2$-iron oxide in a controlled atmosphere; the same as that used in the reducing part of the standard ash fushion test i.e. $CO_2:H_2$ mixture 1:1 v/v. The range of iron oxide content in coal ashes is wider than that of magnesia and hence glasses were prepared with up to 20 wt% equivalent FeO. Two series of glasses were produced based on the five ternary compositions with 5 and 10 wt% equivalent FeO with another two series of glasses based on three of the five composition with 15 and 20 wt% equivalent FeO. The glasses were ground to a fine powder and each was

results of the model compositions indicated that ferric iron present in the liquid phase reduced the solubility of iron oxide which could account for the behaviour.

CONCLUSIONS

Therefore the system $CaO-FeO-Al_2O_3-SiO_2$, governs the initial crystallisation of the ash melts studied. The major aim of this study was to be able to predict the crystallisation of ash melts and relate the behaviour to boiler deposit growth. The phases present in six boiler deposits are compared with that predicted from the corresponding normalised composition in the presentation and shows that for all six (three western and three eastern type) the quaternary system predicts the primary phase. Furthermore the change in composition of the liquid phase for two of the ashes (one slagging the other non-slagging) for a range of degrees of crystallisation shows a great difference in terms of the relative concentration of the components which govern viscosity. While the liquid phase for the non-slagging ash became enriched predominantly in silica (the major viscosity-increasing component) the slagging ash became enriched in viscosity reducing components. This relates directly to the model of deposit growth discussed above and is a confirmation of the model.

The results of the study presented indicate the use of phase equilibria data to be phenomena of p.f. boiler deposits and the possible extension to the prediction of boiler fouling and slagging.

REFERENCES:

1. Barrett, E. P., "The fusion, flow and clinkering of coal ash. A survey of the chemical background." Chemistry of Coal Utilization, Ed. E. Lowry, Vol. 1, 1945, Ch. 15, pp 496-576.

2. British Standard 1016, Pt. 15, 1970. "Methods for the analysis of coal and coke, Fusibility of coal ash and coke ash", pp 14.

3. Kalmanovitch, D. P., "Reactions in coal ash melts", PhD Thesis, Univ. London 1983.

4. Lauf, R. J., "cenospheres in fly ash and conditions favouring their formation". Fuel, 60, 1981, p. 1177-79.

5. Padia, A. S., "The behaviour of ash in pulverised coal under simulated combustion conditions". D.Sc. Thesis, M.I.T., 1976.

6. Raask, E., "Flame imprinted characteristics of ash relevant to boiler slagging, corrosion, and erosion". J. Eng. Power, 104, 1982, p. 858-66.

7. Reid, W. T., method given in "Influence of coal mineral matter on slagging of utility boilers". E.P.R.I. report 736, 1981, p. D-1-4.

8. Watt, J. D. & Fereday, F., "The flow properties of slags formed from the ashes of British coals. Pt. I. Viscosity of homogeneous slags in relation to slag composition". J. Inst. Fuel, 42, 1969, p. 99-103.

9. Winegartner, E. C. "Coal fouling and slagging parameters". A.S.M.E. Special Publication, 1974.

THERMAL CONDUCTIVITY AND HEAT TRANSFER IN COAL SLAGS

K C MILLS

National Physical Laboratory, Teddington, Middlesex, TW11 OLW, UK

1. INTRODUCTION

During the gasification of coal, both molten and solid slags are formed in the converter, and the heat transfer within the gasification chamber is governed to a large extent by the thermal properties of the slag phase. Thus in order to carry out either heat balance or modelling calculations it is necessary to have reliable data for the thermal properties of both solid and liquid coal slags. However, the thermal transfer mechanisms in high temperature processes involving slags are exceedingly complex since heat can be transported by convection, radiation and thermal conduction. The total thermal conductivity (k_{eff}) is, in turn, made up from contributions from (i) the thermal ("phonon") conductivity, k_c, (ii) radiation conductivity, k_R and (iii) electronic conductivity, k_{el}. Heat balance calculations must take account of all these thermal transport mechanisms; consequently it is necessary to study the effects of the various mechanisms for not only do they determine the heat transfer in the gasifier, but they can also critically affect the experimental values derived for the thermal conductivity of the slag. Hence the factors affecting the thermal conductivity of slags will be examined and their effect on the various methods available for the measurement of thermal conductivities will be assessed. Finally, experimental data for the thermal conductivity of slags, glasses and magmas will be evaluated to provide a reliable data base for the thermal conductivity of slags, and to determine the likely effects of variations in chemical composition upon values for coal slags.

2. THERMAL CONDUCTION MECHANISMS

2.1 Thermal "phonon" conductivity (k_c)

Heat is transferred through a medium by phonons, which are quanta of energy associated with each mode of vibration in the sample. This mode of conduction is thus referred to as thermal, phonon or lattice conduction. Scattering of the phonons causes a decrease in the thermal conductivity and hence the conductivity is sensitive to the structure of the sample. Scattering of the phonons can occur by collisions of the phonons with one another, or by impact with grain boundaries or crystal imperfections, such as pores. Thus a low-density, highly-porous material will have a low thermal conductivity. In glassy, non-crystalline materials it has been suggested (1) that thermal conductivity decreases as the disordering of the silicate network increases.

2.2 Radiation conductivity (k_R)

Measurements of the thermal conductivity of glasses were found to be dependent upon the thickness of the specimens used, and this is shown in Figure 1. This behaviour was ascribed to the contribution from radiation conductivity, k_R, which can occur in semi-transparent media like slags and glasses. Radiation conductivity occurs by a mechanism involving absorption and emittance of radiant energy by various sections through the medium. Consider a thin section in the slag, radiant energy absorbed by the section will cause it to increase in temperature and consequently radiant heat will be emitted to cooler sections. This process can occur right through the medium and it is obvious that the energy transferred in this way will increase with increasing number of sections (ie increasing thickness) until the point where k_R attains a constant value. At this point the slag is said to be "optically thick", and this is usually considered to occur when $\alpha d > 3.5$, where α and d are the absorption coefficient and thickness of the slag, respectively.

At high temperatures, radiation conductivity can be the predominant mode of conduction, eg in glassmaking more than 90% of the total conductivity occurs by radiation conduction. The radiation conductivity can be calculated for an optically-thick sample if steady-state conditions apply and if it is assumed that the absorption coefficient of the medium, α, is independent of wavelength, λ, ie grey-body conditions obtain. For these conditions k_R can be calculated by use of equation 1), where σ and n are the Stefan-Boltzmann constant and refractive index, respectively.

$$k_R = \frac{16\sigma n^2 T^3}{3\alpha} \quad . \qquad 1)$$

Values of k_R cannot be calculated for optically-thin samples ($\alpha d < 3.5$) and for some measurement techniques involving non-steady state conditions. Thus it is obvious that reliable values of thermal conductivity can only be obtained when either k_R is negligible, or where it can be calculated reliably for optically-thick conditions.

Absorption coefficient (α)

The absorption coefficient is a very important parameter, as it determines (i) the magnitude of k_R (equation 1) and (ii) the thickness at which a slag becomes optically thick ($\alpha d > 3.5$). Hence increasing α has the effect of decreasing k_R and decreasing the depth at which a slag becomes optically thick. If a particular slag sample were optically thin, these two factors would operate in opposition to one another.

The absorption coefficient is markedly dependent upon the amounts of FeO and MnO present in the slag [2]; although Fe_2O_3 absorbs infra-red radiation, its effect on α is much less pronounced than that of FeO. An empirical rule has been derived[2] for glasses containing less than 5% FeO, the absorption coefficient at room temperature is given by the relationship, $\alpha = 11.$ (% FeO).

A basic assumption adopted in deriving equation 1) was that α was independent of wavelength; however, in practice the spectral absorption coefficient (α_λ) varies with the wavelength (λ) as shown in Figure 2 for a glass containing ca. 5% FeO[3]. It can be seen from this figure that there is strong absorption by FeO at ca. 1 μm and by SiO_2 at ca. 4.4 μm. At high temperatures this restricts absorption by the slag to a "window", in the wavelength range 1-4.4 μm. However, even within this wavelength band there is some variation in α_λ and the average absorption coefficient, α_m, is determined by weighting of the α_λ values.

The average absorption coefficient, α_m, can be affected by temperature in two different ways. Firstly, the absorption spectrum, ie. (α_λ), can change markedly with temperature and consequently alter the value of α_m. Secondly, even if the absorption spectrum is unaffected by temperature, α_m would continue to be a function of temperature because the wavelength distribution used in deriving α_m is itself a function of temperature. This can be seen in Figure 3 where the fraction of total energy emitted in the "window" 1-4.4 μm constitutes 61.1%, 79.5% and 81.9% of the total energy emitted at 1073K, 1573K and 1773K, respectively. In a similar manner, the various α_λ values of the spectrum will have to be weighted differently in the calculation of α_m for the three temperatures in question.

It can be seen from Figure 2 that α_m increases with increasing temperature, and similar behaviour has been observed in rocks and minerals [4,5,6]. By contrast, the absorption coefficients (α_m) of amber glass have been found to decrease with increasing temperature.

Extinction coefficient (E)

In solids, radiant energy can be scattered by grain boundaries, pores and cracks in the material. In these cases, it is necessary to use the extinction coefficient (E) which is given by the relationship $E = \alpha + s$, where s is the scattering coefficient.

2.3 Electronic conductivity (k_{el})

It has been reported that glasses which contain significant concentrations of Fe^{2+} ions behave in a similar manner to semi-conductors and hence thermal conduction via conduction electrons, holes, etc. could be significant, according to Fine et al[7]. Little is known of this mechanism in relation to the heat transfer in slags and consequently the contribution of k_{el} to the measured thermal conductivities has been ignored in this review.

2.4 Total thermal conductivity (k_{eff})

In practice, the radiation and conduction contributions to the heat flux (Q) are interactive, and the interpretation of the combined conductive-radiative heat transfer is exceedingly complex. Various models have therefore been proposed to simplify the theory of the heat transfer process. One widely-used model is the diffusion approximation which assumes that the heat flux (Q) is given by equation 2), where k_{eff} is the effective thermal conductivity and is defined by equation 3) where x is the distance. Gardon [8] has pointed out that this model only applies strictly when (i) k_R is small and (ii) $\alpha d > 8$.

$$Q = -k_{eff} (dT/dx) \qquad 2)$$

$$k_{eff} = k_c + k_R \qquad 3)$$

3. EXPERIMENTAL METHODS FOR DETERMINING THERMAL CONDUCTIVITY

The experimental methods available for measuring thermal conductivities are summarised below; more detailed reviews of the experimental techniques are available elsewhere [3,9,10,11]. The techniques can be divided into three classes: (i) steady-state methods, (ii) non-steady state methods, and (iii) indirect methods for the determination of k_R. The steady-state methods usually yield k_{eff} values and the non-steady state techniques usually produce thermal diffusivity (a_{eff}) values, which can be converted to thermal conductivity values by use of equation 4), where ρ and Cp are the density and heat capacity of the slag.

$$k = a . Cp . \rho \qquad 4)$$

3.1 Steady-state methods

These methods all yield k_{eff} values provided that the specimen is optically thick.

In the linear heat-flow method two disc-shaped specimens are placed on either side of an electrically-heated plate and the temperature profiles across the samples are monitored by thermocouples sited on both faces of the specimens. The apparatus is well insulated to minimise heat losses. In some versions of this method, the total heat fluxes passing through the samples are determined by calorimeters in contact with the specimens. When high-temperature measurements are required, this technique is usually operated as a comparative method [12].

In the radial heat-flow method the specimen is in the shape of a hollow cylinder, which is sited in the annulus between two coaxial cylinders with the internal cylinder acting as a radial heat source [13]. The temperature profile across the specimen is determined by thermocouples placed on the inside walls of the two cylinders. This method requires a large isothermal zone in the furnace, which is difficult to achieve at high temperatures. When this technique is used for measurements on liquids it is prone to errors from convective heat transfer.

3.2 Non-steady state methods

In the radial wave method the slag is placed in a cylindrical crucible sited in the isothermal zone of a furnace, and thermocouples are located on the walls and along the geometric axis of the crucible (the slag). The outside wall of the

of the crucible is then subjected to a sinusoidal variation of temperature and the variation in temperature of the central thermocouple is monitored. There is a phase shift between the input and output which is related to the thermal diffusivity of the slag. In the modification of this apparatus used by Elliott and co-workers[7,14] the periodic variation in temperature is produced in a wire running along the central axis of the cylindrical crucible, and the phase shift is measured in the signal of the thermocouples sited on the walls of the crucible. The thermal diffusivity values obtained with this method may be vulnerable to errors arising from convective heat transfer.

In the modulated beam method the specimen is in the form of a disc, which is maintained at a constant temperature, whilst the front face of the disc is subjected to a laser beam which produces a periodic variation in temperature of constant frequency. The phase shift between this input and the signal from a temperature sensor in contact with the back face is determined. By carrying out measurements at two or more frequencies, Schatz and Simmons[6] were able to derive values of both a_{eff} and the extinction coefficient. If this method were applied to measurements in liquids, it too would be prone to errors caused by convection.

The laser pulse method[15,16] when applied to solids uses a disc-shaped slag specimen coated with metallic films on both planar surfaces. A laser pulse is directed on to the front face of the specimen and the temperature of the back face is monitored continuously. The maximum temperature rise of the back face (ΔT_{max}) usually occurs after ca. 10 seconds, and a_{eff} may be computed from the time taken ($t_{0.5}$) for the back face to attain a temperature rise of ($0.5\ \Delta T_{max}$). The method has also been applied to measurements on liquid slags[15,17] which were contained in Al_2O_3 or BN crucibles. The major advantage of this technique is that the short duration of the experiment minimises the errors due to convection. The major disadvantage is that the maximum specimen thickness is about 4 mm, and consequently optically-thick conditions only apply when the extinction coefficient is greater than 9 cm^{-1}. A second disadvantage is that the laser pulse method is a transient technique and k_R cannot be calculated by equation 1), which is applicable to steady-state conditions; at the present time no formulae exist for the calculation of k_R for this method. Thus this technique is most useful when applied to specimens which have (i) very small values of αd (ie $\alpha d \ll 3.5$) where $a_{eff} \simeq a_c$, or (ii) large extinction coefficients where k_R is negligible and thus $a_{eff} = a_c$.

The line source method is also a transient technique and is the standard method for measuring the thermal conductivities of liquids at lower temperatures. In the high-temperature versions, this method consists of a fine Pt wire (ca. 0.1 mm dia) which is sited centrally in a crucible of molten slag. This wire acts as both heating element and temperature sensor. When an AC or DC current is applied to the wire, the temperature rise of the wire (ΔT) is monitored continuously during the heating period (ca. 1 second). A linear relationship exists between ΔT and ln (time), the slope of which is proportional to (1/k). This method has the advantage that convectional heat transfer is eliminated (if convection does occur it results in a non-linear ΔT-ln (time) plot and can therefore be readily detected). Routines are available for calculating the value of k_R for optically-thick conditions[18]; however, de Castro et al.[19] have recently proposed that k_R is negligible in the values of k_{eff} measured by this technique at ambient temperatures (ie $k_R \simeq 0$, $k_{eff} = k_c$). There is evidence to support the view that $k_R \simeq 0$, as measurements made with this technique at higher temperatures[20,21,22] yield much lower values of k_{eff} for slags than those obtained by steady-state techniques. Furthermore, Powell and Mills[23] have pointed out that the thermal conductivity data for molten salts become more consistent if k_R is taken to be zero in the various line-source determinations.

3.3 Indirect measurements of k_R

The absorption (or extinction) coefficient can be determined by measurement of the optical transmissivity (τ) of the slag as a function of wavelength; the absorption coefficient (α) is given by equation 5), where d is the thickness of the specimen.

Measurements at high temperatures are carried out by using

$$\alpha_\lambda = -\ln(\tau_\lambda)/d \qquad 5)$$

an assembly of mirrors to direct a beam of radiation of known frequency on to a disc-shaped specimen sited in a tube furnace. The transmitted beam is diverted into an infrared spectrophotometer where the transmissivity is determined. Blazek and Endrys[3] have reported that k_R values for glasses calculated from absorption coefficient data are in good agreement with values of $(k_{eff} - k_c)$ determined experimentally.

3.4 Summary of experimental limitations

(i) It is important to ensure that the thermal conductivity measurements on semi-transparent media should be carried out with optically-thick specimens, as k_R cannot be calculated for optically-thin conditions. It is recommended that absorption coefficient measurements should also be carried out to determine the slag thickness required to produce an optically-thick specimen.

(ii) The non-transient techniques are prone to errors due to convectional heat transfer.

(iii) At the present time no reliable routines are available for calculating the k_R contribution to the overall thermal conductivity measured in transient techniques; there is some evidence to suggest that k_R is negligible in measurements obtained by the line source method.

4. REVIEW OF THE EXTANT DATA FOR SLAGS

There is a paucity of data for coal slags; it is therefore necessary to study a much broader range of slags in order to determine the effects of compositional change on the thermal conductivity of the slag. One problem continually encountered is that the distribution of Fe in slags between (Fe^{3+}), (Fe^{2+}) and free iron is not reported, and this can have a marked effect on the absorption coefficient and consequently k_R. Furthermore, the ratio of $((Fe^{2+})/(Fe^{3+}))$ is known to vary with (i) temperature, (ii) $p(O_2)$ and (iii) the composition of the slag, (Fe^{2+}) increasing with increasing SiO_2 and TiO_2, and decreasing CaO and Na_2O.

4.1 $CaO + SiO_2 + FeOx$

Fine et al[7] determined the absorption spectra at room temperature of three slags containing 0, 7 and 14% FeO (Figure 4). The absorption coefficients of the slags containing 7 and 14% FeO will probably increase with increasing temperature as the (Fe^{2+}/Fe^{3+}) ratio increases with increasing temperature. An increase in α with increasing temperature can also be seen in Figure 2. Fine et al[7] used the radial wave method to determine a_{eff} of solid and liquid slags containing 0 to 25% FeO; their results are summarised in equation 6), where B represents the basicity, ie (CaO/SiO_2) ratio and T is the temperature in (°C).

$$a_{eff} = 10^{-7}\,(1.5 - 0.5\,B) + 1.8 \times 10^{-6}\,\frac{(T/1500)^3}{(\%FeO)^{0.8}}\ m^2 s^{-1} \qquad 6)$$

This equation indicates that increasing the FeO content results in a reduction of a_{eff}; this behaviour is due presumably to the increase in α and hence the consequent decrease in k_R with increasing FeO content. However, Nauman et al[24] using the same experimental technique as Fine et al[7] obtained the k_{eff} - (% FeO) relationship shown in Figure 5 for molten slags with high FeO contents. The density of slags are known to increase with increasing (FeO_x, MnO) content, thus $k(= a.C_p.\rho)$ would be expected to increase as the level of FeO increases[25]. However, calculations have shown that this increase in k would be ca. 30%, and this alone would not account for the increase in k shown in Figure 5. Thus it must be concluded that FeO additions do increase the thermal diffusivity of the

system. In these slags with high FeO content, the absorption coefficient must be very high and thus k_R must be negligible and $k_{eff} = k_c$.

4.2 $CaO + Al_2O_3 + SiO_2$

Measurements on solid slags have been reported by Kingery[12] (comparative linear heat-flow method), Osinovskikh[25] and Susa et al[21] (line source method), and for the liquid phase by Susa et al[21] and Ogino et al[13] (radial heat-flow); the results are summarised in Figure 6. The data recorded by Osinovskikh[25] appear to be too low, but there is some measure of agreement between the data obtained for the liquid near the liquidus temperature (T_{liq}). However, the reported, thermal conductivity values diverge as the temperature increases, and this is possibly due to the negligible contribution of k_R in the line source measurements[20] and the effects of k_R and convective heat transfer on the value due to Ogino[13]. The value due to Kingery[12] for the compound $3Al_2O_3.SiO_2$ is appreciably higher than that for the slags of the ternary system.

4.3 $MgO + Al_2O_3 + SiO_2$

Values for the various binary compounds occurring in this system have been reported by Rudkin[26] and by Kingery[12] (comparative linear heat-flow method), and by Schatz and Simmons[6] (modulated beam method) for temperatures up to 1300 °C; there is excellent agreement between the values due to the latter two groups of workers. Schatz and Simmons[6] reported that extinction coefficient of $2MgO.SiO_2$ increases from 5 cm^{-1} at 270 °C to 25 cm^{-1} at 1300 °C.

4.4 $Na_2O + SiO_2$

Susa et al[21] (line source method) reported thermal conductivity data for solid and liquid slags for three compositons; the single value obtained by Ogino et al[13] (radial heat-flow method) is in reasonable agreement with these data.

4.5 Glasses

Blazek and Endrys[3] have reviewed the thermal conductivity data for glasses. The lattice thermal conductivity, k_c, for glasses is relatively unaffected by composition and was found to increase with temperature from $1 Wm^{-1}K^{-1}$ at 25 °C to $2.7 Wm^{-1}K^{-1}$ at 1300 °C. However, the radiation conduction is frequently the dominant mode of heat conduction in glasses at high temperatures.

4.6 CaF_2-based slags

Extinction coefficients have been reported (1.3 cm^{-1} for 1000-1300 °C) by Keene and Mills[27], and absorption coefficients (1.3 cm^{-1}) for the liquid state by Mitchell and Wadier[22].

The thermal conductivity values for polycrystalline (optically-thick) CaF_2 obtained by Kingery[12] (comparative linear flow method) and by Taylor and Mills[16] are in reasonable agreement (Figure 7). However, there is an appreciable discrepancy between the values of k obtained by the line source method[20-22] and the single value due to Ogino et al[13] (radial heat source method).

The reason for the discrepancy probably lies in the magnitude of the k_R values measured in the two experiments, as k_R is probably negligible for the line source technique, in contrast to the steady-state method where k_R would be appreciable despite the fact that the sample was probably optically thin ($\alpha d \simeq 0.8$).

4.7 TiO_2-based slags

Values of thermal diffusivity, a_{eff}, of ca. 3×10^{-7} m^2s^{-1} have been reported by Raflovich and Denisova[28] for slags based on TiO_2 (>45%) and SiO_2 with small

amounts of Al_2O_3 and Fe_2O_3. The data reported by Osinoskikh et al[25] for slags with less than 15% TiO_2 are much lower, this is probably due to the high porosity of the sample used.

4.8 Continuous casting slags

These slags have the approximate composition (CaO = SiO_2 = 35%; Al_2O_3 ≃ 7%; Na_2O (4-15%) and CaF_2 (5-8%). Olusanya[29] has reported that the absorption coefficients lie in the range (0.5 - 5 cm^{-1}) and thus k_R could be appreciable in these slags. Values for a_{eff} were obtained for ten glassy-slags by Taylor and Mills[30] (laser pulse method) which lay between 4 and 5 x 10^{-7} m^2s^{-1} (Figure 8); these slags were optically thin (αd = 0.4) and thus we might expect k_R to be small and $k_{eff} \simeq k_c$. Some crystallisation of the samples occurred at temperatures above the glass temperature in these experiments, and this resulted in an initial decrease in a_{eff}, which was subsequently followed by an increase in the thermal diffusivity. Taylor and Mills reported that a_{eff} of a crystallised specimen had a value of 6 x 10^{-7} m^2s^{-1}, which is higher than that of the glassy specimens; the crystalline samples would have a higher extinction coefficient and thus k_R would be low and hence $a_{eff} = a_c$. Thermal conductivity values for the liquid phase have been obtained by Nagata et al[31] and by Powell et al[32] (line source method), and by Taylor and Edwards[17] (laser pulse method) and by Ohmiya et al (33) interpretation of thermal flux data). As can be seen from Figure 8, the results from the line source technique are lower than the other data, and this probably reflects the fact that k_R is negligible in the line source experiements. The increase in k_{eff} observed by Taylor and Edwards[17] above the solidus temperature is probably due to the decrease in α (and increase in k_R), as liquid is formed from crystallised slag.

4.9 Blast furnce slags

Values of k_{eff} have been reported by Ischenko[34] and by Vargaftik and Oleschuk[35] for temperatures in the range (200-1000 °C). The values cited are lower than those reported for other slags, which is presumably due to the high porosity of the samples used by these workers.

4.10 Rocks and Minerals

Absorption and extinction coefficients for several rocks and minerals[4,5,6] were found to increase appreciably at high temperatures, eg α_M (peridot) increases from 0.5 cm^{-1} at 25 °C to 4.3 cm^{-1} at 1240°C. Values of k_{eff} (or a_{eff}) have been recorded by Kingery[12], by Kawada[36] (comparative linear flow method), by Murase and McBirney[37] (radial heat flow), and Schatz and Simmons[6] (modulated beam method). The results are given in Figure 9, and Schatz and Simmons[6] reported that for forsterite and olivine at 1300 °C, approximately half of the measured k_{eff} value was due to the contribution of k_R. There is good agreement between the results reported by Kingery[12] and by Schatz and Simmons[6] for k_{eff} of forsterite. The values of k_{eff} reported by Murase and McBirney[37] are appreciably lower than those reported by other investigators, which may indicate systematic errors in the method, or may merely be due to the higher SiO_2 content of the samples studied by Murase and McBirney. The sharp increase in k recorded above 1100 °C for some samples probably indicates the onset of melting, which causes the extinction coefficient to decrease and hence k_R to increase appreciably. It is noticeable that Kawada[36] recorded no marked increase in k_{eff} for dunite (DU), which has an FeO content of 13% and where k_R would be negligible.

4.11 Coal slags

The experimental details of various investigations concerned with these slags are summarised in Table 1. The results are presented in Figure 10; only the upper and lower a-(T) curves reported by Gibby and Bates have been plotted.

The absorption coefficients of these slags are probably quite high, as they contain appreciable levels of FeO and free Fe. Thus the radiation contribution, k_R, will

be relatively small. There is good agreement between the results of the investigations when the appreciable differences in the composition of the slags is taken into account. Gibby and Bates[15] reported that for solid slags the value of a_{eff} varied appreciably from run to run and appeared to be dependent upon the thermal history of the sample. This behaviour was attributed to the crystallinity of the sample and the fact that a_{eff} (crystalline) $>$ a(glass), which is in agreement with the observations on continuous-casting slags. Gibby and Bates[15] also observed that K_2O additions resulted in a decrease in a_{eff} up to 900 °C, and that the a_{eff}-(T) relationship showed a sharp inflection around 950 °C, which was attributed to the crystallisation of the slags.

These workers also reported that a_{eff} appeared to decrease with increasing SiO_2 content or with the ratio (SiO_2/(SiO_2 + Fe_2O_3 + MgO + CaO)). This implies that k_c is probably dependent upon the structure of the silicate slag, and thus it should be possible to build up a reliable model for the estimation of k_c in due course. However, it is also possible that the decrease in a_{eff} with increasing SiO_2 content may simply reflect the lower fraction of crystalline phase present in the slag.

5. DISCUSSION

The thermal conductivity data for slags, magmas and glasses have been collated in Figure 11. It can be seen that k_{eff} values for solid coal slags are similar to those for slags from the systems CaO + Al_2O_3 + SiO_2 and CaO + SiO_2 + FeO and for those used in continuous casting. Thus it would appear that the chemical composition of the slag has little effect on the values of k_{eff}; however, certain oxides (eg SiO_2, CaO) could exert some influence on the conductivity by altering the crystallinity of the slag. Furthermore, the radiation conduction will also be affected by the crystallinity of the sample as the extinction coefficient will be high for crystalline materials.

It is more difficult to evaluate the thermal conductivity of molten slags, although the data obtained for coal slags[15] and for slags of the system CaO + FeO + SiO_2 [7][14] indicate that k_{eff} for the liquid near the melting-point is similar to that for the solid phase . It is noticeable that the k_{eff} values obtained for liquid slags by the line source method are considerably lower than the values obtained with other techniques. It is possible that the line source method is prone to systematic errors when applied to molten slags, but a more likely explanation is that the k_R is negligible in these experiments. As coal slags contain relatively high levels of (FeO + Fe_2O_3), it would be expected that the absorption coefficient of the slag would be high and that the k_R contribution would be small. However k_R increases dramatically with temperature and even a slag with a relatively high absorption coefficient of 100 cm^{-1} would give rise to a contribution of k_R of 0.4 $Wm^{-1}K^{-1}$ at 1800 K.

However as the absorption coefficient is very dependent upon the (Fe^{2+}) concentration the value of k_R will be dependent upon the various factors affecting the (Fe^{2+}/Fe^{3+}) ratio in the slag viz. the ratio increases with (i) increasing temperature (ii) decreasing p (O_2) (iii) increasing SiO_2 and TiO_2 contents and decreasing CaO, Na_2O and K_2O contents in the slag. This review has revealed the urgent need for absorption coefficient data for coal slags at high temperatures and for information relating the absorption coefficient to the FeO content of the slag.

The heat transfer process in the coal gasifier can also be affected by the layer of slag which lines the walls of the gasifier. Recently, Grieveson and Bagha [38] have developed a simple experiment for measuring the thermal flux (Q) in various slags used in the continuous casting of steel. A water-cooled, copper finger is lowered into a crucible containing molten iron covered with a layer of slag and a layer of solidfied slag forms around the cold finger. The thermal flux is determined by measuring the

temperature rise of the cooling water flowing through the copper finger. It was found that the heat flux was related to (i) the thickness of the slag layer and (ii) the thermal resistance of the Cu/slag interface. The thickness of the slag layer is, in turn, dependent upon the viscosity of the slag and upon other factors determining the "melt back" of the slag layer. Grieveson and Bagha [38] observed that the thermal resistance of the Cu/slag interface appeared to be related to (i) the mineralogical constitution of the slag and (ii) the strength of the adhesion between the copper and the slag eg. Q (glass from $CaO.SiO_2$ field giving good Cu/slag adhesion) $>$ Q (glass from $CaO.Al_2O_3.2SiO_2$ phase field with poor Cu/slag adhesion). Thus relatively simple experiments like these simulation tests can provide us with a valuable insight into the factors affecting heat transfer mechanisms occurring in industrial processes.

CONCLUSIONS

(i) Experimental data for the thermal conductivities of slags must be carefully analysed to establish the boundary conditions of the experiment (eg. optical thickness of the specimen, magnitude of k_R etc.) This evaluation of the data allows one to determine the suitability of a specific thermal conductivity value for subsequent use in heat balance calculations for the gasifier.

(ii) The thermal conductivities of coal slags are not very dependent upon the chemical composition of the slag.

(iii) The thermal conductivity of a slag is dependent upon the degree of crystallization and consequently upon the thermal history of the specimen; the thermal conductivity of the crystalline phase is greater than that of the glassy phase.

(iv) The radiation conduction, k_R, is principally determined by the magnitude of the absorption (or extinction) coefficient. As the absorption coefficient of the slag is largely dependent upon the (Fe^{2+}) concentration in the slag, it will also be dependent upon the factors affecting the (Fe^{2+}/Fe^{3+}) ratio viz. temperature, $p(O_2)$ and the SiO_2, CaO and Na_2O contents of the slag.

(v) Experimental data are required for the absorption coefficients of coal slags at high temperatures so that the relationship between α_m and the FeO content can be established.

(vi) Heat transfer in the coal gasifier will be partially dependent upon the thermal resistance of the slag/wall interface and this, in turn, will be dependent upon the mineralogical constitution of the slag adjacent to the wall.

ACKNOWLEDGEMENTS

Valuable discussions with B J Keene, (National Physical Laboratory) Professor P Grieveson (Imperial College) and Dr R Taylor (UMIST) are gratefully acknowledged.

REFERENCES

(1) AMMAR, M M., GHARIB, S, HALAWA, M M, E L BADRY, K, GHONEIM, N A and E L BATAL, H A. J. Non-Cryst. Solids 1982, 53, 165.

(2) STEELE, F N and DOUGLAS, R W. Phys. Chem. Glasses 1965, 6, 246.

(3) BLAZEK, A and ENDRYS, J. Review of thermal conductivity data in glass, Part II Thermal conductivity at high temperatures published Intl. Commission on Glass, 1983.

(4) FUKAO, Y., MITZUTANI, H. and UYEDA, S. Phys. Earth Planet Interiors 1968, 1, 57.

(5) ARONSON, J R, BELLOTI, L H ., ECROAD, S W, EMSLIE, A G., MCCONNEL, R K and THUNA, P C von. J Geophys. Res. 1970, 75, 3443.

(6) SCHATZ, J F and SIMMONS, G. J. Geophys. Res. 1972, 77, 6966.

(7) FINE, H A; ENGH, T, and ELLIOTT, J H; Metall. Trans B, 1976, 7B, 277.

(8) GARDON, R; paper presented at 2nd Intl. Thermal Conductivity Conference, Ottawa, 1962, 167.

(9) GARDON, R Review of thermal conductivity data in glass, Part 1 Thermal conductivity at low and moderate temperatures published Intl. Commission on Glass, 1983.

(10) TOULOUKIAN, Y S , POWELL, R W, H O, C Y and KLEMENS, P G. Thermophysical Properties of Matter, volumes 1 (1970) and volume 10 (1973) published by IFI/Plenum, New York

(11) TYE, R P, Thermal conductivity, volumes 1 and 2, 1969, published by Academic Press, New York.

(12) KINGERY, W D, FRANCL, J, COBLE, R L and VASILOS, T. J. Amer. Ceram. Soc., 1954, 37, 107.

(13) OGINO, K, NISHIWAKI, A, YAMAMOTO, K and HAMA, S. Paper presented at Intl. Symp. Phys. Chem. Steelmaking, Toronto, 1982, III-33.

(14) NAUMAN, J; FOO, G; and ELLIOTT, J F; Extractive Metallurgy of Copper, Chapter 12, 237.

(15) GIBBY, R L and BATES, J L; 10th Thermal Conductivity Conference, held Newton, Mass., Sept. 1970, IV-7,8. see also BATES, J L, Final Report to National Science Foundation, Grant GI-44100 Properties of Molten coal slags relating to open cycle MHD, Dec. 1975.

(16) TAYLOR, R and MILLS, K C; Arch. f. Eisenhuttenw., 1982, 53, 55.

(17) TAYLOR, R and EDWARDS, R. cited by MILLS, K C and GRIEVESON, P, a paper presented at the Centenary Conference 1984, "Perspectives in Metallurgy" Sheffield University,July 1984.

(18) SAITO, A; Bull. Jap. Soc. Mech. Engr., 1980, 23, 1459.

(19) de CASTRO, C.A.N, L I, S.F.Y., MAITLAND, G.C. and WAKEHAM, W.A, in press Intl. J Thermophys. (1984)

(20) MILLS, K C; POWELL, J S; BRYANT, J W and KEENE, B J, Canad, Metall. Q, 1981, 20, 93.

(21) SUSA, M, NAGATA, K and GOTO, K S; Trans, Iron Steel Inst. Japan, 1982 22 B42.

(22) MITCHELL, A and WADIER, J F; Canad. Metall. Q, 1981, 20, 373.

(23) POWELL, J S, and MILLS, K C. Paper to be presented at the Ninth European Conference on Thermophysical Properties to be held in Manchester, Sept. 1984.

(24) MILLS, K C. Paper entitled "Estimation of physico-chemical properties of coal slags and ashes" to be presented at this conference.

(25) OSINOVSKIKH, L L, KOCHETOV, N N and BRATCHIKOV, S G; Trudy Urals N-I Chern. Met., 1968 (8), 71.

(26) RUDKIN, R L; Report US AF., ASD-TDR-62-24 II.

(27) KEENE, B J and MILLS, K C. Arch f Eisenhuttenw. 1981, 52, 311.

(28) RAFALOVICH, I M and DENISOVA, I A; Fiz. Khim Rasplav. Schlakov, 1970, 181.

(29) OLUSANYA, A, "The Fundamental Properties of Continuous Casting Fluxes" PhD Thesis, Imperial College, London, 1983.

(30) TAYLOR, R, GRIEVESON, P, TAYLOR, R. Paper entitled "Thermal and Physico-chemical properties of continuous-casting slags" to be presented at Ninth European Conference on Thermophysical Properties to be held in Manchester Sept. 1984.

(31) NAGATA, K and GOTO, K S. private communication, Tokyo Inst. of Technology, 1984.

(32) POWELL, J. S., MILLS, K C unpublished thermal conductivity data on casting powders, National Physical Laboratory, 1984.

(33) OHMIYA, S; TACKE, K H and SCHWERDTFEGER, K; Ironmaking and Steelmaking, 1983, 10, 24.

(34) VARGAFTIK, N B and OLESHCHUK, O N; Teploenergetika, 1955, 4, 13.

(35) ISCHENKO, K D; Met. Kobosokhim, 1970, (21) 82.

(36) KAWADA, K; Bull. Earthquake Res. Inst., 1966, 44, 1071.

(37) MURASE, T. and McBIRNEY, A R; Science, 1970, 170, 16S.

(38) GRIEVESON, P and BAGHA, S cited by MILLS, K C and GRIEVESON, P in a paper presented at the Centenary Conference 1984, "Perspectives in Metallurgy", Sheffield University, July 1984

Table I

Reference	No	Slag composition					Sample	Method	Temperature Range °C
		%CaO + MgO	%SiO_2	%FeO	%Fe_2O_3	%Al_2O_3			
Vargaftik[34]	A	12.8	35.9	29.0	5.3	14.3	Liquid, solidfied slag; (10 mm) *softening point* - ca. 1000 °C	Radial heat flow method. Pt and stainless steel crucibles	25 - 1348
	B	3.8	53.5	14.1	6.0	22.7			25 - 1283
	C	2.2	50.8	21.0	-	13.0			25 - 1151
Gibby and Bates[15]			33-61	6-9	6-36	14-32	6 samples, liquid and solid	Laser pulse method	100 - 1600
Taylor[30]		27	34	6.5	4.5% free Fe	22 + 3% Na_2O	Glass, (1 mm)	Laser pulse method	200 - 950

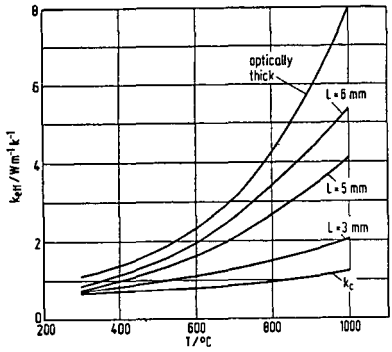

Figure 1. The dependence of k_{eff} upon the thickness of the sample.

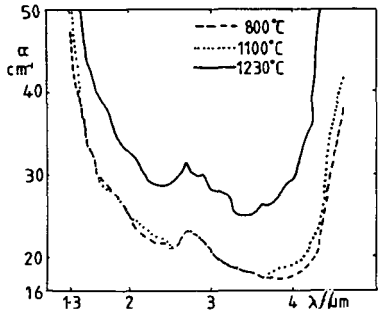

Figure 2. The wavelength of dependence of a glass containing 67 % SiO_2, 16 % Na_2O + 9 % (FeO + Fe_2O_3)

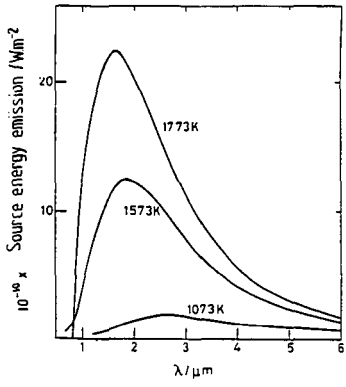

Figure 3. Wavelength distribution of the source energy emission for a black body.

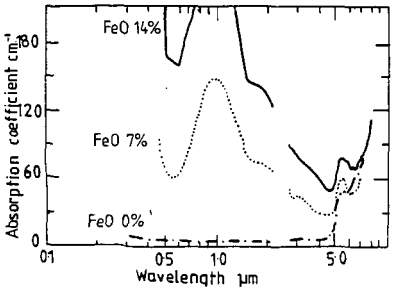

Figure 4. The absorption spectra at room temperature for slags containing FeO_x + CaO + SiO_2.

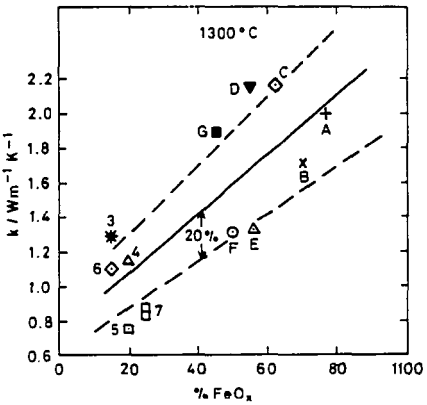

Figure 5. The thermal conductivity of slags of the system FeO_x + CaO + SiO_2 as a function of the FeO_x content. The letters and numerals refer to the specimen numbers (14).

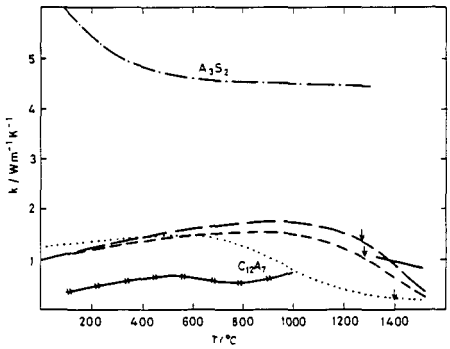

Figure 6. Thermal conductivities of slags from the system, CaO + Al_2O_3 + SiO_2, —·—·—, Kingery for $3Al_2O_3.2SiO_2$; ———, Ogino et al ; Susa et al, ..., 50% CaO + 50% Al_2O_3; — — — — —, 40% CaO + 40% SiO_2 + 20% Al_2O_3; ——— ———, 25½ CaO + 60% SiO_2 + 15% Al_2O_3; —||—, Osinovskikh; ↓, T_{liq}.

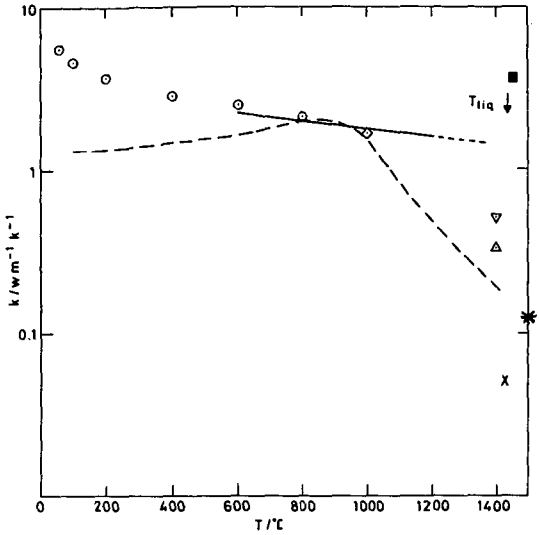

Figure 7. The thermal conductivity of CaF_2 and CaF_2- based slags; CaF_2; *, Powell; ⊙, Charvat; ——— - - -, Taylor; x, Nagata; ■, Ogino; ▽, Mitchell; CaF_2-based slags, - - - -, Susa et al; △, Mitchell.

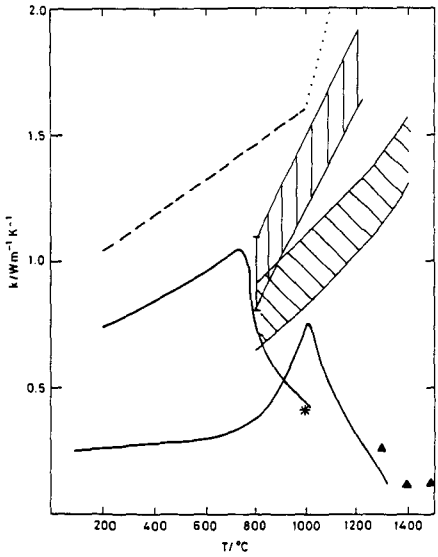

Figure 8. Thermal conductivity of continuous-casting slags; - - - - ; •••• Taylor, and Taylor and Edwards; ——, Nagata; ▥, Ohmiya; *, average k_c value, Ohmiya; ▲, Powell.

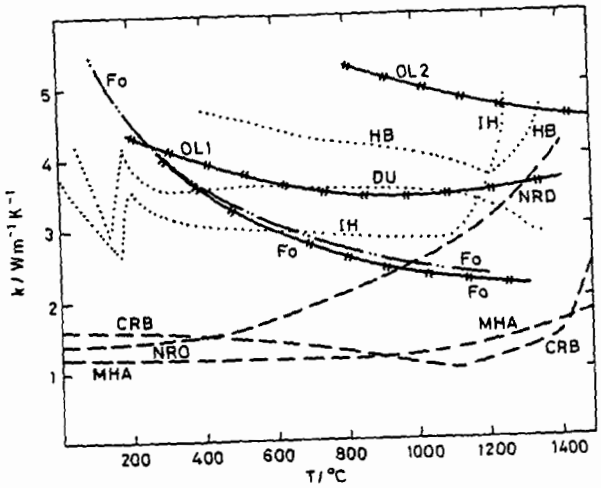

Figure 9. The thermal conductivity of rocks and minerals; — — —, Murase; —·—, Schatz; — ··— , Kingery; ....., Kawada; the letters refer to samples.

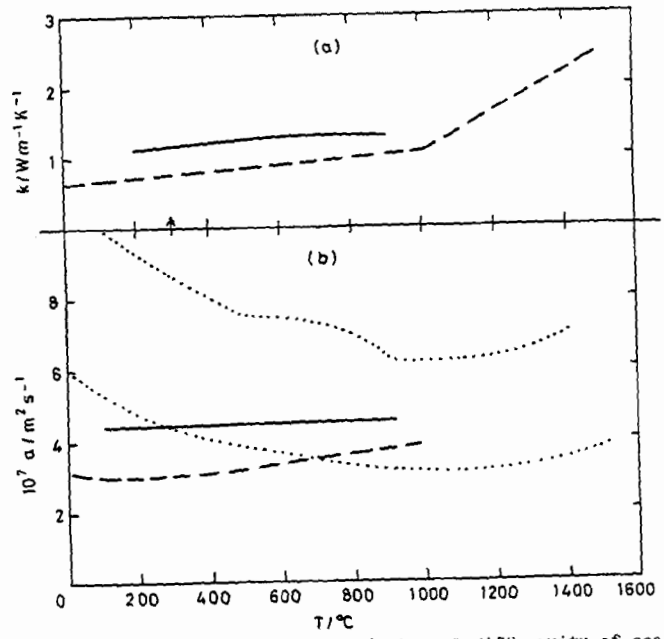

Figure 10. (a) Thermal conductivity (b) thermal diffusivity of coal slags; ——, Taylor; — — —, Vargoftik; ....., upper and lower limits of a values reported by Gibby and Bates.

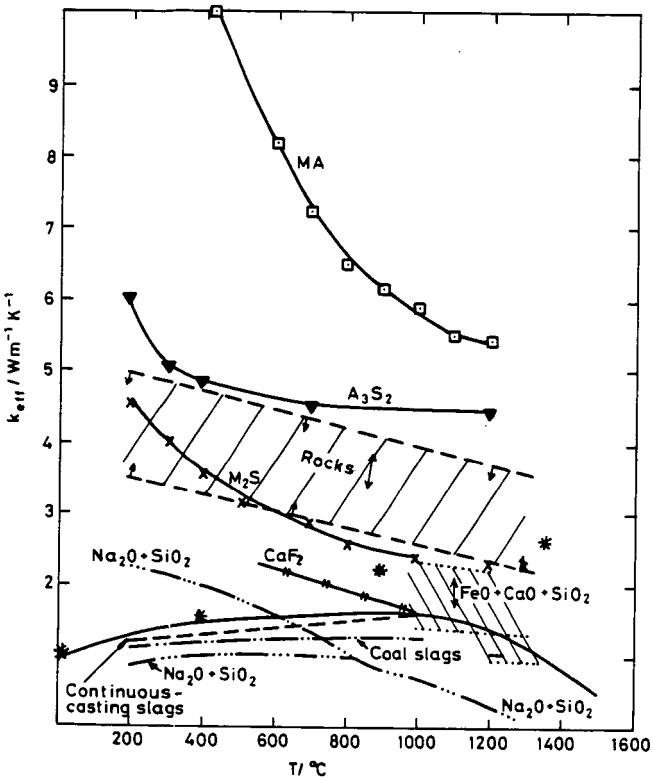

Figure 11. The thermal conductivity of various slag systems; ____, $MgO.Al_2O_3$; _____., $3Al_2O_3.2SiO_2$; _____, $2MgO.SiO_2$; , upper and lower limits for data on rocks; _____, CaF_2; , data for the FeO_x + CaO + SiO_2 system; __ ... __, Na_2O + SiO_2 system; ____, CaO + SiO_2 + Al_2O_3 system; ___ ___ ___, continuous casting powders; __ .. __, coal slags; *, k_c (glass).

SOLID-LIQUID-VAPOR INTERACTIONS IN ALKALI-RICH COAL SLAGS

L. P. Cook and J. W. Hastie

National Bureau of Standards, Washington, D.C. 20234

I. INTRODUCTION

Sodium and potassium are important constituents of the clay minerals found in most coals. As the coal is combusted these metals may be vaporized, transported and reabsorbed by slag in the cooler portions of the system, leading to the production of slags having concentrations of alkalies several times that of the primary mineral matter. Without doubt the most marked concentrations occur in slags from magnetohydrodynamic generators, where potassium is deliberately added to the combustion gases to enhance electrical conductivity of the plasma. Slags from MHD generators have K_2O concentrations approaching 20 wt%.

The corrosive effects of these high alkali slags on ceramic components of combustion systems are well known. Corrosion arises from the fact that such slags are good solvents for a wide range of materials. Furthermore, when many ceramics come into contact with high alkali slags, destructive reactions producing new solids may occur. For example, alumina, a widely used refractory, may react to produce $NaAlSiO_4$, $KAlSiO_4$ or beta alumina, depending upon the activities of silica and the alkalies. In most situations, reactions of this type would result in loss of structural integrity of the ceramic.

For these and related reasons, there is need for detailed knowledge of the physical chemistry of high alkali coal ash - derived slags. NBS has an ongoing theoretical and experimental program to systematically determine the nature of solid-liquid-vapor equilibria in high alkali coal slags. Given the wide variability of coal slag, this necessitates a close interaction between theory and experiment, if significant progress is to be made.

Experimentally, three principal methods are being utilized. Application of the high temperature quenching method, with examination of results by x-ray diffraction and electron microprobe methods, is facilitated by the fact that most silicate melts quench readily to glasses, preserving the textural and chemical relationships which prevailed under equilibrium at high temperatures. On the other hand, the relatively slow kinetics makes necessary great care in the determination of alkali vapor pressures by the Knudsen effusion/mass spectrometric method. Nonetheless the technique has been used successfully at NBS in determining vapor pressures by closely correlating effusion experiments with on-going quench experiments. Similarly, the application of the third principal experimental method, high temperature differential thermal-thermogravimetric analysis, requires a degree of caution.

There has long been interest in the development of models for the prediction of coal slag phase equilibria. While silicate phase diagrams of limited compositional range have been successfully modeled, a single model for accurate prediction of slag phase equilibra in general will require that considerably more progress be made not only in our understanding of the structural chemistry of slags but also in the availability of thermochemical data needed for such models. Progress to date is related to the realization that treatment of silicate liquids as polymerized melts may be necessary for very precise prediction of phase relationships. Also important is the discovery that alkali activities can be modeled over a wide range of compositions by treating slags as composed of mixtures of complex mineral melts such as $CaAl_2Si_2O_8$, $KAlSiO_4$, $NaAlSi_3O_8$, etc.

Thus coal slags, while not chemically ideal mixtures of the oxide components, appear to be much more ideal with respect to a choice of more complex components.

II. PHASE EQUILIBRIA IN COAL SLAGS

(A) Coal Slag As A 7-Component System

The variability of coal ash composition is directly related to variations in the proportions of mineral impurities such as SiO_2, $CaCO_3$, $CaMg(CO_3)_2$, $CaSO_4 \cdot 2H_2O$, Fe_2O_3, FeS_2, and the clay minerals which comprise a complex group of hydrated alkali aluminosilicates. Coal ashes may vary widely in their contents of iron, calcium and magnesium, but do not vary as greatly in the amount of silica and alumina they contain. In fact, of the 323 coal ash analyses reported in U.S. Bureau of Mines Bull. 567 (1), the great majority have a $SiO_2/(SiO_2+Al_2O_3)$ mole ratio between .67 and .80, with a well defined maximum near .75 (2). The bulk chemistry of the ash is related to the conditions of formation of the coal. In general lignites and subbituminous coals of the western U.S.A. are high in calcium while bituminous coals of the eastern U.S.A. contain more iron. Table 1 gives typical analyses for ashes from these coals, and includes for comparison an analysis of coal slag from a magnetohydrodynamic generator. From this table, it can be seen that, in general, coal slag must be regarded as a seven component substance, if minor constituents such as TiO_2 and P_2O_5 are ignored and if sulfur is assumed to vaporize at high temperature.

Table 1. Typical Coal Ash Analyses (wt %).

	Montana Coal[3]	Illinois Coal[3]	MHD Slag[4]
K_2O	0.4	1.4	20.2
Na_2O	0.4	1.6	0.5
CaO	11.9	8.2	3.9
MgO	3.9	0.8	1.1
Al_2O_3	21.4	16.2	12.4
Fe_2O_3	10.0	23.7	14.7
SiO_2	42.5	37.5	48.3
TiO_2	0.8	0.8	0.5
P_2O_5	0.3	0.1	-
SO_3	8.1	8.9	0.2

To account for the fact that Fe_2O_3 reduces partially to FeO with increasing temperature would require an added component. However this may be reduced again to seven if the oxygen partial pressure is included as an intensive variable along with temperature and composition. By doing this the need to specify both FeO and Fe_2O_3 in defining the bulk composition is eliminated; these are replaced by FeO_x, where x is determined by the oxygen partial pressure.

(B) Representation of Solid-Liquid-Vapor Equilibria

Ready visualization of a range of phenomena is one of the attributes making phase diagrams indispensable in understanding the chemistry of heterogeneous systems. However, although advanced multidimensional projective methods have been derived for the representation of n-component systems (5), these do not

in general lead to easily visualized diagrams. Thus for the seven component coal slag system, alternative methods must be used.

It is useful to subdivide the slag system into smaller systems. The system Al_2O_3-SiO_2 is perhaps the most fundamental system for all slags, and to this one may think of adding progressively combinations of the alkalies and CaO, MgO and FeO_x, until the desired degree of complexity is reached. Constituent systems making up the slag system are summarized in Table 2. Data are available for parts of many of these systems (6-10), but as the number of components increases, data become progressively fewer.

At NBS, experimental work is presently concentrating on the system K_2O-CaO-Al_2O_3-SiO_2. This along with K_2O-FeO_x-Al_2O_3-SiO_2 and K_2O-MgO-Al_2O_3-SiO_2, forms the basis for modeling potassium-rich slags. The approach has been to establish subsolidus equilibria (Figure 1) and then to combine these data with literature thermochemical data via solid state reactions of the type

$$A(s) + B(s) \leftrightarrow C(s) + D(s) + 2K(g) + 1/2\ O_2(g)$$

At the temperature of minimum melting, such calculations provide direct links between the phase diagram and the measurements of potassium vapor pressure which are independent of any solution model (Figure 2). This approach aides greatly in the determination of an internally consistent set of thermochemical data.

As the systems investigated become more complex (more components), other techniques may be used to reduce the number of variables, so that results can be portrayed graphically. For example, in principle phase equilibria at 1 atm in the system K_2O-CaO-FeO_x-Al_2O_3-SiO_2 could be portrayed in three dimensions graphically as a tetrahedral diagram at constant μ_{K_2O} or P_{K_2O}, T and P_{O_2}. Another way of reducing the dimensionality of the representational problem is to deal with saturation surfaces - this is actually a form of projection. For example by considering the equilibria in which Al_2O_3 participated as a phase, the need to use Al_2O_3 as a representational component would be eliminated.

(C) Role of Polymerization Theory

One of the major problems in prediction and calculation of phase equilibria is the formulation of accurate expressions for the free energy of mixing of silicate melts. Relatively few calorimetric measurements are available, and hence the importance of sound methods of estimation and prediction of mixing data to within the required degree of accuracy. Polymer theory, extended in the 1960's to include silicate melts by Masson (11) and others holds promise. It is perhaps the only general theory for silicate melts which deals quantitatively with the problem of melt structure. This has been used, with a surprising degree of success, to calculate phase equilibria in binary oxide systems (12,13). Preliminary calculations on multicomponent slags have shown that polymer theory, when treated in a quasichemical fashion, is highly flexible, and can accommodate seven component liquid immiscibility by making relatively few estimates and assumptions (Figure 3). However, attempts to fit liquidus surfaces in the system K_2O-CaO-Al_2O_3-SiO_2 have met with only partial success. Further applications and extensions of polymer theory in this quaternary system are hampered by a lack of experimental data, and an attempt is being made to rectify this situation.

Table 2. Breakdown of Lower Order Systems Comprising 7-Component Coal Slag System.

		(+CaO)	(+MgO)	(+FeO_x)	(+CaO +MgO)	(+CaO +FeO_x)	(+MgO +FeO_x)	(+CaO +MgO +FeO_x)
	Al_2O_3-SiO_2 BASE SYSTEM	CaO-Al_2O_3-SiO_2	MgO-Al_2O_3-SiO_2	FeO_x-Al_2O_3-SiO_2	CaO-MgO-Al_2O_3 -SiO_2	CaO-FeO_x-Al_2O_3 -SiO_2	MgO-FeO_x-Al_2O_3 -SiO_2	CaO-MgO-FeO_x -Al_2O_3-SiO_2
(+K_2O)	K_2O-Al_2O_3-SiO_2	K_2O-CaO-Al_2O_3 -SiO_2	K_2O-MgO-Al_2O_3 -SiO_2	K_2O-FeO_x-Al_2O_3 -SiO_2	K_2O-CaO-MgO -Al_2O_3-SiO_2	K_2O-CaO-FeO_x -Al_2O_3-SiO_2	K_2O-MgO-FeO_x -Al_2O_3-SiO_2	K_2O-CaO-MgO -FeO_x-Al_2O_3-SiO_2
(+Na_2O)	Na_2O-Al_2O_3-SiO_2	Na_2O-CaO-Al_2O_3 -SiO_2	Na_2O-MgO-Al_2O_3 -SiO_2	Na_2O-FeO_x-Al_2O_3 -SiO_2	Na_2O-CaO-MgO -Al_2O_3-SiO_2	Na_2O-CaO-FeO_x -Al_2O_3-SiO_2	Na_2O-MgO-FeO_x -Al_2O_3-SiO_2	Na_2O-CaO-MgO -FeO_x-Al_2O_3-SiO_2
(+K_2O +Na_2O)	K_2O-Na_2O-Al_2O_3 -SiO_2	K_2O-Na_2O-CaO -Al_2O_3-SiO_2	K_2O-Na_2O-MgO -Al_2O_3-SiO_2	K_2O-Na_2O-FeO_x -Al_2O_3-SiO_2	K_2O-Na_2O-CaO -MgO-Al_2O_3-SiO_2	K_2O-Na_2O-CaO -FeO_x-Al_2O_3 -SiO_2	K_2O-Na_2O-MgO -FeO_x-Al_2O_3 -SiO_2	K_2O-Na_2O-CaO-MgO -FeO_x-Al_2O_3-SiO_2 COAL SLAG SYSTEM

III. SOLUTION MODEL FOR THE PREDICTION OF ALKALI VAPOR PRESSURES

(A) Basis of the Model

The model employed for prediction of vapor pressures in multicomponent coal slags has been outlined in (14). Briefly, large negative deviations from ideal thermodynamic activity behavior are attributed to the formation of complex liquids and solids (actual components) such as K_2SiO_3, $KAlSiO_4$, etc. The free energies of formation (ΔG_f) are either known or can be estimated for these liquids and solids. By minimizing the total system free energy, one can calculate the equilibrium composition with respect to these components. Thus, for instance the mole fraction of K_2O present ($X^*_{[K_2O]}$) in equilibrium with K_2SiO_3, and other complex liquids (and solids) containing K_2O, is known. As has been shown previously for the ternary systems, the component activities can, to a good approximation, be equated to these mole fraction quantities (15). From this assumption it also follows that potassium partial pressures can be obtained from the relationship

$$P_K = \left\{2 \cdot X^*_{[K_2O]} K_p\right\}^{0.4},$$

where K_p is the stoichiometric dissociation constant for pure K_2O (liquid or solid) to K and O_2. In the following discussion the model is tested by comparing predicted P_K data determined in this manner with experimental values. Thermodynamic activities and phase compositions were also calculated using this model. The experimental K-pressure data were obtained by Knudsen effusion mass spectrometry as discussed in detail elsewhere (16).

(B) Method of Calculation

The SOLGASMIX computer program (17) used for calculation of the equilibrium composition and hence activities utilizes a data base of the type given in (14). The coefficients to the ΔG_f equation were obtained by fitting ΔG_f vs T data available in JANAF (18), Robie et al (19), Barin and Knacke (20), Rein and Chipman (21) and Kelley (22). In some cases no literature data were available and we estimated functions in the manner described earlier (16). Many of the compounds used in the calculation are mineral phases such as mullite ($Al_6Si_2O_{13}$), kaliophilite ($KAlSiO_4$), leucite ($KAlSi_2O_6$), feldspar ($KAlSi_3O_8$), and gehlenite ($Ca_2Al_2SiO_7$).

(C) Application to the K_2O-CaO-Al_2O_3-SiO_2 System

Figure 4 shows results of calculations for potassium pressures made using the model. As can be seen these agree with experimental results within limits of experimental error over a wide range of temperature. The calculations also indicate temperatures of precipitation of various solids in the quaternary system. These predictions are being checked by experiment. Other potassium pressure calculations (not shown) show similarly good agreement with experiment in the system K_2O-CaO-Al_2O_3-SiO_2.

IV. SUMMARY

An integrated experimental/theoretical approach to the problem of non-condensed (solid-liquid-vapor) phase equilibria in multicomponent coal slags has been outlined, including methods for the presentation of results. This relies upon prediction as an important tool in planning experimental work. Theory in turn benefits from experimental feedback, resulting in a continual evolution of models. Hopefully this will lead to generalized solution models capable of predicting slag phase equilibria with a high degree of accuracy.

V. REFERENCES

1. Selvig, W. A. and Gibson, F. H.: 1956, Bureau of Mines Bull. 567.
2. Cook, L. P.: 1978, Proc. 17th Symposium on Engineering Aspects of Magnetohydrodynamics, Stanford Univ., Stanford, Calif., p. C.1.2-C.1.6.
3. Petrick, M. and Shumyatsky, B. Ya., editors: "Open-Cycle Magnetohydrodynamic Electrical Power Generation" (Argonne, Illinois: Argonne National Lab.), p. 420-421.
4. Long, W.: 1978, Pers. Commun., Univ. Tenn. Space Inst.
5. Palatink, L. S. and Landau, A. I.: 1964, "Phase Equilibria in Multicomponent Systems" (New York: Holt, Rinehart and Winston).
6. Levin, E. M., Robbins, C. R. and McMurdie, H. F.: 1964, "Phase Diagrams for Ceramists" (Columbus: The American Ceramic Society).
7. Levin, E. M., Robbins, C. R. and McMurdie, H. F.: 1969, "Phase Diagrams for Ceramists, 1969 Supplement" (Columbus: The American Ceramic Society).
8. Levin, E. M., Robbins, C. R. and McMurdie, H. F.: 1975, "Phase Diagrams for Ceramists, 1975 Supplement" (Columbus: The American Ceramic Society).
9. Roth, R. S., Negas, T. and Cook, L. P.: 1981, "Phase Diagrams for Ceramists, Volume IV" (Columbus: The American Ceramic Society).
10. Roth, R. S., Negas, T. and Cook, L. P.: 1983, "Phase Diagrams for Ceramists, Volume V" (Columbus: The American Ceramic Society).
11. Masson, C. K., Smith, I. B. and Whiteway, S. G.: 1970, Canad. J. Chem., 48 1456.
12. Fraser, D. G., editor: 1976, "Thermodynamics in Geology" (Oxford, England: NATO Adv. Study Inst.).
13. Lin, P. L. and Pelton, A. D.: 1979, Metall. Trans. 10B, 667.
14. Hastie, J. W., Bonnell, D. W. and Plante, E. R.: 1983, Proc. Annual Meeting of Electrochem. Society, San Francisco, Calif.
15. Hastie, J. W., Horton, W. S., Plante, E. R., and Bonnell, D. W.: Thermodynamic Models of Alkali Vapor Transport in Silicate Systems, IUPAC Conf., Chemistry of Materials at High Temperatures, Harwell, U.K., August 1981; High Temp. High Press, in press.
16. Hastie, J. W., Plante, E. R. and Bonnell, D. W.: 1982, Alkali Vapor Transport in Coal Conversion and Combustion Systems. ACS Symp. Series, 179, p. 543-600, Gole, J. L., and Stwalley, W. C., eds. Metal Bonding and Interactions in High Temperature Systems with Emphasis on Alkali Metals (see also NBSIR 81-2279).
17. Eriksson, G.: 1975, Chemica Scripta, 8, p. 100.
18. JANAF: 1971, Joint Army, Navy, Air Force Thermochemical Tables, 2nd Ed. NSRDS-NBS 37. See also later supplements for 1971-1981.
19. Robie, R. A., Hemingway, B. S., Fisher, J. R.: 1979, Thermodynamic Properties of Minerals and Related Substances at 298.15 K and 1 Bar (10^5 Pascals) Pressure and at Higher Temperatures, Geol. Survey Bull. 1452 (Washington, D.C.: U.S. Govt. Printing Office).
20. Barin, I. and Knacke, O.: 1973, "Thermochemical Properties of Inorganic Substances" (New York: Springer Verlag).
21. Rein, R. H. and Chipman, J.: 1965, Trans. Metall. Soc. AIME, 233, p. 415.
22. Kelley, K. K.: 1962, U.S. Bur. Mines Rep. Invest., No. 5901.
23. Cook, L. P.: 1980: Proc. Seventh International Conference on MHD Electrical Power Generation, MIT, Cambridge, Mass., p. 212-219.

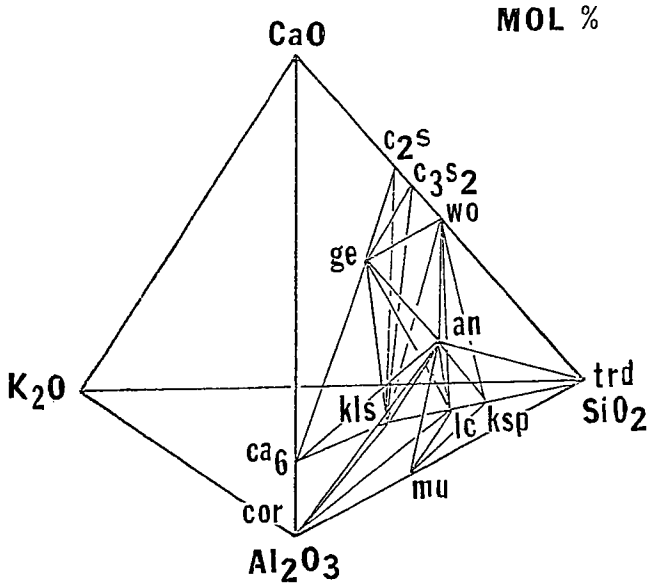

Figure 1. Experimentally determined subsolidus phase relations in the system K_2O-CaO-Al_2O_3-SiO_2.

c_2s = Ca_2SiO_4	trd = SiO_2
c_3s_2 = $Ca_3Si_2O_7$	ksp = $KAlSi_3O_8$
wo = $CaSiO_3$	lc = $KAlSi_2O_6$
ge = $Ca_2Al_2SiO_7$	kls = $KAlSiO_4$
an = $CaAl_2Si_2O_8$	mu = $3Al_2O_3 \cdot 2SiO_2$
ca_6 = $CaAl_{12}O_{19}$	cor = Al_2O_3

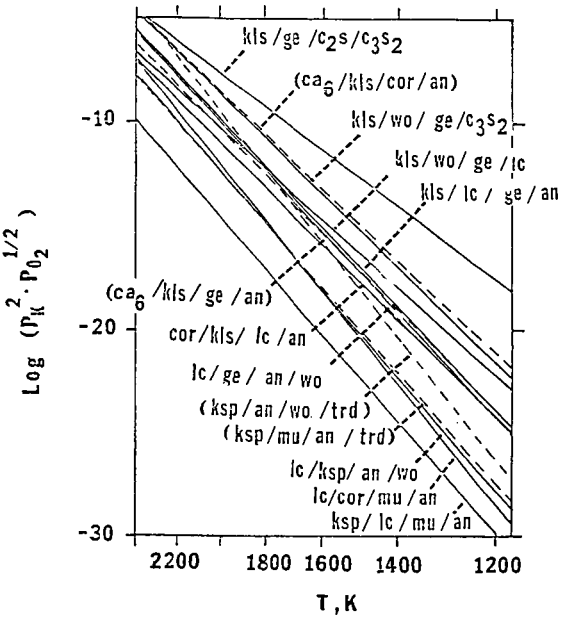

Figure 2. Calculated potassia pressures for solid assemblages in K_2O-CaO-Al_2O_3-SiO_2 (see Figure 1). Thermochemical data used were from (19). Equilibria are metastable above the minimum melting temperatures.

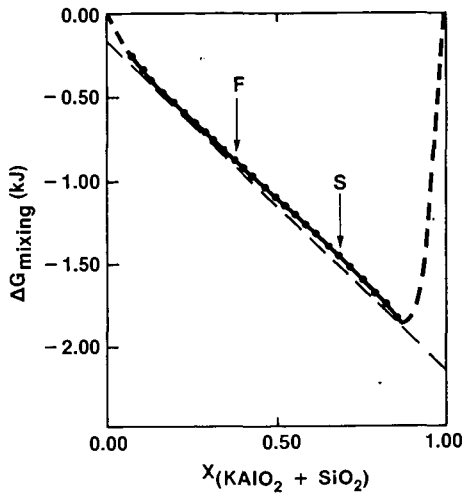

Figure 3. Calculated free energy of mixing along a compositional vector in the system K_2O-CaO-MgO-FeO_x-Al_2O_3-SiO_2 passing through experimentally determined compositions of immiscible melts (F and S). Calculations were made using the quasi-chemical melt polymerization theory (23). The compositions of predicted and observed immiscible melts can be made to agree reasonably well by adjustments in polymerization equilibrium constants and in the ratio $Fe^{+3}/(Fe^{+3} + Fe^{+2})$.

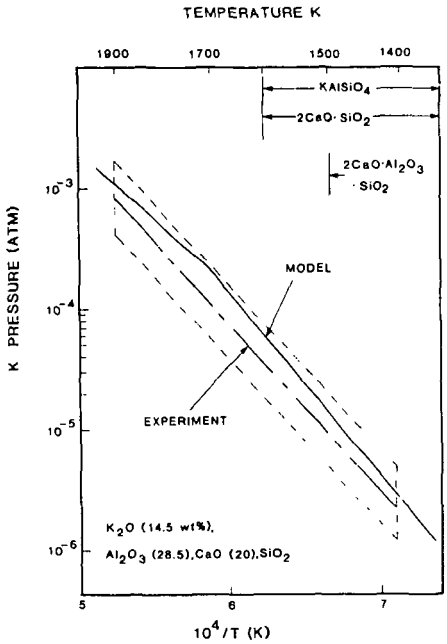

Figure 4. Comparison of ideal mixing of complex components solution model (solid curve) and experimental (broken curve) K-pressure data as a function of reciprocal temperature, for a composition in the K_2O-CaO-Al_2O_3-SiO_2 system. Compounds listed are solid precipitates formed over the temperature interval indicated.

OVERVIEW OF COAL ASH DEPOSITION IN BOILERS

R. W. Borio and A. A. Levasseur

COMBUSTION ENGINEERING, INC.
1000 Prospect Hill Road, Windsor, CT 06095

INTRODUCTION

The management of coal ash in utility boilers continues to be one of the most important fuel property considerations in the design and operation of commercial boilers. The behavior of mineral matter in coal can significantly influence furnace sizing, heat transfer surface placement, and convection pass tube spacing. Ironically, many of the more reactive, low rank U. S. coals must have larger furnaces than the less reactive higher rank coals. This is strictly a requirement based on the mineral matter behavior; Figure 1 illustrates this point. Given the same mineral matter behavior the more reactive, lower rank coals would require less residence time and therefore smaller furnace volumes than the less reactive, higher rank coals.

Although pulverized coal has been fired for more than 50 years and much is known about combustion behavior there are still a number of boilers experiencing operational problems from coal ash effects. Ash-related problems are one of the primary causes of unscheduled outages, unit derating and unavailability. Because of variability in a given coal seam and since many boiler operators may experience changes in their coal supply during the life of a boiler, operational problems caused by changes in coal ash properties can significantly affect boiler performance. Not only must the initial boiler design be correctly determined based on the specification coal but reliable judgements must be made regarding the suitability of other candidate coals and their effect on operation during the lifetime of the boiler.

The increased emphasis on coal usage in this country and, indeed, the significant effort underway to consider coal water mixtures as possible oil substitutes in oil-designed boilers underscores the need to improve the prediction of mineral matter behavior in a boiler environment.

Coal is a very heterogeneous, complex material which produces heterogeneous, complex products during combustion. Since, during pulverized coal combustion, coal particles of various organic and mineral matter compositions can behave in completely different manners, prediction based upon the overall or average composition may be misleading. Like many of the currently-used ASTM coal analyses, the method for determining ash fusibility temperatures was developed when stoker firing was a predominant coal firing technique; the methodologies and conditions employed during many of the ASTM tests reflect this. It is not surprising that the usefulness of some ASTM test results may be limited when used for a pulverized coal firing application. In recent years researchers have developed methodologies for characterizing coal ash behavior that better reflect the fundamental mechanisms controlling behavior and more closely simulate the conditions that exist in a pulverized coal fired boiler.

Clearly there is a need for improved mineral matter behavior predictive techniques. This paper will provide a statement of the ash deposition problem in pulverized coal fired boilers, it will present an assessment of the older, traditional methods for predicting mineral matter behavior and it will address some of the newer techniques that have been suggested as better ways of characterizing coal ash behavior. Additionally some areas of uncertainty will be identified as requiring the development of better predictive techniques.

STATEMENT OF THE PROBLEM

The presence of ash deposits and flyash can create the following problems in a boiler:

1. Reduced heat transfer
2. Impedance of gas flow
3. Physical damage to pressure parts
4. Corrosion of pressure parts
5. Erosion of pressure parts

These problems can result in reduced generating capacity, unscheduled outages, reduced availability, and costly modifications.

Ash which deposits on boiler walls in the radiant section of a furnace is generally referred to as slagging. Ash deposition on convection tube sections downstream of the furnace radiant zone is typically referred to as fouling. Ash slagging and fouling can result in problems listed in items 1 through 4; item 5, erosion, is the result of impingement of abrasive ash on pressure parts. Often coal ash deposit effects are inter-related. For example, slagging will restrict waterwall heat absorption changing the temperature distribution in the boiler which in turn influences the nature and quantity of ash deposition in downstream convective sections. Ash deposits accumulated on convection tubes can reduce the cross-sectional flow area increasing fan requirements and also creating higher local gas velocities which accelerates flyash erosion. In situ deposit reactions can produce liquid phase components which are instrumental in tube corrosion.

One of the most common manifestations of a deposition problem is reduced heat transfer in the radiant zone of a furnace. Decreased heat transfer due to a reduction in surface absorptivity is a result of the combination of radiative properties of the deposit (emissivity/absorptivity) and thermal resistance (conductivity) of a deposit. Thermal resistance (thermal conductivity and deposit overall thickness) is usually more significant because of its effect on absorbing surface temperature.

Previous work has indicated that the physical state of the deposit can have a significant effect on the radiative properties, specifically molten deposits show higher emissivities/absorptivities than sintered or powdery deposits (Ref. 1). Although thin, molten deposits are less troublesome from a heat transfer aspect than thick, sintered deposits, molten deposits are usually more difficult to remove and cause frozen deposits to collect in the lower reaches of the furnace; physical removal then becomes a problem for the wall blowers.

Impedance to gas flow is the result of heavy fouling on tubes in the convective section. Problems of this type are most likely to occur with coals having high sodium contents, usually found in low rank coal deposits in Western U.S. seams. Hard, bonded deposits can occur which are resistant to removal by the retract soot-blowers.

Physical damage to pressure parts can occur if large deposits have accumulated in the upper furnace and proceed to become dislodged or blown off and drop onto the slopes of the lower furnace. Such deposits are usually characterized by their relatively high bonding strengths and their heavily sintered structure.

Fireside corrosion can occur on both waterwall and superheater tube surfaces. Normal sulfates and pyrosulfates are frequently the cause of waterwall corrosion, although reducing conditions can also cause depletion of protective oxide coatings on tube surfaces. On higher temperature metal surfaces, (superheaters/reheaters) alkali-iron-trisulfates are often the cause of corrosion. Chlorine can also be a contributing factor toward superheater metal corrosion. While exact mechanisms can be argued there have been examples of both liquid phase and gas phase corrosion when chlorides have been present (Ref. 2).

Erosion of convective pass tubes, while not a function of deposits, is caused by the abrasive components in flyash. Flyash size and shape, ash particle composition and concentration, and local gas velocities play important roles concerning erosion phenomenon. Recent work has shown that quartz particles above a certain particle size are very influential in the erosion process and that furnace temperature history plays an important role in determining erosive characteristics of the particles (Ref. 3 & 4).

FUNDAMENTAL CONSIDERATIONS IN ASH DEPOSITION

The coal ash deposition process is extremely complex and involves numerous aspects of coal combustion and mineral transformation/reaction. The following all play a role in the formation of ash and the depositon process.

- Coal Organic Properties
- Coal Mineral Matter Properties
- Combustion Kinetics
- Mineral Transformation and Decomposition
- Fluid Dynamics
- Ash Transport Phenomena
- Vaporization and Condensation of Ash Species
- Deposit Chemistry - Specie Migration and Reaction
- Heat Transfer To and From the Deposit

Despite considerable research in these areas, there are many gaps in our fundamental understanding of the mechanisms responsible for mineral matter behavior. Although substantial knowledge exists concerning the deposition process, the complexity of the subject does not allow detailed discussion here. However, the importance of furnace operating conditions on the combined results of each of the above areas must be stressed. For a given coal composition, furnace temperatures and residence times generally dictate the physical and chemical transformations which occur. The ash formation process is primarily dependent on the time/temperature history of the coal particle. The resultant physical properties of a given ash particle generally determine whether it will adhere to heat transfer surfaces. Local stoichiometries can also influence the transformation process and thereby the physical characteristics of ash particles; iron-bearing particles are a prime example of this.

Aerodynamics can play a role in the ash deposition process in all furnaces regardless of the type of firing; recent interest in microfine grinding of coal is testimony to this fact. It has been postulated that smaller ash particles will follow gas streamlines and be less likely to strike heat transfer surfaces. This is a logical hypothesis for those ash particles that cause deposition due to an impact mechanism. In addition to particle size, particle density and shape also affect aerodynamic behavior. Molten, spherical particles will be less likely to follow gas streamlines than angular or irregular particles of the same mass due to the difference in drag forces.

Most coal ash will result in deposits of increasing severity with increasing gas temperature. This is not a linear relationship, as illustrated in Figure 2, but rather shows a progressively more severe ash deposit condition with increasing gas temperature (Ref. 5). Boilers are normally designed so that cleanable, sintered deposits will be formed. This is a reasonable compromise between a very large, economically uncompetitive boiler that may produce very dry, dusty deposits and a very small, highly loaded boiler that would produce molten, running ash deposits.

The key governing factor, then, is determining how small a furnace can be, for a given MW output, and still result in deposits that are cleanable with conventional sootblowing equipment.

Because of the complexity of the ash formation and ash deposition process, it seems logical to deal first with those key coal constituents most responsible for ash deposition. The iron and sodium contents of an ash have typically been considered key constituents. Techniques have been developed to determine how these key constituents are contained in the coal, i.e., the particular mineral forms that are present or the grain size of the constituent in question. Obviously the remainder of the mineral matter has an effect, but depending on the concentration and form in which iron and/or sodium constituents are present, the remaining mineral matter often has second order effects.

As previously discussed, ash formation and the resulting ash size distribution is extremely complex and is dependent on several factors including initial coal size, coal burning characteristics, mineral content, mineral grain size, volatile ash species, melting behavior of the mineral matter, and temperature history of the particle. Generally, coal containing lower melting mineral matter has a greater potential for ash agglomeration as the particle burns and yields fewer ash particles per coal particle which results in coarser ash particles than those of coal with higher melting ash. Obviously things like ash quantity, and mineral grain sizes could influence this hypothesis. The way a coal particle burns may also influence the number of ash particles generated, i.e., a shrinking sphere burning mode may produce a different result from a constant diameter, decreasing density mode of burning; swelling coals may behave differently than non-swelling coals.

In reflecting on the above discussion, it becomes apparent that one cannot completely divorce the predictive techniques employed, from the particular coal burning application. Pulverized coal firing will require a sensitivity to different conditions than stoker firing, or a slagging combustor. Failure to address the specific conditions inherent in each type of firing system will lead to lower resolution in one's predictive abilities than desired.

ASSESSMENT OF TRADITIONAL PREDICTIVE METHODS

ASTM measurements such as ash fusibility (D1857) have formed the basis for traditional ash behavior predictive techniques. These bench-scale tests provide relative information on a fuel; this is used in a comparative fashion with similar data on fuels of known behavior. Unfortunately, the commonly used tests do not always provide sufficient information to permit accurate comparison.

The fusibility temperature measurement technique attempts to recognize the fact that mineral matter is made up of a mixture of compounds each having their own melting point. As a cone of ash is heated some of the compounds melt before others and a mixture of melted and unmelted material results. The structural integrity or deformation of the traditional ash cone changes with increasing temperature as more

of the minerals melt. However, more recent results indicate that significant melting/sintering can occur before initial deformation is observed (Ref. 6). The fact that the time/temperature history of laboratory ash is quite different from conditions experienced in the boiler can result in difference in melting behavior. In addition, the ash used in this technique may not represent the composition of ash deposits that actually stick to the tube surfaces. Often there is a major discrepancy between the composition of as-fired ash and that which is found as deposits (See Table I). This is a major criticism of the ash fusibility temperatures. The discrepancies between fusibility temperature predictions and actual slagging performance is usually greater on ashes that may look reasonably good based on fusibility temperature results. One can usually assume, with reasonable confidence, that the melting temperature of the waterwall deposits will be no higher than ASTM fusibility temperatures; but deposit melting temperatures can be and are often lower than ASTM melting temperatures. This is because selective deposition of lower melting constituents can and does occur; hence there is an enrichment of lower melting material in the deposit.

Ash viscosity measurements suffer similar criticism to the fusibility measurements. These tests are conducted on laboratory ash and on a composite ash sample. Viscosity measurements are less subjective and more definitive than fluid temperature determination for the assessment of ash flow characteristics. However, these measurements reflect the properties of a totally dissolved solution of ash constituents and may not be representative of slag deposit properties in pulverized coal-fired boilers. During pulverized coal firing, a severe problem may already exist before slag deposits reach the fluid/running state. Generally, only a small quantity of liquid phase material exists in deposits and it is the particle-to-particle surface bonding which is most important.

Much use is made of the ash composition which is normally a compilation of the major elements in coal ash expressed as the oxide form. From this compilation of elements, expressed as oxides, judgements are often made based on the quantity of certain key constitutents like iron and sodium. Base/acid ratios are computed and used as indicators of ash behavior; normally lower melting ashes fall in the 0.4 to 0.6 range. It has been shown that base/acid ratios generally correlate with ash softening temperatures, so although base/acid ratios have helped explain why ash softening temperatures varied, it has not improved predictive capabilities in the authors' opinion. Other ratios such as Fe/Ca and Si/Al have been used as indicators of ash deposit behavior. Ratios like these have helped to explain deposit characteristics, but their use as a prime predictive tool is questionable especially since these ratios do not take into account selective deposition nor do they consider the total quantities of the constituents present. An Fe/Ca ratio of 2 could result from 6/3 or 30/15; the latter numbers would generally indicate a far worse situation than the former, but ratios don't show this.

Many slagging and fouling indices are based upon certain ash constituent ratios and corrected using such factors as geographical area, sulfur content, sodium content, etc. One commonly used slagging index uses Base/Acid ratio and sulfur content. Factoring in sulfur content is likely to improve the sensitivity of this index to the influence of pyrite on slagging. (As previously discussed, iron-rich minerals often play an important role in slagging.) However, the use of such "correction" factors is often a crude substitute for more detailed knowledge of the fundamental fuel properties. Another example of this is the use of chlorine content in a coal as a fouling index. This can be true if the chlorine is present as NaCl thereby indicating the concentration of sodium which is in an active form and that will, in fact, cause the fouling. Chlorine present in other forms may or may not adversely affect fouling.

Sintering strength tests have been used as an indication of fouling potential. Assuming that correct ash compositions have been represented (which is less of a problem in the convection section than in the radiant section) worthwhile information may be obtained relative to a time/temperature vs. bonding strength relationship. In order for sintering tests to accurately predict actual behavior it is necessary that tests be conducted with ash produced under representative furnace conditions (time-temperature history). Fouling behavior is often greatly influenced by sodium reactions. Sodium which vaporizes in the furnace can condense in downstream convection sections thereby concentrating on flyash surfaces. Particle surface reactions are primarily responsible for convection deposit bonding.

In summary, traditional methods for prediction ash deposit characteristics are heavily based upon ash chemistry. These convectional analyses do not provide definitive information concerning the mineral forms present in the coals and the distribution of inorganic species within the coal matrix. Such information can be extremely important in extrapolating previous experience, since the nature in which the inorganic constituents are contained in the coal can be the determining factor in their behavior during the ash deposition process.

ASSESSMENT OF NEW PREDICTIVE TECHNIQUES

Generally speaking the newer bench scale predictive techniques are far more sensitive to the conditions that exist in commercial furnaces than the older predictive methods. Selective deposition, for example, has been recognized as a phenomenon which cannot be ignored. More attention is being paid to fundamentals of the ash formation and deposition processes. New tools, such as Scanning Electron Microscopy (SEM), are being considered as ways to improve predictive capabilities. Other, more specialized bench scale apparatuses are being developed to simulate important aspects of commercial conditions and provide quantitative information on parameters that influence bonding strength.

Recent work has shown that pulverized coal, if separated by gravity fractionation, can yield important information relative to slagging potential due to the iron content. (Ref. 6, 7). Results of this work have shown that the percentage of iron in the heavy fractions correlates very well to the slagging behavior in commercial boilers. (See Figure 3). This technique appears to identify the proportion of relatively pure pyrites particles that are generated in the pulverized coal feed and that are capable of melting at relatively low temperatures and that would account for enrichment of iron in lower furnace waterwall deposits.

A method for measuring active alkalies has been developed as a means for improved prediction of fouling potential (Ref. 8). Previous wisdom held that fouling potential was directly related to the total sodium content. Much of this early work was done on low rank coals in which case it was not uncommon for all of the alkalies to be present as an active sodium form (Ref. 9). However, there were many occasions where the fouling potential was not adequately predicted by the total sodium content. (Table II provides some examples of anomalous fouling behavior.) The mechanism postulated for sodium-related fouling was one of a vaporization/condensation mechanism. Simple forms of sodium compounds resulted in the vaporization of sodium in the radiant zone of the furnace where peak temperatures are generated. Subsequent condensation of the sodium on the relatively cool tube surfaces effected a process for deposition of sodium. Sodium is a known, effective fluxing agent that can create hard, bonded deposits. The referenced method relied on the use of weak acid to preferentially leach out sodium from simple compounds like NaCl and/or organically-bound alkali as would be present in many of the lower rank coals. This method gives results that correlate well with field performance on coals having significant sodium contents (See Table II).

The use of new analytical techniques promises to give results that allow mineral matter to be identified according to composition, mineral form, distribution within the coal matrix, and grain size.

Techniques such as computer-controlled scanning electron microscopy (CCSCM) transmission electron microscopy (STEM), X-ray diffracton can be used to characterize these properties on individual particle by particle basis. New spectroscopies such as extended X-ray absorption of fine structure spectroscopy (EXAFS), and electron energy loss spectroscope, (EELS) are capable of determining electronic bonding structure and local atomic environment for organically associated inorganics like calcium, sodium and sulfur. Other new techniques such as Fourier transform infrared spectroscopy (FTIR), electron microprobe, electron spectroscopy for chemical analysis (ESCA), etc. all provide methods of improving present capabilities. By development and application of these techniques a much better fundamental assessment of coal mineral matter behavior is possible. The authors believe these results, coupled with those of other existing methods, can make a significant improvement to predictive capabilities.

AREAS OF UNCERTAINTY

Prediction of ash deposit characteristics based solely on bench-scale fuel properties always requires substantial judgement and allows only a certain level of confidence. As discussed, the ash deposition process is so complex that detailed modelling of commercial systems based on fundamental data is presently unrealistic. However, current techniques can provide relative data which in most cases is sufficient to make accurate assessment of slagging and fouling potentials relative to other fuels.

There remains many areas of uncertainty where experienced judgements must fill the gap between good laboratory results/predictions and boiler design decisions. One of these areas concerns the extent of deposit coverage in a boiler. Though the fuels researcher may adequately characterize a given coal ash in terms of its potential deposit effects, he is often at a loss to adequately describe the extent of coverage of deposits in the boiler. It is necessary to accurately describe furnace conditions in order to assess resulting deposits in particular boiler regions. Though some good work is underway in this area, the question of bonding strength and cleanability remains a problem as far as its prediction from bench scale tests. Though some good correlations have been developed between iron content of heavy gravity fractions and slagging, there does not exist a bench scale technique that can simulate what the ash deposit composition shall be when burned in a commercial boiler.

It is possible to increase the level of confidence for prediction of deposit effects by conducting pilot-scale combustion studies in test rigs which more closely simulate the conditions present in commercial boilers. Combustion testing allows evaluation of the ash formation and deposition process and permits detailed characterization of deposits generated. Results can allow determination of deposit characteristics as a function of fundamental boiler design parameters (such as gas temperature, velocity, etc.). Combustion test rigs also serve as valuable tools for assessment of fuels with very unusual properties and can significantly reduce uncertainties in extrapolation of their behavior from past experience.

Whenever test results are assessed and used to establish boiler design parameters, the representativeness of the test sample must be carefully considered. The degree of variability in the coal deposit and its impact on the day-to-day fuel properties

are very important factors which must be evaluated. Judgements are also required on long term coal supply properties.

In summary, it can be stated that the ash formation and deposition process is not fully understood. Traditional ASTM analyses do not always provide information that can be used to make predictive judgements at the confidence levels desired. Newer techniques have been developed and are being developed that are more sensitive to the conditions that exist in the boiler environment, and that recognize the heterogeneity of the inorganic constituents in the coal matrix. There appears to be a recognition that no one test can adequately describe coal ash behavior; a combination of tests, each designed to focus on a particular aspect of ash behavior seems to be a logical approach. Based on the results from many of these newer tests, on coals that are presently being burned in existing units, the authors feel certain that significant improvements have been made in predicting ash behavior. Finally the authors suggest that attention be given, by cognizant people, to the idea of standardizing some of the newer predictive techniques and incorporating them as supplements to existing ASTM tests.

REFERENCES

1. G. J. Goetz, N. Y. Nsakala, and R.W. Borio, "Development of Method for Determining Emissivities and Absorptivities of Coal Ash Deposits," paper presented at the 1978 Winter Annual ASME Meeting, Dec. 1978, TIS-5890.

2. R. W. Borio, et.al., "The Control of High Temperature Fireside Corrosion in Utility Coal-Fired Boilers," ORC R&D Report No. 41 (1969).

3. F. Raask, "Flame Imprinted Characteristics of Ash Relevant to Boiler Slagging Corrosion and Erosion," presented at the 1981 Joint Power Generation Conference, ASME Paper No. 81-JPGC-Fu-1.

4. W. P. Bauver, J. D. Bianca, J. D. Fishburn, and J. G. McGowan, "Characterization of Erosion of Heat Transfer Tubes in Coal-Fired Power Plants," paper to be presented at 1984 Joint Power Generation Conference, Toronto, Canada, September 1984.

5. R. W. Borio, G. J. Goetz, and A. A. Levasseur, "Slagging and Fouling Properties of Coal Ash Deposits as Determined in a Laboratory Test Facility," paper presented at the ASME Winter Annual Meeting, December 1977, Combustion Engineering publication TIS-5155.

6. J. P.Huffman and F.E. Higgins, "Investigations of Partial Ash Melting by Phase Analysis of Quenched Samples," presented at 1981 Engineering Foundation Conference-Fouling and Slagging Resulting From Impurities in Combustion Gases, July 1981, Henniker, NH.

7. R. W. Borio, R. R. Narciso, Jr., "The Use of Gravity Fractionation Techniques for Assessing Slagging and Fouling Potential of Coal Ash," paper presented at the ASME Winter Annual Meeting, December 10-15, 1978, San Francisco, CA; available as Combustion Engineering publications TIS-5823.

8. R. W. Bryers, "The Physical and Chemical Characteristics of Pyrites and Their Influence on Fireside Problems in Steam Generators, "ASME Paper No. 75-WA/CD-2, 1976.

9. G. L. Hale, A. A. Levasseur, A. L. Tyler and R. P.Hensel, "The Alkali Metals in Coal: A Study of Their Nature and Their Impact on Ash Fouling," paper presented at Coal Technology '80, November 1980, TIS-6645.

10. G. H. Gronhovd, W. Beckering, and P. H. Tlufte, "Study of Factors Affecting Ash Deposition from Lignite and Other Coals," an ASME publication presented at the ASME Winter Annual Meeting, November 16-20, 1969, Los Angeles, CA.

FIGURE 1

EFFECT OF COAL PROPERTIES ON FURNACE SIZE

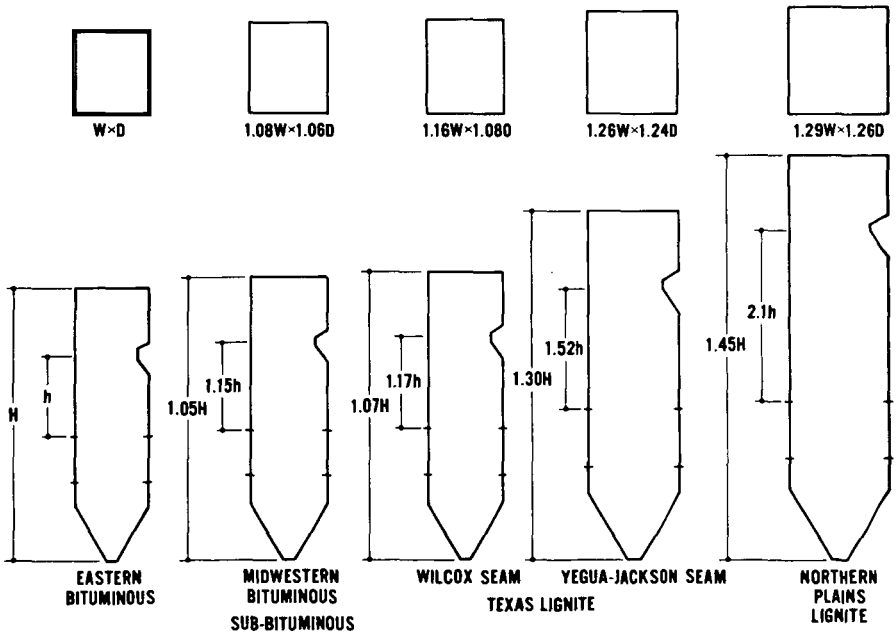

FIGURE 2

SUPERHEATER DEPOSIT BUILDUP vs FLUE GAS TEMPERATURE

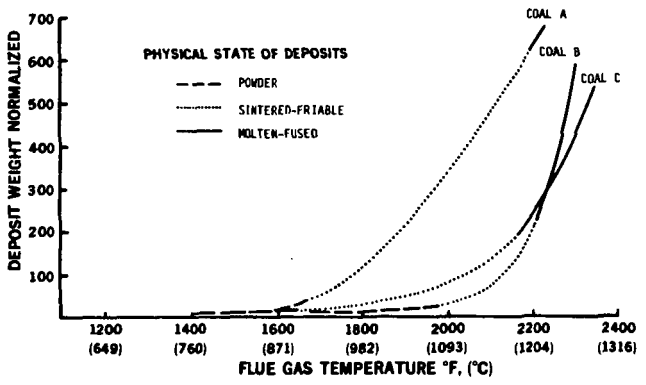

FIGURE 3

EFFECT OF SEGREGATED IRON ON COAL ASH SLAGGING
SLAGGING POTENTIAL
VERSUS
PERCENT IRON IN 2.9 GRAVITY FRACTION

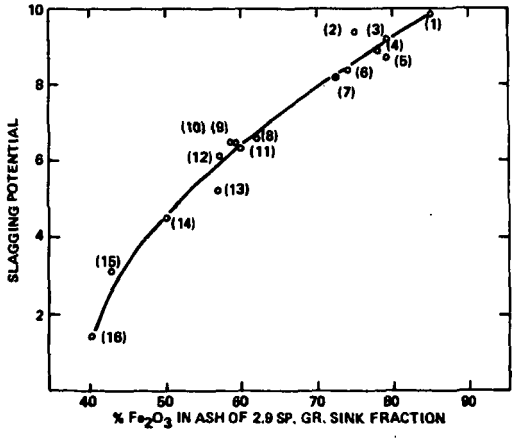

TABLE I

ENRICHMENT OF IRON IN BOILER WALL DEPOSITS
COMPARISON OF COMPOSITION OF ASH
DEPOSITS AND AS-FIRED COAL ASHES

UNIT	1		2		3	
SAMPLE	AS-FIRED COAL ASH	WATERWALL DEPOSIT	AS-FIRED COAL ASH	WATERWALL DEPOSIT	AS-FIRED COAL ASH	WATERWALL DEPOSIT
Ash Composition						
SiO_2	47.0	33.3	50.2	55.1	49.7	41.8
Al_2O_3	26.7	18.0	16.9	14.6	16.5	15.8
Fe_2O_3	14.6	43.5	5.9	18.3	12.0	28.5
CaO	2.2	1.2	12.8	7.2	6.5	9.0
MgO	0.7	0.5	3.5	2.0	0.9	0.9
Na_2O	0.4	0.2	0.6	0.5	1.1	0.6
K_2O	2.3	1.6	0.8	0.6	1.5	0.9
TiO_2	1.3	0.8	0.9	0.8	1.1	0.7
SO_3	1.1	0.5	12.0	0.1	2.0	0.2

TABLE 2 **ANALYTICAL DATA ON U.S. COALS**

Rank Region	**Lignite N. Dakota**	**Sub B Montana**	**Lignite Texas (Yegua)**	**Lignite Texas (Wilcox)**	**hvBb Utah**	**hvAb Penn**	**Lignite Texas (Wilcox)**
(Dry Basis)							
Volatile	44.4	42.2	39.6	41.0	41.5	32.5	38.1
Fixed C	46.0	52.0	26.9	39.5	48.3	54.0	33.0
Ash	9.6	5.6	33.5	19.5	10.2	13.5	28.9
HHV (Btu/lb) (Dry Basis)	10640	12130	7750	9710	12870	13200	8420
Ash Fusibility							
I.D. (°F)	2130	1980	1940	2150	2190	2370	2210
S.T.	2180	2020	2200	2250	2270	2510	2300
H.T.	2190	2060	2430	2340	2390	2560	2420
F.T.	2200	2170	2610	2530	2620	2660	2620
Ash Composition							
SiO_2 (%)	20.0	33.9	62.1	52.3	52.5	51.1	57.9
Al_2O_3	9.1	11.4	15.1	17.4	18.9	30.7	21.8
Fe_2O_3	10.3	10.8	3.5	5.3	1.1	10.0	3.9
CaO	22.4	21.0	6.2	9.4	13.2	1.6	7.1
MgO	6.4	2.7	0.7	3.2	1.3	0.9	2.1
Na_2O	5.0	5.8	3.6	0.9	3.8	0.4	0.9
K_2O	0.5	1.6	2.1	1.2	0.9	1.7	0.8
TiO	0.4	0.7	0.9	1.2	1.2	2.0	1.1
SO_3	21.9	12.0	6.1	9.6	6.2	1.4	4.4
Total alkali, %, ash basis							
Na_2O	5.0	5.8	3.6	0.9	3.8	0.4	0.7
K_2O	0.5	1.6	1.9	1.2	0.9	1.7	0.8
Soluble Alkali, %, ash basis							
Na_2O	5.58	6.45	3.88	0.71	1.49	0.15	0.16
K_2O	—	—	0.44	0.04	0.08	—	0.05
Relative Soluble Alkali, %							
Na_2O	112%	111%	108%	79%	39%	38%	23%
K_2O	—	—	—	3%	9%	—	6%
Fouling Potential	**Severe**	**High**	**High**	**Moderate**	**Moderate**	**Low**	**Low**

DEPOSIT CONSTITUENT PHASE SEPARATION AND ADHESION

E. RAASK

Technology Planning and Research Division, Central Electricity Generating Board, Kelvin Avenue, Leatherhead, Surrey, UK

The initial deposit material on coal fired boiler tubes consist largely of silicate, sulphate and iron oxide particles. The fused silicates and molten sulphates form immiscible phases at high temperatures first on the micro-scale in individual particles and subsequently as separate layers in the deposit. The adhesion of ash deposit constituents to boiler tubes starts with the small particle retention as a result of the van der Waals, electrostatic and liquid film surface tension forces. Subsequently a strong bond will develop between the oxidized metal surface and iron saturated layer of ash deposit.

The pulverized coal fired boilers at electricity utility power stations are designed for "dry" ash operation where the bulk of mineral matter residue is removed in the electrical precipitators in the form of particulate ash. However, it is inevitable that some deposits of sintered ash and semi-fused slag form on the heat exchange tubes and between 20 and 30 per cent of coal ash is discharged from the combustion chamber as clinker. The high temperature cyclone fired boilers are designed for "wet" ash operation and up to 80 per cent of coal ash is discharged from the furnace as molten slag.

The build-up of sintered ash and fused slag deposits depends chiefly on the rate of ash particle impaction and the adhesive characteristics of the collecting surface. The initial deposit on the heat exchange tubes in pulverized coal fired boilers consists of ash particles of diameter ranging from less than 0.1 μm to 100 μm. Subsequently the deposited ash may be re-entrained in the flue gas or it may form first a sintered matrix and later a fused slag deposit chiefly by viscous flow. For the deposit formation the ash particles must be first held at the collecting surface and subsequently the deposit matrix bonded to the boiler tubes by adhesive forces sufficiently strong to overcome the gravitational pull, boiler vibration and eventually the sootblower jet impaction. This work sets out to examine the adhesive characteristics of different constituents of the flame heated ash and the formation of sintered deposits and slag bonded to the heat exchange tubes.

INITIAL DEPOSIT CONSTITUENTS

The mineral matter in coal consists chiefly of silicate, sulphide, carbonate species, and chlorides and organo-metal compounds associated with the fuel substance (1,2). The silicate mineral particles vitrify partially or completely, in the pulverized coal flame (3), and thus the silicate ash fraction of the initial deposit consists of particles of variable amounts of a glassy phase and crystalline species (4).

The sulphide, carbonate, chloride and organo-metal species dissociate and oxidize in the flame. The oxides may remain as discrete particles, chiefly iron oxide (magnetite), can dissolve in the glassy phase of silicates, and a fraction of calcium and sodium oxides are sulphated (5). Thus the initial deposit material will contain some calcium, sodium and potassium sulphate. The latter originates from the release of potassium in the flame heated alumino-silicate particles (6).

The relative concentrations of flame heated ash constituents, namely silicates, iron oxide and sulphate can be estimated from the ash analysis. However, the composition of the initial deposit material can be markedly different as a result of selective deposition. In particular, the deposit material can be enriched in sulphate as shown in Fig. 1. The relative concentrations of different deposit constituents were obtained by analysing the material on a cooled metal tube probe inserted in boiler flue gas for short, 2 to 15 minute duration (7). The sulphate content of the flue gas borne ash and probe deposits in a cyclone fired boiler was higher than that in the pulverized coal fired boiler ash and deposits. This was because in cyclone boilers the bulk of silicate ash is discharged as molten slag but the residual ash is relatively rich in sulphate.

The rate of alkali-metal sulphate deposition will decrease when the temperature of collecting target surface exceeds 1075 K as shown in Fig. 2. The decrease in the deposition of alkali-metal sulphates is related to the concentration of the volatile alkali-metals in the flue gas and the saturation vapour pressure of sodium and potassium sulphates (8). The initial deposit on cooled surfaces contains a small amount of chloride as shown in Fig. 2.

In a reducing atmosphere the deposit material may contain iron sulphide (FeS) formed on dissociation of coal pyrite mineral. This is likely to occur on the combustion chamber wall tubes near the burners where the reaction time is short, below one second, for oxidation of FeS residue to the oxide. It has been suggested that calcium sulphide (CaS) may also be present in the ash material deposited from a reducing atmosphere gas stream as a result of sulphidation of calcium oxide (9).

THERMAL STABILITY OF SULPHATES AND IMMISCIBILITY WITH SILICATES

Bituminous coals usually leave a highly silicious ash on combustion. That is, fused alumino-silicates constitute an acidic media at high temperatures that is capable of absorbing large quantities of basic metals in the form of oxides, chiefly those of sodium, calcium and magnesium. At lower temperatures the corresponding sulphates are thermodynamically more stable in the presence of sulphur gases. The equilibrium distribution of alkaline oxides between molten sulphates and fused silicates at different temperatures can be calculated from the appropriate thermodynamic data. However, the residence time of the flame borne mineral species before deposition is short and the alkali-metal distribution does not reach the equilibrium state.

The fused silicate particles will absorb the flame volatilized sodium to the depth of about 0.05 μm (10), and the remainder is converted to sulphate partly in the flue gas and partly at the surface of ash particles. The distribution of sodium in the silicate and sulphate phases can be expressed in a form:

$$m_{sul} = m_o - kw^{2/3} \qquad \text{... 1)}$$

where $$m_{sil} + m_{sul} = m_o \qquad \text{... 2)}$$

m_{sil}, m_{sul} and m_o denote the amount of sodium in silicate and sulphate fractions, and the total sodium in ash respectively; k is a constant and w is the ash content of coal. When the sodium to ash ratio is below 1 to 100 the bulk of sodium is captured by the silicate particles and equation 2 reduces to:

$$m_{sil} \simeq m_o \qquad \ldots 3)$$

and consequently the amount of sodium available for the formation of sulphate is small.

The molten sodium sulphate/sodium silicate system of composition Na_2SO_4/Na_2O-SiO_2 has one liquid phase at 1475 K, but as the proportion of silica increases, the melt separates into two layers (11,12). The change from the miscible to immiscible phase of the system has been explained by alterations in the silicate structure as the ratio of Na_2O to SiO_2 decreases. In more basic, less viscous melts, the silicate ions exist in the form of SiO_4^{4-} tetrahedrons which have the same mobility as sulphate ions, and thus homogeneity of the system is to be expected. As the silica content is increased the complexity of the silicate structure reaches a point where the silica anions become relatively immobile for a separation of sulphate from silica to take place.

The miscibility of the corresponding potassium sulphate-silicate system has been studied by the usual crucible method as well as by a technique of a hanging droplet (13). The droplets of potassium sulphate/silicate mixtures, 3 mm in diameter, were suspended from 0.5 mm platinum wire which had a semi-spherical head 1.5 mm in diameter. Separation of the silicate (internal) and sulphate phases in the droplets can be observed directly in the Leitz heating microscope which is used, in its conventional mode of operation, to assess the fusion characteristics of coal ashes (14). Fig. 3 shows the two phase separation of $2K_2SO_4-K_2O-2.1SiO_2$ system at 1575 K where the outside envelope is the transparent sulphate phase through which the platinum wire heats (top) and a globule of molten silicate (bottom) can be seen. As the temperature was increased to 1725 K the two phases became miscible because of the increased solubility of sulphate in the silicate melt at the higher temperature.

The $K_2SO_4-K_2O-SiO_2$ phase diagram is depicted in Fig. 4 which shows that the system is miscible at 1575 K when the molar ratio of K_2O to SiO_2 is above 0.5. As in the corresponding sodium sulphate/sodium silicate system, less basic melts separate into two immiscible liquids. This is the case with most coal ash slags where the molar ratio of basic oxides (sum of Na_2O, K_2O, CaO and MgO) to SiO_2 is well below 0.5. Exceptions to this are the sodium and calcium rich ashes of some lignite and non-bituminous coals, which can have sufficient amounts of alkalis to form a single phase melt of miscible sulphates and silicates at high temperatures.

ADHESION BY VAN DER WAALS AND ELECTROSTATIC FORCES

The ash particles deposited on boiler tubes are initially held in place by surface forces, i.e. van der Waals and electrostatic attraction forces. Van der Waals forces become important when molecules or solid surfaces are brought close together without a chemical interaction taking place. For a hemispherical particle of rsdius (r) held at a distance of nearest approach (h) from a plane, the resultant forces (F) is given by:

$$F = \frac{Ar}{6h^2} \qquad \ldots 4)$$

where A is the Hamaker constant (15).

Equation 4 applies over short distances, up to 150 A (1.5×10^{-8} m) and for longer distances the "retarded" van der Waals forces decay rapidly (16). An equation based on the dielectric properties of solids for the retarded

van der Waals forces (F') between a sphere of radius (r) at the distance (h) from a flat surface is (17):

$$F' = \frac{2B\pi r}{3h^3} \qquad \ldots 5)$$

where B is the appropriate constant for the given material.

The changeover from the unretarded to retarded van der Waals forces occurs at a distance of about 150 A (1.5×10^{-8} m), and the corresponding value of the Hamaker constant (A) in equation 4 was found to be 10^{-19} N (Newton), and that of the Lifshitz constant (B) in equation 5 was 8.9×10^{-29} N m (16,18). These values have been used to compute the ratio of van der Waals forces to the gravitational force on small ash particles approaching a flat surface.

The gravitational force (F_g) on an ash particle of radius (r) and the density (D) is given by:

$$F_g = \frac{4\pi r^3 Dg}{3} \qquad \ldots 6)$$

where g is the gravity acceleration constant (9.81 m s^{-2}). Thus, the ratio (F_r) of the short distance van der Waals forces (F) to the gravitational force (F_g) on a particle is:

$$\frac{F}{F_g} = F_r = \frac{A}{8\pi Dgr^2h^2} = \frac{1.62 \times 10^{-25}}{r^2h^2} \qquad \ldots 7)$$

where the value of D for ash was taken to be 2500 kg m^{-3} and when $h < 1.5 \times 10^{-8}$ m. The corresponding ratio (F_r') of the retarded van der Waals forces (F') to the gravitational force is given by:

$$\frac{F'}{F_g} = F_r' = \frac{2B}{Dgr^2h^3} = \frac{8.15 \times 10^{-34}}{r^2h^3} \qquad \ldots 8)$$

where $h > 1.5 \times 10^{-8}$ m.

Fig. 5 shows a comparison of van der Waals and the gravitational forces on small ash particles as these approach a collecting surface. Plots A and B indicate that the sub-micron sized particles are readily held on a surface by van der Waals forces. The capture of small particles of ash on boiler tubes is further enhanced by surface irregularities of oxidized metal (19). Also, it has been suggested that an electrostatic attraction force enhance the transport and retention of sub-micron sized particles on steel probes inserted in the flue gas of coal fired boilers (7,20). A layer of electrically precipitated deposit of ash can have a cohesive strength between 5 and 40 times higher than that formed by sedimentation because particles in an electric field have permanent dipole characteristics which lead to these being orientated to form a cohesive layer of ash (21). It appears therefore that the combined effects of van der Waals and electrostatic forces of attraction, and surface irregularities are sufficient to hold the sub-micron diameter particles on the surface of boiler tubes for the subsequent liquid phase adhesion, and chemical and mechanical bond formation.

ADHESION BY SURFACE TENSION FORCE

The formation of strong adhesive bonds of enamel coatings and glass/metal seals on heating requires the presence of a liquid phase (22,23,24). The role of the liquid film is to provide the initial adhesion of solid particles as a result of surface tension. The work of adhesion (W_a) is given by:

$$W_a = \pi + \gamma (1 + \cos \theta) \qquad \text{... 9)}$$

where γ is the surface tension of the liquid, and θ is the contact angle at the solid/liquid interface. With perfect wetting, i.e. when θ equals zero, W_a has the highest value:

$$W_a = \pi + 2\gamma \qquad \text{... 10)}$$

The work of cohesion of a liquid (W_c) is given by:

$$W_c = 2\gamma \qquad \text{... 11)}$$

With wetting liquids, therefore, W_a can be higher than W_c and failure will take place within the liquid layer, whereas with non-wetting liquids the rupture occurs at the solid/liquid interface.

Alkali-metal sulphates frequently constitute a liquid phase in ash deposits, and the molten sulphates readily wet and spread on the surface of boiler tubes. In a reducing atmosphere and when in contact with carbon, sulphates are reduced to sulphides which wet and spread on any surface. The coefficient of surface tension of sulphates is fairly high, 0.20 N m^{-1} for Na_2SO_4 and 0.14 N m^{-1} for K_2SO_4 near their respective melting point temperatures (25,26). Thus work of cohesion of molten sulphate layer in boiler deposit is between 0.3 and 0.4 N m^{-1} and the work of adhesion is higher because of a low contact angle at the sulphate/tube surface interface. It is therefore to be expected and it is observed in practice that when the deposit is removed, e.g. by sootblowing, there remains a film of sulphate adhering to boiler tubes. The surface tension of coal ash slag has been measured previously by the sessile drop method (27) and a typical value was 0.3 N m^{-1}. It is about twice that of sulphates and thus the work of adhesion (Equation 9) and the cohesive bond strength are corresponding higher at the slag/solid interface.

Only a small amount of liquid, about a hundred molecule thick layer, is sufficient for the adhesion contact of sub-micron diameter particles (28). In the case of a volatile liquid, the equilibrium thickness of the film, and thus the adhesion, varies with partial pressure of the vapour in the surrounding atmosphere. When evaporation from a liquid film occurs, as a result of increased temperature, the adhesion first rises to a maximum value due to the meniscus effect but it breaks down as the film thickness is reduced to molecular dimensions. However, before the break-down of the surface tension chemical and mechanical bonds may develop between the deposited ash and boiler tube surface.

MECHANICAL AND CHEMICAL BONDING

Ash deposits on boiler tubes can be keyed to the surface of metal oxide by mechanical and chemical bonds. Mechanical bonding is enhanced by extending surface at the interface as shown in Fig. 6a. Boiler tubes are not polished and thus have an extended surface that is further increased by oxidation and chemical reactions between the oxide layer and ash deposits. It is therefore evident that a comparatively rough surface of boiler tubes constitute an anchorage for keying ash deposits to the heat exchange elements.

Dietzel (29) and Staley (30) have proposed that the chemical reactions at a enamel/metal interface can be considered in terms of electrolytic cells set up between the metals of different electro-chemical potential. It has been suggested that cobalt or nickel precipitated in the enamel when in contact with steel surface, forms short-circuited local cells in which iron is the anode. The current flows from iron through the melt to cobalt and back to iron. The result is that iron goes into solution, the surface becomes roughened, and the enamel material anchors itself into the cavities as shown in Fig. 6b.

The galvanic reactions will take place at a much faster rate in the low viscosity phase of sulphates in boiler deposit than that in highly viscous silicate glass. However, rapid reactions at the tube surface/deposit interface may not be necessary or appropriate for development of a strong bond between the ash deposit and boiler tubes. In metal/glass seal and metal/enamel coating technology, the adhesive bonds formed on heating have to be completed in a few hours, whereas those in boiler deposits can form over a period of days or weeks. The adhesive bond between the metal surface and a silicate material can be high when there is a gradual rather than abrupt change in the glass phase composition near the interface (31).

When the ash deposit is brought in intimate contact with the surface of boiler tubes either by the action of surface tension or by the galvanic reactions, the controlling parameter in mechanical bonding is the strength of the glassy phase at the narrowest cross sectional area of contact cavities (Fig. 6b). The annealed glass may have a tensile strength of around 50 MN m^{-2} giving a maximum bond strength of 35 MN m^{-2}. However, the glass at the interface may be stronger or weaker depending on whether the conditions in the keying cavities increase or decrease local flaws and resultant stresses.

Chemical bonds, covalent or ionic as shown in Fig. 6c and d, at the metal oxide/deposit surface are potentially strong with theoretical values over 10^9 N m^{-2}. It is, however, impossible to estimate the number of sites and the size of contact areas at the interface where the chemical bonds may be effective. In any case, the cohesive strength of the deposit matrix is the limiting factor since it is lower than that of chemical bonds by several orders of magnitude. In practice, this means that when a strongly adhering deposit is subjected to a destructive force, e.g. sootblower jet, failure occurs within the deposit matrix and there remains a residual layer of ash material firmly bonded to the tube surface.

ADHESION OF ASH DEPOSITS ON FERRITIC AND AUSTENITIC STEELS

The adhesion bond strength of soda glass on a metal substrate has been determined by heating a glass disc sandwiched between two metal discs in a vertical furnace (32). The technique has been adopted for measuring the strength of the adhesive bond developed when a boiler deposit was sandwiched between two discs of ferritic or austenitic steels (33). The deposit material was taken immediately after boiler shut-down from the superheater tubes of a pulverized coal fired boiler fuelled with a mixture of East Midlands, UK coals. The flue gas temperature in the superheater prior to boiler shut-down was about 1300 K and the tube metal temperature was 850 K. The deposit material consisted of 30 per cent of alkali-metal sulphates in weight ratio of 2 to 1 of Na_2SO_4 to K_2SO_4, the remainder being silicate ash. A layer of deposit, 3 mm thick, was sandwiched between two metal discs, 20 mm in diameter, made of boiler tube steels and then heated in a vertical furnace. After a time interval lasting from one to 25 days the bond was ruptured by applying a tensile force without prior cooling.

The results in Fig. 7 show that the strength of adhesive bond between the ferritic steel sample and boiler deposit increased exponentially with

temperature in the range of 775 to 900 K. Similar results were obtained by Moza et al. (34) who used a droplet technique to measure the adhesive bond of coal ash slag on a ferritic steel target in the temperature range of 700 to 950 K.

The results plotted in Fig. 8 shows that the strength of adhesive bond of ash deposit on both the ferritic and austenitic steels increased approximately linearly with time at 900 K. However, the bond strength of deposit on the austenitic steel (Type 18Cr13NiNb) was significantly lower than that between the deposit and 9Cr-ferritic steel. The latter resulted from the thermal and chemical compatibility of the steel oxide layer and deposit material (35). Table 1 shows approximate values of the coefficient of thermal expansion of the ferritic and austenitic steels, some oxides and silicate materials (36).

Table 1: Coefficient of Thermal Expansion of Boiler Tube Steels, Oxides and Silicates

Material	Thermal Expansion, $\frac{\Delta m}{m} K^{-1}$
Steels	
Mild Steel and Ferritic Steels	11 to 12 × 10^{-6}
Austenitic Steels	16 to 18 × 10^{-6}
Oxides	
Tube Metal Oxides	8 to 10 × 10^{-6}
(Fe_3O_4, Cr_2O_3, NiO)	
Deposit Constituents	
Glassy Material	6 to 9 × 10^{-6}
Quartz (Crystalline)	5 to 8 × 10^{-6}
Silicates in Fired Brick	7 to 8 × 10^{-6}

The data in Table 1 show that the coefficient of thermal expansion of mild steel and ferritic steels is not greatly different from that of their oxides and the ash deposit constituents. It is therefore evident that there is no gross incompatibility in the thermal expansion characteristics and strongly bonded ash deposits once formed on mild steel tubes are not easily dislodged on thermal cycling.

In contrast, the thermal expansion of austenitic steel is significantly higher than that of the oxides and deposit material. In the absence of boiler deposit, the oxide material in the form of thin layer is able to absorb thermal stresses and the adhesive layer remains intact on cooling. However, it appears that the oxide layer is unable to absorb thermal stresses in a similar manner when contaminated and constrained by bonded ash deposits. It is therefore a usual occurrence that ash deposits peel off the austenitic steel tubes on cooling whereas the deposit formed on ferritic steels under the same conditions remain firmly attached to the tubes.

King et al. (22) have suggested that in order to obtain good adherence of enamel coatings on metals, the enamel material at the interface must become saturated with the metal oxide, e.g. FeO of ferrit steels. Coal ash deposit on boiler tubes contains between 5 and 25 per cent iron oxide (Fig. 1) and thus the layer at the tube/deposit interface becomes saturated with FeO. The chromium and nickel contents of ash deposit are low and thus the same chemical compatibility stage is not reached at the austenitic steel/deposit interface.

The adhesive bond between boiler ash deposit and the surface of ferritic steels can attain exceptionally high strengths. This was found on examining the deposits formed on different steel specimens tested in an experimental superheater loop. Favourable conditions for the formation of firmly bonded deposits were as follows:

(a) The iron oxide content of coal was above 20 per cent expressed as Fe_2O_3 giving an iron saturated layer of deposit on the tube specimens.

(b) The ash collecting surface was a 5 per cent chromium ferritic steel which formed an oxide layer strongly adhering to metal for a firm anchorage of deposits.

(c) The tube metal temperature was high, 950 K, which enhanced the formation of strong adhesive bond. The flue gas temperature at that position was approximately 1250 K.

(d) The ferritic test piece in the experimental loop was sheltered from direct action of sootblower. Weak turbulence caused by the jet removed some of the unsintered silica ash leaving iron rich deposit firmly bonded to the tube. The iron rich deposit had grown in thickness to about 20 mm after nine months, and cohesive strength of the deposit material increased towards the surface of tube metal. The microscopic examination showed that there was no marked interface boundary between the ash deposit and metal oxide.

FORMATION OF LAYER STRUCTURE DEPOSITS AND SLAG MASSES

The coal ash deposits on boiler tubes have frequently a separate zone structure with a sulphate rich layer up to 2 mm thick under the matrix of sintered ash (35). The outer layer is porous and it constitutes a pathway for the enrichment of alkali-metals in the deposit layer next to tube surface. The diffusable species may be sulphate, chloride, oxide or hydroxide, but the thermodynamic data (8) and the results of deposition measurements in coal fired boilers (Fig. 3) suggest that sodium and potassium sulphates are the principal vapour species which diffuse through a porous matrix of silicate ash deposit.

The relative amounts of Na_2SO_4 and K_2SO_4 which diffuse through the sintered matrix of silicate ash depend on the temperature gradient across the deposit layer, vapour pressure of the species and thermodynamic stability of the sulphates in the presence of silicates. Potassium sulphate has a higher temperature stability limit when compared with that of sodium sulphate and as a result K_2SO_4 can be preferentially transported to the surface of cooled boiler tubes when there is a steep temperature gradient across the ash deposit. The K_2SO_4 rich phase, when molten, can cause severe corrosion of tube metal.

The corrosion product, a mixture of oxide, sulphide at the metal interface and sulphate outside, has a weak adhesive bond to the metal surface and cannot support large deposit masses. It is therefore unusual to find excessive amounts of sintered ash deposits and fused slag in the exact localities where severe high temperature corrosion occurs. Conversely, a strongly adhering matrix

of sintered ash deposit in the absence of sulphate, sulphide or chloride phases is not markedly corrosive.

The build-up of boiler tube deposits is a continuously changing process as depicted in Fig. 9. When the deposit material reaches a thickness of 2 to 3 mm (Fig. 9a) the separate sulphate and silicate phases occur (Fig. 9b). Subsequently, the sulphate layer disappears in the middle section (Fig. 9c) allowing a strong bond to be established between the sintered ash deposit and ferritic steel boiler tubes. This is the "classical" mode of formation of superheater tube deposit when the metal temperature is in the range of 750 to 900 K. Above 950 K the layer structured deposits are less likely to occur and a strong adhesive bond is rapidly formed between the silicate ash deposits and the high temperature tube surface.

A notable feature of slag formed in pulverized coal fired boiler is its variable gas hole porosity. Burning coal particles are incapsulated in the deposit layer and generate CO and CO_2 inside the silicate material (27) resulting in a highly porous slag. The density of slag will increase when the encapsulated coal particles are consumed and gas bubbles have escaped.

It has been observed that new boilers have an "immunity" period lasting weeks or months before severe slag build-up occurs. This is partly due to the fact that during the commissioning period the boiler rarely reaches full load output. However, it may also be partly due to a slow rate of formation of the interface layer on boiler tubes which is able to have a strong adhesive bond to rapidly forming ash slag and thus able to support large masses of deposit.

CONCLUSIONS

Initial Deposit

The initial deposit material on cooled tubes in coal fired boilers consists largely of flame vitrified silicate ash, iron oxide, and calcium and alkali-metal sulphates. Trace amounts of chloride will also deposit and under reducing conditions some iron and calcium sulphides can be present.

Phase Separation

Most coals leave an ash residue which is pyrochemically acidic, and the alkali-metals and calcium are distributed in the silicate and sulphate phases under oxidizing conditions. The fused silicates and molten sulphates are immiscible and separate into two phases. The phase separation enhances the adhesion of ash to boiler tubes and leads to the formation of layer structured deposits.

Initial Particle Adhesion

Initially the small particles of ash, below 1 μm in diameter are held at the surface of boiler tubes by the van der Waals and electrostatic attraction forces. Subsequently a film of molten sulphate may form at the tube surface/deposit interface and only a small amount of liquid, about one hundred molecules thick is sufficient for bonding.

Strong Adhesive Bond of Deposits on Ferritic Steels

Strong adhesive bonds can form between the oxidized surface of ferritic steels and iron rich ash because of the composition and thermal expansion compatibility of the metal oxide and silicate ash deposit. The adhesive bond strength increases exponentially with temperature of the target surface in the

range of 750 to 950 K. The bond strength can reach high values, that is, higher than the cohesive strength of sintered ash deposits at temperatures above 850 K.

Weak Adhesive Bond of Deposits on Austenitic Steels

The adhesive bond between the austenitic steel surface and ash deposit is relatively weak as a result of the composition and thermal incompatibility of the steel oxide and the silicate material. The temperature fluctuations on changeable boiler load conditions can cause sufficiently high thermal stresses for deposit to skid off the austenitic steel tubes.

Boiler Tube/Ash Deposit Interface

The boiler tube/ash deposit interface layer which can support large masses of slag formed in the combustion chamber takes several months to develop. Thus the full extent of boiler slagging may not become evident during the commissioning period of new boiler plant.

ACKNOWLEDGEMENT

The work was carried out at the Central Electricity Research Laboratories and the paper is published by permission of the Central Electricity Generating Board.

LITERATURE CITED

1. Lowry, H.H., Editor, "Chemistry of Coal Utilization", John Wiley and Sons, Inc., New York, (1963)

2. Francis, W., "Fuels and Fuel Technology", Vol. I, Pergamon Press, London, (1965)

3. Raask, E., "Fusion of Silicate Particles in Coal Flames", Fuel, (1969), 48, 366

4. Raask, E. and Goetz, L., "Characterization of Captured Ash, Chimney Stack Solids and Trace Elements", Jour. Inst. Energy, (1981), 54, 163

5. Raask, E., "Sulphate Capture in Ash and Boiler Deposits in Relation to SO_2 Emission", Proc. Ener. Comb. Sci., (1982), 8, 261

6. Raask, E., "The Behaviour of Potassium Silicates in Pulverized Coal Firing", VGB Mitteilungen, (1968), 18, 348

7. Raask, E., "Reactions of Coal Impurities during Combustion and Deposition of Ash Constituents on Cooled Surfaces", Conf., Mechanism of Corrosion by Fuel Impurities, p. 145, Marchwood, UK, Butterworth Publ., London, (1963)

9. Halstead, W.D. and Raask, E., "The Behaviour of Sulphur and Chlorine Compounds in Pulverized Coal Fired Boilers", Jour. Inst. Fuel, (1969), 43, 344

9. Hein, K., "Chemical and Mineralogical Aspects of Fouling of Heat Exchange Surfaces in Non-Bituminous Coal Fired Boilers", VGB Kraftwerkstechnik, (1979), 59, 576

10. Hosegood, E.A. and Raask, E., "Reactions and Properties of Alkalis and Ash in Pulverized Fuel Combustion", CERL Note No. RD/L/N 49/64, Leatherhead, UK, (1964)

11. Kordes, E., Zofelt, B. and Proger, H.J., "Reactions in the Melting of Glass with Na_2SO_4: Immicibility Gap in Liquid State between Na-Ca-Silicates and Na_2SO_4", Zeitschr. Anorg. Allgem. Chem., (1951), 264, 255

12. Pearce, M.L. and Beisler, J.F., "Miscibility Gap in the System Sodium Oxide-Silica-Sodium Sulphate at 1473 K", Jour. Am. Cer. Soc., (1965), 48, 40

13. Raask, E. and Jessop, R., "Miscibility Gap in the Potassium Sulphate-Potassium Silicate System at 1575 K", Phys. and Chem. Glasses, (1966), 7, 200

14. DIN, "Determination of Ash Fusion Behaviour", German Standard, DIN 51 730, (1976)

15. Casimir, H.B.G. and Polder, D., "The Influence of Retardation on the London-van der Waals Forces", Phys. Rev., (1948), 73, 360

16. Tabor, D., "Surface Forces", Chem. Ind., (1971), No. 35, p 969

17. Lifshitz, E.M., "The Theory of Molecular Attractive Forces Between Solids", Soviet Physics, JETP, (1956), 2, 73

18. Tabor, D. and Winterton, R.S.H., "Surface Forces: Direct Measurement of Normal and Retarded van der Waals Forces", Nature, (1968), 219, 1120

19. Pfefferkorn, G. and Vahl, J., "Investigation of Corrosion Layers on Steel Using Electron Microscopy and Electron Diffraction", Conf., Mechanism of Corrosion by Fuel Impurities, p. 366, Marchwood, UK, Butterworths Publ., London, (1963)

20. Steel, J.S. and Brandes, E.A., "Growth and Adhesion of Oxides in Furnace Deposits and Their Influence on Subsequent Deposition of Ash Particles as Combustion Products", Conf., Mechanism of Corrosion by Fuel Impurities, p 374, Marchwood, UK, Butterworths, London, (1963)

21. Penney, G.W. and Klinger, E.H., "Contact Potentials and the Adhesion of Dust", Trans. A.I.E.E., (1962), 81, 200

22. King, B.W., Tripp, H.P. and Duckworth, W.H., "Nature of Adherence of Porcelain Enamels to Metals", Jour. Am. Cer. Soc., (1959), 42, 504

23. Holland, L., "The Properties of Glass Surfaces", Chapman and Hall, London, (1964)

24. Klomp, J.T., "Interfacial Reactions Between Metals and Oxides During Sealing", Am. Ceram. Soc. Bull., (1979), 10, 887

25. International Critical Tables, "Surface Tension of Molten Sulphates", 4, 443, McGraw-Hill Book Co., New York, (1928)

26. Bertozzi, G. and Soldani, G., "Surface Tension of Molten Salts, Alkali Sulphate and Chloride Binary Systems", Jour. Phys. Chem., (1967), 71, 1536

27. Raask, E., "Slag/Coal Interface Phenomena", Trans. ASME for Power, Jan., (1966), p 40

28. Cross, N.L. and Picknett, R.G., "Particle Adhesion in the Presence of Liquid Film", Conf. Mechanism of Corrosion by Fuel Impurities, p 383, Marchwood, UK, Butterworths, Publ., London, (1963)

29. Dietzel, A., "Explanation of Adhering Problem in Sheet Iron Enamels", Emailwaren-Industrie, (1934), 11, 161

30. Staley, H.F., "Electrolytic Reactions in Vitreous Enamels and Their Reaction to Adherence of Enamels to Steel", Jour. Am. Ceram. Soc., (1934), 17, 163

31. Weyl, W.A., "Wetting of Solids as Influenced by Polarizability of Surface Ions", Structure and Properties of Solid Surfaces, p 147, Edited by R. Gomer and C.S. Smith, University of Chicago Press, USA, (1953)

32. Oel, H.J. and Gottschalk, A., "The Adhesion Temperature Between Glass and Metals", Glastechnische Berichte, (1966), 39, 319

33. Raask, E., "Boiler Fouling - The Mechanism of Slagging and Preventive Measures", VGB Kraftwerkstechnik, (1973), 53, 248

34. Moza, A.K., Shoji, K. and Austin, L.G., "The Sticking Temperature and Adhesion Force of Slag Droplets from Four Coals on Oxidized Mild Steel", Jour. Inst. Fuel, (1980), 53, 17

35. Raask, E., "Mineral Impurities in Coal Combustion", Hemisphere Publishing Corp., New York, (1984)

36. Hodgman, C.D., (Editor), "Handbook of Chemistry and Physics", The Chemical Rubber Publishing Co., Ohio, USA, (1962)

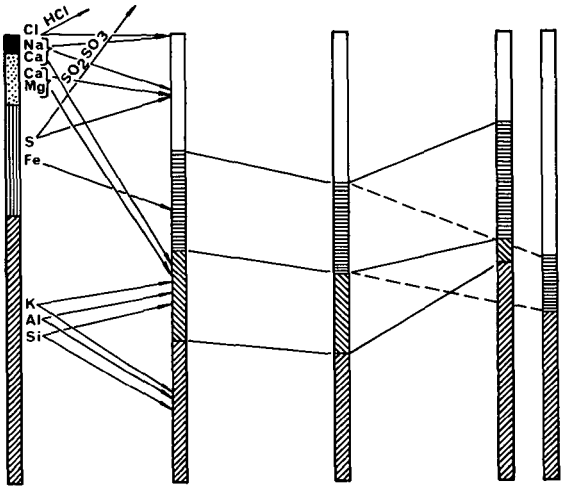

A – COAL MINERALS B – GAS BORNE ASH C – PROBE DEPOSIT D1 D2 OUTER AND INNER LAYERS OF BOILER DEPOSIT

FIG. 1 ASH COMPOSITION CHANGES ON ROUTE FROM MINERAL MATTER TO BOILER TUBE DEPOSITS

IN SOLUBLE SILICATES SOLUBLE SILICATES

PYRITES IRON OXIDES CARBONATES

CHLORIDES SULPHATES

ER/AWS(17.12.1981)RL 4.3.3840

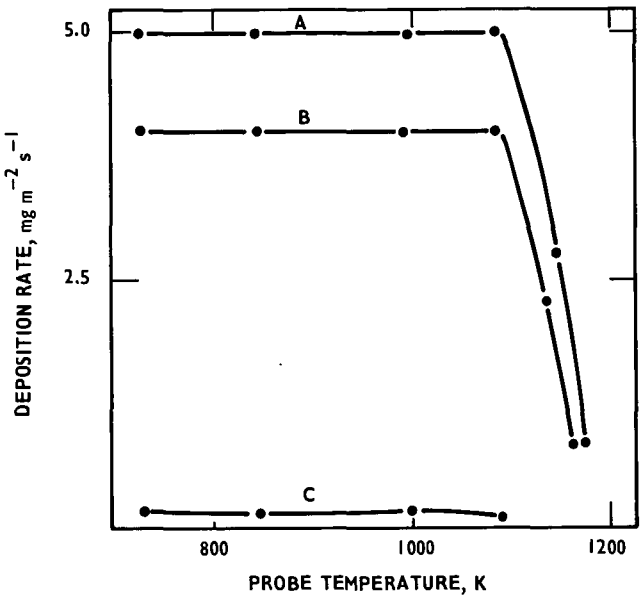

FIG. 2 DEPOSITION OF SULPHATE AND CHLORIDE IN CYCLONE FIRED BOILER – 0.28 PER CENT CHLORINE IN COAL

A – NA_2SO_4 B – K_2SO_4 C – NaCl

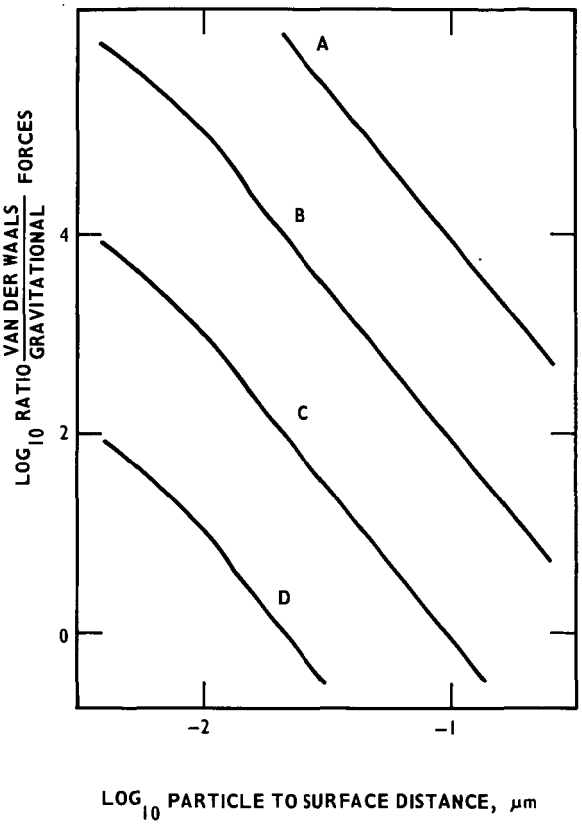

FIG. 5 COMPARISON OF VAN DER WAALS AND GRAVITATIONAL FORCES ON ASH PARTICLES NEAR COLLECTING SURFACES

PARTICLE DIAMETER, μm
A – 0.01; B – 0.1; C – 1.0; D – 10.0

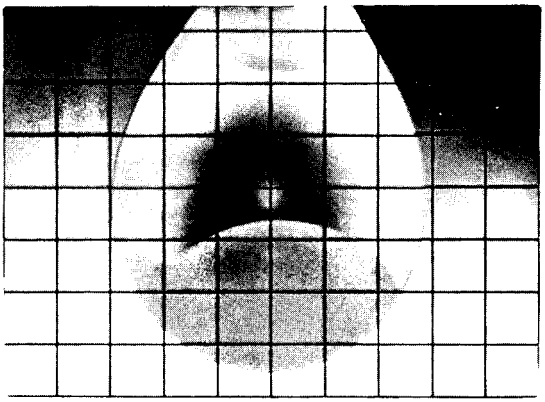

TWO PHASES AT 1575K

FIG. 3 $2K_2SO_4 - K_2O - 2.1\ SiO_2$ DROPLET IN HEATING MICROSCOPE (0.5 mm GRID)

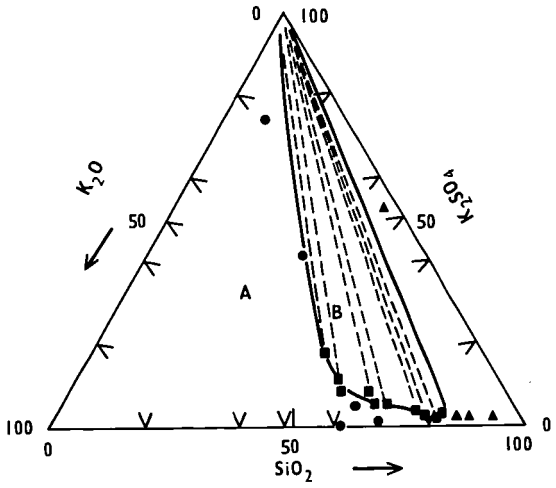

FIG. 4 MISCIBILITY GAP IN K_2SO_4–K_2O–SiO_2 SYSTEM AT 1575 K

A, SINGLE PHASE B, TWO PHASES C, LIQUID + SOLID SiO_2

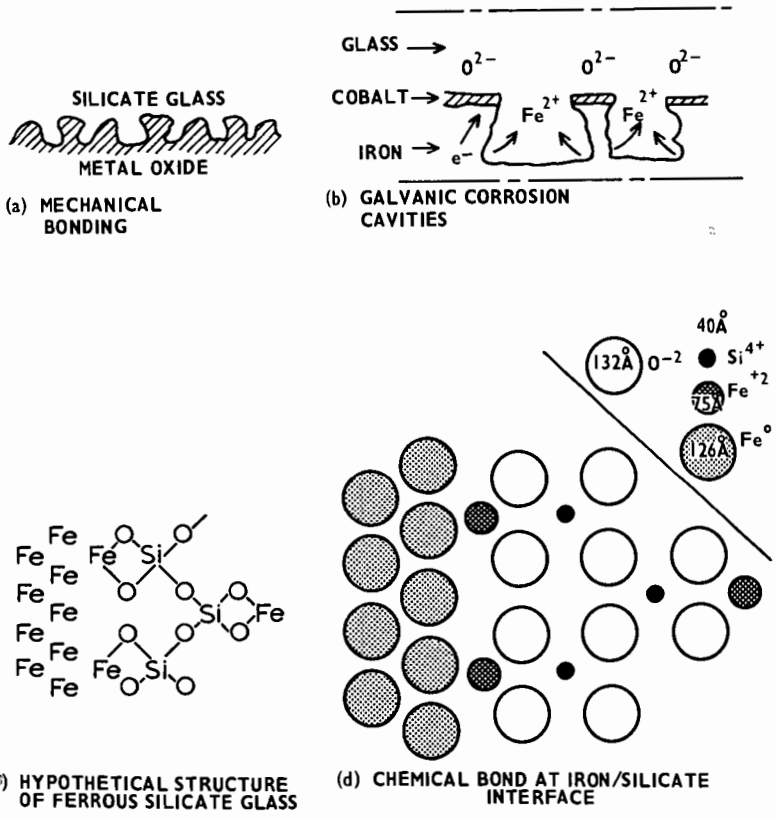

FIG. 6 SCHEMATIC REPRESENTATION OF MECHANICAL AND CHEMICAL BONDS AT BOILER TUBE/ASH DEPOSIT INTERFACE

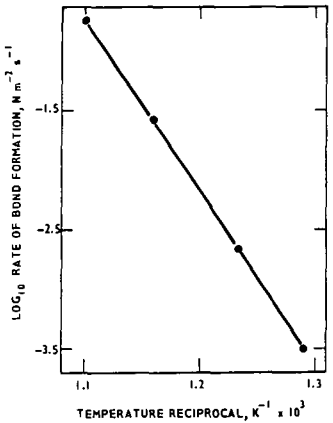

FIG. 7 THE EFFECT OF TEMPERATURE ON ASH DEPOSIT/FERRITIC STEEL BOND

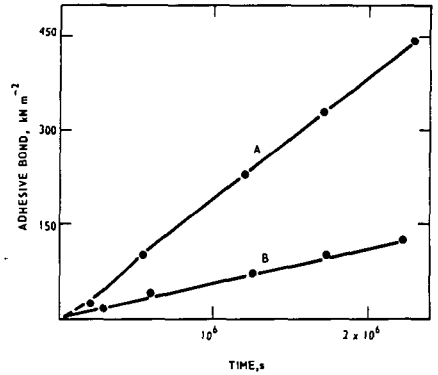

FIG. 8 BOND STRENGTH BETWEEN ASH DEPOSIT AND BOILER TUBE STEELS AT 900 K

A – FERRITIC STEEL B – AUSTENITIC STEELS

(R)

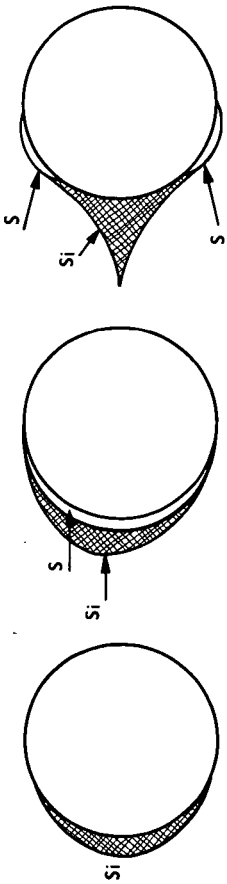

(a) INITIAL UNSEGREGATED ASH DEPOSIT

(b) SEPARATED S-SULPHATE AND Si-SILICATE PHASES

(c) DISPLACED SULPHATE PHASE AND SILICATE/ METAL OXIDE BOND

FIG. 9 SEQUENTIAL STAGES IN THE FORMATION OF LAYER-STRUCTURED AND FIRMLY ADHERING SUPERHEATER DEPOSIT

USE OF GLASS FOR MODELING THE DEPOSITION OF COAL ASH IN HOT CYCLONES

D. M. Mason and A. G. Rehmat

Institute of Gas Technology
IIT Center
3424 South State Street
Chicago, Illinois 60616

K. C. Tsao

University of Wisconsin — Milwaukee
P.O. Box 7841
Milwaukee, Wisconsin 53201

ABSTRACT

Tests have been conducted in a laboratory hot cyclone to obtain an estimate of the temperature below which spherical glass particles do not form a firmly attached deposit. A temperature of 800° to 850°C, corresponding to a viscosity between 6.3 X 10^5 and 2.9 X 10^6 poises, as calculated from the composition of the glass, was found. We take this viscosity to be approximately that of coal ash above which particles will not deposit in cyclones of fluidized-bed coal gasifiers.

INTRODUCTION

A cyclone operating at temperatures near those of the fluidized bed of the reactor has been used in the gasifier of the U-GAS® pilot plant to remove entrained char particles from the product gas and return them to the bed. Essentially pure coal ash has been found to deposit in this hot cyclone (1). The deposits have been analyzed chemically and examined by optical and scanning electron microscopy. Ferrous sulfide is responsible for deposition under adverse conditions, but deposition of iron-rich ferrous aluminosilicates is the more serious problem. In deposits from Western Kentucky coal, for example, the selective deposition of high-iron siliceous particles is indicated by an Fe_2O_3/Al_2O_3 ratio (calculated after excluding the iron contribution of iron sulfide) ranging from 2.2 to 4.6 in the ash of deposits, compared with a ratio of 1.2 in the ash of the coal. The effect of gas temperature (which equals particle temperature) and cyclone-wall temperature on the deposition of such particles was studied in a laboratory hot cyclone in the laboratories of the Mechanical Engineering Department of the University of Wisconsin at Milwaukee (1,2). The particles used in these tests were prepared from pilot plant deposits. The results indicated that the borderline temperature, below which the particles do not form a firm deposit, is about 900°C when gas and wall temperatures are equal.

We envision that the mechanism of deposition involves viscous or plastic flow following collision of particle and deposition surface to create a neck exerting enough surface tension to prevent rebound. We consider that the main cause of flow is impact. Flow driven by surface tension, as postulated by Raask (3) for deposition of coal ash on heat exchange surfaces of boilers, constitutes an additional mechanism leading to firm adhesion. Deposition at the inlet impingement area in the laboratory hot cyclone tests, massiveness of deposits at regions of high gas velocity and acceleration in or near the pilot plant cyclone, and virtual absence of deposits at low-gas-velocity regions of the gasification reactor all indicate that impact of deposition-prone particles plays an important role in the mechanism.

For both mechanisms, however, the effect of temperature on deposition can be attributed to change in viscosity, as surface tension does not vary much with temperature. Investigation of the effect of viscosity with ash particles is difficult, because little is known about the viscosities of iron aluminosilicates and ferrous sulfide at temperatures from 850° to 1050°C and, in sny case, the ash particles vary in composition and presence of high melting phases. Therefore, we have chosen to use glass spheres as a homogeneous model material of known viscosity for the study of deposition. We report here a few results of a preliminary nature.

EXPERIMENTAL

The test apparatus consists of a natural gas burner to provide hot flue gas, a dust feeder, and a 9.68-cm ID cyclone (Figure 1). Calculations indicate that the residence time of particles in the hot flue gas is sufficient to heat the particles to the temperature of the flue gas at the cyclone entrance. The inlet section of the cyclone is jacketed to allow cooling of the wall; or alternatively, it can be heated to achieve substantially equal gas and wall temperatures. Temperature readings of the gas during a run are taken by a bare wire thermocouple projecting into the gas just upstream from the inlet section of the cyclone; it is calibrated before the run by an aspiration thermocouple in the inlet section. Temperature of the wall is measured by a thermocouple embedded in it at the spot where the entering gas impinges, where coherent deposits typically form (1,2). The surface of the inlet section is smoothed with No. 320-grit emery paper before each test.

The feed dust in these tests was supplied by the Cataphote Division of Ferro Corporation as Class IV-A uncoated Unispheres of soda-lime glass in a nominal 13-44 μm diameter. A Coulter counter size distribution analysis indicated that the size ranged only between 20 and 51 μm, with 14% greater than 40 μm and 3% smaller than 25 μm.

To determine the borderline of deposition we have made a total of nine runs with the glass spheres, of which seven were within about 50°C of a borderline region obtained by plotting wall temperature against gas temperature (Figure 2). The burner was operated to yield an oxidizing atmosphere at rates giving cyclone inlet velocities ranging from 30 to 50 f/s; these velocities are comparable to those of laboratory tests with particles of pilot plant deposits. Very light but firm deposits of the spheres were observed at the jet impingement area in three of these tests. The results indicate that the borderline for firm deposition with equal gas and wall temperatures is between 800° and 850°C. The slope of the borderline, which should depend mostly on the specific heat of the dust, is assumed to be parallel to the better-established borderline for the pilot plant deposits, which is also shown in Figure 2. In the future, we expect to make additional tests to establish the borderline more precisely and to determine the effect of variables such as velocity and size of particles.

We have chemically analyzed the glass spheres and from this estimated the viscosity at 800° and 850°C by means of the correlation equations of Lyon (4,5). The range of viscosity thus obtained over the above temperature range is 6.3×10^5 to 2.9×10^6 poises. This is near the geometric mean of the viscosities at the softening and working temperatures of glass (5).

DISCUSSION

According to Dietzel's correlation of the surface tension of glasses, glazes, and enamels with composition (6), the surface tension of the pilot plant deposits is up to about 25% higher than that of the glass used here. Neglecting this difference and the effect of particle shape, we may conclude that the effective viscosity of the pilot plant deposit for borderline deposition in the laboratory hot cyclone is in the range reported above for the glass spheres. In the pilot plant or in a commercial plant with much larger cyclones, considerable scale-up is required for application of our results, but we think it likely that they apply there also.

REFERENCES CITED

1. Mason, D. M.; Rehmat, A.; Tsao, K. C. "Chemistry of Ash Deposits in the U-GAS Process." In Fouling of Heat Exchange Surfaces, Bryers, R. W., Ed. Engineering Foundation: New York, 1983.

2. Tsao, K. C.; Tabrizi, H.; Rehmat, A.; Mason, D. M. "Coal-Ash Agglomeration in a High-Temperature Cyclone," Am. Soc. Mech. Eng. [Pap], ASME Annual Meeting, November 1982, ASME Preprint No. 82-WA/HT-29.

3. Raask, E. VGB Kraftwerkstechnik 1973, 53(4), 248.

4. Lyon, K. C. J. Res. Nat. Bur. Stand. Section A, 78A, 1974, 497.

5. Boyd, D. C.; Thompson, D. A. "Glass," in Encyclopedia of Chemical Technology, 11, 807-80. Wiley: New York, 1980.

6. Scholze, H. "Glas-Natur, Struktur and Eigenschaften," 213-21. Vieweg: Braunschweig, 1965.

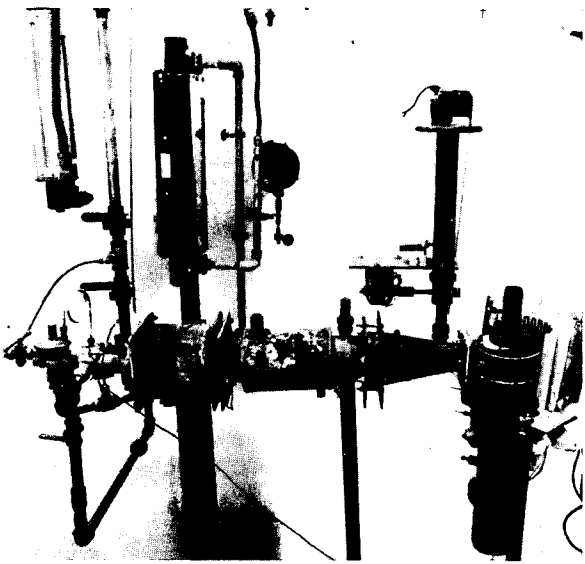

Figure 1. LABORATORY HOT CYCLONE APPARATUS

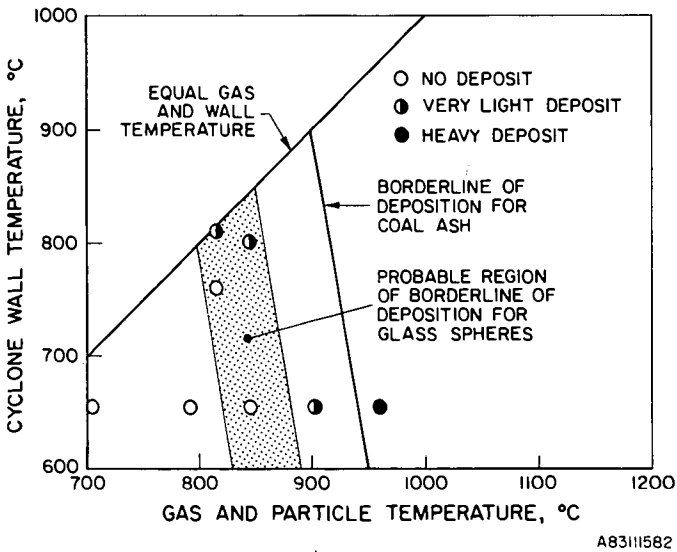

Figure 2. BORDERLINE OF DEPOSITION

A STUDY OF SLAG DEPOSIT INITIATION IN A DROP-TUBE TYPE FURNACE

Murray F. Abbott* & Leonard G. Austin

Fuel Science Section and Department of Mineral Engineering
The Pennsylvania State University
University Park, PA 16802

ABSTRACT

A drop-tube furnace was designed and constructed for the purpose of simulating the time/temperature environment for p.c. combustion in a utility furnace. The ash produced was impacted on oxidized boiler steel coupons at gas and metal temperatures similar to upper furnace waterwall tubes. Both fly ash and deposits were similar to those of a pilot-scale (7-9 kg/hr) combustor. Iron-rich slag droplets produced from pyrite-rich p.c. particles bonded strongly with the oxidized steel surface. These particle types were found at the base of ash deposits after removal of sintered and loose ash for both eastern and western coals. Adhesion of iron-rich droplets was a function of both flame and metal surface temperatures. Also, volatile species, i.e., alkali and exchangeable cations influenced the "sticking" behavior of the iron-rich droplets. These trends are in qualitative agreement with previous sticking test results.

INTRODUCTION

All coals contain inorganic matter which is converted to ash when the coal is burned. The management of this ash constitutes one of the principal limiting design considerations for a p.c. steam generator. Operational problems occur if ash deposition and build-up on heat exchange surfaces becomes unmanageable. A single day's outage for an 800 MW unit for ash removal and repair can cost the utility as much as $600,000 in lost electrical generation (1).Derating of the boiler system to manage ash deposition problems can cost millions of dollars annually. This investigation is part of an ongoing research program to gain a better fundamental understanding of the initiation of slag deposits on the upper walls of a boiler furnace enclosure. This paper reports on the development of a gas-fired vertical muffle tube (drop-tube) furnace as a new research tool.

A previous laboratory test, the sticking test (2-7) led to a number of conclusions concerning the mechanism and chemistry of molten slag drop adhesion to oxidized boiler steels. However, this test had several inherent disadvantages. It required the use of comparatively large molten ash drops (2 mm in diameter) and there was no proof that the conclusions applied equally well to the smaller size droplets (submicron to 250 m) produced in p.c.-fired furnaces. Also, the large drops formed from a coal ash contained all of the constituents of the ash (mean ash composition) which cannot accurately simulate the variety of mineral associations occurring on a particle-by-particle basis in a pulverized coal (8). Thus, the purpose of the drop-tube furnace was to produce coal fly ash particles under the same time/temperature environment experienced in full-scale boiler combustion followed by impaction on an oxidized boiler steel coupon simulating an upper furnace waterwall surface.

EXPERIMENTAL

Three Pennsylvania bituminous coals, designated Keystone, Montour and Tunnelton and a Decker, Montana subbituminous coal were studied in this investigation. All are current steam coals. Semi-quantitative mineralogical analysis of LTA and spectrochemical analysis of ASTM HTA are given in Table 1 for the three

*Current Address: Babcock & Wilcox R&D, 1562 Beeson Street, Alliance, OH 44601

Pennsylvania coals and raw (untreated) and acid washed Decker coal samples.

The drop-tube furnace system in which the test coals were burned is shown in Figure 1. It consisted of four major component parts: (i) a gas-fired hot zone, (ii) a fluid-bed feeding system, (iii) a preheat section and injector, and (iv) a water-cooled ash collector probe. The conditions inside the heated muffle tube simulated those of a utility furnace combustion zone: (i) maximum gas temperatures of 1500 to 1750°C, (ii) particle residence times between one and two seconds, and (iii) ash sampling temperatures ranging from 1000 to 1300°C. The fluid-bed feeder delivered between 0.2 and 0.3 grams of pulverized coal with slightly less than 1 liter of primary air per minute. In the preheat section the secondary air stream (roughly 2 liters/min) was heated to about 1000°C before a honeycomb flow straightener distributed it in streamlines across the muffle tube cross-section. The cold p.c./primary air mixture was carried by the injector to the hot combustion zone. A thin pencil-like p.c. stream was burned as it passed through the heated muffle tube. The fly ash produced was accelerated and impacted onto a water-cooled boiler steel coupon at surface temperatures of 300 to 450°C.

The ash deposits were characterized physically by observation under both a Zeiss optical and IDS-130 scanning electron microscope (SEM). Chemical characteristics were determined by energy dispersive x-ray fluorescence equipment associated with the SEM.

RESULTS AND DISCUSSION

Physical characteristics for all ash deposits were similar. Figure 2 shows a typical ash deposit structure on both a macro and microscale. The top photograph (A) shows an ash deposit collected from the raw Decker coal on a Croloy 1/2 steel coupon. The lower optical photomicrograph shows the strongly bonded material remaining on the surface after the comparatively loosely adhered ash had been brushed away. The opaque black droplets are rich in iron (85 to 100 wt. %) and the light colored transparent glassy spheres are predominantly alumino-silicates. The deposit build-up mechanism appeared to be similar for all coals. All originated with the relatively strong bonding of iron-rich slag drops to the oxidized steel surface. Alumino-silicates were only found in this layer for the raw Decker coal. In addition, there was always a layer of very fine particles (submicron) covering the entire coupon surface. It was not possible to brush or blow this layer from the surface. A region of loosely bonded ash particles often containing most all of the major constituents of the ash then built upon the more strongly adhered droplets. There was little if any interaction between the loose ash and adhesive particles. As the distance from the steel surface increased the ash particles began to sinter, eventually forming a fluid mass in some instances.

Preferential deposition of iron-rich species has been suggested by other investigators (9,10). It was also observed in a pilot-scale p.c. test combustor (11). The fine particle layer probably formed on the coupon surface due to convective diffusion to the relatively cold steel coupon (12). Presumably the scouring action of the ash laden gases in a utility furnace would prevent formation of the loose ash layer until the iron-rich layer is more extensively developed and interaction with successive layers can occur.

The iron-rich deposit base particles formed from the Keystone coal at flame temperatures of 1470 (A) and 1500°C (B) are shown in the SEM photomicrographs in Figure 3. The concentration of these particles increased with increasing flame temperature. Note that the particles flattened more on impact at the higher temperature, probably due to a decrease in particle viscosity. There appeared to be two different iron-rich particle types in each deposit: (i) a porous particle with a rougher surface texture, and (ii) a more glassy appearing particle with a very smooth surface texture. X-ray fluorescence spectrograms are also shown in Figure 3. The porous type particles were found to contain exclusively iron (see analysis of Point 1 in Figure 3B), whereas the more glassy particle types contained smaller amounts of silicon, aluminum and potassium (Point 2).

The two furnace operating parameters which most influenced ash deposition rates

were flame and coupon surface temperatures. Both of these trends are shown in Tables 2 and 3. Deposit build-up rates increased between two and six times with each increase in flame temperature and ten-fold for a 30 degree rise in coupon surface temperature. Removing exchangeable cations from the Decker coal caused a three-fold decrease in the ash deposition rate, see Table 4. The exchangeable cations appeared to play a significant role in both the initial iron-rich deposit and the sintering properties exhibited by the ash deposit. The sintered ash collected from the raw Decker coal was yellow-brown in color and comparatively difficult to break apart requiring a force of nearly 20 psi. The acid form sinter was coral colored and broke apart while removing the coupon from the collector probe.

CONCLUSIONS AND FUTURE WORK

The drop-tube furnace closely simulated the time/temperature history of a utility boiler furnace. One type of slag deposit initiating particle which strongly bonds to oxidized boiler steels is low melting iron-rich droplets produced from pyrite-rich p.c. particles. Flame and metal surface temperatures strongly influence ash deposit build-up rates. Sufficient evidence exits to suggest that alkalis and calcium enhance the "sticking" behavior of iron-rich and other fly ash droplets. This investigation revealed a qualitative relationship between results obtained from several different apparatus used to study slag initiation: (i) sticking apparatus, (ii) drop-tube furnace, and (iii) pilot-scale p.c. test combustor.

Future work in the drop-tube furnace will include: (i) developing a method for defining the relative adhesion properties of ash particle types, and (ii) more clearly defining the role of volatile species in deposit initiation and growth. This second goal can be accomplished by investigating controlled composition synthetic polymer/mineral combinations.

ACKNOWLEDGEMENTS

This study was funded by grants from the Department of Energy, Contract No. DE-FG22-80PC-30199 and Babcock and Wilcox.

REFERENCES

1) Williams, N., Sharbaugh, R., Van Tiggerler, D. and Kadlec, R., Electric Light and Power, 25 (1983).

2) Moza, A.K. and Austin L.G., Fuel, 60, 1057-64 (1981).

3) Abbott, M.F., Moza, A.K. and Austin, L.G., Fuel, 60, 1065-72 (1981).

4) Moza, A.K. and Austin, L.G., Fuel, 61, 161-5 (1982).

5) Abbott, M.F. and Austin, L.G., Fuel, 61, 765-70 (1982).

6) Abbott, M.F., Conn, R.E. and Austin, L.G., "Studies on slag deposit formation in pulverized coal combustors. 5. The effect of flame temperature, thermal cycling of the steel substrate, and time on the adhesion of slag drops to boiler steels", in preparation.

7) Abbott, M.F. and Austin, L.G.,"Studies on slag deposit formation in pulverized coal combustors. 6. The sticking behavior of slag from three Pennsylvania steam coals", in preparation.

8) Moza, A.K., Austin, L.G. and Johnson, G.G., Jr., SEM/1979/1, p. 473, SEM Inc, AMF O'Hare, IL, 1979.

9) Borio, R.W. and Narcisco, R.R., Journal of Engineering for Power, 101, 500 (1979).

10) Bryers, R.W., Journal of Engineering for Power, 101, 517 (1979).

11) Austin, L.G., Abbott, M.F. and Kinneman, W.P., Jr., ASME 83-JPGC-Pwr-42.

12) Rosner, D.E., Chen, B.K., Fryburg, G.C. and Kohl, F.J., Combustion Science and Technology, 20, 87-106 (1979).

TABLE 1. MINERALOGICAL AND ELEMENTAL ASH COMPOSITION FOR TEST COALS

Procedure/Coals	Montour	Keystone	Tunnelton	Raw Decker	Acid-Washed Decker
Mineralogical (wt. % LTA)					
Quartz	25	25	22	20	30
Pyrite	15	10	15	5	10
Calcite	5	--	5	5	--
Gypsum	--	5	--	30	--
Kaolinite	17	30	18	11	16
Illite	30	20	30-40	--	--
Feldspan	--	--	5-10	--	--
LTA (wt. % as received coal)	18.0	21.6	22.9	6.3	3.3
HTA (wt. % as received coal)	15.8	18.0	20.1	4.0	2.2
Spectrochemical (wt. % HTA)					
SiO_2	51.7	54.1	50.3	26.5	53.0
Al_2O_3	25.6	25.9	26.8	15.5	28.5
TiO_2	1.3	1.3	1.3	0.9	2.7
Fe_2O_3	14.1	9.7	11.0	5.3	9.2
CaO	2.4	1.8	2.5	14.3	4.1
MgO	0.9	1.0	1.0	2.5	0.7
Na_2O	0.2	0.3	0.4	0.03	0.01
K_2O	2.4	2.9	2.9	5.0	0.4
SO_3	1.5	1.1	2.3	0.97	0.6
P_2O_5	0.4	0.4	0.4	21.6	--

TABLE 2. DEPOSIT BUILD-UP RATES FOR THE THREE PENNSYLVANIA STEAM COALS AT THREE FLAME TEMPERATURES

Coal	Flame Temperature °C	Deposit Mass mg	Relative Build-up Rates mg/min	mg/gr Coal	Percent of Total Ash (Based on HTA)
Montour	1465	26.5	2.2	11.0	6.9
	1518	64.5	5.4	22.5	14.2
	1561	133.0	11.1	46.3	29.2
Keystone	1470	24.0	2.0	7.1	3.9
	1500	117.7	9.8	40.8	22.7
	1560	286.1	23.8	99.2	47.3
Tunnelton	1467	39.7	3.3	11.8	3.1
	1510	252.6	21.1	75.4	19.7
	1518	297.1	24.8	103.3	51.3

TABLE 3. DEPOSIT BUILD-UP RATES FOR THE KEYSTONE COAL AT A FLAME TEMPERATURE OF 1500°C AND TWO DIFFERENT COUPON SURFACE TEMPERATURES

Coupon Surface Temperature °C	Deposit Mass mg	Relative Build-up Rates mg/min	mg/gr Coal	Percent of Total Ash (Based on HTA)
310-318	11.7	6.98	29.1	2.3
340-345	117.7	9.8	40.8	18.0

TABLE 4. DEPOSIT BUILD-UP RATES FOR RAW AND ACID WASHED DECKER COAL SAMPLES AT A FLAME TEMPERATURE OF 1500°C

Coal Sample	Deposit Mass mg	Relative Build-up Rates mg/min	mg/gr Coal	Percent of Total Ash (Based on HTA)
Raw Decker	82	4.1	14.6	36.6
Acid Washed Decker	25	1.3	5.4	23.7

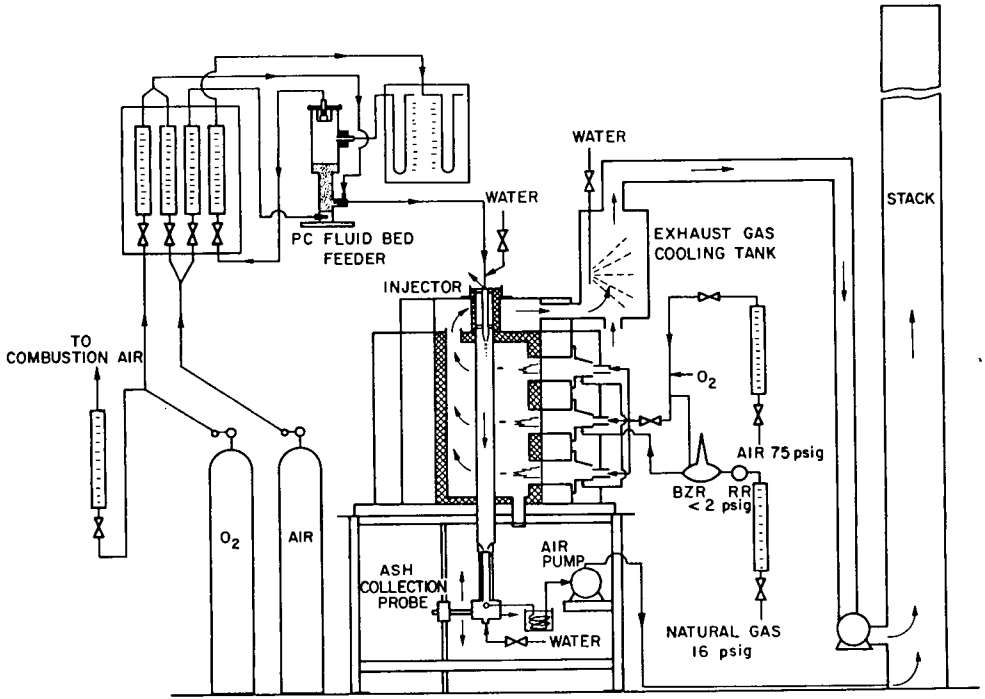

FIGURE 1 DROP-TUBE FURNACE SYSTEM

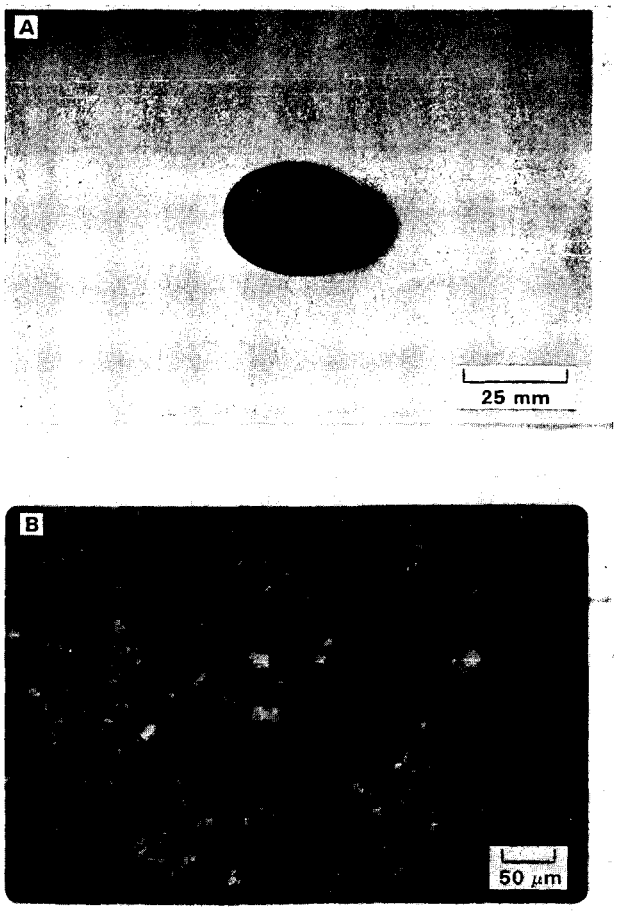

FIGURE 2 RAW DECKER COAL ASH DEPOSIT:
A) TOTAL DEPOSIT AFTER TWENTY MINUTES,
B) OPTICAL PHOTOMICROGRAPH OF BONDED ASH PARTICLES

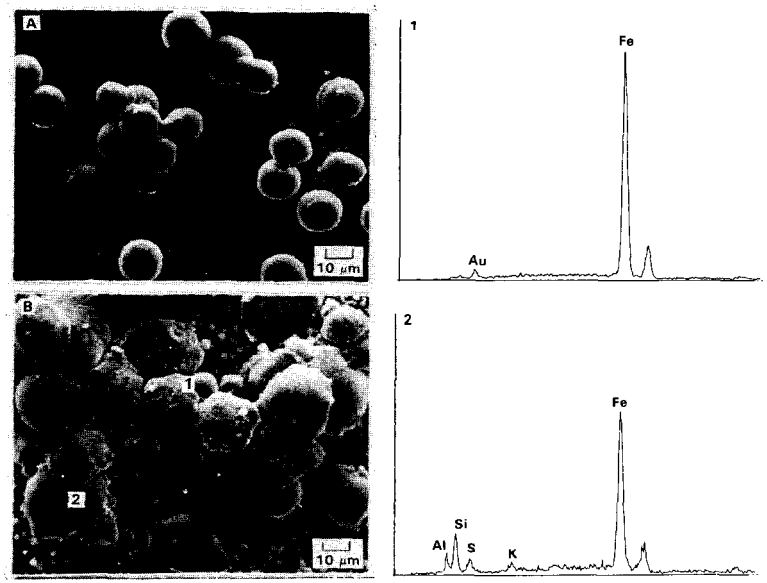

FIGURE 3 KEYSTONE COAL ASH DEPOSITS: A&B) SEM PHOTOMICROGRAPHS SHOWING IRON-RICH SLAG DROPLETS COLLECTED FROM FLAME TEMPERATURES OF 1470°C (A) AND 1550°C (B). X-RAY FLUORESCENCE SPECTROGRAMS CORRESPONDING TO POINTS 1 AND 2 IN PHOTO B.

INFLUENCE OF SEGREGATED MINERAL MATTER IN COAL ON SLAGGING

R. W. Bryers

Foster Wheeler Development Corporation
12 Peach Tree Hill Road
Livingston, New Jersey 07039

INTRODUCTION

The mineral content of any given rank of coal is a key factor in sizing and designing a steam generator or reactor. The mineral content becomes even more important as the premium solid fuels are consumed, leaving reserves with continual increasing mineral concentrations and lower quality ash. The problem of dealing with lower quality ash in coal is compounded by the increase in size of steam generators and refinements imposed by economic constraints. Empirical indices, based on coal ash chemistry and ASTM ash fusion temperatures or viscosity, are presently used to rank coals according to the fireside behavior of the mineral matter. Unfortunately, the indices are only marginally satisfactory, as they do not relate to operating or design parameters and frequently are based on a coal ash chemistry quite different from that deposited on the furnace wall. Frequently, different coals with identical ash chemistry produce decidedly different slagging conditions in steam generators of identical design operated in the same mode. Variations in composition of the slag, when compared with the coal ash, suggest specific minerals are being selectively deposited on furnace walls depending upon their specific gravity, size, composition, and physicochemical properties. It is quite apparent there is a need for a better understanding of the impact of mineral composition, its size, and its association with other minerals and carbonaceous matter on fireside deposits.

MINERAL MATTER IN COAL

Minerals occurring in coal may be classified into five main groups. These include shale, clay, sulfur, and carbonates. The fifth group includes accessory minerals such as quartz and minor constituents like the feldspars (1).

Shale, usually the result of the consolidation of mud, silt, and clay, consists of many minerals including illite and muscovite--these are forms of mica. Kaolinite is the most common clay material (1).

The sulfur minerals include pyrites with some marcasite. Marcasite has the same chemical composition as pyrites but a different mineralogical structure. Sulfur is also present as organic matter and occasionally as sulfate. The latter usually occurs in weathered coal such as in outcrops. The amount of sulfate sulfur in coal is generally less than 0.01 percent.

Generally, 60 percent of the sulfur in coal is pyritic, particularly when the sulfur concentration is low. At higher concentrations it may run as high as 70 to 90 percent. Pyrite occurs in coal in discrete particles in a wide variety of shapes and sizes. The principal forms are (1-6):

- Rounded masses called sulfur balls or nodules an inch or more in size.
- Lens-shaped masses which are thought to be flattened sulfur balls.
- Vertical, inclined veins or fissures filled with pyrite ranging in

thickness from thin flakes up to several inches thick.

- Small, discontinuous veinlets of pyrite, a number of which sometimes radiate from a common center.

- Small particles, <72μ, or veinlets disseminated in the coal. Microscopic pyrite occurs in five basic morphology types: (a) framboids, (b) isolated euhedral crystals, (c) nonspherical aggregates of euhedral cyrstals, (d) irregular shapes, and (e) fractured fillings (7).

All coals contain some of the third and fifth forms of pyrite, and some coals contain all five of the principal forms (6,8,9).

The carbonates are mainly calcite, dolomite, or siderite. The occurrence of calcite is frequently bimodal. Some calcite occurs as inherent ash, while other calcite appears as thin layers in cleats and fissures. Iron can be present in small quantities as hematite, ankorite, and in some of the clay minerals such as illite. In addition to the more common minerals, silica is present sometimes as sand particles or quartz. The alkalies are sometimes found as chlorides or as sulfates but probably most often as feldspars, typically orthoclase and albite. In the case of lignites, unlike bituminous and subbituminous, sodium is not present as a mineral but is probably distributed throughout the lignite as the sodium salt of a hydroxyl group or a carboxylic acid group in humic acid. Calcium, like sodium, is bound organically to humic acid. Therefore, it too is uniformly distributed in the sample.

The term, "mineral matter," usually applies to all inorganic, noncarbonaceous material in the coal and includes those inorganic elements which may occur in organic combination. Physically, the inorganic matter can be divided into two groups--inherent mineral matter and extraneous mineral matter. Inherent mineral matter originates as part of the growing plant life from which coal was formed. Under the circumstances, it has a uniform distribution within the coal. Inherent mineral matter seldom exceeds 2 - 3 percent of the coal (10).

Extraneous mineral matter generally consists of large bits and pieces of inorganic material typical of the surrounding geology. In some cases the extraneous matter is so finely divided and uniformly dispersed within the coal it behaves as inherent mineral matter. Coal preparation can separate some of the extraneous ash from the coal substance, but it seldom removes any of the inherent mineral matter.

The physical differences between inherent and extraneous ash are important not only to those interested in cleaning coal but also to those concerned with the fireside behavior of coal ash. Inherent material is so intimately mixed with coal that its thermal history is linked to the combustion of the coal particle in which it is contained. Therefore, it will most likely reach a temperature in excess of the gas in the immediate surroundings. The close proximity of each species with every other species permits chemical reaction and physical changes to occur so rapidly that the subsequent ash particles formed will behave as a single material whose composition is defined by the mixture of minerals contained within the coal particle. The atmosphere under which the individual transformations take place will, no doubt, approach a reducing environment. Figure 1 illustrates a model of the coal and mineral matter as fed to the combustor and the fate of the minerals after combustion (11).

Extraneous materials can behave as discrete mineral particles comprised of a single species or a multiplicity of species. As already indicated, a portion of this material may be so finely divided it can behave as inherent mineral matter.

During combustion the larger particles respond individually to the rising temperature of the environment. In the absence of carbon or other exothermic reactants, the particle should always be somewhat less than the local gas temperature. However, the particles may be subjected to either reducing or oxidizing conditions. As each particle rises in temperature, it loses water of hydration, evolves gas, becomes oxidized or reduced, and eventually sinters or melts, depending on its particular composition or temperature level.

It is evident, then, that there can be a great difference in the final state of each particle, depending upon its composition and whether it is inherent or extraneous ash. Figure 2 summarizes the phase transformations which pure mineral matter commonly found in coal undergoes during heating (12,13,14). Since this data was developed primarily by mineralogists performing differential thermal analysis under air at slow heating rates, it must be used only as a guideline for predicting the thermal behavior of minerals in coal. Thermal shocking these minerals in the presence of carbon and other mineral forms at very high temperatures, no doubt, will alter some of these transformations and may defer others until postcombustion deposition on heat transfer surfaces.

Clays and Shale

The melting temperatures of most pure minerals are in the vicinity of or greatly exceed the maximum flame temperature encountered during combustion. Therefore, the fused spheroidal fly ash, generated from the mineral matter in coal, primarily forms as the result of the fluxing action between pure minerals contained within each particle. Illite and biotite appear to be an exception. Both minerals contain small concentrations of iron and potassium and form a glassy phase at 950°C and 1100°C, respectively. Depending upon its fluidity, this glassy phase could be responsible for surface deformation at a relatively low temperature and provide the necessary sticking potential to prevent reentrainment upon contacting heat transfer surfaces. Low temperature ash of a gravity fraction containing illite was heated in a thermal analyzer under air to 600 and 1000°C, respectively, and compared to the low temperature ash of a gravity fraction void of illite. The scanning electron photomicrographs, appearing in Figure 3, indicate the minerals containing illite did, indeed, show signs of the formation of a melt.

Quartz

The inherent silica retained in the char as quartz or silica released from kaolinite and illite at low temperatures (i.e., 950°C) is partially reduced to silica monoxide. Unlike silica which boils at 2230°C, silica monoxide melts at 1420°C and boils at 2600°C (15). The vapor pressure of silicon is low--in the range of temperatures experienced during combustion. Honig reports values ranging from 0.01m Hg at 1157°C to 1m Hg pressure at 1852°C (15,16). The presence of other mineral matter and carbonaceous material appears to alter vapor pressure substantially. When a mixture of alumina silicate and graphite was heated, the volatilization of silicon monoxide began at about 1150°C and reached a maximum at 1400°C. Mackowsky reports that volatilization of silicon monoxide starts at about 1649°C in the presence of carbonates and clays and reaches a maximum at 1704°C (17). In the presence of pyrite or metallic iron, volatilization begins at about 1560°C and continues at a rapid rate as the temperature rises until practically all the silica in the mineral is volatilized. Sarofin has shown that about 1.5 to 2.0 percent of the ASTM ash in bituminous coals volatilize (18). Approximately 35 - 40 percent of the volatilized material was silica. The next largest component was iron. Extraneous quartz appears to be relatively innocuous unless contaminated by Fe_2O_3, CaO, or K_2O.

Pyrites

The decomposition of pyrite has been examined by numerous investigators under oxidizing, neutral, and reducing environments. TGA, rather than DTA, has been used by most investigators. Acquisition of representative data is difficult, as the decomposition process is complex and sensitive to many variables including the chemical composition of pyrites, its grain size, its origin, the presence of adventitious impurities, the composition of the local environment, and diffusion rates through sulfated layers. Under oxidizing conditions it is believed that pyrites decompose directly to an iron oxide and SO_2 or SO_3 or iron sulfate and SO_2, depending upon the final temperature level. Under reducing conditions pyrrhotite and either carbon or hydrogen sulfide form. Complete reduction results in elemental iron and carbon disulfide. There is also a possibility that pyrrhotite may form under oxidizing conditions as an intermediate step in the presence of sufficient adventitious carbon. Pure pyrites ignite at about 500°C in the thermal analyzer at 20°C/min and burn out by 550°C in a single-step process, as shown in Figure 5. Pure pyrites do ignite as readily as bituminous coal; however, the burnout time is comparable. Although pyrrhotite ignites readily, it requires as much time as anthracite to complete combustion. Pyrites containing small quantities of adventitious carbon, as might be found in the -1.80 +2.85 gravity fraction, appear to form pyrrhotite, deferring burnout until 800°F. Within the combustor the problem is compounded by the fact that pyrite particles do not shrink during the combustion process as do coal particles, and hence, their burnout time is extended. The burnout time of particles in excess of 40μ appears to exceed the residence time available in most combustors.

TGA reveals decomposition rates but tells little about the physical state during the combustion process. Phase diagrams for the Fe-S-O and FeS-FeO system, representing transitory states at the particle surface, imply the formation of a temporary melt at low temperatures. SEM photomicrographs, appearing in Figure 5, of pure pyrites heated to 600°C, 800°C, and 1000°C under reducing conditions clearly reveal the formation of a melt at temperatures as low as 600°C. Large particles of partially-spent pyrites, which may be molten on contact with the heat transfer surface, complete the oxidation process in situ, forming a solid fused deposit with a very high melting temperature.

An examination of the thermal behavior of the mineral matter in coal indicates the mineral origin of the elements found in coal ash and their juxtaposition with regard to each other, as well as other mineral forms, and determines their physical fate during combustion. As indicated in Figure 1, the physical state (i.e., vapor or solid) and the size of solidified ash will determine the mode and rates of migration to the heat transfer surface. The physical state at the tube surface will depend upon the local surface temperature and the composition of the particulate depositing. In the case of pyrites residence time and environment conditions may also play a significant role.

CHARACTERIZATION OF MINERALS IN COAL

The fireside behavior of mineral matter in coal has been investigated by characterizing the mineral content of several bituminous coals, using size and gravity fractionation analysis of pulverized coal and then firing the coal in a vertically fired combustor. High sulfur coals containing pyrites of varying size and varying association with carbonaceous and other mineral forms were selected for examination. A comparison was also made with western subbituminous coals to assess the impact of potassium in the mineral illite on furnace slagging.

Each coal was analyzed for proximate, ultimate, ash chemistry, and ash fusion temperatures to permit evaluation using conventional data. The pulverized coal samples were then divided into four sizes representing equal weights (i.e., +105μ, -105μ +74μ, -74μ +44μ, and -44μ). Each size fraction was separated into four weight classes, thereby, partitioning the coal into groups dominated by coal, nonpyritic mineral matter, and pyrites. The partitioned coal was analyzed for ash chemistry, ash fusion temperature, combustion profile, and mineral content.

The analytical data is summarized in Figure 6. The enclosed data points represent the composite analysis. The open data points represent the fractionated species. Ash softening temperatures and percent basic constituents were selected as the variables to characterize the coal, as they appear most frequently in the indices used to express the slagging or fouling potential of the fuel. It is quite evident the combustor is exposed to ash with a wide range of chemical compositions and melting temperatures not adequately identified by a composite coal analysis. The data indicates slagging was most severe with coals having the highest melting temperature and demonstrating the greatest degree of separation of ash from coal and pyrites from other mineral matter. The two coals with the lowest composite ash softening, having the highest slagging index by conventional evaluation, caused the least slagging. Liberation of mineral matter from these two coals was also the lowest.

The data was replotted on fusibility diagrams, appearing in Figure 7, typifying the coal with the greatest partitioning of mineral matter and highest degree of slagging and the coal with the least liberation of mineral matter and degree of slagging. The fusibility diagram illustrates the size and weighted contribution of each ash specie. It also shows the degree of liberation of nonpyritic and pyritic mineral matter. By washing the worst coal at 1.80 sp. gr. and 14M x 0, thereby minimizing extraneous ash as well as total sulfur, the degree of slagging of the Upper Freeport coal was greatly reduced.

COMBUSTION TESTING

Deposits were removed from various locations in the combustor after firing each coal for ≅14 - 16 hours. Samples were removed from slagging probes at 398 - 510°C, fouling probes at 510 - 537°C, and refractory surfaces at 537 - 1204°C and examined using the scanning electron microscope and energy dispersive x-ray. Fly ash samples were also examined for carbon loss, surface morphology, and chemical composition.

The deposits forming on the slagging probes were initiated by a thin layer of powdery fly ash, <8μ in size, enriched with small quantities of potassium. Beads of slag formed on top of this thin layer when the surface temperature approached the initial deformation temperature of the deposit. Growth progressed with the formation of rivulets from which a continuous phase of molten slag formed. Deposits forming on the refractory surface represent an advanced stage of slag due to the higher surface temperatures which could only be achieved on the cooler probes after the initial dust layer formed. The composite ash chemistry and ash fusion temperatures of the slag resemble that of the heaviest gravity fraction (i.e., >1.80 sp. gr.) in most cases. Macrophotographs of the deposit formation on the furnace probes subjected to axial symmetric flow at low gas velocities (5 - 6 ft/s), illustrated in Figure 8, show that the initial layer of dust, upon which further slagging depends, formed only when firing coals whose ash contained more than 1 percent potassium. Continued deposit growth resulting in serious slagging is dependent upon the total pyrites liberated from the coal.

SEM microphotographs and EDAX scans of the cross section and outer surface of the slag deposit, illustrated in Figure 9, indicate the chemistry of the deposit is not uniform. The bulk of the fused material is rich in silica, low in iron, and virtually depleted of potassium. The outermost layers, no more than 2 to 3μ thick, are very rich in iron and frequently also rich in calcium. On occasions, the outer surface is covered with small particulate several microns in diameter or undissolved cubic or octahedral crystals whose origin is pyrites. Similar formations have been observed in full-scale operation. The evidence indicates deposits form under axial symmetric flow conditions in the furnace by the fluxing action at the heat transfer surface of small particles, <8μ in diameter, of decidedly different chemical composition and mineral source. Migration of the fly ash to the surface is by means of eddy diffusion, thermophoresis, or Brownian motion.

Sintered deposits form at the furnace exit at lower gas temperatures and in zones subject to rapid changes in direction. The deposit is composed of spheroidal particles <40μ bound together by a molten substance. In those cases where substantial quantities of coarse pyrites are liberated from the pulverized coal, the spheroids are nearly pure Fe_2O_3, as shown in Figure 10. The matrix contained silica, alumina, iron, and potassium and has an initial deformation temperature of 1000°C, as determined by differential thermal analysis. The heavier pure iron spheroids deposit as a result of inertial impact. The mineral source of the molten phase is most likely illite.

Deposits also form on the leading edge of the first row of tubes in the convection pass when firing coals which liberate pure, coarse pyrites. These tubes are subjected to high gas velocities and have moderate to high collection efficiencies for particles between 40 and 100μ. The deposits are nearly pure Fe_2O_3. They are hard and fused despite being at gas temperatures below their initial deformation temperature. No doubt, the final stages of decomposition of the pyrites takes place at the tube surface.

CONCLUSIONS

The formation of fireside deposits in furnaces depends on the composition, size, and association of mineral matter liberated from the coal. Selective deposition of specific mineral species depends on their size, thermal behavior, the local gas temperatures, and their mode of transport to the surface. Consequently, the composition of the sintered deposit or molten slag may vary with time at a given location and will most probably vary throughout the combustor, depending on local temperatures and fluidynamics. The composition of the slag may be substantially different from the composite coal ash, depending upon its heterogeneity. Illite is a likely candidate as the mineral most responsible for initiating deposits. The molten phases are frequently part of the $FeO-SiO_2$ or $FeO-CaO-SiO_2$ system and depend on the interaction of quartz, calcite, or pyrites at the heat transfer surface. Liberated pyrite crystals and small particles are primary candidates for slag formation subjected to parallel flow regimes at low velocities. Coarse pyrites can be selectively deposited and solely responsible for deposit formation on surfaces subjected to flue gas impingement at high velocities.

ACKNOWLEDGMENTS

Substantial portions of this study were sponsored by the U. S. Department of Energy, Pittsburgh Energy Technology Center, Contract DE-AC22-81PC40268, under the direction of Mr. J. Hickerson, Mr. H. Ritz, and Dr. R. Walker. I am grateful to Mr. O. R. Walchuk for supervising the combustion program; Mr. G. Lantos, who

directed laboratory analyses; Messrs. G. Stanko and I. Dojcsanszky for SEM and EDAX analyses; and Mrs. J. Betyeman for preparing the manuscript.

REFERENCES

1. R. W. Bryers, "The Physical and Chemical Characteristics of Pyrites and Their Influence on Fireside Problems in Steam Generators," Trans. of the ASME, Journal of Engineering for Power, October 1976.

2. F. E. Walker and E. F. Hartner, "Forms of Sulfur in U.S. Coals," IC830, Bu. Mines, U.S. Dept. of the Interior, 1966.

3. H. J. Gluskoter and J. A. Simon, "Sulfur in Illinois Coals," Circular 432, Illinois State Geological Survey, Urbana, Illinois, 1968.

4. P. Nicholls and W. A. Selvig, "Clinker Formation as Related to the Fusibility of Coal Ash," U.S. Bureau of Mines Bulletin 364, 1932.

5. J. F. Barkley, "The Sulfur Problem in Burning Coal," Technical Paper 436, Bu. of Mines, U.S. Dept. of the Interior, 1928.

6. "Sulfur Codes Pose Dilemma for Coal," Environmental Science and Technology, Vol. 11, No. 12, December 1970.

7. Hobart M. King and John J. Renton, "The Mode of Occurrence and Distribution of Sulfur in West Virginia Coals," Carboniferous Coal Guide Book, A. Donaldson, M. W. Presley, and J. J. Renton, Editors, West Virginia Geological and Economic Survey Bulletin B-37-1, 1929.

8. M. Deul, "Preliminary Observation of the Mode of Occurrence of Pyrite in Coal," Second Conference, Eastern American Anthraologist, University Park, Pennsylvania, May 26, 1958, p. 27.

9. Hobart M. King, "Sulfide Minerals in West Virginia Coals," Mountain State Geology, West Virginia Geological and Economic Survey, December 1980.

10. R. W. Bryers, "Influence of the Distribution of Mineral Matter in Coal on Fireside Ash Deposition," Trans. of the ASME, Journal of Engineering for Power, October 1979.

11. R. C. Flagan and A. F. Sarofim, "Transformation of Mineral Matter in Coal," Progress in Energy and Combustion, to be published.

12. H. R. Hoy, A. G. Roberts, and D. M. Wilkins, "Behavior of Mineral Matter in Slagging Gasification Processes," I.G.E. Journal, June 1965.

13. P. Jackson, "From Mineral Matter to Deposits in PF-Fired Boilers, Part I: The Behavior of Mineral Matter in the Flame," Pulverized Coal Firing - The Effects of Mineral Matter, T. Wall, ed., University of Newcastle, August 1979.

14. J. D. Watt, "The Physical and Chemical Behavior of the Mineral Matter in Coal Under the Conditions Met in Combustion Plants: A Literature Survey--Part I: The Occurrence, Origin, Identity, Distribution, and Estimation of the Mineral Species in British Coals," BCURA Industrial Laboratories, Leatherhead, Surrey, England, August 1979.

15. N. W. Nelson, et al., "A Review of Available Information on Corrosion and Deposits in Coal- and Oil-Fired Boilers and Gas Turbines," ASME, 1954.

16. R. E. Honig, "Sublimation Studies of Silicon in the Mass Spectrometer," Journal of Chemistry and Physics, Vol. 77, 1954, pp. 1610-1611.

17. M. Th. Mackowsky, "The Behavior of Coal Minerals at High-Combustion Temperatures with Consideration of Slow and Rapid Heating," Paper Given at The Annual Meeting of the Association of Large Boiler Owners, Nürnberg, Germany, July 1955.

18. R. J. Quann and A. F. Sarofim, "Vaporization of Refractory Oxides During Pulverized Coal Combustion," Nineteenth Symposium International on Combustion, The Combustion Institute, 1982.

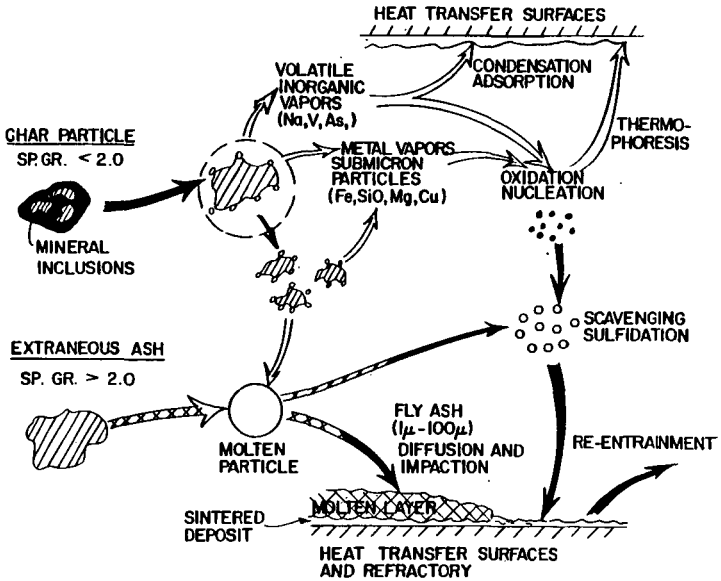

Figure 1 Fate of Mineral Matter in Coal During Combustion, as Proposed by Dr. Sarofin

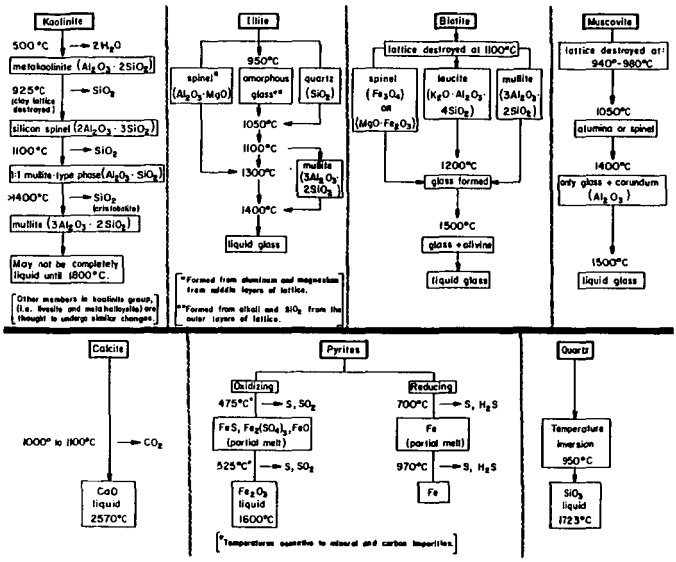

Figure 2 Phase Transformation of Some Mineral Matter Commonly Found in Coal

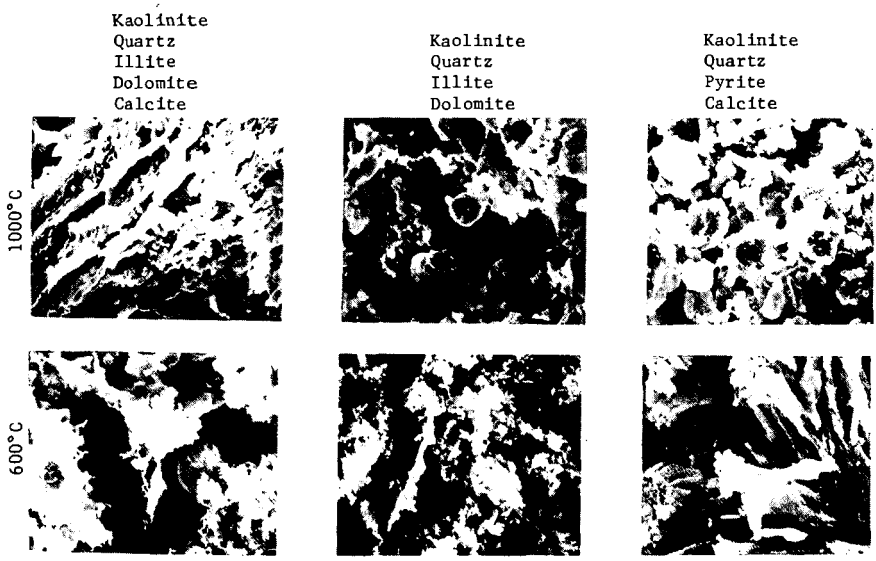

Mag. 3000X

Figure 3 SEM Photomicrographs Showing the Impact of Illite on the Thermal Behavior of Low Temperature Ash

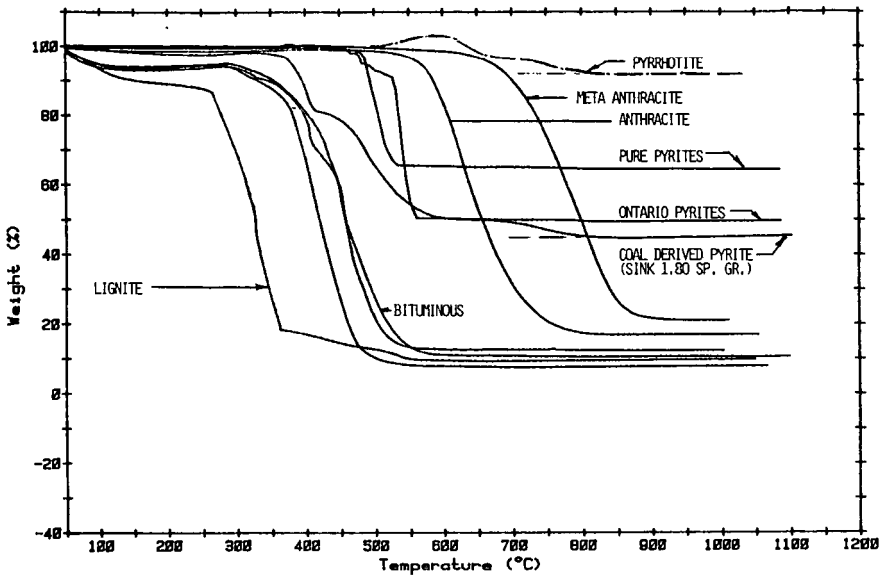

Figure 4 TGA Thermograms Comparing the Decomposition of Various Grades of Pyrites with Various Ranks of Coal

Mag. 3000X

600°C 800°C 1000°C

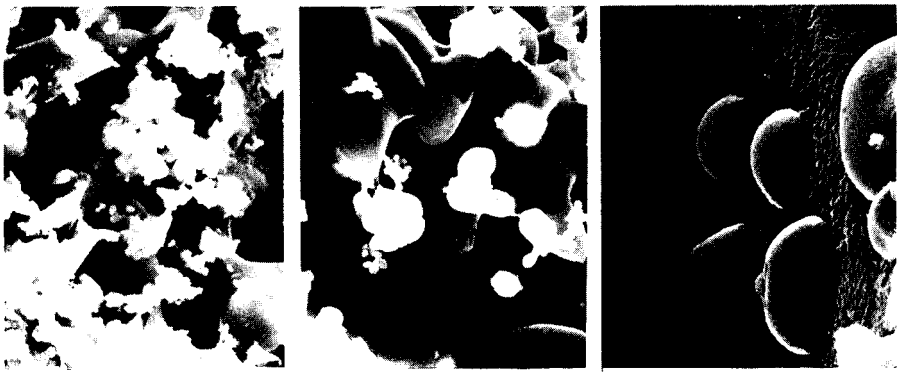

Figure 5 Pure Pyrites Heated Under Reducing Conditions to 600, 800, and 1000°C

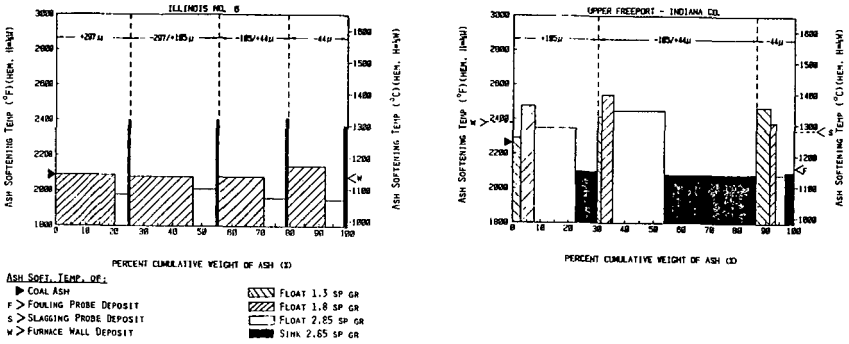

Figure 7 Fusibility Diagrams

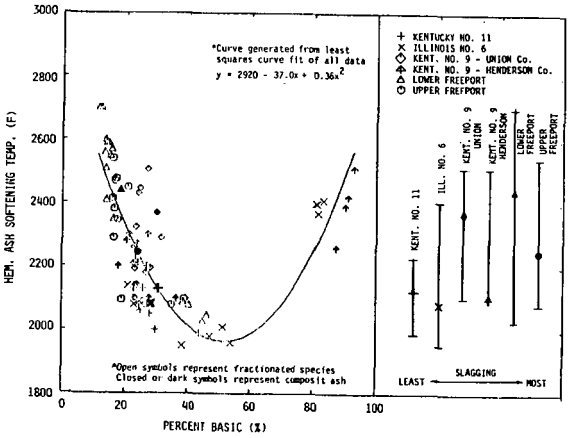

Figure 6 Ash Softening Temperature Vs. Percent Basic for Composite and Fractionated Coal Species

Ash Soften. Temp. (Red) and % Ash	% Liberated Fe_2O_3 in Coal			%Kin Ash	Ash Soften. Temp. (Red) and % Ash
2130°F 14.9	Kentucky No. 11 0.225			Western Fuel 1 0.2	2165°F 6.7
2080°F 9.4	Illinois No. 6 0.159	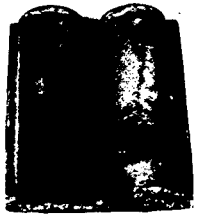		Western Fuel 2 1.0	2252°F 16.67
2443°F 16.4	Lower Freeport 1.56			Western Fuel 3 1.2	2232°F 25.73
2245°F 23.5	Upper Freeport 1.67			Lower Freeport 2.5	2443°F 16.4

Figure 8 Slagging on Furnace Probes after 14 - 16 Hours Operations

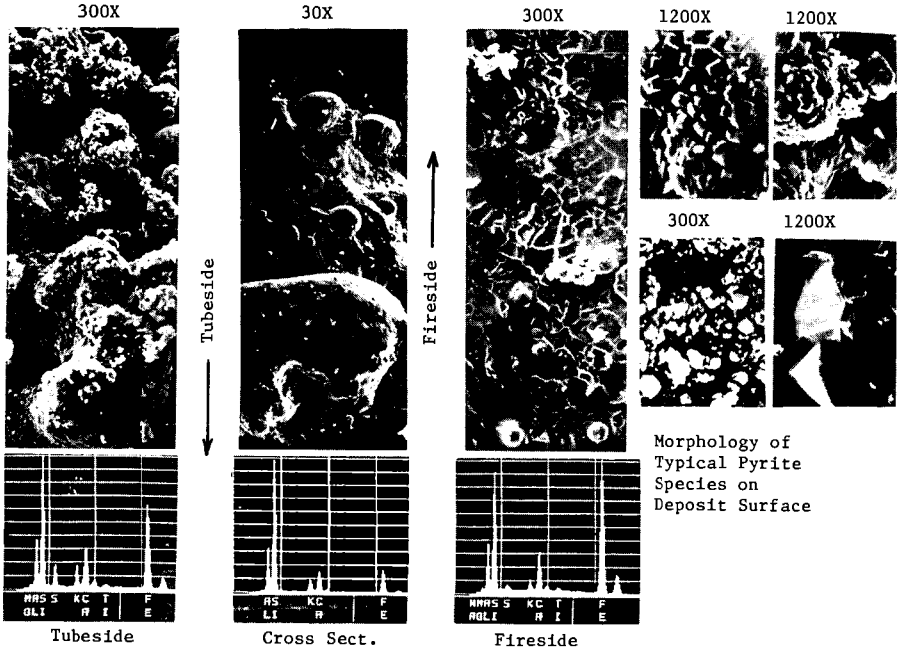

Figure 9 Slag Formation on Furnace Slag Probe

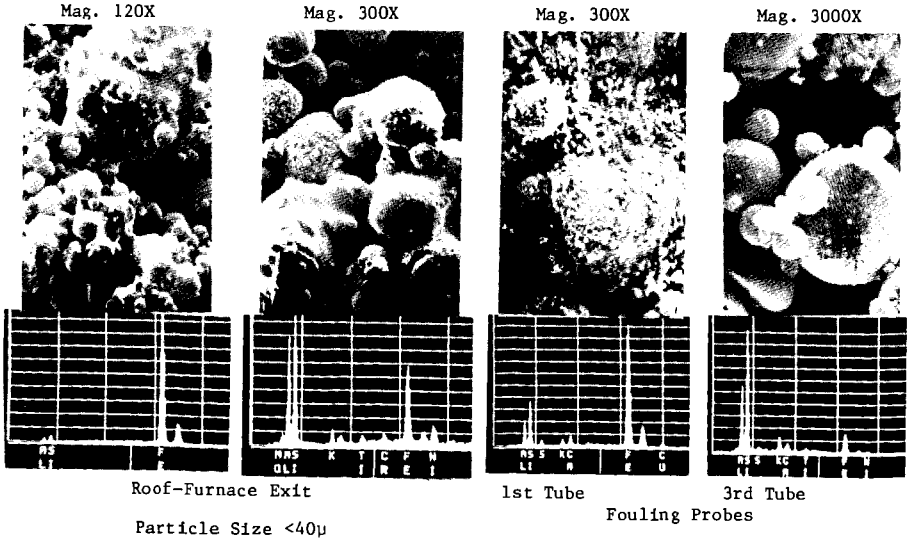

Figure 10 Iron-Rich Sintered Deposits Formed on Furnace Roof and 1st Tube of Convection Pass Probes by Coarse Pyrites

INFLUENCE OF THERMAL PROPERTIES OF WALL DEPOSITS ON PERFORMANCE OF P.F. FIRED BOILER COMBUSTION CHAMBERS

W. Richter, R. Payne, and M.P. Heap

Energy and Environmental Research Corporation
Irvine, CA 92714

1.0 INTRODUCTION

The build-up of ash deposit layers on tube walls and superheaters in dry bottom p.f. boiler combustion chambers not only deteriorates furnace and overall boiler efficiency, but increases the temperature level in furnace and convective passages and aggravates existing deposit problems. This can finally lead to expensive outages when deposit formation cannot be controlled by soot blowing alone. Since errors in furnace design with respect to slagging and fouling or wrong estimation of impact of fuel conversion on deposit formation are so costly in large boilers, there is considerable financial incentive to develop analytical methods in order to predict furnace performance for a wide range of coal types and operating conditions. It is clear that such methods must take quantitatively into account, among other things, the thermal properties of ash deposits.

The properties which determine heat transfer through a deposit layer of given thickness are thermal conductivity, emissivity, and absorptivity. The current paper presents results from various studies carried out by the authors at Energy and Environmental Research Corporation (EER) to show the sensitivity of overall furnace performance, local temperature and heat flux distributions on the properties of deposits in large p.f. fired furnaces.

2.0 PARAMETRIC STUDY OF OVERALL FURNACE PERFORMANCE

The most important parameters for overall furnace heat absorption are the adiabatic flame temperature, the firing density per heat sink area, the emissivity of the furnace volume, temperature and emissivity of the heat sinks and the flow and heat release patterns. Figure 1 shows how these quantities are related in a complex manner to each other, to fuel characteristics and to operating and boundary conditions of the furnace. Some of the relationships of Figure 1 were approximately quantified utilizing a simple well-stirred furnace model (1) which assumed transport of grey radiation. Two important results for furnace performance with respect to formation of deposits are shown in Figures 2 and 3, in which furnace efficiencies η_f,

$$\eta_f \equiv 1 - \frac{\dot{M}_o \, c_p \Big|_{T_o}^{T_{ex}} (T_{ex} - T_o)}{\dot{Q}_o} \qquad 1)$$

are plotted over furnace height L with surface temparatures T_w of deposits and surface emissivities ε_w as parameters. The calculations were carried out for a rectangular furnace box of width L/3. Other input parameters are

listed in the Figures. The grey absorption coefficient K_a of 0.1 1/m used in the examples corresponds to an emissivity ε_f = 0.55 for a furnace volume with a height of L = 30m. The effect of deposit surface temperature T_w on furnace efficiency η_f is considerable for values larger than 700 K (Fig. 2). For instance a furnace efficiency of 0.40 (corresponding to T_{ex} = 1440 K according to Equation 1) was obtained for T_w = 700 K (see Section 3 and 4). The L must be increased by 16.5m or 53% of the original height with clean walls to achieve the same furnace efficiency for a furnace with wall deposit of surface temperature 1300 K.* The impact of wall temperature on η_f will be even stronger for adiabatic flame temperatures less than 2200 K. Such adiabatic flame temperatures can occur when firing lignite or high-moisture coals. For furnaces operated with the same thermal input at low efficiencies, the presence of wall deposits requires only a moderate increase in size.

A reduction of surface emissivities from 1 (clean "sooty" walls) to 0.4 (which is the lowest range reported for ash deposits (see Section 3) also causes a drop of η_f (Fig. 2). However, the required increase in size to maintain η_f is smaller than for the change of deposit surface temperatures from 700 K to 1300 K mentioned above. The size changes non-linear with changes of surface temperature but nearly linearly with ε_w between ε_w = 1 and ε_w = 0.5. Beyond ε_w = 0.2, L must increase non-linearly to maintain furnace efficiency.

When a deposit layer is formed, surface temperature is increased and wall emissivity decreased. However, the superposition of these effects on η_f is less than a pure summation; since, by decreasing ε_w, the net heat flux to the layer is reduced, thus retarding the increase of surface temperature to a certain extent.

3.0 AVAILABLE DATA OF THERMAL PROPERTIES OF ASH DEPOSITS AND DATA ANALYSIS

Thermal Conductivity. A comprehensive review of literature data for thermal conductivity k of ash deposits was published by Wall et al. (2). The thermal conductance, k, of the ash material increases reversibly with temperature until sintering or fusion occurs. At this stage, a rapid and irreversible increase of k is observed. Typical values of k for non-sintered deposits from Australian coals in actual furnaces vary between 0.1 10^{-3} KW/mK at 500 K up to 0.4 10^{-3} KW/mK at 1300 K. The factors contributing to the thermal conductance in the powdered deposits are: Conductance in the solid particles, gas conduction in the voids and radiative transfer through the voids. Fetters et al. recently measured k for boiler deposits of an Indiana coal (3) and point out that the dominant mode of heat trasfer through the deposit layer is by radiation at high temperature. The values of k measured for powdery deposits by Fetters et al. are about 2 times larger than those of

* 1m of furnace height corresponds to ≈ 500,000$.

Wall et al. (2) at the same temperature. This is contributed to the relative large particle sizes of the Indiana coal ash (75% in the 100μm range) compared to the Australian coal ash with mean weight particle diameters of 50μm and less.

Thermal conductivity of sintered and fused deposits found by the Australian researchers range from 0.5 10^{-3} KW/ mK at 800 K to 1.2 10^{-3} KW/mK at 1500 K. This is consistent with the recent findings of Fetters et al. (3) for crushed deposits from a boiler fired with Indiana coal and other literature values (4). The increase of thermal conductivity of sintered and fused deposits is due to a decrease of void space and increased transmissivity of the material. Assuming uniform mean conductivity, the thickness of a sintered deposit layer which maintains fusion at its surface can be estimated by

$$\Delta s_{fu} = \frac{k\,(T_{fu} - T_{t,a})}{\varepsilon_\omega q_{in} - \varepsilon_\omega \sigma T_{fu}^4} \qquad 2)$$

where T_{fu} is the ash fusion temperature, $T_{t,a}$ the temperature of the outer surface of the tubes and q_{in} the incident heat flux density. With typical values k = 0.8 10^{-3} KW/mK, T_{fu} = 1550 K, ε_w = 0.7, $T_{t,a}$ = 750 K and q_{in} = 400 KW/m^2 the layer thickness with a wet surface would be about 8 mm. Wall et al. emphasize that values of k obtained from ground deposits in laboratory studies are questionable since bounding of the deposit occurs in situ which leads to an increase of k. This agrees with our results for a 700 MW_e boiler which yielded an overall value of k = 3.2 KW/m^{2}K for deposits which could not be removed by soot blowing (see Section 4).

Emissivity and Absorptivity

Reviews of emissivity data of ash deposits were given by Wall et al. (2) and recently by Becker (5). The literature data has a considerable spread of emissivity, between values of ε_w = 0.9 and ε_w = 0.3 depending on temperatures, ash origin and probe preparation. However, general agreement exists that, for non-sintered material ε_w decreases reversibly with surface temperature. After sintering, the emissivity changes irreversiblely to higher values (2). This agrees with measurements of furnace generated deposits of American coals carried out by Goetz et al. (6). These authors report values between 0.38 and 0.67 for powdery (initial) deposits, values between 0.76 and 0.93 for sintered deposits and values 0.65 and 0.85 for glassy and or molten deposits. The increase of emissivity with sintering and fusion is due to increased transmission of radiation into the surface of the deposit layer. In the range of surface temperatures of interest, namely between 800 K and 1400 K, measured total emissivities on probes of sintered real furnace deposits exhibit only slight variations with surface temperature (5), (6). However, measurements by Becker of spectral emissivities of deposits on laboratory prepared probes showed distinctive non-grey behavior. For typical flame temperatures of 1700 K and typical surface temperatures of 1100 K, up to 0.2 higher values were found for emissivities than for absorptivites. Non-greyness of emission and absorption is typical for glassy material and is due to the low spectral absorptivities at short wavelengthes which becomes dominant for radiative transfer at more elevated flame

temperatures. The assumption of grey radiation of furnace deposits and consequent use of grey emissivity values for determination of absorption may lead to errors in heat transfer calculations for furnaces with moderate deposits since at lower surface temperatures absorption is several times larger than re-emission. By performing detailed one-dimensional spectral calculations, Becker showed that for a 10 m path length, typical of furnaces, and relatively cool walls errors up to +30% in predicted net heat flux densities would result from the assumption that the deposits were grey. However, these findings are based on spectral values found for laboratory prepared probes. Spectral measurements of real furnace deposits show reduced non-grey behavior (5), (6) and higher emissivities than the laboratory probes (6). Moreover, coloring agents such as unburnt carbon as well as the rough surface structure of real deposits and tube curvatures tend to make boiler surfaces more closely approximate grey behavior. Thus, the importance of non-grey deposits is uncertain in boiler chambers and, in any case, insufficient information is available to recommend replacing the assumption of grey radiation of deposits currently used in 3-D furnace models (see Section 4) by expensive more rigorous spectral models.

4.0 PREDICTIONS OF INFLUENCE OF WALL DEPOSITS ON HEAT TRANSFER IN EXISTING BOILERS

On the basis on the literature values of thermal properties discussed above a considerable number of performance predictions have been carried out for existing boiler combustion chambers in the past two years. Some results of those calculations with relevance to the impact of ash deposits on heat transfer follow. The tool used for the analysis is an extreme flexible 3-D Monte-Carlo type zone model (7), (8). In this model, the emissive power of each volume and surface zone is distributed into a discrete number of radiative beams. Taking multiple reflection at furnace walls into account, the beams are traced throughout the furnace volume until final absorption. Non-greyness of the combustion produts is modeled with a weighted grey gas approach. The radiating species considered are H_2O, CO_2 and particulates (soot, char and ash). Currently, char and ash particles are treated as grey radiators. The model of radiative exchange is directly coupled with a total heat balance of volume and surface (deposit) zones with unknown temperatures. The calculation of convective heat fluxes through the furnace is based on mass flow vectors at the boundary of each zone obtained from isothermal modeling. The heat release pattern is based on this flow field. The heat release due to volatile combustion is based on observed visible flame length and the heat release due to burnout of char particles is calculated from carbon and oxygen balances solved simultaneously with the heat balance.

Example 1: Tangentially Coal-Fired Boiler

This study was carried out to investigate the influence of ash deposits in a twin furnace of a boiler originally designed to fire No. 6 oil at a net thermal input of 1000 MW_t. However, the thermal input of the furnace was reduced to 590 MW_t to investigate the prospects of firing coal in this unit. The coal considered was a Utah coal with 8.8% ash content fired with 30% excess air. Figure 4 shows the zoning of the furnace and the assumed flow

patterns. The heat release due to combustion is indicated by the shaded area. The surface conditions were specified by the following input data:

Case A Clean surfaces, emissivity of tubes $\varepsilon_w = 0.9$
Case B Powdery ash deposit, $\varepsilon_w = 0.6$, $\Delta s = 0.5$mm, $k = 0.3\ 10^{-3}$ KW/mK
Case C Properties of ash deposit layer in upper part of the furnace (above heat-release zone) as specified for Case B; glassy ash deposit layer in lower part of the furnace with $\varepsilon_t = 0.8$, $\Delta s = 7$mm, $K = 1\ 10^{-3}$ KW/mK.

The properties for the powdery (primary) and for the glassy (molten) deposit layer of the Cases B and C correspond to average data from literature as cited above. The actual calculations were carried out with an effective emissivity of the tube walls taking the shadow effect of the gap between adjacent tubes into account.

Table 1 and Figures 5 through 7 show that the build-up of ash deposits seriously affects overall and local heat transfer. The difference ($\Delta\eta_f$) in computed furnace efficiencies for the extreme cases, A (clean walls) and C (highest thermal resistance), is 6.2 percentage points. The formation of a first initial deposit layer (Case B) has a stronger impact on heat transfer than subsequent increase of deposits in the lower furnace (Case C). The increase of the thickness of ash deposit opposite to the heat release zone displaces the peak heat fluxes up into the regions of the thinner deposits (Fig. 6). This is one reason why the build up of deposit layers, once started, spreads into adjacent wall zones. Once the deposit layers begin growing, surface temperatures can soon reach values in the range between softening (1400 K) and fusion temperature (1500 K) as indicated by shaded areas in Fig. 7. The furnace model is also able to predict, for a given coal ash fusion temperature approximately the development and extent of molten slag layers.

Another investigation showed for the same boiler fired with COM at a rate of 875 MW_t, showed that a decrease of surface emissivity from 0.9 (clean) to 0.6 (initial deposit) raised mean furnace exit temperature by 55 K.

Example 2 Opposed P.F. Fired Boiler

This study was carried out in order to verify the 3-D furnace heat transfer model with performance data available from a coal-fired, boiler combustion chamber of 1732 MW_t fuel heat input. The coal had a medium volatile content, an ash content of 6.6%, and was fired with 28% excess air. In this case, the flow pattern was based on detailed distribution of mass mean flow vectors measured in a physical isothermal model. However, turbulent components were superimposed on these vectors with the help of a simple model of turbulence. Fig. 8 shows a comparison of the profiles of gas temperatures measured and predicted for 100% Load in one half of the furnace outlet plane. The difference between predicted and measured values was less than 25 K. The good agreement is partially due to a reasonable assumption of the effective heat conduction coefficient $(k/\Delta s)_{eff}$ of the deposit layers. Fig. 9 shows how the predicted mean furnace exit temperature varied with (k/Δ

$s)_{eff}$ and compares those predictions with two data points obtained from measured heat balances of the boiler immediately after soot blowing and 20 h after soot blowing. Since measurements and observations yielded approximately a 2mm deposit layer, which could not be removed by soot blowing an effective thermal conductivity of 3.2 10^{-3} /mK can be deduced. An assumed value of k = 0.8 10^{-3} KW/mK for a dry partially sintered deposit would suggest the build-up of an additional layer of 1.5 mm, 20 h after soot blowing for a total layer of 3.5 mm thickness.

Fig. 9 also contains the relationship of $T_{ex} = f(k/\Delta s)$ for a similar boiler of 1250 MW_t heat input in which slagging and fouling problems are encountered. Further applications of the 3-D furnace model with respect to impact of wall deposits on heat transfer in CWM and COM fired furnaces may be found in (5), (10).

5.0 CONCLUSIONS

Thermal conductivity and emissivity of wall deposits have a considerable effect on heat transfer in large boilers. This results in temperature differences of furnace exit temperatures which influence furnace height, performance and costs. More exact values of deposit thermal properites, which vary over a wide range of temperatures and conditions, than currently available are needed for detailed prediction of the initial formation of deposit layers. However, gross characteristics of thermal properties can be assumed and are sufficient to estimate the performance of furnaces, since the model contains other major uncertainties such as, thickness and inhomogenous distribution of deposits at furnace walls and superheaters. This is especially true between soot blowing cycles. The 3-D heat-transfer model used in the present study has the potential to form the basis of a more comprehensive model of slagging and fouling because it can provide reliable predictions of flame and deposit temperatures. A model of ash transport is currently being coupled with the furnace heat transfer model which will account for time-temperature histories of ash and wall collisions.

6.0 LITERATURE

(1) Richter, W.: Parametric Screening Studies for the Calculation of Heat Transfer in Combustion Chambers. Topical Report, prepared for Pittsburgh Energy Technology Center, Department of Energy, under Contract No. DE-AC22-80PC30297, January 1982.

(2) Wall, T. F., A. Lowe, L. J. Wibberley, and McC. Stewart: Mineral Matter in Coal and the Thermal Performance of Large Boilers. Prog. Energy Combust., Science, Vol. 5, pp. 129, 1979.

(3) Fetters, G. D., R. Viskanta, and F. P. Incropera: Experimental Study of Heat Transfer Through Coal Ash Deposits. 1982 ASME Winter Annual Meeting, Paper 82-WA/HT-30.

(4) Singer, J. G., Editor: Combustion: Fossil Power Systems, 3rd Edition, Combustion Engineering Inc., Windsor, p. C-16, 1981.

(5) Becker, H. B. : Spectral Band Emissivities of Ash Deposits and Radiative Heat Transfer in Pulverised-Coal-Fired Furnaces. Ph.D. Thesis, University of Newcastle, Australia, February 1982.
(6) Goetz, G. J., N. Y. Nsakala, and R. W. Borio: Development of Method for Determining Emissivities and Absorptivities of Coal Ash Deposits. Journal of Engineering for Power, Vol. 101, pp. 607-619, 1979.
(7) Richter, W., and M. P. Heap: A Semistochastic Method for the Prediction of Radiative Heat Transfer in Combustion Chambers. Western States Section, The Combustion Institute, 1981 Spring Meeting, Paper 81-17, 1981.
(8) Richter, W., and M. P. Heap: The Impact of Heat Release Pattern and Fuel Properties on Heat Transfer in Boilers, 1981 ASME Winter Annual Meeting, Paper 81 WA/HT27, 1981.
(9) England, G. C., Y. Kwan, W. Richter and K. Fujimura: Studies to Evaluate the Impact of Conversion from Fuel-Oil to Coal-Oil Mixtures on Thermal Performance and Pollutant Emissions. Pittsburgh Energy Technology Center, Proc. of the Fourth International Symposium on Coal Slurry Combustion, Vol. 3, 1982.
(10) Payne, R., S. L. Chen and W. Richter: A Procedure for the Evaluation of the Combustion Performance of Coal-Water Slurries. Fifth International Symposium on Coal Slurry Combustion and Technology, Session VII, DOE, PETC, 1983.

Table 1. Thermal Performance of 590 MW_t Coal-Fired Combustion Chamber For Various Slagging And Fouling Conditions

No.	Case	Furnace Efficiency	Mean Furnace Exit Temperature	Mean Net Heat Flux Density	Max. Net Heat Flux Density	Vertical Position of Max. Net Heat Flux Density	Max. Flame Temp.	Max. Furnace Exit Temp.	Unburnt C_{fix}	Carbon Content of Fly Ash
		%	K	KW/m^2	KW/m^2	m	K	K	%	%
A	Clean Surfaces	40.3	1436	168	304	14.9	1661	1515	1.35	6.43
B	Powdery Ash Deposit	35.6	1519	148	235	16.7	1728	1582	0.89	4.33
C	Slagging Lower Half	34.1	1541	143	239	19.2	1776	1610	0.75	3.68

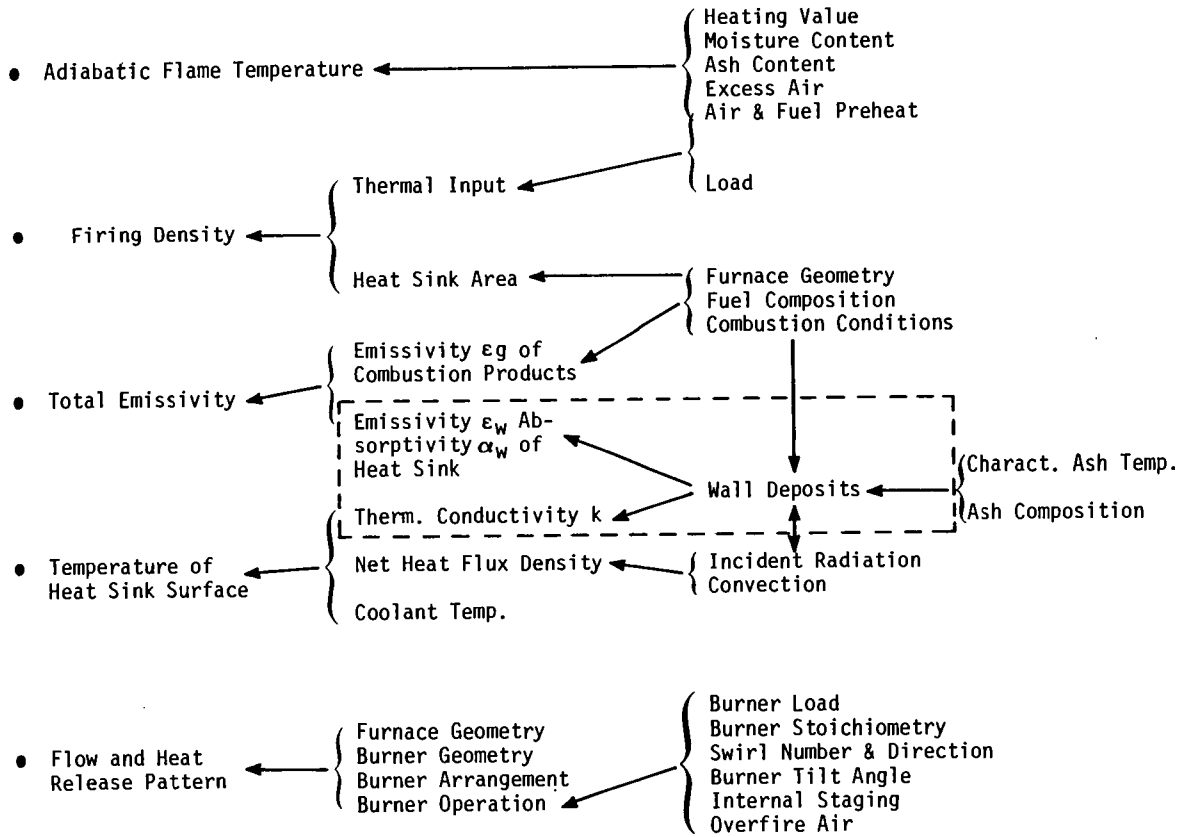

Figure 1. Major Factors Influencing Thermal Performance of Furnaces

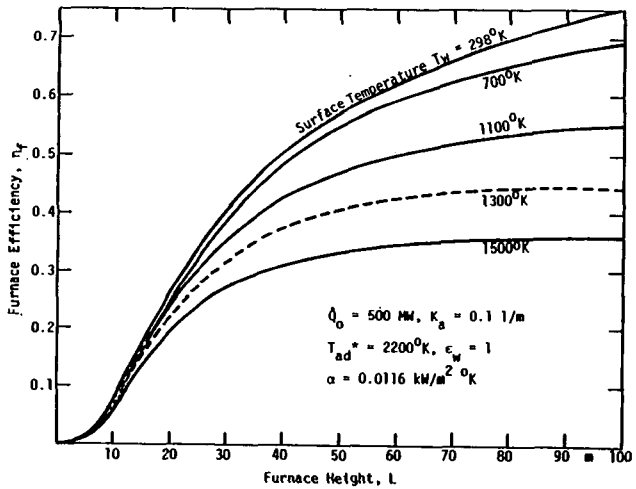

Figure 2. Dependency of Furnace Efficiency on Furnace Dimensions for Various Surface Temperatures.

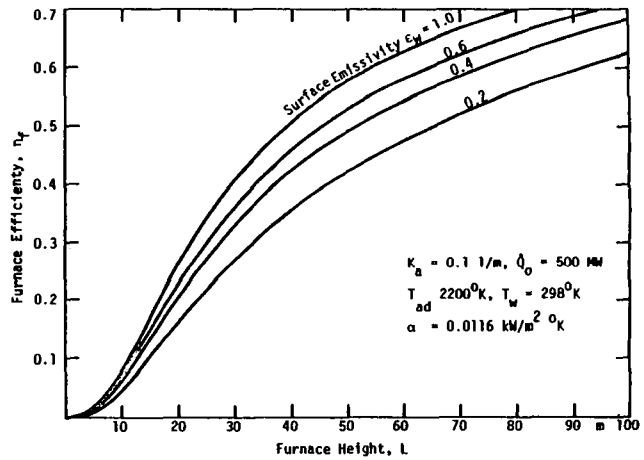

Figure 3. Dependency of Furnace Efficiency on Furnace Height With Surface Emissivity as Parameter.

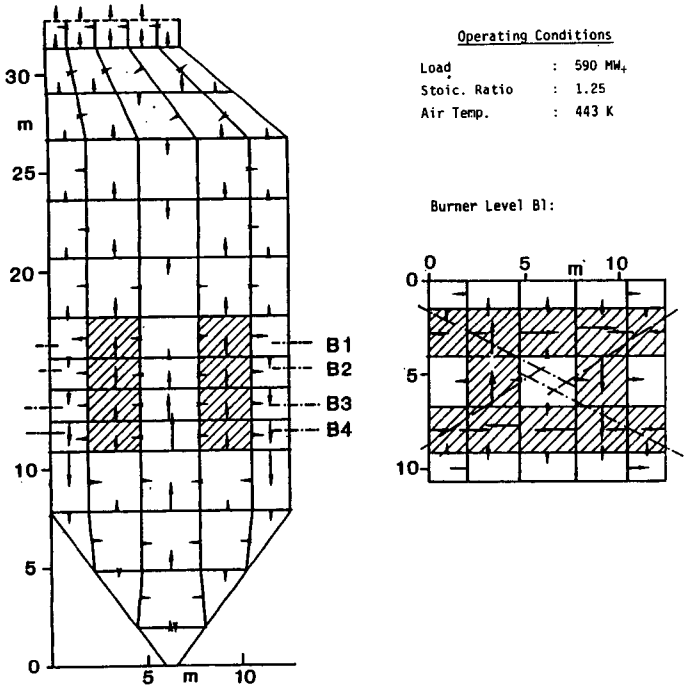

Figure 4. Geometry and Zoning of Tangentially Fired Boiler Originally Designed for Oil Firing with 1000 MW_t Thermal Input.

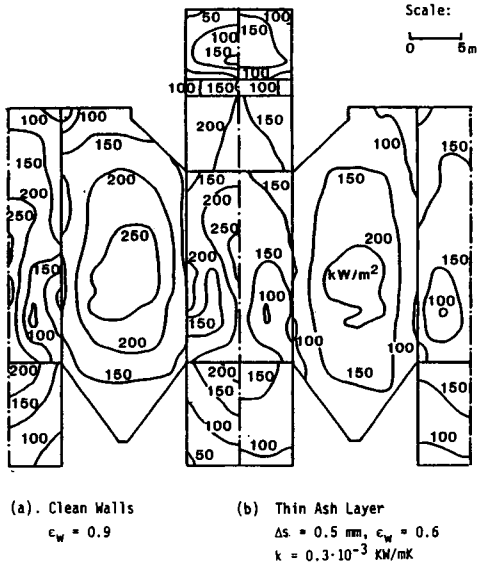

Figure 5. Influence of Wall Deposits on Predicted Net Heat Flux Distribution in Boiler Combustion Chamber Fired with Coal at a Rate of 590 MW_t.

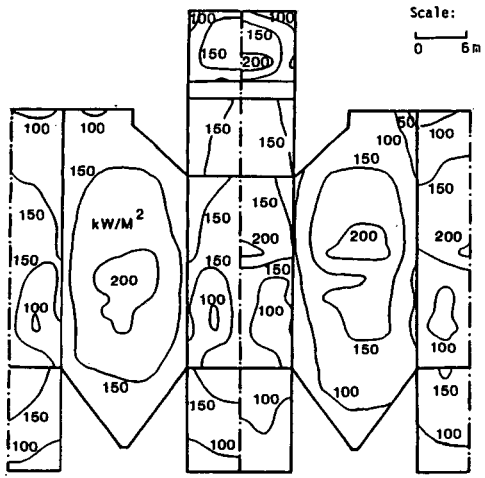

(a) Thin Ash Layer
$\Delta s = 0.5$ mm, $\varepsilon_w = 0.6$
$k = 0.3 \cdot 10^{-3}$ KW/mK

(b) Slagging Lower Half
$\Delta s = 7$ mm, $\varepsilon_w = 0.8$
$k = 1 \cdot 10^{-3}$ KW/mK
Upper Half as in (a)

Figure 6. Influence of Slagging in Lower Furnace Half on Predicted Net Heat Flux Distribution in Boiler Combustion Chamber Fired with Coal at a Rate of 590 MW_t.

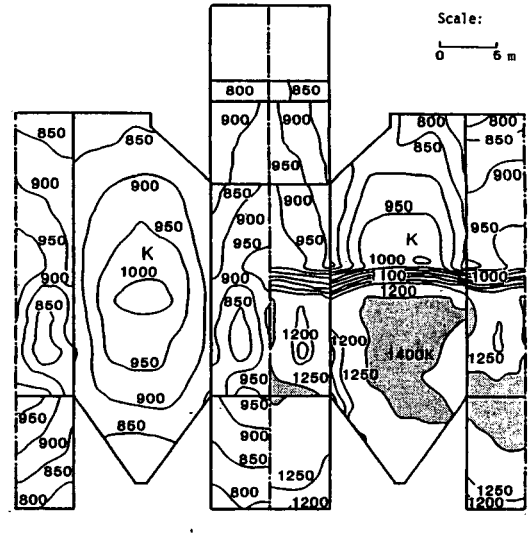

(a) Thin Ash Layer
$\Delta s = 0.5$ mm, $\varepsilon_w = 0.6$
$k = 0.3 \cdot 10^{-3}$ KW/mK

(b) Slagging Lower Half
$\Delta s = 7$ mm, $\varepsilon_w = 0.8$
$k = 1 \cdot 10^{-3}$ KW/mK
Upper Half as in (a)

Figure 7. Influence of Slagging in Lower Furnace Half on Predicted Surface Temperatures of Deposits in Boiler Combustion Chamber Fired with Coal at a Rate of 590 MW_t.

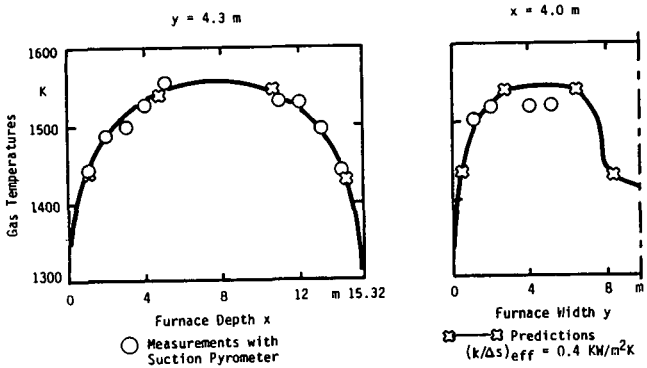

Figure 8. Comparison of Temperature Profiles Predicted and Measured Near Furnace Exit (z = 68.6 m) of 1730 MW_t Opposed Coal- Fired Boiler Combustion Chamber.

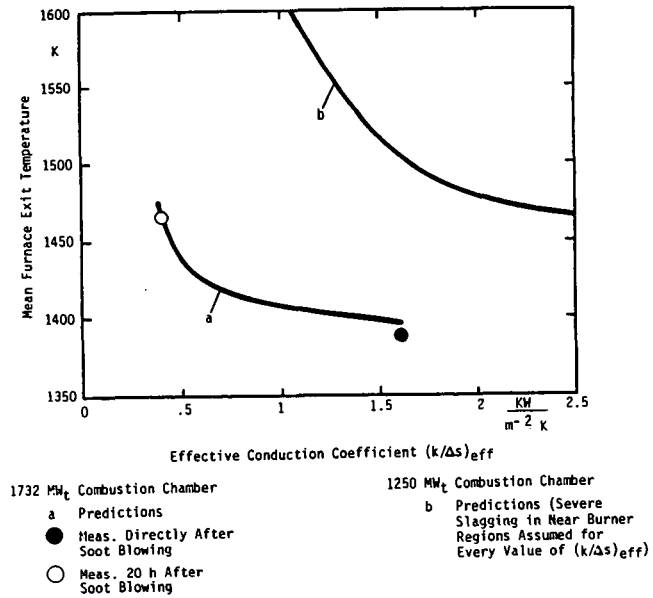

Figure 9. Dependance of Mean Furnace Exit Temperature on Effective Conduction Coefficient for Two Opposed Coal-Fired Boiler Combustion Chambers.

The Prediction of the Tendency of Slagging and Fouling of European Lignites by New Statistical and Experimental Methods

W. Altmann
Technical University of Dresden
Mommenstrasse 13
8027 Dresden
German Democratic Republic
Communicated by:
John H. Pohl
Energy and Environmental Research Corporation
18 Mason
Irvine, California 92714

Introduction

Proper design and operation of coal-fired boilers requires prediction of the tendency of the fuels to foul and slag. A large number of correlations based on the oxides of an ash produced in the laboratory exist (1,2). The success of these correlations has been limited to the range of ash properties for which they were developed, and even then, these relationships may be unreliable. For instance, existing correlations can predict whether a fuel will create deposition problems in boilers rarely, occassionally, or frequently for approximately 50 percent of the fuels. An accuracy only slightly better than random guess (3).

Potential problems using available techniques have been discussed in the literature (2,3,4,5). The problems result from:

- Preparation and analysis of the ash (6)
- Ignoring the distribution and individual nature of mineral matter (4,6)
- Neglecting the influence of ash content (7)
- Ignoring the design of the boilers including heat release rate, heat fluxes and velocity profiles (3,8,9)

In addition the correlation should not be used for coals with properties outside the range for which the correlations were developed.

This paper describes the limited success of applying such techniques to predict performance, efforts to develop and verify new techniques to predict preformance, and application of these techniques to predict the slagging and fouling behavior of European brown coals.

Prediction of Slagging Performance

Slagging performance of coals in boilers has been predicted by:

- temperature of critical viscosity,
- the base to acid ratio,
- and the base to acid ratio multiplied by the sulfur content of the coal.

Predictions of slagging and fouling using these relationships are compared to boiler performance for the six European brown coals listed in Table 1. The calculated indicies and estimated and actual performance of the fuels are shown in Table 2.

The temperature of critical viscosity is the temperature at which the slag changes from plastic to Newtonian behavior. Plastic slags are difficult to remove by soot blowing. As a consequence, fuels with low temperatures of critical vis-

cosity are expected to form difficult to remove plastic and molten slags more readily than other fuels.

The temperature at critical viscosity can be measured in a viscometer, but the measurements are time consuming and expensive and the temperature at critical viscosity is usually estimated using emperical formulae. For instance, Watt and Fereday (10) developed

$$T_{cv} = \sqrt{\frac{107.m}{2.398-c}} + 150 \text{ in } ^{o}C \qquad 1).$$

where $SiO_2 + A\ell_2O_3 + Fe_2O_3 + CaO + MgO = 1$ 2).

and $m = 0.835\ SiO_2 + 0.601\ A\ell_2O_3 - 0.109$ 3).

$c = 4.15\ SiO_2 + 1.92\ A\ell_2O_3$ 4).

The temperature at critical viscosity probably does not adequately predict slagging behavior of the six European brown coals of this study. The qualitative relationship between deposits formed in a boiler and the temperature of critical viscosity estimated by the technique of Watt and Fereday (10) is shown in Figure 1a. The data appear to correlate with observations, but predict improved performance at an intermediate temperature of critical viscosity. No reason is known for this and the correlation may be fortuitious.

The base to acid ratio is the reverse of the previous relationship and probably does not correlate the slagging data either. Figure 1b shows that the base to acid ratio appears to correlate the prediction of performance of brown coals in boilers. This relationship predicts optimum performance at a base to acid ratio of 0.3. This is quite possible with the formation of eutetics. However, comparison of Figure 1a and 1b shows the curves are reversed and the prediction of performance of all the fuels fall in the same relative position on both curves. This again leads to uncertainty as to the reasonableness and the reliability of the correlations in Figure 1.

The standard slagging factor, R_s, could not correlate the performance of all the fuels in the boilers. The slagging factor is defined as

$$R_s = B/A \cdot S \qquad 5).$$

by Attig and Duzy (11). This equation is suggested for ashes which have $Fe_2O_3 >$ CaO + MgO but is applied to all ashes in this study. Only two of the ashes in this study have $Fe_2O_3 >$ CaO + MgO. Leipzig has about equal amounts and Nordbohmen has greater Fe_2O_3 than CaO + MgO. The base to acid ratio (shown in Figure 2a) is recommended to correlate slagging behavior of ashes with CaO + MgO $> Fe_2O_3$ (11). Five of the fuels correlate reasonably with R_s but the slagging of Nordbohmen was greatly underestimated. However, this fuel was the only one with significantly greater Fe_2O_3 than CaO + MgO and might not correlate with the other five fuels.

A good correlation of all six fuels was developed by modifying the slagging factor. The relationship is shown in Figure 2b where the slagging factor, f_s, is defined as:

$$f_s = 1.7 + 1.7\ SiO_2^* + 0.8\ A\ell_2O_3^* - 6.0\ (S)^0 r_{Fe}^2 \qquad 6).$$
$$-2.2\ (CaO^* + MgO^*) - 1.9SO_3^* - 1.3\ (Alk)^*$$

where f_s = 0 is strong slagging

and f_s = 1 is no slagging

and $$[\quad]^* = \frac{[\quad]^*}{1 - SiO_2 + SiO_{2corr}} \qquad 7).$$

$$SiO_{2corr} = 823\ \Gamma_{SO3}^{2.65} \cdot \exp(-9.45\ \Gamma_{SO3})\ Fe_2O_3 \qquad 8).$$

$$\Gamma_{SO3} = \frac{SO_3}{1 - SiO_2} \qquad 9).$$

where S is the weight percent sulfer in the coal as received and all other compositions are weight percent of the ash.

Predictions of Fouling Performance

The fouling performance of the six brown coals of this study could not be adequately predicted by existing or new techniques. The fouling performance of coals with $CaO + MgO > Fe_2O_3$ is usually predicted by the sodium content of the ash. Figure 3a shows the correlation of the qualitative observation of fouling in boilers with the alkali (Na_2O plus K_2O) content of the ash. All the coals except Ungarn correlate with the alkali content of the ash. However, no explanation is available for the fouling of the Ungarn which had 0.0 alkali content in the ash. A new fouling factor, f_F,

$$f_F = \exp\left[\frac{-5.\ Alk^*}{f_s + 0.3}\right]$$

where Alk* is defined by equation (7) was moderately successful, Figure 3b, in correlating the fouling performance of coals. However, considerable scatter still exists in the relationship.

Pilot Scale Prediction of Fouling and Slagging Performance

The limited success of predicting fouling and slagging performance based upon the analysis of the oxides of ashes produced in laboratory apparatus has prompted the Technical University of Dresden to develop pilot scale tests to predict slagging and fouling of ashes in boilers. Two tests are currently being evaluated which determine slagging and fouling characteristics of fuels not determined by current laboratory or other small scale tests. The first, determines the fouling and slagging of the fuel under different combustion conditions. In this test, the coal is burned in a small drop tube furnace. The level of oxygen and the thermal environment of combustion are changed. The particle temperatures are measured with thermographic techniques and the nature and deposition rate evaluated. Such a technique can simulate the limits of the time temperature concentration history in boilers and avoids production of an artifical mean ash. This technique does not account for ash trajectories in boilers.

The tendency of ash to follow streamlines or deposit on surfaces is determined in a second test. In this test, the coal is burned in a small cyclone combustion chamber. This chamber can also simulate the limits of time and temperature history of ashes in boilers. In addition, a cyclone chamber subjects the coal to centrifugal forces, which allows the ability of the fly ash particles to follow streamlines to be assessed.

The ability of these pilot scaled tests to predict the slagging and fouling performance of European brown coals is currently being evaluated. Preliminary results are promising.

TABLE I ASH COMPOSITION OF EUROPEAN BROWN COALS
WEIGHT PERCENT IN THE ASH

	UNGARN	LEIPZIG	NIEDERLAUSITZ	OBERLAUSITZ	NORDBOHMEN	SULZROHLE
SiO_2	47.9	25.5	46.2	41.8	52.9	11.9
Al_2O_3	26.1	3.5	6.8	30.0	25.3	6.9
Fe_2O_3	8.6	24.0	13.4	8.3	12.6	3.0
CaO	8.0	19.5	11.4	9.5	3.4	15.2
MgO	1.7	3.5	7.6	4.0	1.5	2.2
SO_3	4.8	22.5	12.9	3.6	2.5	31.5
Alkali	0.0	1.5	1.3	0.2	1.8	22.0
Not Determined	2.9	0.0	0.4	2.6	0.0	7.3

TABLE II COMPARISON OF ESTIMATED AND OBSERVED PERFORMANCE OF EUROPEAN BROWN COALS

	Performance		Watt & Fereday Critical Viscosity	Prediction									
Coal	slagging	fouling	°C	Slagging B/A		Slagging R_s		Slagging f_s		Fouling f_F		% Alkali	Fouling
Ungarn	considerable	medium	1395	0.247	low	1.088	medium	0.384	medium	1.000	none	0.0	low
Leipzig	strong	medium	904	1.621	high-severe	4.539	very high	0.106	strong	0.863	low	1.5	medium
Niederlausitz	medium	low	1268	0.611	medium	0.734	medium	0.456	medium	0.900	low	1.3	medium
Oberlausitz	none	none	1312	0.304	low	0.061	little	0.963	none	0.988	none	0.2	low
Nordbohmen	very strong	low	1440	0.224	low	0.246	little	0.086	very strong	0.627	medium	1.8	medium
Salzkohle	strong	very strong	963	1.085	high-severe	3.038	very high	0.189	strong	0.091	very strong	22.0	severe

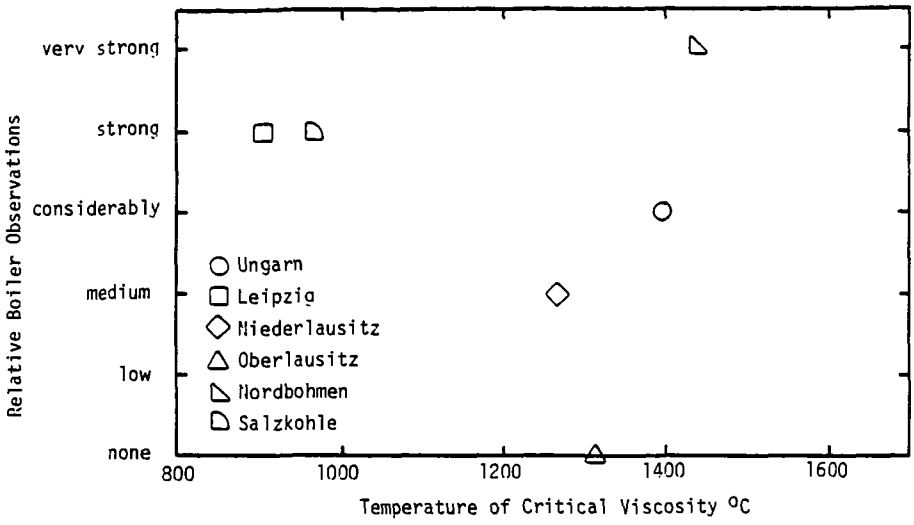

Figure 1a. Comparison of observed and predicted (T_{CV}) slagging performance of brown coal.

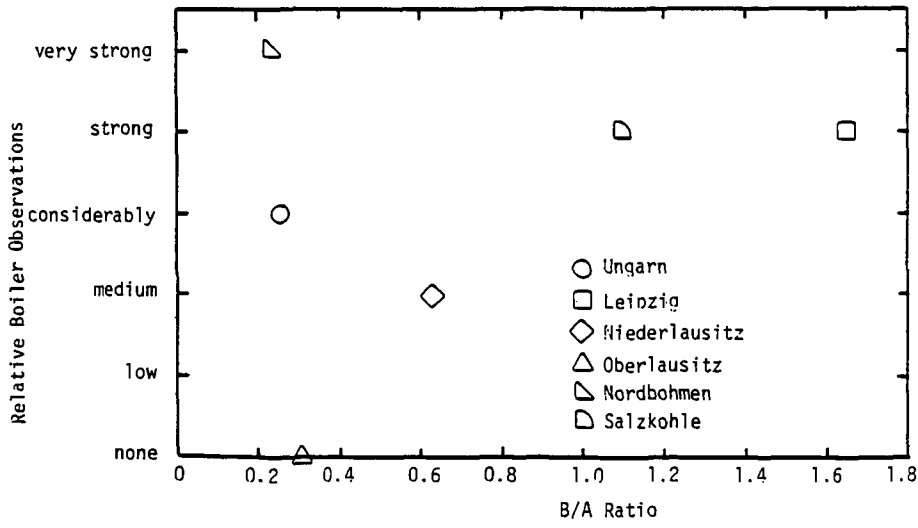

Figure 1b. Comparison of observed and predicted (B/A) slagging performance of brown coal.

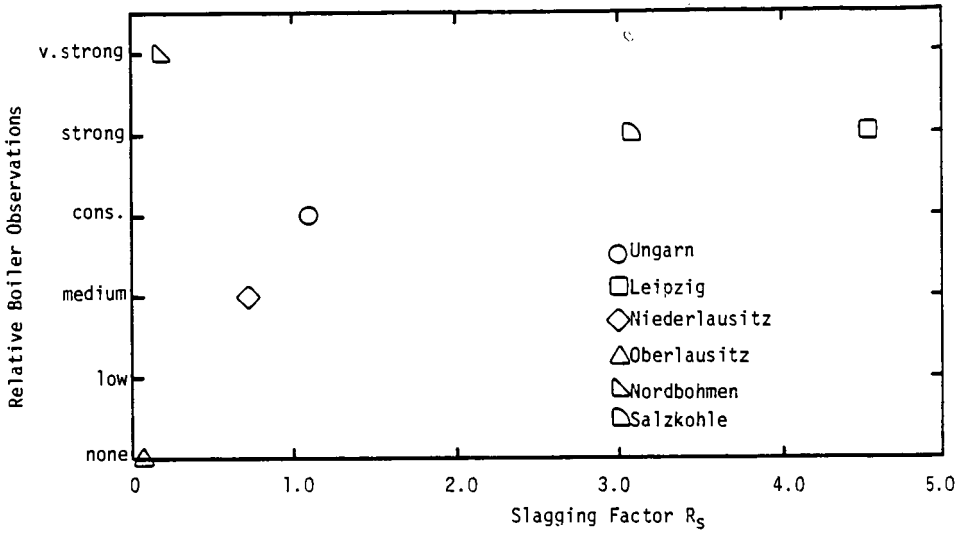

Figure 2a. Comparison of observed and predicted (R_S) slagging performance of brown coal.

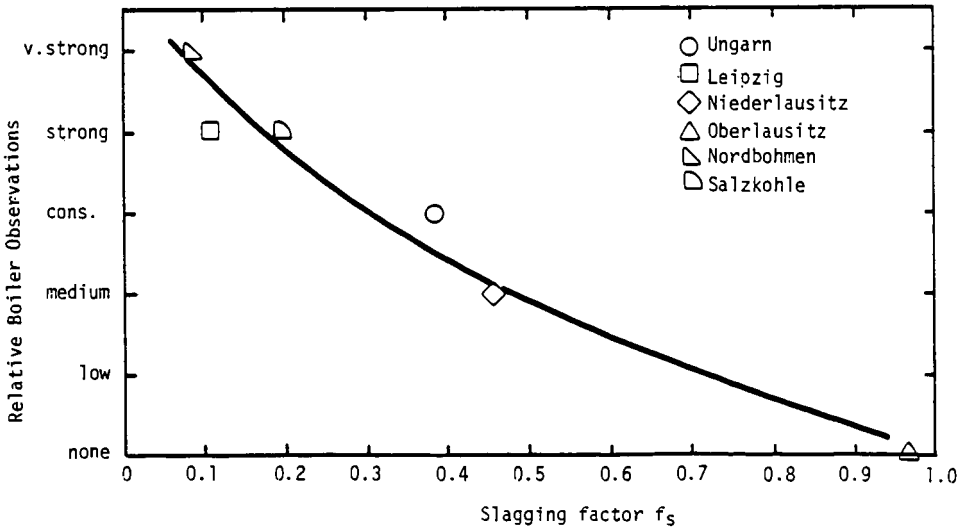

Figure 2b. Comparison of observed and predicted (f_S) slagging performance of brown coal.

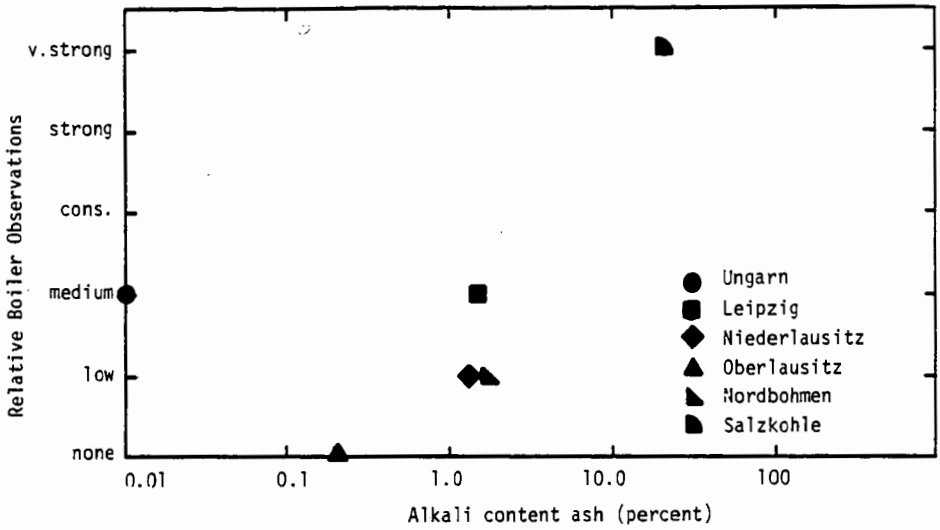

Figure 3a. Comparison of observed and predicted (Alkali content) fouling performance of brown coal.

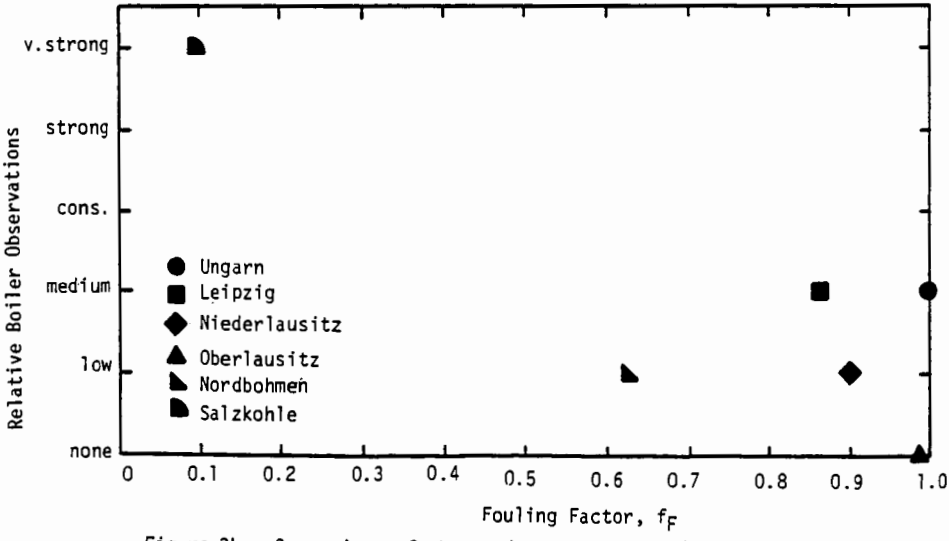

Figure 3b. Comparison of observed and predicted (f_F) fouling performance of brown coal.

References

(1) Winegarteaer, E. C., "Coal Fouling and Slagging Parameters," Book No. H-86 ASME, 1974.

(2) Bryers, R. W., "On-Line Measurements of Fouling and Slagging (Full-Scale and Pilot Units) and Correlation with Predictive Indices in Conventionally Fired Steam Generators." Proceedings of the Low Rank Coal Technology Development Workshop, San Antonio, Texas, June, 1981.

(3) Barrett, R. E., J. M. Murin, and G. A. Mack, and J. P. Dimmer, "Evaluating Slagging and Fouling Parameters," presented at the American Flame Research Committee Fall Meeting, Akron, Ohio, October, 1983.

(4) Pollmann, S. and W. Albrecht, "Investigations of the Slagging Behavior of Bituminous Coals in Large Dry-Bottom Steam Generators," p. 85., in R. W. Bryers, "Fouling and Slagging Resulting from Impurities in Combustion Gases," Engineering Foundation, New York, 1983.

(5) Altmann, W. "Beurteilung der Verschlackungs - und Verschmutzungsneigung fester Brennstoffe." XIV Kraftwerkstechnischen Kolloquium, Dresden, German Democratic Republic, October, 1982.

(6) Pohl, J. H., "Errors in Predicting the Slagging and Fouling Behavior of Coals Based on Standard Techniques", XIV Kraftwerkstechnichen Kolloquium, Dresden, German Democratic Republic, October, 1982.

(7) Blackmore, G., "Quality Coal for Electric Utility Use," Ninth Annual International Conference on Coal Gasification, Liquidification, and Conversion to Electricity," Pittsburgh, PA, August 1982.

(8) Bryers, R. W., Private Communication, Foster Wheeler Development Corporation, 1984.

(9) Richter, W., Private Communication, Energy and Environmental Research Corporation, 1984.

(10) Watt, J. D. and F. Fereday, "The Flow Properties of Slags formed from the Ashes of British Coals: Part 1: Viscosity of Homogeneous Liquid Slags in Relation to Slag Composition." J. Inst. Fuel, v. 42, p.99, 1969.

(11) Attig, R. C., and A. F. Duzy, "Coal Ash Deposition Studies and Applications to Boiler Design, Proceedings of the American Power Conference", v. 31, p. 299, 1969.

AN OVERVIEW OF MINERAL MATTER CATALYSIS OF COAL CONVERSION*

Thomas D. Padrick
Sandia National Laboratories, Albuquerque, NM 87185

INTRODUCTION

Since the 1920's, several studies have focused on the catalytic effects of inherent mineral matter on coal conversion.[1] In recent years, we have witnessed an increase in the level of coal research and the development of new coal utilization processes. In parallel with this activity, there have been reports on the effects of coal minerals on coal liquefaction, coal gasification, in-situ coal gasification, and other areas of coal utilization.[2-5] This overview will deal primarily with recent results of mineral matter effects in coal liquefaction and coal gasification. The terms minerals, mineral matter, and ash will be used synonymously. An attempt will not be made to review the effects of all classes of minerals, but will only consider those minerals which have shown a large effect on coal conversion processes. A good review of the specific minerals present in a variety of coals can be found in the work of Gluskoter et al.[6]

COAL LIQUEFACTION

The Germans used coal liquefaction on a commercial scale from 1930 to the end of the second World War. They found that a catalyst could enhance liquid yields and help remove heteroatoms. The Bergius process used an iron oxide-aluminum catalyst at a 2-3% by coal weight concentration.

In recent years, it has been realized that mineral matter plays an important role in coal liquefaction,[7,8,9] similar to the role of the added catalyst in the Bergius process. Several experimental techniques have been used to study the effects of minerals on coal liquefaction and to identify the specific catalytic phase.[10] Most studies[11,12] strongly imply that the iron sulfides are the most active species, and the other minerals appear to have little effect on enhancement of liquid yield or quality.

The specific role of pyrite (FeS_2) as a catalyst has been under investigation since pyrite was identified as the most active inherent mineral for coal liquefaction. Under liquefaction conditions, FeS_2 is transformed into a nonstoichiometric iron sulfide, $Fe_{1-X}S$ ($0 \leq X \leq 0.125$). Thomas et al.[13] studied the kinetics of this decomposition under coal liquefaction conditions, and concluded that the catalytic activity of FeS_2 is associated with radical initiation resulting from the pyrite-pyrrhotite transformation.

Several studies have investigated the possibility that defects in the pyrrhotite structure provide the sites for catalyst activity. A recent study[14] found a linear correlation between the conversion to benzene or THF solubles and the atomic percent iron in

* This work supported by the U. S. Dept. of Energy at Sandia National Laboratories under contract no. DE-AC04-76DP00789.

the liquefaction residues. Montano et al.[15] used in situ Mössbauer spectroscopy to study transformation of FeS_2 to $Fe_{1-x}S$. They observed a large pyrrhotite surface area at the reaction temperature (above 350°C).

Stohl and Granoff[16] investigated the effects of pyrite particle sizes, pyrite defects and surface areas on coal liquefaction. They observed no effect due to surface area and concluded that the observed particle size effect was due to diffusional limitations in the transformation of pyrite to pyrrhotite.

While many studies indicate that pyrrhotites are probably involved in the liquefaction process, the exact mechanism by which pyrrhotite catalyzes the conversion of coal to oil is not clear. Based on the works of Thomas et al.[13] and Derbyshire et al.,[11] one can suggest that a possible role of pyrrhotite is as a hydrogenation catalyst. However, more work is necessary on the surface properties of the pyrrhotites and the interaction with model compounds before a definite catalytic mechanism can be proposed.

COAL GASIFICATION

The gasification of coal involves two distinct stages: (1) devolatilization and (2) char gasification. Devolatilization occurs quite rapidly as the coal is heated above 400°C. During this period, the coal structure is altered, producing a less reactive solid (char), tars, condensible liquids and light gases. Nominally 40% of the coal is volatilized during this period. The less reactive char then gasifies at a much slower rate. We will discuss the effects of coal minerals on both devolatilization and char gasification.

A large volume of work has been reported on rapid devolatilization of coal (heating rates approximating process conditions).[17,18] Recently, the effects of coal minerals on the rapid pyrolysis of a bituminous coal were reported by Franklin, et al.[19] They found that only the calcium minerals affected the pyrolysis products. Addition of $CaCO_3$ reduced the tar, hydrocarbon gas and liquid yields by 20-30%. The calcium minerals also altered the oxygen release mechanism from the coal. Franklin, et al. attribute these effects to $CaCO_3$ reduction to CaO, which acts as a solid base catalyst for a keto-enol isomerization reaction that produces the observed CO and H_2O.

Walker and co-workers at the Pennsylvania State University have investigated the reactivity of a variety of coals during gasificaton in air, CO_2, H_2 and steam.[20-23] Hippo and Walker[21] found a linear correlation between reactivity and CaO content in the ash. They also observed an increase in reactivity with MgO, up to about 1%. They found no correlation between reactivity and iron content or total K or Na content. In their studies on hydrogen and steam gasification, the Penn State group used coals demineralized by acid washing to study mineral matter effects. While changes were observed in these studies, it was difficult to attribute these changes to catalytic effects or physical effects.

Mahajan et al.[24] observed that the presence of pyrite in coal had a beneficial catalytic effect on hydrogenation at 570°C. They suggested that the catalytic activity was due to pyrrhotite formation. Hüttinger and Krauss[25] reached a similar conclusion concerning the catalytic activity of pyrite, and concluded that

above 850°C, iron enhanced the methane formation if the H_2 pressure was sufficiently high.

Padrick et al.[26] observed enhancement of the hydrogasification rate of a Pittsburgh Seam coal at 1000°C when various iron-containing minerals were mixed with the coal. They investigated the chemical effect of the minerals by measuring H_2/D_2 exchange rates, and also determined the physical effect of the mineral addition on the resultant surface areas and pore volumes of the chars. While the correlation of 1000°C hydrogasification rates with measured parameters was somewhat better including the chemical effects of the minerals, it was concluded that the gasification rates for the various sources of reduced iron were primarily due to the physical iteraction of the minerals with the coal.

REFERENCES

1. Marson, C. B. and Cobb, J. W., Gas J. 171, 39 (1925).

2. Davidson, R. M., "Mineral Effects in Coal Conversion," Rept. No. ICTIS/TR22, IEA Coal Research, London, January 1983.

3. Otto, K., Bortosiewicz, L., and Shelef, M., Fuel 58, 85 (1979).

4. Fisher, J., Young, J. E., Johnson, J. E., and Jonke, A. A., Report ANL 77-7 (1977).

5. Plogman, H. and Kuhn, L., Proceedings of the International Conference on Coal Science, Düsseldorf, Germany, September 7-9 (1981).

6. Gluskoter, H. J., Shimp, N. F. and Ruch, R. R., in "Chemistry of Coal Utilization. 2nd Supplementary Volume," John Wiley and Sons, New York, NY, pp. 369-424 (1981).

7. Granoff, B. and Traeger, R. K., Coal Process. Technol. 15, (1979).

8. Mukherjee, D. K. and Chowdhury, P. A., Fuel 55, 4 (1976).

9. Gray, David, Fuel 57, 213 (1978).

10. Gray, J. and Shah, Y. T. in "Reaction Engineering in Direct Liquefaction," Adison Wesley Pub. Co., New York, NY (1981).

11. Derbyshire, F. J., Varghese, P. and Whitehurst, D. D., Preprints, Amer. Chem. Soc., Div. Fuel Chem. 26, No. 1, 84 (1981).

12. Whitehurst, D. D., Mitchell, F. U. and Farcasiu, M., in "Coal Liquefaction. The Chemistry and Technology of Thermal Processes," Academic Press, New York, NY, pp. 163-177 (1980).

13. Thomas, M. G., Padrick, T. D., Stohl, F. V. and Stephens, H. P., Fuel 61, 761 (1982).

14. Montano, P. A. and Granoff, B., Fuel 59, 214 (1980).

15. Montano, P. A., Bommannavar, A. S., and Shah, V., Fuel 60, 703 (1981).

16. Stohl, F. V. and Granoff, B., 90th Annual Meeting of the AIChE, Houston, TX (1981).

17. Anthony, D. B. and Howard, J. B., AIChE J. 22, 625 (1976).

18. Stangby, P. C. and Sears, P. L., Fuel 60, 131 (1980).

19. Franklin, H. D., Peters, W. A. and Howard, J. B., Preprints, Amer. Chem. Soc., Div. Fuel Chem. 26, No. 2, 121 (1981).

20. Jenkins, R. G., Nandi, S. P. and Walker, P. L. Jr., Fuel 52, 288 (1973).

21. Hippo, E. J. and Walker, P. L. Jr., Fuel 54, 245 (1975).

22. Tomita, A., Mahajan, O. P. and Walker, P. L. Jr., Fuel 56, 137 (1977).

23. Linares-Solano, A., Mahajan, O. P. and Walker, P. L. Jr., Fuel 58, 327 (1979).

24. Mahajan, O. P., Tomita, A., Nelson, J. R. and Walker, P. L. Jr., Fuel 56, 33 (1977).

25. Hüttinger, K. J. and Krauss, W., Fuel 60, 93 (1981).

26. Padrick, T. D., Rice, J. K. and Massis, T. M., Preprints, Amer. Chem. Soc., Div. Fuel Chem. 27, No. 3, 300 (1982).

EFFECTS OF EXCHANGEABLE CATIONS ON THE CONVERSION OF LOW RANK COALS TO GASES AND LIQUIDS

Robert G. Jenkins

Fuel Science Program
Department of Materials Science and Engineering
The Pennsylvania State University, University Park, PA 16802

INTRODUCTION

It has become evident that for low rank coals (generally of subbituminous C and lower) the inorganic constituents play major roles in their utilization. These coals are partly characterized by the presence of significant quantities of carboxyl and phenolic groups which are, to varying degrees, associated with alkali and alkaline-earth metal cations (1,2,3,4). As an example, in an earlier study (2) we reported that these exchangeable metal cations can account for approximately 3 wt% (dmmf) of a Montana Lignite. The dominant exchangeable metal cation in US low rank coals is calcium. However, appreciable concentrations of sodium and magnesium are found (2,3). Generally, approximately between 30 to 60% of the carboxyl groups are associated with metal cations (2,3).

It is important to differentiate between these exchangeable inorganic species and the mineralogical components when considering the behavior of low rank coals under processing conditions. The most significant differentiation is, of course, their dispersion throughout the coal matrix. In the case of the exchangeable cations, they are dispersed on an atomic basis; that is, each metal cation is associated with one or two carboxylic acid groups. There have been many electron microprobe studies (5), for example, which have shown that the inorganic elements under investigation are extremely uniformly distributed through a lignite. In essence, in that type of study, it is impossible to resolve precisely the distribution because the cations are of an atomic size, much lower than the resolution of the instrument. When considering the mineralogical species, it is well established that the great majority of the minerals exist in size ranges greater than 1 μm. Thus, they are several orders of magnitude greater in size than the cations. This size differentiation has, of course, ramifications on the chemical behavior of the species as well as physical considerations. It is extremely likely that the exchangeable metal cations are of much different chemical reactivity than a like atom in the lattice of some mineralogical species. Finally, it must be realized that on pyrolysis (which accompanies combustion, gasification and liquefaction processes) that the carboxylic acid salts will decompose to liberate a metal cation as some chemically reactive entity. Even after some degree of sintering, or agglomeration, the cation derived species will be finely dispersed, i.e., still much smaller than the vast majority of mineralogical particles.

It is the goal of this presentation to review several recent studies which have shown the importance of understanding the nature of the exchangeable cations in the utilization of low rank coals.

DIRECT LIQUEFACTION

It is well known that during direct liquefaction there is always some amount of material which appears as insoluble, residual solids (6,7). These solids are composed of a wide range of carbonaceous and inorganic materials. However, in this case we are only interested in those generated during the liquefaction of low rank coals. The most important feature of reactor deposits obtained from these coals is the formation of calcium carbonate as calcite and/or metastable vaterite (6,7,8,9). Detailed optical and SEM studies on these solids indicates that carbonate is precipitated and is not related to calcite grains which may occur in the feed low

rank coal (6,7). The source of the calcium is the exchangeable calcium present in these coals. A semi-quantitative relationship can be found between the amount of deposited solids and the ion-exchangeable calcium content of the feed coal (6). Liquefaction experiments made on an acid washed coal resulted in no production of calcium carbonate. A series of experiments were made on a Wyodak subbituminous coal which was first demineralized and then back exchanged with calcium acetate solution. The calcium loaded (5 wt%), dried coal was then reacted at 400°C in tetralin (N_2, CO_2 and H_2S atmospheres) for periods varying from 10 to 60 min. The quantity of calcium carbonate was determined quantitatively by measuring the volume of CO_2 evolved on treating the reaction products with 1N HCl. The results of this series of experiments are shown in Figure 1. The data are expressed as a first-order plot in terms of the conversion of carboxylates to the theoretical amount of $CaCO_3$ that could be produced. It is obvious that these data fit the first order plot rather well. Under these conditions 50% of the exchangeable calcium is converted to carbonate after about 23 mins. The calculated rate constant is 5×10^{-4} sec^{-1}. In all cases, the crystallographic form of calcium carbonate produced was found to be a mixture of calcite and vaterite. From the data plotted in Figure 1, it can be seen that the rate of conversion of calcium cations to carbonate, under these conditions, is not affected by the presence of the three gaseous atmospheres utilized (H_2O, N_2 and CO_2).

COAL PYROLYSIS

In any investigation dealing with the role of exchangeable metal cations in coal pyrolysis one has to be concerned with several gauges of pyrolysis behavior. As examples, it is important to gain understanding of the effects of the cations on total weight loss, tar evolution, product gas composition, decarboxylation and kinetics. Several investigations have been made into this general area. Tyler and Schafer (10), Franklin et al. (11), and Otake (12) studied the effects of exchangeable cations on total weight loss and tar yield over a wide range of reaction conditions. They found, in general, that replacement of the metal cations by protons leads to an increase in weight loss. Murray (14) and Schafer (15,16) studied the decarboxylation of low-rank coals in fixed-bed reactors at slow heating rates. They found that removing the metal cations does result in an increase in the amount of decarboxylation at any given temperature.

In recent studies in these laboratories (17,18,19), Morgan found profound effects of the metal cations on rapid pyrolysis of a Montana lignite in an entrained flow apparatus. Total weight loss, at 1173 K in N_2/He, was found to be a function of the presence of metal exchangeable cations for a residence time of about 250 ms (Table 1).

TABLE 1

EFFECT OF CATIONS ON MAXIMUM WEIGHT LOSS IN ENTRAINED FLOW REACTOR, 1173 K, DICF* BASIS (17,18)

Sample	mmoles cation/g DICF Coal	wt Loss
Raw	0.94	31
Ca A	1.11	30
Ca B	0.84	29
Ca C	0.75	35
Ca D	0.49	39
Acid Washed	--	49

* DICF: Dry Inorganic Constituent Free

As can be seen from Table 1, as the loading of calcium increases there is a drop in the total yield. The most significant reductions takes place after the initial

loadings. After a certain level of calcium cations the effects become essentially constant. Morgan's studies also suggested that presence of exchangeable cations caused a reduction in the amount of tars evolved when compared to the acid-washed sample. FTIR spectra of the tars evolved in these cases indicated that tars from the raw coal contain three times the amount of aliphatic hydrogen as do the tars from the acid-washed sample. Finally, it was found that the presence of the metal cations retarded the decomposition of the carboxylic acid groups. In this study, the carboxylic acid concentrations were determined directly on the pyrolyzed lignite samples.

GASIFICATION REACTIVITY

It has been well recognized that the measured gasification reactivities of coal chars, prepared under similar conditions, are a function of the rank of the parent coal (20,21). The chars of highest reactivities are those derived from lignites. Correlation have been made between the reactivities and the amount of exchangeable calcium cations in the coals or calcium in the chars (20,21,22). However, it was not until the work of Radovic et al. (23,24,25,26,27) that it was shown, in the case of calcium loaded onto a North Dakota Lignite, the catalytic species was calcium oxide. In addition, it was established that the observation that reactivity was a function of the severity of pyrolysis conditions was due to catalyst crystallite growth (sintering). As pyrolysis severity increased then the measured reactivities were reduced. A correlation was drawn between the observed gasification reactivities and the dispersion (as measured by crystallite size) of the catalytically active calcium oxide. Thus, the gasification reactivity of lignite chars was shown to be dominated by the concentration of their inherent catalyst sites.

It is important to recognize that the aforementioned reactivity measurements have been made on chars and not the corresponding raw or pretreated lignites. It is becoming evident that the exchangeable cations can have significant effects on combustion and gasification of the coals themselves. Some data reported by Morgan and Jenkins (19) and Morgan and Scaroni (28) have indicated relationships between the presence/absence of exchangeable metal cation and the rates of gasification/combustion of lignites. It is apparent from their data that the effects of the cations on rapid pyrolysis rates can ultimately result in enhancements in oxidation reactivity.

SUMMARY

As research proceeds in the area of low rank coal utilization, it is becoming obvious that the inherent inorganic constituents of these coals have profound influences on their behavior. The reason for this influence is related to the fact that a significant proportion of the inorganic components are in the form of atomically dispersed exchangeable metal cations. It is evident that variations in the metal cation content can bring about significant differences in the performance and behavior of these coals. With that in mind, it may well be that we should be looking in more depth at the "benefication" of low rank coals by effecting alterations in the chemical distributions of the cations associated with their carboxylic acid functionalities.

ACKNOWLEDGEMENTS

The author would like to acknowledge all his colleagues with whom he has been associated. Financial support for the research studies were provided by the Gas Research Institute, Electric Power Research Institute, Department of Energy, and The Pennsylvania State University Cooperative Program in Coal Research.

REFERENCES

1. Schafer, H. N. S., Fuel 49, 197 (1970) and Fuel 49, 271 (1970).

2. Morgan, M. E., Jenkins, R. G., and Walker, P. L., Jr., Fuel 60, 189 (1980).

3. Bobman, M. H., Golden, T. C., and Jenkins, R. G., Solvent Extraction and Ion Exchange 1(4), 791 (1983).

4. Bobman, M. H., Golden, T. C., and Jenkins, R. G., Solvent Extraction and Ion Exchange 1(4), 813 (1983).

5. Fowkes, W. W., "Separation and Identification of Minerals from Lignites," Chapter 27, in Analytical Methods for Coal and Coal Products, Volume 2, Ed. C. Karr, Jr., Academic Press (1978).

6. Walker, P. L., Jr., Spackman, W., Given, P. H., Davis, A., Jenkins, R. G., and Painter, P. C., "Characterization of Mineral Matter in Coals and Coal Liquefaction Residues," Final Report to EPRI, AP-1634, November 1980.

7. Wakely, L. D., Davis, A., Jenkins, R. G., Mitchell, G. D., and Walker, P. L., Jr., Fuel 58, 379 (1979).

8. Brunson, R. J., Chabach, J. J., Chem. Geol. 25(4), 333 (1979).

9. Stone, J. B., Trachte, K. L., Poddar, S. K., Amer. Chem. Soc. (Fuel Chem. Div.) Preprints 24(2), 255 (1979).

10. Tyler, R. J. and Schafer, H. N. S., Fuel 59, 487 (1980).

11. Franklin, H. D., Cosway, R. G., Peters, W. A., and Howard, J. B., Ind. Eng. Chem. Process Des. Dev. 22, 39 (1983).

12. Otake, Y., M.S. Thesis, The Pennsylvania State University (1982).

13. Murray, J. B., Fuel 57, 605 (1978).

14. Schafer, H. N. S., Fuel 58, 667 (1979).

15. Schafer, H. N. S., Fuel 58, 673 (1979).

16. Morgan, M. E., Ph.D. Thesis, The Pennsylvania State University (1983).

17. Morgan, M. E., and Jenkins, R. G., Amer. Chem. Soc. (Fuel Chem. Div.) Preprints 28(4), 138 (1983).

18. Morgan, M. E., and Jenkins, R. G., Amer. Chem. Soc. (Fuel Chem. Div.) Preprints 29(2), 141 (1984).

19. Jenkins, R. G., Nandi, S. P., and Walker, P. L., Jr., Fuel 52, 288 (1973).

20. Hippo, E. J., and Walker, P. L., Jr., Fuel 54, 245 (1975).

21. Hippo, E. J., Jenkins, R. G., and Walker, P. L., Jr., Fuel 58, 338 (1979).

22. Radovic, L. R., Ph.D. Thesis, The Pennsylvania State University (1982).

23. Radovic, L. R., Walker, P. L., Jr., and Jenkins, R. G., Fuel 62, 209 (1983).

24. Radovic, L. R., Walker, P. L., Jr., and Jenkins, R. G., J. Catal. 82, 382 (1983).

25. Radovic, L. R., Walker, P. L., Jr., and Jenkins, R. G., Fuel 62, 849 (1983).

26. Radovic, L. R., Steczko, K., Walker, P. L., Jr., and Jenkins, R. G., submitted to Fuel.

27. Morgan, B. A., and Scaroni, A. W., Amer. Chem. Soc. (Fuel Chem. Div.) Preprints 28(4), 164 (1983).

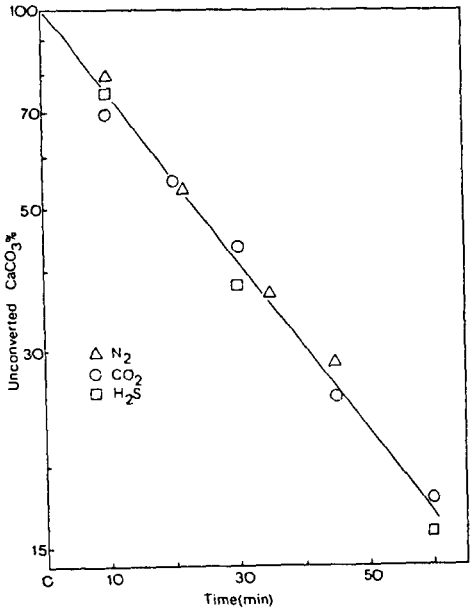

Figure 1. First Order Plot for Calcium Carbonate Formation at 400°C Under Pseudo-Liquefaction Conditions

Iron Sulfide Catalysis in Coal Liquefaction

P.A. Montano, Y.C. Lee, A. Yeye-Odu and C.H. Chien

Department of Physics, West Virginia University, P.O. Box 6023
Morgantown, WV 26506-6023

I. Introduction

The direct liquefaction of coal is a process that involves the interaction between coal, hydrogen, solvent, and catalysts. Mineral matter has been known to enhance the conversion of coal to liquid products.[1,2,3] Addition of pyrite, pyrrhotite, and liquefaction residues[4] to coal has been shown to affect the coal conversion yields and the viscosity of the products.[5] Of all the minerals present in coal, pyrite (and marcasite) are the most important for coal utilization, especially in direct coal liquefaction.[1,5] However, one has to remember that under coal liquefaction conditions pyrite rapidly transforms to a non stoichiometric iron sulfide $Fe_{1-x}S(0<x<0.125)$. It is noted that the sulfur formed as a result of the decomposition of pyrite is able to extract hydrogen from poor donor solvents. The stoichiometry of the pyrrhotite formed from FeS_2 depends strongly on the partial pressure of H_2S.[6]

A correlation between the conversion of coal to benzene soluble, and the stoichiometry of the iron sulfides was observed by Montano and Granoff[7]. Higher conversion is accomplished by a more iron-deficient pyrrhotite. Stephens et al[8] studied the effect of additives to an IL#6 conversion to liquid products. Their work strongly suggests that $Fe_{1-x}S$ and H_2S play a catalytic role in the conversion of coal to oils. These results are in good agreement with the ones obtained from <u>in situ</u> Mössbauer measurements,[6,9,10] where there was clear evidence of interaction between the iron sulfides and some coal components. Many questions remain unanswered concerning the catalytic roles of H_2S and $Fe_{1-x}S$. Lambert[11] suggested that the catalytic activity observed for pyrite is solely due to H_2S acting as a hydrogen-transfer catalyst. In a recent study by Anderson and Bockrath[12] on direct coal liquefaction more conversion was obtained when the ratio of sulfur added to an iron solution (the catalyst) was equal to the one needed to obtain pyrrhotite ($Fe_{1-x}S$). A very recent work by Ogawa, Stenberg, and Montano[13] reporting the hydrogenation of diphenylmethane in the presence of pyrrhotite clearly shows that maximum activity is obtained when the partial pressure of H_2S is enough to maintain an iron deficient surface. Too high a partial pressure of H_2S in the reactor moves the composition of the surface towards FeS_2 and the conversion of diphyenylmethane is reduced. Too low a partial pressure of H_2S leads to the formation of troilite (FeS) and lower conversion. These results indicate that optimum conditions are obtained when the surface of the sulfide is rich in metal vacancies, where dissociation of H_2S can take place forming highly reactive species.[13] It is obvious that the understanding of the catalytic role of the iron sulfides lies in the investigation of their surface properties. We report in the present paper such a study, where surface techniques were used to observe the reaction of gases found under liquefaction conditions with the sulfides surfaces. A special reactor was developed to study the surface composition of the iron sulfides after reaction with oxygen containing compounds using conversion electron Mössbauer spectroscopy (CEMS). Extended X-ray Absorption Fine Structure (EXAFS) and X-ray Absorption Near Edge Structure (XANES) were used for determining the environment of iron species in the residues obtained from the study of the interaction of iron sulfides (FeS_2,Fe_7S_8) with pyrene.[14]

II. Experimental

Auger and electron energy loss spectroscopy measurements were performed using an UHV system with a base pressure of 10^{-10} torr. The system was attached to a reactor cell where the samples were exposed to high temperatures and gases. The reactions of FeS_2, Fe_7S_8, and FeS with CO, H_2, O_2, NH_3, CH_4, C_2H_4, and higher hydrocarbons were studied between room temperature and 450 °C. Figure 1 shows a schematic diagram of the system used in these measurements.

The CEMS measurements were carried out in a specially designed reactor to be described elsewhere. In this reactor the samples of ^{57}Fe foil were studied and treated with H_2/H_2S to obtain the iron sulfides. The detector employed for the detection of the electrons was a He/10% CH_4 flow counter connected in line with the reactor. The reaction of pure iron and iron sulfide with naphtoquinone were studied with this cell. The EXAFS and XANES measurements of the residues of the reactions of FeS_2 and Fe_7S_8 with model compounds were made at the Cornell High Energy Synchrotron Source.

Experimental Results

1. Auger and Electron Energy Loss Measurements on FeS_2, Fe_7S_8, FeS

Natural crystals of FeS_2 (pyrite) and Fe_7S_8 (monoclinic pyrrhotite) were used for the measurements. The (100) face of pyrite and the (0001) face of pyrrhotite were studied in the reactor, using a polycrystalline sample of FeS. All the samples show a characteristic $M_{2,3}$ VV Auger doublet with a separation of 5.0 eV (Figure 2). Two additional peaks (3 and 4 in Figure 2) are also observed for FeS. Peak 1 may correspond to transitions involving the s-3p ($2\sigma_y$) valence band while peak 2 may correspond to transitions involving the d-band. A typical set of Electron Loss spectra for FeS_2 is shown in Figure 3. Peak a is assigned to interband transitions from the Fe-3d band to an empty state above the Fermi level. Peaks b and c may be assigned to transitions for one s-3p-like valence band (peak b to $1\pi g \rightarrow 2\sigma_y$ and c to $2\sigma_g$, $1\pi_u \rightarrow 1\sigma_u$ transitions.) Peaks d and e are attributed to collective oscillations of the conduction or valence electrons. Peaks f and g are assigned to surface and volume plasmons respectively. Peaks j and k are transitions involving the Fe-3p electrons ($M_{2,3}$ level). Peak ℓ is due to transition from the M_1 level. The EEL spectra for the other sulfides are similar but the position and intensities of the peaks vary.[15] In our measurements we observed EEL peaks with strong iron or sulfur character. Damaged iron sulfide surfaces show evidence of reconstruction through migration of sulfur after heating to 450 °C. For undamaged sulfides, heating results in changes in the chemical composition of the surface; migration of sulfur also occurs. There is clear evidence of the presence of elemental sulfur on the pyrite and pyrrhotite surface but not on troilite (FeS). Since the maximum temperature attained was 450 °C we do not expect that reduction of the FeS surface will take place. Essentially if the partial pressure of H_2S is low in the reactor the formation of FeS will occur by removal of sulfur from the $Fe_{1-x}S$ surface. Once this state is reached no further loss of sulfur occurs and a fairly stable surface is obtained.

The interaction of the pyrrhotite with simple gases is more complex, damaged surfaces of FeS_2 and Fe_7S_8 react with CO at 450 °C. We understand that as the result of the interaction of CO with Fe on the sulfide surface. This interaction is not detected with undamaged surfaces (pure single crystals) and with FeS. The formation of oxides on the surface is easily detected for FeS_2, and Fe_7S_8 after reaction with CO. It has been observed that CO undergoes a desproportionation reaction on Fe, $2CO \rightarrow C + CO_2$, with the formation of surface oxide due to the

dissociation of CO.[16] The surface oxide is rapidly removed by H_2. The surfaces of the sulfides do not show any evidence in the Auger and EEL spectra of reactions with NH_3, CH_4, and C_2H_4. However, they interact strongly with molecular oxygen forming a surface oxide. Figure 4 shows the surface oxide formed on pyrite after interaction with oxygen, for comparison purposes the EEL spectrum for α-Fe_2O_3 is also shown. The present measurements indicate a high reactivity of the sulfide surfaces towards oxygen containing compound and very little towards light hydrocarbons and ammonia.

2. CEMS Measurements of the Surface Interaction of Naphthoquinone with Iron and Iron Sulfide Surfaces

A high purity ^{57}Fe foil was used for these measurements, such a foil was necessary in order to record rapidly a Mössbauer spectrum (less than one-half hour). The sample was placed in the holder inside of the reactor and H_2 was flown for 2 hours at 350 °C to reduce the surface and clean off any residual contamination. Figure 5a shows the Mössbauer spectrum at room temperature inside the reactor after cleaning. We studied the hydrogenation of naphthoquinone by introducing about 20 mg of the compound and flowing hydrogen at about 0.5 cc/sec. The temperature of the reaction was 305 °C and 405 °C and the time of reaction was one-half hour. After reaction the CEM spectrum was taken inside the reactor. No evidence of the formation of any known oxide was detected (Figure 5b). The same experiment was repeated using a sulfided sample (produced from the ^{57}Fe foil by flowing H_2/H_2S (10%) at 400 °C). The spectrum for such a sample is shown in Figure 6a before reaction. After reaction with naphtoquinone we see clear evidence of the formation of Fe_3O_4 on the surface (Figure 6b). Magnetite is formed at the expense of the iron sulfide. This observation is in very good agreement with our earlier <u>in situ</u> Mossbauer work,[14] where a less surface sensitive technique was used for the measurements. We interpret these results as evidence of a greater reactivity of the iron sulfides surfaces towards oxygen containing organic molecules than the pure metal. It is noted that magnetite can be easily removed by further flow of H_2/H_2S. The magnetite layer is formed in the first few surface layers of the iron sulfide (see Figure 6).

3. EXAFS and XANES Measurements

Measurements were performed on the residues of the reaction of FeS_2 and Fe_7S_8 with pyrene. Pyrite and monoclinic pyrrhotite were used as chemical standards for the measurements. In Figure 7 the XANES spectra are shown for the residues of the reactions of pyrene with Fe_7S_8 and FeS_2. The reactions were performed([14]) at 440 °C in the presence of H_2. One notices that the near edge structure is different for both residues, we attributed the difference to the presence of FeS in the reaction residues of Fe_7S_8 and pyrene. A compound that is not present in the residues of the pyrite run. The total EXAFS spectrum were analyzed and the Fourier transform for the residues of the FeS_2 run is shown in Figure 8a. (The peak positions are not corrected for phase shifts.) For comparison purposes the Fourier transform for pure pyrite and monoclinic pyrrhotite are also shown. The first prominent peak in all the spectra is due to Fe-S distances (2.262 A for pure FeS_2). The second peak in pyrite (Figure 8b) is due to the other iron neighbors. For Fe_7S_8 the spectrum is complicated since there are many iron distances present (Figure 8c). For the residues of the reaction of FeS_2 with pyrene practically no Fe-Fe can be identified. This means that the iron atoms and vacancies in the $Fe_{1-x}S$ structure[14] (atomic % iron is 47.8) are extremely disordered and randomly distributed and that the only well defined coordination of the iron ions are the sulfur atoms. This is a striking result since we should have expected as a result of the Mössbauer study[14] a better defined pyrrhotite structure.

III. Conclusions

We have observed that the behavior of iron sulfide surfaces depends strongly on the stoichiometry. Iron deficient surfaces show a higher reactivity than the troilite surface. At high temperatures (450 °C) there is elemental sulfur present on the iron sulfide surfaces. The metal vacancies can serve as centers for the dissociation of H_2S thus facilitating the transfer of hydrogen to organic entities. The pyrrhotite surface shows a great reactivity towards oxygen containing compounds. The surface oxide formed on the pyrrhotite surface are easily reduced when H_2 and H_2S are present in the reactor. The interaction between the pyrrhotites surfaces and light hydrocarbons is minimal.

Acknowledgement: The authors wish to thank the U.S. DOE for their support.

REFERENCES

1. R.M. Davidson "Mineral Effects in Coal Conversion," Report No. ICTIS/TR22, IEA Coal Research London.

2. D.K. Mukherjee and P.B. Chowdbury FUEL 55, 4(1976).

3. W. Hodek, Chemical and Physical Valorization of Coal Meeting, Liege, EUR-5954-d/e/f/i, Luxembourg, 87, 1978.

4. B. Granoff, M.G. Thomas, P.M. Baca and G.T. Noles, Am. Chem. Soc. Div. FUEL Chem. Prepr. 23, 23(1978).

5. E. Illig, "Disposable Catalysts in Coal Liquefaction," DOE, Albuquerque, NM (1978).

6. P.A. Montano, A.S. Bommannavar and V. Shah, FUEL 60, 703(1981).

7. P.A. Montano and B. Granoff, FUEL, 59, 214(1980).

8. H.P. Stephens, F.V. Stohl and T.D. Padrick, Proc. Int. Conf. Coal Sci., Dusseldorf, Sept. 1981, Verlag Gluck Auf Essen; pp368 (1981).

9. A.S. Bommannavar and P.A. Montano FUEL, 61, 1289(1982).

10. A.S. Bommannavar and P.A. Montano FUEL, 61, 523(1982).

11. J.M. Lambert, Jr., FUEL, 61, 777(1982).

12. R.R. Anderson and B.C. Bockrath, "Effect of Sulfur on Coal Liquefaction in the Presence of DispersedIron and Molybdenum Catalysts," PETC, Pittsburgh 1982.

13. T. Ogawa, V. I. Stenberg, and P.A. Montano, FUEL (in press).

14. P.A. Montano and A.S. Bommannavar, J. of Molecular Catalysis, 20, 393(1983).

15. Y.C. Lee and P.A. Montano, Surface Science 142, 27(1984).

16. K. Jagannathan, S. Srinivasan, M.S. Hedge and C.N.R. Rao Surface Sci. 99, 309(1980).

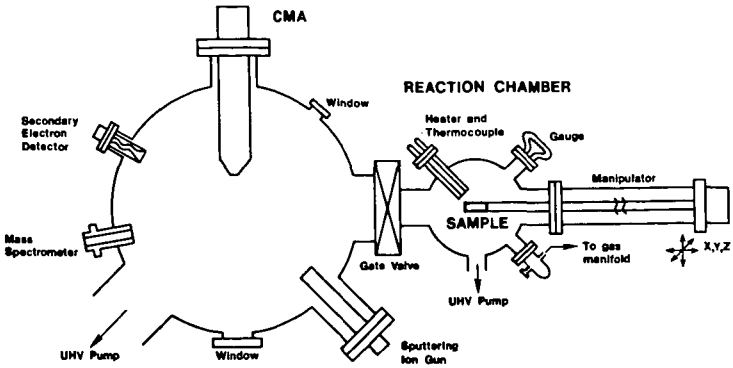

Figure 1. Schematic diagram of the UHV system used for the surface measurements

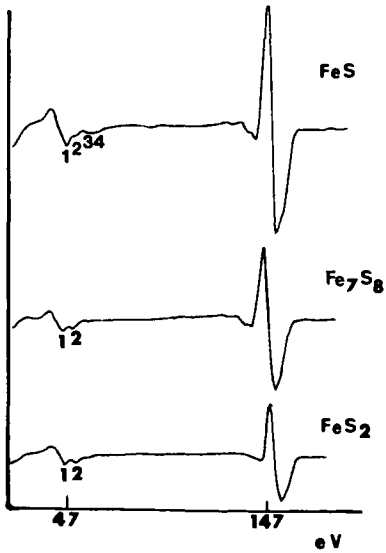

Figure 2. Low energy Auger spectra for the iron sulfides

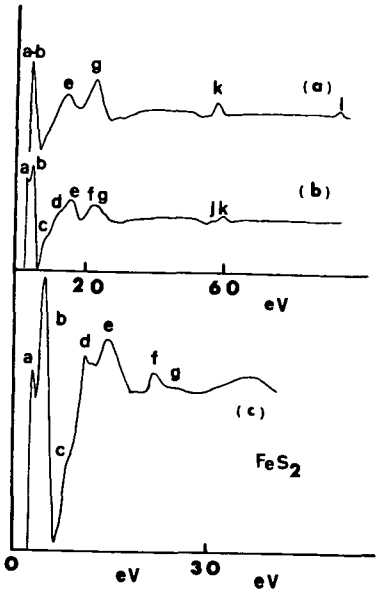

Figure 3. EEL spectra for FeS_2
a) $E_{primary}$ = 300 eV b) E_p = 150 eV c) E_p = 50 eV

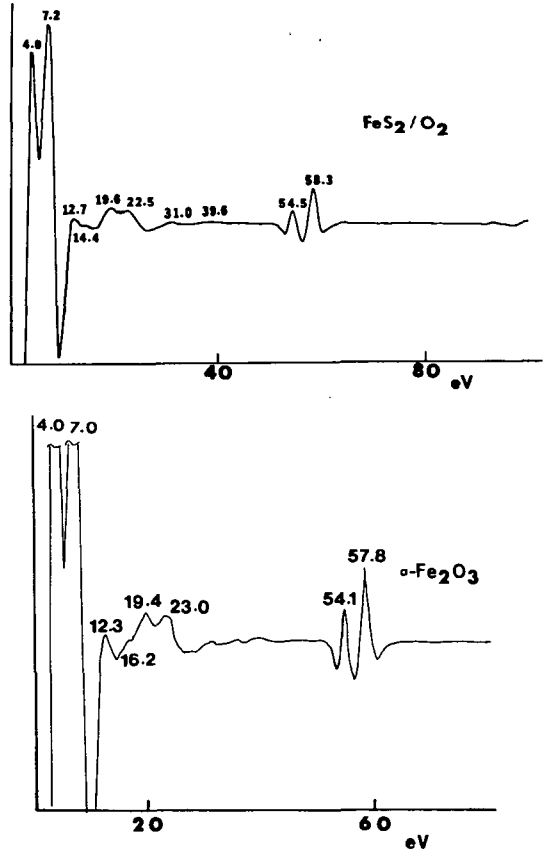

Figure 4. EEL spectra of FeS_2 after reaction with oxygen (a) and of α-Fe_2O_3 (b)

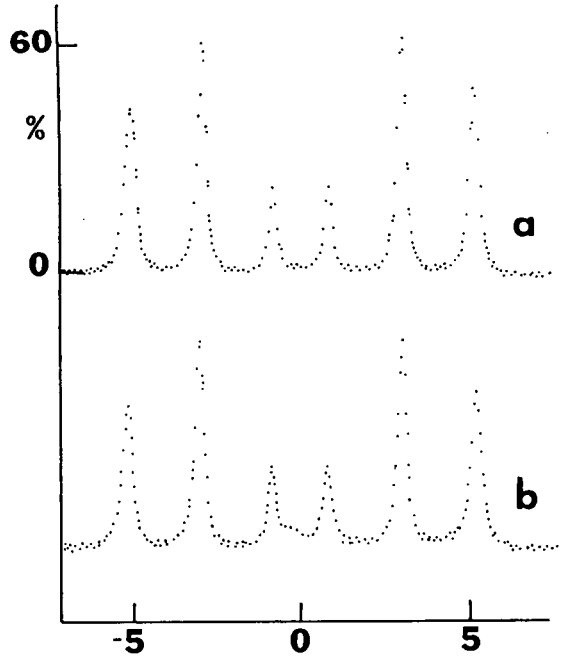

Figure 5. CEM spectra of ^{57}Fe foil (a) and after reaction with naphthoquinone(b). X-axis is in mm/sec.

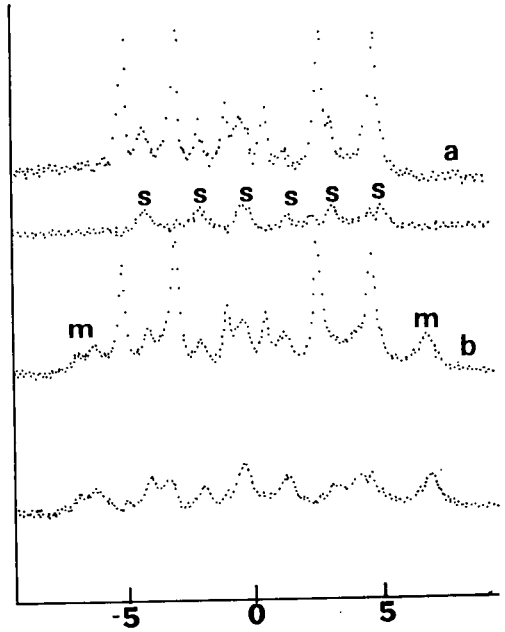

Figure 6. CEM spectra of a) sulfided ^{57}Fe foil, s: indicates the sulfide surface b) After reaction with naphtoquinone m: magnetic, bottom spectrum is the surface layers after reaction. x-axis is mm/sec.

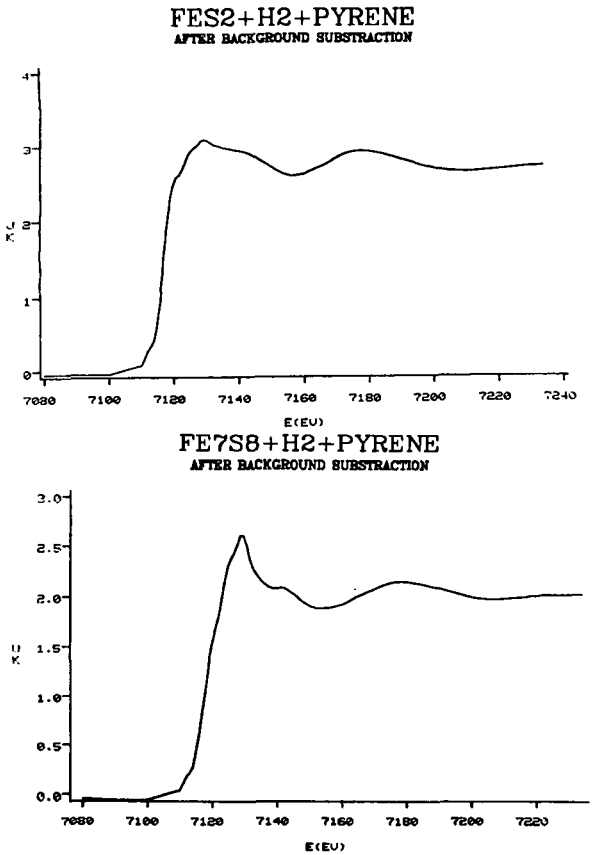

Figure 7. XANES spectra of the residues of the reactions of pyrene with a) FeS_2 and b) Fe_7S_8

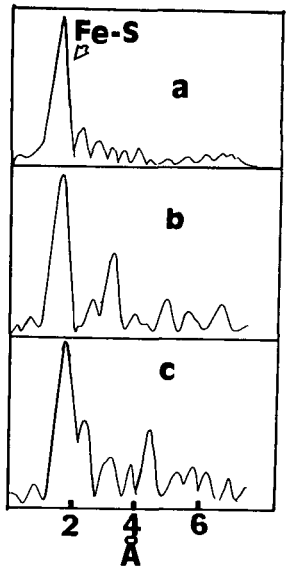

Figure 8. Fourier transforms of $\chi \cdot k$ (x EXAFS structure) for a) FeS_2 after reaction b) pure FeS_2 and c) Fe_7S_8. X-axis is in A and without corrections for phase shifts.

NEW IRON OXIDE CATALYST REDUCTION ACTIVITIES WITH HYDROGEN SULFIDE AND HYDROGEN

H. Hattori, F.A. Jones, T. Ogawa, C.L. Knudson,
L.J. Radonovich and V.I. Stenberg

University of North Dakota Energy Research Center
and the Department of Chemistry
University of North Dakota, Grand Forks, ND 58202

INTRODUCTION

Various types of catalysts have been used for coal liquefaction. Among these catalysts, molybdenum and iron catalysts are most frequently used and they are usually combined with other metal oxides. Molybdenum catalysts, in the form of $Co/Mo/Al_2O_3$ wherein this notation represents some form of the metal oxides and the last species is the support, have been used in the H-Coal process. In others, iron catalysts have been used in the form of red mud which is mixed with elemental sulfur. The activity of iron catalysts has generally been regarded as low when compared with that of molydenum catalysts. However, iron oxide catalysts became highly active for the conversion of coal-related model compounds when used in the presence of H_2S and H_2. For coal liquefaction in the absence of a heterogeneous catalysts, the use of a mixture of H_2S and H_2 instead of H_2 resulted in an increase in conversion.[1] Because of the interaction of H_2S with Fe_2O_3[2] and the fact that iron is presently the lowest cost transition metal, iron was selected as the basis metal for a new set of heterogeneous catalysts specifically designed for coal liquefaction using the H_2S-H_2 reducing gas medium.

EXPERIMENTAL

A series of 26 iron oxide catalysts were designed and synthesized. The supported iron catalysts prepared are listed in Table 1. The selection of the supports were based on the following objectives.

1. To clarify the effect of SiO_2 surface area, SiO_2 supports for catalysts 1, 2, and 3 were prepared at different pH's from a Na-free SiO_2 source.
2. To examine the effect caused by use of a different starting material to prepare SiO_2, catalysts 4, 5, and 6 were prepared from sodium metasilicate at different pH's and can be compared to catalysts 1-3.

3. To examine the effect of the precipitating reagent, catalysts 7 and 8 were prepared from $Si(OC_2H_5)_4$ with H_2SO_4 or NaOH, respectively. Catalysts 7 and 8 results are to be compared with those of catalysts 1 and 3.
4. To examine the effect of basic supports, metal oxides with basic properties were used for the supports of catalysts 9, 10, 11, 12, 13 and 14.
5. To examine the effect of the sulfate ion on the TiO_2 support, it was prepared in the presence of sulfate ions and the resulting catalyst 15 is to be compared with catalyst 14.
6. To examine the effect of additives to Fe/SiO_2, small amounts of Mo, W, Co, and Ni oxides were added (catalysts 16, 17, 18, and 19) to the Fe_2O_3 on the surface of the catalyst.
7. To examine the effect of the sulfate and nitrate anions on the deposition of the iron layer, catalysts 20 and 21 were prepared.
8. To examine the effect of acidic sites on the Fe/SiO_2 catalyst, sodium- and potassium-poisoned catalysts were prepared (catalysts 22 and 23).
9. To examine the effects of the commercial TiO_2 and SiO_2 supports, catalysts 20 and 24 were prepared to be compared to catalysts 1 and 14, respectively.
10. To examine the effect of activated carbon which possesses an extremely high surface area as the Fe_2O_3 supports, catalyst 26 was prepared to be compared to catalyst 20 (SiO_2) and 24 (TiO_2).
11. To examine the effect of a simple admixture of Fe_2O_3 and SiO_2, catalyst 28 was prepared to be compared with catalyst 20.
12. To enable comparison to a known commerical hydrogenation catalyst, $Co/Mo/Al_2O_3$ (catalyst 29) was included as a part of the series.

The catalysts were subjected to two reactions: hydrocracking of diphenylmethane to toluene and benzene, a model compound for the Ar-C bond cleavage of the coal structure, and hydrocracking of diphenyl ether to phenol and benzene, a model compound for the Ar-O bond cleavage of the coal structure. The reaction conditions for these reactions are summarized in Table 2.

RESULTS AND DISCUSSION

The design of the iron oxide catalysts was based on the following experimental findings.

1. For the hydrocracking of diphenylmethane, the effect of H_2S addition was augmented with iron oxide catalysts.[3]

2. The promotional effect of the H_2S addition on the catalytic activity varied with the preparative method for iron catalyst.[3] Among Fe catalysts supported on SiO_2, ZrO_2, and TiO_2, the Fe/SiO_2 showed the highest activity for the hydrocracking of diphenylmethane.
3. The Fe/TiO_2 catalyst was active not only for hydrocracking of diphenylmethane but also for hydrocracking of diphenyl ether.[3]

Besides these findings, it has been generally observed that the catalytic behavior of active components vary with the types of supports.

The time dependence of the diphenylmethane conversion is depicted in Figure 1. The value of 20 minutes reaction time was selected for the tubing bomb tests in order to differentiate catalyst effects.

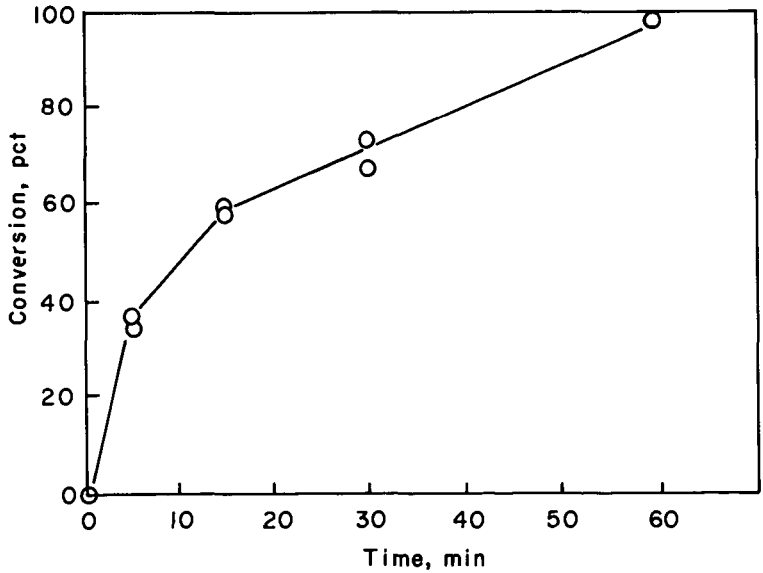

Fig. 1. Time dependence of conversion for hydrocracking of diphenylmethane. Catalyst, Fe_2O_3/SiO_2 (catalyst 20); catalyst/reactant, 50 mg/500 mg; reaction temperature, 425°C; pressure at room temperature, H_2 700 psi, H_2S 100 psi; and reactor, 12-ml capacity.

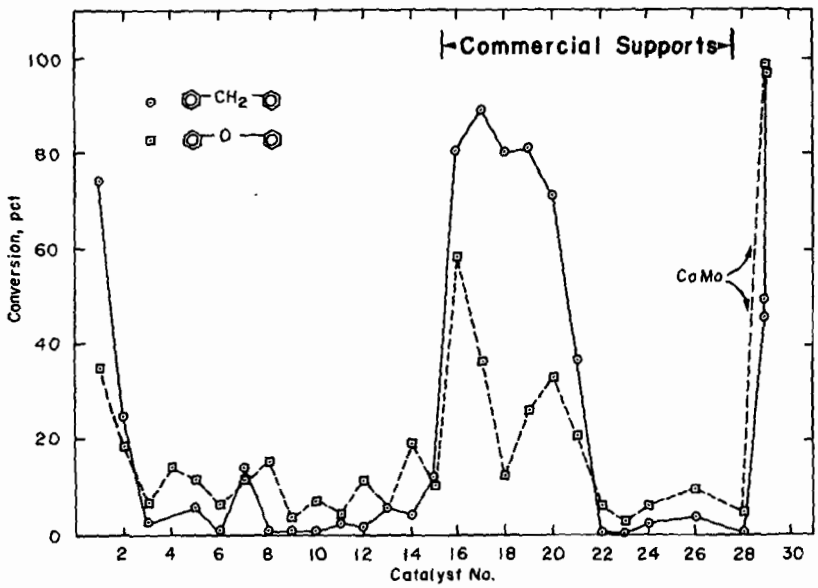

Fig. 2. Conversion of diphenylmethane (—) and diphenylether (---) with various catalysts.

The results of the catalytic reactions are given in Figure 2. For hydrocracking of diphenylmethane, the activities vary with different supports. This indicates that an interaction of Fe_2O_3 with the support occurred. The activity increased with an increase in surface area of support (catalysts 1, 2, and 3). Enhanced catalytic activity was observed by addition of Mo (no. 16), W (no. 17), Co (no. 18), and Ni (no. 19) oxides to the surface Fe_2O_3 as compared to Fe/SiO_2 (no. 20). The introduction of sodium or potassium to Fe/SiO_2 eliminated the catalytic activity (nos. 22 and 23 vs. no. 20). Similar phenomena were observed for catalysts 5, 6, and 8, which possibly contain sodium on the support. The sulfate ion had a negative influence on catalytic activity, cf. catalyst 5 with 2.

For the hydrocracking of diphenyl ether, the catalyst containing Mo and Fe (catalyst 16) was twice as active as the iron oxide catalyst. However, hydrogenated products such as methylcyclopentane and cyclohexane were produced in larger quantities with catalyst 16 than with 20. The Fe/SiO_2 catalyst activity increased with increased surface area of the support (catalysts 1-3), and was poisoned by sodium and potassium ions, cf. catalysts 22 and 23 with 20. The presence of the sulfate ion again retarded the Fe/SiO_2 activity, cf. nos. 15 to 14 and 20 to 21, as it did with diphenylmethane.

In general the catalysts required the presence of hydrogen sulfide[4] and the commercially supplied sample of silica with its high surface area worked very well. The pH of the silica preparation method proved to be crucial to generating high surface area silica. The catalysts in which the iron oxides were deposited on silica exceeded or equaled the activity of a simple admixture of iron oxide and silica (catalyst 28). The iron oxide catalysts were the better than the commercial hydrogenation-hydrocracking catalyst $Co/Mo/Al_2O_3$ for the hydrocracking of diphenylmethane (e.g., catalyst 20 vs. 29) but the latter exhibited both hydrocracking and hydrogenation ability. However, the $Co/Mo/Al_2O_3$ was more active in the conversion of diphenyl ether.

ACKNOWLEDGEMENT

We are grateful for the financial support of the Department of Energy.

REFERENCES

1. (a) Sondreal, E.A.; Wilson, W.G., and Stenberg, V.I., Mechanisms Leading to Process Improvements in Lignite Liquefaction Using CO and H_2S, Fuel, 1982, 61, 926. (b) Baldwin, R.M. and Viciguerra, Fuel, 1982, 62, 498. (c) Abdel-Baset, M. and Ratcliffe, C.T., Preprints Amer. Chem. Soc. Div. Fuel Chem., 1979, 25, 1. (d) Satterfield, C.M. and Model, M., U.S. NTIS, P.B. Rept., 1975, 248101.
2. (a) Ogawa, T.; Stenberg, V.I., and Montano, P.A., Fuel, 1984, in press. (b) Stenberg, V.I.; Tanabe, K.; Ogawa, T.; Sweeny, P. and Hei, R., Iron-Based Catalysts, H_2S and Liquefaction, Preprints, Fuel Division, American Chemical Society, 1983, National Meeting of the American Chemical Society, Washington, D.C.
3. Stenberg, V.I.; Ogawa, T.; Willson, W.G. and Miller, D., Hydrocracking of Dephenylmethane, Fuel, 1982, 62, 1487.

4. (a) Stenberg, V.I.; Srinivas, V.R.; Sweeny, P.; Baltisberger, R.J. and Woolsey, N.F., Dealkylation of N,N-dimethylaniline with Sulphur and Hydrogen Sulphide, Fuel, 1983, 62, 913. (b) Baker, G.G.; Willson, W.G.; Farnum, B.W., and Stenberg, V.I., Homogeneous Catalysis of Lignite Liquefaction with Hydrogen Sulfide, 1983 Spring National AIChE Meeting, Utilizing Texas Lignite, Session 16D, Fuels and Petrochemicals Division, March 27-31, Houston, Texas.

Table 2. Reaction conditions

Reaction	Temperature (°/C)	Ratio of reactant/catalyst by wt.	Pressure (psi cold charge)		Reaction time (1 min)
			H_2S	H_2	
Hydrocracking of diphenylmethane	425	10/1	100	700	20
Hydrocracking of diphenyl ether	425	10/1	100	1400	60

Table 1. List of catalysts prepared

Catalyst		Source of Fe_2O_3	Surface area (M^2/g)	Support		
No.	Composition (wt. ratio)			Starting Material	Precipitation Reagent	pH
1	Fe/SiO_2 (1/9)	$Fe(NO_3)_3$	579	$Si(OC_2H_5)_4$	HNO_3	1
2	Fe/SiO_2 (1/9)	$Fe(NO_3)_3$	382	$Si(OC_2H_5)_4$	HNO_3	5
3	Fe/SiO_2 (1/9)	$Fe(NO_3)_3$	28	$Si(OC_2H_5)_4$	NH_4OH	11
4	Fe/SiO_2 (1/9)	$Fe(NO_3)_3$	578	Na_2SiO_3	H_2SO_4	1
5	Fe/SiO_2 (1/9)	$Fe(NO_3)_3$	349	Na_2SiO_3	H_2SO_4	5
6	Fe/SiO_2 (1/9)	$Fe(NO_3)_3$	318	Na_2SiO_3	H_2SO_4	11
7	Fe/SiO_2 (1/9)	$Fe(NO_3)_3$	568	$Si(OC_2H_5)_4$	H_2SO_4	1
8	Fe/SiO_2 (1/9)	$Fe(NO_3)_3$	39	$Si(OC_2H_5)_4$	NaOH	11
9	Fe/CaO (1/9)	$Fe(NO_3)_3$	1	$Ca(OH)_2$	-(calcined at 500°C)-	
10	Fe/La_2O_3 (1/9)	$Fe(NO_3)_3$	11	$La(NO_3)_3$	NH_4OH	9
11	Fe/ZrO_2 (1/9)	$Fe(NO_3)_3$	74	$ZrOCl_2$	NH_4OH	9
12	Fe/ZnO (1/9)	$Fe(NO_3)_3$	5	$Zn(NO_3)_2$	NH_4OH	9
13	Fe/SnO_2 (1/9)	$Fe(NO_3)_3$	28	$SnCl_2$	NH_4OH	9
14	Fe/TiO_2 (1/9)	$Fe(NO_3)_3$	41	$TiCl_4$	NH_4OH	9
15	Fe/TiO_2 (1/9)	$Fe(NO_3)_3$	56	$TiCl_4 + (NH_4)_2SO_4$	NH_4OH	9

Table 1. (continued)

Catalyst		Source of	Surface area	Support		
No.	Composition (wt. ratio)	Fe_2O_3	(M^2/g)	Starting Material	Precipitation Reagent	pH
16	$Mo/Fe/SiO_2$ (1/9/90)	$Fe(NO_3)_3$ + $(NH_4)_6Mo_7O_{24}$	477	Commercial. Fisher Sci. Co.		
17	$W/Fe/SiO_2$ (1/9/90)	$Fe(NO_3)_3$ + $(NH_4)_{12}W_{12}O_{42}$	496	Catalog No. S-156. 14-20 mesh Lot No. 744571		
18	$CoFe/SiO_2$ (1/9/90)	$Fe(NO_3)_2$ + $Co(NO_3)_3$	550			
19	$Ni/Fe/SiO_2$ (1/9/90)	$Fe(NO_3)_3$ + $Ni(NO_3)_2$	502			
20	Fe/SiO_2 (1/9)	$Fe(NO_3)_3$	521			
21	Fe/SiO_2 (1/9)	$Fe_2(SO_4)_3$	344			
22	$Na/Fe/SiO_2$ (2/10/90)	$Fe(NO_3)_3$	200			
23	$K/Fe/SiO_2$ (2/10/90)	$Fe(NO_3)_3$	205			
24	Fe/TiO_2 (1/9)	$Fe(NO_3)_3$	11	Commercial, MCB, TX068501, Anatase		
26	Fe/Activated C (1/9)	$Fe(NO_3)_3$	946	Commercial, Union Carbide, LCK, Columbia[R]		
28	Fe_2O_3 + SiO_2			Commercial JMC, Puratronic + Fisher SiO_2		
29	$Co/Mo/Al_2O_3$	(Co, 3%; Mo, 9%)		Harshaw Co-Mo-0401		

The Influence of Mineral Matter on The Rate of Coal Char Combustion

John H. Pohl
Energy and Environmental Research Corporation
18 Mason
Irvine, California 92714

Introduction

The rate of coal combustion can, in some instances, influence the design of boilers. The intrinsic rate of char combustion is, however, poorly known. Figure 1 shows that estimated intrinsic rate of char combustion can vary by a factor of 10^4 (1). The largest uncertainties are (2):

Property	Factor of Uncertainity
Surface Area	100
Effectiveness Factor	50
Catalysis	100
Crystal Structure	30

Other uncertainities account for less than a factor of four in the estimated intrinsic rate of coal char combustion.

Changes in the apparent rate of char combustion by a factor of 10 can influence the predicted performance of boilers. An example of these changes for a 660 MWe boiler is shown in Table 1. These figures were calculated using a well tested model of boiler performance (3). Increasing the accepted apparent rate constant by a factor of 10 predicts slightly improved performance, but decreasing the accepted rate constant by a factor 10 predicts severely degraded and unacceptable boiler performance.

This paper assesses one of the major uncertainity in estimating intrinsic rate constants, the influence of catalysis of the combustion rate of coal char.

Mineral Matter

Mineral matter contained in the coal could influence the rate of char combustion by blocking part of the coal surface or by catalytically increasing the rate of combustion. Figure 2 shows that the measured rate of combustion of purified nonporous graphics is uncertain by less than a factor of 3. This is a small difference compared to the spread in the overall rate data and suggests that some of the scatter in the measured rates of coal combustion are caused by the mineral matter in the coal.

Blocking of the surface area of coal by ash is unlikely to significantly change the rate of char reaction. Calculations for a coal with 25 percent ash indicate that, except at high levels of burnout, much less that 1 percent of the surface area of char will be blocked with ash particles.

Experiments have shown that small amounts of certain metals can accelerate the rate of char combustion (4,5,6,7,8,9). A number of anions and cations have been shown to accelerate the combustion of carbons at concentrations of 10 to 1000 ppm. Table 2 shows the relative influence on the combustion rate of various salts added as solutions to purified graphite. Relatively small amounts of metals can accelerate the rate of combustion by many orders of magnitude. Metals which appear in coal in significant concentrations which will accelerate the combustion of coal are 1) sodium and 2) calcium. Sodium can be present in coal in concentrations of 100-6000 ppm and calcium at concentrations of 50-12,000 ppm. The in-

fluence of relatively minor levels of sodium on the combustion rate of graphite is shown in Figure 3. Addition of sodium to a concentration of 15 ppm accelerates the reaction by one to two orders of magnitude; higher levels of sodium accelerate the reaction at a lower rate. Calculations show that the sodium must be distributed on nearly the molecular level to be effective. In addition, the influence of catalysis will be less pronounced at the higher temperatures of combustion where noncatalytic combustion proceeds much faster. No data exists at these higher temperatures. The available data indicates that combustion of carbon is accelerated by up to two orders of magnitude by levels of sodium normally present in coals at temperatures only slightly lower than combustion temperatures.

Summary

Minerals present in coal can accelerate the rate of char combustion by as much as a factor of 100. Molecularly attached Sodium and Calcium Compounds are likely to increase the char combustion substantially at low temperatures. However, information is not available and work should be undertaken to assess the acceleration of char combustion by minerals at the temperatures of combustion.

References

(1) Smith, I. W. "The Intrinsic Reactivity of Carbons to Oxygen." Fuel, Vol. 57, 1978, pp. 409-414.

(2) Pohl, J. H., R. W. Richter, M. P. Heap and B. A. Folsom, "Influence of Coal Char Combustion Rate on Power Plant Performance," Special Report Prepared Under EPRI Contract EPRI RP 2256-1, 1983.

(3) Pohl, J. H., W.Ricter, R. Payne, K. Fujimura, T. C. Derbidge, "Coal Particle Size and the Performance of Coal-Water Slurries," Presented at ASME Winter Annual Meeting, New Orleans, Louisiana, December, 1984.

(4) Smith, I. W. and R. J. Tyler, "Internal Burning of Pulverized Semi-Anthracite: The Relation Between Particle Structure and Reactivity." Fuel, Vol. 51, 1972, pp. 312-321.

(5) Essenhigh, R. H. "Fundamentals of Coal Combustion." In M.A. Elliott, ed, Chemistry of Coal Utilization, Second Supplementary Volume. John Wiley & Sons, New York, 1981, pp. 1153-1312.

(6) Patai, S., E. Hoffman, and L. Rajbenback. "The Oxidation of Carbon by Air I. Catalysis in the Oxidation of Carbon Black by Air." J. Appl. Chem., Vol. 2, 1952, pp. 306-310.

(7) Lang, F. M., P. Magnier, and S. May. "Etude de L'Oxydation des Carbones par et L'Anhydride Carbonique en Fonction de Leur Texture ef d Leur Etat de Purete." 5th Proc. Conf. on Carbon, Vol. 1, 1961, pp. 171-191.

(8) Heuchamps, C. and X. Duval. "Effet des Catalyseurs sur Les Charcteristiques Cinetiques de la Combustion du Graphite." Carbon, Vol. 4, 1966, pp. 243-253.

(9) A Mariglio, H. and X. Duval. "Etude de la Combustion Catalytique du Graphite." Carbon, Vol. 4, 1966, pp. 323-332.

TABLE I INFLUENCE OF COMBUSTION RATE ON POWER PLANT PERFORMANCE FOR A 660 MW_e COAL-FIRED BOILER

Kinetic Constant, g/cm's Atmosphere	Furnace Efficiences (%)	Mean Furnace Exit Temp °F	Mean Net Heat Flux Btu/ft^{2}hr	Maximum Net Heat Flux Btu/ft^{2}hr	Position of Maximum Heat Flux (ft)	Maximum Flame Temp (°F)	Percent Unburned Fixed Carbon	Percent Combustibles In Ash (%)
$40e^{-21,450/RT}$ [a]	43.1	2190	39,000	61,500	116	2650	0.66	5.97
$400e^{-21,450/RT}$	44.2	2160	40,300	62,800	102	2670	0.04	0.38
$4e^{-21,450/RT}$	33.6	2200	26,000	64,700	224[b]	2350	32.17	69.03

[a]Normal Value

[b]Boiler Exit Plane

TABLE 2 INFLUENCE OF METALS ON THE RATE OF GRAPHITE COMBUSTION(9)

Metal	ppm	Relative Reactivity
Be	120	1
B	80	1
Al	70	3
Ca	120	4
mg	120	6
Sr	120	8
Ni	150	32
Cd	120	90
Ba	120	100
Na	120	230
Au	120	240
V	120	340
Cu	120	500
Ag	120	1,340
Cs	120	64,000
Mn	80	86,000
Pb	130	470,000

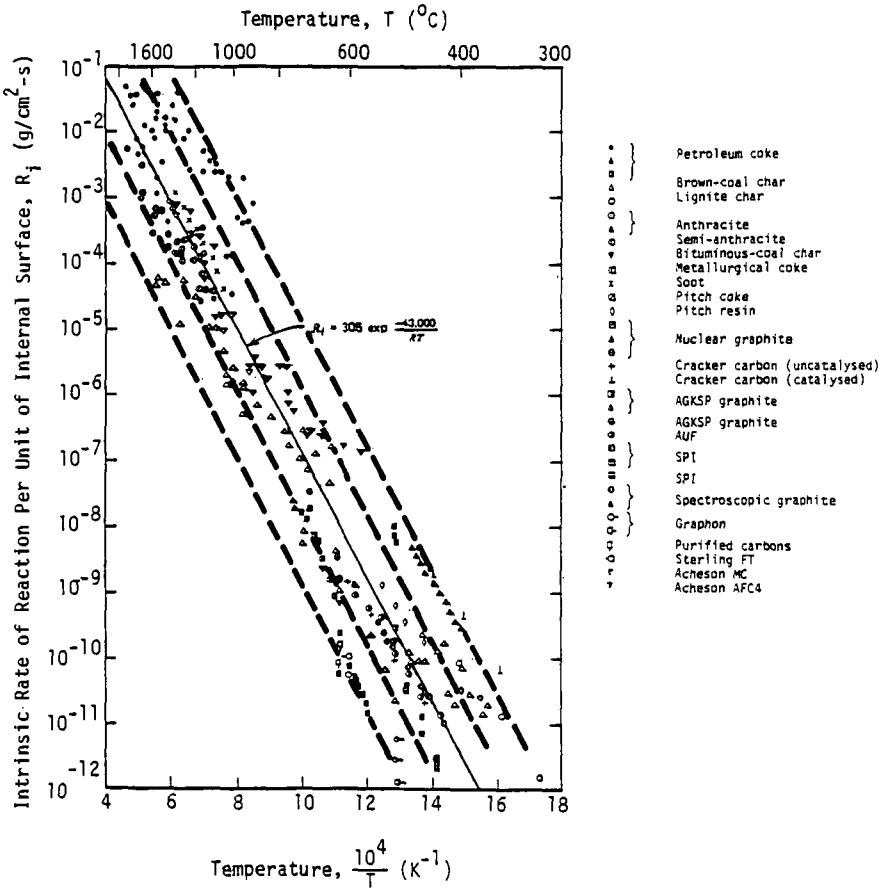

Figure 1. Intrinsic Rate of Reaction of Chars (1)

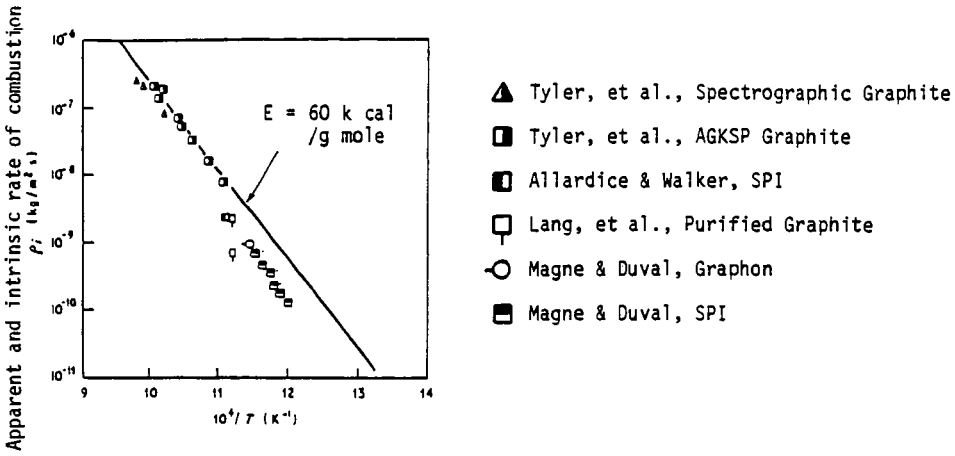

Figure 2. Combustion Rates of Highly Purified Graphite (4)

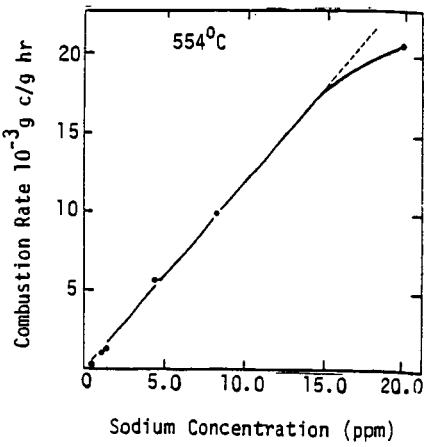

Figure 3. Catalysis of Graphite Combustion by Sodium (9)

BEHAVIOR OF MINERAL MATTER DURING COAL BENEFICIATION

Harold L. Lovell

The Pennsylvania State University
Department of Mineral Engineering
University Park, Pennsylvania 16802

Each coal beneficiation unit operation responds to the physical and chemical properties of its feed. The response is as a "collage" of the individual particles but specifically as the frequency distribution of the component particle properties. These particle responses are not totally independent with particle property-process parameter interactions, but are also significantly controlled by the overall distribution of particle properties. Diligence is appropriately applied to establish the "collage" distribution by certain particle properties of the plant feed. This distribution provides the design bases for each unit operation in the flow sheet - including its capacity, flow rate, and unit loading: thus ultimately defining the separational performance, efficiency, and unit costs. Each unit operation should be sized and operated such that its optimum performance is well within the sensitivity range of its feed property distribution. The concern that the feed distributions may, at times, exceed the sensitivity range for some unit operation within in the system, is normally related to in situ coal variability, which can be extreme. The concern may extend to coal feeds from differ -rent seams and/or paleo-geological origin, mining system, or handling-storage system. Unfortunately, seldom are the concerns extensive and rarely are the feed characterizations detailed to each down stream operation.

The plant feed characterization usually is limited to particle size distribution and, if detailed, will include a particle gravity distribution for several size groupings greater than 28 or 16 mesh (washability). There is no generally accepted range for either the size or density groupings. The characterization of the individual particle fractions are usually limited to moisture, high temperature ash, and total sulfur content. In some unusal instances the low temperature ash and sulfide sulfur content may be determined. Pragmatism, procedures, and economics prevent the direct determination of minerals whose concentrations will be modified in the process. These levels are expressed in terms of ash content. If there is any characterization of the individual macerals or minerals, they are evaluated on the basis of the "total-composite" feed sample. Should flotation processes be anticipated, some "laboratory floatability" studies (1), may be carried out on some minus 16 or 28 mesh or other sized fraction. The origin of the particular fraction thus tested, seldom relates to that which will exist within the plant flow sheet. Feed hardness or friability tests (as Hardgrove Grindability Index, Drop-Shatter, etc.) may also be determined on the composite feed sample. If any comminution evaluations are made for the particular feed coal in the course of selecting a particular comminution device, they are usually made on a sample purported to be representative of the plant feed. Attempts to evaluate variations of particle strength or stability, maceral, mineral, or elemental composition, have been limited to research characterizations, as those reported by the author (2). We are almost totally devoid of pragmatic techniques to establish the particle sizes or volumes of individual components within a given individual coal particle (Richardson and Lovell (3).

These observations can but lead to the conclusion that, in contrast, to typical unit operations in chemical engineering, the coal processing engineer assumes a feed to each unit operation within the plant system based upon the defined plant feed. Further, it is assumed that the collage of particles entering the plant as feed DOES NOT CHANGE in passing through the processing system and that the same number of particles 2 by 1-inch having densities between 1.40 and 1.45 gm/cc (or any other fraction) leaves the plant as enters! We know that this is not

correct even if we ignore the comminution operations within the plant designed to make such changes!

The composition of any individual coal beneficiation feed particle ranges from a nearly uniform metamorphized, phyto component through an almost infinite mixture series with macerals-minerals to an opposite end member as a nearly uniform mineral component. The behavior of a beneficiation feed during processing is determined by this almost limitless (and changing) distribution of individual particle compositions whose responses to process parameters are established by the particle properties as size, shape, density, hardness, porosity, and gas-liquid-solid interfaces. The particle responses establishes its direction and rate of movement toward one of the process product ports.

With coals as sedimentary rocks of paleophyto origin, their inorganic contents incorporate those components which were part of the original phyto system and associated substances, as well as those that have been introduced through all the subsequent geologic events. Accordingly, the mineral components found in coals reflect the nature of the originating plant systems, their environment, degree of water existing (whether of fresh or marine water character), oxidation-reduction conditions, temperatures, and pressures as well as those conditions to which the coal-forming strata have been subject during all the ensuing geologic epochs, including past and current circulating ground waters. Thus the observed complexity of the resulting physical characteristics is to be expected.

The minerals found in United States coals continue to be studied with the availability of improved instrumental procedures as X-ray diffraction, infrared absorption, and scanning electron microscopy beyond the traditional optical and chemical mineralogical techniques as applied to thin sections, polished pellets, and isolated particles. The minerals may be grouped into the silicates (kaolinite, illite, monmorillonite, and chlorite); the oxides (quartz, chalcedony, hematite); the sulfides (pyrite, marcasite, and sphalerite); the sulfates (jarosite, gypsum, barite, and numerous iron sulfate minerals); the carbonates (ankerite, calcite, dolomite, and siderite); and numerous accessory minerals as apatite, phosphorite, zircon, rutile, chlorides, nitrates, and trace minerals).

The greatest interest in mineral occurrences in coal particles for processing engineers relates to their potential liberation as an essential first step for their physical removal. Further the concern relates to the mineral behavoir in each of the unit operations within the preparation plant and environmental implications within the preparation operations, for utilization of the clean coal product and the disposal of the refuse materials. The greatest attention has been given to the former interests, especially as applied to the liberation of pyrite in efforts to achieve the greatest possible sulfur reduction during processing.

Specific Responses of Coal Mineral Components During Processing

The "collage " of particles entering a coal processing plant are subject to a series of unit operations designed to achieve the desired level of quality improvement. The development of the initial set of particles is determined by the mining and preprocessing storage and handling systems. Undoubtedly these operations introduces stresses within the coal particles that lead to subsequent fracture failures. Any potential control of the nature of this particle set is usually extremely limited - being determined by production and economic factors. Situations which lead to oxdiation, decripitation, and absorption of excessive levels of moisture may be modified. The introduction of moisture prior to processing probably enhances clay swelling, tends to increase the amount of mineral fines (usually clays) into the plant stream, and may enhance localized heating, swelling, and oxidation. Initiation of dispersion of clays may begin here. Uncontrolled comminution during the handling and storage due to dropping from stackers, compaction by graders, etc. tend to create fines and probably selectively favors reduction of

the softer particles, especially certain clays. Other handling steps as particle movement through pumps, jigs, etc. tend to accent the production of fines. The oxidation of coal and temperature increases may favor the production of water soluble salts leading to acid plant waters and potential corrosion.

Primary crushing which usually involves breakers or single roll crushers may be preceeded by a scalping operation to remove large particles of hard shales and sandstones. Such operations though not rejecting large amounts of refuse, do prevent wear, save energy, and prevent the introduction of additional refuse fines into the plant feed. The primary comminution devices usually are designed to control top size rather than achieve particle liberation, as such, they offer an opportunity to minimize fines production and show some selectivity toward the large, harder particles as shales and sandstones. Pre operational testing of comminution devices should consider the production of minimal amount of mineral fines. In coal processing systems where classifying rotating mills may be used, the selective build up of harder components within the mill can affect system performance.

In coarse coal sorting operations, as jigs and heavy media vessels, the softer minerals will tend to comminute due to attritional actions of particle movements and result in further dispersion into the plant circulating water system. In jigs, the production of mineral fines may be desirable to enhance hindered settling effects. In the Haldex heavy media system (4) and water only cyclones, the presence of mineral fines are essential to serve as an autogeneous heavy media system. Operational care must be taken to prevent the build up of unacceptable levels of fines leading to unacceptable fluid viscosity levels. Although quartz, clays, and other very fine mineral particles enhance these conditions, several type of clays, notably kaolinite and montmorillonite (especially sodium), are especially responsive. Suspended clay levels above five percent in such systems are most undesirable and may limit control of density in magnetite heavy media systems. The viscosity effect increases with decreasing particle size and with spherical shape which enhances settling rates. These concerns can also become critical in coal-water transport systems.

In fine coal sorting systems, heavy media cyclones, water only cyclones, tables and spirals the density and viscosity responses of suspensions are even more critical. In froth fltoation the presence of clay fines is undesirable and usually require a desliming step ahead of flotation if their concentration becomes excessive.

It is in the water circuit that the build up of fines, especially clays must be controlled. The responses become evident in dewatering devices as centrifuges and filters. In the latter case, clays may enhance blinding resulting in unacceptable water contents of the filter cake, thin watery cakes, and unacceptable performance. Difficulties in the filtration of refuse fines has lead recently to the introduction of expensive processes as pressure and belt filters to meet environmental standards. In thickeners, excessive clay fines may reduce settling rates, minimize the formation of desirable underflow slurry densities, and lead to plant failure. It is in the dewatering stages and water circuit, as processes at the end of the flow sheet that these responses become acute. Although the use of one or more polymeric flocculants can usually control these situations, unexpected changes in plant feeds may require feed rate reductions or plant shut down.

Recent environmental regulations which essentially require closed water circuits make the problems of mineral fines buildup especially severe. Similar difficulties are associated with the disposal of refuse fines.

These examples describe some of the more prominent responses of mineral components in coal processing operations. Control of these problems can be achieved with better detection and analytical systems to identify the problems.

LITERATURE CITED

1a). Cavallaro, J. A. and A. W. Deurbrouck. Froth Flotation Washability Data of Various Appalachian Coals Using The Time Release Analysis Technique. Report of Investigations 6652. U. S. Bureau of Mines. 1965.

1b). Alderman, J. K. Evaluating Flotation Washability Data. Coal Mining and Processing. pp 70-73. 1981.

2). Lovell, Harold L. The Characteristics of American Coals. Final Report. U.S. Department of Energy. FE-2030-11. 1976.

3a). Richardson, D. and H. L. Lovell. Pyrite Liberation - Key to Sulfur Reduction During Beneficiation. Proceedings of Coal Conference and Expo V. Symposium on Coal Preparation and Utilization. October 1979.

3b). Richardson, D. L. A Study of the Occurrence of Pyrite in Coal and Its Relationship to Liberation in Coal Preparation and Mine Drainage Formation. M. S. Thesis in Mining Engineering. 1979. The Pennsylvania State University.

4). Anon. Investigation of the Haldex (Simdex) Process for Beneficiating Coal Refuse: Hungarian Practice - 1969. Special Report 80. The Coal Research Section. The Pennsylvania State University. University Park, Pennsylvania.

MINERALOGICAL CHARACTERISTICS OF COAL IN VARIOUS CLEANING CIRCUITS

Richard B. Muter and William F. Lawrence

Coal Research Bureau
College of Mineral and Energy Resources
West Virginia University, P. O. Box 6070
Morgantown, West Virginia 26506-6070

The optimum utilization of our national coal resources while still affording the protection of our environment can not be achieved without beneficiation. However, our most common ways of measuring the success or failure of beneficiation processes are not truly representative and may well be responsible for unnecessary economic and energy resource losses. This is the result of several factors, the most important of which are:

1. The analyses which we perform do not really measure the materials which are being beneficiated. Rather, they are indirect measurements.

One of the most common quality criteria is that of ash. However, we do not remove ash from coal during beneficiation processes; we really change distribution of the minerals or rock consist of the coal material, and thereby change the "ash" as measured. Also, we do not remove sulfur as such, we remove sulfur containing minerals such as pyrite, marcasite, etc.

2. Mineral properties, not elemental properties, are what effect combustion and beneficiation processes up until the time when the minerals are broken down; yet it is the elemental composition which we seem to be most concerned about.

Seemingly obvious, this point is often overlooked in all stages of beneficiation and utilization until major problems occur. Two coals may have the same SiO_2 content when analyzed, but the physical properties of quartz (sand) are quite different from those of clays (illite, kaolinite, etc.). Different minerals, even of similar compositions, require different cleaning processes and have different effects upon process equipment.

3. Common analytical methods, because they destroy the mineralogical structures, give the impression that coals are to a large extent homogeneous and consistent in mineral content. This impression is markedly false and often leads to major false assumptions.

The two most obvious, i.e. most studied, examples of this error are the forms of sulfur and the siliceous contents of coal. Conventional analyses will give the same silica content for a carbonaceous shale as for a calcareous one, but they will react quite differently during beneficiation and combustion. Total sulfur is the most common analysis for this element of environmental concern, but occasionally a "sulfur breadown" analysis will be performed. Although knowing whether the sulfur is "pyritic", "organic" or "sulfate" is helpful; it is not enough, Knowing that the sulfur is predominately "pyritic" is insufficient, we must know other factors such as size, distribution within the coal matrix, and whether the particles are attached to the coal material as well as the degree of liberation. All these factors affect the beneficiation processes.

Physical beneficiation is generally considered to be a "mature" subject in that most changes which have occurred over the past few years have been in terms of equipment design or the order in which particular operations are performed. These

operations are generally based on physical characteristics such as specific gravity or hardness and brittleness difference between the minerals of interest and the coaly materials. However, these processes are still measured on element reduction bases rather than one of specific mineral concentration or reduction.

Froth flotation, considered a higher lever of sophistication in beneficiation, is also based on differences in mineralogical properties. Based upon particle surface characteristics it tends to be more chemical than physical in nature. Tendencies of particles to be hydrophilic or hydrophobic in nature are enhanced through the use of chemical additives and then a physical separation is made.

The next level of sophistication in coal beneficiation will most likely be that of chemical coal cleaning. It will also be the most costly level, especially when the large tonnage amounts involved in coal utilization are considered. In order to keep these costs to a minimum, while still attaining desired results, process operations will have to be carefully planned and closely monitored. Process designers will have to know exactly what minerals will be involved and in what amounts. Acquiring a better knowledge of what minerals occur in specific coals and how they are affected by less expensive physical beneficiation is an obvious first step.

As part of a much larger effort by the U. S. Department of Energy, the Coal Research Bureau of the College of Mineral and Energy Resources at West Virginia University has been characterizing the mineralogy and petrography of three major bituminous coals in an effort to determine whether the mineralogical associations can be closely followed through common physical beneficiation processes. A listing of the minerals commonly present in these coals is provided in Table 1. Also included are the chemical formulas with the elements of most interest to the beneficiation plant operator underlined. This listing is based upon bituminous coals as most sub-bituminous coals and lignites meet current emission specifications and are not cleaned to a large extent.

Mineralogical analyses were performed using a number of different techniques including x-ray powder diffraction analysis, infrared spectroscopy, normative calculations, and optical petrography. All met with limited success although each had limitations as to the number of minerals which could be identified or accurately quantified. X-ray powder diffraction proved to be the most versatile as to accuracy, ease of implementation and number of different minerals identified versus misidentifications. Mineralogical sink-float (washability) curves were prepared (Figure 1) and compared with actual equipment operations (Table 2). It can be seen, that their predicted value varied for specific minerals and specific processes. However, the indication is that further effort in this area is justified and that a strong potential exists for tracing of specific mineral assemblages through the beneficiation processes and that these processes may be more efficiently designed and monitored. Such monitoring in the future could lead to multi-stream, multi-product plants with only a minimum amount of coal being subjected to more intensive cleaning processes. With careful planning, such a plant could provide a maximum fuel yield while providing maximum environmental protection at a minimum cost.

TABLE 1

MINERALS OF THE DISTRICT #3 PITTSBURGH COAL.
SYMBOLS INDICATE ANALYTICAL PROCEDURES AVAILABLE FOR EACH MINERAL AND WHETHER THE PROCEDURE CAN BE USED FOR QUANTITATIVE, SEMIQUANTITATIVE, OR QUALITATIVE MINERAL ANALYSIS.

	X-ray Powder Diffraction	*Infrared Spectroscopy*	*Normative Calculations*	*Optical Petrography*	*Scanning Electron Microscopy*	*Formulae*
ILLITE	S		Q	S	I	variable
KAOLINITE	Q	Q	Q	S	I	$Al_4(Si_4O_{10})(OH)_8$
QUARTZ	Q		Q	S	I	SiO_2
FELDSPARS	S				I	variable
MUSCOVITE				S	I	$KAl_4(AlSi_3O_{10})(OH)_2$
CARBONATES		Q		S		variable
CALCITE	Q	Q	S	I	I	$CaCO_3$
DOLOMITE	Q		S	I	I	$CaMg(CO_3)_2$
BASSANITE	S				I	$CaSO_4 \cdot \frac{1}{2}H_2O$
GYPSUM		I		I		$CaSO_4 \cdot 2H_2O$
IRON DISULFIDES	Q		Q	S	I	FeS_2
PYRITE				S		FeS_2
MARCASITE				S		FeS_2
APATITE	S				I	$Ca_5(F,Cl,OH)(PO_4)_3$
HEMATITE				S		Fe_2O_3
RUTILE				S	I	TiO_2

Q = Quantitative determinations (±10%)

S = Semiquantitative determinations (±10-30%)

I = Identification only possible

TABLE 2

Mineral weights in the products of the commercial preparation plant and the pilot plant scale coal cleaning equipment. Actual mineral weights are compared to weights predicted from the mineral washability curves of the Pittsburgh coal.

	Deister Table 3/16" X 100M		"Baum" Jig 1" X 3/16"		WEMCO HMS Drum Separator 2" x 10M		Heavy Media Cyclone 10 X 100M	
	Actual	Curve	Actual	Curve	Actual	Curve	Actual	Curve
YIELD	85%	83%	71%	93%	89%	85%	94%	95%
S.G.	?	1.35	?	>1.80	?	1.38	?	>1.80
ASH	5.9%	5.9%	7.7%	7.7%	6.2%	6.2%	8.4%	8.4%
M.M.	126#	120#	133#	185#	138#	135#	183#	210#
ILLITE	16#	29#	28#	46#	55#	31#	6#	58#
KAOLINITE	34#	30#	29#	38#	39#	31#	32#	41#
QUARTZ	21#	20#	25#	30#	23#	22#	26#	34#
CALCITE	13#	4#	12#	8#	10#	4#	9#	12#
PYRITE	30#	23#	28#	36#	0#	26#	36#	44#

= pounds of the mineral in the cleaned coal when one short tone of feed coal is cleaned.

M.M. = mineral matter.

S.G. = specific gravity of the washing medium.

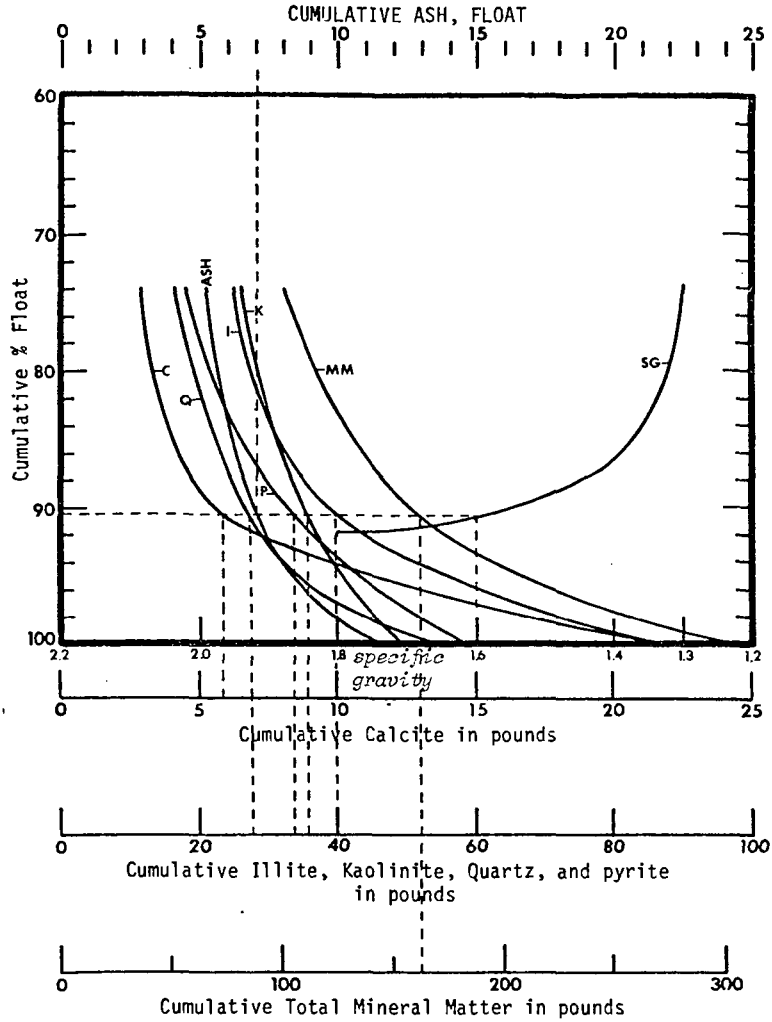

FIGURE 1

Washability curves for the minerals in the District 3 Pittsburgh coal (See the footnote on the next page for explanations of this diagram).

Automated Image Analysis of Mineral Matter in Raw and Supercleaned Coals

Warren E. Straszheim and Richard Markuszewski

Ames Laboratory[1] and Department of Engineering Science and Mechanics
Iowa State University, Ames, IA 50011

The advent of highly sophisticated and automated microscopic techniques, together with powerful mini- and microcomputers, makes it now possible to characterize the mineral components of coal in-situ. Combined automated image analysis (AIA) and scanning electron microscopy (SEM) allows detailed characterization of minerals in coal for size, shape, composition, and relation to the coal matrix. For a statistically significant number of particles, both size distribution and volume fraction can be estimated and used to characterize independently the mineral matter content. The corresponding chemical analyses for the bulk coal samples, provided by more conventional techniques, may be related to the AIA-SEM data for comparison.

Conventional analytical techniques such as x-ray diffraction (XRD) and Fourier transform infrared spectroscopy (FTIR) can identify the mineral phases present in coal and can sometimes provide an estimation of the amount present. However, such techniques use bulk samples; they are limited to calculating only an "average" cleaning effectiveness and do not offer information on the size distribution of those mineral phases identified. On the other hand, AIA-SEM permits cleaning effectiveness to be evaluated with respect to both particle size and mineral phase. Thus, problems associated with removing a particle size or chemical class of particles can be detected and addressed. Such information is important for any coal preparation process, especially since it relates grinding and liberation of mineral particles to washability tests (1).

To evaluate coal particles produced by fine grinding for washability tests, the AIA-SEM technique provides information on the elemental distribution among the various mineral phases. The minerals are classified using a chemistry definition file based on the relative amounts of elements present as determined by energy-dispersive x-ray spectroscopy.

The AIA-SEM technique has been used in Ames Laboratory to study the effect of grinding on washability of fine coal. Several series of coals have been characterized by this technique in the past two years, thus demonstrating its usefulness. In this work, the AIA-SEM technique was applied to determine the coal mineral character before and after cleaning.

---

[1]Ames Laboratory is operated for the U. S. Department of Energy by Iowa State University under Contract No. W-7405-Eng-82.

EXPERIMENTAL

Sample Description and Preparation

The analyses were performed on two bituminous coals being tested for washability by conventional means. The coals were from the Illinois No. 6 seam, Randolph county, Illinois, and from the Pittsburgh No. 8 seam, Lewis county, West Virginia. The coals were ground to a typical power plant grind (i.e., 70-80% less than 200 mesh or 75 μm). The coals were then supercleaned by float-sink separation (using halogenated hydrocarbons) at 1.3 specific gravity to produce a very low-ash, clean coal fraction (ash content <3%). The raw and clean coal fractions were analyzed for moisture, ash, and sulfur forms by the usual ASTM procedures (see Table 1).

Table 1. ASTM analyses of raw and supercleaned coal samples for moisture, ash, forms of sulfur, and mineral matter[a].

	Illinois No. 6		Pittsburgh No. 8	
	Raw	Clean	Raw	Clean
Moisture	16.90	1.95	1.97	1.12
Ash	16.11	2.61	6.75	2.97
Total S	5.10	2.54	3.17	1.82
Pyritic S	2.37	0.22	1.35	0.03
Sulfate S	0.36	0.04	0.41	0.12
Organic S	2.36	2.27	1.42	1.67
Mineral Matter[b]	19.32	3.05	8.26	3.37

[a] Values are expressed as wt. % on a dry basis, except for moisture.
[b] Mineral matter = 1.13x ash + 0.47x (pyritic sulfur).

The raw and clean coal samples were prepared for AIA-SEM analyses by casting two grams of the sample with an epoxy resin into molds one inch in diameter. The hardened pellets were polished to reveal a cross section, with final polishing being done with 0.3 μm alumina powder. The pellets were coated with approximately 500 angstroms of carbon to render sample surfaces electrically conductive for examination in the electron microscope.

AIA-SEM Analysis

The AIA-SEM system consists of a JEOL (Japan Electron Optics Laboratory) model JSM-U3 scanning electron microscope, a LeMont Scientific B-10 image analyzer, and a Tracor Northern TN-2000 energy-dispersive x-ray analyzer. The image analyzer is a software-based system with associated electronics for SEM beam control, image amplification, and thresholding. The software base for image analysis allows the appropriate analysis algorithm to be selected for the particular sample and image conditions encountered. Particle extents are determined from the

points at which horizontal scans cross a feature, and particle outline is reconstructed from these adjacent chords of a particle. Once the outline has been determined, the x-ray data are collected from the center of the particles.

Samples were analyzed in the SEM using 25 kV beam voltage, 1-2 nA sample currents, 300x magnification, and backscattered electron imaging. A point density of 1024 pixels across the screen was used to provide ±10% accuracy on measurements as small as 1% of the field of view. X-ray data were collected for four seconds per particle at a typical counting rate of 1000 counts per second. Regions of interest were set to monitor the intensities of 30 elements; however, only these 11 elements occurred with significant frequency: Na, Mg, Al, Si, P, S, Cl, K, Ca, Ti, and Fe. Approximately 4000 particles were analyzed per sample at a rate of 200 particles per hour.

Data Handling

Based on the relative amounts of the elements present, the particles were classified into one of nine mineral categories according to the definitions given in Table 2. The categories derived from previously established guidelines (2,3) and included the common coal minerals pyrite, quartz, calcite, siderite, kaolinite, and illite. Several other minerals were identified, but they occurred in such small amounts that they were classified together into one common category titled "MINORS". This category included the minerals gypsum, dolomite,

Table 2. Chemical limits for mineral phase definitions

Mineral Phase	Chemical Definition in % Range[a]	Specific Gravity
PYRITE	S 10-80; Fe 10-70	5.00
KAOLINITE	Al 15-80; Si 15-85; Al/Si 0.33-3.0	2.65
ILLITE	Al 10-50; Si 20-85; Mg 0-15; Ca 0-35; Fe 0-40; Ti 0-15	2.75
QUARTZ	Si 65-100	2.65
CALCITE	Ca 70-100	2.80
SIDERITE	Fe 70-100; Mn 0-30; Ni 0-30	5.00
MINORS (includes the following categories)		
GYPSUM	S 10-80; Ca 10-70	2.30
DOLOMITE	Mg 10-60; Ca 60-100	2.90
RUTILE	Ti 70-100	4.50
ALUMINA	Al 65-100	4.00
APATITE	P 15-40; Ca 30-100	3.20
SILICATES	Si 20-80	2.70
MISCELLANEOUS	(no restrictions, all particles accepted)	2.00

[a]Specifications may be given for the amount of other elements that are allowed to be present. Such specifications allow minor amounts of elements not specifically listed in the class definition to be present, but they place an upper limit on the allowable amount.

rutile, alumina, and apatite. In addition, several other categories were defined to accommodate particles not corresponding to any of the above definitions. For example, a "SILICATES" category was defined to include particles with significant silicon content, yet with the balance of the elements in such proportions that the particle would not fit into either the quartz, kaolinite, or illite categories. A "MISCELLANEOUS" category was provided to include those particles whose composition did not allow them to fall into any of the above-mentioned categories. Further descriptions of the instrumental, statistical, classifying, and processing techniques will be given in another publication being readied for submission.

The AIA procedures classified mineral particles into both size and chemical classes. Area-equivalent diameter was used as the size parameter for data presentation. This measurement is the diameter of a circle with the same area as that measured for the mineral particle. Area-equivalent diameter was used instead of a simple length or width measurement because the outline of mineral particles in coal is often complex enough to render such measurements meaningless. The equivalent diameter measurement allows particles to be classified by the area of the particle and yet reported in terms of a linear dimension. Using available literature values for the specific gravity of the individual minerals, the data were then expressed as the weight fraction of the mineral matter within a given mineral/size category. The weight fraction data were then normalized using the mineral matter content to present the mineralogical estimates on a dry coal basis. Such a presentation provides a common base for comparing the coals before and after processing.

The data are presented in Tables 3a and 3b for the raw and clean Illinois coal respectively, and in Tables 4a and 4b for the raw and clean Pittsburgh coal, respectively. Percent removal of the mineral matter calculated for each mineral phase and size category for both coal samples is presented in Tables 3c and 4c.

RESULTS AND DISCUSSION

Conventional analytical data, obtained by ASTM procedures and presented in Table 1, indicate that the float-sink separation achieved an 84% and a 56% removal of ash from the Illinois and Pittsburgh coals, respectively, with corresponding decreases in total and pyritic sulfur of 50 and 91% and of 43 and 97%, respectively. If expressed as a reduction in the total mineral matter content, based on using a modified Parr formula (4), the corresponding values are 84% for the Illinois coal and 59% for the Pittsburgh coal.

The AIA data for the Illinois coal (Tables 3a-c) and for the Pittsburgh coal (Tables 4a-c) are much more interesting. Results for the raw Illinois coal show that pyrite, quartz, and two clays (kaolinite and illite in approximately equal proportions) make up the bulk (86%) of the mineral matter. The mineral phases are rather uniformly distributed over the entire range of particle size from less than 4 μm to more than 36 μm in diameter.

Table 3a. AIA results for Illinois No. 6 raw coal (200 x 0 mesh), expressed as weight percent of dry coal.

Mineral Phase	Particle Size <4 μm	<7 μm	<12 μm	<21 μm	<36 μm	>36 μm	Totals
Pyrite	0.71	0.77	1.16	1.44	1.62	1.27	6.97
Kaolinite	0.57	0.67	0.65	0.38	0.36	0.20	2.83
Illite	0.32	0.38	0.42	0.42	0.45	0.47	2.47
Quartz	0.84	0.90	1.02	0.71	0.35	0.61	4.43
Siderite	0.10	0.10	0.08	0.14	0.00	0.00	0.42
Calcite	0.04	0.04	0.14	0.11	0.10	0.41	0.83
Silicates	0.23	0.16	0.17	0.10	0.03	0.19	0.89
Minors	0.02	0.03	0.05	0.01	0.04	0.00	0.15
Miscellaneous	0.05	0.06	0.11	0.03	0.07	0.00	0.32
Totals	2.87	3.12	3.79	3.36	3.02	3.15	19.32

Table 3b. AIA results for Illinois No. 6 coal floated at 1.3 specific gravity, as expressed as weight percent of dry coal.

Mineral Phase	Particle Size <4 μm	<7 μm	<12 μm	<21 μm	<36 μm	>36 μm	Totals
Pyrite	0.19	0.28	0.42	0.21	0.07	0.00	1.17
Kaolinite	0.10	0.16	0.09	0.02	0.03	0.00	0.40
Illite	0.12	0.12	0.11	0.07	0.00	0.00	0.42
Quartz	0.16	0.19	0.18	0.09	0.01	0.00	0.63
Siderite	0.02	0.01	0.01	0.02	0.02	0.00	0.08
Calcite	0.00	0.00	0.00	0.00	0.00	0.00	0.01
Silicates	0.08	0.05	0.03	0.02	0.02	0.00	0.20
Minors	0.02	0.02	0.01	0.00	0.00	0.00	0.04
Miscellaneous	0.04	0.03	0.02	0.00	0.00	0.00	0.08
Totals	0.72	0.86	0.87	0.44	0.16	0.00	3.05

Table 3c. Use of AIA results to estimate percent removal of mineral matter from Illinois No. 6 coal. The numbers are based on values in Tables 3a and 3b before they were rounded off.

Mineral Phase	Particle Size <4 μm	<7 μm	<12 μm	<21 μm	<36 μm	>36 μm	Totals
Pyrite	73	64	64	85	95	100	83
Kaolinite	83	77	86	94	91	100	86
Illite	61	69	74	82	100	100	83
Quartz	81	79	83	88	96	100	86
Siderite	81	85	86	89	--	100	80
Calcite	98	93	97	96	100	100	99
Silicates	67	67	81	77	45	100	77
Minors	38	51	75	100	100	100	72
Miscellaneous	30	58	83	100	100	100	75
Total	75	73	77	87	95	100	84

Table 4a. AIA results for Pittsburgh No. 8 raw coal (200 x 0 mesh), expressed as weight percent of dry coal.

Mineral Phase	Particle Size <4 μm	<7 μm	<12 μm	<21 μm	<36 μm	>36 μm	Totals
Pyrite	0.13	0.62	0.72	0.81	1.00	1.19	4.47
Kaolinite	0.08	0.38	0.24	0.12	0.08	0.04	0.94
Illite	0.06	0.26	0.17	0.14	0.16	0.20	0.98
Quartz	0.03	0.13	0.12	0.08	0.01	0.15	0.52
Siderite	0.02	0.10	0.06	0.08	0.14	0.06	0.46
Calcite	0.00	0.02	0.01	0.02	0.00	0.00	0.05
Silicates	0.01	0.02	0.01	0.02	0.07	0.00	0.13
Minors	0.05	0.22	0.12	0.02	0.00	0.00	0.41
Miscellaneous	0.02	0.10	0.05	0.04	0.02	0.09	0.31
Totals	0.40	1.84	1.50	1.33	1.47	1.72	8.26

Table 4b. AIA results for Pittsburgh No. 8 Coal floated at 1.3 specific gravity, as expressed as weight percent of dry coal.

Mineral Phase	Particle Size <4 μm	<7 μm	<12 μm	<21 μm	<36 μm	>36 μm	Totals
Pyrite	0.21	0.33	0.35	0.08	0.00	0.00	0.96
Kaolinite	0.28	0.45	0.21	0.04	0.00	0.00	0.98
Illite	0.24	0.35	0.11	0.01	0.00	0.00	0.70
Quartz	0.07	0.17	0.07	0.02	0.00	0.00	0.34
Siderite	0.00	0.01	0.01	0.03	0.00	0.00	0.05
Calcite	0.00	0.01	0.01	0.01	0.00	0.00	0.02
Silicates	0.02	0.02	0.01	0.00	0.00	0.00	0.05
Minors	0.02	0.03	0.01	0.04	0.00	0.00	0.10
Miscellaneous	0.06	0.08	0.03	0.00	0.00	0.00	0.17
Totals	0.91	1.43	0.80	0.22	0.00	0.00	3.37

Table 4c. Use of AIA results to estimate percent removal of mineral matter from Pittsburgh No. 8 coal. The numbers are based on values in Tables 4a and 4b before they were rounded off.

Mineral Phase	Particle Size <4 μm	<7 μm	<12 μm	<21 μm	<36 μm	>36 μm	Totals
Pyrite	--	46	51	89	100	100	78
Kaolinite	--	--	12	64	100	100	--
Illite	--	--	37	96	100	100	28
Quartz	--	--	39	75	100	100	35
Siderite	76	95	80	63	100	100	88
Calcite	80	62	41	69	100	100	60
Silicates	--	--	32	100	100	100	62
Minors	57	86	89	--	100	100	75
Miscellaneous	--	17	42	100	100	100	45
Total	--	22	46	83	100	100	59

In the supercleaned Illinois coal, the levels of almost all minerals have been reduced by 60-85% somewhat uniformly for most of the particle size ranges up to 21 μm. Above that size, the removal increases sharply, with nearly complete removal for the larger sizes. The 21 μm cut-off seems reasonable for pyrite when the following calculation is considered. A 21 μm pyrite phase (specific gravity of 5.0) embedded in a 200 mesh (i.e. 75 μm) coal particle (specific gravity of 1.25) accounts for only 2.2% of the total volume. However, because it accounts for 8.2% of the total weight of such a particle, it increases the specific gravity of the total assemblage to over 1.33; it is thus rejected in the float-sink separation. A 12 μm pyrite phase, however, accounts for about 1% of the volume of the 74-μm assemblage, while the specific gravity is 1.29; thus it is carried along with the float fraction. Of course, since the size consist is 200 mesh x 0, there are many small pyrite particles completely liberated or attached to smaller sized coal particles; however, the cut-off at 21 μm is still remarkably sharp. Furthermore, since the specific gravities for the other minerals are lower than for pyrite, similar calculations for the other minerals should yield a higher value for the particle size at the cut-off point.

When the overall removal of 84% of the total mineral matter is broken down by particle size, it shows an expected trend of increasing with increasing particle size. The cleaning effectiveness ranges from about 75% for the smaller particles (4-12 μm) to 87% at 21 μm and to 100% for particles larger than 36 μm.

The AIA results for the Pittsburgh No. 8 coal (Tables 4a-c) show a distinctly different character of this coal. The mineral matter in the raw sample is more than 50% pyrite. Although the total amount of clay plus quartz is only one-fourth that of the Illinois No. 6 coal, the clay-to-quartz ratio is much higher. In addition, a substantially larger fraction of the mineral content is present in the larger size ranges. This coal exhibits a much sharper cut-off in the effectiveness of cleaning as a function of particle size. The superclean coal fraction contains no particles larger than 21 μm in diameter. The smaller size fractions show only small amounts of mineral matter removed. For the two smallest sizes, even a slight enrichment can be seen for several mineral phases. This apparent enrichment is partially the result of a mathematical anomaly of the normalization process and partially due to the decrease in the total weight by the removal of other mineral matter from the larger fractions. In any case, the absolute mineral content in these very small size fractions is so minute that the allowed analytical errors can account for the discrepancy, and the overall differences become negligible.

Another observation, however, should be scrutinized more closely. In both coals, the content of pyrite as determined by AIA is consistently higher than that calculated from the pyritic sulfur values obtained by ASTM. Since the accuracy (reproducibility between different labs) for ASTM analyses can be within 0.30 or 0.40% (for less than or more than 2.0% pyritic sulfur, respectively)(5), part of the discrepancy could be explained by the possible analytical error. A more plausible interpretation can be given if the ASTM leachings with nitric acid

do not remove all of the pyrite. Significant residues of pyrite have been observed previously in such leached coal samples (6). Another possible explanation can reside in the specific gravity of pyrite used. Although 5.0 is the literature value for mineral-grade pyrite, past work in this laboratory established that coal-derived pyrite can have a specific gravity significantly lower, ranging from about 3.60 for hand-picked samples to 4.25-4.50 for samples which have been extensively cleaned with hot hydrochloric acid (7). Although the absolute values for the pyrite content are divergent, the relative amounts removed (on a wt. % basis) are relatively comparable for both methods of analysis. However, further work is in progress to resolve this issue.

CONCLUSIONS

Automated image analysis used in conjunction with scanning electron microscopy and energy-dispersive x-ray analysis has been shown to be an effective tool to characterize in-situ the mineral matter in raw and cleaned coal. Both mineral phase analysis and particle size distribution were obtained for two coals (200 mesh x 0) before and after processing. For Illinois No. 6 coal, which contained mostly pyrite, quartz, kaolinite, and illite rather uniformly distributed among the various particle sizes, the cleaning effectiveness increased gradually with increasing particle size of the mineral phases. The levels of removal ranged from about 75% for the smallest particles to 100% for particles larger than 36 μm. For the Pittsburgh coal, more than half of the mineral matter was pyrite, and the pyrite was relatively coarse. The other minerals were smaller in size. During cleaning of the Pittsburgh coal, most of the large-sized mineral matter was removed, while the finer-sized mineral matter was relatively untouched. The cut-off size was approximately 21 μm.

ACKNOWLEDGEMENT

This work was supported by the Assistant Secretary for Fossil Energy, Division of Coal Utilization, through the Pittsburgh Energy Technology Center, Coal Preparation Branch. The authors wish to thank J. Cavallaro (PETC) for float-sink separation of the coal samples and D. L. Biggs (ISU) for sample collections.

REFERENCES

1. T. D. Wheelock and R. Markuszewski, "Coal Preparation and Cleaning," Chapter 3 in The Science and Technology of Coal and Coal Utilization, ed. by B. R. Cooper and W. A. Ellingson, Plenum Press, New York, 1984, pp. 47-123.

2. F. E. Huggins, B. A. Kosmack, G. P. Huffman, and R. J. Lee, "Coal Mineralogies by SEM Automated Image Analysis," Scanning Electron Microscopy/1980, Vol. I, pp. 531-540.

3. J. Lebiedzik, LeMont Scientific, Inc., State College, PA, personal communication, Fall 1980.

4. P. H. Given and R. F. Yarzab, "Analysis of the Organic Substance of Coals: Problems Posed by the Presence of Mineral Matter," Chapter 20 in Analytical Methods for Coal and Coal Products, Vol. II, ed. by C. Karr, Jr., Academic Press, New York, 1978, pp. 3-41.

5. American Society for Testing and Materials, Annual Book of ASTM Standards, Section 5: Petroleum Products, Lubricants, and Fossil Fuels, Philadelphia, 1983, Method D2492.

6. R. T. Greer, "Organic and Inorganic Sulfur in Coal," Scanning Electron Microscopy/1979, Vol. I, pp. 477-485.

7. K. C. Chuang, M.-C. Chen, R. T. Greer, R. Markuszewski, Y. Sun, and T. D. Wheelock, "Pyrite Desulfurization by Wet Oxidation in Alkaline Solutions," Chem. Eng. Commun. 7, 79-94 (1980).

BEHAVIOR OF MINERAL MATTER DURING ALKALINE LEACHING OF COAL

C.-W. Fan, R. Markuszewski, and T. D. Wheelock

Chemical Engineering Department and
Energy and Mineral Resources Research Institute
Iowa State University
Ames, Iowa 50011

Introduction

A process for producing premium quality coal with a very low ash content was demonstrated recently (1). This process involves reacting the material with a hot alkaline solution to dissolve quartz and to convert clay minerals and iron pyrite into acid-soluble compounds which are removed in a second step by treatment with acid. To understand this process better, several minerals which generally make up a major portion of the ash-forming mineral matter in many coals were reacted individually with hot alkaline solutions, and the solid reaction products were characterized by X-ray diffraction (XRD). In this study, quartz, kaolinite, and iron pyrite were reacted individually with Na_2CO_3, $NaHCO_3$, and NaOH solutions using various concentrations and temperatures. The solid products were identified and their solubility in dilute mineral acids demonstrated. In addition, the extent of conversion of quartz and pyrite to acid-soluble species was demonstrated for various alkaline treatment conditions.

Experimental Methods

The materials used for this study, obtained from sources listed in Table 1, were checked for impurities by XRD. Using this method, no impurities were detected in the quartz, but the kaolin appeared to contain a significant amount of quartz and trace quantities of illite and titania. The iron pyrite was obtained as nodules by handpicking the refuse produced in cleaning coal from Mahaska County, Iowa. The nodules were crushed and ball-milled to -38 μm size. Part of the ground pyrite was treated for 1 hr. with excess 1.2 M HCl at 70°C under a nitrogen atmosphere (to remove acid-soluble impurities) and then washed and dried. This acid-cleaned material contained about 88% FeS_2, based on total sulfur content, and significant amounts of quartz and kaolinite plus a trace of titania. In addition, it seemed to contain some amorphous material which may have been coal. The raw pyrite which had not been treated with acid contained all of these impurities plus significant amounts of calcite and iron oxides.

Table 1. Materials which were leached

Material	Source	Impurities
Quartz	Ottawa sand (Ill.)	None
Kaolin	Old Hickory No. 5 ball clay (Ky.)	SiO_2, Illite, TiO_2
Raw pyrite	Coal, Mahaska County (Ia.)	$CaCO_3$, iron oxides SiO_2, kaolinite, TiO_2
Cleaned pyrite	Same as above	SiO_2, kaolinite, TiO_2

For the leaching experiments, a weighed amount of finely divided mineral matter was mixed with 120 ml. of alkaline solution in a 300 ml. stainless steel autoclave equipped with a turbine agitator. The system was flushed with nitrogen and then heated to the desired leaching temperature. A nitrogen overpressure of 3.4 atm. was maintained throughout the leaching process. The mixture was stirred continuously while leaching was conducted at constant temperature and pressure for a specified period. After this treatment, the autoclave was cooled quickly, and the contents of the autoclave were filtered to recover any undissolved solids. The solids were washed with water, dried in an oven, weighed, and divided into two parts. One portion was analyzed by XRD with a Siemens D500 diffractometer using copper Kα radiation. The other portion was usually subjected to an acid treatment and washing step in order to determine the proportion of acid-soluble material.

For the acid treatment step, up to 3 g. of alkali-leached material was mixed with 300 ml. of mineral acid (approximately 2.0 M) in a stirred, three-neck Pyrex reaction flask for 30 min. The treatment was conducted either at room temperature (25°C) or at the boiling point (100°C). After the treatment the mixture was filtered, and any undissolved solids were washed with water, dried, weighed, and analyzed by XRD.

Experimental Results

In one set of experiments, -38 μm size quartz particles were leached with various hot alkaline solutions to study the effects of alkali type, alkali concentration, ratio of alkali to quartz, temperature, and leaching time on dissolution. After each leaching, the reactor contents were filtered with Whatman No. 40 filter paper using suction, and the residue was washed with cold water, dried at 350°C for 2 hr., and weighed. The percentage of material extracted was calculated using the following expression:

$$\text{Extraction (\%)} = 100 - \frac{\text{wt. of residue}}{\text{wt. of feed}} \times 100 \qquad 1)$$

The results of leaching quartz with Na_2CO_3 solutions having different concentrations are shown in Figure 1. For each point, 2.0 g. of quartz was leached with 120 ml. of solution at 250°C for the indicated time. It can be seen that the amount of material extracted increased linearly with time for about the first hour. During this period the rate of extraction also increased with alkali concentration to approximately the 0.5 power. Following the constant rate period, the extraction stopped. Apparently the solubility limit was reached, and it seemed to be the solubility limit at room temperature rather than at the leaching temperature. The following evidence pointed to the lower temperature limit. The residue remaining after leaching quartz for 2 hr. or more was an amorphous, non-crystalline solid which was insoluble in hot HCl. The results suggested that quartz had dissolved in the hot solution, and upon cooling some of the silica and possibly some of the soda had reprecipitated as an amorphous or glassy material. On the other hand, the residue remaining after quartz had been leached for less than 1 hr. appeared to be largely quartz. Furthermore when quartz was leached for 1 hr. at 300°C with a 1.0 M solution, the amount of material extracted was only 69% which was no greater than the maximum amount extracted at 250°C. From published solubility data (2) for silica in various alkaline solutions, one would expect the solubility of quartz in a Na_2CO_3 solution to increase markedly with temperature.

Even though the amount of silica extracted seemed to be limited by the room temperature solubility limit, this limit was raised by increasing either the alkali concentration or the ratio of alkali to quartz. Thus by increasing the alkali concentration from 1.0 M to 2.0 M, the maximum amount extracted was raised from 70% to 98.5%. Moreover when the quantity of quartz leached in 1 hr. with a 1.0 M solution at 250°C was reduced from 1 g. to 2 g., the percentage extracted increased from 58% to 95%.

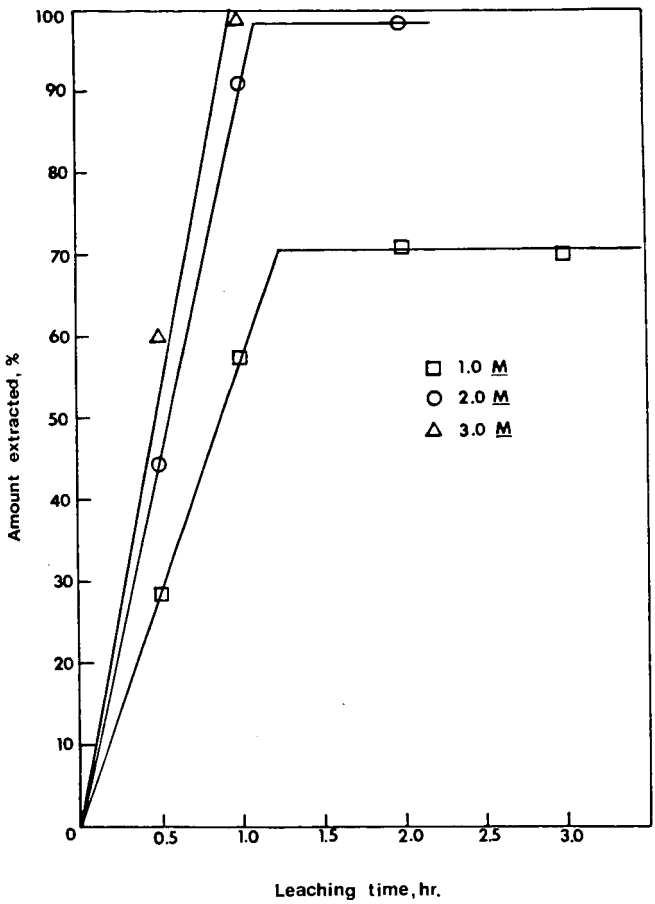

Figure 1. Dissolution of quartz (2.0 g.) by hot (250°C) sodium carbonate solutions (120 ml.) having different concentrations (1.0-3.0 M).

Quartz was also leached for 1 hr. at 250°C with either 2.0 M NaOH or $NaHCO_3$. In each case 2.0 g. of quartz was leached with 120 ml. of solution. Most of the quartz (99.5%) was converted to soluble sodium silicates and extracted by the hot caustic. On the other hand, only 10% of the quartz was extracted by the $NaHCO_3$ solution, and the residue appeared to be entirely quartz. These values were noticeably different from the 58% extracted by 1.0 M Na_2CO_3 under similar conditions. Therefore, these leachants were not equivalent even though each provided the same number of moles of sodium.

None of the residues remaining after leaching quartz with any of the alkalis were acid-soluble.

In a second set of experiments, -74 μm size kaolin particles were leached with hot alkaline solutions to study the conversion of kaolinite to various sodium hydroaluminosilicate compounds (Table 2) under different leaching conditions. In each experiment, 15 g. of kaolin was leached with 120 ml. of alkaline solution. The solid reaction product was recovered by filtration, washed with water, dried in an oven at 95°C, and analyzed by XRD. Although this method of analysis identified the minerals present, it provided only an approximate indication of the relative proportions of the various minerals present. Quartz was particularly misleading because the method of detection was very sensitive to this mineral. Therefore, the results are reported only in terms of major, minor, and trace quantities present in the product as indicated by XRD (Table 3). Because the small amount of titania in the kaolin was apparently not affected by even the most rigorous leaching conditions, the product always contained a trace of this material so no further mention seems necessary.

When kaolin was leached with 1.0 M Na_2CO_3 at 200°C for 1 hr., most of the kaolinite was converted to the sodalite-type natrodavyne (NS) while the quartz and illite impurities were not affected noticeably (Table 3). Increasing the leaching temperature to 250°C resulted in the conversion of the kaolinite to a mixture of mixed-type natrodavyne (NCS) and analcime (A) and complete dissolution of the quartz impurity. The illite impurity was not affected. Leaching at 300°C and above resulted in the conversion of the kaolinite to the cancrinite-type natrodavyne (NC). Only at 350°C did the illite impurity appear to be affected.

A similar trend was observed when kaolin was leached for 1 hr. at 250°C with Na_2CO_3 solutions of different concentrations (Table 3). At the lowest concentration (0.2 M), part of the kaolinite was converted to the sodalite-type natrodavyne while the impurities were untouched. At the highest concentration (2.0 M), the kaolinite was converted to the cancrinite-type natrodavyne, and although the quartz was extracted, the illite remained.

Somewhat similar changes were observed when the leaching time was varied while holding the concentration of Na_2CO_3 at 1.0 M and the temperature at 250°C. With a leaching time of 0.5 hr. the kaolinite was converted to a mixture of analcime and sodalite-type natrodavyne, whereas with a leaching time of 2.0 hr. the kaolinite was largely converted to the cancrinite-type natrodavyne. Not all of the quartz was extracted when leaching was conducted for 0.5 hr., but all of the quartz appeared to be removed when leaching was conducted for longer periods. However, the illite remained even after 2 hr. of leaching.

When kaolin was leached with 1.0 M NaOH at 250°C for 1 hr., most of the kaolinite appeared to be converted to analcime (Table 3). Increasing the concentration to 2.0 M resulted in converting most of the kaolinite to hydroxycancrinite (HC). In either case the quartz impurity was extracted but the illite impurity remained.

Leaching kaolin with 2.0 M $NaHCO_3$ at 250°C for 1 hr. converted the kaolinite to the sodalite-type natrodavyne, but it had no apparent effect on the impurities.

Table 2. Various sodium hydroaluminosilicates produced in leaching kaolinite with hot alkaline solutions

Mineral	Chemical formula	Symbol
Analcime	$Na_2O \cdot Al_2O_3 \cdot 4(SiO_2) \cdot 2(H_2O)$	A
Hydroxycancrinite	$Na_2O \cdot Al_2O_3 \cdot 2(SiO_2) \cdot \frac{2}{3}(NaOH) \cdot n(H_2O)$	HC
Hydroxysodalite	(same as above)	HS
Natrodavyne (sodalite-type)	$Na_2O \cdot Al_2O_3 \cdot 2(SiO_2) \cdot \frac{1}{3}(Na_2CO_3) \cdot n(H_2O)$	NS
Natrodavyne (cancrinite-type)	(same as above)	NC
Natrodavyne (mixed type)	(same as above)	NCS

Table 3. Results of leaching 15 g. kaolin (-74 μm) with 120 ml. alkaline solution

Leaching conditions				Mineral products excluding TiO_2, type, (amount)[a]
Alkali	Conc., M	Temp., °C	Time, hr.	
Na_2CO_3	1.0	200	1.0	NS(maj), SiO_2(maj), kaolinite(min), illite(tr)
Na_2CO_3	1.0	250	1.0	NCS(maj), A(maj), illite(tr)
Na_2CO_3	1.0	300	1.0	NC(maj), A(min), illite(tr)
Na_2CO_3	1.0	350	1.0	NC(maj)
Na_2CO_3	0.2	250	1.0	SiO_2(maj), kaolinite(min), NS(min), illite(tr)
Na_2CO_3	0.5	250	1.0	SiO_2(maj), NS(maj), illite(tr)
Na_2CO_3	1.0	250	1.0	NCS(maj), A(maj), illite(tr)
Na_2CO_3	2.0	250	1.0	NC(maj), illite(tr)
Na_2CO_3	1.0	250	0.5	A(maj), NS(maj), SiO_2(min), illite(tr)
Na_2CO_3	1.0	250	1.0	NCS(maj), A(maj), illite(tr)
Na_2CO_3	1.0	250	2.0	NC(maj), A(min), illite(tr)
NaOH	1.0	250	1.0	A(maj), HS(min), illite(tr)
NaOH	2.0	250	1.0	HC(maj), A(min), illite(tr)
$NaHCO_3$	2.0	250	1.0	NS(maj), SiO_2(maj), illite(tr)

[a]Amount: maj = major quantity, min = minor quantity, tr = trace quantity.

To investigate the dissolution of the sodium hydroaluminosilicates produced by alkaline leaching, 3.0 g. portions of the leached product were treated with 300 ml. of acid in a stirred flask for 30 min. Either 2.0 M HCl or 1.8 M H_2SO_4 were utilized. While HCl was always used at the boiling point, H_2SO_4 was sometimes used at the boiling point and sometimes at room temperature. From XRD analysis of the solid residue remaining after the acid treatment, it was found that all of the sodalite-type and cancrinite-type compounds were dissolved by the acids whether hot or cold. On the other hand, analcime was completely dissolved only by the boiling acids.

In a third set of experiments, -38 μm pyrite particles were leached with hot alkaline solutions to study the conversion of iron pyrite to iron oxide and soluble sulfur species. In each experiment, 5 g. of acid-cleaned pyrite was leached with 120 ml. of alkaline solution for 1 hr. In addition to analyzing the solid residue by XRD, the total sulfur content of the leachate was determined in order to estimate pyrite conversion.

When iron pyrite was leached for 1 hr. with 1.0 M Na_2CO_3 at 250°C, only 12.7% of the pyrite was converted to iron oxide and soluble sulfur species (Table 4). Increasing the leaching temperature to 300°C raised the conversion to 26.4%, and increasing the temperature to 350°C raised the conversion to 44.8%. In each case the solid residue consisted principally of hematite and unreacted pyrite.

Increasing the Na_2CO_3 concentration, while maintaining the leaching time at 1 hr. and temperature at 250°C, increased the pyrite conversion only slightly (Table 4). On the other hand, when pyrite was leached with 2.0 M NaOH at 300°C for 1 hr., a conversion of 62% was achieved. Again, hematite appeared to be the principal solid reaction product.

When the pyrite residue from the alkaline leaching step was treated with acid, all of the hematite dissolved in either hot HCl or H_2SO_4. However, the hematite appeared to dissolve incompletely or very slowly in cold H_2SO_4. Unreacted pyrite was not touched by the acid whether hot or cold.

Conclusions

The solubilization of several of the most prevalent minerals in coal was demonstrated by a one- or two-step treatment process. The first step involves treatment with a hot alkaline solution while the second step involves treatment with a dilute mineral acid.

It was shown that fine-size quartz particles readily dissolve in 1-2 M Na_2CO_3 or NaOH at 250°C. However, when quartz is extracted by a hot Na_2CO_3 solution which is then cooled, an amorphous, acid-insoluble material is produced under some conditions. A likely possibility is that amorphous silica precipitates when the room temperature solubility limit of the material is exceeded. Formation of the amorphous material is prevented by using higher concentrations of alkali or a higher ratio of alkali to silica.

It was also shown that kaolinite reacts with hot alkaline solutions to form various sodium hydroaluminosilicates which are acid-soluble. The particular sodium hydroaluminosilicate formed depends on the type of alkali employed, the alkali concentration, the treatment temperature, and length of treatment. When Na_2CO_3 is employed, kaolinite is largely converted to the sodalite-type natrodavyne under less rigorous conditions and to the cancrinite-type natrodavyne under more rigorous conditions. Under intermediate treatment conditions, the mixed-type natrodavyne and analcime are produced. When NaOH is employed, kaolinite is largely converted to analcime and hydroxycancrinite with the latter being favored by higher alkali concentrations.

Table 4. Results of leaching 5 g. acid-cleaned pyrite (~38 μm) with 120 ml. alkaline solution for 1 hr.

Leaching conditions			Conv.,	Residue
Alkali	Conc., M	Temp., °C	%	
Na_2CO_3	1.0	250	12.7	FeS_2, Fe_2O_3
Na_2CO_3	1.0	300	26.4	FeS_2, Fe_2O_3
Na_2CO_3	1.0	350	44.8	FeS_2, Fe_2O_3
Na_2CO_3	1.0	250	12.7	FeS_2, Fe_2O_3
Na_2CO_3	2.0	250	14.5	----
Na_2CO_3	3.0	250	15.8	----
NaOH	2.0	300	62.0	FeS_2, Fe_2O_3

It was further shown that iron pyrite reacts with hot alkaline solutions to form hematite and soluble sulfur species. NaOH is considerably more effective than Na_2CO_3 for this reaction. However, the effectiveness of Na_2CO_3 solutions can be increased by increasing the treatment temperature and to a lesser extent by increasing the alkali concentration. The hematite produced is readily dissolved by hot mineral acids.

Work is in progress to extend the described reactions to other minerals associated with coal. Further studies are also directed to leaching of coal itself. The results will be used to relate the behavior of the individual minerals when leached alone to their behavior when leached together in their natural occurrence with coal. The studies will shed light on the potential of demineralizing coal for use in low-ash, low-sulfur coal-water mixtures as fuel for replacing oil.

Literature Cited

1. Fan, C.-W., Markuszewski, R., and Wheelock, T. D., Process for producing low-ash, low-sulfur coal, Am. Chem. Soc. Div. of Fuel Chem. Preprints 29(1): 114-119 (1984).

2. Iler, R. K., The Chemistry of Silica, John Wiley and Sons, New York, 1979.

THE SEPARATION OF MINERAL MATTER FROM PITTSBURGH COAL BY WET MILLING

Douglas V. Keller, Jr.

Otisca Industries, Ltd.
P. O. Box 127, Salina Station
Syracuse, New York 13208

Introduction

The term "inherent mineral matter, or ash" is a commonly used phrase in the coal literature (1). The phrase refers to that fraction of the mineral matter bound organically to the carbonaceous structure of the coal and estimates of its content suggest that it is in the range of two weight percent of the whole mineral matter (1). Common classical physical separation schemes such as differential specific gravity separations or froth flotation which are directed at demineralizing the coal never approach that lower limit. For example, at the outset of this investigation one could receive a raw Pittsburgh seam coal at 30 weight percent ash and through careful float-sink processes reduce that ash content into the range of four to five weight percent. Practically reducing that ash content, however, to below three weight percent with a reasonable yield was quite unlikely (2). One consequence of the large weight fraction differential between the practical limit of demineralization, and if you like, the true "inherent" limit of demineralization was a total lack of understanding as to whether or not that mineral fraction could indeed be extracted by physical means. With this as a basis, further questions could be raised as to whether or not that retained mineral matter was a true distinct mineral phase, or if so, could it be bound chemically along the interfaces to the coal structure rendering those particles inseparable. Most simply, in all cases one could ask the question does a separation of mineral matter from the coal take place in all cases when coal is fractured and to what extent, or limit, can the fracture process be utilized in the demineralization of coal.

A series of experiments was assigned to explore the extraction of mineral matter from coal in the size ranges below 0.25 mm. The raw coal samples were obtained from three different sources in the Pittsburgh seam which permitted a degree of comparison over a rather large geographic area. The results are interesting in that they allow a new perspective in the demineralization of coal.

Experimental

The Pittsburgh seam coals used in this investigation has a nominal analysis as illustrated in Table 1.

Lots of Pittsburgh seam coal in excess of 1000 pounds each were received from three different sources in Washington County: Mine (A) was located about 20 miles west of Pittsburgh; Mine (B) was located just south of Pittsburgh; and Mine (C) was located about 40 miles south of Pittsburgh. Representative samples from each source were obtained by ASTM procedures and subjected to the following processing.

A raw coal sample was reduced to 250 μm x 0 by dry mechanical crushing in a hammermill and then ground in a laboratory sample mill.

The mechanically ground coal was then mixed with water to form a slurry with 30 weight percent solids and placed in a standard laboratory ball mill. All of ball milling variables were held constant except for the duration of milling which permitted a variation of the particle size distribution. In the event that chemicals were employed during the ball milling operation those chemicals were incorporated in an excess of the amount of the standard mill content.

The coal water slurry was removed from the mill, diluted with water to ten weight percent solids and the coal fraction removed utilizing the Otisca T-Process (2,3). Separations by the T-Process are unique in that agglomeration results in the recovery of virtually 100% of the carbonaceous material leaving a full dispersed mineral phase in the residue water. Many detailed investigations of this type have concluded that mineral matter recovered with the coal phase is included in the coal that is the ash content of the product coal represents only that mineral matter mechanically attached to or enveloped by the coal.

Analytical procedures for ash (high temperature, HT) and sulfur contents were conducted according to ASTM procedures. Low temperature ash procedures were conducted at 550°C in an oven with an adequate supply of oxygen. The difference in mineral matter morphology and chemistry between this technique and the low temperature ashing method described by Gluskoter (3), can be anticipated from the paper by Mitchell and Gluskoter (4). Principally the higher temperature ashing process will convert pyrite to hematite and kaolinite to metakaolinite. Between 30% and 50% of the mineral matter in the Pittsburgh coal is considered to be kaolinite (5), and in this investigation we presumed that the 550°C ashing procedure did not significantly alter the particle size distribution of the original kaolinite particles.

A Micromeritics 5500L unit was used to obtain the particle size distribution data for this investigation. Data from the Micromeretics unit using a one μm mode sample was compared with the data developed by the manufacturer from a Coulter Counter on the same sample to within ten percent. Even with this in hand there was no attempt to characterize the particles on an absolute basis. The observed area percent data from the Micromeretics unit was transposed to a mass percent base at data points y (in μm) for all of the points $y = 2^x$ where $x = n + 0.5$ and $n = -3, -2.5, \cdots 0 \cdots, +7, +7.5$. The data point at y represents that mass fraction of material lying in the size range $x \pm 0.25$ μm. Thus a summation of all of the data points represents the mass fraction of ash, or product coal, as the case might be.

The following particle size distribution data are given as a log distribution in particle diameter (μm) where the mass points are interconnected for convenience of comparison at the expense of rigor. Typical distributions are bell-shaped where the mode is defined as the particle diameter at that point of half width of the curve at the half height of the maximum. The Micromeritic unit is based on a Stokes' Law settling to the particles where one must choose an average specific gravity of particles under investigation before the data are recorded. In those cases where low temperature ash particles were investigated, the iron minerals with a density larger than 4 gms/cc were separated from the clay minerals with densities less than 3 gms/cc, the distributions measured individually and then the size distributions were recombined mathematically. The product coals demonstrated a very narrow specific gravity distribution in the range of 1.33.

Results and Discussion

Figure 1 illustrates the particles size distribution of the mineral matter that results from the low temperature ashing of three 5 cm cubes of bright coal that were hand-picked from the various samples. The ash contents were in the range of five weight percent. It is of interest to note that band of mineral matter particles that lie in the particle diameter range between one and 50 μm with a mode between four and eight μm. The particle size distribution data from the low temperature ashing of the 5 cm cubes of coal show that raw coal from each source has a unique "fingerprint" of mineral matter particles distributed in the particle size range below 0.25 mm.

Investigations of many other coal seams and coals within a particular seam indicate that indeed the mineral matter distribution varies widely both in shape and magnitude and as such cannot be anticipated from other coal properties. The mineral matter distribution is a fundamental property of that coal which is an uncontrolled natural variable in the extraction of mineral matter.

In order to demonstrate that the 5 cm cube was constituted of an accumulation of much smaller unit volumes each of which represented the whole coal in mineral matter particle size distribution a study of a series of size classified particles was undertaken. For example, if raw coal (C) were ground to 250 μm x 0, and then separated with standard sieves into the size fraction 53 x 44 μm, we would be afforded a dry mixture of raw coal particles and mineral particles with an average size of 48 ± 4 μm. Figure 2 illustrates the particle size distribution of the low temperature ash product of the product coal after the free mineral matter particles were removed. The free mineral matter particles in that size range must have evolved from larger coal particles. Again we have the characteristic curve very similar to the curve shown in Figure 1(C). In fact, that portion of the curve that lies below 3 μm can most usually be superimposed on other curves obtained in a similar manner from the other size fractions of coal (C). Providing, that is, that the coal particle diameters are larger than 10 μm.

The conclusion of that study indicated that product coal particles larger in diameter than the band of microparticles seemed to contain the whole particle distribution of the small microparticles of mineral matter. That is, there appeared to be a relatively homogenious distribution of particles throughout limited in top size by the largest particle in the test. To explore that aspect in more depth, a raw coal was wet milled to smaller sizes.

When a raw coal is wet ball-milled for a sufficient time to produce a slurry with a particle diameter mode in the range of 4 μm there results two forms of mineral matter: That fractured away from the coal and that which is still enveloped in the coal particles. Figure 3 illustrates a typical particle size distribution for the separated product coal as compared to the separated free mineral matter (90 weight percent ash) from one milling test. The separated mineral matter is clearly smaller in diameter than the coal which is probably due to its more brittle properties. Note that in Figures 3 and 4 an integration of the curves will yield 100% of the mineral matter (or ash) under consideration rather than the ash content of the coal as was the case in Figures 1 and 2.

When the product coal shown in Figure 3 was subjected to low temperature ashing as described above and that product subjected to particle size analysis, a curve as is illustrated in Figure 4 results. Clearly the enveloped mineral matter in the product coal particles is considerably smaller in diameter than the coal particles from which they came and as such are not released for separation.

Two very important points are illustrated in Figures 1-4: Firstly, it appears that as coal fracture takes place in this system, mineral matter particles are ejected from the fractured coal system and most without attached coal. Coal attached to mineral matter is recovered as product coal. The implication is that the coal-mineral matter interfaces are not chemically bound. If those interfaces were chemically bound one would observe mineral matter rejection with a large increase in the sub-micron particle population in the released mineral matter, cf. Figure 3, as well as that in the low temperature ash of the product coal. The latter is not observed as is illustrated below.

Secondly, given the low temperature ash distribution of the raw coal and a knowledge of the raw coal particle size distribution after wet milling, we are in a position to predict the ash content of the product coal. Consider Figure 5 where a hypothetical low temperature ash particle size distribution is superimposed on a T-Process product coal size distribution. The product coal particles with diameters lying between x and dx contain no mineral matter particles larger than dx as those particles were removed during the separation process. The mineral matter retained in the product coal particles is the cumulative mineral matter content represented by the low temperature ash curve. Since the mineral content given on the ordinate in Figure 5 is based on 100%, the ash content in each size range can be estimated by multiplying the mass fraction of that point by the total ash content in the raw coal sample, i.e. 250 m x 0, that was used to generate the low temperature ash curve.

A specific case is examined in Table 2 where the particle size distribution data from the low temperature ashing of a 5 cm cube of coal and 44-53 μm coal was related to two product coal samples milled under different conditions all of which originated from the same source coal (C). The first column in Table 2 provides the average particle diameter points (y) at which the data were observed. A comparison of the low temperature ash data for the 5 cm cube, column 2, and for the 44-53 μm coal, column 3, illustrate that the fracture of coal from a 5 cm cube to 48 μm does not significantly disturb the mineral matter particles lying in the range of diameters below 6 μm. Since a 4 μm particle of product coal ought to have the complete mineral matter particle distribution smaller than 4 μm enveloped in that particle, a cumulative ash fraction of the lessor particle diameter ash should be equivalent to the ash content within the 4 μm particles, that is, 2.67 weight percent ash, cf. column 4 at 4 μm.

A test of this relationship is afforded in column 5 where we observe the mass fraction of particles at various diameters of a product coal from a standard mill run with no chemicals added. The predicted ash content of the product coal is determined by a summation, over all particle diameters of the product of the ash content of each diameter cumulated by increasing diameter, (X) times the mass fraction of the product coal at that particular diameter (y). The predicted ash content for this case is 1.19 weight percent ash which can be compared to

the observed value using ASTM procedures of 1.12 weight percent ash. Following identical milling procedures, except for the addition of 20 pounds per ton ligninsulfonate, a dispersant, we obtain a much finer size distribution as is illustrated in column 6, Table 2. The predicted ash content in that case is 0.68 weight percent ash while the observed value was 0.91 weight percent ash. The large discrepancy in the finer coal case was probably due to imperfect separation procedures that were caused by the presence of the dispersant. The ability to predict ash contents using this procedure has been applied to several different coals from different seams and the same seam with results usually within ten percent. A careful examination of these data lends credence to the observation that for the most part the mineral matter included in coal to the micron particle size range is indeed a distinct separable phase capable of physical separation by fracture.

The extent to which milling can be carried out and still attain effective demineralization is to a degree limited by our knowledge of milling. Coal B was reduced in ash into the range of 0.5 weight percent, however, that limit appeared to be a function of milling phenomena rather than fracture phenomena. Clearly, according to the analysis shown in column 5 of Table 2 and the subsequent discussion, one might expect a monotonic decrease in product coal ash content with particle size distribution mode to zero mineral matter which has not been observed. What was not anticipated was the observation that that relation appeared to be insensitive to what might be considered as rather severe changes in the chemical environment during the milling process even though some of the chemical additives made significant changes in the milling efficiency, i.e., specific area increase per unit input energy. Consider the effect of three chemical additives: calcium hydroxide, sodium ligninsulfonate, and sodium sulfosuccinate, as compared to the case of no additives on the particle size distribution of the product coal from a standard mill run shown in Figure 6 where all conditions were identical. Clearly, there were no obvious effects. In the next series, shown in Figure 7, we investigated the additives ammonium hydroxide, sodium hydroxide, and a higher concentration of sodium ligninsulfonate. Clearly, a dynamic difference in specific surface area per unit input energy was observed. The explanation of the differences is beyond the scope of this paper, but what was interesting was the effect that the chemicals had on the fracture mechanism that effects the release of mineral matter. Figure 8 illustrates a plot of the ash content in the product coal versus the mode of the particle size distribution of the product coal. All of the tests utilizing chemical additives were milled under identical conditions utilized in the test which produced the "no additive" data with a 2 μm mode. The three other "no additive" tests were milled for extended times to achieve smaller particle size distributions. The chemical additive calcium hydroxide when used at 20 pounds per ton is above the saturation limit and the solid particles have become imbedded in the coal structure, hence increasing the ash content of the product coal well removed from its anticipated location on the curve. A mild acid etch of that product coal to remove the calcium hydroxide allows recovery of its anticipated position in the scheme. Some of the chemical additives do alter the specific milling rate during the process, but that change does not alter the relationship between particle fracture and mineral matter released. Such lends support to the presumed model that the ultrafine mineral matter is to some degree homogeneously distributed and is only released with the fracture of the coal particle.

Conclusion

High ranked bituminous coals like those of the Pittsburgh seam contain a distribution of discrete mineral matter particles in the size range from 50 to 1 μm which can be released and physically separated from the coal by normal fracture mechanisms experienced in wet ball milling. Demineralization of coal by this mechanism appears to be a predictable process with an error in the range of 10 percent. The demineralization of Pittsburgh seam coal has been achieved to the range of 0.5 weight percent ash, a limit which appears to be controlled by the mechanics of the ball mill.

Acknowledgments

The author extends his sincere appreciation to W. Burry and D. S. Keller for their efforts in the development of the experimental procedures and data analysis.

References

1. Leonard, J. W., "Coal Preparation", Amer. Inst. Mining Met. Pet. Eng., Inc., New York (1979).

2. Keller,Jr., D. V., "Otisca T-Process, A New Coal Beneficiation Approach for the Preparation of Coal Slurries", Coal Gasification, Liquifaction, and Conversion to Electricity Conference, University of Pittsburgh, August 1982.

3. Keller,Jr., D.V., "Coal Refining by Physical Methods for the Preparation of Coal Slurries With Less Than 1 wt.% Ash", Fifth International Symposium on Coal Slurry for Combustion and Technology, Tampa, Florida, April 1983, U.S. DOE, Pittsburgh, p 269.

4. Gluskoter, H.L., Fuel, 44, 285 (1965).

5. Mitchell, R.S. and Gluskoter, H.L., Fuel, 55, 90 (1976).

6. O'Gorman, J.V. and Walker, P.L., "Mineral Matter and Trace Elements in U.S. Coals", U.S. Office of Coal Research, R& D Report No. 61, (1972).

TABLE 1

NOMINAL ANALYSIS OF PITTSBURGH SEAM COAL

	Weight Percent (Dry Basis)
Volatile Matter	35
Fixed Carbon	58
BTU/lb	14,200
Carbon	77.3
Hydrogen	5.2
Nitrogen	1.5
Chlorine	0.1
Sulfur	1.5
Oxygen (diff)	7.6
Ash	6.8

TABLE 2

PARTICLE SIZE DATA FOR LOW TEMPERATURE ASH PRODUCTS AND PRODUCT COALS

Data Point	Low Temperature Ash - Wt.%			Product Coal - Wt.%	
µm (y)	5 cm Cube	44-53µm	44-53µm (Cumulative X)	Standard No Additives (Y)	Standard 20 pounds/ton Ligninsulfonate (Z)
0.35	0.03	0.06	0.06	0.08	0.14
0.50	0.06	0.1	0.16	0.05	0.08
0.71	0.19	0.18	0.34	0.085	0.13
1.00	0.35	0.28	0.62	0.13	0.20
1.41	0.49	0.38	1.0	0.2	0.14
2.0	0.67	0.52	1.52	0.18	0.10
2.83	0.63	0.60	2.12	0.145	0.05
4.0	0.66	0.55	2.67	0.06	0.03
5.66	0.66	0.55	3.22	0.04	0.01

No Additives $\sum_{y=0.35}^{y=5.66} (X_y \times Y_y) =$ 1.19 Wt.% Ash Predicted; 1.12 Wt.% Ash Observed

Ligninsulfonate $\sum_{y=0.35}^{y=5.66} (X_y \times Z_y) =$ 0.68 Wt.% Ash Predicted; 0.91 Wt.% Ash Observed

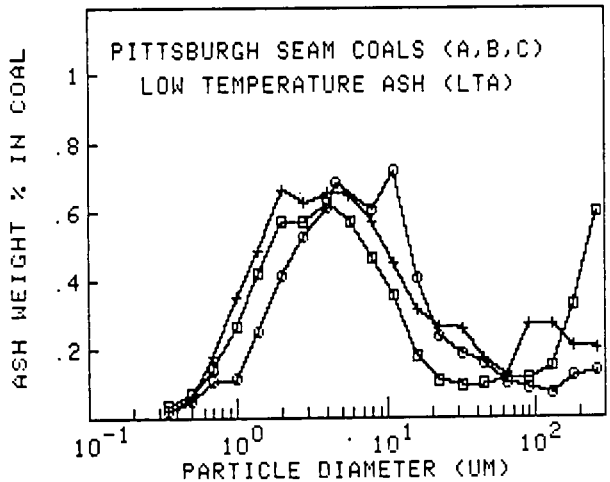

FIGURE 1: PARTICLE SIZE DISTRIBUTIONS OF THE LOW TEMPERATURE ASH PRODUCTS FROM THREE DIFFERENT 5 cm BLOCKS OF PITTSBURGH SEAM COAL: (+) Coal A; (□) Coal B; and (O) Coal C.

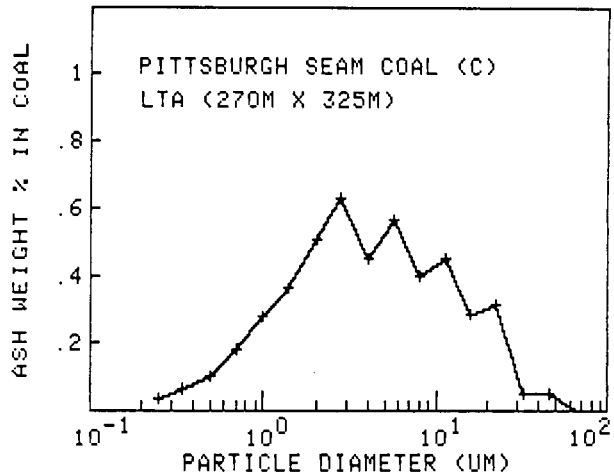

FIGURE 2: PARTICLE SIZE DISTRIBUTION OF THE LOW TEMPERATURE ASH PRODUCT OF A 48 ± 4 μm PRODUCT COAL.

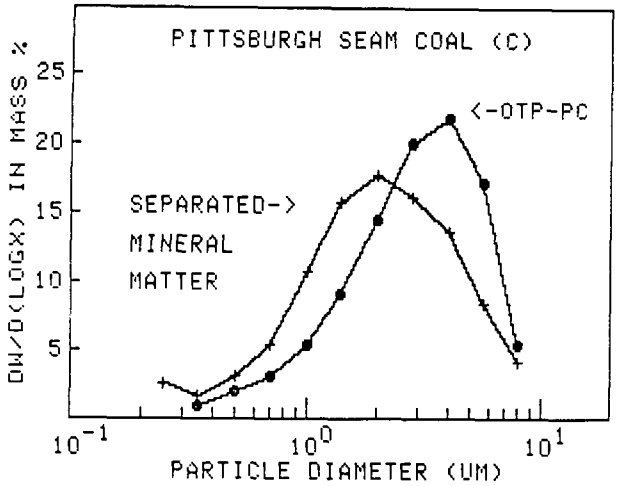

FIGURE 3: WHEN THE PRODUCTS OF WET MILLING 250 μm x 0 PITTSBURGH COAL (C) ARE SEPARATED, TWO PRODUCTS EVOLVE: PRODUCT COAL AND SEPARATED MINERAL MATTER. THE PARTICLE SIZE DISTRIBUTIONS FOR EACH ARE ILLUSTRATED.

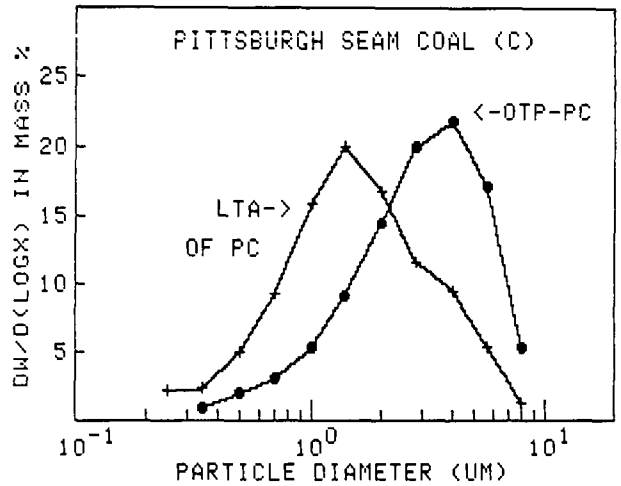

FIGURE 4: PARTICLE SIZE DISTRIBUTION OF THE LOW TEMPERATURE ASH PRODUCT FROM THE SAME PRODUCT COAL SAMPLE SHOWN IN FIGURE 3.

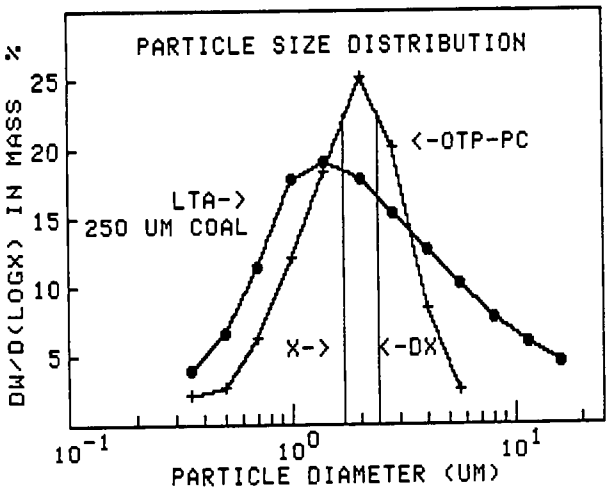

FIGURE 5: A HYPOTHETICAL PARTICLE SIZE DISTRIBUTION CURVE OF LOW TEMPERATURE ASH AND PRODUCT COAL.

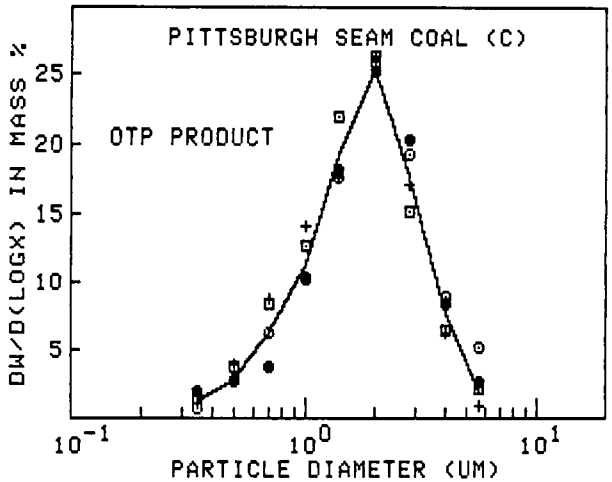

FIGURE 6: THE EFFECTS ON PRODUCT COAL PARTICLE SIZE DISTRIBUTION OF THREE CHEMICAL ADDITIVES WHILE MILLING AT CONSTANT CONDITIONS. (●) No Additives; (⊙) 2 lbs/ton Calcium Hydroxide; (⊡) 2 lbs/ton Sodium Ligninsulfonate; and (+) 20 lbs/ton Sodium Sulfosuccinate.

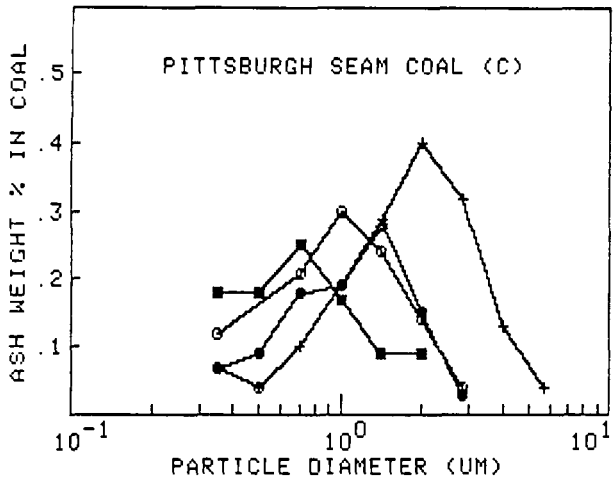

FIGURE 7: THE EFFECTS ON PRODUCT COAL PARTICLE SIZE DISTRIBUTION OF THREE CHEMICAL ADDITIVES WHILE MILLING AT CONSTANT CONDITIONS. (+) No Additives; (●) 36 lbs/ton Ammonium Hydroxide; (○) 7.9 lbs/ton Sodium Hydroxide; and (■) 20 lbs/ton Sodium Ligninsulfonate.

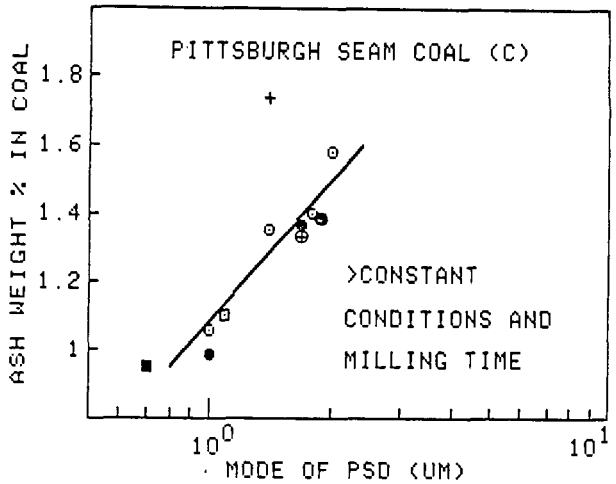

FIGURE 8: WEIGHT PERCENT ASH IN PRODUCT COAL VERSUS THE MODE OF THE PARTICLE SIZE DISTRIBUTION OF THE PRODUCT COAL. (⊙) No Additives; (◆) 7.9 lbs/ton Sodium Hydroxide; (⊡) 36 lbs/ton Ammonium Hydroxide; (■) 20 lbs/ton Sodium Ligninsulfonate; (+) 20 lbs/ton Calcium Hydroxide, (●) 2 lbs/ton Calcium Hydroxide; (⊕) 2 lbs/ton Sodium Ligninsulfonate; and (+) 20 lbs/ton Sodium Sulfosuccinate.

CHEMICAL TREATMENT PRIOR TO PHYSICAL COAL BENEFICIATION

A. B. Walters

Florida Power & Light Company
P.O. Box 14000
Juno Beach, Florida 33408

ABSTRACT

Conventional wisdom dictates that chemical treatment of coal should follow physical beneficiation. This ordering is expected to achieve reduced consumption and improved access of chemical reagents to the smaller, partially demineralized coal particles which result from physical cleaning. The advantages of reversing this conventional order of treatment, particularly for coal demineralization, are often overlooked. Chemical pretreatment can greatly improve the grindability of coal prior to the final size reduction required for physical beneficiation. The use of inexpensive chemical reagents can greatly reduce the disadvantage of higher reagent consumption. Prior chemical treatment can also selectively remove inorganic components which adversely affect coal ash behavior in combustion equipment. The effectiveness of subsequent physical coal demineralization can be improved by chemical pretreatment, especially for physical processes which exploit surface chemistry. Examples describing the advantages of chemical processing prior to physical coal beneficiation are included in this talk.

INTRODUCTION

Coal beneficiation research and development programs are commonly targeted to the dual objectives of sulfur and gross mineral matter removal. Many programs are primarily guided by environmental new source performance standards (NSPS) for coal-burning facilities. Attractive technical approaches to coal beneficiation which cannot meet NSPS are given limited attention. Beneficiation objectives in addition to sulfur and gross mineral matter removal, such as improved combustion behavior, reduced slagging and fouling, improved grindability, and compatibility with emission control equipment, are often ignored.

Earlier efforts to meet NSPS and restrictive oil-backout requirements concentrated on coal hydroliquefaction. These efforts yielded conceptual processes capable of producing highly desulfurized and demineralized coal-based fuels suitable for replacing petroleum-based fuels or feedstocks. High projected process capital costs and modest overall energy yields have discouraged the further development of these conceptual processes.

Relatively high energy yields and relatively low capital and operating costs are achievable with many commercially available coal beneficiation processes. Unfortunately, these processes are capable of only modest reductions in sulfur and gross mineral matter. Newer, conceptual processes are again embarking on the path of "super-clean" coal, the same path that led to

non-competitive product costs in the case of hydroliquefaction. Other, less ambitious approaches capable of improving the performance of coal-burning equipment via coal beneficiation may be more practical. In particular, inexpensive chemical treatment prior to near-conventional physical coal beneficiation may achieve many coal beneficiation objectives.

COAL BENEFICIATION OBJECTIVES

Coal can be beneficiated to meet a variety of objectives related to its use as a heat-producing fuel. These objectives include:

- reducing sulfur content for reduced SO_x emissions;
- reducing gross mineral matter content for reduced total particulate emissions and ash production;
- reducing moisture levels for improved efficiency;
- improving grindability for reduced grinding costs;
- preserving combustible volatiles content for needed combustion behavior;
- improving carbon burnout characteristics for improved efficiency and compatibility with particulate control equipment; and
- reducing selected mineral components to reduce slagging and fouling characteristics of the coal ash.

Many of these objectives are in conflict. Reduced SO_x in flue gases can reduce the efficiency of electrostatic precipitators due to high particulate electrical resistivities. Gross mineral matter reduction can change the composition of resulting coal ash leading to lower coal ash fusion temperatures and increased slagging and fouling; this may in some cases be the result of contamination by beneficiation aids, such as magnetite fines carried-over during heavy media separations. Severe chemical treatments to remove sulfur and mineral matter may significantly reduce the combustible volatiles content of the coal. Very low mineral matter levels can lead to high unburned carbon levels in fly ash particulates which may reduce the efficiency of electrostatic precipitators due to low particle electrical resistivity.

Despite these conflicts, a few general objectives can be selected for top priority. Coal pyrites contribute to increased SO_x and particulate emissions and to increased slagging and fouling due to increased iron in the coal ash. Pyrite removal is an important objective for coal beneficiation. Modern coal burning applications typically require fine coal grinding (ca. $<$200 mesh). This is true for dry, pulverized coal firing or for coal-water mixture fuels intended for oil-backout. Improved coal grindability would significantly reduce the subsequent costs of coal utilization. The preservation of combustible volatiles in the coal is also important. It is especially important for coal/water mixture fuels due to the high moisture levels (ca. 30-40 weight percent

water) in these fuels. The preservation of combustible volatiles limits the severity, particularly temperatures, which can be employed in coal beneficiation. Pyrite removal from many coals can be improved by fine grinding. It can also be improved if fresh pyrite particle surfaces can be rendered more hydrophilic prior to froth flotation for mineral matter removal. The selective removal of alkali and alkaline earth minerals would also be desirable due to the resulting increase in coal ash fusion temperatures which would reduce slagging and fouling. In the case of dry, pulverized coal firing, the high costs of dewatering fine coal prior to burning might preclude the application of froth flotation following fine grinding.

These refined coal beneficiation objectives point towards a chemical treatment aimed at coal mineral matter, particularly the interfaces between mineral matter and the carbonaceous coal macerals. This treatment, not so very distinct from developing chemical comminution technologies should greatly improve subsequent grindability, significantly increase coal ash fusion temperatures, and preserve combustible volatiles. An additional objective of low costs requires that inexpensive reagents and treatment equipment be employed. An approach which may achieve these coal beneficiation objectives is currently under investigation at the Brookhaven National Laboratory (BNL). A pressurized carbon dioxide/water mixture is used as the chemical reagent for chemico-physical coal beneficiation[1].

CHEMICO-PHYSICAL COAL BENEFICIATION

Gaseous carbon dioxide is known to penetrate coal[2] and to improve coal grindability[3]. Unlike chemical comminution caused by ammonia[4], water enhances the swelling and fracturing of coal caused by carbon dioxide[1]. The carbon dioxide/water mixture is reported to have a synergy which enhances the carbon dioxide fracturing of coal while selectively removing alkali and alkaline earth minerals. Significant improvements in coal grindability with very high retention of overall energy content and coal volatiles are reported. Subsequent sink/float studies have indicated selective fracturing of the interfaces of the mineral matter and the carbonaceous coal macerals[5]. Treatment effects on pyrite surface hydrophilicity for coal ground in the pressurized carbon dioxide/water mixture remain to be determined. Such improvements in the hydrophilic nature of fresh pyrite surfaces have been reported for aqueous sodium carbonate treatment at the same temperatures used in the BNL chemico-physical treatment (ca. 80°C)[6].

A major drawback to this potentially effective coal beneficiation treatment is the costs of achieving the treatment conditions (ca. 750 psi, 80°C). An investigation of the effects of treatment conditions on coal beneficiation is being initiated to allow for an engineering study to evaluate the commercial potential of the BNL approach to coal beneficiation.

CONCLUSIONS

The BNL carbon dioxide/water coal beneficiation treatment shows promise for meeting important coal beneficiation objectives. This treatment appears suitable for beneficiating coals for dry, pulverized coal firing without subsequent physical coal beneficiation or for coal/water mixture fuels with subsequent physical beneficiation, e.g. froth flotation. Froth flotation is already included in the processes for some of the proposed commercial coal/water mixture preparation facilities. The effectiveness of the BNL treatment for enhancing pyrite surface hydrophilicity needs further study. Also needed is further study of the commercial potential of this coal beneficiation approach. Engineering studies await the results of more detailed investigations of the effects of varied treatment conditions.

REFERENCES

1. Sapienza, R. S., Slegeir, W. A., Butcher, T., and Healy, F., I. Chem. E. Symp. Ser. No. 83, 85 (1983).

2. Fuller, E. L., Jr. "Coal Structure" M. L. Gorbaty and K. Ouchi, Eds., Adv. Chem. Ser., 192, 293 (1981).

3. Czaplinski, A., and Holda, S., Fuel, 61 (12), 1281-2 (1982).

4. Silveston, P. L., Hudgins, R. R., Spink, D. R., Smith, B., and Mathieu, G, "Coal: Phoenix '80's" A. M. Al Taweel, Ed., Proc. 64th CIC Coal Symp., 1, 277-83 (1982).

5. Sapienza, R. S., personal communication.

6. Patterson, E. C., Report No. IS-ICP-64, EMRRI, Iowa State University, Ames, Iowa, Sept. 1978.

DECOMPOSITION OF PYRITE IN A COAL MATRIX DURING PYROLYSIS OF COAL

I. Stewart and S. G. Whiteway
Atlantic Research Laboratory, National Research Council

AND

P. J. Cleyle and W. F. Caley
Technical University of Nova Scotia

The high sulphur content of Eastern Canadian coals has led to a number of studies aimed at reducing these sulphur levels[1]. In general about two thirds of the sulphur is pyritic, often occuring as small inclusions, and therefore difficult to remove by conventional beneficiation techniques.

In general when coal is pyrolysed the pyrite decomposes to pyrrhotite and H_2S is emitted. It has been reported[2] that not all of the sulphur from the pyrite/pyrrhotite transformation is emitted; some becomes trapped in the organic matrix as 'bound' sulphur. In investigations of the pyrolysis of Nova Scotian coal, Brothers[3] noted that when 95% of the pyritic sulphur was removed prior to pyrolysis, the residual organic sulphur in the char decreased by about 50% in comparison to that of char formed from the raw coal.

The present study deals with the pyrolysis of coal from the Prince Colliery in Cape Breton Island, Nova Scotia (Table 1). This particular coal was chosen both because of its high sulphur content (~4 wt.% S) and because it is typical of much of the proven reserves of the field.

Experimental

The coal was crushed and sieved on Tyler screens to -8 + 16 mesh, (1-2.4 mm). Approximately 2 g of coal was placed in an alumina boat and pyrolysed under argon in a tube furnace at a variety of temperatures and times.

After pyrolysis pieces of the coal were mounted using Fisher Chemical Co. 'Quickmount' cold-mounting resin, and polished in preparation for scanning electron microscopy (SEM). Representative pyrite crystals about 20 μm in diameter, and not near macropores or other discontinuities, were selected for study.

A Jeol-35 SEM microprobe equipped with energy- and wavelength-dispersive spectrometers was used for elemental analysis. Point analyses were carried out; these covered approximately 0.5 μm for the

pyrite and 1 μm for the coal. The standard atomic number, absorption and fluorescence (ZAF) corrections were applied to all analysis, using counting times of 200 seconds, an accelerating voltage of 15 KV, and a pyrite crystal as standard.

Results

The extent of pyrite decomposition was followed by obtaining S/Fe atomic ratios at various points across selected pyritic inclusions. Figure 1 is a plot of this ratio vs. "distance from the edge of the inclusion" for seven particles pyrolysed at different temperatures. The duration of pyrolysis was 15 - 20 hours. It is apparent that the transformation from pyrite to pyrrhotite in Prince coal mainly occurs in the temperature range 500-550°.

Figure 2 is a plot of wt.% S as a function of distance from the inclusion/coal interface into the matrix. This demonstrates the constant background level of organic sulphur in the coal matrix surrounding undecomposed pyrite particles at 400 and 500°. In contrast, it is clear that the sulphur content is enhanced around pyrite particles that had been pyrolysed at 550, 600 and 700°C, and that sulphur transfer has occurred.

Figure 3 shows the effect of time on this sulphur transfer during pyrolysis at 600°C. It can be seen that the total amount of sulphur transferred remains approximately constant after 15.5 hours and that the depth of penetration of sulphur into the surrounding organic matrix does not increase with time of pyrolysis.

Discussion

A. Transformation Temperature

At 400°C and 500°C very little decomposition occurred, while at 600°C and 700°C transformation was virtually complete. At 550°C, however, the transformation was incomplete within the 20 hours given for pyrolysis, the results indicating a pyrite core surrounded by a pyrrhotite shell. These results indicate that pyrite in Prince coal begins to pyrolyse between 500 and 550°C; this is in general agreement with temperatures reported by other authors[4].

B. Sulphur Transfer

The results of this study indicated that there was little transfer of sulphur from pyrite to the surrounding organic matrix of coal not heated beyond 500°C. This is similar to the findings of Raymond and Hagan[5] who examined unreacted coal by SEM.

The extra sulphur observed around the decomposed pyrite in the present study therefore was formed as a result of the pyrolysis reactions. Radio-tracer work using ^{35}S-doped pyrite has shown that some of the sulphur released combines with the organic matrix with the formation of carbon-sulphur bonds[6]. It has been suggested[7] that during pyrolysis sulphur migrates within the iron sulphide as $S^{=}$. At the surface of the FeS charge transfer, reaction and desorption would lead to a variety of compounds.

Considering the hydrogen-rich environment presented by the decomposing coal matrix, one important sulphur compound would be H_2S, which would begin to diffuse away from the FeS/coal interface through the pores of the matrix. Active carbon sites, that are being generated simultaneously by devolatilization of the coal matrix, also could react with the sulphur trapping it as newly formed and strongly bound "organic" sulphur. In the ^{35}S tracer work referred to above, 38% of the overall sulphur liberated in the decomposition of the pyrite became fixed as "organic" sulphur.

Figure 1 shows that at 600°C a typical pyrite grain has decomposed entirely to pyrrhotite within 15.5 hours. Referring to Fig. 3 it is significant that the depth of penetration did not increase with increasing time, which indicates that the trapped sulphur was not mobile. In addition, therefore, we may conclude that diffusion in the matrix is not an important mechanism for migration of sulphur from the pyrite/coal interface. The main transfer mechanism for the sulphur that does escape probably is pore-diffusion of H_2S.

The data of Fig. 2 can be used to estimate the amount of sulphur trapped in a spherical shell around a pyrite particle, and to compare it with the amount of sulphur known to be released by the pyrite/pyrrhotite decomposition. Within the uncertainties of this order-of-magnitude calculation we concluded that all the sulphur released from a small, well-embedded, pyrite particle in Prince coal becomes trapped in the coal matrix. However, it should be pointed out again that during the pyrolysis of macro amounts of coal a considerable amount of pyritic sulphur is released into the gas phase as H_2S; presumably this originates with pyrite of a more massive nature or which is not so well embedded in the matrix.

Summary

The decomposition temperature of pyrite in Prince coal was found to be between 500 and 550°C as determined using a SEM-microprobe. In addition, some of the sulphur liberated in this decomposition became trapped in the coal matrix surrounding the pyrite crystals. For small crystals, well embedded in the coal matrix, all the sulphur released by the decomposing pyrite becomes trapped as "organic" sulphur.

References

1. Tibbetts, T. E. and Montgomery, W. J.
   Canmet Rep. 76-40 (publ. 1976).

2. Yergey, A. L., Lampe, F. W., Vestal, M. L., Day, A. G., Fergusson, G. J., Johnston, W. H., Synderman, J. S., Essenhigh, R. H. and Hudos, J. E.
   Ind. Eng. Chem. Process. Des. Develop. 1974, 13, 233.

3. Brothers, J. A.
   Proceedings of 1983 International Conference on Coal Science, Pittsburgh, 1983, p. 537.

4. Luganov, V. A. and Shabalin, V. I.
   Can. Met. Quart. 1982, 21, 157.

5. Raymond, R. and Hagan, R. C.
   Scanning Electron Microscopy. 1982, 2, 619.

6. Medvedev, K. P. and Petropolskaya
   UKHIN. 1968, 19, 137.

7. Attar, A.
   Fuel. 1978, 57, 201.

Table 1. Proximate Analysis and Sulphur Forms of Prince Coal

Constituent	Weight Percent (moisture free basis)
Moisture	5.5*
Volatiles	27.8
Ash	19.9
Carbon	52.4
Sulphur:	
Pyritic	3.33
Sulphatic	0.34
Organic	1.13
Total	4.80

*On "as received" basis

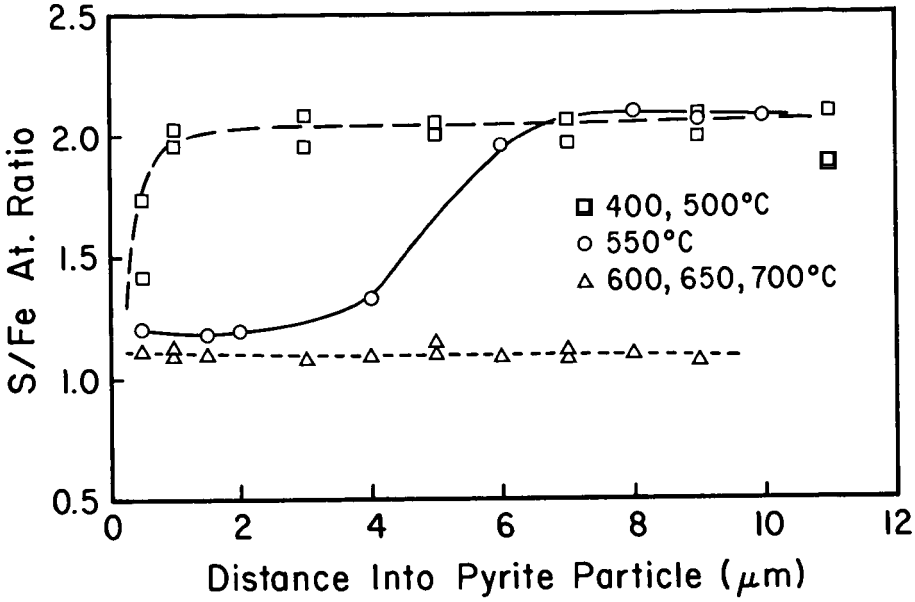

Fig. 1 Decomposition of FeS_2 to FeS as coal is heated above 500°.

Fig.2 Sulphur from decomposed pyrite trapped in matrix of coal.

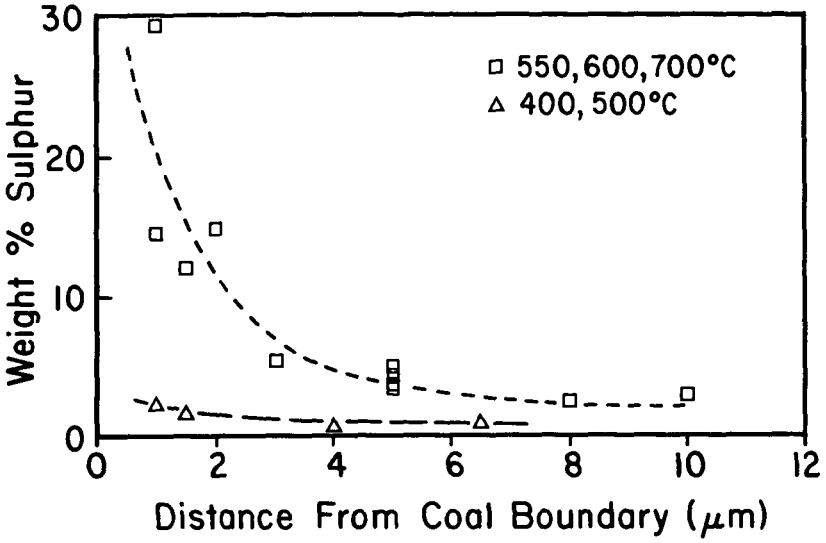

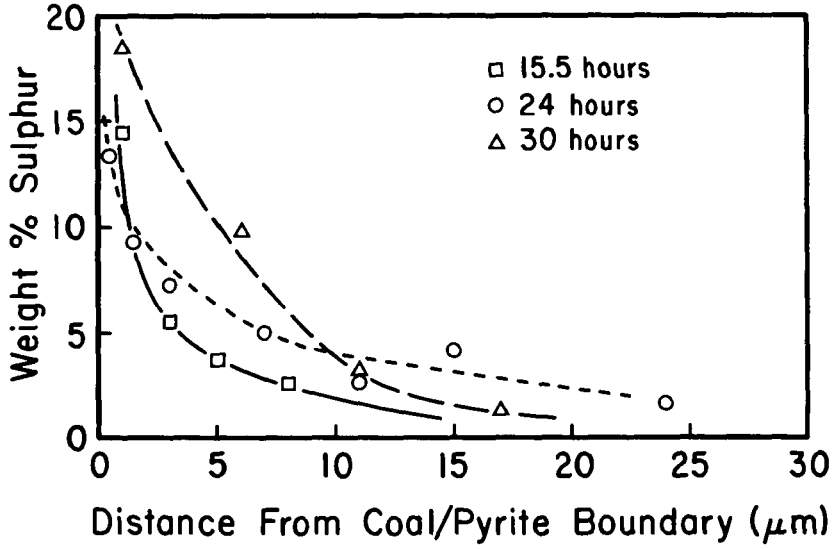

Fig.3 Stability with time of sulphur trapped in matrix of coal.

Water Air Soil Pollut (2010) 213:27–45
DOI 10.1007/s11270-010-0364-6

Geochemical Mobility and Bioavailability of Heavy Metals in a Lake Affected by Acid Mine Drainage: Lake Hope, Vinton County, Ohio

Dina L. López · Elizabeth Gierlowski-Kordesch · Carol Hollenkamp

Received: 13 August 2009 / Accepted: 10 February 2010 / Published online: 2 March 2010
© Springer Science+Business Media B.V. 2010

Abstract Sandy Run (Vinton County, southeastern Ohio, USA) is a stream receiving acid mine drainage (AMD) from an abandoned coal mine complex. This stream has been dammed to form Lake Hope. The heavy metal composition of waters (benthic and pore), sediments, and macroinvertebrates in the lake reservoir sediments were analyzed. Lake waters contained Mn as the heavy metal present in higher concentrations followed by Fe, Al, and Zn. Depletion of Fe and Al occurred from precipitation of less soluble Fe and Al oxides and hydroxides along Sandy Run before entering the lake, producing a high Mn water input into the reservoir. Concentrations of heavy metals in the sediments increased toward the dam area. Sequential extraction of metals in the sediments showed that the highest fractions of metals corresponded to the detrital fraction or eroded material from the watershed and metals associated with iron and manganese hydroxides. Heavy metals in the organic sediment fraction were low. Heavy metals from the AMD source, as well as sediments rich in heavy metals eroded from the watershed, were transported to the downstream dam area and stored at the bottom, producing the observed chemistry. Heavy metals in benthic waters also were sourced from the diffusion of ions from sediments and lake waters as variation in pH and redox conditions determined the flux at the sediment–water interface. Metal concentrations were measured within two deposit feeders, oligochaetes and chironomids, and compared to trends in physical metal concentration across the lake. For the four heavy metals with higher concentration in both benthic animals, the concentrations followed the trend: Fe>Al>Mn>Zn, which were similar to the bioavailable metals in the sediments rather than the pore or the benthic water where Mn was the most abundant heavy metal. Ingestion of sediment, not exposure to pore or benthic waters, appeared to be the main transfer mechanism for metals into the biota. Trends and patterns in animal metal concentrations across the lake were probably a complex process controlled by metabolic needs and metallic regulation and tolerance. Even when Mn was the highest concentration heavy metal in the pore waters, it was the lowest to bioconcentrate in the organisms. In comparison, Cd, the lowest concentration metal in the sediments, presented one of the highest bioaccumulation factors.

Keywords Acid mine drainage · Sequential extraction · Lake sediments · Heavy metal · Contamination · Macroinvertebrates

D. L. López (✉) · E. Gierlowski-Kordesch · C. Hollenkamp
Department of Geological Sciences,
316 Clippinger Laboratories, Ohio University,
Athens, OH 45701-2979, USA
e-mail: lopezd@ohio.edu

1 Introduction

Lake Hope is a 0.6-km^2 impoundment with 9.2 km of shoreline located in northeastern Brown Township, Vinton County, southeastern Ohio (USA; Fig. 1). It was created in 1939 when Sandy Run was dammed 0.40 km upstream from its confluence with Raccoon Creek (Tobin and Youger 1977). This lake has been affected by inputs of acid mine drainage (AMD) from abandoned, underground coal mines in the headwaters of the watershed since its creation. Mining Complex 88 (Fig. 1), approximately 6.0 km upstream from Lake Hope, was sealed in 1979 to reduce the flow of AMD into Sandy Run. Mining Complex 47, located in the same upstream area, was not sealed. The purpose of this paper is to determine the geochemical mobility and bioavailability of the AMD contaminants and the impact on the lake sediments produced by the continuous influx of AMD from abandoned coal mines. Geochemical mobility is the tendency of an element to become soluble based on the geologic and chemical properties of the system. The specific chemical form and binding state of the metals determine the mobility, bioavailability, and toxicity of metals, rather than the total metal concentration (Power and Chapman 1992; Kersten and Förstner 1995; Gleyzes et al. 2002).

AMD is formed when sulfide-bearing minerals, formed under reducing conditions, are exposed to oxygen and water, resulting in the oxidation of sulfides and the subsequent release of acidity, metals, and sulfates (Kleinmann et al. 1995). The rock strata found in the vicinity of Lake Hope are part of the Allegheny Group of the Pennsylvanian System (Marple 1954). The Allegheny Group has valuable deposits of coal, clay, and limestone (Stout 1927). The primary source of the AMD into Lake Hope is from abandoned coal mines in the Middle Kittanning No. 6 coal seam (Harris 1973) with a mean sulfur content of 3.34% (Stout 1927).

1.1 Previous Studies and Objectives

Orciari and Hummon (1975) first investigated the benthic oligochaete population of AMD-impacted Lake Hope, comparing its fauna to that of a nearby unaffected reservoir. The benthic oligochaete fauna of Lake Hope at the downstream dam area was found to be as abundant as the same area in the unaffected lake, but the diversity was moderately lower. The oligochaete *Limnodrilus hoffmeisteri* comprised 75% of the population. Lower diversity of macroinvertebrate fauna is generally associated with AMD in lakes (e.g., Dills and Rogers 1974) and rivers (e.g., Van Damme et al. 2008).

Hughes (1999) compared pre-seal and post-seal data upstream and downstream of AMD discharges from Mine Complexes 88 (sealed) and 47 (unsealed)

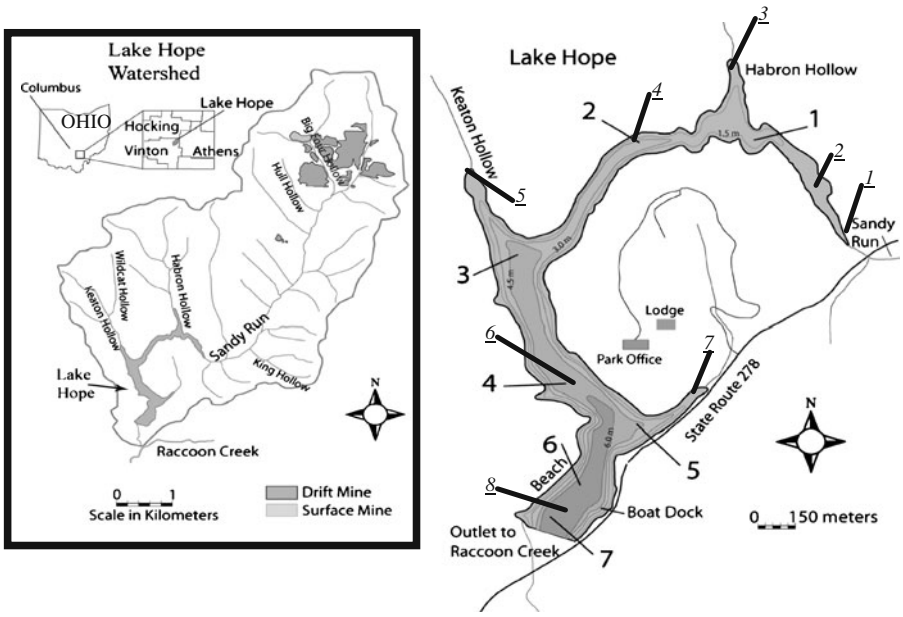

Fig. 1 The Lake Hope Watershed in Vinton County, Ohio. *Large numbers* indicate sampling points for this work. *Underlined smaller numbers* delineate sampling points from Prim (1999). See Table 1 for Prim's data

located approximately 6 km upstream from Lake Hope. Comparison with the pre-sealing data showed that the unsealed mine decreased 46% in acidity loading attributed to natural attenuation, while the sealed mine showed a 75% decrease due to the inundation of the sealed mine.

Prim (1999) conducted a study from August 1997 to June 1998 to assess the impact of AMD on the sedimentation processes and water quality of Lake Hope. Profiles of temperature, pH, and dissolved oxygen at different times of the year did not show the typical seasonal stratification observed in temperate lakes (Wetzel 2001). Vertical isotherms and lines of equal concentration were observed showing the general movement of water from upstream to the downstream dam as in a river. Only the lake area closest to the dam showed incipient stratification during the summer. Sampling points for the Prim study are in Fig. 1 (sampling points 1, 2, 4, 6, and 8), and the benthic water quality collected at 0.3 m above the sediment–water interface are shown in Table 1. Alkalinity along the lake from the input of Sandy Run to the dam showed that the rise in pH is probably due to the input of alkaline groundwater. A longitudinal gradient of metal concentrations in the sediments of Lake Hope, with concentrations generally increasing with proximity to the dam, was observed. Prim (1999) proposed three possible mechanisms for the increase of sediment metal concentrations with proximity to the dam: (1) the physical transport of lake sediments downstream with deposition and accumulation near the dam, (2) the input of metal-rich groundwaters, and (3) the sequestration of metals by algae in the water with a substantial deposition occurring closer to the dam. The third mechanism of sequestration was thought to be the most probable.

The present study has the following objectives: (a) to examine the metal concentrations within the sediments, pore, and benthic waters of Lake Hope from the Sandy Run input to the dam in order to better understand the processes of metal deposition—Patterns in metal accumulation across the lake bottom from the Sandy Run input to the dam may help determine whether metals are added to the sediment through biologic or physical processes—and (b) to compare the bioavailability of the contaminants and their bioconcentration with respect to pore waters and bioaccumulation within the lake sediments for the most common benthic macroinvertebrates, oligochaetes, and chironomids.

1.2 Chemical Speciation and Binding State

Tessier and Campbell (1988) summarized the significant trace metal associations in sediments as those (1) adsorbing to the surfaces of clays, iron and manganese oxyhydroxides, or organic matter; (2) occurring in the lattice of secondary minerals like carbonates or sulfides; (3) occluded in amorphous materials such as iron and manganese oxyhydroxides, iron sulfides, or remains of organisms; and (4) occurring in the lattice of primary minerals. In order to better assess the partitioning of trace metals among the different phases of sediment, Tessier et al. (1979) developed one of the most used sequential extraction methods, in which the sediment was separated into five operationally defined fractions:

1. Exchangeable fraction (SQ-1): The weakly sorbed metals and the reagents used were electrolytes at neutral pH.
2. Acid-soluble fraction (carbonates) (SQ-2): These are metals dissolved at a pH close to 5 and

Table 1 Chemical composition of filtered Lake Hope waters sampled by Prim (1999)

Site	pH	T (°C)	Alkalinity	Acidity	Sulfate	Chloride	Na	K	Ca	Mg	Fe	Mn	Al
1	6.7	25	24	31	65	14	12.5	2.6	19.6	7.8	0.46	0.98	<0.1
2	6.8	24	24	14	40	<5	5.4	1.4	10.0	5.4	0.29	0.10	<0.1
3	5.8	25	0	5	39	<5	5.0	1.0	8.3	4.4	0.25	0.04	0.2
4	6.4	22	24	16	38	<5	5.5	1.4	9.4	4.9	0.34	0.24	0.1
5	6.7	25	0	48	38	<5	5.0	1.2	8.0	4.0	0.08	0.06	0.1
6	6.4	24	24	24	21	<5	3.9	1.4	6.0	4.0	0.92	2.27	0.2
7	6.8	25	20	20	26	<5	4.0	1.4	7.0	4.0	0.02	0.13	0.1
8	6.7	19	16	10	38	<5	3.8	1.2	6.9	3.4	0.05	1.99	<0.1

Site locations shown in Fig. 1. Alkalinity and acidity are in milligrams of $CaCO_3$/l, and other ions in milligrams/liter

released using a buffered acetic acid/sodium acetate solution.

3. Reducible fraction (Fe and Mn oxides) (SQ-3): Hydroxylamine hydrochloride in 25% acetic acid at a pH of 2 was used.
4. Oxidizable fraction (organic matter and sulfides) (SQ-4): Hydrogen peroxide in a dilute nitric acid solution at pH 2 was applied. Ammonium acetate was added to prevent adsorption of the dissolved metals onto the oxidized sediment.
5. Residual fraction (SQ-5): These are metals present in the crystalline lattice of the primary and secondary minerals. Digestion with strong acids, such as HF, $HClO_4$, HCl, and HNO_3, was done.

1.3 Chironomidae and Oligochaeta Ecology and Metal Pollution

Most chironomid larvae (insect Order Diptera) are not restricted to a specific mode of feeding, but the most common feeding mode for *Chironomus* sp. larvae is reported to be deposit feeding in the upper 1–2 cm of subaqueous sediment, up to a depth of 10 cm, in which they feed on recently deposited material (McCall and Tevesz 1982; Berg 1995). Chironomids living in muddy lake sediments typically build burrows in a variety of different shapes, which they irrigate with oxygenated surface water by undulations of their bodies (McCall and Tevesz 1982; Berg 1995). *Chironomus* sp. larvae are also known to filter feed, which includes construction of catchnets from salivary silk secretions across their burrows to catch particulate matter that is carried by the current induced by their body undulations (McCall and Tevesz 1982; Berg 1995). Hence, the feeding habits of chironomids occur primarily in the oxidized zone of the sediment, and they are exposed to the overlying surface water due to their burrow irrigation.

However, chironomid larvae can tolerate low oxygen conditions, low pH, and high iron concentrations (Roback 1974). *Chironomus* sp. from acidic lakes retain different concentrations of metals depending on the instar age of the larvae, with older larger specimens having high Fe, Al, and Ca concentrations. On the other hand, Zn, Cd, and Ni concentrations are lower in older larvae, and Cu and Mn concentrations do not change with larval age. These patterns were all attributed to body size and the changing ability to eliminate or absorb certain metals as the larvae grew, and metabolic needs changed.

Tubificid oligochaetes (Phylum: Annelida) feed primarily in the top 2–8 cm (Davis 1974; Fisher et al. 1980; McCall and Fisher 1980; McCall and Tevesz 1982) but can bioturbate up to the top 20 cm of sediment (McCall and Tevesz 1982). The feeding habit of tubificid oligochaetes is termed as "conveyor belt" feeding, in which they feed at depth in the reduced areas with their head in the substratum and have their posterior portion above the sediment surface, where they respire and defecate (McCall and Fisher 1980; Matisoff 1995). In this way, tubificid oligochaetes are recognized as connecting the reduced zone to the oxidized zone (McCall and Fisher 1980) with more contact with the reduced zone of the sediment and the pore water, and less contact with the overlying water.

Oligochaetes are tolerant of organic pollutants but are less tolerant of heavy metal pollutants in comparison to crustaceans (Brinkhurst and Cook 1974); *L. hoffmeisteri*, however, can adapt to very high levels of Cd and Ni (Klerks and Levinton 1989; Klerks and Bartholomew 1991) with this ability related to genetic architecture (Martínez and Levinton 1996). The uptake of Cr by this tubificid was found experimentally to increase with the metal concentration of the sediment as well as exposure time (Flores-Tena and Martínez-Tabche 2001). A comparison of the metal concentrations of pore waters versus sediment to concentrations in these benthic organisms may shed light on metal transfer from the lake environment into its food chain.

2 Methodology

2.1 Sample Sites and Water Sampling

Seven sampling sites in Lake Hope were selected in offshore areas (Fig. 1) of low energy with fine-grained particle deposition in order to obtain more homogenous samples. The sampling sites were chosen specifically to investigate the evolution of the water and sediments along the water path from Sandy Run to the dam. With the exception of site 1, all sample sites were free of vegetation. The vegetation at site 1 was composed primarily of root wads of lily pads. Lake Hope was frozen from approximately late December 2002 until early March 2003. Sampling began on March 18, 2003, approximately 1 week

after the lake thawed, and ended April 8, 2003. Water samples were collected within approximately 0.3 m above the sediment–water interface (benthic waters). Two hundred fifty-milliliter filtered (0.45 μm) and unfiltered samples, two each, were collected from the composite sample at each site. One filtered and one unfiltered sample each was acidified with 50 drops of 4 N nitric acid. These samples were used for metal analysis. The non-acidified samples were used for analysis of alkalinity, acidity, sulfate, and chloride.

2.2 Sediments and Pore Waters

A MUCK corer (a trigger gravity corer designed by K. Kelts at the University of Minnesota) was used to collect three sediment cores at each site, collecting up to 20–30 cm of fine-grained sediment (Fig. 1). Samples were refrigerated until analysis. The top 5 cm of sediment of each of the three cores were separated and mixed. Half of the sediment was reserved for sequential extraction and for total metal analysis, and the other half of the sediment was placed into acid-cleaned centrifuge tubes and centrifuged for 30 min to extract the pore water. Pore water was decanted, filtered, and then acidified for metal analysis.

A nitric acid-hydrochloric acid digestion was used for digestion of pore water samples. Sediment samples were digested using the EPA method 3050B for total metal analysis (USEPA 1995). Five operationally defined fractions were sequentially extracted using 1 g of dried sediment, following the procedure used by Gunn et al. (1988). Concentrations of Al, Cd, Co, Cu, Cr, Fe, Mn, Ni, Pb, and Zn in sediments and pore water were measured by inductively coupled plasma mass spectrometry. Percent organic matter was determined using the loss on ignition method. Particle size distribution was analyzed by wet sieving to determine the percentage of sand and silt/clay. Before wet sieving, organic matter in the sediments was broken down by treatment with hydrogen peroxide, and aggregates were dispersed by agitation with distilled water and Calgon™.

2.3 Macroinvertebrates

To collect the benthic macroinvertebrates, large surficial samples of sediment were taken with an Ekman dredge in order to obtain sufficient numbers of benthics for trace metal analysis. Sediment was sieved through a 595-μm sieve, and macroinvertebrates were collected from the sieve and transferred to containers with lake water, which were then placed on ice for transport back to the laboratory.

In the lab, macroinvertebrates were separated into groups of *Chironomus* sp. and tubificid and possibly lumbriculid oligochaete worms, as these were the only organisms found in sufficient quantities for metal analysis. They were placed into Petri dishes with distilled water for 48 h in order to purge their digestive systems of sediment. The Petri dishes were changed regularly to prevent coprophagy. The macroinvertebrates were then frozen until acid digestion. In addition, representative specimens isolated for metal analysis and other fauna not found in sufficient quantities for metal analysis were placed in 70% ethyl alcohol for identification.

Approximately 500 mg of frozen macroinvertebrates (oligochaetes or *Chironomus* sp.) was placed in preweighed, acid-washed digestion tubes. This resulted in one to three replicate samples per site. Macroinvertebrates were digested according to the methodology of Newman (1996). They were then dried at 105°C for 1 h, and dry weight was recorded. Five milliliters of concentrated, ultraclean nitric acid was added to each tube. The tubes were then covered and allowed to sit for 1 h at room temperature in order to predigest the tissue.

3 Results

3.1 Anions in Benthic Waters

The analysis of acidity, alkalinity, sulfate, and chloride in the benthic waters (Table 2) produced values that were random and did not have a definite statistically significant trend, with values ranging from 6.7 to 11.1 (average, 8.8) and 4.2 to 5.8 mg (average, 5.2) CaCO3/l, for acidity and alkalinity. Sulfate and chloride ranged from 39 to 45 (average, 42) and 6 to 20 mg/l (average, 13), respectively. The pH of the waters was slightly acidic varying from 5.5 to 6.2 (average, 5.8). The spatial trends that Prim (1999) observed for the waters were not present at the time of sampling for this study. The values for pH, alkalinity, acidity, and sulfate were also slightly lower in this work than the values obtained by Prim in 1999. This difference was attributed to the diluting effects of

Table 2 Acidity, alkalinity, pH, and anions in filtered benthic water of Lake Hope

Site	1	2	3	4	5	6	7
Acidity	11.1	8.6	6.7	9.9	8.0	9.4	8.2
Alkalinity	4.4	4.2	6.4	5.3	5.3	4.8	5.8
pH	5.9	6.0	5.5	5.7	5.9	6.2	5.7
Sulfate	45	44	38	43	42	39	45
Chloride	20	14	9	4	20.	16	6
Dissolved O_2	9.5	8.0	7.7	7.4	6.7	6.5	5.7
Temp. (°C)	9.9	11.3	3.9	4.3	5.8	6.4	5.3

Concentration units for acidity and alkalinity are in milligrams of $CaCO_3$/l. Sulfate, chloride, and oxygen are in milligrams/liter

the winter melt waters reaching Lake Hope in March, as well as seasonal variations in the influx of contaminants, surface water flow, and groundwater to the lake. Prim's data were taken during the summer (June 1998), when precipitation inputs were lower in this region due to higher evapotranspiration (Pigati and López 1999). Note that the water column in this study was relatively oxygenated at all depths, but with a decrease in dissolved oxygen towards the dam.

3.2 Heavy Metals

3.2.1 Benthic and Pore Waters

Benthic and pore water concentrations are presented in Table 3. Heavy metal concentrations are listed in Fig. 2a for the benthic waters and Fig. 2b for the pore waters. For the seven sites, in order of decreasing average concentrations, the metals in the benthic waters of Lake Hope followed the trend: Mn>Fe>Al>Zn>Cu>Cr>Ni>Pb~Co. In a similar way for the pore waters, the average metal concentrations followed the trend: Mn>Fe>Al>Zn>Cu>Ni>Pb≈Cr>Co. The higher concentration ions (Mn, Fe, Al, Zn, and Cu) followed the same trend in both waters. Only Ni, Cr, and Pb presented a different position in both waters. Co was the lowest concentration metal in the two cases. Cd was not detected in both waters.

The numbers on top of the bars of Fig. 2 refer to the sampling sites in Fig. 1. Al, Mn, Fe, Co, Cu, and Zn showed a decrease in concentration in site 3 (Fig. 2a), at the confluence of Lake Hope with Keaton Hollow stream (Fig. 1), suggesting dilution by the water input of this stream. The concentrations of the pore waters were significantly higher than the concentrations of the benthic waters (Fig. 2a, b). The spatial trends in concentrations in the pore waters were also different. Al presented an increasing trend from sites 1 to 7, as well as Fe, Co, and Ni. These increasing correlations were statistically significant at a confidence level higher than 95% (Spearman's test).

Metal concentrations in the water column were compared to the Ohio Water Quality Criteria for the Protection of Aquatic Life and the USEPA National Recommended Water Quality Criteria. Of all the heavy metals in the benthic waters, only Cu (range from 1.2 to 11.6 μg/l) exceeded the Ohio Water Quality Criteria for the Protection of Aquatic Life (4.95 μg/l), the USEPA National Recommended Water Quality Criteria Maximum Concentration (7 μg/l), and the Criteria Continuous Concentration (4.95 μg/l).

3.2.2 Sediments

Organic matter percentage varied from 9.2% to 11.1%. Site 1 had the highest percent organic matter, and site 2 had the lowest percent organic matter. After the low value at site 2, percent organic matter increased with proximity to the dam. Site 1 was the only site where vegetation was prominent on the substrate. For the seven sample sites, the clay fraction (<63 μm) comprised 97.1% to 100.0% of the sediment. Sand fractions were minor, only representing greater than 1% of sediment at site 2.

Table 4 lists the total elemental concentration recovered in the five sequential extraction steps, and the distribution of the elements among the five sequential extraction steps is recorded in Table 5. Several observations about the total sediment metal concentrations presented in Table 4 and Fig. 3a can be summarized:

(a) The concentrations were from highest to lowest: Al>Fe>Mn>Zn>Ni≈Cr>Co≈Cu>Pb>Cd. Al and Fe concentrations were relatively close in value at each site. This sequence for the four higher concentration metals was different in comparison to the pore and benthic waters. Al was the most abundant metal in the total sediment, but Mn dominated in the benthic waters and pore waters.

Table 3 Metal concentrations in benthic and pore water of Lake Hope sediments. Pore water was separated from sediments by centrifugation, and then filtered and acidified. Concentrations in micrograms per liter

	Site 1	Site 2	Site 3	Site 4	Site 5	Site 6	Site 7
Benthic water							
Al	12.3±1.2	24.5±2.4	13.6±1.3	14.8±1.4	14.3±1.4	13.7±1.3	10.1±1
Pb	0.6±0.1	0.3±0	0.4±0	0.2±0	0.3±0	0.3±0	0.6±0.1
Cr	5.9±0.5	1±0.1	3±0.2	2.1±0.2	5.7±0.4	5.3±0.4	6.1±0.5
Mn	832±66	571±45	371±29	550±44	718±57	663±52	731±58
Fe	40.4±3.5	43±3.7	20.6±1.8	20.8±1.8	41.9±3.6	33.8±2.9	38±3.3
Co	0.7±0.1	0.3±0	0.3±0	0.3±0	0.4±0	0.3±0	0.4±0
Ni	3.7±0.3	1.4±0.1	2±0.2	1.6±0.1	3.5±0.3	3.4±0.3	3.5±0.3
Cu	11.6±1	7.8±0.7	2.6±0.2	4.1±0.3	4.7±0.4	1.2±0.1	2.7±0.2
Zn	9.8±0.8	9.5±0.7	8.6±0.7	8.2±0.6	6.9±0.5	3.8±0.3	6.1±0.5
Cd	BDL	BDL	BDL	BDL	BDL	BDL	BDL
Pore water							
Al	25.6±3.2	86.9±11	196±25	462±58	711±90	875±112	886±114
Pb	1.3±0.2	0.6±0.1	2.2±0.3	2.2±0.3	1.3±0.2	1.1±0.1	1.3±0.2
Cr	1.3±0.1	0.6±0.1	0.9±0.1	1.1±0.1	2.3±0.2	1.3±0.1	1.6±0.2
Mn	7,340±794	4,020±434	4,530±490	4,110±445	6,950±752	4,730±512	7,450±806
Fe	90.2±10.4	192.4±22.2	72.5±8.4	754.1±86.9	1,164±134	1,189±137	2,076±239
Co	0.5±0.1	0.2±0	0.8±0.1	1±0.1	1.2±0.1	0.8±0.1	2.2±0.2
Ni	0.9±0.1	1.3±0.1	2.2±0.2	2.1±0.2	3.1±0.3	2±0.2	2.8±0.3
Cu	10.4±1.2	7.4±0.8	8.3±0.9	11.9±1.3	12.9±1.5	7.5±0.8	10±1.1
Zn	9.7±1	9.4±1	26.6±2.9	22.8±2.5	13.5±1.5	13.7±1.5	9.8±1.1
Cd	BDL	BDL	BDL	BDL	BDL	BDL	BDL

BDL below detection limit

(b) All metal concentrations in the sediments except for Cd were positively correlated with distance from Sandy Run at confidence levels higher than 95% (Spearman's test). Fe, Co, Ni, and Cu all exhibited a small decrease in concentration at site 3, probably due to the input of water and sediments from Keaton Hollow.

Sequential extractions 1 to 4 were considered the bioavailable metals (Han et al. 2001; Knox et al. 2006) or metals that were more weakly attached to the solid substrate. The percentages of the five sequential extractions with respect to the total metals in the sediments are in Table 5. The sum of all four sequential extractions concentrations is in Fig. 3b. Several observations are possible with these data and graph:

(a) Over 75% of Al, and Cr; over 50% of Fe; and between 40% to 70% of Ni, Cu, and Pb occurred in SQ-5, the residual phase. The next largest concentration occurred in SQ-3, representing those metals released under reducing conditions or attached to the Mn and Fe oxides and hydroxides. SQ-4 (organic matter fraction) accounted for only 9–14% of the relative concentration of Cu, 3–7% of the relative concentration of Co, and less than 4% for all other metals. Cd was present in the sediments but at low concentrations.

(b) For the bioavailable metals in the sediments, the ions followed the next trend: Fe>Mn>Al>Zn>Ni>Co~Pb>Cu>Cr>Cd. The sequence was similar to the pore and benthic waters for the four metals with higher concentrations, except for Mn, which was the most abundant heavy metal in the waters but not in the sediments. The bioavailable concentration of every heavy metal in the sediments did not present a high variability from sites 1 to 7. However, for the total metals, an increasing spatial trend was observed for Fe, Mn, Al, Zn, Co, and Cr (Fig. 3b), even with a logarithmic graph. Site 3 showed a decrease in concentration for Al, Pb, Cr, Co, Ni, Cu, Zn, and Cd, suggesting dilution of these sediments by the inputs of Keaton Hollow stream.

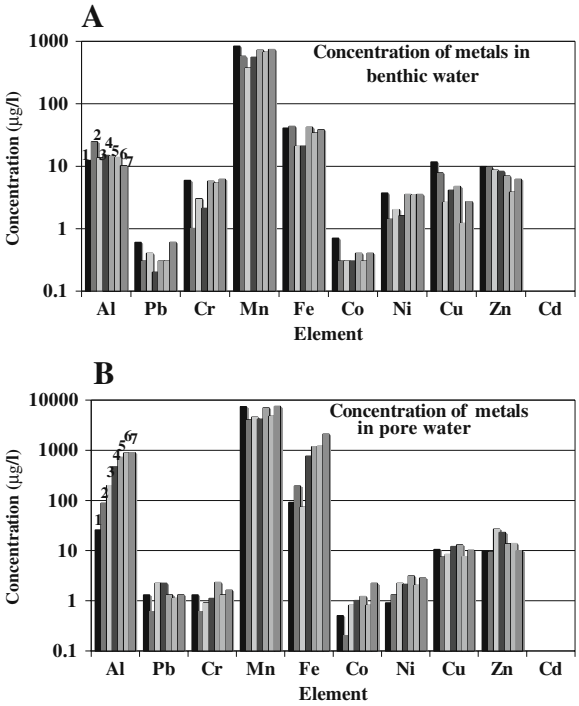

Fig. 2 Composition of heavy metals in (**a**) benthic water and (**b**) pore water of Lake Hope. *Numbers on graph* indicate sampling sites as shown in Fig. 1

In order to assess the degree of contamination of the sediments, metal concentrations of the sediments in this study were compared to sediment criteria utilized historically by the Ohio EPA (OEPA 1992), the New York State Department of Environmental Conservation (NYSDEC 1999), and consensus-based sediment quality guidelines recommended by the USEPA (MacDonald et al. 2000). Cr (range, from 30.5 to 48.4 mg/kg), Cu (range, from 17.0 to 27.1 mg/kg), Fe (range, from 28,990 to 42,730 mg/kg), Mn (range, from 3,107 to 5,111 mg/kg), Ni (range, from 32.9 to 46.2), and Zn (range, from 10 to 157) had sampling points with concentrations higher than at least one of the criteria. Cr, Cu, Fe, Ni, and Zn had values higher than the NYSDEC Lowest Effect Level (26, 16, 20,000, 16, and 120, respectively). Fe had values higher than the NYSDEC Severe Effect Level (40,000), and Cr, Ni, and Zn were higher than the USEPA Threshold Effect Concentration (43.4, 22.7, and 121, respectively).

3.2.3 Macroinvertebrates

The composition of heavy metals in the benthic macroinvertebrates of Lake Hope was assessed. The following fauna were identified in the sediments: for the order Diptera and family Chironomidae: *Chironomus* sp., *Cryptochironomus* sp., *Procladius* sp., *Ceratopogon* sp., *Sphaeromias* sp., and *Chaoborus* sp., and for the order Oligochaeta and family Tubificidae: *Branchiura sowerbyi* and *Limnodrilus claparedeianus*. However, only *Chironomus* sp. and Oligochaeta were selected for metal analysis because of their relative abundance in the sediments. These macroinvertebrates were not present in all the sites. *Chironomus* sp. was present only at sites 1, 3, 4, and 5, and Oligochaeta only at sites 2, 3, 5, 6, and 7. The concentrations of the different heavy metals in *Chironomus* sp. and Oligochaeta are presented in Tables 6 and 7 and Fig. 4a, b. On average, the concentrations of heavy metals found in Oligochaeta were higher for Mn, Fe, and Co and lower for Al, Pb, Cu, Cr, Ni, Cd, and Zn than for *Chironomus* sp. The

Table 4 Metal concentrations in sediments of Lake Hope in milligram per kilogram sediment

	Site 1	Site 2	Site 3	Site 4	Site 5	Site 6	Site 7
Al	29,220±3,180	31,500±3,420	30,640±3,330	38,730±4,200	37,590±4,080	48,820±5,300	46,520±5,050
Pb	13.9±1.5	14.6±1.6	14.2±1.6	17±1.9	17.3±1.9	21.6±2.3	20.8±2.3
Cr	30.5±1.6	32.4±1.7	32.3±1.7	37.9±2	37.5±2	48.4±2.5	45.7±2.4
Mn	3,107±94	3,345±101	3,595±109	3,503±106	3,601±109	5,062±153	5,111±154
Fe	28,990±1,320	32,460±1,470	29,920±1,360	33,950±1,550	35,550±1,620	42,730±1,940	42,620±1,940
Co	18.4±1.2	19.6±1.3	16.7±1.1	19±1.3	19.3±1.3	23.9±1.6	23.6±1.6
Ni	35±2.7	36.5±2.8	32.9±2.6	37.4±2.9	37.3±2.9	46.2±3.6	45.3±3.5
Cu	17.8±1.8	18.2±1.8	17±1.7	21.1±2	20.9±2	27.1±2.4	25.3±2.3
Zn	102±10	124±11	101±10	127±11	130±12	155±14	157±14
Cd	0.37±0.08	0.52±0.09	0.26±0.07	0.29±0.07	0.31±0.07	0.43±0.08	0.39±0.08

Table 5 Percent of total elemental concentration recovered in the five sequential extraction steps

	Site 1	Site 2	Site 3	Site 4	Site 5	Site 6	Site 7
Pb							
1-SQ	11.7%	0.7%	0.6%	0.6%	0.5%	0.5%	0.7%
2-SQ	5.0%	6.2%	3.8%	6.7%	3.5%	4.8%	3.4%
3-SQ	43.6%	44.8%	41.7%	45.5%	46.5%	46.7%	41.6%
4-SQ	0.1%	0.2%	0.2%	0.2%	0.2%	0.2%	0.2%
5-SQ	39.5%	48.0%	53.8%	47.1%	49.3%	47.8%	54.1%
Cr							
1-SQ	BDL	BDL	BDL	BDL	BDL	BDL	BDL
2-SQ	1.3%	0.6%	0.4%	0.8%	0.9%	1.1%	0.8%
3-SQ	13.7%	12.5%	11.1%	12.1%	12.5%	12.3%	9.3%
4-SQ	3.5%	2.4%	2.2%	1.7%	2.0%	2.2%	1.8%
5-SQ	81.5%	84.6%	86.3%	85.4%	84.6%	84.4%	88.1%
Mn							
1-SQ	29.7%	30.1%	39.3%	33.4%	32.6%	43.6%	41.9%
2-SQ	21.7%	21.7%	19.6%	26.4%	24.3%	22.4%	21.8%
3-SQ	25.4%	22.4%	20.4%	19.1%	22.2%	17.7%	16.5%
4-SQ	1.1%	0.8%	0.7%	0.7%	0.8%	0.7%	0.6%
5-SQ	22.1%	25.1%	20.1%	20.4%	20.1%	15.7%	19.2%
Fe							
1-SQ	0.0%	0.0%	0.0%	0.0%	0.0%	0.0%	0.0%
2-SQ	2.6%	3.1%	2.9%	3.7%	3.6%	4.6%	3.5%
3-SQ	39.5%	32.8%	33.8%	35.1%	40.6%	37.1%	32.3%
4-SQ	2.0%	0.7%	0.6%	0.5%	0.6%	0.6%	0.6%
5-SQ	55.9%	63.4%	62.7%	60.7%	55.2%	57.6%	63.6%
Co							
1-SQ	BDL	BDL	BDL	BDL	BDL	BDL	BDL
2-SQ	7.9%	9.9%	11.1%	12.3%	10.9%	13.1%	11.1%
3-SQ	53.4%	51.9%	48.4%	50.8%	53.5%	51.3%	47.0%
4-SQ	6.6%	4.1%	3.5%	3.1%	3.1%	3.8%	3.6%
5-SQ	32.1%	34.2%	37.0%	33.8%	32.5%	31.7%	38.3%
Ni							
1-SQ	1.8%	1.6%	1.8%	1.4%	1.4%	2.0%	1.5%
2-SQ	9.9%	8.4%	7.4%	8.7%	8.5%	8.3%	6.9%
3-SQ	36.7%	36.1%	31.1%	31.8%	33.7%	30.9%	27.9%
4-SQ	3.9%	3.8%	3.0%	2.5%	2.7%	3.3%	3.0%
5-SQ	47.7%	50.1%	56.7%	55.5%	53.6%	55.5%	60.7%
Cu							
1-SQ	5.5%	7.8%	3.0%	14.7%	6.9%	4.0%	9.5%
2-SQ	7.6%	1.0%	0.6%	3.7%	4.5%	2.9%	2.4%
3-SQ	33.5%	18.4%	22.7%	17.6%	18.7%	16.2%	10.4%
4-SQ	14.3%	10.7%	9.3%	9.9%	10.3%	12.5%	9.9%
5-SQ	39.0%	62.0%	64.4%	54.2%	59.5%	64.4%	67.9%
Zn							
1-SQ	1.5%	1.5%	1.4%	1.5%	1.2%	0.9%	1.4%
2-SQ	8.0%	8.1%	8.1%	10.0%	10.6%	10.6%	8.8%
3-SQ	49.5%	46.3%	42.3%	46.3%	47.5%	47.9%	42.3%
4-SQ	3.6%	4.2%	2.7%	2.2%	2.3%	2.6%	2.5%
5-SQ	37.5%	39.9%	45.4%	40.1%	38.3%	37.9%	44.9%
Cd							
1-SQ	12.8%	7.7%	5.0%	7.9%	7.8%	4.8%	9.1%
2-SQ	20.2%	12.7%	0.7%	9.8%	25.5%	18.5%	16.2%
3-SQ	34.4%	38.9%	47.5%	38.6%	33.6%	39.2%	33.4%
4-SQ	0.7%	1.3%	0.1%	0.5%	0.8%	0.7%	0.1%
5-SQ	31.9%	39.4%	46.7%	43.3%	32.4%	36.8%	41.2%

The sum of the five steps is used as the total elemental concentration

BDL below detection limit

concentrations were higher at sites 1 and 3 and lower at sites 4 and 5 for *Chironomus* sp. for all the metals except Co. For Oligochaeta, the concentrations were more variable with Al, Pb, Fe, Ni, and Cu, higher at

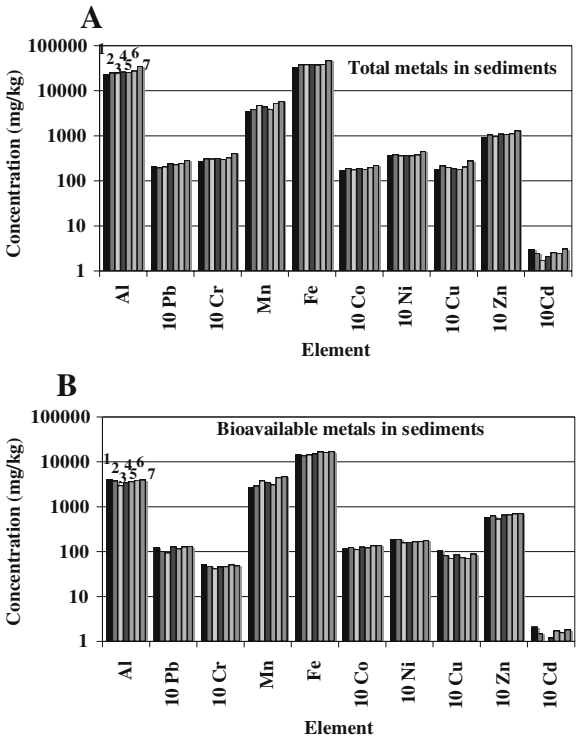

Fig. 3 **a** Total concentration of heavy metals in sediments and (**b**) bioavailable concentration of heavy metals in sediments of Lake Hope. *Numbers on graph* indicate sampling sites as shown in Fig. 1

Table 6 Metal concentrations in oligochaetes at Lake Hope

	Oligochaeta				
	Site 2 $n=1$	Site 3 $n=3$	Site 5 $n=2$	Site 6 $n=2$	Site 7 $n=2$
Al	127±15	130±14	340±40	790±93	81±11
Pb	1.38±0.16	1±0.12	1.34±0.18	2.5±0.32	1.3±0.17
Cr	0.251±0.038	0.166±0.026	0.38±0.06	1.6±0.2	0.76±0.09
Mn	360±32	207±18	170±16	260±25	71±6
Fe	919±88	1,160±108	920±94	1,500±152	520±53
Co	1.16±0.11	1.15±0.1	0.76±0.08	0.94±0.1	1.3±0.13
Ni	0.73±0.08	0.397±0.047	1±0.12	1.7±0.2	0.57±0.08
Cu	11.5±1.2	12.5±1.2	15±2	15±2	13±1
Zn	39.6±3.7	35.3±3.2	36±4	34±4	32±3
Cd	0.08±0.01	0.06±0.01	0.03±0	0.08±0.01	0.23±0.02

Sufficient biomass for metal analysis was found only at sites 2, 3, 5, 6, and 7. Units are in milligrams per kilogram

site 6. Comparison of Fig. 4a, b with Fig. 2a, b and Fig. 3b allowed the following observations:

(a) For the four heavy metals with higher concentration in both benthic animals, the concentrations followed the next trend: Fe>Al>Mn>Zn which was similar to the bioavailable metals in the sediments rather than the pore or the benthic water where Mn was the most abundant heavy metal.
(b) The heavy metals Cu, Pb, Ni, Cr, Co, and Cd did not follow similar trends in the waters, sediments, and macroinvertebrates. However, in all the samples, those metals presented the lower concentrations in comparison with Fe, Al, Mn, and Zn. In addition, Cd was the lowest in

Table 7 Metal concentrations in *Chironomus* sp. in Lake Hope

	Chironomus sp.			
	Site 1 $n=1$	Site 3 $n=1$	Site 4 $n=2$	Site 5 $n=2$
Al	1,200±135	270±32	100±12	140±18
Pb	1.5±0.2	3.5±0.4	1±0.1	1.8±0.2
Cr	2.4±0.3	0.56±0.08	0.2±0.04	0.28±0.05
Mn	92±9	140±13	65±6	60±5
Fe	470±50	910±93	400±40	430±43
Co	0.26±0.03	0.26±0.03	0.32±0.04	0.18±0.02
Ni	1.9±0.2	0.68±0.09	0.36±0.05	0.72±0.09
Cu	16±2	44±5	17±2	16±2
Zn	140±14	47±5	34±3	35±4
Cd	0.4±0.04	0.38±0.03	0.2±0.02	0.26±0.02

Sufficient biomass for metal analysis is found only at sites 1, 3, 4, and 5. Units are in milligrams per kilogram

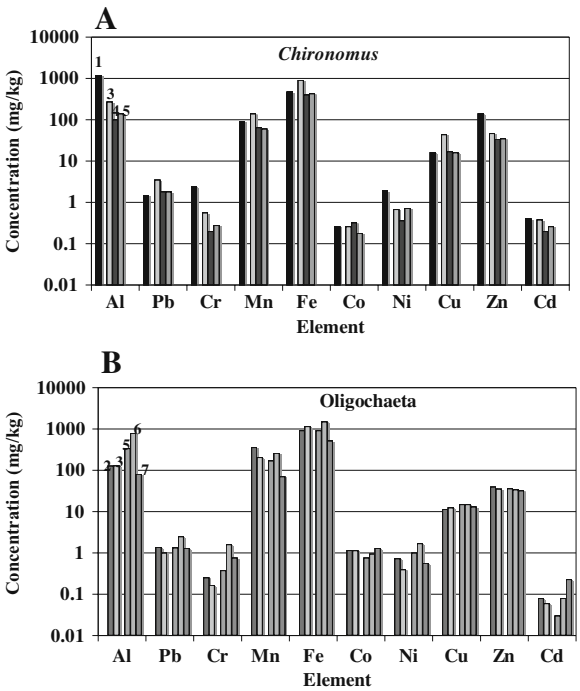

Fig. 4 Composition of heavy metals of (**a**) *Chironomus* sp. and (**b**) Oligochaeta in Lake Hope. *Numbers on graph* indicate sampling sites as shown in Fig. 1

concentration, except for *Chironomus* sp. who had Co in lowest concentration followed by Cd.

3.2.4 Bioconcentration and Bioaccumulation Factors

Bioconcentration factors (BCF; concentration in organism/concentration in pore water) and bioaccumulation factors (BAF) for sediments (concentration in organism/concentration in sediments) are graphed in Fig. 5a–d. Trends among metal concentrations of the oligochaetes and chironomids in Lake Hope differed greatly, illustrating the biologic variability among species in metal regulation.

For chironomids, the BAF and BCF values for Al, Cr, Ni, and Zn followed a pattern in which these metals peaked at site 1, and then decreased in value until site 4 or 5. Cu, Pb, Fe, and Mn followed a different trend for chironomid BAF and BCF, with a peak at site 3, and the lowest value generally occurred at site 4 or 5. Co followed a different pattern than both groups of metals with the peak value at site 1 for BCF, but not for BAF. Trends for oligochaetes were less clear, but in general, values for BCF and BAF for all metals tended to be highest either at site 2 or 6 where both were close in value. Mn generally exhibited a decreasing trend with distance from Sandy Run, with the exception of a minor peak at site 6 in both BCF and BAF.

The average BCF for *Chironomus* sp. followed the decreasing order of Al>Fe>Zn>Cu>Pb>Ni>Cr>Co>Mn, and for the Oligochaeta, the order was Fe>Co>Zn>Cu>Pb>Al>Cr>Ni>Mn. Even when Mn was the highest concentration heavy metal in the waters, it was the lowest to bioconcentrate in the organisms. The BAFs for the organisms and the sediments presented higher values for Cd, Cu, Zn, and Pb for both animals and lower values for the other metals. The more abundant heavy metals in the sediments were Fe, Al, and Mn, but they were not the highest to bioaccumulate in the organisms. Cd, the lowest concentration metal in the sediments, had one of the highest BAFs.

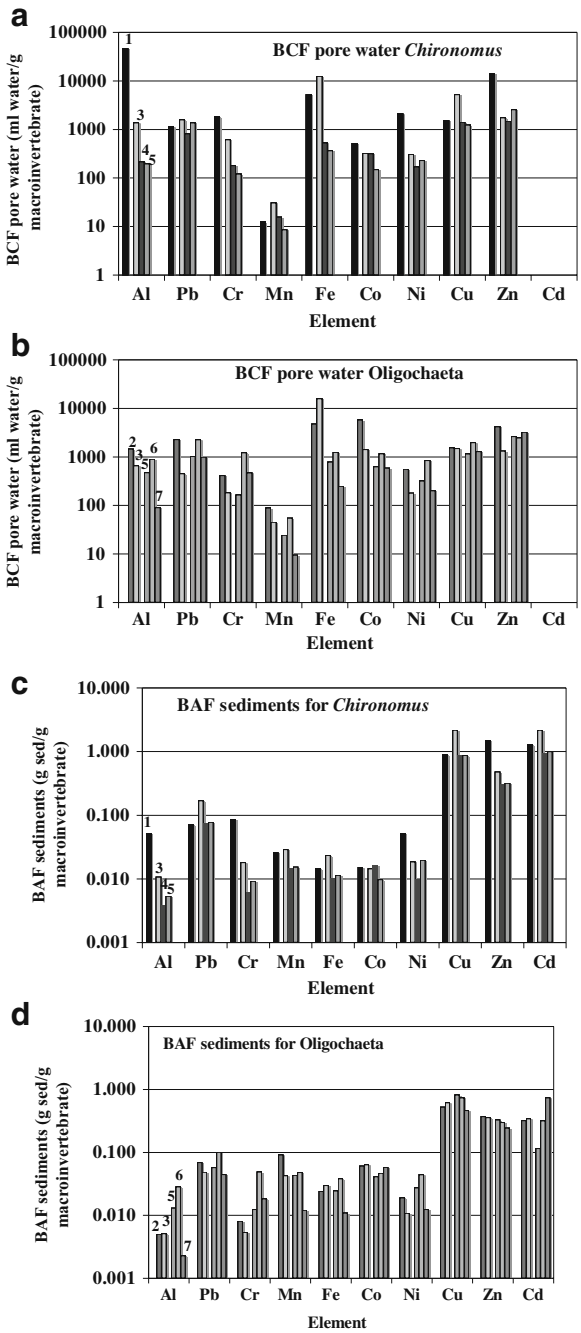

Fig. 5 Bioconcentration factors for (**a**) *Chironomus* sp. and (**b**) Oligochaeta, and bioaccumulation factors for (**c**) *Chironomus* sp. and (**d**) Oligochaeta in Lake Hope. *Numbers on graph* indicate sampling sites as shown in Fig. 1

4 Discussion

4.1 Sediment and Pore Water Chemistry

Other studies have documented gradients along elongated reservoirs and lakes in which clay and/or silt fractions and chemical constituents such as metals, phosphorus, or organic carbon increased with either increasing distance from the main inlet, increasing depth, or both (e.g., Sager and Pucsko

1991; Timmermans et al. 1991; Reynolds 1999). Compared to lakes, reservoirs typically have an elongated geometry; they are shallow near the inlet with a regularly increasing depth towards the dam (Morris and Fan 1998). Lake Hope fits the description of reservoir zonation in that it occupies a well-defined stream valley, with the majority of the overland flow coming from Sandy Run and Habron Hollow in the upper reaches of the lake (see Fig. 1). The depth of Lake Hope gradually increased with proximity to the dam, favoring the accumulation of fine sediments. The structure of Lake Hope promoted the development of a longitudinal gradient.

AMD waters discharging from the mine complex in the headwaters of Sandy Run are rich in Fe, Mn, and Al (Hughes 1999). As pH rises due to neutralization, precipitates of Fe, Al, and Mn minerals form, such as Al hydroxides and Fe and Mn oxides and hydroxides in colloidal form. At low pH, these colloids have a net positive surface charge. As pH increases, it reaches the point of zero charge for each hydroxide (net charge equal to zero). For pH higher than the point of zero charge, the more abundant oxydril produces colloids with a negative charge. The net negative electric charge on the particles surface attracts cations, such as heavy metals (Krauskopf and Bird 1995). Mechanisms for the incorporation of heavy metal cations into colloids include co-precipitation and sorption (Stumm and Morgan 1996). Several researchers have demonstrated that the precipitation of iron and manganese hydroxides incorporates other heavy metals into the produced colloids (e.g., Hem and Skougstad 1960; Webster et al. 1998; Butler 2006). This mechanism explains why the increased concentration of Fe in the sediments of Lake Hope produced increasing concentrations of heavy metals, as illustrated in Fig. 3a. The lake from Sandy Run to the dam increased in depth (Table 2), but the oxygen levels in the benthic water decreased slowly toward the dam. However, the sediments closer to the dam could be more reducing at depth. The increasing concentration of Fe in the pore waters closer to the terminal dam can be explained by the partition coefficient between sediments and pore water that required higher concentration in the pore water as the concentration in the sediments increased. In addition, a greater release of Fe occurred as the conditions became more reducing. The Fe (III) minerals precipitated in more oxidizing conditions released the iron that became partially reduced towards the sediment–water interface.

The relative enrichment of Mn in the waters of Lake Hope contrasted with the waters richer in iron that discharged from the abandoned mines in the upper regions of the watershed (Hughes 1999). However, this behavior can be explained if the relative solubility of Mn and Fe oxides and hydroxides is considered to be a function of pH. Mn is more soluble in slightly acidic to neutral waters than Fe, and a large fraction remains in solution in a neutralized drainage (Kimball et al. 1995; Verplanck et al. 2000). Previous work has shown that even when manganese oxides and hydroxides precipitated from oxidized waters at slightly alkaline pH values, the reaction rates were slower than those of iron (Lind and Hem 1996; Stumm and Morgan 1996). This explains why the benthic and pore waters of Lake Hope had lower Fe than Mn. Most of the Fe precipitated along the path from the mine complexes to the lake in the Sandy Run stream, leaving the waters enriched in Mn.

The precipitation of Mn oxides is slow compared to the precipitation of Fe oxides, even when both reactions are thermodynamically possible (Maynard 2003). The reason for this behavior is that the precipitation of Mn oxides requires the conversion of Mn^{2+} to Mn^{4+}. The kinetics of this reaction is heterogeneous depending not only on the solution species but also on the concentration of previously formed solid manganese oxide (Maynard 2003). Fe oxide surfaces have also the ability to sorb Mn ions from the solution. The formation of Fe oxides is fast at pH values higher than 6. However, the rate of formation of Mn oxides accelerates until pH reaches values higher than 8.5. At Lake Hope, pH values ranged from 5.5 to 6.2, considerable lower than the value needed for fast Mn oxide precipitation. Accordingly, sorption on Fe oxides phases seems to be the possible mechanisms for Mn removal from solution.

Sequential extraction results indicated that the largest concentration of the majority of metals (Al, Cr, Cu, Fe, Ni, and Pb) occurred in SQ-5; these were the least bioavailable and least mobile phase. Total Al concentrations in Lake Hope sediments exhibited a positive correlation with distance from Sandy Run, increasing from 29,220 mg/kg near Sandy Run to as high as 48,820 mg/kg at site 6, near the dam. The only sequential extraction fraction to exhibit a

significant increase in Al concentrations was SQ-5, the lithogenous detrital fraction of the sediment. Aluminum is a component of many clay minerals, and its concentration is highly correlated with the percentage of the fine fraction of sediment (Donoghue et al. 1998). The substantial increase in Al concentrations with proximity to the Lake Hope dam suggested the deposition of more clay particles near the dam. SQ-3, the fraction of sediments sensitive to reducing conditions, accounted for the second highest phase concentration. This high concentration can be attributed to the formation of AMD minerals.

The relatively low concentrations of metals from the organic matter fraction (SQ-4) suggested that this phase did not seem to accumulate a high fraction of metals. This result is surprising due to the well-recognized importance of organic matter in sorbing metals (Horowitz 1991; Bendell-Young and Harvey 1992; Reuther 1999). Cu was the only metal in which SQ-4 accounted for greater than 9% of the total metal concentration of the sediment. Cu was recognized as having one of the highest affinities for organic matter (McBride 1994). The low metal concentrations associated with organic matter could be a seasonal effect. Sampling occurred in the early spring immediately after winter thawing, and organic matter flux due to algal production was likely at a minimum over the winter (Cole 1994; Wetzel 2001). Mn was unique in that SQ-1 accounted for the greatest proportion of Mn in the sediments. Several investigations have found Mn to be highest in the easily exchangeable and/or acido-soluble fraction (SQ-1 and SQ-2, respectively; e.g., Tessier et al. 1979; Van Ryssen et al. 1999).

4.2 Diffusion of Heavy Metals at the Sediment–Water Interface of Lake Hope

The concentrations of heavy metals in the pore waters of Lake Hope were significantly different from the concentrations in the benthic waters, suggesting that diffusion processes should occur between the sediments and the benthic water. The diffusive fluxes of heavy metals at this interface can be calculated using Fick's first law for diffusion (Drever 1997). Since the lake waters were moving relatively slowly compared to river waters, it can be assumed that molecular diffusion was the mechanism responsible for the vertical movement of the ions. The concentration of the heavy metals in the pore water in the upper 5 cm is known, as well as the concentration at around 30 cm above the sediment–water interface. We can assume that the concentrations of the pore water correspond to an average depth of 2.5 cm. In that way, the ions travel 2.5 cm (equal to x_2) within the sediments and 30 cm (equal to x_1) within the benthic water. We can assume that diffusion occurred only in the vertical direction. If C_w is the concentration in the benthic water, C_s is the concentration in the pore water, and C' is the concentration at the sediment–water interface (unknown), then the vertical flux of heavy metal is given by:

$$F = -D'\frac{\mathrm{C}' - \mathrm{C_s}}{\mathrm{x_1}} = -\mathrm{D}\frac{\mathrm{C_w} - \mathrm{C}'}{\mathrm{x_2}} \tag{1}$$

if we assume that the fluxes reaching the interface are the same as those reaching x_1 and vice versa. In Eq. 1, D is the diffusion coefficient in water for the ion, and D' is the diffusion coefficient for the ion in the porous media. We can use the relationship: $D'=D\phi^2$ (Lerman 1988) to find D', where ϕ is the porosity of the sediment.

From Eq. 1 we find that

$$F = -\frac{\frac{D'}{x_1}(C_w - C_s)}{1 + \left(\frac{D'x_2}{Dx_1}\right)} \tag{2}$$

For porosity, Freeze and Cherry (1979) gave a range of 35% to 50% for silt and 40% to 70% for clay. As the sediments were fine and well sorted, a value of 40% was selected for this work.

The diffusion coefficient for each ion at the sampling temperature was calculated by interpolating data at the temperatures of 0°C, 18°C, and 25°C (Li and Gregory 1974). Cr diffusion coefficients were reported only for 18°C and 25°C. The other ions presented a change in slope between 0 and 18 as compared to 18°C and 25°C. For that reason, extrapolation was not possible, and the diffusion coefficient for Cr at 18°C was used. Results of the diffusion coefficients and diffusive fluxes are presented in Table 8 and Fig. 6.

Inspection of the data in Table 8 showed that the fluxes from the different ions can be divided into three types: (1) fluxes that were always positive (upward from the sediments to the benthic water)—these were for Fe, Mn, Al, and Pb (Fig. 6a); (2) fluxes

Table 8 Diffusion coefficients and diffusive fluxes of metals from the pore water to the benthic water in Lake Hope

Diffusive coefficient	Site 1	Site 2	Site 3	Site 4	Site 5	Site 6	Site 7
Diffusion coefficients, units=×E-6 cm^2/s							
Al	2.97	3.05	2.60	2.62	2.71	2.75	2.68
Pb	6.42	6.69	5.29	5.37	5.65	5.77	5.56
Cr	3.90	3.90	3.90	3.90	3.90	3.90	3.90
Mn	4.54	4.75	3.64	3.70	3.92	4.01	3.85
Fe	4.74	4.92	3.93	3.99	4.19	4.27	4.12
Co	4.68	4.86	3.91	3.96	4.15	4.23	4.09
Ni	4.60	4.81	3.70	3.76	3.98	4.07	3.91
Cu	4.77	4.96	3.95	4.00	4.21	4.29	4.14
Zn	4.88	5.10	3.95	4.01	4.25	4.34	4.17
Diffusive flux, units=$\mu g/m^2$day							
Al	0.75	3.60	8.97	22.21	35.81	44.87	44.52
Pb	0.09	0.04	0.18	0.20	0.11	0.09	0.07
Cr	−0.34	−0.03	−0.16	−0.07	−0.25	−0.30	−0.33
Mn	558.90	309.91	286.29	249.10	462.62	308.84	489.23
Fe	4.47	13.93	3.86	55.35	88.96	93.34	158.99
Co	−0.02	−0.01	0.04	0.05	0.06	0.04	0.14
Ni	−0.24	−0.01	0.01	0.04	−0.03	−0.11	−0.05
Cu	−0.11	−0.04	0.43	0.59	0.65	0.51	0.57
Zn	−0.01	−0.01	1.35	1.11	0.53	0.81	0.29

that were negative (downward) for the first two sampling points and then positive for the rest of the lake—these were for Cu, Zn, and Co (Fig. 6b); and (3) fluxes that were negative for the majority of the sampling points—these were for Cr and Ni (Fig. 6c). Cr had negative fluxes for all the sampling points, and Ni only had positive small fluxes for sampling points 3 and 4.

For Fe, Al, Co, and Cu, an increasing trend in the flux can be observed, suggesting that the increased concentration in the solid phase and more reducing conditions closer to the dam promoted the efflux of these ions from the sediments to the pore water and from there to the benthic water. In comparison, the behavior of Pb, Zn, Ni, and Cr was very different from Fe and Al. They presented an initial increase in fluxes (smaller negative fluxes for Ni and Cr), which further decreased (larger negative flux for Ni and Cr) closer to the dam. The variations in pH for the different sampling points at Lake Hope are shown in Fig. 6c. Comparison of the graphs for Pb, Zn, Ni, and Cr suggests that variations in pH could affect the release of these ions from the sediments. The test of significance of the correlation coefficient (Swan and Sandilands 1995) was applied for the fluxes of the different metals and pH. A negative, statistically significant correlation between pH and the fluxes of Pb, Co, Ni, and Zn was concluded with p values equal to 0.001, 0.05, 0.02, and 0.02, respectively. Cr did not show a significant correlation. The negative correlation with pH for these ions suggests that as the pH decreased, the sediments increased the release of these heavy metals to the pore waters, and the fluxes to the benthic zone increased as well.

Sorption as well as dissolution of minerals depended strongly on the pH, with higher sorption partition coefficients at a higher pH (e.g., Young et al. 1992). Cr fluxes were always negative because concentrations in the benthic zone were higher than in the pore waters, and for the first four sampling points (Fig. 6c), the flux seems to be positively correlated with pH, except for points 5 to 7 where the fluxes behaved differently. The behavior for points 1 to 4 can be explained by the higher concentration of Cr in the pore water as the pH decreased, which produced a smaller negative flux. Leaching of Cr from sediments increased with decreasing pH. However, if the Cr (VI) was converted to Cr (III), the solubility decreased, immobilizing Cr in the sediments (Mattuck and Nikolaidis 1996). The behavior

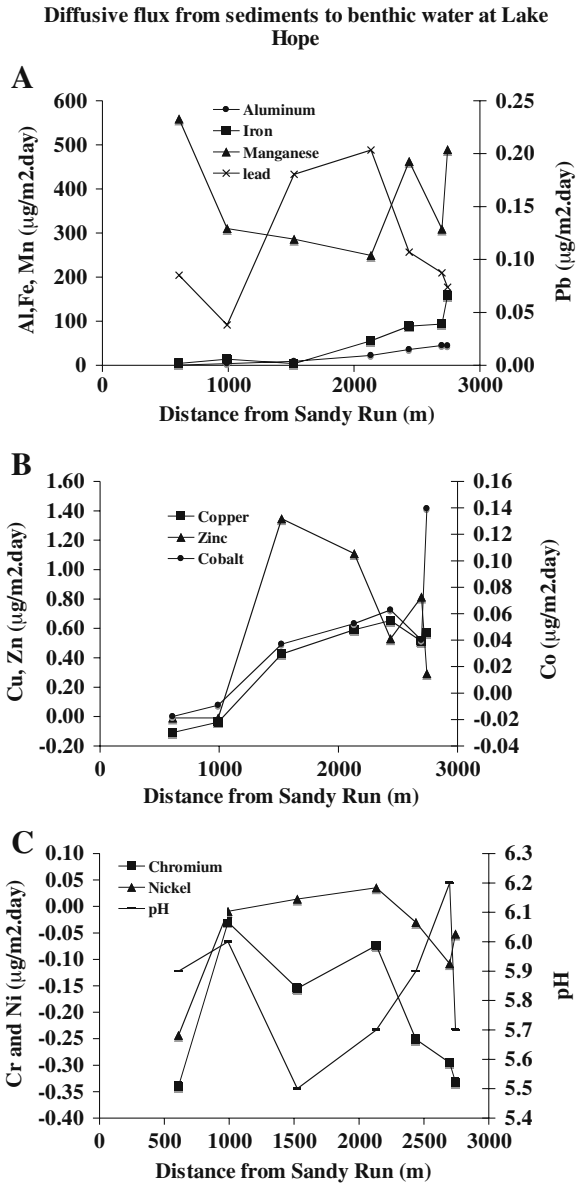

Fig. 6 Vertical diffusive fluxes of metal ions at the sediment–water interface of Lake Hope versus distance from Sandy Run outlet. Positive values indicate fluxes from the sediments to the benthic water and negative fluxes indicate the inverse direction. **a** Fe, Mn, Al, and Pb; (**b**) Cu, Zn, and Co; and (**c**) Cr and Ni as well as the variation of pH in the benthic waters versus distance from Sandy Run outlet

from points 5 to 7 was possibly related to increased reducing conditions that changed the oxidation state and behavior of Cr.

Mn presented a different behavior compared to all the other ions. The fluxes of Mn from the sediments to water decreased from site 1 to 4 and increased from site 5 to 7. The decrease in fluxes from site 1 to 4 corresponded to a general decrease in concentration in the benthic and the pore water along the length of the lake (Table 3), probably because of sorption or co-precipitation in the sediment phase. An increase in concentration occurred from site 5 to 7 in the pore and benthic waters, with a higher increase in the pore waters, explaining the increased positive flux. This increase in concentrations of Mn was probably due to increasing reducing conditions along the lake towards the dam or to possible inputs of Mn-rich groundwater.

4.3 Bioavailability and Macroinvertebrates

Bioavailability is the degree to which a chemical is able to move into or onto an organism (Benson et al. 1994). Routes of exposure to an aquatic organism include uptake from pore water and water above the sediment/water interface, across body walls and respiratory surfaces, as well as ingestion of sediment particles and other food sources (Timmermans et al. 1989; Power and Chapman 1992). Metal uptake may be influenced by the water column above the sediment, which is much more stagnant in lakes and reservoirs than flowing rivers (Bervoets et al. 1998). Upon exposure, organisms may take up bioavailable compounds, which may or may not elicit a measurable biologic effect, such as toxicity, bioaccumulation, or release/elimination (Power and Chapman 1992; Roesijadi and Robinson 1994). A multitude of factors affect the bioavailability of a chemical to an organism, including the chemical and physical composition of the environment and biologic processes, such as feeding habits, living habits, biochemistry, and physiology (Adriano 2001).

Bervoets et al. (1997) found differences among tubificid oligochaete and chironomid larvae bioaccumulation patterns and attributed them to differences in the structural and functional organization of the animals. Differences in feeding behavior and lifestyle are also known to be important factors in bioaccumulation differences (Timmermans et al. 1989; Langston and Spence 1995). Even though the zone of habitation in lake sediment is similar for the oligochaetes and chironomids, differences in their feeding and respiration habits may account for some of the variability in metal accumulation patterns. In general, oligochaetes have less contact with overlying benthic waters than chironomids. Even though lake water above the

sediment was clearly oxic throughout Lake Hope and only slightly lower in the dam area in comparison to the Sandy Run input area (see Table 1), pore waters may have been more reducing and dysoxic (terminology from Potter et al. 2005) at several centimeters depth in the lake sediments. This also potentially could have affected BAFs for the depauperate benthic fauna, especially the oligochaetes when in contact with dysaerobic conditions within the sediment. More testing is needed.

BAFs in the Lake Hope sediments were generally less than 1 g sediment/g macroinvertebrate, indicating a relatively low level of bioaccumulation. Exceptions were Zn, Cu, and Cd for chironomid BAF at site 1, and Cu and Cd for chironomid BAF at site 3. Oligochaetes collected at site 3 had a much lower Cu and Cd BAF than the chironomids. Overall, Zn, Cu, and Cd had the highest BAF for both chironomids and oligochaetes. Cu, Zn, and Cd concentrations in both benthic animals in other studies had the highest BAF among a suite of metals (Chapman et al. 1980; Timmermans et al. 1989, 1992; Reinhold et al. 1999). Radwan et al. (1990) found that for a mixture of macroinvertebrates, including chironomids and oligochaetes, Zn, Mn, and Fe had the highest BAF values, then Cu and Pb, with Co and Cd BAF values ranked lowest of the seven metals. Cu, Zn, Mn, and Fe are essential metals, so some accumulation of these metals was expected to occur.

The magnitude of metal accumulation in Lake Hope sediments was much greater than that in the benthic or sediment pore waters. BAF values near 1 g sediment/g macroinvertebrate indicated that the biota accumulated metals to the same degree as the sediments. BCF values significantly greater than 1 indicated a large difference in the metal concentration of the benthic organisms in relation to the benthic and pore waters. The ingestion of sediment appears to be the major transfer point of metals from the environment into the food chain; exposure to benthic and pore waters does not seem to be an important factor.

5 Conclusions

The benthic waters of Lake Hope did not present concentrations of contaminants higher than the Ohio and USEPA Criteria for Aquatic Life for aquatic life, except for Cu. This metal also presented one of the highest bioconcentration and BAF for the macroinvertebrates analyzed in this work. In comparison, the sediments were contaminated with AMD products as evidenced by the high concentrations of Cr, Cu, Fe, Mn, Ni, and Zn, which ranged above the NYSDEC and/or USEPA criteria. This information is valuable for the use and management of the lake and fishing rules, especially considering the trophic transfer of metals from benthic organisms to fish (e.g., Ng and Wood 2008).

The benthic and pore waters of Lake Hope were higher in Mn than any other heavy metal. The source of Mn in the lake was the AMD discharged from mine complexes located in the upper portions of the watershed. AMD was transported along Sandy Run and discharged into Lake Hope. Possible contributions of alkaline groundwater helped to increase the pH along Sandy Run and Lake Hope. As the pH increased, colloidal particles of Fe, and to some degree Mn hydroxides/oxides, were formed, sequestering the other heavy metals from the waters throughout the process of sorption and co-precipitation. However, as Mn minerals have slower precipitation kinetics than Fe minerals, the water in Lake Hope was enriched in Mn. Sequential extraction results showed that the majority of metals in Lake Hope were in the least geochemically mobile phase or crystalline phases. Fe and Mn oxides/hydroxides were the next most significant phase within the sediments. This suggested the potential for a significant fraction of Pb, Fe, Co, Ni, Cd, and Zn to be released from the sediments under reducing conditions. The concentrations of heavy metals in the benthic waters seem to be the result not only of the water transport of AMD chemicals from Sandy Run but also of the diffusion of ions from or to the benthic waters from or to the sediments. Variations in pH and redox conditions along the lake probably determine the fluxes of heavy metals at the sediment–water interface, with positive fluxes for Fe, Al, Mn, and Pb and negative diffusion at points 1 and 2 as well as further positive fluxes for Cu, Zn, and Co and predominantly negative fluxes for Cr and Ni.

Mn was the most geochemically mobile metal in the sediments of Lake Hope with the potential for release in a variety of environmental processes, such as cation exchange, acidification, and reduction. In comparison, the organic phase in Lake Hope did not seem to accumulate a large fraction of heavy metals,

decreasing the chance of algae transport and deposition as the main processes for heavy metal accumulation close to the dam. Instead, transport and deposition of detrital material from the watershed and AMD products seem to be the responsible processes.

Interspecific and intraspecific variability among the oligochaetes and chironomids appeared to supersede site-specific environmental factors and external bioavailabilities in importance in affecting tissue concentrations. Patterns of bioaccumulation and bioconcentration appeared to be dependent on the biology of the organisms in relation to the bioavailable metals in each part of the lake. For example, even though Cd was not a major metal in the physical environment, it was present in much higher quantities within the tissues of the benthic animals tested. This clearly illustrated the biologic variability among species in metal regulation and tolerance. For the two deposit feeders, the main mechanism for transfer of metals from the environment into the food chain was the ingestion of sediment more than exposure to metal-polluted waters. This was evidenced by BAF values near 1, showing that the organisms accumulated metals to the same degree as the sediments.

Acknowledgments This work was supported by a Baker grant from Ohio University.

References

Adriano, D. C. (2001). *Trace elements in terrestrial environments: Biogeochemistry, bioavailability, and risks of metals* (p. 866). New York: Springer-Verlag.

Bendell-Young, L., & Harvey, H. H. (1992). The relative importance of manganese and iron oxides and organic matter in the sorption of trace metals by surficial lake sediments. *Geochimica et Cosmochimica Acta, 56*, 1175–1186.

Benson, W. H., Alberts, J. J., Allen, H. E., Hunt, C. D., & Newman, M. C. (1994). Synopsis of discussion session on the bioavailability of inorganic contaminants. In J. L. Hamelink, P. F. Landrum, & H. L. Bergman (Eds.), *Bioavailability: Physical, chemical, and biological interactions* (pp. 63–71). Boca Raton: Lewis Publishers.

Berg, M. B. (1995). Larval food and feeding behavior. In P. D. Armitage, P. S. Cranston, & L. C. V. Pinder (Eds.), *The chironomidae: Biology and ecology of non-biting midges* (pp. 136–168). London: Chapman & Hall.

Bervoets, L., Blust, R., de Wit, M., & Verheyen, R. (1997). Relationships between river sediment characteristics and trace metal concentrations in tubificid worms and chironomid larvae. *Environmental Pollution, 95*, 345–356.

Bervoets, L., Solis, D., Romero, A. M., Van Damme, P. A., & Ollevier, F. (1998). Trace metal levels in chironomid larvae and sediments from a Bolivian river: Impact of mining activities. *Ecotoxicology and Environmental Safety, 41*, 275–283.

Brinkhurst, R. O., & Cook, D. G. (1974). Aquatic earthworms (Annelida: Oligochaeta). In C. W. Hart Jr. & S. L. H. Fuller (Eds.), *Pollution ecology of freshwater invertebrates* (pp. 143–156). New York: Academic.

Butler, T. W., II. (2006). Geochemical and biological controls in trace metal transport in an acid mine impacted watershed. *Environmental Geochemistry and Health, 28*, 231–241.

Chapman, P. M., Churchland, L. M., Thomson, P. A., & Michnowsky, E. (1980). Heavy metal studies with oligochaetes. In R. O. Brinkhurst & D. G. Cook (Eds.), *Aquatic oligochaete biology* (pp. 477–502). New York: Plenum Press.

Cole, G. A. (1994). *Textbook of limnology* (4th ed., p. 412). Prospect Heights, IL: Waveland Press, Inc.

Davis, R. B. (1974). Stratigraphic effects of tubificids in profundal lake sediments. *Limnology and Oceanography, 19*, 466–488.

Dills, G., & Rogers, D. T., Jr. (1974). Macroinvertebrate community structure as an indicator of acid mine pollution. *Environmental Pollution, 6*, 239–262.

Donoghue, J. F., Ragland, P. C., Chen, Z. Q., & Trimble, C. A. (1998). Standardization of metal concentrations in sediments using regression residuals: An example from a large lake in Florida, USA. *Environmental Geology, 36*, 65–76.

Drever, J. I. (1997). *The geochemistry of natural waters* (3rd ed., p. 436). New Jersey: Prentice Hall, Upper Saddle River.

Fisher, J. B., Lick, W. J., McCall, P. L., & Robbins, J. A. (1980). Vertical mixing of lake sediments by Tubificid Oligochaetes. *J Geophys Res, 85C*, 3997–4006.

Flores-Tena, F. J., & Martínez-Tabche, L. (2001). The effect of chromium on the hemoglobin concentration of *Limnodrilus hoffmeisteri* (Oligochaeta: Tubificidae). *Ecotoxicology and Environmental Safety, 50*, 196–202.

Freeze, R. A., & Cherry, J. A. (1979). *Groundwater* (p. 604). New Jersey: Prentice Hall, Upper Saddle River.

Gleyzes, C., Tellier, S., & Astruc, M. (2002). Fractionation studies of trace elements in contaminated soils and sediments: A review of sequential extraction procedures. *Trends in Analytical Chemistry, 21*, 451–467.

Gunn, A. M., Winnard, D. A., & Hunt, D. T. E. (1988). Trace metal speciation in sediments and soils. In J. R. Kramer & H. E. Allen (Eds.), *Metal speciation: Theory, analysis, and application* (pp. 261–294). Chelsea, MI: Lewis Publishers.

Han, F. X., Hargreaves, J. A., Kingery, W. L., Hugget, D. B., & Schlenk, D. K. (2001). Accumulation, distribution, and toxicity of copper in sediments of catfish ponds receiving periodic copper sulfate applications. *Journal of Environmental Quality, 30*, 912–919.

Harris, E. F. (1973). Feasibility study, Lake Hope Mine Drainage Demonstration Project 14010 HJQ. US Environmental Protection Agency, Environmental Protection Technology Series, EPA-R2-73-151. 97 pp.

Hem, J. D., & Skougstad, M. W. (1960). *Coprecipitation effects in solutions containing ferrous, ferric, and cupric ions.*

Chemistry of iron in natural water. Geological survey water-supply paper 1459-E. Washington: United States Government Printing Office.

Horowitz, A. J. (1991). *A primer on sediment-trace element chemistry* (2nd ed., p. 136). Chelsea, MI: Lewis Publishers, Inc.

Hughes, M. L. (1999). The impact of acid mine drainage on the hydrogeochemistry of the Lake Hope Watershed, Vinton Co., Ohio. M.S. Thesis, Ohio University. 111 pp.

Kersten, M., & Förstner, U. (1995). Speciation of trace metals in sediments and combustion waste. In A. M. Ure & C. M. Davidson (Eds.), *Chemical speciation in the environment* (pp. 234–275). New York: Blackie Academic & Professional.

Kimball, B. A., Callender, E., & Axtmann, E. V. (1995). Effects of colloids on metal transport in a river receiving acid mine drainage, upper Arkansas River, Colorado, U.S.A. *Applied Geochemistry, 10*, 285–306.

Kleinmann, R. L. P., Allwes, R. A., Jeran, P. W., Jones, P. M., Matetic, R. J., & Statnick, R. (1995). Environmental issues of the Appalachian coal region. *Mining Engineering, 4*, 1120–1123.

Klerks, P. L., & Bartholomew, P. R. (1991). Cadmium accumulation and detoxification in a Cd-resistant population of the oligochaete *Limnodrilus hoffmeisteri*. *Aquatic Toxicology, 19*, 97–112.

Klerks, P. L., & Levinton, J. S. (1989). Rapid evolution of metal resistance in a benthic oligochaete inhabiting a metal-polluted site. *Biological Bulletin, 176*, 135–141.

Knox, A. S., Paller, M. H., Nelson, F. A., Specht, W. L., Halverton, N. V., & Gladden, J. B. (2006). Metal distribution and stability in constructed wetland sediment. *Journal of Environmental Quality, 35*, 1948–1959.

Krauskopf, K. B., & Bird, D. K. (1995). *Introduction to geochemistry* (3rd ed., p. 640). New York: McGraw-Hill, Inc.

Langston, W. J., & Spence, S. K. (1995). Biological factors involved in metal concentrations observed in aquatic organisms. In A. Tessier & D. R. Turner (Eds.), *Metal speciation and bioavailability in aquatic systems* (pp. 407–477). New York: Wiley.

Lerman, A. (1988). Geochemical processes—water and sediment environments. Wiley Interscience, New York. 480 pp. Reprint edition, Krieger Publishing Company, Malabar, Fla., 481 pp.

Li, Y. H., & Gregory, S. (1974). Diffusion of ions in seawater and in deep-sea sediments. *Geochemica et Cosmochimica Acta, 38*, 703–714.

Lind, C. J., & Hem, J. D. (1996). Manganese and iron oxide deposits and trace metal associations in stream sediments, Pinal Creek Basin, Arizona. In J. G. Brown, B. Favor (Eds.), *Hydrology and geochemistry of aquifer and stream contamination related to acidic water in pinal creek near globe Arizona* (pp. 81–103). *US Geological Survey Water-Supply Paper 2466*

MacDonald, D. D., Ingersoll, C. G., & Berger, T. A. (2000). Development and evaluation of consensus-based sediment quality guidelines for freshwater ecosystems. *Archives of Environmental Contamination and Toxicology, 39*, 20–31.

Marple, M. F. (1954). *The geology of Lake Hope State Park* (p. 30). Columbus, OH: Division of geological survey information circular No. 13, Ohio Department of Natural Resources.

Martínez, D. E., & Levinton, J. (1996). Adaptation to heavy metals in the aquatic oligochaete *Limnodrilus hoffmeisteri*: evidence for control by one gene. *Evolution, 50*, 1339–1343.

Matisoff, G. (1995). Effects of bioturbation on solute and particle transport in sediments. In H. E. Allen (Ed.), *Metal contaminated aquatic sediments* (pp. 201–272). Chelsea MI: Ann Arbor Press.

Mattuck, R., & Nikolaidis, N. P. (1996). Chromium mobility in freshwater wetlands. *Journal of Contaminant Hydrology, 23*, 213–232.

Maynard, J. B. (2003). Manganiferous sediments, rocks, and ores. *Treatise in Geochemistry, 7*, 289–308.

McBride, M. B. (1994). *Environmental chemistry of soils* (p. 406). New York: Oxford University Press.

McCall, P. L., & Fisher, J. B. (1980). Affects of tubificid oligochaetes on physical and chemical properties of the Lake Erie sediments. In R. O. Brinkhurst & D. G. Cook (Eds.), *Aquatic oligochaete biology* (pp. 253–318). New York: Plenum Press.

McCall, P. L., & Tevesz, M. J. S. (1982). The effects of benthos on physical properties of freshwater sediments. In P. L. McCall & M. J. S. Tevesz (Eds.), *Animal-sediment relations: The biogenic alteration of sediments* (pp. 105–176). New York: Plenum Press.

Morris, G. L., & Fan, J. (1998). Reservoir sedimentation handbook. Design and management of dams, reservoirs, and watersheds for sustainable use. In *Chapter 10: Sediment deposits in reservoirs* (pp. 10.1–10.42). New York: McGraw-Hill.

Newman, M. C. (1996). Measuring metals and metalloids in water, sediments, and biological tissues. In G. K. Ostrander (Ed.), *Techniques in aquatic toxicology* (pp. 493–516). Boca Raton, FL: Lewis Publishers.

Ng, T. Y.-T., & Wood, C. M. (2008). Trophic transfer and dietary toxicity of Cd from the oligochaete to the rainbow trout. *Aquatic Toxicology, 87*, 47–59.

NYSDEC. (1999). *Technical guidance for screening contaminated sediments*. New York State Department of Environmental Conservation, Division of Fish, Wildlife, and Marine Resources. 39 pp.

OEPA. (1992). *Ohio water resource inventory, volume 3: Ohio's public lakes, ponds, and reservoirs*. Columbus, OH: Ohio Environmental Protection Agency. 24 pp.

Orciari, R. D., & Hummon, W. D. (1975). A comparison of benthic oligochaete populations in acid and neutral lentic environments in southeastern Ohio. *Ohio Journal of Science, 75*, 44–49.

Pigati, E., & López, D. L. (1999). Effect of subsidence on recharge at abandoned coal mines generating acidic drainage: The Majestic Mine, Athens County, Ohio. *Mine Waters and the Environment, 18*, 45–66.

Potter, P. E., Maynard, J. B., & Depetris, P. J. (2005). *Mud and mudstones* (p. 297). Berlin: Springer.

Power, E. A., & Chapman, P. M. (1992). Assessing sediment quality. In G. A. Burton Jr. (Ed.), *Sediment toxicity assessment* (pp. 1–18). Ann Arbor, MI: Lewis Publishers, Inc.

Prim, D. L. (1999). *The effect of acid mine drainage on sedimentation processes and water quality at Lake Hope,*

Lake Hope State Park, Vinton County, Ohio. M.S. Thesis, Athens: Ohio University. 158 pp.

Radwan, S., Kowalik, W., & Kornijow, R. (1990). Accumulation of heavy metals in a lake ecosystem. *Science of the Total Environment, 96*, 121–129.

Reinhold, J. O., Hendricks, A. J., Slager, L. K., & Ohm, M. (1999). Transfer of microcontaminants from sediment to chironomids, and the risk for the Pond bat *Myotis dasycneme* (Chiroptera) preying on them. *Aquatic Ecology, 33*, 363–376.

Reuther, R. (1999). Trace metal speciation in aquatic sediments: methods, benefits, and limitations. In A. Mudroch, J. M. Azcue, & P. Mudroch (Eds.), *Manual of bioassessment of aquatic sediment quality* (pp. 1–54). New York: CRC Press.

Reynolds, S. A. (1999). Sedimentation and contaminants in O'Shaughnessy and Griggs Reservoirs, Scioto River, Delaware and Franklin Counties, Ohio. M.S. Thesis, Athens: Ohio State University. 175 pp.

Roback, S. S. (1974). Insects (Arthropoda: Insecta). In C. W. Hart Jr. & S. L. H. Fuller (Eds.), *Pollution ecology of freshwater invertebrates* (pp. 313–376). New York: Academic.

Roesijadi, G., & Robinson, W. E. (1994). Metal regulation in aquatic animals: Mechanisms of uptake, accumulation, and release. In D. C. Malins & G. K. Ostrander (Eds.), *Aquatic toxicology. Molecular, biochemical, and cellular perspectives* (pp. 387–420). Boca Raton: Lewis Publishers.

Sager, M., & Pucsko, R. (1991). Trace element concentrations of oligochaetes and relations to sediment characteristics in the reservoir at Altenwörth/Austria. *Hydrobiologia, 226*, 39–49.

Stout, W. (1927). *Geology of Vinton County. Bulletin 31* (p. 402). Columbus, OH: Ohio Department of Natural Resources, Division of Geological Survey.

Stumm, W., & Morgan, J. J. (1996). *Aquatic chemistry* (3rd ed., p. 1040). New York: Wiley Interscience.

Swan, A. R. H., & Sandilands, M. (1995). *Introduction to geological data analysis* (p. 446). Oxford: Blackwell Science.

Tessier, A., & Campbell, P. G. C. (1988). Partitioning of trace metals in sediments. In J. Kramer & H. E. Allen (Eds.), *Metal speciation: Theory, analysis, and application* (pp. 183–199). Chelsea, Michigan: Lewis Publishers, Inc.

Tessier, A., Campbell, P. G. C., & Bisson, M. (1979). Sequential extraction procedure for the speciation of particulate trace metals. *Analytical Chemistry, 51*, 844–851.

Timmermans, K. R., Peeters, W., & Tonkes, M. (1992). Cadmium, zinc, lead, and copper in *Chironomus riparius* (Meigen) larvae (Diptera, Chironomidae): Uptake and effects. *Hydrobiologia, 241*, 119–134.

Timmermans, K. R., Van Hattum, B., Kraak, M. H. S., & Davids, C. (1989). Trace metals in a littoral food web: Concentrations in organisms, sediment, and water. *Science of the Total Environment, 87*(88), 477–494.

Timmermans, K. R., Van Hattum, B., Peeters, W., & Davids, K. (1991). Trace metals in the benthic habitat of the Maarsseveen Lakes System, the Netherlands. *Hydrobiology Bulletin, 24*, 153–164.

Tobin, R., & Youger, J. D. (1977). *Limnology of selected Lakes in Ohio-1975*. U.S. Geological Survey Water-Resources Investigations Report 77–105. 205 pp.

USEPA. (1995). EPA Method 3050B: Acid digestion of sediments, sludges, and soils. In *SW-846: Test methods for evaluating solid waste, physical/chemical methods*.

Van Damme, P. A., Hamel, C., Ayala, A., & Bervoets, L. (2008). Macroinvertebrate community response to acid mine drainage in rivers of the High Andes (Bolivia). *Environmental Pollution, 156*, 1061–1068.

Van Ryssen, R., Leermakers, M., & Baeyens, W. (1999). The mobilization potential of trace metals in aquatic sediments as a tool for sediment quality classification. *Environmental Science and Policy, 2*, 75–86.

Verplanck, P. L., Nordstrom, D. K., & Kimball, B. A. (2000). Behavior of iron and aluminum colloids and the attenuation of metals in a stream receiving acid mine drainage, Boulder, Montana. *Geological Society of America Abstracts with Programs, 32*(7), A-78.

Webster, J. G., Swedlund, P. J., & Webster, K. S. (1998). Trace metal absorption onto an acid mine drainage iron (III) oxy hydroxy sulfate. *Environmental Science and Technology, 32*, 1361–1368.

Wetzel, R. G. (2001). *Limnology: Lakes and river ecosystems* (p. 1006). New York: Academic.

Young, T. C., Waltman, M. R., Theis, T. L., & DePinto, J. V. (1992). Studies of heavy metal sorption by trenton channel (Detroit River) sediments. *Hydrobiologia, 235*(236), 649–660.

Marine Pollution Bulletin 64 (2012) 1012–1017

Contents lists available at SciVerse ScienceDirect

Marine Pollution Bulletin

journal homepage: www.elsevier.com/locate/marpolbul

Grounded or submerged bulk carrier: The potential for leaching of coal trace elements to seawater

Steven Andrew Lucas [a,*], John Planner [b]

[a] The Tom Farrell Institute for the Environment, The University of Newcastle, NSW 2308, Australia
[b] Introspec Consulting, Epping, NSW 2121, Australia

ARTICLE INFO

Keywords:
Coal in seawater
Trace elements
Leaching
Ecological impact

ABSTRACT

This study investigates the potential for leaching of coal trace elements to seawater from a grounded bulk carrier. The coal type and ecological scenario was based on the grounding of the "Shen Neng" (April 2010) at Douglas Shoal located within the Great Barrier Reef (Queensland, Australia). The area is of high ecological value and the Queensland Water Quality Guidelines (2009) provided threshold limits to interpret potential impacts.

Coal contains many trace elements that are of major and moderate concern to human health and the environment although many of these concerns are only realised when coal is combusted. However, "unburnt" coal contains trace elements that may be leached to natural waterways and few studies have investigated the potential ecological impact of such an occurrence. For example, coal maritime transport has increased by almost 35% over the last five reported years (Jaffrennou et al., 2007) and as a result there is an increased inherent risk of bulk carrier accidents.

Upon grounding or becoming submerged, coal within a bulk carrier may become saturated with seawater and potentially leach trace elements to the environment and impact on water quality and ecological resilience. The worst case scenario is the breakup of a bulk carrier and dispersal of cargo to the seafloor.

Crown Copyright © 2012 Published by Elsevier Ltd. All rights reserved.

1. Introduction

Due to increased coal maritime transport, information is needed to predict coal behaviour and the potential for coal trace elements to be leached into seawater after a bulk carrier accident. This is a fundamental step in interpreting potential ecological impacts from coal in seawater, however, information is relatively sparse. The study by Alcaro et al. (2002) interpreted the consequences of a bulk carrier accident (Eurobulker IV, 17 kt in Italy in 2000) but the focus was primarily on the smothering of benthic flora and fauna and not the leaching behaviour of coal in seawater.

Ohki et al. (2004) investigated the leaching of various metals from coal into aqueous solutions containing an acid or a chelating agent. Twelve coals were subjected to leaching where the susceptibility of each metal in coal was roughly divided into three classes; largely leached (Ca, Mg and Mn), moderately leached (Cu, Fe, Pb and Zn) and little leached (Al, Co, Cr and Ni). However, these results were undertaken at pH 2 and pH 4 in aqueous solutions that differ from the chemical composition and pH of seawater (high salinity with pH $\approx$ 8.1). Cabon et al. (2007) provided a range of leaching results in seawater for South African reference coal types (SARM) and found that only a few trace elements were leached from coal to seawater. Cabon et al. (2007) explained the leaching dynamics (for Mn in particular) as a function of the bicarbonate (HCO_3^-) system present in seawater. However the leach tests used a few grams of milled (<212 μm) coal samples in 20 mL of seawater and this is not typically representative of the top-size of exported coal in a bulk carrier.

Australian coal is typically exported at a nominal particle size of −50 mm + 0.063 mm. The ways in which trace elements are bound within different minerals in product coal mean that the surface area available for leaching is dependent on the particle size distribution. Furthermore, coal "fines" are likely to float and/or form "froth" on the surface, therefore the particle size distribution is also likely to indicate the percentage of coal that may initially be entrained in local currents and removed from a bulk carrier accident site.

Table 1 shows the major and minor trace elements of concern found in coal that could potentially be leached into seawater.

Sulphur (S), chlorine (Cl) and fluorine (F) in coal are usually measured due to their harmful properties in air after combustion however these elements are relatively abundant in nature and are in relatively low concentrations in coal. These elements were not tested for in this study due to the low concentrations of S, Cl and F in the Bowen Basin coal type present on the "Shen Neng".

* Corresponding author. Tel.: +61 412 954000.
E-mail address: Steven.lucas@newcastle.edu.au (S.A. Lucas).

0025-326X/$ - see front matter Crown Copyright © 2012 Published by Elsevier Ltd. All rights reserved.
doi:10.1016/j.marpolbul.2012.02.001

Table 1
Trace elements in coal of major and minor concern.

Major concern							
Arsenic (As)	Boron (B)	Cadmium (Cd)	Mercury (Hg)	Molybdenum (Mo)	Lead (Pb)	Selenium (Se)	Sulphur (S) (%)
Minor concern							
Chromium (Cr)	Copper (Cu)	Nickel (Ni)	Vanadium (V) (in mg/kg, except S)	Zinc (Zn)	Fluorine (F)	Chlorine (Cl)	Sn + Mn[a]

[a] Tin (Sn) was also added to the list due its potential presence in the anti-fouling agent Copper Tributyl Tin. Manganese (Mn) was included because of its known leaching behaviour in some coals (Jaffrennou et al., 2007).

This study aimed to provide information on the potential ecological impact of coal in seawater as a result of a bulk carrier accident in open-water (as opposed to a closed-water scenario such as coal loading basins). This study investigated the export coal type (Bowen Basin coal type) present on the "Shen Neng" at the time of the grounding in April 2010. However, the particle size distribution, trace element content and associated mineralogy will all influence the leaching behaviour of different coal types and the extent to which they may impact on the environment and is the focus of this study. Furthermore, it is important to note that during the grounding incident of the "Shen Neng", coal in the holds was not saturated with seawater.

2. Methods

2.1. Seawater collection

The seawater used in the following tests was obtained (100 L) from a location approximately 10 nautical miles east of Fingal Island (NSW) (32°44′46.26S–152°23′52.00E). The reason for this was to reduce the likelihood of anthropogenic sources of trace elements sometimes found in coastal seawater (potentially from urban wastewater and stormwater runoff). This sample also represented the "control-sample" used in the leaching tests.

2.2. Particle sizing and sample preparation

An initial coal bulk sample of 150 kg of Bowen Basin coal was sub-sampled using a rotary sample divider to obtain sub-samples of approximately 10 kg (wet mass). One of the 10 kg sub-samples was dried at 40 °C to constant weight before a particle sizing was undertaken. The dried coal was sized at 50 mm, 31.5 mm, 16 mm, 2 mm, 1 mm, 0.5 mm, 0.25 mm, 0.125 mm and 0.063 mm using standard sieves. These size fractions were subsequently used in the flotation tests. A representative sub-sample (all size fractions) and a <0.5 mm sub-sample was dried and crushed to 212 μm for trace element and X-ray Diffraction (XRD) analysis.

2.3. Determination of trace elements in coal and mineralogy

Trace element analysis was undertaken by the Australian Coal Industry Research Laboratories (ACIRL) facilities in Brisbane (QLD) and Maitland (NSW). Trace elements in the Bowen Basin coal (export top-size) were determined using standard methods (AS1038.10, 2002). Trace element analysis was also undertaken on the −0.5 mm size fraction as this proved to have a higher likelihood of being transported from a grounded bulk carrier (see flotation test results in 4.4). XRD techniques (at the University of Newcastle) were utilised to determine the mineralogy of a representative sub-sample (all size fractions) and a <0.5 mm sub-sample of the Bowen Basin coal.

2.4. Flotation tests

A flotation test was undertaken on each size fraction. Coal particle sizes > 2 mm were tested using seawater in a 2 L glass beaker as observations and sample recovery (to air dry samples) was relatively simple. For smaller coal particle sizes, approximately 200 g of each size fraction was placed in a 2 L separation flask filled with 750 mL of seawater and slightly agitated to "wet" the coal. After 1 h the lower 200 mL was allowed to run out of the flask and, after being dried (at 40 °C) and weighed, represented the "sinks". The remaining 550 mL was dried and weighed to constant-weight to determine "floats" (and suspended coal particles).

2.5. Leach tests

One of the 10 kg sub-samples was placed in a large polyethylene bucket and then filled with 20 L of seawater. This step was designed to reflect a bulk mass of export coal in a confined cargo-hold filled with seawater (submerged or grounded bulk carrier). The bucket (and lid) was placed on a large "shaker", similar to that used for the coal particle sizing, and shaken for 2 h to remove air-bubbles and maximise contact between coal particles and seawater. The bucket was allowed to rest for 24 h then the leaching solution (seawater) was filtered for analysis.

This was repeated on two other 10 kg sub-samples to complete the triplicate analysis in determining the potential of trace elements in coal being leached to seawater. A control-sample and the triplicate leaching tests were submitted for analyses which were undertaken by the NATA accredited Australian Laboratory Services (Sydney–ALS). All trace elements were determined using inductively coupled plasma-mass spectrometry (ICP–MS) techniques.

3. Results and discussion

3.1. Seawater analysis

So what trace elements are found naturally in seawater? The Artis Zoo Aquarium in Amsterdam relies on good quality seawater so research undertaken by them provides suitable indicators for potential impacts on marine life. Sondervan (2001) describes how the Artis Zoo Aquarium obtains its seawater from the middle of the Atlantic Ocean on the co-ordinates within small ranges from 45°41′N, 24°42′W. This area lies on the route of the large Hual Benelux b.v. Automobile carriers that travel regularly from Amsterdam to Halifax (NS, Canada) and New York (NY, USA). The seawater is taken in from a depth of 9 m and remains no longer than 4 days in the ballast tanks. In Amsterdam, 160,000 L of that seawater is brought by a vessel through the canals near the aquarium building and pumped into the aquarium reservoirs.

Table 2 shows elements and approximate concentrations of water obtained from the North Atlantic. The transport of seawater to the Artis Zoo is similar, in a maritime sense, to bulk carrier

Table 2
Trace elements in natural seawater (from Sondervan (2001).

Element	Reference (mg/L)	Average (mg/L)
Ca	400	422
K	383	393
Mg	1319	1312
Na	10590	10731
S	878	945
B	4.53	4
Fe	0.01	1
P	0.067	0
Sr	8	7
Br	60	69
	(μg/L)	(μg/L)
Li	176	119
Al	10	26
Ti	0.67	13
Cr	0.6	1
Mn	1.4	28
Co	0.1	1
Ni	4.29	9
Cu	2.07	30
Zn	6.68	353
Rb	121	126
Y	0.11	0
Mo	10.33	2
Ru	?	<0.1
Rh	?	0
Pd	?	<0.1
Ag	0.21	0
Cd	0.1	0
In	10	0
Sn	1.27	0
Sb	0.28	0
I	59	50
Cs	0.37	0
Ba	24	6
La	0.0034	<0.1
Ce	0.14	<0.1
Pr	?	<0.1
W	0.11	<0.1
Pt	?	<0.1
Au	0.005	<0.1
Hg	0.05	<0.1
Tl	0.1	0
Pb	0.03	2
Bi	0.02	<0.1

transport. For example, the seawater is transported in a large container ship as ballast, much like coal, and provides a suitable surrogate for evaluating seawater quality with respect to sampling and storage of seawater.

Seawater used in this study was sampled from open-water and the initial water quality is shown in Table 3. While sampled from the other side of the world, the seawater sampled off Fingal Island (NSW) resided within the average range values shown in Table 2, and thus validated as "typical seawater" for use in the leaching tests.

Table 4 gives the pH, temperature and electrical conductivity (EC) of the seawater both before and after the leach tests and indicated negligible variation in these parameters due to the leaching test. This highlights that S, F and Cl did not change pH and the ionic composition of the seawater was not significantly altered by the leached trace elements.

Table 4
Seawater pH, temperature and EC before and after the leaching tests indicating negligible variation due to the leaching test.

	pH (No units)	Temp (°C)	EC (μS/cm)
Seawater (control)	8.14	21.8	48,500
After Leach A	8.09	22.2	48,400
After Leach B	8.11	22.1	48,500
After Leach C	8.09	22.1	48,500
Average	8.11	22.1	48,475
Maximum	8.14	22.2	48,500
Minimum	8.09	21.8	48,400
Standard deviation	0.02	0.2	50

3.2. Particle sizing and flotation tests

Fig. 1 shows results from the particle sizing and flotation tests.

The >2 mm size fraction represented approximately 50% of the total sample mass and readily sank in seawater during the flotation tests. Coal particle sizes <0.250 mm formed "froth" on the seawater surface. These size fractions are likely to be entrained by local currents and transported away from a grounded/submerged bulk carrier, particularly with a hull breach. Results also indicate that some of the −2 + 1 mm and −1 + 0.5 mm size fractions, and all coal particles <0.5 mm, are likely to be suspended and would be particularly susceptible to transport by ocean currents. The mass of coal that floats means that approximately 15.5% of the cargo may be potentially lost to ocean currents.

Jaffrennou et al. (2007) found that coal particles (1–10 mm in size) could be displaced 1 km away from the dumping point in about 10 h at current velocity (0.46–0.66 knots) however bottom inclination and roughness could modulate the extrapolation from their "polludrome" results. The leaching tests by Cabon et al. (2007) were undertaken using milled samples (<212 μm) and small analysis masses (<2 g). The bulk transport of product coal occurs at a nominal particle size of 50 mm with an associated particle size distribution down to 0.063 mm and, while the lab tests of Cabon et al. (2007) provide valuable insight into the leaching trace elements in coal into seawater, the nominal top-size tested was not typical of bulk coal export in bulk carriers.

3.3. Determination of trace elements in coal (Bowen Basin) and mineralogy

Trace elements in Bowen Basin coal (export nominal top-size and the <0.5 mm size fraction) are shown in Table 5. The trace element range for Australian coals, International coals, Earth's crust and Earth shales are also shown to highlight their relative abundance in nature and the fact that Bowen Basin coal typically has lower average trace element concentrations than other Australian coals and international coals.

X-ray diffraction (XRD) allowed the mineralogy of the coal to be determined. The dominant minerals found in the composite sample (nominal top-size −50 + 0.063 mm) were quartz, kaolinite and siderite (refer Table 6). The <0.5 mm size fraction contained similar minerals, however included Calcium Sulfate Hydrate (hydrated gypsum) and synthetic Magnetite, both of which were likely additives to "fines" during the coal washing and fines recovery process. Muscovite was also present in the <0.5 mm size fraction (refer Table 7).

Table 3
Trace elements found in the seawater used in this study (in μg/L).

Se	Cr	Sn	Hg	As	B	V	Cd	Cu	Pb	Mn	Mo	Ni	Zn
<2	<0.5	<5	<0.1	2.3	5100	1.6	0.4	3	0.4	1.8	13.8	0.6	5

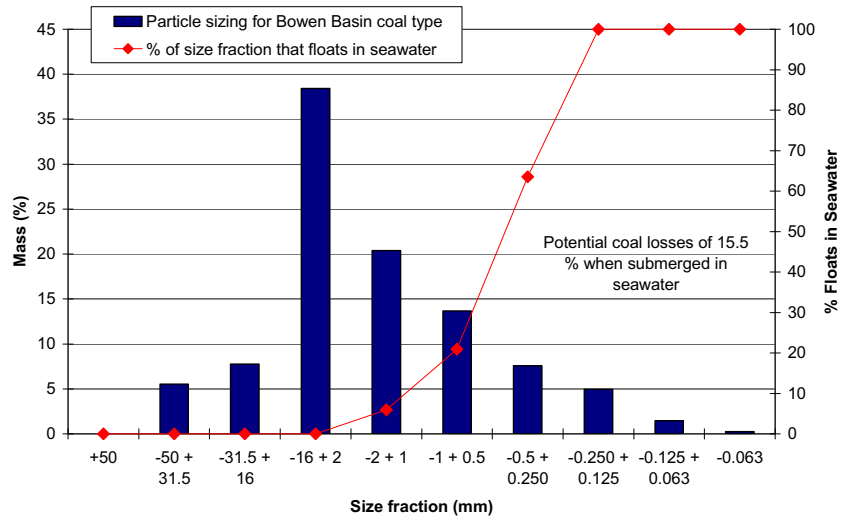

Fig. 1. Particle size distribution and associated percentage that floated in seawater.

Table 5
Trace element analysis for Bowen Basin coal (export nominal top-size and the <0.5 mm size fraction) where the trace element range for Australian coals, International coals, the Earth's crust and Earth shales are also shown.

Element	Symbol	Degree of concern	Units	Bowen Basin (top-size)	Bowen Basin (<0.5 mm)	Range for Australian coals	Range in coal around the world	Earth's crust	Earth shales
Selenium	Se	Major	mg/kg	1	1.1	0.1–1	0.1–5.3	0.05	0.6
Chromium	Cr	Moderate	mg/kg	4	4	2–25	1–35	100	100
Tin	Sn	?	mg/kg	<2	<2	nd	nd	nd	nd
Mercury	Hg	Major	mg/kg	0.02	0.02	0.1–0.11	0.1–0.19	0.08	0.5
Arsenic	As	Major	mg/kg	0.7	0.6	0.2–2.2	3–26	1.8	15
Boron	B	Major	mg/kg	16	19	5–70	6–146	10	100
Vanadium	V	Moderate	mg/kg	41	40	7–75	1–60	135	130
Cadmium	Cd	Major	mg/kg	0.05	0.05	0.01–0.32	0.1–0.31	0.2	0.2
Copper	Cu	Moderate	mg/kg	15	15	6–27	<1–28	55	50
Lead	Pb	Major	mg/kg	5.3	6	2–14	<1–22	12	20
Manganese	Mn	?	mg/kg	42	45	nd	nd	nd	nd
Molybdenum	Mo	Major	mg/kg	<2	<2	0.1–2.6	0.1–4	1.5	3
Nickel	Ni	Moderate	mg/kg	2	2	4–23	2–21	75	70
Zinc	Zn	Moderate	mg/kg	18	18	3–26	1–55	70	100

? Not currently considered as minor, moderate or major concern in the Australian coals.

Table 6
XRD analysis from nominal top-size sample (−50 + 0.063 mm).

Ref. code	Compound name	Chemical formula
01-085-0798	Quartz	SiO_2
01-080-0885	Kaolinite-1A	$Al_2(Si_2O_5)(OH)_4$
01-083-1764	Siderite	$Fe(CO_3)$

Table 7
XRD analysis from <0.5 mm size fraction.

Ref. code	Compound name	Chemical formula
00-001-0385	Calcium Sulfate Hydrate	$CaSO_4 \cdot 2H_2O$
01-070-3755	Quartz	SiO_2
01-080-0885	Kaolinite-1A	$Al_2(Si_2O_5)(OH)_4$
01-083-1764	Siderite	$Fe(CO_3)$
01-087-0245	Magnetite, syn	$Fe_2 \cdot 93O_4$
01-072-1503	Muscovite	$K\ Al_2(Si_3Al)O_{10}(OH)_2$

Table 8
Leaching results–coal in seawater.

	Units	LOR	CONTROL	SW1A	SW1B	SW1C	(Difference)			Trace elements leached from coal to seawater?
							SW1A	SW1B	SW1C	
Selenium (Se)	μg/L	2	<2	<2	<2	<2	0	0	0	No leaching
Chromium (Cr)	μg/L	0.5	<0.5	<0.5	<0.5	<0.5	0	0	0	No leaching
Tin (Sn)	μg/L	5	<5	<5	<5	<5	0	0	0	No leaching
Mercury (Hg)	μg/L	0.1	<0.1	<0.1	<0.1	<0.1	0	0	0	No leaching
Arsenic (As)	μg/L	0.5	2.3	1.2	1.2	1.4	−1.1	−1.1	−0.9	Net removal from seawater
Boron (B)	μg/L	100	5100	4500	4700	4700	−600	−400	−400	Net removal from seawater
Vanadium (V)	μg/L	0.5	1.6	0.5	0.5	0.5	−1.1	−1.1	−1.1	Net removal from seawater
Cadmium (Cd)	μg/L	0.2	0.4	0.6	0.8	0.6	0.2	0.4	0.2	Leaching
Copper (Cu)	μg/L	1	3	12	11	11	9	8	8	Leaching
Lead (Pb)	μg/L	0.2	0.4	0.9	0.8	0.8	0.5	0.4	0.4	Leaching
Manganese (Mn)	μg/L	0.5	1.8	37.1	36.5	37	35.3	34.7	35.2	Leaching
Molybdenum (Mo)	μg/L	0.1	13.8	17	16.8	16.7	3.2	3	2.9	Leaching
Nickel (Ni)	μg/L	0.5	0.6	5.6	5.9	6.2	5	5.3	5.6	Leaching
Zinc (Zn)	μg/L	5	5	23	27	54	18	22	49	Leaching

LOR = limit of reading.

3.4. Leach tests

Table 8 shows results from the leaching tests. The "Control" sample represents the seawater used in the leaching tests and SW1A, SW1B and SW1C represent the triplicate leaching results. The difference between pre and post leaching to seawater is also shown.

No leaching from coal to seawater was observed for Se, Hg, Sn and Cr. There was net removal of As, B and V from seawater, that is, these elements were adsorbed to the coal resulting in a lower concentration in seawater. Leaching from coal to seawater was observed for Cd, Cu, Pb, Mn, Mo, Ni and Zn. How much is leached from coal? A mass balance approach was used to quantify the difference between trace elements in Bowen Basin coal and trace elements found in the seawater leachate. For example, if 10 kg of coal contains 0.05 mg/kg Cd then there was 0.5 mg (500 μg) in the test coal sample. If the initial seawater concentration was 0.4 μg/L (8 μg in 20 L), and it increased by 0.3 μg/L (6 μg in 20 L), then the % leached represents approximately 1.2% of the total Cd content in coal. Table 9 summarises the mass balance for all trace elements that leached from coal to seawater.

The mass balance approach showed that the leaching of trace elements in coal to seawater ranged from 0.03% to 1.2% of the total trace element content in coal. The relatively low amount of trace elements leached from unburnt coal suggests that many trace elements are strongly bound to mineral matrices, particularly when submerged in seawater with a high electrical conductivity and relatively high pH (~8.1). Elemental substitution may occur, for example, such as processes that result in net removal of some elements (As, B and V) and leaching of others (Cd, Cu, Mn, Ni and Zn) from coal in seawater and further research is warranted into such processes.

But what is the ecological threat of such leaching to seawater? Table 10 shows a comparison of water quality guidelines (recommended range) (DERM, 2009) and leachate results, highlighting elements of concern in aquatic environments.

Cu and Mn were the only elements that exceeded guideline values. Fortunately, dilution would be expected in open-waters (like Douglas Shoal on the Great Barrier Reef) that are likely to negate any ecological impact due to leaching of Cu and Mn in coal to seawater. When a semi-enclosed coal loading basin is considered there is likely to be a cumulative impact, however this was outside the scope of this preliminary study. The accumulative ecological impact in such locations also warrants further research.

It is important to note that Mn and Sn are not considered trace elements of major/minor concern in the coal industry. These

Table 10
Comparison of water quality guidelines (recommended range) and leachate results (showing elements of concern in aquatic environments).

Element	Recommended range QLD WQ Guidelines 2009 μg/L	Leach test Average μg/L	Less than Guideline?
As	<50	Net removal	Y
Cd	<3	0.7	Y
Cr	<100	No leaching	Y
Cu	<6	11	N
Mn	<10	37	N
Hg	<0.05	No leaching	Y
Ni	<40	5.9	Y
Sn	<1	<5[a]	?[a]
Zn	<200	35	Y

[a] Likely to be <1 but could not achieve desired limit of reading during analysis.

Table 9
Leaching results–coal in seawater.

Element	Symbol	Degree of concern	Bowen Basin (top-size) (mg/kg)	In 10 kg of coal (μg)	Initial seawater concentration in 20 L (μg)	Increase after leach test (μg in 20 L)	% leached from total mass in coal
Cadmium	Cd	Major	0.05	500	8	6	1.20
Copper	Cu	Moderate	15	150,000	60	160	0.11
Lead	Pb	Major	5.3	53,000	8	16	0.03
Manganese	Mn	?	42	420,000	36	720	0.17
Molybdenum	Mo	Major	<2	20,000	276	62	0.31
Nickel	Ni	Moderate	2	20,000	12	106	0.53
Zinc	Zn	Moderate	18	180,000	100	620	0.34

? = "No concern". Mn is not considered an element of concern in the coal industry.

elements were added to the analysis in this study because of their inclusion in water quality guidelines and the leaching behaviour of Mn as noted in the literature (Cabon et al., 2007; Jaffrennou et al., 2007; Ohki et al., 2004). Cabon et al. (2007) found that few trace elements of concern were leached into seawater, however noted the relationship between the calcite and gypsum content of coal and the leaching of Mn. In this respect, both Mn and Sn should be added to existing Australian Coal Association Research Projects (ACARP), particularly the trace element database (CSIRO and ACARP, 2007). Furthermore, their inclusion would assist in interpreting the impact of coal immersion in seawater as highlighted in the literature and in this study.

4. Conclusion

This study was commissioned by Xstrata Coal to provide preliminary information on the potential ecological impact of coal in seawater after an open-water incident. In context of the Bowen Basin coal type on the "Shen Neng" and the open-water incident on Douglas Shoal, leaching results indicated negligible impact to water quality and ecological resilience as a result of trace elements in this coal type being leached to seawater. Ocean currents are highly likely to disperse and dilute leached trace elements in an open-water incident.

This study also highlighted that particle size distribution, trace element content and mineralogy will all influence the leaching behaviour of different coal types and the extent to which they may impact on the environment and warrants further research. Since this study investigated just one export coal type there may be a need for further research on other coal types as all Australian export coals could have certification concerning their ecological impact in case of a bulk carrier accident. Further research is also required on the potential cumulative impacts of coal "spills" in closed-water systems.

Acknowledgements

The authors wish to acknowledge the services of the Australian Coal Industry Research Laboratories (ACIRL, Maitland, NSW) and Australian Laboratory Services (ALS, Sydney) for coal analysis and water analysis respectively. Thanks also to TUNRA Bulk Solids for coal preparation and the team at the Tom Farrell Institute for the Environment for reviewing the paper (both at the University of Newcastle, NSW Australia).

References

Alcaro, L., Chieruzzi, T., Farchi, C., Penna, M., Tufano, M., Amato, E., 2002. Assessment of the environmental damage resulting from the loss at sea of the M/V Eurobulker IV steam coal cargo. Phase One. Biologia Marina Mediterranea 9, 61–64.

AS1038.10, 2002. Coal and Coke – Analysis and Testing, Part 10: Determination of Trace Elements – Guide to the Determination of Trace Elements, Standards Australia.

Cabon, J-Y., Burel, L., Jaffrennou, C., Giamarchi, P., Bautin, F., 2007. Study of trace metal leaching from coals into seawater. Chemosphere 69, 1100–1110.

CSIRO and ACARP, 2007. Trace Elements in Australian Export Coals, Partnership Study. http://www.csiro.au/partnerships/TraceElements.html.

DERM, 2009. Queensland Water Quality Guidelines – Version 3. Department of the Environment and Resource Management, Queensland Government.

Jaffrennou, C., Giamarchi, P., Cabon, J-Y., Stephan, L., Burel-Deschamps, L., Bautin, F., Thomas, A., Dumont, J., Le Floch, S., 2007. Simulations of accidental coal immersion. Marine Pollution Bulletin 54, 1932–1939.

Ohki, A., Nakajima, T., Yamashita, H., Iwasshita, A., Takanashi, H., 2004. Leaching of various metals from coal into aqueous solutions containing an acid or a chelating agent. Fuel Processes Technology 85, 1089–1102.

Sondervan, P., 2001. The relationship of Calcium loss with trace element concentrations in seawater life systems. Bulletin de l'Institut Océanographique, Monaco, n Spécial 20, Fascicule 1.

USGS
science for a changing world

A Critical Review of Published Coal Quality Data From the Southwestern Part of the Powder River Basin, Wyoming

Open-File Report 2011–1148

U.S. Department of the Interior
U.S. Geological Survey

Cover image. Shot coal from the highwall face at a mine in the Powder River Basin, Wyoming (photograph by Lames A. Luppens, U.S. Geological Survey).

A Critical Review of Published Coal Quality Data From the Southwestern Part of the Powder River Basin, Wyoming

By James A. Luppens

Open-File Report 2011–1148

U.S. Department of the Interior
U.S. Geological Survey

U.S. Department of the Interior
KEN SALAZAR, Secretary

U.S. Geological Survey
Marcia K. McNutt, Director

U.S. Geological Survey, Reston, Virginia: 2011

For more information on the USGS—the Federal source for science about the Earth, its natural and living resources, natural hazards, and the environment, visit http://www.usgs.gov or call 1-888-ASK-USGS

For an overview of USGS information products, including maps, imagery, and publications, visit http://www.usgs.gov/pubprod

To order this and other USGS information products, visit http://store.usgs.gov

Any use of trade, product, or firm names is for descriptive purposes only and does not imply endorsement by the U.S. Government.

Although this report is in the public domain, permission must be secured from the individual copyright owners to reproduce any copyrighted materials contained within this report.

Suggested citation:
Luppens, J.A., 2011, A critical review of published coal quality data from the southwestern part of the Powder River Basin, Wyoming: U.S. Geological Survey Open-File Report 2011–1148, 23 p.

Contents

Abstract 1
Introduction 1
In-Place Coal Quality 1
Fort Union Formation Coal Quality 4
Estimation of the Quality of Deep Fort Union Formation Resources 10
Wasatch Formation Coal Quality 14
Conclusions 21
References Cited 21

Figures

1. Location of Southwestern Wyoming Powder River Basin, Northern Wyoming Powder River Basin, and Gillette coal field, Wyoming 2
2. Location of coal fields in the Southwestern Powder River Basin 3
3. Variation in moist, mineral-matter-free British thermal units in the Wyodak-Anderson coal zone in the Powder River Basin, Wyoming, showing a trend towards increasing apparent rank of the coal from subbituminous C at shallow depths to subbituminous B, and finally subbituminous A in the deepest part of the basin 9
4. Estimated variability of as-received gross calorific values versus depth from table 3 data for the Wyodak coal beds in the Powder River Basin, Wyoming 13
5. Coal bed and coal zone names used in different publications in the Powder River Basin, including current SWPRB coal assessment area 15
6. Estimated variability of as-received and moist, mineral-matter-free gross calorific values versus depth from table 4 for the Wyodak coal beds in the Powder River Basin, Wyoming 17
7. Core log for core hole USGS-1 in the Lake De Smet coal field, Wyoming, illustrating core intervals analyzed, shale intervals excluded from the analyses, and lost-recovery intervals 20

Tables

1. Available as-received coal quality data from the Fort Union formation in the SWPRB assessment area 5
2. A comparison of reported coal quality data in the Sussex coal field, Wyoming, from successive publications 8
3. Properties and composition of coal beds cored in the Powder River Basin, Wyoming. 11
4. Edited version of table 3 in which core holes with anomalous data were deleted 16
5. Available as-received coal quality data from the Wasatch Formation in the Lake De Smet area and other Watsatch coal beds 18
6. Estimated impacts of compositing the originally excluded shale, pyrite, and other high-ash parting material with the coal analyses for the USGS-1 core hole from the Lake De Smet coal field, Wyoming 21

A Critical Review of Published Coal Quality Data From the Southwestern Part of the Powder River Basin, Wyoming

By James A. Luppens

Abstract

A review of publicly available coal quality data during the coal resource assessment of the southwestern part of the Powder River Basin, Wyoming (SWPRB), revealed significant problems and limitations with those data. Subsequent citations of data from original sources often omitted important information, such as moisture integrity and information needed to evaluate the issue of representativeness. Occasionally, only selected data were quoted, and some data were misquoted. Therefore, it was important to try to resolve issues concerning both the accuracy and representativeness of each available dataset. The review processes demonstrated why it is always preferable to research and evaluate the circumstances regarding the sampling and analytical methodology from the original data sources when evaluating coal quality information, particularly if only limited data are available.

Use of the available published data at face value would have significantly overestimated the coal quality for all the coal fields from both the Fort Union and Wasatch Formations in the SWPRB assessment area. However, by using the sampling and analytical information from the original reports, it was possible to make reasonable adjustments to reported data to derive more realistic estimates of coal quality.

Introduction

A review of publicly available coal quality data during the 2010 coal resource assessment of the southwestern part of the Powder River Basin, Wyo. (SWPRB; fig. 1), revealed problems and limitations with those data. Because a detailed discusion of the coal quality data issues exceeded the scope of the assessment, a more thorough discussion of the coal quality data review is presented separately in this report.

Coal quality is one of the major factors in the marketability of coal and is an important parameter in economic evaluations. Coal quality directly impacts the cost of generating electric power. Quality parameters such as increased ash content, which lowers the gross calorific value (British thermal units per pound [Btu/lb]), increase the operating and maintenance costs at coal-fired powerplants. Coals with lower ash content, and therefore higher gross calorific values, command a premium selling price.

Furthermore, the Clean Air Act Amendments (CAAA) have enforced emission limits to reduce certain air pollutants such as sulfur dioxide. The sulfur dioxide emissions limits for all new powerplants built after 1976 were capped at 1.2 pounds of sulfur dioxide per million Btu (U.S. Environmental Protection Agency, 1980). Any coal that could be burned and meet the sulfur dioxide emission standards for air quality (emitting less than 0.6 pound of sulfur per million Btu or 1.2 pounds of sulfur dioxide per million Btu) without the need for flue-gas desulfurization was designated “compliance coal,” also known as low-sulfur coal (U.S. Energy Information Administration, 2010). Subsequent phases of the CAAA have further restricted sulfur dioxide emissions. Currently, New Source Performance Standards (NSPS) establish uniform national U.S. Environmental Protection Agency air emission standards that limit the amount of pollution allowed from new sources or from modified existing sources. Under NSPS, Best Available Control Technology (BACT) emission limitations are based on the maximum degree of reduction of each pollutant subject to regulation under the Clean Air Act (U.S. Environmental Protection Agency, 2006). The minimum BACT standard for sulfur dioxide emissions is 90 percent regardless of the sulfur content. The abundance of low-ash and low-sulfur coal in the Powder River Basin (PRB) has been a significant factor in the steadily growing demand for coal from this region.

In-Place Coal Quality

There are currently no active mines in the SWPRB assessment area, but historically, very limited production from coal beds in both the Fort Union and Wasatch Formations has occurred. Lacking the relatively thick, shallow coal beds found in the Gillette coal field (fig. 1) on the eastern flank of the PRB, mining has not been widespread. As a result, publicly available coal quality information from coal exploration cores and mines is sparse, with the notable exception of the now abandoned Dave Johnston Mine near Glenrock, Wyo. (figs. 1 and 2). Limited coal quality data from deeper coal beds have been generated from a few wells during recent coal bed methane development (Stricker and others, 2007).

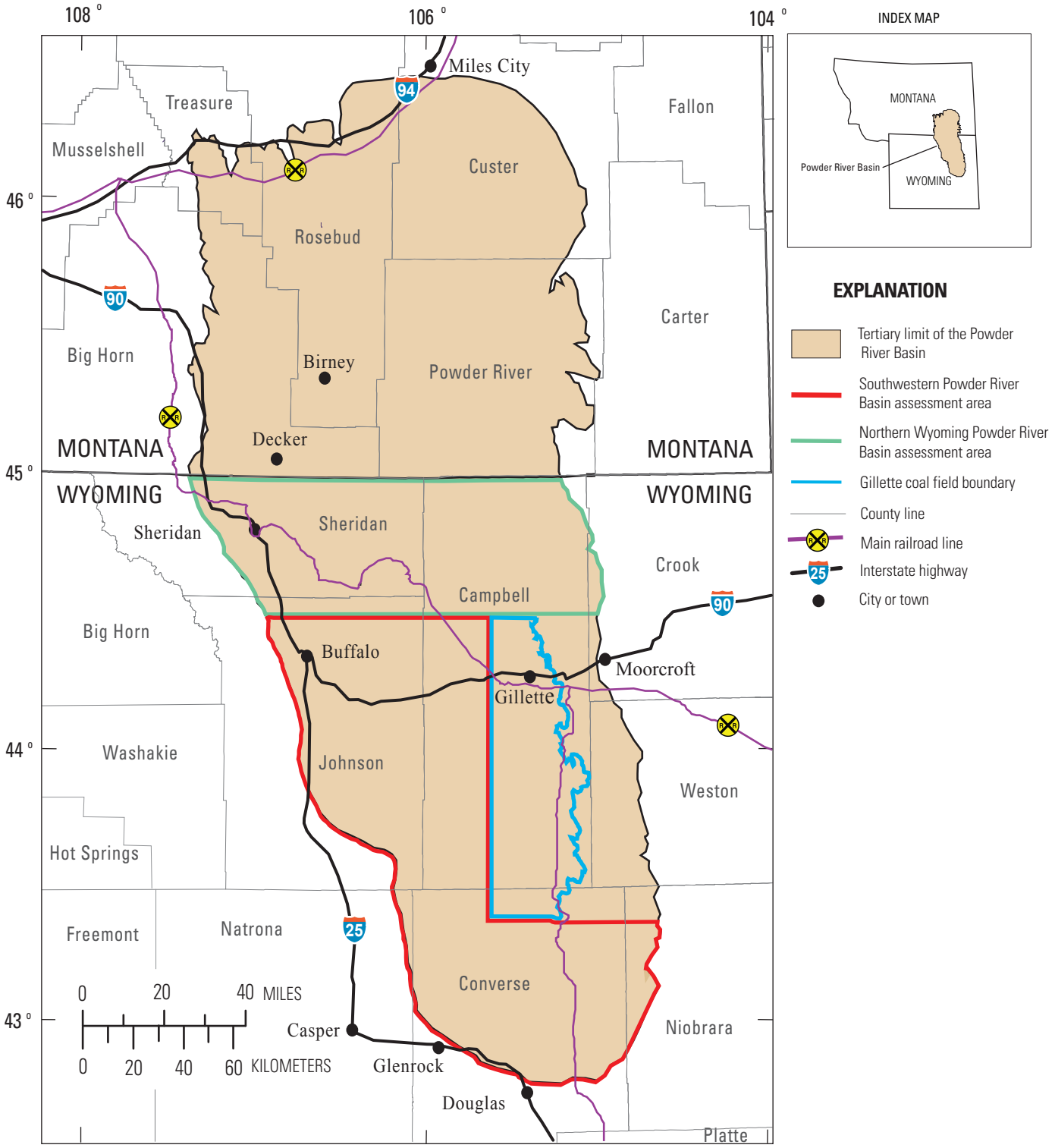

Figure 1. Location of Southwestern Wyoming Powder River Basin, Northern Wyoming Powder River Basin, and Gillette coal field, Wyoming.

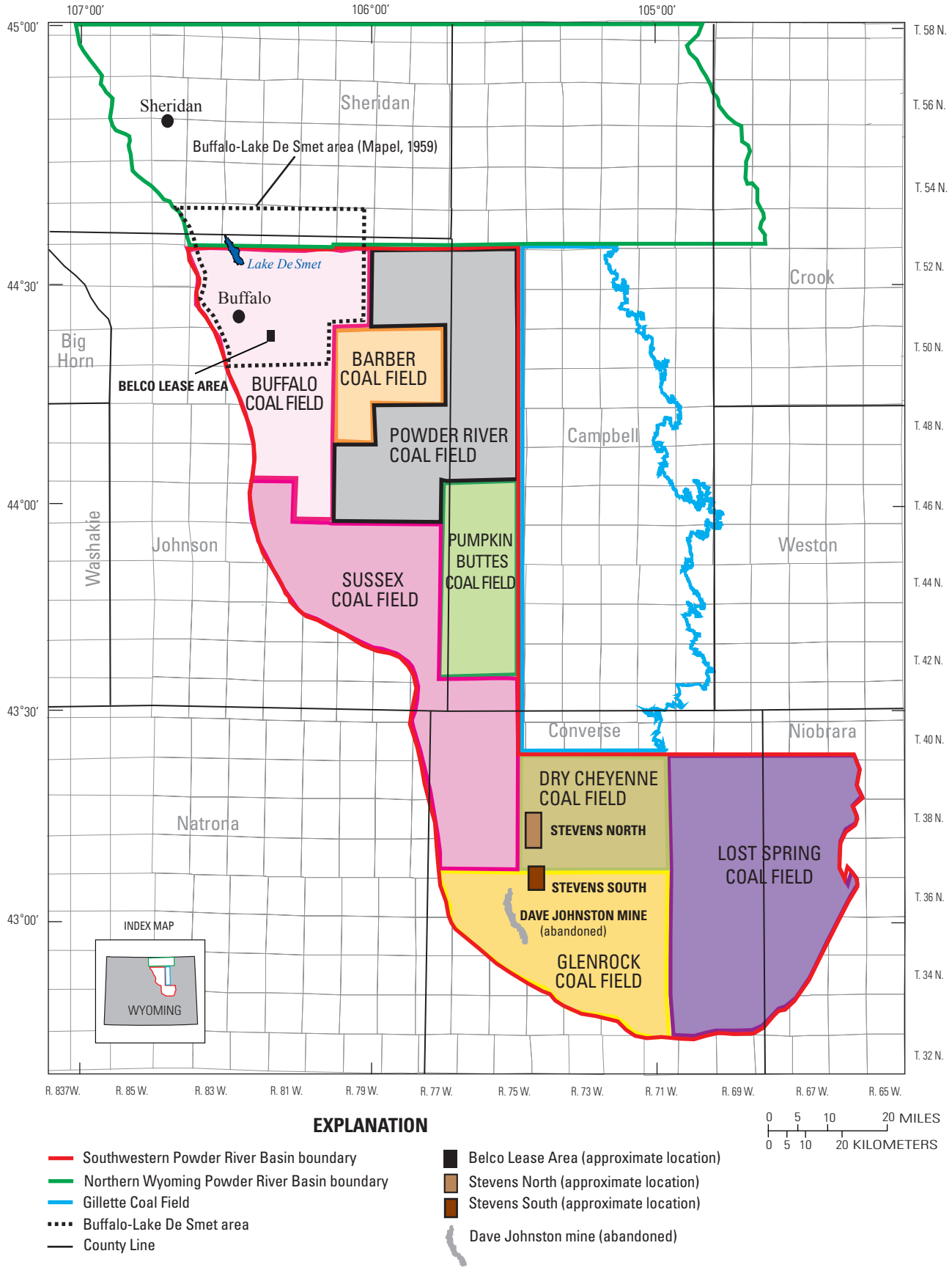

Figure 2. Location of coal fields in the Southwestern Powder River Basin (modified from Glass, 1976).

Assessing the coal quality variations is usually straightforward for regions like the Gillette coal field, where mining has been extensive and coal analytical data are abundant. However, when dealing with relatively few coal analyses, as is the case of the SWPRB, it is especially important to try to assess both the accuracy and the representativeness of each available dataset. During the review of published coal quality data for the SWPRB, two recurring problems were apparent. These problems were either anomalously low moisture values, representativeness issues, or both. The anomalous moisture problems are due to unexplained moisture loss during sampling, shipment, or processing the samples or from the sampling of partially dried coal beds. The issue of representativeness is related to partial coal bed samples, whole bed core samples with significant core loss, or deliberate exclusion of high-ash partings. Because coal quality differs between the Fort Union and Wasatch Formations, they are discussed separately.

Fort Union Formation Coal Quality

The available in-place coal quality data for the Fort Union Formation coal beds in the SWPRB assessment area are summarized in table 1. Essentially all of the shallow coal bed data in the SWPRB are from the Dry Cheyenne and Glenrock coal fields in the south and the Sussex coal field in the west (fig. 2). An initial review of the data from table 1 reveals a relatively wide range in coal quality, especially for moisture contents (18.8 to 28.8 percent). The higher gross calorific values (7,581 to 9,160 Btu/lb) are directly dependent on what appears to be an unusually wide range in as-received moisture values for a single coal field. Typically, variations in the degree of coalification within individual coal fields or adjacent fields are not significant. Luppens (1988) demonstrated that a linear, inverse relationship exists between moisture and ash values in low-rank coals (lignite and subbituminous C ranks) for a single coal field. Any moisture values with similar ash contents that fell more than 1.5 to 2 percent from a best-fit trendline through an ash versus moisture data crossplot were reanalyzed. A similar linear, inverse relationship exists between gross calorific and ash values in low-rank coals for a single coal field (Hoeft and others, 1983). Because of these linear relationships, coal analyses with similar ash values will also have similar moisture and gross calorific values.

As moisture or ash contents, or both, decrease, gross calorific values increase and vice versa. As a general rule of thumb for low-rank coals, a 1-percent change in ash or moisture value is equivalent to a change in the gross calorific value of approximately100 to 120 Btu/lb (J.A. Luppens, unpub. data, 2011). For example, a 5-percent decrease in moisture would result in an increase in the gross calorific value of about 500 Btu/lb. A 5-percent decrease in moisture (+500 Btu/lb) coupled with an increased ash content of 2 percent (−200 Btu/lb) would result in a net increase in the gross calorific value of about 300 Btu/lb. Knowledge of these coal quality data relationships is particularly useful in identifying potentially anomalous data (Hoeft and others, 1983).

Three sets of published coal quality data from the Dry Cheyenne and Glenrock coal fields (fig. 2) were found. The analyses from the Stevens North and South areas (table 1) were performed on coal cores (Western Fuels Association, Inc., 1983). The sample types from the Roland and Smith coal beds from the Dave Johnston Mine (table 1) were either face channel or coal core samples (Glass, 1975).

The analytical data from the Dry Cheyenne and Glenrock coal fields should be very similar because of the relative proximity of the samples (fig. 2). Therefore, samples with similar ash contents should also have similar moisture and gross calorific values. The published average moisture content of 26.6 percent for the produced coal from the Dave Johnston mine (Keystone Coal Industry Manual, 1997), owned by Pacific Power and Light Company (PPL), is the most reliable estimate of the moisture content (at 12.1 percent ash) in the Glenrock and Dry Cheyenne coal fields (table 1). However, 5 of the 10 moisture values from those coal fields, which range from 19.5 to 23.5 percent (table 1), appear to be anomalously low.

In 1974, an extensive face channeling program was initiated by the Geological Survey of Wyoming to collect coal samples to characterize the coal quality in 4 of the 10 major coal-bearing regions in the state (Glass, 1975). The extensive suite of coal analyses performed on these samples included proximate and ultimate analyses, plus tests for gross calorific values, sulfur forms, major and minor oxides, ash fusion temperatures, Hardgrove grindability, and trace elements. As part of that sampling program, Glass (1975) collected two face channel samples (74-36 and 74-37, table 1) totaling 37 and 38 feet in thickness, respectively, from the Smith coal bed (originally correlated as the School coal bed) at the Dave Johnston mine. The “typical” core analyses for the Smith bed supplied by PPL also were presented by Glass (1975) to compare the results of the face channeling results to the expected quality at the mine.

Sampling the vertical highwalls of thick beds in the PRB posed significant logistical and safety challenges from trying to cut a uniform channel through the thick coal beds and collecting the coal by use of multiple 30-foot-long extension ladders. Typically, highwall faces in PRB mines will be exposed for weeks to a month or more before the coal is actually recovered. As soon as the face is exposed, weathering effects begin, initially as moisture loss. This moisture loss results in blocky fracturing due to coal shrinkage, which can extend into the exposed coal faces for up to several feet. Prolonged exposure can result in a decrease in the gross calorific values due to oxidation. Normally, the width and depth of the face channels were gauged to yield a minimum of 6 pounds of coal per vertical foot of channel (Glass, 1975). A 3.5-inch by 3.5-inch channel will yield just over 6 pounds per channel foot. Therefore, the relatively shallow depth of the face channels would most certainly mean that sampling was limited to the zone subjected to partial drying.

Table 1. Available as-received coal quality data from the Fort Union formation in the SWPRB assessment area. Average values are shown in bold type.

Area and coal bed name	No. of analyses	Moisture (percent)	Sulfur (percent)	Ash (percent)	Gross calorific value (Btu/lb)	Pounds of SO_2 per million Btu	Gross calorific value[9] ($Btu/lb_{m,mmf}$)	Apparent rank[10]
Dry Cheyenne coal field–Stevens North area[3]								
Roland (Baker) coal bed	5	28.7	0.51	7.7	7,831	1.30	8,540	subC
Smith coal bed	2	26.1	0.47	7.5	8,247	1.14	8,974	subC
Glenrock coal field–Stevens South area[3]								
Roland (Baker) coal bed	1	22.2	0.42	14.7	7,860	1.07	9,344	subC
Smith coal bed	1	23.5	0.38	4.4	9,010	0.84	9,460	subC
Glenrock coal field–Dave Johnston Mine								
Roland (Baker) coal bed[4]	5	27.4	0.45	7.9	7,950	1.13	8,690	subC
Smith coal bed face channel sample 74-36[4]	1	20.7	0.5	15.7	7,850			
Smith coal bed face channel sample 74-37[4]	1	19.5	0.7	8.8	8,870			
"Typical" Smith coal bed core sample analyses from Dave Johnston Mine[4]	1	26.4	0.5	9.7	7,830			
Smith coal bed[5,7] (average of 3 analyses above from Glass, 1975)	3	**22.2**	**0.6**	**11.4**	**8,180**	**1.47**	**9,329**	**subC**
Dave Johnston Mine (produced averages)[7]	–	**26.6**	**0.45**	**12.1**	**7,581**	**1.19**	**8,720**	**subC**
Sussex coal field[4,5]								
Reported value[1,4]	1	23.5	0.49	5.2	9,160	1.07	9,707	subB
Basin 2[1,6]	1	28.8	0.56	6.7	7,930	1.41	8,547	subC
Basin 3[1,6]	1	23.6	0.68	7.8	8,450	1.61	9,228	subC
Basin 4[1,6]	1	18.8	0.57	7.8	9,160	1.24	10,006	subB
Basin 5[1,6]	1	23.5	0.49	5.2	9,050	1.08	9,590	subB
Basin 6[1,6]	1	28.1	0.45	4.6	8,350	1.08	8,786	subC
Average of 5 basin analyses		**24.6**	**0.55**	**6.4**	**8,588**	**1.28**	**9,228**	**subC**
Estimated average of 5 basin analyses (adjusted to 30 percent moisture)[1]		**30.0**	**0.51**	**6.0**	**7,969**	**1.28**	**8,515**	**subC**
Deep basin coal bed								
Smith (Big George) coal bed[2,8]	–	22.6	0.25	3.5	9,750	0.51	10,135	subB

[1]Partial bed sample.

[2]Unweighted average of 30 incremental samples from a 200-foot-thick cored portion of the bed below 1,000 feet.

[3]Western Fuels Association, Inc. (1983).

[4]Glass (1975).

[5]Glass and Jones (1992).

[6]Wegemann (1912).

[7]Keystone Coal Industry Manual (1997).

[8]Keystone Coal Industry Manual (2010).

[9]Moist, mineral-matter-free (m,mmf) basis.

[10]Subbituminous C (subC), subbituminous B (subB).

The coal from both face channel samples was described as having "blocky" or "cubical fractures," which is consistent with the blocky fractures caused by shrinkage due to moisture loss. Additionally, the condition of sample 74-36 was listed as "weathered" (Glass, 1975), which corroborates the assumption that the as-received moisture content of sample 74-36 was not representative of the true in-place moisture. Although the condition of sample 74-37 was listed as "fresh," its moisture content was over 1 percent lower than that for sample 74-36, which confirms that moisture integrity of both channel samples was compromised by significant moisture loss. In fact, Glass (1975, p. 164) states that "the routine analysis of Sample No. 74-37 compares favorably with the company [PPL] analyses except in as-received moisture and heat values [gross calorific values]. Like Sample No. 74-36, the moisture is lower than the company analyses [19.5 versus 26.4 percent] while the heat content is over 1,000 Btu/lb higher [8,870 versus 7,830 Btu/lb]" (table 1).

Using the simple rule of thumb of 100 to 120 Btu/lb change per for each 1-percent change in moisture or ash contents, the approximately 7-percent difference in moisture would equate to a difference in the gross calorific values of about 700 to 840 Btu/lb. There was also about a 1-percent difference in ash (table 1), which would account for an additional 100 to 120 Btu/lb. The combined estimated difference in moisture and ash contents in terms of impacts to the gross calorific value is 800 to 960 Btu/lb, which closely approximates the "over 1,000 Btu/lb difference" noted by Glass (1975).

Glass and Jones (1992) characterized the coal quality of the Smith bed in the Glenrock coal field using only the two face channel analyses, 74-36 and 74-37, and the core hole analyses provided by PPL (table 1; Glass, 1975), even though it was acknowledged that the face channel samples were described as weathered and had anomalously low moisture contents. Additionally, the coal quality summary was simply an average of those three samples, with data ranges, without any critical information concerning the sample type, condition of the samples, limitations of the data, or source of the data. Only the author's personal knowledge of the 1974 channel sampling program allowed tracing of the average values in Glass and Jones (1992) back to Glass (1975). The use of data that are not representative of the coal to characterize coal quality of a given area is disappointing from a professional standpoint because of the ripple effect. The three-sample summary, with little documentation from Glass and Jones (1992), was cited in subsequent publications (Keystone Coal Industry Manual, 1997, 2005), thus perpetuating the impression that the coal quality in the Glenrock coal field is better than it actually is. The inclusion of samples with anomalously low moisture increased the average gross calorific value.

The moisture values for the two cores from the Stevens South area of the Glenrock coal field (table 1) also look anomalously low. Because this area lies between the Stevens North area and the Dave Johnston Mine, the moisture contents should be similar. It is assumed that unaccounted-for moisture loss during the coring or core handling occurred, but no documentation was available. Additionally, the ash content of 4.4 percent for the Smith bed analysis (table 1) in the Stevens South area also appears to be especially low, especially when compared to other Wyoming PRB coal quality. The Gillette coal field, which produces coal with some of the lowest ash content in the Nation, has as-received ash contents from the south to the north areas that range from 5.2 to 6.4 percent, respectively. Ranges for other as-received coal quality parameters from the south to the north areas in the Gillette coal field were moisture, 26.7 to 30.0 percent; and gross calorific values, 8,200 to 8,810 Btu/lb.

Given the documented problems with the use of samples with anomalously low moisture contents from Glass (1975) and Glass and Jones (1992), more realistic ranges in coal quality from these two coal fields are estimated to be moisture, 26 to 29 percent; ash, 7.5 to 12 percent; sulfur, 0.4 to 0.6 percent; and gross calorific values, 7,500 to 8,000 Btu/lb. The range in moisture is more consistent with that for the Gillette coal field. The gross calorific values are also consistent with those for the Gillette area, given that the average ash content in the Glenrock and Dry Cheyenne coal fields is significantly higher than in the Gillette coal field. It is interesting to note that one of the reasons for closing the Dave Johnston Mine in 2000 was deteriorating coal quality due to higher ash (PacifiCorp, 2008).

The author encountered a similar situation while evaluating purchase of a coal property in the Gillette coal field near Gillette, Wyo. (J.A. Luppens, unpub data, 1998). The seller provided coal quality data from cores drilled in the 1960s, with moisture values ranging from 18 to 34 percent and averaging about 28 percent. However, moisture values from adjacent mines ranged from 30 to 32 percent. A coring program was initiated to resample over 20 original core sites with suspect analyses. The result of the recoring program was a revised average moisture content of about 31.5 percent, consistent with that from the neighboring mines. Subsequent interviews with laboratory personnel who conducted the original analyses confirmed suspicions regarding the conditions of the core samples as received at the laboratory. Many samples had been stored for weeks before shipment to the laboratory in unlined cardboard boxes without plastic bags or other means of preventing moisture loss. Problems caused by unaccountable moisture loss are more common than often realized, especially with coal samples collected years ago when neither materials to prevent moisture loss nor expedited shipping options were available.

The problems with the published coal quality data from the Sussex coal field (fig. 2) stem not only from moisture issues similar to those for the Dry Cheyenne and Glenrock coal fields but also from representativeness issues. Additionally, only select data were reported in more recent publications, and citation errors were introduced.

Table 2 illustrates the progression of reported coal quality data over the past nearly 100 years since the original data were reported. The original assessment of the Sussex coal field reported a total of six coal sample analyses (Wegemann,

1912). Smith and others (1972) reported three of the original six analyses. More recently, only a single coal analysis for the Sussex coal field was reported by Glass and Jones (1992; tables 1 and 2), and it does not exactly match any of the analyses from the original data (table 2). Evidently, the moisture, ash, volatile, fixed carbon, and sulfur contents from sample 10827 were combined with the gross calorific value from sample 10804. It is unknown whether this reporting was due to intentional compositing or was a result of a typographical error. Nevertheless, it demonstrates the value in reviewing the original reports rather than relying on subsequent interpretations. The quotation of the single erroneous analysis from Glass and Jones (1992) by the Keystone Coal Industry Manual (2005) demonstrates how misleading and incorrect citations can easily be perpetuated.

Based on this single reported proximate analysis (Glass and Jones, 1992), the coal quality of the Sussex field appears to be relatively high for the PRB. However, after one reviews the original report on the Sussex coal field (Wegemann, 1912), a different perspective is gained. A total of five analyses from various "basins" within the Sussex coal field with at least as-received moisture, ash, sulfur, and gross calorific values was given in the original report (table 1). The analytical results show a fairly wide range in moisture (and consequently gross calorific values), whereas ash contents are all fairly low. The lower moisture analyses (less than 28 percent moisture) likely reflect unaccountable moisture loss. This conclusion is supported by the nature of the samples. All of the analyses were performed on samples collected at small, shallow, wagon mines along the coal bed outcrops. The author even cautioned "this form [as-received] is not well suited for comparison, because the amount of moisture as it comes from the mine is largely a matter of accident, and consequently analyses of the same coal in this form may vary widely" (Wegemann, 1912, p. 468).

The averages of the five individual basin analyses from the Sussex coal field are also presented in table 1. Although the average gross calorific value of 8,588 Btu/lb is significantly lower than the 9,160 Btu/lb reported by Glass and Jones (1992), the average moisture values still appear to be anomalously low. Assuming that all samples encountered at least some unaccounted-for moisture loss is reasonable, given the nature of the samples as well as the logistics and time required to ship the samples from the field to the laboratory in 1910; an average moisture content of 30 percent would be more realistic. The 30 percent moisture estimate is only about 1 percent higher than the moisture content for the Basin 2 sample. With an as-received moisture level of 30 percent, the 9,160 Btu/lb reported by Glass and Jones (1992) would be reduced to 8,380 Btu/lb. More realistic estimated average values of the basin samples for all parameters adjusted to an as-received moisture level of 30 percent (ASTM International, 2008c) are also shown in table 1.

The issue of anomalously low moisture data was not the major problem encountered in assessing the coal quality of the Sussex coal field. It is important to recognize that the analytical data for the Sussex coal field presented in table 1 should not be considered representative of average values for the whole field. All of the samples are partial coal bed samples. For example, the Basin 6 sample (Laboratory No. 11048) came from a 5-foot-thick bench of lower-ash coal in the middle of an approximately 13-foot-thick coal bed which has several high-ash layers (up to 1 foot thick) in the upper and lower benches of the coal bed. Similarly, the other four samples are from lower-ash coal bed benches, the higher-ash benches being avoided at each sampling location. In fact, the presence of higher-ash coal layers and mineral partings within the coal measures described by Wegemann (1912) are the rule rather than the exception. Statements such as "too broken by shale partings to be minable" are common. The presence of partings and higher-ash layers is consistent with the coal bed geology in the southwestern part of the PRB. On the western flank, the thick coal beds in the eastern and deep central parts of the basin thin, split, and pinch out (Flores and others, 1999). Unlike problems associated with anomalously low moisture contents, which can be straightforwardly adjusted to more realistic levels, the analytical results on coal samples that are not representative of the entire coal bed are especially difficult to assess.

The high frequency and discontinuous nature of these high-ash layers mean that the typical quality of coals in the Sussex coal field is expected to be even lower than the average values adjusted to 30 percent moisture shown in table 1 (higher ash contents and lower gross calorific values). It is impossible to reasonably predict the impacts of inclusion of higher-ash benches on the average coal quality. The same is true for sulfur content predictions. However, it is not unreasonable to expect that the average ash content of 6.0 percent (at the estimated 30 percent moisture basis) would increase to at least 10 percent given the abundance of high-ash layers in the Sussex coal field. At 10 percent ash, the calorific value would decrease to about 7,550 Btu/lb. This calorific value adjustment assumes a decrease of about 100 Btu/lb per 1-percent ash increase. An estimated coal quality of 30 percent moisture, 10 percent ash, and a calorific value of 7,550 Btu/lb is markedly dissimilar from the reported analysis by Glass and Jones (1992; tables 1 and 2).

Excluding the samples with anomalously low moisture contents (table 1), the near-surface Fort Union Formation coal beds have an apparent rank of subbituminous C (subC; ASTM International, 2008a). However, the apparent rank increases with depth as evidenced by the deep Smith (Big George) bed analysis in table 1. The apparent rank reaches subbituminous A (subA) in the deepest part of the basin (fig. 3; Stricker and others, 2007).

Table 2. A comparison of reported coal quality data in the Sussex coal field, Wyoming, from successive publications. Analyses not reported are indicated by NR.

Basin – coal bed	Laboratory number	Analysis	Wegemann (1912)	Smith and others (1972)	Glass and Jones (1992)	Keystone Coal Industry Manual (2005)
Basin 2 – ?	10683	Moisture (%)	28.8			
		Ash (%)	6.7			
		Volatile matter (%)	NR			
		Fixed carbon (%)	NR			
		Sulfur (%)	0.56			
		Calorific value (Btu/lb)	7,930			
Basin 3 – ?	10728	Moisture (%)	23.6			
		Ash (%)	7.8			
		Volatile matter (%)	NR			
		Fixed carbon (%)	NR			
		Sulfur (%)	0.68			
		Calorific value (Btu/lb)	8,450			
Basin 3 – ?	10694	Moisture (%)	NR			
		Ash (%)	14.6			
		Volatile matter (%)	NR			
		Fixed carbon (%)	NR			
		Sulfur (%)	0.56			
		Calorific value (Btu/lb)	7,980			
Basin 4 – Upper bed	10804	Moisture (%)	18.8	18.8		
		Ash (%)	7.6	7.6		
		Volatile matter (%)	35.7	35.7		
		Fixed carbon (%)	37.9	37.9		
		Sulfur (%)	0.57	0.57		
		Calorific value (Btu/lb)	9,160	9,160		
Basin 4 – Lower bed	10827	Moisture (%)	23.5	23.5	23.5	23.5
		Ash (%)	5.17	5.17	5.17	5.2
		Volatile matter (%)	35.6	35.6	35.6	35.6
		Fixed carbon (%)	35.7	35.7	35.7	35.7
		Sulfur (%)	0.49	0.49	0.49	0.49
		Calorific value (Btu/lb)	9,050	9,050	9,160	9,160
Basin 6 – Upper bed	11048	Moisture (%)	28.1	28.1		
		Ash (%)	4.62	4.62		
		Volatile matter (%)	31.6	31.6		
		Fixed carbon (%)	35.7	35.7		
		Sulfur (%)	0.45	0.45		
		Calorific value (Btu/lb)	8,350	8,350		
Additional information	Assessment of moisture validity		YES	NO	NO	NO
	Data to assess representativeness		YES	NO	NO	NO

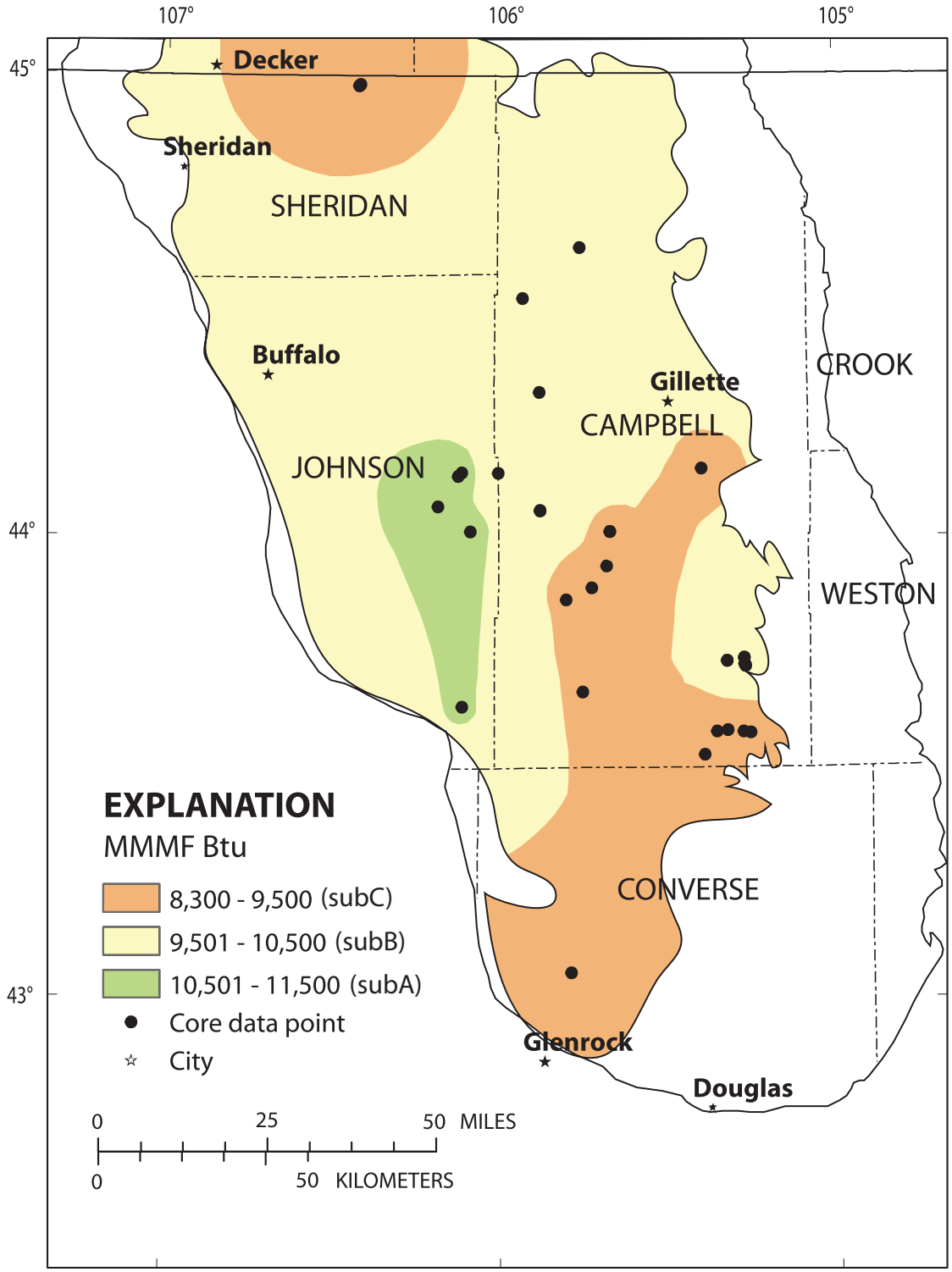

Figure 3. Variation in moist, mineral-matter-free (m, mmf) British thermal units (Btu) in the Wyodak-Anderson coal zone in the Powder River Basin, Wyoming (Stricker and others, 2007), showing a trend towards increasing apparent rank of the coal (ASTM International, 2008a) from subbituminous C (subC) at shallow depths to subbituminous B (subB), and finally subbituminous A (subA) in the deepest part of the basin.

Estimation of the Quality of Deep Fort Union Formation Resources

The SWPRB contains significant volumes of thick Fort Union Formation coal beds that are too deep to mine by means of conventional surface mining technology. As an integral part of the assessment of these deep coal resources, an estimation of the coal quality by depth is an important parameter in assessing the viability of resources potentially recoverable by underground mining methods. Coal quality data for the deeper coal resources are especially limited to a relatively few coal cores sampled for coal-bed natural gas assessment work. Furthermore, the results from the analyses of core samples following gas desorption testing require critical evaluation from the standpoint of both representativeness and sample degradation during the desorption process.

The coal quality dataset from Stricker and others (2007) is a compilation of analyses from 963 core samples from 37 core holes that were placed in sealed canisters for gas desorption measurements. Each sample was 2 feet long and 4.0 inches in diameter. The coal, after gas desorption in the canisters, was split into subsamples for an extensive analytical suite including proximate analyses, ultimate analyses, and gross calorific value determinations. The analytical results from the 37 core holes representing 52 beds were summarized by Stricker and others (2007, table 2, p. 11–14). Those data were then imported into a spreadsheet (table 3) to determine whether a relationship between sample depth and gross calorific values could be established by creating crossplots of depth versus gross calorific values.

The process of analyzing coal quality data from desorbed canister samples can be challenging. The desorption process can take several months or longer. During that time, coal may be partially oxidized, resulting in lower gross calorific values. Furthermore, samples tend to dry out during gas desorption (Mavor and Pratt, 1996). Moisture losses result in anomalously higher as-received gross calorific values. Perhaps one of the greatest challenges is deciding whether or not the canister samples are representative of the entire coal bed. For example, for Bore Hole No. 26 (table 3), a total of fifty-one 2-foot-long canister samples from the Smith (Big George) bed were desorbed, but proximate and gross calorific value analyses were performed on only three of those canister samples.

Representativeness refers not only to parameters like ash but also to the maceral assemblages of each canister sample. Although North American coals tend to be rich in vitrinite (Mathews and others, 2007), there are typically petrographic facies or layers within a coal bed where exinite or inertinite may be enriched relative to vitrinite (Flores and others, 1989). Exinite has a markedly higher calorific value and volatile matter content than vitrinite due to its high hydrogen content. Conversely, the relatively low calorific value of inertinite is due to its lower hydrogen content (Stach and others, 1982). Thus, a canister from a facies enriched in exinite might have an anomalously higher calorific value compared to a whole bed sample from the same sampling location, and the opposite would be true for a facies enriched in inertinite.

Given all the challenges and limitations of interpreting coal quality data from canister samples, it is not surprising that the first attempt to establish a trend of depth versus as-received gross calorific values from table 3 was unsatisfactory (fig. 4). The plot exhibits fairly poor agreement between the two parameters. The least squares trendline had an R^2 of only 0.255. Furthermore, the trendline projection of about 7,000 Btu/lb at shallow depths does not reflect typical values for the PRB at similar depths (table 1).

A review of the data from table 3 suggests that the previously discussed problems of moisture loss, sample oxidation, anomalously high and low calorific values, and representativeness were all encountered to at least some degree. Equilibrium moisture values will typically be lower than the respective inherent (bed) moisture values for a sample that has been collected at its inherent moisture level (Luppens, 1982; Luppens and Hoeft, 1991). In fact, ASTM D1412 ("Standard Test Method for Equilibrium Moisture of Coal at 96 to 97 Percent Relative Humidity and 30°C") states that "based on experience with low rank coals, equilibrium moisture values that exceed inherent moisture values are due to one or both of two situations, either the sample was not collected with its full complement of inherent moisture (partially dried) or an analytical problem occurred, or both" (ASTM International, 2008b, p. 290). For Wyoming subbituminous coals, equilibrium moisture values ranged from 0.5 to 1.3 percent lower than inherent moisture levels (Luppens and Hoeft, 1991). Therefore, equilibrium moisture values that are higher than total moisture values in table 3 indicate moisture was lost during gas desorption for some samples. Additionally, the 2,557-Btu/lb range between the maximum and minimum moisture- and ash-free (DAF) calorific values for coal beds within the same area is quite large. This is probably due in large part to the impact of atypical maceral assemblages on the relatively few canister intervals with calorific analyses and perhaps the effects of sample oxidation, which lowers DAF calorific values.

An additional tool for verifying coal quality is data interrelationships. The verification process is based on the fact that data interrelationships are almost axiomatic in coal analyses. As the analytical result for one parameter changes, the esults for some other parameter usually changes too. The pair of test results may vary inversely or in direct proportion to each other. Correlations based on these data interrelationships can be used to identify possible outliers or estimate missing data (Hoeft and others, 1983). For example, moisture and ash have an inverse linear relationship (Luppens, 1982). As the ash content increases, moisture content decreases. Thus, for two analyses with similar ash contents from the same coal bed and depth, the moisture contents should be similar as well.

Table 3. Properties and composition of coal beds cored in the Powder River Basin, Wyoming (modified from Stricker and others, 2007,table 2). Figure 4 shows the plot of the depth versus as-received calorific values for these data.

Core hole	Mean depth, in feet	Coal zone	Coal bed name as used by gas operators	Number of samples	Moisture		Ash yield (%)	As-received calorific value (Btu/lb)	Dry ash yield (Btu/lb)	Dry colorific value	Dry, ash free (DAF) calorific value (Btu/lb)
					Total (%)	Equilibrium (%)					
9	143.4	Wyodak-Anderson	Upper Wyodak	5	19.27	22.18	12.22	9,280	15.14	11,495	13,095
10	167.0	Wyodak-Anderson	Upper Wyodak	2	26.46	27.45	9.31	8,910	12.66	12,116	13,360
9	181.5	Wyodak-Anderson	Middle/Lower Wyodak	26	22.69	25.57	4.52	8,790	5.85	11,370	11,908
10	209.2	Wyodak-Anderson	Middle/Lower Wyodak	27	27.53	26.78	4.59	8,750	6.33	12,074	12,655
13	212.0	Wyodak-Anderson	Upper Wyodak	8	27.25	----	8.88	8,790	12.21	1,2082	13,260
20	248.9	Wyodak-Anderson	Middle/Lower Wyodak	34	27.81	24.77	4.50	8,990	6.23	12,453	13,040
13	252.4	Wyodak-Anderson	Middle/Lower Wyodak	27	28.86	----	4.56	8,750	6.41	12,300	12,887
14	289.0	Wyodak-Anderson	Middle/Lower Wyodak	30	28.88	25.18	3.46	8,890	4.87	12,500	12,948
15	293.1	Wyodak-Anderson	Middle/Lower Wyodak	32	27.93	25.61	3.69	8,740	5.12	12,127	12,592
17	293.1	Wyodak-Anderson	Middle/Lower Wyodak	39	26.54	25.49	3.82	8,770	5.20	11,938	12,413
16	319.4	Wyodak-Anderson	Middle/Lower Wyodak	28	27.13	26.13	4.22	8,600	5.79	11,802	12,322
28	329.3	Wyodak-Anderson	Anderson	8	27.46	27.23	4.22	8,820	5.82	12,159	12,695
34	345.0	Wyodak-Anderson	Anderson	17	24.98	25.35	4.68	9,010	6.24	12,010	12,600
23	346.0	Wyodak-Anderson	School	9	25.49	26.25	12.20	8,020	16.37	10,764	12,259
18	360.2	Wyodak-Anderson	Middle/Lower Wyodak	40	25.56	----	3.75	9,090	5.04	12,211	12,687
8	385.0	Wyodak-Anderson	Smith	15	26.13	----	5.87	9,080	7.95	12,292	13,058
34	519.5	Wyodak-Anderson	Canyon	13	26.31	24.26	3.71	9,090	5.03	12,335	12,811
30	640.0	Wyodak-Anderson	Canyon	7	25.31	25.53	3.74	9,120	5.01	12,210	12,685
6	648.7	Wyodak-Anderson	Canyon	7	32.01	----	5.20	7,630	7.65	11,222	11,838
6	952.0	----	Cook	8	27.77	----	4.54	8,670	6.29	12,003	12,574
33	960.2	Wyodak-Anderson	Big George	10	24.77	23.83	4.22	9,180	5.61	12,203	12,740
8	990.0	Wyodak-Anderson	Canyon	4	25.82	----	4.19	9,340	5.65	12,591	13,142
6	1,074.0	----	Wall	4	27.40	----	5.67	8,760	7.81	12,066	12,791
5	1,076.0	Wyodak-Anderson	Big George	13	26.42	----	3.95	8,920	5.37	12,123	12,621
2	1,138.9	Wyodak-Anderson	Big George	50	19.78	----	3.38	10,300	4.21	12,840	13,289
4	1,142.0	----	Wall	16	25.55	----	5.78	9,440	7.76	12,680	13,457
37	1,166.1	----	Pawnee	7	21.60	20.91	5.58	9,740	7.12	12,423	13,158
3	1,192.0	Wyodak-Anderson	Anderson	2	27.76	26.40	6.30	7,790	8.72	10,783	11,509
35	1,230.9	Wyodak-Anderson	Big George	20	25.55	24.77	3.65	9,150	4.90	12,290	12,756
25	1,243.0	----	Pawnee	5	25.19	24.34	8.14	8,120	10.88	10,854	11,816

Table 3. Properties and composition of coal beds cored in the Powder River Basin, Wyoming (modified from Stricker and others, 2007,table 2). Figure 4 shows the plot of the depth versus as-received calorific values for these data.—Continued

Core hole	Mean depth, in feet	Coal zone	Coal bed name as used by gas operators	Number of samples	Moisture		Ash yield (%)	As-received calorific value (Btu/lb)	Dry ash yield (Btu/lb)	Dry colorific value	Dry, ash free (DAF) calorific value (Btu/lb)
					Total (%)	Equilibrium (%)					
36	1,266.4	----	Pawnee	4	22.01	34.07	6.09	10,030	7.81	12,861	13,695
5	1,276.5	Wyodak-Anderson	Wyodak	24	24.61	----	4.50	9,440	5.97	12,522	13,112
1	1,287.2	Wyodak-Anderson	Big George	60	19.22	18.50	3.67	10,440	4.54	12,924	13,416
19	1,308.0	Wyodak-Anderson	Big George	6	23.49	23.69	3.36	9,420	4.39	12,312	12,740
26	1,365.2	Wyodak-Anderson	Big George	51	19.23	17.67	3.86	10,330	4.78	12,789	13,303
11	1,366.4	Wyodak-Anderson	Big George	12	24.33	23.48	4.51	9,510	5.96	12,568	13,161
12	1,401.0	Wyodak-Anderson	Big George	32	21.90	19.89	4.58	9,300	5.86	11,908	12,479
31	1,440.3	Wyodak-Anderson	Big George	32	17.94	18.15	5.97	9,870	7.28	12,028	12,791
27	1,537.6	----	Pawnee	11	23.43	20.41	4.55	9,200	5.94	12,015	12,588
32	1,541.8	Wyodak-Anderson	Big George	17	17.95	16.51	3.41	10,440	4.16	12,724	13,173
27	1,709.8	----	Cache	16	23.10	22.24	4.77	9,100	6.20	11,834	12,426
11	1,769.0	Wyodak-Anderson	Werner	13	24.60	22.81	2.69	9,570	3.57	12,692	13,043
29	2,197.5	----	Roberts	7	22.64	16.85	9.75	9,820	12.60	12,694	14,065
Average					24.78	23.62	5.22	9,140	**6.94**	**12,144**	**12,813**
Maximum value (MAX)					32.01	34.07	12.22	10,440	**16.37**	**12,924**	**14,065**
Minimum value (MIN)					17.94	16.51	2.69	7,630	**3.57**	**10,764**	**11,509**
MAX-MIN range					14.07	17.56	9.53	2,810	**12.81**	**2,160**	**2,557**

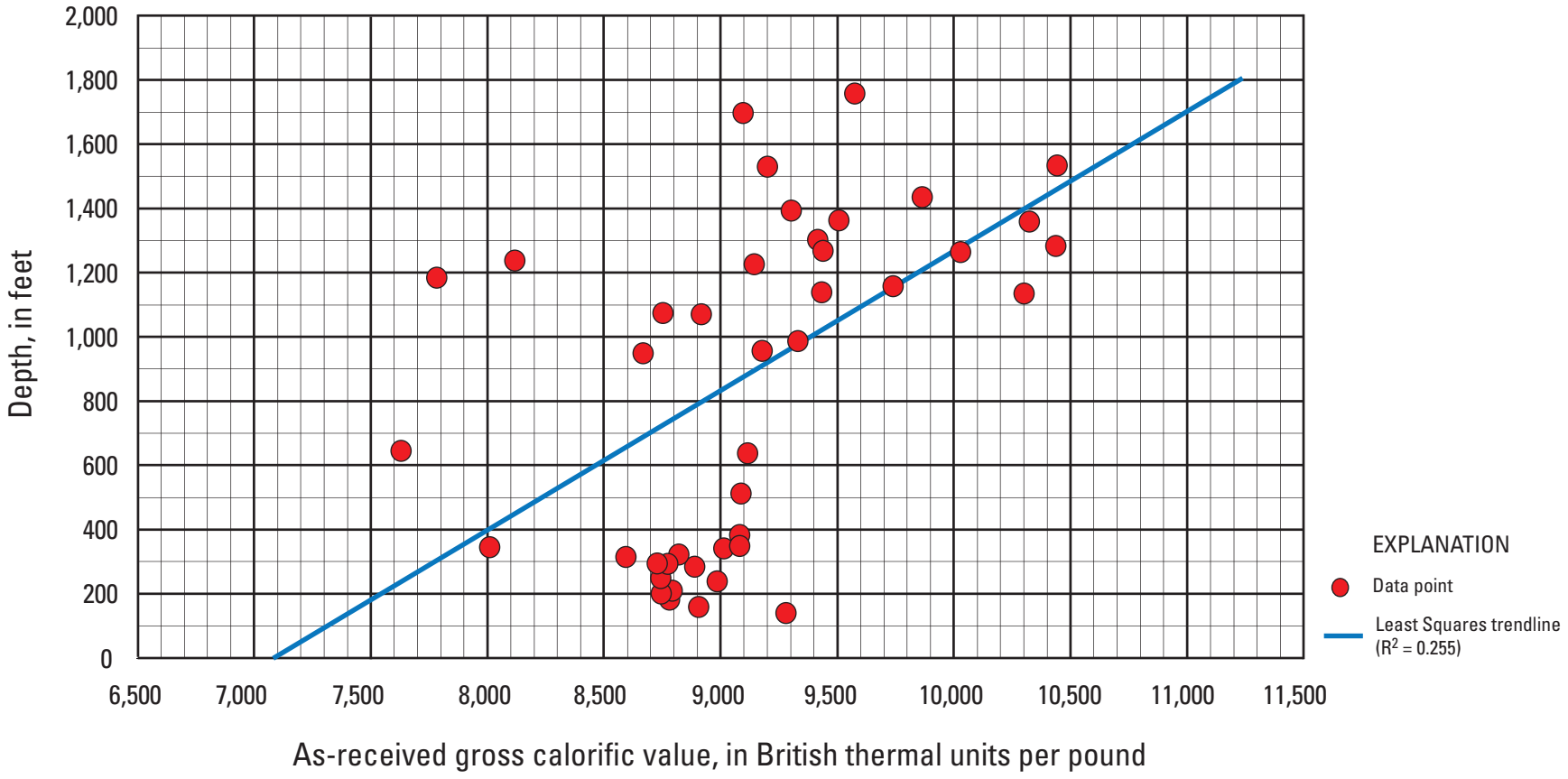

Figure 4. Estimated variability of as-received gross calorific values versus depth from table 3 data for the Wyodak coal beds in the Powder River Basin, Wyoming.

For Core Holes 30 and 6 (table 3), the ash contents and depths are very similar, but the moisture contents are significantly different (25.31 versus 32.01, respectively). Furthermore, the relatively high moisture content for Core Hole 6 resulted in anomalously lower dry and DAF calorific values. Therefore, Core Hole 6 was considered suspect. Core hole samples with equilibrium moisture values that were more than 1 percent higher than the total moisture values also were discarded. The remaining data in table 3 were similarly edited, and coal bed analyses that appeared to be anomalous (mostly because of suspect moisture and calorific values) also were discarded. Also, to reduce variations due to differences in bed characteristics, only coal beds in the Wyodak-Anderson coal zone (Smith through the Werner beds) were used (fig. 5).

Of the 43 coal bed analyses in table 3, only 25 were retained as a result of the editing process (table 4). All the ranges in the maximum and minimum values in table 4 are much more realistic. For example, the range in DAF calorific values was reduced from 2,557 Btu/lb (table 3) to 938 Btu/lb (table 4). More importantly, the plot of depth versus calorific values from the edited data (fig. 6) visually demonstrates a more reliable relationship than the plot made from the unedited data (fig. 4). Additionally, the R^2 of 0.744 from figure 6 represents a significant improvement over that in figure 4. A trendline based on the moist, mineral-matter-free calorific values from table 4 was also plotted on figure 6 to illustrate the relationship between apparent coal rank and depth. It must be stressed that, given the limitations of the desorbed-gas-canister analyses combined with the discarding of analyses through an editing process based solely on author experience with coal quality relationships in the PRB, the results should be refined as more data become available.

Two sources of independent data verification shown on figure 6 corroborate the relationship between calorific values and depth. Testa and Pratt (2003) also examined the relationship between calorific values and depth. The trendline of their depth versus moist, mineral-matter-free calorific values was added to figure 6. The two trendlines exhibit marked concurrence. The slopes are nearly parallel, and calorific values generally agree within 100 Btu/lb. The second source of verification is the published deep basin analyses of the Smith bed (Big George) from table 1. The calorific value of 9,750 Btu/lb represents the "unweighted average of 30 incremental samples from a 200-ft thick cored portion of the bed below 1000 feet" (Keystone Coal Industry Manual, 2010, p. 617). Further investigation revealed that the exact depth interval for this Smith bed was 1,580 to 1,780 feet (N.R. Jones, unpub. data, 2010). This 200-foot sample interval with an average calorific value is plotted on figure 6 as a box, which the trendline for the calorific values versus depth trendline nearly bisects. Although the depth versus calorific values plot in figure 6 is based on relatively few selected data points, the multiple sources of independent data verification support the use of that trendline as a reasonable technique for estimating the expected coal quality of the thick coals to a depth of 2,000 feet.

Wasatch Formation Coal Quality

As with the Fort Union Formation, only limited coal quality data for the Wasatch Formation are available. No significant, large-scale mining has occurred in the Wasatch coal beds in the PRB despite the fact that the Healy bed in the Lake De Smet coal field (fig. 2) is the thickest known coal bed in the contiguous United States (Keystone Coal Industry Manual, 2010). A summary of coal quality data for the Wasatch Formation is presented in table 5.

In general, Wasatch coal beds have higher ash and sulfur contents and lower calorific values than the Fort Union Formation coals currently being produced in the PRB (Luppens and others, 2008). Partings are common and fairly persistent in many Wasatch coal beds (Mapel and others, 1953; Mapel, 1959; Keystone Coal Industry Manual, 2010), which probably accounts, in part, for the lower quality. The apparent rank of Wasatch coal beds based on published data ranges from lignite A to subbituminous C (table 5). As with the Fort Union Formation coal quality for the SWPRB, limitations with existing published Wasatch coal quality information stem from both the accuracy and the representativeness of the data.

The issue of accuracy is, again, basically one of the reliability of the moisture results. The total moisture contents forthe Lake De Smet coal cores in table 5 ranges from 23.6 to 30.5 percent. This range in moisture values for cores with similar ash contents from the same area seems large, especially because the face channel samples from the mine in the Lake De Smet area indicate moisture contents exceeding 30 percent (table 5). The USGS-2A core had a moisture content of 30.5 percent, which is comparable to the two mine face channel samples. It was recognized that moisture in the Bureau of Reclamation (BOR) core (table 5) was at least 5 percent below that of the other cores, which was attributed to moisture loss during handling and shipping (Mapel and others, 1953). Yet, despite this core having an acknowledged anomalously low moisture content, it was used as reported in the calculation of the average coal quality parameters, biasing the average calculated coal quality.

The fluids used in the coring process can add excess surface moisture to the cores (Luppens and others, 1992). Therefore, it would be expected that the average total moisture of the cores should be at or at least slightly higher than—rather than significantly less than—the total moisture values of the mine face channel samples. It is suspected that moisture was lost during shipping and that subsequent partial drying occurred through handling and processing of the core. All the cores were either coated with paraffin wax or wrapped in wax paper to preserve the moisture in the core samples; however, both practices are imperfect barriers to moisture loss. Any additional core breakage during shipping could have compromised the wax coating. Furthermore, the cores were sliced in half by means of a saw with a dry blade (Mapel and others, 1953) prior to core logging and analysis, which also could have contributed to additional, unaccounted-for moisture loss.

Formation name	Kent and others (1980)	Pierce and others (1990)	USGS Fort Union Coal Assessment Team (1999) and Glass (1997)	Ellis and others (2002)	Gillette coal field (Luppens and others, 2008)	Northern Wyoming Powder River Basin (Scott and others, 2010)	Current SWPRB assessment area
	Bed names						
Wasatch		Felix			Upper Felix Felix	Upper Healy Healy Ucross Felix Lower Felix	Upper Healy, Healy Murray Ucross Felix Lower Felix
Fort Union (Tongue River Member)	Smith	Roland/ Badger	Roland	Wyodak Rider	Roland	Roland (Upper Rider) Roland of Baker, 1929 Roland of Taff, 1929	Roland (Upper Rider) Roland (Lower Rider) Roland of Baker, 1929
	Upper Wyodak	Wyodak or Upper Wyodak (Anderson/ Canyon)	Wyodak-Anderson coal zone=Smith (Swartz), Badger, School, Sussex, Big George, Wyodak, Anderson, Dietz, Canyon (Monarch), Werner	Upper Wyodak	Smith Anderson Rider, Anderson Dietz	Smith Anderson Lower Anderson Dietz 1, Dietz 2, Dietz 3, Dietz 4	Smith Anderson Dietz 3 Upper Canyon
	Canyon			Canyon	Canyon	Canyon	Canyon
				Lower Wyodak	Werner	Lower Canyon Ferry Werner	Lower Canyon Werner
	Werner	Lower Wyodak					
						Otter	Otter
	Gates/ Kennedy	Upper Kennedy		Gates/ Kennedy	Gates	Gates	Gates
					Pawnee	Pawnee	Pawnee
						Odell	
							Deep 1
							Deep 2
							Deep 3
						Roberts	Roberts

Wyodak-Anderson coal zone

Figure 5. Coal bed and coal zone names used in different publications in the Powder River Basin, including current SWPRB coal assessment area (L. Osmonson, U.S. Geological Survey, unpub. data, 2010).

Table 4. Edited version of table 3 in which core holes with anomalous data were deleted. Of the total of the 43 coal bed analyses in table 3, only 25 were retained as a result of the editing process. Figure 6 shows the plot of the depth versus as-received calorific values for these data. A trendline for the calculated moist, mineral-matter-free calorific value is also shown on figure 6 to illustrate the relationship with apparent rank versus depth.

Core hole	Mean depth, in feet	Coal zone	Coal bed name as used by gas operators	Number of samples	Moisture		Ash yield (%)	As-received calorific value (Btu/lb)	Dry ash yield (Btu/lb)	Dry colorific value	Dry, ash free (DAF) calorific value (Btu/lb)
					Total (%)	Equilibrium (%)					
10	167.0	Wyodak-Anderson	Upper Wyodak	2	26.46	27.45	9.18	8,790	12.49	11,953	13,162
10	209.2	Wyodak-Anderson	Middle/Lower Wyodak	27	27.53	26.78	4.59	8,750	6.33	12,074	12,655
13	212.0	Wyodak-Anderson	Upper Wyodak	8	27.25	----	8.88	8,790	12.21	12,082	13,260
20	248.9	Wyodak-Anderson	Middle/Lower Wyodak	34	27.81	24.77	4.50	8,990	6.23	12,453	13,040
13	252.4	Wyodak-Anderson	Middle/Lower Wyodak	27	28.86	----	4.56	8,750	6.41	12,300	12,887
14	289.0	Wyodak-Anderson	Middle/Lower Wyodak	30	28.88	25.18	3.46	8,890	4.87	12,500	12,948
15	293.1	Wyodak-Anderson	Middle/Lower Wyodak	32	27.93	25.61	3.69	8,740	5.12	12,127	12,592
17	293.1	Wyodak-Anderson	Middle/Lower Wyodak	39	26.54	25.49	3.82	8,770	5.20	11,938	12,413
16	319.4	Wyodak-Anderson	Middle/Lower Wyodak	28	27.13	26.13	4.22	8,600	5.79	11,802	12,322
28	329.3	Wyodak-Anderson	Anderson	8	27.46	27.23	4.22	8,820	5.82	12,159	12,695
34	345.0	Wyodak-Anderson	Anderson	17	24.98	25.35	4.68	9,010	6.24	12,010	12,600
18	360.2	Wyodak-Anderson	Middle/Lower Wyodak	40	25.56	----	3.75	9,090	5.04	12,211	12,687
8	385.0	Wyodak-Anderson	Smith	15	26.13	----	5.87	9,080	7.95	12,292	13,058
34	519.5	Wyodak-Anderson	Canyon	13	26.31	24.26	3.71	9,090	5.03	12,335	12,811
30	640.0	Wyodak-Anderson	Canyon	7	25.31	25.53	3.74	9,120	5.01	12,210	12,685
33	960.2	Wyodak-Anderson	Big George	10	24.77	23.83	4.22	9,180	5.61	12,203	12,740
8	990.0	Wyodak-Anderson	Canyon	4	25.82	----	4.19	9,340	5.65	12,591	13,142
5	1,076.0	Wyodak-Anderson	Big George	13	26.42	----	3.95	8,920	5.37	12,123	12,621
35	1,230.9	Wyodak-Anderson	Big George	20	25.55	24.77	3.65	9,150	4.90	12,290	12,756
5	1,276.5	Wyodak-Anderson	Wyodak	24	24.61	----	4.50	9,440	5.97	12,522	13,112
19	1,308.0	Wyodak-Anderson	Big George	6	23.49	23.69	3.36	9,420	4.39	12,312	12,740
11	1,366.4	Wyodak-Anderson	Big George	12	24.33	23.48	4.51	9,510	5.96	12,568	13,161
12	1,401.0	Wyodak-Anderson	Big George	32	21.90	19.89	4.58	9,300	5.86	11,908	12,479
31	1,440.3	Wyodak-Anderson	Big George	32	17.94	18.15	5.97	9,870	7.28	12,028	12,791
11	1,769.0	Wyodak-Anderson	Werner	13	24.60	22.81	2.69	9,570	3.57	12,692	13,043
Average					**25.74**	24.47	**4.58**	**9,079**	**6.17**	**12,227**	**12,816**
Maximum value (MAX)					**28.88**	27.45	**9.18**	**9,870**	**12.49**	**12,692**	**13,260**
Minimum value (MIN)					**17.94**	18.15	**2.69**	**8,600**	**3.57**	**11,802**	**12,322**
MAX-MIN range					**10.94**	9.30	**6.49**	**1,270**	**8.92**	**890**	**938**

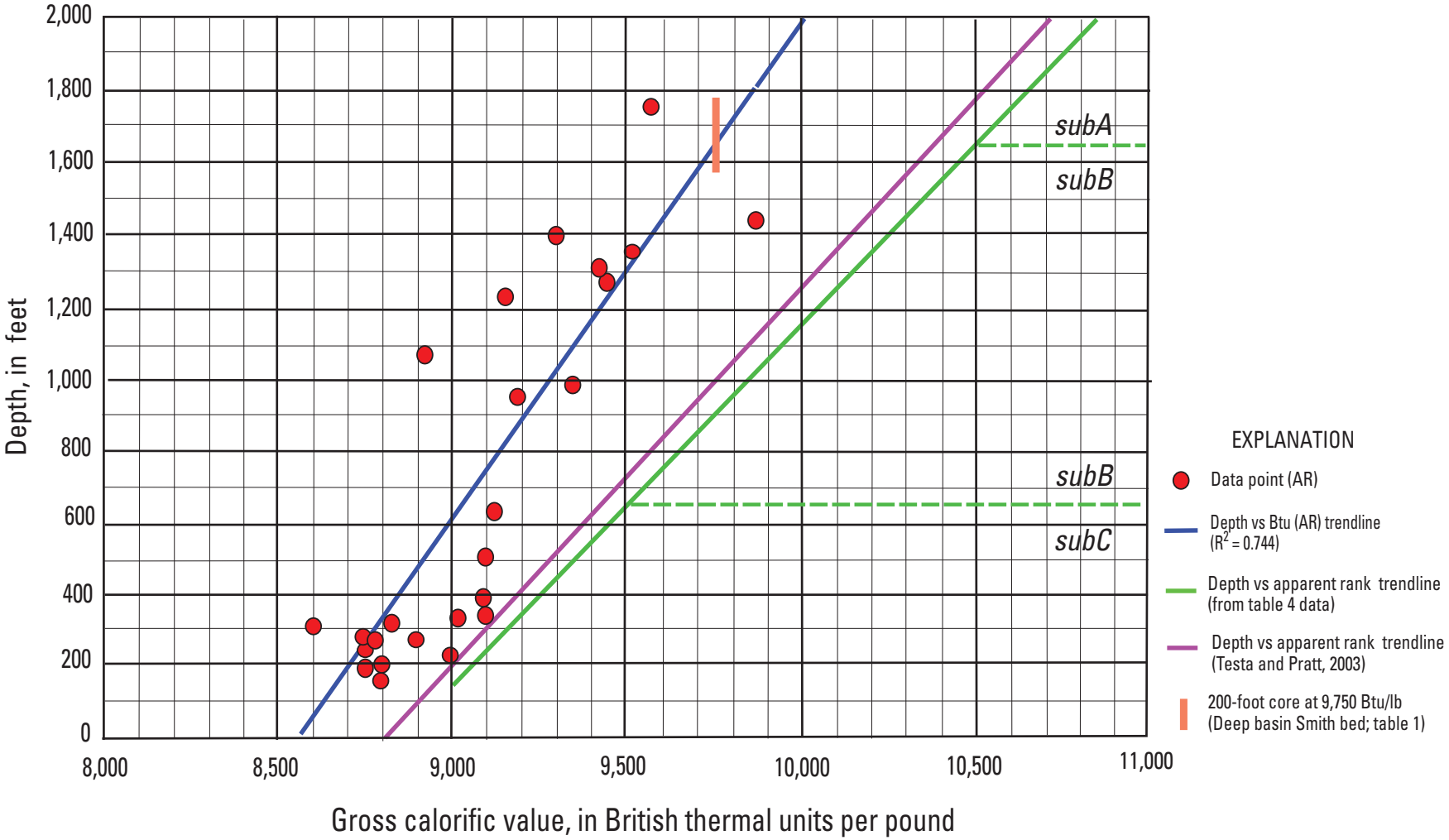

Figure 6. Estimated variability of as-received (AR) and moist, mineral-matter-free (m,mmf) gross calorific values versus depth from table 4 for the Wyodak coal beds in the Powder River Basin, Wyoming. The m,mmf gross calorific values calculated from the table 4 data are used to determine apparent rank, and the ranges are subbituminous C (subC), less than 9,500 Btu/$lb_{m,mmf}$; subbituminous B (subB), 9,500–10,500 Btu/$lb_{m,mmf}$; and subbituminous A (subA), greater than 10,500 Btu/$lb_{m,mmf}$.

Table 5. Available as-received coal quality data from the Wasatch Formation in the Lake De Smet area and other Watsatch coal beds. Average values are shown in bold type.

Area and coal bed name	No. of analyses	Coal bed interval		Total coal bed interval cored	Total feet shale, pyrite excluded	Net total coal feet analyzed[6]	Percent of excluded shale to total recovered core	Percent of core interval analyzed	Moisture (%)	Sulfur (%)	Ash (%)	Calorific value (Btu/lb)	Pounds of SO_2 per million Btu	Calorific value ($Btu/lb_{m.mmf}$)[4]	Apparent rank[5]
		From	To												
Lake De Smet area															
Healy coal bed[1,2]	15								28.5	0.60	7.6	7,880	1.52	8,583	subC
USGS-1 core[1,3]	1	59.0	141.7	82.7	7.1	47.1	13.1	57.0	29.1	0.60	5.1	7,970	1.51	8,432	subC
USGS-2A core[1,3]		66.0	119.0	53.0	1.8	40.8	4.2	77.0	30.5	0.50	6.1	7,845	1.27	8,396	subC
USGS-3 core[1,3]		101.0	159.7	58.7	1.1	37.2	2.9	63.4	28.3	0.60	7.7	7,890	1.52	8,604	subC
USGS-6 core[1,3]		172.0	292.0	120.0	33.8	68.1	33.2	56.8	29.3	0.60	9.2	7,515	1.60	8,341	subC
Bureau of Reclamation core[1,3]		95.0	224.9	129.9	20.2	101.6	16.6	78.2	23.6	1.00	9.7	8,270	2.42	9,239	subC
Average of all 5 core holes[3]	5				**12.8**		**14.0**	**66.5**	**27.0**	**0.70**	**8.1**	**7,940**	**1.76**	**8,700**	subC
Estimated average of 5 core holes (at 30.5% moisture)	5								**30.5**	**0.67**	**7.7**	**7,559**	**1.76**	**8,243**	ligA
Healy bed (face channel mine sample)	1								30.7	0.40	5.1	7,900	1.01	8,359	subC
Bed 120 feet below Healy bed (face channel mine sample)	1								31.1	1.40	8.8	7,350	3.81	8,114	ligA
Other Wasatch coal beds															
Felix coal bed[2]	42								28.0	0.89	7.8	8,050	2.21	8,789	subC
Murray/Ucross beds[2]	15								30.2	1.50	4.3	8,000	3.75	8,383	subC

[1]Partial bed sample.

[2]Keystone Coal Manual (2010).

[3]Mapel and others (1953). (Individual cores from Healy beds.)

[4]Moist, mineral-matter-free (m,mmf) basis.

[5]Subbituminous C (subC), subbituminous B (subB), lignite A (ligA).

[6]Total coal recovered minus shale partings deliberately excluded from analytical samples.

To derive a more realistic estimate of the coal quality for the Lake De Smet coal field, the weighted average of the five cores in table 5 was normalized to 30.5 percent moisture. The 30.5-percent moisture estimate was based largely on the moisture levels of the mine face channel samples and USGS-2A core (table 5). The moisture adjustment resulted in a decrease of more than 300 Btu/lb in the average calorific value to 7,559 Btu/lb and lowered the estimated apparent rank to the lignite A/subbituminous C boundary (table 5). Because the Wasatch Formation is younger than the underlying Fort Union Formation, the slightly lower apparent rank of the Wasatch coal beds relative to the Fort Union coal beds in the nearby Sussex coal field (fig. 1, table 1) is consistent with their relative burial depths.

Unlike the moisture issue, the representativeness of the data is much more difficult to evaluate because of a combination of incomplete core recovery for all core holes and the intentional exclusion of all high-ash intervals. The percentage of the coal bed recovered ranged from about 57 to 78 percent (table 5). This range of core loss is significant (Luppens and others, 1992) and certainly raises questions about the representativeness of the core samples. Frequently, higher-ash zones with interbedded coal and non-coal lamina sustain lower recovery rates during the coring process. The dissimilar lamina create more bedding-plane weaknesses, leading to more fractured core and greater potential for core loss. If this situation contributed to increased core loss, the recovered samples would be biased towards lower-ash contents. However, without corroborating data such as geophysical logs, it is impossible to evaluate the recovered cores from a representativeness perspective.

The most serious problem from a representativeness standpoint was the systematic removal of all high-ash zones and partings greater than 3/8 inch in thickness from all core samples (Mapel and others, 1953). U.S. Geological Survey guidelines in place at the time of sampling mandated that their samplers strictly follow the exclusionary procedure for partings and pyrite of certain thicknesses (Golightly and Simon, 1989). The elimination of the high-ash layers follows the practices in the ASTM D388 standard on the classification of coals by rank (ASTM International, 2008b). This standard specifies excluding mineral partings more than 1 centimeter (3/8 inch) for samples used for the determination of coal rank. The excluded intervals were not analyzed separately. By analyzing both the retained and the excluded materials as well as the coal quality for each, whole bed core could have been mathematically composited. Whole bed core analyses are a fundamental component for all coal resource assessments. Despite the exclusionary practice, the detailed documentation of the core sampling process (Mapel and others, 1953) makes it possible to at least estimate the magnitude of the effect on the reported average coal quality (table 5) if the excluded high ash and pyrite partings were reconstituted with the analyzed core samples. The total thickness of the excluded shale partings for the five cores ranged from 1.1 to 33.8 feet and averaged 12.8 feet (table 5).

Because the total percentage of excluded shale to total coal core analyzed for drill core USGS-1 was very close to the average of the five cores (table 5), USGS-1 was studied more closely to better understand impacts of this exclusionary sampling methodology. To begin, the laboratory descriptions of drill core USGS-1 were reviewed. The USGS-1 core hole spanned a total of 18 black shale partings totaling 7.1 feet, which were removed and discarded prior to analyzing the core samples. The thickness of individual partings ranged from 1/2 inch to 16 3/4 inches. Figure 7 illustrates the distribution and magnitude of the excluded partings, as well as the intervals of lost core. As indicated by this figure, it seems unlikely that selective mining to exclude these parting would be practical given the range in parting thicknesses and their interbedded relationship with the coal layers throughout the entire bed; therefore, from the standpoint of a coal resource assessment, a predicted quality for the whole coal bed is needed.

The first step in arriving at the composited quality is estimating ash and calorific values for the excluded shale fraction. Based on the analyses of numerous coal bed roof and floor samples from Texas, Louisiana, Mississippi, and Wyoming (J.A. Luppens, unpub. data, 2010), the as-received ash and calorific values chosen were 65 percent and 1,500 Btu/lb, respectively. When compositing analyses, it is also important to consider the method by which the proportional amounts of each sample are calculated. Often, one can make the mistake of simply using a volumetric approach (dividing the length of each sample by the total length of the interval to be composited). If the densities of each interval are similar, the volumetric method is appropriate; however, in cases where there are significant density differences (such as partings composed of mineral matter versus coal), the volumetric method is flawed (Luppens and others, 1992). The density of mineral matter should be determined for each lithology and then used to calculate composite values. To evaluate compositing on a mass basis, the average densities of the coal and shale are estimated to be 1.3 grams per cubic centimeter (g/cm^3) and 1.9 g/cm^3.

Table 6 illustrates the differences between results from volume (thickness) weighting versus density weighting to calculate coal quality averages for the USGS-1 core hole interval samples. The volumetric method overestimates the calorific value of the recovered core by nearly 300 Btu/lb and underestimates the ash by 2.7 percent. Most important are the significant differences between the estimated quality from the composited results (table 6) and the original reported values in table 5 for the USGS-1 core hole from Mapel and others (1953). The combined effects of adjusting the moisture level to a more realistic value of 30.5 percent and estimating the impact of including the discarded shale partings was an increase in ash from 5.1 to over 15 percent and a decrease in the calorific value from 7,970 to about 6,700 Btu/lb.

With a significant volume of unrecovered core (fig. 7) for USGS-1 (28.5 feet, or 34.4 percent of the total interval cored), the issue of representativeness cannot be fully resolved (table 6). A compositing case that assumed that the entire unrecovered core was coal is presented in table 6 as a

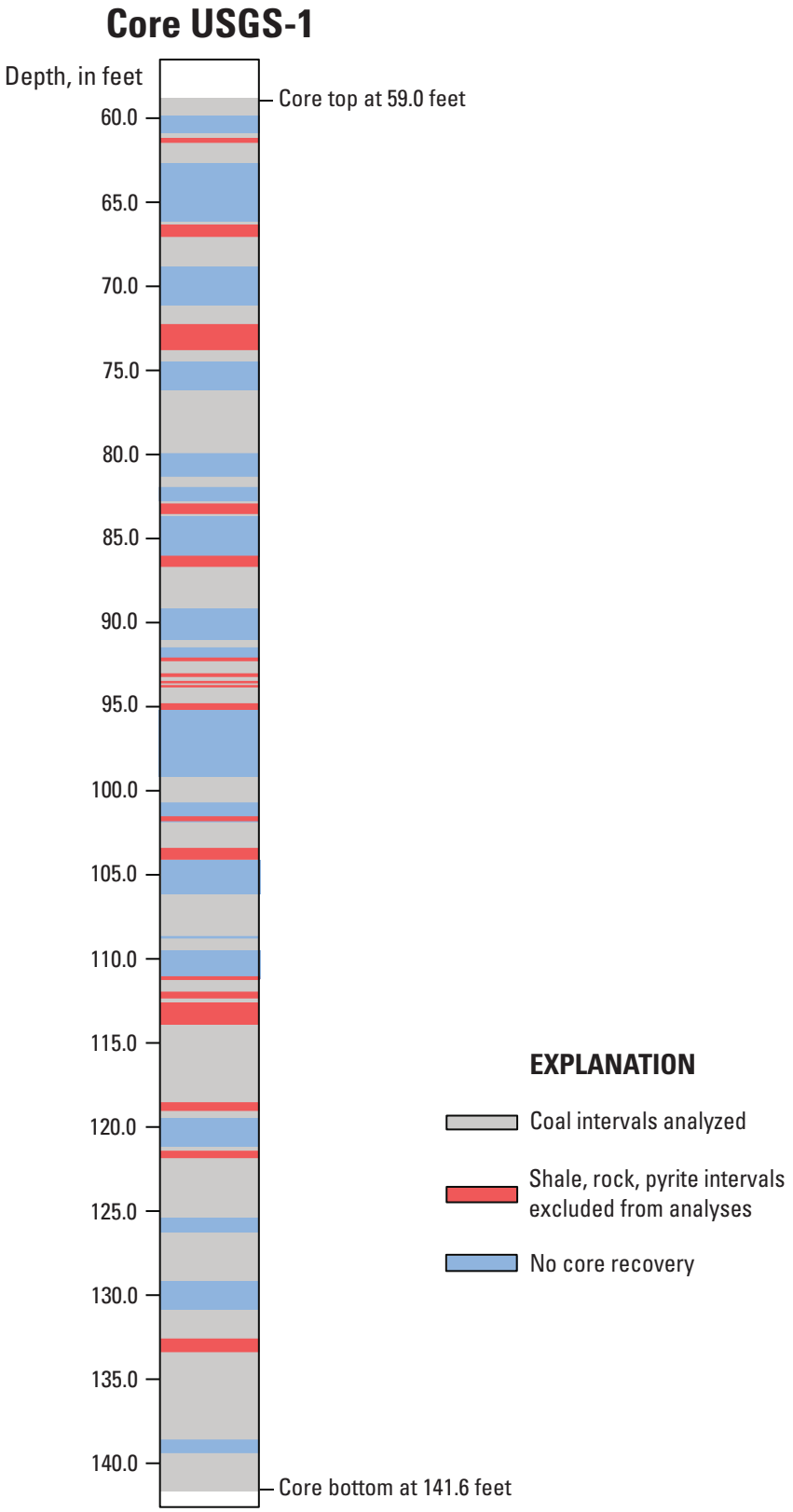

Figure 7. Core log for core hole USGS-1 in the Lake De Smet coal field, Wyoming, illustrating core intervals analyzed, shale intervals excluded from the analyses, and lost-recovery intervals (from Mapel and others, 1953).

Table 6. Estimated impacts of compositing the originally excluded shale, pyrite, and other high-ash parting material with the coal analyses for the USGS-1 core hole (Mapel and others, 1953) from the Lake De Smet coal field, Wyoming. Because these coal quality parameters are reported on a weight basis, mass weighting is the more appropriate method of mathematically compositing samples (Luppens and others, 1992).

Lithologies	Total core thickness (ft)	Analytical parameters		Volumetric weighting			Mass weighting				
		Ash (%)[a]	Calorific value[a] (Btu/lb)	Volume	Ash % × vol %	Calorific value × vol % (Btu/lb)	Density (g/cm³)[b]	Thick-ness × density	Mass	Ash % × mass %	Calorific value × mass % (Btu/lb)
Shale excluded	7.1	65.0	1,500	13.1%	8.5	196	1.9	13.5	17.7%	11.5	266
Total coal analyzed	47.1	5.0	7,813	86.9%	4.3	6,790	1.3	62.6	82.3%	4.1	6,429
Total	54.2			100.0%	**12.9**	**6,986**		76.1	100.0%	**15.6**	**6,694**

[a]Ash and calorific values are the averages for USGS-1 core adjusted to 30.5 percent moisture and estimated values for the excluded shale.

[b]Density values are estimated.

best-case scenario in terms of deriving a whole coal bed estimate. However, this best-case estimate still more than doubles the average ash content from the original reported value. More than likely, the actual quality of the whole coal bed interval is somewhere between the volumetric and mass-weighted estimates in table 6. Additionally, the effects on the average sulfur content of the composited estimates were impossible to assess because of a lack of data; but intuitively, the sulfur content for the whole bed should be higher than reported given the deliberate exclusion of the black shale and pyrite-rich partings.

The thorough review of the original report for the Lake De Smet coal field resulted in a projected average coal quality that was significantly lower than the published data. With estimated values of 12 to nearly 16 percent ash, calorific values of about 6,700 to 7,000 Btu/lb, and sulfur contents perhaps as high as 1.0 percent or higher, the coal quality of this coal field is not competitive with any other coal currently being produced in the PRB. Despite the thickness of the coal bed, no significant, large-scale mining has occurred to date. It is suspected that the relatively inferior coal quality might be a contributing factor to the lack of development in the area.

Conclusions

From the previous discussion, it is demonstrated why it is always preferable to research and evaluate the circumstances regarding the sampling and analytical results from the original data sources when evaluating coal quality information, especially if only limited data are available. Cited data often omit important information, such as moisture integrity and the information needed to evaluate the issue of representativeness. Furthermore, only selected data may be quoted or data may be misquoted, as in the case of Glass and Jones (1992).

Using the available published data at face value would have significantly overestimated the coal quality for all the coal fields from both the Fort Union and the Wasatch Formations in the SWPRB assessment area. However, if sufficient sampling information is provided, it may be possible to make adjustments to reported data to derive more reasonable estimates of coal quality.

References Cited

ASTM International, 2008a, Standard classification of coals by rank: Annual Book of ASTM Standards, v. 05.06, chap. D 388–05, p. 250–256.

ASTM International, 2008b, Standard test method for equilibrium moisture of coal at 96 to 97 percent relative humidity and 30°C: Annual Book of ASTM Standards, v. 05.06, chap. D 1412–07, p. 286–290.

ASTM International, 2008c, Standard practice for calculating coal and coke analyses from as-determined to different bases: Annual Book of ASTM Standards, v. 05.06, chap. D 3180–07, p. 286–290.

Baker, A.A., 1929, The northward extension of the Sheridan coal field, Big Horn and Rosebud counties, Montana: U.S. Geological Survey Bulletin 806–B, p. 15–67.

Flores, R.M., Ochs, A.M., Bader, L.R., Johnson, R.C., and Vogler, D., 1999, Framework geology of the Fort Union coal in the Powder River Basin: U.S. Geological Survey Professional Paper 1625–A, chap. PF, 40 p., accessed November 12, 2010, at *http://pubs.usgs.gov/pp/p1625a/pp1625A.html.*

Flores, R.M. Warwick, P.D., and Moore, T., 1989, Tertiary and Cretaceous coals in the Rocky Mountain region: Washington, D.C., American Geophysical Union Field Trip Guidebook T132, 60 p.

Fort Union Coal Assessment Team, 1999, 1999 resource assessment of selected Tertiary coal beds and zones in the Northern Rocky Mountains and Great Plains Region: U.S. Geological Survey Professional Paper 1625–A, 2 CD-ROMs.

Glass, G.B., 1975, Analyses and measured sections of 54 Wyoming coal samples: Geological Survey of Wyoming Report of Investigation 11, 219 p.

Glass, G.B., 1976, Update on the Powder River Coal Basin, *in* Laudon, R.B., Curry, W.H., III, and Runge, J.S., eds., Geology and energy resources of the Powder River—Wyoming Geological Association Guidebook, 28th Annual Field Conference, Casper, Wyoming: p. 209–220.

Glass, G.B., 1997, Coal geology of Wyoming: Wyoming State Geological Survey Reprint 63, 21 p.

Glass, G.B., and Jones, R.J., 1992, Coal fields and coal beds of Wyoming: Wyoming Geological Survey Reprint 47, p. 133–167.

Golightly, D.W., and Simon, F.O., 1989, Methods for sampling and inorganic analysis of coal: U.S. Geological Survey Bulletin 1823, 72 p., accessed November 12, 2010, at *http://pubs.usgs.gov/bul/b1823/index.htm*.

Hoeft, A.P., Luppens, J.A., Fuller, R.I., and Tucker, C.R., 1983, Coal analysis data interrelationships and crossplots, *in* Proceedings of the 3d International Coal Testing Conference, Lexington, Ky.: p. 95–100.

Kent, B.H., Berlage, L.J., and Boucher, E.M., 1980, Stratigraphic framework of coal beds underlying the western part of the Recluse 1 × ½-degree quadrangle, Campbell County, Wyoming: U.S. Geological Survey Coal Investigations Map C–81C, 2 plates.

Keystone Coal Industry Manual, 1997: Chicago, Intertech Publishing Co. (Sanda, A.P., ed.), 799 p.

Keystone Coal Industry Manual, 2005: Jacksonville, Fla., Mining Media, Inc. (Johnson, Peter, ed.), 618 p.

Keystone Coal Industry Manual, 2010: Jacksonville, Fla., Mining Media, Inc. (Johnson, Peter, ed.), 618 p.

Luppens, J.A., 1982, Experience with the application of the equilibrium moisture test to lignite, *in* Proceedings of the 2d Annual Coal Testing Conference, Lexington, Ky.: p. 1–6.

Luppens, J.A., 1988, The equilibrium moisture problem: Journal of Coal Quality, v. 7, no. 2, p. 39–44.

Luppens, J.A., and Hoeft, A.P., 1991, Relationship between inherent and equilibrium moisture contents in coals by rank: Journal of Coal Quality, v. 10, no. 4, p. 133–141.

Luppens, J.A., Scott, D.C., Haacke, J.E., Osmonson, L.M., Rohrbacher, T.J., and Ellis, M.S., 2008, Assessment of coal geology, resources, and reserves in the Gillette coalfield, Powder River Basin, Wyoming: U.S. Geological Survey Open-File Report 2008–1202, 127 p.

Luppens, J.A., Wilson, S.E., and Stanton, R.W., eds., 1992, Manual on drilling, sampling, and analysis of coal: Philadelphia, Pa., ASTM International, MNL 11, 74 p.

Mapel, W.J., 1959, Geology and coal resources of the Buffalo-Lake De Smet area, Johnson and Sheridan Counties, Wyoming: U.S. Geological Survey Bulletin 1078, 148 p.

Mapel, W.J., Schopf, J.M., and Gill, J.R., 1953, A thick coal bed near Lake De Smet, Johnson County, Wyoming; U.S. Geological Survey Circular 228, 47 p.

Mathews, J.P., Eser, Semih, Hatcher, P.G., and Scaroni, A.W., 2007, The shape of pulverized bituminous vitrinite coal particles: KONA Powder and Particle, 2007, no. 25, p. 145–152, accessed April 22, 2011, at *http://www.kona.or.jp/search/25_145.pdf*.

Mavor, M.J., and Pratt, T.J., 1996, Improved methodology for determining total gas content, Volume II—Comparative evaluation of the accuracy of gas-in-place estimates and review of lost gas models: Chicago, Ill., Gas Research Institute, Topical Report GRI–94/0429, 166 p.

PacifiCorp, 2008, Dave Johnston Power Plant 50th anniversary and Glenrock Wind Farm community celebration: Portland, Oreg., PacifiCorp, accessed October 6, 2010, at *http://www.pacificorp.com/about/newsroom/2008nrl/djpp5aagwfcc.html*.

Pierce, F.W., Johnson, E.A., Molnia, C.L., and Sigleo, W.R., 1990, Cross sections showing coal stratigraphy of the southeastern Powder River Basin, Wyoming: U.S. Geological Survey Miscellaneous Investigations Series Map I–1959–B, 2 plates, scale 1:500,000.

Scott, D.C., Haacke, J.E., Osmonson, L.M., Luppens, J.A., Pierce, P.E., and Rohrbacher, T.J., 2011, Assessment of coal geology, resources, and reserves in the northern Wyoming Powder River Basin: U.S. Geological Survey Open-File Report 2010–1294, 136 p.

Smith, J.B., Ayler, M.F., Knox, C.C., and Pollard, B.C., 1972, Strippable coal reserves of Wyoming: U.S. Bureau of Mines Information Circular IC 8538, 51 p.

Stach, E., Mackowsky, M.T., Teichmuller, M., Taylor, G.H., and Chandra, D., 1982, Stach's textbook of coal petrology: Berlin, Germany, Gebruder Borntraeger, 535 p.

Stricker, G.D., Flores, R.M., Trippi, M.H., Ellis, M.S., Olson, C.M., Sullivan, J.E., and Takahashi, K.I., 2007, Coal quality and major, minor, and trace elements in the Powder River, Green River, and Williston basins, Wyoming and North Dakota: U.S. Geological Survey Open-File Report 2007–1116, 31 p., accessed April 22, 2011, at *http://pubs.usgs.gov/of/2007/1116/.*

Taff, J.A., 1909, The Sheridan coal field, Wyoming, *in* Campbell, M.R., Contributions to economic geology, 1907, Pt. 2, Coal and lignite: U.S. Geological Survey Bulletin 341–B, p. 123–150.

Testa, S.M., and Pratt, T.J., 2003, Sample preparation for coal and shale gas resource assessment, *in* Proceedings, International Coalbed Methane Symposium, Tuscaloosa, Ala., May 5–9, 2003: University of Alabama, Paper 356, 12 p.

U.S. Energy Information Administration, 2010, Energy glossary: Accessed February 5, 2011, at *http://www.eia.doe.gov/glossary/index.cfm.*

U.S. Environmental Protection Agency, 1980, Standards of performance for new stationary source—A compilation as of July 1, 1980: Washington. D.C., U.S. Environmental Protection Agency, Office of Enforcement, Office of General Enforcement, Division of Stationary Source Enforcement, 868 p., accessed February 5, 2011, at *http://nepis.epa.gov/Exe/ZyNET.exe/2000WROU.txt?ZyActionD=ZyDocument&Client=EPA&Index=1976%20Thru%201980&Docs=&Query=340180001A&Time=&EndTime=&SearchMethod=1&TocRestrict=n&Toc=&TocEntry=&QField=pubnumber%5E%22340180001A%22&QFieldYear=&QFieldMonth=&QFieldDay=&UseQField=pubnumber&IntQFieldOp=1&ExtQFieldOp=1&XmlQuery=&File=D%3A%5CZYFILES%5CINDEX%20DATA%5C76THRU80%5CTXT%5C00000006%5C2000WROU.txt&User=ANONYMOUS&Password=anonymous&SortMethod=h%7C-&MaximumDocuments=10&FuzzyDegree=0&ImageQuality=r105g16/r105g16/x150y150g16/i600&Display=p%7Cf&DefSeekPage=x&SearchBack=ZyActionL&Back=ZyActionS&BackDesc=Results%20page&MaximumPages=1&ZyEntry=1.*

U.S. Environmental Protection Agency, 2006, AirControlNET Documentation report; Pechan Report No. 05.09.009/9010.463: Springfield, Va., E.H. Pechan & Associates, 1,633 p., accessed February 5, 2011, at *http://www.epa.gov/ttnecas1/models/DocumentationReport.pdf.*

Wegemann, C.H., 1912, The Sussex coal field, Johnson, Natrona, and Converse counties, Wyoming: U.S. Geological Survey Bulletin 471–F, Part II—Mineral Fuels, p. 441–471.

Western Fuels Association, Inc., 1983, Final showing report Stevens Properties Prospecting Permits, Converse County, Wyoming: Western Fuels Association, Inc., Denver, Colo., 25 p.

Altered growth and related physiological responses in juvenile Chinook salmon...
J P Meador; F C Sommers; G M Ylitalo; C A Sloan
Canadian Journal of Fisheries and Aquatic Sciences; Oct 2006; 63, 10;
CBCA Reference and Current Events
pg. 2364

Altered growth and related physiological responses in juvenile Chinook salmon (*Oncorhynchus tshawytscha*) from dietary exposure to polycyclic aromatic hydrocarbons (PAHs)

J.P. Meador, F.C. Sommers, G.M. Ylitalo, and C.A. Sloan

Abstract: A dietary feeding study with polycyclic aromatic hydrocarbons (PAHs) was conducted with juvenile Chinook salmon (*Oncorhynchus tshawytscha*) to mimic exposure from urban estuaries during their transition from freshwater to seawater. A significant reduction in mean fish dry weight was observed only for the highest doses; however, analysis of variance (ANOVA) using standard deviations and examination of the cumulative frequency plots revealed high variability among all treatments. The skewed fish weight distribution revealed a large number of small fish in several treatments compared with control fish. Analyses of whole-body lipids and several parameters in blood plasma related to growth and metabolism indicated alterations for most treatments. These results and trends in growth, plasma chemistry, and lipids as a consequence of PAH exposure were similar to those in fish exhibiting starvation, which we have termed "toxicant-induced starvation". Based on these results, we conclude that PAHs are toxic to salmonids at this life stage and the reduction in biomass and lipid stores observed here would have the potential to cause increased mortality for individuals during their first winter.

Résumé : Nous avons mené une étude d'alimentation diététique avec des hydrocarbures aromatiques polycycliques (PAHs) chez de jeunes saumons chinook (*Oncorhynchus tshawytscha*) afin de mimer leur exposition aux estuaires urbains durant leur transition de l'eau douce vers la mer. Une réduction significative de la masse sèche des poissons s'observe seulement avec les doses les plus élevées; cependant, une analyse de variance (ANOVA), qui utilise les écarts types et qui examine les graphiques de fréquences cumulées, montre qu'il existe une forte variabilité dans tous les traitements expérimentaux. La distribution asymétrique des masses des poissons montre qu'il y a un grand nombre de petits poissons dans plusieurs groupes expérimentaux par comparaison aux groupes témoins. Les analyses des lipides du corps entier et de plusieurs variables du plasma sanguin reliées à la croissance et au métabolisme indiquent qu'il y a des modifications dans la plupart des groupes expérimentaux. Ces résultats et les tendances dans la croissance, la chimie du plasma et les lipides qui se développent à la suite de l'exposition aux PAH font penser aux conditions de poissons qui manquent de nourriture; nous qualifions cet état de « disette provoquée par les produits toxiques ». Sur la foi de ces résultats, nous concluons que les PAHs sont toxiques pour les salmonidés à cette étape de leur vie et que la réduction de biomasse et de réserves lipidiques observée peut potentiellement causer une augmentation de la mortalité individuelle durant leur premier hiver.

[Traduit par la Rédaction]

Introduction

Several studies and reviews have shown that polycyclic aromatic hydrocarbons (PAHs) are ubiquitous in aquatic systems, especially estuaries, and can often occur at high concentrations in sediment, water, and tissue (Meador et al. 1995; Eisler 2000; van Metre et al. 2000). These contaminants come from multiple sources, such as stormwater runoff, atmospheric transport, petroleum operations (including drilling, refining, transport, combustion, spills, and natural seeps),

Received 26 April 2006. Accepted 14 June 2006. Published on the NRC Research Press Web site at http://cjfas.nrc.ca on 3 October 2006.
J19293

J.P. Meador[1] and F.C. Sommers. Ecotoxicology and Environmental Fish Health Program, Environmental Conservation Division, Northwest Fisheries Science Center, National Marine Fisheries Service, NOAA, 2725 Montlake Boulevard East, Seattle, WA 98112, USA.
G.M. Ylitalo and C.A. Sloan. Environmental Assessment Program, Environmental Conservation Division, Northwest Fisheries Science Center, National Marine Fisheries Service, NOAA, 2725 Montlake Boulevard East, Seattle, WA 98112, USA.

[1]Corresponding author (e-mail: james.meador@noaa.gov).

 doi:10.1139/F06-127 © 2006 NRC Canada

Reproduced with permission of the copyright owner. Further reproduction prohibited without permission.

municipal and industrial wastewater, and combustion of most organic material.

During smoltification, juvenile salmonids, especially wild fish, lose significant amount of lipids, usually falling to 1%–3% of wet weight (Brett 1995; Beckman et al. 2000; Meador et al. 2002). While in the estuary and nearshore environment, juvenile Chinook salmon are voracious consumers of invertebrates and small fish (Weatherley and Gill 1995), leading to a rapid increase in growth and accumulated lipid stores that will be beneficial for their first winter (Burrows 1969; Healey 1980; Biro et al. 2004). This stage in the life cycle of juvenile Chinook salmon is one of the most critical for determining its survival and reproductive success (Spromberg and Meador 2005) and even slight impedance in growth or lipid storage may have severe consequences for survival.

Even though PAHs are ubiquitous and abundant in the environment, very few studies have examined organismal-level responses to these compounds. Only a handful of studies have considered growth impairment or energetics as a response in fish and a few of these reported severe effects at low exposure concentrations (Carls et al. 1996; Rice et al. 2000). This study was designed to examine growth and a selected number of associated metabolic parameters in juvenile Chinook salmon (*Oncorhynchus tshawytscha*) exposed to dietary PAHs. Our main focus was the juvenile stage that enters the estuary for several weeks to acclimate to seawater, increase in size, and accumulate lipid stores before migrating to open water. We selected fish growth, whole-body lipids, and several associated parameters in blood plasma as metrics for assessing toxic effects. The goal was to gauge the magnitude of effect on organismal properties such as body weight and whole-body lipid content that directly affect the survival of juvenile salmonids, in addition to several related blood chemistry parameters that may be useful as early indicators of adverse effects.

Materials and methods

Fish husbandry, experimental design, environmental parameters, and execution of these experiments followed the procedures described in Meador et al. (2005). The following is an abbreviated discussion of our methods.

Husbandry

Chinook salmon were cultured in our lab from eggs obtained from a local hatchery. Before the toxicity experiment, Chinook salmon fry were fed ad libitum with commercial food. Once large enough to consume pellets, juvenile Chinook salmon were fed at a rate of 1.5%–2.0% body weight (bw)·day^{-1} with fish pellets from Rangen Inc. (Buhl, Idaho). When juvenile fish weighed approximately 3 g, they were switched to a specially prepared fish pellet (Rangen Inc.) that contained a total lipid content of 11% dry weight that was formulated to mimic the lipid content of prey for wild fish. Water quality parameters (pH, dissolved oxygen, alkalinity, and hardness) were measured at least once every week and adjusted if outside the accepted range (Meador et al. 2005). Fish were raised in freshwater and introduced to saltwater during the new moon in June. The rate of change from freshwater to saltwater was approximately 5‰·day^{-1} until full-strength seawater was attained.

Experimental design

Individual fish were weighed and selected from a size window of 10.0 to 16.0 g wet weight (ww) (2.2–3.5 g dry weight (dw)), which was the range determined to provide the best achievable variance given the available pool of fish. Approximately 40% of the available fish fit the size selection criteria. Each tank contained 50 fish and the order of filling the tanks, as well as the assignment of treatment to each tank, was done randomly as determined with a random number generator.

Juvenile Chinook salmon were fed a mixture of PAHs intended to mimic those found in the stomach contents of field-collected fish both in magnitude and proportionality. Pellets were dosed using a stock solution of PAHs in dichloromethane ($MeCl_2$) (50 mg·mL^{-1}) that consisted of 21 PAHs (Table 1) at percentages similar to those found for stomach contents from field-collected fish (Varanasi et al. 1993) (Fig. 1). All fish food for a given treatment was made in one 3500 g batch. Fish pellets were placed in a stainless steel bowl, a calculated amount of stock solution was added to 4 L of $MeCl_2$, and the entire amount was added to the bowl covering all the pellets. The mixture was stirred occasionally and allowed to air dry. Once dried, the pellets were placed into plastic tubs with a tight-fitting lid and kept in a freezer at –20 °C until needed to feed fish.

An appropriate amount of food was weighed and supplied in two feedings (morning and afternoon). Fish in each experimental tank were fed 1.9% bw·day^{-1} based on their average day 0 wet weight, and that amount was increased each week by a quantity determined with a growth equation that assumed a conversion efficiency of 20%. In a separate tank, 50 fish were weighed frequently to determine their rate of growth, which allowed us to keep the amount that was to be fed to all tanks at 1.9% bw·day^{-1}. In treatments where growth was inhibited (or enhanced), those fish actually received a higher (or lower) percentage of food to body weight because the amount fed to each tank was incremented according the expected growth rate for control fish. Observations for each tank found that there was no aversion to pellets by fish in any treatment, and the entire allocation of pellets was consumed within a few seconds. Feeding was conducted 5 days per week; therefore, fish were fed 39 times over the 53-day dosing period starting on 27 July 2004 (day 0). The control fish were fed with pellets that were treated identically to those containing PAHs, including $MeCl_2$ soaking. The length of time for dosing was patterned after several studies showing estuarine residence time for juvenile salmonids ranging up to 60 days before migration to open water (Healey 1991; Thorpe 1994). The PAHs provided to fish are considered the administered dose. The administered dose is the amount given to an organism, whereas the acquired dose is the amount found within the tissues. Although food was delivered to the water in each tank, all pellets were consumed and therefore considered as the administered or ingested dose.

This study consisted of one control and five treatments, each with four replicate tanks. The Fiberglas tanks were round with a diameter of 1.3 m and contained 500 L of sea-

© 2006 NRC Canada

Reproduced with permission of the copyright owner. Further reproduction prohibited without permission.

Table 1. Measured doses of each polycyclic aromatic hydrocarbon (PAH) in the experimental diet.

		Dose (μg·g fish^{-1}·day^{-1})				
	Control	0.7	2.3	6.1	18	22.1
Naphthalene (NPH)	0.0016	0.018	0.049	0.12	0.28	0.34
2-Methylnaphthalene	0.0036	0.038	0.106	0.28	0.70	0.85
Dimethylnaphthalene	0.0094	0.057	0.161	0.40	1.11	1.34
Total naphthalenes	**0.0146**	**0.112**	**0.315**	**0.80**	**2.10**	**2.53**
Dibenzothiophene (DBT)	0.0019	0.036	0.113	0.28	0.85	1.02
Acenaphthene (ACE)	0,0004	0.021	0.066	0.18	0.49	0.60
Fluorene (FLU)	0.0004	0.087	0.283	0.79	2.27	2.83
1,8-Dimethyl(9H)fluorene	0.0004	0.002	0.007	0.02	0.05	0.07
Total fluorenes	**0.0009**	**0.089**	**0.290**	**0.81**	**2.32**	**2.90**
Phenanthrene (PHN)	0.0032	0.102	0.321	0.87	2.64	3.21
9-Ethylphenanthrene	0.0004	0.006	0.019	0.05	0.15	0.18
9-Ethyl-10-methylphenanthrene	0.0004	0.003	0.010	0.03	0.08	0.10
1-Methyl-7-isopropylphenanthrene	0.0004	0.002	0.007	0.02	0.06	0.07
Total phenanthrenes	**0.0045**	**0.11**	**0.36**	**0.96**	**2.93**	**3.55**
Anthracene (ANT)	nd	0.023	0.072	0.19	0.59	0.72
Fluoranthene (FLA)	0.0002	0.117	0.378	1.02	3.02	3.78
Pyrene (PYR)	0.0002	0.094	0.321	0.83	2.46	3.02
Methyl pyrene	0.0004	nd	nd	nd	0.003	0.003
Total pyrenes	**0.0006**	**0.094**	**0.321**	**0.83**	**2.46**	**3.03**
Benz[a]anthracene (BAA)	0.0004	0.032	0.111	0.28	0.91	1.15
Chrysene (CHR)	0.0005	0.057	0.185	0.49	1.53	1.89
Benz[a]pyrene (BaP)	0.0004	0.015	0.053	0.13	0.40	0.49
Benzo(k)fluoranthene (BKF)	0.0005	0.009	0.032	0.09	0.25	0.28
Benzo(g,h,i)perylene (BZP)	0.0004	0.002	0.007	0.02	0.06	0.07
Dibenzanthracene (DBA)	0.0003	0.003	0.009	0.02	0.07	0.09

Note: Each value is expressed in micrograms of PAH per gram of wet fish per day. Values in bold are totals for groups of PAHs. The top line is the summed dose for each treatment. nd is not detected.

water. The tanks were inside a building and arranged in a grid pattern. The flow-through seawater system provided 4 L·min^{-1} of sand-filtered and ultraviolet (UV) sterilized water to each tank. Fish were maintained at 10–11 °C for the entire experiment. At the end of the dosing period (17 September 2004), the fish were not fed for 3 days before samples were taken for bile, blood chemistry, and tissue concentrations on day 56. Fish were fed uncontaminated food once on day 56 (after sampling) to prevent starvation conditions, but not again before weighing. All fish were weighed individually on day 58 on a Sartorius 4000 balance to 0.1 g accuracy. Fish length was not analyzed in this study because we consider fish weight to be a more important variable for assessing growth impacts resulting from toxicant exposure. This is supported by a few studies noting that fish weight was more affected than fish length for salmonids exposed to toxicants (Moles and Rice 1983; Heintz et al. 2000).

Samples

Chemical analyses were conducted with composite samples or a combination of individual fish and composites. For all bile, whole-body lipid, and plasma chemistry analyses, each value was determined on a composite of three fish. Whole-body lipids for each treatment were determined for three individual fish from one of the blood chemistry composites in addition to the two composites (three fish each) used for PAH determination for a total of five values. Tissue moisture content was determined for two of the PAH chemistry composites, and each was analyzed in duplicate with two separate aliquots from each composite. In all cases, each composite sample was composed of three fish from a given tank. Three of the four replicate tanks per treatment were chosen at random to make up the three separate composites.

Blood chemistry

Blood plasma samples were analyzed using an automated blood chemistry analyzer (Idexx VetTest 8008 Chemistry Analyzer; IDEXX Laboratories, Inc., Westbrook, Maine). Eleven blood chemistry parameters were measured simultaneously for each plasma sample. A quality control procedure (Idexx Vetrol control lot number J00951101) was run before samples to verify both the VetTest optics groups and the integrity of the test slides.

Blood was taken from stunned juvenile Chinook salmon by transection of the caudal peduncle and direct transfer of blood to heparinized 1.3 mL sample vials (heparin grade 1-A, 25 000 units). When approximately 1 mL was collected from three fish (one composite replicate), samples were immediately centrifuged at 18 800 rpm for 150 s in a Statspin veterinary centrifuge (Iris Sample Processing, Norwood, Mass.). Plasma was transferred via pipette to a sample cup, which allowed for aliquots to be taken up with the VetTest auto pipette and injected into the machine. The minimum amount of sample required was 40 μL, which was used for initiation and the first parameter tested. Each additional parameter

© 2006 NRC Canada

Reproduced with permission of the copyright owner. Further reproduction prohibited without permission.

Fig. 1. Percent occurrence of each polycyclic aromatic hydrocarbon (PAH) in stomach contents of field-collected Chinook salmon (*Oncorhynchus tshawytscha* (open bar)), and dosed fish pellets used in this experiment (shaded bar). Mean and standard error percentages (error bars shown) are for PAHs in stomachs of juvenile Chinook salmon collected from the Duwamish and Hylebos waterways near Seattle, Washington. Data are from Varanasi et al. (1993). Each value is the mean of 12 composite samples, each with 10 fish. Fish food PAHs are mean measured percentages for this study (no error bars). C1, C2, C3, and C4 designate the total number of carbons in the alkylated homologs. ACY, acenaphthylene; BBF, benzo[b]fluoranthene; INP, indenopyrene. See Table 1 for all other abbreviations. Bars for total NPH, FLU, DBT, PHN, PYR, and CHR show summed percentages for parent plus alkyl homologs. ANT was not measured in stomach contents.

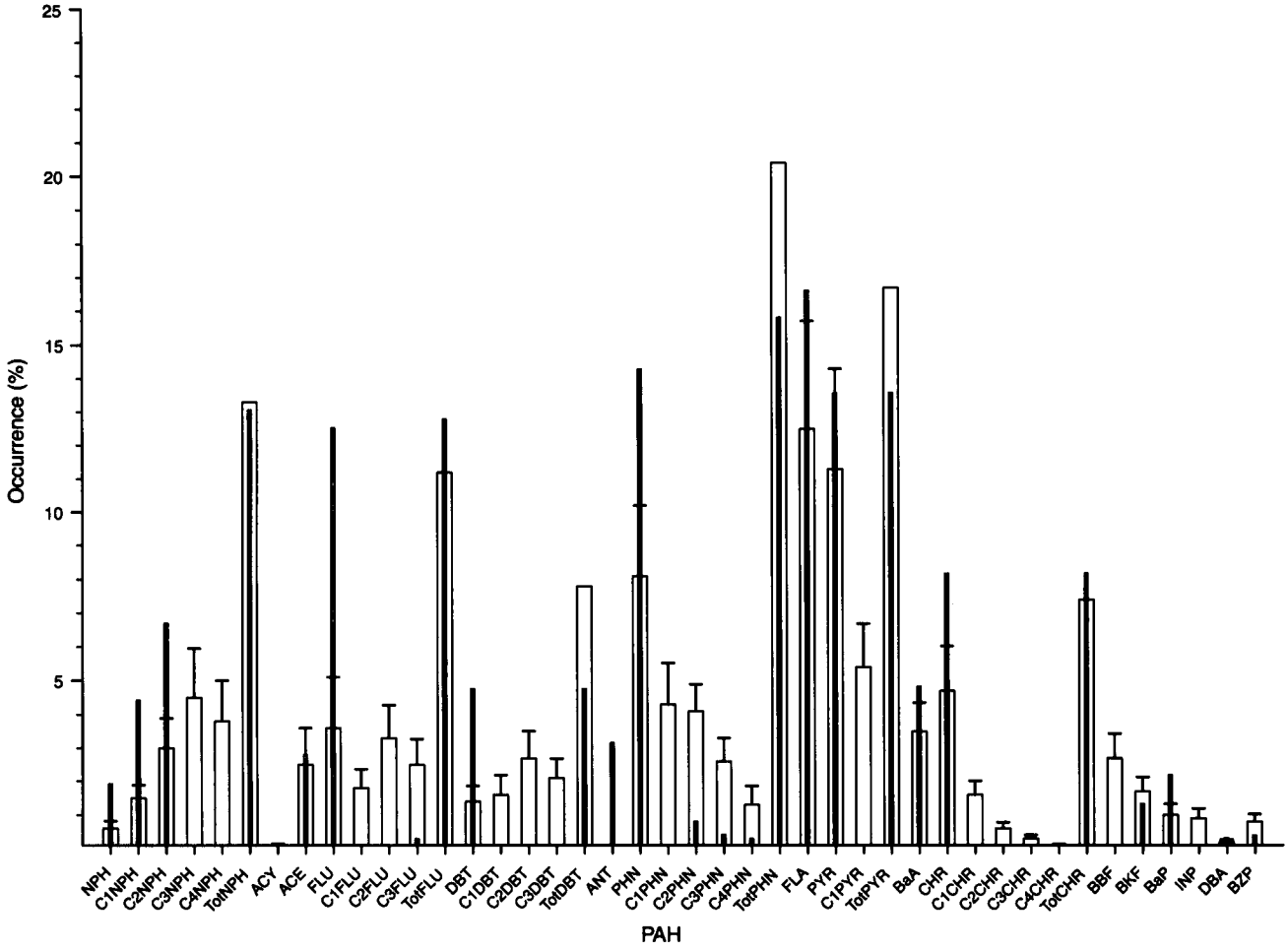

required 10 µL. The time lag between sampling plasma and analysis was less than 20 min. Blood plasma was analyzed for albumin (ALB), alanine aminotransferase (ALT), amylase (AMYL), calcium (CA), cholesterol (CHOL), creatinine (CREA), glucose (GLU), lipase (LIPA), inorganic phosphate (PHOS), total protein (TP), and triacylglycerols (TAG).

Lipid analysis for whole bodies

Whole-body fish were homogenized and analyzed for triacylglycerols (TAGs), cholesterol (CHOL), free fatty acids (FFA), sterol esters – wax esters (SE–WE), and polar lipids (PL). Total lipid concentrations (reported as percent total lipid) were calculated by summing the concentrations of the five lipid classes for each sample. Lipids were determined by a thin-layer chromatography – flame ionization detection (TLC–FID) method (Ylitalo et al. 2005) using an Iatroscan Mark 6 (Iatron Laboratories, Tokyo, Japan). In this method, fish whole bodies were mixed with sodium sulfate and magnesium sulfate and extracted with dichloromethane using an accelerated solvent extractor (Sloan et al. 2005). Various classes of lipids were separated based on polarity, with the nonpolar compounds eluting before the more polar lipids (e.g., phospholipids). Duplicate TLC–FID analyses were performed for each sample extract and the mean value was reported.

Whole-body PAHs and metabolites in fish bile

Composite bile samples of Chinook salmon were analyzed by high performance liquid chromatography (HPLC) for PAH metabolites as described in Krahn et al. (1986). Biliary fluorescent aromatic compounds (FACs) are determined by fluorescence at excitation/emission (ex/em) wavelength pairs. For this study we analyzed for biliary metabolites fluorescing at PHN (ex/em 260/380 nm) and BaP (ex/em 380/430 nm) wavelengths. Whole-body concentrations of PAHs were determined according to the methods of Sloan et

© 2006 NRC Canada

Reproduced with permission of the copyright owner. Further reproduction prohibited without permission.

al. (2005) using a gas chromatograph – mass spectrometer (GC–MS). Fish were not sampled for 3 days after the last dose to allow for gut purging. At the time of sampling, the stomach and alimentary canal were removed; however, it was difficult to assure total removal of these organs.

Because fish were not fed for 3 days before sampling for tissue concentrations, a large percentage of the PAHs were likely metabolized after the dosing period. From these data and the estimated half lives for selected PAHs found in the literature for salmonids (Niimi 1987; Niimi and Dookhran 1989), we calculated an expected whole-body tissue concentration for total PAHs (excluding metabolites) using eq. 1:

$$(1) \qquad [\text{tissue}_{t=0}] = [\text{tissue}_{t=\text{end}}]/e^{-k_2 T}$$

where $[\text{tissue}_{t=0}]$ and $[\text{tissue}_{t=\text{end}}]$ are the beginning and ending tissue concentrations, respectively, for the time period T and k_2 (elimination rate constant) = half live in days/0.693.

Analysis of treatment effects

Fish weights, wet to dry weight ratios, whole-body lipids, and blood chemistry were analyzed by analysis of variance (ANOVA). To test for effects on fish growth, an ANOVA was used to examine treatment differences based on mean fish weights for replicate tanks. To avoid pseudoreplication (Hurlbert 1984), the tank, not individual fish, was treated as the experimental unit. Therefore, replicate tanks in each treatment were not pooled and individual fish were not part of the statistical analysis. The hypothesis of equal variance among tank means (homoscedasticity) was tested with Levene's test. Simple linear regression was also conducted for several parameters as a function of dose.

The ANOVA is generally used to test for differences in treatment means. Performing only this test misses important information that characterizes the growth response in these treatments. Testing for differences in variance heterogeneity can be informative and useful as evidence for adverse effects (Green and Montagna 1996). To test for treatment differences caused by variability in fish weight resulting from PAH exposure, a second ANOVA was performed using tank standard deviation (SD) of fish weights. For this ANOVA, the SD was computed among fish within a tank. The hypothesis we tested was that treatment had no effect on the variability of weight among fish. As with testing for mean fish weight, tanks are the experimental units and each tank yielded a single observation, in this case, the SD of fish weight. This procedure is not an alternative to Levene's test, which examines equality of variances across experimental units, in this case replicate tank means.

All comparisons were considered significantly different from the control at the $\alpha = 0.05$ level. Additionally, a number of p values in the range of $0.05 < p \leq 0.15$ were noted because these low values indicate a substantial response. The α value to determine the level of significance is not a bright line separating significance from nonsignificance. For example, a p value of 0.1 indicates that there is only a 10% chance that the observed treatment effect or one more extreme (i.e., a larger difference between treatment means) would be obtained if there were indeed no treatment effect (a true null hypothesis). This low probably indicates that it is likely that the null hypothesis is not true. Based on this, we believe that these low p values ($p \leq 0.15$) provide a reasonable level of certainty for concluding that there are real treatment effects for many of these parameters.

Control versus treatment differences were determined with Fisher's protected least significant difference (PLSD) post-hoc test. Standard deviations were reported to show the range in the data, and the standard error of the mean (SEM, a statistic of the mean) was reported when comparisons of means were intended. Statistical analyses were conducted with SYSTAT (Systat Software Inc. 2004), JMP (SAS Institute Inc. 2004), and Statview (SAS Institute Inc. 1998).

Results

Chemistry

The measured concentrations in fish pellets were very close to nominal values. The mean (SD) for the ratio of observed to expected concentrations was 1.0 (0.08) for all five treatments. The percentage contribution of each compound in the experimental diet is shown along with the percentages found in stomach concentrations of field-collected fish (Fig. 1). For many PAHs, our measured percentages for pellets were very close to the percentages of PAHs in the stomach contents observed in field-collected fish. Because we could not obtain many of the alkylated homologs, we increased the amounts for some parent and alkyl compounds so that totals (e.g., TotNPH, TotFLU, TotPHN) were similar to the field values. The dose for each PAH is shown by treatment (Table 1), as are the total PAH concentration for fish pellets and total administered dose (as μg and nmol·g fish^{-1}·day^{-1}; Table 2). A few compounds were detected in control food, which resulted in an overall dose to fish of 0.026 μg·g fish^{-1}·day^{-1}.

Overall, whole-body tissue concentrations were very low (Table 2). Based on eq. 2 and an average half-life of 2 days for PAHs in salmonids, the concentrations of total PAHs measured in the whole body on day 56 would have been approximately three times higher if the sampling had been done immediately after the dosing period ended. This would lead to adjusted whole-body concentrations ranging from 0.06 to 2.3 μg·g^{-1} ww (0.4 to 12.4 nmol·g^{-1} ww) total PAHs (Table 2). The results for biliary FACs (Table 2) indicated a highly positive correlation with dose (PHN r^2 = 0.98 and BaP r^2 = 0.97). The proportional increases in biliary FACs over treatment indicate that fish in all treatments were consuming the dosed food, which was supported by behavioral observations.

Fish weights

Mean fish weight for each tank on day 0 (start of dosing) varied from 12.8 to 13.1 g ww (2.8 to 2.9 g dw) with an average SD of 1.5 g ww (0.31 g dw) (Table 3). The ANOVA using all individual fish weights on day 0 indicated that there were no differences among any of the tanks (p = 0.99). The post-hoc test (Fisher's PLSD) found no differences in mean weights between any of the tanks, when examined as pairwise comparisons for all tanks (n = 276; mean (SD) p value = 0.66 (0.21)). When replicate tanks were grouped by treatment, an ANOVA showed no difference between treatments (p = 0.47) for the day 0 mean weights (Table 3). The distribution is shown for day 0 fish by treatment (n = 200;

© 2006 NRC Canada

Reproduced with permission of the copyright owner. Further reproduction prohibited without permission.

Table 2. Polycyclic aromatic hydrocarbons (PAHs) in food and fish tissue.

Treatment	Mortality (%)	Fish dose (µg [nmol]·g^{-1}·day^{-1})	Pellet concentration (µg [nmol]·g^{-1})	Whole-body concentration µg·g^{-1} (obs)	µg·g^{-1} (adj)	nmol·g^{-1} (adj)	Biliary FACs (µg·mg protein^{-1}) PHN	BAP
Control	0	0.026 [0.15]	1 [7]	0.023	0.065	0.41	2.5 (0.3)	0.20 (0.03)
1	1.5	0.7 [3.9]	38 [210]	na	na	na	3.5 (0.1)	0.11 (0.02)
2	2.5	2.3 [12.3]	122 [650]	0.025	0.073	0.47	6.3 (0.6)	0.23 (0.03)
3	2.0	6.1 [32.7]	324 [1730]	0.13 (0.10)	0.38 (0.28)	2.1 (1.5)	11.7 (1.2)	0.25 (0.02)
4	0	18.0 [95.2]	951 [5040]	0.81 (0.46)	2.3 (1.3)	12.4 (7.0)	35.8 (5.5)	0.72 (0.11)
5	0	22.1 [117.1]	1171 [6200]	0.67 (0.25)	1.9 (0.73)	9.9 (3.5)	36.8 (8.2)	0.85 (0.14)

Note: Dose is expressed in µg [nmol] total PAH·g wet fish^{-1}·day^{-1} that was ingested. Pellet concentration is the observed dry weight concentration of total PAHs for fish pellets. Observed (obs) whole-body PAH concentrations shown for day 56 along with the metabolism adjusted (adj) concentrations (µg·g^{-1} and nmol·g^{-1}). Whole-body concentration is the mean and standard error of the mean (SEM) concentration (wet weight) of total PAHs measured in one or two composites (n = 3 fish·composite^{-1}). Biliary FACs (fluorescent aromatic compounds) are the mean (SEM) phenanthrene (PHN) and benzo[a]pyrene (BaP) equivalents in bile (µg·mg protein^{-1}). na, not analyzed.

Fig. 2), which are expressed as dry weights using the wet to dry weight ratio for our control fish (Table 3).

The ANOVA for mean fish wet weight (by tanks) at the end of the experiment (day 58) was highly significant, with a p value of <0.0001. Based on Levene's test (p = 0.16), the null hypothesis of equal variances was accepted. A Fisher's PLSD post-hoc test determined that only the 22.1 µg·g fish^{-1}·day^{-1} treatment was significantly lower than the control (p = 0.0009); however, the mean weight for the 18.0 µg·g fish^{-1}·day^{-1} treatment was substantially reduced (p = 0.17) (Table 3). When dry weights were considered, an ANOVA determined that the two highest treatments (4 and 5) exhibited significantly lower weights (p < 0.0001 and p = 0.01, respectively) (Table 3) when compared with the control.

An analysis of the moisture content of fish from each treatment revealed an increasing trend with treatment concentration on day 58. An ANOVA determined that fish from the two highest doses exhibited substantially elevated ratios of wet weight to dry weight compared with the control fish (p = 0.16 and p = 0.04 for the 18.0 and 22.1 µg·g fish^{-1}·day^{-1} treatments, respectively). Because of the extensive randomization during the experiment setup, there was no reason to suspect differences in ratios of wet weight to dry weight among treatments on day 0. This ratio was determined instead of moisture content because it is a useful multiplier for interconverting between wet and dry weight concentrations.

Although only the two highest doses produced significant reductions in overall fish weight, considerable variability among experimental units (tanks) occurred in all PAH treatments. The ANOVA using tank SD as an indicator of variability in fish weights was significantly different (overall ANOVA p = 0.0098). The result of Levene's test for this ANOVA was not significant (p = 0.9), indicating equal variances. Pairwise comparison of treatments with Fisher's PLSD determined that all control versus treatment comparisons were significantly different (Table 3) because the variability among replicate tanks was higher for each treatment compared with the control. An ANOVA using tank SD was conducted for day 0 fish weights and was not significant (p = 0.75).

Another indication of the increased variability for the day 58 fish is evident in Fig. 2. The cumulative distributions show that all treatments contained fish that were smaller than those in the control tanks when the lower percentiles were considered but were as large or larger in the higher percentile groups. Statistical tests were run for several percentile groups (Table 4), and the results show generally lower weights for those percentiles below the median and higher weights in the upper percentiles. In general, fish in the upper percentiles (e.g., 75th and 95th) of most treatments (except 22.1 µg·g fish^{-1}·day^{-1}) were larger than control fish. Treatment 3 (6.1 µg·g fish^{-1}·day^{-1}) stands out with a significant increase in fish weight for the 95th percentile fish. Also shown is the treatment variance (Table 3), which was determined using the data for all individual fish from a treatment ($n \approx 200$).

Whole-body lipids

Whole-body lipid content in our control fish was very similar to values observed in wild (and some hatchery) juve-

© 2006 NRC Canada

Reproduced with permission of the copyright owner. Further reproduction prohibited without permission.

Table 3. Summary statistics for fish weights.

		Day 0	Day 58				
Treatment	Dose	Mean tank wet weight	Mean tank wet weight	Mean tank dry weight	Mean tank SD (dry weight)	Treat Var	Wet:dry
Control		13.1 (0.10)	27.6 (0.36)	6.18 (0.08)	0.91 (0.06)	0.85	4.47 (0.05)
1	0.7	13.1 (0.07)	28.2 (0.07)	6.15 (0.02)	**1.09** (0.04)	1.1	4.59 (0.04)
2	2.3	12.8 (0.07)	26.9 (0.55)	5.95 (0.12)	**1.19** (0.09)	1.41	4.53 (0.15)
3	6.1	12.9 (0.19)	28.3 (0.64)	6.20 (0.14)	**1.10** (0.07)	1.25	4.47 (0.09)
4	18.0	13.0 (0.17)	26.3 (0.77)	**5.63** (0.17)	**1.28** (0.05)	1.56	4.67 (0.04)
5	22.1	13.0 (0.17)	**22.3** (1.0)	**4.66** (0.21)	**1.09** (0.04)	1.16	**4.80** (0.17)

Note: Dose is expressed in μg total polycyclic aromatic hydrocarbons (PAHs)·gram wet fish^{-1}·day^{-1}. Table shows the mean fish weight for day 0 (wet weight) and day 58 (dry and wet weight) in addition to the mean tank standard deviation (SD) on day 58 (dry weight only) for each treatment (n = 4 experimental units per treatment). Treat Var shows the variance for all individual fish weights in a treatment (all tanks combined, $n \approx 200$ fish). Analysis of variance was conducted for each, except Treat Var. Wet:dry is the ratio of fish wet weight to dry weight. All bold values were significantly different from the control at $\alpha = 0.05$. Most values are presented as mean with standard error of the mean (SEM) in parentheses.

Fig. 2. Cumulative frequency distribution of fish weights by treatment. Plots are shown for day 0 and day 58 (end of experiment). All fish from a treatment were combined for each line ($n \approx 200$). All treatments are shown for day 0, which occur on the left side of the figure. Day 0 wet weights were converted to dry weights by a constant factor of 0.22.

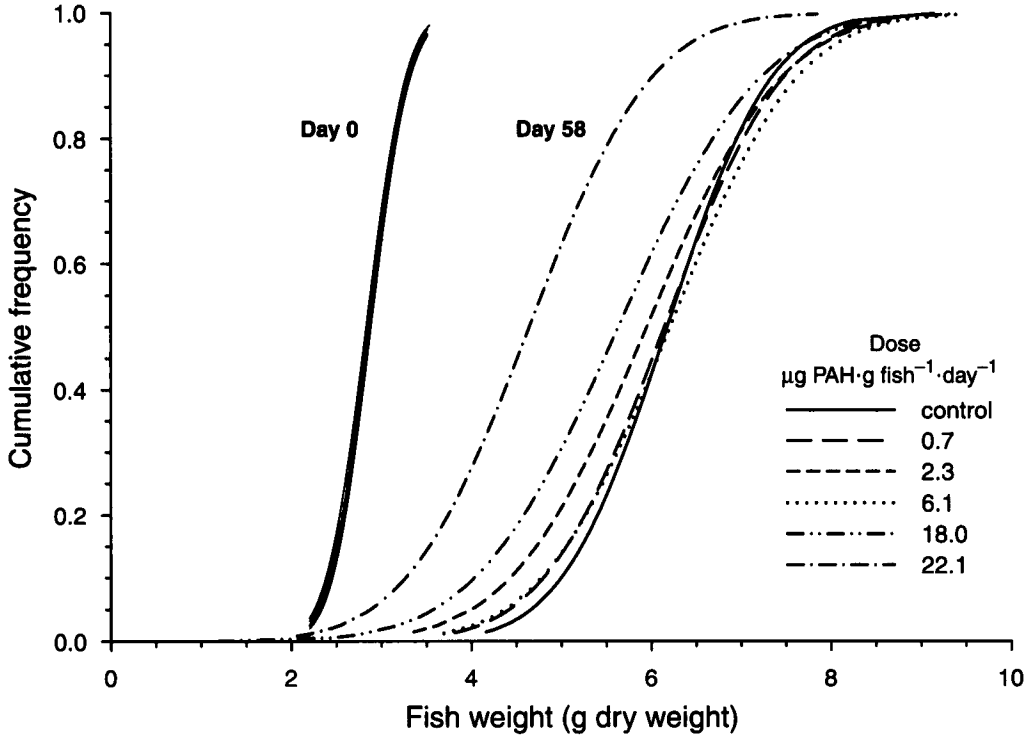

nile Chinook salmon at this life stage (11.2% dry weight ≈ 2.5% wet weight) (Meador et al. 2002). Whole-body lipids generally follow the same pattern as that seen for fish weights. Based on ANOVA, the two highest doses exhibit significant reductions in whole-body lipids and triacylglycerols (Table 5). Other noteworthy values are for CHOL and SE–WE for the 6.1 μg·g fish^{-1}·day^{-1} dose and the general downward trend for TAGs in all PAH treatments (Table 5). No trend was observed for whole-body CHOL. Also, the large increase in free fatty acids and elevated cholesterol for the 6.1 μg·g fish^{-1}·day^{-1} treatment are responsible for the boost in total lipid (TotLip). Significant regression equations were observed for total lipid and TAG in whole body, which were best fit by linear equations. TAG = 49.86 – 1.59Dose, r^2 = 0.73, p = 0.018. TotLip = 11.0 – 0.242Dose, r^2 = 0.49, p = 0.07. Without the 6.1 μg·g fish^{-1}·day^{-1} dose, TotLip = 10.19 – 0.229Dose, r^2 = 0.89, p = 0.01.

Plasma chemistry

Plasma lipids exhibited similar results to those observed for whole-body lipids (Table 6). A declining trend was observed over all treatments for both CHOL and TAGs in plasma, and linear regression equations were the best fit for each. The regression equations are TAG = 107.1 – 2.37Dose, r^2 = 0.72, p = 0.02, and CHOL = 119.4 – 2.24Dose, r^2 = 0.96, p = 0.0004. Several noteworthy patterns were seen in the other blood chemistry parameters analyzed, many significantly different from the control. A declining trend was

© 2006 NRC Canada

Reproduced with permission of the copyright owner. Further reproduction prohibited without permission.

Table 4. Fish weights by percentile.

Dose	5th	10th	25th	50th	75th	95th
Control	4.72 (0.17)	5.00 (0.23)	5.55 (0.11)	6.16 (0.08)	6.76 (0.10)	7.71 (0.12)
0.7	4.53 (0.11)	4.78 (0.13)	5.35 (0.03)	6.10 (0.04)	6.93 (0.06)	7.82 (0.03)
2.3	4.34 (0.19)	*4.52* (0.22)	**4.98** (0.24)	5.84 (0.22)	6.85 (0.10)	7.87 (0.10)
6.1	4.51 (0.12)	4.91 (0.09)	5.51 (0.15)	6.06 (0.18)	6.90 (0.18)	**8.18** (0.22)
18.0	**3.71** (0.38)	**4.18** (0.23)	**4.90** (0.11)	**5.56** (0.14)	*6.37* (0.21)	7.84 (0.20)
22.1	**3.17** (0.12)	**3.35** (0.14)	**3.96** (0.19)	**4.66** (0.24)	**5.30** (0.27)	**6.41** (0.23)

Note: Dose is expressed in μg total polycyclic aromatic hydrocarbons (PAHs)·g wet fish^{-1}·day^{-1}. Values are presented as mean fish dry weight (grams) with standard error of the mean (SEM) in parentheses for all four replicate tanks per treatment. All bold values were significantly different from the control at $\alpha = 0.05$. Italicized values indicate $0.05 < p \leq 0.15$. Each Levene's test was not significant.

Table 5. Whole-body lipids.

Dose	Total lipid (%)	TAG	FFA	CHOL	PL	SE–WE
Control	11.2 (1.2)	58.6 (17.1)	31.7 (14.7)	15.9 (2.2)	5.2 (0.9)	0.35 (0.25)
0.7	9.8 (1.5)	49.9 (17.3)	27.0 (13.0)	16.9 (2.5)	3.8 (0.6)	0.40 (0.26)
2.3	8.7 (2.2)	32.9 (13.4)	28.8 (12.9)	20.0 (4.1)	4.9 (1.1)	0.35 (0.15)
6.1	12.9 (2.0)	43.4 (8.9)	53.8 (12.0)	**25.4** (4.7)	5.6 (1.3)	**1.1** (0.38)
18.0	**6.8** (1.5)	**20.5** (9.2)	25.4 (11.3)	16.4 (2.1)	5.2 (0.7)	0.43 (0.26)
22.1	**4.9** (1.3)	**16.5** (11.3)	14.0 (7.3)	14.7 (1.4)	3.4 (0.9)	0.46 (0.19)

Note: Dose is expressed in μg total polycyclic aromatic hydrocarbons (PAHs)·g wet fish^{-1}·day^{-1}. Values are presented as mean with SEM in parentheses for all five samples per treatment (six for control). TAG, triacylglycerols; FFA, free fatty acids; CHOL, cholesterol; PL, polar lipids; SE–WE, sterol esters and wax esters. Total lipids are expressed as percent of dry weight; all others are expressed in mg·g dry weight^{-1}. Bold values are significantly different from the control at $\alpha = 0.05$. Each Levene's test for these variables was not significant.

Table 6. Plasma chemistry.

	Treatment					
Blood chemistry	Control	0.72	2.3	6.1	18.0	22.1
Albumin (g·dL^{-1})	0.38 (0.07)	*0.20* (0.06)	**0.12** (0.06)	*0.16* (0.09)	**0.12** (0.07)	*0.13* (0.10)
ALT (U·L^{-1})	25.3 (6.3)	26.7 (3.3)	30.3 (6.9)	30.3 (12)	21.7 (6.9)	16.3 (1.3)
Amylase (U·L^{-1})	599 (14)	561 (19)	*526* (48)	614 (42)	568 (17)	**507** (27)
Calcium (mg·dL^{-1})	12.1 (0.2)	11.6 (0.5)	11.6 (0.4)	12.1 (0.07)	11.7 (0.17)	*11.3* (0.5)
Cholesterol (mg·dL^{-1})	125 (11)	118 (10)	110 (2)	*104* (3)	**79** (7)	**72** (14)
Creatinine (mg·dL^{-1})	0.15 (0.02)	0.17 (0.04)	0.22 (0.03)	0.20 (0.03)	0.20 (0.05)	**0.29** (0.03)
Glucose (mg·dL^{-1})	79 (2.9)	77 (3.2)	79 (5.4)	79 (2.1)	**64** (1.1)	**65** (4.0)
Lipase (U·L^{-1})	74 (12.5)	*44.7* (11.5)	**32.3** (5.3)	**30.7** (8.8)	**30.7** (21.1)	**11.0** (11.0)
PHOS (mg·dL^{-1})	13.1 (0.3)	13.0 (0.5)	12.9 (0.5)	13.2 (0.14)	12.4 (0.4)	*11.8* (0.5)
Total protein (g·dL^{-1})	3.1 (0.11)	2.7 (0.08)	2.7 (0.14)	2.7 (0.13)	2.6 (0.3)	*2.5* (0.5)
Triacylglycerols (mg·dL^{-1})	122 (13)	105 (14)	**81** (10)	*95* (10)	**72** (8)	**52** (30)

Note: Mean and standard error of the mean (SEM) in parentheses for various parameters measured in blood plasma. Treatments are expressed in μg polycyclic aromatic hydrocarbon (PAH)·g wet fish^{-1}·day^{-1}. Composite samples ($n = 3$) are from different replicate tanks and each contained plasma from three fish. Bold values are statistically different from the control at $\alpha = 0.05$. Italicized values show those parameters that exhibited a p value between 0.05 and 0.15. ALT, alanine transaminase; PHOS, inorganic phosphate; U·L^{-1}, units per liter; dL, deciliter. None of the Levene's tests for these variables was significant.

generally observed for albumin, amylase, and lipase over PAH treatments; however, other blood parameters were relatively constant across treatments, declining only at the highest doses (ALT, phosphorus, and glucose) (Table 6). Only creatinine exhibited an increasing trend with dose (Table 6). Because the post-hoc power ranged from 0.2 to 0.5 for these ANOVAs, there was a higher probably of type II error, meaning that there was an increased likelihood of false negatives (i.e., accepting the null hypothesis of no treatment effect when in fact there is an effect). With additional statistical power, these parameters would have likely exhibited much lower p values. Even with low power, several parameters exhibited low p values (0.05–0.15) that were considered noteworthy because of the trend observed for other doses (Table 6). Significant regression equations were observed for albumin and lipase, which were best fit with an inverse first-order polynomial:

$$\text{albumin} = 0.144 + (0.0047/\text{Dose}),\ r^2 = 0.89,\ p = 0.003$$

$$\text{lipase} = 29.44 + (0.898/\text{Dose}),\ r^2 = 0.69,\ p = 0.025$$

© 2006 NRC Canada

Reproduced with permission of the copyright owner. Further reproduction prohibited without permission.

Discussion

PAH concentrations

The PAH concentrations tested here were environmentally realistic because of the similar proportions and magnitude of individual compounds observed in stomach contents for juvenile Chinook salmon in contaminated estuaries. This is based on the data in Varanasi et al. (1993) showing a median stomach contents concentration of 23.8 μg total PAH·g^{-1} ww (range 3–365 μg·g^{-1} ww) for 12 composite samples (each with 10 fish) from two contaminated estuaries around Puget Sound, Washington. When based on this median concentration, the dose for field-collected fish would translate to approximately 3.8 μg total PAH·g fish^{-1}·day^{-1}, which is comparable to our middle dose. This dose was determined with the data from Varanasi et al. (1993) for mean fish weight (7 g) and PAHs in stomach contents, in addition to published growth rates of 3%–5%·day^{-1} (Healey 1980; Weatherley and Gill 1995) for this life stage. The growth rates reported by these authors for Chinook salmon and the reported food conversion efficiency for ingested prey of ≈25% (Weatherley and Gill 1995) would imply an average consumption rate of 16% body weight·day^{-1} (based on wet weights), or more, for many salmonids (Weatherley and Gill 1995). In our study, the food conversion efficiency was 23% for the control fish.

The doses calculated above are based on dietary exposure only. Concentrations of PAHs in water also need to be considered when calculating the dose. For many species that have high ventilation rates, such as salmonids, a substantial dose can be obtained with relatively low water concentrations. Water concentrations of PAHs in the low parts-per-billion range, which are not unusual in urban environments and oil spills (Eisler 2000), can lead high doses of PAHs in fish (micrograms of total PAH per gram fish per day) (J.P. Meador, unpublished data). Therefore, it is necessary to consider both dietary and ventilatory sources for determination of dose to salmonids and other species of fish.

The PAH profile for the dosed food was very similar to that observed for PAHs in stomach contents from field-collected fish when most compounds and major classes were considered. Many of the compounds found in stomach contents were not represented in the dosed food. The missing compounds included many of the alkylated PAHs, which comprised from 12% to 88% (mean (SEM) = 48.5% (7.5%)) of the total PAH concentration in stomach contents from juvenile Chinook salmon residing in two different urban estuaries (Varanasi et al. 1993). Because the alkylated PAHs are generally more persistent and toxic than their parent compound (Irwin et al. 1997; Jonsson et al. 2004), our doses (mean alkylated component of 16%) likely underestimated the effects that would be observed in the fish from urban estuaries exposed to dietary PAHs with a higher percentage of alkylated homologs.

The expected concentrations for total whole-body PAHs indicate that more than 99% of the assimilated PAHs were metabolized. Based on the PAH values presented here and the high elimination rates determined by Niimi and Dookhran (1989), these adjusted values are likely close to the maximum that would be observed for this exposure. This implies that the observed adverse responses occurred at very low tissue concentrations. As seen in the results section, whole-body tissue concentrations at low exposure concentrations provide very little information regarding toxic exposure to PAHs. A better approach may be to assess PAH toxicity in fish based on throughput (micrograms of PAH per gram fish per day) or biliary FACs, which shows promise as a metric for PAH exposure in salmonids.

Fish growth

Although the ANOVA and post-hoc tests for mean dry weight determined significant reductions only for the two highest doses, evidence of altered growth on day 58 was observed in most treatments with the distribution plots, ANOVA with SDs, and ANOVA of dry weight by percentile. The observation that fish dry weight was a more accurate indicator of reduced growth and adverse effects is an important observation for the higher doses in this study. In general, the moisture content increased with increasing dose, which was likely due to altered lipid metabolism (Navarro and Gutierrez 1995). At the highest doses (18 and 22.1 μg·g fish^{-1}·day^{-1}), the reduction in mean weight compared with that of control fish was magnified when dry weight was considered. This observation is noteworthy because the higher moisture content indicates that these fish would exhibit a lower energy content per gram wet weight, which is important physiological information that would not be readily apparent if wet weights were considered.

We consider the significant ANOVA using standard deviations and the post-hoc tests showing significant differences for each treatment compared with the control an important result. Although no significant differences in mean fish weights were observed for the low doses, the observed variability and general trend of small fish below the median and larger fish above the median is noteworthy. If exposure had continued for a longer period of time, it is likely that fish from these treatments would have further diverged from the control fish, leading to significant differences in growth. As noted by Green and Montagna (1996), heterogeneity of variance can be an indicator of impact. A very similar experiment in our lab with a different toxicant was also analyzed by ANOVA with SDs, and no significant differences were observed (J.P. Meador, unpublished data), indicating that PAHs are potent inhibitors of metabolic pathways relating to organismal growth.

Comparison to other studies

Only a few studies have examined the toxicity of PAHs to fish from dietary sources and the results are mixed. Wu et al. (2003) examined several responses to dietary exposure of one PAH, benzo[a]pyrene, and concluded that their high dose of 12 μg·g fish^{-1}·day^{-1} did not affect growth or metabolic processes related to growth for the grouper *Epinephelus areolatus*. Another feeding study exposed polychaetes to creosote-contaminated sediment and then fed these worms to juvenile English sole (*Parophrys vetulus*; ≈1 g ww) (Rice et al. 2000). In one experiment from that study, fish exposed to a dose of 0.12 μg total PAH·g fish^{-1}·day^{-1} exhibited a significant reduction in growth rate that was 10-fold lower than the observed rate for control fish (Rice et al. 2000; C. Rice,

© 2006 NRC Canada

Reproduced with permission of the copyright owner. Further reproduction prohibited without permission.

NOAA Fisheries, 2725 Montlake Blvd. East, Seattle, WA 98112, USA, personal communication, 2006). Another dietary study by Carls et al. (1996) examined the responses in pink salmon (*O. gorbuscha*) exposed to oil-contaminated food. These authors reported growth inhibition at their lowest dose of 0.14 μg PAHs·g fish^{-1}·day^{-1}, which is based on the published data and data from M. Carls (NOAA Fisheries, Auke Bay Laboratory, 11305 Glacier Highway, Juneau, AK 99801, USA, personal communication, 2006).

In another study on Chinook salmon, Palm et al. (2003) fed PAH-dosed pellets to juvenile fish for 28 days and reported no effects on growth. The doses in that study (approximately 0.33, 1.3, and 5 μg·g fish^{-1}·day^{-1}) were similar to our low and midrange doses. The methods in Palm et al. (2003) differed substantially from those in our experiment in that no alkylated PAHs were included, a limited subset of fish were weighed, the exposure period was substantially shorter, and no attempt was made to start the experiment with statistically indistinguishable experimental units with low variance.

A field study (Willette 1996) found a significant decrease in growth for pink salmon that were released in moderately oiled areas compared with those released in a lightly oiled area. This reduction in growth was associated with an increase in cytochrome P4501A, which is used as an indicator of PAH exposure. This study ruled out prey density, prey abundance, and feeding rate as possible causes of reduced growth. Willette (1996) concluded that the reduction in growth was likely the cause of the observed reduction in survival to adulthood for these fish.

Plasma chemistry

Several of the blood chemistry parameters for our control fish were in the same range as those reported for migrating juvenile Chinook salmon by Wagner and Congleton (2004). These included lipase, total protein, TAGs, calcium, and total phosphorus. For example, the mean lipase values for our control fish (74 U·L^{-1}) were very similar to the values observed in migrating juvenile Chinook salmon (64–93 U·L^{-1}) (Wagner and Congleton 2004). A few parameters (glucose, cholesterol, and ALT) were lower in our control fish compared with the observed values in that study. Downward trends for cholesterol, TAGs, and lipase are all indicative of impairment to the pathways involved with lipid storage and utilization. Because several of these parameters are interrelated, many are expected to be altered. For example, albumin functions as a transport protein for free fatty acids in the blood stream (Tocher 2003) and will exhibit decline during starvation (Mommsen 1998; Wagner and Congleton 2004).

Very few studies have examined the effects of PAHs on fish by measuring parameters in blood plasma. A review by Folmar (1993) reported only two studies that had examined plasma chemistry as a result of PAH exposure and both had studied English sole. This review also lists control values for several serum and plasma parameters; however, very few values for salmonids are reported. As seen in the review by Folmar (1993), the responses of blood chemistry parameters to toxicant exposure are quite varied. This is no doubt a result of differences among researchers using a variety of tests, life stages, and exposure times. Additionally, the variability in mechanism of action among the different toxicants will elicit increases in some parameters and declines in others. The results presented here are from one time point, which does not capture the potential dynamics of increases and decreases in blood chemistry parameters. Relative responses of the metabolic system to short-term exposure are expected to produce the pattern in blood chemistry parameters seen in our study, whereas longer-term exposure that results in tissue damage would likely produce increases in several blood parameters, especially enzymes.

Physiological condition and implications for the population

The high values for mean fish weight, fish weight by percentile, and total lipid for the 6.1 μg·g fish^{-1}·day^{-1} dose imply hormesis, which is defined as low dose stimulation (Calabrese and Baldwin 2003). Based on these parameters, it appears that fish in this treatment were in better health than the control fish. Examination of other parameters, such as lipid classes and plasma chemistry, indicate that fish from this treatment were strongly affected by PAHs and were not resistant to the toxic effects. The metrics that indicated no toxic effects were likely enhanced by physiological parameters (e.g., mobilized TAGs) or a shift in energy allocation that allowed a boost in growth that would likely not persist over time.

For the PAH-dosed fish, several of the lipid and blood chemistry parameters were depressed and exhibited similar patterns to those observed in fish undergoing starvation. For example, a number of studies report a reduction in lipids, glucose, lipase, and albumin in plasma, in addition to whole-body lipids, in salmonids that have been subjected to fasting (Navarro and Gutierrez 1995; Mommsen 1998; Krogdahl et al. 1999). In this experiment, many of these starvation-like alterations in physiology occurred even though these fish consumed all food supplied to them.

The proximal cause(s) of the starvation-like physiological parameters from PAH exposure in these juvenile Chinook salmon is not known. The physiological and biochemical factors that control and regulate growth and metabolism are diverse and only partially understood (Mommsen 1998). The enzyme lipase may be a key component for this "toxicant-induced" starvation syndrome. Several forms of lipase are known (Mommsen 1998; Tocher 2003) and these are regulated by transcription or phosphorylation. The enzyme responsible for triacylglycerol mobilization is hormone-sensitive lipase (HSL) (Tocher 2003). Under conditions of starvation, the activity of most forms of lipase is severely reduced (70%–90%) (Mommsen 1998).

Although the actual toxic mechanism(s) is not known, it is likely that these toxicants are acting on one or more components creating a cascade of interrelated abnormal physiological responses leading to toxicant-induced starvation. One hypothesis is that some or all of the PAHs absorbed from the diet are affecting lipase via the aryl hydrocarbon receptor (AhR). One study has shown that 2,3,7,8-tetrachlorodibenzo-*p*-dioxin (TCDD) and some PCB congeners reduce lipase activity as a result of interaction with the AhR and may be responsible for TCDD-induced "wasting syndrome" (Olsen et al. 1998). PAHs are also well-known agonists of the AhR (Varanasi et al. 1989) and may affect lipase activity via the

© 2006 NRC Canada

Reproduced with permission of the copyright owner. Further reproduction prohibited without permission.

AhR. Barron et al. (2004) have published fish potency factors (FPF) for PAHs based on their function as AhR agonists, which are based on toxic equivalent factors (TEFs) indexed to TCDD potency.

The reduction in fish size and altered physiological parameters have important ramifications for survival of juvenile salmonids (Burrows 1969; West and Larkin 1987; Beamish and Mahnken 2001) and other species of fish (Cowan et al. 2000). A critical period in the salmonid life cycle occurs during their first winter in lakes, streams, or the marine environment. For many salmonid species, prey availability is greatly reduced during the winter months (Cooney et al. 2001) and fish often need to survive on lipid reserves. Additionally, predation is an important factor for first-year survival, which has been shown to be a function of size. According to Beamish and Mahnken (2001), juvenile salmon that do not attain a critical size during their first summer do not survive the winter.

Reduced lipid stores, which often occur in salmonids during winter months (Gardiner and Geddes 1980; Biro et al. 2004), can directly affect survival. For example, Burrows (1969) found that juvenile fall-run Chinook salmon with a lipid content of 4.1% (wet weight) exhibited a return rate to the hatchery that was approximately half of that for fish with a lipid content of 7.9%. As shown by Biro et al. (2004), the critical lipid level for *O. mykiss* is approximately 1% wet weight (≈5% dry weight), which was determined in lab and field studies. Below this critical level, mortality was very high. This value is supported by Finstad et al. (2004), who determined a critical body energy level of approximately 4400–4800 joules·g^{-1} for winter survival of Atlantic salmon, which translates to a TAG value of approximately 23 mg·g^{-1} dw. Some of the whole-body lipid and TAG values measured in our fish were at or below these critical levels determined by Biro et al. (2004) and Finstad et al. (2004).

The combination of reduced size and lipid content are critical for first year fish. For example, MacFarlane and Norton (2002) demonstrated a large increase in growth rate and a concomitant decline in TAGs when juvenile Chinook salmon exited the estuary to the open ocean. These high growth rates are likely beneficial to juvenile fish by decreasing predation and increasing their success for taking prey; however, they depend on ample prey for lipid accumulation before the winter months of low productivity. If juvenile fish exit the estuary with reduced lipid reserves, they will likely be unable to increase their growth rate and will be more susceptible to predation and less able to catch prey.

Based on the data from Biro et al. (2004) and Finstad et al. (2004), the rate of mortality for fish from our two highest treatments (18.0 and 22.1 μg·g $fish^{-1}$·day^{-1}) would likely approach 100%. Additionally, Biro et al. (2004) demonstrated that even small differences in fish size and lipid content led to increased mortality over winter months. Because of the reduction in size and lipid content observed for many of the fish in our experiment, especially from the lower percentiles, an increased probability for mortality would be expected for their first winter over that predicted for control fish. An increase in mortality for juvenile fish exposed to relatively low levels of PAHs would be an important stress for those populations that already experience myriad habitat alterations.

Acknowledgements

We gratefully acknowledge the following people for assistance with this study: Tiffany Linbo and O. Paul Olson for help with sample collection and Karl Shearer and Lyndal Johnson for their thorough and thoughtful review of this manuscript. We extend a special thanks to Stuart Hurlbert, Michael Paine, and Susan Picquelle for statistical advice and for recommending the ANOVA with standard deviations procedure.

References

Barron, M.G., Heintz, R., and Rice, S.D. 2004. Relative potency of PAHs and heterocycles as aryl hydrocarbon receptor agonists in fish. Mar. Environ. Res. **58**: 95–100.

Beamish, R.J., and Mahnken, C. 2001. A critical size and period hypothesis to explain natural regulation of salmon abundance and the linkage to climate and climate change. Prog. Oceanogr. **49**: 423–437.

Beckman, B.R., Larsen, D.A., Sharpe, C., Lee-Pawlak, B., Schreck, C.B., and Dickhoff, W.W. 2000. Physiological status of naturally reared juvenile spring chinook salmon in the Yakima River: seasonal dynamics and changes associated with smolting. Trans. Am. Fish. Soc. **129**: 727–753.

Biro, P.A., Morton, A.E., Post, J.R., and Parkinson, E.A. 2004. Over-winter lipid depletion and mortality of age-0 rainbow trout (*Oncorhynchus mykiss*). Can. J Fish. Aquat. Sci. **61**: 1513–1519.

Brett, J.R. 1995. Energetics. *In* Physiological ecology of Pacific salmon. *Edited by* C. Groot, L. Margolis, and W.C. Clarke. UBC Press, Vancouver, B.C. pp. 3–68.

Burrows, R.E. 1969. The influence of fingerling quality on adult salmon survivals. Trans. Am. Fish. Soc. **98**: 777–784.

Calabrese, E.J., and Baldwin LA. 2003. Hormesis: the dose-response revolution. Annu. Rev. Pharmacol. Toxicol. **43**: 175–97

Carls, M.G., Holland, L., Larsen, M., Lum, J.L., Mortensen, D.G., Wang, S.Y., and Wertheimer, A.C. 1996. Growth, feeding, and survival of pink salmon fry exposed to food contaminated with crude oil. Am. Fish. Soc. Symp. **18**: 608–618.

Cooney, R.T., Allen, J.R., Bishop, M.A., Eslinger, D.L., Kline, T., Norcross, B.L., McCroy, C.P., Milton, J., Olsen, J., Patrick, V., Paul, A.J., Salmon, D., Scheel, D., Thomas, G.L., Vaughan S.L., and Willette, T.M. 2001. Ecosystem controls of juvenile pink salmon (*Oncorhynchus gorbuscha*) and Pacific herring (*Clupea pallasi*) populations in Prince William Sound, Alaska. Fish. Oceanogr. **10**(Suppl. 1): 1–13.

Cowan, J.H., Rose, K.A., and DeVries, D.R. 2000. Is density-dependent growth in young-of-the-year fishes a question of critical weight? Rev. Fish Biol. Fish. **10**: 61–89.

Eisler, R. 2000. Polycyclic aromatic hydrocarbons. *In* Handbook of chemical risk assessment: health hazards to humans, plants, and animals. Vol 2. Organics. Lewis Publishers Inc., Boca Raton, Fla. pp. 1343–1411.

Finstad, A.G., Ugedal, O., Forseth, T., and Næsje, T.F. 2004. Energy-related juvenile winter mortality in a northern population of Atlantic salmon (*Salmo salar*). Can. J. Fish. Aquat. Sci. **61**: 2358–2368.

Folmar, L.C. 1993. Effects of chemical contaminants on blood chemistry of teleost fish: a bibliography and synopsis of selected effects. Environ. Toxicol. Chem. **12**: 337–375.

Gardiner, W.R., and Geddes, P. 1980. The influence of body composition on the survival of juvenile salmon. Hydrobiologia, **69**: 67–72.

© 2006 NRC Canada

Reproduced with permission of the copyright owner. Further reproduction prohibited without permission.

Green, R.H., and Montagna, P. 1996. Implications for monitoring: study designs and interpretation of results. Can. J. Fish. Aquat. Sci. **53**: 2629–2636.

Healey, M.C. 1980. Utilization of the Nanaimo River estuary by juvenile chinook salmon, *Oncorhynchus tshawytscha*. Fish. Bull **77**: 653–668.

Healey, M.C. 1991. Life history of chinook salmon (*Oncorhynchus tshawytscha*). *In* Pacific salmon life histories. *Edited by* C. Groot and L. Margolis. UBC Press, Vancouver, B.C. pp. 313–393.

Heintz, R.A., Rice, S.D., Wertheimer, A.C., Bradshaw, R.F., Thrower, F.P., Joyce, J.E., and Short, J.W. 2000. Delayed effects on growth and marine survival of pink salmon, *Oncorhynchus gorbuscha*, after exposure to crude oil during embryonic development. Mar. Ecol. Prog. Ser. **208**: 205–216.

Hurlbert, S.H. 1984. Pseudoreplication and the design of ecological field experiments. Ecol. Monogr. **54**: 187–211.

Irwin, R.J., Van Mouwerik, M., Stevens, L., Seese, M.D., and Basham, W. 1997. Entry on alkyl PAHs (alkyl homologs of PAHs). Environmental contaminants encyclopedia. National Park Service, Water Resources Division, Fort Collins, Colorado. *Available from* http://www.nature.nps.gov/hazardssafety/toxic/index.cfm.

Jonsson, G., Bechmann, R.K., Bamber, S.D., and Baussant, T. 2004. Bioconcentration, biotransformation, and elimination of polycyclic aromatic hydrocarbons in sheepshead minnows (*Cyprinodon variegatus*) exposed to contaminated seawater. Environ. Toxicol. Chem. **23**: 1538–1548.

Krahn, M.M., Moore L.K., and MacLeod, W.D., Jr. 1986. Standard analytical procedures of the NOAA National Analytical Facility, 1986: metabolites of aromatic compounds in fish bile. US Department of Commerce Tech. Memo. No. NMFS F/NWC-102.

Krogdahl, A., Nordrum, S., Sorensen, M., Brudseth, L., and Rosjo, C. 1999. Effects of diet composition on apparent nutrient absorption along the intestinal tract and of subsequent fasting on mucosal disaccharidase activities and plasma nutrient concentration in Atlantic salmon, *Salmo salar* L. Aquac. Nutr. **5**: 121–133.

MacFarlane, R.B., and Norton, E.C. 2002. Physiological ecology of juvenile chinook salmon (*Oncorhynchus tshawytscha*) at the southern end of their distribution, the San Francisco Estuary and Gulf of the Farallones, California. Fish. Bull. **100**: 244–257.

Meador, J.P., Stein, J.E., Reichert, W.L., and Varanasi, U. 1995. A review of bioaccumulation of polycyclic aromatic hydrocarbons by marine organisms. Rev. Environ. Contam. Toxicol. **143**: 79–165.

Meador, J.P., Collier, T.K., and Stein, J.E. 2002. Use of tissue and sediment based threshold concentrations of polychlorinated biphenyls (PCBs) to protect juvenile salmonids listed under the U.S. Endangered Species Act. Aquat. Conserv. Mar. Freshw. Ecosyst. **12**: 493–516.

Meador, J.P., Sommers, F.C., Wolotira, R.J., and Kubin, L. 2005. Conducting dose-response feeding studies with salmonids: growth as an endpoint. *In* Techniques in aquatic toxicology. Vol. 2. *Edited by* G.K. Ostrander. CRC Press, Boca Raton, Fla. pp. 93–115.

Moles, A., and Rice, S.D. 1983. Effects of crude oil and naphthalene on growth, caloric content, and fat content of pink salmon in seawater. Trans. Am. Fish. Soc. **112**: 205–211.

Mommsen, T.P. 1998. Growth and metabolism. *In* The physiology of fishes. *Edited by* D.H. Evans. CRC Press, Boca Raton, Fla. pp. 65–97.

Navarro, I., and Gutierrez, J. 1995. Fasting and starvation. *In* Biochemistry and molecular biology of fishes. *Edited by* P.W. Hochachka and T.P. Mommsen. Elsevier, Amsterdam, the Netherlands. pp. 393–434.

Niimi, A.J. 1987. Biological half-lives of chemicals in fishes. Rev. Environ. Contam. Toxicol. **99**: 1–46.

Niimi, A.J., and Dookhran, G.P. 1989. Dietary absorption efficiencies and elimination rates of polycyclic aromatic hydrocarbons (PAHs) in rainbow trout (*Salmo gairdneri*). Environ. Toxicol. Chem. **8**: 719–722.

Olsen, H., Enan, E., and Matsumura, F. 1998. 2,3,7,8-Tetrachlorodibenzo-*p*-dioxin mechanism of action to reduce lipoprotein lipase activity in the 3T3-L1 preadipocyte cell line. J. Biochem. Mol. Toxicol. **12**: 29–39.

Palm, R.C., Powell, D.B., Skillman, A., and Godtfredsen K. 2003. Immunocompetence of juvenile chinook salmon against *Listonella anguillarium* following dietary exposure to polycyclic aromatic hydrocarbons. Environ. Toxicol. Chem. **22**: 2986–2994.

Rice, C.A., Myers, M.S., Willis, M.L, French, B.L., and Casillas, E. 2000. From sediment bioassay to fish biomarker — connecting the dots using simple trophic relationships. Mar. Environ. Res. **50**: 527–533.

SAS Institute Inc. 1998. Statview statistical software. SAS Institute Inc., Cary, N.C.

SAS Institute Inc. 2004. JMP software. SAS Institute Inc., Cary, N.C.

Sloan, C.A., Brown, D.W., Pearce, R.W., Boyer, R.H., Bolton, J.L., Burrows, D.G., Herman, D.P., and Krahn, M.M. 2005. Determining aromatic hydrocarbons and chlorinated hydrocarbons in sediments and tissues using accelerated solvent extraction and gas chromatography/mass spectrometry. *In* Techniques in aquatic toxicology. Vol. 2. *Edited by* G.K. Ostrander. CRC Press, Boca Raton, Fla. pp. 631–651.

Spromberg, J.A., and Meador, J.P. 2005. Population-level effects on chinook salmon from chronic toxicity test measurement endpoints. Integr. Environ. Assess. Manag. **1**: 9–21.

Systat Software Inc. 2004. SYSTAT 11. Systat Software Inc., Richmond, Calif.

Thorpe, J.E. 1994. Salmonid fishes and the estuarine environment. Estuaries, **17**: 76–93.

Tocher, D.R. 2003. Metabolism and functions of lipids and fatty acids in teleost fish. Rev. Fish. Sci. **11**: 107–184.

van Metre, P.C., Mahler, B.J., and Furlong, E.T. 2000. Urban sprawl leaves its PAH signature. Environ Sci. Technol. **34**: 4064–4070.

Varanasi, U., Stein, J.E., Nishimoto, M. 1989. Biotransformation and disposition of polycyclic aromatic hydrocarbons (PAH) in fish. *In* Metabolism of polycyclic aromatic hydrocarbons in the aquatic environment. *Edited by* U. Varanasi. CRC Press, Boca Raton, Fla. pp. 94–149.

Varanasi, U., Casillas, E., Arkoosh, M.R., Hom, T., Misitano, D.A., Brown, D.W., Chan, S-L., Collier, T.K., McCain, B.B., and Stein, J.E. 1993. Contaminant exposure and associated biological effects in juvenile chinook salmon (*Oncorhynchus tshawytscha*) from urban and nonurban estuaries of Puget Sound. NOAA Technical Memorandum NMFS NWFSC-8.

Wagner, T., and Congleton, J.L. 2004. Blood chemistry correlates of nutritional condition, tissue damage, and stress in migrating chinook salmon (*Oncorhynchus tshawytscha*). Can. J. Fish. Aquat. Sci. **61**: 1066–1074.

Weatherley, A.H., and Gill, H.S. 1995. Growth. *In* Physiological ecology of pacific salmon. *Edited by* C. Groot, L. Margolis, and W.C. Clarke. UBC Press, Vancouver. pp. 103–158.

West, C.J., and Larkin, P.A. 1987. Evidence for size-selective mortality of juvenile sockeye salmon (*Oncorhynchus nerka*) in Babine Lake, British Columbia. Can. J. Fish. Aquat. Sci. **44**: 721–722.

Willette, M. 1996. Impacts of the *Exxon Valdez* oil spill on the migration, growth, and survival of juvenile pink salmon in Prince William Sound. Am. Fish. Soc. Symp. **18**: 533–550.

Wu, R.S.S., Carmel, P.A., Au, D.W.T., Zheng, G.J., Yuen, B.B.H., and Lam, P.K.S. 2003. Evaluation of biomarkers of exposure

© 2006 NRC Canada

Reproduced with permission of the copyright owner. Further reproduction prohibited without permission.

and effect in juvenile areolated grouper (*Epinephelus areolatus*) on food borne exposure to benzo[a]pyrene. Environ. Toxicol. Chem. **22**: 1568–1573.

Ylitalo, G.M., Yanagida, G.K., Hufnagle, L., Jr., and Krahn, M.M. 2005. Determination of lipid classes and lipid content in tissues of aquatic organisms using a thin layer chromatography/flame ionization detection (TLC/FID) microlipid method. *In* Techniques in aquatic toxicology. Vol. 2. *Edited by* G.K. Ostrander. CRC Press, Boca Raton, Fla. pp. 227–237.

© 2006 NRC Canada

Reproduced with permission of the copyright owner. Further reproduction prohibited without permission.

Environ. Sci. Technol. **2008,** *42,* 2656–2662

Effects of Diesel on Survival, Growth, and Gene Expression in Rainbow Trout (*Oncorhynchus mykiss*) Fry

LIZZY MOS,*,† GLENN A. COOPER,‡ KERRIE SERBEN,§ MARC CAMERON,† AND BEN F. KOOP‡

Hemmera, Fourth Floor 19 Bastion Square, Victoria BC V8W 1J1 Canada, Centre for Biomedical Research, University of Victoria, Victoria, BC V8W 3P6, Canada, and Ecotoxicology Group, Cantest Ltd., 3650 Wesbrook Mall, Vancouver, BC V6S 2L2, Canada

Received September 7, 2007. Revised manuscript received January 16, 2008. Accepted January 16, 2008.

Diesel spills are all too frequent disturbances of freshwater ecosystems, largely as a result of the quantities transported and consumed. Assessing the risk that such events may pose to aquatic life remains a difficult process, because of the complexity of this hydrocarbon mixture and our limited knowledge of its toxicity. A diesel spike experiment with rainbow trout (*Oncorhynchus mykiss*) fry was carried out to fill this knowledge gap. Survival, growth, and gene expression changes were assessed and toxicity thresholds were determined. Whereas the biological end points were consistent in the determination of (sub)lethal doses, microarrays supplied additional information on the mechanism of toxicity (oxygen deprivation) and potential long-term effects (feminization, immune system alterations) of diesel exposure on salmonids. Hemoglobins, prostaglandins, cytochromes, and gluthathion-S-transferases were among the molecular biomarkers proposed for use in future risk assessments based on microarray results. By bridging traditional toxicity testing with recent microarray technologies, this study shows the potential of genomics tools in ecotoxicity studies as well as industrial applications, including risk assessment, in the near future.

Introduction

Oil continues to be the primary source of energy, accounting for approximately 40% of total energy use worldwide. The total world petroleum consumption was estimated to exceed 84 million barrels (or 3 billion gallons) per day during 2005. Canada represents one of the nations with the largest oil reserves, extensive oil production, and a high level of oil consumption per capita (*1*). The resulting revenues and other economic benefits have often overshadowed the negative impacts of petroleum hydrocarbons spilled into terrestrial, marine, and freshwater ecosystems during production, transportation, and use. In British Columbia, Canada, approximately 4000 spills yearly affect aquatic habitat over half of which are hydrocarbon related (Duncan Ferguson, Hazard Management Section, BC Ministry of the Environment, personal communication). Many of the inland events are from smaller spills of petroleum hydrocarbons into freshwater habitat, thus representing an imminent threat to the spawning habitat of salmonids. With salmonids as an important food item in aquatic food chains, a contributor of nutrients to riparian zones, and a valued economic resource to humans, the impacts of oil spills could affect multiple levels of ecosystems.

Although spill events are frequent and abundant, incidents in freshwater ecosystems are often localized, and hence attract much less public attention than those in marine environments. Consequently, concern and scientific studies of petroleum impacts on freshwater environments have lagged behind. To date, very little information has been published on the potential problems of oil, and little is known about the toxicology of the complex petroleum hydrocarbon mixtures on aquatic life. The objectives of this study are to (1) establish toxicity threshold levels for the effects of the most frequently spilled hydrocarbon product (diesel) on aquatic organisms, using rainbow trout (*Oncorhynchus mykiss*) as a model species; (2) to address the potential long-term impacts of diesel exposure by including sublethal effect end points and elucidate the mechanism of diesel toxicity using genomics tools; and (3) to identify molecular biomarkers of diesel exposure in fish, as tools in future assessments of the ecological risks associated with spills.

Materials and Methods

Test Conditions. Rainbow trout fry (*Oncorhynchus mykiss*; ~11 days post swim up and 100 mg in weight) were obtained from a government certified hatchery (Sun Valley Trout Farm, Langley, BC, Canada) two days before test initiation for acclimatization. The test was carried out at Cantest (Burnaby BC, Canada) facilities. Fish were subjected to a lake water control or a test solution consisting of lake water spiked with Ultra Low Sulfur (ULS) Diesel No. 2 (CAS 68476-34-6). Six replicates, each containing five fish, were tested per loading rate in 1-L glass jars containing 80 mL of test solution per fish, according to the method described by Lazorchak and Smith (*2*). Over the 14-day exposure period, test solutions were renewed daily, constantly aerated, and kept under a photoperiod of 16 h light−8 h dark with a light intensity of 100–500 lx at the water surface. Throughout the test, fish were fed brine shrimp (*Artemia*) twice daily.

Lake water was collected at Marie Lake, Queen Charlotte Islands, BC, Canada, to reflect conditions where biological components of freshwater may interact with contaminants. Lake water was shipped and stored cold (4 °C). Volumes required for next day's water renewal were kept at test temperature overnight, and as necessary, temperature-adjusted and aerated for 30 min before use in preparation of the test solutions. Test concentrations were expressed as loading rates, i.e. the ratio of diesel to dilution water, reflective of the poor solubility of hydrocarbon mixtures. Specific gravity for diesel (0.84 @ 15.6 °C) was used to estimate the volume of diesel. Six loading rates were tested, namely 0.3, 1.5, 8, 40, 200, and 1000 mg/L (based on a 96-h range finding test), including lethal and sublethal exposure concentrations. To obtain the specific concentrations, a stock solution was prepared, mixed for 30 min on a magnetic stir plate, and diluted into lake water. All test solutions were mixed for 30 min to create dispersion before being divided among the test vessels.

Fish survival was recorded over the 14-day period, with half of the replicates being removed at day 7 to assess growth by dry weight analysis. Other replicates were maintained for

* Corresponding author tel: (1-250) 388 3584; fax: (1-250) 388 3517; e-mail: LMos@Hemmera.com.
† Hemmera.
‡ University of Victoria.
§ Cantest Ltd.

10.1021/es702215c CCC: $40.75
© 2008 American Chemical Society
Published on Web 02/20/2008

an additional 7 days, after which the liver was dissected out and the carcass was subjected to dry weight analysis. The presence of unusual behavior or appearance was recorded over the duration of the test, and dissolved oxygen, temperature, pH, and conductivity were monitored to ensure consistent water quality.

RNA Isolation from Fish Livers. Livers were isolated from surviving fish at day 14, and processed in order of increasing exposure concentration. Test vessels were placed into a water bath (15 °C), wrapped in foil, and covered, to minimize stress. The test vessels were emptied into a sieve, and the sieve containing the fish was quickly put into MS222 solution in an ice bath. After a few minutes, when the fish were immobile, fish were dissected on a dissecting pan. Using a scalpel, the head was cut off behind the gills, the belly was opened with scissors, and the liver was removed. Livers were collected in labeled cryovials, which were immediately immersed in liquid nitrogen.

Five fish livers per treatment replicate were combined before RNA isolation into a 1.5 mL safe-lock microcentrifuge tube (Eppendorf, Canada), containing 1 mL of frozen TRIzol reagent (Invitrogen, Canada) and a 3-mm-diameter tungsten-carbide bead (Eppendorf, Canada). For any given sample, the homogenization period consisted of 2 repetitions of 3 min at 20 Hz in a Retsch MM301 mixer mill (Retsch GmbH Co., Germany). From the homogenates, total RNA was isolated per manufacturer's instructions for the use of TRIzol reagent with the following modifications: After phase separation, 1 μL of glycogen (Roche Diagnostics, Canada) was added to each aqueous phase, before RNA was precipitated with 500 μL of isopropanol (Sigma-Aldrich, Canada), and incubated overnight at −80 °C. Samples were centrifuged for 1 h at 12000*g* at 4 °C the following day to obtain a RNA precipitate. Precipitates were gently dried and resuspended in ultraclean DMQ (20 μL; Gibco, Canada), subjected to a 10 min incubation at 55 °C to facilitate resuspension, and stored at −80 °C until further use. Total RNA concentrations were determined using spectrophotometry, and RNA quality was assessed by gel electrophoresis. If sufficient quantities of intact RNA were identified, samples were selected for cDNA synthesis and labeling.

cDNA Synthesis and Labeling. The microarray experiments were designed to comply with MIAME guidelines. The direct method experimental design was employed whereby fish exposed to diesel were compared to control fish each labeled with different cyanine fluors (Cy3 or Cy5) and hybridized simultaneously on the same array. The experimental design for the microarray experiment consisted of 3 biological replicate arrays with their corresponding dye flips (total $n = 6$) for each diesel treatment. Each biological replicate represented the pooled RNA from 5 different individual livers for both exposed and control fish.

Dye flips were performed to remove systematic bias due to dye incorporation. Fabrication and details of the salmonid cDNA microarrays utilized in this study are described elsewhere (*3*). A complete description and list of spotted cDNA probes on the arrays is available at http://web.uvic.ca/cbr/grasp/array.html or at NCBI's GEO repository under GEO platform number GPL2716.

Fluorescently labeled cDNA for use in microarray screening was generated from total RNA using the SuperScript III Indirect cDNA Labeling System (Invitrogen). Briefly, exactly 5 μg of total RNA was reverse transcribed with 2 μL of 25 μg/μL oligo(dT)20 primer and incubated at 46 °C for 3 h to synthesize first-strand cDNA according to the manufacturer's instructions. The original RNA was hydrolyzed by addition of 1 N NaOH, and the pH was neutralized subsequently by 1 N HCl and 3 M sodium acetate (pH 5.2). Amino-modified first-strand cDNA was purified of unincorporated dNTPs and hydrolyzed RNA using a S.N.A.P. Column Purification kit (Invitrogen). Purified cDNA was precipitated with ethanol, and redissolved in 2× coupling buffer and incubated for 2 h at room temperature with their respective Cy3 and Cy5 fluoros (Amersham Biosciences). Unreacted dye was removed from the labeled cDNA sample by a second S.N.A.P. Column procedure. Respective eluted sample pairs were pooled, precipitated with ethanol overnight, and resuspended in 27 μL of nuclease free water. For each pooled sample, 1 μL was removed to quantify the cDNA and dye incorporation using a Nanodrop spectrometer (Nanodrop Technologies, Wilmington, DE).

Array Hybridization and Quantification. Post processing of arrays consisted of washing them twice in 0.2% SDS solution for 5 min, then rinsing 5 times for 1 min in MilliQ dH_2O. Residual dH_2O was removed by centrifugation at 514*g* for 5 min. Arrays were prehybridized for 1.5 h at 49 °C in 5× SSC, 0.1% SDS, 3% BSA solution. Prehybridization solution was removed by 3 washes in MilliQ dH_2O for 20 s and dried by centrifugation.

A total of 60 uL of hybridization buffer consisting of 26 μL of labeled cDNA, 4 μL of LNA dT blocker (Genisphere), 25% formamide, 4× SSC, 0.5% SDS, and 2× Denhardt's solution was applied to each microarray, and placed in a Corning hybridization chamber for 16 h at 49 °C. Coverslips were removed and the slides were washed in 2× SSC, 0.2% SDS at 49 °C, with subsequent washes at room temperature as follows: twice for 5 min in 2× SSC, twice for 5 min in 1× SSC, four times for 5 min in 0.1× SSC. The arrays were dried by centrifugation and scanned immediately at 10 μm resolution, using ScanArray Express (PerkinElmer, Wellesley, MA).

Chemical Analysis of Diesel and Diesel-Spiked Lake Water. A pure diesel sample was submitted to Cantest (Burnaby, BC, Canada) and analyzed using their standard operating procedures. Those are for volatile hydrocarbon compounds and benzene, toluene, ethylbenzene, and xylene (BTEX) U.S. EPA Methods 624/8240/8260, involving sparging with a purge and trap apparatus and analysis by GC-MS, and for polycyclic aromatic hydrocarbons (PAHs) and extractable petroleum hydrocarbons (EPHs) by U.S. EPA Methods 625/8270, involving extraction, cleanup steps, and analysis by GC-MS. Light (C_{10}−C_{19}) and heavy (C_{19}−C_{32}) EPH fractions (LEPH and HEPH, respectively) were then calculated from EPHs by subtraction of PAHs. Results were reported on a percentage by weight basis.

To provide additional information on diesel components in spiked lake water, a set of mock test solutions was prepared and treated similarly to those used for fish exposures. All six loading rates and the control were sampled as initial solutions before aeration and after 24 h. These samples were also analyzed by Cantest for BTEX, PAHs, and LEPH/HEPH to provide actual exposure concentrations.

Data Analysis. Dose–response curves were interpolated from survival, growth, and gene expression results, including survival percentages, growth by weight, and number of genes altered (by an average of up- and downregulated genes). Tests of normality and equality of variance were followed by statistical testing accordingly (data transformation, significance testing), using TOXCALC software (Tidepool Scientific Software, McKinleyville, CA).

Quantified data from the microarrays were analyzed using Genespring 7.3.1 software (Agilent Technologies Inc., Santa Clara, CA) to detect gene expression changes in exposed trout compared to nonexposed controls. Genes were filtered based upon having a present value for at least 3 of 6 arrays for individual exposure conditions. Remaining genes were only retained if they were significantly differently expressed between exposed versus control based upon having a *t* test *p* value lesser or equal to 0.05, and were at least 1.5 fold or greater up- or downregulated. A multiple testing correction

TABLE 1. Rainbow Trout Fry Survival, Growth, and Gene Expression Assessed upon Exposure to Diesel Doses Ranging from 0.3 to 1000 mg/L[a]

	survival (%)		growth (mg/fish dry weight)		gene expression (no. of genes altered ≥1.5-fold)	
loading rate (mg/L)	day 7	day 14	day 7	day 14	upregulated	downregulated
control[b]	100 ± 0	93 ± 12[c]	21.89 ± 3.28	32.35 ± 3.92	NA	NA
0.3	100 ± 0	100 ± 0	25.49 ± 1.54	32.15 ± 0.65	11	17
1.5	100 ± 0	100 ± 0	25.67 ± 1.34	33.88 ± 3.76	20	19
8	97 ± 8	100 ± 0	23.41 ± 3.35	33.75 ± 2.88	28	32
40	93 ± 10	67 ± 31*	16.69 ± 5.48	27.31 ± 5.16	90	161
200	0 ± 0[d]*	0 ± 0*	NA	NA	NA	NA
1000	0 ± 0[d]*	0 ± 0*	NA	NA	NA	NA

[a] Survival and gene expression were significantly altered at the 40 mg/L diesel exposure dose and above. Growth was not significantly affected in surviving fish. [b] Control consists of lake water. [c] One fish death not associated with diesel exposure on Day 12. [d] Mortality of 100% within 3 days. NA = Not applicable. * = Significantly different from control at $p \leq 0.05$.

was not employed in the statistical evaluation. The remaining signature was analyzed by gene function using the Protein Knowledgebase (http://beta.uniprot.org/uniprot) at the 40 mg/L exposure dose. Potential biomarkers were determined by generating expression profiles which were flat for initial diesel concentrations and significantly altered (greater than 1.5 fold in either direction with $p < 0.05$) at the 40 mg/L concentration; genes with a 0.9 Pearson correlation to this profile were retained.

Results and Discussion

Diesel Composition and Toxicity. The ULS Diesel No. 2, as a "light" petroleum hydrocarbon mixture, contained primarily short chain aliphatic hydrocarbons (69%) and lesser amounts of longer chain components (22%), as well as minor contributions of VH (5%), BTEX (0.3%), and PAHs (0.2%) on a percentage by weight basis. Approximately 3.5% of the constituents remained unidentified, but may have consisted of alkylated PAHs and/or additives. Low molecular weight (2–3 rings) PAHs (naphtalene and phenanthrene) were more abundant than the heavy molecular weight PAHs (Table S1 in the Supporting Information). The nature of diesel contributed to its rapid volatilization and breakdown in the test (~50% reductions in BTEX and naphthalene, and ~30% in VHs and PAHs over the course of 24 h; Table S2), as could be expected upon release in the environment. Natural lighting conditions and realistic contaminant exposure durations in the context of recovery and remediation (14 days) were used. Daily renewal represented further realism to spill events, due to the nature of freshwater spills that often result from land activities, whereby oil is repeatedly introduced into a stream or lake for a period of time, facilitated by changes in water levels, runoff, and other environmental conditions. The diesel spike test thereby represented a relevant laboratory simulation of a spill event in a freshwater environment.

The test indicated little effect of diesel on rainbow trout health at doses ≤8 mg/L, as evidenced by no significant effects on survival and growth rates, and only minor changes in liver gene expression (i.e., a low number of unrelated genes; Table 1). Diesel doses of 40 mg/L were associated with a gradual increase in mortality over the duration of the test, and a sharp increase in the number of genes and functional groups of genes with altered expression. Exposures ≥200 mg/L of diesel resulted in 100% mortality of rainbow trout fry (Table 1). Based upon dose–response curves interpolated from data for individual end points, toxicity reference values of 4−45 mg/L were determined (Table 2).

Primary Mechanism of Action Associated with Diesel Toxicity. At the highest diesel dosage tested in the microarray experiment (40 mg/L), 161 genes were significantly downregulated whereas 90 genes were upregulated (Table 1).

TABLE 2. Toxicity Reference Values, in the Form of 20 and 50% Effect Concentrations (EC_{20}, EC_{50}), Derived from Dose–Response Curves for Survival, Growth, and Gene Expression in Rainbow Trout Fry

	EC_{20} (mg/L)	EC_{50} (mg/L)
survival	26.7	44.8
growth	>40.0	>40.0
gene expression	4.1	17.7

Although this represented only 1% of the total number of genes on the array, alterations in the expression of functionally related genes reflected potential physiological consequences of diesel exposure. The multiple functional gene groups affected (Figure 1) were indicative of mechanisms of toxicity that may affect fish in the short and longer term.

Mechanisms of diesel toxicity have not been investigated in great detail, but fish mortality following spills has often been attributed to the formation of a layer of oil (sheen) on the water. Sheen limits the oxygen exchange between air and water, and both sheen and dissolved constituents may coat the gills of fish causing lesions on respiratory surfaces affecting respiration (*4*). In the diesel spike test, observations of fish remaining in the upper level of the water column, swimming sideways, and widely opening their gills are consistent with lack of oxygen. Measurements of dissolved oxygen in test water showed (slightly) lower dissolved oxygen concentrations (9.3 versus 9.8 mg/L on average in test water versus control; Table S2). However, the microarray results indicated the downregulation of the hemoglobin gene, which encodes the protein part of the oxygen transporting molecule in blood. If this in turn decreased the abundance of hemoglobins, it would be a limiting factor in oxygen exchange.

In fish, the larval liver is involved in erythropoiesis, but the kidney, and to a lesser extent the spleen, become the primary hemoglobin producers in the adult. The decreased hemoglobin transcription in exposed fish may therefore be an indirect observation of effects taking place in the kidney. If the extent of hemoglobin downregulation and consistency of downregulation of multiple subunits (hemoglobin alpha, beta, and epsilon chains) in the liver is reflective of the mRNA and protein changes occurring elsewhere, diesel may affect the circulatory oxygen transporting ability, and the associated oxygen delivery to major organs. Additional observations of the upregulation of haptoglobin, making the hemoglobin accessible to degradative enzymes, and downregulation of hemopexin and ferritin, binding heme for iron recovery, would put further stress on oxygen homeostasis. This is consistent with observations by Crider et al. that naphthalene concentrations of 5 mg/L and above reduced circulatory hemoglobin concentrations and oxygen uptake in the wa-

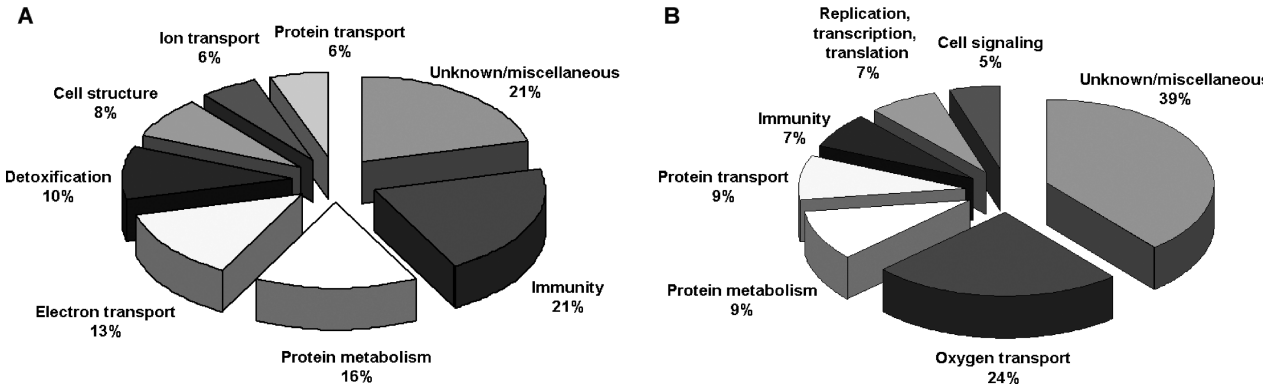

FIGURE 1. At the diesel exposure dose of 40 mg/L, a number of related genes showed altered expression. The following categories were recognized to be represented among the genes (based on their function listed in the Protein Knowledge database): immunity, protein metabolism (including modification and degradation), protein transport, detoxification, cell signaling, cell structure, endocrine function, oxygen transport (including iron storage and recovery from heme), electron transport, metal and ion transport, and replication, transcription, and translation. Large proportions of genes related to immunity and protein metabolism represented the altered upregulated gene functions (A), whereas the primary functional group of downregulated genes was oxygen transport (B). Note: Functional groups that contributed less than 5% to the total were grouped as miscellaneous. These included the following for upregulated genes: cell signaling (3%), endocrine function (2%), oxygen transport (1%), and replication/transcription/translation (2%); and for downregulated genes they included metal/ion transport (3%), cell structure (3%), detoxification (2%), endocrine function (1%), and electron transport (1%).

terflea (*Daphnia magna*) within 24 h (*5*), but has not been previously described in fish.

Diminished energy dedicated to oxygen homeostasis is contradictory to what would be physiologically expected from organisms in a low oxygen environment (*6*). Although this could represent a stress response or secondary toxicity (e.g., cardiovascular toxicity), microarray results supported the hypothesis that this may be a result of altered priorities in the liver. A number of genes associated with normal metabolic liver functions (i.e., the production of hemoglobins, protein transporters, and structural proteins) were downregulated, whereas liver products associated with adaptive responses (immunity) and/or xenobiotic stresses (detoxification) were elevated (Table S3). Others have documented previously that the liver of naphthalene-exposed trout had decreased capacity for exporting glucose, and covering energy demands related to reproductive processes (*7*), and increased internal use of energy associated with detoxification activities (*8*). The liver may therefore divert its energy away from certain functions to be able to attend to contaminant-related processes.

Detoxification is a defense mechanism present in all vertebrates that is rapidly induced upon exposure, to aid in the elimination of toxicants, with the liver being the primary organ for this activity. Increased detoxification activity in diesel-exposed fish was supported by upregulated transcription of typical phase I (cytochrome (CYP) P450 1A1 and 1B1, 9- and 12-fold upregulated, respectively) and phase II (glutathione-S-transferases (GST), 2–3 fold higher) detoxification enzyme genes, and in measured ethoxy-resorufin-O-deethylase (EROD) activity (*9*). These effects are attributed to the minority of PAHs present in diesel (Table S1), consistent with the upregulated transcription of the aryl hydrocarbon receptor 2 (AhR2, 1.7-fold higher copy numbers). AhR2, the functional counterpart of the mammalian AhR, binds PAHs and subsequently mediates the upregulation of AhR-dependent genes such as CYP and GST enzymes (*10–12*). The higher abundance of electron carrier transcripts may also be related to elevated detoxification activity. Detoxification requires significantly higher oxygen consumption in order to support the (phase I) oxygenation of contaminants (*13*), which may represent an additional stress on fish in diesel-contaminated waters. Second, the oxygenation reactions associated with detoxification may produce reactive oxygen species that may result in oxidative stress, damage of cell structure, and eventually cell death (*10*).

The oxygen limitations resulting from (1) decreased environmental oxygen availability in spill areas, (2) downregulation of hemoglobin transcription, and (3) increased oxygen consumption during detoxification and possibly other contaminant-related stresses, observed during the diesel spike test and in microarray experiments, would lead to anoxia in fish. With consistent behavioral observations and the dose at which mortality gradually starts to occur and changes in gene expression are taking place, it is likely that physiologically induced anoxia is the primary mechanism of mortality in fish exposed to diesel products.

Effects of Diesel on the Immune System. Diesel exposure was accompanied by downregulation as well as upregulation of genes associated with immunity. The majority of downregulated genes were components of the complement cascade, serum components whose assembly and activation facilitate inflammation, phagocytosis, and cell lysis. The specific complement cascade components identified are part of the classical complement pathway (including C7 and C2) rather than the alternative pathway. In juvenile fish, the complement system represents an important component of immunity, awaiting lymphoid organ maturation and steadily increasing from fertilization to hatch (*14*).

Immune system alterations may present a nonspecific reaction from the immune system to direct contact and/or ingestion of diesel components, poor general health of exposed fish and an associated increased susceptibility to bacteria/viruses, immunotoxic properties of diesel components (PAHs), or stress associated with contaminant exposure in general (*15, 16*). Our observations of such effects at the molecular level underlie previously documented decreases in fish immune responses upon exposure to diesel oil-contaminated drilling muds (*17*), and the increased prevalence of external abnormalities, including lesions of gills, skin, and fins caused by opportunistic infections, in fish inhabiting PAH-contaminated sediments (*18*). Alteration in immune system function, in either an upregulated or downregulated manner, may disturb the delicate balance under which the multiple immune system components are employed and may affect fish health and survival over prolonged exposure durations.

TABLE 3. Molecular Biomarkers Selected from Genes That Followed an Upregulated (A) or Downregulated (B) Threshold Dose Response Curve Based upon the Knowledge That Diesel Adversely Affects Rainbow Trout Fry Survival and Gene Expression at the 40 mg/L Dose (These Genes May Represent Suitable Biomarkers of Diesel Toxicity in Environmental Monitoring Programs and Risk Assessments)

(A) Upregulated genes following a threshold dose–response curve

putative gene ID	accession no.	diesel exposure dose (mg/L)				*P* value	organism EST derived
		0.3	1.5	8	40		
Cytochrome P450IA1	CB497960	3.28	2.59	2.53	8.61	0.003	*O. mykiss*
Sulfotransferase 6B1	CA042631	1.81	1.65	2.74	6.31	0.003	*S. salar*
Carbonyl reductase	CA064229	1.53	1.95	1.91	4.03	0.003	*S. salar*
Thioredoxin	CA041451	1.30	1.30	1.43	3.65	0.005	*S. salar*
Thioredoxin	CB498297	1.15	1.43	1.62	3.52	0.008	*O. mykiss*
Glutathione S-transferase	CB497579	1.53	1.57	1.83	2.76	0.002	*O. mykiss*
Complement factor H precursor	CB497097	0.98	1.18	1.44	2.57	0.000	*O. mykiss*
Protein disulfide-isomerase A4 precursor	CA064165	1.31	1.72	1.43	2.48	0.000	*S. salar*
Glutathione S-transferase	CA057063	1.37	1.43	1.64	2.43	0.024	*S. salar*
Transaldolase	CA063027	0.82	0.81	1.02	2.35	0.000	*S. salar*
Complement component C7–2	CA049855	0.79	0.63	1.13	2.32	0.017	*S. salar*
Intelectin 1a precursor	CB496555	1.10	1.24	0.90	2.29	0.004	*O. mykiss*
Properdin	CA053493	0.97	1.23	1.31	2.12	0.000	*S. salar*
CD209 antigen-like protein E	CB496842	1.11	0.86	0.99	2.12	0.006	*O. mykiss*
Leukocyte cell-derived chemotaxin 2 precursor	CX984314	0.94	1.23	1.16	2.10	0.003	*S. salar*
Nucleoside diphosphate kinase B	CB497381	1.17	1.03	1.03	1.96	0.002	*O. mykiss*
Complement C1r subcomponent precursor	CB510300	0.94	1.08	1.25	1.91	0.000	*S. salar*
Complement factor H precursor	CA037616	1.07	1.15	1.38	1.87	0.001	*S. salar*
Eukaryotic translation initiation factor	CA050996	1.04	1.07	1.22	1.85	0.018	*S. salar*
Cofilin, muscle isoform	CA060055	0.88	0.75	1.07	1.84	0.004	*S. salar*
Aryl hydrocarbon receptor 2 gamma	CB511953	1.01	1.28	1.09	1.74	0.006	*S. salar*
KIAA1279 protein	CB496780	1.01	1.08	1.06	1.70	0.011	*O. mykiss*
Cytochrome c oxidase subunit IV	CB505449	1.03	1.10	1.19	1.55	0.007	*S. salar*
40S ribosomal protein	CB486904	0.81	0.99	0.82	1.54	0.001	*O. mykiss*
Endoplasmin precursor	CA059329	0.78	0.98	1.04	1.53	0.022	*S. salar*
HSP 90-beta	CA767842	1.12	1.00	1.12	1.49	0.020	*S. salar*

(B) Downregulated genes following a threshold dose–response curve

putative gene ID	accession no.	diesel exposure dose (mg/L)				*P* value	organism EST derived
		0.3	1.5	8	40		
DNA-directed RNA polymerases I, II, and III	CB496981	0.89	0.78	0.97	0.47	0.001	*O. mykiss*
Hemoglobin epsilon-Y2 chain	CB510387	0.80	0.74	0.90	0.46	0.000	*S. salar*
60S ribosomal protein L28	CA051001	0.77	0.75	0.93	0.47	0.020	*S. salar*
Apolipoprotein B	CB497703	0.80	0.80	0.89	0.63	0.002	*O. mykiss*
Apolipoprotein B-100 precursor ($n = 5$)[a]	CB502972, CA043130, CA042944, CK990689, CB509797	0.71	0.91	2.34	8.41	0.008	*S. salar*
Cell division protein kinase 5	CA057215	0.71	0.76	0.69	0.46	0.015	*S. salar*
Coatomer epsilon subunit	CB502159	0.83	0.71	0.76	0.45	0.005	*S. salar*
Felis catus myocyte specific enhancer factor	CA058539	0.82	0.80	0.65	0.40	0.001	*S. salar*
Gastrotropin	CB493070	1.11	0.95	0.90	0.65	0.002	*O. mykiss*
Glyceraldehyde-3-phosphate dehydrogenase	CB498361	0.98	0.94	0.87	0.65	0.002	*O. mykiss*
Hemoglobin alpha chain	CA064277	0.82	0.82	1.04	0.49	0.009	*S. salar*
Hemoglobin alpha chain ($n = 2$)[a]	CA049318,CA770045	0.88	0.71	0.97	0.40	0.004	*S. salar*
Hemoglobin alpha chain	CA058603	0.80	0.74	0.82	0.47	0.003	*S. salar*
Hemoglobin alpha chain	CA058361	0.83	0.83	1.05	0.42	0.001	*S. salar*
Hemoglobin beta-2 chain	CK990563	0.63	0.98	0.75	0.32	0.000	*S. salar*
Hemoglobin beta-2 chain	CK990457	0.81	0.76	0.94	0.38	0.001	*S. salar*
Hemoglobin beta-2 chain	CB498665	0.76	0.86	0.92	0.58	0.003	*O. mykiss*
Hemoglobin beta-2 chain	CB498416	0.82	0.81	1.10	0.41	0.000	*O. mykiss*
Hemoglobin beta-2 chain ($n = 2$)[a]	CB497723, CB494536	0.79	0.84	1.01	0.49	0.002	*O. mykiss*
Hemoglobin beta-2 chain ($n = 2$)[a]	CB498575, CB497309	0.80	0.82	1.06	0.45	0.003	*O. mykiss*
Hemoglobin beta-2 chain	CB496604	0.82	0.81	1.05	0.46	0.000	*O. mykiss*
Hemoglobin epsilon-Y2 chain	CA049313	0.87	0.73	0.89	0.48	0.008	*S. salar*
Hemoglobin epsilon-Y2 chain	CB509758	0.82	0.82	1.03	0.47	0.002	*S. salar*
Hemoglobin epsilon-Y2 chain	CB501013	0.74	0.72	0.88	0.45	0.000	*S. salar*
Hemopexin precursor ($n = 2$)[a]	CB509819, CA037805	1.03	0.94	0.82	0.53	0.045	*S. salar*
Histone H2A variant	CB491527	1.10	1.17	1.00	0.62	0.003	*O. mykiss*
Homo sapiens ARP1 Actin-related protein 1 homologue B	CA051011	0.76	0.81	0.85	0.44	0.005	*S. salar*
Interalpha-inhibitor heavy chain 3	CA063392	0.87	0.78	0.77	0.54	0.008	*S. salar*
Interalpha-trypsin inhibitor heavy chain H2 precursor	CB510131	0.98	0.88	0.87	0.61	0.007	*S. salar*
Liver carboxylesterase 22 precursor	CB496876	0.76	0.87	0.70	0.44	0.001	*O. mykiss*
Liver carboxylesterase 22 precursor	CA057214	0.81	0.78	0.70	0.44	0.000	*S. salar*

TABLE 3. Continued

(B) Downregulated genes following a threshold dose–response curve

putative gene ID	accession no.	diesel exposure dose (mg/L) 0.3	1.5	8	40	*P* value	organism EST derived
Metalloproteinase inhibitor 2 precursor	CB507385	0.97	0.88	0.90	0.62	0.016	*S. salar*
Microsomal glutathione S-transferase 3	CA061668	0.80	0.83	0.97	0.50	0.005	*S. salar*
Prostaglandin-H2 D-isomerase precursor	CB497818	1.01	0.99	0.82	0.55	0.008	*O. mykiss*
Prostaglandin-H2 D-isomerase precursor	CA038730	0.89	0.81	1.00	0.61	0.013	*S. salar*
Salmo salar prion protein	CA059926	0.97	1.00	0.80	0.54	0.015	*S. salar*
Secreted phosphoprotein 24 precursor ($n = 2$)[a]	CB510628, CA037380	0.87	0.95	0.89	0.58	0.007	*S. salar*
Secreted phosphoprotein 24 precursor	CB492943	0.94	0.92	0.84	0.60	0.006	*O. mykiss*
Selenoprotein Pa precursor	CA040124	0.93	0.83	0.83	0.60	0.037	*S. salar*
Selenoprotein Pa precursor	CA044104	0.86	0.90	0.85	0.59	0.003	*S. salar*
Serum albumin precursor	CA038058	0.91	0.79	0.86	0.63	0.022	*S. salar*
Smac protein	CA039356	0.90	1.06	0.74	0.47	0.000	*S. salar*
Transforming growth factor-beta-inducible early growth response protein 2	CB516494	0.76	0.77	0.90	0.42	0.003	*S. salar*
Transposase	CA037517	1.21	0.88	0.93	0.50	0.019	*S. salar*
Type IV antifreeze protein precursor ($n = 2$)[a]	CA044945, CK991076	0.89	0.88	1.00	0.66	0.035	*S. salar*
Ubiquitin carboxyl-terminal hydrolase isozyme L1	CA053740	0.73	0.74	0.92	0.47	0.003	*S. salar*
WD and tetratricopeptide repeats protein 1	CA043849	0.94	0.89	0.80	0.64	0.006	*S. salar*

[a] Number of duplicate elements to calculate the average normalized values.

Endocrine-Disrupting Properties of Diesel. Endocrine-disrupting effects upon diesel exposure were observed in the form of upregulated estrogen-dependent genes, and downregulated testosterone-related and thyroid hormone-dependent genes. The elevated expression of genes under estrogenic regulation included zona pellucida sperm-binding protein (or sperm receptor) and vitellogenin (or egg yolk protein). Under natural conditions, these genes are not expressed by fry, but are associated with fish in a reproductive state (3−4 years of age in rainbow trout). Whereas ethylbenzenes or certain petroleum additives may exert estrogenic properties, PAHs are well studied examples of components able to induce estrogenic effects through the AhR. A number of studies have documented crosstalk between the AhR and estrogen receptor (ER) as a direct toxicity pathway (reviewed in (*19*)). Alternatively, estrogenic effects can be caused by upregulated cytochrome P450 enzymes, which play roles in the biosynthesis of sex steroids (*20*). Testosterone 16-alpha hydroxylase, on the other hand, was downregulated. This cytochrome is primarily expressed in adult males where it catalyzes the breakdown of testosterone. Testosterone, androgens, and their regulatory enzymes have been known to be inhibited by AhR-binding compounds (*21*) and linked to permanent behavioral changes in mammals (*22*).

The decrease in a thyroid hormone dependent gene, thyroid hormone inducible protein or SPOT14, may be due to PAH interference with thyroid hormone physiology at the circulatory or tissue level (*23*).

Implications for Risk Assessment. Diesel may represent an acute toxicity risk to fish present in waters at the time of a spill, during remediation, and during natural attenuation. However, the subacute hazard that diesel may pose to the health of wild fish populations lies in a gradual mortality from anoxia, increased susceptibility to disease, and possibly, endocrine disruption. In areas where fish and fisheries are highly valued, including those inhabited by protected fish species and fish-eating wildlife, and where subsistence fisheries, recreational fishing, and aquaculture takes place, an extra level of protection addressing long-term impacts may be relevant within the context of a risk assessment. Consistency among laboratory observations, survival rates, and molecular changes suggest that molecular biomarkers can provide such a protective action level.

Using trend analysis of microarray data, genes that followed a threshold dose–response curve were selected as biomarkers,—representative indicators of following effects on survival. These genes included hemoglobin subunits, apolipoproteins, prostaglandins, phase I and II detoxification enzymes, and complement proteins (Table 3).The identified gene suite may represent a sensitive screening tool in the early detection of diesel exposure in fish in future studies when a more rapid and cost-effective genomics tool would be needed.

Genomic technologies may be applicable to many scenarios of environmental contamination affecting fish (*24, 25*), as well as other species. Waterfleas (*Daphnia magna*), nematodes, frogs (*Rana* spp.), and mallard ducks (*Anas platyrhynchos*) represent some of the species with a growing genomic toolbox and potential value to risk assessment (*26–29*). The further development of genomics information and tools, experimental verification of its outcomes, and their validation under laboratory and field conditions in the near future will greatly benefit risk assessments in aquatic habitat.

Acknowledgments

This study was financially supported by Hemmera through the Scientific Research & Development (SRED) tax credit program of the Government of Canada, and resources provided by Genome BC and Genome Canada to BK. North Arm Transportation is gratefully acknowledged for providing the diesel sample, and Dr. Peter Hodson is acknowledged for technical review. We also thank Eric Pringle, Paul Hemsley, Geoff Wickstrom, Michael Choi, John Taylor, Christine Lussier, and Erin Bigelow (Hemmera), the Koop lab (University of Victoria), and Curtis Eickhoff, Pam Howes, Christie MacKinley, Tam Vo, and Jeremy Keating (Cantest) for support during the project.

Supporting Information Available

Table S1 contains the chemical composition of the pure diesel sample; Table S2 shows the general water quality parameters and chemical analysis of diesel constituents in test water at test initiation and after 24 h of exposure (upon which water was renewed); Table S3 represents a complete list of all genes of which the expression was significantly altered ($p < 0.05$) equal to or greater than 1.5-fold at each of the exposure doses. This information is available free of charge via the Internet at http://pubs.acs.org.

Literature Cited

(1) Energy Information Administration. *Annual Energy Review 2006*; Energy Information Administration, Office of Markets and End Use, U.S. Department of Energy: Washington, DC, 2007.

(2) Lazorchak, J. M.; Smith, M. E. Rainbow Trout (*Oncorhynchus mykiss)* and Brook Trout (*Salvelinus fontinalis)* 7-day Survival and Growth Test Method. *Arch. Environ. Contam. Toxicol.* **2007**, *53*, 397–405.

(3) von Schalburg, K. R.; Rise, M. L.; Cooper, G. A.; Brown, G. D.; Gibbs, A. R.; Nelson, C. C.; Davidson, W. S.; Koop, B. F. Fish and chips: various methodologies demonstrate utility of a 16,006-gene salmonid microarray. *BMC Genomics* **2005**, *6*, 126.

(4) Green, J.; Trett, M. W. *Fate and Effects of Oil in Freshwater*; Elsevier: London, 1989.

(5) Crider, J. Y.; Wilhm, J.; Harmon, H. J. Effects of naphtalene on the hemoglobin concentration and oxygen uptake of *Daphnia magna. Bull. Environ. Contam. Toxicol.* **1982**, *28*, 52–57.

(6) Hardison, R. Hemoglobins from bacteria to man: evolution of different patterns of gene expression. *J. Exp. Biol.* **1998**, *201*, 1099–1117.

(7) Tintos, A.; Gesto, M.; Alvarez, R.; Miguez, J. M.; Soengas, J. L. Interactive effects of naphtalene treatment and the onset of vitellogenesis on energy metabolism in liver and gonad, and plasma steroid hormones of rainbow trout *Oncorhynchus mykiss. Comp. Biochem. Physiol., C* **2006**, *144*, 155–165.

(8) Tintos, A.; Gesto, M.; Miguez, J. M.; Soengas, J. L. Naphtalene treatment alters liver intermediary metabolism and levels of steroid hormones in plasma of rainbow trout (*Oncorhynchus mykiss*). *Ecotoxicol. Environ. Saf.* **2007**, *66*, 139–147.

(9) Schein, A.; Scott, J.; Mos, L.; Hodson, P. V. Chemical dispersant increases the toxicity of diesel to rainbow trout (*Oncorhynchus mykiss*). *In preparation.*

(10) Dalton, T. P.; Puga, A.; Shertzer, H. G. Induction of cellular oxidative stress by aryl hydrocarbon receptor activation. *Chem.-Biol. Interact.* **2002**, *141*, 77–95.

(11) Mantyla, E.; Ahotupa, M. Polychlorinated biphenyls and naphthalenes - long-lasting induction of oxidative stress in the rat. *Chemosphere* **1993**, *27*, 383–390.

(12) Nebert, D. W.; Roe, A. L.; Dieter, M. Z.; Solis, W. A.; Yang, Y.; Dalton, T. P. Role of the aromatic hydrocarbon receptor and [Ah] gene battery in the oxidative stress response, cell cycle control, and apoptosis. *Biochem. Pharmacol.* **2000**, *59*, 65–85.

(13) Cohen, A.; Nugegoda, D.; Gagnon, M. M. Metabolic responses of fish following exposure to two different oil spill remediation techniques. *Ecotoxicol. Environ. Saf.* **2001**, *48*, 306–310.

(14) Lovoll, M.; Kilvik, T.; Boshra, H.; Bogwald, J.; Sunyer, J. O.; Dalmo, R. A. Maternal transfer of complement components C3-1, C3-3, C3-4, C4, C5, C7, Bf, and Df to offspring in rainbow trout (*Oncorhynchus mykiss*). *Immunogenetics* **2006**, *58*, 168–179.

(15) Reynaud, S.; Deschaux, P. The effects of polycyclic aromatic hydrocarbons on the immune system of fish: A review. *Aquat. Toxicol.* **2006**, *77*, 229–238.

(16) Irwin, M. Stress-induced immune suppression - role of brain corticotropin releasing hormone and autonomic nervous system mechanisms. *Adv. Neuroimmunol.* **1994**, *4*, 29–47.

(17) Tahir, A.; Secombes, C. J. The effects of diesel oil-based drilling mud extracts on immune responses of rainbow trout. *Arch. Environ. Contam. Toxicol.* **1995**, *29*, 27–32.

(18) Hylland, K. Polycyclic aromatic hydrocarbon (PAH) ecotoxicology in marine ecosystems. *J. Toxicol. Environ. Health, Part A* **2006**, *69*, 109–123.

(19) Ohtake, F.; Takeyama, K.; Matsumoto, T.; Kitagawa, H.; Yamamoto, Y.; Nohara, K.; Tohyama, C.; Krust, A.; Mimura, J.; Chambon, P.; Yanagisawa, J.; Fujii-Kuriyama, Y.; Kato, S. Modulation of oestrogen receptor signaling by association with the activated dioxin receptor. *Nature* **2003**, *423*, 545–550.

(20) Sanderson, J. T. The steroid hormone biosynthesis pathway as a target for endocrine-disrupting chemicals. *Toxicol. Sci.* **2006**, *94*, 3–21.

(21) Toppari, J.; Larsen, J. C.; Christiansen, P.; Giwercman, A.; Grandjean, P.; Guillette, L. J., Jr.; Jégou, B.; Jensen, J. K.; Jouannet, P.; Keiding, N.; et al. Male reproductive health and environmental xenoestrogens. *Environ. Health Perspect.* **1996**, *104*, 741–803.

(22) Haake-McMillan, J. M.; Safe, S. H. Neonatal exposure to Aroclor 1254: effects on adult hepatic testosterone hydroxylase activities. *Xenobiotica* **1991**, *21*, 481–489.

(23) Brouwer, A.; Morse, D. C.; Lans, M. C.; Schuur, A. G.; Murk, A. J.; Klasson, W. E.; Bergman, A.; Visser, T. J. Interactions of persistent environmental organohalogens with the thyroid hormone system: mechanisms and possible consequences for animal and human health. *Toxicol. Ind. Health* **1998**, *14*, 59–84.

(24) Finne, E. F.; Cooper, G. A.; Koop, B. F.; Hylland, K.; Tollefsen, K. E. Toxicogenomic responses in rainbow trout (*Oncorhynchus mykiss*) hepatocytes exposed to model chemicals and a synthetic mixture. *Aquat. Toxicol.* **2007**, *81*, 293–303.

(25) Hook, S. E.; Skillman, A. D.; Small, J. A.; Schultz, I. R. Gene expression patterns in rainbow trout, *Oncorhynchus mykiss*, exposed to a suite of model toxicants. *Aquat. Toxicol.* **2006**, *77*, 372–385.

(26) Alvarez, O. A.; Jager, T.; Redondo, M.; Kammenga, J. E. Physiological modes of action of toxic chemicals in the nematode *Acrobeloides nanus. Environ. Toxicol. Chem.* **2006**, *25*, 3230–3237.

(27) Poynton, H. C.; Varshavsky, J. R.; Chang, B.; Cavigiolo, G.; Chan, S.; Holman, P. S.; Loguinov, A. V.; Bauer, D. J.; Komachi, K.; Theil, E. C.; Perkins, E. J.; Hughes, O.; Vulpe, C. D. *Daphnia magna* ecotoxicogenomics provides mechanistic insights into metal toxicity. *Environ. Sci. Technol.* **2007**, *41*, 1044–1050.

(28) Zhang, F.; Degitz, S. J.; Holcombe, G. W.; Kosian, P. A.; Tietge, J.; Veldhoen, N.; Helbing, C. C. Evaluation of gene expression endpoints in the context of a *Xenopus laevis* metamorphosis-based bioassay to detect thyroid hormone disruptors. *Aquat. Toxicol.* **2006**, *76*, 24–36.

(29) Hamilton, M. J.; Yan, T.; Sadowsky, M. J. Development of goose- and duck-specific DNA markers to determine sources of *Escheria coli* in waterways. *Appl. Environ. Microbiol.* **2006**, *72*, 4012–4019.

ES702215C

Wetlands Ecology and Management (2005) 13: 509–515
DOI 10.1007/s11273-004-3939-4
© Springer 2005

Coal dust pollution effects on wetland tree species in Richards Bay, South Africa

G. Naidoo* and Y. Naidoo
*School of Biological and Conservation Sciences, University of KwaZulu-Natal, Private Bag X 54001, Durban 4000, South Africa; *Author for correspondence (e-mail: naidoogn@ukzn.ac.za; phone: +27-31-260-7367; fax: +27-31-260-7364)*

Received 24 February 2003; accepted in revised form 27 September 2004

Key words: Avicennia marina, *Bruguiera gymnorrhiza*, Chlorophyll fluorescence, *Hibiscus tiliaceus*, Mangroves, Photosynthesis, *Rhizophora mucronata*

Abstract

In this study, the effects of coal dust on four, sympatric, wetland tree species in Richards Bay Harbour were investigated. We tested the hypothesis that leaf micromorphology influenced dust accumulation and that coal dust occluded stomata and reduced photosynthetic performance of three mangroves, *Avicennia marina, Bruguiera gymnorrhiza* and *Rhizophora mucronata*, and a mangrove associate, *Hibiscus tiliaceus*. To investigate leaf micromorphology, leaf blade material of the four species was prepared following standard procedures and viewed under scanning electron microscopy. Gas exchange and chlorophyll fluorescence measurements were made at saturating light (>1000 μmol m^{-2} s^{-1}) and high temperature (>25 °C) on leaves that were either covered or uncovered with coal dust. There was no evidence of occlusion of stomata by dust. Dust accumulation in *A. marina* and *H. tiliaceus* was exacerbated by the presence of a dense mat of trichomes on the undersurface of the leaves, as well as by the sticky brine secreted by salt glands in the former species.
Coal dust significantly reduced CO_2 exchange, Photosystem II (PS II) quantum yield and electron transport rate (ETR) through PS II in *A. marina* and *H. tiliaceus* but not in the other two mangroves. Reduction in photosynthetic performance was attributed to reduction in light energy incident on the photosynthetic tissues.

Introduction

Mangroves thrive in a stressful and naturally changing intertidal environment. These trees and shrubs grow luxuriantly in saline wetlands along tropical and subtropical coasts and are considered among the most productive ecosystems (Alongi et al. 1992). Increasingly, mangrove ecosystems are also being subjected to anthropogenic changes due to intense pressure from human activities. For purposes of management it is important to separate natural from anthropogenic changes.

In South Africa, mangrove vegetation occurs along many of the protected estuaries on the east coast extending from Mozambique in the north to East London in the south (Macnae 1962). In Richards Bay Harbour, three mangrove species (*Avicennia marina* (Forsk.) Vierh., *Bruguiera gymnorrhiza* (L.) Lam. and *Rhizophora mucronata* Lam.) and a mangrove associate (*Hibiscus tiliaceus* L.), are important components of tidal saline wetlands. Located in Richards Bay Harbour, in close proximity to these wetland species, is Richards Bay Coal Terminal (RBCT), the largest coal

export terminal in the world with a storage capacity of 6.7 million tons, stacked to a height of 21 m and a width of 78 m. Despite the adoption of several dust abatement mechanisms such as water sprays and wind breaks, the coal operations, which involve shunting, stockpiles, conveyer belts and ship loading, create dust which is a problem in the harbour and surrounding areas, not only on wetland species, but also on other plant communities in the vicinity, as well as on human health. Tidal wetland tree species in close proximity to the coal terminal appear to be in poorer health than those in distant areas. Visual observations indicated that some species were more prone to coal dust accumulation than others.

In a previous study, we were the first to demonstrate that coal dust significantly reduced photosynthetic performance of *A. marina*, the reduction being greater on lower leaf surfaces and at higher elevations in the swamp that supported isolated dwarfed trees (Naidoo and Chirkoot 2004). In this investigation, the effect of coal dust on four sympatric, wetland tree species within 3 km of the coal stockpile, was determined. Others have shown that dust may occlude stomata (Ricks and Williams 1974; Hirano et al. 1995), reduce light incident on leaves (Sharifi et al. 1997), reduce CO_2 uptake (Ernst 1982; Naidoo and Chirkoot 2004) and reduce growth (Sharifi et al. 1997).

We tested the hypothesis that leaf micromorphology influenced coal dust accumulation and that dust occluded stomata, and reduced photosynthetic performance of three mangroves *Avicennia marina* (Forsk.) Vierh., *Bruguiera gymnorrhiza* (L.) Lam. and *Rhizophora mucronata* Lam., and a mangrove associate, *Hibiscus tiliaceus* L.

Materials and methods

This work was undertaken in Richards Bay Harbour (28°48′ S; 32°05′ E) between September 2001 and August 2002. The study site was located in the southern portion of the harbour, within 3 km of the RBCT coal storage facility. The mangrove area is dominated by an almost pure stand of *A. marina*. On the landward fringes of the *Avicennia* zone, *B. gymnorrhiza*, *R. mucronata* and *H. tiliaceus* occur.

In the study site, all four species co-occurred, thereby allowing the assumption that environmental conditions were similar. In this area, portions of trees facing RBCT were covered with dust and appeared black, while those on the leeward side were green and relatively uncovered. Five trees of each species were tagged and five mature leaves on each tree marked for measurements as being covered or uncovered with coal dust. Measurements were made on four separate days. Although there were differences in the degree of dust loading, only leaves that were extensively covered and appeared black were selected for measurements. All trees sampled received full sunlight. Mean soil water potential at the study site, measured with a WP4 Dew Point Potential Meter (Decagon Devices Inc, Pullman, Washington, USA) was -1.12 ± 0.48 MPa ($n = 25$).

CO_2 exchange

Gas exchange measurements were made with a portable infrared gas analyser (Licor-6400, Licor, Lincoln, Nebraska, USA). Five trees of each species were selected and tagged for measurements. On each of five trees of each species, five gas exchange measurements were made on mature leaves that were either covered or uncovered with coal dust, resulting in 25 measurements per treatment per species per day. Measurements were made on 4 days at saturating light (1000–1500 μmol m^{-2} s^{-1}) and ambient temperature (28–30 °C). In total there were 100 measurements per treatment. Gas exchange rates were calculated on a leaf area basis for the upper leaf surface. Leaf temperatures were marginally above ambient by less than 1 °C.

Chlorophyll fluorescence

Fluorescence measurements were determined with a field portable, pulse amplitude, modulated fluorometer, PAM-2000 (H. Walz, GmbH, Effeltrich, Germany; see Schreiber et al. 1995). Operation of the fluorometer and data processing were conducted with a Hewlett Packard HP200 LX Palmtop Computer. The instrument was protected from direct sunlight to prevent heating of

the emitter/detector (E/D)-unit. Control measurements using a fluorescence standard (Walz, GmbH, Effeltrich, Germany) indicated that these precautions prevented a shifting of the fluorescence signal due to temperature changes in the E/D-unit, which was reported previously by Herppich et al. (1994).

All measurements were made on the lamina, midway between the tip and base of mature, attached leaves. Quantum yield of PSII electron transport ($\Delta F/F_{m'}$) was measured using a leaf clip with integrated microquantum sensor (H. Walz, GmbH, Effeltrich, Germany) and calculated according to Genty et al. (1989). The electron transport rate (ETR) through PSII was calculated as ETR = 0.5* 84* PDF*$\Delta F/F_{m'}$, assuming that 84% of the incident light is absorbed by the leaves and that photons are equally distributed between PSII and PSI (Schreiber et al. 1995). The maximum quantum yield of PSII (F_v/F_m) was measured after 20 min dark adaptation, using a dark leaf clip with a shutter (H. Walz, GmbH, Effeltrich, Germany). The period of predarkening was sufficient for a complete relaxation of the fast relaxing components of non-photochemical quenching (Krause and Weis 1991).

All chlorophyll fluorescence measurements were made under ambient conditions at saturating light on the same or similar leaves on which gas exchange measurements were made. For each species, 25 measurements were made per treatment per day over 4 days.

Scanning electron microscopy (SEM)

To investigate surface leaf morphology, pieces of freshly harvested leaf blade material of all four species were rapidly quenched in liquid nitrogen, fractured and then freeze-dried at −60 °C at a vacuum of 10^{-2} Torr for 72 h. Samples were secured with carbon conductive tape onto brass stubs and coated with gold. Leaf segments were viewed in a Philips SEM 500 at 12 kV. Stomatal apertures were measured from the micrographs. Coal dust particles, removed under water from leaf surfaces, were analysed for elemental composition by Energy Dispersive X-ray microanalysis (EDX) using the Noran 'Voyager' 2100 EDX system interfaced with a Joel SEM 6100. During analysis, working distance was 15 mm, data collection time 60 s and accelerating voltage 15 kV.

Statistical analyses

All data, which satisfied the assumptions of ANOVA, were analysed by unpaired *t*-tests to detect for significant differences between pairs of means ($p < 0.05$) using GraphPad Instat Version 3.00 (Mustek).

Results

Leaf morphology

Field observations indicated that leaves of *A. marina* and *H. tiliaceus* were more prone to coal dust accumulation than the other two species, especially on the abaxial surfaces, which may appear completely black on exposed sites. The SEM data showed that adaxial leaf surfaces of *B. gymnorrhiza* and *R. mucronata* were glabrous, being covered by a thick smooth cuticle and did not accumulate much dust. In *A. marina*, the adaxial surface is smooth with numerous salt glands (Figure 1A). In *H. tiliaceus*, occasional tentacle-like trichomes, which were appressed to the leaf, occurred on the adaxial surface (Figure 2A).

While the abaxial leaf surfaces of *B. gymnorrhiza* and *R. mucronata* are glabrous, those of *A. marina* and *H. tiliaceus* are covered by a dense mat of multicellular trichomes which are tentacle-like in *H. tiliaceus* (Figure 2B) and peltate in *A. marina* Figure 1B). Coal dust particles accumulate on and in-between these trichomes (Figures 1C and 2C). Fully open stomatal apertures of the four species were less than 5 μm while dust particles were generally larger and ranged from 5 to 12 μm. EDX microanalysis of coal dust collected from the leaves revealed that coal dust was 99.53% carbon with negligible amounts of toxic elements.

CO_2 exchange

Coal dust significantly decreased CO_2 exchange in *A. marina* by 39% and in *H. tiliaceus* by 32%, but

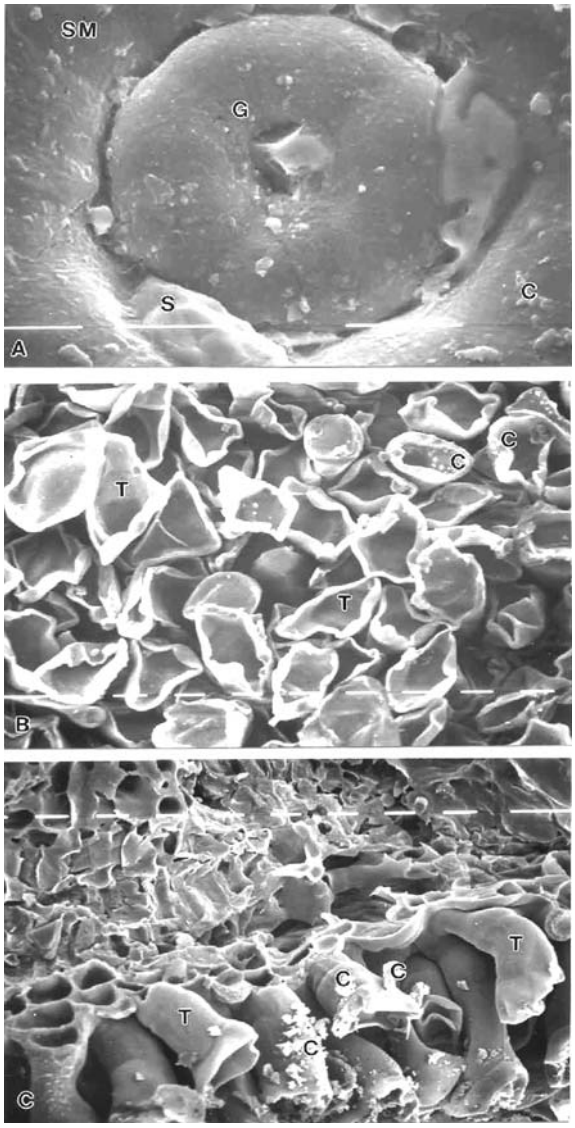

Figure 1. SEM of upper (A) and lower (B) leaf surface and freeze-fractured lower leaf surface (C) of *A. marina*. C – coal dust, G – salt gland, SM – smooth leaf surface, T – trichome. Bars represent 10 μm.

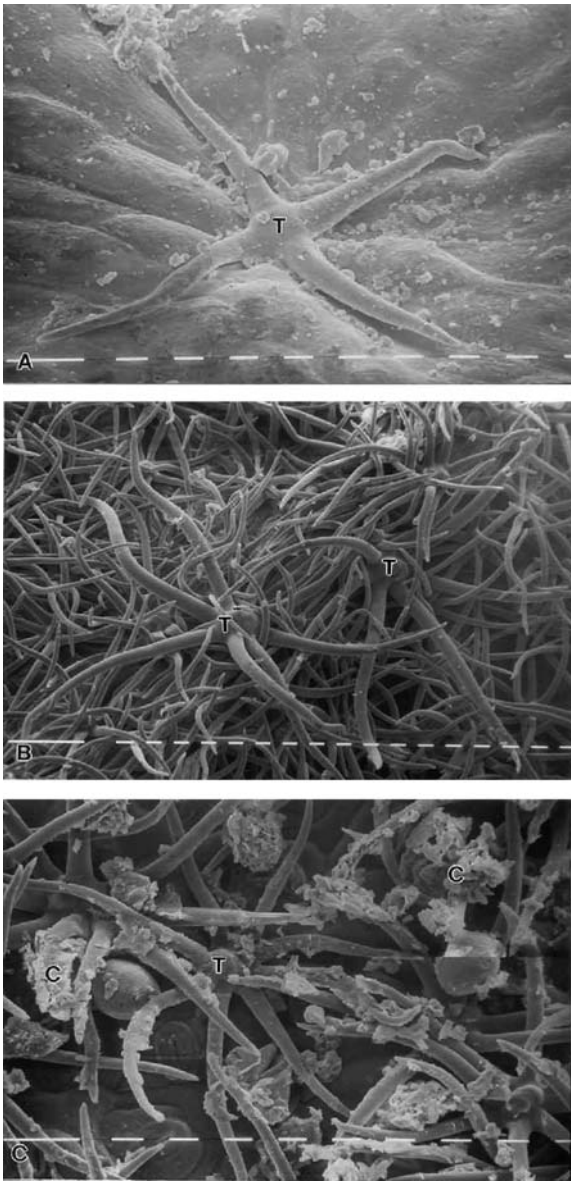

Figure 2. SEM of upper (A) and lower (B) leaf surfaces of *H. tiliaceus* uncovered (B) and covered (C) with dust. Other details as for Figure 1. Bars represent 10 μm.

had no effect on the other two species (Figure 3). Decreases in CO_2 exchange in *A. marina* and *H. tiliaceus* were associated with significant decreases in leaf conductance (35 and 19%, respectively) and transpiration (28 and 29%, respectively). There were no decreases in internal CO_2 concentration between leaves that were covered or uncovered with coal dust, except for *A. marina* where CO_2 concentration decreased by 35% (Table 1).

Chlorophyll fluorescence

Coal dust reduced quantum yield of PSII in *H. tiliaceus* and *A. marina* by 36 and 40%, respectively (Table 1). ETR through PS II was reduced in dust-coated leaves of *H. tiliaceus* and *A. marina* by 39 and 36%, respectively. Coal dust had no effect on quantum yield or ETR in *B. gymnorrhiza* and *R. mucronata*. Maximum

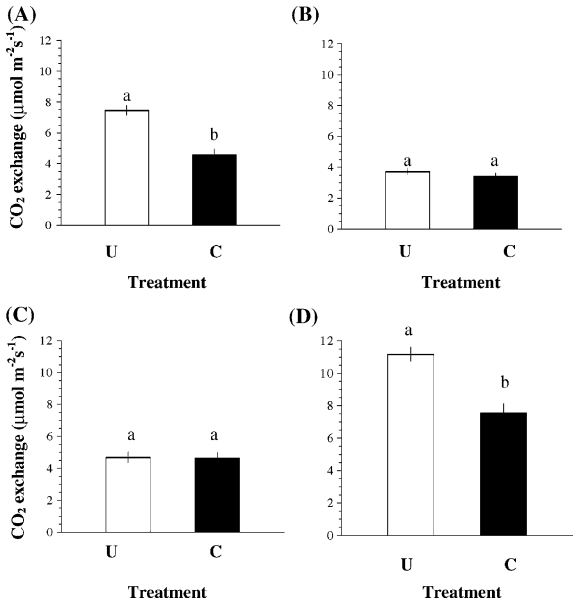

Figure 3. CO_2 exchange in *A. marina* (A), *B. gymnorrhiza* (B), *R. mucronanta* (C) and *H. tiliaceus* (D) leaves uncovered (U) and covered (C) with coal dust. Measurements were made at saturating light (> 1000 μmol m^{-2} s^{-1}), $n = 100$, vertical bars indicate standard error of the mean. Bars with different letters are significantly different at $p < 0.05$ using unpaired '*t*' tests.

photochemical efficiency (F_v/F_m) was unaffected by coal dust except for *A. marina* (Table 1).

Table 1. Leaf conductance (g), transpiration (E), internal carbon dioxide (c_i), quantum yield of PS II electron transport ($\Delta F_v/F_m$) ETR through PSII and maximum photochemical efficiency (F_v/F_m) in *A. marina, B. gymnorrhiza, R. mucronata* and *H. tiliaceus* leaves uncovered or covered with coal dust, $n = 100$, except for F_v/F_m where $n = 20$.

	Uncovered	Covered
A. marina		
g (mol m^{-2} s^{-1})	0.058 ± 0.018	0.043 ± 0.015*
E (mmol m^{-2} s^{-1})	1.16 ± 0.409	0.830 ± 0.342*
c_i (μl l^{-1})	135.1 ± 61.5	183.0 ± 45.6*
$\Delta F_v/F_m$	0.391 ± 0.052	0.243 ± 0.022*
ETR (μmol m^{-2} s^{-1})	86.4 ± 8.2	55.1 ± 4.7*
F_v/F_m	0.782 ± 0.006	0.721 ± 0.027*
B. gymnorrhiza		
g (mol m^{-2} s^{-1})	0.038 ± 0.008	0.032 ± 0.009*
E (mmol m^{-2} s^{-1})	1.23 ± 0.31	0.94 ± 0.26*
c_i (μl l^{-1})	176.5 ± 52.2	157.9 ± 69.6^{ns}
$\Delta F_v/F_m$	0.22 ± 0.02	0.19 ± 0.02^{ns}
ETR (μmol m^{-2} s^{-1})	77.2 ± 9.4	75.4 ± 8.3^{ns}
F_v/F_m	0.766 ± 0.007	0.762 ± 0.011^{ns}
R. mucronata		
g (mol m^{-2} s^{-1})	0.048 ± 0.013	0.043 ± 0.016 ^{ns}
E (mmol m^{-2} s^{-1})	1.34 ± 0.35	1.34 ± 0.51^{ns}
c_i (μl l^{-1})	185.4 ± 20.5	163.0 ± 51.7^{ns}
$\Delta F_v/F_m$	0.14 ± 0.02	0.14 ± 0.01^{ns}
ETR (μmol m^{-2} s^{-1})	60.3 ± 9.1	52.2 ± 5.1^{ns}
F_v/F_m	0.793 ± 0.004	0.792 ± 0.005^{ns}
H. tiliaceus		
g (mol m^{-2} s^{-1})	0.123 ± 0.04	0.080 ± 0.04*
E (mmol m^{-2} s^{-1})	3.22 ± 0.85	2.30 ± 1.19*
c_i (μl l^{-1})	174.8 ± 38.6	168.5 ± 43.3^{ns}
$\Delta F_v/F_m$	0.25 ± 0.01	0.15 ± 0.01*
ETR (μmol m^{-2} s^{-1})	98.7 ± 5.2	60.3 ± 5.6*
F_v/F_m	0.790 ± 0.006	0.781 ± 0.009^{ns}

*Significant differences between leaves uncovered and covered with coal dust using unpaired "*t*" tests, $p < 0.05$.
ns – not significant.

Discussion

Leaf morphology

SEM indicated that micromorphological characteristics of the leaves influence dust accumulation. Dust effects were minimal in species with glabrous leaves, such as *B. gymnorrhiza* and *R. mucronata*, as much of the dust that settles on the leaves is removed by rain and wind. In those species where the hairs are located only on the undersurface (*A. marina*) or predominantly on the lower surface (*H. tiliaceus*) the dust particles are trapped in-between the hairs and cannot be removed by wind or rain. Furthermore, in *A. marina*, the sticky salt secretion from salt glands on both leaf surfaces tended to accumulate dust still further. In a study on the effect of iron ore dust on mangroves in Western Australia, Paling et al. (2001), also reported that the hairy undersurface of *A. marina* leaves accumulated more dust than five other species with glabrous leaves.

Coal dust particles were larger than the fully open stomatal apertures of the four species and were unlikely to occlude stomata. In *A. marina* and *H. tiliaceus* the dense mat of trichomes shielded stomata from wind-blown coal dust so that dust accumulated on trichomes with little penetration to the leaf surface where stomata are located. Elemental analysis of coal dust particles by EDX showed that dust was predominantly carbon and therefore unlikely to be toxic to plants.

Photosynthetic characteristics

The gas exchange data clearly indicated that species with hairy leaves, such as *A. marina* and *H. tiliaceus* were more susceptible to dust-induced reduction in CO_2 exchange than those with glabrous leaves. Reduction in CO_2 exchange may be mediated through increases in temperature of leaves coated with black dust leading to stomatal closure and increased photoinhibition. Differences in temperature between leaves covered and uncovered with dust, however, were less than 1 °C and therefore unlikely to account for the decrease in CO_2 exchange of dust-coated leaves. Decreases in CO_2 exchange in dust-covered leaves of *A. marina* and *H. tiliaceus* were probably mediated through reduction in light incident on the leaves, resulting in subsequent reduction in conductance and transpiration. Lack of differences in internal CO_2 concentration may be attributed to high cuticular transpiration (Kirschbaum and Pearcy 1988; Boyer et al. 1997) and patchy stomatal closure, which have been demonstrated to overestimate internal CO_2 concentration when averaged over large areas (Terashima 1992).

In other reports (Ricks and Williams 1974) atmospheric pollution was shown to increase stomatal diffusive resistance in *Quercus petraes*, while species with hairy leaves were reported to be at greater risk from dust than those with glabrous leaves (Semenuik 1987; Paling et al. 2001). Moreover, in several Mojave Desert shrubs, dust loading on leaves reduced gas exchange (Sharifi et al. 1997).

Decreases in quantum yield of PSII and ETR through PSII (Table 1), supported the gas exchange data that photosynthetic performance of dust-coated *A. marina* and *H. tiliaceus* leaves was reduced. Photochemical efficiency of PSII in *A. marina* was significantly reduced in dust-covered leaves suggesting photoinhibitory damage (Table 1). In the other three species, photochemical efficiency values were similar and ranged from 0.76 to 0.79, which are typical of nearly completely relaxed PSII. Mangroves have been shown to possess effective mechanisms to dissipate excess light (Bjorkman et al. 1988) and avoid chronic photoinhibition (Lovelock and Clough 1992; Cheeseman et al. 1997; Tuffers et al. 1999; Naidoo et al. 2002).

General

In the vicinity of the RBCT site, dust permeates all surfaces, including leaves, stems, aerial roots and soil. In the long term, dust is bound to have adverse effects on health, growth, productivity and mortality of species, as well as changes in community structure. *A. marina* is by far the most dominant tree, thriving in monospecific stands and tends to accumulate more dust than the other three species. Dust significantly reduces photosynthetic performance of species with hairy leaves and in the long term would reduce growth and productivity.

In a previous study, it was demonstrated that coal dust effects on *A. marina* are greater at high salinities because of the combined stress effects of salinity and dust (Naidoo and Chirkoot 2004). In highly saline areas (>35%). *A. marina* trees are dwarfed and extremely slow growing and these effects are exacerbated by coal dust. Mortality of *A. marina* in highly saline areas will contribute to barren zones as few other species can tolerate hypersaline conditions. In areas of low salinity, however, changes in community structure may occur with *A. marina* and *H. tiliaceus* being replaced *by B. gymnorrhiza* and *R. mucronata*.

Acknowledgements

This research was funded by Richards Bay Coal Terminal, National Research Foundation, South Africa and the University of Durban-Westville Research Fund. The authors gratefully acknowledge the assistance of D. Chirkoot and R. Jimmy for field assistance, O. Hiralal for the micrographs and A. Rajh for photography.

References

Alongi B.M., Boto K.G. and Robertson A.I. 1992. Nitrogen and phosphorus cycles. In: Robertson A.I. and Alongi B.M. (eds), Tropical Mangrove Ecosystems. American Geophysical Union, Washington D.C.

Bjorkman O., Demming B. and Andrews T.J. 1988. Mangrove photosynthesis: response to high irradiance stress. Aust. J. Plant Physiol. 15: 43–61.

Boyer J.S., Chin Wong S. and Farquhar G.D. 1997. CO_2 and water vapour exchange across leaf cuticle (epidermis) at various water potentials. Plant Physiol. 114: 185–191.

Cheeseman J.M., Herendeen L.B., Cheeseman A.T. and Clough B.F. 1997. Photosynthesis and photoprotection in mangroves under field conditions. Plant Cell Environ. 20: 579–588.

Ernst W.H.O. 1982. Monitoring of particulate pollutants. In: Steubing L. and Jager H.J. (eds), Monitoring of Air Pollutants by Plants: Methods and Problems Proceedings of the International Workshop, Osnabriick (F.R.G.), September 24–25, 1981. Dr. W. Junk Publishers, The Hague.

Genty B., Briantais J.M. and Baker N.R. 1989. The relationship between the quantum yield of photosynthetic electron transport and quenching of chlorophyll fluorescence. Biochem. Biophys. Acta 990: 87–92.

Herppich M., Herppich W. and von Willert D.J. 1994. Influence of water availability on photosynthesis, gas exchange and water relations of a dwarf fynbos protea. Bot. Acta 107: 440–449.

Hirano T., Kiyota M. and Aiga I. 1995. Physical effects of dust on leaf physiology of cucumber and kidney bean plants. Environ. Pollut. 89: 255–261.

Kirschbaum M.U.F. and Pearcy R. W. 1988. Gas exchange analysis of the relative importance of stomatal and biochemical factors in photosynthetic induction in *Alocasia macrorrhiza*. Plant Physiol. 86: 782–785.

Krause G.H. and Weis E. 1991. Chlorophyll fluorescence and photosynthesis: the basics. Annu. Rev. Plant Physiol. Plant Mol. Biol. 42: 313–349.

Lovelock C.E. and Clough B.F. 1992. Influence of solar radiation and leaf angle on xanthophyll concentrations in mangroves. Oecologia 91: 518–525.

Macnae W. 1962. The fauna and flora of the eastern coasts of southern Africa in relation to ocean currents. S. Afr. J. Sci. 58: 208–212.

Naidoo G. and Chirkoot D. 2004. The effects of coal dust on photosynthetic performance of the mangrove *Avicennia marina* in Richards Bay, South Africa. Environ. Pollut. 127: 359–366.

Naidoo G., Tuffers A.V. and von Willert D.J. 2002. Changes in gas exchange and chlorophyll fluorescence characteristics of two mangroves and a mangrove associate in response to salinity in the natural environment. Trees 16: 140–146.

Paling E.I., Humphries G., McCardle I. and Thomson G. 2001. The effects of iron ore dust on mangroves in Western Australia: lack of evidence for stomatal damage. Wetlands Ecol. Manage. 9: 363–370.

Ricks G.R. and Williams R.J.H. 1974. Effects of atmospheric pollution on deciduous woodland Part 2: effects of particulate matter upon stomatal diffusion resistance in leaves of *Quercus petraes* (Mattuschka) Leibl. Environ. Pollut. 6: 87–109.

Schreiber U., Bilger W. and Neubauer C. 1995. Chlorophyll fluorescence as a non-intrusive indicator for rapid assessment of *in vivo* photosynthesis. In: Schulze E.D. and Caldwell W.W. (eds), Ecophysiology of Photosynthesis. Springer Verlag, Berlin/Heidelberg, pp. 49–70.

Semenuik V. 1987. Threats to, and exploitation and destruction of mangrove systems in Western Australia. In: Field C.D. and Dartnell A.J. (eds), Mangrove Ecosystems of Asia and the Pacific-Status, Exploitation and Management Proceedings on Research for Development, Seminar, AIMS, May 1985 pp. 228–240.

Sharifi M.R., Gibson A.C. and Rundel P.W. 1997. Surface dust impacts on gas exchange in Mojave Desert shrubs. J. Appl. Ecol. 34: 837–846.

Terashima I. 1992. Anatomy of non-uniform leaf photosynthesis. Photosyn. Res. 31: 195–212.

Tuffers A.V., Naidoo G. and von Willert D.J. 1999. The contribution of leaf angle to photoprotection in the mangroves *Avicennia marina* (Forssk.) Vierh. and *Bruguiera gymnorrhiza* (L.) Lam. under field conditions in South Africa. Flora 194: 267–275.

EXHIBIT 12

UNITED STATES DEPARTMENT OF COMMERCE
National Oceanic and Atmospheric Administration
NATIONAL MARINE FISHERIES SERVICE
Washington State Habitat Office
510 Desmond Drive SE, Suite 103
Lacey, WA 98503

July 15, 2009

Mr. Mike Gearheard
Director, Office of Water and Watersheds
U.S. Environmental Protection Agency, Region 10
(OWW130)
1200 Sixth Avenue
Seattle, Washington 98101

Dear Mr. Gearheard:

The State of Washington Department of Ecology (Ecology) has recently issued a Public Notice Draft National Pollution Discharge Elimination System (NPDES) Industrial Stormwater General Permit for public review and comment. The National Marine Fisheries Service (NMFS) offers the following brief comments on the proposed permit reissuance pursuant to our role as providers of biological and technical assistance under the Endangered Species Act of 1973 (16 U.S.C. 1531 *et seq*.), as amended (ESA) and the Fish and Wildlife Coordination Act (16 U.S.C. 661 *et seq.*). We are sending these comments to you because of EPA's acknowledged oversight role in the issuance of this permit under Section 402(d) of the Clean Water Act (CWA), and acknowledged responsibility to comply with Section 7(a)(2) of the Endangered Species Act (ESA). In addition, these comments are provided per the processes outlined in the Memorandum of Agreement between the EPA and the NMFS regarding enhanced coordination under the CWA and ESA (hereafter "MOA") (May 22, 2001, 66FR 11202-11217).

With the CWA authority delegated from the EPA, Ecology proposes to reissue the Industrial Stormwater General Permit to over 1,200 industrial facilities in Washington State, replacing the current permit. The permit uses the concept of benchmarks and action levels (levels of industrial contaminants that will require the permittee to take further actions) rather than requiring compliance with State water quality standards. In addition, the permit relies heavily a water quality risk evaluation (Herrera Environmental Consultants 2009) to justify their proposed benchmark and action levels.

The geographic area covered by the permit overlaps the range of 15 federally-listed threatened or endangered salmon, as well as designated critical habitat for 13 of these populations. The permit area overlaps areas addressed by the Puget Sound Shared Strategy Recovery Plans, Lower Columbia River Fish Recovery Board, the Upper and

Mid-Columbia Fish Recovery Boards, the Governor's Salmon Plan, and the Puget Sound Partnership. Most of these plans have identified stormwater runoff as a significant factor in reaching salmon recovery. In addition, the Puget Sound Partnership has developed recommendations for addressing stormwater effects with the goal of achieving a healthy Puget Sound by the year 2020. Also, a recent report supported by your agency, identified stormwater runoff as the greatest contributor of the worst pollutants in Puget Sound (Hart Crowser, Inc. et al. 2007).

We support Ecology's objectives in permitting this large number of industrial facilities, with the hope that the discharge of contaminated stormwater from industrial activities into receiving waters will be reduced, and fish and wildlife resources including threatened and endangered salmon will receive additional protection. However in our review of the draft permit we are not assured that protection for listed salmon will be improved. We have identified three main issues that contribute to this concern:

1) the copper and zinc benchmark levels,
2) using zinc as a surrogate for copper and limiting copper monitoring, and
3) the reliance on risk assessment calculations to protect listed species.

We have identified in the past through meetings, e-mails, and correspondence (between NMFS, EPA and Ecology) our concerns about copper and zinc levels allowed by this permit. Adverse effects of dissolved copper and zinc on listed salmon occur at very low levels (values ranging from 0.18 to 2.1 µg/L in freshwater for copper (Hecht et. al, 2007) and at 5.6 µg/L in freshwater for zinc (Sprague 1968)). Adverse effects of copper include interference with fish sensory systems and important behaviors that underlie predator avoidance, juvenile growth and migratory success. These effects occur at pollutant levels that are 6 to 77 times lower than the proposed benchmark level for total copper (14 µg/L). Similarly, adverse effects of zinc include altered behavior, blood and serum chemistry, impaired reproduction, and reduced growth. These effects occur at pollutant levels that are 35 and 45 times lower than the proposed total zinc benchmark levels (200 µg/L for Western Washington and 255 µg/L for Eastern Washington). In addition, the proposed benchmark level for zinc in this permit (200 and 255µg/L total Zn) is higher than the level proposed for the 2007 Industrial permit (115 µg/L total Zn). We do not believe these proposed benchmark levels avoid more than minor detrimental effects to listed salmon and steelhead.

Given that copper has adverse effects on listed fish at very low levels, we are surprised that Ecology has proposed in this permit to eliminate the requirement for facilities to conduct monitoring for copper when zinc benchmarks are exceeded in stormwater discharges. Instead Ecology is proposing to use total zinc as the representative metal for core sampling and apply copper sampling requirements to only 5 sectors of industrial facilities. With the proposed benchmark level for zinc set at a level that does not provide protection necessary for salmon growth and survival, and with copper being identified as a widespread pollutant in industrial facilities, we do not believe using zinc as a surrogate of copper and limiting copper monitoring to 5 sectors will adequately protect listed salmon.

The proposed permit targets for the Industrial permit are based on a water quality risk evaluation that examines the risk of exceeding acute water quality standards (Herrera Environmental Consultants 2009). For this analysis, Ecology determined that the proposed benchmarks and action levels should be considered based on a dilution factor of 5 and a 10 percent risk for exceeding the applicable water quality standard for each metal. While this may be a viable approach for setting benchmark levels across a broad range of facility types and receiving waters, it is not an approach that provides adequate protection for listed salmon. We cannot accurately assume that a dilution factor of 5 will always be provided where listed salmon are present. Nor can we accurately assume that a 10 percent risk of exceeding applicable water quality standards will not have adverse effects on listed fish, particularly when we know that current water quality standards for some pollutants (particularly copper and zinc) already exceed levels that result in adverse effects for listed salmon and steelhead. Therefore, we do not believe more than minor detrimental effects to listed salmon and steelhead will be avoided.

We thank you for the opportunity to provide these comments under the process identified in the MOA. We look forward to continued coordination with EPA and Ecology on NPDES permits, as well as completing our ESA consultations on Water Quality Standards as they are revised in Washington State, in part to meet the needs of listed salmon. Please call me at (360) 753-6054 if you would like to discuss this issue further.

Sincerely,

Steven W. Landino
Washington State Director
for Habitat Conservation

cc: Kelly Susewind, P.E., P.G. Ecology
Ken Berg, USFWS

References:

Hart Crowser, Inc. 2007. Control of Toxic Chemicals in Puget Sound. Phase 1: Initial Estimate of Loadings. Prepared for Washington State Department of Ecology, U.S. Environmental Protection Agency, and Puget Sound Partnership. Publication No. 07-10-079.

Hecht, S.A., D.H. Baldwin, C.A. Mebane, T. Hawkes, S.J. Gross, and N.L. Scholz. 2007. An Overview of sensory effects on juvenile salmonids exposed to dissolved copper: Applying a benchmark concentration approach to evaluate sublethal neuro behavioral toxicity. U.S. Dept. Commer., NOAA Tech. Memo. NMFS-NWFSC-83, 39p.

Herrera Environmental Consultants. 2009. Water Quality Risk Evaluation for Proposed Benchmarks/Action Levels in the Industrial Stormwater General Permit. Analysis Report prepared for Washington State Department of Ecology. 40 pgs.

Sprague, J. B. 1968. Avoidance reactions of rainbow trout to zinc sulphate solutions. Water Research Pergamon Press. Vol 2, pp. 367-372.

Bc: WSHO – Chron File
WSHO – File Copy
WSHO – Landino

Cc addresses:

Kelly Susewind, P.E., P.G. Ecology
Program Manager
Water Quality Program
PO Box 47600
Olympia, WA. 98504-7600

Ken Berg, USFWS

Environmental Biology of Fishes **70:** 169–174, 2004.
© 2004 *Kluwer Academic Publishers. Printed in the Netherlands.*

An assessment of the potential for selenium to impair reproduction in bull trout, *Salvelinus confluentus*, from an area of active coal mining

Vince P. Palace[a], Christopher Baron[a], Robert E. Evans[a], Jodi Holm[b], Suzanne Kollar[a], Kerry Wautier[a], Jeffrey Werner[a], Paula Siwik[c], George Sterling[c] & Craig F. Johnson[d]
[a]*Department of Fisheries and Oceans, Freshwater Institute, Winnipeg Canada R3T 2N6 (e-mail: palacev@dfo-mpo.gc.ca)*
[b]*Department of Zoology, University of Manitoba, Winnipeg, Canada R3T 2N2*
[c]*Alberta Sustainable Resource Development, Fisheries and Wildlife Division, Edson, Canada T7E 1T2*
[d]*Alberta Conservation Association, Edson, Canada T7E 1T2*

Received 13 May 2003 Accepted 3 September 2003

Key words: fish, contaminants, teratogen, muscle biopsy

Synopsis

Selenium (Se) is an essential nutrient, but in higher concentrations can reduce recruitment in fish populations by increasing rates of deformities during early development. Recent work has identified elevated levels of Se in water and biota collected downstream from coal mining activity in Alberta's northeast slopes region. We also recently identified increased incidence of terata and edema in rainbow trout and brook trout with elevated tissue Se from this area. However, there is currently no information regarding the potential for Se to contribute to declining stocks of bull trout, a species of concern in the area. The present study provides an assessment of the potential for Se to contribute to low recruitment in bull trout downstream from coal mining activity. Non-destructive muscle biopsy sampling and a sensitive atomic fluorescence analysis technique are used to determine Se. Results indicate that most bull trout (>90%) captured immediately downstream from coal mining activity in the region have concentrations of Se that would be expected to impair recruitment. Additional work is required to determine the extent of Se's contribution to low recruitment in bull trout.

Introduction

Bull trout, *Salvelinus confluentus*, have declined in numbers and range in the eastern slopes region of Alberta, Canada during the past several decades (Fish & Wildlife 2001). In the United States, bull trout are listed as a threatened species under the federal Endangered Species Act (Hansen et al. 2002a). Habitat fragmentation, overfishing and competition from introduced species may all have contributed to declines in both countries (Fish & Wildlife 2001, Hansen et al. 2002). In the United States exposure to contaminants has also been cited as a possible factor in the decline of bull trout populations (Hansen et al. 2002).

Recently, elevated levels of selenium (Se) were identified in waters downstream from coal mining activity in the northeast slopes region of Alberta (Casey & Siwik 2000). Se is a naturally occurring metalloid that is typically present in uncontaminated waters at concentrations of 0.1–0.4 $\mu g\,l^{-1}$ (Lemly 1985, Dobbs et al. 1996). Casey & Siwik (2000) reported values near this range for waters collected from reference streams in the northeast slopes region, but found Se concentrations as high as 5–47 $\mu g\,l^{-1}$ in waters downstream from active coal mining.

Field and laboratory studies in fish have demonstrated that excessive tissue Se can result in a variety of toxic effects including reduced growth, tissue damage, reproductive effects and increased mortality (Hodson et al. 1980, Hodson & Hilton 1983, Lemly 1993b). A hallmark of Se toxicity is the appearance of teratogenic deformities in the progeny of exposed females that result from the deposition of Se to their eggs. Teratogenesis is restricted to the egg–larval stage of

development when the larvae utilize yolks contaminated with Se (Lemly 1997a). The most common types of terata include spinal curvatures (lordosis, scoliosis, or kyphosis), missing or deformed fins, gills, opercula and eyes, as well as abnormally shaped heads and mouths (Lemly 1993b, 1997a). Other symptoms of Se poisoning include pericardial and abdominal edema, exopthalmus (bulging or protrusion of eyes), and cataracts (Lemly 1996). Based on extensive population sampling and the existing literature, Lemly (1993b) has suggested toxic effects thresholds for the appearance of reproductive effects for several tissues in fish including liver ($12\,\mu g\,g^{-1}$), skeletal muscle ($8\,\mu g\,g^{-1}$), ovary and egg ($10\,\mu g\,g^{-1}$), and whole body ($4\,\mu g\,g^{-1}$). These values are given on a dry weight basis. It should be noted that a wide array of essential and non-essential trace elements and micronutrients can affect the toxicity of Se (Hamilton & Palace 2001).

We recently identified increased incidence of terata and edema in rainbow trout, *Oncorhynchus mykiss*, and brook trout, *Salvelinus fontinalis*, with elevated tissue Se that were captured downstream from coal mining activity in the northeast slopes region of Alberta (Holm et al. 2003). This area is also critical habitat for bull trout and they too could be affected by exposure to elevated Se concentrations. To evaluate this potential, we non-destructively sampled the dorsal epaxial region of white muscle in bull trout using 2 mm diameter biopsy needles. The samples, collected from fish captured over two years in the Northeast Slopes Region of Alberta (McLeod River drainage system) (Figure 1) were analyzed for their content of Se using a sensitive atomic fluorescence hydride generation technique (PSA Analytical 1999). One sample location, Luscar Creek, is immediately downstream from active coal mining, while the other location, MacKenzie Creek, is removed from direct mine drainage but still accessible to fish from exposed sites (Figure 1). Our results indicate that the majority of bull trout captured from Luscar Creek, and many of the fish from MacKenzie Creek, have Se concentrations that exceed established toxicity threshold limits for negatively impacting reproductive success.

Materials and methods

Fish

Bull trout were captured incidentally from Luscar Creek in October 2001 and June 2002 while electrofishing for brook trout or rainbow trout, respectively. Fish were captured using hand held dip nets after being briefly stunned with a Smith-Root type VII back pack electroshocker at settings I-5 and 200 V. Bull trout were captured from McKenzie Creek in August and September 2001 in an in-stream live trap used by the provincial agency, Alberta Sustainable Resource Development, for stock assessments. In both cases, after fish were captured they were anesthetized in water from the site containing clove oil ($0.05\,ml\,l^{-1}$). After fin movement ceased (<3 min) three biopsy samples were obtained from the dorsal muscle of each fish (1–3 cm behind the dorsal fin) using sterile 2.0 mm disposable biopsy punches (Fray Products Corp., Buffalo, NY). Samples were dispensed into labeled 1.5 ml microcentrifuge tubes and kept cool on ice until they could be frozen on dry ice and then stored at −90°C until analyzed.

Se analysis

Each set of biopsy samples were weighed into a clean, acid washed Pyrex tube and 2 ml of trace metals grade HNO_3 (Fisher Scientific, Whitby, ON), 0.50 ml of environmental grade $HClO_4$ (Anachemia, Montreal, QC), and 0.25 ml of Baker analyzed trace metal grade H_2SO_4 (JT Baker, St. Leonard, QC) were added to the sample. After vortexing the samples were allowed to settle out for 12 h. Each sample was then mixed and heated at 135 ± 5°C for 5 h followed by 200°C for 2 h in a Thermolyne type 2200 benchtop hotblock (Barnstead International, Dubuque, IW) in a designated perchloric fumehood. The samples were allowed to cool and then 7.50 ml DDW and 3.75 ml environmental grade HCl (Anachemia, Montreal, QC) were added and the samples were again heated at 90°C for 1 h. After cooling the samples were diluted to a final volume of 12.5 ml with DDW and analyzed by atomic fluorescence hydride generation spectroscopy using a PSA Analytical Millenium Excalibur Model 10.005 instrument (PSA Analytical, Kent, U.K.) as described previously.[1] Concentrations of Se were determined by comparison of the peak areas against a standard curve constructed with commercially available Se standards (SCP Science, Baie D'Urfe, QC). Analysis of standard reference materials CRM 2796 and Tort-2 from the

[1] PS Analytical. 1999. Determination of Se in oyster tissue using hydride generation atomic fluorescence spectrometry. Technical Note APP050. PSA Analytical, Kent U.K. Available from the internet URL http://www.psanalytical.com/applications.htm.

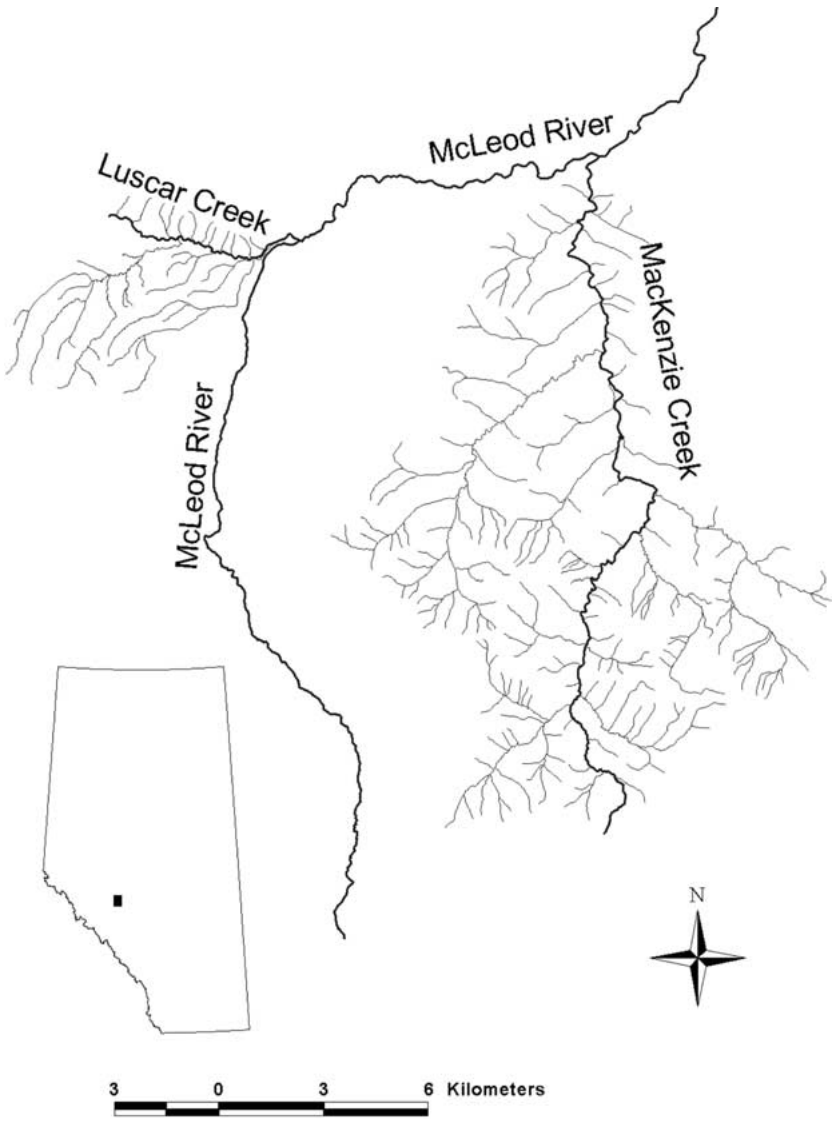

Figure 1. Study site in Alberta's northeastern slopes region.

National Research Council of Canada (Ottawa, ON) were included in each series of analysis and values of Se returned were 97% and 94% of the expected certified values respectively.

Data analysis

Linear regression analysis was used to evaluate relationships between Se concentrations in muscle and egg in rainbow trout and brook trout. Muscle concentrations in bull trout were then used in these regression models to calculate potential concentrations of Se in eggs. Significance was accepted at the $p < 0.05$ level for all regressions.

Results and discussion

Selenium concentrations ranged from a minimum of $0.6\,\mu g\,g^{-1}$ to a maximum of $5.5\,\mu g\,g^{-1}$ in the muscle of bull trout captured in MacKenzie Creek and between 1.2 and $9.4\,\mu g\,g^{-1}$ in bull trout from Luscar Creek, on a wet mass basis. While bioaccumulation and bioconcentration of Se in aquatic systems are known to occur for

the most part at the level of primary producer and consumer (Besser et al. 1989, 1993), several studies have also shown that fish can accumulate Se (Baumann & Gillespie 1986, Saiki & Palawski 1990, Coyle et al. 1993, Hopkins et al. 2000). In wild fish, accumulation of Se is thought to occur primarily from the diet but also by direct uptake from the surrounding water (Hermanutz et al. 1992). Based on this information it could be expected that larger fish would contain higher concentrations of Se than smaller fish. However, there were no significant relationships between fish length and the concentration of Se in bull trout muscle tissue from either of the sample locations.

At least two other studies have documented accumulation and the potential effects of Se on threatened species of fish using muscle biopsies as an alternative to lethal sampling techniques. Osmundson et al. (2000) found average concentrations of 17 $\mu g\, g^{-1}$ in Colorado Pikeminnow, *Pychochelius lucius*, collected from the Colorado River. Hamilton & Waddell (1994) reported that razorback suckers, *Xyrauchen texanus*, from Ashley Creek in the Green River area of Utah, had muscle concentrations of Se ranging from 4 to 32 $\mu g\, g^{-1}$, on a dry weight basis. Based on Lemly's (1993a) proposal that 8 $\mu g\, g^{-1}$ in muscle and 10 $\mu g\, g^{-1}$ in ovary and eggs should be considered toxic effects thresholds for freshwater and anadromous fishes, these authors speculated that Se could be limiting survival and recruitment of larvae to the juvenile stage. It should be noted that values that we have reported for Se in bull trout from this study are given on a wet weight basis. By applying Lemly's (1993a) conversion factor of 75% water content in muscle, the toxicity threshold for muscle becomes 2 $\mu g\, g^{-1}$ as depicted in Figure 2. Many of the bull trout from this study have Se concentrations above the toxicity threshold limit and Luscar Creek has proportionally more fish above that limit than MacKenzie Creek. More than 91% of the bull trout captured in Luscar Creek exceeded the toxicity threshold limit and 39% of the fish from MacKenzie Creek exceeded the limit.

Berdusco et al. (2000) suggested that toxicity thresholds derived for fish inhabiting warm waters are not generally applicable to cold-water fishes and Lemly (1994,1996) has also speculated that cold-water species could be more sensitive to Se than warm water fish. However, Brix et al. (2000) fit statistical models to the toxicity data for cold and warm water species and found that cold-water anadromous salmoninds may be slightly more sensitive than fish that inhabit warm waters. We have recently reported similar toxicity

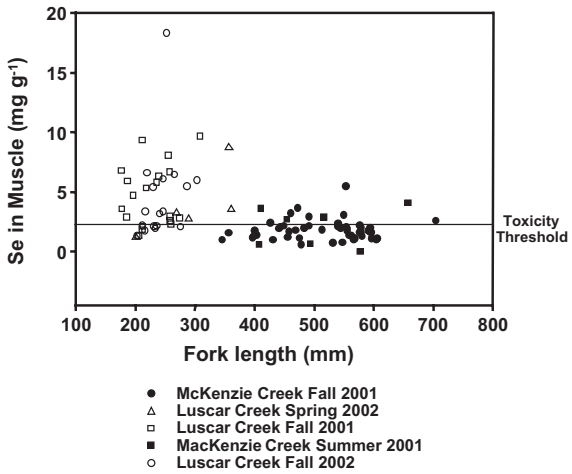

Figure 2. Se concentrations in muscle relative to fork length of bull trout, *Salvelinus confluentus*, captured in MacKenzie Creek and Luscar Creek during 2001 and 2002.

thresholds to those proposed by Lemly (1993a) for two cold-water species, rainbow trout and brook trout exposed to elevated concentrations of Se downstream from coal mining activity in Alberta (Holm et al. 2003).

The first adverse effects of Se on fish populations are likely to arise from maternal deposition of Se into eggs and the assimilation of that Se by the developing embryos prior to their beginning exogenous feeding (Lemly 1996). For this reason, measuring concentrations of Se in eggs is the most relevant measure of the potential for Se to disrupt recruitment in a given population. However, failing the ability to obtain eggs, as in the case of threatened species, muscle biopsies may provide the necessary information for an initial assessment. In fact, Hamilton and Waddell (1994) found a strong correlation between the concentrations of Se in muscle biopsies and eggs of razorback suckers ($r^2 = 0.99$). We have also found a strong correlation between concentrations of Se in muscle and eggs of rainbow trout and brook trout (Figure 3) (Holm 2002). By applying the regression for Se in muscle *versus* eggs from brook trout, a species from the same genus as bull trout, average egg concentrations of 7.82 ± 1.14 and 3.22 ± 0.05 $\mu g\, g^{-1}$ would be expected in the Luscar and Mackenzie creek populations respectively. Using this relationship, the vast majority of bull trout from Luscar Creek (92%) and many of the fish from MacKenzie Creek (64%) would be expected to exceed the toxicity threshold value of 2.5 $\mu g\, g^{-1}$ Se in eggs (on a wet mass basis) (Lemly 1993b). Higher estimates for Se in eggs of bull trout are obtained when the

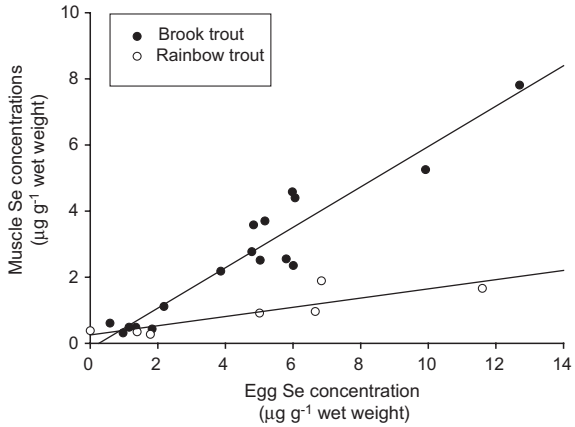

Figure 3. Regressions of Se in muscle and eggs of rainbow trout, *Oncorhynchus mykiss*, and brook trout, *Salvelinus fontinalis*, captured from several sites in the McLeod River drainage basin.

regression for rainbow trout is applied (31.35 ± 2.05 and $11.17 \pm 0.96\,\mu g\,g^{-1}$ from Luscar and MacKenzie Creek fish, respectively). Specific analysis of bull trout muscle and eggs are required to determine the precise regression formula for that species.

There are at least two limitations of using muscle biopsies to determine Se concentrations and potential toxicity from Se in eggs. The first is that only a small amount of tissue is available for analysis. This is a relatively serious issue in the case of Se, because Se toxicity in fish can be altered by the presence or absence of other elements (Hamilton & Palace 2001). Limited tissue precludes analysis for other elements. The most extensively studied elemental interaction with Se is that of mercury (reviewed in Cuvin-Aralar & Furness 1991), but other elements including antimony, arsenic, cadmium, cobalt, copper, germanium, lead, silver, tellurium and tungsten can interact additively, antagonistically or synergistically (Dilpock & Hoekstra 1976, Whanger 1981, Maier & Jaworski 1983, Sorensen 1991). The second limitation of biopsy sampling is that Se accumulation kinetics in muscle tissue may not necessarily predict those in other tissues. Hodson & Hilton (1983) demonstrated relatively short biological half lives for Se (21–28 d) and important differences in the uptake kinetics of Se by carcass, liver and kidney of rainbow trout. The labile nature of tissue Se and differences in tissue uptake and depuration dictate caution when deriving toxicity predictions from muscle biopsies alone. Nonetheless, results from these studies indicate that further investigation of the potential for Se to limit recruitment in bull trout from coal mine impacted waters is warranted.

Acknowledgements

This work was funded by grants from DFO-Fish Habitat Management and Environmental Science Strategic Research Fund (ESSRF). Ms. Holm was supported by graduate student fellowship from the National Science and Engineering Research Council (NSERC) and by matching funds from the University of Manitoba and DFO. The authors would like to acknowledge the excellent technical assistance of Rudy Hawryluk and Don Hildebrandt.

References

Baumann, P.C. & R.B. Gillespie. 1986. Selenium bioaccumulation in gonads of largemouth bass and bluegill from three power plant cooling reservoirs. Environ. Toxicol. Chem. 5: 695–701.

Berdusco, R., B. Dixon, J. Lant, R. Jones & M. Cole. 2000. Selenium studies in the Elk River basin of the east Kootenay. pp. 174–183. *In*: R. Rosentreter & K. Bittman (ed.) Planning for End Land Uses in Mine Reclamation. Proceedings of the 24th Annual British Columbia Mine Reclamation Symposium, Williams Lake, B.C.

Besser, J.M., J.N. Huckins, E.E. Little & T.W. LaPoint. 1989. Distribution and bioaccumulation of selenium in aquatic microorganisms. Environ. Pollut. 62: 1–12.

Besser, J.M., T.J. Canfield & T.W. LaPoint. 1993. Bioaccumulation of organic and inorganic selenium in a laboratory food chain. Environ. Toxicol. Chem. 12: 57–72.

Brix, K.V., D.K. Deforest, A. Fairbrother & W.J. Adams. 2000. Critical review of tissue-based selenium toxicity thresholds for fish and birds. pp. 220–230. *In*: R. Rosentreter & K. Bittman (ed.) Proceedings of the 24th Annual British Columbia Mine Reclamation Symposium. Williams Lake, B.C.

Casey, R. & P. Siwik. 2000. Overview of selenium in surface waters, sediment and biota in river basins of west central Alberta. pp. 184–194. *In*: R. Rosentreter & K. Bittman (ed.) Proceedings of the 24th Annual British Columbia Mine Reclamation Symposium, Williams Lake, B.C.

Coyle, J.J., D.R. Buckler, C.G. Ingersoll, J.F. Fairchild & T.W. May. 1993. Effect of dietary selenium on the reproductive success of bluegill sunfish (*Lepomis macrochirus*). Environ. Toxicol. Chem. 12: 551–565.

Cuvin-Aralar, M.L.A. & R.W. Furness. 1991. Mercury and selenium interaction: A review. Ecotoxicol. Environ. Safety 21: 348–364.

Diplock, A.T. & W.G. Hoekstra. 1976. Metabolic aspects of selenium action and toxicity. CRC Crit. Rev. Toxicol. 5: 271–329.

Dobbs, M.G., D.S. Cherry & J. Cairns. 1996. Toxicity and bioaccumulation of selenium to a three-trophic level food chain. Environ. Toxicol. Chem. 15: 340–347.

Fish & Wildlife Division. 2001. Alberta species at risk program and projects 2000–2001. Alberta Sustainable Resource Development, Fish and Wildlife Division, Alberta Species at Risk Report No. 1, Edmonton, AB. 82pp.

Hamilton, S.J. & V.P. Palace. 2001. Assessment of selenium effects in lotic ecosystems. Ecotoxicol. Environ. Safety 50: 161–166.

Hamilton, S.S.J. & B.Waddell. 1994. Selenium in eggs and milt of razorback sucker (*Xyrauchen texanus*) in the middle Greeen River, Utah. Arch. Environ. Contam. Toxicol. 27: 195–201.

Hansen, J.A., J. Lipton & P.G. Welsh. 2002. Relative sensitivity of bull trout (*Salvelinus confluentus*) and rainbow trout (*Oncorhynchus mykiss*) to acute copper toxicity. Environ. Toxicol. Chem. 21: 633–639.

Hansen, J.A., P.G. Welsh, J. Lipton, D. Cacela & A.D. Daley. 2002a. Relative sensitivity of bull trout (*Salvelinus confluentus*) and rainbow trout (*Oncorhynchus mykiss*) to acute exposures of cadmium and zinc. Environ. Toxicol. Chem. 21: 67–75.

Hermanutz, R.O., K.N. Allen, T.H. Roush & S.F. Hedtke. 1992. Effects of elevated selenium concentrations on bluegills (*Lepomis macrochirus*) in outdoor experimental streams. Environ. Toxicol. Chem. 11: 217–224.

Hodson, P.V. & J.W. Hilton. 1983. The nutritional requirements and toxicity to fish of dietary and waterborne selenium. Ecol. Bull. 35: 335–340.

Hodson, P.V., D.J. Spry & B.R. Blunt. 1980. Effects on rainbow trout (*Salmo gairdneri*) of a chronic exposure to waterborne selenium. Can. J. Fish. Aquat. Sci. 37: 233–240.

Holm, J. 2002. Sublethal effects of selenium on rainbow trout (*Oncorhynchus mykiss*) and brook trout (*Salvelinus fontinalis*). M.Sc. Thesis. University of Manitoba. November 2002. 174 pp.

Holm, J., V.P. Palace, K. Wautier, R.E. Evans, C.L. Baron, P. Siwik & G. Sterling. 2003. An assessment of the development and survival of wild rainbow trout (*Oncorhynchus mykiss*) and brook trout (*Salvelinus fontinalis*) exposed to elevated selenium in an area of active coal mining. *In*: H.I. Browman & A.B. Skiftesvik (ed.) "The Big Fish Bang." Proceedings of the 26th Annual Larval Fish Conference, July 22–26, Bergen, Norway. pp. 1–17.

Hopkins, W.A., J.W. Snodgrass, J.H. Roe, B.P. Jackson, J.C. Gariboldi & J.D. Congdon. 2000. Detrimental effects associated with trace element uptake in lake chubsuckers (*Erimyzon sucetta*) exposed to polluted sediments. Arch. Environ. Contam. Toxicol. 39: 193–199.

Lemly, A.D. 1985. Ecological basis for regulating aquatic emissions from the power industry. The case with selenium. Regul. Toxicol. Pharmacol. 5: 465–486.

Lemly, A.D. 1993a. Teratogenic effects of selenium in natural populations of freshwater fish. Ecotoxicol. Environ. Safety 26: 181–204.

Lemly, A.D. 1993b. Guidelines for evaluating selenium data from aquatic monitoring and assessment studies. Environ. Monitor. Assess. 28: 83–100.

Lemly, A.D. 1994. Mining in Northern Canada: Expanding the industry while protecting arctic fishes – a review. Ecotoxicol. Environ. Safety 29: 229–242.

Lemly, A.D. 1996. Selenium in aquatic organisms. pp. 427–445. *In*: W.N. Beyer, G.H. Heinz & A.W. Redmon-Norwood (ed.) Environmental Contaminants in Wildlife. CRC Press, Boca Raton, FL, U.S.A.

Lemly, A.D. 1997a. A teratogenic deformity index for evaluating impacts of selenium on fish populations. Ecotoxicol. Environ. Safety 37: 259–266.

Lemly, AD. 1997b. Ecosystems recovery following selenium contamination in a freshwater reservoir. Ecotoxicol. Environ. Safety 36: 275–281.

Maier, J.R. & J.F. Jaworski. 1983. Interactions of Selenium, Pub. No. NRCC 20643. National Research Council of Canada. 85 pp.

Osmundson, B.C., T.W. May & D.B. Osmundson. 2000. Selenium concentrations in the Colorado pikeminnow (*Pychocheilus lucius*): Relationships with flows in the upper Colorado River. Arch. Environ. Contam. Toxicol. 38: 479–485.

Saiki, M.K. & D.U. Pawlawski. 1990. Selenium and other elements in juvenile striped bass from the San Joaquin Valley and San Francisco estuary, California. Arch. Environ. Contam. Toxicol. 19: 717–730.

Sorensen, E.M.B. (ed.) 1991. Metal Poisoning in Fish. CRC Press, Boca Raton, FL, U.S.A. 384 pp.

Whanger, P.D. 1981. Selenium and heavy metal toxicity. pp. 230–255. *In*: J.E. Spallholz, J.L. Martin & H.E. Ganther (ed.) Selenium in Biology and Medicine, AVI Press, Westport CT, U.S.A.

BioOne RESEARCH EVOLVED

Ecotoxicological Effects of Combined UVB and Organic Contaminants in Coastal Waters: A Review

Author(s): É Pelletier, P. Sargian, J. Payet, and S. Demers
Source: Photochemistry and Photobiology, 82(4):981-993. 2006.
Published By: American Society for Photobiology
DOI: 10.1562/2005-09-18-RA-688.1
URL: http://www.bioone.org/doi/full/10.1562/2005-09-18-RA-688.1

BioOne (www.bioone.org) is an electronic aggregator of bioscience research content, and the online home to over 160 journals and books published by not-for-profit societies, associations, museums, institutions, and presses.

Your use of this PDF, the BioOne Web site, and all posted and associated content indicates your acceptance of BioOne's Terms of Use, available at www.bioone.org/page/terms_of_use.

Usage of BioOne content is strictly limited to personal, educational, and non-commercial use. Commercial inquiries or rights and permissions requests should be directed to the individual publisher as copyright holder.

BioOne sees sustainable scholarly publishing as an inherently collaborative enterprise connecting authors, nonprofit publishers, academic institutions, research libraries, and research funders in the common goal of maximizing access to critical research.

Photochemistry and Photobiology, 2006, 82: 981–993

Symposium-in-Print: UV Effects on Aquatic and Coastal Ecosystems

Ecotoxicological Effects of Combined UVB and Organic Contaminants in Coastal Waters: A Review

É. Pelletier*, P. Sargian, J. Payet and S. Demers

Institut des Sciences de la Mer de Rimouski, Université du Québec à Rimouski, Rimouski, Canada

Received 18 September 2005; accepted 4 April 2006; published online 7 April 2006 DOI: 2005-09-18-RA-688

ABSTRACT

Organisms living in coastal waters are exposed to anthropogenic contaminants from terrestrial drainage, ice melting and maritime traffic and to enhanced UVB radiation (UVBR; 280–320 nm) caused by decreased concentrations of ozone in the stratosphere. This article reviews available information about the combined effects of UVBR and selected hydrosoluble contaminants potentially present in surface waters on marine species and especially on plankton community structure in high-latitude coastal zones. Effects of UVBR on three selected pesticides (Atrazine, carbaryl and Acifluorfen) and possible induction of phototoxicity are reviewed. Most toxicological studies have been conducted under laboratory conditions with questionable relevance for coastal marine ecosystems. Similarly, photoactivation of polycyclic aromatic hydrocarbons (PAHs) has been closely examined and reported effects on aquatic species summarized. Experiments with field-sampled communities demonstrated the complexity and the difficulty in determining the impact of multiple stressors on an aquatic ecosystem, even for ecosystems simplified by eliminating large grazers and fish. Nutrient status, specific composition and light history have influenced the different responses of planktonic assemblages exposed to enhanced UVBR and water-soluble fraction (WSF) from crude oil or to tributyltin. Plankton assemblages subjected to changes in the ozone hole were physiologically stressed and more susceptible to WSF toxicity than communities from less enhanced UVBR-impacted sites. A close relationship between phytoplankton assemblages and bacteria was observed in all experiments in mesocosms. A contaminant-induced phytoplankton crash after a bloom event may release important carbon and nutrient sources for bacteria. The magnitude of phytoplanktonic mortality induced by a contaminant probably influenced how rapidly bacteria grew over time. The transition from a herbivorous food web to a microbial food web has significant ecological implications for carbon cycling and energy flow in pelagic systems. A high phytoplankton mortality implies a situation in which the potential for downward carbon export from surface waters is high. In contrast, high bacterial enrichment implies that the phytoplankton carbon is largely recycled in surface waters through a microbial loop and does not contribute significantly to sinking particle flux. The most ecologically relevant results were obtained with mesocosm studies using field-collected communities. The enhancement of hydrocarbon toxicity in the presence of a high level of UVBR cannot be described as being a synergistic or an additive effect, because the WSF alone is not toxic and may even be beneficial by increasing bacterial activity. This is a case in which one stressor has the ability to modify another stressor to cause it to be toxic to target organisms. These abiotically induced interactions may be important for biological communities exposed to extreme conditions when physical, chemical or photochemical reactions modify the nature of environmental stressors before they interact with biological functions. The need for models on the impacts of multiple stressors on biodiversity and ecosystem functioning is emphasized.

INTRODUCTION

A decrease in the concentration of ozone in the stratosphere may significantly increase the level of UVB radiation (UVBR; 280–320 nm) reaching the Earth's surface. These modifications have raised concern among scientists and policy makers during the past 2 decades. Numerous laboratory and field experiments have been conducted illustrating deleterious effects of UVBR on aquatic species and communities (1,2). In addition to UVBR enhancement (mainly at high latitudes), anthropogenic impacts also include the direct release of contaminants (such as heavy metals and organometals, chlorinated pesticides, brominated flame retardants, estrogens and complex mixtures of petrogenic and pyrogenic hydrocarbons) into rivers, estuaries and coastal waters. Many of these chemicals are known to have deleterious effects on aquatic organisms because they provide an additional stress on aquatic communities. It is crucial therefore to identify interactions of multiple stressors on biodiversity and ecosystem functioning.

Some recent experimental studies have focused on the toxic effects of simultaneous exposure to solar UV radiation (UVR; natural and/or artificially enhanced) and water-soluble contaminants and indicate that both stressors can act either additively or synergistically on aquatic microbes (3,4), algae (5–7), plants (8,9), amphipods (10–12), crustaceans (13,14) molluscs (15), echinoderms (4), fish (16–18) and amphibians (19). Laboratory tests involving single species or unrealistic concentrations of contaminants with artificial UV lamps have been subject to severe criticism (20,21) for their lack of ecological relevance and their lack of usefulness in determining real risks for species and whole

*Corresponding author email: emilien_pelletier@uqar.qc.ca (É. Pelletier)
© 2006 American Society for Photobiology 0031-8655/06

ecosystems. Very few studies have examined the combined effects of solar radiation and contaminants on field-collected communities (22). Only a recent study examined the effects of water-soluble fractions (WSFs) of heavy oil on marine enclosed ecosystems in large mesocosms (23) in which experimental tanks were covered with acrylic plates to filter sunlight.

The aim of this article is to provide an overview of reported observations and findings about interactions between UVBR and soluble organic pollutants potentially present in marine coastal waters and their combined effects on marine biota. Special attention has been paid to our recent findings on the combined effects of UVBR and water-soluble hydrocarbons from petroleum (24) and the antifouling agent tributyltin (TBT) (25) on the plankton marine communities sampled in a northern ecosystem (St. Lawrence Estuary, Canada) and sub-Antarctic environment (Southern Argentina).

UVBR AND SELECTED PESTICIDES

Pesticides are toxic substances widely used to control or eradicate viruses, fungi and bacteria, algae and plants, insects, molluscs, fish, rodents and many other living organisms considered as detrimental to human activities. More than 6500 chemical pesticides are currently listed in the PAN (Pesticides Action Network) database (available from: http://www.pesticideinfo.org/Index.html). Unlike aromatic hydrocarbons discussed hereafter, aqueous photochemistry of pesticides has received little attention from research laboratories and only a limited number of studies on photomodified toxicity of pesticides by UVBR has been published.

Carbaryl (1-naphthyl-N-methylcarbamate) is an insecticide best known as Sevin® and is commonly used on fruit and vegetable crops, lawns and ornamental trees. Carbaryl is not considered to be persistent in the environment. Photodegradation of carbaryl in natural coastal waters is unknown but Samanidou *et al.* (26) determined the photolysis rate of some carbamate pesticides in seawater under laboratory conditions and found a rapid degradation within a few hours or days.

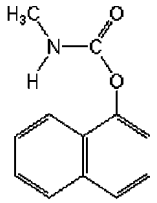

Scheme 1: Chemical structure of carbaryl

A recent study by Miller and Chin (27) conducted in wetland surface waters indicated that, when the nitrate concentration was low (which is often the case in coastal waters during summer), natural organic matter played the role of photosensitizer and enhanced the production of unidentified transient species. The main photoproduct is 1-naphthol, a known cytotoxic metabolite that is also a polycyclic aromatic hydrocarbon (PAH) photoproduct requiring high concentrations for toxicity (28). A similar process may apply in brackish and estuarine waters where fulvic and humic acids are known to play an important role in the photochemistry of many natural and anthropogenic chemicals.

In early work by Zaga *et al.* (19) the photoenhanced toxicity of the insecticide carbaryl was examined in laboratory exposure glass chambers using embryos and tadpoles of two frogs (*Xenopus laevis* and *Hyla versicolor*) under controlled UVBR. All of the UVBR–carbaryl experiments revealed a significant interactive effect between carbaryl, UVBR and day of exposure. Differences observed between carbaryl treatments with and carbaryl treatments without UVBR were attributed to the formation of photolytic by-products as the main breakdown product of carbaryl was 1-naphthol. However, Bridges and Boone (29) re-examined the joint toxicity of carbaryl and UVBR in leopard frog (*Rana sphenocephala*) tadpoles in outdoor artificial ponds and found that tadpole survival to metamorphosis was positively influenced by the level of UVBR intensity. Tadpoles in ponds exposed to carbaryl contained more than three times as much algae and yielded larger metamorphs than control ponds. Bridges and Boone (29) suggested that dissolved organic carbon in the ponds may have played a protective role by increasing photodegradation of carbaryl and naphthol and they emphasized the importance of conducting field studies to more accurately predict what occurs under natural conditions.

Atrazine is a strong herbicide that inhibits photosystem II (PS II) and is widely used to control broadleaf and some grassy weeds for a variety of major and minor crops (*e.g.* corn, sugarcane and winter wheat) and nonagricultural uses (*e.g.* golf courses and residential lawns).

Atrazine and photoproducts have been detected in surface waters

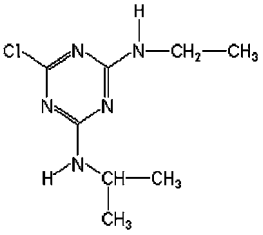

Scheme 2: Chemical structure of atrazine

and coastal waters (30,31) but their toxicity toward marine communities is still unexplored. Lin *et al.* (32) reported the toxicity of atrazine and metolachlor after exposure to simulated sunlight in the marine luminescent bacterium *Vibrio fishcheri* (known as the Microtox test) and observed a decrease in toxicity with increasing intensity of light and an even lower toxicity in estuarine waters with high concentrations of organic and suspended matter. Their study showed a rapid photodegradation of atrazine and a low toxicity for photoproducts. However, these results were challenged by Konstantinou *et al.* (33), who studied photolysis of pesticides in the laboratory and observed an increased optical filter effect as the concentration of dissolved organic matter (DOM) increased, leading to a lower photodegradation rate in natural waters. The half-life of atrazine in marine waters (using glass beakers and incident solar radiation) reached 56 days, compared with 34 days in distilled water.

A more realistic experiment was conducted in flow-through freshwater mesocosms using atrazine concentrations (5–75 μg/L) typical of surface waters in the midwestern region of the United States (34). End points measured included nutrients, periphyton biomass and productivity, growth of macrophytes and survival and growth of *Daphnia magna*, *Rana pipiens* and *Pimephales promelas* larvae and adults. The atrazine half-life in the experimental wetlands was 8–14 days. Only periphyton species were significantly affected by atrazine at any of the concentrations tested but they developed resistance at concentrations greater than 50 μg/L. Losses of atrazine from the water column were greater than those predicted by kinetic models and half-lives were *ca* 3 times shorter

than calculated values. Both atrazine and sunlight exposures significantly decreased *D. magna* survival but the authors (34) found no significant interaction between these two stressors. The lack of potentiated atrazine toxicity by sunlight was attributed to a mitigation effect of naturally occurring humic substances (particularly from plant litter), which likely reduced the bioavailability of atrazine as previously observed for anthracene (35).

The role of humic substances on the photodegradation of dissolved chemicals has often been often mentioned in recent years but little is yet known about the molecular mechanisms that could have a beneficial or detrimental effect on the toxicity of metabolites or their parent compounds. It is generally recognized that UVBR induces photochemical reactions in DOM and generates reactive oxygen species that, in turn, may oxidize organic pollutants (36). The photodegradation rate of atrazine in fresh water with different types and concentrations of humic substances under outdoor sunlight conditions was recently reported (37). Increasing concentration of river humic acid induced an increasing photodegradation rate of atrazine although fulvic acid (low molecular weight) had no significant effect. A comparable field experiment with special attention to DOM has not yet been reported for a marine ecosystem although the presence of atrazine in coastal waters is expected to be too low to produce appreciable phototoxicity except very close to the shore.

The activity of diphenyl-ether herbicides, a family of pesticides introduced in 1990s, may represent a real case of photoinduced toxicity (38). Diphenyl-ethers are broad-spectrum herbicides registered for use on soybeans, peanuts and rice for postemergent weed control. They are light-dependent peroxydizing herbicides (LDPHs) that act in plants by inhibiting the enzyme protoporphyrinogen oxidase, which is a key enzyme in the chlorophyll biosynthetic pathway. Photochemistry and photoinduced toxicity of Acifluorfen® were studied in the laboratory by exposing herbicide solutions to a solar simulator (1.1 kW xenon lamp with a passing wavelength of 300–800 nm) for 140 h (38).

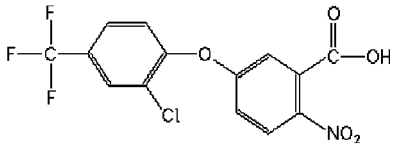

Scheme 3: Chemical structure of Acifluorfen®

Toxicity tests using *D. magna* indicated a significant increase of toxicity toward Acifluorfen® for solutions in which the parent molecule was entirely transformed in photodegraded by-products. Leo (39) used structural data to calculate that K_{OW} (octanol-water partition coefficients) of some well-identified photoproducts were much higher than that for Acifluorfen®. High K_{OW} provide reasonable indices that photoproducts were much more bioavailable than the parent compound and were able to interact with biological functions of *D. magna*. The relevance of these results needs to be assessed by carefully designed field experiments in which a whole freshwater or marine ecosystem is considered.

UVBR AND HYDROCARBONS

Hydrocarbons form a very rich and complex family of organic molecules comprising linear and cyclic saturated hydrocarbons, single and polycyclic rings with or without side chains and heterocycles containing sulfur (thiophenes) and nitrogen (porphyrines) atoms. The lighter PAHs exhibit relatively high solubility in water (Table 1) and are readily available (high log K_{OW}) to phytoplankton and swimming aquatic organisms ranging from microzooplankton to fish. Most abundant sources of aromatic hydrocarbons at sea are petroleum residues and crude oil accidentally spilled or intentionally discharged by tankers and other vessels navigating across oceans, along continental coastlines and in narrow estuaries, fjords and river channels.

PAHs are also emitted in the air as gases and soot by combustion of fossil fuel, plastics, wood and other natural materials. Most hydrosoluble PAHs (Table 1) can be released in coastal waters by desorption from falling soot particles, suspended particulate matter and sediment carried by storm water runoff and sewage discharges (40). Data on photodegradation of PAHs in water (including photolysis and photooxidation by reaction with hydroxyl radicals) are sparse and often broadly distributed after source and determination techniques (41,42). Table 1 shows that smaller molecules are generally more resistant to photodegradation than larger ones are.

UVR activation of PAHs has been intensively studied because of their ability to absorb both UVBR and UVAR, by virtue of their extensive π-orbital system (43). This UVR absorption can lead to the photodegradation of the PAH molecules (photooxidation and photodissociation), thereby resulting in new photoproducts. However, many studies have shown that an important aspect of the photoinduced PAH toxicity is derived from such photodegradation processes (8,22,44–47). In these studies chemical compounds were irradiated before toxicity testing, allowing demonstration of whether photomodified PAHs were contributing to toxicity.

Huang *et al.* (8) investigated the photoinduced toxicity of anthracene, phenanthrene and benzo(a)pyrene to the aquatic higher plant *Lemna gibba* (a duckweed) with chemicals irradiated before toxicity testing in which inhibition of growth and the extent of chlorosis were measured. They found that light activated the phytotoxicity of PAHs (UVR being more effective than visible light), with compounds becoming more toxic as they were converted to new structures by radiation. Comparable results were obtained by Ren *et al.* (45) with fluoranthene, pyrene and naphthalene, demonstrating that the photomodification process could be rapid under environmentally relevant levels of actinic radiation. So in many instances it was found that photomodification of any given PAH leads to a wide variety of oxidation products that are often difficult to analyze and identify (9,48–50).

The investigation of the toxicity of photoproducts was extended by Mallakin *et al.* (51), who determined which photoproducts in the mixture of photoproducts made the most significant contributions to toxicity, using anthracene as the test compound. Application of different radiation conditions demonstrates that the toxicity of the photoproducts of anthracene can also be photoinduced. This is in contrast to phenanthrenequinone (the major photoproduct of phenanthrene), the toxicity of which is greater than that of phenanthrene but not greatly photoinduced (50). Certain anthracene photoproducts are themselves subject to photooxidation, with a concomitant increase in toxicity. Conversely, some of the photoproducts of anthracene, although not readily photooxidized, are nonetheless phototoxic, indicating photosensitization activity. Interestingly, one of these photoproducts (2-hydroxyanthraquinone), which was not subject to photooxidation, appeared as the most toxic of the compounds tested. As a light-stable compound it presents the risk of a persistent environmental hazard.

Table 1. Chemical properties of selected aromatic hydrocarbons commonly found in the water-soluble fraction (WSF) obtained by contact of oil products with seawater.*

Chemical name	Molecular weight	Water solubility† (mg/L)	Henry's law constant† (Pa m^3/mol)	Partition coefficient† (log K_{OW})	Photodegradation half-life in water (hours)
Benzene	78	1780	557	2.13	>8000
Toluene	92	535	680	2.69	321–1284
Ethylbenzene	106	152	854	3.15	15
1,4-dimethylbenzene	106	156	754	3.15	NA
1,3,5-trimethylbenzene	120	97	849	3.42	3208–12 800
1,2,4,5-tetramethylbenzene	134	3.5	2540	4.1	NA
Naphthalene	128	30	43	3.37	71
1-methylnaphthalene	142	28	45	3.87	22
1,3-dimethylnaphthalene	156	8	NA	4.42	NA
2,6-dimethylnaphthalene	156	2	6.5	4.31	15.5
2-ethylnaphthalene	156	8	82	4.37	18.4
1,4,5-trimethylnaphthalene	170	2.1	23.5	4.9	NA
Acenaphthene	154	3.9	24	3.92	3
Acenaphthylene	152	3.9	11.5	4.06	NA
Fluorene	166	1.9	8.5	4.18	NA
Phenanthrene	178	1.6	4.0	4.46	8
1-methylphenanthrene	192	0.26	NA	5.14	6
Anthracene	178	0.05	6	4.45	<1 to 110
9-methylanthracene	192	0.26	NA	5.07	<1
Pyrene	202	0.135	1.2	5.0	98
Fluoranthene	202	0.24	NA	5.22	160
Chrysene	228	0.002	0.45	5.91	4.4

*Data were gathered by Mackay *et al.* (41,42). NA = data not available. †Most likely or recommended value by Mackay *et al.* (41,42).

Thus, it is believed that comprehensive PAH load assessments should now include such photoproducts as indicators of the presence of hazardous PAH photooxidation products.

On the basis of this study and previous work it is clear that a significant part of photoinduced toxicity of aromatic hydrocarbons can be attributed to the photomodification products that are more water soluble and therefore potentially more bioavailable than parent compounds for aquatic microbes (50), algae (22,44), plants (8,9,45,51,52), amphipods (10), crustaceans (15,47) and fish (16). However, bioavailability and direct toxicity of photo-oxidized PAHs is only a part of the problem, because the same photoproducts can become active photosensitizers and/or can be further photomodified (52).

Many other studies have shown that photosensitization processes also represent important aspects of the photoinduced toxicity of PAHs (10,11,13,18,53–56). Such processes imply activation of the chemicals that have bioaccumulated in biological matrices after radiant energy absorption, generating reactive oxygen species (ROS) (57) that can disrupt cell membranes via lipid peroxidation (46). PAHs and solar radiation can therefore interact to induce a broad range of effects in aquatic animals and plants. After coexposure to adequate amounts of solar radiation and PAH the lethal effects are likely due to massive cellular and tissue damage that cannot be repaired at an adequate rate. For example, exposure of juvenile fathead minnows, *Pimephales promelas*, to the PAH fluoranthene and solar UVR resulted in disruption of the integrity and function of gill tissue, suggesting that lethality was likely due to decreased oxygen diffusion capacity of the gills (58). Bluegill fish, *Lepomis macrochirus*, exposed to anthracene and solar UVR for 96 h exhibited significant increases in hematocrit, decreases in whole-blood levels of hemoglobin, evidence of hemolysis and inhibition of NaK–ATPase and Mg–ATPase enzyme activity in gill tissue (59). In the presence of simulated UVR individual PAHs, such as anthracene, fluoranthene, and pyrene, were 12 to >50 000 times as toxic to the juvenile marine bivalve *Mulinia lateralis* and juvenile mysid shrimp than they were in the absence of simulated UVR (14).

COMBINED EFFECTS OF UVBR AND HYDROCARBONS ON MARINE COMMUNITIES

Photoenhanced toxicity of PAHs is well documented in laboratory studies in which single plant or animal species have been tested under well-controlled conditions but it is often not ecologically relevant, although these studies provided pivotal information in our understanding of phototoxic mechanisms at molecular and cellular levels. As pointed out by McDonald and Chapman (21) very few studies can be considered as representative of field conditions in which organisms and/or assemblages of organisms can adopt protective behaviors and react to stressors to reduce their effects.

In an attempt to fulfill, at least partially, this gap for marine plankton communities, in June 2000 we initiated a series of microcosm experiments in which field-sampled planktonic assemblages were exposed to enhanced UVBR in the presence of the WSF of hydrocarbons from crude oil. Such an experimental setup was applied in order to mimic simultaneous ozone depletion and increasing traffic of commercial ships and tourist boats in coastal and estuarine waters at high latitudes. The ecological relevance of phototoxicity of small and soluble PAHs from petroleum was closely examined for phytoplankton and bacteria assemblages proliferating in the near-surface layer of the ocean and forming the first trophic levels of the marine food web (24).

A microcosm approach was used on natural plankton assemblages because it allows some control of experimental conditions, such as UVBR and/or contamination level. Microcosm experiments were performed using surface seawater collected near the two experimental sites. The first site was the south shore of the lower St. Lawrence Estuary (Québec, Canada [lat 48.4°N, long 68.5°W]) (Fig. 1A). This first experiment (Expt I) was performed during a 5-

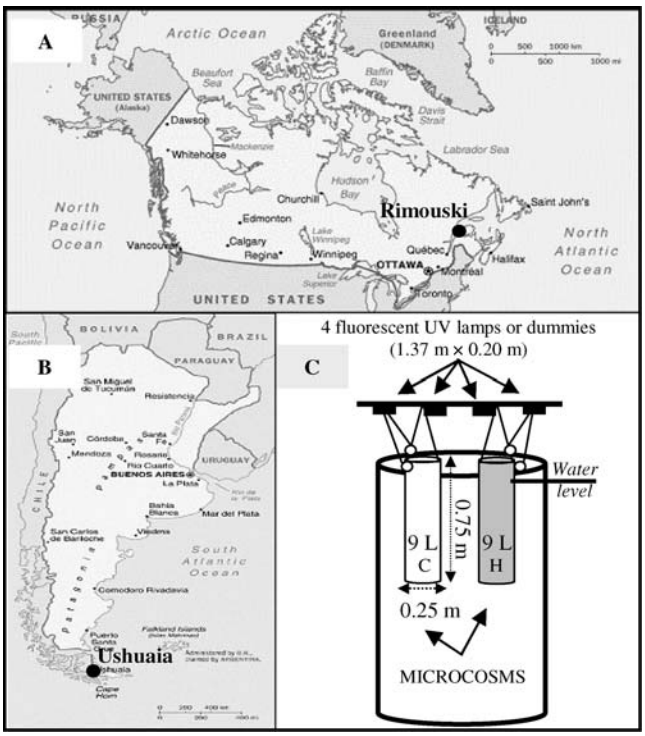

Figure 1. Schematic view of the location of the experimental sites of (A) Expt I (Rimouski, Canada) and (B) Expt II (Ushuaia, Argentina). The experimental set-up for both studies is also shown (C).

day period in June 2000. The second 5-day experiment (Expt II) was performed in Beagle Channel Bay near the city of Ushuaia (Tierra del Fuego, Argentina [lat 54.8°S, long 68.2°W]) (Fig. 1B) and was performed in early November 2001. A third experiment (Expt III) was conducted in mid-August 2001 near Rimouski and used experimental parameters similar to those used in Expt I.

For Expt I and Expt II, microcosms (9l-cylindrical Teflon® bags [75 cm tall × 25 cm wide]) (Fig. 1C) were placed in larger mesocosms before filling with natural water collected in each specific site and were screened through a 500 μm Nitex™ mesh in order to exclude large grazers. Larger mesocosms consisted of clear polyethylene bags (*ca* 2.3 m deep, with a volume of *ca* 1800 L) attached to a wharf structure and immersed in the water column. In each experiment microcosms were exposed in triplicate to the following UVR regimes: natural UVBR (NUVBR) and enhanced UVBR (HUVBR). UVBR enhancement was provided by four fluorescent UV lamps (TL40W-12RS, Philips) with an emission peak at 313 nm. Wavelengths shorter than 290 nm (UVC radiation) were screened out by means of 0.13 mm cellulose acetate films that were changed daily. Compared with the NUVBR, the weighted irradiance in the UV region was 2.15-fold greater for the HUVBR treatment each day for a period of 6 h.

In order to determine possible interactive effects of UVBR and hydrocarbons a stock solution of WSF of crude oil was prepared with crude oil *Forties* from North Sea oil fields (for the specimens from Rimouski) and an Argentinean crude (for the specimens from Ushuaia). The resulting WSF was then added to the microcosms to yield realistic concentrations according to the experiment and crude oil used (*ca* 10 mg/L in Expt I and *ca* 5 mg/L in Expt II). Microcosms were identified according to their UVBR treatment and WSF addition as follows: NUVBR and HUVBR, respectively, for microcosms without dissolved hydrocarbons, and NUVBR+WSF and HUVBR+WSF, respectively, for microcosms with dissolved hydrocarbons added.

During these 5-day experiments, incident UVBR, WSF and nutrient concentrations, as well as abundance and production of heterotrophic bacteria and phytoplankton were monitored. Therefore, these microcosm experiments, which were performed in different seasons and at different latitudes, revealed the relative short-term impact of UVBR and of WSF on a natural planktonic assemblage. However, the extent of both UVBR effects and WSF effects was different between the two specific sites, which explains the different results observed under simultaneous exposure to dual stress for Expt I and Expt II.

An increase in UVBR alone induced no significant effects on total phytoplanktonic biomass of the St. Lawrence Estuary, as determined by Chl *a* concentration (Fig. 2). However, a decrease in phytoplankton abundance (as determined by flow cytometry) was observed (Fig. 3), with a greater decrease in growth rates for nanophytoplanktonic cells than for picophytoplanktonic cells (Fig. 4). A decrease in photochemical efficiency given by the *Fv*/*Fm* value, as determined with a PAM fluorometer on the final day of the experiment, was also observed (60). For Expt II phytoplankton was much less abundant and both total biomass and phytoplankton cells abundance were negatively affected (Figs. 2 and 3) with a greater decrease in growth rates for picophytoplankton cells than for nanophytoplankton cells. According to *Fv*/*Fm* values an inhibition of *ca* 50% was observed after exposure to enhanced UVBR. However, by the end of the experiment the photochemical yield reached values equal to those observed under natural light conditions.

Many factors can govern the impact of UVBR and may explain differences observed in these two experiments. Nutritional status must be considered first. Initial concentrations were relatively high in Expt I (nitrate–nitrite concentration, 14.15 μmol/L; silicate concentration, 19 μmol/L), allowing the phytoplanktonic bloom (mainly diatoms) to occur. Previous studies have demonstrated the greater resistance of diatoms to deal with UVBR (61). By the end of Expt I the phytoplanktonic bloom had resulted in nutrient depletion and, therefore, an increasing sensitivity to UVBR effects. In the Ushuaia experiment the planktonic assemblage was characterized by lower nutrient concentrations (nitrate–nitrite concentration, 5 μmol/L; silicate concentration, 4.3 μmol/L) because the experiment took place just after the spring bloom. Large cells were less abundant and/or in a senescent state, resulting in a greater UVBR effect on the total biomass. Such limited nutrient status can indeed impede repair mechanisms to cope with UVBR effects, because repair enzyme synthesis and photoprotective pigments require energy and nutrients. Therefore, it is unlikely that phytoplankton assemblages of the St. Lawrence Estuary could have synthesized photoprotective compounds, as revealed by the decrease in photochemical yield by the end of the experiment associated with nutrient depletion.

In Expt II the diel periodicity of the photochemical yield (with a significant decrease during the day and recovery at night) could be related to synthesis of photoprotective compounds by nanophytoplankton, thus explaining the increase in the mean cell size of this phytoplanktonic fraction. However, photoprotective synthesis requires energy that was no longer available for physiological processes, resulting in the observed diminution of growth rates. Synthesis of such compounds is not expected in picophytoplankton

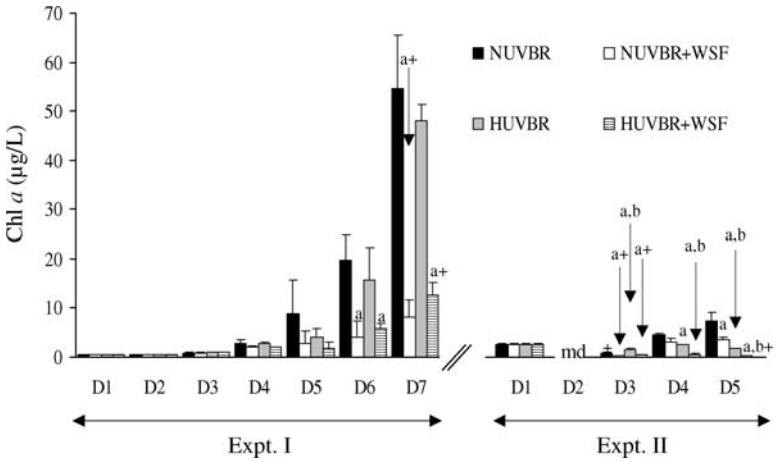

Figure 2. Temporal changes in total chlorophyll *a* concentrations. a: Significant differences relative to NUVBR (closed box). a,b: Significant differences relative to NUVBR plus WSF (open box). +: Significant differences relative to HUVBR (shaded box). md = missing data for day 2, Expt II. Data are means ± SD.

cells, which seem to be affected more by DNA damage, resulting in a higher inhibition of their growth rates.

Similar observations can be made about bacterioplankton responses. UVBR induces direct effects on this biological component, as well as indirect effects due to trophic interactions between bacterioplankton and phytoplankton assemblage (62). Bacterial abundance increased in Expt I after UVBR exposure (Fig. 5A), probably because of a greater bioavailability of growth substrates (*e.g.* from phytoplanktonic cells affected by UVBR). It is also possible that ciliates were affected by UVBR stress, resulting in decreased predation on bacterioplankton (62). A diel periodicity was observed and likely due to the co-occurrence of DNA damage and repair processes. These results suggest a cellular UVBR effect rather than a population effect. Such UVBR effects on total bacterial abundance were not found in Expt II, suggesting that bacteria were already at an advantage, because the experiment took place just after the phytoplanktonic bloom. However, it was possible in Expt II to distinguish between HNA bacteria (*i.e.* bacteria with a high nucleic acid content) and LNA bacteria (*i.e.* bacteria with a low nucleic acid content) (63). Recent studies have demonstrated the deleterious effects of UVBR on the abundance of LNA bacteria (Fig. 5B) (Sargian *et al.*, unpublished).

The influence of the addition of WSF differed between the two experiments, primarily because of a difference in the initial WSF concentration (*ca* 10 mg/L at Rimouski and *ca* 5 mg/L at Ushuaia) obtained from two different crude oils with different physicochemical characteristics, but were specific to each site in terms of crude oil spill risks. WSF addition was detrimental to the total phytoplanktonic biomass, because diatoms are highly sensitive to hydrocarbons (64), and to the abundance of cells (<20 µm). Indeed, bioaccumulated hydrocarbons can have direct toxic effects or can interfere with photosynthetic processes (*e.g.* decrease in photochemical yield; (60)). Naphthalene toxicity, which was the main compound identified in the WSF can be associated with its conversion in related naphthoquinones and hydroxylated compounds (65). These degradation products can potentially block photosynthesis, especially where plastoquinone is used as an electron acceptor or donor (9), because of their structural similarity with the Q_b-binding niche in PS II.

Whatever the processes could be, it seems that WSF addition did not induce any structural modification in cells (*e.g.* cell size) in either experiment, suggesting a direct toxic effect of hydrocarbons for cell death. Phytoplankton growth rates were affected in a different way according to the experimental site considered. For the St. Lawrence Estuary assemblage, growth rates of nanophytoplanktonic cells were more affected (*e.g. ca* 80% inhibition) than those of picophytoplanktonic cells (*ca* 38% inhibition) (Fig. 4). For the Ushuaia assemblage, only the smallest cells demonstrated a

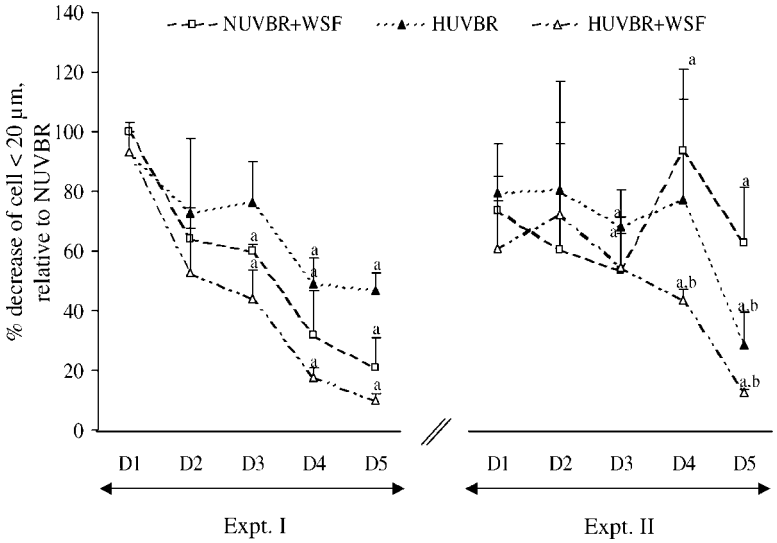

Figure 3. Percentages of total abundance of phytoplankton cells (<20 µm) relative to natural UVBR level uncontaminated with WSF. a: Significant differences relative to NUVBR. a,b: Significant differences relative to NUVBR plus WSF. Data are mean values ± SD.

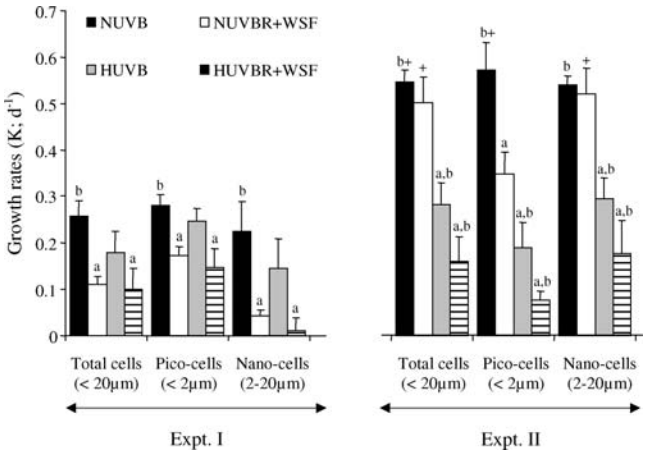

Figure 4. Growth rates (K; d^{-1}) for total cells (<20 µm), picophytoplankton and nanophytoplankton cells. a: Significant differences relative to NUVBR (closed box). b: Significant differences relative to NUVBR plus WSF (open box). +: Significant differences relative to HUVBR (shaded box). Data are mean values ± SD.

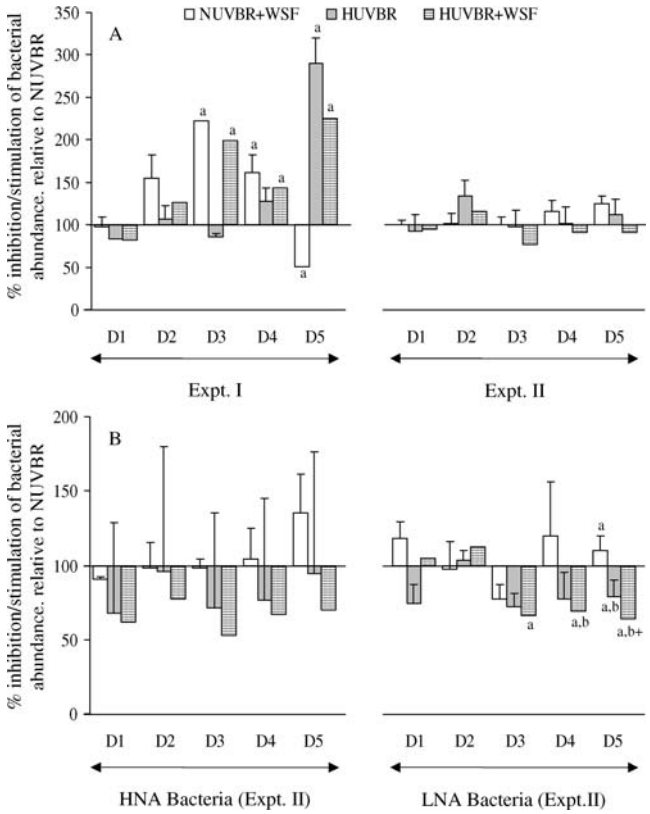

Figure 5. Percentage inhibition/stimulation of total bacterial abundance in Expt I and II (A) and HNA and LNA bacteria (B) as determined by flow cytometry (for Expt II only) and relative to NUVBR. a: Significant differences relative to NUVBR. a,b: Significant differences relative to NUVBR+WSF (open box). +: Significant differences relative to HUVBR (shaded box). Data are mean values ± SD.

decrease in their growth rate (*e.g. ca* 22% inhibition). These results can be explained by the initial WSF used which was different between the two sites.

According to the bacterioplankton, the apparent stimulation of the bacterial abundance observed in the Rimouski experiment was not recorded in Ushuaia (Fig. 5A). However, for the first experiment, the increase in bacterial biomass was associated with a decrease in bacterial activity during the first days, and conversely by the end of the experiment (*e.g.* decrease in abundance with increase in activity). From these results, it can be hypothesized that addition of soluble hydrocarbons induced a change in the specific composition of the bacterioplankton, with the establishment of specialized bacteria degrading hydrocarbons.

For Ushuaia, no significant effects of WSF addition were observed on the total bacterial abundance. However, according to the distinction between HNA and LNA bacteria, a WSF addition resulted in a stimulation of the abundance of LNA bacteria (Fig. 5B), associated with an increase in colony-forming units (Sargian *et al.*, unpublished). Therefore, the hypothesis advanced for Expt I seems to be confirmed for a change in the bacterial specific composition.

Simultaneous exposure to enhanced UVBR and WSF did not induce the same impact at both experimental sites. Moreover, the plankton assemblage of the St. Lawrence Estuary was first exposed to UVBR before WSF addition whereas in Ushuaia the plankton assemblage was first exposed to WSF, and then to UVBR. For Expt I the deleterious effects of hydrocarbons exceeded the potential deleterious effects of UVBR, resulting in no measurable effect (*e.g.* additive or synergistic effects) due to the co-occurrence of both stressors. UVBR and WSF present similar phytotoxicity mechanisms, affecting especially the photosynthetic apparatus, damaging DNA and leading to reactive oxygen species formation. For Expt II, the more moderated effects of the WSF and the stronger impact of UVBR on the natural plankton assemblage caused a synergistic interaction between the two stressors, leading to a change in phytoplanktonic composition as well as in bacterial composition.

As seen from Expt I and II at least two factors—the status of the planktonic population and the concentration of WSF—seem to play the determining role in the behavior of a natural planktonic assemblage submitted to the enhanced UVBR stress and dissolved hydrocarbons. To obtain more insight about these factors an additional experiment with WSF (Expt III) was conducted during a 7-day period with samples from St. Lawrence Estuary's planktonic assemblage obtained in mid-summer (August 2001), instead of at the end of spring (June 2000) as in Expt I. The experimental setup was similar to that in Expt I: the same microcosms were used but were immersed in a 1300 L plastic tank onshore with circulating water to maintain the temperature of microcosms at 15.6 ± 0.6°C. This study used the following three WSF concentrations: *ca* 10, *ca* 20 and *ca* 50 mg/L prepared with the same crude oil used in Expt I. The average increase of UVBR in HUVBR treatment was *ca* 1.49-fold higher than the ambient level throughout the experiment. The level of inorganic nutrients were very low, compared with the level in Expt I, but was quite similar to that in Expt II, with a nitrate–nitrite concentration starting at 3.16 µmol/L and decreasing to 1.47 µmol/L over 7 days and a silicate concentration of 4.42–2.33 µmol/L. Detailed results are reported in Payet (66); only the main features are summarized here. The ratio of 2-methylnaphthalene to 1-methylnaphthalene (2-MN : 1-MN) was calculated from chromatographic data and was used to characterize the weathering process affecting dissolved oil in different microcosms (67). The ratio decreases under bacterial degradation because 1-MN is preferably degraded to 2-MN.

During Expt III the mean 2-MN : 1-MN ratio (±SD) decreased from 0.7 ± 0.2 on day 0 to 0.5 ± 0.2 on day 6 (results not shown).

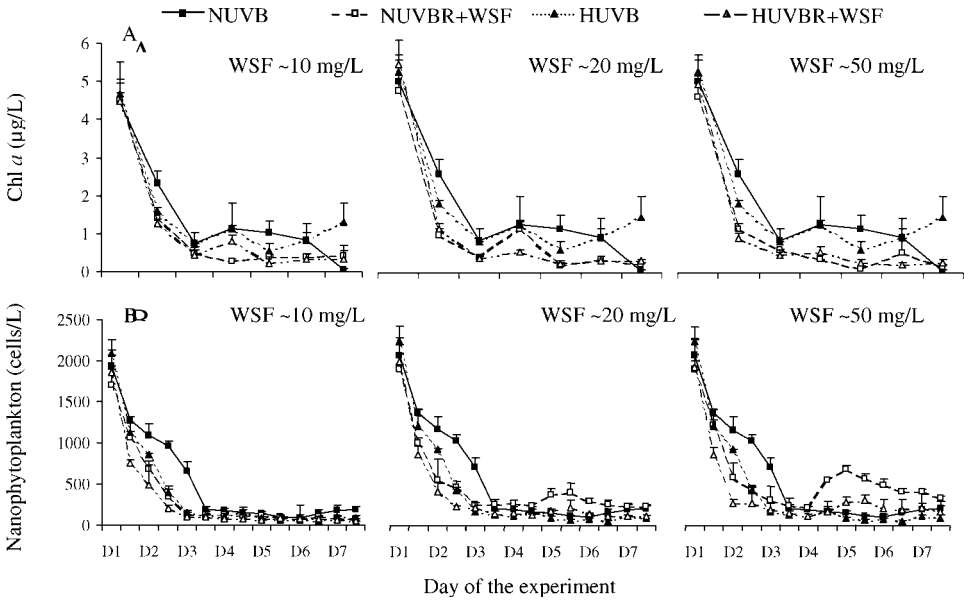

Figure 6. Temporal changes in total chlorophyll *a* (A) and nanophytoplanktonic abundance (B), according to the three initial WSF concentrations used (Expt III). Data are mean values ± SD.

No multivariate effects between UVBR and WSF treatments were detected over time but a 2-way analysis of variance indicated that WSF had a statistically significant degradative effect on the ratio during days 2–6 ($P < 0.01$). There was a significant decrease in the 2-MN : 1-MN ratio under LWSF (concentration, 2 mg/L), compared with MWSF (concentration, 10 mg/L) and HWSF (concentration, 50 mg/L). Although no significant UVBR effect was found on degradation activities the treatment kept in dark seemed to result in a greater degradation for 10 and 20 mg of WSF/L, compared with UVBR treatments. It might be a first indication that hydrocarbon-specific bacteria stimulated by the presence of WSF were affected by UVBR.

Total phytoplankton population, which was estimated on the basis of the Chl *a* concentration, was usually high at that time of the year; it drastically decreased in the first 48 h and remained at a low level until the end of the experiment in all microcosms, including those with natural light and without WSF (Fig. 6). High phytoplankton abundance and low nutrient concentrations made the assemblage particularly sensitive to environmental stressors, such as sampling and water transfer, changes in light intensity and presence of dissolved hydrocarbons. Throughout the experiment combined UVBR and WSF treatments did not induce large changes in both Chl *a* and nanophytoplankton abundance (Fig. 6). UVBR effects appeared to be more detrimental than WSF contamination. Indeed, nanophytoplankton abundance was reduced under enhanced UVBR, whereas WSF contamination seemed to stimulate their growth rate (especially at concentrations of *ca* 20 and *ca* 50 mg/L), relative to uncontaminated NUVBR environment (Fig. 6). Previous studies have also observed such an effect with hydrocarbon contamination (64,68) and this could be attributed to a shift in the phytoplanktonic assemblage with the appearance of tolerant species, such as flagellates. The community structure was probably the most important factor related to the sensitivity observed during Expt III. For instance, in a study performed in Argentina (69) only postbloom assemblages were significantly affected by UVBR, compared to the prebloom and bloom periods, and this was attributed to a different population located in the natural phytoplanktonic community.

Thus, the observed drastic decrease of nanophytoplankton abundance under NUVBR and HUVBR can be at least partly be attributed to the occurrence of more-vulnerable species, such as nanoplanktonic flagellates, that generally dominate during post-bloom events in the St. Lawrence Estuary (70–72). Many studies have demonstrated the sensitivity of phytoflagellates exposed to UVBR (61,69,72). Overall, the effect of HUVBR was significantly stronger than that of NUVBR on nanophytoplankton cell values during days 3–6, whereas both total Chl *a* and nanophytoplankton abundance remained almost constant and significantly higher under the dark treatment, compared with the UVBR treatments.

The bacterial community in Expt III was not affected in the same way as phytoplankton. The initial population (concentration, *ca* 1.9×10^6 cells mL^{-1}) started to grow within 48 h and reached a concentration of 6.9×10^6 cells mL^{-1} by the end of the experiment, with a peak at 10×10^6 cells mL^{-1} during treatment with 50 mg WSF/L while in the dark. For comparison the bacterial count in Expt I started at 0.2×10^2 cells mL^{-1} and increased by a factor of 10 in microcosms treated with WSF. In Ushuaia (Expt II) the total count ranged from 3.0×10^6 to 7.4×10^6 cells mL^{-1}.

The abundance of bacteria increased with increasing WSF levels, most likely because of the development of an opportunistic bacterial community on dead phytoplankton cells and the development of hydrocarbon-specific bacteria that are able to grow on the additional carbon source provided by dissolved hydrocarbons (Fig. 7). However, when WSF was considered jointly with enhanced UVBR exposure, the lowest values of bacterial abundance were recorded and more drastically under the highest WSF level. It was likely that enhanced UVBR exposure was enough to induce phototoxicity of the WSF. As a general trend differences between UVBR and WSF treatments increased with time. The effects of fluctuations in UVBR conditions and WSF treatments on bacteria were more important at the end of the experiment (days 5–6) than at the beginning (days 0–1). Bacteria appeared more sen-

sitive to combined high UVBR conditions and WSF levels during the last 2 days of the experiment.

All together, these three experiments with field-sampled communities demonstrated the complexity and the difficulty in determining the impact of multiple stressors on an aquatic ecosystem, even when the system was simplified by eliminating large grazers and fish. A range of environmental variables (with their spatial and temporal variability) determines the importance of UVBR and WSF effects, both of which demonstrated similarity in their mode of action. Nutrient status, specific composition and light history each influenced the different responses of planktonic assemblages.

The lack of synergistic effects between UVBR and WSF observed in Expt I was mainly attributed to the greater impact of WSF, which was strong enough to exceed the potential deleterious effects of UVBR, resulting in no detectable combined (*e.g.* additive or synergistic) effects. On the basis of these results it was hypothesized that synergistic or additive effects could probably take place at lower concentrations of WSF (*e.g.* chronic inputs of hydrocarbons into aquatic ecosystems) representative of more typical situations in coastal areas. Expt II confirmed this hypothesis with a lower initial WSF concentration. Moreover, this study illustrated that plankton assemblages influenced by a periodic decrease in stratospheric ozone concentration and enhanced UVBR were physiologically stressed and more susceptible to WSF toxicity than sites that received lower levels of UVBR (as shown in both Rimouski experiments). Expt III highlighted a close relationship between phytoplankton assemblages and bacteria. A phytoplankton crash after a bloom event may release important carbon and nutrient sources for bacteria. Subsequently, bacteria grew, accumulated and took advantage of those favorable conditions through a dynamic feedback system.

The magnitude of phytoplanktonic mortality probably influenced how rapidly bacteria grew over time. A close inverse relationship was found between bacteria and nanophytoplankton, supporting the idea that the initial trophic food web status shifted from a postbloom algal state to a microbial food web in which bacteria were numerically dominant. In addition, it seems that UVBR and WSF treatments were important factors that enhanced this transition, probably because of the high phytoplankton sensitivity. The degree of this transition throughout the experiment has significant ecological implications for carbon cycling and energy flow in pelagic systems. This high phytoplankton mortality implies a situation in which the potential for carbon export from surface waters is high. In contrast, a high bacterial enrichment implies that the phytoplankton carbon is largely recycled in surface waters through a microbial loop and does not contribute significantly to sinking particle flux. In addition, UVBR and WSF treatments could also influence the food web structure and sinking flux in a pelagic planktonic community, favoring a system dominated by a microbial loop from which there is very little downward export.

These findings open an interesting window in the field of multiple interactions in ecotoxicology. The enhancement of hydrocarbon toxicity in the presence of high UVBR cannot be described as a synergistic or an additive effect, because WSF without enhanced UVBR is not toxic and may even be beneficial by increasing bacterial activity. Actually, there is a case in which one of the stressors has the ability to modify (photochemically, in this case) one of the other stressors and turn it into a harmful compound for target organisms. This type of interaction is difficult to categorize and has received little attention to date. These abiotic-induced interactions might be important for biological communities exposed to extreme conditions in which physical, chemical or photochemical reactions could modify the nature of environmental stressors before they interact with biological functions.

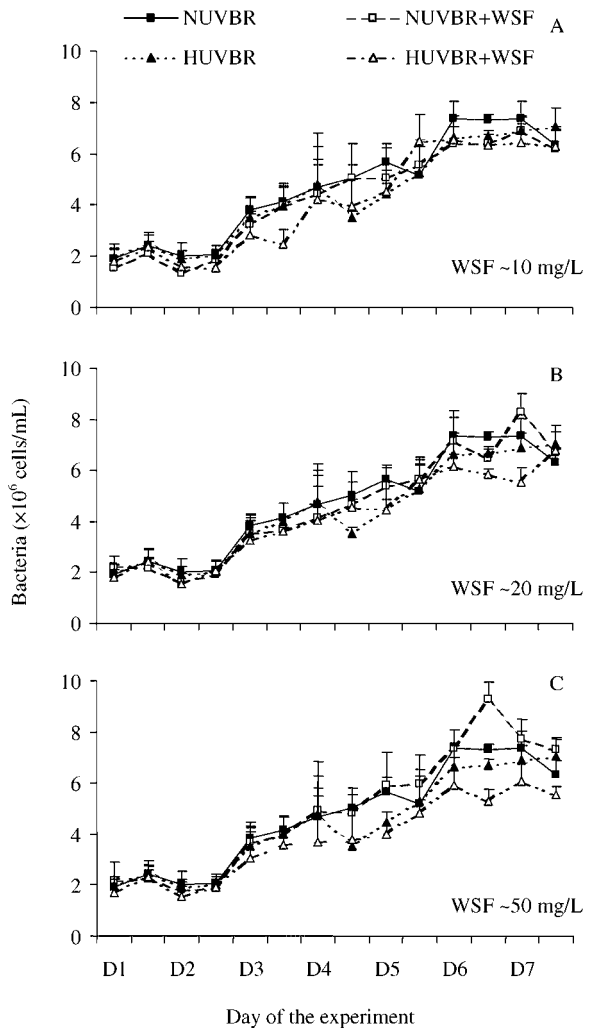

Figure 7. Temporal changes in bacterial abundance exposed to low WSF (A; *ca* 10 mg/L), medium WSF (B; *ca* 20 mg/L), and high WSF (C; *ca* 50 mg/L) concentrations (Expt III). Data are mean values ± SD.

UVBR AND BUTYLTIN COMPOUNDS

The sensitivity of aquatic organisms to heavy metals (cadmium, copper, chromium, mercury, nickel, lead and zinc) can be increased in the presence of UVBR. This was shown in laboratory and field studies that involved a variety of organisms, such as algae, rotifers and invertebrates (6,73–75). Again, most toxicological results for trace metals and UVR have been obtained in laboratory under unrealistic concentrations of dissolved metals and single species.

Among trace metals, tin (Sn) exhibits a peculiar chemical behavior, because it can form stable organotin compounds in which Sn (IV) is covalently bound to one, two, three or four alkyl or aryl groups. This property was used to synthesize a large groups of organotins with various uses in plastic and pesticide industries. Among them, tributyltin (TBT) is used as a biocide in antifouling

Table 2. Summary of effects of tributyltin (TBT) and UVBR on field-collected plankton community exposed over 5 days in mesocosms.*

Measured parameter	Observations	Ecotoxicological significance
Nutrients	Significant differences in N and P concentrations between TBT treatments and normal UVBR where nutrients are depleted in 5 days	A rapid shift of the community from autotrophs to heterotrophs and low assimilation of nitrate
Chlorophyll *a*	Steady decrease of Chl *a* in all TBT treatments and increase of Chl *a* in TBT-free treatments; significant photoinhibition of PS II, especially in TBT-positive enhanced UVBR.	Highly significant inhibitory effect induced by TBT on phytoplankton cells
Abundance of phytoplankton cells (<20 μm)	Significant decrease of total abundance of cells in TBT treatments with a worse situation in enhanced UVBR treatment	Synergetic effects of TBT-positive enhanced levels of UVBR on the abundance of cells
Cell characteristics	TBT increased cell size of nanoautotrophs and induced high SSC values; indices of picoautotrophs not significantly affected in the first days	TBT inhibition of photophosphorylation and subsequent inhibition of ATP-positive Pi exchange activities
Growth rates	Growth rates of larger cells are much more affected than those of smaller cells	Shift from large autotrophs to small autotrophs as a transition step before heterotrophy takes place
Bacterial abundance	Bacterial abundance was significantly higher in all TBT treatments toward normal UVBR	Respiration of suddenly available organic carbon by bacteria
Bacterial-specific activity	Inhibition of the specific activity in TBT treatments	Adaptation of the bacterial community to a toxic environment

*Data are from Sargian *et al.* (25). SSC = side-light scattering related to refractive index, granularity and cell shape.

paints for ship hulls. TBT exhibits a high toxic activity toward a variety of aquatic nontargeted organisms (76), including phytoplankton (77,78) and bacterioplankton (79). Despite the current restrictions on TBT in antifouling paints and a total ban expected by January 2008, this organometallic compound persists in coastal areas at concentrations considered to be chronically toxic (80). Butyltin compounds absorb radiant energy only in the UV region and essentially in the UVBR component of sunlight (280–320 nm), which can cause photodegradation of butyltins in surface waters (81). It can be hypothesized that contamination of estuaries and coastal environments by TBT and its degradation by-products (dibutyltin and monobutyltin) can increase the susceptibility of planktonic assemblages to enhanced UVBR levels.

Using the previously described setup for Expt I on UVBR and PAHs, we exposed a field-collected planktonic community to dissolved TBT (0.3 n*M*) and UVBR for 5 days (25). Single and combined toxic effects were investigated by determining bacterial abundance and productivity, phytoplankton abundance, cellular characteristics and growth rates and Chl *a* fluorescence. The main findings and their interpretation are summarized in Table 2. The results clearly demonstrated that TBT addition resulted in a decrease in photosynthesis, an increase in the mean phytoplankton cell size and changes in cell shape, with ultimately a significant decrease in cell abundance. The toxic effects of TBT were magnified when cells were jointly exposed to enhanced UVBR. Sargian *et al.* (25) have described cellular mechanisms by which UVBR and TBT lead to these catabolic cellular changes.

The bacterial component of the natural plankton assemblage showed a different behaviour, with an apparent stimulation of the bacterial abundance (*i.e.* additional available carbon) associated with an inhibition of the bacterial activity, suggesting a shift in the specific composition of the bacterial community toward a consortium more resistant to butyltins.

The synergistic mechanism of TBT and UVBR on a natural plankton community could imply either a UVBR-associated increase in TBT sensitivity or a TBT-associated increase in UVBR sensitivity of cells but it was not possible to define the exact synergistic mechanism involved. However, it was evident that both environmental stressors acted together to induce negative effects reflected in the continuously decreasing total abundance of phytoplankton cells (<20 μm), as well as in the inhibition of the bacterial productivity. As previously mentioned for PAHs, the combined effects of UVBR and TBT favor the microbial food web characterized by ammonium-based production (*i.e.* ''regenerated production''), dominance of small organisms (flagellates, bacteria and microzooplankton) and low carbon export.

PERSPECTIVES

Identifying interactions between stressors is a challenging task because the potential effects of two or more stressors acting simultaneously are often astonishingly complex and could include abiotic induced interactions, biodegradation and bioactivation, food availability, seasonal and annual cycles, interspecific interactions, tolerance and protective behavior, population shifts and biodiversity losses. Models have been developed to assess effects of multiple stressors (82–85) but most authors agree that the predictive success of a given model is first governed by the quality of data used to test the model. Many results reported in our review show how problematic the extrapolation of laboratory results is, because most laboratory experiments do not account for interspecific interactions, autoprotective behavior of sensitive species and chemical interactions with naturally occurring organic matter. Even water temperature is often neglected. On the other hand, results obtained with field-sampled communities and mesocosms appear to be much more relevant to a proper evaluation of the ecological impacts of UVBR and anthropogenic pollutants released in coastal waters. A shift toward small species seems to be a generalized stress response because the ability to survive various stressors might depend on a rapid reproductive rate and a small body size (86,87). A shift toward heterotrophic assemblages is an unsuspected adverse effect that reduces the sink of CO_2 and most probably reduces the biodiversity of coastal waters. The tolerance of plankton species to multiple stressors, particularly enhanced UVBR and pollutants, should be determined and models on impacts of multiple stressors on biodiversity and ecosystem functioning (88) should be developed in the near future.

Acknowledgements—This work was supported by the National Sciences and Engineering Research Council of Canada, the Fonds Québecois de Recherche sur la Nature et les Technologies, the Inter American Institute for Global Change Research and the Canada Research Chairs Program.

REFERENCES

1. De Mora, S., S. Demers and M. Vernet (2000) *The Effects of UV Radiation in the Marine Environment*. Cambridge University Press Environmental Chemistry Series, Cambridge.
2. Helbling, E. W. and H. Zagarese (2003) *UV Effects in Aquatic Organisms and Ecosystems*. Springer-Verlag, New York.
3. El-Alawi, Y. S., D. G. Dixon and B. M. Greenberg (2001) Effects of pre-incubation period on the photoinduced toxicity of polycyclic aromatic hydrocarbons to the luminescent bacterium *Vibrio fischeri*. *Environ. Toxicol.* **16**, 277–286.
4. Steevens, J. A., M. Slaterry, D. Schlenk, A. Aryl and W. H. Benson (1999) Effects of ultraviolet-B light and polyaromatic hydrocarbon exposure on sea urchin development and bacterial bioluminescence. *Mar. Environ. Res.* **48**, 439–457.
5. Gala, W. R. and J. P. Giesy (1992) Photo-induced toxicity of anthracene to the green alga, *Selenastrum capricornutum*. *Arch. Environ. Contam. Toxicol.* **23**, 316–323.
6. Rai, P. K. and L. G. Rai (1997) Interactive effects of UV-B and Cu on photosynthesis, uptake and metabolism of nutrients in a green alga *Chlorella vulgaris* under simulated ozone column. *J. Gen. Appl. Microbiol.* **43**, 281–288.
7. Southerland, H. A. and A. J. Lewitus (2004) Physiological responses of estuarine phytoplankton to ultraviolet light-induced fluoranthene toxicity. *J. Exp. Mar. Biol. Ecol.* **298**, 303–322.
8. Huang, X. D., D. G. Dixon and B. M. Greenberg (1993) Impacts of UV radiation and photomodification on the toxicity of PAHs to the higher plant *Lemna gibba* (duckweed). *Environ. Toxicol. Chem.* **12**, 1067–1077.
9. Huang, X. D., B. J. McConkey, S. T. Babu and B. M. Greenberg (1997) Mechanisms of photoinduced toxicity of photomodified anthracene to plants: Inhibition of photosynthesis in the aquatic higher plant *Lemna gibba* (duckweed). *Environ. Toxicol. Chem.* **16**, 1707–1715.
10. Ankley, G. T., S. A. Collyard, P. D. Monson and P. A. Kosian (1994) Influence of ultraviolet light on results of toxicity tests conducted with sediments contaminated with polycyclic aromatic hydrocarbons. *Environ. Toxicol. Chem.* **13**, 1791–1796.
11. Boese, B. L., J. O. Lamberson, R. C. Swartz, R. Ozretich and F. Cole (1998) Photoinduced toxicity of PAHs and alkylated PAHs to a marine infaunal amphipod (*Rhepoxynius abronius*). *Arch. Environ. Contam. Toxicol.* **34**, 235–240.
12. Diamond, S. A., N. J. Milroy, V. R. Mattson, L. J. Heinis and D. R. Mount (2003) Photoactivated toxicity in amphipods collected from polycyclic aromatic hydrocarbon-contaminated sites. *Environ. Toxicol. Chem.* **22**, 2752–2760.
13. Cleveland, L., E. E. Little, R. D. Calfee and M. G. Barron (2000) Photoenhanced toxicity of weathered oil to *Mysidopsis bahia*. *Aquat. Toxicol.* **49**, 63–76.
14. Pelletier, M. C., R. M. Burgess, K. T. Ho, A. Kuhn, R. A. McKinney and S. A. Ryba (1997) Phototoxicity of individual polycyclic aromatic hydrocarbons and petroleum to marine invertebrate larvae and juveniles. *Environ. Toxicol. Chem.* **16**, 2190–2199.
15. Peachey, R. B. M. (2005) The synergism between hydrocarbon pollutants and UV radiation: Potential link between coastal pollution and larval mortality. *J. Exp. Mar. Biol. Ecol.* **315**, 103–114.
16. Barron, M. G., M. G. Carls, J. W. Short, S. D. Rice, R. A. Heintz, M. Rau and R. Di Giulio (2005) Assessment of the phototoxicity of weathered Alaska North Slope crude oil to juvenile pink salmon. *Chemosphere* **60**, 105–110.
17. Bowling, J. W., G. J. Leversee, P. F. Landrum and J. P. Giesy (1983) Acute mortality of anthracene-contaminated fish exposed to sunlight. *Aquat. Toxicol.* **3**, 79–90.
18. Little, E. E., L. Cleveland, R. Calfee and M. G. Barron (2000) Assessment of the photoenhanced toxicity of a weathered oil to the tidewater silverside. *Environ. Toxicol. Chem.* **19**, 926–932.
19. Zaga, A., E. E. Little, C. F. Rabeni and M. R. Ellersieck (1998) Photoenhanced toxicity of a carbamate insecticide to early life stage anuran amphibians. *Environ. Toxicol. Chem.* **17**, 2543–2553.
20. Boese, B. L., J. O. Lamberson, R. C. Swartz, F. A. Cole, J. Pelletier and J. Jones (1999) Toxicity and phototoxicity of mixture of highly lipophilic PAH compounds in marine sediment: Can the sum PAH model be extrapolated? *Arch. Environ. Contam. Toxicol.* **36**, 270–280.
21. McDonald, B. G. and P. M. Chapman (2002) PAH phototoxicity—An ecologically irrelevant phenomenon? *Mar. Pollut. Bull.* **44**, 1321–1326.
22. Marwood, C. A., R. E. H. Smith, K. R. Solomon, M. N. Charlton and B. M. Greenberg (1999) Intact and photomodified polycyclic aromatic hydrocarbons inhibit photosynthesis in natural assemblage of Lake Erie phytoplankton exposed to solar radiation. *Ecotoxicol. Environ. Saf.* **44**, 322–327.
23. Ohwada, K., M. Nishumura, M. Wada, H. Nomura, A. Shibata, K. Okamoto, K. Toyoda, A. Yoshida, H. Takada and M. Yamada (2003). Study of the effect of water-soluble fractions of heavy-oil on coastal marine organisms using enclosed ecosystems, mesocosms. *Mar. Pollut. Bull.* **47**, 78–84.
24. Sargian, P., B. Mostajir, K. Chatila, G. A. Ferreyra, É. Pelletier and S. Demers (2005a) Non-synergistic effects of water-soluble crude oil and enhanced ultraviolet-B radiation on a natural plankton assemblage. *Mar. Ecol. Prog. Ser.* **294**, 63–77.
25. Sargian, P., É. Pelletier, B. Mostajir, G. A. Ferreyra and S. Demers (2005b) TBT toxicity on a natural planktonic assemblage exposed to enhanced ultraviolet-B radiation. *Aquat. Toxicol.* **73**, 299–314.
26. Samanidou, V., K. Fytianos, G. Pfister and M. Bahair (1988). Photochemical decomposition of carbamate pesticides in natural waters of Northern Greece. *Sci. Total Environ.* **76**, 85–92.
27. Miller, P. L. and Y. P. Chin (2002) Photoinduced degradation of carbaryl in a wetland surface water. *J. Agric. Food Chem.* **50**, 6758–6765.
28. Tringle, M. D., M. Pirmohamed, E. Templeton, A. S. Wilson, S. Wadden, N. R. Kitteringham and B. K. Park (1993) An investigation of the formation of cytotoxic, genotoxic, protein-reactive and stable metabolites from naphthalene by human liver microsomes. *Biochem. Pharmacol.* **46**, 1529–1538.
29. Bridges, C. M. and M. D. Boone (2003) The interactive effects of UV-B and insecticide exposure on tadpole survival, growth and development. *Biol. Conserv.* **113**, 49–54.
30. Readmen, J. W., T. A. Albanis, D. Barcelo, S. Galissi, J. Tronczynski and G. P. Gabrielides (1993) Herbicide contamination in Mediterranean estuarine waters. Results from a MEDPOL pilot survey. *Mar. Pollut.* **26**, 613–619.
31. Albanis, T. A. and D. G. Hela (1998) Pesticide concentrations in Louros river and their fluxes into the marine environment. *Int. J. Environ. Anal. Chem.* **70**, 105–120.
32. Lin, Y.-J., M. Karuppiah, A. Shaw and G. Gupta (1999) Effect of simulated sunlight on atrazine and metolachlor toxicity of surface waters. *Ecotoxicol. Environ. Saf.* **43**, 35–37.
33. Konstantinou, I. K., A. K. Zarkadis and T. A. Albanis (2001) Photodegradation of selected herbicides in various natural waters and soils under natural conditions. *J. Environ. Qual.* **30**, 121–130.
34. Detenbeck, N. E., R. Hermanutz, K. Allen and M. C. Swift (1996) Fate and effects of the herbicide atrazine in flow-through wetland mesocosms. *Environ. Toxicol. Chem.* **15**, 937–946.
35. Oris, J. T., A. T. Hall and J. D. Tylka (1990) Humic acids reduce the photo-induced toxicity of anthracene to fish and daphnia. *Environ. Toxicol. Chem.* **9**, 575–583.
36. Zepp, R. G. (1988) Environmental photoprocesses involving natural organic matter. In *Humic Substances and their Role in the Environment* (Edited by F. H. Frimmel R. F. Christman), pp. 193–214. Wiley, New York.
37. Zeng, K., H. Hwang and H. Yu (2002) Effect of dissolved humic substances on the photochemical degradation rate of 1-aminopyrene and atrazine. *Int. J. Mol. Sci.* **3**, 1048–1057.
38. Scrano, L., S. A. Bufo, M. D'Auria, O. Meallier, A. Behechti and K. W. Shramm (2002) Photochemistry and photoinduced toxicity of Acifluorfen, a diphenyl-ether herbicide. *J. Environ. Qual.* **31**, 268–274.
39. Leo, A. J. (1993) Calculating log P_{oct} from structures. *Chem. Rev.* **93**, 1281–1306.
40. Neff, J. (1979) *Polycyclic Aromatic Hydrocarbons in the Aquatic Environment*. Applied Science Publishers, Essex, United Kingdom.
41. Mackay, D., W. Y. Shiu and K. C. Ma (1991a) *Illustrated Handbook of Physical-chemical Properties and Environmental Fate for Organic*

Chemicals. Volume I: Monoaromatic Hydrocarbons, Chlorobenzenes and PCBs. Lewis Publishers, Chelsea, MI.
42. Mackay, D., W. Y. Shiu and K. C. Ma (1991b) *Illustrated Handbook of Physical-chemical Properties and Environmental Fate for Organic Chemicals. Volume II: Polycyclic Aromatic Hydrocarbons, Polychlorinated Dioxins, and Dibenzofurans*. Lewis Publishers, Chelsea, Michigan.
43. Dabestani, R. and I. N. Ivanov (1999) A compilation of physical, spectroscopic and photophysical properties of polycyclic aromatic hydrocarbons. *Photochem. Photobiol.* **70**, 10–34.
44. Karydis, M. (1982) Toxicity of a photooxidised crude oil on two marine microalgae. *Bot. Mar.* **25**, 25–29.
45. Ren, L., X.-D. Huang, B. J. McConkey, D. G. Dixon and B. M. Greenberg (1994) Photoinduced toxicity to three polycyclic aromatic hydrocarbons (fluoranthene, pyrene and naphthalene) to the duckweed *Lemna gibba* L. G-3. *Ecotoxicol. Environ. Saf.* **28**, 160–171.
46. Arfsten, D. P., D. J. Schaffer and D. C. Mulveny (1996) The effects of near ultraviolet radiation on the toxic effects of PAH in animals and plants: A review. *Ecotox. Environ. Saf.* **33**, 1–24.
47. Nikkilä, A., S. Penttinen and J. V. K. Kukkonen (1999) UV-B induced acute toxicity of pyrene to the waterflea *Daphnia magna* in natural freshwaters. *Ecotoxicol. Environ. Saf.* **44**, 271–279.
48. Duxbury, C. I., D. G. Dixon and B. M. Greenberg (1997) The effects of simulated solar radiation on the bioaccumulation of polycyclic aromatic hydrocarbons by the duckweed *Lemna gibba*. *Environ. Toxicol. Chem.* **16**, 1739–1748.
49. Krylov, S. N., X.-D. Huang, L. F. Zeiler, D. G. Dixon and B. M. Greenberg (1997) Mechanism quantitative structure-activity relationship model for the photoinduced toxicity of polycyclic aromatic hydrocarbons. I. Physical model based on chemical kinetics in a two-compartment system. *Environ. Toxicol. Chem.* **16**, 2283–2295.
50. McConkey, B. J., C. L. Duxbury, D. G. Dixon and B. M. Greenberg (1997) Toxicity of a PAH photooxidation product to the bacteria *Photobacterium phosphoreum* and the duckweed *Lemna gibba*: Effects of phenanthrene and its primary photoproduct, phenanthrenequinone. *Environ. Toxicol. Chem.* **16**, 892–899.
51. Mallakin, A., B. J. McConkey, G. Miao, B. McKibben, V. Snieckus, D. G. Dixon and B. M. Greenberg (1999) Impacts of structural photomodification on the toxicity of environmental contaminants: Anthracene photooxidation products. *Ecotoxicol. Environ. Saf.* **43**, 204–212.
52. Newsted, J. L. and J. P. Giesy (1987) Predictive models for photoinduced acute toxicity of polycyclic aromatic hydrocarbons to *Daphnia magna*, Strauss (Cladocera, Crustacea). *Environ. Toxicol. Chem.* **6**, 445–461.
53. Boese, B. L., J. O. Lamberson, R. C. Swartz and R. J. Ozretich (1997) Photoinduced toxicity of fluoranthene to seven benthic crustaceans. *Arch. Environ. Contam. Toxicol.* **32**, 389–393.
54. Huovinen, P. S., M. R. Soimasuo and A. O. J. Oikari (2001) Photoinduced toxicity of retene to *Daphnia magna* under enhanced UV-B radiation. *Chemosphere* **45**, 683–691.
55. Monson, P. D., G. T. Ankley and P. A. Kosian (1995) Phototoxic response of *Lumbriculus variegates* to sediments contaminated by polycyclic aromatic hydrocarbons. *Environ. Toxicol. Chem.* **14**, 891–894.
56. Swartz, R. C., S. P. Ferraro, J. O. Lamberson, F. A. Cole, R. J. Ozretich, B. L. Boese, D. W. Schults, M. Behrenfeld and G. T. Ankley (1997) Photoactivation and toxicity of mixtures of polycyclic aromatic hydrocarbon compounds in marine sediment. *Environ. Toxicol. Chem.* **16**, 2151–2157.
57. Foote, C. S. (1991) Definition of type I and type II photosensitized oxidation. *Photochem. Photobiol.* **54**, 659.
58. Weinstein, J. W., J. T. Oris and D. H. Tayler (1997) An ultrastructural examination of the mode of UV-induced toxic action of fluoranthene in the fathead minnow, *Pimephales promelas*. *Aquat. Toxicol.* **39**, 1–22.
59. McCloskey, J. T. and J. T. Oris (1993) Effects of anthracene and solar ultraviolet radiation exposure on gill ATPase and selected hematologic measurements in bluegill sunfish (*Lepomis macrochirus*). *Aquat. Toxicol.* **24**, 207–218.
60. Sargian, P. (2005) Comportement des premiers maillons du réseau trophique marin exposés au rayonnement ultraviolet-B et aux contaminants dissous. Ph.D. thesis, Université du Québec à Rimouski, Quebec.
61. Vernet, M. (2000) Effects of UV radiation on the physiology and ecology of marine phytoplankton. In *The Effects of UV Radiation in the Marine Environment* (Edited by S. De Mora, S. Demers and M. Vernet), pp. 237–278. Cambridge Environmental Chemistry, University Press.
62. Mostajir, B., S. Demers, S. de Mora, C. Belzile, J.-P. Chanut, M. Gosselin, S. Roy, P. Zulema Villegas, J. Fauchot, J. Bouchard, D. Bird, P. Monfort and M. Levasseur (1999) Experimental test of the effect of ultraviolet-B radiation on a planktonic community. *Limnol. Oceanogr.* **44**, 586–596.
63. Lebaron, P., P. Servais, H. Agogué, C. Courties and F. Joux (2001) Does the high nucleic acid content of individual bacterial cells allow us to discriminate between active cells and inactive cells in aquatic systems? *Appl. Environ. Microbiol.* **67**, 1775–1782.
64. Siron, R., É. Pelletier and S. Roy (1996) Effects of dispersed and adsorbed crude oil on microalgal and bacterial communities of cold seawater. *Ecotoxicol.* **5**, 229–251.
65. Bagchi, M., D. Bagchi, J. Balmoori, X. Ye and S. J. Stohs (1998) Naphthalene-induced oxidative stress and DNA damage in cultured macrophage J774A.1 cells. *Free Rad. Biol. Med.* **25**, 137–143.
66. Payet, J. (2003) Effets combinés du rayonnement ultraviolet-B et des hydrocarbures dissous sur les communautés microbiennes d'un écosystème côtier naturel. M.S. thesis, Université du Québec à Rimouski, Québec.
67. Siron, R., É. Pelletier, D. Delille and S. Roy (1993). Fate and effects of dispersed crude oil under icy conditions simulated in mesocosms. *Mar. Environ. Res.* **35**, 273–302.
68. Roy, S., R. Siron and É. Pelletier (1991) Comparison of radiocarbon uptake and DCMU-fluorescence techniques in evaluating dispersed oil effects on phytoplankton photosynthetic activity. *Water Res.* **25**, 1249–1254.
69. Barbieri, E., V. Villafañe and E. W. Helbling (2002) Experimental assessment of UV effects on temperate marine phytoplankton when exposed to variable radiation regimes. *Limnol. Oceanogr.* **47**, 1648–1655.
70. Levasseur, M., J.-C. Therriault and L. Legendre (1984) Hierarchical control of phytoplankton succession by physical factors. *Mar. Ecol. Prog. Ser.* **19**, 211–222.
71. Ferreyra, G. (1995) Effets du rayonnement ultraviolet sur le plancton des régions froides tempérées et polaires. Ph.D. thesis, Université du Québec à Rimouski, Québec.
72. Roy, S., J.-P. Chanut, M. Gosselin and T. Sime-Ngando (1996) Characterization of phytoplankton communities in the lower St. Lawrence Estuary using HPLC-detected pigments and cell microscopy. *Mar. Ecol. Prog. Ser.* **142**, 55–73.
73. Duquesne, S. and M. Liess (2003) Increased sensitivity of the macroinvertebrate *Paramorea walkeri* to heavy-metal contamination in the presence of solar UV radiation in Antarctic shoreline waters. *Mar. Ecol. Prog. Ser.* **255**, 183–191.
74. Preston, B. L., T. W. Snell and R. Kneisel (1999) UV-B exposure increases acute toxicity of pentachlorophenol and mercury to the rotifer *Brachionus calycyflorus*. *Environ. Pollut.* **106**, 23–31.
75. Ray, L. C., B. Tyagi, P. K. Ray and N. Mallick (1998) Interactive effects of UV-B and heavy-metals (Cu and Pb) on nitrogen and phosphorus metabolism of a N_2-fixing cyanobacterium *Anabaena doliolum*. *Environ. Exp. Bot.* **39**, 221–231.
76. Maguire, R. J. (2000) Review of the persistence, bioaccumulation and toxicity of tributyltin in aquatic environments in relation to Canada's Toxic Substances Management Policy. *Wat. Qual. Res. J. Can.* **35**, 633–679.
77. Huang, G., S. Dai and H. Sun (1996) Toxic effects of organotin species on algae. *Appl. Organomet. Chem.* **10**, 377–387.
78. Sidharthan, M., K. S. Young, L. H. Woul, P. K. Soon and H. W. Shin (2002) TBT toxicity on the marine microalga *Nannochloropsis oculata*. *Mar. Pollut. Bull.* **45**, 177–182.
79. Cooney, J. J. and S. Wuertz (1989) Toxic effects of tin compounds on microorganisms. *J. Ind. Microbiol.* **4**, 375–402.
80. Viglino, L., É. Pelletier and R. St-Louis (2004) Highly persistent butyltins in northern marine sediments: A long-term threat for the Saguenay Fjord (Canada). *Environ. Toxicol. Chem.* **23**, 2673–2681.
81. Navio, J. A., F. J. Marchena and C. Cerrillos (1993) UV photolytic degradation of butyltin chlorides in water. *J. Photochem. Photobiol. A. Chem.* **71**, 97–102.

82. Bruland, K. W., J. R. Donat and D. A. Hutchins (1991) Interactive influences of bioactive trace metals on biological production in oceanic waters. *Limnol. Oceanogr.* **36**, 1555–1577.
83. Hay, M. E., Q. E. Kappel and W. Fenical (1994). Synergisms in plant defenses against herbivores: Interactions of chemistry, calcification, and plant quality. *Ecology* **75**, 1714–1727.
84. Soluk, D. A. (1993) Multiple predator effects: Predicting combined functional response of stream fish and invertebrate predators. *Ecology.* **74**, 219–225
85. Folt, C. L., C. Y. Chen, M. V. Moore and J. Burnaford (1999) Synergism and antagonism among multiple stressors. *Limnol. Oceanogr.* **44**, 864–877.
86. Moore, M. V. and C. L. Folt (1993) Zooplankton body size and community structure: Effects of thermal and contaminant stress. *Trends Ecol. Evol.* **8**, 178–183.
87. Hanazota, T. (1998) Response of a zooplankton community to insecticide application in experimental ponds: A review and the implications of the effects of chemicals on the structure and functioning of freshwater communities. *Environ. Pollut.* **101**, 361–373.
88. Vinebrooke, R. D., K. L. Cottingham, J. Norberg, M. Scheffer, S. I. Dodson, S. C. Maberly and U. Sommer (2004) Impacts of multiple stressors on biodiversity and ecosystem functioning: The role of species co-tolerance. *Oikos* **104**, 451–457.